ISSN 1007-9327 (print)
ISSN 2219-2840 (online)

World Journal of *Gastroenterology*

World J Gastroenterol 2021 January 7; 27(1): 1-142



Published by Baishideng Publishing Group Inc

World Journal of Gastroenterology

Contents

Weekly Volume 27 Number 1 January 7, 2021

REVIEW

1 Experimental models of metabolic and alcoholic fatty liver disease

Buyco DG, Martin J, Jeon S, Hooks R, Lin C, Carr R

19 Human hepatitis viruses-associated cutaneous and systemic vasculitis

Wang CR, Tsai HW

MINIREVIEWS

37 Lipidome is lipids regulator in gastrointestinal tract and it is a life collar in COVID-19: A review

Koriem KMM

ORIGINAL ARTICLE

Basic Study

55 Long non-coding ribonucleic acid W5 inhibits progression and predicts favorable prognosis in hepatocellular carcinoma

Lei GL, Fan HX, Wang C, Niu Y, Li TL, Yu LX, Hong ZX, Yan J, Wang XL, Zhang SG, Ren MJ, Yang PH

Retrospective Study

69 Predictors of pain response after endoscopic ultrasound-guided celiac plexus neurolysis for abdominal pain caused by pancreatic malignancy

Han CQ, Tang XL, Zhang Q, Nie C, Liu J, Ding Z

80 Evaluation of controlled attenuation parameter in assessing hepatic steatosis in patients with autoimmune liver diseases

Ni XX, Lian M, Wu HM, Li XY, Sheng L, Bao H, Miao Q, Xiao X, Guo CJ, Li H, Ma X, Hua J

92 Valuable clinical indicators for identifying infantile-onset inflammatory bowel disease patients with monogenic diseases

Su W, Yu Y, Xu X, Wang XQ, Huang JB, Xu CD, Xiao Y

Randomized Controlled Trial

107 Effect of probiotic *Lactobacillus plantarum* Dad-13 powder consumption on the gut microbiota and intestinal health of overweight adults

Rahayu ES, Mariyatun M, Putri Manurung NE, Hasan PN, Therdtatha P, Mishima R, Komalasari H, Mahfuzah NA, Pamungkaningtyas FH, Yoga WK, Nurfiana DA, Liwan SY, Juffrie M, Nugroho AE, Utami T

CASE REPORT

129 Spontaneous regression of gastric gastrinoma after resection of metastases to the lesser omentum: A case report and review of literature

Okamoto T, Yoshimoto T, Ohike N, Fujikawa A, Kanie T, Fukuda K

World Journal of Gastroenterology

Weekly Volume 27 Number 1 January 7, 2021

Contents

ABOUT COVER

Editorial Board Member of *World Journal of Gastroenterology*, King-Wah Chiu is a Distinguished Professor at the Cheng Shui University in Kaohsiung, Taiwan, Republic of China. Having received his Bachelor's degree from China Medical University College of Medicine in 1985, he rose to Chief in the Gastroenterology Division of the Kaohsiung Chang Gung Memorial Hospital Affiliated to Chang Gung University of College of Medicine in 2002. Dr. Chiu is a recognized expert in hepato-gastroenterology, having practiced for 30 years, and the pioneer of transplant hepatology in the field of liver transplantation, practicing in Kaohsiung Chang Gung Memorial Hospital since 1998. His ongoing research interests involve the application of molecular biology in transplant hepatology, particularly to study the effects of integrative basic medicine on and management of living-donor liver transplantation establishment. (L-Editor: Filipodia)

AIMS AND SCOPE

The primary aim of *World Journal of Gastroenterology* (*WJG*, *World J Gastroenterol*) is to provide scholars and readers from various fields of gastroenterology and hepatology with a platform to publish high-quality basic and clinical research articles and communicate their research findings online. *WJG* mainly publishes articles reporting research results and findings obtained in the field of gastroenterology and hepatology and covering a wide range of topics including gastroenterology, hepatology, gastrointestinal endoscopy, gastrointestinal surgery, gastrointestinal oncology, and pediatric gastroenterology.

INDEXING/ABSTRACTING

The *WJG* is now indexed in Current Contents®/Clinical Medicine, Science Citation Index Expanded (also known as SciSearch®), Journal Citation Reports®, Index Medicus, MEDLINE, PubMed, PubMed Central, and Scopus. The 2020 edition of Journal Citation Report® cites the 2019 impact factor (IF) for *WJG* as 3.665; IF without journal self cites: 3.534; 5-year IF: 4.048; Ranking: 35 among 88 journals in gastroenterology and hepatology; and Quartile category: Q2.

RESPONSIBLE EDITORS FOR THIS ISSUE

Production Editor: *Yu-Jie Ma*; **Production Department Director:** *Xiang Li*; **Editorial Office Director:** *Ze-Mao Gong*.

NAME OF JOURNAL
World Journal of Gastroenterology

ISSN
ISSN 1007-9327 (print) ISSN 2219-2840 (online)

LAUNCH DATE
October 1, 1995

FREQUENCY
Weekly

EDITORS-IN-CHIEF
Andrzej S Tarnawski, Subrata Ghosh

EDITORIAL BOARD MEMBERS
http://www.wjgnet.com/1007-9327/editorialboard.htm

PUBLICATION DATE
January 7, 2021

COPYRIGHT
© 2021 Baishideng Publishing Group Inc

INSTRUCTIONS TO AUTHORS
https://www.wjgnet.com/bpg/gerinfo/204

GUIDELINES FOR ETHICS DOCUMENTS
https://www.wjgnet.com/bpg/GerInfo/287

GUIDELINES FOR NON-NATIVE SPEAKERS OF ENGLISH
https://www.wjgnet.com/bpg/gerinfo/240

PUBLICATION ETHICS
https://www.wjgnet.com/bpg/GerInfo/288

PUBLICATION MISCONDUCT
https://www.wjgnet.com/bpg/gerinfo/208

ARTICLE PROCESSING CHARGE
https://www.wjgnet.com/bpg/gerinfo/242

STEPS FOR SUBMITTING MANUSCRIPTS
https://www.wjgnet.com/bpg/GerInfo/239

ONLINE SUBMISSION
https://www.f6publishing.com

© 2021 Baishideng Publishing Group Inc. All rights reserved. 7041 Koll Center Parkway, Suite 160, Pleasanton, CA 94566, USA

E-mail: bpgoffice@wjgnet.com https://www.wjgnet.com

World Journal of Gastroenterology

Submit a Manuscript: https://www.f6publishing.com

World J Gastroenterol 2021 January 7; 27(1): 1-18

DOI: 10.3748/wjg.v27.i1.1

ISSN 1007-9327 (print) ISSN 2219-2840 (online)

REVIEW

Experimental models of metabolic and alcoholic fatty liver disease

Delfin Gerard Buyco, Jasmin Martin, Sookyoung Jeon, Royce Hooks, Chelsea Lin, Rotonya Carr

ORCID number: Delfin Gerard Buyco 0000-0001-5477-0316; Jasmin Martin 0000-0002-6581-2005; Sookyoung Jeon 0000-0002-3620-0851; Royce Hooks 0000-0003-0899-9907; Chelsea Lin 0000-0003-3696-121X; Rotonya Carr 0000-0003-0235-6994.

Author contributions: Buyco DG wrote the first draft of the paper; Buyco DG, Martin J, Jeon S, Hooks R, Lin C and Carr RM performed the research for the manuscript and edited all drafts of the paper.

Conflict-of-interest statement: The authors report no conflicts of interest.

Open-Access: This article is an open-access article that was selected by an in-house editor and fully peer-reviewed by external reviewers. It is distributed in accordance with the Creative Commons Attribution NonCommercial (CC BY-NC 4.0) license, which permits others to distribute, remix, adapt, build upon this work non-commercially, and license their derivative works on different terms, provided the original work is properly cited and the use is non-commercial. See: http://creativecommons.org/Licenses/by-nc/4.0/

Manuscript source: Unsolicited Manuscript

Specialty type: Gastroenterology and hepatology

Delfin Gerard Buyco, Jasmin Martin, Sookyoung Jeon, Royce Hooks, Chelsea Lin, Rotonya Carr, Division of Gastroenterology, University of Pennsylvania, Philadelphia, PA 19104, United States

Corresponding author: Rotonya Carr, MD, Assistant Professor, Division of Gastroenterology, University of Pennsylvania, 421 Curie Boulevard 907 Biomedical Research Center, Philadelphia, PA 19104, United States. rotonya.carr@pennmedicine.upenn.edu

Abstract

Non-alcoholic fatty liver disease (NAFLD) is a multi-systemic disease that is considered the hepatic manifestation of metabolic syndrome (MetS). Because alcohol consumption in NAFLD patients is common, there is a significant overlap in the pathogenesis of NAFLD and alcoholic liver disease (ALD). Indeed, MetS also significantly contributes to liver injury in ALD patients. This "syndrome of metabolic and alcoholic steatohepatitis" (SMASH) is thus expected to be a more prevalent presentation in liver patients, as the obesity epidemic continues. Several pre-clinical experimental models that couple alcohol consumption with NAFLD-inducing diet or genetic obesity have been developed to better understand the pathogenic mechanisms of SMASH. These models indicate that concomitant MetS and alcohol contribute to lipid dysregulation, oxidative stress, and the induction of innate immune response. There are significant limitations in the applicability of these models to human disease, such as the ability to induce advanced liver injury or replicate patterns in human food/alcohol consumption. Thus, there remains a need to develop models that accurately replicate patterns of obesogenic diet and alcohol consumption in SMASH patients.

Key Words: Non-alcoholic fatty liver disease; Alcoholic liver disease; Non-alcoholic steatohepatitis; Animal models; Insulin resistance; Oxidative stress

©The Author(s) 2021. Published by Baishideng Publishing Group Inc. All rights reserved.

Core Tip: Experimental animal and cell culture models have been developed to study the "syndrome of metabolic and alcoholic steatohepatitis" (SMASH), in which concomitant non-alcoholic fatty liver disease and alcoholic liver disease risk factors play a role in liver injury. These models demonstrate that obesity, metabolic syndrome, and alcohol consumption synergistically contribute to lipid dysregulation, oxidative stress, inflammation, and fibrogenesis. The pathogenesis of SMASH in these

Country/Territory of origin: United States

Peer-review report's scientific quality classification
Grade A (Excellent): 0
Grade B (Very good): 0
Grade C (Good): C
Grade D (Fair): 0
Grade E (Poor): 0

Received: September 3, 2020
Peer-review started: September 3, 2020
First decision: October 17, 2020
Revised: November 1, 2020
Accepted: December 6, 2020
Article in press: December 6, 2020
Published online: January 7, 2021

P-Reviewer: Jin H
S-Editor: Zhang H
L-Editor: A
P-Editor: Liu JH



experimental models is dependent on obesogenic diet composition, alcohol consumption patterns, alcohol dosage, and genetic background.

Citation: Buyco DG, Martin J, Jeon S, Hooks R, Lin C, Carr R. Experimental models of metabolic and alcoholic fatty liver disease. *World J Gastroenterol* 2021; 27(1): 1-18
URL: https://www.wjgnet.com/1007-9327/full/v27/i1/1.htm
DOI: https://dx.doi.org/10.3748/wjg.v27.i1.1

INTRODUCTION

The two most common causes of liver disease worldwide are non-alcoholic fatty liver disease (NAFLD) and alcoholic liver disease (ALD)[1]. NAFLD is a multi-system disease whose major risk factors are genetic susceptibility, obesity, insulin resistance, and metabolic syndrome (MetS). MetS is the constellation of obesity, insulin resistance, hypercholesterolemia, hypertriglyceridemia, and hypertension; and NAFLD is considered the hepatic manifestation of MetS[2-4]. ALD also has a multi-factorial etiology, including alcohol consumption quantity and pattern, environmental factors, and genetics. Alcohol consumption patterns can be described in terms of long-term (chronic) or acute (binge) drinking episodes.

Clinicians recognize the existence of an overlap condition between NAFLD and ALD, despite the absence of significant alcohol intake in NAFLD diagnostic criteria[5]. For example, among ALD patients, obesity increases the likelihood for the development of alcoholic cirrhosis[6], while both long-term alcohol consumption and obesity have been found to independently promote advanced fibrosis[7]. Obesity and MetS also increase mortality in ALD[8]. Obesity, insulin resistance, and MetS are the most significant contributors to ALD severity, with as many as 50% of ALD patients estimated to have liver disease as a consequence of both alcohol overconsumption and obesity[9,10]. Obese individuals who overconsume alcohol are more likely to develop hepatic steatosis and cirrhosis compared to normal weight individuals[7]. As the obesity epidemic persists, this "syndrome of metabolic and alcoholic steatohepatitis" or SMASH is expected to become a more common presentation in liver patients[11].

Several experimental models have been developed to understand the metabolic factors that exacerbate liver disease in patients with coexistent NAFLD and ALD risk factors. Studies that incorporated both obesogenic diet (*e.g.*, high-fat, high-fructose) or genetic obesity and some form of alcohol consumption in a rodent model were included in this critical review, while human retrospective studies, human clinical trials, and *in vitro* models were excluded. While these models couple NAFLD risk factors with alcohol exposure, they differ in the animal genetic background, obesogenic diet composition, type and duration of alcohol consumption, and ability to induce significant liver injury. Here, we review the pre-clinical experimental models developed to study the interactive effects of NAFLD and ALD risk factors on hepatic injury, as well as limitations of the various models with regards to human disease.

PATHOLOGICAL OVERLAP BETWEEN NAFLD AND ALD

Lipid dysregulation

Lipid metabolism dysregulation is a key factor in the pathogenesis of NAFLD and ALD. *De novo* lipogenesis and fatty acid oxidation (FAO) are implicated in NAFLD pathogenesis, although lipid uptake, storage, and export also play a role[12]. Meanwhile, experimental models indicate that alcohol (EtOH) consumption further exacerbates lipid dysregulation in MetS. AMP-activated protein kinase (AMPK) is a key regulator of lipid metabolism, and its inhibition has been implicated in both NAFLD and ALD[13-15]. AMPK has reciprocal effects on *de novo* lipogenesis and fatty acid (FA) uptake through the regulation of the transcription factor sterol response element binding protein 1 (SREBP-1)[16]. SREBP-1 is upregulated in NAFLD patients and in high-fat diet (HFD)-induced NAFLD rodent models[17]. Pharmacological inhibition of SREBP-1 increases insulin sensitivity and suppresses FA synthesis[18]. AMPK also modulates FAO by regulating peroxisome proliferator-activated receptor

(PPAR) α and sirtuin 1 (SIRT-1), the latter of which is inhibited by EtOH consumption[19-22]. FAO is induced in NAFLD as a compensatory effect of increased lipid uptake and *de novo* lipogenesis[23]. In obese patients, EtOH is also known to increase adiponectin levels, which induces AMPK activation[24].

Oxidative stress

NAFLD risk factors and EtOH consumption also contribute to oxidative stress in fatty liver disease by dysregulating oxidative biochemical processes and producing reactive oxygen species (ROS). Obesogenic diet contributes to the formation of ROS such as hydrogen peroxide (H_2O_2), superoxide (O_2-), 4-hydroxynonenal (4-HNE), malondialdehyde (MDA), and oxysterols as byproducts of FAO[25]. EtOH metabolism by alcohol and acetaldehyde dehydrogenases, and cytochrome P450 2E1 (CYP2E1) also produces ROS[26]. CYP2E1, in particular, is implicated in the pathogenesis of both NAFLD and ALD in humans[5,27]. CYP2E1 metabolizes EtOH and other xenobiotics in a nicotinamide adenine dinucleotide phosphate ($NADP^+$/NADPH)-mediated process and produces H_2O_2 and O_2^-[28]. Mouse models also indicate that CYP2E1 plays a role in lipid dysregulation[29] and diabetes[30]. Inhibition of CYP2E1 has been found to be protective against lipid metabolism dysregulation and oxidative stress induced by combined FA and EtOH treatment *in vitro*[31].

Concomitant NAFLD risk factors and EtOH consumption also dysregulate the unfolded protein response (UPR), resulting in the production of ROS in the endoplasmic reticulum (ER)[32]. In the UPR, misfolded proteins sequester binding immunoglobulin protein (BIP), inducing the protein kinase R-like ER kinase (PERK), activating transcription factor 6 (ATF-6), and inositol-requiring kinase (IRE-1) transduction pathways. The UPR involves the formation of disulfide bonds, an oxidative process that produces H_2O_2 and other ROS[32]. Protein folding dysregulation is associated with oxidative stress in fatty liver disease[33]; saturated FA, oleic acid, and cholesterol interact with the UPR and induce ER stress[34]. Lipids and EtOH have a reciprocal relationship with the ER: PERK induces protein and lipid metabolism, and apoptosis, while ATF-6 and IRE-1 mediate protein trafficking and inflammation[35,36].

Three enzymes are key to the elimination of ROS: Superoxide dismutase (SOD) metabolizes O_2- to O_2 and H_2O_2; while catalase and glutathione peroxidase (GPx) metabolize H_2O_2 to O_2 and H_2O[37,38]. H_2O_2 oxidation by GPx is coupled to the metabolism of reduced glutathione (GSH) to oxidized glutathione disulfide (GSSG). GSSG is reduced back to GSH by glutathione reductase (GR), which requires NADPH[39,40]. Clinical observations indicate that patients with NAFLD have increased SOD, GPx, and GR activities, as well as elevated levels of GSH[41,42]. Similarly, patients with ALD have upregulated SOD activity[43], although GSH/GSSG ratio is decreased[44].

Immune response

Macrophage and neutrophil activation play important roles in liver injury in the context of MetS and EtOH consumption[45,46]. Macrophages adopt a number of functional states that are traditionally categorized into two groups. Pro-inflammatory M1 polarization is distinguished by the presence of cell surface marker CD68, and secretion of interleukin (IL) 6, tumor necrosis factor α (TNFα), and other cytokines. Conversely, anti-inflammatory M2 polarization is distinguished by CD163, transforming growth factor β (TGFβ), IL-10, and arginase 1 (ARG-1)[47]. Saturated FAs and cholesterol are known to induce a predominantly M1-like phenotype in Kupffer cells, liver-resident macrophages[48]. M1 polarization is associated with severity of disease, CD68+ Kupffer cells, and TNFα expression were both found to be significantly higher in non-alcoholic steatohepatitis (NASH) patients compared to patients with simple steatosis[49]. However, CD45+ leukocytes and CD163+ Kupffer cells are also increased in pediatric NAFLD patients[50]. Meanwhile, hepatocyte damage in ALD increases lipopolysaccharide (LPS) leakage into the liver by enhancing intestinal permeability, resulting in TNFα and IL-10 secretion by Kupffer cells[51,52]. The two-state model of macrophage polarization may thus be insufficient to describe immune response under concomitant NAFLD and ALD risk factors. Kupffer cells also release IL-1β in response to hepatic tissue damage and necrosis, which results in neutrophil recruitment from bone marrow to the liver[53]. Neutrophil infiltration, distinguished by upregulation in TNFα, IL-1, and osteopontin (OPN), contributes to hepatocyte death and correlates with ALD severity[54].

Apoptosis and fibrosis

NAFLD pathogenesis involves hepatocellular apoptosis, which occurs *via* the extrinsic

and intrinsic pathways. In the intrinsic pathway, apoptosis occurs as a result of cellular, ER, or mitochondrial stress[55]. In the extrinsic pathway, apoptosis arises as a response to extracellular signaling[56]. One particularly important extrinsic mechanism in NAFLD is the tumor necrosis factor α (TNFα) pathway. TNFα activates anti-apoptotic NF-κB and apoptotic caspase-3[57,58].

Oxidative stress, inflammation, and hepatocyte apoptosis contribute to hepatic fibrosis in NAFLD and ALD, and these pathways are mediated by hepatic stellate cells (HSC)[59]. One important fibrogenic mechanism in NAFLD and ALD is the TGFβ pathway, which induces the expression of collagens, a component of extracellular matrix (ECM), *via* the signal transducer SMAD-3. Another important signaling pathway is that of toll-like receptor 4 (TLR-4), which responds to LPS, and produces pro-inflammatory cytokines[60,61]. TLR-4 is upregulated in obese patients with NAFLD[62]; and in patients with ALD, alcohol increases gut permeability and promotes LPS-producing Gram-negative bacteria[63]. However, in one study, mRNA expression of TLR-4 tended to decrease in biopsy-diagnosed NAFLD patients who drank at most 20 g/kg/d EtOH compared to those who did not drink[64]. Activated HSCs also produce tissue inhibitor of metalloproteinases (TIMP), which inhibits ECM-degrading matrix metalloproteinases (MMPs)[65].

EXPERIMENTAL MODELS OF NAFLD AND ALD

Despite the pathological overlap between NAFLD and ALD, most studies model NAFLD risk factors and EtOH consumption independent of each other. Although individually these models are limited in their capacity to recapitulate SMASH pathogenesis, they form the foundation for many SMASH models.

NAFLD models

A variety of animal models have been proposed for studying NAFLD, which can be largely divided into three categories: dietary, genetic, and combined models. Dietary manipulations can induce NAFLD development by using obesogenic or nutrient-deficient diets[66]. Obesogenic diets are typically rich in fat with additional sugar and/or cholesterol, representing metabolic and histological features of human NAFLD. There are a number of obesogenic diets, varying in the macronutrient composition, sources of fat, types of sugar, and cholesterol content. Nutrient-deficient diets, such as methionine- and choline-deficient, and choline-deficient L-amino acid-defined (CDAA) diets, are also capable of inducing NAFLD[66-68]. Choline-deficient and CDAA diets are used because methionine and choline are required for phosphatidylcholine synthesis, and are thus intimately involved in lipoprotein synthesis, lipid storage, and lipid regulation[69]. Nutrient-deficient diets can rapidly induce NAFLD within a few weeks of feeding, but some metabolic features including body weight, hyperglycemia, and insulin sensitivity do not manifest as they do in human NAFLD.

Various genetic animal models have also been created to study NAFLD, and are especially valuable for studying the mechanisms of NAFLD pathogenesis[67,70]. Genetic mouse models of NAFLD include leptin-deficient (ob/ob), leptin receptor-deficient (db/db), insulin resistant (KK-A^{y}), SREBP-1c transgenic, PPARα null, phosphatase and tensin homolog (PTEN) null, and acyl-coenzyme A oxidase (ACOX) null mice. For rats, genetic models include leptin receptor-deficient (fa/fa) and cholecystokinin knockout (OLETF). Dietary and genetic models are also combined to replicate the multifactorial nature of human NAFLD. A detailed discussion of NAFLD animal models is beyond the scope of this review and described in other reviews[66-68,70].

ALD models

Pre-clinical models have also been developed to understand the pathogenesis of ALD. EtOH can be administered to animals either orally or intravenously. Four models have been developed for studying ALD: (1) Binge feeding, in which animals are acutely administered EtOH by gavage; (2) Chronic feeding, in which animals are given access to EtOH through diet or drinking water for a prolonged period of time (*e.g.*, Lieber-DeCarli diet model[71]); (3) Intragastric (iG) infusion feeding (*e.g.*, Tsukamoto-French model[72-74]); and (4) Chronic-binge feeding, in which animals are given chronic EtOH for a certain period of time, then administered EtOH acutely (*e.g.*, Gao model[75,76]). Variations in these models exist, such as multiple binge feeding and combined models. In addition, experimental models vary in EtOH concentration and feeding period. Animal models should thus be selected depending on the purpose of the study, as

there have been no animal models that fully recapitulate the full spectrum of ALD.

EXPERIMENTAL MODELS OF SMASH

Experimental rodent models (Table 1) of SMASH couple one of the dietary or genetic models of NAFLD described above with EtOH consumption models of ALD. While obesity and EtOH consumption models vary considerably, studies that combine the two generally indicate a synergistic increase in steatosis, inflammation, and fibrosis by obesity and EtOH.

Dietary models of SMASH

The most common type of dietary SMASH model couples HFD with either chronic or binge (acute) EtOH consumption. For example, Gäbele *et al*[77] gave Balb/c mice *ad libitum* access to either chow diet or HFD, along with water or 5% EtOH in drinking water. HFD-EtOH diet upregulated TNFα, TGFβ, collagen I, α smooth muscle actin (αSMA) expression, synergistically contributing to inflammation and fibrosis. HFD upregulated TLR-4 expression, but EtOH did not have an effect on TLR-4. However, combined HFD-EtOH increased serum LPS levels and had increased fibrosis compared to the other groups, suggesting that obesity increases LPS sensitivity by upregulating TLR-4, while EtOH promotes fibrosis by increasing intestinal permeability and LPS leakage.

Wang *et al*[78] used high-fat (HF) Lieber-DeCarli (LD) diet and observed increased inflammation and apoptosis in HF-EtOH treated rats. Sprague-Dawley rats were given *ad libitum* access to control LD or HF LD diet for 6 wk. The HF LD-fed rats were then given either HF LD and HF-EtOH LD for another 4 wk. HF-EtOH LD increased hepatic steatosis and number of inflammatory foci compared to controls. HF-EtOH LD also increased TUNEL+ apoptotic hepatocytes compared to control diet, but EtOH did not significantly affect TUNEL+ hepatocyte count, suggesting that obesogenic diet contributes more to apoptosis than EtOH in this model. There was no difference in B-cell lymphoma (BCL) 2 or BCL-2-associated X protein (Bax) between the groups, while Fas death receptor and Fas ligand were upregulated in the HF-EtOH LD group, suggesting that hepatocyte apoptosis occurs *via* the extrinsic pathway in SMASH.

Similarly, Gopal *et al*[79] developed a model using both solid diet and LD to determine the effect of exogenous SOD-1 on inflammation and fibrosis in SMASH. C57BL/6 mice were fed either chow or HFD for 10 wk, then either control LD or 5% EtOH LD for an additional 4 wk. The HFD-fed mice were also administered SOD-1 for 2 wk. HFD-EtOH upregulated CYP2E1, ADH, catalase, FA oxidizing ACOX-1, pro-inflammatory CCL-2, and pro-fibrotic MMP-12 compared to controls. These results corroborate the findings in the other aforementioned HFD-EtOH models that dietary obesity and EtOH both contribute to lipid dysregulation, inflammation, and fibrosis. SOD-1 treatment attenuated the increases in CYP2E1, ADH, CCL-2, and MMP-12, but further upregulated catalase, PPARα, and ACOX-1. The effects of SOD indicate that dysregulation of antioxidant mechanisms plays a role in SMASH pathogenesis, but targeting these mechanisms pharmacologically may have adverse effects on lipid metabolism (Figure 1).

The aforementioned models used chronic EtOH feeding to induce liver injury, but Duly *et al*[80] took a different approach to modeling SMASH by coupling HFD to repeated binge EtOH consumption. C57BL/6 mice were fed chow or HFD for 12 wk, and administered saline or 2 g EtOH/kg BW twice per week. ALT/AST activity did not differ between experimental groups, but HFD-EtOH increased hepatic TG levels compared to controls. HFD-EtOH also upregulated SREBP-1 and stearoyl-CoA desaturase 1, a transcriptional target of SREBP-1 involved in FA synthesis[16], compared to controls. HFD-EtOH also increased vimentin+ cells in the hepatic parenchyma and collagen deposition compared to controls, but did not affect expression of pro-fibrotic collagen I, TGFβ, and plasminogen activator inhibitor (PAI-1). These results suggest that obesity and EtOH synergistically contribute to lipid dysregulation and fibrosis, although through a yet unknown mechanism. The application of this study to human disease is also limited because HFD alone did not promote TG accumulation, a diagnostic criterion for NAFLD.

HFD intragastric infusion is also used in overfeeding models of SMASH. For example, Lazaro *et al*[81] fed C57BL/6 mice high saturated fat, high cholesterol (HFHC) diet for 2 wk, then liquid HFD or HFD-EtOH by intragastric infusion for 8 wk, with some HFD-EtOH-fed mice also receiving additional EtOH by gavage. HFHC and chronic-binge EtOH upregulated myeloperoxidase, CXCL-1, and OPN, and increased

Table 1 Experimental studies modeling the effect of metabolic syndrome risk factors and alcohol consumption on liver injury outcomes in rodent and cell culture models

Ref.	Experimental model details	Biochemistry	Anatomy and histology	mRNA and protein expression
Alwahsh *et al*[84]	(1) Animal: 10 wk male Sprague- Dawley rat; (2) Initial weight: 270-310 g; (3) Diet: LD control, LD with 30% kcal from fructose, 30% kcal from EtOH, or LD with both fructose and EtOH; and (4) Duration: 28 d	(1) ↑ ALT; (2) ↑ liver and plasma TG; (3) ↑ plasma leptin; (4) ↓ plasma HDL; (5) ↓ plasma albumin; and (6) No dif. in leptin or hepatic TG between LD-EtOH and LD- fructose-EtOH	(1) Portal inflammatory infiltration and stage 1 fibrosis (LD-EtOH); (2) Periportal macrosteatosis (LD-fructose); and (3) Portal inflammation, periportal macrosteatosis, fibrosis (LD-fructose-EtOH)	(1) ↑ leptin; (2) ↑ ACC-2; (3) ↑ lipase in LD-EtOH, but ↓ in LD-fructose and LD-fructose-EtOH; (4) ↓ IRS-1, IRS-2 (fructose groups); and (5) ↑ CD36, CPT-1α, PPARα in LD- EtOH and LD-fructose, but no change in LD-fructose-EtOH
Bucher *et al*[112]	(1) Animal: 7 wk male C57BL/6J Mouse; (2) Initial weight: 20-23 g; (3) Diet: Control (3 kcal/g food; 16% kcal protein) or HFD (5.5 kcal/g; 60% kcal SFA); 10 g/kg/d EtOH in drinking water; and (4) Duration: 4 mo	(1) ↑ ALT, but ↓ ALT compared to EtOH-naïve HFD; (2) ↑ cholesterol, but ↓ cholesterol compared to EtOH-naïve HFD; (3) ↑ TG↑ serum glucose; (4) ↑ serum insulin; and (5) ↑ MUFA and ↓ SFA (compared to HFD)	(1) Mediovesicular and macrovacular steatosis and (2) No dif. in necroinflammation or perisinusoidal fibrosis between HFD and HFD-EtOH	(1) ↑ genes for apoptosis inhibition, acetyl-CoA synthesis, lipogenesis, mitochondrial functions (NADH dehydrogenase, COX, ATP synthase), and proteolysis; (2) ↓ genes for apoptosis (BCL-2 homologs), fibrosis (collagen), chemotaxis, oxidative stress (GPx, HMOX-1, SOD); and (3) ↓ CYP2E1 protein levels
Carmiel-Haggai *et al*[94]	(1) Animal: 15 wk male fa/fa Zucker Rat; (2) Initial weight: 595 ± 35 g (obese), 316 ± 32 g (lean controls); and (3) Diet: 35% v/v EtOH in saline every 12 h for 3 d; final dose was 4 g/kg EtOH	(1) ↑ ALT; (2) ↑ NEFA; (3) ↑ LPO by-products (4-HNE, MDA); and (4) ↓ CYP2E1 activity	(1) Macrovesicular steatosis (EtOH-naïve fa/fa) and (2) Lobular microvesicular, central macrosteatosis, inflammation (EtOH-fed fa/fa)	(1) ↓ GSH, GPx, GR; (2) ↓ GSSG (EtOH-fed and EtOH-naïve fa/fa); (3) ↓ catalase, SOD; (4) ↑ iNOS; (5) ↑ caspase 3, caspase 8; (6) ↑ BCL-XL, FAS ligand; and (7) ↑ BCL-2, BAX (EtOH-fed and EtOH-naïve fa/fa)
Duly *et al*[80]	(1) Animal: 6-8 wk male C57BL/6 Mouse; (2) Initial weight: 20 g; (3) Diet: chow (12% kcal fat) or HFD (45% kcal fat, 0.25% cholesterol); 2 g/kg EtOH in saline twice per wk; and (4) Duration: 12 wk	(1) ↑ TG (chow-EtOH, but not HFD or HFD-EtOH); (2) ↑ cholesterol, HDL, LDL (but no difference between HFD and HFD- EtOH); and (3) ↑ serum insulin	(1) Steatosis and lipid accumulation; (2) Collagen deposition; (3) ↑ cellular infiltration; (4) ↑ CD45+ leukocytes; (5) ↑ F4/80+ Kupffer cells; and (6) ↑ vimentin+ HSCs	(1) ↑ SREBP-1; (2) ↑ SCD-1; (3) ↑ PPARα; (4) ↓ ACOX-1; (5) No dif. in TGFβ or HSP90; and (6) ↑ collagen I, PAI-1 (EtOH-naïve HFD)
Everitt *et al*[87]	(1) Animal: 12 wk male ob/ob C57BL/6-J/Rj-ob mouse; (2) Diet: PUFA-enriched LD with 27.5% EtOH or isocaloric maltodextrin; and (3) Duration: 4 wk	(1) ↑ ALT/AST; (2) ↑ hepatic TG; (3) ↑ hepatic cholesterol; (4) ↑ hepatic lactate; (5) ↓ hepatic pyruvate; (6) No dif. in BAL between EtOH-fed; and (7) ob/ob and EtOH-fed lean mice	Steatosis in EtOH-fed ob/ob	(1) ↑ mTOR, PPARγ, FGF-21, FSP-27; (2) ↑ SIRT-1, pAMPKα, AMPKα, pACC (ob compared to lean; EtOH did not have an effect); (3) ↑ adipose TNFα, ↓ hepatic TNFα; (4) ↑ cytosolic lipin-1 protein levels; (5) ↓ nuclear lipin-1 protein levels; (6) ↓ PGC-1α; and (7) ↓ ACOX-1
Gäbele *et al*[77]	(1) Animal: 12 wk female Balb/c mouse; (2) Diet: Chow or HFD [17% fat (50% lard, 50% cacao-butter), 1.25% cholesterol, 0.5% cholate]; 5% EtOH in *ad libitum*; and (3) Duration: 6 wk	(1) ↑ hepatic TG; (2) ↑ portal blood LPS; and (3) ↓ BAL (not statistically significant)	(1) Steatosis in HFD-fed mice; (2) ↑ 4-HNE; (3) ↑ αSMA+ cells; (4) ↑ collagen I; and (5) ↑ ECM deposition	(1) ↑ p47phox, TNF, TGFβ, collagen I; (2) ↑ TLR-4 in HFD mice, with no effect by EtOH; (3) ↑ αSMA protein levels; and (4) ↓ CYP2E1 protein levels in HFD
Gopal *et al*[79]	(1) Animal: 6-8 wk male C57BL/6 mouse; (2) Diet: Chow or HFD (45% kcal fat) for 10 wk, then LD control or 5% v/v EtOH LD for 4 wk additionally; and (3) Drug: HFD mice also given 1000 U/kg Cu/Zn SOD-1 with polylysine- PEG copolymer in 10 mM HEPES every 2 d for 2 wk	(1) ↑ ALT; (2) ↑ FFA; (3) ↓ leptin; (4) nanoSOD treatment counteracted the above effects; and (5) No dif. in MDA between groups	(1) ↑ adipose mass by HFD, but ↓ fat/body weight ratio by HFD- EtOH; (2) ↑ microvesicular steatosis (in all mice); (3) ↑ macrovesicular steatosis; (4) ↑ inflammatory nodules; (5) ↑ hepatocyte ballooning; and (6) ↑ MCP-1 protein levels, ↓ MCP-1 in HFD-EtOH mice treated with nanoSOD	(1) ↑ adipose CYP2E1 protein levels, ↓ CYP2E1 by nanoSOD; (2) ↑ hepatic CYP2E1, ADH, catalase, ↓ CYP2E1 and ADH, but ↑ catalase by nanoSOD; (3) ↑ PPARα, ACOX-1 in HFD, further ↑ ACOX-1 by EtOH, further ↑ for both by nanoSOD; and (4) ↑ CCL-2, MMP-12; ↓ by nanoSOD
Jung *et al*[108]	(1) Animal: Female C57BL/6J mouse; (2) Diet: Control (69% carbohydrates, 12% fat, 19% protein) or FFC (60% carbohydrates, 25% fat, 15% protein, 50% wt/wt	(1) ↑ TG; ↓ in beer-treated FFC compared to EtOH-treated or naïve and (2) ↓ glucose tolerance in all FFC-fed groups	(1) ↑ neutrophil granulocytes; ↓ by beer in FFC-fed mice; (2) ↑ NAS; ↓ by beer in FFC-fed mice; (3) ↑ iNOS protein levels; ↓ by beer and EtOH in FFC-fed mice; and (4) ↑ 4-HNE; ↓ by beer and EtOH in FFC-fed mice	(1) ↑ IR, IRS-2 in FFC-EtOH and FFC- beer compared to naïve; no dif. in IRS-1; (2) ↓ adiponectin in FFC and FFC- EtOH, but ↑ in FFC-beer; (3) ↑ hepatic AdipoR1 and SIRT-1 in FFC-beer; and (4)

	fructose, 0.16% wt/wt cholesterol); Diets enriched with 2.5 g/kg EtOH, isocaloric beer (4.9% v/v EtOH), or isocaloric diet; and (3) Duration: 7 wk			No dif. in PPARγ, AdipoR2, FASN, SREBP-1c, ACOX-1 between groups
Kanuri *et al*[106]	(1) Animal: 6 wk male ob/ob C57BL/6 mouse; (2) Diet: 2.5 g/kg/d EtOH in drinking water; and (3) Duration: 6 wk	(1) ↑ ALT/AST in ob/ob, but ↓ slightly by EtOH in ob/ob; (2) ↑ TG, cholesterol, HDL, LDL in ob/ob, but no effect by EtOH; and (3) No dif. in FFA	(1) Steatosis, hepatomegaly in ob/ob; (2) Macrovesicular steatosis in EtOH-naïve ob/ob; (3) Microvesicular steatosis in EtOH- fed ob/ob; and (4) ↓ hepatic neutrophils	(1) ↑ PLIN-2, PLIN-3, TNFα, PAI-1 in ob/ob, ↓ PAI-1, PLIN-2, PLIN-3 by EtOH; (2) ↓ IRS-1, IRS-2, adiponectin, SIRT- 1 in ob/ob; ↑ adiponectin, SIRT-1 by EtOH; (3) No effect by EtOH on PPARγ, ACOX-1, SREBP-1c, IRS-1, IRS02, GLUT-4, glucokinase, PEPCK; and (4) No dif. in hepatic ACOX-1, PPARγ
Kitagawa *et al*[95]	(1) Animal: 8 wk female KK-A^{y} mouse; (2) Diet: LD with 5% EtOH or isocaloric maltodextrin; Single gavage of 4 g/kg EtOH or gavage on after 11 d; (3) Drug: 0.1 g/L rifaximin (RFX); and (4) Duration: 10 d	(1) ↑ ALT; (2) ↑ serum and hepatic TG; (3) ↑ portal blood LPS; (4) ↑ CYP2E1 activity; and (5) ↓ ALT, TG, LPS (but not to basal levels) in EtOH-fed treated with RFX	(1) Lipid droplet accumulation in hepatic lobule; (2) Hepatomegaly; (3) ↑ 4-HNE; and (4) RFX counteractedthe aboveeffects	(1) ↑ ACCα, FASN; TNFα, IL-6, ILNγ; CCL-2; CD14, TLR-4, TLR-2; HMOX- 1, NOX-1; (2) ↓ CPT-1α; (3) ↑ CYP2E1 protein levels; no effect by RFX; and (4) RFX counteracted effects of EtOH on ACCα, FASN, TNFα, IFNγ, TLR-4, HMOX-1, and NOX-2, CPT-1α
Lazaro *et al*[81]	(1) Animal: Male WT and OPN- knockout C57BL/6 mice and (2) Diet: High-fat, high-cholesterol diet for 2 wk, then iG liquid HFD-EtOH (36% kcal from corn oil; 27 g/kg/d EtOH) or isocaloric HFD for 8 wk; Some HFD-EtOH given 4-5 g/kg/wk EtOH by gavage	(1) ↑ ALT, but ↓ with binge EtOH; ↓ ALT in binge-treated OPN KO compared to binge-treated WT; (2) ↑ bilirubin, ↓ albumin; (3) ↑ TG; and (4) No dif. in BAL	(1) Steatosis, hepatomegaly, mononuclear cell inflammation, neutrophil infiltration, perisinusoidal and percellular fibrosis in HFD-EtOH and (2) Splenomegaly, ↑ TLR-4 in binge-treated mice; effect of binge greater in OPN KO	(1) ↑ collagen I, αSMA, TIMP-1 by EtOH; further ↑ by EtOH binge; (2) ↑ myeloperoxidase, CXCL-1, OPN in binge-treated; and (3) ↑ myeloperoxidase, IL-17α in binge-treated OPN KO
Minato *et al*[96]	(1) Animal: 30 wk male OLET and OLETF rat; (2) Initial weight: 620 ± 15 g (OLETF), 460 ± 10 g (OLET); (3) Diet: 10 mL 10% EtOH by gavage for 1-5 d/wk; and (4) Duration: 3 wk	(1) ↑ ALT/AST; (2) ↑ serum and hepatic TG; (3) ↑ serum glucose; (4) ↑ serum insulin in OLETF, with no effect from EtOH; and (5) ↑ serum adiponectin in OLETF, ↓ by EtOH in OLETF	(1) Mild pericentral microvesicular steatosis in EtOH-naïve OLETF; (2) Steatohepatitis, focal hepatic necrosis, and hepatocyte ballooning in EtOH-treated OLETF; (3) ↑ hepatic CYP2E1; and (4) ↑ 4-HNE	(1) ↑ PPARγ in OLETF, with no effect from EtOH and (2) ↑ TNFα
Nieto *et al*[85]	(1) Animal: 12 wk male Lewis rat; (2) Initial weight: 100 g; (3) Diet: Choline deficient (CD) diet; (4) 15 mL/kg whiskey by gavage 3 times per wk; and (5) Duration: 3 mo	(1) ↑ ALT/AST; (2) ↑ TG; (3) ↑ NEFA; (4) ↑ MDA, protein carbonyls; (5) ↑ serum TNFα, but ↓ in CD- whiskey; (6) ↑ CYP2E1 activity; (7) ↑ caspase-3, caspase-8 activity	(1) Minimal steatosis in whiskey-naïve CD rats and (2) Periportal and percentral microvesicular steatosis in CD-whiskey rats	(1) ↑ collagen 1, αSMA, cytochrome *c*, HSP47, CYP2E1; (2) ↑ leptin, TIMP-1, and BAX protein levels by CD, with no effect by whiskey; and (3) ↓ MMP-2, MMP-9, MMP-13, BCL-2, BCL-XL by CD, with no effect by whiskey
Osaki *et al*[101]	(1) Animal: Male Sprague-Dawley rat; (2) Initial weight: 106 g; (3) Diet: HFD (30% beef tallow, 20% casein, 20% sucrose); 1%-2% v/v EtOH *ad libitum*; and (4) Duration: 12 wk	(1) ↓ ALT; no dif. in AST; (2) ↓ ammonia, urate; (3) No dif. in serum glucose, FFA, cholesterol, HDL, bilirubin, alkaline phosphatase levels, urea, creatinine, lactate, acetate; (4) No dif. in hepatic TG, MDA; (5) No dif. in hepatic, renal, or pulmonary thiobarbituric acid-reactive substances	No dif. in hepatic TG, MDA No dif. in weight of liver, epididymal adipose tissue, perirenal adipose tissue, or gastrocnemius muscle	No dif. in TNFα, adiponectin, insulin-like growth factor binding protein 1, hemoglobin
Robin *et al*[86]	(1) Animal: Male ob/ob C57BL/6J mouse; (2) Initial weight: 49-56 g (obese), 26-30 g (lean); (3) Diet: 2.5 g/kg/d EtOH by gastric intubation; (4) Drug: 100 mg/kg/d pentoxifylline (PTX) by iP; and (5) Duration: 4 d	(1) ↑ ALT in ob/ob; no effect by EtOH; (2) ↑ caspase-3,CYP2E1, SOD activities; ↓ caspase 3 by PTX; (3) ↓ GPx, cytosolic GT activity in ob/ob, but no effect by EtOH; (4) ↓ mitochondrial GT activity by EtOH; and (5) No dif. in GR activity	(1) Steatosis, caspase-3 activation in ob/ob; (2) TUNEL+ hepatocytes; and (3) Necrosis, inflammation in EtOH-naïve ob/ob	(1) ↑ TNFα protein levels; ↓ by PTX; (2) ↑ IκBα protein levels, ↓ NF-κB p65; ↓ NF-κB activity; (3) ↓ iNOS, BCL-XL; (4) ↓ cytosolic GSH, mitochondrial GSSG; and (5) ↑ HSP70
Song *et al*[124]	(1) Animal: 6 wk male C57BL/6J mouse; (2) Diet: high-fructose diet (20.2% kcal protein, 66.96% kcal carbohydrates, 12.9% kcal fat); 10% v/v EtOH for 2 d,	(1) ↑ ALT/AST; (2) ↑ plasma TG, NEFA, cholesterol by EtOH, but not fructose; (3) ↑ plasma glucose by fructose diet, ↓ glucose by EtOH; (4) ↑ insulin by fructose and EtOH, but not combined	(1) ↑ microvesicular steatosis and (2) ↑ macrovesicular steatosis in EtOH-naïve fructose; ↓ by fructose-EtOH diet	(1) ↑ hepatic CYP2E1 protein levels; (2) ↑ KHK in EtOH-naïve fructose; (3) ↑ F4/80, CD68, and TNFα, MyD88, IRF-3, and TRAF-6; (4) ↑ CCL-2, TLR-4, and IRF-7 only in fructose-EtOH; (5) ↑

	15% for 5 d, 20% for 17 wk; and (3) Duration: 18 wk	fructose-EtOH; (5) ↓ copper by fructose and EtOH, but not combined fructose-EtOH		CD163, IL-1β, or ARG-1 by EtOH, but no effect by fructose; and (6) No dif. in IL-6, IL-10
Sun *et al*[107]	(1) Animal: Male Sprague-Dawley rats; (2) Initial weight: 80-100 g; (3) Diet: HFD (38% fat, 2% cholesterol, 1% cholate) or control (38% kcal from fat); 4 g/kg/d EtOH by gavage beginning after 3 wk; and (4) Duration: 12 wk	No dif. in plasma LPS levels	(1) ↑ steatosis, fibrosis in HFD mice compared to HFD-EtOH and (2) ↑ Kupffer cell and HSC activation in HFD mice compared to HFD- EtOH	↑ inflammatory cytokines (TNFα, CXCL-1, CXCL-2, IL-1β, IL-6), pro- fibrotic markers (αSMA, collagen, TGF-β, TIMP-1, MMP-2, MMP-9) in HFD compared to HFD-EtOH
Suzuki *et al*[92]	(1) Animal: 8 wk male KK-A^{y} mouse; (2) Diet: LD containing 5% EtOH or isocaloric maltodextrin; 4 g/kg EtOH or isocaloric maltodextrin by gavage on day 11; (3) Drug: 120 mg/kg/d phenylbutyric acid (PBA); and (4) Duration: 10 d	(1) ↑ ALT/AST in chronic-binge mice; no dif. in ALT/AST between chronic-only and controls; (2) ↑ serum and hepatic TG; (3) No dif. in blood glucose; and (4) PBA ↓ ALT/AST, TG in EtOH-fed mice compared to PBA-naïve	(1) ↑ steatosis, PMN infiltration, ccCK18+ hepatocytes, 4-HNE+ cells in chronic-binge mice and (2) PBA alleviated liver injury, but did not decrease 4-HNE+ cell count	(1) ↑ inflammatory cytokines (TNFα, IL-6), ER stress markers (BiP, uXBP-1, sXBP-1, IP3R1, CHOP), and HMOX-1 by chronic-binge; PBA ↓ aforementioned genes; (2) ↑ BiP, uXBP-1 in chronic, but not sXBP-1, IP3R1, CHOP, HMOX-1; and (3) ↑ CYP2E1; PBA had no effect
Wang *et al*[78]	(1) Animal: 8 wk male Sprague-Dawley rat; (2) Diet: LD control (35% kcal from fat) or LD HFD (71% kcal from fat) for 6 wk; then LD HFD were given either solid HFD (55% kcal fat) or HF-EtOH diet (55% kcal fat, 16% kcal EtOH) for 4 wk; (3) Duration: 10 wk	(1) ↑ TUNEL+ hepatocytes; (2) ↑ cleaved caspase-3 levels; and (3) No dif. in 4-HNE or MDA levels between HFD and HFD-EtOH, but ↑ compared to controls	(1) Lipid droplet accumulation; (2) ↑ steatosis; and (3) ↑ number of inflammatory foci	(1) ↑ Fas death receptor and ligand; (2) No dif. in caspase-3 expression; (3) No dif. in CYP2E1, TNFα, TNFR-1, IL-1β, IL-12 between HFD and HFD-EtOH, but ↑ compared to controls
Xu *et al*[83]	(1) Animal: 8 wk male C57BL/6J mouse; (2) Diet: 580 kcal/kg/d (control) or 986 kcal/kg/d (overfed) of liquid HFD (37% kcal corn oil) by iG infusion for 45 d; 23 g/kg/d (low dose) or 32 g/kg/d (high dose) *via* iG infusion added to diet after 45; controls received isocaloric amount of diet; and (3) Duration: 10 wk	(1) ↑ hepatic TG, hepatic MDA, BAL in EtOH-treated overfed mice and (2) ↑ ALT in overfed mice; dose- dependent ↑ ALT by EtOH	(1) Steatosis, mononuclear cell infiltration in EtOH-treated (high dose) control mice; (2) Steatohepatitis and pericellular fibrosis in EtOH-treated (high dose) overfed mice; (3) ↑ macrophage infiltration in WAT in EtOH-treated overfed mice; and (4) No dif. in liver histology between EtOH-naïve overfed mice and controls	(1) ↑ M1 polarization markers (iNOS, TNFα) in liver and WAT for overfed-EtOH mice; (2) ↑ M2 markers (IL-10, ARG-1) in WAT, but ↓in liver for overfed- EtOH mice; (3) ↓ AdipoR, mitochondrial function genes (PGC-1α, PPARα, COX, cytochrome *c*, ACOX-1), in overfed-EtOH; (4) ↑ SREBP-1, ↓ pACC in EtOH; and (5) No effect on AMPK, PPARδ by overfeeding or EtOH

Results listed refer to experimental groups with concomitant metabolic syndrome risk factor and alcohol consumption compared to healthy or EtOH-naïve controls, unless stated otherwise. ACC: Acetyl-CoA carboxylase; ACOX: Acyl-CoA oxidase; AdipoR: Adiponectin receptor; ALT: Alanine aminotransferase; αSMA: Alpha smooth muscle actin; AUC: Area under the curve; ARG: Arginase; AST: Aspartate aminotransferase; BCL: B-cell lymphoma; BAX: BCL-2-associated X protein; BiP: Binding immunoglobulin protein; BAL: Blood alcohol level; CPT: Carnitine palmitoyltransferase; CHOP: C/EBP homologous protein; DGAT-2: Diacylglycerol O-acyltransferase 1; ER: Endoplasmic reticulum; EtOH: Ethanol; FA: Fatty acid; FASN: Fatty acid synthase; FAO: Fatty acid oxidation; FGF: Fibroblast growth factor; GTT: Glucose tolerance test; GSSG: Glutathione, oxidized; GSH: Glutathione, reduced; GPx: Glutathione peroxidases; GR: Glutathione reductase; GT: Glutathione transferase; H&E: Hematoxylin and eosin stain; HMOX: Heme oxygenase; HSP: Heat shock protein; HSC: Hepatic stellate cells; HCC: Hepatocellular carcinoma; HDL: High density lipoprotein; HFD: High-fat diet; HFHC: High-fat, high cholesterol diet; FFC: High-fat, high-fructose, high-cholesterol diet; 4-HNE: 4-hydroxynonenal; iNOS: Inducible nitric oxide synthase; IP3R1: Inositol trisphosphate receptor type 1; IR: Insulin receptor; IRS: Insulin receptor substrate; IFN: Interferon; IRF: Interferon regulatory factor; IL: Interleukin; iG: Intragastric; iP: Intraperitoneal; JNK: c-Jun N-terminal kinase; KHK: Ketohexokinase; LD: Lieber- DeCarli; LDL: Low density lipoprotein; MDA: Malondialdehyde; MMP: Matrix metallopeptidase; MCP: Monocyte chemoattractant protein; MUFA: Monounsaturated fatty acids; MyD88: Myeloid differentiation primary response 88; NOX: NADPH oxidase; NOX: NAFLD activity score; OLET: Otsuka Long-Evans Tokushima; OLETF: Otsuka Long-Evans Tokushima fatty; PLIN: Perilipin; PPAR: Peroxisome proliferator-activated receptor; PEPCK: Phosphoenolpyruvate carboxykinase; PAI-1: Plasminogen activator inhibitor 1; PUFA: Polyunsaturated fatty acids; PGC-1α: PPARγ coactivator 1 α; PHH: Primary human hepatocytes; Akt: Protein kinase B; SFA: Saturated fatty acids; SIRT-1: Sirtuin 1; SCD-1: Stearoyl-CoA desaturase 1; SREBP-1: Steroid response-element binding protein 1; SOD: Superoxide dismutase; TGFβ: Transforming growth factor β; TG: Triglycerides; TNFα: Tumor necrosis factor α; TRAF: TNF receptor associated factor; WAT: White adipose tissue; XBP-1: X-box binding protein 1.

the presence of necrotic hepatocytes, suggesting increased hepatic neutrophil infiltration. HFHC-EtOH with additional EtOH binge also upregulated collagen I, αSMA, and TIMP-1 compared to controls. Unlike the Gäbele study, EtOH also upregulated TLR-4 expression in HFHC-fed mice. Since OPN is associated with increased ALD severity[82], HFHC-EtOH diet was also given to OPN-knockout (KO) mice to determine the role of OPN in liver disease. HFHC-EtOH diet increased neutrophil infiltration, plasma ALT activity, and αSMA in OPN KO mice, suggesting

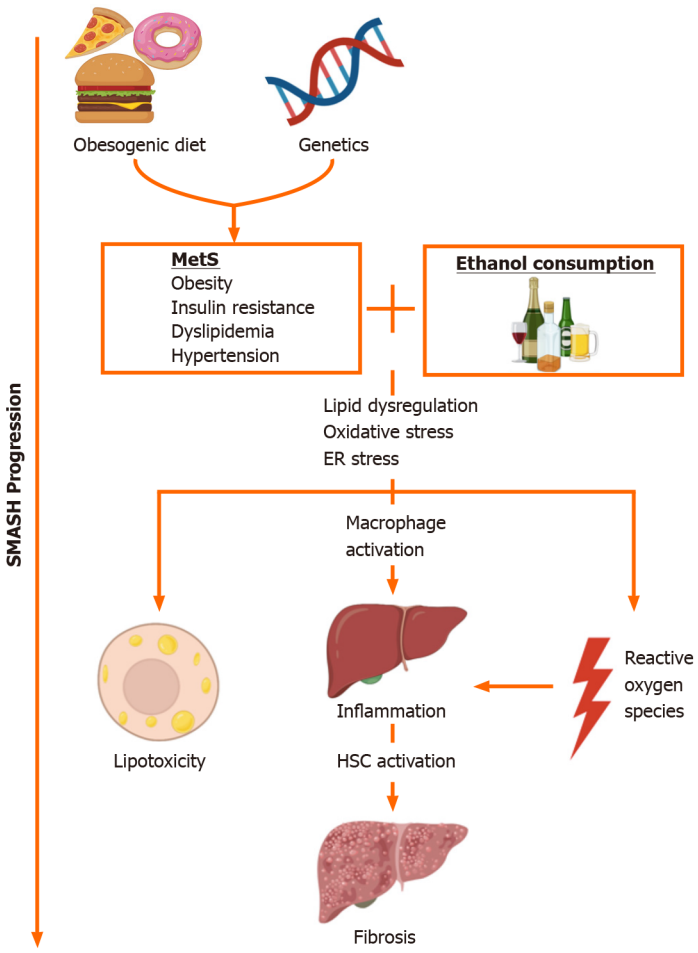


Figure 1 Pathogenesis and progression of the syndromes of metabolic and alcoholic steatohepatitis. Metabolic syndrome (MetS) is a cluster of factors–obesity, insulin resistance, hypertension, high triglyceride levels, and low high-density lipoproteins cholesterol levels–that arise from obesogenic diet and genetic factors. Coupled with heavy alcohol consumption, MetS promotes lipid dysregulation, oxidative stress, and endoplasmic reticulum stress. These biochemical processes reciprocally mediate each other and contribute to lipotoxic cellular dysfunction, immune response, inflammation, and fibrosis in syndromes of metabolic and alcoholic steatohepatitis.

that OPN plays a protective role in fatty liver disease. Similarly, Xu *et al*[83] overfed C57BL/6 mice HFD by iG infusion for 45 d, after which different dosages of EtOH was introduced for another 4 wk. Compared to controls, overfeeding and EtOH elevated hepatic TG levels, increased fibrosis, upregulated induced nitric oxide synthase (iNOS) activity, and induced the PERK and IRE-1 pathways. HFD and high-dose EtOH increased liver weight, hepatic TG levels, plasma adiponectin levels, ALT activity, and fibrosis compared to low-dose EtOH treatment. These results suggest that concomitant overfeeding and EtOH consumption induce fibrosis, oxidative stress, and ER stress. Furthermore, these results indicate that the effects of EtOH on NAFLD progression are dose-dependent, as evidenced by the differential effects on liver injury by low and high dose EtOH.

To recapitulate SMASH pathogenesis, EtOH is also coupled with other dietary models of NAFLD other than HFD. These other dietary models of SMASH are similar to the HFD-based models in that they induce lipid dysregulation, oxidative stress, apoptosis, and fibrosis. Alwahsh *et al*[84] fed Sprague-Dawley rats either control LD, fructose LD, EtOH LD, or combined fructose-EtOH LD diet for 28 d. EtOH and fructose independently elevated hepatic TG and cholesterol, and upregulated PPARα and carnitine palmitoyltransferase I (CPT-1) compared to controls. However, combined fructose-EtOH decreased cholesterol, and downregulated PPARα and CPT-1 compared to controls. Combined treatment also upregulated leptin receptor and acetyl-CoA carboxylase (ACC). This study suggests that in either NAFLD or ALD, PPARα compensates for the increase in lipid accumulation, but FAO capacity is diminished under concomitant in SMASH. Nieto *et al*[85] developed a model in which Lewis rats were administered a choline-deficient (CD) diet and multiple whiskey gavages. Compared to controls, CD-whiskey treatment elevated MDA and protein carbonyl levels, upregulated TNFα, collagen I, αSMA, and β-tubulin, increased

collagen deposition, and increased caspase-3 and caspase-8 activity. These results suggest that CD-whiskey induces oxidative stress, inflammation, and fibrosis. CD diet also downregulated BCL-XL, suggesting greater susceptibility to apoptosis, although whiskey did not affect its expression.

Genetic models of SMASH

Experimental rodent models of SMASH also employ genetic models of NAFLD coupled with EtOH consumption. One commonly used genetic mouse model is ob/ob leptin deficiency. For example, Robin *et al*[86] developed a model in which ob/ob mice were administered EtOH daily by gavage for 4 d. EtOH upregulated TNFα and heat shock protein 70 (HSP70) expression, increased caspase-3 activity, and downregulated NF-κB expression and activity in obese mice compared to controls. Treatment with TNFα inhibitor pentoxifylline attenuated these effects in EtOH-treated obese mice. These results suggest that combined multiple binge EtOH dysregulates TNFα signaling and induces hepatocellular apoptosis in genetic obesity. However, EtOH did not increase serum ALT in either lean or obese mice, suggesting that it does not contribute to acute liver injury in this model.

Everitt *et al*[87] also used ob/ob mice to determine the effect of polyunsaturated fatty acids (PUFA) and chronic EtOH on obesity. EtOH increased ALT/AST, TG and cholesterol levels, and AMPK expression in obese mice compared to controls. EtOH also downregulated SIRT-1 and SFRS-10, a SIRT-1 target. SFRS-10 modulates splicing for the transcription factor lipin 1, which has two isoforms: FA oxidizing lipin 1α and TG synthetic lipin 1β[88]. The decrease in SFRS-10 resulted in an upregulation of the β isoform, which is also seen in human obesity and *in vitro* models[89]. In PUFA-fed ob/ob mice, EtOH also upregulated PPARγ which regulates adipocyte differentiation, glucose homeostasis, lipogenesis, and lipid droplet formation[90]. Although PPARγ is not upregulated in NASH patients[91], increased PPARγ and lipin-1β in the Everitt model underscores the potential synergistic effects of obesogenic factors and EtOH on AMPK-mediated *de novo* lipogenesis in human disease.

Another genetic mouse model is KK-A^{y}, which induces obesity and hyperinsulinemia by dysregulating appetite suppression. Suzuki *et al*[92] fed KK-A^{y} mice control or 5% EtOH LD diet for 10 d, then administered a single 4 g/kg EtOH dose by gavage in a chronic-binge EtOH model. In obese mice, EtOH upregulated spliced and unspliced XBP-1, BIP, inositol trisphosphate receptor, and C/EBP homologous protein, and oxidative stress markers CYP2E1 and heme oxygenase 1 (HMOX-1). Treatment with the chemical chaperone 4-phenylbutyric acid decreased the aforementioned UPR genes, ALT/AST activity, and hepatic TG levels. These results suggest that EtOH induces the UPR, exacerbates ER stress, and promotes oxidative stress in genetic obesity. In another study from the same lab, Kitagawa *et al*[93] used a similar feeding regiment and found elevated serum LPS, and upregulated inflammatory cytokines TNFα, IL-1β, and interferon γ, and upregulated TLR-4. Furthermore, with regards to the small intestinal microbiota, EtOH decreased *Lactobacillales* and increased *Erysipelotrichales* in the KK-A^{y} mice. Treatment with rifaximin, an antibiotic, restored the *Erysipelotrichales* population and increased *Bacteroidales*, while restoring cytokine expression to basal levels.

In rat studies, one commonly used genetic model is the fa/fa Zucker rat. For example, Carmiel-Haggai *et al*[94] administered fa/fa Zucker rats multiple binges of 35% EtOH or saline over 3 days to determine the effect of concomitant genetic obesity and EtOH consumption on oxidative stress. In obese fa/fa rats, EtOH decreased basal GSH levels, increased GSSG levels, and upregulated CYP2E1 and iNOS compared to controls. EtOH also decreased SOD, catalase, and GR activity in obese rats, suggesting that EtOH exacerbates oxidative stress in obesity by straining antioxidant mechanisms. Another genetic rat model is the Otsuka Long Evans Tokushima Fatty (OLETF) rat, which is a cholecystokinin KO model that dysregulates appetite suppression[95]. Minato *et al*[96] administered lean OLET and obese OLETF rats 10% EtOH gavage every few days for 3 wk in a multiple binge EtOH model of SMASH. In obese rats, EtOH increased inflammation, CYP2E1 protein levels, TNFα expression, 4-HNE levels compared to controls. However, EtOH did not affect PPARγ expression or steatosis in OLETF rats compared to EtOH-naïve OLETF rats. These results suggest that while this model recapitulates inflammation and oxidative stress in SMASH, it does not feature lipid metabolism dysregulation.

Apparent alleviation of NAFLD/NASH by ethanol

Some experimental models that couple obesity and EtOH consumption do not induce severe liver injury, and instead show evidence for a possible protective effect by moderate EtOH consumption in NAFLD. The amount of alcohol that constitutes "mild

or moderate" (referred to as "moderate" hereafter) consumption is difficult to define, and there are varied definitions of moderate alcohol consumption in both humans and rodent models. In retrospective studies of NAFLD, moderate alcohol consumption is less than 20-40 g EtOH daily[97-99], although other studies define it as less than 2 alcoholic drinks per day[100]. Moderate alcohol consumption is associated with improved insulin sensitivity, decreased fibrosis, and improved cardiovascular outcomes in NAFLD/NASH patients[101-103], which is a significant finding because fibrosis is a major factor in NAFLD mortality[104]. However, the effects of BMI, insulin resistance, socioeconomic status, drinking pattern, or type of alcoholic beverage on human fatty liver disease have not been fully elucidated[103]. Nevertheless, there are rodent models that describe an apparent alleviation of NAFLD symptoms associated with moderate alcohol consumption. Moderate alcohol consumption is less rigorously defined for rodent models, although of the studies reviewed in this paper, those that model "moderate alcohol consumption" generally have less than a daily 5 g EtOH/kg body weight dosage for rodents[105-108].

Osaki *et al*[105] developed a model in which chronic consumption of 1%-2% v/v EtOH reduced blood markers for liver injury in HFD-fed Sprague-Dawley rats for 12 wk. EtOH did not affect body weight, liver mass, or adipose tissue mass, nor did it affect serum cholesterol, FFA, or TG levels. EtOH decreased serum ALT activity, lactate dehydrogenase, urate, and ammonia levels. In a similar study by Sun *et al*[107], a 4 g/kg EtOH binge by gavage downregulated expression of pro-inflammatory TNFα, CXCL-1, CXCL-2, and IL-1β, and pro- fibrotic αSMA, collagen, TGFβ, TIMP1, MMP2, and MMP9 in Sprague-Dawley rats fed HFHC for 12 wk. Using a genetic obesity model, Kanuri *et al*[106] determined the effect of chronic EtOH consumption on lipid storage and thrombosis. *Ad libitum* access to 2.5 g/kg EtOH was not found to affect TNFα, insulin receptor substrate (IRS)-1, or IRS-2 expression in ob/ob C57BL/6 mice. EtOH downregulated the expression of lipid droplet-associated proteins perilipin (PLIN) 2 and PLIN-3, suggesting decreased lipid accumulation due to EtOH. PLIN2 expression and lipid accumulation are known to be upregulated in ALD[109,110], but PLIN3 may instead play a protective role by facilitating lipid export from the ER[111]. Expression of pro-thrombotic PAI-1 was comparable between EtOH- treated ob/ob mice and control WT mice, despite upregulation of PAI-1 in EtOH-naïve ob/ob mice compared to WT.

Experimental animal studies have suggested the possible role of adiponectin signaling and sensitivity in apparent EtOH-mediated amelioration of NAFLD. For example, Bucher *et al*[112] found a decrease in serum adiponectin levels in C57BL/6 mice administered HFD and 10 g/kg/d EtOH in drinking water compared to mice fed HFD only. Decreased adiponectin in EtOH-treated mice accompanied lower serum TG and cholesterol levels, and downregulated collagen I, collagen III, and CYP2E1 expression. Similarly, Jung *et al*[108] found upregulated SIRT-1 and insulin receptor expression in high-fat, high-fructose, high-cholesterol-fed C57BL/6 mice administered pure EtOH or beer, compared to alcohol-naïve mice. Beer, but not pure EtOH, also upregulated adiponectin and adiponectin receptor 1 expression. In both of the aforementioned studies, AMPK activation by adiponectin suggests a possible compensatory effect in response to concomitant EtOH and lipid intake. However, the differential effects of beer and pure EtOH suggest that the alcohol-associated alleviation of fatty liver may instead be due to other components in alcoholic beverages. In an intervention study, serum adiponectin was elevated, although not significantly, in overweight (BMI ≥ 27 kg/m^2) adults who consumed 100 mL whiskey daily for 4 wk, compared to overweight adults who were asked to drink mineral water[24].

CONCLUSION

Various pre-clinical experimental models have been developed to study the interactive effects of NAFLD and ALD risk factors on hepatic injury resulting in SMASH. While each model differs in obesity etiology, as well as pattern and duration of alcohol consumption, they all demonstrate that obesity and heavy alcohol consumption synergistically contribute to hepatic injury. The models suggest that both sets of risk factors contribute to increased steatosis and fibrosis, as well as an M1-like phenotype in activated macrophages. There is also evidence that obesity and alcohol consumption synergistically interfere with antioxidant defense, but the effect of alcohol seems to be dose-dependent. Despite the advantages of these animal models, there are still limitations with regards to replicating what we understand from human disease.

New models should consider the effect of alcohol consumption patterns on fatty liver disease pathogenesis. For example, the highest risk group for ALD are

individuals who already drink heavily, then dramatically increase alcohol intake in a short period[113]. There are already models, such as the NIAAA model[75], that replicate chronic-binge alcohol consumption patterns in ALD. In the NIAAA model, mice are fed Lieber-DeCarli EtOH diet for 10 d and given EtOH gavage on the eleventh day, with a set of chronic-binge feedings that can repeated multiple times. However, repeated sets of chronic-binge feedings only slightly elevate ALT/AST levels compared to a single set, and does not result in liver fibrosis. Thus, future models should also induce advanced liver injury in the context of repeated chronic-binge alcohol consumption to fully recapitulate fatty liver disease in humans.

Furthermore, while most current experimental models use high-fat diets to induce obesity, future models should more closely replicate the diets that are composed of high-fat and high glycemic index foods that are commonly found in Western countries and have been identified as risk factors for NAFLD/NASH[114]. Fructose, in particular, is known to increase hepatic *de novo* lipogenesis and impair fatty acid oxidation in humans, and promote gut permeability in mice. Fructose also promotes insulin resistance in both the liver and skeletal muscle[115]. There are studies that model NAFLD progression that combine saturated fats, cholesterol, and fructose into a single diet[116,117], but the specific composition of fats and fructose source (*e.g.*, sucrose or high fructose corn syrup) varies between studies. Future experimental models should thus also determine the effect of fructose on multi-system lipid dysregulation, insulin resistance, and inflammation.

Animal studies are also limited in replicating the genetic factors for NAFLD and ALD. For example, genetic models for obesity and insulin resistance in mice include ob/ob (leptin), db/db (leptin receptor), and foz/foz (ALMS-1)[118]. These do not parallel genetic polymorphisms known to predispose humans to NAFLD/NASH. Human genetic predispositions to fatty liver disease include polymorphisms in PNPLA3, TM6SF2, GCKR, MBOAT7, HSD17B3, PPARγ, IRS-1, PLIN2, and adiponectin, among others[119-121]. Furthermore, different rodent strains may also have an inherent bias towards certain disease states. For example, TNFα and iNOS are upregulated in C57BL/6 mice compared to Balb/c mice, despite being administered the same diet. Likewise, ARG-1 is increased in Balb/c compared to C57BL/6[122]. C57BL/6 mice may thus have a bias towards M1 polarization; and Balb/c, to M2 polarization. Future studies should further compare the roles that different human polymorphisms play in fatty liver disease pathogenesis, while also controlling for possible bias in the animal model used.

Finally, further research is needed to determine the interaction between multiple factors in fatty liver disease pathogenesis. In the established "two-hit" model of NAFLD pathogenesis, lipid accumulation results in a cascade of other dysfunctions, such as inflammation and fibrogenesis. Meanwhile, in the competing "multi-hit" model, multiple factors, such as insulin resistance and gut microbiome dysregulation, along with lipid metabolism dysregulation, synergistically result in liver injury[123]. For example, approximately 70% of all patients with insulin resistance will develop NAFLD. To determine possible interactions or causal relationships between these factors and alcohol, future experimental models should monitor fatty liver disease progression over time.

The development of novel pre-clinical experimental models may help elucidate new mechanisms and the interactions between alcohol and metabolic abnormalities in fatty liver disease. Specifically, feeding regimens that better model food and alcohol consumption in patients with SMASH should be developed. These models should incorporate both chronic-binge alcohol consumption and Western diet and also consider how those dietary factors interact with human genetics.

REFERENCES

1 **Asrani SK**, Devarbhavi H, Eaton J, Kamath PS. Burden of liver diseases in the world. *J Hepatol* 2019; **70**: 151-171 [PMID: 30266282 DOI: 10.1016/j.jhep.2018.09.014]

2 **Rinella ME**. Nonalcoholic fatty liver disease: a systematic review. *JAMA* 2015; **313**: 2263-2273 [PMID: 26057287 DOI: 10.1001/jama.2015.5370]

3 **Younossi ZM**, Marchesini G, Pinto-Cortez H, Petta S. Epidemiology of Nonalcoholic Fatty Liver Disease and Nonalcoholic Steatohepatitis: Implications for Liver Transplantation. *Transplantation* 2019; **103**: 22-27 [PMID: 30335697 DOI: 10.1097/TP.0000000000002484]

4 **Marchesini G**, Brizi M, Bianchi G, Tomassetti S, Bugianesi E, Lenzi M, McCullough AJ, Natale S, Forlani G, Melchionda N. Nonalcoholic fatty liver disease: a feature of the metabolic syndrome. *Diabetes* 2001; **50**: 1844-1850 [PMID: 11473047 DOI: 10.2337/diabetes.50.8.1844]

5 **Chalasani N**, Gorski JC, Asghar MS, Asghar A, Foresman B, Hall SD, Crabb DW. Hepatic

cytochrome P450 2E1 activity in nondiabetic patients with nonalcoholic steatohepatitis. *Hepatology* 2003; **37**: 544-550 [PMID: 12601351 DOI: 10.1053/jhep.2003.50095]

6 **Naveau S**, Giraud V, Borotto E, Aubert A, Capron F, Chaput JC. Excess weight risk factor for alcoholic liver disease. *Hepatology* 1997; **25**: 108-111 [PMID: 8985274 DOI: 10.1002/hep.510250120]

7 **Hart CL**, Morrison DS, Batty GD, Mitchell RJ, Davey Smith G. Effect of body mass index and alcohol consumption on liver disease: analysis of data from two prospective cohort studies. *BMJ* 2010; **340**: c1240 [PMID: 20223873 DOI: 10.1136/bmj.c1240]

8 **Stepanova M**, Rafiq N, Younossi ZM. Components of metabolic syndrome are independent predictors of mortality in patients with chronic liver disease: a population-based study. *Gut* 2010; **59**: 1410-1415 [PMID: 20660697 DOI: 10.1136/gut.2010.213553]

9 **Raynard B**, Balian A, Fallik D, Capron F, Bedossa P, Chaput JC, Naveau S. Risk factors of fibrosis in alcohol-induced liver disease. *Hepatology* 2002; **35**: 635-638 [PMID: 11870378 DOI: 10.1053/jhep.2002.31782]

10 **Åberg F**, Puukka P, Salomaa V, Männistö S, Lundqvist A, Valsta L, Perola M, Jula A, Färkkilä M. Combined Effects of Alcohol and Metabolic Disorders in Patients With Chronic Liver Disease. *Clin Gastroenterol Hepatol* 2020; **18**: 995-997. e2 [PMID: 31255807 DOI: 10.1016/j.cgh.2019.06.036]

11 **Carr RM**, Correnti J. Insulin resistance in clinical and experimental alcoholic liver disease. *Ann N Y Acad Sci* 2015; **1353**: 1-20 [PMID: 25998863 DOI: 10.1111/nyas.12787]

12 **Lambert JE**, Ramos-Roman MA, Browning JD, Parks EJ. Increased de novo lipogenesis is a distinct characteristic of individuals with nonalcoholic fatty liver disease. *Gastroenterology* 2014; **146**: 726-735 [PMID: 24316260 DOI: 10.1053/j.gastro.2013.11.049]

13 **Mihaylova MM**, Shaw RJ. The AMPK signalling pathway coordinates cell growth, autophagy and metabolism. *Nat Cell Biol* 2011; **13**: 1016-1023 [PMID: 21892142 DOI: 10.1038/ncb2329]

14 **You M**, Matsumoto M, Pacold CM, Cho WK, Crabb DW. The role of AMP-activated protein kinase in the action of ethanol in the liver. *Gastroenterology* 2004; **127**: 1798-1808 [PMID: 15578517 DOI: 10.1053/j.gastro.2004.09.049]

15 **Smith BK**, Marcinko K, Desjardins EM, Lally JS, Ford RJ, Steinberg GR. Treatment of nonalcoholic fatty liver disease: role of AMPK. *Am J Physiol Endocrinol Metab* 2016; **311**: E730-E740 [PMID: 27577854 DOI: 10.1152/ajpendo.00225.2016]

16 **Jung EJ**, Kwon SW, Jung BH, Oh SH, Lee BH. Role of the AMPK/SREBP-1 pathway in the development of orotic acid-induced fatty liver. *J Lipid Res* 2011; **52**: 1617-1625 [PMID: 21757781 DOI: 10.1194/jlr.M015263]

17 **Kohjima M**, Higuchi N, Kato M, Kotoh K, Yoshimoto T, Fujino T, Yada M, Yada R, Harada N, Enjoji M, Takayanagi R, Nakamuta M. SREBP-1c, regulated by the insulin and AMPK signaling pathways, plays a role in nonalcoholic fatty liver disease. *Int J Mol Med* 2008; **21**: 507-511 [PMID: 18360697]

18 **Tang JJ**, Li JG, Qi W, Qiu WW, Li PS, Li BL, Song BL. Inhibition of SREBP by a small molecule, betulin, improves hyperlipidemia and insulin resistance and reduces atherosclerotic plaques. *Cell Metab* 2011; **13**: 44-56 [PMID: 21195348 DOI: 10.1016/j.cmet.2010.12.004]

19 **Pawlak M**, Lefebvre P, Staels B. Molecular mechanism of PPARα action and its impact on lipid metabolism, inflammation and fibrosis in non-alcoholic fatty liver disease. *J Hepatol* 2015; **62**: 720-733 [PMID: 25450203 DOI: 10.1016/j.jhep.2014.10.039]

20 **Schug TT**, Li X. Sirtuin 1 in lipid metabolism and obesity. *Ann Med* 2011; **43**: 198-211 [PMID: 21345154 DOI: 10.3109/07853890.2010.547211]

21 **Lin J**, Yang R, Tarr PT, Wu PH, Handschin C, Li S, Yang W, Pei L, Uldry M, Tontonoz P, Newgard CB, Spiegelman BM. Hyperlipidemic effects of dietary saturated fats mediated through PGC-1beta coactivation of SREBP. *Cell* 2005; **120**: 261-273 [PMID: 15680331 DOI: 10.1016/j.cell.2004.11.043]

22 **You M**, Liang X, Ajmo JM, Ness GC. Involvement of mammalian sirtuin 1 in the action of ethanol in the liver. *Am J Physiol Gastrointest Liver Physiol* 2008; **294**: G892-G898 [PMID: 18239056 DOI: 10.1152/ajpgi.00575.2007]

23 **Ipsen DH**, Lykkesfeldt J, Tveden-Nyborg P. Molecular mechanisms of hepatic lipid accumulation in non-alcoholic fatty liver disease. *Cell Mol Life Sci* 2018; **75**: 3313-3327 [PMID: 29936596 DOI: 10.1007/s00018-018-2860-6]

24 **Beulens JW**, van Loon LJ, Kok FJ, Pelsers M, Bobbert T, Spranger J, Helander A, Hendriks HF. The effect of moderate alcohol consumption on adiponectin oligomers and muscle oxidative capacity: a human intervention study. *Diabetologia* 2007; **50**: 1388-1392 [PMID: 17492425 DOI: 10.1007/s00125-007-0699-8]

25 **Bellanti F**, Villani R, Facciorusso A, Vendemiale G, Serviddio G. Lipid oxidation products in the pathogenesis of non-alcoholic steatohepatitis. *Free Radic Biol Med* 2017; **111**: 173-185 [PMID: 28109892 DOI: 10.1016/j.freeradbiomed.2017.01.023]

26 **Peter Guengerich F**, Avadhani NG. Roles of Cytochrome P450 in Metabolism of Ethanol and Carcinogens. *Adv Exp Med Biol* 2018; **1032**: 15-35 [PMID: 30362088 DOI: 10.1007/978-3-319-98788-0_2]

27 **Niemelä O**, Parkkila S, Juvonen RO, Viitala K, Gelboin HV, Pasanen M. Cytochromes P450 2A6, 2E1, and 3A and production of protein-aldehyde adducts in the liver of patients with alcoholic and non-alcoholic liver diseases. *J Hepatol* 2000; **33**: 893-901 [PMID: 11131450 DOI: 10.1016/s0168-8278(00)80120-8]

28 **Chen Y**, Han M, Matsumoto A, Wang Y, Thompson DC, Vasiliou V. Glutathione and Transsulfuration in Alcohol-Associated Tissue Injury and Carcinogenesis. *Adv Exp Med Biol* 2018; **1032**: 37-53 [PMID: 30362089 DOI: 10.1007/978-3-319-98788-0_3]

29 **Kamada Y**, Matsumoto H, Tamura S, Fukushima J, Kiso S, Fukui K, Igura T, Maeda N, Kihara S, Funahashi T, Matsuzawa Y, Shimomura I, Hayashi N. Hypoadiponectinemia accelerates hepatic tumor formation in a nonalcoholic steatohepatitis mouse model. *J Hepatol* 2007; **47**: 556-564 [PMID: 17459514 DOI: 10.1016/j.jhep.2007.03.020]

30 **Leclercq IA**, Field J, Enriquez A, Farrell GC, Robertson GR. Constitutive and inducible expression of hepatic CYP2E1 in leptin-deficient ob/ob mice. *Biochem Biophys Res Commun* 2000; **268**: 337-344 [PMID: 10679205 DOI: 10.1006/bbrc.2000.2125]

31 **Mahli A**, Thasler WE, Patsenker E, Müller S, Stickel F, Müller M, Seitz HK, Cederbaum AI, Hellerbrand C. Identification of cytochrome CYP2E1 as critical mediator of synergistic effects of alcohol and cellular lipid accumulation in hepatocytes in vitro. *Oncotarget* 2015; **6**: 41464-41478 [PMID: 26497211 DOI: 10.18632/oncotarget.6203]

32 **Ozgur R**, Uzilday B, Iwata Y, Koizumi N, Turkan I. Interplay between the unfolded protein response and reactive oxygen species: a dynamic duo. *J Exp Bot* 2018; **69**: 3333-3345 [PMID: 29415271 DOI: 10.1093/jxb/ery040]

33 **Liu X**, Green RM. Endoplasmic reticulum stress and liver diseases. *Liver Res* 2019; **3**: 55-64 [PMID: 32670671 DOI: 10.1016/j.livres.2019.01.002]

34 **Henkel A**, Green RM. The unfolded protein response in fatty liver disease. *Semin Liver Dis* 2013; **33**: 321-329 [PMID: 24222090 DOI: 10.1055/s-0033-1358522]

35 **Liu Z**, Lv Y, Zhao N, Guan G, Wang J. Protein kinase R-like ER kinase and its role in endoplasmic reticulum stress-decided cell fate. *Cell Death Dis* 2015; **6**: e1822 [PMID: 26225772 DOI: 10.1038/cddis.2015.183]

36 **Han J**, Kaufman RJ. The role of ER stress in lipid metabolism and lipotoxicity. *J Lipid Res* 2016; **57**: 1329-1338 [PMID: 27146479 DOI: 10.1194/jlr.R067595]

37 **Marí M**, Morales A, Colell A, García-Ruiz C, Fernández-Checa JC. Mitochondrial glutathione, a key survival antioxidant. *Antioxid Redox Signal* 2009; **11**: 2685-2700 [PMID: 19558212 DOI: 10.1089/ARS.2009.2695]

38 **He L**, He T, Farrar S, Ji L, Liu T, Ma X. Antioxidants Maintain Cellular Redox Homeostasis by Elimination of Reactive Oxygen Species. *Cell Physiol Biochem* 2017; **44**: 532-553 [PMID: 29145191 DOI: 10.1159/000485089]

39 **Weydert CJ**, Cullen JJ. Measurement of superoxide dismutase, catalase and glutathione peroxidase in cultured cells and tissue. *Nat Protoc* 2010; **5**: 51-66 [PMID: 20057381 DOI: 10.1038/nprot.2009.197]

40 **Moreno-Sánchez R**, Marín-Hernández Á, Gallardo-Pérez JC, Vázquez C, Rodríguez-Enríquez S, Saavedra E. Control of the NADPH supply and GSH recycling for oxidative stress management in hepatoma and liver mitochondria. *Biochim Biophys Acta Bioenerg* 2018; **1859**: 1138-1150 [PMID: 30053395 DOI: 10.1016/j.bbabio.2018.07.008]

41 **Świderska M**, Maciejczyk M, Zalewska A, Pogorzelska J, Flisiak R, Chabowski A. Oxidative stress biomarkers in the serum and plasma of patients with non-alcoholic fatty liver disease (NAFLD). Can plasma AGE be a marker of NAFLD? *Free Radic Res* 2019; **53**: 841-850 [PMID: 31234658 DOI: 10.1080/10715762.2019.1635691]

42 **Asghari S**, Hamedi-Shahraki S, Amirkhizi F. Systemic redox imbalance in patients with nonalcoholic fatty liver disease. *Eur J Clin Invest* 2020; **50**: e13211 [PMID: 32017057 DOI: 10.1111/eci.13211]

43 **Chien YW**, Chen YL, Peng HC, Hu JT, Yang SS, Yang SC. Impaired homocysteine metabolism in patients with alcoholic liver disease in Taiwan. *Alcohol* 2016; **54**: 33-37 [PMID: 27565754 DOI: 10.1016/j.alcohol.2016.06.002]

44 **Szuster-Ciesielska A**, Daniluk J, Kandefer-Szerszeń M. Oxidative stress in the blood of patients with alcohol-related liver cirrhosis. *Med Sci Monit* 2002; **8**: CR419-CR424 [PMID: 12070432]

45 **Bieghs V**, Trautwein C. Innate immune signaling and gut-liver interactions in non-alcoholic fatty liver disease. *Hepatobiliary Surg Nutr* 2014; **3**: 377-385 [PMID: 25568861 DOI: 10.3978/j.issn.2304-3881.2014.12.04]

46 **Byun JS**, Yi HS. Hepatic Immune Microenvironment in Alcoholic and Nonalcoholic Liver Disease. *Biomed Res Int* 2017; **2017**: 6862439 [PMID: 28852648 DOI: 10.1155/2017/6862439]

47 **Zhou D**, Huang C, Lin Z, Zhan S, Kong L, Fang C, Li J. Macrophage polarization and function with emphasis on the evolving roles of coordinated regulation of cellular signaling pathways. *Cell Signal* 2014; **26**: 192-197 [PMID: 24219909 DOI: 10.1016/j.cellsig.2013.11.004]

48 **Kitade H**, Chen G, Ni Y, Ota T. Nonalcoholic Fatty Liver Disease and Insulin Resistance: New Insights and Potential New Treatments. *Nutrients* 2017; **9** [PMID: 28420094 DOI: 10.3390/nu9040387]

49 **Park JW**, Jeong G, Kim SJ, Kim MK, Park SM. Predictors reflecting the pathological severity of non-alcoholic fatty liver disease: comprehensive study of clinical and immunohistochemical findings in younger Asian patients. *J Gastroenterol Hepatol* 2007; **22**: 491-497 [PMID: 17376039 DOI: 10.1111/j.1440-1746.2006.04758.x]

50 **De Vito R**, Alisi A, Masotti A, Ceccarelli S, Panera N, Citti A, Salata M, Valenti L, Feldstein AE, Nobili V. Markers of activated inflammatory cells correlate with severity of liver damage in children with nonalcoholic fatty liver disease. *Int J Mol Med* 2012; **30**: 49-56 [PMID: 22505182 DOI:

10.3892/ijmm.2012.965]
51 **Kazankov K**, Jørgensen SMD, Thomsen KL, Møller HJ, Vilstrup H, George J, Schuppan D, Grønbæk H. The role of macrophages in nonalcoholic fatty liver disease and nonalcoholic steatohepatitis. *Nat Rev Gastroenterol Hepatol* 2019; **16**: 145-159 [PMID: 30482910 DOI: 10.1038/s41575-018-0082-x]
52 **Hosseini N**, Shor J, Szabo G. Alcoholic Hepatitis: A Review. *Alcohol Alcohol* 2019; **54**: 408-416 [PMID: 31219169 DOI: 10.1093/alcalc/agz036]
53 **Xu R**, Huang H, Zhang Z, Wang FS. The role of neutrophils in the development of liver diseases. *Cell Mol Immunol* 2014; **11**: 224-231 [PMID: 24633014 DOI: 10.1038/cmi.2014.2]
54 **Gao B**, Bataller R. Alcoholic liver disease: pathogenesis and new therapeutic targets. *Gastroenterology* 2011; **141**: 1572-1585 [PMID: 21920463 DOI: 10.1053/j.gastro.2011.09.002]
55 **Alkhouri N**, Carter-Kent C, Feldstein AE. Apoptosis in nonalcoholic fatty liver disease: diagnostic and therapeutic implications. *Expert Rev Gastroenterol Hepatol* 2011; **5**: 201-212 [PMID: 21476915 DOI: 10.1586/egh.11.6]
56 **Youle RJ**, Strasser A. The BCL-2 protein family: opposing activities that mediate cell death. *Nat Rev Mol Cell Biol* 2008; **9**: 47-59 [PMID: 18097445 DOI: 10.1038/nrm2308]
57 **Yang YM**, Seki E. TNFα in liver fibrosis. *Curr Pathobiol Rep* 2015; **3**: 253-261 [PMID: 26726307 DOI: 10.1007/s40139-015-0093-z]
58 **Luedde T**, Schwabe RF. NF-κB in the liver--linking injury, fibrosis and hepatocellular carcinoma. *Nat Rev Gastroenterol Hepatol* 2011; **8**: 108-118 [PMID: 21293511 DOI: 10.1038/nrgastro.2010.213]
59 **Wallace MC**, Friedman SL, Mann DA. Emerging and disease-specific mechanisms of hepatic stellate cell activation. *Semin Liver Dis* 2015; **35**: 107-118 [PMID: 25974897 DOI: 10.1055/s-0035-1550060]
60 **Seki E**, Brenner DA. Recent advancement of molecular mechanisms of liver fibrosis. *J Hepatobiliary Pancreat Sci* 2015; **22**: 512-518 [PMID: 25869468 DOI: 10.1002/jhbp.245]
61 **Tsuchida T**, Friedman SL. Mechanisms of hepatic stellate cell activation. *Nat Rev Gastroenterol Hepatol* 2017; **14**: 397-411 [PMID: 28487545 DOI: 10.1038/nrgastro.2017.38]
62 **Sharifnia T**, Antoun J, Verriere TG, Suarez G, Wattacheril J, Wilson KT, Peek RM Jr, Abumrad NN, Flynn CR. Hepatic TLR4 signaling in obese NAFLD. *Am J Physiol Gastrointest Liver Physiol* 2015; **309**: G270-G278 [PMID: 26113297 DOI: 10.1152/ajpgi.00304.2014]
63 **Petrasek J**, Mandrekar P, Szabo G. Toll-like receptors in the pathogenesis of alcoholic liver disease. *Gastroenterol Res Pract* 2010; **2010** [PMID: 20827314 DOI: 10.1155/2010/710381]
64 **Yamada K**, Mizukoshi E, Seike T, Horii R, Kitahara M, Sunagozaka H, Arai K, Yamashita T, Honda M, Kaneko S. Light alcohol consumption has the potential to suppress hepatocellular injury and liver fibrosis in non-alcoholic fatty liver disease. *PLoS One* 2018; **13**: e0191026 [PMID: 29342182 DOI: 10.1371/journal.pone.0191026]
65 **Gandhi CR**. Hepatic stellate cell activation and pro-fibrogenic signals. *J Hepatol* 2017; **67**: 1104-1105 [PMID: 28939135 DOI: 10.1016/j.jhep.2017.06.001]
66 **Denk H**, Abuja PM, Zatloukal K. Animal models of NAFLD from the pathologist's point of view. *Biochim Biophys Acta Mol Basis Dis* 2019; **1865**: 929-942 [PMID: 29746920 DOI: 10.1016/j.bbadis.2018.04.024]
67 **Santhekadur PK**, Kumar DP, Sanyal AJ. Preclinical models of non-alcoholic fatty liver disease. *J Hepatol* 2018; **68**: 230-237 [PMID: 29128391 DOI: 10.1016/j.jhep.2017.10.031]
68 **Hebbard L**, George J. Animal models of nonalcoholic fatty liver disease. *Nat Rev Gastroenterol Hepatol* 2011; **8**: 35-44 [PMID: 21119613 DOI: 10.1038/nrgastro.2010.191]
69 **Sherriff JL**, O'Sullivan TA, Properzi C, Oddo JL, Adams LA. Choline, Its Potential Role in Nonalcoholic Fatty Liver Disease, and the Case for Human and Bacterial Genes. *Adv Nutr* 2016; **7**: 5-13 [PMID: 26773011 DOI: 10.3945/an.114.007955]
70 **Lau JK**, Zhang X, Yu J. Animal models of non-alcoholic fatty liver disease: current perspectives and recent advances. *J Pathol* 2017; **241**: 36-44 [PMID: 27757953 DOI: 10.1002/path.4829]
71 **Lieber CS**, DeCarli LM. Liquid diet technique of ethanol administration: 1989 update. *Alcohol Alcohol* 1989; **24**: 197-211 [PMID: 2667528]
72 **Tsukamoto H**, French SW, Benson N, Delgado G, Rao GA, Larkin EC, Largman C. Severe and progressive steatosis and focal necrosis in rat liver induced by continuous intragastric infusion of ethanol and low fat diet. *Hepatology* 1985; **5**: 224-232 [PMID: 3979954 DOI: 10.1002/hep.1840050212]
73 **French SW**, Miyamoto K, Tsukamoto H. Ethanol-induced hepatic fibrosis in the rat: role of the amount of dietary fat. *Alcohol Clin Exp Res* 1986; **10**: 13S-19S [PMID: 3544925 DOI: 10.1111/j.1530-0277.1986.tb05175.x]
74 **Ueno A**, Lazaro R, Wang PY, Higashiyama R, Machida K, Tsukamoto H. Mouse intragastric infusion (iG) model. *Nat Protoc* 2012; **7**: 771-781 [PMID: 22461066 DOI: 10.1038/nprot.2012.014]
75 **Bertola A**, Mathews S, Ki SH, Wang H, Gao B. Mouse model of chronic and binge ethanol feeding (the NIAAA model). *Nat Protoc* 2013; **8**: 627-637 [PMID: 23449255 DOI: 10.1038/nprot.2013.032]
76 **Mathews S**, Xu M, Wang H, Bertola A, Gao B. Animals models of gastrointestinal and liver diseases. Animal models of alcohol-induced liver disease: pathophysiology, translational relevance, and challenges. *Am J Physiol Gastrointest Liver Physiol* 2014; **306**: G819-G823 [PMID: 24699333 DOI: 10.1152/ajpgi.00041.2014]
77 **Gäbele E**, Dostert K, Dorn C, Patsenker E, Stickel F, Hellerbrand C. A new model of interactive

effects of alcohol and high-fat diet on hepatic fibrosis. *Alcohol Clin Exp Res* 2011; **35**: 1361-1367 [PMID: 21463337 DOI: 10.1111/j.1530-0277.2011.01472.x]

78 **Wang Y**, Seitz HK, Wang XD. Moderate alcohol consumption aggravates high-fat diet induced steatohepatitis in rats. *Alcohol Clin Exp Res* 2010; **34**: 567-573 [PMID: 20028348 DOI: 10.1111/j.1530-0277.2009.01122.x]

79 **Gopal T**, Kumar N, Perriotte-Olson C, Casey CA, Donohue TM Jr, Harris EN, Talmon G, Kabanov AV, Saraswathi V. Nanoformulated SOD1 ameliorates the combined NASH and alcohol-associated liver disease partly *via* regulating CYP2E1 expression in adipose tissue and liver. *Am J Physiol Gastrointest Liver Physiol* 2020; **318**: G428-G438 [PMID: 31928222 DOI: 10.1152/ajpgi.00217.2019]

80 **Duly AM**, Alani B, Huang EY, Yee C, Haber PS, McLennan SV, Seth D. Effect of multiple binge alcohol on diet-induced liver injury in a mouse model of obesity. *Nutr Diabetes* 2015; **5**: e154 [PMID: 25915743 DOI: 10.1038/nutd.2015.4]

81 **Lazaro R**, Wu R, Lee S, Zhu NL, Chen CL, French SW, Xu J, Machida K, Tsukamoto H. Osteopontin deficiency does not prevent but promotes alcoholic neutrophilic hepatitis in mice. *Hepatology* 2015; **61**: 129-140 [PMID: 25132354 DOI: 10.1002/hep.27383]

82 **Seth D**, Duly A, Kuo PC, McCaughan GW, Haber PS. Osteopontin is an important mediator of alcoholic liver disease *via* hepatic stellate cell activation. *World J Gastroenterol* 2014; **20**: 13088-13104 [PMID: 25278703 DOI: 10.3748/wjg.v20.i36.13088]

83 **Xu J**, Lai KKY, Verlinsky A, Lugea A, French SW, Cooper MP, Ji C, Tsukamoto H. Synergistic steatohepatitis by moderate obesity and alcohol in mice despite increased adiponectin and p-AMPK. *J Hepatol* 2011; **55**: 673-682 [PMID: 21256905 DOI: 10.1016/j.jhep.2010.12.034]

84 **Alwahsh SM**, Xu M, Schultze FC, Wilting J, Mihm S, Raddatz D, Ramadori G. Combination of alcohol and fructose exacerbates metabolic imbalance in terms of hepatic damage, dyslipidemia, and insulin resistance in rats. *PLoS One* 2014; **9**: e104220 [PMID: 25101998 DOI: 10.1371/journal.pone.0104220]

85 **Nieto N**, Rojkind M. Repeated whiskey binges promote liver injury in rats fed a choline-deficient diet. *J Hepatol* 2007; **46**: 330-339 [PMID: 17156887 DOI: 10.1016/j.jhep.2006.09.010]

86 **Robin MA**, Demeilliers C, Sutton A, Paradis V, Maisonneuve C, Dubois S, Poirel O, Lettéron P, Pessayre D, Fromenty B. Alcohol increases tumor necrosis factor alpha and decreases nuclear factor-kappab to activate hepatic apoptosis in genetically obese mice. *Hepatology* 2005; **42**: 1280-1290 [PMID: 16317704 DOI: 10.1002/hep.20949]

87 **Everitt H**, Hu M, Ajmo JM, Rogers CQ, Liang X, Zhang R, Yin H, Choi A, Bennett ES, You M. Ethanol administration exacerbates the abnormalities in hepatic lipid oxidation in genetically obese mice. *Am J Physiol Gastrointest Liver Physiol* 2013; **304**: G38-G47 [PMID: 23139221 DOI: 10.1152/ajpgi.00309.2012]

88 **Bi L**, Jiang Z, Zhou J. The role of lipin-1 in the pathogenesis of alcoholic fatty liver. *Alcohol Alcohol* 2015; **50**: 146-151 [PMID: 25595739 DOI: 10.1093/alcalc/agu102]

89 **Pihlajamäki J**, Lerin C, Itkonen P, Boes T, Floss T, Schroeder J, Dearie F, Crunkhorn S, Burak F, Jimenez-Chillaron JC, Kuulasmaa T, Miettinen P, Park PJ, Nasser I, Zhao Z, Zhang Z, Xu Y, Wurst W, Ren H, Morris AJ, Stamm S, Goldfine AB, Laakso M, Patti ME. Expression of the splicing factor gene SFRS10 is reduced in human obesity and contributes to enhanced lipogenesis. *Cell Metab* 2011; **14**: 208-218 [PMID: 21803291 DOI: 10.1016/j.cmet.2011.06.007]

90 **Lefterova MI**, Haakonsson AK, Lazar MA, Mandrup S. PPARγ and the global map of adipogenesis and beyond. *Trends Endocrinol Metab* 2014; **25**: 293-302 [PMID: 24793638 DOI: 10.1016/j.tem.2014.04.001]

91 **Gross B**, Pawlak M, Lefebvre P, Staels B. PPARs in obesity-induced T2DM, dyslipidaemia and NAFLD. *Nat Rev Endocrinol* 2017; **13**: 36-49 [PMID: 27636730 DOI: 10.1038/nrendo.2016.135]

92 **Suzuki M**, Kon K, Ikejima K, Arai K, Uchiyama A, Aoyama T, Yamashina S, Ueno T, Watanabe S. The Chemical Chaperone 4-Phenylbutyric Acid Prevents Alcohol-Induced Liver Injury in Obese KK-A^{y} Mice. *Alcohol Clin Exp Res* 2019; **43**: 617-627 [PMID: 30748014 DOI: 10.1111/acer.13982]

93 **Kitagawa R**, Kon K, Uchiyama A, Arai K, Yamashina S, Kuwahara-Arai K, Kirikae T, Ueno T, Ikejima K. Rifaximin prevents ethanol-induced liver injury in obese KK-A^{y} mice through modulation of small intestinal microbiota signature. *Am J Physiol Gastrointest Liver Physiol* 2019; **317**: G707-G715 [PMID: 31509430 DOI: 10.1152/ajpgi.00372.2018]

94 **Carmiel-Haggai M**, Cederbaum AI, Nieto N. Binge ethanol exposure increases liver injury in obese rats. *Gastroenterology* 2003; **125**: 1818-1833 [PMID: 14724834 DOI: 10.1053/j.gastro.2003.09.019]

95 **Moran TH**. Unraveling the obesity of OLETF rats. *Physiol Behav* 2008; **94**: 71-78 [PMID: 18190934 DOI: 10.1016/j.physbeh.2007.11.035]

96 **Minato T**, Tsutsumi M, Tsuchishima M, Hayashi N, Saito T, Matsue Y, Toshikuni N, Arisawa T, George J. Binge alcohol consumption aggravates oxidative stress and promotes pathogenesis of NASH from obesity-induced simple steatosis. *Mol Med* 2014; **20**: 490-502 [PMID: 25180626 DOI: 10.2119/molmed.2014.00048]

97 **Dunn W**, Sanyal AJ, Brunt EM, Unalp-Arida A, Donohue M, McCullough AJ, Schwimmer JB. Modest alcohol consumption is associated with decreased prevalence of steatohepatitis in patients with non-alcoholic fatty liver disease (NAFLD). *J Hepatol* 2012; **57**: 384-391 [PMID: 22521357 DOI: 10.1016/j.jhep.2012.03.024]

98 **Cotrim HP**, Freitas LA, Alves E, Almeida A, May DS, Caldwell S. Effects of light-to-moderate alcohol consumption on steatosis and steatohepatitis in severely obese patients. *Eur J Gastroenterol*

Hepatol 2009; **21**: 969-972 [PMID: 19194305 DOI: 10.1097/MEG.0b013e328328f3ec]
99 **Kwon HK**, Greenson JK, Conjeevaram HS. Effect of lifetime alcohol consumption on the histological severity of non-alcoholic fatty liver disease. *Liver Int* 2014; **34**: 129-135 [PMID: 23809459 DOI: 10.1111/liv.12230]
100 **Ascha MS**, Hanouneh IA, Lopez R, Tamimi TA, Feldstein AF, Zein NN. The incidence and risk factors of hepatocellular carcinoma in patients with nonalcoholic steatohepatitis. *Hepatology* 2010; **51**: 1972-1978 [PMID: 20209604 DOI: 10.1002/hep.23527]
101 **Hsu CC**, Kowdley KV. The Effects of Alcohol on Other Chronic Liver Diseases. *Clin Liver Dis* 2016; **20**: 581-594 [PMID: 27373618 DOI: 10.1016/j.cld.2016.02.013]
102 **Ajmera VH**, Terrault NA, Harrison SA. Is moderate alcohol use in nonalcoholic fatty liver disease good or bad? *Hepatology* 2017; **65**: 2090-2099 [PMID: 28100008 DOI: 10.1002/hep.29055]
103 **Weng G**, Dunn W. Effect of alcohol consumption on nonalcoholic fatty liver disease. *Transl Gastroenterol Hepatol* 2019; **4**: 70 [PMID: 31620652 DOI: 10.21037/tgh.2019.09.02]
104 **Hagström H**. Alcohol Consumption in Concomitant Liver Disease: How Much is Too Much? *Curr Hepatol Rep* 2017; **16**: 152-157 [PMID: 28706775 DOI: 10.1007/s11901-017-0343-0]
105 **Osaki A**, Okazaki Y, Kimoto A, Izu H, Kato N. Beneficial effect of a low dose of ethanol on liver function and serum urate in rats fed a high-fat diet. *J Nutr Sci Vitaminol (Tokyo)* 2014; **60**: 408-412 [PMID: 25866304 DOI: 10.3177/jnsv.60.408]
106 **Kanuri G**, Landmann M, Priebs J, Spruss A, Löscher M, Ziegenhardt D, Röhl C, Degen C, Bergheim I. Moderate alcohol consumption diminishes the development of non-alcoholic fatty liver disease (NAFLD) in ob/ob mice. *Eur J Nutr* 2016; **55**: 1153-1164 [PMID: 26003186 DOI: 10.1007/s00394-015-0929-7]
107 **Sun F**, Zhuang Z, Zhang D, Chen Y, Liu S, Gao N, Shi J, Wang B. Chronic moderate alcohol consumption relieves high-fat high-cholesterol diet-induced liver fibrosis in a rat model. *Clin Exp Pharmacol Physiol* 2018; **45**: 1046-1055 [PMID: 29851129 DOI: 10.1111/1440-1681.12976]
108 **Jung F**, Lippmann T, Brandt A, Jin CJ, Engstler AJ, Baumann A. Moderate consumption of fermented alcoholic beverages diminishes diet-induced non-alcoholic fatty liver disease through mechanisms involving hepatic adiponectin signaling in mice. *Eur J Nutr* 2020; **59**: 787-799 [PMID: 30879098 DOI: 10.1007/s00394-019-01945-2]
109 **Carr RM**, Dhir R, Yin X, Agarwal B, Ahima RS. Temporal effects of ethanol consumption on energy homeostasis, hepatic steatosis, and insulin sensitivity in mice. *Alcohol Clin Exp Res* 2013; **37**: 1091-1099 [PMID: 23398239 DOI: 10.1111/acer.12075]
110 **Carr RM**, Peralta G, Yin X, Ahima RS. Absence of perilipin 2 prevents hepatic steatosis, glucose intolerance and ceramide accumulation in alcohol-fed mice. *PLoS One* 2014; **9**: e97118 [PMID: 24831094 DOI: 10.1371/journal.pone.0097118]
111 **Jeon S**, Carr R. Alcohol effects on hepatic lipid metabolism. *J Lipid Res* 2020; **61**: 470-479 [PMID: 32029510 DOI: 10.1194/jlr.R119000547]
112 **Bucher S**, Begriche K, Catheline D, Trak-Smayra V, Tiaho F, Coulouarn C, Pinon G, Lagadic-Gossmann D, Rioux V, Fromenty B. Moderate chronic ethanol consumption exerts beneficial effects on nonalcoholic fatty liver in mice fed a high-fat diet: possible role of higher formation of triglycerides enriched in monounsaturated fatty acids. *Eur J Nutr* 2020; **59**: 1619-1632 [PMID: 31161349 DOI: 10.1007/s00394-019-02017-1]
113 **Choi G**, Runyon BA. Alcoholic hepatitis: a clinician's guide. *Clin Liver Dis* 2012; **16**: 371-385 [PMID: 22541704 DOI: 10.1016/j.cld.2012.03.015]
114 **Hosseini Z**, Whiting SJ, Vatanparast H. Current evidence on the association of the metabolic syndrome and dietary patterns in a global perspective. *Nutr Res Rev* 2016; **29**: 152-162 [PMID: 27955720 DOI: 10.1017/s095442241600007x]
115 **Weber KS**, Simon MC, Strassburger K, Markgraf DF, Buyken AE, Szendroedi J, Müssig K, Roden M; GDS Group. Habitual Fructose Intake Relates to Insulin Sensitivity and Fatty Liver Index in Recent-Onset Type 2 Diabetes Patients and Individuals without Diabetes. *Nutrients* 2018; **10** [PMID: 29914103 DOI: 10.3390/nu10060774]
116 **Dorn C**, Engelmann JC, Saugspier M, Koch A, Hartmann A, Müller M, Spang R, Bosserhoff A, Hellerbrand C. Increased expression of c-Jun in nonalcoholic fatty liver disease. *Lab Invest* 2014; **94**: 394-408 [PMID: 24492282 DOI: 10.1038/labinvest.2014.3]
117 **Ganz M**, Bukong TN, Csak T, Saha B, Park JK, Ambade A, Kodys K, Szabo G. Progression of non-alcoholic steatosis to steatohepatitis and fibrosis parallels cumulative accumulation of danger signals that promote inflammation and liver tumors in a high fat-cholesterol-sugar diet model in mice. *J Transl Med* 2015; **13**: 193 [PMID: 26077675 DOI: 10.1186/s12967-015-0552-7]
118 **Stephenson K**, Kennedy L, Hargrove L, Demieville J, Thomson J, Alpini G, Francis H. Updates on Dietary Models of Nonalcoholic Fatty Liver Disease: Current Studies and Insights. *Gene Expr* 2018; **18**: 5-17 [PMID: 29096730 DOI: 10.3727/105221617X15093707969658]
119 **Miyaaki H**, Nakao K. Significance of genetic polymorphisms in patients with nonalcoholic fatty liver disease. *Clin J Gastroenterol* 2017; **10**: 201-207 [PMID: 28290069 DOI: 10.1007/s12328-017-0732-5]
120 **Anstee QM**, Reeves HL, Kotsiliti E, Govaere O, Heikenwalder M. From NASH to HCC: current concepts and future challenges. *Nat Rev Gastroenterol Hepatol* 2019; **16**: 411-428 [PMID: 31028350 DOI: 10.1038/s41575-019-0145-7]
121 **Eslam M**, George J. Genetic contributions to NAFLD: leveraging shared genetics to uncover

systems biology. *Nat Rev Gastroenterol Hepatol* 2020; **17**: 40-52 [PMID: 31641249 DOI: 10.1038/s41575-019-0212-0]

122 **Maina V**, Sutti S, Locatelli I, Vidali M, Mombello C, Bozzola C, Albano E. Bias in macrophage activation pattern influences non-alcoholic steatohepatitis (NASH) in mice. *Clin Sci (Lond)* 2012; **122**: 545-553 [PMID: 22142284 DOI: 10.1042/CS20110366]

123 **Buzzetti E**, Pinzani M, Tsochatzis EA. The multiple-hit pathogenesis of non-alcoholic fatty liver disease (NAFLD). *Metabolism* 2016; **65**: 1038-1048 [PMID: 26823198 DOI: 10.1016/j.metabol.2015.12.012]

124 **Song M**, Chen T, Prough RA, Cave MC, McClain CJ. Chronic alcohol consumption causes liver injury in high-fructose-fed male mice through enhanced hepatic inflammatory response. *Alcohol Clin Exp Res* 2016; **40**: 518-528 [PMID: 26858005 DOI: 10.1111/acer.12994]

World Journal of Gastroenterology

Submit a Manuscript: https://www.f6publishing.com

World J Gastroenterol 2021 January 7; 27(1): 19-36

DOI: 10.3748/wjg.v27.i1.19

ISSN 1007-9327 (print) ISSN 2219-2840 (online)

REVIEW

Human hepatitis viruses-associated cutaneous and systemic vasculitis

Chrong-Reen Wang, Hung-Wen Tsai

ORCID number: Chrong-Reen Wang 0000-0001-9881-7024; Hung-Wen Tsai 0000-0001-9223-2535.

Author contributions: Wang CR designed the report and wrote the paper; Wang CR and Tsai HW collected and analyzed the clinical data.

Conflict-of-interest statement: The authors declare no conflicts of interest.

Open-Access: This article is an open-access article that was selected by an in-house editor and fully peer-reviewed by external reviewers. It is distributed in accordance with the Creative Commons Attribution NonCommercial (CC BY-NC 4.0) license, which permits others to distribute, remix, adapt, build upon this work non-commercially, and license their derivative works on different terms, provided the original work is properly cited and the use is non-commercial. See: http://creativecommons.org/Licenses/by-nc/4.0/

Manuscript source: Invited manuscript

Specialty type: Gastroenterology and hepatology

Country/Territory of origin: Taiwan

Peer-review report's scientific

Chrong-Reen Wang, Department of Internal Medicine, National Cheng Kung University Hospital, Tainan 70403, Taiwan

Hung-Wen Tsai, Department of Pathology, National Cheng Kung University Hospital, Tainan 70403, Taiwan

Corresponding author: Chrong-Reen Wang, MD, PhD, Department of Internal Medicine, National Cheng Kung University Hospital, No. 138 Sheng-Li Road, Tainan 70403, Taiwan. wangcr@mail.ncku.edu.tw

Abstract

Human hepatitis viruses (HHVs) include hepatitis A virus, hepatitis B virus (HBV), hepatitis C virus (HCV), hepatitis delta virus, and hepatitis E virus and can cause liver inflammation in their common human host. Usually, HHV is rapidly cleared by the immune system, following acute HHV invasion. The morbidities associated with hepatitis A virus and hepatitis E virus infection occur shortly after their intrusion, in the acute stage. Nevertheless, the viral infectious process can persist for a long period of time, especially in HBV and HCV infection, leading to chronic hepatitis and further progressing to hepatic cirrhosis and liver cancer. HHV infection brings about complications in other organs, and both acute and chronic hepatitis have been associated with clinical presentations outside the liver. Vascular involvement with cutaneous and systemic vasculitis is a well-known extrahepatic presentation; moreover, there is growing evidence for a possible causal relationship between viral pathogens and vasculitis. Except for hepatitis delta virus, other HHVs have participated in the etiopathogenesis of cutaneous and systemic vasculitis *via* different mechanisms, including direct viral invasion of vascular endothelial cells, immune complex-mediated vessel wall damage, and autoimmune responses with stimulation of autoreactive B-cells and impaired regulatory T-cells. Cryoglobulinemic vasculitis and polyarteritis nodosa are recognized for their association with chronic HHV infection. Although therapeutic guidelines for HHV-associated vasculitis have not yet been established, antiviral therapy should be initiated in HBV and HCV-related systemic vasculitis in addition to the use of corticosteroids. Plasma exchange and/or combined cyclophosphamide and corticosteroid therapy can be considered in patients with severe life-threatening vasculitis manifestations.

Key Words: Human hepatitis viruses; Hepatitis B virus; Hepatitis C virus; Cryoglobulinemic vasculitis; Polyarteritis nodosa; Antiviral therapy

quality classification
Grade A (Excellent): 0
Grade B (Very good): B, B
Grade C (Good): 0
Grade D (Fair): 0
Grade E (Poor): 0

Received: November 21, 2020
Peer-review started: November 21, 2020
First decision: December 17, 2020
Revised: December 19, 2020
Accepted: December 27, 2020
Article in press: December 27, 2020
Published online: January 7, 2021

P-Reviewer: Liang XS, Wang K
S-Editor: Zhang L
L-Editor: A
P-Editor: Ma YJ

©The Author(s) 2021. Published by Baishideng Publishing Group Inc. All rights reserved.

Core Tip: The human hepatitis viruses (HHVs) hepatitis A virus, hepatitis B virus, hepatitis C virus, hepatitis delta virus, and hepatitis E virus can cause liver inflammation in their common human host. With the exception of hepatitis delta virus, all other HHVs can participate in the pathogenesis of cutaneous and systemic vasculitis *via* different mechanisms like direct viral invasion of vascular endothelial cells and immune complex-mediated vessel wall damage. Cryoglobulinemic vasculitis and polyarteritis nodosa are recognized for their association with chronic HHV infection. Antiviral therapy should be initiated in hepatitis B virus and hepatitis C virus-related systemic vasculitis.

Citation: Wang CR, Tsai HW. Human hepatitis viruses-associated cutaneous and systemic vasculitis. *World J Gastroenterol* 2021; 27(1): 19-36
URL: https://www.wjgnet.com/1007-9327/full/v27/i1/19.htm
DOI: https://dx.doi.org/10.3748/wjg.v27.i1.19

INTRODUCTION

Hepatocellular injury caused by acute or chronic inflammation of the liver is derived from adverse factors, including alcohol consumption, autoimmune response, drug use, steatosis, and viruses[1]. Hepatotropic viruses are known for their role in the etiology of viral hepatitis, and, from the public health perspective, the disease is associated with heavy health burden and higher annual mortality[2]. In addition to uncommon herpes viruses-related hepatitis due to Epstein-Barr virus, cytomegalovirus, and herpes simplex virus infection[3], human hepatitis viruses (HHVs) are the most common causes of acute and chronic hepatitis in their human host[4]. The discovery of HHV starts with clinical description of disease, antigen/antibody reaction establishment, virus-like particles visualization, and finally viral genomes sequencing[5]. Early experiments illustrated two types, infectious hepatitis and serum hepatitis[6]. Australia antigens in serum hepatitis yielded the detection of 42-nm Dane particles[7,8]. Subsequently, deoxyribonucleic acid (DNA) sequencing was performed and hepatitis B virus (HBV) was found[9]. Later, virus-like particles were observed in infectious hepatitis, and complementary DNA (cDNA) from hepatitis A virus (HAV) was sequenced[10,11]. Hepatitis C virus (HCV) was identified in non-A, non-B hepatitis patients receiving multiple transfusions[12], transmission to chimpanzees[13], and cDNA library screens[14]. Hepatitis delta virus (HDV), a HBV-associated virus[15], is a separate defective virus requiring the help of HBV for its infection[16]. After elucidating the hepatitis E virus (HEV) cDNA[17], an endemic non-A, non-B hepatitis[18], there are five members of HHVs[5].

Typically following HHV invasion into humans, there is rapid clearance of viruses by the host defense system, with a self-limiting disease course[4]. The morbidities associated with HAV and HEV infection, commonly transmitted *via* the fecal-oral route, occur shortly after their intrusion in the acute stage[19-21]. The infectious processes can persist for a long period of time in HBV, HCV, and HDV infection, progressing to chronic hepatitis and leading to liver fibrosis, irreversible cirrhosis, and hepatocellular carcinoma[22-24]. Table 1 summarizes and compares the common characteristics of the five HHV members[4,5,19-29].

EXTRAHEPATIC MANIFESTATIONS OF HUMAN HEPATITIS VIRUSES INFECTION

Although HHVs primarily affect hepatocytes, they can cause extrahepatic manifestations, with damage to other organs[30-34]. Both acute and chronic forms of viral hepatitis are associated with various clinical presentations outside of the liver, which may precede or follow hepatic dysfunction. The crucial pathogenic mechanism is caused by the immune responses against viral pathogens, with the deposition of immune complexes (IC) in targeted tissues.

Table 1 Common characteristics and comparative features in five members of human hepatitis viruses

	HAV	HBV	HCV	HDV[1]	HEV
Family; Genus	*Picornaviridae Hepatovirus*	*Hepadnavirida Orthohepadnavirus*	*Flaviviridae Hepacivirus*	*Deltaviridae Deltavirus*	*Hepeviridae Orthohepevirus*
Discovery[2]; Frequency	1983 Highest in AH	1979 Highest in CH	1989 Second in CH	1986 Less in CH	1990 Less in AH
Genome[3]; Length; Diameter[4]; Envelope[5]; Receptor	Linear ssRNA; 7500 nt; 27-32 nm; Quasi-envelope; Unknown	Circular dsDNA; 3200 nt; 42 nm; Envelope; NTCP, HSP	Linear ssRNA; 9600 nt; 55-65 nm; Envelope; CD81, SR-BI	Circular ssRNA; 1700 nt; 36-43 nm; Envelope; NTCP, HSP	Linear ssRNA; 7200 nt; 30-34 nm; Quasi-envelope; Unknown
Incubation; Age[6]; Course	14-30 d; Children; Acute	30-180 d; Any; Acute/chronic	14-180 d; Any; Acute/chronic	14-160 d; Any; Acute/chronic[7]	14-70 d; Adults; Acute
Route of spread	Enteric, sexual	Parental, sexual, vertical	Parental, sexual	Parental, sexual, vertical	Enteric, vertical, parenteral
Hepatitis diagnosis	Anti-HAV IgM	Anti-HBc IgM, HBs antigen, DNA by PCR	Anti-HCV IgG, RNA by PCR	Anti-HDV IgM, RNA by PCR	Anti-HEV IgM, RNA by PCR
Vaccine; Post-exp; Av agent	Available; Ig/vaccine; Not available	Available; Ig/vaccine; NA, IFN-α	Not available; Not effective; DAA agent	HBV vaccine; Not available; IFN-α	Available in China; Not available; Not available
FH[8]; LC/HCC; Prognosis[9]	Very rare; Nil; Full recovery	Very rare; Yes; Chronic carrier	Extremely rare; Yes; High carrier rate	Yes; Yes; Chronic carrier	Yes; Nil; Full recovery

[1]Co-infection/superinfection with hepatitis B virus.
[2]By cloning and sequencing.
[3]Partial dsRNA in hepatitis B virus.
[4]Diameter of virion.
[5]Quasi-envelop with internal protein rather than viral glycoprotein.
[6]Commonly affected age.
[7]Progress to chronicity in 80% superinfection/5% co-infection hepatitis B virus.
[8]Up to 20% in superinfection with hepatitis B virus and pregnant women.
[9]Poorer in hepatitis B virus superinfection with hepatitis delta virus and pregnant woman with hepatitis E virus. AH: Acute hepatitis; Av: Antiviral; CH: Chronic hepatitis; DAA: Direct-acting antiviral; DNA: Deoxyribonucleic acid; ds: Double-stranded; Post-exp: Post-exposure; FH: Fulminant hepatitis; HBc: Hepatitis B virus core antigen; HBs: Hepatitis B virus surface antigen; HCC: Hepatocellular carcinoma; HSP: Heparan sulfate proteoglycans; IFN: Interferon; Ig: Immunoglobulins; LC: Liver cirrhosis; NA: Nucleoside/nucleotide analogues; nt: Nucleotide; NTCP: Sodium taurocholate co-transporting polypeptide, PCR: Polymerase chain reaction; RNA: Ribonucleic acid; SR-BI: Scavenger receptor class B type I; ss: Single-stranded.

Extrahepatic manifestations with evanescent rash and transient arthralgia that develop in acute HAV infection are rare[35]. In the protracted clinical course with cholestasis or relapsing disease, cutaneous vasculitis and arthritis occur with a predilection for lower extremities[36-38], and usually there is spontaneous recovery after the clearance of HAV. Other infrequently observed presentations include glomerulonephritis, myocarditis, thrombocytopenia, and neurological complications like Guillain-Barre syndrome[20,32,39-41].

Acute HEV infection can be asymptomatic or manifest as fulminant hepatitis[21]. Neurological involvement is the most frequently encountered extrahepatic disorder, followed by hematological and gastrointestinal manifestations, possibly caused by autoimmune responses related to molecular mimicry[42,43]. Neuralgic amyotrophy and Guillain-Barre syndrome are two common neuromuscular disorders[44,45], and other uncommon presentations include mononeuritis multiplex, meningoradiculitis, and encephalitis[46-48]. Thrombocytopenia is a frequently identified hematological disorder[49,50], and pancreatitis is the most common gastrointestinal abnormality[51,52]. Myocarditis and glomerulonephritis are rarely observed complications[53,54]. Although there is evidence to support the treatment of HEV-related neurological manifestations with corticosteroids[42,55], the currently recommended therapy is plasma exchange and immune modulation with intravenous immunoglobulin[42,56].

Although extrahepatic manifestations exist with acute infection of all HHVs, such presentations are more commonly identified in HBV, with up to 20% occurrence[57]. Acute HBV infection is often subclinical and asymptomatic in around two-thirds of cases[58]. In the pre-icteric prodromal phase, there is serum sickness-like illness with arthritis and dermatitis due to the deposition of circulating IC composed of HBV surface (HBs) antigen and further activation of complements[59]. These manifestations are usually transient and are resolved after the onset of jaundice. Guillain-Barre syndrome has been reported to be associated with acute HBV infection, and both

plasma exchange and intravenous immunoglobulin are effective treatments[60], implying that there is autoimmune-mediated damage to the myelin sheath of peripheral nerves.

Owing to the availability of viral markers and our understanding of pathogenic pathways, extrahepatic manifestations of chronic HBV infection have been well-elucidated for a while[33,57]. The etiopathogenesis outside the liver in the chronic phase involves the deposition of IC comprised of HBs and/or HBe antigens, followed by the local activation of complement cascades and the recruitment of inflammatory cells[61]. Notably, higher viral load or persistent infection can promote the production of IC, leading to deposition at small or medium-sized arteries[62]. In addition, viral replication has been demonstrated in the endothelium of targeted vessels[63]. Taken together, both mechanisms suggest that inhibition of viral replication, either spontaneously or under antiviral therapy, can reduce extrahepatic manifestations. Up to one-fifth of victims with chronic HBV infection have morbidities outside the liver[61], and these are comprised of arthritis, glomerulonephritis, uveitis, peripheral neuropathy, Raynaud phenomenon, Sjögren syndrome, cutaneous vasculitis, and systemic vasculitis, including polyarteritis nodosa and cryogobulinemic vasculitis[57,62,64,65]. Since the administration of immunosuppressive agents increases the risk of additional hepatic HBV replication with worsening liver disease[61], the treatment of HBV-associated glomerulonephritis and vasculitis is mainly based on antiviral agents, interferon (IFN)-α or nucleoside/nucleotide analogues (NAs)[66-70].

In most cases, symptomatic manifestations are uncommon during acute HCV infection[71]. Extrahepatic presentations include arthralgia, myalgia, and rash[72]. Patients with HCV infection usually progress to chronic stage without recovery[71,72]. Nevertheless, antiviral therapy is highly effective for the acute infection, resulting in the clearance of HCV with sustained virological response (SVR)[72,73].

Persistent HCV infection is a leading cause of chronic liver disease[74]. Although essentially curable with direct-acting antiviral (DAA) therapy, only a portion of patients are diagnosed. Notably, extrahepatic manifestations occur in up to three-quarter of victims with chronic HCV infection[75], and cryoglobulinemia is the most frequently encountered presentation (in 40% to 60% of infected patients)[76]. Direct viral invasion and deposits of soluble IC are two pathogenic processes involved in the development of disease outside the liver[75,76]. The clinical presentations include arthralgia, myalgia, glomerulonephritis, Raynaud phenomenon, Sjögren's syndrome, Hashimoto's thyroiditis, Graves' disease, ulcerative keratitis, peripheral neuropathy, and cryoglobulinemia vasculitis[74-78]. Occasionally, extrahepatic-related autoimmune comorbidities such as cryoglobulinemia vasculitis can lead to the diagnosis of HCV infection[76]. Sustained eradication of HCV by IFN-α or DAA agents has shown to be beneficial for outcomes following these manifestations[78,79]. Notably, a prospective study with 9895 HCV-infected cases receiving DAA medications revealed that viral clearance is responsible for a significant decrease in HCV extrahepatic mortality[80].

VASCULITIS MANIFESTATION IN HUMAN HEPATITIS VIRUSES INFECTION

There is growing evidence demonstrating a causal relationship between viral pathogens and vasculitis. Except for HDV[24,25], other HHVs have been shown to participate in the etiopathogenesis of cutaneous and systemic vasculitis *via* different mechanisms, including direct viral invasion of vascular endothelium, IC-mediated vessel wall damage, and autoimmune responses with stimulation of autoreactive B-cells and impaired regulatory T cells[81-83].

Cutaneous leukocytoclastic vasculitis (CLV) rarely occurs during acute HAV infection, and it may resolve after the regression of hepatitis[36-38,84]. In chronic HBV infection, CLV is rarely observed, with an 1% incidence[62]. HBs antigen has been identified in affected skin lesions[85]. Notably, IFN-α therapy is effective against HBV-associated CLV[86]. The histopathological picture of HHV-triggered CLV shows relatively less eosinophils and lymphocytes compared with those in drug-induced CLV[81].

Acute HAV or HEV infection can induce Henoch-Schönlein purpura (referred to as HSP)[87-89], a systemic vasculitis caused by the widespread deposition of circulating immunoglobulin (Ig)A IC in small-sized blood vessels of skin, joint, lung, kidney, testis, gastrointestinal tract, and nervous system[90]. HAV- and HEV-related HSP usually have a spontaneous recovery. Owing to the defective liver catabolism of IgA IC with further tissue deposits, HSP occurs in HBV or HCV chronic liver diseases,

usually requiring antiviral and corticosteroid therapy[91-94].

Vascular involvement with systemic vasculitis in HHV infection is a recognized extrahepatic morbidity with potential life-threatening organ dysfunction[31,95]. Among them, cryoglobulinemic vasculitis and polyarteritis nodosa are well-known vascular comorbidities in HHV infection[96,97].

HUMAN HEPATITIS VIRUSES-ASSOCIATED CRYOGLOBULINEMIC VASCULITIS

Cryoglobulinemic vasculitis is caused by IC-mediated inflammation of small-sized blood vessels and is accompanied by the activation of complements[96]. Cryoglobulins are circulating antibodies that precipitate *in vitro* at temperatures less than 37 °C and dissolve after rewarming, and these are either Ig or a mixture of Ig and complement components[98]. Individuals with cryoglobulinemia may remain asymptomatic without clinical abnormalities[96,98]. A typical triad of purpura, arthralgia, and weakness associated with organic dysfunction and elevated levels of rheumatoid factor (RF) was defined as cryoglobulinemic disease in 1966 by Meltzer *et al*[99]. Based on the composition of Ig, cryoglobulinemia can be classified into type I with monoclonal Ig (usually IgM), type II with polyclonal IgG and monoclonal IgM RF, and type III with polyclonal IgG and polyclonal IgM RF[100]. Type I is an infrequently encountered subgroup and is only found in hematological malignancies[101], whereas mixed types II and III can be associated with viral hepatitis caused by HBV, most commonly observed with HCV, and rarely identified with HAV infection[96,102-104]. Despite the presence of cryoglobulins in up to 60% of chronic HCV patients, cryoglobulinemic vasculitis only appears in around 10% of cases[76]. In chronic HHV infection, envelope glycoproteins can help the virus enter intrahepatic and circulating B lymphocytes to produce Ig with RF activity, resulting in the generation of cryoglobulins and formation of IC with vascular wall deposition[105,106].

Recurrent palpable purpura with the characteristic histopathological finding of leukocytoclastic vasculitis is the most common clinical manifestation[107]. Other cutaneous presentations are ischemic ulcers, digital gangrene, and Raynaud's phenomenon. In Figure 1, the presence of leukocytoclastic vasculitis in biopsied skin lesions from a HCV-infected patient with cryoglobulinemia-associated purpura is shown. In addition, the presence of Meltzer triad was identified in most patients at the onset of disease[108], and skin, joint, kidney, and peripheral nerve are frequently affected organs in cryoglobulinemic vasculitis[96,108]. Renal involvement with membranoproliferative glomerulonephritis as the most common finding is associated with significant morbidity and even mortality[109]. HCV core protein and Ig are major components of IC and are distributed along the capillary walls of glomeruli[110]. Peripheral neuropathy with mononeuritis multiplex is commonly observed, which can be the first clinical manifestation[111]. Other rarely involved organs include the central nervous system, gastrointestinal tract, myocardium, and lung, and their involvement leads to the clinical presentations of impaired cognitive function, intestinal ischemia, hypertrophic cardiomyopathy, and diffuse alveolar hemorrhage[96,108,112-115].

Sporadic cases with cryoglobulinemic vasculitis, either in adults or children, have been observed during acute HAV infection[36,84,104,116,117]. These patients had biopsy-proven CLV plus arthritis or glomerulonephritis, and the use of corticosteroids were required to control these complications.

Based on clinical observations, the Meltzer triad had been regarded as an IC-mediated disease secondary to the HBV infection[118]. Since then, HBs antigen in biopsied vessel wall and HBs antigen/anti-HBs in circulating cryoprecipitates have been identified in cryoglobulinemic vasculitis[119]. A retrospective study from 913 cases with cryoglobulinemia demonstrated a HBs antigen positivity of 5.8%[120], whereas analyzed data from 231 patients with mixed cryoglobulinemia only revealed an HBV infection rate of 1.8%[107]. Nevertheless, HBV is among three common infectious etiologies in patients with cryoglobulinemia[108]. This virus is predominantly associated with type II cryoglobulinemia, and its common extrahepatic manifestations are purpura, arthralgia, and neuropathy[121]. Furthermore, compared to adults, children with symptomatic cryogobulinemia have a lower occurrence of HBV infection but higher frequencies of articular and cutaneous involvement[122]. Notably, the presence of HBs antigen represents one of the main independent predictors of mortality in cryogobulinemic vasculitis[70].

Accumulated evidence indicates that the use of NAs for viral suppression in HBV-related cryogobulinemic vasculitis can cause the disappearance of cryoglobulins,

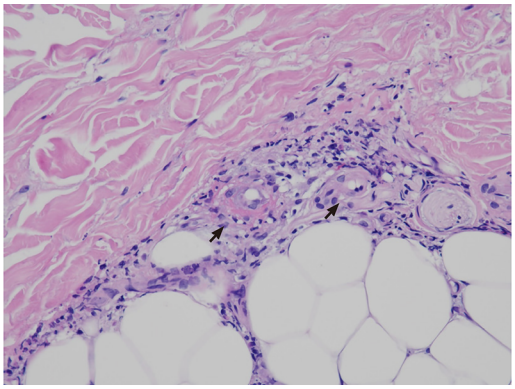


Figure 1 Cryoglobulinemic vasculitis. The small vessels show neutrophilic inflammation, with fibrinoid necrosis and fragmented neutrophil nuclei (black arrows). Hematoxylin and eosin staining, 400 ×.

normalize liver function, and significantly clinically improve most patients with mild disease, indicating a role for HBV replication in the pathogenesis[70,123]. Antiviral therapy with NAs should be a life-long prescription, and discontinuation is considered only after persistent HBs antigen loss with the seroconversion and undetectable HBV DNA[70,124]. Despite an observation with ineffective responses[70], IFN-α can be an alternative therapeutic modality[123]. The use of corticosteroids without NA therapy is ineffective for suppression of HBV viremia, resulting in refractory or relapsing disease[121]. Nevertheless, only a portion of patients with severe disease, including peripheral neuropathy and renal involvement, can achieve clinical regression under NA therapy[70,123,125]. CD20-positive B-cells are expanded and activated in mixed cryogobulinemia, and they participate in the production of cryoglobulins[126]. Clinical remission has been reported in patients with glomerulonephritis treated with NA in combination with rituximab, a monoclonal antibody against CD20 on the surface of B-cells[127,128]. Considering the risk of viral reactivation in patients with positive HBs or an occult infection with negative HBs and positive anti-HBc, prophylaxis with NAs should be initiated before the rituximab treatment[70,124,129]. Because of a potentially fatal complication, its use should be avoided during an active flare of HBV infection[70,130]. Prescription of this biologic as a second-line agent can be considered in patients with severe disease refractory to NA therapy[70,123].

Among the underlying diseases in cryoglobulinemia, HCV infection is the most common cause, with a 73% positive frequency of anti-HCV and a 86% occurrence of HCV ribonucleic acid[102,108,131]. Nevertheless, only a small portion of cryoglobulinemia with HCV infection develops significant vasculitis manifestations[96]. Similar to HBV infection, HCV is mainly associated with type II cryoglobulinemia[108]. The interaction of HCV envelope proteins with CD81 surface receptor can stimulate B-cells to expand clonally and produce monoclonal IgM RF that binds polyclonal anti-HCV core antigen, which suggests that cryoglobulinemia is due to host immune responses against HCV infection[132-134]. Although the HCV-related mixed cryoglobulinemia is a benign B-cell lymphoproliferative condition, chronic viral stimulation on the immune system leads to the selection of abnormal clones[135]. An epidemiological survey elucidated a link between HCV infection and B-cell non-Hodgkin's lymphoma (NHL)[135]. A large-scale cohort with 146394 HCV-infected patients demonstrated a more than 20% increased risk of this malignancy[136]. Furthermore, the overall risk of B-cell NHL in mixed cryoglobulinemia patients was estimated to be 35 times higher than that in the general population[137]. Collectively, these observations have indicated a pathogenic role of HCV in B-cell NHL.

Since HCV-related cryoglobulinemic vasculitis is an antigen-driven process and its activity usually correlates with viremia, the most effective treatment is the eradication of underlying viral infection[96]. Anti-HCV therapy can follow the existing guideline as cryoglobulinemia does not specifically influence the choice of antiviral drug[138]. DAA agents alone induce SVR with less adverse events and are more effective than the combined IFN-α and ribavirin regimen in cryoglobulinemic vasculitis[79]. In a prospective multicenter study carried out in these patients, all achieved SVR with a 90% complete clinical response after DAA therapy for 12 wk or more[139]. Altogether, patients with HCV-associated cryoglobulinemic vasculitis had higher SVR (74%-100%) and clinical remission (61%-100%) rates after receiving DAA medications[79]. Higher complete response rates (75%-100%) were observed in cutaneous and musculoskeletal

presentations, while lower responses (30%-70%) were identified in peripheral nerve and renal involvement[139]. In addition, DAA therapy is beneficial for HCV-associated B-cell malignancy, resulting in higher SVR and lymphoproliferative disease response rates in indolent NHL patients[140].

In addition to optimized DAA agents, corticosteroids in combination with cyclophosphamide are also considered as first-line therapy in severe fulminant manifestations, such as intestinal necrotizing vasculitis, rapid progressive glomerulonephritis, and diffuse alveolar hemorrhage[108,141]. Plasma exchange with warm apheresis solution to avoid cryoglobulin precipitation is an adjunct treatment that is useful in life-threatening disease by removing circulating cryoglobulins to interrupt the IC-mediated pathogenesis[141]. An earlier investigation showed that the addition of rituximab to the combined IFN-α and ribavirin regimen can enhance the clearance of cryoglobulins and shorten the time to clinical remission[142]. A subsequent randomized controlled trial in patients with severe disease revealed that rituximab monotherapy is as effective as conventional immunosuppressive treatment[143]. Despite the promise of rituximab as a therapeutic agent[144], there is a substantial risk for IC formation between this biologic and RF-positive IgM to exacerbate the vasculitis activity in HCV-associated type II cryoglobulinemic vasculitis[145].

HUMAN HEPATITIS VIRUSES-ASSOCIATED POLYARTERITIS NODOSA

Polyarteritis nodosa is a rare disease, with an annual incidence ranging from 0 to 2 cases per million population[97]. It is a necrotizing vasculitis affecting small- and medium-sized arteries, with systemic involvement but usually sparing the lungs. A skin-restricted form involving the area below the knees can progress to the systemic form, suggesting the same entity for both forms[146,147]. Most patients with polyarteritis nodosa belong to the idiopathic type with autoimmune-mediated mechanisms[97,148]. The secondary type is often observed in viral diseases, like cytomegalovirus, human immunodeficiency virus, and HHV infections. The association between HBV and polyarteritis nodosa was first recognized in 1970[149,150], and since then a substantial portion of cases have been identified after HBV infection. Later on, owing to the introduction of the vaccination protocol, the occurrence of HBV-related polyarteritis nodosa has gradually disappeared from clinical practice[151]. Although HCV positivity has been observed in this disorder, it is not a dominant etiological factor[152]. The occlusion and rupture of inflamed arteries can produce ischemia and hemorrhage in various organs and tissues, including skin, joint, kidney, testis, gastrointestinal tract, and peripheral nerve[97,148]. The most frequently involved organ system is the skin, presenting manifestations of palpable purpura, livedoid lesions, subcutaneous nodules, and necrotic ulcers[153]. Figure 2 demonstrates the histopathological findings of transmural necrotizing arteritis with neutrophilic infiltration and fibrinoid necrosis in a cutaneous biopsy specimen from a patient with polyarteritis nodosa-associated nodules (Case No. 2 in Table 2). Mononeuritis multiplex and symmetrical polyneuropathy are common neurological complications[154]. Gastrointestinal manifestations are usually associated with significant morbidity and can manifest as an acute surgical abdomen[155]. Renal involvement without glomerulonephritis is related to infarction or hemorrhage caused by the rupture of renal micro-aneurysms[97]. Although rare as an initial presentation, orchitis due to testicular ischemia is a characteristic finding of polyarteritis nodosa[156].

As supported by clinical evidence, the idiopathic type benefits from combined corticosteroids and cyclophosphamide therapy, which induce remission in severe disease with organ dysfunction; whereas, mild manifestations can be treated with corticosteroids alone[97,148]. After the completion of cyclophosphamide therapy, azathioprine or methotrexate can be prescribed as a remission-maintenance agent[97]. Currently, small-molecule targeted drugs and biologics have been used in refractory patients naïve to HBV infection with successful outcomes, including Janus kinase inhibitor, B-cell targeted agent, tumor necrosis factor blocker, and interleukin-6 blockade[157-161]. The clinical data and medication profiles with biologics in polyarteritis nodosa patients recently diagnosed by authors are shown in Table 2. Although poor prognosis in earlier years is due to a delayed diagnosis[97], the overall outcome has improved to a 5-year survival rate of 80%. Outcomes are significantly worsened in association with HBV infection, age above 65 years, new-onset hypertension, renal impairment with high creatinine levels, gastrointestinal involvement requiring surgery, and peripheral nerve involvement[153].

There are no available reports related to the association of polyarteritis nodosa with

Table 2 Clinical and medication profiles in five polyarteritis nodosa patients naïve to human hepatitis virus infection[1]

No	Age/sex	Initial symptom	Diagnosisperiod[2]	BVAS/FFS[3]	HHV status[4]	Follow-up manifestation	Therapy	Outcome
1	23/F	Arthralgia, rash[5]	2 mo	6/0	Negative	Joint, PN, skin	Az, Cs	Survival, remission
2	29/F	Arthralgia, fever, rash[5]	1 yr	11/0	Negative	FN, GI, joint, PN, skin	Az, Cs	Survival, remission
3	38/F	Fever, rash[5]	1 yr 5 mo	14/0	Negative	Joint, PN, skin	Az, Cs, Cy	Survival, remission
4	39/M	Rash	3 yr 10 mo	18/1	Negative	Kidney, skin	Az, Cs, RTX	Survival, chronic renal insufficiency
5	42/M	Arthralgia, rash	6 mo	7/0	Negative	Joint, PN, skin, kidney, testis	ADA, Az, Cs, Cy	Survival, remission

[1]Enrollment from 2012 to 2019.
[2]Time period from initial symptoms to the established diagnosis.
[3]Calculation at the disease diagnosis.
[4]Human hepatitis virus status, including examinations for hepatitis A virus, hepatitis B virus, hepatitis C virus, and hepatitis delta virus.
[5]Erythematous nodosum-like skin lesions. ADA: Adalimumab; Az: Azathioprine; BVAS: Birmingham vasculitis activity score; Cs: Corticosteroids, Cy: Cyclophosphamide; F: Female; FFS: Four-factor score, including age above 65 years, cardiac symptoms, gastrointestinal involvement, and renal insufficiency; FN: Foot necrosis; GI: Gastrointestinal; HHV: Human hepatitis virus; M: Male; PAN: Polyarteritis nodosa; PN: Peripheral neuropathy; RTX: Rituximab.

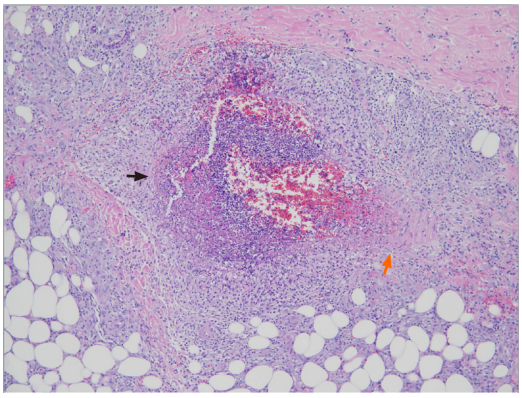


Figure 2 Polyarteritis nodosa. The vascular wall shows transmural necrotizing inflammation, with intense neutrophilic infiltration and fibrinoid necrosis (black arrow). There is residual muscular wall of the vessel (orange arrow). Hematoxylin and eosin staining, 100 ×.

HAV. Nevertheless, published cases with cutaneous or renal manifestations have shown histopathological evidence of medium-sized blood vessels' involvement compatible with the diagnosis of polyarteritis nodosa[162,163].

Simultaneous development of mixed cryoglobulinemia and polyarteritis nodosa has been documented in patients with coinfection of HCV and HBV[164,165]. In a clinical survey on polyarteritis nodosa, the positive frequency of anti-HCV was 20% (5% with detectable HCV ribonucleic acid and they were more likely to have cutaneous manifestation)[166]. In a large cohort with 161 cases of HCV-related vasculitis (19% polyarteritis nodosa and 81% cryoglobulinemic vasculitis), there were more acute and severe clinical presentations in the former group, including constitutional symptoms, new-onset hypertension, gastrointestinal tract involvement, and mononeuritis multiplex[167]. Despite no differences in the 5-year survival rates, there was a higher complete remission rate for polyarteritis nodosa than for cryoglobulinemic vasculitis. The therapeutic guidelines for HCV-related polyarteritis nodosa have not been established yet. Reported cases have received various combinations of corticosteroids, cyclophosphamide, and antiviral agents. B-cell targeted therapy has been applied to patients with HCV-related polyarteritis nodosa[167,168]. A higher clinical relapse rate was observed for rituximab treatment than for a combined regimen with IFN-α and ribavirin in this disease[167].

During the 1970s to 1980s, HBV was a major cause of polyarteritis nodosa, with

nearly half of cases having this infection, but the frequency has decreased due to improved blood safety and a viral vaccine campaign since early the 1990s, indicating HBV as a causal etiology[169]. Although histopathological studies have rarely confirmed the presence of HBV antigens in the vessel wall[151], the pathogenesis of HBV-related type is related to the deposits of IC, different from the idiopathic disease[169]. When comparing HBV- with HCV-associated polyarteritis nodosa[167,169], the former group has more general symptoms and orchitis, less cutaneous manifestation and new-onset hypertension, a lower survival rate, and a much shorter average period from viral infection to vasculitis development, 7 mo *vs* 20 years. In the HBV-related type, most cases have higher viral replication and HBV DNA levels, leading to the persistent presence of circulating IC[169].

The prevalence of HBs antigen in the general Taiwan population used to be near 20%, but the HBV seropositive rate in children has decreased dramatically from 11% to less than 1% after the initiation of the national vaccination program in 1984[170]. Despite a high inpatient prevalence with more than 10 cases per 100000 discharges in the United States[171], polyarteritis nodosa has been very rarely encountered by practicing physicians in Taiwan. In particular, even with more than 2 million infected patients, there is no reported association between HBV and polyarteritis nodosa[159,172-177]. Perinatal mother-to-infant HBV transmission is the most important factor responsible for a high carriage rate of HBs antigen in Taiwan[178]. Vertical transmission in infants is asymptomatic until adulthood and associated with a greater risk of chronic infection, suggesting that HBV infection causes an immunotolerant status in children who are less prone to develop full immune responses[179]. Parenteral HBV infection during adult life can induce polyarteritis nodosa within 1 year after viral infection, indicating an early post-infectious disease *via* this transmission route[169]. In Table 3, polyarteritis nodosa from various larger-number case series with different HBV-associated frequencies is compared[153,172-177,180-184]. Patients reported from Taiwan have no HBV infection, younger female predominance, and more cutaneous or testicular manifestation than those from other series with a HBV association.

After initial therapy with corticosteroids to reduce acute vascular inflammation, the therapeutic approach in HBV-associated polyarteritis nodosa is to clear circulating IC and suppress HBV replication by plasma exchange and antiviral agents with NAs or IFN-α[169]. Since the addition of cyclophosphamide to corticosteroids has shown to benefit patients presenting with poor prognostic factors[185], this regimen can be considered in patients with severe disease. Notably, plasma exchange has not been shown to be beneficial in polyarteritis nodosa patients without HBV infection[186]. Furthermore, antiviral agents can be used concurrently with corticosteroids or combined cyclophosphamide and corticosteroids therapy[97,148]. Contradictory to the idiopathic disease, relapses have rarely been observed in HBV-related type, especially when viral replication has ceased and seroconversion from HBe antigen to antibody has been achieved after antiviral therapy[148,169].

CONCLUSION

Although HHVs primarily affect hepatocytes, they can also cause complications in other organs, and both acute and chronic viral hepatitis are associated with clinical presentations outside the liver. Vascular involvement with cutaneous and systemic vasculitis is a well-known extrahepatic morbidity. There is growing evidence suggesting a causal relationship between viral pathogens and vasculitis. Except for HDV, other HHVs have participated in the etiopathogenesis of cutaneous and systemic vasculitis *via* different mechanisms, including direct viral invasion of vascular endothelial cells, IC-mediated vessel wall damage, and autoimmune responses with stimulation of autoreactive B-cells and impaired regulatory T cells. Cryoglobulinemic vasculitis and polyarteritis nodosa are recognized for their association with chronic HHV infection. Therapeutic guidelines for HHV-associated vasculitis have not been established yet. Antiviral therapy should be initiated in HBV and HCV-related systemic vasculitis in addition to the use of corticosteroids. Plasma exchange and/or combined cyclophosphamide and corticosteroid therapy can be considered in patients with severe life-threatening vasculitis manifestations.

Table 3 Comparisons of clinical and outcome profiles in polyarteritis nodosa from various case series with different hepatitis B virus-infected frequencies

Source of cases	No/age[1] F%	HBV status	Fever	AM	Skin	PN	GI	Renal	TestisM%	Therapy	Death
Taiwan	12/31, 67%	0%	67%	58%	75%	42%	50%	75%	50%	Az, Cs, Cy, Bio	33%
United Kingdom	17/49, 24%	31%	76%	77%	65%	59%	65%	77%	NA	Cs, Is	38%
United States	53/54, 34%	11%	31%	55%	58%	60%	25%	66%	NA	Cs, Cy	42%
Canada	45/54, 47%	19%	63%	51%	44%	51%	53%	44%	4%	Cs, Cy	53%
South Korea	27/47, 37%	56%	52%	30%	44%	63%	48%	48%	24%	Az, Cs, Cy, Is	15%
France	348/51,37%	35%	64%	59%	50%	74%	38%	51%	17%	Av, Cs, Cy, Is	25%
India	27/38, 26%	26%	52%	37%	37%	82%	30%	59%	30%	Av, Az, Cs, Cy	11%

[1]Mean age at disease diagnosis. AM: Articulomuscular; Az: Azathioprine; Av: Antiviral agent; Bio: Biologics; Cs: Corticosteroids; Cy: Cyclophosphamide; F: Female; GI: Gastrointestinal; Is: Immunosuppressive agent, M: Male; NA: Not available; PN: Peripheral neuropathy.

ACKNOWLEDGEMENTS

The authors are indebted to Dr. Wu IC, Division of Gastroenterology and Hepatology, for his valuable comments on HHV-related clinical manifestations, and to other physicians at the National Cheng Kung University Hospital involved in the diagnosis and management of reported patients. The Institutional Review Board of National Cheng Kung University Hospital approved this study (No. B-ER-105-108).

REFERENCES

1 **Arroyo V**, Moreau R, Jalan R. Acute-on-Chronic Liver Failure. *N Engl J Med* 2020; **382**: 2137-2145 [PMID: 32459924 DOI: 10.1056/NEJMra1914900]
2 **Razavi H**. Global Epidemiology of Viral Hepatitis. *Gastroenterol Clin North Am* 2020; **49**: 179-189 [PMID: 32389357 DOI: 10.1016/j.gtc.2020.01.001]
3 **Noor A**, Panwala A, Forouhar F, Wu GY. Hepatitis caused by herpes viruses: A review. *J Dig Dis* 2018; **19**: 446-455 [PMID: 29923691 DOI: 10.1111/1751-2980.12640]
4 **Rasche A**, Sander AL, Corman VM, Drexler JF. Evolutionary biology of human hepatitis viruses. *J Hepatol* 2019; **70**: 501-520 [PMID: 30472320 DOI: 10.1016/j.jhep.2018.11.010]
5 **Khuroo MS**, Sofi AA. The Discovery of Hepatitis Viruses: Agents and Disease. *J Clin Exp Hepatol* 2020; **10**: 391-401 [PMID: 32655240 DOI: 10.1016/j.jceh.2020.04.006]
6 **Krugman S**, Giles JP, Hammond J. Infectious hepatitis. Evidence for two distinctive clinical, epidemiological, and immunological types of infection. *JAMA* 1967; **200**: 365-373 [PMID: 4164595 DOI: 10.1001/jama.200.5.365]
7 **BLUMBERG BS**, ALTER HJ, VISNICH S. A "NEW" ANTIGEN IN LEUKEMIA SERA. *JAMA* 1965; **191**: 541-546 [PMID: 14239025 DOI: 10.1001/jama.1965.03080070025007]
8 **Dane DS**, Cameron CH, Briggs M. Virus-like particles in serum of patients with Australia-antigen-associated hepatitis. *Lancet* 1970; **1**: 695-698 [PMID: 4190997 DOI: 10.1016/s0140-6736(70)90926-8]
9 **Burrell CJ**, Mackay P, Greenaway PJ, Hofschneider PH, Murray K. Expression in Escherichia coli of hepatitis B virus DNA sequences cloned in plasmid pBR322. *Nature* 1979; **279**: 43-47 [PMID: 377093 DOI: 10.1038/279043a0]
10 **Koff RS**. Feinstone SM, Kapikian AZ, Purcell RH. Hepatitis A: detection by immune electron microscopy of a virus like antigen associated with acute illness [Science 1973;182:1026-1028]. *J Hepatol* 2002; **37**: 2-6 [PMID: 12076855 DOI: 10.1016/s0168-8278(02)00169-1]
11 **Ticehurst JR**, Racaniello VR, Baroudy BM, Baltimore D, Purcell RH, Feinstone SM. Molecular cloning and characterization of hepatitis A virus cDNA. *Proc Natl Acad Sci USA* 1983; **80**: 5885-5889 [PMID: 6310601 DOI: 10.1073/pnas.80.19.5885]
12 **Alter HJ**, Holland PV, Morrow AG, Purcell RH, Feinstone SM, Moritsugu Y. Clinical and serological analysis of transfusion-associated hepatitis. *Lancet* 1975; **2**: 838-841 [PMID: 53329 DOI: 10.1016/s0140-6736(75)90234-2]
13 **Alter HJ**, Purcell RH, Holland PV, Popper H. Transmissible agent in non-A, non-B hepatitis. *Lancet* 1978; **1**: 459-463 [PMID: 76017 DOI: 10.1016/s0140-6736(78)90131-9]

14 **Choo QL**, Kuo G, Weiner AJ, Overby LR, Bradley DW, Houghton M. Isolation of a cDNA clone derived from a blood-borne non-A, non-B viral hepatitis genome. *Science* 1989; **244**: 359-362 [PMID: 2523562 DOI: 10.1126/science.2523562]

15 **Rizzetto M**, Canese MG, Aricò S, Crivelli O, Trepo C, Bonino F, Verme G. Immunofluorescence detection of new antigen-antibody system (delta/anti-delta) associated to hepatitis B virus in liver and in serum of HBsAg carriers. *Gut* 1977; **18**: 997-1003 [PMID: 75123 DOI: 10.1136/gut.18.12.997]

16 **Rizzetto M**, Hoyer B, Canese MG, Shih JW, Purcell RH, Gerin JL. delta Agent: association of delta antigen with hepatitis B surface antigen and RNA in serum of delta-infected chimpanzees. *Proc Natl Acad Sci USA* 1980; **77**: 6124-6128 [PMID: 6934539 DOI: 10.1073/pnas.77.10.6124]

17 **Khuroo MS**. Study of an epidemic of non-A, non-B hepatitis. Possibility of another human hepatitis virus distinct from post-transfusion non-A, non-B type. *Am J Med* 1980; **68**: 818-824 [PMID: 6770682 DOI: 10.1016/0002-9343(80)90200-4]

18 **Reyes GR**, Purdy MA, Kim JP, Luk KC, Young LM, Fry KE, Bradley DW. Isolation of a cDNA from the virus responsible for enterically transmitted non-A, non-B hepatitis. *Science* 1990; **247**: 1335-1339 [PMID: 2107574 DOI: 10.1126/science.2107574]

19 **Hofmeister MG**, Foster MA, Teshale EH. Epidemiology and Transmission of Hepatitis A Virus and Hepatitis E Virus Infections in the United States. *Cold Spring Harb Perspect Med* 2019; **9** [PMID: 29712684 DOI: 10.1101/cshperspect.a033431]

20 **Abutaleb A**, Kottilil S. Hepatitis A: Epidemiology, Natural History, Unusual Clinical Manifestations, and Prevention. *Gastroenterol Clin North Am* 2020; **49**: 191-199 [PMID: 32389358 DOI: 10.1016/j.gtc.2020.01.002]

21 **Aslan AT**, Balaban HY. Hepatitis E virus: Epidemiology, diagnosis, clinical manifestations, and treatment. *World J Gastroenterol* 2020; **26**: 5543-5560 [PMID: 33071523 DOI: 10.3748/wjg.v26.i37.5543]

22 **Yuen MF**, Chen DS, Dusheiko GM, Janssen HLA, Lau DTY, Locarnini SA, Peters MG, Lai CL. Hepatitis B virus infection. *Nat Rev Dis Primers* 2018; **4**: 18035 [PMID: 29877316 DOI: 10.1038/nrdp.2018.35]

23 **Kaplan DE**. Hepatitis C Virus. *Ann Intern Med* 2020; **173**: ITC33-ITC48 [PMID: 32866406 DOI: 10.7326/AITC202009010]

24 **Gilman C**, Heller T, Koh C. Chronic hepatitis delta: A state-of-the-art review and new therapies. *World J Gastroenterol* 2019; **25**: 4580-4597 [PMID: 31528088 DOI: 10.3748/wjg.v25.i32.4580]

25 **Taylor JM**. Infection by Hepatitis Delta Virus. *Viruses* 2020; **12** [PMID: 32560053 DOI: 10.3390/v12060648]

26 **Feng Z**, Hirai-Yuki A, McKnight KL, Lemon SM. Naked Viruses That Aren't Always Naked: Quasi-Enveloped Agents of Acute Hepatitis. *Annu Rev Virol* 2014; **1**: 539-560 [PMID: 26958733 DOI: 10.1146/annurev-virology-031413-085359]

27 **Cheung A**, Kwo P. Viral Hepatitis Other than A, B, and C: Evaluation and Management. *Clin Liver Dis* 2020; **24**: 405-419 [PMID: 32620280 DOI: 10.1016/j.cld.2020.04.008]

28 **Cao Y**, Bing Z, Guan S, Zhang Z, Wang X. Development of new hepatitis E vaccines. *Hum Vaccin Immunother* 2018; **14**: 2254-2262 [PMID: 29708836 DOI: 10.1080/21645515.2018.1469591]

29 **World Health Organization**. Hepatitis 2020. https://www.who.int/health-topics/hepatitis#tab=tab_1

30 **Schiff ER**. Atypical clinical manifestations of hepatitis A. *Vaccine* 1992; **10** Suppl 1: S18-S20 [PMID: 1475999 DOI: 10.1016/0264-410x(92)90534-q]

31 **Pyrsopoulos NT**, Reddy KR. Extrahepatic manifestations of chronic viral hepatitis. *Curr Gastroenterol Rep* 2001; **3**: 71-78 [PMID: 11177698 DOI: 10.1007/s11894-001-0044-1]

32 **Amarapurkar DN**, Amarapurkar AD. Extrahepatic manifestations of viral hepatitis. *Ann Hepatol* 2002; **1**: 192-195 [PMID: 15280806]

33 **Han SH**. Extrahepatic manifestations of chronic hepatitis B. *Clin Liver Dis* 2004; **8**: 403-418 [PMID: 15481347 DOI: 10.1016/j.cld.2004.02.003]

34 **Romano C**, Cuomo G, Ferrara R, Del Mastro A, Esposito S, Sellitto A, Adinolfi LE. Uncommon immune-mediated extrahepatic manifestations of HCV infection. *Expert Rev Clin Immunol* 2018; **14**: 1089-1099 [PMID: 30338718 DOI: 10.1080/1744666X.2018.1538790]

35 **Shin EC**, Jeong SH. Natural History, Clinical Manifestations, and Pathogenesis of Hepatitis A. *Cold Spring Harb Perspect Med* 2018; **8** [PMID: 29440324 DOI: 10.1101/cshperspect.a031708]

36 **Inman RD**, Hodge M, Johnston ME, Wright J, Heathcote J. Arthritis, vasculitis, and cryoglobulinemia associated with relapsing hepatitis A virus infection. *Ann Intern Med* 1986; **105**: 700-703 [PMID: 3021038 DOI: 10.7326/0003-4819-105-5-700]

37 **Ilan Y**, Hillman M, Oren R, Zlotogorski A, Shouval D. Vasculitis and cryoglobulinemia associated with persisting cholestatic hepatitis A virus infection. *Am J Gastroenterol* 1990; **85**: 586-587 [PMID: 2337062]

38 **Dan M**, Yaniv R. Cholestatic hepatitis, cutaneous vasculitis, and vascular deposits of immunoglobulin M and complement associated with hepatitis A virus infection. *Am J Med* 1990; **89**: 103-104 [PMID: 2368780 DOI: 10.1016/0002-9343(90)90107-o]

39 **Shenoy R**, Nair S, Kamath N. Thrombocytopenia in hepatitis A--an atypical presentation. *J Trop Pediatr* 2004; **50**: 241-242 [PMID: 15357567 DOI: 10.1093/tropej/50.4.241]

40 **Allen O**, Edhi A, Hafeez A, Halalau A. A Very Rare Complication of Hepatitis A Infection: Acute Myocarditis-A Case Report with Literature Review. *Case Rep Med* 2018; **2018**: 3625139 [PMID:

30302093 DOI: 10.1155/2018/3625139]
41 **Stübgen JP**. Neuromuscular complications of hepatitis A virus infection and vaccines. *J Neurol Sci* 2011; **300**: 2-8 [PMID: 20920814 DOI: 10.1016/j.jns.2010.09.015]
42 **Dalton HR**, Kamar N, van Eijk JJ, Mclean BN, Cintas P, Bendall RP, Jacobs BC. Hepatitis E virus and neurological injury. *Nat Rev Neurol* 2016; **12**: 77-85 [PMID: 26711839 DOI: 10.1038/nrneurol.2015.234]
43 **Rawla P**, Raj JP, Kannemkuzhiyil AJ, Aluru JS, Thandra KC, Gajendran M. A Systematic Review of the Extra-Hepatic Manifestations of Hepatitis E Virus Infection. *Med Sci (Basel)* 2020; **8** [PMID: 32033102 DOI: 10.3390/medsci8010009]
44 **Avila JD**, Lacomis D, Lam EM. Neuralgic Amyotrophy Associated With Hepatitis E Virus Infection: First Case in the United States. *J Clin Neuromuscul Dis* 2016; **18**: 96-100 [PMID: 27861224 DOI: 10.1097/CND.0000000000000137]
45 **Loly JP**, Rikir E, Seivert M, Legros E, Defrance P, Belaiche J, Moonen G, Delwaide J. Guillain-Barré syndrome following hepatitis E. *World J Gastroenterol* 2009; **15**: 1645-1647 [PMID: 19340910 DOI: 10.3748/wjg.15.1645]
46 **Perrin HB**, Cintas P, Abravanel F, Gérolami R, d'Alteroche L, Raynal JN, Alric L, Dupuis E, Prudhomme L, Vaucher E, Couzigou P, Liversain JM, Bureau C, Vinel JP, Kamar N, Izopet J, Peron JM. Neurologic Disorders in Immunocompetent Patients with Autochthonous Acute Hepatitis E. *Emerg Infect Dis* 2015; **21**: 1928-1934 [PMID: 26490255 DOI: 10.3201/eid2111.141789]
47 **Dalton HR**, van Eijk JJJ, Cintas P, Madden RG, Jones C, Webb GW, Norton B, Pique J, Lutgens S, Devooght-Johnson N, Woolson K, Baker J, Saunders M, Househam L, Griffiths J, Abravanel F, Izopet J, Kamar N, van Alfen N, van Engelen BGM, Hunter JG, van der Eijk AA, Bendall RP, Mclean BN, Jacobs BC. Hepatitis E virus infection and acute non-traumatic neurological injury: A prospective multicentre study. *J Hepatol* 2017; **67**: 925-932 [PMID: 28734938 DOI: 10.1016/j.jhep.2017.07.010]
48 **Despierres LA**, Kaphan E, Attarian S, Cohen-Bacrie S, Pelletier J, Pouget J, Motte A, Charrel R, Gerolami R, Colson P. Neurologic disorders and hepatitis E, France, 2010. *Emerg Infect Dis* 2011; **17**: 1510-1512 [PMID: 21801637 DOI: 10.3201/eid1708.102028]
49 **Marion O**, Abravanel F, Del Bello A, Esposito L, Lhomme S, Puissant-Lubrano B, Alric L, Faguer S, Izopet J, Kamar N. Hepatitis E virus-associated cryoglobulinemia in solid-organ-transplant recipients. *Liver Int* 2018; **38**: 2178-2189 [PMID: 29845733 DOI: 10.1111/liv.13894]
50 **Woolson KL**, Forbes A, Vine L, Beynon L, McElhinney L, Panayi V, Hunter JG, Madden RG, Glasgow T, Kotecha A, Dalton HC, Mihailescu L, Warshow U, Hussaini HS, Palmer J, Mclean BN, Haywood B, Bendall RP, Dalton HR. Extra-hepatic manifestations of autochthonous hepatitis E infection. *Aliment Pharmacol Ther* 2014; **40**: 1282-1291 [PMID: 25303615 DOI: 10.1111/apt.12986]
51 **Nayak HK**, Kamble NL, Raizada N, Garg S, Daga MK. Acute pancreatitis complicating acute hepatitis e virus infection: a case report and review. *Case Reports Hepatol* 2013; **2013**: 531235 [PMID: 25374721 DOI: 10.1155/2013/531235]
52 **Raj M**, Kumar K, Ghoshal UC, Saraswat VA, Aggarwal R, Mohindra S. Acute Hepatitis E-Associated Acute Pancreatitis: A Single Center Experience and Literature Review. *Pancreas* 2015; **44**: 1320-1322 [PMID: 26390412 DOI: 10.1097/MPA.0000000000000402]
53 **Sengupta P**, Biswas S, Roy T. Hepatitis E-Induced Acute Myocarditis in an Elderly Woman. *Case Rep Gastroenterol* 2019; **13**: 342-349 [PMID: 31572104 DOI: 10.1159/000501998]
54 **Del Bello A**, Guilbeau-Frugier C, Josse AG, Rostaing L, Izopet J, Kamar N. Successful treatment of hepatitis E virus-associated cryoglobulinemic membranoproliferative glomerulonephritis with ribavirin. *Transpl Infect Dis* 2015; **17**: 279-283 [PMID: 25708383 DOI: 10.1111/tid.12353]
55 **van Eijk JJ**, van Alfen N, Berrevoets M, van der Wilt GJ, Pillen S, van Engelen BG. Evaluation of prednisolone treatment in the acute phase of neuralgic amyotrophy: an observational study. *J Neurol Neurosurg Psychiatry* 2009; **80**: 1120-1124 [PMID: 19321467 DOI: 10.1136/jnnp.2008.163386]
56 **Osman C**, Jennings R, El-Ghariani K, Pinto A. Plasma exchange in neurological disease. *Pract Neurol* 2020; **20**: 92-99 [PMID: 31300488 DOI: 10.1136/practneurol-2019-002336]
57 **Trepo C**, Guillevin L. Polyarteritis nodosa and extrahepatic manifestations of HBV infection: the case against autoimmune intervention in pathogenesis. *J Autoimmun* 2001; **16**: 269-274 [PMID: 11334492 DOI: 10.1006/jaut.2000.0502]
58 **McMahon BJ**, Alward WL, Hall DB, Heyward WL, Bender TR, Francis DP, Maynard JE. Acute hepatitis B virus infection: relation of age to the clinical expression of disease and subsequent development of the carrier state. *J Infect Dis* 1985; **151**: 599-603 [PMID: 3973412 DOI: 10.1093/infdis/151.4.599]
59 **Kappus MR**, Sterling RK. Extrahepatic manifestations of acute hepatitis B virus infection. *Gastroenterol Hepatol (N Y)* 2013; **9**: 123-126 [PMID: 23983659]
60 **Yimam KK**, Merriman RB, Todd Frederick R. A rare case of acute hepatitis B virus infection causing guillain-barré syndrome. *Gastroenterol Hepatol (N Y)* 2013; **9**: 121-123 [PMID: 23983658]
61 **Cacoub P**, Terrier B. Hepatitis B-related autoimmune manifestations. *Rheum Dis Clin North Am* 2009; **35**: 125-137 [PMID: 19481001 DOI: 10.1016/j.rdc.2009.03.006]
62 **Cacoub P**, Saadoun D, Bourlière M, Khiri H, Martineau A, Benhamou Y, Varastet M, Pol S, Thibault V, Rotily M, Halfon P. Hepatitis B virus genotypes and extrahepatic manifestations. *J Hepatol* 2005; **43**: 764-770 [PMID: 16087273 DOI: 10.1016/j.jhep.2005.05.029]
63 **Mason A**, Theal J, Bain V, Adams E, Perrillo R. Hepatitis B virus replication in damaged

endothelial tissues of patients with extrahepatic disease. *Am J Gastroenterol* 2005; **100**: 972-976 [PMID: 15784044 DOI: 10.1111/j.1572-0241.2005.41308.x]

64 **Levo Y**, Gorevic PD, Kassab HJ, Zucker-Franklin D, Franklin EC. Association between hepatitis B virus and essential mixed cryoglobulinemia. *N Engl J Med* 1977; **296**: 1501-1504 [PMID: 865530 DOI: 10.1056/NEJM197706302962605]

65 **Stübgen JP**. Neuromuscular disorders associated with hepatitis B virus infection. *J Clin Neuromuscul Dis* 2011; **13**: 26-37 [PMID: 22361623 DOI: 10.1097/CND.0b013e3181df2b2b]

66 **Guillevin L**, Lhote F, Sauvaget F, Deblois P, Rossi F, Levallois D, Pourrat J, Christoforov B, Trépo C. Treatment of polyarteritis nodosa related to hepatitis B virus with interferon-alpha and plasma exchanges. *Ann Rheum Dis* 1994; **53**: 334-337 [PMID: 7912504 DOI: 10.1136/ard.53.5.334]

67 **Guillevin L**, Mahr A, Cohen P, Larroche C, Queyrel V, Loustaud-Ratti V, Imbert B, Hausfater P, Roudier J, Bielefeld P, Petitjean P, Smadja D; French Vasculitis Study Group. Short-term corticosteroids then lamivudine and plasma exchanges to treat hepatitis B virus-related polyarteritis nodosa. *Arthritis Rheum* 2004; **51**: 482-487 [PMID: 15188337 DOI: 10.1002/art.20401]

68 **Tang S**, Lai FM, Lui YH, Tang CS, Kung NN, Ho YW, Chan KW, Leung JC, Lai KN. Lamivudine in hepatitis B-associated membranous nephropathy. *Kidney Int* 2005; **68**: 1750-1758 [PMID: 16164651 DOI: 10.1111/j.1523-1755.2005.00591.x]

69 **Chung DR**, Yang WS, Kim SB, Yu E, Chung YH, Lee Y, Park JS. Treatment of hepatitis B virus associated glomerulonephritis with recombinant human alpha interferon. *Am J Nephrol* 1997; **17**: 112-117 [PMID: 9096440 DOI: 10.1159/000169083]

70 **Mazzaro C**, Dal Maso L, Visentini M, Gitto S, Andreone P, Toffolutti F, Gattei V. Hepatitis B virus-related cryogobulinemic vasculitis. The role of antiviral nucleot(s)ide analogues: a review. *J Intern Med* 2019; **286**: 290-298 [PMID: 31124596 DOI: 10.1111/joim.12913]

71 **Martinello M**, Hajarizadeh B, Grebely J, Dore GJ, Matthews GV. Management of acute HCV infection in the era of direct-acting antiviral therapy. *Nat Rev Gastroenterol Hepatol* 2018; **15**: 412-424 [PMID: 29773899 DOI: 10.1038/s41575-018-0026-5]

72 **Loomba R**, Rivera MM, McBurney R, Park Y, Haynes-Williams V, Rehermann B, Alter HJ, Herrine SK, Liang TJ, Hoofnagle JH, Heller T. The natural history of acute hepatitis C: clinical presentation, laboratory findings and treatment outcomes. *Aliment Pharmacol Ther* 2011; **33**: 559-565 [PMID: 21198704 DOI: 10.1111/j.1365-2036.2010.04549.x]

73 **Morin T**, Pariente A, Lahmek P, Rabaud C, Silvain C, Cadranel JF; Association Nationale des Hépato-gastroentérologues des Hôpitaux généraux (ANGH) Société de Pathologie Infectieuse de Langue Française (SPILF) Fédération des Pôles de Référence et Réseaux Hépatites (FPRRH). Acute hepatitis C: analysis of a 126-case prospective, multicenter cohort. *Eur J Gastroenterol Hepatol* 2010; **22**: 157-166 [PMID: 19734798 DOI: 10.1097/MEG.0b013e328330a8e8]

74 **Spearman CW**, Dusheiko GM, Hellard M, Sonderup M. Hepatitis C. *Lancet* 2019; **394**: 1451-1466 [PMID: 31631857 DOI: 10.1016/S0140-6736(19)32320-7]

75 **Cacoub P**, Poynard T, Ghillani P, Charlotte F, Olivi M, Piette JC, Opolon P. Extrahepatic manifestations of chronic hepatitis C. MULTIVIRC Group. Multidepartment Virus C. *Arthritis Rheum* 1999; **42**: 2204-2212 [PMID: 10524695 DOI: 10.1002/1529-0131(199910)42:10<2204::AID-ANR24>3.0.CO;2-D]

76 **Kuna L**, Jakab J, Smolic R, Wu GY, Smolic M. HCV Extrahepatic Manifestations. *J Clin Transl Hepatol* 2019; **7**: 172-182 [PMID: 31293918 DOI: 10.14218/JCTH.2018.00049]

77 **Zegans ME**, Anninger W, Chapman C, Gordon SR. Ocular manifestations of hepatitis C virus infection. *Curr Opin Ophthalmol* 2002; **13**: 423-427 [PMID: 12441848 DOI: 10.1097/00055735-200212000-00014]

78 **Petta S**, Craxì A. Extrahepatic Manifestations of Chronic Viral C Hepatitis. *Gastroenterol Clin North Am* 2020; **49**: 347-360 [PMID: 32389367 DOI: 10.1016/j.gtc.2020.01.012]

79 **Comarmond C**, Cacoub P, Saadoun D. Treatment of chronic hepatitis C-associated cryoglobulinemia vasculitis at the era of direct-acting antivirals. *Therap Adv Gastroenterol* 2020; **13**: 1756284820942617 [PMID: 32782479 DOI: 10.1177/1756284820942617]

80 **Carrat F**, Fontaine H, Dorival C, Simony M, Diallo A, Hezode C, De Ledinghen V, Larrey D, Haour G, Bronowicki JP, Zoulim F, Asselah T, Marcellin P, Thabut D, Leroy V, Tran A, Habersetzer F, Samuel D, Guyader D, Chazouilleres O, Mathurin P, Metivier S, Alric L, Riachi G, Gournay J, Abergel A, Cales P, Ganne N, Loustaud-Ratti V, D'Alteroche L, Causse X, Geist C, Minello A, Rosa I, Gelu-Simeon M, Portal I, Raffi F, Bourliere M, Pol S; French ANRS CO22 Hepather cohort. Clinical outcomes in patients with chronic hepatitis C after direct-acting antiviral treatment: a prospective cohort study. *Lancet* 2019; **393**: 1453-1464 [PMID: 30765123 DOI: 10.1016/S0140-6736(18)32111-1]

81 **Thomas K**, Vassilopoulos D. Infections and vasculitis. *Curr Opin Rheumatol* 2017; **29**: 17-23 [PMID: 27662570 DOI: 10.1097/BOR.0000000000000348]

82 **Lidar M**, Lipschitz N, Langevitz P, Shoenfeld Y. The infectious etiology of vasculitis. *Autoimmunity* 2009; **42**: 432-438 [PMID: 19811260 DOI: 10.1080/08916930802613210]

83 **Vergani D**, Mieli-Vergani G. Autoimmune manifestations in viral hepatitis. *Semin Immunopathol* 2013; **35**: 73-85 [PMID: 23010889 DOI: 10.1007/s00281-012-0328-6]

84 **Cozzani E**, Herzum A, Burlando M, Parodi A. Cutaneous manifestations of HAV, HBV, HCV. *G Ital Dermatol Venereol* 2019 [PMID: 31804053 DOI: 10.23736/S0392-0488.19.06488-5]

85 **Grigorescu I**, Dumitrascu DL. Spontaneous and antiviral-induced cutaneous lesions in chronic hepatitis B virus infection. *World J Gastroenterol* 2014; **20**: 15860-15866 [PMID: 25400473 DOI:

10.3748/wjg.v20.i42.15860]
86 **Glück T**, Weber P, Wiedmann KH. [Hepatitis-B-associated vasculitis. Clinical course with glucocorticoid and alpha-interferon therapy]. *Dtsch Med Wochenschr* 1994; **119**: 1388-1392 [PMID: 7924948 DOI: 10.1055/s-2008-1058850]
87 **Chemli J**, Zouari N, Belkadhi A, Abroug S, Harbi A. [Hepatitis A infection and Henoch-Schonlein purpura: a rare association]. *Arch Pediatr* 2004; **11**: 1202-1204 [PMID: 15475276 DOI: 10.1016/j.arcped.2004.06.014]
88 **Altinkaynak S**, Ertekin V, Selimoglu MA. Association of Henoch-Schonlein purpura and hepatitis A. *J Emerg Med* 2006; **30**: 219-220 [PMID: 16567262 DOI: 10.1016/j.jemermed.2005.12.011]
89 **Thapa R**, Biswas B, Mallick D. Henoch-Schönlein purpura triggered by acute hepatitis E virus infection. *J Emerg Med* 2010; **39**: 218-219 [PMID: 19201130 DOI: 10.1016/j.jemermed.2008.10.004]
90 **Heineke MH**, Ballering AV, Jamin A, Ben Mkaddem S, Monteiro RC, Van Egmond M. New insights in the pathogenesis of immunoglobulin A vasculitis (Henoch-Schönlein purpura). *Autoimmun Rev* 2017; **16**: 1246-1253 [PMID: 29037908 DOI: 10.1016/j.autrev.2017.10.009]
91 **Maggiore G**, Martini A, Grifeo S, De Giacomo C, Scotta MS. Hepatitis B virus infection and Schönlein-Henoch purpura. *Am J Dis Child* 1984; **138**: 681-682 [PMID: 6731386 DOI: 10.1001/archpedi.1984.02140450063019]
92 **Ergin S**, Sanli Erdoğan B, Turgut H, Evliyaoğlu D, Yalçin AN. Relapsing Henoch-Schönlein purpura in an adult patient associated with hepatitis B virus infection. *J Dermatol* 2005; **32**: 839-842 [PMID: 16361739 DOI: 10.1111/j.1346-8138.2005.tb00856.x]
93 **Ogawa M**, Makino Y, Ueda S, Ohto M, Akikusa B. Rapidly progressive glomerulonephritis in association with Henoch-Schönlein purpura in a patient with advanced liver cirrhosis. *Nephron* 1995; **71**: 365-366 [PMID: 8569993 DOI: 10.1159/000188750]
94 **Madison DL**, Allen E, Deodhar A, Morrison L. Henoch-Schönlein purpura: a possible complication of hepatitis C related liver cirrhosis. *Ann Rheum Dis* 2002; **61**: 281-282 [PMID: 11830445 DOI: 10.1136/ard.61.3.281-a]
95 **Nishida N**, Kudo M. Clinical features of vascular disorders associated with chronic hepatitis virus infection. *Dig Dis* 2014; **32**: 786-790 [PMID: 25376297 DOI: 10.1159/000368023]
96 **Silva F**, Pinto C, Barbosa A, Borges T, Dias C, Almeida J. New insights in cryoglobulinemic vasculitis. *J Autoimmun* 2019; **105**: 102313 [PMID: 31383568 DOI: 10.1016/j.jaut.2019.102313]
97 **De Virgilio A**, Greco A, Magliulo G, Gallo A, Ruoppolo G, Conte M, Martellucci S, de Vincentiis M. Polyarteritis nodosa: A contemporary overview. *Autoimmun Rev* 2016; **15**: 564-570 [PMID: 26884100 DOI: 10.1016/j.autrev.2016.02.015]
98 **Desbois AC**, Cacoub P, Saadoun D. Cryoglobulinemia: An update in 2019. *Joint Bone Spine* 2019; **86**: 707-713 [PMID: 30731128 DOI: 10.1016/j.jbspin.2019.01.016]
99 **Meltzer M**, Franklin EC. Cryoglobulinemia--a study of twenty-nine patients. I. IgG and IgM cryoglobulins and factors affecting cryoprecipitability. *Am J Med* 1966; **40**: 828-836 [PMID: 4956870 DOI: 10.1016/0002-9343(66)90199-9]
100 **Brouet JC**, Clauvel JP, Danon F, Klein M, Seligmann M. Biologic and clinical significance of cryoglobulins. A report of 86 cases. *Am J Med* 1974; **57**: 775-788 [PMID: 4216269 DOI: 10.1016/0002-9343(74)90852-3]
101 **Harel S**, Mohr M, Jahn I, Aucouturier F, Galicier L, Asli B, Malphettes M, Szalat R, Brouet JC, Lipsker D, Fermand JP. Clinico-biological characteristics and treatment of type I monoclonal cryoglobulinaemia: a study of 64 cases. *Br J Haematol* 2015; **168**: 671-678 [PMID: 25363150 DOI: 10.1111/bjh.13196]
102 **Trejo O**, Ramos-Casals M, García-Carrasco M, Yagüe J, Jiménez S, de la Red G, Cervera R, Font J, Ingelmo M. Cryoglobulinemia: study of etiologic factors and clinical and immunologic features in 443 patients from a single center. *Medicine (Baltimore)* 2001; **80**: 252-262 [PMID: 11470986 DOI: 10.1097/00005792-200107000-00004]
103 **Charles ED**, Dustin LB. Hepatitis C virus-induced cryoglobulinemia. *Kidney Int* 2009; **76**: 818-824 [PMID: 19606079 DOI: 10.1038/ki.2009.247]
104 **Cheema SR**, Arif F, Charney D, Meisels IS. IgA-dominant glomerulonephritis associated with hepatitis A. *Clin Nephrol* 2004; **62**: 138-143 [PMID: 15356971 DOI: 10.5414/cnp62138]
105 **Chen PP**, Fong S, Goni F, Silverman GJ, Fox RI, Liu MF, Frangione B, Carson DA. Cross-reacting idiotypes on cryoprecipitating rheumatoid factor. *Springer Semin Immunopathol* 1988; **10**: 35-55 [PMID: 3137675 DOI: 10.1007/]
106 **Quartuccio L**, Fabris M, Salvin S, Isola M, Soldano F, Falleti E, Beltrami CA, De Re V, De Vita S. Bone marrow B-cell clonal expansion in type II mixed cryoglobulinaemia: association with nephritis. *Rheumatology (Oxford)* 2007; **46**: 1657-1661 [PMID: 17893101 DOI: 10.1093/rheumatology/kem209]
107 **Ferri C**, Sebastiani M, Giuggioli D, Cazzato M, Longombardo G, Antonelli A, Puccini R, Michelassi C, Zignego AL. Mixed cryoglobulinemia: demographic, clinical, and serologic features and survival in 231 patients. *Semin Arthritis Rheum* 2004; **33**: 355-374 [PMID: 15190522 DOI: 10.1016/j.semarthrit.2003.10.001]
108 **Ramos-Casals M**, Stone JH, Cid MC, Bosch X. The cryoglobulinaemias. *Lancet* 2012; **379**: 348-360 [PMID: 21868085 DOI: 10.1016/S0140-6736(11)60242-0]
109 **Roccatello D**, Fornasieri A, Giachino O, Rossi D, Beltrame A, Banfi G, Confalonieri R, Tarantino A, Pasquali S, Amoroso A, Savoldi S, Colombo V, Manno C, Ponzetto A, Moriconi L, Pani A,

Rustichelli R, Di Belgiojoso GB, Comotti C, Quarenghi MI. Multicenter study on hepatitis C virus-related cryoglobulinemic glomerulonephritis. *Am J Kidney Dis* 2007; **49**: 69-82 [PMID: 17185147 DOI: 10.1053/j.ajkd.2006.09.015]

110 **Johnson RJ**, Gretch DR, Yamabe H, Hart J, Bacchi CE, Hartwell P, Couser WG, Corey L, Wener MH, Alpers CE. Membranoproliferative glomerulonephritis associated with hepatitis C virus infection. *N Engl J Med* 1993; **328**: 465-470 [PMID: 7678440 DOI: 10.1056/NEJM199302183280703]

111 **Ammendola A**, Sampaolo S, Ambrosone L, Ammendola E, Ciccone G, Migliaresi S, Di Iorio G. Peripheral neuropathy in hepatitis-related mixed cryoglobulinemia: electrophysiologic follow-up study. *Muscle Nerve* 2005; **31**: 382-385 [PMID: 15515001 DOI: 10.1002/mus.20184]

112 **Casato M**, Saadoun D, Marchetti A, Limal N, Picq C, Pantano P, Galanaud D, Cianci R, Duhaut P, Piette JC, Fiorilli M, Cacoub P. Central nervous system involvement in hepatitis C virus cryoglobulinemia vasculitis: a multicenter case-control study using magnetic resonance imaging and neuropsychological tests. *J Rheumatol* 2005; **32**: 484-488 [PMID: 15742440]

113 **Retamozo S**, Díaz-Lagares C, Bosch X, Bové A, Brito-Zerón P, Gómez ME, Yagüe J, Forns X, Cid MC, Ramos-Casals M. Life-Threatening Cryoglobulinemic Patients With Hepatitis C: Clinical Description and Outcome of 279 Patients. *Medicine (Baltimore)* 2013; **92**: 273-284 [PMID: 23974248 DOI: 10.1097/MD.0b013e3182a5cf71]

114 **Cavalli G**, Berti A, Fragasso G, De Cobelli F. Hypertrophic cardiomyopathy secondary to hepatitis C virus-related vasculitis. *J Cardiovasc Med (Hagerstown)* 2016; **17** Suppl 2: e156-e157 [PMID: 24979124 DOI: 10.2459/JCM.0000000000000109]

115 **Terrier B**, Saadoun D, Sène D, Scerra S, Musset L, Cacoub P. Presentation and outcome of gastrointestinal involvement in hepatitis C virus-related systemic vasculitis: a case-control study from a single-centre cohort of 163 patients. *Gut* 2010; **59**: 1709-1715 [PMID: 20841367 DOI: 10.1136/gut.2010.218123]

116 **Muñoz-Martínez SG**, Díaz-Hernández HA, Suárez-Flores D, Sánchez-Ávila JF, Gamboa-Domínguez A, García-Juárez I, Torre A. Atypical manifestations of hepatitis A virus infection. *Rev Gastroenterol Mex* 2018; **83**: 134-143 [PMID: 29685743 DOI: 10.1016/j.rgmx.2017.10.004]

117 **Nassih H**, Bourrahouat A, Sab IA. Hepatitis A Virus Infection Associated with Cryoglobulinemic Vasculitis. *Indian Pediatr* 2020; **57**: 71-72 [PMID: 31937705]

118 **Levo Y**, Gorevic PD, Kassab HJ, Tobias H, Franklin EC. Liver involvement in the syndrome of mixed cryoglobulinemia. *Ann Intern Med* 1977; **87**: 287-292 [PMID: 900672 DOI: 10.7326/0003-4819-87-3-287]

119 **Gower RG**, Sausker WF, Kohler PF, Thorne GE, McIntosh RM. Small vessel vasculitis caused by hepatitis B virus immune complexes. Small vessel vasculitis and HBsAG. *J Allergy Clin Immunol* 1978; **62**: 222-228 [PMID: 701656 DOI: 10.1016/0091-6749(78)90211-7]

120 **Monti G**, Galli M, Invernizzi F, Pioltelli P, Saccardo F, Monteverde A, Pietrogrande M, Renoldi P, Bombardieri S, Bordin G. Cryoglobulinaemias: a multi-centre study of the early clinical and laboratory manifestations of primary and secondary disease. GISC. Italian Group for the Study of Cryoglobulinaemias. *QJM* 1995; **88**: 115-126 [PMID: 7704562]

121 **Mazzaro C**, Dal Maso L, Urraro T, Mauro E, Castelnovo L, Casarin P, Monti G, Gattei V, Zignego AL, Pozzato G. Hepatitis B virus related cryoglobulinemic vasculitis: A multicentre open label study from the Gruppo Italiano di Studio delle Crioglobulinemie - GISC. *Dig Liver Dis* 2016; **48**: 780-784 [PMID: 27106525 DOI: 10.1016/j.dld.2016.03.018]

122 **Liou YT**, Huang JL, Ou LS, Lin YH, Yu KH, Luo SF, Ho HH, Liou LB, Yeh KW. Comparison of cryoglobulinemia in children and adults. *J Microbiol Immunol Infect* 2013; **46**: 59-64 [PMID: 22237397 DOI: 10.1016/j.jmii.2011.12.027]

123 **Mazzaro C**, Dal Maso L, Visentini M, Ermacora A, Tonizzo M, Gattei V, Andreone P. Recent news in the treatment of hepatitis B virus-related cryogobulinemic vasculitis. *Minerva Med* 2020; **111**: 566-572 [PMID: 32573522 DOI: 10.23736/S0026-4806.20.06771-3]

124 **European Association for the Study of the Liver**. ; European Association for the Study of the Liver. EASL 2017 Clinical Practice Guidelines on the management of hepatitis B virus infection. *J Hepatol* 2017; **67**: 370-398 [PMID: 28427875 DOI: 10.1016/j.jhep.2017.03.021]

125 **Kamimura H**, Setsu T, Kimura N, Yokoo T, Sakamaki A, Kamimura K, Tsuchiya A, Takamura M, Yamagiwa S, Terai S. Renal Impairment in Chronic Hepatitis B: A Review. *Diseases* 2018; **6** [PMID: 29921773 DOI: 10.3390/diseases6020052]

126 **Ferri C**, Antonelli A, Mascia MT, Sebastiani M, Fallahi P, Ferrari D, Giunti M, Pileri SA, Zignego AL. B-cells and mixed cryoglobulinemia. *Autoimmun Rev* 2007; **7**: 114-120 [PMID: 18035320 DOI: 10.1016/j.autrev.2007.02.019]

127 **Pasquet F**, Combarnous F, Macgregor B, Coppere B, Mausservey C, Ninet J, Hot A. Safety and efficacy of rituximab treatment for vasculitis in hepatitis B virus-associated type II cryoglobulinemia: a case report. *J Med Case Rep* 2012; **6**: 39 [PMID: 22284897 DOI: 10.1186/1752-1947-6-39]

128 **Terrier B**, Marie I, Lacraz A, Belenotti P, Bonnet F, Chiche L, Graffin B, Hot A, Kahn JE, Michel C, Quemeneur T, de Saint-Martin L, Hermine O, Léger JM, Mariette X, Senet P, Plaisier E, Cacoub P. Non HCV-related infectious cryoglobulinemia vasculitis: Results from the French nationwide CryoVas survey and systematic review of the literature. *J Autoimmun* 2015; **65**: 74-81 [PMID: 26320984 DOI: 10.1016/j.jaut.2015.08.008]

129 **Tsutsumi Y**, Yamamoto Y, Ito S, Ohigashi H, Shiratori S, Naruse H, Teshima T. Hepatitis B virus

reactivation with a rituximab-containing regimen. *World J Hepatol* 2015; **7**: 2344-2351 [PMID: 26413224 DOI: 10.4254/wjh.v7.i21.2344]

130 **Khan ZH**, Ilyas K, Ghazanfar H, Khan HH, Hussain Q, Hammad S, Munir A, Asim R. Fatal Fulminant Hepatitis from Rituximab-induced Hepatitis B Reactivation in a Patient with Follicular Lymphoma: A Case Report and a Brief Review of Literature. *Cureus* 2018; **10**: e2257 [PMID: 29725560 DOI: 10.7759/cureus.2257]

131 **Ferri C**, Greco F, Longombardo G, Palla P, Moretti A, Marzo E, Mazzoni A, Pasero G, Bombardieri S, Highfield P. Association between hepatitis C virus and mixed cryoglobulinemia [see comment]. *Clin Exp Rheumatol* 1991; **9**: 621-624 [PMID: 1662567]

132 **Rosa D**, Saletti G, De Gregorio E, Zorat F, Comar C, D'Oro U, Nuti S, Houghton M, Barnaba V, Pozzato G, Abrignani S. Activation of naïve B lymphocytes *via* CD81, a pathogenetic mechanism for hepatitis C virus-associated B lymphocyte disorders. *Proc Natl Acad Sci* 2005; **102**: 18544-18549 [PMID: 16339892 DOI: 10.1073/pnas.0509402102]

133 **Charles ED**, Green RM, Marukian S, Talal AH, Lake-Bakaar GV, Jacobson IM, Rice CM, Dustin LB. Clonal expansion of immunoglobulin M+CD27+ B cells in HCV-associated mixed cryoglobulinemia. *Blood* 2008; **111**: 1344-1356 [PMID: 17942751 DOI: 10.1182/blood-2007-07-101717]

134 **Ferri C**, La Civita L, Zignego AL, Pasero G. Viruses and cancers: possible role of hepatitis C virus. *Eur J Clin Invest* 1997; **27**: 711-718 [PMID: 9352239 DOI: 10.1046/j.1365-2362.1997.1790728.x]

135 **Mele A**, Pulsoni A, Bianco E, Musto P, Szklo A, Sanpaolo MG, Iannitto E, De Renzo A, Martino B, Liso V, Andrizzi C, Pusterla S, Dore F, Maresca M, Rapicetta M, Marcucci F, Mandelli F, Franceschi S. Hepatitis C virus and B-cell non-Hodgkin lymphomas: an Italian multicenter case-control study. *Blood* 2003; **102**: 996-999 [PMID: 12714514 DOI: 10.1182/blood-2002-10-3230]

136 **Giordano TP**, Henderson L, Landgren O, Chiao EY, Kramer JR, El-Serag H, Engels EA. Risk of non-Hodgkin lymphoma and lymphoproliferative precursor diseases in US veterans with hepatitis C virus. *JAMA* 2007; **297**: 2010-2017 [PMID: 17488966 DOI: 10.1001/jama.297.18.2010]

137 **Monti G**, Pioltelli P, Saccardo F, Campanini M, Candela M, Cavallero G, De Vita S, Ferri C, Mazzaro C, Migliaresi S, Ossi E, Pietrogrande M, Gabrielli A, Galli M, Invernizzi F. Incidence and characteristics of non-Hodgkin lymphomas in a multicenter case file of patients with hepatitis C virus-related symptomatic mixed cryoglobulinemias. *Arch Intern Med* 2005; **165**: 101-105 [PMID: 15642884 DOI: 10.1001/archinte.165.1.101]

138 **Bunchorntavakul C**, Mitrani R, Reddy KR. Advances in HCV and Cryoglobulinemic Vasculitis in the Era of DAAs: Are We at the End of the Road? *J Clin Exp Hepatol* 2018; **8**: 81-94 [PMID: 29743799 DOI: 10.1016/j.jceh.2017.11.012]

139 **Saadoun D**, Pol S, Ferfar Y, Alric L, Hezode C, Si Ahmed SN, de Saint Martin L, Comarmond C, Bouyer AS, Musset L, Poynard T, Resche Rigon M, Cacoub P. Efficacy and Safety of Sofosbuvir Plus Daclatasvir for Treatment of HCV-Associated Cryoglobulinemia Vasculitis. *Gastroenterology* 2017; **153**: 49-52. e5 [PMID: 28288791 DOI: 10.1053/j.gastro.2017.03.006]

140 **Arcaini L**, Besson C, Frigeni M, Fontaine H, Goldaniga M, Casato M, Visentini M, Torres HA, Loustaud-Ratti V, Peveling-Oberhag J, Fabris P, Rossotti R, Zaja F, Rigacci L, Rattotti S, Bruno R, Merli M, Dorival C, Alric L, Jaccard A, Pol S, Carrat F, Ferretti VV, Visco C, Hermine O. Interferon-free antiviral treatment in B-cell lymphoproliferative disorders associated with hepatitis C virus infection. *Blood* 2016; **128**: 2527-2532 [PMID: 27605512 DOI: 10.1182/blood-2016-05-714667]

141 **Ramos-Casals M**, Zignego AL, Ferri C, Brito-Zerón P, Retamozo S, Casato M, Lamprecht P, Mangia A, Saadoun D, Tzioufas AG, Younossi ZM, Cacoub P; International Study Group of Extrahepatic Manifestations related to HCV (ISG-EHCV). Evidence-based recommendations on the management of extrahepatic manifestations of chronic hepatitis C virus infection. *J Hepatol* 2017; **66**: 1282-1299 [PMID: 28219772 DOI: 10.1016/j.jhep.2017.02.010]

142 **Saadoun D**, Resche Rigon M, Sene D, Terrier B, Karras A, Perard L, Schoindre Y, Coppéré B, Blanc F, Musset L, Piette JC, Rosenzwajg M, Cacoub P. Rituximab plus Peg-interferon-alpha/ribavirin compared with Peg-interferon-alpha/ribavirin in hepatitis C-related mixed cryoglobulinemia. *Blood* 2010; **116**: 326-34; quiz 504 [PMID: 20439619 DOI: 10.1182/blood-2009-10-248518]

143 **De Vita S**, Quartuccio L, Isola M, Mazzaro C, Scaini P, Lenzi M, Campanini M, Naclerio C, Tavoni A, Pietrogrande M, Ferri C, Mascia MT, Masolini P, Zabotti A, Maset M, Roccatello D, Zignego AL, Pioltelli P, Gabrielli A, Filippini D, Perrella O, Migliaresi S, Galli M, Bombardieri S, Monti G. A randomized controlled trial of rituximab for the treatment of severe cryoglobulinemic vasculitis. *Arthritis Rheum* 2012; **64**: 843-853 [PMID: 22147661 DOI: 10.1002/art.34331]

144 **Desbois AC**, Comarmond C, Saadoun D, Cacoub P. Cryoglobulinemia vasculitis: how to handle. *Curr Opin Rheumatol* 2017; **29**: 343-347 [PMID: 28368978 DOI: 10.1097/BOR.0000000000000390]

145 **Sène D**, Ghillani-Dalbin P, Amoura Z, Musset L, Cacoub P. Rituximab may form a complex with IgMkappa mixed cryoglobulin and induce severe systemic reactions in patients with hepatitis C virus-induced vasculitis. *Arthritis Rheum* 2009; **60**: 3848-3855 [PMID: 19950292 DOI: 10.1002/art.25000]

146 **Ishiguro N**, Kawashima M. Cutaneous polyarteritis nodosa: a report of 16 cases with clinical and histopathological analysis and a review of the published work. *J Dermatol* 2010; **37**: 85-93 [PMID: 20175828 DOI: 10.1111/j.1346-8138.2009.00752.x]

147 **Morgan AJ**, Schwartz RA. Cutaneous polyarteritis nodosa: a comprehensive review. *Int J Dermatol* 2010; **49**: 750-756 [PMID: 20618492 DOI: 10.1111/j.1365-4632.2010.04522.x]

148 **Hernández-Rodríguez J**, Alba MA, Prieto-González S, Cid MC. Diagnosis and classification of polyarteritis nodosa. *J Autoimmun* 2014; **48-49**: 84-89 [PMID: 24485157 DOI: 10.1016/j.jaut.2014.01.029]

149 **Gocke DJ**, Hsu K, Morgan C, Bombardieri S, Lockshin M, Christian CL. Association between polyarteritis and Australia antigen. *Lancet* 1970; **2**: 1149-1153 [PMID: 4098431 DOI: 10.1016/s0140-6736(70)90339-9]

150 **Trepo C**, Thivolet J. Hepatitis associated antigen and periarteritis nodosa (PAN). *Vox Sang* 1970; **19**: 410-411 [PMID: 4396040]

151 **Ozen S**. The changing face of polyarteritis nodosa and necrotizing vasculitis. *Nat Rev Rheumatol* 2017; **13**: 381-386 [PMID: 28490787 DOI: 10.1038/nrrheum.2017.68]

152 **Sharma A**, Sharma K. Hepatotropic viral infection associated systemic vasculitides-hepatitis B virus associated polyarteritis nodosa and hepatitis C virus associated cryoglobulinemic vasculitis. *J Clin Exp Hepatol* 2013; **3**: 204-212 [PMID: 25755502 DOI: 10.1016/j.jceh.2013.06.001]

153 **Pagnoux C**, Seror R, Henegar C, Mahr A, Cohen P, Le Guern V, Bienvenu B, Mouthon L, Guillevin L; French Vasculitis Study Group. Clinical features and outcomes in 348 patients with polyarteritis nodosa: a systematic retrospective study of patients diagnosed between 1963 and 2005 and entered into the French Vasculitis Study Group Database. *Arthritis Rheum* 2010; **62**: 616-626 [PMID: 20112401 DOI: 10.1002/art.27240]

154 **Imboden JB**. Involvement of the Peripheral Nervous System in Polyarteritis Nodosa and Antineutrophil Cytoplasmic Antibodies-Associated Vasculitis. *Rheum Dis Clin North Am* 2017; **43**: 633-639 [PMID: 29061248 DOI: 10.1016/j.rdc.2017.06.011]

155 **Pagnoux C**, Mahr A, Cohen P, Guillevin L. Presentation and outcome of gastrointestinal involvement in systemic necrotizing vasculitides: analysis of 62 patients with polyarteritis nodosa, microscopic polyangiitis, Wegener granulomatosis, Churg-Strauss syndrome, or rheumatoid arthritis-associated vasculitis. *Medicine (Baltimore)* 2005; **84**: 115-128 [PMID: 15758841 DOI: 10.1097/01.md.0000158825.87055.0b]

156 **Brimo F**, Lachapelle J, Epstein JI. Testicular vasculitis: a series of 19 cases. *Urology* 2011; **77**: 1043-1048 [PMID: 21419476 DOI: 10.1016/j.urology.2011.01.021]

157 **Rimar D**, Alpert A, Starosvetsky E, Rosner I, Slobodin G, Rozenbaum M, Kaly L, Boulman N, Awisat A, Ginsberg S, Zilber K, Shen-Orr SS. Tofacitinib for polyarteritis nodosa: a tailored therapy. *Ann Rheum Dis* 2016; **75**: 2214-2216 [PMID: 27558986 DOI: 10.1136/annrheumdis-2016-209330]

158 **Seri Y**, Shoda H, Hanata N, Nagafuchi Y, Sumitomo S, Fujio K, Yamamoto K. A case of refractory polyarteritis nodosa successfully treated with rituximab. *Mod Rheumatol* 2017; **27**: 696-698 [PMID: 25671401 DOI: 10.3109/14397595.2015.1014153]

159 **Wang CR**, Yang CC. Adalimumab therapy in hepatitis B virus-negative polyarteritis nodosa: A case report. *Medicine (Baltimore)* 2018; **97**: e11053 [PMID: 29923995 DOI: 10.1097/MD.0000000000011053]

160 **Ginsberg S**, Rosner I, Slobodin G, Rozenbaum M, Kaly L, Jiries N, Boulman N, Awisat A, Hussein H, Novofastovski I, Silawy A, Rimar D. Infliximab for the treatment of refractory polyarteritis nodosa. *Clin Rheumatol* 2019; **38**: 2825-2833 [PMID: 30972576 DOI: 10.1007/s10067-019-04474-9]

161 **Krusche M**, Ruffer N, Kötter I. Tocilizumab treatment in refractory polyarteritis nodosa: a case report and review of the literature. *Rheumatol Int* 2019; **39**: 337-344 [PMID: 30465270 DOI: 10.1007/s00296-018-4210-2]

162 **Press J**, Maslovitz S, Avinoach I. Cutaneous necrotizing vasculitis associated with hepatitis A virus infection. *J Rheumatol* 1997; **24**: 965-967 [PMID: 9150090]

163 **Candan F**, Ayan S, Tas F, Gökce G, Elagoz S. Spontaneous renal laceration as the presenting feature of polyarteritis nodosa in a patient with familial Mediterranean fever after hepatitis A infection. *Rheumatol Int* 2005; **25**: 475-477 [PMID: 15765217 DOI: 10.1007/s00296-005-0597-7]

164 **Della Rossa A**, Tavoni A, Lorefice P, Casula F, Bombardieri S. HBV and HCV infection, polyarteritis nodosa and mixed cryoglobulinaemia: a case report. *Clin Rheumatol* 2000; **19**: 502-504 [PMID: 11147768 DOI: 10.1007/s100670070018]

165 **Garcia de La Peña Lefebvre P**, Mouthon L, Cohen P, Lhote F, Guillevin L. Polyarteritis nodosa and mixed cryoglobulinaemia related to hepatitis B and C virus coinfection. *Ann Rheum Dis* 2001; **60**: 1068-1069 [PMID: 11602482 DOI: 10.1136/ard.60.11.1068]

166 **Carson CW**, Conn DL, Czaja AJ, Wright TL, Brecher ME. Frequency and significance of antibodies to hepatitis C virus in polyarteritis nodosa. *J Rheumatol* 1993; **20**: 304-309 [PMID: 8097250]

167 **Saadoun D**, Terrier B, Semoun O, Sene D, Maisonobe T, Musset L, Amoura Z, Rigon MR, Cacoub P. Hepatitis C virus-associated polyarteritis nodosa. *Arthritis Care Res (Hoboken)* 2011; **63**: 427-435 [PMID: 20981809 DOI: 10.1002/acr.20381]

168 **Néel A**, Masseau A, Hervier B, Bossard C, Cacoub P, Pagnoux C, Hamidou MA. Life-threatening hepatitis C virus-associated polyarteritis nodosa successfully treated by rituximab. *J Clin Rheumatol* 2011; **17**: 439-441 [PMID: 22089995 DOI: 10.1097/RHU.0b013e31823a58d7]

169 **Guillevin L**, Mahr A, Callard P, Godmer P, Pagnoux C, Leray E, Cohen P; French Vasculitis Study Group. Hepatitis B virus-associated polyarteritis nodosa: clinical characteristics, outcome, and

impact of treatment in 115 patients. *Medicine (Baltimore)* 2005; **84**: 313-322 [PMID: 16148731 DOI: 10.1097/01.md.0000180792.80212.5e]

170 **Lin CL**, Kao JH. Perspectives and control of hepatitis B virus infection in Taiwan. *J Formos Med Assoc* 2015; **114**: 901-909 [PMID: 26184565 DOI: 10.1016/j.jfma.2015.06.003]

171 **Ungprasert P**, Koster MJ, Cheungpasitporn W, Wijarnpreecha K, Thongprayoon C, Kroner PT. Inpatient burden and association with comorbidities of polyarteritis nodosa: National Inpatient Sample 2014. *Semin Arthritis Rheum* 2020; **50**: 66-70 [PMID: 31362895 DOI: 10.1016/j.semarthrit.2019.07.009]

172 **Chen WY**, Lin KT, Chuang CY, Chen CY. Clinical studies of polyarteritis nodosa. *Taiwan Yi Xue Hui Za Zhi* 1977; **76**: 982-989 [PMID: 25312]

173 **Wang CR**, Liu MF, Tsai RT, Chuang CY, Chen CY. Circulating intercellular adhesion molecules-1 and autoantibodies including anti-endothelial cell, anti-cardiolipin, and anti-neutrophil cytoplasma antibodies in patients with vasculitis. *Clin Rheumatol* 1993; **12**: 375-380 [PMID: 8258240 DOI: 10.1007/BF02231583]

174 **Tsai WL**, Tsai IC, Lee T, Hsieh CW. Polyarteritis nodosa: MDCT as a "one-stop shop" modality for whole-body arterial evaluation. *Cardiovasc Intervent Radiol* 2008; **31** Suppl 2: S26-S29 [PMID: 17508232 DOI: 10.1007/s00270-007-9059-9]

175 **Huang MN**, Wu CH. Polyarteritis nodosa and antiphospholipid syndrome causing bilateral renal infarction. *J Rheumatol* 2009; **36**: 197 [PMID: 19208533 DOI: 10.3899/jrheum.080601]

176 **Li KJ**, Hsieh SC, Toh YC, Yu CL. Clinical images: non-hepatitis B virus-related polyarteritis nodosa presenting with fever and diffuse intra-abdominal microaneurysms. *Arthritis Rheum* 2011; **63**: 3597 [PMID: 21834065 DOI: 10.1002/art.30579]

177 **Tsai HC**, Liao HT, Tsai CY. Polyarteritis nodosa with intra-hepatic arterial haemorrhage. *Liver Int* 2020; **40**: 2858-2859 [PMID: 32810375 DOI: 10.1111/liv.14641]

178 **Lu FT**, Ni YH. Elimination of Mother-to-Infant Transmission of Hepatitis B Virus: 35 Years of Experience. *Pediatr Gastroenterol Hepatol Nutr* 2020; **23**: 311-318 [PMID: 32704492 DOI: 10.5223/pghn.2020.23.4.311]

179 **Hong M**, Bertoletti A. Tolerance and immunity to pathogens in early life: insights from HBV infection. *Semin Immunopathol* 2017; **39**: 643-652 [PMID: 28685270 DOI: 10.1007/s00281-017-0641-1]

180 **Travers RL**, Allison DJ, Brettle RP, Hughes GR. Polyarteritis nodosa: a clinical and angiographic analysis of 17 cases. *Semin Arthritis Rheum* 1979; **8**: 184-199 [PMID: 34221 DOI: 10.1016/s0049-0172(79)80007-4]

181 **Cohen RD**, Conn DL, Ilstrup DM. Clinical features, prognosis, and response to treatment in polyarteritis. *Mayo Clin Proc* 1980; **55**: 146-155 [PMID: 6101626]

182 **Fortin PR**, Larson MG, Watters AK, Yeadon CA, Choquette D, Esdaile JM. Prognostic factors in systemic necrotizing vasculitis of the polyarteritis nodosa group--a review of 45 cases. *J Rheumatol* 1995; **22**: 78-84 [PMID: 7699687]

183 **Bae YD**, Choi HJ, Lee JC, Park JJ, Lee YJ, Lee EB, Song YW. Clinical features of polyarteritis nodosa in Korea. *J Korean Med Sci* 2006; **21**: 591-595 [PMID: 16891798 DOI: 10.3346/jkms.2006.21.4.591]

184 **Sharma A**, Pinto B, Dhooria A, Rathi M, Singhal M, Dhir V, Sharma K, Parkash M, Modi M, Vijayvergiya R, Sinha SK, Nada R, Minz RW, Singh S. Polyarteritis nodosa in north India: clinical manifestations and outcomes. *Int J Rheum Dis* 2017; **20**: 390-397 [PMID: 27990777 DOI: 10.1111/1756-185X.12954]

185 **Guillevin L**, Lhote F, Gayraud M, Cohen P, Jarrousse B, Lortholary O, Thibult N, Casassus P. Prognostic factors in polyarteritis nodosa and Churg-Strauss syndrome. A prospective study in 342 patients. *Medicine (Baltimore)* 1996; **75**: 17-28 [PMID: 8569467 DOI: 10.1097/00005792-199601000-00003]

186 **Guillevin L**, Lhote F, Cohen P, Jarrousse B, Lortholary O, Généreau T, Léon A, Bussel A. Corticosteroids plus pulse cyclophosphamide and plasma exchanges versus corticosteroids plus pulse cyclophosphamide alone in the treatment of polyarteritis nodosa and Churg-Strauss syndrome patients with factors predicting poor prognosis. A prospective, randomized trial in sixty-two patients. *Arthritis Rheum* 1995; **38**: 1638-1645 [PMID: 7488285 DOI: 10.1002/art.1780381116]

World Journal of Gastroenterology

Submit a Manuscript: https://www.f6publishing.com

World J Gastroenterol 2021 January 7; 27(1): 37-54

DOI: 10.3748/wjg.v27.i1.37

ISSN 1007-9327 (print) ISSN 2219-2840 (online)

MINIREVIEWS

Lipidome is lipids regulator in gastrointestinal tract and it is a life collar in COVID-19: A review

Khaled Mohamed Mohamed Koriem

ORCID number: Khaled Mohamed Mohamed Koriem 0000-0002-1323-1700.

Author contributions: Koriem KMM designed the review study, conceived of the manuscript, conducted the literature search and wrote the first and final versions of the manuscript.

Conflict-of-interest statement: The author declares no conflict of interest.

Open-Access: This article is an open-access article that was selected by an in-house editor and fully peer-reviewed by external reviewers. It is distributed in accordance with the Creative Commons Attribution NonCommercial (CC BY-NC 4.0) license, which permits others to distribute, remix, adapt, build upon this work non-commercially, and license their derivative works on different terms, provided the original work is properly cited and the use is non-commercial. See: http://creativecommons.org/Licenses/by-nc/4.0/

Manuscript source: Invited manuscript

Specialty type: Gastroenterology and hepatology

Country/Territory of origin: Egypt

Khaled Mohamed Mohamed Koriem, Medical Physiology Department, Medical Research Division, National Research Centre, Dokki 12622, Cairo, Egypt

Corresponding author: Khaled Mohamed Mohamed Koriem, PhD, Professor, Medical Physiology Department, Medical Research Division, National Research Centre, 33 El-Buhouth Street, Dokki 12622, Cairo, Egypt. kkoriem@yahoo.com

Abstract

The term lipidome is mentioned to the total amount of the lipids inside the biological cells. The lipid enters the human gastrointestinal tract through external source and internal source. The absorption pathway of lipids in the gastrointestinal tract has many ways; the 1st way, the lipid molecules are digested in the lumen before go through the enterocytes, digested products are re-esterified into complex lipid molecules. The 2nd way, the intracellular lipids are accumulated into lipoproteins (chylomicrons) which transport lipids throughout the whole body. The lipids are re-synthesis again inside the human body where the gastrointestinal lipids are: (1) Transferred into the endoplasmic reticulum; (2) Collected as lipoproteins such as chylomicrons; or (3) Stored as lipid droplets in the cytosol. The lipids play an important role in many stages of the viral replication cycle. The specific lipid change occurs during viral infection in advanced viral replication cycle. There are 47 lipids within 11 lipid classes were significantly disturbed after viral infection. The virus connects with blood-borne lipoproteins and apolipoprotein E to change viral infectivity. The viral interest is cholesterol- and lipid raft-dependent molecules. In conclusion, lipidome is important in gastrointestinal fat absorption and coronavirus disease 2019 (COVID-19) infection so lipidome is basic in gut metabolism and in COVID-19 infection success.

Key Words: Lipidome; Gastrointestinal tract; Fat metabolism; COVID-19; Viral infection; Future therapy

©The Author(s) 2021. Published by Baishideng Publishing Group Inc. All rights reserved.

Core Tip: The lipidome is mentioned to the total amount of the lipids inside the biological cells. The lipid enters the human gastrointestinal tract through external

Peer-review report's scientific quality classification
Grade A (Excellent): A, A
Grade B (Very good): 0
Grade C (Good): 0
Grade D (Fair): 0
Grade E (Poor): 0

Received: November 16, 2020
Peer-review started: November 16, 2020
First decision: November 25, 2020
Revised: December 2, 2020
Accepted: December 17, 2020
Article in press: December 17, 2020
Published online: January 7, 2021

P-Reviewer: Alberca RW
S-Editor: Fan JR
L-Editor: A
P-Editor: Ma YJ

source and internal source. The tissue distribution of lipid is completely different among different species. The lipids play an important role in many stages of the viral replication cycle. The specific lipid change occurs during viral infection. The virus connects with blood-borne lipoproteins and apolipoprotein E. The viral interest is cholesterol- and lipid raft-dependent molecules. This review focuses on the important of lipidome in both gastrointestinal fat absorption and coronavirus disease 2019 infection.

Citation: Koriem KMM. Lipidome is lipids regulator in gastrointestinal tract and it is a life collar in COVID-19: A review. *World J Gastroenterol* 2021; 27(1): 37-54
URL: https://www.wjgnet.com/1007-9327/full/v27/i1/37.htm
DOI: https://dx.doi.org/10.3748/wjg.v27.i1.37

INTRODUCTION

The term lipidome or lipidomic is mentioned to the total amount of the lipids inside the biological cells. There are 4 principal constituents occurs inside the biological cells or organs and these 4 constituents are lipids, proteins, sugars and nucleic acids. Lipids are the most important compounds in the living organisms, where they build blocks for cellular membranes, energy storage, and signaling molecules. The technique used in lipidome is generally mass spectrometry (MS)[1]. Lipid metabolism plays an important role in the regulation of cellular homeostasis. Lipid compositions are often used to evaluate lipid metabolism though the application of lipodome[2]. The lipidome or lipidomic is one of the omics science applies in modern biology[3]. There are a tight correlation between lipidomic, metabolomics, genomic and proteomic especially in protective and therapeutic studies[4-6]. Figure 1 explores different types of omics. The lipidome technique applies either by MS or by bioinformatics or ordinary lab-based methods[7,8]. The repeated doses of the drug to micro-tissues lead to collect lipid molecules for 5 time points (2, 4, 7, 9, and 11 d) and hepatotoxic effect occurs[9]. The absorption pathway of lipids in the gastrointestinal tract has many ways; the 1st way, the lipid molecules are digested in the lumen before go through the enterocytes (inside the enterocytes), digested products are re-esterified into complex lipid molecules. The 2nd way, the intracellular lipids are accumulated into lipoproteins (chylomicrons) which transport lipids throughout the whole body[10]. The chylomicrons carrying most of lipids which secreted into the intercellular space, then into the lamina propria, then the lipids enter into the lacteals, and then into the lymphatic system. Thus, the gastrointestinal lymphatic system has a principal role in the absorption of lipids[11-13]. The gastrointestinal lipid metabolism is important to supply of energy (in the form of lipids) to the different organs in the body where the defects in the process of lipid absorption can lead to severe pathological diseases.

Coronavirus disease 2019 (COVID-19) is the last coronavirus outbreak. Coronavirus is derived its name from Latin corona word. Corona virus is first discovered in 1930, while first diagnostic in 1940 in animal models. The first human case of coronavirus is reported in China in 2003 but the COVID-19 was discovered in 2019. This is 3rd serious coronavirus outbreak during the last 20 years, after severe acute respiratory syndrome-related coronavirus (SARS-CoV) in 2002-2003 and Middle East respiratory syndrome-related coronavirus (MERS-CoV) in 2012[14]. There are 7 coronaviruses induce human infections (4 of which, cause cold symptoms in humans while the other 3 coronaviruses called SARS-CoV, MERS-CoV, and COVID-19) cause severe respiratory illness[15]. The coronavirus RNA genome size = 27-34 kilo-bases and this size is the largest RNA genome size. The life cycle of coronavirus is summarized into 3 successive steps: (1) Viral entry; (2) Viral replication; and (3) Viral release. The transmission of COVID-19 in human is occurred though a specific connection process between viral protein and host cell receptor. There are 4 types of coronavirus: (1) *Alphacoronavirus*; (2) *Betacoronavirus*; (3) *Gammacoronavirus*; and (4) *Deltacoronavirus*. Table 1 reveals different genus of coronaviruses. *Betacoronavirus* is the dangerous one because it contains Human coronavirus *e.g.*,., COVID-19, MERS, and severe acute respiratory syndrome-related coronavirus-2 (SARS-CoV-2, SARS-CoV-2). In COVID-19 cases, the attention of blood safety is recommended where coronaviruses have globally arisen especially in endemic areas[16].

Table 1 Different genus of coronaviruses

Coronaviruses	Genus	Type species	Species
Coronaviruses	Alphacoronavirus	Alphacoronavirus 1	Alphacoronavirus 1
			Human coronavirus 229E
			Human coronavirus NL63
			Miniopterus bat coronavirus 1
			Miniopterus bat coronavirus HKU8
			Porcine epidemic diarrhea virus
			Rhinolophus bat coronavirus HKU2
			Scotophilus bat coronavirus 512
	Betacoronavirus	Murine coronavirus	Betacoronavirus 1 (Bovine , Human coronavirus OC43)
			Hedgehog coronavirus 1
			Human coronavirus HKU1
			MERS-CoV
			Murine coronavirus
			Pipistrellus bat coronavirus HKU5
			Rousettus bat coronavirus HKU9
			SARS-CoV, SARS-CoV-2
			Tylonycteris bat coronavirus HKU4
	Gammacoronavirus	Avian coronavirus	Avian coronavirus
			Beluga whale coronavirus SW1
	Deltacoronavirus	Bulbul coronavirus	Bulbul coronavirus HKU11
			Porcine coronavirus HKU15

MERS-CoV: Middle East respiratory syndrome-related coronavirus; SARS-CoV: Severe acute respiratory syndrome-related coronavirus.

The aim of this review is to provide a link between the lipid important in both gastrointestinal fat absorption and COVID-19 infection success. So, this review deals with lipidome in gastrointestinal metabolism and in COVID-19 infection success.

GASTROINTESTINAL UPTAKE OF LIPIDS

The lipid enters the human gastrointestinal tract through 2 sources; external source such as dietary food and internal source such as enterocytes emerge from the gastrointestinal mucosa and from liver bile[17]. The dietary lipids include non-polar lipids, triacylglycerols, cholesterol esters, and polar phospholipids. The liver bile lipids are dissolved in bile acid (include cholesterols and phospholipids). In the gut, the external lipids in diet are hydrolysis by gut lipase to diacylglycerols and fatty acids. The gastrointestinal lipids such as high density lipoproteins, very low density lipoprotein excretion, cytosolic lipid drops and fatty acid oxidation are also included in gastrointestinal lipids[18]. The lipids, as well as, proteins and mucins adhere to plastic particles such as polyvinyl chloride, polyethylene, polyethylene terephthalate polypropylene, and polystyrene. The human gastrointestinal tract do not decays these particles[19]. The high lipid containing-diet for 1 d declined the number of small intestinal intraepithelial lymphocytes and lamina propria lymphocytes. The effect of high lipid containing-diet on the intestinal immune system was independent of the gut microbes. The oral intake of free fatty acids declined the number of small intestinal intraepithelial lymphocytes and lamina propria lymphocytes. So, free fatty acids damaged the intestines and intestinal lipotoxicity occurred as in the case of colorectal cancer or food allergy[20]. The deficiency of fatty acid lead to tissue-resident memory T (Trm) cells death. The gastric adenocarcinoma cells pushed Trm cells for lipid uptake

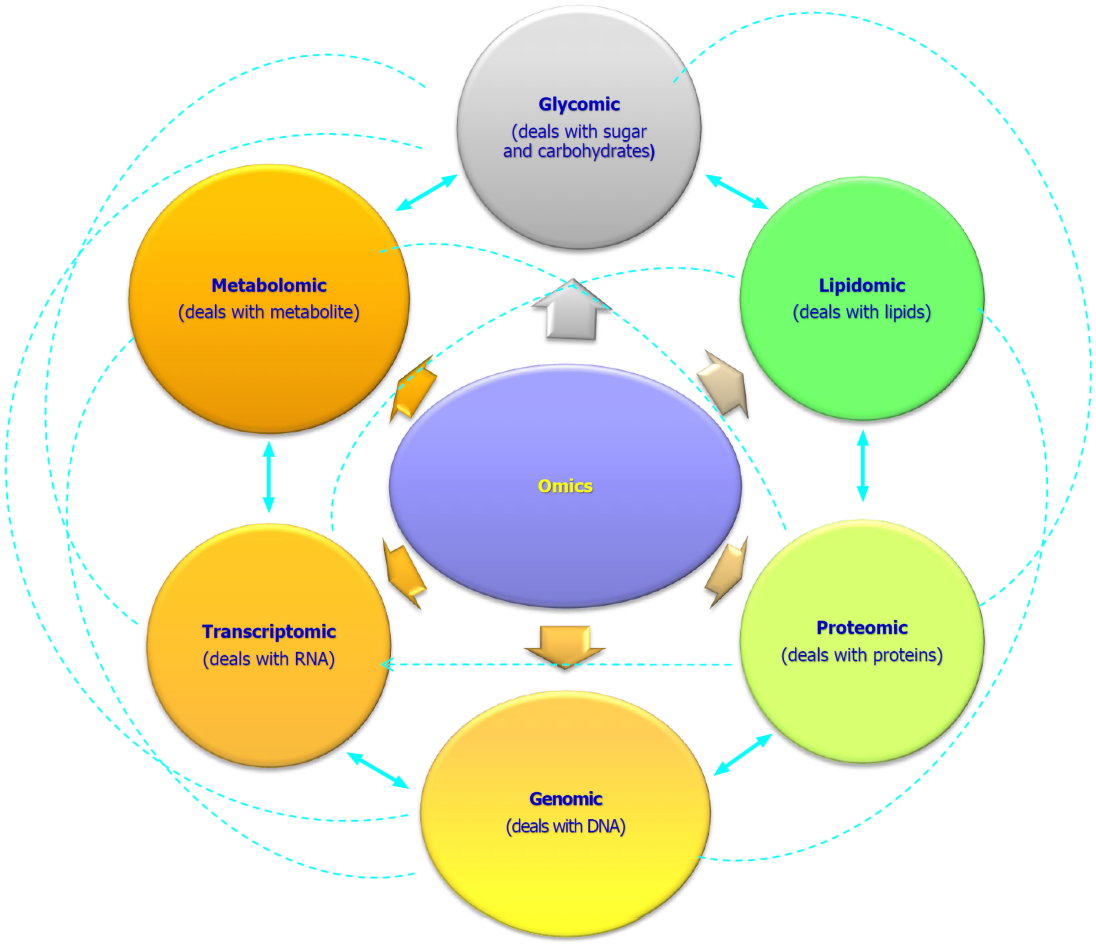


Figure 1 Different types of omics.

and caused Trm cell death[21]. The cancer-associated fibroblasts, through lipidomic technique, accumulate more fatty acids and phospholipids in colorectal cancer cells that plays a principal role in colorectal cancer progress. The fatty acids synthase enzyme, which increased fatty acids synthesis, is considerably increased in cancer-associated fibroblasts[22]. The lipidomics technique in dextran sulfate sodium-induced intestinal barrier dysfunction inhibited the transport and uptake of most of bee pollen lipids such as glycerophospholipids, sphingomyelins, and glycosylsphingolipids. The administration with bee pollen lipids controlled glycerophospholipid and sphingolipid metabolisms that correlated with gastrointestinal permeability barriers and improving gastrointestinal oxidative stress[23]. The gastrointestinal-fatty acid binding protein connected with high-fat diet, leads to changes in gut motility and morphology which caused thinner phenotype occurring at the human whole body. So, gastrointestinal-fatty acid binding protein is incorporated in dietary lipid sensing and signaling which effecting gastrointestinal motility, intestinal configuration, and nutrient absorption and consequently effecting total energy metabolism[24].

GASTROINTESTINAL UPTAKE OF FATTY ACIDS

Fatty acids are uptake by the gastrointestinal tract through 2 ways; the 1st way, fatty acids transfer from the intestinal membrane from higher concentration to lower concentration inside the cell while the 2nd way occurs from the cell to the lumen when the fatty acids concentration inside the cell is higher than lumen fatty acids concentration. The gastrointestinal bile acids are essential for the conservation of their enterohepatic flow. Most of the bile acids are absorbed by gastrointestinal tract *via* certain carrier proteins. These proteins are up-regulate in the distal ileum. The bile acids uptake by gastrointestinal cells reduces the stimulation of cytosolic and membrane receptors (farnesoid X receptor and guanine nucleotide-binding proteins-coupled bile acid receptor 1). These receptors effect on hepatic synthesis of bile acids,

glucose, and lipid metabolism. The increase in bile acid absorption leads to the pathophysiology of liver and metabolic disorders such as fatty liver diseases and type 2 diabetes mellitus[25]. Short-chain fatty acids *e.g.*,. butyrates are bacterial metabolites formed in the gastrointestinal tract and these fatty acids are benefit for host cells. These short-chain fatty acids are stimulators of gastrointestinal cellular gene expression. The propionate and butyrate exert higher efficacy for controlling cell differentiation and gene expression[26]. The tumor necrosis factor-α (TNF-α) is an inflammatory agent associated with gastrointestinal inflammation while omega-3 polyunsaturated fatty acids exert anti-inflammatory activities and stop TNF-α inhibition of sugar uptake by gastrointestinal tract in the human colon cancer cell line (Caco-2). In Caco-2 cancer cells, TNF-α reduces glutamine uptake which counteracts by pro-resolving lipid mediators. So, pro-resolving lipid mediators are favorable biomolecules to restore intestinal nutrients transport during intestinal inflammation[27]. The long-chain fatty acids uptake is an essential physiological process that controls cellular energy homeostasis. The 5' adenosine monophosphate-activated protein kinase accelerates the gastrointestinal long-chain fatty acids uptake by up-regulating human protein is encoded by the CD36 gene (CD36 protein) and stimulating its membrane translocation in the same time[28]. The metabolite of intestinal microbes (TMAVA) level increased in plasma from subjects with liver steatosis compared with controls. The TMAVA declined synthesis of carnitine. The TMAVA changed fecal microbiomes and declined cold tolerance. The TMAVA decreased plasma and liver levels of carnitine and acyl-carnitine. The hepatocytes possessed lower liver fatty acid oxidation. The high fat diet stimulated liver steatosis which declined by carnitine administration. The decrease levels of carnitine and fatty acid oxidation leads to the increase of uptake and liver accumulation of free fatty acids[29]. The colorectal cancer is correlated with the change of fatty acids level in serum and tumor tissues. The colorectal cancer tissues had higher levels of polyunsaturated fatty acids than normal large intestinal mucosa. The change in tumor and serum polyunsaturated fatty acids level is due to the uptake of these fatty acids by cancer cells. The polyunsaturated fatty acids are essential for formation of cell membrane phospholipids during rapid multiplying of cancer cells[30]. The fatty acid system possessed a memory. The memory of the fatty acid system consists of small intestine enterocytes [CD36, scavenger receptor class B type 1, long-chain fatty acid transport protein 4 (FATP4), fatty acid-binding protein 1 (FABP1), FABP2] and hepatocytes. In these cells, the short-term memory fatty acids are found. These short-term fatty acids consist of cytoplasmic lipid droplet cycles. The short-term memory of enterocytes and hepatocytes are united together to form long-term fatty acids memory. These long-term fatty acids memory are found in the adipocyte and in cellular membranes. The formation of fatty acids memory depend on sensing environmental material, encoding, consolidation, long-term storage, retrieval, re-encoding, re-consolidation, and renewed long-term storage[31]. The gastrointestinal microbiome controls many homeostatic processes in the healthy host such as immune function and gut barrier protection. Loss of normal gastrointestinal microbial configuration and function correlated with diseases such as clostridioides difficile infection, asthma, and epilepsy. The change of gastrointestinal microbiome stimulate sepsis by many processes such as: (1) Stimulates pathogenic intestinal bacteria; (2) Instructs the immune system for inflammatory response; and (3) Decreases section of beneficial microbial products such as short-chain fatty acids[32]. 2 meal/d against 12 meal/d declined peri-renal fat weight and serum triglyceride and liposaccharide levels in high fat diet-fed pigs. The decline of meal frequncy down-regulated mRNA expression of lipoprotein lipase, CD36 molecule, interleukin 1 beta, tumor necrosis factor alpha, toll-like receptor 4, myeloid differentiation factor 88, and nuclear factor kappa beta 1 as well as protein expression of myeloid differentiation primary response 88 (MYD88) in perirenal fat of high fat diet-fed pigs. So, the 2 meal/d against the 12 meal/d enhanced high fat diet-induced fat deposition and inflammatory response by decreasing fatty acid uptake[33].

GASTROINTESTINAL UPTAKE OF CHOLESTEROL

The aryl hydrocarbon receptor (AHR) modifies hepatic expression of cholesterol synthesis. Niemann-Pick C1-like intracellular cholesterol transporter (NPC1L1) facilitates the intestinal absorption of dietary cholesterol. The transcription of NPC1L1 involved in the cholesterol synthesis pathway is controlled by sterol-regulatory element-binding protein-2. So, the AHR possessed a role in the homeostatic regulation of cholesterol synthesis and absorption which referred to the application of this

receptor in the treatment of hyperlipidosis-associated metabolic diseases[34]. The decrease of gastrointestinal microbiota diminished albuminuria and tubulointerstitial damage. The serum acetate level was declined in antibiotics-treated diabetic rats and associated with the cholesterol level in the kidney. The acetate increased cholesterol increase in human kidney-2 (HK-2) cells which was induced by higher expression of proteins that reducing cholesterol synthesis and uptake. So, the acetate formed from gastrointestinal microbiota facilitated the imbalance of cholesterol homeostasis and consequently gastrointestinal microbiota reprogramming helping in diabetic nephropathy prevention and therapy[35]. Higher secretion of bile salts into the canalicular lumen increases bile formation and promotes biliary cholesterol and phospholipid output. Disturbing hepatic bile salt uptake was found to limit bile salt flux *via* the liver and consequently decrease biliary lipid excretion. Higher lysosomal discharge into bile increased biliary lipid secretion. The higher bile salts exposed to canalicular membrane leads to more cholesterol and phospholipid molecules to be excreted per bile salt. The increase of biliary lipid secretion is independent on variations in bile salt output, biliary bile salt hydrophobicity, or cholesterol and phospholipid transporters activities. Consequently, increase exposure of the canalicular membrane to bile salts associated with increased biliary cholesterol secretion and this process controls biliary cholesterol and phospholipid secretion[36]. The low-density lipoprotein, high-density lipoprotein and cholesterol levels in the blood become low in Plasmodium falciparum parasites infections in humans. These parasites import cholesterol from the surrounding environment. So, cholesterol import by Plasmodium falciparum includes hepatocytes and cholesterol uptake by the parasites[37]. Lipid structure of liposome alters the cell response for permeability, transport, and uptake in small intestine. The surface statuses of cholesterol-containing liposomes were smooth but they did not affect their transport and uptake through Caco-2 cell and microfold cells monolayers[38]. The sterols occur in the blood circulation either from cholesterol synthesis or gastrointestinal uptake. They are esterified or oxygenated. The cholesterol, cholesterol precursors, plant sterols and oxysterols accumulated in carotid artery plates. The circulating sterols were not reflected sterols levels. The normal cholesterol level occurs when plant sterol (but not oxysterol level) connected between plasma and plates. The oxysterols were lower in plates. Both cholesterol and plant sterols were lower esterified in plates than in plasma. The cholesterol, cholesterol precursors, plant sterols, and oxysterols were increased in symptomatic compared to asymptomatic patients[39]. The brown fat stimulation increases the uptake of cholesterol by the liver and so lowers plasma cholesterol and protects against atherosclerosis occurs. The hepatic cholesterol is converted into bile acids which secreted into the intestine. The bile acids seizure prevents the higher level of plasma bile acids which induced by brown fat activation. This process improves cholesterol metabolism and declines atherosclerosis occurs. Consequently, the collection of both brown fat activation and bile acids seizure is a favorable new therapeutic strategy to decline hyperlipidaemia and cardiovascular diseases[40]. The human Caco-2 cell line is well known *in vitro* model of the gastrointestinal epithelial barrier. The intestine is a major border in cholesterol uptaking and represents a non-biliary way for cholesterol excretion. The Caco-2 cells are a valuable model for investigating cholesterol homeostasis such as cholesterol uptake and efflux[41]. The Caco-2 cells signify the structure and functional properties of small intestinal cells. It is able of expressing brush borders, tight junctions, intestinal efflux and uptake and this control infusion of drugs and food extracts from intestinal lumen to blood circulation. The functional foods and their constituents had anti-proliferative and anti-cancer effects through apoptosis, cell cycle halt and decrease of all signal paths include in Caco-2 cell lines. The transportation, bioavailability, metabolism, mechanisms of actions, cellular paths created by food stuffs in Caco-2 cell lines are affected by their molecular weight, structures and physicochemical properties[42]. The cholesterol homeostasis is controlled by external factors such as diet and internal factors such as certain receptors, enzymes and transcription factors. The receptor 36 (CD36) is a membrane receptor takes place in fatty acid uptake, lipid metabolism, atherothrombosis and inflammation. The CD36 is vital molecule for cholesterol homeostasis in many processes such as absorption/reabsorption, synthesis, and transport of cholesterol and bile acids. The amount of fatty acids and fatty acid structure in the diet affects the CD36 Level and CD36 facilitated cholesterol metabolism in the liver, intestine and macrophages. The CD36 facilitated cholesterol and lipoprotein homeostasis counteracted by dietary saturated fatty acids and *trans*-fatty acids in the diet[43].

UPTAKE OF LYSOPHOSPHOLIPIDS

The bee venom caused skin inflammation which includes erythema, blisters, edemas, pain, and itching. The bee venom has an inhibitory effect on toll-like receptors. The toll-like receptors caused by secretory phospholipase A2. This secretory phospholipase A2 facilitates the hydrolysis of membrane phospholipids into lysophospholipids and free fatty acids[44]. The metabolic analysis in human cancers increased uptake of lysophospholipids and lipid storage, associated with increased fatty acid oxidation that maintains both adenosine triphosphate (ATP) levels and reactive oxygen species (ROS)-detoxifying reduced form of nicotinamide adenine dinucleotide phosphate (NADPH)[45]. The glycerol phosphate process creates higher than 90% of the hepatic triacylglycerol. The lysophosphatidic acid (an intermediate in this process) is created by glycerol-3-phosphate acyltransferase domain containing 3. The glycerophosphodiester phosphodiesterase creates lysophosphatidic acid from lysophospholipids. In human, liver glycerophosphodiester phosphodiesterase overexpression caused increased both lysophosphatidic acid and fatty acids uptake. The liver steatosis patients have increased glycerol-3-phosphate acyltransferase domain containing 3 mRNA levels compared with normal one. Consequently, the glycerol-3-phosphate acyltransferase domain containing 3 overexpression have a vital role in liver triacylglycerol increase and controls liver steatosis[46]. The microalga (Chlorella vulgaris) when exposed to the flame retardant triphenyl phosphate increase the synthesis of membrane lipids but decrease of lysoglycerolipids, fatty acids, and glyceryl-glucoside. On the other side, the microalga Scenedesmus obliquus when exposed to the flame retardant triphenyl phosphate increase lipolysis process such as accumulation of fatty acids, lysophospholipids, and glycerol phosphate[47]. The breathing of sphingosine increased the levels of sphingosine in the luminal membrane of bronchi and the trachea. The breathing of sphingosine without any side effects even with high doses[48]. The lysophosphatidic acid (LPA) is a bioactive lipid mediator which is incorporated in development, physiology, and pathological processes of the cardiovascular system. The LPA created both inside the cells and in the biological fluids. Most of the LPA is created by the secreted lysophospholipase D, autotaxin, *via* its binding to various β integrins or heparin sulfate on cell surface and hydrolyzing many lysophospholipids. The LPA possessed many effects on many blood cells and vascular cells that associated in the development of cardiovascular diseases such as atherosclerosis and aortic valve sclerosis. The LPA caused diversity of monocytes into macrophages and arouses oxidized low-density lipoproteins uptake by macrophages to form foam cells during atherosclerosis[49]. The docosahexaenoic acid-associated lysophosphatidyl choline declined triacylglycerol level due to the increase of carnitine palmitoyltransferase 2 and acyl-CoA oxidase levels and the decrease of acetyl-CoA carboxylase and glucose-6-phosphate dehydrogenase levels in the liver. So, the docosahexaenoic acid-associated lysophosphatidylcholine rich oil has hypolipidemic effect[50].

GASTROINTESTINAL METABOLISM OF ABSORBED LIPIDS

The tissue distribution of lipid is completely different among different species. Tiger puffer possesses lipid storage in the liver. There are 29 lipid metabolism-associated genes. These genes are included in lipogenesis, fatty acid oxidation, biosynthesis and hydrolysis of glycerides, lipid transport, and lipid transcription control. The intestine possesses the high transcription of lipogenic genes while the liver and muscle possesses low lipid gene expression. The intestine also has the highest transcription genes of most apolipoproteins and lipid metabolism-associated transcription factors. The fatty acid oxidation occurs in the mitochondrial β-oxidation in the liver and intestine. The re-acylation of absorbed lipids occurs in the intestine. In conclusion, the intestine is the center of lipid metabolism while the liver is the pure storage organ for lipid[51]. The highly lipophilic food stuffs are occurred in higher concentrations in the medium-chain triglycerides than the long-chain triglycerides. The 30% of the lipophilic food stuffs in medium-chain triglycerides are crossed the Caco-2 cells and 50% of the lipophilic food stuffs in medium-chain triglycerides were metabolized. The 60% of the lipophilic food stuffs in long-chain triglycerides were crossed the Caco-2 cells and 10% of the lipophilic food stuffs in long-chain triglycerides were metabolized. The higher lipid droplets and chylomicrons were formed for the long-chain triglycerides referring to of the lipophilic food stuffs transported through lymph. Although the medium-chain triglycerides possesses the higher of the lipophilic food stuffs, the final amount

of the lipophilic food stuffs absorbed and transported to the lymph was lower to that of the long-chain triglycerides formulation[52]. Vitamin B_6 is found in the diet in many forms but only pyridoxal 5'-phosphate (PLP) can serve as an enzymes cofactor. The intestine absorbs nonphosphorylated B_6 vitamers, which are changed to the active PLP form. Many human processes dependent on PLP such as amino acid and neurotransmitter metabolism, folate metabolism, protein and polyamine synthesis, carbohydrate and lipid metabolism, mitochondrial function and erythropoiesis. There are many roles of PLP beside the role of PLP as a cofactor B_6 vitamers and these roles are antioxidants, altering expression and action of steroid hormone receptors, affecting immune function, and antagonist of adenosine-5'-triphosphate (ATP)[53]. The oxysterols are oxidized forms of cholesterol which created by enzymes or by reactive oxygen species or both. The cholesterol or oxysterols are absorbed and stored in lipoproteins by hepatic cells. Inside the liver, additional cholesterol is metabolized to form bile acids. The endoplasmic reticulum is the main place for bile acid synthesis process. The metabolized sterols from this process are stored in the other places and in the cell membrane. The changes in membrane oxysterol: Sterol ratio affects the cell membrane stucture. The oxysterols changes membrane flexibility and receptor location. The hydroxylase enzymes in the mitochondria expedite oxysterol formation by an acidic process. In lysosomes, the oxysterols are also detected. The biochemical and physiological properties of oxysterols are many and important. Oxysterol levels are associated in many diseases such as chronic inflammatory diseases (Alzheimer's disease, atherosclerosis, and bowel disease), cancer and many neurodegenerative diseases[54]. The lipins possess vital roles in adipogenesis, insulin sensitivity, and gene regulation/mutation in these genes induces lipodystrophy, myoglobinuria, and inflammatory disorders. The lipids (lipid 1, 2, and 3) serve as phosphatidic acid phosphatase enzymes (need for triacylglycerol synthesis). The alteration of fatty acids in diet into triglycerides has been done by lipid 2 and 3. These 2 Lipids phosphatidic acid phosphatase enzymes activities have an important role in phospholipid homeostasis and chylomicron accumulation in enterocytes[55].

THE FINAL FORMS OF GASTROINTESTINAL LIPIDS

The lipids are re-synthesis again inside the human body where the gastrointestinal lipids are: (1) Transferred into the endoplasmic reticulum; (2) Collected as lipoproteins such as chylomicrons; or (3) Stored as lipid droplets in the cytosol. Both chylomicrons and cytosolic lipid droplets possess similar structure. The decrease of the microbiota which produces acetyl-CoA from acetate leads to suppress the change of fructose into hepatic acetyl-CoA and fatty acids. So, the higher fructose consumption facilitates fructose absorption in the small intestine and citrate breakdown in hepatocytes through lipogenesis process. But, the lipogenic transcriptional program stimulates by fructose that is independent of acetyl-CoA metabolism. Consequently, 2 mechanisms regulate hepatic lipogenesis by fructose inside the hepatocytes and these 2 mechanisms are: (1) The expression of lipogenic genes; and (2) The generation of microbial acetate feeds lipogenic pools of acetyl-CoA[56]. There are lower small intestine muscle mass, increase Bacteroidetes, decrease Firmicutes in the large intestine, and decrease of circulating short-chain fatty acids (SCFA) values in non-obese diabetic animals. These changes are correlated with increase body weight, hyperlipidemia, and severe insulin and glucose intolerance. Also, insulin resistance disturbances which related to energy metabolism such as decrease overall respiratory exchange rates but increase liver oxidative activity. There are changes related to gut and microbiota structure which accompanied with decrease of circulating SCFA that leads to metabolic disorders occurs[57]. Vitamin E includes 8 compounds; α-, β-, γ-, and delta-tocopherol and α-, β-, γ-, and delta-tocotrienol. α-tocopherol is found in the human diet. All the above forms of the vitamin E are absorbed in the small intestine, and then the liver metabolizes only α-tocopherol. The liver then removes and excretes the remaining vitamin E forms. Vitamin E deficiency is caused by a diet with low vitamin E or is caused by irregularities in dietary fat absorption or metabolism. Vitamin E is a lipid-soluble vitamin. Vitamin E reduces atherosclerosis and decrease rates of cardiac disease[58]. The different lipids during passage in gastrointestinal tract depend on lipid type and the microenvironment surrounding. The protein is the problem for pancreas lipase to catalyze lipid hydrolysis following gastric digestion. The higher free fatty acids secretion level and rate persistent in small intestine digestion in triacylglycerols (glycerol tripalmitate, glycerol tristearate, glycerol trioleate) in the order of glycerol tripalmitate > glycerol tristearate > glycerol trioleate, respectively[59]. The free fatty

acids secretion during 240 min in-vitro gastrointestinal digestion were measured, and the results proved that the release rate of short-chain saturated fatty acids were higher than the long-chain poly-unsaturated fatty acids. Also, the location of fatty acids inside triacylglycerols possesses an effect on the lipid hydrolysis process through pancreas lipase in gastrointestinal tract using in-vitro digestion model[60]. In the biological system, the gasotransmitters [nitric oxide (NO), hydrogen sulfide (H_2S), and carbon monoxide (CO)] are molecules do neural purposes in the whole body. Also, the gasotransmitters are small and lipid molecules control the changes in lipids rates of production or consumption. Moreover, tissue levels of the gasotransmitters are controlled by the level of O_2 and reactive oxygen species[61]. The changes in intestinal barrier permeability cause severe gastrointestinal disturbances. The leaky gut syndrome is caused by intestinal hyperpermeability due to changes in the expression levels and functioning of tight junctions. The diseases linked to intestinal hyperpermeability are found in Western countries, where a diet possesses higher fats. The fructose is a key that incorporated in the control of the intestinal permeability and induced harmful effects (such as tight junction protein dysfunction). The short chain fatty acids (such as butyrate) cause decrease of intestinal permeability but long chain fatty acids (such as *n*-3 and *n*-6 polyunsaturated fatty acids) have unknown effects[62]. The transepithelial transport rates in the Caco-2 cell were as follows: Scoparone > hydroxycinnamic acid > rutin > quercetin. The main metabolism of hydroxycinnamic acid (quercetin, and scoparone) in transepithelial transport was found to be methylation. Also, triglyceride, low-density lipoprotein cholesterol, total cholesterol, aspartate aminotransferase, and alanine aminotransferase levels in human liver cancer cell line (HepG2 cells) were suppressed by 53.64%, 23.44%, 36.49%, 27.98%, and 77.42% compared to the oleic acid-induced group[63].

COVID-19 AND LIPIDOME

The COVID-19 pandemic presents a global threat to global public health. The plasma lipidome is analyzed in mild, moderate, and severe COVID-19 patients and healthy subjects. Plasma lipidome of COVID-19 contains monosialodihexosyl ganglioside (GM3)-enriched exosomes, with sphingomyelins (SMs) and GM3s, and decrease diacylglycerols (DAGs). The COVID-19 patients with increase disease severity have an increase in GM3s. So, GM3-enriched exosomes participate in pathological cases of COVID-19 and presents the higher source on the plasma lipidome to COVID-19[64]. There is a change in lipid metabolism especially short and medium chain saturated fatty acids, acyl-carnitines, and sphingolipids in COVID-19 patients. But, there are no changes in hematological parameters (red blood cells, hematocrit, and mean corpuscular hemoglobin concentration, with slight increase in mean corpuscular volume) is observed[65,66]. MS-related methods such as lipidomics has been applied in COVID-19 disease outbreaks. Ultra-high-pressure liquid chromatographies with high-resolution mass spectrometry (UHPLC-HRMS)-based lipidomics are used to identify infectious pathogens and biomarkers related in COVID-19. Polymerase chain reaction-mass spectrometry (PCR-MS) is a new technology to determine known pathogens from the clinical specimens. Also, miniaturized MS provides an application with fast, high sensitive and easy way to analyze for COVID-19. Consequently, MS-related methods are an easy and sensitive way in studying corona outbreaks such as COVID-19[67]. MS-related, lipidomics method provides a suitable way of virus-induced changes to the host after infection and can lead to the determination of new therapeutic agents for preventing disease spreading. The omics study with MERS-CoV is used lipid extraction to develop a single sample in lipids determination in COVID-19 infection[68]. The lipidomic changes such as structural-lipids, the eicosanoids, and docosanoids lipid mediators (LMs) are important for the diagnosis of COVID-19 disease severity. The progression from moderate to severe disease is accompanied with loss of specific immune regulatory LMs and increased pro-inflammatory cytokines[69,70]. COVID-19 exerts higher effect on the metabolism. The lipidomic analysis showed pathogenic redistribution of the lipoprotein particle size and composition to increase the atherosclerotic danger. The metabolomic analysis showed abnormal high levels of ketone bodies such as acetoacetic acid, 3-hydroxybutyric acid, and acetone. Also, higher increase of 2-hydroxybutyric acid (an indication of hepatic glutathione synthesis and oxidative stress marker). So, SARS-CoV-2 infection caused liver damage correlated with dyslipidemia and oxidative stress[71]. The viral infection is depended on the lipid metabolism of the infected cells. From a lipidomics view, there are many mechanisms connecting to viral infection such as viral entry, the disorder of host cell

lipid metabolism, and the role related to different lipids in the infection efficiency. So, lipids play an important role in COVID-10 infection success especially the role of cholesterol in the success of viral infection[72]. Figure 2 exhibits lipidome and COVID-19 in gastrointestinal tract.

LIPIDOME VIEW IN VIRAL REPLICATION CYCLES

COVID-19 is a virus and this virus is dependent on its lipid cover which possesses high capability to detergent. The lipids play an important role in many stages of the virus replication cycle. The definite lipid change occurs during viral infection in higher viral replication cycle. There are 47 lipids within 11 lipid classes were significantly disturbed after viral infection. There are 4 polyunsaturated fatty acids (PUFAs): (1) Arachidonic acid (AA); (2) Docosahexaenoic acid (DHA); (3) Docosapentaenoic acid (DPA); and (4) Eicosapentaenoic acid (EPA) were upregulated during viral infection. The 3 of these 4 fatty acids (PUFAs; AA, DHA, and EPA) declined viral replication. Consequently, enteroviruses modify the host lipid pathways for higher virus replication. Higher exogenous lipids prevent effective viral replication. The control of the host lipid profile is a host-targeting antiviral strategy for enterovirus infection[73]. In hepatitis C virus (HCV) infection, the HCV reproduction depends on many lipid metabolic processes during viral life cycle. The HCV induces cells' lipidomic profile changes by controlling many key pathways of lipid synthesis, remodeling and utilization. So, the lipids play a significant role in HCV RNA replication, meeting and entrance. In viral process, there are many changes in the cell fatty acid content and variations of the membrane lipid composition during replication of the virus. In viral process, the lipids represent lipid provider during replication and as an essential hub for HCV meeting. The lipoproteins play an important role in HCV maturation and entrance[74]. There is an increase in the levels of many phosphatidylethanolamine (PE) lipids in the serum of Zika virus patients, most of them plasmenyl-phosphatidylethanolamine (pPE) (or plasmalogens) correlated with polyunsaturated fatty acids. The plasmalogens correlated with polyunsaturated fatty acids are abundant in neural membranes of the brain and these represent 20% of total phospholipids in humans. The biosynthesis of plasmalogens is necessary for efficient peroxisomes, which are important sites for Zika virus replication[75]. A stable benzoic derivative of retinoic acid (AM580) and retonic acid receptor-αagonist has greater effective in disturbing the life cycle of many viruses such as MERS-coronavirus and influenza A virus. The sterol regulatory element binding protein (SREBP) connect with AM580 and exerts antiviral effect. Consequently, lipidome technique plays a major role in human viral infections where SREBP is an effective agent in the antiviral strategies development[76]. The glycerophospholipids and fatty acids increased in human coronavirus 229E-infected cells and the linoleic acid (LA) to AA metabolism was disturbed in HCoV-229E infection by using high performance liquid chromatography-associated with lipidome technique. Supplementation with LA or AA in HCoV-229E-infected cells depressed HCoV-229E virus replication. The inhibition of LA and AA on virus replication can be seen in MERS-CoV. So, the host lipid metabolic processes correlated with human-coronavirus proliferation. Consequently, the control of lipid metabolism is the main goal for coronavirus infections[77]. The cell lipidome technique shows an increase in phospholipase A2 (PLA2) activity to produce lyso-phosphatidylcholine (lyso-PChol). The PLA2 enzyme family is activated in West Nile virus strain Kunjin virus-infected cells and produces lyso-PChol lipid molecules that need for viral reproduction. The production of lyso-PChol is increased by inhibition of PLA2 in West Nile virus strain Kunjin virus reproduction and production of infectious virus is occurred. The lyso-PChol related to the formation of the West Nile virus strain Kunjin virus replication complex (RC). Consequently, lipid homeostasis enables the researchers to understand flaviviruses replication[78]. The HCV-infected cells contain higher amounts of phosphatidylcholines and triglycerides with longer fatty acyl chains and increased use of C18 fatty acids especially oleic acid. So, decrease of fatty acid elongases and desaturases reduces HCV reproduction. There is an increase in the levels of polyunsaturated fatty acids (PUFAs) in HCV infection. The decrease of the PUFA synthesis path damaged viral reproduction, indicating that higher PUFAs are needed for viral replication. Consequently, the control of the host cell lipid metabolism is needed and caused by HCV to increase viral replication[79].

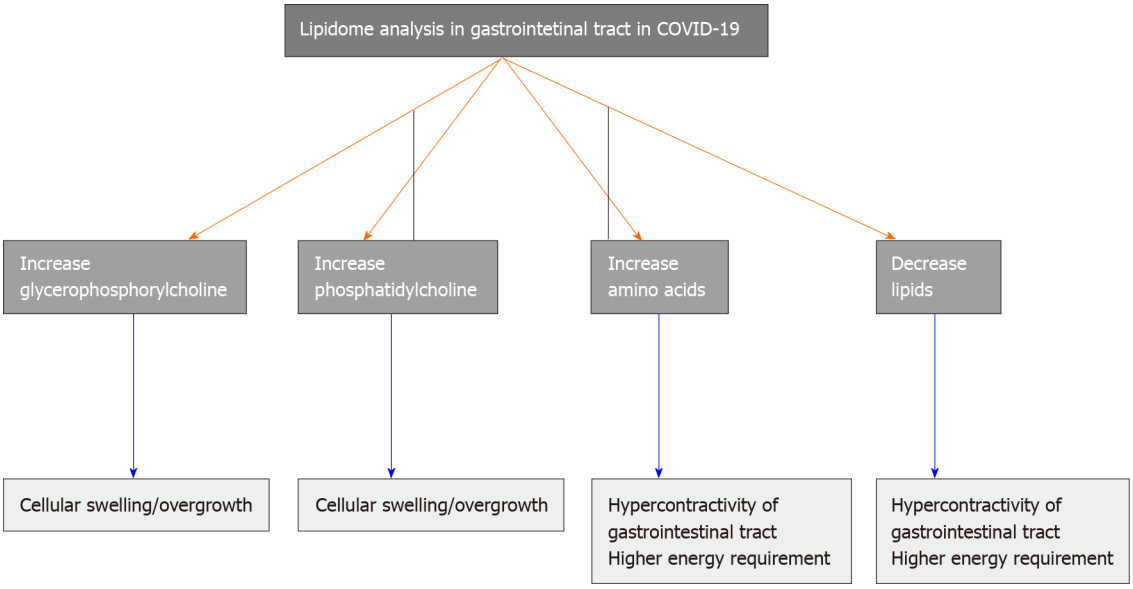


Figure 2 Lipidome and COVID-19 in gastrointestinal tract.

THE ROLE OF LIPIDOME DURING THE HOST-VIRAL INTERACTIONS

In the recent century, researches using genetic, cell biological, and biochemical techniques has led to huge increase in molecular and biological insight into interaction of virus with their hosts. Cell biological studies depend on microscope as a principal technique, of basic microbiology methods so these researches added more data to host-viral interactions. On the other hand, the biomedical researches, the main focus was on the determination of genes and proteins necessary for activity. Based on these findings there is now increased consciousness that lipids (both of host and of virus) play vital roles in regulating infection stability, entry into host cells, as well as, replication and persistence of the virus. There is a connection between the host protein disulfide isomerase (PDI) with dengue virus protein and role of lipid raft in viral infection. The PDI correlates with dengue virus nonstructural protein 1 (NS1) inside the biological cell as well as on the surface in the lipid raft molecule. Disturbance of this relation between PDI and NS1 is important in treatment strategy to stop dengue virus infection[80]. The virus connects with blood-borne lipoproteins and apolipoprotein E (apoE) to change viral infectivity. Viral interest is cholesterol- and lipid raft-dependent (24-dehydrocholesterol reductase, 3-hydroxy-3-methylglutaryl-CoA reductase, fibrin degradation products, raft-linking protein, Sterol regulatory element-binding transcription factor 1). The virus is gone to the nucleus through the dynein and kinesin motors. Amyloid precursor protein has a role nucleus invention by the virus. The viral protein removes mitochondrial DNA as in Alzheimer's disease case. The virus connects with the host transcription factors transcription factor CP2 and POU domain, class 2, transcription factor 1 that control many other genes. Viral inactivity is controlled by interleukin 6 (IL6) and IL1β. Viral avoidance occurs by inhibition of the antigen processor human gene that encodes the protein antigen peptide transporter 2, the production of an Fc immunoglobulin receptor mimic and inhibition of the viral-activated kinase eukaryotic interferon-inducible factor 2 alpha kinase[81]. The role of lipidome during the host-viral interactions includes 2 main categories: (1) cell and chemical biology in the viral-host interaction; and (2) lipid profiling in the viral-host interaction.

Cell and chemical biology in the viral-host interaction

There is an important host factor (CPSF6) connects with nuclear protein (NP1). The CPSF6 increases the nuclear production of NP1 in the same time CPSF6 possesses an important role in progress of capsid mRNAs inside the nucleus. The connection between viral NP1 and host CPSF6 gives the scientist the mechanism enables viral protein increases the viral gene expression and replication as well as antiviral drug discovery[82]. The virus infection causes spreading of the distraction of transcription termination (DoTT) of RNA polymerase II (RNAPII) in host genes. The herpes simplex virus-1 (HSV-1) immediate early protein (ICP27) causes widespread DoTT through connection with essential mRNA 3' processing factor (CPSF). The ICP27 stimulates

mRNA 3' processing for viral and host transcription. So, ICP27 possesses an important role in HSV-1-causes viral infection while CPSF stimulates regulation of transcription end[83]. The RNA binding-deficient stores in nucleoprotein (NP) bodies and the nuclear RNA export factor 1 (NXF1) is necessary for viral protein expression but not for viral RNA synthesis. The NXF1 connects with viral mRNAs but not with viral RNAs. Consequently, the NXF1 promotes the export of viral mRNA:NXF1 complexes from inclusion bodies. This provides a basis for new therapeutic approaches for viruses[84]. The ribosomal proteins (RPs) contain 60S subunit control translation of specific mRNAs. The translation process of the RPs in this process controls in the catalyzing peptide bond formation. The ribosomal protein L13 (RPL13) is a regulator of viral translation and infection. Consequently, understanding this process gives rise to the effects for the translation of viral mRNA and thus for the development of viral prevention[85]. The influenza A viruses contain RNA genome include 8 segments. Each RNA segment correlated with the NP and viral RNA polymerase to and from a viral ribonucleoprotein (vRNP) molecule. The formation of viral mRNA is dependent on the host RNA transcription and for these processes to be occurred; the vRNPs must pass through the cell nuclear pore complex (NPC) to the nucleus. The influenza A virus NS2 protein, also called the nuclear export protein and this protein connects with the host cellular nucleoporins during the nuclear export of vRNPs. The human nucleoporin 214 (Nup214) is called NS2-binding protein and NS2 protein coonects with the amino terminal FG domain of the Nup214 protein. The influenza viral replication was decreased by the Nup214 protein. Consequently, the FG domains of nucleoporins have an important role in the connection of the influenza NS2 protein with host NPC for viral RNA (vRNA) spread[86]. The importin-α3 (one of the main nuclear factor kappa-light-chain-enhancer of activated B cells (NF-κB) transporters) is the expressed nuclear factor in the mammalian respiratory tract. Importin-α3 promoter effect is controlledby TNF-α-induced NF-κB. The increasing of TNF-α increasing pathogenic avian influenza A viruses (HPAIVs) in serious human cases protecting human polymerase signatures (PB2 627K, 701N) which downregulate importin-α3 mRNA expression in the lung cells. The decrease of Importin-α3 is returned by the mutating of the HPAIV polymerase into an avian-type signature (PB2 627E, 701D) which suppresses the high TNF-α levels. The decrease of importin-α3 decreased the NF-κB antiviral gene expression and increased influenza dangerous. Consequently, importin-α3 possesses a role in antiviral immunity in influenza and so importin-α3 in the lung help in the strategy to fight respiratory virus infections[87]. During rotavirus infection, the small interfering RNA (siRNA) facilitates genetic exhaustion of ATP5B or other ATP synthase molecules (ATP5A1 and ATP5O) decreases the production of viral new generations without modification of viral RNA amounts and translation. The ATP5B controls the late-stage rotavirus growth in intestinal cells. Consequently, the role of host proteins in rotavirus RNA identifies ATP5B as a novel pro-rotavirus RNA-binding protein that help scientists to understand virus growth and pathogenesis[88]. The host protein (hnRNP C1/C2) decreases viral RNA translation. The hnRNP C1/C2 connects with stem-loop V in the Internal Ribosome Entry Site' (IRES) and transfers binding protein where this protein controls of viral translation. The hnRNP C1/C2 causes changing of viral translation to replication. Consequently, the hnRNP C1/C2 controls of viral RNA translation to replication by a specific mechanism[89]. The connection of glycyl-tRNA synthetase (GARS) increases the environmental of the initiation area of the internal IRES in the mRNA binding site of the ribosome that increasing IRES effect at the step of initiation formation[90].

Lipid profiling in the viral-host interaction

The studies of viral lipids are not new trends. The main developments in analytical biochemistry have added new information to these studies. The liquid chromatography and MS are the most important techniques applied in the field of lipidome. These techniques allow detection, characterization, and quantification of huge molecules of lipids (although it is currently not possible to determine the full "lipidome" of a cell or tissue in one study). The major biochemical information of lipid lists (*e.g.*,. of mycobacteria) is now applied to investigate the details of lipid biosynthesis and lipid transporters. Potato is a natural host of Potato spindle tuber viroid (PSTVd) which causes arresting phenotype and alteration of leaves and tubers. The PSTVd virus replicates in the nucleus and moves in the plant. The host possesses defense, stress and sugar metabolism correlated genes which alters expression levels in infection and the hormone-related genes showed up- or down-regulation. Consequently, gibberellin and brassinosteroid paths possess an important role in tuber development upon PSTVd infection[91]. In dengue virus infection, there is an increase in mRNA, myeloid differentiation 2-related lipid recognition protein (ML) and Niemann

Pick-type C1 (NPC1) genes. These 3 genes translate lipid-binding proteins which play an important role in host-viral connection. The RNA interference (RNAi)-mediated gene stops the ML and NPC1 genes. In viral infection, ML and NPC1 increase viral infection by reducing the host immune ability. Consequently, the dengue virus effects the expression of these genes to stimulate viral infection of the mosquito host[92].

FUTURE THERAPY OF CORONAVIRUS

No vaccines or antiviral drug to prevent or treat human coronavirus infections is available. The coronavirus treatment is only caring. There are many antiviral agents used *e.g.*, viral proteases, polymerases and entry proteins. Coronavirus is capable to replicate in invitro study such as human lung cancer cell line (Calu-3 cells) and causes lower transcriptomic variations before 12 h after viral infection. As infection progress, coronavirus causes a significant dysregulation of the host transcriptome greater than SARS virus. Both viruses induced a similar stimulation of host receptors and the interleukin 17 paths but coronavirus inhibits the expression of many genes such as type I and II major histocompatibility complex genes. This viral effect identifies the ability of the host response to viral infection. There are 207 genes was inhibited following coronavirus infection, and was used to detect the antiviral secretions such as kinase inhibitors and glucocorticoids. Consequently, coronavirus and SARS virus possesses host gene expression reactions that effect on *in vivo* pathogenesis and therapeutic strategies[93]. In coronavirus infection, the whole blood cytokine investigations increased the cytokine expression in the viral cell infected case. The inflammatory gene expression increased after dysfunction of respiratory function, except the expression in the IL1 path. The investigations of CD4 and CD8 expression showed that the pro-inflammatory factors increased with T cell initiation that leads to prolong the disease or prolong the infection. Consequently, the pro-inflammatory factors such as IL1 and related pro-inflammatory paths analyzes and uses as therapeutic agents for COVID-19[94].

CONCLUSION

The term lipidome is mentioned to the total amount of the lipids inside the biological cells. The lipid enters the human gastrointestinal tract through external source and internal source. The lipids are re-synthesis again inside the human body where the gastrointestinal lipids are: (1) Transferred into the endoplasmic reticulum; (2) Collected as lipoproteins such as chylomicrons; or (3) Stored as lipid droplets in the cytosol. The tissue distribution of lipid is completely different among different species. Fatty acids are uptake by the gastrointestinal tract through 2 ways; the 1st way, fatty acids transfer from the intestinal membrane from higher concentration to lower concentration inside the cell while the 2nd way occurs from the cell to the lumen when the fatty acids concentration inside the cell is higher than lumen fatty acids concentration. The lipids play an important role in many stages of the viral replication cycle. There are 47 Lipids within 11 Lipid classes were significantly disturbed after viral infection. The virus connects with blood-borne lipoproteins and apolipoprotein E to change viral infectivity. The viral interest is cholesterol- and lipid raft-dependent molecules. The future therapy of coronavirus includes the investigations of CD4 and CD8 expression where these pro-inflammatory factors increased with T cell initiation that leads to prolong the infection.

REFERENCES

1 **Züllig T**, Trötzmüller M, Köfeler HC. Lipidomics from sample preparation to data analysis: a primer. *Anal Bioanal Chem* 2020; **412**: 2191-2209 [PMID: 31820027 DOI: 10.1007/s00216-019-02241-y]

2 **Schlame M**, Xu Y, Erdjument-Bromage H, Neubert TA, Ren M. Lipidome-wide ^{13}C flux analysis: a novel tool to estimate the turnover of lipids in organisms and cultures. *J Lipid Res* 2020; **61**: 95-104 [PMID: 31712250 DOI: 10.1194/jlr.D119000318]

3 **Quehenberger O**, Armando AM, Brown AH, Milne SB, Myers DS, Merrill AH, Bandyopadhyay S, Jones KN, Kelly S, Shaner RL, Sullards CM, Wang E, Murphy RC, Barkley RM, Leiker TJ, Raetz CR, Guan Z, Laird GM, Six DA, Russell DW, McDonald JG, Subramaniam S, Fahy E, Dennis EA. Lipidomics reveals a remarkable diversity of lipids in human plasma. *J Lipid Res* 2010; **51**: 3299-3305 [PMID: 20671299 DOI: 10.1194/jlr.M009449]

4 **Koriem KMM**. A lipidomic concept in infectious diseases. *Asian Pac J Trop Biomed* 2017; **7**: 265-274 [DOI: 10.1016/j.apjtb.2016.12.010]
5 **Koriem KMM**. Protective effect of natural products and hormones in colon cancer using metabolome: A physiological overview. *Asian Pac J Trop Biomed* 2017; **7**: 957-966 [DOI: 10.1016/j.apjtb.2017.09.002]
6 **Koriem KMM**. Proteomic approach in human health and disease: Preventive and cure studies. *Asian Pac J Trop Biomed* 2018; **8**: 226-236 [DOI: 10.4103/2221-1691.231285]
7 **Subramaniam S**, Fahy E, Gupta S, Sud M, Byrnes RW, Cotter D, Dinasarapu AR, Maurya MR. Bioinformatics and systems biology of the lipidome. *Chem Rev* 2011; **111**: 6452-6490 [PMID: 21939287 DOI: 10.1021/cr200295k]
8 **Seppänen-Laakso T**, Oresic M. How to study lipidomes. *J Mol Endocrinol* 2009; **42**: 185-190 [PMID: 19060177 DOI: 10.1677/JME-08-0150]
9 **Goracci L**, Valeri A, Sciabola S, Aleo MD, Moritz W, Lichtenberg J, Cruciani G. A Novel Lipidomics-Based Approach to Evaluating the Risk of Clinical Hepatotoxicity Potential of Drugs in 3D Human Microtissues. *Chem Res Toxicol* 2020; **33**: 258-270 [PMID: 31820940 DOI: 10.1021/acs.chemrestox.9b00364]
10 **Tso P**, Balint JA. Formation and transport of chylomicrons by enterocytes to the lymphatics. *Am J Physiol* 1986; **250**: G715-G726 [PMID: 3521320 DOI: 10.1152/ajpgi.1986.250.6.G715]
11 **D'Aquila T**, Hung YH, Carreiro A, Buhman KK. Recent discoveries on absorption of dietary fat: Presence, synthesis, and metabolism of cytoplasmic lipid droplets within enterocytes. *Biochim Biophys Acta* 2016; **1861**: 730-747 [PMID: 27108063 DOI: 10.1016/j.bbalip.2016.04.012]
12 **Hung YH**, Carreiro AL, Buhman KK. Dgat1 and Dgat2 regulate enterocyte triacylglycerol distribution and alter proteins associated with cytoplasmic lipid droplets in response to dietary fat. *Biochim Biophys Acta Mol Cell Biol Lipids* 2017; **1862**: 600-614 [PMID: 28249764 DOI: 10.1016/j.bbalip.2017.02.014]
13 **Hussain MM**. Intestinal lipid absorption and lipoprotein formation. *Curr Opin Lipidol* 2014; **25**: 200-206 [PMID: 24751933 DOI: 10.1097/MOL.0000000000000084]
14 **Yang Y**, Peng F, Wang R, Yange M, Guan K, Jiang T, Xu G, Sun J, Chang C. The deadly coronaviruses: The 2003 SARS pandemic and the 2020 novel coronavirus epidemic in China. *J Autoimmun* 2020; **109**: 102434 [PMID: 32143990 DOI: 10.1016/j.jaut.2020.102434]
15 **Hasöksüz M**, Kiliç S, Saraç F. Coronaviruses and SARS-COV-2. *Turk J Med Sci* 2020; 549-556 [PMID: 32293832 DOI: 10.3906/sag-2004-127]
16 **Chang L**, Yan Y, Wang L. Coronavirus Disease 2019: Coronaviruses and Blood Safety. *Transfus Med Rev* 2020; **34**: 75-80 [PMID: 32107119 DOI: 10.1016/j.tmrv.2020.02.003]
17 **Shiau YF**, Popper DA, Reed M, Umstetter C, Capuzzi D, Levine GM. Intestinal triglycerides are derived from both endogenous and exogenous sources. *Am J Physiol* 1985; **248**: G164-G169 [PMID: 3970197 DOI: 10.1152/ajpgi.1985.248.2.G164]
18 **Ko CW**, Qu J, Black DD, Tso P. Regulation of intestinal lipid metabolism: current concepts and relevance to disease. *Nat Rev Gastroenterol Hepatol* 2020; **17**: 169-183 [PMID: 32015520 DOI: 10.1038/s41575-019-0250-7]
19 **Stock V**, Fahrenson C, Thuenemann A, Dönmez MH, Voss L, Böhmert L, Braeuning A, Lampen A, Sieg H. Impact of artificial digestion on the sizes and shapes of microplastic particles. *Food Chem Toxicol* 2020; **135**: 111010 [PMID: 31794801 DOI: 10.1016/j.fct.2019.111010]
20 **Tanaka S**, Nemoto Y, Takei Y, Morikawa R, Oshima S, Nagaishi T, Okamoto R, Tsuchiya K, Nakamura T, Stutte S, Watanabe M. High-fat diet-derived free fatty acids impair the intestinal immune system and increase sensitivity to intestinal epithelial damage. *Biochem Biophys Res Commun* 2020; **522**: 971-977 [PMID: 31810607 DOI: 10.1016/j.bbrc.2019.11.158]
21 **Lin R**, Zhang H, Yuan Y, He Q, Zhou J, Li S, Sun Y, Li DY, Qiu HB, Wang W, Zhuang Z, Chen B, Huang Y, Liu C, Wang Y, Cai S, Ke Z, He W. Fatty Acid Oxidation Controls $CD8^+$ Tissue-Resident Memory T-cell Survival in Gastric Adenocarcinoma. *Cancer Immunol Res* 2020; **8**: 479-492 [PMID: 32075801 DOI: 10.1158/2326-6066.CIR-19-0702]
22 **Gong J**, Lin Y, Zhang H, Liu C, Cheng Z, Yang X, Zhang J, Xiao Y, Sang N, Qian X, Wang L, Cen X, Du X, Zhao Y. Reprogramming of lipid metabolism in cancer-associated fibroblasts potentiates migration of colorectal cancer cells. *Cell Death Dis* 2020; **11**: 267 [PMID: 32327627 DOI: 10.1038/s41419-020-2434-z]
23 **Li Q**, Liang X, Xue X, Wang K, Wu L. Lipidomics Provides Novel Insights into Understanding the Bee Pollen Lipids Transepithelial Transport and Metabolism in Human Intestinal Cells. *J Agric Food Chem* 2020; **68**: 907-917 [PMID: 31842537 DOI: 10.1021/acs.jafc.9b06531]
24 **Lackey AI**, Chen T, Zhou YX, Bottasso Arias NM, Doran JM, Zacharisen SM, Gajda AM, Jonsson WO, Córsico B, Anthony TG, Joseph LB, Storch J. Mechanisms underlying reduced weight gain in intestinal fatty acid-binding protein (IFABP) null mice. *Am J Physiol Gastrointest Liver Physiol* 2020; **318**: G518-G530 [PMID: 31905021 DOI: 10.1152/ajpgi.00120.2019]
25 **Ticho AL**, Malhotra P, Dudeja PK, Gill RK, Alrefai WA. Intestinal Absorption of Bile Acids in Health and Disease. *Compr Physiol* 2019; **10**: 21-56 [PMID: 31853951 DOI: 10.1002/cphy.c190007]
26 **Pearce SC**, Weber GJ, van Sambeek DM, Soares JW, Racicot K, Breault DT. Intestinal enteroids recapitulate the effects of short-chain fatty acids on the intestinal epithelium. *PLoS One* 2020; **15**: e0230231 [PMID: 32240190 DOI: 10.1371/journal.pone.0230231]
27 **Castilla-Madrigal R**, Gil-Iturbe E, López de Calle M, Moreno-Aliaga MJ, Lostao MP. DHA and its derived lipid mediators MaR1, RvD1 and RvD2 block TNF-α inhibition of intestinal sugar and

glutamine uptake in Caco-2 cells. *J Nutr Biochem* 2020; **76**: 108264 [PMID: 31760230 DOI: 10.1016/j.jnutbio.2019.108264]

28 **Wu W**, Wang S, Liu Q, Shan T, Wang X, Feng J, Wang Y. AMPK facilitates intestinal long-chain fatty acid uptake by manipulating CD36 expression and translocation. *FASEB J* 2020; **34**: 4852-4869 [PMID: 32048347 DOI: 10.1096/fj.201901994R]

29 **Zhao M**, Zhao L, Xiong X, He Y, Huang W, Liu Z, Ji L, Pan B, Guo X, Wang L, Cheng S, Xu M, Yang H, Yin Y, Garcia-Barrio MT, Chen YE, Meng X, Zheng L. TMAVA, a Metabolite of Intestinal Microbes, Is Increased in Plasma From Patients With Liver Steatosis, Inhibits γ-Butyrobetaine Hydroxylase, and Exacerbates Fatty Liver in Mice. *Gastroenterology* 2020; **158**: 2266-2281. e27 [PMID: 32105727 DOI: 10.1053/j.gastro.2020.02.033]

30 **Mika A**, Kobiela J, Pakiet A, Czumaj A, Sokołowska E, Makarewicz W, Chmielewski M, Stepnowski P, Marino-Gammazza A, Sledzinski T. Preferential uptake of polyunsaturated fatty acids by colorectal cancer cells. *Sci Rep* 2020; **10**: 1954 [PMID: 32029824 DOI: 10.1038/s41598-020-58895-7]

31 **Straub RH**. The memory of the fatty acid system. *Prog Lipid Res* 2020; **79**: 101049 [PMID: 32589906 DOI: 10.1016/j.plipres.2020.101049]

32 **Adelman MW**, Woodworth MH, Langelier C, Busch LM, Kempker JA, Kraft CS, Martin GS. The gut microbiome's role in the development, maintenance, and outcomes of sepsis. *Crit Care* 2020; **24**: 278 [PMID: 32487252 DOI: 10.1186/s13054-020-02989-1]

33 **Yan H**, Cao S, Li Y, Zhang H, Liu J. Reduced meal frequency alleviates high-fat diet-induced lipid accumulation and inflammation in adipose tissue of pigs under the circumstance of fixed feed allowance. *Eur J Nutr* 2020; **59**: 595-608 [PMID: 30747271 DOI: 10.1007/s00394-019-01928-3]

34 **Muku GE**, Kusnadi A, Kuzu G, Tanos R, Murray IA, Gowda K, Amin S, Perdew GH. Selective Ah receptor modulators attenuate NPC1L1-mediated cholesterol uptake through repression of SREBP-2 transcriptional activity. *Lab Invest* 2020; **100**: 250-264 [PMID: 31417158 DOI: 10.1038/s41374-019-0306-x]

35 **Hu ZB**, Lu J, Chen PP, Lu CC, Zhang JX, Li XQ, Yuan BY, Huang SJ, Ruan XZ, Liu BC, Ma KL. Dysbiosis of intestinal microbiota mediates tubulointerstitial injury in diabetic nephropathy *via* the disruption of cholesterol homeostasis. *Theranostics* 2020; **10**: 2803-2816 [PMID: 32194836 DOI: 10.7150/thno.40571]

36 **Roscam Abbing RLP**, Slijepcevic D, Donkers JM, Havinga R, Duijst S, Paulusma CC, Kuiper J, Kuipers F, Groen AK, Oude Elferink RPJ, van de Graaf SFJ. Blocking Sodium-Taurocholate Cotransporting Polypeptide Stimulates Biliary Cholesterol and Phospholipid Secretion in Mice. *Hepatology* 2020; **71**: 247-258 [PMID: 31136002 DOI: 10.1002/hep.30792]

37 **Hayakawa EH**, Kato H, Nardone GA, Usukura J. A prospective mechanism and source of cholesterol uptake by Plasmodium falciparum-infected erythrocytes co-cultured with HepG2 cells. *Parasitol Int* 2021; **80**: 102179 [PMID: 32853776 DOI: 10.1016/j.parint.2020.102179]

38 **Konishi K**, Du L, Francius G, Linder M, Sugawara T, Kurihara H, Takahashi K. Lipid Composition of Liposomal Membrane Largely Affects Its Transport and Uptake through Small Intestinal Epithelial Cell Models. *Lipids* 2020; **55**: 671-682 [PMID: 32770855 DOI: 10.1002/lipd.12269]

39 **Ceglarek U**, Dittrich J, Leopold J, Helmschrodt C, Becker S, Staab H, Richter O, Rohm S, Aust G. Free cholesterol, cholesterol precursor and plant sterol levels in atherosclerotic plaques are independently associated with symptomatic advanced carotid artery stenosis. *Atherosclerosis* 2020; **295**: 18-24 [PMID: 31981947 DOI: 10.1016/j.atherosclerosis.2019.12.018]

40 **Zhou E**, Hoeke G, Li Z, Eibergen AC, Schonk AW, Koehorst M, Boverhof R, Havinga R, Kuipers F, Coskun T, Boon MR, Groen AK, Rensen PCN, Berbée JFP, Wang Y. Colesevelam enhances the beneficial effects of brown fat activation on hyperlipidaemia and atherosclerosis development. *Cardiovasc Res* 2020; **116**: 1710-1720 [PMID: 31589318 DOI: 10.1093/cvr/cvz253]

41 **Hiebl V**, Schachner D, Ladurner A, Heiss EH, Stangl H, Dirsch VM. Caco-2 Cells for Measuring Intestinal Cholesterol Transport - Possibilities and Limitations. *Biol Proced Online* 2020; **22**: 7 [PMID: 32308567 DOI: 10.1186/s12575-020-00120-w]

42 **Iftikhar M**, Iftikhar A, Zhang H, Gong L, Wang J. Transport, metabolism and remedial potential of functional food extracts (FFEs) in Caco-2 cells monolayer: A review. *Food Res Int* 2020; **136**: 109240 [PMID: 32846508 DOI: 10.1016/j.foodres.2020.109240]

43 **Ulug E**, Nergiz-Unal R. Dietary fatty acids and CD36-mediated cholesterol homeostasis: potential mechanisms. *Nutr Res Rev* 2020; 1-14 [PMID: 32308181 DOI: 10.1017/S0954422420000128]

44 **Nakashima A**, Tomono S, Yamazaki T, Inui M, Morita N, Ichimonji I, Takagi H, Nagaoka F, Matsumoto M, Ito Y, Yanagishita T, Miyake K, Watanabe D, Akashi-Takamura S. Phospholipase A2 from bee venom increases poly(I:C)-induced activation in human keratinocytes. *Int Immunol* 2020; **32**: 371-383 [PMID: 31957789 DOI: 10.1093/intimm/dxaa005]

45 **Qiao S**, Koh SB, Vivekanandan V, Salunke D, Patra KC, Zaganjor E, Ross K, Mizukami Y, Jeanfavre S, Chen A, Mino-Kenudson M, Ramaswamy S, Clish C, Haigis M, Bardeesy N, Ellisen LW. REDD1 loss reprograms lipid metabolism to drive progression of *RAS* mutant tumors. *Genes Dev* 2020; **34**: 751-766 [PMID: 32273287 DOI: 10.1101/gad.335166.119]

46 **Key CC**, Bishop AC, Wang X, Zhao Q, Chen GY, Quinn MA, Zhu X, Zhang Q, Parks JS. Human GDPD3 overexpression promotes liver steatosis by increasing lysophosphatidic acid production and fatty acid uptake. *J Lipid Res* 2020; **61**: 1075-1086 [PMID: 32430316 DOI: 10.1194/jlr.RA120000760]

47 **Wang L**, Huang X, Lim DJ, Laserna AKC, Li SFY. Uptake and toxic effects of triphenyl phosphate

on freshwater microalgae Chlorella vulgaris and Scenedesmus obliquus: Insights from untargeted metabolomics. *Sci Total Environ* 2019; **650**: 1239-1249 [PMID: 30308812 DOI: 10.1016/j.scitotenv.2018.09.024]

48 **Carstens H**, Schumacher F, Keitsch S, Kramer M, Kühn C, Sehl C, Soddemann M, Wilker B, Herrmann D, Swaidan A, Kleuser B, Verhaegh R, Hilken G, Edwards MJ, Dubicanac M, Carpinteiro A, Wissmann A, Becker KA, Kamler M, Gulbins E. Clinical Development of Sphingosine as Anti-Bacterial Drug: Inhalation of Sphingosine in Mini Pigs has no Adverse Side Effects. *Cell Physiol Biochem* 2019; **53**: 1015-1028 [PMID: 31854953 DOI: 10.33594/000000194]

49 **Zhao Y**, Hasse S, Zhao C, Bourgoin SG. Targeting the autotaxin - Lysophosphatidic acid receptor axis in cardiovascular diseases. *Biochem Pharmacol* 2019; **164**: 74-81 [PMID: 30928673 DOI: 10.1016/j.bcp.2019.03.035]

50 **Hosomi R**, Fukunaga K, Nagao T, Shiba S, Miyauchi K, Yoshida M, Takahashi K. Effect of Dietary Oil Rich in Docosahexaenoic Acid-Bound Lysophosphatidylcholine Prepared from Fishery By-Products on Lipid and Fatty Acid Composition in Rat Liver and Brain. *J Oleo Sci* 2019; **68**: 781-792 [PMID: 31366855 DOI: 10.5650/jos.ess19103]

51 **Xu H**, Meng X, Jia L, Wei Y, Sun B, Liang M. Tissue distribution of transcription for 29 lipid metabolism-related genes in Takifugu rubripes, a marine teleost storing lipid predominantly in liver. *Fish Physiol Biochem* 2020; **46**: 1603-1619 [PMID: 32415410 DOI: 10.1007/s10695-020-00815-7]

52 **Yao M**, Li Z, Julian McClements D, Tang Z, Xiao H. Design of nanoemulsion-based delivery systems to enhance intestinal lymphatic transport of lipophilic food bioactives: Influence of oil type. *Food Chem* 2020; **317**: 126229 [PMID: 32078989 DOI: 10.1016/j.foodchem.2020.126229]

53 **Wilson MP**, Plecko B, Mills PB, Clayton PT. Disorders affecting vitamin B_6 metabolism. *J Inherit Metab Dis* 2019; **42**: 629-646 [PMID: 30671974 DOI: 10.1002/jimd.12060]

54 **Dias IH**, Borah K, Amin B, Griffiths HR, Sassi K, Lizard G, Iriondo A, Martinez-Lage P. Localisation of oxysterols at the sub-cellular level and in biological fluids. *J Steroid Biochem Mol Biol* 2019; **193**: 105426 [PMID: 31301352 DOI: 10.1016/j.jsbmb.2019.105426]

55 **Goldberg IJ**, Hussain MM. To absorb fat - supersize my lipid droplets. *J Clin Invest* 2019; **129**: 58-59 [PMID: 30507609 DOI: 10.1172/JCI125318]

56 **Zhao S**, Jang C, Liu J, Uehara K, Gilbert M, Izzo L, Zeng X, Trefely S, Fernandez S, Carrer A, Miller KD, Schug ZT, Snyder NW, Gade TP, Titchenell PM, Rabinowitz JD, Wellen KE. Dietary fructose feeds hepatic lipogenesis *via* microbiota-derived acetate. *Nature* 2020; **579**: 586-591 [PMID: 32214246 DOI: 10.1038/s41586-020-2101-7]

57 **Simon MC**, Reinbeck AL, Wessel C, Heindirk J, Jelenik T, Kaul K, Arreguin-Cano J, Strom A, Blaut M, Bäckhed F, Burkart V, Roden M. Distinct alterations of gut morphology and microbiota characterize accelerated diabetes onset in nonobese diabetic mice. *J Biol Chem* 2020; **295**: 969-980 [PMID: 31822562 DOI: 10.1074/jbc.RA119.010816]

58 **Kemnic TR**, Coleman M. Vitamin E Deficiency. 2020 Jul 10. In: StatPearls [Internet]. Treasure Island (FL): StatPearls Publishing; 2020 Jan– [PMID: 30085593]

59 **Ye Z**, Cao C, Liu Y, Cao P, Li Q. Triglyceride Structure Modulates Gastrointestinal Digestion Fates of Lipids: A Comparative Study between Typical Edible Oils and Triglycerides Using Fully Designed in Vitro Digestion Model. *J Agric Food Chem* 2018; **66**: 6227-6238 [PMID: 29845858 DOI: 10.1021/acs.jafc.8b01577]

60 **Ye Z**, Li R, Cao C, Xu YJ, Cao P, Li Q, Liu Y. Fatty acid profiles of typical dietary lipids after gastrointestinal digestion and absorbtion: A combination study between in-vitro and in-vivo. *Food Chem* 2019; **280**: 34-44 [PMID: 30642504 DOI: 10.1016/j.foodchem.2018.12.032]

61 **Liu T**, Mukosera GT, Blood AB. The role of gasotransmitters in neonatal physiology. *Nitric Oxide* 2020; **95**: 29-44 [PMID: 31870965 DOI: 10.1016/j.niox.2019.12.002]

62 **Binienda A**, Twardowska A, Makaro A, Salaga M. Dietary Carbohydrates and Lipids in the Pathogenesis of Leaky Gut Syndrome: An Overview. *Int J Mol Sci* 2020; **21**: 8368 [PMID: 33171587 DOI: 10.3390/ijms21218368]

63 **Yao Y**, Xu F, Ju X, Li Z, Wang L. Lipid-Lowering Effects and Intestinal Transport of Polyphenol Extract from Digested Buckwheat in Caco-2/HepG2 Coculture Models. *J Agric Food Chem* 2020; **68**: 4205-4214 [PMID: 32141744 DOI: 10.1021/acs.jafc.0c00321]

64 **Song JW**, Lam SM, Fan X, Cao WJ, Wang SY, Tian H, Chua GH, Zhang C, Meng FP, Xu Z, Fu JL, Huang L, Xia P, Yang T, Zhang S, Li B, Jiang TJ, Wang R, Wang Z, Shi M, Zhang JY, Wang FS, Shui G. Omics-Driven Systems Interrogation of Metabolic Dysregulation in COVID-19 Pathogenesis. *Cell Metab* 2020; **32**: 188-202 e5 [PMID: 32610096 DOI: 10.1016/j.cmet.2020.06.016]

65 **Thomas T**, Stefanoni D, Dzieciatkowska M, Issaian A, Nemkov T, Hill RC, Francis RO, Hudson KE, Buehler PW, Zimring JC, Hod EA, Hansen KC, Spitalnik SL, D'Alessandro A. Evidence for structural protein damage and membrane lipid remodeling in red blood cells from COVID-19 patients. *medRxiv* 2020.06.29.20142703 [PMID: 32637980 DOI: 10.1101/2020.06.29.20142703]

66 **Thomas T**, Stefanoni D, Dzieciatkowska M, Issaian A, Nemkov T, Hill RC, Francis RO, Hudson KE, Buehler PW, Zimring JC, Hod EA, Hansen KC, Spitalnik SL, D'Alessandro A. Evidence of Structural Protein Damage and Membrane Lipid Remodeling in Red Blood Cells from COVID-19 Patients. *J Proteome Res* 2020; **19**: 4455-4469 [PMID: 33103907 DOI: 10.1021/acs.jproteome.0c00606]

67 **Mahmud I**, Garrett TJ. Mass Spectrometry Techniques in Emerging Pathogens Studies: COVID-19 Perspectives. *J Am Soc Mass Spectrom* 2020; **31**: 2013-2024 [PMID: 32880453 DOI: 10.1021/jasms.0c00238]

68 **Nicora CD**, Sims AC, Bloodsworth KJ, Kim YM, Moore RJ, Kyle JE, Nakayasu ES, Metz TO.

Metabolite, Protein, and Lipid Extraction (MPLEx): A Method that Simultaneously Inactivates Middle East Respiratory Syndrome Coronavirus and Allows Analysis of Multiple Host Cell Components Following Infection. *Methods Mol Biol* 2020; **2099**: 173-194 [PMID: 31883096 DOI: 10.1007/978-1-0716-0211-9_14]

69 **Schwarz B**, Sharma L, Roberts L, Peng X, Bermejo S, Leighton I, Massana AC, Farhadian S, Ko A, DelaCruz C, Bosio CM. Severe SARS-CoV-2 infection in humans is defined by a shift in the serum lipidome resulting in dysregulation of eicosanoid immune mediators. *medRxiv* 2020; 2020.07.09. 20149849 [PMID: 32676616 DOI: 10.1101/2020.07.09.20149849]

70 **Schwarz B**, Sharma L, Roberts L, Peng X, Bermejo S, Leighton I, Massana AC, Farhadian S, Ko AI; Yale IMPACT Team; Cruz CSD; Bosio CM. Severe SARS-CoV-2 infection in humans is defined by a shift in the serum lipidome resulting in dysregulation of eicosanoid immune mediators. *Res Sq* 2020; rs.3. rs-42999 [PMID: 32743565 DOI: 10.21203/rs.3.rs-42999/v1]

71 **Bruzzone C**, Bizkarguenaga M, Gil-Redondo R, Diercks T, Arana E, García de Vicuña A, Seco M, Bosch A, Palazón A, San Juan I, Laín A, Gil-Martínez J, Bernardo-Seisdedos G, Fernández-Ramos D, Lopitz-Otsoa F, Embade N, Lu S, Mato JM, Millet O. SARS-CoV-2 Infection Dysregulates the Metabolomic and Lipidomic Profiles of Serum. *iScience* 2020; **23**: 101645 [PMID: 33043283 DOI: 10.1016/j.isci.2020.101645]

72 **Balgoma D**, Gil-de-Gómez L, Montero O. Lipidomics Issues on Human Positive ssRNA Virus Infection: An Update. *Metabolites* 2020; **10**: 356 [PMID: 32878290 DOI: 10.3390/metabo10090356]

73 **Yan B**, Zou Z, Chu H, Chan G, Tsang JO, Lai PM, Yuan S, Yip CC, Yin F, Kao RY, Sze KH, Lau SK, Chan JF, Yuen KY. Lipidomic Profiling Reveals Significant Perturbations of Intracellular Lipid Homeostasis in Enterovirus-Infected Cells. *Int J Mol Sci* 2019; **20**: 5952 [PMID: 31779252 DOI: 10.3390/ijms20235952]

74 **Bley H**, Schöbel A, Herker E. Whole Lotta Lipids-from HCV RNA Replication to the Mature Viral Particle. *Int J Mol Sci* 2020; **21**: 2888 [PMID: 32326151 DOI: 10.3390/ijms21082888]

75 **Queiroz A**, Pinto IFD, Lima M, Giovanetti M, de Jesus JG, Xavier J, Barreto FK, Canuto GAB, do Amaral HR, de Filippis AMB, Mascarenhas DL, Falcão MB, Santos NP, Azevedo VAC, Yoshinaga MY, Miyamoto S, Alcantara LCJ. Lipidomic Analysis Reveals Serum Alteration of Plasmalogens in Patients Infected With ZIKA Virus. *Front Microbiol* 2019; **10**: 753 [PMID: 31031729 DOI: 10.3389/fmicb.2019.00753]

76 **Yuan S**, Chu H, Chan JF, Ye ZW, Wen L, Yan B, Lai PM, Tee KM, Huang J, Chen D, Li C, Zhao X, Yang D, Chiu MC, Yip C, Poon VK, Chan CC, Sze KH, Zhou J, Chan IH, Kok KH, To KK, Kao RY, Lau JY, Jin DY, Perlman S, Yuen KY. SREBP-dependent lipidomic reprogramming as a broad-spectrum antiviral target. *Nat Commun* 2019; **10**: 120 [PMID: 30631056 DOI: 10.1038/s41467-018-08015-x]

77 **Yan B**, Chu H, Yang D, Sze KH, Lai PM, Yuan S, Shuai H, Wang Y, Kao RY, Chan JF, Yuen KY. Characterization of the Lipidomic Profile of Human Coronavirus-Infected Cells: Implications for Lipid Metabolism Remodeling upon Coronavirus Replication. *Viruses* 2019; **11**: 73 [PMID: 30654597 DOI: 10.3390/v11010073]

78 **Liebscher S**, Ambrose RL, Aktepe TE, Mikulasova A, Prier JE, Gillespie LK, Lopez-Denman AJ, Rupasinghe TWT, Tull D, McConville MJ, Mackenzie JM. Phospholipase A2 activity during the replication cycle of the flavivirus West Nile virus. *PLoS Pathog* 2018; **14**: e1007029 [PMID: 29709018 DOI: 10.1371/journal.ppat.1007029]

79 **Hofmann S**, Krajewski M, Scherer C, Scholz V, Mordhorst V, Truschow P, Schöbel A, Reimer R, Schwudke D, Herker E. Complex lipid metabolic remodeling is required for efficient hepatitis C virus replication. *Biochim Biophys Acta Mol Cell Biol Lipids* 2018; **1863**: 1041-1056 [PMID: 29885363 DOI: 10.1016/j.bbalip.2018.06.002]

80 **Diwaker D**, Mishra KP, Ganju L, Singh SB. Protein disulfide isomerase mediates dengue virus entry in association with lipid rafts. *Viral Immunol* 2015; **28**: 153-160 [PMID: 25664880 DOI: 10.1089/vim.2014.0095]

81 **Carter CJ**. Interactions between the products of the Herpes simplex genome and Alzheimer's disease susceptibility genes: relevance to pathological-signalling cascades. *Neurochem Int* 2008; **52**: 920-934 [PMID: 18164103 DOI: 10.1016/j.neuint.2007.11.003]

82 **Wang X**, Xu P, Cheng F, Li Y, Wang Z, Hao S, Wang J, Ning K, Ganaie SS, Engelhardt JF, Yan Z, Qiu J. Cellular Cleavage and Polyadenylation Specificity Factor 6 (CPSF6) Mediates Nuclear Import of Human Bocavirus 1 NP1 Protein and Modulates Viral Capsid Protein Expression. *J Virol* 2020; **94**: e01444-19 [PMID: 31666379 DOI: 10.1128/JVI.01444-19]

83 **Wang X**, Hennig T, Whisnant AW, Erhard F, Prusty BK, Friedel CC, Forouzmand E, Hu W, Erber L, Chen Y, Sandri-Goldin RM, Dölken L, Shi Y. Herpes simplex virus blocks host transcription termination *via* the bimodal activities of ICP27. *Nat Commun* 2020; **11**: 293 [PMID: 31941886 DOI: 10.1038/s41467-019-14109-x]

84 **Wendt L**, Brandt J, Bodmer BS, Reiche S, Schmidt ML, Traeger S, Hoenen T. The Ebola Virus Nucleoprotein Recruits the Nuclear RNA Export Factor NXF1 into Inclusion Bodies to Facilitate Viral Protein Expression. *Cells* 2020; **9**: 187 [PMID: 31940815 DOI: 10.3390/cells9010187]

85 **Han S**, Sun S, Li P, Liu Q, Zhang Z, Dong H, Sun M, Wu W, Wang X, Guo H. Ribosomal Protein L13 Promotes IRES-Driven Translation of Foot-and-Mouth Disease Virus in a Helicase DDX3-Dependent Manner. *J Virol* 2020; **94**: e01679-19 [PMID: 31619563 DOI: 10.1128/JVI.01679-19]

86 **Şenbaş Akyazi B**, Pirinçal A, Kawaguchi A, Nagata K, Turan K. Interaction of influenza A virus NS2/NEP protein with the amino-terminal part of Nup214. *Turk J Biol* 2020; **44**: 82-92 [PMID:

32256144 DOI: 10.3906/biy-1909-49]

87 **Thiele S**, Stanelle-Bertram S, Beck S, Kouassi NM, Zickler M, Müller M, Tuku B, Resa-Infante P, van Riel D, Alawi M, Günther T, Rother F, Hügel S, Reimering S, McHardy A, Grundhoff A, Brune W, Osterhaus A, Bader M, Hartmann E, Gabriel G. Cellular Importin-α3 Expression Dynamics in the Lung Regulate Antiviral Response Pathways against Influenza A Virus Infection. *Cell Rep* 2020; **31**: 107549 [PMID: 32320654 DOI: 10.1016/j.celrep.2020.107549]

88 **Ren L**, Ding S, Song Y, Li B, Ramanathan M, Co J, Amieva MR, Khavari PA, Greenberg HB. Profiling of rotavirus 3'UTR-binding proteins reveals the ATP synthase subunit ATP5B as a host factor that supports late-stage virus replication. *J Biol Chem* 2019; **294**: 5993-6006 [PMID: 30770472 DOI: 10.1074/jbc.RA118.006004]

89 **Dave P**, George B, Balakrishnan S, Sharma DK, Raheja H, Dixit NM, Das S. Strand-specific affinity of host factor hnRNP C1/C2 guides positive to negative-strand ratio in Coxsackievirus B3 infection. *RNA Biol* 2019; **16**: 1286-1299 [PMID: 31234696 DOI: 10.1080/15476286.2019.1629208]

90 **Andreev DE**, Hirnet J, Terenin IM, Dmitriev SE, Niepmann M, Shatsky IN. Glycyl-tRNA synthetase specifically binds to the poliovirus IRES to activate translation initiation. *Nucleic Acids Res* 2012; **40**: 5602-5614 [PMID: 22373920 DOI: 10.1093/nar/gks182]

91 **Katsarou K**, Wu Y, Zhang R, Bonar N, Morris J, Hedley PE, Bryan GJ, Kalantidis K, Hornyik C. Insight on Genes Affecting Tuber Development in Potato upon Potato spindle tuber viroid (PSTVd) Infection. *PLoS One* 2016; **11**: e0150711 [PMID: 26937634 DOI: 10.1371/journal.pone.0150711]

92 **Jupatanakul N**, Sim S, Dimopoulos G. Aedes aegypti ML and Niemann-Pick type C family members are agonists of dengue virus infection. *Dev Comp Immunol* 2014; **43**: 1-9 [PMID: 24135719 DOI: 10.1016/j.dci.2013.10.002]

93 **Josset L**, Menachery VD, Gralinski LE, Agnihothram S, Sova P, Carter VS, Yount BL, Graham RL, Baric RS, Katze MG. Cell host response to infection with novel human coronavirus EMC predicts potential antivirals and important differences with SARS coronavirus. *mBio* 2013; **4**: e00165-e00113 [PMID: 23631916 DOI: 10.1128/mBio.00165-13]

94 **Ong EZ**, Chan YFZ, Leong WY, Lee NMY, Kalimuddin S, Haja Mohideen SM, Chan KS, Tan AT, Bertoletti A, Ooi EE, Low JGH. A Dynamic Immune Response Shapes COVID-19 Progression. *Cell Host Microbe* 2020; **27**: 879-882. e2 [PMID: 32359396 DOI: 10.1016/j.chom.2020.03.021]

World Journal of Gastroenterology

Submit a Manuscript: https://www.f6publishing.com

World J Gastroenterol 2021 January 7; 27(1): 55-68

DOI: 10.3748/wjg.v27.i1.55

ISSN 1007-9327 (print) ISSN 2219-2840 (online)

ORIGINAL ARTICLE

Basic Study

Long non-coding ribonucleic acid W5 inhibits progression and predicts favorable prognosis in hepatocellular carcinoma

Guang-Lin Lei, Hong-Xia Fan, Cheng Wang, Yan Niu, Tie-Ling Li, Ling-Xiang Yu, Zhi-Xian Hong, Jin Yan, Xi-Liang Wang, Shao-Geng Zhang, Ming-Ji Ren, Peng-Hui Yang

ORCID number: Guang-Lin Lei 0000-0002-2092-2251; Hong-Xia Fan 0000-0001-9068-8459; Cheng Wang 0000-0001-6213-7027; Yan Niu 0000-0002-1536-8663; Tie-Ling Li 0000-0003-0683-8659; Ling-Xiang Yu 0000-0002-0727-400X; Zhi-Xian Hong 0000-0002-0187-3351; Jin Yan 0000-0002-3743-9477; Xi-Liang Wang 0000-0002-2652-6874; Shao-Geng Zhang 0000-0002-0479-7569; Ming-Ji Ren 0000-0001-6259-1158; Peng-Hui Yang 0000-0001-6519-5927.

Author contributions: Zhang SG and Yang PH contributed to conception and intellectual input; Lei GL, Fan HX, Li TL, Hong ZX and Ren MJ contributed to designing and performing the experiments; Fan HX and Lei GL contributed to sample collection and manuscript drafting; Yan J and Wang XL contributed to statistical analyses and data interpretation; all authors read and approved the final manuscript.

Supported by National High Technology Research and Development Program of China, No. 2015AA020924; Natural Science Foundation of Beijing, China, No. 7202194 and No. 7162185.

Institutional animal care and use committee statement: All animal

Guang-Lin Lei, Hong-Xia Fan, Ling-Xiang Yu, Zhi-Xian Hong, Jin Yan, Shao-Geng Zhang, Peng-Hui Yang, Fifth Medical Center of Chinese PLA General Hospital, Beijing 100039, China

Hong-Xia Fan, Yan Niu, Ming-Ji Ren, College of Basic Medicine, Inner Mongolia Medical University, Hohhot 010110, Inner Mongolia, China

Cheng Wang, Tie-Ling Li, First Medical Center of Chinese PLA General Hospital, Beijing 100853, China

Xi-Liang Wang, Peng-Hui Yang, State Key Laboratory of Pathogens and Biosecurity, Beijing Institute of Microbiology and Epidemiology, Beijing 100071, China

Corresponding author: Peng-Hui Yang, MD, Professor, Fifth Medical Center of Chinese PLA General Hospital, No. 100 Xisihuan Zhong Lu, Fengtai District, Beijing 100039, China. yph3022017@163.com

Abstract

BACKGROUND

Accumulating evidence has revealed that several long non-coding ribonucleic acids (lncRNAs) are crucial in the progress of hepatocellular carcinoma (HCC).

AIM

To classify a long non-coding RNA, *i.e.*, lncRNA W5, and to determine the clinical significance and potential roles of lncRNA W5 in HCC.

METHODS

The results showed that lncRNA W5 expression was significantly downregulated in HCC cell lines and tissues. Analysis of the association between lncRNA W5 expression levels and clinicopathological features suggested that low lncRNA W5 expression was related to large tumor size ($P < 0.01$), poor histological grade ($P < 0.05$) and serious portal vein tumor thrombosis ($P < 0.05$). Furthermore, Kaplan-Meier survival analysis showed that low expression of lncRNA W5 predicts poor overall survival ($P = 0.016$).

RESULTS

Gain-of-loss function experiments, including cell counting kit8 assays, colony formation assays, and transwell assays, were performed *in vitro* to investigate the

biological roles of lncRNA W5. *In vitro* experiments showed that ectopic overexpression of lncRNA W5 suppressed HCC cell proliferation, migration and invasion; conversely, silencing of lncRNA W5 promoted cell proliferation, migration and invasion. In addition, acting as a tumor suppressor gene in HCC, lncRNA W5 inhibited the growth of HCC xenograft tumors *in vivo*.

CONCLUSION

These results showed that lncRNA W5 is down-regulated in HCC, and it may suppress HCC progression and predict poor clinical outcomes in patients with HCC. LncRNA W5 may serve as a potential HCC prognostic biomarker in addition to a therapeutic target.

Key Words: Hepatocellular carcinoma; Long non-coding ribonucleic acid; Long non-coding ribonucleic acid W5

©The Author(s) 2021. Published by Baishideng Publishing Group Inc. All rights reserved.

Core Tip: Our results showed that the expression of long non-coding ribonucleic acid (lncRNA) W5 was considerably reduced in hepatocellular carcinoma (HCC) tissues, which suppressed proliferation, migration and invasion of tumor cells *in vitro*. It was also shown that low expression of lncRNA W5 correlated with tumor progression and poor prognosis. Furthermore, manipulation of lncRNA W5 expression affected the biological behavior of HCC. These results suggest that lncRNA W5 may serve as a tumor suppressor in the development and progression of HCC, and has the potential to be a diagnostic and therapeutic target in the clinical management of HCC.

Citation: Lei GL, Fan HX, Wang C, Niu Y, Li TL, Yu LX, Hong ZX, Yan J, Wang XL, Zhang SG, Ren MJ, Yang PH. Long non-coding ribonucleic acid W5 inhibits progression and predicts favorable prognosis in hepatocellular carcinoma. *World J Gastroenterol* 2021; 27(1): 55-68
URL: https://www.wjgnet.com/1007-9327/full/v27/i1/55.htm
DOI: https://dx.doi.org/10.3748/wjg.v27.i1.55

INTRODUCTION

Around 90% of primary liver cancer cases are hepatocellular carcinoma (HCC)[1], approximately 600000 deaths occur globally each year, and half of all deaths occur in China[2,3]. In addition to hepatic resection, liver transplantation, chemotherapy and molecular targeted therapy are often carried out to improve outcomes in patients with HCC; however, the 5-year survival rate of patients with HCC still remains poor[4,5]. The specific signaling mechanisms underlying the development and progression of HCC remain to be defined.

The long non-coding ribonucleic acids (lncRNAs) are a class of noncoding RNAs with more than 200 nucleotides which have no protein-coding potential. Several reports have shown that lncRNAs are critical in numerous biological processes, including tumor development, differentiation, and tumorigenesis[6-10]. The expression of lncRNAs is dysregulated in cancer. Of note, specific lncRNAs are related to cancer recurrence, metastasis and prognosis in various cancers, including HCC[11-14]. To date, several lncRNA have been reported to be associated with the growth and advance of HCC, such as HULC[15], H19[16], MEG3[17], ZFAS1[18], P7[19], ATB[20], GAS8-AS1[21], and so on. In our previous study, we profiled the the expression of lncRNAs in influenza virus infected patients and identified panels of uncharacterized lncRNAs. In the current study, we classified the lncRNA W5 (mitochondrial translation optimization 1homologue; hsa_lncRNA_0007874/hsa_lncRNA_104135) which is notably down-regulated in HCC tissues and strictly associated with the prognosis of HCC patients. Furthermore, we investigated its roles, underlying mechanisms and clinical significance in HCC progression.

experiments were conducted with the approval of the Fifth Medical Center of Chinese PLA General Hospital's Animal Care and Use Committee.

Conflict-of-interest statement: All authors declare no financial or commercial conflicts of interest.

Data sharing statement: All data generated or analyzed during this study are included in this published article.

Open-Access: This article is an open-access article which was selected by an in-house editor and fully peer-reviewed by external reviewers. It is distributed in accordance with the Creative Commons Attribution Non Commercial (CC BY-NC 4.0) license, which permits others to distribute, remix, adapt, build upon this work non-commercially, and license their derivative works on different terms, provided the original work is properly cited and the use is non-commercial. See: http://creativecommons.org/licenses/by-nc/4.0/

Manuscript source: Unsolicited manuscript

Specialty type: Gastroenterology and hepatology

Country/Territory of origin: China

Peer-review report's scientific quality classification
Grade A (Excellent): 0
Grade B (Very good): B
Grade C (Good): 0
Grade D (Fair): 0
Grade E (Poor): 0

Received: August 25, 2020
Peer-review started: August 25, 2020
First decision: September 12, 2020
Revised: October 27, 2020
Accepted: November 13, 2020
Article in press: November 13, 2020
Published online: January 7, 2021

P-Reviewer: Zhang L
S-Editor: Zhang L
L-Editor: Webster JR
P-Editor: Ma YJ

MATERIALS AND METHODS

Clinical samples

A total of 86 resected HCC tissues and matched tumor-adjacent tissues were kindly provided by the Department of Hepatobiliary Surgery of the Fifth Medical Center, Chinese PLA General Hospital between October 2013 and June 2018. Tumor tissues and adjacent non-tumor tissue specimens were obtained from the patients after informed consent in accordance with the institutional guidelines of the hospital's Ethics Committee. Table 1 indicates the clinical and pathological characteristics of HCC patients obtained from clinical records.

Cell lines

All human cell lines were provided by the Experimental Center of the Fifth Medical Center, Chinese PLA General Hospital (Beijing, China), and included the normal non-malignant liver cell line LO2 and HCC cell lines Huh7, MHCC-97L, MHCC-97H, PLC, Hep3B and HCCLM3. All cell lines were maintained in DMEM (Gibco, Beijing, China) and were supplemented with 10% fetal bovine serum (Gibco, Beijing, China) in an incubator at 37°C with 5% CO_2.

RNA extraction and reverse transcription-polymerase chain reaction

TRIzol reagent (Invitrogen, United States) was used to isolate total RNA from HCC cells and tissues, and first strand complementary deoxyribonucleic acid (cDNA) was synthesized by the use of reverse transcriptase. Quantitative real-time polymerase chain reaction (PCR) was conducted using the SYBR Green PCR kit (Thermo Fisher Scientific, United States). All reactions were performed on the ABI 7500 system (Applied Biosystems). The lncRNA W5-specific reverse transcription-polymerase chain reaction (qRT-PCR) primers used were as follows: forward: 5'-AAGGAGAACACAAAACAGGCAT-3', reverse: 5'-TGTGAAGCCCTAG ATTTCCCAT-3'; GAPDH forward: 5'-AAG GAGAACACAAAACAG GCAT-3' reverse: 5'-TGTGAAGCCCTAGATTTCCCAT-3'. Human *GAPDH* gene was amplified as an internal control.

Vector construction

The lncRNA W5 vector was constructed and sub-cloned into the pcDNA3.1 (+) vector at the BamHI and EcoRI sites, which produced pcDNA3.1-lncRNA W5. The primers used were as follows: forward: 5'-GCGCGGATCCACTGACTCTTTTCGTTAAGC-3', reverse: 5'-CGCGCGGAATTCATGTTGACTTAAGTTCAGG-3'. Empty vector pcDNA3.1 (+) was used as a negative control. The lncRNA W5 and control were transfected into HCC cells using Polyplus (Invitrogen) according to the manufacturer's instructions and cultured on six-well plates, respectively.

Cell proliferation assay

Cell proliferation experiments were performed using the CCK-8 kit (Dojindo Laboratories) according to the manufacturer's protocol. Briefly, a Huh7 or LM3 cell suspension was adjusted to a final cell concentration of 5×10^3/mL and then added to a 96-well plate. HCC cells were cultured for the indicated time points, and then 10 μL of CCK-8 (5 mg/mL) was added to each well. The cell culture plate was placed in the incubator for 1 h, and the absorbance was measured at 450 nm per well using a Thermomax plate reader (Thermo Fisher, China).

Colony formation assay

Huh7 or LM3 cells were completely dispersed into individual cells in 6-well plates and incubated at 37°C in DMEM with 10% fetal bovine serum, respectively. After 14 d, the cell colonies were washed with PBS, fixed in 4% paraformaldehyde for 20 min, and stained with crystal violet for 20 min. Photographs were subsequently taken and only colonies containing more than 50 cells were recorded.

Cell migration and invasion assays

A chamber assay with Matrigel (invasion) or without Matrigel (migration) was performed at least in triplicate. Twenty-four-well chambers with 8 μm pore size were used in this experiment. Briefly, cells were added to the top chamber without Matrigel (migration) or with Matrigel (invasion) in the 24-well plate (Corning). The medium with 15% forward-based system was added to the lower chambers. After incubator for 48-72 h, the DMEM medium was removed and the cells were washed with PBS, and

Table 1 Association of long non-coding ribonucleic acid W5 expression with clinicopathologic features in hepatocellular carcinoma patients

Parameters	Group	Total	W5 expression		*P* value
			Low	High	
Gender	Male	70	34	36	0.791
	Female	16	10	6	
Age (yr)	≤ 60	30	15	15	0.579
	> 60	56	28	28	
Tumor size (cm)	< 3 cm	21	6	15	0.007[b]
	≥ 3 cm	65	38	27	
AFP	< 20	39	21	18	0.328
	≥ 20	47	22	25	
Histological grade	Well/moderate-poor	52/34	5/28	47/6	0.046[a]
Clinical stage	I/II	50	23	27	0.501
Tumor number	III	36	20	16	
	Solitary	76	36	40	0.312
	Multiple	10	7	3	
Drinking status	Yes	42	24	18	0.276
	No	44	19	25	
Smoking status	Yes	36	18	18	0.584
	No	50	24	26	
PVTT	Yes	32	22	10	0.024[a]
	No	54	21	33	
Microvascular invasion	Yes	70	36	34	0.568
	No	16	6	10	
Liver cirrhosis	Absence	59	30	29	0.489
HBV	Yes	55	25	30	0.365
	No	31	18	13	

[a]$P < 0.05$.
[b]$P < 0.01$. PVTT: Portal vein tumor thrombosis; HBV: Hepatitis B virus.

carefully removed from the top chamber with a cotton swab. The cells were fixed with 4% paraformaldehyde, stained with crystal violet, and then photographed in five randomly selected microscope fields.

In vivo tumor growth

Athymic BALB/C mice (4-6 wk old) were purchased from the Beijing Vital River Laboratory Animal Technology Co., Ltd (Beijing, China) and maintained in a SPF facility. Huh7 cells (5×10^6) over-expressing lncRNA W5 were subcutaneously injected into the flanks of nude mice. Tumor length (L) and width (W) were measured using calipers every 3 d up to 6 wk. Tumor volume was estimated using the formula: π × length × width 2/6. After 6 wk, the mice were sacrificed, and tumor volumes and weights were examined. Proliferation progression was examined and quantified using a noninvasive bioluminescence *in vivo* Imaging System (Xenogen Corporation, Alameda, CA, United States). All animal experiments were conducted with the approval of the Fifth Medical Center of Chinese PLA General Hospital's Animal Care and Use Committee.

Statistical analysis

All statistical analyses were performed using the SPSS 20.0 software package (Chicago, IL, United States). Data were expressed as the mean ± SD. Kaplan-Meier analysis was used to determine whether there was a correlation between the expression of lncRNA W5 and overall survival rate of HCC patients. $P < 0.05$ was considered significant.

RESULTS

HCC cancer tissues and cell lines have low expression of lncRNA W5

Initially, to investigate the potential role of lncRNA W5 in HCC tumorigenesis, we determined the expression of lncRNA W5 in 86 sets of HCC tissues and non-tumor tissues by qRT-PCR. As shown in Figure 1, the expression of lncRNA W5 was significantly reduced in HCC tissues compared with adjacent non-tumor tissues ($P < 0.001$, Figure 1A and B). In addition, we determined the expression of lncRNA W5 in regular liver cells (LO2) and six HCC cancer cell lines (Huh7, MHCC-97L, MHCC-97H, PLC, Hep3B and HCCLM3). The results revealed that lncRNA W5 expression was significantly downregulated in the six HCC cancer cells compared with the regular liver cell line LO2 (Figure 1C). Levels of lncRNA W5 expression were relatively lower in the Huh7 and LM3 HCC cell lines, and were used in subsequent studies. More importantly, a Kaplan-Meier survival analysis indicated that HCC patients with low expression of lncRNA W5 had shorter overall survival than those patients with high expression of lncRNA W5 ($P = 0.016$) (Figure 1D). Cox survival analysis was then used to further confirm the prognostic value of lncRNA W5 in HCC. Univariate analysis showed that the analyzed variables (lncRNA W5 expression, Pathologic-stage and Pathologic-TMN) were markedly associated with the overall survival time of HCC patients. Furthermore, multivariate analysis revealed that lncRNA W5 expression ($P = 0.027$), Pathologic-T ($P = 0.014$) and Pathologic-M ($P = 0.005$) were promising independent prognostic factors of HCC (Table 2). Thus, lncRNA W5 could be used as an independent prognostic factor. Finally, we also measured the expression of lncRNA W5 in nuclear and cytosolic fractions of Huh7 cells by qRT-PCR. The differential enrichments of GAPDH, β-actin and U1 RNA were used as fractionation indicators. Subcellular fractionation location results showed that lncRNA W5 was mainly located in the nucleus (Figure 1E), thus suggesting that lncRNA W5 might play an essential regulatory function at the transcriptional level.

To investigate the relationship between the expression of lncRNA W5 and clinicopathological characteristics, lncRNA W5 expression was detected in 86 HCC patients and distributed into two groups (high–high expression of lncRNA W5 and low–low expression of lncRNA W5) based on the median lncRNA W5 expression. The correlations between lncRNA W5 expression and clinical parameters were analyzed and it was found that low expression of lncRNA W5 was linked to large tumor size ($P < 0.01$), poor histological grade ($P < 0.05$) and serious portal vein tumor thrombosis ($P < 0.05$). Nevertheless, no significant correlation was observed between the expression of lncRNA W5 and other clinicopathological features, such as age, gender, AFP levels, tumor number and with/without HBV infection.

In vitro effects of lncRNA W5 on HCC cell proliferation

To assess the role of lncRNA W5 in regulating the biological behavior of HCC cells, we used the lncRNA W5 expression vector pcDNA3.1-lncRNA W5 and overexpressed lncRNA W5 in the HCC cell lines Huh7 and LM3. LncRNA W5 overexpression in the two cell lines was verified by RT-qPCR (Figure 2A). CCK-8 assays, which were used to show overexpression of lncRNA W5 in the HCC cell lines Huh7 and LM3, demonstrated a significant reduction in cell proliferation from 48 h to 96 h (Figure 2B). Accordingly, colony formation assays, which showed that Huh7 and LM3 cells transfected with lncRNA W5, resulted in significantly decreased clonogenic survival than empty vector control Huh7 and LM3 cell lines (Figure 2C). In addition, we constructed shRNA-1 and shRNA-2 containing the back-splicing region of lncRNA W5 for silencing. The efficiency of lncRNA W5 silencing was confirmed by qPCR following transfection with lncRNA W5 shRNA-1 or-2 in Huh7 and LM3 cells (Figure 2D). As expected, we found that lncRNA W5 silencing significantly promoted cell proliferation of Huh7 and LM3 cells as indicated by MTS (Figure 2E). Furthermore, a clone formation assay verified that following lncRNA W5 knockdown, the HCC population dependence and proliferation ability were considerably increased (Figure 2F). Overall, these data demonstrated that lncRNA W5 may inhibit HCC cell proliferation *in vitro*.

Table 2 Cox proportional hazards model analysis of clinicopathologic features related to overall survival in terms of long non-coding ribonucleic acid W5 expression in hepatocellular carcinoma patients

Variables	Univariate analysis			Multivariate analysis		
	P value	HR	95%CI	*P* value	HR	95%CI
Expression (high/low)	0.041[a]	1.672	1.032-2.159	0.027[a]	1.285	0.867-2.155
Pathologic-Stage (I + II/III + IV)	0.001[a]	2.584	1.934-4.162	0.159	2.436	0.715-7.667
Pathologic-T (T1 + T2/T3 + T4)	0.004[a]	4.068	1.573-8.869	0.014[a]	10.638	2.314-57.649
Pathologic-M (M0/M1)	0.007[a]	5.294	3.195-7.657	0.005[a]	3.082	1.726-5.342
Pathologic-N (N0/N1 + N2 + N3)	0.002[a]	2.413	1.519-3.969	0.246	0.719	0.312-1.911
Age (< 60/ ≥ 60 yrs)	0.342	1.402	0.914-2.357			
Gender (female/male)	0.258	1.324	0.849-1.905			

[a]$P < 0.05$. HR: Hazard ratio; CI: Confidence interval.

In vitro effects of lncRNA W5 on HCC cell migration and invasion

To evaluate the potential role of lncRNA W5 in HCC metastasis, and investigate the effect of lncRNA W5 on cell migration and invasion capacity, we performed transwell assays using Huh7 and LM3 cells. The results revealed that the migration and invasion ability of HCC cells that over-expressed lncRNA W5 was significantly decreased compared with the empty vector group (Figure 3A). On the contrary, lncRNA W5 knockdown with shRNA-1 or-2 significantly promoted cell migration and enhanced cell invasion of Huh7 and LM3 cells, respectively (Figure 3B). These results strongly suggest that lncRNA W5 has a critical effect on the inhibition of HCC cell migration and invasion.

lncRNA W5 inhibits tumor growth in vivo

To elucidate the *in vivo* role of lncRNA W5 in tumorigenesis, we subcutaneously injected the flanks of nude mice with Huh7 cells over-expressing lncRNA W5 and stably expressing luciferase and monitored tumor growth every three days. As shown in Figure 4, mice injected with lncRNA W5 over-expressing cells had a significant decrease in tumor growth at 36 d post-injection as compared with mice injected with control cells. Six weeks after injection, the volumes and weights of tumors examined in mice injected with pcDNA3.1-lncRNA W5 were notably smaller than those in mice injected with the control. At 6 wk after injection, bioluminescent signals were weaker in mice with lncRNA W5 over-expression than in control mice, suggesting that lncRNA W5 may inhibit the growth of HCC xenograft tumors *in vivo*.

DISCUSSION

Increasing evidence has shown that aberrant expression of numerous lncRNAs has been discovered in HCC. Previous studies showed that amplification of lncRNA ZFAS1 promotes metastasis in HCC[18]. Sun SH's group observed in HCC that the lncRNA-activated by TGF-β (lncRNA-ATB) promoted the invasion-metastasis cascade[20]. Hur K's group also reported that lncRNA-ATB could have potential as a biomarker for the prognosis of HCC and as a targeted therapy for HCC patients[22]. Another study showed that the MBNL3 splicing factor promoted HCC by increasing the expression of PXN by the alternative splicing of lncRNA-PXN-AS1[23]. The lncRNA lncHDAC2 may drive the self-renewal of liver cancer stem cells through the activation of Hedgehog signaling[24]. Super-enhancer associated lncRNA HCCL5 is activated by ZEB1 and promotes the malignancy of HCC[25]. Recently, Huang *et al*[26] identified oncofetal lncRNA Ptn-dt which might promote HCC proliferation by regulating the Ptn receptor[26]. These results indicate that lncRNAs may have critical roles in HCC progression and development and can be used in clinical applications.

In this study, we reported an uncharacterized low expression of lncRNA W5 in HCC specimens and cell lines, suggesting that lncRNA W5 expression might be related to HCC carcinogenesis. Decreased expression of lncRNA W5 was associated with aggressive clinicopathological features of HCC tissues, including tumor size,

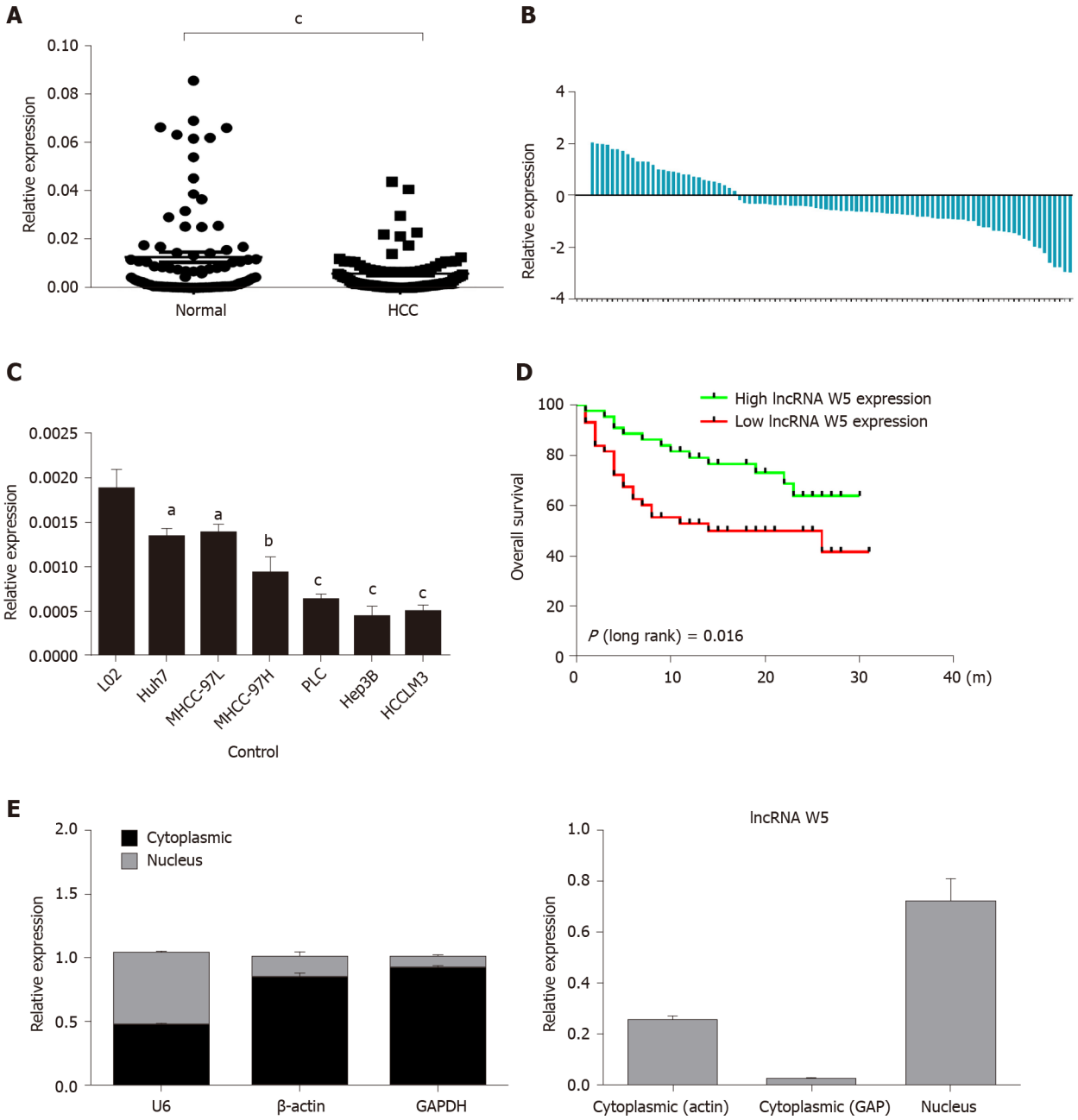
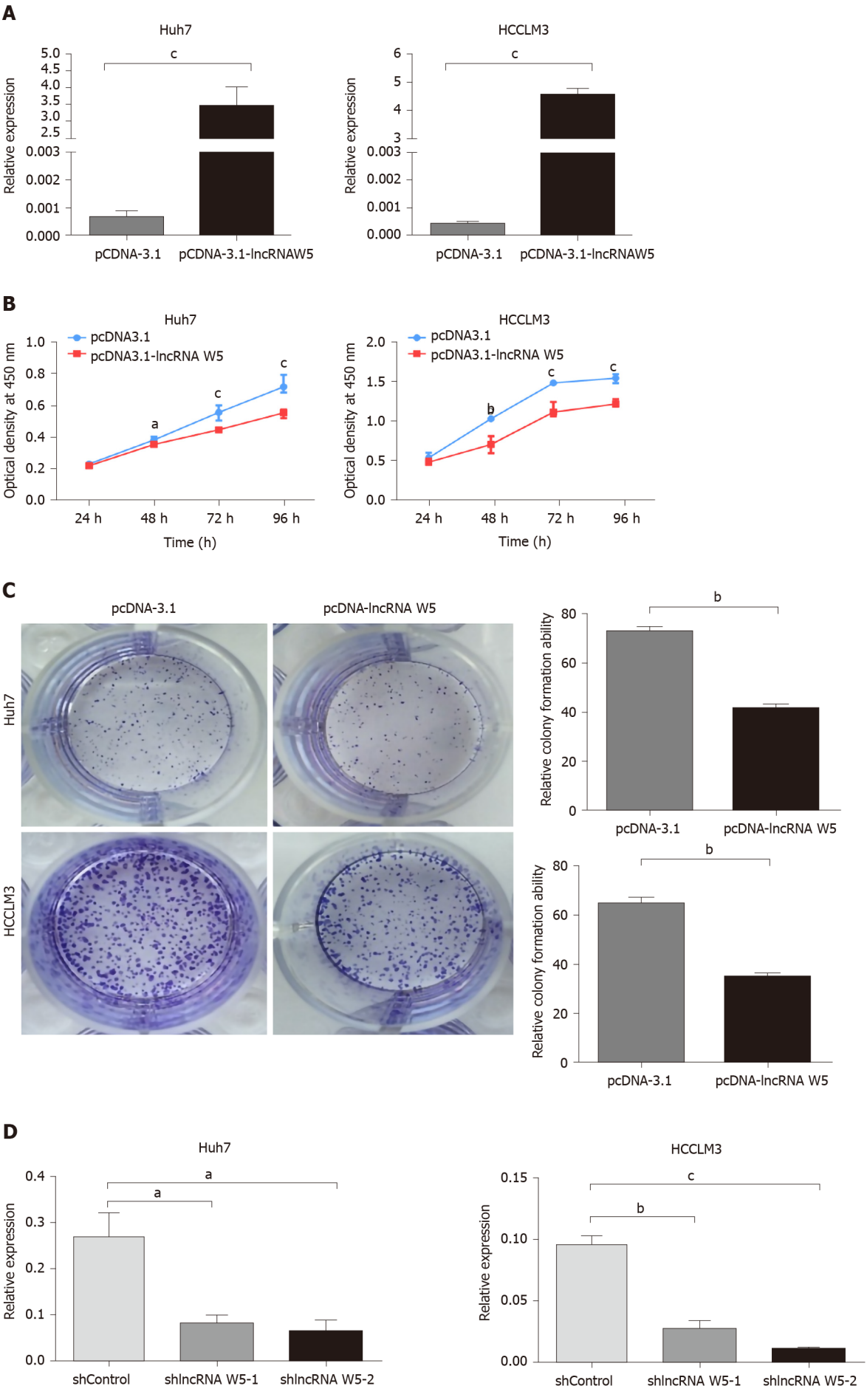


Figure 1 Expression of long non-coding ribonucleic acid W5 is downregulated in hepatocellular carcinoma tissues and cells. A: The expression of long non-coding ribonucleic acid (lncRNA) W5 was detected by reverse transcription-polymerase chain reaction (qRT-PCR) in tumor tissues and non-adjacent normal tissues of hepatocellular carcinoma (HCC) patients (n = 86). LncRNA W5 expression was normalized to GAPDH expression; B: The expression of lncRNA W5 was detected by qRT-PCR in tumor tissues and non-adjacent normal tissues of 86 HCC patients; C: The expression levels of lncRNA W5 in a series of HCC cell lines were reduced compared to that in LO2 cells; D: Analysis of overall survival based on lncRNA W5 expression levels is shown in 86 HCC patients; and E: Subcellular localization of lncRNA W5 in Huh7 cells was examined by qRT-PCR. GAPDH, β-actin and U1 were considered as the control markers, respectively. $^{a}P < 0.05$; $^{b}P < 0.01$; $^{c}P < 0.001$. HCC: Hepatocellular carcinoma; lncRNA: Long non-coding ribonucleic acid; qRT-PCR: Reverse transcription-polymerase chain reaction.

histological grade and the presence of portal vein tumor thrombosis. Gain-and loss function experiments showed that over-expression of lncRNA W5 in Huh7 and LM3 cells decreased cell proliferation, and impaired cell migration and invasion. Moreover, lncRNA W5 over-expression inhibited tumor growth in HCC xenograft-bearing mice. These results demonstrated that lncRNA W5 is involved in the progression of HCC and may be a potential target for therapy. Furthermore, our studies showed that HCC patients with low expression of lncRNA W5 had shorter overall survival than patients with high expression of lncRNA W5, suggesting that lncRNA W5 might be a potential prognostic predictor. Of course, down-regulation of lncRNA W5 should be validated in more HCC cohorts. The interactions of this protein and downstream pathways also warrant further investigation in subsequent studies. In addition, whether lncRNA W5


A
Huh7
HCCLM3
Relative expression
pCDNA-3.1
pCDNA-3.1-lncRNAW5
B
Huh7
HCCLM3
pcDNA3.1
pcDNA3.1-lncRNA W5
Optical density at 450 nm
24 h
48 h
72 h
96 h
Time (h)
C
pcDNA-3.1
pcDNA-lncRNA W5
Huh7
HCCLM3
Relative colony formation ability
D
Huh7
HCCLM3
shControl
shlncRNA W5-1
shlncRNA W5-2

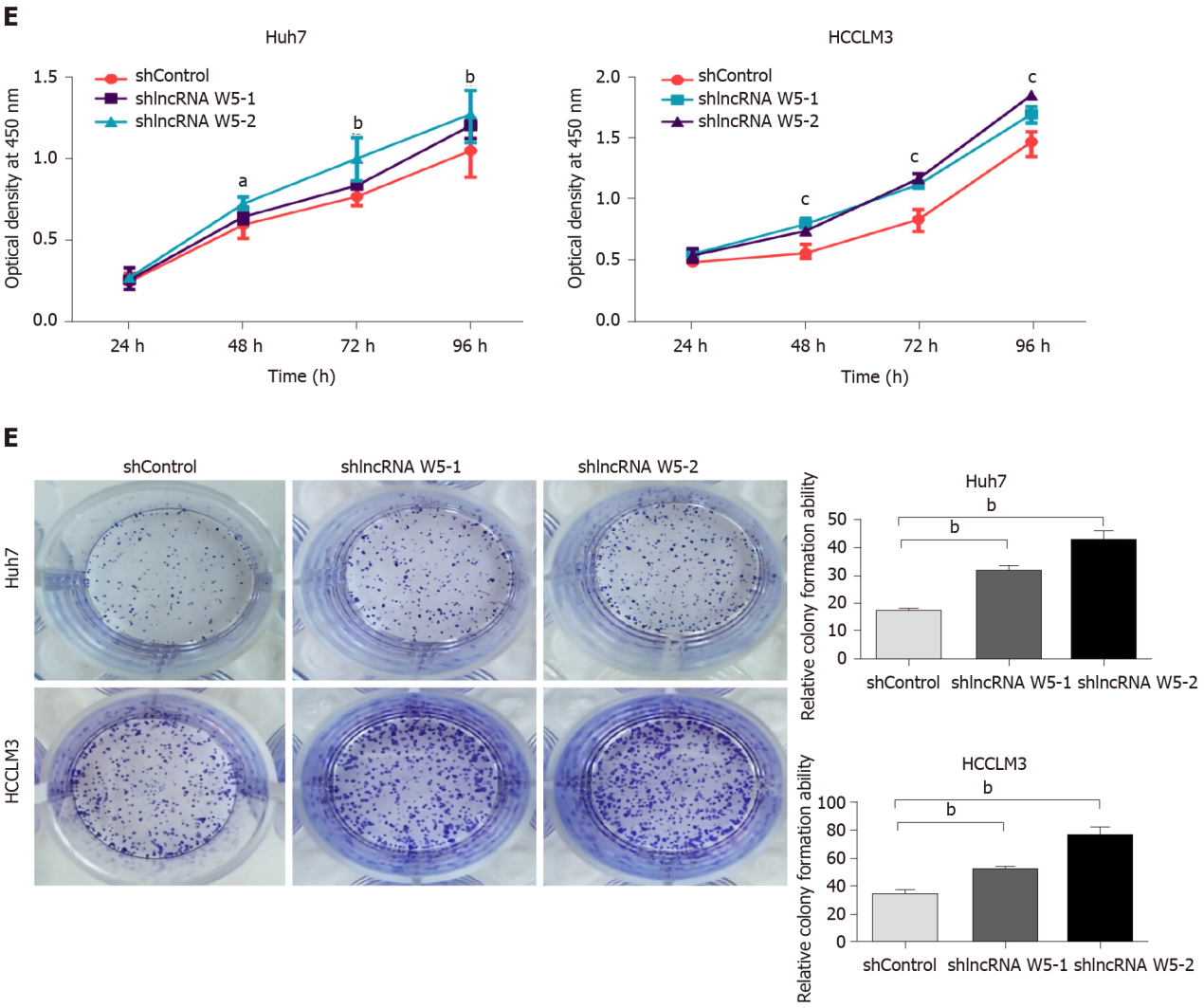
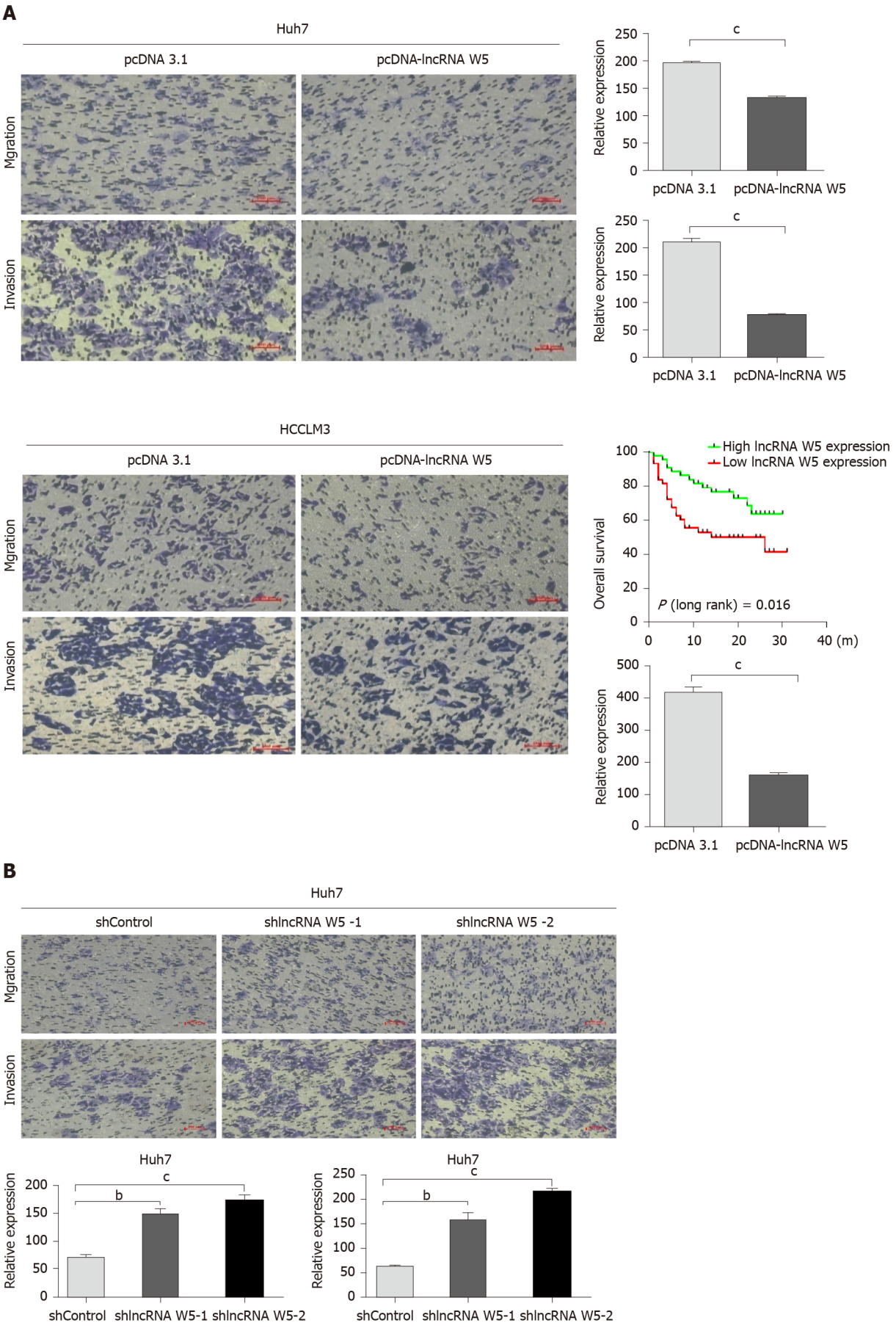


Figure 2 ***In vitro*** **suppression of long non-coding ribonucleic acid W5 in hepatocellular carcinoma proliferation.** A: Increased long non-coding ribonucleic acid (lncRNA) W5 expression in Huh7 and LM3 cells was confirmed after over-expressed lncRNA W5 transfection by reverse transcription-polymerase chain reaction. LncRNA W5 expression was normalized to GAPDH. $^{c}P < 0.001$; B: Cell viability of pCDNA-3.1 LncRNAW5-transfected Huh7 and LM3 cells were detected by CCK-8 assays. Cell number was determined every 24 h up to 96 h. The results are shown as the mean ± SE from three independent experiments. $^{a}P < 0.05$; $^{b}P < 0.01$. $^{c}P < 0.001$, compared with the control by two-sided *t*-test; C: Colony-forming assay was used to determine the effect of lncRNA W5 on the proliferation in Huh7 and LM3 cells; D: Decreased lncRNA W5 expression in Huh7 and LM3 cells was confirmed after sh-1 or sh-2 LncRNAW5 transfection by reverse transcription-polymerase chain reaction. LncRNA W5 expression was normalized to GAPDH. $^{a}P < 0.05$; $^{b}P < 0.01$. $^{c}P < 0.001$; E: Cell viability of sh-1 or sh-2 LncRNAW5-transfected Huh7 and LM3 cells were detected by CCK-8 assays. Cell number was determined every 24 h up to 96 h. The results are shown as the mean ± SE from at least three independent experiments. $^{a}P < 0.05$; $^{b}P < 0.01$. $^{c}P < 0.001$, compared with the control by two-sided *t*-test; and F: Colony-forming assay was used to determine the effect of sh-1 or sh-2 LncRNA W5 on the proliferation of Huh7 and LM3 cells.

exists in other solid tumors remains to be elucidated.

CONCLUSION

In conclusion, our results showed that the expression of lncRNA W5 was considerably reduced in HCC tissues, which suppressed proliferation, migration and invasion of tumor cells *in vitro*. The results also showed that low expression of lncRNA W5 correlated with tumor progression and poor prognosis. Furthermore, manipulation of lncRNA W5 expression impacted the biological behavior of HCC. These results suggest that lncRNA W5 may serve as a tumor suppressor in the development and progression of HCC, and has potential as a diagnostic and therapeutic target in the clinical management of HCC.


A
Huh7
pcDNA 3.1
pcDNA-lncRNA W5
Mgration
Invasion
Relative expression
c
pcDNA 3.1
pcDNA-lncRNA W5
HCCLM3
High lncRNA W5 expression
Low lncRNA W5 expression
Overall survival
P (long rank) = 0.016
40 (m)
B
shControl
shlncRNA W5 -1
shlncRNA W5 -2
b
shlncRNA W5-1
shlncRNA W5-2

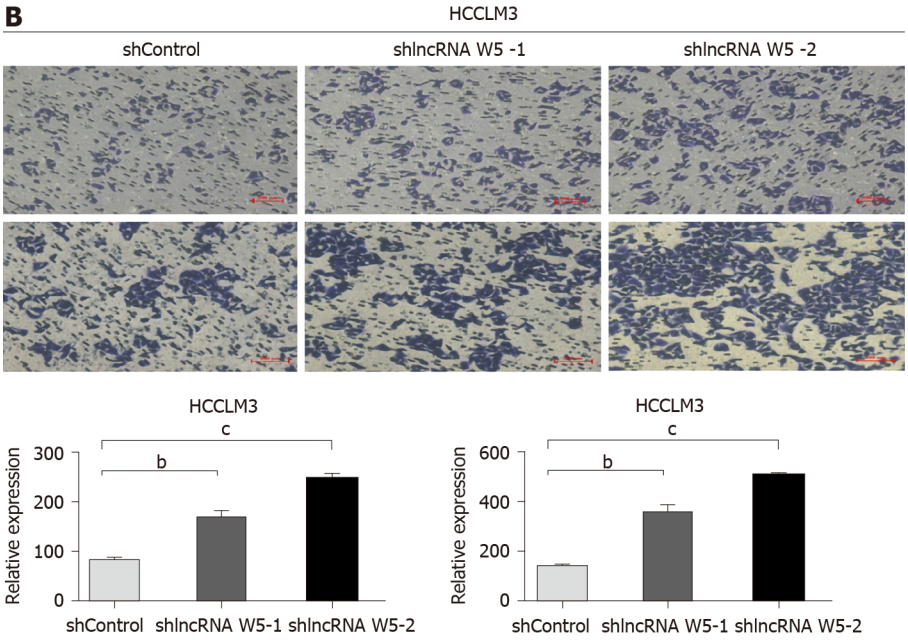


Figure 3 Effects of long non-coding ribonucleic acid W5 on hepatocellular carcinoma migration and invasion. A: Cell migration and invasion abilities were determined after transfection with pcDNA-3.1 and pcDNA-3.1 long non-coding ribonucleic acid W5 in Huh7 and LM3 cell lines, respectively; B: Cell migration and invasion abilities were determined after transfection with sh-1 or sh-2 LncRNA W5 in Huh7 and LM3 cell lines, respectively. All experiments were performed in triplicate. $^{a}P < 0.05$; $^{b}P < 0.01$; $^{c}P < 0.001$.

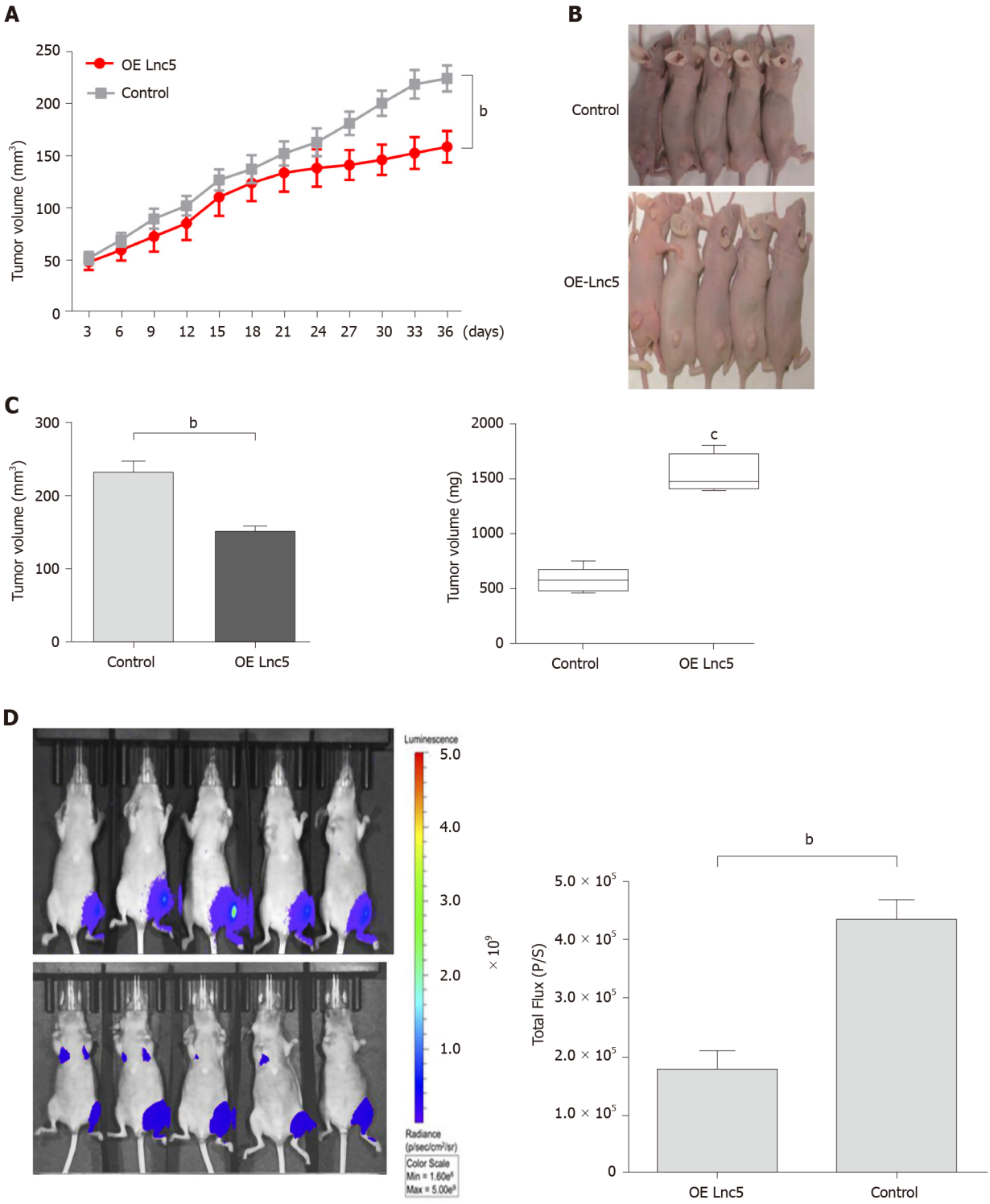


Figure 4 Long non-coding ribonucleic acid W5 inhibits tumor growth *in vivo*. A: Huh7 cells (5×10^6) stably expressed with long non-coding ribonucleic acid W5 (lncRNA W5) were subcutaneously injected into the left flank of nude mice, and the effect of lncRNA W5 on hepatocellular carcinoma tumor growth was examined every 3 d during the course of the experiment ($n = 5$); B: A representative image of the xenograft-bearing mice; C: Tumors were isolated from the nude mice after sacrifice. The effects of lncRNA W5 on hepatocellular carcinoma growth were determined by tumor volume and tumor weight; D: LncRNA W5-overexpressing Huh7 cells which stably expressed luciferase were injected into nude mice ($n = 5$). The bioluminescence photographs of tumor were recorded with the *in vivo* 200 Imaging System. A representative luciferase signal was recorded from each group at 6 wk after injection. $^bP < 0.01$.

ARTICLE HIGHLIGHTS

Research background

Accumulating evidence has revealed that several long non-coding RNAs (lncRNAs) are crucial in the progress of hepatocellular carcinoma (HCC).

Research motivation

To determine the clinical significance and potential roles of lncRNA W5 in HCC.

Research objectives

We classified the long non-coding RNA, lncRNA W5, and examined its clinical significance and potential roles in HCC.

Research methods

Analysis of the association between lncRNA W5 expression levels and clinico-pathological features was performed. In addition, overall survival was determined using Kaplan-Meier survival analysis.

Research results

The results showed that lncRNA W5 was down-regulated in HCC, and it may suppress HCC progression and predict a poor clinical outcome in patients with HCC.

Research conclusions

lncRNA W5 may serve as a potential prognostic biomarker and therapeutic target in HCC.

Research perspectives

lncRNA W5 may serve as a tumor suppressor in the development and progression of HCC, and have potential as a diagnostic and therapeutic target in the clinical management of HCC.

REFERENCES

1 **Hindupur SK**, Colombi M, Fuhs SR, Matter MS, Guri Y, Adam K, Cornu M, Piscuoglio S, Ng CKY, Betz C, Liko D, Quagliata L, Moes S, Jenoe P, Terracciano LM, Heim MH, Hunter T, Hall MN. The protein histidine phosphatase LHPP is a tumour suppressor. *Nature* 2018; **555**: 678-682 [PMID: 29562234 DOI: 10.1038/nature26140]

2 **Zhu J**, Yin T, Xu Y, Lu XJ. Therapeutics for advanced hepatocellular carcinoma: Recent advances, current dilemma, and future directions. *J Cell Physiol* 2019; **234**: 12122-12132 [PMID: 30644100 DOI: 10.1002/jcp.28048]

3 **Okusaka T**, Ikeda M. Immunotherapy for hepatocellular carcinoma: current status and future perspectives. *ESMO Open* 2018; **3**: e000455 [PMID: 30622744 DOI: 10.1136/esmoopen-2018-000455]

4 **Ghouri YA**, Mian I, Rowe JH. Review of hepatocellular carcinoma: Epidemiology, etiology, and carcinogenesis. *J Carcinog* 2017; **16**: 1 [PMID: 28694740 DOI: 10.4103/jcar.JCar_9_16]

5 **Escudier B**, Worden F, Kudo M. Sorafenib: key lessons from over 10 years of experience. *Expert Rev Anticancer Ther* 2019; **19**: 177-189 [PMID: 30575405 DOI: 10.1080/14737140.2019.1559058]

6 **Maracaja-Coutinho V**, Paschoal AR, Caris-Maldonado JC, Borges PV, Ferreira AJ, Durham AM. Noncoding RNAs Databases: Current Status and Trends. *Methods Mol Biol* 2019; **1912**: 251-285 [PMID: 30635897 DOI: 10.1007/978-1-4939-8982-9_10]

7 **Lorenzi L**, Avila Cobos F, Decock A, Everaert C, Helsmoortel H, Lefever S, Verboom K, Volders PJ, Speleman F, Vandesompele J, Mestdagh P. Long noncoding RNA expression profiling in cancer: Challenges and opportunities. *Genes Chromosomes Cancer* 2019; **58**: 191-199 [PMID: 30461116 DOI: 10.1002/gcc.22709]

8 **Zeng Y**, Ren K, Zhu X, Zheng Z, Yi G. Long Noncoding RNAs: Advances in Lipid Metabolism. *Adv Clin Chem* 2018; **87**: 1-36 [PMID: 30342708 DOI: 10.1016/bs.acc.2018.07.001]

9 **Rafiee A**, Riazi-Rad F, Havaskary M, Nuri F. Long noncoding RNAs: regulation, function and cancer. *Biotechnol Genet Eng Rev* 2018; **34**: 153-180 [PMID: 30071765 DOI: 10.1080/02648725.2018.1471566]

10 **Idda ML**, Munk R, Abdelmohsen K, Gorospe M. Noncoding RNAs in Alzheimer's disease. *Wiley Interdiscip Rev RNA* 2018; **9** [PMID: 29327503 DOI: 10.1002/wrna.1463]

11 **Yu WD**, Wang H, He QF, Xu Y, Wang XC. Long noncoding RNAs in cancer-immunity cycle. *J Cell Physiol* 2018; **233**: 6518-6523 [PMID: 29574911 DOI: 10.1002/jcp.26568]

12 **Cheng D**, Deng J, Zhang B, He X, Meng Z, Li G, Ye H, Zheng S, Wei L, Deng X, Chen R, Zhou J.

LncRNA HOTAIR epigenetically suppresses miR-122 expression in hepatocellular carcinoma *via* DNA methylation. *EBioMedicine* 2018; **36**: 159-170 [PMID: 30195653 DOI: 10.1016/j.ebiom.2018.08.055]

13 **Sun QM**, Hu B, Fu PY, Tang WG, Zhang X, Zhan H, Sun C, He YF, Song K, Xiao YS, Sun J, Xu Y, Zhou J, Fan J. Long non-coding RNA 00607 as a tumor suppressor by modulating NF-κB p65/p53 signaling axis in hepatocellular carcinoma. *Carcinogenesis* 2018; **39**: 1438-1446 [PMID: 30169594 DOI: 10.1093/carcin/bgy113]

14 **Noh JH**, Gorospe M. AKTions by Cytoplasmic lncRNA CASC9 Promote Hepatocellular Carcinoma Survival. *Hepatology* 2018; **68**: 1675-1677 [PMID: 30014487 DOI: 10.1002/hep.30165]

15 **Wang Y**, Chen F, Zhao M, Yang Z, Li J, Zhang S, Zhang W, Ye L, Zhang X. The long noncoding RNA HULC promotes liver cancer by increasing the expression of the HMGA2 oncogene *via* sequestration of the microRNA-186. *J Biol Chem* 2017; **292**: 15395-15407 [PMID: 28765279 DOI: 10.1074/jbc.M117.783738]

16 **Zhou Y**, Fan RG, Qin CL, Jia J, Wu XD, Zha WZ. LncRNA-H19 activates CDC42/PAK1 pathway to promote cell proliferation, migration and invasion by targeting miR-15b in hepatocellular carcinoma. *Genomics* 2019; **111**: 1862-1872 [PMID: 30543848 DOI: 10.1016/j.ygeno.2018.12.009]

17 **Zheng Q**, Lin Z, Xu J, Lu Y, Meng Q, Wang C, Yang Y, Xin X, Li X, Pu H, Gui X, Li T, Xiong W, Lu D. Long noncoding RNA MEG3 suppresses liver cancer cells growth through inhibiting β-catenin by activating PKM2 and inactivating PTEN. *Cell Death Dis* 2018; **9**: 253 [PMID: 29449541 DOI: 10.1038/s41419-018-0305-7]

18 **Li T**, Xie J, Shen C, Cheng D, Shi Y, Wu Z, Deng X, Chen H, Shen B, Peng C, Li H, Zhan Q, Zhu Z. Amplification of Long Noncoding RNA ZFAS1 Promotes Metastasis in Hepatocellular Carcinoma. *Cancer Res* 2015; **75**: 3181-3191 [PMID: 26069248 DOI: 10.1158/0008-5472.CAN-14-3721]

19 **Cheng S**, Li T, Wang C, Wang K, Lai C, Yan J, Fan H, Sun F, Wang Z, Zhang P, Yu L, Hong Z, Lei G, Sun B, Gao Y, Xiao Z, Ji X, Wang R, Wu J, Wang X, Zhang S, Yang P. Decreased long intergenic noncoding RNA P7 predicts unfavorable prognosis and promotes tumor proliferation *via* the modulation of the STAT1-MAPK pathway in hepatocellular carcinoma. *Oncotarget* 2018; **9**: 36057-36066 [PMID: 30546827 DOI: 10.18632/oncotarget.23282]

20 **Yuan JH**, Yang F, Wang F, Ma JZ, Guo YJ, Tao QF, Liu F, Pan W, Wang TT, Zhou CC, Wang SB, Wang YZ, Yang Y, Yang N, Zhou WP, Yang GS, Sun SH. A long noncoding RNA activated by TGF-β promotes the invasion-metastasis cascade in hepatocellular carcinoma. *Cancer Cell* 2014; **25**: 666-681 [PMID: 24768205 DOI: 10.1016/j.ccr.2014.03.010]

21 **Pan W**, Zhang N, Liu W, Liu J, Zhou L, Liu Y, Yang M. The long noncoding RNA *GAS8-AS1* suppresses hepatocarcinogenesis by epigenetically activating the tumor suppressor *GAS8*. *J Biol Chem* 2018; **293**: 17154-17165 [PMID: 30228180 DOI: 10.1074/jbc.RA118.003055]

22 **Jang SY**, Kim G, Park SY, Lee YR, Kwon SH, Kim HS, Yoon JS, Lee JS, Kweon YO, Ha HT, Chun JM, Han YS, Lee WK, Chang JY, Park JG, Lee B, Tak WY, Hur K. Clinical significance of lncRNA-ATB expression in human hepatocellular carcinoma. *Oncotarget* 2017; **8**: 78588-78597 [PMID: 29108251 DOI: 10.18632/oncotarget.21094]

23 **Yuan JH**, Liu XN, Wang TT, Pan W, Tao QF, Zhou WP, Wang F, Sun SH. The MBNL3 splicing factor promotes hepatocellular carcinoma by increasing PXN expression through the alternative splicing of lncRNA-PXN-AS1. *Nat Cell Biol* 2017; **19**: 820-832 [PMID: 28553938 DOI: 10.1038/ncb3538]

24 **Wu J**, Zhu P, Lu T, Du Y, Wang Y, He L, Ye B, Liu B, Yang L, Wang J, Gu Y, Lan J, Hao Y, He L, Fan Z. The long non-coding RNA LncHDAC2 drives the self-renewal of liver cancer stem cells *via* activation of Hedgehog signaling. *J Hepatol* 2019; **70**: 918-929 [PMID: 30582981 DOI: 10.1016/j.jhep.2018.12.015]

25 **Peng L**, Jiang B, Yuan X, Qiu Y, Peng J, Huang Y, Zhang C, Zhang Y, Lin Z, Li J, Yao W, Deng W, Zhang Y, Meng M, Pan X, Li C, Yin D, Bi X, Li G, Lin DC. Super-Enhancer-Associated Long Noncoding RNA HCCL5 Is Activated by ZEB1 and Promotes the Malignancy of Hepatocellular Carcinoma. *Cancer Res* 2019; **79**: 572-584 [PMID: 30482773 DOI: 10.1158/0008-5472.CAN-18-0367]

26 **Huang JF**, Jiang HY, Cai H, Liu Y, Zhu YQ, Lin SS, Hu TT, Wang TT, Yang WJ, Xiao B, Sun SH, Ma LY, Yin HR, Wang F. Genome-wide screening identifies oncofetal lncRNA Ptn-dt promoting the proliferation of hepatocellular carcinoma cells by regulating the Ptn receptor. *Oncogene* 2019; **38**: 3428-3445 [PMID: 30643194 DOI: 10.1038/s41388-018-0643-z]

World Journal of Gastroenterology

Submit a Manuscript: https://www.f6publishing.com

World J Gastroenterol 2021 January 7; 27(1): 69-79

DOI: 10.3748/wjg.v27.i1.69

ISSN 1007-9327 (print) ISSN 2219-2840 (online)

ORIGINAL ARTICLE

Retrospective Study

Predictors of pain response after endoscopic ultrasound-guided celiac plexus neurolysis for abdominal pain caused by pancreatic malignancy

Chao-Qun Han, Xue-Lian Tang, Qin Zhang, Chi Nie, Jun Liu, Zhen Ding

ORCID number: Chao-Qun Han 0000-0003-1338-865X; Xue-Lian Tang 0000-0002-1695-7371; Qin Zhang 0000-0001-9156-0772; Chi Nie 0000-0001-6897-2138; Jun Liu 0000-0003-4436-5729; Zhen Ding 0000-0001-8575-5282.

Author contributions: Han CQ performed the literature search and data extraction and drafted of the manuscript; Tang XL and Zhang Q collected the data; Nie C and Liu J contributed important intellectual content; Ding Z designed the study and edited the manuscript as corresponding author.

Supported by National Natural Science Foundation of China, No. 81800467 and No. 81770637.

Institutional review board statement: The study was approved by the Ethics Committee of Tongji Medical College, Huazhong University of Science and Technology (IORG No: IORG0003571).

Informed consent statement: Written informed consent was obtained from the patients.

Conflict-of-interest statement: There is no conflict of interest in this study.

Chao-Qun Han, Xue-Lian Tang, Qin Zhang, Chi Nie, Jun Liu, Zhen Ding, Division of Gastroenterology, Union Hospital, Tongji Medical College, Huazhong University of Science and Technology, Wuhan 430022, Hubei Province, China

Corresponding author: Zhen Ding, MD, PhD, Doctor, Professor, Teacher, Division of Gastroenterology, Union Hospital, Tongji Medical College, Huazhong University of Science and Technology, No. 1277 Jiefang Avenue, Wuhan 430022, Hubei Province, China. 2017xh0122@hust.edu.cn

Abstract

BACKGROUND

Endoscopic ultrasound-guided celiac plexus neurolysis (EUS-CPN) has gained popularity as a minimally invasive approach and is currently widely used to treat pancreatic cancer-associated pain. However, response to treatment is variable.

AIM

To identify the efficacy of EUS-CPN and explore determinants of pain response in EUS-CPN for pancreatic cancer-associated pain.

METHODS

A retrospective study of 58 patients with abdominal pain due to inoperable pancreatic cancer who underwent EUS-CPN were included. The efficacy for palliation of pain was evaluated based on the visual analog scale pain score at 1 wk and 4 wk after EUS-CPN. Univariable and multivariable logistic regression analyses were performed to explore predictors of pain response.

RESULTS

A good pain response was obtained in 74.1% and 67.2% of patients at 1 wk and 4 wk, respectively. Tumors located in the body/tail of the pancreas and patients receiving bilateral treatment were weakly associated with a good outcome. Multivariate analysis revealed patients with invisible ganglia and metastatic disease were significant factors for a negative response to EUS-CPN at 1 wk and 4 wk, respectively, particularly for invasion of the celiac plexus (odds ratio (OR) = 13.20, P = 0.003 for 1 wk and OR = 15.11, P = 0.001 for 4 wk). No severe adverse events were reported.

Data sharing statement: Dataset available from the corresponding author at 271914799@qq.com.

Open-Access: This article is an open-access article that was selected by an in-house editor and fully peer-reviewed by external reviewers. It is distributed in accordance with the Creative Commons Attribution NonCommercial (CC BY-NC 4.0) license, which permits others to distribute, remix, adapt, build upon this work non-commercially, and license their derivative works on different terms, provided the original work is properly cited and the use is non-commercial. See: http://creativecommons.org/Licenses/by-nc/4.0/

Manuscript source: Unsolicited manuscript

Specialty type: Gastroenterology and Hepatology

Country/Territory of origin: China

Peer-review report's scientific quality classification

Grade A (Excellent): 0
Grade B (Very good): B
Grade C (Good): C
Grade D (Fair): D
Grade E (Poor): 0

Received: July 4, 2020
Peer-review started: July 4, 2020
First decision: August 8, 2020
Revised: August 15, 2020
Accepted: November 12, 2020
Article in press: November 12, 2020
Published online: January 7, 2021

P-Reviewer: Kozarek RA, Thandassery RB
S-Editor: Liu M (Part-Time Editor)
L-Editor: Filipodia
P-Editor: Ma YJ

CONCLUSION

EUS-CPN is a safe and effective form of treatment for intractable pancreatic cancer-associated pain. Invisible ganglia, distant metastasis, and invasion of the celiac plexus were predictors of less effective response in EUS-CPN for pancreatic cancer-related pain. For these patients, efficacy warrants attention.

Key Words: Endoscopic ultrasound; Celiac plexus neurolysis; Pancreatic cancer; Pain; Predictor

©The Author(s) 2021. Published by Baishideng Publishing Group Inc. All rights reserved.

Core Tip: Endoscopic ultrasound-guided celiac plexus neurolysis (EUS-CPN) is widely used to treat pancreatic cancer-associated pain. However, response to treatment is variable. The procedure is not always effective, is often variable, and yields transient results. The data on determinants of pain relief response following EUS-CPN are limited and still need to undergo further exploration. Our study found that invisible ganglia, presence of distant metastases, and celiac plexus invasion were considered to be significantly negative variables. The strongest predictor of response was celiac plexus invasion. Moreover, tumors located at the body/tail predicted a better response than those with tumors at the pancreatic head/neck.

Citation: Han CQ, Tang XL, Zhang Q, Nie C, Liu J, Ding Z. Predictors of pain response after endoscopic ultrasound-guided celiac plexus neurolysis for abdominal pain caused by pancreatic malignancy. *World J Gastroenterol* 2021; 27(1): 69-79
URL: https://www.wjgnet.com/1007-9327/full/v27/i1/69.htm
DOI: https://dx.doi.org/10.3748/wjg.v27.i1.69

INTRODUCTION

Up to 90% advanced pancreatic cancer patients experience difficult-to-control pain syndromes[1]. Conventionally, pain is alleviated using a three-step analgesic ladder approach beginning with nonsteroidal anti-inflammatory agents followed by escalating doses of opiates[2]. However, pain is always refractory in some cases, posing a challenge to the physician. A high dose of such drugs still cannot provide adequate analgesia, especially for those patients experiencing intolerable drug-related side effects that can markedly reduce survival. In these patients, interventional pain techniques may be indicated.

In endoscopic ultrasound-guided celiac plexus neurolysis (EUS-CPN), a neurolytic agent disrupts the pain signal transductions from the afferent nerves to the spinal cord, and it has been widely applied as a minimally invasive approach. This procedure is able to decrease significantly the daily usage of morphine medications and relieve pain. The current National Comprehensive Cancer Network guidelines recommends EUS-CPN for treatment of severe cancer-associated pain[3]. Varied studies have reported that over 80% of patients achieved sustainable pain relief after treatment, and many even to the time of death[4,5].

However, the procedure is not always effective, is often variable, and has transient results. Subsequent studies showed the proportion of patients benefiting from pain amelioration is quite variable at 50% to 80%[6-8]. Optimization of treatment outcomes for the technique of neurolysis involves direct injection into the celiac ganglia, broad injection to involve the area around the superior mesenteric artery, and bilateral *vs* unilateral injection; lesion characteristics for optimization have been reported as well, but findings are controversial[7,9-12]. EUS-CPN is not recommended for patients suspected of having unfavorable outcomes. Moreover, the data on determinants of pain relief response following EUS-CPN are limited and still need to undergo further exploration. In this study, we attempt to summarize the predictive factors for response to EUS-CPN in pancreatic cancer with the goal of providing rational selection of the therapeutic strategies to alleviate pancreatic cancer-associated pain.

MATERIALS AND METHODS

Study population

A total of 58 patients who were diagnosed with pancreatic cancer and underwent EUS-CPN over a 4-year period (from January 2015 to December 2018) were included in this study. The inclusion criteria were as follows: (1) Patients over the age of 18 years; (2) Complete information; (3) Presence of unresectable or metastatic pancreatic cancer; (4) No receiving any palliative chemotherapy or radiation therapy; (5) No bleeding tendency (international normalized ratio ≤ 1.5 or platelet count ≥ 50,000 × 10^9/L); (6) No esophageal or gastric varices; and (7) Enduring abdominal or back pain due to confirmed pancreatic malignancy diagnosed by EUS guided fine-needle aspiration/biopsy or percutaneous biopsy. The study was approved by the Ethics Committee of Tongji Medical College, Huazhong University of Science and Technology (IORG No: IORG0003571). All patients signed informed consent for EUS operation, and data were anonymized and de-identified.

Endoscopic procedure in EUS-CPN

Patients were hydrated with 500-1000 mL saline solution during the procedure to minimize the risk of hypotension. They were placed in the left lateral decubitus position, and propofol was administered for deep sedation. Vital signs were continuously monitored with an automated non-invasive blood pressure measurement, electrocardiogram, and pulse oximetry.

EUS-CPN was performed by using the Olympus processor EU-ME2 with a linear array endoscopic ultrasonography (GF-UCT 260; Olympus, Tokyo, Japan). By tracing the aorta under real-time EUS guidance, the base of the celiac artery was identified. Celiac ganglia could be visualized between the celiac artery and the left adrenal gland. Typically for CPN unilateral injection, an Echo Tip 22-gauge needle (Cook Medical, Inc., Winston-Salem, NC, United States) primed with normal saline solution was inserted into the operating channel, affixed to the hub, and placed adjacent to the base of the celiac trunk at its origin from the aorta. In cases with bilateral injection, the same procedure was done, but injections were done at both sides of the celiac trunk with clockwise and counter-clockwise rotation (half of the dehydrated 98% absolute alcohol was injected in each side)[13,14]. After confirming no backflow of blood occurred, the celiac plexus injection by dehydrated 98% absolute alcohol was directly applied. A dense hyperechoic cloud was usually seen in the area of injection, and the injection was continued until spilling to the periganglionic space (Supplemental material). Whether a bilateral injection was carried out depended on the locations of intervening vessels, the tumor status, and invasion of the celiac plexus or not. Tumors extending to the para-aortic region from the level of the celiac axis to the origin of SMA were considered invasive of the celiac plexus. No antibiotics were administered before or post-CPN. All procedures were performed by a single endosonographer.

Pain scores

Pain intensity was evaluated by telephone interview and done objectively using a continuous visual analog scale (VAS), with 0 as no pain and 10 as worst possible pain. Detailed instructions explaining how to assess the VAS were read and the patients then informed the best VAS score that reflected their pain status. Good pain relief was defined as a decrease in the pain score by ≥ 3 or a ≥ 30% reduction in baseline pain without any increase in the narcotic daily dosing[15]. If the patients had no pain improvement or markedly increased pain or required additional doses of narcotic agents 1 wk after the procedure, the procedure was considered to be a failure.

Outcomes measures

Primary outcomes included the efficacy of EUS-CPN and the difference in pain control by VAS was compared. Pain management was evaluated at 1 wk and 4 wk after the CPN procedure. Secondary outcomes included analgesia requirement and adverse events. To minimize subjective variations in the evaluation of outcomes, the same authorized staff who was unaware of the detailed endoscopic procedures collected the outcomes of all patients.

Data collection

To analyze all possible factors that could affect the determinants of pain response in patients undergoing EUS-CPN for abdominal pain caused by pancreatic cancer, the following data were collected for each patient: Information regarding tumor characteristics (*i.e.* size, location, vascular invasion, and distant metastasis), procedure

details (including procedure method, dehydrated alcohol dose, visible or invisible ganglia, and intra-procedural heart rate change), the incidence of adverse events, and the dose of morphine medications administered before and after the assignment intervention. Heart rate change was defined as a decrease of ≥ 5 beats for ≥ 10 s during alcohol injection. Other covariates, including demographics (*i.e.* age, gender, initial VAS score), symptom *(i.e.* abdominal pain concomitant with jaundice and presence of ascites), were also collected.

Statistical analysis

Categorical data are presented as counts and percentages. Continuous variable results were presented as mean ± standard deviation. Associations among various categorical variables were constructed by Pearson's chi-squared test, and non-categorical variables were analyzed by *t* tests. Subsequently, univariable and multivariable logistic regression analyses were carried out to examine potential predictors of pain response to the CPN procedure. All statistical analyses were performed using IBM SPSS software20.0 (SPSS, Armonk, NY, United States). Values were considered to be statistically significant if the *P* value was less than 0.05 (two-sided).

RESULTS

Patient demographic and clinical characteristics

A total of 58 patients with abdominal pain due to inoperable pancreatic cancer who underwent EUS-CPN were included. These cases consisted of 33 men and 25 women with a mean age of 67 years (range: 54-73 years). Predominant distribution of tumor location in pancreas was located in the body/tail (69.0%), and mean tumor diameter was 44.3 mm (range: 24-100 mm). Fifty-one patients were referred for initial evaluation of suspected pancreatic cancer and were first confirmed *via* EUS-fine needle aspiration (FNA) before undergoing EUS-CPN in the same session. The seven remaining patients had been previously diagnosed with pancreatic malignancy and were referred to our center for palliation with EUS-CPN only. The 51 patients had malignant tumors histologically confirmed by EUS-FNA of pancreas (n = 36), enlarged lymph nodes (n = 8), and liver metastases (n = 3) or ascites cytology (n = 4). Of the entire group of patients, visible pre-procedural celiac ganglia were present in 42 patients (72.4%) during the EUS session. Direct invasion of the celiac plexus was detected in 16 (27.6%) patients, whereas 26 (44.8%) patients had distant metastasis. The patient clinical demographics, disease, and treatment characteristics are summarized in Table 1 and Figure 1.

Efficacy for palliation of pain after EUS-CPN

With regard to therapeutic effect, the mean dose of alcohol injection was 10 mL (range: 5-20 mL). The mean initial VAS score was 8, and 51 patients (87.9%) were already taking narcotic analgesics prior to EUS-CPN. The tramadol dose used was 50 mg per time (range: 0–300). The rates of good pain response, defined as a drop of VAS score by ≥ 3 points in pain scale with subjective pain improvements without additional narcotics, were 74.1% and 67.2% of patients at 1 wk and 4 wk after EUS-guided neurolysis, respectively. The other patients were regarded as treatment failures, because either the pain was not better by ≥ 3 points from the baseline VAS score or they were feeling not better and increased their dose of tramadol medication after EUS-CPN. In the successful-treatment group, there was clearly a persistent treatment effect where pain relief lasted for 1–16 wk (until death in eight patients). Overall, there was a significant reduction in pain score from a mean of 8.2 at baseline to 4.4 at 1 wk (P = 0.004) and to 4.9 at 4 wk (P = 0.012) in all patients.

Predictors associated with pain response after EUS-CPN

To assess the predictive factors for pain response at 1 wk and 4 wk in patients who underwent EUS-CPN, variable data between the successful-treatment and the insufficient groups were compared. At 1 wk, tumors located in the body/tail of the pancreas and patients receiving bilateral procedure were weakly associated with a good response, but this was not statistically significant (P = 0.094; P = 0.087, respectively) (Table 2). However, invisible ganglia and presence of distant metastasis were significant negative predictive factors in the univariable analysis [odds ratio (OR) = 3.574, 95% confidence interval (CI): 1.80-14.24, P = 0.003; OR = 5.940, 95%CI: 1.31-11.82, P = 0.015]. Moreover, invasion of the celiac plexus was significantly associated

Table 1 Baseline characteristics of patients who underwent endoscopic ultrasound-guided celiac plexus neurolysis [*n* (%), *n* = 58]

Independent variables	Total number
Age in yr, range (mean)	54–73 (67)
Gender, female/male	25/33
Symptom	
Abdominal pain concomitant with jaundice Tumor largest dimension in mm, range (mean)	6 (10.3)
Ascites, slight or mild	24–100 (44.3)
Tumor location	4 (6.9)
Pancreatic head/neck	
Pancreatic body/tail	18 (31.0)
Initial VAS score, range (mean)	40 (69.0)
Tramadol use before EUS-CPN	6-10 (8)
Dose in mg, range (mean)	51 (87.9)
Ganglia visualized	0-240 (40)
Invasion of celiac plexus	42 (72.4)
Distant metastasis	16 (27.6)
Injected alcohol dose in mL, range (mean)	26 (44.8)
Procedure method	5–20 (10)
Unilateral	
Bilateral	33 (56.9)
Intra-procedural decrease in heart rate	25 (43.1)
decrease of ≥ 5 beats for ≥ 10 s	
	48 (82.8)

EUS-CPN: Endoscopic ultrasound-guided celiac plexus neurolysis; VAS: Visual analog scale.

with a poor pain response (OR = 7.922, P = 0.001). When these factors were subjected to multivariable logistic regression analysis, invisible ganglia, presence of distant metastases, and celiac plexus invasion were identified as significant negative independent pain response factors to EUS-CPN (Table 3). The other factors age, gender, symptom, tumor size, presence of ascites, and initial pain scores did not differ significantly between the two groups (Table 2). Furthermore, neither the pre-intervention tramadol dose use nor injected alcohol dose correlated with the outcome of EUS-CPN. Finally, there was no statistical difference in response to diagnosis between patients who were presenting for initial evaluation by EUS-FNA and those who already had a biopsy-proven pancreatic cancer.

Similarly, at 4 wk, invisible ganglia, presence of distant metastases, and celiac plexus invasion were significant negative predictive factors in univariable analysis (P = 0.003, P = 0.009 and P = 0.001, respectively) (Table 4). At multivariate regression analysis of potential predictors, invisible ganglia, presence of distant metastases, and celiac plexus invasion were associated with a bad pain response (P = 0.037, P = 0.019 and P = 0.001, respectively). The strongest predictor of response was celiac plexus invasion, which yielded a 15-fold higher chance of response for those patients compared with those without celiac plexus invasion (Table 5).

Complication after EUS-CPN

Complications occurred in 10.3% of enrolled patients. No serious adverse events including ischemic, inebriation, and acute paraplegia related to EUS-CPN occurred. Most of the complications were minor and transitory self-limited and included hypotension (1.7%), increase of pain (5.2%), and transient loose stools (3.4%).

Table 2 Univariable analysis of variables associated with pain response after 1 wk in the enrolled cohort of 58 patients

Independent variables	OR	95%CI	*P* value
Age in yr	1.084	0.60-3.88	0.212
Gender, female/male	1.39	0.43-3.79	0.64
Symptom			
Abdominal pain concomitant with jaundice	1.29	0.53–3.26	0.581
Tumor largest dimension	1.32	0.45-4.69	0.665
Ascites	1.772	0.59–6.84	0.437
Tumor location			
Pancreatic head/neck	2.071	0.60-7.09	0.232
Pancreatic body/tail	0.617	0.65-10.40	0.094
Initial VAS score	2.231	0.76-5.41	0.132
Tramadol use before EUS-CPN	1.339	0.54-15.39	0.327
Invisible ganglia	3.574	1.80-14.24	**0.003**
Invasion of celiac plexus	7.922	2.24-25.93	**0.001**
Distant metastasis	5.94	1.31–11.82	**0.015**
Injected alcohol dose	3.825	1.12–13.42	0.437
Procedure method			
Unilateral	1.677	0.84–11.48	0.591
Bilateral	0.489	0.11–1.12	0.087
Intra-procedural decrease in heart rate	1.011	0.91–2.08	0.933

OR: Odds ratio; CI: Confidence interval; EUS-CPN: Endoscopic ultrasound-guided celiac plexus neurolysis; VAS: Visual analogue scale.

Table 3 Multivariate analysis for predictors affecting pain response after 1 wk by endoscopic ultrasound-guided celiac plexus neurolysis

Independent variables	OR	95%CI	*P* value
Ganglia invisible	4.9	2.25-17.91	0.011
Invasion of celiac plexus	13.2	3.02-46.27	0.003
Distant metastasis	6.84	2.34–19.15	0.022

Summarizes the results of the multivariate analyses of the predictive factors associated with pain relief by EUS-CPN. The only independent predictive factors that achieved statistical significance in the univariate analysis were included. CI: Confidence interval; EUS-CPN: Endoscopic ultrasound-guided celiac plexus neurolysis; OR: Odds ratio.

DISCUSSION

Pancreatic cancer is often associated with intense and refractory pain. EUS-CPN was demonstrated to be safe and significantly improved pain control in 88% of patients with pancreatic cancer[16]. However, subsequent studies showed substantial variation in the proportion of patients experiencing pain relief[17]. This wide range is mainly attributable to differences in the characteristics of patients and the lack of standardized operation. For these reasons, it is difficult to compare the efficacy rate of EUS-CPN. Therefore, the current study was designed to analyze potential factors influencing EUS-CPN efficacy in patients with pancreatic cancer. Our data revealed that patients with invisible ganglia, distant metastasis, and invasion of the celiac plexus were predictors of less effective response in EUS-guided neurolysis for pancreatic cancer-related pain.

Our results demonstrated that invisible ganglia, presence of distant metastases, and

Table 4 Univariable analysis of variables associated with pain response after 4 wk in the enrolled cohort of 58 patients

Independent variables	OR	95%CI	*P* value
Age in yr	1.091	0.63-3.94	0.209
Gender, female/male	1.124	0.47-3.99	0.532
Symptom			
Abdominal pain concomitant with	1.384	0.43–4.82	0.618
jaundice	1.496	0.32-5.92	0.701
Tumor largest dimension	1.921	0.79–9.34	0.408
Ascites			
Tumor location	3.59	0.40-10.06	0.184
Pancreatic head/neck	0.42	0.15-12.77	0.082
Pancreatic body/tail	2.93	0.42-8.17	0.101
Initial VAS score	2.91	0.24-19.40	0.149
Tramadol use before EUS-CPN	4.02	1.62-13.27	0.003
Invisible ganglia	8.84	2.11-23.32	0.001
Invasion of celiac plexus	7.83	1.81–15.77	0.009
Distant metastasis	4.90	1.32–17.91	0.394
Injected alcohol dose			
Procedure method	2.87	0.44–17.41	0.502
Unilateral	0.54	0.16–1.99	0.093
Bilateral	0.94	0.42–3.12	0.858
Intra-procedural decrease in heart rate			

CI: Confidence interval; EUS-CPN: Endoscopic ultrasound-guided celiac plexus neurolysis; OR: Odds ratio; VAS: Visual analogue scale.

Table 5 Multivariate analysis for predictors affecting pain response after 4 wk by endoscopic ultrasound-guided celiac plexus neurolysis

Independent variables	OR	95%CI	*P* value
Invisible ganglia	5.85	2.66-22.73	0.037
Invasion of celiac plexus	15.11	4.01-51.22	0.001
Distant metastasis	8.59	2.16–27.02	0.019

Summarizes the results of the multivariate analyses of the predictive factors associated with pain relief by EUS-CPN. The only independent predictive factors that achieved statistical significance in the univariate analysis were included. CI: Confidence interval; EUS-CPN: Endoscopic ultrasound-guided celiac plexus neurolysis; OR: Odds ratio.

celiac plexus invasion were significant negative variables at 1 wk and 4 wk after EUS-CPN by univariable analysis and multivariate regression analysis. The strongest predictor of response was celiac plexus invasion, which may be related to perineural invasion of pancreatic nerves by tumor cells. Direct invasion of the ganglia or plexus may result in patients with pain not mediated by the celiac plexus[1]. In fact, FNA of the celiac ganglia has confirmed invasion by malignant cells in some patients with pancreatic cancer[18]. The reason also may be that cancer invasion restricts the spread of neurolytic solution and limits the subsequent pain relief[19]. Iwata *et al*[20] also suggested that EUS-CPN seems to be less effective in patients with direct invasion of the celiac plexus.

There are mixed findings regarding bilateral or unilateral approach, and a recent meta-analysis showed that the short-term analgesic effect and general risk of bilateral EUS-CPN are comparable with those of unilateral EUS-CPN[9]. There were no

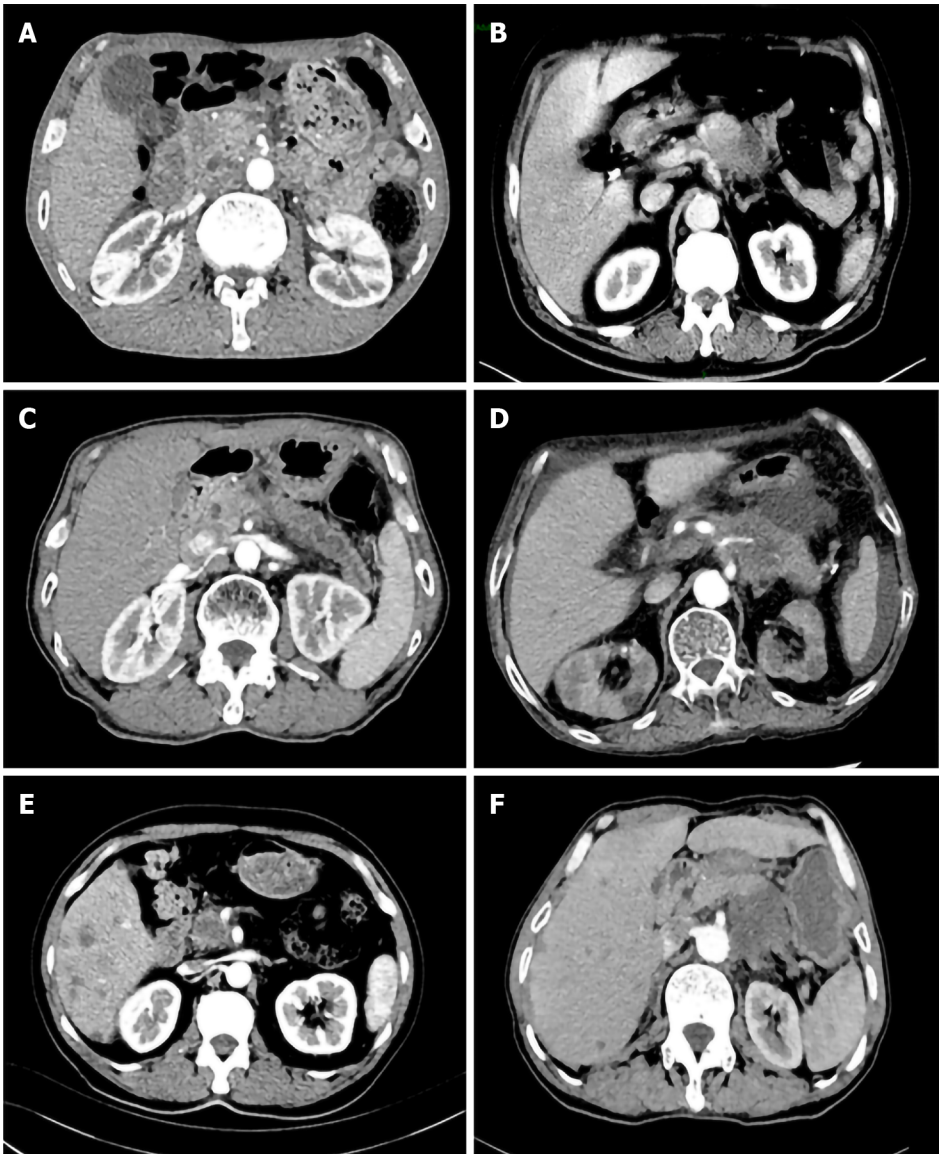


Figure 1 Varied pancreatic lesions are shown by contrast-enhanced computed tomography image. A: The lesion was located in head/neck of pancreas; B: The lesion was located in body/tail of pancreas; C: Pancreatic head lesion was associated with celiac trunk and celiac plexus invasion; D: The image showed a pancreatic body/tail invading the celiac plexus; E: Pancreatic head/neck lesion was accompanied with hepatic metastasis; F: Pancreatic body/tail lesion was accompanied with hepatic metastasis.

differences in onset or duration of pain relief when either one or two injections were used[13,14,21]. In our cohort patients, the bilateral method was associated with a good pain response but no statistical significance (P = 0.087). With regard to the dose of alcohol used in EUS-CPN, the amount of alcohol used in EUS-CPN ranged from 2 mL to 20 mL[22-24]. Our results found that there was no difference in the dose of alcohol used in EUS-CPN, which is consistent with the results described by Leblanc *et al*[25]. Leblanc *et al*[25] indicated that similar clinical outcomes were seen in the 10 mL and 20 mL alcohol groups with respect to overall pain relief, weekly pain scores, onset of pain relief, and proportion of complete responders.

However, according to our data, tumors located at the body/tail predicted a better response than those with tumors at the pancreatic head/neck after 1 wk or 4 wk, although there were no significant differences (P = 0.094 and P = 0.082 L, respectively). This is in contrast to previous literature reports[26]. Ascunce *et al*[1] reported that tumors located outside the head of the pancreas were weakly associated with a good response. Rykowski *et al*[27] also reported that the posterior transcutaneous CPN technique was more effective in tumors involving the pancreatic head than in those affecting the body and tail of the pancreas. On the other hand, our finding was inconsistent with a previous study on heart rate change. Recently, Bang *et al*[28] discussed a direct correlation between the increase in heart rate during alcohol injection and treatment outcomes. They found that during EUS-CPN, the heart rate change cohort had

significantly better adjusted scores for pain, financial difficulties, weight loss, and satisfaction with body image. Especially, a rise in heart rate during alcohol injection appeared to signal successful targeting of the celiac plexus and may be a simple predictor of treatment outcome. However, during alcohol injection in our cohort, the intra-procedural heart rate was decreased in ≥ 80% of patients. The heart rate always decreased when the alcohol was injected into the celiac plexus, and it returned to baseline level after several seconds.

Certainly, the present study has its inherent limitations that should be considered. First, the study is retrospective and the samples of patients are relatively small, suggesting restricted application of the results. A second limitation is the difficulty in measuring pain score, which was variable and a subjective measure. Finally, we failed to supply any results beyond 4 wk, because over time the efficacy of CPN decreased. Also, beyond 4 wk to 16 wk, there were fewer patients for analyzing these data. Therefore, we did not include these patients who received treatment more than 4 wk in the study (data not shown). We also could not compare the survival of patients who did CPN and those who did not. In order to evaluate objectively the significance of these parameters, a large group of multicenter, prospective, randomized trials are required.

CONCLUSION

Our study found that EUS-CPN is a safe and effective form of treatment for intractable pancreatic cancer-associated pain. EUS-CPN seems to be less effective in patients with invisible ganglia, distant metastasis, and direct invasion of the celiac plexus. For these patients, additional attention should be paid to efficacy.

ARTICLE HIGHLIGHTS

Research background

Endoscopic ultrasound-guided celiac plexus neurolysis (EUS-CPN) is widely used to treat pancreatic cancer-associated pain.

Research motivation

Response to the treatment of EUS-CPN is variable.

Research objectives

To explore determinants of pain response in EUS-CPN for pancreatic cancer-associated pain.

Research methods

Univariable and multivariable logistic regression analyses were performed to explore predictors of pain response.

Research results

Invisible ganglia, metastatic disease, and invasion of the celiac plexus were identified as significant factors for a negative response to EUS-CPN. No severe adverse events were reported.

Research conclusions

Invisible ganglia, distant metastasis, and invasion of the celiac plexus were predictors of less effective response in EUS-CPN for pancreatic cancer-related pain. For these patients, attention should be given regarding efficacy.

Research perspectives

These findings could be helpful to endoscopists or oncologists to develop an appropriate treatment scheme for pain management in pancreatic cancer patients.

REFERENCES

1 **Ascunce G**, Ribeiro A, Reis I, Rocha-Lima C, Sleeman D, Merchan J, Levi J. EUS visualization and direct celiac ganglia neurolysis predicts better pain relief in patients with pancreatic malignancy (with video). *Gastrointest Endosc* 2011; **73**: 267-274 [PMID: 21295640 DOI: 10.1016/j.gie.2010.10.029]

2 **Minaga K**, Takenaka M, Kamata K, Yoshikawa T, Nakai A, Omoto S, Miyata T, Yamao K, Imai H, Sakamoto H, Kitano M, Kudo M. Alleviating Pancreatic Cancer-Associated Pain Using Endoscopic Ultrasound-Guided Neurolysis. *Cancers (Basel)* 2018; **10**: 50 [PMID: 29462851 DOI: 10.3390/cancers10020050]

3 **Tempero MA**, Malafa MP, Al-Hawary M, Asbun H, Bain A, Behrman SW, Benson AB, Binder E, Cardin DB, Cha C, Chiorean EG, Chung V, Czito B, Dillhoff M, Dotan E, Ferrone CR, Hardacre J, Hawkins WG, Herman J, Ko AH, Komanduri S, Koong A, LoConte N, Lowy AM, Moravek C, Nakakura EK, O'Reilly EM, Obando J, Reddy S, Scaife C, Thayer S, Weekes CD, Wolff RA, Wolpin BM, Burns J, Darlow S. Pancreatic Adenocarcinoma, Version 2.2017, NCCN Clinical Practice Guidelines in Oncology. *J Natl Compr Canc Netw* 2017; **15**: 1028-1061 [PMID: 28784865 DOI: 10.6004/jnccn.2017.0131]

4 **Eisenberg E**, Carr DB, Chalmers TC. Neurolytic celiac plexus block for treatment of cancer pain: a meta-analysis. *Anesth Analg* 1995; **80**: 290-295 [PMID: 7818115 DOI: 10.1097/00000539-199502000-00015]

5 **Nagels W**, Pease N, Bekkering G, Cools F, Dobbels P. Celiac plexus neurolysis for abdominal cancer pain: a systematic review. *Pain Med* 2013; **14**: 1140-1163 [PMID: 23802777 DOI: 10.1111/pme.12176]

6 **Levy MJ**, Gleeson FC, Topazian MD, Fujii-Lau LL, Enders FT, Larson JJ, Mara K, Abu Dayyeh BK, Alberts SR, Hallemeier CL, Iyer PG, Kendrick ML, Mauck WD, Pearson RK, Petersen BT, Rajan E, Takahashi N, Vege SS, Wang KK, Chari ST. Combined Celiac Ganglia and Plexus Neurolysis Shortens Survival, Without Benefit, *vs* Plexus Neurolysis Alone. *Clin Gastroenterol Hepatol* 2019; **17**: 728-738. e9 [PMID: 30217513 DOI: 10.1016/j.cgh.2018.08.040]

7 **Koulouris AI**, Banim P, Hart AR. Pain in Patients with Pancreatic Cancer: Prevalence, Mechanisms, Management and Future Developments. *Dig Dis Sci* 2017; **62**: 861-870 [PMID: 28229252 DOI: 10.1007/s10620-017-4488-z]

8 **Yasuda I**, Wang HP. Endoscopic ultrasound-guided celiac plexus block and neurolysis. *Dig Endosc* 2017; **29**: 455-462 [PMID: 28160344 DOI: 10.1111/den.12824]

9 **Lu F**, Dong J, Tang Y, Huang H, Liu H, Song L, Zhang K. Bilateral vs. unilateral endoscopic ultrasound-guided celiac plexus neurolysis for abdominal pain management in patients with pancreatic malignancy: a systematic review and meta-analysis. *Support Care Cancer* 2018; **26**: 353-359 [PMID: 28956176 DOI: 10.1007/s00520-017-3888-0]

10 **Wyse JM**, Battat R, Sun S, Saftoiu A, Siddiqui AA, Leong AT, Arturo Arias BL, Fabbri C, Adler DG, Santo E, Kalaitzakis E, Artifon E, Mishra G, Okasha HH, Poley JW, Guo J, Vila JJ, Lee LS, Sharma M, Bhutani MS, Giovannini M, Kitano M, Eloubeidi MA, Khashab MA, Nguyen NQ, Saxena P, Vilmann P, Fusaroli P, Garg PK, Ho S, Mukai S, Carrara S, Sridhar S, Lakhtakia S, Rana SS, Dhir V, Sahai AV. Practice guidelines for endoscopic ultrasound-guided celiac plexus neurolysis. *Endosc Ultrasound* 2017; **6**: 369-375 [PMID: 29251270 DOI: 10.4103/eus.eus_97_17]

11 **Wyse JM**, Carone M, Paquin SC, Usatii M, Sahai AV. Randomized, double-blind, controlled trial of early endoscopic ultrasound-guided celiac plexus neurolysis to prevent pain progression in patients with newly diagnosed, painful, inoperable pancreatic cancer. *J Clin Oncol* 2011; **29**: 3541-3546 [PMID: 21844506 DOI: 10.1200/JCO.2010.32.2750]

12 **Doi S**, Yasuda I, Kawakami H, Hayashi T, Hisai H, Irisawa A, Mukai T, Katanuma A, Kubota K, Ohnishi T, Ryozawa S, Hara K, Itoi T, Hanada K, Yamao K. Endoscopic ultrasound-guided celiac ganglia neurolysis vs. celiac plexus neurolysis: a randomized multicenter trial. *Endoscopy* 2013; **45**: 362-369 [PMID: 23616126 DOI: 10.1055/s-0032-1326225]

13 **Téllez-Ávila FI**, Romano-Munive AF, Herrera-Esquivel Jde J, Ramírez-Luna MA. Central is as effective as bilateral endoscopic ultrasound-guided celiac plexus neurolysis in patients with unresectable pancreatic cancer. *Endosc Ultrasound* 2013; **2**: 153-156 [PMID: 24949384 DOI: 10.7178/eus.06.007]

14 **LeBlanc JK**, Al-Haddad M, McHenry L, Sherman S, Juan M, McGreevy K, Johnson C, Howard TJ, Lillemoe KD, DeWitt J. A prospective, randomized study of EUS-guided celiac plexus neurolysis for pancreatic cancer: one injection or two? *Gastrointest Endosc* 2011; **74**: 1300-1307 [PMID: 22000795 DOI: 10.1016/j.gie.2011.07.073]

15 **Si-Jie H**, Wei-Jia X, Yang D, Lie Y, Feng Y, Yong-Jian J, Ji L, Chen J, Liang Z, De-Liang F. How to improve the efficacy of endoscopic ultrasound-guided celiac plexus neurolysis in pain management in patients with pancreatic cancer: analysis in a single center. *Surg Laparosc Endosc Percutan Tech* 2014; **24**: 31-35 [PMID: 24487155 DOI: 10.1097/SLE.0000000000000032]

16 **Wiersema MJ**, Wiersema LM. Endosonography-guided celiac plexus neurolysis. *Gastrointest Endosc* 1996; **44**: 656-662 [PMID: 8979053 DOI: 10.1016/s0016-5107(96)70047-0]

17 **Puli SR**, Reddy JB, Bechtold ML, Antillon MR, Brugge WR. EUS-guided celiac plexus neurolysis for pain due to chronic pancreatitis or pancreatic cancer pain: a meta-analysis and systematic review. *Dig Dis Sci* 2009; **54**: 2330-2337 [PMID: 19137428 DOI: 10.1007/s10620-008-0651-x]

18 **Levy MJ**, Topazian M, Keeney G, Clain JE, Gleeson F, Rajan E, Wang KK, Wiersema MJ, Farnell M, Chari S. Preoperative diagnosis of extrapancreatic neural invasion in pancreatic cancer. *Clin*

Gastroenterol Hepatol 2006; **4**: 1479-1482 [PMID: 17101297 DOI: 10.1016/j.cgh.2006.08.012]

19 **De Cicco M**, Matovic M, Bortolussi R, Coran F, Fantin D, Fabiani F, Caserta M, Santantonio C, Fracasso A. Celiac plexus block: injectate spread and pain relief in patients with regional anatomic distortions. *Anesthesiology* 2001; **94**: 561-565 [PMID: 11379673 DOI: 10.1097/00000542-200104000-00006]

20 **Iwata K**, Yasuda I, Enya M, Mukai T, Nakashima M, Doi S, Iwashita T, Tomita E, Moriwaki H. Predictive factors for pain relief after endoscopic ultrasound-guided celiac plexus neurolysis. *Dig Endosc* 2011; **23**: 140-145 [PMID: 21429019 DOI: 10.1111/j.1443-1661.2010.01046.x]

21 **Sahai AV**, Lemelin V, Lam E, Paquin SC. Central vs. bilateral endoscopic ultrasound-guided celiac plexus block or neurolysis: a comparative study of short-term effectiveness. *Am J Gastroenterol* 2009; **104**: 326-329 [PMID: 19174816 DOI: 10.1038/ajg.2008.64]

22 **Levy MJ**, Topazian MD, Wiersema MJ, Clain JE, Rajan E, Wang KK, de la Mora JG, Gleeson FC, Pearson RK, Pelaez MC, Petersen BT, Vege SS, Chari ST. Initial evaluation of the efficacy and safety of endoscopic ultrasound-guided direct Ganglia neurolysis and block. *Am J Gastroenterol* 2008; **103**: 98-103 [PMID: 17970834 DOI: 10.1111/j.1572-0241.2007.01607.x]

23 **Sakamoto H**, Kitano M, Kamata K, Komaki T, Imai H, Chikugo T, Takeyama Y, Kudo M. EUS-guided broad plexus neurolysis over the superior mesenteric artery using a 25-gauge needle. *Am J Gastroenterol* 2010; **105**: 2599-2606 [PMID: 20823834 DOI: 10.1038/ajg.2010.339]

24 **Gunaratnam NT**, Sarma AV, Norton ID, Wiersema MJ. A prospective study of EUS-guided celiac plexus neurolysis for pancreatic cancer pain. *Gastrointest Endosc* 2001; **54**: 316-324 [PMID: 11522971 DOI: 10.1067/mge.2001.117515]

25 **Leblanc JK**, Rawl S, Juan M, Johnson C, Kroenke K, McHenry L, Sherman S, McGreevy K, Al-Haddad M, Dewitt J. Endoscopic Ultrasound-Guided Celiac Plexus Neurolysis in Pancreatic Cancer: A Prospective Pilot Study of Safety Using 10 mL *vs* 20 mL Alcohol. *Diagn Ther Endosc* 2013; **2013**: 327036 [PMID: 23365492 DOI: 10.1155/2013/327036]

26 **Minaga K**, Kitano M, Sakamoto H, Miyata T, Imai H, Yamao K, Kamata K, Omoto S, Kadosaka K, Sakurai T, Nishida N, Chiba Y, Kudo M. Predictors of pain response in patients undergoing endoscopic ultrasound-guided neurolysis for abdominal pain caused by pancreatic cancer. *Therap Adv Gastroenterol* 2016; **9**: 483-494 [PMID: 27366217 DOI: 10.1177/1756283X16644248]

27 **Rykowski JJ**, Hilgier M. Efficacy of neurolytic celiac plexus block in varying locations of pancreatic cancer: influence on pain relief. *Anesthesiology* 2000; **92**: 347-354 [PMID: 10691219 DOI: 10.1097/00000542-200002000-00014]

28 **Bang JY**, Hasan MK, Sutton B, Holt BA, Navaneethan U, Hawes R, Varadarajulu S. Intraprocedural increase in heart rate during EUS-guided celiac plexus neurolysis: Clinically relevant or just a physiologic change? *Gastrointest Endosc* 2016; **84**: 773-779.e3 [PMID: 27048974 DOI: 10.1016/j.gie.2016.03.1496]

World Journal of Gastroenterology

Submit a Manuscript: https://www.f6publishing.com

World J Gastroenterol 2021 January 7; 27(1): 80-91

DOI: 10.3748/wjg.v27.i1.80

ISSN 1007-9327 (print) ISSN 2219-2840 (online)

ORIGINAL ARTICLE

Retrospective Study

Evaluation of controlled attenuation parameter in assessing hepatic steatosis in patients with autoimmune liver diseases

Xi-Xi Ni, Min Lian, Hui-Min Wu, Xiao-Yun Li, Li Sheng, Han Bao, Qi Miao, Xiao Xiao, Can-Jie Guo, Hai Li, Xiong Ma, Jing Hua

ORCID number: Xi-Xi Ni 0000-0003-3361-3703; Min Lian 0000-0003-2122-1614; Hui-Min Wu 0000-0002-3991-3857; Xiao-Yun Li 0000-0003-4706-6114; Li Sheng 0000-0002-3641-5211; Han Bao 0000-0003-2934-3990; Qi Miao 0000-0003-3370-9692; Xiao Xiao 0000-0002-7936-336X; Can-Jie Guo 0000-0001-5951-299X; Hai Li 0000-0002-2510-5103; Xiong Ma 0000-0002-2640-2708; Jing Hua 0000-0002-6100-9477.

Author contributions: Ni XX, Lian M, Wu HM, and Li XY contributed equally to this work, and collected and analyzed the data; Sheng L coordinated the research; Bao H and Xiao X performed the transient elastography and coordinated the liver biopsy; Miao Q contributed to histological examination; Ma X, Hua J, Li H, and Guo CJ analyzed the data; Hua J designed the study; Ni XX, Lian M, and Hua J wrote the manuscript; all authors have read and approved the final manuscript.

Supported by National Natural Science Foundation of China, No. 81470842 and No. 81770572.

Institutional review board statement: This study was reviewed and approved by the Ethics Committee of Renji Hospital.

Xi-Xi Ni, Hui-Min Wu, Xiao-Yun Li, Xiao Xiao, Jing Hua, Department of Gastroenterology and Hepatology, Renji Hospital, School of Medicine, Shanghai Jiao Tong University, Shanghai Institute of Digestive Disease, Shanghai 200127, China

Min Lian, Han Bao, Can-Jie Guo, Department of Gastroenterology and Hepatology, Renji Hospital, School of Medicine, Shanghai Jiao Tong University, Shanghai 200127, China

Li Sheng, Xiong Ma, School of Medicine, Shanghai Jiao Tong University, Shanghai Cancer Institute, Shanghai Institute of Digestive Disease, Shanghai 200127, China

Qi Miao, School of Medicine, Shanghai Jiao Tong University, Shanghai Institute of Digestive Disease, Shanghai 200127, China

Hai Li, Department of Gastroenterology, Renji Hospital, Shanghai Jiao Tong University School of Medicine, Shanghai 200127, China

Xiong Ma, Department of Gastroenterology, Renji Hospital, School of Medicine, Shanghai Jiao Tong University, Shanghai Institute of Digestive Disease, Shanghai 200001, China

Corresponding author: Jing Hua, MD, PhD, Professor, Department of Gastroenterology and Hepatology, Renji Hospital, School of Medicine, Shanghai Jiao Tong University, Shanghai Institute of Digestive Disease, No. 160 Pujian Road, Shanghai 200127, China.
hua_jing88@163.com

Abstract

BACKGROUND

Hepatic steatosis commonly occurs in some chronic liver diseases and may affect disease progression.

AIM

To investigate the performance of controlled attenuation parameter (CAP) for the diagnosis of hepatic steatosis in patients with autoimmune liver diseases (AILDs).

METHODS

Patients who were suspected of having AILDs and underwent liver biopsy were consistently enrolled. Liver stiffness measurement (LSM) and CAP were performed by transient elastography. The area under the receiver operating

Informed consent statement: Patients were not required to give informed consent to the study because the analysis used anonymous clinical data that were obtained after each patient agreed to treatment by written consent.

Conflict-of-interest statement: The authors have no financial relationships to disclose.

Data sharing statement: No additional data are available.

Open-Access: This article is an open-access article that was selected by an in-house editor and fully peer-reviewed by external reviewers. It is distributed in accordance with the Creative Commons Attribution NonCommercial (CC BY-NC 4.0) license, which permits others to distribute, remix, adapt, build upon this work non-commercially, and license their derivative works on different terms, provided the original work is properly cited and the use is non-commercial. See: http://creativecommons.org/Licenses/by-nc/4.0/

Manuscript source: Unsolicited manuscript

Specialty type: Gastroenterology and hepatology

Country/Territory of origin: China

Peer-review report's scientific quality classification

Grade A (Excellent): 0
Grade B (Very good): 0
Grade C (Good): C
Grade D (Fair): 0
Grade E (Poor): 0

Received: September 11, 2020
Peer-review started: September 11, 2020
First decision: November 23, 2020
Revised: December 1, 2020
Accepted: December 11, 2020
Article in press: December 11, 2020
Published online: January 7, 2021

P-Reviewer: Kita K
S-Editor: Huang P
L-Editor: Wang TQ
P-Editor: Li JH

characteristic (AUROC) curve was used to evaluate the performance of CAP for diagnosing hepatic steatosis compared with biopsy.

RESULTS

Among 190 patients with biopsy-proven hepatic steatosis, 69 were diagnosed with autoimmune hepatitis (AIH), 18 with primary biliary cholangitis (PBC), and 27 with AIH-PBC overlap syndrome. The AUROCs of CAP for the diagnosis of steatosis in AILDS were 0.878 (0.791-0.965) for S1, 0.764 (0.676-0.853) for S2, and 0.821 (0.716-0.926) for S3. The CAP value was significantly related to hepatic steatosis grade ($P < 0.001$). Among 69 patients with AIH, the median CAP score was 205.63 ± 47.36 dB/m for S0, 258.41 ± 42.83 dB/m for S1, 293.00 ± 37.18 dB/m for S2, and 313.60 ± 27.89 dB/m for S3. Compared with patients with nonalcoholic fatty liver disease (NAFLD) presenting with autoimmune markers, patients with AIH concomitant with NAFLD were much older and had higher serum IgG levels and LSM values.

CONCLUSION

CAP can be used as a noninvasive diagnostic method to evaluate hepatic steatosis in patients with AILDs. Determination of LSM combined with CAP may help to identify patients with AIH concomitant with NAFLD from those with NAFLD with autoimmune phenomena.

Key Words: Controlled attenuation parameter; Hepatic steatosis; Autoimmune liver diseases; Nonalcoholic fatty liver disease; Liver stiffness measurement; Autoimmune hepatitis

©The Author(s) 2021. Published by Baishideng Publishing Group Inc. All rights reserved.

Core Tip: This retrospective study determined that controlled attenuation parameter (CAP) could be used as a noninvasive diagnostic tool to evaluate hepatic steatosis effectively and accurately in patients with autoimmune liver diseases. Patients with autoimmune hepatitis concomitant with nonalcoholic fatty liver disease (NAFLD) had higher IgG levels and liver stiffness measurement values, while patients with NAFLD with autoimmune phenomena had higher gamma-glutamyl transferase levels and CAP values, which benefits the identification of these two kinds of patients.

Citation: Ni XX, Lian M, Wu HM, Li XY, Sheng L, Bao H, Miao Q, Xiao X, Guo CJ, Li H, Ma X, Hua J. Evaluation of controlled attenuation parameter in assessing hepatic steatosis in patients with autoimmune liver diseases. *World J Gastroenterol* 2021; 27(1): 80-91
URL: https://www.wjgnet.com/1007-9327/full/v27/i1/80.htm
DOI: https://dx.doi.org/10.3748/wjg.v27.i1.80

INTRODUCTION

Hepatic steatosis is the accumulation of lipids within hepatocytes and is considered pathologic when it affects more than 5% of hepatocytes[1]. The most common cause of steatosis is insulin resistance associated with nonalcoholic fatty liver disease (NAFLD)[2]. It also occurs in alcoholic liver disease and chronic viral hepatitis, defined as a "cofactor" capable of affecting disease progression and treatment perspectives[3]. Autoimmune liver diseases (AILDs) are a group of autoimmune diseases associated with the liver and are characterized by dysregulation of immune cell homeostasis and inflammation, including autoimmune hepatitis (AIH), primary biliary cholangitis (PBC), primary sclerosing cholangitis, and their overlapping subtypes[4,5]. When hepatic steatosis is present in subjects with AILDs, this coexisting scenario may cause a synergistic combination of steatosis, cellular adaptation, and oxidative damage that aggravates liver injury and affects the treatment effect[6]. Moreover, the standard regimen for AIH involves glucocorticoids[7], the long-term administration of which will further aggravate hepatic steatosis. However, the incidence of AILDs combined with hepatic steatosis has not been reported. Therefore, the evaluation of hepatic steatosis is

a component that cannot be ignored in the management of patients with AILDs.

Liver biopsy is considered the standard method for staging hepatic inflammation, steatosis, and fibrosis. Thus, it plays a vital role in the diagnosis and follow-up of AILDs[7,8]. However, liver biopsy is an invasive procedure, which bears a potential risk of severe complications and is of limited acceptance among patients. Furthermore, the severity of hepatic steatosis may change within weeks after treatment that cannot be sufficiently monitored by repetitive invasive procedures. Accordingly, noninvasive assessments are urgently needed[9].

The controlled attenuation parameter (CAP) measured by transient elastography (TE) is an easy and rapid noninvasive examination method for the detection of hepatic steatosis. It is based on the physical phenomenon that the amplitude of ultrasound waves is attenuated more quickly when they traverse across a steatotic liver[10,11]. TE can also quantify the speed of a mechanically induced shear wave in liver tissue and hence generate a parameter called liver stiffness measurement (LSM) to estimate liver fibrosis[12]. CAP is measured simultaneously with LSM, making it possible to assess hepatic steatosis and fibrosis at the same time. Studies with CAP have been performed in NAFLD, alcoholic liver disease, and viral hepatitis, but very few data are available on AILDs[13-15]. It has been showed that in patients with chronic viral hepatitis and advanced liver fibrosis, CAP performed better than ultrasound for assessing liver steatosis[16]. Besides, a recent meta-analysis showed that CAP diagnosed moderate and severe hepatic steatosis with diagnostic accuracies above 0.85 in patients with liver disease of mixed etiology. However, the analysis did not include patients with AILDs[17].

In this study, we assessed the performance of CAP for evaluating hepatic steatosis in AILDs to determine whether it could be regarded as a reliable tool to monitor disease course.

MATERIALS AND METHODS

Patients

Patients who were suspected of having AILDs and eventually underwent liver biopsy at Shanghai Jiao Tong University Renji Hospital were consistently enrolled from January 2016 to November 2018. A total of 800 patients were analyzed for steatosis in liver histology.

Diagnostic criteria

Diagnosis was made according to the diagnostic criteria described in the clinical practice guidelines for AIH, PBC, AIH-PBC overlap syndrome, and NAFLD. AIH[18] was diagnosed according to a simple score based on four measurements: Liver histology, autoantibody titers, gamma-globulin/IgG levels, and the absence of viral hepatitis. The diagnosis of PBC[19] required fulfilment of two or more of the following criteria: (1) Biochemical evidence of cholestasis based mainly on alkaline phosphatase (AKP) elevation; (2) Detection of anti-mitochondrial autoantibodies (AMA); and (3) Typical histologic evidence of nonsuppurative destructive cholangitis and destruction of interlobular bile ducts. AIH-PBC overlap syndrome[20] was diagnosed based on clinical, biochemical, serological, and histological features overlapping those of PBC and AIH. The diagnosis of NAFLD[21] required imaging or histological evidence of diffuse hepatic steatosis and ruling out other causes of hepatic steatosis, such as excessive alcohol consumption.

Histological examination

Percutaneous liver biopsy guided by ultrasound was performed under local anesthesia using a 16G disposable needle. Liver specimens at least 1 cm in length with eight complete portal tracts were included. The specimens were immediately fixed in 10% neutral formalin and embedded in paraffin. Hematoxylin and eosin staining was used to observe the morphology of the liver, and Masson's trichrome and reticulin staining was performed to detect fibrosis. One single experienced pathologist who was blinded to the patients' clinical data assessed liver histology using a METAVIR-derived scoring system. Hepatic steatosis was scored as S0: < 5%, S1: 5%-33%, S2: > 33%-66%, and S3: > 66%. Fibrosis was staged as follows: F0, no fibrosis; F1, portal fibrosis without septa; F2, portal and periportal fibrosis with few septa; F3, portal and periportal fibrosis with numerous septa without cirrhosis; and F4, cirrhosis. Hepatic inflammatory activity was graded as follows: A0, none; A1, mild; A2, moderate; and A3, severe.

Clinical measurements

Medical records of the patients who were finally included were reviewed, and clinical data and laboratory findings were collected and analyzed. Body mass index (BMI) was calculated. Laboratory evaluations included liver biochemistry [*i.e.*, alanine aminotransferase (ALT), aspartate aminotransferase, AKP, gamma-glutamyl transferase (GGT), total bilirubin, direct bilirubin, globulin, and albumin], serum immunoglobulins (IgG, IgM, and IgA), routine blood tests (white blood cell count and platelet count), and prothrombin time. Serum autoantibodies, including anti-nuclear antibody (ANA), AMA, and anti-smooth muscle actin antibody (ASMA), were detected by indirect immunofluorescence (Euroimmun AG, Hangzhou, China).

CAP and LSM by TE

TE measured with a FibroScan device and an M probe ultrasound transducer (Echosens, Paris, France) was performed in all patients who underwent liver biopsy on the same day. Subjects were placed in the supine position with the right arm in maximal abduction, and measurements were taken over the right hepatic lobe through an intercostal space. We obtained ten valid CAP and LSM measurements from each participant and considered LSM with an interquartile range ≤ 30% and a success rate ≥ 60% as reliable. The median CAP and LSM were taken as the estimates for hepatic steatosis and fibrosis, expressed in dB/m and kilopascals (kPa), respectively.

Statistical analysis

Data were analyzed using SPSS software version 22.0 (SPSS Inc, Chicago, IL, United States). Summary data are reported as the mean ± SD or median (interquartile range) according to distribution. Quantitative variables were compared using independent samples Student's *t*-test or one-way analysis of variance when appropriate. Spearman's rank correlation test was used to explore the correlation between CAP and hepatic steatosis grade. The diagnostic accuracy of CAP for the prediction of hepatic steatosis grade was calculated using a receiver operator characteristic (ROC) curve. Optimal CAP cut-off values for each steatosis stage were determined based on the highest combined sensitivity and specificity (Youden index). The area under the ROC curve (AUROC), sensitivity, specificity, positive predictive value, and negative predictive value for the predefined cut-off values were calculated. A P value < 0.05 was considered statistically significant.

RESULTS

Characteristics of the patients

In 800 patients with liver biopsy, a total of 190 patients were finally included in the study according to the existence of various grades of hepatic steatosis in liver histology, with a mean age of 46.36 ± 12.82 years, including 45 males (23.68%) and 145 females (76.32%). Among these patients, 69 were diagnosed with AIH, 18 with PBC, 27 with AIH-PBC overlap syndrome, 66 with NAFLD, and 10 with other liver diseases. In all patients, the prevalence of autoantibodies, including ANA, AMA, and ASMA, was 70.53%. The average BMI was 23.97 ± 2.69 kg/m^2.

Diagnostic accuracy of CAP to grade hepatic steatosis in patients with mixed etiology liver disease

In all 190 patients, the median CAP score was 270.17 ± 54.52 dB/m, and the median LSM score was 7.66 ± 5.57 kPa (Table 1). The distribution of the CAP value for each steatosis grade in all patients with mixed etiology liver disease is as follows. The median CAP score was 201.6 ± 46.78 dB/m for S0, 260.5 ± 47.92 dB/m for S1, 293.6 ± 40.13 dB/m for S2, and 307.4 ± 45.31 dB/m for S3. The CAP value was significantly related to hepatic steatosis grade (ρ = 0.549, P < 0.001) (Figure 1A).

The AUROCs of CAP for the diagnosis of steatosis were 0.883 (0.807-0.958) for S1, 0.772 (0.705-0.838) for S2, and 0.732 (0.640-0.824) for S3 (Figure 1B-D and Table 2). The optimal cut-off values of CAP for steatosis grades were 229 dB/m for S ≥ 1, 259 dB/m for S ≥ 2, and 283.5 dB/m for S3 with the highest combined sensitivity and specificity (Table 2).

Diagnostic accuracy of CAP for grading hepatic steatosis in AILDs

Next, we further assessed the performance of CAP for evaluating hepatic steatosis in AILDs. The median CAP score for each steatosis grade in AILDs was very similar to

Table 1 Baseline patient characteristics

Variable	All (*n* = 190)	AILDs (*n* = 114)	NAFLD (*n* = 66)
Age, yr	46.36 ± 12.82	48.72 ± 11.57	42.15 ± 13.80
Male sex, *n* (%)	45 (23.68)	23 (20.18)	18 (27.27)
BMI, kg/m^2	23.97 ± 2.69	24.33 ± 1.80	23.63 ± 2.34
Prevalence of autoantibodies, *n* (%)	134 (70.53)	89 (78.07)	37 (56.06)
Laboratory			
AST, U/L	63.96 ± 86.42	72.54 ± 102.23	54.6 ± 59.10
ALT, U/L	83.86 ± 86.42	81.98 ± 92.78	92.81 ± 78.67
LDH, U/L	182.70 ± 35.43	183.02 ± 37.39	182.64 ± 32.86
AKP, U/L	80.00 (63.00, 108.50)	85.00 (62.25, 129.5)	75.00 (64.00, 94.00)
GGT, U/L	103.67 ± 126.83	126.00 ± 151.92	76.82 ± 73.15
Total bilirubin, mg/dL	10.90 (8.10, 15.30)	11.20 (8.30, 16.70)	9.80 (6.95, 14.15)
Direct bilirubin, mg/dL	3.60 (2.80, 4.90)	3.70 (2.90, 5.70)	3.45 (2.52, 4.50)
Histological steatosis stage, *n* (%)			
S0 (< 5%)	22 (11.6)	20 (11.1)	0 (0.0)
S1 (5%-33%)	85 (44.7)	61 (33.9)	16 (24.2)
S2 (> 33%-66%)	55 (28.9)	28 (15.6)	27 (40.9)
S3 (> 66%)	28 (14.7)	5 (2.8)	23 (34.8)
Histological fibrosis stage, *n* (%)			
F0 (no fibrosis)	12 (6.3)	1 (0.9)	10 (15.2)
F1 (portal fibrosis without septa)	70 (36.8)	38 (33.3)	30 (45.5)
F2 (portal and periportal fibrosis with few septa)	64 (33.7)	40 (35.1)	18 (27.3)
F3 (portal and periportal fibrosis with numerous septa without cirrhosis)	35 (18.4)	26 (22.8)	8 (12.1)
F4 (cirrhosis)	9 (4.7)	9 (7.9)	0 (0.0)
CAP, dB/m	270.17 ± 54.52	261.73 ± 53.80	290.97 ± 50.68
LSM, kPa	7.66 ± 5.57	8.48 ± 6.50	6.61 ± 3.66

Distributions are expressed as the mean ± SD or median (interquartile range) or number (percentage). AIH: Autoimmune hepatitis; NAFLD: Nonalcoholic fatty liver disease; BMI: Body mass index; AKP: Alkaline phosphatase; ALT: Alanine aminotransferase; AST: Aspartate aminotransferase; CAP: Controlled attenuation parameter; GGT: Gamma-glutamyl transferase; LDH: Lactate dehydrogenase; LSM: Liver stiffness measurement.

that in all patients. The CAP value was also significantly related to hepatic steatosis grade (ρ = 0.553, P < 0.001) (Figure 2A). The AUROCs of CAP for the diagnosis of steatosis in AILDs were 0.878 (0.791-0.965) for S1, 0.764 (0.676-0.853) for S2, and 0.821 (0.716-0.926) for S3 (Figure 2D-F and Table 2). The optimal cut-off values of CAP for steatosis grades were 220.5 dB/m for S ≥ 1, 271.5 dB/m for S ≥ 2, and 283.5 dB/m for S3 (Table 2).

Considering the relatively high incidence and clinical significance of AIH, we focused on calculating the median CAP value for patients with AIH. Among 69 patients with AIH, the median CAP score was 205.63 ± 47.36 dB/m for S0, 258.41 ± 42.83 dB/m for S1, 293.00 ± 37.18 dB/m for S2, and 313.60 ± 27.89 dB/m for S3 (Figure 2B). Furthermore, there was no significant difference in the median CAP value between patients with AIH and NAFLD in each hepatic steatosis grade (Figure 2C).

Factors affecting the performance of CAP

Univariate and multivariate analyses showed that the CAP value was significantly correlated with BMI and hepatic steatosis (P < 0.001, P < 0.001). When patients were divided into three subgroups according to BMI < 24 kg/m^2, 24-27 kg/m^2, and BMI ≥ 27 kg/m^2, patients with BMI ≥ 27 kg/m^2 had a significantly higher CAP value than the

Table 2 Diagnostic performance of controlled attenuation parameter for assessment of hepatic steatosis in patients with mixed etiology liver disease and in patients with autoimmune liver diseases

Etiology	Grade	AUROC (95%CI)	Cut-off, dB/m (kPa)	Sensitivity	Specificity	PPV	NPV
Mixed etiology	S ≥ 1	0.883 (0.807-0.958)	229	0.852	0.714	0.960	0.375
	S ≥ 2	0.772 (0.705-0.838)	259	0.875	0.636	0.636	0.875
	S = 3	0.732 (0.640-0.824)	283.5	0.750	0.654	0.273	0.938
AILDs	S ≥ 1	0.878 (0.791-0.965)	220.5	0.874	0.737	0.937	0.538
	S ≥ 2	0.764 (0.676-0.853)	271.5	0.818	0.704	0.510	0.937
	S = 3	0.821 (0.716-0.926)	283.5	1.000	0.688	0.128	1.000

AUROC: Area under receiver operating characteristic; CAP: Controlled attenuation parameter; NPV: Negative predictive value; PPV: Positive predictive value.

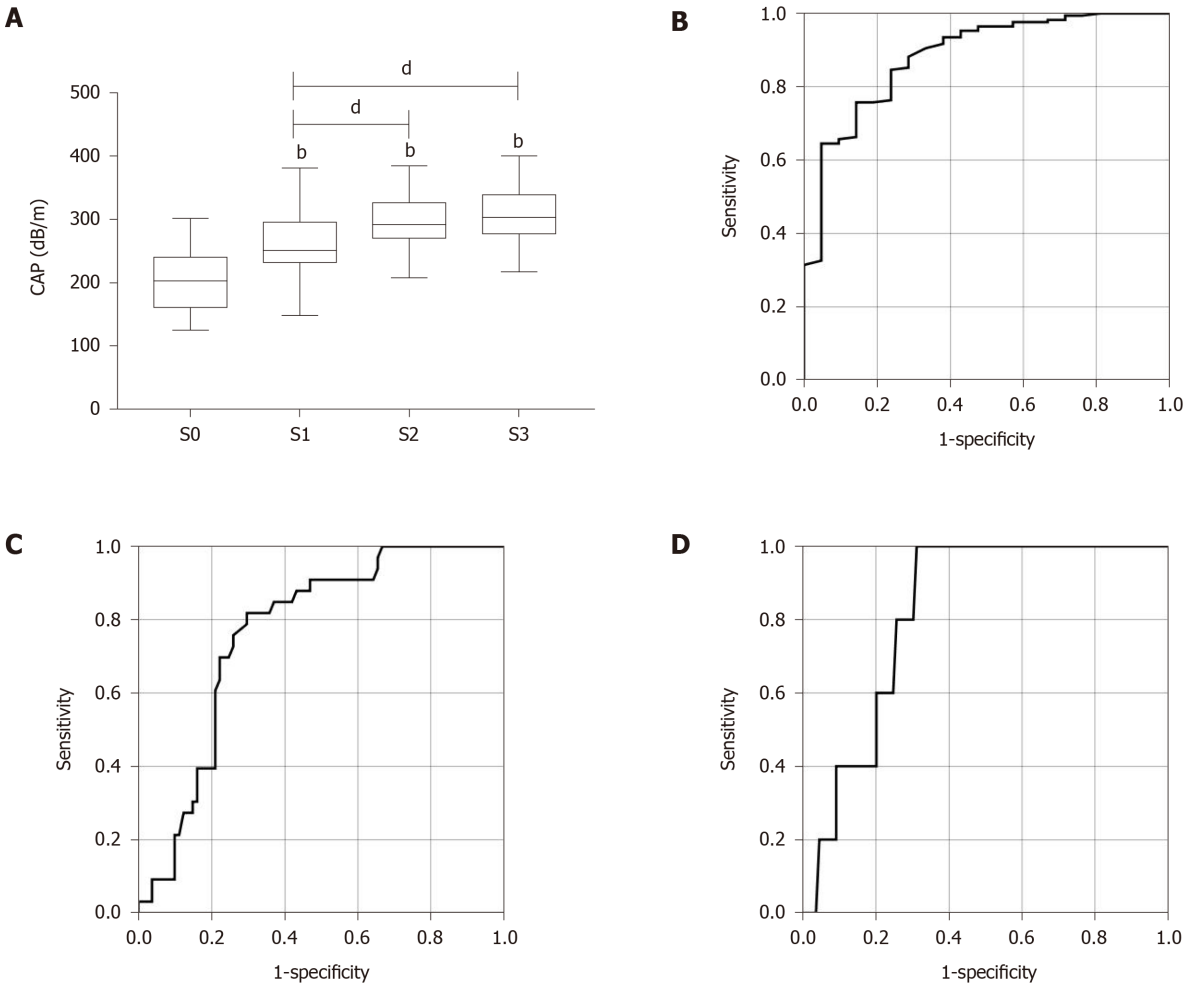


Figure 1 The receiver operator characteristic curve of controlled attenuation parameter for diagnosis of hepatic steatosis grade in patients with mixed etiology liver disease. A: Correlation between the controlled attenuation parameter (CAP) and the grade of hepatic steatosis (ρ = 0.549, P < 0.001); B-D: The receiver operator characteristic curve of CAP for diagnosis of (B) steatosis grade ≥ S1, (C) steatosis grade ≥ S2, and (D) steatosis grade ≥ S3 in patients with mixed etiology liver disease. ^{b}P < 0.01 *vs* S0; ^{d}P < 0.01. CAP: Controlled attenuation parameter.

other two groups (Figure 3). The performance of CAP was stable across fibrosis stages. In addition, traditional factors affecting the performance of LSM, such as bilirubin and serum ALT level, did not affect the performance of CAP (data not shown).

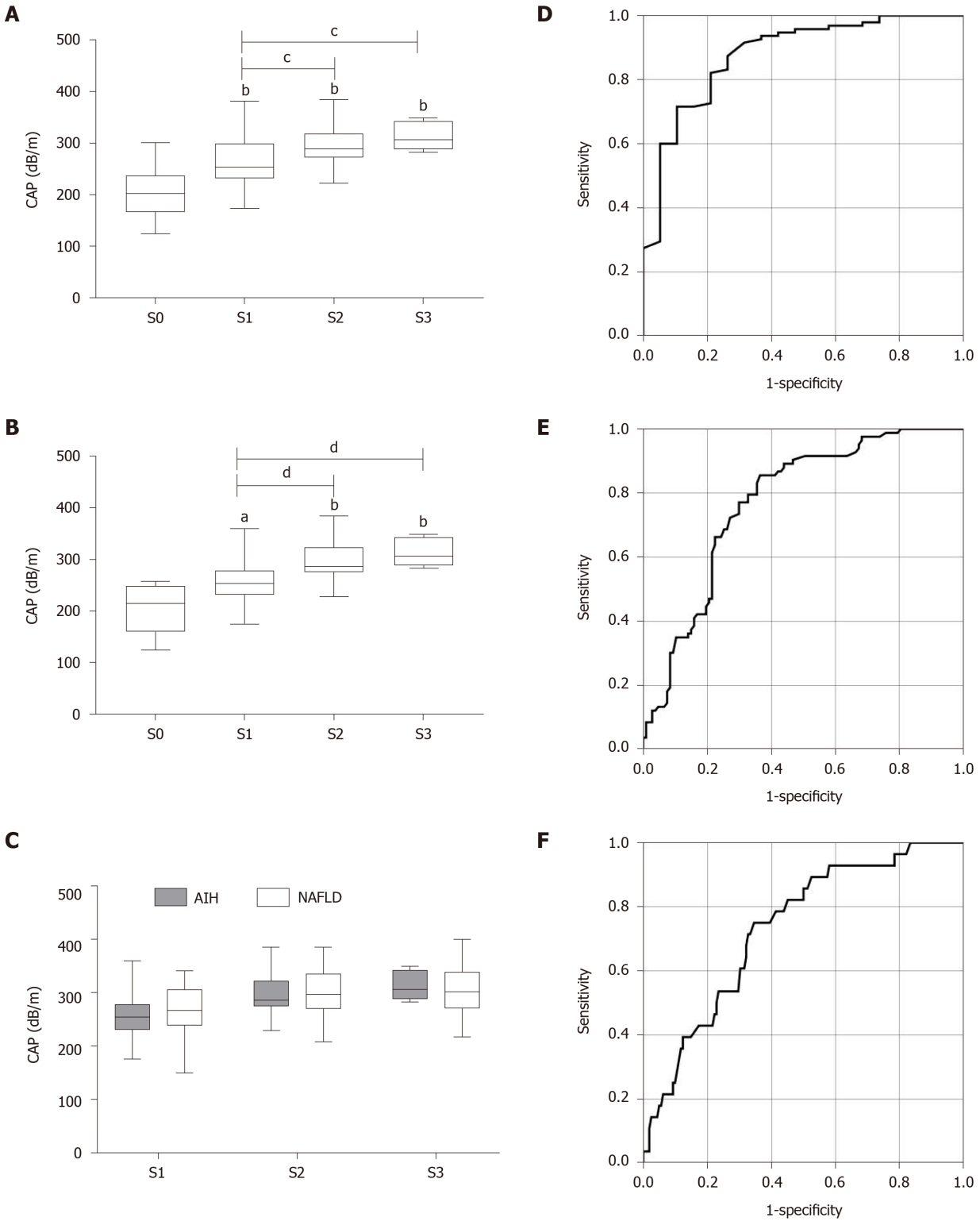


Figure 2 Controlled attenuation parameter value in different hepatic steatosis grades and etiologies and the receiver operator characteristic curve of controlled attenuation parameter for diagnosis of hepatic steatosis grade in patients with autoimmune liver diseases. A and B: Correlation between the controlled attenuation parameter (CAP) and the grade of hepatic steatosis in patients with (A) autoimmune liver diseases (AILDs) or (B) autoimmune hepatitis (AIH); C: Comparison of the CAP value in patients with AIH and nonalcoholic fatty liver disease in different hepatic steatosis grades; D-F: The receiver operator characteristic curve of CAP for diagnosis of (D) steatosis grade ≥ S1, (E) steatosis grade ≥ S2, and (F) steatosis grade ≥ S3 in patients with AILDs. $^{a}P < 0.05$; $^{b}P < 0.01$ *vs* S0; $^{c}P < 0.05$; $^{d}P < 0.01$. CAP: Controlled attenuation parameter; AIH: Autoimmune hepatitis; NAFLD: Nonalcoholic fatty liver disease.

Comparative analysis of patients with AIH concomitant with NAFLD and patients with NAFLD with autoimmune phenomena

In this study, we defined patients with histologic evidence of both AIH and NAFLD as patients with AIH concomitant with NAFLD and patients with histologic evidence of NAFLD and positive autoantibodies or elevated IgG or IgM as patients with NAFLD with autoimmune phenomena.

The results showed that patients with AIH concomitant with NAFLD were older and had higher IgG levels and LSM values than patients with NAFLD with autoimmune phenomena. In contrast, the GGT level and CAP value were higher in patients with NAFLD with autoimmune phenomena (Table 3). Interestingly, when we compared the LSM value in each steatosis grade of the two groups, patients with AIH concomitant with NAFLD were higher in both S1 and S3 grades, suggesting a potential diagnostic marker for patients with AIH concomitant with NAFLD.

DISCUSSION

The prevalence of hepatic steatosis is rising in association with the global increase in obesity. The overall prevalence of NAFLD over the past two decades is 29.6%, up to 46.4% in heavy drinkers and 50%-80% in the obese population[22]. Close attention was paid to the potential interactions between chronic liver disease and hepatic steatosis with the growing NAFLD prevalence. However, the particular role of hepatic steatosis has been less of a focus of attention in AILDs than in other chronic liver diseases, partly due to the lack of proper evaluation tools. Herein, we demonstrated that CAP measured by TE could be used as a noninvasive diagnostic tool to evaluate hepatic steatosis effectively and accurately in patients with AILDs.

In this study, we confirmed that CAP correlated well with hepatic steatosis on histology, and we were able to establish cut-off values with high diagnostic accuracies. The cut-off values for each steatosis grade in patients with mixed etiology liver disease were similar to the previously proposed cut-off values in an individual patient data meta-analysis (229 dB/m for S ≥ 1, 258 dB/m for S ≥ 2)[17]. However, the accuracy of CAP in separating steatosis grades 2 and 3 was suboptimal, which was similar to prior reports[13]. Nevertheless, in clinical practice, the identification of moderate steatosis is of greater utility than distinctions between S2 and S3, and thus, the Youden cut-off for S2 of 258 dB/m is sufficient.

Given the high risk of glycolipid metabolism disorder and increased possibility of hepatic steatosis in patients with AIH due to the long-term administration of immunosuppressive drugs such as glucocorticoids, the noninvasive method may be particularly suited for monitoring current hepatic histological changes and therapeutic effects[7,23]. Here, we found that CAP was closely related to hepatic steatosis in patients with AILDs, as well as patients with AIH. Surprisingly, the performance of CAP for the diagnosis of hepatic steatosis grade in patients with AIH remained stable, which supported that CAP can be used as a noninvasive and reliable diagnostic method to monitor steatosis and disease course.

Notably, we found a strong correlation between CAP and BMI, in agreement with previous studies[24,25]. The skin capsular distance (SCD) has also been shown to be associated with increased CAP values[26]. Since BMI and SCD are both surrogate markers of adiposity, it is difficult to determine the mechanism underlying the association. However, we did not find a correlation between CAP and LSM as reported for patients with NAFLD[27].

It is found in the clinic that elevated immunoglobulin and/or positive autoantibodies may occur during the progression of NAFLD, which we defined as "patients with NAFLD with autoimmune phenomena" here. On the other hand, patients with AIH can also have NAFLD, thereby affecting the diagnosis and treatment. In this study, we found that patients with AIH concomitant with NAFLD were older and had higher IgG levels and LSM values than patients with NAFLD with autoimmune phenomena, which could be related to the repeated and long-term course of AILDs. In contrast, the GGT level was higher in patients with NAFLD with autoimmune phenomena. Therefore, serum IgG and GGT levels and the LSM value can benefit the identification of these two kinds of patients.

There are a few limitations in this study. First, our study is retrospective in nature due to the data collection despite the "blinded" analysis of histology. Second, the sample size is limited due to the low prevalence of AILDs, especially PBC and AIH-PBC overlap syndrome. Third, for historical reasons, CAP was measured only using the M probe. However, a recent multicenter prospective study has shown that there

Table 3 Comparative analysis of patients with autoimmune hepatitis concomitant with nonalcoholic fatty liver disease and patients with nonalcoholic fatty liver disease with autoimmune phenomena

Variable	Patients with AIH concomitant with NAFLD (*n* = 61)	Patients with NAFLD with autoimmune phenomena (*n* = 34)	*P* value
Age, yr	52.05 ± 11.11	43.68 ± 13.71	< 0.001
Male sex, *n* (%)	13 (21.3)	6 (17.6)	
BMI, kg/m^2	24.21 ± 3.10	24.65 ± 2.02	
Laboratory			
AST, U/L	55.03 ± 47.31	50.03 ± 29.26	
ALT, U/L	66.62 ± 74.94	86.01 ± 62.59	
AKP, U/L	63.00 (45.00, 84.00)	75.00 (54.00, 87.00)	
GGT, U/L	49.27 ± 32.24	69.26 ± 44.07	< 0.05
Total bilirubin, mg/dL	10.20 (8.60, 14.10)	10.25 (7.40, 13.67)	
Direct bilirubin, mg/dL	4.20 (3.20, 5.00)	3.70 (2.92, 4.65)	
IgG	15.60 ± 4.57	13.81 ± 2.67	< 0.05
IgM	1.18 ± 0.45	1.28 ± 0.57	
Histological steatosis stage, *n* (%)			
S1	39 (63.9)	8 (23.5)	
S2	17 (27.9)	10 (29.4)	
S3	5 (8.2)	16 (47.1)	
Histological fibrosis stage, *n* (%)			
F1	17 (27.9)	6 (17.6)	
F2	22 (36.1)	14 (41.2)	
F3	16 (26.2)	11 (32.4)	
F4	6 (9.8)	3 (8.8)	
CAP, dB/m	272.57 ± 44.39	293.41 ± 51.04	< 0.05
LSM in total, kPa	9.34 ± 7.14	6.49 ± 2.44	< 0.05
In steatosis S1	9.19 ± 8.11	5.28 ± 1.88	< 0.05
In steatosis S2	7.80 ± 3.47	6.31 ± 2.18	
In steatosis S3	15.76 ± 6.25	7.20 ± 2.69	< 0.01

Distributions are expressed as the mean ± SD or median [interquartile range] or number (percentage). AKP: Alkaline phosphatase; ALT: Alanine aminotransferase; AST: Aspartate aminotransferase; BMI: Body mass index; CAP: Controlled attenuation parameter; GGT: Gamma-glutamyl transferase; LSM: Liver stiffness measurement; AIH: Autoimmune hepatitis; NAFLD: Nonalcoholic fatty liver.

was no significant difference in diagnostic accuracy between the two probes to diagnose liver fibrosis and steatosis in patients with NAFLD[28].

CONCLUSION

In summary, this study revealed that CAP could be used as a noninvasive diagnostic method to evaluate hepatic steatosis in patients with AILDs. Determination of LSM combined with CAP may help to identify patients with AIH concomitant with NAFLD from those with NAFLD with autoimmune phenomena.

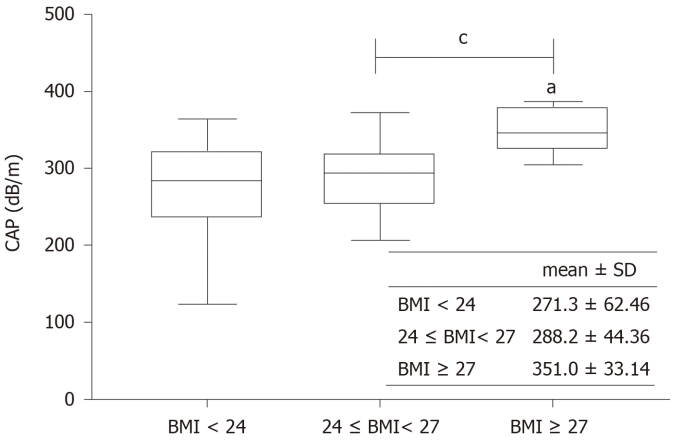


Figure 3 Controlled attenuation parameter in patients with different body mass indexes. [a]*P* < 0.05 *vs* S0; [c]*P* < 0.05. CAP: Controlled attenuation parameter; BMI: Body mass index.

ARTICLE HIGHLIGHTS

Research background

The controlled attenuation parameter (CAP) assesses hepatic steatosis with high diagnostic accuracies among several chronic liver diseases. However, it has not been studied in patients with autoimmune liver diseases (AILDs).

Research motivation

This study aimed to investigate the performance of CAP for the diagnosis of hepatic steatosis in patients with AILDs.

Research objectives

We evaluated the performance and usefulness of CAP for detection of hepatic steatosis in patients with AILDs.

Research methods

The area under the receiver operating characteristic curve was used to evaluate the performance of CAP for diagnosing hepatic steatosis compared with biopsy. Optimal CAP cut-off values were determined based on the highest combined sensitivity and specificity.

Research results

CAP can accurately detect hepatic steatosis as a noninvasive method in patients with AILDs. Compared with patients with nonalcoholic fatty liver disease (NAFLD) presenting with autoimmune markers, patients with autoimmune hepatitis (AIH) concomitant with NAFLD were much older and had higher serum IgG levels and liver stiffness measurement (LSM) values.

Research conclusions

CAP can be used as a noninvasive diagnostic method to evaluate hepatic steatosis in patients with AILDs. Determination of LSM combined with CAP may help to identify patients with AIH concomitant with NAFLD from patients with NAFLD with autoimmune phenomena.

Research perspectives

Larger multicenter studies using both M and XL probes are needed to confirm our results.

REFERENCES

1 **Yeh MM**, Brunt EM. Pathological features of fatty liver disease. *Gastroenterology* 2014; **147**: 754-764 [PMID: 25109884 DOI: 10.1053/j.gastro.2014.07.056]

2 **Sasso M**, Miette V, Sandrin L, Beaugrand M. The controlled attenuation parameter (CAP): a novel tool for the non-invasive evaluation of steatosis using Fibroscan. *Clin Res Hepatol Gastroenterol* 2012; **36**: 13-20 [PMID: 21920839 DOI: 10.1016/j.clinre.2011.08.001]

3 **Persico M**, Iolascon A. Steatosis as a co-factor in chronic liver diseases. *World J Gastroenterol* 2010; **16**: 1171-1176 [PMID: 20222159 DOI: 10.3748/wjg.v16.i10.1171]

4 **Tanaka A**, Mori M, Matsumoto K, Ohira H, Tazuma S, Takikawa H. Increase trend in the prevalence and male-to-female ratio of primary biliary cholangitis, autoimmune hepatitis, and primary sclerosing cholangitis in Japan. *Hepatol Res* 2019; **49**: 881-889 [PMID: 30932290 DOI: 10.1111/hepr.13342]

5 **Beringer A**, Miossec P. IL-17 and IL-17-producing cells and liver diseases, with focus on autoimmune liver diseases. *Autoimmun Rev* 2018; **17**: 1176-1185 [PMID: 30321671 DOI: 10.1016/j.autrev.2018.06.008]

6 **Powell EE**, Jonsson JR, Clouston AD. Steatosis: co-factor in other liver diseases. *Hepatology* 2005; **42**: 5-13 [PMID: 15962320 DOI: 10.1002/hep.20750]

7 **European Association for the Study of the Liver**. EASL Clinical Practice Guidelines: Autoimmune hepatitis. *J Hepatol* 2015; **63**: 971-1004 [PMID: 26341719 DOI: 10.1016/j.jhep.2015.06.030]

8 **European Association for the Study of the Liver**. European Association for the Study of the Liver. EASL Clinical Practice Guidelines: The diagnosis and management of patients with primary biliary cholangitis. *J Hepatol* 2017; **67**: 145-172 [PMID: 28427765 DOI: 10.1016/j.jhep.2017.03.022]

9 **Castera L**, Vilgrain V, Angulo P. Noninvasive evaluation of NAFLD. *Nat Rev Gastroenterol Hepatol* 2013; **10**: 666-675 [PMID: 24061203 DOI: 10.1038/nrgastro.2013.175]

10 **Sasso M**, Beaugrand M, de Ledinghen V, Douvin C, Marcellin P, Poupon R, Sandrin L, Miette V. Controlled attenuation parameter (CAP): a novel VCTE™ guided ultrasonic attenuation measurement for the evaluation of hepatic steatosis: preliminary study and validation in a cohort of patients with chronic liver disease from various causes. *Ultrasound Med Biol* 2010; **36**: 1825-1835 [PMID: 20870345 DOI: 10.1016/j.ultrasmedbio.2010.07.005]

11 **Sasso M**, Audière S, Kemgang A, Gaouar F, Corpechot C, Chazouillères O, Fournier C, Golsztejn O, Prince S, Menu Y, Sandrin L, Miette V. Liver Steatosis Assessed by Controlled Attenuation Parameter (CAP) Measured with the XL Probe of the FibroScan: A Pilot Study Assessing Diagnostic Accuracy. *Ultrasound Med Biol* 2016; **42**: 92-103 [PMID: 26386476 DOI: 10.1016/j.ultrasmedbio.2015.08.008]

12 **Sandrin L**, Fourquet B, Hasquenoph JM, Yon S, Fournier C, Mal F, Christidis C, Ziol M, Poulet B, Kazemi F, Beaugrand M, Palau R. Transient elastography: a new noninvasive method for assessment of hepatic fibrosis. *Ultrasound Med Biol* 2003; **29**: 1705-1713 [PMID: 14698338 DOI: 10.1016/j.ultrasmedbio.2003.07.001]

13 **Eddowes PJ**, Sasso M, Allison M, Tsochatzis E, Anstee QM, Sheridan D, Guha IN, Cobbold JF, Deeks JJ, Paradis V, Bedossa P, Newsome PN. Accuracy of FibroScan Controlled Attenuation Parameter and Liver Stiffness Measurement in Assessing Steatosis and Fibrosis in Patients With Nonalcoholic Fatty Liver Disease. *Gastroenterology* 2019; **156**: 1717-1730 [PMID: 30689971 DOI: 10.1053/j.gastro.2019.01.042]

14 **Seto WK**, Hui RWH, Mak LY, Fung J, Cheung KS, Liu KSH, Wong DK, Lai CL, Yuen MF. Association Between Hepatic Steatosis, Measured by Controlled Attenuation Parameter, and Fibrosis Burden in Chronic Hepatitis B. *Clin Gastroenterol Hepatol* 2018; **16**: 575-583. e2 [PMID: 28970146 DOI: 10.1016/j.cgh.2017.09.044]

15 **Thiele M**, Rausch V, Fluhr G, Kjærgaard M, Piecha F, Mueller J, Straub BK, Lupşor-Platon M, De-Ledinghen V, Seitz HK, Detlefsen S, Madsen B, Krag A, Mueller S. Controlled attenuation parameter and alcoholic hepatic steatosis: Diagnostic accuracy and role of alcohol detoxification. *J Hepatol* 2018; **68**: 1025-1032 [PMID: 29343427 DOI: 10.1016/j.jhep.2017.12.029]

16 **Ferraioli G**, Tinelli C, De Silvestri A, Lissandrin R, Above E, Dellafiore C, Poma G, Di Gregorio M, Maiocchi L, Maserati R, Filice C. The clinical value of controlled attenuation parameter for the noninvasive assessment of liver steatosis. *Liver Int* 2016; **36**: 1860-1866 [PMID: 27439331 DOI: 10.1111/liv.13207]

17 **Karlas T**, Petroff D, Sasso M, Fan JG, Mi YQ, de Lédinghen V, Kumar M, Lupsor-Platon M, Han KH, Cardoso AC, Ferraioli G, Chan WK, Wong VW, Myers RP, Chayama K, Friedrich-Rust M, Beaugrand M, Shen F, Hiriart JB, Sarin SK, Badea R, Jung KS, Marcellin P, Filice C, Mahadeva S, Wong GL, Crotty P, Masaki K, Bojunga J, Bedossa P, Keim V, Wiegand J. Individual patient data meta-analysis of controlled attenuation parameter (CAP) technology for assessing steatosis. *J Hepatol* 2017; **66**: 1022-1030 [PMID: 28039099 DOI: 10.1016/j.jhep.2016.12.022]

18 **Hennes EM**, Zeniya M, Czaja AJ, Parés A, Dalekos GN, Krawitt EL, Bittencourt PL, Porta G, Boberg KM, Hofer H, Bianchi FB, Shibata M, Schramm C, Eisenmann de Torres B, Galle PR, McFarlane I, Dienes HP, Lohse AW; International Autoimmune Hepatitis Group. Simplified criteria for the diagnosis of autoimmune hepatitis. *Hepatology* 2008; **48**: 169-176 [PMID: 18537184 DOI: 10.1002/hep.22322]

19 **Lindor KD**, Gershwin ME, Poupon R, Kaplan M, Bergasa NV, Heathcote EJ; American Association for Study of Liver Diseases. Primary biliary cirrhosis. *Hepatology* 2009; **50**: 291-308 [PMID: 19554543 DOI: 10.1002/hep.22906]

20 **Chazouillères O**, Wendum D, Serfaty L, Montembault S, Rosmorduc O, Poupon R. Primary biliary cirrhosis-autoimmune hepatitis overlap syndrome: clinical features and response to therapy. *Hepatology* 1998; **28**: 296-301 [PMID: 9695990 DOI: 10.1002/hep.510280203]

21 **National Workshop on Fatty Liver and Alcoholic Liver Disease CSoH**; Chinese Medical

Association. Guidelines of prevention and treatment for nonalcoholic fatty liver disease: a 2018 update. *Linchuang Gandan Bing Zazhi* 2018; **34**: 947-957

22 **Zhou J**, Zhou F, Wang W, Zhang XJ, Ji YX, Zhang P, She ZG, Zhu L, Cai J, Li H. Epidemiological Features of NAFLD From 1999 to 2018 in China. *Hepatology* 2020; **71**: 1851-1864 [PMID: 32012320 DOI: 10.1002/hep.31150]

23 **Mieli-Vergani G**, Vergani D, Czaja AJ, Manns MP, Krawitt EL, Vierling JM, Lohse AW, Montano-Loza AJ. Autoimmune hepatitis. *Nat Rev Dis Primers* 2018; **4**: 18017 [PMID: 29644994 DOI: 10.1038/nrdp.2018.17]

24 **Wong VW**, Petta S, Hiriart JB, Cammà C, Wong GL, Marra F, Vergniol J, Chan AW, Tuttolomondo A, Merrouche W, Chan HL, Le Bail B, Arena U, Craxì A, de Lédinghen V. Validity criteria for the diagnosis of fatty liver by M probe-based controlled attenuation parameter. *J Hepatol* 2017; **67**: 577-584 [PMID: 28506907 DOI: 10.1016/j.jhep.2017.05.005]

25 **de Lédinghen V**, Vergniol J, Capdepont M, Chermak F, Hiriart JB, Cassinotto C, Merrouche W, Foucher J, Brigitte le B. Controlled attenuation parameter (CAP) for the diagnosis of steatosis: a prospective study of 5323 examinations. *J Hepatol* 2014; **60**: 1026-1031 [PMID: 24378529 DOI: 10.1016/j.jhep.2013.12.018]

26 **Shen F**, Zheng RD, Shi JP, Mi YQ, Chen GF, Hu X, Liu YG, Wang XY, Pan Q, Chen GY, Chen JN, Xu L, Zhang RN, Xu LM, Fan JG. Impact of skin capsular distance on the performance of controlled attenuation parameter in patients with chronic liver disease. *Liver Int* 2015; **35**: 2392-2400 [PMID: 25689614 DOI: 10.1111/liv.12809]

27 **Petta S**, Wong VW, Cammà C, Hiriart JB, Wong GL, Marra F, Vergniol J, Chan AW, Di Marco V, Merrouche W, Chan HL, Barbara M, Le-Bail B, Arena U, Craxì A, de Ledinghen V. Improved noninvasive prediction of liver fibrosis by liver stiffness measurement in patients with nonalcoholic fatty liver disease accounting for controlled attenuation parameter values. *Hepatology* 2017; **65**: 1145-1155 [PMID: 27639088 DOI: 10.1002/hep.28843]

28 **Oeda S**, Takahashi H, Imajo K, Seko Y, Ogawa Y, Moriguchi M, Yoneda M, Anzai K, Aishima S, Kage M, Itoh Y, Nakajima A, Eguchi Y. Accuracy of liver stiffness measurement and controlled attenuation parameter using FibroScan® M/XL probes to diagnose liver fibrosis and steatosis in patients with nonalcoholic fatty liver disease: a multicenter prospective study. *J Gastroenterol* 2020; **55**: 428-440 [PMID: 31654131 DOI: 10.1007/s00535-019-01635-0]

World Journal of Gastroenterology

Submit a Manuscript: https://www.f6publishing.com

World J Gastroenterol 2021 January 7; 27(1): 92-106

DOI: 10.3748/wjg.v27.i1.92

ISSN 1007-9327 (print) ISSN 2219-2840 (online)

ORIGINAL ARTICLE

Retrospective Study

Valuable clinical indicators for identifying infantile-onset inflammatory bowel disease patients with monogenic diseases

Wen Su, Yi Yu, Xu Xu, Xin-Qiong Wang, Jie-Bin Huang, Chun-Di Xu, Yuan Xiao

ORCID number: Wen Su 0000-0002-7853-4606; Yi Yu 0000-0002-5680-1195; Xu Xu 0000-0002-5720-945X; Xin-Qiong Wang 0000-0003-0057-3653; Jie-Bin Huang 0000-0001-9362-3511; Chun-Di Xu 0000-0002-2314-9188; Yuan Xiao 0000-0002-4927-8199.

Author contributions: Su W and Yu Y contributed equally to this work; Su W and Yu Y were in charge of the data analysis and writing; Xu X and Wang XQ contributed to data collection; Huang JB contributed to literature search and figure preparation; Xu CD and Xiao Y contributed to study design and data interpretation, and they contributed equally to this work; all authors have read and approved the final manuscript.

Supported by Scientific Research Fund of Shanghai Municipal Health Commission, No. 201640368; National Natural Science Foundation of China, No. 81741103; and The Shanghai Plan for Women and Children's Health Service Capacity Construction (Enhancing the Service Capacity of Shanghai Women and Children Health Care Institutions).

Institutional review board statement: This study was approved by the ethics committee of Ruijin Hospital, Shanghai

Wen Su, Yi Yu, Xu Xu, Xin-Qiong Wang, Jie-Bin Huang, Chun-Di Xu, Yuan Xiao, Department of Pediatrics, Ruijin Hospital, Shanghai Jiao Tong University, School of Medicine, Shanghai 200025, China

Corresponding author: Yuan Xiao, MD, PhD, Associate Chief Physician, Doctor, Department of Pediatrics, Ruijin Hospital, Shanghai Jiao Tong University, School of Medicine, No. 197 Ruijin 2 Road, Shanghai 200025, China. yxiao.penicilinum@gmail.com

Abstract

BACKGROUND

Infantile-onset inflammatory bowel disease (IO-IBD) occurs in very young children and causes severe clinical manifestations, which has poor responses to traditional inflammatory bowel disease (IBD) treatments. At present, there are no simple and reliable laboratory indicators for early screening IO-IBD patients, especially those in whom the disease is caused by monogenic diseases.

AIM

To search for valuable indicators for early identifying IO-IBD patients, especially those in whom the disease is caused by monogenic diseases.

METHODS

A retrospective analysis was performed in 73 patients with IO-IBD admitted to our hospital in the past 5 years. Based on the next-generation sequencing results, they were divided into a monogenic IBD group (M-IBD) and a non-monogenic IBD group (NM-IBD). Forty age-matched patients with allergic proctocolitis (AP) were included in a control group. The clinical manifestations and the inflammatory factors in peripheral blood were evaluated. Logistic regression analysis and receiver operating characteristic (ROC) curve analysis were used to identify the screening factors and cut-off values of IO-IBD as well as monogenic IO-IBD, respectively.

RESULTS

Among the 44 M-IBD patients, 35 carried *IL-10RA* mutations, and the most common mutations were c.301C>T (p.R101W, 30/70) and the c.537G>A (p.T179T, 17/70). Patients with higher serum tumor necrosis factor (TNF)-α value were more likely to have IBD [odds ratio (OR) = 1.25, 95% confidence interval (CI): 1.05-1.50, P = 0.013], while higher serum albumin level was associated with lower risk of IBD (OR = 0.86, 95%CI: 0.74-1.00, P = 0.048). The cut-off values of TNF-α and

Jiaotong University School of Medicine.

Informed consent statement: All guardians of the enrolled pediatric patients who experienced the gene test signed an informed consent form.

Conflict-of-interest statement: The authors have no conflicts of interest to declare.

Data sharing statement: No additional data are available.

Open-Access: This article is an open-access article that was selected by an in-house editor and fully peer-reviewed by external reviewers. It is distributed in accordance with the Creative Commons Attribution NonCommercial (CC BY-NC 4.0) license, which permits others to distribute, remix, adapt, build upon this work non-commercially, and license their derivative works on different terms, provided the original work is properly cited and the use is non-commercial. See: http://creativecommons.org/Licenses/by-nc/4.0/

Manuscript source: Unsolicited manuscript

Specialty type: Gastroenterology and hepatology

Country/Territory of origin: China

Peer-review report's scientific quality classification
Grade A (Excellent): 0
Grade B (Very good): B
Grade C (Good): 0
Grade D (Fair): 0
Grade E (Poor): 0

Received: October 16, 2020
Peer-review started: October 16, 2020
First decision: November 23, 2020
Revised: December 2, 2020
Accepted: December 11, 2020
Article in press: December 11, 2020
Published online: January 7, 2021

P-Reviewer: Tanabe S
S-Editor: Gao CC
L-Editor: Wang TQ

albumin were 17.40 pg/mL (sensitivity: 0.78; specificity: 0.88) and 36.50 g/L (sensitivity: 0.80; specificity: 0.90), respectively. The increased ferritin level was indicative of a genetic mutation in IO-IBD patients. Its cut-off value was 28.20 ng/mL (sensitivity: 0.93; specificity: 0.92). When interleukin (IL)-10 level was higher than 33.05 pg/mL (sensitivity: 1.00; specificity: 0.84), or the onset age was earlier than 0.21 mo (sensitivity: 0.82; specificity: 0.94), the presence of disease-causing mutations in *IL-10RA* in IO-IBD patients was strongly suggested.

CONCLUSION
Serum TNF-α and albumin level could differentiate IO-IBD patients from allergic proctocolitis patients, and serum ferritin and IL-10 levels are useful indicators for early diagnosing monogenic IO-IBD.

Key Words: Infantile-onset inflammatory bowel disease; Immunodeficiency; Clinical indicators; Interleukin 10; Ferritin; *IL10RA*

©The Author(s) 2021. Published by Baishideng Publishing Group Inc. All rights reserved.

Core Tip: It is very important to identify infantile-onset inflammatory bowel disease (IO-IBD) patients, especially those in whom the disease is caused by monogenic diseases, as early as possible because these patients have poor responses to traditional inflammatory bowel disease treatments. However, there are no simple and reliable laboratory indicators for early differential diagnosis. This is the first study focusing on the laboratory indicators that could be used to distinguish O-IBD patients from allergic enteritis patients and screening IO-IBD patients with monogenic diseases. We believe that these results may be valuable in the initial investigations and diagnosis of IO-IBD.

Citation: Su W, Yu Y, Xu X, Wang XQ, Huang JB, Xu CD, Xiao Y. Valuable clinical indicators for identifying infantile-onset inflammatory bowel disease patients with monogenic diseases. *World J Gastroenterol* 2021; 27(1): 92-106
URL: https://www.wjgnet.com/1007-9327/full/v27/i1/92.htm
DOI: https://dx.doi.org/10.3748/wjg.v27.i1.92

INTRODUCTION

Inflammatory bowel disease (IBD) is a chronic recurrent gastrointestinal inflammatory disease, which could be classified into Crohn's disease (CD), ulcerative colitis (UC), and IBD-unclassified (IBD-U)[1]. Common clinical manifestations include diarrhea, hematochezia, abdominal pain, growth retardation, and weight loss. Many studies have reported that the phenotypic characteristics are different in very early onset-IBD (VEO-IBD, the onset age was younger than 6 years old) children from those in adolescent-onset or adult-onset IBD patients[2]. An increasing number of studies[3] have indicated the presence of monogenic defects in VEO-IBD children, especially in infantile patients (< 2 years old). Gene sequencing, especially next generation-sequencing (NGS), could help to find the mutations to explain the cause of the disease; however, this method has high costs, and is time-consuming and not suitable for regular application at the early stage of the disease, particularly in economically underdeveloped areas. Besides, many variants of uncertain significance (VUS) after NGS was applied need laboratory indicators to verify their pathogenicity. However, there have been no reliable clinical indicators reported to identify pediatric IBD patients early, especially those who have potential gene mutations. In this retrospective study, we intended to search for early diagnostic indicators for IO-IBD children with or without the gene mutation, in order to shorten the diagnosis time, reduce medical costs, simplify the analysis of NGS, and administer targeted intervention as early as possible.

P-Editor: Wang LL

MATERIALS AND METHODS

Study participants and groups

This study was approved by the ethics committee of Ruijin Hospital, Shanghai Jiaotong University School of Medicine. All guardians of the enrolled pediatric patients who experienced the gene test signed an informed consent form. This study retrospectively analyzed 73 IO-IBD patients with a disease onset before 2 years of age who were admitted to the Department of Pediatrics, Ruijin Hospital, Shanghai Jiaotong University School of Medicine from January 2014 to February 2019. The diagnostic criteria were based on the Consensus on the Diagnosis and Management of Pediatric Inflammatory Bowel Disease[4] formulated by the Chinese Society of Pediatric Gastroenterology, the Chinese Medical Association. According to the NGS results, the patients were divided into either a monogenic IBD (M-IBD) group, which comprised IO-IBD patients caused by Mendelian diseases, or a non-monogenic IBD (NM-IBD) group, which comprised IO-IBD patients without disease-causing gene mutations. Forty age-matched children who were hospitalized due to diarrhea and hematochezia during the same period and ultimately diagnosed with allergic proctocolitis (AP) were enrolled in the study as a control group.

Clinical data analysis

The clinical data of all patients were collected, including sex, age of onset, body weight and height on admission, average daily frequency of diarrhea, hematochezia, perianal lesions, recurrent fever, and treatment outcomes (remission, non-remission, and death). The results of complete blood count, C-reactive protein (CRP), erythrocyte sedimentation rate (ESR), serum albumin, and serum iron levels were collected and analyzed. Tumor necrosis factor (TNF)-α, interleukin (IL)-6, and IL-10 levels were determined using chemiluminescence immunoassays with a commercial kit (Siemens). The serum ferritin concentration was detected using a double-site enzyme immunoassay with a commercial ferritin kit (ACCES).

Next-generation sequencing and validation

Peripheral blood was collected from all IO-IBD patients for the genetic test. A FlexiGene DNA Kit (Qiagen GmbH, D-40724 Hilden) was used to extract DNA according to the manufacturer's instructions. NGS of targeted genes including primary immunodeficiency diseases and congenital diarrheal diseases (20 cases) was performed by Beijing Mygeno Gene Technology Co., Ltd and whole-exome sequencing (53 cases) was performed by Beijing Berry Genomics Co., Ltd. For the mutations found *via* NGS, Sanger sequencing was used to retest the corresponding gene sequences of the patients and their parents to verify and confirm the genetic origin. The genetic variations were identified using online databases, such as the Single Nucleotide Polymorphism Database (dbSNP), Clinvar, the Human Gene Mutation Database (HGMD), the 1000 Genomes Project, and Online Mendelian Inheritance in Man (OMIM), to verify whether they were the known pathogenic mutations. For novel mutations not included in the databases, pathogenicity was further evaluated according to the American College of Medical Genetics and Genomics (ACMG) guidelines[5].

Statistical analysis

Z scores for height and weight were calculated using WHO Anthro V3.2.2 software. All data were statistically analyzed using IBM SPSS Statistics 25.0. Measurement data with a normal distribution are expressed as the mean ± standard deviation (SD), and nonnormally distributed data are expressed as the median and interquartile range (IQR). Data with a normal distribution and homogeneity of variance were analyzed using ANOVA analysis, and abnormally distributed data were analyzed by nonparametric Kruskal-Wallis analysis. Categorical data were analyzed using the chi-square test, or Fisher's exact Chi-square test. Multivariate binary logistic regression analysis was performed to identify risk factors for IO-IBD and monogenic IO-IBD. Receiver operating characteristic (ROC) curve analysis was performed to assess the diagnostic value of the identified indicators. *P* values were adjusted using the Bonferroni method for pairwise comparison. $P < 0.05$ was considered statistically significant. The statistical methods of this study were reviewed by Li J from the Clinical Research Center, Ruijin Hospital, Shanghai Jiao Tong University School of Medicine.

RESULTS

Genotypes of IO-IBD patients

Among the 73 IO-IBD patients, 24 did not carry any disease-causing mutations in IBD-associated genes, and 49 had the gene mutations related to the disease. Among 49 patients with mutations, 39 carried *IL-10RA* mutations, 2 carried *CYBB* mutations, and *WAS*, *IKBKG*, *SLC37A4*, *CD40LG*, *LIG4*, *CARD11*, *PIK3CD*, and *CXCR4* mutations were observed in one patient each (Table 1). Four of them carried the *IL-10RA* heterozygous mutation which did not meet the criteria of Mendelian disease, and one of them had a heterozygous *CXCR4* mutation which was inherited from his father with ankylosing spondylitis and recognized as a VUS according to the ACMG guidelines because of absence of typical manifestations of autosome dominant WHIM syndrome. Therefore, these five patients were included in the NM-IBD group. There were 14 different missense mutations found in *IL-10RA* among M-IBD patients. Two variations, the c.301C>T (p.R101W) and the c.537G>A (p.T179T), were considered hotspot mutations in the M-IBD patient cohort, the mutation frequencies were 42.86% (30/70) and 24.29% (17/70) respectively. We also found nine novel mutations: c.109G>T, c.302G>A, c.569T>G, and c.787C>T in *IL-10RA* gene; c.674+2T>C in *CYBB* gene; c.267delC in *CD40LG* gene; c.1144_1145delCT in *LIG4* gene; c.155T>C in *CARD11* gene; and c.1001G>A in *CXCR4* gene. The amino acid substitutions and pathogenicity of these variations that were assessed according to the ACMG guidelines are summarized in Table 1.

Clinical characteristics

As shown in Table 2, the proportions of male patients in the AP group, the M-IBD group, and the NM-IBD group was higher than those of female patients; however, no significant difference was observed among the three groups. The median onset age of patients in the M-IBD group was 0.51 (0.04-1.79) mo, which was much younger than that in the AP group [4.44 (1.25-11.76) mo; $P = 0.003$] and the NM-IBD group [3.99 (3-9) mo; $P = 0.001$]. The proportions of all IO-IBD patients who had severe diarrhea (more than 8 times/d, 86.4% in the M-IBD group and 58.6% in the NM-IBD group) and recurrent fever (63.6% in the M-IBD group and 41.4% in the NM-IBD group) were significantly higher than those in AP patients (25% of patients had severe diarrhea [$P < 0.001$] and 5% of patients had a recurrent fever [$P = 0.01$]). The percentages of the patients who had severe diarrhea and perianal lesions in the M-IBD group (86.4% and 79.5%, respectively) were much higher than those in the NM-IBD group (58.6% [$P = 0.007$] and 24.1% [$P = 0.005$]). The anthropometric results showed that the *Z* scores for body weight (-1.95 ± 0.26 for the M-IBD group and -1.15 ± 0.29 for the NM-IBD group) and body height (-1.95 ± 0.25 for the M-IBD group and -1.32 ± 0.31 for the NM-IBD group) of the IBD patients were all lower than those of the children in the AP group (-0.05 ± 0.21 for weight [$P < 0.001$] and 0.17 ± 0.19 for height [$P < 0.001$]), while there was no significant difference between the M-IBD group and the NM-IBD group. Regarding the outcomes of treatment, mortality in the M-IBD group was significantly higher than that in the NM-IBD group (20.5% *vs* 3.4%, $P = 0.001$), whereas no death occurred in the AP group.

As shown in Table 3, the blood test results showed that peripheral white blood cell count (WBC), platelet count (PLT), CRP, ESR, TNF-α, and IL-6 levels in the IO-IBD group were significantly higher than those in the AP group ($P < 0.01$ for all), while serum albumin level was lower than that in the AP group ($P < 0.001$). Differences in serum iron levels were not significant among the three groups. Notably, serum IL-10 [85.50 (42.75-127.25) pg/mL] and ferritin [55.90 (36.10-231.20) ng/mL] levels in the M-IBD group were significantly higher than those in the AP group [IL-10: 5.00 (5.00-5.00) pg/mL, $P < 0.001$; ferritin: 22.90 (14.90-37.05) ng/mL, $P = 0.002$] and in the NM-IBD group [IL-10: 6.37 (5.00-14.80) pg/mL, $P < 0.001$; ferritin: 15.30 (9.40-27.60) ng/mL, $P < 0.001$].

Binary logistic regression analysis and ROC curve analysis

Clinical indicators for risk of IO-IBD: Binary logistic regression analysis was performed for the parameters with significant differences between the AP group and the IO-IBD group [including diarrhea (> 8 times/d), recurrent fever, *Z*-scores for weight, *Z*-scores for height, WBC, hemoglobin (Hb), PLT, CRP, ESR, TNF-α, IL-6, and albumin levels]. The results showed that increased peripheral WBC (odds ratio [OR] = 1.19, 95% confidence interval [CI]: 1.01-1.40, $P = 0.040$), ESR (OR = 1.10, 95%CI: 1.01-1.20, $P = 0.037$) and levels of TNF-α (OR =1.25, 95%CI: 1.05-1.50, $P = 0.013$), as well as reduced albumin levels were risk factors (OR = 0.86, 95%CI: 0.74-1.00, $P = 0.048$) for

Table 1 Genotypes of 49 infantile-onset inflammatory bowel disease patients

Patient	Gene	Variant (allele 1)	Amino acid	ACMG (P/LP)	Variant (allele 2)	Amino acid	ACMG (P/LP)
1	*IL10RA*	c.301C>T	R101W	P (PS1+PS3+PM1+PM2+PP3+PP4)	c.301C>T	R101W	P (PS1+PS3+PM1+PM2+PP3+PP4)
2	*IL10RA*	c.299T>G	V100G	P (PS1+PS3+PM2+PP3+PP4)	c.301C>T	R101W	P (PS1+PS3+PM1+PM2+PP3+PP4)
3	*IL10RA*	c.191A>G	Y64C	LP (PM1+PM2+PM3+PP3+PP4)	c.537G>A	T179T	P (PS1+PS3+PM2+PP3+PP4)
4	*IL10RA*	c.301C>T	R101W	P (PS1+PS3+PM1+PM2+PP3+PP4)	c.537G>A	T179T	P (PS1+PS3+PM2+PP3+PP4)
5	*IL10RA*	c.301C>T	R101W	P (PS1+PS3+PM1+PM2+PP3+PP4)	c.301C>T	R101W	P (PS1+PS3+PM1+PM2+PP3+PP4)
6	*IL10RA*	c.493C>T	R165X	P (PVS1+PS1+PM2+PP4)	c.301C>T	R101W	P (PS1+PS3+PM1+PM2+PP3+PP4)
7	*IL10RA*	c.301C>T	R101W	P (PS1+PS3+PM1+PM2+PP3+PP4)	c.537G>A	T179T	P (PS1+PS3+PM2+PP3+PP4)
8	*IL10RA*	c.350G>A	R117H	P (PS1+PM1+PM2+PP3+PP4)	c.493C>T	R165X	P (PVS1+PS1+PM2+PP4)
9	*IL10RA*	c.301C>T	R101W	P (PS1+PS3+PM1+PM2+PP3+PP4)	c.436delC	P146fs	P (PVS1+PS1+PM2+PP4)
10	*IL10RA*	c.301C>T	R101W	P (PS1+PS3+PM1+PM2+PP3+PP4)	c.537G>A	T179T	P (PS1+PS3+PM2+PP3+PP4)
11	*IL10RA*	c.421G>A	G141R	P (PS1+PM2+PM3+PP3+PP4)	c.537G>A	T179T	P (PS1+PS3+PM2+PP3+PP4)
12	*IL10RA*	c.301C>T	R101W	P (PS1+PS3+PM1+PM2+PP3+PP4)	c.301C>T	R101W	P (PS1+PS3+PM1+PM2+PP3+PP4)
13	*IL10RA*	c.301C>T	R101W	P (PS1+PS3+PM1+PM2+PP3+PP4)	c.350G>A	R117H	P (PS1+PM1+PM2+PP3+PP4)
14	*IL10RA*	c.537G>A	T179T	P (PS1+PS3+PM2+PP3+PP4)	c.537G>A	T179T	P (PS1+PS3+PM2+PP3+PP4)
15	*IL10RA*	c.301C>T	R101W	P (PS1+PS3+PM1+PM2+PP3+PP4)	c.537G>A	T179T	P (PS1+PS3+PM2+PP3+PP4)
16	*IL10RA*	c.99G>A	W33X	P (PVS1+PS1+PM2+PP4)	c.301C>T	R101W	P (PS1+PS3+PM1+PM2+PP3+PP4)
17	*IL10RA*	c.493C>T	R165X	P (PVS1+PS1+PM2+PP4)	c.493C>T	R165X	P (PVS1+PS1+PM2+PP4)
18	*IL10RA*	c.109G>T	E37X	LP (PVS1+PM2+PM3+PP4)	c.301C>T	R101W	P (PS1+PS3+PM1+PM2+PP3+PP4)
19	*IL10RA*	c.301C>T	R101W	P (PS1+PS3+PM1+PM2+PP3+PP4)	c.537G>A	T179T	P (PS1+PS3+PM2+PP3+PP4)
20	*IL10RA*	c.301C>T	R101W	P (PS1+PS3+PM1+PM2+PP3+PP4)	c.537G>A	T179T	P (PS1+PS3+PM2+PP3+PP4)
21	*IL10RA*	c.301C>T	R101W	P (PS1+PS3+PM1+PM2+PP3+PP4)	c.537G>A	T179T	P (PS1+PS3+PM2+PP3+PP4)
22	*IL10RA*	c.301C>T	R101W	P (PS1+PS3+PM1+PM2+PP3+PP4)	c.350G>A	R117H	P (PS1+PM1+PM2+PP3+PP4)
23	*IL10RA*	c.99G>A	W33X	P (PVS1+PS1+PM2+PP4)	c.299T>G	V100G	P (PS1+PS3+PM2+PP3+PP4)
24	*IL10RA*	c.301C>T	R101W	P (PS1+PS3+PM1+PM2+PP3+PP4)	c.537G>A	T179T	P (PS1+PS3+PM2+PP3+PP4)
25	*IL10RA*	c.301C>T	R101W	P (PS1+PS3+PM1+PM2+PP3+PP4)	c.537G>A	T179T	P (PS1+PS3+PM2+PP3+PP4)
26	*IL10RA*	c.301C>T	R101W	P(PS1+PS3+PM1+PM2+PP3+PP4)	c.493C>T	R165X	P (PVS1+PS1+PM2+PP4)
27	*IL10RA*	c.301C>T	R101W	P (PS1+PS3+PM1+PM2+PP3+PP4)	c.537G>A	T179T	P (PS1+PS3+PM2+PP3+PP4)
28	*IL10RA*	c.493C>T	R165X	P (PVS1+PS1+PM2+PP4)	c.537G>A	T179T	P (PS1+PS3+PM2+PP3+PP4)
29	*IL10RA*	c.301C>T	R101W	P (PS1+PS3+PM1+PM2+PP3+PP4)	c.301C>T	R101W	P (PS1+PS3+PM1+PM2+PP3+PP4)
30	*IL10RA*	c.302G>A	R101Q	LP (PM1+PM2+PM3+PM5+PP3+PP4)	c.349C>T	R117C	P (PS1+PM1+PM2+PP3+PP4)
31	*IL10RA*	c.301C>T	R101W	P (PS1+PS3+PM1+PM2+PP3+PP4)	c.301C>T	R101W	P (PS1+PS3+PM1+PM2+PP3+PP4)
32	*IL10RA*	c.301C>T	R101W	P (PS1+PS3+PM1+PM2+PP3+PP4)	c.301C>T	R101W	P (PS1+PS3+PM1+PM2+PP3+PP4)
33	*IL10RA*	c.299T>G	V100G	P (PS1+PS3+PM2+PP3+PP4)	c.569T>G	F190C	LP (PS1+PM2+PM3_VeryStrong+PP3+PP4)
34	*IL10RA*	c.537G>A	T179T	P (PS1+PS3+PM2+PP3+PP4)	c.537G>A	T179T	P (PS1+PS3+PM2+PP3+PP4)
35	*IL10RA*	c.299T>G	V100G	P (PS1+PS3+PM2+PP3+PP4)	c.299T>G	V100G	P (PS1+PS3+PM2+PP3+PP4)
36	*WAS*	IVS8: +3- +6 GAGT del		LP (PS1+PM2+PP3+PP4)			
37	*IKBKG*	c.1217A>T	D406V	P (PS1+PM1+PM2+PP3+PP4)			
38	*SLC37A4*	c.310 ins T		P (PVS1+PM2+PP4)	c.1014-1120 del107		P (PVS1+PM2+PP4)

39	*CYBB*	c.674+2T>C		P (PVS1+PM2+PP4)			
40	*CYBB*	c.1272G>A	W424X	P (PVS1+PS1+PM2+PP4)			
41	*CD40LG*	c.267delC	Q90Sfs*6	LP (PVS1+PM2+PP4)			
42	*LIG4*	c.833G>T	R278L	LP (PM1+PM2+PM3+PM5+PP3+PP4)	c.1144_1145delCT	L382Efs*5	LP (PVS1+PS1+PM2+PP4)
43	*CARD11*	c.155T>C	I52T	LP (PS2+PM2+PP4)			
44	*PIK3CD*	c.3061G>A	E1021K	P (PS1+PS3+PM2+PP3+PP4)			
45	*IL10RA*	c.350G>A	R117H	P (PS1+PM1+PM2+PP3+PP4)			
46	*IL10RA*	c.537G>A	T179T	P (PS1+PS3+PM2+PP3+PP4)			
47	*IL10RA*	c.787C>T	R263X	LP (PVS1+PM2+PP4)			
48	*IL10RA*	c.301C>T	R101W	P (PS1+PS3+PM1+PM2+PP3+PP4)			
49	*CXCR4*	c.1001G>A	R334Q	VUS (PM2+PP3+PP4:BS4)			

ACMG: American College of Medical Genetics and Genomics; P/LP: Pathogenic/likely pathogenic; VUS: Variants of uncertain significance.

Table 2 Clinical features and growth parameters among three groups of patients

	AP	M-IBD	NM-IBD	*P* value
Total number	40	44	29	
Male (%)	25 (62.50)	27 (61.36)	21 (72.41)	0.591
Median onset age (mo, IQR)	4.44 (1.25,11.76)	0.51 (0.04,1.79)[1]	3.99 (3.00,9.00)	< 0.001
Diarrhea (≥ 8 times/d, %)	10 (25.00)[1]	38 (86.40)[1]	17 (58.60)	< 0.001
Diarrhea with blood (%)	30 (75.00)	29 (65.90)	24 (82.80)	0.320
Perianal disease (%)	0 (0)	35 (79.54)[1]	7 (24.14)	0.005
Fever (%)	2 (5.00)[1]	28 (63.63)	12 (41.38)	< 0.001
Death (%)	0 (0.00)	9 (20.45)	1 (3.45)[2]	0.001
Z scores for weight (mean ± SD)	-0.05 ± 0.21[1]	-1.95 ± 0.26	-1.15 ± 0.29	< 0.001
Z scores for height (mean ± SD)	0.19 ± 0.19[1]	-1.95 ± 0.25	-1.32 ± 0.31	< 0.001
Z scores for BMI (mean ± SD)	-0.21 ± 0.24[2]	-1.30 ± 0.28	-0.52 ± 0.27	0.026

[1]Compared with the other two groups, adjusted *P* value < 0.05.
[2]Compared with the monogenic inflammatory bowel disease (M-IBD) group, adjusted *P* value < 0.05. AP: Allergic proctocolitis; M-IBD: Monogenic inflammatory bowel disease; NM-IBD: Non-monogenic inflammatory bowel disease; IQR: Interquartile range; SD: Standard deviation; BMI: Body mass index.

the diagnosis of IO-IBD (Table 4). We further investigated these four indicators using ROC curve analysis to explore their diagnostic value. The areas under the curves (AUCs) and the cut-off values are shown in Figure 1A and B. For WBC, the AUC was 0.78 (95%CI: 0.69-0.86, $P < 0.001$) and the cut-off value was 11.96 × 10^9/L (sensitivity: 0.66; specificity: 0.88). For ESR, the AUC was 0.81 (95%CI: 0.73-0.89, $P < 0.001$), and the cut-off value was 12.50 mm/h (sensitivity: 0.70; specificity: 0.90). For TNF-α, the AUC was 0.80 (95%CI: 0.72-0.89, $P < 0.001$) and the cut-off value was 17.40 pg/mL (sensitivity: 0.78; specificity: 0.88). For albumin, the AUC was 0.88 (95%CI: 0.81-0.94, $P < 0.001$), and the cut-off value was 36.50 g/L (sensitivity: 0.80; specificity: 0.90). Based on the results, WBC and ESR had a low sensitivity for recognizing IO-IBD. While TNF-α and albumin level had a higher sensitivity and specificity, and we speculated they may be used for early identifying IO-IBD patients.

Clinical indicators for risk of M-IBD: Binary logistic regression analysis was performed using the parameters with significant differences between the M-IBD group and the NM-IBD group [including median onset age, diarrhea (> 8 times/d), perianal disease, CRP, IL-10, and ferritin levels]. The results showed that very early onset age

Table 3 Results of blood test and inflammatory factors among three groups of patients (median, interquartile range)

	AP	M-IBD	NM-IBD	*P* value
WBC (× 10^9)	8.77 (6.78, 10.75)[1]	14.88 (9.84, 19.37)	13.77 (8.87,18.51)	< 0.001
Hemoglobin (mg/L)	119 (115, 126)[1]	98 (90, 113)	100 (80.50,116)	< 0.001
PLT (× 10^9)	304 (254, 383)[1]	447 (306.75, 591.50)	477 (323.50, 601.50)	0.002
CRP (mg/L)	1 (0.20, 1.00)[1]	48 (7.98, 75.23)[1]	21 (1.00, 44.35)	< 0.001
ESR (mm/h)	6 (4, 8)[1]	18.50 (8, 39)	21 (6, 42)	< 0.001
TNF-α (pg/mL)	14.60 (10.68, 17.03)[1]	21.50 (17.58, 27.88)	22.90 (14.48, 61.28)	< 0.001
IL-6 (pg/mL)	2.85 (2.00, 3.35)[1]	21.00 (10.20, 50.30)	14.55 (6.81, 30.00)	< 0.001
IL-10 (pg/mL)	500 (5, 5)	85.50 (42.75, 127.25)[1]	6.37 (5.00, 14.80)	< 0.001
Ferritin (ng/mL)	22.90 (14.90, 37.05)	55.90 (36.10, 231.20)[1]	15.50 (10.60, 27.72)	< 0.001
Albumin (g/L)	41 (38, 43)[1]	31 (27, 35)	33 (27.00, 36.50)	< 0.001
Serum iron (μmol/L)	8.00 (5.90, 10.20)	3.90 (2.60, 6.88)	5.70 (4.35, 11.38)	0.069

[1]Compared with the other two groups, adjusted *P* value < 0.05. AP: Allergic proctocolitis; M-IBD: Monogenic inflammatory bowel disease; NM-IBD: Non-monogenic inflammatory bowel disease; WBC: White blood cells; PLT: Platelets; CRP: C-reactive protein; ESR: Erythrocyte sedimentation rate; TNF: Tumor necrosis factor; IL: Interleukin.

Table 4 Binary logistic analysis for identifying risk factors for infantile-onset inflammatory bowel disease

	AP (median, IQR)	IO-IBD (median, IQR)	Adjusted OR (95%CI)	*P* value
WBC (× 10^9)	8.77 (6.78, 10.75)	14.12 (8.85, 18.27)	1.19 (1.01, 1.40)	0.040
ESR (mm/h)	6 (4, 8)	19.00 (8.00, 39.00)	1.10 (1.01, 1.20)	0.037
TNF-α (pg/mL)	14.60 (10.68, 17.03)	21.65 (17.33, 29.45)	1.25 (1.05, 1.50)	0.013
Albumin (g/L)	41 (38, 43)	32 (27, 36)	0.86 (0.74, 1.00)	0.048

Binary logistic analysis showed that white blood cell (WBC) count, erythrocyte sedimentation rate (ESR), tumor necrosis factor (TNF)-α, and albumin in peripheral blood could be used to identify the infantile-onset inflammatory bowel disease from AP if a child had diarrhea and hematochezia in early childhood. Higher WBC, ESR, and TNF-α, as well as lower level of albumin suggested a higher probability of inflammatory bowel disease. AP: Allergic proctocolitis; IO-IBD: Infantile-onset inflammatory bowel disease; IQR: Interquartile range; OR: Odds ratio; CI: Confidence interval; WBC: White blood cells; ESR: Erythrocyte sedimentation rate; TNF: Tumor necrosis factor.

(OR = 3.47, 95%CI: 1.29-9.29, *P* = 0.013], presence of perianal diseases (OR = 11.42, 95%CI: 1.71-76.23, *P* = 0.012), and high levels of serum ferritin (OR = 1.14, 95%CI: 1.06-1.24, *P* = 0.001) and IL-10 (OR = 1.04, 95%CI: 1.01-1.08, *P* = 0.005) were the main risk factors for M-IBD diagnosis (Table 5). Because the *IL-10RA* mutations in this study accounted for a dominant proportion (79.6%) in the M-IBD group, to avoid bias caused by sample selection, we further compared the above high-risk factors among patients with *IL-10RA* mutations or non-*IL-10RA* mutations in the M-IBD group, and those without any disease-causing mutations in the NM-IBD group. The results showed that only serum ferritin could discriminate M-IBD and NM-IBD regardless of genotypes. The level of serum ferritin was significantly lower in the NM-IBD group than in the other two groups (Table 6) and could be used as an indicator for recognizing IO-IBD children with genetic mutations. The ROC curve analysis was also performed to explore the indicators for the diagnosis of M-IBD. Using gene sequencing results as the gold standard, all IO-IBD patients were included in the analysis. The AUC of ferritin for diagnosing M-IBD was 0.94 (95%CI: 0.87-1.00, *P* < 0.001), with a cut-off value of 28.20 ng/mL (sensitivity: 0.93; specificity: 0.92; Figure 1C), which showed high diagnostic value. Besides, we further analyzed the value of serum IL-10 level and onset age for early noticing *IL-10RA* mutation in M-IBD patients. The AUC for IL-10 was 0.91 (95%CI: 0.86-0.99, *P* < 0.001), and the cut-off value was 33.05 pg/mL (sensitivity: 1.00; specificity: 0.84); the AUC for onset age was 0.87 (95%CI: 0.78-0.96, *P* < 0.001), and the cut-off value was 0.21 mo (sensitivity: 0.82; specificity: 0.94; Figure 1D and E). These results indicated that the two indicators had high diagnostic value and may be

Table 5 Binary logistic analysis for identifying risk factors for monogenic inflammatory bowel disease

	M-IBD (median, IQR)	NM-IBD (median, IQR)	Ajusted OR (95%CI)	*P* value
Ferritin (ng/mL)	55.90 (36.10, 231.20)	15.30 (9.40, 27.60)	1.14 (1.06, 1.24)	0.001
IL-10 (pg/mL)	85.20 (43.30, 126.50)	5.00 (5.00, 9.11)	1.04 (1.01, 1.08)	0.005
Median onset age (mo)	0.51 (0.04, 1.79)	3.99 (3.00, 9.00)	3.47 (1.29, 9.29)	0.013
Perianal disease (%)	35 (79.50)	7 (24.10)	11.42 (1.71, 76.23)	0.012

Binary logistic analysis showed that higher levels of ferritin and interleukin (IL)-10 in peripheral blood, earlier onset age, and presence of perianal disease suggested that inflammatory bowel disease children may have the gene mutation. However, most of the mutations (79.6%) in this study occurred in *IL-10RA*, and in order to avoid the bias, we did further analyses as showed in Table 6. M-IBD: Monogenic inflammatory bowel disease; NM-IBD: Non-monogenic inflammatory bowel disease; IL: Interleukin; IQR: Interquartile range; OR: Odds ratio; CI: Confidence interval.

Table 6 Comparison of risk factors among infantile-onset inflammatory bowel disease patients with or without *IL-10RA* mutation and non-monogenic inflammatory bowel disease (median, interquartile range)

	IL-10RA M-IBD	Non-*IL-10RA* M-IBD	NM-IBD	*P* value
Ferritin (ng/mL)	55.90 (53.12, 74.73)	45.25 (16.58, 68.70)	15.30 (14.55, 17.95)[1]	< 0.001
IL-10 (pg/mL)	85.20 (66.20, 125.00)[1]	8.90 (5.00, 85.20)	5.00 (5.00, 9.11)	< 0.001
Median onset age (mo)	0.04 (0.00, 0.08)[1]	2 (0.41, 4.08)	3.99 (3, 9)	< 0.001
Perianal disease (%)	32 (91.43)[1]	3 (33.33)	7 (24.14)	0.002

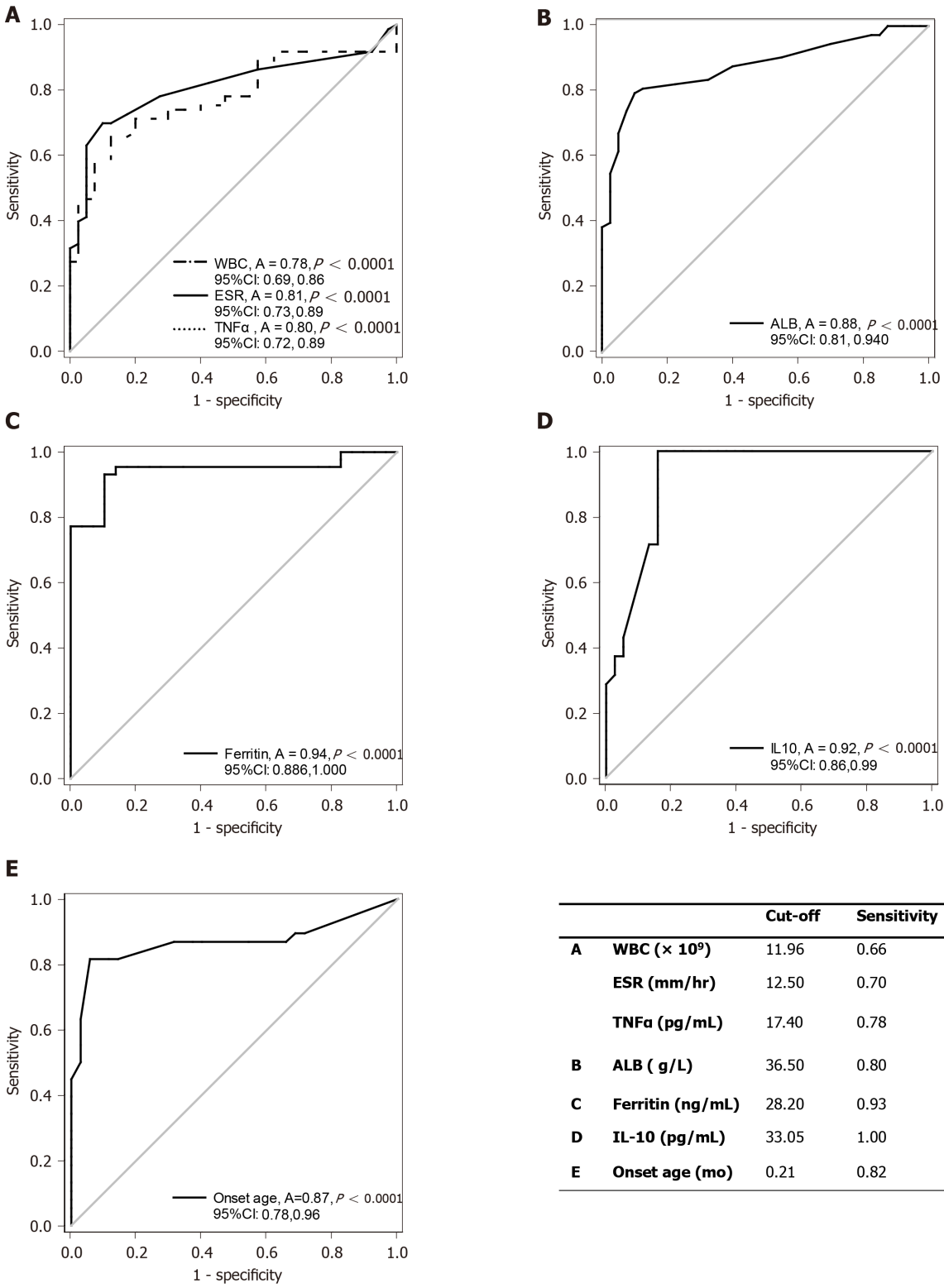
[1]Compared with the other two groups, adjusted *P* value < 0.01. M-IBD: Monogenic inflammatory bowel disease; NM-IBD: Non-monogenic inflammatory bowel disease; IL: Interleukin.

used in clinical practice. All above results suggested that, when serum ferritin levels were higher than 28.20 ng/mL, it might indicate the existence of pathogenic gene mutations in IO-IBD patients. If the infant got IO-IBD within 1 wk after the birth or their serum IL-10 levels were higher than 33.05 pg/mL, it might strongly suggest the presence of *IL-10RA* gene mutations.

DISCUSSION

Approximately 15% of pediatric patients were categorized as having VEO-IBD[2], and approximately 1% of pediatric patients developed symptoms during infancy (IO-IBD). Over the past decade, the prevalence of VEO-IBD had increased by more than 50%[6,7]. Increasing studies believed that genetic factors, such as monogenic diseases, play important roles in the development of VEO-IBD, especially IO-IBD. Currently, there is no epidemiological data for IO-IBD patients in China. However, in the past 5 years, more than 200 cases of VEO-IBD have been reported by our hospital and other hospitals in China[8-13], and more than half of the patients presented genetic defects. Among the 73 pediatric patients in this study, 49 (67.12%) carried disease-related gene mutations, which was much higher than the reported proportions in European and American countries[14,15] but similar to the proportion reported by Huang *et al*[10], suggesting that the presence of monogenic diseases is more common in Chinese VEO-IBD patients.

A total of ten mutated genes were identified in this study, among which the *IL-10RA* mutation was the most common (39/49). This finding was similar to those reported by other researchers in China[8], while *IL-10RB* and *IL-10* mutations were not observed. Among the 14 *IL-10RA* variants, ten have been reported previously, among which c.537G>A, c.493C>T, c.436delC, c.299T>G, and c.191A>G mutations were observed in children only in China or other Asian countries[11,16,17] but have not been reported in Western countries, suggesting a genetic founder effect in *IL-10RA*. The four identified novel variants were c.109G>T, c.302G>A, c.569T>G, and c.787C>T, which were likely pathogenic mutations according to the ACMG guidelines. In this study, the most common *IL-10RA* mutation locus was c.301C>T, followed by c.537G>A, which was



		Cut-off	Sensitivity	Specipicity
A	**WBC (× 10⁹)**	11.96	0.66	0.88
	ESR (mm/hr)	12.50	0.70	0.90
	TNFα (pg/mL)	17.40	0.78	0.88
B	**ALB (g/L)**	36.50	0.80	0.90
C	**Ferritin (ng/mL)**	28.20	0.93	0.92
D	**IL-10 (pg/mL)**	33.05	1.00	0.84
E	**Onset age (mo)**	0.21	0.82	0.94

Figure 1 Receiver operating characteristic curve analysis for diagnostic indicators. A and B: Parameters that may be used to distinguish allergic proctocolitis from infantile-onset inflammatory bowel disease (IO-IBD). The increased peripheral white blood cell count, erythrocyte sedimentation, rate and tumor necrosis factor (TNF)-α, as well as the reduced albumin levels were risk factors for the diagnosis of IO-IBD, and TNF-α and albumin levels had higher sensitivity and specificity; C: Serum ferritin level has high diagnostic value in discriminating IO-IBD patients with gene mutation (M-IBD) or without (NM-IBD) when serum ferritin levels are above 28.20 ng/mL. It might indicate the existence of pathogenic gene mutations in IO-IBD patients; D and E: Serum interleukin (IL)-10 level and onset age can be used to screen *IL-10RA* mutation in M-IBD patients. If an infant got IO-IBD within a week in life or a patient's serum IL-10 levels were higher than 33.05 pg/mL, the presence of *IL-10RA* gene mutations was strongly suggested. WBC: White blood cell; ESR: Erythrocyte sedimentation rate; TNF: Tumor necrosis factor; ALB: Albumin; IL: Interleukin; CI: Confidence interval.

consistent with the previous reports in Asian children[8]. Notably, c.537G>A mutation was located in exon 4, which was always missed in the reports as it was mistaken for a synonymous mutation; however, it had been confirmed as a splicing mutation that has a deleterious effect on IL-10 receptor[11]. For IBD children who are highly suspected of having abnormal IL-10 signaling pathways, especially those who have a heterozygous *IL-10RA* mutation after gene sequencing, clinicians should be aware of the sequencing report and not to miss the c.537G>A mutation.

In addition to *IL-10RA*, the other eight genetic mutations that could cause immunodeficiency diseases were also observed in this study. These included *CYBB* mutation, which caused X-linked chronic granulomatous disease[18], *IKBKG* mutation, which caused ectodermal dysplasia and immunodeficiency[19,20], *PIK3CD* mutation, which caused activated phosphoinositide 3-kinase δ syndrome[21], *CD40LG* mutation, which caused X-linked hyper-IgM syndrome[22], *SLC37A4* mutation, which caused glycogen storage disease type 1B[23], *LIG4* mutation, which caused LIG4 syndrome[24], *WAS* mutation, which caused Wiskott-Aldrich syndrome[25], and *CARD11* mutation, which caused immunodeficiency type 11B with atopic dermatitis[26]. These diseases have been confirmed to cause IBD-like colitis in infants, such as recurrent diarrhea, hematochezia, infections, perianal abscess, and growth retardation.

Because of an insufficient understanding of IO-IBD, especially that caused by monogenic diseases, most patients could not be diagnosed as early as possible. It has been reported that the median time from the occurrence of symptoms to disease diagnosis was approximately 6 mo[15]. The most common misdiagnosis was allergic diseases, therefore, this study included a group of age-matched patients who were admitted to the hospital due to diarrhea and hematochezia and were eventually diagnosed as allergic proctocolitis. Although the AP children had diarrhea, hematochezia, or other similar symptoms with the IBD children, there was less onset of failure to thrive, perianal lesions, and death in AP patients; meanwhile, the daily frequency of diarrhea was significantly higher in IO-IBD children than in AP children. Inflammatory markers in peripheral blood such as WBC, CRP, ESR, PLT, TNF-α, and IL-6 in IO-IBD children were significantly higher than those in AP children, while the nutritional indicators such as albumin and hemoglobin were lower in IBD patients than in AP patients. Logistic regression analysis further confirmed that increased levels of WBC, ESR, and TNF-α, as well as lower serum albumin level were associated with a higher likelihood of IBD. Although it has been reported that hematological examinations had little value in the differential diagnosis of food allergy and IBD[15],the ROC curve analysis in this study showed that TNF-α and serum albumin level had moderate value for differentiating IBD from allergic disease. Moreover, the high sensitivities and specificities of cut-off values for TNF-α and serum albumin may help clinicians, especially those in areas with limited medical resources, to identify IO-IBD patients earlier.

Genetic diagnosis is currently the gold standard for the diagnosis of IO-IBD caused by gene defects. However, the economic and time costs of this detection are relatively high in China. Most parents are not willing to choose this method at initial visits, and this would delay the diagnosis and treatment. The binary logistic regression analysis showed the serum ferritin (OR = 1.14) and IL-10 (OR = 1.04) may indicate the presence of gene defects in IO-IBD children; however, in view of the high proportion of IL-10RA mutations in our cohort, we further compared these factors among patients with *IL-10RA* mutations, those with non-*IL-10RA* mutations, and those without any disease-causing mutations. The final results showed that serum ferritin was abnormally elevated in IO-IBD patients with gene mutations and was not affected by the genotypes. Further ROC curve analysis showed that serum ferritin might be a valuable diagnostic indicator for monogenic IBD. Serum ferritin was acknowledged as an inflammatory marker, which would reflect the acute and chronic inflammatory state in infectious diseases, immunological diseases, hematological diseases, and malignant diseases[27]. A variety of cells could synthesize and secrete ferritin, of which macrophages were the main source and could induce diseases[27]. The role of ferritin in inflammatory responses is still unclear. It was hypothesized that in the inflammatory state, the Toll-like receptor (TLR) 9 signaling pathway is activated, IL-1β and IL-18 levels increased, then macrophages were activated, and synthesized more ferritin, which could further amplify the inflammatory response through the TLR9 signaling pathway, thereby forming a positive feedback loop and resulting in continuous aggravation of inflammation[28-32]. Some researchers believed that serum ferritin could bind to T and B lymphocytes directly[32,33], then inhibit T cell proliferation, B cell maturation, and immunoglobulin synthesis[33-35]. In addition, serum ferritin could also promote regulatory T cell differentiation through the IL-10 signaling pathway and play an immunoregulatory role[36]. In our study, the serum ferritin level was

significantly elevated in M-IBD children, but whether it plays a pro-inflammatory or immunomodulatory role needs further study.

Both in our study and other studies in China, *IL-10RA* is the most common mutated gene in Chinese VEO-IBD patients. We also found that compared to the patients with other gene mutations, patients with the *IL-10RA* deficiency had unique features. First, the age of onset was particularly early. The median onset age was 0.04-mo-old, while it was 2-mo-old in patients with other gene mutations, indicating that diarrhea and hematochezia existed from birth in *IL-10RA* mutated children. Second, serum IL-10 level in these patients was particularly high. IL-10 is an important anti-inflammatory factor secreted by a variety of immune cells. After binding to IL-10R, IL-10 can activate a series of cascade reactions to maintain immune homeostasis by inhibiting inflammatory factors such as TNF-α[37]. IL-10R is composed of two subunits, IL-10RA and IL-10RB, and IL-10RA only binds to IL-10[38]. It was previously believed that the increased expression of IL-10 in IBD patients indicated a good steroid response and prognosis[39]. However, when IL-10R is deficient, the anti-inflammatory function of IL-10 could not be achieved. Glocker *et al*[40] confirmed that human peripheral blood mononuclear cells (PBMCs) could secrete large amounts of TNF-α after stimulation with lipopolysaccharide (LPS) *in vitro*, but its level decreased significantly when exogenous IL-10 was added into the culture medium, while this phenomenon could not be observed in the PBMC culture supernatant from *IL-10RA* deficient children, indicating the important role of the IL-10 signaling pathway in anti-inflammatory processes. In our study, both high IL-10 and TNF-α levels were observed in patients with *IL-10RA* mutation, which indicated that even such a high level of IL-10 could not inhibit TNF-α release and alleviate the inflammation in these children. These findings were similar to the *in vitro* research mentioned above. Therefore, we speculated that IL-10 level could be used as an *in vivo* detective indicator to verify the function of novel mutations of the *IL-10RA* gene. In this study, ROC curve analysis also confirmed that serum IL-10 level had a high sensitivity and specificity for identifying the presence of *IL-10RA* mutations, which suggested that if IO-IBD patients have a remarkably elevated IL-10 level, the gene sequencing is strongly recommended to identify the existence of *IL-10RA* deficiency. In fact, we did further investigation by whole-genome sequencing (WGS) in two patients of this cohort, whose clinical manifestations were similar to those of *IL-10RA* mutated patients, especially the increased significantly IL-10 level but whole-exsome sequencing only found heterozygous mutations in *IL-10RA*. However, the results of WGS showed that there was another heterozygous deletion of 333bp in *IL-10RA* which led to exon 1 absence. This result further supported that serum IL-10 level may help distinguish *IL-10RA* mutated patients.

IO-IBD patients, especially those caused by gene mutations, are rare. Although the cohort included in this study was larger than many published studies, the absolute number was not large, which may lead to statistical bias. Besides, we needed further prospective studies to evaluate the diagnostic value of the indicators identified in this study.

CONCLUSION

Children with IO-IBD have a higher proportion of Mendelian diseases. For Chinese Han pediatric patients, *IL-10RA* mutation is the most common pathogenic gene. A complete medical history and clinical evaluation are necessary to differentiate IBD and allergic proctocolitis earlier. Diarrhea frequency, body weight, height, serum albumin, and TNF-α level could help distinguish IO-IBD and allergy. Elevated serum ferritin level could be used for identifying IO-IBD caused by gene mutations, and the remarkably increased serum IL-10 level strongly suggests the presence of *IL-10RA* gene mutation. These clinical characteristics and hematological parameters would help to shorten the time of diagnosis so that the patients are able to receive timely and correct treatment and then reduce social and financial burdens.

ARTICLE HIGHLIGHTS

Research background

Infantile-onset inflammatory bowel disease (IO-IBD) causes severe clinical manifestations and responds poorly to traditional inflammatory bowel disease (IBD)

treatments. At present, there are no simple and reliable laboratory indicators for early screening IO-IBD patients, especially those in whom the disease is caused by monogenic diseases.

Research motivation

Because of an insufficient understanding of IO-IBD, especially that caused by monogenic diseases, most patients could not be diagnosed as early as possible. It is hard to persuade the parents to accept endoscopic examination or genetic diagnosis at initial visits, especially those in areas with limited medical resources.

Research objectives

We intended to search for early diagnostic indicators for IO-IBD children with or without gene mutations, in order to shorten the diagnosis time, reduce medical costs, simplify the analysis of next generation-sequencing, and administer targeted intervention as early as possible.

Research methods

A retrospective analysis was performed in 73 patients with IO-IBD admitted to our hospital in the past 5 years. Based on the next-generation sequencing results, they were divided into either a monogenic IBD group (M-IBD) or non-monogenic IBD group (NM-IBD). Forty age-matched patients with allergic proctocolitis (AP) were included as a control group. The clinical manifestations and the inflammatory factors in peripheral blood were evaluated. Logistic regression analysis and receiver operating characteristic (ROC) curve analysis were performed to find the screening factors and cut-off values of IO-IBD as well as monogenic IO-IBD.

Research results

Among the 44 M-IBD patients, 35 carried *IL-10RA* mutations, and the most common mutations were c.301C>T (p.R101W, 30/70) and c.537G>A (p.T179T, 17/70). Patients with higher serum tumor necrosis factor (TNF)-α value were more likely have IBD [odds ratio (OR) = 1.25, 95% confidence interval (CI): 1.05-1.50, P = 0.013), while higher serum albumin level was associated with lower risk of IBD (OR = 0.86, 95%CI: 0.74-1.00, P = 0.048). The cut-off values of TNF-α and albumin were 17.40 pg/mL (sensitivity: 0.78; specificity: 0.88) and 36.50 g/L (sensitivity: 0.80; specificity: 0.90), respectively. The increased ferritin level was indicative of a genetic mutation in IO-IBD patients. Its cut-off value was 28.20 ng/mL (sensitivity: 0.93; specificity: 0.92). When interleukin (IL)-10 level was higher than 33.05 pg/mL (sensitivity: 1.00; specificity: 0.84), or the onset age was earlier than 0.21 mo (sensitivity: 0.82; specificity: 0.94), the presence of disease-causing mutations in *IL-10RA* in IO-IBD patients was strongly suggested.

Research conclusions

Serum TNF-α and albumin level could differentiate IO-IBD patients from allergic proctocolitis patients, and serum ferritin and IL-10 level are useful indicators for early diagnosing monogenic IO-IBD.

Research perspectives

Using serum TNF-α and albumin level may contribute to distinguishing IO-IBD which needs further investigations, such as gastrointestinal endoscopy. High levels of serum ferritin and IL-10 can infer a monogenic disease in IO-IBD patients, especially the mutations in the *IL-10RA* gene. The diagnostic value of the indicators identified in this study should be evaluated by prospective studies.

ACKNOWLEDGEMENTS

We thank Li J at the Ruijin Hospital for statistics assistance and Chen XY at the Ruijin Hospital for pathological diagnosis.

REFERENCES

1 **Levine A**, Koletzko S, Turner D, Escher JC, Cucchiara S, de Ridder L, Kolho KL, Veres G, Russell RK, Paerregaard A, Buderus S, Greer ML, Dias JA, Veereman-Wauters G, Lionetti P, Sladek M,

Martin de Carpi J, Staiano A, Ruemmele FM, Wilson DC; European Society of Pediatric Gastroenterology; Hepatology; and Nutrition. ESPGHAN revised porto criteria for the diagnosis of inflammatory bowel disease in children and adolescents. *J Pediatr Gastroenterol Nutr* 2014; **58**: 795-806 [PMID: 24231644 DOI: 10.1097/MPG.0000000000000239]

2 **Heyman MB**, Kirschner BS, Gold BD, Ferry G, Baldassano R, Cohen SA, Winter HS, Fain P, King C, Smith T, El-Serag HB. Children with early-onset inflammatory bowel disease (IBD): analysis of a pediatric IBD consortium registry. *J Pediatr* 2005; **146**: 35-40 [PMID: 15644819 DOI: 10.1016/j.jpeds.2004.08.043]

3 **Chandrakasan S**, Venkateswaran S, Kugathasan S. Nonclassic Inflammatory Bowel Disease in Young Infants: Immune Dysregulation, Polyendocrinopathy, Enteropathy, X-Linked Syndrome, and Other Disorders. *Pediatr Clin North Am* 2017; **64**: 139-160 [PMID: 27894441 DOI: 10.1016/j.pcl.2016.08.010]

4 **Pediatircs' Inflammation bowl diesease collaborating group attached to the Chinese society of pediatric gastroenterology of Chinese Medical Association**, Chen J, Xu CD, Huang ZH, Gong ST, Dong YS, Dong M, Sun M, Ye LY, Huang YK, Wang BX, Wang LL, Xu XW, Jiang MZ, Yang WL, Zhu CM, You JY, Wu QB, Jiang LR, Li ZL, Shao CH, Huang Y, Zhang YL, Xu XH, Liu FL, Mang M. Consensus on the Diagnosis and Management of Pediatric Inflammatory Bowel Disease. *Zhongguo Shiyong Erke Zazhi* 2010; **25**: 263-265

5 **Richards S**, Aziz N, Bale S, Bick D, Das S, Gastier-Foster J, Grody WW, Hegde M, Lyon E, Spector E, Voelkerding K, Rehm HL; ACMG Laboratory Quality Assurance Committee. Standards and guidelines for the interpretation of sequence variants: a joint consensus recommendation of the American College of Medical Genetics and Genomics and the Association for Molecular Pathology. *Genet Med* 2015; **17**: 405-424 [PMID: 25741868 DOI: 10.1038/gim.2015.30]

6 **Benchimol EI**, Guttmann A, Griffiths AM, Rabeneck L, Mack DR, Brill H, Howard J, Guan J, To T. Increasing incidence of paediatric inflammatory bowel disease in Ontario, Canada: evidence from health administrative data. *Gut* 2009; **58**: 1490-1497 [PMID: 19651626 DOI: 10.1136/gut.2009.188383]

7 **Benchimol EI**, Mack DR, Nguyen GC, Snapper SB, Li W, Mojaverian N, Quach P, Muise AM. Incidence, outcomes, and health services burden of very early onset inflammatory bowel disease. *Gastroenterology* 2014; **147**: 803-813. quiz e14-5 [PMID: 24951840 DOI: 10.1053/j.gastro.2014.06.023]

8 **Zheng C**, Huang Y, Hu W, Shi J, Ye Z, Qian X, Huang Z, Xue A, Wang Y, Lu J, Tang Z, Wu J, Wang L, Peng K, Zhou Y, Miao S, Sun H. Phenotypic Characterization of Very Early-Onset Inflammatory Bowel Disease with Interleukin-10 Signaling Deficiency: Based on a Large Cohort Study. *Inflamm Bowel Dis* 2019; **25**: 756-766 [PMID: 30212871 DOI: 10.1093/ibd/izy289]

9 **Su W**, Xu CD, Wang XQ, Yu Y, Guo Y, Xu X, Xiao Y. Analysis of clinical phenotype and genotype of 30 Chinese pediatric patients suffering very early onset inflammatory bowel disease. *Zhonghua Yanxingchangbing Zazhi* 2018; **2**: 83-88 [DOI: 10.3760/cma.j.issn.2096-367X.2018.02.003]

10 **Huang Z**, Peng K, Li X, Zhao R, You J, Cheng X, Wang Z, Wang Y, Wu B, Wang H, Zeng H, Yu Z, Zheng C, Wang Y, Huang Y. Mutations in Interleukin-10 Receptor and Clinical Phenotypes in Patients with Very Early Onset Inflammatory Bowel Disease: A Chinese VEO-IBD Collaboration Group Survey. *Inflamm Bowel Dis* 2017; **23**: 578-590 [PMID: 28267044 DOI: 10.1097/MIB.0000000000001058]

11 **Xu YB**, Chen YB, Zeng P, Chen HS, Zeng HS. Interleukin-10 receptor mutations in children with neonatal onset inflammatory bowel disease: genetic diagnosis and pathogenesis. *Zhonghua Erke Zazhi* 2015; **53**: 348-354 [DOI: 10.3760/cma.j.issn.0578-1310.2015.05.007]

12 **Liu LL**, Jiang Y, HOU XL, Tang ZZ, Zhou CL, Sun GW. Clinical characteristics and genetic diagnosis of infantile inflammatory bowel disease within four months after birth: seven case report. *Zhongguo Xunzheng Erke Zazhi* 2016; **11**: 285-289 [DOI: 10.3969/j.issn.1673-5501.2016.04.009]

13 **Xiao Y**, Wang XQ, Yu Y, Guo Y, Xu X, Gong L, Zhou T, Li XQ, Xu CD. Comprehensive mutation screening for 10 genes in Chinese patients suffering very early onset inflammatory bowel disease. *World J Gastroenterol* 2016; **22**: 5578-5588 [PMID: 27350736 DOI: 10.3748/wjg.v22.i24.5578]

14 **Kotlarz D**, Beier R, Murugan D, Diestelhorst J, Jensen O, Boztug K, Pfeifer D, Kreipe H, Pfister ED, Baumann U, Puchalka J, Bohne J, Egritas O, Dalgic B, Kolho KL, Sauerbrey A, Buderus S, Güngör T, Enninger A, Koda YK, Guariso G, Weiss B, Corbacioglu S, Socha P, Uslu N, Metin A, Wahbeh GT, Husain K, Ramadan D, Al-Herz W, Grimbacher B, Sauer M, Sykora KW, Koletzko S, Klein C. Loss of interleukin-10 signaling and infantile inflammatory bowel disease: implications for diagnosis and therapy. *Gastroenterology* 2012; **143**: 347-355 [PMID: 22549091 DOI: 10.1053/j.gastro.2012.04.045]

15 **Kammermeier J**, Dziubak R, Pescarin M, Drury S, Godwin H, Reeve K, Chadokufa S, Huggett B, Sider S, James C, Acton N, Cernat E, Gasparetto M, Noble-Jamieson G, Kiparissi F, Elawad M, Beales PL, Sebire NJ, Gilmour K, Uhlig HH, Bacchelli C, Shah N. Phenotypic and Genotypic Characterisation of Inflammatory Bowel Disease Presenting Before the Age of 2 years. *J Crohns Colitis* 2017; **11**: 60-69 [PMID: 27302973 DOI: 10.1093/ecco-jcc/jjw118]

16 **Yanagi T**, Mizuochi T, Takaki Y, Eda K, Mitsuyama K, Ishimura M, Takada H, Shouval DS, Griffith AE, Snapper SB, Yamashita Y, Yamamoto K. Novel exonic mutation inducing aberrant splicing in the IL10RA gene and resulting in infantile-onset inflammatory bowel disease: a case report. *BMC Gastroenterol* 2016; **16**: 10 [PMID: 26822028 DOI: 10.1186/s12876-016-0424-5]

17 **Oh SH**, Baek J, Liany H, Foo JN, Kim KM, Yang SC, Liu J, Song K. A Synonymous Variant in

IL10RA Affects RNA Splicing in Paediatric Patients with Refractory Inflammatory Bowel Disease. *J Crohns Colitis* 2016; **10**: 1366-1371 [PMID: 27177777 DOI: 10.1093/ecco-jcc/jjw102]

18 **Schäppi MG**, Smith VV, Goldblatt D, Lindley KJ, Milla PJ. Colitis in chronic granulomatous disease. *Arch Dis Child* 2001; **84**: 147-151 [PMID: 11159292 DOI: 10.1136/adc.84.2.147]

19 **Mizukami T**, Obara M, Nishikomori R, Kawai T, Tahara Y, Sameshima N, Marutsuka K, Nakase H, Kimura N, Heike T, Nunoi H. Successful treatment with infliximab for inflammatory colitis in a patient with X-linked anhidrotic ectodermal dysplasia with immunodeficiency. *J Clin Immunol* 2012; **32**: 39-49 [PMID: 21993693 DOI: 10.1007/s10875-011-9600-0]

20 **Orange JS**, Jain A, Ballas ZK, Schneider LC, Geha RS, Bonilla FA. The presentation and natural history of immunodeficiency caused by nuclear factor kappaB essential modulator mutation. *J Allergy Clin Immunol* 2004; **113**: 725-733 [PMID: 15100680 DOI: 10.1016/j.jaci.2004.01.762]

21 **Nunes-Santos CJ**, Uzel G, Rosenzweig SD. PI3K pathway defects leading to immunodeficiency and immune dysregulation. *J Allergy Clin Immunol* 2019; **143**: 1676-1687 [PMID: 31060715 DOI: 10.1016/j.jaci.2019.03.017]

22 **Levy J**, Espanol-Boren T, Thomas C, Fischer A, Tovo P, Bordigoni P, Resnick I, Fasth A, Baer M, Gomez L, Sanders EA, Tabone MD, Plantaz D, Etzioni A, Monafo V, Abinun M, Hammarstrom L, Abrahamsen T, Jones A, Finn A, Klemola T, DeVries E, Sanal O, Peitsch MC, Notarangelo LD. Clinical spectrum of X-linked hyper-IgM syndrome. *J Pediatr* 1997; **131**: 47-54 [PMID: 9255191 DOI: 10.1016/s0022-3476(97)70123-9]

23 **Gerin I**, Veiga-da-Cunha M, Achouri Y, Collet J-F, Van Schaftingen E. Sequence of a putative glucose 6-phosphate translocase, mutated in glycogen storage disease type Ib1. *FEBS Lett* 1997; **419**: 235-238 [DOI: 10.1016/s0014-5793(97)01463-4]

24 **Felgentreff K**, Perez-Becker R, Speckmann C, Schwarz K, Kalwak K, Markelj G, Avcin T, Qasim W, Davies EG, Niehues T, Ehl S. Clinical and immunological manifestations of patients with atypical severe combined immunodeficiency. *Clin Immunol* 2011; **141**: 73-82 [PMID: 21664875 DOI: 10.1016/j.clim.2011.05.007]

25 **Catucci M**, Castiello MC, Pala F, Bosticardo M, Villa A. Autoimmunity in wiskott-Aldrich syndrome: an unsolved enigma. *Front Immunol* 2012; **3**: 209 [PMID: 22826711 DOI: 10.3389/fimmu.2012.00209]

26 **Dorjbal B**, Stinson JR, Ma CA, Weinreich MA, Miraghazadeh B, Hartberger JM, Frey-Jakobs S, Weidinger S, Moebus L, Franke A, Schäffer AA, Bulashevska A, Fuchs S, Ehl S, Limaye S, Arkwright PD, Briggs TA, Langley C, Bethune C, Whyte AF, Alachkar H, Nejentsev S, DiMaggio T, Nelson CG, Stone KD, Nason M, Brittain EH, Oler AJ, Veltri DP, Leahy TR, Conlon N, Poli MC, Borzutzky A, Cohen JI, Davis J, Lambert MP, Romberg N, Sullivan KE, Paris K, Freeman AF, Lucas L, Chandrakasan S, Savic S, Hambleton S, Patel SY, Jordan MB, Theos A, Lebensburger J, Atkinson TP, Torgerson TR, Chinn IK, Milner JD, Grimbacher B, Cook MC, Snow AL. Hypomorphic caspase activation and recruitment domain 11 (CARD11) mutations associated with diverse immunologic phenotypes with or without atopic disease. *J Allergy Clin Immunol* 2019; **143**: 1482-1495 [PMID: 30170123 DOI: 10.1016/j.jaci.2018.08.013]

27 **Kernan KF**, Carcillo JA. Hyperferritinemia and inflammation. *Int Immunol* 2017; **29**: 401-409 [PMID: 28541437 DOI: 10.1093/intimm/dxx031]

28 **Gray CP**, Arosio P, Hersey P. Heavy chain ferritin activates regulatory T cells by induction of changes in dendritic cells. *Blood* 2002; **99**: 3326-3334 [PMID: 11964300 DOI: 10.1182/blood.v99.9.3326]

29 **Carcillo JA**, Sward K, Halstead ES, Telford R, Jimenez-Bacardi A, Shakoory B, Simon D, Hall M; Eunice Kennedy Shriver National Institute of Child Health and Human Development Collaborative Pediatric Critical Care Research Network Investigators. A Systemic Inflammation Mortality Risk Assessment Contingency Table for Severe Sepsis. *Pediatr Crit Care Med* 2017; **18**: 143-150 [PMID: 27941423 DOI: 10.1097/PCC.0000000000001029]

30 **Fautrel B**, Le Moël G, Saint-Marcoux B, Taupin P, Vignes S, Rozenberg S, Koeger AC, Meyer O, Guillevin L, Piette JC, Bourgeois P. Diagnostic value of ferritin and glycosylated ferritin in adult onset Still's disease. *J Rheumatol* 2001; **28**: 322-329 [PMID: 11246670]

31 **Garcia PC**, Longhi F, Branco RG, Piva JP, Lacks D, Tasker RC. Ferritin levels in children with severe sepsis and septic shock. *Acta Paediatr* 2007; **96**: 1829-1831 [PMID: 18001337 DOI: 10.1111/j.1651-2227.2007.00564.x]

32 **Recalcati S**, Invernizzi P, Arosio P, Cairo G. New functions for an iron storage protein: the role of ferritin in immunity and autoimmunity. *J Autoimmun* 2008; **30**: 84-89 [PMID: 18191543 DOI: 10.1016/j.jaut.2007.11.003]

33 **Fargion S**, Fracanzani AL, Brando B, Arosio P, Levi S, Fiorelli G. Specific binding sites for H-ferritin on human lymphocytes: modulation during cellular proliferation and potential implication in cell growth control. *Blood* 1991; **78**: 1056-1061 [PMID: 1831058 DOI: 10.1182/blood.V78.4.1056.bloodjournal7841056]

34 **Broxmeyer HE**, Williams DE, Geissler K, Hangoc G, Cooper S, Bicknell DC, Levi S, Arosio P. Suppressive effects *in vivo* of purified recombinant human H-subunit (acidic) ferritin on murine myelopoiesis. *Blood* 1989; **73**: 74-79 [PMID: 2910370 DOI: 10.1182/blood.V73.1.74.bloodjournal73174]

35 **Yamashita M**, Harada G, Matsumoto SE, Aiba Y, Ichikawa A, Fujiki T, Udono M, Kabayama S, Yoshida T, Zhang P, Fujii H, Shirahata S, Katakura Y. Suppression of immunoglobulin production in human peripheral blood mononuclear cells by monocytes *via* secretion of heavy-chain ferritin.

Immunobiology 2014; **219**: 149-157 [PMID: 24157279 DOI: 10.1016/j.imbio.2013.08.011]

36 **Li R**, Luo C, Mines M, Zhang J, Fan GH. Chemokine CXCL12 induces binding of ferritin heavy chain to the chemokine receptor CXCR4, alters CXCR4 signaling, and induces phosphorylation and nuclear translocation of ferritin heavy chain. *J Biol Chem* 2006; **281**: 37616-37627 [PMID: 17056593 DOI: 10.1074/jbc.M607266200]

37 **Hutchins AP**, Diez D, Miranda-Saavedra D. The IL-10/STAT3-mediated anti-inflammatory response: recent developments and future challenges. *Brief Funct Genomics* 2013; **12**: 489-498 [PMID: 23943603 DOI: 10.1093/bfgp/elt028]

38 **Commins S**, Steinke JW, Borish L. The extended IL-10 superfamily: IL-10, IL-19, IL-20, IL-22, IL-24, IL-26, IL-28, and IL-29. *J Allergy Clin Immunol* 2008; **121**: 1108-1111 [PMID: 18405958 DOI: 10.1016/j.jaci.2008.02.026]

39 **Santaolalla R**, Mañé J, Pedrosa E, Lorén V, Fernández-Bañares F, Mallolas J, Carrasco A, Salas A, Rosinach M, Forné M, Espinós JC, Loras C, Donovan M, Puig P, Mañosa M, Gassull MA, Viver JM, Esteve M. Apoptosis resistance of mucosal lymphocytes and IL-10 deficiency in patients with steroid-refractory Crohn's disease. *Inflamm Bowel Dis* 2011; **17**: 1490-1500 [PMID: 21674705 DOI: 10.1002/ibd.21507]

40 **Glocker EO**, Kotlarz D, Boztug K, Gertz EM, Schäffer AA, Noyan F, Perro M, Diestelhorst J, Allroth A, Murugan D, Hätscher N, Pfeifer D, Sykora KW, Sauer M, Kreipe H, Lacher M, Nustede R, Woellner C, Baumann U, Salzer U, Koletzko S, Shah N, Segal AW, Sauerbrey A, Buderus S, Snapper SB, Grimbacher B, Klein C. Inflammatory bowel disease and mutations affecting the interleukin-10 receptor. *N Engl J Med* 2009; **361**: 2033-2045 [PMID: 19890111 DOI: 10.1056/NEJMoa0907206]

World Journal of Gastroenterology

Submit a Manuscript: https://www.f6publishing.com

World J Gastroenterol 2021 January 7; 27(1): 107-128

DOI: 10.3748/wjg.v27.i1.107

ISSN 1007-9327 (print) ISSN 2219-2840 (online)

ORIGINAL ARTICLE

Randomized Controlled Trial

Effect of probiotic *Lactobacillus plantarum* Dad-13 powder consumption on the gut microbiota and intestinal health of overweight adults

Endang Sutriswati Rahayu, Mariyatun Mariyatun, Nancy Eka Putri Manurung, Pratama Nur Hasan, Phatthanaphong Therdtatha, Riko Mishima, Husnita Komalasari, Nurul Ain Mahfuzah, Fathyah Hanum Pamungkaningtyas, Wahyu Krisna Yoga, Dina Aulia Nurfiana, Stefanie Yolanda Liwan, Mohammad Juffrie, Agung Endro Nugroho, Tyas Utami

ORCID number: Endang Sutriswati Rahayu 0000-0002-6101-3433; Mariyatun Mariyatun 0000-0002-7998-2531; Nancy Eka Putri Manurung 0000-0002-5182-7433; Pratama Nur Hasan 0000-0001-7780-2421; Phatthanaphong Therdtatha 0000-0002-1443-5270; Riko Mishima 0000-0003-0961-1628; Husnita Komalasari 0000-0001-8399-6015; Nurul Ain Mahfuzah 0000-0002-2156-8645; Fathyah Hanum Pamungkaningtyas 0000-0002-2106-0040; Wahyu Krisna Yoga 0000-0002-7350-0589; Dina Aulia Nurfiana 0000-0003-0192-8217; Stefanie Yolanda Liwan 0000-0001-5753-233X; Mohammad Juffrie 0000-0002-2862-3897; Agung Endro Nugroho 0000-0001-7840-8493; Tyas Utami 0000-0003-3600-6060.

Author contributions: Rahayu ES leaded the research project and together with Utami T designed the study; Juffrie M supervised the ethical approval and acted as the consultant for the clinical trial; Nugroho AE supervised the production of probiotic powder; Mariyatun M and Hasan PN supervised the on-site study; Putri Manurung NE, Komalasari H, Yoga WK, Therdtatha P, Mishima

Endang Sutriswati Rahayu, Mariyatun Mariyatun, Nancy Eka Putri Manurung, Pratama Nur Hasan, Husnita Komalasari, Nurul Ain Mahfuzah, Fathyah Hanum Pamungkaningtyas, Wahyu Krisna Yoga, Dina Aulia Nurfiana, Stefanie Yolanda Liwan, Tyas Utami, Department of Food and Agricultural Technology, Faculty of Agricultural Technology, Universitas Gadjah Mada, Yogyakarta 55281, Indonesia

Endang Sutriswati Rahayu, Mariyatun Mariyatun, Nancy Eka Putri Manurung, Pratama Nur Hasan, Fathyah Hanum Pamungkaningtyas, Dina Aulia Nurfiana, Tyas Utami, Center for Food and Nutrition Studies, Universitas Gadjah Mada, Yogyakarta 55281, Indonesia

Phatthanaphong Therdtatha, Riko Mishima, Department of Bioscience and Biotechnology, Faculty of Agriculture, Kyushu University, 774 Motooka, Nishi-ku, Fukuoka, Japan

Mohammad Juffrie, Department of Public Health, Faculty of Medicine, Public Health and Nursery, Universitas Gadjah Mada, Yogyakarta 55281, Indonesia

Agung Endro Nugroho, Department of Pharmacology and Clinical Pharmacy, Faculty of Pharmacy, Universitas Gadjah Mada, Yogyakarta 55281, Indonesia

Corresponding author: Endang Sutriswati Rahayu, Dr, Professor, Department of Food and Agricultural Technology, Faculty of Agricultural Technology, Universitas Gadjah Mada, Jalan Flora No. 1, Bulaksumur, Sleman, Yogyakarta 55281, Yogyakarta, Indonesia.
endangsrahayu@ugm.ac.id

Abstract

BACKGROUND

Shifting on lifestyle, diet, and physical activity contributed on increasing number of obese people around the world. Multiple factors influence the development of obesity. Some research suggested that gut microbiota (GM) plays an important role in nutrient absorption and energy regulation of individuals, thus affecting their nutritional status. Report of Indonesia Basic Health Research showed that the prevalence of obesity in every province tended to increase. Although the root

R performed the work on-site and maintained the coordination with subject as well as conducted sampling; Nurfiana DA, Mahfuzah NA, Liwan SY performed analysis at the laboratory; Mariyatun M and Pamungkaningtyas FH analysed the laboratory data and took part in preparing the manuscript.

Supported by Ristekdikti Kalbe - Science Awards, No. 048/KF-Legal/RKSA/I/2019.

Institutional review board statement: The study was reviewed and approved by the Ethic Comittee Faculty of Medicine Universitas Gadjah Mada, Institutional Review Board, Approval No. KE/1267/11/2018.

Clinical trial registration statement: This study is registered on the Health Research and Development Agency, Ministry of Health of the Republic of Indonesia, registration No. INA-2A8RG4R.

Informed consent statement: All subjects agreed to participate in this study after informed consent and ethical permission was obtained.

Conflict-of-interest statement: The authors declare that they have no conflicts of interest related to this manuscript.

Data sharing statement: No additional data are available.

CONSORT 2010 statement: The authors have read the CONSORT 2010 Statement, and the manuscript was prepared and revised according to the CONSORT 2010 Statement.

Open-Access: This article is an open-access article that was selected by an in-house editor and fully peer-reviewed by external reviewers. It is distributed in accordance with the Creative Commons Attribution NonCommercial (CC BY-NC 4.0) license, which permits others to distribute, remix, adapt, build upon this work non-commercially, and license their derivative works on different terms, provided the

cause of obesity is excessive calorie intake compared with expenditure, the differences in gut microbial ecology between healthy and obese humans may affect energy homeostasis. GM affect body weight, especially obesity. Probiotics that are consumed while alive and able to colonize in the intestine are expected to increase the population of good bacteria, especially *Bifidobacteria* and Lactobacilli, and suppress pathogens such as *Enterobacteriaceae* and *Staphylococcus*. The strain of *L. plantarum* Dad-13 has been demonstrated to survive and colonize in the gastrointestinal tract of healthy Indonesian adults who consume fermented milk containing *L. plantarum* Dad-13. The consumption of probiotic *L. plantarum* Dad-13 powder decreased *E. coli* and non-*E. coli* coliform bacteria in school-aged children in Indonesia. *L. plantarum* is a dominant bacterium in the average Indonesian's GM. For this reason, this bacterium is probably a more suitable probiotic for Indonesians.

AIM

To determine the effect of the consumption of indigenous probiotic *Lactobacillus plantarum* Dad-13 powder in overweight adults in Yogyakarta (Indonesia).

METHODS

Sixty overweight volunteers with a body mass index (BMI) equal to or greater than 25 consume indigenous probiotic powder *L. plantarum* Dad-13 (2×10^9 CFU/gram/sachet) for 90 d. The study was a randomized, double-blind, placebo-controlled study. The volunteers filled in a diary on a daily basis, which consisted of questions on study product intake (only during ingestion period), other food intake, number of bowel movements, fecal quality (consistency and color), any medications received, and any symptom of discomfort, such as diarrhea, constipation, vomiting, gassing, sensation of illness, *etc.* Fecal samples and the subjects' diaries were collected on the morning of day 10 + 1, which was marked as the end of the baseline period and the start of the ingestion period. During the ingestion period (from day 11 to day 101), several parameters to measure and analyze the results included body weight and height (once a month), the lipid profile, GM analysis using MiSeq, short-chain fatty acid (SCFA) analysis using gas chromatography, and the measurement of fecal pH using a pH meter.

RESULTS

The consumption of indigenous probiotic powder *L. plantarum* Dad-13 caused the average body weight and BMI of the probiotic group to decrease from 84.54 ± 17.64 kg to 83.14 ± 14.71 kg and 33.10 ± 6.15 kg/m^2 to 32.57 ± 5.01 kg/m^2, respectively. No significant reduction of body weight and BMI in the placebo group was observed. An analysis of the microbiota showed that the number of *Bacteroidetes*, specifically *Prevotella*, increased significantly, while that of *Firmicutes* significantly decreased. No significant change in lipid profile in both groups was found. Also, no significant change in SCFAs (*e.g.*, butyrate, propionate, acetic acid) and pH level was found after the consumption of the probiotic.

CONCLUSION

No significant differences in pH before and after ingestion were observed in both the probiotic and placebo groups as well as in the lipid profile of both cholesterol and triglyceride, high-density lipoprotein (HDL), low-density lipoprotein (LDL), and the LDL/HDL ratio. In addition, no significant changes in the concentration of SCFAs (*e.g.*, acetic acid, propionate, and butyrate) were found after consumption. Interestingly, a significant decrease in body weight and BMI ($P < 0.05$) was determined in the treatment group. An analysis of GM shows that *L. plantarum* Dad-13 caused the *Firmicutes* population to decrease and the *Bacteroidetes* population (especially *Prevotella*) to increase.

Key Words: Obesity; Body mass index; Lipid profile; Gut microbiota; Short chain fatty acid; Probiotic *Lactobacillus plantarum* Dad-13

©The Author(s) 2021. Published by Baishideng Publishing Group Inc. All rights reserved.

original work is properly cited and the use is non-commercial. See: http://creativecommons.org/Licenses/by-nc/4.0/

Manuscript source: Unsolicited manuscript

Specialty type: Gastroenterology and hepatology

Country/Territory of origin: Indonesia

Peer-review report's scientific quality classification

Grade A (Excellent): 0
Grade B (Very good): 0
Grade C (Good): C
Grade D (Fair): 0
Grade E (Poor): 0

Received: November 9, 2020
Peer-review started: November 9, 2020
First decision: November 23, 2020
Revised: December 7, 2020
Accepted: December 16, 2020
Article in press: December 16, 2020
Published online: January 7, 2021

P-Reviewer: Jin X
S-Editor: Huang P
L-Editor: A
P-Editor: Ma YJ

Core Tip: Obesity and overweight are corelated with unhealthy lifestyle that affect the health of intestine and affect the ecosystem of gut microbiota (GM). Consumption of probiotics help to maintain the ecosystem of GM to stay balance and healthy. *L. plantarum* Dad-13 is potential probiotics for Indonesians to maintain health of the gastrointestinal ecosystem. This research was conducted to investigate and determine the effect of consumption of indigenous probiotic *L. plantarum* Dad-13 powder in overweight adults in Yogyakarta (Indonesia). The results show decreasing body mass index and weight on overweight subject and increasing of *Bacteroidetes* specifically *Prevotella*.

Citation: Rahayu ES, Mariyatun M, Putri Manurung NE, Hasan PN, Therdtatha P, Mishima R, Komalasari H, Mahfuzah NA, Pamungkaningtyas FH, Yoga WK, Nurfiana DA, Liwan SY, Juffrie M, Nugroho AE, Utami T. Effect of probiotic *Lactobacillus plantarum* Dad-13 powder consumption on the gut microbiota and intestinal health of overweight adults. *World J Gastroenterol* 2021; 27(1): 107-128
URL: https://www.wjgnet.com/1007-9327/full/v27/i1/107.htm
DOI: https://dx.doi.org/10.3748/wjg.v27.i1.107

INTRODUCTION

Changes in lifestyle, diet, and physical activity have resulted in an exponential increase in the number of obese people around the world. Multiple factors influence the development of this disease, and gut microbiota (GM) have been suggested to play an important role in the nutrient absorption and energy regulation of individuals, thus affecting their nutritional status. Different levels of GM have been observed between individuals with normal nutritional status and those who are obese.

The World Health Organization defines obesity as an accumulation of abnormal or excessive fat that can interfere with health[1]. Body mass index (BMI) is the easiest way to identify whether someone is obese or not, namely, by calculating body weight (kg) divided by height squared (m^2). A person is categorized as overweight if his/her BMI is greater than or equal to 25.0, while an obese person is someone with a BMI greater than or equal to 30.0[2]. A report from Indonesia Basic Health Research showed that the prevalence of obesity in every province tended to increase from 2007 to 2013 to 2018. In addition, it reported that adult women had higher obesity prevalence compared with adult men[3].

Although the root cause of obesity is excessive calorie intake compared with expenditure, the differences in gut microbial ecology between healthy and obese humans may affect energy homeostasis. In other words, individuals predisposed to obesity may have gut microbial communities that promote the more efficient extraction and/or storage of energy from a given diet compared with the communities in lean individuals[4].

GM affect body weight, especially obesity. A study showed that after the GM of fat mice were moved to thin mice, the latter gradually increased in weight and became fat[5]. A link is presumed to exist between GM and body weight. The biomarker of the GM of obesity is high-phylum *Firmicutes* bacteria[6]. Delzenne *et al*[7] found that the number of *Bifidobacteria* in obese individuals is lower than that in normal individuals. Other bacteria that were reported to consistently increase in obese individuals include *Enterobacteriaceae*, *Escherichia coli*, and *Staphylococcus* aureus[7].

Bifidobacteria are known as good bacteria as they produce short-chain fatty acids (SCFAs), such as acetate, propionate, butyrate, and lactate. This metabolite result has important effects on host metabolism. SCFAs can regulate (suppress or activate) the expression of specific genes associated with adiposity and inflammation that somewhat benefits the host. Given this description, we know that the population of *Bifidobacteria* is decreasing and that some pathogen bacteria, such as *Enterobacteriaceae* and *Staphylococcus*, are inclined to increase in obese individuals. Probiotics that are consumed while alive and able to colonize in the intestine are expected to increase the population of good bacteria, especially *Bifidobacteria* and Lactobacilli, and suppress pathogens such as *Enterobacteriaceae* and *Staphylococcus*. Kobyliak *et al*[8] proved that the consumption of probiotics, especially Lactobacilli, for nine weeks could suppress body weight gain and reduce adipose tissue in obese mice.

The probiotic research team of Universitas Gadjah Mada (UGM) came up with an indigenous probiotic from Indonesia that was obtained from various sources, but it has not been thoroughly studied. A study by Rahayu *et al*[9] revealed that the Indonesian indigenous probiotic strains have been molecularly confirmed and could inhibit the growth of pathogenic bacteria. In addition, the indigenous probiotic strains were shown to be resistant to pH 2 and bile salt of 3% concentration. Some probiotic cultures owned by the UGM research team are *Lactobacillus plantarum* Dad-13 (obtained from dadih, fermented buffalo milk), *L. plantarum* Mut-7 and Mut-13 (taken from gatot, fermented cassava), *L. plantarum* T3 (obtained from growol, fermented raw cassava), and *Lactobacillus paracasei* SNP-2 (taken from healthy baby feces).

The strain of *L. plantarum* Dad-13 has been demonstrated to survive and colonize in the gastrointestinal tract of healthy Indonesian adults who consume fermented milk containing *L. plantarum* Dad-13[10]. A safety assessment of *L. plantarum* Dad-13 on Sprague Dawley rats reported no adverse effects in general health, organ weight, leukocyte profiles, GOT activity, MDA concentration, and intestinal morphology after the consumption of the probiotic[11]. The indigenous probiotic *L. plantarum* Dad-13 also did not cause translocation in the organs and blood of the rats[11].

Apart from significantly increasing the population of *L. plantarum* and *Lactobacillus*, the consumption of probiotic *L. plantarum* Dad-13 powder decreased *E. coli* and non–*E. coli* coliform bacteria in school-aged children in Indonesia[12]. *L. plantarum* is a dominant bacterium in the average Indonesian's GM[13]. For this reason, this bacterium is probably a more suitable probiotic for Indonesians. Thus, this study aimed to determine the effect of the consumption of indigenous probiotic *L. plantarum* Dad-13 powder in overweight adults in Yogyakarta (Indonesia).

MATERIALS AND METHODS

Study subjects

This study involved 60 overweight volunteers, consisting of 24 males and 36 females. The age of the subjects ranged between 35 and 56 years old. The inclusion criteria of the subjects covered having a BMI equal to or greater than 25, no history of gastrointestinal disorder (such as constipation, diarrhea, abdominal pain, and irritable bowel syndrome), and no allergies to certain foods. The subjects had not taken antibiotics/antimycotics or any specific drugs and did not consume antidiarrheal or laxative medicine for 100 d during the study.

Ethical approval

This study was conducted in accordance with Good Clinical Practice (GCP) as defined by the International Conference of Harmonization (ICH) and in accordance with the Indonesian National Agency for Drug and Food Control Guidance. Approval by the Ethics Committee of the Faculty of Medicine, Public Health, and Nursing of UGM, Yogyakarta, was received on January 2, 2018, as stated in the committee's letter, with reference number KE/FK/0002/2018.

Study products

The product of this study was 1 g of skimmed milk powder containing the probiotic *L. plantarum* Dad-13 of 2×10^9 CFU in sachet packing. The product was prepared using a halal medium by the Center for Food and Nutrition Studies, UGM. One gram of skimmed milk obtained from a local supermarket was used in the placebo group. The study products were stored in a refrigerator (< 4 °C) before being consumed. *L. plantarum* Dad-13, the indigenous probiotic strain, was deposited in ampoules at the Food and Nutrition Culture Collection (FNCC), Center for Food and Nutrition Studies, UGM. Labelling and product blinding were prepared by the Unit Production of Probiotics and Starter Cultures, Center for Food and Nutrition Studies, UGM.

Materials

DNA fecal extraction was performed using phenol–chloroform extraction. The SsoFast™ Evagreen®Supermix Kit from PT Sciencewerke (Indonesia) was used as a mixture of DNA extracts in super-mix real-time PCR. The primers for qPCR analysis consisted of *Bifidobacteria*[14], the *L. plantarum* subgroup[15], *Clostridium coccoides*[15], and *Enterobacteriaceae*[14]. The main instrument used for GM analysis was real-time PCR. Stool sampling equipment included stool tubes, sterile tissue paper, gloves, masks, ice gel, and cool boxes. DNA extraction equipment included a centrifuge, a vortex,

analytical scales, and other kinds of glassware. The equipment for the probiotic powder included freeze dryers and vacuum sealing.

Study design

The study was a randomized, placebo-controlled study; 60 volunteers were divided into an intervention group (probiotic) and a control group (placebo). All the subjects and the researcher were blinded to the treatment administrated (double-blind study). This study used simple randomization, performed in such a way that leaves no significant difference between the study groups (BMI, age, or sex). The placebo product used was skimmed milk without probiotics. The study consisted of 10 d without the consumption of the study product (baseline period) followed by 90 d of ingestion, as shown in Figure 1. During the baseline period, the volunteers consumed their normal dietaries with the exception of probiotic products. The baseline period was a "washout" period to eliminate the effect of previously used probiotics. The volunteers filled in a diary on a daily basis, which consisted of questions on study product intake (only during the ingestion period), other food intake, number of bowel movements, fecal quality (consistency and color), any medications received, and any symptom of discomfort, such as diarrhea, constipation, vomiting, gassing, sensation of illness, *etc*. Fecal samples and the subjects' diaries were collected on the morning of day 10 ± 1, which was marked as the end of the baseline period and the start of the ingestion period. During the ingestion period (from day 11 to day 101), the volunteers consumed one sachet of the study product per day after having lunch for 90 consecutive days. The volunteers were not allowed to consume any other probiotic products. They were requested to fill in a new diary on a daily basis. Upon the completion of the ingestion period, on the morning of day 100 ± 1, fecal samples and the subjects' diaries were collected.

Fecal collection

A fecal sample was collected into a sterile tube with a kind of scoop built into the inside of the lid by the subjects at home, and the sample was immediately transported to the laboratory in a cold storage container (< 10 °C). Two tubes were used to collect the samples, containing buffer/stabilizer RNA later and glass beads, one tube for GM analysis and the other for SCFA analysis. The materials and instructions for fecal sample collection were provided to the subjects prior to the fecal collection schedule. The subjects were instructed to defecate on the trail paper (smooth side up) and were prevented from wetting the fecal paper with urine or water. Then they were required to immediately take a sample by scraping the feces with the scooper and capping the tube tightly.

Analysis

Several parameters to measure and analyze the results included: (1) The measurement of body weight and height once a month; (2) The lipid profile; (3) GM analysis; (4) SCFA analysis using gas chromatography; and (5) The measurement of fecal pH using a pH meter.

GM analysis using next-genome sequencing - MiSeq

A high-throughput analysis of 16 rRNA gene sequences was carried out according to the previous method. Areas V3-V4 of the sequences from the bacteria were amplified with the fecal DNA genome (approximately 1 ng) using TaKaRa Ex TaqTM HS (Takara Bio, Japan) and universal primer Bakt_341F (5'-CGCTCTTCCGATCTCTG CCTACGGGGGGGCWGCAG-355)GGCTATICCCACCATTCCCCATTCCACCA CCACCACCACCACCACCACCACCA UTAA. The amplification results were used as a template for the second PCR using barcode-tag primers. The second PCR results were purified using the FastGene Gel/PCR Extraction Kit (NIPPON Genetics, Japan) according to company protocol. The purified products were quantified using the PicoGreen® dsDNA Assay Kit (Life Technologies, United States) based on company protocol. All the PCR samples were of the same total amount (approximately 200 ng total), and they were purified using electrophoresis in 2% (w/v) agarose gel (classic-type Agarose-LE: Nacalai Tesque, Japan), followed by extraction from the gel by the FastGene Gel/PCR Extraction Kit. The purified mixture was applied to the final-pair sequence of Illumina MiSeq v3 (Illumina, United States).

Statistical analysis

The data was displayed as mean ± standard deviation unless stated otherwise. IBM Statistic SPSS 20.0 with a 95% confidence interval (a = 5%) was used to perform

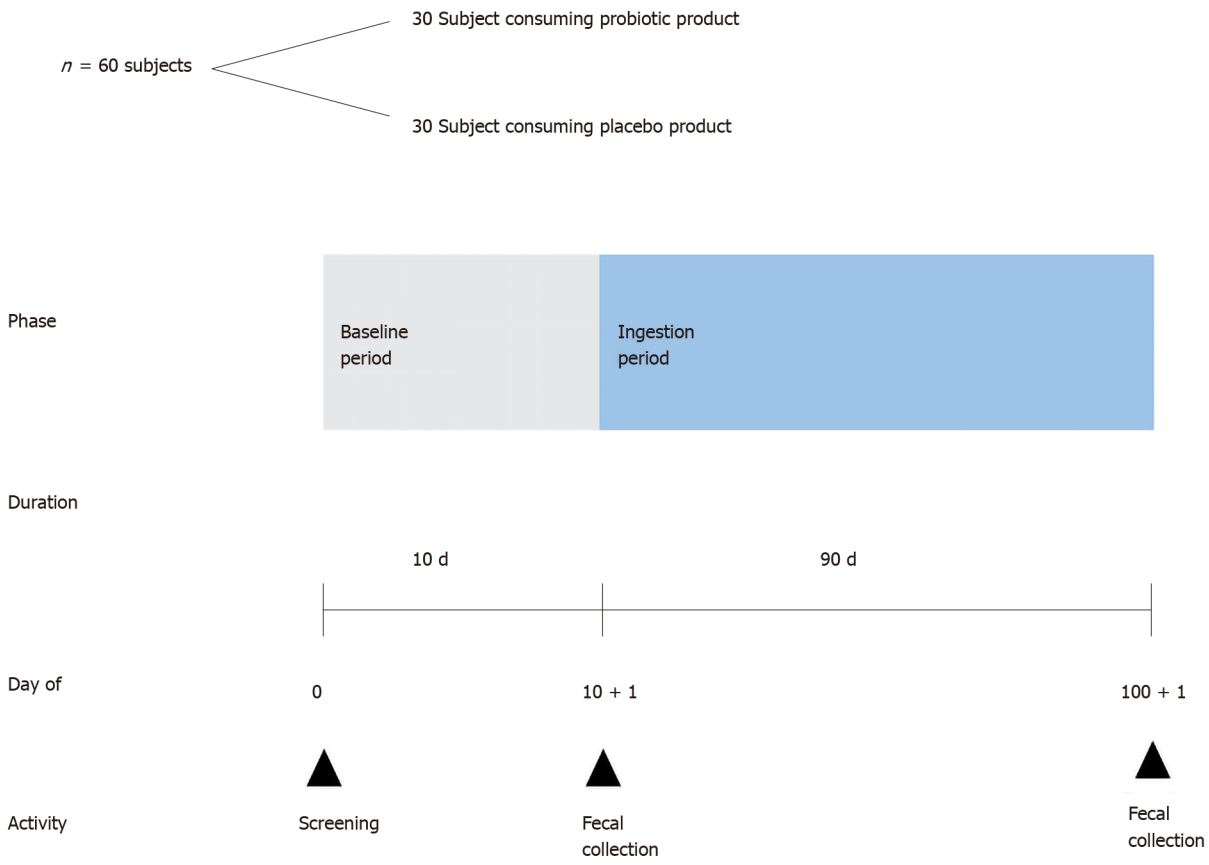


Figure 1 Study design.

statistical analysis. A chi-square test or independent *t*-test or Wilcoxon test was carried out to evaluate the significant differences of the observed parameters between the probiotic-treated group and the placebo group depending on the normality and equality of variance of the data. In addition, a paired *t*-test was used to analyze the observed parameters before and after the consumption of the indigenous probiotic powder or placebo powder.

RESULTS

Demographic data of study subjects

Sixty overweight subjects who participated in the research signed informed consent forms. The subjects were divided into two groups, namely, the probiotic-treated group and the placebo group. Neither the researcher nor the participants knew which subject entered the probiotic group or the placebo group. The research began on January 5, 2019. Fifteen days were allotted for the prescreening period, and the baseline period started on January 21-30, 2019, the intervention period started on January 31 and ended on April 30, 2019. The research ended when all the subjects finished giving their fecal samples to the researcher. The demographic data of the subjects showed no significant differences in age, height, weight, and BMI, and the number of female participants was higher than that of male participants (Table 1).

Body weight, height, and BMI

The body weight, height, and BMI of the subjects were measured every 10 d. Table 2 presents a significant decrease ($P < 0.05$) in the body weight and BMI of the subjects after 90 d of probiotic ingestion. Table 3 further shows the different effects of consuming probiotics between the female and male subjects.

Some studies also reported that probiotics could reduce body weight. Kadooka *et al*[16] found that the probiotic *Lactobacillus gasseri* SBT2055 (LG2055) caused abdominal adiposity, body weight, and other measures to decrease, suggesting its

Table 1 Demographic data of study subjects

	Probiotic-treated group (*n* = 30)	Placebo group (*n* = 30)	*P* value
Age (yr)	44.07 ± 6.23	44.67 ± 5.66	0.42[1]
Height (cm)	159.66 ± 8.27	157.92 ± 9.58	0.40[1]
Weight (kg)	83.45 ± 14.61	79.58 ± 11.79	0.21[1]
BMI (kg/m^2)	32.69 ± 5.07	31.88 ± 3.77	0.18[1]
Women, *n* (%)	18 (60)	18 (60)	0.00[2]
Men, *n* (%)	12 (40)	12 (40)	0.00[2]

[1]Independent sample *t*-test.
[2]Chi-square. BMI: Body mass index.

Table 2 Changes of body weight, height, and body mass index

	Group	Baseline period	Ingestion period	*P* value
Weight	Probiotic-treated	84.54 ± 17.62	83.14 ± 14.71	0.04[2a]
	Placebo	79.37 ± 11.76	78.80 ± 11.77	0.12[1]
Height	Probiotic-treated	159.66 ± 8.27	159.66 ± 8.27	1.00[2]
	Placebo	157.92 ± 9.58	157.92 ± 9.58	1.00[2]
BMI	Probiotic-treated	33.10 ± 6.15	32.57 ± 5.01	0.04[2a]
	Placebo	31.80 ± 3.71	31.56 ± 3.67	0.18[1]

[1]Independent sample *t*-test.
[2]Wilcoxon signed-rank test. A significantly different ([a]$P < 0.05$). BMI: Body mass index.

beneficial influence on metabolic disorders. According to Higashikawa *et al*[17], the heat-killed *Pediococcus pentosaceus* LP28 displayed an anti-obesity effect that reduced BMI, body fat, and waist circumference. Another study revealed that the mean of weight loss in female subjects consuming *Lactobacillus rhamnosus* CGMCC1.3724 (LPR) supplementation was significantly higher than that in women who belonged to the placebo group after the first 12 wk. The body weight and fat mass of the male subjects were not affected by the treatment[18].

Lipid profile

The lipid profile showed that in both groups, there was no significant difference in each parameter measured after consuming the study product. The results of the lipid profile are shown in Table 4.

Fecal characteristics and defecation frequency

Fecal characteristics indicate intestinal conditions in humans. These characteristics include volume, type, color, odor, and pH. The fecal volume of 1 is equal to the volume of a chicken egg. The color is indicated in four scales (1: yellow; 2: brownish yellow; 3: brown; 4: green). The Bristol stool chart was used to identify the type of feces. The aroma of the feces was expressed using a three-point scale (1: normal; 2: strong; 3: very strong). Table 5 shows the fecal characteristics and defecation frequency.

Table 5 indicates that in both the probiotic-treated group and the placebo group, the volume, type, color, odor, and pH of the feces during the baseline and ingestion periods were not significantly changed. The defecation frequency was expressed as the total number or frequency of defecation in 10 d. Overall, the fecal samples from both groups had the following characteristics: Banana-like shape, brownish yellow color, normal odor, and pH of 5.58-5.76.

SCFA

An analysis of SCFAs was performed using gas chromatography. The SCFAs analyzed

Table 3 Different changes of body weight, height, and body mass index in female and male subjects

Gender		Group	Baseline period	Ingestion period	*P* value
Women	Weight	Probiotic-treated	77.91 ± 14.16	77.08 ± 13.68	0.01[1a]
		Placebo	73.20 ± 9.93	72.69 ± 9.93	0.33[1]
	Height	Probiotic-treated	153.82 ± 4.05	153.82 ± 4.05	1.00[2]
		Placebo	151.42 ± 5.92	151.42 ± 5.92	1.00[2]
	BMI	Probiotic-treated	32.90 ± 5.73	32.58 ± 5.58	0.02[1a]
		Placebo	31.96 ± 4.25	31.72 ± 4.14	0.31[1]
Men	Weight	Probiotic-treated	94.48 ± 18.11	92.22 ± 11.45	0.38[1]
		Placebo	88.63 ± 7.51	87.97 ± 7.77	0.16[1]
	Height	Probiotic-treated	168.42 ± 3.92	168.42 ± 3.92	1.00[2]
		Placebo	167.67 ± 3.87	167.67 ± 3.87	1.00[2]
	BMI	Probiotic-treated	33.39 ± 6.98	32.54 ± 4.25	0.37[1]
		Placebo	31.56 ± 2.87	31.32 ± 2.96	0.15[1]

[1]Independent sample *t*-test.
[2]Wilcoxon signed-rank test. A significantly different ([a]$P < 0.05$). BMI: Body mass index.

Table 4 Lipid profile

Lipid profile	Group	Baseline period	Ingestion period	*P* value
Cholesterol (mg/dL)	Probiotic-treated	194.93 ± 37.64	192.20 ± 36.55	0.46[2]
	Placebo	193.70 ± 29.47	192.37 ± 29.75	0.41[2]
Triglyceride (mg/dL)	Probiotic-treated	151.50 ± 63.92	166.83 ± 75.02	0.16[2]
	Placebo	191.40 ± 133.60	187.73 ± 111.58	0.54[2]
HDL (mg/dL)	Probiotic-treated	40.33 ± 9.77	40.00 ± 9.28	0.69[1]
	Placebo	39.93 ± 7.29	40.60 ± 8.18	0.39[1]
LDL (mg/dL)	Probiotic-treated	141.43 ± 32.17	136.97 ± 33.12	0.18[2]
	Placebo	134.50 ± 24.84	133.50 ± 27.06	0.71[1]
Ratio of LDL/HDL	Probiotic-treated	3.63 ± 0.95	3.55 ± 0.87	0.38[1]
	Placebo	3.44 ± 0.70	3.39 ± 0.84	0.61[1]

[1]Paired *t*-test.
[2]Wilcoxon signed-rank test. A significantly different ($P < 0.05$). LDL: Low-density lipoprotein; HDL: High-density lipoprotein.

in this study included acetic acid, propionate, and butyrate. Table 6 shows the SCFA concentration of the probiotic-treated and placebo groups. It also shows that the SCFAs did not significantly change ($P > 0.05$) in both groups after the ingestion period. The SCFAs function *via* diverse host molecular mechanisms to regulate host energy intake, energy expenditure, and storage[19]. The production of SCFAs by bacteria that ferment carbohydrates contribute 10% of the total energy to be absorbed in the colon, and the rest would be lost through the feces[20]. One study proved that the administration of *L. salivarius* Ls-33 to obese adolescent subjects did not have a significant effect[21]. Likewise, the administration of *L. plantarum* Dad-13 in this study did not affect the SCFA concentration of the overweight subjects. The pH value in the treatment group was 5.72 ± 0.31 before ingestion and 5.76 ± 0.28 after ingestion. The pH value in the placebo group was 5.58 ± 0.40 before ingestion and 5.75 ± 0.34 after ingestion. This insignificant change of fecal pH was attributed to insignificant SCFA concentration, so the intestines' condition did not change.

Table 5 Fecal characteristic (volume, type, color, odor, pH) and defecation frequency

	Group	Baseline period	Ingestion period	*P* value
Volume	Probiotic-treated	2.20 ± 0.79	2.23 ± 0.96	0.86[1]
	Placebo	2.37 ± 0.95	2.29 ± 0.90	0.23[2]
Type	Probiotic-treated	3.59 ± 0.93	3.22 ± 1.17	0.08[1]
	Placebo	4.02 ± 1.14	3.89 ± 0.93	0.34[2]
Color	Probiotic-treated	1.86 ± 0.57	1.73 ± 0.55	0.20[1]
	Placebo	2.00 ± 0.59	1.95 ± 0.54	0.70[1]
Odor	Probiotic-treated	1.11 ± 0.37	1.10 ± 0.28	0.93[2]
	Placebo	1.26 ± 0.35	1.32 ± 0.41	0.57[2]
pH	Probiotic-treated	5.72 ± 0.31	5.76 ± 0.28	0.51[3]
	Placebo	5.58 ± 0.40	5.75 ± 0.34	0.07[3]
Defecation frequency[4]	Probiotic-treated	12.93 ± 3.61	13.40 ± 4.52	0.58[2]
	Placebo	14.67 ± 4.93	15.70 ± 7.57	0.51[2]

[1]Independent sample *t*-test.
[2]Wilcoxon signed-rank test.
[3]Paired *t*-test.
[4]Every 10 d.

Table 6 Short-chain fatty acid (acetic acid, propionic acid, and butyrate acid) of feces

	Group	Baseline period	Ingestion period	*P* value[a]
Acetic acid (mmol/kg)	Probiotic-treated	63.19 ± 34.97	64.76 ± 17.61	0.89
	Placebo	67.09 ± 19.56	63.76 ± 13.05	0.65
Propionic acid (mmol/kg)	Probiotic-treated	22.02 ± 14.17	20.65 ± 9.76	0.67
	Placebo	21.98 ± 10.44	17.16 ± 2.04	0.17
Butyrate acid (mmol/kg)	Probiotic-treated	14.78 ± 6.68	14.97 ± 7.24	0.95
	Placebo	19.45 ± 8.60	15.59 ± 9.40[a]	0.33

[a]Paired *t*-test with significance level of 5%.

Diet profile

Diet or food intake is associated with obesity. This study also recorded the daily diet of the subjects. The dietary records were analyzed using the NutriSurvey 2007 software. The household size based on the standard issued by the Republic of Indonesia Ministry of Health in 2014 was used to measure the amount of food intake. Table 7 below summarizes the diet profile of the subjects.

Based on the analysis of the dietary patterns of the subjects, the standard deviation was high, which indicates that the nutrient intake of the subjects was very diverse. Compared to the intake during the baseline period, both the probiotic-treated group and the placebo group consumed less energy, protein, lipid, carbohydrate, and PUFA sources in the last month of the ingestion period. In addition, the average daily energy intake of the subjects was around 1518.17-1642.88 kcal/d, less than that of a normal adult (around 2000 kcal/d)[22]. The consumption of dietary fiber sources experienced a gradual drop from day 41 to the end of the study period. Meanwhile, no significant differences were observed in the intake of cholesterol between the baseline period and the end of the ingestion period in both the probiotic-treated group and the placebo group.

Table 7 Diet profile of subjects

	Group	Baseline period	Ingestion day 11-20	Ingestion day 21-30	Ingestion day 31-40	Ingestion day 41-60	Ingestion day 61-80	Ingestion day 81-100
Energy (kcal)	Probiotic-treated	1518.17 ± 484.46	1322.04 ± 431.90	1338.23 ± 376.17	1274.13 ± 390.37	1124.89 ± 378.82[a]	1060.65 ± 286.86[a]	1103.54 ± 311.74[a]
	Placebo	1642.88 ± 599.33	1660.02 ± 611.62	1562.79 ± 1144.53	1396.65 ± 476.01[a]	1085.16 ± 346.08[a]	1047.90 ± 313.37[a]	1105.73 ± 313.58[a]
Water (g)	Probiotic-treated	744.06 ± 526.92	633.17 ± 397.27	593.60 ± 377.72	691.70 ± 470.44	720.66 ± 551.62	656.24 ± 419.94	712.81 ± 438.11
	Placebo	1122.19 ± 615.82	1016.66 ± 665.44	1041.80 ± 568.23	1100.16 ± 601.35	688.97 ± 533.39[a]	813.86 ± 565.46	841.27 ± 595.64
Protein (g)	Probiotic-treated	52.72 ± 19.49	44.69 ± 16.73	46.23 ± 14.61	46.81 ± 12.61	38.49 ± 14.10[a]	38.30 ± 10.23[a]	39.62 ± 11.30[a]
	Placebo	53.92 ± 24.02	55.03 ± 25.52	47.12 ± 33.52	47.02 ± 18.70	38.38 ± 12.95[a]	35.67 ± 10.98[a]	39.09 ± 9.72[a]
Lipid (g)	Probiotic-treated	61.41 ± 30.24	47.15 ± 26.32	47.60 ± 21.41	49.86 ± 19.25	40.78±15.24[a]	39.63 ± 12.02[a]	40.78 ± 12.99[a]
	Placebo	64.15 ± 34.36	63.17 ± 38.78	54.22 ± 36.98	52.15 ± 25.09[a]	36.99 ± 13.85[a]	36.88 ± 12.74[a]	37.68 ± 9.70[a]
Carbo-hydrate (g)	Probiotic-treated	190.85 ± 68.00	179.93 ± 57.44	180.95 ± 65.23	160.50 ± 59.23	150.80 ± 56.88	137.97 ± 43.53[a]	144.63 ± 46.33[a]
	Placebo	216.39 ± 88.21	221.71 ± 83.07	224.10 ± 190.74	186.27 ± 71.98	149.82 ± 48.91[a]	144.70 ± 49.45[a]	153.74 ± 60.37[a]
Fiber (g)	Probiotic-treated	10.96 ± 5.88	8.66 ± 3.04	8.71 ± 2.91	8.49 ± 2.63	7.08 ± 2.16[a]	6.24 ± 2.01[a]	6.61 ± 2.48[a]
	Placebo	12.17 ± 7.15	13.34 ± 9.00	11.90 ± 8.61	10.20 ± 4.67	6.96 ± 2.99[a]	7.17 ± 2.30[a]	7.45 ± 2.30[a]
PUFA (g)	Probiotic-treated	16.87 ± 13.02	12.80 ± 7.73	12.17 ± 5.87	13.03 ± 7.64	12.17 ± 7.36	10.91 ± 4.50	10.86 ± 4.31
	Placebo	18.20 ± 13.73	18.49 ± 15.71	15.70 ± 13.47	16.29 ± 13.52	10.50 ± 5.94[a]	10.03 ± 4.70[a]	9.73 ± 3.1[a]
Choles-terol (mg)	Probiotic-treated	191.39 ± 163.58	163.28 ± 83.55	168.44 ± 92.31	182.29 ± 68.95	160.32 ± 84.56	172.70 ± 77.78	179.23 ± 57.13
	Placebo	170.42 ± 154.32	168.91 ± 169.50	142.45 ± 159.96	164.19 ± 124.86	173.22 ± 86.80	165.31 ± 85.03	182.64 ± 81.91

[a]$P < 0.05$ based on Independent sample *t*-test compared to the nutrient intake in baseline. PUFA: Polyunsaturated fatty acid.

Population of GM in overweight subjects

Based on the results of the 16 RNA sequences using MiSeq performed in both the probiotic-treated and placebo groups, the bacterial group was dominated by the phyla *Firmicutes*, *Bacteroidetes*, *Actinobacteria*, *Proteobacteria*, *Fusobacteria*, and *Verrucomicrobia* (Figure 2). A small portion of the phyla *Cyanobacteria*, *Lentisphaerae*, *Elusimicrobia*, and *Synergistetes* appeared in both the treatment and control groups (Table 8).

The phylum distribution composition of each subject from both the treatment and control groups can be seen in Figure 3. Three genera - *Firmicutes*, *Bacteroidetes*, and *Actinobacteria* - are the most dominant genera appearing on almost all the subjects, while some phyla, such as *Proteobacteria* and *Fusobacteria*, appear dominantly in only a few subjects.

Concerning the two dominant phyla, the number of *Bacteroidetes* significantly increased ($P < 0.05$) in both the treatment and placebo groups after the ingestion period (Table 9), and the number of *Firmicutes* significantly decreased ($P < 0.05$) in the treatment group (Figure 4). Meanwhile, the *Fusobacteria* population was only found in a few subjects. The *Verrucomicrobia* population significantly decreased in both the treatment and placebo groups after the ingestion period. *Verrucomicrobia* was often associated with gastrointestinal health and glucose homeostasis. No significant changes ($P > 0.05$) were found in the phyla of *Cyanobacteria*, *Elusimicrobia*, *Lentisphaerae*, and *Synergistetes* in the treatment and placebo groups before and after the ingestion period. The changes in phylum of bacterial composition in both the probiotic-treated and placebo groups before and after the ingestion period are presented in Figure 4.

At the genus level (as shown in Table 8), some microbiota showed some changes in

Table 8 Gut microbiota composition based on genus

Phylum	Genus	Probiotic-treated			Placebo		
		Baseline, mean (%) ± SD	Ingestion, mean (%) ± SD	*P* value	Baseline, mean (%) ± SD	Ingestion, mean (%) ± SD	*P* value
Firmicutes	*Faecalibacterium*	11.43 ± 5.03	10.94 ± 4.21	0.614	15.30 ± 7.07	11.82 ± 5.50	0.01[a]
	Coprococcus	7.53 ± 3.55	6.23 ± 1.85	0.037[a]	7.34 ± 3.71	5.82 ± 2.67	0.116
	Other	7.63 ± 5.05	8.22 ± 4.15	0.491	6.03 ± 4.13	8.40 ± 4.56	0.012[a]
	Ruminococcus	4.49 ± 4.06	3.69 ± 2.90	0.271	3.80 ± 3.84	3.70 ± 4.79	0.572
	Roseburia	1.36 ± 1.31	1.54 ± 1.10	0.072[b]	1.49 ± 1.55	2.04 ± 1.28	0.037[a]
	Clostridium	0.16 ± 0.22	0.16 ± 0.27	0.829	0.25 ± 0.53	0.35 ± 0.49	0.202
	Paenibacillus	0.01 ± 0.01	0.00 ± 0.01	0.1	0.03 ± 0.06	0.00 ± 0.01	0.002[a]
Bacteroidetes	*Prevotella*	14.56 ± 11.57	19.25 ± 13.03	0.066[b]	14.15 ± 13.69	14.28 ± 14.13	0.75
	Bacteroides	3.78 ± 5.43	5.57 ± 8.21	0.019[a]	5.59 ± 9.97	10.30 ± 13.83	0.04[a]
Actino-bacteria	*Bifidobacterium*	3.38 ± 4.96	2.74 ± 4.01	0.6	3.07 ± 3.95	2.71 ± 2.91	0.957
	Collinsella	2.02 ± 1.40	1.52 ± 0.94	0.069[b]	2.00 ± 1.80	1.51 ± 0.98	0.271
	Brevibacterium	0.01 ± 0.01	0.00 ± 0.01	0.307	0.03 ± 0.07	0.01 ± 0.02	0.082[b]
Proteo-bacteria	*Succinivibrio*	2.19 ± 4.51	1.44 ± 3.37	0.548	2.06 ± 5.29	2.51 ± 6.89	0.534
	Phyllobacterium	0.02 ± 0.04	0.02 ± 0.02	0.037[a]	0.01 ± 0.03	0.01 ± 0.03	0.167
	Sphingomonas	0.02 ± 0.03	0.02 ± 0.02	0.75	0.01 ± 0.03	0.01 ± 0.03	0.833
Verrucomicrobia	*Akkermansia*	0.13 ± 0.56	0.04 ± 0.18	0.028[a]	0.35 ± 1.64	0.02 ± 0.07	0.024[a]

[a]Paired *t*-test with significance level of 5% ($P < 0.05$).
[b]Significance level 10% ($P < 0.1$).

composition. However, not all genera of the whole phylum experienced some changes. In the phylum *Firmicutes*, *Faecalibacterium* was quite significant in the placebo group compared with the treatment group ($P < 0.05$). One species of *Faecalibacterium* that is quite abundant in the human digestive tract is *Faecalibacterium prausnitzii*. *Faecalibacterium* is a fairly dominant digestive microbiota, as indicated by the fact that 5%-15% of total bacteria are *F. prausnitzii* species[23]. *F. prausnitzii* is also considered one of the health indicators of gastrointestinal health. Healthy subjects normally showed an abundance of *F. prausnitzii* compared with subjects with Crohn's disease[24]. The genus *Coprococcus* showed a significant decrease in the treatment group ($P < 0.05$). *Coprococcus* is characterized as comprising anaerobic microbes able to produce butyrate acid. Countless studies have associated *Coprococcus* with the health conditions of the human digestive tract. One study showed that its healthy subjects had a high abundance of *Coprococcus* compared with subjects with colorectal cancer[25]. Other studies showed that the number of *Bacteroides* and *Coprococcus* in subjects with colorectal pre-cancerous conditions was much lower than that in healthy subjects[26]. Body conditions in humans, such as obesity or being overweight, can also affect the conditions of microbiota. The populations of *Blautia*, *Coprococcus*, and *Enterobacteriaceae* were quite high in overweight children in Mexico compared with those with normal conditions[27].

Table 8 shows that *Roseburia* significantly increased in both the treatment ($P < -0.01$) and placebo groups ($P < 0.05$). *Roseburia* is a microbiota of the genus *Firmicutes* that has the characteristics of gram-positive, obligate anaerobes and can produce the SCFA butyrate. In the human digestive tract, one of the species of *Roseburia* - namely, *Roseburia hominis* - can regulate immunity[28]. An increase in the population of *Roseburia* can also be attributed to the type of food consumed. The consumption of resistant starch is said to increase *Eubacterium rectale* and *Roseburia*[29]. The *Roseburia* population in humans is quite varied. A study of groups of obese and overweight children showed a fairly high *Roseburia* population compared with the normal group[27].

The *Paenibacillus* genus, as shown in Table 8, decreased in both groups, but only the placebo control group experienced a significant decrease. The genus *Clostridium* did not significantly change in both groups, but the placebo group experienced a slight

Table 9 Composition of gut microbiota (based on the most abundant in phylum population) in the probiotic-treated and placebo groups before and after ingestion period

No.	Phylum	Group	Baseline period	Ingestion period	*P* value[a]
1	*Firmicutes*	Probiotic-treated	69.90 ± 15.95	64.13 ± 15.22	0.037[a]
		Placebo	70.66 ± 14.41	65.30 ± 14.52	0.153
2	*Bacteroidetes*	Probiotic-treated	20.63 ± 11.49	28.27 ± 14.26	0.008[a]
		Placebo	21.30 ± 12.72	26.71 ± 13.93	0.045[a]
3	*Actinobacteria*	Probiotic-treated	6.11 ± 5.37	5.07 ± 5.48	0.237
		Placebo	5.55 ± 4.90	4.63 ± 3.61	0.453
4	*Proteobacteria*	Probiotic-treated	2.87 ± 6.39	2.04 ± 6.05	0.491
		Placebo	1.84 ± 4.32	1.69 ± 3.77	0.572
5	*Fusobacteria*	Probiotic-treated	0.23 ± 0.57	0.34 ± 0.86	0.701
		Placebo	0.20 ± 0.94	1.58 ± 6.57	0.044[a]
6	*Verrucomicrobia*	Probiotic-treated	0.13 ± 0.57	0.04 ± 1.66	0.028[a]
		Placebo	0.35 ± 0.19	0.02 ± 0.07	0.024[a]
7	*Cyanobacteria*	Probiotic-treated	0.09 ± 0.29	0.07 ± 0.21	0.537
		Placebo	0.06 ± 0.24	0.04 ± 0.10	0.427
8	*Lentisphaerae*	Probiotic-treated	0.02 ± 0.05	0.01 ± 0.08	0.681
		Placebo	0.03 ± 0.02	0.03 ± 0.11	0.334
9	*Elusimicrobia*	Probiotic-treated	0.00 ± 0.01	0.00 ± 0.03	0.655
		Placebo	0.01 ± 0.02	0.00 ± 0.00	0.317
10	*Synergistetes*	Probiotic-treated	0.00 ± 0.00	0.00 ± 0.00	0.655
		Placebo	0.00 ± 0.00	0.00 ± 0.01	0.273

[a]Paired *t*-test with significance level of 5%.

increase in abundance. The genus *Ruminococcus* decreased significantly in the probiotic-treated group.

The *Coprococcus* genus experienced a significant decrease in the treatment group after consumption, inversely proportional to the genus *Roseburia*, which experienced a significant increase in the treatment group after consumption. *Roseburia* also experienced a significant increase in the control group after the ingestion period. The genera *Faecalibacterium* and *Paenibacillus* experienced a decrease in the placebo group after the ingestion period. No significant differences were observed in the genera *Clostridium* and *Ruminococcus* in both the treatment and placebo groups after the ingestion period.

The second dominant phylum (Table 9) is *Bacteroidetes*, which increased in the treatment group. The genus *Bacteroides* significantly increased in both the probiotic-treated and placebo groups ($P < 0.05$). However, the genus *Prevotella* significantly increased ($P < 0.1$) in the probiotic-treated group. Previous papers mentioned that *Prevotella* is the dominant genus in the phylum *Bacteroidetes* for healthy school-aged children (Murugesan *et al*[27] 2015) and adult Indonesians (Rahayu *et al*[13] 2019). In this study, the population of *Prevotella* is much higher than that of *Bacteroides*. This finding supports previous reports stating that Indonesians have the *Prevotella* enterotype.

The relative abundance of the phylum *Actinobacteria* - namely, the genera Brevibacterium, *Bifidobacteria*, and *Collinsella* - is shown in Table 8. *Brevibacterium* in the treatment group significantly decreased after the ingestion period and showed a significant decrease in the genus *Collinsella* in the treatment group ($P < 0.1$) compared with the placebo group. *Collinsella* is a microbiota of the phylum *Actinobacteria*. These microbiota were often said to be pathobionts, which have the potential to influence the nature of the pathogen to its host[30]. Subjects with obesity and having type 2 diabetes are said to have a high abundance of *Collinsella* compared with healthy people[31].

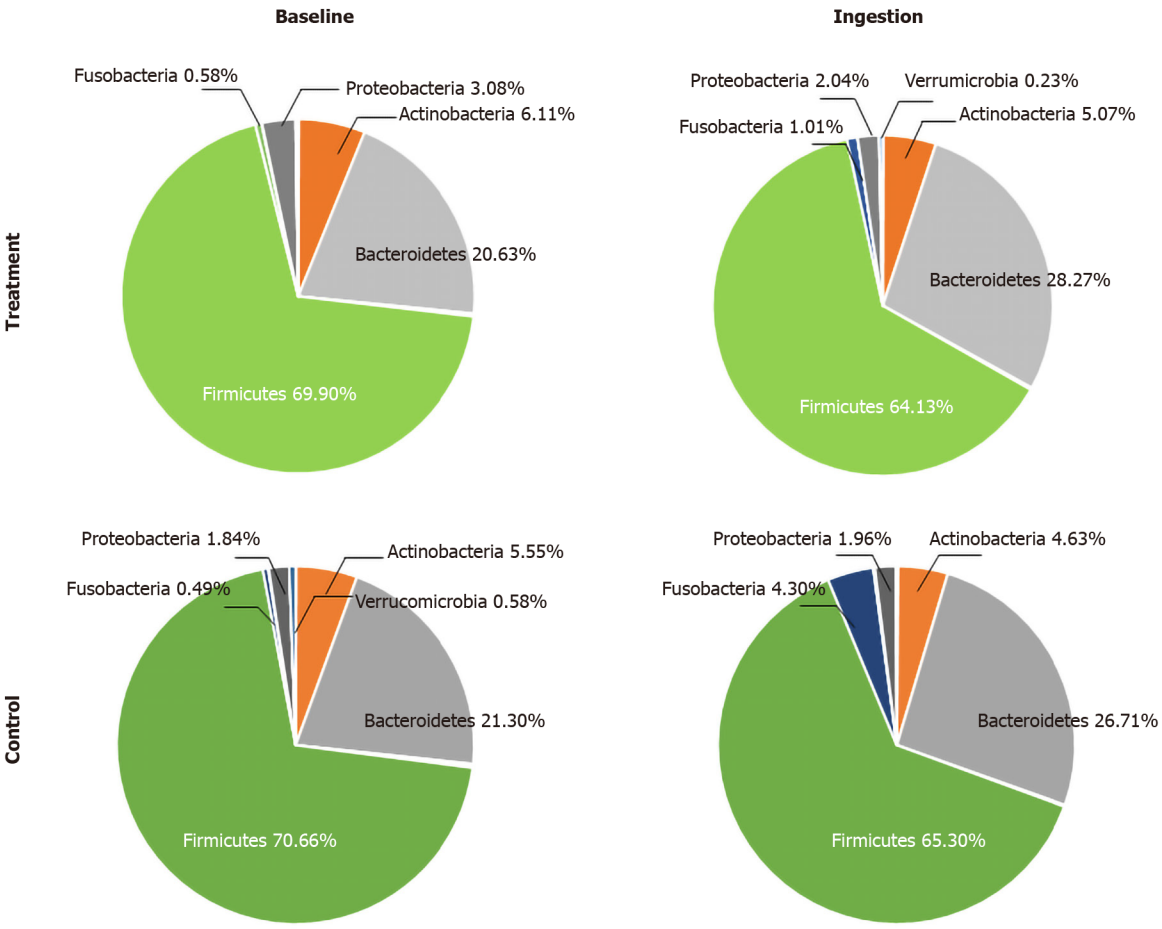


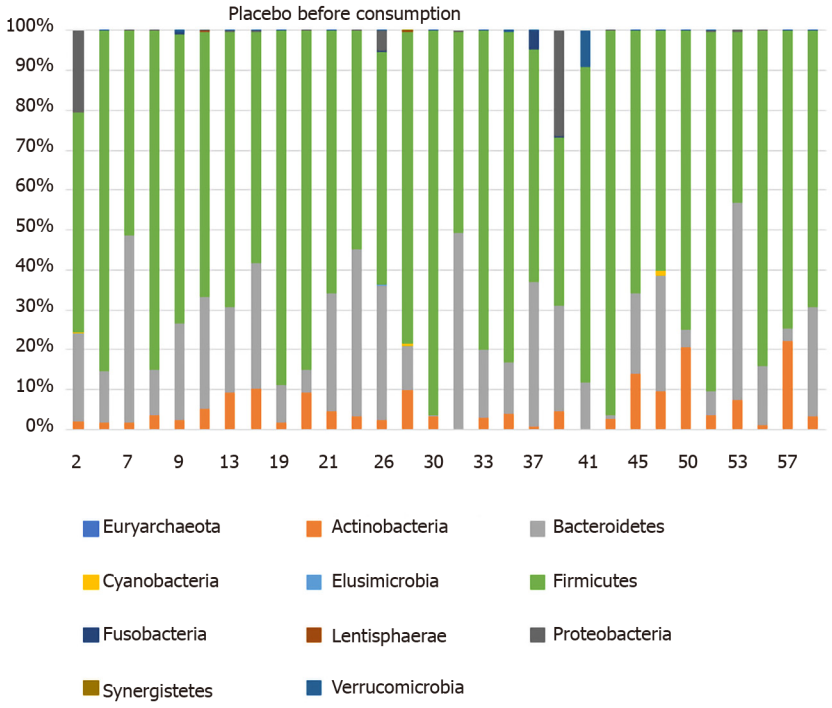
Figure 2 The composition of gut microbiota [relative abundance (%) in the probiotic-treated and placebo groups before and after ingestion period].

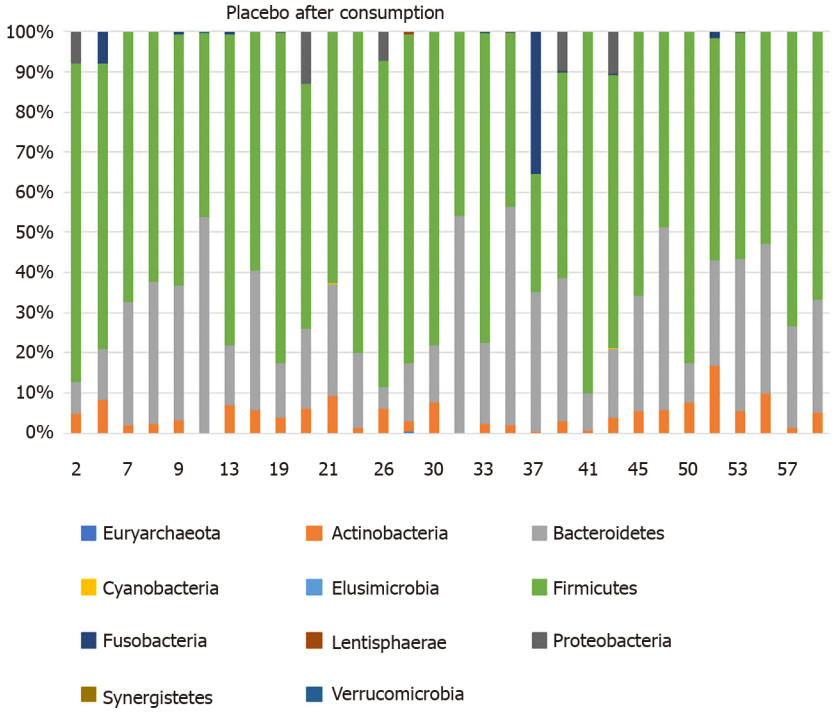
Table 8 shows that the genus Phyllobacterium of the phylum *Proteobacteria* increased significantly in the treatment group, while no significant change in the genera *Succinivibrio* and *Sphingomonas* was found in both the treatment and placebo groups. Meanwhile, the abundance of the genus *Akkermansia* in the phylum *Verrucomicrobia* decreased significantly.

From the analyses using LeSfe with a *P* value of < 0.05 (LDA > 2.0), one against all showed a significant difference in bacterial abundance in the probiotic-treated and placebo groups before and after the ingestion period. Alpha diversity analysis (Figure 5) showed that the abundance of bacteria in the probiotic-treated group significantly increased after they consumed the probiotic powder. This indicates that the consumption of probiotics could increase the abundance of bacteria in obese people, who have a diversity and wealth of microbiota gut components compared with eutrophic subjects[32]. At the genus level, a significant increase was observed in the abundance of the genus Phyllobacterium in the probiotic-treated group after consumption, whereas in the control group, *Roseburia* abundance increased significantly after consumption. The Brevibacterium, *Paenibacillus*, *Bacillales*, and *Faecalibacterium* groups were abundant in the placebo group before the consumption of the placebo product.

DISCUSSION

Ley *et al*[33] authored one of the first studies linking GM to obesity in humans[4]. The results from the 16 rRNA gene sequences in mouse models indicated that the two most abundant bacterial phyla were *Firmicutes* (60%-80%) and *Bacteroidetes* (20%-40%). In particular, the *ob*/*ob* mice had a 50% decrease in the population of *Bacteroidetes* and a proportional increase in *Firmicutes*. These changes indicate that obesity affects the diversity of GM and suggest that the intentional manipulation of the community


Placebo before consumption
100%
90%
80%
70%
60%
50%
40%
30%
20%
10%
0%
2 7 9 13 19 21 26 30 33 37 41 45 50 53 57
Euryarchaeota
Actinobacteria
Bacteroidetes
Cyanobacteria
Elusimicrobia
Firmicutes
Fusobacteria
Lentisphaerae
Proteobacteria
Synergistetes
Verrucomicrobia


Placebo after consumption
100%
90%
80%
70%
60%
50%
40%
30%
20%
10%
0%
2 7 9 13 19 21 26 30 33 37 41 45 50 53 57
Euryarchaeota
Actinobacteria
Bacteroidetes
Cyanobacteria
Elusimicrobia
Firmicutes
Fusobacteria
Lentisphaerae
Proteobacteria
Synergistetes
Verrucomicrobia

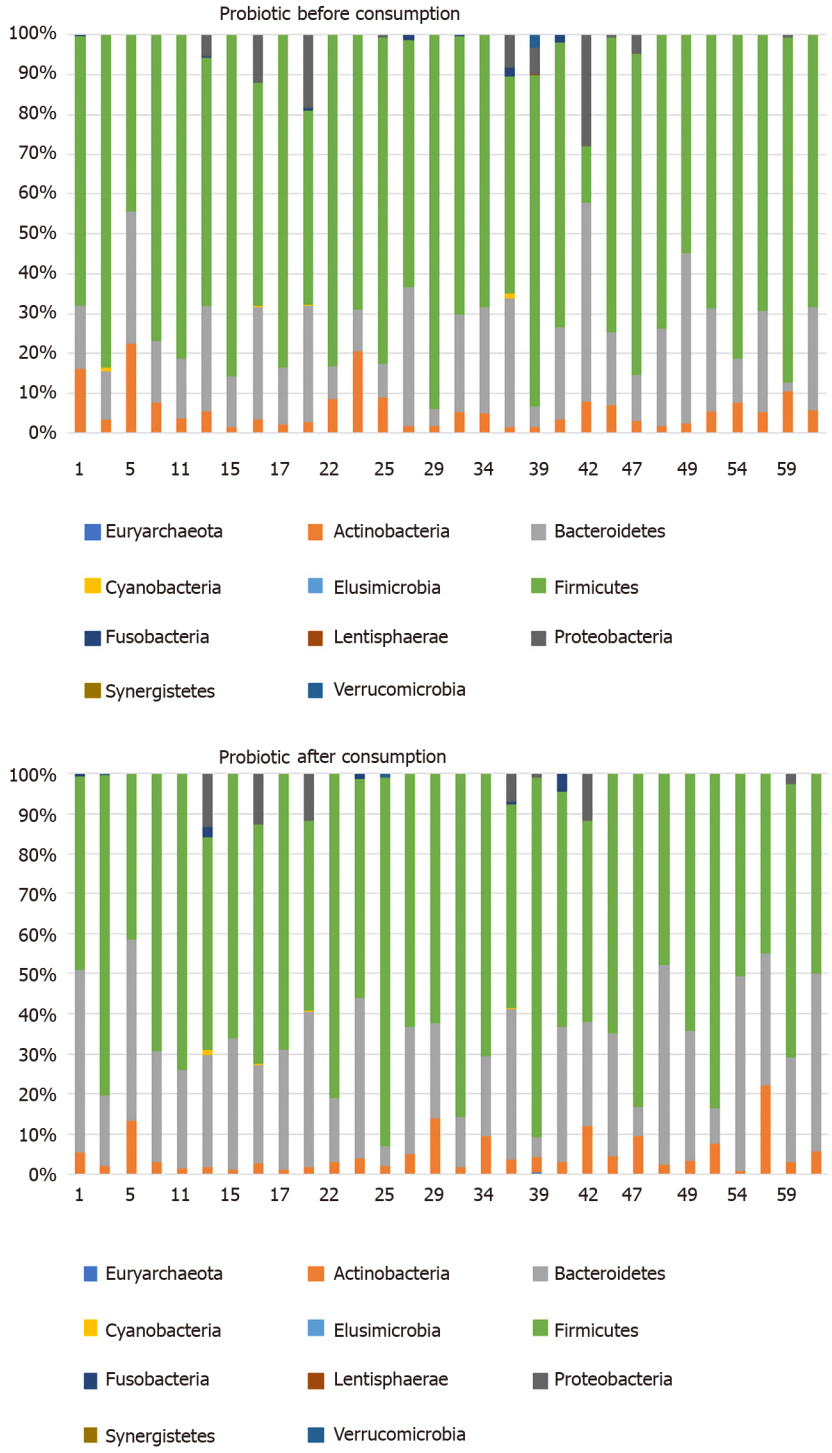


Figure 3 The phylum distribution composition of each subject from both probiotic-treated and placebo groups. The number on the X-axis represents the code of subject.

structure may be useful to regulate the energy balance in the obese individual[4,33]. Meanwhile, Turnbaugh *et al*[34] and Furet *et al*[35] found a lower representation of *Bacteroidetes* (*Bacteroides*/*Prevotella*) in obese individuals, with no differences in the *Firmicutes phylum*.

In addition, an ongoing review of GM and obesity found evidence of the association between gut bacteria and obesity[36,37]. Normally, the subclass distributions of GM are composed of the following: *Bacteroidetes* (23%), comprising the genus *Bacteroides*; *Firmicutes* (64%), including *Bacilli*, *Clostridia*, and *Mollicutes*; *Proteobacteria* (8%), gram-negative bacteria, such as *E. coli* and *Helicobacter pylori*; *Fusobacteria*, *Verrucomicrobia*, and *Actinobacteria* (3%), which include species such as *Bifidobacteria*; and only about 2% of other phyla. Our findings also indicate that an obese person has a different microbial proportion of the dominant phyla, which consists of the higher *Firmicutes* of

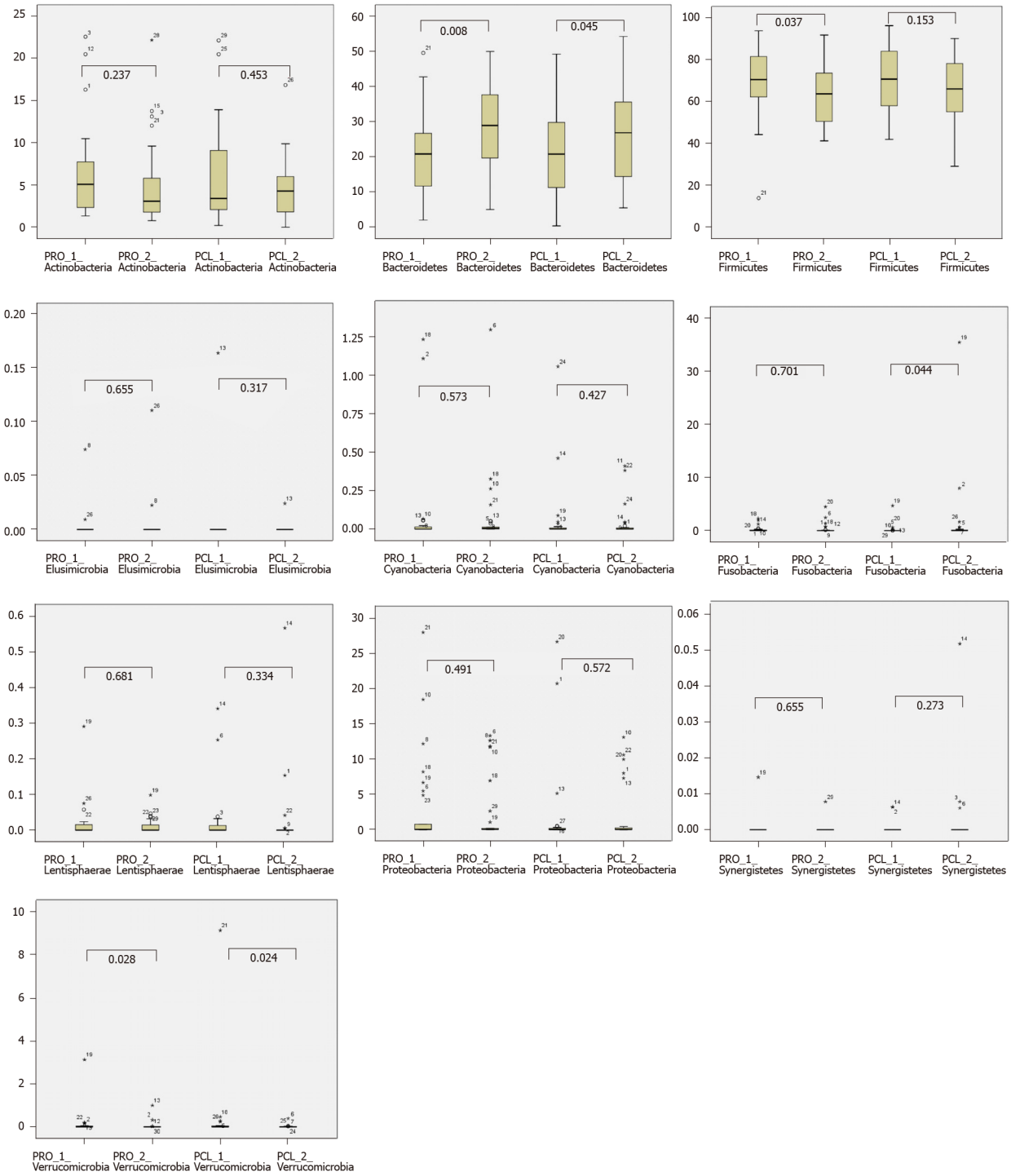


Figure 4 The changes in phylum of bacterial composition in both probiotic-treated and placebo groups before and after ingestion period.
PRO1: Probiotic before ingestion; PRO2: Probiotic after ingestion; PLC1: Placebo before ingestion; PLC2: Placebo after ingestion.

about 70% and the lower *Bacteroidetes* of about 21%, compared with a normal person, as mentioned in another study by Abenavoli *et al*[37]. The other phyla comprise *Actinobacteria* at about 6%, *Proteobacteria* at 3%, and less than 1% of other bacteria, such as *Fusobacteria*, *Verrucomicrobia*, *Cyanobacteria*, and *Lentisphaerae*.

Jumpertz *et al*[38] investigated the dynamic changes of GM during diets that varied in caloric content in the feces of lean and obese individuals by measuring ingested and stool calories using bomb calorimetry. The alteration of the nutrient load induced rapid changes in the GM. These changes were directly correlated with stool energy loss in lean individuals, such as a 20% increase in *Firmicutes* and a corresponding decrease in *Bacteroidetes*, which were associated with an increased energy harvest. A high degree of overfeeding in lean individuals was accompanied by a greater fractional decrease in stool energy loss. These results show that the nutrient load is a

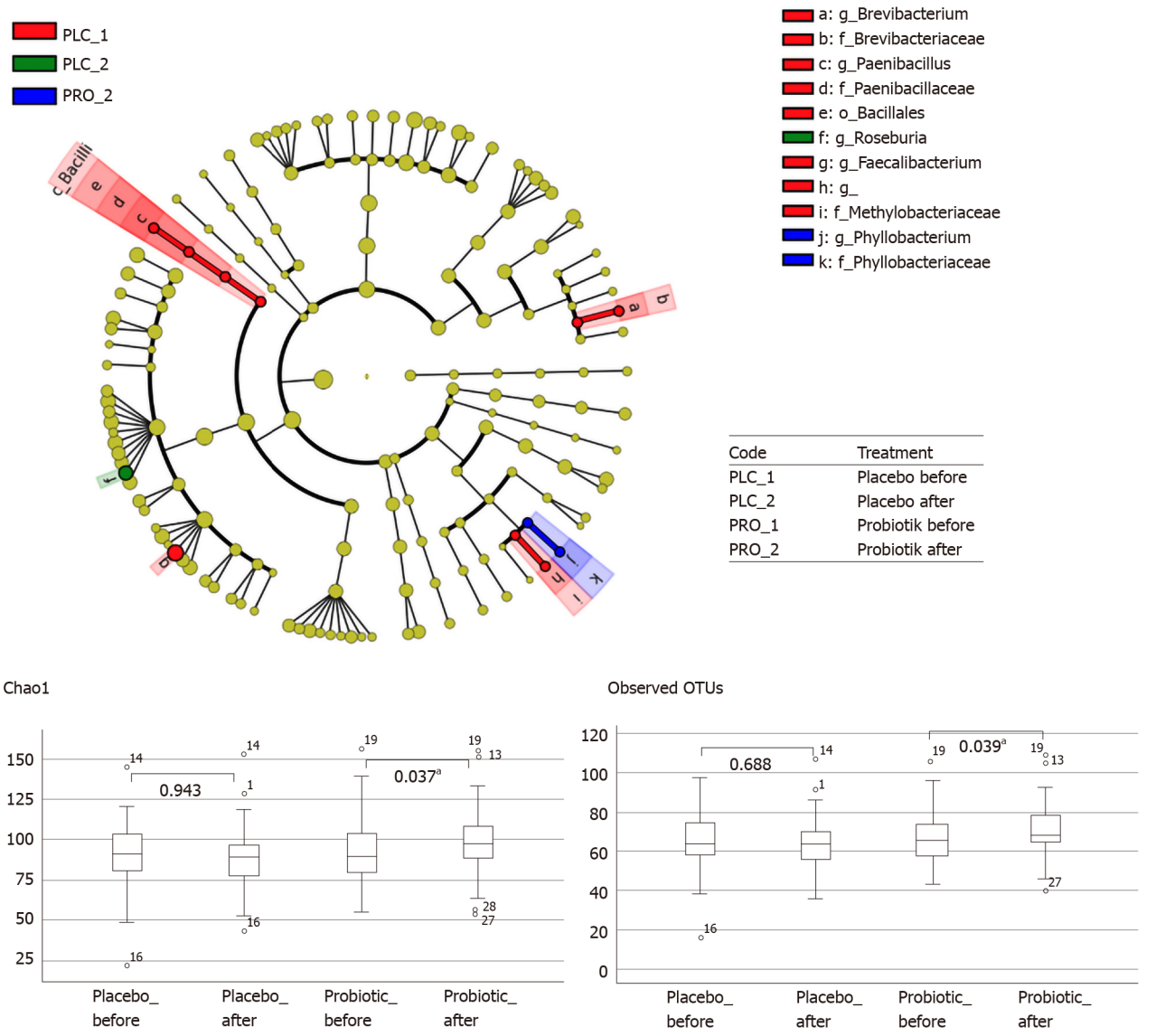


Figure 5 Cladogram and Alpha diversity on the treatment group and placebo group before and after the ingestion period. PRO1: Probiotic before ingestion; PRO2: Probiotic after ingestion; PLC1: Placebo before ingestion; PLC2: Placebo after ingestion.

key variable that can influence the gut (fecal) bacterial community structure over short periods. Furthermore, the observed associations between gut microbes and nutrient absorption indicate a possible role of the human GM in the regulation of the nutrient harvest. Recent studies have shown that the increase of bile acids in the intestine when comparing sterile rats with normal rats would show that the GM are related to not only obesity but also a diverse range of metabolic diseases[39].

Several mechanisms have been proposed for GM causative action in obesity physiopathology. In fact, gut commensal bacteria interact with our metabolism at several points. They help convert ingested complex nutrients to SCFAs, transform mucins and dietary fibers into simple sugars ready for absorption, stimulate intestinal epithelial proliferation, and favor nutrient absorption and metabolism. They are the main actor in shaping the gut crucial defense barrier constituted by the systemic and mucosal immune system and activate bio-inactive compounds[40]. Nevertheless, GM play an important role in human adipose tissue formation and deposition. Indeed, our intestinal bacteria can maintain the human body's energy balance mainly because of their ability to share the otherwise indigestible components of a mammalian's diet[41]. In this study, the average daily energy intake of the subjects was around 1518.17-1642.88 kcal/d, less than that of a normal adult (around 2000 kcal/d). No significant differences were observed in the diet profile of the subjects in both the probiotic-treated and placebo groups.

Abenavoli *et al*[37] mentioned in their review that evidence of the association between gut bacteria and obesity exists in both infants and adults. Several genetic, metabolic,

and inflammatory pathophysiological mechanisms are involved in the interplay between gut microbes and obesity. Microbial changes in the human gut can be considered a factor in obesity development in humans. The modulation of the bacterial strains in the digestive tract can help reshape the metabolic profile in the human obese host, as suggested by data from several animal and human studies. Several reports have also been conducted on the probiotic treatment of obese individuals. In adults, different strains of *Lactobacillus* and *Bifidobacterium*, alone or in combination, as well as *P. pentosaceus* led to a significant reduction of body weight, BMI, waist circumference, and fat mass[17,42-46].

As the administered dosage of probiotics affects the efficacy of the treatment, reduced visceral adiposity and waist circumference were observed after exposure to a high dose of *L. gasseri* BNR17[44]. These results were not so unambiguous given the different doses of Ecologic® (a mixture of multi-strains of *Lactobacillus* and *Bifidobacterium*), although this study was only conducted on obese women[47]. Interestingly, a report by Sanchez *et al*[48] showed the gender-specific effects of probiotics in human obese subjects. Indeed, the administration of *L. rhamnosus* CGMCC1.3724 and a restricted caloric diet resulted in significantly higher weight loss in obese women than in men. This finding can be explained by a greater impact on satiety, eating habits, and mood in women *vs* men[48]. Finally, scant evidence exists on the potential preventive effect on obesity of some probiotics in non-obese subjects. Specifically, VSL#3 can reduce body weight and fat accumulation *via L. gasseri* SBT2055 administration[16,49].

CONCLUSION

No significant differences in pH were found before and after ingestion in both the probiotic and placebo groups as well as in the lipid profile of both cholesterol and triglyceride, high-density lipoprotein (HDL), low-density lipoprotein (LDL), and the LDL/HDL ratio. In addition, no significant changes in the concentration of SCFAs (acetic acid, propionate, and butyrate) were observed after the consumption of the probiotic powder *L. plantarum* Dad-13.

An interesting finding is a significant decrease in body weight and BMI ($P < 0.05$) in the treatment group. This weight loss was particularly observed in the female subjects. GM analysis shows that *L. plantarum* Dad-13 was able to decrease *Firmicutes* and increase *Bacteroidetes* (especially *Prevotella*).

ARTICLE HIGHLIGHTS

Research background

Gut microbiota (GM) play an important role in the nutrient absorption and energy regulation of individuals, thus affecting their nutritional status. GM also affect body weight, especially obesity, a condition wherein the accumulation of abnormal or excessive fat can interfere with health. Obesity in Indonesia showed an increasing prevalence in every province from 2007 to 2018. One study found a link between GM and body weight. Probiotics, as healthy bacteria, can improve an individual's health status by affecting GM composition. The consumption of probiotics may maintain this status and reduce the weight gain of adults with obesity in Indonesia.

Research motivation

This research aimed to investigate the effect of the consumption of an indigenous probiotic on overweight people. The results obtained may be used to determine the condition of GM in overweight people and the effect of indigenous probiotics on the GM of overweight adults. These results may also be used to determine the treatment of probiotic consumption that is most suitable and effective for overweight individuals in Indonesia to improve their health status.

Research objectives

The objective of this study was to determine the effect of the consumption of the indigenous probiotic powder *L. plantarum* Dad-13 on overweight adults in Indonesia.

Research methods

Sixty overweight volunteers with body mass index (BMI) equal to or greater than 25 consumed indigenous probiotic powder *L. plantarum* Dad-13 (2×10^9 CFU/gram/sachet) for 90 d. The study was a randomized, double-blind, placebo-controlled study. The volunteers filled in a diary on a daily basis, which consisted of questions on study product intake (only during the ingestion period), other food intake, number of bowel movements, fecal quality (consistency and color), any medications received, and any symptom of discomfort, such as diarrhea, constipation, vomiting, gassing, sensation of illness, *etc*. Fecal samples and the subjects' diaries were collected on the morning of day 10 + 1, marked as the end of the baseline period and the start of the ingestion period. During the ingestion period (from day 11 to day 101), several parameters to measure and analyze the results included body weight and height (once a month), the lipid profile, GM analysis using MiSeq, short-chain fatty acid (SCFA) analysis using gas chromatography, and the measurement of fecal pH using a pH meter.

Research results

The consumption of indigenous probiotic powder *L. plantarum* Dad-13 by overweight people caused the average body weight and BMI of the probiotic group to decrease from 84.54 ± 17.64 kg to 83.14 ± 14.71 kg and from 33.10 ± 6.15 kg/m^2 to 32.57 ± 5.01 kg/m^2, respectively. No significant reduction in the body weight and BMI of the placebo group was found. An analysis of the microbiota showed that the number of *Bacteroidetes*, specifically *Prevotella*, increased significantly, while *Firmicutes* significantly decreased. No significant change in lipid profile was observed in both groups. Also, no significant change in SCFAs (butyrate, propionate, acetic acid) and pH level were found after the consumption of the probiotic.

Research conclusions

No significant differences in pH were found before and after ingestion in both the probiotic and placebo groups as well as in the lipid profile of both cholesterol and triglyceride, high-density lipoprotein (HDL), low-density lipoprotein (LDL), and the LDL/HDL ratio. In addition, no significant changes were observed in the concentration of SCFAs (acetic acid, propionate, and butyrate) after consumption. Interestingly, a significant decrease in body weight and BMI ($P < 0.05$) was found in the treatment group. An analysis of the GM shows that *L. plantarum* Dad-13 was able to decrease *Firmicutes* and increase *Bacteroidetes* (especially *Prevotella*).

Research perspectives

These results proved that the consumption of probiotics among overweight adults helps significantly reduce body weight, especially in women, and affects the composition of GM.

ACKNOWLEDGEMENTS

The researchers would like to sincerely thank the Indonesian Ministry of Research and Higher Education and Kalbe PT for providing support, as well as the study subjects for their participation.

REFERENCES

1 **World Health Organization**. What is malnutrition? [Internet]. 2020. Available from: https://www.who.int/features/qa/malnutrition/en/
2 **World Health Organization**. Obesity and overweight [Internet]. 2020. Available from: https://www.who.int/news-room/fact-sheets/detail/obesity-and-overweight
3 **Ministry of Health of the Republic of Indonesia**. Report of Indonesia Basic Health Research in 2018. 2018. Available from: https://www.litbang.kemkes.go.id/Laporan-riset-kesehatan-dasar-riskesdas/
4 **Ley RE**, Bäckhed F, Turnbaugh P, Lozupone CA, Knight RD, Gordon JI. Obesity alters gut microbial ecology. *Proc Natl Acad Sci USA* 2005; **102**: 11070-11075 [PMID: 16033867 DOI: 10.1073/pnas.0504978102]
5 **Turnbaugh PJ**, Bäckhed F, Fulton L, Gordon JI. Diet-induced obesity is linked to marked but reversible alterations in the mouse distal gut microbiome. *Cell Host Microbe* 2008; **3**: 213-223

[PMID: 18407065 DOI: 10.1016/j.chom.2008.02.015]
6 **De Filippo C**, Cavalieri D, Di Paola M, Ramazzotti M, Poullet JB, Massart S, Collini S, Pieraccini G, Lionetti P. Impact of diet in shaping gut microbiota revealed by a comparative study in children from Europe and rural Africa. *Proc Natl Acad Sci USA* 2010; **107**: 14691-14696 [PMID: 20679230 DOI: 10.1073/pnas.1005963107]
7 **Delzenne NM**, Cani PD. Interaction between obesity and the gut microbiota: relevance in nutrition. *Annu Rev Nutr* 2011; **31**: 15-31 [PMID: 21568707 DOI: 10.1146/annurev-nutr-072610-145146]
8 **Kobyliak N**, Conte C, Cammarota G, Haley AP, Styriak I, Gaspar L, Fusek J, Rodrigo L, Kruzliak P. Probiotics in prevention and treatment of obesity: a critical view. *Nutr Metab (Lond)* 2016; **13**: 14 [PMID: 26900391 DOI: 10.1186/s12986-016-0067-0]
9 **Rahayu ES**, Yogeswara A, Mariyatun, Windiarti L, Utami T, Watanabe K. Molecular characteristics of indigenous probiotic strains from Indonesia. *Int J Probiotics Prebiotics* 2016; **11**: 109-116
10 **Rahayu ES**, Cahyanto M, Windiarti L, Sutriyanto J, Kandarina T, Utami T. Effects of Consumption of Fermented Milk Containing Indigenous Probiotic Lactobacillus Plantarum Dad-13 on the Fecal Microbiota of Healthy Indonesian Volunteers. *Int J Probiotics Prebiotics* 2016; **11**: 91-98
11 **Rahayu ES**, Rusdan IH, Athennia A, Kamil RZ, Pramesi PC, Marsono Y, Utami T, Widada J. Safety Assessment of Indigenous Probiotic Strain Lactobacillus plantarum Dad-13 Isolated from Dadih Using Sprague Dawley Rats as a Model. *Am J Pharmacol Toxicol* 2019; **1**: 38-47 [DOI: 10.3844/ajptsp.2019.38.47]
12 **Maghfirotin Marta B**, Tyas U, Muhammad Nur C, Jaka W, Endang Sutriswati R. Effects of Consumption of Probiotic Powder Containing Lactobacillus Plantarum Dad-13 on Fecal Bacterial Population in School-Age Children in Indonesia. *Int J Probiotics Prebiotics* 2019; **14**: 1-8 [DOI: 10.37290/ijpp2641-7197.14:1-8]
13 **Rahayu ES**, Utami T, Mariyatun M, Hasan PN, Kamil RZ, Setyawan RH, Pamungkaningtyas FH, Harahap IA, Wiryohanjoyo DV, Pramesi PC, Cahyanto MN, Sujaya IN, Juffrie M. Gut microbiota profile in healthy Indonesians. *World J Gastroenterol* 2019; **25**: 1478-1491 [PMID: 30948911 DOI: 10.3748/wjg.v25.i12.1478]
14 **Matsuki T**, Watanabe K, Fujimoto J, Kado Y, Takada T, Matsumoto K, Tanaka R. Quantitative PCR with 16S rRNA-gene-targeted species-specific primers for analysis of human intestinal bifidobacteria. *Appl Environ Microbiol* 2004; **70**: 167-173 [PMID: 14711639 DOI: 10.1128/AEM.70.1.167-173.2004]
15 **Matsuda K**, Tsuji H, Asahara T, Matsumoto K, Takada T, Nomoto K. Establishment of an analytical system for the human fecal microbiota, based on reverse transcription-quantitative PCR targeting of multicopy rRNA molecules. *Appl Environ Microbiol* 2009; **75**: 1961-1969 [PMID: 19201979 DOI: 10.1128/AEM.01843-08]
16 **Kadooka Y**, Sato M, Imaizumi K, Ogawa A, Ikuyama K, Akai Y, Okano M, Kagoshima M, Tsuchida T. Regulation of abdominal adiposity by probiotics (Lactobacillus gasseri SBT2055) in adults with obese tendencies in a randomized controlled trial. *Eur J Clin Nutr* 2010; **64**: 636-643 [PMID: 20216555 DOI: 10.1038/ejcn.2010.19]
17 **Higashikawa F**, Noda M, Awaya T, Danshiitsoodol N, Matoba Y, Kumagai T, Sugiyama M. Antiobesity effect of Pediococcus pentosaceus LP28 on overweight subjects: a randomized, double-blind, placebo-controlled clinical trial. *Eur J Clin Nutr* 2016; **70**: 582-587 [PMID: 26956126 DOI: 10.1038/ejcn.2016.17]
18 **Sanchez M**, Darimont C, Drapeau V, Emady-Azar S, Lepage M, Rezzonico E, Ngom-Bru C, Berger B, Philippe L, Ammon-Zuffrey C, Leone P, Chevrier G, St-Amand E, Marette A, Doré J, Tremblay A. Effect of Lactobacillus rhamnosus CGMCC1.3724 supplementation on weight loss and maintenance in obese men and women. *Br J Nutr* 2014; **111**: 1507-1519 [PMID: 24299712 DOI: 10.1017/S0007114513003875]
19 **Shen J**, Obin MS, Zhao L. The gut microbiota, obesity and insulin resistance. *Mol Aspects Med* 2013; **34**: 39-58 [PMID: 23159341 DOI: 10.1016/j.mam.2012.11.001]
20 **Flint HJ**, Scott KP, Duncan SH, Louis P, Forano E. Microbial degradation of complex carbohydrates in the gut. *Gut Microbes* 2012; **3**: 289-306 [PMID: 22572875 DOI: 10.4161/gmic.19897]
21 **Larsen N**, Vogensen FK, Gøbel RJ, Michaelsen KF, Forssten SD, Lahtinen SJ, Jakobsen M. Effect of Lactobacillus salivarius Ls-33 on fecal microbiota in obese adolescents. *Clin Nutr* 2013; **32**: 935-940 [PMID: 23510724 DOI: 10.1016/j.clnu.2013.02.007]
22 **Institute of Medicine**, Food and Nutrition Board. A Report of the Panel on Macronutrients, Subcommittees on Upper Reference Levels of Nutrients and Interpretation and Uses of Dietary Reference Intakes, Standing Committee on the Scientific Evaluation of Dietary Reference Intakes. Dietary Reference intakes for energy, carbohydrates, fiber, fat, fatty acids, cholesterol, protein and amino acids. The National Academies Press. 2005 [DOI: 10.17226/10490]
23 **Duncan SH**, Hold GL, Harmsen HJM, Stewart CS, Flint HJ. Growth requirements and fermentation products of Fusobacterium prausnitzii, and a proposal to reclassify it as Faecalibacterium prausnitzii gen. nov., comb. nov. *Int J Syst Evol Microbiol* 2002; **52**: 2141-2146 [PMID: 12508881 DOI: 10.1099/00207713-52-6-2141]
24 **Miquel S**, Martín R, Rossi O, Bermúdez-Humarán LG, Chatel JM, Sokol H, Thomas M, Wells JM, Langella P. Faecalibacterium prausnitzii and human intestinal health. *Curr Opin Microbiol* 2013; **16**: 255-261 [PMID: 23831042 DOI: 10.1016/j.mib.2013.06.003]
25 **Ai D**, Pan H, Li X, Gao Y, Liu G, Xia LC. Identifying Gut Microbiota Associated With Colorectal Cancer Using a Zero-Inflated Lognormal Model. *Front Microbiol* 2019; **10**: 826 [PMID: 31068913

DOI: 10.3389/fmicb.2019.00826]

26 **Brugère JF**, Borrel G, Gaci N, Tottey W, O'Toole PW, Malpuech-Brugère C. Archaebiotics: proposed therapeutic use of archaea to prevent trimethylaminuria and cardiovascular disease. *Gut Microbes* 2014; **5**: 5-10 [PMID: 24247281 DOI: 10.4161/gmic.26749]

27 **Murugesan S**, Ulloa-Martínez M, Martínez-Rojano H, Galván-Rodríguez FM, Miranda-Brito C, Romano MC, Piña-Escobedo A, Pizano-Zárate ML, Hoyo-Vadillo C, García-Mena J. Study of the diversity and short-chain fatty acids production by the bacterial community in overweight and obese Mexican children. *Eur J Clin Microbiol Infect Dis* 2015; **34**: 1337-1346 [PMID: 25761741 DOI: 10.1007/s10096-015-2355-4]

28 **Patterson AM**, Mulder IE, Travis AJ, Lan A, Cerf-Bensussan N, Gaboriau-Routhiau V, Garden K, Logan E, Delday MI, Coutts AGP, Monnais E, Ferraria VC, Inoue R, Grant G, Aminov RI. Human Gut Symbiont *Roseburia hominis* Promotes and Regulates Innate Immunity. *Front Immunol* 2017; **8**: 1166 [PMID: 29018440 DOI: 10.3389/fimmu.2017.01166]

29 **Walker AW**, Ince J, Duncan SH, Webster LM, Holtrop G, Ze X, Brown D, Stares MD, Scott P, Bergerat A, Louis P, McIntosh F, Johnstone AM, Lobley GE, Parkhill J, Flint HJ. Dominant and diet-responsive groups of bacteria within the human colonic microbiota. *ISME J* 2011; **5**: 220-230 [PMID: 20686513 DOI: 10.1038/ismej.2010.118]

30 **Chow J**, Tang H, Mazmanian SK. Pathobionts of the gastrointestinal microbiota and inflammatory disease. *Curr Opin Immunol* 2011; **23**: 473-480 [PMID: 21856139 DOI: 10.1016/j.coi.2011.07.010]

31 **Bunney PE**, Zink AN, Holm AA, Billington CJ, Kotz CM. Orexin activation counteracts decreases in nonexercise activity thermogenesis (NEAT) caused by high-fat diet. *Physiol Behav* 2017; **176**: 139-148 [PMID: 28363838 DOI: 10.1016/j.physbeh.2017.03.040]

32 **Al-Assal K**, Martinez AC, Torrinhas RS, Cardinelli C, Waitzberg D. Gut microbiota and obesity. *Clin Nutr Exp* 2018; **20**: 60-64 [DOI: 10.1016/j.yclnex.2018.03.001]

33 **Ley RE**, Turnbaugh PJ, Klein S, Gordon JI. Microbial ecology: human gut microbes associated with obesity. *Nature* 2006; **444**: 1022-1023 [PMID: 17183309 DOI: 10.1038/4441022a]

34 **Turnbaugh PJ**, Gordon JI. The core gut microbiome, energy balance and obesity. *J Physiol* 2009; **587**: 4153-4158 [PMID: 19491241 DOI: 10.1113/jphysiol.2009.174136]

35 **Furet JP**, Kong LC, Tap J, Poitou C, Basdevant A, Bouillot JL, Mariat D, Corthier G, Doré J, Henegar C, Rizkalla S, Clément K. Differential adaptation of human gut microbiota to bariatric surgery-induced weight loss: links with metabolic and low-grade inflammation markers. *Diabetes* 2010; **59**: 3049-3057 [PMID: 20876719 DOI: 10.2337/db10-0253]

36 **Yu M**, Stott S, Toner M, Maheswaran S, Haber DA. Circulating tumor cells: approaches to isolation and characterization. *J Cell Biol* 2011; **192**: 373-382 [PMID: 21300848 DOI: 10.1083/jcb.201010021]

37 **Abenavoli L**, Scarpellini E, Colica C, Boccuto L, Salehi B, Sharifi-Rad J, Aiello V, Romano B, De Lorenzo A, Izzo AA, Capasso R. Gut Microbiota and Obesity: A Role for Probiotics. *Nutrients* 2019; **11**: 2690 [PMID: 31703257 DOI: 10.3390/nu11112690]

38 **Jumpertz R**, Le DS, Turnbaugh PJ, Trinidad C, Bogardus C, Gordon JI, Krakoff J. Energy-balance studies reveal associations between gut microbes, caloric load, and nutrient absorption in humans. *Am J Clin Nutr* 2011; **94**: 58-65 [PMID: 21543530 DOI: 10.3945/ajcn.110.010132]

39 **Devaraj S**, Hemarajata P, Versalovic J. The human gut microbiome and body metabolism: implications for obesity and diabetes. *Clin Chem* 2013; **59**: 617–628 [PMID: 23401286 DOI: 10.1373/clinchem.2012.187617]

40 **Sanmiguel C**, Gupta A, Mayer EA. Gut Microbiome and Obesity: A Plausible Explanation for Obesity. *Curr Obes Rep* 2015; **4**: 250-261 [PMID: 26029487 DOI: 10.1007/s13679-015-0152-0]

41 **Stephens RW**, Arhire L, Covasa M. Gut Microbiota: From Microorganisms to Metabolic Organ Influencing Obesity. *Obesity (Silver Spring)* 2018; **26**: 801-809 [PMID: 29687647 DOI: 10.1002/oby.22179]

42 **Jung S**, Lee YJ, Kim M, Kim M, Kwak JH, Lee JW, Ahn YT, Sim JH, Lee JH. Supplementation with two probiotic strains, Lactobacillus curvatus HY7601 and Lactobacillus plantarum KY1032, reduced body adiposity and Lp-PLA2 activity in overweight subjects. *J Funct Foods* 2015; **19**: 744-752 [DOI: 10.1016/j.jff.2015.10.006]

43 **Gomes AC**, de Sousa RG, Botelho PB, Gomes TL, Prada PO, Mota JF. The additional effects of a probiotic mix on abdominal adiposity and antioxidant Status: A double-blind, randomized trial. *Obesity (Silver Spring)* 2017; **25**: 30-38 [PMID: 28008750 DOI: 10.1002/oby.21671]

44 **Kim J**, Yun JM, Kim MK, Kwon O, Cho B. Lactobacillus gasseri BNR17 Supplementation Reduces the Visceral Fat Accumulation and Waist Circumference in Obese Adults: A Randomized, Double-Blind, Placebo-Controlled Trial. *J Med Food* 2018; **21**: 454-461 [PMID: 29688793 DOI: 10.1089/jmf.2017.3937]

45 **Minami J**, Iwabuchi N, Tanaka M, Yamauchi K, Xiao JZ, Abe F, Sakane N. Effects of *Bifidobacterium breve* B-3 on body fat reductions in pre-obese adults: a randomized, double-blind, placebo-controlled trial. *Biosci Microbiota Food Health* 2018; **37**: 67-75 [PMID: 30094122 DOI: 10.12938/bmfh.18-001]

46 **Pedret A**, Valls RM, Calderón-Pérez L, Llauradó E, Companys J, Pla-Pagà L, Moragas A, Martín-Luján F, Ortega Y, Giralt M, Caimari A, Chenoll E, Genovés S, Martorell P, Codoñer FM, Ramón D, Arola L, Solà R. Effects of daily consumption of the probiotic Bifidobacterium animalis subsp. lactis CECT 8145 on anthropometric adiposity biomarkers in abdominally obese subjects: a randomized controlled trial. *Int J Obes (Lond)* 2019; **43**: 1863-1868 [PMID: 30262813 DOI: 10.1038/s41366-018-0220-0]

47 **Szulińska M**, Łoniewski I, van Hemert S, Sobieska M, Bogdański P. Dose-Dependent Effects of Multispecies Probiotic Supplementation on the Lipopolysaccharide (LPS) Level and Cardiometabolic Profile in Obese Postmenopausal Women: A 12-Week Randomized Clinical Trial. *Nutrients* 2018; **10**: 773 [PMID: 29914095 DOI: 10.3390/nu10060773]

48 **Sanchez M**, Darimont C, Panahi S, Drapeau V, Marette A, Taylor VH, Doré J, Tremblay A. Effects of a Diet-Based Weight-Reducing Program with Probiotic Supplementation on Satiety Efficiency, Eating Behaviour Traits, and Psychosocial Behaviours in Obese Individuals. *Nutrients* 2017; **9**: 284 [PMID: 28294985 DOI: 10.3390/nu9030284]

49 **Osterberg KL**, Boutagy NE, McMillan RP, Stevens JR, Frisard MI, Kavanaugh JW, Davy BM, Davy KP, Hulver MW. Probiotic supplementation attenuates increases in body mass and fat mass during high-fat diet in healthy young adults. *Obesity (Silver Spring)* 2015; **23**: 2364-2370 [PMID: 26466123 DOI: 10.1002/oby.21230]

World Journal of Gastroenterology

Submit a Manuscript: https://www.f6publishing.com

World J Gastroenterol 2021 January 7; 27(1): 129-142

DOI: 10.3748/wjg.v27.i1.129

ISSN 1007-9327 (print) ISSN 2219-2840 (online)

CASE REPORT

Spontaneous regression of gastric gastrinoma after resection of metastases to the lesser omentum: A case report and review of literature

Takeshi Okamoto, Takaaki Yoshimoto, Nobuyuki Ohike, Aoi Fujikawa, Takayoshi Kanie, Katsuyuki Fukuda

ORCID number: Takeshi Okamoto 0000-0001-9719-0282; Takaaki Yoshimoto 0000-0003-3014-1392; Nobuyuki Ohike 0000-0001-8631-821X; Aoi Fujikawa 0000-0003-2299-3931; Takayoshi Kanie 0000-0002-6955-0671; Katsuyuki Fukuda 0000-0001-6273-4227.

Author contributions: Okamoto T cared for the patient, performed endoscopic procedures, wrote the manuscript, and reviewed the literature; Yoshimoto T cared for the patient and contributed to manuscript drafting; Ohike N interpreted the pathological findings and contributed to manuscript drafting; Fujikawa A performed the surgical procedure and contributed to manuscript drafting; Kanie T cared for the patient, performed cardiology procedures and contributed to manuscript drafting; Fukuda K provided oversight for the manuscript and revised the manuscript for important intellectual content; and all authors issued final approval for the version to be submitted.

Informed consent statement: The patient has provided written informed consent for the publication of this article and associated images.

Takeshi Okamoto, Takaaki Yoshimoto, Katsuyuki Fukuda, Department of Gastroenterology, St. Luke's International Hospital, Tokyo 104-8560, Japan

Nobuyuki Ohike, Department of Pathology, Shizuoka Cancer Center, Shizuoka 411-8777, Japan

Aoi Fujikawa, Department of Surgery, St. Luke's International Hospital, Tokyo 104-8560, Japan

Takayoshi Kanie, Department of Cardiology, St. Luke's International Hospital, Tokyo 104-8560, Japan

Corresponding author: Takeshi Okamoto, MD, Staff Physician, Department of Gastroenterology, St. Luke's International Hospital, 9-1 Akashicho, Chuo-ku, Tokyo 104-8560, Japan. tak@afia.jp

Abstract

BACKGROUND

Gastric gastrinoma and spontaneous tumor regression are both very rarely encountered. We report the first case of spontaneous regression of gastric gastrinoma.

CASE SUMMARY

A 37-year-old man with a 9-year history of chronic abdominal pain was referred for evaluation of an 8 cm mass in the lesser omentum discovered incidentally on abdominal computed tomography. The tumor was diagnosed as grade 2 neuroendocrine neoplasm (NEN) on endoscopic ultrasound-guided fine-needle aspiration. Screening esophagogastroduodenoscopy revealed a 7 mm red polypoid lesion with central depression in the gastric antrum, also confirmed to be a grade 2 NEN. Laparoscopic removal of the abdominal mass confirmed it to be a metastatic gastrinoma lesion. The gastric lesion was subsequently diagnosed as primary gastric gastrinoma. Three months later, the gastric lesion had disappeared without treatment. The patient remains symptom-free with normal fasting serum gastrin and no recurrence of gastrinoma during 36 mo of follow-up.

CONCLUSION

Gastric gastrinoma may arise as a polypoid lesion in the gastric antrum. Spontaneous regression can rarely occur after biopsy.

Conflict-of-interest statement: The authors have no financial disclosures or conflicts of interest to declare.

CARE Checklist (2016) statement: The authors have read the CARE Checklist (2016), and the manuscript was prepared and revised according to the CARE Checklist (2016).

Open-Access: This article is an open-access article that was selected by an in-house editor and fully peer-reviewed by external reviewers. It is distributed in accordance with the Creative Commons Attribution NonCommercial (CC BY-NC 4.0) license, which permits others to distribute, remix, adapt, build upon this work non-commercially, and license their derivative works on different terms, provided the original work is properly cited and the use is non-commercial. See: http://creativecommons.org/Licenses/by-nc/4.0/

Manuscript source: Unsolicited manuscript

Specialty type: Gastroenterology and hepatology

Country/Territory of origin: Japan

Peer-review report's scientific quality classification

Grade A (Excellent): 0
Grade B (Very good): B
Grade C (Good): 0
Grade D (Fair): 0
Grade E (Poor): 0

Received: October 11, 2020
Peer-review started: October 11, 2020
First decision: November 23, 2020
Revised: November 28, 2020
Accepted: December 16, 2020
Article in press: December 16, 2020
Published online: January 7, 2021

P-Reviewer: Sun Q
S-Editor: Huang P
L-Editor: A
P-Editor: Liu JH

Key Words: Neuroendocrine neoplasm; Functional tumor; Biopsy; Gastrin; Stomach; Case report

©The Author(s) 2021. Published by Baishideng Publishing Group Inc. All rights reserved.

Core Tip: Gastrinoma is a functional neuroendocrine tumor which can cause refractory gastrointestinal symptoms. We present a rare case of gastrinoma originating in the stomach, with metastasis to the lesser omentum. Tumors including neuroendocrine tumors are rarely known to regress spontaneously following biopsy or surgical insult. This is the first report of spontaneous regression of a gastric gastrinoma. We also review the literature on gastric gastrinoma, gastrinoma arising in the lesser omentum, and spontaneous regression of gastrinomas and other neuroendocrine tumors.

Citation: Okamoto T, Yoshimoto T, Ohike N, Fujikawa A, Kanie T, Fukuda K. Spontaneous regression of gastric gastrinoma after resection of metastases to the lesser omentum: A case report and review of literature. *World J Gastroenterol* 2021; 27(1): 129-142
URL: https://www.wjgnet.com/1007-9327/full/v27/i1/129.htm
DOI: https://dx.doi.org/10.3748/wjg.v27.i1.129

INTRODUCTION

Gastrinoma is a type of neuroendocrine neoplasm (NEN) with high malignant potential. It is known to cause Zollinger-Ellison syndrome (ZES), a state of gastrin hypersecretion causing peptic ulcers in over 90% of affected cases[1]. The annual incidence has been reported at 0.5-2 per million. About 25% are associated with multiple endocrine neoplasia (MEN) type 1, while the remainder are sporadic[2]. Most arise in the gastrinoma triangle, an area with borders formed by the porta hepatis, duodenum, and pancreatic head[1]. Duodenal and pancreatic gastrinomas make up over 80% of all gastrinomas; other potential sites for primary lesions include the liver, biliary tree, ovary, kidney, jejunum, greater and lesser omentum, heart, and stomach[2-4].

Gastric NENs have an annual incidence of 2-5 per 100000 persons and account for 0.3%-1.8% of all gastric tumors, 5.6%-7.4% of NENs, and 6.9%-8.7% of all digestive NENs[5-8]. A large majority arise from enterochromaffin-like (ECL) cells which are stimulated by gastrin and secrete histamines[9-11]. As ECL cells are distributed in the gastric fundus and corpus, antral NENs are rare and originate from G-cells (which produce gastrin), D-cells (somatostatin) and enterochromaffin cells (serotonin).

NENs arising from ECL cells (ECLomas) are classified into 3 types based on etiology[5,6]. Type 1 is the most common and often presents with small, multiple polypoid lesions in the setting of autoimmune atrophic gastritis. Type 2 is the rarest type, accounting for 5%-6% of gastric NENs. It also commonly presents with small, multiple polypoid lesions in the fundus or body, but arises in the setting of gastrinoma or MEN type 1. Both type 1 and type 2 have high fasting serum gastrin (FSG) but type 2 has lower gastric pH and higher rates of metastasis (10%-30%). Type 3 commonly presents with large neuroendocrine carcinoma, has normal FSG, and metastatic disease is observed in a majority of cases. More recently, a fourth type involving multiple lesions associated with hypergastrinemia, endocrine cell hyperplasia, and parietal cell hypertrophy has been reported[12]. Gastric NENs originate in the deep mucosa and invade the submucosa, creating dome-like protrusions with or without central depressions when observed endoscopically[13].

Gastric gastrinomas do not fit into this framework, as they are not ECLomas. To the extent of our search, there are only 12 reports of gastric gastrinoma in the English literature[4,5,14-23]. While gastrinomas can occur sporadically or in connection with MEN type 1, all reported gastric cases in the English language are sporadic gastrinomas. There is one French report of a gastric gastrinoma associated with the latter[24].

Spontaneous regression is defined as the complete or partial disappearance of a tumor with no or inadequate treatment[25]. It is not equivalent to cure; the tumor may reappear in the same location or elsewhere in the body. While initially estimated to occur once in every 60000-100000 cases, recent studies suggest that at least partial

regression may be much more common[26-28]. The frequency of spontaneous regression varies widely depending on the tumor, with a large number of reports in renal cell carcinoma, melanoma, and neuroblastoma[25,26,28]. Reports in gastric NENs are scarce[29-31]. Immunological response by tumor infiltrating leukocytes such as cytotoxic T lymphocytes has been implicated as a possible explanation, while the impact of hormones, infection, diet and nutrition, toxins, genetics, and invasive procedures such as biopsies and surgery have also been suggested[26,28,32,33].

Here, we present a case of gastric gastrinoma with large metastases to the lesser omentum. The primary gastric lesion regressed spontaneously following biopsy of the gastric lesion and surgical resection of the metastatic lesion. We also review the existing literature on gastric gastrinomas, gastrinomas of the lesser omentum, and spontaneous regression of NENs.

CASE PRESENTATION

Chief complaints

A 37-year-old man presented to the emergency department after sudden cardiopulmonary arrest while outdoors.

History of present illness

Return of spontaneous circulation was achieved due to bystander cardiopulmonary resuscitation and 2 electric shocks from an automated external defibrillator.

History of past illness

His medical history was only significant for gastric mucosal erosions diagnosed 9 years prior to admission. The patient had chronic abdominal pain and occasional reflux symptoms despite continued treatment with proton pump inhibitors (PPIs).

Personal and family history

He had never consumed alcohol or smoked cigarettes. He had no known food or drug allergies. He had also never experienced syncope or palpitations in the past.

Physical examination

Body temperature of 36.2 degrees Celsius, blood pressure of 139/111 mmHg, sinus tachycardia with a heart rate of 130 beats/min, and respiratory rate of 32 times/min were noted upon arrival. The patient's eyes were open but he could not speak (Glasgow Coma Scale: E4V1M4). Physical examination was otherwise unremarkable.

Laboratory examinations

Laboratory values were significant for leukocytosis, mild increase in liver enzymes and creatinine, lactic acidosis (pH of 7.118 and lactate of 8.1 mmol/L on arterial blood gas analysis), and a severely elevated D-dimer of over 100 mcg/mL. Electrolytes were within their normal ranges. Rapid improvement was observed on serial follow-up examinations.

Imaging examinations

Computed tomography (CT) with contrast at admission revealed an incidental 8 cm mass in the lesser omentum (Figure 1). The mass appeared to result from the fusion of 3 similar solid tumors, of which 1 contained a non-enhancing, low-density area suggestive of necrosis or hematoma.

Further diagnostic work-up

Esophagogastroduodenoscopy (EGD) incidentally revealed a red, 7 mm submucosal tumor with central depression, which was biopsied (Figure 2A). Prominent gastric folds and shallow duodenal ulcers were also noted despite prolonged intravenous PPI treatment during admission (Figure 2B and C). No signs of gastroesophageal reflux disease or duodenal submucosal tumors were observed. Endoscopic ultrasound revealed 3 clearly delineated, hyperechoic masses with uniform texture, of which 1 had a hypoechoic center (Figure 2D). No pancreatic tumors were noted. Endoscopic ultrasound-guided fine-needle aspiration was performed. Pathology of both the gastric and lesser omentum specimens stained positive for chromogranin A and synaptophysin and were diagnosed as grade 2 NENs.

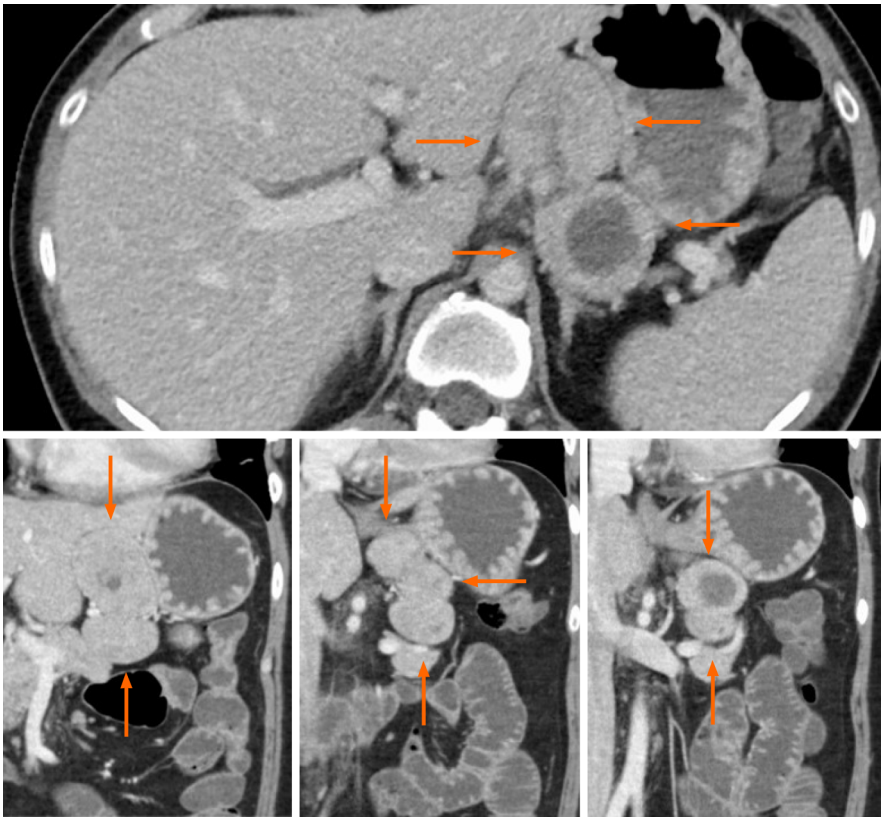


Figure 1 Axial (top) and coronal (bottom) views of computed tomography with contrast at admission revealed an incidental 8 cm mass in the lesser omentum (orange arrows). The mass appeared to result from the fusion of 3 similar tumors, of which 1 contained a non-enhancing, low-density area suggestive of necrosis or hematoma.

MULTIDISCIPLINARY EXPERT CONSULTATION

Takayoshi Kanie, MD, Department of Cardiology, St. Luke's International Hospital

After admission, targeted temperature management was performed under total anesthesia. The patient recovered completely after 2 d, with no neurological sequelae. While coronary angiogram including various stress tests was unremarkable, electrocardiogram findings were suggestive of Brugada's syndrome. An implantable cardiac defibrillator (EMBLEM MRI S-ICD System, Boston Scientific, Marlborough, MA, United States) was implanted during admission.

Aoi Fujikawa, MD, Department of Surgery, St. Luke's International Hospital

As the gastric and omental lesions were initially assumed to be independent lesions, laparoscopic omental tumor resection with possible gastrectomy was planned. The intention was to perform endoscopic submucosal dissection (ESD) to treat the gastric lesion once post-operative recovery was confirmed. The patient provided informed consent for the surgery and the overall treatment plan based on an adequate understanding of the risks involved in each procedure, particularly given his post-resuscitation status.

Laparoscopic surgery revealed an 83 mm × 80 mm × 37 mm mass in the lesser omentum which appeared to be formed from the fusion of 3 spherical tumors (Figure 3). No adhesion to the stomach was observed, enabling *en bloc* resection without partial gastrectomy. A macroscopic examination of the resected specimen revealed a brown, well-defined, encapsulated 75 mm × 40 mm solid tumor inside adipose tissue of the lesser omentum with a central hematoma. Pathology revealed nests of tumor cells characterized by small ovoid nuclei and mildly eosinophilic cytoplasms with intervening dilated capillary networks (Figure 4A). The tumor was positive for chromogranin A, synaptophysin, and gastrin (Figure 4B-D). Mitotic count was less than 2 per 2 mm^2 and the Ki67 index was 6%. No lymphatic or vascular invasion was noted. While initially suspected to be lymph nodes, the fused tumor was completely composed on uniform tumor cells with almost no lymphocytes except outside the encapsulated tumor. The differential at the time included primary

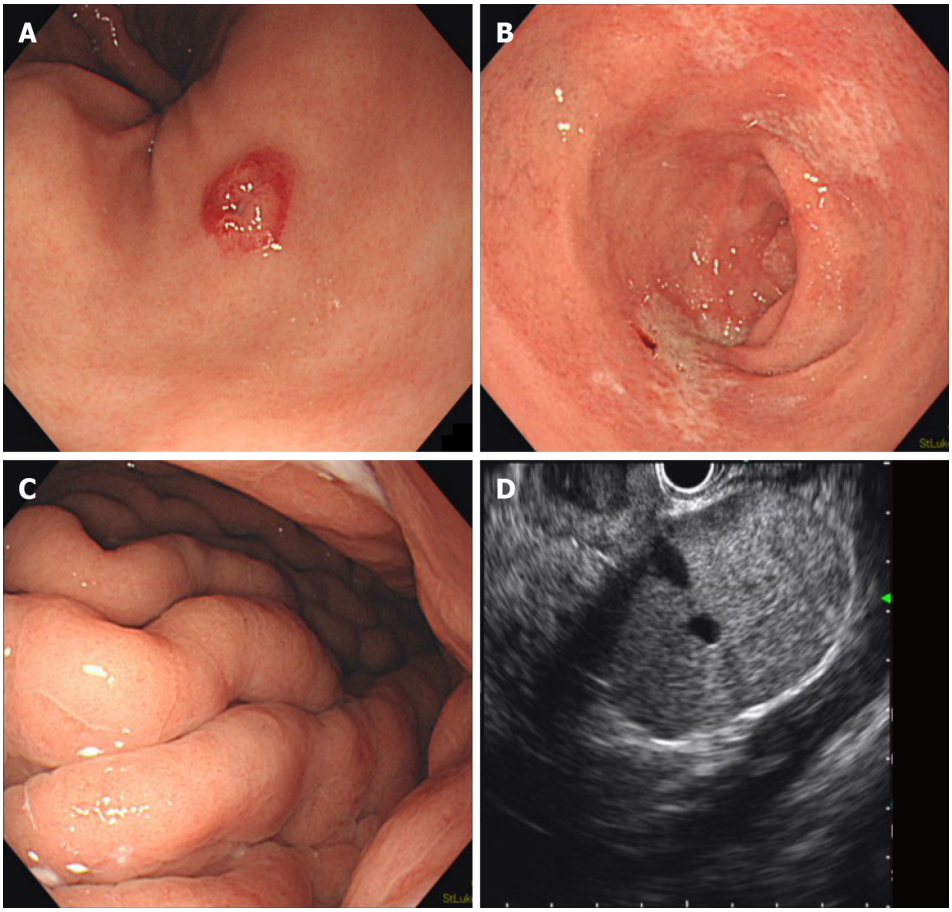


Figure 2 Esophagogastroduodenoscopy incidentally revealed a red, 7 mm submucosal tumor with a central depression (A); prominent gastric folds (B) and shallow duodenal ulcers (C) were also noted; endoscopic ultrasound revealed 3 clearly delineated, hyperechoic masses with uniform texture, of which 1 had a hypoechoic center with clear borders (D).

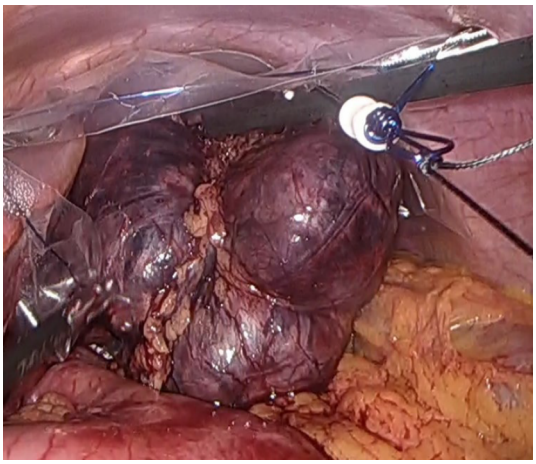


Figure 3 Laparoscopic surgery revealed an 83 mm × 80 mm × 37 mm mass in the lesser omentum which appeared to be formed from the fusion of 3 spherical tumors.

gastrinoma of lesser omentum lymph node, lymph node metastasis from primary gastric or undetected duodenal gastrinoma, and tumor-forming hematogenous spread of gastrinoma. While the gastric lesion had not been resected, the Tumor-Node-Metastasis staging was clinically considered to be T1N1M0, stage III (Union for International Cancer Control, 8th edition) assuming the lesion was a locoregional lymph node metastasis from a gastric NEN primary.

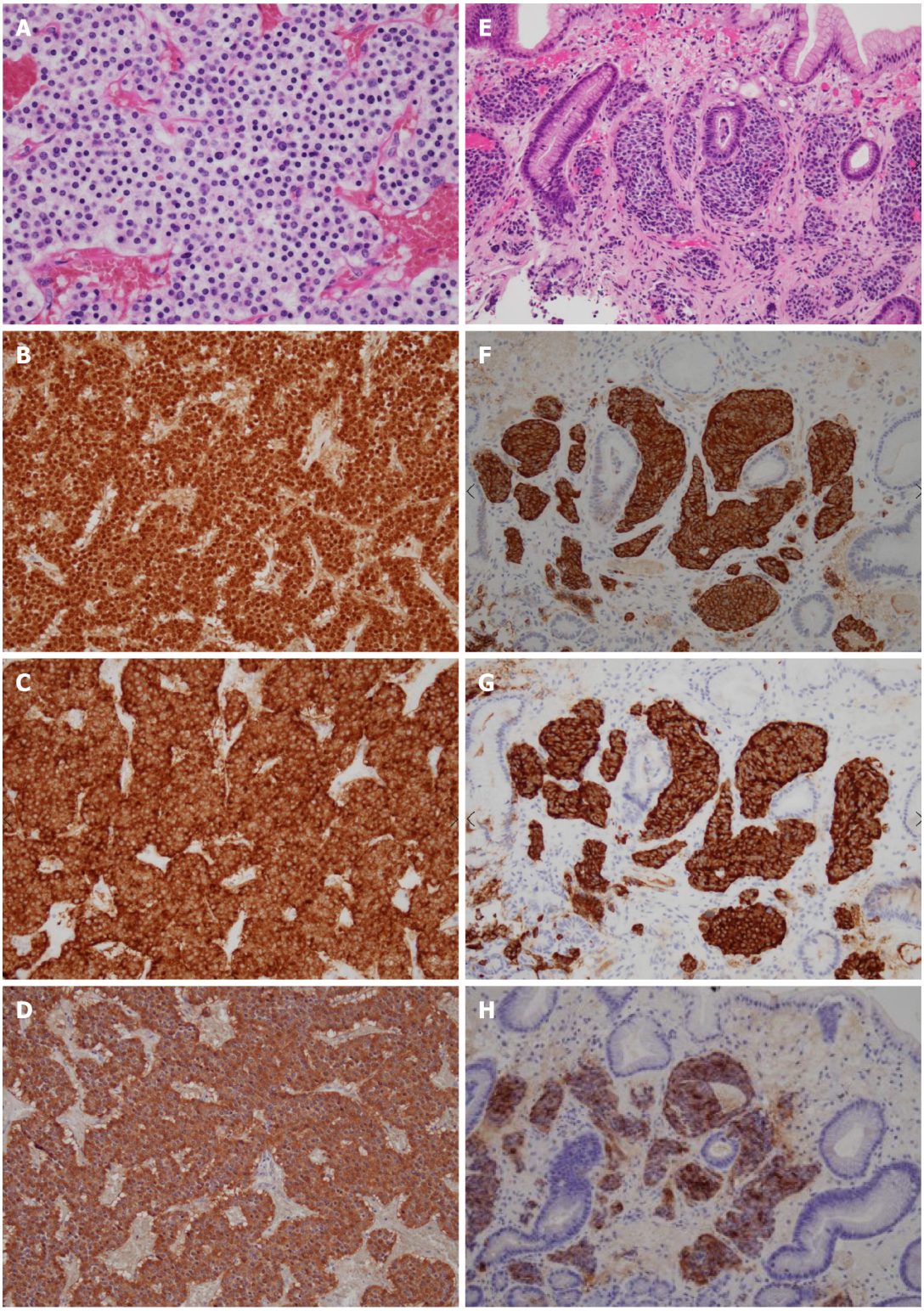


Figure 4 Pathology of the surgical specimen (A-D) and gastric biopsy (E-H). Nests of tumor cells characterized by small ovoid nuclei and mildly eosinophilic cytoplasms with intervening dilated capillary networks were observed in the omental lesion (A). The tumor was positive for chromogranin A (B), synaptophysin (C), and gastrin (D) stains. Biopsy of the gastric lesion showed similar cells in the mucosal layer (E) which were also positive for chromogranin A (F), synaptophysin (G), and gastrin (H) stains.

Nobuyuki Ohike, MD, PhD, Department of Pathology, Shizuoka Cancer Center

After the surgery, results of the pre-operative FSG test returned and showed marked elevation (41100 pg/mL without discontinuation of PPIs; reference range: 37-172 pg/mL). Pathology of the stomach biopsy was re-evaluated by an expert pathologist specializing in gastrointestinal tumors and was found to have a striking resemblance to the resected lesser omentum mass (Figure 4E-G). Strong immunoreactivity with gastrin was also confirmed for the first time (Figure 4H).

FINAL DIAGNOSIS

The patient denied a family history of MEN type 1, of pituitary, parathyroid, or pancreatic tumors, or of peptic ulcers. Gastric pH was not evaluated as the primary cardiology team believed PPIs should not be withheld for testing. Calcium, parathyroid hormone, vitamin B12, and thyroid function tests were within their normal ranges. Parietal cell and intrinsic factor antibodies and *Helicobacter pylori* antibodies were negative. Brain, neck, and abdominal imaging showed no pituitary, parathyroid, or pancreatic tumors.

As a result, the patient was diagnosed with sporadic gastric gastrinoma with metastases to the lesser omentum.

TREATMENT

In part due to stress from a long hospital stay, the patient left the hospital against medical advice after surgery.

OUTCOME AND FOLLOW-UP

He voluntarily returned for follow-up EGD 3 mo later to be re-evaluated before a possible distal gastrectomy. However, the gastric gastrinoma had reduced to a red dot with no visible elevation and was barely identifiable (Figure 5A). Biopsy of the lesion was negative for tumor, with only regenerative and fibrous changes (Figure 5B). Chromogranin A and synaptophysin stains were also negative (Figure 5C). In addition, duodenal ulcers had healed completely, allowing the patient to discontinue PPIs for the first time in 9 years. The prominent gastric folds observed in the gastric corpus had also normalized. FSG decreased dramatically to the normal range (167 pg/mL) and somatostatin-receptor scintigraphy (Octreoscan) showed no focal uptake throughout the body, including the stomach and lesser omentum. Based on a careful discussion of the risks involved, the patient decided to forgo surgery and opted for close observation.

Subsequent endoscopic findings have remained unchanged, FSG has remained within the normal range, and CT and scintigraphy have shown no recurrence of gastrinoma during 36 mo of follow-up. The patient remains asymptomatic without PPIs. No shocks from his implantable cardiac defibrillator have been triggered to date.

DISCUSSION

Gastric gastrinoma

G-cells are neuroendocrine cells which secrete gastrin. G-cells are stimulated by vagal stimulation *via* gastrin-releasing peptide, producing gastrin which in turn stimulate ECL cells to produce histamines. While G-cell NENs are strongly positive for the gastrin stain, they are not considered gastrinomas unless they present with symptoms consistent with ZES; gastrinoma is a clinical diagnosis[4-6]. Primary gastric gastrinoma is a rare clinical entity, even though most G-cells in the human body residing in the gastric antrum. La Rosa *et al*[11] found only 1 case of gastric gastrinoma among 8 antral G-cell NENs and among 209 gastric NENs.

Huang *et al*[14] reported an exceptionally high rate of gastrinomas among NENs at their institution: 20 cases of gastrinoma, of which 9 were gastric gastrinomas, out of 109 upper gastrointestinal NENs studied. However, they state in their discussion that type 1 and type 2 gastric NENs were considered gastrinomas. Their report appears to be focused on NENs (ECLomas) induced by hypergastrinemia instead of gastrin-producing primary NENs, which is our topic of discussion.

We conducted a PubMed search using the search terms "gastrinoma AND (stomach OR gastric)" and investigated all sources cited in each relevant report. We found 12 reports in the English language (excluding abstracts), mostly from the twentieth century (Table 1)[4,5,15-23]. Among the 13 reports including our case, there was a male preponderance (83%). Ages varied broadly, from 11 to 91 years of age. Most had a long history of abdominal symptoms and all lesions with specified locations were found in the distal half of the stomach, mainly in the antrum. Surgery was generally the treatment of choice, after which FSG normalized in a majority of cases. Lymph nodes

Table 1 Case reports of gastric gastrinoma

Case	Ref.	Year	Age	Gender	Symptoms	Symptom duration (yr)	History of peptic ulcer	Location	Size (mm)	Metastases	Gastrin before surgery (pg/mL)	Gastrin after surgery (pg/mL)	Treatment	Follow-up (mo)	Recurrence
1	Royston *et al*[16]	1972	65	M	Abdominal pain	14	+	Whole stomach	Large	-	> 1000	Undetectable	Total gastrectomy	15	-
2	Larsson *et al*[17]	1973	65	M	Abdominal pain, hematemesis	10	+	Antro-pylorus	10	-	NA	NA	Gastrectomy	12	-
3	Bhagavan *et al*[18]	1974	11	M	Acute peritonitis	0	-	Antrum (multiple)	Micro-scopic	-	> 1000	11000	Total gastrectomy	12	NA
4	Russo *et al*[19]	1980	51	F	Dyspepsia	7	-	Antrum-body junction	10	-	265	< 100	Polypectomy, antrectomy + splenectomy	36	-
5	Thompson *et al*[20]	1985	19	M	NA	3	+	Antrum	20	Liver	3000-4000	Normal	Total gastrectomy + segmental hepatectomy	NA	-
6	Liu *et al*[21]	1989	50	M	Pain, diarrhea, vomiting, weight loss	1.5	+	Antrum	< 10	Lymph node	1100-3000	153	Total gastrectomy	36	+
7	Liu *et al*[21]	1989	36	F	Pain, diarrhea, vomiting, weight loss	3.5	+	Lower body/antrum-body junction (multiple)	60	Lymph node, liver	518	4900	Subtotal gastrectomy	29 (dead)	NA
8	Werbel *et al*[22]	1989	72	M	Nausea, vomiting, anorexia, weight loss	8	+	Antrum	15	-	340	40	Antrectomy + vagotomy	12	-
9	Rindi *et al*[5]	1993	NA	NA	NA	NA	+	Pylorus	20	-	Elevated	Normal	Distal gastrectomy	NA	-
10	Wu *et al*[4]	1997	40	M	NA	NA	NA	Pylorus	NA	-	373	250	Enucleation	140	+
11	de Leval *et al*[23]	2002	91	M	Nausea, vomiting, anorexia, weight loss	4	+	Antrum	55	Lymph node, liver	3500	NA	None	0 (dead)	NA
12	Tartaglia *et al*[15]	2005	37	M	Abdominal pain, nausea	8	+	Angulus	7	Hepatogastric ligament	420	95	Endoscopic resection, subtotal gastrectomy + left hepatic lobectomy, lanreotide	72	+
13	Our case	2020	37	M	Abdominal pain	9	+	Antrum	7	Lesser omentum	41100	167	Tumor resection	30	-

and the liver were the most common sites for metastases.

Treatment for gastric gastrinoma has not been elucidated due to its rarity.

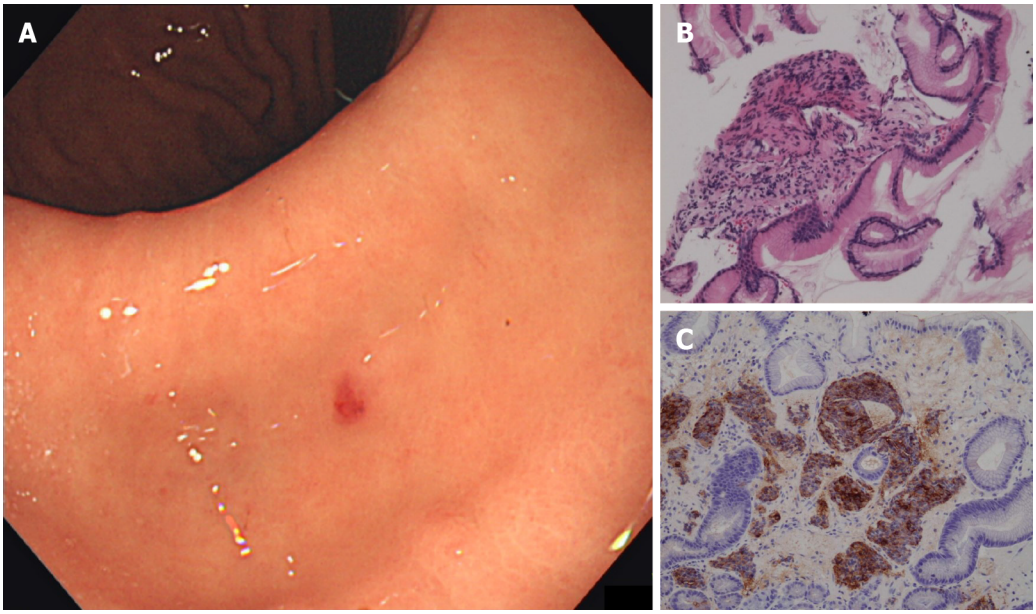


Figure 5 The gastric neuroendocrine neoplasm was barely identifiable on follow-up esophagogastroduodenoscopy, reducing to a red dot with no visible elevation (A); biopsy of the lesion was negative for tumor, with only regenerative and fibrous changes (B); synaptophysin (C) stain was also negative.

Guidelines from the National Comprehensive Cancer Network (NCCN) and the European Neuroendocrine Tumor Society (ENETS) both recommend radical resection with lymph node sampling for duodenal and pancreatic gastrinomas[7,34]. While both NCCN and ENETS guidelines permit endoscopic resection for certain types of small gastric NENs, radical resection with lymph node sampling should be performed for gastric gastrinomas due to the potential for metastases. Although some authors suggest a role for endoscopic resection of gastric gastrinomas[35], our preferred approach is open surgery with intraoperative digital and ultrasound exploration to investigate undetected duodenal primaries. In the present case, laparoscopy was performed instead of open surgery as the diagnosis of gastrinoma was not reached before surgery.

A gastrinoma work-up is generally considered when encountering NENs in the gastric fundus or corpus. We propose that gastric gastrinoma should be included in the differential diagnosis for a NEN in the gastric antrum, particularly when accompanied by peptic ulcers and prominent gastric folds.

Relationship between the gastric and omental lesions

Before reaching the final diagnosis of primary gastric gastrinoma with metastasis to the lesser omentum, we considered several other possibilities for the relationship between the gastric and lesser omentum lesions.

Primary omental gastrinoma with gastric NEN from ectopic ECL cells: While ECL cells generally do not exist in the gastric antrum, type 2 antral NENs arising from ectopic ECL cells were observed in at least 2 of 4 antral NEN cases in one report[36]. However, the positive gastrin stain in our case supports a G-cell origin.

Primary gastrinoma of the lesser omentum with gastric metastasis: We initially entertained the possibility that the large lesser omentum lesion was the primary site. Primary tumors of the lesser omentum are rare. Most are benign tumors such as lymphangiomas and hemangiomas, with isolated reports of gastrointestinal stroma tumors and malignancies such as soft tissue sarcoma, lymphoma, and small cell carcinoma[37-40]. There are 5 reports of primary gastrinoma of the lesser omentum (Table 2)[41-44]. Four cases were relatively young males (average age: 26.3 years) including 2 teenagers, while the fifth was an elderly woman. All had solitary tumors and none had any evidence of MEN type 1. Tumors in most cases exceeded 4 cm but had no metastases. Normalization of serum gastrin and recurrence-free status was achieved in all cases. Tumor resection without gastrectomy was possible in 3 cases, while total gastrectomy was performed in 2 cases. These is also one report of primary gastrinoma of the greater omentum in which serum gastrin similarly normalized after

Table 2 Case reports of primary gastrinoma of the lesser omentum

Case	Ref.	Year	Age	Gender	Symptoms	Size (mm)	Gastrin before surgery (pg/mL)	Gastrin after surgery (pg/mL)	Treatment	Follow-up (mo)	Recurrence
1	Wolfe *et al*[41]	1982	51	M	Recurrent duodenal ulcer	NA	753	112	Total gastrectomy	60	-
2	Wolfe *et al*[41]	1982	15	M	Hematemesis, abdominal pain, diarrhea	25	455	41	Tumor resection	12	-
3	Kohyama *et al*[42]	2007	74	F	Abdominal pain	40	1850	118	Resection of remnant stomach with tumor	24	-
4	Chang *et al*[43]	2010	13	M	Abdominal pain, diarrhea	45 × 37	1263	Normal	Tumor resection	36	-
5	Labidi *et al*[44]	2018	26	M	Melena, abdominal pain	50 × 40	306	Normal	Tumor resection	6	-

surgery and no recurrence was observed[45].

There is no known method of determining whether the gastric lesion or the omental lesion was the primary gastrinoma. However, both sub-centimeter duodenal gastrinomas and sub-centimeter gastric NENs have been reported to metastasize[11,15]. To the extent of our search, there are no reports of gastrinomas metastasizing to the stomach. It therefore appears natural to consider the gastric lesion as the primary site.

Primary lymph node gastrinoma with gastric metastasis: The existence of primary lymph node gastrinoma remains in dispute among experts. Sub-centimeter duodenal primaries commonly exhibit distant metastases and may be undetected despite careful evaluation, including autopsy. In a study of 176 ZES patients, lymph nodes were the only lesions discovered initially in 45 cases[46]. While small duodenal gastrinomas had been missed in several cases, 26 appeared to be completely cured after surgical resection of the involved lymph node. None of these cases arose in the omentum.

Furthermore, primary lymph node gastrinoma is currently diagnosed when diagnostic criteria for gastrinoma are met without any confirmed lesions other than lymph nodes and their resection leads to normalization of FSG and other laboratory or radiological findings suggestive of gastrinoma. This definition fails to account for spontaneous regression of an undetected primary after surgery, discussed below.

Gastric and omental metastases from undiscovered primary duodenal tumor: Most gastrinomas arise in the duodenum and small duodenal gastrinomas undetected by endoscopic or imaging studies are known to metastasize. As surgery was not performed in our patient, this possibility is the most difficult to rule out. There is no way to confirm whether or not spontaneous regression, which occurred in the stomach, also occurred in the duodenum. However, as stated previously, we found no reports of gastrinoma metastasizing to the stomach.

Gastric NEN triggered by chronic PPI use: Chronic PPI use is widely known to cause ECL cell hyperplasia as well as hypergastrinemia, albeit at mild levels of approximately 1-3 times the upper limit of normal which generally plateaus after 1-2 years. A systematic review of 1920 patients on PPIs found no found gastric NENs[47]. On the other hand, a single center study reported that 3 of 31 gastric NENs arose in patients with long-term PPI use in the absence of autoimmune atrophic gastritis, *Helicobacter pylori* infection, or ZES. ECL hyperplasia was not observed in 1 of the 3 cases, while another was a 6 mm, grade 2 NEN with normal FSG[48]. A study of 66 gastric NENs in long-term PPI users reported that 9% of NENs arose in the antrum or pylorus, but did not specify whether these were ECL-cell NENs[49]. In any event, the strongly positive gastrin stain and strong resemblance to the omental lesion makes this an unlikely explanation in our case.

Multicentric or incidental simultaneous occurrence of gastric and omental NENs: Simultaneous multicentric occurrence of NENs is another possibility. The negative tests for MEN type 1 and the strong pathological resemblance between the gastric primary and omental metastasis does not allow us to rule this out completely.

Additional molecular genetic testing, not available at our institution, may shed light on this possibility[50].

It is also possible for sporadic NENs in 2 separate organs to be discovered incidentally at the same time. This premature assumption led to a delay in the diagnosis in our patient. There are no reports on this phenomenon and other possibilities should be considered first, particularly in young patients with no apparent risk factors for NEN development. Had gastrinoma been suspected in advance, open laparotomy with digital and ultrasound exploration would have been selected over laparoscopy. The pathological resemblance between the 2 lesions was too strong for them to be considered unrelated lesions.

Spontaneous regression

Complete and partial spontaneous regressions of NENs have been observed in various organs. Most reports involve Merkel cell carcinomas and neuroblastomas, which are neuroendocrine carcinomas of the skin and sympathetic nervous system, respectively[51,52]. Isolated cases of spontaneous regression of NENs in the pancreas, lung, bile duct, thymus, and pelvis have been reported, as well as in metastatic disease[53-58]. Biopsy, surgery for another condition, and pregnancy have been suggested as possible triggers[54-56].

Focusing on this placebo arms of randomized controlled trials conducted from 1980 to 2014, Ghatalia *et al*[27] investigated spontaneous regression in various solid tumors including 2 trials relating to pancreatic NENs. Partial spontaneous regression was observed in 4 of 252 patients receiving placebo, for an overall response ratio (ORR) of 1.6%. Amoroso expanded this idea to include 5 trials on NENs and found an ORR of 1.52% among 531 patients receiving placebo[53]. The authors also found minor response, defined as a 10%-30% reduction in tumor size from baseline, in almost 6% of NEN patients receiving placebo. While no complete spontaneous regressions were observed in these studies, partial spontaneous regressions may not be as rare as once believed.

Spontaneous regression of metastatic gastrinomas after biopsy and/or surgery was reported as far back as the 1960s. Disappearance of biopsy-proven liver and/or lung metastases on imaging or during second-look operations were observed in 2 out of 44 gastrinoma patients in one study and 4 out of 267 metastatic reports in another, all following total gastrectomy[59,60]. There are also sparse reports of spontaneous regression of gastric NENs. An Indian report detailed the complete spontaneous regression of an 11 cm gastric NEN after exploratory laparotomy[29]. Another report from Hong Kong found no residual tumor in the gastrectomy specimen after biopsy revealed a 4 cm high-grade large-cell neuroendocrine carcinoma in the gastric cardia[30]. Complete spontaneous regression was observed in both cases after either biopsy or surgical insult. Three cases of autoimmune atrophic gastritis in which multiple small gastric carcinoids regressed spontaneously during follow-up have also been reported[31].

In our case, we believe that complete spontaneous regression was achieved based on normalized FSG, cure of peptic ulcers, no signs of recurrence on imaging, and the negative biopsy of the gastric lesion. However, the biopsy was limited to the mucosal layer and remnants of tumor in the submucosal layer cannot be completely ruled out without surgery or ESD. While the patient did not consent to such additional treatment, at least a partial spontaneous regression was clearly achieved. We speculate biopsy of the primary lesion and subsequent surgery triggered the spontaneous regression.

To the extent of our search, we could not find any relationship between ZES and Brugada's syndrome, which was the cause of our patient's cardiopulmonary arrest. While cardiopulmonary arrest due to carcinoid syndrome has been reported, there were no clinical manifestations to raise any suspicion of this rare event[61]. We suspect that the gastrinoma was unrelated to the cardiopulmonary arrest.

CONCLUSION

In conclusion, we report a case of gastric gastrinoma which regressed spontaneously after biopsy and resection of a metastatic lesion in the lesser omentum. ZES can be left undetected for years and should be suspected in longstanding reflux disease or abdominal pain refractory to PPIs. NENs in the antrum should alert the physician for possible gastrinoma as well as NENs of other non-ECL cell origins. Further research is

required to further clarify the mechanisms behind spontaneous regression and to determine the characteristics of lesions or patients who may experience this extraordinary phenomenon. Such research may contribute to the discovery of new immunotherapies and to the reduction of unnecessary surgeries.

REFERENCES

1 **Jensen RT**, Cadiot G, Brandi ML, de Herder WW, Kaltsas G, Komminoth P, Scoazec JY, Salazar R, Sauvanet A, Kianmanesh R; Barcelona Consensus Conference participants. ENETS Consensus Guidelines for the management of patients with digestive neuroendocrine neoplasms: functional pancreatic endocrine tumor syndromes. *Neuroendocrinology* 2012; **95**: 98-119 [PMID: 22261919 DOI: 10.1159/000335591]

2 **Gibril F**, Schumann M, Pace A, Jensen RT. Multiple endocrine neoplasia type 1 and Zollinger-Ellison syndrome: a prospective study of 107 cases and comparison with 1009 cases from the literature. *Medicine (Baltimore)* 2004; **83**: 43-83 [PMID: 14747767 DOI: 10.1097/01.md.0000112297.72510.32]

3 **Jensen RT**, Niederle B, Mitry E, Ramage JK, Steinmuller T, Lewington V, Scarpa A, Sundin A, Perren A, Gross D, O'Connor JM, Pauwels S, Kloppel G; Frascati Consensus Conference; European Neuroendocrine Tumor Society. Gastrinoma (duodenal and pancreatic). *Neuroendocrinology* 2006; **84**: 173-182 [PMID: 17312377 DOI: 10.1159/000098009]

4 **Wu PC**, Alexander HR, Bartlett DL, Doppman JL, Fraker DL, Norton JA, Gibril F, Fogt F, Jensen RT. A prospective analysis of the frequency, location, and curability of ectopic (nonpancreaticoduodenal, nonnodal) gastrinoma. *Surgery* 1997; **122**: 1176-1182 [PMID: 9426435 DOI: 10.1016/s0039-6060(97)90224-5]

5 **Rindi G**, Luinetti O, Cornaggia M, Capella C, Solcia E. Three subtypes of gastric argyrophil carcinoid and the gastric neuroendocrine carcinoma: a clinicopathologic study. *Gastroenterology* 1993; **104**: 994-1006 [PMID: 7681798 DOI: 10.1016/0016-5085(93)90266-f]

6 **Rindi G**, Klimstra DS, Abedi-Ardekani B, Asa SL, Bosman FT, Brambilla E, Busam KJ, de Krijger RR, Dietel M, El-Naggar AK, Fernandez-Cuesta L, Klöppel G, McCluggage WG, Moch H, Ohgaki H, Rakha EA, Reed NS, Rous BA, Sasano H, Scarpa A, Scoazec JY, Travis WD, Tallini G, Trouillas J, van Krieken JH, Cree IA. A common classification framework for neuroendocrine neoplasms: an International Agency for Research on Cancer (IARC) and World Health Organization (WHO) expert consensus proposal. *Mod Pathol* 2018; **31**: 1770-1786 [PMID: 30140036 DOI: 10.1038/s41379-018-0110-y]

7 **Delle Fave G**, O'Toole D, Sundin A, Taal B, Ferolla P, Ramage JK, Ferone D, Ito T, Weber W, Zheng-Pei Z, De Herder WW, Pascher A, Ruszniewski P; Vienna Consensus Conference participants. ENETS Consensus Guidelines Update for Gastroduodenal Neuroendocrine Neoplasms. *Neuroendocrinology* 2016; **103**: 119-124 [PMID: 26784901 DOI: 10.1159/000443168]

8 **Grozinsky-Glasberg S**, Alexandraki KI, Angelousi A, Chatzellis E, Sougioultzis S, Kaltsas G. Gastric Carcinoids. *Endocrinol Metab Clin North Am* 2018; **47**: 645-660 [PMID: 30098721 DOI: 10.1016/j.ecl.2018.04.013]

9 **WHO of Tumours Editorial Board**. Digestive system tumors. Lyon: International Agency for Research on Cancer. 5th ed. 2019; 1: 104-109. Available from: https://publications.iarc.fr/Book-And-Report-Series/Who-Classification-Of-Tumours/Digestive-System-Tumours-2019

10 **La Rosa S**, Vanoli A. Gastric neuroendocrine neoplasms and related precursor lesions. *J Clin Pathol* 2014; **67**: 938-948 [PMID: 25053544 DOI: 10.1136/jclinpath-2014-202515]

11 **La Rosa S**, Inzani F, Vanoli A, Klersy C, Dainese L, Rindi G, Capella C, Bordi C, Solcia E. Histologic characterization and improved prognostic evaluation of 209 gastric neuroendocrine neoplasms. *Hum Pathol* 2011; **42**: 1373-1384 [PMID: 21531442 DOI: 10.1016/j.humpath.2011.01.018]

12 **Ooi A**, Ota M, Katsuda S, Nakanishi I, Sugawara H, Takahashi I. An Unusual Case of Multiple Gastric Carcinoids Associated with Diffuse Endocrine Cell Hyperplasia and Parietal Cell Hypertrophy. *Endocr Pathol* 1995; **6**: 229-237 [PMID: 12114744 DOI: 10.1007/BF02739887]

13 **Sato Y**, Hashimoto S, Mizuno K, Takeuchi M, Terai S. Management of gastric and duodenal neuroendocrine tumors. *World J Gastroenterol* 2016; **22**: 6817-6828 [PMID: 27570419 DOI: 10.3748/wjg.v22.i30.6817]

14 **Huang SF**, Kuo IM, Lee CW, Pan KT, Chen TC, Lin CJ, Hwang TL, Yu MC. Comparison study of gastrinomas between gastric and non-gastric origins. *World J Surg Oncol* 2015; **13**: 202 [PMID: 26077245 DOI: 10.1186/s12957-015-0614-6]

15 **Tartaglia A**, Vezzadini C, Bianchini S, Vezzadini P. Gastrinoma of the stomach: a case report. *Int J Gastrointest Cancer* 2005; **35**: 211-216 [PMID: 16110123 DOI: 10.1385/IJGC:35:3:211]

16 **Royston CM**, Brew DS, Garnham JR, Stagg BH, Polak J. The Zollinger-Ellison syndrome due to an infiltrating tumour of the stomach. *Gut* 1972; **13**: 638-642 [PMID: 4562021 DOI: 10.1136/gut.13.8.638]

17 **Larsson LI**, Ljungberg O, Sundler F, Håkanson R, Svensson SO, Rehfeld J, Stadil R, Holst J. Antor-pyloric gastrinoma associated with pancreatic nesidioblastosis and proliferation of islets. *Virchows Arch A Pathol Pathol Anat* 1973; **360**: 305-314 [PMID: 4201098 DOI: 10.1007/BF00548351]

18 **Bhagavan BS**, Hofkin GA, Woel GM, Koss LG. Zollinger-Ellison syndrome. Ultrastructural and histochemical observations in a child with endocrine tumorlets of gastric antrum. *Arch Pathol* 1974; **98**: 217-222 [PMID: 4416924]

19 **Russo A**, Buffa R, Grasso G, Giannone G, Sanfilippo G, Sessa F, Solcia E. Gastric gastrinoma and diffuse G cell hyperplasia associated with chronic atrophic gastritis. Endoscopic detection and removal. *Digestion* 1980; **20**: 416-419 [PMID: 6250933 DOI: 10.1159/000198484]

20 **Thompson NW**, Vinik AI, Eckhauser FE, Strodel WE. Extrapancreatic gastrinomas. *Surgery* 1985; **98**: 1113-1120 [PMID: 4071387]

21 **Liu TH**, Zhong SX, Chen YF, Lin Y, Chen J, Li DC, Wang DT, Gu CF, Yie SF. Gastric gastrinoma. *Chin Med J (Engl)* 1989; **102**: 774-782 [PMID: 2517058]

22 **Werbel GB**, Nelson SP, Robinson PG, Anastasi J, Joehl RJ, Rege RV. A foregut carcinoid tumor causing Zollinger-Ellison syndrome. *Arch Surg* 1989; **124**: 381-384 [PMID: 2919971 DOI: 10.1001/archsurg.1989.01410030131022]

23 **de Leval L**, Hardy N, Deprez M, Delwaide J, Belaïche J, Boniver J. Gastric collision between a papillotubular adenocarcinoma and a gastrinoma in a patient with Zollinger-Ellison syndrome. *Virchows Arch* 2002; **441**: 462-465 [PMID: 12447676 DOI: 10.1007/s00428-002-0707-9]

24 **Buyse S**, Charachon A, Petit T, Marmuse JP, Mignon M, Soule JC. [The gastric antrum: a rare primitive location of a gastrinoma within a type I multiple endocrine neoplasia]. *Gastroenterol Clin Biol* 2006; **30**: 625-628 [PMID: 16733391 DOI: 10.1016/s0399-8320(06)73240-7]

25 **COLE WH**, EVERSON TC. Spontaneous regression of cancer: preliminary report. *Ann Surg* 1956; **144**: 366-383 [PMID: 13363274 DOI: 10.1097/00000658-195609000-00007]

26 **Cole WH**. Efforts to explain spontaneous regression of cancer. *J Surg Oncol* 1981; **17**: 201-209 [PMID: 6166811 DOI: 10.1002/jso.2930170302]

27 **Ghatalia P**, Morgan CJ, Sonpavde G. Meta-analysis of regression of advanced solid tumors in patients receiving placebo or no anti-cancer therapy in prospective trials. *Crit Rev Oncol Hematol* 2016; **98**: 122-136 [PMID: 26597016 DOI: 10.1016/j.critrevonc.2015.10.018]

28 **Challis GB**, Stam HJ. The spontaneous regression of cancer. A review of cases from 1900 to 1987. *Acta Oncol* 1990; **29**: 545-550 [PMID: 2206563 DOI: 10.3109/02841869009090048]

29 **Sawant PD**, Nanivadekar SA, Shroff CP, Srinivas A, Dewoolkar VV. Spontaneous regression of large gastric carcinoid. *Indian J Gastroenterol* 1989; **8**: 289-290 [PMID: 2689331]

30 **Ip YT**, Pong WM, Kao SS, Chan JK. Spontaneous complete regression of gastric large-cell neuroendocrine carcinoma: mediated by cytomegalovirus-induced cross-autoimmunity? *Int J Surg Pathol* 2011; **19**: 355-358 [PMID: 21665860 DOI: 10.1177/1066896911404412]

31 **Harvey RF**. Spontaneous resolution of multifocal gastric enterochromaffin-like cell carcinoid tumours. *Lancet* 1988; **1**: 821 [PMID: 2895334 DOI: 10.1016/s0140-6736(88)91677-7]

32 **Bodey B**. Spontaneous regression of neoplasms: new possibilities for immunotherapy. *Expert Opin Biol Ther* 2002; **2**: 459-476 [PMID: 12079483 DOI: 10.1517/14712598.2.5.459]

33 **Abdelrazeq AS**. Spontaneous regression of colorectal cancer: a review of cases from 1900 to 2005. *Int J Colorectal Dis* 2007; **22**: 727-736 [PMID: 17146588 DOI: 10.1007/s00384-006-0245-z]

34 **National Comprehensive Cancer Network: NCCN Clinical Practice Guidelines in Oncology (NCCN Guidelines®)**. Neuroendocrine and Adrenal Tumors Version 2.2020 – July 24, 2020. Available from: https://www.nccn.org/

35 **Shao QQ**, Zhao BB, Dong LB, Cao HT, Wang WB. Surgical management of Zollinger-Ellison syndrome: Classical considerations and current controversies. *World J Gastroenterol* 2019; **25**: 4673-4681 [PMID: 31528093 DOI: 10.3748/wjg.v25.i32.4673]

36 **Bordi C**, Corleto VD, Azzoni C, Pizzi S, Ferraro G, Gibril F, Delle Fave G, Jensen RT. The antral mucosa as a new site for endocrine tumors in multiple endocrine neoplasia type 1 and Zollinger-Ellison syndromes. *J Clin Endocrinol Metab* 2001; **86**: 2236-2242 [PMID: 11344233 DOI: 10.1210/jcem.86.5.7479]

37 **Ninomiya S**, Hiroishi K, Shiromizu A, Ueda Y, Shiraishi N, Inomata M, Arita T. Gastrointestinal stromal tumor of the lesser omentum: a case report and review of the literature. *J Surg Case Rep* 2019; **2019**: rjz035 [PMID: 30792845 DOI: 10.1093/jscr/rjz035]

38 **Feng JF**, Guo YH, Chen WY, Chen DF, Liu J. Primary small cell carcinoma of the lesser omentum. *Kaohsiung J Med Sci* 2012; **28**: 115-119 [PMID: 22313540 DOI: 10.1016/j.kjms.2011.10.028]

39 **Wang B**, Ren KW, Yang YC, Wan DL, Li XJ, Zhai ZL, Zhang LL, Zheng SS. Carcinosarcoma of the Lesser Omentum: A Unique Case Report and Literature Review. *Medicine (Baltimore)* 2016; **95**: e3246 [PMID: 27057865 DOI: 10.1097/MD.0000000000003246]

40 **Onodera H**, Maetani S, Imamura M, Hayashi K, Nakayama T, Aoki T. [A case of a huge malignant lymphoma in the lesser omentum showing a long-term survival after combined treatment of surgery and VEP-THP chemotherapy]. *Gan To Kagaku Ryoho* 1994; **21**: 689-692 [PMID: 8154894]

41 **Wolfe MM**, Alexander RW, McGuigan JE. Extrapancreatic, extraintestinal gastrinoma: effective treatment by surgery. *N Engl J Med* 1982; **306**: 1533-1536 [PMID: 6281644 DOI: 10.1056/NEJM198206243062506]

42 **Kohyama A**, Shibata C, Funayama Y, Fukushima K, Takahashi K, Ueno T, Kobayashi T, Kinouchi M, Sasaki I, Moriya T. Primary Gastrinoma in the Lesser Omentum: A Case Report. *Jpn J Gastroenterol Surg* 2007; **40**: 1582-1586 [DOI: 10.5833/jjgs.40.1582]

43 **Chang FY**, Liao KY, Wu L, Lin SP, Lai YT, Liu CS, Tsay SH, Wu TC. An uncommon cause of abdominal pain and diarrhea-gastrinoma in an adolescent. *Eur J Pediatr* 2010; **169**: 355-357 [PMID:

19565263 DOI: 10.1007/s00431-009-1013-1]
44 **Labidi A**, Hamdi S, Ben Othman A, Chelly B, Daghfous A, Fekih M. A rare cause of upper gastrointestinal bleeding: Primary gastrinoma of the lesser omentum. *Presse Med* 2018; **47**: 913-915 [PMID: 30361100 DOI: 10.1016/j.lpm.2018.08.013]
45 **Pisegna JR**, Norton JA, Slimak GG, Metz DC, Maton PN, Gardner JD, Jensen RT. Effects of curative gastrinoma resection on gastric secretory function and antisecretory drug requirement in the Zollinger-Ellison syndrome. *Gastroenterology* 1992; **102**: 767-778 [PMID: 1537514 DOI: 10.1016/0016-5085(92)90157-t]
46 **Norton JA**, Alexander HR, Fraker DL, Venzon DJ, Gibril F, Jensen RT. Possible primary lymph node gastrinoma: occurrence, natural history, and predictive factors: a prospective study. *Ann Surg* 2003; **237**: 650-7; discussion 657 [PMID: 12724631 DOI: 10.1097/01.SLA.0000064375.51939.48]
47 **Lundell L**, Vieth M, Gibson F, Nagy P, Kahrilas PJ. Systematic review: the effects of long-term proton pump inhibitor use on serum gastrin levels and gastric histology. *Aliment Pharmacol Ther* 2015; **42**: 649-663 [PMID: 26177572 DOI: 10.1111/apt.13324]
48 **Cavalcoli F**, Zilli A, Conte D, Ciafardini C, Massironi S. Gastric neuroendocrine neoplasms and proton pump inhibitors: fact or coincidence? *Scand J Gastroenterol* 2015; **50**: 1397-1403 [PMID: 26059834 DOI: 10.3109/00365521.2015.1054426]
49 **Trinh VQ**, Shi C, Ma C. Gastric neuroendocrine tumours from long-term proton pump inhibitor users are indolent tumours with good prognosis. *Histopathology* 2020; **77**: 865-876 [PMID: 32702178 DOI: 10.1111/his.14220]
50 **Ahmadi Moghaddam P**, Cornejo KM, Hutchinson L, Tomaszewicz K, Dresser K, Deng A, O'Donnell P. Complete Spontaneous Regression of Merkel Cell Carcinoma After Biopsy: A Case Report and Review of the Literature. *Am J Dermatopathol* 2016; **38**: e154-e158 [PMID: 27759689 DOI: 10.1097/DAD.0000000000000614]
51 **Wang B**, Xia CY, Lau WY, Lu XY, Dong H, Yu WL, Jin GZ, Cong WM, Wu MC. Determination of clonal origin of recurrent hepatocellular carcinoma for personalized therapy and outcomes evaluation: a new strategy for hepatic surgery. *J Am Coll Surg* 2013; **217**: 1054-1062 [PMID: 24246620 DOI: 10.1016/j.jamcollsurg.2013.07.402]
52 **De Bernardi B**, Gerrard M, Boni L, Rubie H, Cañete A, Di Cataldo A, Castel V, Forjaz de Lacerda A, Ladenstein R, Ruud E, Brichard B, Couturier J, Ellershaw C, Munzer C, Bruzzi P, Michon J, Pearson AD. Excellent outcome with reduced treatment for infants with disseminated neuroblastoma without MYCN gene amplification. *J Clin Oncol* 2009; **27**: 1034-1040 [PMID: 19171711 DOI: 10.1200/JCO.2008.17.5877]
53 **Amoroso V**, Agazzi GM, Roca E, Fazio N, Mosca A, Ravanelli M, Spada F, Maroldi R, Berruti A. Regression of advanced neuroendocrine tumors among patients receiving placebo. *Endocr Relat Cancer* 2017; **24**: L13-L16 [PMID: 27965278 DOI: 10.1530/ERC-16-0475]
54 **Venkatram S**, Sinha N, Hashmi H, Niazi M, Diaz-Fuentes G. Spontaneous Regression of Endobronchial Carcinoid Tumor. *J Bronchology Interv Pulmonol* 2017; **24**: 70-74 [PMID: 27367850 DOI: 10.1097/LBR.0000000000000232]
55 **Sewpaul A**, Bargiela D, James A, Johnson SJ, French JJ. Spontaneous Regression of a Carcinoid Tumor following Pregnancy. *Case Rep Endocrinol* 2014; **2014**: 481823 [PMID: 25587468 DOI: 10.1155/2014/481823]
56 **Rayson D**, Pitot HC, Kvols LK. Regression of metastatic carcinoid tumor after valvular surgery for carcinoid heart disease. *Cancer* 1997; **79**: 605-611 [PMID: 9028374]
57 **Sano I**, Kuwatani M, Sugiura R, Kato S, Kawakubo K, Ueno T, Nakanishi Y, Mitsuhashi T, Hirata H, Haba S, Hirano S, Sakamoto N. Hepatobiliary and Pancreatic: A rare case of a well-differentiated neuroendocrine tumor in the bile duct with spontaneous regression diagnosed by EUS-FNA. *J Gastroenterol Hepatol* 2017; **32**: 11 [PMID: 28052461 DOI: 10.1111/jgh.13585]
58 **Kawaguchi K**, Usami N, Okasaka T, Yokoi K. Multiple thymic carcinoids. *Ann Thorac Surg* 2011; **91**: 1973-1975 [PMID: 21619996 DOI: 10.1016/j.athoracsur.2010.11.067]
59 **Delcore R**, Friesen SR. Zollinger-Ellison syndrome. A new look at regression of gastrinomas. *Arch Surg* 1991; **126**: 556-558 [PMID: 2021333 DOI: 10.1001/archsurg.1991.01410290028004]
60 **Fox PS**, Hofmann JW, Decosse JJ, Wilson SD. The influence of total gastrectomy on survival in malignant Zollinger-Ellison tumors. *Ann Surg* 1974; **180**: 558-566 [PMID: 4416322 DOI: 10.1097/00000658-197410000-00020]
61 **Magabe PC**, Bloom AL. Sudden death from carcinoid crisis during image-guided biopsy of a lung mass. *J Vasc Interv Radiol* 2014; **25**: 484-487 [PMID: 24581473 DOI: 10.1016/j.jvir.2013.10.054]

Published by **Baishideng Publishing Group Inc**
7041 Koll Center Parkway, Suite 160, Pleasanton, CA 94566, USA
Telephone: +1-925-3991568
E-mail: bpgoffice@wjgnet.com
Help Desk: https://www.f6publishing.com/helpdesk
https://www.wjgnet.com

© 2021 Baishideng Publishing Group Inc. All rights reserved.

ISSN 1007-9327 (print)
ISSN 2219-2840 (online)

World Journal of *Gastroenterology*

World J Gastroenterol 2021 January 14; 27(2): 143-232



Published by Baishideng Publishing Group Inc

World Journal of Gastroenterology

Contents

Weekly Volume 27 Number 2 January 14, 2021

MINIREVIEWS

143 Hepatotropic viruses: Is Roma population at risk?

Mrzljak A, Bajkovec L, Vilibic-Cavlek T

ORIGINAL ARTICLE

Basic Study

152 Triolein emulsion infusion into the hepatic artery increases vascular permeability to doxorubicin in rabbit liver

Kim YW, Kim HJ, Cho BM, Choi SH

Case Control Study

162 Detection of fucosylated haptoglobin using the 10-7G antibody as a biomarker for evaluating endoscopic remission in ulcerative colitis

Motooka K, Morishita K, Ito N, Shinzaki S, Tashiro T, Nojima S, Shimizu K, Date M, Sakata N, Yamada M, Takamatsu S, Kamada Y, Iijima H, Mizushima T, Morii E, Takehara T, Miyoshi E

Retrospective Cohort Study

176 Repeatedly elevated γ-glutamyltransferase levels are associated with an increased incidence of digestive cancers: A population-based cohort study

Lee CH, Han K, Kim DH, Kwak MS

Retrospective Study

189 Development of a computed tomography-based radiomics nomogram for prediction of transarterial chemoembolization refractoriness in hepatocellular carcinoma

Niu XK, He XF

Observational Study

208 Real-world disease activity and sociodemographic, clinical and treatment characteristics of moderate-to-severe inflammatory bowel disease in Brazil

Zaltman C, Parra RS, Sassaki LY, Santana GO, Ferrari MLA, Miszputen SJ, Amarante HMBS, Kaiser Junior RL, Flores C, Catapani WR, Parente JML, Bafutto M, Ramos O, Gonçalves CD, Guimaraes IM, da Rocha JJR, Feitosa MR, Feres O, Saad-Hossne R, Penna FGC, Cunha PFS, Gomes TN, Nones RB, Faria MAG, Parente MPPD, Scotton AS, Caratin RF, Senra J, Chebli JM

Randomized Controlled Trial

224 Effect of probiotics on length of hospitalization in mild acute pancreatitis: A randomized, double-blind, placebo-controlled trial

Wan YD, Zhu RX, Bian ZZ, Sun TW

World Journal of Gastroenterology

Weekly Volume 27 Number 2 January 14, 2021

Contents

ABOUT COVER

Stanislav Sitkin, MD, PhD, Associate Professor, Senior Researcher, Department of Internal Diseases, Gastroenterology and Dietetics, North-Western State Medical University named after I.I. Mechnikov, St. Petersburg 191015, Russia. drsitkin@gmail.com

AIMS AND SCOPE

The primary aim of *World Journal of Gastroenterology* (*WJG*, *World J Gastroenterol*) is to provide scholars and readers from various fields of gastroenterology and hepatology with a platform to publish high-quality basic and clinical research articles and communicate their research findings online. *WJG* mainly publishes articles reporting research results and findings obtained in the field of gastroenterology and hepatology and covering a wide range of topics including gastroenterology, hepatology, gastrointestinal endoscopy, gastrointestinal surgery, gastrointestinal oncology, and pediatric gastroenterology.

INDEXING/ABSTRACTING

The *WJG* is now indexed in Current Contents®/Clinical Medicine, Science Citation Index Expanded (also known as SciSearch®), Journal Citation Reports®, Index Medicus, MEDLINE, PubMed, PubMed Central, and Scopus. The 2020 edition of Journal Citation Report® cites the 2019 impact factor (IF) for *WJG* as 3.665; IF without journal self cites: 3.534; 5-year IF: 4.048; Ranking: 35 among 88 journals in gastroenterology and hepatology; and Quartile category: Q2.

RESPONSIBLE EDITORS FOR THIS ISSUE

Production Editor: *Ji-Hong Liu*; **Production Department Director:** *Yun-Xiaojian Wu*; **Editorial Office Director:** *Ze-Mao Gong*.

NAME OF JOURNAL
World Journal of Gastroenterology

ISSN
ISSN 1007-9327 (print) ISSN 2219-2840 (online)

LAUNCH DATE
October 1, 1995

FREQUENCY
Weekly

EDITORS-IN-CHIEF
Andrzej S Tarnawski, Subrata Ghosh

EDITORIAL BOARD MEMBERS
http://www.wjgnet.com/1007-9327/editorialboard.htm

PUBLICATION DATE
January 14, 2021

COPYRIGHT
© 2021 Baishideng Publishing Group Inc

INSTRUCTIONS TO AUTHORS
https://www.wjgnet.com/bpg/gerinfo/204

GUIDELINES FOR ETHICS DOCUMENTS
https://www.wjgnet.com/bpg/GerInfo/287

GUIDELINES FOR NON-NATIVE SPEAKERS OF ENGLISH
https://www.wjgnet.com/bpg/gerinfo/240

PUBLICATION ETHICS
https://www.wjgnet.com/bpg/GerInfo/288

PUBLICATION MISCONDUCT
https://www.wjgnet.com/bpg/gerinfo/208

ARTICLE PROCESSING CHARGE
https://www.wjgnet.com/bpg/gerinfo/242

STEPS FOR SUBMITTING MANUSCRIPTS
https://www.wjgnet.com/bpg/GerInfo/239

ONLINE SUBMISSION
https://www.f6publishing.com

© 2021 Baishideng Publishing Group Inc. All rights reserved. 7041 Koll Center Parkway, Suite 160, Pleasanton, CA 94566, USA
E-mail: bpgoffice@wjgnet.com https://www.wjgnet.com

World Journal of Gastroenterology

Submit a Manuscript: https://www.f6publishing.com

World J Gastroenterol 2021 January 14; 27(2): 143-151

DOI: 10.3748/wjg.v27.i2.143

ISSN 1007-9327 (print) ISSN 2219-2840 (online)

MINIREVIEWS

Hepatotropic viruses: Is Roma population at risk?

Anna Mrzljak, Lucija Bajkovec, Tatjana Vilibic-Cavlek

ORCID number: Anna Mrzljak 0000-0001-6270-2305; Lucija Bajkovec 0000-0002-6727-1353; Tatjana Vilibic-Cavlek 0000-0002-1877-5547.

Author contributions: Mrzljak A and Vilibic-Cavlek T made contributions to the concept, design and writing of the manuscript; Bajkovec L was involved in writing the manuscript and creating the image; all authors approved the final manuscript.

Conflict-of-interest statement: No potential conflicts of interest.

Open-Access: This article is an open-access article that was selected by an in-house editor and fully peer-reviewed by external reviewers. It is distributed in accordance with the Creative Commons Attribution NonCommercial (CC BY-NC 4.0) license, which permits others to distribute, remix, adapt, build upon this work non-commercially, and license their derivative works on different terms, provided the original work is properly cited and the use is non-commercial. See: http://creativecommons.org/Licenses/by-nc/4.0/

Manuscript source: Invited manuscript

Specialty type: Gastroenterology and hepatology

Country/Territory of origin: Croatia

Anna Mrzljak, Department of Gastroenterology, University Hospital Merkur, Zagreb 10000, Croatia

Anna Mrzljak, Tatjana Vilibic-Cavlek, School of Medicine, University of Zagreb, Zagreb 10000, Croatia

Lucija Bajkovec, Department of Medicine, County Hospital Cakovec, Cakovec 40000, Croatia

Tatjana Vilibic-Cavlek, Department of Virology, Croatian Institute of Public Health, Zagreb 10000, Croatia

Corresponding author: Anna Mrzljak, MD, PhD, Associate Professor, Department of Gastroenterology, University Hospital Merkur, Zajčeva 19, Zagreb 10000, Grad Zagreb, Croatia. anna.mrzljak@gmail.com

Abstract

Roma people make up a significant ethnic minority in many European countries, with the vast majority living in Central and Eastern Europe. Roma are a vulnerable population group in social, economic, and political terms. Frequent migrations, life in segregated communities, substandard housing, poverty, and limited access to quality health care, including low immunization coverage, affect their health status and predispose them to various diseases, including viral hepatitis. Hepatitis A, B, and E are highly prevalent among Roma and mainly associated with low socioeconomic status. In contrast, hepatitis C does not seem to be more frequent in the Roma population. Enhanced efforts should be directed towards the implementation of screening programs, preventive measures, and treatment of viral hepatitis in Roma communities throughout Europe.

Key Words: Roma population; Hepatitis A virus; Hepatitis B virus; Hepatitis C virus; Hepatitis E virus; Europe

©The Author(s) 2021. Published by Baishideng Publishing Group Inc. All rights reserved.

Core Tip: Roma people constitute the most important transnational minority in Europe. They are a vulnerable population group in social, economic, and political terms. Low socioeconomic conditions and lack of quality health care predispose them to viral hepatitis, especially hepatitis A, B, and E. In the global attempt to eliminate viral hepatitis, Roma should be considered a high priority group for screening and treatment

Peer-review report's scientific quality classification
Grade A (Excellent): A
Grade B (Very good): B
Grade C (Good): 0
Grade D (Fair): 0
Grade E (Poor): 0

Received: October 25, 2020
Peer-review started: October 25, 2020
First decision: November 13, 2020
Revised: November 13, 2020
Accepted: November 29, 2020
Article in press: November 29, 2020
Published online: January 14, 2021

P-Reviewer: Schiff ER
S-Editor: Fan JR
L-Editor: A
P-Editor: Liu JH

based on the epidemiological and social context.

Citation: Mrzljak A, Bajkovec L, Vilibic-Cavlek T. Hepatotropic viruses: Is Roma population at risk? *World J Gastroenterol* 2021; 27(2): 143-151
URL: https://www.wjgnet.com/1007-9327/full/v27/i2/143.htm
DOI: https://dx.doi.org/10.3748/wjg.v27.i2.143

INTRODUCTION

Roma people are a distinct ethnic minority dispersed worldwide, with an estimated population of around 12 million. In Europe, they are the largest minority group (5.2 million), with the vast majority living in Central and Eastern Europe (Figure 1)[1-3]. However, the exact number is uncertain due to their nomadic life and historical lack of birth and death records[4]. Roma are a vulnerable population group in social, economic, and political terms. This vulnerability is manifested in widespread poverty, unemployment, illiteracy, lack of formal education, segregation in the educational system, and substandard housing[5,6]. Roma people have worse health status, higher infant mortality rates, shorter (10-15 years) life expectancy, and a higher prevalence of chronic diseases than the non-Roma[2,7,8]. Unhealthy habits, smoking, and lack of physical activity are common in Roma population[9,10]. Moreover, Roma experience difficulties accessing healthcare due to fear, lack of trust, and previous bad experiences with health providers[11]. Poor socioeconomic factors predispose Roma to a number of various infectious diseases, including viral hepatitis[6,12,13]. Moreover, many Roma believe in folk medicine and prefer home-made remedies, resulting in low immunization coverage and outbreaks of infectious diseases[4].

In the attempt of global elimination of viral hepatitis[14], preventive measures, linkage to care, and treatment process may be challenging in vulnerable populations. In this opinion review, we aim to summarize available data and address practical issues related to viral hepatitis in the European Roma population.

HEPATITIS A

According to the European Centre for Disease Prevention and Control[15], there were 11296 hepatitis A cases in 2019 in the European Union. The incidence of hepatitis A globally decreases, but it is still high in developing countries and among minorities living in low socioeconomic conditions in developed countries[16]. In low-income countries, almost 100% of older children and adults are seropositive[17]. As hepatitis A virus (HAV) is transmitted by person-to-person contact or through contaminated water and food[16], access to clean water and hygiene facilities contributes to the reduction of HAV prevalence[18]. Socioeconomic factors are the most important predictors of HAV infection. Better living standards, including higher incomes and higher education degrees, as well as better housing conditions, significantly decrease the risk of HAV infection[17]. Hepatitis A can be prevented with a vaccine that provides long-term immunity[16].

Roma people are recognized as a high-risk group for HAV infection, in addition to migrants, travelers to endemic countries, and men who have sex with other men[19,20]. In Slovakia and Greece, the countries with a significant number of Roma residents, several hepatitis A outbreaks were reported over the last 15 years[16,19,21]. In the period between 2009 and 2018, 1193 cases of HAV infection were reported in Greece. Roma people accounted for approximately 20% of all infections, with 80.7% of cases affecting Roma children under 15 years old, whereas in the non-Roma population, the percentage of children was significantly lower (5.3%)[19]. Even though the HAV vaccine is mandatory for all children in Greece since 2008, the study from 2013 showed that only 22.6% of Roma children were vaccinated against HAV[22]. In the Roma population, both genders were equally affected, whereas in the non-Roma population, infection predominantly occurred in males. Almost half of HAV clusters (2009-2018) were reported in the Roma population, which accounts for the minority of the Greek population[19]. The study on the HAV outbreak in south-eastern Greece (2007) demonstrated that Roma are susceptible to HAV infection, which appears at an earlier

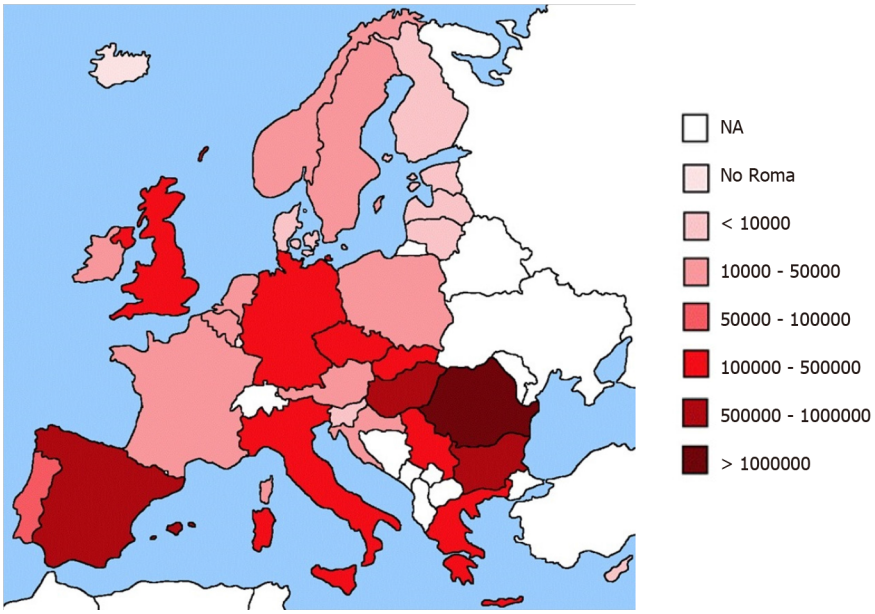


Figure 1 Distribution of Roma population in Europe according to the European Commission: Roma Health Report[1]. NA: No available data.

age than in non-Roma[16,20]. In Portugal, an outbreak of HAV was reported in 2005, which involved Roma children[23]. In 2008, there were 9 HAV outbreaks in Slovakia, and four of them took place in the districts predominantly inhabited by the Roma population. The biggest outbreak was registered in Lomnička village (298 cases), where 99% of the residents are Roma. Living conditions in the village, inadequate clean water supplies, and sewage systems predisposed the outbreak[21]. The only data on hepatitis A in Roma from the Czech Republic derives from the European Commission Roma Health Report (2014), stating two epidemics; one in 2009 and the other in 2010 when 30%-50% of Roma from all reported cases developed symptoms[1]. In the Czech Republic, the vaccination against HAV is easily accessible but not obligatory and not free. The HAV vaccination rates among Roma are estimated as low[1]. In the Plovdiv region in Bulgaria, 3911 cases of HAV were documented between 2005 and 2008, most of them associated with Roma. Notification rate in groups of respondents living in worse socioeconomic conditions, mostly Roma, was remarkably higher than in those living in good sanitary conditions[24]. In France, the hepatitis A outbreak involved a total of 492 cases over the 2008-2009 period, including eight clusters of cases among communities living in sites with poor sanitation[1]. A seroepidemiological study conducted in 1995 in San Sebastian, Spain, showed that 82.2% of Roma children were HAV seropositive compared to 9.3% of non-Roma children[25].

HAV infection in Roma differs from the non-Roma population in terms of the lower age of infection and equal distribution among genders[16,19]. The high prevalence is mainly due to poor socioeconomic factors, inadequate sanitary conditions, and sewage systems, contributing to easier transmission of the disease. Additionally, the vaccination coverage in Roma children is low[22,26,27]. In the attempt to lower the HAV incidence, better vaccination coverage and improvement of living conditions in Roma communities should be continuously and decisively implemented.

HEPATITIS B

Hepatitis B virus (HBV) infection has a chronic course and leads to fibrosis, cirrhosis, and hepatocellular carcinoma. The pattern of HBV transmission is vertical and horizontal by infected blood or sexual contact[28]. The HBV vaccine prevents HBV infection and has significantly decreased HBV-related mortality[29]. As HBV infection is associated with poor socioeconomic conditions[28,30], Roma living in communities with poor hygiene are predisposed to have a higher incidence of HBV infection[31,32].

Several studies addressed the prevalence of HBV in Slovakia, where the Roma minority is very numerous. It is estimated that approximately 400000 Roma people live in Slovakia, which accounts for 7.5% of the Slovak population[8]. Their socio-

economic (lower education, unemployment, social benefits) and living conditions (lack of standard household facilities such as sewage system, water supply, flush toilet, bathroom or shower, electricity) are significantly worse compared with the majority[14]. In 2008-2009, a study was conducted in 9 districts of Eastern Slovakia, comparing districts with higher (> 5%) and lower (< 5%) Roma population. There was no significant difference in the overall prevalence of HBsAg (1.95% *vs* 1.62%). However, pregnant women showed a higher prevalence of HBV infection in districts with a higher Roma population (2.72% *vs* 0.98%)[33]. In addition, a cross-sectional epidemiological study on hepatitis B was conducted in 2011 among randomly sampled Roma and non-Roma populations. Roma population had a significantly higher prevalence of HBsAg (12.4% *vs* 2.8%) and anti-HBc (52.8% *vs* 15.9%) than the non-Roma population. Furthermore, HBsAg positive Roma population was more commonly HBV DNA positive compared to HBsAg positive non-Roma population (94.3% *vs* 70.0%). Tattooing, economic factors (unemployment, elementary education, poverty), and male sex were found to be risk factors for HBV positivity[34]. Furthermore, targeted testing in primary care demonstrated a high prevalence of HBV infection within the Slovak-Roma population in Sheffield, United Kingdom. The HBsAg positivity was found to be 9.4%, while 28% had evidence of cleared past HBV infection (anti-HBc positive)[35].

One Greek study (2002) analyzed the prevalence and risk factors of hepatitis B in Roma and non-Roma children who lived in a deprived suburb of Athens. Among Roma children, 22.0% were identified with evidence of past HBV infection (anti-HBc positive), of whom 4.2% were chronic carriers (HBsAg positive), whereas no past infection was detected among the non-Roma. The evidence of HBV vaccination (anti-HBs positive) was detected in only 13.6% Roma, but in 95.9% non-Roma children. Among possible risk factors, unfavorable living conditions, frequent residency change, lack of child insurance and primary healthcare delivery were significantly associated with HBV seroprevalence among Roma[36]. Although overall vaccination coverage in Roma children is low[22], it varies in different European countries. For instance, in Slovakia, 59.2% of Roma children are vaccinated against HBV[23]. In the Doctors of the World report (2011) the HBV vaccination coverage in Roma children under two years of age was 43.5%[37]. On the other hand, in the Czech Republic, 95% of Roma children are vaccinated for obligatory diseases, including HBV[1].

Tattooing, blood transfusions, drug use, and imprisonment carry a high risk for HBV and are more common in Roma people[38]. However, it is considered that sexual intercourse is more significant for horizontal transmission of HBV among Roma, since a minority of them use preventive methods against sexually transmitted diseases[34,38]. Vaccination against HBV is less common in Roma; it is not completed because of lack of compliance[38]. Lastly, the efficacy of HBV treatment in Roma is concerning, mainly due to non-compliance and poor availability of healthcare[34].

HEPATITIS C

Hepatitis C virus (HCV) is a widespread cause of acute and chronic hepatitis and a significant risk factor for liver cirrhosis and hepatocellular carcinoma. Around 71 million people worldwide are suffering from chronic hepatitis C infection[39]. It is a blood-borne virus, most commonly transmitted by contaminated needles (intravenous drug users), through blood transfusions or sexual intercourse[40,41]. Vertical transmission is also possible[39].

Some of the risky behaviors appear to be common among Roma. For instance, studies reported an increase in Roma women participating in sex work and a higher prevalence of injection drug use among Roma[3,42,43].

In 2010, a seroprevalence study on HCV was conducted among Roma youth aged 15–24 years in two cities in Serbia-Belgrade (the nation's capital and largest city with 1.2% of residents estimated to be Roma) and Kragujevac (the fourth largest city in Serbia with up to 14% Roma by estimates). Although some of the risk factors were highly prevalent (intravenous drug use, 0.5%-3%; experience with sex workers, 5%-10%; tattooing in non-sterile conditions, 2%-14%; the use of a condom with a constant partner, 1%-25%), only four of 240 (1.7%) participants tested positive for HCV antibodies. Two reported intravenous drug use and three reported having a tattoo[44].

Similar results were found in Slovakia among 441 Roma with HCV seropositivity of 0.7% (1.5% in the general population). Predisposing factors for HCV were tattooing, blood transfusions, and having more sexual partners[32]. In a study conducted among students of two elementary schools in Greece (2002), none of the 118 Roma children

involved were positive for HCV antibodies[36]. According to these studies, HCV infection is not as frequent as other hepatitis viruses among Roma.

HEPATITIS E

Hepatitis E virus (HEV) is an emerging viral disease, with 20 million infection cases and 55000 deaths worldwide. Its prevalence is higher in developing countries; however, lately, it has been recognized as a significant cause of hepatitis in resource-rich countries[45]. HEV can be transmitted through contaminated water; however, food-borne, blood transfusion-related transmission by gained significant attention in recent decades[45,46].

The data about HEV among Roma in Europe are scarce and conducted only in Slovakia. The Roma population's HEV prevalence ranged from 21.5% to 45.5%, and the only significant risk factor appeared to be the consumption of raw meat[47,48].

CONCLUSION

In 2016, the World Health Organization adopted the first Global Health Sector Strategy on Viral Hepatitis, calling for its elimination as a public health threat. The strategy presented a target for 2030–of reducing new hepatitis B and C infections by 90% and mortality by 65%[14]. Roma constitute the most important transnational minority in Europe and a highly vulnerable population affected by viral hepatitis. Based on their epidemiological and social context, living conditions, lack of access to clean water, safe food, and medical services to maintain effective infection control measures, Roma should be considered a high priority group in managing viral hepatitis.

Screening is of particular importance as data on viral hepatitis prevalence in European Roma are scarce and limited to specific regions (Table 1). In Roma, hepatitis B prevalence is high, and mother-to-child transmission is likely a major mode of transmission and early childhood infection based on low vaccination. In addition, the fecal-oral and/or food-borne hepatitis (HAV and HEV) are more common in Roma than in the non-Roma population. In contrast, HCV infection does not seem to be more frequent in Roma.

The challenges in the Roma population are high. However, in the attempt to improve Roma's health and reduce health inequalities, viral hepatitis screening programs, facilitated linkage to care with access to affordable antivirals and vaccines should be continuously implemented through Roma communities. Effectively combating viral hepatitis may also reduce maternal and child mortality, as the mortality from non-communicable diseases. This strategy and its far-fetched implications may alleviate poverty and facilitate further development in terms of managing sanitation and water, reducing inequality in access to services, and promoting non-discrimination.

All European countries approved the WHO strategy, and now we have just one decade left to reach the goals and fulfill these promises.

Table 1 The epidemiology of hepatitis A, B, C and E among Roma population in Europe

Region	Year	Population, *N*	(Sero) Prevalence	Acute cases/outbreaks	Ref.
Northeastern Greece	2007	124 inhabitants of Xanthi, Rodopi and Evros, mostly Roma		54% males, 46% females, age 2–17 yr	Vantarakis *et al*[16], 2010
Greece	2004–2013	295 Roma/995 confirmed cases		Median age 5.9 yr; 2007 outbreak: 139 cases, 82% Roma	Mellou *et al*[20], 2015
Greece	2009-2018	240 Roma/1193 confirmed cases		51.2% males, 80.4% < 15 years old, median age 7 yr; 20 clusters recorded among Roma; 2013: Greatest outbreak, 112 cases among Roma	Mellou *et al*[19], 2020
Athens, Greece	1999-2013	467 children hospitalized with hepatitis A, age 0-14 yr		HAV hospitalization rates *per* 1000 admissions, among Roma: 233.1 (1999-2008), 54.3 (2009-2013)	Papaevangelou *et al*[27], 2016
Western Athens, Greece	2002	216 children from two elementary schools, 118 Roma	Anti-HAV IgG: Roma children 98%, non-Roma children 33%		Michos *et al*[36], 2008
Slovakia	2008	667 cases reported to Epidemiological Information System database		536 cases in "low hygienic standards" areas; considered Roma; 4/9 outbreaks in areas with mostly Roma population; Lomnička outbreak (99% Roma population): 298 cases, 297 < 18 years old	Hrivniaková *et al*[21], 2009
South Bulgaria	2005-2008	3911 patients with hepatitis A treated in Clinics of Infectious Diseases, Plovdiv		Incidence rate in group living in poor hygienic conditions (mostly Roma): 450.66/100000; Outbreak in Stolipinovo quarter (2006); 1004 cases, mostly Roma	Stoycheva *et al*[24], 2011
San Sebastian, Spain	1995	73 Roma, age 2-16 yr	Total anti-HAV 82.2 %, total anti-HAV 50% in children 2-5 yr, total anti-HAV 92.7% in children > 5 yr		Cilla *et al*[25], 1995
Eastern Slovakia (9 regions)	2008-2009	59279 serum samples (13798were part of the pregnancy screening)	HBsAg overall 2.18%-9.07%; pregnant women 0.82%-4.13%		Kristian *et al*[33], 2013
Eastern Slovakia	2011	452 Roma, adult population	HBsAg 12.4%; anti-HBc 52.8%; HBV DNA 94.3%		Drazilova *et al*[34], 2018
Sheffield, United Kingdom	2007-2013	436 Slovak-Roma adult population	HBsAg 9.4%; anti-HBc 28%		Gregory *et al*[35], 2014
Western Athens, Greece	2002	118 Roma children	HBsAg 4.2%; anti-HBs 13.6%; anti-HBc 22.0%		Michos *et al*[36], 2008
Serbia (Belgrade and Kragujevac)	2010	240 Roma, age 20-24 yr	Anti-HCV 1.7%		Djonic *et al*[44], 2013
Eastern Slovakia, Košice region	2011	441 Roma, age 18-55 yr	Anti-HCV 0.7%		Veselíny *et al*[32], 2014
Western Athens, Greece	2002	216 children from two elementary schools, age 5-15 yr, 118 Roma	Anti-HCV 0%		Michos *et al*[36], 2008
Eastern Slovakia	2011	195 Roma living in Roma settlements, age 18-55 yr	Total anti-HEV 21.5%, highest in Roma men–29.4%		Halánová *et al*[47], 2018
Košice, eastern	2018	175 patients hospitalized in Department of	Total anti-HEV 45.5%		Paraličová *et al*[48],

Slovakia	Infectology and Travel Medicine, age 19-94 yr, 11 Roma	2020

HAV: Hepatitis A virus; HBV: Hepatitis B virus; HCV: Hepatitis C virus; HEV: Hepatitis E virus.

REFERENCES

1 European Commission: Roma Health Report [Internet]. 2014 [cited 2020 Oct. 25]. Available from: https://ec.europa.eu/health/sites/health/files/social_determinants/docs/2014_roma_health_report_en.pdf

2 **Sepkowitz KA**. Health of the world's Roma population. *Lancet* 2006; **367**: 1707-1708 [PMID: 16731250 DOI: 10.1016/S0140-6736(06)68746-1]

3 **Hajioff S**, McKee M. The health of the Roma people: a review of the published literature. *J Epidemiol Community Health* 2000; **54**: 864-869 [PMID: 11027202 DOI: 10.1136/jech.54.11.864]

4 **Vivian C**, Dundes L. The crossroads of culture and health among the Roma (Gypsies). *J Nurs Scholarsh* 2004; **36**: 86-91 [PMID: 15098424 DOI: 10.1111/j.1547-5069.2004.04018.x]

5 **European Union Agency for Fundamental Rights**. Roma and travellers in six countries [Internet]. 2020 [cited 2020 Oct. 25]. Available from: https://fra.europa.eu/sites/default/files/fra_uploads/fra-2020-roma-travellers-six-countries_en.pdf

6 **Jarcuska P**, Bobakova D, Uhrin J, Bobak L, Babinska I, Kolarcik P, Veselska Z, Madarasova Geckova A; HEPA-META team. Are barriers in accessing health services in the Roma population associated with worse health status among Roma? *Int J Public Health* 2013; **58**: 427-434 [PMID: 23546390 DOI: 10.1007/s00038-013-0451-8]

7 **Rosicova K**, Madarasova Geckova A, van Dijk JP, Kollarova J, Rosic M, Groothoff JW. Regional socioeconomic indicators and ethnicity as predictors of regional infant mortality rate in Slovakia. *Int J Public Health* 2011; **56**: 523-531 [PMID: 20976517 DOI: 10.1007/s00038-010-0199-3]

8 **Sedláková D**. Low socioeconomic status and unhealthy lifestyle lead to high morbidity in young Roma of East Slovakia. *Cent Eur J Public Health* 2014; **22** Suppl: S3-S5 [PMID: 24847606 DOI: 10.21101/cejph.a4008]

9 **Babinská I**, Gecková AM, Jarcuska P, Pella D, Mareková M, Stefková G, Veselská ZD; HepaMeta Team. Does the population living in Roma settlements differ in physical activity, smoking and alcohol consumption from the majority population in Slovakia? *Cent Eur J Public Health* 2014; **22** Suppl: S22-S27 [PMID: 24847610 DOI: 10.21101/cejph.a3897]

10 **Petek D**, Rotar Pavlic D, Svab I, Lolić D. Attitudes of Roma toward smoking: qualitative study in Slovenia. *Croat Med J* 2006; **47**: 344-347 [PMID: 16625703]

11 **Shaaf M**. Roma Health Mediators: Successes and Challenges [Internet]. 2011 [cited 2020 Oct. 25]. Available from: https://www.opensocietyfoundations.org/publications/roma-health-mediators-successes-and-challenges#publications_download

12 **Janicko M**, Senajová G, Drazilová S, Veselíny E, Fedacko J, Siegfried L, Kristian P, Virág L, Pella D, Mareková M, Gecková AM, Kalanin P, Jarcuska P, Halánová M; HepaMeta Team. Association between metabolic syndrome and hepatitis B virus infection in the Roma population in eastern Slovakia: a population-based study. *Cent Eur J Public Health* 2014; **22** Suppl: S37-S42 [PMID: 24847613 DOI: 10.21101/cejph.a3900]

13 **Gecková AM**, Babinská I, Bobáková D, Veselská ZD, Bosáková L, Kolarcik P, Jarcuska P, Pella D,

Halánová M; HepaMeta Team. Socioeconomic characteristics of the population living in Roma settlements and their association with health and health-related behaviour. *Cent Eur J Public Health* 2014; **22** Suppl: S57-S64 [PMID: 24847616 DOI: 10.21101/cejph.a3903]

14 **World Health Organization**. Global health sector strategy on viral hepatitis, 2016–2021 [Internet]. 2016 [cited 2020 Oct. 25]. Available from: https://apps.who.int/iris/bitstream/handle/10665/246177/WHO-HIV-2016.06-eng.pdf?sequence=1

15 **European Centre for Disease Prevention and Control**. Surveillance Atlas of Infectious Diseases [Internet]. 2020 [cited 2020 Oct. 6]. Available from: https://atlas.ecdc.europa.eu/public/index.aspx

16 **Vantarakis A**, Nearxou A, Pagonidis D, Melegos F, Seretidis J, Kokkinos P, Zarkadis I, Parasidis T, Alamanos Y. An outbreak of hepatitis A in Roma populations living in three prefectures in Greece. *Epidemiol Infect* 2010; **138**: 1025-1031 [PMID: 19941688 DOI: 10.1017/S0950268809991257]

17 **Jacobsen KH**, Wiersma ST. Hepatitis A virus seroprevalence by age and world region, 1990 and 2005. *Vaccine* 2010; **28**: 6653-6657 [PMID: 20723630 DOI: 10.1016/j.vaccine.2010.08.037]

18 **Jacobsen KH**. Globalization and the Changing Epidemiology of Hepatitis A Virus. *Cold Spring Harb Perspect Med* 2018; **8**: a031716 [PMID: 29500305 DOI: 10.1101/cshperspect.a031716]

19 **Mellou K**, Chrysostomou A, Sideroglou T, Kyritsi M, Georgakopoulou T, Tsiodras S, Hadjichristodoulou C. Epidemiology of hepatitis A in Greece in the last decade: management of reported cases and outbreaks and lessons learned. *Epidemiol Infect* 2020; **148**: e58 [PMID: 32052723 DOI: 10.1017/S0950268820000382]

20 **Mellou K**, Sideroglou T, Papaevangelou V, Katsiaflaka A, Bitsolas N, Verykouki E, Triantafillou E, Baka A, Georgakopoulou T, Hadjichristodoulou C. Considerations on the current universal vaccination policy against hepatitis A in Greece after recent outbreaks. *PLoS One* 2015; **10**: e0116939 [PMID: 25590132 DOI: 10.1371/journal.pone.0116939]

21 **Hrivniaková L**, Sláciková M, Kolcunová S. Hepatitis A outbreak in a Roma village in eastern Slovakia, August-November 2008. *Euro Surveill* 2009; **14**: 19093 [PMID: 19161727]

22 **Papamichail D**, Petraki I, Arkoudis C, Terzidis A, Smyrnakis E, Benos A, Panagiotopoulos T. Low vaccination coverage of Greek Roma children amid economic crisis: national survey using stratified cluster sampling. *Eur J Public Health* 2017; **27**: 318-324 [PMID: 27694159 DOI: 10.1093/eurpub/ckw179]

23 **Rodrigues L**, Pista A, Oliveira A, Agua-Doce I, Manita C, Paixão MT. Molecular epidemiology of hepatitis A virus in a group of Portuguese citizens living in Lisbon area. *J Med Virol* 2007; **79**: 483-487 [PMID: 17387747 DOI: 10.1002/jmv.20851]

24 **Stoycheva M**, Vatev N, Petrov A, Venchev C, Atanasova M. Epidemiological Study of Hepatitis A in Plovdiv Region – Bulgaria, 2005-2008. *World J Vaccines* 2011; **1**: 162-168 [DOI: 10.4236/wjv.2011.14017]

25 **Cilla G**, Perez-Trallero E, Marimon JM, Erdozain S, Gutierrez C. Prevalence of hepatitis A antibody among disadvantaged gypsy children in northern Spain. *Epidemiol Infect* 1995; **115**: 157-161 [PMID: 7641829 DOI: 10.1017/s0950268800058210]

26 **Stojanovski K**, McWeeney G, Emiroglu N, Ostlin P, Koller T, Licari L, Kaluski DN. Risk factors for low vaccination coverage among Roma children in disadvantaged settlements in Belgrade, Serbia. *Vaccine* 2012; **30**: 5459-5463 [PMID: 22776215 DOI: 10.1016/j.vaccine.2012.06.072]

27 **Papaevangelou V**, Alexopoulou Z, Hadjichristodoulou C, Kourlamba G, Katsioulis A, Theodoridou K, Spoulou V, Theodoridou M. Time trends in pediatric hospitalizations for hepatitis A in Greece (1999-2013): Assessment of the impact of universal infant immunization in 2008. *Hum Vaccin Immunother* 2016; **12**: 1852-1856 [PMID: 27141813 DOI: 10.1080/21645515.2016.1151589]

28 **Polaris Observatory Collaborators**. Global prevalence, treatment, and prevention of hepatitis B virus infection in 2016: a modelling study. *Lancet Gastroenterol Hepatol* 2018; **3**: 383-403 [PMID: 29599078 DOI: 10.1016/S2468-1253(18)30056-6]

29 **Zanetti AR**, Van Damme P, Shouval D. The global impact of vaccination against hepatitis B: a historical overview. *Vaccine* 2008; **26**: 6266-6273 [PMID: 18848855 DOI: 10.1016/j.vaccine.2008.09.056]

30 **Nardone A**, Anastassopoulou CG, Theeten H, Kriz B, Davidkin I, Thierfelder W, O'Flanagan D, Bruzzone B, Mossong J, Boot HJ, Butur D, Slaciková M, Panait ML, Hellenbrand W, DE Melker H, Sobotová Z, Icardi G, Andrews N, Pebody RG, VAN Damme P, Kafatos G, Miller E, Hatzakis A. A comparison of hepatitis B seroepidemiology in ten European countries. *Epidemiol Infect* 2009; **137**: 961-969 [PMID: 19102797 DOI: 10.1017/S0950268808001672]

31 **Babinska I**, Veselska ZD, Bobakova D, Pella D, Panico S, Reijneveld SA, Jarcuska P, Jarcuska P, Zezula I, Geckova AM; HEPA-META team. Is the cardiovascular risk profile of people living in Roma settlements worse in comparison with the majority population in Slovakia? *Int J Public Health* 2013; **58**: 417-425 [PMID: 23564005 DOI: 10.1007/s00038-013-0463-4]

32 **Veselíny E**, Janicko M, Drazilová S, Siegfried L, Pastvová L, Schréter I, Kristian P, Viág L, Jarcuska P, Valková I, Cáriková K, Senajová G, Fedacko J, Pella D, Mareková M, Gecková AM, Jarcuska P; HepaMeta Team. High hepatitis B and low hepatitis C prevalence in Roma population in eastern Slovakia. *Cent Eur J Public Health* 2014; **22** Suppl: S51-S56 [PMID: 24847615 DOI: 10.21101/cejph.a3902]

33 **Kristian P**, Veselská ZD, Paralicová Z, Jarcuska P, Virág L, Valková I, Schréter I. Regional and ethnic aspects of viral hepatitis B among pregnant women. *Cent Eur J Public Health* 2013; **21**: 22-25 [PMID: 23741894]

34 **Drazilova S**, Janicko M, Kristian P, Schreter I, Halanova M, Urbancikova I, Madarasova-Geckova A,

Marekova M, Pella D, Jarcuska P; HepaMeta Team. Prevalence and Risk Factors for Hepatitis B Virus Infection in Roma and Non-Roma People in Slovakia. *Int J Environ Res Public Health* 2018; **15**: 1047 [PMID: 29789486 DOI: 10.3390/ijerph15051047]

35 **Gregory A**, Vedio A, Stone B, Green S, Bronsdon C. Targeted testing in primary care demonstrates high prevalence of hepatitis B infection within the Slovak-Roma population in Sheffield, UK. *J Viral Hepat* 2014; **21**: e138-e139 [PMID: 25056611 DOI: 10.1111/jvh.12287]

36 **Michos A**, Terzidis A, Kalampoki V, Pantelakis K, Spanos T, Petridou ET. Seroprevalence and risk factors for hepatitis A, B, and C among Roma and non-Roma children in a deprived area of Athens, Greece. *J Med Virol* 2008; **80**: 791-797 [PMID: 18360892 DOI: 10.1002/jmv.21134]

37 **Medicines du Monde**. Rapport d'enquête sur la couverture vaccinale des populations rroms rencontrées par les équipes de Médecins du Monde en France [Internet]. 2011 [cited 2020 Oct. 25]. Available from: https://fnasat.centredoc.fr/doc_num.php?explnum_id=208

38 **Drazilova S**, Kristian P, Janicko M, Halanova M, Safcak D, Dorcakova PD, Marekova M, Pella D, Madarasova-Geckova A, Jarcuska P, HepaMeta Team. What is the Role of the Horizontal Transmission of Hepatitis B Virus Infection in Young Adult and Middle-Aged Roma Population Living in the Settlements in East Slovakia? *Int J Environ Res Public Health* 2020; **17**: 3293 [PMID: 32397342 DOI: 10.3390/ijerph17093293]

39 **World Health Organization**. Hepatitis C [Internet]. 2020 [cited 2020 Oct. 12]. Available from: https://www.who.int/news-room/fact-sheets/detail/hepatitis-c

40 **Cavlek TV**, Margan IG, Lepej SZ, Kolaric B, Vince A. Seroprevalence, risk factors, and hepatitis C virus genotypes in groups with high-risk sexual behavior in Croatia. *J Med Virol* 2009; **81**: 1348-1353 [PMID: 19551819 DOI: 10.1002/jmv.21530]

41 **Vilibic-Cavlek T**, Kucinar J, Kaic B, Vilibic M, Pandak N, Barbic L, Stevanovic V, Vranes J. Epidemiology of hepatitis C in Croatia in the European context. *World J Gastroenterol* 2015; **21**: 9476-9493 [PMID: 26327756 DOI: 10.3748/wjg.v21.i32.9476]

42 **Iraurgi I**, Jiménez-Lerma JM, Landabaso MA, Arrazola X, Gutiérrez-Fraile M. Gypsies and drug addictions. Study of the adherence to treatment. *Eur Addict Res* 2000; **6**: 34-41 [PMID: 10729741 DOI: 10.1159/000019007]

43 **Casals M**, Pila P, Langohr K, Millet JP, Caylà JA; Roma Population Working Group. Incidence of infectious diseases and survival among the Roma population: a longitudinal cohort study. *Eur J Public Health* 2012; **22**: 262-266 [PMID: 21217119 DOI: 10.1093/eurpub/ckq204]

44 **Djonic D**, Djuric M, Bassioni-Stamenic F, McFarland W, Knezevic T, Nikolic S, Zivkovic V, Vallabhaneni S. HIV-related risk behaviors among Roma youth in Serbia: results of two community-based surveys. *J Adolesc Health* 2013; **52**: 234-240 [PMID: 23332490 DOI: 10.1016/j.jadohealth.2012.05.012]

45 **European Association for the Study of the Liver**. EASL Clinical Practice Guidelines on hepatitis E virus infection. *J Hepatol* 2018; **68**: 1256-1271 [PMID: 29609832 DOI: 10.1016/j.jhep.2018.03.005]

46 **Mrzljak A**, Dinjar-Kujundzic P, Jemersic L, Prpic J, Barbic L, Savic V, Stevanovic V, Vilibic-Cavlek T. Epidemiology of hepatitis E in South-East Europe in the "One Health" concept. *World J Gastroenterol* 2019; **25**: 3168-3182 [PMID: 31333309 DOI: 10.3748/wjg.v25.i25.3168]

47 **Halánová M**, Veseliny E, Kalinová Z, Jarčuška P, Janičko M, Urbančíková I, Pella D, Dražilová S, Babinská I; HepaMeta Team. Seroprevalence of Hepatitis E Virus in Roma Settlements: A Comparison with the General Population in Slovakia. *Int J Environ Res Public Health* 2018; **15**: 904 [PMID: 29751522 DOI: 10.3390/ijerph15050904]

48 **Paraličová Z**, Halánová M, Schréter I, Kalinová Z, Novotný M, Sekula J, Paralič J, Kristian P. Seroprevalence of hepatitis E among hospitalized patients in Slovakia: first report. *Cent Eur J Public Health* 2020; **28**: 70-73 [PMID: 32228821 DOI: 10.21101/cejph.a5346]

World Journal of Gastroenterology

Submit a Manuscript: https://www.f6publishing.com

World J Gastroenterol 2021 January 14; 27(2): 152-161

DOI: 10.3748/wjg.v27.i2.152

ISSN 1007-9327 (print) ISSN 2219-2840 (online)

ORIGINAL ARTICLE

Basic Study

Triolein emulsion infusion into the hepatic artery increases vascular permeability to doxorubicin in rabbit liver

Yong-Woo Kim, Hak Jin Kim, Byung Mann Cho, Seon Hee Choi

ORCID number: Yong-Woo Kim 0000-0002-1703-7753; Hak Jin Kim 0000-0002-6532-4896; Byung Mann Cho 0000-0003-0893-3617; Seon Hee Choi 0000-0001-7682-0361.

Author contributions: Kim YW and Kim HJ designed the research and wrote the paper; Kim YW, Kim HJ and Choi SH performed the research and acquired the data; Cho BM, Kim YW and Kim HJ analyzed and interpreted the data, revised the manuscript critically for important intellectual content and approved the final version for submission.

Supported by Biomedical Research Institute, Pusan National University Hospital, No. 2018B008.

Institutional animal care and use committee statement: Animal experiments were performed according to our Institutional Laboratory Animal Protocol Guidelines (Approval No. PNUH-2019-139).

Conflict-of-interest statement: Hak Jin Kim has received research funding from Pusan National University Hospital.

Data sharing statement: Technical appendix, statistical code, and dataset available from the corresponding author at

Yong-Woo Kim, Department of Radiology, Research Institute for Convergence of Biomedical Science and Technology, Pusan National University Yangsan Hospital, Pusan National University College of Medicine, Yangsan 50612, South Korea

Hak Jin Kim, Department of Radiology, Biomedical Research Institute, Pusan National University Hospital, Pusan National University College of Medicine, Busan 49241, South Korea

Byung Mann Cho, Preventive Medicine and Occupational Medicine, Pusan National University School of Medicine, Yangsan 50612, South Korea

Seon Hee Choi, Department of Radiology, Pusan National University, Busan 49241, South Korea

Corresponding author: Hak Jin Kim, PhD, Professor, Department of Radiology, Biomedical Research Institute, Pusan National University Hospital, Pusan National University College of Medicine, 179 Gudeok-ro, Seo-gu, Busan 49241, South Korea. hakjink@pusan.ac.kr

Abstract

BACKGROUND

The infusion of triolein emulsion (TE) induced increased vascular permeability and a negligible and temporary decrease in liver function without specific histopathological damage.

AIM

To assess changes in doxorubicin concentration according to the percentage of TE infused *via* a hepatic artery to study the vascular permeability in the rabbit liver.

METHODS

Thirty-nine healthy rabbits were divided into five groups according to the concentration of emulsified triolein infused into the hepatic arteries: Group 0, saline infusion (control group, $n = 5$); group 1, 0.3% TE ($n = 13$); group 2, 0.6% TE ($n = 6$); group 3, 0.9% TE ($n = 8$); and group 4, 1.5% TE ($n = 6$). Doxorubicin (2.4 mg/kg) was infused immediately after TE injection *via* the hepatic arteries. After 2 h, the livers were harvested, and doxorubicin concentrations were calculated fluorometrically. The doxorubicin concentrations were compared between TE groups and the control group, and the optimal concentrations within the TE groups were calculated. Statistical analysis was performed using the

hakjink@pusan.ac.kr. Informed consent was not obtained because this study is animal research. No additional data are available.

ARRIVE guidelines statement: The authors have read the ARRIVE guidelines, and the manuscript was prepared and revised according to the ARRIVE guidelines.

Open-Access: This article is an open-access article that was selected by an in-house editor and fully peer-reviewed by external reviewers. It is distributed in accordance with the Creative Commons Attribution NonCommercial (CC BY-NC 4.0) license, which permits others to distribute, remix, adapt, build upon this work non-commercially, and license their derivative works on different terms, provided the original work is properly cited and the use is non-commercial. See: http://creativecommons.org/Licenses/by-nc/4.0/

Manuscript source: Unsolicited manuscript

Specialty type: Gastroenterology and hepatology

Country/Territory of origin: South Korea

Peer-review report's scientific quality classification

Grade A (Excellent): 0
Grade B (Very good): 0
Grade C (Good): C
Grade D (Fair): 0
Grade E (Poor): 0

Received: October 14, 2020
Peer-review started: October 14, 2020
First decision: December 3, 2020
Revised: December 15, 2020
Accepted: December 22, 2020
Article in press: December 22, 2020
Published online: January 14, 2021

P-Reviewer: Fu T
S-Editor: Fan JR
L-Editor: A
P-Editor: Liu JH

nonparametric Mann-Whitney *U* test and Kruskal–Wallis test. $P < 0.05$ were considered statistically significant.

RESULTS

In the liver, doxorubicin concentrations were 2.06, 2.07, 2.16 and 1.66 times higher in groups 1 through 4, respectively, and significantly higher in the TE groups than in the control group (all $P < 0.05$). However, there were no significant differences in the mean doxorubicin concentrations between the four TE groups ($P = 0.642$). In the lungs, the mean doxorubicin concentrations were not significantly different between the control and TE groups ($P > 0.05$).

CONCLUSION

TE infusion into the hepatic arteries significantly increased the doxorubicin concentration approximately twofold but was not different between the TE groups. These findings suggest that TE infusion might be a useful adjuvant treatment of liver cancers.

Key Words: Triolein emulsion; Liver tumor; Chemotherapy; Drug delivery; Vascular permeability; Dexorubicin

©The Author(s) 2021. Published by Baishideng Publishing Group Inc. All rights reserved.

Core Tip: Triolein emulsion infused intra-arterially increases vascular permeability transiently and reversibly. This could be applicable for adjuvant treatment to enhance chemotherapy using an angiographic technique. This study assessed changes in doxorubicin concentration *per* the percentage of TE infused *via* hepatic arteries to study vascular permeability in rabbit liver.

Citation: Kim YW, Kim HJ, Cho BM, Choi SH. Triolein emulsion infusion into the hepatic artery increases vascular permeability to doxorubicin in rabbit liver. *World J Gastroenterol* 2021; 27(2): 152-161
URL: https://www.wjgnet.com/1007-9327/full/v27/i2/152.htm
DOI: https://dx.doi.org/10.3748/wjg.v27.i2.152

INTRODUCTION

Sinusoidal capillaries in the liver have a lumen of almost 30 μm or more in diameter, which is much greater than that of normal capillaries. They also have irregular, tortuous walls, not formed by a continuous layer of endothelial cells, and have wide gaps of approximately 100 nm in diameter between cells. There are an incomplete basal lamina and no morphologic barrier between the perisinusoidal space and sinusoids. Therefore, plasma has direct access to the cell surface of the liver, which is a functionally very important structural characteristic for active metabolic exchange between the liver and blood[1].

In our previous study[2], the infusion of triolein emulsion (TE) in rabbit livers induced increased vascular permeability and a negligible and temporary decrease in liver function without specific histopathological damages. The gross findings revealed evans blue staining in 33% of the TE infusion group. In that study[2], we used only a single triolein volume (0.2 mL triolein in 20 mL of normal saline), whereas other previous studies[3,4] related to TE used 0.05 or 1 mL triolein in 20 mL of normal saline. Vascular permeability is possibly related to the volume of infused triolein. However, there have been no researches on this reciprocal relationship between the infused triolein volume and vascular permeability in the liver. Therefore, it is required to determine the appropriate volume of infused triolein in order to maximize the increase in vascular permeability as required. A direct quantitative demonstration is required to determine the degree of vascular permeability increase after infusion of TE into the hepatic artery.

Doxorubicin, a widely used anticancer agent, was one of the first and most commonly used chemotherapeutic drugs for the treatment of hepatocellular carcinoma

(HCC)[5,6]. Intermediate HCC is treated with angiography-guided transcatheter therapy by selectively infusing a chemotherapeutic drug, a technique called transarterial chemoembolization[7-10]. This treatment method has two purposes: To deliver the drug close to the tumor and to cause an arterial embolization close to the cancer location[5,11]. The tumor is exposed to a high concentration of the drugs when infused close to it, leading to an increase in antitumor effect, while also reducing systemic exposure and side effects[12]. Furthermore, doxorubicin and its metabolites have specific fluorescence features and can be used for follow-up on the outcome of doxorubicin[13,14]. However, if TE infusion into the liver could be used to open the sinusoids or sinusoidal capillaries in the liver, this might increase the doxorubicin concentration and lead to an increased antitumor effect, which would subsequently reduce the total dosage and side effects of chemotherapeutic drugs. Moreover, doxorubicin can be extracted from the samples of liver tissue and quantified with a fluorometer at excitation and emission wavelengths of 470 and 585 nm, respectively[15-17].

The purpose of the present study was to evaluate changes in doxorubicin concentrations in rabbit liver tissues according to the percentage of TE infused *via* the hepatic arteries in a rabbit liver model.

MATERIALS AND METHODS

Animal preparation

Animal experiments were performed according to our institutional laboratory animal protocol guidelines (Approval No. PNUH-2019-139). The animal house was maintained at 22 ± 2 °C with a room humidity of 50% ± 15% under a 12 h dark/light cycle. Animals were kept in an environmentally controlled breeding room and supplied with standard laboratory food and water for 3 d before the experiments.

Before drug administration, animals were subjected to a 12-hour fast with free access to water. Thirty-nine New Zealand White rabbits (Samtaco, Osan, South Korea), weighing 2.6-3 kg each, were used in this doxorubicin study. The rabbits were anesthetized intramuscularly, in the groin muscles, with ketamine HCl (2.5 mg/kg; Huons, Jecheon, South Korea) and xylazine (0.125 mg/kg; Bayer Korea, Seoul, South Korea). During the procedure, the rabbits were ventilated using room air. Body temperature was monitored using a rectal probe (MGA-III 219; Shibaura Electronics, Tokyo, Japan) and was maintained at 35.5 °C to 36.5 °C with a heating pad. After anesthesia, each rabbit was placed in a supine position on a laboratory-fabricated wooden holding table that allowed each of the four extremities to be fixed with straps.

Transauricular approach

Short hairs on the dorsal ear surfaces were shaved and a dressing placed on the puncture sites. After tapping the central auricular artery repeatedly to dilate its lumen, the artery was punctured randomly in the right or left ears using a 20-gauge intravenous catheter (Insyte, Becton Dickinson, Sandy, UT, United States). After advancing the plastic sheath and simultaneously removing the inner stylet needle of the IV catheter, a 2.0-F microcatheter (Progreat α®; Terumo, Tokyo, Japan) with a 0.016-inch guidewire (GT Wire; Terumo, Tokyo, Japan) was introduced through the IV catheter and advanced to the aortic arch. Microcatheter and guidewire manipulations were performed under fluoroscopic guidance to permit selection of the celiac trunk, and angiography was performed by manual injection of contrast media (Xenetix®; donated by Guerbet Korea, Seoul, South Korea). The microcatheter tip was positioned in the proper hepatic artery following fluoroscopic guidance (Figure 1).

Infusion of TE and doxorubicin

TE was performed as described by Kim *et al*[3]. The rabbits were classified according to the TE concentration infused into the hepatic artery as follows: Group 1 (0.3% TE; n = 13), group 2 (0.6% TE; n = 6), group 3 (0.9% TE; n = 8), and group 4 (1.5% TE; n = 6). TE (20 mL) was infused into each rabbit *via* the microcatheter at a speed of 4 mL/min. Normal saline (20 mL) was infused instead of TE in the control group (group 0, n = 5). Immediately after the infusion of TE (groups 1-4) or saline (group 0), doxorubicin hydrochloride (2.4 mg/kg; Boryung Pharmacy, Kyungkido, South Korea) was injected *via* the same catheter at the same speed, in all rabbits of all experimental groups. Subsequently, 3 mL of evans blue (Sigma-Aldrich, St. Louis, MO, United States) was infused through the same catheter just after the doxorubicin injection to mark targeted areas for liver tissue extraction.

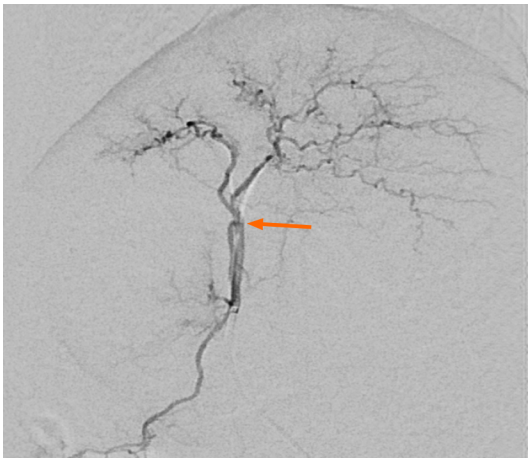


Figure 1 Angiographic findings of the hepatic artery in the rabbit. The hepatic angiogram shows both lobar hepatic arteries. The catheter tip is located in the proper hepatic artery and passes through the gastroduodenal artery. Triolein emulsion or normal saline, doxorubicin, and evans blue were injected through a microcatheter at this level.

Doxorubicin extraction and fluorometric analysis

Doxorubicin concentrations in the liver and lungs were determined by fluorometric examination. Two hours after the infusion of TE, the rabbits were perfused transcardially with saline to flush unabsorbed doxorubicin from the vasculature. Liver (100 mg), identified by evans blue staining, and basal segments of both lungs were harvested in all groups (Figure 2). In the absence of a stained area, the anteroinferior portions of both lobes of the liver were selected. Tissues were soaked in four volumes of HCl (0.3 N) in 50% ethanol. The tissues were homogenized in a tissue blender and refrigerated for 24 h at 4 °C and then centrifuged (14000 × g for 25 min). For fluorescence intensities, the supernatants were measured with a fluorometer (Synergy H1, BioTek, Winooski, VT, United States) with excitation/emission of 470/585 nm. For quantitative measurement of doxorubicin concentrations, a standard curve was used, and three readings were performed *per* tissue sample and averaged. To prove the effect of increased vascular permeability caused by TE in the hepatic and pulmonary arteries, the concentrations in the liver and lungs were calculated.

Statistical analysis

Nonparametric tests are statistical methods used for studies with small sample sizes or non-normal distributions. Owing to the small sample size in our study, statistical analysis was conducted using the nonparametric Mann–Whitney *U* test and Kruskal–Wallis test (SPSS version 26.0; IBM Corp, Armonk, United States). *P* values of < 0.05 were considered statistically significant.

RESULTS

Liver vascular permeability change by evans blue staining

The hepatic surfaces showed blue staining after injecting evans blue in 12/34 rabbits in the TE groups, and the blue staining was patchy (Figure 2). However, the hepatic surface did not show blue staining in the control group. Lungs were not grossly stained in any of the rabbits in all groups (TE and control).

Fluorometric analysis of doxorubicin extraction

In the liver, doxorubicin concentrations were 943.27 ± 261.94 (group 1), 950.82 ± 403.11 (group 2), 989.49 ± 404.48 (group 3), and 762.55 ± 236.24 (group 4) in the TE groups and 458.68 ± 37.63 (group 0) in control group. The mean doxorubicin concentrations were 2.06, 2.07, 2.16 and 1.66 times higher in group 1 through group 4, respectively, than in the control group (Table 1 and Figure 3). The Kruskal–Wallis test showed a significant difference in doxorubicin concentration between the control and TE groups ($P < 0.05$). Also, the Mann–Whitney U test with Bonferroni correction compared the control group with each TE group, and all results were significantly different (all $P < 0.05$). However, there were no significant differences in the mean doxorubicin

Table 1 The concentration of doxorubicin in the liver of triolein emulsion groups

	Group 0 NS (*n* = 5)	Group 1 0.3% TE (*n* = 13)	Group 2 0.6% TE (*n* = 6)	Group 3 0.9% TE (*n* = 8)	Group 4 1.5% TE (*n* = 6)
1	429.5	1177.0	1553.4	642.7	1096.1
2	417.4	720.3	1306.8	910.5	526.2
3	487.9	629.7	632.0	1466.2	526.3
4	505.8	1402.3	788.6	822.0	924.0
5	452.8	1017.9	912.9	1088.1	873.4
6		768.2	511.2	751.4	629.3
7		918.9		1693.8	
8		1017.7		541.2	
9		898.0			
10		724.9			
11		1449.4			
12		746.1			
13		792.1			
Mean	458.68	943.27	950.81	989.49	762.56
SD	37.63	261.94	403.12	404.48	236.24

TE: Triolein emulsion; NS: Normal saline.

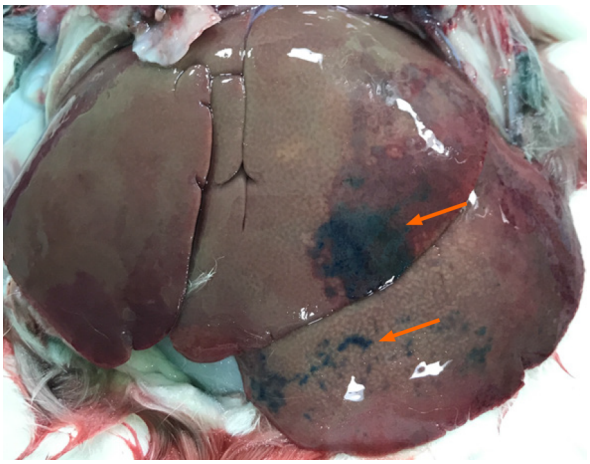


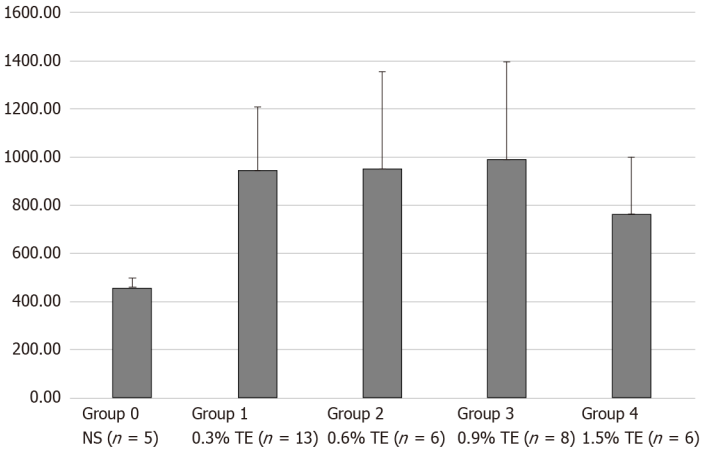
Figure 2 Gross finding of the hepatic surface from a rabbit in the triolein emulsion group after evans blue staining. The anterior surface of the left lobe shows patchy blue staining by evans blue.

concentrations between the four TE groups (P = 0.642).

In the lungs, the doxorubicin concentrations in the TE groups were 340.23 ± 97.68 (group 1), 315.63 ± 67.24 (group 2), 382.18 ± 92.36 (group 3), and 319.85 ± 70.34 (group 4); while it was 361.40 ± 62.74 (group 0) in the control group. The mean doxorubicin concentrations were not significantly different (P > 0.05) between the control and TE groups (Figure 4).

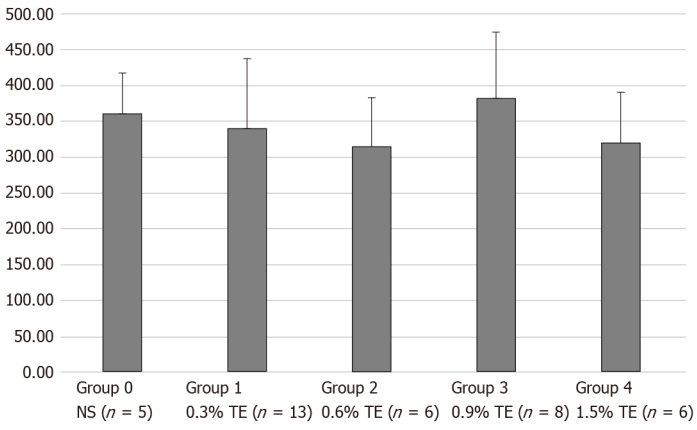
DISCUSSION

In the present study, doxorubicin concentrations were increased after TE infusion into the hepatic arteries, compared with normal saline infusion, in a rabbit liver model. This indicates that TE increases vascular permeability in the sinusoidal capillaries in the liver, which is similar to skeletal muscle with capillaries without a blood–organ



	Group 0 NS (n = 5)	Group 1 0.3% TE (n = 13)	Group 2 0.6% TE (n = 6)	Group 3 0.9% TE (n = 8)	Group 4 1.5% TE (n = 6)
Mean	458.68	943.27	950.81	989.49	762.56
SD	37.63	261.94	403.12	404.48	236.23

Figure 3 Longitudinal plot of mean doxorubicin concentration in the liver in the control and triolein emulsion groups. NS: Normal saline; TE: Triolein emulsion.



	Group 0 NS (n = 5)	Group 1 0.3% TE (n = 13)	Group 2 0.6% TE (n = 6)	Group 3 0.9% TE (n = 8)	Group 4 1.5% TE (n = 6)
Mean	361.40	340.23	315.61	382.16	319.83
SD	56.12	97.68	67.24	92.36	70.34

Figure 4 Longitudinal plot of mean doxorubicin concentration in the lungs in the control and triolein emulsion groups. NS: Normal saline; TE: Triolein emulsion.

barrier, and increases vascular permeability without significant histological changes[18]. Doxorubicin, the most popular single chemotherapeutic drug in transarterial catheter treatment for hepatic malignancy, can be easily extracted from the obtained tissues and quantified by fluorometric analysis (excitation/emission wavelength, 470/585 nm)[14,16]. HCl (0.3N) in ethanol (50%) enables highly efficient recovery of doxorubicin from tissues[14], and doxorubicin concentrations in liver tissues can then be easily measured using a fluorometer. Because the high molecular weight of doxorubicin (579.98 Da) prevents its crossing the blood–organ barrier, it is not effective to treat primary or metastatic brain tumors[19]. However, a delivery study in animal models using TE revealed that doxorubicin concentrations increased in a dose-dependent manner in the brain 2 h after TE injection[13]. Unlike the brain, testis, and orbit with blood–organ barriers, the liver has no barriers between the sinusoids and adjacent hepatic tissues. In our previous study, no significant histological and biochemical changes were found in the liver tissue after TE infusion. The results of the study suggested that the infusion of TE into the hepatic artery may lead to no specific

histopathological changes in the liver if the volume of injected triolein is limited[2]. Thus, although TE is used as an adjunctive agent in the chemotherapeutic treatment of liver malignancy, TE may not damage the liver and lung histopathologically but may increase doxorubicin concentration in the liver, which does not have a blood–organ barrier, rather than in the brain, which has a blood–organ barrier.

In the present study, the mean doxorubicin concentration in the liver samples of the TE groups was increased approximately twofold and was significantly higher than that in the normal saline control group ($P < 0.05$). However, there were no significant differences in mean doxorubicin concentrations between the four TE groups ($P = 0.642$). Many experimental studies on TE performed in organs with[3,4,13,15,20-25] or without[2,18] a blood–organ barrier have reported transient and reversible changes with no significant lesions, which could have been due to the particle sizes of triolein in the emulsion. Increased vascular permeability of the blood-brain barrier could be applicable to studies on drug reactions in the brain or in research on the treatment of central nervous system diseases. However, severe cerebral edema has been reported in many TE studies, and this could be an unpredictable side effect. Thus, the dosage of TE required to increase vascular permeability should be optimized to reduce unpredictable side effects. In previous studies, the concentration of TE (0.25%-1.0%) administered varied widely[4,24,25], and the optimal dosage of TE required to increase vascular permeability with minimal edema was 0.5% in a cat brain model, and this should be increased in a dose-dependent manner[26]. The present study was unable to elucidate why there were no differences in the mean doxorubicin concentrations between the TE groups. A possible explanation for this is that the pattern of increased vascular permeability may differ between the liver and brain because of the size of each organ, the vessel size for TE injection, and the difference in the type of capillary. The volume of the liver is 66.7 ± 13.7 mL, whereas that of the brain is 9.55 ± 0.35 mL. The vessel size is also larger in the liver than in the brain (1.68 ± 0.55 mm in the proper hepatic artery *vs* 1.13 ± 0.25 mm in the internal carotid artery). The liver has fenestrated-type capillaries without a barrier, whereas the brain has continuous-type capillaries with a barrier[18,27,28]. In the liver, sinusoids or sinusoidal capillaries are found, and the luminal diameters of these capillaries are greater than those of normal capillaries. In fact, sinusoids may be larger than 30 μm in diameter and have irregular, tortuous walls without a continuous layer of endothelial cells and with wide gaps (approximately 100 nm in diameter) between cells. The sinusoids have incomplete basal lamina, and there is no morphologic barrier between the sinusoids and the perisinusoidal space[1,2]. In the brain, continuous capillaries are found. The endothelial cells have a large amount of cytoplasm in connection with the nucleus, fine filaments, and numerous pinocytotic vesicles. The pinocytotic vesicles are 50-70 nm in diameter and are most likely related to the transport of fluid across the capillary wall, respecting the sites of the so-called large-pore system of capillary permeability. The endothelial cells are connected with either simple or interdigitated junctions and have a narrow gap between the adjacent cell membranes. However, in certain areas, opposing cell membranes are fused to form tight junctions[1,2]. Capillaries without barriers in the liver are permeable to plasma proteins. Thus, they are different from the capillaries in the brain. The increased vascular permeability in the liver did not increase in a dose-dependent manner after the infusion of TE.

In the lungs, the mean doxorubicin concentration was not significantly different between the control and TE groups. This result is associated with the high molecular weight of doxorubicin and the characteristics of the sinusoidal capillary that lacks a blood-organ barrier, causing doxorubicin concentration to increase mainly in the liver but preventing its passage into the lungs.

A limitation of the current study was that TE was infused into the proper hepatic artery. A 2.0-F microcatheter is not suitable for use in a lobar hepatic artery, and the deep insertion of the guidewire for the selection caused a vasospasm and a flow disturbance of the lobar hepatic artery. For further evaluation of the therapeutic effects of anticancer agents in liver cancer, catheters that can be used in one lobar branch of the hepatic artery are required. The use of a microcatheter with a smaller diameter would possibly overcome this limitation. Another limitation was that the concentration and amount of TE used in this study were 0.3%-1.5% and 20 mL, respectively. These values are similar to those reported in previous studies conducted on the brain[4,24-26]. In the present study, vascular permeability in the liver was increased by TE injection; however, it did not differ by TE concentration. It is possible that vascular permeability in the liver would change if different volumes of the same TE percentage were infused. Therefore, further studies using an increased amount of TE in a rabbit liver model are required.

CONCLUSION

In the present study, TE infusion into the hepatic arteries increased the doxorubicin concentration approximately twofold, a statistically significant difference in the TE groups compared with the control group. However, the differences in doxorubicin concentration between the TE groups were not statistically significant. That is, in the TE groups, doxorubicin concentrations increased in a non-dose-dependent manner. We believe our study results will be useful in the research on vascular permeability in the liver and could be useful in future studies assessing the effect and dosage of TE as adjuvant chemotherapy for the treatment of liver cancers.

ARTICLE HIGHLIGHTS

Research background

The infusion of triolein emulsion (TE) induced increased vascular permeability and a negligible and temporary decrease in liver function without specific histopathological damage.

Research motivation

A technique of increased vascular permeability could be used for chemotherapy in hepatic malignancy.

Research objectives

The present study aimed to assess changes in doxorubicin concentration with TE infused *via* the hepatic artery in rabbit liver.

Research methods

The TE was infused into each rabbit through a microcatheter *via* the hepatic artery. Immediately after the infusion of emulsified triolein (group 1, 0.3% TE, $n = 13$; group 2, 0.6% TE, $n = 6$; group 3, 0.9% TE, $n = 8$; group 4, 1.5% TE, $n = 6$) or saline (group 0), doxorubicin was infused through the same catheter. The concentrations of doxorubicin in the liver and lungs were measured by fluorometry. Two hours after the injection of TE, 100 mg of liver tissue, identified by evans blue staining, was harvested from all rabbits. Doxorubicin concentrations were quantified using a fluorometer. Statistical analysis was performed using the nonparametric Mann–Whitney *U* test and Kruskal–Wallis test (SPSS version 26.0; IBM Corp., Armonk, United States). *P*-values of < 0.05 were considered statistically significant.

Research results

The mean doxorubicin concentrations were 1.66 to 2.16 times higher in the TE groups than in the control group and significantly different in the TE groups ($P < 0.05$).

Research conclusions

TE infusion into the hepatic arteries significantly increased the doxorubicin concentration.

Research perspectives

TE infusion might be a useful adjuvant treatment for liver tumors.

REFERENCES

1 **Leeson THLC**. The Liver. In: Leeson THLC, editor. Histology. Philadelphia, London, Toronto: WB Saunders; 1981: 383-397

2 **Kim YW**, Park YM, Yoon S, Kim HJ, Park DY, Cho BM, Choi SH. Effect of intra-arterial infusion with triolein emulsion on rabbit liver. *World J Gastroenterol* 2014; **20**: 14442-14449 [PMID: 25339830 DOI: 10.3748/wjg.v20.i39.14442]

3 **Kim HJ**, Lee CH, Kim HG, Lee SD, Son SM, Kim YW, Eun CK, Kim SM. Reversible MR changes in the cat brain after cerebral fat embolism induced by triolein emulsion. *AJNR Am J Neuroradiol* 2004; **25**: 958-963 [PMID: 15205130]

4 **Kim YW**, Kim HJ, Cho BM, Moon TY, Eun CK. The study of cerebral hemodynamics in the hyperacute stage of fat embolism induced by triolein emulsion. *AJNR Am J Neuroradiol* 2006; **27**:

398-401 [PMID: 16484418]
5 **Dubbelboer IR**, Pavlovic N, Heindryckx F, Sjögren E, Lennernäs H. Liver Cancer Cell Lines Treated with Doxorubicin under Normoxia and Hypoxia: Cell Viability and Oncologic Protein Profile. *Cancers (Basel)* 2019; **11** [PMID: 31330834 DOI: 10.3390/cancers11071024]
6 **Lencioni R**, de Baere T, Soulen MC, Rilling WS, Geschwind JF. Lipiodol transarterial chemoembolization for hepatocellular carcinoma: A systematic review of efficacy and safety data. *Hepatology* 2016; **64**: 106-116 [PMID: 26765068 DOI: 10.1002/hep.28453]
7 **Pecorelli A**, Lenzi B, Gramenzi A, Garuti F, Farinati F, Giannini EG, Ciccarese F, Piscaglia F, Rapaccini GL, Di Marco M, Caturelli E, Zoli M, Borzio F, Sacco R, Cabibbo G, Felder M, Morisco F, Gasbarrini A, Baroni GS, Foschi FG, Biasini E, Masotto A, Virdone R, Bernardi M, Trevisani F; Italian LiverCancer (ITA. LI.CA) group. Curative therapies are superior to standard of care (transarterial chemoembolization) for intermediate stage hepatocellular carcinoma. *Liver Int* 2017; **37**: 423-433 [PMID: 27566596 DOI: 10.1111/liv.13242]
8 **Galle PR**, Tovoli F, Foerster F, Wörns MA, Cucchetti A, Bolondi L. The treatment of intermediate stage tumours beyond TACE: From surgery to systemic therapy. *J Hepatol* 2017; **67**: 173-183 [PMID: 28323121 DOI: 10.1016/j.jhep.2017.03.007]
9 **Gaba RC**, Lewandowski RJ, Hickey R, Baerlocher MO, Cohen EI, Dariushnia SR, Janne d'Othée B, Padia SA, Salem R, Wang DS, Nikolic B, Brown DB; Society of Interventional Radiology Technology Assessment Committee. Transcatheter Therapy for Hepatic Malignancy: Standardization of Terminology and Reporting Criteria. *J Vasc Interv Radiol* 2016; **27**: 457-473 [PMID: 26851158 DOI: 10.1016/j.jvir.2015.12.752]
10 **European Association for the Study of the Liver**. EASL Clinical Practice Guidelines: Management of hepatocellular carcinoma. *J Hepatol* 2018; **69**: 182-236 [PMID: 29628281 DOI: 10.1016/j.jhep.2018.03.019]
11 **Hepatocellular Carcinoma: Diagnosis and Treatment**, 3rd ed. Springer International Publishing: Cham, Switzerland, 2016
12 **El Fouly A**, Ertle J, El Dorry A, Shaker MK, Dechêne A, Abdella H, Mueller S, Barakat E, Lauenstein T, Bockisch A, Gerken G, Schlaak JF. In intermediate stage hepatocellular carcinoma: radioembolization with yttrium 90 or chemoembolization? *Liver Int* 2015; **35**: 627-635 [PMID: 25040497 DOI: 10.1111/liv.12637]
13 **Kim HJ**, Kim YW, Choi SH, Cho BM, Bandu R, Ahn HS, Kim KP. Triolein Emulsion Infusion Into the Carotid Artery Increases Brain Permeability to Anticancer Agents. *Neurosurgery* 2016; **78**: 726-733 [PMID: 26540353 DOI: 10.1227/NEU.0000000000001104]
14 **Bachur NR**, Moore AL, Bernstein JG, Liu A. Tissue distribution and disposition of daunomycin (NCS-82151) in mice: fluorometric and isotopic methods. *Cancer Chemother Rep* 1970; **54**: 89-94 [PMID: 5527015]
15 **Lee IS**, Kim HJ, Choi SH, Kim YW, Choi KJ. Doxorubicin concentration in brain remains high for one day after triolein emulsion infusion induced BBB opening. *Int J Neurosci* 2020; **130**: 770-776 [PMID: 31842703 DOI: 10.1080/00207454.2019.1705809]
16 **Treat LH**, McDannold N, Vykhodtseva N, Zhang Y, Tam K, Hynynen K. Targeted delivery of doxorubicin to the rat brain at therapeutic levels using MRI-guided focused ultrasound. *Int J Cancer* 2007; **121**: 901-907 [PMID: 17437269 DOI: 10.1002/ijc.22732]
17 **Park J**, Zhang Y, Vykhodtseva N, Jolesz FA, McDannold NJ. The kinetics of blood brain barrier permeability and targeted doxorubicin delivery into brain induced by focused ultrasound. *J Control Release* 2012; **162**: 134-142 [PMID: 22709590 DOI: 10.1016/j.jconrel.2012.06.012]
18 **Kim HJ**, Kim YW, Lee IS, Song JW, Jeong YJ, Choi SH, Choi KU, Suh KT, Cho BM. Intra-arterial delivery of triolein emulsion increases vascular permeability in skeletal muscles of rabbits. *Acta Vet Scand* 2009; **51**: 30 [PMID: 19604410 DOI: 10.1186/1751-0147-51-30]
19 **von Holst H**, Knochenhauer E, Blomgren H, Collins VP, Ehn L, Lindquist M, Norén G, Peterson C. Uptake of adriamycin in tumour and surrounding brain tissue in patients with malignant gliomas. *Acta Neurochir (Wien)* 1990; **104**: 13-16 [PMID: 2386084 DOI: 10.1007/BF01842886]
20 **Kim HJ**, Lee CH, Lee SH, Cho BM, Kim HK, Park BR, Ye SY, Jeon GR, Chang KH. Early development of vasogenic edema in experimental cerebral fat embolism in cats: correlation with MRI and electron microscopic findings. *Invest Radiol* 2001; **36**: 460-469 [PMID: 11500597 DOI: 10.1097/00004424-200108000-00005]
21 **Kim HJ**, Lee JH, Lee CH, Lee SH, Moon TY, Cho BM, Kim HK, Park BR, Chang KH. Experimental cerebral fat embolism: embolic effects of triolein and oleic acid depicted by MR imaging and electron microscopy. *AJNR Am J Neuroradiol* 2002; **23**: 1516-1523 [PMID: 12372741]
22 **Kim HJ**, Lee CH, Lee SH, Moon TY. Magnetic resonance imaging and histologic findings of experimental cerebral fat embolism. *Invest Radiol* 2003; **38**: 625-634 [PMID: 14501490 DOI: 10.1097/01.rli.0000077055.48406.e2]
23 **Kim YW**, Kim HJ, Choi SH, Cho B, Hwangbo L, Kim DC. Hemorrhage in cerebral fat embolisms in a cat model using triolein dependent on the physical properties of triolein. *Jpn J Radiol* 2014; **32**: 30-37 [PMID: 24288099 DOI: 10.1007/s11604-013-0265-x]
24 **Baik SK**, Kim YW, Kim HJ, Lee JW, Cho BM, Kim DH, Choi SH, Lee SH, Chang KH. Proton magnetic resonance spectroscopic findings of cerebral fat embolism induced by triolein emulsion in cats. *Acta Radiol* 2008; **49**: 1174-1181 [PMID: 19031181 DOI: 10.1080/02841850802512449]
25 **Kim KN**, Kim HJ, Lee SD, Moon TY, Lee SH, Lee JW, Lee TH. Effect of triolein emulsion on the blood-testis barrier in cats. *Invest Radiol* 2004; **39**: 445-449 [PMID: 15194916 DOI:

10.1097/01.rli.0000129466.33263.8c]
26 **Choi SH**, Kim HJ, Hwangbo L, Kim YW. The minimum percentage of triolein emulsion for studying cerebral vascular permeability with least brain edema. *Iran J Radiol* 2014; **11**: e14887 [PMID: 25780547 DOI: 10.5812/iranjradiol.14887]
27 **Tam AL**, Melancon MP, Ensor J, Liu Y, Dixon K, McWatters A, Gupta S. Rabbit hepatic arterial anatomy variations: implications on experimental design. *Acta Radiol* 2014; **55**: 1226-1233 [PMID: 24292899 DOI: 10.1177/0284185113514050]
28 **Lee JS**, Hamilton MG, Zabramski JM. Variations in the anatomy of the rabbit cervical carotid artery. *Stroke* 1994; **25**: 501-503 [PMID: 8303763 DOI: 10.1161/01.str.25.2.501]

World Journal of Gastroenterology

Submit a Manuscript: https://www.f6publishing.com

World J Gastroenterol 2021 January 14; 27(2): 162-175

DOI: 10.3748/wjg.v27.i2.162

ISSN 1007-9327 (print) ISSN 2219-2840 (online)

ORIGINAL ARTICLE

Case Control Study

Detection of fucosylated haptoglobin using the 10-7G antibody as a biomarker for evaluating endoscopic remission in ulcerative colitis

Kei Motooka, Koichi Morishita, Nami Ito, Shinichiro Shinzaki, Taku Tashiro, Satoshi Nojima, Kayoko Shimizu, Mutsuhiro Date, Natsumi Sakata, Momoko Yamada, Shinji Takamatsu, Yoshihiro Kamada, Hideki Iijima, Tsunekazu Mizushima, Eiichi Morii, Tetsuo Takehara, Eiji Miyoshi

ORCID number: Kei Motooka 0000-0002-9799-2020; Koichi Morishita 0000-0002-9350-5504; Nami Ito 0000-0001-5132-6260; Shinichiro Shinzaki 0000-0002-7051-618X; Taku Tashiro 0000-0002-7801-8230; Satoshi Nojima 0000-0002-9305-8409; Kayoko Shimizu 0000-0003-0470-6468; Mutsuhiro Date 0000-0002-3336-1764; Natsumi Sakata 0000-0002-8761-0172; Momoko Yamada 0000-0002-6473-5810; Shinji Takamatsu 0000-0003-1996-7740; Yoshihiro Kamada 0000-0001-5485-902X; Hideki Iijima 0000-0002-5423-3059; Tsunekazu Mizushima 0000-0002-0825-6823; Eiichi Morii 0000-0001-8490-3650; Tetsuo Takehara 0000-0001-5036-3457; Eiji Miyoshi 0000-0002-9430-2362.

Author contributions: Miyoshi E contributed to the conception and design of the study; Motooka K, Morishita K, Ito N, Sakata N, Yamada M, Takamatsu S and Kamada Y contributed to the acquisition and analysis of data; Shimizu K and Date M produced ELISA kits and interpretation of data; Shinzaki S, Tashiro T, Nojima S, Iijima H, Mizushima T, Morii E and Takehara T provided clinical samples and data; Motooka K, Morishita K and Miyoshi E contributed to the drafting the article or revising it critically for

Kei Motooka, Koichi Morishita, Nami Ito, Natsumi Sakata, Momoko Yamada, Shinji Takamatsu, Yoshihiro Kamada, Eiji Miyoshi, Department of Molecular Biochemistry and Clinical Investigation, Osaka University Graduate School of Medicine, Suita 565-0871, Osaka, Japan

Shinichiro Shinzaki, Taku Tashiro, Hideki Iijima, Tetsuo Takehara, Department of Gastroenterology and Hepatology, Osaka University Graduate School of Medicine, Suita 565-0871, Osaka, Japan

Satoshi Nojima, Eiichi Morii, Department of Pathology, Osaka University Graduate School of Medicine, Suita 565-0871, Osaka, Japan

Kayoko Shimizu, Mutsuhiro Date, FUJIFILM Wako Pure Chemical Corporation, Amagasaki 661-0963, Hyogo, Japan

Tsunekazu Mizushima, Department of Gastroenterological Surgery, Osaka University Graduate School of Medicine, Suita 565-0871, Osaka, Japan

Corresponding author: Eiji Miyoshi, MD, PhD, Professor, Department of Molecular Biochemistry and Clinical Investigation, Osaka University Graduate School of Medicine, 1-7 Yamada-oka, Suita 565-0871, Osaka, Japan. emiyoshi@sahs.med.osaka-u.ac.jp

Abstract

BACKGROUND

Inflammatory bowel disease (IBD) is a chronic, relapsing inflammation of the digestive tract. Although fecal and serum biomarkers have been extremely important and supportive for monitoring of IBD, their low sensitivity and high variability characteristics limit clinical efficacy. Thus, the establishment of better biomarkers is expected. Fucosylation is one of the most important glycosylation modifications of proteins. Fucosylated haptoglobin (Fuc-Hpt) is used as a biomarker for several cancers and inflammation-related diseases. We recently established a novel glycan monoclonal antibody (mAb), designated 10-7G, which recognizes Fuc-Hpt. We developed an enzyme-linked immunosorbent assay (ELISA) to measure serum levels of Fuc-Hpt (10-7G values).

AIM

To investigate the usefulness of the serum 10-7G values as a potential biomarker

important intellectual content; all authors approved the final version of the article.

Supported by Ministry of Education, Culture, Sports, Science and Technology of Japan, No. 19H03562; and FUJIFILM Wako Pure Chemical Corporation, No. J770701626.

Institutional review board statement: This study was approved by the ethics committee of Osaka University Hospital and conducted in accordance with approved guidelines (Approval No. 14107-10).

Informed consent statement: Written informed consent was obtained from all subjects in this study at the time of enrollment or blood sampling.

Conflict-of-interest statement: Shimizu K and Date M are employees of FUJIFILM Wako Pure Chemical Corporation and the authors received approximately $5000 per year from a collaboration grant with FUJIFILM Wako Pure Chemical Corporation. The authors declare no other conflicts of interest.

Data sharing statement: No additional data are available.

STROBE statement: The authors have read the STROBE Statement-checklist of items, and the manuscript was prepared and revised according to the STROBE Statement-checklist of items.

Open-Access: This article is an open-access article that was selected by an in-house editor and fully peer-reviewed by external reviewers. It is distributed in accordance with the Creative Commons Attribution NonCommercial (CC BY-NC 4.0) license, which permits others to distribute, remix, adapt, build upon this work non-commercially, and license their derivative works on different terms, provided the original work is properly cited and the use is non-commercial. See: http://creativecommons.org/License

for monitoring disease activity in IBD.

METHODS

This was a case control study. Intestinal tissues of IBD patients (n = 10) were examined immunohistochemically using the 10-7G mAb. We determined 10-7G values using serum from patients with ulcerative colitis (UC, n = 110), Crohn's disease (n = 45), acute enteritis (AE, n = 11), and healthy volunteers (HVs) who exhibited normal (n = 20) or high (n = 79) C-reactive protein (CRP) levels at medical check-up. We investigated the correlation between the 10-7G value and various clinical parameters of IBD patients by correlation analysis. Receiver operating characteristic (ROC) curve analysis was performed to evaluate the usefulness of the 10-7G values as a biomarker for clinical and endoscopic remission of UC compared to conventional serum biomarkers.

RESULTS

In the immunohistochemical analysis, positive 10-7G mAb staining was observed in lymphocytes infiltrating into inflammatory sites of the mucosal layer and lymphoid follicles. The 10-7G values were significantly higher in patients with IBD (P < 0.001) and AE (P < 0.05) compared with HVs. In addition, 10-7G values were correlated with clinical examination parameters related to inflammation in patients with UC, particularly the CRP level (rs = 0.525, P = 0.003) and clinical activity index score (rs = 0.435, P = 0.038). However, there was no correlation between 10-7G values and CRP in HVs with high CRP levels, suggesting that the 10-7G values is not the same as a general inflammation biomarker. ROC curve analysis showed that area under the curve (AUC) value of 10-7G values for the diagnosis of endoscopic remission was higher than other biomarkers (AUC value = 0.699).

CONCLUSION

The serum 10-7G value is a novel biomarker for evaluating intestinal inflammation and endoscopic mucosal healing in UC.

Key Words: Inflammatory bowel disease; Biomarkers; Glycosylation; Fucosylated haptoglobin; Prohaptoglobin; Endoscopic remission

©The Author(s) 2021. Published by Baishideng Publishing Group Inc. All rights reserved.

Core Tip: Fucosylation is one of the most important glycosylation involved in cancer and inflammation. Recently, we have succeeded to establish a novel glycan antibody 10-7G mAb which directly recognizes fucosylated haptoglobin (Fuc-Hpt), and developed its enzyme-linked immunosorbent assay (ELISA) system. In this study, we demonstrated the serum 10-7G values (Fuc-Hpt levels determined with 10-7G mAb ELISA) were significantly higher in patients with inflammatory bowel disease. We also found that Fuc-Hpt was produced by lymphocytes infiltrating into inflammatory sites of intestine. Moreover, statistical analyses showed that the 10-7G value could evaluate intestinal inflammation and endoscopic mucosal healing in ulcerative colitis.

Citation: Motooka K, Morishita K, Ito N, Shinzaki S, Tashiro T, Nojima S, Shimizu K, Date M, Sakata N, Yamada M, Takamatsu S, Kamada Y, Iijima H, Mizushima T, Morii E, Takehara T, Miyoshi E. Detection of fucosylated haptoglobin using the 10-7G antibody as a biomarker for evaluating endoscopic remission in ulcerative colitis. *World J Gastroenterol* 2021; 27(2): 162-175

URL: https://www.wjgnet.com/1007-9327/full/v27/i2/162.htm

DOI: https://dx.doi.org/10.3748/wjg.v27.i2.162

INTRODUCTION

Inflammatory bowel disease (IBD), which comprises Crohn's disease (CD) and

s/by-nc/4.0/

Manuscript source: Unsolicited manuscript

Specialty type: Gastroenterology and hepatology

Country/Territory of origin: Japan

Peer-review report's scientific quality classification

Grade A (Excellent): 0
Grade B (Very good): 0
Grade C (Good): C, C
Grade D (Fair): 0
Grade E (Poor): 0

Received: September 23, 2020
Peer-review started: September 23, 2020
First decision: November 8, 2020
Revised: November 11, 2020
Accepted: December 23, 2020
Article in press: December 23, 2020
Published online: January 14, 2021

P-Reviewer: Yang B
S-Editor: Gao CC
L-Editor: A
P-Editor: Wang LL

ulcerative colitis (UC), is a chronic recurrent intestinal inflammatory disease of unknown etiology, and the number of individuals affected is increasing worldwide[1]. Although the etiology of IBD remains unknown, the disease is known to involve complex interactions between genetic, environmental, and microbial factors and the immune response[2,3]. For proper management and selection of appropriate treatment strategy, it is essential to evaluate disease activity of IBD accurately. Endoscopy is the gold standard for the diagnosis and monitoring status of IBD patients, but cannot be frequently performed because of the cost and invasiveness. Although fecal and serum biomarkers, such as fecal calprotectin and serum C-reactive protein (CRP), have been important and supportive for monitoring of IBD, their low sensitivity and high variability characteristics limit clinical efficacy[4,5]. Thus, the establishment of better biomarkers is expected.

Haptoglobin, an acute-phase protein produced primarily in the liver, is rapidly upregulated following stimulation with cytokines such as tumor necrosis factor alpha, interleukin (IL)-6, and IL-1[6]. Haptoglobin modulates inflammation *via* its systemic anti-inflammatory activity[7]. A major function of haptoglobin is binding free plasma hemoglobin produced due to hemolysis, thereby preventing damage associated with oxidative stress[8]. Haptoglobin is an α- and β-chain heterodimer linked by disulfide bonds, with all four N-glycans located in the β chain and no potential N-glycosylation sites in the α chain[9,10].

Fucosylation is one of the most important glycosylation modifications of proteins involved in inflammation and cancer[11]. We previously reported that fucosylated haptoglobin (Fuc-Hpt) is found in the serum of patients with pancreatic cancer[12] and established a lectin–antibody enzyme-linked immunosorbent assay (ELISA) to determine serum Fuc-Hpt levels[13]. Recently, we established a novel glycan antibody [10-7G monoclonal antibody (mAb)] that directly recognizes Fuc-Hpt[14]. Epitope analysis of the 10-7G mAb indicated that the peptide recognized by this antibody is in the haptoglobin α-chain, and the epitope appears as a result of aberrant glycosylation, which induces a conformational change in mature haptoglobin[15]. In human serum, the 10-7G mAb recognizes not only fucosylated mature haptoglobin (Fuc-mHpt) but also fucosylated prohaptoglobin (Fuc-pHpt), a precursor molecule. Moreover, affinity chromatography using the 10-7G mAb followed by lectin blotting and mass spectrometry analysis revealed that the 10-7G mAb predominantly recognizes both Fuc-mHpt and Fuc-pHpt[14]. The novel ELISA we developed using the 10-7G mAb enables measurement of both types of Fuc-Hpt in the serum. Here, we use Fuc-Hpt to describe both Fuc-mHpt and Fuc-pHpt, and Fuc-Hpt levels determined using the 10-7G mAb ELISA are reported as 10-7G values (Figure 1). As expected, 10-7G values are increased in pancreatic cancer patients compared with healthy volunteers (HVs)[14,16].

We recently found that the 10-7G mAb can be used for immunohistochemical staining of lymphocytes and macrophages associated with pancreatic cancer tissues. In immunoblotting analyses using the 10-7G mAb, we demonstrated that some immune cell lines produce Fuc-Hpt and that several inflammatory cytokines induce its secretion (manuscript submitted). These results suggest that the production of Fuc-Hpt by immune cells is related to local immune conditions, such as those associated with cancer and inflammation. With respect to inflammatory diseases, IBD is one of the most representative diseases in terms of the relationship between immune cells and local immunity.

In general, serum haptoglobin levels increase during acute inflammation, as do levels of CRP[6], and fucosylation of serum proteins increases dramatically in chronic inflammation[11]. As described above, the 10-7G mAb we developed recognizes characteristic types of haptoglobin, including Fuc-mHpt and Fuc-pHpt. In the present study, we investigated the usefulness of the 10-7G value as a potential serum biomarker for monitoring disease activity of IBD, comparing 10-7G values with several conventional serum biomarkers.

MATERIALS AND METHODS

Clinical samples

Serum samples were obtained from patients with CD (n = 45), UC (n = 110), and acute enteritis (AE; n = 11) at Osaka University and Osaka University Hospital. Serum samples were also obtained from HVs with normal serum CRP levels (≤ 0.3 mg/dL; n = 20) and high serum CRP levels (> 0.3 mg/dL; n = 79) who underwent medical health examinations at aMs New Otani Clinic, Osaka, Japan. Detailed characteristics of HVs and UC, CD, and AE patients are presented in Table 1. Resected intestinal tissue

Table 1 Characteristics of patients with ulcerative colitis, Crohn's disease, and acute enteritis and healthy volunteers

Characteristic	Patients with UC	Patients with CD	Patients with AE	HVs	CRP-high HVs
Number (male:female)	110 (63:47)	45 (36:9)	11 (5:6)	20 (14:6)	79 (56:26)
Age, yr, mean (SD)	48.79 (15.08)	46.24 (11.75)	42.89 (20.20)	53.05 (6.58)	56.01 (11.23)
Age at IBD diagnosis, yr, mean (SD)	34.74 (16.64)	26.89 (8.36)			
UC disease location, extensive colitis/left-sided colitis/proctitis	52/40/18				
CD location, colic/ileal/ileo-colic		5/17/23			
Alb, g/dL, mean (SD)	4.14 (0.31)	3.71 (0.51)	3.84 (0.41)	4.41 (0.19)	4.28 (0.24)
ALT, U/L, mean (SD)	20.27 (17.49)	16.00 (6.04)		37.00 (22.19)	16.96 (5.22)
ALP, U/L, mean (SD)	212.58 (69.81)	244.79 (88.12)		214.35 (54.46)	209.84 (56.33)
T-Bil, mg/dL, mean (SD)	0.51 (0.36)	0.45 (0.24)		0.77 (0.22)	0.63 (0.23)
γ-GTP, U/L, mean (SD)	30.75 (23.66)	22.67 (15.61)		42.78 (25.20)	28.97 (17.30)
CRP, mg/dL, mean (SD)	0.38 (0.61)	0.68 (1.16)	8.15 (2.46)	0.10 (0.08)	1.35 (0.85)
Hb, g/dL, mean (SD)	12.79 (1.87)	12.78 (1.75)	13.08 (1.75)	14.53 (1.05)	13.96 (1.32)
Ht, %, mean (SD)	38.91 (7.58)	39.65 (4.77)	39.11 (4.59)	42.6 (2.68)	40.79 (3.66)
WBC, $10^3/\mu L$, mean (SD)	7.35 (2.48)	6.75 (2.17)	12.50 (5.18)		
Plt, $10^4/\mu L$, mean (SD)	27.58 (7.07)	28.90 (6.21)	27.34 (6.22)	21.60 (5.62)	23.43 (6.45)
Mayo, mean (SD)	3.27 (2.83)				
CDAI, mean (SD)		129.18 (70.48)			

UC: Ulcerative colitis; CD: Crohn's disease; AE: Acute enteritis; HVs: Healthy volunteers; Alb: Albumin; ALT: Alanine aminotransferase; ALP: Alkaline phosphatase; T-Bil: Total-bilirubin; γ-GTP: γ-Glutamyl transpeptidase; CRP: C-reactive protein; Hb: Hemoglobin; Ht: Hematocrit; WBC: White blood cells; Plt: Platelets; Mayo: Full Mayo score; CDAI: Crohn's disease activity index; SD: Standard deviation.

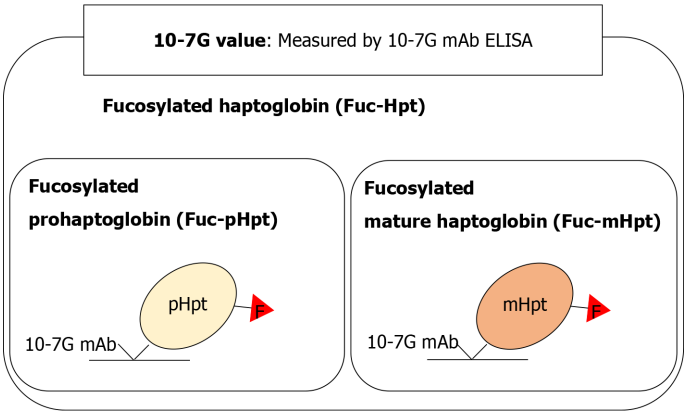


Figure 1 Schematic illustration of fucosylated haptoglobin detection using the 10-7G mAb. ELISA: Enzyme-linked immunosorbent assay.

sections from patients with severe CD (n = 5) or UC (n = 5) were embedded in paraffin at the Department of Pathology of Osaka University Graduate School of Medicine. This study was approved by the ethics committee of Osaka University Hospital and conducted in accordance with approved guidelines (approval number 14107-10). Written informed consent was obtained from all subjects in this study at the time of enrollment or blood sampling.

Immunohistochemistry

Tissue sample sections (4-μm thickness) were fixed in 10% formaldehyde and embedded in paraffin. Sections were then deparaffinized using a xylene alternative, Hemo-De (Falma, Tokyo, Japan), and then rehydrated in 100% ethanol (FUJIFILM Wako Pure Chemical Corporation, Osaka, Japan). The sections were rinsed with

phosphate-buffered saline [PBS; 137 mmol/L NaCl, 10 mmol/L Na_2HPO_4, 2.7 mmol/L KCl, 1.76 mmol/L KH_2PO_4 (pH 7.4)]. For antigen retrieval, sections were submerged in antigen-retrieval buffer [10 mmol/L $Na_3C_6H_5O_7$ (pH 6.0)] for 30 s at 125 °C and then submerged for 10 s at 90°C in a Pascal decloaking chamber (Dako, Glostrup, Denmark). The sections were cooled for 10 min in the chamber and 10 min at room temperature (RT) following antigen retrieval. After rinsing in Tris-buffered saline containing Tween 20 [TBST; 136 mmol/L NaCl, 2.6 mmol/L KCl, 24 mmol/L Tris, 0.005% Tween 20 (pH 7.4)], endogenous peroxidase activity was blocked by incubation in Dako REAL peroxidase-blocking solution (Dako) for 5 min at RT. The sections were incubated overnight at 4 °C with 0.22 μg/mL of the 10-7G mAb diluted in Dako REAL antibody diluent (Dako). Next, the sections were incubated with Dako ChemMate ENVISION kit/HRP (DAB) (Dako) for 30 min at RT. After each incubation step, the sections were washed with TBST three times for 5 min each. Subsequently, the sections were incubated with DAB+ chromogen solution (Dako) diluted with DAB substrate buffer (Dako) for 3 min to develop the stain. Finally, the slides were counterstained with hematoxylin (CHROMA, Nordrhein-Westfalen, Germany), dehydrated, cleared, and mounted. Images were acquired using a BZ-9000 microscope (KEYENCE, Osaka, Japan).

ELISAs

The 10-7G mAb ELISA was performed according to our previously reported method, with slight modifications[14]. 3,3′,5,5′-Tetramethylbiphenyl-4-4′-diamine solution was used for color development, as described previously[17]. The chromogen and the optical density were measured at 450 nm using an iMark™ microplate absorbance reader (Bio-Rad, Hercules, CA, United States).

A lectin-antibody ELISA was used to determine serum Fuc-mHpt levels, as described previously[13]. The Fab fragment of anti-haptoglobin polyclonal antibody (pAb) (Dako) was coated onto an ELISA plate to capture serum haptoglobin, and fucosylation of haptoglobin was detected using biotinylated *Aleuria aurantia* lectin (AAL). Serum Fuc-mHpt levels determined using this lectin-antibody ELISA are reported as AAL-mHpt.

Serum levels of leucine-rich alpha-2 glycoprotein (LRG) were determined using a human LRG assay kit (IBL, Gunma, Japan), according to the manufacturer's instructions.

pHpt plasmid construction

A pcDNA3.1-Hyg (+) vector (Invitrogen, Carlsbad, CA, United States) encoding the human haptoglobin transcript variant 1 (Hpt2) gene was prepared as previously described[18]. To construct the human pHpt expression vector, site-directed mutagenesis was employed to replace arginine with glutamine at residue 161, which is important for digestion by complement C1r subcomponent-like protein (C1RL). Amino acid substitution was carried out by polymerase chain reaction (PCR). In brief, the cycle parameters were as follows: initial denaturation at 95 °C for 3 min, one cycle of 98 °C for 10 s, 50 °C for 2 min, and 68 °C for 8 min, followed by 35 cycles of 10 s of denaturation at 98 °C, 15 s annealing at 57 °C, and an 8-min extension at 68 °C. The resulting DNA fragments were ligated with T4 DNA ligase (Promega, Madison, WI, United States). Primer sequences were as follows: sense, CCAAGAATCCGGCAAA-CCCAGTGCAGCAGATCCTGGGTGGAC; anti-sense, GGCATCCAGGTGTCCACCC-AGGATCTGCTGCACTGGGTTTGCC. The mutated sequences were confirmed by sequencing analysis.

Purification of Fuc-pHpt from HEK293T cells

Human embryonic kidney cells (HEK293T) were obtained from the American Type Culture Collection (Manassas, VA, United States) and maintained at 37 °C in a humidified atmosphere with 5% CO_2 and 95% air in DMEM high-glucose (Nacalai Tesque Inc., Kyoto, Japan) medium supplemented with 10% heat-inactivated fetal bovine serum (HyClone, Logan, UT, United States), 100 units/mL of penicillin, and 100 μg/mL of streptomycin (Nacalai Tesque Inc.).

HEK293T cells were transfected with the expression vector pcDNA3.1-Hyg(+) containing the mutated Hpt2 gene. After 24 h of incubation, transfected cells were selected using hygromycin B (Wako) for 2-3 wk to obtain the pHpt-overexpressing stable transfectants.

Fuc-pHpt products were collected from the conditioned medium of pHpt-overexpressing HEK293T cells and purified using an affinity chromatography column coupled with 10-7G mAb, as previously described[14]. The concentration of Fuc-pHpt

was determined using a Nano Drop 1000 spectrophotometer (Thermo Fisher Scientific, Waltham, MA, United States).

Fuc-pHpt semi-quantification by Western blotting

A 0.25-μL aliquot of serum in 10 μL of PBS was electrophoresed on a 10% polyacrylamide gel and transferred onto a polyvinylidene difluoride membrane. After blocking with 5% skim milk for 1 h, the membrane was incubated with 1/7500-diluted 10-7G mAb at 4 °C overnight. After three 10-min washes with TBST, the membrane was incubated with peroxidase-conjugated anti-mouse immunoglobulin G (IgG) for 1 h. After three 10-min washes with TBST, bound immunoglobulins were visualized using ImmunoStar® Zeta (Wako), according to standard protocols. Chemiluminescence signal detection and quantification were using a FUSION chemiluminescence imaging system (Vilber-Lourmat, Collegien, France). The quantity of Fuc-pHpt in each serum sample was calculated based on the ratio of the chemiluminescence signal intensity of the sample to that of the positive control. A fixed amount (5.0 ng) of purified Fuc-pHpt was used as a positive control sample for every Western blot analysis.

Haptoglobin phenotyping

For haptoglobin phenotyping, serum samples were subjected to Western blotting using anti-human haptoglobin pAb, as described previously[16]. Haptoglobin phenotypes for each sample were determined after antibody signals were developed using ImmunoStar® Zeta (Wako) and detection of α-1 and/or α-2.

Statistical analysis

Statistical analyses were performed using JMP Pro 14.0 software (SAS Institute Inc., Cary, NC, United States). Data were analyzed using the Wilcoxon test, Spearman rank correlation analysis, and receiver operating characteristic (ROC) curve analysis. As the 10-7G value, AAL-mHpt, Fuc-pHpt amount, CRP levels, hemoglobin (Hb), and albumin (Alb) data did not exhibit a Gaussian distribution, these parameters were common log-transformed before correlation diagrams were drawn. In the statistical analyses, samples of the Hpt1-1 phenotype were excluded because the 10-7G values were below the level of detection. P values < 0.05 were considered indicative of a statistically significant difference.

RESULTS

Immunohistochemical identification of Fuc-Hpt–producing cells in IBD patient tissues

To identify Fuc-Hpt–producing cells in UC and CD intestinal tissues collected from IBD patients, we performed immunohistochemical analyses using the 10-7G mAb. As shown in Figure 2A and B, positive 10-7G mAb staining was observed in lymphocytes infiltrating into inflammatory sites of the mucosal layer and lymph nodules in the intestinal tissues of UC patients. Similar but much more diffuse 10-7G mAb staining was observed in comparable cells in CD tissues (Figure 2C and D).

Determination of the serum 10-7G value in patients with IBD and AE

We determined serum 10-7G values for HVs and patients with UC, CD, or AE. As expected, 10-7G values were significantly higher in patients with UC, CD, and AE as compared to HVs (Figure 3A). To determine whether the 10-7G mAb primarily recognized Fuc-mHpt or Fuc-pHpt, we assessed serum Fuc-pHpt levels by immunoblot analysis using the 10-7G mAb, whereas serum Fuc-mHpt levels were determined using the lectin-antibody ELISA. Data regarding the semi-quantification of serum Fuc-pHpt levels by immunoblot analysis using the 10-7G mAb are described as Fuc-pHpt amount, whereas serum Fuc-mHpt levels determined using the lectin-antibody ELISA are described as AAL-mHpt.

Data regarding 10-7G values and Fuc-pHpt amount or AAL-mHpt were statistically analyzed using Spearman's rank correlation coefficient (rs). As shown in Figure 3B, a marked positive correlation was observed between the 10-7G value and Fuc-pHpt amount (rs = 0.695, P < 0.0001). In contrast, a lower positive correlation was observed between serum AAL-mHpt levels and 10-7G values (rs = 0.386, P = 0.0002) (Figure 3C). These results indicate that the 10-7G value depends primarily on serum Fuc-pHpt and partly reflects serum Fuc-mHpt in patients with intestinal inflammatory diseases.

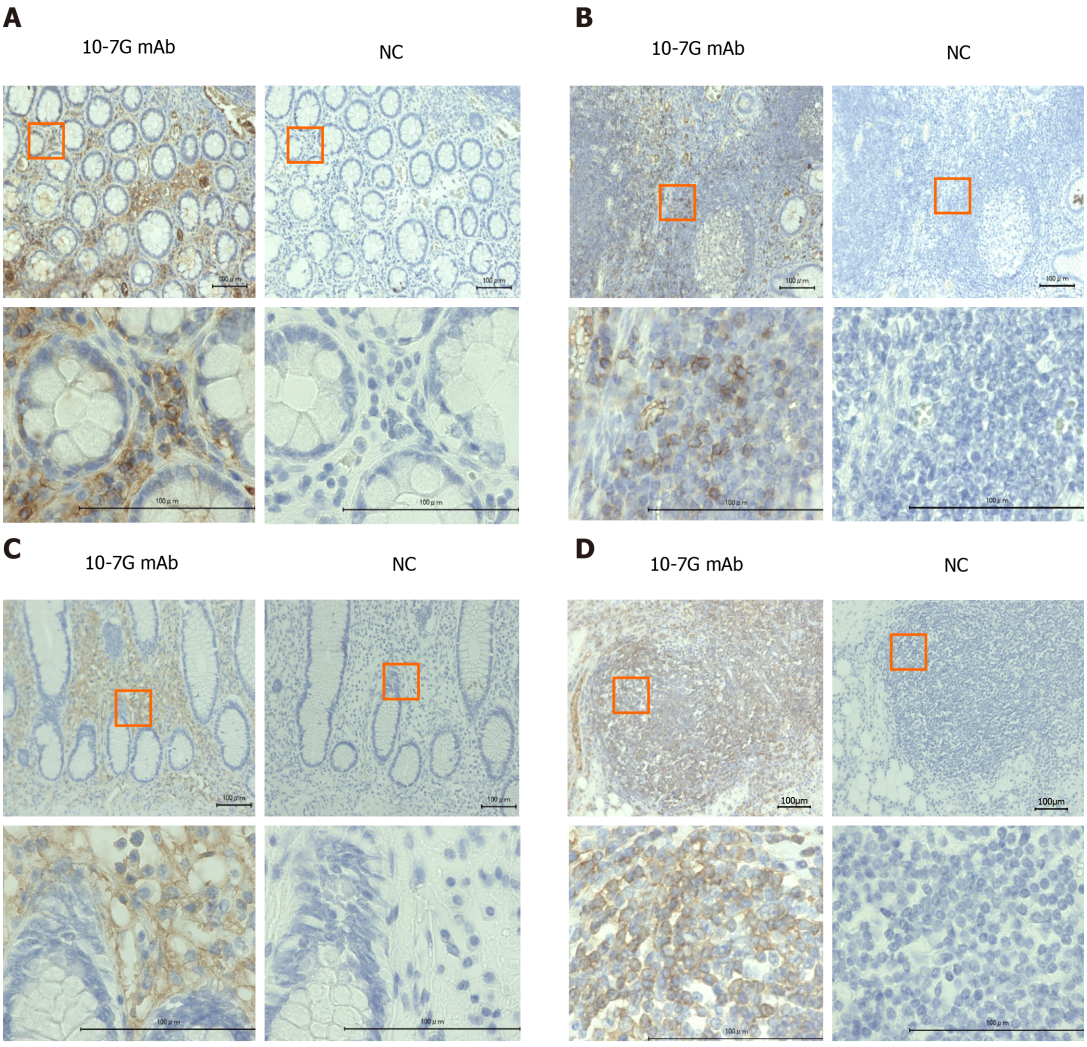


Figure 2 Immunohistochemical study of ulcerative colitis and Crohn's disease intestinal tissues using the 10-7G mAb. A and B: Lymphocytes infiltrating into inflammatory sites of the mucosal layer (A) and lymph nodules in intestinal tissues (B) of patients with ulcerative colitis (n = 5) were stained using the 10-7G mAb; C and D: Lymphocytes infiltrating into inflammatory sites of the mucosal layer (C) and lymph nodules in intestinal tissues (D) of patients with Crohn's disease (n = 5) were also stained. Photographs were acquired using a 20 × (upper) or 100 × (lower) objective. Scale bar, 100 μm. Positive staining was judged by comparison to the negative control. NC: Negative control.

Correlation between the 10-7G value and various clinical parameters

To elucidate the pathophysiologic significance of 10-7G values in IBD, we investigated the correlation between the 10-7G value and various clinical parameters of IBD patients, including Alb, alanine aminotransferase, alkaline phosphatase, total-bilirubin, γ-glutamyl transpeptidase, CRP, Hb, hematocrit, white blood cell count, platelet count, IBD activity index score, and full Mayo score (Mayo) for UC or Crohn's disease activity index (CDAI) for CD (Table 2). As shown in Figure 4A-C the 10-7G values of UC patients were negatively correlated with Hb (rs = -0.308, P = 0.0419) and positively correlated with CRP (rs = 0.525, P = 0.0003) and Mayo (rs = 0.435, P = 0.038). In contrast, as shown in Figure 4D and E, the 10-7G values of CD patients were negatively correlated with Alb (rs = -0.376, P = 0.014) and positively correlated with CRP (rs = 0.595, P < 0.0001). However, no significant correlation was observed between 10-7G values and CDAI (Figure 4F). These results indicate that 10-7G values are correlated with some inflammation-related biomarkers, especially CRP, in both UC and CD patients and reflect an inflammatory condition.

To determine whether the 10-7G value is a suitable inflammation marker similar to CRP, we also determined 10-7G values of HVs who were found to have elevated CRP levels during routine medical examinations (CRP-high HVs, n = 79). As shown in Figure 5A, there was no significant difference in 10-7G values in CRP-high or normal HVs. In addition, there was no significant correlation between the 10-7G value and CRP level in CRP-high HVs (Figure 5B). In contrast, the 10-7G values of CRP-high IBD patients were significantly higher than those of CRP-normal IBD patients, and there

Table 2 Correlation coefficients between 10-7G value and clinical parameters in ulcerative colitis and Crohn's disease patients

	UC			CD		
	rs	*P* value	*n*	*rs*	*P* value	*n*
Alb	-0.182	0.254	41	-0.376[a]	0.014	42
ALT	-0.214	0.339	22	-0.148	0.51	22
ALP	0.453	0.052	19	0.329	0.169	19
T-Bil	-0.419	0.059	21	-0.081	0.728	21
γ-GTP	-0.06	0.801	20	0.392	0.079	21
CRP	0.525[a]	0.0003	44	0.595[a]	< 0.0001	44
Hb	-0.308[a]	0.0419	44	-0.287	0.072	40
Ht	-0.304	0.064	38	-0.261	0.091	43
WBC	0.289	0.057	44	0.215	0.177	41
Plt	0.06	0.712	40	0.145	0.387	38
Mayo	0.435[a]	0.038	23			
CDAI				0.134	0.392	43

rs: Spearman's rank correlation coefficient.

[a]$P < 0.05$. UC: Ulcerative colitis; CD: Crohn's disease; Alb: Albumin; ALT: Alanine aminotransferase; ALP: Alkaline phosphatase; T-Bil: Total-bilirubin; γ-GTP: γ-Glutamyl transpeptidase; CRP: C-reactive protein; Hb: Hemoglobin; Ht: Hematocrit; WBC: White blood cells; Plt: Platelets; Mayo: Full Mayo score; CDAI: Crohn's disease activity index.

was a significant correlation between 10-7G values and CRP in IBD patients (Figure 5C and D). These data suggest that the 10-7G value mainly reflects intestinal inflammation, whereas CRP reflects systemic inflammation.

Usefulness of the 10-7G value as a biomarker of UC disease activity

As the 10-7G value was found to correlate with IBD activity index score in a small number of UC patients (Figure 4C and Table 2), we investigated the usefulness of the 10-7G value as an indicator of UC disease activity using a larger number of serum samples (n = 110). We compared the 10-7G value with CRP and LRG, a novel serum biomarker for UC disease activity[19]. We first analyzed the correlation between the 10-7G value, LRG, CRP, and three clinical activity index scores: the partial Mayo score (pMayo), an evaluation of symptomatic severity; the Mayo endoscopic subscore (MES), an evaluation of endoscopic severity; and Mayo, the sum of pMayo and MES, which is an indicator of clinical severity (Supplementary Table 1). Although the 10-7G value was significantly correlated with three of the scores (pMayo: rs = 0.2433, P = 0.0224, MES: rs = 0.3540, P = 0.0064, Mayo: rs = 0.2273, P = 0.0440), the correlation coefficients were slightly lower than those for CRP (pMayo: rs = 0.2947, P = 0.0053, MES: rs = 0.4375, P = 0.0006, Mayo: rs = 0.2597, P = 0.0208) and LRG (pMayo: rs = 0.3108, P = 0.0032, MES: rs = 0.3665, P = 0.0047, Mayo: rs = 0.3010, P = 0.0070).

The sensitivity and specificity of the serum 10-7G value, LRG, and CRP for diagnosis of endoscopic remission and clinical remission based on MES and Mayo were determined using ROC curve analysis. Endoscopic remission (*i.e.*, mucosal healing) was defined as MES ≤ 1[20], and clinical remission was defined as Mayo ≤ 2 (pMayo ≤ 1 and MES ≤ 1)[21]. For the diagnosis of endoscopic remission, the area under the curve (AUC) of the 10-7G value (MES ≤ 1: 0.699) (Figure 6A) was higher than that of both LRG (MES ≤ 1: 0.659) (Figure 6B) and CRP (MES ≤ 1: 0.663) (Figure 6C). In terms of clinical remission, the AUC value of the 10-7G value (Mayo ≤ 2: 0.626) (Supplementary Figure 1A) was lower than that of both LRG (Mayo ≤ 2: 0.714) (Supplementary Figure 1B) and CRP (Mayo ≤ 2: 0.678) (Supplementary Figure 1C). These results indicate that the 10-7G value is a useful biomarker for evaluating endoscopic mucosal healing in UC patients.

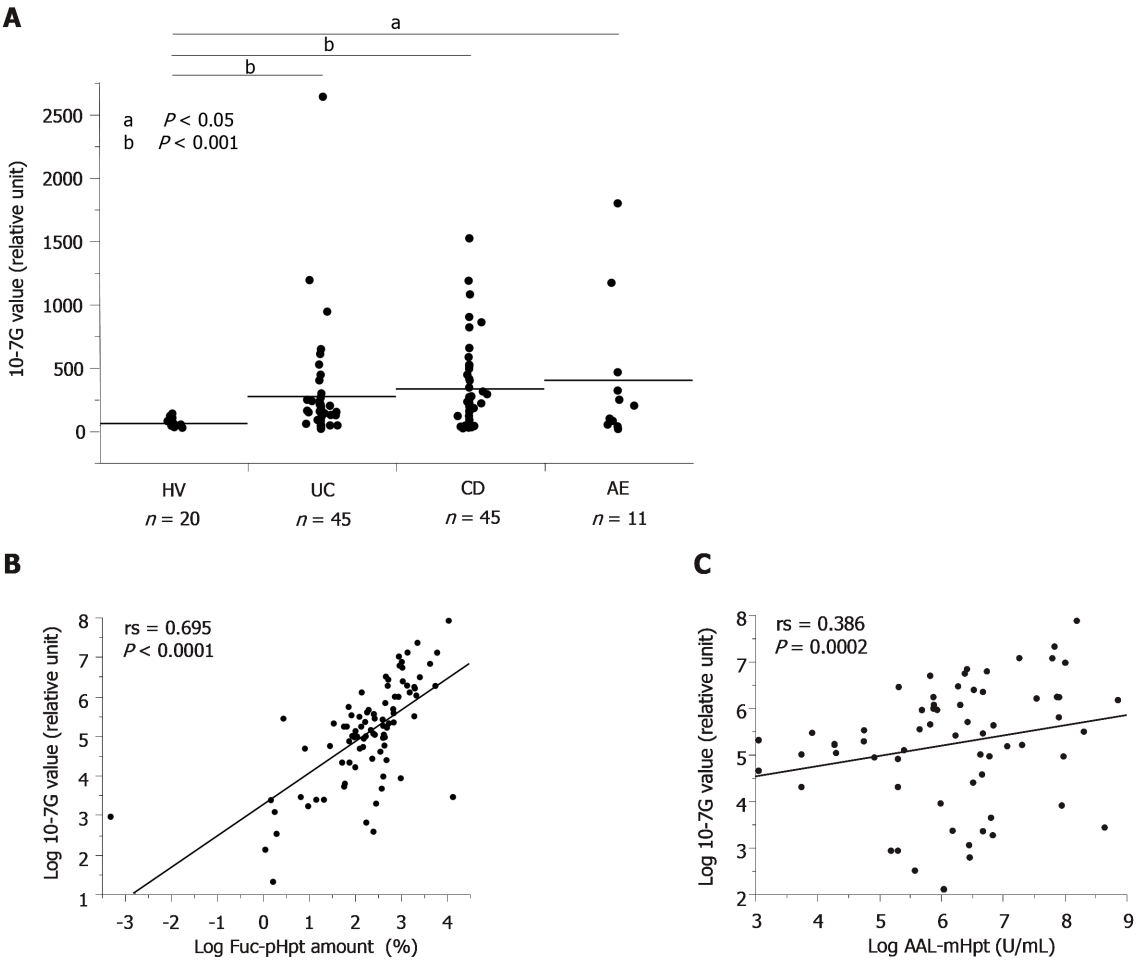


Figure 3 Measurement of the serum 10-7G value and fucosylated prohaptoglobin amount in patients with inflammatory bowel disease. A: Serum 10-7G value of healthy volunteers and patients with ulcerative colitis, Crohn's disease, or acute enteritis. Values are shown in relative units; B and C: Coefficients of correlation (B) between the 10-7G value and Fuc-pHpt amount and (C) between the 10-7G value and AAL-mHpt level. HV: Healthy volunteer; UC: Ulcerative colitis; CD: Crohn's disease; AE: Acute enteritis.

DISCUSSION

In this study, we demonstrated that the 10-7G value reflects intestinal inflammation. We found that the 10-7G value was not increased in the serum of HVs with elevated CRP levels, but it was significantly increased in the serum of patients with IBD and AE (Figures 3A and 5A). In addition, there was a significant correlation between 10-7G values and CRP in IBD patients, whereas no significant correlation in HVs with elevated CRP levels (Figure 5B and D). We previously reported agalactosyl IgG as a diagnostic biomarker of IBD[22]. Agalactosyl IgG is also an indicator of chronic inflammation associated with conditions such as rheumatoid arthritis[23]. The 10-7G value, on the other hand, is associated with acute and/or chronic intestinal inflammation.

We also demonstrated that the 10-7G value is a useful biomarker of disease activity in IBD patients, especially those with UC. Correlation analyses revealed that the 10-7G value is correlated with UC activity index score, non-CD Mayo score, and CDAI (Figure 4C and F). We concluded that this difference was due to the specificity of the 10-7G value for intestinal inflammation. Whereas the inflammatory lesions associated with UC are localized in the large intestine, those associated with CD can occur throughout the gastrointestinal tract, from the oral cavity to the anal canal[24]. The CDAI reflects not only intestinal inflammation but also lesions related to extraintestinal complications, such as arthritis, stomatitis, and anal fistulas[25]. Furthermore, calculation of the Mayo includes endoscopic findings that enable accurate evaluation of the intestinal condition, but the CDAI does not consider these findings. Therefore, the 10-7G value may not be correlated with the CDAI.

We also compared the 10-7G value and the LRG level, a promising tool for monitoring disease activity in IBD patients that was recently accepted for insurance

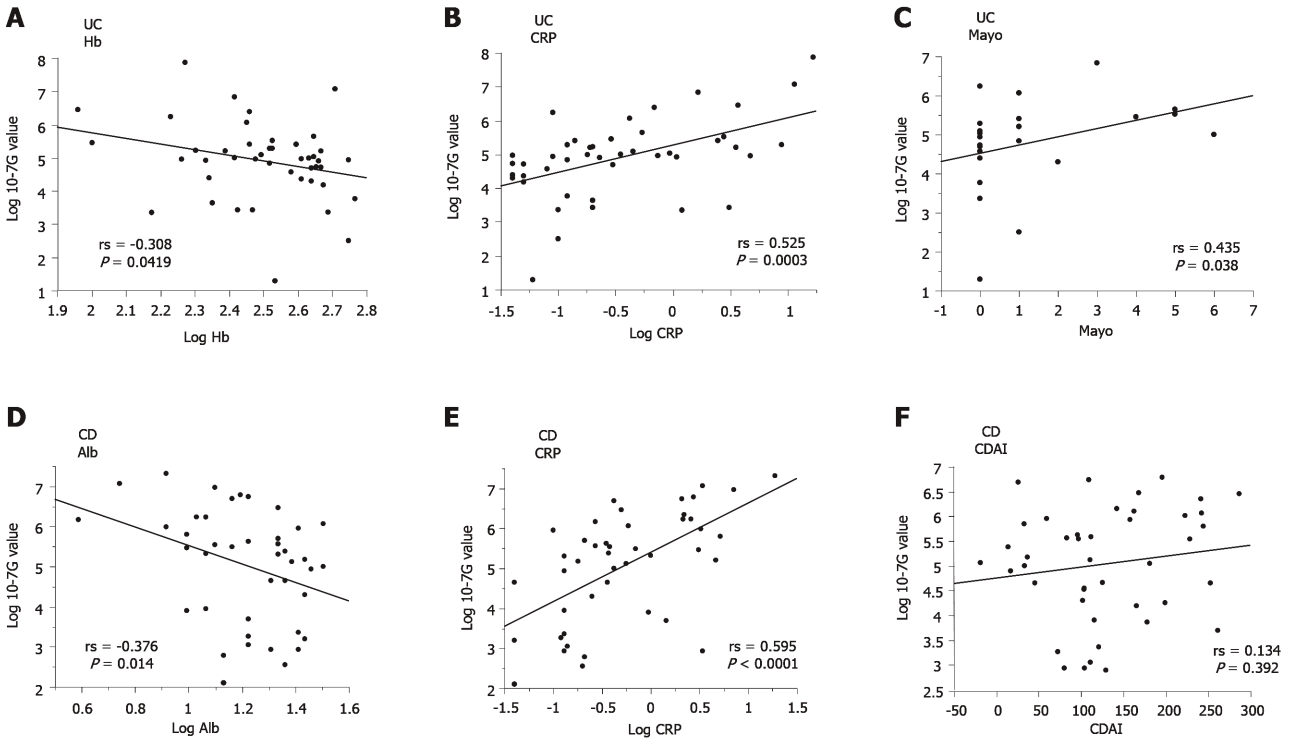


Figure 4 Correlations between 10-7G values and clinical parameters in inflammatory bowel disease patients. A-C: In ulcerative colitis patients, the 10-7G value was negatively correlated with hemoglobin and positively correlated with C-reactive protein (CRP) level and full Mayo score; D and E: In Crohn's disease patients, the 10-7G value was negatively correlated with albumin and positively correlated with CRP level; F: The 10-7G value was not correlated with the Crohn's disease activity index. UC: Ulcerative colitis; CD: Crohn's disease; Hb: Hemoglobin; CRP: C-reactive protein; Mayo: Mayo score; Alb: Albumin; CDAI: Crohn's disease activity index.

coverage in Japan. As indicated in Figure 6, the AUC of the 10-7G value for a diagnosis of endoscopic remission (MES ≤ 1) was higher than that of LRG. In contrast, the AUC of LRG for the diagnosis of symptomatic remission (pMayo ≤ 1) was higher than that of the 10-7G value (Supplementary Figure 1D and E). In other words, the 10-7G value is superior to LRG for evaluating the endoscopic mucosal condition, and LRG is superior to the 10-7G value for evaluating general symptoms such as stool frequency and hematochezia. As indicated in Figure 3B, the 10-7G value of IBD patients primarily reflects Fuc-pHpt levels, and some studies have reported that pHpt increases epithelial permeability[26]. Based on our results and other reports, we attributed the usefulness of the 10-7G value for evaluating the mucosal condition of UC patients to the detection of Fuc-pHpt.

To identify Fuc-Hpt–producing cells in intestinal tissues of IBD patients, we performed immunohistochemical staining with the 10-7G mAb. As shown in Figure 2, lymphocytes infiltrating into areas of inflammation in the mucosal layer were stained with the 10-7G mAb. The staining signal was thought to depend primarily on Fuc-pHpt rather than Fuc-mHpt. Cleavage of pHpt by C1RL is required for haptoglobin maturation. C1RL is a serine protease that cleaves αβ-junctions within pHpt[27]. C1RL expression is reportedly markedly elevated in the liver[28]. Therefore, most haptoglobin produced in hepatocytes matures before it is secreted into the blood. The expression of C1RL in other tissues is typically much lower than in hepatocytes; therefore, synthesized haptoglobin does not fully mature. In addition, in an immunoblotting analysis using 10-7G mAb, we recently demonstrated that some lines of non-adherent cells produce Fuc-pHpt and that several inflammatory cytokines facilitate Fuc-pHpt secretion (manuscript submitted). These data support our hypothesis that infiltrating lymphocytes produce Fuc-pHpt in sites of intestinal inflammation and that the 10-7G value is an indicator of Fuc-pHpt production. Further studies are needed to fully elucidate the mechanism underlying the secretion of Fuc-pHpt by immune cells, however.

Considering our findings in this study, we proposed the flow chart of non-invasive detection methods of clinical activity of IBD, especially UC, using 10-7G value based on the cutoff value of 211 defined as ROC curve analysis (Figure 6A), the point of the best split of endoscopic remission (Figure 7). Since clinical symptoms appear after

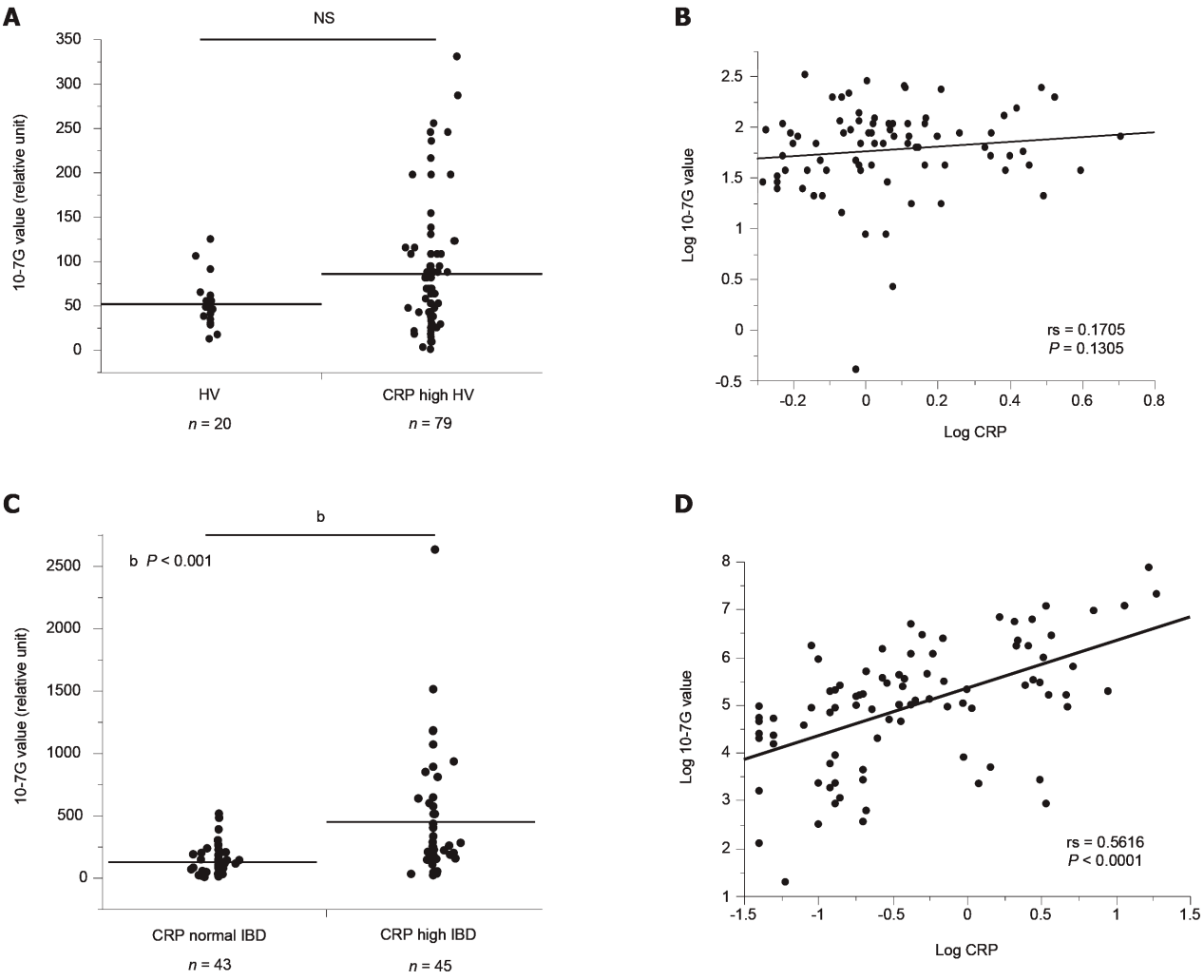


Figure 5 Measurement of serum 10-7G values and correlation between 10-7G values and C-reactive protein in healthy volunteers who underwent a medical examination. A: The 10-7G value of healthy volunteers (HVs) who had elevated C-reactive protein (CRP) levels (> 0.3 mg/dL) diagnosed during routine medical examination (CRP-high HVs); B: Coefficient of correlation between the 10-7G value and CRP level in CRP-high HVs; C: 10-7G values of inflammatory bowel disease (IBD) patients with normal CRP level (≤ 0.3 mg/dL) (CRP-normal IBD) or high CRP level (> 0.3 mg/dL) (CRP-high IBD); D: Coefficient of correlation between the 10-7G value and CRP level in IBD patients. HV: Healthy volunteer; CRP: C-reactive protein; IBD: Inflammatory bowel disease; NS: Not significant.

changes in mucosal inflammation status of the intestine and colonoscopy itself has a risk of exacerbating mucosal inflammation, non-invasive biomarkers such as 10-7G value are required to follow up the patients with IBD.

CONCLUSION

In conclusion, we demonstrated that the serum 10-7G value reflects intestinal inflammation and is a useful biomarker for evaluating endoscopic mucosal healing in UC, as Fuc-Hpt detected by the 10-7G mAb is produced by lymphocytes infiltrating into sites of inflammation in the intestinal mucosal layer.

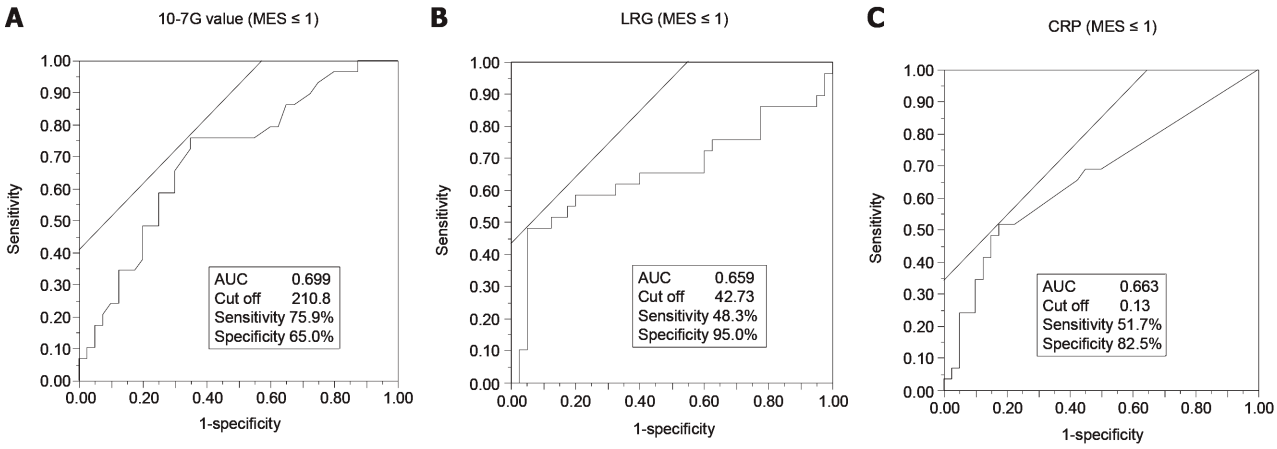


Figure 6 Evaluation of the usefulness of the 10-7G value for pathologic diagnosis of ulcerative colitis compared to C-reactive protein and leucine-rich alpha-2 glycoprotein. A-C: Analysis of receiver operating characteristic curves for 10-7G value, leucine-rich alpha-2 glycoprotein, and C-reactive protein for differentiation between ulcerative colitis (UC) patients with endoscopic mucosal remission by Mayo endoscopic subscore (MES). AUC: Area under the curve; MES: Mayo endoscopic subscore; LRG: Leucine-rich alpha-2 glycoprotein; CRP: C-reactive protein.

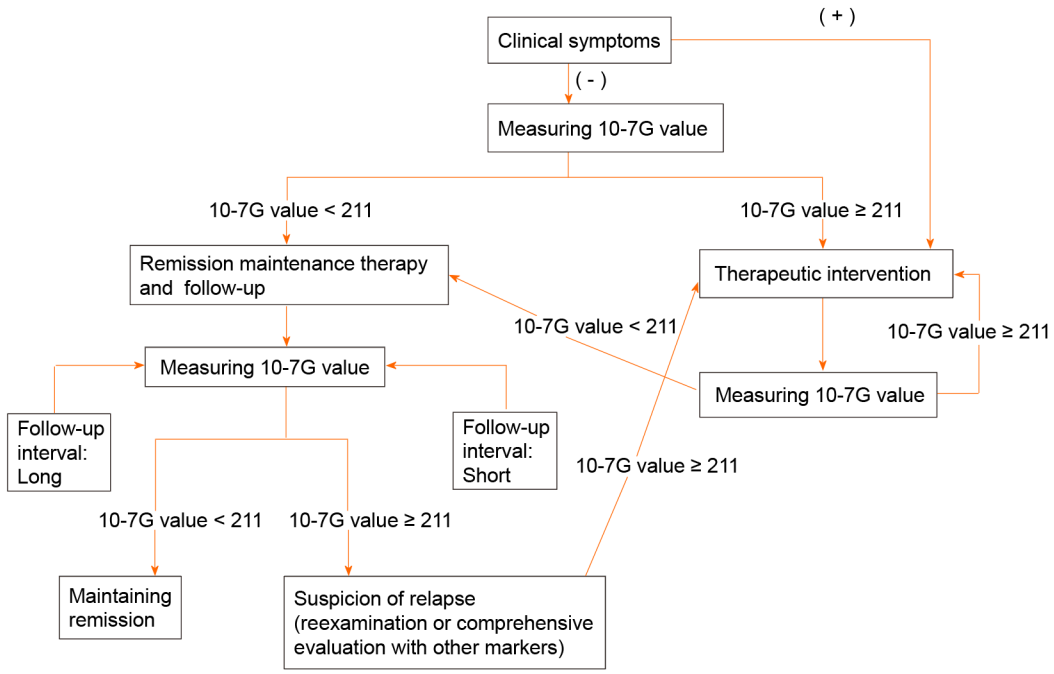


Figure 7 Non-invasive follow-up chart of patients with ulcerative colitis using 10-7G value.

ARTICLE HIGHLIGHTS

Research background

Fucosylation is one of the most important glycosylation involved in cancer and inflammation. Recently, we have succeeded to establish a novel glycan antibody 10-7G mAb which directly recognizes fucosylated haptoglobin (Fuc-Hpt), and developed its enzyme-linked immunosorbent assay system.

Research motivation

Although fecal and serum biomarkers have been extremely important and supportive for monitoring of Inflammatory bowel disease (IBD), their low sensitivity and high variability characteristics limit clinical efficacy. Thus, the establishment of better biomarkers is expected.

Research objectives

This research aimed to investigate the usefulness of the serum levels of Fuc-Hpt (10-7G values) as a potential biomarker for monitoring disease activity in IBD.

Research methods

Intestinal tissues of IBD patients were examined immunohistochemically using the 10-7G mAb. The 10-7G values were measured using serum from patients with IBD, acute enteritis (AE), and healthy volunteers. Correlation analysis and Receiver operating characteristic curve analysis were performed to evaluate the usefulness of the 10-7G values as a biomarker for IBD compared to conventional serum biomarkers and various clinical parameters.

Research results

Positive 10-7G mAb staining was observed in lymphocytes infiltrating into inflammatory sites of the mucosal layer. The 10-7G values were significantly higher in patients with IBD and AE. Statistical analyses showed that the 10-7G values could evaluate intestinal inflammation and endoscopic mucosal healing in ulcerative colitis (UC).

Research conclusions

Fuc-Hpt is produced by lymphocytes infiltrating into sites of inflammation in the intestine and the serum 10-7G value is a non-invasive biomarker for evaluating endoscopic remission in UC.

Research perspectives

Further studies are needed to fully elucidate the mechanism underlying the secretion of Fuc-Hpt by immune cells. In addition, we will measure serum 10-7G values of same patients with UC in follow-up study.

ACKNOWLEDGEMENTS

The authors would like to thank Dr. Yamada M (aMs NEW OTANI CLINIC, Osaka, Osaka 540-8570, Japan) for the excellent assistance.

REFERENCES

1 **Xavier RJ**, Podolsky DK. Unravelling the pathogenesis of inflammatory bowel disease. *Nature* 2007; **448**: 427-434 [PMID: 17653185 DOI: 10.1038/nature06005]
2 **Uhlig HH**. Monogenic diseases associated with intestinal inflammation: implications for the understanding of inflammatory bowel disease. *Gut* 2013; **62**: 1795-1805 [PMID: 24203055 DOI: 10.1136/gutjnl-2012-303956]
3 **Geremia A**, Biancheri P, Allan P, Corazza GR, Di Sabatino A. Innate and adaptive immunity in inflammatory bowel disease. *Autoimmun Rev* 2014; **13**: 3-10 [PMID: 23774107 DOI: 10.1016/j.autrev.2013.06.004]
4 **Carlson CS**, Aldred SF, Lee PK, Tracy RP, Schwartz SM, Rieder M, Liu K, Williams OD, Iribarren C, Lewis EC, Fornage M, Boerwinkle E, Gross M, Jaquish C, Nickerson DA, Myers RM, Siscovick DS, Reiner AP. Polymorphisms within the C-reactive protein (CRP) promoter region are associated with plasma CRP levels. *Am J Hum Genet* 2005; **77**: 64-77 [PMID: 15897982 DOI: 10.1086/431366]
5 **Soubières AA**, Poullis A. Emerging role of novel biomarkers in the diagnosis of inflammatory bowel disease. *World J Gastrointest Pharmacol Ther* 2016; **7**: 41-50 [PMID: 26855811 DOI: 10.4292/wjgpt.v7.i1.41]
6 **Eckersall PD**, Bell R. Acute phase proteins: Biomarkers of infection and inflammation in veterinary medicine. *Vet J* 2010; **185**: 23-27 [PMID: 20621712 DOI: 10.1016/j.tvjl.2010.04.009]
7 **Yang H**, Wang H, Levine YA, Gunasekaran MK, Wang Y, Addorisio M, Zhu S, Li W, Li J, de Kleijn DP, Olofsson PS, Warren HS, He M, Al-Abed Y, Roth J, Antoine DJ, Chavan SS, Andersson U, Tracey KJ. Identification of CD163 as an antiinflammatory receptor for HMGB1-haptoglobin complexes. *JCI Insight* 2016; **1** [PMID: 27294203 DOI: 10.1172/jci.insight.85375]
8 **Kristiansen M**, Graversen JH, Jacobsen C, Sonne O, Hoffman HJ, Law SK, Moestrup SK. Identification of the haemoglobin scavenger receptor. *Nature* 2001; **409**: 198-201 [PMID: 11196644 DOI: 10.1038/35051594]
9 **Yang F**, Brune JL, Baldwin WD, Barnett DR, Bowman BH. Identification and characterization of human haptoglobin cDNA. *Proc Natl Acad Sci USA* 1983; **80**: 5875-5879 [PMID: 6310599 DOI: 10.1073/pnas.80.19.5875]

10 **Black JA**, Chan GF, Hew CL, Dixon GH. Gene action in the human haptoglobins. 3. Isolation of the alpha-chains as single gene products. Isolation, molecular weight, and amino acid composition of alpha and beta chains. *Can J Biochem* 1970; **48**: 123-132 [PMID: 5512535 DOI: 10.1139/o70-019]

11 **Miyoshi E**, Moriwaki K, Nakagawa T. Biological function of fucosylation in cancer biology. *J Biochem* 2008; **143**: 725-729 [PMID: 18218651 DOI: 10.1093/jb/mvn011]

12 **Okuyama N**, Ide Y, Nakano M, Nakagawa T, Yamanaka K, Moriwaki K, Murata K, Ohigashi H, Yokoyama S, Eguchi H, Ishikawa O, Ito T, Kato M, Kasahara A, Kawano S, Gu J, Taniguchi N, Miyoshi E. Fucosylated haptoglobin is a novel marker for pancreatic cancer: a detailed analysis of the oligosaccharide structure and a possible mechanism for fucosylation. *Int J Cancer* 2006; **118**: 2803-2808 [PMID: 16385567 DOI: 10.1002/ijc.21728]

13 **Kamada Y**, Kinoshita N, Tsuchiya Y, Kobayashi K, Fujii H, Terao N, Kamihagi K, Koyama N, Yamada S, Daigo Y, Nakamura Y, Taniguchi N, Miyoshi E. Reevaluation of a lectin antibody ELISA kit for measuring fucosylated haptoglobin in various conditions. *Clin Chim Acta* 2013; **417**: 48-53 [PMID: 23262369 DOI: 10.1016/j.cca.2012.12.014]

14 **Nishino K**, Koda S, Kataoka N, Takamatsu S, Nakano M, Ikeda S, Kamamatsu Y, Morishita K, Moriwaki K, Eguchi H, Yamamoto E, Kikkawa F, Tomita Y, Kamada Y, Miyoshi E. Establishment of an antibody specific for cancer-associated haptoglobin: a possible implication of clinical investigation. *Oncotarget* 2018; **9**: 12732-12744 [PMID: 29560105 DOI: 10.18632/oncotarget.24332]

15 **Morishita K**, Maki Y, Takamatsu S, Ito N, Koda S, Motooka K, Kamada Y, Kajihara Y, Miyoshi E. Identification of the epitope of 10-7G glycan antibody to recognize cancer-associated haptoglobin. *Anal Biochem* 2020; **593**: 113588 [PMID: 31981485 DOI: 10.1016/j.ab.2020.113588]

16 **Morishita K**, Ito N, Koda S, Maeda M, Nakayama K, Yoshida K, Takamatsu S, Yamada M, Eguchi H, Kamada Y, Miyoshi E. Haptoglobin phenotype is a critical factor in the use of fucosylated haptoglobin for pancreatic cancer diagnosis. *Clin Chim Acta* 2018; **487**: 84-89 [PMID: 30189188 DOI: 10.1016/j.cca.2018.09.001]

17 **Roberts IM**, Jones SL, Premier RR, Cox JC. A comparison of the sensitivity and specificity of enzyme immunoassays and time-resolved fluoroimmunoassay. *J Immunol Methods* 1991; **143**: 49-56 [PMID: 1919036 DOI: 10.1016/0022-1759(91)90271-g]

18 **Narisada M**, Kawamoto S, Kuwamoto K, Moriwaki K, Nakagawa T, Matsumoto H, Asahi M, Koyama N, Miyoshi E. Identification of an inducible factor secreted by pancreatic cancer cell lines that stimulates the production of fucosylated haptoglobin in hepatoma cells. *Biochem Biophys Res Commun* 2008; **377**: 792-796 [PMID: 18951869 DOI: 10.1016/j.bbrc.2008.10.061]

19 **Serada S**, Fujimoto M, Terabe F, Iijima H, Shinzaki S, Matsuzaki S, Ohkawara T, Nezu R, Nakajima S, Kobayashi T, Plevy SE, Takehara T, Naka T. Serum leucine-rich alpha-2 glycoprotein is a disease activity biomarker in ulcerative colitis. *Inflamm Bowel Dis* 2012; **18**: 2169-2179 [PMID: 22374925 DOI: 10.1002/ibd.22936]

20 **Colombel JF**, Rutgeerts P, Reinisch W, Esser D, Wang Y, Lang Y, Marano CW, Strauss R, Oddens BJ, Feagan BG, Hanauer SB, Lichtenstein GR, Present D, Sands BE, Sandborn WJ. Early mucosal healing with infliximab is associated with improved long-term clinical outcomes in ulcerative colitis. *Gastroenterology* 2011; **141**: 1194-1201 [PMID: 21723220 DOI: 10.1053/j.gastro.2011.06.054]

21 **Lewis JD**, Chuai S, Nessel L, Lichtenstein GR, Aberra FN, Ellenberg JH. Use of the noninvasive components of the Mayo score to assess clinical response in ulcerative colitis. *Inflamm Bowel Dis* 2008; **14**: 1660-1666 [PMID: 18623174 DOI: 10.1002/ibd.20520]

22 **Shinzaki S**, Iijima H, Nakagawa T, Egawa S, Nakajima S, Ishii S, Irie T, Kakiuchi Y, Nishida T, Yasumaru M, Kanto T, Tsujii M, Tsuji S, Mizushima T, Yoshihara H, Kondo A, Miyoshi E, Hayashi N. IgG oligosaccharide alterations are a novel diagnostic marker for disease activity and the clinical course of inflammatory bowel disease. *Am J Gastroenterol* 2008; **103**: 1173-1181 [PMID: 18177457 DOI: 10.1111/j.1572-0241.2007.01699.x]

23 **Parekh RB**, Dwek RA, Sutton BJ, Fernandes DL, Leung A, Stanworth D, Rademacher TW, Mizuochi T, Taniguchi T, Matsuta K. Association of rheumatoid arthritis and primary osteoarthritis with changes in the glycosylation pattern of total serum IgG. *Nature* 1985; **316**: 452-457 [PMID: 3927174 DOI: 10.1038/316452a0]

24 **Abraham C**, Cho JH. Inflammatory bowel disease. *N Engl J Med* 2009; **361**: 2066-2078 [PMID: 19923578 DOI: 10.1056/NEJMra0804647]

25 **Best WR**, Becktel JM, Singleton JW, Kern F Jr. Development of a Crohn's disease activity index. National Cooperative Crohn's Disease Study. *Gastroenterology* 1976; **70**: 439-444 [PMID: 1248701 DOI: 10.1016/S0016-5085(76)80163-1]

26 **Tripathi A**, Lammers KM, Goldblum S, Shea-Donohue T, Netzel-Arnett S, Buzza MS, Antalis TM, Vogel SN, Zhao A, Yang S, Arrietta MC, Meddings JB, Fasano A. Identification of human zonulin, a physiological modulator of tight junctions, as prehaptoglobin-2. *Proc Natl Acad Sci USA* 2009; **106**: 16799-16804 [PMID: 19805376 DOI: 10.1073/pnas.0906773106]

27 **Wicher KB**, Fries E. Prohaptoglobin is proteolytically cleaved in the endoplasmic reticulum by the complement C1r-like protein. *Proc Natl Acad Sci USA* 2004; **101**: 14390-14395 [PMID: 15385675 DOI: 10.1073/pnas.0405692101]

28 **Ligoudistianou C**, Xu Y, Garnier G, Circolo A, Volanakis JE. A novel human complement-related protein, C1r-like protease (C1r-LP), specifically cleaves pro-C1s. *Biochem J* 2005; **387**: 165-173 [PMID: 15527420 DOI: 10.1042/bj20041196]

World Journal of Gastroenterology

Submit a Manuscript: https://www.f6publishing.com

World J Gastroenterol 2021 January 14; 27(2): 176-188

DOI: 10.3748/wjg.v27.i2.176

ISSN 1007-9327 (print) ISSN 2219-2840 (online)

ORIGINAL ARTICLE

Retrospective Cohort Study

Repeatedly elevated γ-glutamyltransferase levels are associated with an increased incidence of digestive cancers: A population-based cohort study

Chang-Hoon Lee, Kyungdo Han, Da Hye Kim, Min-Sun Kwak

ORCID number: Chang-Hoon Lee 0000-0001-9960-1524; Kyungdo Han 0000-0002-6096-1263; Da Hye Kim 0000-0002-2241-3960; Min-Sun Kwak 0000-0003-0353-6460.

Author contributions: Kwak MS and Lee CH contributed to the conception and design of the study, interpretation of the data, and drafting of the manuscript; Han K and Kim DH contributed to the acquisition of the data, statistical analysis, table and figure creation and critical revision of the manuscript for important intellectual content.

Institutional review board statement: This study protocol was exempted from review by the Seoul National University Hospital Institutional Review Board because of the retrospective design of the study, and the researchers accessed only de-identified open clinical data for analytical purposes (No. H-1912-022-1085).

Informed consent statement: The subjects' information in the database was de-identified before the investigator accessed the data, thus informed consent was waived.

Conflict-of-interest statement: The authors declare no conflicts of

Chang-Hoon Lee, Department of Internal Medicine, Seoul National University Hospital, Seoul 03080, South Korea

Kyungdo Han, Department of Statistics and Actuarial Science, Soongsil University, Seoul 06978, South Korea

Da Hye Kim, Department of Biostatistics, College of Medicine, Catholic University of Korea, Seoul 06591, South Korea

Min-Sun Kwak, Department of Internal Medicine, Healthcare Research Institute, Healthcare System Gangnam Center, Seoul National University Hospital, Seoul 06236, South Korea

Corresponding author: Min-Sun Kwak, MD, PhD, Assistant Professor, Department of Internal Medicine, Healthcare Research Institute, Healthcare System Gangnam Center, Seoul National University Hospital, 39th FL. Gangnam Finance Center, 737 Yeoksam-dong, Gangnam-gu, Seoul 06236, South Korea. kms39@snuh.org

Abstract

BACKGROUND

The association between elevated γ-glutamyltransferase (GGT) at a certain point and incident cancer has been suggested; however, no study has evaluated the association between repeatedly elevated GGT and cancer incidence.

AIM

To investigate the effects of repeatedly elevated GGT on the incidence of digestive cancers.

METHODS

Participants who had undergone health screening from 2009 to 2012 and 4 consecutive previous examinations were enrolled. GGT points were calculated as the number of times participants met the criteria of quartile 4 of GGT in four serial measurements (0-4 points). Multivariable Cox proportional hazard regression models were applied.

RESULTS

In total, 3559109 participants were included; among them, 43574 digestive cancers

interest for this article.

Data sharing statement: No additional data are available.

STROBE statement: The authors have read the STROBE Statement-checklist of items, and the manuscript was prepared and revised according to the STROBE Statement-checklist of items.

Open-Access: This article is an open-access article that was selected by an in-house editor and fully peer-reviewed by external reviewers. It is distributed in accordance with the Creative Commons Attribution NonCommercial (CC BY-NC 4.0) license, which permits others to distribute, remix, adapt, build upon this work non-commercially, and license their derivative works on different terms, provided the original work is properly cited and the use is non-commercial. See: http://creativecommons.org/licenses/by-nc/4.0/

Manuscript source: Unsolicited manuscript

Specialty type: Gastroenterology and hepatology

Country/Territory of origin: South Korea

Peer-review report's scientific quality classification

Grade A (Excellent): 0
Grade B (Very good): 0
Grade C (Good): C, C
Grade D (Fair): 0
Grade E (Poor): 0

Received: October 12, 2020
Peer-review started: October 12, 2020
First decision: November 23, 2020
Revised: December 5, 2020
Accepted: December 16, 2020
Article in press: December 16, 2020
Published online: January 14, 2021

P-Reviewer: Sharma K
S-Editor: Gao CC
L-Editor: A
P-Editor: Liu JH

developed during a median of 6.8 years of follow-up. The incidence of total digestive cancers increased in a dose-response manner in men [adjusted hazard ratio (aHR) compared with those with 0 GGT points = 1.28 and 95% confidence interval (CI) = 1.24-1.33 in those with 1 point; aHR = 1.40 and 95%CI = 1.35-1.46 in those with 2 points; aHR = 1.52 and 95%CI = 1.46-1.58 in those with 3 points; aHR = 1.88 and 95%CI = 1.83-1.94 in those with 4 points; *P* for trend < 0.001]. This trend was more prominent in men than in women and those with healthy habits (no smoking, no alcohol consumption, and a low body mass index) than in those with unhealthy habits.

CONCLUSION

Repeatedly elevated GGT levels were associated with an increased risk of incident digestive cancer in a dose-responsive manner, particularly in men and those with healthy habits. Repeated GGT measurements may be a good biomarker of incident digestive cancer and could help physicians identify high-risk populations.

Key Words: Gamma-glutamyltransferase; Cancer; Digestive organ; Serial exam; Incident cancer; Biomarker

©The Author(s) 2021. Published by Baishideng Publishing Group Inc. All rights reserved.

Core Tip: We evaluate whether repeatedly elevated γ-glutamyltransferase (GGT) levels on four consecutive exams were associated with an increased incidence of digestive cancers using the population-based cohort data. In total, 3559109 participants were included with a median of 6.8 years of follow-up. Repeatedly elevated GGT levels on four consecutive exams were associated with an increased incidence of digestive cancers in a dose-response manner. This trend was more prominent in men than women and in those with healthy habits (no smoking, no alcohol consumption, and a low body mass index) than those with unhealthy habits.

Citation: Lee CH, Han K, Kim DH, Kwak MS. Repeatedly elevated γ-glutamyltransferase levels are associated with an increased incidence of digestive cancers: A population-based cohort study. *World J Gastroenterol* 2021; 27(2): 176-188
URL: https://www.wjgnet.com/1007-9327/full/v27/i2/176.htm
DOI: https://dx.doi.org/10.3748/wjg.v27.i2.176

INTRODUCTION

Gamma-glutamyltransferase (GGT) is the enzyme responsible for the extracellular catabolism of glutathione by catalyzing the transfer of the glutamyl residue from glutathione to an acceptor amino acid[1]. GGT is present on the external surface of most cells but is mainly present in biliary epithelial cells[2]. GGT is a well-known marker of hepatic dysfunction, cholestasis or excessive alcohol consumption[3]. However, elevated serum levels of GGT are also associated with various diseases, including non-hepatobiliary diseases, such as type 2 diabetes mellitus (DM)[4], obesity, dyslipidemia, metabolic syndrome[5], hypertension[4], chronic kidney disease[6] and cardiovascular disease[7].

Several studies have suggested that elevated serum levels of GGT are also associated with an increased incidence of digestive cancers. A population-based study showed that elevated serum GGT is associated with an increased risk of esophageal cancer[8]. Another population-based study in Korea showed that the baseline GGT had a dose-response association with incident cancers, including liver cancer and several gastrointestinal cancers[9]. A meta-analysis including 14 cohort studies showed that the overall cancer risk increased by 1.04 times per 5-U/L increment in serum GGT[10]. Nevertheless, most of these studies used a single measurement of GGT, although the GGT levels fluctuate over time. The within-subject biological variation in GGT was reported to be 13.8% (range, 3.9%-14.5%)[11]. Several other longitudinal follow-up studies also showed dynamic changes in GGT[12-14]. Furthermore, many factors affect

the level of GGT, such as age, sex, ethnicity, region, alcohol consumption, smoking, underlying diseases and drugs[15,16]. Therefore, a single measurement of GGT does not fully reflect the current status of GGT, limiting the understanding of the actual relationship between GGT and diseases. We hypothesized that multiple measurements of GGT over several years could mitigate the limitations of a single measurement. In this study, we investigated whether repeatedly elevated serum GGT levels on serial measurements over 3-4 years were associated with an increased risk of incident digestive cancer using population-based data.

MATERIALS AND METHODS

National Health Insurance Service data source

We used the National Health Insurance Service (NHIS) database, which is managed by the Korean government. The NHIS covers almost all Koreans (97.2% of the Korean population)[8]. The NHIS supports annual or biennial standardized national health check-ups for all insured Koreans older than 40 years and employees older than 20 years. The NHIS contains information for each participant on their demographics, examinations, disease diagnosis codes claims according to the International Classification of Diseases (ICD-10), and treatments, including medication prescribed and procedures performed[17].

This study protocol was exempted from review by the Seoul National University Hospital Institutional Review Board because of the retrospective design of the study, and the researchers accessed only de-identified open clinical data for analytical purposes (H-1912-022-1085). Informed consent from participants was also waived by the Institutional Review Board of Seoul National University Hospital because of the retrospective nature of the study, and the researchers accessed only anonymous clinical data for analytical purposes.

Study population

We initially included participants who had undergone the Korean Health screening from 2009 to 2012. Among them, we selected participants who had 4 previous serial health screening examinations, as presented in Figure 1. Next, those with missing data were excluded. Participants who were diagnosed with any cancers at baseline were excluded based on C-codes and registration programs for serious diseases before the index date. The Korean government provides co-payment reductions for registered cancer patients. Only patients with a confirmed diagnosis of cancer after a thorough evaluation by a physician can be registered in this program.

Participants who died or had an event within 1 year ("lag period") were also excluded. The included participants were followed until December 2017.

Measurement of clinical variables and biochemical analysis

Standardized self-administered questionnaires were collected. They included questions on age (years), sex, alcohol consumption (amount and frequency), smoking (never, former and current), regular physical activity, yearly income, and underlying diseases, including malignancy. Heavy alcohol consumption was defined as > 21 standard drinks per week based on the self-administered questionnaire[18].

Body weight (kg) and height (m^2) were measured using an electronic scale, and the body mass index (BMI) was calculated as follows: BMI = body weight (kg)/height^2 (m^2). A BMI greater than 25 kg/m^2 was used to define the obese population in the subgroup analysis. The waist circumference (WC) was measured using a tape measure at the midpoint between the iliac crest and the lower costal margin by a well-trained examiner. Systolic blood pressure (SBP) and diastolic blood pressure (DBP) were measured after 5 min of rest.

After overnight fasting, blood samples were collected from each participant and analyzed using a standardized laboratory method. The baseline laboratory examinations included GGT, total cholesterol, triglycerides, low-density lipoprotein cholesterol, high-density lipoprotein cholesterol, fasting glucose, aspartate aminotransferase (AST), and alanine aminotransferase (ALT).

The diagnoses of hypertension, dyslipidemia and DM were defined using anthropometric measurements or laboratory data (SBP = 140 mmHg or DBP = 90 mmHg; total cholesterol level ≥ 240 mg/dL; fasting glucose level ≥ 126 mg/dL) or ICD codes (ICD I10 to I13 or I15; E78; E11 to E14) and medication use, including antihypertensive medication, dyslipidemia medication or insulin or oral hypoglycemic agents. In the subgroup analysis, the definition of chronic liver disease or liver

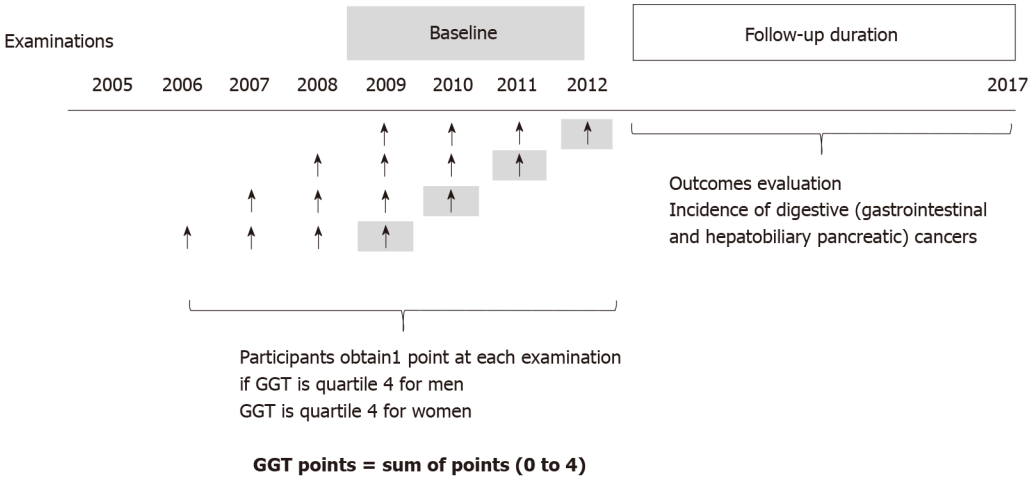


Figure 1 Definition of the γ-glutamyltransferase points and study design. The participants received one point if γ-glutamyltransferase (GGT) was in quartile 4 at each examination. The GGT points were defined as the sum of points of four examinations. GGT: Gamma-glutamyltransferase.

cirrhosis was based on ICD codes (B15-B19, K70.3, K74.6).

Definition of GGT points

Participants were assigned "GGT points" based on 4 consecutive examinations. They obtained 1 point if GGT was considered quartile 4 at each measurement. Participants who had GGT levels in quartile 4 in all four examinations received 4 GGT points; however, participants who had all GGT levels in quartiles 1-3 in the four examinations received 0 GGT points (Figure 1).

Outcomes

We evaluated the incidence of digestive cancers using the claim records of the NHIS during the follow-up period. The primary outcome was newly developed cancer in the gastrointestinal and hepatobiliary pancreas. Cancer was defined based on both the registration codes for serious diseases and the following ICD-10 codes: C15 (esophageal); C16 (stomach); C18-20 (colorectal); C22.0, 22.2, 22.3, 22.4, 22.7, and 22.9 (liver); C22.1, C23, and C24 (gallbladder and biliary tract); and C25 (pancreatic). Codes for reimbursement for serious diseases were also reviewed to reduce the error in studies with claims data; that is, both codes were required for the identification of cancer patients[19].

"Total digestive cancers" included both "gastrointestinal cancers" and "hepatobiliary pancreatic cancers". "Gastrointestinal cancers" included esophageal, stomach, and colorectal cancers. "Hepatobiliary pancreatic cancers" included liver, biliary (gallbladder and biliary tract), and pancreatic cancers.

Statistical analysis

Categorical variables were expressed as numbers and percentages, and continuous variables were expressed as means ± SD. For non-normally distributed variables, log transformation was performed, and geometric means were calculated. Group comparisons were performed using chi-squared tests for categorical variables and one-way analysis of variance for continuous variables.

The incidence rate of cancers was calculated as the number of events divided by the summation of person-years (per 1000). Multivariable Cox proportional hazards regression models were used to adjust covariates, and adjusted hazard ratios (aHRs) and 95% confidence intervals (CIs) were presented. We also performed subgroup analyses according to the age, smoking status, alcohol consumption status, BMI, liver cirrhosis or hepatitis to evaluate whether there were effect modifications of the impact of GGT on cancer incidence in each subgroup.

Statistical analyses were performed using SAS version 9.3 (SAS Institute Inc., Cary, NC, United States) and R version 3.2.3 (The R Foundation for Statistical Computing, Vienna, Austria). A two-sided *P* value less than 0.05 was considered statistically significant.

RESULTS

The flowchart of the study enrolment is presented in Supplementary Figure 1. Among the total 3559109 included participants, 2569773 were men, and 989336 were women. More than half of both men (62.1%) and women (57.3%) had 0 GGT points. In other words, 37.9% of men and 42.7% of women had a high GGT level in at least one of the four time evaluations. In total, 10.1% of men and 15.5% of women had one point, 6.9% of men and 8.4% of women had 2 points, 7.1% of men and 7.1% of women had 3 points, and 13.8% of men and 11.7% of women had 4 points. Older age, current smoking, heavy drinking, hypertension, dyslipidemia, diabetes, high BMI, high waist circumference, elevated levels of fasting glucose, total cholesterol, triglycerides, AST, ALT and low physical activity were associated with increased GGT points in both men and women (P for trend < 0.001 for all; Table 1). The median follow-up duration was 6.8 years (5.3-7.4 years, mean 6.3 years). The univariate and multivariate analyses of the incidence of total digestive cancers, gastrointestinal cancers (esophageal, stomach and colorectal) and hepatobiliary pancreatic cancers according to the GGT points are presented in Table 2. The incidence of total digestive cancers increased as the GGT points increased. In men, the incidence of total digestive cancers increased in a dose-responsive manner as the GGT points increased compared with those who had 0 GGT points (aHR = 1.28, 95%CI = 1.24-1.33 in those with 1 GGT point; aHR = 1.40, 95%CI = 1.35-1.46 in those with 2 points; aHR = 1.52, 95%CI = 1.46-1.58 in those with 3 points; aHR = 1.88, 95%CI = 1.83-1.94 in those with 4 points; P for trend < 0.001). In women, this trend was similar, although the effect sizes were smaller than those in men (aHR = 0.99 and 95%CI = 0.93-1.06 in participants with 1 GGT point; aHR = 1.02 and 95%CI = 0.94-1.11 in those with 2 points; aHR = 1.11 and 95%CI = 1.02-1.21 in those with 3 points; aHR = 1.27 and 95%CI = 1.19-1.36 in those with 4 points; P for trend < 0.001).

This increasing trend according to the GGT points was consistent for each digestive cancer, including esophageal, stomach, colorectal, liver, pancreatic, and biliary cancers (Table 3 and Figure 2). In particular, this trend was the most prominent for liver cancer (6.89 times the increased risk), followed by esophageal cancer (3.07 times increased risk) in the 4-GGT-point group compared with the 0-point group in men. Similarly, the risk for liver cancers was mostly increased in women (aHR = 3.91 and 95%CI = 3.25-4.71 in those with 4 GGT points *vs* 0 points). However, no significant association was found between each type of gastrointestinal cancer and GGT points in women.

We performed subgroup analyses (Figure 3 and Supplementary Table 1). In men, the increasing trend in GGT points was consistent in all subgroups. This trend was most evident in those with healthy lifestyles (P for interaction < 0.001 among non-smokers; P for interaction < 0.001 among non-drinkers; P for interaction < 0.001 in the non-obese group) and those with hepatitis or liver cirrhosis (P for interaction < 0.001). There was no effect modification, with only one exception in the association of GGT points and cancer incidence among women. Only the presence of hepatitis or liver cirrhosis showed a significant interaction with the association between GGT points and liver cancer and stomach cancer incidence (aHR = 11.81, 95%CI = 6.95-20.07, P for interaction < 0.001; aHR = 1.94, 95%CI = 0.96-3.93, P for interaction = 0.043).

DISCUSSION

This large-scale population-based study showed that repeatedly elevated GGT levels (meeting the criteria of quartile 4) on four consecutive examinations over three years were associated with an increased incidence of digestive cancers, including esophageal, stomach, colorectal, liver, biliary and pancreatic cancers, during a median 6.8-year follow-up period. The higher was the number of GGT points, the higher was the risk of each cancer in a dose-response manner. The risk of liver cancer mostly increased as the GGT points increased. This trend was more prominent in men than in women and those with healthy habits (no smoking, no alcohol consumption, and a low BMI) than in those with unhealthy habits.

Several previous studies have shown an association between the GGT levels and incident digestive cancer. The Swedish Amoris cohort study showed the association between baseline GGT levels and the incidence of cancer, including liver cancer[20]. The Ohsaki cohort study in Japan showed the association of GGT levels and colorectal cancer incidence[21]. A meta-analysis including 1.7 million participants reported pooled relative risks of 1.32 (1.15-1.52) for overall cancers and 1.94 (1.35-2.79) for digestive cancers in the highest quartile *vs* the bottom third of baseline GGT levels[10]. However, these studies used a single measurement of GGT to investigate the relationship

Table 1 Baseline characteristics according to the γ-glutamyltransferase points

	Total	GGT points[1]				
		0	1	2	3	4
Men	2569773	1595879	260084	177029	181702	355079
Age, yr	42.41 ± 10.53	41.64 ± 10.84	43.19 ± 10.47	43.31 ± 10.13	43.64 ± 9.82	44.19 ± 9.29
Smoking						
Non-smoker	720342 (28.03)	511103 (32.03)	65347 (25.13)	39900 (22.54)	37994 (20.91)	65998 (18.59)
Ex-smoker	662215 (25.77)	410064 (25.7)	70316 (27.04)	47571 (26.87)	47955 (26.39)	86309 (24.31)
Current	1187216 (46.2)	674712 (42.28)	124421 (47.84)	89558 (50.59)	95753 (52.7)	202772 (57.11)
Alcohol consumption						
No	720354 (28.03)	540201 (33.85)	64798 (24.91)	36701 (20.73)	32092 (17.66)	46562 (13.11)
Mild	1583612 (61.62)	952992 (59.72)	165116 (63.49)	114805 (64.85)	118787 (65.37)	231912 (65.31)
Heavy	265807 (10.34)	102686 (6.43)	30170 (11.6)	25523 (14.42)	30823 (16.96)	76605 (21.57)
Lowest quartile of yearly income (Q1)	399370 (15.54)	244182 (15.3)	42615 (16.39)	28596 (16.15)	28873 (15.89)	55104 (15.52)
Regular PA	790381 (30.76)	496084 (31.09)	80897 (31.1)	54551 (30.81)	55753 (30.68)	103096 (29.03)
BMI (kg/m^2)	24.19 ± 3.01	23.55 ± 2.79	24.71 ± 2.91	25.1 ± 2.98	25.34 ± 3.03	25.64 ± 3.13
WC (cm)	83.14 ± 7.56	81.48 ± 7.16	84.46 ± 7.22	85.43 ± 7.25	86.08 ± 7.33	86.96 ± 7.45
SBP (mmHg)	123.78 ± 12.99	122 ± 12.45	124.88 ± 12.85	125.93 ± 13.02	126.8 ± 13.23	128.37 ± 13.68
DBP (mmHg)	77.98 ± 9.17	76.71 ± 8.79	78.75 ± 9.07	79.51 ± 9.16	80.19 ± 9.32	81.27 ± 9.6
Hypertension	543619 (21.15)	249986 (15.66)	63584 (24.45)	48861 (27.6)	55827 (30.72)	125361 (35.31)
Dyslipidemia	394282 (15.34)	169026 (10.59)	47739 (18.36)	37512 (21.19)	42552 (23.42)	97453 (27.45)
Diabetes						
No	1747553 (68)	1178083 (73.82)	168406 (64.75)	108469 (61.27)	105608 (58.12)	186987 (52.66)
IFG	633865 (24.67)	343650 (21.53)	69127 (26.58)	50151 (28.33)	54139 (29.8)	116798 (32.89)
DM	188355 (7.33)	74146 (4.65)	22551 (8.67)	18409 (10.4)	21955 (12.08)	51294 (14.45)
Fasting glucose (mg/dL)	97.2 ± 22.15	94.38 ± 18.25	98.47 ± 22.98	100.13 ± 24.85	101.84 ± 26.59	105.13 ± 29.72
Total cholesterol (mg/dL)	195.09 ± 34.85	190.25 ± 32.83	198.57 ± 34.96	201.16 ± 35.5	202.95 ± 36.32	207.29 ± 37.85
LDL (mg/dL)	112.94 ± 32.32	112.28 ± 30.41	114.88 ± 33.13	114.76 ± 34.14	114.17 ± 35.16	112.95 ± 37.16
HDL (mg/dL)	52.16 ± 13.63	52.38 ± 13.38	51.6 ± 13.93	51.57 ± 14.01	51.58 ± 13.9	52.18 ± 14.14
Triglyceride (mg/dL)[2]	129.81 (129.72-129.9)	112.69 (112.6-112.78)	141.48 (141.19-141.77)	154 (153.61-154.38)	164.57 (164.16-164.98)	187.2 (186.86-187.54)
AST (IU/L)[2]	25.9 (25.89-25.91)	23.64 (23.63-23.65)	27.11 (27.08-27.15)	28.47 (28.43-28.51)	29.84 (29.79-29.89)	33.52 (33.47-33.56)
ALT (IU/L)[2]	26.41 (26.4-26.43)	22.44 (22.43-22.46)	29.54 (29.49-29.6)	32.15 (32.07-32.22)	34.42 (34.34-34.51)	40.07 (40-40.14)
GGT (U/L)[2]	36.3 (36.28-36.33)	24.79 (24.78-24.81)	43.21 (43.14-43.27)	53.64 (53.54-53.73)	66.15 (66.02-66.28)	107.44 (107.26-107.61)
Women	989336	566518	153299	83247	70183	116089
Age, yr	41.61 ± 11.55	39.36 ± 11.04	42.51 ± 11.54	44.13 ± 11.57	45.34 ± 11.47	47.33 ± 10.9
Smoking						
Non-smoker	950040 (96.03)	547422 (96.63)	147238 (96.05)	79376 (95.35)	66593 (94.88)	109411 (94.25)
Ex-smoker	16273 (1.64)	8976 (1.58)	2493 (1.63)	1454 (1.75)	1294 (1.84)	2056 (1.77)
Current	23023 (2.33)	10120 (1.79)	3568 (2.33)	2417 (2.9)	2296 (3.27)	4622 (3.98)
Alcohol consumption						

	No	661884 (66.9)	383621 (67.72)	103332 (67.41)	55147 (66.25)	45838 (65.31)	73946 (63.7)
	Mild	318233 (32.17)	179199 (31.63)	48446 (31.6)	26984 (32.41)	23345 (33.26)	40259 (34.68)
	Heavy	9219 (0.93)	3698 (0.65)	1521 (0.99)	1116 (1.34)	1000 (1.42)	1884 (1.62)
Lowest quartile of yearly income (Q1)		365612 (36.96)	181102 (31.97)	61625 (40.2)	35775 (42.97)	31499 (44.88)	55611 (47.9)
Regular PA		270758 (27.37)	155736 (27.49)	42388 (27.65)	22839 (27.44)	18923 (26.96)	30872 (26.59)
BMI (kg/m^2)		22.45 ± 3.22	21.79 ± 2.82	22.56 ± 3.15	23.14 ± 3.39	23.64 ± 3.53	24.36 ± 3.71
WC (cm)		73.52 ± 8.28	71.77 ± 7.42	73.86 ± 8.07	75.36 ± 8.49	76.6 ± 8.78	78.47 ± 9.09
SBP (mmHg)		116.17 ± 13.59	114.11 ± 12.72	116.63 ± 13.55	118.33 ± 14.04	119.76 ± 14.23	121.91 ± 14.56
DBP (mmHg)		72.92 ± 9.26	71.68 ± 8.83	73.17 ± 9.25	74.2 ± 9.46	75.08 ± 9.54	76.39 ± 9.73
Hypertension		130992 (13.24)	45016 (7.95)	21361 (13.93)	15255 (18.32)	15700 (22.37)	33660 (28.99)
Dyslipidemia		128796 (13.02)	45810 (8.09)	21112 (13.77)	14928 (17.93)	15084 (21.49)	31862 (27.45)
Diabetes							
	No	805990 (81.47)	489351 (86.38)	124149 (80.98)	64211 (77.13)	51316 (73.12)	76963 (66.3)
	IFG	148818 (15.04)	68823 (12.15)	24264 (15.83)	15071 (18.1)	14042 (20.01)	26618 (22.93)
	DM	34528 (3.49)	8344 (1.47)	4886 (3.19)	3965 (4.76)	4825 (6.87)	12508 (10.77)
Fasting glucose (mg/dL)		91.41 ± 16.31	89.21 ± 12.41	91.39 ± 15.32	93.13 ± 17.79	94.99 ± 20.38	98.8 ± 25.3
Total cholesterol (mg/dL)		190.33 ± 34.94	185.48 ± 32.85	191.82 ± 35.03	195.68 ± 35.98	198.31 ± 36.74	203.37 ± 37.76
LDL (mg/dL)		110.02 ± 31.3	106.75 ± 29.16	111.38 ± 31.72	113.91 ± 33.05	115.34 ± 33.97	118.18 ± 35.21
HDL (mg/dL)		60.82 ± 15.16	61.63 ± 14.7	60.57 ± 15.3	59.93 ± 15.73	59.3 ± 15.65	58.74 ± 16.1
Triglyceride (mg/dL)[2]		85.34 (85.25-85.42)	76.5 (76.4-76.59)	87.69 (87.47-87.91)	95.8 (95.47-96.13)	103.29 (102.89-103.69)	115.13 (114.78-115.49)
AST (IU/L)[2]		21.38 (21.36-21.39)	20.06 (20.05-20.08)	21.64 (21.61-21.67)	22.58 (22.54-22.63)	23.6 (23.55-23.66)	25.95 (25.89-26)
ALT (IU/L)[2]		16.82 (16.81-16.84)	14.74 (14.73-14.76)	17.38 (17.34-17.41)	19.11 (19.05-19.17)	20.85 (20.78-20.92)	24.6 (24.53-24.67)
GGT (U/L)[2]		17.53 (17.51-17.54)	13.52 (13.51-13.53)	18.15 (18.12-18.18)	21.94 (21.89-21.99)	26.28 (26.21-26.35)	39.57 (39.46-39.69)

[1]Participants receive 1 point at each examination if γ-glutamyltransferase (GGT) is in the highest quartile at each examination. GGT points were calculated as the sum of points at 4 consecutive examinations.

[2]Geometric mean. Categorical variables are expressed as numbers (%); continuous variables are expressed means ± SD. PA: Physical activity; BMI: Body mass index; WC: Waist circumference; SBP: Systolic blood pressure; DBP: Diastolic blood pressure; IFG: Impaired fasting glucose; DM: Diabetes mellitus; LDL: Low-density lipoprotein; HDL: High-density lipoprotein; AST: Aspartate aminotransferase; ALT: Alanine aminotransferase; GGT: Gamma-glutamyltransferase.

between GGT and the risk of digestive cancers. A single measurement of GGT has limitations, as described above in the introduction. Our study showed that repeated measurements have the benefit of mitigating the limitations of a single measurement of GGT in the screening of those at risk of cancer. In the current study, 37.9% of men and 42.7% of women had a high GGT level in at least one of four measurements. Among them, 27% of men (10.1% of men in total) and 36% of women (15.5% of women in total) had a high GGT level only once. Thus, most of them would have been classified into a low-level GGT group if they had undergone a single measurement during that period. Additionally, participants who had 2 or more GGT points had a higher risk of incident digestive cancer than those with 1 GGT point who had a high GGT level only once. A dose-response relationship was found between the GGT points and risk of incident digestive cancer. Those with 1 GGT point did not show a higher risk of cancer than those with 0 GGT points, but those with higher GGT points showed a higher risk of cancer than those with 0 GGT points for several cancers. (*e.g.*, biliary and pancreatic cancers in women, as shown in Table 3). In one study, the GGT levels were measured several times; however, the main outcome was the association between only the baseline GGT and site-specific cancers, and the changing status of GGT was not fully evaluated. Moreover, alcohol consumption, which is the most important confounder, was not adjusted[22,23] In the current study, we adjusted for various major

Table 2 Incidence of all digestive cancers, gastrointestinal cancers (including esophagus, stomach and colorectal cancers), and hepatobiliary pancreatic cancers (including liver, biliary tract and pancreas) according to the γ-glutamyltransferase points

GGT points	Number	Event	Duration	IR per 1000	Age-adjusted	Model 1	Model 2	Model 3
					IR (95%CI)	HR (95%CI)	HR (95%CI)	HR (95%CI)
Men								
Total digestive cancer								
0	1595879	17789	10257993.68	1.734	3.20 (3.14, 3.26)	1 (reference)	1 (reference)	1 (reference)
1	260084	4058	1667865.93	2.433	4.19 (3.88, 4.52)	1.40 (1.36, 1.45)	1.30 (1.26, 1.34)	1.28 (1.24, 1.33)
2	177029	2982	1133122.25	2.632	4.70 (4.25, 5.19)	1.52 (1.46, 1.58)	1.43 (1.38, 1.49)	1.40 (1.35, 1.46)
3	181702	3341	1161757.06	2.876	5.06 (4.63, 5.53)	1.66 (1.60, 1.72)	1.57 (1.51, 1.62)	1.52 (1.46, 1.58)
4	355079	8106	2250566.91	3.602	6.36 (6.14, 6.59)	2.08 (2.03, 2.13)	1.96 (1.91, 2.01)	1.88 (1.83, 1.94)
P for trend						< 0.001	< 0.001	< 0.001
Gastrointestinal cancer								
0	1595879	14709	10263671.88	1.433	2.64 (2.59, 2.69)	1 (reference)	1 (reference)	1 (reference)
1	260084	3023	1669790.42	1.810	3.11 (2.87, 3.37)	1.26 (1.22, 1.31)	1.17 (1.12, 1.22)	1.12 (1.08, 1.17)
2	177029	2169	1134702.18	1.912	3.39 (3.03, 3.78)	1.33 (1.28, 1.40)	1.26 (1.20, 1.32)	1.18 (1.13, 1.24)
3	181702	2372	1163597.98	2.039	3.55 (3.21, 3.93)	1.42 (1.36, 1.49)	1.34 (1.28, 1.40)	1.24 (1.19, 1.30)
4	355079	5075	2256426.45	2.249	3.94 (3.76, 4.12)	1.57 (1.52, 1.62)	1.48 (1.43, 1.53)	1.34 (1.29, 1.39)
P for trend						< 0.001	< 0.001	< 0.001
Hepatobiliary pancreatic cancer								
0	1595879	5616	10294767.52	0.546	1.01 (0.98, 1.03)	1 (reference)	1 (reference)	1 (reference)
1	260084	1584	1675373.07	0.945	1.62 (1.49, 1.76)	1.73 (1.64, 1.83)	1.60 (1.52, 1.70)	1.65 (1.56, 1.75)
2	177029	1217	1138317.76	1.069	1.92 (1.73, 2.13)	1.96 (1.84, 2.09)	1.86 (1.75, 1.98)	1.93 (1.82, 2.06)
3	181702	1399	1167524.64	1.198	2.13 (1.95, 2.34)	2.20 (2.07, 2.33)	2.08 (1.96, 2.21)	2.18 (2.05, 2.32)
4	355079	4109	2262184.82	1.816	3.22 (3.13, 3.32)	3.34 (3.20, 3.47)	3.16 (3.04, 3.29)	3.35 (3.21, 3.50)
P for trend						< 0.001	< 0.001	< 0.001
Women								
Total digestive cancer								
0	566518	3367	3558510.54	0.946	1.81 (1.77, 1.85)	1 (reference)	1 (reference)	1 (reference)
1	153299	1124	959235.81	1.172	1.75 (1.65, 1.86)	1.24 (1.16, 1.33)	1.00 (0.93, 1.07)	0.99 (0.93, 1.06)
2	83247	694	519023.27	1.337	1.80 (1.63, 1.98)	1.42 (1.30, 1.54)	1.03 (0.95, 1.12)	1.02 (0.94, 1.11)
3	70183	682	435747.09	1.565	1.95 (1.78, 2.15)	1.66 (1.53, 1.80)	1.12 (1.03, 1.22)	1.11 (1.02, 1.21)
4	116089	1431	714960.09	2.002	2.25 (2.15, 2.35)	2.12 (1.99, 2.26)	1.30 (1.22, 1.38)	1.27 (1.19, 1.36)
P for trend						< 0.001	< 0.001	< 0.001
Gastrointestinal cancer								
0	566518	2891	3559398.08	0.812	1.55 (1.51, 1.59)	1 (reference)	1 (reference)	1 (reference)
1	153299	913	959636.19	0.951	1.43 (1.33, 1.53)	1.17 (1.09, 1.26)	0.95 (0.88, 1.03)	0.95 (0.88, 1.02)
2	83247	548	519282.68	1.055	1.44 (1.28, 1.61)	1.30 (1.19, 1.43)	0.96 (0.88, 1.05)	0.95 (0.87, 1.04)
3	70183	526	436048.99	1.206	1.51 (1.34, 1.69)	1.49 (1.36, 1.63)	1.03 (0.93, 1.13)	1.01 (0.92, 1.11)
4	116089	1006	715795.75	1.405	1.58 (1.49, 1.68)	1.74 (1.62, 1.86)	1.08 (1.01, 1.17)	1.06 (0.98, 1.14)
P for trend						< 0.001	0.052	0.232
Hepatobiliary pancreatic cancer								
0	566518	884	3565741.17	0.248	0.47 (0.45,0.49)	1 (reference)	1 (reference)	1 (reference)

1	153299	337	961504.59	0.350	0.53 (0.48, 0.57)	1.42 (1.25, 1.60)	1.11 (0.98, 1.25)	1.10 (0.97, 1.25)
2	83247	238	520353.15	0.457	0.58 (0.52, 0.66)	1.85 (1.60, 2.13)	1.29 (1.12, 1.49)	1.29 (1.11, 1.49)
3	70183	241	437047.77	0.551	0.69 (0.62, 0.77)	2.23 (1.94, 2.57)	1.44 (1.25, 1.66)	1.43 (1.23, 1.65)
4	116089	608	717322.51	0.848	0.95 (0.91, 0.99)	3.44 (3.10, 3.81)	1.98 (1.78, 2.20)	1.95 (1.74, 2.18)
P for trend						< 0.001	< 0.001	< 0.001

Model 1: Unadjusted model. Model 2: Age-adjusted model. Model 3: Age, smoking, drinking, income, hypertension, diabetes, dyslipidemia, body mass index, and physical activity-adjusted model. IR: Incidence rate; HR: Hazard ratio; CI: confidence interval; GGT: Gamma-glutamyltransferase.

confounders, including alcohol consumption and physical activity, in a nationwide, population-based, large-scale study.

The underlying biological mechanisms of the effect of repeatedly elevated levels of GGT and cancer incidence cannot be fully explained considering the epidemiologic study design of this study. GGT is a marker of oxidative stress[24]. The involvement of the pro-oxidant activity of GGT can serve as an additional source of endogenous reactive oxygen species in cancer cells. This activity can contribute to persistent oxidative stress, modulate important redox-sensitive processes, affect the proliferation and apoptosis of cells, and cause genomic instability and carcinogenesis[25,26]. This mechanism might explain the possible role of GGT in cancer incidence.

The association between GGT and total digestive cancer incidence was more prominent in men than in women, and the association between GGT and gastrointestinal cancers was present in only men. The cause might be the higher level of GGT in men than in women, as presented in other studies[9,20,21,27]. The GGT levels were lower in women than in men (mean 17.5 *vs* 36.3) in this study; thus, the relative effect sizes were smaller in women than in men. Another plausible explanation is that a sex effect modification may exist regarding the association between GGT and cancer incidence. The sex-related variability of the effect of GGT on cancer incidence may be due to sex-specific genetic variations or mutations or sex-specific responses to exposed carcinogens or environmental factors[27,28].

Another interesting finding is that GGT points had a greater association with incident digestive cancer in the subgroup with a healthy lifestyle (no smoking, no alcohol consumption, no obesity) than in the subgroup with an unhealthy lifestyle, although the difference in each site-specific cancer should be considered. The risk of cancer was the highest in liver cancer, followed by esophageal cancer according to the GGT points in men. Because these two cancers are well-known alcohol-associated cancers, some may hypothesize that the association between GGT points and cancer may be attributable to residual confounding by alcohol intake. A previous study in Japan showed a positive association between GGT and alcohol-related cancers among only current drinkers[21]. However, another study conversely showed an association between baseline GGT and cancer incidence regardless of the drinking and smoking status[9]. Our study found similar results to the latter and even showed a highly prominent association between GGT and cancer in the never smoker and no drinking groups. The exact underlying mechanism of this phenomenon is unknown. However, one possible explanation is that the effect of GGT points on cancer incidence might have been weakened by other well-known cancer risk factors in participants with unhealthy habits. This result suggests that elevated GGT, which can be detected using an inexpensive and simple test is a risk factor in those without other commonly known cancer risk factors, such as smoking, alcohol or obesity. Additional attention should be given to patients with repeatedly elevated GGT levels on serial examinations, particularly those who are not smokers, heavy alcohol consumers or obese.

CONCLUSION

Our nationwide population-based study showed an association between repeatedly elevated GGT and the incidence of digestive cancers in a dose-response manner, even after adjustment for major confounders, including alcohol consumption. A single measurement of serum GGT is an easy and inexpensive test but has limitations; thus, repeated measurements could provide more useful information in the health screening setting. The repeated measurement of GGT may be a good biomarker for predicting cancer incidence and could help physicians identify those at high-risk for digestive

Table 3 Incidence of site-specific digestive cancers according to the γ-glutamyltransferase points based on four consecutive examinations

	Esophagus		Stomach		Colorectal		Liver		Biliary		Pancreas	
	IR per 1000	HR (95%CI)	IR per 1000	HR (95%CI)	IR per 1000	HR (95%CI)	IR per 1000	HR (95%CI)	IR per 1000	HR (95%CI)	IR per 1000	HR (95%CI)
Men												
0	0.037	1 (reference)	0.772	1 (reference)	0.757	1 (reference)	0.215	1 (reference)	0.126	1 (reference)	0.293	1 (reference)
1	0.073	1.78 (1.45, 2.18)	0.968	1.12 (1.06, 1.19)	0.938	1.09 (1.03, 1.15)	0.505	2.39 (2.21, 2.59)	0.203	1.46 (1.29, 1.64)	0.389	1.18 (1.08, 1.28)
2	0.082	1.99 (1.58, 2.51)	1.011	1.18 (1.10, 1.25)	0.984	1.14 (1.07, 1.21)	0.624	3.13 (2.87, 3.41)	0.203	1.49 (1.30, 1.72)	0.392	1.19 (1.08, 1.32)
3	0.103	2.43 (1.97, 3.00)	1.063	1.22 (1.15, 1.29)	1.051	1.19 (1.12, 1.27)	0.727	3.74 (3.45, 4.06)	0.203	1.49 (1.30, 1.72)	0.425	1.27 (1.15, 1.40)
4	0.134	3.07 (2.61, 3.62)	1.127	1.26 (1.21, 1.33)	1.209	1.34 (1.28, 1.40)	1.293	6.89 (6.49, 7.32)	0.257	1.91 (1.72, 2.12)	0.501	1.48 (1.37, 1.59)
Women												
0	0.005	1 (reference)	0.319	1 (reference)	0.534	1 (reference)	0.067	1 (reference)	0.065	1 (reference)	0.150	1 (reference)
1	0.007	1.00 (0.42, 2.39)	0.345	0.87 (0.77, 0.99)	0.651	0.99 (0.90, 1.08)	0.114	1.41 (1.12, 1.77)	0.102	1.12 (0.88, 1.42)	0.186	0.97 (0.81, 1.14)
2	0.008	0.92 (0.31, 2.74)	0.390	0.89 (0.77, 1.04)	0.720	0.99 (0.89, 1.11)	0.150	1.70 (1.32, 2.20)	0.138	1.30 (0.99, 1.70)	0.238	1.10 (0.90, 1.34)
3	0.009	1.01 (0.34, 3.02)	0.462	0.98 (0.84, 1.14)	0.804	1.03 (0.92, 1.16)	0.199	2.14 (1.66, 2.74)	0.162	1.36 (1.03, 1.78)	0.279	1.18 (0.96, 1.44)
4	0.014	1.38 (0.61, 3.12)	0.542	1.04 (0.92, 1.17)	0.924	1.06 (0.97, 1.17)	0.396	3.91 (3.25, 4.71)	0.203	1.45 (1.16, 1.80)	0.354	1.32 (1.13, 1.55)

Multivariate analysis was adjusted for age, smoking, drinking, income, hypertension, diabetes, dyslipidemia, body mass index and physical activity. IR: Incidence rate; HR: Hazard ratio; CI: Confidence interval.

cancers, even in those with healthy habits.

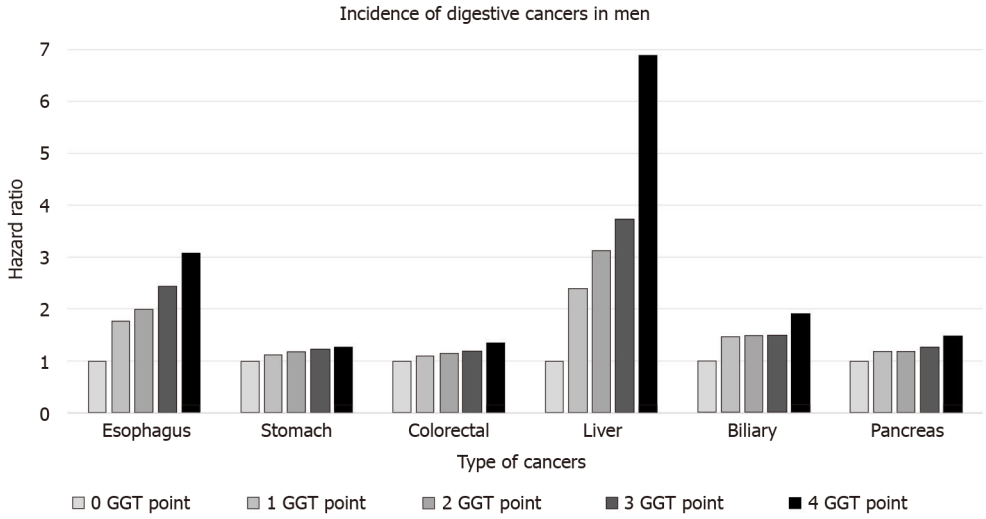


Figure 2 Incidence of site-specific digestive cancers according to the γ-glutamyltransferase points based on four consecutive examinations in men. GGT: Gamma-glutamyltransferase.

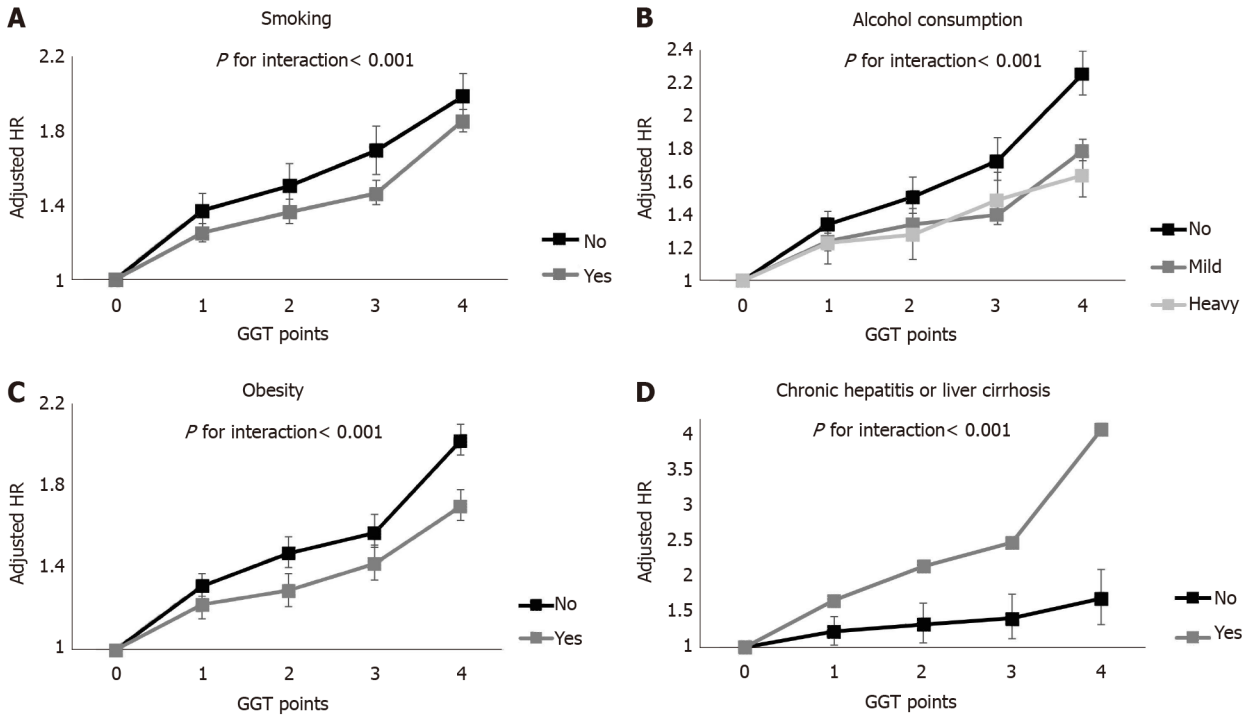


Figure 3 Subgroup analysis of the association of γ-glutamyltransferase points and the total digestive cancer incidence. A: Smoking (no smoking *vs* ever smoking); B: Alcohol consumption; C: Obesity (body mass index ≥ 25); D: Chronic hepatitis or liver cirrhosis in men. GGT: Gamma-glutamyltransferase; HR: hazard ratio.

ARTICLE HIGHLIGHTS

Research background

The association between elevated γ-glutamyltransferase (GGT) at a certain point and incident cancer has been suggested; however, no study has studied the association between repeatedly elevated GGT and cancer incidence.

Research motivation

GGT levels are not fixed but dynamic, and many factors affect the level of GGT. Therefore, a single measurement of GGT does not fully reflect the current status of GGT, limiting the understanding of the actual relationship between GGT and diseases. We hypothesized that multiple measurements of GGT over several years could

mitigate the limitations of a single measurement.

Research objectives

To elucidate whether repeatedly elevated GGT levels, which are commonly practiced in routine health examinations, can be used as a biomarker of subsequent incidence of digestive cancer.

Research methods

A population-based longitudinal cohort study was conducted with the participants who had undergone health screening from 2009 to 2012 and 4 consecutive previous examinations. GGT points were calculated as the number of times participants met the criteria of quartile 4 of GGT in four serial measurements (0-4 points). Multivariable Cox proportional hazard regression models were applied.

Research results

Among 3559109 participants, 43574 digestive cancers developed during a median of 6.8 years of follow-up. The incidence of total digestive cancers increased according to GGT points in a dose-response manner in men [adjusted hazard ratio (aHR) compared with those with 0 GGT points = 1.28 and 95% confidence interval (CI) = 1.24-1.33 in those with 1 point; aHR = 1.40 and 95%CI = 1.35-1.46 in those with 2 points; aHR = 1.52 and 95%CI = 1.46-1.58 in those with 3 points; aHR = 1.88 and 95%CI = 1.83-1.94 in those with 4 points; P for trend < 0.001]. This trend was more prominent in men than in women and those with healthy habits (no smoking, no alcohol consumption, and a low body mass index) than in those with unhealthy habits.

Research conclusions

Repeatedly elevated GGT levels were associated with an increased risk of incident digestive cancer in a dose-responsive manner, particularly in men and those with healthy habits.

Research perspectives

Repeated GGT measurements may be a good biomarker of incident digestive cancer and could help physicians identify high-risk populations.

REFERENCES

1 **Whitfield JB**. Gamma glutamyl transferase. *Crit Rev Clin Lab Sci* 2001; **38**: 263-355 [PMID: 11563810 DOI: 10.1080/20014091084227]

2 **Smith GS**, Walter GL, Walker RM. Haschek and Rousseaux's Handbook of Toxicologic Pathology. 3rd ed. Academic Press; 2013: 565-594

3 **Teschke R**, Rauen J, Neuefeind M, Petrides AS, Strohmeyer G. Alcoholic liver disease associated with increased gamma-glutamyltransferase activities in serum and liver. *Adv Exp Med Biol* 1980; **132**: 647-654 [PMID: 6106999 DOI: 10.1007/978-1-4757-1419-7_67]

4 **Lee DH**, Jacobs DR Jr, Gross M, Kiefe CI, Roseman J, Lewis CE, Steffes M. Gamma-glutamyltransferase is a predictor of incident diabetes and hypertension: the Coronary Artery Risk Development in Young Adults (CARDIA) Study. *Clin Chem* 2003; **49**: 1358-1366 [PMID: 12881453 DOI: 10.1373/49.8.1358]

5 **Lee MY**, Hyon DS, Huh JH, Kim HK, Han SK, Kim JY, Koh SB. Association between Serum Gamma-Glutamyltransferase and Prevalence of Metabolic Syndrome Using Data from the Korean Genome and Epidemiology Study. *Endocrinol Metab (Seoul)* 2019; **34**: 390-397 [PMID: 31884739 DOI: 10.3803/EnM.2019.34.4.390]

6 **Ryu S**, Chang Y, Kim DI, Kim WS, Suh BS. gamma-Glutamyltransferase as a predictor of chronic kidney disease in nonhypertensive and nondiabetic Korean men. *Clin Chem* 2007; **53**: 71-77 [PMID: 17110470 DOI: 10.1373/clinchem.2006.078980]

7 **Wannamethee G**, Ebrahim S, Shaper AG. Gamma-glutamyltransferase: determinants and association with mortality from ischemic heart disease and all causes. *Am J Epidemiol* 1995; **142**: 699-708 [PMID: 7572939 DOI: 10.1093/oxfordjournals.aje.a117699]

8 **Choi YJ**, Lee DH, Han KD, Yoon H, Shin CM, Park YS, Kim N. Elevated serum gamma-glutamyltransferase is associated with an increased risk of oesophageal carcinoma in a cohort of 8,388,256 Korean subjects. *PLoS One* 2017; **12**: e0177053 [PMID: 28475598 DOI: 10.1371/journal.pone.0177053]

9 **Mok Y**, Son DK, Yun YD, Jee SH, Samet JM. γ-Glutamyltransferase and cancer risk: The Korean cancer prevention study. *Int J Cancer* 2016; **138**: 311-319 [PMID: 26111622 DOI: 10.1002/ijc.29659]

10 **Kunutsor SK**, Apekey TA, Van Hemelrijck M, Calori G, Perseghin G. Gamma glutamyltransferase,

alanine aminotransferase and risk of cancer: systematic review and meta-analysis. *Int J Cancer* 2015; **136**: 1162-1170 [PMID: 25043373 DOI: 10.1002/ijc.29084]

11 **Carobene A**, Braga F, Roraas T, Sandberg S, Bartlett WA. A systematic review of data on biological variation for alanine aminotransferase, aspartate aminotransferase and γ-glutamyl transferase. *Clin Chem Lab Med* 2013; **51**: 1997-2007 [PMID: 24072574 DOI: 10.1515/cclm-2013-0096]

12 **André P**, Balkau B, Born C, Charles MA, Eschwège E; D. E.S.I.R. study group. Three-year increase of gamma-glutamyltransferase level and development of type 2 diabetes in middle-aged men and women: the D.E.S.I.R. cohort. *Diabetologia* 2006; **49**: 2599-2603 [PMID: 16969645 DOI: 10.1007/s00125-006-0418-x]

13 **Hong SH**, Han K, Park S, Kim SM, Kim NH, Choi KM, Baik SH, Park YG, Yoo HJ. Gamma-Glutamyl Transferase Variability and Risk of Dementia in Diabetes Mellitus: A Nationwide Population-Based Study. *J Clin Endocrinol Metab* 2020; **105** [PMID: 31955208 DOI: 10.1210/clinem/dgaa019]

14 **Strasak AM**, Kelleher CC, Klenk J, Brant LJ, Ruttmann E, Rapp K, Concin H, Diem G, Pfeiffer KP, Ulmer H; Vorarlberg Health Monitoring and Promotion Program Study Group. Longitudinal change in serum gamma-glutamyltransferase and cardiovascular disease mortality: a prospective population-based study in 76,113 Austrian adults. *Arterioscler Thromb Vasc Biol* 2008; **28**: 1857-1865 [PMID: 18617645 DOI: 10.1161/ATVBAHA.108.170597]

15 **Tynjälä J**, Kangastupa P, Laatikainen T, Aalto M, Niemelä O. Effect of age and gender on the relationship between alcohol consumption and serum GGT: time to recalibrate goals for normal ranges. *Alcohol Alcohol* 2012; **47**: 558-562 [PMID: 22753786 DOI: 10.1093/alcalc/ags072]

16 **Koenig G**, Seneff S. Gamma-Glutamyltransferase: A Predictive Biomarker of Cellular Antioxidant Inadequacy and Disease Risk. *Dis Markers* 2015; **2015**: 818570 [PMID: 26543300 DOI: 10.1155/2015/818570]

17 **Song SO**, Jung CH, Song YD, Park CY, Kwon HS, Cha BS, Park JY, Lee KU, Ko KS, Lee BW. Background and data configuration process of a nationwide population-based study using the korean national health insurance system. *Diabetes Metab J* 2014; **38**: 395-403 [PMID: 25349827 DOI: 10.4093/dmj.2014.38.5.395]

18 **Chalasani N**, Younossi Z, Lavine JE, Charlton M, Cusi K, Rinella M, Harrison SA, Brunt EM, Sanyal AJ. The diagnosis and management of nonalcoholic fatty liver disease: Practice guidance from the American Association for the Study of Liver Diseases. *Hepatology* 2018; **67**: 328-357 [PMID: 28714183 DOI: 10.1002/hep.29367]

19 **Choi YJ**, Lee DH, Han KD, Yoon H, Shin CM, Park YS, Kim N. Adult height in relation to risk of cancer in a cohort of 22,809,722 Korean adults. *Br J Cancer* 2019; **120**: 668-674 [PMID: 30778143 DOI: 10.1038/s41416-018-0371-8]

20 **Van Hemelrijck M**, Jassem W, Walldius G, Fentiman IS, Hammar N, Lambe M, Garmo H, Jungner I, Holmberg L. Gamma-glutamyltransferase and risk of cancer in a cohort of 545,460 persons - the Swedish AMORIS study. *Eur J Cancer* 2011; **47**: 2033-2041 [PMID: 21486691 DOI: 10.1016/j.ejca.2011.03.010]

21 **Tsuboya T**, Kuriyama S, Nagai M, Hozawa A, Sugawara Y, Tomata Y, Kakizaki M, Nishino Y, Tsuji I. Gamma-glutamyltransferase and cancer incidence: the Ohsaki cohort study. *J Epidemiol* 2012; **22**: 144-150 [PMID: 22277791 DOI: 10.2188/jea.je20110071]

22 **Strasak AM**, Rapp K, Brant LJ, Hilbe W, Gregory M, Oberaigner W, Ruttmann E, Concin H, Diem G, Pfeiffer KP, Ulmer H; VHM&PP Study Group. Association of gamma-glutamyltransferase and risk of cancer incidence in men: a prospective study. *Cancer Res* 2008; **68**: 3970-3977 [PMID: 18483283 DOI: 10.1158/0008-5472.CAN-07-6686]

23 **Strasak AM**, Pfeiffer RM, Klenk J, Hilbe W, Oberaigner W, Gregory M, Concin H, Diem G, Pfeiffer KP, Ruttmann E, Ulmer H; Vorarlberg Health Monitoring and Promotion Program Study Group. Prospective study of the association of gamma-glutamyltransferase with cancer incidence in women. *Int J Cancer* 2008; **123**: 1902-1906 [PMID: 18688855 DOI: 10.1002/ijc.23714]

24 **Lee DH**, Blomhoff R, Jacobs DR Jr. Is serum gamma glutamyltransferase a marker of oxidative stress? *Free Radic Res* 2004; **38**: 535-539 [PMID: 15346644 DOI: 10.1080/10715760410001694026]

25 **Toyokuni S**, Okamoto K, Yodoi J, Hiai H. Persistent oxidative stress in cancer. *FEBS Lett* 1995; **358**: 1-3 [PMID: 7821417 DOI: 10.1016/0014-5793(94)01368-b]

26 **Corti A**, Franzini M, Paolicchi A, Pompella A. Gamma-glutamyltransferase of cancer cells at the crossroads of tumor progression, drug resistance and drug targeting. *Anticancer Res* 2010; **30**: 1169-1181 [PMID: 20530424]

27 **Zheng D**, Trynda J, Williams C, Vold JA, Nguyen JH, Harnois DM, Bagaria SP, McLaughlin SA, Li Z. Sexual dimorphism in the incidence of human cancers. *BMC Cancer* 2019; **19**: 684 [PMID: 31299933 DOI: 10.1186/s12885-019-5902-z]

28 **Czene K**, Lichtenstein P, Hemminki K. Environmental and heritable causes of cancer among 9.6 million individuals in the Swedish Family-Cancer Database. *Int J Cancer* 2002; **99**: 260-266 [PMID: 11979442 DOI: 10.1002/ijc.10332]

World Journal of Gastroenterology

Submit a Manuscript: https://www.f6publishing.com

World J Gastroenterol 2021 January 14; 27(2): 189-207

DOI: 10.3748/wjg.v27.i2.189

ISSN 1007-9327 (print) ISSN 2219-2840 (online)

ORIGINAL ARTICLE

Retrospective Study

Development of a computed tomography-based radiomics nomogram for prediction of transarterial chemoembolization refractoriness in hepatocellular carcinoma

Xiang-Ke Niu, Xiao-Feng He

ORCID number: Xiang-Ke Niu 0000-0002-7025-7587; Xiao-Feng He 0000-0002-7426-9032.

Author contributions: He XF designed the research study; He XF and Niu XK performed the research; Niu XK analyzed the data; Niu XK and He XF wrote the paper; all authors have read and approved the final manuscript.

Supported by Health and Family Planning Commission of Sichuan Province, China, No. 17PJ430 and No. 18PJ150.

Institutional review board statement: This study was reviewed and approved by the Ethics Committee of Affiliated Hospital of Chengdu University, approval No. PJ2019-019-01.

Informed consent statement: Patients were not required to give informed consent to the study because the analysis used anonymous data that were obtained after each patient agreed to treatment by written consent.

Conflict-of-interest statement: The authors declare that there is no conflict of interest related to this study.

Xiang-Ke Niu, Xiao-Feng He, Department of Interventional Radiology, Nanfang Hospital, Southern Medical University, Guangzhou 510515, Guangdong Province, China

Xiang-Ke Niu, Department of Interventional Radiology, Affiliated Hospital of Chengdu University, Chengdu 610081, Sichuan Province, China

Corresponding author: Xiao-Feng He, MD, Chief Doctor, Professor, Department of Interventional Radiology, Nanfang Hospital, Southern Medical University, No. 1838 North Guangzhou Avenue, Guangzhou 510515, Guangdong Province, China. ozonetherapy@163.com

Abstract

BACKGROUND

Some patients with hepatocellular carcinoma (HCC) are more likely to experience disease progression despite continuous transarterial chemoembolization (TACE), which is called TACE refractoriness. At present, it is still difficult to predict TACE refractoriness, although some models/scoring systems have been developed. At present, radiological-based radiomics models have been successfully applied to predict cancer patient prognosis.

AIM

To develop and validate a computed tomography (CT)-based radiomics nomogram for the pre-treatment prediction of TACE refractoriness.

METHODS

This retrospective study consisted of a training dataset (n = 137) and an external validation dataset (n = 81) of patients with clinically/pathologically confirmed HCC who underwent repeated TACE from March 2009 to March 2016. Radiomics features were retrospectively extracted from preoperative CT images of the arterial phase. The pre-treatment radiomics signature was generated using least absolute shrinkage and selection operator Cox regression analysis. A CT-based radiomics nomogram incorporating clinical risk factors and the radiomics signature was built and verified by calibration curve and decision curve analyses. The usefulness of the CT-based radiomics nomogram was assessed by Kaplan-Meier curve analysis. We used the concordance index to conduct head-to-head comparisons of the radiomics nomogram with the other four models (Assessment for Retreatment with Transarterial Chemoembolization score; α-fetoprotein,

Data sharing statement: No additional data are available.

Open-Access: This article is an open-access article that was selected by an in-house editor and fully peer-reviewed by external reviewers. It is distributed in accordance with the Creative Commons Attribution NonCommercial (CC BY-NC 4.0) license, which permits others to distribute, remix, adapt, build upon this work non-commercially, and license their derivative works on different terms, provided the original work is properly cited and the use is non-commercial. See: http://creativecommons.org/Licenses/by-nc/4.0/

Manuscript source: Unsolicited manuscript

Specialty type: Gastroenterology and hepatology

Country/Territory of origin: China

Peer-review report's scientific quality classification
Grade A (Excellent): A
Grade B (Very good): 0
Grade C (Good): 0
Grade D (Fair): 0
Grade E (Poor): 0

Received: November 2, 2020
Peer-review started: November 2, 2020
First decision: December 3, 2020
Revised: December 7, 2020
Accepted: December 16, 2020
Article in press: December 16, 2020
Published online: January 14, 2021

P-Reviewer: Donadon M
S-Editor: Huang P
L-Editor: Wang TQ
P-Editor: Ma YJ

Barcelona Clinic Liver Cancer, Child-Pugh, and Response score; CT-based radiomics signature; and clinical model). All analyses were conducted according to the transparent reporting of a multivariable prediction model for individual prognosis or diagnosis statement.

RESULTS
The median duration of follow-up was 61.3 mo (interquartile range, 25.5-69.3 mo) for the training cohort and 67.1 mo (interquartile range, 32.4-71.3 mo) for the validation cohort. The median number of TACE sessions was 4 (range, 3-7) in both cohorts. Eight radiomics features were chosen from 869 candidate features to build a radiomics signature. The CT-based radiomics nomogram included the radiomics score (hazard ratio = 3.9, 95% confidence interval: 3.1-8.8, $P < 0.001$) and four clinical factors and classified patients into high-risk (score > 3.5) and low-risk (score ≤ 3.5) groups with markedly different prognoses (overall survival: 12.3 mo *vs* 23.6 mo, $P < 0.001$). The accuracy of the nomogram was considerably higher than that of the other four models. The calibration curve and decision curve analyses verified the usefulness of the CT-based radiomics nomogram for clinical practice.

CONCLUSION
The newly constructed CT-based radiomics nomogram can be used for the pre-treatment prediction of TACE refractoriness, which may provide better guidance for decision making regarding further TACE treatment.

Key Words: Hepatocellular carcinoma; Transarterial chemoembolization; Refractoriness; Radiomics; Nomogram; Computed tomography

©The Author(s) 2021. Published by Baishideng Publishing Group Inc. All rights reserved.

Core Tip: At present, it is still difficult to predict transarterial chemoembolization (TACE) refractoriness. The main finding of this study is that our computed tomography (CT)-based radiomics nomogram can be used to individually predict patients' refractory state before the first session of TACE. The predictive calibration curves of the training and validation datasets demonstrated agreement with the ideal curve. This CT-based radiomics nomogram may provide an unprecedented opportunity to improve clinical decision making for the patients who are repeatedly treated by TACE and, eventually, improve the overall survival of these patients.

Citation: Niu XK, He XF. Development of a computed tomography-based radiomics nomogram for prediction of transarterial chemoembolization refractoriness in hepatocellular carcinoma. *World J Gastroenterol* 2021; 27(2): 189-207
URL: https://www.wjgnet.com/1007-9327/full/v27/i2/189.htm
DOI: https://dx.doi.org/10.3748/wjg.v27.i2.189

INTRODUCTION

Transarterial chemoembolization (TACE) has been established as the mainstay treatment for intermediate-stage hepatocellular carcinoma (HCC)[1]. Depending on the heterogeneity of the tumour, including the size, number, growth pattern, and anatomical location, a treatment response is not always easy to obtain from a single session of TACE[2,3]. Thus, repeated TACE is often performed to achieve a sufficient outcome. Nevertheless, in some cases, despite an initial response induced by TACE, repetitive TACE treatments could gradually impair liver function and, even worse, have adverse effects on patient survival[4]. This state was initially termed TACE refractoriness and was first recommended by the Japan Society of Hepatology (JSH) in 2010[5]. Furthermore, intermediate HCC patients whose disease was refractory to TACE who received sorafenib experienced an increase in survival compared with those who continued TACE[6,7]. Therefore, it is very important to identify patients who could benefit from consecutive TACE sessions early to improve their outcome.

To predict TACE refractoriness early, some scoring systems have been developed. Sieghart *et al*[8] developed a scoring system known as the Assessment for Retreatment with Transarterial Chemoembolization (ART) score. The ART score is composed of radiologic tumour response, Child-Pugh increase, and aspartate aminotransferase increase by 25%. Adhoute *et al*[9] contructed the ABCR score, which included α-fetoprotein (AFP) level, Barcelona Clinic Liver Cancer (BCLC) stage, Child–Pugh score, and Response score. Subsequent studies in Italian and Japanese cohorts have failed to demonstrate the usefulness of the ART score[10,11]. The Milan group criticized the ABCR score for its "overfitting"[12]. Recently, Kloeckner *et al*[13] also demonstrated that both scores were not sufficient to support clear-cut clinical decisions, and further efforts are needed to determine TACE refractoriness.

Computed tomography (CT) is the most frequently used imaging technique due to its excellent spatial resolution, tissue contrast, and availability. Compared with conventional CT-based imaging features, radiomics signatures reveal the tumour phenotype and tumour biological heterogeneity and therefore can quantitatively estimate patient survival pre-operatively by transforming traditional medical images into high-throughput quantitative imaging features[14,15]. Radiological-based radiomics models have been successfully applied to predict cancer patient survival[16,17]. Unfortunately, Park *et al*[18] found that the overall scientific quality of radiomics studies is currently insufficient. To improve the reporting of studies on clinical prediction models, a strict guideline called the transparent reporting of a multivariable prediction model for individual prognosis or diagnosis (TRIPOD) was released in January 2015[19]. Therefore, following the TRIPOD statement, our study aimed to develop and validate a novel CT-based radiomics nomogram to select patients who could benefit from consecutive TACE cycles.

MATERIALS AND METHODS

This study was performed retrospectively in compliance with the Health Insurance Portability and Accountability Act, and a waiver for the requirement of informed patient consent was obtained from the institutional review board.

Study population

Training cohort: Patients with a diagnosis of HCC who were treated by TACE at the Southern Medical University Nanfang Hospital from March 2009 to March 2016 were included in this study. The inclusion criteria of this retrospective study were as follows: (1) Patients underwent more than two TACE sessions during their therapeutic course (the first two sessions were performed within 3 mo. Then, the rest of the TACE procedures were performed "on-demand"); (2) HCC was diagnosed according to the European Association for the Study of the Liver criteria or histological examination; (3) TACE was performed as monotherapy; (4) patients were ≥ 18 years old and had an ECOG performance status score of ≤ 2 at the time of the first TACE session; (5) patients had HCC at BCLC stage A or B (TACE was chosen by the patient voluntarily after the treatment options had been presented) and well-preserved liver function (Child-Pugh class A or B); and (6) preoperative CT imaging was performed within 0-7 d before the first session of TACE. The exclusion criteria were as follows: (1) Patients had BCLC stage C or Child-Pugh class C disease; (2) Patients had another percutaneous treatment combined with TACE (including radiofrequency/microwave ablation, *etc.*); and (3) The raw CT data could not be processed (Figure 1). Finally, 137 patients (median age, 54.3 years; range, 19-79 years) were included in the training cohort.

Validation cohort: An independent external validation cohort comprised patients who underwent TACE procedures at the Affiliated Hospital of Chengdu University. Consecutive patients who underwent TACE between March 2009 and March 2016 were identified from the local electronic patient recording system. The selection and exclusion criteria for the validation cohort were the same as those for the training cohort. Overall, 81 patients (median age, 57.1 years; range, 21-78 years) were included.

TACE procedure: All TACE procedures were conducted under local anaesthesia *via* a traditional femoral artery approach. Our method of TACE was consistent with the practical standard method of TACE in Asian countries, which was previously reported[20]. After the first two TACE sessions, both institutions used treatment "on demand", and TACE was scheduled upon the detection of viable tumours (local or distant intra-/extra-hepatic recurrences) in patients with Child-Pugh A/B, which can still be treated by TACE.

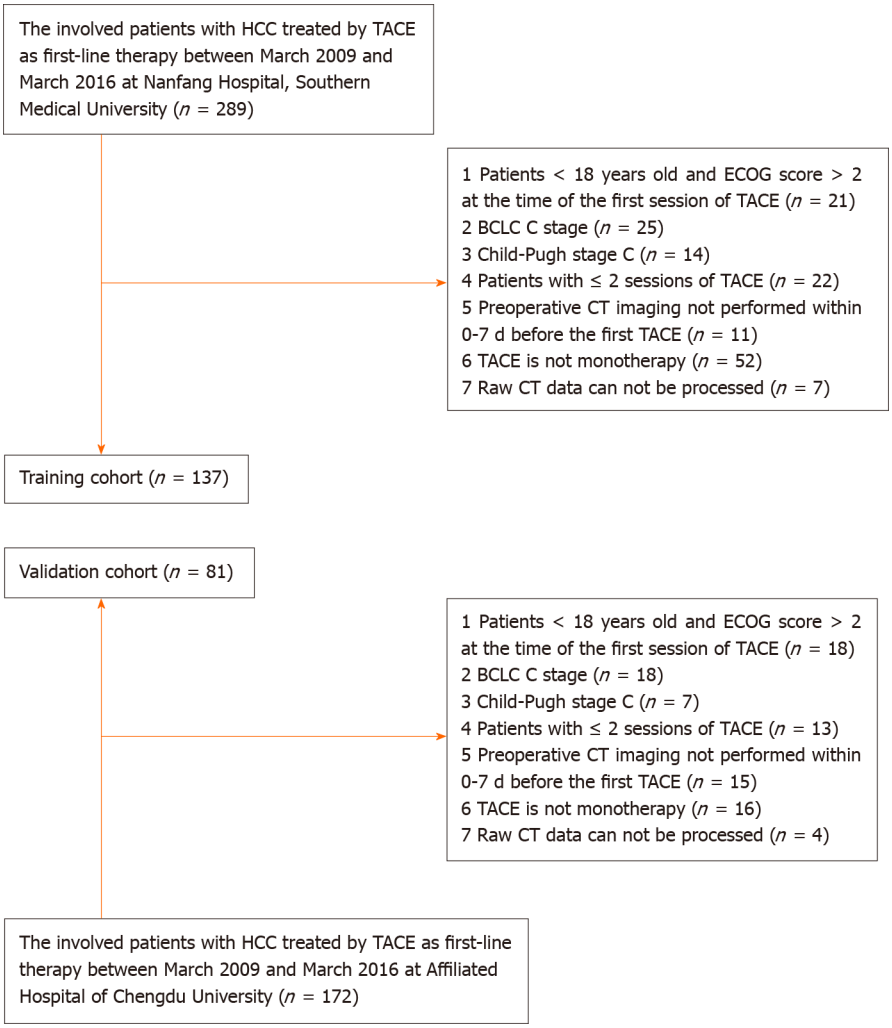


Figure 1 Flowchart for inclusion and exclusion of patients within the training and validation cohort. TACE: Transarterial chemoembolization; ECOG: Eastern Cooperative Oncology Group; BCLC: Barcelona Clinic Liver Cancer; CT: Computed tomography; HCC: Hepatocellular carcinoma.

Factors analysed

Primary outcome: Overall survival (OS) was defined as the period from 1 d before the first TACE procedure to death or the last follow-up (March 2020). Survival data were obtained by one researcher who was blinded to the study purpose. There was no loss to follow-up in the present study.

TACE refractoriness: In the present study, TACE refractoriness was defined according to the JSH and the Liver Cancer Study Group of Japan (JSH-LCSGJ) criteria[21] as follows: Two or more consecutive insufficient responses of the treated tumour (viable lesion > 50%) or an increase in tumour number after changing the chemotherapeutic agents and/or reanalysis of the feeding artery seen on the response evaluation CT/MRI at 1-3 mo after having adequately performed selective TACE; the appearance of vascular invasion; the appearance of extrahepatic spread; or a continuous elevation in tumour markers immediately after TACE even though a slight transient decrease was observed.

Candidate clinical variables: Based on the ART and ABCR scores, we collected as much clinical data as possible. Before the first TACE session, the presence or absence of a tumour capsule was evaluated according to Liver Imaging Reporting and Data System version 2018 (LI-RADS v2018) ancillary features[22]. Irregular tumour margins were defined as non-smooth margins, presenting as the multinodular confluent type, and nodular type with extranodular extension and/or with an infiltrative appearance[23]. Those radiologic imaging evaluations were assessed by two senior radiologists (more than 10 years in interpreting abdominal imaging) with consensus.

Radiomics feature selection: All patients underwent multidetector CT examination (Siemens Somatom Definition 64; VCT 64; GE Medical Systems). A 1.5 mL/kg body

weight bolus of iohexol (Omnipaque, GE Healthcare Co., Ltd.) was injected intravenously at a flow rate of 2.5 mL/s, followed by a 20-mL saline flush. Images of the arterial phase, portal venous phase, and delay phase were obtained at 35 s, 65 s, and 120 s, respectively, after intravenous contrast material injection. The scanning parameters used in this study were as follows: Tube voltage, 120 kVp; detector collimation, 128 mm × 0.625 mm; field of view, 250-400 mm; pixel size, 512 × 512; rotation time, 0.5 s; slice interval, 0 mm; slice thickness, 5 mm; and reconstructed section thicknesses, 1 mm. The processing flow of the radiomics analysis included the following four steps: Tumour segmentation, feature extraction, model building, and model evaluation. Radiomics features were extracted from CT images of the pre-treatment arterial phase. The largest tumours were manually delineated on each transverse image by using ITK-SNAP software (http://www.itksnap.org/pmwiki/pmwiki.php) (Figure 2). Two researchers (with 5 and 8 years of experience in abdominal imaging) who were blinded to the research purpose independently performed tumour delineation and feature extraction with the open-source PyRadiomics package (version 2.2.0). Images were standardized to a voxel size of 1 mm × 1 mm × 1 mm, and voxel intensity values were discretized by using a fixed bin width of 10 HU to reduce image noise and normalize intensities, allowing for a constant intensity resolution across all tumour images[24]. The interobserver reproducibility of the radiomics features was evaluated by the intraclass correlation coefficient (ICC).

Statistical analysis

The image features and clinical data were evaluated by applying the Student's *t*-test, the chi-squared test, or the Mann-Whitney *U*-test, where appropriate. Missing data were considered at random and handled using multiple imputations by the iterative Markov chain Monte Carlo method (10 iterations)[25]. All statistical analyses were conducted by using R software (http://www.Rproject.org). A two-tailed $P < 0.05$ was regarded as statistically significant.

Step 1 - construct radiomics score: Radiomics features that had ICCs greater than 0.80 were used for subsequent analysis. We used the least absolute shrinkage and selection operator (LASSO) Cox regression method to determine radiomics features that predicted OS. The radiomics score (Rad-score) cut-off value was determined with the "surv_cutpoint" function of the "survminer" R package.

Step 2 - construct the clinical model/CT-based radiomics nomogram: Univariate and multivariate Cox proportional hazards analyses were used to identify clinical factors related to patient survival. The B regression coefficients of the Cox regression model were multiplied by 2 and rounded to obtain the risk score calculation. A CT-based radiomics nomogram was constructed by incorporating the clinical risk factors and radiomics signature by the use of a multivariable Cox regression model. The radiomics model used the median value of the total score to stratify patients into high- and low-risk groups, and ultimately, a nomogram was built.

Step 3 - model evaluation: The OS of different groups was estimated by using the Kaplan-Meier method and compared by the log-rank test. The performance of each model was evaluated by the concordance index (C-index). The C-index is the area under the curve for continuous time-to-event survival data used to measure the discrimination of a prognostic model. The calibration curve was established, and the Hosmer-Lemeshow test was used to analyse the prognostic performance of the CT-based radiomics nomogram in both cohorts. Decision curve analysis (DCA) was conducted to determine the clinical usefulness of the nomogram in the validation cohort.

RESULTS

Patient characteristics

Between March 2009 and March 2016, a total of 461 HCC patients underwent TACE as first-line therapy. A total of 137 patients were included in the training cohort, and 81 were included in the validation cohort. The median duration of follow-up was 61.3 mo (interquartile range, 25.5-69.3 mo) for the training cohort and 67.1 mo (interquartile range, 32.4-71.3 mo) for the validation cohort. The median number of TACE sessions was 4 (range, 3-7) in both cohorts. The median survival time for the training cohort

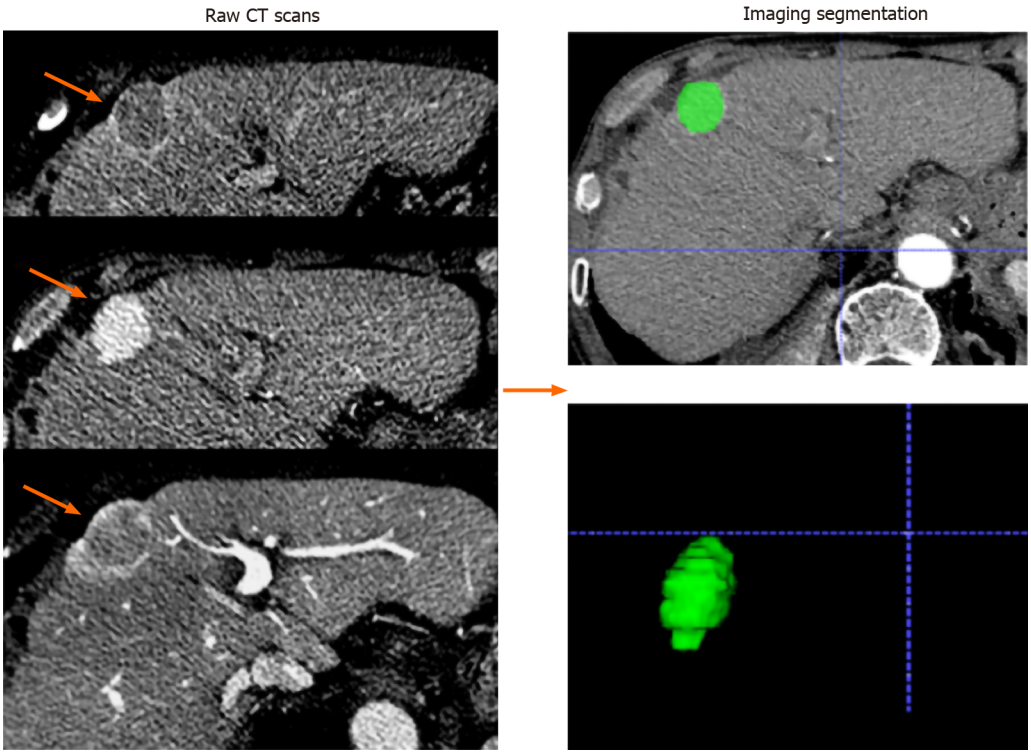


Figure 2 Imaging segmentation. The images were acquired form a 65-year-old man with hepatocellular carcinoma (orange arrows). Serial raw computed tomography scans obtained before transarterial chemoembolization treatment; regions of interest were manually depicted along with the tumor outline on each axial slice and automatically merged into a volume of interest (green area).

was 21.6 mo (95% confidence interval [CI]: 13.6-28.1), while that of the validation cohort was 19.7 mo (95%CI: 12.3-25.2) (training *vs* validation, $P = 0.324$).

In the training cohort, 67% of patients were male, and most (80.0%) patients tested positive for HBsAg. The majority of patients were graded as having Child-Pugh A (61%) and BCLC stage B (85%). The proportion of patients with a tumour size of 5 cm or greater was 34%. The included variables were not significantly different between the two cohorts (Table 1).

Radiomics score building

A total of 869 radiomics features were extracted. Sixty-five radiomics features remained in the arterial phase after the reproducibility test (Figure 3A). All the selected features were entered into the LASSO Cox regression analysis. Eight features were selected to build the radiomics signature using the LASSO regression model (Figure 3B): Two volumetric texture features and six wavelet texture features, respectively. The CT-based radiomics signature can be calculated with the following formula: Radiomics score = 0.174 + 0.432 × Shape_Maximum 3D Diameter - 0.432 × Shape_Elongation + 0.017 × wavelet-HHH_GLSZM_Gray Level Variance - 0.263 × wavelet-HHL_GLSZM_Size Zone Non-Uniformity Normalized + 0.046 × wavelet-HLH_GLSZM_Gray Level Non-Uniformity Normalized - 0.367 × wavelet-HLH_GLSZM_Zone Variance + 0.562 × wavelet-HHH_GLRLM_Low Gray Level Zone Emphasis - 0.214 × wavelet- LHL_GLDM_Dependence Non-Uniformity Normalized. The median Rad-score was 0.75 (range, -1.3-1.7). The cut-off value of the Rad-score was 0.1.

Development of a clinical model/CT-based radiomics nomogram

Clinical model: A multivariate model based on Cox analyses revealed four clinical factors affecting OS: BCLC stage, irregular tumour margin, largest tumour size, and tumour number. These factors were combined to create a clinical score (Table 2).

CT-based radiomics nomogram: The results of the univariate analysis showed that Rad-score, BCLC stage, irregular tumour margin, largest tumour size, tumour number, irregular tumour margin, and AFP level had significant effects on OS (Table 3). Multivariate Cox regression analysis showed that the following five factors affected OS: Rad-score, BCLC stage, irregular tumour margin, largest tumour size, and tumour

Table 1 Patient characteristics

Characteristic	Training cohort		Validation cohort		*P* value
	n	%	*n*	%	
Before treatment	137		81		
Age (yr)					0.778
< 60	87	63	49	60	
≥ 60	50	37	32	40	
Sex					0.159
Male	91	67	45	55	
Female	46	33	36	45	
HBsAg status					0.950
Positive	110	80	65	80	
Negative	27	20	16	20	
Child-Pugh class					0.879
A	84	61	51	62	
B	53	39	30	38	
Largest tumor size (mean ± SD, cm)					0.321
< 5	91	66	47	58	
≥ 5	46	34	34	42	
Tumor distribution					0.360
Solitary	89	64	45	56	
Multiple	48	36	36	44	
BCLC stage					0.249
A	20	15	16	19	
B	117	85	65	81	
AFP (IU/mL)					0.410
< 200	29	21	21	26	
≥ 200	108	79	60	74	
ECOG performance status score					0.321
0	42	30	31	38	
1	85	62	43	53	
2	10	8	7	9	
AST (U/L)					0.106
< 40	50	36	37	46	
≥ 40	87	64	44	54	
Irregular tumor margin					0.579
Absent	62	45	33	41	
Present	75	55	48	59	
Capsule					0.165
Absent	67	48	31	38	
Present	70	52	50	62	

BCLC: Barcelona Clinic Liver Cancer; AST: Aspartate aminotransferase; AFP: Alpha fetoprotein; ECOG: Eastern Cooperative Oncology Group.

number (Table 4). The median value of the CT-based radiomics nomogram was 3.5 (Figure 4). We used the median value to classify our patients into high- and low-risk groups.

Model evaluation

The CT-based radiomics nomogram stratified the patients in the training cohort into two subgroups with distinct prognoses. Patients with a score ≤ 3.5 (low-risk group) had a median OS of 23.6 mo (95%CI: 16.3-28.7), whereas patients with a score > 3.5 (high-risk group) had a median OS of 12.3 mo (95%CI: 7.9-16.4; $P < 0.001$). In the validation cohort, the same trend was observed. The Hosmer-Lemeshow test demonstrated that there was no significant difference between the predictive curve (CT-based radiomics nomogram) and the ideal curve in the training and validation cohorts ($P = 0.137$ and 0.165, respectively) (Figure 5A and B). DCA indicated that the CT-based radiomics nomogram adds more net benefit than the other four models/scoring systems in the validation cohort (Figure 5C). We used the ART and ABCR scores to identify TACE refractoriness in our cohorts. In both the ART and ABCR groups, the median OS duration did not show a significant difference in either the training or validation cohorts (Figure 6). The C-indexes of the CT-based radiomics nomogram were 0.844 (0.762-0.901) and 0.831 (0.742-0.881) in the training and validation cohorts, respectively, and the nomogram significantly better predicted OS than the other models (the ART score, the ABCR score, our newly constructed clinical model, and the radiomics score) (Table 5).

DISCUSSION

The main finding of this study is that our CT-based radiomics nomogram can be used to individually predict a patient's refractory state before the first session of TACE. The predictive calibration curves of the training and validation datasets demonstrated agreement with the ideal curve. Compared with the existing ART and ABCR scores, our new model showed the best discrimination for selecting patients who could benefit from consecutive TACE sessions, and DCA proved that our newly constructed nomogram was clinically useful in the current study.

Our newly developed CT-based radiomics nomogram includes four clinical parameters: BCLC stage, irregular tumour margin, largest tumour size, and tumour number. These four clinical parameters mainly emphasize tumour burden and tumour aggressiveness before initial treatment. Currently, BCLC staging is the most commonly used method worldwide for HCC treatment allocation. Despite the limitations of the BCLC staging system, *e.g.*, it does not include tumour characteristics (including tumour distribution and heterogeneity), it remains the most validated and reliable system for HCC prognostication. Tumour size has been broadly recognized as a major predictive factor for response to TACE[26-28]. The blood supply of HCC is mainly from the hepatic artery. Large tumours always have a more abundant blood supply, grow faster, break through the capsule more easily, and readily infiltrate the surrounding liver tissue. Large tumours also more easily cause invasion of the portal vein, increasing the probability of post-TACE intrahepatic recurrence. Katayama *et al*[29] proved that pre-treatment tumour number is a useful factor for predicting TACE response. Multiple tumours in the liver are mostly due to intrahepatic metastasis, and an increase in tumour number usually indicates more rapid metastasis. For these patients, even if the visible tumours are totally embolized, small metastases may also be present in the liver, which is consistent with the finding of this study that patients with multiple tumours had a higher rate of TACE treatment failure. Irregular tumour margin was confirmed as a reliable predictor of microvascular invasion (MVI)[30]. MVI has been regarded as an important risk factor affecting the prognosis of HCC patients after treatment[31]. In our study, irregular tumour margin had a significant effect on patient survival, indicating that it also had an increasing trend in the development of TACE refractoriness.

CT imaging is commonly used in clinical procedures for HCC patients, such as tumour detection and staging. However, since conventional imaging evaluation relies on semantic features and provides relatively few metrics, the large amount of additional useful information about tumour heterogeneity has been underutilized[32]. Radiomics is a rapidly advancing form of medical image analysis that enables the quantification of tumour phenotypic characteristics to provide prognostic information[33]. To facilitate the clinical use of a radiomics model, we constructed a

Table 2 Univariate and multivariate-Cox regression analyses of prognostic factors in hepatocellular carcinoma patients treated by transarterial chemoembolization in the training cohort

Variable	Univariate analysis			Multivariate analysis				Score
Before first TACE	Hazard ratio	95%CI	*P* value	Hazard ratio	95%CI	*P* value	B	
Age (yr), < 60/≥ 60	0.781	0.324-1.012	0.124					
Sex, male/female	0.891	0.456-1.213	0.211					
HBsAg status, positive/negative	0.671	0.319-0.987	0.121					
Child-Pugh class, A/B	1.178	0.614-1.418	0.256					
Largest tumor size (cm), < 5/≥ 5	1.619	1.671-2.341	0.005	1.312	0.981-1.992	< 0.001	0.4168	1
Tumor number, solitary/multiple	1.987	1.561-2.354	0.007	1.289	1.481-2.002	< 0.001	0.3178	1
BCLC stage, A/B	1.671	1.319-1.987	<0.001	1.789	1.289-2.112	< 0.001	0.4288	1
AFP (IU/mL), < 200/≥ 200	0.678	0.214-1.018	0.128					
ECOG performance status score, 0/1/2	1.102	0.781-1.456	0.199					
AST (U/L), < 40/≥ 40	0.543	0.178-0.967	0.089					
Irregular tumor margin, absent/present	1.562	1.211-1.897	< 0.001	1.457	1.090-2.089	< 0.001	0.404	1
Capsule, absent/present	1.432	1.121-1.976	0.032	1.321	1.007-1.764	0.082		

The regression coefficients (B) in multivariate-Cox regression analysis were multiplied by 2 and rounded to calculate the clinical score. The clinical model used the median value (2) of total score (4) to stratify patients into high and low-risk group. HCC: Hepatocellular carcinoma; TACE, Transarterial chemoembolization; BCLC, Barcelona Clinic Liver Cancer; AST: Aspartate aminotransferase; AFP: Alpha fetoprotein; ECOG: Eastern Cooperative Oncology Group; CI: Confidence interval.

nomogram to visualize and quantify the results of the complex radiomics analysis. Considering the weaknesses of the preceding radiomics models and the doubts about their reproducibility and robustness, we took effective measures to guarantee the objectivity and reproducibility of our radiomics model. First, we applied voxel intensity discretization and voxel size resampling to reduce the dependency of differences in image specifications, in accordance with recent CT radiomics studies[34,35]. Second, two radiologists carried out the tumour segmentation step, and ICCs were used to minimize subjectivity and operator error. Both the segmentation software and feature extraction software that we used were commonly adopted in earlier investigations and had been verified by those studies[36,37]. With all the above measures, a relatively evidence-based radiomics-clinical model was constructed for the pre-treatment evaluation of patients who are likely to develop TACE refractoriness.

The LASSO method is a powerful method for the regression of high-dimensional predictors[38]. In our study, 65 potential features were chosen from 869 candidate radiomics features of the arterial phase *via* the LASSO test method to build a radiomics signature. The majority of previous studies[34,35,39] applied morphological features and grey-level texture features [such as histograms and grey-level co-occurrence matrices (GLCM)] extracted from regions of interest. Morphological features have limited value in predicting tumour treatment response, and GLCM features mainly represent the heterogeneity of peripheral tumour regions. Alternatively, wavelet transformation can provide comprehensive spatial and frequency distributions for characterizing intratumoural and peritumoural regions in terms of low- and high-frequency signals. These properties may improve the performance of the radiomics model[40,41]. Not surprisingly, in the present study, the CT-based radiomics signature was composed primarily of wavelet-transformed textures. The wavelet transformation decomposes images into high frequency signals (heterogeneity) and low frequency signals (homogeneity) for both intratumoural and peritumoural regions, which is a strong suggestion of the tumour microenvironment heterogeneity. Recently, Chun *et al*[42] and Zhou *et al*[43] also proved that wavelet-based features can be used for disease diagnosis and the prediction of therapy response.

There are several limitations to our study. First, because this was a retrospective

Table 3 Univariate analysis of prognostic factors in hepatocellular carcinoma patients treated by transarterial chemoembolization in the training cohort

Variable	*n*	Overall survival (mo)		*P* value
		Median	95%CI	
Before treatment				
Age (yr)				0.213
< 60	87	19.8	16.8-23.4	
≥ 60	50	17.6	14.3-21.1	
Sex				0.178
Male	91	15.4	12.5-19.6	
Female	46	19.6	14.3-23.1	
HBsAg status				0.121
Positive	110	14.9	12.3-19.2	
Negative	27	18.1	14.1-22.8	
Child-Pugh stage				
Child-Pugh class				0.301
A	84	23.5	19.1-32.4	
B	53	19.8	13.7-23.8	
Largest tumor size (cm)				0.032
< 5	91	19.6	19.7-24.2	
≥ 5	46	14.1	14.1-18.8	
Tumor number				0.029
Solitary	89	19.1	17.4-22.7	
Multiple	48	14.7	13.8-18.1	
BCLC stage				0.033
A	20	26.7	22.3-31.2	
B	117	16.1	13.7-24.2	
AFP (IU/mL)				0.041
< 200	29	20.7	17.2-29.4	
≥ 200	108	16.8	9.5-18.2	
ECOG performance status score				0.195
0	42	21.6	13.2-26.7	
1	85	19.3	10.3-24.4	
2	10	17.1	9.1-22.3	
AST (U/L)				0.261
< 40	50	18.3	15.2-23.7	
≥ 40	87	16.9	12.3-22.9	
Irregular tumor margin				0.018
Absent	62	20.5	14.7-27.2	
Present	75	12.6	8.7-16.4	
Capsule				0.087
Absent	67	16.7	12.1-22.4	
Present	70	19.3	13.5-25.1	

Radiomics score				0.003
< 0.1	102	23.3	19.8-28.6	
≥ 0.1	35	10.3	6.5-14.3	

HCC: Hepatocellular carcinoma; TACE: Transarterial chemoembolization; BCLC: Barcelona Clinic Liver Cancer; AST: Aspartate aminotransferase; AFP: Alpha fetoprotein; ECOG: Eastern Cooperative Oncology Group; CI: Confidence interval.

Table 4 Multivariate stepwise backward Cox regression analysis of prognostic factors in hepatocellular carcinoma patients treated by transarterial chemoembolization in the training cohort

Variable	Hazard ratio ratio	95%CI	B	Score	*P* value (Cox regression)
Before treatment					
BCLC stage					
A	1		0	0	
B	2.3	1.2-3.1	0.39	1	0.032
Irregular tumor margin					
Absent	1		0	0	
Present	1.9	0.7-3.3	0.42	1	0.028
Largest tumor size (cm)					
< 5	1		0	0	
≥ 5	1.7	0.6-2.9	0.47	1	0.017
Tumor number					
Solitary	1		0	0	
Multiple	2.1	1.1-3.1	0.33	1	0.021
Radiomics score					
< 0.1	1		0	0	
≥ 0.1	3.9	3.1-8.8	1.72	3	< 0.001

The regression coefficients (B) in multivariate-Cox regression analysis were multiplied by 2 and rounded to calculate the radiomics-clinical score. The radiomics-clinical model used the median value (3.5) of total score (7) to stratify patients into high and low-risk group. HCC: Hepatocellular carcinoma; TACE: Transarterial chemoembolization; BCLC: Barcelona Clinic Liver Cancer; B: B regression coefficient; CI: Confidence interval.

study, the selection bias may exist. Further large external validation cohort should be used to testify the robustness and reproducibility of the model. Second, we cannot obtain genomic data of each tumor, which may hinder better interpretation of radiomics features. Last, other clinical features may also be valuable for the construction of the predictive model, but we excluded them from the present study for reasons of data integrity and only selected the most reasonable features. In spite of these limitations, we believe that our approach offers advantages for the following reasons: (1) We performed the study in accordance with the TRIPOD statement, which may improve clinical utility of our results; and (2) In addition to the clinical data, the combination of radiomics and traditional imaging characteristics may improve the clinical acceptability of our newly constructed model.

CONCLUSION

In conclusion, based on CT-radiomics, we developed a novel and externally validated, noninvasive, objective nomogram for the pre-treatment prediction of patients who are likely to have TACE refractoriness. This may provide an unprecedented opportunity to improve clinical decision making for patients who are repeatedly treated by TACE and, therefore, improve the OS of these patients.

Table 5 Predictive performance of each model/score

Prediction model	Training cohort C-index (95%CI)	Validation cohortC-index (95%CI)	*P* value			
			3 *vs* 1	3 *vs* 2	3 *vs* 4	*vs* 5
1 Clinical model	0.643 (0.613-0.712)	0.629 (0.601-0.678)	0.025[a]/0.023[b]	0.003[a]/0.002[b]	0.007[a]/0.006[b]	0.009[a]/0.004[b]
2 Radiomics score	0.723 (0.634-0.778)	0.734 (0.641-0.793)				
3 CT-based radiomics nomogram	0.844 (0.762-0.901)	0.831 (0.742-0.881)				
4 ART score	0.714 (0.632-0.771)	0.690 (0.601-0.761)				
5 ABCR score	0.732 (0.646-0.801)	0.701 (0.632-0.789)				

[a]Significant difference of C-index between computed tomography (CT)-based radiomics nomogram *vs* other models/scores in the training cohort.
[b]Significant difference of C-index between CT-based radiomics nomogram *vs* other models/scores in the validation cohort. CI: Confidence interval; CT: Computed tomography; ART: Assessment for Retreatment with Transarterial Chemoembolization; ABCR: α-Fetoprotein, Barcelona Clinic Liver Cancer, Child-Pugh, and Response.

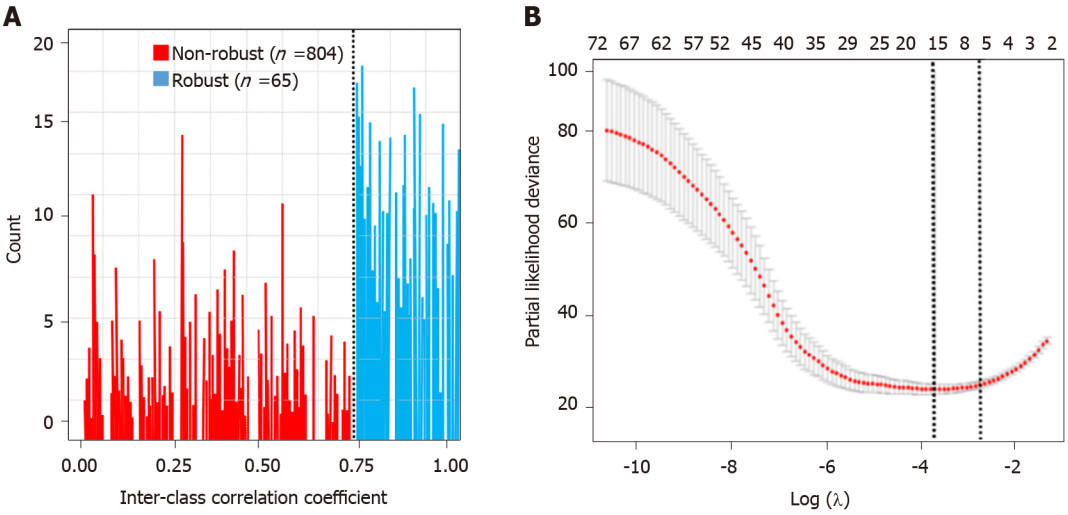


Figure 3 Feature selection. A: Histogram of the inter-class correlation coefficient. The intraclass correlation coefficient (ICC) was used to determine the stability of the features. Features with an ICC < 0.8 were excluded from the analysis. After robustness test, 65 of the initial 869 computed tomography image features in the arterial phase were retained; B: Partial likelihood deviance was drawn *vs* log (λ) in the arterial phase.

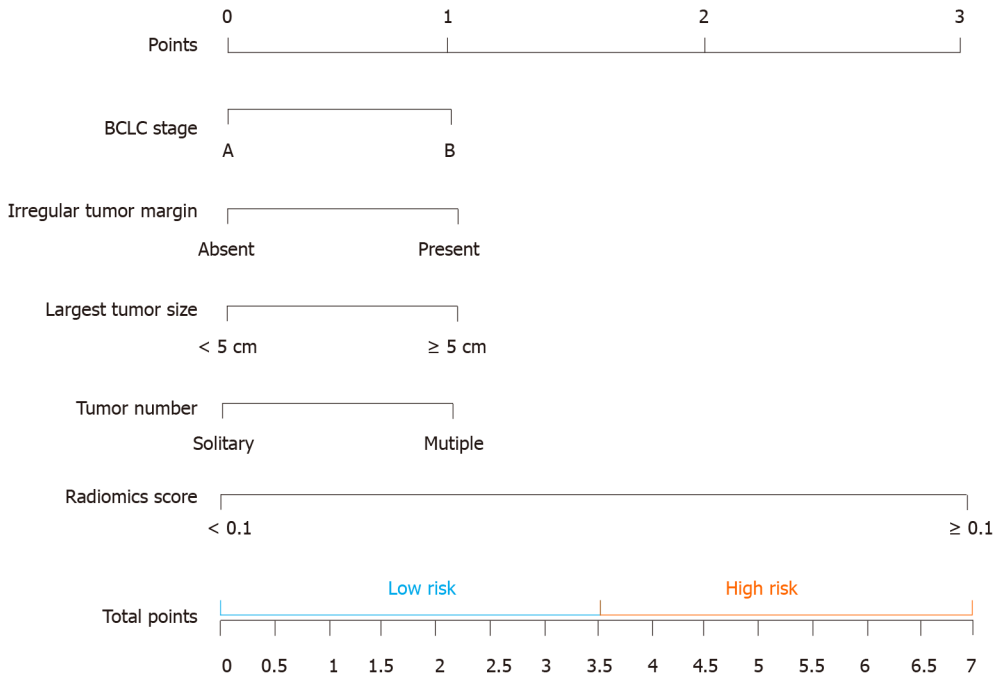


Figure 4 The computed tomography-based nomogram was built. The computed tomography (CT)-based nomogram was obtained by combining the effective clinical factors and radiomics signature of artery phase contrast-enhanced CT images. We choose the median value (3.5) to classify our patients into high and low-risk groups. BCLC: Barcelona Clinic Liver Cancer.

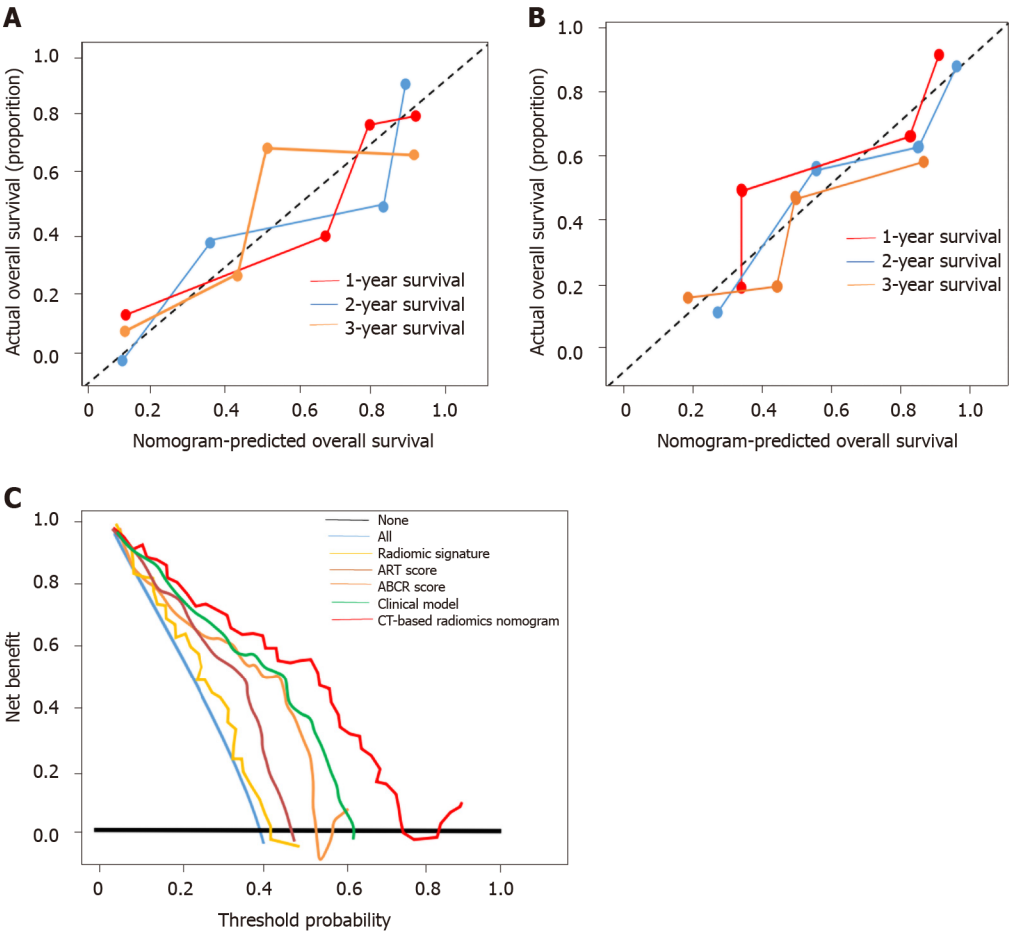


Figure 5 Calibration curve and clinical utility analyses. A: Calibration curves of the nomogram on the training dataset. The Hosmer-Lemeshow test yielded a *P* value of 0.137 in the training dataset; B: Calibration curves of the nomogram on the validation dataset. The Hosmer-Lemeshow test yielded a *P* value of 0.165 in the validation dataset; C: Decision curve analysis for each model in the validation dataset. The Y-axis measures the net benefit, which is calculated by summing the benefits (true-positive findings) and subtracting the harms (false-positive findings). The decision curve showed that if the threshold probability is over 10%, the application of computed tomography-based radiomics nomogram to predict transarterial chemoembolization-refractoriness adds more benefit compared with the other scores/models. ART: Assessment for Retreatment with Transarterial Chemoembolization; ABCR: α-Fetoprotein, Barcelona Clinic Liver Cancer, Child-Pugh, and Response; CT: Computed tomography.

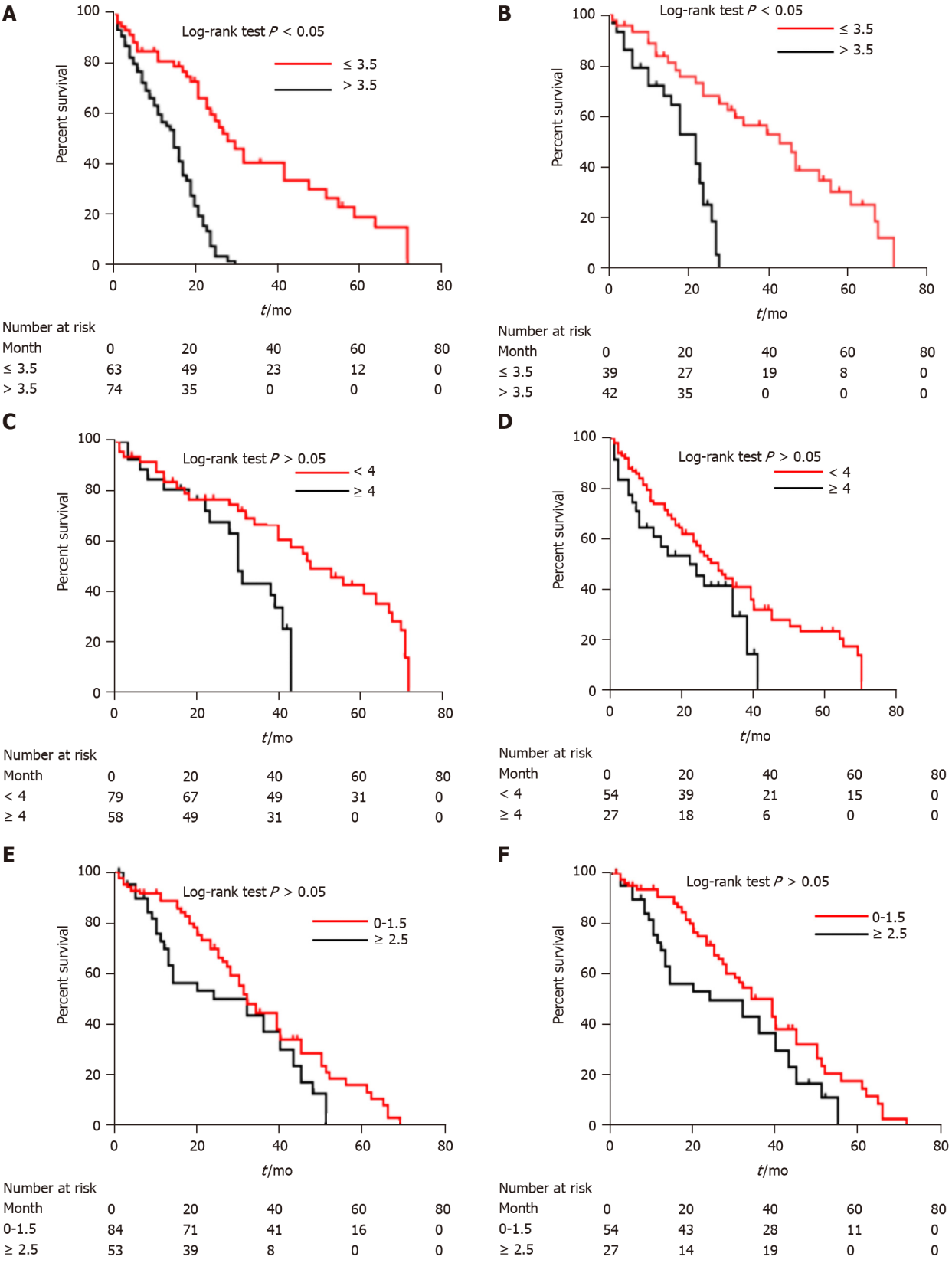


Figure 6 Kaplan-Meier curves of survival outcomes in different patient groups. A: Kaplan-Meier analysis of overall survival of high-risk (> 3.5) and low-risk (≤ 3.5) patients according to computed tomography (CT)-based radiomics nomogram in the training cohort; B: Kaplan-Meier analysis of overall survival of high-risk (> 3.5) and low-risk (≤ 3.5) patients according to CT-based radiomics nomogram in the validation cohort; C: Kaplan-Meier analysis of overall survival of high-risk (≥ 4) and low-risk (< 4) patients according to α-fetoprotein, Barcelona Clinic Liver Cancer, Child-Pugh, and Response (ABCR) score in the training cohort; D: Kaplan-Meier analysis of overall survival of high-risk (≥ 4) and low-risk (< 4) patients according to ABCR score in the validation cohort; E: Kaplan-Meier analysis of overall survival of high-risk (≥ 2.5) and low-risk (0-1.5) patients according to Assessment for Retreatment with Transarterial Chemoembolization (ART) score in the training cohort; F: Kaplan-Meier analysis of overall survival of high-risk (≥ 2.5) and low-risk (0-1.5) patients according to ART score in the validation cohort.

ARTICLE HIGHLIGHTS

Research background

The point at which transarterial chemoembolization (TACE) should be continued or stopped is currently not addressed by any guideline to our knowledge. Repeated TACE cycles are, however, associated with an increase of related side effects and liver damage, potentially preventing an even greater survival advantage. In the era of personalized oncology, radiomics has allowed digitally encrypted medical images to be transformed into high-throughput quantitative features that provide information on patient prognosis.

Research motivation

In previous studies, patients with high Assessment for Retreatment with Transarterial Chemoembolization (ART) or α-fetoprotein, Barcelona Clinic Liver Cancer, Child-Pugh, and Response score (ABCR) scores tended to have a poor prognosis. Nonetheless, in terms of predictive ability, neither score was reliable enough to allow for clinical decision-making. Although previous studies have shown the prognostic value of computed tomography (CT) radiomic features for different cancer sites, there is scarcity of multi-centre radiomics research on TACE refractoriness.

Research objectives

The purpose of this study was to develop and validate a CT-based radiomics nomogram for the pre-treatment prediction of TACE refractoriness.

Research methods

Our study consisted of a training dataset (n = 137) and an external validation dataset (n = 81) of patients with clinically/pathologically confirmed hepatocellular carcinoma who underwent repeated TACE from March 2009 to March 2016. The radiomics features were retrospectively extracted from preoperative CT images of the arterial phase. The radiomics signature was built by least absolute shrinkage and selection operator (LASSO) regression. The CT-based radiomics nomogram incorporating clinical risk factors was built by multivariable logistic regression analysis. The performance of the nomogram was assessed with respect to its calibration, discrimination, and clinical usefulness. We used the concordance index to conduct head-to-head comparisons of the radiomics nomogram with the other four models (ART score, ABCR score, CT-based radiomics signature, and clinical model).

Research results

Eight features were selected to build the radiomics signature using the LASSO regression model. The CT-based radiomics nomogram included the radiomics score (HR = 3.9, 95% confidence interval: 3.1-8.8, P < 0.001) and four clinical factors and classified patients into high-risk (score > 3.5) and low-risk (score ≤ 3.5) groups with markedly different prognoses (overall survival: 12.3 mo *vs* 23.6 mo, P < 0.001). The accuracy of the nomogram was considerably higher than that of the other four models (ART score, ABCR score, CT-based radiomics signature, and clinical model). The calibration curve and decision curve analyses verified the usefulness of the CT-based radiomics nomogram for clinical practice.

Research conclusions

The CT-based radiomics nomogram is valuable in preoperatively predicting TACE refractoriness, which may aid interventional radiologist in determining the optimal treatment approach.

Research perspectives

First, additional information, such as gene sequence data or the molecular pathway, might be necessary for better interpretation of radiomics features, and this issue is left for future research. Second, larger prospective multicenter studies are needed to externally validate our newly constructed model in the future.

REFERENCES

1 **Llovet JM**, Real MI, Montaña X, Planas R, Coll S, Aponte J, Ayuso C, Sala M, Muchart J, Solà R, Rodés J, Bruix J; Barcelona Liver Cancer Group. Arterial embolisation or chemoembolisation *versus*

symptomatic treatment in patients with unresectable hepatocellular carcinoma: a randomised controlled trial. *Lancet* 2002; **359**: 1734-1739 [PMID: 12049862 DOI: 10.1016/S0140-6736(02)08649-X]

2 **Terzi E**, Golfieri R, Piscaglia F, Galassi M, Dazzi A, Leoni S, Giampalma E, Renzulli M, Bolondi L. Response rate and clinical outcome of HCC after first and repeated cTACE performed "on demand". *J Hepatol* 2012; **57**: 1258-1267 [PMID: 22871502 DOI: 10.1016/j.jhep.2012.07.025]

3 **Bolondi L**, Burroughs A, Dufour JF, Galle PR, Mazzaferro V, Piscaglia F, Raoul JL, Sangro B. Heterogeneity of patients with intermediate (BCLC B) Hepatocellular Carcinoma: proposal for a subclassification to facilitate treatment decisions. *Semin Liver Dis* 2012; **32**: 348-359 [PMID: 23397536 DOI: 10.1055/s-0032-1329906]

4 **Hu K**, Lu S, Li M, Zhang F, Tang B, Yuan J, Shan Y, Xu P, Chen R, Ren Z, Yin X. A Novel Pre-treatment Model Predicting Risk of Developing Refractoriness to Transarterial Chemoembolization in Unresectable Hepatocellular Carcinoma. *J Cancer* 2020; **11**: 4589-4596 [PMID: 32489476 DOI: 10.7150/jca.44847]

5 **Kudo M**, Izumi N, Kokudo N, Matsui O, Sakamoto M, Nakashima O, Kojiro M, Makuuchi M; HCC Expert Panel of Japan Society of Hepatology. Management of hepatocellular carcinoma in Japan: Consensus-Based Clinical Practice Guidelines proposed by the Japan Society of Hepatology (JSH) 2010 updated version. *Dig Dis* 2011; **29**: 339-364 [PMID: 21829027 DOI: 10.1159/000327577]

6 **Arizumi T**, Ueshima K, Minami T, Kono M, Chishina H, Takita M, Kitai S, Inoue T, Yada N, Hagiwara S, Minami Y, Sakurai T, Nishida N, Kudo M. Effectiveness of Sorafenib in Patients with Transcatheter Arterial Chemoembolization (TACE) Refractory and Intermediate-Stage Hepatocellular Carcinoma. *Liver Cancer* 2015; **4**: 253-262 [PMID: 26734579 DOI: 10.1159/000367743]

7 **Ogasawara S**, Chiba T, Ooka Y, Kanogawa N, Motoyama T, Suzuki E, Tawada A, Kanai F, Yoshikawa M, Yokosuka O. Efficacy of sorafenib in intermediate-stage hepatocellular carcinoma patients refractory to transarterial chemoembolization. *Oncology* 2014; **87**: 330-341 [PMID: 25227534 DOI: 10.1159/000365993]

8 **Sieghart W**, Hucke F, Pinter M, Graziadei I, Vogel W, Müller C, Heinzl H, Trauner M, Peck-Radosavljevic M. The ART of decision making: retreatment with transarterial chemoembolization in patients with hepatocellular carcinoma. *Hepatology* 2013; **57**: 2261-2273 [PMID: 23316013 DOI: 10.1002/hep.26256]

9 **Adhoute X**, Penaranda G, Naude S, Raoul JL, Perrier H, Bayle O, Monnet O, Beaurain P, Bazin C, Pol B, Folgoc GL, Castellani P, Bronowicki JP, Bourlière M. Retreatment with TACE: the ABCR SCORE, an aid to the decision-making process. *J Hepatol* 2015; **62**: 855-862 [PMID: 25463541 DOI: 10.1016/j.jhep.2014.11.014]

10 **Terzi E**, Terenzi L, Venerandi L, Croci L, Renzulli M, Mosconi C, Allegretti G, Granito A, Golfieri R, Bolondi L, Piscaglia F. The ART score is not effective to select patients for transarterial chemoembolization retreatment in an Italian series. *Dig Dis* 2014; **32**: 711-716 [PMID: 25376288 DOI: 10.1159/000368007]

11 **Arizumi T**, Ueshima K, Iwanishi M, Minami T, Chishina H, Kono M, Takita M, Kitai S, Inoue T, Yada N, Hagiwara S, Ida H, Minami Y, Sakurai T, Nishida N, Kitano M, Kudo M. Evaluation of ART Scores for Repeated Transarterial Chemoembolization in Japanese Patients with Hepatocellular Carcinoma. *Oncology* 2015; **89** Suppl 2: 4-10 [PMID: 26584030 DOI: 10.1159/000440625]

12 **Facciorusso A**, Bhoori S, Sposito C, Mazzaferro V. Repeated transarterial chemoembolization: An overfitting effort? *J Hepatol* 2015; **62**: 1440-1442 [PMID: 25678386 DOI: 10.1016/j.jhep.2015.01.033]

13 **Kloeckner R**, Pitton MB, Dueber C, Schmidtmann I, Galle PR, Koch S, Wörns MA, Weinmann A. Validation of Clinical Scoring Systems ART and ABCR after Transarterial Chemoembolization of Hepatocellular Carcinoma. *J Vasc Interv Radiol* 2017; **28**: 94-102 [PMID: 27562621 DOI: 10.1016/j.jvir.2016.06.012]

14 **Gillies RJ**, Kinahan PE, Hricak H. Radiomics: Images Are More than Pictures, They Are Data. *Radiology* 2016; **278**: 563-577 [PMID: 26579733 DOI: 10.1148/radiol.2015151169]

15 **Zheng BH**, Liu LZ, Zhang ZZ, Shi JY, Dong LQ, Tian LY, Ding ZB, Ji Y, Rao SX, Zhou J, Fan J, Wang XY, Gao Q. Radiomics score: a potential prognostic imaging feature for postoperative survival of solitary HCC patients. *BMC Cancer* 2018; **18**: 1148 [PMID: 30463529 DOI: 10.1186/s12885-018-5024-z]

16 **Ji GW**, Zhang YD, Zhang H, Zhu FP, Wang K, Xia YX, Zhang YD, Jiang WJ, Li XC, Wang XH. Biliary Tract Cancer at CT: A Radiomics-based Model to Predict Lymph Node Metastasis and Survival Outcomes. *Radiology* 2019; **290**: 90-98 [PMID: 30325283 DOI: 10.1148/radiol.2018181408]

17 **Park H**, Lim Y, Ko ES, Cho HH, Lee JE, Han BK, Ko EY, Choi JS, Park KW. Radiomics Signature on Magnetic Resonance Imaging: Association with Disease-Free Survival in Patients with Invasive Breast Cancer. *Clin Cancer Res* 2018; **24**: 4705-4714 [PMID: 29914892 DOI: 10.1158/1078-0432.CCR-17-3783]

18 **Park JE**, Kim D, Kim HS, Park SY, Kim JY, Cho SJ, Shin JH, Kim JH. Quality of science and reporting of radiomics in oncologic studies: room for improvement according to radiomics quality score and TRIPOD statement. *Eur Radiol* 2020; **30**: 523-536 [PMID: 31350588 DOI: 10.1007/s00330-019-06360-z]

19 **Collins GS**, Reitsma JB, Altman DG, Moons KG. Transparent Reporting of a multivariable prediction model for Individual Prognosis or Diagnosis (TRIPOD): the TRIPOD statement. *Ann Intern Med*

2015; **162**: 55-63 [PMID: 25560714 DOI: 10.7326/M14-0697]
20 **Ikeda M**, Arai Y, Park SJ, Takeuchi Y, Anai H, Kim JK, Inaba Y, Aramaki T, Kwon SH, Yamamoto S, Okusaka T; Japan Interventional Radiology in Oncology Study Group (JIVROSG); Korea Interventional Radiology in Oncology Study Group (KIVROSG). Prospective study of transcatheter arterial chemoembolization for unresectable hepatocellular carcinoma: an Asian cooperative study between Japan and Korea. *J Vasc Interv Radiol* 2013; **24**: 490-500 [PMID: 23466316 DOI: 10.1016/j.jvir.2013.01.003]
21 **Kudo M**, Matsui O, Izumi N, Kadoya M, Okusaka T, Miyayama S, Yamakado K, Tsuchiya K, Ueshima K, Hiraoka A, Ikeda M, Ogasawara S, Yamashita T, Minami T; Liver Cancer Study Group of Japan. Transarterial chemoembolization failure/refractoriness: JSH-LCSGJ criteria 2014 update. *Oncology* 2014; **87** Suppl 1: 22-31 [PMID: 25427730 DOI: 10.1159/000368142]
22 **Chernyak V**, Fowler KJ, Kamaya A, Kielar AZ, Elsayes KM, Bashir MR, Kono Y, Do RK, Mitchell DG, Singal AG, Tang A, Sirlin CB. Liver Imaging Reporting and Data System (LI-RADS) Version 2018: Imaging of Hepatocellular Carcinoma in At-Risk Patients. *Radiology* 2018; **289**: 816-830 [PMID: 30251931 DOI: 10.1148/radiol.2018181494]
23 **Kim H**, Park MS, Choi JY, Park YN, Kim MJ, Kim KS, Choi JS, Han KH, Kim E, Kim KW. Can microvessel invasion of hepatocellular carcinoma be predicted by pre-operative MRI? *Eur Radiol* 2009; **19**: 1744-1751 [PMID: 19247666 DOI: 10.1007/s00330-009-1331-8]
24 **Ji GW**, Zhu FP, Xu Q, Wang K, Wu MY, Tang WW, Li XC, Wang XH. Radiomic Features at Contrast-enhanced CT Predict Recurrence in Early Stage Hepatocellular Carcinoma: A Multi-Institutional Study. *Radiology* 2020; **294**: 568-579 [PMID: 31934830 DOI: 10.1148/radiol.2020191470]
25 **Sterne JA**, White IR, Carlin JB, Spratt M, Royston P, Kenward MG, Wood AM, Carpenter JR. Multiple imputation for missing data in epidemiological and clinical research: potential and pitfalls. *BMJ* 2009; **338**: b2393 [PMID: 19564179 DOI: 10.1136/bmj.b2393]
26 **Vesselle G**, Quirier-Leleu C, Velasco S, Charier F, Silvain C, Boucebci S, Ingrand P, Tasu JP. Predictive factors for complete response of chemoembolization with drug-eluting beads (DEB-TACE) for hepatocellular carcinoma. *Eur Radiol* 2016; **26**: 1640-1648 [PMID: 26455721 DOI: 10.1007/s00330-015-3982-y]
27 **Sun S**, Wang X, Chen J. Using Pre-Treatment Neutrophil-to-Lymphocyte Ratio to Predict the Prognosis of Young Patients with Hepatocellular Carcinoma Implemented Minimally Invasive Treatment. *J Adolesc Young Adult Oncol* 2020; **9**: 85-89 [PMID: 31621472 DOI: 10.1089/jayao.2019.0046]
28 **Kim JY**, Sinn DH, Gwak GY, Choi GS, Saleh AM, Joh JW, Cho SK, Shin SW, Carriere KC, Ahn JH, Paik YH, Choi MS, Lee JH, Koh KC, Paik SW. Transarterial chemoembolization *versus* resection for intermediate-stage (BCLC B) hepatocellular carcinoma. *Clin Mol Hepatol* 2016; **22**: 250-258 [PMID: 27377909 DOI: 10.3350/cmh.2016.0015]
29 **Katayama K**, Imai T, Abe Y, Nawa T, Maeda N, Nakanishi K, Wada H, Fukui K, Ito Y, Yokota I, Ohkawa K. Number of Nodules but not Size of Hepatocellular Carcinoma Can Predict Refractoriness to Transarterial Chemoembolization and Poor Prognosis. *J Clin Med Res* 2018; **10**: 765-771 [PMID: 30214648 DOI: 10.14740/jocmr3559w]
30 **Reginelli A**, Vanzulli A, Sgrazzutti C, Caschera L, Serra N, Raucci A, Urraro F, Cappabianca S. Vascular microinvasion from hepatocellular carcinoma: CT findings and pathologic correlation for the best therapeutic strategies. *Med Oncol* 2017; **34**: 93 [PMID: 28401484 DOI: 10.1007/s12032-017-0949-7]
31 **Xu W**, Li R, Liu F. Novel Prognostic Nomograms for Predicting Early and Late Recurrence of Hepatocellular Carcinoma After Curative Hepatectomy. *Cancer Manag Res* 2020; **12**: 1693-1712 [PMID: 32214844 DOI: 10.2147/CMAR.S241959]
32 **Bi WL**, Hosny A, Schabath MB, Giger ML, Birkbak NJ, Mehrtash A, Allison T, Arnaout O, Abbosh C, Dunn IF, Mak RH, Tamimi RM, Tempany CM, Swanton C, Hoffmann U, Schwartz LH, Gillies RJ, Huang RY, Aerts HJWL. Artificial intelligence in cancer imaging: Clinical challenges and applications. *CA Cancer J Clin* 2019; **69**: 127-157 [PMID: 30720861 DOI: 10.3322/caac.21552]
33 **Wakabayashi T**, Ouhmich F, Gonzalez-Cabrera C, Felli E, Saviano A, Agnus V, Savadjiev P, Baumert TF, Pessaux P, Marescaux J, Gallix B. Radiomics in hepatocellular carcinoma: a quantitative review. *Hepatol Int* 2019; **13**: 546-559 [PMID: 31473947 DOI: 10.1007/s12072-019-09973-0]
34 **Sun R**, Limkin EJ, Vakalopoulou M, Dercle L, Champiat S, Han SR, Verlingue L, Brandao D, Lancia A, Ammari S, Hollebecque A, Scoazec JY, Marabelle A, Massard C, Soria JC, Robert C, Paragios N, Deutsch E, Ferté C. A radiomics approach to assess tumour-infiltrating CD8 cells and response to anti-PD-1 or anti-PD-L1 immunotherapy: an imaging biomarker, retrospective multicohort study. *Lancet Oncol* 2018; **19**: 1180-1191 [PMID: 30120041 DOI: 10.1016/S1470-2045(18)30413-3]
35 **van Griethuysen JJM**, Fedorov A, Parmar C, Hosny A, Aucoin N, Narayan V, Beets-Tan RGH, Fillion-Robin JC, Pieper S, Aerts HJWL. Computational Radiomics System to Decode the Radiographic Phenotype. *Cancer Res* 2017; **77**: e104-e107 [PMID: 29092951 DOI: 10.1158/0008-5472.CAN-17-0339]
36 **Zhou Y**, He L, Huang Y, Chen S, Wu P, Ye W, Liu Z, Liang C. CT-based radiomics signature: a potential biomarker for preoperative prediction of early recurrence in hepatocellular carcinoma. *Abdom Radiol (NY)* 2017; **42**: 1695-1704 [PMID: 28180924 DOI: 10.1007/s00261-017-1072-0]
37 **Gao J**, Han F, Jin Y, Wang X, Zhang J. A Radiomics Nomogram for the Preoperative Prediction of Lymph Node Metastasis in Pancreatic Ductal Adenocarcinoma. *Front Oncol* 2020; **10**: 1654 [PMID:

32974205 DOI: 10.3389/fonc.2020.01654]

38 **Zhang JX**, Song W, Chen ZH, Wei JH, Liao YJ, Lei J, Hu M, Chen GZ, Liao B, Lu J, Zhao HW, Chen W, He YL, Wang HY, Xie D, Luo JH. Prognostic and predictive value of a microRNA signature in stage II colon cancer: a microRNA expression analysis. *Lancet Oncol* 2013; **14**: 1295-1306 [PMID: 24239208 DOI: 10.1016/S1470-2045(13)70491-1]

39 **Mosconi C**, Cucchetti A, Bruno A, Cappelli A, Bargellini I, De Benedittis C, Lorenzoni G, Gramenzi A, Tarantino FP, Parini L, Pettinato V, Modestino F, Peta G, Cioni R, Golfieri R. Radiomics of cholangiocarcinoma on pretreatment CT can identify patients who would best respond to radioembolisation. *Eur Radiol* 2020; **30**: 4534-4544 [PMID: 32227266 DOI: 10.1007/s00330-020-06795-9]

40 **Majeed Alneamy JS**, A Hameed Alnaish Z, Mohd Hashim SZ, Hamed Alnaish RA. Utilizing hybrid functional fuzzy wavelet neural networks with a teaching learning-based optimization algorithm for medical disease diagnosis. *Comput Biol Med* 2019; **112**: 103348 [PMID: 31356992 DOI: 10.1016/j.compbiomed.2019.103348]

41 **Das DK**, Dutta PK. Efficient automated detection of mitotic cells from breast histological images using deep convolution neutral network with wavelet decomposed patches. *Comput Biol Med* 2019; **104**: 29-42 [PMID: 30439598 DOI: 10.1016/j.compbiomed.2018.11.001]

42 **Chun SH**, Suh YJ, Han K, Park SJ, Shim CY, Hong GR, Lee S, Lee SH, Kim YJ, Choi BW. Differentiation of left atrial appendage thrombus from circulatory stasis using cardiac CT radiomics in patients with valvular heart disease. *Eur Radiol* 2020 [PMID: 32812175 DOI: 10.1007/s00330-020-07173-1]

43 **Zhou J**, Lu J, Gao C, Zeng J, Zhou C, Lai X, Cai W, Xu M. Predicting the response to neoadjuvant chemotherapy for breast cancer: wavelet transforming radiomics in MRI. *BMC Cancer* 2020; **20**: 100 [PMID: 32024483 DOI: 10.1186/s12885-020-6523-2]

World Journal of Gastroenterology

Submit a Manuscript: https://www.f6publishing.com

World J Gastroenterol 2021 January 14; 27(2): 208-223

DOI: 10.3748/wjg.v27.i2.208

ISSN 1007-9327 (print) ISSN 2219-2840 (online)

ORIGINAL ARTICLE

Observational Study

Real-world disease activity and sociodemographic, clinical and treatment characteristics of moderate-to-severe inflammatory bowel disease in Brazil

Cyrla Zaltman, Rogério Serafim Parra, Ligia Yukie Sassaki, Genoile Oliveira Santana, Maria de Lourdes Abreu Ferrari, Sender J Miszputen, Heda M B S Amarante, Roberto Luiz Kaiser Junior, Cristina Flores, Wilson R Catapani, José Miguel Luz Parente, Mauro Bafutto, Odery Ramos, Carolina D Gonçalves, Isabella Miranda Guimaraes, Jose J R da Rocha, Marley R Feitosa, Omar Feres, Rogerio Saad-Hossne, Francisco Guilherme Cancela Penna, Pedro Ferrari Sales Cunha, Tarcia NF Gomes, Rodrigo Bremer Nones, Mikaell Alexandre Gouvea Faria, Mírian Perpétua Palha Dias Parente, António S Scotton, Rosana Fusaro Caratin, Juliana Senra, Júlio Maria Chebli

ORCID number: Cyrla Zaltman 0000-0002-5236-6501; Rogério Serafim Parra 0000-0002-5566-9284; Ligia Yukie Sassaki 0000-0002-7319-8906; Genoile Oliveira Santana 0000-0001-5936-9791; Maria de Lourdes Abreu Ferrari 0000-0002-2122-5538; Sender J Miszputen 0000-0003-4487-5004; Heda M B S Amarante 0000-0001-7449-1138; Roberto Luiz Kaiser Junior 0000-0003-1952-1255; Cristina Flores 0000-0003-1623-4525; Wilson R Catapani 0000-0002-0412-2182; José Miguel Luz Parente 0000-0003-4563-2784; Mauro Bafutto 0000-0001-5585-3957; Odery Ramos 0000-0002-9730-6860; Carolina D Gonçalves 0000-0003-3663-4390; Isabella Miranda Guimaraes 0000-0003-3401-6580; Jose J R da Rocha 0000-0001-7118-0545; Marley R Feitosa 0000-0002-4440-2023; Omar Feres 0000-0003-3593-0526; Rogerio Saad-Hossne 0000-0002-8166-0304; Francisco Guilherme Cancela Penna 0000-0002-2338-5367; Pedro Ferrari Sales Cunha 0000-0003-4384-2606; Tarcia NF Gomes 0000-0003-2897-0327; Rodrigo Bremer Nones 0000-0002-6256-2629; Mikaell Alexandre Gouvea Faria 0000-0003-4121-0306;

Cyrla Zaltman, Carolina D Gonçalves, Isabella Miranda Guimaraes, Department of Internal Medicine, Federal University of Rio de Janeiro, Rio de Janeiro 21941-913, Brazil

Rogério Serafim Parra, Jose J R da Rocha, Marley R Feitosa, Omar Feres, Department of Surgery and Anatomy, Ribeirão Preto Medical School, University of São Paulo, Ribeirao Preto 14049-900, São Paulo, Brazil

Ligia Yukie Sassaki, Department of Internal Medicine, São Paulo State University (UNESP), Medical School, Botucatu 18618-687, São Paulo, Brazil

Genoile Oliveira Santana, IBD Unit, Federal University of Bahia, Salvador 41150-000, Bahia, Brazil

Maria de Lourdes Abreu Ferrari, Francisco Guilherme Cancela Penna, Pedro Ferrari Sales Cunha, Department of Clinical Medicine, Medical School, Universidade Federal de Minas Gerais, Belo Horizonte 30130-100, Minas Gerais, Brazil

Sender J Miszputen, Department of Gastroenterology, Escola Paulista de Medicina, São Paulo 04023-900, Brazil

Heda M B S Amarante, Odery Ramos, Hospital de Clinicas, Universidade Federal do Parana, Curitiba 80060-900, Parana, Brazil

Roberto Luiz Kaiser Junior, Department of Proctology, Beneficencia Portuguesa Hospital/Kaiser Day Hospital, Sao Jose do Rio Preto 15015110, São Paulo, Brazil

Cristina Flores, Department of Gastroenterology and Hepatology Sciences, Hospital de Clínicas, Universidade Federal do Rio Grande do Sul, Porto Alegre 90560002, Rio Grande do Sul, Brazil

Wilson R Catapani, Department of Gastroenterology, Faculdade de Medicina do ABC, Santo Andre 09060-870, São Paulo, Brazil

Mírian Perpétua Palha Dias Parente 0000-0002-0176-717X; António S Scotton 0000-0001-9247-0904; Rosana Fusaro Caratin 0000-0003-0922-8530; Juliana Senra 0000-0001-6787-806X; Júlio Maria Chebli 0000-0003-1527-0663.

Author contributions: Zaltman C, Parra RS, Sassaki LY, Santana GO, Ferrari MLA, Miszputen SJ, Amarante HMBS, Junior RLK, Flores C, Catapani WR, Parente JML, Bafutto M, Ramos O, Scotton AS and Chebli JM provided substantial contributions to the concept and design, acquisition of data, and analysis and interpretation of data; Gonçalves CD, Guimaraes IM, da Rocha JJR, Feitosa MR, Feres O, Saad-Hossne R, Penna FGC, Cunha PFS, Gomes TNF, Nones RB, Faria MAG, Parente MPPD, Caratin RF and Senra J contributed to the analysis and interpretation of data; all authors contributed to the editing of the manuscript, revised it critically for important intellectual content, granted approval of the version to be published and agreed to be accountable for all aspects of the work in ensuring that questions related to the accuracy or integrity of any part of the work are appropriately investigated and resolved.

Supported by Takeda Pharmaceuticals Brazil.

Institutional review board statement: The study protocol was reviewed and approved by the ethics committees of the participating centers.

Informed consent statement: All study participants provided written informed consent prior to study enrollment.

Conflict-of-interest statement: Cyrla Zaltman has received speaker fees from AbbVie, Janssen, Pfizer, UCB Pharma and Takeda, and received research funding from AbbVie, Takeda, and Janssen; Rogerio Serafim Parra has received fees for serving as speaker or as an advisory board member for AbbVie, Ferring Pharmaceuticals, Janssen, UCB Pharma and Takeda;

José Miguel Luz Parente, Department of General Medicine, Gastroenterology Unit, University Hospital, Federal University of Piaui, Teresina 64049-550, Piauí, Brazil

Mauro Bafutto, Department of Gastroenterology, Faculdade de Medicina, Universidade Federal de Goiás, Goiania 74535-170, Goias, Brazil

Rogerio Saad-Hossne, Department of Surgery, Botucatu Medical School at São Paulo State University (UNESP), Botucatu 18618687, São Paulo, Brazil

Tarcia NF Gomes, Department of Gastroenterology, UNIFESP, São Paulo 04040-002, Brazil

Rodrigo Bremer Nones, IBD unit, Gastroenterology Department, Hospital Nossa Senhora das Graças, Curitiba 80810-040, Parana, Brazil

Mikaell Alexandre Gouvea Faria, Department of Proctology, Kaiser Hospital Dia, Sao Jose do Rio Preto 15015-110, São Paulo, Brazil

Mírian Perpétua Palha Dias Parente, Health Sciences Center, Epidemiology Unit, State University of Piaui, Teresina 64001-280, Piauí, Brazil

António S Scotton, Department of Gastroenterology, CMIP Centro Mineiro de Pesquisa, Juiz de Fora 36010-570, Minas Gerais, Brazil

Rosana Fusaro Caratin, Scientific Affairs, Takeda Pharmaceuticals Brazil, São Paulo 04709-011, Brazil

Juliana Senra, Clinical Research, Takeda Pharmaceuticals Brazil, São Paulo 04709-011, Brazil

Júlio Maria Chebli, Department of Medicine, University Hospital of Federal University of Juiz de Fora, Juiz de Fora 36036-247, Minas Gerais, Brazil

Corresponding author: Cyrla Zaltman, MD, PhD, Associate Professor, Internal Medicine, Federal University of Rio de Janeiro, Hospital Universitario Clementino Fraga Filho - Rua Prof. Rodolpho Paulo Rocco 255 - 4 andar - Ilha do Fundao, Rio de Janeiro 21941-913, Brazil.
c.zaltman@gmail.com

Abstract

BACKGROUND

Understanding the treatment landscape of inflammatory bowel diseases (IBD) is essential for improving disease management and patient outcomes. Brazil is the largest Latin American country, and it presents socioeconomic and health care differences across its geographical regions. This country has the highest increase in IBD incidence and prevalence in Latin America, but information about the clinical and treatment characteristics of IBD is scarce.

AIM

To describe the sociodemographic, clinical, and treatment characteristics of IBD outpatients in Brazil overall and in the Southeast, South and Northeast/Midwest regions.

METHODS

Multicenter, cross-sectional study with a 3-year retrospective chart review component. Patients with moderate-to-severe Crohn's disease (CD) or ulcerative colitis (UC) were consecutively enrolled between October 2016 and February 2017. Active CD at enrollment was defined as a Harvey Bradshaw Index ≥ 8 or a CD Activity Index ≥ 220 or a calprotectin level > 200 μg/g or an active result based on colonoscopy suggestive of inadequate control during the previous year; active UC was defined as a partial Mayo score ≥ 5. Descriptive statistics were used to analyze all variables.

RESULTS

In a total of 407 included patients, CD was more frequent than UC, both overall (264 CD/143 UC patients) and by region (CD:UC ratios of 2.1 in the Southeast, 1.6 in the South and 1.2 in the Northeast/Midwest). The majority of patients were

Ligia Yukie Sassaki has received speaker fees from AbbVie and Takeda; Genoile Oliveira Santana has received speaker fees from AbbVie, Janssen, Takeda and UCB Pharma; and received research funding from Celgene, Roche and Takeda; Maria de Lourdes Abreu Ferrari has received fees for serving as a speaker or as an advisory board member for AbbVie, Ferring Pharmaceuticals, Janssen, UCB Pharma, and Takeda; Sender Jankiel Miszputen has received fees for serving as speaker or as a consultant for Farmoquimica, Janssen and Marjan, and received research funding from Ache, Roche and Takeda; Cristina Flores has received speaker fees from Janssen, Takeda, and AbbVie; and received fees for serving as an advisory board member for Janssen; Wilson Roberto Catapani has received fees for serving as a speaker or as an advisory board member for Janssen and Takeda; Jose Miguel Luz Parente has received speaker fees from Takeda; Mauro Bafutto has received speaker fees from Takeda, AbbVie, Janssen, UCB and Farmoquimica; and received fees for serving as an advisory board member for AbbVie and Janssen; Jose Joaquim Ribeiro da Rocha has received speaker fees from Nestle; Marley Ribeiro Feitosa has received speaker fees from Janssen and Nestle, and fees for scientific congresses' support by Janssen, AbbVie, Takeda, Ferring and Nestle and was a subinvestigator in scientific studies sponsored by Janssen, AbbVie and Takeda; Rogerio Saad Hossne has received speaker fees from AbbVie, Janssen, Pfizer and Takeda; Francisco Guilherme Cancela e Penna has received speaker fees from Janssen, Takeda, AbbVie and UCB; Tarcia Nogueira Ferreira Gomes has received research funding from Coordenacao de Aperfeicoamento de Pessoal de Nivel Superior and Takeda; and has received speaker fees from Janssen; Rodrigo Bremer Nones has received speaker fees from AbbVie, Ferring Pharmaceuticals, Janssen, Nestle, Novartis, Pfizer, UCB Pharma and

female (54.2% of CD; 56.6% of UC), and the mean ages were 45.9 ± 13.8 years (CD) and 42.9 ± 13.0 years (UC). The median disease duration was 10.0 (range: 0.5-45) years for both IBD types. At enrollment, 44.7% [95% confidence interval (CI): 38.7-50.7] of CD patients and 25.2% (95%CI: 18.1-32.3) of UC patients presented with active disease. More than 95% of IBD patients were receiving treatment at enrollment; CD patients were commonly treated with biologics (71.6%) and immunosuppressors (67.4%), and UC patients were commonly treated with mesalazine [5-Aminosalicylic acid (5-ASA)] derivates (69.9%) and immunosuppressors (44.1%). More than 50% of the CD patients had ileocolonic disease, and 41.7% presented with stricturing disease. One-quarter of CD patients had undergone CD-related surgery in the past 3 years, and this proportion was lower in the Northeast/Midwest region (2.9%).

CONCLUSION

In Brazil, there are regional variations in IBD management. CD outweighs UC in both frequency and disease activity. However, one-quarter of UC patients have active disease, and most are receiving 5-ASA treatment.

Key Words: Inflammatory bowel disease; Crohn's disease; Ulcerative colitis; Disease activity; Epidemiology; Treatment

©The Author(s) 2021. Published by Baishideng Publishing Group Inc. All rights reserved.

Core Tip: In this multicenter study from Brazil, a substantial proportion (45%, and less pronounced in the South) of Crohn's disease patients had active disease despite being treated with biologics and immunosuppressors. One-quarter (higher in the Northeast/Midwest region) of ulcerative colitis patients had active disease, with the majority treated with 5-Aminosalicylic acid derivatives. In the largest Latin American country, regional differences were observed regarding inflammatory bowel diseases (IBD) activity and treatment patterns. Findings from this study can further elucidate about variations in clinical practice, ultimately promoting debate among specialists regarding the optimal management of IBD patients.

Citation: Zaltman C, Parra RS, Sassaki LY, Santana GO, Ferrari MLA, Miszputen SJ, Amarante HMBS, Kaiser Junior RL, Flores C, Catapani WR, Parente JML, Bafutto M, Ramos O, Gonçalves CD, Guimaraes IM, da Rocha JJR, Feitosa MR, Feres O, Saad-Hossne R, Penna FGC, Cunha PFS, Gomes TN, Nones RB, Faria MAG, Parente MPPD, Scotton AS, Caratin RF, Senra J, Chebli JM. Real-world disease activity and sociodemographic, clinical and treatment characteristics of moderate-to-severe inflammatory bowel disease in Brazil. *World J Gastroenterol* 2021; 27(2): 208-223
URL: https://www.wjgnet.com/1007-9327/full/v27/i2/208.htm
DOI: https://dx.doi.org/10.3748/wjg.v27.i2.208

INTRODUCTION

Inflammatory bowel diseases (IBDs) comprise mainly Crohn's disease (CD) and ulcerative colitis (UC)[1]. Signs and symptoms of active IBD may include abdominal pain, rectal bleeding, diarrhea and fatigue[2]. The global incidence of UC varies from 0.5 to 24.5 *per* 1000000 inhabitants, while the CD incidence ranges from 0.1 to 16 *per* 1000000 inhabitants[3,4]. Although the incidence of IBD has been stable in European and North American regions, the incidence and prevalence of IBD is steadily rising across Latin American (LA) countries[5,6].

Brazil is the largest LA country, with a 2017 Human Development Index of 0.759[7]. However, socioeconomic and health care disparities reduce this index to 0.578 when it is adjusted for inequality[7]. These disparities are also observed among Brazilian states or regions. States in the South and Southeast regions have higher socioeconomic levels and a large influence of European immigrant communities than the Northeastern states[8].

Takeda; Antonio Scafuto Scotton has received speaker fees from Janssen, Novartis, AbbVie, MSD, and EMS, and has received research funding from Janssen, Novartis, AbbVie, Roche, Pfizer, Bristol, Lilly, Novo Nordisk, Anthera, AstraZeneca, GSK, UCB, Sanofi, Takeda, Parexel, IQVIA, PPD, PRA, ICON, INP Research, Covance, and In Trials; Rosana Fusaro Caratin was an employee at Takeda Pharmaceuticals Brazil at the time of the study and when this manuscript was written; Juliana Tosta Senra is an employee at Takeda Pharmaceuticals Brazil; Julio Maria Fonseca Chebli has received speaker fees from AbbVie, Janssen, UCB Pharma and Takeda; Heda Maria Barska dos Santos Amarante, Roberto Kaiser Junior, Odery Ramos, Carolina Dias Gonçalves, Isabella de Miranda Guimaraes, Omar Feres, Mikaell Alexandre Gouvea Faria, Pedro Ferrari Sales da Cunha, Mírian Perpétua Palha Dias Parente declare that they have no conflict of interest

STROBE statement: The authors have read the STROBE Statement—checklist of items, and the manuscript was prepared and revised according to the STROBE Statement—checklist of items.

Open-Access: This article is an open-access article that was selected by an in-house editor and fully peer-reviewed by external reviewers. It is distributed in accordance with the Creative Commons Attribution NonCommercial (CC BY-NC 4.0) license, which permits others to distribute, remix, adapt, build upon this work non-commercially, and license their derivative works on different terms, provided the original work is properly cited and the use is non-commercial. See: http://creativecommons.org/Licenses/by-nc/4.0/

Manuscript source: Unsolicited manuscript

Specialty type: Gastroenterology and hepatology

Epidemiologic information about IBD in Brazil is limited[4,9,10]. This country has one of the highest increases in IBD incidence among newly industrialized countries, with annual percentage increases of 11.1% in CD incidence and 14.9% in UC incidence from 1988 to 2012[5,6]. In addition, the incidence of IBD in Brazil was estimated at 0.08 *per* 100000 inhabitants in 1988, but the CD incidence rose from 0.68 (1991-1995) to 3.5 (2001-2005), being observed a peak incidence of 5.5 *per* 100000 inhabitants in 2015[11]. The same trend can be observed at a regional level, with Sao Paulo State showing the highest IBD incidence when compared to other areas of Brazil[12-14].

Given the complexity and heterogeneity of IBD, treatment decisions should consider the disease activity and severity, the extent of the inflammatory process, steroid dependency and risk factors for poor prognosis, among other factors[9,15,16]. Treatments are effective in relieving symptoms and can alter the natural debilitating course of these diseases, and several strategies are available[1,17].

In Brazil, current treatment options include mesalazine [5-Aminosalicylic acid (5-ASA)] derivates, steroids, immunosuppressors and biologics therapy, such as antitumor necrosis factor (anti-TNF), anti-integrin drugs, anti-interleukin (IL)12 and IL-23 (only for CD treatment) and Janus Kinase inhibitor (tofacitinib, for UC treatment)[17-20]. Biologic therapy has been increasingly used, especially for moderate-to-severe IBD or for patients with no response to conventional treatments[9]. Infliximab[17,21], adalimumab[22,23], certolizumab, vedolizumab[18,20] and ustekinumab[19,24] are effective for the induction and maintenance of IBD clinical remission. However, some constraints on the Public Health System have been reported regarding access to biologic drugs for UC (e.g., costs and distance from health care facilities), which may compromise the achievement and maintenance of disease control.

Due to the increased incidence and prevalence of IBD and the diversity of IBD treatments in Brazil, this study aimed to describe the sociodemographic, clinical and therapeutic characteristics of IBD outpatients in Brazil overall and in three major geographical regions of Brazil: The Southeast (SE), South and Northeast/Midwest (NE/MW).

MATERIALS AND METHODS

Study design and participants

The Real-world Data of Moderate to Severe Inflammatory Bowel Disease in Brazil (RISE BR) study was a multicenter, noninterventional, cross-sectional study with a 3-year retrospective chart review component. Patients were enrolled consecutively from October 2016 until February 2017 at scheduled clinical appointments at 14 Brazilian IBD reference centers in both the public (9 centers) and private (5 centers) health systems and from across different areas in Brazil: SE (8 centers from the states of Sao Paulo, Rio de Janeiro and Minas Gerais), South (3 centers from the states of Parana and Rio Grande do Sul) and NE/MW (3 from Bahia, Piaui and Goias states, the latter from Midwest region).

Eligible participants had an established diagnosis of UC or CD, were aged ≥ 18 years old and had a previous event suggesting moderate-to-severe IBD at least 6 mo prior to enrollment, irrespective of disease activity at enrollment. Exclusion criteria were presenting indeterminate or unclassified colitis, participation in an interventional study within 3 years prior to enrollment, mental incapacity, unwillingness to participate or language barriers precluding adequate understanding or cooperation with the study protocol. Patients who were hospitalized at enrollment or under off-label treatment with vedolizumab were also excluded.

The study was approved by local ethics committees, and all participants provided written informed consent prior to the study (ClinicalTrials.gov Identifier: NCT02822235).

Data variables

Sociodemographic data (sex, age, educational level, and professional status) and smoking habits were collected from the medical records. The clinical variables related to IBD included the time since IBD diagnosis, Montreal classification (*i.e.*, location and severity/behavior)[25], steroid status (dependent or refractory), familial history of IBD and the presence of extraintestinal manifestations (EIMs). Steroid-dependent disease was defined in patients who either (1) were unable to reduce steroid use to below the equivalent of prednisolone 10 mg/d within 3 mo of starting steroids, without recurrent disease; or (2) had a relapse within 3 mo of stopping glucocorticoids. Steroid-refractory disease was defined as active disease despite the use of up to 0.75 mg/kg/d

Country/Territory of origin: Brazil

Peer-review report's scientific quality classification
Grade A (Excellent): 0
Grade B (Very good): 0
Grade C (Good): C
Grade D (Fair): 0
Grade E (Poor): 0

Received: October 26, 2020
Peer-review started: October 26, 2020
First decision: December 3, 2020
Revised: December 17, 2020
Accepted: December 28, 2020
Article in press: December 28, 2020
Published online: January 14, 2021

P-Reviewer: Chang YY
S-Editor: Fan JR
L-Editor: A
P-Editor: Li JH

of prednisolone over 4 wk.

At enrollment, CD activity was assessed by the investigator, and active disease was defined according to one of the following criteria: Harvey Bradshaw Index (HBI) ≥ 8[26] or Crohn's Disease Activity Index (CDAI) ≥ 220[2] or calprotectin > 200 μg/g or colonoscopy suggestive of inadequate control performed during the previous year. UC activity at enrollment was assessed with the 9-item partial Mayo (pMayo) score. This score results from the scores for the three categories of the total Mayo score (bleeding, stool frequency, physician assessment) without the endoscopic subscore[27]. When available, the endoscopic findings at enrollment were assessed using the Mayo endoscopic subscore, where a score ≥ 2 corresponds to moderate-to-severe UC[27]. Active UC was defined as pMayo ≥ 5.

Current and prior IBD treatment (*i.e.*, 5-ASA derivates, immunosuppressors, biologics, steroids and antibiotics) and the number of previous outpatient visits, surgeries and hospitalizations due to IBD were collected from medical records for the previous 3 years.

Statistical analysis

Overall, 400 patients were expected to be enrolled, irrespective of IBD type. This sample size allowed estimates of disease activity with a 95% confidence interval (CI) and a margin of error < 5%. All analyses were broken down by IBD type (UC or CD) and by geographic region (South, SE and NE/MW).

Descriptive statistics (mean, median, standard deviation and minimum-maximum) were used to analyze sociodemographic, clinical and treatment-related variables. Student's t-test for independent samples or the Mann-Whitney test were used to compare CD and UC patients in terms of quantitative variables. Statistical tests were two-tailed, and significance was set at 5%. There was no imputation of missing values. Statistical analysis was performed using SAS® (version 9.4, SAS Institute, Inc., Cary, NC, United States).

RESULTS

Sociodemographic and clinical characteristics of the sample, overall and by region

Overall, 407 patients – 264 (64.9%) with CD and 143 (35.1%) with UC – were included in the study (Figure 1). The ratio of CD:UC patients was 1.85 for the overall sample, 2.09 in the SE, 1.62 in the South and 1.21 in the NE/MW.

The median age at enrollment was 41.0 (20-72) years for CD and 45.0 (19-84) years for UC (P = 0.029), and the majority of patients were female (54.2% and 56.6% in CD and UC, respectively) (Table 1). Approximately 12.5% of the CD patients and 10.5% of the UC patients had a family history of IBD. The median disease duration was 10.0 years for both CD and UC. No statistically significant differences were observed for any sociodemographic or CD or UC clinical characteristics except for age at enrollment.

The South region had a lower prevalence of females with CD (41.2%) than the SE and NE/MW regions did (56.6% and 52.9%, respectively) (Table 1). The median age at CD diagnosis was higher in the NE/MW group (42.0 years) than in the South and SE groups (29.0 and 28.0 years, respectively). The South had a higher proportion of CD patients with higher education (65.2%) and a lower proportion of unemployed CD patients (16.7%) than the SE (28.6%) and NE/MW (30.4%) regions. Most CD patients in the South region were treated at private hospitals (67.6%), while in the NE/MW and SE regions, public hospitals were the most frequent treatment setting (81.1% and 79.4% of patients, respectively). Over 70% of CD patients in the SE region had never smoked, compared to 53.6% in the South and 65.2% in the NE/MW. The presence of EIMs in CD patients was higher in the NE/MW (53.8%) and lower in the South (25.1%).

The NE/MW region had a higher prevalence of females with UC (64.3%) than the SE and South regions did (57.4% and 42.9%, respectively) (Table 1). The median disease duration of UC was higher in the South (14.0 years) and lower in the NE/MW (6.0 years). Half of the UC patients in the South (50.0%) had a higher education, compared to 21.2% in the SE and 6.2% in the NE/MW. The proportion of unemployment among UC patients was higher in the SE (26.6%) and lower in NE/MW (14.8%). Most UC patients in the SE and NE/MW regions were treated at public hospitals (87.2% and 89.3%, respectively), while in the South, private hospitals were the most frequently used treatment settings (85.7% of patients). Over 70% of UC patients in the SE and South regions had never smoked, compared to 45.5% in the NE/MW. The prevalence of EIMs in UC patients was lower in the South (25.0%) and

Table 1 Sociodemographic characteristics and clinical features of Crohn's disease and ulcerative colitis patients by geographic region of Brazil

	Total		Southeast		South		Northeast/Midwest	
	CD (*n* = 264)	UC (*n* = 143)	CD (*n* = 196)	UC (*n* = 94)	CD (*n* = 34)	UC (*n* = 21)	CD (*n* = 34)	UC (*n* = 28)
Age (yr)	41.0 [20-72]	45.0 [19-84]	41.0 [21-72]	44.0 [20-78]	37.5 [20-67]	44.0 [19-66]	41.0 [24-68]	51.0 [26-84]
Female	143 (54.2)	81 (56.6)	111 (56.6)	54 (57.4)	14 (41.2)	9 (42.9)	18 (52.9)	18 (64.3)
Disease duration (yr)	10.0 [0.5-45.0]	10.0 [0.5-31.0]	11.0 [1.0-45.0]	10.0 [0.5-31.0]	8.0 [1.0-30.0]	14.0 [1.0-29.0]	9.0 [1.0-31.0]	6.0 [1.0-22.0]
Age at diagnosis (yr)	29.0 [12-70]	34.0 [14-70]	28.0 [12-70]	33.0 [15-64]	29.0 [18-63]	32.0 [14-64]	42.0 [20-70]	32.0 [18-60]
Educational level[1]								
Not literate	3 (1.4)	0 (0.0)	2 (1.2)	0 (0.0)	0 (0.0)	0 (0.0)	1 (4.3)	0 (0.0)
Primary school	52 (25.1)	38 (38.8)	47 (29.2)	26 (39.4)	3 (13.0)	2 (12.5)	2 (8.7)	10 (62.5)
Secondary school	83 (40.1)	37 (37.7)	66 (41.0)	26 (39.4)	5 (21.7)	6 (37.5)	13 (56.5)	5 (31.3)
Higher education	69 (33.3)	23 (23.5)	46 (28.6)	14 (21.2)	15 (65.2)	8 (50.0)	7 (30.4)	1 (6.2)
Missing	57	45	35	28	11	5	11	12
Professional situation								
Employed	101 (44.3)	53 (42.7)	77 (44.0)	32 (40.5)	13 (54.2)	13 (72.2)	11 (37.9)	8 (29.6)
Unemployed	61 (26.8)	33 (26.6)	44 (25.1)	21 (26.6)	4 (16.7)	3 (16.7)	13 (44.8)	9 (33.3)
Retired	30 (13.2)	15 (12.1)	24 (13.7)	11 (13.9)	5 (20.8)	0 (0.0)	1 (3.4)	4 (14.8)
Student	10 (4.4)	5 (4.0)	8 (4.6)	3 (3.8)	2 (8.3)	1 (5.6)	0 (0.0)	1 (3.7)
Other	26 (11.4)	18 (14.5)	22 (12.6)	12 (15.2)	0 (0.0)	1 (5.6)	4 (13.8)	5 (18.5)
Missing	36	19	21	15	10	3	5	1
Health system								
Public	197 (74.6)	110 (76.9)	159 (81.1)	82 (87.2)	11 (32.4)	3 (14.3)	27 (79.4)	25 (89.3)
Private	67 (33.3)	33 (23.1)	37 (18.9)	12 (12.8)	23 (67.6)	18 (85.7)	7 (20.6)	3 (10.7)
Family history of IBD	33 (12.5)	15 (10.5)	27 (13.8)	10 (10.6)	3 (8.9)	3 (14.3)	3 (8.8)	2 (7.1)
Smoking habits[2]								
Current smoker	24 (9.9)	3 (2.3)	20 (10.5)	3 (3.3)	3 (10.7)	0 (0.0)	1 (4.3)	0 (0.0)
Former smoker	47 (19.4)	38 (28.8)	30 (15.7)	21 (23.1)	10 (35.7)	5 (26.3)	7 (30.4)	12 (54.5)
Never smoked	171 (70.7)	91 (68.9)	141 (73.8)	67 (73.6)	15 (53.6)	14 (73.7)	15 (65.2)	10 (45.5)
Missing	22	11	5	3	6	2	11	6
Any EIM[3]	54 (37.8)	30 (38.0)	41 (38.7)	21 (42.0)	6 (25.0)	4 (25.0)	7 (53.8)	5 (38.5)
Use of steroids[4]								
Steroid dependent	31 (14.8)	23 (19.3)	21 (13.8)	9 (11.8)	6 (19.4)	11 (55.0)	4 (15.4)	3 (13.0)
Steroid refractory	16 (7.7)	11 (9.2)	10 (6.6)	7 (9.2)	2 (6.5)	2 (10.0)	4 (15.4)	2 (8.7)
No previous use	87 (41.6)	36 (30.3)	66 (43.4)	22 (28.9)	10 (32.3)	3 (15.0)	11 (42.3)	11 (47.8)
Unknown	75 (35.9)	49 (41.2)	55 (36.2)	38 (50.0)	13 (41.9)	4 (20.0)	7 (26.9)	7 (30.4)
Missing	55	24	44	18	3	1	8	5

Data are shown as *n* (%) or median [range].

[1]Highest level attended.

[2]Current smokers: patients who were smoking at enrollment and had smoked 100 cigarettes in their lifetime. Former smokers: Patients who were not smoking at enrollment but had smoked 100 cigarettes in their lifetime.

[3]Extraintestinal manifestations observed: For the Crohn's disease population–arthralgia (reported in all regions), arthritis (in the Southeast and

Northeast/Midwest), sacroiliitis (only in the Southeast), erythema nodosum (only in the Southeast), pyoderma gangrenosum (only in the Southeast), uveitis (only in the Southeast), cholelithiasis (only in the Southeast), nephrolithiasis (only in the Southeast), hypertension (only in the Southeast), other (not specified) (reported in all regions); for the Ulcerative colitis population–arthralgia (reported in the Southeast and Northeast/Midwest), arthritis (only in the Southeast), sacroiliitis (in the South and Northeast/Midwest), pyoderma gangrenosum (only in the Northeast/Midwest), psoriasis (only in the Southeast), uveitis (only in Southeast), sclerosing cholangitis (in the Southeast and South), nephrolithiasis (only in Southeast), hypertension (in Southeast and Northeast/Midwest), other (not specified) (in the Southeast and South).

[4]Steroid-dependent disease: Patients who either (1) were unable to reduce steroid use to below the equivalent of prednisolone 10 mg/d within 3 mo of starting steroids, without recurrent disease; or (2) had a relapse within 3 mo of stopping glucocorticoids; steroid-refractory disease: Active disease despite the use of up to 0.75 mg/kg/d of prednisolone over 4 wk. CD: Crohn's disease; EIM: Extraintestinal manifestations; UC: Ulcerative colitis; IBD: Inflammatory bowel diseases.

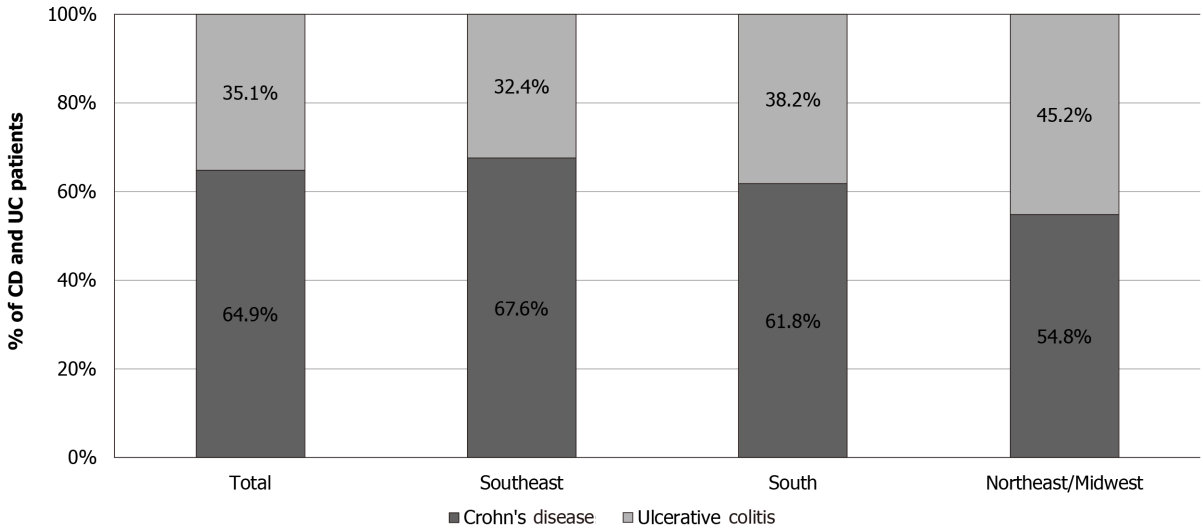


Figure 1 Frequency (%) of Crohn's disease and ulcerative colitis, overall and by Brazilian region. CD: Crohn's disease; UC: Ulcerative colitis.

higher in the SE (42.0%). The presence of steroid-dependent behavior was highest in the South at 55.0% of patients, compared to 13.0% in the NE/MW and 11.8% in the SE.

Regarding the Montreal classification and disease activity at enrollment (Table 2), most CD patients (56.8%) had an ileocolonic location, and this location was most frequent in the SE region (59.2%). The most frequent CD phenotype was stricturing disease (41.7%), and the rate was higher in the SE group (45.4%). A total of 105 (39.8%) CD patients had symptomatic perianal disease. Overall, 44.7% (95%CI: 38.7%-50.7%) of CD patients presented with active disease at enrollment: 17.4% scored HBI ≥ 8 or CDAI ≥ 220, 15.2% had fecal calprotectin > 200 μg/g, and 26.1% had a colonoscopy result suggestive of disease activity (presence of ulcerative lesions in any segment of the gut) during the previous year. The proportion of patients with active CD did not vary substantially across the regions. Nevertheless, only half of the patients had undergone CDAI evaluations.

Approximately half of UC patients presented with pancolitis (51.7%), and this prevalence was lower in the NE/MW region (28.6%) (Table 2). Over half (52.1%) of the UC patients had moderate or severe disease according to the Mayo endoscopic subscore (although nearly half of the patients had missing data). Approximately 40% of UC patients were asymptomatic according to the Montreal classification. The median total Mayo score was 2.0 (0.0-10.0, n = 71), although data were missing for nearly half of the patients. A quarter of UC patients (25.2%; 95%CI: 18.1%-32.3%) had active disease at enrollment. Active UC was most predominant in the NE/MW (42.9% of patients), compared to 23.8% and 20.2% of patients in the South and SE regions, respectively.

IBD treatment patterns and health care resource utilization

The vast majority of CD and UC patients were on treatment at enrollment (97.0% of CD patients and 96.5% of UC patients) (Table 3). The most common treatments among CD patients were biologics (71.6% of patients), followed by immunosuppressors (67.4%). This pattern was similar across the regions. The most frequent treatment among UC patients was 5-ASA derivatives (69.9% of patients), followed by

Table 2 Montreal classification and activity scores at enrollment by inflammatory bowel diseases type and geographic region

CD classification	CD patients (*n* = 264)	Southeast (*n* = 196)	South (*n* = 34)	Northeast/Midwest (*n* = 34)
Location[1]				
L1-ileal	67 (25.4)	50 (25.5)	10 (29.4)	7 (20.6)
L2-colonic	42 (15.9)	26 (13.3)	5 (14.7)	11 (32.4)
L3-ileocolonic	150 (56.8)	116 (59.2)	18 (52.9)	16 (47.1)
L4-upper GI tract disease	17 (6.4)	11 (5.6)	2 (5.9)	4 (11.8)
Behavior				
B1-Nonstricturing/nonpenetrating	58 (22.0)	33 (16.8)	9 (26.5)	16 (47.1)
B2-Stricturing	110 (41.7)	89 (45.4)	14 (41.2)	7 (20.6)
B3-Penetrating	91 (34.5)	70 (35.7)	10 (29.4)	11 (32.4)
Perianal disease	105 (39.8)	87 (44.4)	12 (35.3)	6 (17.6)
HBI score	2.0 [0-37]	2.0 [0-37]	2.0 [0-17]	3.5 [0-12]
Missing	34	32	0	2
CDAI	137.0 [-25-495]	141.0 [-25-495]	NA	93.0 [-22-292]
Missing	187	137	34	16
Active CD[2]	118 (44.7)	89 (45.4)	13 (38.2)	16 (47.0)
HBI ≥ 8 or CDAI ≥ 220	46 (17.4)	UNK	UNK	UNK
Fecal calprotectin > 200 μg/g	40 (15.2)	UNK	UNK	UNK
Colonoscopy result suggestive of disease activity during the previous year	69 (26.1)	UNK	UNK	UNK
UC classification	**UC patients (*n* = 143)**	**Southeast (*n* = 94)**	**South (*n* = 21)**	**Northeast/Midwest (*n* = 28)**
Extension				
E1-distal UC	43 (30.1)	27 (28.7)	8 (38.1)	8 (28.6)
E2-left-sided	26 (18.2)	12 (12.8)	2 (9.5)	12 (42.9)
E3-pancolitis	74 (51.7)	55 (58.5)	11 (52.4)	8 (28.6)
Severity				
S0-asymptomatic	57 (39.9)	36 (38.3)	9 (42.9)	12 (42.9)
S1-mild UC	32 (22.4)	25 (26.6)	3 (14.3)	4 (14.3)
S2-moderate UC	40 (28.0)	25 (26.6)	7 (33.3)	8 (28.6)
S3-severe UC	14 (9.8)	8 (8.5)	2 (9.5)	4 (14.3)
Mayo endoscopic subscore (*n* = 71)				
Normal	16 (22.5)	9 (19.1)	1 (12.5)	6 (37.5)
Mild disease	18 (25.4)	13 (27.7)	2 (25.0)	3 (18.8)
Moderate disease	28 (39.4)	20 (42.6)	3 (37.5)	5 (31.3)
Severe disease	9 (12.7)	5 (10.6)	2 (25.0)	2 (12.5)
Missing	72	47	13	12
Total Mayo score	2.0 [0.0-10.0]	3.0 [0.0-9.0]	2.5 [0.0-10.0]	2.0 [0.0-8.0]
Missing	72	47	13	12
Partial Mayo score	1.0 [0.0-9.0]	1.5 [0.0-9.0]	1.0 [0.0-9.0]	1.5 [0.0-8.0]
Active UC[2]	36 (25.2)	19 (20.2)	5 (23.8)	12 (42.9)

Data are shown as *n* (%) or median [range].
[1]More than one possible option: L4 includes isolated upper gastrointestinal (GI) tract disease or upper GI tract disease combined with L1, L2 or L3.
[2]Active disease at enrollment was defined as presenting Harvey-Bradshaw index ≥ 8 or Crohn's disease activity index ≥ 220 or fecal calprotectin > 200 mg/g or colonoscopy suggestive of inadequate control during the previous year (for Crohn's disease patients) and partial Mayo score ≥ 5 (for ulcerative colitis patients). CD: Crohn's disease; CDAI: Crohn's disease activity index; HBI: Harvey-Bradshaw index; UC: Ulcerative colitis; UNK: Unknown; GI: Gastrointestinal.

immunosuppressors (44.1%). Most UC patients in the NE/MW region (96.4%) were being treated with 5-ASA derivatives, while over half (57.1%) of patients in the South region were being treated with immunosuppressors.

Approximately one-quarter (25.4%) of patients had undergone CD-related surgery in the past 3 years, and this proportion was lower in the NE/MW region (2.9% of patients). The median number of CD-related surgeries *per* patient in the previous 3 years was 1.0 (range 1-5). The median number of CD-related hospitalizations in the previous 3 years was 1.0 (range 1-5) *per* patient, and the median number of CD specialist appointments was 11.0 (range 1-45) *per* patient.

Only 2.8% of patients, all from the SE region, had undergone UC-related surgery in the previous 3 years, and the median number of surgeries *per* patient was 2.0 (range 1-2). The median number of UC-related hospitalizations in the previous 3 years was 1.0 (range 1-5), and the median number of UC specialist appointments was 10.0 (range 1-39), which was higher in the South (median 14.0 appointments) than in the SE and NE/MW (median 10.0 and 9.0, respectively). The proportion of patients with at least one hospitalization in the previous 3 years was higher among the CD patients than among the UC patients (38.3% *vs* 19.6%, respectively; $P < 0.001$).

DISCUSSION

The objective of the RISE BR study was to characterize IBD patients in terms of their sociodemographic and clinical features and their treatment patterns. As Brazil is a large country with known inequalities, this study allowed us to understand variations across the South, SE and NE/MW regions.

Although UC is more prevalent than CD in most LA countries[28], including Brazil[10,12,13,29], we found a predominance of CD compared to UC, both overall and by region. Nevertheless, our findings are aligned with the CD and UC prevalence (24.1 and 14.1/100000, respectively) reported in a systematic review from LA[11] and those reported in a recent epidemiological characterization of 579 IBD patients from a Southeastern Brazilian tertiary care center, which found a CD prevalence of 56.1%[30].

The sociodemographic and clinical features of IBD patients varied across the three Brazilian regions. Females were more predominant in the SE and NE/MW regions (for both diseases), a finding that is in line with previous studies[13,14,29-31]. In the NE/MW region, the majority of IBD patients had a lower educational level and lower employment status. The latter finding could be attributed not only to the incapacity associated with the disease but also to the difficulty of obtaining work opportunities in the region. In the South, IBD patients were mostly men, had higher education and employment rates and were more likely to be followed up in the private setting than patients in the other regions.

Patients from the SE had fewer EIMs, and a lower proportion had active UC. These findings may suggest socioeconomic disparities among the regions, which can translate into differences in access to and use of health care services and medicines.

A substantial proportion of CD patients (44.7%) showed active disease based on clinical (HBI or CDAI), biomarker (fecal calprotectin) or endoscopic outcomes (presence of ulcerative lesions in any segment of the gut). Similar proportions were found across the three Brazilian regions, although the proportions were somewhat lower in the South region. On the other hand, a quarter of UC patients had active disease based on pMayo or Mayo endoscopic subscores, and this proportion was substantially higher in the NE/MW region (42.9%). These results highlight the importance of adopting treatment targets for IBD that can be used as a "treat-to-target" management strategy, which will ultimately improve disease outcomes[32].

Most CD patients (56.8%) had ileocolonic disease, and a substantial proportion of patients showed a complicated phenotype (41.7% with stricturing disease), particularly in the SE and South regions. Lima Martins *et al*[29] reported a lower prevalence of ileocolonic location (30.9%) and a less stricturing phenotype (21.0%).

Table 3 Inflammatory bowel diseases treatment at enrollment and use of health care resources during the previous 3 years by inflammatory bowel diseases type and by geographic region

	CD patients (*n* = 264)	Southeast (*n* = 196)	South (*n* = 34)	Northeast/Midwest (*n* = 34)
Any CD treatment at enrollment[1]	256 (97.0)	189 (96.4)	33 (97.1)	34 (100.0)
CD treatment at enrollment[2]				
5-ASA derivates	39 (14.8)	24 (12.2)	7 (20.6)	8 (23.5)
Biological therapy	189 (71.6)	140 (71.4)	21 (61.8)	28 (82.4)
Infliximab	106 (40.2)	NA	NA	NA
Adalimumab	78 (29.5)	NA	NA	NA
Vedolizumab	4 (1.5)	NA	NA	NA
Certolizumab	1 (0.4)	NA	NA	NA
Ustekinumab	1 (0.4)	NA	NA	NA
Immunosuppressors	178 (67.4)	133 (67.9)	18 (52.9)	27 (79.4)
Thiopurines	165 (62.5)	NA	NA	NA
Methotrexate	14 (5.3)	NA	NA	NA
Corticosteroids	30 (11.4)	21 (10.7)	2 (5.9)	7 (20.6)
Prednisone	29 (11.0)	NA	NA	NA
Hydrocortisone	1 (0.4)	NA	NA	NA
Methylprednisolone	1 (0.4)	NA	NA	NA
Antibiotics	14 (5.3)	9 (4.6)	1 (2.9)	4 (11.8)
Any previous CD-related surgery[3]	67 (25.4)	58 (29.6)	8 (23.5)	1 (2.9)
CD-related surgeries *per* patient	1.0 [1-5]	1.0 [1-5]	1.5 [1-3]	2.0
Any previous CD-related hospitalization	101 (38.3)	71 (36.2)	14 (41.2)	16 (47.0)
CD-related hospitalizations *per* patient	1.0 [1-5]	1.0 [1-5]	1.0 [1-4]	1.0 [1-3]
Previous CD appointments *per* patient	11.0 [1-45]	11.0 [1-45]	13.5 [4-43]	10.0 [1-21]
	UC patients (*n* = 143)	**Southeast (*n* = 94)**	**South (*n* = 21)**	**Northeast/Midwest (*n* = 28)**
Any UC treatment at enrollment[1]	138 (96.5)	89 (94.7)	21 (100.0)	28 (100.0)
UC treatment at enrollment[2]				
5-ASA derivates	100 (69.9)	60 (63.8)	13 (61.9)	27 (96.4)
Biological therapy	41 (28.7)	30 (31.9)	7 (33.3)	4 (14.3)
Infliximab	31 (21.7)	NA	NA	NA
Adalimumab	9 (6.3)	NA	NA	NA
Vedolizumab	2 (1.4)	NA	NA	NA
Immunosuppressors	63 (44.1)	41 (43.6)	12 (57.1)	10 (35.7)
Thiopurines	59 (41.3)	NA	NA	NA
Methotrexate	3 (2.1)	NA	NA	NA
Tacrolimus	1 (0.7)	NA	NA	NA
Corticosteroids	26 (18.2)	15 (16.0)	6 (28.6)	5 (17.9)
Prednisone	24 (16.8)	NA	NA	NA
Hydrocortisone	2 (1.4)	NA	NA	NA
Prednisolone	2 (1.4)	NA	NA	NA
Antibiotics	7 (4.9)	6 (6.4)	1 (4.8)	NA
Any previous UC-related surgery[4]	4 (2.8)	4 (4.3)	0 (0.0)	0 (0.0)

UC-related surgeries *per* patient	2.0 [1-2]	2.0 [1-2]	-	-
Any previous UC-related hospitalization	28 (19.6)	13 (13.8)	9 (42.9)	6 (21.4)
UC-related hospitalizations *per* patient	1.0 [1-5]	1.0 [1-2]	2.0 [1-5]	1.0 [1-2]
Previous UC appointments *per* patient	10.0 [1-39]	10.0 [1-39]	14.0 [4-38]	9.0 [1-17]

Data are shown as *n* (%) or median [range]. Percentages were calculated for the total group of patients.
[1]Any inflammatory bowel diseases treatment ongoing or initiated at the study appointment.
[2]More than one possible option: patients could have combined treatment.
[3]The most common surgeries were fistulectomy/anal fistulectomy (20.4% of patients), partial colectomy (12% of patients) and enterotomy and/or enterorrhaphy with suture/resection (12%).
[4]Two total colectomies and two enterostomy closures.
CD: Crohn's disease; 5-ASA: 5-Aminosalicylic acid; NA: Not available; UC: Ulcerative colitis.

However, Parra *et al*[30] found a predominance of ileocolonic location (53.0%) and penetrating phenotype (52.0%) in the SE region that was higher than that usually reported by European studies[33]. Other studies, including ones from Hungary, the Netherlands, Australia and Asia, reported proportions of ileocolonic disease ranging from 38.8% to 45%[34]. Parente *et al*[13] reported a frequency of colonic location of 36.0% and a frequency of nonstricturing/nonpenetrating disease of 69.0% in the Northeast region. In our study, 47.1% of patients from the NE/MW region had nonstricturing/nonpenetrating disease, 47.1% showed ileocolonic location, and 32.4% had colonic location (approximately two times higher than the prevalence in the other two regions). The higher proportions of CD patients with a worse phenotype that we observed in our study – compared to others – could have resulted from differences in study populations, as we included patients that had a previous moderate-to-severe episode and that were followed at IBD referential centers – which, in general, receive patients with more complicated disease.

UC patients seemed to present less severe disease than CD patients, while most CD patients were receiving standard care with immunosuppressive drugs. Although the median disease duration was quite similar for both IBD types (approximately 10 years), in the NE/MW region, the disease duration for UC patients was lower (6 years). The median age at diagnosis in CD patients in this region was higher than that in other regions, exceeding 40 years old. The extent of UC influences the disease behavior and prognosis of the disease[35]. In a 7-year follow-up study, approximately half of UC patients had inflammation that extended to the proximal transverse colon and beyond (pancolitis), a suggested risk factor for colectomy[36]. For the three geographic regions, the results were similar to other Brazilian studies[14,30,31], with UC patients in the NE/MW showing predominantly left-sided disease (42.9%), while patients from SE had more frequent pancolitis, which is aligned with findings from Uruguay (a 40.0% prevalence of extensive UC in Montevideo)[37]. Even so, the rates of UC-related surgeries, including colectomies, and UC-related hospitalizations were low in the SE region. This may be because the reference IBD surgery centers in Brazil (*i.e.*, centers that perform a high number of IBD surgeries) are located in the South and SE regions.

One quarter of CD patients underwent surgery (fistulectomy being the most common) and had, on average, one hospitalization due to the disease in the previous 3 years, with no variations observed across the three regions. A very small percentage of UC patients underwent surgery (colectomy or closures of enterostomy) and had, on average, one hospitalization over the past three years. Hospitalization rates were substantially higher in the centers in the South, but for both CD or UC patients, few hospitalizations and surgeries were observed across the three regions during the previous three years.

Several risk factors for higher activity and a worse prognosis have been described, including genetics, environmental factors and factors related to early diagnosis and treatment[38,39]. Family history is a window to both the genetic background and shared environment, and some authors suggest that having a relative with IBD is an important risk factor for the onset of IBD[13,40]; however, this is a controversial issue, especially in a country with a mixed ethnic background such as Brazil[35,41]. A systematic review with pooled data from several countries (excluding LA) showed a prevalence of family history ranging from 11%-13%[42]. In our study, approximately 12% of CD patients (higher in SE) and 10% of UC patients (higher in South) reported a family history of the disease. One study conducted in northeastern Brazil showed that 7.9% of UC patients had a family history[14]. Similarly, in a case-control study

conducted in the southeastern region of Brazil, 9.0% of the 145 CD patients had a family history, although this finding was not statistically associated with CD (OR = 1.51; 95%CI: 0.64-3.54)[38]. Based on these results, we hypothesize that genetic background may play a smaller role in the increase in IBD incidence in Brazil, in addition to characteristics such as a high education level, urban residency, smaller family size and use of treated water[38,43].

Smoking is an environmental factor that negatively affects the prognosis of some types of IBD, although evidence is also conflicting[13,14,35,38]. In our sample, 9.9% of CD patients and only 2.3% of UC patients were current smokers, with similar rates across regions. Public health strategies that promote smoking cessation can partially explain the low rate of smoking observed if we consider that approximately 19% of CD patients and 29% of UC patients were former smokers. Although one should be cautious regarding this interpretation due to the volume of missing data regarding smoking status, this variable may be particularly relevant as smoking cessation might slow CD development and attenuate its severity, in contrast to UC, where smoking is considered a protective factor against the development of disease[44].

Treatment is a major determinant of IBD prognosis, and several treatment strategies are available in Brazil[1,22]. Considering that the study included moderate-to-severe patients, it is not surprising that almost all patients were on treatment at enrollment. UC patients were predominantly prescribed 5-ASA derivatives (approximately 70%), while biologics (71.6%) and immunosuppressors (67.4%) were the most common treatments among CD patients. A systematic review of studies from LA reported that less than 13% of UC patients used anti-TNF drugs, with the most common treatment being mesalazine (5-ASA compound), a lower-cost medicine[28].

When considering Brazilian regions, the proportion of biologics users in the SE (71.4%) was similar to that previously reported by Parra *et al*[30]. All CD patients from the NE/MW region, a region with a higher proportion of patients with active CD, were taking medication. Notably, the proportion of UC patients with active disease was also higher in this region (42.9%) compared to the other regions, but even though the large majority of patients were medicated with 5-ASA derivatives (96.4%), the proportion of biologics users was much lower than that in the SE and South regions. In 2015, da Silva *et al*[14] reported that UC patients from two reference centers in Bahia state (Northeastern) were even less frequently prescribed biologic drugs (only 1.5% of the 267 patients). Together, these findings suggest that NE/MW UC patients may face some barriers regarding access to more advanced therapies, such as biologics therapy, which is not currently available for UC patients as part of the Brazilian public reimbursement system[14]. Greater access to medical care and therapy for IBD patients in the South region (who were mainly recruited from private centers) may contribute to improving clinical, endoscopic and other outcomes in IBD patients.

One of the major strengths of this study was the number and diversity of IBD settings included, which covered the more densely populated regions of Brazil. In fact, the sociodemographic characteristics found in our study, overall and by region, corroborate the findings observed in other studies.

One of the study limitations is its cross-sectional nature, making it difficult to interpret associations between IBD activity at enrollment and sociodemographic and clinical features and treatments. Methodological and setting differences can partially explain the inclusion of more severe cases in our study, particularly among CD patients, when compared with other regional/single-center studies. In fact, the study sample included IBD patients from reference centers (including tertiary care centers) from both public and private settings with moderate-to-severe disease and an average of ten years of disease duration, which may reflect a heavily treated population, more prone to refractoriness, or with a more progressed/severe IBD but also represent a subgroup with higher medical needs. Since the scope of this study was to capture information in the outpatient setting only, one may not exclude the potential bias associated with exclusion of hospitalized patients, where information on more severe cases could have been captured. Capturing information on hospitalizations would require another sampling approach that would affect the study's recruitment rate. Due to the way data capture was designed, it was not possible to obtain robust information regarding treatment combinations (challenging to know whether treatments were done concomitantly or not). Moreover, some of the medical and treatment histories were captured from chart reviews, resulting in a substantial volume of missing data for some variables. Therefore, one should be cautious in interpreting the treatment patterns and medical data captured from this study. Finally, the small samples obtained for the South and NE/MW regions limited comparisons among the three regions.

CONCLUSION

In conclusion, this study provided a picture of IBD in private and public settings in three important regions of Brazil. CD patients predominated over UC patients. Some differences were observed across the regions regarding sociodemographic characteristics. The SE region presented a higher proportion of females and higher levels of education and employment. Sao Paulo, which is located in the SE, is the most developed state in Brazil, with higher economic activity and greater opportunities for employment. Based on public health system records from 2012-2015, the state of Sao Paulo recorded the highest IBD incidence, namely, 6.14 and 7.16 *per* 100000 inhabitants/year for CD and UC, respectively[12].

A substantial proportion of the CD patients had active disease (though the proportion was less pronounced in the South) and were being treated primarily with biologics and immunosuppressors. A quarter of the UC patients had active disease (the proportion was considerably higher in the NE/MW), and most were treated with 5-ASA derivatives. Although the Brazilian public health system is free and universal, patient access to specialized care is frequently delayed and difficult. Furthermore, biological therapy, until very recently, was available through the government health system only to CD, which could justify the low use by UC patients. As the prevalence of infectious disease – an IBD risk factor in Brazil[43] – is high in NE/MW region, the physicians from primary health care and also specialists from other areas (*e.g.*, dermatologists, rheumatologists), should be informed and aware about IBD, in order to perform an earlier diagnosis and/or referral to centers with expertise in IBD. We suggest that, with more timely diagnosis of UC and with the improvement of patient access to biologic drugs in this region, a better control of UC activity can be achieved. Future studies in this region should also address other IBD risk factors such as education level, local geographic features, urban residency, family size and use of treated water, on a context of public health strategy.

By characterizing the sociodemographic and clinical features of the IBD population across different settings and regions, describing the treatment patterns and the use of health care resources, the findings from this study can further contribute to understanding practices and variations, with the ultimate goal of promoting discussion among specialists regarding the optimal management of IBD patients in Brazil.

ARTICLE HIGHLIGHTS

Research background

Inflammatory bowel diseases (IBD) incidence and prevalence has been consistently increasing in Latin American countries. Brazil is the largest country in South America, with regional sociodemographic and heath care disparities that can impact IBD epidemiology and treatment.

Research motivation

IBD incidence and prevalence have been increasing in Brazil but the information about IBD epidemiology and setting is still scarce in this continent-sized country. On the other hand, multiple treatments are currently available but some constraints on the access to biologic drugs have been reported. A real-world characterization of the IBD patient profile, disease activity and uptake of IBD treatments in Brazil is required to support the optimization of IBD management.

Research objectives

This study aimed to describe the sociodemographic, clinical and therapeutic characteristics of IBD outpatients in Brazil, overall and by three major geographical regions of Brazil: The Southeast (SE), South and Northeast/Midwest (NE/MW).

Research methods

A multicenter, cross-sectional study with a 3-year retrospective chart review component was conducted in 14 Brazilian IBD reference centers. Adult patients with moderate-to-severe Crohn's disease (CD) or ulcerative colitis (UC) were consecutively enrolled between October 2016 and February 2017, during routinely scheduled in-office appointments. Active IBD at enrolment was defined as presenting, for CD patients, Harvey Bradshaw Index ≥ 8, Crohn's Disease Activity Index ≥ 220,

calprotectin level > 200 μg/g or an active result based on colonoscopy suggestive of inadequate control during the previous year, and, for UC patients, presenting a partial Mayo score ≥ 5. Descriptive statistics were used to analyze study variables, overall and by geographical region.

Research results

We observed that, in Brazil, CD was more frequent than UC, overall and by region. Almost half of CD patients and one quarter of UC patients presented active disease at enrolment and, while CD patients were commonly treated with biologic drugs, UC patients were mostly treated with 5-Aminosalicylic acid (5-ASA) derivates and immunosuppressors. CD patients showed a worse phenotype, namely ileocolonic disease and stricturing disease, and one-quarter had undergone CD-related surgery in the past 3 years. In the South, IBD patients were mostly men, had higher education and employment rates and were more likely to be followed up in the private setting than patients in the other regions. In the NE/MW region, the majority of IBD patients had a lower educational level and lower employment status. In this region, more UC patients had active disease compared to the SE and South regions, but the proportion of biologics users was much lower than that in the other regions.

Research conclusions

In Brazil, CD frequency, activity and severity outweighs those of UC. Nevertheless, one-quarter of UC patients have active disease, and most are receiving 5-ASA treatment. Regional variations in IBD management were observed, with the NE/MW region presenting more UC patients with active disease and less treated.

Research perspectives

Findings from this study can elucidate about differences in clinical practice across Brazilian regions, thus promoting discussion among specialists regarding the optimal management of IBD patients.

ACKNOWLEDGEMENTS

We would like to express our gratitude to the study participants and site staff who collaborated in the study. In addition, the authors acknowledge CTI Clinical Trial & Consulting Services for the study monitoring and statistical and writing assistance.

REFERENCES

1 **Moreau J**, Mas E. Drug resistance in inflammatory bowel diseases. *Curr Opin Pharmacol* 2015; **25**: 56-61 [PMID: 26645664 DOI: 10.1016/j.coph.2015.11.003]
2 **Vilela EG**, Torres HO, Martins FP, Ferrari Mde L, Andrade MM, Cunha AS. Evaluation of inflammatory activity in Crohn's disease and ulcerative colitis. *World J Gastroenterol* 2012; **18**: 872-881 [PMID: 22408345 DOI: 10.3748/wjg.v18.i9.872]
3 **Loftus EV Jr**. Clinical epidemiology of inflammatory bowel disease: Incidence, prevalence, and environmental influences. *Gastroenterology* 2004; **126**: 1504-1517 [PMID: 15168363 DOI: 10.1053/j.gastro.2004.01.063]
4 **Kaplan GG**. The global burden of IBD: from 2015 to 2025. *Nat Rev Gastroenterol Hepatol* 2015; **12**: 720-727 [PMID: 26323879 DOI: 10.1038/nrgastro.2015.150]
5 **Ng SC**, Shi HY, Hamidi N, Underwood FE, Tang W, Benchimol EI, Panaccione R, Ghosh S, Wu JCY, Chan FKL, Sung JJY, Kaplan GG. Worldwide incidence and prevalence of inflammatory bowel disease in the 21st century: a systematic review of population-based studies. *Lancet* 2018; **390**: 2769-2778 [PMID: 29050646 DOI: 10.1016/S0140-6736(17)32448-0]
6 **Selvaratnam S**, Gullino S, Shim L, Lee E, Lee A, Paramsothy S, Leong RW. Epidemiology of inflammatory bowel disease in South America: A systematic review. *World J Gastroenterol* 2019; **25**: 6866-6875 [PMID: 31885427 DOI: 10.3748/wjg.v25.i47.6866]
7 United Nations Development Programme. Human development indices and indicators: 2018 Statistical update. New York: UNDP. 2018 [accessed 2020 Oct 26]. In: Human Development Reports [Internet]. Available from: http://hdr.undp.org/en/content/human-development-indices-indicators-2018-statistical-update
8 **Programa das Nações Unidas para o Desenvolvimento**, Instituto de Pesquisa Econômica Aplicada, Fundação João Pinheiro. O índice de desenvolvimento humano municipal brasileiro. Brasília: Programa das Nações Unidas para o Desenvolvimento, 2013. Available from: http://www.atlasbrasil.org.br/acervo/biblioteca

9 **Brazilian Study Group of Inflammatory Bowel Diseases**. Consensus guidelines for the management of inflammatory bowel disease. *Arq Gastroenterol* 2010; **47**: 313-325 [PMID: 21140096 DOI: 10.1590/s0004-28032010000300019]

10 **Quaresma AB**, Kaplan GG, Kotze PG. The globalization of inflammatory bowel disease: the incidence and prevalence of inflammatory bowel disease in Brazil. *Curr Opin Gastroenterol* 2019; **35**: 259-264 [PMID: 30973356 DOI: 10.1097/MOG.0000000000000534]

11 **Kotze PG**, Underwood FE, Damião AOMC, Ferraz JGP, Saad-Hossne R, Toro M, Iade B, Bosques-Padilla F, Teixeira FV, Juliao-Banos F, Simian D, Ghosh S, Panaccione R, Ng SC, Kaplan GG. Progression of Inflammatory Bowel Diseases Throughout Latin America and the Caribbean: A Systematic Review. *Clin Gastroenterol Hepatol* 2020; **18**: 304-312 [PMID: 31252191 DOI: 10.1016/j.cgh.2019.06.030]

12 **Gasparini RG**, Sassaki LY, Saad-Hossne R. Inflammatory bowel disease epidemiology in São Paulo State, Brazil. *Clin Exp Gastroenterol* 2018; **11**: 423-429 [PMID: 30464570 DOI: 10.2147/CEG.S176583]

13 **Parente JM**, Coy CS, Campelo V, Parente MP, Costa LA, da Silva RM, Stephan C, Zeitune JM. Inflammatory bowel disease in an underdeveloped region of Northeastern Brazil. *World J Gastroenterol* 2015; **21**: 1197-1206 [PMID: 25632193 DOI: 10.3748/wjg.v21.i4.1197]

14 **da Silva BC**, Lyra AC, Mendes CM, Ribeiro CP, Lisboa SR, de Souza MT, Portela RC, Santana GO. The Demographic and Clinical Characteristics of Ulcerative Colitis in a Northeast Brazilian Population. *Biomed Res Int* 2015; **2015**: 359130 [PMID: 26509150 DOI: 10.1155/2015/359130]

15 **Harbord M**, Eliakim R, Bettenworth D, Karmiris K, Katsanos K, Kopylov U, Kucharzik T, Molnár T, Raine T, Sebastian S, de Sousa HT, Dignass A, Carbonnel F; European Crohn's and Colitis Organisation [ECCO]. Third European Evidence-based Consensus on Diagnosis and Management of Ulcerative Colitis. Part 2: Current Management. *J Crohns Colitis* 2017; **11**: 769-784 [PMID: 28513805 DOI: 10.1093/ecco-jcc/jjx009]

16 **Gomollón F**, Dignass A, Annese V, Tilg H, Van Assche G, Lindsay JO, Peyrin-Biroulet L, Cullen GJ, Daperno M, Kucharzik T, Rieder F, Almer S, Armuzzi A, Harbord M, Langhorst J, Sans M, Chowers Y, Fiorino G, Juillerat P, Mantzaris GJ, Rizzello F, Vavricka S, Gionchetti P; ECCO. 3rd European Evidence-based Consensus on the Diagnosis and Management of Crohn's Disease 2016: Part 1: Diagnosis and Medical Management. *J Crohns Colitis* 2017; **11**: 3-25 [PMID: 27660341 DOI: 10.1093/ecco-jcc/jjw168]

17 **Mowat C**, Cole A, Windsor A, Ahmad T, Arnott I, Driscoll R, Mitton S, Orchard T, Rutter M, Younge L, Lees C, Ho GT, Satsangi J, Bloom S; IBD Section of the British Society of Gastroenterology. Guidelines for the management of inflammatory bowel disease in adults. *Gut* 2011; **60**: 571-607 [PMID: 21464096 DOI: 10.1136/gut.2010.224154]

18 **Sandborn WJ**, Feagan BG, Rutgeerts P, Hanauer S, Colombel JF, Sands BE, Lukas M, Fedorak RN, Lee S, Bressler B, Fox I, Rosario M, Sankoh S, Xu J, Stephens K, Milch C, Parikh A; GEMINI 2 Study Group. Vedolizumab as induction and maintenance therapy for Crohn's disease. *N Engl J Med* 2013; **369**: 711-721 [PMID: 23964933 DOI: 10.1056/NEJMoa1215739]

19 **Feagan BG**, Sandborn WJ, Gasink C, Jacobstein D, Lang Y, Friedman JR, Blank MA, Johanns J, Gao LL, Miao Y, Adedokun OJ, Sands BE, Hanauer SB, Vermeire S, Targan S, Ghosh S, de Villiers WJ, Colombel JF, Tulassay Z, Seidler U, Salzberg BA, Desreumaux P, Lee SD, Loftus EV Jr, Dieleman LA, Katz S, Rutgeerts P; UNITI–IM-UNITI Study Group. Ustekinumab as Induction and Maintenance Therapy for Crohn's Disease. *N Engl J Med* 2016; **375**: 1946-1960 [PMID: 27959607 DOI: 10.1056/NEJMoa1602773]

20 **Mosli MH**, MacDonald JK, Bickston SJ, Behm BW, Tsoulis DJ, Cheng J, Khanna R, Feagan BG. Vedolizumab for induction and maintenance of remission in ulcerative colitis: a Cochrane systematic review and meta-analysis. *Inflamm Bowel Dis* 2015; **21**: 1151-1159 [PMID: 25844963 DOI: 10.1097/MIB.0000000000000396]

21 **Rutgeerts P**, Sandborn WJ, Feagan BG, Reinisch W, Olson A, Johanns J, Travers S, Rachmilewitz D, Hanauer SB, Lichtenstein GR, de Villiers WJ, Present D, Sands BE, Colombel JF. Infliximab for induction and maintenance therapy for ulcerative colitis. *N Engl J Med* 2005; **353**: 2462-2476 [PMID: 16339095 DOI: 10.1056/NEJMoa050516]

22 **Cassinotti A**, Ardizzone S, Porro GB. Adalimumab for the treatment of Crohn's disease. *Biologics* 2008; **2**: 763-777 [PMID: 19707457 DOI: 10.2147/btt.s3292]

23 **Zhang ZM**, Li W, Jiang XL. Efficacy and Safety of Adalimumab in Moderately to Severely Active Cases of Ulcerative Colitis: A Meta-Analysis of Published Placebo-Controlled Trials. *Gut Liver* 2016; **10**: 262-274 [PMID: 26780088 DOI: 10.5009/gnl15042]

24 **Sands BE**, Sandborn WJ, Panaccione R, O'Brien CD, Zhang H, Johanns J, Adedokun OJ, Li K, Peyrin-Biroulet L, Van Assche G, Danese S, Targan S, Abreu MT, Hisamatsu T, Szapary P, Marano C; UNIFI Study Group. Ustekinumab as Induction and Maintenance Therapy for Ulcerative Colitis. *N Engl J Med* 2019; **381**: 1201-1214 [PMID: 31553833 DOI: 10.1056/NEJMoa1900750]

25 **Satsangi J**, Silverberg MS, Vermeire S, Colombel JF. The Montreal classification of inflammatory bowel disease: controversies, consensus, and implications. *Gut* 2006; **55**: 749-753 [PMID: 16698746 DOI: 10.1136/gut.2005.082909]

26 **Harvey RF**, Bradshaw JM. A simple index of Crohn's-disease activity. *Lancet* 1980; **1**: 514 [PMID: 6102236 DOI: 10.1016/s0140-6736(80)92767-1]

27 **Lewis JD**, Chuai S, Nessel L, Lichtenstein GR, Aberra FN, Ellenberg JH. Use of the noninvasive components of the Mayo score to assess clinical response in ulcerative colitis. *Inflamm Bowel Dis*

2008; **14**: 1660-1666 [PMID: 18623174 DOI: 10.1002/ibd.20520]
28 **Calderón M**, Minckas N, Nuñez S, Ciapponi A. Inflammatory Bowel Disease in Latin America: A Systematic Review. *Value Health Reg Issues* 2018; **17**: 126-134 [PMID: 29936359 DOI: 10.1016/j.vhri.2018.03.010]
29 **Lima Martins A**, Volpato RA, Zago-Gomes MDP. The prevalence and phenotype in Brazilian patients with inflammatory bowel disease. *BMC Gastroenterol* 2018; **18**: 87 [PMID: 29914399 DOI: 10.1186/s12876-018-0822-y]
30 **Parra RS**, Feitosa MR, Ferreira SC, Caetano BE, Favoretto A, Jr, Ribeiro da Rocha JJ, Féres O, Troncon LEdA. P236 Inflammatory bowel disease epidemiology a tertiary centre in Brazil. *J Crohns Colitis* 2019; **13**: S214-S215 [DOI: 10.1093/ecco-jcc/jjy222.360]
31 **Souza MH**, Troncon LE, Rodrigues CM, Viana CF, Onofre PH, Monteiro RA, Passos AD, Martinelli AL, Meneghelli UG. [Trends in the occurrence (1980-1999) and clinical features of Crohn's disease and ulcerative colitis in a university hospital in southeastern Brazil]. *Arq Gastroenterol* 2002; **39**: 98-105 [PMID: 12612713 DOI: 10.1590/s0004-28032002000200006]
32 **Peyrin-Biroulet L**, Sandborn W, Sands BE, Reinisch W, Bemelman W, Bryant RV, D'Haens G, Dotan I, Dubinsky M, Feagan B, Fiorino G, Gearry R, Krishnareddy S, Lakatos PL, Loftus EV Jr, Marteau P, Munkholm P, Murdoch TB, Ordás I, Panaccione R, Riddell RH, Ruel J, Rubin DT, Samaan M, Siegel CA, Silverberg MS, Stoker J, Schreiber S, Travis S, Van Assche G, Danese S, Panes J, Bouguen G, O'Donnell S, Pariente B, Winer S, Hanauer S, Colombel JF. Selecting Therapeutic Targets in Inflammatory Bowel Disease (STRIDE): Determining Therapeutic Goals for Treat-to-Target. *Am J Gastroenterol* 2015; **110**: 1324-1338 [PMID: 26303131 DOI: 10.1038/ajg.2015.233]
33 **Burisch J**, Munkholm P. The epidemiology of inflammatory bowel disease. *Scand J Gastroenterol* 2015; **50**: 942-951 [PMID: 25687629 DOI: 10.3109/00365521.2015.1014407]
34 **Moran C**, Sheehan D, Shanahan F. The Changing Phenotype of Inflammatory Bowel Disease. *Gastroenterol Res Pract* 2016; **2016**: 1619053 [PMID: 28050166 DOI: 10.1155/2016/1619053]
35 **da Silva BC**, Lyra AC, Rocha R, Santana GO. Epidemiology, demographic characteristics and prognostic predictors of ulcerative colitis. *World J Gastroenterol* 2014; **20**: 9458-9467 [PMID: 25071340 DOI: 10.3748/wjg.v20.i28.9458]
36 **Vester-Andersen MK**, Prosberg MV, Jess T, Andersson M, Bengtsson BG, Blixt T, Munkholm P, Bendtsen F, Vind I. Disease course and surgery rates in inflammatory bowel disease: a population-based, 7-year follow-up study in the era of immunomodulating therapy. *Am J Gastroenterol* 2014; **109**: 705-714 [PMID: 24642581 DOI: 10.1038/ajg.2014.45]
37 **Iade B**, Buenavida GB, Casañas A. Incidence of inflammatory bowel disease in two medical centers in Uruguay, during the period 2007-2011. *Acta Gastroenterol Latinoam* 2018; **48**: 263-270
38 **Salgado VCL**, Luiz RR, Boechat N, Schorr BC, Leão IS, Nunes T, Zaltman C. Crohn's disease environmental factors in the developing world: A case-control study in a statewide catchment area in Brazil. *World J Gastroenterol* 2017; **23**: 5549-5556 [PMID: 28852314 DOI: 10.3748/wjg.v23.i30.5549]
39 **Zaltman C**. Inflammatory bowel disease: how relevant for Brazil? *Cad Saude Publica* 2007; **23**: 992-993 [PMID: 17486222 DOI: 10.1590/s0102-311x2007000500001]
40 **Wang PQ**, Hu J, Al Kazzi ES, Akhuemonkhan E, Zhi M, Gao X, de Paula Pessoa RH, Ghazaleh S, Cornelius T, Sabunwala SA, Ghadermarzi S, Tripathi K, Lazarev M, Hu PJ, Hutfless S. Family history and disease outcomes in patients with Crohn's disease: A comparison between China and the United States. *World J Gastrointest Pharmacol Ther* 2016; **7**: 556-563 [PMID: 27867689 DOI: 10.4292/wjgpt.v7.i4.556]
41 **Lins TC**, Vieira RG, Abreu BS, Grattapaglia D, Pereira RW. Genetic composition of Brazilian population samples based on a set of twenty-eight ancestry informative SNPs. *Am J Hum Biol* 2010; **22**: 187-192 [PMID: 19639555 DOI: 10.1002/ajhb.20976]
42 **Childers RE**, Eluri S, Vazquez C, Weise RM, Bayless TM, Hutfless S. Family history of inflammatory bowel disease among patients with ulcerative colitis: a systematic review and meta-analysis. *J Crohns Colitis* 2014; **8**: 1480-1497 [PMID: 24974207 DOI: 10.1016/j.crohns.2014.05.008]
43 **Salgado VCL**, Luiz RR, Boéchat NLF, Leão IS, Schorr BDC, Parente JML, Lima DC, Silveira Júnior ES, Silva GOS, Almeida NP, Vieira A, de Bueno MLQ, Chebli JM, Bertges ÉR, Brugnara LMDC, Junqueira Neto C, Campbell SBG, Discacciati LL, Cézar JPS, Nunes T, Kaplan GG, Zaltman C. Risk factors associated with inflammatory bowel disease: A multicenter case-control study in Brazil. *World J Gastroenterol* 2020; **26**: 3611-3624 [PMID: 32742130 DOI: 10.3748/wjg.v26.i25.3611]
44 **Nunes T**, Etchevers MJ, García-Sánchez V, Ginard D, Martí E, Barreiro-de Acosta M, Gomollón F, Arroyo M, Bastida G, Gonzalez B, Monfort D, García-Planella E, Figueroa C, Panés J, Sans M. Impact of Smoking Cessation on the Clinical Course of Crohn's Disease Under Current Therapeutic Algorithms: A Multicenter Prospective Study. *Am J Gastroenterol* 2016; **111**: 411-419 [PMID: 26856753 DOI: 10.1038/ajg.2015.401]

World Journal of Gastroenterology

Submit a Manuscript: https://www.f6publishing.com

World J Gastroenterol 2021 January 14; 27(2): 224-232

DOI: 10.3748/wjg.v27.i2.224

ISSN 1007-9327 (print) ISSN 2219-2840 (online)

ORIGINAL ARTICLE

Randomized Controlled Trial

Effect of probiotics on length of hospitalization in mild acute pancreatitis: A randomized, double-blind, placebo-controlled trial

You-Dong Wan, Rui-Xue Zhu, Zhong-Zheng Bian, Tong-Wen Sun

ORCID number: You-Dong Wan 0000-0003-4270-9213; Rui-Xue Zhu 0000-0002-9432-5556; Zhong-Zheng Bian 0000-0003-2240-1342; Tong-Wen Sun 0000-0001-5228-8710.

Author contributions: Wan YD wrote the paper; Wan YD and Zhu RX collected and analyzed the data; Wan YD, Zhu RX, Bian ZZ, and Sun TW designed the study, critically reviewed the manuscript, and approved the final version.

Supported by National Natural Science Foundation of China, No. 81370364.

Institutional review board statement: The study was ethically approved by the Ethics Committee of The Affiliated Hospital of Qingdao University.

Clinical trial registration statement: The trial was registered in the Chinese Clinical Trial Registry (ChiCTR2000030425).

Informed consent statement: All study participants, or their legal guardian, provided informed written consent prior to study enrollment.

Conflict-of-interest statement: The authors declare no conflict of interests for this article.

You-Dong Wan, Tong-Wen Sun, Integrated Intensive Care Unit, The First Affiliated Hospital of Zhengzhou University, Zhengzhou 450052, Henan Province, China

Rui-Xue Zhu, Health Management Centre, The Affiliated Hospital of Qingdao University, Qingdao 266000, Shandong Province, China

Zhong-Zheng Bian, Department of Emergency Medicine, The Affiliated Hospital of Qingdao University, Qingdao 266000, Shandong Province, China

Corresponding author: Tong-Wen Sun, MD, Chief Doctor, Professor, Integrated Intensive Care Unit, The First Affiliated Hospital of Zhengzhou University, No. 1 Jianshe East Road, Zhengzhou 450052, Henan Province, China. wanyoudong123@163.com

Abstract

BACKGROUND

Acute pancreatitis is the leading cause of hospitalization for acute gastrointestinal disease worldwide. The effects of probiotics in mild acute pancreatitis have not been studied. We hypothesized that the administration of probiotics may accelerate the recovery of intestinal function and shorten the length of hospital stay (LOS) in patients with mild pancreatitis.

AIM

To investigate the value of probiotics in reducing the LOS in patients with mild acute pancreatitis.

METHODS

We conducted a double-blind randomized clinical trial to evaluate the effects of probiotics administered to patients with mild acute pancreatitis at a tertiary medical center. The patients were given probiotics capsules (a mixed preparation of *Bacillus subtilis* and *Enterococcus faecium*) or placebo. The primary study endpoint was the LOS. The secondary endpoints included time to abdominal pain relief, recurrent abdominal pain, and time to successful oral feeding.

RESULTS

A total of 128 patients were included, with 64 patients in each arm. The severity of illness and the etiological distribution of disease were similar in the two groups. There was a significant reduction in the LOS in the probiotics treatment group *vs* the placebo group (5.36 ± 0.15 *vs* 6.02 ± 0.17 d, $P < 0.05$). The probiotics group was

CONSORT 2010 statement: The authors have read the CONSORT Statement—checklist of items, and the manuscript was prepared and revised according to the CONSORT Statement—checklist of items.

Open-Access: This article is an open-access article that was selected by an in-house editor and fully peer-reviewed by external reviewers. It is distributed in accordance with the Creative Commons Attribution NonCommercial (CC BY-NC 4.0) license, which permits others to distribute, remix, adapt, build upon this work non-commercially, and license their derivative works on different terms, provided the original work is properly cited and the use is non-commercial. See: http://creativecommons.org/Licenses/by-nc/4.0/

Manuscript source: Unsolicited manuscript

Specialty type: Gastroenterology and hepatology

Country/Territory of origin: China

Peer-review report's scientific quality classification

Grade A (Excellent): 0
Grade B (Very good): 0
Grade C (Good): C, C
Grade D (Fair): 0
Grade E (Poor): 0

Received: November 5, 2020
Peer-review started: November 5, 2020
First decision: November 25, 2020
Revised: November 29, 2020
Accepted: December 16, 2020
Article in press: December 16, 2020
Published online: January 14, 2021

P-Reviewer: Plaza MA
S-Editor: Fan JR
L-Editor: Wang TQ
P-Editor: Liu JH

associated with a shorter time to abdominal pain relief and time to successful oral feeding ($P < 0.01$ for both) than the placebo group. No statistical difference was found in recurrent abdominal pain between the two groups.

CONCLUSION

The study results showed that the administration of probiotics capsules is associated with a shorter duration of hospitalization in patients with mild acute pancreatitis.

Key Words: Acute pancreatitis; Probiotics; Length of hospitalization; Randomized study; Placebo; Mild

©The Author(s) 2021. Published by Baishideng Publishing Group Inc. All rights reserved.

Core Tip: Acute pancreatitis is the leading cause of hospitalization for acute gastrointestinal diseases. Probiotics are widely used for intestinal diseases, although its effect on mild acute pancreatitis has not been studied. This is the first study to explore the effect of probiotics in mild pancreatitis patients. The results indicated that probiotics were associated with decreased length of hospitalization.

Citation: Wan YD, Zhu RX, Bian ZZ, Sun TW. Effect of probiotics on length of hospitalization in mild acute pancreatitis: A randomized, double-blind, placebo-controlled trial. *World J Gastroenterol* 2021; 27(2): 224-232
URL: https://www.wjgnet.com/1007-9327/full/v27/i2/224.htm
DOI: https://dx.doi.org/10.3748/wjg.v27.i2.224

INTRODUCTION

Acute pancreatitis is one of the most common causes of acute abdominal pain, resulting in a huge clinical and financial burden worldwide. A nationwide retrospective analysis involving two million acute pancreatitis patients from the United States found that there was a 13.2% increase in admissions in the years 2009-2012 compared to that in 2002–2005[1]. In 2012, the annual cost of acute pancreatitis hospitalizations was about $2.6 billion[2]. Most patients (80%) with acute pancreatitis present with mild disease, which is characterized by a short hospital stay, no or few complications, and rapid resumption of oral feeding[3]. Allowing for the very low mortality rate (about 0.79%) of mild acute pancreatitis[1], shortening the length of hospital stay (LOS), and reducing medical financial expenditure have become the research priority.

More and more studies have shown that intestinal microbial communities are closely related to the occurrence and progression of gastrointestinal diseases, such as inflammatory bowel disease, irritable bowel syndrome, and colorectal cancer[4,5]. Altering the microbiota to decrease the severity of disease or even cure the disease has become a sought-after research direction. Probiotics play an important role in a variety of microecologic interventions. Probiotics were defined as "live microorganisms that, when administered in adequate amounts, confer a health benefit on the host"[6]. The mechanisms of probiotics in the treatment of intestinal disease include improving barrier function, modulating cell-mediated and humoral immune functions, interacting with the gut microbiota through competition for nutrients, antagonism, cross-feeding, and supporting microbiota stability, *etc*.[7]. In a multicenter randomized, placebo-controlled trial, 298 patients predicted with severe acute pancreatitis were randomly assigned to receive a multispecies probiotic or placebo; it was found that probiotic prophylaxis did not reduce the risk of infectious complications and was associated with an increased risk of mortality[8]. Subsequently, a meta-analysis involving six trials with 536 patients showed that probiotics supplementation did not significantly affect the pancreatic infection rate, LOS, or mortality[9]. In contrast, another meta-analysis showed reduced LOS in Chinese patients with severe acute pancreatitis[10]. However, the effect of probiotics in mild acute pancreatitis has not been studied. Considering the potential benefits of probiotics in the treatment of

gastrointestinal disease, we hypothesized that probiotics may accelerate the recovery of intestinal function and shorten the LOS in patients with mild pancreatitis. Thus, we conducted a randomized, double-blind, placebo-controlled trial to evaluate the effect of the administration of probiotics in patients with mild pancreatitis.

MATERIALS AND METHODS

Study design

This 1:1 randomized, controlled, double-blind clinical trial was conducted at the emergency ward of a tertiary teaching hospital with 5186 beds in China from July 2017 to July 2019. The study protocol was defined in accordance with the declaration of Helsinki and was approved by the Ethics Committee of our institution. The trial was registered in the Chinese Clinical Trial Registry (ChiCTR2000030425) and is reported in accordance with the CONSORT guidelines. All patients provided written informed consent before study participation. All study authors had access to the data and approved the final manuscript.

Patients were randomly allocated to a probiotics capsules or placebo group, and probiotics capsules or placebo were given orally from study inclusion to discharge. Considering the safety and efficacy shown in other clinical research[11], we chose a probiotics commercial preparation, a mixed preparation of *Bacillus subtilis* and *Enterococcus faecium*, which has been widely used in China (Meichangan, national medicine permission number S20030087). A computer-generated random-number table was prepared by statisticians to assign patients to receive either the probiotics capsules or placebo. The random-number table was unknown to the investigators, who enrolled the patients. To ensure blinding, placebo capsules identical to the probiotics capsules were manufactured (same appearance, color, and odor). The patients, clinicians, evaluators, and statisticians were blinded to the study treatment.

Inclusion and exclusion criteria

The inclusion criteria[12] were patients who (1) were 18-75 years old; and (2) met two of the following three diagnostic criteria for acute pancreatitis, including typical upper abdominal pain, serum amylase and/or lipase activity more than three times, and imaging manifestations of pancreatitis. Patients who presented with any indication of severe acute pancreatitis were excluded from our study. The indications of severe acute pancreatitis included: (1) Evidence of organ failure (oxygen saturation less than 90% on room air, mean arterial pressure less than 70 mmHg, the requirement for vasopressors or inotropic support, serum creatinine greater than 2.0 mg/dL, and Glasgow coma score less than 15)[12]; (2) Suspected or confirmed infected pancreatic necrosis; (3) C-reactive protein (CRP) over 150 mg/L[8]; and (4) Acute Physiology and Chronic Health Evaluation score ≥ 8[8]. Patients were included only for the first episode of mild pancreatitis. Patients receiving probiotics therapy during the 3 mo preceding the index admission were excluded. Additionally, pregnant or breastfeeding women were not allowed to participate.

Data collection

We extracted clinical data from the hospital electronic medical record systems. We collected the clinical data including basic information at admission such as sex, age, CRP, body mass index (BMI), Charlson score, disease etiology (gallstones-related, hypertriglyceridemia, alcohol-related, others, or unknown), relevant diagnostic and therapeutic interventions, and outcomes including LOS, time to successful oral feeding, rate of recurrent abdominal pain, time to abdominal pain relief, 30-d readmissions, and mortality. Successful oral feeding means that patients could take food through the mouth without any abdominal pain or other discomforts. Rate of recurrent abdominal pain means the failure rate of the patient's initial attempt to take food orally characterized as abdominal pain, nausea, vomiting, or other abdominal discomforts after the attempt. Abdominal pain relief means the time when abdominal pain symptoms completely disappeared for the first time. Previously reported adverse effects of probiotics in our study were closely monitored, including exacerbating abdominal discomfort (abdominal pain, nausea, vomiting, flatulence, or diarrhea)[13], anaphylactic reaction[14], probiotic-related infections[13], and lactic acidosis[15].

Outcomes

We used LOS as our primary endpoint. It is generally believed that patients with mild

pancreatitis, characterized by complete abdominal pain relief, no abdominal discomfort (such as nausea and vomiting), and successfully eating solid or semi-liquid foods, could be discharged from the hospital[16]. Thus, we chose the following indexes as our secondary endpoint: Time to first abdominal pain relief, rate of recurrent abdominal pain, and time to successful oral feeding. Patients were followed for 30 d for mortality and 30-d readmissions. All these outcomes were prespecified in the protocol.

Sample size estimation

According to a previous study[16,17], assuming the median LOS of mild pancreatitis patients was 5 d, we needed 128 patients (64 in each group) to obtain 80% power for detecting a 1-d relative decrease in the LOS with the one-sided alpha risk of 0.05.

Statistical analysis

Continuous variables are expressed as the mean ± SD if they were normally distributed. Categorical variables are expressed as percentages. The Kolmogorov–Smirnov test was used to assess whether continuous data were normally distributed ($P > 0.05$). For continuous variables, differences between groups were tested by Student's *t*-test for normally distributed data or Mann–Whitney *U* test for non-normally distributed data and the c2 test for categorical variables. All analyses were done according to the intention-to-treat principle. Results were considered significant at $P < 0.05$. Statistical analyses were carried out using SPSS version 23.0 (IBM Inc., Chicago, Illinois, United States).

RESULTS

Participant characteristics

We assessed 234 patients for eligibility, and 106 were excluded. The patients were excluded for having severe acute pancreatitis, suspected or confirmed infected pancreatic necrosis, and Acute Physiology and Chronic Health Evaluation score ≥ 8. Fifty-one patients refused to participate in the study, mainly because of concerns about the safety of the drugs. The remaining 128 patients were randomized, and 64 were allocated to each group. The CONSORT standardized flow diagram shows the enrollment process (Figure 1). We followed the patients for 30 d for mortality or readmissions through telephone calls, of whom eight were lost to follow-up due to change of contact number, or non-response.

Thus, 128 patients were included in the intention-to-treat analysis. The baseline demographics of the study population are shown in Table 1. The average age of the collective group was 52.73 years, with 64.1% male. The mean CRP level was 54.9 mg/L. There were no significant differences in age, sex, BMI, CRP, Charlson score, or disease etiology distribution between the two groups. The most common etiology overall for acute pancreatitis in this study was gallstones-related (50%).

Primary endpoint

The mean LOS in the probiotics group was 5.36 ± 0.15 d, and in the placebo group was 6.02 ± 0.17 d. Patients in the probiotics group had a significantly shorter LOS than the placebo group by about 0.65 d ($P < 0.05$). The result are shown in Figure 2.

Secondary end points

The study endpoints between the probiotics and placebo groups are listed in Table 2. Recurrent abdominal pain was noted in six patients in the probiotics group and nine patients in the placebo group, with no significant difference between the two groups ($P = 0.41$). Notably, the time to abdominal pain relief in the probiotics group was significantly shorter than that in the placebo group by about 1 d (2.98 ± 0.74 d *vs* 4.14 ± 1.32 d, $P < 0.01$). Additionally, the probiotics group had a significantly shorter time to successful oral feeding than the placebo group (4.56 ± 1.13 d *vs* 5.37 ± 1.13 d, $P < 0.01$). No patient mortality was noted in our study. One patient was re-hospitalized within 30 d of discharge because of hyperlipidemic pancreatitis, which was caused by repeated overeating in the probiotics group; and one patient in the placebo group was re-admitted for pancreatitis secondary to repeated heavy alcohol drinking.

Safety and harm

The adverse effects of probiotics administration in our study were closely monitored.

Table 1 Baseline characteristics of participants

Parameter	Probiotics (*n* = 64)	Placebo (*n* = 64)	*P* value
Age (yr) (mean ± SD)	50.25 ± 16.79	54.72 ± 14.86	0.16
Sex (female)	24 (37%)	22 (34%)	0.71
BMI (mean ± SD)	25.75 ± 3.40	26.29 ± 2.82	0.33
CRP (mg/L) (mean ± SD)	57.32 ± 28.21	52.55 ± 24.47	0.31
Charlson score	3.02 ± 1.12	2.96 ± 0.29	0.32
Disease etiology			
Gallstones-related	30 (46%)	34 (53%)	0.48
Hypertriglyceridemia	11 (17%)	10 (16%)	0.81
Alcohol-related	9 (14%)	6 (9%)	0.41
Others or unknown	12 (19%)	12 (19%)	1.0
Time from first symptoms to admission (d)	2 (1–4)	3 (1–5)	0.10
Follow-up period (d)	31.67 ± 1.97	31.32 ± 2.13	0.33

BMI: Body mass index; CRP: C-reactive protein.

Table 2 Comparison of secondary endpoints between probiotics and placebo groups

	Probiotics (*n* = 64)	Placebo (*n* = 64)	*P* value
Time to successful oral feeding (d, mean ± SD)	4.56 ± 1.13	5.37 ± 1.13	< 0.01
Rate of recurrent abdominal pain	6 (9%)	9 (14%)	0.41
Time to abdominal pain relief (d, mean ± SD)	2.98 ± 0.74	4.14 ± 1.32	< 0.01
30-d readmissions	1 (1.5%)	1 (1.5%)	1
Mortality	0	0	

The results are shown in Table 3. The most common adverse effect was exacerbating abdominal discomfort. In the probiotics group, about 18.7% (12/64) of patients experienced transient abdominal discomfort, such as abdominal pain (4.7%), flatulence (7.8%), and nausea (4.7%). The proportion was lower in that of the placebo group [14.1% (9/64)]. There was no significant difference between the two groups in the rate of exacerbating abdominal discomfort (P = 0.47). The symptoms were mild and transient despite the high abdominal discomfort rate. No anaphylactic reaction, probiotic-related infections, or lactic acidosis secondary to probiotics administration was found in our study.

DISCUSSION

The present study investigated the effect of the administration of probiotics on patients with mild pancreatitis. We found that probiotics were associated with decreased LOS. The possible reasons were that probiotics may accelerate successful oral feeding and abdominal pain relief. The safety of probiotics in the treatment of mild pancreatitis in our study was also considered. Transient abdominal discomfort was the most common adverse effect found in our study, but no significant difference was found between the probiotics and placebo groups.

At present, studies on pancreatitis tend to focus on severe cases, including management of early acute inflammatory response, fluid resuscitation, and management of late infectious complications[18]. There are relatively fewer studies on mild acute pancreatitis because of its low mortality rate. However, mild acute pancreatitis accounts for up to 80% of all pancreatitis cases[3]. With the increasing pressure of medical costs due to mild acute pancreatitis, shortening the LOS and reducing the medical cost have become the primary target of acute pancreatitis

Table 3 Comparison of side effects between probiotics and placebo groups

	Probiotics (*n* = 64)	Placebo (*n* = 64)	*P* value
Exacerbating abdominal discomfort	12	9	0.47
Abdominal pain	3	2	1
Nausea	3	4	1
Vomiting	1	1	1
Flatulence	5	2	0.44
Diarrhea	0	0	
Anaphylactic reaction	0	0	
Probiotic-related infections	0	0	
Lactic acidosis	0	0	

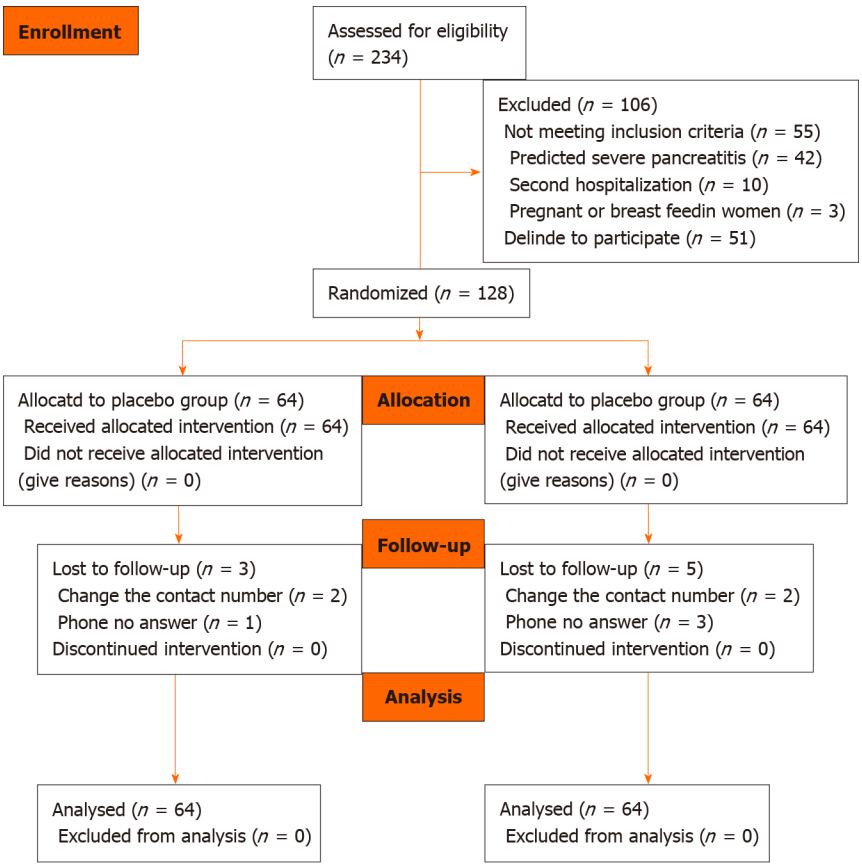


Figure 1 CONSORT diagram.

treatment. At present, probiotics are mainly used to treat diarrhea, constipation, enteritis, abdominal distension, dyspepsia, and loss of appetite caused by intestinal flora imbalance. Some studies[10,19] suggested that probiotics were associated with decreased LOS, but these reports were of low quality and included a small sample of patients with severe acute pancreatitis. Besselink *et al*[8] conducted a study with the largest sample size of 298 randomized patients with severe acute pancreatitis; they found that probiotic prophylaxis did not reduce the risk of infectious complications and was associated with an increased risk of mortality. No difference was found in intensive care stay and hospital stay between their probiotics and non-probiotics groups.

In our randomized placebo-controlled study, probiotics were associated with a decreased LOS in patients with mild acute pancreatitis. In mild acute pancreatitis, rapid relief of abdominal pain and successful oral feeding were the main indications for hospital discharge. Based on previous gastrointestinal disease studies[20,21], we

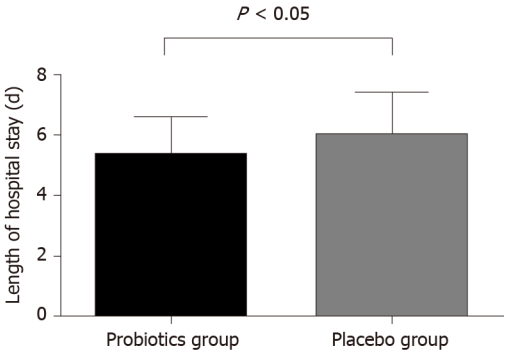


Figure 2 Comparison of length of hospital stay between probiotics and placebo groups.

hypothesized that probiotics may improve intestinal microecology and food tolerance, reduce the inflammatory response, and consequently improve the possibility of successful oral feeding. Consistent with previous research results, our study showed accelerated successful oral feeding and abdominal pain relief after the administration of probiotics capsules consisting of *Bacillus subtilis* and *Enterococcus faecium*.

Adverse reactions to probiotics were closely observed in this study. The most frequent adverse effect was exacerbating abdominal discomfort (7%–9%), mostly experienced as flatulence. The reasons may be as follows: First, probiotic supplements are packaged as capsules that need to be taken orally with water, which contradicts the usual practice of diet prohibition before abdominal pain relief. As recommended in the 2013 International Association of Pancreatology and the American Pancreatic Association Evidence-Based Guidelines[22], and the 2018 American Gastroenterological Association Institute Guideline[23], oral feeding in mild pancreatitis can be restarted only when abdominal pain is decreasing and inflammatory markers are improving. The early administration of probiotic capsules may aggravate the gastrointestinal condition. Second, the role and target of probiotics on the intestinal flora in patients with disease states are not yet fully understood[24]. Rao *et al*[25] concluded that probiotics-fermented carbohydrates in the proximal small bowel induce intestinal bacterial overgrowth, resulting in increased gas output, and abdominal bloating.

The present study had several limitations. First, our results may not be generalizable to all patients with acute pancreatitis because we only included patients with mild acute pancreatitis. Although we showed that probiotics may be beneficial to patients with mild pancreatitis, the adverse reactions of probiotics should prompt clinician concern. Second, the results of this study are not generalizable to all probiotics since we only used *Bacillus subtilis* and *Enterococcus faecium* probiotic strains. At present, there are many types of probiotics with different clinical therapeutic and adverse effects that may be different or opposite to the findings of our study. Therefore, caution is advised in considering the results of this study.

CONCLUSION

In conclusion, probiotics supplementation appears to be safe and effective in reducing the length of hospitalization for patients with mild acute pancreatitis in this double-blinded randomized clinical trial. However, the sample size is small and the follow-up time is short in this study. In future studies, a randomized study with a larger sample using different types and doses of probiotics can be conducted to further clarify the role of probiotics in acute pancreatitis and other uninvestigated gastrointestinal diseases.

ARTICLE HIGHLIGHTS

Research background

Acute pancreatitis is one of the most common causes of acute abdominal pain, resulting in a huge clinical and financial burden worldwide. Most patients (80%) with acute pancreatitis present with mild disease, which is characterized by a short hospital stay, no or few complications, and rapid resumption of oral feeding. Allowing for the

very low mortality rate (about 0.79%) of mild acute pancreatitis, shortening the length of hospital stay (LOS), and reducing medical financial expenditure have become the research priority.

Research motivation

Probiotics play an important role in a variety of microecologic interventions. The effects of probiotics in mild acute pancreatitis have not been studied. Considering the potential benefits of probiotics in the treatment of gastrointestinal disease, we hypothesized that probiotics may accelerate the recovery of intestinal function and shorten the LOS in patients with mild pancreatitis. Thus, we conducted a randomized, double-blind, placebo-controlled trial to evaluate the effect of the administration of probiotics in patients with mild pancreatitis.

Research objectives

This study was designed to investigate the value of probiotics in reducing the LOS in patients with mild acute pancreatitis.

Research methods

We conducted a double-blind randomized clinical trial to evaluate the effects of probiotics administered to patients with mild acute pancreatitis at a tertiary medical center. The patients were given probiotics capsules (a mixed preparation of *Bacillus subtilis* and *Enterococcus faecium*) or placebo. The primary study endpoint was the LOS. The secondary endpoints included time to abdominal pain relief, recurrent abdominal pain, and time to successful oral feeding.

Research results

A total of 128 patients were included, with 64 patients in each arm. The severity of illness and the etiological distribution of disease were similar in the two groups. There was a significant reduction in the LOS in the probiotics treatment group *vs* the placebo group (5.36 ± 0.15 *vs* 6.02 ± 0.17 d, $P < 0.05$). The probiotics group was associated with a shorter time to abdominal pain relief and time to successful oral feeding ($P < 0.01$ for both) than the placebo group. No statistical difference was found in recurrent abdominal pain between the two groups.

Research conclusions

The study results showed that the administration of probiotics capsule is associated with a shorter duration of hospitalization in patients with mild acute pancreatitis.

Research perspectives

Probiotics supplementation appears to be safe and effective in reducing the length of hospitalization for patients with mild acute pancreatitis in this double-blinded randomized clinical trial. However, the sample size is small and the follow-up time is short in this study. In future studies, a randomized study with a larger sample using different types and doses of probiotics can be conducted to further clarify the role of probiotics in acute pancreatitis and other uninvestigated gastrointestinal diseases.

REFERENCES

1 **Krishna SG**, Kamboj AK, Hart PA, Hinton A, Conwell DL. The Changing Epidemiology of Acute Pancreatitis Hospitalizations: A Decade of Trends and the Impact of Chronic Pancreatitis. *Pancreas* 2017; **46**: 482-488 [PMID: 28196021 DOI: 10.1097/MPA.0000000000000783]

2 **Peery AF**, Dellon ES, Lund J, Crockett SD, McGowan CE, Bulsiewicz WJ, Gangarosa LM, Thiny MT, Stizenberg K, Morgan DR, Ringel Y, Kim HP, DiBonaventura MD, Carroll CF, Allen JK, Cook SF, Sandler RS, Kappelman MD, Shaheen NJ. Burden of gastrointestinal disease in the United States: 2012 update. *Gastroenterology* 2012; **143**: 1179-1187. e3 [PMID: 22885331 DOI: 10.1053/j.gastro.2012.08.002]

3 **van Dijk SM**, Hallensleben NDL, van Santvoort HC, Fockens P, van Goor H, Bruno MJ, Besselink MG; Dutch Pancreatitis Study Group. Acute pancreatitis: recent advances through randomised trials. *Gut* 2017; **66**: 2024-2032 [PMID: 28838972 DOI: 10.1136/gutjnl-2016-313595]

4 **Nardone G**, Compare D, Rocco A. A microbiota-centric view of diseases of the upper gastrointestinal tract. *Lancet Gastroenterol Hepatol* 2017; **2**: 298-312 [PMID: 28404159 DOI: 10.1016/S2468-1253(16)30108-X]

5 **Kong F**, Cai Y. Study Insights into Gastrointestinal Cancer through the Gut Microbiota. *Biomed Res Int* 2019; **2019**: 8721503 [PMID: 31341907 DOI: 10.1155/2019/8721503]

6 **Hill C**, Guarner F, Reid G, Gibson GR, Merenstein DJ, Pot B, Morelli L, Canani RB, Flint HJ, Salminen S, Calder PC, Sanders ME. Expert consensus document. The International Scientific Association for Probiotics and Prebiotics consensus statement on the scope and appropriate use of the term probiotic. *Nat Rev Gastroenterol Hepatol* 2014; **11**: 506-514 [PMID: 24912386 DOI: 10.1038/nrgastro.2014.66]

7 **Sanders ME**, Merenstein DJ, Reid G, Gibson GR, Rastall RA. Probiotics and prebiotics in intestinal health and disease: from biology to the clinic. *Nat Rev Gastroenterol Hepatol* 2019; **16**: 605-616 [PMID: 31296969 DOI: 10.1038/s41575-019-0173-3]

8 **Besselink MG**, van Santvoort HC, Buskens E, Boermeester MA, van Goor H, Timmerman HM, Nieuwenhuijs VB, Bollen TL, van Ramshorst B, Witteman BJ, Rosman C, Ploeg RJ, Brink MA, Schaapherder AF, Dejong CH, Wahab PJ, van Laarhoven CJ, van der Harst E, van Eijck CH, Cuesta MA, Akkermans LM, Gooszen HG; Dutch Acute Pancreatitis Study Group. Probiotic prophylaxis in predicted severe acute pancreatitis: a randomised, double-blind, placebo-controlled trial. *Lancet* 2008; **371**: 651-659 [PMID: 18279948 DOI: 10.1016/S0140-6736(08)60207-X]

9 **Gou S**, Yang Z, Liu T, Wu H, Wang C. Use of probiotics in the treatment of severe acute pancreatitis: a systematic review and meta-analysis of randomized controlled trials. *Crit Care* 2014; **18**: R57 [PMID: 24684832 DOI: 10.1186/cc13809]

10 **Tian X**, Pi YP, Liu XL, Chen H, Chen WQ. Supplemented Use of Pre-, Pro-, and Synbiotics in Severe Acute Pancreatitis: An Updated Systematic Review and Meta-Analysis of 13 Randomized Controlled Trials. *Front Pharmacol* 2018; **9**: 690 [PMID: 30002627 DOI: 10.3389/fphar.2018.00690]

11 **Li SR**, Wang HH, Wu ZY, Liu RH, Tong MH, Wang CH, Wang RL, Zhao HC, Wei W. [Efficacies of lactulose plus live combined Bacillus subtilis and Enterococcus faecium capsules in the treatment of functional constipation: a multicenter, randomized, double blind, controlled trial]. *Zhonghua Yi Xue Za Zhi* 2012; **92**: 2955-2960 [PMID: 23328283 DOI: 10.3760/cma.j.issn.0376-2491.2012.42.002]

12 **Banks PA**, Bollen TL, Dervenis C, Gooszen HG, Johnson CD, Sarr MG, Tsiotos GG, Vege SS; Acute Pancreatitis Classification Working Group. Classification of acute pancreatitis--2012: revision of the Atlanta classification and definitions by international consensus. *Gut* 2013; **62**: 102-111 [PMID: 23100216 DOI: 10.1136/gutjnl-2012-302779]

13 **Doron S**, Snydman DR. Risk and safety of probiotics. *Clin Infect Dis* 2015; **60** Suppl 2: S129-S134 [PMID: 25922398 DOI: 10.1093/cid/civ085]

14 **Sanders ME**, Akkermans LM, Haller D, Hammerman C, Heimbach J, Hörmannsperger G, Huys G, Levy DD, Lutgendorff F, Mack D, Phothirath P, Solano-Aguilar G, Vaughan E. Safety assessment of probiotics for human use. *Gut Microbes* 2010; **1**: 164-185 [PMID: 21327023 DOI: 10.4161/gmic.1.3.12127]

15 **Rao SSC**, Rehman A, Yu S, Andino NM. Brain fogginess, gas and bloating: a link between SIBO, probiotics and metabolic acidosis. *Clin Transl Gastroenterol* 2018; **9**: 162 [PMID: 29915215 DOI: 10.1038/s41424-018-0030-7]

16 **Moraes JM**, Felga GE, Chebli LA, Franco MB, Gomes CA, Gaburri PD, Zanini A, Chebli JM. A full solid diet as the initial meal in mild acute pancreatitis is safe and result in a shorter length of hospitalization: results from a prospective, randomized, controlled, double-blind clinical trial. *J Clin Gastroenterol* 2010; **44**: 517-522 [PMID: 20054282 DOI: 10.1097/MCG.0b013e3181c986b3]

17 **Riquelme F**, Marinkovic B, Salazar M, Martínez W, Catan F, Uribe-Echevarría S, Puelma F, Muñoz J, Canals A, Astudillo C, Uribe M. Early laparoscopic cholecystectomy reduces hospital stay in mild gallstone pancreatitis. A randomized controlled trial. *HPB (Oxford)* 2020; **22**: 26-33 [PMID: 31235428 DOI: 10.1016/j.hpb.2019.05.013]

18 **Boxhoorn L**, Voermans RP, Bouwense SA, Bruno MJ, Verdonk RC, Boermeester MA, van Santvoort HC, Besselink MG. Acute pancreatitis. *Lancet* 2020; **396**: 726-734 [PMID: 32891214 DOI: 10.1016/S0140-6736(20)31310-6]

19 **Karakan T**, Ergun M, Dogan I, Cindoruk M, Unal S. Comparison of early enteral nutrition in severe acute pancreatitis with prebiotic fiber supplementation versus standard enteral solution: a prospective randomized double-blind study. *World J Gastroenterol* 2007; **13**: 2733-2737 [PMID: 17569144 DOI: 10.3748/wjg.v13.i19.2733]

20 **Wilkins T**, Sequoia J. Probiotics for Gastrointestinal Conditions: A Summary of the Evidence. *Am Fam Physician* 2017; **96**: 170-178 [PMID: 28762696]

21 **Parker EA**, Roy T, D'Adamo CR, Wieland LS. Probiotics and gastrointestinal conditions: An overview of evidence from the Cochrane Collaboration. *Nutrition* 2018; **45**: 125-134. e11 [PMID: 28870406 DOI: 10.1016/j.nut.2017.06.024]

22 **Working Group IAP/APA Acute Pancreatitis Guidelines**. IAP/APA evidence-based guidelines for the management of acute pancreatitis. *Pancreatology* 2013; **13**: e1-15 [PMID: 24054878 DOI: 10.1016/j.pan.2013.07.063]

23 **Crockett SD**, Wani S, Gardner TB, Falck-Ytter Y, Barkun AN; American Gastroenterological Association Institute Clinical Guidelines Committee. American Gastroenterological Association Institute Guideline on Initial Management of Acute Pancreatitis. *Gastroenterology* 2018; **154**: 1096-1101 [PMID: 29409760 DOI: 10.1053/j.gastro.2018.01.032]

24 **Lerner A**, Shoenfeld Y, Matthias T. Probiotics: If It Does Not Help It Does Not Do Any Harm. Really? *Microorganisms* 2019; **7**: 104 [PMID: 30979072 DOI: 10.3390/microorganisms7040104]

25 **Rao SSC**, Yu S, Tetangco EP, Yan Y. Probiotics can Cause D-Lactic Acidosis and Brain Fogginess: Reply to Quigley *et al*. *Clin Transl Gastroenterol* 2018; **9**: 207 [PMID: 30449886 DOI: 10.1038/s41424-018-0077-5]

Published by **Baishideng Publishing Group Inc**
7041 Koll Center Parkway, Suite 160, Pleasanton, CA 94566, USA
Telephone: +1-925-3991568
E-mail: bpgoffice@wjgnet.com
Help Desk: https://www.f6publishing.com/helpdesk
https://www.wjgnet.com

© 2021 Baishideng Publishing Group Inc. All rights reserved.

ISSN 1007-9327 (print)
ISSN 2219-2840 (online)

World Journal of *Gastroenterology*

World J Gastroenterol 2021 January 21; 27(3): 233-304



Published by Baishideng Publishing Group Inc

World Journal of Gastroenterology

Contents

Weekly Volume 27 Number 3 January 21, 2021

EDITORIAL

233 Screening colonoscopy: The present and the future

Hayman CV, Vyas D

ORIGINAL ARTICLE

Basic Study

240 Circular RNA AKT3 governs malignant behaviors of esophageal cancer cells by sponging miR-17-5p

Zang HL, Ji FJ, Ju HY, Tian XF

Retrospective Study

255 Serum vitamin D and vitamin-D-binding protein levels in children with chronic hepatitis B

Huang CZ, Zhang J, Zhang L, Yu CH, Mo Y, Mo LY

267 Trends in the management of anorectal melanoma: A multi-institutional retrospective study and review of the world literature

Bleicher J, Cohan JN, Huang LC, Peche W, Pickron TB, Scaife CL, Bowles TL, Hyngstrom JR, Asare EA

Observational Study

281 Comparative study on artificial intelligence systems for detecting early esophageal squamous cell carcinoma between narrow-band and white-light imaging

Li B, Cai SL, Tan WM, Li JC, Yalikong A, Feng XS, Yu HH, Lu PX, Feng Z, Yao LQ, Zhou PH, Yan B, Zhong YS

CASE REPORT

294 Peritoneal dissemination of pancreatic cancer caused by endoscopic ultrasound-guided fine needle aspiration: A case report and literature review

Kojima H, Kitago M, Iwasaki E, Masugi Y, Matsusaka Y, Yagi H, Abe Y, Hasegawa Y, Hori S, Tanaka M, Nakano Y, Takemura Y, Fukuhara S, Ohara Y, Sakamoto M, Okuda S, Kitagawa Y

World Journal of Gastroenterology

Weekly Volume 27 Number 3 January 21, 2021

Contents

ABOUT COVER

Michael Linnebacher, PhD, Academic Fellow, Research Fellow, Research Scientist, Senior Researcher, Senior Scientist, Molecular Oncology and Immunotherapy, Department of General, Visceral, Vascular and Transplantation Surgery, University Medical Center Rostock, Schillingallee 69, Rostock 18057, Germany. michael.linnebacher@med.uni-rostock.de

AIMS AND SCOPE

The primary aim of *World Journal of Gastroenterology* (*WJG*, *World J Gastroenterol*) is to provide scholars and readers from various fields of gastroenterology and hepatology with a platform to publish high-quality basic and clinical research articles and communicate their research findings online. *WJG* mainly publishes articles reporting research results and findings obtained in the field of gastroenterology and hepatology and covering a wide range of topics including gastroenterology, hepatology, gastrointestinal endoscopy, gastrointestinal surgery, gastrointestinal oncology, and pediatric gastroenterology.

INDEXING/ABSTRACTING

The *WJG* is now indexed in Current Contents®/Clinical Medicine, Science Citation Index Expanded (also known as SciSearch®), Journal Citation Reports®, Index Medicus, MEDLINE, PubMed, PubMed Central, and Scopus. The 2020 edition of Journal Citation Report® cites the 2019 impact factor (IF) for *WJG* as 3.665; IF without journal self cites: 3.534; 5-year IF: 4.048; Ranking: 35 among 88 journals in gastroenterology and hepatology; and Quartile category: Q2. The *WJG*'s CiteScore for 2019 is 7.1 and Scopus CiteScore rank 2019: Gastroenterology is 17/137.

RESPONSIBLE EDITORS FOR THIS ISSUE

Production Editor: *Yu-Jie Ma*; **Production Department Director:** *Xiang Li*; **Editorial Office Director:** *Ze-Mao Gong*.

NAME OF JOURNAL
World Journal of Gastroenterology

ISSN
ISSN 1007-9327 (print) ISSN 2219-2840 (online)

LAUNCH DATE
October 1, 1995

FREQUENCY
Weekly

EDITORS-IN-CHIEF
Andrzej S Tarnawski, Subrata Ghosh

EDITORIAL BOARD MEMBERS
http://www.wjgnet.com/1007-9327/editorialboard.htm

PUBLICATION DATE
January 21, 2021

COPYRIGHT
© 2021 Baishideng Publishing Group Inc

INSTRUCTIONS TO AUTHORS
https://www.wjgnet.com/bpg/gerinfo/204

GUIDELINES FOR ETHICS DOCUMENTS
https://www.wjgnet.com/bpg/GerInfo/287

GUIDELINES FOR NON-NATIVE SPEAKERS OF ENGLISH
https://www.wjgnet.com/bpg/gerinfo/240

PUBLICATION ETHICS
https://www.wjgnet.com/bpg/GerInfo/288

PUBLICATION MISCONDUCT
https://www.wjgnet.com/bpg/gerinfo/208

ARTICLE PROCESSING CHARGE
https://www.wjgnet.com/bpg/gerinfo/242

STEPS FOR SUBMITTING MANUSCRIPTS
https://www.wjgnet.com/bpg/GerInfo/239

ONLINE SUBMISSION
https://www.f6publishing.com

© 2021 Baishideng Publishing Group Inc. All rights reserved. 7041 Koll Center Parkway, Suite 160, Pleasanton, CA 94566, USA

E-mail: bpgoffice@wjgnet.com https://www.wjgnet.com

World Journal of Gastroenterology

Submit a Manuscript: https://www.f6publishing.com

World J Gastroenterol 2021 January 21; 27(3): 233-239

DOI: 10.3748/wjg.v27.i3.233

ISSN 1007-9327 (print) ISSN 2219-2840 (online)

EDITORIAL

Screening colonoscopy: The present and the future

Chelsea V Hayman, Dinesh Vyas

ORCID number: Chelsea V Hayman 0000-0002-5555-6861; Dinesh Vyas 0000-0002-5330-9429.

Author contributions: Hayman CV and Vyas D contributed to this paper; Vyas D designed the overall concept and outline of this manuscript; Hayman CV and Vyas D contributed to the discussion and design of the manuscript; Hayman CV contributed to the writing, and editing of the manuscript, illustrations, and review of the literature

Conflict-of-interest statement: Chelsea V Hayman and Dinesh Vyas have nothing to disclose.

Open-Access: This article is an open-access article that was selected by an in-house editor and fully peer-reviewed by external reviewers. It is distributed in accordance with the Creative Commons Attribution NonCommercial (CC BY-NC 4.0) license, which permits others to distribute, remix, adapt, build upon this work non-commercially, and license their derivative works on different terms, provided the original work is properly cited and the use is non-commercial. See: http://creativecommons.org/Licenses/by-nc/4.0/

Manuscript source: Unsolicited manuscript

Specialty type: Gastroenterology

Chelsea V Hayman, Dinesh Vyas, College of Medicine, California Northstate University, Elk Grove, CA 95757, United States

Dinesh Vyas, Department of Surgery, San Joaquin General Hospital, French Camp, CA 95231, United States

Corresponding author: Dinesh Vyas, MD, MSc, Associate Professor, Director, Surgeon, Department of Surgery, San Joaquin General Hospital, 500 West Hospital Road, French Camp, CA 95231, United States. dineshvyas@yahoo.com

Abstract

In the United States, colorectal cancer (CRC) is the second leading cause of mortality in men and women. We are now seeing an increasing number of patients with advanced-stage diagnosis and mortality from colorectal cancer before 50 years of age, which requires earlier screening. With the increasing need for CRC screening through colonoscopy, and thus endoscopists, easier and simpler techniques are needed to train proficient endoscopists. The most widely used approach by endoscopists is air insufflation colonoscopy, where air distends the colon to allow visualization of the colonic mucosa. This technique is uncomfortable for patients and requires an anesthetist to administer sedation. In addition, patients commonly complain about discomfort post-op as air escapes into the small bowel and cannot be adequately removed. Current research into the use of water insufflation colonoscopies has proved promising in reducing the need for sedation, decreasing discomfort, and increasing the visibility of the colonic mucosa. Future direction into water insufflation colonoscopies which have shown to be simpler and easier to teach may increase the number of proficient endoscopists in training to serve our aging population.

Key Words: Colorectal cancer; Water-insufflation colonoscopy; Air-insufflation colonoscopy; Adenomatous polyps; Adenoma detection rate

©The Author(s) 2021. Published by Baishideng Publishing Group Inc. All rights reserved.

Core Tip: Training residents in water-insufflation colonoscopy techniques are simpler and easier to teach and lead to a reduction in patient pain, need for sedation, and increased visibility of the colonic mucosa. As more endoscopists are comfortable with this technique, more people in our growing population will be able to obtain the

and hepatology

Country/Territory of origin: United States

Peer-review report's scientific quality classification
Grade A (Excellent): 0
Grade B (Very good): B
Grade C (Good): 0
Grade D (Fair): 0
Grade E (Poor): 0

Received: October 16, 2020
Peer-review started: October 16, 2020
First decision: October 27, 2020
Revised: November 10, 2020
Accepted: December 11, 2020
Article in press: December 11, 2020
Published online: January 21, 2021

P-Reviewer: Mizukami T
S-Editor: Liu M
L-Editor: A
P-Editor: Ma YJ

necessary screening colonoscopies.

Citation: Hayman CV, Vyas D. Screening colonoscopy: The present and the future. *World J Gastroenterol* 2021; 27(3): 233-239
URL: https://www.wjgnet.com/1007-9327/full/v27/i3/233.htm
DOI: https://dx.doi.org/10.3748/wjg.v27.i3.233

INTRODUCTION

In the United States, colorectal cancer (CRC) is the second leading cause of mortality in men and women. The most effective tool for reducing the morbidity and mortality associated with CRC is the use of colonoscopy. With nearly 14.2 million procedures performed in the United States alone[1], the colonoscopy is one of the most common procedures performed. However, colonoscopies can only benefit the population with endoscopists who have proficiency in both technical and cognitive skills. The guidelines for training in colonoscopy techniques and grading proficiency continue to evolve as new advances in the tools used by endoscopists are discovered. In the 1960s, retrograde colonoscopy and endoscopic excision of polyps were developed in Japan to advance the visualization and removal of polyps from the entire large intestine[2]. Previous techniques such as the barium enema were challenging without considerable training and practice, and the presence of polypoid tumors could not be reliably excluded. As it was demonstrated that CRC did not occur *de-novo* but arose from a premalignant polyp, the use of the colonoscopy as a screening technique increased. Research into the use of the colonoscopy and the colonoscopy polypectomy proved that the detection of cancer at an earlier, pre-symptomatic stage was associated with better survival[3].

For a successful screening colonoscopy, partial distention of the lumen is needed to allow proper visualization and inspection of the colonic mucosa. The current standard technique for colonic distention is the use of air insufflation (AI) using an integrated air pump[4,5]. However, one of the major sources of pain and discomfort for patients undergoing a colonoscopy is the volume of air insufflated which causes significant abdominal distention and looping of the instrument. Potential risks for this procedure include perforation, bleeding, and infection. To minimize discomfort and pain during the procedure, patients undergoing colonoscopy with AI often require sedation which adds additional risks including medication side effects, higher medical costs, and longer recovery time when compared with unsedated colonoscopy[6]. At the end of the procedure, the air can only be partially removed, as some of it escapes into the small bowel. This leads to post-procedure cramping, gas, and bloating which can only be relieved by passing gas.

Recent clinical trials have proposed that using water infusion to distend the colon may reduce patient pain and discomfort and improve colonic visualization through difficult segments of the colon. This was first described by Falchuk and Griffin in 1984 in patients who could not undergo AI due to severe diverticular disease[7]. For water infusion colonoscopy, instead of expanding the colon, the water weighs it down utilizing gravity. It was Japanese endoscopists who evolved this technique by using syringes for water infusion and complete air suction to "collapse" the colonic lumen and continuously infusing water to advance the colonoscope[8]. This method straightens the colon and allows for better navigation of the scope through less extreme angles. As no air is left behind, this technique reduces post-procedure pain and allows for faster recovery. The first randomized control trial in 2010 showed that using the water immersion technique compared to standard AI increases the success rate of minimal sedation colonoscopy[9]. This along with other studies has shown the use of water improves the rate and time of cecal intubation, alleviates abdominal pain, and increases patients' willingness to undergo a repeat procedure[7]. This technique is shown in Figure 1.

The overall effectiveness of colonoscopy is the achievement of various quality measurements. The most important quality measurement is the adenoma detection rate (ADR) which is the frequency with which adenomas are detected in asymptomatic, average-risk individuals in a screening colonoscopy[10]. Another quality measurement is cecal intubation or the ability to pass the colonoscope through the tip

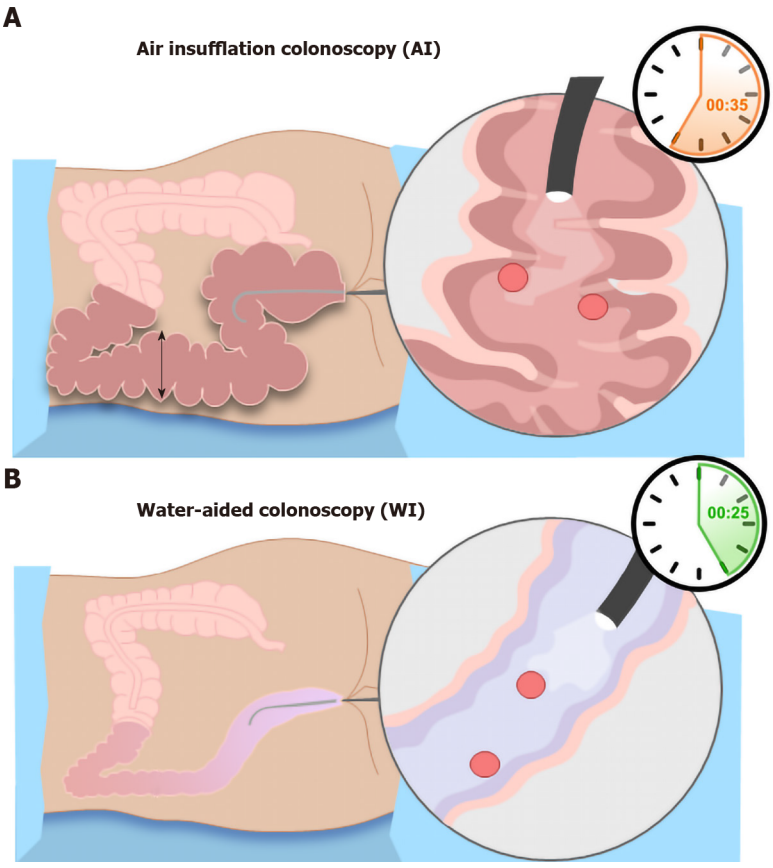


Figure 1 Image of colonic distension and bowel looping in air insufflation colonoscopy *vs* water-aided colonoscopy. A: Air insufflation colonoscopy causes significant distention of the colon in both length and width. The air promotes looping of the bowl at the flexure points leading to difficult navigation of the colonoscope; B: Water insufflation utilizes gravity to pull the colon down while providing minimal distention and looping. AI: Air insufflation; WI: Water insufflation.

of the ileocecal valve. This ensures adequate visualization of the entire colonic mucosa. Bowel preparation is an important measure as its effectiveness rests in the hands of the patient. Without adequate bowel preparation, clear visualization of the colon is difficult and may require repeat procedures. Sedation and the use of an anesthetist decrease intra-op and post-op pain, yet it is associated with increased cost.

New advances in colonoscopy have led to the development of virtual colonoscopy and robotic colonoscopy. Virtual colonoscopies, or computed tomography colonography (CTC), use helical CT scanners and AI to take 3D images of the colon. This technique is non-invasive, requires no sedation, can be completed in 10-15 min, and is overall much safer[11]. However, there are some limitations to this approach. Incomplete distention of colonic segments and flat lesions can lead to false-negative diagnoses. In addition, CTC does not allow for removal or biopsy of lesions. Robotic colonoscopy has benefits over the traditional endoscope approach including better viewing of the gastrointestinal tract, decreased pain, and the ability to navigate tortuous colons successfully. Multiple models of robotic instruments are currently being studied including robotic capsules and robotically controlled advanced colonoscopies. These new advances and the ease with which they can be used may aid in the training of future endoscopists. New research shows that training residents in water insufflation colonoscopic technique leads to increased patient comfort and decreased complications with comparable success rates[12]. As the number of people needing screening colonoscopies continues to grow, so will the need for competent endoscopists and successful endoscopic techniques.

ADR

ADR is the proportion of screening colonoscopies that detect at least one adenoma[13]. The goal of endoscopic screening is checking for CRC, so detection of adenoma in the large bowel can limit the advancement to larger adenomas. The recommended ADR is

20%, based on studies that showed adenoma prevalence in asymptomatic adults to be between 25% to 40%[14,15]. In a study with over 10000 patients, the overall ADR (95% confidence interval) for water insufflation was 34.4% and 30.2% for AI[16]. ADRs are inversely correlated with interval cancers which makes them an important measure in colonoscopies. Interval cancers, or post-colonoscopy CRCs, are cancers detected within the surveillance interval, or 6-36 mo post-cleared colonoscopy. The incidence of interval cancers is 3.4%-9.2%, and improving ADR and colonoscopy techniques can decrease this number substantially[17].

CECAL INTUBATION

Cecal intubation is successfully achieved when the tip of the colonoscope is passed through the ileocecal valve into the caput. This allows for a complete examination of the colonic mucosa at the medial wall of the cecum. AI distends the length of the colon, often farther than the length of the colonoscope. This attributes to the difficulty of adequate cecal intubation with AIC. Gravity allows water infusion into the sigmoid colon to open a passage through the loops and bends of the colon. In addition, abdominal compression and proper positioning of the patient facilitates the passage of the colonoscope and enhances cecal intubation. Some studies have reported that warm water insulation reduces colonic spasms which may also contribute to a higher cecal intubation rate. Some studies have shown that WIC improved cecal intubation time compared with AIC[7,18]. Increasing cecal intubation time can decrease the total OR time and thus, decrease the overall cost.

BOWEL PREP QUALITY

In order to optimize the effectiveness of colonoscopy as a screening tool, patients need to accept the procedure and the necessity of adequate bowel preparation[19]. Preparation quality affects the mucosal visualization, the ability to complete the exam, and the procedure duration. Only three-quarters of colonoscopies have adequate colon preparation[20]. Poor bowel prep can lead to lower ADRs and may force patients to undergo follow-up colonoscopies sooner. In water insufflation (WI), the suction of dirty water and infusion of clean water in the colonic lumen provides serendipitously salvage bowel cleaning in patients with suboptimal bowel preparation[21]. Ineffective bowel preparation may lead to cancelations or rescheduling procedures, which is a major contributor to costs[22].

SEDATION

Sedation for colonoscopy procedure increases the cost and post-procedure recovery time for patients. Patients who have more challenging anatomy often require more sedation as they experience more pain. Studies have shown that water exchange has minimized the requirement for sedation compared with AI. In one study, only 11.5% of patients required on-demand sedation with water exchange compared with 26% in the AI group[23]. Another benefit of limiting sedation is to decrease the risk of cardiopulmonary complications associated with anesthesia. In a study that used the Clinical Outcomes Research Initiative database, cardiopulmonary complications occurred in 0.9% of procedures and made up 67% of unplanned events in endoscopic procedures with sedation[24]. Patients with increased risk of CVP complications include those with advanced age and presence of comorbidities. These patients could benefit greatly from water insufflation colonoscopy, which requires little if any, pain management.

LIMITING PRE AND POST-PROCEDURE PAIN

Intraoperatively, AI causes more pain during colonoscopy as it elongates and distends the colon. Post-operatively, patients experience discomfort as the gas escapes the colon into the small bowel and leads to abdominal distention. Water insufflation reduces intraoperative pain by weighing down and straightening the sigmoid and decreasing

colonic spasm[25]. Fewer patients require sedation with water insufflation compared with AI[26]. Several studies revealed that WIC significantly increased the number of patients who were willing to undergo another colonoscopy due to limited pain during the procedure; this was found to be significantly higher in WIC than in AIC[18,27,28]. With AI, undesired outcomes including perforation and bleeding are partly due to increased colonic distention, angulations exaggeration at flexures, and the increased looping of the instrument. The current rate of perforation is low, ranging from 0.08% to 0.3% in various studies[29]. Pain during colonoscopy indicates the risk of perforation, but sedation can mask this important warning[30]. WI colonoscopy minimizes colonic distention, improves visibility, and reduces the need for sedation, thus reducing the risk of perforation.

TEACHING ENDOSCOPY TECHNIQUES IN TRAINING PROGRAMS

There are multiple different methods currently used for colonoscopy training, including mechanical simulators, virtual reality simulators, computer-simulating endoscopy, magnetic endoscopic imaging, and composite and explanted animal organ simulators. One of the main factors that leads to a lack of polyp discovery is the inexperience of the endoscopist[30,31]. However, there have been some limitations to colonoscopy instruction, including time management and potential trauma to patients involved. Endoscopists in training may benefit from learning the water insufflation technique, as the scope becomes easier to navigate through a minimally looped colon. In addition, detorsion becomes easier for trainees with water insufflation as there is a decreased risk of perforation from AI. Studies have shown that WIC has significantly shorter cecal intubation time for endoscopists in training compared with AIC[7]. The increasing need for colonoscopy screening has increased the demand for high-quality training. Stimulation models are a key tool that many programs use to ease the learning curve of colonoscopy techniques. Another tool that should be introduced into training programs is the use of water insufflation colonoscopy. Trainees may benefit from training with the water insufflation technique as there is the ease of insertion, reduced cecal intubation time, more comfort for the patient, and less looping of the bowel[12]. The strengths and weaknesses of these two techniques are shown in Table 1.

CONCLUSION

Colorectal cancer is the second leading cause of mortality in men and women in the United States. Since the onset of screening colonoscopies, the conventional colonoscope has not changed much since its development. Many colonoscopy practices use deep sedation to provide comfort for the patients, which adds to the overall cost of the procedure. There is still a lack of widespread acceptance of the use of colonoscopies (*vs* other non-invasive screening techniques), as up to 75% of patients diagnosed with colon cancer present with locally advanced disease[32]. In addition, 1 in 10 patients has developed interval cancers after clear colonoscopies. Beyond the water insufflation technique, there have been new advances in the use of robotic endoscopic techniques for screening colonoscopies. These devices can give a more in-depth view of the gastrointestinal tract, decrease pain associated with endoscopy, and perform well in more challenging colons[33]. Future directions should aim at getting a true 360-degree view of the colon with minimal pain, sedation, and total procedure time. In addition, colonoscopy practices should be geared toward practices that can be safely done during the COVID pandemic without the risk of aerosolizing viral particles.

Table 1 Strengths and weaknesses of air insufflation *vs* water insufflation

AI: Strengths	AI: Weaknesses	WI: Strengths	WI: Weaknesses
Distended bowel allows for better visualization	Increased pain on insertion	Increased ADR	Decreased visualization through fluid
More widely accepted	Increased postoperative pain	Decreased looping of bowel	Longer insertion time
Current teaching method	Increased sedation requirement	Decreased sedation requirement	Not widely accepted or utilized
Current patient preference	Increased risk of perforation	Increased cecal intubation rate	

AI: Air insufflation; WI: Water insufflation; ADR: Adenoma detection rate.

REFERENCES

1 **Seeff LC**, Richards TB, Shapiro JA, Nadel MR, Manninen DL, Given LS, Dong FB, Winges LD, McKenna MT. How many endoscopies are performed for colorectal cancer screening? *Gastroenterology* 2004; **127**: 1670-1677 [PMID: 15578503 DOI: 10.1053/j.gastro.2004.09.051]

2 **Wolff WI**. Colonoscopy: history and development. *Am J Gastroenterol* 1989; **84**: 1017-1025 [PMID: 2672788]

3 **Muto T**, Bussey HJ, Morson BC. The evolution of cancer of the colon and rectum. *Cancer* 1975; **36**: 2251-2270 [PMID: 1203876 DOI: 10.1002/cncr.2820360944]

4 **Phaosawasdi K**, Cooley W, Wheeler J, Rice P. Carbon dioxide-insufflated colonoscopy: an ignored superior technique. *Gastrointest Endosc* 1986; **32**: 330-333 [PMID: 3095169 DOI: 10.1016/s0016-5107(86)71877-4]

5 **Janssens F**, Deviere J, Eisendrath P, Dumonceau JM. Carbon dioxide for gut distension during digestive endoscopy: technique and practice survey. *World J Gastroenterol* 2009; **15**: 1475-1479 [PMID: 19322921 DOI: 10.3748/wjg.15.1475]

6 **Stock C**, Ihle P, Sieg A, Schubert I, Hoffmeister M, Brenner H. Adverse events requiring hospitalization within 30 days after outpatient screening and nonscreening colonoscopies. *Gastrointest Endosc* 2013; **77**: 419-429 [PMID: 23410698 DOI: 10.1016/j.gie.2012.10.028]

7 **Hafner S**, Zolk K, Radaelli F, Otte J, Rabenstein T, Zolk O. Water infusion *vs* air insufflation for colonoscopy. *Cochrane Database Syst Rev* 2015; **26**: CD009863 [PMID: 26011829 DOI: 10.1002/14651858.CD009863.pub2]

8 **Mizukami T**, Yokoyama A, Imaeda H, Kumai K. Collapse-submergence method: simple colonoscopic technique combining water infusion with complete air removal from the rectosigmoid colon. *Digest Endosc* 2007; **19**: 43-48 [DOI: 10.1111/j.1443-1661.2007.00670.x]

9 **Leung CW**, Kaltenbach T, Soetikno R, Wu KK, Leung FW, Friedland S. Water immersion *vs* standard colonoscopy insertion technique: randomized trial shows promise for minimal sedation. *Endoscopy* 2010; **42**: 557-563 [PMID: 20593332 DOI: 10.1055/s-0029-1244231]

10 **Rex DK**, Schoenfeld PS, Cohen J, Pike IM, Adler DG, Fennerty MB, Lieb JG 2nd, Park WG, Rizk MK, Sawhney MS, Shaheen NJ, Wani S, Weinberg DS. Quality indicators for colonoscopy. *Gastrointest Endosc* 2015; **81**: 31-53 [PMID: 25480100 DOI: 10.1016/j.gie.2014.07.058]

11 **Heiken JP**, Peterson CM, Menias CO. Virtual colonoscopy for colorectal cancer screening: current status. *Cancer Imaging* 2005; **5** Spec No A: S133-S139 [PMID: 16361129 DOI: 10.1102/1470-7330.2005.0108]

12 **Vyas D**, Chang J, Goyal M, Obad N, Ramdass P, Sodavarapu S. Training surgery residents in underwater colonoscopies is more effective than training them in air-insufflation colonoscopies. *medRxiv* 2020; Epub ahead of print [DOI: 10.1101/2020.06.06.20124339]

13 **Rex DK**, Bond JH, Winawer S, Levin TR, Burt RW, Johnson DA, Kirk LM, Litlin S, Lieberman DA, Waye JD, Church J, Marshall JB, Riddell RH; U. S. Multi-Society Task Force on Colorectal Cancer. Quality in the technical performance of colonoscopy and the continuous quality improvement process for colonoscopy: recommendations of the U.S. Multi-Society Task Force on Colorectal Cancer. *Am J Gastroenterol* 2002; **97**: 1296-1308 [PMID: 12094842 DOI: 10.1111/j.1572-0241.2002.05812.x]

14 **Lieberman DA**, Weiss DG, Bond JH, Ahnen DJ, Garewal H, Chejfec G. Use of colonoscopy to screen asymptomatic adults for colorectal cancer. Veterans Affairs Cooperative Study Group 380. *N Engl J Med* 2000; **343**: 162-168 [PMID: 10900274 DOI: 10.1056/NEJM200007203430301]

15 **Imperiale TF**, Wagner DR, Lin CY, Larkin GN, Rogge JD, Ransohoff DF. Risk of advanced proximal neoplasms in asymptomatic adults according to the distal colorectal findings. *N Engl J Med* 2000; **343**: 169-174 [PMID: 10900275 DOI: 10.1056/NEJM200007203430302]

16 **Faccio L**, Frazzoni L, Hassan C, La Marca M, Paci V, Smania V, De Bortoli N, Bazzoli F, Repici A, Rex D, Cadoni S. Water exchange colonoscopy increases adenoma detection rate: a systematic review with network meta-analysis of randomized controlled studies. *Gastrointest Endosc* 2018; **88**: 589-597.e11 [PMID: 29981753 DOI: 10.1016/j.gie.2018.06.028]

17 **Jang HJ**. Training in Endoscopy: Colonoscopy. *Clin Endosc* 2017; **50**: 322-327 [PMID: 28783920 DOI: 10.5946/ce.2017.077]

18 **Leung FW**, Harker JO, Jackson G, Okamoto KE, Behbahani OM, Jamgotchian NJ, Aharonian HS, Guth PH, Mann SK, Leung JW. A proof-of-principle, prospective, randomized, controlled trial demonstrating improved outcomes in scheduled unsedated colonoscopy by the water method. *Gastrointest Endosc* 2010; **72**: 693-700 [PMID: 20619405 DOI: 10.1016/j.gie.2010.05.020]

19 **McLachlan SA**, Clements A, Austoker J. Patients' experiences and reported barriers to colonoscopy in the screening context--a systematic review of the literature. *Patient Educ Couns* 2012; **86**: 137-146 [PMID: 21640543 DOI: 10.1016/j.pec.2011.04.010]

20 **Harewood GC**, Sharma VK, de Garmo P. Impact of colonoscopy preparation quality on detection of suspected colonic neoplasia. *Gastrointest Endosc* 2003; **58**: 76-79 [PMID: 12838225 DOI: 10.1067/mge.2003.294]

21 **Ramirez FC**, Leung FW. A head-to-head comparison of the water vs. air method in patients undergoing screening colonoscopy. *J Interv Gastroenterol* 2011; **1**: 130-135 [PMID: 22163084 DOI: 10.4161/jig.1.3.18512]

22 **Rex DK**, Imperiale TF, Latinovich DR, Bratcher LL. Impact of bowel preparation on efficiency and cost of colonoscopy. *Am J Gastroenterol* 2002; **97**: 1696-1700 [PMID: 12135020 DOI: 10.1111/j.1572-0241.2002.05827.x]

23 **Cadoni S**, Gallittu P, Sanna S, Fanari V, Porcedda ML, Erriu M, Leung FW. A two-center randomized controlled trial of water-aided colonoscopy *vs* air insufflation colonoscopy. *Endoscopy* 2014; **46**: 212-218 [PMID: 24218307 DOI: 10.1055/s-0033-1353604]

24 **Sharma VK**, Nguyen CC, Crowell MD, Lieberman DA, de Garmo P, Fleischer DE. A national study of cardiopulmonary unplanned events after GI endoscopy. *Gastrointest Endosc* 2007; **66**: 27-34 [PMID: 17591470 DOI: 10.1016/j.gie.2006.12.040]

25 **Rapelli S**, Montorfano G, Gornati R, Berra B. Tissue and serum gangliosides determination in patients with meningiomas. *Ital J Biochem* 1989; **38**: 289A-291A [PMID: 2583983 DOI: 10.1016/j.giec.2014.11.002]

26 **Chaubal A**, Pandey V, Patel R, Poddar P, Phadke A, Ingle M, Sawant P. Difficult colonoscopy: air, carbon dioxide, or water insufflation? *Intest Res* 2018; **16**: 299-305 [PMID: 29743844 DOI: 10.5217/ir.2018.16.2.299]

27 **Ransibrahmanakul K**, Leung J, Mann S; Siao-Salera R; Lim B; Hasyagar C; Yen D; Nastaskin I; Leung F. Water Infusion in Lieu of Air Insufflation (Water Method) Diminished Discomfort in Patients Undergoing Minimal Sedation Colonoscopy in the Hands of Supervised Trainees. *Am J Gastroenterol* 2009; **104**: S509-S510

28 **Hsieh YH**, Lin HJ, Tseng KC. Limited water infusion decreases pain during minimally sedated colonoscopy. *World J Gastroenterol* 2011; **17**: 2236-2240 [PMID: 21633535 DOI: 10.3748/wjg.v17.i17.2236]

29 **ASGE Standards of Practice Committee**, Fisher DA, Maple JT, Ben-Menachem T, Cash BD, Decker GA, Early DS, Evans JA, Fanelli RD, Fukami N, Hwang JH, Jain R, Jue TL, Khan KM, Malpas PM, Sharaf RN, Shergill AK, Dominitz JA. Complications of colonoscopy. *Gastrointest Endosc* 2011; **74**: 745-752 [PMID: 21951473 DOI: 10.1016/j.gie.2011.07.025]

30 **Leung FW**, Aljebreen AM, Brocchi E, Chang EB, Liao WC, Mizukami T, Schapiro M, Triantafyllou K. Sedation-risk-free colonoscopy for minimizing the burden of colorectal cancer screening. *World J Gastrointest Endosc* 2010; **2**: 81-89 [PMID: 21160707 DOI: 10.4253/wjge.v2.i3.81]

31 **Papanikolaou IS**, Karatzas PS, Varytimiadis LT, Tsigaridas A, Galanopoulos M, Viazis N, Karamanolis DG. Effective colonoscopy training techniques: strategies to improve patient outcomes. *Adv Med Educ Pract* 2016; **7**: 201-210 [PMID: 27099542 DOI: 10.2147/AMEP.S99617]

32 **Johnston PG**. The Colorectal Cancer Coalition: reflections on the future. *Oncologist* 2006; **11**: 970-972 [PMID: 17030636 DOI: 10.1634/theoncologist.11-9-970]

33 **Cater D**, Vyas A, Vyas D. Robotics in Colonoscopy. *Am J Robot Surg* 2014; **1**: 48-54 [PMID: 26380845 DOI: 10.1166/ajrs.2014.1008]

World Journal of Gastroenterology

Submit a Manuscript: https://www.f6publishing.com

World J Gastroenterol 2021 January 21; 27(3): 240-254

DOI: 10.3748/wjg.v27.i3.240

ISSN 1007-9327 (print) ISSN 2219-2840 (online)

ORIGINAL ARTICLE

Basic Study

Circular RNA AKT3 governs malignant behaviors of esophageal cancer cells by sponging miR-17-5p

Hong-Liang Zang, Fu-Jian Ji, Hai-Ying Ju, Xiao-Feng Tian

ORCID number: Hong-Liang Zang 0000-0002-9837-0805; Fu-Jian Ji 0000-0002-6041-6089; Hai-Ying Ju 0000-0001-8243-5224; Xiao-Feng Tian 0000-0002-6544-0395.

Author contributions: Zang HL contributed to the study design and reviewed the manuscript; Ji FJ and Tian XF analyzed the data and wrote the manuscript; Ju HY and Zang HL contributed to the data collection, data interpretation, and manuscript writing; all authors read and approved the final manuscript.

Institutional review board statement: This research was reviewed and approved by the Ethics Committee of China-Japan Union Hospital of Jilin University and complied with the guidelines of Declaration of Helsinki.

Institutional animal care and use committee statement: The procedures were in accordance with guidelines of Animal Use and Care Committee of China-Japan Union Hospital of Jilin University.

Conflict-of-interest statement: All the authors have no conflict of interest related to the manuscript.

Data sharing statement: No additional data are available.

Hong-Liang Zang, Xiao-Feng Tian, Department of Hepatobiliary and Pancreatic Surgery, China-Japan Union Hospital of Jilin University, Changchun 130033, Jilin Province, China

Fu-Jian Ji, Department of Colorectal Surgery, China-Japan Union Hospital of Jilin University, Changchun 130033, Jilin Province, China

Hai-Ying Ju, Department of Hematology, Jilin Province Blood Center, Changchun 130000, Jilin Province, China

Corresponding author: Xiao-Feng Tian, MD, Chief Doctor, Department of Hepatobiliary and Pancreatic Surgery, China-Japan Union Hospital of Jilin University, No. 126 Xiantai Street, Erdao District, Changchun 130033, Jilin Province, China. fengwykctut4210@163.com

Abstract

BACKGROUND

Recent studies have demonstrated that circular RNA AKT3 (circAKT3) plays a crucial role in regulating the malignant phenotypes of tumor cells. However, the potential effects of circAKT3 on esophageal cancer have not been investigated.

AIM

To illuminate the role of circAKT3 in malignant behaviors of esophageal cancer cells and its underlying mechanism.

METHODS

Clinical samples were collected to detect the expression of *circAKT3*. The role of circAKT3 in proliferation, migration, invasion, and apoptosis of esophageal cancer cells was evaluated using Cell Counting Kit-8, wound healing assays, Transwell assays, and fluorescence analysis, respectively. The target of circAKT3 was screened and identified using an online database and luciferase reporter assay. A xenograft nude mouse model was established to investigate the role of circAKT3 *in vivo*.

RESULTS

In vitro assays showed that proliferative, migratory, and invasive capacities of esophageal cancer cells were significantly enhanced by *circAKT3* overexpression. Furthermore, miR-17-5p was screened as the target of circAKT3, and miR-17-5p antagonized the effects of circAKT3 on esophageal cancer cells. Moreover, we identified RHOC and STAT3 as the direct target molecules of miR-17-5p, and

ARRIVE guidelines statement: The authors have read the ARRIVE guidelines, and the manuscript was prepared and revised according to the ARRIVE guidelines.

Open-Access: This article is an open-access article that was selected by an in-house editor and fully peer-reviewed by external reviewers. It is distributed in accordance with the Creative Commons Attribution NonCommercial (CC BY-NC 4.0) license, which permits others to distribute, remix, adapt, build upon this work non-commercially, and license their derivative works on different terms, provided the original work is properly cited and the use is non-commercial. See: http://creativecommons.org/licenses/by-nc/4.0/

Manuscript source: Unsolicited manuscript

Specialty type: Gastroenterology and hepatology

Country/Territory of origin: China

Peer-review report's scientific quality classification

Grade A (Excellent): A
Grade B (Very good): 0
Grade C (Good): 0
Grade D (Fair): 0
Grade E (Poor): 0

Received: October 30, 2020
Peer-review started: October 30, 2020
First decision: November 30, 2020
Revised: December 4, 2020
Accepted: December 16, 2020
Article in press: December 16, 2020
Published online: January 21, 2021

P-Reviewer: Kravtsov V
S-Editor: Chen XF
L-Editor: Filipodia
P-Editor: Ma YJ

circAKT3 facilitated expression of *RHOC* and *STAT3* by inhibiting miR-17-5p. *In vivo* assays showed *circAKT3* knockdown inhibited growth of esophageal cancer.

CONCLUSION

CircAKT3 contributed to the malignant behaviors of esophageal cancer *in vitro* and *in vivo* by sponging miR-17-5p thus providing a potential target for treatment of esophageal cancer.

Key Words: Esophageal cancer; Circular RNA AKT3; miR-17-5p; Proliferation; Migration; Invasion

©The Author(s) 2021. Published by Baishideng Publishing Group Inc. All rights reserved.

Core Tip: Circular RNA AKT3 was overexpressed in esophageal cancer and enhanced proliferative, migratory, and invasive capacities of esophageal cancer cells by sponging miR-17-5p to exert protumor effects. Downregulation of circular RNA AKT3 inhibited xenograft tumor growth of esophageal cancer *in vivo*. This research provided a potential target for better understanding the underlying mechanism of esophageal cancer.

Citation: Zang HL, Ji FJ, Ju HY, Tian XF. Circular RNA AKT3 governs malignant behaviors of esophageal cancer cells by sponging miR-17-5p. *World J Gastroenterol* 2021; 27(3): 240-254
URL: https://www.wjgnet.com/1007-9327/full/v27/i3/240.htm
DOI: https://dx.doi.org/10.3748/wjg.v27.i3.240

INTRODUCTION

As one of the most malignant tumors, esophageal cancer ranks in the top ten in morbidity and mortality of the tumors worldwide[1]. However, the exact mechanism is still in discussion. Currently, surgery is the predominant approach for treatment of esophageal cancer in combination with some other alternatives[2,3]. Although great progress has been made in the diagnosis and treatment of esophageal cancer, the prognosis has not been improved satisfactorily with a 5-year survival rate of less than 30%[4]. Thus, investigating the underlying mechanism is conducive to deepening the pathogenesis of esophageal cancer and developing targeted therapies.

Circular RNAs (circRNAs) belong to endogenous noncoding RNAs, which could be expressed in eukaryotic cells[5]. Unlike other RNA molecules, circRNAs possess the structure of a closed loop and cannot be degraded by RNase R[6]. Accumulating evidence has demonstrated that circRNAs participate in the modulation of protein expression by sponging microRNAs (miRNAs) or interacting with RNA binding proteins[7,8]. In tumor tissues and cell lines, the aberrant expression of circRNAs is involved in the regulation of malignant phenotypes of tumor cells. Wang *et al*[9] reported that circLMTK2 is overexpressed in gastric cancer, which could also be a predictor for a poor prognosis in patients with gastric cancer. In colorectal cancer, *circFBXW7* is significantly downregulated, and *circFBXW1* overexpression suppresses proliferative, migratory, and invasive abilities of colorectal cancer cells[10]. Therefore, differential expression of circRNAs exerts the opposite effects on tumor cells. However, only a few studies have concentrated on the effects of circRNAs on esophageal cancer.

Circular RNA AKT3 (circAKT3) is a novel molecule, which is derived from the *AKT3* gene and identified in gastric cancer with cisplatin resistance[11]. The *in vitro* and *in vivo* assays have revealed that circAKT3 is overexpressed in cisplatin resistant-gastric cancer and leads to the increased expression of *PIK3R1* to mediate resistance of gastric cancer cells to cisplatin[11]. However, Xia *et al*[12] demonstrated that glioblastoma expressed a low level of *circAKT3*, and *circAKT3* overexpression suppressed proliferation and promoted sensitivity to radiation of glioblastoma cells. The contradictory findings remind us of the potential role of circAKT3 in esophageal cancer.

MATERIALS AND METHODS

Collection of clinical samples

The clinical tissue samples were acquired from patients with esophageal cancer (n = 82) who underwent surgery at China-Japan Union Hospital of Jilin University. The relative expression of *circAKT3* less than the mean value was classified into the circAKT3 low group (n = 43), and the relative expression of *circAKT3* more than the mean value was classified into the circAKT3 high group (n = 39).

In vivo assay

The nude mice (n = 12) were purchased from Experimental Animal Center of China-Japan Union Hospital of Jilin University, housed in cages under the condition of the 12-h shift of light-dark cycles, and randomly divided into two groups. Negative control short hairpin RNA and short hairpin RNA against circAKT3, purchased from Integrated Biotech Solutions Co. (China), were transfected into TE-1 cells in the presence of puromycin (3 mg/mL; Thermo Fisher Scientific, United States) to establish the *circAKT3* knockdown cell lines. The mice injected with the negative control short hairpin RNA-transfected TE-1 cells were designated as the negative control short hairpin RNA group, and mice injected with the short hairpin RNA against circAKT3-transfected TE-1 cells were designated as the short hairpin RNA against circAKT3 group. After feeding for 30 d, the mice were anesthetized with pentobarbital sodium (25 mg/kg; Sigma-Aldrich, United States) intraperitoneally and killed by decapitation. The xenografts were isolated carefully and weighed.

Cell culture

Human esophageal cancer cell lines (KYSE-150, TE-10, TE-1) and human embryonic kidney cell line (HEK-293T) were cultured in Dulbecco's Modified Eagle Medium containing 10% fetal bovine serum (Gibco, United States). Human normal esophageal epithelial cell line (HEEC) was cultured in Dulbecco's Modified Eagle Medium with high glucose containing 10% fetal bovine serum (Gibco, United States). All of the cells were cultured in a CO_2 incubator chamber (Thermo Fisher Scientific, United States).

Quantitative real time-polymerase chain reaction

TRIzol (Ambion, United States) was utilized to extract the total RNA. SuperScript III (Invitrogen, United States) was used to obtain cDNA. SYBR Premix Ex Taq II (Takara, Japan) was utilized to perform quantitative real time(qRT)-PCR. The primer sequences of circAKT3 and U6 were adopted as previously reported[11]. The primer sequences of miR-17-5p were obtained from recent research[13]. The primer sequences of AKT3, RHOC, STAT3, and GAPDH were obtained from the NCBI online database (https://www.ncbi.nlm.nih.gov/gene/). CircAKT3 (forward, 5′-TCCAAATAAACGCCTTGGTGG-3′; reverse, 5′-CCTCAGAGAACACCCGCTCT-3′); miR-17-5p (forward, 5′-CGGCGGCAAAGTGCTTACAG-3′; reverse, 5′-GTGCAGGGTCCGAGGT-3′); U6 (forward, 5′-CTCGCTTCGGCAGCACA-3′; reverse, 5′-AACGCTTCACGAATTTGCGT-3′); AKT3 (forward, 5′-CGGCTTTCTCACGGATCACA-3′; reverse, 5′-CGGGACACTTTCCTTCCTCC-3′); RHOC (forward, 5′-AAGTTCCCTTTGCCCGTCTG-3′; reverse, 5′-ACAGTGGCAACTCAAGGGTC-3′); STAT3 (forward, 5′-CCAGGTACCGTGTGTCAAGC-3′; reverse, 5′-CAGACCTGACACCTGTGTTG-3′); GAPDH (forward, 5′-TGAAATGTGCACGCACCAAG-3′; reverse, 5′-GGGAAGCAGCATTCAGGTCT-3′). All of the primers were synthesized by Sangon (China).

Cell transfection

The siRNAs against circAKT3, miR-17-5p mimics, miR-17-5p inhibitor, indicated negative control, and plasmids were synthesized and purchased from Sangon (China). Lipofectamine 3000 (Invitrogen, United States) was used to conduct the transfection. RNase R (Epicentre, United States) was used to digest linear RNAs (but not circRNAs) in line with the manufacturer's instruction.

Fluorescence analysis

The Hoechst Staining Kit (Beyotime, China) was used to evaluate apoptotic cells. In brief, TE-1 cells were seeded at a density of 2.0×10^5 cells per well. After cell transfection with indicated vectors, 4% paraformaldehyde was used to fix the cultured TE-1 cells, followed by using Hoechst 33258 to stain the cells. A fluorescence microscope (Olympus, Japan) was utilized to observe the cells.

Measurement of cell viability

The Cell Counting Kit-8 (CCK-8; Beyotime, China) was utilized to measure cell viability. After transfection, TE-1 cells were seeded at a density of 1×10^4 cells per well for the indicated time. CCK-8 solution was added into each well for 2 h, and the Microplate Reader (Bio-Rad, United States) was used to record the value at 450 nm.

Wound healing assay

The wound healing assay was used to measure the migratory ability. After transfection, TE-1 cells were seeded into a 6-well plate for 24 h. The cells were scratched by a 10 mL Finntip and cultured in serum-free medium. Images were captured at 0 h and 24 h and analyzed by ImageJ software.

Measurement of invasive ability

The Transwell assay was conducted to evaluate the invasive ability. TE-1 cells with indicated transfection were cultured in Millicell Standing Cell Culture 24 well (Millipore, United States). After incubation for 24 h, glutaraldehyde solution was used to fix the cells, and crystal violet was used to stain the cells.

Luciferase reporter assay

ENCORI database was used to acquire the predicted binding sites between circAKT3 and miR-17-5p. TargetScanHuman database was utilized to acquire the potential binding sites of miR-17-5p with RHOC or STAT3. The procedures of the luciferase reporter assay were conducted in line with the previous study[11]. In our research, HEK-293T cells were utilized to detect the binding ability by cotransfecting the indicated vectors (Sangon, China) with Lipofectamine 3000 (Invitrogen, United States). The luciferase activity was evaluated by Bio-Glo™ Luciferase Assay System (Promega, United States).

Western blot

Western blot was carried out in line with the previous report[14]. In brief, the total protein was lysed by RIPA lysis buffer (Beyotime, China), and the BCA Kit (Thermal Fisher Scientific, United States) was used to detect the precise concentration. The total protein was added into SDS-PAGE gel (Beyotime, China). Primary antibodies [STAT3 rabbit monoclonal antibody (Cell Signaling Technology, United States); RHOC rabbit monoclonal antibody (Cell Signaling Technology, United States); GAPDH mouse monoclonal antibody (Cell Signaling Technology, United States)] were used overnight at 4 °C. Secondary antibodies with horseradish peroxidase (Beyotime, China) were applied for 2 h, and the indicated proteins were monitored by ChemDoc™ XRS+ System (Bio-Rad, United States).

Statistical analysis

The data in our research were displayed as mean ± standard deviation and analyzed by GraphPad Prism 8.0 Software (GraphPad, United States). The *t*-test, two-way ANOVA or Chi-squared test was used. Statistical significance was set as the *P* value less than 0.05.

RESULTS

CircAKT3 was overexpressed in esophageal cancer

First, we detected the expression of *circAKT3* in the esophageal cancer tissue samples and cell lines. The qRT-PCR results showed that circAKT3 was significantly upregulated in esophageal cancer tissue samples (Figure 1A). The characteristic analysis of the patients with esophageal cancer indicated that the tumor size, lymphatic metastasis, and clinical tumor node metastasis staging were positively related to the upregulation of circAKT3 in the tissue samples (Table 1). We also found that human esophageal cancer cell lines TE-1 cells, TE-10 cells, and KYSE-150 cells expressed a significantly higher level of circAKT3 compared to human normal esophageal epithelial cell line HEEC cells (Figure 1B).

CircAKT3 promoted malignant behaviors of TE-1 cells

Next, siRNAs against circAKT3 were transfected into TE-1 cells, and qRT-PCR analysis revealed a marked efficiency of *circAKT3* knockdown (Figure 1C). As the differential structure between circAKT3 and AKT3 mRNA, circAKT3 was resistant to RNase R,

Table 1 Characteristics of patients with esophageal cancer

Characteristic	CircAKT3 low	CircAKT3 high	*P* value
Age in yr			0.824
< 50	19	19	
≥ 50	24	20	
Tumor diameter in cm			0.026
< 3	27	14	
≥ 3	16	25	
Lymphatic metastasis			0.027
No	24	12	
Yes	19	27	
TNM staging			0.016
I-II	26	13	
III-IV	17	26	

CircAKT3: Circular RNA AKT3; TNM: Tumor node metastasis.

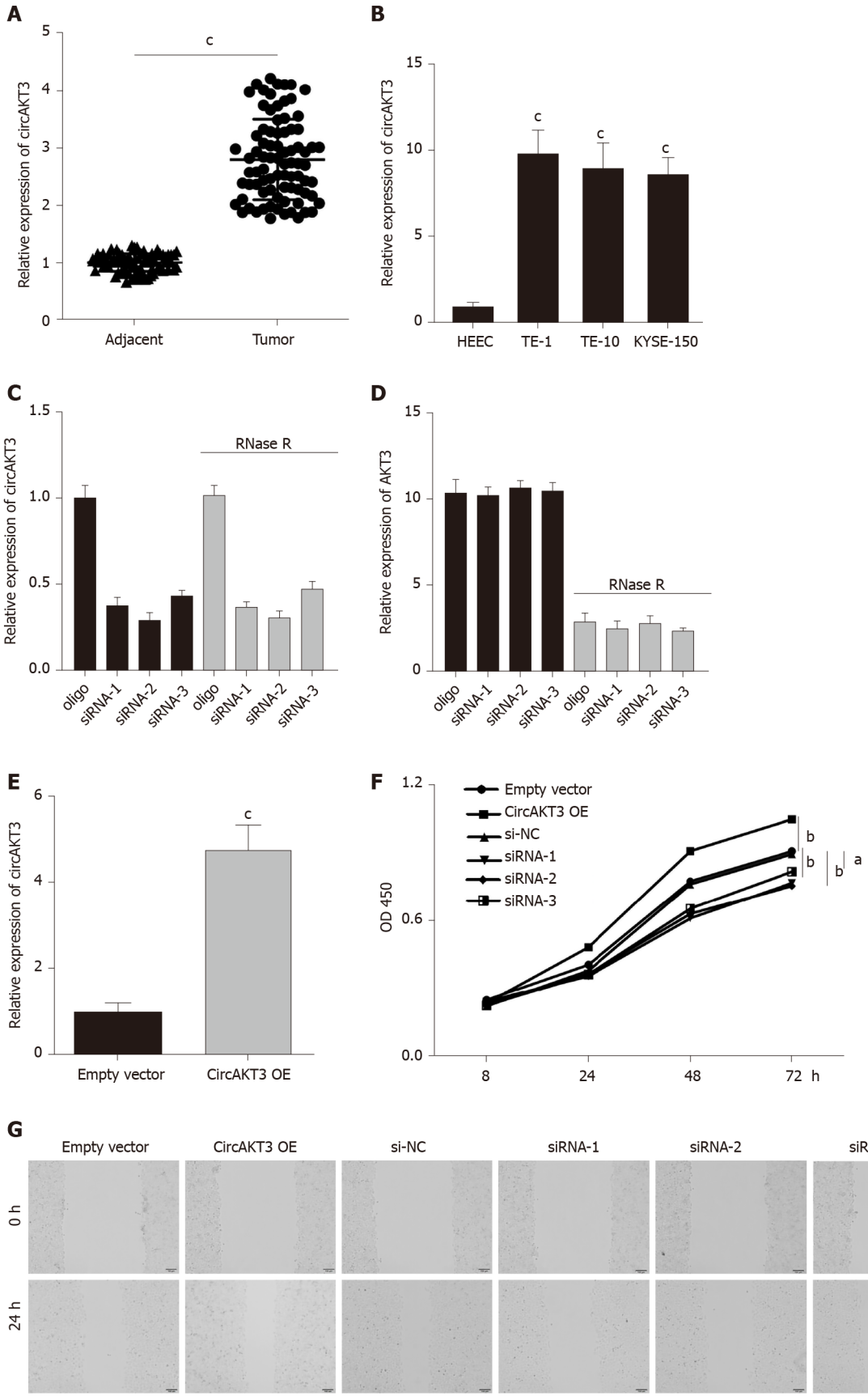
while AKT3 mRNA was sensitive to RNase R (Figure 1C and 1D), which confirmed the circular structure of circAKT3. Moreover, the *circAKT3* overexpression plasmids were transfected into TE-1 cells and could significantly increase the expression of *circAKT3* (Figure 1E). CCK-8 assay showed that circAKT3 siRNAs inhibited proliferation of TE-1 cells, while *circAKT3* overexpression plasmids facilitated proliferation of TE-1 cells (Figure 1F). We also found that *circAKT3* knockdown suppressed migration and invasion of TE-1 cells, while *circAKT3* overexpression exerted the opposite role by conducting the wound healing assay and Transwell assay, respectively (Figure 1G and 1H). We also measured the effect of circAKT3 on apoptosis. The fluorescence analysis indicated that circAKT3 siRNAs increased the number of condensed nuclei in TE-1 cells; however, *circAKT3* overexpression had no effect on the apoptotic rate of TE-1 cells (Figure 1I). These findings suggested that circAKT3 facilitated proliferative, migratory, and invasive capacities of esophageal cancer cells.

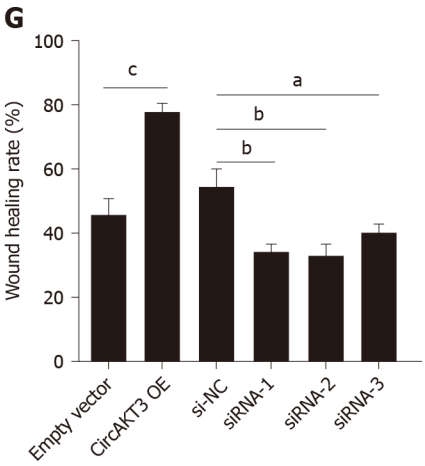
miR-17-5p acted as the downstream molecule of circAKT3 to antagonize the effects of circAKT3 on TE-1 cells

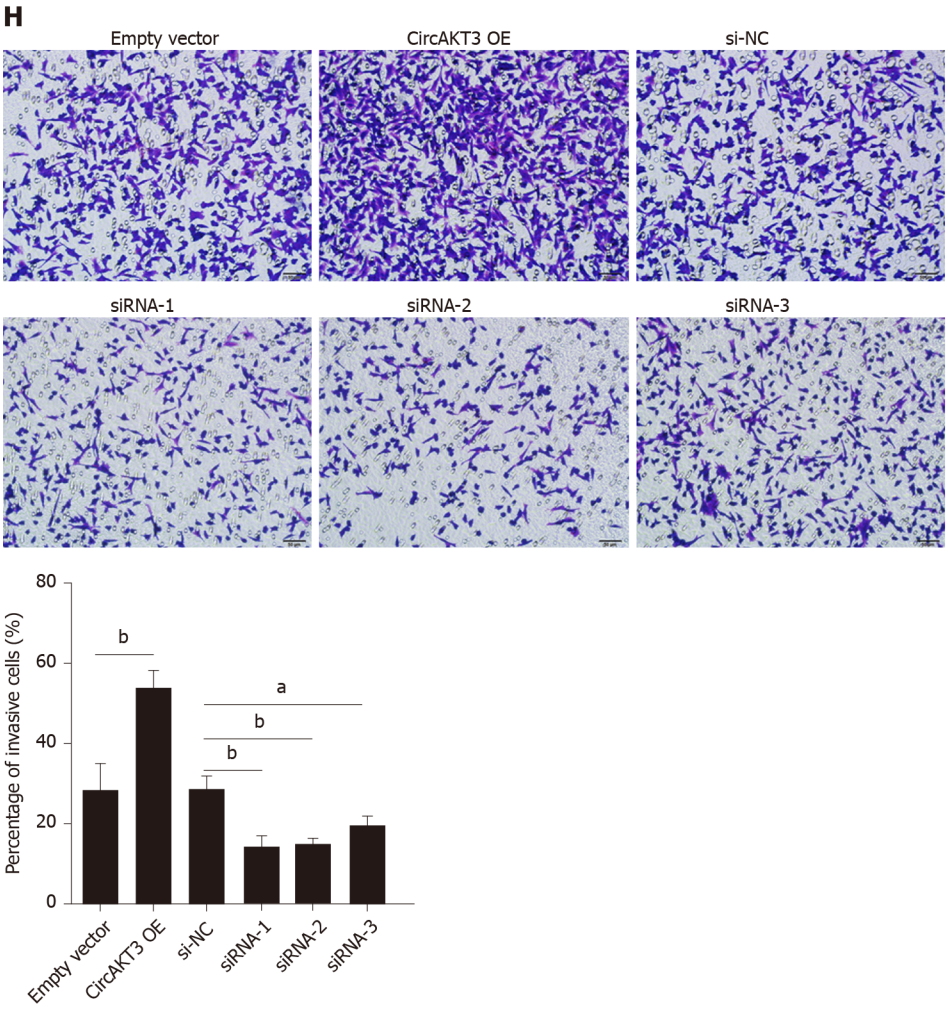
Accumulating evidence has reported that circRNAs regulate cell functions by sponging miRNAs[7]. The ENCORI database (http://starbase.sysu.edu.cn/index.php) was utilized to predict the potential target of circAKT3, and we identified miR-17-5p as the target of circAKT3. We carried out a luciferase reporter assay and found that TE-1 cells with wild-type circAKT3 and miR-17-5p mimics cotransfection presented a remarkably decreased luciferase activity (Figure 2A). Next, we detected the expression of *miR-17-5p* and found a lower level of miR-17-5p in esophageal cancer tissue samples (Figure 2B). Moreover, *miR-17-5p* expression was inversely associated with the expression of *circAKT3* in clinical tissue samples (Figure 2C). Meanwhile, esophageal cancer cell lines showed decreased expression of *miR-17-5p* (Figure 2D). These results indicated that miR-17-5p was inhibited by circAKT3. We then explored the role of miR-17-5p functioning as a downstream molecule of circAKT3 in TE-1 cells. CCK-8 assay showed that cell viability of TE-1 cells with cotransfection of *circAKT3* overexpression plasmids and miR-17-5p mimics was decreased compared to that with *circAKT3* overexpression plasmids transfection (Figure 2E). Moreover, miR-17-5p mimics suppressed migratory and invasive abilities of *circAKT3* overexpression plasmids-transfected TE-1 cells by the wound healing assay and Transwell assay, respectively (Figure 2F and 2G). In parallel, miR-17-5p mimics increased the apoptotic rate of *circAKT3* overexpression plasmids-transfected TE-1 cells (Figure 2H).

RHOC and STAT3 were modulated by the circAKT3/miR-17-5p axis

We then identified RHOC and STAT3 as the potential targets of miR-17-5p by using TargetScanHuman database (http://www.targetscan.org/vert_72/). The luciferase


A
Relative expression of circAKT3
c
Adjacent
Tumor
B
Relative expression of circAKT3
c
c
c
HEEC
TE-1
TE-10
KYSE-150
C
Relative expression of circAKT3
RNase R
oligo
siRNA-1
siRNA-2
siRNA-3
D
Relative expression of AKT3
RNase R
E
Relative expression of circAKT3
c
Empty vector
CircAKT3 OE
F
OD 450
Empty vector
CircAKT3 OE
si-NC
siRNA-1
siRNA-2
siRNA-3
b
b
b
a
8
24
48
72 h
G
Empty vector
CircAKT3 OE
si-NC
siRNA-1
siRNA-2
siRNA-3
0 h
24 h


G
Wound healing rate (%)
100
80
60
40
20
0
c
a
b
b
Empty vector
CircAKT3 OE
si-NC
siRNA-1
siRNA-2
siRNA-3


H
Empty vector
CircAKT3 OE
si-NC
siRNA-1
siRNA-2
siRNA-3
Percentage of invasive cells (%)
80
60
40
20
0
b
a
b
b
Empty vector
CircAKT3 OE
si-NC
siRNA-1
siRNA-2
siRNA-3

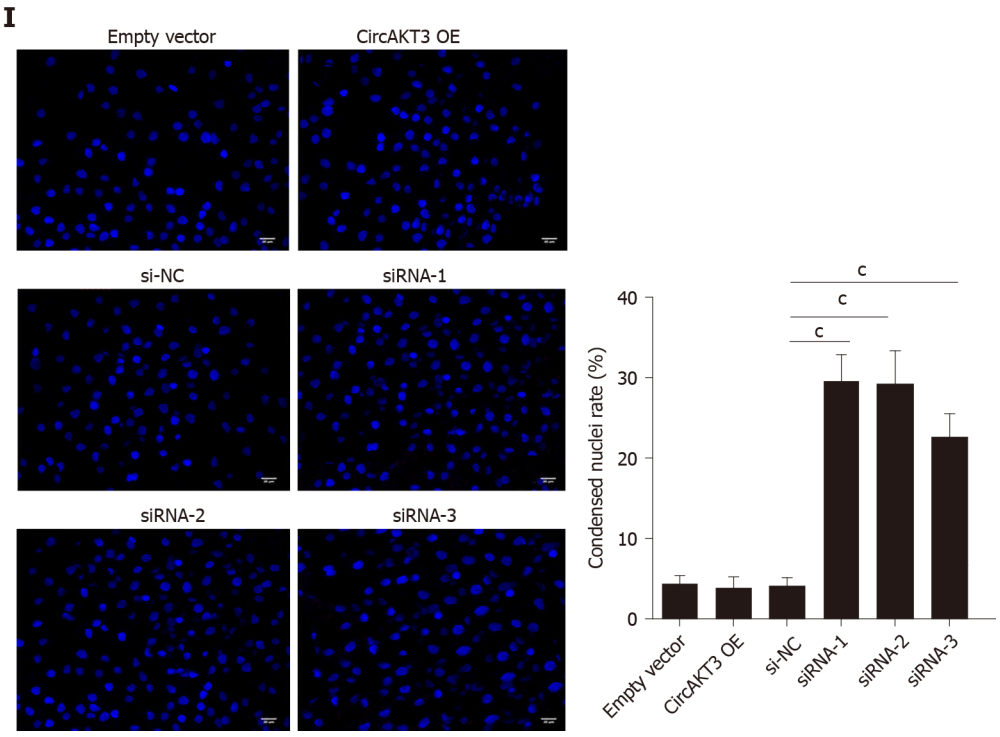


Figure 1 Circular RNA AKT3 promoted malignant phenotypes of TE-1 cells. A: The expression of *circular RNA AKT3* (*circAKT3*) in tissue samples; B: The expression of *circAKT3* human normal esophageal epithelial cell line (HEEC) and human esophageal cancer cell lines; C and D: TE-1 cells were transfected with control oligo and circAKT3 siRNAs in the presence or absence of RNase R to detect the expression of *circAKT3* and *AKT3*; E: The expression of *circAKT3* in TE-1 cells with *circAKT3* overexpression (OE); F: Cell viability of TE-1 cells as detected by the Cell Counting Kit-8 assay was performed to detect cell viability of TE-1 cells with indicated transfection; G: Migratory capacity of TE-1 cells with *circAKT3* OE and knockdown; H: Invasive ability of TE-1 cells with *circAKT3* OE and knockdown; I: Apoptosis of TE-1 cells with *circAKT3* OE and knockdown by Hoechst staining. $^{a}P < 0.05$; $^{b}P < 0.01$; $^{c}P < 0.001$. NC: Negative control; OD: Optical density.

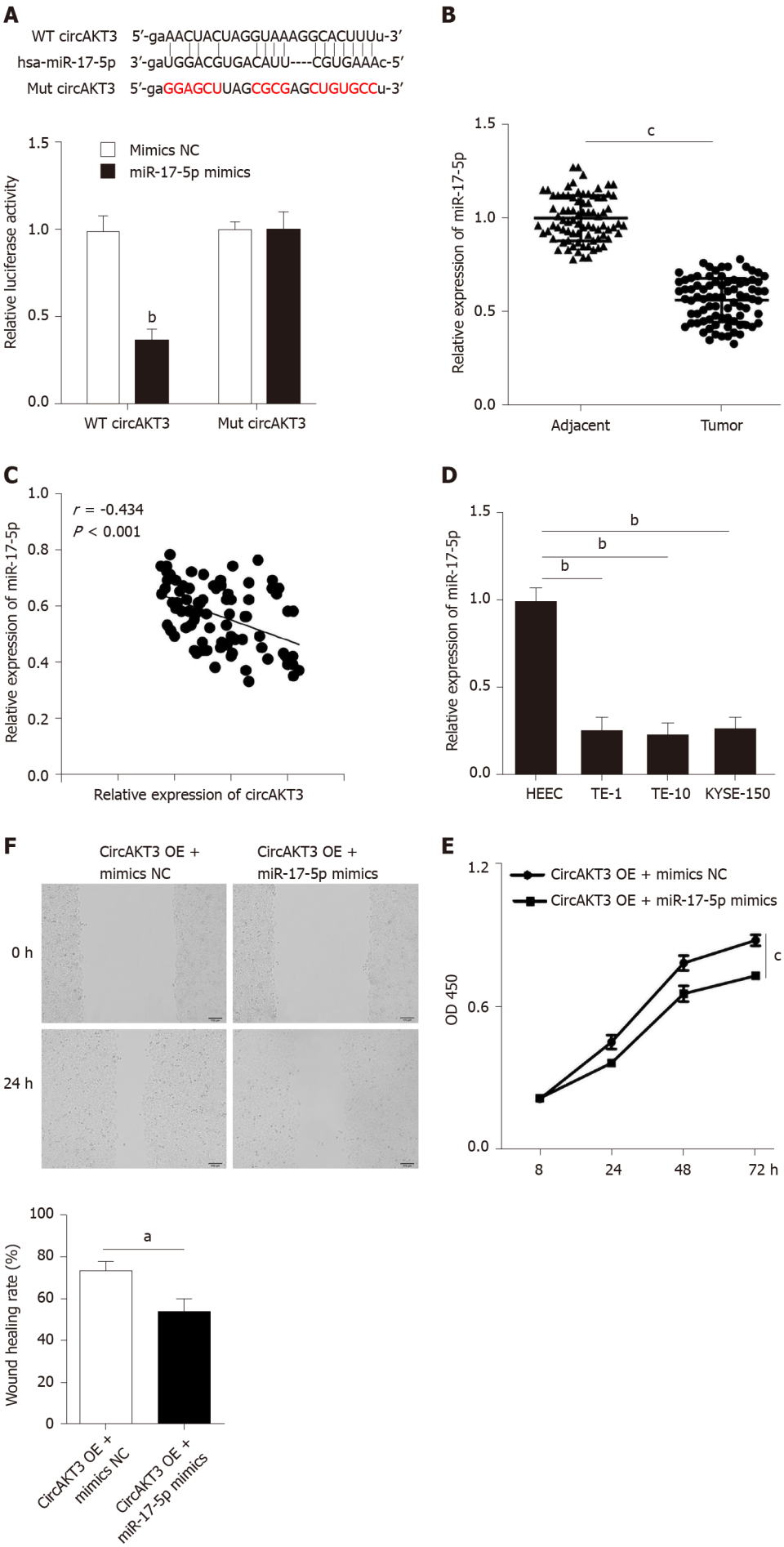
reporter assay showed that TE-1 cells with cotransfection of wild-type RHOC and miR-17-5p mimics presented a lower luciferase activity (Figure 3A). In addition, the decreased luciferase activity was also shown in TE-1 cells with cotransfection of wild-type STAT3 and miR-17-5p mimics (Figure 3B). Next, we detected the mRNA level of RHOC and STAT3 in clinical samples and found that both RHOC and STAT3 were upregulated in esophageal cancer tissue samples (Figure 3C and 3D). Moreover, the expression of *RHOC* and *STAT3* was increased in TE-1 cells, TE-10 cells, and KYSE-150 cells (Figure 3E and 3F). Western blot analysis showed that circAKT3 promoted the expression of RHOC and STAT3 in TE-1 cells, and miR-17-5p led to the reduced expression of RHOC and STAT3, which was reversed by circAKT3 overexpression plasmids cotransfection (Figure 3G). Conversely, circAKT3 siRNA inhibited the expression of RHOC and STAT3 in TE-1 cells, and a miR-17-5p inhibitor promoted the expression of RHOC and STAT3, which was reverted by circAKT3 siRNA cotransfection (Figure 3H). In consequence, circAKT3 facilitated the expression of RHOC and STAT3 by sponging miR-17-5p in esophageal cancer cells.

CircAKT3 knockdown suppressed growth of esophageal cancer in vivo

CircAKT3 shRNA was transfected into TE-1 cells to establish the stable *circAKT3* knockdown cell line (Figure 4A). The *in vivo* assay showed that the size and weight of the xenograft tumor injected with circAKT3 shRNA-transfected TE-1 cells were smaller and lighter (Figure 4B and 4C). The qRT-PCR analysis indicated that the xenograft tumor injected with circAKT3 shRNA-transfected TE-1 cells expressed a lower level of circAKT3, RHOC, and STAT3 and a higher level of miR-17-5p (Figure 4D-G). In parallel, the protein levels of RHOC and STAT3 were decreased in the xenograft tumor injected with circAKT3 shRNA-transfected TE-1 cells (Figure 4H).

DISCUSSION

Increased proliferative, migratory, and invasive abilities are hallmarks of tumor cells[15]. Thus, exploring the exact mechanism of malignant phenotypes of tumor cells


A
WT circAKT3 5′-gaAACUACUAGGUAAAGGCACUUUu-3′
hsa-miR-17-5p 3′-gaUGGACGUGACAUU----CGUGAAAc-5′
Mut circAKT3 5′-gaGGAGCUUAGCGCGAGCUGUGCCu-3′
B
C
D
E
F
Mimics NC
miR-17-5p mimics
Relative luciferase activity
WT circAKT3
Mut circAKT3
Relative expression of miR-17-5p
Adjacent
Tumor
r = -0.434
P < 0.001
Relative expression of circAKT3
HEEC
TE-1
TE-10
KYSE-150
CircAKT3 OE + mimics NC
CircAKT3 OE + miR-17-5p mimics
0 h
24 h
OD 450
Wound healing rate (%)

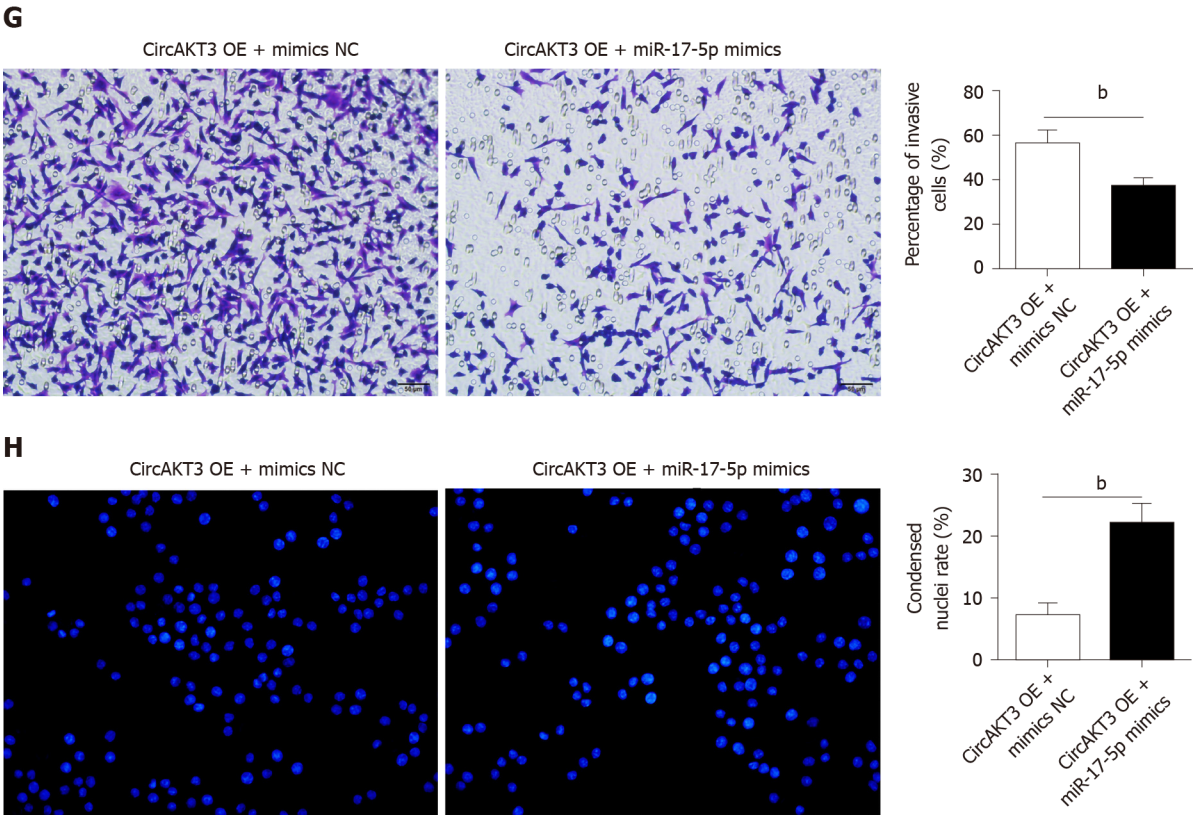


Figure 2 miR-17-5p acted as the downstream molecule of *circular RNA AKT3* to antagonize the effects of circular RNA AKT3 on TE-1 cells. A: Schematic of the miR-17-5p binding sites in wild-type (WT) *circular RNA AKT3* (*circAKT3*) and the mutant (Mut) *circAKT3* (up). Luciferase reporter assay was performed in HEK-293T cells to determine the binding ability between miR-17-5p and circAKT3 (down); B: The expression of *miR-17-5p* in tissue samples; C: CircAKT3 was negatively correlated with miR-17-5p in esophageal cancer tissue samples; D: *miR-17-5p* expression in indicated cell lines; E-H: Cell viability (E), migratory ability (F), invasive ability (G), and apoptosis (H) of *circAKT3* overexpression (OE)-transfected TE-1 cells in the presence or absence of miR-17-5p mimics. [a] $P < 0.05$; [b] $P < 0.01$; [c] $P < 0.001$. HEEC: Human normal esophageal epithelial cell line; NC: Negative control; OD: Optical density.

contributes to clarifying the pathogenesis of tumorigenesis. Herein, we reported the protumor role of circAKT3 in esophageal cancer cells by measuring the proliferative, migratory, and invasive abilities. In addition, miR-17-5p acted as a sponge molecule to inhibit the effects of circAKT3 on esophageal cancer cells. Furthermore, two protumor molecules, RHOC and STAT3, were the direct downstream targets of miR-17-5p, and circAKT3 upregulated RHOC and STAT3 by inhibiting miR-17-5p in esophageal cancer cells. Finally, we found *circAKT3* knockdown inhibited growth of esophageal cancer *in vivo*.

CircRNAs function among the complex molecular network and are implicated in the expression of functional proteins[5,7]. Mechanistically, the inhibitory effect of circRNAs on miRNAs is one of the predominant mechanisms involving regulation of proteins[7]. Increasing evidence has focused on the effects of circRNAs on the modulation of malignant phenotypes of tumor cells; however, only a few studies explore the relationship between circRNAs and esophageal cancer. A recent study reported that circZNF292 is upregulated in the esophageal cancer cell line Eca-109, and inhibition of circZNF292 enhanced the expression of *miR-206* to limit the proliferative, migratory, and invasive ability of Eca-109 cells[16]. In addition, Shi *et al*[17] demonstrated that overexpressed circPRKCI promoted the expression of *AKT3* by inhibiting miR-3680-3p to facilitate proliferation and migration of esophageal cancer cells. In addition, circSMAD7[18] and circFOXO3[19] could sponge different miRNAs to suppress malignant phenotypes of esophageal cancer cells. Therefore, it can be inferred that circRNAs exert the opposite roles in development and progression of esophageal cancer.

Our research identified circAKT3 as a motivator in development and progression of esophageal cancer cells. The gene symbol of circAKT3 is *AKT3*, which is a key member of the PI3K/AKT signaling pathway[11,20]. Previously, Huang *et al*[11] reported that *circAKT3* overexpression in gastric cancer participated in cisplatin resistance by restraining miR-198. However, the contradiction about the effects of circAKT3 on tumors is that circAKT3 could suppress development of glioblastoma[12] and

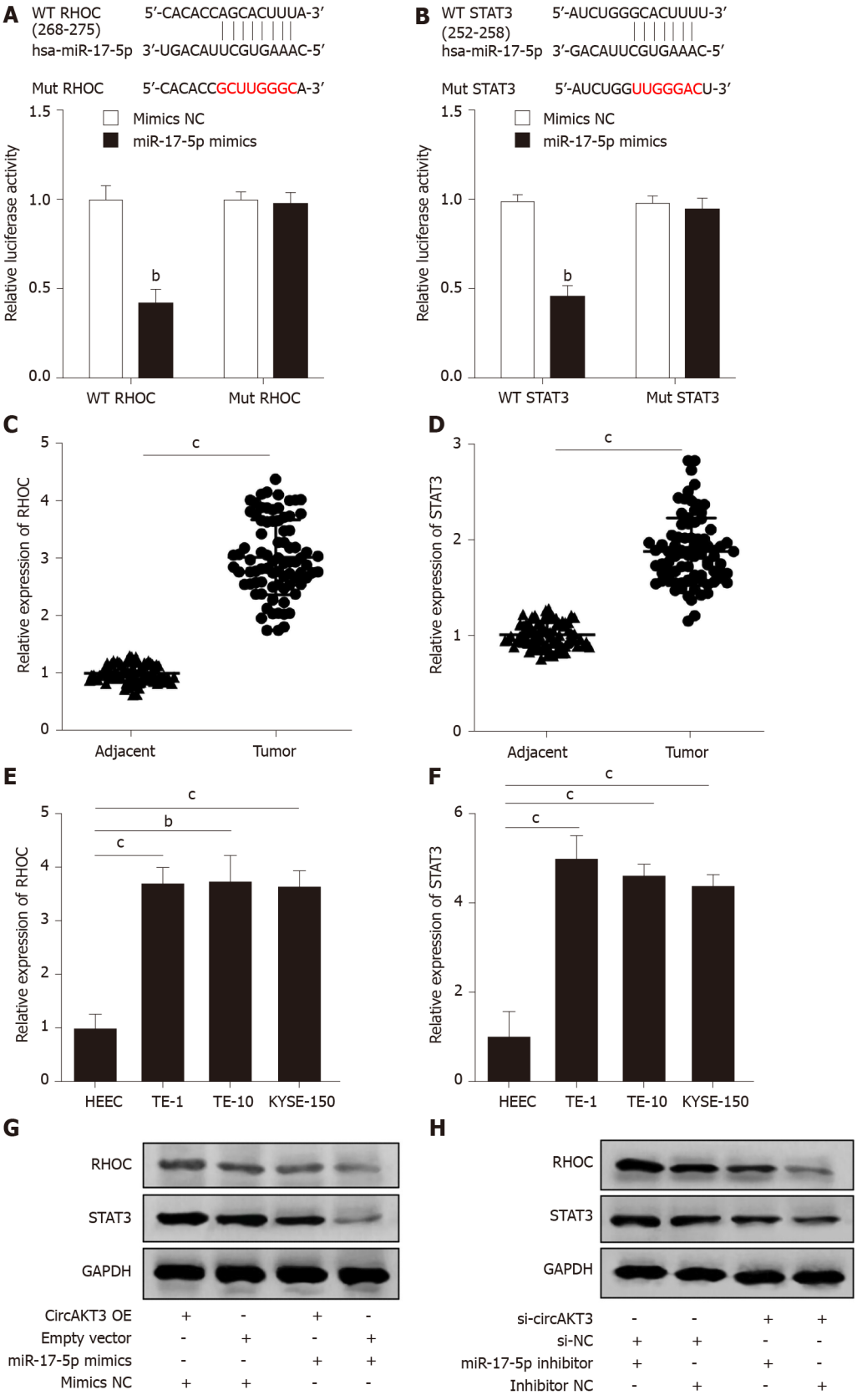


Figure 3 RHOC and STAT3 were modulated by the circular RNA AKT3/miR-17-5p axis. A: Schematic of the miR-17-5p binding sites in wild-type (WT) *RHOC* and the mutant (Mut) *RHOC* (up). Luciferase reporter assay was performed in HEK-293T cells to determine the binding ability between miR-17-5p and RHOC (down); B: Schematic of the miR-17-5p binding site in WT *STAT3* and the Mut *STAT3* (up). Luciferase reporter assay was performed in HEK-293T cells to determine the binding ability between miR-17-5p and STAT3 (down); C and D: The expression of *RHOC* (C) and *STAT3* (D) in tissue samples; E and F: The expression of *RHOC* (E) and *STAT3* (F) in indicated cell lines; G and H: Protein level of RHOC and STAT3 in TE-1 cells with indicated transfection. $^{b}P < 0.01$; $^{c}P < 0.001$. circAKT3: Circular RNA AKT3; HEEC: Human normal esophageal epithelial cell line; NC: Negative control; OE: Overexpression.

progression of clear cell renal cell carcinoma[20]. These findings, combined with our results, indicate a tumor specificity of circAKT3. Moreover, we identified miR-17-5p as a downstream molecule of circAKT3 to suppress the effects of circAKT3 on esophageal cancer cells by evaluating proliferation, migration, and invasion of TE-1 cells and found that esophageal cancer tissue samples and cell lines showed a significantly lower level of miR-17-5p. It has been reported that the expression of *miR-17-5p* decreased esophageal cancer stem-like cells and mediated radiation resistance[13], which further reinforced our findings.

Additionally, we screened two protumor molecules RHOC and STAT3 as the direct downstream targets of miR-17-5p. RHOC is one of the Ras homolog family members and functions as a protumor molecule in multiple tumors[21,22]. Clinical data shows that RHOC is positively expressed in esophageal cancer tissue samples and could be regarded as a predictor for patients with a poor prognosis of esophageal cancer[23,24]. The *in vitro* and *in vivo* experiments manifest that RHOC enhanced the proliferative and invasive capacity of esophageal cancer cells[25]. Similar to RHOC, STAT3 is a pivotal molecule that accelerates development and progression of malignant tumors[26,27]. In esophageal cancer cells, activation of STAT3 dramatically reduced apoptotic rate and contributed to increased proliferative ability[28]. Moreover, STAT3 promoted the expression of programmed death ligand 1 to mediate immune evasion of esophageal cancer cells[29].

CONCLUSION

Taken together, our research discovered that circAKT3 enhanced proliferative, migratory, and invasive capacities of esophageal cancer cells by sponging miR-17-5p to exert protumor effects, and downregulation of circAKT3 inhibited xenograft tumor growth of esophageal cancer *in vivo*, providing a potential target for better understanding the underlying mechanism of esophageal cancer.

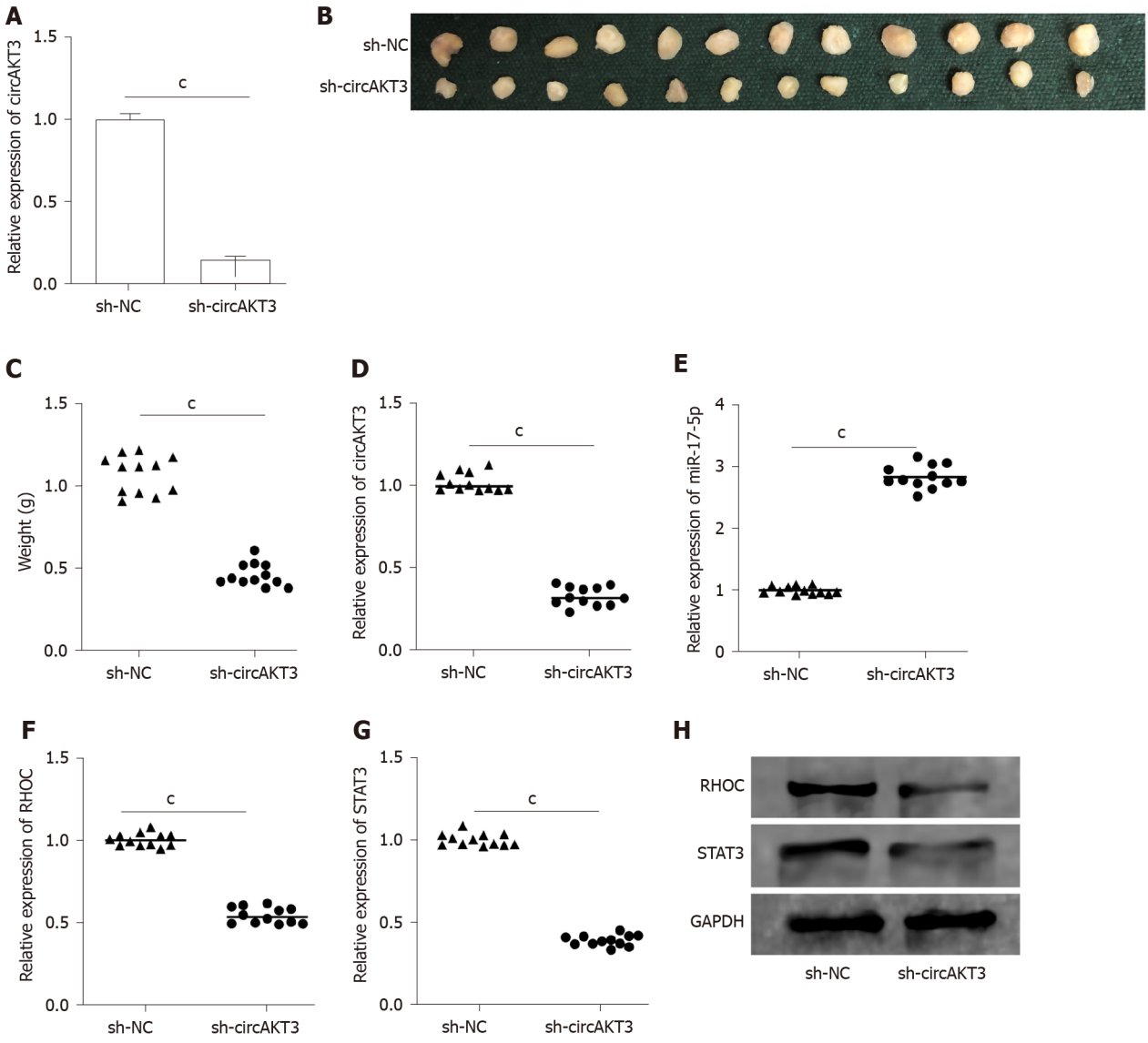


Figure 4 *Circular RNA AKT3* knockdown suppressed growth of esophageal cancer *in vivo*. A: The expression of *circular RNA AKT3* (*circAKT3*) in TE-1 cells with circAKT3 short hairpin (sh)RNA transfection; B and C: The size (B) and weight (C) of the xenograft tumor injected with circAKT3 shRNA-transfected TE-1 cells; D-G: The expression of *circAKT3* (D), *miR-17-5p* (E), *RHOC* (F) and *STAT3* (G) in the xenograft tumor injected with circAKT3 shRNA-transfected TE-1 cells by quantitative real time-polymerase chain reaction; H: The protein levels of RHOC and STAT3 in the xenograft tumor injected with circAKT3 shRNA-transfected TE-1 cells. $^{c}P < 0.001$. sh-NC: Negative control shRNA; sh-circAKT3: Circular RNA AKT3 shRNA.

ARTICLE HIGHLIGHTS

Research background

Esophageal cancer is one of the most malignant tumors in the digestive system and exploring the underlying mechanism is a key issue that needs to be addressed. Circular RNA AKT3 (circAKT3) is a novel noncoding RNA participating in the development and progression of multiple tumors.

Research motivation

To identify biomarkers for the diagnosis and treatment of esophageal cancer.

Research objectives

To explore the mechanism of the role of circAKT3 in the development of esophageal cancer.

Research methods

Cell Counting Kit-8, wound healing assay, Transwell assay, and fluorescence analysis

were used to evaluate the circAKT3 effect on proliferation, migration, invasion, and apoptosis of esophageal cancer cells.

Research results

In vitro assays results revealed that proliferative, migratory, and invasive capacities of esophageal cancer cells were significantly enhanced by *circAKT3* overexpression. miR-17-5p was screened as the target of circAKT3, and miR-17-5p antagonized the effects of circAKT3 on esophageal cancer cells. Moreover, we identified RHOC and STAT3 as the direct target molecules of miR-17-5p, and circAKT3 facilitated expression of *RHOC* and *STAT3* by inhibiting miR-17-5p. *In vivo* assays showed *circAKT3* knockdown inhibited growth of esophageal cancer.

Research conclusions

CircAKT3 enhanced proliferative, migratory, and invasive capacities of esophageal cancer cells by sponging miR-17-5p to exert protumor effects, and downregulation of circAKT3 inhibited xenograft tumor growth of esophageal cancer *in vivo*, providing a potential target for better understanding the underlying mechanism of esophageal cancer.

Research perspectives

The role of circAKT3 in other tumors may be uncovered in the future, and its application in anticancer therapy will be promoted.

REFERENCES

1 **Bray F**, Ferlay J, Soerjomataram I, Siegel RL, Torre LA, Jemal A. Global cancer statistics 2018: GLOBOCAN estimates of incidence and mortality worldwide for 36 cancers in 185 countries. *CA Cancer J Clin* 2018; **68**: 394-424 [PMID: 30207593 DOI: 10.3322/caac.21492]

2 **Lagergren J**, Smyth E, Cunningham D, Lagergren P. Oesophageal cancer. *Lancet* 2017; **390**: 2383-2396 [PMID: 28648400 DOI: 10.1016/S0140-6736(17)31462-9]

3 **van Rossum PSN**, Mohammad NH, Vleggaar FP, van Hillegersberg R. Treatment for unresectable or metastatic oesophageal cancer: current evidence and trends. *Nat Rev Gastroenterol Hepatol* 2018; **15**: 235-249 [PMID: 29235549 DOI: 10.1038/nrgastro.2017.162]

4 **Ohashi S**, Miyamoto S, Kikuchi O, Goto T, Amanuma Y, Muto M. Recent Advances From Basic and Clinical Studies of Esophageal Squamous Cell Carcinoma. *Gastroenterology* 2015; **149**: 1700-1715 [PMID: 26376349 DOI: 10.1053/j.gastro.2015.08.054]

5 **Kristensen LS**, Andersen MS, Stagsted LVW, Ebbesen KK, Hansen TB, Kjems J. The biogenesis, biology and characterization of circular RNAs. *Nat Rev Genet* 2019; **20**: 675-691 [PMID: 31395983 DOI: 10.1038/s41576-019-0158-7]

6 **Xia L**, Song M, Sun M, Wang F, Yang C. Circular RNAs as Biomarkers for Cancer. *Adv Exp Med Biol* 2018; **1087**: 171-187 [PMID: 30259366 DOI: 10.1007/978-981-13-1426-1_14]

7 **Qu S**, Yang X, Li X, Wang J, Gao Y, Shang R, Sun W, Dou K, Li H. Circular RNA: A new star of noncoding RNAs. *Cancer Lett* 2015; **365**: 141-148 [PMID: 26052092 DOI: 10.1016/j.canlet.2015.06.003]

8 **Zang J**, Lu D, Xu A. The interaction of circRNAs and RNA binding proteins: An important part of circRNA maintenance and function. *J Neurosci Res* 2020; **98**: 87-97 [PMID: 30575990 DOI: 10.1002/jnr.24356]

9 **Wang S**, Tang D, Wang W, Yang Y, Wu X, Wang L, Wang D. circLMTK2 acts as a sponge of miR-150-5p and promotes proliferation and metastasis in gastric cancer. *Mol Cancer* 2019; **18**: 162 [PMID: 31722712 DOI: 10.1186/s12943-019-1081-4]

10 **Lu H**, Yao B, Wen X, Jia B. FBXW7 circular RNA regulates proliferation, migration and invasion of colorectal carcinoma through NEK2, mTOR, and PTEN signaling pathways in vitro and in vivo. *BMC Cancer* 2019; **19**: 918 [PMID: 31519156 DOI: 10.1186/s12885-019-6028-z]

11 **Huang X**, Li Z, Zhang Q, Wang W, Li B, Wang L, Xu Z, Zeng A, Zhang X, Zhang X, He Z, Li Q, Sun G, Wang S, Li Q, Wang L, Zhang L, Xu H, Xu Z. Circular RNA AKT3 upregulates PIK3R1 to enhance cisplatin resistance in gastric cancer *via* miR-198 suppression. *Mol Cancer* 2019; **18**: 71 [PMID: 30927924 DOI: 10.1186/s12943-019-0969-3]

12 **Xia X**, Li X, Li F, Wu X, Zhang M, Zhou H, Huang N, Yang X, Xiao F, Liu D, Yang L, Zhang N. A novel tumor suppressor protein encoded by circular AKT3 RNA inhibits glioblastoma tumorigenicity by competing with active phosphoinositide-dependent Kinase-1. *Mol Cancer* 2019; **18**: 131 [PMID: 31470874 DOI: 10.1186/s12943-019-1056-5]

13 **Lynam-Lennon N**, Heavey S, Sommerville G, Bibby BA, Ffrench B, Quinn J, Gasch C, O'Leary JJ, Gallagher MF, Reynolds JV, Maher SG. MicroRNA-17 is downregulated in esophageal adenocarcinoma cancer stem-like cells and promotes a radioresistant phenotype. *Oncotarget* 2017; **8**: 11400-11413 [PMID: 28002789 DOI: 10.18632/oncotarget.13940]

14 **Zhan N**, Li B, Xu X, Xu J, Hu S. Inhibition of FASN expression enhances radiosensitivity in human non-small cell lung cancer. *Oncol Lett* 2018; **15**: 4578-4584 [PMID: 29541228 DOI: 10.3892/ol.2018.7896]

15 **Pastushenko I**, Blanpain C. EMT Transition States during Tumor Progression and Metastasis. *Trends Cell Biol* 2019; **29**: 212-226 [PMID: 30594349 DOI: 10.1016/j.tcb.2018.12.001]

16 **Liu Z**, Hu G, Zhao Y, Xiao Z, Yan M, Ren M. Silence of cZNF292 suppresses the growth, migration, and invasion of human esophageal cancer Eca-109 cells *via* upregulating miR-206. *J Cell Biochem* 2020; **121**: 2354-2362 [PMID: 31680303 DOI: 10.1002/jcb.29458]

17 **Shi N**, Shan B, Gu B, Song Y, Chu H, Qian L. Circular RNA circ-PRKCI functions as a competitive endogenous RNA to regulate AKT3 expression by sponging miR-3680-3p in esophageal squamous cell carcinoma. *J Cell Biochem* 2019; **120**: 10021-10030 [PMID: 30659640 DOI: 10.1002/jcb.28285]

18 **Zhang Y**, Wang Q, Zhu D, Rong J, Shi W, Cao X. Up-regulation of circ-SMAD7 inhibits tumor proliferation and migration in esophageal squamous cell carcinoma. *Biomed Pharmacother* 2019; **111**: 596-601 [PMID: 30611100 DOI: 10.1016/j.biopha.2018.12.116]

19 **Xing Y**, Zha WJ, Li XM, Li H, Gao F, Ye T, Du WQ, Liu YC. Circular RNA circ-Foxo3 inhibits esophageal squamous cell cancer progression *via* the miR-23a/PTEN axis. *J Cell Biochem* 2020; **121**: 2595-2605 [PMID: 31680314 DOI: 10.1002/jcb.29481]

20 **Xue D**, Wang H, Chen Y, Shen D, Lu J, Wang M, Zebibula A, Xu L, Wu H, Li G, Xia L. Circ-AKT3 inhibits clear cell renal cell carcinoma metastasis *via* altering miR-296-3p/E-cadherin signals. *Mol Cancer* 2019; **18**: 151 [PMID: 31672157 DOI: 10.1186/s12943-019-1072-5]

21 **Guan X**, Chen S, Zhao Y. The role of RhoC in malignant tumor invasion, metastasis and targeted therapy. *Histol Histopathol* 2018; **33**: 255-260 [PMID: 28664531 DOI: 10.14670/HH-11-915]

22 **Thomas P**, Pranatharthi A, Ross C, Srivastava S. RhoC: a fascinating journey from a cytoskeletal organizer to a Cancer stem cell therapeutic target. *J Exp Clin Cancer Res* 2019; **38**: 328 [PMID: 31340863 DOI: 10.1186/s13046-019-1327-4]

23 **Faried A**, Faried LS, Usman N, Kato H, Kuwano H. Clinical and prognostic significance of RhoA and RhoC gene expression in esophageal squamous cell carcinoma. *Ann Surg Oncol* 2007; **14**: 3593-3601 [PMID: 17896152 DOI: 10.1245/s10434-007-9562-x]

24 **Zhao ZH**, Tian Y, Yang JP, Zhou J, Chen KS. RhoC, vascular endothelial growth factor and microvascular density in esophageal squamous cell carcinoma. *World J Gastroenterol* 2015; **21**: 905-912 [PMID: 25624724 DOI: 10.3748/wjg.v21.i3.905]

25 **Faried A**, Faried LS, Kimura H, Nakajima M, Sohda M, Miyazaki T, Kato H, Usman N, Kuwano H. RhoA and RhoC proteins promote both cell proliferation and cell invasion of human oesophageal squamous cell carcinoma cell lines in vitro and in vivo. *Eur J Cancer* 2006; **42**: 1455-1465 [PMID: 16750623 DOI: 10.1016/j.ejca.2006.02.012]

26 **Huynh J**, Chand A, Gough D, Ernst M. Therapeutically exploiting STAT3 activity in cancer - using tissue repair as a road map. *Nat Rev Cancer* 2019; **19**: 82-96 [PMID: 30578415 DOI: 10.1038/s41568-018-0090-8]

27 **Thilakasiri PS**, Dmello RS, Nero TL, Parker MW, Ernst M, Chand AL. Repurposing of drugs as STAT3 inhibitors for cancer therapy. *Semin Cancer Biol* 2019 [PMID: 31711994 DOI: 10.1016/j.semcancer.2019.09.022]

28 **Liu Y**, Zhi Y, Song H, Zong M, Yi J, Mao G, Chen L, Huang G. S1PR1 promotes proliferation and inhibits apoptosis of esophageal squamous cell carcinoma through activating STAT3 pathway. *J Exp Clin Cancer Res* 2019; **38**: 369 [PMID: 31438989 DOI: 10.1186/s13046-019-1369-7]

29 **Zhang W**, Pang Q, Yan C, Wang Q, Yang J, Yu S, Liu X, Yuan Z, Wang P, Xiao Z. Induction of PD-L1 expression by epidermal growth factor receptor-mediated signaling in esophageal squamous cell carcinoma. *Onco Targets Ther* 2017; **10**: 763-771 [PMID: 28243112 DOI: 10.2147/OTT.S118982]

World Journal of Gastroenterology

Submit a Manuscript: https://www.f6publishing.com

World J Gastroenterol 2021 January 21; 27(3): 255-266

DOI: 10.3748/wjg.v27.i3.255

ISSN 1007-9327 (print) ISSN 2219-2840 (online)

ORIGINAL ARTICLE

Retrospective Study

Serum vitamin D and vitamin-D-binding protein levels in children with chronic hepatitis B

Cai-Zhi Huang, Jie Zhang, Lin Zhang, Cui-Hua Yu, Yi Mo, Li-Ya Mo

ORCID number: Cai-Zhi Huang 0000-0001-9122-1199; Jie Zhang 0000-0001-9637-8961; Lin Zhang 0000-0002-4273-0592; Cui-Hua Yu 0000-0002-9685-2990; Yi Mo 0000-0002-0623-9309; Li-Ya Mo 0000-0002-1154-6899.

Author contributions: All authors contributed to the conceptualization of the study; Mo LY designed the research; Huang CZ and Zhang J performed the research; Zhang L and Yu CH contributed to data collection; Huang CZ and Mo Y analyzed the data; Huang CZ and Mo LY wrote and revised the paper.

Supported by Hunan Provincial Health Commission Science Foundation of China, No. 20200017.

Institutional review board statement: This research was reviewed and approved by Ethics Committee of Hunan Children's Hospital.

Informed consent statement: Informed consent was obtained from all subjects.

Conflict-of-interest statement: All authors have no conflict of interest to declare.

Data sharing statement: No

Cai-Zhi Huang, Jie Zhang, Lin Zhang, Yi Mo, Li-Ya Mo, Department of Laboratory Medicine, Hunan Children's Hospital, Changsha 410007, Hunan Province, China

Cui-Hua Yu, Department of GCP Certified Sites, The Third Hospital of Changsha City, Changsha 410005, Hunan Province, China

Corresponding author: Li-Ya Mo, MBBS, Chief Technician, Director, Professor, Department of Laboratory Medicine, Hunan Children's Hospital, No. 86 Ziyuan Road, Changsha 410007, Hunan Province, China. 643183753@qq.com

Abstract

BACKGROUND

Vitamin D is an essential fat-soluble secosteroid hydroxylated by the liver to form the intermediate metabolite calcidiol {25-hydroxy vitamin D [25(OH)D]}, which is a reliable indicator to investigate individual vitamin D status. Vitamin-D-binding protein (VDBP) is a multifunctional glycoprotein mainly synthesized in the liver and the major transport protein for vitamin D and its metabolites. Serum vitamin D and VDBP are both associated with hepatitis B. However, few studies have reported the relationship and clinical significance of vitamin D and VDBP with hepatitis B virus (HBV) replication and hepatic fibrosis in children with chronic hepatitis B (CHB).

AIM

To explore vitamin D and VDBP serum levels in children with CHB and the association of vitamin D and VDBP with HBV replication and hepatic fibrosis.

METHODS

We enrolled 204 children with CHB admitted to Hunan Children' Hospital in summer and autumn between 2018 and 2019 and 170 healthy controls. CHB patients included: 164 hepatitis B e antigen (HBeAg) positive and 40 HBeAg negative; 193 hepatitis B surface antigen (HBsAg) positive and 11 HBsAg negative; 164 with detectable HBV deoxyribonucleic acid (DNA) and 40 with undetectable HBV DNA; 131 with HBV genotype B and 23 with HBV genotype C; and 27 without hepatic fibrosis and 97 with hepatic fibrosis. Serum levels of 25(OH)D, VDBP, liver function markers, and other clinical parameters were collected to analyze their association with vitamin D and VDBP. Mann-Whitney *U* test, Kruskal-Wallis *H* test, or *t* test was used to analyze serum 25(OH)D and VDBP levels in different groups. Spearman rank correlation test was utilized to

analyze the correlation of 25(OH)D and VDBP with other markers. Statistically significant factors determined by univariate analysis were further analyzed by binary multivariate logistic regression analysis. $P < 0.05$ was considered statistically significant.

RESULTS

Children with CHB had lower serum 25(OH)D (56.64 ± 17.89 nmoL/L) and VDBP [122.40 (70.74-262.84 μg/L)] levels than healthy controls had ($P < 0.001$). Serum 25(OH)D and VDBP levels were significantly different among the different grades of hepatic fibrosis ($P < 0.05$). VDBP levels in children with HBV genotype C, HBsAg, HBeAg, and detectable HBV DNA were significantly lower than those in children with HBV genotype B, no HBsAg, no HBeAg, and undetectable HBV DNA ($P < 0.05$). Serum 25(OH)D level was negatively correlated with age and serum total bilirubin level ($r = -0.396$ and -0.280, respectively, $P < 0.001$). Serum VDBP level was negatively correlated with HBV DNA ($\log_{10}$ IU/mL) ($r = -0.272$, $P < 0.001$). Serum 25(OH)D level was not correlated with VDBP level ($P > 0.05$). Univariate ($P < 0.05$) and multivariate logistic regression analysis showed that low level of 25(OH)D (odds ratio = 0.951, 95% confidence interval: 0.918-0.985) and high level of HBV DNA (odds ratio = 1.445, 95% confidence interval: 1.163-1.794) were independently correlated with hepatic fibrosis ($P < 0.01$).

CONCLUSION

Serum levels of 25(OH)D and VDBP are decreased in children with CHB. Serum VDBP level is negatively correlated with HBV replication. Low level of 25(OH)D is independently associated with hepatic fibrosis in children with CHB. There is no significant association between serum levels of 25(OH)D and VDBP.

Key Words: Chronic hepatitis B; Children; Vitamin D; Vitamin-D-binding protein; Hepatitis B virus

©The Author(s) 2021. Published by Baishideng Publishing Group Inc. All rights reserved.

Core Tip: Serum vitamin D and vitamin-D-binding protein (VDBP) levels are associated with hepatitis B. The association of vitamin D and VDBP with hepatitis B virus replication and hepatic fibrosis in children with chronic hepatitis B (CHB) has rarely been reported. We found that low level of serum 25-hydroxy vitamin D is an independent factor associated with development of hepatic fibrosis, and it could be valuable for maintaining sufficient 25-hydroxy vitamin D level to prevent or delay hepatic fibrosis in children with CHB. VDBP is negatively correlated with hepatitis B virus replication, and VDBP analogs might be considered for management of CHB.

Citation: Huang CZ, Zhang J, Zhang L, Yu CH, Mo Y, Mo LY. Serum vitamin D and vitamin-D-binding protein levels in children with chronic hepatitis B. *World J Gastroenterol* 2021; 27(3): 255-266
URL: https://www.wjgnet.com/1007-9327/full/v27/i3/255.htm
DOI: https://dx.doi.org/10.3748/wjg.v27.i3.255

INTRODUCTION

Vitamin D is a fat-soluble secosteroid and is essential for humans. Vitamin D is mainly produced in the skin by means of sunlight exposure or retrieved from dietary components. In order to become biologically active, vitamin D needs to be combined with vitamin-D-binding protein (VDBP), which is the major transport protein of vitamin D and its metabolites, and it sequentially converts to its intermediate metabolite calcidiol {25-hydroxy vitamin D [25(OH)D]} and the final active form calcitriol (1,25-dihydroxy vitamin D) by hydroxylation in the liver and kidneys. Twenty-five (OH)D is the main metabolite of vitamin D and is relatively stable in serum. Precise quantification of calcitriol is problematic because of its short half-life and serum concentrations are 1000 times lower compared to those of 25(OH)D. In

additional data are available.

Open-Access: This article is an open-access article that was selected by an in-house editor and fully peer-reviewed by external reviewers. It is distributed in accordance with the Creative Commons Attribution NonCommercial (CC BY-NC 4.0) license, which permits others to distribute, remix, adapt, build upon this work non-commercially, and license their derivative works on different terms, provided the original work is properly cited and the use is non-commercial. See: http://creativecommons.org/Licenses/by-nc/4.0/

Manuscript source: Unsolicited manuscript

Specialty type: Gastroenterology and hepatology

Country/Territory of origin: China

Peer-review report's scientific quality classification
Grade A (Excellent): 0
Grade B (Very good): B, B
Grade C (Good): 0
Grade D (Fair): 0
Grade E (Poor): 0

Received: November 4, 2020
Peer-review started: November 4, 2020
First decision: December 24, 2020
Revised: December 29, 2020
Accepted: January 6, 2021
Article in press: January 6, 2021
Published online: January 21, 2021

P-Reviewer: Fraga RS
S-Editor: Fan JR
L-Editor: Filipodia
P-Editor: Ma YJ

contrast, 25(OH)D has a half-life of approximately 3 wk, making it a suitable and largely reliable indicator to investigate the individual vitamin D status. Vitamin D promotes absorption of calcium and regulates skeletal function. It is also a powerful modulator of the immune response and is closely associated with many diseases such as immune disease[1], inflammatory bowel disease[2], cancer[3], and metabolic disorders[4].

Hepatitis B virus (HBV) is a serious threat to human health and life. HBV infection is one of the major contributors to the development of chronic hepatitis, fibrosis, cirrhosis, and hepatocellular carcinoma. About 1 million people die from HBV infection every year[5,6]. One-third of the population around the world are infected by HBV, and it was estimated by the World Health Organization in 2015 that 257 million people were living with chronic hepatitis B infection. Newborn infants and children with acute HBV infection are prone to developing chronic hepatitis B (CHB), and the rate of chronicity in newborn infants, children aged < 6 years, and adults is 80%-90%, 25%-30%, and 1%-5%[7], respectively.

Immune and inflammatory responses participate in chronic liver injuries and fibrogenesis of CHB *via* activating hepatic stellate cells. Due to the heterogeneity of CHB, patients may have different levels of viral replication and severity of hepatic disease. Pathologically, patients infected with HBV are characterized by impairment of T-cell function. The elimination of HBV in CHB patients largely depends on the cellular immune response mediated by T helper (Th)1 cells. Combination of the active form of vitamin D and vitamin D receptor (VDR) may inhibit the proliferation of Th1 cells and the release of cytokines and concurrently activate Th2 cells, thus regulating the immune response. However, HBV-transfected cells downregulate VDR expression, thereby preventing vitamin D from inhibiting transcription and translation of HBV *in vitro*, and HBV might use this mechanism to avoid the immune system[8]. Therefore, it is believed that vitamin D is closely linked to hepatitis B. In recent years, it has been shown that vitamin D deficiency is related to CHB in adults, and vitamin D level might affect the antiviral effect and disease progression and prognosis[9,10]. Nevertheless, the association of HBV replication and vitamin D level is not consistent[11,12], and there have been few studies about the relationship among vitamin D, VDBP, and CHB in children. Thus, we carried out this study to investigate the association of vitamin D and VDBP with HBV replication and hepatic fibrosis in children with CHB.

MATERIALS AND METHODS

Study population

This research was approved by the Ethics Committee of Hunan Children's Hospital. The study protocol conformed to the provisions of the Declaration of Helsinki. The diagnostic criteria and definitions for CHB were in accordance with the American Association for the Study of Liver Diseases 2018 Hepatitis B Guidance[13]. Hepatic fibrosis was classified according to the Scheuer Scoring System: Grade 0, no fibrosis; grade 1, enlarged and fibrotic portal tracts; grade 2, periportal or portal-portal septal fibrosis but intact architecture; grade 3, fibrosis with architectural distortion but no obvious cirrhosis; and grade 4, probable or definite cirrhosis.

We selected 257 children with CHB who were admitted to Hunan Children's Hospital in summer and autumn between 2018 and 2019, along with 170 randomly selected healthy controls. Patients were excluded from the present analysis if they met the following exclusion criteria: (1) Patients with infectious liver disease caused by pathogens other than HBV and with other liver diseases such as autoimmune liver disease; (2) Patients with malignant tumors; (3) Patients who have received immunomodulatory therapy or taken vitamin D preparations in the past 4 wk; (4) Patients with comorbidities that may affect the serum levels of vitamin D and VDBP, including malnutrition, renal disease, and diabetes; and (5) Repeated patients during the study period. Lastly, 53 of the patients were excluded, and a total of 204 children were enrolled in the analysis.

The enrolled patients included: 193 hepatitis B surface antigen (HBsAg) positive and 11 HBsAg negative; 164 hepatitis B e antigen (HBeAg) positive and 40 HBeAg negative; 164 with detectable HBV deoxyribonucleic acid (DNA) and 40 with undetectable HBV DNA; 131 with HBV genotype B, 23 with HBV genotype C, and 50 without genotyping due to refusal of guardians; and 124 with histopathological determination of grade of hepatic fibrosis (27 grade 0, 74 grade 1, 12 grade 2, 9 grade 3, and 2 grade 4), and 80 without histopathological examination because of refusal of

guardians. The flow chart of the study is shown in Figure 1.

Data collection

All blood tests were provided by the Department of Laboratory Medicine of Hunan Children's Hospital. Serum 25(OH)D level was determined by chemiluminescent immunoassay (ADVIA Centaur XP; Siemens, Erlangen, Germany). Serum VDBP level was detected by ELISA (reagent kit from China). After collection, the human serum samples for 25(OH)D examination were stored at 4 °C and tested within 24 h, and the samples for VDBP examination were stored at -70 °C and tested within 1 wk. The definition of vitamin D levels in Hunan Children's Hospital included deficiency (< 37.50 nmoL/L), insufficiency (37.5-50.0 nmoL/L), and sufficiency (50.0-250.0 nmoL/L). Other clinical parameters including liver function tests, serum HBV DNA level, and serological markers of HBV, such as HBsAg and HBeAg, were collected for analysis of the association with 25(OH)D and VDBP levels.

Statistical analysis

Statistical analysis was performed using SPSS version 19.0 software (Armonk, NY, United States). Normal distribution measurement data were expressed as mean ± standard deviation and analyzed by the *t* test to determine the difference between two groups. Non-normal distribution measurement data were expressed as median (interquartile range) and analyzed by Mann-Whitney *U* test or Kruskal-Wallis *H* test. Numerical data were expressed as rate or percentage and analyzed by χ^2 test. The Spearman's rank correlation test was used to determine the correlation between the two groups. Binary multivariate logistic regression analysis was applied to analyze further the statistically significant factors determined by univariate analysis. Statistical analysis was based on the actual number of completed cases if values were missing. $P < 0.05$ by two-tailed tests was considered statistically significant for tests of all variables.

RESULTS

Analysis of serum levels of 25(OH)D and VDBP in patients with CHB and healthy controls

Serum levels of 25(OH)D, VDBP, calcium, and phosphorus and liver function test results in patients with CHB and healthy controls are shown in Table 1. Patients with CHB had higher serum levels of alanine aminotransferase (ALT), aspartate aminotransferase (AST), and total bilirubin (TBil); longer prothrombin time (PT); and lower serum levels of 25(OH)D, VDBP, calcium, and phosphorus. No difference in albumin (ALB) level was found between patients with CHB and healthy controls. There were 25 cases (12.25%) of vitamin D deficiency, 44 (21.57%) of vitamin D insufficiency, and 135 (66.18%) of vitamin D sufficiency in children with CHB. The cases of vitamin D deficiency, insufficiency, and sufficiency in healthy controls were 3 (1.76%), 12 (7.06%), and 155 (91.18%), respectively. The distribution frequency of vitamin D in CHB patients and healthy controls is shown in Figure 2.

Differences in serum levels of 25(OH)D and VDBP in CHB children with different conditions

Serum levels of 25(OH)D and VDBP in different groups of children with CHB are shown in Table 2. In children with CHB, no significant difference was found in serum 25(OH)D levels between HBeAg-positive and -negative ($P = 0.091$), between HBsAg-positive and -negative ($P = 0.076$), between patients with HBV genotype B and genotype C ($P = 0.753$), or between patients with detectable and undetectable HBV DNA ($P = 0.441$). Serum level of 25(OH)D was significantly different among groups with various grades of hepatic fibrosis ($P < 0.001$). The levels of serum 25(OH)D decreased successively in patients with grade 0, 1, 2, and 3 of hepatic fibrosis, and the difference between any two groups was significant ($P < 0.05$).

Serum levels of VDBP in children with HBeAg, HBsAg, HBV genotype C, and detectable HBV DNA were significantly lower than those in children without HBeAg and HBsAg and with HBV genotype B and undetectable HBV DNA. There was a significant difference in serum VDBP levels among patients with various grades of hepatic fibrosis ($P = 0.032$). Patients with grade 2 hepatic fibrosis had higher serum VDBP levels than those with grade 0 or 3 hepatic fibrosis ($P < 0.05$), and no significant difference was found between any other two groups. The data for hepatic fibrosis

Table 1 Serum levels of 25-hydroxy vitamin D and vitamin-D-binding protein in patients with chronic hepatitis B and healthy controls

Factor	CHB, *n* = 204	Healthy controls, *n* = 170	χ^2/Z/*t* value[1]	*P* value[1]
Sex, M/F	133/71	108/62	0.11	0.737
Age in mo	61.00 (37.0-97.75)	56.00 (32.75-82.25)	1.27	0.205
ALT in IU/L	30.22 (17.80-63.36)	15.00 (8.75-24.25)	9.37	< 0.001
AST in IU/L	38.25 (28.70-64.98)	25.00 (17.00-31.50)	10.44	< 0.001
TBil in μmoL/L	8.67 (6.61-12.65)	7.00 (5.60-9.25)	4.57	< 0.001
ALB in g/L	42.52 ± 3.53	42.10 ± 5.39	0.88	0.383
PT in s	13.34 ± 0.80	11.37 ± 0.91	22.22	< 0.001
25(OH)D, nmoL/L	56.64 ± 17.89	75.48 ± 28.28	7.52	< 0.001
VDBP, μg/L	122.40 (70.74-262.84)	643.25 (415.74-1034.43)	14.89	< 0.001
Calcium, mmoL/L	2.24 ± 0.15	2.44 ± 0.16	11.99	< 0.001
Phosphorus, mmoL/L	1.47 ± 0.12	1.69 ± 0.16	14.80	< 0.001

[1]Normal distribution measurement data were expressed as mean ± SD and analyzed by the *t* test to determine the difference between two groups. Non-normal distribution measurement data were expressed as median (interquartile range) and analyzed by Mann-Whitney *U* test to determine the difference between two groups. Numerical data were expressed as rate and analyzed by χ^2 test. 25(OH)D: 25-hydroxy vitamin D; ALB: Albumin; ALT: Alanine aminotransferase; AST: Aspartate aminotransferase; F: Female; M: Male; PT: Prothrombin time; TBil: Total bilirubin; VDBP: Vitamin-D-binding protein.

grade 4 were not involved in statistical analysis because there were only 2 cases.

Correlation between serum levels of 25(OH)D and VDBP and other clinical parameters in patients with CHB

Spearman's rank correlation test revealed that serum levels of 25(OH)D were negatively correlated with age and serum TBil level in children with CHB (r = -0.396, -0.280, P < 0.001), but serum 25(OH)D level was not correlated with sex or serum levels of ALT, AST, ALB, PT, calcium, phosphorus, HBV DNA, and VDBP. Serum VDBP level was negatively correlated with serum HBV DNA ($\log_{10}$ IU/mL) (r = -0.272, P < 0.001) in children with CHB (Figure 3). No significant correlation was found between VDBP levels and age, sex, or levels of ALT, AST, TBil, ALB, PT, calcium, and phosphorus.

Univariate and multivariate analyses of factors associated with hepatic fibrosis

Univariate analysis revealed that CHB patients with hepatic fibrosis had higher levels of TBil, VDBP, and HBV DNA, lower levels of 25(OH)D, and lower rate of HBeAg-positive to -negative than CHB patients without hepatic fibrosis. Multivariate logistic regression analysis showed that low level of serum 25(OH)D [odds ratio = 0.951, 95% confidence interval: 0.918-0.985] and high level of HBV DNA (odds ratio = 1.445, 95% confidence interval: 1.163-1.794) were both independently correlated with hepatic fibrosis in children with CHB (Table 3).

DISCUSSION

In the present study, the serum levels of 25(OH)D in children with CHB was investigated, along with its correlation with other factors. Children with CHB were found to have lower serum 25(OH)D levels than healthy controls; CHB patients with hepatic fibrosis had lower levels of 25(OH)D than patients without hepatic fibrosis; and low level of serum 25(OH)D was independently correlated with hepatic fibrosis. The results demonstrate the value of maintaining normal levels of 25(OH)D for the prevention and delay of hepatic fibrosis in children with CHB.

Compared with healthy controls, patients with CHB had higher rates of vitamin D deficiency and insufficiency. This may be due to the decrease of vitamin D hydroxylation in the liver in the context of impaired liver function and the increase of vitamin D consumption on account of immune response mediated by vitamin D in patients with CHB.

Table 2 Serum levels of 25-hydroxy vitamin D and vitamin-D-binding protein in different groups of children with chronic hepatitis B

Group (*n*)	25(OH)D, nmoL/L	*Z*/*t*/*H* value[1]	*P* value[1]	VDBP, μg/L	*Z*/*H* value[1]	*P* value[1]
HBeAg		1.70	0.091		3.81	< 0.001
Positive (164)	57.69 ± 18.06			106.95 (68.44-203.21)		
Negative (40)	52.35 ± 16.73			257.23 (135.61-342.96)		
HBV genotype[2]		0.32	0.753		2.51	0.012
Genotype B (131)	55.69 ± 17.63			105.00 (69.30-199.35)		
Genotype C (23)	56.93 ± 17.69			75.40 (42.75-123.10)		
HBsAg		1.77	0.076		4.32	< 0.001
Positive (193)	56.26 ± 18.17			113.87 (69.90-217.03)		
Negative (11)	56.60 (54.37-72.96)			439.65 (259.27-510.45)		
HBV DNA		0.77	0.441		4.75	< 0.001
Detectable (164)	57.12 ± 18.14			105.75 (66.39-193.73)		
Undetectable (40)	54.69 ± 16.91			284.18 (152.64-406.14)		
Fibrosis grades[2]		29.81	< 0.001		8.81	0.032
Grade 0 (27)	61.86 ± 13.63			90.00 (61.20-121.45)		
Grade 1 (74)	54.97 ± 13.63			117.03 (65.74-275.76)		
Grade 2 (12)	43.99 (35.79-55.15)			174.88 (121.34-292.94)		
Grade 3 (9)	32.95 (28.61-35.20)			78.13 (35.05-176.75)		

[1]Normal distribution measurement data were analyzed by *t* test to determine the difference between two groups. For non-normal distribution measurement data, Mann-Whitney *U* test was used to compare serum levels of 25-hydroxy vitamin D and vitamin-D-binding protein between two groups, and Kruskal-Wallis *H* test was applied to analyze the difference among multiple groups.
[2]Statistical analysis was based on the actual number of completed cases because of the missing values. 25(OH)D: 25-hydroxy vitamin D; HBeAg: Hepatitis B e antigen; HBsAg: Hepatitis B surface antigen; HBV: Hepatitis B virus; VDBP: Vitamin-D-binding protein.

Some investigations have indicated that serum 25(OH)D level is negatively correlated with HBV load, and low 25(OH)D level is associated with HBV genotype B, HBsAg, and HBeAg[11,14]. Other studies have shown inconsistent results[8,10,12]. In the present study, 25(OH)D was not correlated with HBV DNA in patients with CHB, and serum levels of 25(OH)D did not differ significantly between patients with or without HBeAg, patients with HBV genotype B or C, patients with or without HBsAg, and patients with or without detectable HBV DNA. These results indicate that serum 25(OH)D levels are not associated with HBV genotype and virus replication. The discrepancy between various studies may have been caused by the different disease course and stage and study population.

A previous study revealed that vitamin D can reduce profibrotic factors and collagen expression and that it has immunomodulatory effects on immune cells, including T cells[15]. Vitamin D has been found to have an antifibrotic effects on human primary transforming-growth-factor-β-stimulated hepatic stellate cells[16]. In the present study, serum levels of 25(OH)D in CHB children with hepatic fibrosis were markedly decreased, and the higher the grade of hepatic fibrosis, the lower the level of serum 25(OH)D. Multivariate logistic regression analysis also revealed that low level of 25(OH)D was independently associated with hepatic fibrosis, which suggested that maintaining normal levels of 25(OH)D in children with CHB may have a positive effect on the prevention and delay of hepatic fibrosis.

VDBP, also known as gc-globulin, is a plasma glycoprotein with a molecular weight of 56-58 kDa, composed of 458 amino acids. VDBP is primarily synthesized in the liver and expressed in several organs and tissues, including the liver, kidneys, gonads and fat, and neutrophils. Unlike serum vitamin D following seasonal variation, serum concentration of VDBP is stable during the year[17]. VDBP has numerous physiological roles, including transporting vitamin D and its metabolites, regulating bone development, scavenging actin, and regulating immune and inflammation process[18].

In the present study, serum VDBP levels in CHB children were significantly lower

Table 3 Univariate and multivariate analyses of hepatic fibrosis in children with chronic hepatitis B

Factor	Without hepatic fibrosis, *n* = 27	Hepatic fibrosis, *n* = 97	Univariate analysis		Multivariate analysis	
			Z/*t*/χ^2 value[1]	*P* value[1]	OR (95%CI)[1]	*P* value[1]
Age in mo	54.00 (32.0-98.0)	63.00 (40.00-95.00)	0.83	0.407		
Male/female	18/9	63/34	0.03	0.868		
ALT in IU/L	32.03 (16.40-57.0)	43.48 (20.15-88.64)	0.98	0.330		
AST in IU/L	39.11 (27.50-65.30)	47.30 (30.65-83.10)	1.14	0.254		
TBil in μmoL/L	6.77 (6.10-8.80)	9.20 (6.98-14.20)	2.86	0.004	1.053 (0.938-1.182)	0.384
ALB in g/L	42.98 ± 2.17	42.30 ± 3.27	1.27	0.209		
PT in s	13.29 ± 0.76	13.26 ± 0.78	0.18	0.860		
25(OH)D, nmoL/L	61.86 ± 13.63	51.22 ± 14.67	3.38	0.001	0.951 (0.918-0.985)	0.005
VDBP, μg/L	90.00 (61.20-121.45)	134.50 (71.25-267.18)	1.98	0.047	1.001 (0.999-1.003)	0.316
Calcium, mmoL/L	2.30 ± 0.16	2.27 ± 0.15	0.88	0.383		
Phosphorus, mmoL/L	1.48 ± 0.12	1.45 ± 0.12	1.19	0.237		
HBV DNA in $\log_{10}$ IU/mL	5.40 (2.00-7.31)	6.88 (5.53-7.64)	2.40	0.017	1.445 (1.163-1.794)	0.001
HBeAg positive/negative	26/1	73/24	5.81	0.016	0.138 (0.017-1.160)	0.068

[1]Normal distribution measurement data, non-normal distribution measurement data and numerical data were analyzed by *t* test, Mann-Whitney *U* test and χ^2 test to determine the difference between two groups, respectively. Binary multivariate logistic regression analysis was applied to further analyze the statistically significant factors determined by univariate analysis. 25(OH)D: 25-hydroxy vitamin D; ALB: Albumin; ALT: Alanine aminotransferase; AST: Aspartate aminotransferase; CI: Confidence interval; DNA: Deoxyribonucleic acid; HBeAg: Hepatitis B e antigen; HBV: Hepatitis B virus; OR: Odds ratio; PT: Prothrombin time; TBil: Total bilirubin; VDBP: Vitamin-D-binding protein.

than those in healthy controls, and the levels of VDBP were markedly decreased in patients with HBV genotype C, HBsAg, HBeAg, and detectable HBV DNA. VDBP levels were negatively correlated with HBV DNA levels in children with CHB. The results demonstrated that serum levels of VDBP were associated with HBV genotype and negatively correlated with HBV replication. The reasons for the decrease in VDBP may be lower production in impaired hepatic cells and greater consumption of scavenging actin, mediating monocyte and neutrophil chemotaxis to inflammatory foci caused by HBV replication[18].

Children with CHB and hepatic fibrosis had higher VDBP level, and VDBP levels increased in patients with grade 1 and 2 but decreased in patients with grade 3 fibrosis. Although it has been reported that hepatocytes are compensatory in the early stage of fibrosis and that the remaining normal hepatocytes produce more VDBP to replenish the shortage in the circulation caused by massive consumption[19], the detailed mechanism of VDBP variation in different stages of hepatic fibrosis is still unknown. The association between VDBP and hepatic fibrosis and the underlying mechanisms warrant further investigation.

Serum levels of 25(OH)D and VDBP were both decreased in children with CHB, but there was no significant correlation between the two markers. This may be due to the multifunctional property of VDBP. VDBP has many other important physiological functions other than being a transporter and < 5% of the binding sites on VDBP are occupied by 25(OH)D[18]. Most VDBP may be involved in the immune response and inflammatory process caused by HBV infection. The different biological functions of the two markers result in the incompletely consistent variation.

CONCLUSION

Both serum 25(OH)D and VDBP levels are significantly decreased in children with CHB, VDBP may be negatively correlated with HBV replication, and low level of serum 25(OH)D is an independent factor associated with the development of hepatic fibrosis. Therefore, maintaining sufficient 25(OH)D level in children with CHB could be valuable to prevent or delay the process of fibrosis, and the development and

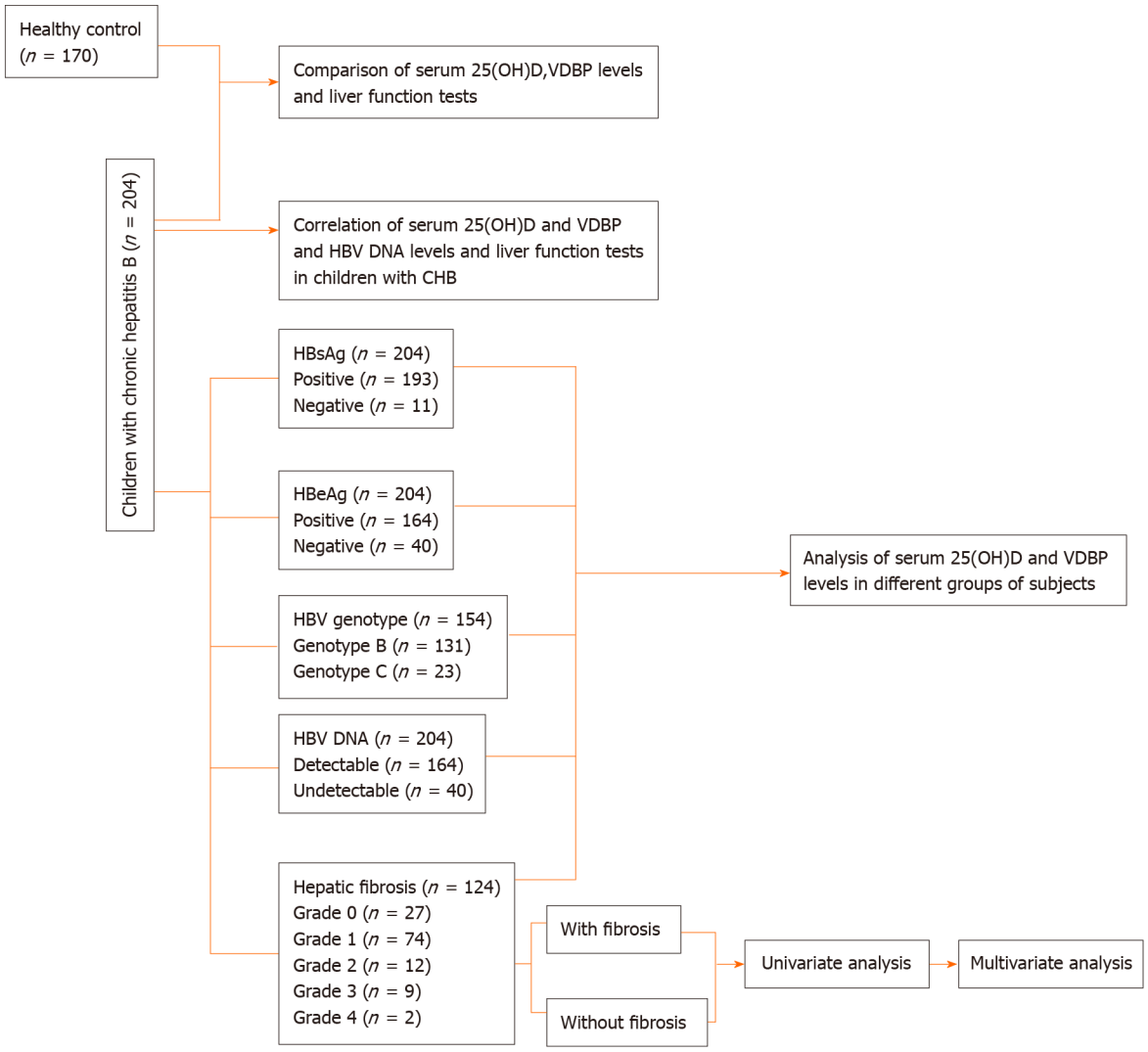


Figure 1 Flow chart of the study. 25(OH)D: 25-hydroxy vitamin D; CHB: Chronic hepatitis B; HBeAg: Hepatitis B e antigen; HBsAg: Hepatitis B surface antigen; HBV: Hepatitis B virus; VDBP: Vitamin D binding protein.

application of VDBP analogues might be a consideration for the management of CHB.

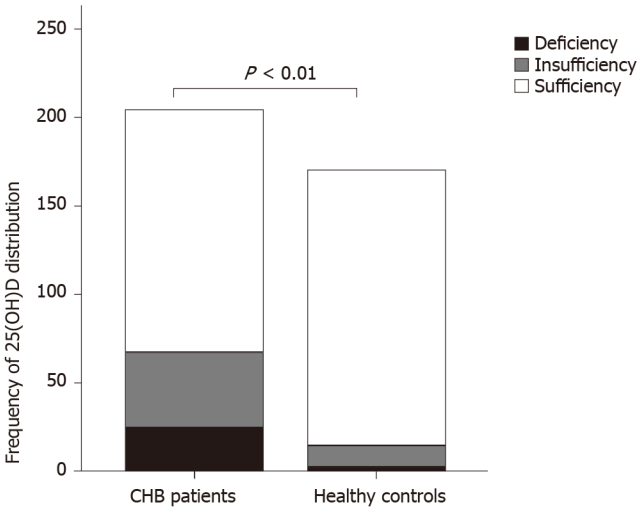


Figure 2 Distribution frequency of serum 25-hydroxy vitamin D in chronic hepatitis B patients and healthy controls. 25(OH)D: 25-hydroxy vitamin D; CHB: Chronic hepatitis B.

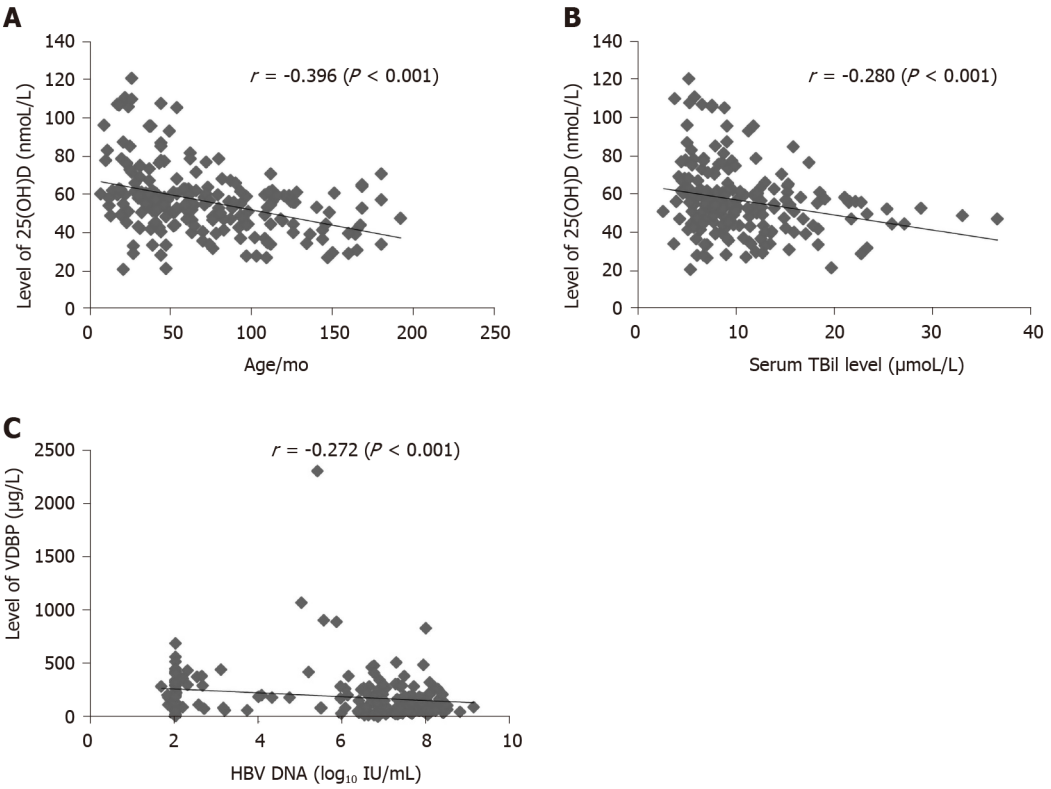


Figure 3 Distribution and correlation of serum 25-hydroxy vitamin D and vitamin-D-binding protein levels with other parameters in children with chronic hepatitis B. A: Correlation of serum 25-hydroxy vitamin D [25(OH)D] level with age; B: Correlation of serum 25(OH)D level with serum total bilirubin level; C: Correlation of serum vitamin-D-binding protein level with serum hepatitis B virus deoxyribonucleic acid. 25(OH)D: 25-hydroxy vitamin D; DNA: Deoxyribonucleic acid; HBV: Hepatitis B virus; TBil: Total bilirubin; VDBP: Vitamin-D-binding protein.

ARTICLE HIGHLIGHTS

Research background

Vitamin D is an essential fat-soluble secosteroid hydroxylated by the liver to form the intermediate metabolite {calcidiol, 25-hydroxy vitamin D [25(OH)D]}, which is a reliable indicator for investigating individual vitamin D status. Vitamin D is known to promote absorption of calcium and regulate skeletal function and is a powerful modulator of the immune response. Vitamin-D-binding protein (VDBP) as the major

transport protein of vitamin D and its metabolites is mainly synthesized by the liver, and VDBP has many other physiological roles, including regulation of bone development, scavenging actin, and regulation of immune and inflammatory processes. Immune and inflammatory responses are involved in chronic liver injuries and fibrogenesis of chronic hepatitis B (CHB). It has been demonstrated that serum levels of vitamin D and VDBP are associated with the development and progress of CHB. However, few studies have been reported about the relationship of vitamin D and VDBP with hepatitis B virus (HBV) replication and hepatic fibrosis in children with CHB. It is of interest to investigate the clinical significance of serum vitamin D and VDBP levels in children with CHB.

Research motivation

Few studies have been reported about the serum levels of vitamin D and VDBP and their clinical significance in children with CHB. Some studies have revealed that vitamin D can reduce profibrotic factors and collagen expression and that they have immunomodulatory effects on immune cells, including T cells. Patients infected with HBV is pathologically characterized as the functional impairment of T cells. The elimination of HBV in CHB patients largely depends on the cellular immune response mediated by T helper (Th)1 cells. Combination of the active form of vitamin D and vitamin D receptor may inhibit the proliferation of Th1 cells and the release of cytokines, and concurrently activate Th2 cells, thus regulating immune responses. Vitamin D and its metabolites in the circulation are mainly transported by VDBP, which is a multifunctional plasma glycoprotein that can mediate monocyte and neutrophil chemotaxis to inflammatory foci caused by HBV replication. The present study aimed at exploring the clinical significance of serum 25(OH)D and VDBP levels in children with CHB. The results will help to illustrate whether vitamin D and VDBP levels are associated with HBV replication and hepatic fibrosis.

Research objectives

The main objective of this study was to investigate the serum levels of vitamin D and VDBP in children with CHB and analyze the association of vitamin D and VDBP with HBV replication and hepatic fibrosis.

Research methods

We enrolled 204 children with CHB who were admitted to Hunan Children's Hospital in summer and autumn between 2018 and 2019 and 170 healthy controls. Children with CHB included: 164 hepatitis B e antigen (HBeAg) positive and 40 HBeAg negative; 193 hepatitis B surface antigen (HBsAg) positive and 11 HBsAg negative; 164 with detectable HBV DNA and 40 with undetectable HBV DNA; 131 with HBV genotype B and 23 with HBV genotype C; and 97 with hepatic fibrosis and 27 without hepatic fibrosis. Serum levels of 25(OH)D, VDBP, liver function markers, and other clinical parameters were collected for analysis of the association with vitamin D and VDBP. Mann-Whitney *U* test, Kruskal-Wallis *H* test, or *t* test was used to analyze serum 25(OH)D and VDBP levels in different groups of subjects. Spearman rank correlation test was utilized to analyze the correlation of 25(OH)D and VDBP with other markers. Finally, statistically significant factors for hepatic fibrosis determined by univariate analysis were further analyzed by binary multivariate logistic regression analysis.

Research results

Children with CHB had lower serum 25(OH)D (56.64 ± 17.89 nmoL/L) and VDBP [122.40 (70.74-262.84 μg/L)] levels than healthy controls had ($P < 0.001$). Serum 25(OH)D and VDBP levels were significantly different among the stages of hepatic fibrosis ($P < 0.05$). Patients with HBV genotype C, HBsAg, HBeAg, and detectable HBV DNA had lower VDBP levels than patients with HBV genotype B, without HBsAg and HBeAg, and undetectable HBV DNA ($P < 0.05$). Serum 25(OH)D level was negatively correlated with age and serum total bilirubin level ($r = -0.396$ and -0.280, respectively, $P < 0.001$). Serum VDBP level was negatively associated with HBV DNA ($\log_{10}$ IU/mL) ($r = -0.272$, $P < 0.001$). Serum 25(OH)D level was not correlated with VDBP level ($P > 0.05$). Univariate ($P < 0.05$) and multivariate logistic regression analysis showed that low level of 25(OH)D (odds ratio = 0.951, 95% confidence interval: 0.918-0.985) and high level of HBV DNA (odds ratio = 1.445, 95% confidence interval: 1.163-1.794) were independently associated with hepatic fibrosis ($P < 0.01$).

Research conclusions

Children with CHB have lower serum levels of 25(OH)D and VDBP. Serum VDBP level is negatively correlated with replication of HBV. Low level of 25(OH)D is independently associated with hepatic fibrosis in CHB children. There is no significant association between serum levels of 25(OH)D and VDBP.

Research perspectives

Previous studies and our data indicate that vitamin D and VDBP are involved in the inflammatory response and immunological regulation in children with CHB. Vitamin D may play an antifibrotic role by reducing stimulation of hepatic stellate cells, profibrotic factors, and collagen expression. VDBP may have a positive effect on alleviating liver injury caused by HBV replication. We speculate that sufficient concentration of vitamin D and VDBP in children with CHB may be beneficial for the progress and prognosis of the disease. The potential value of vitamin D detection in monitoring hepatic fibrosis development and VDBP detection in evaluating the degree of inflammation and liver injury, more detailed mechanism of vitamin D and VDBP on the progression of CHB, and whether VDBP analogs may become a treatment measure for children with CHB warrant further investigation.

ACKNOWLEDGEMENTS

The authors thank Professor Lian Tang from the Department of Liver Disease in Hunan Children's Hospital, China for her advice and language modification of this manuscript.

REFERENCES

1 **Vanherwegen AS**, Gysemans C, Mathieu C. Regulation of Immune Function by Vitamin D and Its Use in Diseases of Immunity. *Endocrinol Metab Clin North Am* 2017; **46**: 1061-1094 [PMID: 29080635 DOI: 10.1016/j.ecl.2017.07.010]

2 **Barbalho SM**, Goulart RA, Gasparini RG. Associations between inflammatory bowel diseases and vitamin D. *Crit Rev Food Sci Nutr* 2019; **59**: 1347-1356 [PMID: 29236523 DOI: 10.1080/10408398.2017.1406333]

3 **Hu K**, Callen DF, Li J, Zheng H. Circulating Vitamin D and Overall Survival in Breast Cancer Patients: A Dose-Response Meta-Analysis of Cohort Studies. *Integr Cancer Ther* 2018; **17**: 217-225 [PMID: 28589744 DOI: 10.1177/1534735417712007]

4 **Schmitt EB**, Nahas-Neto J, Bueloni-Dias F, Poloni PF, Orsatti CL, Petri Nahas EA. Vitamin D deficiency is associated with metabolic syndrome in postmenopausal women. *Maturitas* 2018; **107**: 97-102 [PMID: 29169589 DOI: 10.1016/j.maturitas.2017.10.011]

5 **Terrault NA**, Bzowej NH, Chang KM, Hwang JP, Jonas MM, Murad MH; American Association for the Study of Liver Diseases. AASLD guidelines for treatment of chronic hepatitis B. *Hepatology* 2016; **63**: 261-283 [PMID: 26566064 DOI: 10.1002/hep.28156]

6 **Nannini P**, Sokal EM. Hepatitis B: changing epidemiology and interventions. *Arch Dis Child* 2017; **102**: 676-680 [PMID: 27986700 DOI: 10.1136/archdischild-2016-312043]

7 **Komatsu H**, Inui A. Hepatitis B virus infection in children. *Expert Rev Anti Infect Ther* 2015; **13**: 427-450 [PMID: 25724218 DOI: 10.1586/14787210.2015.1019867]

8 **Gotlieb N**, Tachlytski I, Lapidot Y, Sultan M, Safran M, Ben-Ari Z. Hepatitis B virus downregulates vitamin D receptor levels in hepatoma cell lines, thereby preventing vitamin D-dependent inhibition of viral transcription and production. *Mol Med* 2018; **24**: 53 [PMID: 30326825 DOI: 10.1186/s10020-018-0055-0]

9 **Hoan NX**, Tong HV, Song LH, Meyer CG, Velavan TP. Vitamin D deficiency and hepatitis viruses-associated liver diseases: A literature review. *World J Gastroenterol* 2018; **24**: 445-460 [PMID: 29398866 DOI: 10.3748/wjg.v24.i4.445]

10 **Yu R**, Tan D, Ning Q, Niu J, Bai X, Chen S, Cheng J, Yu Y, Wang H, Xu M, Shi G, Wan M, Chen X, Tang H, Sheng J, Dou X, Shi J, Ren H, Wang M, Zhang H, Gao Z, Chen C, Ma H, Jia J, Hou J, Xie Q, Sun J. Association of baseline vitamin D level with genetic determinants and virologic response in patients with chronic hepatitis B. *Hepatol Res* 2018; **48**: E213-E221 [PMID: 28834607 DOI: 10.1111/hepr.12972]

11 **Hu YC**, Wang WW, Jiang WY, Li CQ, Guo JC, Xun YH. Low vitamin D levels are associated with high viral loads in patients with chronic hepatitis B: a systematic review and meta-analysis. *BMC Gastroenterol* 2019; **19**: 84 [PMID: 31185932 DOI: 10.1186/s12876-019-1004-2]

12 **Zhao XY**, Li J, Wang JH, Habib S, Wei W, Sun SJ, Strobel HW, Jia JD. Vitamin D serum level is associated with Child-Pugh score and metabolic enzyme imbalances, but not viral load in chronic hepatitis B patients. *Medicine (Baltimore)* 2016; **95**: e3926 [PMID: 27399065 DOI:

10.1097/MD.0000000000003926]
13 **Terrault NA**, Lok ASF, McMahon BJ, Chang KM, Hwang JP, Jonas MM, Brown RS Jr, Bzowej NH, Wong JB. Update on prevention, diagnosis, and treatment of chronic hepatitis B: AASLD 2018 hepatitis B guidance. *Hepatology* 2018; **67**: 1560-1599 [PMID: 29405329 DOI: 10.1002/hep.29800]
14 **Chen EQ**, Bai L, Zhou TY, Fe M, Zhang DM, Tang H. Sustained suppression of viral replication in improving vitamin D serum concentrations in patients with chronic hepatitis B. *Sci Rep* 2015; **5**: 15441 [PMID: 26486883 DOI: 10.1038/srep15441]
15 **Artaza JN**, Norris KC. Vitamin D reduces the expression of collagen and key profibrotic factors by inducing an antifibrotic phenotype in mesenchymal multipotent cells. *J Endocrinol* 2009; **200**: 207-221 [PMID: 19036760 DOI: 10.1677/JOE-08-0241]
16 **Beilfuss A**, Sowa JP, Sydor S, Beste M, Bechmann LP, Schlattjan M, Syn WK, Wedemeyer I, Mathé Z, Jochum C, Gerken G, Gieseler RK, Canbay A. Vitamin D counteracts fibrogenic TGF-β signalling in human hepatic stellate cells both receptor-dependently and independently. *Gut* 2015; **64**: 791-799 [PMID: 25134788 DOI: 10.1136/gutjnl-2014-307024]
17 **Oleröd G**, Hultén LM, Hammarsten O, Klingberg E. The variation in free 25-hydroxy vitamin D and vitamin D-binding protein with season and vitamin D status. *Endocr Connect* 2017; **6**: 111-120 [PMID: 28179376 DOI: 10.1530/EC-16-0078]
18 **Lisowska-Myjak B**, Jóźwiak-Kisielewska A, Łukaszkiewicz J, Skarżyńska E. Vitamin D-binding protein as a biomarker to confirm specific clinical diagnoses. *Expert Rev Mol Diagn* 2020; **20**: 49-56 [PMID: 31795772 DOI: 10.1080/14737159.2020.1699064]
19 **Schiødt FV**, Clemmesen JO, Bondesen S, Dahl B, Ott P. Increased turnover of Gc-globulin in patients with hepatic encephalopathy. *Scand J Gastroenterol* 2001; **36**: 998-1003 [PMID: 11521994 DOI: 10.1080/00365520175030555 8]

World Journal of Gastroenterology

Submit a Manuscript: https://www.f6publishing.com

World J Gastroenterol 2021 January 21; 27(3): 267-280

DOI: 10.3748/wjg.v27.i3.267

ISSN 1007-9327 (print) ISSN 2219-2840 (online)

ORIGINAL ARTICLE

Retrospective Study

Trends in the management of anorectal melanoma: A multi-institutional retrospective study and review of the world literature

Josh Bleicher, Jessica N Cohan, Lyen C Huang, William Peche, T Bartley Pickron, Courtney L Scaife, Tawnya L Bowles, John R Hyngstrom, Elliot A Asare

ORCID number: Josh Bleicher 0000-0001-6137-4426; Jessica N Cohan 0000-0002-5461-4716; Lyen C Huang 0000-0002-8605-2631; William Peche 0000-0001-9770-2137; T Bartley Pickron 0000-0002-0880-1959; Courtney L Scaife 0000-0003-2497-4961; Tawnya L Bowles 0000-0002-1883-1510; John R Hyngstrom 0000-0002-4833-3838; Elliot A Asare 0000-0002-0176-3865.

Author contributions: Bleicher J, Bowles TL, Hyngstrom JR and Asare EA designed the study and created the methodology; Bleicher J and Asare EA performed data analysis; Bleicher J created the first draft of the manuscript; Asare EA supervised the research; all authors participated in data acquisition and provided edits and helped with subsequent writing.

Institutional review board statement: The Institutional Review Boards of the University of Utah and Intermountain Health Care approved this study.

Conflict-of-interest statement: I confirm that I have no financial disclosures to declare. As the corresponding author for this manuscript, I also declare that none of my co-authors have financial disclosures to declare.

Josh Bleicher, Jessica N Cohan, Lyen C Huang, William Peche, T Bartley Pickron, Courtney L Scaife, Tawnya L Bowles, John R Hyngstrom, Elliot A Asare, Department of Surgery, Huntsman Cancer Institute at the University of Utah, Salt Lake City, UT 84114, United States

William Peche, John R Hyngstrom, Department of Surgery, George E Wahlen Department of Veterans Affairs Medical Center, Salt Lake City, UT 84114, United States

Tawnya L Bowles, Elliot A Asare, Department of Surgery, Intermountain Medical Center, Murray, UT 84107, United States

Corresponding author: Elliot A Asare, MD, MS, Assistant Professor, Surgical Oncologist, Department of Surgery, Huntsman Cancer Institute at the University of Utah, 1950 Circle of Hope Drive, Suite N6345, Salt Lake City, UT 84114, United States. elliot.asare@hci.utah.edu

Abstract

BACKGROUND

Anorectal melanoma (ARM) is a rare disease with a poor prognosis. Evidence on optimal treatment is limited and surgical management varies widely. We hypothesized that the frequency of abdominoperineal resection used as primary treatment of ARM has decreased over the past several decades.

AIM

To update our understanding of outcomes for patients with ARM and analyze management trends around the world.

METHODS

This is a multi-institutional, retrospective study of patients treated for ARM at 7 hospitals. Hospitals included both large, academic, tertiary care centers and smaller, general community hospitals. Using prospectively maintained institutional tumor registries, we identified 24 patients diagnosed with ARM between January 2000 and May 2019. We analyzed factors prognostic for recurrence and survival. We then used Cox regression to measure overall survival (OS) and melanoma-specific survival. We also performed a literature review to assess trends in surgical management and outcomes.

RESULTS

Of the 24 patients diagnosed with ARM, 12 (50.0%) had local, 8 (33.3%) regional,

Data sharing statement: Because of the small number of participants involved in this cohort and the inability to obtain informed consent, it is difficult to ensure patient anonymity in our dataset and this will not be made available. Statistical code is available from the first author at josh.bleicher@hsc.utah.edu.

Open-Access: This article is an open-access article that was selected by an in-house editor and fully peer-reviewed by external reviewers. It is distributed in accordance with the Creative Commons Attribution NonCommercial (CC BY-NC 4.0) license, which permits others to distribute, remix, adapt, build upon this work non-commercially, and license their derivative works on different terms, provided the original work is properly cited and the use is non-commercial. See: http://creativecommons.org/Licenses/by-nc/4.0/

Manuscript source: Unsolicited manuscript

Specialty type: Gastroenterology and hepatology

Country/Territory of origin: United States

Peer-review report's scientific quality classification

Grade A (Excellent): 0
Grade B (Very good): B, B, B, B
Grade C (Good): 0
Grade D (Fair): 0
Grade E (Poor): 0

Received: December 1, 2020
Peer-review started: December 1, 2020
First decision: December 21, 2020
Revised: December 28, 2020
Accepted: January 7, 2021
Article in press: January 7, 2021
Published online: January 21, 2021

P-Reviewer: Gong N, Taher M
S-Editor: Fan JR
L-Editor: A
P-Editor: Li JH

and 4 (16.7%) distant disease at diagnosis. Median time to recurrence was 10.4 mo [interquartile range (IQR) 7.5-17.2] with only 2 patients (9.3%) not developing recurrence following surgical resection. Median OS was 18.8 mo (IQR 13.5-33.9). One patient is still alive without recurrence at 21.4 mo from diagnosis; no other patient survived 5 years. Primary surgical management with abdominoperineal resection (APR) *vs* wide excision (WE) did not lead to differences in OS [hazard ratio = 1.4 (95%CI: 0.3-6.8)]. Review of the literature revealed geographic differences in surgical management of ARM, with increased use of WE in the United States and Europe over time and more frequent use of APR in Asia and India. There was no significant improvement in survival over time.

CONCLUSION

There is wide variation in the management of ARM and survival outcomes remain poor regardless of approach. Surgical management should aim to minimize morbidity.

Key Words: Melanoma; Anorectal melanoma; Literature review; Melanoma surgery; Surgical oncology; Colorectal surgery

©The Author(s) 2021. Published by Baishideng Publishing Group Inc. All rights reserved.

Core Tip: This is a retrospective study to evaluate current trends in management of anorectal melanoma (ARM). On review of 24 patients from 7 hospitals in Utah, we found that ARM is a highly lethal disease with overall survival of 18.8 mo (interquartile range 13.5-33.9) and no 5-year survivors. Only 2 patients underwent abdominoperineal resection (APR) as primary surgical management. Review of the literature demonstrated wide variation in surgical management of ARM over time and around the world. Whether APR or wide excision was used, outcomes remained poor. With this data, we recommend that surgical management should aim to minimize morbidity.

Citation: Bleicher J, Cohan JN, Huang LC, Peche W, Pickron TB, Scaife CL, Bowles TL, Hyngstrom JR, Asare EA. Trends in the management of anorectal melanoma: A multi-institutional retrospective study and review of the world literature. *World J Gastroenterol* 2021; 27(3): 267-280
URL: https://www.wjgnet.com/1007-9327/full/v27/i3/267.htm
DOI: https://dx.doi.org/10.3748/wjg.v27.i3.267

INTRODUCTION

Anorectal melanoma (ARM) is a rare malignancy with a poor prognosis. The estimated annual incidence in the United States is less than 5 cases per 10 million[1]. Overall 5-year survival is between 10% and 20%[2]. This low survival is due to the late diagnosis of most tumors and aggressive biology of ARM[3]. Most tumors are first recognized from symptoms such as bleeding, obstruction, pain, or changes in bowel habits[4-6]. When these tumors are recognized, they are often misdiagnosed as hemorrhoids or other benign anorectal pathology[7].

National Clinical Cancer Network (NCCN) guidelines on melanoma do not currently include recommendations for treatment of ARM[8]. Without guidelines, and due to the rare nature of the tumor, treatment is highly variable. Controversy exists over optimal primary surgical therapy. Some advocate abdominoperineal resection (APR) for initial treatment, while others report similar oncologic outcomes with wide excision (WE) alone[9,10]. As outcomes are universally poor, many providers recommend the less invasive and lower morbidity WE as primary treatment[11]. Optimal primary nodal management strategy is also unknown. Non-surgical therapy is even more varied. Radiotherapy, chemotherapy, and targeted therapies (including interferon, checkpoint-inhibitors, anti-BRAF therapy, and tyrosine kinase inhibitors) have all been used alone or in various combinations[12-17]. No clear treatment strategy has emerged as the gold standard for treatment of this rare but aggressive disease.

Given the lack of guidelines and variability in reported practice patterns, we analyzed outcomes from a multi-institutional cohort of patients with ARM. We also provide an updated review of the literature to compare outcomes from across the decades and around the world. This review allows for analysis of overall trends to help guide treatment decisions for patients with ARM.

MATERIALS AND METHODS

Study design

We retrospectively reviewed patients diagnosed with ARM between January 1, 2000 and January 1, 2019. This allowed for at least 12 mo of follow-up for all patients. Patients were identified using international classification of diseases-9/10 codes in prospectively maintained institutional tumor registries at 7 centers near Salt Lake City, Utah. These centers included the University of Utah Huntsman Cancer Institute and 6 hospitals affiliated with Intermountain Health Care. All names were linked across institutions to ensure only unique patients were included in the study.

Data Collection

We abstracted data from the electronic medical record and institutional tumor registries. Manual chart review was performed for all records to verify data and obtain additional information. Data abstracted includes patient demographics, primary tumor characteristics, treatment details, and cancer-related outcomes. Both adjuvant therapy and therapy at time of relapse were recorded. Specific chemotherapy and immunotherapy agents were noted. Vital status was available for all but one patient.

Extent of disease was categorized into local, regional, or distant depending on whether disease was confined to the anorectum, involved regional lymph nodes, or other organs[3]. Extent of disease classification was based on clinical documentation. The extent of primary surgical therapy was also determined by clinical documentation. The Institutional Review Boards of the University of Utah and Intermountain Health Care approved this study.

Statistical analyses

Statistical analyses were performed using Stata Version 15.1 (Stata Corp, College Station, TX, United States). We analyzed patient demographics, initial tumor characteristics, and treatment details using descriptive statistics. We calculated median time to recurrence, melanoma-specific survival (MSS), and overall survival (OS) for the cohort and determined MSS and OS at 2, 3, and 5-year intervals. Patients with unknown survival outcomes were excluded from OS analysis and patients with unknown cause of death were excluded from MSS analysis. We graphically evaluated these outcomes using the Kaplan-Meier method. Time-zero for all time-to-event outcomes was the date of diagnosis. Recurrence was defined as re-appearance of disease on physical exam or radiographically in patients who had been initially rendered free of disease after initial treatment. Patients were determined to be free of disease following initial therapy based on intention to treat, as described in clinical documentation.

Cox regression was used to assess for any factors associated with survival. Results were considered statistically significant if the two-sided $P < 0.05$. Analysis of outcomes associated with different surgical and non-surgical treatment options was performed in a similar fashion. Multivariable analysis was not performed because of the small sample size of this cohort.

Review of the literature

We performed a literature review using the PubMed database. The 2009 PRISMA checklist was used to ensure transparent reporting of search and review methodology[18]. The search term used was "ARM." Search results did not differ significantly when "anal melanoma" or "rectal melanoma" were considered separately. All English language articles were included. Articles were excluded if they did not describe outcomes of a unique cohort of at least 10 patients. When multiple articles described overlapping patient cohorts, the most recent and inclusive article was used. Studies describing patient outcomes from national databases in the United States were excluded, as these patients are often represented in other institutional studies. National database studies from other countries were included when other cohorts from these countries did not exist. All titles and abstracts were reviewed for

inclusion.

Once this review was complete, all full-length articles were reviewed. Outcomes of interest were surgical management of patients, median OS, and 5-year OS. No summary of outcomes was performed because of the significant heterogeneity among the various studies.

RESULTS

Twenty-four patients met inclusion criteria. Two-thirds of patients were female, with median age of 65.5 [interquartile range (IQR) 54-76] (Table 1). Patients were from five different states (UT, ID, WY, NV, CO) and approximately 20% of patients were from rural communities. Of 13 patients with information on Breslow depth, 7 (53.8%) were > 5 mm. There were 9 (37.5%) patients whose melanoma exhibited ulceration (Table 1). Half of the patients had advanced disease at diagnosis; 8 with nodal disease and 4 with distant metastases.

Fifteen patients (62.5%) underwent WE at diagnosis and 2 patients (8.3%) underwent APR (Table 2). Seven patients (29.2%) received biopsy alone, including 2/4 patients with distant disease at diagnosis. The primary operation took place at a median of 27 d after diagnosis (IQR 0-47). Sentinel lymph node biopsy (SLNB) was performed in 6 (25%) patients. Of those with local or nodal disease, nearly half of patients received surgery alone as primary management. The remainder of patients received systemic therapy of some form following surgical resection. There was wide variation in adjuvant treatment. Some patients received chemotherapy, radiation, interferon, or checkpoint-inhibitor therapy alone; others received these in various combinations (Table 2).

Of 21 patients with complete follow-up data, only 2 (9.5%) remained free of disease after resection. One of these patients died of metastatic colon adenocarcinoma 13.9 mo after ARM diagnosis. The other patient was alive at last follow-up with no evidence of disease 21.4 mo from diagnosis. Excluding the 4 patients with distant disease at diagnosis, 3 (20.0%) of the remaining 15 patients were never free of disease and the remaining 12 (80.0%) recurred after initial treatment. One patient who was never free of disease underwent APR as salvage therapy. Median time to recurrence was 10.4 mo (IQR 7.5-17.2). At the time of recurrence, 4 patients (33.3%) opted not to pursue further therapy given their age, comorbidities, and/or overall prognosis. Of those who received further treatment (n = 8), only 1 patient had surgery (repeat WE and bilateral inguinal lymph node dissection). Use of systemic therapy was highly variable. Individual patient treatments and outcomes are shown in Supplementary Table 1.

Survival status was known for all but 1 patient. Of these 23 patients, 1 (4.3%) was alive at last follow-up (21.4 mo from diagnosis). Fourteen (60.9%) died from ARM. The cause of death was unknown for 7 (30.4%) patients. Median OS was 18.8 mo (IQR 13.5-33.9) with 0 survivors at 5 years (Figure 1A). Two-year OS was 21.0% (95%CI: 6.8%-40.3%) and 3-year OS was 10.4% (95%CI: 1.8%-27.9%). Median MSS was 19.5 mo (IQR 14.8-35.1) (Figure 1B). Two-year MSS was 29.1% (95%CI: 9.1%-53.0%) and 3-year MSS was 14.6% (95%CI: 2.4%-37.0%). Excluding patients with distant disease at diagnosis, median OS was 19.9 mo (IQR 16.0-35.1) with 2-year OS of 25.5% (95%CI: 8.2%-47.3%) and 3-year OS of 12.7% (95%CI: 2.2%-33.0%). Median MSS was 19.9 mo (IQR 16.4-39.8) with 2-year MSS of 36.4% (95%CI: 11.2%-62.7%) and 3-year MSS of 18.2% (95%CI: 2.9%-44.2%).

Age, sex, rural location, mitoses, ulceration, and Breslow depth were not prognostic of OS. Patients with distant disease at diagnosis had higher risk of mortality than patients with local disease [hazard ratio (HR) = 14.6 (95%CI: 2.5-86.7)] or nodal disease [HR = 14.4 (95%CI: 2.2-92.1)]. No differences in OS were noted for patients who underwent APR *vs* WE as their primary operation [HR = 1.4 (95%CI: 0.3-6.8)]. There was no significant difference in OS between patients who underwent nodal surgery [SLNB or completion lymph node dissection (CLND)] and those who did not [HR = 0.4 (95%CI: 0.1-1.1)]. Exclusion of patients with distant disease at diagnosis did not alter these results. No individual adjuvant therapy (immunotherapy, radiation, or chemotherapy) demonstrated a benefit over another therapy for patients with local or nodal disease treated with surgery as initial treatment.

Review of the literature

This search revealed 360 unique articles, of which 33 were included for review (Figure 2). Cohorts differed across studies, with some including all patients diagnosed with ARM and others limited to only patients with local or nodal disease or patients

Table 1 Demographics and primary tumor characteristics for cohort with anorectal melanoma (*n* = 24)

Classification		*n*
Age, years (median, IQR)		65.5 (54-76)
	≤ 50	3 (12.5)
	51–60	7 (29.2)
	61–70	6 (25.0)
	71–80	6 (25.0)
	> 80	2 (8.3)
Sex	M	8 (33.3)
	F	16 (66.7)
Race	White	23 (95.8)
	Latino	1 (4.2)
Rural	Yes	5 (20.8)
	No	19 (79.2)
Breslow depth (mm)	≤ 5	6 (25.0)
	> 5	7 (29.2)
	Unknown	11 (45.8)
Ulceration	Present	9 (37.5)
	Absent	2 (8.3)
	Unknown	13 (54.2)
Mitoses	> 1	7 (29.2)
	Unknown	17 (70.8)
Stage	I	12 (50.0)
	II	8 (33.3)
	III	4 (16.7)

IQR: Interquartile range.

treated with curative intent. Twenty-five studies reported median OS (Table 3). Median OS ranged from 7-49.5 mo and 21 (84%) studies had median OS < 25 mo. There was wide variation in the type of surgical management across studies. At some centers, all patients received WE while other centers treated all patients with APR[10,19,20].

Eight studies achieved a 5-year OS rate of 20%. Three of these studies included patients diagnosed before 1980, with 1 study including patients from the 1930s[10,21,22]. The other five study cohorts spanned into the 2000s. Surgical management of patients was mixed in this subset of studies. In a study of 54 patients with ARM treated at MD Anderson Cancer Center (MDACC) from 1989-2008, all patients with local disease underwent WE followed by radiation therapy and a 5-year OS of 30% was reported[10]. In another study from South Korea, authors described 12 patients who underwent APR and 7 who underwent WE with significantly improved OS with APR compared to WE[9]. In the remainder of studies, 3 studies reported no significant differences between APR and WE and 3 did not report results of this comparison[7,21-24]. No other dominant themes in surgical or non-surgical treatment were noted across these studies with superior survival outcomes.

Across all studies, the number of APRs was similar to WEs. In total, 427 patients had APR and 436 underwent WE. Studies from the same institution at different time points showed a trend towards performing fewer APRs with time. In two studies from Memorial Sloan Kettering Cancer Center (MSKCC) looking at cohorts from 1950-1977 and 1984-2003, 73.3% of patients underwent APR in the older cohort compared to 41.3% in the more recent cohort[25,26]. At MDACC, Ross *et al*[27] reported APR in 53.8% of patients from 1952-1988 while Kelly *et al*[10] reported exclusive treatment with WE

Table 2 Treatment details for cohort with anorectal melanoma (*n* = 24)

	Treatment	
Primary operation, *n*	WE	15 (62.5)
	APR	2 (8.3)
	Biopsy alone	7 (29.2)
Primary nodal operation, *n*	SLNB	6 (25.0)
	CLND	3 (12.5)
	None	15 (62.5)
Adjuvant therapy, *n*[1]	Chemotherapy alone	0 (0)
	Radiation alone	1 (4.2)
	Interferon alone	3 (12.5)
	Checkpoint Inhibitor	3 (12.5)
	Combination chemotherapy/radiation	2 (8.3)
	Combination chemotherapy/immunotherapy	3 (12.5)
	Combination radiation/immunotherapy	1 (4.2)
	None	11 (45.8)
Surgery at recurrence[2]	APR	1 (9.1)
	WE	1 (9.1)
Non-operative therapies at recurrence[2]	Chemotherapy	1 (9.1)
	Radiation	0 (0)
	Interferon	0 (0)
	Checkpoint Inhibitor	2 (18.2)
	Combination chemotherapy/radiation	4 (26.7)
	Combination chemotherapy/immunotherapy	2 (13.3)
	Combination radiation/immunotherapy	2 (13.3)

[1]Excluding patients with distant disease at diagnosis (*n* = 4).
[2]Percentages calculated from total patients with recurrence who underwent treatment (*n* = 8).
APR: Abdominoperineal resection; WE: Wide excision; SLNB: Sentinel lymph node biopsy; CLND: Completion lymph node dissection.

between 1989-2008, as noted previously[10,27].

Geographic variation in surgical management exists. In United States cohorts, 45.7% (132/289) of surgical patients underwent APR, down to 24.3% over the past 40 years (35/144). European cohorts were similar with 45.1% of patients undergoing APR (123/273). Asian (China, South Korea, Japan, and Taiwan) and Indian cohorts had higher rates of APR with 69.9% (200/286) and 79.7% (51/64) of patients receiving APR as primary surgical therapy respectively. Das *et al*[19] and Ranjith *et al*[20] report cohorts from India with 100% of patients undergoing APR[19,20].

DISCUSSION

Dr. George Pack wrote in 1967, "cures are possible although they do not occur with encouraging frequency[19]". This study confirms the dismal prognosis associated with ARM. Only 1 patient from our study cohort was alive at last follow up, and there were no 5-year survivors. Only 6/33 studies reviewed reported a 5-year OS > 20%, and some of these studies included only patients with local disease. Most studies reported median OS of less than 2 years, and many less than 1 year. There is no compelling evidence from this review that a significant improvement in survival has been made for patients with ARM since 1967.

This study also demonstrates the wide variation in surgical treatment for ARM, both

Table 3 Studies included in literature review and select outcomes

Ref.	Date published	Location	Dates included	Sample size	Median age	M/F (*n*)	APR/WE (*n*)	Median OS	APR *vs* WE (% survival to 5 yr)	Overall 5 yr survival (%)
Pack *et al*[40]	1967	Pack Medical Foundation, United States	1930-1965	20	53.5[1]	5/15	11/3	-	-	5
Abbas *et al*[41]	1980	Roswell Park Memorial Institute, United States	1930-1979	20	61.7	4/16	11/7	18.8[1]	20.1 mo *vs* 8.5 mo[3]	7
Ward *et al*[42]	1986	St. Mark's Hospital, United Kingdom	1932-1982	21	-	12/9	9/6	8.8[1]	-	0
Thibault *et al*[21]	1996	Mayo Clinic, United States	1939-1993	50	63[1]	15/35	26/10	26[1,2]	18 *vs* 19	22
Wanebo *et al*[25]	1990	Memorial Sloan Kettering Cancer Center, United States	1950-1977	36	60	15/21	22/8	14	16/7 mo *vs* 21.5 mo[3,4]	8
Ross *et al*[27]	1990	MD Anderson Cancer Center, United States	1952-1988	32	-	-	14/12	18.6	19.5 mo *vs* 18.9 mo[3]	3
Dodds *et al*[43]	2019	Melanoma Institute Australia, Australia	1958-2016	43	61	21/22	20/15	24	-	16
Siegal *et al*[44]	1983	Sheba Medical Center, Israel	1960-1981	30	64[1]	13/17	15/9	10.5[1]	-	7
Roumen *et al*[45]	1996	Eindhoven Cancer Registry, Netherlands	1960-1995	63	66	27/36	21/18	-	-	6
Nilsson *et al*[46]	2010	Swedish National Cancer Registry, Sweden	1960-1999	251	73	101/150	66/86	11.2	7 *vs* 15, *P* = 0.08	
Podnos *et al*[47]	2006	City of Hope National Medical Center, United States	1973-2001	126	69.2[1]	39/87	-	15	-	19
Slingluff *et al*[48]	1990	Duke University Medical Center, United States	1974-1988	24	64[1]	7/17	13/8	18	18 *vs* 12	8
Belli *et al*[49]	2008	National Institute of Cancer, Italy	1975-2006	40	63	19/21	13/18	17	18.5 *vs* 18.5, *P* = 0.97	-
Che *et al*[22]	2011	Peking Union Medical College, China	1975-2008	56	-	22/34	36/20	21	24.6 *vs* 9.9, *P* = 0.65	20
Pessaux *et al*[50]	2004	Institut Gustave Roussy, France	1977-2002	30	58.1	7/23	9/21	17	16 *vs* 33	17
Ramakrishnan *et al*[51]	2008	Cancer Institue (WIA), India	1980-2004	63	-	34/29	3/8	9.5[2]	-	5
Yeh *et al*[26]	2006	Memorial Sloan Kettering Cancer Center, United States	1984-2003	46	59	18/28	19/27	39[5]	32 *vs* 35, *P* = 0.66[5]	-
Homsi *et al*[52]	2007	H. Lee Moffitt Cancer Center, United States	1987-2004	12	67	3/9	5/6	-	-	-
Bullard *et al*[53]	2003	University of Minnesota, United States	1988-2002	15	65[1]	6/9	4/11	18[6]	14 mo *vs* 19 mo[3]	-
Kelly *et al*[10]	2010	MD Anderson Cancer Center, United States	1989-2008	54	61	19/35	0/54	29	-	30
Das *et al*[19]	2003	Tata Memorial Hospital, India	1990-2001	72	49[1]	20/52	24/0	13[2,5]	-	8[2]
Hicks *et al*[28]	2014	John Hopkins Hospital, United States	1991-2012	18	64	10/8	7/11	15.5	11.5 mo *vs* 13.5 mo, *P* = 0.75[3]	-
Yen *et al*[54]	2013	Chang Gung Memorial Hospital, China	1993-2011	22	58.4[1]	8/14	12/8	-	0 *vs* 28.6, *P* = 0.06	9
Zhang *et al*[7]	2010	First Affiliated Hospital of Guangxi Medical University, China	1995-2007	54	54	21/33	39/15	25	30 *vs* 16, *P* = 0.28	26

Aytac *et al*[55]	2010	Uludag University, Turkey	1997-2004	14	58	8/6	11/3	7.5	-	0
Ishizone *et al*[32]	2008	Shinshu University Hospital, Japan	1997-2006	79	65.8[1]	34/45	63/14	22	-	29
Belbaraka *et al*[56]	2012	National Institute of Oncology, Morocco	1998-2007	17	58[1]	12/5	7/3	8	-	-
Choi *et al*[9]	2010	Samsung Medical Center, South Korea	1999-2008	19	61	8/11	12/7	45.9	50 *vs* 0	32
Miguel *et al*[23]	2015	IPOFG, Portugal	2000-2011	10	70.5	2/8	5/1	9.3	-	20
Ranjith *et al*[20]	2018	Regional Cancer Center Thiruvanathapuram, India	2001-2013	31	56	12/19	9/0	9	-	0
Ren *et al*[24]	2018	Fudan University Shanghai Cancer Center, China	2005-2017	60	61	18/42	38/22	-	-	33.3[5]
Nusrath *et al*[57]	2018	Basavatakrakam Indo American Cancer Hospital, India	2010-2015	30	50	15/15	15/5	13	13 *vs* 36, P = 0.48	-
Sahu *et al*[58]	2017	Tata Memorial Hospital, India	2013-2015	37	54	25/12	-	7	-	-

[1]Mean reported instead of median.
[2]Only cases treated with curative intent included in analysis.
[3]Median overall survival (OS) [abdominoperineal resection (APR) *vs* wide excision].
[4]APR OS grouped as lymph node negative/lymph node positive.
[5]Melanoma specific survival.
[6]Mean OS of deceased patients only.
APR: Abdominoperineal resection; WE: Wide excision; mo: Month; OS: Overall survival.

within and between medical centers. Geographic variation also exists, with United States and European centers more likely to perform WE and Asian and Indian centers more likely to perform APR. This finding was true in our cohort, with few patients undergoing APR. While low sample size limits analysis, there was no difference in survival outcomes between patients undergoing WE *vs* APR. Multiple other groups have demonstrated similar or better outcomes with WE compared to APR[10,28]. This same conclusion has been reached using larger cohorts from Surveillance, Epidemiology, and End Results and National Cancer Database (NCDB)[1,11,12]. A prior systematic review concluded that while APR may reduce local recurrence, there is no improvement in OS or recurrence-free survival compared to WE[29].

WE allows for avoidance of a colostomy and significantly reduced morbidity compared to APR. A study of 49 patients undergoing WE demonstrated the safety of this procedure; 3 patients had minor infections requiring antibiotics and 1 patient required a second operation for postoperative bleeding. No other complications from surgery occurred[10]. While most studies of APR for ARM have not reported complication rates, APR for other indications is known to be associated with significant morbidities. Perineal wound complications occur in up to 40% of patients and 50% of patients develop genitourinary and/or sexual dysfunction postoperatively[30]. No studies currently exist in ARM that compare quality of life between WE and APR[31]. Some centers continue to routinely perform APR for ARM patients; however, we did not find evidence in this review to support this practice[9,19,20,32].

Nodal management also differs widely. In our cohort, there were no significant differences in survival outcomes between patients who underwent initial nodal surgery (SLNB or CLND) and those who did not. Nearly 2/3 of patients did not receive any nodal staging or treatment. Older studies hypothesized that the benefit of APR was largely secondary to the mesorectal lymphadenectomy performed with this procedure[25]. However, Yeh *et al*[26] found that the presence of lymph node metastases had no prognostic significance on survival in 19 patients who underwent APR at MSKCC[26]. Many patients in this cohort received local surgery alone and did not receive additional therapy until the time of recurrence. Some of these patients likely had unidentified nodal disease at the time of initial surgery. If patients had undergone SLNB and were found to have positive nodal disease, adjuvant systemic therapy could have been initiated sooner. The impact this may have had on survival is unknown. This review did not find studies with large enough patient numbers to make

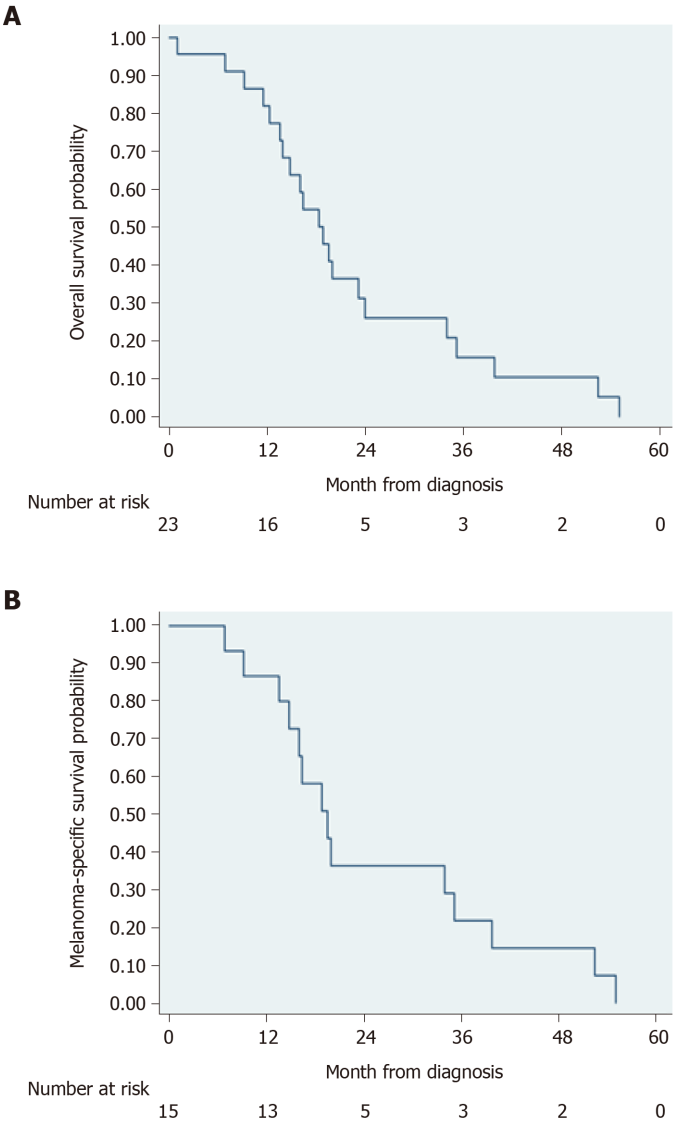


Figure 1 Overall mortality and melanoma-specific mortality in cohort of patients with anorectal melanoma. A: Overall mortality; B: Melanoma-specific mortality.

conclusions regarding the benefits of nodal surgery.

Use of immune checkpoint inhibitors and targeted therapies is also controversial and evidence is lacking to help with decision making. While checkpoint inhibitors, tyrosine kinase inhibitors, and BRAF/MEK inhibitors have significantly improved outcomes for cutaneous melanoma over the past decade, their role in treatment of ARM remains unknown[33-36]. Results of immune checkpoint inhibitor therapy for ARM are limited and show mixed outcomes. Tokuhara *et al*[13] reported a case of a 67-year-old male with ARM who had no oncologic progression of disease for 17 mo after initiation of anti- programmed death 1 (PD-1) therapy[13]. Conversely, Faure *et al*[37] reported a case of a 77 year-old male with ARM who progressed rapidly on anti-PD-1 therapy[37]. Higher level evidence of the effectiveness of immune checkpoint inhibitor therapy in treating ARM is lacking[13,38]. While immune checkpoint inhibitor therapy has helped individual patients with ARM, the efficacy of this treatment in most ARMs has been questioned as most ARMs do not exhibit 1-PD-ligand expression and few have tumor-infiltrating lymphocytes[25]. Evidence for other targeted therapies is similarly poor[2]. The genomic profiles of ARMs differ from cutaneous melanomas, with very low BRAF expression and few NRAS and KIT mutations[39]. ARM likely has different drivers of metastases with fewer targetable mutations. Although a rare disease, clinical trials are necessary to determine what therapies are most useful for ARM.

This study is limited by its retrospective nature and small cohort size. ARM is an extremely rare disease and only 24 cases were identified over a 20-year period. Additionally, the lack of a synoptic report for this disease has resulted in many

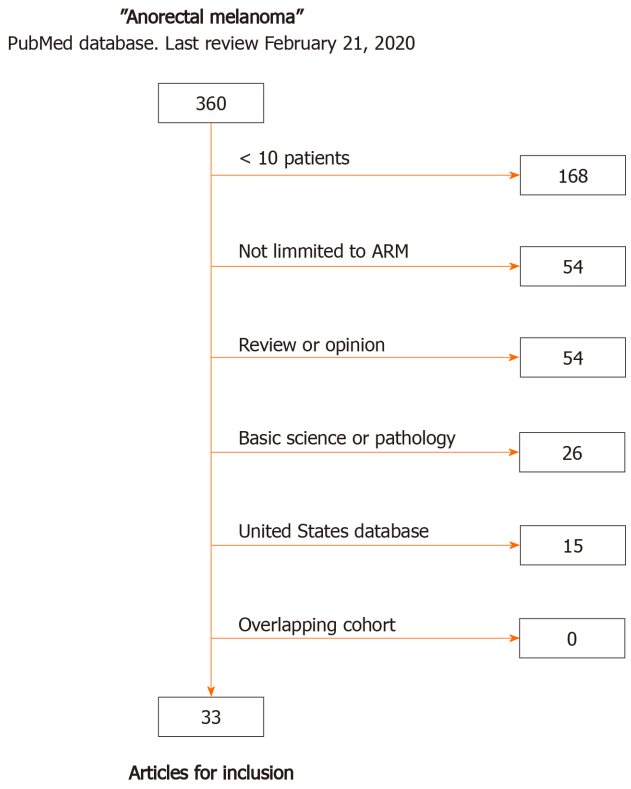


Figure 2 Flow diagram of selection of articles for literature review. ARM: Anorectal melanoma.

missing pertinent variables which would have strengthened this study.

CONCLUSION

ARM is a highly lethal disease. Over the past 50 years, outcomes have remained largely unchanged. Without good evidence to drive treatment decisions, surgical and non-surgical management remains highly variable across the United States and the world. Even within our own cohort, management differed between patients. Review of the literature was also unable to resolve many questions on ARM. There does not appear to be survival benefit of APR over WE. With no clear advantage to APR, surgical management should aim to minimize morbidity. Many other questions on ARM management remain unanswered. Improving the quality of data on ARM is necessary. A consensus meeting of experts aimed at the identification of pertinent variables to collect would be a good first step. Additionally, clinical trials to assess the role of sentinel lymph node biopsy, targeted therapies, radiation therapy, and treatment sequencing are needed.

ARTICLE HIGHLIGHTS

Research background

Anorectal melanoma (ARM) is a rare disease with poor outcomes. 5-year survival remains < 20%.

Research motivation

Optimal surgical management of ARM remains unknown. Abdominoperineal resection (APR) and wide excision (WE) are both used and no gold standard for primary tumor management currently exists. Understanding trends in management and outcomes is critical to determining appropriate surgical management.

Research objectives

We aimed to update our understanding of treatment outcomes for patients with ARM

and analyze trends across countries and time.

Research methods

We performed a retrospective study of patients who were diagnosed with ARM at 7 hospitals in the Salt Lake City, UT region. We analyzed factors prognostic for recurrence and survival. We also performed a review of the literature to assess regional and temporal trends in ARM management.

Research results

We identified 24 patients diagnosed with ARM between 2000-01 and 2019-05. 12 (50.0%) had local, 8 (33.3%) regional, and 4 (16.7%) distant disease at diagnosis. Only 2 patients who had surgical resection of their primary tumor with curative intent failed to recur. Median time to recurrence was 10.4 mo [interquartile range (IQR) 7.5–17.2] and median overall survival was 18.8 mo (IQR 13.5–33.9). No patients survived to 5 years. No survival differences were noted for patients managed with WE *vs* APR. Review of the literature demonstrated regional trends in surgical management of ARM, with WE favored in the United States and Europe and APR used more frequently in Asia.

Research conclusions

ARM remains a highly lethal disease regardless of surgical treatment. Patients who undergo WE and APR have poor outcomes. No convincing evidence exists to favor APR over WE. Despite this, APR continues to be used for primary surgical management, although with decreasing frequency in the United States and Europe in recent years. We feel that surgical management should aim to minimize morbidity. WE should be favored over APR for primary surgical treatment.

Research perspectives

Further research should focus on better risk stratification and the role of targeted therapies, radiation therapy, and treatment sequencing. Improving non-surgical therapies will be critical to improving survival for patients with ARM.

ACKNOWLEDGEMENTS

We thank Emily Z. Keung, MD, MD Anderson Cancer Center, Houston, TX, United States.

REFERENCES

1 **Chen H**, Cai Y, Liu Y, He J, Hu Y, Xiao Q, Hu W, Ding K. Incidence, Surgical Treatment, and Prognosis of Anorectal Melanoma From 1973 to 2011: A Population-Based SEER Analysis. *Medicine (Baltimore)* 2016; **95**: e2770 [PMID: 26886623 DOI: 10.1097/MD.0000000000002770]

2 **Paolino G**, Didona D, Macrì G, Calvieri S, Mercuri SR. Anorectal Melanoma. In: Scott JF, Gerstenblith MR, editors. Noncutaneous Melanoma [Internet]. *Brisbane (AU): Codon Publications* 2018; **6**: 83-98 [PMID: 29874013 DOI: 10.15586/codon.noncutaneousmelanoma.2018.ch6]

3 **Patrick RJ**, Fenske NA, Messina JL. Primary mucosal melanoma. *J Am Acad Dermatol* 2007; **56**: 828-834 [PMID: 17349716 DOI: 10.1016/j.jaad.2006.06.017]

4 **Mihajlovic M**, Vlajkovic S, Jovanovic P, Stefanovic V. Primary mucosal melanomas: a comprehensive review. *Int J Clin Exp Pathol* 2012; **5**: 739-753 [PMID: 23071856]

5 **van Schaik PM**, Ernst MF, Meijer HA, Bosscha K. Melanoma of the rectum: a rare entity. *World J Gastroenterol* 2008; **14**: 1633-1635 [PMID: 18330962 DOI: 10.3748/wjg.14.1633]

6 **Khan M**, Bucher N, Elhassan A, Barbaryan A, Ali AM, Hussain N, Mirrakhimov AE. Primary anorectal melanoma. *Case Rep Oncol* 2014; **7**: 164-170 [PMID: 24748866 DOI: 10.1159/000360814]

7 **Zhang S**, Gao F, Wan D. Effect of misdiagnosis on the prognosis of anorectal malignant melanoma. *J Cancer Res Clin Oncol* 2010; **136**: 1401-1405 [PMID: 20130908 DOI: 10.1007/s00432-010-0793-z]

8 **National Comprehensive Cancer Network**. Cutaneous Melanoma: Clinical Practice Guidelines in Oncology. 2019

9 **Choi BM**, Kim HR, Yun HR, Choi SH, Cho YB, Kim HC, Yun SH, Lee WY, Chun HK. Treatment outcomes of anorectal melanoma. *J Korean Soc Coloproctol* 2011; **27**: 27-30 [PMID: 21431094 DOI: 10.3393/jksc.2011.27.1.27]

10 **Kelly P**, Zagars GK, Cormier JN, Ross MI, Guadagnolo BA. Sphincter-sparing local excision and hypofractionated radiation therapy for anorectal melanoma: a 20-year experience. *Cancer* 2011; **117**: 4747-4755 [PMID: 21446049 DOI: 10.1002/cncr.26088]

11 **Ciarrocchi A**, Pietroletti R, Carlei F, Amicucci G. Extensive surgery and lymphadenectomy do not improve survival in primary melanoma of the anorectum: results from analysis of a large database (SEER). *Colorectal Dis* 2017; **19**: 158-164 [PMID: 27317493 DOI: 10.1111/codi.13412]

12 **Taylor JP**, Stem M, Yu D, Chen SY, Fang SH, Gearhart SL, Safar B, Efron JE. Treatment Strategies and Survival Trends for Anorectal Melanoma: Is it Time for a Change? *World J Surg* 2019; **43**: 1809-1819 [PMID: 30830243 DOI: 10.1007/s00268-019-04960-w]

13 **Tokuhara K**, Nakatani K, Tanimura H, Yoshioka K, Kiyohara T, Kon M. A first reported case of metastatic anorectal amelanotic melanoma with a marked response to anti-PD-1 antibody nivolumab: A case report. *Int J Surg Case Rep* 2017; **31**: 188-192 [PMID: 28171845 DOI: 10.1016/j.ijscr.2017.01.028]

14 **Knowles J**, Lynch AC, Warrier SK, Henderson M, Heriot AG. A case series of anal melanoma including the results of treatment with imatinib in selected patients. *Colorectal Dis* 2016; **18**: 877-882 [PMID: 26546509 DOI: 10.1111/codi.13209]

15 **Shoushtari AN**, Bluth MJ, Goldman DA, Bitas C, Lefkowitz RA, Postow MA, Munhoz RR, Buchar G, Hester RH, Romero JA, Fitzpatrick LJ, Weiser MR, Panageas KS, Wolchok JD, Chapman PB, Carvajal RD. Clinical features and response to systemic therapy in a historical cohort of advanced or unresectable mucosal melanoma. *Melanoma Res* 2017; **27**: 57-64 [PMID: 27792058 DOI: 10.1097/CMR.0000000000000306]

16 **Kim KB**, Sanguino AM, Hodges C, Papadopoulos NE, Eton O, Camacho LH, Broemeling LD, Johnson MM, Ballo MT, Ross MI, Gershenwald JE, Lee JE, Mansfield PF, Prieto VG, Bedikian AY. Biochemotherapy in patients with metastatic anorectal mucosal melanoma. *Cancer* 2004; **100**: 1478-1483 [PMID: 15042682 DOI: 10.1002/cncr.20113]

17 **Lian B**, Si L, Cui C, Chi Z, Sheng X, Mao L, Li S, Kong Y, Tang B, Guo J. Phase II randomized trial comparing high-dose IFN-α2b with temozolomide plus cisplatin as systemic adjuvant therapy for resected mucosal melanoma. *Clin Cancer Res* 2013; **19**: 4488-4498 [PMID: 23833309 DOI: 10.1158/1078-0432.CCR-13-0739]

18 PRISMA. Systematic Review and Meta-analysis Checklist. 2009

19 **Das G**, Gupta S, Shukla PJ, Jagannath P. Anorectal melanoma: a large clinicopathologic study from India. *Int Surg* 2003; **88**: 21-24 [PMID: 12731727]

20 **Ranjith S**, Muralee M, Sajeed A, Arun PM, Cherian K, Nair CK, Augustine P, Ahamed I. Anorectal melanoma: experience from a tertiary cancer care centre in South India. *Ann R Coll Surg Engl* 2018; **100**: 185-189 [PMID: 29046101 DOI: 10.1308/rcsann.2017.0184]

21 **Thibault C**, Sagar P, Nivatvongs S, Ilstrup DM, Wolff BG. Anorectal melanoma--an incurable disease? *Dis Colon Rectum* 1997; **40**: 661-668 [PMID: 9194459 DOI: 10.1007/BF02140894]

22 **Che X**, Zhao DB, Wu YK, Wang CF, Cai JQ, Shao YF, Zhao P. Anorectal malignant melanomas: retrospective experience with surgical management. *World J Gastroenterol* 2011; **17**: 534-539 [PMID: 21274385 DOI: 10.3748/wjg.v17.i4.534]

23 **Miguel I**, Freire J, Passos MJ, Moreira A. Anorectal malignant melanoma: retrospective analysis of management and outcome in a single Portuguese Institution. *Med Oncol* 2015; **32**: 445 [PMID: 25502089 DOI: 10.1007/s12032-014-0445-2]

24 **Ren M**, Lu Y, Lv J, Shen X, Kong J, Dai B, Kong Y. Prognostic factors in primary anorectal melanoma: a clinicopathological study of 60 cases in China. *Hum Pathol* 2018; **79**: 77-85 [PMID: 29763716 DOI: 10.1016/j.humpath.2018.05.004]

25 **Wanebo HJ**, Woodruff JM, Farr GH, Quan SH. Anorectal melanoma. *Cancer* 1981; **47**: 1891-1900 [PMID: 6164474 DOI: 10.1002/1097-0142(19810401)47:7<1891::aid-cncr2820470730>3.0.co;2-k]

26 **Yeh JJ**, Shia J, Hwu WJ, Busam KJ, Paty PB, Guillem JG, Coit DG, Wong WD, Weiser MR. The role of abdominoperineal resection as surgical therapy for anorectal melanoma. *Ann Surg* 2006; **244**: 1012-1017 [PMID: 17122627 DOI: 10.1097/01.sla.0000225114.56565.f9]

27 **Ross M**, Pezzi C, Pezzi T, Meurer D, Hickey R, Balch C. Patterns of failure in anorectal melanoma. A guide to surgical therapy. *Arch Surg* 1990; **125**: 313-316 [PMID: 2306178 DOI: 10.1001/archsurg.1990.01410150035007]

28 **Hicks CW**, Pappou EP, Magruder JT, Gazer B, Fang S, Wick EC, Gearhart SL, Ahuja N, Efron JE. Clinicopathologic Presentation and Natural History of Anorectal Melanoma: A Case Series of 18 Patients. *JAMA Surg* 2014; **149**: 608-611 [PMID: 24848283 DOI: 10.1001/jamasurg.2013.4643]

29 **Matsuda A**, Miyashita M, Matsumoto S, Takahashi G, Matsutani T, Yamada T, Kishi T, Uchida E. Abdominoperineal resection provides better local control but equivalent overall survival to local excision of anorectal malignant melanoma: a systematic review. *Ann Surg* 2015; **261**: 670-677 [PMID: 25119122 DOI: 10.1097/SLA.0000000000000862]

30 **Peterson CY**, Garcia-Aguilar J. Abdominoperineal resection for rectal cancer. In: Fischer's Mastery of Surgery. 2019: 1841-1852

31 **Smith HG**, Glen J, Turnbull N, Peach H, Board R, Payne M, Gore M, Nugent K, Smith MJF. Less is more: A systematic review and meta-analysis of the outcomes of radical *vs* conservative primary resection in anorectal melanoma. *Eur J Cancer* 2020; **135**: 113-120 [PMID: 32563895 DOI: 10.1016/j.ejca.2020.04.041]

32 **Ishizone S**, Koide N, Karasawa F, Akita N, Muranaka F, Uhara H, Miyagawa S. Surgical treatment for anorectal malignant melanoma: report of five cases and review of 79 Japanese cases. *Int J Colorectal Dis* 2008; **23**: 1257-1262 [PMID: 18633625 DOI: 10.1007/s00384-008-0529-6]

33 **Freeman M**, Laks S. Surveillance imaging for metastasis in high-risk melanoma: importance in individualized patient care and survivorship. *Melanoma Manag* 2019; **6**: MMT12 [PMID: 31236204

DOI: 10.2217/mmt-2019-0003]
34 **Joseph RW**, Elassaiss-Schaap J, Kefford R, Hwu WJ, Wolchok JD, Joshua AM, Ribas A, Hodi FS, Hamid O, Robert C, Daud A, Dronca R, Hersey P, Weber JS, Patnaik A, de Alwis DP, Perrone A, Zhang J, Kang SP, Ebbinghaus S, Anderson KM, Gangadhar TC. Baseline Tumor Size Is an Independent Prognostic Factor for Overall Survival in Patients with Melanoma Treated with Pembrolizumab. *Clin Cancer Res* 2018; **24**: 4960-4967 [PMID: 29685882 DOI: 10.1158/1078-0432.CCR-17-2386]
35 **Long GV**, Flaherty KT, Stroyakovskiy D, Gogas H, Levchenko E, de Braud F, Larkin J, Garbe C, Jouary T, Hauschild A, Chiarion-Sileni V, Lebbe C, Mandalà M, Millward M, Arance A, Bondarenko I, Haanen JBAG, Hansson J, Utikal J, Ferraresi V, Mohr P, Probachai V, Schadendorf D, Nathan P, Robert C, Ribas A, Davies MA, Lane SR, Legos JJ, Mookerjee B, Grob JJ. Dabrafenib plus trametinib *vs* dabrafenib monotherapy in patients with metastatic BRAF V600E/K-mutant melanoma: long-term survival and safety analysis of a phase 3 study. *Ann Oncol* 2017; **28**: 1631-1639 [PMID: 28475671 DOI: 10.1093/annonc/mdx176]
36 **Kaufman H**, Amatruda T, Nemunaitis JJ, Chesney JA, Delman KA, Spitler LE, Collichio FA, Ross MI, Zhang Y, Shilkrut M, Andtbacka RHI. Tumor size and clinical outcomes in melanoma patients (MEL pts) treated with talimogene laherparepvec (T-VEC). *J Clin Oncol* 2015; **33**: 9074 [DOI: 10.1200/jco.2015.33.15_suppl.9074]
37 **Faure M**, Rochigneux P, Olive D, Taix S, Brenot-Rossi I, Gilabert M. Hyperprogressive Disease in Anorectal Melanoma Treated by PD-1 Inhibitors. *Front Immunol* 2018; **9**: 797 [PMID: 29725330 DOI: 10.3389/fimmu.2018.00797]
38 **Cai YT**, Cao LC, Zhu CF, Zhao F, Tian BX, Guo SY. Multiple synchronous anorectal melanomas with different colors: A case report. *World J Clin Cases* 2019; **7**: 1337-1343 [PMID: 31236398 DOI: 10.12998/wjcc.v7.i11.1337]
39 **Yang HM**, Hsiao SJ, Schaeffer DF, Lai C, Remotti HE, Horst D, Mansukhani MM, Horst BA. Identification of recurrent mutational events in anorectal melanoma. *Mod Pathol* 2017; **30**: 286-296 [PMID: 27739435 DOI: 10.1038/modpathol.2016.179]
40 **Pack GT**, Oropeza R. A comparative study of melanoma and epidermoid carcinoma of the anal canal: A review of 20 melanomas and 29 epidermoid carcinomas (1930 to 1965). *Dis Colon Rectum* 1967; **10**: 161-176 [PMID: 6026797 DOI: 10.1007/BF02617173]
41 **Abbas JS**, Karakousis CP, Holyoke ED. Anorectal melanoma: clinical features, recurrence and patient survival. *Int Surg* 1980; **65**: 423-426 [PMID: 7451062]
42 **Ward MW**, Romano G, Nicholls RJ. The surgical treatment of anorectal malignant melanoma. *Br J Surg* 1986; **73**: 68-69 [PMID: 3947881 DOI: 10.1002/bjs.1800730127]
43 **Dodds TJ**, Wilmott JS, Jackett LA, Lo SN, Long GV, Thompson JF, Scolyer RA. Primary anorectal melanoma: clinical, immunohistology and DNA analysis of 43 cases. *Pathology* 2019; **51**: 39-45 [PMID: 30497801 DOI: 10.1016/j.pathol.2018.09.060]
44 **Siegal B**, Cohen D, Jacob ET. Surgical treatment of anorectal melanomas. *Am J Surg* 1983; **146**: 336-338 [PMID: 6614323 DOI: 10.1016/0002-9610(83)90410-5]
45 **Roumen RM**. Anorectal melanoma in The Netherlands: a report of 63 patients. *Eur J Surg Oncol* 1996; **22**: 598-601 [PMID: 9005147 DOI: 10.1016/S0748-7983(96)92346-X]
46 **Nilsson PJ**, Ragnarsson-Olding BK. Importance of clear resection margins in anorectal malignant melanoma. *Br J Surg* 2010; **97**: 98-103 [PMID: 20013935 DOI: 10.1002/bjs.6784]
47 **Podnos YD**, Tsai NC, Smith D, Ellenhorn JD. Factors affecting survival in patients with anal melanoma. *Am Surg* 2006; **72**: 917-920 [PMID: 17058735]
48 **Slingluff CL Jr**, Vollmer RT, Seigler HF. Anorectal melanoma: clinical characteristics and results of surgical management in twenty-four patients. *Surgery* 1990; **107**: 1-9 [PMID: 2296748]
49 **Belli F**, Gallino GF, Lo Vullo S, Mariani L, Poiasina E, Leo E. Melanoma of the anorectal region: the experience of the National Cancer Institute of Milano. *Eur J Surg Oncol* 2009; **35**: 757-762 [PMID: 18602790 DOI: 10.1016/j.ejso.2008.05.001]
50 **Pessaux P**, Pocard M, Elias D, Duvillard P, Avril MF, Zimmerman P, Lasser P. Surgical management of primary anorectal melanoma. *Br J Surg* 2004; **91**: 1183-1187 [PMID: 15449271 DOI: 10.1002/bjs.4592]
51 **Ramakrishnan AS**, Mahajan V, Kannan R. Optimizing local control in anorectal melanoma. *Indian J Cancer* 2008; **45**: 13-19 [PMID: 18453735 DOI: 10.4103/0019-509x.40641]
52 **Homsi J**, Garrett C. Melanoma of the anal canal: a case series. *Dis Colon Rectum* 2007; **50**: 1004-1010 [PMID: 17468984 DOI: 10.1007/s10350-007-0242-5]
53 **Bullard KM**, Tuttle TM, Rothenberger DA, Madoff RD, Baxter NN, Finne CO, Spencer MP. Surgical therapy for anorectal melanoma. *J Am Coll Surg* 2003; **196**: 206-211 [PMID: 12595048 DOI: 10.1016/S1072-7515(02)01538-7]
54 **Yen CI**, Chen HH, Chiang SF, Yeh CY, Chen JS, Hsieh PS, Chiang JM, Tsai WS, Tang R, Changchien CR, Wang JY. Anorectal melanoma: review of 22 consecutive cases. *Hepatogastroenterology* 2013; **60**: 89-93 [PMID: 22829553 DOI: 10.5754/hge12453]
55 **Aytac B**, Adim SB, Yerci O, Yilmazlar T. Anorectal malignant melanomas: experience of Uludag University. *Kaohsiung J Med Sci* 2010; **26**: 658-662 [PMID: 21186014 DOI: 10.1016/S1607-551X(10)70100-5]
56 **Belbaraka R**, Elharroudi T, Ismaili N, Fetohi M, Tijami F, Jalil A, Errihani H. Management of anorectal melanoma: report of 17 cases and literature review. *J Gastrointest Cancer* 2012; **43**: 31-35 [PMID: 20886311 DOI: 10.1007/s12029-010-9216-2]

57 **Nusrath S**, Thammineedi SR, Patnaik SC, Raju KVVN, Pawar S, Goel V, Chavali RN, Murthy S. Anorectal Malignant Melanoma-Defining the Optimal Surgical Treatment and Prognostic Factors. *Indian J Surg Oncol* 2018; **9**: 519-523 [PMID: 30538382 DOI: 10.1007/s13193-018-0791-1]

58 **Sahu A**, Ramaswamy A, Singhal N, Doshi V, Mirani J, Desouza A, Banavali S, Saklani A, Ostwal V. Metastatic anorectal melanomas - An exploratory retrospective analysis on the benefits of systemic therapy *vs* best supportive care in a resource-limited setting from India. *South Asian J Cancer* 2017; **6**: 147-150 [PMID: 29404289 DOI: 10.4103/sajc.sajc_276_16]

World Journal of Gastroenterology

Submit a Manuscript: https://www.f6publishing.com

World J Gastroenterol 2021 January 21; 27(3): 281-293

DOI: 10.3748/wjg.v27.i3.281

ISSN 1007-9327 (print) ISSN 2219-2840 (online)

ORIGINAL ARTICLE

Observational Study

Comparative study on artificial intelligence systems for detecting early esophageal squamous cell carcinoma between narrow-band and white-light imaging

Bing Li, Shi-Lun Cai, Wei-Min Tan, Ji-Chun Li, Ayimukedisi Yalikong, Xiao-Shuang Feng, Hon-Ho Yu, Pin-Xiang Lu, Zhen Feng, Li-Qing Yao, Ping-Hong Zhou, Bo Yan, Yun-Shi Zhong

ORCID number: Bing Li 0000-0001-9802-5860; Shi-Lun Cai 0000-0002-5000-9658; Wei-Min Tan 0000-0001-7677-4772; Ji-Chun Li 0000-0003-4906-8244; Ayimukedisi Yalikong 0000-0002-7328-8354; Xiao-Shuang Feng 0000-0002-7933-3996; Hon-Ho Yu 0000-0002-9580-345X; Pin-Xiang Lu 0000-0001-5941-9584; Zhen Feng 0000-0003-0424-4726; Li-Qing Yao 0000-0001-6900-6791; Ping-Hong Zhou 0000-0002-5434-0540; Bo Yan 0000-0003-0256-9682; Yun-Shi Zhong 0000-0002-3128-3168.

Author contributions: Zhong YS and Yan B conceived the study design; Li B, Cai SL, Tan WM, Li JC, Yalikong A, Yu HH, Lu PX, and Feng Z acquired the data; Li B, Cai SL, Yalikong A, Tan WM, Feng XS, Yao LQ, Zhou PH, and Zhong YS analyzed and interpreted the data; Li B, Tan WM, and Cai SL drafted the manuscript; Zhong YS critically revised the manuscript for important intellectual content; Li B, Cai SL, Tan WM, Li JC, Yalikong A, Feng XS, Yu HH, Lu PX, Feng Z, Yao LQ, Zhou PH, Yan B, and Zhong YS approved the final version of the manuscript; Li B, Cai SL and Tan WM contributed equally to this article.

Supported by National Key R&D

Bing Li, Shi-Lun Cai, Ayimukedisi Yalikong, Li-Qing Yao, Ping-Hong Zhou, Yun-Shi Zhong, Department of Endoscopy Center, Zhongshan Hospital of Fudan University, Shanghai 200032, China

Wei-Min Tan, Ji-Chun Li, Bo Yan, School of Computer Science, Fudan University, Shanghai 200433, China

Xiao-Shuang Feng, Clinical Statistical Center, Shanghai Cancer Center of Fudan University, Shanghai 200032, China

Hon-Ho Yu, Department of Gastroenterology, Kiang Wu Hospital, Macau SAR 999078, China

Pin-Xiang Lu, Zhen Feng, Department of Endoscopy Center, Xuhui Hospital, Zhongshan Hospital of Fudan University, Shanghai 200031, China

Corresponding author: Yun-Shi Zhong, MD, PhD, Professor, Department of Endoscopy Center, Zhongshan Hospital of Fudan University, No. 180 Fenglin Road, Shanghai 200032, China. zhongyunshi@yahoo.com

Abstract

BACKGROUND

Non-magnifying endoscopy with narrow-band imaging (NM-NBI) has been frequently used in routine screening of esophagus squamous cell carcinoma (ESCC). The performance of NBI for screening of early ESCC is, however, significantly affected by operator experience. Artificial intelligence may be a unique approach to compensate for the lack of operator experience.

AIM

To construct a computer-aided detection (CAD) system for application in NM-NBI to identify early ESCC and to compare it with our previously reported CAD system with endoscopic white-light imaging (WLI).

METHODS

A total of 2167 abnormal NM-NBI images of early ESCC and 2568 normal images were collected from three institutions (Zhongshan Hospital of Fudan University,

Program of China, No. 2018YFC1315000, No. 2018YFC1315005, No. 2019YFC1315800, and No. 2019YFC1315802; National Natural Science Foundation of China, No. 81861168036 and No. 81702305; Science and Technology Commission Foundation of Shanghai Municipality, No. 19411951600, and No. 19411951601; Macao SAR Science and Technology Development Foundation, No. 0023/2018/AFJ; and Dawn Program of Shanghai Education Commission, No. 18SG08.

Institutional review board statement: This study was reviewed and approved by the Ethics Committee of Zhongshan Hospital, Fudan University.

Informed consent statement: Patients were not required to give informed consent to the study because the analysis used anonymous clinical data that were obtained after each patient agreed to undergo treatment by written consent.

Conflict-of-interest statement: The authors declare that they have no competing interests.

Data sharing statement: The datasets used and analyzed during the current study are available from the corresponding author on reasonable request.

STROBE statement: The authors have read the STROBE Statement checklist of items, and the manuscript was prepared and revised according to the STROBE Statement-checklist of items.

Open-Access: This article is an open-access article that was selected by an in-house editor and fully peer-reviewed by external reviewers. It is distributed in accordance with the Creative Commons Attribution NonCommercial (CC BY-NC 4.0) license, which permits others to distribute, remix, adapt, build upon this work non-commercially, and license their derivative works

Xuhui Hospital, and Kiang Wu Hospital) as the training dataset, and 316 pairs of images, each pair including images obtained by WLI and NBI (same part), were collected for validation. Twenty endoscopists participated in this study to review the validation images with or without the assistance of the CAD systems. The diagnostic results of the two CAD systems and improvement in diagnostic efficacy of endoscopists were compared in terms of sensitivity, specificity, accuracy, positive predictive value, and negative predictive value.

RESULTS

The area under receiver operating characteristic curve for CAD-NBI was 0.9761. For the validation dataset, the sensitivity, specificity, accuracy, positive predictive value, and negative predictive value of CAD-NBI were 91.0%, 96.7%, 94.3%, 95.3%, and 93.6%, respectively, while those of CAD-WLI were 98.5%, 83.1%, 89.5%, 80.8%, and 98.7%, respectively. CAD-NBI showed superior accuracy and specificity than CAD-WLI ($P = 0.028$ and $P \leq 0.001$, respectively), while CAD-WLI had higher sensitivity than CAD-NBI ($P = 0.006$). By using both CAD-WLI and CAD-NBI, the endoscopists could improve their diagnostic efficacy to the highest level, with accuracy, sensitivity, and specificity of 94.9%, 92.4%, and 96.7%, respectively.

CONCLUSION

The CAD-NBI system for screening early ESCC has higher accuracy and specificity than CAD-WLI. Endoscopists can achieve the best diagnostic efficacy using both CAD-WLI and CAD-NBI.

Key Words: Computer-aided detection; Esophageal squamous cell carcinoma; Endoscopy; Screening; Narrow-band imaging; White-light imaging

©The Author(s) 2021. Published by Baishideng Publishing Group Inc. All rights reserved.

Core Tip: The computer-assisted diagnosis (CAD) system under conventional endoscopic white-light imaging (WLI) for screening of early esophagus squamous cell carcinoma (ESCC) has high accuracy. However, few studies have examined different characteristics of CAD application in WLI and narrow-band imaging (NBI) models. In this study, the CAD system we constructed under the NBI model for screening of early ESCC had higher accuracy and specificity than the CAD-WLI system. Endoscopists could achieve the best diagnostic efficacy by using both CAD-WLI and CAD-NBI. The two CAD systems have different advantages in avoiding missed diagnosis and excessive biopsy, which could help endoscopists, especially those with less experience, in more efficient screening of early ESCC.

Citation: Li B, Cai SL, Tan WM, Li JC, Yalikong A, Feng XS, Yu HH, Lu PX, Feng Z, Yao LQ, Zhou PH, Yan B, Zhong YS. Comparative study on artificial intelligence systems for detecting early esophageal squamous cell carcinoma between narrow-band and white-light imaging. *World J Gastroenterol* 2021; 27(3): 281-293
URL: https://www.wjgnet.com/1007-9327/full/v27/i3/281.htm
DOI: https://dx.doi.org/10.3748/wjg.v27.i3.281

INTRODUCTION

Upper gastrointestinal endoscopy combined with biopsy is the method of choice to diagnose esophagus squamous cell carcinoma (ESCC), and it has been widely adopted in population screening for ESCC[1,2]. However, it is not always easy to identify early-stage ESCC, especially for unexperienced doctors, during examination with white-light imaging (WLI)[3,4]. The narrow-band imaging (NBI) system improves the visualization of microvasculature and mucosal patterns in the alimentary tract[5]. Non-magnifying endoscopy with NBI (NM-NBI) has been used frequently in routine screening examinations with higher accuracy and specificity[6,7]. However, the sensitivity of NBI for screening of mucosal high-grade neoplasia is significantly

on different terms, provided the original work is properly cited and the use is non-commercial. See: http://creativecommons.org/licenses/by-nc/4.0/

Manuscript source: Unsolicited manuscript

Specialty type: Gastroenterology and hepatology

Country/Territory of origin: China

Peer-review report's scientific quality classification

Grade A (Excellent): A
Grade B (Very good): 0
Grade C (Good): C
Grade D (Fair): 0
Grade E (Poor): 0

Received: October 9, 2020
Peer-review started: October 9, 2020
First decision: November 23, 2020
Revised: December 5, 2020
Accepted: December 22, 2020
Article in press: December 22, 2020
Published online: January 21, 2021

P-Reviewer: Kishida Y, Zavras N
S-Editor: Fan JR
L-Editor: Filipodia
P-Editor: Liu JH

different between experienced and less experienced endoscopists[8,9]. Early lesions missed at screening may not be identified until they become more advanced and less amenable to treatment. Thus, the experience of the operator plays a critical role in the screening result for early ESCC.

Artificial intelligence (AI) may be uniquely poised to compensate for the lack of operator experience. Studies have demonstrated the ability of AI to meet or exceed the performance of human experts as a triage or screening tool for gastrointestinal diseases[10,11]. In our previous research, we reported a novel system of computer-aided detection (CAD) to localize and identify early ESCC under conventional endoscopic WLI with sensitivity above 97%[12]. Here, another system of CAD for application in NM-NBI for screening of early ESCC was constructed and validated. More importantly, we compared the effectiveness of the two systems based on WLI or NM-NBI in helping endoscopists to detect early ESCC. On the basis of the results, we can determine which technique is most effective to help endoscopists, *i.e.* whether to use CAD-NBI or CAD-WLI alone or both.

MATERIALS AND METHODS

Study design

This study was performed at the Endoscopy Center of three general hospitals (Zhongshan Hospital of Fudan University, Xuhui Hospital, and Kiang Wu Hospital) in partnership with the School of Computer Science of Fudan University. Patient data were anonymized, and any personal identifying information was excluded. This study was approved by the Institutional Review Board of Zhongshan Hospital, Fudan University (approval No. B2019-141R). All authors had access to the study data and reviewed and approved the final manuscript.

Datasets used for training and validation of the CAD-NBI system

First, we retrospectively obtained esophagoscopic NM-NBI images for the development of the CAD system for NBI images (CAD-NBI system). In the training dataset, a total of 2167 abnormal NM-NBI images of early ESCCs in 235 cases and 2568 normal NM-NBI images in 412 cases were collected between January 2016 and April 2018 from three institutions. Then, we collected 316 pairs of images (133 abnormal and 183 normal), each pair including WLI and NBI at the same location and at the same angle, from 112 consecutive cases. The purpose of establishing this paired image dataset includes: (1) All NBI images are used to test our newly established CAD-NBI system; (2) White light images paired with NBI in the same situation are used to test the CAD system for WLI (CAD-WLI system)[12] that has been reported previously to compare the differences between the two CAD systems; and (3) Endoscopists are asked to review all the images from this validation dataset to evaluate their diagnostic ability with or without the help of these two CAD systems.

The criteria for normal and abnormal images refer to the previous study on CAD for screening of early ESCC from our team[12]. The criteria for choosing normal image data were as follows: (1) The initial endoscopic inspection results for the esophagus were negative; (2) The abovementioned patients had no newly detected lesions until September 2019; and (3) The normal images were confirmed by endoscopists with ≥ 15 years of experience in endoscopy, and all the endoscopists believed that the image is normal. All patients with abnormal endoscopic images underwent endoscopic submucosal dissection procedures, and three gastrointestinal pathologists (two with > 10 years of experience and one with > 15 years of experience) conducted histological assessments in the pathology departments of both centers. Early ESCC includes low-grade and high-grade intraepithelial neoplasia and esophageal cancer (EC) that has invaded mucosal or superficial submucosal layer.

Design and development of the CAD-NBI system

In this study, we consider the esophagus lesions in endoscopic images to be semantic objects. We demonstrate the development and validation of an endoscopist-level CAD-NBI system based on deep learning algorithm for screening esophagus lesions. We propose to use fully convolutional neural network based on Visual Geometry Group model for semantic segmentation, where semantics denote the esophagus lesions. Therefore, the CAD-NBI system is used to predict the location and irregular shape of esophagus lesions, which is helpful for endoscopists to judge the size, area, and location of lesions more effectively.

To obtain an accurate predictor based on limited esophagoscopic images, some

preprocessing is conducted on the esophagoscopic images before training. First, some irrelevant regions for lesion detection, such as black background, are cropped automatically using a simple image processing algorithm developed by us. Second, we randomly flip the esophagoscopic images horizontally and vertically to augment data diversity. Third, for further data augmentation, esophagoscopic images and the corresponding lesion masks are resized to 300 × 300 and randomly cropped to 224 × 224. During training, the network parameters are updated with the initial learning rate of 0.0001 and decayed every 2000 iterations with a decay rate of 0.9 in the staircase mode. During inference, given an esophagoscopic image that the CAD-NBI system has never seen previously, the system outputs the segmentation result of esophagoscopic lesion directly.

Comparison of the improvement of diagnostic capability of endoscopists under CAD-WLI and CAD-NBI

The accuracy of the CAD-NBI system was evaluated by the validation dataset established previously. We invited 20 endoscopists with varying experience from three centers to participate in this study in order to compare diagnostic performance between the CAD system and endoscopists. Moreover, we wanted to know the effectiveness of the two systems, CAD-WLI and CAD-NBI, for the improvement of diagnostic capabilities of endoscopists. Among the endoscopists, four were classified as highly experienced endoscopists who had performed more than 10000 conventional endoscopy examinations and 5000 NBI endoscopy examinations, eight were classified as mid-level endoscopists who had performed more than 5000 conventional endoscopy examinations and 2500 NBI endoscopy examinations, and eight were classified as junior endoscopists who had performed more than 2000 conventional endoscopy examinations and 1000 NBI endoscopy examinations.

To test the effectiveness of the two CAD systems, we designed a four-phase trial. In the first phase, the 20 endoscopists were asked to review every pair image of the validation dataset in digital format on a laptop. All of them were blinded to the histological data and asked to review the esophagoscopic images independently. The CAD-NBI system scanned and analyzed each NM-NBI image of every pair saved in JPEG/PNG format on the hard drive, and the CAD-WLI system did the same for NM-WLI images. In the second phase, after the WLI images had been marked using the CAD-WLI system (NBI images were not marked), we invited these endoscopists to again screen every pair of images in the validation dataset. This action was noteworthy as the review sequence of images was altered randomly by computer to minimize the impact of impression from the last performance in each phase. In the third phase, endoscopists were asked to review every pair of images in the validation dataset once again, after all NBI images were marked by the CAD-NBI system while WLI images were not. In the last phase, the endoscopists completed their final diagnosis for the validation paired images by referring to the results from both CAD-WLI and CAD-NBI systems. Between each two continuous phases, we set the wash-out phase as 1-1-2 mo, respectively. Moreover, these 20 endoscopists were unaware of the performance of the CAD-WLI and CAD-NBI systems. A flowchart depicting the processes used during the study is shown in Figure 1.

Outcome measures

The ability of the CAD-NBI system to identify early ESCC was mathematically assessed by the area under the curve of the receiver operating characteristic curve, and the sensitivity, specificity, accuracy, positive predictive value (PPV), and negative predictive value (NPV) were determined. The accuracy, sensitivity, specificity, PPV, and NPV were also compared between CAD-NBI, CAD-WLI, and the endoscopists.

Statistical analysis

The chi-square test and t test were used wherever applicable. A P value of < 0.05 was considered to be statistically significant. A two-sided McNemar test with a significance level of 0.05 was used to compare differences in accuracy, sensitivity, specificity, PPV, and NPV. All statistical analyses were performed using SPSS version 18.0 (SPSS Inc., Chicago, IL, United States).

RESULTS

The detailed characteristics of the patients and lesions in the validation image dataset

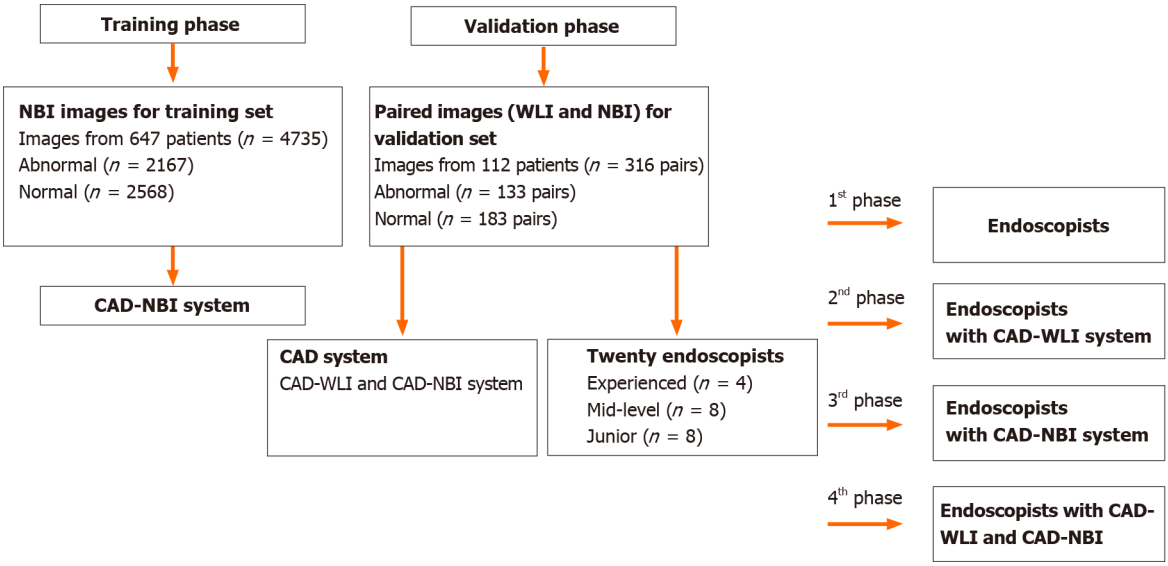


Figure 1 Flowchart of the procedures. CAD: Computer-assisted detection; NBI: Narrow-band imaging; WLI: White -light imaging.

are listed in Table 1.

Performance of the CAD-NBI and CAD-WLI systems

The receiver operating characteristic curve of the CAD-NBI system is shown in Figure 2, and the area under the curve was 0.9761. For 316 NBI images in the validation dataset, the sensitivity, specificity, accuracy, PPV, and NPV of CAD-NBI were 91.0%, 96.7%, 94.3%, 95.3%, and 93.6%, respectively. For 316 WLI images in the validation dataset, CAD-WLI correctly identified 131 of the 133 early ESCC lesions, with sensitivity, specificity, and accuracy of 98.5%, 83.1%, and 89.5%, respectively. The PPV and NPV of the CAD-WLI system were 80.8% and 98.7%, respectively.

Comparison of the two CAD systems (Figure 3) revealed that the accuracy and specificity of CAD-NBI were superior to those of CAD-WLI ($P = 0.028$ and $P \leq 0.001$). However, the sensitivity of the CAD-WLI system was higher than that of the CAD-NBI system ($P = 0.006$). The CAD-WLI and CAD-NBI system recognized and marked the lesion with a blue square in paired images (Figure 4A and B). In addition, when CAD-WLI mistakenly identified the normal mucosa as lesion (blue square) in WLI, CAD-NBI with high specificity could correct it in NBI (Figure 4C and D).

Comparison between CAD systems and the endoscopists

Table 2 compares the performance of the two CAD systems and the endoscopists for diagnosing early ESCC. The overall accuracy, sensitivity, specificity, PPV, and NPV of the 20 endoscopists were 73.9%, 87.7%, 81.9%, 81.7%, and 82.7%, respectively. Apparently, the experienced endoscopists achieved significantly better diagnostic results than the less experienced ones, including mid-level and junior endoscopists. The average accuracy value of the experienced endoscopists for early ESCC was 93.6%, which was similar to that of the CAD-NBI system and higher than that of the CAD-WLI system. CAD-WLI achieved the highest sensitivity (98.5%), whereas its specificity was lower than that of CAD-NBI with the highest value of 96.7% and the average value of all the endoscopists (87.7%).

Improvement after referring to the results from CAD-WLI and CAD-NBI

With the assistance of either CAD-WLI or CAD-NBI, all the three groups of endoscopists showed improvement in accurately diagnosing early ESCC (Figure 5). Table 3 shows the average diagnostic performance of endoscopists in the detection of early ESCC after referring to the results from the CAD-WLI system in the second phase and from the CAD-NBI system in the third phase. Next, we compared the advantages of the two systems in different aspects. The CAD-NBI system helped the endoscopists to achieve higher value than that achieved with the assistance of CAD-WLI system, especially in the mid-level group with a significant difference (85.3% *vs* 88.4%, $P = 0.012$). Experienced and mid-level endoscopists showed no significant differences in their sensitivity for lesions in the two phases, while the CAD-WLI system helped junior endoscopists to achieve higher sensitivity than that achieved

Table 1 Patient and lesion characteristics in the validation image set

Patient characteristics, *n* = 112	Value
Median age, yr (range)	59 (19-86)
Sex, male/female	67/45
Lesion characteristics, *n* = 42	
Median size, mm (range)	23 (9-42)
Location, Ce/Ut/Mt/Lt/Ae	0/3/24/15/0
Pathological diagnosis	
LGIN/HGIN	6/18
Cancer, M/SM1	15/3

Ae: Abdominal esophagus; Ce: Cervical esophagus; HGIN: High-grade intraepithelial neoplasia; LGIN: Low-grade intraepithelial neoplasia; Lt: Lower thoracic esophagus; M: Mucosal; Mt: Middle thoracic esophagus; SM1: Submucosal; Ut: Upper thoracic esophagus.

Table 2 Diagnostic performance of computer-assisted detection systems *vs* endoscopists

	CAD systems		Endoscopists			
	CAD-NBI	CAD-WLI	All, *n* = 20	Experienced, *n* = 4	Mid-level, *n* = 8	Junior, *n* = 8
Sensitivity, % (95%CI)	91.0	98.5	73.9 (68.1-79.7)	94.7 (85.0-100)	73.9 (71.9-75.8)	63.5 (59.7-67.3)
Specificity, % (95%CI)	96.7	83.1	87.7 (84.9-90.5)	92.8 (81.2-100)	83.4 (81.1-85.7)	89.4 (85.0-93.8)
Accuracy, % (95%CI)	94.3	89.5	81.9 (78.9-84.8)	93.6 (89.1-98.1)	79.4 (78.3-80.5)	78.5 (76.6-80.4)
PPV, % (95%CI)	95.3	80.8	81.7 (78.0-85.5)	91.4 (78.0-100)	76.5 (74.2-78.8)	82.2 (76.1-88.2)
NPV, % (95%CI)	93.6	98.7	82.7 (79.2-86.3)	96.4 (90.1-100)	81.5 (80.5-82.4)	77.2 (75.8-78.6)

CAD: Computer-assisted detection; CI: Confidence interval; NBI: Narrow-band imaging; NPV: Negative predictive value; PPV: Positive predictive value; WLI: White-light imaging.

using the CAD-NBI system (83.0% *vs* 77.3%, P = 0.008). In addition, there were no significant differences in the specificity of experienced endoscopists when using CAD-WLI or CAD-NBI. However, a significant improvement in diagnostic specificity was shown by mid-level (85.9% *vs* 92.6%, P = 0.000) and junior endoscopists (88.6% *vs* 94.9%, P = 0.003).

Table 4 shows the average diagnostic performance of endoscopists after referring to the results from both the CAD-WLI and CAD-NBI systems. In the fourth phase, the diagnostic capability of all the endoscopists improved to the highest level, with the accuracy, sensitivity, and specificity of 94.9%, 92.4%, and 96.7%, respectively. The accuracy of junior endoscopists was 92.9%, and it was significantly higher than that in the first (*vs* 78.5%, P = 0.000), second (*vs* 86.2%, P = 0.000), and third (*vs* 87.5%, P = 0.000) phases. The accuracy of mid-level endoscopists was 94.8%, and it was significantly higher than that in the first (*vs* 79.4%, P = 0.000), second (*vs* 85.3%, P = 0.000), and third (*vs* 88.4%, P = 0.000) phases. In the experienced endoscopist group, the average accuracy value was 98.8%, and it was also significantly higher than that in the first (*vs* 93.6%, P = 0.011), second (*vs* 95.5%, P = 0.015), and third (*vs* 96.5%, P = 0.049) phases (Figure 6A). In terms of sensitivity and specificity for lesions, the average values of the mid-level and junior groups also increased to the highest value after using CAD-WLI and CAD-NBI (Figure 6B and C).

DISCUSSION

CAD has been developed to overcome the limitation of less experience of diagnosis in young doctors. A recent study presented an AI system that can surpass human experts in breast cancer prediction[13]. In the field of gastroenterology, several CAD systems have shown excellent diagnostic potential compared with human endoscopists in

Table 3 Comparison of the improvement of endoscopists under computer-assisted detection-white-light imaging and computer-assisted detection-narrow-band imaging

	2nd phase CAD-WLI assistance	3rd phase CAD-NBI assistance	*P* value
Sensitivity, % (95%CI)			
All, *n* = 20	86.4 (83.1-89.6)	83.1 (79.6-86.6)	0.162
Experienced, *n* = 4	96.8 (94.4-99.2)	95.7 (91.8-99.5)	0.454
Mid-level, *n* = 8	84.5 (80.0-89.0)	82.6 (79.4-85.9)	0.435
Junior, *n* = 8	83.0 (79.3-86.6)	77.3 (74.9-79.7)	0.008
Specificity, % (95%CI)			
All, *n* = 20	88.7 (86.5-90.8)	94.4 (93.0-95.8)	0.000
Experienced, *n* = 4	94.5 (87.9-100)	97.2 (93.6-100)	0.310
Mid-level, *n* = 8	85.9 (84.3-87.4)	92.6 (90.7-94.5)	0.000
Junior, *n* = 8	88.6 (85.1-92.1)	94.9 (92.5-97.2)	0.003
Accuracy, % (95%CI)			
All, *n* = 20	87.7 (85.5-89.9)	89.7 (87.8-91.5)	0.156
Experienced, *n* = 4	95.5 (92.4-98.6)	96.5 (93.6-99.4)	0.469
Mid-level, *n* = 8	85.3 (83.1-87.5)	88.4 (87.1-89.7)	0.012
Junior, *n* = 8	86.2 (84.2-88.3)	87.5 (86.0-89.0)	0.261
PPV, % (95%CI)			
All, *n* = 20	84.9 (82.2-87.5)	91.6 (89.7-93.6)	0.000
Experienced, *n* = 4	93.0 (85.1-100)	96.1 (91.4-100)	0.325
Mid-level, *n* = 8	81.3 (79.4-83.2)	89.2 (86.7-91.7)	0.000
Junior, *n* = 8	84.4 (80.5-88.2)	91.8 (88.4-95.2)	0.004
NPV, % (95%CI)			
All, *n* = 20	90.1 (87.9-92.3)	88.7 (86.5-90.9)	0.361
Experienced, *n* = 4	97.7 (96.0-99.3)	96.9 (94.2-99.6)	0.465
Mid-level, *n* = 8	88.5 (85.6-91.4)	88.1 (86.2-89.9)	0.755
Junior, *n* = 8	87.8 (85.6-90.1)	85.2 (83.9-86.5)	0.031

CAD: Computer-assisted detection; CI: Confidence interval; NBI: Narrow-band imaging; NPV: Negative predictive value; PPV: Positive predictive value; WLI: Whit-light imaging.

colorectal polyp classification, determination of the invasion depth of gastric cancer, and identification of small bowel diseases[14-16]. The application of AI in automatically detecting and classifying lesions, especially in the context of medical imaging, is expected to help physicians provide more accurate diagnoses[17].

Squamous cell carcinoma is the predominant histologic subtype of EC in Asia, where the rate of EC is quite high[18]. Several research studies on CAD for improving the screening efficiency for ESCC have been reported. Horie *et al*[19] first evaluated the ability of the CNN to detect EC in endoscopic images of superficial and advanced cancer and achieved a sensitivity of 98%. Zhao *et al*[20] developed a deep learning model based on magnifying NBI images to investigate the automated classification of intrapapillary capillary loops and assist endoscopic diagnosis of early ESCC. In a recent study by Guo *et al*[21], the authors developed a CAD system for real-time automated diagnosis of precancerous lesions and ESCC. In 2019, our team reported a novel system using deep neural network (DNN) to localize and identify early ESCC under endoscopic WLI with high accuracy and sensitivity[12]. Moreover, after referring to the results of DNN-CAD, the average diagnostic ability of the endoscopists improved significantly. However, this CAD system could only identify early ESCC in WLI, and the specificity was only 85.4%, which may lead to unnecessary biopsies. As NBI is also an accurate diagnostic tool for early ESCC, a better CAD system that can be

Table 4 Diagnostic performance of endoscopists in screening of esophagus squamous cell carcinoma after referring to the results from computer-assisted detection-white-light imaging and computer-assisted detection-narrow-band imaging

	Sensitivity, % (95%CI)	Specificity, % (95%CI)	Accuracy, % (95%CI)	PPV, % (95%CI)	NPV, % (95%CI)
All, *n* = 20	92.4 (90.3-94.5)	96.7 (95.7-97.7)	94.9 (93.6-96.1)	95.3 (93.9-96.7)	94.7 (93.2-96.1)
Experienced, *n* = 4	98.5 (96.3-100)	99.1 (97.5-100)	98.8 (98.2-99.4)	98.7 (96.7-100)	98.9 (97.4-100)
Mid-level, *n* = 8	93.2 (91.3-95.1)	96.0 (94.5-97.6)	94.8 (93.7-95.9)	94.5 (92.5-96.6)	95.2 (93.8-96.5)
Junior, *n* = 8	88.5 (86.2-90.8)	96.1 (94.3-97.9)	92.9 (91.2-94.6)	94.3 (91.8-96.8)	92.0 (90.5-93.6)

CI: Confidence interval; NPV: Negative predictive value; PPV: Positive predictive value.

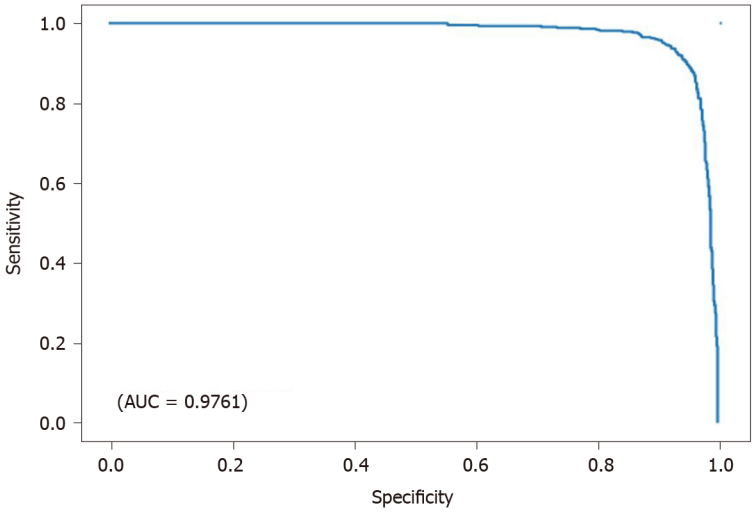


Figure 2 Receiver operating characteristic curve for the test dataset. The area under the curve (AUC) was above 97%.

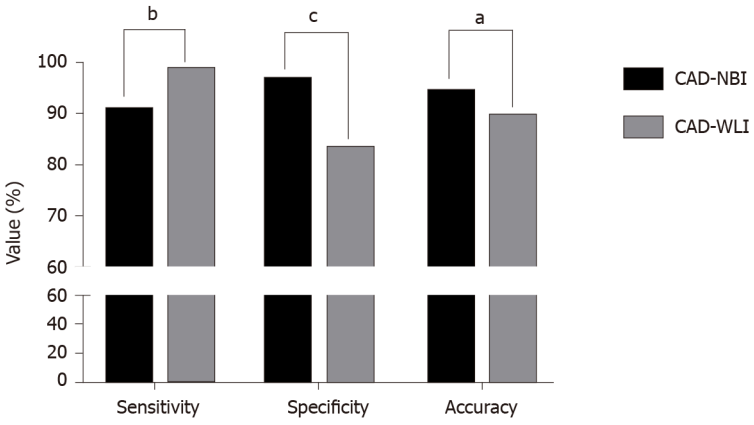


Figure 3 A comparison between the computer-assisted detection-narrow-band imaging and computer-assisted detection-white-light imaging systems in detecting early esophageal squamous cell carcinoma. [a]*P* < 0.05; [b]*P* < 0.01; [c]*P* < 0.001. CAD: Computer-assisted detection; NBI: Narrow-band imaging; WLI: White-light imaging.

used in the NBI model of endoscopy needs to be developed. In addition, a comparative study of AI application in WLI and NBI models is lacking.

In the present study, we developed a CAD system to detect early ESCC under the NBI model of endoscopy. Considering our previously developed CAD system for WLI, we wanted to compare the different characteristics of CAD-NBI and CAD-WLI systems to validate the usefulness of CAD-NBI. Therefore, 316 pairs of images, each pair including WLI and NBI at the same location and at the same angle, were collected from three institutions. The results showed that CAD for NM-NBI images of the esophagus had a good ability to diagnose early ESCC, with an accuracy of 94.3%. For

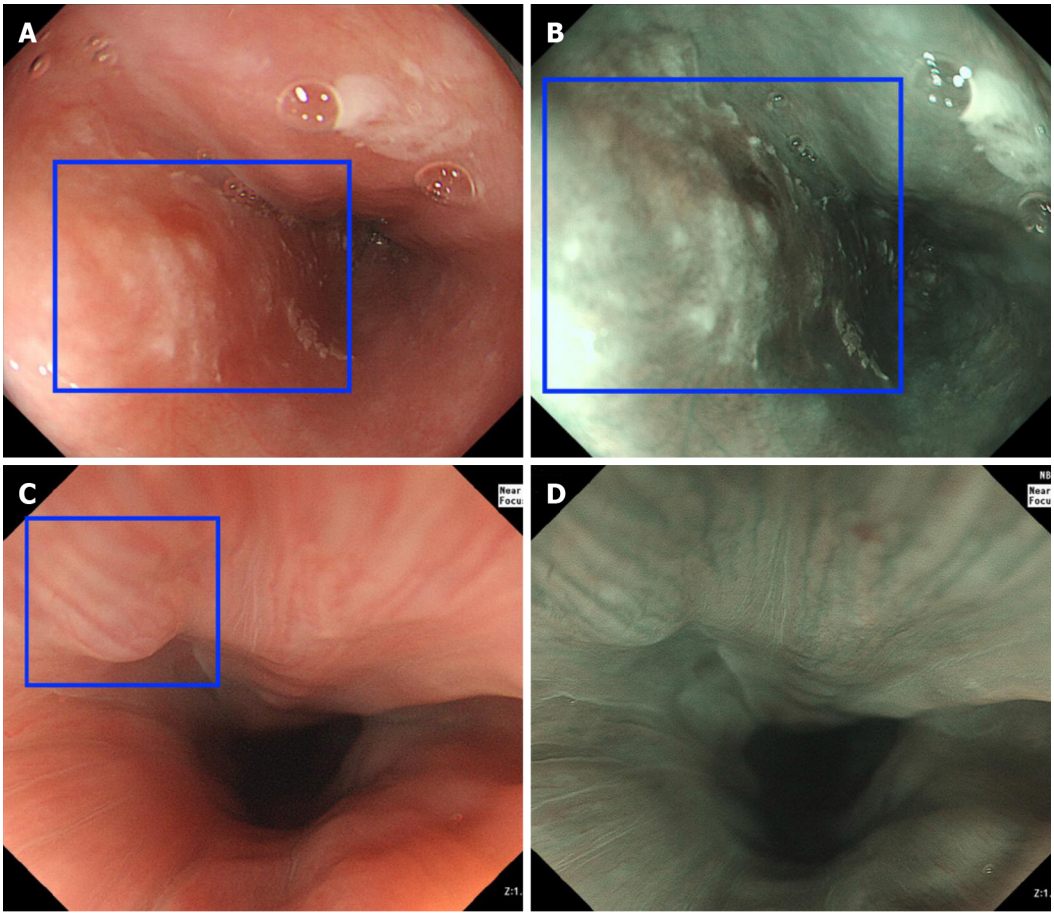


Figure 4 Examples of computer-assisted detection system-diagnosed images. A and B: under white-light imaging (WLI) and narrow-band imaging (NBI), computer-assisted detection (CAD)-WLI and CAD-NBI recognized the esophageal cancer lesion (blue square); C and D: CAD-WLI mistakenly identified the normal mucosa as a lesion (blue square) in WLI, while CAD-NBI corrected it in NBI.

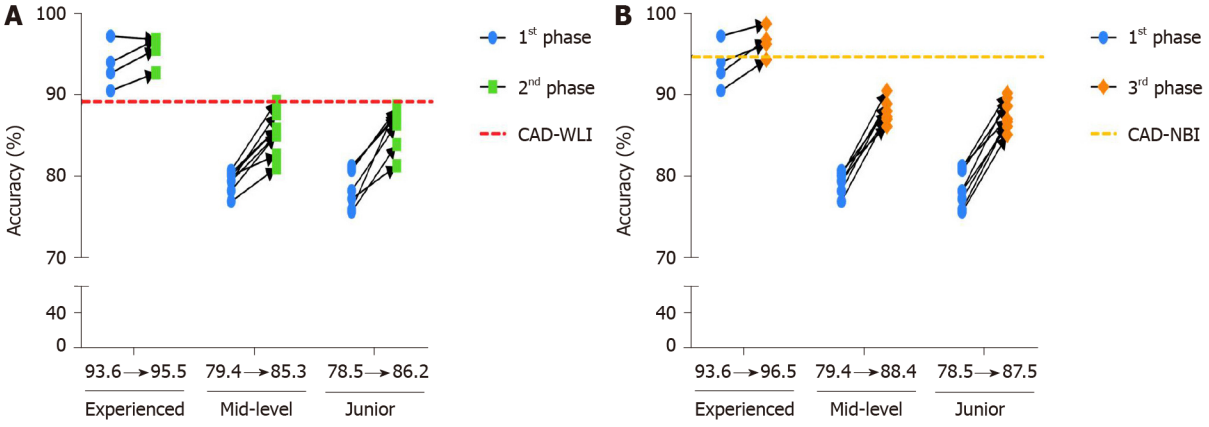


Figure 5 Improved accuracy of diagnosis with the assistance of the two computer-assisted detection systems according to the groups. A: Improvement of endoscopists' accuracy in the second phase with the assistance of computer-assisted detection (CAD)-white-light imaging; B: Improvement of endoscopists' accuracy in the third phase with the assistance of CAD-narrow-band imaging. WLI: White-light imaging.

WLI images in the validation dataset, CAD-WLI correctly identified 131 of the 133 lesions. The diagnostic ability of CAD-WLI for this validation image dataset was similar to that reported in our previous study[12]. Comparison of the two systems showed that CAD-NBI had superior accuracy and specificity compared to CAD-WLI, while the CAD-WLI system had higher sensitivity than the CAD-NBI system. The results showed that CAD-NBI may compensate for the feature of low specificity of CAD-WLI and make the overall accuracy higher, but its own sensitivity still needs to be improved further.

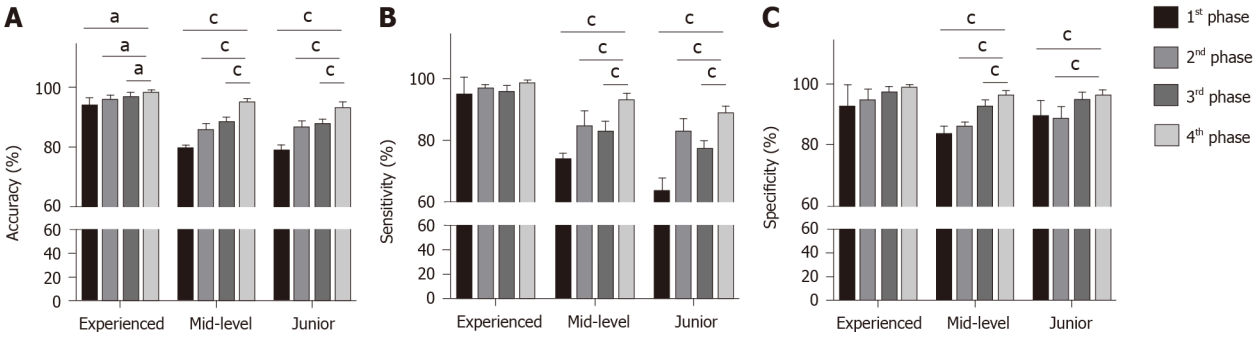


Figure 6 Average diagnostic performance of the three groups of endoscopists in four phases. A: Accuracy; B: Sensitivity; C: Specificity. $^{a}P < 0.05$; $^{c}P < 0.001$.

Endoscopists were asked to review the images from this validation dataset to evaluate their diagnostic ability. In the first phase, the average accuracy value of the experienced endoscopists for early ESCC was 93.6%, which was similar to that of the CAD-NBI system and higher than that of the CAD-WLI system. However, the average diagnostic accuracy of the less experienced endoscopists, including the mid-level (79.4%) and junior groups (78.5%), was lower. Subsequently, the less experienced endoscopists in particular showed improvement in their diagnostic ability with the help of both CAD-WLI in the second phase and CAD-NBI in the third phase. Junior endoscopists made a greater improvement in terms of sensitivity with the CAD-WLI system when their diagnostic specificity was further improved after referring to the results from CAD-NBI. In addition, mid-level endoscopists showed higher values of specificity and accuracy with the assistance of the CAD-NBI system than with the CAD-WLI system. In the fourth phase, by using both CAD-WLI and CAD-NBI, the average values of the three groups increased to the highest value. After simulating the clinical use of the two CAD systems through four different situations, we found that the two systems had different advantages in terms of avoiding missed diagnosis and performing excessive biopsy, and thus, endoscopists could achieve the best diagnostic efficacy by using both CAD-WLI and CAD-NBI.

The sensitivity of a previous system reported by Horie *et al*[19] for the diagnosis of ESCC on WLI and NBI was 72% and 86%, respectively, and our CAD-WLI and CAD-NBI systems provided higher sensitivity of 98.5% and 91.0%, respectively. We have continuously developed the two CAD systems for WLI and NBI based on DNN and conducted for the first time a comparative study to reveal the respective advantages of both systems. The ultimate goal is to integrate the two systems into one to meet the needs of different equipment in a hospital at all levels from different regions. Although Guo *et al*[21] reported that their system for the automated diagnosis of early ESCC under NBI had sensitivity and specificity of 98.04% and 95.03%, respectively, the sensitivity of CAD-WLI and specificity of CAD-NBI were similar to their reported values. In addition, our study invited 20 endoscopists to review the images of the validation dataset with or without the help of the two CAD systems; 10 of the 20 endoscopists (2 mid-level and 8 junior) are from Xuhui Hospital, which is a secondary hospital where the number of patients is much less than that in the tertiary hospital. As secondary hospitals have lower capability to diagnose and treat ESCC than tertiary hospitals, we wanted to assess fully the effectiveness of our CAD system in helping less experienced endoscopists to detect early ESCC, especially doctors in basic hospitals. Our results confirmed that the improvement of diagnosis capability was most pronounced in less experienced endoscopists.

Next, we will explain the reasons for the differences in the diagnostic characteristics of the two CAD systems. CAD-WLI and CAD-NBI are based on different concepts. CAD-WLI uses a bounding box method to detect the location of esophagus lesions in endoscopic images. The detection result of the CAD-WLI system unavoidably includes unnecessary areas such as background regions and parts of other lesions. In contrast, CAD-NBI uses the object semantic segmentation method based on the FCN model, which only outputs the regions of esophagus lesions. Therefore, the accuracy of the CAD-NBI system is higher than that of the CAD-WLI system. In addition, the CAD-NBI system is developed by an end-to-end trainable approach, which is different from the sliding window approach of the CAD-WLI system that densely generates a large number of candidate boxes with different sizes and ratios on a given image. Thus, the CAD-NBI system has the advantage of computational speed when compared with the

CAD-WLI system. Finally, NBI and WLI have different characteristics, which can help us obtain high accuracy, sensitivity, and specificity simultaneously. On the basis of the key observation, we can develop a multichannel DNN to extract and fuse the features of NBI and WLI simultaneously in future studies.

The present study has several limitations. First, the sample size, including images in the training and validation datasets, was small. The low detection rate of early ESCC limits our ability to obtain more images. In addition, our work on CAD for the early detection of ESCC was validated only on still images with a limited scale. Second, the performance of endoscopists in the latter phase may be slightly affected by the image impression of the previous phase. Third, the CAD diagnosis was based on high-quality images, and bias might occur with poor-quality images such as out-of-focus images or blurred images caused by mucus during real-time gastroscopy.

CONCLUSION

In conclusion, we have constructed a CAD system under the NBI model for screening early ESCC, and this CAD-NBI system has higher accuracy and specificity than the CAD-WLI system reported previously. Endoscopists could achieve the best diagnostic efficacy by using both CAD-WLI and CAD-NBI. Therefore, a novel system combining the characteristics of these two systems under WLI and NBI is needed.

ARTICLE HIGHLIGHTS

Research background

Non-magnifying endoscopy with narrow-band imaging (NM-NBI) has been frequently used in routine screening of esophagus squamous cell carcinoma (ESCC). The performance of NBI for screening of early ESCC is, however, significantly affected by operator experience. Artificial intelligence may be a unique approach to compensate for the lack of operator experience.

Research motivation

In our previous research, we reported a novel system of computer-aided detection (CAD) to localize and identify early ESCC under conventional endoscopic white-light imaging (WLI) with sensitivity of above 97%. The construction of another CAD system for application in NM-NBI was the next step in the continuation of our research.

Research objectives

To construct a CAD system for application in NM-NBI to identify early ESCC and compare it with our previously reported CAD system with endoscopic WLI.

Research methods

We collected a total of 2167 abnormal NM-NBI images of early ESCC and 2568 normal images from three institutions (Zhongshan Hospital of Fudan University, Xuhui Hospital, and Kiang Wu Hospital) as the training dataset, and 316 pairs of images, each pair including images obtained with WLI and NBI (same part), were collected for validation. Twenty endoscopists participated in this study to review the validation images with or without the assistance of the CAD systems. The diagnostic results of the two CAD systems and the improvement in the diagnostic efficacy of endoscopists were compared in terms of sensitivity, specificity, accuracy, positive predictive value, and negative predictive value.

Research results

The area under receiver operating characteristic curve for CAD-NBI was 0.9761. For the validation dataset, the sensitivity, specificity, accuracy, positive predictive value, and negative predictive value of CAD-NBI were 91.0%, 96.7%, 94.3%, 95.3%, and 93.6%, respectively, while those of CAD-WLI were 98.5%, 83.1%, 89.5%, 80.8%, and 98.7%, respectively. CAD-NBI showed superior accuracy and specificity than CAD-WLI (P = 0.028 and $P \leq 0.001$, respectively), while CAD-WLI had higher sensitivity than CAD-NBI (P = 0.006). By using both CAD-WLI and CAD-NBI, the endoscopists could improve their diagnostic efficacy to the highest level, with accuracy, sensitivity, and specificity of 94.9%, 92.4%, and 96.7%, respectively.

Research conclusions

The CAD-NBI system for screening early ESCC has higher accuracy and specificity than CAD-WLI. Endoscopists can achieve the best diagnostic efficacy by using both CAD-WLI and CAD-NBI.

Research perspectives

According to the results, the two CAD systems had different advantages in avoiding missed diagnosis and excessive biopsy, which could help endoscopists, especially those with less experience, in screening of early ESCC more efficiently. As the two CAD systems have unique characteristics, we plan to develop a multichannel deep neural network to extract and combine the features of NBI and WLI simultaneously in our future work.

REFERENCES

1 **Wei WQ**, Chen ZF, He YT, Feng H, Hou J, Lin DM, Li XQ, Guo CL, Li SS, Wang GQ, Dong ZW, Abnet CC, Qiao YL. Long-Term Follow-Up of a Community Assignment, One-Time Endoscopic Screening Study of Esophageal Cancer in China. *J Clin Oncol* 2015; **33**: 1951-1957 [PMID: 25940715 DOI: 10.1200/JCO.2014.58.0423]

2 **He Z**, Liu Z, Liu M, Guo C, Xu R, Li F, Liu A, Yang H, Shen L, Wu Q, Duan L, Li X, Zhang C, Pan Y, Cai H, Ke Y. Efficacy of endoscopic screening for esophageal cancer in China (ESECC): design and preliminary results of a population-based randomised controlled trial. *Gut* 2019; **68**: 198-206 [PMID: 29306867 DOI: 10.1136/gutjnl-2017-315520]

3 **Lee YC**, Wang CP, Chen CC, Chiu HM, Ko JY, Lou PJ, Yang TL, Huang HY, Wu MS, Lin JT, Hsiu-Hsi Chen T, Wang HP. Transnasal endoscopy with narrow-band imaging and Lugol staining to screen patients with head and neck cancer whose condition limits oral intubation with standard endoscope (with video). *Gastrointest Endosc* 2009; **69**: 408-417 [PMID: 19019362 DOI: 10.1016/j.gie.2008.05.033]

4 **Morita FH**, Bernardo WM, Ide E, Rocha RS, Aquino JC, Minata MK, Yamazaki K, Marques SB, Sakai P, de Moura EG. Narrow band imaging versus lugol chromoendoscopy to diagnose squamous cell carcinoma of the esophagus: a systematic review and meta-analysis. *BMC Cancer* 2017; **17**: 54 [PMID: 28086818 DOI: 10.1186/s12885-016-3011-9]

5 **Muto M**, Katada C, Sano Y, Yoshida S. Narrow band imaging: a new diagnostic approach to visualize angiogenesis in superficial neoplasia. *Clin Gastroenterol Hepatol* 2005; **3**: S16-S20 [PMID: 16012987 DOI: 10.1016/s1542-3565(05)00262-4]

6 **Nagami Y**, Tominaga K, Machida H, Nakatani M, Kameda N, Sugimori S, Okazaki H, Tanigawa T, Yamagami H, Kubo N, Shiba M, Watanabe K, Watanabe T, Iguchi H, Fujiwara Y, Ohira M, Hirakawa K, Arakawa T. Usefulness of non-magnifying narrow-band imaging in screening of early esophageal squamous cell carcinoma: a prospective comparative study using propensity score matching. *Am J Gastroenterol* 2014; **109**: 845-854 [PMID: 24751580 DOI: 10.1038/ajg.2014.94]

7 **Muto M**, Minashi K, Yano T, Saito Y, Oda I, Nonaka S, Omori T, Sugiura H, Goda K, Kaise M, Inoue H, Ishikawa H, Ochiai A, Shimoda T, Watanabe H, Tajiri H, Saito D. Early detection of superficial squamous cell carcinoma in the head and neck region and esophagus by narrow band imaging: a multicenter randomized controlled trial. *J Clin Oncol* 2010; **28**: 1566-1572 [PMID: 20177025 DOI: 10.1200/JCO.2009.25.4680]

8 **Ishihara R**, Takeuchi Y, Chatani R, Kidu T, Inoue T, Hanaoka N, Yamamoto S, Higashino K, Uedo N, Iishi H, Tatsuta M, Tomita Y, Ishiguro S. Prospective evaluation of narrow-band imaging endoscopy for screening of esophageal squamous mucosal high-grade neoplasia in experienced and less experienced endoscopists. *Dis Esophagus* 2010; **23**: 480-486 [PMID: 20095991 DOI: 10.1111/j.1442-2050.2009.01039.x]

9 **Rodríguez de Santiago E**, Hernanz N, Marcos-Prieto HM, De-Jorge-Turrión MÁ, Barreiro-Alonso E, Rodríguez-Escaja C, Jiménez-Jurado A, Sierra-Morales M, Pérez-Valle I, Machado-Volpato N, García-Prada M, Núñez-Gómez L, Castaño-García A, García García de Paredes A, Peñas B, Vázquez-Sequeiros E, Albillos A. Rate of missed oesophageal cancer at routine endoscopy and survival outcomes: A multicentric cohort study. *United European Gastroenterol J* 2019; **7**: 189-198 [PMID: 31080603 DOI: 10.1177/2050640618811477]

10 **Topol EJ**. High-performance medicine: the convergence of human and artificial intelligence. *Nat Med* 2019; **25**: 44-56 [PMID: 30617339 DOI: 10.1038/s41591-018-0300-7]

11 **Mori Y**, Kudo SE, Misawa M, Saito Y, Ikematsu H, Hotta K, Ohtsuka K, Urushibara F, Kataoka S, Ogawa Y, Maeda Y, Takeda K, Nakamura H, Ichimasa K, Kudo T, Hayashi T, Wakamura K, Ishida F, Inoue H, Itoh H, Oda M, Mori K. Real-Time Use of Artificial Intelligence in Identification of Diminutive Polyps During Colonoscopy: A Prospective Study. *Ann Intern Med* 2018; **169**: 357-366 [PMID: 30105375 DOI: 10.7326/M18-0249]

12 **Cai SL**, Li B, Tan WM, Niu XJ, Yu HH, Yao LQ, Zhou PH, Yan B, Zhong YS. Using a deep learning system in endoscopy for screening of early esophageal squamous cell carcinoma (with video). *Gastrointest Endosc* 2019; **90**: 745-753. e2 [PMID: 31302091 DOI:

10.1016/j.gie.2019.06.044]
13 **McKinney SM**, Sieniek M, Godbole V, Godwin J, Antropova N, Ashrafian H, Back T, Chesus M, Corrado GS, Darzi A, Etemadi M, Garcia-Vicente F, Gilbert FJ, Halling-Brown M, Hassabis D, Jansen S, Karthikesalingam A, Kelly CJ, King D, Ledsam JR, Melnick D, Mostofi H, Peng L, Reicher JJ, Romera-Paredes B, Sidebottom R, Suleyman M, Tse D, Young KC, De Fauw J, Shetty S. International evaluation of an AI system for breast cancer screening. *Nature* 2020; **577**: 89-94 [PMID: 31894144 DOI: 10.1038/s41586-019-1799-6]
14 **Chen PJ**, Lin MC, Lai MJ, Lin JC, Lu HH, Tseng VS. Accurate Classification of Diminutive Colorectal Polyps Using Computer-Aided Analysis. *Gastroenterology* 2018; **154**: 568-575 [PMID: 29042219 DOI: 10.1053/j.gastro.2017.10.010]
15 **Zhu Y**, Wang QC, Xu MD, Zhang Z, Cheng J, Zhong YS, Zhang YQ, Chen WF, Yao LQ, Zhou PH, Li QL. Application of convolutional neural network in the diagnosis of the invasion depth of gastric cancer based on conventional endoscopy. *Gastrointest Endosc* 2019; **89**: 806-815. e1 [PMID: 30452913 DOI: 10.1016/j.gie.2018.11.011]
16 **Ding Z**, Shi H, Zhang H, Meng L, Fan M, Han C, Zhang K, Ming F, Xie X, Liu H, Liu J, Lin R, Hou X. Gastroenterologist-Level Identification of Small-Bowel Diseases and Normal Variants by Capsule Endoscopy Using a Deep-Learning Model. *Gastroenterology* 2019; **157**: 1044-1054. e5 [PMID: 31251929 DOI: 10.1053/j.gastro.2019.06.025]
17 **He J**, Baxter SL, Xu J, Xu J, Zhou X, Zhang K. The practical implementation of artificial intelligence technologies in medicine. *Nat Med* 2019; **25**: 30-36 [PMID: 30617336 DOI: 10.1038/s41591-018-0307-0]
18 **Arnold M**, Soerjomataram I, Ferlay J, Forman D. Global incidence of oesophageal cancer by histological subtype in 2012. *Gut* 2015; **64**: 381-387 [PMID: 25320104 DOI: 10.1136/gutjnl-2014-308124]
19 **Horie Y**, Yoshio T, Aoyama K, Yoshimizu S, Horiuchi Y, Ishiyama A, Hirasawa T, Tsuchida T, Ozawa T, Ishihara S, Kumagai Y, Fujishiro M, Maetani I, Fujisaki J, Tada T. Diagnostic outcomes of esophageal cancer by artificial intelligence using convolutional neural networks. *Gastrointest Endosc* 2019; **89**: 25-32 [PMID: 30120958 DOI: 10.1016/j.gie.2018.07.037]
20 **Zhao YY**, Xue DX, Wang YL, Zhang R, Sun B, Cai YP, Feng H, Cai Y, Xu JM. Computer-assisted diagnosis of early esophageal squamous cell carcinoma using narrow-band imaging magnifying endoscopy. *Endoscopy* 2019; **51**: 333-341 [PMID: 30469155 DOI: 10.1055/a-0756-8754]
21 **Guo L**, Xiao X, Wu C, Zeng X, Zhang Y, Du J, Bai S, Xie J, Zhang Z, Li Y, Wang X, Cheung O, Sharma M, Liu J, Hu B. Real-time automated diagnosis of precancerous lesions and early esophageal squamous cell carcinoma using a deep learning model (with videos). *Gastrointest Endosc* 2020; **91**: 41-51 [PMID: 31445040 DOI: 10.1016/j.gie.2019.08.018]

World Journal of Gastroenterology

Submit a Manuscript: https://www.f6publishing.com

World J Gastroenterol 2021 January 21; 27(3): 294-304

DOI: 10.3748/wjg.v27.i3.294

ISSN 1007-9327 (print) ISSN 2219-2840 (online)

CASE REPORT

Peritoneal dissemination of pancreatic cancer caused by endoscopic ultrasound-guided fine needle aspiration: A case report and literature review

Hideaki Kojima, Minoru Kitago, Eisuke Iwasaki, Yohei Masugi, Yohji Matsusaka, Hiroshi Yagi, Yuta Abe, Yasushi Hasegawa, Shutaro Hori, Masayuki Tanaka, Yutaka Nakano, Yusuke Takemura, Seiichiro Fukuhara, Yoshiyuki Ohara, Michiie Sakamoto, Shigeo Okuda, Yuko Kitagawa

ORCID number: Hideaki Kojima 0000-0003-2449-9726; Minoru Kitago 0000-0002-4909-1199; Eisuke Iwasaki 0000-0001-8010-5117; Yohei Masugi 0000-0002-6952-4043; Yohji Matsusaka 0000-0003-3471-2762; Hiroshi Yagi 0000-0002-9897-8108; Yuta Abe 0000-0003-4746-0584; Yasushi Hasegawa 0000-0002-4990-0419; Shutaro Hori 0000-0001-9213-0758; Masayuki Tanaka 0000-0003-0335-3912; Yutaka Nakano 0000-0003-3228-3474; Yusuke Takemura 0000-0003-3791-9902; Seiichiro Fukuhara 0000-0003-1675-5670; Yoshiyuki Ohara 0000-0002-0013-8726; Michiie Sakamoto 0000-0003-3507-7369; Shigeo Okuda 0000-0002-7874-9527; Yuko Kitagawa 0000-0001-6469-2155.

Author contributions: Kojima H interpreted the patient data based on the case notes and drafted the manuscript; Kitago M performed the surgery and supervised the manuscript; Masugi Y, Ohara Y, and Sakamoto M evaluated the pathological findings; all other members equally contributed to the medical treatment.

Informed consent statement: Written informed consent was obtained from the patient for the publication of this case report and

Hideaki Kojima, Minoru Kitago, Hiroshi Yagi, Yuta Abe, Yasushi Hasegawa, Shutaro Hori, Masayuki Tanaka, Yutaka Nakano, Yusuke Takemura, Yuko Kitagawa, Department of Surgery, Keio University School of Medicine, Tokyo 160-8582, Japan

Eisuke Iwasaki, Seiichiro Fukuhara, Division of Gastroenterology and Hepatology, Department of Internal Medicine, Keio University School of Medicine, Tokyo 160-8582, Japan

Yohei Masugi, Yoshiyuki Ohara, Michiie Sakamoto, Department of Pathology, Keio University School of Medicine, Tokyo 160-8582, Japan

Yohji Matsusaka, Shigeo Okuda, Department of Radiology, Keio University School of Medicine, Tokyo 160-8582, Japan

Corresponding author: Minoru Kitago, PhD, Reader (Associate Professor), Department of Surgery, Keio University School of Medicine, 35 Shinanomachi, Shinjuku-ku, Tokyo 160-8582, Japan. dragonpegasus@keio.jp

Abstract

BACKGROUND

Endoscopic ultrasound-guided fine needle aspiration (EUS-FNA) is a biopsy technique widely used to diagnose pancreatic tumors because of its high sensitivity and specificity. Although needle-tract seeding caused by EUS-FNA has been recently reported, dissemination of pancreatic cancer cells is generally considered to be a rare complication that does not affect patient prognosis. However, the frequency of dissemination and needle-tract seeding appears to have been underestimated. We present a case of peritoneal dissemination of pancreatic cancer due to preoperative EUS-FNA.

CASE SUMMARY

An 81-year-old man was referred to the Department of Surgery of our hospital in Japan owing to the detection of a pancreatic mass on computed tomography during medical screening. Trans-gastric EUS-FNA revealed that the mass was an adenocarcinoma; hence laparoscopic distal pancreatectomy with lympha-denectomy was performed. No intraoperative peritoneal dissemination and liver

metastasis were visually detected, and pelvic lavage cytology was negative for carcinoma cells. The postoperative surgical specimen was negative for carcinoma cells at the dissected margin and the cut end margin; however, pathological findings revealed adenocarcinoma cells on the peritoneal surface proximal to the needle puncture site, and the cells were suspected to be disseminated *via* EUS-FNA. Hence, the patient received adjuvant therapy with S-1 (tegafur, gimeracil, and oteracil potassium); however, computed tomography performed 5 mo after surgery revealed liver metastasis and cancerous peritonitis. The patient received palliative therapy and died 8 mo after the operation.

CONCLUSION
The indications of EUS-FNA should be carefully considered to avoid iatrogenic dissemination, especially for cancers in the pancreatic body or tail.

Key Words: Case report; Pancreatic carcinoma; Endoscopic ultrasound-guided fine needle aspiration; Peritoneal dissemination; Cancerous peritonitis; Biopsy

©The Author(s) 2021. Published by Baishideng Publishing Group Inc. All rights reserved.

Core Tip: Along with the development of preoperative chemotherapy, there is an increasing need for tissue sample collection using endoscopic ultrasound-guided fine needle aspiration (EUS-FNA). Peritoneal dissemination and needle-tract seeding caused by EUS-FNA were previously considered rare events with minimal prognostic impact. However, we experienced a case of peritoneal dissemination of pancreatic cancer—secondary to EUS-FNA—that markedly affected postoperative survival. We provide suggestions for the use of EUS-FNA along with a review of literature.

Citation: Kojima H, Kitago M, Iwasaki E, Masugi Y, Matsusaka Y, Yagi H, Abe Y, Hasegawa Y, Hori S, Tanaka M, Nakano Y, Takemura Y, Fukuhara S, Ohara Y, Sakamoto M, Okuda S, Kitagawa Y. Peritoneal dissemination of pancreatic cancer caused by endoscopic ultrasound-guided fine needle aspiration: A case report and literature review. *World J Gastroenterol* 2021; 27(3): 294-304
URL: https://www.wjgnet.com/1007-9327/full/v27/i3/294.htm
DOI: https://dx.doi.org/10.3748/wjg.v27.i3.294

INTRODUCTION

Endoscopic ultrasound-guided fine needle aspiration (EUS-FNA) is a type of biopsy procedure to collect tissue from mass lesions or body fluid inside and outside the gastrointestinal tract wall. It was first clinically used for pancreatic cancer in 1992 by Vilmann *et al*[1] and has been widely used for the qualitative diagnosis of pancreatic tumors, as it has a high sensitivity of 85%-92% and a high specificity of 96%-98% for the diagnosis of pancreatic cancer[2,3]. The main indications of EUS-FNA are the differentiation of benign and malignant tumors, acquisition of histological evidence for introducing chemotherapy and selecting an appropriate drug regimen, and diagnosis of cancer progression. Considering recently developed therapies, such as neoadjuvant chemotherapy and chemoradiotherapy for pancreatic cancer, the need for collecting tissue samples *via* EUS-FNA will increase in the future[4-6]. EUS-FNA is a relatively safe method with few complications[7,8]. The incidence rate of complications is approximately 1%-2%, and complications mainly include abdominal pain, pancreatitis, hematoma, bleeding, fever, and abdominal discomfort. Although peritoneal dissemination and needle-tract seeding are rare events among the limited complications, they are an issue because they can influence patient prognosis. In this regard, previous studies concluded that EUS-FNA does not affect postoperative survival or peritoneal recurrence[9-11]. However, cases of dissemination or needle-tract seeding caused by EUS-FNA have been recently reported, with most cases being intra-gastric wall metastases due to needle tract seeding; peritoneal dissemination is rare[9,12-31]. Herein, we report a case of peritoneal dissemination of pancreatic cancer that was revealed to be caused by preoperative EUS-FNA based on pathological findings

the accompanying images.

Conflict-of-interest statement: The authors declare that they have no competing interests.

CARE Checklist (2016) statement: The guidelines of the "CARE Checklist-2016: Information for writing a case report" have been adopted by the authors.

Open-Access: This article is an open-access article that was selected by an in-house editor and fully peer-reviewed by external reviewers. It is distributed in accordance with the Creative Commons Attribution NonCommercial (CC BY-NC 4.0) license, which permits others to distribute, remix, adapt, build upon this work non-commercially, and license their derivative works on different terms, provided the original work is properly cited and the use is non-commercial. See: http://creativecommons.org/Licenses/by-nc/4.0/

Manuscript source: Unsolicited manuscript

Specialty type: Gastroenterology and hepatology

Country/Territory of origin: Japan

Peer-review report's scientific quality classification
Grade A (Excellent): A, A
Grade B (Very good): B, B
Grade C (Good): 0
Grade D (Fair): 0
Grade E (Poor): 0

Received: December 5, 2020
Peer-review started: December 5, 2020
First decision: December 17, 2020
Revised: December 28, 2020
Accepted: January 6, 2021
Article in press: January 6, 2021
Published online: January 21, 2021

P-Reviewer: Geramizadeh B, Krishna SG, Park WS
S-Editor: Zhang H
L-Editor: A
P-Editor: Ma YJ

and resulted in radical disease progression, along with a review of the literature.

CASE PRESENTATION

Chief complaints

An 81-year-old man was found to have a 16-mm hypodense mass lesion at the pancreatic tail region as well as dilation of the main pancreatic duct on undergoing computed tomography (CT) performed during the course of an annual medical check-up in Japan. The patient was then referred to the Department of Surgery for further examination and treatment.

History of present illness

The patient did not have any specific subjective or objective symptoms.

History of past illness

The patient had a history of diabetes.

Personal and family history

There was no family history of malignant tumors.

Physical examination

No jaundice or palpable masses were observed.

Laboratory examinations

A blood test revealed normal protein levels, including carbohydrate antigen 19-9 (15 U/mL; normal range, 0-37 U/mL), carcinoembryonic antigen (1.7 ng/mL; normal, < 5 ng/mL), s-pancreas-1 antigen (11 U/mL; normal, < 30 U/mL), duke pancreatic monoclonal antigen type 2 (< 25 U/mL; normal, < 150 U/mL), and elastase-1 (40 ng/dL; normal, < 300 ng/dL).

Imaging examinations

Contrast-enhanced CT of the chest, abdomen, and pelvis and magnetic resonance cholangiopancreatography revealed a pancreatic mass at the pancreatic tail region with a prolonged contrast effect, as well as dilation of the main pancreatic duct (Figure 1A and B). Positron emission tomography-CT (PET-CT) revealed abnormal accumulation of fluorodeoxyglucose in the same lesion (Figure 1C). These findings were strongly suspected to be pancreatic cancer and associated obstructive pancreatitis; however, there remained a possibility that the tumor was benign, such as mass-forming pancreatitis or autoimmune pancreatitis.

FURTHER DIAGNOSTIC WORK-UP

Hence, trans-gastric EUS-FNA was performed with a 22-gauge needle to obtain a qualitative diagnosis by an experienced gastroenterologist. During the procedure, the needle passed four times through the gastric wall. Tumor tissue was then successfully collected, with no early complications (Figure 1D). The pathological findings indicated a diagnosis of adenocarcinoma (Figure 2A). PET-CT and contrast-enhanced CT scans showed no evidence of distant metastasis, no infiltration into the anterior or posterior adipose tissue, and no involvement of the major arteries (celiac axis, superior mesenteric artery, common hepatic artery) or veins (superior mesenteric vein, portal vein) in the tumor. The preoperative diagnosis was pancreatic invasive ductal adenocarcinoma, cT1c, cN0, and cM0 cStage IA, per both the 7th edition of the Japanese Pancreas Society classification (JPS 7th ed) and the 8th edition of the Union for International Cancer Control (UICC 8th ed). After establishing the diagnosis, laparoscopic distal pancreatectomy with lymphadenectomy was performed. No intra-operative peritoneal dissemination and liver metastasis were visually observed, and pelvic lavage cytology was negative for carcinoma cells (P0, CY0). The pancreatic tumor did not invade the surrounding organs or adipose tissue, which was confirmed by intra-operative ultrasound examination of the pancreas. The operation was successfully performed as planned without exposing the tumor during surgery. The patient had an uneventful postoperative recovery and was discharged on

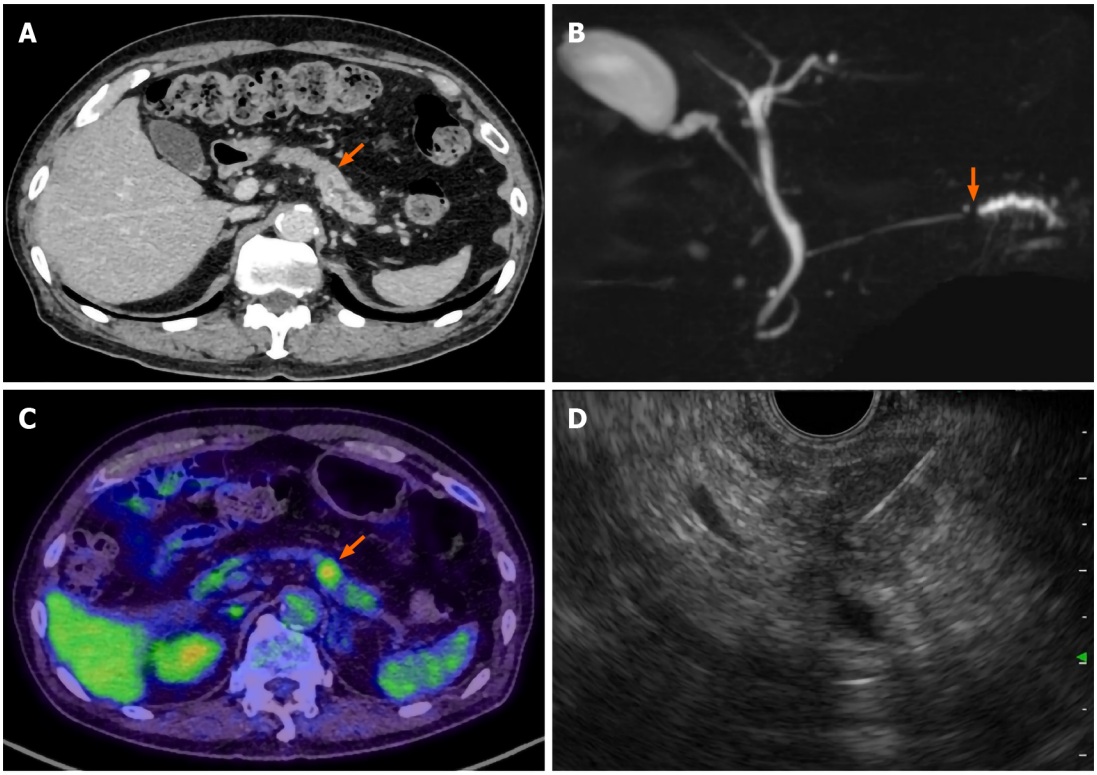


Figure 1 Pre-operative imaging findings. A: Contrast-enhanced computed tomography (CT) scan showing a hypodense mass lesion (arrow) in the pancreatic tail region as well as dilation of the main pancreatic duct; B: Magnetic resonance cholangiopancreatography showing obstruction (arrow) and dilation of the main pancreatic duct; C: Positron emission tomography-CT scan showing the high uptake (arrow) of fluorodeoxyglucose by the pancreatic tail mass; D: Endoscopic ultrasound-guided fine needle aspiration performed using a 22-gauge needle through the posterior gastric wall.

postoperative day 13. The final pathological findings revealed that the dissected and cut end margins were negative for carcinoma cells. The tumor was observed to be a poorly circumscribed whitish mass that was located within the pancreatic parenchyma, and direct infiltration into the anterior and posterior adipose tissues was not observed (Figure 2B). There were two areas of peritoneal thickening with reddish and whitish appearance at a distance from the main tumor site, where a trabecular fibrotic scar associated with peritoneal surface hemorrhage owing to needle puncture *via* EUS-FNA was observed under a high-power view (Figure 2B, E and F). In this area, small aggregates of tumor cells were observed that were similar to those of the main tumor, indicating that these tumor cells were disseminated *via* EUS-FNA from the main lesion (Figure 2D, G and H).

FINAL DIAGNOSIS

The final diagnosis was Pt, TS1 (13 × 12 × 10 mm), infiltrative, ductal adenocarcinoma, pT1c, int, INFc, ly1, v3, ne1, mpd0, pS0, pCHX, pDUX, pPVsp0, pAsp0, pPL0, pPCM0, pDPM0, N1a (1/36, #11p), M1 (P), pStage IV (JPS 7th ed) and pT1c, pN1, and pM1 pStage IV (UICC 8th ed).

TREATMENT

Accordingly, the patient underwent adjuvant therapy with S-1 (tegafur, gimeracil, and oteracil potassium). However, a CT scan of the chest, abdomen, and pelvis obtained 5 mo after the operation revealed liver metastasis and cancerous peritonitis (Figure 3). The patient was offered a more effective chemotherapy regimen for recurrent pancreatic cancer; however, he did not want further treatment.

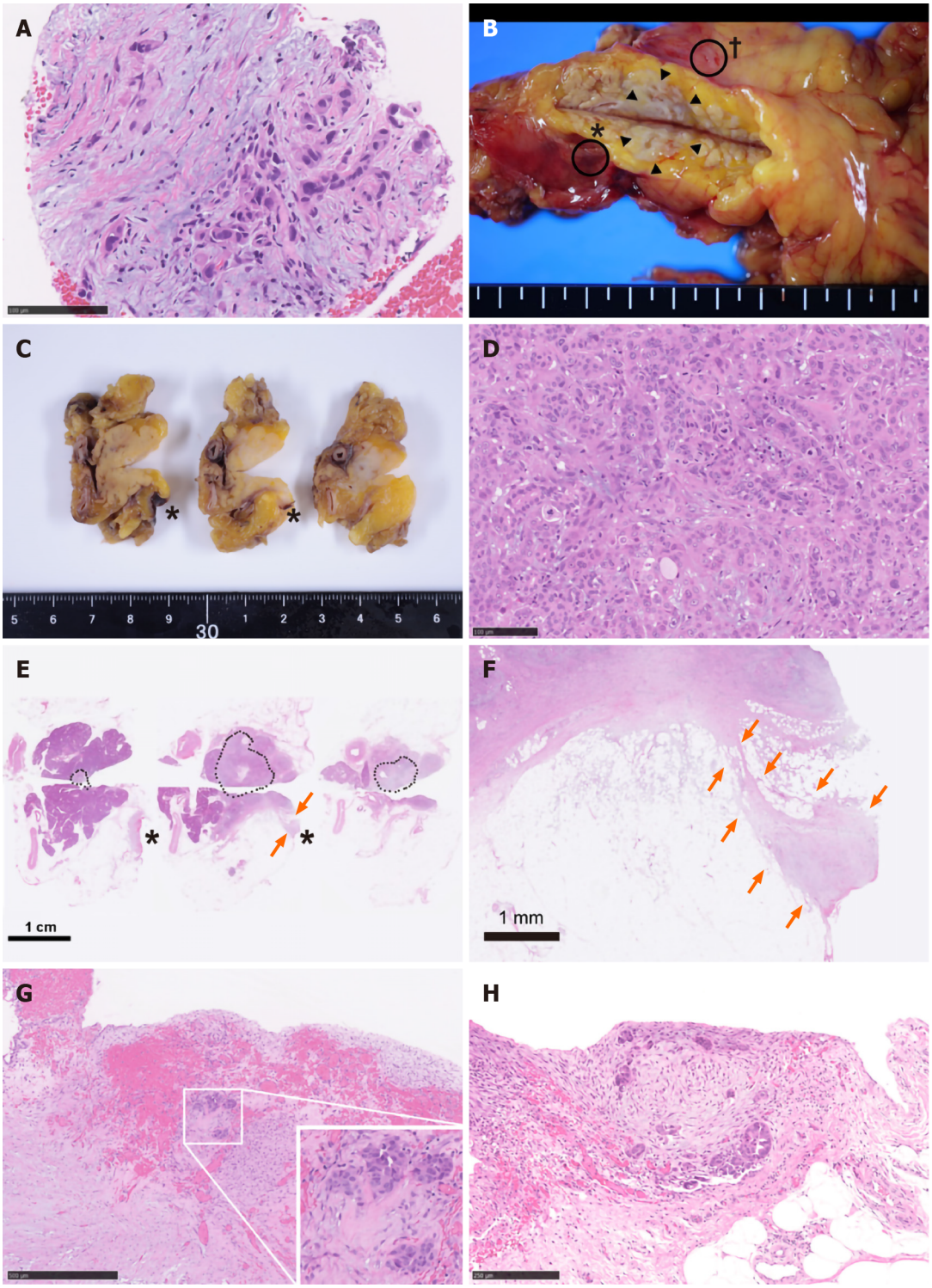


Figure 2 Pathological findings. A: Specimens obtained *via* endoscopic ultrasound-guided fine needle aspiration (EUS-FNA) biopsy. Atypical cells with enlarged and hyperchromatic nuclei infiltrating the fibrous stroma are visible; B: A fresh gross image of the resected pancreas: a poorly circumscribed whitish tumor mass (arrowheads) is observed within pancreas parenchyma at the cut surface. Two areas of peritoneal thickening with reddish (asterisk) and whitish (dagger) appearance are observed at a distance from the tumor site; C: The cut surface of the formalin-fixed specimen: the peritoneal side is on the right, and the retroperitoneal side on the left; D: Histological image of the main tumor: the tumor is predominantly composed of poorly differentiated carcinoma cells with ill-defined ductular structures; E: A loupe image correspondence to the macroscopic image observed in panel C: the area surrounded by black dots is the main tumor lesion. A trabecular fibrotic scar (arrows) associated with peritoneal surface hemorrhage (asterisks) is observed; F: A low-power view of the fibrotic scar (arrows in E) possibly due to the needle tract injected during EUS-FNA; G: A high-magnification image of hemorrhagic peritoneum (asterisks in B, C, and E) proximal to the fibrotic scar. In this area (considered to be the needle puncture site), small aggregates of tumor cells (inset) are embedded in the fibrotic stroma; H: A high-power microscopic view of the whitish thickened peritoneum (dagger in B). Disseminated tumor cells focally forming the ductular structures are seen on the surface of the serosa.

OUTCOME AND FOLLOW-UP

He received palliative therapy and died 8 mo after the operation.

DISCUSSION

Peritoneal dissemination or needle-tract seeding *via* EUS-FNA is an issue because it impairs patient survival. However, the frequency of dissemination is extremely low. Moreover, several studies have evaluated the long-term prognosis of patients with pancreatic cancer; the results showed that EUS-FNA was not associated with recurrence in the gastric or peritoneal wall or with overall survival of patients who underwent resection for pancreatic cancer[9-11]. Similar to the results of previous studies, Yane *et al*[32] reported that EUS-FNA does not affect recurrence-free survival and overall survival. However, the authors also mentioned non-negligible effects of needle-tract seeding after EUS-FNA as 6 of 176 (3.4%) patients had recurrences in the intra-gastric wall[32]. Furthermore, some researchers have indicated that EUS-FNA might promote distant metastasis by blood dissemination and puncture dissemination. Levy *et al*[33] analyzed cell-free DNA (cfDNA) before and after EUS-FNA of pancreatic adenocarcinoma to assess the risk of the distant metastasis due to EUS-FNA. cfDNA is the nuclear material from a tumor that disseminates into the bloodstream (tumoremia); it has been developed a useful biomarker for various tumors (including pancreatic cancer) to predict the therapeutic response and prognosis[34,35]. Levy *et al*[33] reported an insignificant increase in the plasma concentration of cfDNA and increased detection of *KRAS* mutations in cfDNA after EUS-FNA. Additionally, a significant number of new distant metastases were detected in patients with tumoremia. Although the study was a preliminary evaluation with only a small number of patients, the findings suggest that EUS-FNA might contribute to increased distant metastases. Accordingly, we are planning to evaluate cfDNA in preserved plasma from the case presented in this report.

Considering the findings of these studies, the frequency of dissemination and needle-tract seeding due to EUS-FNA appears to have been underestimated. There are several possible causes of underestimation, as clarified in the previously reported 24 cases including the present case (Table 1). First, upper endoscopy is not performed, and EUS-FNA puncture sites are not examined if patients have no symptoms. Second, the needle tract could be also resected with the main tumor lesion; hence, dissemination does not tend to be evaluated. Third, peritoneal dissemination may be unlikely in cases of pancreatic head tumors, because there is no space between the pancreatic head and the duodenum. Finally, it is difficult to distinguish between procedure-related dissemination and disease progression *via* imaging. These reasons may explain why most cases reported needle-tract seeding into the intra-gastric wall and not the peritoneal wall, and there was no case of the primary tumor being in the pancreatic head. From a prognostic point of view, additional gastrectomy seemed to be effective for cases of intra-gastric wall recurrence[17,29,30]; therefore, the puncture site should be regularly investigated postoperatively, and surgical intervention should be considered in cases of local recurrence. In contrast, some cases develop inoperative short-term recurrences[25], as observed in the current case. Therefore, the indications for a trans-gastric biopsy from the pancreatic body and tail should be carefully considered before being performed. Cumulative case reports and a large prospective cohort study are needed to clarify the frequency of procedure-related dissemination and its effect on long-term outcomes.

To the best of our knowledge, the current case is the first report in which peritoneal dissemination associated with EUS-FNA was pathologically proven by using a post-operative specimen. In the current case, some small peritoneal disseminations were observed that were discontinuous from the main lesion. Similar pathological findings and dismal prognoses have been observed in cases of intra-pancreatic metastasis or multi-centric carcinogenesis[36,37]. Therefore, if a small cancerous lesion is observed within the pancreatic parenchyma, it needs to be differentiated from needle tract seeding. Unlike previous reports that state that preoperative EUS-FNA does not affect the prognosis, the current patient showed aggressive disease progression. Although the liver metastasis might be explained by the high degree of pathological vascular invasion, it is clinically unusual to present with such acute cancerous peritonitis when the intra-operative cytology results were negative for carcinoma cells. In addition to the pathological findings, the unusual disease progression is also consistent with EUS-FNA-related dissemination.

Table 1 Clinical features of 24 previous cases of dissemination after endoscopic ultrasound-guided fine needle aspiration

No	Author [ref.], year	Primary lesion					EUS-FNA		Recurrence				
		Diagnosis	size, mm	Location	Initial therapy	Cystic lesion	Puncture site	Passes, *n*	Interval from EUS-FNA, mo	Location	size, mm	Treatment	Outcomes
1	Hirooka *et al*[12], 2003	IPMC	20	Pb	DP+LG	(+)	Trans-gastric		0	G/Wserosa	7		Died 25 mo after surgery
2	Paquin *et al*[13], 2005	IPMC	8	Pt	DP	(+)	Trans-gastric	5	21	G/W	30	Palliative Chemotherapy	Died 12 mo after diagnosis
3	Ahmed *et al*[14], 2011	PDAC		Pb	MPAdj gefinitiveRadiation	(+)	Trans-gastric	multiple	48	G/W	45	TG	Died of another malignancy
4	Chong *et al*[15], 2011	IDC	28	Pt	DP	(+)	Trans-gastric	2	26	G/W	40		
5	Katanuma *et al*[16], 2012	IDC	20	Pb	DP	(-)	Trans-gastric	4	22	G/W			
6	Ngamruengphong *et al*[9], 2013	IDC		Pb, Pt	Subtotal PancreatomyRadiation	(+)	Trans-gastric	3	27	G/W			
7	Ngamruengphong *et al*[9], 2013	IDC	40	Pt	DP+LGAdj Chemoradiation	(+)	Trans-gastric	3	26	G/W			
8	Sakurada *et al*[17], 2015	Adeno-squamous	25	Pb	DP	(-)	Trans-gastric		19	G/W	20	LG	No recurrence after 16 mo follow-up
9	Tomonari *et al*[18], 2015	IDC	20	Pb	DPAdj S-1	(-)	Trans-gastric	2	28	G/W	32	Subtotal Gastrectomy	
10	Minaga *et al*[19], 2015	IDC	20	Pt	DP	(-)	Trans-gastric	3	8	G/W	12	LG	
11	Hirohito *et al*[20], 2015	IDC	20	Pb	GEM⇒S-1	(-)	Trans-gastric	4	9	G/W	16	Palliative Chemotherapy	Died 11 mo after diagnosis
12	Yamauchi *et al*[21], 2016	IDC	25	Pb	DP	(-)	Trans-gastric	1	23	G/W	30	LG	
13	Iida *et al*[22], 2016	IDC			DP	(-)	Trans-gastric	3	6	G/W	18	DGAdj S-1	Recurrence after 21 mo follow-up
14	Kita *et al*[23], 2016	IDC		Pb, Pt	Radiation	(-)	Trans-gastric	2	7	G/W			
15	Minaga *et al*[24], 2016	IDC	10	Pb	DP	(-)	Trans-gastric		24	G/W	30		
16	Yamabe *et al*[25], 2016	IPMC	30	Pb	GEM	(+)	Trans-gastric		3	G/W	24	Palliative Chemotherapy	Died 26 months after diagnosis
17	Yasumoto *et al*[26], 2018	IDC	10	Pb	DPAdj S-1	(-)	Trans-gastric		22	G/W		LG	
19	Sakamoto *et al*[27], 2018	IDC	38	Pt	DPAdj S-1+Gem	(-)	Trans-gastric	2	24	G/W	20	LG	

18	Matsumoto *et al*[28], 2018	IDC	25	Pb	Chemotherapy	(-)	Trans-gastric	3	8	G/W		DP+LG	
20	Matsui *et al*[29], 2019	IDC	15	Pb	DPPartial Gx	(-)	Trans-gastric	4	0	G/Wserosa		Adj S-1	Recurrence 6 mo after surgery; Died 18 mo after surgery
21	Matsui *et al*[29], 2019	IDC	15	Pb	DP+LG	(-)	Trans-gastric	1	0	G/Wserosa		Adj S-1	No recurrence after 18 mo follow-up
22	Sato *et al*[30], 2020	IDC	25	Pb	DPAdj S-1	(-)	Trans-gastric	2	25	G/W	23	LG	No recurrence after 5 mo follow-up
23	Yamaguchi *et al*[31], 2020	SPN	60	Pb	DP	(+)	Trans-gastric	4	60	G/W	40	DG	
24	Current case	IDC	16	Pb	DP	(-)	Trans-gastric	4	0	Peritoneum			Cancerous peritonitis and liver metastasis 5 mo after surgeryDied 8 mo after surgery

EUS-FNA: Endoscopic ultrasound-guided fine needle aspiration; IDC: Invasive ductal carcinoma; IPMC: Intraductal papillary mucinous carcinoma; SPN: Solid-pseudopapillary neoplasm; Pb: Pancreatic body; Pt: Pancreatic tail; DP: Distal pancreatectomy; MP: Middle pancreatectomy; LG: Local gastrectomy; DG: Distal gastrectomy; TG: Total gastrectomy; Adj: Adjuvant; S-1: Tegafur, gineracil, oteracil potassium; GEM: Gemcitabine hydrochloride; G/W: Gastric wall.

EUS-FNA is widely used when it is difficult to distinguish between benign and malignant tumors *via* imaging, because it helps to avoid unnecessary surgery. In addition, EUS-FNA is recommended for both resectable cases and unresectable advanced cases because a histological diagnosis is needed to select an appropriate drug regimen for neoadjuvant chemotherapy or palliative chemotherapy. However, it is not always necessary to obtain a definitive preoperative pathological diagnosis when the tumor is strongly suspected to be pancreatic cancer and when up-front surgery has been already planned.

This case highlights the importance of recognizing the risk of disease dissemination associated with EUS-FNA. Thorough discussion should be conducted on individual cases prior to performing EUS-FNA.

CONCLUSION

The indications for EUS-FNA should be thoroughly discussed with radiologists and endoscopists to avoid iatrogenic dissemination, especially for cancers in the pancreatic body or tail. In addition, careful observation is required not only of the surgical site but also of the puncture site.

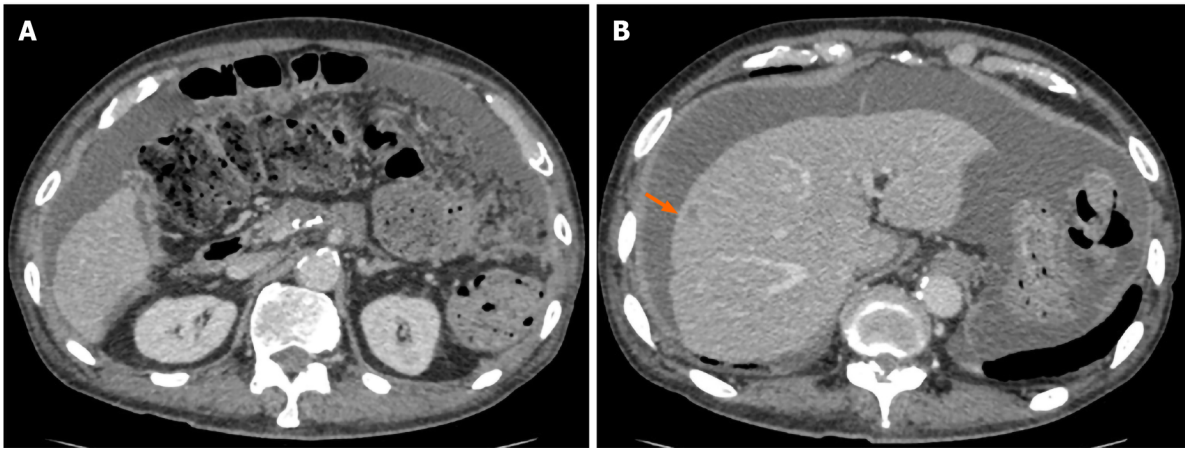


Figure 3 Computed tomography obtained 5 mo after surgery. An ascites associated with cancerous peritonitis and liver metastasis (arrow) was observed.

ACKNOWLEDGEMENTS

We would like to thank Kazumasa Fukuda, a staff member of the Department of Surgery at Keio University School of Medicine, for her help in preparing this manuscript.

REFERENCES

1 **Vilmann P**, Jacobsen GK, Henriksen FW, Hancke S. Endoscopic ultrasonography with guided fine needle aspiration biopsy in pancreatic disease. *Gastrointest Endosc* 1992; **38**: 172-173 [PMID: 1568614 DOI: 10.1016/s0016-5107(92)70385-x]

2 **Hewitt MJ**, McPhail MJ, Possamai L, Dhar A, Vlavianos P, Monahan KJ. EUS-guided FNA for diagnosis of solid pancreatic neoplasms: a meta-analysis. *Gastrointest Endosc* 2012; **75**: 319-331 [PMID: 22248600 DOI: 10.1016/j.gie.2011.08.049]

3 **Puli SR**, Bechtold ML, Buxbaum JL, Eloubeidi MA. How good is endoscopic ultrasound-guided fine-needle aspiration in diagnosing the correct etiology for a solid pancreatic mass? *Pancreas* 2013; **42**: 20-26 [PMID: 23254913 DOI: 10.1097/MPA.0b013e3182546e79]

4 **Motoi F**, Kosuge T, Ueno H, Yamaue H, Satoi S, Sho M, Honda G, Matsumoto I, Wada K, Furuse J, Matsuyama Y, Unno M; Study Group of Preoperative Therapy for Pancreatic Cancer (Prep) and Japanese Study Group of Adjuvant Therapy for Pancreatic cancer (JSAP). Randomized phase II/III trial of neoadjuvant chemotherapy with gemcitabine and S-1 versus upfront surgery for resectable pancreatic cancer (Prep-02/JSAP05). *Jpn J Clin Oncol* 2019; **49**: 190-194 [PMID: 30608598 DOI: 10.1093/jjco/hyy190]

5 **Endo Y**, Kitago M, Aiura K, Shinoda M, Yagi H, Abe Y, Oshima G, Hori S, Nakano Y, Itano O, Fukada J, Masugi Y, Kitagawa Y. Efficacy and safety of preoperative 5-fluorouracil, cisplatin, and mitomycin C in combination with radiotherapy in patients with resectable and borderline resectable pancreatic cancer: a long-term follow-up study. *World J Surg Oncol* 2019; **17**: 145 [PMID: 31420046 DOI: 10.1186/s12957-019-1687-4]

6 **Fujii-Nishimura Y**, Nishiyama R, Kitago M, Masugi Y, Ueno A, Aiura K, Kawachi S, Kawaida M, Abe Y, Shinoda M, Itano O, Tanimoto A, Sakamoto M, Kitagawa Y. Two Cases of Pathological Complete Response to Neoadjuvant Chemoradiation Therapy in Pancreatic Cancer. *Keio J Med* 2015; **64**: 26-31 [PMID: 26118369 DOI: 10.2302/kjm.2014-0014-CR]

7 **Yamao K**, Sawaki A, Mizuno N, Shimizu Y, Yatabe Y, Koshikawa T. Endoscopic ultrasound-guided fine-needle aspiration biopsy (EUS-FNAB): past, present, and future. *J Gastroenterol* 2005; **40**: 1013-1023 [PMID: 16322944 DOI: 10.1007/s00535-005-1717-6]

8 **Jenssen C**, Alvarez-Sánchez MV, Napoléon B, Faiss S. Diagnostic endoscopic ultrasonography: assessment of safety and prevention of complications. *World J Gastroenterol* 2012; **18**: 4659-4676 [PMID: 23002335 DOI: 10.3748/wjg.v18.i34.4659]

9 **Ngamruengphong S**, Xu C, Woodward TA, Raimondo M, Stauffer JA, Asbun HJ, Wallace MB. Risk of gastric or peritoneal recurrence, and long-term outcomes, following pancreatic cancer resection with preoperative endosonographically guided fine needle aspiration. *Endoscopy* 2013; **45**: 619-626 [PMID: 23881804 DOI: 10.1055/s-0033-1344216]

10 **Ngamruengphong S**, Swanson KM, Shah ND, Wallace MB. Preoperative endoscopic ultrasound-guided fine needle aspiration does not impair survival of patients with resected pancreatic cancer. *Gut* 2015; **64**: 1105-1110 [PMID: 25575893 DOI: 10.1136/gutjnl-2014-307475]

11 **Tsutsumi H**, Hara K, Mizuno N, Hijioka S, Imaoka H, Tajika M, Tanaka T, Ishihara M, Yoshimura

K, Shimizu Y, Niwa Y, Sasaki Y, Yamao K. Clinical impact of preoperative endoscopic ultrasound-guided fine-needle aspiration for pancreatic ductal adenocarcinoma. *Endosc Ultrasound* 2016; **5**: 94-100 [PMID: 27080607 DOI: 10.4103/2303-9027.180472]

12 **Hirooka Y**, Goto H, Itoh A, Hashimoto S, Niwa K, Ishikawa H, Okada N, Itoh T, Kawashima H. Case of intraductal papillary mucinous tumor in which endosonography-guided fine-needle aspiration biopsy caused dissemination. *J Gastroenterol Hepatol* 2003; **18**: 1323-1324 [PMID: 14535994 DOI: 10.1046/j.1440-1746.2003.03040.x]

13 **Paquin SC**, Gariépy G, Lepanto L, Bourdages R, Raymond G, Sahai AV. A first report of tumor seeding because of EUS-guided FNA of a pancreatic adenocarcinoma. *Gastrointest Endosc* 2005; **61**: 610-611 [PMID: 15812422 DOI: 10.1016/s0016-5107(05)00082-9]

14 **Ahmed K**, Sussman JJ, Wang J, Schmulewitz N. A case of EUS-guided FNA-related pancreatic cancer metastasis to the stomach. *Gastrointest Endosc* 2011; **74**: 231-233 [PMID: 21168837 DOI: 10.1016/j.gie.2010.10.008]

15 **Chong A**, Venugopal K, Segarajasingam D, Lisewski D. Tumor seeding after EUS-guided FNA of pancreatic tail neoplasia. *Gastrointest Endosc* 2011; **74**: 933-935 [PMID: 21951481 DOI: 10.1016/j.gie.2010.10.020]

16 **Katanuma A**, Maguchi H, Hashigo S, Kaneko M, Kin T, Yane K, Kato R, Kato S, Harada R, Osanai M, Takahashi K, Shinohara T, Itoi T. Tumor seeding after endoscopic ultrasound-guided fine-needle aspiration of cancer in the body of the pancreas. *Endoscopy* 2012; **44** Suppl 2 UCTN: E160-E161 [PMID: 22622721 DOI: 10.1055/s-0031-1291716]

17 **Sakurada A**, Hayashi T, Ono M, Ishiwatari H, Ogino J, Kimura Y, Kato J. A case of curatively resected gastric wall implantation of pancreatic cancer caused by endoscopic ultrasound-guided fine-needle aspiration. *Endoscopy* 2015; **47** Suppl 1 UCTN: E198-E199 [PMID: 26062146 DOI: 10.1055/s-0034-1377592]

18 **Tomonari A**, Katanuma A, Matsumori T, Yamazaki H, Sano I, Minami R, Sen-yo M, Ikarashi S, Kin T, Yane K, Takahashi K, Shinohara T, Maguchi H. Resected tumor seeding in stomach wall due to endoscopic ultrasonography-guided fine needle aspiration of pancreatic adenocarcinoma. *World J Gastroenterol* 2015; **21**: 8458-8461 [PMID: 26217099 DOI: 10.3748/wjg.v21.i27.8458]

19 **Minaga K**, Kitano M, Yamashita Y. Surgically resected needle tract seeding following endoscopic ultrasound-guided fine-needle aspiration in pancreatic cancer. *J Hepatobiliary Pancreat Sci* 2015; **22**: 708-709 [PMID: 26084566 DOI: 10.1002/jhbp.269]

20 **Naruse H**, Yamato H, Yamamoto Y, Hatanaka K, Yamamoto K, Horimoto M, Matsuda K, Yamanashi K, Kudou K, Shimoyama N. An autopsy-confirmed case of needle tract seeding of pancreatic cancer following EUS-guided FNA. *Gastroenterol Endosc* 2015; **57**: 1616-1622 [DOI: 10.11280/gee.57.1616]

21 **Yamauchi J**, Kobayashi S, Miyazaki K, Ajiki T, Tsuchihara K, Ishiyama S. A case of curative resection of needle tract seeding after EUS-guided fine needle aspiration for pancreatic body cancer. *J Jpn Surg Assoc* 2016; **77**: 2994-2999 [DOI: 10.3919/jjsa.77.2994]

22 **Iida T**, Adachi T, Ohe Y, Nakagaki S, Yabana T, Kondo Y, Nakase H. Re-recurrence after distal gastrectomy for recurrence caused by needle tract seeding during endoscopic ultrasound-guided fine-needle aspiration of a pancreatic adenocarcinoma. *Endoscopy* 2016; **48**: E304-E305 [PMID: 27669534 DOI: 10.1055/s-0042-116431]

23 **Kita E**, Yamaguchi T, Sudo K. A case of needle tract seeding after EUS-guided FNA in pancreatic cancer, detected by serial positron emission tomography/CT. *Gastrointest Endosc* 2016; **84**: 869-870 [PMID: 26853299 DOI: 10.1016/j.gie.2016.01.060]

24 **Minaga K**, Kitano M, Enoki E, Kashida H, Kudo M. Needle-Tract Seeding on the Proximal Gastric Wall After EUS-Guided Fine-Needle Aspiration of a Pancreatic Mass. *Am J Gastroenterol* 2016; **111**: 1515 [PMID: 27808133 DOI: 10.1038/ajg.2016.307]

25 **Yamabe A**, Irisawa A, Shibukawa G, Hoshi K, Fujisawa M, Igarashi R, Sato A, Maki T, Hojo H. Rare condition of needle tract seeding after EUS-guided FNA for intraductal papillary mucinous carcinoma. *Endosc Int Open* 2016; **4**: E756-E758 [PMID: 27556091 DOI: 10.1055/s-0042-107072]

26 **Yasumoto M**, Okabe Y, Ishikawa H, Kisaki J, Akiba J, Naito Y, Ishida Y, Ushijima T, Tsuruta O, Torimura T. A case of gastric wall implantation caused by EUS-FNA 22 months after pancreatic cancer resection. *Endosc Ultrasound* 2018; **7**: 64-66 [PMID: 29451172 DOI: 10.4103/eus.eus_58_17]

27 **Sakamoto U**, Fukuba N, Ishihara S, Sumi S, Okada M, Sonoyama H, Ohshima N, Moriyama I, Kawashima K, Kinoshita Y. Postoperative recurrence from tract seeding after use of EUS-FNA for preoperative diagnosis of cancer in pancreatic tail. *Clin J Gastroenterol* 2018; **11**: 200-205 [PMID: 29392646 DOI: 10.1007/s12328-018-0822-z]

28 **Matsumoto K**, Kato H, Tanaka N, Okada H. Preoperative Detection of Tumor Seeding after Endoscopic Ultrasonography-guided Fine Needle Aspiration for Pancreatic Cancer. *Intern Med* 2018; **57**: 1797-1798 [PMID: 29434140 DOI: 10.2169/internalmedicine.0321-17]

29 **Matsui T**, Nishikawa K, Yukimoto H, Katsuta K, Nakamura Y, Tanaka S, Oiwa M, Nakahashi H, Shomi Y, Haruki Y, Taniguchi K, Shimomura M, Isaji S. Needle tract seeding following endoscopic ultrasound-guided fine-needle aspiration for pancreatic cancer: a report of two cases. *World J Surg Oncol* 2019; **17**: 134 [PMID: 31382964 DOI: 10.1186/s12957-019-1681-x]

30 **Sato N**, Takano S, Yoshitomi H, Furukawa K, Takayashiki T, Kuboki S, Suzuki D, Sakai N, Kagawa S, Mishima T, Nakadai E, Mikata R, Kato N, Ohtsuka M. Needle tract seeding recurrence of pancreatic cancer in the gastric wall with paragastric lymph node metastasis after endoscopic ultrasound-guided fine needle aspiration followed by pancreatectomy: a case report and literature

review. *BMC Gastroenterol* 2020; **20**: 13 [PMID: 31941458 DOI: 10.1186/s12876-020-1159-x]

31 **Yamaguchi H**, Morisaka H, Sano K, Nagata K, Ryozawa S, Okamoto K, Ichikawa T. Seeding of a Tumor in the Gastric Wall after Endoscopic Ultrasound-guided Fine-needle Aspiration of Solid Pseudopapillary Neoplasm of the Pancreas. *Intern Med* 2020; **59**: 779-782 [PMID: 31787691 DOI: 10.2169/internalmedicine.3244-19]

32 **Yane K**, Kuwatani M, Yoshida M, Goto T, Matsumoto R, Ihara H, Okuda T, Taya Y, Ehira N, Kudo T, Adachi T, Eto K, Onodera M, Sano I, Nojima M, Katanuma A. Non-negligible rate of needle tract seeding after endoscopic ultrasound-guided fine-needle aspiration for patients undergoing distal pancreatectomy for pancreatic cancer. *Dig Endosc* 2020; **32**: 801-811 [PMID: 31876309 DOI: 10.1111/den.13615]

33 **Levy MJ**, Kipp BR, Milosevic D, Schneider AR, Voss JS, Avula R, Kerr SE, Henry MR, Highsmith E Jr, Liu MC, Gleeson FC. Analysis of Cell-Free DNA to Assess Risk of Tumoremia Following Endoscopic Ultrasound Fine-Needle Aspiration of Pancreatic Adenocarcinomas. *Clin Gastroenterol Hepatol* 2018; **16**: 1632-1640. e1 [PMID: 29526691 DOI: 10.1016/j.cgh.2018.02.048]

34 **Shinozaki M**, O'Day SJ, Kitago M, Amersi F, Kuo C, Kim J, Wang HJ, Hoon DS. Utility of circulating B-RAF DNA mutation in serum for monitoring melanoma patients receiving biochemotherapy. *Clin Cancer Res* 2007; **13**: 2068-2074 [PMID: 17404088 DOI: 10.1158/1078-0432.CCR-06-2120]

35 **Nakano Y**, Kitago M, Matsuda S, Nakamura Y, Fujita Y, Imai S, Shinoda M, Yagi H, Abe Y, Hibi T, Fujii-Nishimura Y, Takeuchi A, Endo Y, Itano O, Kitagawa Y. KRAS mutations in cell-free DNA from preoperative and postoperative sera as a pancreatic cancer marker: a retrospective study. *Br J Cancer* 2018; **118**: 662-669 [PMID: 29360815 DOI: 10.1038/bjc.2017.479]

36 **Fujita Y**, Kitago M, Masugi Y, Itano O, Shinoda M, Abe Y, Hibi T, Yagi H, Fujii-Nishimura Y, Sakamoto M, Kitagawa Y. Two cases of pancreatic ductal adenocarcinoma with intrapancreatic metastasis. *World J Gastroenterol* 2016; **22**: 9222-9228 [PMID: 27895409 DOI: 10.3748/wjg.v22.i41.9222]

37 **Fujita Y**, Matsuda S, Sasaki Y, Masugi Y, Kitago M, Yagi H, Abe Y, Shinoda M, Tokino T, Sakamoto M, Kitagawa Y. Pathogenesis of multiple pancreatic cancers involves multicentric carcinogenesis and intrapancreatic metastasis. *Cancer Sci* 2020; **111**: 739-748 [PMID: 31799787 DOI: 10.1111/cas.14268]

Published by **Baishideng Publishing Group Inc**
7041 Koll Center Parkway, Suite 160, Pleasanton, CA 94566, USA
Telephone: +1-925-3991568
E-mail: bpgoffice@wjgnet.com
Help Desk: https://www.f6publishing.com/helpdesk
https://www.wjgnet.com

© 2021 Baishideng Publishing Group Inc. All rights reserved.

ISSN 1007-9327 (print)
ISSN 2219-2840 (online)

World Journal of *Gastroenterology*

World J Gastroenterol 2021 January 28; 27(4): 305-376



Published by Baishideng Publishing Group Inc

World Journal of Gastroenterology

Contents

Weekly Volume 27 Number 4 January 28, 2021

MINIREVIEWS

305 Pleiotropy within gene variants associated with nonalcoholic fatty liver disease and traits of the hematopoietic system

Pirola CJ, Salatino A, Sookoian S

ORIGINAL ARTICLE

Retrospective Study

321 Preoperative maximal voluntary ventilation, hemoglobin, albumin, lymphocytes and platelets predict postoperative survival in esophageal squamous cell carcinoma

Hu SJ, Zhao XK, Song X, Lei LL, Han WL, Xu RH, Wang R, Zhou FY, Wang L, Wang LD

336 Clinic-pathological features of metabolic associated fatty liver disease with hepatitis B virus infection

Wang MF, Wan B, Wu YL, Huang JF, Zhu YY, Li YB

Clinical Trials Study

345 Effect of remote ischemic preconditioning among donors and recipients following pediatric liver transplantation: A randomized clinical trial

Qi B, Wang XQ, Pan ST, Li PY, Chen LK, Xia Q, Yang LQ, Yu WF

Prospective Study

358 Could saline irrigation clear all residual common bile duct stones after lithotripsy? A self-controlled prospective cohort study

Lin YY, Wang YD, Yue P, Zhang XZ, Leung JW, Jiao PP, Yang M, Wang HP, Bai B, Liu Y, Zhang JD, Chen HB, Meng WB, Li X

CASE REPORT

371 Duplication of the common bile duct manifesting as recurrent pyogenic cholangitis: A case report

Hwang JS, Ko SW

World Journal of Gastroenterology

Weekly Volume 27 Number 4 January 28, 2021

Contents

ABOUT COVER

Wei-Dong Tong, MD, PhD, Professor, Chief, Department of Gastric & Colorectal Surgery, Daping Hospital, Army Medical University, No. 10 Changjiang Zhi Lu, Daping, Chongqing 400042, China. vdtong@163.com

AIMS AND SCOPE

The primary aim of *World Journal of Gastroenterology* (*WJG*, *World J Gastroenterol*) is to provide scholars and readers from various fields of gastroenterology and hepatology with a platform to publish high-quality basic and clinical research articles and communicate their research findings online. *WJG* mainly publishes articles reporting research results and findings obtained in the field of gastroenterology and hepatology and covering a wide range of topics including gastroenterology, hepatology, gastrointestinal endoscopy, gastrointestinal surgery, gastrointestinal oncology, and pediatric gastroenterology.

INDEXING/ABSTRACTING

The *WJG* is now indexed in Current Contents®/Clinical Medicine, Science Citation Index Expanded (also known as SciSearch®), Journal Citation Reports®, Index Medicus, MEDLINE, PubMed, PubMed Central, and Scopus. The 2020 edition of Journal Citation Report® cites the 2019 impact factor (IF) for *WJG* as 3.665; IF without journal self cites: 3.534; 5-year IF: 4.048; Ranking: 35 among 88 journals in gastroenterology and hepatology; and Quartile category: Q2. The *WJG*'s CiteScore for 2019 is 7.1 and Scopus CiteScore rank 2019: Gastroenterology is 17/137.

RESPONSIBLE EDITORS FOR THIS ISSUE

Production Editor: *Ji-Hong Liu*; **Production Department Director:** *Yun-Xiaojian Wu*; **Editorial Office Director:** *Ze-Mao Gong*.

NAME OF JOURNAL
World Journal of Gastroenterology

ISSN
ISSN 1007-9327 (print) ISSN 2219-2840 (online)

LAUNCH DATE
October 1, 1995

FREQUENCY
Weekly

EDITORS-IN-CHIEF
Andrzej S Tarnawski, Subrata Ghosh

EDITORIAL BOARD MEMBERS
http://www.wjgnet.com/1007-9327/editorialboard.htm

PUBLICATION DATE
January 28, 2021

COPYRIGHT
© 2021 Baishideng Publishing Group Inc

INSTRUCTIONS TO AUTHORS
https://www.wjgnet.com/bpg/gerinfo/204

GUIDELINES FOR ETHICS DOCUMENTS
https://www.wjgnet.com/bpg/GerInfo/287

GUIDELINES FOR NON-NATIVE SPEAKERS OF ENGLISH
https://www.wjgnet.com/bpg/gerinfo/240

PUBLICATION ETHICS
https://www.wjgnet.com/bpg/GerInfo/288

PUBLICATION MISCONDUCT
https://www.wjgnet.com/bpg/gerinfo/208

ARTICLE PROCESSING CHARGE
https://www.wjgnet.com/bpg/gerinfo/242

STEPS FOR SUBMITTING MANUSCRIPTS
https://www.wjgnet.com/bpg/GerInfo/239

ONLINE SUBMISSION
https://www.f6publishing.com

© 2021 Baishideng Publishing Group Inc. All rights reserved. 7041 Koll Center Parkway, Suite 160, Pleasanton, CA 94566, USA
E-mail: bpgoffice@wjgnet.com https://www.wjgnet.com

World Journal of Gastroenterology

Submit a Manuscript: https://www.f6publishing.com

World J Gastroenterol 2021 January 28; 27(4): 305-320

DOI: 10.3748/wjg.v27.i4.305

ISSN 1007-9327 (print) ISSN 2219-2840 (online)

MINIREVIEWS

Pleiotropy within gene variants associated with nonalcoholic fatty liver disease and traits of the hematopoietic system

Carlos Jose Pirola, Adrian Salatino, Silvia Sookoian

ORCID number: Carlos Jose Pirola 0000-0001-8234-4058; Adrian Salatino 0000-0002-0091-1678; Silvia Sookoian 0000-0001-5929-5470.

Author contributions: Pirola CJ contributed to study concept and design, data acquisition, data analysis and interpretation, statistical analysis, manuscript drafting, general study supervision and securing funding; Salatino A contributed to data acquisition and bioinformatic support; Sookoian S contributed to study concept and design, data acquisition, data analysis and interpretation, general study supervision, manuscript drafting, securing funding; Pirola CJ and Sookoian S should be considered joint senior authors.

Conflict-of-interest statement: No potential conflicts of interest. No financial support.

Open-Access: This article is an open-access article that was selected by an in-house editor and fully peer-reviewed by external reviewers. It is distributed in accordance with the Creative Commons Attribution Non Commercial (CC BY-NC 4.0) license, which permits others to distribute, remix, adapt, build upon this work non-commercially, and license their derivative works on different terms, provided the

Carlos Jose Pirola, Adrian Salatino, Department of Molecular Genetics and Biology of Complex Diseases, National Scientific and Technical Research Council (CONICET), University of Buenos Aires, Institute of Medical Research (IDIM), Ciudad Autónoma de Buenos Aires C1427ARO, Argentina

Carlos Jose Pirola, Adrian Salatino, Silvia Sookoian, Institute of Medical Research A Lanari, University of Buenos Aires, School of Medicine, Ciudad Autónoma de Buenos Aires, Ciudad Autónoma de Buenos Aires C1427ARO, Argentina

Silvia Sookoian, Department of Clinical and Molecular Hepatology, National Scientific and Technical Research Council (CONICET), University of Buenos Aires, Institute of Medical Research (IDIM), Ciudad Autónoma de Buenos Aires C1427ARO, Argentina

Corresponding author: Silvia Sookoian, FAASLD, MD, PhD, Senior Scientist, Department of Clinical and Molecular Hepatology, National Scientific and Technical Research Council (CONICET), University of Buenos Aires, Institute of Medical Research (IDIM), Combatientes de Malvinas 3150, Ciudad Autónoma de Buenos Aires 1427, Argentina.
ssookoian@intramed.net

Abstract

Genome-wide association studies of complex diseases, including nonalcoholic fatty liver disease (NAFLD), have demonstrated that a large number of variants are implicated in the susceptibility of multiple traits — a phenomenon known as pleiotropy that is increasingly being explored through phenome-wide association studies. We focused on the analysis of pleiotropy within variants associated with hematologic traits and NAFLD. We used information retrieved from large public National Health and Nutrition Examination Surveys, Genome-wide association studies, and phenome-wide association studies based on the general population and explored whether variants associated with NAFLD also present associations with blood cell-related traits. Next, we applied systems biology approaches to assess the potential biological connection/s between genes that predispose affected individuals to NAFLD and nonalcoholic steatohepatitis, and genes that modulate hematological-related traits—specifically platelet count. We reasoned that this analysis would allow the identification of potential molecular mediators that link NAFLD with platelets. Genes associated with platelet count are most highly expressed in the liver, followed by the pancreas, heart, and muscle. Conversely, genes associated with NAFLD presented high expression levels in the brain, lung, spleen, and colon. Functional mapping, gene prioritization, and

original work is properly cited and the use is non-commercial. See: http://creativecommons.org/Licenses/by-nc/4.0/

Manuscript source: Invited manuscript

Specialty type: Gastroenterology and hepatology

Country/Territory of origin: Argentina

Peer-review report's scientific quality classification
Grade A (Excellent): 0
Grade B (Very good): B
Grade C (Good): 0
Grade D (Fair): 0
Grade E (Poor): 0

Received: November 9, 2020
Peer-review started: November 9, 2020
First decision: December 8, 2020
Revised: December 19, 2020
Accepted: December 27, 2020
Article in press: December 27, 2020
Published online: January 28, 2021

P-Reviewer: Elshaarawy O
S-Editor: Zhang L
L-Editor: Webster JR
P-Editor: Liu JH

functional analysis of the most significant loci ($P < 1 \times 10^{-8}$) revealed that loci involved in the genetic modulation of platelet count presented significant enrichment in metabolic and energy balance pathways. In conclusion, variants in genes influencing NAFLD exhibit pleiotropic associations with hematologic traits, particularly platelet count. Likewise, significant enrichment of related genes with variants influencing platelet traits was noted in metabolic-related pathways. Hence, this approach yields novel mechanistic insights into NAFLD pathogenesis.

Key Words: Nonalcoholic fatty liver disease; Nonalcoholic steatohepatitis; Platelets; Leukocytes; Hematologic traits; Genetics

©The Author(s) 2021. Published by Baishideng Publishing Group Inc. All rights reserved.

Core Tip: Pleiotropy within variants associated with hematologic traits and nonalcoholic fatty liver disease.

Citation: Pirola CJ, Salatino A, Sookoian S. Pleiotropy within gene variants associated with nonalcoholic fatty liver disease and traits of the hematopoietic system. *World J Gastroenterol* 2021; 27(4): 305-320
URL: https://www.wjgnet.com/1007-9327/full/v27/i4/305.htm
DOI: https://dx.doi.org/10.3748/wjg.v27.i4.305

INTRODUCTION

Nonalcoholic fatty liver disease and pleiotropic associations

Nonalcoholic fatty liver disease (NAFLD) is regarded as the most prevalent chronic liver disease[1]. A worldwide increase in NAFLD prevalence is acknowledged not only in the adult but also the pediatric population[1]. Consequently, NAFLD has become a serious health issue on a global scale.

Like many other complex diseases, NAFLD develops due to the combined effect of environmental and genetic factors[2-4]. NAFLD presents phenotypic complexity and inter-individual variability, implying that its natural course is characterized by different histological stages-from simple fat accumulation to steatohepatitis (NASH), cirrhosis, and eventually to hepatocellular carcinoma[1]—and considerable variability in disease progression exists among affected patients. One of the proposed factors contributing to the observed inter-patient differences in the disease prognosis and severity is genetic susceptibility[2-4], which might explain up to approximately 20% of the disease variance[5].

Furthermore, NAFLD has not only a high degree of comorbidity with disorders of the metabolic syndrome, including type 2 diabetes, obesity, and cardiovascular disease, but also shared disease mechanisms and disease pathways[6]. These comorbidities have a strong negative impact on the course of NAFLD and vice versa, whereby the presence of NAFLD substantially modifies the course and prognosis of metabolic syndrome-associated diseases[6]. More importantly, the impact of long-term consequences of these comorbidities on cardiovascular health is, at least in part, independent of the presence of general obesity. In fact, it was shown that lean patients with NAFLD have an altered metabolic profile mostly related to increased visceral adiposity that predispose them to cardiovascular risks[7].

Notably, knowledge gained from genome-wide and exon-wide association studies [Genome-wide association studies (GWAS) and EWAS, respectively] of complex diseases, including NAFLD, shows that a large number of single nucleotide polymorphisms are implicated in the susceptibility of multiple traits, which is known as pleiotropy. Phenome-wide association studies (PheWAS) that exploit a significant amount of clinical characteristics gathered mostly from electronic clinical records have thus become a powerful strategy for uncovering pleiotropy.

Among the many traits explored to date in large GWAS/EWAS and PheWAS, including disease traits and biochemical parameters, pleiotropy within gene variants associated with NAFLD and biochemical traits of the hematopoietic system is remarkably consistent across different datasets, specifically those concerning platelet

count and platelet volume[8-10]. However, the mechanisms behind the biological connection between NAFLD and platelet-related traits remain poorly understood.

Therefore, in this review, we focused on the analysis of pleiotropy within variants associated with biochemical hematologic traits and NAFLD. We took advantage of information retrieved from large public GWAS and PheWAS based on the general population and examined whether variants known to be associated with NAFLD also exhibit associations with blood cell-related traits, specifically platelet-related phenotypes. After collecting that information, we adopted systems biology approaches to assess the potential biological connection/s between genes that predispose to NAFLD and NASH, and genes that modulate related hematological traits, including platelet count and platelet crit. We reasoned that focusing on clinically meaningful traits for which associations with liver disorders would be plausible from the biological perspective may help elucidate NAFLD biology. Likewise, these analyses would conceptually allow the identification of potential molecular mediators that link NAFLD with platelets.

NAFLD AND HEMATOLOGICAL TRAITS

Recent observations shed light on the concept that NAFLD not only co-exists with cardiovascular disease, including functional and structural myocardial abnormalities[11], but is also associated with other diseases, including cancer, kidney disease, and hematological disorders, among many others[5]. To illustrate the relevance of the association between NAFLD and hematological traits, we analyzed data from the National Health and Nutrition Examination Surveys (NHANES) 2017-2018 database. The dataset and further information are freely available online https://www.cdc.gov/nchs/nhanes/index.htm). The NHANES are population-based surveys conducted by the National Center for Health Statistics of the Centers for Disease Control and Prevention of the United States. They are frequently used to study liver disease. The National Center for Health Statistics Research Ethics Review Board approved the NHANES protocol, and informed consent was obtained from all participants. Liver steatosis was defined by the controlled attenuation parameter (CAP) obtained *via* transient elastography (FibroScan®). Liver steatosis was diagnosed when CAP >268 dB/m was obtained, which is the threshold for significant steatosis based on a large study[12]. We modeled the relationship between NAFLD and relevant factors by linear logistic regression with an interaction term for the specific hematologic trait and gender while adjusting for subjects' demographic and clinical characteristics. Figure 1 shows the effect of white blood cells (WBC), including lymphocytes (Figure 1A), eosinophils (Figure 1B), neutrophils (Figure 1C), and platelet (Figure 1D) count number by gender. Myeloid and lymphoid lineages, as well as platelets show interaction effects with gender even after adjusting for log-transformed confounding factors such as age, waist circumference, diabetes, glycohemoglobin, total cholesterol, and systolic blood pressure. More importantly, NAFLD risk increased steadily with the number of different blood cell types, particularly in men.

These results are reproducibly observed in the Asian population. Wang *et al*[13] reported that WBC count is a significant factor associated with incident NAFLD in Han Chinese[13]. The authors observed that the association between WBC count and NAFLD remained valid after adjusting for confounding factors including age, gender, smoking, regular exercise, BMI, hypertension, hyperglycemia, and lipid traits[13]. Similarly, WBC count was found to be independently associated with NAFLD regardless of components of the metabolic syndrome in the Korean population[14,15].

PLATELETS AND LIVER DISORDERS—A CONCISE APPRAISAL OF THE RELATIONSHIP

For many biological reasons, the liver and platelets are biologically connected. For example: (1) The fetal liver is a privileged organ of megakaryocyte progenitor differentiation[16]; (2) Thrombocytopenia is a major and debilitating complication of liver cirrhosis[17]; (3) Platelets are involved in the process of fibrogenesis by remodeling the extracellular matrix[18] and secretion of cytokines, including platelet-derived growth factors[19]; and (4) Platelets functioning in the liver exhibit a collaborative effect with endothelial and Kupffer cells in liver regeneration[20]. A more comprehensive update on the role of platelets in liver disorders has been recently published[21].

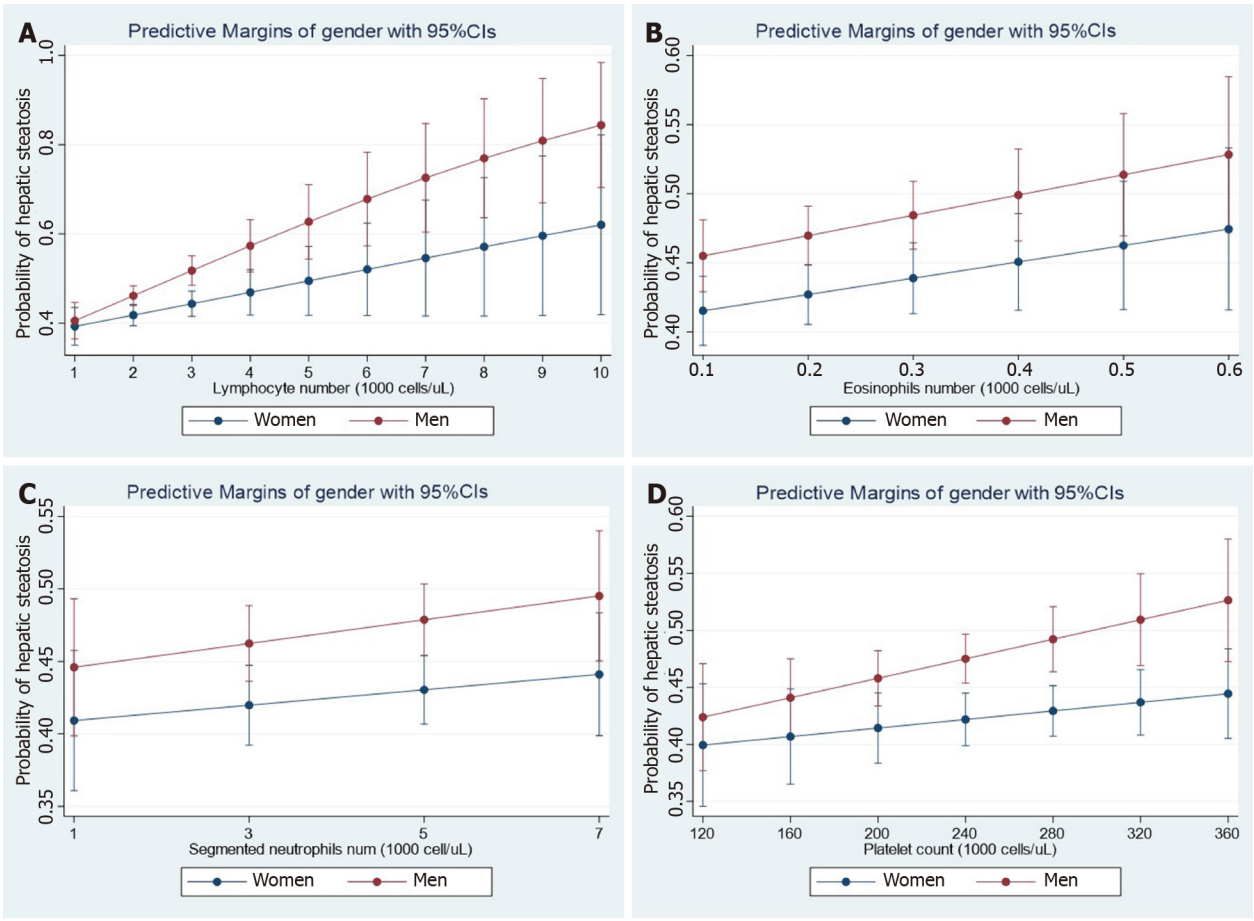


Figure 1 Steatosis and hematological traits. Panels show the interaction effects between hepatic steatosis and hematological traits (A: Lymphocyte number; B: Eosinophil number; C: Neutrophil number; D: Platelet number) on the probability of having hepatic steatosis according to gender. Interaction analyses were performed by linear logistic regression for the presence of steatosis (no = 0, yes = 1) as the dependent variable adding an interaction term among gender (women = 0, men = 1) and the specific continuous variable. Diabetes and log-transformed age, waist, HgbA1c, total cholesterol, systolic blood pressure, and triglycerides were also included as cofactors. The probability of liver fibrosis was estimated by margins as implemented in the STATA software. Data analysis was based on National Health and Nutrition Examination Surveys 2017-2018; the National Center for Health Statistics Research Ethics Review Board approved the National Health and Nutrition Examination Surveys protocol, and participants gave informed consent. Datasets and further information are available online (https://www.cdc.gov/nchs/nhanes/index.htm). Liver steatosis was defined by the controlled attenuation parameter[12]. Only participants that consumed less than 30 g and 20 g of alcohol for men and women, respectively, were included in the present analysis. Those participants with positive tests for viral hepatitis were excluded.

Earlier evidence also demonstrates that platelets are involved in NASH-related complications. For example, we have observed that patients with NASH have high expression of *TGFB1* (transforming grown factor β1)-mRNA in circulating platelets[22]. Platelets are also involved in the process of atherogenesis by upregulating many molecules[23], including *TGFB1*[24], which is also related to NAFLD and the risk of cardiovascular disease. Results yielded by a recent study suggest that platelet-mediated inflammation in NAFLD drives hepatocellular carcinogenesis[25].

PLEIOTROPIC EFFECTS OF THE NONSYNONYMOUS *PNPLA3*-RS738409 (P.ILE148MET) VARIANT

The nonsynonymous rs738409 C/G variant in *PNPLA3* (patatin-like phospholipase domain containing protein 3, also known as adiponutrin or calcium-independent phospholipase A2-epsilon), which encodes the amino acid substitution I148M, is regarded as the major genetic variant associated with the susceptibility to NAFLD and NASH[26,27].

The rs738409 has also been associated with alcoholic liver disease[28-30], hepatitis C[31], hepatitis B[32], and hepatocellular carcinoma[33],[34].

Results of a large PheWAS performed in subjects of European ancestry (816903 participants) with genome-wide genotyped data linked to phenotypic information, including the United Kingdom Biobank cohort, 23andMe cohort, FINRISK (working-

age population of Finland), and Children's Hospital of Philadelphia, confirmed that rs738409 presents pleiotropic effects beyond the liver. For instance, rs738409-G was associated with increased risk of type 2 diabetes and decreased risk of high total cholesterol, acne, gout, and gallstones; all these associations remained significant after adjusting for elevated transaminases[35].

In addition, it was suggested that rs738409 might be used to predict race-related hepatotoxicity in pediatric patients with acute lymphoblastic leukemia[9].

Another study revealed the association of rs738409 with mean corpuscular hemoglobin ($P = 6 \times 10^{-9}$) based on the analysis of individuals of 116666 British ancestry[36]. Consistently, Kichaev *et al*[37] established the association of rs738409 with mean corpuscular hemoglobin ($P = 4 \times 10^{-25}$) by using genome-wide genotyping array in a sample of 443000 individuals of European ancestry[37]. Variants in or near *PNPLA3* have also been associated with the aspartate transaminase-to-platelet ratio index[38].

A summary picture illustrating the genetic associations with *PNPLA3* locus, including its pleiotropic effects on diverse laboratory measurements, is shown in Figure 2. It reveals that the strength of the association scores of rs738409 and levels of liver enzymes, particularly ALT levels (association score = 1), is shared with the effect of this variant on many blood-related traits, for instance platelet count (association score = 0.8) (Figure 2).

PHEWAS: THE EFFECT OF VARIANTS ASSOCIATED WITH NAFLD ON BLOOD-RELATED TRAITS

We next used information sourced from electronic health records and GWAS data computed from United Kingdom Biobank entries pertaining to 452264 individuals, which was retrieved from the Gene ATLAS (http://geneatlas.roslin.ed.ac.uk) and Neale's database (http://www.nealelab.is/uk-biobank/).

We specifically searched for PheWAS associations of variants influencing NAFLD, including *PNPLA3*-rs738409, *TM6SF2*-rs58542916, *MBOAT7-TMC4* rs641738, *GCKR*-rs780094, and *HSD17B13*-rs72613567. As expected, rs738409, rs58542916, and rs72613567 were associated with liver-related traits in the United Kingdom-Biobank GWAS (Table 1).

Of note, all aforementioned variants showed GWAS-significant associations ($P < 5 \times 10^{-8}$) with blood-related traits. The strongest associations pertained to platelet traits, including platelet crit (which represents the proportion of blood volume that is occupied by platelets, expressed as a percentage), platelet volume, and platelet count (Table 1). Specifically, *PNPLA3*-rs738409 was associated with platelet count ($P = 2.9 \times 10^{-45}$) and platelet crit ($P = 3.6 \times 10^{-29}$) with the *P* values for association exceeding those for association with liver diseases (Table 1). A similar pattern was obtained for *TM6SF2*-rs58542926 and *HSD17B13*-rs72613567 (Table 1) variants and their associations with platelet traits.

GENES ASSOCIATED WITH NAFLD AND PLATELET COUNT SHARE PATHWAYS INVOLVED IN EXTRACELLULAR MATRIX REMODELING AND CYTOSKELETAL SIGNALING PROTEINS

To explore shared pathways between NAFLD and platelet-related traits, we retrieved from the Open Target Genetics platform (https://genetics.opentargets.org) the list of genes (human protein-coding genes) associated with phenotypes of interest. Specifically, we focused on platelet count, which expresses the number of platelets per unit volume in a sample of venous blood.

The genetic associations in the Open Target platform are derived from GWAS Catalog (https://www.ebi.ac.uk/gwas) and PheWAS (https://phewascatalog.org/), whereby the former contains publications indexed in PubMed and the latter is a repository of electronic medical records with links to the Vanderbilt DNA biobank. The list of genes associated with platelet count ($n = 305$) and NAFLD ($n = 161$) is shown in Supplementary Table 1 and Supplementary Table 2, respectively.

To analyze and interpret the pathways shared between genes associated with NAFLD and those associated with platelet count, we used the FUMA platform available at https://fuma.ctglab.nl/. FUMA utilizes positional expression quantitative trait loci and chromatin interaction mappings to build gene-based pathways and tissue

Table 1 Phenome-wide association studies associations of variants influencing nonalcoholic fatty liver disease and their effect on blood-related traits

Variant	Trait[1]	Effect (beta)	*P* value
***PNPLA3*-rs738409. Chromosomal position: 44324727. Allele C MAF: 0.21**			
Blood-related trait	Platelet count	1.5369	2.8659e-45
	Hemoglobin concentration	-0.025607	9.0819e-35
	Platelet crit	0.0010141	3.6242e-29
	Mean corpuscular volume	-0.069237	9.4452e-16
	Hematocrit percentage	-0.063676	2.9494e-25
	Mean corpuscular hemoglobin	-0.031471	2.2846e-19
	Monocyte percentage	-0.035411	4.7043e-15
	Mean platelet (thrombocyte) volume	-0.016089	9.5385e-18
Liver diseases	K76 Other diseases of liver	-0.0022213	4.5111e-22
	K70 Alcoholic liver disease	-0.00087844	1.7073e-14
	K70-K77 Diseases of liver	-0.0028804	3.3855e-25
	K74 Fibrosis and cirrhosis of liver	-0.00075775	2.3186e-11
***TM6SF2*-rs58542926. Chromosomal position: 19379549. Allele C MAF: 0.975**			
Blood-related trait	Lymphocyte percentage	0.22273	1.8966e-19
	Neutrophil percentage	-0.20618	8.0938e-13
	Platelet crit	-0.001243	2.6606e-18
	Platelet count	-0.96935	1.5736e-08
	Red blood cell (erythrocyte) count	-0.008401	4.1569e-14
Liver diseases	K76 Other diseases of liver	-0.0020969	5.9013e-09
	K74 Fibrosis and cirrhosis of liver	-0.00078964	8.6924e-06
	K70-K77 Diseases of liver	-0.0023442	7.1296e-08
***HSD17B13*-rs72613567. Chromosomal position: 88231392. Allele T MAF: 0.27**			
Blood-related trait	Platelet count	-1.0628	6.675e-26
	Platelet crit	-0.00068946	2.0658e-16
	Mean platelet (thrombocyte) volume	0.012228	2.4506e-12
	Mean corpuscular hemoglobin	0.020281	2.7946e-10
Liver diseases	K70-K77 Diseases of liver	0.00095351	0.0002012
	K74 Fibrosis and cirrhosis of liver	0.00032971	0.0016351
	K70 Alcoholic liver disease	0.00030904	0.0034794
***MBOAT7*-TMC4 rs641738. Chromosomal position: 54676763. Allele T MAF: 0.44**			
Blood-related trait	Platelet crit	0.00079482	1.0509e-25
	Platelet count	0.84392	2.3213e-20
	White blood cell (leukocyte) count	-0.012957	3.4321e-05
	Mean platelet (thrombocyte) volume	0.0013881	0.37852
Liver diseases	K76 Other diseases of liver	0.0005036	0.0086505
	K70-K77 Diseases of liver	0.00058356	0.011748
	K74 Fibrosis and cirrhosis of liver	0.00019063	0.043702
	K70 Alcoholic liver disease	0.00017298	0.069988

***GCKR*-rs780094. Chromosomal position: 27741237. Allele C MAF: 0.38**			
Blood-related trait	Mean reticulocyte volume	0.16064	5.9197e-33
	Neutrophil percentage	-0.14035	2.7743e-19
	Neutrophil count	-0.037139	6.3804e-47
	Monocyte percentage	0.073076	7.914e-79
	Mean platelet (thrombocyte) volume	0.014342	1.3297e-18
	Platelet crit	-0.0013887	1.3581e-71
	Platelet count	-1.9052	6.2404e-92
	Hematocrit percentage	0.049511	4.3172e-21
Liver diseases	K76 Other diseases of liver	-0.00058708	0.0026207
	K70-K77 Diseases of liver	-0.0004415	0.060918
	K74 Fibrosis and cirrhosis of liver	-0.00011872	0.2169
	K75 Other inflammatory liver diseases	-0.00012854	0.13954
	K70 Alcoholic liver disease	9.7922e-05	0.31331

[1]Letters and numbers such as K70, K76, K74 and K75 represent the codes for diseases (ICD10) in the United Kingdom Biobank. Approximately 30 million variants in the United Kingdom Biobank from the Gene ATLAS (http://geneatlas.roslin.ed.ac.uk) and Neale's database (http://www.nealelab.is/uk-biobank/) resources were comprehensively tested for their association with liver (ICD10 codes: K70, K76, K74 and K75) and blood cell-associated traits, including platelet, leukocyte and neutrophil counts. *PNPLA3*: Patatin-like Phospholipase Domain Containing protein 3; *TM6SF2*: Transmembrane 6 Superfamily Member 2; *HSD17B13*: Hydroxysteroid 17-Beta Dehydrogenase 13; *MBOAT7*: Membrane Bound O-Acyltransferase Domain Containing 7; *TMC4*: Transmembrane channel like 4; *GCKR*: Glucokinase regulator.

enrichment heatmaps[39]. Hence, we first tested the tissue specificity of the list of genes/proteins associated with each phenotype, namely NAFLD and platelet count. Specifically, we explored tissues in which those genes/proteins present higher expression levels (differentially expressed genes are defined for each label of each expression dataset). Genes showing a $P \leq 0.05$ after Bonferroni correction and absolute log fold change ≥ 0.58 were defined as differentially expressed. Interestingly, genes associated with platelet count were most highly expressed in the liver, followed by the pancreas, heart, and muscle (Figure 3A). Conversely, genes associated with NAFLD presented high expression levels in the brain, lung, spleen, and colon (Figure 3B).

The Venn diagram provided in Figure 3C shows the genes shared between NAFLD and platelet count according to the information retrieved from GWAS and PheWAS catalogs, as explained earlier, among which we found eleven shared loci that included *PNPLA3*. Next, we performed pathway analysis on the list of shared genes, which revealed an enrichment of genes (*ACTN1* and *TNFRSF13B*) belonging to the predicted pathway "Syndecan 4 pathway" (PID_SYNDECAN_4_PATHWAY) (Figure 3D). The Syndecan 4 pathway is involved in cell growth, differentiation, and adhesion, and in the modulation of extracellular matrix proteins[40]. Syndecans are type I transmembrane proteins with an N-terminal ectodomain that contains several consensus sequences for attachment to glycosaminoglycan, heparan sulfate, and to a lesser extent chondroitin sulfate chains, and a short C-terminal cytoplasmic domain. Syndecans may act as integrin co-receptors. Interactions between fibronectin and syndecans are modulated by tenascin-C. Syndecans bind a wide variety of soluble and insoluble ligands, including extracellular matrix components, cell adhesion molecules, and growth factors, including VEGFs, cytokines, and proteinases[41]. It is worth noting that parvin beta (*PARVB*), which has been significantly associated with NAFLD[42,43] and hematological traits[44], encodes a member of the parvin family of actin-binding proteins that play a role in cytoskeleton organization and cell adhesion. This family member binds to alphaPIX and alpha-actinin, and can inhibit the activity of integrin-linked kinase. This protein also functions as a tumor suppressor. As the *PARVB* locus is located near *PNPLA3*, further studies are needed to establish whether the association of the locus with NAFLD and hematological traits merely reflects a linkage between the two genetic loci.

We further explored the Gene Ontology (GO) biological processes in which the list of genes associated with platelet count was specifically enriched. We found that, in addition to expected pathways that included hemostasis, response to wound healing, and platelet degranulation, there were pathways that support the plausibility of

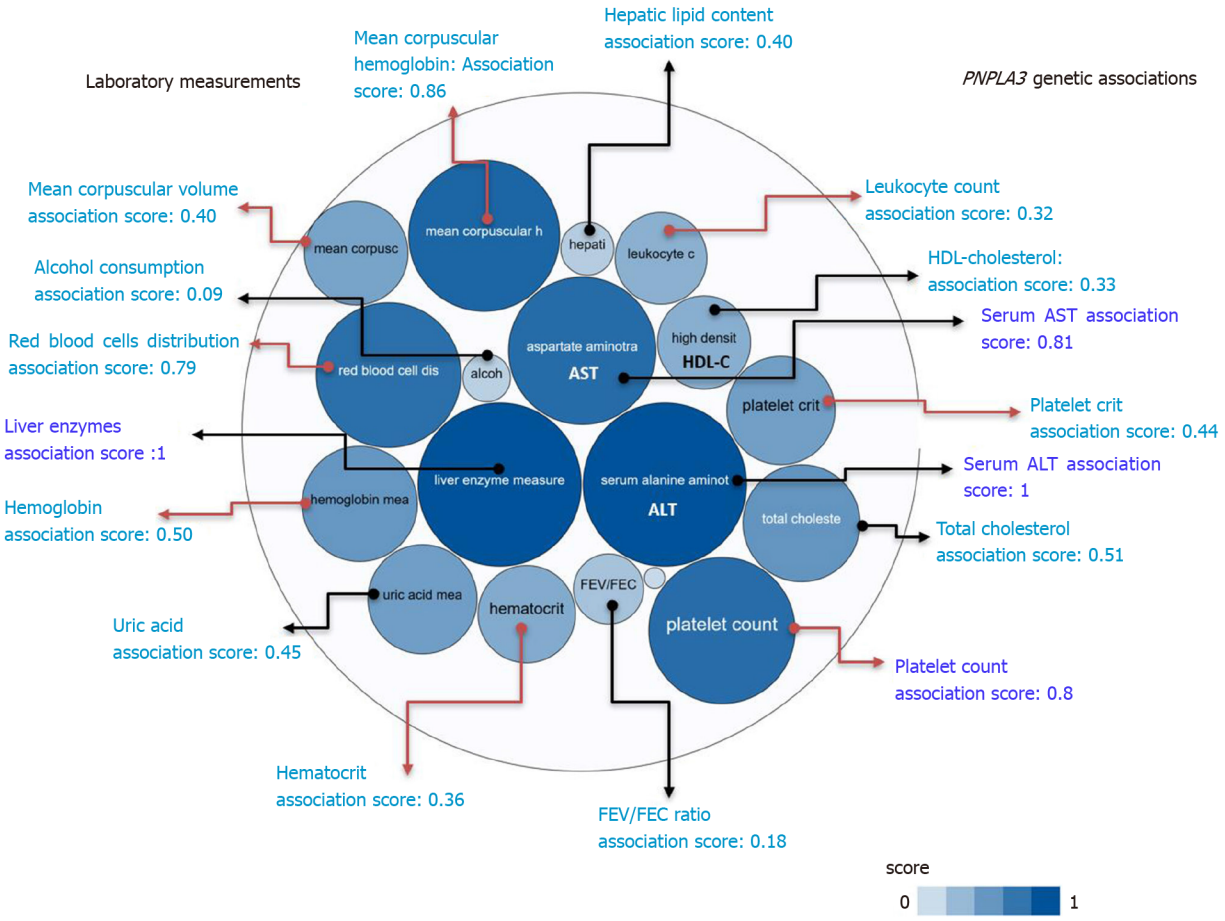


Figure 2 *PNPLA3* and genetic associations with laboratory measurements in genome-wide association studies and phenome-wide association studies. The score for the associations ranges from 0 to 1, with higher scores indicating stronger evidence for an association. Bubbles in the figure represent the different scores with varying shades of blue: the darker the blue, the stronger the association. Red arrows highlight the association of the *rs738409* variant in *PNPLA3* and laboratory measurements related with hematological traits. HDL: High density lipoprotein cholesterol; FEV: The ratio of forced expiratory volume to forced vital capacity, used as a measure of pulmonary function; uric: Uric acid; AST: Aspartate aminotransferase level; ALT: Alanine aminotransferase level; total chol: Total cholesterol. Source: Open Target Database (https://genetics.opentargets.org/gene/ENSG00000100344). Score summaries: Data sources and factors that affect the relative strength of the evidence scores can be found at: https://docs.targetvalidation.org/getting-started/scoring.

sharing genes with NAFLD, for example the triglyceride catalytic process. The GO biological processes associated with the top 50 genes on the list of loci associated with platelet count is shown in Figure 4. Remarkably, *PNPLA3* and *FABP6* (Fatty Acid Binding Protein 6) are the two overlapping loci that would be responsible for the enrichment of triglyceride metabolism (Figure 4).

BIOLOGICAL PATHWAYS OF GENES ASSOCIATED WITH PLATELET COUNT VS GENES ASSOCIATED WITH NAFLD

It is also noteworthy that, despite the shared genes, there are differences in the biological processes in which the sets of genes associated with platelet count and with NAFLD are involved. To explore these pathways, we performed overrepresentation analysis based on a more comprehensive list of genes associated with each phenotype.

The input list of platelet count-associated variants ($P < 1 \times 10^{-6}$) was generated by searching the United Kingdom Biobank GWAS database as provided by Neale's lab resource (http://www.nealelab.is/uk-biobank/), which shows variants in about 2424 loci with genome-wide significance ($P < 5 \times 10^{-8}$) for an association with platelet count as a continuous trait (10^9 cells/L; mean = 252.023 ± Std.dev = 60.0604). We used the United Kingdom Biobank GWAS database because it provides one of the largest publically available sources of genetic associations with laboratory traits in the general population involving 479367 individuals of both sexes (http://biobank.ctsu.ox.ac.uk/crystal/field.cgi?id=30080).

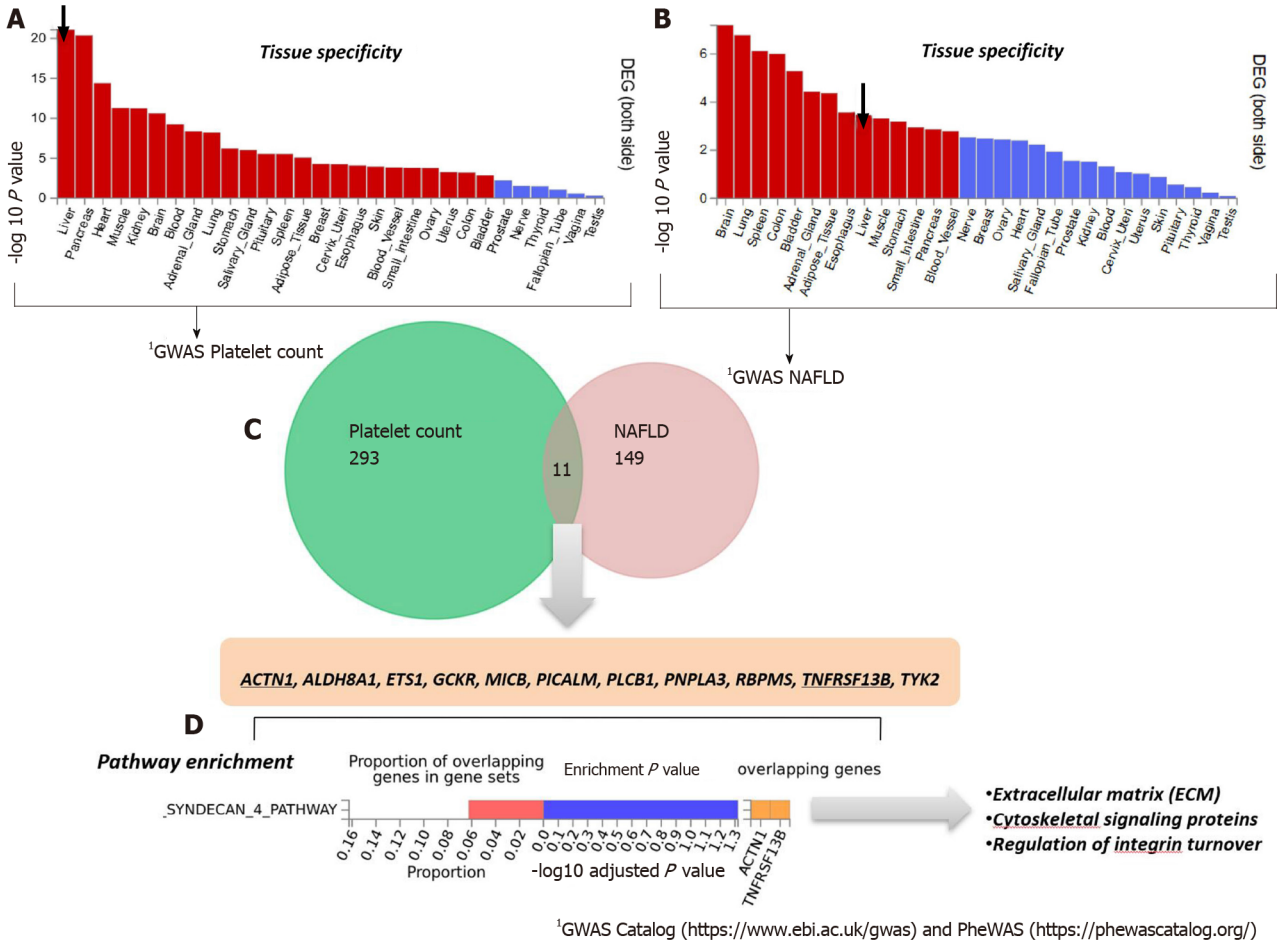


Figure 3 Genes that are shared between nonalcoholic fatty liver disease and platelet count. A and B: Significantly enriched Differentially Expressed Gene (DEG) Sets (P_{bon} < 0.05) are highlighted in red (FUMA). DEG sets were pre-calculated by performing two-sided *t*-test for any one of the labels against all others. For this purpose, expression values were normalized (zero-mean) to obtain a $\log_2$ transformation of expression value (EPKM or TPM). Genes with $P \leq 0.05$ after Bonferroni correction and absolute log fold change ≥ 0.58 were defined as differentially expressed genes in a given label compared to others. In addition to DEG, up-regulated DEG and down-regulated DEG were also pre-calculated by taking the sign of *t*-statistics into account. Input genes were tested against each of the DEG sets using the hypergeometric test. The background genes are genes that have average expression value > 1 in at least one of the labels and exist in the user-selected background genes. Significant enrichment at Bonferroni-corrected $P \leq 0.05$ is colored in red. C: Venn diagram showing the number of genes that are common (overlapping areas) and dissimilar (non-overlapping areas) in nonalcoholic fatty liver disease (NAFLD) and platelet count gene lists. D: Pathway analysis using all Canonical Pathways (MsigDB c2) in the web-based FUMA platform available at http://fuma.ctglab.nl. Overlapping genes (underlined): *ACTN1*: Actinin Alpha 1; *TNFRSF13B:* TNF Receptor Superfamily Member 13B. The input lists of platelet count- and NAFLD-associated variants were generated by searching the Open Target platform, which contains data retrieved from GWAS Catalog (https://www.ebi.ac.uk/gwas) and phenome-wide association studies (https://phewascatalog.org/). The list of genes associated with platelet count contains 305 loci and that associated with NAFLD contains 149 loci, as shown in Supplementary Figures 1 and 2, respectively.

In the case of NAFLD, and to avoid issues arising from the paucity of GWAS/EWAS discovered genes, we included a more comprehensive list of 928 loci obtained by data mining[5] that represents genetic and molecular associations with the disease.

We chose to conduct the overrepresentation analysis on the list of loci obtained from data mining because NAFLD as the disease trait (K76.0 Fatty change of liver: http://biobank.ctsu.ox.ac.uk/crystal/field.cgi?id=41202) is underrepresented in the United Kingdom Biobank GWAS database, affecting only 460 of 410332 individuals whose data are stored in this repository.

Differences in biological pathway enrichment between the two datasets (NAFLD and platelet count) are summarized in Figure 5, which shows specificity in the function of genes in each of the gene lists. For instance, the NAFLD list of associated genes/proteins is enriched in expected pathways, such as metabolism of lipids and amino acids, purine metabolism, and circadian rhythm, among others (Figure 5). The platelet count list is enriched with genes involved in DNA repair, telomere maintenance, and the Hedgehog pathway, among many others, as shown in Figure 5[45]. Interestingly, some pathways related to platelet-derived growth factors, such as the platelet-derived growth factors receptor-alpha signaling pathway, are over-represented in the list of genes associated with NAFLD. The many types of

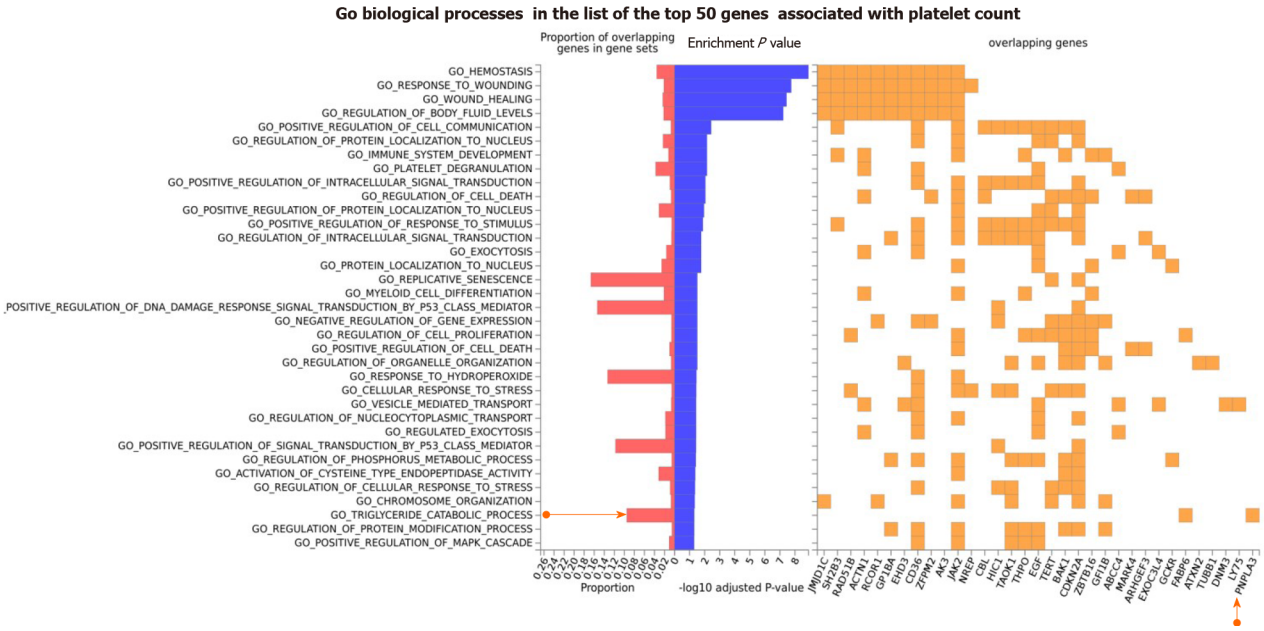


Figure 4 Gene Ontology biological processes of the top 50 genes associated with platelet count. The chart shows fold enrichment in biological processes of genes associated with platelet count with respect to those present in the whole genome. The input list of platelet count-associated variants was generated by conducting a search *via* the Open Target platform, which contains data retrieved from genome-wide association studies Catalog (https://www.ebi.ac.uk/gwas) and phenome-wide association studies (https://phewascatalog.org/). The whole list of genes associated with platelet count contains 305 loci, as shown in Supplementary Figure 2. Gene mapping and analysis was conducted using the FUMA genome-wide association studies tool (https://fuma.ctglab.nl/). Genes belonging to the pathways as overlapping genes are shown as a heatplot to the right.

integrin cell surface interaction pathways seem to play a more important role in NAFLD pathophysiology than in regulating platelet count. Notably, the gene set associated with platelet count presents enrichment in the leukotriene synthesis pathways, which have been linked to the progression of NAFLD[46-49].

FUNCTIONAL ASSESSMENT OF VARIANTS ASSOCIATED WITH LABORATORY HEMATOLOGICAL-RELATED TRAITS

To understand the potential involvement of genes associated with laboratory hematological-related traits in NAFLD biology, we performed functional analysis. Based on the reverse biology premise, we reasoned that genes involved in hematological-related traits might be associated with some metabolic function/s that would presumably affect NAFLD pathogenesis. Thus, the top blood-related associated traits in terms of their statistical significance were further searched for genetic associations in the entire United Kingdom Biobank dataset. Specifically, approximately 30 million variants in the United Kingdom Biobank from the Gene ATLAS (http://geneatlas.roslin.ed.ac.uk) and Neale's database (http://www.nealelab.is/uk-biobank/) resources were comprehensively tested for associations with blood cell-associated traits, including platelet, leukocyte and neutrophil counts. We further explored the pathways in which the lists of genes associated with these traits are involved. For this purpose, we used the FUMA resource that allows using functional and biological information to prioritize genes based on GWAS outcomes.

Interestingly, functional mapping, gene prioritization, and functional analysis using FUMA of the most significant genetic variants ($P < 1 \times 10^{-6}$) revealed 85 mapped genes in the full list of loci associated with hematological traits that are also associated with liver traits, including chronic liver diseases, fibrosis and liver cirrhosis, NAFLD, and other inflammatory liver diseases (Figure 6A). *PNPLA3*, *SAMM50*, *PARVB* and *HSD17B13* are among the ten genes shared by liver traits and platelet count. *TM6SF2* is shared by liver traits, platelet count, and neutrophil count, and *GCKR* is shared by liver and all hematological traits (Figure 6A).

In addition, Figure 6B shows the consistent association of *PNPLA3*, *TM6SF2*, *SAMM50*, and *PARVB* with liver and hematological traits identified *via* FUMA analysis in reported GWAS. Finally, we performed functional enrichment analysis on

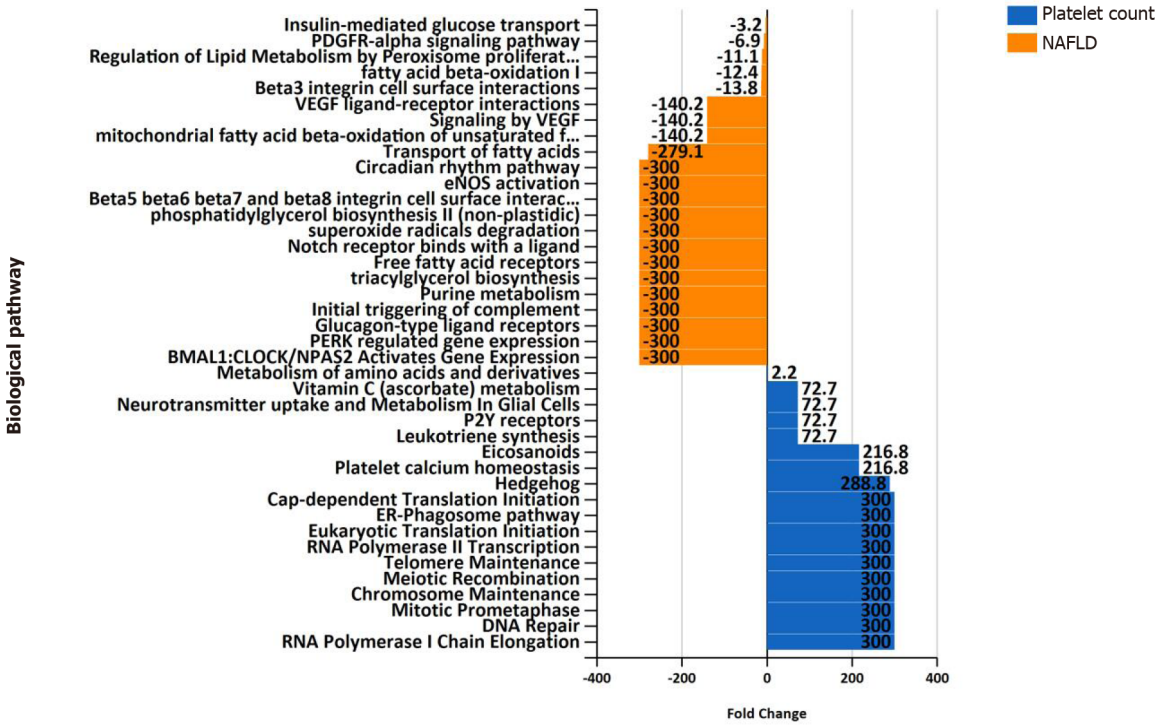


Figure 5 Overrepresentation analysis of biological pathways of genes associated with platelet count *vs.* genes associated with nonalcoholic fatty liver disease. Overrepresentation analysis of biological pathways of platelet count-associated genes in comparison with that pertaining to nonalcoholic fatty liver disease-associated genes. The input list of platelet count-associated variants ($P < 1 \times 10^{-6}$) was generated by searching the United Kingdom Biobank genome-wide association studies database as provided by Neale's lab resource (http://www.nealelab.is/uk-biobank/). The input list associated with nonalcoholic fatty liver disease includes 928 genes/proteins obtained by data mining[5]. The analysis was performed by applying the functional enrichment and interaction network analysis (FunRich) tool[46].

genes significantly associated with platelet count, leukocyte count, and neutrophil count by applying the FunRich tool. Notably, loci involved in the genetic modulation of platelet, leukocyte, and neutrophil counts presented significant enrichment in metabolic, energy balance, xenobiotics, and CYP-450-related pathways (Figure 7A–C). However, platelet-related loci are particularly involved in regulating key aspects of metabolism, while leukocyte and neutrophil counts are related to more general homeostasis regulation processes (Figure 7D–F).

CONCLUSION

PheWas revealed that variants in genes influencing NAFLD present pleiotropic associations with laboratory-related hematologic traits and are relevant to the hematopoietic liver function. Similarly, related genes with variants influencing hematological traits, platelet count in particular, presented significant enrichment in metabolic and energy balance-related pathways.

By using different resources and datasets of variants associated with the genetics of platelet count and NAFLD, we found consistency in the results, suggesting that there are shared mechanisms and pathways between the two phenotypes. In particular, we found metabolic and lipid pathways shared by NAFLD and platelet traits. It is anticipated that potential therapeutic targets, including novel ligands of peroxisome proliferator-activated receptors may also play a role in modulating platelet-related phenotypes such as platelet activation and the cascade of events associated with inflammation and cardiovascular risk.

In summary, our approach provides novel mechanistic insights into NAFLD pathogenesis. Further research is nonetheless necessary to ascertain whether genes associated with liver diseases present ample pleiotropy and, therefore, modify functions of diverse organs simultaneously. If, conversely, some phenotypes are found to act as intermediaries between genes and disease, a Mendelian Randomization approach can be used to study the relationship between, in this case, hematological and liver traits or vice versa.

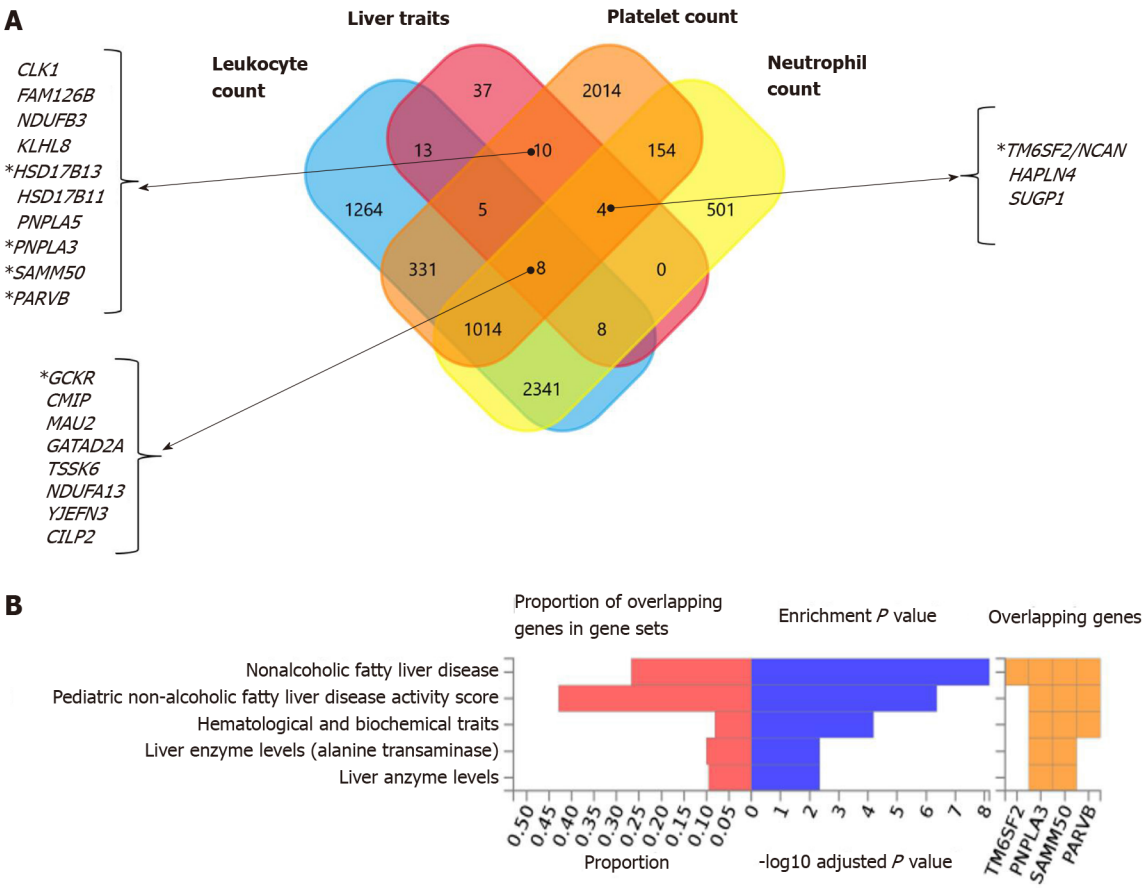


Figure 6 Nonalcoholic fatty liver disease and hematological traits associated genes. A: Venn diagram showing the set of genes associated with liver traits (ICD10 codes: K70, K76, K74 and K75), platelet count, leukocyte count, and neutrophil count, as well as their overlapping genes in the United Kingdom Biobank. Approximately 30 million variants in the United Kingdom Biobank dataset sourced from the Neale's database (http://www.nealelab.is/uk-biobank/) were comprehensively tested for association with liver and blood cell traits, including platelet, leukocyte and neutrophil counts. B: Overlap between nonalcoholic fatty liver disease-associated genes and those associated with hematological traits. The chart shows information on previously known single nucleotide polymorphisms-trait associations reported in the genome-wide association studies (GWAS) catalog for all single nucleotide polymorphisms associated with nonalcoholic fatty liver disease in the United Kingdom Biobank GWAS database; the analysis was conducted using the FUMA GWAS tool (https://fuma.ctglab.nl/).

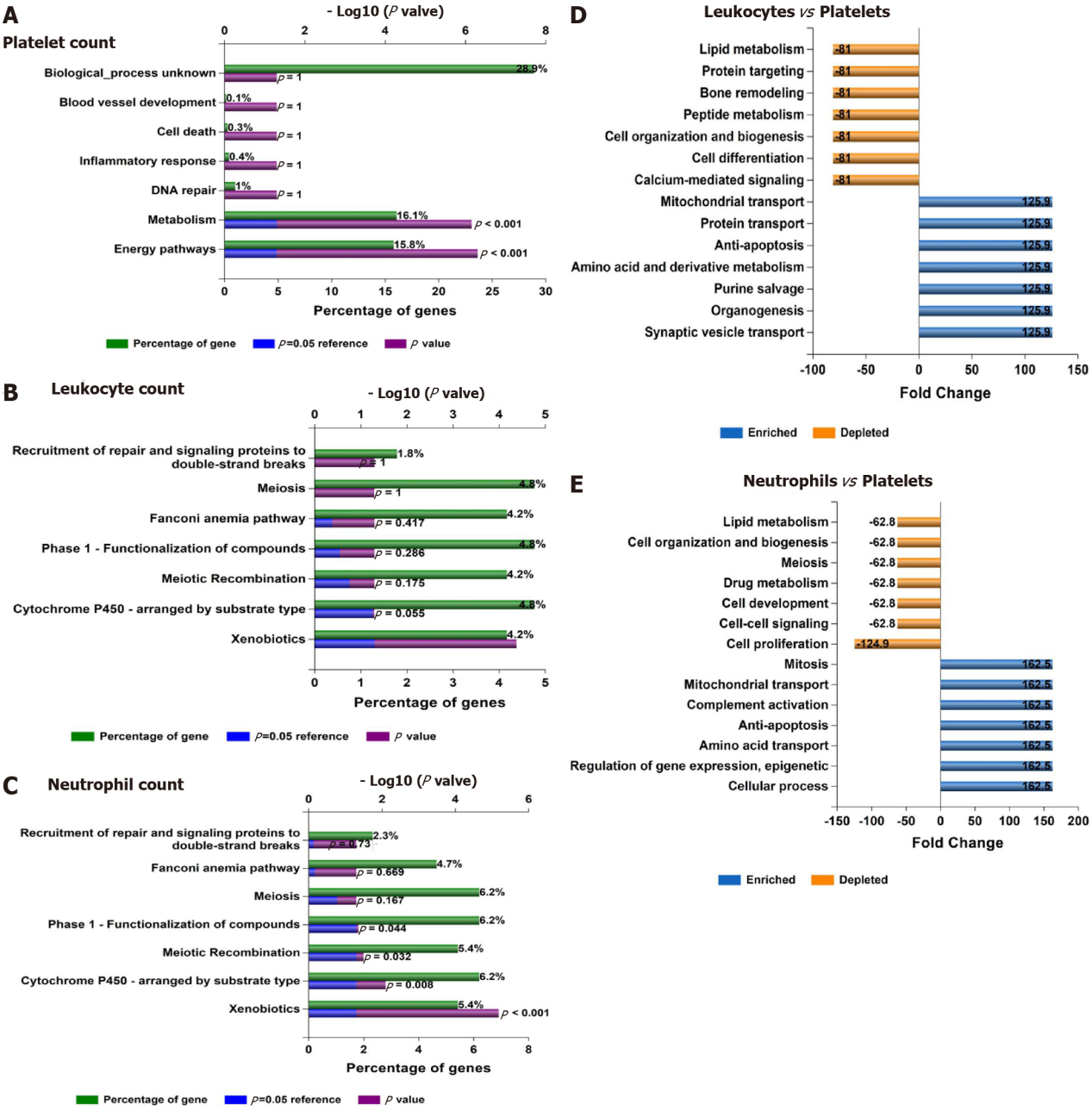


Figure 7 Functional assessment of variants associated with laboratory hematological-related traits. A-C: Functional analysis of genes significantly associated with platelet, leukocyte, and neutrophil count in the whole genome-wide association studies dataset (*452264* individuals whose data are included in the United Kingdom Biobank). Functional enrichment analysis was performed using the FunRich tool, while Bonferroni and Benjamini-Hochberg methods were used to correct for multiple testing. D-E: Charts show fold changes in biological processes of genes associated with leukocyte or neutrophil counts *vs* biological processes of genes associated with platelet count. The input list of genes associated with platelet count, leukocyte count, and neutrophil count ($P < 1 \times 10^{-8}$) was generated by searching the United Kingdom Biobank genome-wide association studies database.

REFERENCES

1 **Brunt EM**, Wong VW, Nobili V, Day CP, Sookoian S, Maher JJ, Bugianesi E, Sirlin CB, Neuschwander-Tetri BA, Rinella ME. Nonalcoholic fatty liver disease. *Nat Rev Dis Primers* 2015; **1**: 15080 [PMID: 27188459 DOI: 10.1038/nrdp.2015.80]

2 **Sookoian S**, Pirola CJ. Precision medicine in nonalcoholic fatty liver disease: New therapeutic insights from genetics and systems biology. *Clin Mol Hepatol* 2020; **26**: 461-475 [PMID: 32906228 DOI: 10.3350/cmh.2020.0136]

3 **Pirola CJ**, Sookoian S. Epigenetics factors in nonalcoholic fatty liver disease. *Expert Rev Gastroenterol Hepatol* 2020; 1-16 [PMID: 32476509 DOI: 10.1080/17474124.2020.1765772]

4 **Sookoian S**, Pirola CJ, Valenti L, Davidson NO. Genetic Pathways in Nonalcoholic Fatty Liver Disease: Insights From Systems Biology. *Hepatology* 2020; **72**: 330-346 [PMID: 32170962 DOI: 10.1002/hep.31229]

5 **Sookoian S**, Pirola CJ. Genetics of Nonalcoholic Fatty Liver Disease: From Pathogenesis to

Therapeutics. *Semin Liver Dis* 2019; **39**: 124-140 [PMID: 30912099 DOI: 10.1055/s-0039-1679920]
6 **Sookoian S**, Pirola CJ. Review article: shared disease mechanisms between non-alcoholic fatty liver disease and metabolic syndrome - translating knowledge from systems biology to the bedside. *Aliment Pharmacol Ther* 2019; **49**: 516-527 [PMID: 30714632 DOI: 10.1111/apt.15163]
7 **Sookoian S**, Pirola CJ. Systematic review with meta-analysis: risk factors for non-alcoholic fatty liver disease suggest a shared altered metabolic and cardiovascular profile between lean and obese patients. *Aliment Pharmacol Ther* 2017; **46**: 85-95 [PMID: 28464369 DOI: 10.1111/apt.14112]
8 **Eicher JD**, Chami N, Kacprowski T, Nomura A, Chen MH, Yanek LR, Tajuddin SM, Schick UM, Slater AJ, Pankratz N, Polfus L, Schurmann C, Giri A, Brody JA, Lange LA, Manichaikul A, Hill WD, Pazoki R, Elliot P, Evangelou E, Tzoulaki I, Gao H, Vergnaud AC, Mathias RA, Becker DM, Becker LC, Burt A, Crosslin DR, Lyytikäinen LP, Nikus K, Hernesniemi J, Kähönen M, Raitoharju E, Mononen N, Raitakari OT, Lehtimäki T, Cushman M, Zakai NA, Nickerson DA, Raffield LM, Quarells R, Willer CJ, Peloso GM, Abecasis GR, Liu DJ; Global Lipids Genetics Consortium; Deloukas P; Samani NJ; Schunkert H; Erdmann J; CARDIoGRAM Exome Consortium; Myocardial Infarction Genetics Consortium; Fornage M; Richard M; Tardif JC; Rioux JD; Dube MP; de Denus S; Lu Y; Bottinger EP; Loos RJ; Smith AV; Harris TB; Launer LJ; Gudnason V; Velez Edwards DR; Torstenson ES; Liu Y; Tracy RP; Rotter JI; Rich SS; Highland HM; Boerwinkle E; Li J; Lange E; Wilson JG; Mihailov E; Mägi R; Hirschhorn J; Metspalu A; Esko T; Vacchi-Suzzi C; Nalls MA; Zonderman AB; Evans MK; Engström G; Orho-Melander M; Melander O; O'Donoghue ML; Waterworth DM; Wallentin L; White HD; Floyd JS; Bartz TM; Rice KM; Psaty BM; Starr JM; Liewald DC; Hayward C; Deary IJ; Greinacher A; Völker U; Thiele T; Völzke H; van Rooij FJ; Uitterlinden AG; Franco OH; Dehghan A; Edwards TL; Ganesh SK; Kathiresan S; Faraday N; Auer PL; Reiner AP; Lettre G; Johnson AD. Platelet-Related Variants Identified by Exomechip Meta-analysis in 157,293 Individuals. *Am J Hum Genet* 2016; **99**: 40-55 [PMID: 27346686 DOI: 10.1016/j.ajhg.2016.05.005]
9 **Liu Y**, Fernandez CA, Smith C, Yang W, Cheng C, Panetta JC, Kornegay N, Liu C, Ramsey LB, Karol SE, Janke LJ, Larsen EC, Winick N, Carroll WL, Loh ML, Raetz EA, Hunger SP, Devidas M, Yang JJ, Mullighan CG, Zhang J, Evans WE, Jeha S, Pui CH, Relling MV. Genome-Wide Study Links PNPLA3 Variant With Elevated Hepatic Transaminase After Acute Lymphoblastic Leukemia Therapy. *Clin Pharmacol Ther* 2017; **102**: 131-140 [PMID: 28090653 DOI: 10.1002/cpt.629]
10 **Verma A**, Bang L, Miller JE, Zhang Y, Lee MTM, Zhang Y, Byrska-Bishop M, Carey DJ, Ritchie MD, Pendergrass SA, Kim D; DiscovEHR Collaboration. Human-Disease Phenotype Map Derived from PheWAS across 38,682 Individuals. *Am J Hum Genet* 2019; **104**: 55-64 [PMID: 30598166 DOI: 10.1016/j.ajhg.2018.11.006]
11 **Lonardo A**, Sookoian S, Pirola CJ, Targher G. Non-alcoholic fatty liver disease and risk of cardiovascular disease. *Metabolism* 2016; **65**: 1136-1150 [PMID: 26477269 DOI: 10.1016/j.metabol.2015.09.017]
12 **Serra-Burriel M**, Graupera I, Torán P, Thiele M, Roulot D, Wai-Sun Wong V, Neil Guha I, Fabrellas N, Arslanow A, Expósito C, Hernández R, Lai-Hung Wong G, Harman D, Darwish Murad S, Krag A, Pera G, Angeli P, Galle P, Aithal GP, Caballeria L, Castera L, Ginès P, Lammert F; investigators of the LiverScreen Consortium. Transient elastography for screening of liver fibrosis: Cost-effectiveness analysis from six prospective cohorts in Europe and Asia. *J Hepatol* 2019; **71**: 1141-1151 [PMID: 31470067 DOI: 10.1016/j.jhep.2019.08.019]
13 **Wang S**, Zhang C, Zhang G, Yuan Z, Liu Y, Ding L, Sun X, Jia H, Xue F. Association between white blood cell count and non-alcoholic fatty liver disease in urban Han Chinese: a prospective cohort study. *BMJ Open* 2016; **6**: e010342 [PMID: 27251683 DOI: 10.1136/bmjopen-2015-010342]
14 **Lee YJ**, Lee HR, Shim JY, Moon BS, Lee JH, Kim JK. Relationship between white blood cell count and nonalcoholic fatty liver disease. *Dig Liver Dis* 2010; **42**: 888-894 [PMID: 20472517 DOI: 10.1016/j.dld.2010.04.005]
15 **Chung GE**, Yim JY, Kim D, Kwak MS, Yang JI, Chung SJ, Yang SY, Kim JS. Associations between White Blood Cell Count and the Development of Incidental Nonalcoholic Fatty Liver Disease. *Gastroenterol Res Pract* 2016; **2016**: 7653689 [PMID: 28070183 DOI: 10.1155/2016/7653689]
16 **Brouard N**, Jost C, Matthias N, Albrecht C, Egard S, Gandhi P, Strassel C, Inoue T, Sugiyama D, Simmons PJ, Gachet C, Lanza F. A unique microenvironment in the developing liver supports the expansion of megakaryocyte progenitors. *Blood Adv* 2017; **1**: 1854-1866 [PMID: 29296832 DOI: 10.1182/bloodadvances.2016003541]
17 **Afdhal N**, McHutchison J, Brown R, Jacobson I, Manns M, Poordad F, Weksler B, Esteban R. Thrombocytopenia associated with chronic liver disease. *J Hepatol* 2008; **48**: 1000-1007 [PMID: 18433919 DOI: 10.1016/j.jhep.2008.03.009]
18 **Bataller R**, Brenner DA. Liver fibrosis. *J Clin Invest* 2005; **115**: 209-218 [PMID: 15690074 DOI: 10.1172/JCI24282]
19 **Pinzani M**, Marra F. Cytokine receptors and signaling in hepatic stellate cells. *Semin Liver Dis* 2001; **21**: 397-416 [PMID: 11586468 DOI: 10.1055/s-2001-17554]
20 **Kurokawa T**, Ohkohchi N. Platelets in liver disease, cancer and regeneration. *World J Gastroenterol* 2017; **23**: 3228-3239 [PMID: 28566882 DOI: 10.3748/wjg.v23.i18.3228]
21 **Chauhan A**, Adams DH, Watson SP, Lalor PF. Platelets: No longer bystanders in liver disease. *Hepatology* 2016; **64**: 1774-1784 [PMID: 26934463 DOI: 10.1002/hep.28526]
22 **Sookoian S**, Gianotti TF, Rosselli MS, Burgueño AL, Castaño GO, Pirola CJ. Liver transcriptional profile of atherosclerosis-related genes in human nonalcoholic fatty liver disease. *Atherosclerosis*

2011; **218**: 378-385 [PMID: 21664615 DOI: 10.1016/j.atherosclerosis.2011.05.014]
23 **Coppinger JA**, Cagney G, Toomey S, Kislinger T, Belton O, McRedmond JP, Cahill DJ, Emili A, Fitzgerald DJ, Maguire PB. Characterization of the proteins released from activated platelets leads to localization of novel platelet proteins in human atherosclerotic lesions. *Blood* 2004; **103**: 2096-2104 [PMID: 14630798 DOI: 10.1182/blood-2003-08-2804]
24 **Assoian RK**, Sporn MB. Type beta transforming growth factor in human platelets: release during platelet degranulation and action on vascular smooth muscle cells. *J Cell Biol* 1986; **102**: 1217-1223 [PMID: 3457014 DOI: 10.1083/jcb.102.4.1217]
25 **Malehmir M**, Pfister D, Gallage S, Szydlowska M, Inverso D, Kotsiliti E, Leone V, Peiseler M, Surewaard BGJ, Rath D, Ali A, Wolf MJ, Drescher H, Healy ME, Dauch D, Kroy D, Krenkel O, Kohlhepp M, Engleitner T, Olkus A, Sijmonsma T, Volz J, Deppermann C, Stegner D, Helbling P, Nombela-Arrieta C, Rafiei A, Hinterleitner M, Rall M, Baku F, Borst O, Wilson CL, Leslie J, O'Connor T, Weston CJ, Adams DH, Sheriff L, Teijeiro A, Prinz M, Bogeska R, Anstee N, Bongers MN, Notohamiprodjo M, Geisler T, Withers DJ, Ware J, Mann DA, Augustin HG, Vegiopoulos A, Milsom MD, Rose AJ, Lalor PF, Llovet JM, Pinyol R, Tacke F, Rad R, Matter M, Djouder N, Kubes P, Knolle PA, Unger K, Zender L, Nieswandt B, Gawaz M, Weber A, Heikenwalder M. Platelet GPIbα is a mediator and potential interventional target for NASH and subsequent liver cancer. *Nat Med* 2019; **25**: 641-655 [PMID: 30936549 DOI: 10.1038/s41591-019-0379-5]
26 **Romeo S**, Kozlitina J, Xing C, Pertsemlidis A, Cox D, Pennacchio LA, Boerwinkle E, Cohen JC, Hobbs HH. Genetic variation in PNPLA3 confers susceptibility to nonalcoholic fatty liver disease. *Nat Genet* 2008; **40**: 1461-1465 [PMID: 18820647 DOI: 10.1038/ng.257]
27 **Sookoian S**, Pirola CJ. Meta-analysis of the influence of I148M variant of patatin-like phospholipase domain containing 3 gene (PNPLA3) on the susceptibility and histological severity of nonalcoholic fatty liver disease. *Hepatology* 2011; **53**: 1883-1894 [PMID: 21381068 DOI: 10.1002/hep.24283]
28 **Chamorro AJ**, Torres JL, Mirón-Canelo JA, González-Sarmiento R, Laso FJ, Marcos M. Systematic review with meta-analysis: the I148M variant of patatin-like phospholipase domain-containing 3 gene (PNPLA3) is significantly associated with alcoholic liver cirrhosis. *Aliment Pharmacol Ther* 2014; **40**: 571-581 [PMID: 25060292 DOI: 10.1111/apt.12890]
29 **Stickel F**, Buch S, Lau K, Meyer zu Schwabedissen H, Berg T, Ridinger M, Rietschel M, Schafmayer C, Braun F, Hinrichsen H, Günther R, Arlt A, Seeger M, Müller S, Seitz HK, Soyka M, Lerch M, Lammert F, Sarrazin C, Kubitz R, Häussinger D, Hellerbrand C, Bröring D, Schreiber S, Kiefer F, Spanagel R, Mann K, Datz C, Krawczak M, Wodarz N, Völzke H, Hampe J. Genetic variation in the PNPLA3 gene is associated with alcoholic liver injury in caucasians. *Hepatology* 2011; **53**: 86-95 [PMID: 21254164 DOI: 10.1002/hep.24017]
30 **Tian C**, Stokowski RP, Kershenobich D, Ballinger DG, Hinds DA. Variant in PNPLA3 is associated with alcoholic liver disease. *Nat Genet* 2010; **42**: 21-23 [PMID: 19946271 DOI: 10.1038/ng.488]
31 **Valenti L**, Rumi M, Galmozzi E, Aghemo A, Del Menico B, De Nicola S, Dongiovanni P, Maggioni M, Fracanzani AL, Rametta R, Colombo M, Fargion S. Patatin-like phospholipase domain-containing 3 I148M polymorphism, steatosis, and liver damage in chronic hepatitis C. *Hepatology* 2011; **53**: 791-799 [PMID: 21319195 DOI: 10.1002/hep.24123]
32 **Viganò M**, Valenti L, Lampertico P, Facchetti F, Motta BM, D'Ambrosio R, Romagnoli S, Dongiovanni P, Donati B, Fargion S, Colombo M. Patatin-like phospholipase domain-containing 3 I148M affects liver steatosis in patients with chronic hepatitis B. *Hepatology* 2013; **58**: 1245-1252 [PMID: 23564580 DOI: 10.1002/hep.26445]
33 **Falleti E**, Fabris C, Cmet S, Cussigh A, Bitetto D, Fontanini E, Fornasiere E, Bignulin S, Fumolo E, Bignulin E, Pirisi M, Toniutto P. PNPLA3 rs738409C/G polymorphism in cirrhosis: relationship with the aetiology of liver disease and hepatocellular carcinoma occurrence. *Liver Int* 2011; **31**: 1137-1143 [PMID: 21745286 DOI: 10.1111/j.1478-3231.2011.02534.x]
34 **Trépo E**, Nahon P, Bontempi G, Valenti L, Falleti E, Nischalke HD, Hamza S, Corradini SG, Burza MA, Guyot E, Donati B, Spengler U, Hillon P, Toniutto P, Henrion J, Franchimont D, Devière J, Mathurin P, Moreno C, Romeo S, Deltenre P. Association between the PNPLA3 (rs738409 C>G) variant and hepatocellular carcinoma: Evidence from a meta-analysis of individual participant data. *Hepatology* 2014; **59**: 2170-2177 [PMID: 24114809 DOI: 10.1002/hep.26767]
35 **Diogo D**, Tian C, Franklin CS, Alanne-Kinnunen M, March M, Spencer CCA, Vangjeli C, Weale ME, Mattsson H, Kilpeläinen E, Sleiman PMA, Reilly DF, McElwee J, Maranville JC, Chatterjee AK, Bhandari A, Nguyen KH, Estrada K, Reeve MP, Hutz J, Bing N, John S, MacArthur DG, Salomaa V, Ripatti S, Hakonarson H, Daly MJ, Palotie A, Hinds DA, Donnelly P, Fox CS, Day-Williams AG, Plenge RM, Runz H. Phenome-wide association studies across large population cohorts support drug target validation. *Nat Commun* 2018; **9**: 4285 [PMID: 30327483 DOI: 10.1038/s41467-018-06540-3]
36 **Pilling LC**, Atkins JL, Kuchel GA, Ferrucci L, Melzer D. Red cell distribution width and common disease onsets in 240,477 healthy volunteers followed for up to 9 years. *PLoS One* 2018; **13**: e0203504 [PMID: 30212481 DOI: 10.1371/journal.pone.0203504]
37 **Kichaev G**, Bhatia G, Loh PR, Gazal S, Burch K, Freund MK, Schoech A, Pasaniuc B, Price AL. Leveraging Polygenic Functional Enrichment to Improve GWAS Power. *Am J Hum Genet* 2019; **104**: 65-75 [PMID: 30595370 DOI: 10.1016/j.ajhg.2018.11.008]
38 **Chen VL**, Chen Y, Du X, Handelman SK, Speliotes EK. Genetic variants that associate with cirrhosis have pleiotropic effects on human traits. *Liver Int* 2020; **40**: 405-415 [PMID: 31815349 DOI: 10.1111/liv.14321]

39 **Watanabe K**, Taskesen E, van Bochoven A, Posthuma D. Functional mapping and annotation of genetic associations with FUMA. *Nat Commun* 2017; **8**: 1826 [PMID: 29184056 DOI: 10.1038/s41467-017-01261-5]

40 **Elfenbein A**, Simons M. Syndecan-4 signaling at a glance. *J Cell Sci* 2013; **126**: 3799-3804 [PMID: 23970415 DOI: 10.1242/jcs.124636]

41 **Morgan MR**, Humphries MJ, Bass MD. Synergistic control of cell adhesion by integrins and syndecans. *Nat Rev Mol Cell Biol* 2007; **8**: 957-969 [PMID: 17971838 DOI: 10.1038/nrm2289]

42 **Kitamoto T**, Kitamoto A, Ogawa Y, Honda Y, Imajo K, Saito S, Yoneda M, Nakamura T, Nakajima A, Hotta K. Targeted-bisulfite sequence analysis of the methylation of CpG islands in genes encoding PNPLA3, SAMM50, and PARVB of patients with non-alcoholic fatty liver disease. *J Hepatol* 2015; **63**: 494-502 [PMID: 25776890 DOI: 10.1016/j.jhep.2015.02.049]

43 **Wu G**, Wang K, Xue Y, Song G, Wang Y, Sun X, Zhong L, Zhou C, Shen B, Chen J, Yu Y, Tang H, Peng Z, Sun P, Wang X. Association of rs5764455 and rs6006473 polymorphisms in PARVB with liver damage of nonalcoholic fatty liver disease in Han Chinese population. *Gene* 2016; **575**: 270-275 [PMID: 26343796 DOI: 10.1016/j.gene.2015.09.007]

44 **Kamatani Y**, Matsuda K, Okada Y, Kubo M, Hosono N, Daigo Y, Nakamura Y, Kamatani N. Genome-wide association study of hematological and biochemical traits in a Japanese population. *Nat Genet* 2010; **42**: 210-215 [PMID: 20139978 DOI: 10.1038/ng.531]

45 **Min HK**, Sookoian S, Pirola CJ, Cheng J, Mirshahi F, Sanyal AJ. Metabolic profiling reveals that PNPLA3 induces widespread effects on metabolism beyond triacylglycerol remodeling in Huh-7 hepatoma cells. *Am J Physiol Gastrointest Liver Physiol* 2014; **307**: G66-G76 [PMID: 24763554 DOI: 10.1152/ajpgi.00335.2013]

46 **Pathan M**, Keerthikumar S, Ang CS, Gangoda L, Quek CY, Williamson NA, Mouradov D, Sieber OM, Simpson RJ, Salim A, Bacic A, Hill AF, Stroud DA, Ryan MT, Agbinya JI, Mariadason JM, Burgess AW, Mathivanan S. FunRich: An open access standalone functional enrichment and interaction network analysis tool. *Proteomics* 2015; **15**: 2597-2601 [PMID: 25921073 DOI: 10.1002/pmic.201400515]

47 **Sookoian S**, Pirola CJ. PNPLA3, the history of an orphan gene of the potato tuber protein family that found an organ: the liver. *Hepatology* 2014; **59**: 2068-2071 [PMID: 24122882 DOI: 10.1002/hep.26895]

48 **Sookoian S**, Pirola CJ. PNPLA3, the triacylglycerol synthesis/hydrolysis/storage dilemma, and nonalcoholic fatty liver disease. *World J Gastroenterol* 2012; **18**: 6018-6026 [PMID: 23155331 DOI: 10.3748/wjg.v18.i42.6018]

49 **Mitsche MA**, Hobbs HH, Cohen JC. Patatin-like phospholipase domain-containing protein 3 promotes transfer of essential fatty acids from triglycerides to phospholipids in hepatic lipid droplets. *J Biol Chem* 2018; **293**: 9232 [PMID: 29907731 DOI: 10.1074/jbc.AAC118.004058]

World Journal of Gastroenterology

Submit a Manuscript: https://www.f6publishing.com

World J Gastroenterol 2021 January 28; 27(4): 321-335

DOI: 10.3748/wjg.v27.i4.321

ISSN 1007-9327 (print) ISSN 2219-2840 (online)

ORIGINAL ARTICLE

Retrospective Study

Preoperative maximal voluntary ventilation, hemoglobin, albumin, lymphocytes and platelets predict postoperative survival in esophageal squamous cell carcinoma

Shou-Jia Hu, Xue-Ke Zhao, Xin Song, Ling-Ling Lei, Wen-Li Han, Rui-Hua Xu, Ran Wang, Fu-You Zhou, Liang Wang, Li-Dong Wang

ORCID number: Shou-Jia Hu 0000-0002-9857-0065; Xue-Ke Zhao 0000-0002-9036-6342; Xin Song 0000-0002-7680-4908; Ling-Ling Lei 0000-0001-7540-7786; Wen-Li Han 0000-0002-3516-2195; Rui-Hua Xu 0000-0002-6914-2168; Ran Wang 0000-0002-2588-5760; Fu-You Zhou 0000-0002-6548-4099; Liang Wang 0000-0002-9364-8572; Li-Dong Wang 0000-0002-7933-0410.

Author contributions: Wang LD and Hu SJ designed and wrote the paper; Lei LL, Han WL, Xu RH, Wang R and Zhou FY performed data collection, interpretation and follow-up; Hu SJ, Zhao XK and Song X contributed to data analysis; Zhou FY, Wang L and Wang LD revised the manuscript; Wang L edited the manuscript for English language.

Supported by National Natural Science Foundation of China, No. U1301227, No. 81872032 and No. U1804262; Doctoral Team Foundation of the First Affiliated Hospital of Zhengzhou University, No. 2016-BSTDJJ-03.

Institutional review board statement: This study was reviewed and approved by the Ethics Committee of Zhengzhou

Shou-Jia Hu, Xue-Ke Zhao, Xin Song, Ling-Ling Lei, Wen-Li Han, Rui-Hua Xu, Ran Wang, Li-Dong Wang, State Key Laboratory of Esophageal Cancer Prevention & Treatment and Henan Key Laboratory for Esophageal Cancer Research of The First Affiliated Hospital, Zhengzhou University, Zhengzhou 450052, Henan Province, China

Fu-You Zhou, Department of Thoracic Surgery, Anyang Tumor Hospital, Anyang 455000, Henan Province, China

Liang Wang, Department of Tumor Biology, H. Lee Moffitt Cancer Center and Research Institute, Tampa, FL 33612, United States

Corresponding author: Li-Dong Wang, MD, PhD, Professor, State Key Laboratory of Esophageal Cancer Prevention & Treatment and Henan Key Laboratory for Esophageal Cancer Research of The First Affiliated Hospital, Zhengzhou University, No. 40 Daxue Road, Zhengzhou 450052, Henan Province, China. ldwang2007@126.com

Abstract

BACKGROUND

Preoperative pulmonary function plays an important role in selecting surgical candidates and assessing postoperative complications. Reduced pulmonary function is associated with poor survival in several cancers, but the prognostic value of preoperative pulmonary function in esophageal squamous cell carcinoma (ESCC) is unclear. Nutritional and systemic inflammation parameters are vital to cancer survival, and the combination of these parameters improves the prognostic value. The hemoglobin, albumin, lymphocytes and platelets (HALP) score is a novel prognostic indicator to reflect the nutritional and inflammation status, but the clinical effects of the HALP score combined with maximal voluntary ventilation (MVV), an important parameter of pulmonary function, have not been well studied in ESCC.

AIM

To investigate the prognostic value of MVV and HALP score for assessing postoperative survival of ESCC patients.

University.

Informed consent statement: Patients were not required to give informed consent to the study because the analysis used anonymous clinical data that were obtained after each patient agreed to treatment by written consent.

Conflict-of-interest statement: We have no potential conflicts of interest to disclose.

Open-Access: This article is an open-access article that was selected by an in-house editor and fully peer-reviewed by external reviewers. It is distributed in accordance with the Creative Commons Attribution NonCommercial (CC BY-NC 4.0) license, which permits others to distribute, remix, adapt, build upon this work non-commercially, and license their derivative works on different terms, provided the original work is properly cited and the use is non-commercial. See: http://creativecommons.org/Licenses/by-nc/4.0/

Manuscript source: Unsolicited manuscript

Specialty type: Gastroenterology and hepatology

Country/Territory of origin: China

Peer-review report's scientific quality classification

Grade A (Excellent): 0
Grade B (Very good): B, B
Grade C (Good): C
Grade D (Fair): 0
Grade E (Poor): 0

Received: October 13, 2020
Peer-review started: October 13, 2020
First decision: December 3, 2020
Revised: December 17, 2020
Accepted: December 24, 2020
Article in press: December 24, 2020
Published online: January 28, 2021

P-Reviewer: Cho YS, De Nardi P
S-Editor: Fan JR
L-Editor: A
P-Editor: Liu JH

METHODS

Data from 834 ESCC patients who underwent radical esophagectomy with R0 resection were collected and retrospectively analyzed. Preoperative MVV and HALP data were retrieved from medical archives. The HALP score was calculated by the formula: Hemoglobin (g/L) × albumin (g/L) × lymphocytes (/L)/platelets (/L). The optimal cut-off values of MVV and HALP score were calculated by the receiver operating characteristic curve analysis. The Kaplan-Meier method with log-rank test was used to draw the survival curves for the variables tested. Multivariate Cox proportional hazard regression models were used to analyze the independent prognostic factors for overall survival.

RESULTS

MVV was significantly associated with gender ($P < 0.001$), age at diagnosis ($P < 0.001$), smoking history ($P < 0.001$), drinking history ($P < 0.001$), tumor length ($P = 0.013$), tumor location ($P = 0.037$) and treatment type ($P = 0.001$). The HALP score was notably associated with gender ($P < 0.001$), age at diagnosis ($P = 0.035$), tumor length ($P < 0.001$) and invasion depth ($P = 0.001$). Univariate Cox regression analysis showed that low MVV and low HALP score were associated with worse overall survival (all $P < 0.001$). Multivariate analysis showed that low MVV and the HALP score were both independent risk factors for overall survival (all $P < 0.001$). The combination of MVV and HALP score improved the prediction performance for overall survival than tumor-node-metastasis. Also, low combination of MVV and HALP score was an independent risk factor for poor overall survival ($P < 0.001$).

CONCLUSION

MVV, HALP score and their combination are simple and promising clinical markers to predict overall survival of ESCC patients.

Key Words: Maximal voluntary ventilation; Hemoglobin, albumin, lymphocytes and platelets score; Nutritional status; Inflammation status; Postoperative survival; Esophageal squamous cell carcinoma

©The Author(s) 2021. Published by Baishideng Publishing Group Inc. All rights reserved.

Core Tip: Reduced pulmonary function is considered a risk factor for cancer survival. The combination score of hemoglobin, albumin, lymphocytes and platelets (HALP) is a novel prognostic indicator to reflect nutritional and inflammatory status. We demonstrated that preoperative maximal voluntary ventilation (MVV), an important parameter of pulmonary function, and HALP score were independent prognostic factors for patients with esophageal squamous cell carcinoma. The combination of MVV and HALP score has a better prognostic value than tumor-node-metastasis alone. The combination of MVV and HALP score reflects the status of inflammation, nutrition and pulmonary function simultaneously and may partly compensate for the limitation of the tumor-node-metastasis staging system.

Citation: Hu SJ, Zhao XK, Song X, Lei LL, Han WL, Xu RH, Wang R, Zhou FY, Wang L, Wang LD. Preoperative maximal voluntary ventilation, hemoglobin, albumin, lymphocytes and platelets predict postoperative survival in esophageal squamous cell carcinoma. *World J Gastroenterol* 2021; 27(4): 321-335
URL: https://www.wjgnet.com/1007-9327/full/v27/i4/321.htm
DOI: https://dx.doi.org/10.3748/wjg.v27.i4.321

INTRODUCTION

Esophageal cancer is the sixth leading cause of cancer-related death in the world[1]. Esophageal squamous cell carcinoma (ESCC) is the predominant type of esophageal cancer in China. Despite improvements in treatment and clinical management, the

prognosis of ESCC is still poor[1]. Surgery remains the preferred method for non-metastatic cancer patients. Although the tumor-node-metastasis (TNM) staging system is well known as a predictive clinical parameter in terms of guiding treatment and clinical prognosis[2], the survival outcomes for esophageal cancer patients with the same TNM stage still vary widely. In addition, accurate TNM stage identification relies on the pathologic result after esophagectomy. Therefore, it is important to identify more effective preoperative clinical factors for early guidance of treatment and for predicting the prognosis of esophageal cancer, particularly in ESCC.

Preoperative pulmonary evaluation is a routine examination used to select potential surgical candidates and assess postoperative respiratory complications[3]. Previous studies have shown that poor pulmonary function is associated with severe postoperative complications in patients undergoing esophagectomy[4-6]. Some studies have reported that reduced pulmonary function is associated with mortality risk in the general population[7,8], lung cancer[9] and gastric cancer[10], while little attention has been given to the correlation between preoperative pulmonary evaluation and the overall survival of esophageal cancer patients. Forced vital capacity (FVC) and vital capacity (VC) are both important parameters in pulmonary evaluation test. Low FVC has been implicated as a risk prognostic predictor in gastric cancer[10], and low VC also predicts the poor survival in Japanese esophageal cancer[11] in previous limited studies. Maximal voluntary ventilation (MVV) is another important parameter in pulmonary evaluation test and is usually used to reflect respiratory muscle strength and lung capacity. Studies report that MVV reflects dysfunction and airway resistance both in inspiratory and expiratory phases, while FVC and VC reflect only the expiratory phase[12], so MVV may better reflects the real capacity of lung function. However, few studies have examined its effects on esophageal cancer patient survival.

Dysphagia is a typical symptom of esophageal cancer patients and may lead to malnutrition. Numerous studies have demonstrated that the parameters of nutrition and inflammation status, including the levels of hemoglobin and albumin and lymphocyte and platelet counts, are vital to cancer survival[13-16]. More importantly, some studies reported that the combination of these parameters such as neutrophil-lymphocyte ratio[17], platelet-to-lymphocyte ratio[18] and prognostic nutritional index[19] could better predict prognosis than nutritional or inflammatory condition status alone. The combination of hemoglobin, albumin, lymphocytes and platelets (HALP) score with four hematological parameters has been demonstrated as a novel and potential prognostic indicator for several types of malignancies[20-22], but the clinical effects of HALP score combined with other prognostic factors in ESCC patients who underwent esophagectomy have not been well studied.

Thus, to address these issues, we investigated the prognostic value of preoperative pulmonary function (MVV) and HALP score for the long-term survival in this group of ESCC patients.

MATERIALS AND METHODS

Patients

A total of 834 ESCC patients who underwent radical esophagectomy with R0 resection between 2011 and 2014 from the 500000 esophageal and gastric cardia carcinoma database (1973-2020), established by Henan Key Laboratory for Esophageal Cancer Research of The First Affiliated Hospital, Zhengzhou University, were enrolled in the retrospective study. Patients were selected according to the following criteria: (1) Patients were diagnosed with ESCC by postoperative histopathology; (2) Patients had tumors located in the thoracic esophagus; (3) Patients had no other malignant tumors except for ESCC; (4) Patients received no chemotherapy or/and radiotherapy before surgery; (5) Patients had no neuromuscular disorders, respiratory diseases, chronic/acute inflammatory disease or autoimmune disease or not received glucocorticoid therapy before surgery; and (6) Preoperative records of pulmonary evaluation test and HALP parameters were obtained.

Clinical data collection and follow-up

The MVV value was determined and collected from routine preoperative pulmonary evaluation, and the values for HALP parameters were obtained from routine blood test before surgery. The HALP score was calculated using the following formula: Hemoglobin (g/L) × albumin (g/L) × lymphocytes (/L)/platelets (/L). The pathological TNM stage of patients was also collected on the basis of the 7th edition of the TNM staging system from the American Joint Committee on Cancer[2]. The time of

diagnosis was the date when patients were confirmed to have ESCC by histopathology. The overall survival time was the interval from the time of diagnosis to death or the last follow-up. The last follow-up was performed in May 2020. Of the total 834 patients, 799 patients (95.8%) had detailed follow-up data. In the first year after esophagectomy, patients were followed up every 3 mo. Then, follow-up was conducted once a year.

Statistical analysis

SPSS software (version 21, IBM, Armonk, NY, United States) and GraphPad Prism version 8.0 (GraphPad Software, San Diego, CA, United States) were used to perform all the statistical analyses. Two-tailed *P* values of less than 0.05 were considered statistically significant. The optimal cut-off values of MVV and HALP score were calculated by the receiver operating characteristic (ROC) curve analysis. The chi-square test was used to analyze the relationship of clinical features with MVV and HALP score for patients with ESCC. A univariate Cox proportional hazard regression model was used to evaluate the prognostic value of each variable for overall survival. The Kaplan-Meier method with log-rank test was used to draw the survival curves for the variables tested. Multivariate Cox proportional hazard regression models were used to analyze the independent prognostic factors for overall survival. Significant prognostic variables in the univariate analysis were chosen for the multivariate analysis.

RESULTS

Patients' basic clinical characteristics

From the archived clinical record, we retrieved the baseline clinic parameters for this group of ESCC patients (Table 1). The ratio of males to females was 1.6:1. The median age was 60 years, ranging from 38 to 84 years. Overall, 756 patients (90.6%) underwent open esophagectomy by the left approach, and 78 patients (9.4%) underwent surgery by the right approach, including 75 patients (9.0%) who were treated with open esophagectomy and three patients (0.4%) who were treated with thoracoscopic esophagectomy. 151 patients (18.1%) had postoperative complications. The median survival time of the ESCC patients was 4.4 years, ranging from 0.19 to 9.5 years. The 1-, 3- and 5-year survival rates of all patients were 91.4%, 64.6% and 42.9%, respectively.

Association of MVV and HALP score with basic clinical characteristics

To assess the potential correlation of MVV and HALP score for overall survival, we first performed ROC analysis using their values in these ESCC patients. We found that the area under the curve (AUC) of MVV and HALP score were 0.631 and 0.646, respectively, indicating that they were both significant for predicting 5-year overall survival (all $P < 0.001$, Figure 1). Then, we determined the optimal cutoff values of MVV and HALP score as 85.2 and 38.8, respectively, by using the maximal Youden index. Based on the two cutoff values, the ESCC patients were divided into high and low groups for both MVV and HALP score, respectively. We then applied the chi square test to evaluate the potential association of MVV and HALP score with basic clinical factors. We found that MVV was significantly associated with gender ($P < 0.001$), age at diagnosis ($P < 0.001$), smoking history ($P < 0.001$), drinking history ($P < 0.001$), tumor length ($P = 0.013$), tumor location ($P = 0.037$) and treatment type ($P = 0.001$). The association between MVV and overall postoperative complications ($P = 0.243$, Table 2) were not observed, and MVV was not associated with postoperative pulmonary complications ($P = 0.843$). The HALP score was notably associated with gender ($P < 0.001$), age at diagnosis ($P = 0.035$), tumor length ($P < 0.001$) and invasion depth ($P = 0.001$). The association of patients' clinical features with MVV and HALP score was shown in Table 2.

Association of MVV and HALP score with overall survival

To evaluate the potential association of clinical factors with overall survival, we performed univariate Cox regression analysis and observed a significant association with age at diagnosis ($P < 0.001$), tumor length ($P < 0.001$), differentiation ($P < 0.001$), invasion depth ($P < 0.001$), lymph node metastasis ($P < 0.001$) and postoperative complications ($P < 0.001$) (Table 3). We also observed an association between survival and MVV ($P < 0.001$) and HALP score ($P < 0.001$) (Table 3). Kaplan-Meier analysis using the log-rank test showed that low MVV ($P < 0.001$, Figure 2) and low HALP

Table 1 Clinical characteristics of patients with esophageal squamous cell carcinoma

Variable	Cases	
	n	%
Gender		
Male	509	61.0
Female	325	39.0
Age at diagnosis in yr		
Median (interquartile range)	60 (55-65)	
Smoking history		
No	434	52.0
Yes	400	48.0
Drinking history		
No	574	68.8
Yes	260	31.2
Tumor length (cm)		
Median (interquartile range)	4.0 (3.0-5.0)	
Tumor location		
Upper	140	16.8
Middle	549	65.8
Lower	145	17.4
Differentiation		
Well	37	4.5
Moderate	459	55.0
Poor	338	40.5
Invasion depth		
pT1	108	12.9
pT2	240	28.8
pT3	486	58.3
Lymph node metastasis		
pN0	494	59.2
pN1	190	22.8
pN2	121	14.5
pN3	29	3.5
TNM stage		
I	100	12.0
II	454	54.4
III	280	33.6
Surgical approach		
Left	756	90.6
Right	78	9.4
Treatment type		
Surgery	650	77.9
Surgery + adjuvant RT/CT	184	22.1

MVV		
Median (interquartile range)	85.1 (68.5-96.6)	
HALP score		
Median (interquartile range)	43.2 (31.6-55.4)	
Overall complications		
No	683	81.9
Yes	151	18.1

CT: Chemotherapy; HALP: Hemoglobin, albumin, lymphocytes and platelets; MVV: Maximal voluntary ventilation; RT: Radiotherapy; TNM: Tumor-node-metastasis.

score ($P < 0.001$, Figure 2) predicted a worse overall survival. By adjusting the clinical factors from the multivariate Cox regression analysis, the association of low MVV and low HALP score with poor survival remained significantly with $P < 0.001$ (hazard ratio: 1.451, 95% confidence interval: 1.208-1.743) and $P < 0.001$ (hazard ratio: 1.537, 95% confidence interval: 1.287-1.836) (Table 3), respectively, suggesting that low MVV and HALP score were independent risk factors for overall survival. Gender, smoking history, drinking history, tumor location, differentiation, surgical approach and treatment type were not independently associated with overall survival (all $P > 0.05$), whereas age at diagnosis, tumor length, invasion depth, lymph node metastasis, MVV, HALP score and postoperative complications were independent predictive factors for overall survival (all $P < 0.05$) (Table 3).

Predictive value of the combination of MVV with HALP score for overall survival

Since both MVV and HALP score were independent predictive factors, we next explored the cumulative effect of MVV and HALP score (coMVV-HALP) on overall survival. We defined the following: (1) The coMVV-HALP score was 0 when patients had both low MVV and HALP score; (2) The coMVV-HALP score was 1 when patients had either low MVV or HALP score; and (3) The coMVV-HALP score was 2 when patients had both high MVV and HALP score. Then, we performed ROC analysis to evaluate the predictive value of the coMVV-HALP score for 5-year overall survival. We found that the AUC for the coMVV-HALP score was 0.681 ($P < 0.001$, Figure 3), which indicated better prognostic value than TNM (AUC: 0.659) and HALP score (AUC: 0.646) or MVV (AUC: 0.631) alone.

Kaplan-Meier analysis using the log-rank test showed that a low coMVV-HALP score predicted poor overall survival ($P < 0.001$, Figure 4) in ESCC patients. As age at diagnosis, tumor length, invasion depth and lymph node metastasis were independent predictive factors for overall survival, we then performed further stratification analysis for the ESCC patients according to age, tumor length and TNM to explore the predictive value of the coMVV-HALP score in different groups. Stratification analysis by age at diagnosis and tumor length accordingly showed that patients with coMVV-HALP score = 0 had a worse overall survival than patients with coMVV-HALP score = 1 or 2 in groups with age < 60 ($n = 379$, $P < 0.001$, Figure 5), age ≥ 60 ($n = 420$, $P < 0.001$, Figure 5), tumor length < 4 cm ($n = 374$, $P = 0.002$, Figure 5) and tumor length ≥ 4 cm ($n = 425$, $P < 0.001$, Figure 5). Stratification analysis by TNM stage showed no significant difference in overall survival among patients with different coMVV-HALP scores (0, 1, 2) in stage I ($n = 98$, $P = 0.096$, Figure 6). However, we found that, among patients in stage II ($n = 437$, $P < 0.001$, Figure 6) and III ($n = 264$, $P < 0.001$, Figure 6), those with coMVV-HALP score = 0 had a worse overall survival than those with coMVV-HALP score = 1 or 2. Multivariate analysis further showed that a low coMVV-HALP score was an independent risk factor for poor overall survival ($P < 0.001$, Supplementary Table 1).

DISCUSSION

Reliable clinical factors that predict patients' overall survival are important for clinicians to make informed treatment decisions. In this study, we investigated the prognostic value of preoperative pulmonary evaluation with MVV and HALP score for predicting the long-term survival of ESCC patients. Our data showed that MVV,

Table 2 Association of maximal voluntary ventilation and hemoglobin, albumin, lymphocytes and platelets score with basic clinical factors, *n* (%)

Variable	MVV			HALP score		
	≥ 85.2	< 85.2	*P* value	≥ 38.8	< 38.8	*P* value
Gender			< 0.001			< 0.001
Male	404 (97.1)	105 (25.1)		319 (66.2)	190 (54.0)	
Female	12 (2.9)	313 (74.9)		163 (33.8)	162 (46.0)	
Age at diagnosis in yr			< 0.001			0.035
< 60	250 (60.1)	149 (35.6)		246 (51.0)	153 (43.5)	
≥ 60	166 (39.9)	269 (64.4)		236 (49.0)	199 (56.5)	
Smoking history			< 0.001			0.107
No	108 (26.0)	326 (78.0)		239 (49.6)	195 (55.4)	
Yes	308 (74.0)	92 (22.0)		243 (50.4)	157 (44.6)	
Drinking history			< 0.001			0.082
No	209 (50.2)	365 (87.3)		320 (66.4)	254 (72.2)	
Yes	207 (49.8)	53 (12.7)		162 (33.6)	98 (27.8)	
Tumor length in cm			0.013			< 0.001
< 4	175 (42.1)	212 (50.7)		249 (51.7)	138 (39.2)	
≥ 4	241 (57.9)	206 (49.3)		233(48.3)	214 (60.8)	
Tumor location			0.037			0.733
Upper	75 (18.0)	65 (15.5)		85 (17.6)	55 (15.6)	
Middle	257 (61.8)	292(69.9)		315 (65.4)	234 (66.5)	
Lower	84 (20.2)	61 (14.6)		82 (17.0)	63 (17.9)	
Differentiation			0.490			0.183
Well	15 (3.6)	22 (5.3)		16 (3.3)	21 (6.0)	
Moderate	229 (55.1)	230 (55.0)		267 (55.4)	192 (54.5)	
Poor	172 (41.3)	166 (39.7)		199 (41.3)	139 (39.5)	
Invasion depth			0.366			0.001
pT1	47 (11.3)	61 (14.6)		69 (14.3)	39 (11.1)	
pT2	122 (29.3)	118 (28.2)		158 (32.8)	82 (23.3)	
pT3	247 (59.4)	239 (57.2)		255 (52.9)	231 (65.6)	
Lymph node metastasis			0.163			0.672
pN0	242 (58.2)	252 (60.3)		290 (60.2)	204 (57.9)	
pN1	107 (25.7)	83 (19.8)		112 (23.2)	78 (22.2)	
pN2	53 (12.7)	68 (16.3)		64 (13.3)	57 (16.2)	
pN3	14 (3.4)	15 (3.6)		16 (3.3)	13 (3.7)	
TNM stage			0.541			0.084
I	45 (10.8)	55 (13.2)		62 (12.9)	38 (10.8)	
II	232 (55.8)	222 (53.1)		273 (56.6)	181 (51.4)	
III	139 (33.4)	141 (33.7)		147 (30.5)	133 (37.8)	
Surgical approach			0.478			0.718
Left	374 (89.9)	382 (91.4)		435 (90.2)	321 (91.2)	
Right	42 (10.1)	36 (8.6)		47 (9.8)	31 (8.8)	

Treatment type			0.001			0.353
Surgery	305 (73.3)	345 (82.5)		370 (76.8)	280 (79.5)	
Surgery + adjuvant RT/CT	111 (26.7)	73 (17.5)		112 (23.2)	72 (20.5)	
Overall complications			0.243			0.525
No	334 (80.3)	349 (83.5)		391 (81.1)	292 (83.0)	
Yes	82 (19.7)	69 (16.5)		91 (18.9)	60 (17.0)	

CT: Chemotherapy; HALP: Hemoglobin, albumin, lymphocytes and platelets; MVV: Maximal voluntary ventilation; RT: Radiotherapy; TNM: Tumor-node-metastasis.

HALP score and their combination were independent prognostic factors. If further validated, this score may be used clinically to overcome some limitations of the TNM staging system in assessing ESCC prognosis.

Numerous studies have focused mainly on the prognostic value of preoperative pulmonary function in lung cancer but rarely in digestive cancers. These studies have clearly shown that preoperative pulmonary evaluation could be used as a predictor for postoperative complications and survival in lung cancer[9,23]. As described previously, FVC and VC have been demonstrated as predictors of postoperative complications and the survival in gastric cancer[10] and Japanese esophageal cancer[11], respectively. In the present study, we did not find the association between MVV and postoperative complications. One possibility was that we had a different source of patients, inclusion and exclusion criteria as well as sample size. In this study, we found that low MVV was an independent risk factor for the overall survival of Chinese ESCC patients. Although the mechanism of this association between lung function and cancer prognosis is unclear, multiple studies have demonstrated that impaired lung function is associated with mortality risk in the general population[7,8]. Additionally, Sarkar *et al*[24] elaborated a mechanism in which abnormal function of the respiratory system could lead to the development of hypoxemia and its detrimental consequences. Muz *et al*[25] have reported that tumor-hypoxia plays a vital role in cell mobility and metastasis in cancer progression. It was also shown that hypoxia was correlated with poor prognosis in cancer patients[26]. Moreover, pulmonary rehabilitation is important for lung cancer patients to improve pulmonary capacity and quality of life[27]. A study has suggested that pulmonary rehabilitation benefits cancer patients and should be applied to the entire process of cancer care[28]. Therefore, MVV may influence the capacity of oxygen supply for the body and then further affect the prognosis.

The HALP score is a new combined index and its prognostic value has been investigated in many cancers, but its role in ESCC patients who underwent esophagectomy has not been studied. Our study showed that the HALP score was an independent factor for overall survival in this group of ESCC patients. The result is further supported by a study that investigated the role of the HALP score in 39 male ESCC patients receiving platinum-based chemotherapy[29]. The survival association may be explained by the following findings: (1) Studies have shown that anemia affects patients' disease progression, treatment, quality of life and survival[13,30], and anemia before radiotherapy predicts poor survival for ESCC patients[31]; (2) Low serum albumin levels are common in many advanced cancers, and some studies suggest that albumin may be a source of energy for cancer growth[32] and metabolism[33]. Importantly, it has been shown that low albumin is a risk factor for the survival outcome in ESCC[14]; (3) A systemic review has demonstrated that lymphocytes play an important role in mediating tumor suppression and controlling tumor growth[34]. A low preoperative lymphocyte count could serve as a risk factor for a variety of cancers including ESCC[35,36]; and (4) Platelets may protect tumor cells from immuno-surveillance and mediate cancer metastasis[37]. Clearly, these accumulated studies have provided strong evidence showing the prognostic value of the HALP score, which partly reflects the status of inflammation and nutrition.

By combining the MVV and HALP score, we developed a predictive coMVV-HALP score for ESCC survival, and it has a better predictive value than TNM. To the best of our knowledge, this study is the first to investigate the value of MVV and HALP score combination, which reflects the status of inflammation, nutrition and pulmonary function of ESCC patients. It is well known that esophageal cancer is a systemic disease that impacts many systems in the human body. CoMVV-HALP score is based on the routine data from the preoperative blood test and pulmonary evaluation. TNM

Table 3 Univariate and multivariate analyses for patients' overall survival with esophageal squamous cell carcinoma

Variable	Univariate analysis		Multivariate analysis	
	HR (95%CI)	*P* value	HR (95%CI)	*P* value
Gender		0.924		
Female	1			
Male	0.991 (0.831-1.183)			
Age at diagnosis in yr		< 0.001		< 0.001
< 60	1		1	
≥ 60	1.613 (1.355-1.920)		1.388 (1.155-1.668)	
Smoking history		0.760		
No	1			
Yes	0.974 (0.821-1.155)			
Drinking history		0.293		
No	1			
Yes	0.905 (0.752-1.090)			
Tumor length in cm		< 0.001		0.018
< 4	1		1	
≥ 4	1.691 (1.419-2.016)		1.259 (1.040-1.525)	
Tumor location		0.064		
Upper	1			
Middle	0.782 (0.623-0.982)			
Lower	0.733 (0.549-0.979)			
Differentiation		< 0.001		0.308
Well	1		1	
Moderate	1.308 (0.839-2.039)		1.189 (0.759-1.865)	
Poor	1.829 (1.169-2.862)		1.334 (0.841-2.118)	
Invasion depth		< 0.001		0.001
pT1	1		1	
pT2	2.100 (1.491-2.958)		1.671 (1.173-2.379)	
pT3	2.769 (2.007-3.819)		1.926 (1.371-2.706)	
Lymph node metastasis		< 0.001		< 0.001
pN0	1		1	
pN1	1.803 (1.463-2.222)		1.695 (1.362-2.109)	
pN2	2.809 (2.224-3.549)		2.281 (1.780-2.922)	
pN3	3.857 (2.571-5.787)		2.945 (1.926-4.504)	
Surgical approach		0.130		
Left	1			
Right	1.250 (0.936-1.669)			
Treatment type		0.512		
Surgery	1			
Surgery + adjuvant RT/CT	1.072 (0.871-1.319)			
MVV		< 0.001		< 0.001
≥ 85.2	1		1	

< 85.2	1.487 (1.252-1.767)		1.451 (1.208-1.743)	
HALP score		< 0.001		< 0.001
≥ 38.8	1		1	
< 38.8	1.617 (1.361-1.922)		1.537 (1.287-1.836)	
Overall complications		< 0.001		< 0.001
No	1		1	
Yes	1.456 (1.179-1.799)		1.515 (1.218-1.884)	

CI: Confidence interval; CT: Chemotherapy; HALP: Hemoglobin, albumin, lymphocytes and platelets; HR: Hazard ratio; MVV: Maximal voluntary ventilation; RT: Radiotherapy.

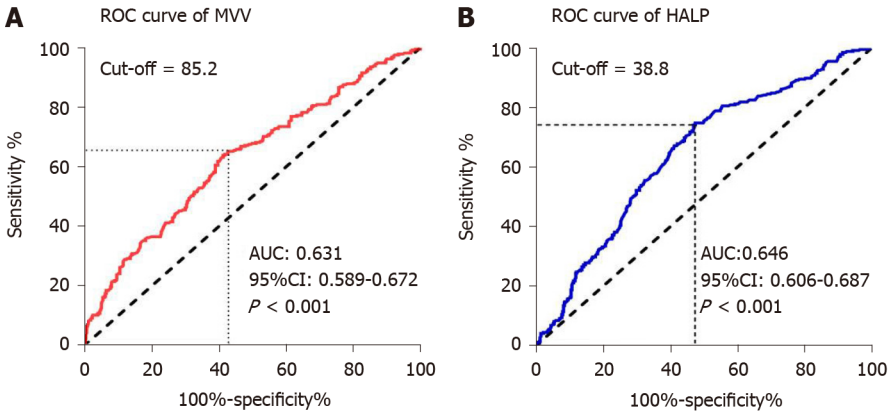


Figure 1 Receiver operating characteristic curves for 5-year overall survival in esophageal squamous cell carcinoma patients. A: Receiver operating characteristic (ROC) curve of maximal voluntary ventilation (MVV) for 5-year overall survival; B: ROC curve of hemoglobin, albumin, lymphocytes and platelets (HALP) score for 5-year overall survival. AUC: Area under the curve; CI: Confidence interval.

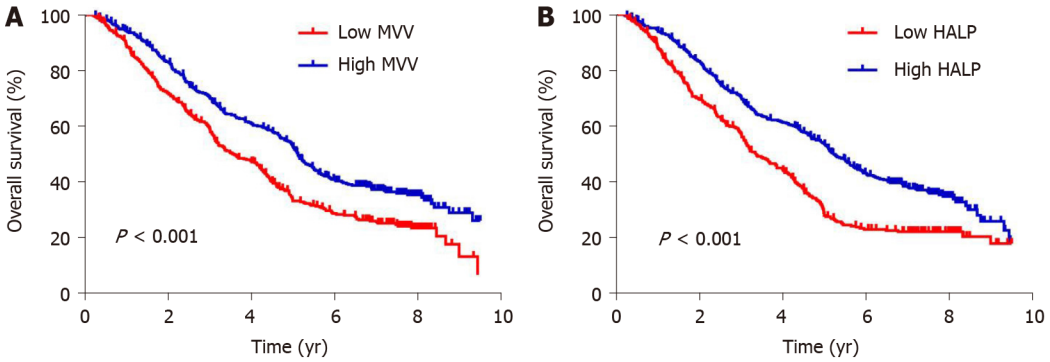
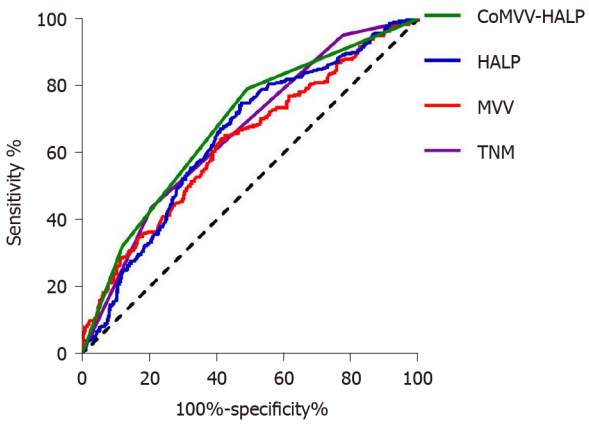


Figure 2 Kaplan-Meier curves for overall survival in esophageal squamous cell carcinoma patients. A: Kaplan-Meier curves of overall survival according to maximal voluntary ventilation (MVV) in esophageal squamous cell carcinoma (ESCC) patients; B: Kaplan-Meier curves of overall survival according to the hemoglobin, albumin, lymphocytes and platelets (HALP) score in ESCC patients.

staging system is well known as the criteria to assess the prognosis of the esophageal cancer patients, but it relies on the complete postoperative pathological information. CoMVV-HALP score may provide a new method to evaluate the prognosis of the patients before surgery. Therefore, the multivariate model integrating MVV with the HALP score may partly compensate for the limitation of the TNM staging system. This score can be easily calculated since individual clinical factors are conveniently available using a less invasive approach. These clinical factors can also be monitored cost-effectively during the course of disease progression.

This study also has some limitations: (1) Since it is a retrospective study from a single center involving different pathologists, physicians and technicians, there might be some bias of the uniformity in determining some clinical factors; and (2) The sample



Variable	AUC	95%CI	*P* value
MVV	0.631	0.589-0.672	< 0.001
HALP	0.646	0.606-0.687	< 0.001
TNM	0.659	0.619-0.699	< 0.001
coMVV-HALP	0.681	0.642-0.721	< 0.001

Figure 3 Receiver operating characteristic curves of maximal voluntary ventilation, hemoglobin, albumin, lymphocytes and platelets score, tumor-node-metastasis and maximal voluntary ventilation and hemoglobin, albumin, lymphocytes and platelets score for predicting 5-year overall survival in esophageal squamous cell carcinoma patients. MVV: Maximal voluntary ventilation; HALP: Hemoglobin, albumin, lymphocytes and platelets; CoMVV-HALP: MVV and HALP; AUC: Area under the curve; CI: Confidence interval; TNM: Tumor-node-metastasis.

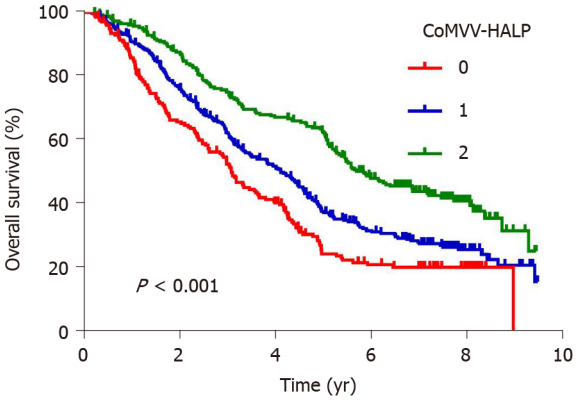


Figure 4 Kaplan-Meier curves of overall survival according to the maximal voluntary ventilation and hemoglobin, albumin, lymphocytes and platelets score in esophageal squamous cell carcinoma patients. MVV: Maximal voluntary ventilation; HALP: Hemoglobin, albumin, lymphocytes and platelets; coMVV-HALP: MVV and HALP.

size was relatively small and included only ESCC with no other types of esophageal cancer. Further prospective studies using a large sample size from more centers are needed to confirm this new finding.

CONCLUSION

MVV and HALP score, alone or in combination are simple and promising clinical predictors. Once validated in large cohorts, these clinical factors should be taken into account when assessing the prognosis of ESCC patients.

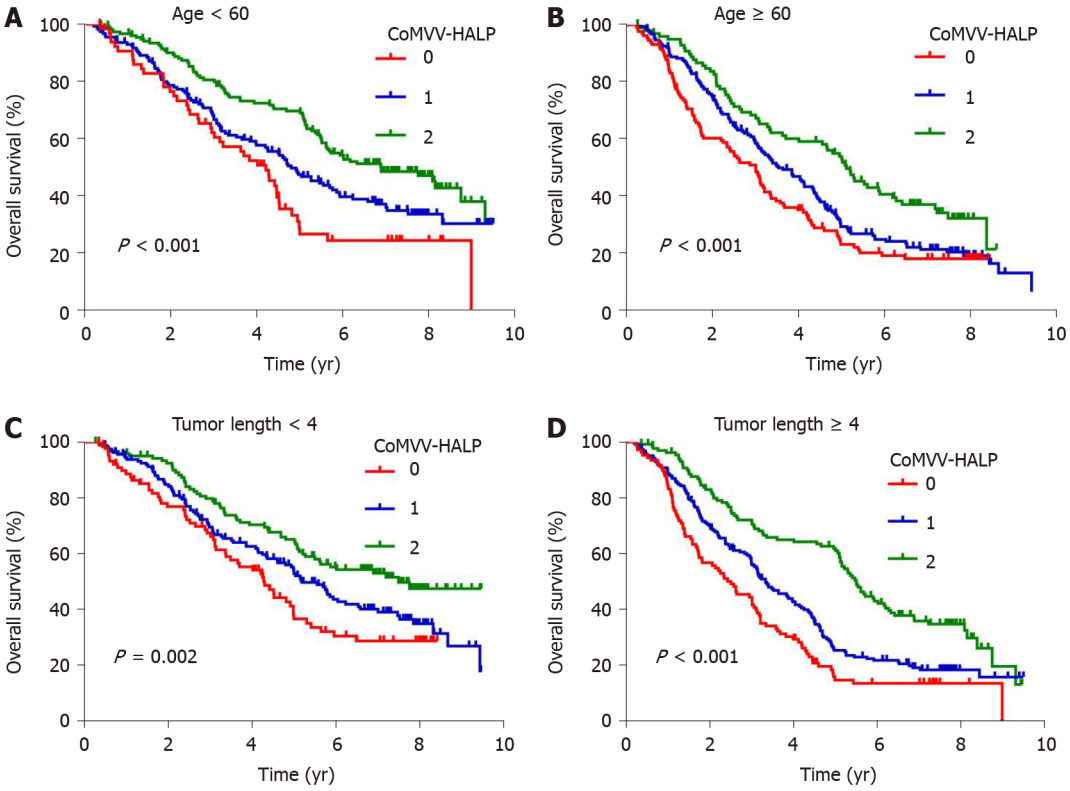


Figure 5 Kaplan-Meier curves of overall survival according to the maximal voluntary ventilation and hemoglobin, albumin, lymphocytes and platelets score in subgroups of esophageal squamous cell carcinoma patients with different ages at diagnosis and tumor lengths. A: Kaplan-Meier curves of overall survival according to maximal voluntary ventilation (MVV) and hemoglobin, albumin, lymphocytes and platelets (coMVV-HALP) score in group with age < 60; B: Kaplan-Meier curves of overall survival according to coMVV-HALP score in the group with age ≥ 60; C: Kaplan-Meier curves of overall survival according to coMVV-HALP score in the group with tumor length < 4 cm; D: Kaplan-Meier curves of overall survival according to coMVV-HALP score in the group with tumor length ≥ 4 cm.

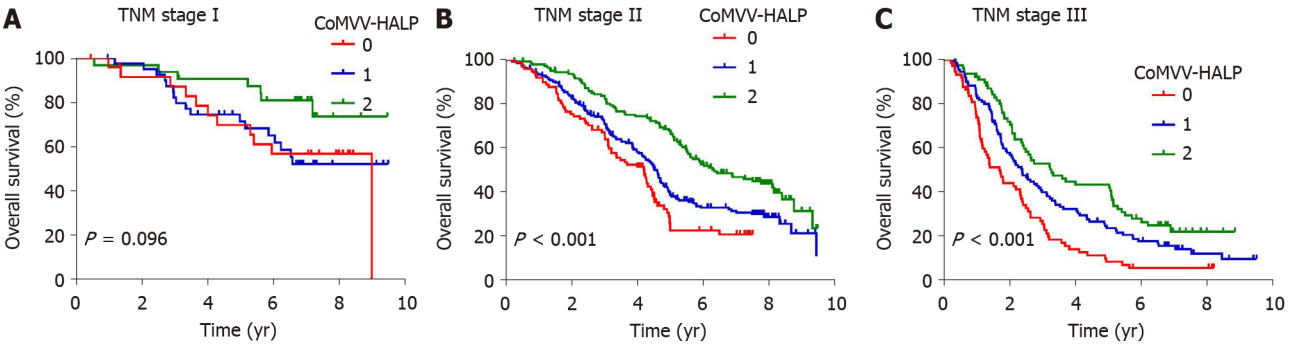


Figure 6 Kaplan-Meier curves of overall survival according to the maximal voluntary ventilation and hemoglobin, albumin, lymphocytes and platelets score in subgroups of esophageal squamous cell carcinoma patients with different tumor-node-metastasis stages. A: Kaplan-Meier curves of overall survival according to maximal voluntary ventilation (MVV) and hemoglobin, albumin, lymphocytes and platelets (coMVV-HALP) score in patients with tumor-node-metastasis (TNM) stage I; B: Kaplan-Meier curves of overall survival according to coMVV-HALP score in TNM stage II; C: Kaplan-Meier curves of overall survival according to coMVV-HALP score in TNM stage III.

ARTICLE HIGHLIGHTS

Research background

Preoperative pulmonary function plays an important role in selecting surgical candidates and assessing postoperative complications. Nutritional and systemic inflammation parameters are vital to cancer survival, and the combination of these parameters improves the prognostic value. The hemoglobin, albumin, lymphocytes and platelets (HALP) score is a novel prognostic indicator to reflect the nutritional and inflammation status.

Research motivation

The prognostic values of preoperative pulmonary function and the HALP score for survival in esophageal squamous cell carcinoma (ESCC) are unclear.

Research objectives

This study aimed to investigate the predictive values of preoperative pulmonary function and the HALP score for survival in ESCC patients.

Research methods

The predictive values of preoperative pulmonary function and the HALP score for long-term overall survival were performed in 834 ESCC patients who underwent radical esophagectomy.

Research results

Low maximal voluntary ventilation (MVV) and the HALP score were both independent risk factors for overall survival (all $P < 0.001$). The combination of MVV and HALP score (coMVV-HALP) improved the prediction performance for overall survival compared to tumor-node-metastasis, and low coMVV-HALP score was an independent risk factor for poor overall survival ($P < 0.001$).

Research conclusions

MVV, HALP score and their combination are simple and promising clinical markers to predict overall survival of ESCC patients.

Research perspectives

MVV and HALP score, alone or in combination, are simple and promising clinical predictors. Once validated in large cohorts, these clinical factors should be taken into account when assessing the prognosis of ESCC patients.

ACKNOWLEDGEMENTS

We thank Dr. Tian YJ (H. Lee Moffitt Cancer Center, United States) for English editing and thoughtful comments for this manuscript; and Professor Shi XZ (Department of Epidemiology and Biostatistics, College of Public Health in Zhengzhou University) for help in statistical analysis.

REFERENCES

1 **Lagergren J**, Smyth E, Cunningham D, Lagergren P. Oesophageal cancer. *Lancet* 2017; **390**: 2383-2396 [PMID: 28648400 DOI: 10.1016/S0140-6736(17)31462-9]
2 **Rice TW**, Blackstone EH, Rusch VW. 7th edition of the AJCC Cancer Staging Manual: esophagus and esophagogastric junction. *Ann Surg Oncol* 2010; **17**: 1721-1724 [PMID: 20369299 DOI: 10.1245/s10434-010-1024-1]
3 **Smetana GW**. Preoperative pulmonary evaluation. *N Engl J Med* 1999; **340**: 937-944 [PMID: 10089188 DOI: 10.1056/NEJM199903253401207]
4 **Ferguson MK**, Celauro AD, Prachand V. Prediction of major pulmonary complications after esophagectomy. *Ann Thorac Surg* 2011; **91**: 1494-1500; discussion 1500 [PMID: 21524462 DOI: 10.1016/j.athoracsur.2010.12.036]
5 **Reinersman JM**, Allen MS, Deschamps C, Ferguson MK, Nichols FC, Shen KR, Wigle DA, Cassivi SD. External validation of the Ferguson pulmonary risk score for predicting major pulmonary complications after oesophagectomy†. *Eur J Cardiothorac Surg* 2016; **49**: 333-338 [PMID: 25724906 DOI: 10.1093/ejcts/ezv021]
6 **Goense L**, Meziani J, Bülbül M, Braithwaite SA, van Hillegersberg R, Ruurda JP. Pulmonary diffusion capacity predicts major complications after esophagectomy for patients with esophageal cancer. *Dis Esophagus* 2019; **32** [PMID: 30239639 DOI: 10.1093/dote/doy082]
7 **Mannino DM**, Buist AS, Petty TL, Enright PL, Redd SC. Lung function and mortality in the United States: data from the First National Health and Nutrition Examination Survey follow up study. *Thorax* 2003; **58**: 388-393 [PMID: 12728157 DOI: 10.1136/thorax.58.5.388]
8 **Godfrey MS**, Jankowich MD. The Vital Capacity Is Vital: Epidemiology and Clinical Significance of the Restrictive Spirometry Pattern. *Chest* 2016; **149**: 238-251 [PMID: 26356330 DOI: 10.1378/chest.15-1045]
9 **Lee SY**, Choi YJ, Seo JH, Lee SY, Kim JS, Kang EJ. Pulmonary function is implicated in the prognosis of metastatic non-small cell lung cancer but not in extended disease small cell lung cancer.

J Thorac Dis 2019; **11**: 4562-4572 [PMID: 31903245 DOI: 10.21037/jtd.2019.10.77]

10 **Feng F**, Tian Y, Zang Y, Sun L, Hong L, Yang J, Guo M, Lian X, Fan D, Zhang H. Low forced vital capacity predicts poor prognosis in gastric cancer patients. *Oncotarget* 2017; **8**: 28897-28905 [PMID: 28423645 DOI: 10.18632/oncotarget.15953]

11 **Sugawara K**, Mori K, Okumura Y, Yagi K, Aikou S, Uemura Y, Yamashita H, Seto Y. Preoperative Low Vital Capacity Influences Survival After Esophagectomy for Patients with Esophageal Carcinoma. *World J Surg* 2020; **44**: 2305-2313 [PMID: 32123980 DOI: 10.1007/s00268-020-05450-0]

12 **Suh MR**, Kim DH, Jung J, Kim B, Lee JW, Choi WA, Kang SW. Clinical implication of maximal voluntary ventilation in myotonic muscular dystrophy. *Medicine (Baltimore)* 2019; **98**: e15321 [PMID: 31045770 DOI: 10.1097/MD.0000000000015321]

13 **Huang XZ**, Yang YC, Chen Y, Wu CC, Lin RF, Wang ZN, Zhang X. Preoperative Anemia or Low Hemoglobin Predicts Poor Prognosis in Gastric Cancer Patients: A Meta-Analysis. *Dis Markers* 2019; **2019**: 7606128 [PMID: 30719182 DOI: 10.1155/2019/7606128]

14 **Wu N**, Chen G, Hu H, Pang L, Chen Z. Low pretherapeutic serum albumin as a risk factor for poor outcome in esophageal squamous cell carcinomas. *Nutr Cancer* 2015; **67**: 481-485 [PMID: 25706773 DOI: 10.1080/01635581.2015.1004726]

15 **Rho SY**, Hwang HK, Chong JU, Yoon DS, Lee WJ, Kang CM. Association of preoperative total lymphocyte count with prognosis in resected left-sided pancreatic cancer. *ANZ J Surg* 2019; **89**: 503-508 [PMID: 30836428 DOI: 10.1111/ans.15030]

16 **Rachidi S**, Li H, Wallace K, Li Z, Balch C, Lautenschlaeger T. Preoperative platelet counts and postoperative outcomes in cancer surgery: a multicenter, retrospective cohort study. *Platelets* 2020; **31**: 79-87 [PMID: 30744463 DOI: 10.1080/09537104.2019.1573977]

17 **Duan H**, Zhang X, Wang FX, Cai MY, Ma GW, Yang H, Fu JH, Tan ZH, Meng YQ, Fu XY, Ma QL, Lin P. Prognostic role of neutrophil-lymphocyte ratio in operable esophageal squamous cell carcinoma. *World J Gastroenterol* 2015; **21**: 5591-5597 [PMID: 25987784 DOI: 10.3748/wjg.v21.i18.5591]

18 **Yodying H**, Matsuda A, Miyashita M, Matsumoto S, Sakurazawa N, Yamada M, Uchida E. Prognostic Significance of Neutrophil-to-Lymphocyte Ratio and Platelet-to-Lymphocyte Ratio in Oncologic Outcomes of Esophageal Cancer: A Systematic Review and Meta-analysis. *Ann Surg Oncol* 2016; **23**: 646-654 [PMID: 26416715 DOI: 10.1245/s10434-015-4869-5]

19 **Xue Y**, Zhou X, Xue L, Zhou R, Luo J. The role of pretreatment prognostic nutritional index in esophageal cancer: A meta-analysis. *J Cell Physiol* 2019; **234**: 19655-19662 [PMID: 31344989 DOI: 10.1002/jcp.28565]

20 **Xu SS**, Li S, Xu HX, Li H, Wu CT, Wang WQ, Gao HL, Jiang W, Zhang WH, Li TJ, Ni QX, Liu L, Yu XJ. Haemoglobin, albumin, lymphocyte and platelet predicts postoperative survival in pancreatic cancer. *World J Gastroenterol* 2020; **26**: 828-838 [PMID: 32148380 DOI: 10.3748/wjg.v26.i8.828]

21 **Peng D**, Zhang CJ, Gong YQ, Hao H, Guan B, Li XS, Zhou LQ. Prognostic significance of HALP (hemoglobin, albumin, lymphocyte and platelet) in patients with bladder cancer after radical cystectomy. *Sci Rep* 2018; **8**: 794 [PMID: 29335609 DOI: 10.1038/s41598-018-19146-y]

22 **Guo Y**, Shi D, Zhang J, Mao S, Wang L, Zhang W, Zhang Z, Jin L, Yang B, Ye L, Yao X. The Hemoglobin, Albumin, Lymphocyte, and Platelet (HALP) Score is a Novel Significant Prognostic Factor for Patients with Metastatic Prostate Cancer Undergoing Cytoreductive Radical Prostatectomy. *J Cancer* 2019; **10**: 81-91 [PMID: 30662528 DOI: 10.7150/jca.27210]

23 **Cho O**, Oh YT, Chun M, Noh OK, Heo JS. Prognostic implication of FEV1/FVC ratio for limited-stage small cell lung cancer. *J Thorac Dis* 2018; **10**: 1797-1805 [PMID: 29707334 DOI: 10.21037/jtd.2018.02.14]

24 **Sarkar M**, Niranjan N, Banyal PK. Mechanisms of hypoxemia. *Lung India* 2017; **34**: 47-60 [PMID: 28144061 DOI: 10.4103/0970-2113.197116]

25 **Muz B**, de la Puente P, Azab F, Azab AK. The role of hypoxia in cancer progression, angiogenesis, metastasis, and resistance to therapy. *Hypoxia (Auckl)* 2015; **3**: 83-92 [PMID: 27774485 DOI: 10.2147/HP.S93413]

26 **Semenza GL**. Defining the role of hypoxia-inducible factor 1 in cancer biology and therapeutics. *Oncogene* 2010; **29**: 625-634 [PMID: 19946328 DOI: 10.1038/onc.2009.441]

27 **Wang H**, Liu X, Rice SJ, Belani CP. Pulmonary Rehabilitation in Lung Cancer. *PM R* 2016; **8**: 990-996 [PMID: 27060645 DOI: 10.1016/j.pmrj.2016.03.010]

28 **Morris GS**, Gallagher GH, Baxter MF, Brueilly KE, Scheetz JS, Ahmed MM, Shannon VR. Pulmonary rehabilitation improves functional status in oncology patients. *Arch Phys Med Rehabil* 2009; **90**: 837-841 [PMID: 19406305 DOI: 10.1016/j.apmr.2008.12.005]

29 **Cong L**, Hu L. The value of the combination of hemoglobin, albumin, lymphocyte and platelet in predicting platinum-based chemoradiotherapy response in male patients with esophageal squamous cell carcinoma. *Int Immunopharmacol* 2017; **46**: 75-79 [PMID: 28268208 DOI: 10.1016/j.intimp.2017.02.027]

30 **Madeddu C**, Gramignano G, Astara G, Demontis R, Sanna E, Atzeni V, Macciò A. Pathogenesis and Treatment Options of Cancer Related Anemia: Perspective for a Targeted Mechanism-Based Approach. *Front Physiol* 2018; **9**: 1294 [PMID: 30294279 DOI: 10.3389/fphys.2018.01294]

31 **Zhang F**, Cheng F, Cao L, Wang S, Zhou W, Ma W. A retrospective study: the prevalence and prognostic value of anemia in patients undergoing radiotherapy for esophageal squamous cell carcinoma. *World J Surg Oncol* 2014; **12**: 244 [PMID: 25085112 DOI: 10.1186/1477-7819-12-244]

32 **Stehle G**, Sinn H, Wunder A, Schrenk HH, Stewart JC, Hartung G, Maier-Borst W, Heene DL. Plasma protein (albumin) catabolism by the tumor itself--implications for tumor metabolism and the genesis of cachexia. *Crit Rev Oncol Hematol* 1997; **26**: 77-100 [PMID: 9298326 DOI: 10.1016/s1040-8428(97)00015-2]

33 **Merlot AM**, Kalinowski DS, Richardson DR. Unraveling the mysteries of serum albumin-more than just a serum protein. *Front Physiol* 2014; **5**: 299 [PMID: 25161624 DOI: 10.3389/fphys.2014.00299]

34 **Ostroumov D**, Fekete-Drimusz N, Saborowski M, Kühnel F, Woller N. CD4 and CD8 T lymphocyte interplay in controlling tumor growth. *Cell Mol Life Sci* 2018; **75**: 689-713 [PMID: 29032503 DOI: 10.1007/s00018-017-2686-7]

35 **Hong J**, Chen X, Gao W, Zhu S, Wu J, Huang O, He J, Zhu L, Chen W, Li Y, Fei X, Lin L, Shen K. A high absolute lymphocyte count predicts a poor prognosis in HER-2- positive breast cancer patients treated with trastuzumab. *Cancer Manag Res* 2019; **11**: 3371-3379 [PMID: 31114373 DOI: 10.2147/CMAR.S187233]

36 **Feng JF**, Liu JS, Huang Y. Lymphopenia predicts poor prognosis in patients with esophageal squamous cell carcinoma. *Medicine (Baltimore)* 2014; **93**: e257 [PMID: 25501097 DOI: 10.1097/MD.0000000000000257]

37 **Schlesinger M**. Role of platelets and platelet receptors in cancer metastasis. *J Hematol Oncol* 2018; **11**: 125 [PMID: 30305116 DOI: 10.1186/s13045-018-0669-2]

World Journal of Gastroenterology

Submit a Manuscript: https://www.f6publishing.com

World J Gastroenterol 2021 January 28; 27(4): 336-344

DOI: 10.3748/wjg.v27.i4.336

ISSN 1007-9327 (print) ISSN 2219-2840 (online)

ORIGINAL ARTICLE

Retrospective Study

Clinic-pathological features of metabolic associated fatty liver disease with hepatitis B virus infection

Ming-Fang Wang, Bo Wan, Yin-Lian Wu, Jiao-Feng Huang, Yue-Yong Zhu, You-Bing Li

ORCID number: Ming-Fang Wang 0000-0001-7306-955X; Bo Wan 0000-0002-8109-1850; Yin-Lian Wu 0000-0001-9298-8367; Jiao-Feng Huang 0000-0003-1383-6897; Yue-Yong Zhu 0000-0002-0746-4911; You-Bing Li 0000-0002-8994-0853.

Author contributions: Wang MF and Li YB designed the study; Huang JF and Wu YL collected and analyzed the data; Wang MF and Wan B drafted the manuscript; Zhu YY and Li YB critically revised the manuscript; Wang MF and Wan B contributed equally to this work; all authors approved the final version of the manuscript prior to submission.

Supported by Chinese National 13th Five-Year Plan's Science and Technology Projects, No. 2017ZX10202201.

Institutional review board statement: This study was reviewed and approved by the Ethics Committee of the First Affiliated Hospital of Fujian Medical University in accordance with the Declaration of Helsinki.

Conflict-of-interest statement: The authors have no conflict of interest to declare.

Open-Access: This article is an open-access article that was

Ming-Fang Wang, Department of Liver Research Center, The First Affiliated Hospital of Fujian Medical University, Fuzhou 350005, Fujian Province, China

Bo Wan, Institute of Neurology, University College London, London WC1N 3BG, United Kingdom

Yin-Lian Wu, Jiao-Feng Huang, Yue-Yong Zhu, You-Bing Li, Department ofLiver Research Center, The First Affiliated Hospital of Fujian Medical University, Fuzhou 350005, Fujian Province, China

Corresponding author: You-Bing Li, PhD, Associate Chief Physician, Department of Liver Research Center, The First Affiliated Hospital of Fujian Medical University, No. 20 Chazhong Road, Taijiang District, Fuzhou 350005, Fujian Province, China. liyoubing1976@sina.com

Abstract

BACKGROUND

Metabolic associated fatty liver disease (MAFLD) is a novel concept proposed in 2020.

AIM

To compare the characteristics of MAFLD and MAFLD with hepatitis B virus (HBV) infection.

METHODS

Patients with histopathologically proven MAFLD from a single medical center were included. Patients were divided into MAFLD group (without HBV infection) and HBV-MAFLD group (with HBV infection). Propensity score matching was utilized to balance the baseline characteristics between two groups.

RESULTS

A total of 417 cases with MAFLD were included, 359 (86.1%) of whom were infected with HBV. There were significantly more males in the HBV-MAFLD group than in the MAFLD group ($P < 0.05$). After propensity score matching, 58 pairs were successfully matched with no significant differences found in gender, age, body mass index, lipid levels, liver enzymes, and the other metabolic associated comorbidities between the two groups ($P > 0.05$). The rank sum test results showed that the degree of liver steatosis in the MAFLD group was more severe than that in the HBV-MAFLD group, while the degree of inflammation and

selected by an in-house editor and fully peer-reviewed by external reviewers. It is distributed in accordance with the Creative Commons Attribution NonCommercial (CC BY-NC 4.0) license, which permits others to distribute, remix, adapt, build upon this work non-commercially, and license their derivative works on different terms, provided the original work is properly cited and the use is non-commercial. See: http://creativecommons.org/Licenses/by-nc/4.0/

Manuscript source: Unsolicited manuscript

Specialty type: Gastroenterology and hepatology

Country/Territory of origin: China

Peer-review report's scientific quality classification

Grade A (Excellent): 0
Grade B (Very good): B
Grade C (Good): C
Grade D (Fair): 0
Grade E (Poor): 0

Received: October 9, 2020
Peer-review started: October 9, 2020
First decision: December 3, 2020
Revised: December 11, 2020
Accepted: December 22, 2020
Article in press: December 22, 2020
Published online: January 28, 2021

P-Reviewer: Exbrayat JM, Fallatah H
S-Editor: Fan JR
L-Editor: Filipodia
P-Editor: Ma YJ

fibrosis in the liver was less severe ($P < 0.05$). In multivariate analysis, HBV infection was associated with significantly lower grade of hepatic steatosis [odds ratio (OR) = 0.088, 95% confidence interval (CI): 0.027-0.291] but higher inflammation level (OR = 4.059, 95%CI: 1.403-11.742) and fibrosis level (OR = 3.016, 95%CI: 1.087-8.370) after adjusting for age, gender, and other metabolic parameters.

CONCLUSION

HBV infection is associated with similar metabolic risks, lower steatosis grade, higher inflammation, and fibrosis grade in MAFLD patients.

Key Words: Fatty liver disease; Metabolic associated fatty liver disease; Hepatitis B virus; Biopsy; Clinic-pathological features

©The Author(s) 2021. Published by Baishideng Publishing Group Inc. All rights reserved.

Core Tip: Metabolic associated fatty liver disease (MAFLD) is a novel concept proposed in 2020 aiming to replace the previous definition of non-alcoholic fatty liver disease. Patients with MAFLD have different features from those with non-alcoholic fatty liver disease because MAFLD does not require the exclusion of other chronic liver disease, such as hepatitis B virus (HBV) infection. In this study, we compared the characteristics of patients with and without HBV infection in a biopsy-proved MAFLD cohort. The results of this study involving 417 participants showed that cases with HBV-MAFLD had similar metabolic features as pure MAFLD, and the presence of HBV infection was associated with lower steatosis grade but higher inflammation and fibrosis grade in MAFLD. These results highlight the importance of the monitoring and managing HBV infection in MAFLD.

Citation: Wang MF, Wan B, Wu YL, Huang JF, Zhu YY, Li YB. Clinic-pathological features of metabolic associated fatty liver disease with hepatitis B virus infection. *World J Gastroenterol* 2021; 27(4): 336-344
URL: https://www.wjgnet.com/1007-9327/full/v27/i4/336.htm
DOI: https://dx.doi.org/10.3748/wjg.v27.i4.336

INTRODUCTION

Fatty liver disease is one of the most common chronic liver diseases, affecting nearly 25% of the population worldwide[1]. Metabolic associated fatty liver disease (MAFLD) is a new definition proposed recently that is different from previous diagnostic criteria for non-alcoholic fatty liver disease (NAFLD)[2,3]. The significant difference between NAFLD and MAFLD is that the diagnosis of MAFLD does not need to exclude other etiology of liver disease, such as excessive alcohol intake or viral infection[4], while the presence of metabolic dysfunction is necessary for MAFLD[5]. These criteria help to identify more cases at high risk[6,7].

Hepatitis B virus (HBV) infection is prevalent in Asia. In China, the HBV infection rate is as high as 5%-6% in the general population[8]. The association between NAFLD and HBV has been controversial for a long time because, theoretically, the diagnosis of NAFLD requires the exclusion of HBV infection[9]. As the MAFLD criteria do not need to exclude chronic hepatitis B, there would be a considerable number of HBV-infected cases diagnosed with MAFLD. In the light of the MAFLD definition, the combination of HBV and MAFLD (HBV-MAFLD) would become an important subtype of MAFLD. The clinicopathological characteristics of this subtype are unclear. To answer this question, this study compared patients with MAFLD and HBV-MAFLD in a large biopsy proven cohort, aiming to characterize MAFLD patients infected with HBV.

MATERIALS AND METHODS

Patients

This study included a consecutive cohort of patients with pathologically proven steatosis from the Liver Research Center of the First Affiliated Hospital of Fujian Medical University from 2005 to 2015. The inclusion criteria were meeting MAFLD diagnostic criteria irrespective of HBV infection.

Patients with excessive alcohol intake (male < 40 g/d or female < 20 g/d) were diagnosed with alcoholic liver disease[10], and they were advised to stop consuming alcohol. None of them received liver biopsy in our department. Thus, this study did not include any case with excessive alcohol consumption.

Diagnostic criteria

MAFLD is diagnosed based on histopathologically proven liver steatosis and the presence of one of the following: Overweight or obesity, diabetes mellitus, or evidence of metabolic dysregulation[5]. Overweight was defined as body mass index (BMI) ≥ 23 kg/m^2 for Asians. The metabolic dysregulation was diagnosed when two of the following criteria were met: (1) Waist circumference ≥ 90/80 cm in Asian men and women; (2) Triglyceride ≥ 1.70 mmoL/L or receiving specific drug treatment; (3) Blood pressure ≥ 130/85 mmHg or specific drug treatment; (4) High-density lipoprotein cholesterol < 1.0 mmoL/L for men and < 1.3 mmoL/L for women; (5) Prediabetes [*i.e.* glycated hemoglobin 5.7%-6.4%, fasting glucose levels (FPG) 5.6 to 6.9 mmoL/L, or 2 h glucose levels 7.8 to 11.0 mmoL/L]; (6) Hypersensitive C-reactive protein level > 2 mg/L; and (7) Homeostasis model assessment-insulin resistance score ≥ 2.5.

Patients were divided into two groups according to the result of HBV surface antigen (HBsAg): MAFLD group (HBsAg negative) and HBV-MAFLD group (HBsAg positive).

Liver biopsy

Liver biopsy was performed with a 16 g Tru-Cut biopsy needle under the guidance of ultrasound. Specimens of 15-20 mm liver tissues were fixed with 10% neutral formalin, embedded in paraffin, and sectioned into 4 μm slices by Ultra-Thin Semiautomatic Microtome. All slides were stained with hematoxylin-eosin-safran and Masson's trichrome. Qualified samples were those with a minimum of six portal tracts. All pathology slides were reviewed by two independent pathologists blind to the clinical history. The stages of liver inflammation and the degree of fibrosis were graded in accordance with the Chinese Guidelines of the Programme of Prevention and Cure for Viral Hepatitis[11]. According to the amount of fat accumulation in the hepatocyte, hepatic steatosis can be classified into four grades: S0 (< 5%), S1 (5%-33%), S2 (33%-66%), S3 (> 66%)[12].

Demographic and laboratory parameters

The following variables were obtained from the clinical records: Sex, age, BMI, and history of hypertension and diabetes. BMI was calculated as weight divided by the square of the height.

Biochemical measurements included alanine transaminase, aspartate aminotransferase, γ-glutamyl transferase, FPG, apolipoprotein A, apolipoprotein B, low-density lipoprotein cholesterol, very low density lipoprotein cholesterol, high-density lipoprotein cholesterol, triglyceride, total cholesterol, free fatty acids, blood urea nitrogen, creatinine, and uric acid. Those assessments were detected by AU2700 automatic biochemical instrument of Olympus Company (Tokyo, Japan).

Statistical analysis

Categorical variables are expressed as percentages and continuous variables are expressed as means ± standard deviation. The Mann-Whitney U-test was used for variables that were non-normally distributed; the student t-test was used for the comparison of variables that were normally distributed; and the Chi-squared test was used for categorical variables. Propensity score matching (PSM) was used to balance the age and gender between the two groups with a ratio of 1:1 and a caliper value of 0.2. Logistic regression analysis was used to investigate odds ratio (OR) of HBV infection for liver inflammation, steatosis, and fibrosis. All tests were two-tailed, and results with *P* value less than 0.05 were considered statistically significant. All data were analyzed with SPSS software (version 24.0, Armonk, NY, United States).

Ethics

This study was reviewed and approved by the Ethics Committee of the First Affiliated Hospital of Fujian Medical University in accordance with the Declaration of Helsinki.

RESULTS

This study included 417 patients with MAFLD, 354 (84.9%) of whom were male, and the average age of this study cohort was 40.5 ± 10.9-years-old. The majority of the cases were infected with HBV (359/417, 86.1%), among whom 184 (51.3%) were HBeAg positive. The average HBVDNA level was 5.69 ± 1.57 Lg IU/mL in the HBV-MAFLD group (Table 1).

There were more males in the HBV-MAFLD group than in the MAFLD group (88.9% *vs* 60.3%, $P < 0.001$). No significant difference was found in BMI, lipids, liver enzymes, and FPG levels between the MAFLD and HBV-MAFLD groups ($P > 0.05$). However, the proportions of hypertriglyceridemia, pre-diabetes, diabetes, and hypertension were higher in the MAFLD group than in the HBV-MAFLD group ($P < 0.05$).

After PSM, 58 pairs were successfully matched with no significant differences found in gender and age between the two groups (Table 1). The percentage of hypertension in the MAFLD group was still significantly higher than that in HBV-MAFLD group (27.6% *vs* 6.9%, $P < 0.05$). The BMI, lipid levels, liver enzymes, and the other metabolic associated comorbidities were comparable between two groups ($P > 0.05$).

Comparison of liver pathology between MAFLD and HBV-MAFLD

After PSM, there were 10 (17.2%) cases with severe steatosis (S3) in the HBV-MAFLD group and 32 (55.2%) cases in the MAFLD group. The average rank of liver steatosis in the HBV-MAFLD group was 43.76, while that in MAFLD group was 73.24 ($P < 0.05$), suggesting that liver steatosis in the HBV-MAFLD group was less severe than that in MAFLD group (Figure 1 and Table 2).

There were 27 (46.6%) cases with severe inflammation (G3-4) in the HBV-MAFLD group and 11 (19.0%) cases in the MAFLD group. The average rank of liver inflammation degree in HBV-MAFLD group was 70.84, while that in MAFLD group was 46.16 ($P < 0.05$). This suggested that the liver inflammation in HBV-MAFLD group was more severe than that in MAFLD group (Figure 2 and Table 2).

Advanced fibrosis (F3-4) was observed in 23 (39.7%) cases in the HBV-MAFLD group and nine (15.5%) cases in the MAFLD group. The fibrosis was more severe in HBV-MAFLD group than that in MAFLD group (average ranks: 71.01 *vs* 45.99, $P < 0.05$) (Table 2).

The Spearman analysis showed in the MAFLD group that the fibrosis and inflammation were positively correlated ($r = 0.757$, $P < 0.001$), while the correlation between fibrosis and steatosis was not statistically significant ($r = 0.209$, $P = 0.115$). Same results were found in the HBV-MAFLD group ($r = 0.696$ for fibrosis and inflammation, $P < 0.001$, and $r = -0.002$ for fibrosis and steatosis, $P = 0.990$).

Impact of HBV infection for the severity of steatosis, inflammation, and steatosis in MAFLD

Multivariate analysis was used to explore the impact of HBV infection for the severity of steatosis, inflammation, and fibrosis. Two different models were utilized to estimate the OR for different outcomes. Model 1 adjusted for the age and gender, while model 2 additionally adjusted for metabolic parameters including BMI, hypertension, diabetes mellitus, lipid levels, glucose level, and free fatty acids. The results showed that, HBV infection was associated with lower grade of hepatic steatosis (OR 0.088-0.157, $P < 0.001$) but higher grade of inflammation (OR 4.087-4.059, $P < 0.01$) and fibrosis (OR 3.016-3.659, $P < 0.05$) in every model (Table 3).

DISCUSSION

MAFLD with HBV infection is a special subtype of MAFLD in Asian countries. This study found that the metabolic components are not different between MAFLD cases with or without HBV infection. However, the presence of HBV is associated with lower steatosis grade and higher fibrosis and inflammation grade.

The relationship between liver steatosis and HBV infection is not yet clear.

Table 1 Comparison of baseline characteristics between metabolic associated fatty liver disease and hepatitis B virus-metabolic associated fatty liver disease groups before and after propensity score matching[1]

Characteristics	Before propensity score matching				After propensity score matching			
	MAFLD	HBV-MAFLD	*t* or χ^2	*P* value	MAFLD	HBV-MAFLD	*t* or χ^2	*P* value
Number	58	359			58	58		
Male, *n* (%)	35 (60.3%)	319 (88.9%)	31.652	< 0.001	35 (60.3%)	36 (62.1%)	0.036	0.849
Age in yr	41.53 ± 15.41	40.39 ± 10.08	0.548	0.586	41.53 ± 15.41	40.90 ± 11.17	0.255	0.799
BMI in kg/m^2	25.24 ± 3.36	25.50 ± 2.51	-0.7	0.484	25.31 ± 3.40	24.97 ± 3.00	0.563	0.575
TC in mmoL/L	4.84 ± 1.03	4.74 ± 1.14	0.621	0.535	4.84 ± 1.03	4.77 ± 1.25	0.363	0.717
TG in mmoL/L	2.13 ± 2.32	1.59 ± 0.97	1.72	0.091	2.13 ± 2.32	1.62 ± 1.02	1.545	0.125
LDL in mmoL/L	2.85 ± 1.00	2.88 ± 0.96	-0.213	0.831	2.85 ± 1.00	2.81 ± 1.10	0.667	0.842
VLDL in mmoL/L	0.65 ± 0.51	0.49 ± 0.35	2.978	0.003	0.65 ± 0.51	0.46 ± 0.33	2.484	0.014
HDL in mmoL/L	1.13 ± 0.35	1.12 ± 0.31	0.127	0.899	1.13 ± 0.35	1.18 ± 0.29	-0.878	0.382
APOA in g/L	1.20 ± 0.30	1.18 ± 0.22	0.408	0.618	1.20 ± 0.30	1.18 ± 0.23	0.348	0.729
APOB in g/L	0.99 ± 0.25	0.96 ± 0.28	0.969	0.333	0.99 ± 0.25	0.94 ± 0.29	1.098	0.274
FPG in mmoL/L	5.44 ± 1.04	5.32 ± 1.53	0.543	0.588	5.44 ± 1.04	5.57 ± 1.94	-0.441	0.660
FFA in mmoL/L	468.21 ± 202.54	466.48 ± 200.66	0.052	0.959	468.21 ± 202.54	458.59 ± 177.92	0.295	0.769
CR in μmoL/L	67.03 ± 13.99	74.51 ± 13.39	-3.836	< 0.001	67.03 ± 13.99	70.12 ± 14.05	-1.197	0.234
BUN in mmoL/L	4.63 ± 1.43	4.79 ± 1.18	-0.885	0.377	4.63 ± 1.43	4.54 ± 0.95	0.407	0.685
UA in mmoL/L	355.81 ± 74.56	370.64 ± 83.20	-1.251	0.212	355.81 ± 74.56	367.00 ± 79.35	-0.789	0.432
ALT in U/L	119.76 ± 118.19	135.82 ± 210.31	-0.567	0.571	119.76 ± 118.19	168.60 ± 208.80	-1.55	0.125
AST in U/L	65.55 ± 63.28	71.70 ± 88.63	-0.507	0.612	65.55 ± 63.28	90.94 ± 99.46	-1.64	0.104
GGT in U/L	179.83 ± 189.39	75.13 ± 82.34	4.147	< 0.001	179.83 ± 189.39	78.93 ± 70.11	3.805	< 0.001
GFR in mL/min	136.22 ± 37.84	117.36 ± 28.91	3.63	0.01	136.22 ± 37.84	127.95 ± 34.19	1.234	0.220
Hypertension, *n* (%)	16 (27.6%)	26 (7.2%)	22.816	0.000	16 (27.6%)	4 (6.9%)	8.700	0.003
DM, *n* (%)	17 (29.3%)	65 (17.5%)	3.968	0.046	17 (29.3%)	17 (29.3%)	0.000	1.000
Low HDL-C, *n* (%)	28 (48.3%)	165 (46.0%)	0.108	0.743	28 (48.3%)	30 (51.7%)	0.138	0.710
Prediabetes, *n* (%)	21 (36.2%)	77 (21.4%)	6.050	0.014	21 (36.2%)	15 (25.9%)	1.450	0.229
Obesity, *n* (%)	50 (86.2%)	328 (91.4%)	1.567	0.211	50 (86.2%)	51 (87.9%)	0.077	0.782
Hypertriglyceridemia, *n* (%)	26 (44.8%)	109 (30.4%)	4.772	0.029	26 (44.8%)	16 (27.6%)	3.732	0.053

[1]The age and sex were matched between two groups. ALT: Alanine aminotransferase; APOA: Apolipoprotein A; APOB: Apolipoprotein B; AST: Aspartate aminotransferase; BMI: Body mass index; BUN: Blood urea nitrogen; CR: Creatinine; DM: Diabetes mellitus; FFA: Free fatty acids; FPG: Fasting plasma glucose; GFR: Glomerular filtration rate; GGT: γ-glutamyl transpeptidase; HBV: Hepatitis B virus; HDL-C: High-density lipoprotein cholesterol; LDL-C: Low-density lipoprotein cholesterol; MAFLD: Metabolic associated fatty liver disease; TC: Total cholesterol; TG: Triglyceride; UA: Uric acid; VLDL-C: Very low-density lipoprotein cholesterol.

Laboratory data showed HBV X protein induces liver fat deposition by activating peroxisome proliferator-activated receptor γ, sterol regulatory element binding protein 1, and liver fatty acid binding protein 1[13,14], suggesting the HBV virus itself may lead to liver steatosis. However, a cross-sectional study showed current HBV infection may reduce the risk of NAFLD, but this effect became no longer significant after spontaneous HBsAg seroclearance[15]. Several large sample-sized studies showed a negative correlation between HBsAg and the risk of NAFLD in the future[16,17]. In addition, higher BMI also helps the seroclearance of HBsAg[18]. Consistent with previous studies[19], our results showed that concomitant HBV infection led to a lower degree of steatosis. This suggests the novel definition of MAFLD does not greatly influence the correlation between HBV infection and fatty liver disease; HBV infection is associated with lower degree of steatosis in MAFLD.

Although HBV was associated with lower degree of steatosis in MAFLD patients,

Table 2 Comparison of histopathological characteristics between metabolic associated fatty liver disease and hepatitis B virus-metabolic associated fatty liver disease groups

	Inflammatory stage					Fibrosis stage					Steatosis stage		
	0	1	2	3	4	0	1	2	3	4	1	2	3
MAFLD; *n* (%)	2 (3.4)	36 (62.2)	9 (15.5)	9 (15.5)	2 (3.4)	15 (25.9)	23 (39.7)	11 (19.0)	7 (12.0)	2 (3.4)	11 (18.9)	15 (25.9)	32 (55.2)
HBV-MAFLD; *n* (%)	0 (0)	16 (27.6)	15 (25.9)	18 (31.0)	9 (15.5)	3 (5.2)	15 (25.9)	17 (29.3)	14 (24.1)	9 (15.5)	37 (63.8)	11 (19.0)	10 (17.2)
Z	-4.193					-4.131					-5.060		
P value	< 0.001					< 0.001					< 0.001		

HBV: Hepatitis B virus; MAFLD: Metabolic associated fatty liver disease.

Table 3 Odds ratio of hepatitis B virus infection for the pathological changes in metabolic associated fatty liver disease population

	Steatosis stage			Inflammatory stage			Fibrosis stage		
	OR	*P* value	95%CI	OR	*P* value	95%CI	OR	*P* value	95%CI
Crude OR	0.169	< 0.001	0.072-0.398	3.721	0.002	1.615-8.577	3.578	0.005	1.478-8.663
Adjusted OR 1	0.157	< 0.001	0.065-0.378	4.087	0.001	1.720-9.713	3.659	0.004	1.501-8.919
Adjusted OR 2	0.088	< 0.001	0.027-0.291	4.059	0.010	1.403-11.742	3.016	0.034	1.087-8.370

Odds ratio (OR) 1 adjusts age and gender; OR 2 adjusts age, gender, hypertension, diabetes mellitus, triglyceride, total cholesterol, very low-density lipoprotein cholesterol, high-density lipoprotein cholesterol, low-density lipoprotein cholesterol, body mass index, fasting plasma glucose, apolipoprotein A, apolipoprotein B and free fatty acids. CI: Confidence interval.

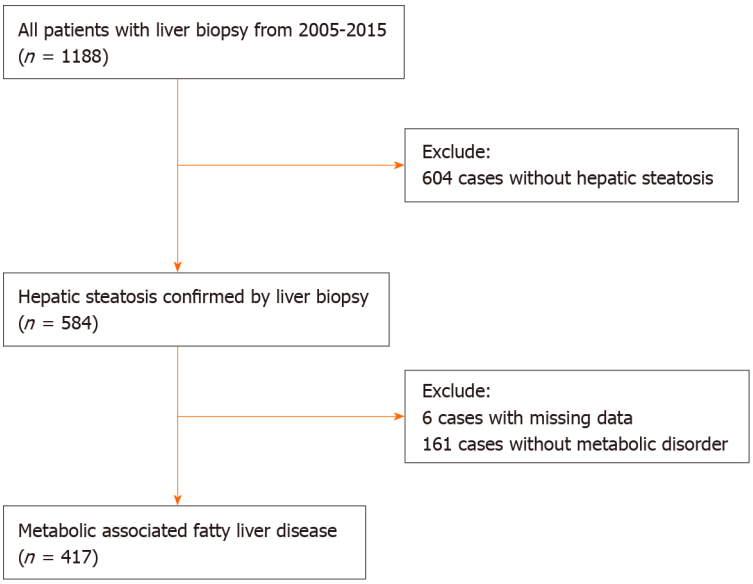


Figure 1 Flow chart of cases selection.

unsurprisingly, HBV infection independently increased the risk of inflammation and fibrosis. HBV-infection in MAFLD increased the odds of advanced fibrosis by at least 3-fold and inflammation by 4-fold. This result was in line with a previous report that HBV infection is an independent risk factor for fibrosis in NAFLD[20]. Therefore, for patients with MAFLD combined with HBV infection, closer monitoring and intervention of both factors are required, as the presence of two pathogenic risks might accelerate disease progression.

The strength of this study is that, to our knowledge, it is the first to focus on the relationship between MAFLD and HBV infection. As MAFLD is a novel, recently

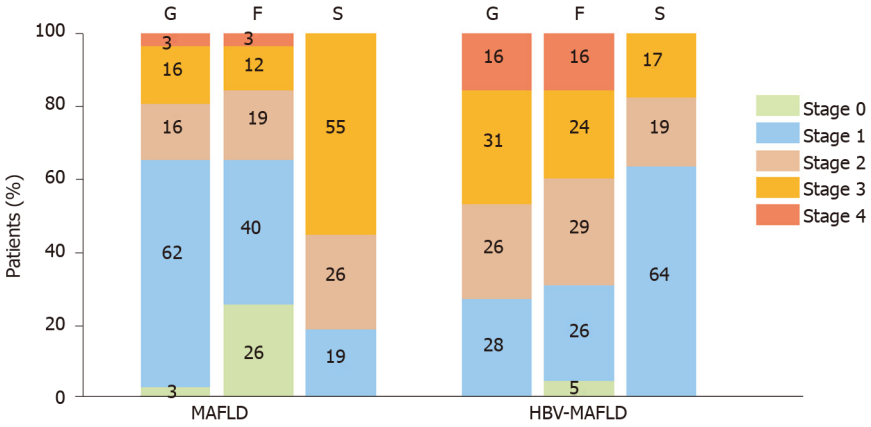


Figure 2 Inflammation, fibrosis, and steatosis stage in metabolic associated fatty liver disease and hepatitis B virus-metabolic associated fatty liver disease groups. F: Fibrosis; S: Steatosis; G: Inflammation; HBV: Hepatitis B virus; MAFLD: Metabolic associated fatty liver disease.

proposed concept and its prevalence will keep increasing in future decades[21], the clarification of the association between MAFLD and HBV is of clinical importance. However, there are some limitations that compromise this study. First, this is a single center study. The lack of waist circumference, homeostatic model assessment of insulin resistance, and C-reactive protein will lead to some missing cases of MAFLD. Second, this cross-sectional study was unable to determine the causal relationship between HBV infection and MAFLD. Lastly, the study population was relatively lean and had less metabolic syndrome. The conclusions should be validated in other populations with higher prevalence of obesity and metabolic syndromes.

CONCLUSION

In summary, cases with HBV-MAFLD have similar metabolic risks compared to pure MAFLD but are associated with lower steatosis grade and higher inflammation and fibrosis grade in histopathology. More attention should be paid to the monitoring and management of MAFLD with HBV infection.

ARTICLE HIGHLIGHTS

Research background

Metabolic associated fatty liver disease (MAFLD) is a novel concept proposed in 2020.

Research motivation

MAFLD does not require the exclusion of hepatitis B virus (HBV) infection, thus the combination of HBV and MAFLD (HBV-MAFLD) would become an important subtype of MAFLD. The clinicopathological characteristics of this subtype are unclear.

Research objectives

This retrospective study aimed to compare the characteristics between MAFLD and HBV-MAFLD.

Research methods

Patients with histopathologically proven MAFLD from a single medical center were included. Patients were divided into MAFLD group (without HBV infection) and HBV-MAFLD group (with HBV infection). Propensity score matching was utilized to balance the baseline characteristics between two groups.

Research results

A total of 417 cases with MAFLD were included, 359 (86.1%) of whom were infected with HBV. There were significantly more males in the HBV-MAFLD group than in MAFLD group ($P < 0.05$). After propensity score matching, 58 pairs were successfully

matched with no significant differences found in gender, age, body mass index, lipid levels, liver enzymes, and the other metabolic associated comorbidities between two groups ($P > 0.05$). The rank sum test results showed that the degree of liver steatosis in the MAFLD group was more severe than that in HBV-MAFLD group, while the degree of inflammation and fibrosis in liver was less severe ($P < 0.05$). In multivariate analysis, HBV infection was associated with lower grade of hepatic steatosis [odds ratio (OR) = 0.088, 95% confidence interval (CI): 0.027-0.291] but higher inflammation (OR = 4.059, 95%CI: 1.403-11.742) and fibrosis grades (OR = 3.016, 95%CI: 1.087-8.370) after adjusting for age, gender, and other metabolic parameters.

Research conclusions

HBV infection is associated with similar metabolic risks, lower steatosis grade, and higher inflammation and fibrosis grade in MAFLD patients.

Research perspectives

The overall body mass index and the prevalence of metabolic disorder were relatively low in this study cohort. The conclusion should be validated in other populations with more metabolic dysfunctions.

REFERENCES

1 **Younossi ZM**, Koenig AB, Abdelatif D, Fazel Y, Henry L, Wymer M. Global epidemiology of nonalcoholic fatty liver disease-Meta-analytic assessment of prevalence, incidence, and outcomes. *Hepatology* 2016; **64**: 73-84 [PMID: 26707365 DOI: 10.1002/hep.28431]

2 **Eslam M**, Sanyal AJ, George J; International Consensus Panel. MAFLD: A Consensus-Driven Proposed Nomenclature for Metabolic Associated Fatty Liver Disease. *Gastroenterology* 2020; **158**: 1999-2014. e1 [PMID: 32044314 DOI: 10.1053/j.gastro.2019.11.312]

3 **Fouad Y**, Waked I, Bollipo S, Gomaa A, Ajlouni Y, Attia D. What's in a name? *Liver Int* 2020; **40**: 1254-1261 [PMID: 32301554 DOI: 10.1111/liv.14478]

4 **European Association for the Study of the Liver (EASL)**. EASL-EASD-EASO Clinical Practice Guidelines for the management of non-alcoholic fatty liver disease. *Diabetologia* 2016; **59**: 1121-1140 [PMID: 27053230 DOI: 10.1007/s00125-016-3902-y]

5 **Eslam M**, Newsome PN, Sarin SK, Anstee QM, Targher G, Romero-Gomez M, Zelber-Sagi S, Wai-Sun Wong V, Dufour JF, Schattenberg JM, Kawaguchi T, Arrese M, Valenti L, Shiha G, Tiribelli C, Yki-Järvinen H, Fan JG, Grønbæk H, Yilmaz Y, Cortez-Pinto H, Oliveira CP, Bedossa P, Adams LA, Zheng MH, Fouad Y, Chan WK, Mendez-Sanchez N, Ahn SH, Castera L, Bugianesi E, Ratziu V, George J. A new definition for metabolic dysfunction-associated fatty liver disease: An international expert consensus statement. *J Hepatol* 2020; **73**: 202-209 [PMID: 32278004 DOI: 10.1016/j.jhep.2020.03.039]

6 **Lin S**, Huang J, Wang M, Kumar R, Liu Y, Liu S, Wu Y, Wang X, Zhu Y. Comparison of MAFLD and NAFLD diagnostic criteria in real world. *Liver Int* 2020; **40**: 2082-2089 [PMID: 32478487 DOI: 10.1111/liv.14548]

7 **Yamamura S**, Eslam M, Kawaguchi T, Tsutsumi T, Nakano D, Yoshinaga S, Takahashi H, Anzai K, George J, Torimura T. MAFLD identifies patients with significant hepatic fibrosis better than NAFLD. *Liver Int* 2020 [PMID: 32997882 DOI: 10.1111/liv.14675]

8 **Jia JD**, Hou JL, Wei L, Zhuang H. [Highlights of the guidelines of prevention and treatment for chronic hepatitis B (2019 version)]. *Zhonghua Gan Zang Bing Za Zhi* 2020; **28**: 21-23 [PMID: 32023693 DOI: 10.3760/cma.j.issn.1007-3418.2020.01.006]

9 **Haga Y**, Kanda T, Sasaki R, Nakamura M, Nakamoto S, Yokosuka O. Nonalcoholic fatty liver disease and hepatic cirrhosis: Comparison with viral hepatitis-associated steatosis. *World J Gastroenterol* 2015; **21**: 12989-12995 [PMID: 26675364 DOI: 10.3748/wjg.v21.i46.12989]

10 **Li YM**, Fan JG, Wang BY, Lu LG, Shi JP, Niu JQ, Shen W; Chinese Association for the Study of Liver Disease. Guidelines for the diagnosis and management of alcoholic liver disease: update 2010: (published in Chinese on Chinese Journal of Hepatology 2010; 18: 167-170). *J Dig Dis* 2011; **12**: 45-50 [PMID: 21276208 DOI: 10.1111/j.1751-2980.2010.00477.x]

11 **Desmet VJ**, Gerber M, Hoofnagle JH, Manns M, Scheuer PJ. Classification of chronic hepatitis: diagnosis, grading and staging. *Hepatology* 1994; **19**: 1513-1520 [PMID: 8188183]

12 **Kleiner DE**, Brunt EM, Van Natta M, Behling C, Contos MJ, Cummings OW, Ferrell LD, Liu YC, Torbenson MS, Unalp-Arida A, Yeh M, McCullough AJ, Sanyal AJ; Nonalcoholic Steatohepatitis Clinical Research Network. Design and validation of a histological scoring system for nonalcoholic fatty liver disease. *Hepatology* 2005; **41**: 1313-1321 [PMID: 15915461 DOI: 10.1002/hep.20701]

13 **Kim KH**, Shin HJ, Kim K, Choi HM, Rhee SH, Moon HB, Kim HH, Yang US, Yu DY, Cheong J. Hepatitis B virus X protein induces hepatic steatosis *via* transcriptional activation of SREBP1 and PPARgamma. *Gastroenterology* 2007; **132**: 1955-1967 [PMID: 17484888 DOI: 10.1053/j.gastro.2007.03.039]

14 **Wu YL**, Peng XE, Zhu YB, Yan XL, Chen WN, Lin X. Hepatitis B Virus X Protein Induces Hepatic

Steatosis by Enhancing the Expression of Liver Fatty Acid Binding Protein. *J Virol* 2016; **90**: 1729-1740 [PMID: 26637457 DOI: 10.1128/JVI.02604-15]

15 **Huang J**, Jing M, Wang C, Wang M, You S, Lin S, Zhu Y. The impact of hepatitis B virus infection status on the prevalence of nonalcoholic fatty liver disease: A population-based study. *J Med Virol* 2020; **92**: 1191-1197 [PMID: 31691993 DOI: 10.1002/jmv.25621]

16 **Joo EJ**, Chang Y, Yeom JS, Ryu S. Hepatitis B virus infection and decreased risk of nonalcoholic fatty liver disease: A cohort study. *Hepatology* 2017; **65**: 828-835 [PMID: 28035771 DOI: 10.1002/hep.28917]

17 **Zhu L**, Jiang J, Zhai X, Baecker A, Peng H, Qian J, Zhou M, Song C, Zhou Y, Xu J, Liu H, Hang D, Hu Z, Shen H, Zhang ZF, Zhu F. Hepatitis B virus infection and risk of non-alcoholic fatty liver disease: A population-based cohort study. *Liver Int* 2019; **39**: 70-80 [PMID: 30025200 DOI: 10.1111/liv.13933]

18 **Cao J**, Gong J, Tsia Hin Fong CJ, Xiao C, Lin G, Li X, Jie Y, Chong Y. Prediction Model of HBsAg Seroclearance in Patients with Chronic HBV Infection. *Biomed Res Int* 2020; **2020**: 6820179 [PMID: 32855968 DOI: 10.1155/2020/6820179]

19 **Worland T**, Apostolov R, Asadi K, Leung C. Hepatitis B virus activity is not associated with degree of liver steatosis in patients with hepatitis B-related chronic liver disease. *Liver Int* 2020; **40**: 1500-1502 [PMID: 31883410 DOI: 10.1111/liv.14344]

20 **Su HJ**, Kao JH, Tseng TC, Yang HC, Su TH, Chen PJ, Liu CJ. Pathologic findings of patients with nonalcoholic fatty liver disease and the impact of concurrent hepatitis B virus infection in Taiwan. *J Formos Med Assoc* 2020; **119**: 1476-1482 [PMID: 32499209 DOI: 10.1016/j.jfma.2020.05.027]

21 **Younossi Z**, Tacke F, Arrese M, Chander Sharma B, Mostafa I, Bugianesi E, Wai-Sun Wong V, Yilmaz Y, George J, Fan J, Vos MB. Global Perspectives on Nonalcoholic Fatty Liver Disease and Nonalcoholic Steatohepatitis. *Hepatology* 2019; **69**: 2672-2682 [PMID: 30179269 DOI: 10.1002/hep.30251]

World Journal of Gastroenterology

Submit a Manuscript: https://www.f6publishing.com

World J Gastroenterol 2021 January 28; 27(4): 345-357

DOI: 10.3748/wjg.v27.i4.345

ISSN 1007-9327 (print) ISSN 2219-2840 (online)

ORIGINAL ARTICLE

Clinical Trials Study

Effect of remote ischemic preconditioning among donors and recipients following pediatric liver transplantation: A randomized clinical trial

Bo Qi, Xiao-Qiang Wang, Shu-Ting Pan, Pei-Ying Li, Ling-Ke Chen, Qiang Xia, Li-Qun Yang, Wei-Feng Yu

ORCID number: Bo Qi 0000-0003-4037-1335; Xiao-Qiang Wang 0000-0002-1002-4693; Shu-Ting Pan 0000-0002-0497-2371; Pei-Ying Li 0000-0002-5721-9914; Ling-Ke Chen 0000-0003-0589-8553; Qiang Xia 0000-0002-6632-1354; Li-Qun Yang 0000-0001-5801-7890; Wei-Feng Yu 0000-0002-8592-5349.

Author contributions: Qi B and Wang XQ contributed equally to this work; Yang LQ and Yu WF contributed to conceptualization and formal analysis; Qi B, Wang XQ, Pan ST and Li PY contributed to data curation and statistical analysis; Wang XQ, Yang LQ and Chen LK contributed to drafting and editing the manuscript; Yu WF and Xia Q contributed to review and editing.

Supported by Renji Hospital Clinical Innovation Foundation, No. PYIII-17-002; Outstanding Academic Leaders' Program of Health and Family Planning Commission of Shanghai, No. 2017BR042; and Investigative Doctor Program (2017) of Shanghai Jiao Tong University School of Medicine; and Joint Project of Health and Family Planning Commission of Pudong District, No. PW2015D-3.

Bo Qi, Xiao-Qiang Wang, Pei-Ying Li, Ling-Ke Chen, Li-Qun Yang, Wei-Feng Yu, Department of Anesthesiology, Renji Hospital, School of Medicine, Shanghai Jiao Tong University, Shanghai 200127, China

Shu-Ting Pan, Clinical Center for Investigation, Renji Hospital, School of Medicine, Shanghai Jiao Tong University, Shanghai 200127, China

Qiang Xia, Department of Transplantation and Hepatic Surgery, Renji Hospital, School of Medicine, Shanghai Jiao Tong University, Shanghai 200120, China

Corresponding author: Wei-Feng Yu, PhD, Chief Doctor, Department of Anesthesiology, Renji Hospital, School of Medicine, Shanghai Jiao Tong University, No. 160 Pujian Road, Shanghai 200127, China. ywf808@yeah.net

Abstract

BACKGROUND

Studies suggested that remote ischemic preconditioning (RIPC) may effectively lessen the harmful effects of ischemia reperfusion injury during organ transplantation surgery.

AIM

To investigate the protective effects of RIPC on living liver donors and recipients following pediatric liver transplantation.

METHODS

From January 2016 to January 2019 at Renji Hospital Affiliated with Shanghai Jiao Tong University School of Medicine, 208 donors were recruited and randomly assigned to four groups: S-RIPC group (no intervention; n = 55), D-RIPC group (donors received RIPC; n = 51), R-RIPC group (recipients received RIPC, n = 51) and DR-RIPC group (both donors and recipients received RIPC; n = 51). We primarily evaluated postoperative liver function among donors and recipients and incidences of early allograft dysfunction, primary nonfunction and postoperative complications among recipients.

RESULTS

RIPC did not significantly improve alanine transaminase and aspartate

Institutional review board statement: The study was reviewed and approved by the Renji Hospital Institutional Review Board (Approval No. 2016-002K).

Clinical trial registration statement: This study is registered at Clinical-Trails.gov. The registration identification number is NCT02830841.

Informed consent statement: All study participants, or their legal guardian, provided informed written consent prior to study enrollment.

Conflict-of-interest statement: The authors have no conflicts of interest to disclose.

Data sharing statement: No additional data are available.

CONSORT 2010 statement: The authors have read the CONSORT 2010 Statement, and the manuscript was prepared and revised according to the CONSORT 2010 Statement.

Open-Access: This article is an open-access article that was selected by an in-house editor and fully peer-reviewed by external reviewers. It is distributed in accordance with the Creative Commons Attribution NonCommercial (CC BY-NC 4.0) license, which permits others to distribute, remix, adapt, build upon this work non-commercially, and license their derivative works on different terms, provided the original work is properly cited and the use is non-commercial. See: http://creativecommons.org/Licenses/by-nc/4.0/

Manuscript source: Unsolicited manuscript

Specialty type: Gastroenterology and hepatology

Country/Territory of origin: China

Peer-review report's scientific quality classification

Grade A (Excellent): A, A
Grade B (Very good): 0
Grade C (Good): C, C

aminotransferase levels among donors and recipients or decrease the incidences of early allograft dysfunction, primary nonfunction, and postoperative complications among recipients. Limited protective effects were observed, including a lower creatinine level in the D-RIPC group than in the S-RIPC group on postoperative day 0 ($P < 0.05$). However, no significant improvements were found in donors who received RIPC. Furthermore, RIPC had no effects on the overall survival of recipients.

CONCLUSION

The protective effects of RIPC were limited for recipients who received living liver transplantation, and no significant improvement of the prognosis was observed in recipients.

Key Words: Pediatric liver transplantation; Remote ischemic preconditioning; Postoperative complications; Ischemia reperfusion injury; Primary nonfunction; Hepatology

©The Author(s) 2021. Published by Baishideng Publishing Group Inc. All rights reserved.

Core Tip: Ischemia reperfusion injury (IRI) has been a well-known underlying cause for inducing or aggravating primary graft nonfunction, vascular complications and biliary complications during liver transplantation (LT). Some studies suggested that remote ischemic preconditioning (RIPC) may effectively lessen the harmful effects of IRI during organ transplantation surgery. However, studies on the effect of RIPC on pediatric LT were rare. The present single-center randomized clinical trial aimed to determine whether RIPC could be beneficial for reducing IRI among both donors and recipients undergoing pediatric LT.

Citation: Qi B, Wang XQ, Pan ST, Li PY, Chen LK, Xia Q, Yang LQ, Yu WF. Effect of remote ischemic preconditioning among donors and recipients following pediatric liver transplantation: A randomized clinical trial. *World J Gastroenterol* 2021; 27(4): 345-357
URL: https://www.wjgnet.com/1007-9327/full/v27/i4/345.htm
DOI: https://dx.doi.org/10.3748/wjg.v27.i4.345

INTRODUCTION

Since first performed by Starzl *et al*[1] in 1963, liver transplantation (LT) has undergone remarkable progress and innovation over the last 50 years. Currently, LT remains the gold standard treatment for patients suffering from end-stage liver disease or metabolic liver disease, with an overall 3-year survival rate exceeding 80% due to advancements in immunosuppressive agents, surgical techniques and perioperative management[2-5]. Approximately 600 pediatric LTs were performed in the United States in 2018[2], with the first pediatric LT successfully performed in 1967 by Starzl *et al*[6]. Meanwhile, the development of pediatric LT in China has been rapid and prominent, with Renji Hospital becoming the major pediatric LT center, performing more than 400 pediatric LTs in 2019. According to recorded data from Renji Hospital, the overall 3-year survival rate of children in recent years had exceeded 90%.

Despite the outstanding achievements in pediatric LT, some complications, such as primary graft nonfunction (PNF), vascular complications, biliary complications and allograft rejection, still exist[3,5,7,8]. Accordingly, ischemia reperfusion injury (IRI) has been a well-known underlying cause for inducing or aggravating PNF, vascular complications and biliary complications[9-11]. Given that IRIs usually occur when temporarily cutting off and then restoring an organ or tissue's blood supply, avoiding it during LT is challenging[12]. Although several studies have attempted to ameliorate hepatic IRI[11,13,14], the mechanisms of IRI still remain largely unclear with no definitive therapies having been established.

Remote ischemic preconditioning (RIPC), a simple noninvasive therapy for alleviating the harmful effects of IRI, has shown promise in protecting multiple organs, such as the kidneys, heart and liver[9,15,16]. RIPC is usually performed by inflating and

Grade D (Fair): 0
Grade E (Poor): 0

Received: October 29, 2020
Peer-review started: October 29, 2020
First decision: November 30, 2020
Revised: December 9, 2020
Accepted: December 26, 2020
Article in press: December 26, 2020
Published online: January 28, 2021

P-Reviewer: de Carvalho JF, Di Pasqua L, Haruma K
S-Editor: Huang P
L-Editor: Filipodia
P-Editor: Liu JH

deflating a standard blood pressure cuff placed on the upper arm or thigh to induce transient ischemia and reperfusion, providing systemic multiorgan protection[17]. A number of fundamental and clinical studies have suggested that RIPC can effectively reduce IRI in the liver[9,18-20]. For instance, Abu-Amara *et al*[19,20] confirmed that RIPC successfully reduced IRI in a mouse model, while Wu *et al*[18] found that RIPC was able to reduce hepatic IRI among patients undergoing liver resection. Moreover, Jung *et al*[9] suggested that RIPC might be beneficial for postoperative liver function among recipients after living donor LT. However, other studies have shown no benefits for RIPC in animal models or patients[17,21,22]. Therefore, more studies are needed to validate the effectiveness of RIPC.

Given the current lack of studies on the effect of RIPC on pediatric LT, the present single-center randomized clinical trial aimed to determine whether RIPC could be beneficial for reducing IRI among both donors and recipients undergoing pediatric LT.

MATERIALS AND METHODS

Study design and intervention

This single-center, randomized controlled study had been approved by the ethics committee of the Renji Hospital (2016-002K) and was registered with Clinical-Trails.gov (NCT02830841). Written informed consent was obtained from the donors and families of recipients. The study was conducted in accordance with the Declaration of Helsinki and the CONSORT criteria[23].

Randomization was achieved by using opaque envelopes in which allocations were stored, and random sequence was generated by an independent data manager. Patients who consent to enter this trial were randomly allocated into the S-RIPC group (no intervention to donors and recipients), D-RIPC group (donors received RIPC), R-RIPC group (recipients received RIPC), and DR-RIPC group (both donors and recipients received RIPC) in a 1:1:1:1 fashion. No masking was applied except for data assessors.

Donors and recipients in the S-RIPC group underwent the same procedure without RIPC. Donors in D-RIPC group underwent RIPC in the right upper limb after induction of anesthesia and before abdominal skin incision. The cuff was placed in the upper third of the right upper limb, after which three 5-min cycles each of inflation at a pressure of 200 mmHg and subsequent reperfusion with the cuff deflated were performed. Recipients in the D-RIPC group underwent the same procedure except without RIPC. Recipients in the R-RIPC group underwent RIPC with the cuff being placed on the left lower limb at an inflation pressure of 150 mmHg. Donors in the R-RIPC group underwent the same procedure except without RIPC. Both donors and recipients in the DR-RIPC group underwent RIPC as described.

Sample size calculation

According to plasma alanine transaminase (ALT) records from 235 children who previously performed LT without RIPC in Renji Hospital, we found that mean natural logarithm of maximum postoperative ALT (ALT_{max}) was 5.86; assuming the mean logarithm of ALT_{max} decreases to 5.3 after performing RIPC in recipients, which leads to effect size $f = 0.25$. Combined with significance level of $a = 0.05$, and power of 80%, each treatment group had to include at least 32 patients[24]. Considering 10% dropout rate, we decided to include at least 144 patients in total.

Participants and inclusion/exclusion criterion

A total of 220 patients with biliary atresia and family liver donors who underwent living pediatric LT from January 2016 to January 2019 at Renji Hospital Affiliated with Shanghai Jiao Tong University School of Medicine were eligible for enrollment. The inclusion criteria were as follows: (1) American society of anesthesiologists score of I-III; (2) Age of 3-72 mo; and (3) Elective living LT surgery. The exclusion criteria were as follows: (1) Peripheral vascular disease; (2) History of thromboembolism; (3) Systemic or local infection before surgery; (4) Autoimmune diseases; (5) Severe congenital heart disease, and (6) History of LT.

Variables and data sources

Donors and recipient characteristics were obtained from the electronic medical record system. Pediatric end-stage liver disease grade was calculated as described previously[25]. Early allograft dysfunction (EAD), PNF and acute kidney injury were

defined according to published studies[26-28]; EAD was defined as in Olthoff *et al*[29]; and PNF was defined as graft loss, re-transplantation or death due to graft nonfunction within 30 d after surgery (except those induced by hepatic artery embolism, bile duct complications or recurrent liver disease)[30]. Postoperative complications were classified according to the modified Clavien Grading System[31]. Moreover, all recipients were followed up until July 1, 2019, while recipient survival was updated every 3 mo. Two trained research assistants oversaw data collection and recorded them using "Excel" or "Epidata".

Anesthetic techniques

Recipients were monitored through regular electrocardiographic monitoring and underwent initial induction with 8% sevoflurane and 5 L/min of O_2. After achieving silence, the peripheral veins of the upper limbs were opened, and tracheal cannulation was performed under induction with 0.05 mg/kg midazolam, 1 mg/kg rocuronium and 1 μg/kg sufentanil. The pressure support ventilation mode was selected, with a respiratory frequency of 16-20 times/min. The end tidal carbon dioxide tension was controlled at 35-40 mmHg. Intraoperative anesthesia was maintained using sevoflurane (anesthesia depth at 0.6 minimum alveolar concentration). Intraoperative analgesia and muscle relaxation were maintained using sufentanil (1 μg/kg/h) and rocuronium (0.15 mg/kg/h). Basic vital signs and circulation capacity were monitored and managed regularly. All recipients were sent to the intensive care unit (ICU) for postoperative care.

Donors were monitored through regular electrocardiographic monitoring. The peripheral veins and radial artery were opened for transfusion and invasive blood pressure measurement. Donors underwent induction with 0.05 mg/kg midazolam, 2 mg/kg propofol, 0.6 mg/kg rocuronium and 0.5 g/kg sufentanil. Endotracheal intubation and mechanical ventilation were performed with a tidal volume of 8 mL/kg, while the end tidal carbon dioxide tension was maintained between 35 mmHg and 45 mmHg. Intraoperative anesthesia was maintained using cisatracurium, sevoflurane and remifentanil. Following the right internal jugular vein puncture, an internal jugular vein catheter with double cavities was inserted for central venous pressure monitoring. After the operation, donors were sent to the anesthesia recovery room for resuscitation and extubation.

Surgical techniques

Donors were placed in the horizontal position with an inverted L abdominal incision being utilized according to the surgeon's preference. Intraoperative doppler ultrasonography was used to confirm the anatomical structure of the hepatic portal vein and hepatic vein, while intraoperative cholangiography was performed to verify the division position of the hepatic parenchyma after cholecystectomy. After completing parenchymal dissection, the anesthetists administered intravenous heparin sodium (0.5 mg/kg). After the left hepatic artery and left portal vein were severed, 50 mg of protamine was used to reverse immediately heparinization. The graft was maintained at 4 °C, after which portal vein perfusion was started. After confirming that the color of the perfusate discharged from the hepatic vein had faded, the graft was transferred to the preserving solution for vascular structure examination and weight measurement. Details regarding the liver graft resection have been described previously[5,9,32].

Recipients were placed in the horizontal position with a straight-line abdominal incision being utilized. The original liver was initially resected, after which the surgery entered the anhepatic phase. Thereafter, the hepatic vein, portal vein and hepatic artery were inosculated and successively opened. The velocity and pattern of blood flow in the new hepatic portal vein, hepatic vein and hepatic artery were determined using color doppler ultrasound. Roux-en-Y biliary jejunostomy was then performed to replace the inosculation of recipients and donors' biliary duct. Recipients were subsequently transferred to the ICU after confirming that all vessels were fluent and vital signs were stable.

Outcomes

Patients were followed up until July 1, 2019. The primary outcomes examined herein included ALT_{max} and maximum aspartate aminotransferase (AST_{max}). Secondary outcomes included EAD, PNF, postoperative complications and overall survival of recipients.

Statistical analysis

Statistical analyses were conducted using the IBM SPSS Statistics 26.0 (SPSS Inc., Armonk, NY, United States) and R software (Version 3.6.1). Categorical variables are presented as frequency (*n*) or proportion (%), while continuous variables were expressed as mean ± standard deviation or median (25% interquartile range, 75% interquartile range). Differences were analyzed through repeated measures/block randomized one-way analysis of variance, followed by post-hoc analysis (Tukey's test) as appropriate. Moreover, non-parametric tests followed by the Kruskal-Wallis test were utilized for multiple groups comparisons. Categorical variables were compared using the ^{2} test with the Yates correction or Fisher's exact test (when the total sample was < 40 or the expected frequency was < 1). Overall survival curves were created using Kaplan-Meier survival analysis, while the log-rank *t* test was used to compare differences between the four groups. Additionally, a post-hoc subgroup analysis was used to investigate possible effect modification of four groups. All statistical tests were two-sided with *P* values < 0.05 being considered statistically significant.

RESULTS

Patients were randomly assigned to the four groups (*n* = 55 per group). Twelve patients were excluded from the study owing to unexpected issues or changes in surgical plans (Figure 1). The remaining 208 patients [S-RIPC group (*n* = 55), D-RIPC group (*n* = 51), R-RIPC group (*n* = 51) and DR-RIPC group (*n* = 51)] were ultimately analyzed.

Demographic and preoperative/intraoperative characteristics of the recipients and donors are presented in Tables 1 and 2, respectively. No significant differences in demographic or preoperative/intraoperative characteristics were observed between recipients and donors. Recipients in all four groups showed good comparability and consistency.

Recipients were continuously monitored for changes in ALT, AST, total bilirubin, albumin, creatinine (Cr), white blood cell, neutrophil %, hemoglobin and platelet after surgery (0 d) until postoperative day 7, with a portion of the results being presented in Supplementary Table 1. Accordingly, our results found no differences in the aforementioned nine variables except for Cr-D0 (*P* = 0.029), suggesting a significant reduction in Cr levels at postoperative day 0, which was mainly attributed to the difference between the D-RIPC and S-RIPC group. For donors, no differences were found in all variables (Supplementary Table 2).

Clinical outcomes among recipients are summarized in Table 3. Accordingly, significant differences in ICU duration were observed (*P* = 0.041). No differences were found for other clinical outcomes. Our results indicated that RIPC did not improve clinical outcomes among recipients or shorten ICU and ventilation duration. On the contrary, those in the DR-RIPC groups seemed to have had longer ICU duration compared to those in the D-RIPC group. In addition, for postoperative complications, no significant differences were observed in donors before discharge (Supplementary Table 3).

Thereafter, the overall survival among recipients was analyzed. Accordingly, the S-RIPC, D-RIPC, R-RIPC and DR-RIPC groups had a 3-year survival rate of 90.9%, 96.1%, 90.2%, and 92.2%, respectively, with no differences between all four groups (Figure 2).

Lastly, subgroup analyses were performed for recipients, with the results being similar to those for the primary endpoint and clinical outcomes among recipients (Table 4).

DISCUSSION

The present randomized clinical trial showed that RIPC did not significantly improve liver functions or decrease incidences of EAD, PNF and postoperative complications among both recipients or donors. The primary end points, ALT_{max} and AST_{max}, did not differ between the four groups regardless of whether donors or recipients received RIPC. Furthermore, no significant differences were found for incidences of EAD, PNF, postoperative complications and the overall survival of recipients. After further analyzing the effects of RIPC on donors, our still results suggested benefits were limited. Nonetheless, some protective effects of RIPC were observed in recipients,

Table 1 Recipient demographics and preoperative and intraoperative characteristics

	DR-RIPC, *n* = 51	D-RIPC, *n* = 51	R-RIPC, *n* = 51	S-RIPC, *n* = 55	*P* value
Demographics					
Sex, male/female	23/28	28/23	25/26	29/26	0.766
Age in mo	7 (6, 8)	7 (6, 8)	7 (6, 9)	7 (6, 9)	0.130
Weight in kg	7.4 ± 1.3	7.2 ± 1.0	7.6 ± 1.4	7.8 ± 1.8	0.190
Height in cm	66.5 ± 5.8	66.3 ± 4.6	67.3 ± 6.1	68.4 ± 6.8	0.245
Kasai operation, yes/no	30/21	31/20	30/21	33/22	0.996
PELD grade	16.7 ± 10.2	17.2 ± 8.9	14.0 ± 10.1	15.3 ± 8.5	0.222
Child-Pugh grade, A/B/C	4/30/17	3/30/18	5/35/11	6/37/12	0.599
Preoperative biochemical data					
ALT in U/L	140.0 (70.0, 220.0)	154.5 (93.5, 237.2)	130.0 (88.67, 201.5)	140.0 (81.0, 268.6)	0.774
AST in U/L	257.7 (166.0, 421.0)	230.1 (161.0, 339.5)	239.0 (114.0, 405.5)	282.0 (153.0, 500.8)	0.385
TB in mmol/L	264.4 ± 153.3	274.6 ± 166.8	243.9 ± 163.0	253.9 ± 141.0	0.839
ALB in g/L	34.3 ± 6.3	33.3 ± 5.4	32.9 ± 6.1	34.1 ± 5.5	0.604
Cr in μmol/L	14.8 ± 5.1	13.9 ± 3.8	15.8 ± 4.8	15.2 ± 6.4	0.256
WBC as 10^9/L	11.6 ± 4.6	13.6 ± 10.7	12.2 ± 5.9	10.4 ± 4.8	0.204
N%	39.4 ± 12.1	39.2 ± 14.6	34.7 ± 11.9	39.9 ± 13.3	0.159
Hgb in g/L	92.4 ± 17.7	94.5 ± 15.8	96.7 ± 15.9	93.3 ± 14.5	0.535
PLT as 10^9/L	215.0 (148.0, 301.0)	207.0 (138.0, 315.0)	202.0 (144.0, 258.0)	188.0 (129.0, 244.0)	0.476
Intraoperative characteristics					
Length of anhepatic phase in min	32.0 (30.0, 38.0)	34.0 (29.0, 38.5)	33.0 (30.25, 39.0)	34.0 (30.0, 42.5)	0.714
Time of cold ischemia in min	65.7 ± 19.2	63.4 ± 21.5	63.5 ± 17.7	66.4 ± 16.8	0.477
Weight of donor liver in g	249.7 ± 36.0	238.4 ± 44.5	247.8 ± 36.8	253.8 ± 54.4	0.333
GRWR, %	3.5 ± 0.7	3.4 ± 0.8	3.3 ± 0.7	3.3 ± 0.9	0.674
Time of anesthesia in min	470.0 (430.0, 502.5)	441.5 (410.2, 509.8)	473.5 (420.0, 524.0)	468.0 (428.5, 503.0)	0.586
Time of surgery in min	373.9 ± 55.6	366.4 ± 72.2	378.4 ± 69.0	384.5 ± 63.4	0.543
Transfusion volume in mL	1550.0 (1285.0, 1715.0)	1485.0 (1210.0, 1750.0)	1658.0 (1302.0, 1850.0)	1580.0 (1325.0, 1748.0)	0.410
ALB transfusion in g	26.3 ± 7.2	24.4 ± 8.2	24.8 ± 9.4	24.5 ± 7.5	0.486
RBC transfusion in U	1.0 (1.0, 2.0)	1.0 (1.0, 2.0)	1.0 (1.0, 1.9)	1.0 (1.0, 1.8)	0.863
Bleeding in mL	100.0 (100.0, 200.0)	100.0 (100.0, 200.0)	100.0 (100.0, 200.0)	100.0 (100.0, 200.0)	0.928
Urine in mL	220.0 (150.0, 300.0)	210.0 (151.2, 300.0)	220.0 (152.5, 300.0)	210.0 (140.0, 305.0)	0.965

Variables are shown as "mean (SD)" or "median (25% quartile, 75% quartile)". ALB: Albumin; ALT: Alanine transaminase; AST: Aspartate aminotransferase; Cr: Creatinine; D-RIPC: Donors received remote ischemic preconditioning; DR-RIPC: Both donors and recipients received remote ischemic preconditioning; GRWR: Graft/recipient's body weight ratio; Hgb: Hemoglobin; N%: Neutrophil%; PLT: Platelet; RBC: Red blood cell; S-RIPC: Remote ischemic preconditioning with no intervention; R-RIPC: Recipients received remote ischemic preconditioning; PELD: Pediatric end-stage liver disease; TB: Total bilirubin; WBC: White blood cell.

including a lower Cr level in the D-RIPC group than the S-RIPC group on postoperative day 0 ($P < 0.05$), although these were limited to alleviating IRI or improving the prognosis for patients who received LT.

The discovery of possible protective effects of RIPC in reducing IRI and improving organ function highlights a new therapy for clinical treatment[33]. The most important advantages of RIPC include its low cost, ease of performance and almost impeccable safety for patients. Thus, numerous clinical studies have been conducted to explore effects and potential mechanism of RIPC in different areas, such as organ transplantation, cardiac surgery, hepatic surgery and neurosurgery[9,18,34-36]. Studies

Table 2 Donor demographics and preoperative and intraoperative characteristics

	DR-RIPC, *n* = 51	D-RIPC, *n* = 51	R-RIPC, *n* = 51	S-RIPC, *n* = 55	*P* value
Demographics					
Sex, male/female	15/36	22/29	20/31	18/37	0.463
Age in yr	31 (27, 36)	29(26, 32)	30 (27, 34.5)	29 (26, 33.5)	0.299
Weight in kg	59.0 ± 8.7	61.9 ± 10.8	58.7 ± 10.8	58.8 ± 10.7	0.427
Height in cm	163.0 (159.5, 168.0)	162.0 (158.0, 171.0)	162.0 (160.0, 169.5)	162.0 (160.0, 167.5)	0.983
Preoperative biochemical data					
ALT in U/L	14.0 (12.0, 18.0)	15.0 (11.0, 21.0)	15.0 (11.0, 21.0)	13.0 (11.5, 16.5)	0.282
AST in U/L	17.0 (15.5, 20.0)	18.0 (15.5, 21.0)	18.0 (14.5, 21.5)	17.0 (15.0, 20.0)	0.850
TB in mmol/L	10.8 (8.9, 13.5)	11.4 (9.5, 15.7)	11.0 (8.0, 12.2)	10.8 (8.8, 12.8)	0.414
ALB in g/L	46.6 ± 4.3	47.1 ± 3.6	46.5 ± 2.7	46.8 ± 3.0	0.473
Intraoperative characteristics					
Time of anesthesia in min	195.0 (164.0, 217.0)	199.0 (181.0, 218.5)	190.0 (162.0, 217.0)	193.0 (180.5, 229.0)	0.428
Time of surgery in min	156.5 ± 35.9	165.7 ± 43.2	156.4 ± 38.0	161.5 ± 41.3	0.758
Transfusion volume in mL	1650.0 (1250.0, 2000.0)	1750.0 (1250.0, 2000.0)	1750.0 (1250.0, 2000.0)	1750.0 (1250.0, 1750.0)	0.936
Bleeding in mL	50.0 (40.0, 80.0)	50.0 (50.0, 100.0)	50.0 (35.0, 100.0)	50.0 (50.0, 100.0)	0.138
Urine in mL	400.0 (300.0, 450.0)	400.0 (300.0, 500.0)	400.0 (300.0, 475.0)	400.0 (300.0, 500.0)	0.983

Variables are shown as "mean ± SD" or "median (25% quartile, 75% quartile)". ALB: Albumin; ALT: Alanine transaminase; AST: Aspartate aminotransferase; D-RIPC: Donors received remote ischemic preconditioning; DR-RIPC: Both donors and recipients received remote ischemic preconditioning; R-RIPC: Recipients received remote ischemic preconditioning; S-RIPC: Remote ischemic preconditioning with no intervention; TB: Total bilirubin.

Table 3 Comparisons of clinical outcomes in recipients

	DR-RIPC, *n* = 51	D-RIPC, *n* = 51	R-RIPC, *n* = 51	S-RIPC, *n* = 55	*P* value
Duration in ICU in h	115.2 (113.6, 126.2)	113.1[a] (91.0, 114.8)	114.6 (91.3, 116.1)	114.3 (92.5, 138.2)	0.041
Time of ventilation in h	17.7 (16.7, 18.7)	17.8 (16.9, 18.9)	17.6 (17.1, 19.0)	17.8 (16.5, 19.2)	0.941
EAD	6	11	5	8	0.350
PNF	0	0	1	2	0.343
AKI	0	0	0	0	/
Postoperative complications					0.870
≤ 3a	46	50	45	50	
> 3a	5	1	6	5	

[a]$P < 0.05$, donors received remote ischemic preconditioning group *vs* Both donors and recipients received remote ischemic preconditioning group. Variables are shown as "median (25% quartile, 75% quartile)". AKI: Acute kidney injury; D-RIPC: Donors received remote ischemic preconditioning; DR-RIPC: Both donors and recipients received remote ischemic preconditioning; EAD: Early allograft dysfunction; ICU: Intensive care unit; PNF: Primary nonfunction; R-RIPC: Recipients received remote ischemic preconditioning; S-RIPC: Remote ischemic preconditioning with no intervention.

have demonstrated that RIPC mainly occurs in two "windows," one of which is the initial period following the preconditioning stimulus, which can last for 1-4 h[37,38], while the other happens at 24 h following preconditioning, which can last for 24-72 h[39]. Therefore, detecting related critical characteristics after surgery (0 d) is necessary until at least postoperative day 3. The present study continuously monitored liver function variables from day 0 to postoperative day 7 among recipients and day 0 to postoperative day 3 among donors. The ample amount of data has certainly helped us understand the dynamic changes in liver function, inflammatory response and kidney function of patients.

Table 4 Subgroup analyses among four groups in recipients

Stratum	Mean difference in postoperative log maximal ALT compared with S-RIPC (95%CI)			Mean difference in postoperative log maximal AST compared with S-RIPC (95%CI)		
	D-RIPC	R-RIPC	DR-RIPC	D-RIPC	R-RIPC	DR-RIPC
Gender						
Male	0.03 (-0.31, 0.38)	0.11 (-0.24, 0.47)	0.11 (-0.25, 0.47)	0.11 (-0.23, 0.44)	0.20 (-0.14, 0.55)	0.15 (-0.21, 0.50)
Female	-0.06 (-0.50, 0.37)	0.21 (-0.21, 0.64)	0.32 (-0.10, 0.73)	-0.06 (-0.41, 0.29)	0.01 (-0.34, 0.35)	0.19 (-0.15, 0.53)
PELD						
≤ 16	-0.03 (-0.40, 0.33)	-0.05 (-0.40, 0.31)	0.11 (-0.27, 0.48)	0.15 (-0.18, 0.47)	-0.06 (-0.38, 0.27)	0.17 (-0.16, 0.51)
> 16	0.02 (-0.40, 0.43)	0.44 (0.02, 0.86)	0.33 (-0.07, 0.73)	-0.11 (-0.46, 0.25)	0.33 (-0.03, 0.69)	0.17 (-0.17, 0.51)
Time of cold ischemia						
< 60	0.28 (-0.07, 0.63)	0.29 (-0.07, 0.64)	0.29 (-0.09, 0.66)	0.25 (-0.13, 0.63)	0.27 (-0.11, 0.66)	0.24 (-0.16, 0.65)
≥ 60	-0.30 (-0.72, 0.12)	0.08 (-0.34, 0.50)	0.18 (-0.22, 0.57)	-0.19 (-0.50, 0.12)	-0.05 (-0.35, 0.26)	0.13 (-0.16, 0.42)
GRWR						
2.5-4	0.08 (-0.22, 0.38)	0.25 (-0.04, 0.53)	0.28 (-0.01, 0.58)	-0.01 (-0.27, 0.25)	0.10 (-0.16, 0.35)	0.19 (-0.07, 0.46)
< 2.5 or > 4	-0.18 (-0.77, 0.40)	0.07 (-0.62, 0.75)	0.13 (-0.48, 0.74)	0.12 (-0.41, 0.64)	0.16 (-0.45, 0.77)	0.14 (-0.40, 0.68)
Kasai operation						
Yes	-0.11 (-0.47, 0.24)	0.06 (-0.29, 0.42)	0.18 (-0.18, 0.54)	0.00 (-0.28, 0.29)	0.00 (-0.29, 0.29)	0.19 (-0.10, 0.48)
No	0.15 (-0.29, 0.58)	0.31 (-0.12, 0.74)	0.28 (-0.15, 0.72)	0.07 (-0.35, 0.50)	0.25 (-0.17, 0.68)	0.15 (-0.27, 0.57)

For maximum alanine transaminase and maximum aspartate aminotransferase, no significant differences were found in subgroup analyses. ALT: Alanine transaminase; AST: Aspartate aminotransferase; CI: Confidential interval; D-RIPC: Donors received remote ischemic preconditioning; DR-RIPC: Both donors and recipients received remote ischemic preconditioning; GRWR: Graft/recipient's body weight ratio; PELD: Pediatric end-stage liver disease; R-RIPC: Recipients received remote ischemic preconditioning; S-RIPC: Remote ischemic preconditioning with no intervention.

Some potential mechanisms whereby RIPC offers protection have been discussed and can be summarized into three components: Triggers, signal transduction and end-effectors[40]. Accordingly, performing RIPC allowed the local release of certain factors, such as adenosine, cytokines and endogenous opioids, termed "triggers," thereby activating related protein kinase mediators (*e.g.*, phosphoinositol 3-kinase, janus kinase and signal transducer and activator of transcription and protein kinase C) and signaling pathways[41,42]. Signal transduction plays a critical role in exerting the protective effects of RIPC, with some hypotheses having been presented. The two main competing hypotheses regarding the mechanism of signal transduction include "humoral hypothesis" and "neural hypothesis"[43-45]. "Humoral hypothesis" is supported by evidence showing that protection can be transferred by serum transfusion from a rabbit that has undergone ischemic preconditioning (IPC) to one that has not[46]. Meanwhile, "neural hypothesis" is also supported by a series of studies, especially in the cardiovascular and neural field. Lieder *et al*[44] found that RIPC could activate efferent vagal nerves to stimulate the spleen, which then releases humoral cardioprotective substances. Another study[47] showed that the cardioprotective effects of IPC were completely abolished by denervation of the limbs. To some extent, both the "humoral hypothesis" and "neural hypotheses" are reasonable and interact. After signal transduction, the end-effectors, which could be specific organs, cells or organelles, will finally be activated, and the protective effects induced by RIPC would be transformed into changes in cellular signal pathways[40,43].

A number of studies have focused on the effects of RIPC on graft transplantation. Accordingly, Jung *et al*[9] found that RIPC might be beneficial for postoperative liver function among recipients after living donor LT. AST level on postoperative day 1 and maximal AST level within 7 postoperative days were significantly lower in recipients who received a preconditioned graft. However, their results did not show any definite beneficial effects among donors. Also, no differences were found in the incidence of EAD or graft failure among recipients. A systematic review[10] that summarized solid organ transplantation and RIPC studies found controversial results, with some studies suggesting improvements in graft function, while others not showing any effects. In

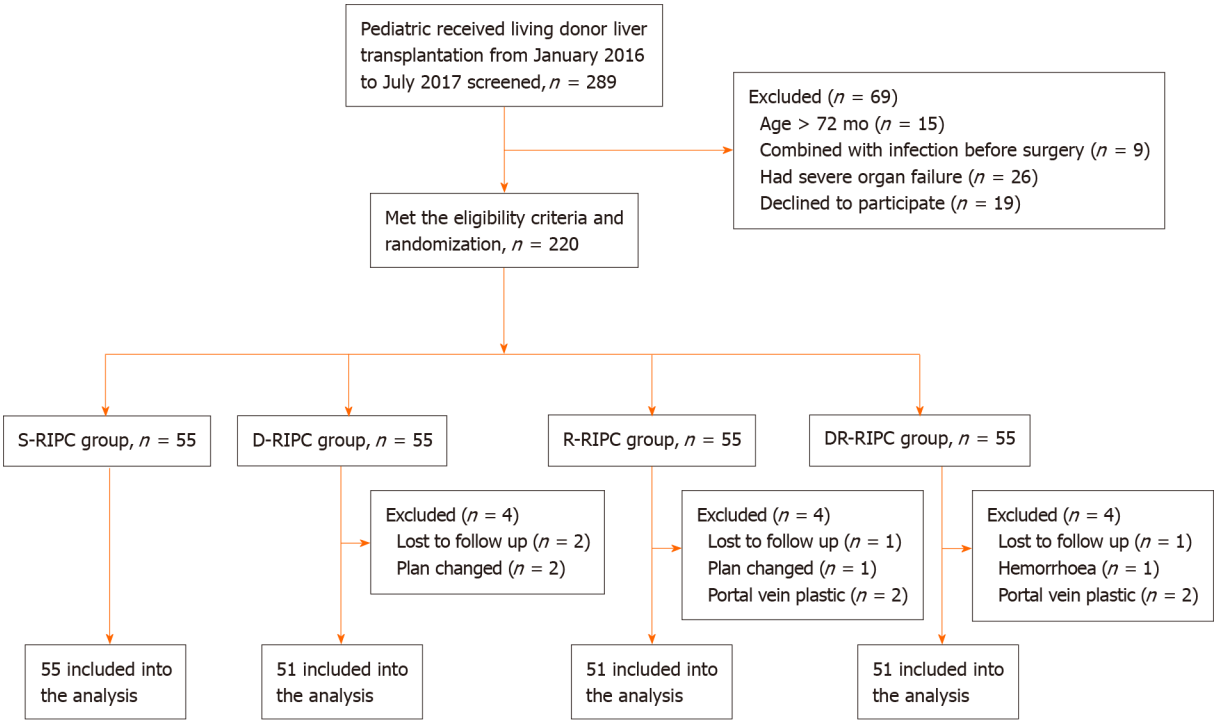


Figure 1 Flow diagram detailing the selection of patients included in the randomized clinical trial. S-RIPC: Remote ischemic preconditioning with no intervention; D-RIPC: Donors received remote ischemic preconditioning; R-RIPC: Recipients received remote ischemic preconditioning; DR-RIPC: Both donors and recipients received remote ischemic preconditioning.

another meta-analysis[48], the researchers found that donor IPC promoted a large reduction in recipient mortality and incidence of PNF. However, still, no statistically significant difference had been observed. Overall, studies regarding RIPC and LT have been insufficient, especially for RIPC and pediatric LT. Stronger and more convincing clinical trials are thus needed to clarify the effects of RIPC on adult and pediatric LT.

To our knowledge, this has been the first randomized clinical trial to explore the effects of RIPC on pediatric LT. Moreover, we had discussed the effects of RIPC on recipients and donors simultaneously. Generally, RIPC had been performed on donors, while the grafts treated with RIPC were subsequently transplanted to recipients. However, the grafts were flushed to cleanse the organ of blood before storage and introduction into the recipients which could flush away potential protective "triggers" for alleviating IRI[49]. Therefore, RIPC among recipients seemed to promote better effects compared to RIPC among donors. Our study was designed such that patients were divided into four groups, which allowed us to understand comprehensively the effects of RIPC on both donors and recipients. Accordingly, our findings showed that RIPC might have fairly limited effects for protecting liver function or reducing incidences of EAD, PNF and postoperative complications among both donors and recipients. Though our study led to a negative result, it was of high significance and helped us understand the effects of RIPC in pediatric LT. Some reasons may help us understand these results. First of all, the muscle and neural system are relatively immature and undeveloped in children. As a result, the effects of RIPC may have been weakened when the RIPC was performed in recipients, compared with adults. Second, the potential protective "triggers" for alleviating IRI in grafts may have been flushed away before storage and introduction into the recipients. Given the differences in recipients, samples, interventions and group design, it is reasonable to assume that our findings may be inconsistent with those presented in studies that showed significant protective effects of RIPC[18,36].

Some limitations of the present study are worth noting. First, this was a single-center study. As such, the inclusion of more centers and more samples would strengthen the clinical significance of the study. Second, measuring more indicators of liver function and IRI, such as interleukin-2, interleukin-6, tumor necrosis factor, malonaldehyde and creatine phosphokinase, would provide more useful information. Third, owing to the lack of consensus regarding the optimal RIPC protocols for adults and children, the cycle and time could have been insufficient to yield the best beneficial effects. In future studies, we would like to attempt more intervention

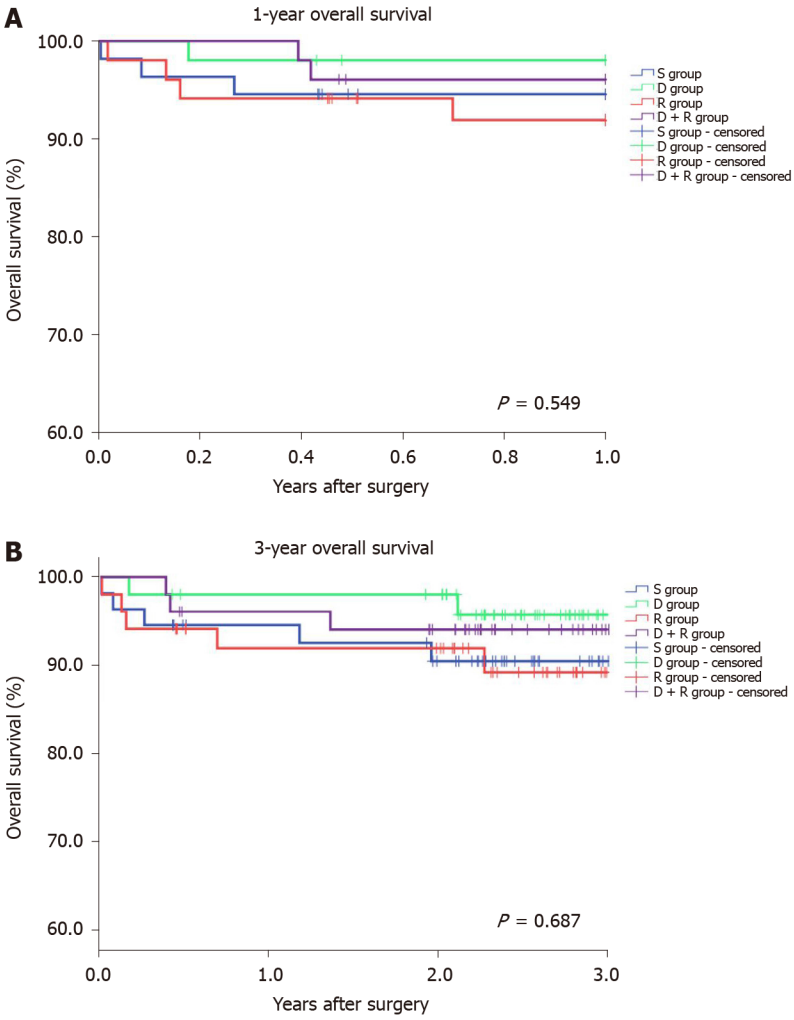


Figure 2 The 1-year (A) and 3-year (B) overall survival analyses of recipients among four groups.

methods.

CONCLUSION

In conclusion, the present study suggested that RIPC may have limited beneficial effects on liver and renal function, overall survival or incidences of EAD, PNF and postoperative complications among recipients undergoing LT, as well as liver function among donors. Nonetheless, more clinical trials regarding the effects of RIPC on pediatric LT are warranted.

ARTICLE HIGHLIGHTS

Research background

Studies suggested that remote ischemic preconditioning (RIPC) may effectively lessen the harmful effects of ischemia reperfusion injury (IRI) during organ transplantation surgery. However, the effect of RIPC on pediatric liver transplantation (LT) was still unknown.

Research motivation

To investigate the protective effects of RIPC on living liver donors and recipients following pediatric LT.

Research objectives

We performed this single-center randomized clinical trial to determine whether RIPC could be beneficial in reducing IRI among both donors and recipients undergoing pediatric living LT.

Research methods

Two-hundred-eight donors were recruited and randomly assigned to four groups: S-RIPC group (no intervention), D-RIPC group (donors received RIPC), R-RIPC group (recipients received RIPC) and DR-RIPC group (both donors and recipients received RIPC). We primarily evaluated postoperative liver function among donors and recipients and incidences of early allograft dysfunction (EAD), primary nonfunction (PNF) and postoperative complications among recipients.

Research results

RIPC did not significantly improve alanine transaminase and aspartate aminotransferase levels among donors and recipients and decrease incidences of EAD, PNF and postoperative complications among recipients. Furthermore, RIPC had no effects on the overall survival of recipients.

Research conclusions

The protective effects of RIPC were limited for recipients who received living LT, and no significant improvement of the prognosis was observed in recipients.

Research perspectives

Our research suggested that RIPC may have limited beneficial effects for recipients undergoing LT as well as donors. Nonetheless, more clinical trials regarding the effects of RIPC on pediatric LT are warranted.

REFERENCES

1 **Starzl TE**, Marchioro TL, Vonkaulla KN, Hermann G, Brittain RS, Waddell WR. Homotransplantation of the liver in humans. *Surg Gynecol Obstet* 1963; **117**: 659-676 [PMID: 14100514]

2 **Kwong A**, Kim WR, Lake JR, Smith JM, Schladt DP, Skeans MA, Noreen SM, Foutz J, Miller E, Snyder JJ, Israni AK, Kasiske BL. OPTN/SRTR 2018 Annual Data Report: Liver. *Am J Transplant* 2020; **20** Suppl: 193-299 [PMID: 31898413 DOI: 10.1111/ajt.15674]

3 **Bodzin AS**, Baker TB. Liver Transplantation Today: Where We Are Now and Where We Are Going. *Liver Transpl* 2018; **24**: 1470-1475 [PMID: 30080954 DOI: 10.1002/lt.25320]

4 **Meirelles Júnior RF**, Salvalaggio P, Rezende MB, Evangelista AS, Guardia BD, Matielo CE, Neves DB, Pandullo FL, Felga GE, Alves JA, Curvelo LA, Diaz LG, Rusi MB, Viveiros Mde M, Almeida MD, Pedroso PT, Rocco RA, Meira Filho SP. Liver transplantation: history, outcomes and perspectives. *Einstein (Sao Paulo)* 2015; **13**: 149-152 [PMID: 25993082 DOI: 10.1590/S1679-45082015RW3164]

5 **Pham YH**, Miloh T. Liver Transplantation in Children. *Clin Liver Dis* 2018; **22**: 807-821 [PMID: 30266163 DOI: 10.1016/j.cld.2018.06.004]

6 **Starzl TE**, Marchioro TL, Porter KA, Brettschneider L. Homotransplantation of the liver. *Transplantation* 1967; **5** Suppl: 790-803 [PMID: 4963511 DOI: 10.1097/00007890-196707001-00003]

7 **Benkö T**, Belker J, Gallinat A, Treckmann JW, Paul A, Minor T, Hoyer DP. Analysis of Data from the Oxygen Persufflation in Liver Transplantation (OPAL) Study to Determine the Role of Factors Affecting the Hepatic Microcirculation and Early Allograft Dysfunction. *Ann Transplant* 2019; **24**: 481-488 [PMID: 31417074 DOI: 10.12659/AOT.915214]

8 **Kohli R**, Cortes M, Heaton ND, Dhawan A. Liver transplantation in children: state of the art and future perspectives. *Arch Dis Child* 2018; **103**: 192-198 [PMID: 28918383 DOI: 10.1136/archdischild-2015-310023]

9 **Jung KW**, Kang J, Kwon HM, Moon YJ, Jun IG, Song JG, Hwang GS. Effect of Remote Ischemic Preconditioning Conducted in Living Liver Donors on Postoperative Liver Function in Donors and Recipients Following Liver Transplantation: A Randomized Clinical Trial. *Ann Surg* 2020; **271**: 646-653 [PMID: 31356262 DOI: 10.1097/SLA.0000000000003498]

10 **Farooqui W**, Pommergaard HC, Rasmussen A. Remote ischemic preconditioning of transplant recipients to reduce graft ischemia and reperfusion injuries: A systematic review. *Transplant Rev (Orlando)* 2018; **32**: 10-15 [PMID: 28637593 DOI: 10.1016/j.trre.2017.06.001]

11 **Robertson FP**, Fuller BJ, Davidson BR. An Evaluation of Ischaemic Preconditioning as a Method of Reducing Ischaemia Reperfusion Injury in Liver Surgery and Transplantation. *J Clin Med* 2017; **6**: 69 [PMID: 28708111 DOI: 10.3390/jcm6070069]

12 **Cannistrà M**, Ruggiero M, Zullo A, Gallelli G, Serafini S, Maria M, Naso A, Grande R, Serra R, Nardo B. Hepatic ischemia reperfusion injury: A systematic review of literature and the role of current drugs and biomarkers. *Int J Surg* 2016; **33** Suppl 1: S57-S70 [PMID: 27255130 DOI: 10.1016/j.ijsu.2016.05.050]

13 **Oliveira THC**, Marques PE, Proost P, Teixeira MMM. Neutrophils: a cornerstone of liver ischemia and reperfusion injury. *Lab Invest* 2018; **98**: 51-62 [PMID: 28920945 DOI: 10.1038/labinvest.2017.90]

14 **Yamada N**, Karasawa T, Wakiya T, Sadatomo A, Ito H, Kamata R, Watanabe S, Komada T, Kimura H, Sanada Y, Sakuma Y, Mizuta K, Ohno N, Sata N, Takahashi M. Iron overload as a risk factor for hepatic ischemia-reperfusion injury in liver transplantation: Potential role of ferroptosis. *Am J Transplant* 2020; **20**: 1606-1618 [PMID: 31909544 DOI: 10.1111/ajt.15773]

15 **Lau JK**, Roy P, Javadzadegan A, Moshfegh A, Fearon WF, Ng M, Lowe H, Brieger D, Kritharides L, Yong AS. Remote Ischemic Preconditioning Acutely Improves Coronary Microcirculatory Function. *J Am Heart Assoc* 2018; **7**: e009058 [PMID: 30371329 DOI: 10.1161/JAHA.118.009058]

16 **Zhang W**, Chen C, Jing R, Liu T, Liu B. Remote Ischemic Preconditioning Protects Cisplatin-Induced Acute Kidney Injury through the PTEN/AKT Signaling Pathway. *Oxid Med Cell Longev* 2019; **2019**: 7629396 [PMID: 31781349 DOI: 10.1155/2019/7629396]

17 **Hausenloy DJ**, Candilio L, Evans R, Ariti C, Jenkins DP, Kolvekar S, Knight R, Kunst G, Laing C, Nicholas J, Pepper J, Robertson S, Xenou M, Clayton T, Yellon DM; ERICCA Trial Investigators. Remote Ischemic Preconditioning and Outcomes of Cardiac Surgery. *N Engl J Med* 2015; **373**: 1408-1417 [PMID: 26436207 DOI: 10.1056/NEJMoa1413534]

18 **Wu G**, Chen M, Wang X, Kong E, Yu W, Sun Y, Wu F. Effect of remote ischemic preconditioning on hepatic ischemia-reperfusion injury in patients undergoing liver resection: a randomized controlled trial. *Minerva Anestesiol* 2020; **86**: 252-260 [PMID: 31808659 DOI: 10.23736/S0375-9393.19.13838-2]

19 **Abu-Amara M**, Yang SY, Quaglia A, Rowley P, Tapuria N, Seifalian AM, Fuller BJ, Davidson BR. Effect of remote ischemic preconditioning on liver ischemia/reperfusion injury using a new mouse model. *Liver Transpl* 2011; **17**: 70-82 [PMID: 21254347 DOI: 10.1002/lt.22204]

20 **Abu-Amara M**, Yang SY, Quaglia A, Rowley P, Fuller B, Seifalian A, Davidson B. Role of endothelial nitric oxide synthase in remote ischemic preconditioning of the mouse liver. *Liver Transpl* 2011; **17**: 610-619 [PMID: 21506249 DOI: 10.1002/lt.22272]

21 **Björnsson B**, Winbladh A, Bojmar L, Sundqvist T, Gullstrand P, Sandström P. Conventional, but not remote ischemic preconditioning, reduces iNOS transcription in liver ischemia/reperfusion. *World J Gastroenterol* 2014; **20**: 9506-9512 [PMID: 25071345 DOI: 10.3748/wjg.v20.i28.9506]

22 **Koneru B**, Shareef A, Dikdan G, Desai K, Klein KM, Peng B, Wachsberg RH, de la Torre AN, Debroy M, Fisher A, Wilson DJ, Samanta AK. The ischemic preconditioning paradox in deceased donor liver transplantation-evidence from a prospective randomized single blind clinical trial. *Am J Transplant* 2007; **7**: 2788-2796 [PMID: 17949458 DOI: 10.1111/j.1600-6143.2007.02009.x]

23 **Schulz KF**, Altman DG, Moher D; CONSORT Group. CONSORT 2010 statement: updated guidelines for reporting parallel group randomized trials. *Ann Intern Med* 2010; **152**: 726-732 [PMID: 20335313 DOI: 10.7326/0003-4819-152-11-201006010-00232]

24 **Cohen J**. Statistical power analysis for the behavioral sciences. 2nd ed. Routledge, 1988 [DOI: 10.4324/9780203771587]

25 **Hsu EK**, Horslen SP, Reyes JD. Pediatric End-stage Liver Disease Scores as a Method of Assessing Mortality Risk or Prioritization to Transplantability: Let Us Save the Children. *JAMA Pediatr* 2018; **172**: 1015-1017 [PMID: 30242376 DOI: 10.1001/jamapediatrics.2018.2889]

26 **Kurian SM**, Fouraschen SM, Langfelder P, Horvath S, Shaked A, Salomon DR, Olthoff KM. Genomic profiles and predictors of early allograft dysfunction after human liver transplantation. *Am J Transplant* 2015; **15**: 1605-1614 [PMID: 25828101 DOI: 10.1111/ajt.13145]

27 **Kennedy EM**, Wood RP, Shaw BW Jr. Primary nonfunction. Is there a contribution from the back table bath? *Transplantation* 1990; **49**: 739-743 [PMID: 2326869]

28 **Li PK**, Burdmann EA, Mehta RL. World Kidney Day 2013: acute kidney injury-global health alert. *Am J Kidney Dis* 2013; **61**: 359-363 [PMID: 23414727 DOI: 10.1053/j.ajkd.2013.01.002]

29 **Olthoff KM**, Kulik L, Samstein B, Kaminski M, Abecassis M, Emond J, Shaked A, Christie JD. Validation of a current definition of early allograft dysfunction in liver transplant recipients and analysis of risk factors. *Liver Transpl* 2010; **16**: 943-949 [PMID: 20677285 DOI: 10.1002/lt.22091]

30 **Adam R**, Karam V, Delvart V, O'Grady J, Mirza D, Klempnauer J, Castaing D, Neuhaus P, Jamieson N, Salizzoni M, Pollard S, Lerut J, Paul A, Garcia-Valdecasas JC, Rodríguez FS, Burroughs A; All contributing centers (www. eltr.org); European Liver and Intestine Transplant Association (ELITA). Evolution of indications and results of liver transplantation in Europe. A report from the European Liver Transplant Registry (ELTR). *J Hepatol* 2012; **57**: 675-688 [PMID: 22609307 DOI: 10.1016/j.jhep.2012.04.015]

31 **Dindo D**, Demartines N, Clavien PA. Classification of surgical complications: a new proposal with evaluation in a cohort of 6336 patients and results of a survey. *Ann Surg* 2004; **240**: 205-213 [PMID: 15273542 DOI: 10.1097/01.sla.0000133083.54934.ae]

32 **Robertson FP**, Goswami R, Wright GP, Fuller B, Davidson BR. Protocol for a prospective randomized controlled trial of recipient remote ischaemic preconditioning in orthotopic liver transplantation (RIPCOLT trial). *Transplant Res* 2016; **5**: 4 [PMID: 27054029 DOI: 10.1186/s13737-016-0033-4]

33 **Przyklenk K**, Bauer B, Ovize M, Kloner RA, Whittaker P. Regional ischemic 'preconditioning' protects remote virgin myocardium from subsequent sustained coronary occlusion. *Circulation* 1993; **87**: 893-899 [PMID: 7680290 DOI: 10.1161/01.cir.87.3.893]

34 **Guo L**, Zhou D, Wu D, Ding J, He X, Shi J, Duan Y, Yang T, Ding Y, Ji X, Meng R. Short-term remote ischemic conditioning may protect monkeys after ischemic stroke. *Ann Clin Transl Neurol* 2019; **6**: 310-323 [PMID: 30847363 DOI: 10.1002/acn3.705]

35 **Flechsig M**, Ruf TF, Troeger W, Wiedemann S, Quick S, Ibrahim K, Pfluecke C, Youssef A, Sveric KM, Winzer R, Heinzel FR, Linke A, Strasser RH, Zhang K, Heidrich FM. Remote Ischemic Preconditioning Neither Improves Survival nor Reduces Myocardial or Kidney Injury in Patients Undergoing Transcatheter Aortic Valve Implantation (TAVI). *J Clin Med* 2020; **9**: 160 [PMID: 31936060 DOI: 10.3390/jcm9010160]

36 **Zarbock A**, Schmidt C, Van Aken H, Wempe C, Martens S, Zahn PK, Wolf B, Goebel U, Schwer CI, Rosenberger P, Haeberle H, Görlich D, Kellum JA, Meersch M; RenalRIPC Investigators. Effect of remote ischemic preconditioning on kidney injury among high-risk patients undergoing cardiac surgery: a randomized clinical trial. *JAMA* 2015; **313**: 2133-2141 [PMID: 26024502 DOI: 10.1001/jama.2015.4189]

37 **Lawson CS**, Downey JM. Preconditioning: state of the art myocardial protection. *Cardiovasc Res* 1993; **27**: 542-550 [PMID: 8324783 DOI: 10.1093/cvr/27.4.542]

38 **Loukogeorgakis SP**, Panagiotidou AT, Broadhead MW, Donald A, Deanfield JE, MacAllister RJ. Remote ischemic preconditioning provides early and late protection against endothelial ischemia-reperfusion injury in humans: role of the autonomic nervous system. *J Am Coll Cardiol* 2005; **46**: 450-456 [PMID: 16053957 DOI: 10.1016/j.jacc.2005.04.044]

39 **Marber MS**, Latchman DS, Walker JM, Yellon DM. Cardiac stress protein elevation 24 hours after brief ischemia or heat stress is associated with resistance to myocardial infarction. *Circulation* 1993; **88**: 1264-1272 [PMID: 8353888 DOI: 10.1161/01.cir.88.3.1264]

40 **Veighey K**, MacAllister R. Clinical applications of remote ischaemic preconditioning in native and transplant acute kidney injury. *Pediatr Nephrol* 2015; **30**: 1749-1759 [PMID: 25280959 DOI: 10.1007/s00467-014-2965-6]

41 **Hausenloy DJ**, Lecour S, Yellon DM. Reperfusion injury salvage kinase and survivor activating factor enhancement prosurvival signaling pathways in ischemic postconditioning: two sides of the same coin. *Antioxid Redox Signal* 2011; **14**: 893-907 [PMID: 20615076 DOI: 10.1089/ars.2010.3360]

42 **Soares ROS**, Losada DM, Jordani MC, Évora P, Castro-E-Silva O. Ischemia/Reperfusion Injury Revisited: An Overview of the Latest Pharmacological Strategies. *Int J Mol Sci* 2019; **20**: 5034 [PMID: 31614478 DOI: 10.3390/ijms20205034]

43 **Basalay MV**, Davidson SM, Gourine AV, Yellon DM. Neural mechanisms in remote ischaemic conditioning in the heart and brain: mechanistic and translational aspects. *Basic Res Cardiol* 2018; **113**: 25 [PMID: 29858664 DOI: 10.1007/s00395-018-0684-z]

44 **Lieder HR**, Kleinbongard P, Skyschally A, Hagelschuer H, Chilian WM, Heusch G. Vago-Splenic Axis in Signal Transduction of Remote Ischemic Preconditioning in Pigs and Rats. *Circ Res* 2018; **123**: 1152-1163 [PMID: 30359199 DOI: 10.1161/CIRCRESAHA.118.313859]

45 **Skyschally A**, Kleinbongard P, Lieder H, Gedik N, Stoian L, Amanakis G, Elbers E, Heusch G. Humoral transfer and intramyocardial signal transduction of protection by remote ischemic perconditioning in pigs, rats, and mice. *Am J Physiol Heart Circ Physiol* 2018; **315**: H159-H172 [PMID: 29569956 DOI: 10.1152/ajpheart.00152.2018]

46 **Dickson EW**, Reinhardt CP, Renzi FP, Becker RC, Porcaro WA, Heard SO. Ischemic preconditioning may be transferable *via* whole blood transfusion: preliminary evidence. *J Thromb Thrombolysis* 1999; **8**: 123-129 [PMID: 10436142 DOI: 10.1023/a:1008911101951]

47 **Steensrud T**, Li J, Dai X, Manlhiot C, Kharbanda RK, Tropak M, Redington A. Pretreatment with the nitric oxide donor SNAP or nerve transection blocks humoral preconditioning by remote limb ischemia or intra-arterial adenosine. *Am J Physiol Heart Circ Physiol* 2010; **299**: H1598-H1603 [PMID: 20802131 DOI: 10.1152/ajpheart.00396.2010]

48 **Robertson FP**, Bessell PR, Diaz-Nieto R, Thomas N, Rolando N, Fuller B, Davidson BR. High serum Aspartate transaminase levels on day 3 postliver transplantation correlates with graft and patient survival and would be a valid surrogate for outcome in liver transplantation clinical trials. *Transpl Int* 2016; **29**: 323-330 [PMID: 26615011 DOI: 10.1111/tri.12723]

49 **Liu C**, Loong CC, Hsia CY, Tsou MY, Tsai HL, Wei C. Retrograde arterial flush of the liver graft in living donor liver transplantation. *J Invest Surg* 2009; **22**: 406-412 [PMID: 20001809 DOI: 10.3109/08941930903410833]

World Journal of Gastroenterology

Submit a Manuscript: https://www.f6publishing.com

World J Gastroenterol 2021 January 28; 27(4): 358-370

DOI: 10.3748/wjg.v27.i4.358

ISSN 1007-9327 (print) ISSN 2219-2840 (online)

ORIGINAL ARTICLE

Prospective Study

Could saline irrigation clear all residual common bile duct stones after lithotripsy? A self-controlled prospective cohort study

Yan-Yan Lin, Yu-Dong Wang, Ping Yue, Xian-Zhuo Zhang, Joseph W Leung, Pan-Pan Jiao, Man Yang, Hai-Ping Wang, Bing Bai, Ying Liu, Jin-Duo Zhang, Hong-Bo Chen, Wen-Bo Meng, Xun Li

ORCID number: Yan-Yan Lin 0000-0001-7417-0190; Yu-Dong Wang 0000-0003-1240-3838; Ping Yue 0000-0001-8736-949X; Xian-Zhuo Zhang 0000-0003-0160-903X; Joseph W Leung 0000-0001-8919-0442; Pan-Pan Jiao 0000-0002-4581-3000; Man Yang 0000-0003-4966-9701; Hai-Ping Wang 0000-0002-7771-5077; Bing Bai 0000-0001-8672-8569; Ying Liu 0000-0002-0997-4480; Jin-Duo Zhang 0000-0002-3425-9614; Hong-Bo Chen 0000-0002-0954-5600; Wen-Bo Meng 0000-0002-9355-0225; Xun Li 0000-0003-3787-1558.

Author contributions: Lin YY, Wang YD, Yue P, and Zhang XZ contributed equally to this work; Lin YY, Wang YD, Yue P, Leung JW, and Meng WB contributed to study conception and design; Chen HB, Meng WB ,and Li X contributed to administrative support; Lin YY, Wang YD, Yue P, Zhang XZ, Jiao PP, Yang M, Bai B, Liu Y, and Zhang JD contributed to provision of study materials or patients; Lin YY, Wang YD, Yue P, Zhang XZ, Jiao PP, Yang M, Bai B, Liu Y, and Zhang JD contributed collection and assembly of the data; Lin YY, Wang YD, Yue P, Zhang XZ, Jiao PP, Leung JW, Wang HP, Chen HB, Meng WB, and Li X contributed to data analysis and interpretation; all authors wrote the manuscript, and

Yan-Yan Lin, Ping Yue, Xian-Zhuo Zhang, Bing Bai, Jin-Duo Zhang, Wen-Bo Meng, Xun Li, Department of General Surgery, The First Hospital of Lanzhou University, Lanzhou 730000, Gansu Province, China

Yan-Yan Lin, Ping Yue, Hai-Ping Wang, Bing Bai, Jin-Duo Zhang, Wen-Bo Meng, Xun Li, Clinical Medical College Cancer Center of Lanzhou University, The First Hospital of Lanzhou University, Lanzhou 730000, Gansu Province, China

Yan-Yan Lin, Ping Yue, Hai-Ping Wang, Bing Bai, Jin-Duo Zhang, Wen-Bo Meng, Xun Li, Key Laboratory of Biological Therapy and Regenerative Medicine Transformation of Gansu Province, The First Hospital of Lanzhou University, Lanzhou 730000, Gansu Province, China

Yu-Dong Wang, Department of General Surgery, The First Affiliated Hospital of Henan Polytechnic University, Jiaozuo 454001, Henan Province, China

Xian-Zhuo Zhang, Pan-Pan Jiao, The First School of Clinical Medicine, Lanzhou University, Lanzhou 730000, Gansu Province, China

Joseph W Leung, Department of Gastroenterology, Sacramento VA Medical Center, Mather, CA 95655-4200, United States

Joseph W Leung, Department of Gastroenterology and Hepatology, UC Davis Medical Center, Sacramento, CA 95817, United States

Man Yang, Department of Gastroenterology, Songgang People's Hospital, Shenzhen 518105, Guangdong Province, China

Ying Liu, School of Foreign Languages and Literatures, Lanzhou University, Lanzhou 730000, Gansu Province, China

Hong-Bo Chen, School of Pharmaceutical Sciences, Sun Yat-sen University, Shenzhen 518105, Guangdong Province, China

Corresponding author: Wen-Bo Meng, MD, PhD, Professor, Department of General Surgery, The First Hospital of Lanzhou University, No. 1 Donggang West Road, Lanzhou 730000, Gansu Province, China. mengwb@lzu.edu.cn

have read and approved the final manuscript.

Supported by National Natural Science Foundation of China, No. 81872036 and No. 82060551.

Institutional review board statement: The study was approved by the ethics committee of The First Hospital of Lanzhou University (No. LDYYMENG2018-1028) and conducted in accordance with the ethical principles of the Declaration of Helsinki.

Clinical trial registration statement: This study is registered at ClinicalTrials.gov. The registration identification number is NCT03701009.

Informed consent statement: The patients were not required to give informed consent to the study because written informed consents were obtained from the patients for using their data anonymously in scientific studies while protecting their anonymity before the procedure.

Conflict-of-interest statement: All authors have no conflicts of interest to declare.

Data sharing statement: No additional data are available.

CONSORT 2010 statement: The authors have read the CONSORT 2010 statement, and the manuscript was prepared and revised according to the CONSORT 2010 statement.

Open-Access: This article is an open-access article that was selected by an in-house editor and fully peer-reviewed by external reviewers. It is distributed in accordance with the Creative Commons Attribution NonCommercial (CC BY-NC 4.0) license, which permits others to distribute, remix, adapt, build upon this work non-commercially, and license their derivative works on different terms, provided the original work is properly cited and the use is non-commercial. See: http://creativecommons.org/Licenses/by-nc/4.0/

Abstract

BACKGROUND

A previous study showed that irrigation with 100 mL saline reduced residual common bile duct (CBD) stones, which potentially cause recurrent stones after endoscopic retrograde cholangiopancreatography.

AIM

To determine whether saline irrigation can improve CBD clearance after lithotripsy.

METHODS

This prospective self-controlled study enrolled patients receiving mechanical lithotripsy for large (> 1.2 cm) CBD stones. After occlusion cholangiography confirmed CBD stone clearance, peroral cholangioscopy (POC) was performed to determine clearance scores based on the number of residual stones. The amounts of residual stones spotted *via* POC were graded on a 5-point scale (score 1, worst; score 5, best). Scores were documented after only stone removal (control) and after irrigation with 50 mL and 100 mL saline, respectively. The stone composition was analyzed using infrared spectroscopy.

RESULTS

Between October 2018 and January 2020, 47 patients had CBD clearance scores of 2.4 ± 1.1 without saline irrigation, 3.5 ± 0.7 with 50 mL irrigation, and 4.6 ± 0.6 with 100 mL irrigation ($P < 0.001$). Multivariate analysis showed that CBD diameter > 15 mm [odds ratio (OR) = 0.08, 95% confidence interval (CI): 0.01-0.49; $P = 0.007$] and periampullary diverticula (PAD) (OR = 6.51, 95%CI: 1.08-39.21; $P = 0.041$) were independent risk factors for residual stones. Bilirubin pigment stones constituted the main residual stones found in patients with PAD ($P = 0.004$).

CONCLUSION

Irrigation with 100 mL of saline may not clear all residual CBD stones after lithotripsy, especially in patients with PAD and/or a dilated (> 15 mm) CBD. Pigment residual stones are soft and commonly found in patients with PAD. Additional saline irrigation may be required to remove retained stones.

Key Words: Endoscopic retrograde cholangiopancreatography; Common bile duct gall stones; Peroral cholangioscopy; Saline irrigation; Periampullary diverticula; Prospective cohort study

©The Author(s) 2021. Published by Baishideng Publishing Group Inc. All rights reserved.

Core Tip: This is a prospective self-controlled study with 47 patients seeking to determine whether saline irrigation can also improve common bile duct (CBD) clearance after mechanical lithotripsy. Irrigation with 100 mL of saline may not clear all residual CBD stones after mechanical lithotripsy, especially in patients with periampullary diverticula (PAD) and/or a dilated (> 15 mm) CBD. Pigment residual stones are soft and commonly found in patients with PAD. Additional saline irrigation may be required to remove the retained stones.

Citation: Lin YY, Wang YD, Yue P, Zhang XZ, Leung JW, Jiao PP, Yang M, Wang HP, Bai B, Liu Y, Zhang JD, Chen HB, Meng WB, Li X. Could saline irrigation clear all residual common bile duct stones after lithotripsy? A self-controlled prospective cohort study. *World J Gastroenterol* 2021; 27(4): 358-370

URL: https://www.wjgnet.com/1007-9327/full/v27/i4/358.htm

DOI: https://dx.doi.org/10.3748/wjg.v27.i4.358

Manuscript source: Unsolicited manuscript

Specialty type: Gastroenterology and hepatology

Country/Territory of origin: China

Peer-review report's scientific quality classification

Grade A (Excellent): 0
Grade B (Very good): 0
Grade C (Good): C, C, C
Grade D (Fair): 0
Grade E (Poor): 0

Received: November 22, 2020
Peer-review started: November 22, 2020
First decision: November 30, 2020
Revised: December 11, 2020
Accepted: December 28, 2020
Article in press: December 28, 2020
Published online: January 28, 2021

P-Reviewer: Cascella M, Maetani I
S-Editor: Gao CC
L-Editor: Wang TQ
P-Editor: Wang LL

INTRODUCTION

Endoscopic retrograde cholangiopancreatography (ERCP) is an effective and relatively minimally invasive technique for common bile duct (CBD) stones[1-3]. It has been reported that the recurrence rate of CBD stones after ERCP has increased from 4% to 24%[4-6]. The incidence of residual stones after mechanical lithotripsy for intractable CBD stones is 24% to 40%[7-10]. A growing number of studies suggest that an important reason for the recurrence of bile duct stones is the presence of stone debris after lithotripsy[11-13]. During ERCP, occluded cholangiography (OC) is often performed after stone removal to determine whether the stone is removed completely, but OC lacks accuracy. Even if no obvious stones are found on cholangiography, the presence of contrast can obscure small stone debris in the bile duct[8,14]. Complete bile duct clearance is necessary to decrease recurrent bile duct stones.

Some studies[15-17] reported that irrigation of the bile duct with saline after stone extraction further improves the clearance of the bile duct and has the advantages of being a simple, low-cost procedure with rare complications. Ang *et al*[16] showed that a mean of 48 mL of saline solution could irrigate and flush out residual stones after the endoscopic removal of CBD stones. Ahn *et al*[17] found that irrigation with 100 mL of saline can flush out residual stone fragments from the bile duct into the duodenum after stone extraction. However, intraductal ultrasound (IDUS) has a high sensitivity and accuracy in diagnosing bile duct stones/debris[11,16]. This modality yields only indirect images of the debris.

The lack of direct evidence to support the efficacy of saline irrigation after lithotripsy prompted us to use peroral cholangioscopy (POC) to examine the bile duct and detect any residual stones/debris. The results of no irrigation after stone extraction were confirmed by OC and were compared to the effectiveness of irrigation with 50 mL or 100 mL saline. To evaluate whether irrigation with 100 mL of saline is more effective in achieving complete clearance of the bile duct after mechanical lithotripsy, we conducted this prospective self-controlled study.

MATERIALS AND METHODS

Study design and participants

Between October 2018 and January 2020, 47 patients with CBD stones were enrolled in a prospective clinical trial conducted in the surgical endoscopy center of The First Hospital of Lanzhou University (Figure 1). All eligible patients or their legal representatives gave informed consent before the treatment. The inclusion criteria were patients with CBD stones undergoing ERCP, able to provide informed consent, with a stone size larger than 1.2 cm and requiring mechanical lithotripsy for stone removal. The exclusion criteria included pre-ERCP acute suppurative cholangitis, acute pancreatitis, gastrointestinal (GI) tract hemorrhage and/or perforation, previous history of ERCP, prior Bilroth II gastrectomy and Roux-en-Y or cholangiojejunostomy, pregnancy or breastfeeding, coagulopathy with international normalized ratio > 1.5 and low platelet count (< 50 × 10^9/L) or active use of anticoagulation drugs, severe liver disease including decompensated liver cirrhosis or liver failure, septic shock, biliary-duodenal fistula confirmed before ERCP cannulation, the presence of intrahepatic duct stones and malignancy, and patient unwillingness or inability to give informed consent.

To assess the number of residual stones, we created a CBD clearance score as follows: (1) A large number of stone fragments and biliary sludge; (2) A moderate number of stone fragments and biliary sludge; (3) A small number of stone fragments and biliary sludge; (4) Presence of biliary sludge without any stones; and (5) Completely cleared CBD without any biliary sludge. The scores were determined by two endoscopists independently (Figure 2).

The study was approved by the ethics committee of The First Hospital of Lanzhou University (No. LDYYMENG2018-1028) and conducted in accordance with the ethical principles of the Declaration of Helsinki. All authors had access to the study data and reviewed and approved the final manuscript.

Procedures

All endoscopic procedures were performed by two experienced endoscopists (each has performed > 1000 ERCPs). Routine prophylactic antibiotics were given in all cases. ERCP was performed with a standard duodenoscope (TJF-260V, Olympus, Tokyo, Japan). The patients received propofol anesthesia without tracheal intubation.

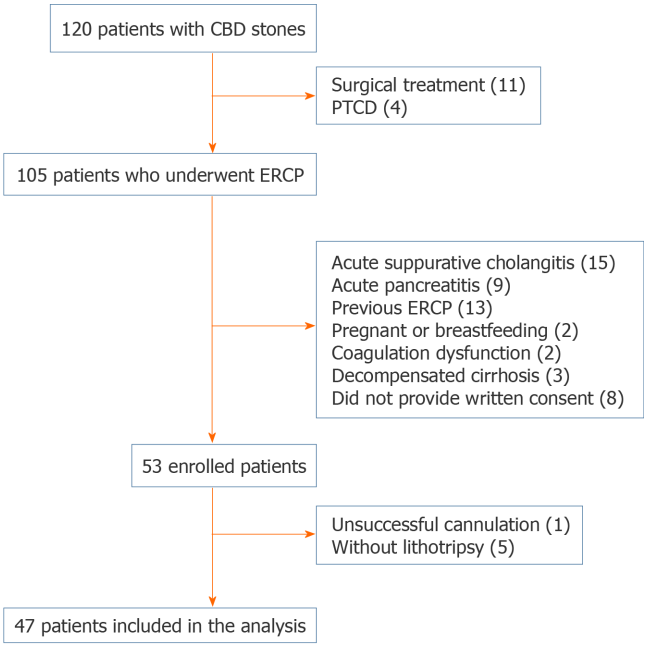


Figure 1 Flow chart of the self-controlled study. CBD: Common bile duct; ERCP: Endoscopic retrograde cholangiopancreatography; PTCD: Percutaneous transhepatic cholangiodrainage.

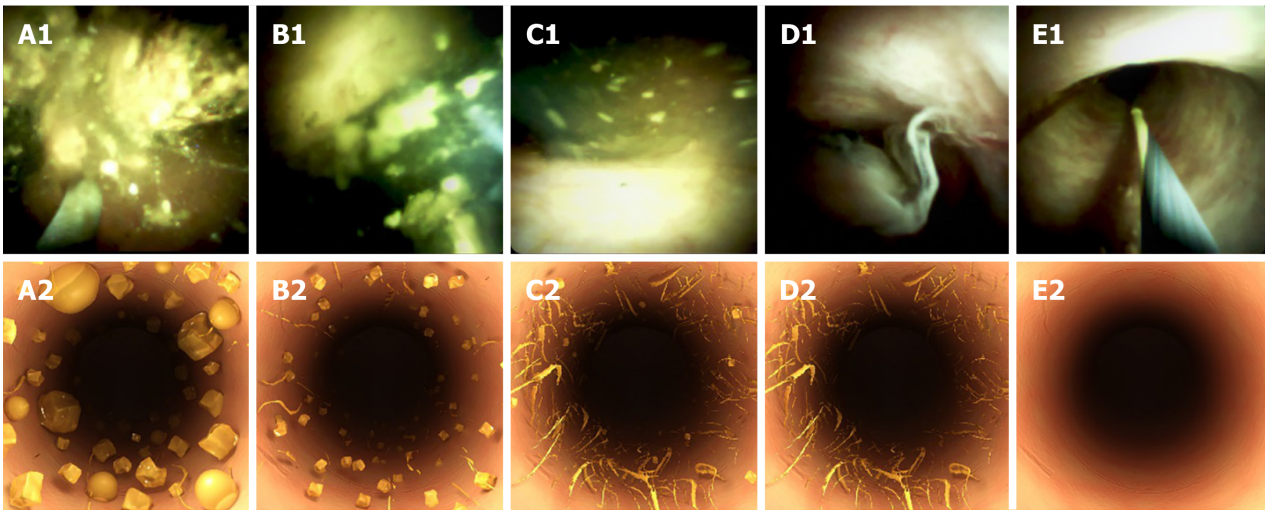


Figure 2 SpyGlass DS images and simulation graphs of the residual stone. A-E: SpyGlass DS images (A1-E1) and simulation graphs (A2-E2). Score 1: A large amount of stone fragments and biliary sludge. Score 2: A moderate amount of stone fragments and biliary sludge. Score 3: A small amount of stone fragments and biliary sludge. Score 4: Presence of biliary sludge without any stones. Score 5: Completely cleared common bile duct without any biliary sludge.

During ERCP, cannulation was performed with a wire-guided sphincterotome. After successful cannulation, contrast was injected to determine the stone size (more or less than 12 mm) and the need for mechanical lithotripsy. All patients underwent a small sphincterotomy with an average length of 3-5 mm using the ENDO CUT mode (power setting 90-120 W; Erbe Elektromedizin, Tuebingen, Germany) followed by balloon sphincteroplasty using a controlled radial expansion (CRE) balloon (10-12 mm in diameter; Boston Scientific, Cork, Ireland). Lithotripsy was performed using an endoscopic lithotripter-compatible basket (Boston Scientific, Marlborough, MA, United States), and stones were removed using the basket and a balloon catheter. Samples of CBD stones were collected using an EndoRetrieval bag (Micro-Tech, Nanjing, China) and placed in a container for subsequent analysis. Occlusion cholangiography was performed by injecting contrast with a balloon catheter. Fluoroscopic assessment using a C-arm X-ray (OEC 9900 Elite, Salt Lake City, Utah, United States) was applied to confirm complete removal of CBD stones and the existence of stone residuals was determined by both endoscopist and radiologist.

Confirmed stone residues by applying occlusion cholangiography were then followed by repeated extraction attempts. If complete stone removal was confirmed, a CBD clearance score was generated by further applying SpyGlass DS (Boston Scientific Corporation, Marlborough, Massachusetts, United States) examination. If the CBD clearance score was less than 5, the bile duct was irrigated intermittently with 50 mL of normal saline using a basket. The basket was shaken during irrigation with slight suction applied to the duodenoscope to promote drainage. The bile duct was then examined again using the SpyGlass DS to detect any residual stones/sludge and document the clearance score. If the clearance score was still less than 5, repeat irrigation of the CBD was performed using another 50 mL of normal saline. The final CBD clearance score was obtained one more time using SpyGlass DS examination. CBD stones that were not irrigated out after double 50 mL-saline irrigations continued to be irrigated with saline until they were fully cleared (Figure 3). Endoscopic nasobiliary drainage (ENBD) or biliary stenting was performed if necessary. The CBD clearance score was assessed by two blinded endoscopists who were masked to the treatment.

The composition of the removed CBD stones was analyzed using infrared ray (IR) spectroscopy. One milligram (mg) of stone samples was mixed with 150 mg of potassium bromide in a mortar and ground into powder. The stone mixture was pressed into a mold and then placed into an automatic IR spectrum analyzer for automated detection to determine the IR spectrogram of the CBD stones. The IR spectrogram showed characteristic absorption peaks at a wavelength of 1460 cm-1, indicating cholesterol-based stones, and those at a wavelength of 1680 cm-1 indicated pigment-based stones.

Definition for complications

Most of the post-ERCP adverse events were detected within 24 h after the procedure. We routinely assessed these adverse events, including cholangitis, oozing/bleeding, pancreatitis, cholecystitis, and perforation, at 24 and 48 h after the ERCP procedure by symptoms, signs, laboratory tests, and imaging examinations if necessary[18,19]. Post-ERCP adverse events were defined as follows: (1) The diagnosis of acute cholangitis was based on Tokyo Guidelines 2018/2013 (TG18/TG13) diagnostic criteria[20]; (2) Oozing was defined as bleeding that was slight and stopped spontaneously; (3) Pancreatitis was described as new or worsening abdominal pain along with an increase in serum amylase levels (> 3 × higher than normal upper limit measured 24 h after surgery); (4) Cholecystitis was defined as pain in the epigastrium or RUQ accompanied by a positive Murphy sign, and abdominal ultrasonography showing a thickened gallbladder wall; and (5) Perforation was defined as sudden abdominal pain accompanied by retroperitoneal air and fluid.

Mechanical lithotripsy was performed by the same assistant for all patients. Stones that were fragmented successfully with only one attempt were defined as soft stones. Stones that required multiple fragmentation attempts or needed to be broken again were defined as hard stones.

Statistical analysis

The sample size calculation was based on the rate of residual stone clearance. According to a previous study[16] and our prior experience, we assumed a success rate of 84.5% for endoscopic extraction of CBD stones and an increase of up to 97% with saline irrigation. We estimated that 47 patients were needed in this analysis to obtain a power of 80% at the 5% level.

Categorical variables are expressed as numbers or percentages (%). Continuous variables are presented as the mean ± SD or median and interquartile range, as appropriate. Continuous variables with a normal distribution were analyzed by paired *t*-test or signed-rank test. Categorical variables were analyzed using the chi-square test or Fisher's exact test. Logistic regression was used to predict risk factors for complications, and the results are presented as odds ratios (ORs) with 95% confidence intervals (Cis). Variables with a P value of < 0.2 in the univariate analysis were included in the multivariate analysis. Linear mixed-effects models were conducted to assess the effect of saline irrigation on the clearance score with a random intercept for each patient and an unstructured covariance structure. A two-sided P value of less than 0.05 was considered statistically significant. The analyses were conducted with statistical software (SAS version 9.4, SAS Institute, Inc., NC, United States).

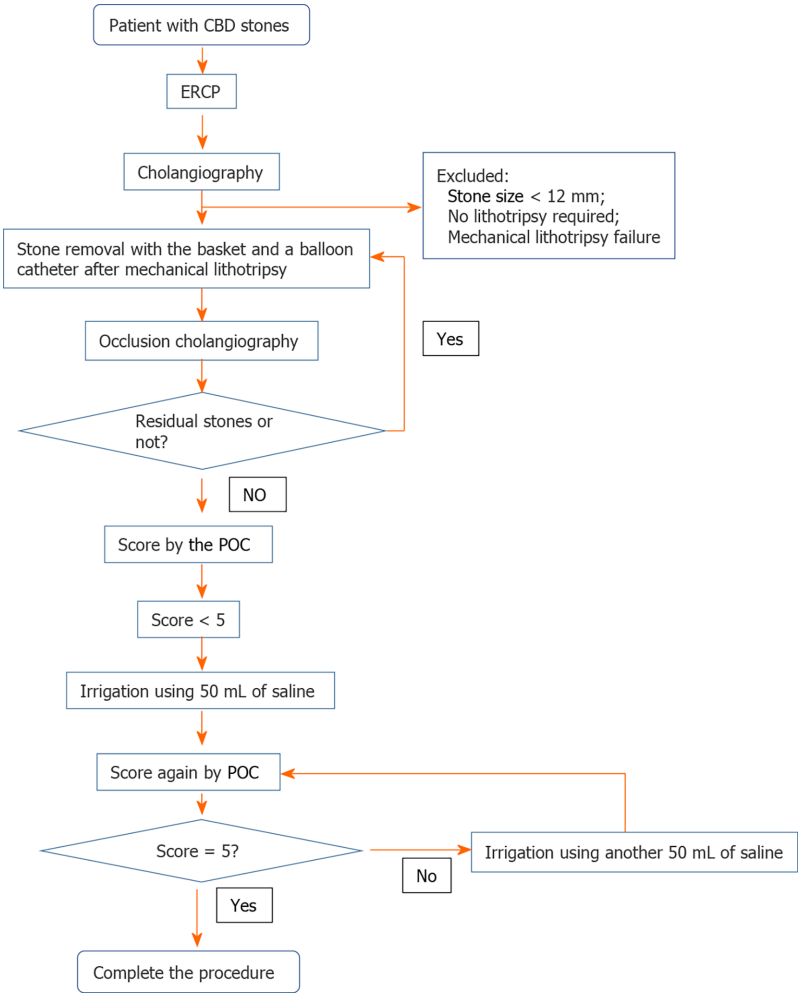


Figure 3 Protocol of evaluation and irrigation procedures. CBD: Common bile duct; ERCP: Endoscopic retrograde cholangiopancreatography; POC: Peroral cholangioscopy.

RESULTS

The patients' average age was 61 ± 16.5 years, and 23 (48.9%) were male. Comorbidities included coronary disease in three (6.4%) patients, hypertension in 14 (29.8%), diabetes in two (4.3%), liver cirrhosis in three (2.1%), and portal hypertension in one (6.4%). The stone analysis showed that 17 (36.2%) cases had cholesterol-based stones, and 30 (63.8%) had pigment-based stones.

Procedure-related adverse events occurred in 11 (23.4%) of 47 patients, with cholangitis in four patients, bleeding in two, pancreatitis in four, and cholecystitis in one. No mortality or perforation occurred. The mean time for ERCP was 40.3 ± 15.4 min (Table 1).

After endoscopic stone extraction, occlusion cholangiography showed that there were no residual CBD stones. Seven patients had a clearance score of 4 identified by POC with the SpyGlass DS, and no patients had a score of 5 before saline irrigation. After irrigation with 50 mL saline, CBD clearance improved to 4 in 28 patients, but none achieved a score of 5. After a total of 100 mL of saline irrigation, there was further improvement in the clearance scores: 12 (26%) patients had a score of 4, and 32 (68%) had a score of 5 identified by the SpyGlass DS. The respective CBD stone clearance rates for the control (no irrigation), 50 mL saline irrigation, and 100 mL saline irrigation were 15%, 60%, and 94%, respectively, and the difference among them was statistically significant ($P < 0.001$) (Table 2). The CBD clearance score (mean ± SD) was 2.4 ± 1.1 in the control, 3.5 ± 0.7 in the 50 mL saline irrigation, and 4.6 ± 0.6 in the 100 mL saline irrigation ($P < 0.001$) (Supplementary Figure 1).

After ERCP, 13 patients had a score of 1 (a large amount of residual stone/sludge) before saline irrigation. Only 15 patients did not reach a score of 5 (complete clearance) after 100 mL of saline irrigation. A dilated CBD diameter > 15 mm (OR = 4.93, 95%CI: 1.13-21.57; $P = 0.034$) was an independent risk factor for significant residual CBD

Table 1 Clinical and procedural characteristics of the patients

Patients	*n* = 47
Age (yr, mean ± SD)	61 ± 16.5
Male	23 (48.9%)
Stone size (mm)	14 (14-15)
Multiple CBD stones	36 (76.6%)
Diameter of CBD (mm)	15 (12-18)
Gallbladder stones	21 (44.7%)
Previous cholecystectomy	24 (51.1%)
Periampullary diverticulum	15 (31.9%)
Total bilirubin (μmol/L)	71.1 (64.9-107.9)
Comorbidities	
Coronary disease	3 (6.4%)
Hypertension	14 (29.8%)
Diabetes	2 (4.3%)
Liver cirrhosis	3 (2.1%)
Portal hypertension	1 (6.4%)
ENBD	40 (85.1%)
Procedure time, min (mean ± SD)	40.3 ± 15.4
Stone texture	
Hard stones	16 (34.0%)
Soft stones	31 (66.0%)
Stone compositions	
Cholesterol-based stones	17 (36.2%)
Pigment-based stones	30 (63.8%)
Procedure-related adverse events	
Cholangitis	4 (8.5%)
Oozing	2 (4.3%)
Pancreatitis	4 (8.5%)
Cholecystitis	1 (2.1%)
Perforation	0
Death	0

Data are expressed as the mean ± SD, median (interquartile range) or *n* (%). ENBD: Endoscopic nasobiliary drainage; CBD: Common bile duct.

stones (score = 1). Multivariate analysis revealed that CBD diameter > 15 mm (OR = 0.08, 95%CI: 0.01-0.49; P = 0.007) and the presence of periampullary diverticula (PAD) (OR = 6.51, 95%CI: 1.08-39.21; P = 0.041) were independent risk factors for failed CBD clearance despite irrigation with 100 mL saline (Table 3).

Further analysis showed that the volume of saline used for irrigation[20] (P < 0.001) was an important factor determining CBD clearance (Supplementary Table 1).

We used IR spectroscopy to analyze the components of stones in the CBD of all patients. IR spectroscopy analysis showed that the proportion of pigment-based stones was significantly higher in patients with PAD (93.3% *vs* 50.0%, P = 0.04), and these stones were mostly soft stones (77.4% *vs* 22.6%, P = 0.01) (Table 4).

Table 2 Common bile duct clear score and stone clearance rate before and after saline irrigation

Score	No irrigation	50 mL	100 mL	*P* value
Score 1	13 (28%)	0 (0%)	0 (0%)	
Score 2	8 (17%)	4 (8%)	0 (0%)	
Score 3	19 (40%)	15 (32%)	3 (6%)	
Score 4	7 (15%)	28 (60%)	12 (26%)	
Score 5	0 (0%)	0 (0%)	32 (68%)	
Clear	7 (15%)	28 (60%)	44 (94%)	< 0.001

DISCUSSION

Fluoroscopic cholangiographic imagery is currently the main method to determine the successful clearance of CBD stones[20]. However, studies involving the use of IDUS have identified residual biliary sludge within the bile duct despite the absence of filling defects on cholangiography. Mechanical lithotripsy produces a large number of stone fragments, and these minor residual CBD stones may lead to recurrent stone formation[21].

It has been reported that residual small CBD stone fragments can be flushed out of the bile duct using saline irrigation with a balloon catheter with a side hole[15]. A study reported that an average of 48 mL of saline could remove residual stones[16]. However, another study found that at least 100 mL of saline was needed to reduce residual stones[17]. Therefore, the effectiveness of saline irrigation on the clearance of residual bile duct stones after lithotripsy is not clear. This study's purpose differs from previous ones in that all of the patients had large stones and were post lithotripsy. In this study, we found that after ERCP and an additional round of lithotripsy were performed to remove CBD stones, POC using the SpyGlass DS showed that only 15% of the patients were relatively cleared of bile duct stones despite a negative occlusion cholangiogram. After irrigation with 50 mL of normal saline, 60% of the patients had relatively cleared bile ducts. After a total of 100 mL saline irrigation, 94% of the patients achieved complete clearance of the bile duct. The results showed that irrigation with 50 mL of saline was not enough to clear the bile duct of residual stones/sludge.

In this series, all patients received mechanical lithotripsy for stone fragmentation, which generates substantial stone fragments/debris, thus increasing the difficulty of clearing the bile duct. Our results showed that a good CBD clearance rate could be achieved with a larger saline irrigation volume. The clearance rate of bile duct stones could be higher for those without lithotripsy.

Residual stones have been found in approximately 1/3 of cases after stone retrieval using endoscopic ultrasound (EUS)[22,23]. In addition to stone detection, the EUS approach might also offer an alternative for treating bile duct stones. However, the use of EUS is very challenging[24-27]. IDUS has also been used to detect small residual stones in 14/59 patients (23.7%) with residual stones[11]. However, the ultrasonic probe is costly and can be easily damaged. In addition, the method is highly operator dependent and often produces poor quality images, and the presence of air in the bile duct can affect the detection of residual stones. Many studies have shown that POC has a high sensitivity in the detection of residual CBD stones, ranging from 25.3% to 34%, where residual stones are missed by standard cholangiography[8,9,28].

In our study, we used the SpyGlass DS system to determine the CBD clearance score. The SpyScope has a 4-way tip deflection and is much smaller (10 French) than conventional choledochoscopes. More importantly, it has a separate and independent irrigation channel that allows intermittent or continuous irrigation of the biliary system. It also offers a direct examination of the bile duct lumen and is more accurate in detecting and diagnosing residual bile duct stones/sludge.

Residual CBD stones can lead to recurrent stone formation. Itoi *et al*[7] reported that PAD and intraoperative lithotripsy were closely related to residual stones ($P < 0.05$), as we observed in our study. We also found that a dilated CBD with a diameter > 15 mm was an independent risk factor for failed CBD clearance and a large number of residual stones. Despite irrigation with 100 mL saline, PAD and a dilated CBD remained independent risk factors for incomplete bile duct clearance. This may be due to the presence of an air-filled duodenum/diverticulum that compresses the distal CBD, making it difficult to wash away the residual stones/sludge[29,30]. CBD clearance can be improved by increasing the volume of saline irrigation.

Table 3 Biliary cleanliness before and after saline irrigation, assessed by logistic regression analysis

		Residual massive stones (score = 1) before saline irrigation					Biliary clearance (score = 5) after 100 mL saline irrigation			
	n/N	Univariable analysis	Multivariable analysis	*n*/N	Univariable analysis	Multivariable analysis				
		OR (95%CI)	*P* value	OR (95%CI)	*P* value		OR (95%CI)	*P* value	OR (95%CI)	*P* value
Age										
≤ 65 yr	6/27	1.00		19/27		19/27	1.00		-	
> 65 yr	7/20	1.89 (0.52-6.86)	0.34	13/20		13/20	0.78 (0.23-2.69)	0.70	-	-
Gender					-					
Female	9/24	1.00		16/24		16/24	1.00		-	
Male	4/23	0.35 (0.09-1.37)	0.13	16/23	0.17	16/23	1.14 (0.34-3.90)	0.83	-	-
CBD diameter										
≤ 15 mm	5/32	1.00		26/32		26/32	1.00		1.00	
> 15 mm	8/15	6.17 (1.53-24.84)	0.01	6/15	0.034	6/15	0.15 (0.04-0.60)	0.007	0.08 (0.01-0.49)	0.007
Stone number										
Single	3/11	1.00		10/11		10/11	1.00		1.00	
Multiple	10/36	1.03 (0.23-4.66)	0.97	22/36	-	22/36	0.16 (0.02-1.37)	0.09	0.08 (0.01-1.09)	0.06
Stone diameter										
≤ 15 mm	8/36	1.00		26/36		26/36	1.00		-	
> 15 mm	5/11	2.92 (0.70-12.11)	0.14	6/11	0.34	6/11	0.46 (0.12-1.86)	0.28	-	-
Pigment-based stones										
No	4/17	1.00		14/17		14/17	1.00		1.00	
Yes	9/30	1.39 (0.36-5.46)	0.63	18/30	-	18/30	0.32 (0.08-1.36)	0.12	0.43 (0.05-3.60)	0.44
PAD										
No	4/15	1.00		26/32		26/32	1.00		1.00	
Yes	9/32	1.08 (0.27-4.28)	0.92	6/15	-	6/15	6.50 (1.67-25.38)	0.007	6.51 (1.08-39.21)	0.041

N: Total number; CBD: Common bile duct; PAD: Periampullary diverticula; CI: Confidence interval; OR: Odds ratio.

Our results showed that PAD not only increased the difficulty of bile duct clearance but can also affect stone composition. We found that pigment-based stones constituted the majority of CBD stones in our patients with PAD (P = 0.004). Song *et al*[31] reported that recurrent bile duct stones were more likely to be brown pigmented stones than cholesterol-based stones. This may be because pigment-based stones are often related to bacterial infection, and the formation of biliary sludge will contribute to recurrent stone formation over time[32-34]. The brown pigmented stones that form as a result of bacterial infection are soft and easy to fragment and generate abundant debris. Our experience showed that soft stones/sludge require more saline irrigation to clear the bile duct. In this study, 26% of cases with biliary sludge were found even with 100 mL saline irrigation. If an effective bile duct cleaning device is used to remove biliary sludge, it may reduce the CBD stone recurrence rate after ERCP.

Table 4 Correlation between the composition of stones and variables

Variable	Pigment-based stones	Cholesterol-based stones		*P* value
PAD				
Yes	14 (93.3%)	1 (6.7%)	8.31	0.004
No	16 (50.0%)	16 (50.0%)		
Diameter of the CBD				
≤ 15 mm	21 (65.6%)	11 (34.4%)	0.14	0.75
> 15 mm	9 (60.0%)	6 (40.0%)		
Diameter of the stone				
≤ 15 mm	25 (69.4%)	11 (30.6%)	2.10	0.17
> 15 mm	5 (45.5%)	6 (54.5%)		
Stone texture				
Hard	6 (37.5%)	10 (62.5%)	7.28	0.01
Soft	24 (77.4%)	7 (22.6%)		

CBD: Common bile duct; PAD: Periampullary diverticula.

Without adequate biliary drainage, saline irrigation can increase the intraductal pressure, causing cholangitis because of contaminated bile[35]. Proper drainage methods can mitigate this stress[36,37]. No serious adverse events were reported in our study except for 10% of patients with cholangitis secondary possibly to saline irrigation. Intermittent irrigation and endoscopic suction to promote biliary drainage may lower the risk in addition to antibiotic coverage. Differences between this study and previous studies include the following: We studied the effect of flushing with saline after lithotripsy; our evaluation method was different from that of previous studies (we used SpyGlass DS examination); and we performed a component analysis related to diverticula. Our study has several methodological advantages. First, it was a prospective study using a self-controlled design, and SpyGlass DS was used to assess the presence of residual stones in the bile ducts. All of the patients showed no stones by imaging even though small residual bile duct stones were observed by SpyGlass DS, indicating that the evaluation of residual bile duct stones using SpyGlass DS is more sensitive than imaging alone. If we observe that there are still stones, it would be unethical not to continue flushing after using 50 mL of saline. Second, this study used objective definitions to assess residual stones identified by POC. Third, this study included objective stone composition analysis using IR spectroscopy.

The study has limitations. This study was not a randomized controlled trial. The use of direct cholangioscopy by the SpyGlass DS increases the procedure time with additional cost. Therefore, we do not recommend routine use of SpyGlass DS to rule out residual stones.

CONCLUSION

In conclusion, in patients with large CBD stones undergoing mechanical lithotripsy, routine irrigation of the bile duct with at least 100 mL of saline is recommended to improve CBD clearance, especially for patients with a dilated bile duct and/or those with PAD. Saline irrigation is simple, inexpensive, and easy to perform to improve bile duct clearance, and it may avoid recurrent stone formation.

ARTICLE HIGHLIGHTS

Research background

Endoscopic retrograde cholangiopancreatography (ERCP) is an effective and relatively minimally invasive technique for common bile duct (CBD) stones. The recurrence rate

of CBD stones after ERCP has increased from 4% to 24%. The incidence of residual stones after mechanical lithotripsy for intractable CBD stones is 24% to 40%. An important reason for the recurrence of CBD stones is the presence of stone debris after lithotripsy.

Research motivation

It has been suggested that saline irrigation of the bile duct after stone removal can increase the cleaning of the bile duct. Complete bile duct clearance is necessary to decrease recurrent bile duct stones. However, the efficacy and dosage of saline are still unclear.

Research objectives

To determine whether saline irrigation can improve CBD clearance after lithotripsy and how much saline solution will remove residual stones/debris.

Research methods

This prospective self-controlled study enrolled patients receiving mechanical lithotripsy for large (> 1.2 cm) CBD stones. After occlusion cholangiography confirmed CBD stone clearance, peroral cholangioscopy (POC) was performed to determine clearance scores based on the number of residual stones. The number of residual stones spotted *via* POC was graded on a 5-point scale (score 1, worst; score 5, best). Scores were documented after only stone removal (control) and after irrigation with 50 mL and 100 mL saline, respectively. The stone composition was analyzed using infrared spectroscopy.

Research results

Between October 2018 and January, 47 patients had CBD clearance scores of 2.4 ± 1.1 without saline irrigation, 3.5 ± 0.7 with 50 mL irrigation, and 4.6 ± 0.6 with 100 mL irrigation. Multivariate analysis showed that CBD diameter > 15 mm and periampullary diverticula (PAD) were independent risk factors for residual stones. Bilirubin pigment stones constituted the main residual stones found in patients with PAD.

Research conclusions

Irrigation with 100 mL of saline may not clear all residual CBD stones after lithotripsy, especially in patients with PAD and/or a dilated (> 15 mm) CBD. Pigment residual stones are soft and commonly found in patients with PAD. Additional saline irrigation may be required to remove retained stones.

Research perspectives

In the future, prospective, large sample, multi-center, well-designed studies are needed to validate the amount of saline needed to completely remove the residual stones/debris of different types of CBD stones after mechanical lithotripsy.

ACKNOWLEDGEMENTS

We thank the clinical and research teams at the Department of General Surgery for providing ongoing support.

REFERENCES

1 **Cheng CL**, Tsou YK, Lin CH, Tang JH, Hung CF, Sung KF, Lee CS, Liu NJ. Poorly expandable common bile duct with stones on endoscopic retrograde cholangiography. *World J Gastroenterol* 2012; **18**: 2396-2401 [PMID: 22654432 DOI: 10.3748/wjg.v18.i19.2396]

2 **Cotton PB**. Fifty years of ERCP: a personal review. *Gastrointest Endosc* 2018; **88**: 393-396 [PMID: 29654739 DOI: 10.1016/j.gie.2018.04.013]

3 **Frossard JL**, Morel PM. Detection and management of bile duct stones. *Gastrointest Endosc* 2010; **72**: 808-816 [PMID: 20883860 DOI: 10.1016/j.gie.2010.06.033]

4 **Baiu I**, Visser B. Endoscopic Retrograde Cholangiopancreatography. *JAMA* 2018; **320**: 2050 [PMID: 30458491 DOI: 10.1001/jama.2018.14481]

5 **Talukdar R**. Complications of ERCP. *Best Pract Res Clin Gastroenterol* 2016; **30**: 793-805 [PMID: 27931637 DOI: 10.1016/j.bpg.2016.10.007]

6 **Cai JS**, Qiang S, Bao-Bing Y. Advances of recurrent risk factors and management of choledocholithiasis. *Scand J Gastroenterol* 2017; **52**: 34-43 [PMID: 27610642 DOI: 10.1080/00365521.2016.1224382]

7 **Itoi T**, Sofuni A, Itokawa F, Shinohara Y, Moriyasu F, Tsuchida A. Evaluation of residual bile duct stones by peroral cholangioscopy in comparison with balloon-cholangiography. *Dig Endosc* 2010; **22** Suppl 1: S85-S89 [PMID: 20590779 DOI: 10.1111/j.1443-1661.2010.00954.x]

8 **Lee YN**, Moon JH, Choi HJ, Min SK, Kim HI, Lee TH, Cho YD, Park SH, Kim SJ. Direct peroral cholangioscopy using an ultraslim upper endoscope for management of residual stones after mechanical lithotripsy for retained common bile duct stones. *Endoscopy* 2012; **44**: 819-824 [PMID: 22791587 DOI: 10.1055/s-0032-1309880]

9 **Sejpal DV**, Trindade AJ, Lee C, Miller LS, Benias PC, Inamdar S, Singh G, Stewart M, George BJ, Vegesna AK. Digital cholangioscopy can detect residual biliary stones missed by occlusion cholangiogram in ERCP: a prospective tandem study. *Endosc Int Open* 2019; **7**: E608-E614 [PMID: 30993165 DOI: 10.1055/a-0842-6450]

10 **Manzoor Ul Haque M**, Hassan Luck N, Ali Tasneem A, Mudassir Laeeq S, Mandhwani R, Hanif FM, Ullah Lail G. Safety and Efficacy of Extracorporeal Shock Wave Lithotripsy for Difficult-to-retrieve Common Bile Duct Stones: A Ten-year Experience. *J Transl Int Med* 2020; **8**: 159-164 [PMID: 33062592 DOI: 10.2478/jtim-2020-0025]

11 **Tsuchiya S**, Tsuyuguchi T, Sakai Y, Sugiyama H, Miyagawa K, Fukuda Y, Ando T, Saisho H, Yokosuka O. Clinical utility of intraductal US to decrease early recurrence rate of common bile duct stones after endoscopic papillotomy. *J Gastroenterol Hepatol* 2008; **23**: 1590-1595 [PMID: 18554235 DOI: 10.1111/j.1440-1746.2008.05458.x]

12 **Konstantakis C**, Triantos C, Theopistos V, Theocharis G, Maroulis I, Diamantopoulou G, Thomopoulos K. Recurrence of choledocholithiasis following endoscopic bile duct clearance: Long term results and factors associated with recurrent bile duct stones. *World J Gastrointest Endosc* 2017; **9**: 26-33 [PMID: 28101305 DOI: 10.4253/wjge.v9.i1.26]

13 **Jang SE**, Ahn DW, Lee SH, Lee BS, Jeong JB, Hwang JH, Ryu JK, Kim YT, Lee KH, Kim YH. Preventive saline irrigation of the bile duct after the endoscopic removal of common bile duct stones. *Dig Dis Sci* 2013; **58**: 2353-2360 [PMID: 23546698 DOI: 10.1007/s10620-013-2647-4]

14 **Huang SW**, Lin CH, Lee MS, Tsou YK, Sung KF. Residual common bile duct stones on direct peroral cholangioscopy using ultraslim endoscope. *World J Gastroenterol* 2013; **19**: 4966-4972 [PMID: 23946602 DOI: 10.3748/wjg.v19.i30.4966]

15 **Komatsu Y**, Toda N, Isayama H, Tsujino T, Tateishi K, Yamagata M, Ohashi M, Tada M, Yoshida H, Shiratori Y, Kawabe T, Omata M. Washout of small stones in the bile duct by saline infusion using a side-holed balloon catheter in patients undergoing endoscopic papillary balloon dilation. *Gastrointest Endosc* 1999; **49**: 101-104 [PMID: 9869732 DOI: 10.1016/s0016-5107(99)70454-2]

16 **Ang TL**, Teo EK, Fock KM, Lyn Tan JY. Are there roles for intraductal US and saline solution irrigation in ensuring complete clearance of common bile duct stones? *Gastrointest Endosc* 2009; **69**: 1276-1281 [PMID: 19249039 DOI: 10.1016/j.gie.2008.10.018]

17 **Ahn DW**, Lee SH, Paik WH, Song BJ, Park JM, Kim J, Jeong JB, Hwang JH, Ryu JK, Kim YT. Effects of Saline Irrigation of the Bile Duct to Reduce the Rate of Residual Common Bile Duct Stones: A Multicenter, Prospective, Randomized Study. *Am J Gastroenterol* 2018; **113**: 548-555 [PMID: 29610513 DOI: 10.1038/ajg.2018.21]

18 **Cotton PB**, Garrow DA, Gallagher J, Romagnuolo J. Risk factors for complications after ERCP: a multivariate analysis of 11,497 procedures over 12 years. *Gastrointest Endosc* 2009; **70**: 80-88 [PMID: 19286178 DOI: 10.1016/j.gie.2008.10.039]

19 **Sugiura R**, Kuwatani M, Hirata K, Kato S, Kawamoto Y, Kawakubo K, Mitsuhashi T, Asano T, Hirano S, Sakamoto N. Synchronous multiple pancreatic cancers developed long after severe postendoscopic retrograde cholangiopancreatography pancreatitis. *Endosc Ultrasound* 2019; **8**: 213-214 [PMID: 30880725 DOI: 10.4103/eus.eus_67_18]

20 **Kiriyama S**, Kozaka K, Takada T, Strasberg SM, Pitt HA, Gabata T, Hata J, Liau KH, Miura F, Horiguchi A, Liu KH, Su CH, Wada K, Jagannath P, Itoi T, Gouma DJ, Mori Y, Mukai S, Giménez ME, Huang WS, Kim MH, Okamoto K, Belli G, Dervenis C, Chan ACW, Lau WY, Endo I, Gomi H, Yoshida M, Mayumi T, Baron TH, de Santibañes E, Teoh AYB, Hwang TL, Ker CG, Chen MF, Han HS, Yoon YS, Choi IS, Yoon DS, Higuchi R, Kitano S, Inomata M, Deziel DJ, Jonas E, Hirata K, Sumiyama Y, Inui K, Yamamoto M. Tokyo Guidelines 2018: diagnostic criteria and severity grading of acute cholangitis (with videos). *J Hepatobiliary Pancreat Sci* 2018; **25**: 17-30 [PMID: 29032610 DOI: 10.1002/jhbp.512]

21 **ASGE Standards of Practice Committee**, Maple JT, Ikenberry SO, Anderson MA, Appalaneni V, Decker GA, Early D, Evans JA, Fanelli RD, Fisher D, Fisher L, Fukami N, Hwang JH, Jain R, Jue T, Khan K, Krinsky ML, Malpas P, Ben-Menachem T, Sharaf RN, Dominitz JA. The role of endoscopy in the management of choledocholithiasis. *Gastrointest Endosc* 2011; **74**: 731-744 [PMID: 21951472 DOI: 10.1016/j.gie.2011.04.012]

22 **Endo R**, Satoh A, Tanaka Y, Shimoda F, Suzuki K, Takahashi K, Okata H, Hiramoto K, Kimura O, Asonuma S, Umemura K, Shimosegawa T. Saline Solution Irrigation of the Bile Duct after Stone Removal Reduces the Recurrence of Common Bile Duct Stones. *Tohoku J Exp Med* 2020; **250**: 173-179 [PMID: 32161251 DOI: 10.1620/tjem.250.173]

23 **Kim YJ**, Chung WC, Jo IH, Kim J, Kim S. Efficacy of endoscopic ultrasound after removal of common bile duct stone. *Scand J Gastroenterol* 2019; **54**: 1160-1165 [PMID: 31491357 DOI:

10.1080/00365521.2019.1660911]
24 **Kaspy MS**, Hassan GM, Paquin SC, Sahai AV. An assessment of the yield of EUS in patients referred for dilated common bile duct and normal liver function tests. *Endosc Ultrasound* 2019; **8**: 318-320 [PMID: 31249161 DOI: 10.4103/eus.eus_21_19]
25 **Ogura T**, Okuda A, Higuchi K. Intrahepatic bile duct stone removal using peroral transluminal cholangioscopy (with videos). *Endosc Ultrasound* 2019; **8**: 131-132 [PMID: 30246711 DOI: 10.4103/eus.eus_26_18]
26 **Cazacu IM**, Singh BS, Saftoiu A, Bhutani MS. Recent developments in hepatopancreatobiliary EUS. *Endosc Ultrasound* 2019; **8**: 146-150 [PMID: 31031329 DOI: 10.4103/eus.eus_20_19]
27 **Wang G**, Liu X, Wang S, Ge N, Guo J, Sun S. Endoscopic Ultrasound-guided Gastroenterostomy: A Promising Alternative to Surgery. *J Transl Int Med* 2019; **7**: 93-99 [PMID: 31637179 DOI: 10.2478/jtim-2019-0021]
28 **Theerasuwipakorn N**, Tasneem AA, Kongkam P, Angsuwatcharakon P, Ridtitid W, Navicharern P, Kitisin K, Wangrattanapranee P, Rerknimitr R, Kullavanijaya P. Walled-off Peripancreatic Fluid Collections in Asian Population: Paradigm Shift from Surgical and Percutaneous to Endoscopic Drainage. *J Transl Int Med* 2019; **7**: 170-177 [PMID: 32010603 DOI: 10.2478/jtim-2019-0032]
29 **Yang JJ**, Liu XC, Chen XQ, Zhang QY, Liu TR. Clinical value of DPOC for detecting and removing residual common bile duct stones (video). *BMC Gastroenterol* 2019; **19**: 135 [PMID: 31349795 DOI: 10.1186/s12876-019-1045-6]
30 **Yue P**, Zhu KX, Wang HP, Meng WB, Liu JK, Zhang L, Zhu XL, Zhang H, Miao L, Wang ZF, Zhou WC, Suzuki A, Tanaka K, Li X. Clinical significance of different periampullary diverticulum classifications for endoscopic retrograde cholangiopancreatography cannulation. *World J Gastroenterol* 2020; **26**: 2403-2415 [PMID: 32476801 DOI: 10.3748/wjg.v26.i19.2403]
31 **Song ME**, Chung MJ, Lee DJ, Oh TG, Park JY, Bang S, Park SW, Song SY, Chung JB. Cholecystectomy for Prevention of Recurrence after Endoscopic Clearance of Bile Duct Stones in Korea. *Yonsei Med J* 2016; **57**: 132-137 [PMID: 26632393 DOI: 10.3349/ymj.2016.57.1.132]
32 **Mu P**, Yue P, Li F, Lin Y, Liu Y, Meng W, Zhou W, Li X. Does periampullary diverticulum affect ERCP cannulation and post-procedure complications? *Turk J Gastroenterol* 2020; **31**: 193-204 [PMID: 32343231 DOI: 10.5152/tjg.2020.19058]
33 **Sung JY**, Leung JW, Shaffer EA, Lam K, Costerton JW. Bacterial biofilm, brown pigment stone and blockage of biliary stents. *J Gastroenterol Hepatol* 1993; **8**: 28-34 [PMID: 8439659 DOI: 10.1111/j.1440-1746.1993.tb01171.x]
34 **Leung JW**, Ling TK, Chan RC, Cheung SW, Lai CW, Sung JJ, Chung SC, Cheng AF. Antibiotics, biliary sepsis, and bile duct stones. *Gastrointest Endosc* 1994; **40**: 716-721 [PMID: 7859970 DOI: 10.1016/S0016-5107(94)70115-6]
35 **Meng W**, Leung JW, Zhang K, Zhou W, Wang Z, Zhang L, Sun H, Xue P, Liu W, Wang Q, Zhang J, Wang X, Wang M, Shao Y, Cai K, Hou S, Li Q, Zhang L, Zhu K, Yue P, Wang H, Zhang M, Sun X, Yang Z, Tao J, Wen Z, Wang Q, Chen B, Shao Q, Zhao M, Zhang R, Jiang T, Liu K, Zhang L, Chen K, Zhu X, Zhang H, Miao L, Wang Z, Li J, Yan X, Wang F, Zhang L, Suzuki A, Tanaka K, Nur U, Weiderpass E, Li X. Optimal dilation time for combined small endoscopic sphincterotomy and balloon dilation for common bile duct stones: a multicentre, single-blinded, randomised controlled trial. *Lancet Gastroenterol Hepatol* 2019; **4**: 425-434 [PMID: 31003961 DOI: 10.1016/S2468-1253(19)30075-5]
36 **Sethi A**, Chen YK, Austin GL, Brown WR, Brauer BC, Fukami NN, Khan AH, Shah RJ. ERCP with cholangiopancreatoscopy may be associated with higher rates of complications than ERCP alone: a single-center experience. *Gastrointest Endosc* 2011; **73**: 251-256 [PMID: 21106195 DOI: 10.1016/j.gie.2010.08.058]
37 **Mu P**, Lin Y, Zhang X, Lu Y, Lu Y, Yang M, Da Z, Gao L, Mi N, Li T, Liu Y, Wang H, Wang F, Leung J, Yue P, Meng W, Zhou W, Li X. The evaluation of ENGBD versus PTGBD in high-risk acute cholecystitis: A single-center prospective randomized controlled trial. *EClinicalMedicine* 2021; **31** [DOI: 10.1016/j.eclinm.2020.100668]

World Journal of Gastroenterology

Submit a Manuscript: https://www.f6publishing.com

World J Gastroenterol 2021 January 28; 27(4): 371-376

DOI: 10.3748/wjg.v27.i4.371

ISSN 1007-9327 (print) ISSN 2219-2840 (online)

CASE REPORT

Duplication of the common bile duct manifesting as recurrent pyogenic cholangitis: A case report

Jun Seong Hwang, Sung Woo Ko

ORCID number: Jun Seong Hwang 0000-0002-0454-7527; Sung Woo Ko 0000-0002-9629-5784.

Author contributions: Hwang JS was the patient's gastroenterologist, and contributed to manuscript drafting; Ko SW was responsible for the revision of the manuscript by providing important intellectual content.

Informed consent statement: Informed written consent was obtained from the patient for publication of this report and any accompanying images.

Conflict-of-interest statement: The authors declare that they have no conflict of interest.

CARE Checklist (2016) statement: The authors have read the CARE Checklist (2016), and the manuscript was prepared and revised according to the CARE Checklist (2016).

Open-Access: This article is an open-access article that was selected by an in-house editor and fully peer-reviewed by external reviewers. It is distributed in accordance with the Creative Commons Attribution NonCommercial (CC BY-NC 4.0) license, which permits others to distribute, remix, adapt, build upon this work non-commercially,

Jun Seong Hwang, Internal Medicine, Inje University Haeundae Paik Hospital, Inje College of Medicine, Busan 48108, South Korea

Sung Woo Ko, Internal Medicine, Eunpyeong St. Mary's Hospital, Catholic University of Korea, Seoul 03312, South Korea

Corresponding author: Sung Woo Ko, MD, Assistant Professor, Internal medicine, Eunpyeong St. Mary's Hospital, Catholic University of Korea, 1021, Tongil-ro, Eunpyeong-gu, Seoul 03312, South Korea. gogo930@catholic.ac.kr

Abstract

BACKGROUND

Duplication of the extrahepatic bile duct (DCBD) is an extremely rare congenital anomaly of the biliary system. There are five types of DCBD according to the latest classification. Among them, Type V is characterized by single drainage of the extrahepatic bile ducts. Reports on DCBD Type V are scarce.

CASE SUMMARY

A 77-year-old woman presented with recurrent epigastric pain but without fever or chills. Computed tomography revealed a dilated common bile duct (CBD) that harboured multiple choledocholithiasis. Endoscopic retrograde cholangiopancreatography (ERCP) was performed, and the stones were extracted using a Dormia basket. She was discharged without any complications; however, she visited the emergency department a day after she was discharged due to epigastric pain and fever. Laboratory findings were suggestive of cholestasis. After urgent ERCP for stone removal, magnetic resonance cholangiopancreatography was performed to evaluate remnant choledocholithiasis. Magnetic resonance cholangiopancreatography revealed a DCBD Type Va and remnant choledocholithiasis in the right CBD. Both CBDs were accessed, and the stones were cleared successfully during a subsequent ERCP.

CONCLUSION

In this article, we report an extremely rare case of DCBD manifesting as recurrent pyogenic cholangitis. This case highlights the importance of recognizing DCBD because stones in the unrecognized bile duct could make the patient's prognosis critical.

Key Words: Double common bile duct; Common bile duct disease; Choledocholithiasis;

and license their derivative works on different terms, provided the original work is properly cited and the use is non-commercial. See: http://creativecommons.org/Licenses/by-nc/4.0/

Manuscript source: Unsolicited manuscript

Specialty type: Gastroenterology and hepatology

Country/Territory of origin: South Korea

Peer-review report's scientific quality classification

Grade A (Excellent): 0
Grade B (Very good): B
Grade C (Good): 0
Grade D (Fair): 0
Grade E (Poor): 0

Received: November 23, 2020
Peer-review started: November 23, 2020
First decision: December 8, 2020
Revised: December 16, 2020
Accepted: January 8, 2021
Article in press: January 8, 2021
Published online: January 28, 2021

P-Reviewer: Lin H
S-Editor: Zhang L
L-Editor: A
P-Editor: Ma YJ



Cholangitis; Endoscopic retrograde cholangiopancreatography; Case report

©The Author(s) 2021. Published by Baishideng Publishing Group Inc. All rights reserved.

Core Tip: Double common bile duct (DCBD) is an extremely rare congenital biliary tract anomaly. We present herein, a rare case of DCBD manifesting as a recurrent pyogenic cholangitis. It is substantial to establish complete stone clearance during endoscopic retrograde cholangiopancreatography because residual stone is a probable risk factor for recurrent cholangitis. However, DCBD, an extremely rare anomaly, can completely mask the presence of remnant bile duct stones for biliary endoscopists. In this case, recurrent cholangitis, which occurred immediately after bile duct stone clearance was a clue to recognize DCBD. Although this is a rare condition, our case highlights the importance of recognizing DCBD because stones in the unrecognized bile duct could make the patient's prognosis critical.

Citation: Hwang JS, Ko SW. Duplication of the common bile duct manifesting as recurrent pyogenic cholangitis: A case report. *World J Gastroenterol* 2021; 27(4): 371-376
URL: https://www.wjgnet.com/1007-9327/full/v27/i4/371.htm
DOI: https://dx.doi.org/10.3748/wjg.v27.i4.371

INTRODUCTION

Double common bile duct (DCBD) is an extremely rare congenital anomaly of the biliary system. Morphological classification of this anomaly was modified by Choi *et al*[1] in 2007 by adding a Type V, which is characterized by single drainage of the extrahepatic bile ducts. Only 7 cases of DCBD Type V have been reported so far. Herein, we report a rare case of DCBD Type V in an elderly woman who presented with recurrent pyogenic cholangitis.

CASE PRESENTATION

Chief complaints

A 77-year-old woman presented to the outpatient department of our hospital complaining of recurrent epigastric pain.

History of present illness

Patient's symptoms started a month ago with recurrent episodes, with no history of fever, chills, or vomiting.

History of past illness

The patient had a history of laparoscopic cholecystectomy for cholelithiasis 2 years earlier at another hospital. She had undergone endoscopic retrograde cholangiopancreatography (ERCP) twice for choledocholithiasis before undergoing cholecystectomy.

Personal and family history

The patient did not have a history of drinking or smoking. There was no remarkable family medical history.

Physical examination

Physical examination did not reveal tenderness or signs of peritoneal irrigation, and the bowel sounds were normal. At the outpatient clinic, her temperature was 36.7 °C, pulse rate was 70 beats/min, and blood pressure was 122/82 mm Hg.

Laboratory examinations

Blood analysis showed normal complete blood cell count, liver function test and C-

reactive protein.

Imaging examinations

Computed tomography (CT) imaging revealed a dilated CBD that harboured multiple choledocholithiasis (Figure 1A). After admission, ERCP was subsequently performed, and the stones were extracted using a Dormia basket (MTW Endoskopie, Wesel, Germany) (Figure 1B) after endoscopic papillary balloon dilatation by a CRE™ balloon dilatation catheters (Boston Scientific Corporation, Natick, MA, United States). A 5 Fr endoscopic nasobiliary drainage (ENBD) catheter (ENBD-5, Cook Medical, Bloomington, IN, United States) was inserted at the end of the procedure. A day after the ERCP, tubography *via* the ENBD catheter was performed to confirm the presence of residual stones in the bile duct. However, no definite filling defects were observed on tubography (Figure 1C). The patient was discharged without any complications of ERCP. A day after discharge, she visited the emergency department with complaints of severe epigastric pain and fever. Her temperature was 38.2 °C, pulse rate was 79 beats/min, and blood pressure was 149/85 mm Hg. Laboratory findings were suggestive of cholestasis [aspartate aminotransferase, 210 U/L (normal: 0–35 U/L); alanine aminotransferase, 134 U/L (0-35); alkaline phosphatase, 201 U/L (30-120); gamma glutamyl transferase, 184 U/L (9-64); total bilirubin, 2.77 mg/dL (0.3-1.2); direct bilirubin, 1.32 mg/dL (0-0.2); and C-reactive protein 6.91 mg/dL]. A CT scan demonstrated another dilated extrahepatic bile duct draining the right lobe of the liver, which also contained stones in the distal portion (Figure 2A). An urgent ERCP was performed as the stones were impacted at the ampulla (Figure 2B), and the stones with pus were retrieved using a balloon catheter (Escort II® Double Lumen Extraction Balloon, Cook Medical, Bloomington, IN, United States). A 10 Fr, 5 cm endoscopic retrograde biliary drainage tube (Cotton-Leung Biliary Stent, Cook Medical, Bloomington, IN, United States) was then placed in the CBD.

Magnetic resonance cholangiopancreatography (MRCP) was performed to evaluate the delicate structures of the CBD and to check for any remnant stones. MRCP revealed DCBD independently draining the left and right lobes of the liver, that created a short segment intrapancreatic CBD (Figure 3A) without a communicating channel, that was consistent with the DCBD Type Va as classified by Choi *et al*[1,2]. Residual choledocholithiasis was also noted in the right CBD. There was no evidence of anomalous union of the pancreaticobiliary duct on MRCP.

FINAL DIAGNOSIS

The final diagnosis was DCBD that manifested as recurrent pyogenic cholangitis due to the residual choledocholithiasis.

TREATMENT

To remove the residual stones, subsequent ERCP was performed, and both CBDs were cannulated successfully under fluoroscopic guidance (Figure 3B). After stone removal, two ENBD tubes were placed separately in both bile ducts to achieve sufficient biliary drainage. Tubography was performed a day after ERCP and did not reveal any definite filling defects suggestive of residual stones in either CBD (Figure 3C).

OUTCOME AND FOLLOW-UP

The patient was discharged after resolution of cholangitis, and is being followed up for 9 mo after the procedure without recurrence of cholangitis.

DISCUSSION

DCBD is an extremely rare congenital anomaly of the biliary system. Since Vesarius first reported it in 1543, only 24 cases had been reported in the western literature until 1986[3]. However, cases of DCBD are reported more often in the eastern literature. A total of 47 patients reported in the Japanese literature were reviewed by Yamashita

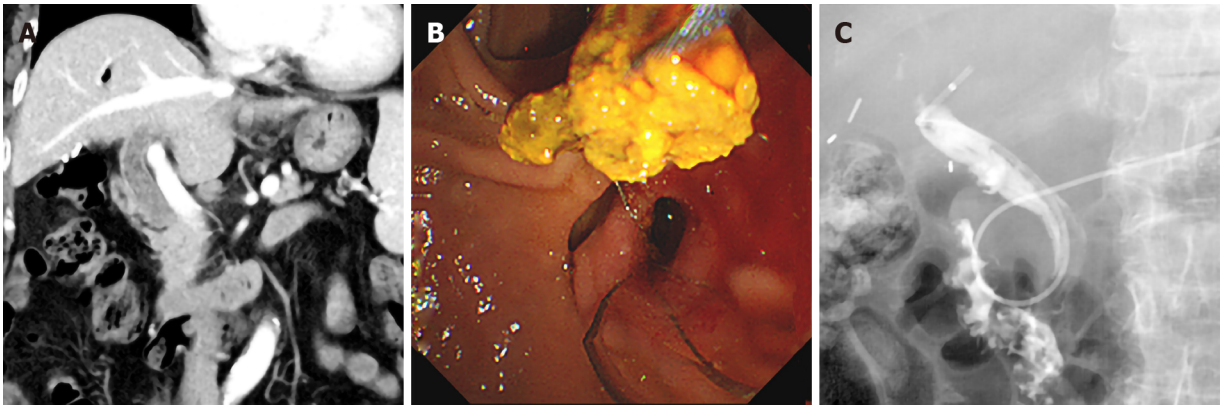


Figure 1 Computed tomography imaging and endoscopic retrograde cholangiopancreatography. A: Computed tomography revealed multiple stones in the common bile duct; B: Stones were removed by Endoscopic retrograde cholangiopancreatography using a Dormia basket; and C: Follow-up tubography using an endoscopic nasobiliary drainage showed no definite filling defects in the common bile duct.

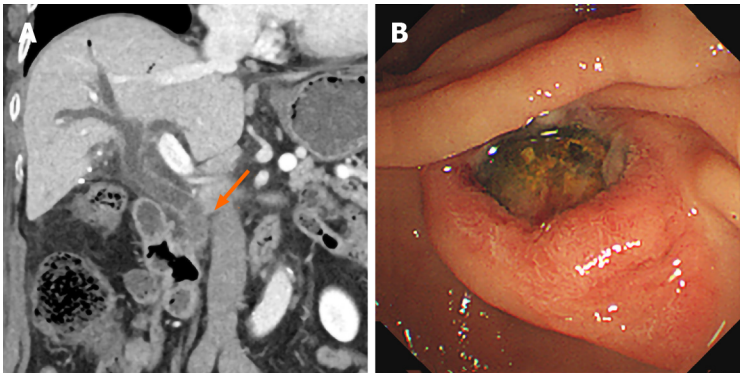


Figure 2 Computed tomography imaging and endoscopic retrograde cholangiopancreatography. A: Follow-up computed tomography demonstrated choledocholithiasis in the extrahepatic bile duct draining the right lobe of the liver; B: An impacted stone was identified at the ampulla of Vater.

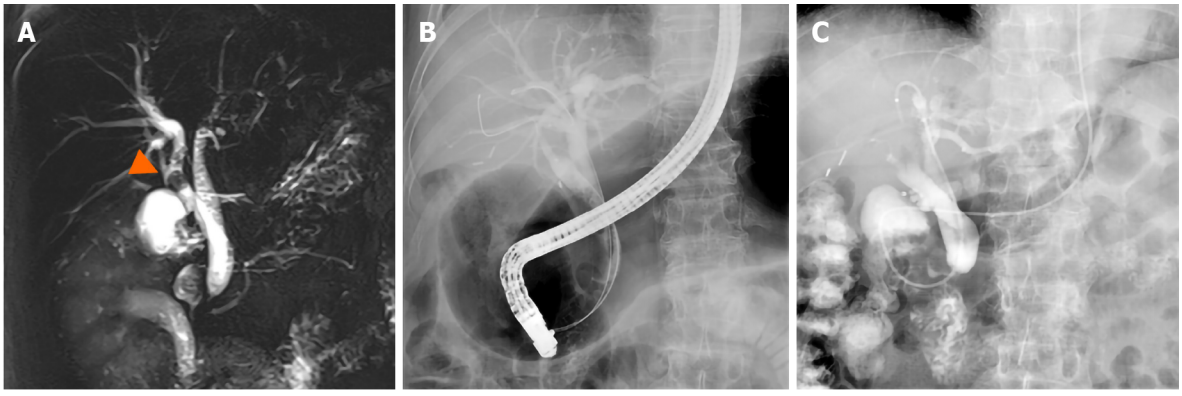


Figure 3 Magnetic resonance cholangiopancreatography. A: Magnetic resonance cholangiopancreatography showed duplicated common bile duct (CBD) independently draining the left and the right robes of the liver, to create a short segment intrapancreatic CBD without communicating channel. Residual stones were identified in the right CBD (white arrowhead); B: Both CBD was accessed using guidewire on Endoscopic retrograde cholangiopancreatography; and C: No definite filling defects were identified in both CBD on tubography using an endoscopic nasobiliary drainage.

et al[4] in 2002; furthermore, Chen *et al*[5], reported 24 Chinese cases in 2014.

The mechanism of this biliary system anomaly is considered to be due to an abnormality during embryogenesis. The presence of two bile ducts is normal anatomically during early human embryogenesis[6]. However, failure of the second bile duct to regress results in the persistence of an accessory extrahepatic bile duct[1].

Morphological classification of this anomaly was first suggested by Goor *et al*[7]. Goor's classification was revised by Saito *et al*[2], and recently Choi *et al*[1], modified it

by adding a Type V, which is characterized by single drainage of the extrahepatic bile ducts. According to the classification by Choi *et al*[1], the types of DCBD are as follows: Type I, CBD divided by septum; Type II, CBD bifurcates at the distal end and drains into each opening independently; Type III, duplicated biliary drainage with (Type IIIa) or without (Type IIIb) intrahepatic communicating channels; Type IV, duplicated biliary drainage with one or more communicating channels; Type V, duplicated extrahepatic bile duct rejoined as a single drainage with (Type Va) or without (Type Vb) communicating channels (Figure 4). Our case corresponds to Type Va in the classification by Choi *et al*[1].

Very few cases of DCBD Type V have been reported. Ever since Choi *et al*[1] reported the first case of DCBD Type V, only 7 cases have been reported[8]. To the best of our knowledge, this patient is the eighth case of DCBD Type V to be reported. Among the previously reported cases, 5 cases were diagnosed with choledocholithiasis[3,8-11]. There were 2 cases[9,11] that had choledocholithiasis in both extrahepatic bile ducts; one underwent surgery as the stones were not completely removed using ERCP[11], and another case successfully underwent stone extraction in one session of ERCP[9]. In our case, the patient presented with recurrent pyogenic cholangitis because a DCBD was not initially suspected due to the rarity of the anomaly. Therefore, two sessions of ERCP were needed to remove all choledochal stones in this case.

MRCP is the examination of choice to evaluate the anatomy of the biliary tree and its variations[12]. It has several advantages over ERCP such as (1) non-invasiveness; (2) no radiation hazard; and (3) less operator dependence[13]. It also has advantages over CT; it does not require intravenous contrast media and provides comprehensive anatomy of the biliary tract in a single image due to its capability to acquire images in any desired plane[14]. As very few biliary endoscopists and radiologists have ever encountered DCBD even in high-volume centres[9], in this case, the right CBD was mistaken for a residual cystic duct on initial CT because the patient had already undergone cholecystectomy. However, the precise anatomy of CBD was clarified through MRCP, and this extremely rare congenital anomaly could be diagnosed. Therefore, MRCP should always be considered in patients with suspected biliary tract anomalies.

Despite the extremely rare nature of this condition, it is crucial to consider the possibility of this congenital anomaly. Goor *et al*[7] reported a case of inadvertent transection of the CBD during laparoscopic cholecystectomy because of the failure to recognize the presence of DCBD. It is substantial to establish complete stone clearance during ERCP, because residual stone is a probable risk factor for recurrent cholangitis[15]. Although we performed ENBD to confirm the residual stones, the stones in the ancillary bile duct were completely concealed because only one of the two CBDs was assessed during the index procedure. It may be quite challenging to access both bile ducts in a DCBD Type V because it shares a short segment of the draining duct. In a case reported by Kim *et al*[11], stones in the right CBD were extracted surgically owing to inadequate access to the right duct. Although only one duct was accessible initially in our case, we were able to successfully cannulate both bile ducts after recognizing DCBD.

CONCLUSION

We herein report an extremely rare case of duplication of the extrahepatic bile duct Type V associated with recurrent cholangitis. Although this condition is rare, it is very crucial for biliary endoscopists to be aware of this disease because choledocholithiasis in the unrecognized ancillary bile duct can significantly affect the prognosis of patients.

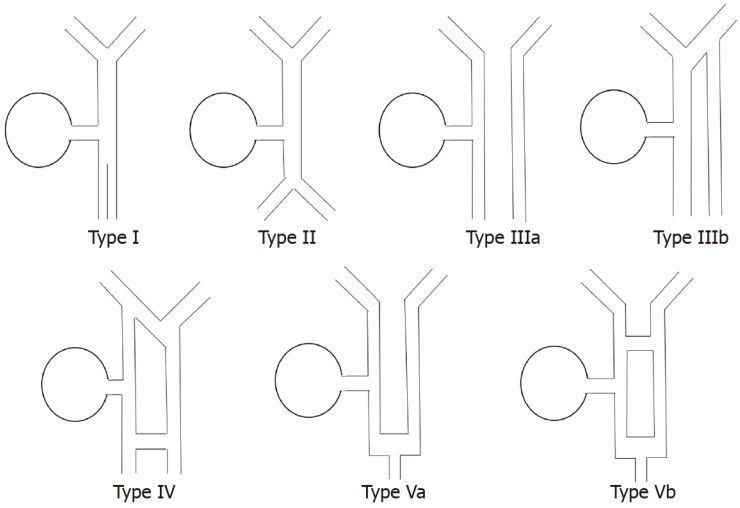


Figure 4 Illustration of Choi's double common bile duct classification.

REFERENCES

1 **Choi E**, Byun JH, Park BJ, Lee MG. Duplication of the extrahepatic bile duct with anomalous union of the pancreaticobiliary ductal system revealed by MR cholangiopancreatography. *Br J Radiol* 2007; **80**: e150-e154 [PMID: 17704313 DOI: 10.1259/bjr/50929809]

2 **Saito N**, Nakano A, Arase M, Hiraoka T. [A case of duplication of the common bile duct with anomaly of the intrahepatic bile duct]. *Nihon Geka Gakkai Zasshi* 1988; **89**: 1296-1301 [PMID: 3054479]

3 **Arora A**, Sureka B, Kasana V, Patidar Y, Bansal K. Common bile duct duplication: the more the murkier. *Saudi J Gastroenterol* 2015; **21**: 51-54 [PMID: 25672240 DOI: 10.4103/1319-3767.151231]

4 **Yamashita K**, Oka Y, Urakami A, Iwamoto S, Tsunoda T, Eto T. Double common bile duct: a case report and a review of the Japanese literature. *Surgery* 2002; **131**: 676-681 [PMID: 12075184 DOI: 10.1067/msy.2002.124025]

5 **Chen G**, Wang H, Zhang L, Li Z, Bie P. Double common bile duct with choledochal cyst and cholelithiasis: report of a case. *Surg Today* 2014; **44**: 778-782 [PMID: 23553420 DOI: 10.1007/s00595-013-0561-1]

6 **Joo YE**, Kim HS, Choi SK, Rew JS, Cho CK, Kim SJ. Congenital anomalous connection between the left intrahepatic bile duct and the stomach. *J Gastroenterol* 2002; **37**: 961-965 [PMID: 12483253 DOI: 10.1007/s005350200161]

7 **Goor DA**, Ebert PA. Anomalies of the biliary tree. Report of a repair of an accessory bile duct and review of the literature. *Arch Surg* 1972; **104**: 302-309 [PMID: 5010841 DOI: 10.1001/archsurg.1972.04180030050012]

8 **Fan X**, He L, Khadaroo PA, Zhou D, Lin H. Duplication of the extrahepatic bile duct: A case report and review of the literatures. *Medicine (Baltimore)* 2018; **97**: e9953 [PMID: 29465584 DOI: 10.1097/MD.0000000000009953]

9 **Chin JL**, Sengupta S, Morrin MM, Murray FE, Patchett SE. Common bile duct duplication: double bile ducts, double trouble. *Gastrointest Endosc* 2017; **85**: 855-856 [PMID: 27179690 DOI: 10.1016/j.gie.2016.05.005]

10 **Gupta V**, Chandra A. Duplication of the extrahepatic bile duct. *Congenit Anom (Kyoto)* 2012; **52**: 176-178 [PMID: 22925219 DOI: 10.1111/j.1741-4520.2011.00341.x]

11 **Kim SW**, Park DH, Shin HC, Kim IY, Park SH, Jung EJ, Kim CH. Duplication of the extrahepatic bile duct in association with choledocholithiasis as depicted by MDCT. *Korean J Radiol* 2008; **9**: 550-554 [PMID: 19039272 DOI: 10.3348/kjr.2008.9.6.550]

12 **Sureka B**, Bansal K, Patidar Y, Arora A. Magnetic resonance cholangiographic evaluation of intrahepatic and extrahepatic bile duct variations. *Indian J Radiol Imaging* 2016; **26**: 22-32 [PMID: 27081220 DOI: 10.4103/0971-3026.178283]

13 **Hekimoglu K**, Ustundag Y, Dusak A, Erdem Z, Karademir B, Aydemir S, Gundogdu S. MRCP vs. ERCP in the evaluation of biliary pathologies: review of current literature. *J Dig Dis* 2008; **9**: 162-169 [PMID: 18956595 DOI: 10.1111/j.1751-2980.2008.00339.x]

14 **Petrescu I**, Bratu AM, Petrescu S, Popa BV, Cristian D, Burcos T. CT vs. MRCP in choledocholithiasis jaundice. *J Med Life* 2015; **8**: 226-231 [PMID: 25866583]

15 **Endo R**, Satoh A, Tanaka Y, Shimoda F, Suzuki K, Takahashi K, Okata H, Hiramoto K, Kimura O, Asonuma S, Umemura K, Shimosegawa T. Saline Solution Irrigation of the Bile Duct after Stone Removal Reduces the Recurrence of Common Bile Duct Stones. *Tohoku J Exp Med* 2020; **250**: 173-179 [PMID: 32161251 DOI: 10.1620/tjem.250.173]

Published by **Baishideng Publishing Group Inc**
7041 Koll Center Parkway, Suite 160, Pleasanton, CA 94566, USA
Telephone: +1-925-3991568
E-mail: bpgoffice@wjgnet.com
Help Desk: https://www.f6publishing.com/helpdesk
https://www.wjgnet.com

© 2021 Baishideng Publishing Group Inc. All rights reserved.

ISSN 1007-9327 (print)
ISSN 2219-2840 (online)

World Journal of *Gastroenterology*

World J Gastroenterol 2021 February 7; 27(5): 377-448



Published by Baishideng Publishing Group Inc

World Journal of Gastroenterology

Contents

Weekly Volume 27 Number 5 February 7, 2021

MINIREVIEWS

377 Liver injury in the era of COVID-19

Cichoż-Lach H, Michalak A

ORIGINAL ARTICLE

Basic Study

391 Changes in gut microbiota composition and diversity associated with post-cholecystectomy diarrhea

Li YD, Liu BN, Zhao SH, Zhou YL, Bai L, Liu EQ

Retrospective Study

404 Histopathology and the predominantly progressive, indeterminate and predominately regressive score in hepatitis C virus patients after direct-acting antivirals therapy

Huang R, Rao HY, Yang M, Gao YH, Wang J, Jin Q, Ma DL, Wei L

416 Comparative study of indocyanine green-R15, Child-Pugh score, and model for end-stage liver disease score for prediction of hepatic encephalopathy after transjugular intrahepatic portosystemic shunt

Wang Z, Wu YF, Yue ZD, Zhao HW, Wang L, Fan ZH, Zhang Y, Liu FQ

Clinical Trials Study

428 Noninferiority clinical trial comparing the bowel cleansing efficacy of sodium phosphate tablets (Quiklean®) with a polyethylene glycol/bisacodyl kit

Hung SY, Chen HC, Ke TW, Chen JH, Hsiao KH, Wang HM, Chiang HC, Chang SC, Chen YC, Hsieh MH, Tsai YY, Hsieh YW, Chen WTL

CASE REPORT

442 Vedolizumab in Crohn's disease with rectal fistulas and presacral abscess: A case report

Yeh H, Kuo CJ, Wu RC, Chen CM, Tsai WS, Su MY, Chiu CT, Le PH

World Journal of Gastroenterology

Weekly Volume 27 Number 5 February 7, 2021

Contents

ABOUT COVER

Yosuke Tsuji, MD, PhD, Assistant Professor, Department of Gastroenterology, Graduate School of Medicine, The University of Tokyo, 7-3-1, Hongo, Bunkyo-ku, Tokyo 113-8655, Japan. ytsuji-tky@umin.ac.jp

AIMS AND SCOPE

The primary aim of *World Journal of Gastroenterology* (*WJG*, *World J Gastroenterol*) is to provide scholars and readers from various fields of gastroenterology and hepatology with a platform to publish high-quality basic and clinical research articles and communicate their research findings online. *WJG* mainly publishes articles reporting research results and findings obtained in the field of gastroenterology and hepatology and covering a wide range of topics including gastroenterology, hepatology, gastrointestinal endoscopy, gastrointestinal surgery, gastrointestinal oncology, and pediatric gastroenterology.

INDEXING/ABSTRACTING

The *WJG* is now indexed in Current Contents®/Clinical Medicine, Science Citation Index Expanded (also known as SciSearch®), Journal Citation Reports®, Index Medicus, MEDLINE, PubMed, PubMed Central, and Scopus. The 2020 edition of Journal Citation Report® cites the 2019 impact factor (IF) for *WJG* as 3.665; IF without journal self cites: 3.534; 5-year IF: 4.048; Ranking: 35 among 88 journals in gastroenterology and hepatology; and Quartile category: Q2. The *WJG*'s CiteScore for 2019 is 7.1 and Scopus CiteScore rank 2019: Gastroenterology is 17/137.

RESPONSIBLE EDITORS FOR THIS ISSUE

Production Editor: *Yu-Jie Ma*; **Production Department Director:** *Xiang Li*; **Editorial Office Director:** *Ze-Mao Gong*.

NAME OF JOURNAL
World Journal of Gastroenterology

ISSN
ISSN 1007-9327 (print) ISSN 2219-2840 (online)

LAUNCH DATE
October 1, 1995

FREQUENCY
Weekly

EDITORS-IN-CHIEF
Andrzej S Tarnawski, Subrata Ghosh

EDITORIAL BOARD MEMBERS
http://www.wjgnet.com/1007-9327/editorialboard.htm

PUBLICATION DATE
February 7, 2021

COPYRIGHT
© 2021 Baishideng Publishing Group Inc

INSTRUCTIONS TO AUTHORS
https://www.wjgnet.com/bpg/gerinfo/204

GUIDELINES FOR ETHICS DOCUMENTS
https://www.wjgnet.com/bpg/GerInfo/287

GUIDELINES FOR NON-NATIVE SPEAKERS OF ENGLISH
https://www.wjgnet.com/bpg/gerinfo/240

PUBLICATION ETHICS
https://www.wjgnet.com/bpg/GerInfo/288

PUBLICATION MISCONDUCT
https://www.wjgnet.com/bpg/gerinfo/208

ARTICLE PROCESSING CHARGE
https://www.wjgnet.com/bpg/gerinfo/242

STEPS FOR SUBMITTING MANUSCRIPTS
https://www.wjgnet.com/bpg/GerInfo/239

ONLINE SUBMISSION
https://www.f6publishing.com

© 2021 Baishideng Publishing Group Inc. All rights reserved. 7041 Koll Center Parkway, Suite 160, Pleasanton, CA 94566, USA
E-mail: bpgoffice@wjgnet.com https://www.wjgnet.com

World Journal of Gastroenterology

Submit a Manuscript: https://www.f6publishing.com

World J Gastroenterol 2021 February 7; 27(5): 377-390

DOI: 10.3748/wjg.v27.i5.377

ISSN 1007-9327 (print) ISSN 2219-2840 (online)

MINIREVIEWS

Liver injury in the era of COVID-19

Halina Cichoż-Lach, Agata Michalak

ORCID number: Halina Cichoż-Lach 0000-0002-7337-835X; Agata Michalak 0000-0003-4426-6321.

Author contributions: Cichoż-Lach H designed and coordinated the study; Michalak A acquired and analyzed the data; Cichoż-Lach H and Michalak A wrote the manuscript; all authors approved the final version of the article.

Conflict-of-interest statement: Authors declare no conflict of interests for this article.

Open-Access: This article is an open-access article that was selected by an in-house editor and fully peer-reviewed by external reviewers. It is distributed in accordance with the Creative Commons Attribution NonCommercial (CC BY-NC 4.0) license, which permits others to distribute, remix, adapt, build upon this work non-commercially, and license their derivative works on different terms, provided the original work is properly cited and the use is non-commercial. See: http://creativecommons.org/Licenses/by-nc/4.0/

Manuscript source: Unsolicited manuscript

Specialty type: Gastroenterology and hepatology

Country/Territory of origin: Poland

Peer-review report's scientific

Halina Cichoż-Lach, Agata Michalak, Department of Gastroenterology with Endoscopy Unit, Medical University of Lublin, Jaczewskiego 8, Lublin 20-954, Poland

Corresponding author: Halina Cichoż-Lach, PhD, Full Professor, Department of Gastroenterology with Endoscopy Unit, Medical University of Lublin, Jaczewskiego 8, Lublin 20-954, Poland. lach.halina@wp.pl

Abstract

Severe acute respiratory syndrome coronavirus-2 (SARS-CoV-2) has undoubtedly revolutionized the whole globe and given a new point of view on respiratory tract infections. Nevertheless, coronavirus disease 2019 (COVID-19) cannot be perceived as a disease limited only to pneumonia with diverse severity. More and more reports have demonstrated a wide range of possible systemic symptoms, including hepatic complications. Liver injury has been observed in a significant proportion of patients, especially in those with a severe or critical illness. COVID-19 might provoke a deterioration of liver function in patients with already diagnosed chronic liver diseases and without pre-existing liver disorders. The deterioration of liver function worsens the prognosis, increases the risk of a severe course of SARS-CoV-2 infection and prolongs the hospital stay. In general, patients who develop liver dysfunction in COVID-19 are mainly males, elderly people, and those with higher body mass index. The underlying mechanisms for hepatic failure in patients infected with SARS-CoV-2 are still unclear, nevertheless liver damage appears to be directly connected with virus-induced cytopathic effects. A liver injury observed during hospitalization might be simultaneously caused by the use of potentially hepatotoxic drugs, mainly antiviral agents. This minireview focuses on a possible relationship between COVID-19 and the liver, potential molecular mechanisms of liver damage, the characteristics of liver injury and suggested factors predisposing to hepatic manifestations in COVID-19 patients.

Key Words: SARS-CoV-2 infection; COVID-19; Acute liver failure; Chronic liver diseases; Inflammation

©The Author(s) 2021. Published by Baishideng Publishing Group Inc. All rights reserved.

Core Tip: The coronavirus disease 2019 (COVID-19) pandemic has revolutionized the priorities of the medical society worldwide. In the natural history of severe acute

quality classification
Grade A (Excellent): 0
Grade B (Very good): B
Grade C (Good): 0
Grade D (Fair): 0
Grade E (Poor): 0

Received: October 20, 2020
Peer-review started: October 20, 2020
First decision: December 18, 2020
Revised: December 25, 2020
Accepted: January 8, 2021
Article in press: January 8, 2021
Published online: February 7, 2021

P-Reviewer: Fan X
S-Editor: Zhang L
L-Editor: Webster JR
P-Editor: Liu JH

respiratory syndrome coronavirus-2 infection, liver injury is relatively frequent but quite mild and it is described as any liver damage occurring during disease progression and treatment of infection in patients with or without pre-existing liver disorders. Direct viral cytopathic injury, secondary liver impairment due to systemic inflammatory response or hypoxia, drug-induced liver failure and finally the exacerbation of chronic liver diseases are enumerated as potential etiologic factors for liver injury in COVID-19.

Citation: Cichoż-Lach H, Michalak A. Liver injury in the era of COVID-19. *World J Gastroenterol* 2021; 27(5): 377-390
URL: https://www.wjgnet.com/1007-9327/full/v27/i5/377.htm
DOI: https://dx.doi.org/10.3748/wjg.v27.i5.377

INTRODUCTION

December 2019 was the crucial time, when the first cases of severe pneumonia and other infections of the respiratory tract were diagnosed in the city of Wuhan, located in Hubei province, central China. Information regarding the causative factor - severe acute respiratory syndrome coronavirus-2 (SARS-CoV-2) emerged and was the beginning of the diagnosis of coronavirus disease 2019 (COVID-19) according to World Health Organization nomenclature[1-3]. Since the start of 2020, COVID-19 has become a pandemic, spreading worldwide, and leading to the disruption of among human societies and significant economic destabilization. Up to October 10th, more than 39.4 million SARS-CoV-2 cases were identified in the world and more than 1.11 million patients died due to its severe course. The situation remains dynamic and new epidemiological data are actualized each day. Current medical knowledge associates SARS-CoV-2 with a spectrum of disorders involving the respiratory tract. COVID-19 mainly presents with dyspnea, pneumonia, dry cough and fever. Nevertheless, a possible manifestation of the disease may be closely related to pathologies of the gastrointestinal tract. Diarrhea, vomiting, abdominal pain or anorexia might precede respiratory symptoms or even behave as isolated signs of the illness[4-6].

INVOLVEMENT OF THE GASTROINTESTINAL TRACT IN COVID-19 PRESENTATION

In a multicenter study performed in Hubei province on 204 patients with COVID-19, researchers showed that the percentage of persons manifesting gastrointestinal symptoms was 50.5%. With the exception of the group with loss of appetite as the dominant complaint (a relatively low specificity for this symptom), gastrointestinal disorders were present in 18.6% of those enrolled in the study. Interestingly, in patients with digestive tract disorders, the period of time from the beginning of COVID-19 manifestations to hospitalization was significantly longer compared to those with typical respiratory infections (9 d and 7.3 d, respectively; P = 0.013). Another observation in this study was that a more severe course of COVID-19 was associated with more marked gastrointestinal symptoms[7]. Recent observations proved that gastrointestinal manifestations of SARS-CoV-2 infection may involve 39.6% to 50% of patients and usually include nausea, diarrhea, anorexia, abdominal pain, belching and emesis[8-10]. A complex presentation of SARS-CoV-2 infection involving skin disorders, impaired taste and smell, kidney dysfunction, acute heart failure and even multiple organ dysfunction syndrome, proves that COVID-19 is a systemic diseases. Early reports from Wuhan showed that only approximately 2%-10% of patients complained of diarrhea as the first symptom of the infection and in such cases, the virus genome could be isolated from stool and blood samples. However, a recent analysis of the clinical manifestations of SARS-CoV-2 infection in 992 patients revealed that 53% had at least one gastrointestinal symptom at any time during their illness, usually diarrhea (34%), nausea (27%), vomiting (16%), and abdominal pain (11%)[11-14]. Similarly, a broad spectrum of abnormalities can be found in laboratory tests, *e.g.*, lymphopenia, monocytopenia, prolonged prothrombin time, hypo-

proteinemia and even hypertransaminasemia. Nowadays, accumulated data suggest a harmful effect of SARS-CoV-2 on the liver; however, the number of available reports is still limited[15,16].

MECHANISMS OF LIVER INJURY IN COVID-19 – WHEN CAN WE SUSPECT THIS COMPLICATION TO OCCUR?

Angiotensin converting enzyme 2 (ACE2) appears to be a key agent in liver injury due to COVID-19. This metallopeptidase, which serves as a functional receptor for SARS-CoV-2, is not only localized on the surface of respiratory tract epithelium (in the lung-specific pulmonary alveolar type II cells), but also on epithelial cells of the upper esophagus, enterocytes of the ileum and colon, in the heart, testicles, cells of smooth muscles and the endothelium of pancreatic, brain and kidney blood vessels[17-20]. Furthermore, increased expression of ACE2 is also observed in cholangiocytes (59.7% of cells) and to a lesser extent in hepatocytes (2.6% of cells). This proves that SARS-CoV-2 infection impairs liver function by direct cytotoxicity due to the continuous replication of the virus in the above-mentioned cell populations[21,22]. Additionally, gene expression of ACE2 transmembrane serine protease 2 together with paired basic amino acid cleaving enzyme have also been proved in cholangiocytes and hepatocytes. Thus, SARS-CoV-2 may exert a cytopathic effect, either by lysis and/or by inducing necrosis and apoptosis[23-27]. ACE2 plays a fundamental role in host cells as a receptor of Spike-I Glycoprotein of COVID-19 which finally leads to infection. A recent finding revealed that the renin-angiotensin system and peroxisome proliferator-activated receptor signaling pathway can even enhance the infection at this stage. Therefore, both angiotensin and peroxisome proliferator-activated receptor family proteins may potentially be perceived as possible therapeutic targets[28,29]. Another survey indicated the potential role of viral-induced cytotoxic T-cells in the severity of the disease[30]. A subsequent pathological pathway responsible for liver dysfunction in COVID-19 is an immunological inflammatory response. This phenomenon has already been confirmed by high levels of inflammatory markers [*e.g.*, C-reactive protein (CRP), ferritin, lactate dehydrogenase (LDH), D-dimers, interleukin-6 (IL-6), IL-2], suggesting a direct link between the presence of the cytokine storm syndrome and disease severity[31]. Furthermore, hepatic anoxia during the course of SARS-CoV-2-related respiratory failure cannot be omitted. On the other hand, antiviral agents in the treatment of COVID-19 (*e.g.*, lopinavir, ritonavir, ramdevpir, umifenovir) or antibiotics used in the case of coexisting bacterial infections, antipyretics or steroids might also cause deterioration of liver function[32,33]. A group of patients with known chronic liver failure is more prone to developing hepatic complications in the presence of SARS-CoV-2 infection. Furthermore, chronic liver disorders are well-known independent causative factors of severe COVID-19. In a recently published survey of 2780 persons with COVID-19, 250 patients with known chronic liver disease (CLD) were at a higher risk of prolonged hospitalization and death[34]. Unfortunately, according to available data, it is difficult to predict which liver diseases are mostly dangerous. Of note, biologics such as tocilizumab and baricitinib administered in severe COVID-19 may lead to a reactivation of HBV infection. Thus, these patients require special supervision. On the other hand, a potential link between SARS-CoV-2 infection and cholestatic liver pathologies still remains an unexplored field[35]. Figure 1 presents the spectrum of mechanisms involved in liver damage accompanying COVID-19.

COVID-19 AND THE LIVER – WHERE ARE WE NOW?

In a great majority of clinical studies, regardless of existing CLD, COVID-19 was associated with mild to moderate liver failure, reflected mainly by hyper-transaminasemia, elevation of gamma-glutamyl transferase (GGT) and alkaline phosphatase (ALP) levels (less frequently), hypoproteinemia and prolonged prothrombin time[36-40]. Accumulated data suggest that more than one-third of patients hospitalized due to SARS-CoV-2 infection might have impaired liver function. An increase in aspartate transaminase (AST) and alanine transaminase (ALT) activity, especially in men, results in a severe course of COVID-19. In general, a higher level of ALT, thrombocytopenia and hypoalbuminemia are indices of increased mortality in COVID-19 patients. Moreover, hypoalbuminemia is recognized as an independent marker of severe SARS-CoV-2 infection, poor prognosis and higher mortality[41-43]. The

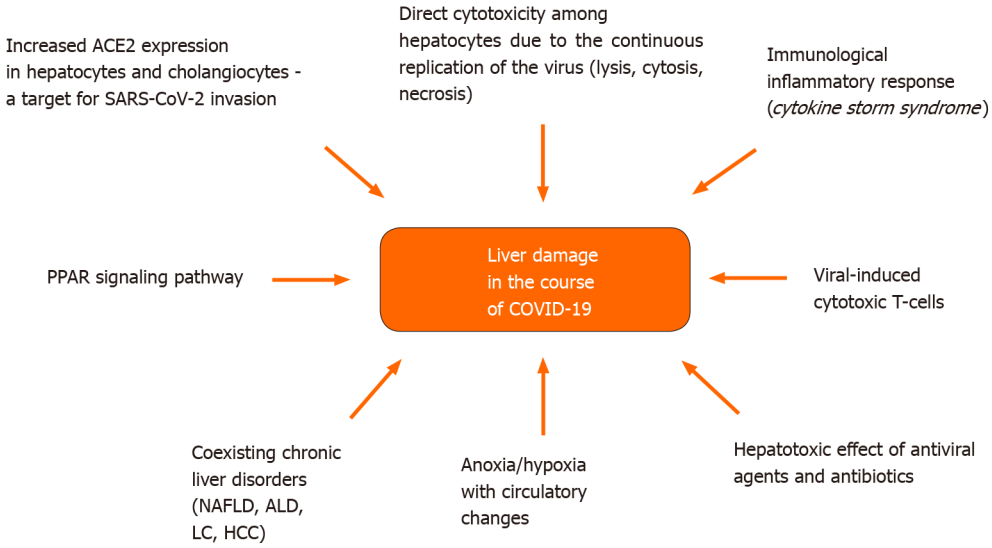


Figure 1 Mechanisms of coronavirus disease 2019-related liver injury. ACE2: Angiotensin converting enzyme 2; SARS-CoV-2: Severe acute respiratory syndrome coronavirus-2; PPAR: Peroxisome proliferator-activated receptors; NAFLD: Non-alcoholic fatty liver disease; ALD: Alcohol-related liver disease; LC: Liver cirrhosis; HCC: Hepatocellular carcinoma.

possible manifestations of liver injury during the course of COVID-19 are shown in Figure 2.

Some reports have even proved the presence of a correlation between abnormal liver tests and coagulation dysfunction in SARS-CoV-2 pneumonia, highlighting the significant role of the liver in this disease[44]. However, the data are too scanty to differentiate an exact background of hypertransaminasemia in COVID-19 patients – a pre-existing chronic liver failure or a certain hepatotoxic impact of SARS-CoV-2 infection.

In large cohort studies of hospitalized patients, an elevation in AST and ALT activity varied from 14% to 53% with reference to the normal range. A study of the clinical profile of COVID-19 patients with abnormal liver test results was performed by Cai *et al*[45]. This study included 417 Chinese patients hospitalized in Shenzhen. Deviations of liver enzymes were classified as parenchymal (a 3-fold increase in the values of ALT and/or AST above the upper limit of normal (ULN), cholestatic (ALP or GGT values 2-fold higher according to the ULN) and mixed (coexisting above-mentioned pathologies). Additionally, researchers identified a group of patients with liver injury defined as a 3-fold increase in AST and/or ALT above the ULN and a 2-fold increase in ALP, GGT and/or bilirubin above the ULN. Parameters of liver function were assessed on admission to the hospital and during hospitalization. 41% of the examined patients had impaired liver function tests on admission; 5% of them fulfilled the criteria mentioned in the identified subgroup. Deterioration of liver function was most common in men, elderly patients and those with a higher body mass index (BMI). Patients with chronic liver disorders [non-alcoholic fatty liver disease (NAFLD), alcohol-related liver disease (ALD), chronic hepatitis-B] also showed abnormal liver test results; however, the percentage of these conditions was not significant. The examined patients manifested cough as the first symptom of COVID-19. A moderate impairment of liver function was noted in a majority of study participants; the level of evaluated markers did not exceed the ULN by more than 2-fold (the results were higher in only 4% of patients). The most marked elevation was seen in GGT; its activity was 2-fold higher than the ULN in 12.71% of patients and 3-fold higher in 2.4%. An analysis of 417 people with COVID-19 revealed abnormal liver test results in 76.3% patients; 21.5% presented with features of liver injury. The presence of these impairments became more visible during the first two weeks of hospitalization with a higher than 3-fold increase in ALT, AST, bilirubin and GGT levels in 23.4%, 14.8%, 11.5%, and 24.4% of patients, respectively. 26.7% of patients with impaired liver function tests developed severe pneumonia. A mixed type of liver injury was the dominant type (43.4% of patients); parenchymal and cholestatic patterns were less common (20.75% and 29.25% of patients, respectively). An elevation in ALT, AST, bilirubin and GGT levels, exceeding a 3-fold increase according to the ULN, was noted in 10.38%, 2.83% and 11.64% of the study participants, respectively. A significant increase in ALP activity was not observed. Furthermore, a mixed type of

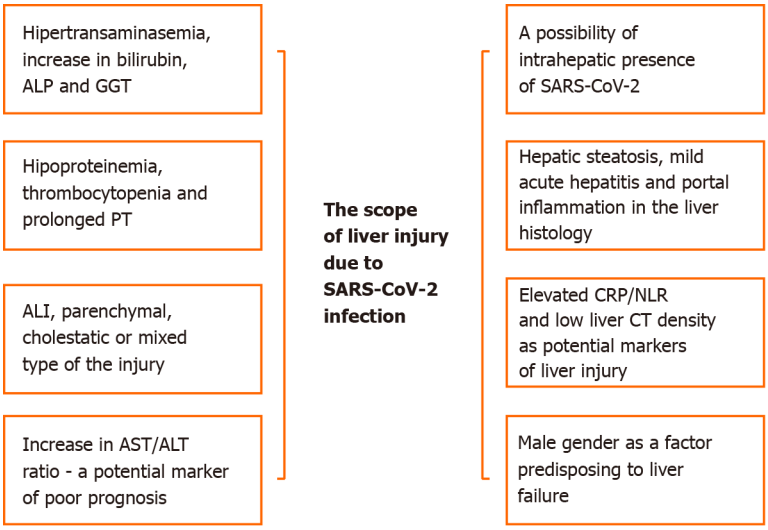


Figure 2 Characteristics of liver injury during the course of severe acute respiratory syndrome coronavirus-2 infection. ALP: Alkaline phosphatase; GGT: Gamma-glutamyl transferase; PT: Prothrombin time; ALI: Acute liver failure; AST: Aspartate transaminase; ALT: Alanine transaminase; SARS-CoV-2: Severe acute respiratory syndrome coronavirus-2; CRP: C-reactive protein; NLR: Neutrophil-to-lymphocyte ratio; CT: Computed tomography.

liver injury dominated in patients with severe pneumonia due to SARS-CoV-2 infection. There was no significant difference in ALP level in this group compared to patients with a less severe disease course. 11.76% of patients were diagnosed with multiorgan insufficiency; 2 patients had liver insufficiency. Interestingly, nearly half of the patients with liver function impairment belonged to a subgroup with severe COVID-19. Activities of ALT and GGT 3-fold higher than the ULN were also more common in severe cases (41% and 37%, respectively). Increases in AST and bilirubin levels were less frequent and were observed in 20% and 10% of patients, respectively. Abnormal ALP levels were uncommon. 23.26% of severe COVID-19 patients (10 cases) developed multiorgan failure; 2 had liver insufficiency. Three patients died, one with liver failure. All systemic complications were directly related to secondary infections in patients hospitalized in intensive care units. Patients with impaired liver function tests (as previously defined) had a significantly higher risk of a severe course of COVID-19 – the group with a parenchymal subtype – 2-fold higher and mixed type – 4.44-fold [Odds ratio (OR): 2.73; confidence interval (CI): 1.19–6.30; $P = 0.02$; OR: 4.44; CI: 1.93–10.23; $P < 0.001$, respectively]. Liver failure (according to the above-mentioned definition) was a factor responsible for a 9-fold higher risk of severe COVID-19 in comparison to patients without hepatic complications (OR: 9.04; 95%CI: 3.19–25.6; $P < 0.001$). Parenchymal and mixed types of liver insufficiency were associated with a higher probability of the development of severe SARS-CoV-2 infection (3.19-fold and 11.22-fold, respectively). The severity of COVID-19 did not depend on the treatment with ACE inhibitors (ACEI) and angiotensin II receptor blockers. Furthermore, the patients treated with other antihypertensives did not have significant differences in SARS-CoV-2 infection presentation compared to those treated with ACEI/angiotensin II receptor blockers. The authors of this report did not find that antibiotics, nonsteroidal anti-inflammatory drugs, ribavirin or interferon provoked hepatic complications. Lopinavir and ritonavir were the only agents proved to deteriorate liver function (4.44-fold to 5.03-fold, respectively) in a dose-dependent manner, according to an analysis. The antivirals mainly caused an increase in bilirubin and GGT values. It is worth emphasizing that the percentage of patients with COVID-19 presenting with liver failure in the study was relatively high compared with previous reports and only a small subgroup of patients had CLD, suggesting the presence of a direct link between SARS-CoV-2 infection and viral infection of hepatocytes.

To date, the pathway of liver injury during the course of SARS-CoV-2 infection has not been fully explained, and this may be due to the pathogenetic mechanism of the virus or as a result of the use of hepatotoxic drugs. The majority of antipyretics used in COVID-19 patients contain acetaminophen, which is can lead to liver failure. The list of potential agents used in COVID-19 treatment is becoming longer and longer. Currently chloroquine phosphate or hydroxychloroquine sulfate, tocilizumab (IL-6 blocker), ribavirin, remdesivir (nucleotide analogue inhibiting viral ribonucleic acid polymerase), lopinavir/ritonavir and oseltamivir have been tested. There are still single reports on their potential hepatotoxic action, nevertheless this harmful effect is

observed more frequently in severe COVID-19, with liver injury at baseline[46-49].

Remdesivir used in the treatment of COVID-19 pneumonia has recently been suspected to induce acute liver injury in two patients, who presented with hypertransaminasemia, features of coagulopathy and encephalopathy between day 3 and day 10 of therapy. The introduction of acetylcysteine infusions restored the normal level of liver enzymes; however, one of the patients recovered and the other died, probably due to septic shock.

Data on a potential relationship between remdesivir and acute liver injury in the COVID-19 population are limited, but worth further exploration[50].

There are first reports in the literature regarding the use of ursodeoxycholic acid for COVID-19. Abdulrab *et al*[51] proposed adding this agent to the standard treatment due to its anti-inflammatory and immunomodulating activity. This strategy may be helpful in the increase in cytokines due to possible regulation of the immune response by ursodeoxycholic acid. The suggested dose is 13-15 mg/kg/day. Nevertheless, further detailed analyses are required[52].

Recently, EASL recommendations concerning hepatic care in the COVID-19 pandemic have been published. They present rules concerning the use of diagnostic procedures, supervision of patients with CLDs and those after liver transplantation[53].

LIVER FAILURE AS A PROGNOSTIC MARKER OF COVID-19 DISEASE COURSE

Fan *et al*[54] tried to determine the potential relationship between liver dysfunction and concomitant treatment, by retrospectively enrolling 148 patients with COVID-19 hospitalized in Shanghai. The authors analyzed liver parameter values, treatment and the length of hospital stay. Impaired liver function (characterized by increased activity of aminotransferases, GGT, ALP and total bilirubin level) was diagnosed in 37.2% of patients on the day of hospital admission. Abnormal AST, ALT, GGT and bilirubin results were found in 21.6%, 18.2%, 17.6%, 6.1%, and 4.1% of patients, respectively. The presence of a high fever was more common in this group of patients. Increased levels of hepatic parameters were characteristic in the male population and were often accompanied by elevated levels of inflammatory markers (CRP and procalcitonin). This may have been related to the systemic inflammatory response due to SARS-CoV-2 infection. Similar to other analyses, increased ALP activity was least often observed[55]. Interestingly, the use of antibiotics (levofloxacin, azithromycin, cephalosporin), antiviral agents (umifenovir, oseltamivir, acyclovir) and antipyretics (ibuprofen) prior to hospitalization, was not related to liver function. 57.8% of patients treated with lopinavir or ritonavir presented with abnormal liver function. The duration of hospital stay in patients with deterioration of liver function was significantly prolonged (approximately 15.1 ± 4.8 d) compared to those without liver dysfunction (approximately 12.8 ± 4.4 d; $P = 0.021$). 48.5% of patients with normal liver function at baseline developed insufficiency approximately 7 d (from 4 to 11 d) after hospitalization. The peak of liver enzymes elevation was noted around day 10 (from 7 to 12 d) after hospital discharge. A less frequently observed peak of increased bilirubin concentration was present on day 5 after hospital discharge (from 4 to 12 d). The authors of the aforementioned publication concluded that abnormal liver function in SARS-CoV-2 infection predisposes to prolonged hospitalization. The observed results of ALT between 41 and 115 U/L and AST between 37 and 107 U/L, suggested mild liver function impairment related to COVID-19.

Comparable conclusions were drawn by Wang *et al*[56]. AST was evaluated in patients with a severe presentation of COVID-19 as a potential diagnostic marker and its level was significantly higher in non-survivors compared with survivors. Receiver operating characteristic (ROC) curve analysis of AST revealed an area under the curve (AUC) of 0.854, indicating the prognostic value of this marker in infected patients[57].

Furthermore, Medetalibeyoglu *et al*[58] stated that an AST/ALT ratio > 1 in 554 COVID-19 patients was associated with more frequent admission to the intensive care unit and with the severity of pneumonia, compared to those with an AST/ALT ratio < 1 ($P = 0.033$ and $P = 0.016$, respectively). An analysis of the AUC value under the ROC curve for the AST/ALT ratio revealed its high diagnostic accuracy in the prediction of mortality, severity of pneumonia and the risk of intensive care unit admission (AUC = 0.713/$P = 0.001$, AUC = 0.577/$P = 0.002$ and AUC = 0.636/$P = 0.001$, respectively)[58].

Accumulated data indicate that patients with severe pneumonia tend to develop liver failure more frequently. It can be assumed that the strong activity of proinflammatory cytokines followed by a strong immune response are the main causative

factors in this association[59,60].

Nevertheless, resources concerning the activity of less frequently assessed enzymes potentially involved in liver function impairment in COVID-19 patients are very sparse. LDH activity has been proved to increase especially in patients with abnormal liver tests. Fan *et al*[54] found an association between high LDH activity and an unfavorable course of COVID-19 in a patient who died due to respiratory insufficiency. Corresponding observations related to hyperactivity of LDH have been reported in patients with acute respiratory failure diagnosed with SARS-CoV and Middle-east respiratory syndrome infections, which resemble SARS-CoV-2 infection. Thus, LDH may be an independent prognostic marker of severe respiratory insufficiency. However, further analyses are required to determine its role among other alarm markers in the course of COVID-19[61,62].

ACUTE LIVER FAILURE AND SARS-CoV-2 - SHOULD MEN BE AFRAID?

The clinical presentation of acute liver injury (ALI) during the course of SARS-CoV-2 infection has been rarely presented in the literature. One of the surveys performed on 187 patients with COVID-19 revealed that 15.4% of patients were affected by ALI[63]. Another analysis by Fu *et al*[64] on the clinical characteristics of ALI due to COVID-19 in 355 patients showed a differential type of this complication. Its course was mild in 211 persons, was severe in 88 and was critical in the remaining 51 patients. Hypoalbuminemia was noted in 62.8% of patients, cholestasis in 42.5% and parenchymal liver failure was found in 28.5% of patients on hospital admission. ALI was frequently present in patients with critical COVID-19, suggesting that liver failure is an unfavorable marker of COVID-19. On the other hand, markers of systemic oxidation and the function of the respiratory tract correlated positively with the serological concentration of proteins, especially albumin. Therefore, a deterioration of respiratory tract function can at least partly induce ALI in COVID-19 patients. Severe cases of COVID-19 followed by death were more often related to hyper-transaminasemia and elevated level of bilirubin, compared to other types of the disease (mild and moderate). Hyperbilirubinemia and increased ALT, ALP and GGT levels were characteristic in the male population - in contrast to hypoalbuminemia. The listed parameters were also higher in elderly patients. Of note, coexisting arterial hypertension was a factor predisposing to greater activity of ALP and GGT. Male gender, older age and lymphopenia were three independent predictors of ALI in SARS-CoV-2 infection. Fu *et al*[64] observed that hypoproteinemia increased the risk of the death by 9-fold and cholestasis by 2-fold in comparison to patients without these pathologies (RR = 9.471, $P < 0.001$, RR = 2.182, $P < 0.05$). Abnormal liver function tests were long-lasting. Appropriate liver function was not restored within 14 d after hospital discharge; a value of at least one of the markers was elevated in two-thirds of patients during this time period. According to the above-listed observations, ALI during the course of COVID-19 is more common in men. It is worth emphasizing that males represent 58% of people infected with SARS-CoV-2[65].

A low concentration of testosterone was proposed by German scientists as one of the risk factors in patients with COVID-19, who were hospitalized in an emergency unit in Hamburg. This hormonal imbalance was noted in two-thirds of male patients on admission[66,67]. This theory is supported by a retrospective study conducted by Naaraayan *et al*[68] of 370 patients with COVID-19. Younger men (< 65 years) were found to be more likely to develop ALI (defined as elevation of AST and ALT levels greater than 3 x the ULN) compared to women ($P = 0.02$). Interestingly, in older patients, sex difference did not influence liver function.

METABOLIC SYNDROME AND INFLAMMATION AS FACTORS PREDISPOSING TO LIVER FAILURE IN COVID-19 PATIENTS

Wang *et al*[69] concluded after studying 657 patients infected with SARS-CoV-2 in Wuhan that not only male sex, but also serum concentration of high sensitivity CRP ≥ 10 mg/L and a neutrophil-to-lymphocyte ratio ≥ 5 predispose to liver injury during the course of COVID-19, defined in this survey as a serum level of ALT or total bilirubin greater than the ULN. Thus, an inflammatory background may be closely related to liver function impairment as a complication of the disease[70,71]. Metabolic syndrome and isolated hepatic steatosis were also evaluated as potential risk factors

for liver dysfunction during the course of SARS-CoV-2 infection. Ji *et al*[72] retrospectively assessed 202 patients diagnosed with COVID-19; in 76 of these patients (37.6%) NAFLD was an accompanying condition. One half of the study participants manifested biochemical features of liver failure on the day of hospital admission and 75.2% of all patients during hospitalization. The majority of cases with liver function impairment had a parenchymal type; only 2.6% had the cholestatic or mixed type. In 33.2% of patients, liver dysfunction was observed during the hospital stay (one month at maximum). In a great majority of patients (80.7%) the course of COVID-19 was stable; only 19.3% of patients had severe disease progression. The group with severe SARS-CoV-2 infection was represented by elderly patients, those with higher BMI and the presence of other comorbidities (together with NAFLD). The risk of disease progression was 3-fold higher in men and close to 5-fold higher in patients aged sixty years and over (OR: 4.8; 95%CI: 1.5–16.2). Moreover, elevated BMI was responsible for a 1.3-fold higher risk of the development of complications (OR: 1.3; 95%CI: 1.0–1.8) and a 6-fold higher risk of comorbidities with NAFLD (OR: 6.3; 95%CI: 2.3–18.8 and OR 6.4; 95%CI: 1.5-31.2, respectively). COVID-19 patients with accompanying NAFLD were shown to have a significantly greater risk of complications during the course of the infection (44.7% *vs* 6.6%, $P < 0.0001$). A similar observation was seen with reference to the probability of prolonged liver function impairment from hospital admission to discharge (70% *vs* 11.1%, $P < 0.0001$). It is worth highlighting that the presence of NAFLD was directly related to the prolonged elimination of SARS-CoV-2 (17.5 ± 5.2 d *vs* 12.1 ± 4.4 d; $P < 0.0001$, respectively)[72]. Elements of the metabolic syndrome such as arterial hypertension, obesity and type 2 diabetes mellitus have been found to be associated with a severe presentation of COVID-19 and as independent markers of poor prognosis[73,74]. Another cohort study of 342 patients with COVID-19 revealed a relationship between hepatic steatosis and both transaminitis and increased disease severity. However, steatosis did not predispose to the development of clinically relevant liver insufficiency during the course of infection[75].

In addition, patients with metabolic syndrome and liver steatosis were found to be more prone to developing drug-induced liver injury after SARS-CoV-2 infection[76].

CHRONIC LIVER DISEASE COMPLICATED BY SARS-CoV-2 INFECTION

A novel observational cohort study by Kim *et al*[77] of 867 patients with CLDs and coexisting COVID-19 revealed that ALD, decompensated cirrhosis and hepatocellular carcinoma may be predictors of higher overall mortality during the course of infection. This observation was recently confirmed in a subsequent large cohort study of 745 patients with CLDs and concomitant SARS-CoV-2 infection (including 386 patients with cirrhosis and 359 without cirrhosis). Mortality among cirrhotic patients was significantly higher (32% *vs* 8%, $P < 0.001$) and increased according to liver function decompensation (Child-Turcotte-Pugh class). Respiratory failure was stated as the key cause of death (71%). Age, liver disease severity and ALD were found to be factors associated with death in all examined patients[78]. Another retrospective analysis of COVID-19 patients in Shanghai revealed that male gender, COVID-19 severity, together with a low liver CT density were causative factors strongly related to liver injury (ORs: 2.936, 6.543, and 3.387, respectively)[79]. In general, CLDs are known to be risk factors for severe COVID-19 infection (57.33%), and higher mortality (17.65%), as shown by Oyelade *et al*[80] among others in a recent meta-analysis. This phenomenon could be related to low platelets and lymphocytes in these patients, indicating that cirrhosis-associated immune dysfunction is a potential factor predisposing to a greater susceptibility of developing liver damage caused by SARS-CoV-2. Another meta-analysis of 11 observational studies involving 2043 COVID-19 positive patients revealed that the prevalence of CLDs ranged between 3% and 11%[81-83].

HISTOLOGICAL APPEARANCE OF THE LIVER DURING THE COURSE OF COVID-19

Data concerning the histological appearance of the liver in patients infected with SARS-CoV-2 are becoming more and more detailed, as the number of studies is increasing and the quality of our insight into the relationship between the infection and histopathological findings in the liver is improving. The first autopsy examinations were casuistic and concerned individual cases. A liver biopsy from a 69-

year-old deceased man revealed mild steatosis of a small number of hepatocytes and their degeneration was probably caused by ischemia and hypoxia. Liver sinusoids were mildly infiltrated by neutrophils, plasmocytes and Kupffer cells[84]. Another autopsy performed in a 50-year-old male patient showed moderate vesicular steatosis and water degeneration in the liver together with a mild inflammatory process within the lobules and portal areas, suggesting that both SARS-CoV-2 and treatment could be the factors leading to this type of liver injury[85]. A study in Milan of 48 liver biopsies from post-mortem COVID-19 patients showed vascular changes in the portal vein, with a coexisting increased number of portal branches, terminal vessel dilations, and thrombi observed in portal and sinusoidal vessels. The features of inflammation were discrete, with mild portal and lobular infiltrates. The authors concluded that histopathological findings in COVID-19 are suggestive of impairments in the intrahepatic blood vessel network secondary to systemic alterations due to SARS-CoV-2. In addition, liver injury in COVID-19 patients might be induced through viral replication itself within hepatocytes, as SARS-CoV-2 binds cells through the ACE2 enzyme, especially in biliary epithelial cells[86]. However, relatively low serum aminotransferase concentrations present in COVID-19 patients do not suggest an exacerbated inflammatory response or direct viral injury to hepatocytes to be of crucial importance. The scheme of the aminotransferase curves in SARS-CoV-2 infection differs from those seen in hepatitis associated with other epidemic viruses that involve dynamic liver function test elevations due to intense parenchymal necrosis (*e.g.*, dengue or yellow fever)[84,87-89]. On the other hand, the pattern of liver injury during the course of COVID-19 resembles that found in patients infected with other viruses, such as SARS, Middle-east respiratory syndrome and influenza[90-92]. Liver histology in other COVID-19 cases presented a mixed inflammatory infiltration with marked bile duct damage, features of endotheliitis and many apoptotic bodies. The intrahepatic presence of SARS-CoV-2 was even suggested in electron microscopy and in-situ hybridization, indicating the possibility of direct cell injury[93]. The ultrastructural assessment of postpartum liver tissue biopsies derived from two deceased COVID-19 patients by Wang *et al*[94] revealed typical coronavirus particles with their spikes in the cytoplasm of hepatocytes. Virus-related hepatocyte injury was described as mitochondrial swelling, endoplasmic reticulum dilatation, and cell membrane dysfunction. Of note, these authors documented viral ability to replicate in hepatocytes. This seems to be the first study showing the SARS-CoV-2 cytopathic liver cell effect as a background of liver function derangement. Viral ribonucleic acid was also identified in hepatocytes by Lagana *et al*[95] in the liver sections of 44 COVID-19 autopsies (in 11 of 20 examined patients). Polymerase chain reaction positivity correlated with peak creatinine and ferritin; however, there were no relationships with histological results or liver enzymes. The main findings in this study corresponded with other observations, as hepatic steatosis (75%), mild acute hepatitis (50%) and portal inflammation (50%) were the most common abnormalities.

CONCLUSION

Impaired liver diagnostic test results constitute common findings in COVID-19 patients and may affect over one-third of inpatients. Deterioration of liver function worsens the prognosis, increases the risk of severe SARS-CoV-2 infection and prolongs the duration of hospitalization. Abnormal liver function test results may be predictors of COVID-19 severity. COVID-19 patients affected by liver dysfunction are mainly male, elderly, and have a higher BMI. Liver injury observed during hospitalization might be simultaneously caused by the use of potentially hepatotoxic drugs, mainly antiviral agents such as lopinavir and ritonavir. Patients with accompanying chronic liver diseases are predisposed to developing a more severe course of COVID-19, but on the other hand, a more complicated presentation of SARS-CoV-2 infection increases the risk of liver failure.

REFERENCES

1 **Zhu N**, Zhang D, Wang W, Li X, Yang B, Song J, Zhao X, Huang B, Shi W, Lu R, Niu P, Zhan F, Ma X, Wang D, Xu W, Wu G, Gao GF, Tan W; China Novel Coronavirus Investigating and Research Team. A Novel Coronavirus from Patients with Pneumonia in China, 2019. *N Engl J Med* 2020; **382**: 727-733 [PMID: 31978945 DOI: 10.1056/NEJMoa2001017]

2 **Coronaviridae Study Group of the International Committee on Taxonomy of Viruses**. The

species Severe acute respiratory syndrome-related coronavirus: classifying 2019-nCoV and naming it SARS-CoV-2. *Nat Microbiol* 2020; **5**: 536-544 [PMID: 32123347 DOI: 10.1038/s41564-020-0695-z]

3 **Asselah T**, Durantel D, Pasmant E, Lau G, Schinazi RF. COVID-19: Discovery, diagnostics and drug development. *J Hepatol* 2021; **74**: 168-184 [PMID: 33038433 DOI: 10.1016/j.jhep.2020.09.031]

4 **Gao QY**, Chen YX, Fang JY. 2019 Novel coronavirus infection and gastrointestinal tract. *J Dig Dis* 2020; **21**: 125-126 [PMID: 32096611 DOI: 10.1111/1751-2980.12851]

5 **Puli S**, Baig M, Walayat S. Gastrointestinal Symptoms and Elevation in Liver Enzymes in COVID-19 Infection: A Systematic Review and Meta-Analysis. *Cureus* 2020; **12**: e9999 [PMID: 32983698 DOI: 10.7759/cureus.9999]

6 **Noor FM**, Islam MM. Prevalence and Associated Risk Factors of Mortality Among COVID-19 Patients: A Meta-Analysis. *J Community Health* 2020; **45**: 1270-1282 [PMID: 32918645 DOI: 10.1007/s10900-020-00920-x]

7 **Pan L**, Mu M, Yang P, Sun Y, Wang R, Yan J, Li P, Hu B, Wang J, Hu C, Jin Y, Niu X, Ping R, Du Y, Li T, Xu G, Hu Q, Tu L. Clinical Characteristics of COVID-19 Patients With Digestive Symptoms in Hubei, China: A Descriptive, Cross-Sectional, Multicenter Study. *Am J Gastroenterol* 2020; **115**: 766-773 [PMID: 32287140 DOI: 10.14309/ajg.0000000000000620]

8 **Dahiya DS**, Kichloo A, Albosta M, Pagad S, Wani F. Gastrointestinal implications in COVID-19. *J Investig Med* 2020; **68**: 1397-1401 [PMID: 32928903 DOI: 10.1136/jim-2020-001559]

9 **Kopel J**, Perisetti A, Gajendran M, Boregowda U, Goyal H. Clinical Insights into the Gastrointestinal Manifestations of COVID-19. *Dig Dis Sci* 2020; **65**: 1932-1939 [PMID: 32447742 DOI: 10.1007/s10620-020-06362-8]

10 **Galanopoulos M**, Gkeros F, Doukatas A, Karianakis G, Pontas C, Tsoukalas N, Viazis N, Liatsos C, Mantzaris GJ. COVID-19 pandemic: Pathophysiology and manifestations from the gastrointestinal tract. *World J Gastroenterol* 2020; **26**: 4579-4588 [PMID: 32884218 DOI: 10.3748/wjg.v26.i31.4579]

11 **Yeo C**, Kaushal S, Yeo D. Enteric involvement of coronaviruses: is faecal-oral transmission of SARS-CoV-2 possible? *Lancet Gastroenterol Hepatol* 2020; **5**: 335-337 [PMID: 32087098 DOI: 10.1016/S2468-1253(20)30048-0]

12 **Elmunzer BJ**, Spitzer RL, Foster LD, Merchant AA, Howard EF, Patel VA, West MK, Qayed E, Nustas R, Zakaria A, Piper MS, Taylor JR, Jaza L, Forbes N, Chau M, Lara LF, Papachristou GI, Volk ML, Hilson LG, Zhou S, Kushnir VM, Lenyo AM, McLeod CG, Amin S, Kuftinec GN, Yadav D, Fox C, Kolb JM, Pawa S, Pawa R, Canakis A, Huang C, Jamil LH, Aneese AM, Glamour BK, Smith ZL, Hanley KA, Wood J, Patel HK, Shah JN, Agarunov E, Sethi A, Fogel EL, McNulty G, Haseeb A, Trieu JA, Dixon RE, Yang JY, Mendelsohn RB, Calo D, Aroniadis OC, LaComb JF, Scheiman JM, Sauer BG, Dang DT, Piraka CR, Shah ED, Pohl H, Tierney WM, Mitchell S, Condon A, Lenhart A, Dua KS, Kanagala VS, Kamal A, Singh VK, Pinto-Sanchez MI, Hutchinson JM, Kwon RS, Korsnes SJ, Singh H, Solati Z, Willingham FF, Yamchimski PS, Conwell DL, Mosier E, Azab M, Patel A, Buxbaum J, Wani S, Chak A, Hosmer AE, Keswani RN, DiMaio CJ, Bronze MS, Muthusamy R, Canto MI, Gjeorgjievski VM, Imam Z, Odish F, Edhi AI, Orosey M, Tiwari A, Patwardhan S, Brown NG, Patel AA, Ordiah CO, Sloan IP, Cruz L, Koza CL, Okafor U, Hollander T, Furey N, Reykhart O, Zbib NH, Damianos JA, Esteban J, Hajidiacos N, Saul M, Mays M, Anderson G, Wood K, Mathews L, Diakova G, Caisse M, Wakefield L, Nitchie H, Waljee AK, Tang W, Zhang Y, Zhu J, Deshpande AR, Rockey DC, Alford TB, Durkalski V; North American Alliance for the Study of Digestive Manifestations of COVID-19. Digestive Manifestations in Patients Hospitalized with COVID-19. *Clin Gastroenterol Hepatol* 2020 [PMID: 33010411 DOI: 10.1016/j.cgh.2020.09.041]

13 **Kotfis K**, Skonieczna-Żydecka K. COVID-19: gastrointestinal symptoms and potential sources of SARS-CoV-2 transmission. *Anaesthesiol Intensive Ther* 2020; **52**: 171-172 [PMID: 32200613 DOI: 10.5114/ait.2020.93867]

14 **Chen N**, Zhou M, Dong X, Qu J, Gong F, Han Y, Qiu Y, Wang J, Liu Y, Wei Y, Xia J, Yu T, Zhang X, Zhang L. Epidemiological and clinical characteristics of 99 cases of 2019 novel coronavirus pneumonia in Wuhan, China: a descriptive study. *Lancet* 2020; **395**: 507-513 [PMID: 32007143 DOI: 10.1016/S0140-6736(20)30211-7]

15 **Mehta P**, McAuley DF, Brown M, Sanchez E, Tattersall RS, Manson JJ; HLH Across Speciality Collaboration; UK. COVID-19: consider cytokine storm syndromes and immunosuppression. *Lancet* 2020; **395**: 1033-1034 [PMID: 32192578 DOI: 10.1016/S0140-6736(20)30628-0]

16 **Shanmugam C**, Mohammed AR, Ravuri S, Luthra V, Rajagopal N, Karre S. COVID-2019 - A comprehensive pathology insight. *Pathol Res Pract* 2020; **216**: 153222 [PMID: 32979742 DOI: 10.1016/j.prp.2020.153222]

17 **Hamming I**, Timens W, Bulthuis ML, Lely AT, Navis G, van Goor H. Tissue distribution of ACE2 protein, the functional receptor for SARS coronavirus. A first step in understanding SARS pathogenesis. *J Pathol* 2004; **203**: 631-637 [PMID: 15141377 DOI: 10.1002/path.1570]

18 **Fierro NA**. COVID-19 and the liver: What do we know after six months of the pandemic? *Ann Hepatol* 2020; **19**: 590-591 [PMID: 32956871 DOI: 10.1016/j.aohep.2020.09.001]

19 **Metawea MI**, Yousif WI, Moheb I. COVID 19 and liver: An A-Z literature review. *Dig Liver Dis* 2020 [PMID: 32988758 DOI: 10.1016/j.dld.2020.09.010]

20 **Wang F**, Wang H, Fan J, Zhang Y, Wang H, Zhao Q. Pancreatic Injury Patterns in Patients With Coronavirus Disease 19 Pneumonia. *Gastroenterology* 2020; **159**: 367-370 [PMID: 32247022 DOI: 10.1053/j.gastro.2020.03.055]

21 **Loganathan S**, Kuppusamy M, Wankhar W, Gurugubelli KR, Mahadevappa VH, Lepcha L, Choudhary AK. Angiotensin-converting enzyme 2 (ACE2): COVID 19 gate way to multiple organ failure syndromes. *Respir Physiol Neurobiol* 2021; **283**: 103548 [PMID: 32956843 DOI: 10.1016/j.resp.2020.103548]

22 **Lizardo-Thiebaud MJ**, Cervantes-Alvarez E, Limon-de la Rosa N, Tejeda-Dominguez F, Palacios-Jimenez M, Méndez-Guerrero O, Delaye-Martinez M, Rodriguez-Alvarez F, Romero-Morales B, Liu WH, Huang CA, Kershenobich D, Navarro-Alvarez N. Direct or Collateral Liver Damage in SARS-CoV-2-Infected Patients. *Semin Liver Dis* 2020; **40**: 321-330 [PMID: 32886936 DOI: 10.1055/s-0040-1715108]

23 **Bourgonje AR**, Abdulle AE, Timens W, Hillebrands JL, Navis GJ, Gordijn SJ, Bolling MC, Dijkstra G, Voors AA, Osterhaus AD, van der Voort PH, Mulder DJ, van Goor H. Angiotensin-converting enzyme 2 (ACE2), SARS-CoV-2 and the pathophysiology of coronavirus disease 2019 (COVID-19). *J Pathol* 2020; **251**: 228-248 [PMID: 32418199 DOI: 10.1002/path.5471]

24 **Pirola CJ**, Sookoian S. COVID-19 and ACE2 in the Liver and Gastrointestinal Tract: Putative Biological Explanations of Sexual Dimorphism. *Gastroenterology* 2020; **159**: 1620-1621 [PMID: 32348773 DOI: 10.1053/j.gastro.2020.04.050]

25 **Wong SH**, Lui RN, Sung JJ. Covid-19 and the digestive system. *J Gastroenterol Hepatol* 2020; **35**: 744-748 [PMID: 32215956 DOI: 10.1111/jgh.15047]

26 **Li J**, Fan JG. Characteristics and Mechanism of Liver Injury in 2019 Coronavirus Disease. *J Clin Transl Hepatol* 2020; **8**: 13-17 [PMID: 32274341 DOI: 10.14218/JCTH.2020.00019]

27 **Machhi J**, Herskovitz J, Senan AM, Dutta D, Nath B, Oleynikov MD, Blomberg WR, Meigs DD, Hasan M, Patel M, Kline P, Chang RC, Chang L, Gendelman HE, Kevadiya BD. The Natural History, Pathobiology, and Clinical Manifestations of SARS-CoV-2 Infections. *J Neuroimmune Pharmacol* 2020; **15**: 359-386 [PMID: 32696264 DOI: 10.1007/s11481-020-09944-5]

28 **Chai X**, Hu L, Zhang Y, Han W, LuZ, Ke A, Zhou J, Shi G, Fang N, Fan J, Cai J, Fan J, Lan F. Specific ACE2 expression in cholangiocytes may cause liver damage after 2019 nCoV infection. *bioRxiv* 2020 [DOI: 10.1101/2020.02.03.931766]

29 **Dey A**, Sen S, Maulik U. Unveiling COVID-19-associated organ-specific cell types and cell-specific pathway cascade. *Brief Bioinform* 2020 [PMID: 32968798 DOI: 10.1093/bib/bbaa214]

30 **Shi H**, Wang W, Yin J, Ouyang Y, Pang L, Feng Y, Qiao L, Guo X, Shi H, Jin R, Chen D. The inhibition of IL-2/IL-2R gives rise to $CD8^+$ T cell and lymphocyte decrease through JAK1-STAT5 in critical patients with COVID-19 pneumonia. *Cell Death Dis* 2020; **11**: 429 [PMID: 32513989 DOI: 10.1038/s41419-020-2636-4]

31 **Fara A**, Mitrev Z, Rosalia RA, Assas BM. Cytokine storm and COVID-19: a chronicle of pro-inflammatory cytokines. *Open Biol* 2020; **10**: 200160 [PMID: 32961074 DOI: 10.1098/rsob.200160]

32 **Gupta R**, Misra A. Contentious issues and evolving concepts in the clinical presentation and management of patients with COVID-19 infectionwith reference to use of therapeutic and other drugs used in Co-morbid diseases (Hypertension, diabetes etc). *Diabetes Metab Syndr* 2020; **14**: 251-254 [PMID: 32247213 DOI: 10.1016/j.dsx.2020.03.012]

33 **Lei P**, Zhang L, Han P, Zheng C, Tong Q, Shang H, Yang F, Hu Y, Li X, Song Y. Liver injury in patients with COVID-19: clinical profiles, CT findings, the correlation of the severity with liver injury. *Hepatol Int* 2020; **14**: 733-742 [PMID: 32886333 DOI: 10.1007/s12072-020-10087-1]

34 **Singh S**, Khan A. Clinical Characteristics and Outcomes of Coronavirus Disease 2019 Among Patients With Preexisting Liver Disease in the United States: A Multicenter Research Network Study. *Gastroenterology* 2020; **159**: 768-771. e3 [PMID: 32376408 DOI: 10.1053/j.gastro.2020.04.064]

35 **Mantovani A**, Beatrice G, Dalbeni A. Coronavirus disease 2019 and prevalence of chronic liver disease: A meta-analysis. *Liver Int* 2020; **40**: 1316-1320 [PMID: 32329563 DOI: 10.1111/liv.14465]

36 **Kullar R**, Patel AP, Saab S. Hepatic Injury in Patients With COVID-19. *J Clin Gastroenterol* 2020; **54**: 841-849 [PMID: 32976196 DOI: 10.1097/MCG.0000000000001432]

37 **Deidda S**, Tora L, Firinu D, Del Giacco S, Campagna M, Meloni F, Orrù G, Chessa L, Carta MG, Melis A, Spolverato G, Littera R, Perra A, Onali S, Zorcolo L, Restivo A. Gastrointestinal coronavirus disease 2019: epidemiology, clinical features, pathogenesis, prevention, and management. *Expert Rev Gastroenterol Hepatol* 2021; **15**: 41-50 [PMID: 32955375 DOI: 10.1080/17474124.2020.1821653]

38 **Napodano C**, Pocino K, Stefanile A, Marino M, Miele L, Gulli F, Basile V, Pandolfi F, Gasbarrini A, Rapaccini GL, Basile U. COVID-19 and hepatic involvement: The liver as a main actor of the pandemic novel. *Scand J Immunol* 2020; e12977 [PMID: 32931622 DOI: 10.1111/sji.12977]

39 **Wong YJ**, Tan M, Zheng Q, Li JW, Kumar R, Fock KM, Teo EK, Ang TL. A systematic review and meta-analysis of the COVID-19 associated liver injury. *Ann Hepatol* 2020; **19**: 627-634 [PMID: 32882393 DOI: 10.1016/j.aohep.2020.08.064]

40 **Ghoda A**, Ghoda M. Liver Injury in COVID-19 Infection: A Systematic Review. *Cureus* 2020; **12**: e9487 [PMID: 32879813 DOI: 10.7759/cureus.9487]

41 **Liu W**, Tao ZW, Wang L, Yuan ML, Liu K, Zhou L, Wei S, Deng Y, Liu J, Liu HG, Yang M, Hu Y. Analysis of factors associated with disease outcomes in hospitalized patients with 2019 novel coronavirus disease. *Chin Med J (Engl)* 2020; **133**: 1032-1038 [PMID: 32118640 DOI: 10.1097/CM9.0000000000000775]

42 **Trevenzoli M**, Guarnaccia A, Alberici I, Fassan M, Di Meco E, Farinati F, Cattelan AM. SARS-CoV-2 and hepatitis. *J Gastrointestin Liver Dis* 2020; **29**: 473-475 [PMID: 32919428 DOI: 10.15403/jgld-2747]

43 **Gholizadeh P**, Safari R, Marofi P, Zeinalzadeh E, Pagliano P, Ganbarov K, Esposito S, Khodadadi E, Yousefi M, Samadi Kafil H. Alteration of Liver Biomarkers in Patients with SARS-CoV-2 (COVID-19). *J Inflamm Res* 2020; **13**: 285-292 [PMID: 32669866 DOI: 10.2147/JIR.S257078]

44 **Chen S**, Liu H, Li T, Huang R, Gui R, Zhang J. Correlation analysis of coagulation dysfunction and liver damage in patients with novel coronavirus pneumonia: a single-center, retrospective, observational study. *Ups J Med Sci* 2020; **125**: 293-296 [PMID: 32990149 DOI: 10.1080/03009734.2020.1822960]

45 **Cai Q**, Huang D, Yu H, Zhu Z, Xia Z, Su Y, Li Z, Zhou G, Gou J, Qu J, Sun Y, Liu Y, He Q, Chen J, Liu L, Xu L. COVID-19: Abnormal liver function tests. *J Hepatol* 2020; **73**: 566-574 [PMID: 32298767 DOI: 10.1016/j.jhep.2020.04.006]

46 **Zhang C**, Shi L, Wang FS. Liver injury in COVID-19: management and challenges. *Lancet Gastroenterol Hepatol* 2020; **5**: 428-430 [PMID: 32145190 DOI: 10.1016/S2468-1253(20)30057-1]

47 **Bertolini A**, van de Peppel IP, Bodewes FAJA, Moshage H, Fantin A, Farinati F, Fiorotto R, Jonker JW, Strazzabosco M, Verkade HJ, Peserico G. Abnormal Liver Function Tests in Patients With COVID-19: Relevance and Potential Pathogenesis. *Hepatology* 2020; **72**: 1864-1872 [PMID: 32702162 DOI: 10.1002/hep.31480]

48 **Zhang C**, Wu Z, Li JW, Zhao H, Wang GQ. Cytokine release syndrome in severe COVID-19: interleukin-6 receptor antagonist tocilizumab may be the key to reduce mortality. *Int J Antimicrob Agents* 2020; **55**: 105954 [PMID: 32234467 DOI: 10.1016/j.ijantimicag.2020.105954]

49 **Li Y**, Hu Y, Yu J, Ma T. Retrospective analysis of laboratory testing in 54 patients with severe- or critical-type 2019 novel coronavirus pneumonia. *Lab Invest* 2020; **100**: 794-800 [PMID: 32341519 DOI: 10.1038/s41374-020-0431-6]

50 **Carothers C**, Birrer K, Vo M. Acetylcysteine for the Treatment of Suspected Remdesivir-Associated Acute Liver Failure in COVID-19: A Case Series. *Pharmacotherapy* 2020; **40**: 1166-1171 [PMID: 33006138 DOI: 10.1002/phar.2464]

51 **Abdulrab S**, Al-Maweri S, Halboub E. Ursodeoxycholic acid as a candidate therapeutic to alleviate and/or prevent COVID-19-associated cytokine storm. *Med Hypotheses* 2020; **143**: 109897 [PMID: 32505909 DOI: 10.1016/j.mehy.2020.109897]

52 **Işık S**, Karaman M, Çilaker Micili S, Çağlayan-Sözmen Ş, Bağrıyanık HA, Arıkan-Ayyıldız Z, Uzuner N, Karaman Ö. Beneficial effects of ursodeoxycholic acid *via* inhibition of airway remodelling, apoptosis of airway epithelial cells, and Th2 immune response in murine model of chronic asthma. *Allergol Immunopathol (Madr)* 2017; **45**: 339-349 [PMID: 28256288 DOI: 10.1016/j.aller.2016.12.003]

53 **Boettler T**, Newsome PN, Mondelli MU, Maticic M, Cordero E, Cornberg M, Berg T. Care of patients with liver disease during the COVID-19 pandemic: EASL-ESCMID position paper. *JHEP Rep* 2020; **2**: 100113 [PMID: 32289115 DOI: 10.1016/j.jhepr.2020.100113]

54 **Fan Z**, Chen L, Li J, Cheng X, Yang J, Tian C, Zhang Y, Huang S, Liu Z, Cheng J. Clinical Features of COVID-19-Related Liver Functional Abnormality. *Clin Gastroenterol Hepatol* 2020; **18**: 1561-1566 [PMID: 32283325 DOI: 10.1016/j.cgh.2020.04.002]

55 **Holshue ML**, DeBolt C, Lindquist S, Lofy KH, Wiesman J, Bruce H, Spitters C, Ericson K, Wilkerson S, Tural A, Diaz G, Cohn A, Fox L, Patel A, Gerber SI, Kim L, Tong S, Lu X, Lindstrom S, Pallansch MA, Weldon WC, Biggs HM, Uyeki TM, Pillai SK; Washington State 2019-nCoV Case Investigation Team. First Case of 2019 Novel Coronavirus in the United States. *N Engl J Med* 2020; **382**: 929-936 [PMID: 32004427 DOI: 10.1056/NEJMoa2001191]

56 **Wang D**, Hu B, Hu C, Zhu F, Liu X, Zhang J, Wang B, Xiang H, Cheng Z, Xiong Y, Zhao Y, Li Y, Wang X, Peng Z. Clinical Characteristics of 138 Hospitalized Patients With 2019 Novel Coronavirus-Infected Pneumonia in Wuhan, China. *JAMA* 2020; **323**: 1061-1069 [PMID: 32031570 DOI: 10.1001/jama.2020.1585]

57 **Zhu Y**, Du Z, Zhu Y, Li W, Miao H, Li Z. Evaluation of organ function in patients with severe COVID-19 infections. *Med Clin (Engl Ed)* 2020; **155**: 191-196 [PMID: 32984539 DOI: 10.1016/j.medcle.2020.05.015]

58 **Medetalibeyoglu A**, Catma Y, Senkal N, Ormeci A, Cavus B, Kose M, Bayramlar OF, Yildiz G, Akyuz F, Kaymakoglu S, Tukek T. The effect of liver test abnormalities on the prognosis of COVID-19. *Ann Hepatol* 2020; **19**: 614-621 [PMID: 32920162 DOI: 10.1016/j.aohep.2020.08.068]

59 **Huang C**, Wang Y, Li X, Ren L, Zhao J, Hu Y, Zhang L, Fan G, Xu J, Gu X, Cheng Z, Yu T, Xia J, Wei Y, Wu W, Xie X, Yin W, Li H, Liu M, Xiao Y, Gao H, Guo L, Xie J, Wang G, Jiang R, Gao Z, Jin Q, Wang J, Cao B. Clinical features of patients infected with 2019 novel coronavirus in Wuhan, China. *Lancet* 2020; **395**: 497-506 [PMID: 31986264 DOI: 10.1016/S0140-6736(20)30183-5]

60 **Yang RX**, Zheng RD, Fan JG. Etiology and management of liver injury in patients with COVID-19. *World J Gastroenterol* 2020; **26**: 4753-4762 [PMID: 32921955 DOI: 10.3748/wjg.v26.i32.4753]

61 **Lee N**, Hui D, Wu A, Chan P, Cameron P, Joynt GM, Ahuja A, Yung MY, Leung CB, To KF, Lui SF, Szeto CC, Chung S, Sung JJ. A major outbreak of severe acute respiratory syndrome in Hong Kong. *N Engl J Med* 2003; **348**: 1986-1994 [PMID: 12682352 DOI: 10.1056/NEJMoa030685]

62 **Assiri A**, Al-Tawfiq JA, Al-Rabeeah AA, Al-Rabiah FA, Al-Hajjar S, Al-Barrak A, Flemban H, Al-Nassir WN, Balkhy HH, Al-Hakeem RF, Makhdoom HQ, Zumla AI, Memish ZA. Epidemiological, demographic, and clinical characteristics of 47 cases of Middle East respiratory syndrome coronavirus disease from Saudi Arabia: a descriptive study. *Lancet Infect Dis* 2013; **13**: 752-761 [PMID: 23891402 DOI: 10.1016/S1473-3099(13)70204-4]

63 **Guo T**, Fan Y, Chen M, Wu X, Zhang L, He T, Wang H, Wan J, Wang X, Lu Z. Cardiovascular

Implications of Fatal Outcomes of Patients With Coronavirus Disease 2019 (COVID-19). *JAMA Cardiol* 2020; **5**: 811-818 [PMID: 32219356 DOI: 10.1001/jamacardio.2020.1017]

64 **Fu L**, Fei J, Xu S, Xiang H, Xiang Y, Tan Z, Li M, Liu F, Li Y, Han M, Li X, Zhao H, Xu D. Acute liver injury and its association with death risk of patients with COVID-19: a hospital-based prospective case-cohort study. *medRxiv* 2020 [DOI: 10.1101/2020.04.02.20050997]

65 **Zhou F**, Yu T, Du R, Fan G, Liu Y, Liu Z, Xiang J, Wang Y, Song B, Gu X, Guan L, Wei Y, Li H, Wu X, Xu J, Tu S, Zhang Y, Chen H, Cao B. Clinical course and risk factors for mortality of adult inpatients with COVID-19 in Wuhan, China: a retrospective cohort study. *Lancet* 2020; **395**: 1054-1062 [PMID: 32171076 DOI: 10.1016/S0140-6736(20)30566-3]

66 **Schroeder M**, Tuku B, Jarczak D, Nierhaus A, Bai T, Jacobsen H, Zickler M, Mueller Z, Stanelle-Bertram S, Meinhardt A, Aberle J, Kluge S, Gabriel G. The majority of male patients with COVID-19 present low testosterone levels on admission to Intensive Care in Hamburg, Germany: a retrospective cohort study. *medRxiv* 2020 [DOI: 10.1101/2020.05.07.20073817]

67 **Pozzilli P**, Lenzi A. Commentary: Testosterone, a key hormone in the context of COVID-19 pandemic. *Metabolism* 2020; **108**: 154252 [PMID: 32353355 DOI: 10.1016/j.metabol.2020.154252]

68 **Naaraayan A**, Nimkar A, Hasan A, Pant S, Durdevic M, Elenius H, Nava Suarez C, Jesmajian S. Analysis of Male Sex as a Risk Factor in Older Adults With Coronavirus Disease 2019: A Retrospective Cohort Study From the New York City Metropolitan Region. *Cureus* 2020; **12**: e9912 [PMID: 32974111 DOI: 10.7759/cureus.9912]

69 **Wang M**, Yan W, Qi W, Wu D, Zhu L, Li W, Wang X, Ma K, Ni M, Xu D, Wang H, Chen G, Yu H, Ding H, Xing M, Han M, Luo X, Chen T, Guo W, Xi D, Ning Q. Clinical characteristics and risk factors of liver injury in COVID-19: a retrospective cohort study from Wuhan, China. *Hepatol Int* 2020; **14**: 723-732 [PMID: 33026573 DOI: 10.1007/s12072-020-10075-5]

70 **Zhang H**, Liao YS, Gong J, Liu J, Zhang H. Clinical characteristics and risk factors for liver injury in COVID-19 patients in Wuhan. *World J Gastroenterol* 2020; **26**: 4694-4702 [PMID: 32884226 DOI: 10.3748/wjg.v26.i31.4694]

71 **Effenberger M**, Grander C, Grabherr F, Griesmacher A, Ploner T, Hartig F, Bellmann-Weiler R, Joannidis M, Zoller H, Weiss G, Adolph TE, Tilg H. Systemic inflammation as fuel for acute liver injury in COVID-19. *Dig Liver Dis* 2020 [PMID: 32873520 DOI: 10.1016/j.dld.2020.08.004]

72 **Ji D**, Qin E, Xu J, Zhang D, Cheng G, Wang Y, Lau G. Non-alcoholic fatty liver diseases in patients with COVID-19: A retrospective study. *J Hepatol* 2020; **73**: 451-453 [PMID: 32278005 DOI: 10.1016/j.jhep.2020.03.044]

73 **Hussain A**, Vasas P, El-Hasani S. Letter to the Editor: Obesity as a risk factor for greater severity of COVID-19 in patients with metabolic associated fatty liver disease. *Metabolism* 2020; **108**: 154256 [PMID: 32360211 DOI: 10.1016/j.metabol.2020.154256]

74 **Bramante C**, Tignanelli CJ, Dutta N, Jones E, Tamariz L, Clark JM, Usher M, Metlon-Meaux G, Ikramuddin S. Non-alcoholic fatty liver disease (NAFLD) and risk of hospitalization for Covid-19. *medRxiv* 2020 [PMID: 32909011 DOI: 10.1101/2020.09.01.20185850]

75 **Chen VL**, Hawa F, Berinstein JA, Reddy CA, Kassab I, Platt KD, Hsu CY, Steiner CA, Louissaint J, Gunaratnam NT, Sharma P. Hepatic Steatosis Is Associated with Increased Disease Severity and Liver Injury in Coronavirus Disease-19. *Dig Dis Sci* 2020 [PMID: 32980956 DOI: 10.1007/s10620-020-06618-3]

76 **Boeckmans J**, Rodrigues RM, Demuyser T, Piérard D, Vanhaecke T, Rogiers V. COVID-19 and drug-induced liver injury: a problem of plenty or a petty point? *Arch Toxicol* 2020; **94**: 1367-1369 [PMID: 32266419 DOI: 10.1007/s00204-020-02734-1]

77 **Kim D**, Adeniji N, Latt N, Kumar S, Bloom PP, Aby ES, Perumalswami P, Roytman M, Li M, Vogel AS, Catana AM, Wegermann K, Carr RM, Aloman C, Chen V, Rabiee A, Sadowski B, Nguyen V, Dunn W, Chavin K, Zhou K, Lizaola-Mayo B, Moghe A, Debes J, Lee TH, Branch A, Viveiros K, Chan W, Chascsa D, Kwo P, Dhanasekaran R. Predictors of Outcomes of COVID-19 in Patients with Chronic Liver Disease: US Multi-center Study. *Clin Gastroenterol Hepatol* 2020 [PMID: 32950749 DOI: 10.1016/j.cgh.2020.09.027]

78 **Marjot T**, Moon AM, Cook JA, Abd-Elsalam S, Aloman C, Armstrong MJ, Pose E, Brenner EJ, Cargill T, Catana MA, Dhanasekaran R, Eshraghian A, García-Juárez I, Gill US, Jones PD, Kennedy J, Marshall A, Matthews C, Mells G, Mercer C, Perumalswami PV, Avitabile E, Qi X, Su F, Ufere NN, Wong YJ, Zheng MH, Barnes E, Barritt AS 4th, Webb GJ. Outcomes following SARS-CoV-2 infection in patients with chronic liver disease: An international registry study. *J Hepatol* 2020 [PMID: 33035628 DOI: 10.1016/j.jhep.2020.09.024]

79 **Guo H**, Zhang Z, Zhang Y, Liu Y, Wang J, Qian Z, Zou Y, Lu H. Analysis of liver injury factors in 332 patients with COVID-19 in Shanghai, China. *Aging (Albany NY)* 2020; **12**: 18844-18852 [PMID: 33001040 DOI: 10.18632/aging.103860]

80 **Oyelade T**, Alqahtani J, Canciani G. Prognosis of COVID-19 in Patients with Liver and Kidney Diseases: An Early Systematic Review and Meta-Analysis. *Trop Med Infect Dis* 2020; **5** [PMID: 32429038 DOI: 10.3390/tropicalmed5020080]

81 **Kumar A**, Arora A, Sharma P, Anikhindi SA, Bansal N, Singla V, Khare S, Srivastava A. Clinical Features of COVID-19 and Factors Associated with Severe Clinical Course: A Systematic Review and Meta-Analysis. *SSRN* 2020; 3566166 [PMID: 32714109 DOI: 10.2139/ssrn.3566166]

82 **Henry BM**, de Oliveira MHS, Benoit S, Plebani M, Lippi G. Hematologic, biochemical and immune biomarker abnormalities associated with severe illness and mortality in coronavirus disease 2019 (COVID-19): a meta-analysis. *Clin Chem Lab Med* 2020; **58**: 1021-1028 [PMID: 32286245 DOI:

10.1515/cclm-2020-0369]
83 **Qi X**, Liu Y, Wang J, Fallowfield JA, Wang J, Li X, Shi J, Pan H, Zou S, Zhang H, Chen Z, Li F, Luo Y, Mei M, Liu H, Wang Z, Li J, Yang H, Xiang H, Li X, Liu T, Zheng MH, Liu C, Huang Y, Xu D, Li X, Kang N, He Q, Gu Y, Zhang G, Shao C, Liu D, Zhang L, Li X, Kawada N, Jiang Z, Wang F, Xiong B, Takehara T, Rockey DC; COVID-Cirrhosis-CHESS Group. Clinical course and risk factors for mortality of COVID-19 patients with pre-existing cirrhosis: a multicentre cohort study. *Gut* 2020 [PMID: 32434831 DOI: 10.1136/gutjnl-2020-321666]
84 **Brito CA**, Barros FM, Lopes EP. Mechanisms and consequences of COVID-19 associated liver injury: What can we affirm? *World J Hepatol* 2020; **12**: 413-422 [PMID: 32952870 DOI: 10.4254/wjh.v12.i8.413]
85 **Xu Z**, Shi L, Wang Y, Zhang J, Huang L, Zhang C, Liu S, Zhao P, Liu H, Zhu L, Tai Y, Bai C, Gao T, Song J, Xia P, Dong J, Zhao J, Wang FS. Pathological findings of COVID-19 associated with acute respiratory distress syndrome. *Lancet Respir Med* 2020; **8**: 420-422 [PMID: 32085846 DOI: 10.1016/S2213-2600(20)30076-X]
86 **Sonzogni A**, Previtali G, Seghezzi M, Alessio MG, Gianatti A, Licini L, Zerbi P, Carsana L, Rossi R, Lauri E, Pellegrinelli A, Nebuloni M. Liver and COVID 19 infection: a very preliminary lesson learnt from histological post-mortem findings in 48 patients. Preprints 2020; 2020040438 [DOI: 10.20944/preprints202004.0438.v1]
87 **Souza LJ**, Alves JG, Nogueira RM, Gicovate Neto C, Bastos DA, Siqueira EW, Souto Filho JT, Cezário Tde A, Soares CE, Carneiro Rda C. Aminotransferase changes and acute hepatitis in patients with dengue fever: analysis of 1,585 cases. *Braz J Infect Dis* 2004; **8**: 156-163 [PMID: 15361994 DOI: 10.1590/S1413-86702004000200006]
88 **Samanta J**, Sharma V. Dengue and its effects on liver. *World J Clin Cases* 2015; **3**: 125-131 [PMID: 25685758 DOI: 10.12998/wjcc.v3.i2.125]
89 **Escosteguy CC**, Pereira AGL, Marques MRVE, Lima TRA, Galliez RM, Medronho RA. Yellow fever: profile of cases and factors associated with death in a hospital in the State of Rio de Janeiro, 2017-2018. *Rev Saude Publica* 2019; **53**: 89 [PMID: 31644770 DOI: 10.11606/s1518-8787.2019053001434]
90 **Chang HL**, Chen KT, Lai SK, Kuo HW, Su IJ, Lin RS, Sung FC. Hematological and biochemical factors predicting SARS fatality in Taiwan. *J Formos Med Assoc* 2006; **105**: 439-450 [PMID: 16801031 DOI: 10.1016/S0929-6646(09)60183-2]
91 **Saad M**, Omrani AS, Baig K, Bahloul A, Elzein F, Matin MA, Selim MA, Al Mutairi M, Al Nakhli D, Al Aidaroos AY, Al Sherbeeni N, Al-Khashan HI, Memish ZA, Albarrak AM. Clinical aspects and outcomes of 70 patients with Middle East respiratory syndrome coronavirus infection: a single-center experience in Saudi Arabia. *Int J Infect Dis* 2014; **29**: 301-306 [PMID: 25303830 DOI: 10.1016/j.ijid.2014.09.003]
92 **Cao B**, Li XW, Mao Y, Wang J, Lu HZ, Chen YS, Liang ZA, Liang L, Zhang SJ, Zhang B, Gu L, Lu LH, Wang DY, Wang C; National Influenza A Pandemic (H1N1) 2009 Clinical Investigation Group of China. Clinical features of the initial cases of 2009 pandemic influenza A (H1N1) virus infection in China. *N Engl J Med* 2009; **361**: 2507-2517 [PMID: 20007555 DOI: 10.1056/NEJMoa0906612]
93 **Fiel MI**, El Jamal SM, Paniz-Mondolfi A, Gordon RE, Reidy J, Bandovic J, Advani R, Kilaru S, Pourmand K, Ward S, Thung SN, Schiano T. Findings of Severe Hepatic Severe Acute Respiratory Syndrome Coronavirus-2 Infection. *Cell Mol Gastroenterol Hepatol* 2020 [PMID: 32992052 DOI: 10.1016/j.jcmgh.2020.09.015]
94 **Wang Y**, Liu S, Liu H, Li W, Lin F, Jiang L, Li X, Xu P, Zhang L, Zhao L, Cao Y, Kang J, Yang J, Li L, Liu X, Li Y, Nie R, Mu J, Lu F, Zhao S, Lu J, Zhao J. SARS-CoV-2 infection of the liver directly contributes to hepatic impairment in patients with COVID-19. *J Hepatol* 2020; **73**: 807-816 [PMID: 32437830 DOI: 10.1016/j.jhep.2020.05.002]
95 **Lagana SM**, Kudose S, Iuga AC, Lee MJ, Fazlollahi L, Remotti HE, Del Portillo A, De Michele S, de Gonzalez AK, Saqi A, Khairallah P, Chong AM, Park H, Uhlemann AC, Lefkowitch JH, Verna EC. Hepatic pathology in patients dying of COVID-19: a series of 40 cases including clinical, histologic, and virologic data. *Mod Pathol* 2020; **33**: 2147-2155 [PMID: 32792598 DOI: 10.1038/s41379-020-00649-x]

World Journal of Gastroenterology

Submit a Manuscript: https://www.f6publishing.com

World J Gastroenterol 2021 February 7; 27(5): 391-403

DOI: 10.3748/wjg.v27.i5.391

ISSN 1007-9327 (print) ISSN 2219-2840 (online)

ORIGINAL ARTICLE

Basic Study

Changes in gut microbiota composition and diversity associated with post-cholecystectomy diarrhea

Yan-Dong Li, Bao-Ning Liu, Si-Hai Zhao, Yong-Li Zhou, Liang Bai, En-Qi Liu

ORCID number: Yan-Dong Li 0000-0001-8927-7230; Bao-Ning Liu 0000-0003-2252-1862; Si-Hai Zhao 0000-0002-5845-6639; Yong-Li Zhou 0000-0002-2061-2990; Liang Bai 0000-0002-4129-8662; En-Qi Liu 0000-0002-2092-3158.

Author contributions: Li YD and Liu EQ designed the study; Li YD, Liu BN, Zhao SH, Zhou YL and Bai L performed the experiments; Liu EQ and Zhao SH provided reagents and materials; Li YD and Liu BN analyzed the data; Li YD, Liu BN and Liu EQ wrote the main manuscript text and prepared the figures; all authors reviewed the manuscript.

Institutional review board statement: The study was undertaken with the approval of the Medical Ethics Board of the First Affiliated Hospital of Xi'an Medical University.

Conflict-of-interest statement: The authors declare no conflict of interest.

Data sharing statement: Technical appendix, statistical code, and dataset available from the corresponding author at email address. Participants gave informed consent for data sharing.

Open-Access: This article is an

Yan-Dong Li, Si-Hai Zhao, Laboratory Animal Center, Xi'an Jiaotong University Health Science Center, Xi'an Jiaotong University, Xi'an 710061, Shaanxi Province, China

Bao-Ning Liu, Research Institute of Atherosclerotic Disease and Laboratory Animal Center, School of Medicine, Xi'an Jiaotong University, Xi'an 710061, Shaanxi Province, China

Yong-Li Zhou, Department of Gastroenterology, The First Affiliated Hospital of Xi'an Medical University, Xi'an 710077, Shaanxi Province, China

Liang Bai, En-Qi Liu, Laboratory Animal Center, Institute of Atherosclerotic Disease, Xi'an Jiaotong University, Xi'an 710061, Shaanxi Province, China

Corresponding author: En-Qi Liu, PhD, Director, Professor, Laboratory Animal Center, Institute of Atherosclerotic Disease, Xi'an Jiaotong University, No. 76 Yanta West Road, Xi'an 710061, Shaanxi Province, China. liuenqi@mail.xjtu.edu.cn

Abstract

BACKGROUND

Post-cholecystectomy diarrhea (PCD) frequently occurs in patients following gallbladder removal. PCD is part of the post-cholecystectomy (PC) syndrome, and is difficult to treat. After cholecystectomy, bile enters the duodenum directly, independent of the timing of meals. The interaction between the bile acids and the intestinal microbes is changed. Therefore, the occurrence of PCD may be related to the change in microbiota. However, little is known about the relationship between the gut microbiota and PCD.

AIM

To better understand the role of the gut microbiota in PCD patients.

METHODS

Fecal DNA was isolated. The diversity and profiles of the gut microbiota were analyzed by performing high-throughput 16S rRNA gene sequencing. The gut microbiota were characterized in a healthy control (HC) group and a PC group. Subsequently, the PC group was further divided into a PCD group and a post-cholecystectomy non-diarrhea group (PCND) according to the patients' clinical symptoms. The composition, diversity and richness of microbial communities were determined and compared.

open-access article that was selected by an in-house editor and fully peer-reviewed by external reviewers. It is distributed in accordance with the Creative Commons Attribution NonCommercial (CC BY-NC 4.0) license, which permits others to distribute, remix, adapt, build upon this work non-commercially, and license their derivative works on different terms, provided the original work is properly cited and the use is non-commercial. See: http://creativecommons.org/Licenses/by-nc/4.0/

Manuscript source: Unsolicited manuscript

Specialty type: Gastroenterology and hepatology

Country/Territory of origin: China

Peer-review report's scientific quality classification

Grade A (Excellent): A
Grade B (Very good): 0
Grade C (Good): 0
Grade D (Fair): 0
Grade E (Poor): 0

Received: October 12, 2020
Peer-review started: October 12, 2020
First decision: November 23, 2020
Revised: November 30, 2020
Accepted: December 17, 2020
Article in press: December 17, 2020
Published online: February 7, 2021

P-Reviewer: Hann HW
S-Editor: Fan JR
L-Editor: Webster JR
P-Editor: Ma YJ

RESULTS

In the PC and HC groups, 720 operational taxonomic units (OTUs) were identified. The PC group had fewer OTUs than the HC group. β-diversity was decreased in the PC group. This indicated decreased microbial diversity in the PC group. Fifteen taxa with differential abundance between the HC and PC groups were identified. In the PCD group compared to the PCND group, significant decreases in microbial diversity, Firmicutes/Bacteroidetes ratio, and richness of probiotic microbiota (Bifidobacterium and Lactococcus), and an increase in detrimental microbiota (Prevotella and Sutterella) were observed. Moreover, a negative correlation was found between Prevotella and Bifidobacterium. Using a Kyoto Encyclopedia of Genes and Genomes functional analysis, it was found that the abundances of gut microbiota involved in lipid metabolism pathways were markedly lower in the PCD group compared to the PCND group.

CONCLUSION

This study demonstrated that gut dysbiosis may play a critical role in PCD, which provides new insights into therapeutic options for PCD patients.

Key Words: Cholecystectomy; Post-cholecystectomy; Diarrhea; 16S rRNA; Microbiota; Bifidobacterium

©The Author(s) 2021. Published by Baishideng Publishing Group Inc. All rights reserved.

Core Tip: Post-cholecystectomy diarrhea (PCD) is difficult to treat. Approximately 12%-35.6% of post-cholecystectomy patients have varying degrees of chronic diarrhea. Little is known regarding the intestinal microbiota characteristics in PCD patients. High-throughput sequencing of the 16S rRNA gene was used to characterize the composition and diversity of the complex intestinal microbial community in PCD patients. The results indicates that decreased diversity and abundance of the microbial community in the PCD group may cause diarrhea. These findings demonstrate the association between PCD and the gut microbiota, especially regarding Prevotella and Bifidobacterium. Thus, this study provides new insights into potential therapeutics that could target the microbiota to attenuate PCD.

Citation: Li YD, Liu BN, Zhao SH, Zhou YL, Bai L, Liu EQ. Changes in gut microbiota composition and diversity associated with post-cholecystectomy diarrhea. *World J Gastroenterol* 2021; 27(5): 391-403
URL: https://www.wjgnet.com/1007-9327/full/v27/i5/391.htm
DOI: https://dx.doi.org/10.3748/wjg.v27.i5.391

INTRODUCTION

Cholecystectomy, surgical removal of the gallbladder, can alter the flow of bile to the intestines. There are approximately 10^{13} bacteria in the human intestines, which can be divided into three categories according to their functions: Beneficial, harmful, and neutral bacteria[1].

After cholecystectomy, bile enters the duodenum directly, independent of the timing of meals. The bile acid metabolism balance is disrupted and primary bile acid production is increased. The interaction between the bile acids and the intestinal microbes is changed[2]. The occurrence of post-cholecystectomy diarrhea (PCD) may be related to the change in the bile flowing into the intestines after cholecystectomy[3,4]. Some studies have provided evidence that the intestinal microbiota maintains normal gastrointestinal function and that alterations in the intestinal microbial community contributes to gastrointestinal symptoms[5-9]. Accumulating evidence indicates that the gut microbiota plays a significant role in the development of a number of disease states, such as immune, metabolic, and even skin diseases[10-13]. Studies have shown that gut dysbiosis may also cause many diseases, such as diarrhea, inflammatory bowel disease, obesity, and diabetes[14-16].

Thus, PCD may be related to the gut microbiota. PCD is part of the post-

cholecystectomy (PC) syndrome, and is difficult to treat[17]. The clinical characteristics of PCD include feeling an urgent need to defecate, an increased frequency of defecation, and diarrhea that mostly occurs in the daytime. According to the definition of diarrhea as three or more bowel movements of liquid stools per day without precipitating factors[18,19], our questionnaire survey of PC patients showed that diarrhea occurred in 32% of patients after 6 mo (data not shown). Studies have reported that cholecystectomy is associated with a higher occurrence of diarrhea[20]. Approximately 12%-35.6% of PC patients have varying degrees of chronic diarrhea[21-25].

Little is known regarding the intestinal microbiota characteristics in PCD patients. To better understand the role of the intestinal microbiota in PCD patients, high-throughput sequencing of the 16S rRNA gene was used to characterize the composition and diversity of the complex intestinal microbial community for the first time. In this study, we identified changes in the fecal microbiota in PCD patients. The results indicated that decreased diversity and abundance of the microbial community in the PCD group may cause diarrhea.

MATERIALS AND METHODS

Study population

We studied 31 PC patients who were divided into two subgroups: The PCD group (n = 16) and the post-cholecystectomy non-diarrhea (PCND) group (n = 15). A group of 20 healthy controls (HC) was also included, who had a similar age range and sex ratio as the PC group (Table 1). Subjects were recruited from the First Affiliated Hospital of Xi'an Medical University, China, and health status was assessed at the participants' annual physical examination appointments. The inclusion criteria for PC patients were as follows: No retained gallstones, no bile duct injury, no stenosis of the bile duct, and ≤ 1 year since cholecystectomy. The exclusion criteria for PC patients were as follows: Alcohol consumption, smoking, history of treatment with antibiotics or anti-inflammatory agents in the previous 3 mo, history of other diseases in the previous 3 mo, and consumption of probiotics in the previous 2 mo.

Ethics statement

The study was undertaken with the approval of the Medical Ethics Board of the First Affiliated Hospital of Xi'an Medical University. All experiments were performed in accordance with the approved guidelines. All participants provided written informed consent before participation in the study.

Sample collection and DNA extraction

Fresh stool samples from each participant were collected in the morning using fecal collection containers. Each sample was immediately transferred to the laboratory where it was homogenized, divided into aliquots, and stored at -80°C before further analysis. Bacterial DNA was extracted from the stool samples using a QIAamp DNA Stool Minikit (Qiagen, Hilden, Germany) following the manufacturer's instructions.

16S rRNA amplicon sequencing

The 16S rRNA gene (V3-V4 region) in the extracted DNA was amplified using the primer pair F (5'-ACTCCTACGGGRSGCAGCAG-3') and R (5'-GGACTACV VGGGTATCTAATC-3'). A KAPA HiFi Hotstart ReadyMix PCR kit was used for the high-fidelity amplification. The rDNA was then sequenced using an Illumina HiSeq 2500 platform (RealgeneBio Co. Ltd., Shanghai, China) with 2 × 250 base pair paired-end sequencing. The read length was centralized on 400-440 base pairs. Raw data are now available at NCBI under the Sequence Read Archive database with accession no. SRP247004.

Sequencing data analysis and statistical analysis

PANDAseq was applied to assemble the overlapping paired-end reads[26]. The 16S rDNA sequences were clustered into operational taxonomic units (OTUs) based on ≥ 97% sequence similarity using USEARCH[27]. A representative sequence for each OTU was chosen for downstream analysis based on the most abundant sequence. OTUs were taxonomically assigned using the Ribosomal Database Project (RDP) database and classifier (RDP, http://rdp.cme.msu.edu)[28,29].

Quantitative Insights Into Microbial Ecology was used to generate the rarefaction curves for testing the sequencing depth. Phylogenetic diversity tree diversity indices

Table 1 Basic information on the healthy control and post-cholecystectomy groups

	HC group	PC group	
		Diarrhea	Non-diarrhea
Number of subjects	20	16	15
Males/females	8/12	6/10	6/9
Age (yr), mean (range)	47.3 (23-66)	46.8 (23-66)	46.4 (24-65)
Body mass index, mean (range)	22.1 (18.7-23.6)	21.9 (18.5-23.2)	22.4 (18.5-23.7)

HC: Healthy control; PC: Post-cholecystectomy.

were used to assess the α-diversity, which represents the species abundance in a single sample, and comparisons between groups were performed. The communities were compared based on phylogenetic distances using the weighted UniFrac metric to assess β-diversity. One-way analysis of similarities (ANOSIM), nonmetric multidimensional scaling (NMDS), and multi-response permutation procedure (MRPP) analyses were also employed to assess the community similarities or dissimilarities between groups. Linear discriminant analysis (LDA) effect size (LefSe) was applied to identify bacteria with differential abundance between groups. LefSe analysis was applied with a logarithmic LDA score cut off of 2. Statistical analysis of microbial differences between groups was performed using the Wilcoxon rank sum test and Kruskal-Wallis rank sum test in R3.1.0. All values of $P < 0.05$ were considered significant. Spearman's correlation coefficient was calculated using R and visualized as a network using corrplot.

Analysis of predicted metagenomes

Phylogenetic Investigation of Communities by Reconstruction of Unobserved States (PICRUSt) was used for analyzing both 16S rRNA gene relative abundances and the predicted metabolic data. The sequences of genes in the merged gene catalogue were aligned to the Kyoto Encyclopedia of Genes and Genomes (KEGG) bioinformatics database.

RESULTS

Diversity and richness of gut microbiota decreased after cholecystectomy

The basic information on the study population is listed in Table 1. The diversity and profiles of the gut microbiota were analyzed by performing high-through put 16S rRNA gene sequencing in the PC and HC groups. In total, 720 OTUs were identified based on a 3% dissimilarity cut-off. To better understand the differences in the microbiota distributions between groups, a Venn diagram was constructed and it was found that the majority of OTUs were shared by the HC and PC groups. However, the PC group had fewer OTUs than the HC group (Figure 1A). We also observed attenuated α-diversity in terms of community richness in the PC group, although the difference was not statistically significant (Figure 1B). Based on the β-diversity indices of the gut microbiota in the PC and HC groups, NMDS was implemented to assess discrepancies regarding different abundances, which indicated that β-diversity was decreased in the PC group (Supplementary Figure 1). Furthermore, the microbiota abundance, from phyla to genera, was different between the PC and HC groups. Based on profiling of bacterial taxa, the abundance of the genus Prevotella was higher and Bacteroides was lower in the PC group compared to the HC group (Figure 1C). There were 20 bacterial taxa (seven at the genus level) that exhibited remarkable differences between the HC and PC groups. At the genus level, Bifidobacterium, Acinetobacter, and Megasphaera were higher in the PC group, while Clostridium XVIII, Brachybacterium, Leucobacter, and Clostridium sensu stricto were higher in the HC group (Supplementary Figure 2). Using LefSe analysis, 15 taxa with differential abundance between the HC and PC groups were identified (Figure 1D).

Diarrhea-associated intestinal microbiota in PC patients

By comparing the OTUs between the PCD and PCND groups, we found attenuated

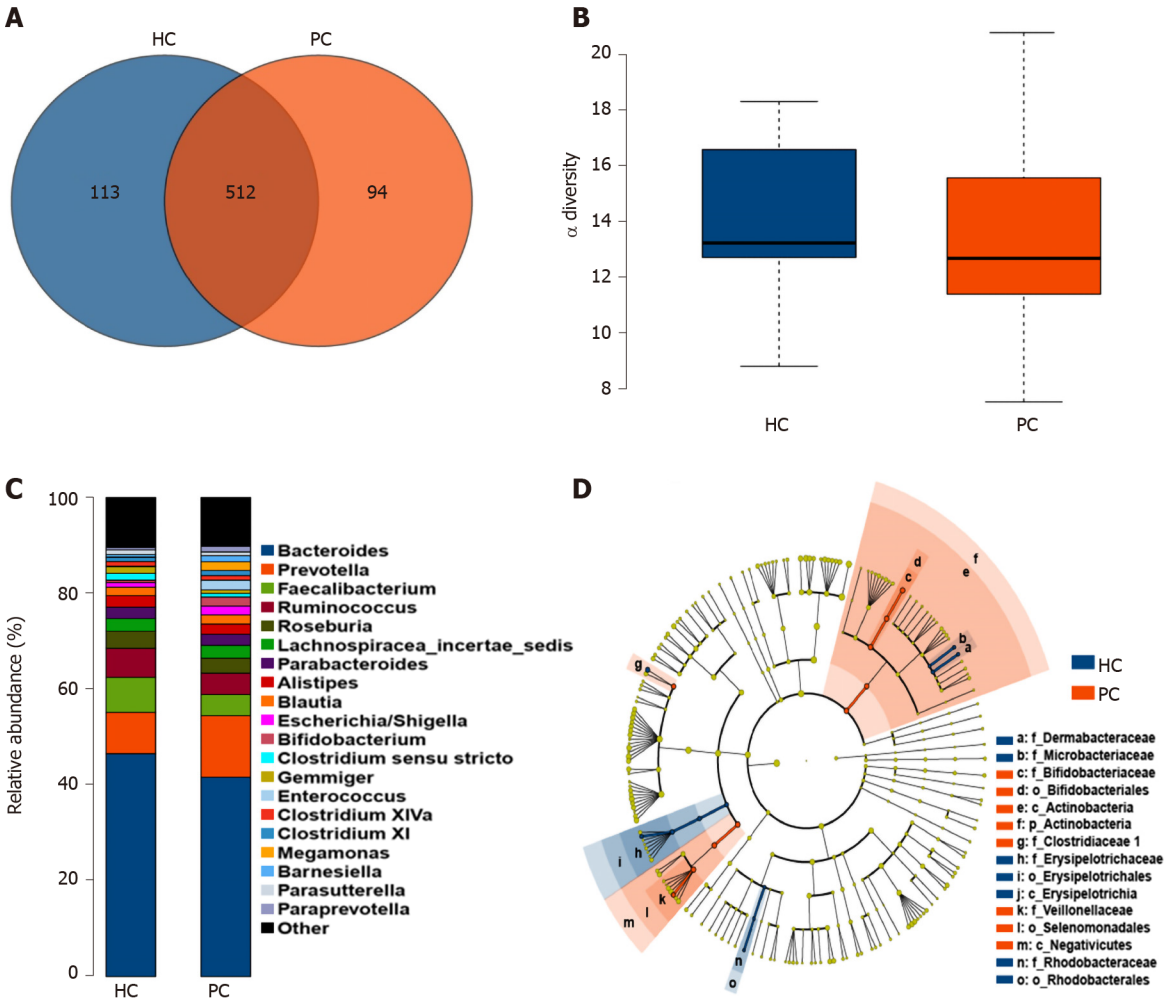
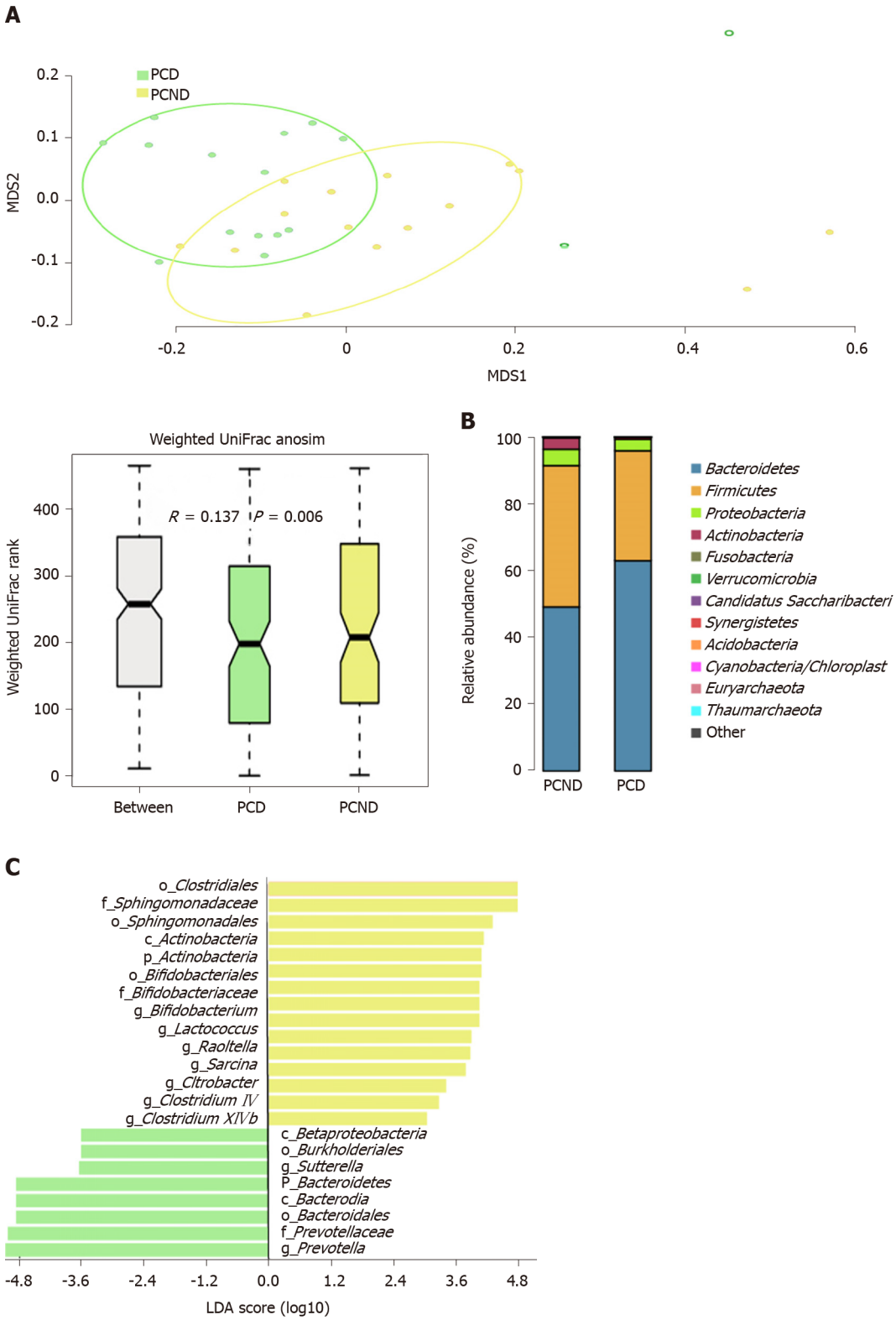


Figure 1 Comparison of gut microbiota structure and abundance between the healthy control and post-cholecystectomy groups. A: Venn diagram comparing the operational taxonomic units in the fecal microbiota between the two groups; B: Phylogenetic diversity tree used to estimate the diversity of the gut microbiota; C: Profiling of bacterial taxa at the genus level; D: Logarithmic linear discriminant analysis score identifying the taxa with the greatest differences in abundance between the healthy control and post-cholecystectomy groups. The brightness of each dot is proportional to the effect size. HC: Healthy control; PC: Post-cholecystectomy.

community richness in the PCD group. It was found that 427 OTUs were shared between the PCD and PCND groups, the PCND group had 75 OTUs more than the PCD group. Significant differences in β-diversity between the PCD and PCND groups were found based on the weighted UniFrac metric (ANOSIM r = 0.137, P = 0.006) (Figure 2A), indicating that the fecal microbial structure and richness in the PCD group were significantly different compared to the PCND group. MRPP analysis also indicated a significant difference between the PCD and PCND groups based on the weighted UniFrac metric (P = 0.009). Based on the NMDS plot, the patients formed two clusters: A tight PCD cluster (Figure 2A, green dots) and a tight PCND cluster (Figure 2A, yellow dots).

Profiling of the bacterial taxa was conducted at the phylum and genus levels. At the phylum level, the abundance of Bacteroidetes was significantly higher in the PCD group than in the PCND group. The ratio of Firmicutes/Bacteroidetes was decreased in the PCD group compared with the PCND group (Figure 2B). However, at the genus level, Bacteroides decreased in the PCD group compared with the PCND group (Supplementary Figure 3). LefSe analysis revealed that 23 bacterial taxa (with nine at the genus level) exhibited remarkable differences between the PCD and PCND groups (Figure 2C). The Wilcoxon and Kruskal-Wallis rank sum tests identified the top 20 differentially abundant microbiota between the PCD and PCND groups, and the relevant eight taxa at the genus level are shown in Figure 2D. At the genus level, Prevotella and Sutterella were higher in the PCD group, while Bifidobacterium, Citrobacter, Clostridium IV, Clostridium XlVb, Lactococcus, and Raoultella were higher in the PCND group (Figure 2D).


A
PCD
PCND
MDS2
MDS1
Weighted UniFrac anosim
R = 0.137
P = 0.006
Weighted UniFrac rank
Between
PCD
PCND
B
Relative abundance (%)
PCND
PCD
Bacteroidetes
Firmicutes
Proteobacteria
Actinobacteria
Fusobacteria
Verrucomicrobia
Candidatus Saccharibacteri
Synergistetes
Acidobacteria
Cyanobacteria/Chloroplast
Euryarchaeota
Thaumarchaeota
Other
C
o_Clostridiales
f_Sphingomonadaceae
o_Sphingomonadales
c_Actinobacteria
p_Actinobacteria
o_Bifidobacteriales
f_Bifidobacteriaceae
g_Bifidobacterium
g_Lactococcus
g_Raoltella
g_Sarcina
g_Citrobacter
g_Clostridium IV
g_Clostridium XlVb
c_Betaproteobacteria
o_Burkholderiales
g_Sutterella
P_Bacteroidetes
c_Bacterodia
o_Bacteroidales
f_Prevotellaceae
g_Prevotella
LDA score (log10)

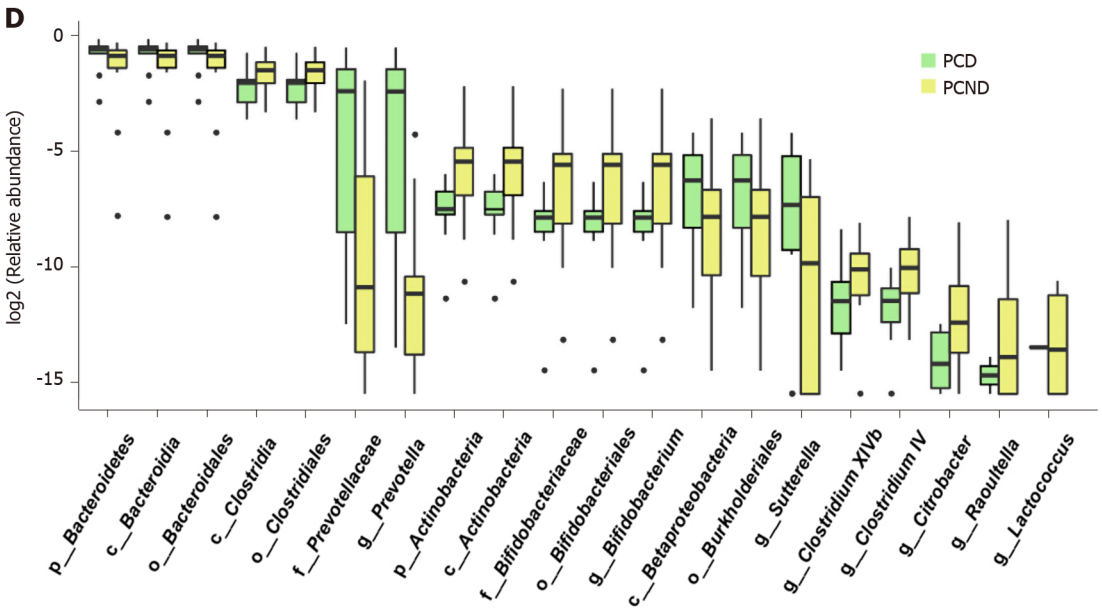


Figure 2 Comparison of gut microbiota structure and abundance between the post-cholecystectomy diarrhea and post-cholecystectomy non-diarrhea groups. A: Differences between and within post-cholecystectomy diarrhea (PCD) and post-cholecystectomy non-diarrhea (PCND) groups were assessed by one-way analysis of similarities and nonmetric multidimensional scaling analysis of the gut microbiota based on the weighted UniFrac metric; B: Comparison of the relative abundance at the phylum level between the PCD and PCND groups; C: Linear discriminant analysis effect size analysis showing the taxa with the greatest differences in abundance between the PCD and PCND groups. Green bars: PCD group-enriched taxa; yellow bars: PCND group-enriched taxa. The brightness of each dot is proportional to the effect size; D: Box plots showing the relative abundance of the top 20 microbial taxa with differential abundance. PCD: Post-cholecystectomy diarrhea; PCND: Post-cholecystectomy non-diarrhea; LDA: Linear discriminant analysis.

Correlations among diarrhea-associated microbes

The differentially abundant microbiota could be used to clearly distinguish the PCD group from the PCND group (Figure 3A). To further characterize the relationships between the bacterial taxa, we calculated the Spearman's correlations of the bacterial genera with differential abundances (Figure 3B). Significant positive correlations were observed among Lactococcus, Citrobacter, and Raoultella, while a significant negative correlation was observed between Prevotella and Bifidobacterium.

Predictive function analysis of bacterial taxa associated with diarrhea

The KEGG analysis suggested that the fecal microbial structures may contribute to functional variation in their hosts. At KEGG levels 2 (Figure 4A) and 3 (Figure 4B), we identified seven and 33 differentially abundant pathways, respectively. At level 2, seven microbial gene functions, including pathways involved with amino acid metabolism, lipid metabolism, and the circulatory system, were higher in the PCND group, whereas microbial gene functions related to the digestive system, metabolism of terpenoids and polyketides, folding, sorting, and degradation, and energy metabolism pathways were higher in the PCD group.

DISCUSSION

Cholecystectomy has become the most common biliary surgery[30], but the main complication of diarrhea has been largely ignored. It affects the quality of life of PC patients to a certain extent[31,32]. Therefore, it is necessary to pay attention to PCD.

In this study, we mainly analyzed and compared the fecal microbiota communities between PCD and PCND patients using 16S rRNA gene sequencing. Our study found a significant reduction in α-diversity in the fecal microbiota of PCD patients, which suggests that the fecal microbiota of PCD patients has lower microbial richness and diversity.

To compare the different fecal microbial structures between groups, we calculated the UniFrac phylogenetic distances related to the microbe composition among subjects. NMDS analysis was used to distinguish the clustering of the PCD group from the PCND group, and distinct bacterial profiles were observed. The β-diversity index (structure) in the PCD group differed significantly from that in the PCND group,

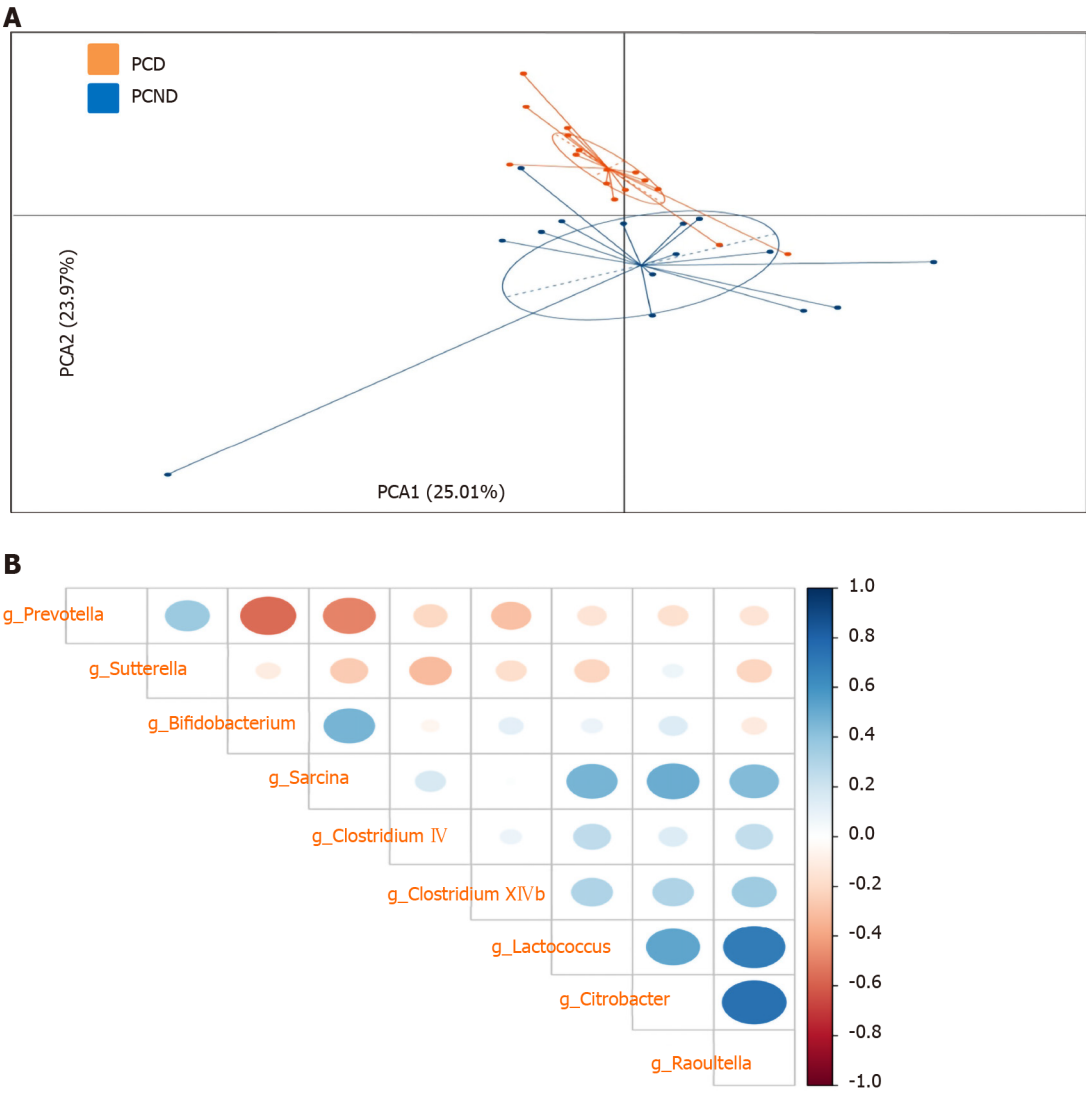


Figure 3 Principal component analyses and correlation plots of different microbial taxa in the post-cholecystectomy diarrhea and post-cholecystectomy non-diarrhea groups. A: Principal component analysis plot of different taxa in the post-cholecystectomy diarrhea and post-cholecystectomy non-diarrhea groups; B: Spearman's correlation plots of the relative abundances of the differentially abundant bacteria at the genus level. Statistical significance was determined for all pairwise comparisons. Positive values (blue circles) indicate positive correlations, and negative values (red circles) indicate negative correlations. The shade and size of each circle indicate the magnitude of the correlation (with darker shades indicating higher correlations). PCD: Post-cholecystectomy diarrhea; PCND: Post-cholecystectomy non-diarrhea.

indicating a significant difference in bacterial diversity between the PCD and PCND groups.

The ratio of Firmicutes/Bacteroidetes is an important parameter in evaluating the composition of the intestinal microbiota. The members of Bacteroidetes have been reported to be associated with immunity and metabolic processes[33], and the relative abundance of the phylum Bacteroidetes increased significantly in the PCD group, whereas that of Firmicutes was decreased, which is consistent with the gut microbiota associated with HIV infection[34,35]. In addition, cholecystectomy increases the abundance of Bacteroidetes, a contributor to colorectal cancer[2]. As the abundance of Bacteroidetes was significantly higher in the PCD group than in the PCND group, this increase in Bacteroidetes may be related to diarrhea. Consistent with previous research[2], our investigation showed that the fecal abundance of Bacteroides decreased in PC patients compared to HCs, Furthermore, our investigation indicated that the genus Bacteroides decreased in the PCD group compared with the PCND group, which is consistent with findings for antibiotic-associated diarrhea[36]. Our study also showed that the genus Sutterella was significantly higher in the PCD group than in the PCND group. Research has shown that the abundance of Sutterella in mice with antibiotic-induced diarrhea is significantly higher than in normal mice, indicating that Sutterella may promote diarrhea; after feeding the Chinese medicine Shenqibai to the

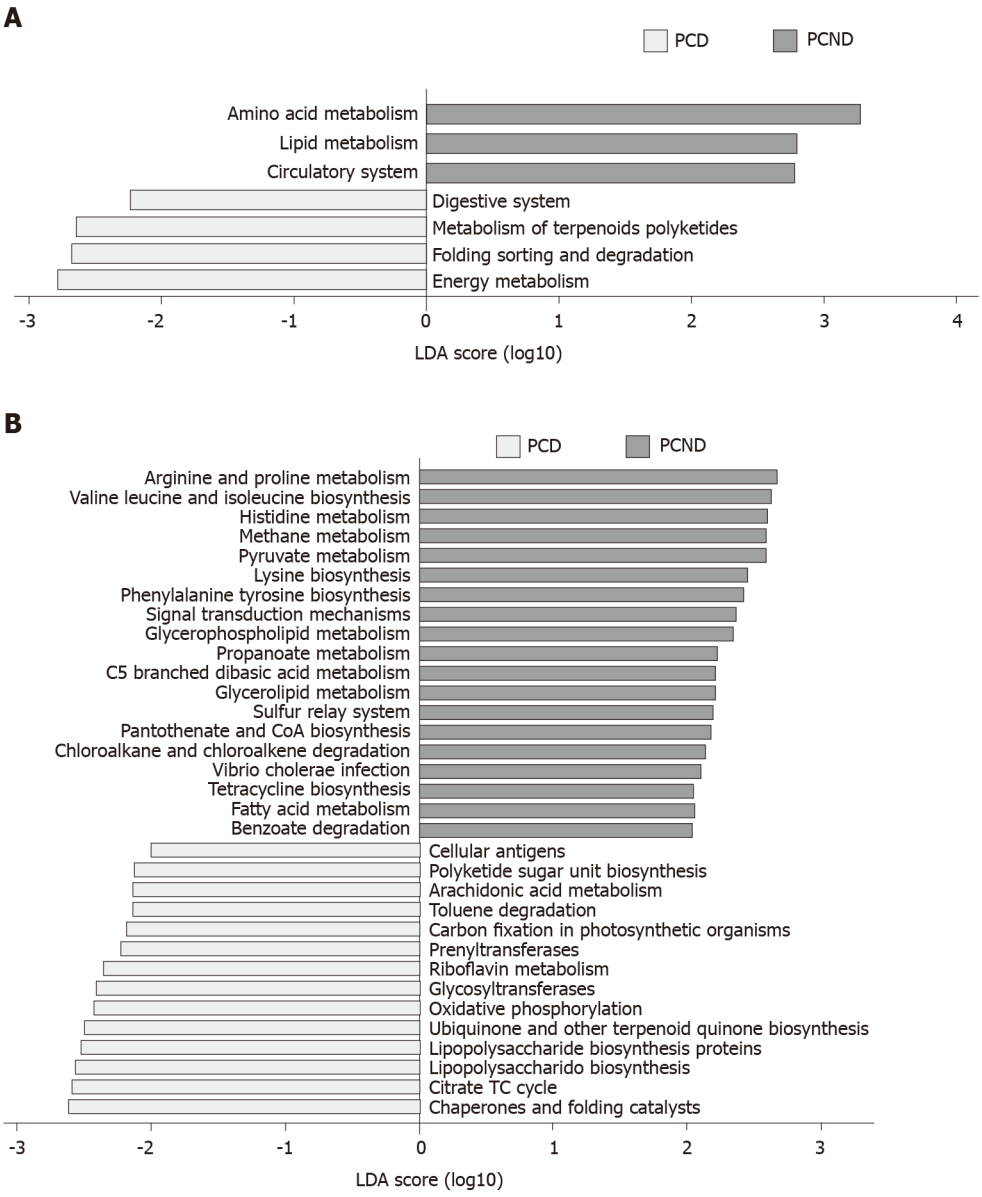


Figure 4 Kyoto Encyclopedia of Genes and Genomes functional categories of microbiota with differential abundance. A: Comparison between the post-cholecystectomy diarrhea-enriched and post-cholecystectomy non-diarrhea-enriched markers regarding the Kyoto Encyclopedia of Genes and Genomes level 2 functional categories; B: Comparison between the post-cholecystectomy diarrhea-enriched and post-cholecystectomy non-diarrhea-enriched markers regarding the Kyoto Encyclopedia of Genes and Genomes level 3 functional categories. PCD: Post-cholecystectomy diarrhea; PCND: Post-cholecystectomy non-diarrhea; LDA: Linear discriminant analysis.

mice, the structure of the flora was normalized, and the number of Sutterella in the mice decreased significantly[36].

Prevotella is a conditional pathogenic bacterial genus. Research has linked the increased abundance of Prevotella to localized and systemic disease, including periodontitis, bacterial vaginosis, rheumatoid arthritis, metabolic disorders, and low-grade systemic inflammation[37]. Our study showed a significant increase in the abundance of Prevotella in the PCD group compared to the PCND group. Therefore, Prevotella may also play a role in promoting diarrhea.

Our results suggested a negative correlation between Prevotella and Bifidobacterium, which may be an important cause of diarrhea. We found a higher abundance of Bifidobacterium in the PC group compared with the HC group, which is consistent with previous research[38]. This may reflect the physiological adjustments in the body following loss of the reservoir function of the gallbladder. However, Bifidobacterium was significantly less abundant in the PCD group than in the PCND group. Therefore, lack of Bifidobacterium may have an important effect in PCD. Bifidobacterium is a beneficial genus and is one of the main bacterial groups found on the surface of the normal intestinal mucosa. It is involved in the detachment of bile

acid, maintaining the composition of normal intestinal flora, and regulating the immune function of the intestinal mucosa[39-41]. Probiotics including Bifidobacterium have been used in the treatment of dysbacteriosis[42-45]. Bifidobacterium is very important in the balance of bacteria[46-48]. This study showed that Bifidobacterium was significantly reduced in patients with PCD, which provides a theoretical basis for the treatment of PCD using Bifidobacteria probiotics.

Our study also showed that the abundance of Lactococcus was higher in the PCND group than in the PCD group. Lactococcus is a genus in the family Lactobacillaceae and the order Lactobacillales, and it is a beneficial bacteria that can produce lactic acid by fermentation, promote intestinal peristalsis, and prevent constipation and diarrhea[49]. Therefore, we believe that the change in Lactococcus plays a role in the process of PCD.

Using a function analysis based on the KEGG database, we found that lipid metabolism pathways were markedly enriched in the PCND group compared to the PCD group. This may explain why the PCD patients who ate too much fat had frequent diarrhea.

CONCLUSION

In conclusion, we report gut dysbiosis in PCD patients, which is a result of differences in microbial structure, diversity, and abundance when compared to PCND patients. Decreased diversity and abundance of the microbial community in PC patients can cause diarrhea. Our study findings demonstrate the association between PCD and the gut microbiota, especially regarding Prevotella and Bifidobacterium. Thus, this study provides new insights into potential therapeutics that could target the microbiota to attenuate PCD.

ARTICLE HIGHLIGHTS

Research background

Post-cholecystectomy diarrhea (PCD) frequently occurs in patients following gallbladder removal. PCD is difficult to treat. After cholecystectomy, bile enters the duodenum directly, independent of the timing of meals. The interaction between the bile acids and the intestinal microbes is changed. Therefore, the occurrence of PCD may be related to the change in microbiota.

Research motivation

Little is known regarding the intestinal microbiota characteristics in PCD patients. High-throughput sequencing of the 16S rRNA gene can be used to characterize the composition and diversity of the complex intestinal microbial community.

Research objectives

To identify changes in the intestinal microbiota and to better understand the role of the intestinal microbiota in PCD patients.

Research methods

The diversity and profiles of the gut microbiota were analyzed by performing high-through put 16S rRNA gene sequencing. The gut microbiota in a healthy control (HC) group and a post-cholecystectomy (PC) group were characterized. Subsequently, the PC group was further divided into a PCD group and a post-cholecystectomy non-diarrhea group (PCND) according to the patients' clinical symptoms. The composition, diversity and richness of microbial communities were detected and compared.

Research results

The PC group had fewer OTUs than the HC group. β-diversity indicated a decreased microbial diversity in the PC group. Fifteen taxa with differential abundance between the HC and PC groups were identified. In the PCD group compared to the PCND group, significant decreases in microbial diversity, Firmicutes/Bacteroidetes ratio, and richness of probiotic microbiota (Bifidobacterium and Lactococcus), and an increase in detrimental microbiota (Prevotella and Sutterella) were observed. Moreover, a negative correlation was observed between Prevotella and Bifidobacterium. By

performing Kyoto Encyclopedia of Genes and Genomes functional analysis, we found that the abundances of gut microbiota involved in lipid metabolism pathways were markedly lower in the PCD group compared to the PCND group.

Research conclusions

These findings demonstrate the association between PCD and the gut microbiota. Gut dysbiosis in PCD patients is a result of differences in microbial structure, diversity, and abundance when compared to PCND patients. Decreased diversity and abundance of the microbial community in PC patients can cause diarrhea.

Research perspectives

This study demonstrated that gut dysbiosis may play a critical role in PCD, especially regarding Prevotella and Bifidobacterium. Thus, this study provides new insights into potential therapeutics that could target the microbiota to attenuate PCD.

REFERENCES

1 **Sender R**, Fuchs S, Milo R. Revised Estimates for the Number of Human and Bacteria Cells in the Body. *PLoS Biol* 2016; **14**: e1002533 [PMID: 27541692 DOI: 10.1371/journal.pbio.1002533]

2 **Keren N**, Konikoff FM, Paitan Y, Gabay G, Reshef L, Naftali T, Gophna U. Interactions between the intestinal microbiota and bile acids in gallstones patients. *Environ Microbiol Rep* 2015; **7**: 874-880 [PMID: 26149537 DOI: 10.1111/1758-2229.12319]

3 **Lamberts MP**, Lugtenberg M, Rovers MM, Roukema AJ, Drenth JP, Westert GP, van Laarhoven CJ. Persistent and de novo symptoms after cholecystectomy: a systematic review of cholecystectomy effectiveness. *Surg Endosc* 2013; **27**: 709-718 [PMID: 23052498 DOI: 10.1007/s00464-012-2516-9]

4 **Sciarretta G**, Furno A, Mazzoni M, Malaguti P. Post-cholecystectomy diarrhea: evidence of bile acid malabsorption assessed by SeHCAT test. *Am J Gastroenterol* 1992; **87**: 1852-1854 [PMID: 1449156]

5 **Caenepeel P**, Janssens J, Vantrappen G, Eyssen H, Coremans G. Interdigestive myoelectric complex in germ-free rats. *Dig Dis Sci* 1989; **34**: 1180-1184 [PMID: 2752868 DOI: 10.1007/bf01537265]

6 **Husebye E**, Hellström PM, Sundler F, Chen J, Midtvedt T. Influence of microbial species on small intestinal myoelectric activity and transit in germ-free rats. *Am J Physiol Gastrointest Liver Physiol* 2001; **280**: G368-G380 [PMID: 11171619 DOI: 10.1152/ajpgi.2001.280.3.G368]

7 **Lesniewska V**, Rowland I, Laerke HN, Grant G, Naughton PJ. Relationship between dietary-induced changes in intestinal commensal microflora and duodenojejunal myoelectric activity monitored by radiotelemetry in the rat in vivo. *Exp Physiol* 2006; **91**: 229-237 [PMID: 16263800 DOI: 10.1113/expphysiol.2005.031708]

8 **Arebi N**, Gurmany S, Bullas D, Hobson A, Stagg A, Kamm M. Review article: the psychoneuroimmunology of irritable bowel syndrome--an exploration of interactions between psychological, neurological and immunological observations. *Aliment Pharmacol Ther* 2008; **28**: 830-840 [PMID: 18637004 DOI: 10.1111/j.1365-2036.2008.03801.x]

9 **Ringel Y**, Carroll IM. Alterations in the intestinal microbiota and functional bowel symptoms. *Gastrointest Endosc Clin N Am* 2009; **19**: 141-150 [PMID: 19232285 DOI: 10.1016/j.giec.2008.12.004]

10 **Palm NW**, de Zoete MR, Flavell RA. Immune-microbiota interactions in health and disease. *Clin Immunol* 2015; **159**: 122-127 [PMID: 26141651 DOI: 10.1016/j.clim.2015.05.014]

11 **Sonnenburg JL**, Bäckhed F. Diet-microbiota interactions as moderators of human metabolism. *Nature* 2016; **535**: 56-64 [PMID: 27383980 DOI: 10.1038/nature18846]

12 **Song H**, Yoo Y, Hwang J, Na YC, Kim HS. Faecalibacterium prausnitzii subspecies-level dysbiosis in the human gut microbiome underlying atopic dermatitis. *J Allergy Clin Immunol* 2016; **137**: 852-860 [PMID: 26431583 DOI: 10.1016/j.jaci.2015.08.021]

13 **Liu B**, Zhang Y, Wang R, An Y, Gao W, Bai L, Li Y, Zhao S, Fan J, Liu E. Western diet feeding influences gut microbiota profiles in apoE knockout mice. *Lipids Health Dis* 2018; **17**: 159 [PMID: 30021609 DOI: 10.1186/s12944-018-0811-8]

14 **Tanemoto S**, Sujino T, Kanai T. [Intestinal immune response is regulated by gut microbe]. *Nihon Rinsho Meneki Gakkai Kaishi* 2017; **40**: 408-415 [PMID: 29367525 DOI: 10.2177/jsci.40.408]

15 **Khanna S**. Microbiota Replacement Therapies: Innovation in Gastrointestinal Care. *Clin Pharmacol Ther* 2018; **103**: 102-111 [PMID: 29071710 DOI: 10.1002/cpt.923]

16 **Gallardo P**, Izquierdo M, Vidal RM, Chamorro-Veloso N, Rosselló-Móra R, O'Ryan M, Farfán MJ. Distinctive Gut Microbiota Is Associated with Diarrheagenic *Escherichia coli* Infections in Chilean Children. *Front Cell Infect Microbiol* 2017; **7**: 424 [PMID: 29075617 DOI: 10.3389/fcimb.2017.00424]

17 **Parfenov AI**, Krums LM, Lychkova AE, Poleva NI. [Cholagenic diarrhea]. *Ter Arkh* 2008; **80**: 33-38 [PMID: 18372593]

18 **Müllhaupt B**. [Diarrhea]. *Praxis (Bern 1994)* 2002; **91**: 1749-1756 [PMID: 12426943 DOI: 10.1024/0369-8394.91.42.1749]

19 **Bajor J**, Beró T. [Diarrhea, from the gastroenterologist's point of view]. *Orv Hetil* 2009; **150**: 1655-

1661 [PMID: 19692310 DOI: 10.1556/OH.2009.28709]
20 **Yueh TP**, Chen FY, Lin TE, Chuang MT. Diarrhea after laparoscopic cholecystectomy: associated factors and predictors. *Asian J Surg* 2014; **37**: 171-177 [PMID: 24647139 DOI: 10.1016/j.asjsur.2014.01.008]
21 **Fisher M**, Spilias DC, Tong LK. Diarrhoea after laparoscopic cholecystectomy: incidence and main determinants. *ANZ J Surg* 2008; **78**: 482-486 [PMID: 18522570 DOI: 10.1111/j.1445-2197.2008.04539.x]
22 **Middelfart HV**, Kristensen JU, Laursen CN, Qvist N, Højgaard L, Funch-Jensen P, Kehlet H. Pain and dyspepsia after elective and acute cholecystectomy. *Scand J Gastroenterol* 1998; **33**: 10-14 [PMID: 9489901 DOI: 10.1080/00365529850166130]
23 **Lublin M**, Crawford DL, Hiatt JR, Phillips EH. Symptoms before and after laparoscopic cholecystectomy for gallstones. *Am Surg* 2004; **70**: 863-866 [PMID: 15529838]
24 **Weinert CR**, Arnett D, Jacobs D Jr, Kane RL. Relationship between persistence of abdominal symptoms and successful outcome after cholecystectomy. *Arch Intern Med* 2000; **160**: 989-995 [PMID: 10761964 DOI: 10.1001/archinte.160.7.989]
25 **Niranjan B**, Chumber S, Kriplani AK. Symptomatic outcome after laparoscopic cholecystectomy. *Trop Gastroenterol* 2000; **21**: 144-148 [PMID: 11084841]
26 **Masella AP**, Bartram AK, Truszkowski JM, Brown DG, Neufeld JD. PANDAseq: paired-end assembler for illumina sequences. *BMC Bioinformatics* 2012; **13**: 31 [PMID: 22333067 DOI: 10.1186/1471-2105-13-31]
27 **Edgar RC**. UPARSE: highly accurate OTU sequences from microbial amplicon reads. *Nat Methods* 2013; **10**: 996-998 [PMID: 23955772 DOI: 10.1038/nmeth.2604]
28 **Cole JR**, Wang Q, Fish JA, Chai B, McGarrell DM, Sun Y, Brown CT, Porras-Alfaro A, Kuske CR, Tiedje JM. Ribosomal Database Project: data and tools for high throughput rRNA analysis. *Nucleic Acids Res* 2014; **42**: D633-D642 [PMID: 24288368 DOI: 10.1093/nar/gkt1244]
29 **Wang Q**, Garrity GM, Tiedje JM, Cole JR. Naive Bayesian classifier for rapid assignment of rRNA sequences into the new bacterial taxonomy. *Appl Environ Microbiol* 2007; **73**: 5261-5267 [PMID: 17586664 DOI: 10.1128/AEM.00062-07]
30 **Coccolini F**, Catena F, Pisano M, Gheza F, Fagiuoli S, Di Saverio S, Leandro G, Montori G, Ceresoli M, Corbella D, Sartelli M, Sugrue M, Ansaloni L. Open versus laparoscopic cholecystectomy in acute cholecystitis. Systematic review and meta-analysis. *Int J Surg* 2015; **18**: 196-204 [PMID: 25958296 DOI: 10.1016/j.ijsu.2015.04.083]
31 **Fort JM**, Azpiroz F, Casellas F, Andreu J, Malagelada JR. Bowel habit after cholecystectomy: physiological changes and clinical implications. *Gastroenterology* 1996; **111**: 617-622 [PMID: 8780565 DOI: 10.1053/gast.1996.v111.pm8780565]
32 **Sauter GH**, Moussavian AC, Meyer G, Steitz HO, Parhofer KG, Jüngst D. Bowel habits and bile acid malabsorption in the months after cholecystectomy. *Am J Gastroenterol* 2002; **97**: 1732-1735 [PMID: 12135027 DOI: 10.1111/j.1572-0241.2002.05779.x]
33 **Lv LX**, Fang DQ, Shi D, Chen DY, Yan R, Zhu YX, Chen YF, Shao L, Guo FF, Wu WR, Li A, Shi HY, Jiang XW, Jiang HY, Xiao YH, Zheng SS, Li LJ. Alterations and correlations of the gut microbiome, metabolism and immunity in patients with primary biliary cirrhosis. *Environ Microbiol* 2016; **18**: 2272-2286 [PMID: 27243236 DOI: 10.1111/1462-2920.13401]
34 **McHardy IH**, Li X, Tong M, Ruegger P, Jacobs J, Borneman J, Anton P, Braun J. HIV Infection is associated with compositional and functional shifts in the rectal mucosal microbiota. *Microbiome* 2013; **1**: 26 [PMID: 24451087 DOI: 10.1186/2049-2618-1-26]
35 **Yu G**, Fadrosh D, Ma B, Ravel J, Goedert JJ. Anal microbiota profiles in HIV-positive and HIV-negative MSM. *AIDS* 2014; **28**: 753-760 [PMID: 24335481 DOI: 10.1097/QAD.0000000000000154]
36 **Lv W**, Liu C, Ye C, Sun J, Tan X, Zhang C, Qu Q, Shi D, Guo S. Structural modulation of gut microbiota during alleviation of antibiotic-associated diarrhea with herbal formula. *Int J Biol Macromol* 2017; **105**: 1622-1629 [PMID: 28219687 DOI: 10.1016/j.ijbiomac.2017.02.060]
37 **Larsen JM**. The immune response to Prevotella bacteria in chronic inflammatory disease. *Immunology* 2017; **151**: 363-374 [PMID: 28542929 DOI: 10.1111/imm.12760]
38 **Wang W**, Wang J, Li J, Yan P, Jin Y, Zhang R, Yue W, Guo Q, Geng J. Cholecystectomy Damages Aging-Associated Intestinal Microbiota Construction. *Front Microbiol* 2018; **9**: 1402 [PMID: 29988510 DOI: 10.3389/fmicb.2018.01402]
39 **Ramery E**, Papakonstantinou S, Pinilla M, McAllister H, Jahns H, Gallagher B, O'Brien PJ. Bacterial cholangiohepatitis in a dog. *Can Vet J* 2012; **53**: 423-425 [PMID: 23024392]
40 **Isolauri E**. Probiotics in human disease. *Am J Clin Nutr* 2001; **73**: 1142S-1146S [PMID: 11393192 DOI: 10.1093/ajcn/73.6.1142S]
41 **Inagaki T**, Choi M, Moschetta A, Peng L, Cummins CL, McDonald JG, Luo G, Jones SA, Goodwin B, Richardson JA, Gerard RD, Repa JJ, Mangelsdorf DJ, Kliewer SA. Fibroblast growth factor 15 functions as an enterohepatic signal to regulate bile acid homeostasis. *Cell Metab* 2005; **2**: 217-225 [PMID: 16213224 DOI: 10.1016/j.cmet.2005.09.001]
42 **Schoster A**, Kokotovic B, Permin A, Pedersen PD, Dal Bello F, Guardabassi L. In vitro inhibition of Clostridium difficile and Clostridium perfringens by commercial probiotic strains. *Anaerobe* 2013; **20**: 36-41 [PMID: 23471038 DOI: 10.1016/j.anaerobe.2013.02.006]
43 **Saint-Cyr MJ**, Haddad N, Taminiau B, Poezevara T, Quesne S, Amelot M, Daube G, Chemaly M, Dousset X, Guyard-Nicodème M. Use of the potential probiotic strain Lactobacillus salivarius SMXD51 to control Campylobacter jejuni in broilers. *Int J Food Microbiol* 2017; **247**: 9-17 [PMID:

27432696 DOI: 10.1016/j.ijfoodmicro.2016.07.003]
44 **Carter A**, Adams M, La Ragione RM, Woodward MJ. Colonisation of poultry by Salmonella Enteritidis S1400 is reduced by combined administration of Lactobacillus salivarius 59 and Enterococcus faecium PXN-33. *Vet Microbiol* 2017; **199**: 100-107 [PMID: 28110775 DOI: 10.1016/j.vetmic.2016.12.029]
45 **Chingwaru W**, Vidmar J. Potential of Zimbabwean commercial probiotic products and strains of Lactobacillus plantarum as prophylaxis and therapy against diarrhoea caused by Escherichia coli in children. *Asian Pac J Trop Med* 2017; **10**: 57-63 [PMID: 28107866 DOI: 10.1016/j.apjtm.2016.12.009]
46 **Hussain SA**, Patil GR, Reddi S, Yadav V, Pothuraju R, Singh RRB, Kapila S. Aloe vera (Aloe barbadensis Miller) supplemented probiotic lassi prevents Shigella infiltration from epithelial barrier into systemic blood flow in mice model. *Microb Pathog* 2017; **102**: 143-147 [PMID: 27914960 DOI: 10.1016/j.micpath.2016.11.023]
47 **Schachtsiek M**, Hammes WP, Hertel C. Characterization of Lactobacillus coryniformis DSM 20001T surface protein Cpf mediating coaggregation with and aggregation among pathogens. *Appl Environ Microbiol* 2004; **70**: 7078-7085 [PMID: 15574903 DOI: 10.1128/AEM.70.12.7078-7085.2004]
48 **Markowiak P**, Śliżewska K. Effects of Probiotics, Prebiotics, and Synbiotics on Human Health. *Nutrients* 2017; **9** [PMID: 28914794 DOI: 10.3390/nu9091021]
49 **Hayes SR**, Vargas AJ. Probiotics for the Prevention of Pediatric Antibiotic-Associated Diarrhea. *Explore (NY)* 2016; **12**: 463-466 [PMID: 27688016 DOI: 10.1016/j.explore.2016.08.015]

World Journal of Gastroenterology

Submit a Manuscript: https://www.f6publishing.com

World J Gastroenterol 2021 February 7; 27(5): 404-415

DOI: 10.3748/wjg.v27.i5.404

ISSN 1007-9327 (print) ISSN 2219-2840 (online)

ORIGINAL ARTICLE

Retrospective Study

Histopathology and the predominantly progressive, indeterminate and predominately regressive score in hepatitis C virus patients after direct-acting antivirals therapy

Rui Huang, Hui-Ying Rao, Ming Yang, Ying-Hui Gao, Jian Wang, Qian Jin, Dan-Li Ma, Lai Wei

ORCID number: Rui Huang 0000-0001-5561-8746; Hui-Ying Rao 0000-0003-2431-3872; Ming Yang 0000-0001-5765-3844; Ying-Hui Gao 0000-0003-4532-3412; Jian Wang 0000-0002-9578-8288; Qian Jin 0000-0002-5213-8680; Dan-Li Ma 0000-0001-9614-6343; Lai Wei 0000-0003-2326-1257.

Author contributions: Huang R, Rao HY and Wei L designed the protocol of this study; Huang R, Rao HY, Yang M, Gao YH, Wang J, Jian Q and Ma DL collected the data; Huang R and Rao HY analyzed and interpreted the patient data and were major contributors in writing the manuscript; all authors read and approved the final manuscript.

Supported by The National Natural Science Foundation of China, No. 81870406; the Beijing Natural Science Foundation, No. 7182174; and the China National Science and Technology Major Project for Infectious Diseases Control during the 13th Five-Year Plan Period, No. 2017ZX10202202.

Institutional review board statement: The study was reviewed and approved by the Institutional Review Board of Peking University People's

Rui Huang, Hui-Ying Rao, Ying-Hui Gao, Jian Wang, Qian Jin, Dan-Li Ma, Peking University Hepatology Institute, Beijing Key Laboratory of Hepatitis C and Immunotherapy for Liver Diseases, Beijing International Cooperation Base for Science and Technology on NAFLD Diagnosis, Peking University People's Hospital, Beijing 100044, China

Ming Yang, Lai Wei, Hepatopancreatobiliary Center, Beijing Tsinghua Changgung Hospital, Tsinghua University, Beijing 102218, China

Corresponding author: Hui-Ying Rao, MD, Chief Doctor, Professor, Peking University Hepatology Institute, Beijing Key Laboratory of Hepatitis C and Immunotherapy for Liver Diseases, Beijing International Cooperation Base for Science and Technology on NAFLD Diagnosis, Peking University People's Hospital, No. 11 Xizhimen South Street, Xicheng District, Beijing 100044, China. raohuiying@pkuph.edu.cn

Abstract

BACKGROUND

Histological changes after direct-acting antivirals (DAAs) therapy in hepatitis C virus (HCV) patients has not been elucidated. Whether the predominantly progressive, indeterminate and predominately regressive (P-I-R) score, evaluating fibrosis activity in hepatitis B virus patients has predictive value in HCV patients has not been investigated.

AIM

To identify histological changes after DAAs therapy and to evaluate the predictive value of the P-I-R score in HCV patients.

METHODS

Chronic HCV patients with paired liver biopsy specimens before and after DAAs treatment were included. Sustained virologic response (SVR) was defined as an undetectable serum HCV RNA level at 24 wk after treatment cessation. The Ishak system and P-I-R score were assessed. Inflammation improvement and fibrosis regression were defined as a ≥ 2-points decrease in the histology activity index (HAI) score and a ≥ 1-point decrease in the Ishak fibrosis score, respectively. Fibrosis progression was defined as a ≥ 1-point increase in the Ishak fibrosis score. Histologic improvement was defined as a ≥ 2-points decrease in the HAI score

Hospital (2019PHB036-01) and informed consent was waived.

Informed consent statement: Patients were not required to give informed consent for this study as the analysis used anonymous clinical data. The Institutional Review Board of Peking University People's Hospital approved waiving informed consent.

Conflict-of-interest statement: Dr. Rao reports grants from National Natural Science Foundation of China (NSFC) (81870406), grants from Beijing Natural Science Foundation (7182174), grants from China National Science and Technology Major Project for Infectious Diseases Control during the 13th Five-Year Plan Period (2017ZX10202202), during the conduct of the study.

Data sharing statement: No additional data are available.

Open-Access: This article is an open-access article which was selected by an in-house editor and fully peer-reviewed by external reviewers. It is distributed in accordance with the Creative Commons Attribution Non Commercial (CC BY-NC 4.0) license, which permits others to distribute, remix, adapt, build upon this work non-commercially, and license their derivative works on different terms, provided the original work is properly cited and the use is non-commercial. See: http://creativecommons.org/licenses/by-nc/4.0/

Manuscript source: Unsolicited manuscript

Specialty type: Gastroenterology and hepatology

Country/Territory of origin: China

Peer-review report's scientific quality classification

Grade A (Excellent): 0
Grade B (Very good): B
Grade C (Good): C
Grade D (Fair): 0
Grade E (Poor): 0

Received: October 28, 2020

without worsening of the Ishak fibrosis score after DAAs therapy. The P-I-R score was also assessed. "absolutely reversing or advancing" was defined as the same directionality implied by both change in the Ishak score and posttreatment P-I-R score; and "probably reversing or advancing" was defined as only one parameter showing directionality.

RESULTS

Thirty-eight chronic HCV patients with paired liver biopsy specimens before and after DAAs treatment were included. The mean age of these patients was 40.9 ± 14.6 years and there were 53% (20/38) males. Thirty-four percent (13/38) of patients were cirrhotic. Eighty-two percent (31/38) of patients achieved inflammation improvement. The median HAI score decreased significantly after SVR (pretreatment 7.0 *vs* posttreatment 2.0, Z = -5.146, P = 0.000). Thirty-seven percent (14/38) of patients achieved fibrosis improvement. The median Ishak score decreased significantly after SVR (pretreatment 4.0 *vs* posttreatment 3.0, Z = -2.354, P = 0.019). Eighty-two percent (31/38) of patients showed histological improvement. The P-I-R score was evaluated in 61% (23/38) of patients. The progressive group showed lower platelet (P = 0.024) and higher HAI scores (P = 0.070) before treatment. In patients with stable Ishak stage after treatment: Progressive injury was seen in 22% (4/18) of patients, 33% (6/18) were classified as indeterminate and regressive changes were seen in 44% (8/18) of patients who were judged as probably reversing by the Ishak and P-I-R systems.

CONCLUSION

Significant improvement of necroinflammation and partial remission of fibrosis in HCV patients occurred shortly after DAAs therapy. The P-I-R score has potential in predicting fibrosis in HCV patients.

Key Words: Hepatitis C virus; Direct-acting antiviral agents; Necroinflammation; Fibrosis; Predominantly progressive, indeterminate and predominately regressive score; Histopathology

©The Author(s) 2021. Published by Baishideng Publishing Group Inc. All rights reserved.

Core Tip: In this retrospective analysis of paired liver biopsy specimens from hepatitis C virus (HCV) patients who achieved sustained virologic response after direct-acting antivirals (DAAs) therapy, clinical and histologic features including the Ishak system and predominantly progressive, indeterminate and predominately regressive (P-I-R) scores were analyzed. Significant improvement of necroinflammation and partial remission of fibrosis in HCV patients occurred shortly after DAAs therapy. The P-I-R score has potential in predicting fibrosis in HCV patients.

Citation: Huang R, Rao HY, Yang M, Gao YH, Wang J, Jin Q, Ma DL, Wei L. Histopathology and the predominantly progressive, indeterminate and predominately regressive score in hepatitis C virus patients after direct-acting antivirals therapy. *World J Gastroenterol* 2021; 27(5): 404-415
URL: https://www.wjgnet.com/1007-9327/full/v27/i5/404.htm
DOI: https://dx.doi.org/10.3748/wjg.v27.i5.404

INTRODUCTION

Direct-acting antivirals (DAAs) have resulted in extraordinary progress in the treatment of hepatitis C virus (HCV) infection. The potential for liver fibrosis of HCV patients to regress following successful treatment has been acknowledged for many years, particularly after eradication of HCV in most patients[1,2]. However, due to the low rate of sustained virologic response (SVR) following the interferon-ribavirin (PR) regimen, and limited indications to perform a liver biopsy after virus eradication, liver biopsy findings after successful HCV eradication have not been elucidated. Previous

Peer-review started: October 28, 2020
First decision: December 3, 2020
Revised: December 14, 2020
Accepted: December 26, 2020
Article in press: December 26, 2020
Published online: February 7, 2021

P-Reviewer: Trifan A
S-Editor: Chen XF
L-Editor: Webster JR
P-Editor: Ma YJ

studies indicated the benefit of HCV eradication by PR therapy[3,4]. As DAAs have only been used in clinical practice for several years, histopathological improvement after successful DAAs therapy has only been described in a few studies and these findings were unclear[5].

Recently, a new classification, consisting of three categories of fibrosis quality: the predominantly progressive, indeterminate and predominately regressive (P-I-R) score was used to evaluate the quality of fibrosis activity based on the balance between progressive and regressive liver disease in patients with hepatitis B virus (HBV) infection, which was called the Beijing classification[6-8]. This classification was predictive of histological outcomes by uniquely incorporating histopathologic features of regressive *vs* progressive fibrosis, *i.e.*, the quality of fibrosis, not only its extent and it performed well in HBV patients[6]. However, whether the Beijing classification has predictive value in HCV patients, especially after SVR, has not been investigated.

We performed this retrospective analysis of paired liver biopsy specimens of HCV patients achieving SVR after DAAs therapy. Paired liver biopsies before and after SVR with clinical and histologic features including the Ishak system and P-I-R scores were measured and analyzed.

MATERIALS AND METHODS

Study population

Chronic HCV patients with paired liver biopsy specimens before and after successful treatment with DAAs in our hospital were included in this study between January 2015 and December 2016. SVR was defined as undetectable serum HCV RNA at 24 wk after the end of treatment (EOT). Patients with other chronic liver disease (*e.g.*, hepatitis B, hemochromatosis *etc.*), unqualified liver samples or incomplete clinical or laboratory data were excluded. We collected all the patients' sociodemographic, clinical and histological information from medical records in our hospital.

Histological evaluation

All available formalin-fixed, paraffin-embedded pretreatment and posttreatment liver biopsy specimens from patients were collected. Pretreatment was defined as 6 mo before DAAs therapy and posttreatment was defined as any time after EOT. The biopsy specimens were then reviewed by two independent experienced hepatopathologists, masked to the clinical information of these patients.

Necroinflammation activity and fibrosis stage were assessed by the Ishak modified histology activity index (HAI) grading and Ishak staging system, respectively[9]. Cirrhosis was defined as an Ishak fibrosis score ≥ 5. Inflammation improvement and fibrosis regression were defined as ≥ a 2-points decrease in the HAI score and a ≥ 1-point decrease in the Ishak fibrosis score, respectively. Fibrosis progression was defined as a ≥ 1-point increase in the Ishak fibrosis score. Histologic improvement was defined as a ≥ 2-points decrease in the HAI score without worsening of the Ishak fibrosis score after DAAs therapy.

The Beijing classification was also assessed, which was applied for liver biopsy specimens with at least focal fibrous septa formation or higher stages of scarring (Ishak staging ≥ F3). The classification consisted of three categories of fibrosis quality: Predominantly progressive, indeterminate and predominately regressive[6]. "Absolutely reversing or advancing" was defined as the same directionality implied by both change in Ishak score and posttreatment P-I-R score; and "probably reversing or advancing" was defined as only one parameter showing directionality.

Statistical analysis

Descriptive statistics were used in the analysis of patients' sociodemographic characteristics, clinical information, histological information and P-I-R scores. Categorical variables (gender, HCV genotype, treatment group, HAI and Ishak score) were measured as percentages while continuous variables were expressed as mean ± SD (age, albumin, platelet and HCV RNA) or median (interquartile range) [alanine aminotransferase (ALT), total bilirubin (TB), international normalized ratio (INR) and liver stiffness measurement (LSM)] as appropriate. Pretreatment and posttreatment HAI grading and Ishak staging were compared using the Wilcoxon sign rank test. One-Way ANOVA (age, albumin, platelet and HCV RNA) and Kruskal-Wallis H test (ALT, TB, INR and LSM) were used to compare continuous variables and the Mantel-Haenszel chi-square test (gender, HAI and Ishak score) was used to compare categorical variables by groups of pretreatment or posttreatment P-I-R score,

respectively. All statistical tests were considered significant at a *P* level less than 0.05. Statistical analysis was performed using SPSS 25.0 (SPSS Inc.; Chicago, IL, United States).

RESULTS

We identified 40 patients with paired liver biopsy specimens and 95% (38/40) of them were included in the analysis with available paired clinical and histological data before and after treatment. Pretreatment biopsy specimens were obtained an average of 3 mo before DAAs therapy (range: 1-6 mo) and posttreatment biopsy specimens were obtained an average of 6 mo after EOT (range: 5-7 mo).

Patient demographics, clinical and laboratory characteristics

The mean age of the patients was 40.9 ± 14.6 years. Fifty-three percent (20/38) of patients were male. Of these, the pretreatment HAI score was judged to be ≥ 10 in 29% (11/38) of patients. Thirty-four percent (13/38) of patients were cirrhotic (Ishak ≥ 5) (Table 1).

Necroinflammation grading

Eighty-two percent (31/38) of patients achieved improvement of HAI ≥ 2. The proportion with mild or no necroinflammation (HAI range: 0-3) increased from pretreatment 16% (6/38) to posttreatment 68% (26/38). The median HAI score decreased significantly after SVR (pretreatment 7.0 *vs* posttreatment 2.0, Z = -5.146, P = 0.000).

Compared to the proportion of pretreatment specimens, the proportion of absent or minimal/focal necroinflammation in individual components of the HAI score significantly decreased after SVR (periportal or periseptal interface hepatitis: 45% and 84%; confluent necrosis: 71% and 95%; focal lytic necrosis: 18% and 76%; portal inflammation: 21% and 68%). The proportion of patients with grade 3 or greater periportal hepatitis decreased from 37% (14/38) before SVR to 5% (2/38) after SVR (Figure 1A). The proportion of patients with grade 3 or greater confluent necrosis decreased from 29% (11/38) to 5% (2/38) after SVR (Figure 1B). Respectively, 71% (27/38) and 26% (10/38) of patients had a decrease or no change in focal lytic necrosis and focal inflammation score before and after SVR (Figure 1C). Eighty-two percent (31/38) of patients had decreased portal inflammation scores after SVR; and 47% (18/38) of patients had a decrease of 2-points or greater. The proportion of patients with grade 3 or greater portal inflammation decreased from 63% (24/38) to 11% (4/38) after SVR (Figure 1D). The median necroinflammation scores decreased significantly after SVR (periportal hepatitis: Pretreatment 2.0 *vs* posttreatment 0.0, Z = -4.620, P = 0.000; confluent necrosis: pretreatment 0.0 *vs* posttreatment 0.0, Z = -2.767, P = 0.006; focal lytic necrosis: pretreatment 2.0 *vs* posttreatment 1.0, Z = -4.670, P = 0.000; portal inflammation: pretreatment 3.0 *vs* posttreatment 1.0, Z = -4.826, P = 0.000).

Ishak staging

Thirty-seven percent (14/38) of patients achieved fibrosis improvement and fibrosis stage in 61% (23/38) patients did not change. Overall, regression of liver fibrosis was documented in 34% (13/38) of patients, including one patient who regressed from F5 to F4. Five percent (2/38) of patients had progression of fibrosis: One progressed from F0 to F3, and the other from F5 to F6. The median Ishak score decreased significantly after SVR (pretreatment 4.0 *vs* posttreatment 3.0, Z = -2.354, P = 0.019).

Histological improvement as shown by the Ishak system

Eighty-two percent (31/38) of patients reached the criterion of histological improvement. Specifically, 100% (3/3), 75% (3/4), 80% (4/5) and 92% (11/12) of patients achieved histological improvement in those with a pretreatment Ishak fibrosis score of 1, 2, 3 and 4, respectively, as did 77% (10/13) of cirrhotic patients.

P-I-R classification of liver fibrosis quality

The P-I-R classification was used to evaluate 23 paired liver biopsies of patients with a pretreatment Ishak score ≥ 3. The progressive group showed lower platelet (P = 0.024) and higher HAI scores (P = 0.070), followed, in turn, by the indeterminate and regressive groups before treatment. Although patients in the regressive group were younger and had less severe necroinflammation than those in the progressive and

Table 1 Clinical and histological characteristic of hepatitis C virus patients before treatment (*n* = 38)

Parameters	
Age (yr)	40.9 ± 14.6
Males, *n* (%)	20 (53)
ALT (U/L)	54 (30)
TBil (μmol/L)	11.5 (6.7)
Albumin (g/L)	45.7 ± 3.5
Platelets (× 10^3 μL)	173.6 ± 63.6
INR	1.00 (0.10)
HCV RNA (log IU/L)	6.24 ± 0.79
LSM, kPa	6.6 (3.6)
HCV genotype	
1	23 (60)
2	3 (8)
3	12 (32)
Treatment, *n* (%)	
SOF + RBV	17 (45)
DCV + ASV	14 (37)
GZR + EBR	7 (18)
HAI score, *n* (%)	
0-3	6 (16)
4-6	12 (32)
7-9	9 (24)
≥ 10	11 (29)
Ishak score, *n* (%)	
F0-2	8 (21)
F3-4	17 (45)
F5-6	13 (34)

ALT: Alanine aminotransferase; TBil: Total bilirubin; INR: International normalized ratio; HCV: Hepatitis C virus; LSM: Liver stiffness measurement; SOF + RBV: Sofosbuvir + ribavirin; DCV + ASV: Daclatasvir + asunaprevir; GZR + EBR: Grazoprevir + elbasvir; HAI: Histology activity index.

indeterminate groups, the differences were not significant after treatment (Table 2).

Posttreatment P-I-R fibrosis quality vs changes in Ishak fibrosis stage between pretreatment and posttreatment

A comparison of posttreatment P-I-R fibrosis quality with changes in Ishak fibrosis stage between pretreatment and posttreatment is shown in Table 3. In 4 of 23 (17%) patients whose Ishak score decreased by 1 stage, none showed progressive injury after treatment, with 25% (1/4) and 75% (3/4) showing regressive and indeterminate, respectively. In those with stable Ishak stages, progressive injury after treatment was seen in 22% (4/18) of patients, 33% (6/18) were classified as indeterminate and regressive changes were seen in 44% (8/18) of patients who were judged as probably reversing by the Ishak and P-I-R systems. Only one patient with an increased Ishak stage in the posttreatment biopsy also showed progressive changes.

Eight "probably reversing" cases are shown in Table 4. Fibrosis staging of these patients was stable after SVR. Histology of two "probably reversing" cases before and after SVR with DAAs is shown in Figure 2.

Table 2 Clinical and pathological parameters of hepatitis C virus patients by pretreatment and posttreatment predominantly progressive, indeterminate and predominately regressive score (*n* = 23)

Parameters	Progressive	Indeterminate	Regressive	*P* value
Pretreatment, *n* (%)	15 (65)	7 (30)	1 (4)	
Age (yr)	50.3 ± 12.3	43.9 ± 12.5	27.0	0.154
Males, *n* (%)	6 (40)	3 (43)	0 (0)	0.709
ALT (U/L)	66 (57)	48 (38)	50 (0)	0.469
TBil (μmol/L)	14.0 (8.0)	12.0 (6.0)	9.0 (0.0)	0.642
Albumin (g/L)	44.0 ± 3.9	47.0 ± 3.1	45.0	0.233
Platelets (× 10^3 μL)	129.3 ± 60.2	188.0 ± 51.5	268.0	0.024
INR	1.04 (0.16)	1.00 (0.2)	1.00 (0.00)	0.307
HCV RNA (log IU/L)	6.01 ± 0.66	6.46 ± 0.90	6.60	0.375
LSM, kPa	8.8 (14.8)	6.6 (2.9)	6.6 (0.0)	0.331
HAI score, *n* (%)				0.070
0-3	0 (1)	1 (14)	0 (0)	
4-6	1 (7)	2 (29)	1 (100)	
7-9	4 (27)	3 (43)	0 (0)	
≥ 10	10 (67)	1 (14)	0 (0)	
Ishak score, *n* (%)				0.072
3-4	4 (27)	5 (71)	1 (100)	
5-6	11 (73)	2 (29)	0 (0)	
Posttreatment, *n* (%)	5 (22)	9 (39)	9 (39)	
Age (yr)	50.4 ± 12.0	47.8±14.1	45.4 ± 13.4	0.802
Males, *n* (%)	1 (20)	3 (33)	5 (56)	0.384
ALT (U/L)	25 (21)	17 (8)	15 (15.5)	0.340
TBil (μmol/L)	19 (10)	10 (6)	14 (9)	0.149
Albumin (g/L)	44.0 ± 4.2	44.9 ± 1.9	46.0 ± 1.8	0.353
Platelets (× 10^3 μL)	156.4 ± 63.3	184.4 ± 80.3	151.1 ± 65.8	0.552
INR	1.13 (0.15)	1.00 (0.14)	1.09 (0.15)	0.052
LSM, kPa	11.5 (22.8)	7.8 (7.4)	6.8 (5.2)	0.683
HAI score, *n* (%)				0.338
0-3	1 (20)	4 (44)	6 (67)	
4-6	2 (40)	4 (44)	3 (33)	
7-9	1 (20)	0 (0)	0 (0)	
≥ 10	1 (20)	1 (11)	0 (0)	
Ishak score, *n* (%)				0.339
3-4	2 (40)	6 (67)	6 (67)	
5-6	3 (60)	3 (33)	3 (33)	

ALT: Alanine aminotransferase; TBil: Total bilirubin; INR: International normalized ratio; HCV: Hepatitis C virus; LSM: Liver stiffness measurement; HAI: Histology activity index.

DISCUSSION

Our study of 38 paired liver biopsy specimens from HCV patients showed the histological changes after successful antiviral therapy with DAAs. Significant improvement of necroinflammation was achieved and fibrosis staging improved or did not worsen in most patients. Eighty-two percent of patients reached the criterion of histological improvement. The analysis of P-I-R classification of 23 paired liver biopsies showed that 65% of biopsies were in the progressive groups before SVR, which reduced to only 22% after SVR. Liver biopsy findings after successful HCV eradication by DAAs therapy have not been elucidated. Our study is important due to the availability of paired histological data before and after SVR.

Previous studies comparing liver biopsies of HCV patients before and after SVR indicated improvements in inflammation and fibrosis scores after SVR[4,10]. However, a small subset of patients display persistent hepatic inflammation and/or progression to cirrhosis despite SVR[5,11,12], and regression of fibrosis varies[4,13,14].

A 5-year follow-up study on HCV patients with 49 paired pre-treatment and long-term follow-up biopsies showed that 45 (92%) patients had a decrease in the combined inflammation score after their 4th year of follow-up[4], and another study demonstrated long-term changes in liver histology following treatment of chronic HCV showed that patients with SVR had a significant decline in mean inflammation[15]. The longest hepatitis C study with paired liver samples had a median interval between the two biopsies of 93 mo: In total, 71% of patients with SVR treated with PR achieved inflammation improvement, while 23% worsened[12]. These studies reached relatively similar conclusions according to paired liver biopsies: Histological inflammation in hepatitis C patients with SVR significantly improved after long-term follow-up. However, in one study with paired liver biopsies from hepatitis C patients after successful interferon therapy, histological improvement was significant, but mild inflammation persisted in 87% of patients even after more than 4 years[16]. In another study of allograft liver biopsy specimens from patients achieving SVR after a liver transplant (LT) for HCV infection, fibrosis continued to progress in 23% of patients[5]. It should be noted that these conclusions were established based on evidence from the PR regimen. Data on the DAAs regimen are limited: A recent study on the histological findings of 25 HCV patients after successful DAAs therapy before LT, showed that 24% (6/25) of patients still had mild inflammation (HAI: 5-8), and 4% (1/25) had moderate inflammation (HAI: 9-12) after SVR. These proportions were similar to those in patients without SVR[11]. Our finding that significant improvement of necroinflammation (improvement of HAI ≥ 2) was achieved in 82% of patients in a very short time after SVR demonstrated the rapid improvement in inflammation following successful DAAs treatment.

Clinical studies have clearly established that most patients demonstrated marked improvements in fibrosis following SVR after PR therapy[1,4,12]. However, in large clinical trials a minority of patients (7%-13%) maintained their level of fibrosis or even progressed to cirrhosis despite achieving SVR[5,10,17,18]. The above results are all derived from clinical studies of PR. The effect of DAAs on fibrosis in HCV patients after SVR has been unclear up to now. Noninvasive methods for assessing fibrosis have been applied[19-22]. However, histological improvement of fibrosis in HCV patients after successful DAAs treatment has not been extensively studied. We found fibrosis regression in 37% (14/38) of patients; however, one study indicated a weak effect of SVR on fibrosis regression in cirrhotic HCV patients after DAAs therapy before LT[11]. In another study of liver histopathology after LT in HCV patients after successful therapy with PR or DAAs, 23% of patients still had fibrosis progression[5]. The fact that only 34% of patients in our study were cirrhotic and were facing more complicated conditions after LT could explain the distinctions between our results and others.

The P-I-R score has been proposed to evaluate the quality of fibrosis activity based on the balance between progressive and regressive liver disease in HBV patients[6-8]. Our research first determined whether the P-I-R score had predictive value in HCV patients especially after SVR with DAAs. In 23 patients with paired liver biopsy samples, 65% of pretreatment biopsies were in the progressive groups, while the proportion decreased to 22% after SVR. Patients with a progressive form of fibrosis showed higher total HAI scores and portal inflammation than those with a regressive form of fibrosis. In 8 patients who were probably reversing, the posttreatment P-I-R scores were almost consistent with the changing tendency of noninvasive measurements of fibrosis indicating that the predictive value of P-I-R may be similar to that of noninvasive measurements. However, further assessment should be performed in future studies.

Table 3 Posttreatment predominantly progressive, indeterminate and predominately regressive score *vs* changes in Ishak stage to evaluate disease progression or regression (*n* = 23)

Ishak (pre-post)	Posttreatment P-I-R score (*n* = 23)		
	Progressive (*n* = 5)	Indeterminate (*n* = 9)	Regressive (*n* = 9)
Increase (*n* = 1)	Absolutely advancing 100% (1 of 1)	0	0
Stable (*n* = 18)	Probably advancing 22% (4 of 18)	33% (6 of 18)	Probably reversing 44% (8 of 18)
Decrease (*n* = 4)	0	75% (3 of 4)	Absolutely reversing 33% (1 of 3)

P-I-R: Predominantly progressive, indeterminate and predominately regressive.

Table 4 The three fibrosis scoring or staging systems of the 8 "probably reversing" cases

Case No.	P-I-R		Ishak score		LSM (kPa)	
	Pre	Post	Pre	Post	Pre	Post
1	P	R	6	6	6.8	6.1
2	P	R	6	6	7.4	5.6
3	I	R	3	3	4.9	4.1
4	P	R	6	6	24.2	27
5	P	R	5	5	6.3	3.6
6	I	R	4	4	5.8	5.6
7	P	R	6	6	14.0	10.7
8	I	R	5	5	6.9	7.6

P-I-R: Predominantly progressive, indeterminate and predominately regressive; P: Progressive; I: Indeterminate; R: Regressive; LSM: Liver stiffness measurement; Pre: Pretreatment; Post: Posttreatment.

CONCLUSION

Our retrospective study of 38 paired liver biopsy specimens showed histological improvements in HCV patients with SVR after successful DAAs treatment. Histological improvement including necroinflammation and fibrosis were seen in most patients within a very short time after SVR. A preliminary examination of the application of the P-I-R score was performed in HCV patients. However, in view of the small sample size and short-term follow-up, larger and longer-term prospective studies and predictive factors for histological improvement after DAAs treatment should be performed in future studies.

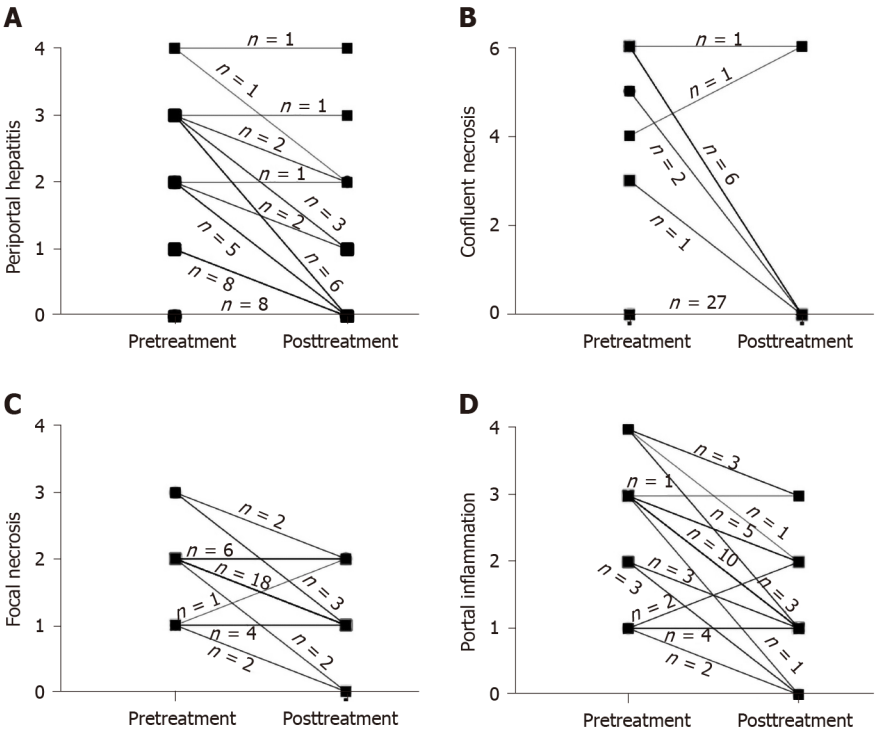


Figure 1 Changes in liver inflammation between pretreatment and posttreatment liver biopsies in individual patients. A: Change in periportal or periseptal interface hepatitis; B: Change in confluent necrosis; C: Change in focal lytic necrosis; D: Change in portal inflammation.

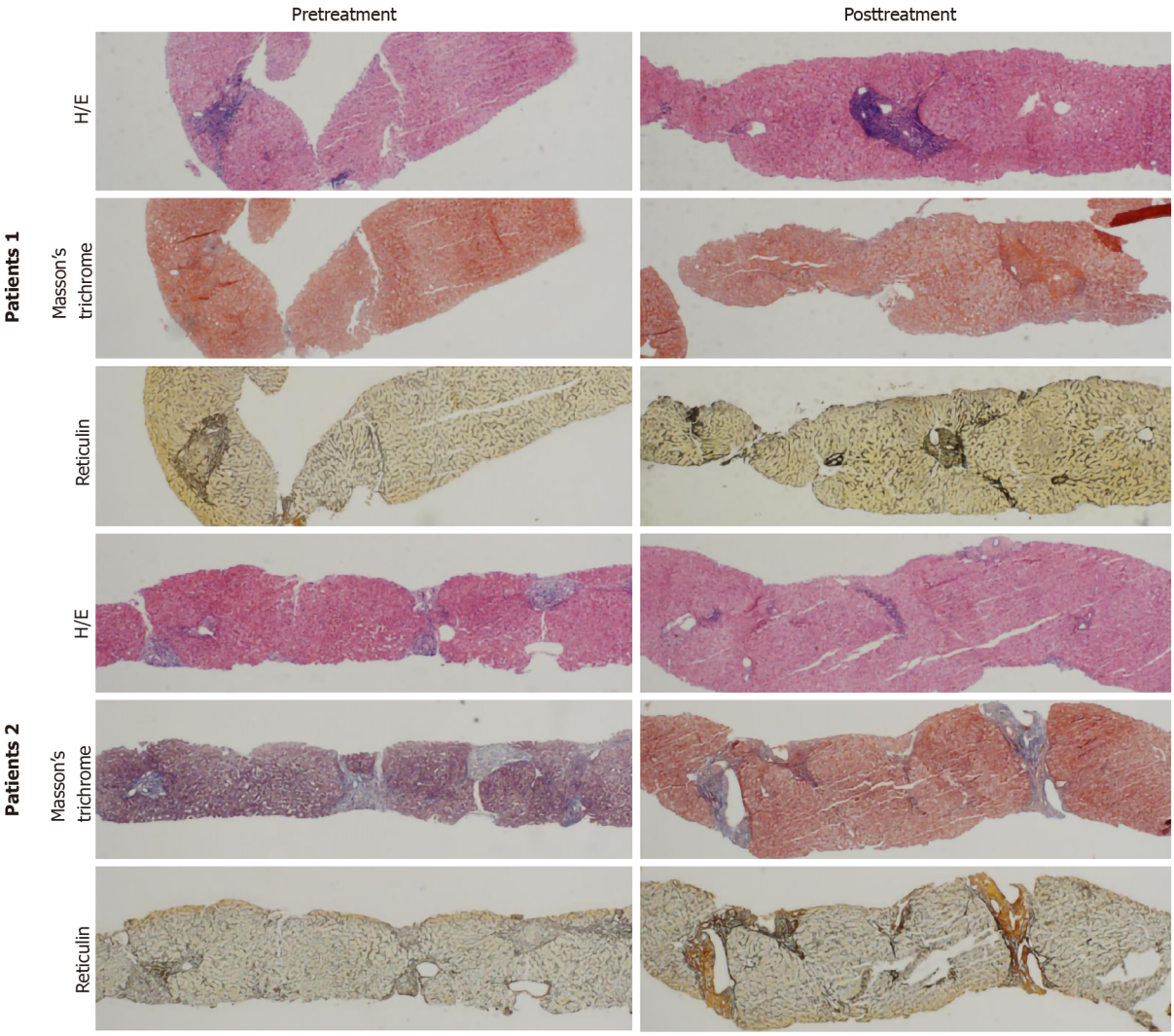


Figure 2 Histology of two "probably reversing" cases before and after sustained virologic response with direct-acting antivirals. Patient 1 is a 55-year-old male with genotype 1b treated with daclatasvir + asunaprevir for 24 wk: Pre-histology activity index (HAI) 14, pre-Ishak 6, pre-predominantly progressive, indeterminate and predominately regressive (P-I-R) predominantly progressive, post-HAI 4, post-Ishak 6, post-P-I-R predominantly progressive. Patient 2 is a 39-year-old female with genotype 3 treated with sofosbuvir + ribavirin for 24 wk: Pre-HAI 6, pre-Ishak 3, pre-P-I-R indeterminate, post-HAI 3, post-Ishak 3, post-P-I-R predominately regressive. Hematoxylin and eosin (10 ×); Masson's trichrome (4 ×); reticulin (4 ×). H/E: hematoxylin and eosin.

ARTICLE HIGHLIGHTS

Research background

Histological changes after direct-acting antivirals (DAAs) therapy in hepatitis C virus (HCV) patients have not been elucidated. Whether the predominantly progressive, indeterminate and predominately regressive (P-I-R) score has predictive value in HCV patients has not been investigated.

Research motivation

The key issues are whether DAAs improve histopathology in HCV patients rapidly and whether the P-I-R score has predictive value in HCV patients. The results will provide important information on the histological response to DAAs therapy and the potential value of the P-I-R score in HCV patients.

Research objectives

To obtain a full understanding of the effect of DAAs on the liver, we assessed the histological changes after DAAs therapy. We also evaluated the predictive value of the P-I-R score in HCV patients.

Research methods

Chronic HCV patients with paired liver biopsy specimens before and after DAAs treatment were included. Sustained virologic response was defined as an undetectable serum HCV RNA level at 24 wk after treatment cessation. The Ishak system and P-I-R score were assessed.

Research results

Thirty-eight chronic HCV patients were included. Their mean age was 40.9 ± 14.6 years and 53% (20/38) were male. Eighty-two percent (31/38) and 37% (14/38) of patients achieved inflammation and fibrosis improvement, respectively. The P-I-R score was evaluated in 61% (23/38) of patients. In patients with stable Ishak stage after treatment: Progressive injury was seen in 22% (4/18) of patients, 33% (6/18) were classified as indeterminate and regressive changes were seen in 44% (8/18) of patients who were judged as probably reversing by the Ishak and P-I-R systems. Our results increased the knowledge on liver biopsy findings after successful HCV eradication by DAAs therapy. However, in view of the small sample size and short-term follow-up, larger and longer-term prospective studies and predictive factors for histological improvement after DAAs treatment should be performed in future studies.

Research conclusions

Significant improvement of necroinflammation and partial remission of fibrosis in HCV patients occurred shortly after DAAs therapy. The P-I-R score has potential in predicting fibrosis in HCV patients.

Research perspectives

Larger and longer-term prospective studies and predictive factors for histological improvement after DAAs treatment should be performed in future studies.

ACKNOWLEDGEMENTS

We thank Liu HX, MD for help with the statistical review.

REFERENCES

1 **Pockros PJ**, Hamzeh FM, Martin P, Lentz E, Zhou X, Govindarajan S, Lok AS. Histologic outcomes in hepatitis C-infected patients with varying degrees of virologic response to interferon-based treatments. *Hepatology* 2010; **52**: 1193-1200 [PMID: 20658462 DOI: 10.1002/hep.23809]

2 **Poynard T**, McHutchison J, Manns M, Trepo C, Lindsay K, Goodman Z, Ling MH, Albrecht J. Impact of pegylated interferon alfa-2b and ribavirin on liver fibrosis in patients with chronic hepatitis C. *Gastroenterology* 2002; **122**: 1303-1313 [PMID: 11984517 DOI: 10.1053/gast.2002.33023]

3 **McHutchison JG**, Gordon SC, Schiff ER, Shiffman ML, Lee WM, Rustgi VK, Goodman ZD, Ling MH, Cort S, Albrecht JK. Interferon alfa-2b alone or in combination with ribavirin as initial treatment for chronic hepatitis C. Hepatitis Interventional Therapy Group. *N Engl J Med* 1998; **339**: 1485-1492 [PMID: 9819446 DOI: 10.1056/nejm199811193392101]

4 **George SL**, Bacon BR, Brunt EM, Mihindukulasuriya KL, Hoffmann J, Di Bisceglie AM. Clinical, virologic, histologic, and biochemical outcomes after successful HCV therapy: a 5-year follow-up of 150 patients. *Hepatology* 2009; **49**: 729-738 [PMID: 19072828 DOI: 10.1002/hep.22694]

5 **Whitcomb E**, Choi WT, Jerome KR, Cook L, Landis C, Ahn J, Te HS, Esfeh J, Hanouneh IA, Rayhill SC, Gibson W, Plesec T, Koo J, Wang HL, Hart J, Pai RK, Westerhoff M. Biopsy Specimens From Allograft Liver Contain Histologic Features of Hepatitis C Virus Infection After Virus Eradication. *Clin Gastroenterol Hepatol* 2017; **15**: 1279-1285 [PMID: 28501538 DOI: 10.1016/j.cgh.2017.04.041]

6 **Sun Y**, Zhou J, Wang L, Wu X, Chen Y, Piao H, Lu L, Jiang W, Xu Y, Feng B, Nan Y, Xie W, Chen G, Zheng H, Li H, Ding H, Liu H, Lv F, Shao C, Wang T, Ou X, Wang B, Chen S, Wee A, Theise ND, You H, Jia J. New classification of liver biopsy assessment for fibrosis in chronic hepatitis B patients before and after treatment. *Hepatology* 2017; **65**: 1438-1450 [PMID: 28027574 DOI: 10.1002/hep.29009]

7 **Theise ND**, Jia J, Sun Y, Wee A, You H. Progression and regression of fibrosis in viral hepatitis in the treatment era: the Beijing classification. *Mod Pathol* 2018; **31**: 1191-1200 [PMID: 29700417 DOI: 10.1038/s41379-018-0048-0]

8 **Wang B**, Sun Y, Zhou J, Wu X, Chen S, Wu S, Liu H, Wang T, Ou X, Jia J, You H. Advanced septa size quantitation determines the evaluation of histological fibrosis outcome in chronic hepatitis B patients. *Mod Pathol* 2018; **31**: 1567-1577 [PMID: 29785021 DOI: 10.1038/s41379-018-0059-x]

9 **Brunt EM**. Grading and staging the histopathological lesions of chronic hepatitis: the Knodell histology activity index and beyond. *Hepatology* 2000; **31**: 241-246 [PMID: 10613753 DOI: 10.1002/hep.510310136]

10 **Lee YA**, Friedman SL. Reversal, maintenance or progression: what happens to the liver after a virologic cure of hepatitis C? *Antiviral Res* 2014; **107**: 23-30 [PMID: 24726738 DOI: 10.1016/j.antiviral.2014.03.012]

11 **Putra J**, Schiano TD, Fiel MI. Histological assessment of the liver explant in transplanted hepatitis C virus patients achieving sustained virological response with direct-acting antiviral agents. *Histopathology* 2018; **72**: 990-996 [PMID: 29235144 DOI: 10.1111/his.13453]

12 **Chu CY**, Cheng CH, Chen HL, Lin IT, Wu CH, Lee YK, Bair MJ. Long-term histological change in chronic hepatitis C patients who had received peginterferon plus ribavirin therapy with sustained virological response. *J Formos Med Assoc* 2019; **118**: 1129-1137 [PMID: 30472042 DOI: 10.1016/j.jfma.2018.11.005]

13 **Shiratori Y**, Imazeki F, Moriyama M, Yano M, Arakawa Y, Yokosuka O, Kuroki T, Nishiguchi S, Sata M, Yamada G, Fujiyama S, Yoshida H, Omata M. Histologic improvement of fibrosis in patients with hepatitis C who have sustained response to interferon therapy. *Ann Intern Med* 2000; **132**: 517-524 [PMID: 10744587 DOI: 10.7326/0003-4819-132-7-200004040-00002]

14 **Tachi Y**, Hirai T, Miyata A, Ohara K, Iida T, Ishizu Y, Honda T, Kuzuya T, Hayashi K, Ishigami M, Goto H. Progressive fibrosis significantly correlates with hepatocellular carcinoma in patients with a sustained virological response. *Hepatol Res* 2015; **45**: 238-246 [PMID: 24655233 DOI: 10.1111/hepr.12331]

15 **Shiffman ML**, Sterling RK, Contos M, Hubbard S, Long A, Luketic VA, Stravitz RT, Fuchs M, Sanyal AJ. Long term changes in liver histology following treatment of chronic hepatitis C virus. *Ann Hepatol* 2014; **13**: 340-349 [PMID: 24927604]

16 **Tsuda N**, Yuki N, Mochizuki K, Nagaoka T, Yamashiro M, Omura M, Hikiji K, Kato M. Long-term clinical and virological outcomes of chronic hepatitis C after successful interferon therapy. *J Med Virol* 2004; **74**: 406-413 [PMID: 15368524 DOI: 10.1002/jmv.20190]

17 **Poynard T**, Moussalli J, Munteanu M, Thabut D, Lebray P, Rudler M, Ngo Y, Thibault V, Mkada H, Charlotte F, Bismut FI, Deckmyn O, Benhamou Y, Valantin MA, Ratziu V, Katlama C; FibroFrance-GHPS group. Slow regression of liver fibrosis presumed by repeated biomarkers after virological cure in patients with chronic hepatitis C. *J Hepatol* 2013; **59**: 675-683 [PMID: 23712051 DOI: 10.1016/j.jhep.2013.05.015]

18 **Maylin S**, Martinot-Peignoux M, Moucari R, Boyer N, Ripault MP, Cazals-Hatem D, Giuily N, Castelnau C, Cardoso AC, Asselah T, Féray C, Nicolas-Chanoine MH, Bedossa P, Marcellin P. Eradication of hepatitis C virus in patients successfully treated for chronic hepatitis C. *Gastroenterology* 2008; **135**: 821-829 [PMID: 18593587 DOI: 10.1053/j.gastro.2008.05.044]

19 **Facciorusso A**, Del Prete V, Turco A, Buccino RV, Nacchiero MC, Muscatiello N. Long-term liver stiffness assessment in hepatitis C virus patients undergoing antiviral therapy: Results from a 5-year cohort study. *J Gastroenterol Hepatol* 2018; **33**: 942-949 [PMID: 28976021 DOI: 10.1111/jgh.14008]

20 **Knop V**, Hoppe D, Welzel T, Vermehren J, Herrmann E, Vermehren A, Friedrich-Rust M, Sarrazin C, Zeuzem S, Welker MW. Regression of fibrosis and portal hypertension in HCV-associated cirrhosis and sustained virologic response after interferon-free antiviral therapy. *J Viral Hepat* 2016; **23**: 994-1002 [PMID: 27500382 DOI: 10.1111/jvh.12578]

21 **Bachofner JA**, Valli PV, Kröger A, Bergamin I, Künzler P, Baserga A, Braun D, Seifert B, Moncsek A, Fehr J, Semela D, Magenta L, Müllhaupt B, Terziroli Beretta-Piccoli B, Mertens JC. Direct antiviral agent treatment of chronic hepatitis C results in rapid regression of transient elastography and fibrosis markers fibrosis-4 score and aspartate aminotransferase-platelet ratio index. *Liver Int* 2017; **37**: 369-376 [PMID: 27678216 DOI: 10.1111/liv.13256]

22 **Singh S**, Facciorusso A, Loomba R, Falck-Ytter YT. Magnitude and Kinetics of Decrease in Liver Stiffness After Antiviral Therapy in Patients With Chronic Hepatitis C: A Systematic Review and Meta-analysis. *Clin Gastroenterol Hepatol* 2018; **16**: 27-38.e4 [PMID: 28479504 DOI: 10.1016/j.cgh.2017.04.038]

World Journal of Gastroenterology

Submit a Manuscript: https://www.f6publishing.com

World J Gastroenterol 2021 February 7; 27(5): 416-427

DOI: 10.3748/wjg.v27.i5.416

ISSN 1007-9327 (print) ISSN 2219-2840 (online)

ORIGINAL ARTICLE

Retrospective Study

Comparative study of indocyanine green-R15, Child-Pugh score, and model for end-stage liver disease score for prediction of hepatic encephalopathy after transjugular intrahepatic portosystemic shunt

Zhong Wang, Yi-Fan Wu, Zhen-Dong Yue, Hong-Wei Zhao, Lei Wang, Zhen-Hua Fan, Yu Zhang, Fu-Quan Liu

ORCID number: Zhong Wang 0000-0003-3575-1982; Yi-Fan Wu 0000-0003-2709-2729; Zhen-Dong Yue 0000-0001-5403-8336; Hong-Wei Zhao 0000-0001-5657-1839; Lei Wang 0000-0003-4080-1630; Zhen-Hua Fan 0000-0001-5417-1997; Yu Zhang 0000-0001-9895-175X; Fu-Quan Liu 0000-0003-1972-7712.

Author contributions: Liu FQ designed the research; Zhang Y, Wu YF, Yue ZD, Zhao HW, Wang L, and Fan ZH performed the research; Wang Z analyzed the data and wrote the paper.

Supported by Beijing Municipal Science and Technology Commision, No. Z181100001718097.

Institutional review board statement: The study was reviewed and approved by the Institutional Review Board of Shijitan Hospital, Capital Medical University.

Conflict-of-interest statement: There are no conflicts of interest related to this study.

Data sharing statement: No additional data are available.

Open-Access: This article is an open-access article that was

Zhong Wang, Yi-Fan Wu, Zhen-Dong Yue, Hong-Wei Zhao, Lei Wang, Zhen-Hua Fan, Yu Zhang, Fu-Quan Liu, Department of Interventional Therapy, Beijing Shijitan Hospital, Capital Medical University, Beijing 100038, China

Corresponding author: Fu-Quan Liu, BCPS, MD, Director, Professor, Department of Interventional Therapy, Beijing Shijitan Hospital, Capital Medical University, No. 10 Tie Yi Road, Yangfangdian, Haidian District, Beijing 100038, China. lfuquan@aliyun.com

Abstract

BACKGROUND

Hepatic encephalopathy (HE) remains an enormous challenge in patients who undergo transjugular intrahepatic portosystemic shunt (TIPS) implantation. The preoperative indocyanine green retention rate at 15 min (ICG-R15), as one of the liver function assessment tools, has been developed as a prognostic indicator in patients undergoing surgery, but there are limited data on its role in TIPS.

AIM

To determine whether the ICG-R15 can be used for prediction of post-TIPS HE in decompensated cirrhosis patients with portal hypertension (PHT) and compare the clinical value of ICG-R15, Child-Pugh score (CPS), and model for end-stage liver disease (MELD) score in predicting post-TIPS HE with PHT.

METHODS

This retrospective study included 195 patients with PHT who underwent elective TIPS at Beijing Shijitan Hospital from January 2018 to June 2019. All patients underwent the ICG-R15 test, CPS evaluation, and MELD scoring 1 wk before TIPS. According to whether they developed HE or not, the patients were divided into two groups: HE group and non-HE group. The prediction of one-year post-TIPS HE by ICG-R15, CPS and MELD score was evaluated by the areas under the receiver operating characteristic curves (AUCs).

RESULTS

A total of 195 patients with portal hypertension were included and 23% (45/195) of the patients developed post-TIPS HE. The ICG-R15 was identified as an independent predictor of post-TIPS HE. The AUCs for the ICG-R15, CPS, and MELD score for predicting post-TIPS HE were 0.664 (95% confidence interval [CI]:

selected by an in-house editor and fully peer-reviewed by external reviewers. It is distributed in accordance with the Creative Commons Attribution NonCommercial (CC BY-NC 4.0) license, which permits others to distribute, remix, adapt, build upon this work non-commercially, and license their derivative works on different terms, provided the original work is properly cited and the use is non-commercial. See: http://creativecommons.org/licenses/by-nc/4.0/

Manuscript source: Unsolicited manuscript

Specialty type: Gastroenterology and hepatology

Country/Territory of origin: China

Peer-review report's scientific quality classification

Grade A (Excellent): A
Grade B (Very good): B, B
Grade C (Good): 0
Grade D (Fair): 0
Grade E (Poor): 0

Received: November 23, 2020
Peer-review started: November 23, 2020
First decision: December 17, 2020
Revised: December 20, 2020
Accepted: January 15, 2021
Article in press: January 15, 2021
Published online: February 7, 2021

P-Reviewer: Joko K, Liem S, Martins VH
S-Editor: Fan JR
L-Editor: Wang TQ
P-Editor: Wang LL

0.557-0.743, P = 0.0046), 0.596 (95%CI: 0.508-0.679, P = 0.087), and 0.641 (95%CI: 0.554-0.721, P = 0.021), respectively. The non-parametric approach (Delong-Delong & Clarke-Pearson) showed that there was statistical significance in pairwise comparison between AUCs of ICG-R15 and MELD score (P = 0.0229).

CONCLUSION

The ICG-R15 has appreciated clinical value for predicting the occurrence of post-TIPS HE and is a choice for evaluating the prognosis of patients undergoing TIPS.

Key Words: Hepatic encephalopathy; Indocyanine green-R15; Child-Pugh score; Model for end-stage liver disease score; Transjugular intrahepatic portosystemic shunt; Portal hypertension

©The Author(s) 2021. Published by Baishideng Publishing Group Inc. All rights reserved.

Core Tip: We studied whether the indocyanine green retention rate at 15 min (ICG-R15) can be used for prediction of post-transjugular intrahepatic portosystemic shunt (TIPS) hepatic encephalopathy (HE) in decompensated cirrhosis patients with portal hypertension (PHT) and compare the clinical value of ICG-R15, Child-Pugh score, and model for end-stage liver disease score in predicting post-TIPS HE with PHT.

Citation: Wang Z, Wu YF, Yue ZD, Zhao HW, Wang L, Fan ZH, Zhang Y, Liu FQ. Comparative study of indocyanine green-R15, Child-Pugh score, and model for end-stage liver disease score for prediction of hepatic encephalopathy after transjugular intrahepatic portosystemic shunt. *World J Gastroenterol* 2021; 27(5): 416-427
URL: https://www.wjgnet.com/1007-9327/full/v27/i5/416.htm
DOI: https://dx.doi.org/10.3748/wjg.v27.i5.416

INTRODUCTION

Portal hypertension (PHT) is a very common and serious complication of chronic liver disease that often causes variceal bleeding and refractory ascites[1]. Transjugular intrahepatic portosystemic shunt (TIPS) is an important treatment option that has been shown to be efficacious in the management of PHT[2]. This procedure can alleviate portal hypertension by creating a large channel between the portal vein and hepatic vein[3]. Unfortunately, TIPS can cause severe complications such as heart failure, liver failure, and hepatic encephalopathy (HE). HE has a high incidence rate and is one of the most debilitating complications, which has a serious effect on the prognosis and survival of patients[4-6]. Although some risk factors are known, the identification of patients at risk of HE needs additional research. It is important to predict post-TIPS HE so that prevention and treatment measures can be implemented in high-risk HE patients to avoid adverse outcomes.

The indocyanine green retention rate at 15 min (ICG-R15), the Child-Pugh score (CPS), and the model for end-stage liver disease (MELD) score have been developed to assess liver function[7,8]. The ICG-R15 is a relatively non-invasive, quick, and inexpensive method that has been widely used in patients with end-stage liver disease[9]. Zipprich *et al*[10] reported that ICG is the most accurate predictor among quantitative liver function tests of the survival of patients with cirrhosis[10]. A recent retrospective study demonstrated that preoperative ICG clearance was predictive of the surgical prognosis in patients undergoing hepatectomy[11]. The CPS was developed to assess the severity of liver cirrhosis in the clinic. This scoring system includes the bilirubin level, the albumin level, the prothrombin time, HE, and ascites[12]. The MELD score is used to predict the survival of patients undergoing TIPS and to evaluate patients with severe liver disease prior to transplantation. It includes three objective variables: The total bilirubin level, the creatinine level, and the international normalized ratio (INR)[13]. However, there are limited data on the use of liver function tools, especially the ICG-R15, to predict post-TIPS HE. Therefore, the aim of this study was to compare the clinical value of the MELD score, CPS, and ICG-R15 for the prediction of post-TIPS HE in patients with PHT.

MATERIALS AND METHODS

This retrospective study was approved by the Ethics Committee of Beijing Shijitan Hospital of Capital Medical University. The need to obtain informed consent was waived due to its retrospective nature.

Patients

All patients who underwent TIPS between January 2018 and June 2019 in the interventional department of Beijing Shijitan Hospital were included in this study.

The following inclusion criteria were set: (1) Patients between 18 and 70 years old; (2) Patients diagnosed with PHT; and (3) Patients who underwent TIPS using a polytetrafluoroethylene-covered stent. The following exclusion criteria were set: (1) Preoperative HE; (2) Liver cancer; (3) Liver transplantation; (4) TIPS retreatment; (5) Non-cirrhotic PHT; (6) Surgical splenectomy; (7) Portal vein thrombosis; and (8) Urgent TIPS.

Definitions

PHT was defined as the radiological presence of significant splenomegaly, umbilical vein recanalization, and/or portosystemic shunts as well as a preoperative platelet count < 100×10^9/L. Portal pressure gradient values greater than or equal to 10 mmHg indicated clinically significant PHT[14].

HE was defined as neuropsychiatric abnormalities ranging from mild neuropsychological dysfunction to deep coma and abnormal ammonia levels, after the exclusion of other possible causes of altered mental status by computed tomography or magnetic resonance imaging[15].

Preoperative ICG-R15, CPS, and MELD score

All patients included in this study underwent the ICG-R15 test with a dye-densitogram (DDG) analyser (Japan, NIHON KOHDEN, model DDG-3300K) and an ICG clearance rate test (Japan, NIHON KOHDEN, model A). Within 30 s after the injection of ICG (0.5 mg/kg) into the median cubital vein, plasma ICG concentrations were monitored *via* a sensor attached to the patients' finger. The ICG-R15 was subsequently assessed by a computer. The CPS score can be divided into three grades depending on the total points: Grade A (5-6 points), B (7-9 points), and C (≥ 10 points). The MELD score was calculated based on the following formula: R = 3.8 × ln (bilirubin mg/dL) + 11.2 × ln (INR) + 9.6 ln (creatinine mg/dL) + 6.4 × aetiology (biliary and alcoholic 0, others 1)[8,16] (Figure 1).

TIPS

Under fluoroscopic guidance, a standard TIPS procedure was performed by an experienced interventional radiologist. A pigtail catheter was inserted into the right internal jugular vein leading to the hepatic veins. After finding the portal vein through the superior mesenteric artery or splenic artery using indirect portal venography, a stent (7, 8, or 10 mm, Fluency, Bard, United States) was placed to create a channel between the hepatic vein and the portal vein. Afterward, the portal vein pressure was measured at least three times, and a pressure transducer system (Combitrans, Braun Melsungen, Germany) with a multichannel monitor (Sirecust, Siemens, Germany) was used to measure the haemodynamic parameters.

Statistical analysis

Clinical and laboratory characteristics were collected from the medical records. SPSS (version 20.0, SPSS Inc., United States) and MedCalc were used for the statistical analyses. Descriptive data are presented as the mean ± SD, and qualitative variables are presented as frequencies or percentages. Student's *t* test or the Mann-Whitney *U* test was used to compare quantitative variables between groups, and the chi-square test or Fisher's exact test was used for qualitative variables. Univariate and multivariable logistic regression analyses were used to determine HE-related risk factors after TIPS. The areas under the receiver operating characteristic curves (AUCs) for the ICG-R15, CPS, and MELD score were evaluated. The non-parametric approach (Delong-Delong & Clarke-Pearson)[17] was used for pairwise comparison among AUCs of ICG-R15, CPS, and MELD score. Statistical significance was established at $P < 0.05$.

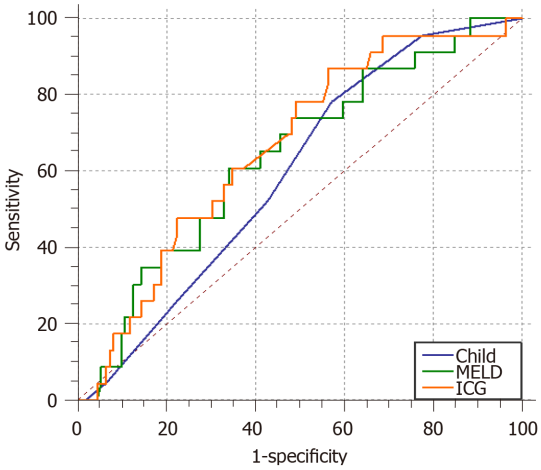


Figure 1 Receive operating characteristic curve analyses of indocyanine green-R15, Child-Pugh score, and model for end-stage liver disease score to predict post-transjugular intrahepatic portosystemic shunt hepatic encephalopathy. ICG: Indocyanine green; MELD: Model for end-stage liver disease.

RESULTS

Patients' preoperative characteristics

A total of 221 patients who underwent TIPS were included in this study. After applying the inclusion and exclusion criteria of the study, data were collected from a total of 195 decompensated cirrhosis patients with PHT who underwent TIPS. The basic clinical characteristics are listed in Table 1. The study population comprised 140 men and 55 women, with a mean age of 51.2 ± 11.4 years. The indications included variceal bleeding in 118 (60.7%) patients, refractory ascites in 36 (18.5%), variceal bleeding combined with ascites in 27 (14.1%), and other (including pleural fluid and hepatorenal syndrome) in 14 (6.7%). The most common cause of cirrhosis was viral cirrhosis (60.7%), followed by alcoholic cirrhosis (15.9%), biliary cirrhosis (4.6%), and drug-induced and autoimmune hepatitis cirrhosis (4.6%). According to the CPS, 108 patients were classified as having grade A, 75 as having grade B and 12 as having grade C. The median MELD score and ICG-R15 were 7 (4.1, 10) and 38.4 (22, 50), respectively.

Univariable and multivariable analyses of post-TIPS HE

Of the 195 patients who underwent TIPS, 45 (23%) developed HE at the 12 mo follow-up. The factors associated with HE in univariable analysis included age, stent size, puncture site, ICG-R15, CPS, MELD score, blood urea nitrogen (BUN) level, and NH_3 level (P = 0.006, 0.019, 0.006, 0.027, 0.022, 0.020, 0.025, and 0.044, respectively). As shown in Table 2, multivariate regression analysis identified the following variables as independent risk factors for post-TIPS HE: Older age, 10 mm stent size, puncture site in the right branch of the portal vein, high ICG-R15, high BUN level, high NH_3 level, high CPS, and high MELD score.

Discriminatory power of the CPS, MELD score, and ICG-R15

The area under the receiver operating characteristic (ROC) curve for the ICG-R15 (AUC = 0.664, 95% confidence interval [CI]: 0.557-0.743, P = 0.0046) for the prediction of post-TIPS HE was larger than those of the CPS (AUC = 0.596, 95%CI: 0.508-0.679, P = 0.087) and the MELD score (AUC = 0.641, 95%CI: 0.554-0.721, P = 0.021). The non-parametric approach (Delong-Delong & Clarke-Pearson)[17] showed that there was no statistical significance in pairwise comparison between AUCs of ICG-R15 and MELD score (P = 0.0229). The cut-off value for the ICG-R15, which was determined by the maximum of Youden index, was 30, with a sensitivity of 86.96% and specificity of 56.25% for the prediction of post-TIPS HE (Table 3). Of the 126 patients with an ICG-R15 > 30, 36 (28.5%) developed post-TIPS HE, while 9 (13%) of 69 patients with an ICG ≤ 30 developed post-TIPS HE.

Table 1 Patients' preoperative characteristics

Parameter	Patients enrolled (*n* = 195)	Patients without post-TIPS HE (*n* = 150)	Patients with post-TIPS HE (*n* = 45)	*P* value
Age (years)[1]	51.2 ± 11.4	49.8 ± 13.2	58.3 ± 9.9	0.004[b]
Gender (F/M), *n*[2]	140/55			0.79
TIPS indication, *n*[2]				0.10
Variceal bleeding	118 (60.7)	93	25	
Ascites	36 (18.5)	29	7	
Bleeding combine with ascites	27 (14.1)	21	6	
Other	14 (6.7)	7	7	
Cirrhotic aetiology, *n*[2]				0.98
Viral	146 (74.9)	111	35	
Alcoholic	31 (15.9)	25	6	
Biliary	9 (4.6)	7	2	
Drug-induced	4 (2)	3	1	
Autoimmune	5 (2.6)	4	1	
Preoperative HVPG, mmHg[3]	17.1 (11, 23)	18 (13, 21)	20 (12, 20)	0.28
Preoperative PPG, mmHg[3]	23 (18, 29)	23 (16, 29)	23 (20, 28)	0.6
Stent size, mm (%)[2]				0.057
7	59 (30.4)	51	8	
8	117 (60)	87	30	
10	19 (9.6)	12	7	
Puncture site of portal vein, *n*[2]				0.013[a]
Left branch	113 (57.7)	96	17	
Bifurcation	22 (11.1)	15	7	
Right branch	60 (31.2)	40	20	
Child-Pugh score[1]	7.1 ± 1.5	7.0 ± 1.6	8.0 ± 2.1	
Child-Pugh grade, *n*[2]				0.029[a]
A	108 (55.6)	89	19	
B	75 (38.5)	55	20	
C	12 (5.9)	6	6	
MELD score[3]	7.0 (4.1, 10.0)	6.5 (3.8, 10.0)	7.9 (5.8, 13.0)	0.07
ICG-R15, %[3]	38.4 (22, 50)	34.6 (21.8, 47.7)	44.4 (35.4, 63.0)	0.013[a]
Total protein, g/L[1]	64.0 ± 9.0	64.6 ± 9.6	61.8 ± 6.9	0.19
Total bilirubin, μmoL/L[3]	24.5 (16.8, 35.4)	24.0 (16.9, 35.2)	29.8 (19.5, 44.5)	0.169
Creatinine, μmoL/L[3]	63 (52, 77)	61 (52, 73)	70 (59, 85)	0.084
ALT, U/L[3]	21 (15, 33)	22 (16, 33)	21 (16, 29)	0.889
AST, U/L[3]	28 (20, 42)	28 (20, 44)	31 (23, 50)	0.442
ALP, U/L[3]	91 (67, 122)	90 (67, 131)	92 (65, 121)	0.39
Albumin, g/L[1]	34.9 ± 5.4	33.4 ± 5.2	35.2 ± 6.9	0.12
Serum potassium, mmoL/L[1]	4.0 ± 0.5	3.9 ± 0.3	4.0 ± 0.4	0.62
Serum clozapine, mmoL/L[1]	105.2 ± 5.8	105.3 ± 5.4	105.5 ± 6.6	0.81
Serum sodium, mmoL/L[1]	138.7 ± 5.1	136.2 ± 4.9	140.7 ± 6.1	0.39

WBC, × 10^9/L[3]	3.27 (2.1, 4.6)	3.1 (2.1, 4.4)	3.3 (2.5, 5.7)	0.26
Platelet count, × 10^9/L[3]	80 (58.3, 120)	85 (61.2, 127.7)	83 (63, 107)	0.49
Hb, g/L[1]	97.4 ± 27.1	95.3 ± 25.5	98.1 ± 27.9	0.9
BUN, mmoL/L[3]	5.7 (4.3, 7.7)	5.4 (4.2, 7.0)	7.6 (5.4, 8.8)	0.07
NH_3, μg/Dl[1]	49.5 ± 19.5	46.6 ± 15.4	54.9 ± 23.8	0.037[a]
APTT, s[3]	33.4 ± 4.4	33.8 ± 4.5	33.5 ± 4.2	0.76
INR[1]	1.4 ± 0.3	1.37 ± 0.3	1.32 ± 0.19	0.50
FIB, g/L[1]	2.17 ± 0.8	2.2 ± 0.8	2.3 ± 0.7	0.39
PT, s[1]	14.8 ± 2.5	14.7 ± 2.6	14.4 ± 2.0	0.69

[1]Values are the mean ± SD.
[2]Values are *n*.
[3]Values are medians (P25, P75).
[a]$P < 0.05$.
[b]$P < 0.01$. TIPS: Transjugular intrahepatic portosystemic shunt; HE: Hepatic encephalopathy; HVPG: Hepatic venous pressure gradient; PPG: Portal pressure gradient; MELD: Model for end-stage liver disease; ICG: Indocyanine green; ALT: Alanine aminotransferase; AST: Aspartate transaminase; ALP: Alkaline phosphatase; Hb: Hemoglobin; BUN: Blood urea nitrogen; APTT: Active partial thromboplastin; INR: International normalized ratio; FIB: Fibrinogen; PT: Prothrombin time; WBC: White blood cells.

Comparison of post-TIPS-HE incidence between patients with an ICG-R15 > 30% and < 30%

The patients were divided into two groups according to the ICG-R15 cut-off value, 30%, determined by the maximal Youden index. Patients with an ICG-R15 > 30% had a higher incidence of HE than those with an ICG-R15 < 30% (13% *vs* 28.5%; $P = 0.014$). There were significant differences in age, CPS, preoperative portal pressure gradient, NH_3, albumin, aspartate transaminase, Cl, Na, white blood cells, active partial thromboplastin, or prothrombin time in patients with different ICG-R15 levels below and above 30% (Table 4).

DISCUSSION

TIPS has been widely used to treat complications of PHT, including varices and ascites, by creating a large channel between the hepatic vein and portal vein. This procedure changes the liver haemodynamics by shunting a fraction of the portal venous blood directly into the systemic circulation, which can lead to decreased liver blood supply and impaired liver function reserve. In addition, HE occurs because of an increase in the amount of natural toxins such as ammonia travelling to the brain as a result of the shunting of the blood directly from the portal vein to the hepatic vein[18]. HE can produce a spectrum of neurological/psychiatric syndromes ranging from subclinical alterations to coma. It remains one of the most common and worrisome complications of end-stage liver disease after TIPS[15].

The ICG-R15 test is simple, fast, less invasive, and inexpensive, and can be performed in less than half an hour. The ICG-R15 retention trial was introduced as a relatively noninvasive tool for the classification of pediatric and adult patients with acute and chronic liver failure[19]. A particular advantage of the ICG-R15 test is that it is more suitable for pediatric patients. In addition, the trial appears to be an ideal way to assess the risks of surgical procedures such as liver resection. In addition to assessing the predictive value of varices and ascites, the results of some papers suggest that the ICG-R15 test may also predict mortality[20].

In this study, univariate and multivariate logistic analyses showed that 10 mm stent size, puncture site in the right branch of the portal vein, age, ICG-R15, BUN level, NH_3 level, CPS, and MELD score were predictors of post-TIPS HE in patients with portal hypertension. Patients with puncture sites in the right portal vein had a high incidence of post-TIPS HE. This is related to the right branch of the portal vein contains more poisons mainly received from the superior mesenteric vein[21-23]. It was reported that choosing the left branch of the portal vein as the puncture site during the placement of TIPS may decrease the incidence of HE significantly[24,25]. HE occurs more often in patients with a stent diameter of 10 mm than in those with smaller-diameter stents. A

Table 2 Univariable and multivariable logistic regression analyses of post-transjugular intrahepatic portosystemic shunt hepatic encephalopathy

Parameter	Univariable logistic regression			Multivariable logistic regression		
	Regression coefficient	OR	*P* value	Regression coefficient	OR	*P* value
Age	0.53	1.055	0.006[b]	0.057	1.059	0.021[a]
Gender (F/M)	0.134	1.143	0.789			
TIPS indication (variceal bleeding/ascites/bleeding combined with ascites/other)	0.147	1.159	0.522			
Cirrhotic aetiology (viral/alcoholic/biliary/drug-induced/autoimmune)	0.053	0.761	0.437			
Preoperative HVPG	0.019	1.019	0.502			
Preoperative PPG	0.022	1.023	0.289			
Stent size (7/8/10)	-0.975	0.377	0.019[a]			
Puncture site of portal vein (left branch/bifurcation/right branch)	0.763	2.145	0.006[b]	0.566	1.762	0.018[a]
Child-Pugh score	0.027	1.027	0.022[a]	0.053	1.055	0.046[a]
Child-Pugh grade (A/B/C)	0.196	0.594	1.216			
MELD score	0.256	1.291	0.020[a]	0.516	1.068	0.043[a]
ICG-R15	0.026	1.027	0.027[a]	0.028	1.029	0.031[a]
Total protein	-0.029	0.972	0.203			
Total bilirubin	0.000	1.000	0.962			
Creatinine	0.006	1.006	0.151			
ALT	0.000	1.000	0.892			
AST	0.003	1.003	0.232			
ALP	0.002	1.002	0.248			
Albumin	-0.058	0.94	0.1364			
Serum potassium	0.233	1.262	0.689			
Serum clozapine	0.007	1.007	0.864			
Serum sodium	-0.035	0.965	0.395			
WBC	0.047	1.049	0.544			
Platelet count	-0.003	0.997	0.359			
Hb	-0.001	0.999	0.908			
BUN	0.084	1.087	0.025[a]	0.085	1.008	0.028[a]
NH_3	0.025	1.025	0.044[a]	0.032	1.033	0.025[a]
APTT	-0.015	0.985	0.768			
INR	-0.644	0.525	0.504			
FIB	0.248	1.281	0.389			
PT	-0.059	0.943	0.559			

[a]$P < 0.05$.

[b]$P < 0.01$. TIPS: Transjugular intrahepatic portosystemic shunt; HVPG: Hepatic venous pressure gradient; PPG: Portal pressure gradient; MELD: Model for end-stage liver disease; ICG: Indocyanine green; ALT: Alanine aminotransferase; AST: Aspartate transaminase; ALP: Alkaline phosphatase; Hb: Hemoglobin; BUN: Blood urea nitrogen; APTT: Active partial thromboplastin; INR: International normalized ratio; FIB: Fibrinogen; PT: Prothrombin time; WBC: White blood cell.

Table 3 Areas under the receiver operating characteristic curves of indocyanine green rentention rate of 15 min, Child-Pugh score, and model for end-stage liver disease score

Parameter	CPS	MELD	ICG-R15
AUC	0.596	0.641	0.664
95%CI	0.508-0.679	0.554-0.721	0.557-0.743
Z statistic	1.709	2.293	2.832
P value	0.087	0.021[a]	0.0046[b]
Youden index J	0.211	0.269	0.307
Cut-off value	6	7.5	30
Sensitivity	78.2	60.87	86.96
Specificity	42.6	66.07	43.75

[b]*P* < 0.01. ICG: Indocyanine green; CPS: Child-Pugh score; MELD: Model for end-stage liver disease; AUS: Areas under the receiver operating characteristic curves.

Table 4 Characteristics of patients with an indocyanine green rentention rate at 15 min ≤ 30% and > 30%

Characteristic	ICG-R15 ≤ 30% (*n* = 69)	ICG-R15 > 30% (*n* = 126)	*P* value
HE/non HE[1]	9 (13%)/60	36 (28.5%)/90	0.014[a]
Age (yr)[2]	48.3 ± 11.6	52.9 ± 14.1	0.033[a]
Child-Pugh score[2]	6.3 ± 1.2	7.6 ± 1.6	< 0.001[c]
Preoperative PPG, mmHg[3]	15.6 (11, 18)	18 (16, 24)	0.005[b]
NH_3, μg/dL[2]	45.0 ± 15.0	52.0 ± 21.2	0.021[a]
Albumin, g/L[2]	38.0 ± 4.4	33.3 ± 5.6	
AST, U/L[3]	25 (18, 36)	28.5 (22, 45.7)	0.018[a]
Serum clozapine, mmoL/L[2]	106.6 ± 4.8	104.5 ± 5.9	0.024[a]
Serum sodium, mmoL/L[2]	140.4 ± 3.7	137.7 ± 5.5	< 0.001[c]
WBC, × 10^9/L[3]	2.77 (1.81, 3.86)	3.6 (2.3, 4.9)	0.031[a]
APTT, s[3]	32.8 ± 3.2	34.3 ± 5.0	0.024[a]
PT, s[2]	14.0 ± 1.9	15.3 ± 2.6	0.043[a]

[1]Values are *n*.
[2]Values are the mean ± SD.
[3]Values are medians (P25, P75).
[a]*P* < 0.05.
[b]*P* < 0.01.
[c]*P* < 0.001. ICG: Indocyanine green; HE: Hepatic encephalopathy; PPG: Portal pressure gradient; AST: Aspartate transaminase; APTT: Active partial thromboplastin; PT: Prothrombin time; WBC: White blood cells.

larger stent can effectively reduce portal vein pressure, but at the same time, more blood that has not been detoxified by the liver directly enters the systemic circulation, which can further impair liver function and lead to HE. However, some studies showed that the incidence of post-TIPS HE was unrelated to stent diameter[26]. Li *et al*[27] also found that age and Child-Pugh classification were independent risk factors for early post-TIPS HE[27], which was in accord with previous studies[28,29]. Fonio *et al*[4] demonstrated that the MELD grade was a risk factor for post-TIPS HE; the results of this study support this finding[4]. Normally, ammonia is detoxified by conversion to urea by Krebs-Henseleit buffer or the urea cycle in the liver. In total, 40% to 60% of the urea nitrogen in the primary urine is absorbed in the renal tubules and collecting tubes. A high incidence of HE was found in patients with high BUN levels, which is related to the aggravation of liver function involving the kidneys, renal decompensation, and azotaemia[30].

Hiwatashi *et al*[31] found that a higher ICG-R15 was significantly correlated with surgical complications and liver dysfunction after surgical resection and chemotherapy in patients with colorectal cancer[31]. Wang *et al*[32] demonstrated that the ICG-R15 could more accurately predict preoperative liver reserve function than the Child-Pugh and MELD scores in patients who suffered from liver cancer[32]. Another study showed that the ALICE scoring system (including serum albumin and ICG-R15) could simply and effectively predict the prognosis of liver cancer patients undergoing surgery[33]. In this study, we analysed and compared the areas under the ROC curves for the ICG-R15, CPS, and MELD score. The results were as follows: $AUC_{ICG\text{-}R15} > AUC_{MELD} > AUC_{CPS}$, and there was statistical significance in pairwise comparison between AUCs of ICG-R15 and MELD score. This suggests that the ICG-R15 has clinical equivalent value to predict post-TIPS HE compared to MELD score. The CPS is relatively restricted because it includes two subjective variables (HE and severity of ascites)[12], and the limited values ranging from 5 to 15 make it imprecise. The boundary values for the five parameters were chosen empirically and have not been formally validated[34]. In some situations, the predictive value of MELD may be reduced. Malabsorption of vitamin K secondary to cholestasis can cause an increase in the INR; starvation and infection can increase the level of bilirubin; and the use of diuretics can increase the level of creatinine[35]. As a quantitative assessment, the ICG-R15 is a simple and practical way to assess liver function and is widely used in patients undergoing liver surgery. The ICG-R15 may play a role in predicting post-TIPS HE; consequently, it may be useful for identifying high-risk patients.

The optimal ICG-R15 cut-off value in our study was 30%, and it divided the patients into two groups with different risks of post-TIPS HE. This difference was highly significant ($P = 0.014$), which implies that TIPS patients with an ICG-R15 > 30% should be given special care during perioperative management. However, we did not compare the role of the CPS, MELD score, and ICG-R15 for predicting the survival of patients after TIPS, which needs further study. In addition, future studies should analyse the incidence of complications and survival between different ICG-R15 groups. A small number of patients with Child-Pugh C cirrhosis and the low median MELD score were limitations of this study. Since this may be related to the small sample size, we will increase the amount of the sample in the future.

In summary, the ICG-R15 can be used for predicting post-TIPS HE in patients with PHT. We propose using the ICG-R15 to evaluate the risk of HE in PHT patients undergoing TIPS.

CONCLUSION

TIPS for PHT in patients with cirrhosis should be considered after careful selection based on patient characteristics and liver function. The ICG-R15 has appreciated clinical value for predicting the occurrence of post-TIPS HE and is a choice for evaluating the prognosis of patients undergoing TIPS.

ARTICLE HIGHLIGHTS

Research background

Transjugular intrahepatic portosystemic shunt (TIPS) is a technique for the treatment of portal hypertension-related complications such as esophageal variceal bleeding and refractory ascites by establishing shunt channels in the hepatic parenchyma between the hepatic vein and the portal vein. It can also be used as a bridging therapy for decompensated patients with cirrhosis and other patients waiting for liver transplantation. However, the high incidence of postoperative hepatic encephalopathy (HE) seriously affects the prognosis and survival of patients, and it is particularly important to find accurate methods to predict post-TIPS HE. Some studies have shown that the clearance rate of indocyanine green before operation has good predictive value for the prognosis of patients undergoing hepatectomy. We hypothesized that indocyanine green retention rate at 15 min (ICG-R15) may can predict postoperative HE after TIPS (post-TIPS HE); therefore, prevention and treatment can be implemented in high-risk HE patients to avoid adverse outcomes.

Research motivation

TIPS is currently used in the management of complications of portal hypertension.

However, the incidence of HE remains an issue in TIPS placement and affects patient quality of life and long-term outcomes. The preoperative ICG-R15 has been developed as a prognostic indicator in patients undergoing surgery, but there are limited data on its role in TIPS. The purpose of this study was to explore whether ICG-R15 can be used as a predictor of post-TIPS HE and compared the clinical value of the ICG-R15, Child-Pugh score (CPS), and model for end-stage liver disease (MELD) score for the prediction of post-TIPS HE in decompensated cirrhosis patients with portal hypertension (PHT).

Research objectives

The aim of this study was to explore whether ICG-R15 can be used as a predictor of post-TIPS HE and compared the clinical value of the ICG-R15, CPS, and MELD score for the prediction of post-TIPS HE in decompensated cirrhosis patients with PHT. According to the ICG-R15 value, appropriate and timely intervention can be implemented in patients with high-risk HE patients.

Research methods

We conducted a prospective study of 195 patients with PHT who underwent elective TIPS. All patients underwent the ICG-R15 test, CPS evaluation, and MELD scoring. According to whether they developed HE or not, the patients were divided into two groups: HE group and non-HE group. Descriptive data are presented as the mean ± SD, and qualitative variables are presented as frequencies or percentages. Student's *t* test or the Mann-Whitney *U* test was utilized to compare quantitative variables between groups, and the chi-square test or Fisher's exact test was used for qualitative variables. Univariate and multivariable logistic regression analyses were used to determine HE-related risk factors after TIPS. The prediction of one-year post-TIPS HE by ICG-R15, CPS, and MELD score was evaluated by the areas under the receiver operating characteristic curves (AUCs). Pairwise comparison of AUCs in three different function tools was analysed.

Research results

A total of 195 patients with PHT were included and 23% (45/195) of the patients developed post-TIPS HE. The ICG-R15 was identified as an independent predictor of post-TIPS HE. The AUCs for the ICG-R15, CPS, and MELD score for predicting post-TIPS HE were 0.664 (95% confidence interval [CI]: 0.557-0.743, P = 0.0046), 0.596 (95%CI: 0.508-0.679, P = 0.087), and 0.641 (95%CI: 0.554-0.721, P = 0.021), respectively. Molodianovitch *et al*[17] showed that there was statistical significance in pairwise comparison between AUCs of ICG-R15 and MELD score (P = 0.0229).

Research conclusions

TIPS for PHT in patients with cirrhosis should be considered after careful selection based on patient characteristics and liver function. The ICG-R15 has appreciated clinical value for predicting the occurrence of post-TIPS HE and is a choice for evaluating the prognosis of patients undergoing TIPS.

Research perspectives

We can learn from this study that monitoring patients who underwent TIPS with an ICG-R15 value above 30% can better prevent adverse outcomes. Future studies will focus on the incidence of complications and survival in terms of the value of ICG-R15 and randomized controlled trials are needed in order to verify our results.

REFERENCES

1 **Tsochatzis EA**, Bosch J, Burroughs AK. Liver cirrhosis. *Lancet* 2014; **383**: 1749-1761 [PMID: 24480518 DOI: 10.1016/S0140-6736(14)60121-5]

2 **Hung ML**, Lee EW. Role of Transjugular Intrahepatic Portosystemic Shunt in the Management of Portal Hypertension: Review and Update of the Literature. *Clin Liver Dis* 2019; **23**: 737-754 [PMID: 31563220 DOI: 10.1016/j.cld.2019.07.004]

3 **Sankar K**, Moore CM. Transjugular Intrahepatic Portosystemic Shunts. *JAMA* 2017; **317**: 880 [PMID: 28245324 DOI: 10.1001/jama.2016.20899]

4 **Fonio P**, Discalzi A, Calandri M, Doriguzzi Breatta A, Bergamasco L, Martini S, Ottobrelli A, Righi D, Gandini G. Incidence of hepatic encephalopathy after transjugular intrahepatic portosystemic shunt (TIPS) according to its severity and temporal grading classification. *Radiol Med* 2017; **122**: 713-721 [PMID: 28510807 DOI: 10.1007/s11547-017-0770-6]

5 **Teng D**, Zuo H, Liu L, Dong J, Ding L. Long-term clinical outcomes in patients with viral hepatitis related liver cirrhosis after transjugular intrahepatic portosystemic shunt treatment. *Virol J* 2018; **15**: 151 [PMID: 30285813 DOI: 10.1186/s12985-018-1067-7]

6 **Zuo L**, Lv Y, Wang Q, Yin Z, Wang Z, He C, Guo W, Niu J, Bai W, Li K, Yu T, Yuan X, Chen H, Liu H, Xia D, Wang E, Luo B, Li X, Yuan J, Han N, Nie Y, Fan D, Han G. Early-Recurrent Overt Hepatic Encephalopathy Is Associated with Reduced Survival in Cirrhotic Patients after Transjugular Intrahepatic Portosystemic Shunt Creation. *J Vasc Interv Radiol* 2019; **30**: 148-153.e2 [PMID: 30638778 DOI: 10.1016/j.jvir.2018.08.023]

7 **Pind ML**, Bendtsen F, Kallemose T, Møller S. Indocyanine green retention test (ICG-r15) as a noninvasive predictor of portal hypertension in patients with different severity of cirrhosis. *Eur J Gastroenterol Hepatol* 2016; **28**: 948-954 [PMID: 27172450 DOI: 10.1097/MEG.0000000000000611]

8 **Haj M**, Rockey DC. Predictors of clinical outcomes in cirrhosis patients. *Curr Opin Gastroenterol* 2018; **34**: 266-271 [PMID: 29846263 DOI: 10.1097/MOG.0000000000000450]

9 **Reinhart MB**, Huntington CR, Blair LJ, Heniford BT, Augenstein VA. Indocyanine Green: Historical Context, Current Applications, and Future Considerations. *Surg Innov* 2016; **23**: 166-175 [PMID: 26359355 DOI: 10.1177/1553350615604053]

10 **Zipprich A**, Kuss O, Rogowski S, Kleber G, Lotterer E, Seufferlein T, Fleig WE, Dollinger MM. Incorporating indocyanin green clearance into the Model for End Stage Liver Disease (MELD-ICG) improves prognostic accuracy in intermediate to advanced cirrhosis. *Gut* 2010; **59**: 963-968 [PMID: 20581243 DOI: 10.1136/gut.2010.208595]

11 **Schwarz C**, Plass I, Fitschek F, Punzengruber A, Mittlböck M, Kampf S, Asenbaum U, Starlinger P, Stremitzer S, Bodingbauer M, Kaczirek K. The value of indocyanine green clearance assessment to predict postoperative liver dysfunction in patients undergoing liver resection. *Sci Rep* 2019; **9**: 8421 [PMID: 31182746 DOI: 10.1038/s41598-019-44815-x]

12 **Kaplan DE**, Dai F, Aytaman A, Baytarian M, Fox R, Hunt K, Knott A, Pedrosa M, Pocha C, Mehta R, Duggal M, Skanderson M, Valderrama A, Taddei TH; VOCAL Study Group. Development and Performance of an Algorithm to Estimate the Child-Turcotte-Pugh Score From a National Electronic Healthcare Database. *Clin Gastroenterol Hepatol* 2015; **13**: 2333-41.e1-6 [PMID: 26188137 DOI: 10.1016/j.cgh.2015.07.010]

13 **Hoekstra LT**, de Graaf W, Nibourg GA, Heger M, Bennink RJ, Stieger B, van Gulik TM. Physiological and biochemical basis of clinical liver function tests: a review. *Ann Surg* 2013; **257**: 27-36 [PMID: 22836216 DOI: 10.1097/SLA.0b013e31825d5d47]

14 **Turco L**, Garcia-Tsao G. Portal Hypertension: Pathogenesis and Diagnosis. *Clin Liver Dis* 2019; **23**: 573-587 [PMID: 31563212 DOI: 10.1016/j.cld.2019.07.007]

15 **Montagnese S**, Russo FP, Amodio P, Burra P, Gasbarrini A, Loguercio C, Marchesini G, Merli M, Ponziani FR, Riggio O, Scarpignato C. Hepatic encephalopathy 2018: A clinical practice guideline by the Italian Association for the Study of the Liver (AISF). *Dig Liver Dis* 2019; **51**: 190-205 [PMID: 30606696 DOI: 10.1016/j.dld.2018.11.035]

16 **Asrani SK**, Kamath PS. Model for end-stage liver disease score and MELD exceptions: 15 years later. *Hepatol Int* 2015; **9**: 346-354 [PMID: 26016462 DOI: 10.1007/s12072-015-9631-3]

17 **Molodianovitch K**, Faraggi D, Reiser B. Comparing the areas under two correlated ROC curves: parametric and non-parametric approaches. *Biom J* 2006; **48**: 745-757 [PMID: 17094340 DOI: 10.1002/bimj.200610223]

18 **Routhu M**, Safka V, Routhu SK, Fejfar T, Jirkovsky V, Krajina A, Cermakova E, Hosak L, Hulek P. Observational cohort study of hepatic encephalopathy after transjugular intrahepatic portosystemic shunt (TIPS). *Ann Hepatol* 2017; **16**: 140-148 [PMID: 28051803 DOI: 10.5604/16652681.1226932]

19 **Lisotti A**, Azzaroli F, Buonfiglioli F, Montagnani M, Cecinato P, Turco L, Calvanese C, Simoni P, Guardigli M, Arena R, Cucchetti A, Colecchia A, Festi D, Golfieri R, Mazzella G. Indocyanine green retention test as a noninvasive marker of portal hypertension and esophageal varices in compensated liver cirrhosis. *Hepatology* 2014; **59**: 643-650 [PMID: 24038116 DOI: 10.1002/hep.26700]

20 **Stauber RE**, Wagner D, Stadlbauer V, Palma S, Gurakuqi G, Kniepeiss D, Iberer F, Smolle KH, Haas J, Trauner M. Evaluation of indocyanine green clearance and model for end-stage liver disease for estimation of short-term prognosis in decompensated cirrhosis. *Liver Int* 2009; **29**: 1516-1520 [PMID: 19732329 DOI: 10.1111/j.1478-3231.2009.02104.x]

21 **Mogicato G**, Vautravers G, Meynaud-Collard P, Deviers A, Sautet J. Blood flows in tributaries of the portal vein: anatomical and angiographic studies in normal beagle dogs. *Anat Histol Embryol* 2015; **44**: 460-467 [PMID: 25376527 DOI: 10.1111/ahe.12161]

22 **Ursic M**, Ravnik D, Hribernik M, Pecar J, Butinar J, Fazarinc G. Gross anatomy of the portal vein and hepatic artery ramifications in dogs: corrosion cast study. *Anat Histol Embryol* 2007; **36**: 83-87 [PMID: 17371378 DOI: 10.1111/j.1439-0264.2006.00719.x]

23 **Maruyama H**, Okugawa H, Ishibashi H, Takahashi M, Kobayashi S, Yoshizumi H, Yokosuka O. Carbon dioxide-based portography: an alternative to conventional imaging with the use of iodinated contrast medium. *J Gastroenterol Hepatol* 2010; **25**: 1111-1116 [PMID: 20594227 DOI: 10.1111/j.1440-1746.2010.06248.x]

24 **Chen SL**, Hu P, Lin ZP, Zhao JB. The Effect of Puncture Sites of Portal Vein in TIPS with ePTFE-Covered Stents on Postoperative Long-Term Clinical Efficacy. *Gastroenterol Res Pract* 2019; **2019**: 2935498 [PMID: 30728835 DOI: 10.1155/2019/2935498]

25 **Luo SH**, Chu JG, Huang H, Zhao GR, Yao KC. Targeted puncture of left branch of intrahepatic

portal vein in transjugular intrahepatic portosystemic shunt to reduce hepatic encephalopathy. *World J Gastroenterol* 2019; **25**: 1088-1099 [PMID: 30862997 DOI: 10.3748/wjg.v25.i9.1088]

26 **Trebicka J**, Bastgen D, Byrtus J, Praktiknjo M, Terstiegen S, Meyer C, Thomas D, Fimmers R, Treitl M, Euringer W, Sauerbruch T, Rössle M. Smaller-Diameter Covered Transjugular Intrahepatic Portosystemic Shunt Stents Are Associated With Increased Survival. *Clin Gastroenterol Hepatol* 2019; **17**: 2793-2799.e1 [PMID: 30940552 DOI: 10.1016/j.cgh.2019.03.042]

27 **Li Y**, He X, Pang H. A model to predict early hepatic encephalopathy in patients undergoing transjugular intrahepatic portosystemic shunt. *Turk J Gastroenterol* 2019; **30**: 702-707 [PMID: 31418414 DOI: 10.5152/tjg.2019.18485]

28 **Casadaban LC**, Parvinian A, Minocha J, Lakhoo J, Grant CW, Ray CE Jr, Knuttinen MG, Bui JT, Gaba RC. Clearing the Confusion over Hepatic Encephalopathy After TIPS Creation: Incidence, Prognostic Factors, and Clinical Outcomes. *Dig Dis Sci* 2015; **60**: 1059-1066 [PMID: 25316553 DOI: 10.1007/s10620-014-3391-0]

29 **Bai M**, Qi X, Yang Z, Yin Z, Nie Y, Yuan S, Wu K, Han G, Fan D. Predictors of hepatic encephalopathy after transjugular intrahepatic portosystemic shunt in cirrhotic patients: a systematic review. *J Gastroenterol Hepatol* 2011; **26**: 943-951 [PMID: 21251067 DOI: 10.1111/j.1440-1746.2011.06663.x]

30 **Bigot A**, Tchan MC, Thoreau B, Blasco H, Maillot F. Liver involvement in urea cycle disorders: a review of the literature. *J Inherit Metab Dis* 2017; **40**: 757-769 [PMID: 28900784 DOI: 10.1007/s10545-017-0088-5]

31 **Hiwatashi K**, Ueno S, Sakoda M, Iino S, Minami K, Mori S, Kita Y, Baba K, Kurahara H, Mataki Y, Maemura K, Shinchi H, Natsugoe S. The Evaluation of Liver Function and Surgical Influence by ICGR15 after Chemotherapy for Colorectal Liver Metastases. *J Cancer* 2016; **7**: 595-599 [PMID: 27053958 DOI: 10.7150/jca.13759]

32 **Wang YY**, Zhao XH, Ma L, Ye JZ, Wu FX, Tang J, You XM, Xiang BD, Li LQ. Comparison of the ability of Child-Pugh score, MELD score, and ICG-R15 to assess preoperative hepatic functional reserve in patients with hepatocellular carcinoma. *J Surg Oncol* 2018; **118**: 440-445 [PMID: 30259515 DOI: 10.1002/jso.25184]

33 **Kokudo T**, Hasegawa K, Amikura K, Uldry E, Shirata C, Yamaguchi T, Arita J, Kaneko J, Akamatsu N, Sakamoto Y, Takahashi A, Sakamoto H, Makuuchi M, Matsuyama Y, Demartines N, Malagó M, Kokudo N, Halkic N. Assessment of Preoperative Liver Function in Patients with Hepatocellular Carcinoma - The Albumin-Indocyanine Green Evaluation (ALICE) Grade. *PLoS One* 2016; **11**: e0159530 [PMID: 27434062 DOI: 10.1371/journal.pone.0159530]

34 **Wong M**, Busuttil RW. Surgery in Patients with Portal Hypertension. *Clin Liver Dis* 2019; **23**: 755-780 [PMID: 31563221 DOI: 10.1016/j.cld.2019.07.003]

35 **Cheng XP**, Zhao J, Chen Y, Meng FK, Xu B, Yu HW, Meng QH, Liu YM, Zhang SB, Meng S, Zhang JY, Zhang JY, Duan ZP, Zheng SJ. Comparison of the ability of the PDD-ICG clearance test, CTP, MELD, and MELD-Na to predict short-term and medium-term mortality in patients with decompensated hepatitis B cirrhosis. *Eur J Gastroenterol Hepatol* 2016; **28**: 444-448 [PMID: 26649802 DOI: 10.1097/MEG.0000000000000538]

World Journal of Gastroenterology

Submit a Manuscript: https://www.f6publishing.com

World J Gastroenterol 2021 February 7; 27(5): 428-441

DOI: 10.3748/wjg.v27.i5.428

ISSN 1007-9327 (print) ISSN 2219-2840 (online)

ORIGINAL ARTICLE

Clinical Trials Study

Noninferiority clinical trial comparing the bowel cleansing efficacy of sodium phosphate tablets (Quiklean®) with a polyethylene glycol/bisacodyl kit

Shih-Ya Hung, Hung-Chang Chen, Tao-Wei Ke, Jiann-Hwa Chen, Koung-Hung Hsiao, Hwei-Ming Wang, Hua-Che Chiang, Sheng-Chi Chang, Yi-Chang Chen, Ming-Hao Hsieh, Yuan-Yao Tsai, Yo-Wen Hsieh, William Tzu-Liang Chen

ORCID number: Shih-Ya Hung 0000-0003-0749-1562; Hung-Chang Chen 0000-0001-9930-7982; Tao-Wei Ke 0000-0001-6847-4008; Jiann-Hwa Chen 0000-0002-8608-6313; Koung-Hung Hsiao 0000-0001-6870-3309; Hwei-Ming Wang 0000-0002-0155-4561; Hua-Che Chiang 0000-0003-0173-3495; Sheng-Chi Chang 0000-0002-7593-6669; Yi-Chang Chen 0000-0003-2958-6773; Ming-Hao Hsieh 0000-0002-8239-4458; Yuan-Yao Tsai 0000-0002-6703-0103; Yo-Wen Hsieh 0000-0002-0523-3482; William Tzu-Liang Chen 0000-0002-6585-2437.

Author contributions: Chen WTL and Chen HC worked on conceptualization, methodology, and project administration; Chen WTL and Hung SY worked on original draft preparation and manuscript editing; Chen HC, Ke TW, Chen JH, Hsiao KH, Wang HM, Chiang HC, Chang SC, Chen YC, Hsieh MH, Tsai YY, and Chen WTL performed colonoscopy, data collection, and data curation; Hsieh YW worked on drug dispensing and pharmaceutical care.

Supported by The China Medical University Hospital, No. DMR-108-125.

Shih-Ya Hung, Graduate Institute of Acupuncture Science, China Medical University, Taichung 40402, Taiwan

Shih-Ya Hung, Department of Medical Research, China Medical University Hospital, Taichung 40447, Taiwan

Hung-Chang Chen, Tao-Wei Ke, Hwei-Ming Wang, Hua-Che Chiang, Sheng-Chi Chang, Yi-Chang Chen, Ming-Hao Hsieh, Yuan-Yao Tsai, Division of Colorectal Surgery, Department of Surgery, China Medical University Hospital, Taichung 40447, Taiwan

Jiann-Hwa Chen, Division of Gastroenterology, Taipei Tzu Chi Hospital, Taipei 23142, Taiwan

Koung-Hung Hsiao, Division of Colorectal Surgery, Taipei Tzu Chi Hospital, Taipei 23142, Taiwan

Yo-Wen Hsieh, Department of Pharmacy, China Medical University Hospital, Taichung 40447, Taiwan

William Tzu-Liang Chen, Department of Colorectal Surgery, China Medical University Hsinchu Hospital, Zhubei 30272, Taiwan

William Tzu-Liang Chen, School of Medicine, China Medical University, Taichung 40402, Taiwan

Corresponding author: William Tzu-Liang Chen, MD, Superintendent, Department of Colorectal Surgery, China Medical University Hsinchu Hospital, No. 199 Sec. 1, Xinglong Road, Zhubei 30272, Taiwan. wtchen@mail.cmuh.org.tw

Abstract

BACKGROUND

Efficient bowel cleansing is essential for a successful colonoscopy, but the ideal cleansing agent, volume, and pharmaceutical dosage form have yet to be determined. Small-volume cleansers enhance patient compliance.

Institutional review board statement: This study was reviewed and approved by the Institutional Review Boards of China Medical University Hospital (CMUH107-REC2-151) and Taipei Tzu Chi Hospital (08-FS-030). Study methods were conducted in accordance with the Institutional Review Board committee guidelines.

Clinical trial registration statement: This study has been registered at https://clinicaltrials.gov/ct2/show/NCT03992365 (ID: NCT03992365).

Informed consent statement: Written informed consent was provided by all study participants.

Conflict-of-interest statement: Quiklean® was provided by Universal Integrated Corporation (Taiwan). The authors have no conflicts of interest to declare.

Data sharing statement: No additional data are available.

CONSORT 2010 statement: The authors have read the CONSORT 2010 Statement, and the manuscript was prepared and revised according to the CONSORT 2010 Statement.

Open-Access: This article is an open-access article which was selected by an in-house editor and fully peer-reviewed by external reviewers. It is distributed in accordance with the Creative Commons Attribution Non Commercial (CC BY-NC 4.0) license, which permits others to distribute, remix, adapt, build upon this work non-commercially, and license their derivative works on different terms, provided the original work is properly cited and the use is non-commercial. See: http://creativecommons.org/licenses/by-nc/4.0/

Manuscript source: Unsolicited manuscript

Specialty type: Gastroenterology and hepatology

Country/Territory of origin: Taiwan

AIM

To compare the bowel cleansing efficacy of 32-tablet sodium phosphate (Quiklean®) with 2-L polyethylene glycol (PEG)/bisacodyl (Klean-Prep/Dulcolax®) under identical dietary recommendations.

METHODS

This multicenter, randomized, parallel-group, noninferiority clinical trial enrolled 472 outpatients, randomized 456 subjects, and scheduled 442 subjects to undergo colonoscopy (Quiklean® = 222 and Klean-Prep/Dulcolax® = 220). After bowel preparation, a colonoscopist performed the colonoscopy with video recorded for rating. The primary efficacy endpoint was the bowel cleansing quality using the Aronchick Scale. The secondary endpoints were the bowel cleansing efficacy of three colon segments, tolerability and acceptability, safety using the Ottawa bowel preparation scale, questionnaires by subjects, and monitoring of adverse events.

RESULTS

Success rates (Excellent + Good) of the bowel cleansing quality by Aronchick Scale were 98.6% (n = 205) and 97.6% (n = 204) in the Quiklean® and Klean-Prep/Dulcolax® groups, respectively. Quiklean® demonstrated noninferiority over Klean-Prep/Dulcolax® in colon cleansing efficacy. Quicken showed better tolerability and acceptability in the overall experience (was rated as excellent; 24.0% *vs* 17.2%; P = 0.0016) and the taste of the study preparation (was rated as excellent, 23.1% *vs* 13.4%; P < 0.0001) than Klean-Prep/Dulcolax®. Safety profiles did not differ between the two groups. Our data indicate that Quiklean® is an adequate, well-tolerated bowel cleansing preparation compared with the standard comparator Klean-Prep/Dulcolax®.

CONCLUSION

Quiklean® is sodium phosphate tablets available on Taiwan's market for bowel preparation; it potentially offers patients an alternative to standard large-volume bowel preparation regimens and may, therefore, increase positive attitudes toward colonoscopies and participation rates.

Key Words: Bowel preparation; Clinical trial; Colonoscopy; Polyethylene glycol; Sodium phosphate

©The Author(s) 2021. Published by Baishideng Publishing Group Inc. All rights reserved.

Core Tip: The bowel cleanser 32-tablet sodium phosphate (Quiklean®) is an adequate bowel cleansing preparation with better tolerability and acceptability than the standard comparator 2-L polyethylene glycol/bisacodyl (Klean-Prep/Dulcolax®).

Citation: Hung SY, Chen HC, Ke TW, Chen JH, Hsiao KH, Wang HM, Chiang HC, Chang SC, Chen YC, Hsieh MH, Tsai YY, Hsieh YW, Chen WTL. Noninferiority clinical trial comparing the bowel cleansing efficacy of sodium phosphate tablets (Quiklean®) with a polyethylene glycol/bisacodyl kit. *World J Gastroenterol* 2021; 27(5): 428-441
URL: https://www.wjgnet.com/1007-9327/full/v27/i5/428.htm
DOI: https://dx.doi.org/10.3748/wjg.v27.i5.428

INTRODUCTION

Optimal bowel cleansing is essential before a colonoscopy, which is the most commonly used and cost-effective method in screening for various diseases, such as colorectal cancer[1]. Bowel preparation is a complex undertaking, involving dietary modifications and laxatives tailored to the individual patient[2]. Several agents are currently available to clean the colon, including sodium picosulfate/magnesium citrate (PSMC), polyethylene glycol (PEG), magnesium citrate, and sodium phosphate products[3]. An adequate bowel preparation that uses effective cleanser results in a high-quality colonoscopy, but the ideal clearing agent, the volume, and the

Peer-review report's scientific quality classification
Grade A (Excellent): 0
Grade B (Very good): 0
Grade C (Good): C
Grade D (Fair): 0
Grade E (Poor): 0

Received: November 5, 2020
Peer-review started: November 5, 2020
First decision: December 13, 2020
Revised: December 24, 2020
Accepted: January 6, 2021
Article in press: January 6, 2021
Published online: February 7, 2021

P-Reviewer: Ho KY
S-Editor: Chen XF
L-Editor: Filipodia
P-Editor: Ma YJ

pharmaceutical dosage form have yet to be determined.

The ideal bowel-cleansing agent should be well-tolerated, easily administered, inexpensive, and produce adequate clearance without allowing explosive gases to form[4]. Bowel preparation quality by different agents is assessed based on their efficacy, safety, and tolerability[5]. Most bowel preparations are either PEG-based or hyperosmotic; many of these regimens are perceived as unpalatable or unpleasant by patients[6]. PEG-containing preparations (*e.g.*, Klean-Prep, GoLYTELY) are large-volume (2-4 L), osmotically-balanced nonabsorbable solutions that act as purgatives to evacuate the intestine; 2-L split-dose PEG preparations are better tolerated than 4-L PEG preparations[3]. Similarly, 2-L PEG/bisacodyl preparations are as effective as the standard 4-L PEG regimens but are better tolerated[3]. Sodium phosphate tablets were developed to improve patient acceptability of the bowel preparation regimen[7]. Sodium phosphate acts as an osmotic purgative, drawing water into the bowel lumen and stimulating peristalsis and evacuation[8]. Sodium phosphate has two oral dosage forms, solution and tablet[9]. Visicol® and OsmoPrep® are sodium phosphate tablets that are used for bowel cleansing before a colonoscopy in the United States[10,11]. However, although sodium phosphate provides excellent cleansing results and is well tolerated by most patients, concerns have been expressed about its safety regarding the osmotic action[8,12]. Moreover, sodium phosphate is not recommended for patients with renal or cardiac disorders or those on diuretic medications[9].

Colonoscopy is an important screening and therapeutic procedure for colon-related diseases[13]. The quality of bowel preparation impacts the success of colonoscopy[13]. Of the various agents available to clean the colon, small-volume cleansers are associated with improved patient compliance (tolerance), which affects bowel-clearing efficacy[14]. However, the efficacy of different small-volume bowel preparation agents has not been clearly defined. Our previous clinical trial found that a small-volume preparation (PSMC 300 mL) had better tolerability, higher acceptability, and compliance than a 2-L PEG/bisacodyl (5 mg)-Klean-Prep/Dulcolax preparation[14]. Tjandra *et al*[9] have shown that a 45-mL sodium phosphate solution was more effective in bowel cleansing than a PSMC preparation. Although these two agents were both accepted well by subjects, the PSMC preparation tasted significantly better than the 45 mL sodium phosphate preparation[9]. In comparison with the 4-L PEG solution, Jung *et al*[7] have shown that sodium phosphate tablets produced equivalent colon cleansing, did not cause more side effects, and had better patient acceptability and satisfaction in relatively young (aged < 60 years), healthy individuals without comorbidities. In 2011, the United States Food and Drug Administration (FDA) withdrew the 2-L PEG bowel cleansing kit HalfLytely containing bisacodyl 10 mg tablets due to safety concerns of ischemic colitis and abdominal cramping compared with the same kit using only bisacodyl 5 mg[15,16].

In Taiwan, 2-L Klean-Prep/bisacodyl (5 mg) is more commonly used than sodium phosphate tablets. The introduction of the 32-tablet sodium phosphate preparation Quiklean® (Universal Integrated Corporation, Taiwan) prompted us to conduct a multicenter, randomized, parallel-group, pre-specified noninferiority study to compare the bowel cleansing efficacy, acceptability, tolerability, and safety of Quiklean® to a 2-L PEG solution Klean-Prep (Helsinn-Birex Pharmaceuticals Limited, Ireland) combined with bisacodyl 5 mg (Dulcolax®, Boehringer Ingelheim, Germany) before the colonoscopy in 422 outpatients of Taiwanese populations. The objective was to compare the bowel cleansing efficacy, acceptability and tolerability, and safety of Quiklean® to Klean-Prep/Dulcolax® for bowel preparation.

MATERIALS AND METHODS

Study design and trial information

This randomized, active-controlled, evaluator-blinded, noninferiority, parallel, multicenter phase III clinical trial (ClinicalTrials.gov Identifier: NCT03992365; first posted date: June 20, 2019) was conducted in China Medical University Hospital (Taiwan) and Taipei Tzu Chi Hospital (Taiwan).

Before trial initiation and subject enrollment, the Institutional Review Boards of China Medical University Hospital (CMUH107-REC2-151) and Taipei Tzu Chi Hospital (08-FS-030) approved the study, and Taiwan's FDA approved the study protocol on January 17, 2019 (version: v2.0).

Sample size calculation, subject information, and selection of study participants

For sample size estimation, we assumed a conservative, successful cleaning response

rate of 85% with Quiklean® and that the true difference in response rates between the Quiklean® and Klean-Prep/Dulcolax® groups would be zero. The sample size calculation was determined by assuming a 10% noninferiority margin, at least 80% power, and a one-sided significance level of 0.025. Based on these assumptions, this trial required 205 subjects per group to verify the noninferiority of Quiklean® over Klean-Prep/Dulcolax®. It was anticipated that up to 10% of randomized subjects were ineligible for the per-protocol population. Approximately 456 subjects were therefore recruited to provide 410 evaluable subjects. After the trial was started, a total number of 472 subjects were enrolled between June 10, 2019 and October 15, 2019; 456 subjects were subsequently randomized to receive either the Quiklean® (n = 228) or Klean-Prep/Dulcolax® (n = 228) regimen. A flow chart detailing the study design and timetable of four visits (screening, randomization, colonoscopy, and post-colonoscopy follow-up) is depicted in Figure 1A. The study event schedule performed during each visit is detailed in Table 1. After undergoing screening for inclusion and exclusion criteria in Visit 1, patients completed informed written consent forms and underwent physical examinations that assessed vital signs, signs of pregnancy, liver and renal functions, and serum electrolyte levels. The inclusion and exclusion criteria of this study are presented in Supplementary Table 1. An overview of subject disposition (enrollment, randomization, study withdrawals, colonoscopy, and post-colonoscopy follow-up) is provided in Figure 1B.

Dietary advice

At the time of randomization, each study subject received standardized dietary advice with a dietary card containing detailed instructions about dietary measures to be taken and Quiklean® or Klean-Prep/Dulcolax® consumption. Subjects were instructed to give the completed dietary card and the empty bag or any remaining package of study regimen on the day of colonoscopy to the unblinded study coordinator, who recorded the following information: (1) Standard dietary advice; (2) The start time, the end time, and the number of bowel movements after the first regimen of the study product before colonoscopy; (3) The number of cups of clear water consumed; and (4) Adverse events experienced during consumption of the bowel preparation.

Drug administration and compliance of the study regimen

The Quiklean® regimen contained 32 tablets, each tablet containing 1.102 g of sodium phosphate monobasic monohydrate (United States Pharmacopoeia grade) and 0.398 g of sodium phosphate dibasic anhydrous (United States Pharmacopoeia grade), for a total of 1.5 g of sodium phosphate per tablet. Subjects were instructed to undertake the following procedures: (1) The evening before the colonoscopy: Ingest four tablets with 250 mL of clear liquids every 15 min, for a total of 20 tablets; and (2) On the day of the colonoscopy: Starting 3-5 h before the procedure, ingest four tablets with 250 mL of clear liquids every 15 min, for a total of 12 tablets. The Klean-Prep/Dulcolax® procedure (two sachets of Klean-Prep with one tablet of Dulcolax®) required subjects to prepare Klean-Prep (ingredients per sachet: 59 g PEG 3350, 5.685 g anhydrous sodium sulfate, 1.685 g sodium bicarbonate, 1.465 g sodium chloride, 0.7425 g potassium chloride, and 0.0494 g aspartame) immediately before each administration, by mixing one sachet of Klean-Prep with 1000 mL of cold water at room temperature, stirring thoroughly until the solution became clear as previously described[14]. The Klean-Prep/Dulcolax® administration was as follows: (1) In the afternoon before the day of colonoscopy: Ingest one 5 mg tablet of Dulcolax® (without chewing or crushing the tablet); (2) About 4 h after taking Dulcolax®, subjects were instructed to drink 1000 mL of Klean-Prep solution over a 2-h period or approximately 250 mL every 15 min; and (3) On the day of the colonoscopy: 3-5 h before the procedure, subjects were instructed to drink the other 1000 mL Klean-Prep solution at a rate of 250 mL every 15 min. The subject's self-completed dietary card supplied details on compliance with Quiklean® or Klean-Prep/Dulcolax®, as to whether the subject drank the required amount of water or solution, as follows: (1) Excellent compliance, claiming ingestion of at least 8 cups of clear water/solution (one cup is equivalent to 250 mL); (2) Good compliance, claiming ingestion of at least 6 cups and fewer than 8 cups of clear water/solution; (3) Medium compliance, claiming ingestion of at least 4 cups and fewer than 6 cups of clear water/solution; (4) Poor compliance, claiming ingestion of fewer than 4 cups of clear water/solution; and (5) Non-compliance, claiming ingestion of 0 cups of clear water/solution.

Subjects and treatment

The study consisted of four clinical visits, according to a predefined schedule. Subjects

Table 1 Study event schedule

	Screening visit	Randomization visit[1]	Regimen start	Colonoscopy visit	Follow-up visit
Visit	1	2		3	4
Day	-8 to -1	-8 to -1	1	2	9-16
Informed consent	X				
Inclusion/exclusion	X	X			
Medical history	X				
Demographic data	X				
Physical examination	X				X
Vital signs	X			X	X
Urine pregnancy test	X				
12-Lead electrocardiogram	X				X
Renal function	X[2]			X[3]	X
Electrolytes	X[2]			X[3]	X
Randomization		X			
Dietary control			X		
Dispensing of study drug		X			
Dosing day			X[4]	X	
Dietary card			X	X	
Subject questionnaire				X[5]	
Colonoscopy				X	
Aronchick scale				X[6]	
Ottawa bowel preparation scale (OBPS)				X[6]	
Bowel preparation compliance				X	
Concomitant medication	X	X	X	X	X
Reported events[7]			X	X	
Unsolicited adverse events and serious adverse events			X	X	X

[1]Indicates that the screening day and randomization day could be the same. However, the activities listed for the Screening Visit had to be completed before randomization.
[2]Indicates that after obtaining baseline laboratory data, the subject was randomized if s/he did not meet exclusion criteria No. 9.
[3]Indicates that laboratory tests were performed after completion of investigation procedures and following the colonoscopy.
[4]Indicates that the first dosing day was scheduled to follow the dispensing of study drug instructions.
[5]Indicates that tolerability and satisfaction of the preparation was measured by a standardized subject questionnaire administered on the day of colonoscopy, prior to the procedure.
[6]Indicates that all colonoscopies were videorecorded. After the colonoscopy, independent blinded colonoscopists rated the video recordings for Aronchick Scale and Ottawa bowel preparation scale scores.
[7]Indicates that reported adverse events were recorded in the dietary card.

were screened on Visit 1 and randomized into the study on Visit 2. Colonoscopy was performed on Visit 3, and post-colonoscopy follow-up was conducted on Visit 4 (Figure 1A). After obtaining informed consent from the subject, the designated assessment was performed. If the eligibility criteria were satisfied, the subjects were randomly assigned (1:1) to either the Quiklean® or Klean-Prep/Dulcolax® regimen and scheduled to undergo colonoscopy. The colonoscopy visit was arranged within 10 d of screening (Figure 1A). Subjects were instructed on how to take the study medication, and each study group was issued with identical standard dietary instructions. After undergoing bowel-clearing preparation, the colonoscopy was performed in the morning by the experienced colonoscopist, with the entire colonoscopy recorded by video. After the completion of colonoscopy, the quality of bowel cleansing in the video

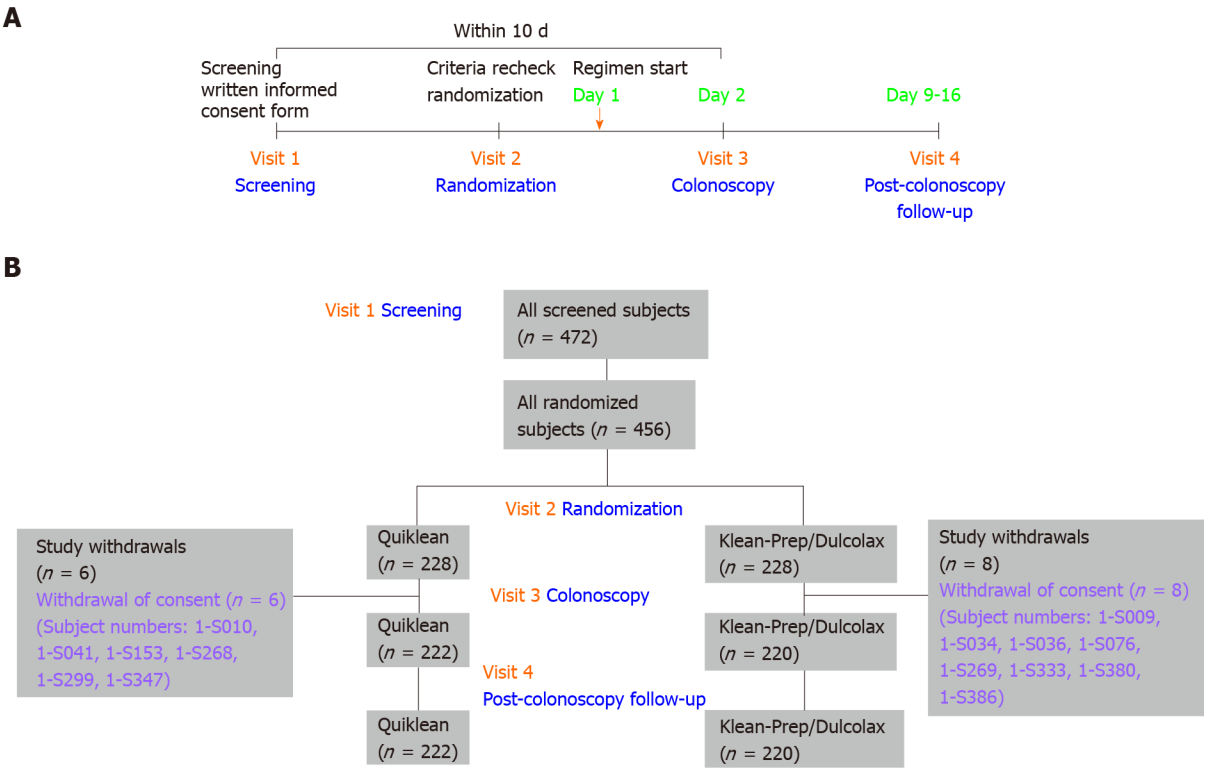


Figure 1 Flow diagram of our randomized trial comparing Quiklean® with Klean-Prep/Dulcolax®. A: Flow chart of the study design and timetable; B: Flow diagram of study subjects and subject numbers, with reasons for withdrawals.

recording was rated by independent colonoscopists blinded to treatment allocation. The colonoscopists jointly evaluated the scoring system before the study commenced in order to minimize interobserver variability.

Efficacy and safety outcome variables

Aronchick Scale and Ottawa bowel preparation scale (OBPS) scores graded colon cleanliness[17,18]. The primary endpoint of this study was the efficiency of colon cleansing according to the modified Aronchick Scale, as follows: Excellent = only a small volume of clear liquid or > 95% of the surface was observed; Good = a large volume of clear liquid covered 5%-25% of the surface, but > 90% of the surface was observed; Fair = some semi-solid stools were found, but these could be suctioned or washed away and > 90% of the surface was observed; Poor = semi-solid stools were found that could not be suctioned or washed away and < 90% of the surface was observed; and Inadequate = the subject was required to undergo a repeat preparation process[17]. Successful and unsuccessful bowel preparations were defined as "Excellent + Good" and "Fair + Poor + Inadequate", respectively. For the secondary endpoint, the OBPS evaluated subjects' acceptance and tolerance of the preparation, as well as cleansing efficacy in the ascending, mid- (transverse and descending), and rectosigmoid segments of the colon[18]. OBPS scores for each colon segment were graded on a 5-point scale, as follows: Excellent = 0; Good = 1; Fair = 2; Poor = 3; and Inadequate = 4[18]. OBPS scores ranged from 0 to 14 (fluid scores, 0-2; scores of ascending + mid + rectosigmoid segments, 0-12)[18]. The colonoscopist rated the overall fluid amount on a 3-point scale (where 0 = mild; 1 = moderate; 2 = large)[18]. Safety was assessed by monitoring adverse events and laboratory examinations. All adverse events were coded using MedDRA Preferred Terms. All study procedures, including efficacy and safety measurements, were performed according to the schedule described in Table 1.

Analysis sets

Our analysis used the International Council for Harmonisation of Technical Requirements for Registration of Pharmaceuticals for Human Use recommendations in guidelines E3 and E9 regarding intent-to-treat, per-protocol, and safety analysis sets. Among 456 randomized subjects, 442 (Quiklean® = 222 and Klean-Prep/Dulcolax® = 220) who received study medications and underwent colonoscopy were included in

the intent-to-treat analysis set and safety analysis set. After excluding 25 subjects from the intent-to-treat analysis set, 417 subjects (Quiklean® = 208 and Klean-Prep/Dulcolax® = 209) were included in the per-protocol analysis set. Supplementary Table 2 (lower) lists the reasons concerning exclusions from the per-protocol analysis set; Supplementary Table 3 lists subjects in the intent-to-treat set who were excluded from the per-protocol analysis set. Supplementary Table 2 also details patient disposition data for each group, each analysis set, and reasons for study withdrawals. No significant between-group differences were identified for baseline characteristics, including sex, age, body weight, height, and body mass index in the per-protocol analysis set (Supplementary Table 4).

Statistical analysis

The statistical analysis in this study was implemented by a contract research organization, StatPlus Inc., which used SAS® Version 9.4 (Cary, NC, United States); the Taiwan FDA approved the results. The primary efficacy variable was the percentage of subjects who achieved "success rate" (Excellent + Good) in overall colon cleansing, based on the Aronchick Scale in both the intent-to-treat and per-protocol analysis sets. The differences in success rates (Excellent + Good) were calculated using Fisher's exact test with associated exact 95% confidence intervals (CIs)[19]. Noninferiority was satisfied if the lower bound of the two-sided 95%CI for the difference in the success rate (Quiklean® minus Klean-Prep/Dulcolax®) was at least −10%; $P < 0.05$ was regarded as statistically significant[14]. The secondary endpoint included bowel cleaning efficacy by OBPS and the subject's responses to acceptability and tolerability. The overall score and each colon segment score of OBPS were used to analyze the secondary endpoint by Fisher's exact test and independent *t*-tests. The total OBPS score was categorized as excellent cleansing (score 0-1), good (score 2-4), sufficient (score 5-7), poor (score 8-10), or inappropriate (score 11-14). The subject's responses in the questionnaire regarding acceptability and tolerability, numbers, and percentages were categorized by the responses on each questionnaire for each group and analyzed by the Fisher's exact test for binary variables and the Cochran-Mantel-Haenszel test with relative to an identified distribution integral transformation scores for ordered categorical variables. All safety parameters, including adverse events, clinical laboratory evaluations, and vital signs, were summarized with descriptive statistics for the two groups, and each scheduled a return visit.

RESULTS

Subject randomization and study withdrawal rates

The study design and visit timetable (screening, randomization, colonoscopy, and post-colonoscopy follow-up) are depicted in the flow chart illustrated in Figure 1A. In the beginning, 472 subjects were screened in Visit 1, and 16 subjects within that did not pass criteria recheck in Visit 2; then 456 subjects were randomized in the trial. Study withdrawal rates were 2.6% and 3.5% for Quiklean® and Klean-Prep/Dulcolax®, respectively (Supplementary Table 2). In both groups, the reason cited for withdrawal was the subjects' withdrawal of consent (Figure 1B, Supplementary Table 2).

Bowel cleansing efficacy by the Aronchick Scale

The primary endpoint of our trial was the "success rate" (Excellent + Good) of bowel cleansing, evaluated by the Aronchick Scale, which graded 24.0%, 74.5%, 1.4%, 0%, and 0% of the Quiklean® per-protocol analysis set and 33%, 64.6%, 1.9%, 0%, and 0% of the Klean-Prep/Dulcolax® per-protocol analysis set as Excellent, Good, Fair, Poor, and Inadequate, respectively (Table 2). Success rates (Excellent + Good) were 98.6% (n = 205) and 97.6% (n = 204) in the Quiklean® and Klean-Prep/Dulcolax® groups, respectively; the between-group difference was 0.95% (95%CI: −8.620%, 10.525%) (Table 2). For the primary endpoint assessed by the Aronchick Scale, Quiklean® demonstrated noninferiority over Klean-Prep/Dulcolax® since the lower confidence bound of the two-sided 95%CI of the treatment difference (Quiklean® minus Klean-Prep/Dulcolax®) was greater than the pre-specified margin of −10%.

Bowel cleansing efficacy of three colonic segments rated by the OBPS

One of our four secondary endpoints was bowel cleansing efficacy in three colonic segments, evaluated by the OBPS. Mean overall OBPS scores were 2.5 ± 1.48 in the Quiklean® cohort (n = 208) and 2.5 ± 1.68 in the Klean-Prep/Dulcolax® cohort (n = 208),

Table 2 The primary endpoint of bowel cleansing efficacy as assessed by the Aronchick Scale (per-protocol analysis set)

	Quiklean®, *n* = 208	Klean-Prep/Dulcolax®, *n* = 209	*P* value
Responses			
Successful (Excellent + Good)	205	204	
Unsuccessful (Fair + Poor + Inadequate)	3	5	
Success rate	98.6%	97.6%	
Between-group difference	0.95%		
95% exact CI	(-8.620%, 10.525%)		
Rating, *n* (%)			
Excellent	50 (24.0)	69 (33.0)	0.1355
Good	155 (74.5)	135 (64.6)	
Fair	3 (1.4)	4 (1.9)	
Poor	0	1 (0.5)	
Inadequate	0	0	

P value was obtained by Chi-Square test. CI: Confidence interval.

without statistical between-group significance (P = 0.733; Table 3). Success rates (Excellent + Good + Fair) for overall bowel cleansing quality were 100% with Quiklean® and 99.0% with Klean-Prep/Dulcolax® (P = 0.4988; Table 3). The success rates for the ascending colon were 100% for both groups (P = 1.0000); 100% for the transverse colon with Quiklean® and 99.5% with Klean-Prep/Dulcolax® (P = 1.0000); 100% for the descending colon with Quiklean® and 98.6% with KleanPrep/Dulcolax® (P = 0.2482).

Acceptability and tolerability

The other three secondary endpoints of our trial were acceptability, tolerability, and safety, as rated by each subject. Subject ratings did not differ between the groups regarding how easy or difficult the preparations were to consume (Table 4). All 208 Quiklean® recipients (100%) and 207 Klean-Prep/Dulcolax® recipients (99%) could consume the study preparation as instructed (P = 0.4988; Table 4). A significantly higher proportion of Quiklean® *vs* Klean-Prep/Dulcolax® recipients rated their overall experience as "Excellent" (24.0% *vs* 17.2%; P = 0.0016; Table 4). The taste of the study preparation was rated as excellent by more Quiklean® than Klean-Prep/Dulcolax® recipients (23.1% *vs* 13.4%; P < 0.0001; Table 4). A total of 80.3% of Quiklean® recipients and 72.7% of Klean-Prep/Dulcolax® recipients stated they would choose the same regimen again in the future (P = 0.0830; Table 4). The proportions of subjects claiming they would refuse the same preparation in the future did not differ significantly between the groups (P = 0.2007; Table 5).

Safety results

Reported adverse events were reported by similar proportions of Quiklean® and Klean-Prep/Dulcolax® recipients (P = 0.4944) including nausea (P = 0.0299), vomiting (P = 0.0126), abdominal pain/cramping (P = 0.0333), abdominal bloating (P = 0.0080), urticaria (P = 1.0000), anal irritation (P = 0.1865), and edema (P = 0.4483). Although Quiklean® recipients had significantly higher rates of nausea, vomiting, and abdominal bloating than Klean-Prep/Dulcolax® recipients, the Klean-Prep/Dulcolax® preparation was associated with higher rates of abdominal pain/cramping than Quiklean®; all reported adverse events were deemed to be mild in intensity. During the study period, 98.2% of Quiklean® recipients and 31.8% of Klean-Prep/Dulcolax® recipients reported at least one treatment-emergent adverse event (P < 0.0001; Table 5); corresponding proportions reporting at least one study drug-related treatment-emergent adverse event were 97.7% and 20.5%, respectively. Although Quiklean® was associated with a significantly higher incidence of any study drug-related treatment-emergent adverse event than Klean-Prep/Dulcolax®, no severe treatment-emergent adverse events resulted in discontinuation or death. The top two reported treatment-emergent adverse events associated with Quiklean® were an increase in blood phosphorus and a

Table 3 The secondary endpoint of overall bowel cleansing efficacy as assessed by the Ottawa bowel preparation scale (per-protocol analysis set)

	Quiklean®, *n* = 208	Klean-Prep/Dulcolax®, *n* = 209	*P* value
Total bowel preparation score			
mean ± SD	2.5 ± 1.48	2.5 ± 1.68[1]	0.7333[2]
Median (Min, Max)	3.0 (0, 7)	3.0 (0, 9)	
Overall bowel cleansing quality, *n* (%)			
Success (Excellent + Good + Fair)	208 (100)	206 (99)[1]	0.4988[3]
Un-success (Poor + Inadequate)	0 (0)	2 (1)	

[1]Indicates that subject 1-S074-R1074 had previously undergone removal of an ascending colon segment.
[2]Indicates that *P* value was obtained by independent *t*-test.
[3]Indicates that *P* value was obtained by Fisher's exact test. SD: Standard deviation.

decrease in blood potassium (97.3% and 49.1%; $P < 0.0001$); the most commonly reported treatment-emergent event with Klean-Prep/Dulcolax® was a decrease in blood phosphorus (19.1%; $P < 0.0001$) (Table 5). Blood electrolytes that differed significantly between the study groups included phosphorous, potassium, and sodium (Table 5). None of these electrolytes differed significantly between the groups at Visit 1/screening (baseline) (Supplementary Tables 5, 6, and 7, respectively). Compared with baseline values at Visit 1 (screening), phosphorus levels were found to be significantly increased with Quiklean® and significantly decreased with Klean-Prep/Dulcolax® at Visit 3 (colonoscopy) ($P < 0.0001$ for both intra-group comparisons); both values were restored to baseline values by Visit 4 (post-colonoscopy follow-up) (Supplementary Table 5). The normal range of serum potassium is 3.5-5.0 mmol/L; the level in patients with moderate hypokalemia is 2.5-3.0 mmol/L[20]. Supplementary Table 6 shows that the means of blood potassium levels were significantly decreased from baseline (Quiklean® = 3.87 mmol/L and Klean-Prep/Dulcolax® = 3.89 mmoL) in both study groups at Visit 3 (Quiklean® = 3.08 mmol/L and Klean-Prep/Dulcolax® = 3.60 mmoL) and had returned to baseline in both groups at Visit 4 (Quiklean® = 3.89 mmol/L and Klean-Prep/Dulcolax® = 3.88 mmoL). Conversely, blood sodium levels were significantly increased in both study groups at Visit 3 and had returned to baseline in both groups at Visit 4 (Supplementary Table 7). On Visits 1, 3, and 4, no statistically significant between-group differences were identified for renal function (serum creatinine and blood urea nitrogen) or vital signs (body temperature, blood pressure, pulse rate, respiration rate, and body weight); all of these values remained within the normal range during the study period.

DISCUSSION

Adequate bowel preparation is essential for high-quality colonoscopies capable of detecting diseases of the colon and rectum. Ideal preparation would rapidly and reliably eliminate all fecal material from the colon without causing any gross or histological alternations of the colonic mucosa[21,22]. Moreover, the preparation would not cause any discomfort and would be safe for the patient[23]. In this study, 32 tablets of Quiklean® (1.5 g sodium phosphate per tablet) demonstrated noninferiority over two sachets of Klean-Prep combined with one tablet of 5 mg Dulcolax® (Klean-Prep/Dulcolax®) for colon cleansing before colonoscopy, according to Aronchick Scale scores. Secondary endpoint evaluations revealed similar success rates for bowel cleansing quality in the overall and individual colon segments, according to OBPS scores. Acceptability and tolerability ratings demonstrated that Quiklean® was easier to consume, tasted better, and was more often rated as an overall excellent experience during bowel preparation than Klean-Prep/Dulcolax®. Patient satisfaction scores indicated that more subjects would prefer Quiklean® over Klean-Prep/Dulcolax® in the future. Visit 3 (colonoscopy) safety data revealed that Quiklean® was associated with increases from baseline in blood phosphorus and sodium, as well as a decrease in blood potassium, while Klean-Prep/Dulcolax® was associated with reductions from baseline in blood phosphorus and potassium, and an increase in blood sodium. In both study groups, all values were restored to baseline by Visit 4 (post-colonoscopy follow-

Table 4 Acceptability and tolerability (per-protocol analysis set), *n* (%)

	Quiklean®, *n* = 208	Klean-Prep/Dulcolax®, *n* = 209	*P* value
1 How easy or difficult was it to consume the study drug?			
Very easy	68 (32.7)	48 (23.0)	0.1201[1]
Easy	96 (46.2)	110 (52.6)	
Tolerable	23 (11.1)	25 (12.0)	
Difficult	18 (8.7)	25 (12.0)	
Very difficult	3 (1.4)	1 (0.5)	
2 Were you able to consume the study preparation as instructed?			
Yes	208 (100)	207 (99.0)	0.4988[2]
No	0	2 (1.0)	
3 Please describe your overall experience with the study preparation.			
Excellent	50 (24.0)	36 (17.2)	0.0016[1]
Good	112 (53.8)	109 (52.2)	
Fair	21 (10.1)	12 (5.7)	
Poor	24 (11.5)	43 (20.6)	
Bad	1 (0.5)	9 (4.3)	
4 The taste of this study preparation was			
Excellent	48 (23.1)	28 (13.4)	< 0.0001[1]
Good	82 (39.4)	82 (39.2)	
Fair	41 (19.7)	17 (8.1)	
Poor	35 (16.8)	65 (31.1)	
Bad	2 (1.0)	17 (8.1)	
5 Would you ask your doctor for this preparation again if you need another colonoscopy in the future?			
Yes	167 (80.3)	152 (72.7)	0.0830[2]
No	41 (19.7)	27.3)	
6 Would you refuse the same preparation again if it were to be prescribed to you in the future?			
Yes	42 (20.2)	54 (25.8)	0.2007[2]
No	166 (79.8)	155 (74.2)	

[1]Indicates that *P* value was obtained by Cochran-Mantel-Haenszel test.
[2]Indicates that *P* value was obtained by Fisher's exact test.

up). Our data suggest that the new bowel-clearing preparation Quiklean® may increase patients' positive attitudes and participation in bowel preparation for colonoscopy.

The quality of bowel preparation can be rated during colonoscopy, and thus the superiority of one bowel preparation method can be effectively compared with others[24]. The Aronchick Scale is one such rating scale that is universally accepted and has been used in pivotal trials that have resulted in new drug application approvals, including that of HalfLytely[17]. The OBPS is associated with high interobserver agreement and reliability, whether used as a total score or for individual colon segments[18]. In the present study, our independent blinded colonoscopists used both the Aronchick Scale and OBPS to rate bowel cleansing quality. Their ratings demonstrate noninferiority for Quiklean® over Klean-Prep/Dulcolax®.

Many bowel-clearing preparations are available on the market. It is advised that the choice of any such regimen should be based on cleansing efficacy first and patient tolerability second, although these factors are undoubtedly closely interrelated[5]. For example, poor tolerability that prevents full compliance with a bowel cleansing regimen may mean inadequate cleansing[5]. Comparing sodium phosphate and other

Table 5 Summary of treatment-emergent adverse events (safety analysis set), *n* (%)

Treatment-emergent adverse events	Quiklean®, *n* = 222	Klean-Prep/Dulcolax®, *n* = 220	*P* value
Any treatment-emergent adverse events	218 (98.2)	70 (31.8)	< 0.0001
Mild	217 (97.7)	70 (31.8)	
Moderate	1 (0.5)	0	
Severe	0	0	
Life threatening	0	0	
Death	0	0	
MedDRA preferred term			
Blood phosphorus increased	216 (97.3)	8 (3.6)	< 0.0001
Blood potassium decreased	109 (49.1)	9 (4.1)	< 0.0001
Blood phosphorus decreased	6 (2.7)	42 (19.1)	< 0.0001
Blood urea decreased	16 (7.2)	7 (3.2)	0.0847
Blood chloride decreased	14 (6.3)	8 (3.6)	0.2740
Blood chloride increased	6 (2.7)	7 (3.2)	0.7867
Blood calcium decreased	6 (2.7)	1 (0.5)	0.1221
Blood sodium decreased	7 (3.2)	0	0.0149
Blood creatinine decreased	2 (0.9)	1 (0.5)	1.0000
Blood urea increased	1 (0.5)	2 (0.9)	0.6224
Blood magnesium increased	2 (0.9)	0	0.4989
Blood sodium increased	1 (0.5)	1 (0.5)	1.0000
Blood creatinine increased	1 (0.5)	0	1.0000
Blood potassium increased	1 (0.5)	0	1.0000
Duodenal ulcer	0	1 (0.5)	0.4977
Nonalcoholic fatty liver disease	0	1 (0.5)	0.4977
Herpes zoster	0	1 (0.5)	0.4977
Pyoderma	0	1 (0.5)	0.4977
Muscle disorder	0	1 (0.5)	0.4977
Calculus urinary	1 (0.5)	0	1.0000
Asthma	1 (0.5)	0	1.0000
Rhinitis allergic	1 (0.5)	0	1.0000

P value: Between-group differences were compared using the Fisher's exact test.

bowel preparation agents has shown that sodium phosphate is better tolerated by patients, making this a preferred method of preparing colonoscopy for specific patient subgroups[25,26]. Sodium phosphate tablets were developed to improve patient acceptability of the bowel preparation and have been reported to be similar or better than PEG solution for patient compliance in Western countries and Japan[11,27,28]. In the present study, Quiklean® had higher acceptability and tolerability than Klean-Prep/Dulcolax®. Quiklean® may offer Taiwanese patients a suitable agent that is very effective and well-tolerated for colon cleansing before colonoscopy.

Significant dehydration and electrolyte abnormalities have been described with the use of oral sodium phosphate[8]. Two major safety issues are related to its use: First, the osmotic action of this agent can draw fluid from the intravascular space and potentially lead to hypovolemia; second, most patients develop transient mild hyperphosphatemia that could potentially result in symptoms caused by hypocalcemia[8]. However, evidence from 26 clinical trials involving 2496 subjects administered oral sodium phosphate solution and 526 subjects who received sodium

phosphate tablets show no major adverse events attributed to sodium phosphate[8]. Most of those studies excluded patients with heart failure, renal failure, ascites, and/or myocardial infarction within the previous 6 mo[8]. In our study, the exclusion criteria also included renal insufficiency, cardiovascular diseases, and myocardial infarction to avoid significant adverse events. Serum potassium is closely regulated physiologically with normal values ranging from 3.5 mmol/L to 5.0 mmol/L, and moderate hypokalemia (2.5-3.0 mmol/L) can be highly arrhythmogenic in normal hearts[20]. In subjects of Quiklean® group, the mean blood potassium levels of Visit 1, Visit 3, and Visit 4 were 3.87 mmol/L, 3.08 mmol/L, and 3.89 mmol/L, respectively. The data in Klean-Prep/Dulcolax® group were 3.89 mmol/L, 3.60 mmol/L, and 3.88 mmol/L, respectively. Indicating the changes in serum potassium levels in subjects of Quiklean® group did not cause severe and life-threatening hypokalemia. In the present study, we identified significantly higher rates of nausea, vomiting, and abdominal bloating with Quiklean® compared with Klean-Prep/Dulcolax®, while abdominal pain/cramping was significantly more likely with Klean-Prep/Dulcolax® than with Quiklean®; all reported adverse events reported in this study were judged to be mild in intensity. Moreover, treatment-emergent adverse events were similar for both study groups. No severe treatment-emergent adverse events occurred.

Our limitations in this study include the fact that during the enrollment process, we included subjects aged between 20 and 74 years and excluded subjects with significant cardiovascular or renal impairment, significant gastrointestinal disease, acute exacerbation of inflammatory bowel disease, or pregnancy. Thus, our safety data for Quiklean® should not be applied to the older elderly (> 75 years) with significant comorbidities. Significant dehydration and electrolyte abnormalities have been described with sodium phosphate. Our study detected changes from baseline (Visit 1/screening) in both study groups for renal function measures and electrolytes at Visit 3 (colonoscopy). Quiklean® induced increases in blood phosphorous and sodium and a decrease in potassium, while Klean-Prep/Dulcolax® induced decreases in blood phosphorous and potassium and an increase in sodium; all values were restored to normal levels in both groups by Visit 4 (post-colonoscopy follow-up). The 7-d to the 14-d interval between colonoscopy and follow-up prevents us from knowing the details about the electrolyte changes over this timeframe.

CONCLUSION

Adequate bowel preparations are critical for high-quality colonoscopy examinations and successful colonoscopy screening or surveillance programs. In conclusion, 32 tablets of Quiklean® (1.5 g per tablet) demonstrated noninferiority over two Klean-Prep sachets combined with one tablet of Dulcolax® for the outcome of effective colon cleansing. Patient satisfaction ratings indicated a higher preference for Quiklean® compared with Klean-Prep/Dulcolax®. Quiklean® may, therefore, increase patients' positive attitudes and participation in bowel preparation for colonoscopy.

ARTICLE HIGHLIGHTS

Research background

Efficient bowel cleansing is essential for a successful colonoscopy.

Research motivation

The ideal cleansing agent, volume, and pharmaceutical dosage form have yet to be determined. Small-volume cleansers enhance patient compliance.

Research objectives

To compare the bowel cleansing efficacy of 32-tablet sodium phosphate (Quiklean®) with 2-L polyethylene glycol (PEG)/bisacodyl (Klean-Prep/Dulcolax®) under identical dietary recommendations.

Research methods

This multicenter, randomized, parallel-group, noninferiority clinical trial enrolled 472 outpatients, randomized 456 subjects, and scheduled 442 subjects to undergo colonoscopy (Quiklean® = 222 and Klean-Prep/Dulcolax® = 220). After bowel

preparation, a colonoscopist performed the colonoscopy with video recorded for rating. The primary efficacy endpoint was the bowel cleansing quality using the Aronchick Scale. The secondary endpoints were the bowel cleansing efficacy of three colon segments, tolerability and acceptability, and safety using the Ottawa bowel preparation scale, questionnaires by subjects, and monitoring of adverse events.

Research results

Success rates (Excellent + Good) of the bowel cleansing quality by Aronchick Scale were 98.6% (n = 205) and 97.6% (n = 204) in the Quiklean® and Klean-Prep/Dulcolax® groups, respectively. Quiklean® demonstrated noninferiority over Klean-Prep/Dulcolax® in colon cleansing efficacy. Quicken showed better tolerability and acceptability in the overall experience (was rated as excellent; 24.0% *vs* 17.2%; P = 0.0016) and taste of the study preparation (was rated as excellent, 23.1% *vs* 13.4%; P < 0.0001) than Klean-Prep/Dulcolax®. Safety profiles did not differ between the two groups. Our data indicate that Quiklean® is an adequate, well-tolerated bowel cleansing preparation compared with the standard comparator Klean-Prep/Dulcolax®.

Research conclusions

Quiklean® is sodium phosphate tablets available on Taiwan's market for bowel preparation; it potentially offers patients an alternative to standard large-volume bowel preparation regimens and may, therefore, increase positive attitudes toward colonoscopies and participation rates.

Research perspectives

The bowel cleanser 32-tablet sodium phosphate (Quiklean®) is an adequate bowel cleansing preparation with better tolerability and acceptability as compared with the standard comparator 2-L polyethylene glycol (PEG)/bisacodyl (Klean-Prep/Dulcolax®).

REFERENCES

1 **Sonnenberg A**, Delcò F, Inadomi JM. Cost-effectiveness of colonoscopy in screening for colorectal cancer. *Ann Intern Med* 2000; **133**: 573-584 [PMID: 11033584 DOI: 10.7326/0003-4819-133-8-200010170-00007]

2 **Hassan C**, Bretthauer M, Kaminski MF, Polkowski M, Rembacken B, Saunders B, Benamouzig R, Holme O, Green S, Kuiper T, Marmo R, Omar M, Petruzziello L, Spada C, Zullo A, Dumonceau JM; European Society of Gastrointestinal Endoscopy. Bowel preparation for colonoscopy: European Society of Gastrointestinal Endoscopy (ESGE) guideline. *Endoscopy* 2013; **45**: 142-150 [PMID: 23335011 DOI: 10.1055/s-0032-1326186]

3 **Barkun A**, Chiba N, Enns R, Marcon M, Natsheh S, Pham C, Sadowski D, Vanner S. Commonly used preparations for colonoscopy: efficacy, tolerability, and safety--a Canadian Association of Gastroenterology position paper. *Can J Gastroenterol* 2006; **20**: 699-710 [PMID: 17111052 DOI: 10.1155/2006/915368]

4 **Atkin WS**, Hart A, Edwards R, Cook CF, Wardle J, McIntyre P, Aubrey R, Baron C, Sutton S, Cuzick J, Senapati A, Northover JM. Single blind, randomised trial of efficacy and acceptability of oral picolax *versus* self administered phosphate enema in bowel preparation for flexible sigmoidoscopy screening. *BMJ* 2000; **320**: 1504-8; discussion 1509 [PMID: 10834891 DOI: 10.1136/bmj.320.7248.1504]

5 **Johnson DA**, Barkun AN, Cohen LB, Dominitz JA, Kaltenbach T, Martel M, Robertson DJ, Boland CR, Giardello FM, Lieberman DA, Levin TR, Rex DK. Optimizing adequacy of bowel cleansing for colonoscopy: recommendations from the U.S. multi-society task force on colorectal cancer. *Gastrointest Endosc* 2014; **80**: 543-562 [PMID: 25220509 DOI: 10.1016/j.gie.2014.08.002]

6 **Rutherford CC**, Calderwood AH. Update on Bowel Preparation for Colonoscopy. *Curr Treat Options Gastroenterol* 2018; **16**: 165-181 [PMID: 29404921 DOI: 10.1007/s11938-018-0165-3]

7 **Jung YS**, Lee CK, Kim HJ, Eun CS, Han DS, Park DI. Randomized controlled trial of sodium phosphate tablets *vs* polyethylene glycol solution for colonoscopy bowel cleansing. *World J Gastroenterol* 2014; **20**: 15845-15851 [PMID: 25400471 DOI: 10.3748/wjg.v20.i42.15845]

8 **Hookey LC**, Depew WT, Vanner S. The safety profile of oral sodium phosphate for colonic cleansing before colonoscopy in adults. *Gastrointest Endosc* 2002; **56**: 895-902 [PMID: 12447305 DOI: 10.1067/mge.2002.129522]

9 **Tjandra JJ**, Chan M, Tagkalidis PP. Oral sodium phosphate (Fleet) is a superior colonoscopy preparation to Picopre (sodium picosulfate-based preparation). *Dis Colon Rectum* 2006; **49**: 616-620 [PMID: 16525746 DOI: 10.1007/s10350-005-0323-2]

10 **US Food and Drug Administration**. Drug Approval Package. Visicol® NDA Medical Review. 2000. Available from: https://www.accessdata.fda.gov/drugsatfda_docs/nda/2000/21097_Visicol.cfm

11 **US Food and Drug Administration**. Drug Approval Package. OsmoPrep® NDA Medical Review. 2006. Available from: https://www.accessdata.fda.gov/drugsatfda_docs/nda/2006/021892_osmoprep_toc.cfm

12 **Vanner SJ**, MacDonald PH, Paterson WG, Prentice RS, Da Costa LR, Beck IT. A randomized prospective trial comparing oral sodium phosphate with standard polyethylene glycol-based lavage solution (Golytely) in the preparation of patients for colonoscopy. *Am J Gastroenterol* 1990; **85**: 422-427 [PMID: 2183591]

13 **Bechtold ML**, Mir F, Puli SR, Nguyen DL. Optimizing bowel preparation for colonoscopy: a guide to enhance quality of visualization. *Ann Gastroenterol* 2016; **29**: 137-146 [PMID: 27065725 DOI: 10.20524/aog.2016.0005]

14 **Hung SY**, Chen HC, Chen WT. A Randomized Trial Comparing the Bowel Cleansing Efficacy of Sodium Picosulfate/Magnesium Citrate and Polyethylene Glycol/Bisacodyl (The Bowklean Study). *Sci Rep* 2020; **10**: 5604 [PMID: 32221332 DOI: 10.1038/s41598-020-62120-w]

15 **Shibata M**, Lu T, Furuya T, Degterev A, Mizushima N, Yoshimori T, MacDonald M, Yankner B, Yuan J. Regulation of intracellular accumulation of mutant Huntingtin by Beclin 1. *J Biol Chem* 2006; **281**: 14474-14485 [PMID: 16522639 DOI: 10.1074/jbc.M600364200]

16 **Clark RE**, Godfrey JD, Choudhary A, Ashraf I, Matteson ML, Bechtold ML. Low-volume polyethylene glycol and bisacodyl for bowel preparation prior to colonoscopy: a meta-analysis. *Ann Gastroenterol* 2013; **26**: 319-324 [PMID: 24714413]

17 **Aronchick CA**, Lipshutz WH, Wright SH, DuFrayne F, Bergman G. Validation of an instrument to assess colon cleansing. *Am J Gastroenterol* 1999; **94**: 2667-2667

18 **Rostom A**, Jolicoeur E. Validation of a new scale for the assessment of bowel preparation quality. *Gastrointest Endosc* 2004; **59**: 482-486 [PMID: 15044882 DOI: 10.1016/s0016-5107(03)02875-x]

19 **Mathus-Vliegen EMH**, van der Vliet K, Wignand-van der Storm IJ, Stadwijk JS. Efficacy and Safety of Sodium Picosulfate/Magnesium Citrate for Bowel Preparation in a Physically Disabled Outpatient Population: A Randomized, Endoscopist-Blinded Comparison With Ascorbic Acid-Enriched Polyethylene Glycol Solution Plus Bisacodyl (The PICO-MOVI Study). *Dis Colon Rectum* 2018; **61**: 239-249 [PMID: 29337780 DOI: 10.1097/DCR.0000000000000956]

20 **Weiss JN**, Qu Z, Shivkumar K. Electrophysiology of Hypokalemia and Hyperkalemia. *Circ Arrhythm Electrophysiol* 2017; **10** [PMID: 28314851 DOI: 10.1161/CIRCEP.116.004667]

21 **ASGE Technology Committee**, Mamula P, Adler DG, Conway JD, Diehl DL, Farraye FA, Kantsevoy SV, Kaul V, Kethu SR, Kwon RS, Rodriguez SA, Tierney WM. Colonoscopy preparation. *Gastrointest Endosc* 2009; **69**: 1201-1209 [PMID: 19481646 DOI: 10.1016/j.gie.2009.01.035]

22 **Wexner SD**, Beck DE, Baron TH, Fanelli RD, Hyman N, Shen B, Wasco KE; American Society of Colon and Rectal Surgeons; American Society for Gastrointestinal Endoscopy; Society of American Gastrointestinal and Endoscopic Surgeons. A consensus document on bowel preparation before colonoscopy: prepared by a task force from the American Society of Colon and Rectal Surgeons (ASCRS), the American Society for Gastrointestinal Endoscopy (ASGE), and the Society of American Gastrointestinal and Endoscopic Surgeons (SAGES). *Gastrointest Endosc* 2006; **63**: 894-909 [PMID: 16733101 DOI: 10.1016/j.gie.2006.03.918]

23 **Koshitani T**, Kawada M, Yoshikawa T. Bowel preparation for colonoscopy using standard *vs* reduced doses of sodium phosphate: A single-blind randomized controlled study. *World J Gastrointest Endosc* 2014; **6**: 379-384 [PMID: 25132922 DOI: 10.4253/wjge.v6.i8.379]

24 **Lee SH**, Lee DJ, Kim KM, Seo SW, Kang JK, Lee EH, Lee DR. Comparison of the efficacy and safety of sodium phosphate tablets and polyethylene glycol solution for bowel cleansing in healthy Korean adults. *Yonsei Med J* 2014; **55**: 1542-1555 [PMID: 25323890 DOI: 10.3349/ymj.2014.55.6.1542]

25 **Aronchick CA**, Lipshutz WH, Wright SH, Dufrayne F, Bergman G. A novel tableted purgative for colonoscopic preparation: efficacy and safety comparisons with Colyte and Fleet Phospho-Soda. *Gastrointest Endosc* 2000; **52**: 346-352 [PMID: 10968848 DOI: 10.1067/mge.2000.108480]

26 **Hsu CW**, Imperiale TF. Meta-analysis and cost comparison of polyethylene glycol lavage *versus* sodium phosphate for colonoscopy preparation. *Gastrointest Endosc* 1998; **48**: 276-282 [PMID: 9744604 DOI: 10.1016/s0016-5107(98)70191-9]

27 **Hosoe N**, Nakashita M, Imaeda H, Sujino T, Bessho R, Ichikawa R, Inoue N, Kanai T, Hibi T, Ogata H. Comparison of patient acceptance of sodium phosphate *versus* polyethylene glycol plus sodium picosulfate for colon cleansing in Japanese. *J Gastroenterol Hepatol* 2012; **27**: 1617-1622 [PMID: 22646064 DOI: 10.1111/j.1440-1746.2012.07190.x]

28 **Kastenberg D**, Chasen R, Choudhary C, Riff D, Steinberg S, Weiss E, Wruble L. Efficacy and safety of sodium phosphate tablets compared with PEG solution in colon cleansing: two identically designed, randomized, controlled, parallel group, multicenter phase III trials. *Gastrointest Endosc* 2001; **54**: 705-713 [PMID: 11726845 DOI: 10.1067/mge.2001.119733]

World Journal of Gastroenterology

Submit a Manuscript: https://www.f6publishing.com

World J Gastroenterol 2021 February 7; 27(5): 442-448

DOI: 10.3748/wjg.v27.i5.442

ISSN 1007-9327 (print) ISSN 2219-2840 (online)

CASE REPORT

Vedolizumab in Crohn's disease with rectal fistulas and presacral abscess: A case report

Heng Yeh, Chia-Jung Kuo, Ren-Chin Wu, Chien-Ming Chen, Wen-Sy Tsai, Ming-Yao Su, Cheng-Tang Chiu, Puo-Hsien Le

ORCID number: Heng Yeh 0000-0002-3908-6927; Chia-Jung Kuo 0000-0003-2845-6248; Ren-Chin Wu 0000-0003-1439-0874; Chien-Ming Chen 0000-0001-7829-1504; Wen-Sy Tsai 0000-0001-6873-2863; Ming-Yao Su 0000-0002-5229-3074; Cheng-Tang Chiu 0000-0002-7347-8052; Puo-Hsien Le 0000-0002-1100-5371.

Author contributions: Yeh H wrote and revised the manuscript; Kuo CJ acquired the data; Wu RC interpreted the pathological result; Chen CM analyzed the radiological images; Tsai WS, Su MY and Chiu CT analyzed the data; Le PH decided the treatment plan, wrote and revised the manuscript.

Informed consent statement: The study participant provided informed written consent prior to study enrollment.

Conflict-of-interest statement: The authors have no conflict of interest to declare.

CARE Checklist (2016) statement: The authors have read the CARE Checklist (2016), and the manuscript was prepared and revised according to the CARE Checklist (2016).

Open-Access: This article is an open-access article that was

Heng Yeh, School of Medicine, Chang Gung University, Taoyuan City 333323, Taiwan

Chia-Jung Kuo, Cheng-Tang Chiu, Puo-Hsien Le, Department of Gastroenterology and Hepatology, Chang Gung Memorial Hospital, Linkou Branch, Taoyuan 333, Taiwan

Chia-Jung Kuo, Ming-Yao Su, Cheng-Tang Chiu, Puo-Hsien Le, Taiwan Association of the Study of Small Intestine Disease, Taoyuan 333, Taiwan

Ren-Chin Wu, Department of Pathology, Chang Gung Memorial Hospital, Linkou Branch, Taoyuan 333, Taiwan

Chien-Ming Chen, Department of Medical Imaging and Intervention, Chang Gung Memorial Hospital, Linkou Branch, Taoyuan 333, Taiwan

Wen-Sy Tsai, Department of Colon and Rectal Surgery, Chang Gung Memorial Hospital, Linkou Branch, Taoyuan 333, Taiwan

Ming-Yao Su, Department of Gastroenterology and Hepatology, New Taipei City Municipal Tucheng Hospital, New Taipei City 236017, Taiwan

Puo-Hsien Le, Liver Research Center, Chang Gung Memorial Hospital, Linkou Branch, Taoyuan 333, Taiwan

Corresponding author: Puo-Hsien Le, MD, Assistant Professor, Department of Gastroenterology and Hepatology, Chang Gung Memorial Hospital, Linkou Branch, No. 5 Fuxing Street, Guishan District, Taoyuan 333, Taiwan. puohsien@gmail.com

Abstract

BACKGROUND

Fistula and intraabdominal abscess are common complications of Crohn's disease (CD), but complex rectal fistula with abscess formation is rare. Tumor necrosis factor antagonists combined with percutaneous drainage or surgical intervention is optimal treatment for fistulizing CD with intraabdominal abscess. There is no study showing the efficacy of vedolizumab in such complicated condition.

CASE SUMMARY

A 47-year-old man has decompensated liver cirrhosis, Child B. He suffered from abdominal pain, bloody diarrhea, fever, and body weight loss. CD with rectoprostatic fistula, rectopresacral fistula, presacral abscess and cyto-

selected by an in-house editor and fully peer-reviewed by external reviewers. It is distributed in accordance with the Creative Commons Attribution NonCommercial (CC BY-NC 4.0) license, which permits others to distribute, remix, adapt, build upon this work non-commercially, and license their derivative works on different terms, provided the original work is properly cited and the use is non-commercial. See: http://creativecommons.org/Licenses/by-nc/4.0/

Manuscript source: Unsolicited manuscript

Specialty type: Gastroenterology and hepatology

Country/Territory of origin: Taiwan

Peer-review report's scientific quality classification

Grade A (Excellent): 0
Grade B (Very good): B, B
Grade C (Good): 0
Grade D (Fair): 0
Grade E (Poor): 0

Received: October 12, 2020
Peer-review started: October 12, 2020
First decision: November 23, 2020
Revised: December 8, 2020
Accepted: January 6, 2021
Article in press: January 6, 2021
Published online: February 7, 2021

P-Reviewer: Funel N, Makhlouf NA
S-Editor: Gao CC
L-Editor: A
P-Editor: Liu JH

megalovirus (CMV) infection were noted. He received antibiotics, anti-viral therapy, transverse colostomy and vedolizumab treatment. Six months later, he had deep remission and complete fistula tracts closure.

CONCLUSION
Early vedolizumab and stool diversion are effective and safe in treating CD with complex rectal fistula with abscess formation.

Key Words: Vedolizumab; Crohn's disease; Rectoprostatic fistula; Rectal presacral fistula; Presacral abscess; Case report

©The Author(s) 2021. Published by Baishideng Publishing Group Inc. All rights reserved.

Core Tip: Fistulas and intraabdominal abscess are common complications of Crohn's disease (CD) and tumor necrosis factor antagonists combined with percutaneous drainage or surgical intervention is the optimal treatment for fistulizing CD with intraabdominal abscess. However, no previous study has reported the efficacy of vedolizumab in this complicated situation. This 47-year-old male presented with CD with complex fistulas and presacral abscess. He received vedolizumab with transverse colostomy and the follow-up sigmoidoscopy 6 mo later showed mucosal healing without any visible fistula tracts. We think early vedolizumab treatment with stool diversion are effective and safe in treating CD with complex fistulas and abscess formation.

Citation: Yeh H, Kuo CJ, Wu RC, Chen CM, Tsai WS, Su MY, Chiu CT, Le PH. Vedolizumab in Crohn's disease with rectal fistulas and presacral abscess: A case report. *World J Gastroenterol* 2021; 27(5): 442-448
URL: https://www.wjgnet.com/1007-9327/full/v27/i5/442.htm
DOI: https://dx.doi.org/10.3748/wjg.v27.i5.442

INTRODUCTION

Fistula affects up to 50% Crohn's disease (CD) patients within 20 years of initial diagnosis[1,2]. It includes perianal, rectovaginal, enterocutaneous and internal fistula, but no rectoprostatic fistula or rectopresacral fistula were reported. The treatment of fistula usually requires a combination of medical and surgical approach[3]. As far as medical treatment is concerned, tumor necrosis factor (TNF) antagonists are the most effective to treat fistulizing CD[4]. However, some studies also noted the beneficial effect of vedolizumab for fistulizing CD[5,6]. We presented the patient of CD, complicated with rectoprostatic fistula, rectopresacral fistula and presacral abscess. He had complete fistula closure and deep remission after transverse colostomy and vedolizumab treatment for six months.

CASE PRESENTATION

Chief complaints

Low abdominal pain and intermittent bloody stool for 6 mo.

History of present illness

A 47-year-old man has decompensated liver cirrhosis, Child B, hepatitis C virus (HCV) and alcoholism related, complicated with hypoalbuminemia, hyperbilirubinemia, coagulopathy, thrombocytopenia, splenomegaly and esophageal varices, Form 1. He complained low abdominal pain and intermittent bloody stool for 6 mo. Appendicitis was diagnosed in local hospital, and he received appendectomy on 16th November 2019. However, he suffered from progressive low abdominal pain, bloody stool, dizziness, and intermittent fever up to 38 °C for four days. He also mentioned body weight loss 20 kg within one year. He was brought to our emergent department.

History of past illness

Decompensated liver cirrhosis, Child B, hepatitis C virus infection and alcoholism.

Personal and family history

Appendicitis was diagnosed in local hospital, and he received appendectomy on 16th November 2019.

Laboratory examinations

Lab data revealed hemoglobin 10.1 g/dL, platelet 66000/μL, white blood cell 7700/μL, segment 68.7%, lymphocyte 23.7%, international normalized ratio (INR) 1.5, aspartate aminotransferase (AST) 55 U/L, alanine aminotransferase (ALT) 95 U/L, total bilirubin 2.1 mg/dL, albumin 2.38 g/dL and CRP 22.81 mg/L. Cytomegalovirus (CMV) immunoglobulin (Ig) M, CMV DNA, Epstein-Barr virus (EBV)-VCA IgM, EBV DNA, human immunodeficiency virus (HIV) antibody (Ab), amebic Ab, Clostridium difficile toxin, culture for *Salmonella*, *Shigella* and *Campylobacter* were all negative. Positive CMV IgG, EBV-VCA IgG, stool pus cell and occult blood were noted.

Imaging examinations

Colonoscopy showed terminal ileal shallow ulcer (Figure 1A) and multiple complex rectal fistula tracts (Figure 1B and C) on 10th December 2019. Magnetic resonance imaging (MRI) noted decompensated liver cirrhosis with ascites (Figure 2A), rectoprostatic fistula (Figure 2B), rectopresacral fistula (Figure 2C) and presacral abscess (Figure 2D) on 21th December 2019. Pathology revealed acute on chronic inflammation with granulation tissue, compactable with CD (Figure 3A). Besides, there was positive result of CMV immunohistochemistry (IHC) staining (Figure 3B), which was performed with a monoclonal antibody directed against the CMV pp65 antigen (Novocastra™ lyophilized mouse monoclonal antibody; Leica Microsystems, Wetzlar, Germany).

FINAL DIAGNOSIS

He was diagnosed to have CD with CMV infection based on endoscopy and pathological findings. The CD activity index (CDAI) was 526 points and Harvey-Bradshaw index (HBI) was 22 points. He also had rectoprostatic fistula, rectopresacral fistula and presacral abscess diagnosed by MRI findings.

TREATMENT

He refused percutaneous abscess fine needle aspiration, and we kept Tazocin for abscess treatment for 27 d. Because of positive CMV IHC staining result, he also received intravenous ganciclovir for 17 d and then valganciclovir oral treatment for two months. Transverse colostomy was performed for stool diversion on 25th December 2019. He couldn't tolerant azathioprine due to pancytopenia and vedolizumab (300 mg) was prescript since 22th January 2020.

OUTCOME AND FOLLOW-UP

Follow-up sigmoidoscopy showed mucosal healing without any fistula tract (Figure 1D) on 9th July 2020. The pathologist reported minimal inflammatory activity (Figure 3C). Lower gastrointestinal series mentioned no more fistula tract (Figure 4) on 21th July 2020. There was no more rectoprostatic or rectopresacral fistula (Figure 5A) and presacral abscess (Figure 5B) in MRI. After vedolizumab treatment for 6 mo, the CDAI was 42 points and HBI score was 0 point. His body weight also increased 20 kg, back to the same level before the episode.

DISCUSSION

Fistulizing CD results in not only high morbidity but also impairs health-related quality of life[4]. Biologics combined with surgical intervention seems to be the best

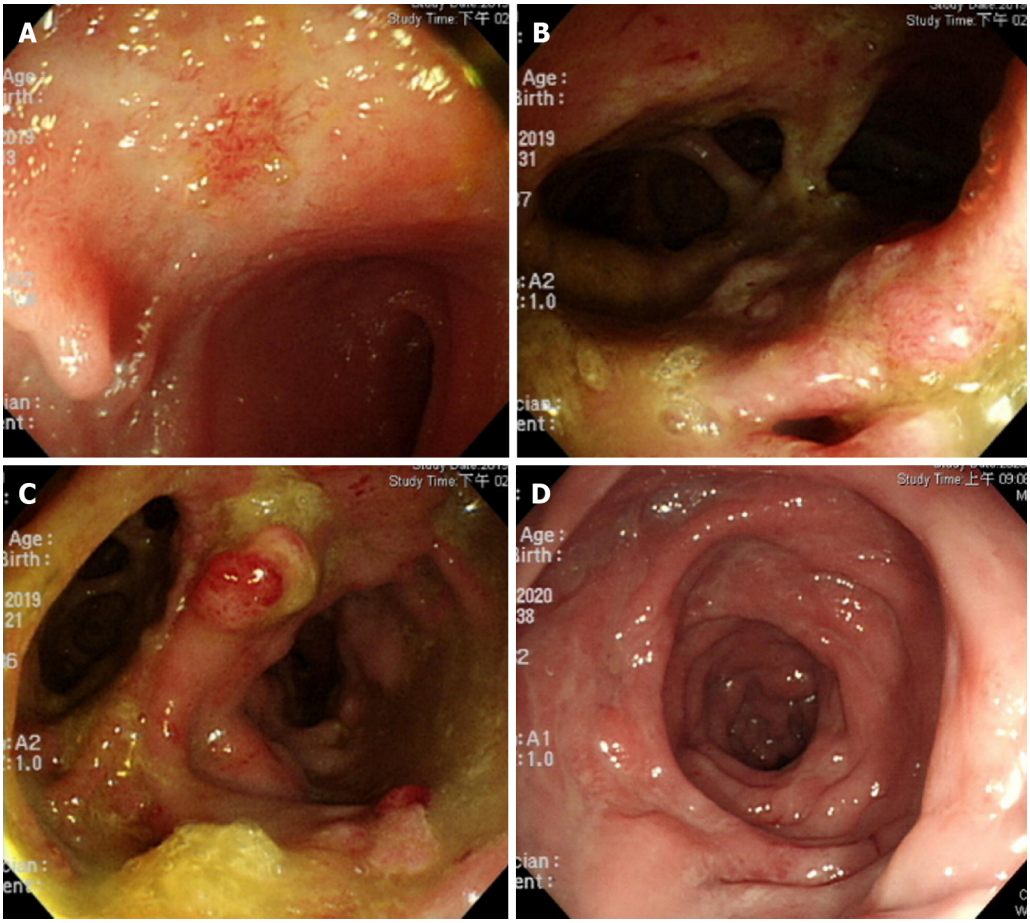


Figure 1 Endoscopic findings. A: Terminal ileal shallow ulcer at diagnosis; B and C: Multiple rectal fistula tracts with inflammation; D: Mucosal healing without fistula tracts six months after vedolizumab treatment, seven months after diagnosis.

solution. Although Infliximab has the strongest evidence in fistulizing CD treatment[7,8], vedolizumab also showed its efficacy in some studies[5,6]. However, vedolizumab has better safety profiles (less severe adverse events and infections) in real world studies[9,10].

Intra-abdominal abscess occurs in up to 20% of patients with CD[11,12]. Adequate percutaneous drainage combined with early adalimumab treatment achieves up to 74% successful rate[13]. In this case, it was difficult to drain the presacral abscess and patient refused, too. Therefore, we chose vedolizumab with transverse colostomy in treating the complex rectal fistula and presacral abscess without abscess drainage.

This patient received vedolizumab treatment one month after the diagnosis. Earlier initiation of biological treatment shortly after diagnosis (less than one year) in patients with moderately to severely active CD improved the long-term clinical outcomes[14]. Besides, early stool diversion with transverse colostomy and early anti-viral treatment for CMV infection were crucial to achieve the good outcome in this case.

CONCLUSION

Vedolizumab with loop transverse colostomy was effective in treating CD with complex rectal fistulas with presacral abscess. Besides, early biological and anti-CMV treatments also lead to the favorable outcome.

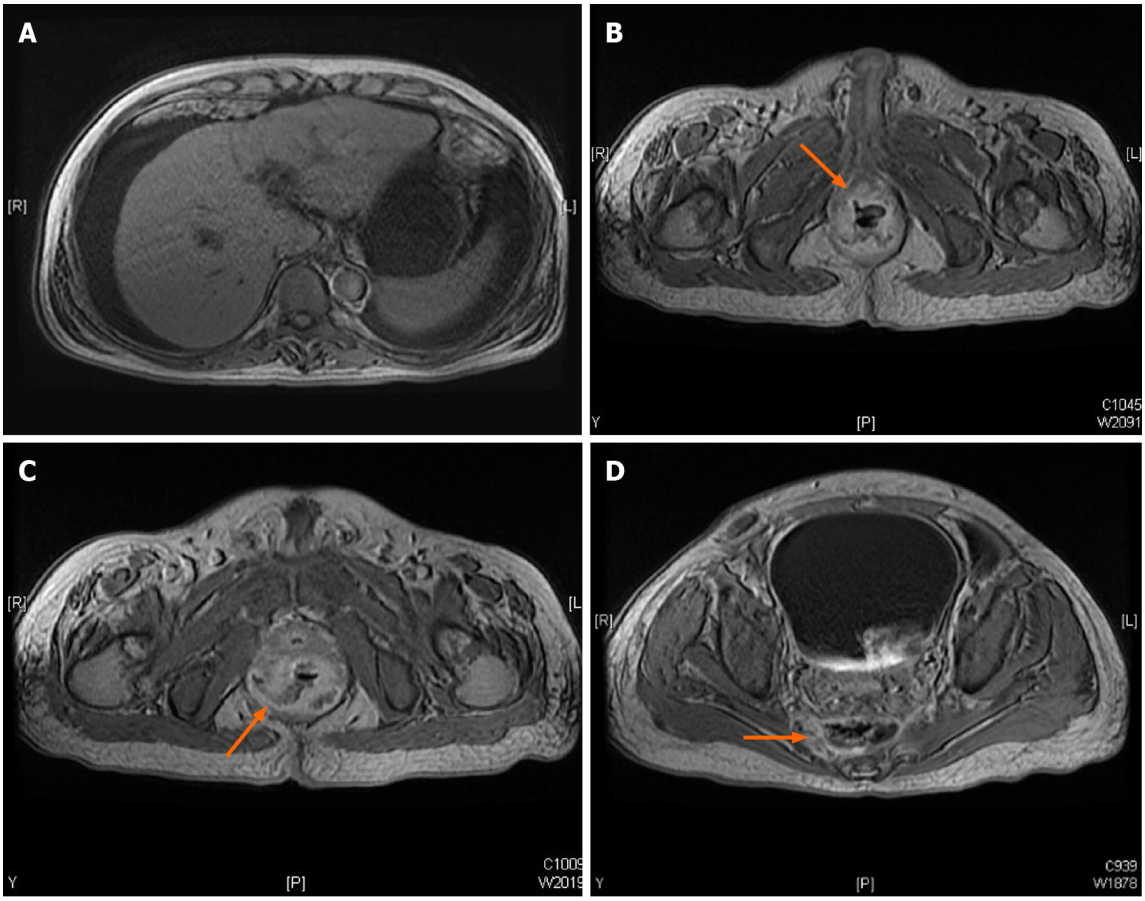


Figure 2 Magnetic resonance imaging at diagnosis. A: Liver cirrhosis with ascites; B: Rectoprostatic fistula; C: Rectopresacral fistula; D: Presacral abscess.

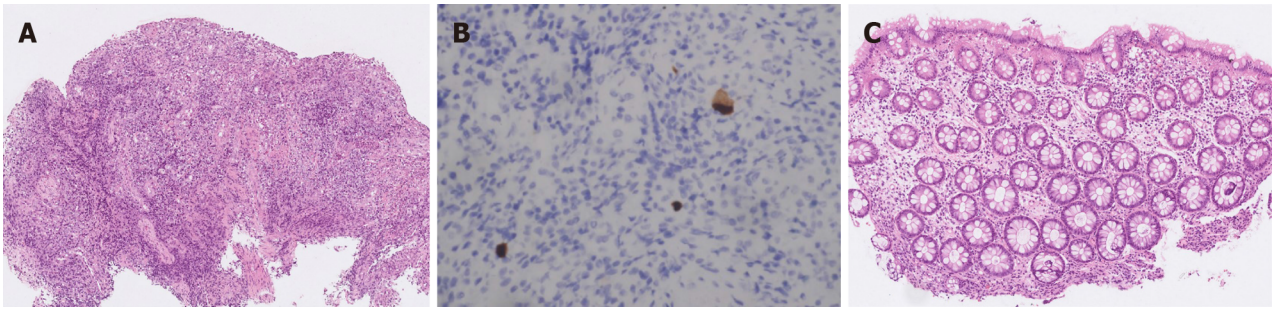


Figure 3 Pathology. A: Ulcer with acute on chronic inflammation and granulation tissue at diagnosis; B: Pathological presentations of cytomegalovirus (CMV) infection, immunohistochemistry stain (20 × objective) was performed with 1:200 diluted Novocastra™ lyophilized mouse monoclonal antibody against CMV pp65 antigen and showed strong focal CMV immunoreactivity with brownish areas; C: Minimal inflammatory cells infiltration six months after vedolizumab treatment, seven months after diagnosis.



Figure 4 Lower gastrointestinal series showed no more rectal fistula tract.

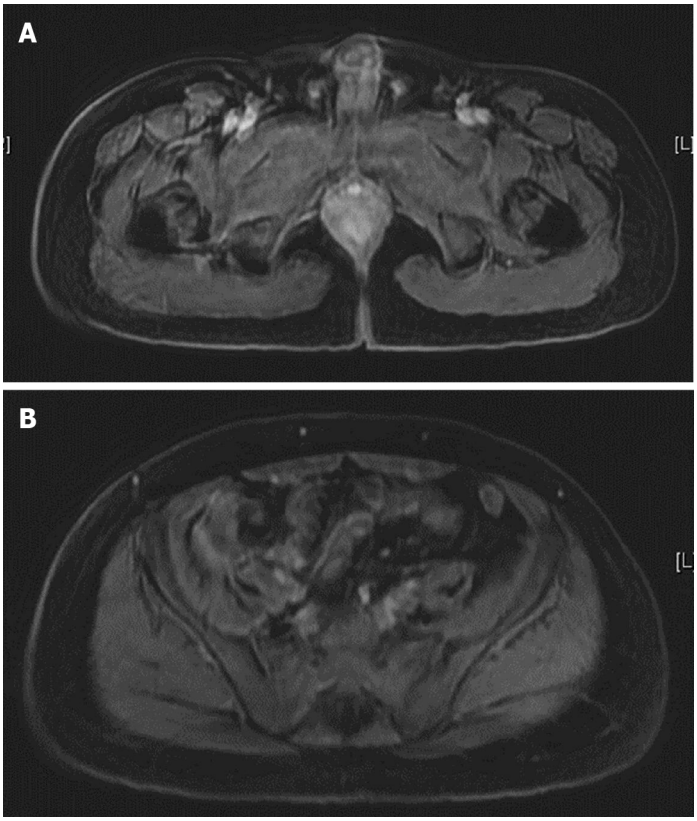


Figure 5 Magnetic resonance imaging seven months after diagnosis. A: No more rectal fistula tract; B: No more presacral abscess.

REFERENCES

1 **Siegmund B**, Feakins RM, Barmias G, Ludvig JC, Teixeira FV, Rogler G, Scharl M. Results of the Fifth Scientific Workshop of the ECCO (II): Pathophysiology of Perianal Fistulizing Disease. *J*

Crohns Colitis 2016; **10**: 377-386 [PMID: 26681764 DOI: 10.1093/ecco-jcc/jjv228]
2 **Schwartz DA**, Loftus EV Jr, Tremaine WJ, Panaccione R, Harmsen WS, Zinsmeister AR, Sandborn WJ. The natural history of fistulizing Crohn's disease in Olmsted County, Minnesota. *Gastroenterology* 2002; **122**: 875-880 [PMID: 11910338 DOI: 10.1053/gast.2002.32362]
3 **Gecse KB**, Bemelman W, Kamm MA, Stoker J, Khanna R, Ng SC, Panés J, van Assche G, Liu Z, Hart A, Levesque BG, D'Haens G; World Gastroenterology Organization; International Organisation for Inflammatory Bowel Diseases IOIBD; European Society of Coloproctology and Robarts Clinical Trials; World Gastroenterology Organization International Organisation for Inflammatory Bowel Diseases IOIBD European Society of Coloproctology and Robarts Clinical Trials. A global consensus on the classification, diagnosis and multidisciplinary treatment of perianal fistulising Crohn's disease. *Gut* 2014; **63**: 1381-1392 [PMID: 24951257 DOI: 10.1136/gutjnl-2013-306709]
4 **Vavricka SR**, Rogler G. Fistula treatment: The unresolved challenge. *Dig Dis* 2010; **28**: 556-564 [PMID: 20926886 DOI: 10.1159/000320416]
5 **Schwartz D**, Peyrin-Biroulet L, Lasch K, Adsul S, Danese S. P476 Efficacy and safety of 2 vedolizumab IV regimens in patients with perianal fistulising Crohn's disease: results of the ENTERPRISE study. *J Crohns Colitis* 2020; **14**: S418-S419 [DOI: 10.1093/ecco-jcc/jjz203.605]
6 **Feagan BG**, Schwartz D, Danese S, Rubin DT, Lissoos TW, Xu J, Lasch K. Efficacy of Vedolizumab in Fistulising Crohn's Disease: Exploratory Analyses of Data from GEMINI 2. *J Crohns Colitis* 2018; **12**: 621-626 [PMID: 29471381 DOI: 10.1093/ecco-jcc/jjy019]
7 **Present DH**, Rutgeerts P, Targan S, Hanauer SB, Mayer L, van Hogezand RA, Podolsky DK, Sands BE, Braakman T, DeWoody KL, Schaible TF, van Deventer SJ. Infliximab for the treatment of fistulas in patients with Crohn's disease. *N Engl J Med* 1999; **340**: 1398-1405 [PMID: 10228190 DOI: 10.1056/nejm199905063401804]
8 **Sands BE**, Anderson FH, Bernstein CN, Chey WY, Feagan BG, Fedorak RN, Kamm MA, Korzenik JR, Lashner BA, Onken JE, Rachmilewitz D, Rutgeerts P, Wild G, Wolf DC, Marsters PA, Travers SB, Blank MA, van Deventer SJ. Infliximab maintenance therapy for fistulizing Crohn's disease. *N Engl J Med* 2004; **350**: 876-885 [PMID: 14985485 DOI: 10.1056/NEJMoa030815]
9 **Yarur A**, Mantzaris G, Silverberg M, Walshe M, Zezos P, Stein D, Bassel M, Lissoos T, Lopez C, Natsios A, Radulescu G, Patel H, Demuth D, Bressler B. P573 Real-world effectiveness and safety of vedolizumab and anti-TNF in biologic-naive ulcerative colitis patients: Results from the EVOLVE study. *J Crohns Colitis* 2019; **13**: S400-S401 [DOI: 10.1093/ecco-jcc/jjy222.697]
10 **Helwig U**, Mross M, Schubert S, Hartmann H, Brandes A, Stein D, Kempf C, Knop J, Campbell-Hill S, Ehehalt R. Real-world clinical effectiveness and safety of vedolizumab and anti-tumor necrosis factor alpha treatment in ulcerative colitis and Crohn's disease patients: a German retrospective chart review. *BMC Gastroenterol* 2020; **20**: 211 [PMID: 32640990 DOI: 10.1186/s12876-020-01332-w]
11 **Hurst RD**, Molinari M, Chung TP, Rubin M, Michelassi F. Prospective study of the features, indications, and surgical treatment in 513 consecutive patients affected by Crohn's disease. *Surgery* 1997; **122**: 661-7; discussion 667 [PMID: 9347840 DOI: 10.1016/s0039-6060(97)90071-4]
12 **Yamaguchi A**, Matsui T, Sakurai T, Ueki T, Nakabayashi S, Yao T, Futami K, Arima S, Ono H. The clinical characteristics and outcome of intraabdominal abscess in Crohn's disease. *J Gastroenterol* 2004; **39**: 441-448 [PMID: 15175942 DOI: 10.1007/s00535-003-1317-2]
13 **Pineton de Chambrun G**, Pariente B, Seksik P, Altwegg R, Vuitton L, Stefasnescu C, Nancey S, Aubourg A, Serrero M, Peyrin-Biroulet L, Filippi J, Viennot S, Abitbol V, Boualit M, Boureille A, Moreau J, Buisson A, Roblin X, Nachury M, Zappa M, Lambert J, Bouhnik Y; GETAID-MICA study group. Adalimumab for patients with Crohn's disease complicated by intra-abdominal abscess: a multicentre, prospective, observational cohort study. *J Crohns Colitis* 2019; **13**: S616 [PMID: 30794285 DOI: 10.1093/ecco-jcc/jjz045]
14 **Panaccione R**, Löfberg R, Rutgeerts P, Sandborn WJ, Schreiber S, Berg S, Maa JF, Petersson J, Robinson AM, Colombel JF. Efficacy and Safety of Adalimumab by Disease Duration: Analysis of Pooled Data From Crohn's Disease Studies. *J Crohns Colitis* 2019; **13**: 725-734 [PMID: 30753371 DOI: 10.1093/ecco-jcc/jjy223]

Published by **Baishideng Publishing Group Inc**
7041 Koll Center Parkway, Suite 160, Pleasanton, CA 94566, USA
Telephone: +1-925-3991568
E-mail: bpgoffice@wjgnet.com
Help Desk: https://www.f6publishing.com/helpdesk
https://www.wjgnet.com

© 2021 Baishideng Publishing Group Inc. All rights reserved.

ISSN 1007-9327 (print)
ISSN 2219-2840 (online)

World Journal of *Gastroenterology*

World J Gastroenterol 2021 February 14; 27(6): 449-544



Published by Baishideng Publishing Group Inc

World Journal of Gastroenterology

Contents

Weekly Volume 27 Number 6 February 14, 2021

REVIEW

449 Current understanding of the impact of COVID-19 on gastrointestinal disease: Challenges and openings

Sahu T, Mehta A, Ratre YK, Jaiswal A, Vishvakarma NK, Bhaskar LVKS, Verma HK

ORIGINAL ARTICLE

Basic Study

470 Demethylation of miR-34a upregulates expression of membrane palmitoylated proteins and promotes the apoptosis of liver cancer cells

Li FY, Fan TY, Zhang H, Sun YM

487 Circular RNA circVAPA promotes chemotherapy drug resistance in gastric cancer progression by regulating miR-125b-5p/STAT3 axis

Deng P, Sun M, Zhao WY, Hou B, Li K, Zhang T, Gu F

Retrospective Cohort Study

501 Validation of serum tumor biomarkers in predicting advanced cystic mucinous neoplasm of the pancreas

Sun LQ, Peng LS, Guo JF, Jiang F, Cui F, Huang HJ, Jin ZD

Retrospective Study

513 Washed microbiota transplantation reduces proton pump inhibitor dependency in nonerosive reflux disease

Zheng YM, Chen XY, Cai JY, Yuan Y, Xie WR, Xu JT, Xia HHX, Zhang M, He XX, Wu LH

Prospective Study

523 Prevalence of advanced liver fibrosis and steatosis in type-2 diabetics with normal transaminases: A prospective cohort study

Makker J, Tariq H, Kumar K, Ravi M, Shaikh DH, Leung V, Hayat U, Hassan MT, Patel H, Nayudu S, Chilimuri S

CASE REPORT

534 Pancreaticoduodenectomy after neoadjuvant chemotherapy for gastric cancer invading the pancreatic head: A case report

Yura M, Takano K, Adachi K, Hara A, Hayashi K, Tajima Y, Kaneko Y, Ikoma Y, Fujisaki H, Hirata A, Hongo K, Yo K, Yoneyama K, Dehari R, Koyanagi K, Nakagawa M

World Journal of Gastroenterology

Weekly Volume 27 Number 6 February 14, 2021

Contents

ABOUT COVER

Michele Barone, MD, PhD, Assistant Professor, Department of Emergency and Organ Transplantation, Polyclinic University Hospital, University of Bari Aldo Moro, Piazza G. Cesare 11, Bari 70124, Italy. michele.barone@uniba.it

AIMS AND SCOPE

The primary aim of *World Journal of Gastroenterology* (*WJG*, *World J Gastroenterol*) is to provide scholars and readers from various fields of gastroenterology and hepatology with a platform to publish high-quality basic and clinical research articles and communicate their research findings online. *WJG* mainly publishes articles reporting research results and findings obtained in the field of gastroenterology and hepatology and covering a wide range of topics including gastroenterology, hepatology, gastrointestinal endoscopy, gastrointestinal surgery, gastrointestinal oncology, and pediatric gastroenterology.

INDEXING/ABSTRACTING

The *WJG* is now indexed in Current Contents®/Clinical Medicine, Science Citation Index Expanded (also known as SciSearch®), Journal Citation Reports®, Index Medicus, MEDLINE, PubMed, PubMed Central, and Scopus. The 2020 edition of Journal Citation Report® cites the 2019 impact factor (IF) for *WJG* as 3.665; IF without journal self cites: 3.534; 5-year IF: 4.048; Ranking: 35 among 88 journals in gastroenterology and hepatology; and Quartile category: Q2. The *WJG*'s CiteScore for 2019 is 7.1 and Scopus CiteScore rank 2019: Gastroenterology is 17/137.

RESPONSIBLE EDITORS FOR THIS ISSUE

Production Editor: *Ji-Hong Liu*; **Production Department Director:** *Yun-Xiaojian Wu*; **Editorial Office Director:** *Ze-Mao Gong*.

NAME OF JOURNAL
World Journal of Gastroenterology

ISSN
ISSN 1007-9327 (print) ISSN 2219-2840 (online)

LAUNCH DATE
October 1, 1995

FREQUENCY
Weekly

EDITORS-IN-CHIEF
Andrzej S Tarnawski, Subrata Ghosh

EDITORIAL BOARD MEMBERS
http://www.wjgnet.com/1007-9327/editorialboard.htm

PUBLICATION DATE
February 14, 2021

COPYRIGHT
© 2021 Baishideng Publishing Group Inc

INSTRUCTIONS TO AUTHORS
https://www.wjgnet.com/bpg/gerinfo/204

GUIDELINES FOR ETHICS DOCUMENTS
https://www.wjgnet.com/bpg/GerInfo/287

GUIDELINES FOR NON-NATIVE SPEAKERS OF ENGLISH
https://www.wjgnet.com/bpg/gerinfo/240

PUBLICATION ETHICS
https://www.wjgnet.com/bpg/GerInfo/288

PUBLICATION MISCONDUCT
https://www.wjgnet.com/bpg/gerinfo/208

ARTICLE PROCESSING CHARGE
https://www.wjgnet.com/bpg/gerinfo/242

STEPS FOR SUBMITTING MANUSCRIPTS
https://www.wjgnet.com/bpg/GerInfo/239

ONLINE SUBMISSION
https://www.f6publishing.com

© 2021 Baishideng Publishing Group Inc. All rights reserved. 7041 Koll Center Parkway, Suite 160, Pleasanton, CA 94566, USA
E-mail: bpgoffice@wjgnet.com https://www.wjgnet.com

World Journal of Gastroenterology

Submit a Manuscript: https://www.f6publishing.com

World J Gastroenterol 2021 February 14; 27(6): 449-469

DOI: 10.3748/wjg.v27.i6.449

ISSN 1007-9327 (print) ISSN 2219-2840 (online)

REVIEW

Current understanding of the impact of COVID-19 on gastrointestinal disease: Challenges and openings

Tarun Sahu, Arundhati Mehta, Yashwant Kumar Ratre, Akriti Jaiswal, Naveen Kumar Vishvakarma, Lakkakula Venkata Kameswara Subrahmanya Bhaskar, Henu Kumar Verma

ORCID number: Tarun Sahu 0000-0002-2721-7432; Arundhati Mehta 0000-0003-2242-0033; Yashwant Kumar Ratre 0000-0002-1488-6653; Akriti Jaiswal 0000-0002-6107-0382; Naveen Kumar Vishvakarma 0000-0002-4691-8015; Lakkakula Venkata Kameswara Subrahmanya Bhaskar 0000-0003-2977-6454; Henu Kumar Verma 0000-0003-1130-8783.

Author contributions: Verma HK contributed to the conceptualization, investigation and supervision; Verma HK and Bhaskar LVKS contributed to the methodology; Verma HK and Vishvakarma NK contributed to the software; Sahu T, Mehta A, Jaiswal A and Ratre YK contributed to the article search and writing the original draft; Sahu T, Ratre YK, Verma HK, Vishvakarma NK and Bhaskar LVKS contributed to the writing, reviewing, and editing of the manuscript.

Conflict-of-interest statement: No conflict of interest.

Open-Access: This article is an open-access article that was selected by an in-house editor and fully peer-reviewed by external reviewers. It is distributed in accordance with the Creative Commons Attribution NonCommercial (CC BY-NC 4.0)

Tarun Sahu, Akriti Jaiswal, Department of Physiology, All India Institute of Medical Science, Raipur 492001, Chhattisgarh, India

Arundhati Mehta, Yashwant Kumar Ratre, Naveen Kumar Vishvakarma, Department of Biotechnology, Guru Ghasidas Vishwavidyalaya, Bilaspur 495001, Chhattisgarh, India

Lakkakula Venkata Kameswara Subrahmanya Bhaskar, Department of Zoology, Guru Ghasidas Vishwavidyalaya, Bilaspur 495001, Chhattisgarh, India

Henu Kumar Verma, Developmental and Stem Cell Biology Lab, Institute of Experimental Endocrinology and Oncology CNR, Naples, Campania 80131, Italy

Corresponding author: Henu Kumar Verma, PhD, Research Scientist, Developmental and Stem Cell Biology Lab, Institute of Experimental Endocrinology and Oncology CNR, *via* Pansini 5, Naples, Campania 80131, Italy. henu.verma@yahoo.com

Abstract

The novel coronavirus disease-2019 (COVID-19) is caused by a positive-sense single-stranded RNA virus which belongs to the Coronaviridae family. In March 2019 the World Health Organization declared that COVID-19 was a pandemic. COVID-19 patients typically have a fever, dry cough, dyspnea, fatigue, and anosmia. Some patients also report gastrointestinal (GI) symptoms, including diarrhea, nausea, vomiting, and abdominal pain, as well as liver enzyme abnormalities. Surprisingly, many studies have found severe acute respiratory syndrome coronavirus 2 (SARS-CoV-2) viral RNA in rectal swabs and stool specimens of asymptomatic COVID-19 patients. In addition, viral receptor angiotensin-converting enzyme 2 and transmembrane protease serine-type 2, were also found to be highly expressed in gastrointestinal epithelial cells of the intestinal mucosa. Furthermore, SARS-CoV-2 can dynamically infect and replicate in both GI and liver cells. Taken together these results indicate that the GI tract is a potential target of SARS-CoV-2. Therefore, the present review summarizes the vital information available to date on COVID-19 and its impact on GI aspects.

Key Words: SARS-CoV-2; COVID-19; Gastrointestinal symptoms; Recommendation; Diagnosis; Therapeutics

©The Author(s) 2021. Published by Baishideng Publishing Group Inc. All rights reserved.

license, which permits others to distribute, remix, adapt, build upon this work non-commercially, and license their derivative works on different terms, provided the original work is properly cited and the use is non-commercial. See: http://creativecommons.org/Licenses/by-nc/4.0/

Manuscript source: Invited manuscript

Specialty type: Gastroenterology and hepatology

Country/Territory of origin: Italy

Peer-review report's scientific quality classification
Grade A (Excellent): 0
Grade B (Very good): 0
Grade C (Good): C
Grade D (Fair): 0
Grade E (Poor): 0

Received: November 21, 2020
Peer-review started: November 21, 2020
First decision: December 3, 2020
Revised: December 28, 2020
Accepted: January 8, 2021
Article in press: January 8, 2021
Published online: February 14, 2021

P-Reviewer: Nabil A
S-Editor: Zhang H
L-Editor: Webster JR
P-Editor: Ma YJ



Core Tip: The landscape of coronavirus disease-2019 (COVID-19) is evolving dramatically, with new information increasing at an alarming rate. It is a challenge to make sense of these data and to interpret what is crucial and high-quality evidence. In this critical circumstance, in-depth work is highly important for the future treatment and management of the disease. In this review, we summarize the vital information available to date on COVID-19 and its impact on gastrointestinal aspects.

Citation: Sahu T, Mehta A, Ratre YK, Jaiswal A, Vishvakarma NK, Bhaskar LVKS, Verma HK. Current understanding of the impact of COVID-19 on gastrointestinal disease: Challenges and openings. *World J Gastroenterol* 2021; 27(6): 449-469
URL: https://www.wjgnet.com/1007-9327/full/v27/i6/449.htm
DOI: https://dx.doi.org/10.3748/wjg.v27.i6.449

INTRODUCTION

Populations worldwide are currently facing an unprecedented health emergency due to the spread of novel coronavirus disease-2019 (COVID-19) caused by severe acute respiratory syndrome coronavirus 2 (SARS-CoV-2). According to the World Health Organization (WHO), the COVID-19 health crisis has spread to over 205 countries including the United States, India, Russia, Brazil, and Colombia[1-3]. The most common symptoms of moderate COVID-19 include fever, dry cough, tiredness, sore throat or dyspnea. However, the pulmonary system is the main system involved in the clinical manifestation of the disease. Patients infected with this virus can suffer potential damage to other vital organs, such as the gastrointestinal (GI), cardiac, renal and nervous systems[4-6]. Before COVID-19, many infectious diseases affected global populations, including the plague, Spanish flu, cholera, swine flu (H1N1), and severe acute respiratory syndrome-coronavirus (SARS-CoV)[7-11]. Recent studies have shown that the mortality ratio (MR) due to COVID-19 in China is 0.66%, on the Diamond Princess ship it is 2.3% and a large meta-analysis of 36 European countries showed that the MR ranged from 4% to 4.5%[12-14].

To date, there are no vaccines or medicines available to combat this pandemic. However, several clinical trials of both therapeutics and vaccine candidates are underway. Furthermore, it was proven that convalescent plasma transfusion (CPT) is useful in patients with severe COVID-19[15,16]. As the landscape of COVID-19 is evolving dramatically, it is becoming a challenge to determine high-quality evidence as data is being generated at an alarming rate.

Several studies have identified SARS-CoV-2 viral RNA in rectal swabs[17,18], and stool specimens of asymptomatic COVID-19 patients[19,20]. This raises the issue of GI viral infection and the route of fecal-oral transmission. Furthermore, viral receptor angiotensin-converting enzyme 2 (ACE2) is expressed in epithelial cells of GI mucosa[21,22]. Taken together, these results indicate that SARS-CoV-2 can dynamically infect and replicate in the GI tract and liver cells. However, this has important implications for the management, transmission and control of the disease. Thus, in-depth research is essential for the future treatment and management of the disease. In this review, we summarized the vital information available to date on COVID-19 and its impact on GI aspects. We recognize the ever-changing literature and aim to update future publications with the most up-to-date information available.

GI MANIFESTATIONS OF COVID-19

There are more than 40 million cases of COVID-19 worldwide, and studies that can confirm the symptoms and manifestations associated with SARS-CoV-2 are now critical. Although the lung is the primary target organ of this virus, this causes discomfort in patients with detrimental oxygen saturation effects, causing shortness of breath. However, GI symptoms have also been observed in COVID patients[23-25]. If the virus enters *via* food it may cause diarrhea. In patients with high viral load, anorexia, anosmia, and dyspepsia are the main GI symptoms[26,27]. Furthermore, anti-viral drugs can give rise to nausea, vomiting and diarrhea (Table 1).

Table 1 Gastrointestinal manifestations of coronavirus disease-2019

Gastrointestinal manifestations	Clinical findings
Lack of appetite	Elevated AST
Anorexia	Elevated ALT
Anosmia	Elevated bilirubin
Vomiting	Elevated LDH
Dysgeusia	
Nausea	
Abdominal pain	
Bloody diarrhea	
Intestinal dysfunction	

AST: Aspartate aminotransferase; ALT: Alanine aminotransferase; LDH: Lactate dehydrogenase.

SARS-CoV-2 can be detected in the GI tract. The virus can invade epithelial cells in the stomach, intestine and colon surface and cause symptoms in the GI tract. As the world is now facing the second wave of this current pandemic, the GI manifestations of COVID-19 require much more attention as there are more possibilities for transmission of the infection due to lack of information/knowledge on GI complications[21,28-30]. The course of alveolar events, GI spread and the manifestations of SARS-CoV-2 infection are shown in Figure 1.

A meta-analysis of 60 studies from 6 countries found that 4243 patients with SARS-CoV-2 infection had GI symptoms, including diarrhea (12.5%), nausea/vomiting (10.2%), anorexia (26.8%) and abdominal pain (9.2%), which were the most common symptoms[31]. Another hospital-based study reported that of 1099 patients, nausea or vomiting and diarrhea occurred in 5% and 3.8% of patients, respectively[21]. Another study showed that in 148 Chinese SARS-CoV-2 positive patients, half of the patients seemed to have abnormal liver function at the time of admission[32]. A further study showed similar results with non-typical findings in hepatic enzymes[33,34]. Patients were expected to have moderate to high fever with elevated liver function, and these tests were remarkably more frequent in male patients (68.67%) than in female patients (38.36%)[35].

CLINICAL SIGNIFICANCE OF COVID-19

SARS-CoV-2 when entering the body causes viremia with associated pneumonia and the main clinical features of this disease are fever, severe headache, fatigue, diarrhea and other potential associated comorbidities[36,37]. The estimated average duration of incubation is 1-14 d (commonly 3-7 d). Viruses enter the body and proliferate mainly in the lungs, GI tract, and heart. SARS-CoV-2 is believed to be concentrated in tissues that express ACE2[38,39]. Recently, studies have reported that anorexia, nausea, vomiting and diarrhea were the most common GI tract symptoms in almost 40% of patients[40,41]. However, one-tenth of patients complained of GI symptoms without major difficulty in breathing or mild fever[42]. SARS-CoV-2 has been correlated with a hyper-coagulable condition with a major risk of venous thromboembolism[43]. Neurological indications such as severe headache, dizziness, and loss of consciousness, stroke, and muscle injury have also been observed[44]. Detailed clinical manifestations are shown in Table 2. GI manifestations of SARS-CoV-2 infection are also indicated to alter nutrient absorption by modulating the expression and activity of nutrient transporters, such as the neutral amino acid transporter BAT1.SARS-CoV-2 infection which potentially triggers physiological and anatomical damage related to the GI tract along with its systemic influence is summarized in Figure 2.

Table 2 Clinical significance of coronavirus disease-2019

Stage	Symptoms
Mild	Initial symptoms are mild or negligible with no sign of pneumonia on imaging.
Moderate	Cough, moderate fever, myalgia, gastrointestinal symptoms, anosmia and respiratory signs with radiological imaging findings of pneumonia.
Severe	The presence of one of the following: (1) Shortness of breath (RR ≥ 30 breaths/min); (2) Oxygen saturation ≤ 93% at rest; (3) Arterial partial pressure of oxygen/fraction of inspired oxygen ≤ 300 mmHg (1 mmHg = 0.133 kPa); and (4) In less than 24-48 h, more than half of patients with radiological imaging show clear lesion progression.
Critical	Any of the following: (1) Lung failure or requiring mechanical ventilation; (2) Septic shock; and (3) Multiple organ failure (other organ failure that requires HDU/ICU critical care.)

RR: Risk ratio; HDU: High dependency unit; ICU: Intensive care unit.

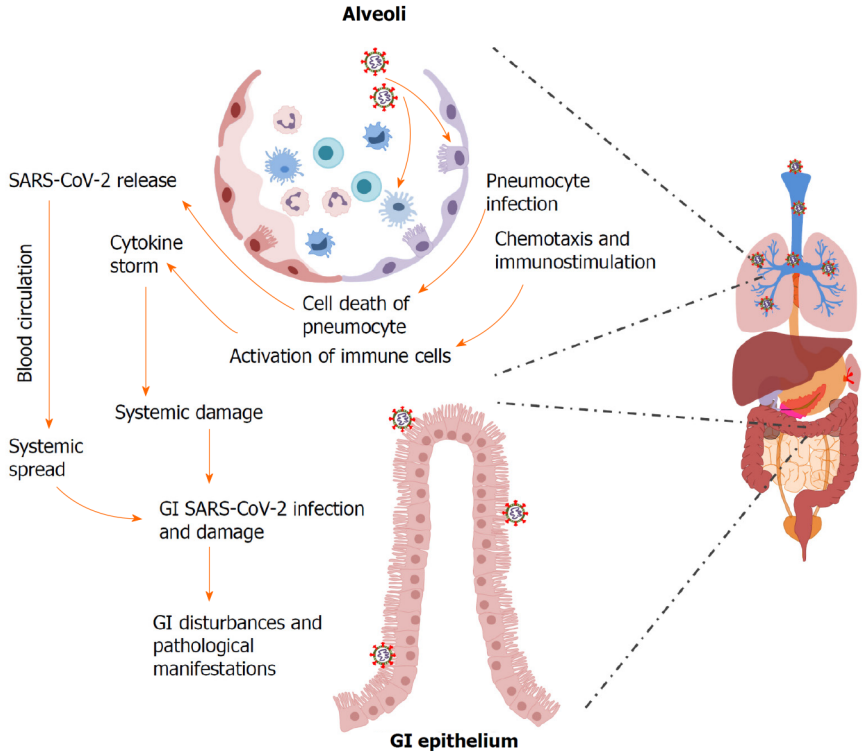


Figure 1 Systematic representation of the course of alveolar events, gastrointestinal spread and manifestations of severe acute respiratory syndrome coronavirus 2 infection. SARS-CoV-2: Severe acute respiratory syndrome coronavirus 2; GI: Gastrointestinal.

CARE OF PATIENTS WITH EXISTING LIVER DISEASE

Non-alcoholic fatty liver

Obesity is a major risk factor for severe COVID-19 because pneumonia is mainly exacerbated in obese people as adipose tissue can act as a viral repository and is, therefore, an immunological center for the inflammatory response[45,46]. Since non-alcoholic fatty liver disease (NAFLD) is associated with metabolic comorbidities such as type 2 diabetes, hypertension and obesity, NAFLD patients are at higher risk of having severe COVID-19[47]. According to a retrospective study, 39 of 202 confirmed COVID-19 patients had higher body mass index (BMI) and higher NAFLD co-morbidity rates. The study also found that NAFLD patients had a higher risk of disease progression to severe COVID-19, and these patients also had a longer duration of viral shedding[48]. Interestingly, patients with NAFLD and SARS-CoV-2 infection less than 60 years of age are associated with an elevated risk of severe disease[49]. NAFLD patients with increased non-invasive liver fibrosis scores are more likely, despite metabolic comorbidities, to develop severe COVID-19 disease[50].

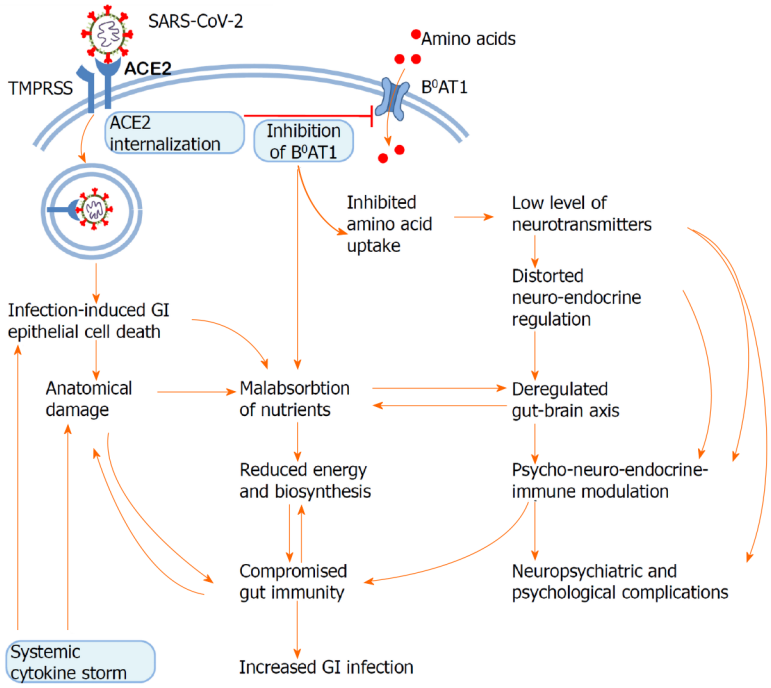


Figure 2 Potential events caused by severe acute respiratory syndrome coronavirus 2 infection in gastrointestinal physiological and anatomical damage with systemic influence. SARS-CoV-2: Severe acute respiratory syndrome coronavirus 2; ACE2: Angiotensin-converting enzyme 2; GI: Gastrointestinal.

Viral hepatitis

Almost 5 billion people in the Asia-Pacific region have chronic viral hepatitis[51]. Unlike metabolic liver disorder, there is little or no evidence that chronic viral hepatitis affects the progression of COVID-19. Corticosteroid and tocilizumab are administered to critically ill patients with COVID-19, which can lead to reactivation of hepatitis B virus (HBV) and to severe liver failure in patients with long-term HBV infection. Therefore, HBsAg screening should be performed in patients with severe COVID-19 with a positive HBsAg test at the time of corticosteroid therapy[52]. It is essential to initiate antiviral medication in newly diagnosed HBV patients affected by COVID-19 when HBV DNA is more than 2000 IU/mL and alanine aminotransferase is above the upper limit of normal. Drug-drug interactions between agents used to treat COVID-19 and HBV may occur. In addition, patients with HBV and HBC should continue to receive antiviral drugs. Considering the uncertain effect of interferon-alpha on the systemic inflammation associated with COVID-19, treatment with alternative drugs in patients with HBV during the pandemic should be addressed prior to medication administration. In COVID-19 patients, initiation of treatment for HBV and hepatitis C virus (HCV) is usually not required and should be delayed until recovery from COVID-19 is achieved. Interactions between the drugs used in the treatment of COVID 19, and those used to treat HBV and HCV should be carefully monitored.

Autoimmune liver disease

Patients with autoimmune liver disease can experience severe liver problems. Therefore, the reduction of immunosuppressive drugs in the prevention of SARS-CoV-2 is generally not recommended. The reduction should only be performed under special conditions (such as drug-induced cytopenia or bacterial super-infection) after consultation with a specialist. Treatment with corticosteroids was found to be promising in hospital patients seeking respiratory support for COVID-19. There is still concern that patients who are taking elevated doses of corticosteroids may be more vulnerable to SARS-CoV-2 infection and serious COVID-19. Patients who are already taking corticosteroids when they develop COVID-19 should have an adequate dose of corticosteroids to prevent adrenal insufficiency. Adding or switching to dexamethasone can only be addressed in patients with COVID-19 who require hospitalization and respiratory assistance. Liver enzymes such as transaminases, alkaline phosphatase and gamma-glutamyltranspeptidase may be increased in patients with confirmed COVID-19 or suspected SARS-CoV-2 infection. Thus, it is

strongly recommended that suspected infection should be confirmed by biopsy. However, if there is a strong suspicion of autoimmune hepatitis, empiric therapy may be initiated without histological confirmation at the standard treatment dose[53-55].

Liver cirrhosis

Patients with cirrhosis are susceptible to SARS-CoV-2 infection, new and worsening hepatic decompensation, severe COVID-19 and death. Patients with new or deteriorating hepatic decompensation should be given priority to SARS-CoV-2 screening even in the absence of respiratory symptoms. For patients with cirrhosis who are infected with SARS-CoV-2, rapid admission must be considered to prevent further worsening of their condition. There is no specific consideration to date for cirrhosis patients who have been infected with SARS-CoV-2 as the drug used to control COVID-19 may increase the risk of other infections and viral shedding[53,56,57].

Liver transplant recipients

Patients who have undergone liver transplantation are at high risk of severe infection with SARS-CoV-2 and death. The risk of transmission of SARS-CoV-2 through liver transplantation is unknown; therefore, it is recommended that all donors should be screened for SARS-CoV-2 infection with real-time reverse transcription polymerase chain reaction (RT-PCR). Considering that SARS-CoV-2 can spread from asymptomatic people, including children, patients undergoing liver transplantation should strictly follow physical distancing or not travel during the COVID-19 pandemic. Telehealth home surveillance is efficient and useful for liver transplant recipients; consequently, it must be available in most transplant centers and applied to pre-transplant patients where telehealth services are available. Unrecognized COVID-19 significantly increases the risk of severe immune suppression and post-transplant infection in liver transplant recipients, leading to multiple organ failure and even death. A reduction of immunosuppressive therapy in liver transplant recipients should not be considered to prevent SARS-CoV-2 infection. Such a reduction can only be carried out under exceptional conditions (including drug-induced lymphopenia or bacterial/fungal super-infection in the event of SARS-CoV-2 infection) after consultation with a specialist. Calcineurin inhibitor dosage levels and mechanistic targeting by rapamycin inhibitors should be closely monitored as they are offered in conjunction with drugs such as hydroxychloroquine, protease inhibitors or recent COVID-19 test drugs[58-61].

DIAGNOSIS OF GI COVID-19 EFFECTS

COVID-19 is spread by air-borne viral particles and affects not only the respiratory tract, cardiovascular, and central nervous systems but also affects the GI system. Previous findings demonstrated that several patients with COVID-19 had many low to moderate GI complications, including diarrhea during the disease course[26]. Until recently, there was no evidence on the potential of anti-GI drugs but sufficient frequent rehydration and potassium ion monitoring were conducted in COVID-19 patients. Therefore, it might be hypothesized that diarrhea should be considered an awareness parameter and must be investigated to reach an early diagnosis in COVID-19 patients. Furthermore, measurement of calprotectin could play an important role in the monitoring, diagnosis, and follow-up of COVID-19-associated diarrhea and GI complications. Therefore, participation of the GI tract in COVID-19 should be considered and explored under several clinical policies and practices such as the incorporation of rectal swab testing before the discharge of COVID-19 patients[62], as well as our future supply of personal protective equipment (PPE) in the endoscopy, ultrasound and another relevant diagnostic settings. These implementations will act as promising tools to eradicate COVID-19[63].

GI endoscopy

Endoscopy is a very complex procedure in GI clinical settings. In COVID-19 patients, it is a high-risk process for healthcare professionals due to potential high exposure while performing upper GI endoscopy, and makes them more prone to infection as a result of the patient's aerosol[64]. A study reported the presence of SARS-CoV-2 RNA in a patient's stool samples. These findings raise suspicion and support the potential fecal-oral transmission route of infection. Furthermore, the novel virus is possibly transmitted through fecal contamination *via* inhalation, conjunctival splash contact, or direct contact with feces during colonoscopy[21]. To restrict the aerosol transmission of

SARS-CoV-2 within/between the endoscopy team, various hospital infection control guidelines and protocols should be established. All endoscopic procedures should be conducted in an isolated aseptic environment with one set of endoscopy equipment and a PPE kit. According to recent data, it was estimated that the half-life of SARS-CoV-2 virus particles in the air is estimated at around 1.1 h[65]. To prevent viral load, patient to patient cross-infection, and transmission, the current guidelines suggest performing endoscopy in a negative pressure isolated room[66]. All COVID-19 patients should undergo prescreening before arrival at the endoscopy room. During this current outbreak of COVID-19, many experts have recommended the indications for urgent endoscopy which are limited to acute GI bleeding, GI obstruction requiring stenting or dilatation, biliary sepsis, repair of GI perforations and leakage, foreign body retrieval, and the establishment of enteral nutrition. According to recent guidelines, we would like to recommend other criteria including a minimum number of staff with specifically one proficient endoscopist and two nurses for each endoscopy platform. Adequate time should be allowed for infection control measures before and after endoscopy. It should be kept in mind that the same staff should serve the same room for the whole session while performing the procedure. However, when it comes to operative and non-operative endoscopic procedures, all safety measures concerning medical health worker exposure should be considered. There are three criteria and routes for the endoscopic procedure: (1) Oral route: any procedure *via* the mouth or nose; (2) Anal or stomal route: any procedure passing through the anus or an entero-cutaneous stoma; and (3) Capsule endoscopy.

The following vital parameters should be documented before performing endoscopy; fever of more than 37.5°C, contact history, travel history, occupational exposure, and clustering[67]. For all suspected and positive cases, the clinical preparation for endoscopy should be reviewed, and preferably patients with a medical emergency, life-threatening conditions should receive endoscopy. Moreover, all endoscopy teams and staff should receive proper training on the use of PPE and infection control management. Various disinfectants such as ethanol (62%-71% concentration), 2% glutaraldehyde, and 0.1%-0.5% sodium hypochlorite are frequently used before and after each case. All these practices can help to reduce the viral load within one minute of the exposure period[68].

Endoscopy is a very advanced tool, and we would like to recommend all elective endoscopies during the current COVID-19 pandemic for diagnosis purposes be limited until there is a promising cure. This diagnostic strategy helps to protect health care capacity to handle many suspected and positive cases of COVID-19 strategically. However, this approach will act as a potential protective measure to reduce the cross-transmission of COVID-19 between patients and healthcare staff, particularly at the early stage of the COVID-19 pandemic[69]. All these measures aid some significant effort to reduce the risk of cross-infection, the spread of the virus and preserve the use of PPE, are essential in overcoming the spread of COVID-19 within healthcare staff.

Abdominal ultrasound and computed tomography imaging

In COVID-19 patients, fever and dry cough are the most commonly observed symptoms? RT-PCR is the most frequently use confirmatory test to diagnose and identify genomic RNA of SARS-CoV-2. However, early radiological studies focused on imaging of the chest using high resolution computed tomography (CT), which measures peripheral patches of ground-glass densities with or without consolidations with bilateral basal predominance, organizing pneumonia pattern, crazy paving, mild bronchiectasis, and vascular engorgement may also be observed[70,71]. Radiography of the chest, apart from its widespread use and low cost, also has low diagnostic sensitivity for pneumonia in COVID-19 patients[72]. Unlike radiography, lung CT is considered a sensitive imaging technique for early detection of pulmonary severity in infected patients[73]. A recent study found that CT imaging is superior to RT-PCR (98% *vs* 71%, respectively, $P < 0.001$) in the diagnosis of COVID-19[74]. However, it is difficult to imagine a situation where CT is systematically performed in all suspected and positive cases due to cost, exposure to radiation, time required, and the probability of cross-contamination.

Ultrasound (US) is a portable, low cost, and relatively fast procedure with real-time visualization. In the current pandemic, US is considered a potent technique for the diagnosis of suspected and confirmed COVID-19 cases to facilitate better treatment strategies. The use of US has advantages as it restricts exposure of multiple staff to confirmed cases. Additionally, point-of-care US has recently been recommended to manage COVID-19 cases to reduce the use of medical equipment and the number of healthcare staff, which ultimately minimizes cross-infection. More recently, some authors have reported the high diagnostic accuracy of US compared with radiography

when evaluating lung abnormalities[75,76]. However, imaging findings may also increase the understanding of abdominal manifestations in COVID-19 patients. Recently, Abdelmohsen and coworkers conducted abdominal imaging studies (sonographic examination) at 30 intensive care units with 41 confirmed COVID-19 patients with abdominal complications. They reported that 51.2% of patients had increased liver function tests, particularly serum bilirubin, followed by elevated renal function tests in 14.6% of patients[77]. Tullie *et al*[78] conducted abdominal US and CT imaging in pediatric COVID-19 confirmed patients and found that US was the best diagnostic imaging tool in patients with GI symptoms.

Furthermore, they reported that US findings were in line with lymphadenopathy and the presence of inflammatory fat throughout the mesentery with visible thickening of the terminal ileum. Thus, US and CT may accelerate the understanding of abdominal complications in COVID-19 patients[78]. Therefore, we strongly recommend the use of abdominal US imaging for the diagnosis of patients with GI manifestations when investigating for possible appendicitis.

RISK FACTORS DURING ENDOSCOPY IN COVID-19 PATIENTS

Endoscopy is a minimally-invasive technique and is usually recommended for the evaluation of ulcers/polyps, gastritis, stomach pain, dysphagia, digestive tract bleeding, and sometimes for biopsy[79]. It is a safe and common practice; however, it does have the risk of adverse events preventing completion of the procedure and can result in complications ranging from low to potentially rare or mild to lethal complications[80]. During clinical practice from pre-procedure to post-procedure, various adverse reactions can occur, such as infections, cardiopulmonary disorders, bleeding, thromboembolism *etc.* To date, more than 44 million COVID-19 cases with over 1 million deaths have been recorded[81]. It has been verified that this infection is contagious and is chiefly transmitted *via* respiratory droplets (> 5 to 10 μm in diameter) or by close contact (usually within 1 m) to an infected individual while coughing or sneezing. The alarming element concerning COVID-19 is its airborne transmission that may also be feasible in some medical circumstances. Certain clinical practices such as endotracheal intubation, bronchoscopy, nebulization *etc*, produces aerosols resulting in aerial spread, while fecal-oral route transmission (fomites) can also result in contamination[82,83].

Paramasivam and his team conducted a review referencing the report of the Quality Committee of American Society for Gastrointestinal Endoscopy where they mentioned the three key rudiments in defining endoscopic risk factors, *i.e.*, the complexity of the procedure (procedure-related), co-morbidity and clinical status (patient-related) and individual expertise (operator-related)[84,85]. Complexity encompasses clinical and perceived risk elements. Technically more sophisticated approaches are often riskier. Treatment with endoscopic retrograde cholangiopancreatography (ERCP) in conjunction with or without sphincter division (sphincterotomy), colonic polyps as well as peptic ulcer elimination, have high complication rates following therapeutic endoscopy procedures[86]. Artificial ventilation or positive insufflation practice may cause significant aerosol generation due to short physical distancing during endoscopy, increasing the risk of infection in staff, medical personnel, anesthesiologist and others[87,88]. Techniques have progressed to endo-luminal from surgical methods with the escalation and advancement of endoscopic expertise, innovation and has accrued considerable experience to combat this pandemic[86,87].

Although, different endoscopic procedures have specific complications, such as post-ERCP pancreatitis in ERCP or asthma and hemoptysis in bronchoscopy[86,89]; however, perforation, hypoxemia and bleeding are the most commonly recorded complications of all forms of endoscopy[86]. It has been documented that the bleeding rate ranges from low to high with the intensification of invasive procedures such as endoscopic biliary sphincterotomy, endoscopy dilatation or colonoscopic polypectomy during diagnosis[90-92]. Medical guidelines recommend that endoscopy is carried out within 24 h of the patient presenting with acute upper GI bleeding[93]. Compared to other risks, endoscopic-mediated bleeding, typically improves after rapid and rigorous treatment and controls or minimizes other risks[90]. However, the debate about endoscopy in COVID-19 patients, gives rise to specific management decisions. A case study by Cavaliere *et al*[88] documented that endotracheal tube intubation during upper endoscopy surgery in a COVID-19 patient is challenging, and may increase the mortality rate. Coagulopathy linked to COVID is another explanation for GI bleeding; therefore, for stratification, prothrombin time, platelet count and D-dimer

measurement are recommended[94]. Since the complications of endoscopy could surpass the benefits, clinicians have agreed to cautiously treat these patients with a blood transfusion (when necessary), proton pump inhibitor drip, and regular surveillance of GI symptoms, hemoglobin level and other vital signs[88].

Similar to bleeding, perforation has also been recognized as an important risk factor due to its high incidence during numerous procedures, it has been studied in GI trials and clinical interventions are often employed[80]. Perforations are frequently found in the sigmoid colon. Three approaches are considered to cause perforations: air insufflation driven barotrauma, therapeutic procedures and colonoscopy or an instrument triggered mechanical injury[95,96]. Perforations occurring during ERCP arise when there is a transmural extension of sphincterotomy beyond the sphincter and are archetypally asymptomatic. Other factors include adhesions, dysfunction of the sphincter of Oddi, biliary stricture dilation, snare polypectomy *etc*[80].

Operator inexperience has also been designated a significant risk factor. Researchers found that prolonged treatment in conjunction with elevated sedation dose could be attributed, in part, to a higher proportion of complications. Over-sedation may increase the risk of severe complications (such as perforation and bleeding), which can inhibit the pain response[97,98]. Due to its short recovery duration, propofol is among the most widely used agents and has lower complication rates than conventional sedative agents as its mean sedation period is shorter and the sedation depth is higher. Propofol is thought to be safe for sedating (senior) patients when given the correct dose, while the risks including hemodynamic and breathing depression occur and accelerate during upper GI endoscopic procedures[80]. Under severe sedation, patients undergoing difficult colonoscopy tend to vomit resulting in pulmonary aspiration. This can lead to needless misperception in medical personnel and caretakers as the signs of pneumonia due to pulmonary aspiration are similar to those in COVID-19[99].

Respiratory and cardiovascular complications have also been observed. Tachycardia and bradycardia can be found during invasive events. Hypertension, hypotension, and syncope were observed during treatment. Clinical micro-aspiration can be considered insignificant if it does not result in pulmonary inflammation or prolonged bronchospasm[80]. As soon as these risk factors have been identified and defined, standard operating procedures and detailed protocols can be set up to reduce the risk of complications before or during the planning phase. The compulsory pre-screening test should be carried out before entry (conditionally carried out to the outbreak of COVID-19) and there should be a discrete unit for 'low-risk' and 'high-risk' patients. Also, healthcare staff and workers must abide by asymptomatic carrier precautions and level 2 biosafety[100].

RECOMMENDATIONS FOR THE MANAGEMENT OF PATIENTS WITH LIVER DISEASE DURING COVID-19

General recommendations

In view of the significant multifaceted effects of the pandemic, especially in chronic diseases, liver damage can be highly variable and complex, leading to the activation of an intra-hepatic immune response, triggering microvascular thrombosis, hepatic obstruction and systemic inflammation in addition to drug toxicity. In conjunction, this systemic disorder is often associated with a phenomenon known as "bystander hepatitis" and the patient can have a lethal course and show no specific signs of hepatic failure[101,102]. The personal care of these patients relies greatly on the regional COVID-19 prevalence and the laws and guidelines imposed[101]. Therefore, the pragmatic structuring of strategies to address this issue must be made by physicians and their organizations by strengthening electronic health records (EHR) and encompassing novel technologies such as remote monitoring and telemedicine to restore treatment levels wherever feasible[103]. The epidemiology of this virus appears uncertain. However, for some time to come, its prevalence may increase and diminish chronologically. Thus, a customized and versatile patient care strategy is needed to align nationwide SARS-CoV-2 infection dynamics, public infrastructure accessibility, and the degree of frequency of existing hepatic disease in an individual. Finally, it is necessary to restart clinical trial registration to make significant progress despite unimaginable global events[53] (Table 3) .

Standard recommendations

Both the American Association for the Study of Liver Diseases[104] and the European

Table 3 Recommendation guidelines for the management of patients with liver disease during coronavirus disease-2019

S. No.	Clinical condition	Consulting organization	Recommendation guidelines for management during COVID-19
1	Out-patient care	AASLD, EASL-ESCMID	(1) Offering telehealth; (2) Mail order of prescriptions & medications; (3) If viral hepatitis occurs: continue medication; (4) Tracking & recording alcohol usage; (5) Limiting testing, imaging & blood withdrawal; and (6) For patients with autoimmune liver disease, immunosuppression medication is continued.
2	In-patient care	AASLD, EASL-ESCMID	(1) Clustering COVID-19 & non-COVID-19 patients separately; (2) Minimizing personnel on rounds; (3) Safe discharge planning; (4) Usage of remote care-telehealth communications & video monitoring; (5) Limiting patient visitors; (6) Minimizing testing, imaging & blood withdrawal; and (7) Avoiding inter/intra-transfer between facilities.
3	Endoscopy	AASLD, EASL, APSDE, AGA, ESGE, ASGE	(1) Limiting emergent indications such as ERCP (for cholangitis), severe GI bleeding or variceal bleeding; (2) Minimizing personnel during procedures; (3) Every clinician/personnel recommended to use N95 masks and PPE as there is high aerosol generation during clinical procedures; and (4) Postponing certain elective procedures such as esophageal variceal screening.
4	NAFLD	AASLD, EASL	(1) Notification to patients regarding adverse hepatic/metabolic implications associated with social isolation & lifestyle; (2) In line with existing directives, arterial hypertension treatment should continue; and (3) All NAFLD patients who may be infected with SARS-CoV-2 should have early admission.
5	Viral hepatitis (HBV & HCV)	AASLD, EASL	(1) If under care, continue treatment for chronic HCV and chronic HBV; (2) For follow-up patients, offer telehealth and laboratory testing; (3) Mail order of direct-acting anti-viral prescriptions & medications, if initiated; (4) Alternative therapy should be considered as associated risks of IFN-α is unknown; (5) Case-by-case basis decision in consultation with a medical specialist should be undertaken for patients with COVID-19 and high disease flare; and (6) Use of anti-viral therapy is considered in individuals with resolved or chronic HBV and COVID-19 conditions undertaking immunosuppressive therapy.
6	Liver cirrhosis	AASLD, EASL	(1) Clustering COVID-19 & non-COVID-19 patients separately; (2) Early admission and prioritized COVID-19 testing for patients with ACLF or deteriorating/chronic hepatic conditions is advised; (3) Every attempt must be made, wherever feasible, to restore highest quality treatment for patients; (4) Prophylactic course of action for GI hemorrhage, hepatic encephalopathy *etc*. must be trialed; (5) Use of vasoconstrictor therapy ought to be undertaken with great consideration and care; and (6) Vaccination recommended for *Streptococcus pneumoniae* and influenza.
7	ALD	AASLD, EASL	(1) It is recommended that there should be no reduction in immunosuppressant dosing in patients with ALD & COVID-19. Under special conditions, dosage may be decreased but, after consultation with a clinician; (2) Monitoring of corticosteroid treatment in patients with elevated doses as they have increase susceptibility to viral infection; (3) Agents such as budesonide is recommended as a primary treatment to reduce the systemic risk of glucocorticoids; and (4) Vaccination is recommended for *Streptococcus pneumoniae* and influenza.
8	ARLD	AASLD, EASL	(1) Reduction in consumption of alcohol; (2) Implementing strategies such as cessation and online (telephone) alcohol liaison services; (3) Monitoring of corticosteroid treatment in patients with elevated doses as they have an increase susceptibility to viral infection; (4) Awareness of online circulation of misinformation or fabrication concerning alcoholic effects.
9	Liver transplantation and surgery	AASLD, EASL, ILTS, LTSI, ATS, TTS	(1) Avoid evaluation of in-patient transplants; (2) Screening of recipients and donors for COVID-19; (3) Reduction in immunosuppression in chronic COVID patients; (4) Routine reduction in immunosuppression doses should not be encouraged; (5) Edge to urgent indications/case-by-case; (6) Minimize workforce during treatment procedures; (7) Safe anesthesia practice with appropriate PPE and N95 masks use is recommended; and (8) Deferring elective procedures such as hepatic resection.
10	Hepatocellular carcinoma	AASLD, EASL, ILCA, ASCO, ESMO	(1) Postponing HCC screening for some months; (2) Pausing enrolment in clinical trials; (3) If surgery or extirpation are delayed, then trans-arterial bridging therapies should be offered; and (4) The patient needs to continue, if already taking tyrosine kinase inhibitor medications.

NAFLD: Non-alcoholic fatty liver disease; ALD: Auto-immune liver disease; ARLD: Alcohol-related liver disease; COVID-19: Coronavirus disease-2019; ERCP: Endoscopic retrograde cholangiopancreatography; GI: Gastrointestinal; PPE: Personal protective equipment; SARS-CoV-2: Severe acute respiratory syndrome coronavirus 2; HBV: Hepatitis B virus; HCV: Hepatitis C virus; ACLF: Acute-on-chronic liver failure; ALD: Alcoholic liver disease; HCC: Hepatocellular carcinoma; AASLD: American Association for the Study of Liver Diseases; EASL: European Association for the Study of the Liver; ESCMID: European Society of Clinical Microbiology and Infectious Diseases; APSDE: Asian Pacific Society for Digestive Endoscopy; AGA: American Gastroenterological Association; ESGE: European Society of Gastrointestinal Endoscopy; ASGE: American Society for Gastrointestinal Endoscopy; ILTS: International Liver Transplantation Society; LTSI: Liver Transplant Society of India; ATS: American Thoracic Society; TTS: Transplantation Society; ILCA:

International Liver Cancer Association; ASCO: American Society of Clinical Oncology; ESMO: European Society for Medical Oncology.

Association for the Study of the Liver (EASL)[101], advocate the use of telemedicine to minimize interaction between patients and health workers by recommending prevention and management interventions that include sectioning of COVID-19 inpatients from other clinically healthy patients and optimization of the use of telemedicine. For COVID-19 adults with chronic disease (particularly if other risk factors are present), the EASL recommends considering early admission and with an upscaled biochemical profile, must be examined for concomitant viral hepatitis B or C infections[105]. In patients with strong clinical suspicion of deep venous thrombosis, or biliary blockage, diagnostic imaging must only be implemented in selected patients, and biopsies should be postponed, but certain cases should be admitted to detect autoimmune hepatitis[101,104,105]. Besides using EHR and telemedicine in some patients as an alternative to in-person care, various medical centers must change their modus operandi to meet the needs of social distancing[106].

Viral hepatitis-HCV and HBV: Medication for HCV and HBV should be administered following the general guidelines in patients without COVID-19[107]. If the patients are already taking medication such as anti-viral therapy for the treatment of chronic HCV/ HBV, telehealthcare, as well as clinical tests, should be conducted in addition to electronic follow-up prescriptions and if initiated, additional resources including a complete course of anti-viral medications with alternative therapies to prevent the uncertain effect of INF-a[53,54]. A case-by-case decision by the consultant should be taken for clients with COVID-19 and a high disease flare or a clinical concern of acute HBV hepatitis, and then patients should undergo antiviral therapy. The use of antiviral therapeutic interventions should be taken into account to avoid viral flares or reactivation in patients with severe, latent or healed HBV and COVID-19 treated with immunosuppressive agents[53].

Liver cirrhosis: The effect of SARS-CoV-2 infection on patients with cirrhosis and the negative impacts of late or amended treatment during the COVID-19 pandemic is especially important and every attempt must be made wherever possible to establish the highest quality treatment for cirrhosis patients in compliance with guidelines[53,108]. The option to postpone all regular screenings or monitoring procedures for patients with compensated cirrhosis should be available. As per the proposal of the Baveno VI consensus, it is recommended that low-risk patients should avoid intrusive variceal blood screening[106]. The risk of infection and associated comorbidities in cirrhosis patients is expanding, and is critical for patients who have decompensated cirrhosis, as a result of immune dysfunction related to cirrhosis. Particular measures should be carried out for those patients with cirrhosis admitted for reasons other than COVID-19 in a designated non-COVID-19 station, ideally side-rooms, in an attempt to mitigate the risk of SARS-CoV-2 nosocomial contamination[53]. Standardized rules and regulations to avoid and deter admission must also be strictly observed concerning GI hemorrhage, hepatic encephalopathy and prophylaxis of spontaneous bacterial peritonitis[53,108].

NAFLD or steatohepatitis: Metabolic complications such as hypertension, obesity and diabetes mellitus (DM) will increase the probability of severe COVID-19 in patients with NAFLD or steatohepatitis (NASH)[101,106]. The associated negative metabolic and hepatic effects due to social repression, including intensified sedentary habits and intake of convenience foods should be made known to patients[53,106]. The development of liver disease may be prevented by activities such as diet guidance, weight loss advice and managing DM, which may minimize severe disease following future infection with SARS-CoV-2. The treatment of arterial hypertension should follow current guidelines. There is currently no indication that angiotensin-converting enzyme blockers or angiotensin receptor antagonists increase either the risk of SARS-CoV-2 or the risk of serious complications or death from COVID-19. All patients with NAFLD and SARS-CoV-2 should be admitted to hospital promptly[53].

Specific recommendations for NAFLD: Patients with NAFLD are considered to be susceptible to COVID-19; therefore, specific recommendations should be followed. Patients with NAFLD should be mindful of the possible detrimental effects of social isolation on metabolic and hepatic function, as more unhealthy lifestyles and excessive intake of refined foods may exacerbate the condition. To prevent the progression of liver disease, good lifestyle choices should be made. Maintaining body weight and avoiding obesity can help to prevent future SARS-CoV-2 infection. Under current

guidelines, treatment of arterial hypertension should be continued as there is no research at present to suggest that angiotensin-converting enzyme inhibitors or angiotensin receptor blockers raise the risk of SARS-CoV-2 infection or the risk of experiencing serious complications or death from COVID-19. For all NAFLD patients who develop COVID-19 admission should be considered. Whenever possible, patients with NAFLD should be hospitalized in areas physically separated from other COVID-19 patients[53].

Alcohol-related liver disease: Alcohol intake can enhance the vulnerability of a person to SARS-CoV-2 infection. Social exclusion can contribute to new and elevated use of alcohol[109], a rise in alcohol consumption may be associated with further liver decompensation. Therefore, physicians and agencies should adopt preventive actions such as patient access to telephone alcohol liaison and abstinence. While therapy with corticosteroids has shown a positive benefit in hospitalized COVID-19 patients[110], there is still uncertainty as to whether patients already on elevated doses of corticosteroids are more likely to be seriously affected by COVID-19. These aspects should be addressed in patients with severe alcoholic hepatitis before the initiation of corticosteroids[53].

Autoimmune liver disease: Experts are currently suggesting that immunosuppression therapy should be avoided in COVID-19 patients with autoimmune liver disease. A decline in medication following lymphopenia/cytopenia or microbial super-infection in patients with severe COVID-19 should be considered only in exceptional circumstances following consultation with a physician[53,106]. Although corticosteroid treatment has had a positive effect in hospitalized COVID-19 patients, it is unknown whether patients treated with high doses of corticosteroids may be more vulnerable to SARS-CoV-2 infection and severe COVID-19. Therefore, we suggest the initial administration of budesonide to reduce systemic glucocorticoid exposure in patients with autoimmune hepatitis flare without cirrhosis[53,101]. Dexamethasone should be introduced or added only in COVID-19 patients who require hospital admission and respiratory assistance[110]. There is insufficient information on patients with IgG4-associated diseases, primary sclerosing cholangitis and biliary cholangitis to formulate specific guidelines. All patients should be vaccinated against *Streptococcus pneumoniae* and influenza[53,101].

Patients who have undergone liver transplantation: Patients with decompensated cirrhosis on the liver transplantation (LT) standby list are at greater risk of serious COVID-19 and death; therefore it is advisable that LT facilities should, as far as appropriate, be restored after the pandemic. Researchers urge the creation and enhancement of LT-donors and recipients' local and global risk pathways, which involve a combination of clinics. LT is a priority for those with a short-term prognosis, such as those with acute liver failure, elevated Model for End-stage Liver Disease score and hepatocellular carcinoma (HCC) at the top of the Milan criteria, in centers with constant resources[53,101,105]. It is currently proposed that all SARS-CoV-2 donors be tested using reverse transcription PCR before using SARS-CoV-2-infected donor livers[60]. It should be noted that patients with SARS infection waiting for LT are associated with a greater risk of COVID-19 and mortality following significant surgery; thus, the possible risk of nosocomial COVID should require consent for diagnostic and therapeutic procedures relating to transplantation[111]. Calcineurin-inhibitor drug levels and rapamycin inhibitor mechanistic targets should be closely monitored when used in combination with medications such as hydroxychloroquine, protease inhibitors or experimental COVID-19 drugs[53]. Case-by-case consideration should include diligent risk stratification of the donor (living) and recipient using a combination of the clinical background, chest X-rays and SARS-CoV-2 monitoring. A COVID-19-free transplant plan, including strict social isolation for patients on a housing list, wireless screening for signs and exposures before admission and peri-operative management in a designated clean intensive care facility and post-LT care unit should be developed in areas with high disease burden[53,101].

HCC: People living with cancer have worse COVID-19 consequences. This is likely to apply to HCC patients as they are usually older, more vulnerable and require several medications including cytotoxic chemotherapy[105,112]. Multi-factorial HCC boards may continue to operate remotely and offer clinical advice, including ongoing systemic treatment and LT assessment. When appropriate, full HCC monitoring shall be restored. Where resource constraints exist, priority should be given, by public HCC risk stratification ratings, to patients at higher risk, including those with elevated alpha-fetoprotein levels, advanced cirrhosis, chronic hepatitis B, NASH/diabetes,

etc[53,101].

Pharmacological management

COVID-19 is a fast-growing area for targeted management, with a wealth of new or repurposed drugs rapidly being in and out of favor. While no medications have been approved at present for SARS-CoV-2, in recent weeks many treatments have been tested and many are still are under investigation. It is encouraged to investigate possible hepatotoxic effects at "LiverTox" and drug interactions at "HEP drug interactions" before beginning any COVID-19 medications[106]. Unique factors in treatment trials for COVID-19 patients with chronic liver disease are briefly summarized here. Trials in COVID-19 patients include research on the following medications:

Remdesivir: Remdesivir is an adenosine nucleotide analogue demonstrated to minimize the length of symptoms following early use as a potential contender for COVID-19 therapy. It induced termination of the RNA chain and was first developed as an anti-Ebola agent[113]. In preclinical studies, remdesivir use in randomized studies demonstrated no major effect on liver function tests relative to a sugar pill, despite evidence of a reversible aminotransferase elevation. The elevation in aminotransferase was seen in patients on remdesivir after exclusion of certain liver conditions[53]. A clinical *in vitro* isolate of SARS-CoV-2 has recently been inhibited and in an *in-vivo* rhesus macaque model, the severity of the associated MERS-CoV infection was decreased by remdesivir[114].

Corticosteroids: The association between corticosteroids and COVID-19 seems inconclusive. Those with an existing serious disease appear to benefit from the addition of corticosteroids, while patients who have already taken corticosteroids may be more at risk of COVID-19 adverse effects[53]. Corticosteroids reduce pro-inflammatory cytokine production, and there is a risk of an increase in co-infection in persons with decompensated cirrhosis[106]. Their use has been related to intensive care unit admission, artificial ventilation or death in patients with inflammatory bowel disease. Similarly, the rheumatological hospitalization rating for maintenance glucocorticoids after SARS-CoV-2 infection has expanded[53]. Standard immunosuppression in patients with autoimmune hepatitis or LT, including steroids where necessary, is currently recommended. However, for patients with severe COVID-19 who require respiratory assistance, corticosteroids are a feasible treatment choice. Dexamethasone decreased mortality in perfusing patients by one-third and in patients who received additional oxygen by one-fifth in June 2020[110]. This agent is likely to be used more and more to treat serious COVID-19 even in patients with pre-existing chronic liver disease[53].

Anticoagulation: The risk of venous thromboembolism is greater in patients with advanced liver disease. The rate of venous thromboembolic disease in patients hospitalized due to COVID-19 is frighteningly high, with an observed 20% incidence on day 7, and 42% on day 21 despite thromboprophylaxis[115]. Therefore extensive analysis of the role of anticoagulation in COVID patients has demonstrated that the results in extreme COVID-19 are strengthened, although there are still coherent stepped care models and processing thresholds. While there are reservations regarding the use of anticoagulation in patients with liver cirrhosis and portal hypertension, there has been no systematic evaluation indicating excess blood disorders in cirrhosis- and portal vein thrombosis anticoagulated patients[53].

Tocilizumab: The main driver of the "cytokine storm," interleukin-6 (IL-6), appears to be significant in lungs and other organs due to severe COVID-19. Tocilizumab, a humanized monoclonal antibody targeting IL-7 has shown value in retrospective series of COVID-19 by reducing the need for and duration of organ support. As this agent is widely used in rheumatoid arthritis and other autoinflammatory diseases, its liver profile is well-established[53,101,106]. Mild serum aminotransferase elevations are common and are generally self-limited and asymptomatic. However, gradual jaundice requiring LT has been reported[53,106]. In rare cases, tocilizumab is associated with HBV reactivation[53].

Others: Several studies have indicated that other drugs have shown clinical effectiveness in patients with COVID-19. Clinical research in patients affected is underway to better determine their effectiveness. Chloroquine phosphate or hydroxychloroquine, ritonavir-boosted lopinavir, baricitinib *etc* are some of the

medications currently being assessed. Hydroxychloroquine impedes lysosomal acidification and autophagy, preventing *in-vitro* viral entry[106,116]. Baricitinib is a JAK 1/2-AAK1 inhibitor resulting in lymphopenia, HBV activation and is not recommended in those with liver impairment[106]. Drugs with natural origins have also been suggested to improve COVID-19-associated clinical manifestations including GI disturbances.

Limitations of existing therapy

At present, there is no evidence from clinical trials which shows the effectiveness of drugs in patients with either suspected or confirmed COVID-19, and there are no clinical trial results available that endorse prophylactic treatments. Therefore, repurposing old drugs is the only option to cope with the current pandemic until vaccines are developed. Chloroquine/hydroxychloroquine, lopinavir, ribavirin, remdesivir, favipiravir, corticosteroids, and tocilizumab are the only Food and Drug Administration approved medications for COVID-19. However, even after identifying old drugs for reutilization, there are several barriers to minimize the severity of COVID-19 such as dose adjustments, route of administration, mechanism of action, GI toxicity, and choice of delivery system to administer these old drugs. The limitations of using these agents are a tendency to cause acute heart and liver toxicity. This acute toxicity can overwhelm the undetermined advantage of a particular antiviral agent. Approximately 50% of patients treated with lopinavir experienced adverse reactions in a recent randomized controlled trial and 14% of patients discontinued treatment due to GI side-effects. Lopinavir may exacerbate hepatotoxicity and liver injury as it elevates alanine transaminase. Ribavirin causes severe dose-dependent hematological toxicity. High doses of ribavirin in SARS trials resulted in hemolytic anemia in more than 60% of patients. Tocilizumab has been linked to HBV reactivation and thus HBV serology should be part of the routine pre-treatment workup. The lack of clinical data suggesting a specific benefit of these agents do not explain their risks[53,117].

CONCLUSION

The recent COVID-19 pandemic has posed an unprecedented burden on human health. The lungs are the primary infection site for the causative agent of this COVID-19 pandemic, *i.e.*, SARS-CoV-2 and, therefore, initial investigations have mainly focused on its community spread and consequent pulmonary disorders. With the quantity of studies from various medical, bio-medical as well as allied fields, it is now established that the effects of SARS-CoV-2 are not limited to only the lungs. Systemic infection and pathological manifestations have been confirmed including those in the GI system. Considering the critical role of the GI system in physiological maintenance, it is essential to combat the SARS-CoV-2 infection-triggered anatomical damage. GI disturbances in COVID-19 also result in complications which are challenging in the clinical management of patients with co-morbidities including obesity, hyperglycemia, hypertensive disorders, liver diseases, cardiovascular disorders, *etc.* Although most of the symptoms in SARS-CoV-2 infected patients are similar to those known to arise in other respiratory viral infections, its novel nature and the degree of uncertainty regarding the outcome of therapeutic interventions make treatment challenging. Moreover, the steps taken to prevent the ongoing pandemic (social distancing, lockdown, stay-home strategies) also drive disturbances in physiological and mental well-being. This will contribute to GI anomalies due to altered daily routine, leisure activities, dietary habits, and hormonal imbalance (reduced vitamin D due to less sunlight exposure).

Due to its severity, rapid rate of spread and associated clinical complications, it is difficult to diagnose the GI ailments associated with COVID-19. Conventional methods and combinatorial strategies are suggested to provide an accurate diagnosis. The presence of SARS-COV-2 in various organs and fecal discharge, even in individuals negative for respiratory infections, indicates that GI organs also serve as a target and reservoir for the virus. As the GI system is involved in nutrient assimilation and physiological processes, viral infection results in diverse clinical manifestations in different systems including cardiovascular, neuropsychiatric, pulmonary, and hepatic, *etc.* Therefore, it is suggested that GI disturbances due to SARS-COV-2 infection must be considered as important as respiratory complications in COVID-19. This warrants the restructuring of medical service priorities to cover GI physiological disturbances in the treatment of COVID-19.

In the absence of any specific medication and prophylactic measures, the recent pandemic is expected to persist. However, the associated clinical manifestations of COVID-19 are not entirely known. Data on the clinical sequelae of COVID-19 in organs other than lungs are expected from ongoing investigations which are likely to increase. This requires the preparedness of health organizations to respond to the probable increase in GI disorders during and after the COVID-19 pandemic.

REFERENCES

1 **Cucinotta D**, Vanelli M. WHO Declares COVID-19 a Pandemic. *Acta Biomed* 2020; **91**: 157-160 [PMID: 32191675 DOI: 10.23750/abm.v91i1.9397]

2 **Mahase E**. Covid-19: WHO declares pandemic because of "alarming levels" of spread, severity, and inaction. *BMJ* 2020; **368**: m1036 [PMID: 32165426 DOI: 10.1136/bmj.m1036]

3 **Ou X**, Liu Y, Lei X, Li P, Mi D, Ren L, Guo L, Guo R, Chen T, Hu J, Xiang Z, Mu Z, Chen X, Chen J, Hu K, Jin Q, Wang J, Qian Z. Characterization of spike glycoprotein of SARS-CoV-2 on virus entry and its immune cross-reactivity with SARS-CoV. *Nat Commun* 2020; **11**: 1620 [PMID: 32221306 DOI: 10.1038/s41467-020-15562-9]

4 **Gavriatopoulou M**, Korompoki E, Fotiou D, Ntanasis-Stathopoulos I, Psaltopoulou T, Kastritis E, Terpos E, Dimopoulos MA. Organ-specific manifestations of COVID-19 infection. *Clin Exp Med* 2020; **20**: 493-506 [PMID: 32720223 DOI: 10.1007/s10238-020-00648-x]

5 **Merad M**, Martin JC. Pathological inflammation in patients with COVID-19: a key role for monocytes and macrophages. *Nat Rev Immunol* 2020; **20**: 355-362 [PMID: 32376901 DOI: 10.1038/s41577-020-0331-4]

6 **Rohollah Valizadeh AB**, Azin Mirzazadeh, Lakkakula VKS Bhaskar. ,. Coronavirus-nephropathy; renal involvement in COVID-19. *J Renal Inj Prev* 2020; **9**: e18 [DOI: 10.34172/jrip.2020.18]

7 **Bramanti B**, Dean KR, Walløe L, Chr Stenseth N. The Third Plague Pandemic in Europe. *Proc Biol Sci* 2019; **286**: 20182429 [PMID: 30991930 DOI: 10.1098/rspb.2018.2429]

8 **Taubenberger JK**, Morens DM. 1918 Influenza: the mother of all pandemics. *Emerg Infect Dis* 2006; **12**: 15-22 [PMID: 16494711 DOI: 10.3201/eid1201.050979]

9 **Chowdhury FR**, Nur Z, Hassan N, von Seidlein L, Dunachie S. Pandemics, pathogenicity and changing molecular epidemiology of cholera in the era of global warming. *Ann Clin Microbiol Antimicrob* 2017; **16**: 10 [PMID: 28270154 DOI: 10.1186/s12941-017-0185-1]

10 **Ratre YK**, Vishvakarma NK, Bhaskar LVKS, Verma HK. Dynamic Propagation and Impact of Pandemic Influenza A (2009 H1N1) in Children: A Detailed Review. *Curr Microbiol* 2020; **77**: 3809-3820 [PMID: 32959089 DOI: 10.1007/s00284-020-02213-x]

11 **Luk HKH**, Li X, Fung J, Lau SKP, Woo PCY. Molecular epidemiology, evolution and phylogeny of SARS coronavirus. *Infect Genet Evol* 2019; **71**: 21-30 [PMID: 30844511 DOI: 10.1016/j.meegid.2019.03.001]

12 **Verity R**, Okell LC, Dorigatti I, Winskill P, Whittaker C, Imai N, Cuomo-Dannenburg G, Thompson H, Walker PGT, Fu H, Dighe A, Griffin JT, Baguelin M, Bhatia S, Boonyasiri A, Cori A, Cucunubá Z, FitzJohn R, Gaythorpe K, Green W, Hamlet A, Hinsley W, Laydon D, Nedjati-Gilani G, Riley S, van Elsland S, Volz E, Wang H, Wang Y, Xi X, Donnelly CA, Ghani AC, Ferguson NM. Estimates of the severity of coronavirus disease 2019: a model-based analysis. *Lancet Infect Dis* 2020; **20**: 669-677 [PMID: 32240634 DOI: 10.1016/S1473-3099(20)30243-7]

13 **Russell TW**, Hellewell J, Jarvis CI, van Zandvoort K, Abbott S, Ratnayake R, Cmmid Covid-Working Group, Flasche S, Eggo RM, Edmunds WJ, Kucharski AJ. Estimating the infection and case fatality ratio for coronavirus disease (COVID-19) using age-adjusted data from the outbreak on the Diamond Princess cruise ship, February 2020. *Euro Surveill* 2020; **25** [PMID: 32234121 DOI: 10.2807/1560-7917.ES.2020.25.12.2000256]

14 **Karadag E**. Increase in COVID-19 cases and case-fatality and case-recovery rates in Europe: A cross-temporal meta-analysis. *J Med Virol* 2020; **92**: 1511-1517 [PMID: 32437052 DOI: 10.1002/jmv.26035]

15 **Verma HK**, Merchant N, Verma MK, Kuru Cİ, Singh AN, Ulucan F, Verma P, Bhattacharya A, Bhaskar LVKS. Current updates on the European and WHO registered clinical trials of coronavirus disease 2019 (COVID-19). *Biomed J* 2020; **43**: 424-433 [PMID: 32792167 DOI: 10.1016/j.bj.2020.07.008]

16 **Verma HK**, Farran B, Bhaskar LVKS. Convalescent plasma transfusion a promising therapy for coronavirus diseases 2019 (COVID-19): current updates. *Antibody Therapeutics* 2020; **3**: 115-125 [DOI: 10.1093/abt/tbaa010]

17 **Lin W**, Xie Z, Li Y, Li L, Wen C, Cao Y, Chen X, Ou X, Hu F, Li F, Tang X, Cai W, Li L. Association between detectable SARS-COV-2 RNA in anal swabs and disease severity in patients with coronavirus disease 2019. *J Med Virol* 2021; **93**: 794-802 [PMID: 32672840 DOI: 10.1002/jmv.26307]

18 **Novazzi F**, Cassaniti I, Piralla A, Di Sabatino A, Bruno R, Baldanti F. SARS-CoV-2 positivity in rectal swabs: implication for possible transmission. *J Glob Antimicrob Resist* 2020; **22**: 754-755 [PMID: 32623000 DOI: 10.1016/j.jgar.2020.06.011]

19 **Holshue ML**, DeBolt C, Lindquist S, Lofy KH, Wiesman J, Bruce H, Spitters C, Ericson K,

Wilkerson S, Tural A, Diaz G, Cohn A, Fox L, Patel A, Gerber SI, Kim L, Tong S, Lu X, Lindstrom S, Pallansch MA, Weldon WC, Biggs HM, Uyeki TM, Pillai SK; Washington State 2019-nCoV Case Investigation Team. First Case of 2019 Novel Coronavirus in the United States. *N Engl J Med* 2020; **382**: 929-936 [PMID: 32004427 DOI: 10.1056/NEJMoa2001191]

20 **Tang A**, Tong ZD, Wang HL, Dai YX, Li KF, Liu JN, Wu WJ, Yuan C, Yu ML, Li P, Yan JB. Detection of Novel Coronavirus by RT-PCR in Stool Specimen from Asymptomatic Child, China. *Emerg Infect Dis* 2020; **26**: 1337-1339 [PMID: 32150527 DOI: 10.3201/eid2606.200301]

21 **Xiao F**, Tang M, Zheng X, Liu Y, Li X, Shan H. Evidence for Gastrointestinal Infection of SARS-CoV-2. *Gastroenterology* 2020; **158**: 1831-1833. e3 [PMID: 32142773 DOI: 10.1053/j.gastro.2020.02.055]

22 **Ni W**, Yang X, Yang D, Bao J, Li R, Xiao Y, Hou C, Wang H, Liu J, Yang D, Xu Y, Cao Z, Gao Z. Role of angiotensin-converting enzyme 2 (ACE2) in COVID-19. *Crit Care* 2020; **24**: 422 [PMID: 32660650 DOI: 10.1186/s13054-020-03120-0]

23 **Huang C**, Wang Y, Li X, Ren L, Zhao J, Hu Y, Zhang L, Fan G, Xu J, Gu X, Cheng Z, Yu T, Xia J, Wei Y, Wu W, Xie X, Yin W, Li H, Liu M, Xiao Y, Gao H, Guo L, Xie J, Wang G, Jiang R, Gao Z, Jin Q, Wang J, Cao B. Clinical features of patients infected with 2019 novel coronavirus in Wuhan, China. *Lancet* 2020; **395**: 497-506 [PMID: 31986264 DOI: 10.1016/S0140-6736(20)30183-5]

24 **Chen N**, Zhou M, Dong X, Qu J, Gong F, Han Y, Qiu Y, Wang J, Liu Y, Wei Y, Xia J, Yu T, Zhang X, Zhang L. Epidemiological and clinical characteristics of 99 cases of 2019 novel coronavirus pneumonia in Wuhan, China: a descriptive study. *Lancet* 2020; **395**: 507-513 [PMID: 32007143 DOI: 10.1016/S0140-6736(20)30211-7]

25 **Zhou F**, Yu T, Du R, Fan G, Liu Y, Liu Z, Xiang J, Wang Y, Song B, Gu X, Guan L, Wei Y, Li H, Wu X, Xu J, Tu S, Zhang Y, Chen H, Cao B. Clinical course and risk factors for mortality of adult inpatients with COVID-19 in Wuhan, China: a retrospective cohort study. *Lancet* 2020; **395**: 1054-1062 [PMID: 32171076 DOI: 10.1016/S0140-6736(20)30566-3]

26 **Pan L**, Mu M, Yang P, Sun Y, Wang R, Yan J, Li P, Hu B, Wang J, Hu C, Jin Y, Niu X, Ping R, Du Y, Li T, Xu G, Hu Q, Tu L. Clinical Characteristics of COVID-19 Patients With Digestive Symptoms in Hubei, China: A Descriptive, Cross-Sectional, Multicenter Study. *Am J Gastroenterol* 2020; **115**: 766-773 [PMID: 32287140 DOI: 10.14309/ajg.0000000000000620]

27 **Giacomelli A**, Pezzati L, Conti F, Bernacchia D, Siano M, Oreni L, Rusconi S, Gervasoni C, Ridolfo AL, Rizzardini G, Antinori S, Galli M. Self-reported Olfactory and Taste Disorders in Patients With Severe Acute Respiratory Coronavirus 2 Infection: A Cross-sectional Study. *Clin Infect Dis* 2020; **71**: 889-890 [PMID: 32215618 DOI: 10.1093/cid/ciaa330]

28 **Xu Y**, Li X, Zhu B, Liang H, Fang C, Gong Y, Guo Q, Sun X, Zhao D, Shen J, Zhang H, Liu H, Xia H, Tang J, Zhang K, Gong S. Characteristics of pediatric SARS-CoV-2 infection and potential evidence for persistent fecal viral shedding. *Nat Med* 2020; **26**: 502-505 [PMID: 32284613 DOI: 10.1038/s41591-020-0817-4]

29 **Gu J**, Han B, Wang J. COVID-19: Gastrointestinal Manifestations and Potential Fecal-Oral Transmission. *Gastroenterology* 2020; **158**: 1518-1519 [PMID: 32142785 DOI: 10.1053/j.gastro.2020.02.054]

30 **Galanopoulos M**, Gkeros F, Doukatas A, Karianakis G, Pontas C, Tsoukalas N, Viazis N, Liatsos C, Mantzaris GJ. COVID-19 pandemic: Pathophysiology and manifestations from the gastrointestinal tract. *World J Gastroenterol* 2020; **26**: 4579-4588 [PMID: 32884218 DOI: 10.3748/wjg.v26.i31.4579]

31 **Cheung KS**, Hung IFN, Chan PPY, Lung KC, Tso E, Liu R, Ng YY, Chu MY, Chung TWH, Tam AR, Yip CCY, Leung KH, Fung AY, Zhang RR, Lin Y, Cheng HM, Zhang AJX, To KKW, Chan KH, Yuen KY, Leung WK. Gastrointestinal Manifestations of SARS-CoV-2 Infection and Virus Load in Fecal Samples From a Hong Kong Cohort: Systematic Review and Meta-analysis. *Gastroenterology* 2020; **159**: 81-95 [PMID: 32251668 DOI: 10.1053/j.gastro.2020.03.065]

32 **Fan Z**, Chen L, Li J, Cheng X, Yang J, Tian C, Zhang Y, Huang S, Liu Z, Cheng J. Clinical Features of COVID-19-Related Liver Functional Abnormality. *Clin Gastroenterol Hepatol* 2020; **18**: 1561-1566 [PMID: 32283325 DOI: 10.1016/j.cgh.2020.04.002]

33 **Shi H**, Han X, Jiang N, Cao Y, Alwalid O, Gu J, Fan Y, Zheng C. Radiological findings from 81 patients with COVID-19 pneumonia in Wuhan, China: a descriptive study. *Lancet Infect Dis* 2020; **20**: 425-434 [PMID: 32105637 DOI: 10.1016/S1473-3099(20)30086-4]

34 **Kim ES**, Chin BS, Kang CK, Kim NJ, Kang YM, Choi JP, Oh DH, Kim JH, Koh B, Kim SE, Yun NR, Lee JH, Kim JY, Kim Y, Bang JH, Song KH, Kim HB, Chung KH, Oh MD; Korea National Committee for Clinical Management of COVID-19. Clinical Course and Outcomes of Patients with Severe Acute Respiratory Syndrome Coronavirus 2 Infection: a Preliminary Report of the First 28 Patients from the Korean Cohort Study on COVID-19. *J Korean Med Sci* 2020; **35**: e142 [PMID: 32242348 DOI: 10.3346/jkms.2020.35.e142]

35 **Zhang C**, Shi L, Wang FS. Liver injury in COVID-19: management and challenges. *Lancet Gastroenterol Hepatol* 2020; **5**: 428-430 [PMID: 32145190 DOI: 10.1016/S2468-1253(20)30057-1]

36 **Zhang W**, Du RH, Li B, Zheng XS, Yang XL, Hu B, Wang YY, Xiao GF, Yan B, Shi ZL, Zhou P. Molecular and serological investigation of 2019-nCoV infected patients: implication of multiple shedding routes. *Emerg Microbes Infect* 2020; **9**: 386-389 [PMID: 32065057 DOI: 10.1080/22221751.2020.1729071]

37 **Ding J**, Fu H, Liu Y, Gao J, Li Z, Zhao X, Zheng J, Sun W, Ni H, Ma X, Feng J, Wu A, Liu J, Wang Y, Geng P, Chen Y. Prevention and control measures in radiology department for COVID-19. *Eur*

Radiol 2020; **30**: 3603-3608 [PMID: 32300968 DOI: 10.1007/s00330-020-06850-5]
38 **Goh Y**, Chua W, Lee JKT, Ang BWL, Liang CR, Tan CA, Choong DAW, Hoon HX, Ong MKL, Quek ST. Operational Strategies to Prevent Coronavirus Disease 2019 (COVID-19) Spread in Radiology: Experience From a Singapore Radiology Department After Severe Acute Respiratory Syndrome. *J Am Coll Radiol* 2020; **17**: 717-723 [PMID: 32298643 DOI: 10.1016/j.jacr.2020.03.027]
39 **Lin L**, Lu L, Cao W, Li T. Hypothesis for potential pathogenesis of SARS-CoV-2 infection-a review of immune changes in patients with viral pneumonia. *Emerg Microbes Infect* 2020; **9**: 727-732 [PMID: 32196410 DOI: 10.1080/22221751.2020.1746199]
40 **Liang W**, Feng Z, Rao S, Xiao C, Xue X, Lin Z, Zhang Q, Qi W. Diarrhoea may be underestimated: a missing link in 2019 novel coronavirus. *Gut* 2020; **69**: 1141-1143 [PMID: 32102928 DOI: 10.1136/gutjnl-2020-320832]
41 **Zhang JJ**, Dong X, Cao YY, Yuan YD, Yang YB, Yan YQ, Akdis CA, Gao YD. Clinical characteristics of 140 patients infected with SARS-CoV-2 in Wuhan, China. *Allergy* 2020; **75**: 1730-1741 [PMID: 32077115 DOI: 10.1111/all.14238]
42 **Wang D**, Hu B, Hu C, Zhu F, Liu X, Zhang J, Wang B, Xiang H, Cheng Z, Xiong Y, Zhao Y, Li Y, Wang X, Peng Z. Clinical Characteristics of 138 Hospitalized Patients With 2019 Novel Coronavirus-Infected Pneumonia in Wuhan, China. *JAMA* 2020; **323**: 1061-1069 [PMID: 32031570 DOI: 10.1001/jama.2020.1585]
43 **Danzi GB**, Loffi M, Galeazzi G, Gherbesi E. Acute pulmonary embolism and COVID-19 pneumonia: a random association? *Eur Heart J* 2020; **41**: 1858 [PMID: 32227120 DOI: 10.1093/eurheartj/ehaa254]
44 **Mao L**, Jin H, Wang M, Hu Y, Chen S, He Q, Chang J, Hong C, Zhou Y, Wang D, Miao X, Li Y, Hu B. Neurologic Manifestations of Hospitalized Patients With Coronavirus Disease 2019 in Wuhan, China. *JAMA Neurol* 2020; **77**: 683-690 [PMID: 32275288 DOI: 10.1001/jamaneurol.2020.1127]
45 **Cai Q**, Chen F, Wang T, Luo F, Liu X, Wu Q, He Q, Wang Z, Liu Y, Liu L, Chen J, Xu L. Obesity and COVID-19 Severity in a Designated Hospital in Shenzhen, China. *Diabetes Care* 2020; **43**: 1392-1398 [PMID: 32409502 DOI: 10.2337/dc20-0576]
46 **Ryan PM**, Caplice NM. Is Adipose Tissue a Reservoir for Viral Spread, Immune Activation, and Cytokine Amplification in Coronavirus Disease 2019? *Obesity (Silver Spring)* 2020; **28**: 1191-1194 [PMID: 32314868 DOI: 10.1002/oby.22843]
47 **Guan WJ**, Ni ZY, Hu Y, Liang WH, Ou CQ, He JX, Liu L, Shan H, Lei CL, Hui DSC, Du B, Li LJ, Zeng G, Yuen KY, Chen RC, Tang CL, Wang T, Chen PY, Xiang J, Li SY, Wang JL, Liang ZJ, Peng YX, Wei L, Liu Y, Hu YH, Peng P, Wang JM, Liu JY, Chen Z, Li G, Zheng ZJ, Qiu SQ, Luo J, Ye CJ, Zhu SY, Zhong NS; China Medical Treatment Expert Group for Covid-19. Clinical Characteristics of Coronavirus Disease 2019 in China. *N Engl J Med* 2020; **382**: 1708-1720 [PMID: 32109013 DOI: 10.1056/NEJMoa2002032]
48 **Ji D**, Qin E, Xu J, Zhang D, Cheng G, Wang Y, Lau G. Non-alcoholic fatty liver diseases in patients with COVID-19: A retrospective study. *J Hepatol* 2020; **73**: 451-453 [PMID: 32278005 DOI: 10.1016/j.jhep.2020.03.044]
49 **Zhou YJ**, Zheng KI, Wang XB, Yan HD, Sun QF, Pan KH, Wang TY, Ma HL, Chen YP, George J, Zheng MH. Younger patients with MAFLD are at increased risk of severe COVID-19 illness: A multicenter preliminary analysis. *J Hepatol* 2020; **73**: 719-721 [PMID: 32348790 DOI: 10.1016/j.jhep.2020.04.027]
50 **Targher G**, Mantovani A, Byrne CD, Wang XB, Yan HD, Sun QF, Pan KH, Zheng KI, Chen YP, Eslam M, George J, Zheng MH. Risk of severe illness from COVID-19 in patients with metabolic dysfunction-associated fatty liver disease and increased fibrosis scores. *Gut* 2020; **69**: 1545-1547 [PMID: 32414813 DOI: 10.1136/gutjnl-2020-321611]
51 **Rizvi SAA**, Saleh AM. Applications of nanoparticle systems in drug delivery technology. *Saudi Pharm J* 2018; **26**: 64-70 [PMID: 29379334 DOI: 10.1016/j.jsps.2017.10.012]
52 **Wong GL**, Yuen BW, Chan HL, Tse YK, Yip TC, Lam KL, Lui GC, Wong VW. Impact of dose and duration of corticosteroid on the risk of hepatitis flare in patients with chronic hepatitis B. *Liver Int* 2019; **39**: 271-279 [PMID: 30179316 DOI: 10.1111/liv.13953]
53 **Boettler T**, Marjot T, Newsome PN, Mondelli MU, Maticic M, Cordero E, Jalan R, Moreau R, Cornberg M, Berg T. Impact of COVID-19 on the care of patients with liver disease: EASL-ESCMID position paper after 6 months of the pandemic. *JHEP Rep* 2020; **2**: 100169 [PMID: 32835190 DOI: 10.1016/j.jhepr.2020.100169]
54 **Wong GL**, Wong VW, Thompson A, Jia J, Hou J, Lesmana CRA, Susilo A, Tanaka Y, Chan WK, Gane E, Ong-Go AK, Lim SG, Ahn SH, Yu ML, Piratvisuth T, Chan HL; Asia-Pacific Working Group for Liver Derangement during the COVID-19 Pandemic. Management of patients with liver derangement during the COVID-19 pandemic: an Asia-Pacific position statement. *Lancet Gastroenterol Hepatol* 2020; **5**: 776-787 [PMID: 32585136 DOI: 10.1016/S2468-1253(20)30190-4]
55 **Polaris Observatory Collaborators**. Global prevalence, treatment, and prevention of hepatitis B virus infection in 2016: a modelling study. *Lancet Gastroenterol Hepatol* 2018; **3**: 383-403 [PMID: 29599078 DOI: 10.1016/S2468-1253(18)30056-6]
56 **Rezasoltani S**, Hatami B, Yadegar A, Asadzadeh Aghdaei H, Zali MR. How Patients With Chronic Liver Diseases Succeed to Deal With COVID-19? *Front Med (Lausanne)* 2020; **7**: 398 [PMID: 32754608 DOI: 10.3389/fmed.2020.00398]

57 **Mantovani A**, Beatrice G, Dalbeni A. Coronavirus disease 2019 and prevalence of chronic liver disease: A meta-analysis. *Liver Int* 2020; **40**: 1316-1320 [PMID: 32329563 DOI: 10.1111/liv.14465]

58 **Ji D**, Zhang D, Yang T, Mu J, Zhao P, Xu J, Li C, Cheng G, Wang Y, Chen Z, Qin E, Lau G. Effect of COVID-19 on patients with compensated chronic liver diseases. *Hepatol Int* 2020; **14**: 701-710 [PMID: 32734407 DOI: 10.1007/s12072-020-10058-6]

59 **Becchetti C**, Zambelli MF, Pasulo L, Donato MF, Invernizzi F, Detry O, Dahlqvist G, Ciccarelli O, Morelli MC, Fraga M, Svegliati-Baroni G, van Vlierberghe H, Coenraad MJ, Romero MC, de Gottardi A, Toniutto P, Del Prete L, Abbati C, Samuel D, Pirenne J, Nevens F, Dufour JF; COVID-LT group. COVID-19 in an international European liver transplant recipient cohort. *Gut* 2020; **69**: 1832-1840 [PMID: 32571972 DOI: 10.1136/gutjnl-2020-321923]

60 **Di Maira T**, Berenguer M. COVID-19 and liver transplantation. *Nat Rev Gastroenterol Hepatol* 2020; **17**: 526-528 [PMID: 32651555 DOI: 10.1038/s41575-020-0347-z]

61 **Lee BT**, Perumalswami PV, Im GY, Florman S, Schiano TD; COBE Study Group. COVID-19 in Liver Transplant Recipients: An Initial Experience From the US Epicenter. *Gastroenterology* 2020; **159**: 1176-1178. e2 [PMID: 32442561 DOI: 10.1053/j.gastro.2020.05.050]

62 **Yeo C**, Kaushal S, Yeo D. Enteric involvement of coronaviruses: is faecal-oral transmission of SARS-CoV-2 possible? *Lancet Gastroenterol Hepatol* 2020; **5**: 335-337 [PMID: 32087098 DOI: 10.1016/S2468-1253(20)30048-0]

63 **Repici A**, Maselli R, Colombo M, Gabbiadini R, Spadaccini M, Anderloni A, Carrara S, Fugazza A, Di Leo M, Galtieri PA, Pellegatta G, Ferrara EC, Azzolini E, Lagioia M. Coronavirus (COVID-19) outbreak: what the department of endoscopy should know. *Gastrointest Endosc* 2020; **92**: 192-197 [PMID: 32179106 DOI: 10.1016/j.gie.2020.03.019]

64 **Tse F**, Borgaonkar M, Leontiadis GI. COVID-19: Advice from the Canadian Association of Gastroenterology for Endoscopy Facilities, as of March 16, 2020. *J Can Assoc Gastroenterol* 2020; **3**: 147-149 [PMID: 32395690 DOI: 10.1093/jcag/gwaa012]

65 **van Doremalen N**, Bushmaker T, Morris DH, Holbrook MG, Gamble A, Williamson BN, Tamin A, Harcourt JL, Thornburg NJ, Gerber SI, Lloyd-Smith JO, de Wit E, Munster VJ. Aerosol and Surface Stability of SARS-CoV-2 as Compared with SARS-CoV-1. *N Engl J Med* 2020; **382**: 1564-1567 [PMID: 32182409 DOI: 10.1056/NEJMc2004973]

66 **Day LW**, Kwok K, Visrodia K, Petersen BT. American Society for Gastrointestinal Endoscopy Infection Control Summit: updates, challenges, and the future of infection control in GI endoscopy. *Gastrointest Endosc* 2021; **93**: 1-10 [PMID: 32819676 DOI: 10.1016/j.gie.2020.06.024]

67 **Wong ATY**, Chen H, Liu SH, Hsu EK, Luk KS, Lai CKC, Chan RFY, Tsang OTY, Choi KW, Kwan YW, Tong AYH, Cheng VCC, Tsang DNC; Central Committee on Infectious Diseases and Emergency Response; Hospital Authority; Hong Kong Special Administrative Region. From SARS to Avian Influenza Preparedness in Hong Kong. *Clin Infect Dis* 2017; **64**: S98-S104 [PMID: 28475794 DOI: 10.1093/cid/cix123]

68 **Siddharta A**, Pfaender S, Vielle NJ, Dijkman R, Friesland M, Becker B, Yang J, Engelmann M, Todt D, Windisch MP, Brill FH, Steinmann J, Steinmann J, Becker S, Alves MP, Pietschmann T, Eickmann M, Thiel V, Steinmann E. Virucidal Activity of World Health Organization-Recommended Formulations Against Enveloped Viruses, Including Zika, Ebola, and Emerging Coronaviruses. *J Infect Dis* 2017; **215**: 902-906 [PMID: 28453839 DOI: 10.1093/infdis/jix046]

69 **Ng K**, Poon BH, Kiat Puar TH, Shan Quah JL, Loh WJ, Wong YJ, Tan TY, Raghuram J. COVID-19 and the Risk to Health Care Workers: A Case Report. *Ann Intern Med* 2020; **172**: 766-767 [PMID: 32176257 DOI: 10.7326/L20-0175]

70 **Kanne JP**. Chest CT Findings in 2019 Novel Coronavirus (2019-nCoV) Infections from Wuhan, China: Key Points for the Radiologist. *Radiology* 2020; **295**: 16-17 [PMID: 32017662 DOI: 10.1148/radiol.2020200241]

71 **Yoon SH**, Lee KH, Kim JY, Lee YK, Ko H, Kim KH, Park CM, Kim YH. Chest Radiographic and CT Findings of the 2019 Novel Coronavirus Disease (COVID-19): Analysis of Nine Patients Treated in Korea. *Korean J Radiol* 2020; **21**: 494-500 [PMID: 32100485 DOI: 10.3348/kjr.2020.0132]

72 **Peng QY**, Wang XT, Zhang LN; Chinese Critical Care Ultrasound Study Group (CCUSG). Findings of lung ultrasonography of novel corona virus pneumonia during the 2019-2020 epidemic. *Intensive Care Med* 2020; **46**: 849-850 [PMID: 32166346 DOI: 10.1007/s00134-020-05996-6]

73 **Wei Y**, Lu Y, Xia L, Yuan X, Li G, Li X, Liu L, Liu W, Zhou P, Wang CY, Zhang H. Analysis of 2019 novel coronavirus infection and clinical characteristics of outpatients: An epidemiological study from a fever clinic in Wuhan, China. *J Med Virol* 2020; **92**: 2758-2767 [PMID: 32544281 DOI: 10.1002/jmv.26175]

74 **Fang Y**, Zhang H, Xie J, Lin M, Ying L, Pang P, Ji W. Sensitivity of Chest CT for COVID-19: Comparison to RT-PCR. *Radiology* 2020; **296**: E115-E117 [PMID: 32073353 DOI: 10.1148/radiol.2020200432]

75 **Smith MJ**, Hayward SA, Innes SM, Miller ASC. Point-of-care lung ultrasound in patients with COVID-19 - a narrative review. *Anaesthesia* 2020; **75**: 1096-1104 [PMID: 32275766 DOI: 10.1111/anae.15082]

76 **Yasukawa K**, Minami T. Point-of-Care Lung Ultrasound Findings in Patients with COVID-19 Pneumonia. *Am J Trop Med Hyg* 2020; **102**: 1198-1202 [PMID: 32333544 DOI: 10.4269/ajtmh.20-0280]

77 **Abdelmohsen MA**, Alkandari BM, Gupta VK, ElBeheiry AA. Diagnostic value of abdominal sonography in confirmed COVID-19 intensive care patients. *EJRNM* 2020; **51**: 198 [DOI:

10.1186/s43055-020-00317-9]
78 **Tullie L**, Ford K, Bisharat M, Watson T, Thakkar H, Mullassery D, Giuliani S, Blackburn S, Cross K, De Coppi P, Curry J. Gastrointestinal features in children with COVID-19: an observation of varied presentation in eight children. *Lancet Child Adolesc Health* 2020; **4**: e19-e20 [PMID: 32442420 DOI: 10.1016/S2352-4642(20)30165-6]
79 **NHS**. Endoscopy. NHS Choices. National Health Service Gov.UK., 2017
80 **Verschoore T**, Vandecandelaere S, Vandecandelaere P, Vanderplancke T, Bergs J. Risk factors for complications and mortality related to endoscopic procedures in adults. *Acta Gastroenterol Belg* 2016; **79**: 39-46 [PMID: 26852762]
81 **WHO**. Weekly Operational Update on COVID-19 - 30 October 2020. Coronavirus disease (COVID-19) Weekly Epidemiological Update and Weekly Operational Update. World Health Organization Situation Reports, 2020
82 **Rana SS**. Risk of COVID-19 Transmission During Gastrointestinal Endoscopy. *J Digest Endosc* 2020; **11**: 27-30 [DOI: 10.1055/s-0040-1712076]
83 **Goenka MK**, Afzalpurkar S, Ghoshal UC, Guda N, Reddy N. Impact of COVID-19 on gastrointestinal endoscopy practice in India: a cross-sectional study. *Endosc Int Open* 2020; **8**: E974-E979 [PMID: 32617401 DOI: 10.1055/a-1181-8391]
84 **Paramasivam RK**, Angsuwatcharakon P, Soontornmanokul T, Rerknimitr R. Management of endoscopic complications, in particular perforation. *Dig Endosc* 2013; **25** Suppl 2: 132-136 [PMID: 23617664 DOI: 10.1111/den.12079]
85 **Cotton PB**, Eisen GM, Aabakken L, Baron TH, Hutter MM, Jacobson BC, Mergener K, Nemcek A Jr, Petersen BT, Petrini JL, Pike IM, Rabeneck L, Romagnuolo J, Vargo JJ. A lexicon for endoscopic adverse events: report of an ASGE workshop. *Gastrointest Endosc* 2010; **71**: 446-454 [PMID: 20189503 DOI: 10.1016/j.gie.2009.10.027]
86 **Ringold DA**, Jonnalagadda S. Complications of Therapeutic Endoscopy: A Review of the Incidence, Risk Factors, Prevention, and Endoscopic Management. *Tech Gastrointest Endosc* 2007; **9**: 90-103 [DOI: 10.1016/j.tgie.2007.02.005]
87 **Chiu PWY**, Ng SC, Inoue H, Reddy DN, Ling Hu E, Cho JY, Ho LK, Hewett DG, Chiu HM, Rerknimitr R, Wang HP, Ho SH, Seo DW, Goh KL, Tajiri H, Kitano S, Chan FKL. Practice of endoscopy during COVID-19 pandemic: position statements of the Asian Pacific Society for Digestive Endoscopy (APSDE-COVID statements). *Gut* 2020; **69**: 991-996 [PMID: 32241897 DOI: 10.1136/gutjnl-2020-321185]
88 **Cavaliere K**, Levine C, Wander P, Sejpal DV, Trindade AJ. Management of upper GI bleeding in patients with COVID-19 pneumonia. *Gastrointest Endosc* 2020; **92**: 454-455 [PMID: 32325065 DOI: 10.1016/j.gie.2020.04.028]
89 **Dumonceau JM**, Andriulli A, Elmunzer BJ, Mariani A, Meister T, Deviere J, Marek T, Baron TH, Hassan C, Testoni PA, Kapral C; European Society of Gastrointestinal Endoscopy. Prophylaxis of post-ERCP pancreatitis: European Society of Gastrointestinal Endoscopy (ESGE) Guideline - updated June 2014. *Endoscopy* 2014; **46**: 799-815 [PMID: 25148137 DOI: 10.1055/s-0034-1377875]
90 **Cappell MS**, Abdullah M. Management of gastrointestinal bleeding induced by gastrointestinal endoscopy. *Gastroenterol Clin North Am* 2000; **29**: 125-167, vi [PMID: 10752020 DOI: 10.1016/S0889-8553(05)70110-2]
91 **Cotton PB**, Lehman G, Vennes J, Geenen JE, Russell RC, Meyers WC, Liguory C, Nickl N. Endoscopic sphincterotomy complications and their management: an attempt at consensus. *Gastrointest Endosc* 1991; **37**: 383-393 [PMID: 2070995 DOI: 10.1016/s0016-5107(91)70740-2]
92 **Frühmorgen P**, Demling L. Complications of diagnostic and therapeutic colonoscopy in the Federal Republic of Germany. Results of an inquiry. *Endoscopy* 1979; **11**: 146-150 [PMID: 446429 DOI: 10.1055/s-0028-1098341]
93 **Laine L**, Jensen DM. Management of patients with ulcer bleeding. *Am J Gastroenterol* 2012; **107**: 345-60; quiz 361 [PMID: 22310222 DOI: 10.1038/ajg.2011.480]
94 **Thachil J**, Tang N, Gando S, Falanga A, Cattaneo M, Levi M, Clark C, Iba T. ISTH interim guidance on recognition and management of coagulopathy in COVID-19. *J Thromb Haemost* 2020; **18**: 1023-1026 [PMID: 32338827 DOI: 10.1111/jth.14810]
95 **Anderson ML**, Pasha TM, Leighton JA. Endoscopic perforation of the colon: lessons from a 10-year study. *Am J Gastroenterol* 2000; **95**: 3418-3422 [PMID: 11151871 DOI: 10.1111/j.1572-0241.2000.03356.x]
96 **Agalar F**, Daphan C, Hayran M, Sayek I. Clinical presentation and management of iatrogenic colon perforations. *Am J Surg* 1998; **175**: 164 [PMID: 9515538 DOI: 10.1016/S0002-9610(96)00236-X]
97 **Schreiner MA**, Fennerty MB. Endoscopy in the obese patient. *Gastroenterol Clin North Am* 2010; **39**: 87-97 [PMID: 20202582 DOI: 10.1016/j.gtc.2009.12.009]
98 **Wehrmann T**, Riphaus A. Sedation with propofol for interventional endoscopic procedures: a risk factor analysis. *Scand J Gastroenterol* 2008; **43**: 368-374 [PMID: 18938664 DOI: 10.1080/00365520701679181]
99 **Rah KH**, Platovsky A. Determining Urgent/Emergent Status of Gastrointestinal Endoscopic Procedures in an Ambulatory Care Setting During the COVID-19 Pandemic: Additional Factors That Need To Be Considered. *Anesth Analg* 2020; **131**: e30-e31 [PMID: 32282390 DOI: 10.1213/ANE.0000000000004861]
100 **Huang WH**, Teng LC, Yeh TK, Chen YJ, Lo WJ, Wu MJ, Chin CS, Tsan YT, Lin TC, Chai JW,

Lin CF, Tseng CH, Liu CW, Wu CM, Chen PY, Shi ZY, Liu PY. 2019 novel coronavirus disease (COVID-19) in Taiwan: Reports of two cases from Wuhan, China. *J Microbiol Immunol Infect* 2020; **53**: 481-484 [PMID: 32111449 DOI: 10.1016/j.jmii.2020.02.009]

101 **Boettler T**, Newsome PN, Mondelli MU, Maticic M, Cordero E, Cornberg M, Berg T. Care of patients with liver disease during the COVID-19 pandemic: EASL-ESCMID position paper. *JHEP Rep* 2020; **2**: 100113 [PMID: 32289115 DOI: 10.1016/j.jhepr.2020.100113]

102 **Yi H**, Lu F, Jin X, Chen R, Liu B, Dong X, Xiong W, Yang D, Guo Y, Zhou M. Clinical characteristics and outcomes of coronavirus disease 2019 infections among diabetics: A retrospective and multicenter study in China. *J Diabetes* 2020 [PMID: 32725691 DOI: 10.1111/1753-0407.13098]

103 **Serper M**, Shaked A, Olthoff KM, Hoteit M, Appolo B, Reddy KR. A local response to COVID-19 for advanced liver disease: Current model of care, challenges and opportunities. *J Hepatol* 2020; **73**: 708-709 [PMID: 32450089 DOI: 10.1016/j.jhep.2020.05.022]

104 **Fix OK**, Hameed B, Fontana RJ, Kwok RM, McGuire BM, Mulligan DC, Pratt DS, Russo MW, Schilsky ML, Verna EC, Loomba R, Cohen DE, Bezerra JA, Reddy KR, Chung RT. Clinical Best Practice Advice for Hepatology and Liver Transplant Providers During the COVID-19 Pandemic: AASLD Expert Panel Consensus Statement. *Hepatology* 2020; **72**: 287-304 [PMID: 32298473 DOI: 10.1002/hep.31281]

105 **Bollipo S**, Kapuria D, Rabiee A, Ben-Yakov G, Lui RN, Lee HW, Kumar G, Siau K, Turnes J, Dhanasekaran R. One world, one pandemic, many guidelines: management of liver diseases during COVID-19. *Gut* 2020; **69**: 1369-1372 [PMID: 32499304 DOI: 10.1136/gutjnl-2020-321553]

106 **Alqahtani SA**, Aljumah AA, Hashim A, Alenazi TH, AlJawad M, Al Hamoudi WK, Alghamdi MY. Principles of Care for Patients with Liver Disease During the Coronavirus Disease 2019 (COVID-19) Pandemic: Position Statement of the Saudi Association for the Study of Liver Disease and Transplantation. *Ann Saudi Med* 2020; **40**: 273-280 [PMID: 32564624 DOI: 10.5144/0256-4947.2020.273]

107 **European Association for the Study of the Liver**. ; European Association for the Study of the Liver. EASL 2017 Clinical Practice Guidelines on the management of hepatitis B virus infection. *J Hepatol* 2017; **67**: 370-398 [PMID: 28427875 DOI: 10.1016/j.jhep.2017.03.021]

108 **European Association for the Study of the Liver**. ; European Association for the Study of the Liver. EASL Clinical Practice Guidelines for the management of patients with decompensated cirrhosis. *J Hepatol* 2018; **69**: 406-460 [PMID: 29653741 DOI: 10.1016/j.jhep.2018.03.024]

109 **Da BL**, Im GY, Schiano TD. Coronavirus Disease 2019 Hangover: A Rising Tide of Alcohol Use Disorder and Alcohol-Associated Liver Disease. *Hepatology* 2020; **72**: 1102-1108 [PMID: 32369624 DOI: 10.1002/hep.31307]

110 **Horby P**, Lim WS, Emberson J, Mafham M, Bell J, Linsell L, Staplin N, Brightling C, Ustianowski A, Elmahi E, Prudon B, Green C, Felton T, Chadwick D, Rege K, Fegan C, Chappell LC, Faust SN, Jaki T, Jeffery K, Montgomery A, Rowan K, Juszczak E, Baillie JK, Haynes R, Landray MJ. Effect of Dexamethasone in Hospitalized Patients with COVID-19: Preliminary Report. *medRxiv* 2020 [DOI: 10.1101/2020.06.22.20137273]

111 **COVIDSurg Collaborative**. Mortality and pulmonary complications in patients undergoing surgery with perioperative SARS-CoV-2 infection: an international cohort study. *Lancet* 2020; **396**: 27-38 [PMID: 32479829 DOI: 10.1016/S0140-6736(20)31182-X]

112 **Lee LY**, Cazier JB, Angelis V, Arnold R, Bisht V, Campton NA, Chackathayil J, Cheng VW, Curley HM, Fittall MW, Freeman-Mills L, Gennatas S, Goel A, Hartley S, Hughes DJ, Kerr D, Lee AJ, Lee RJ, McGrath SE, Middleton CP, Murugaesu N, Newsom-Davis T, Okines AF, Olsson-Brown AC, Palles C, Pan Y, Pettengell R, Powles T, Protheroe EA, Purshouse K, Sharma-Oates A, Sivakumar S, Smith AJ, Starkey T, Turnbull CD, Várnai C, Yousaf N; UK Coronavirus Monitoring Project Team; Kerr R; Middleton G. COVID-19 mortality in patients with cancer on chemotherapy or other anticancer treatments: a prospective cohort study. *Lancet* 2020; **395**: 1919-1926 [PMID: 32473682 DOI: 10.1016/S0140-6736(20)31173-9]

113 **Goldman JD**, Lye DCB, Hui DS, Marks KM, Bruno R, Montejano R, Spinner CD, Galli M, Ahn MY, Nahass RG, Chen YS, SenGupta D, Hyland RH, Osinusi AO, Cao H, Blair C, Wei X, Gaggar A, Brainard DM, Towner WJ, Muñoz J, Mullane KM, Marty FM, Tashima KT, Diaz G, Subramanian A; GS-US-540-5773 Investigators. Remdesivir for 5 or 10 Days in Patients with Severe Covid-19. *N Engl J Med* 2020; **383**: 1827-1837 [PMID: 32459919 DOI: 10.1056/NEJMoa2015301]

114 **de Wit E**, Feldmann F, Cronin J, Jordan R, Okumura A, Thomas T, Scott D, Cihlar T, Feldmann H. Prophylactic and therapeutic remdesivir (GS-5734) treatment in the rhesus macaque model of MERS-CoV infection. *Proc Natl Acad Sci USA* 2020; **117**: 6771-6776 [PMID: 32054787 DOI: 10.1073/pnas.1922083117]

115 **Middeldorp S**, Coppens M, van Haaps TF, Foppen M, Vlaar AP, Müller MCA, Bouman CCS, Beenen LFM, Kootte RS, Heijmans J, Smits LP, Bonta PI, van Es N. Incidence of venous thromboembolism in hospitalized patients with COVID-19. *J Thromb Haemost* 2020; **18**: 1995-2002 [PMID: 32369666 DOI: 10.1111/jth.14888]

116 **Deng Y**, Liu W, Liu K, Fang YY, Shang J, Zhou L, Wang K, Leng F, Wei S, Chen L, Liu HG. Clinical characteristics of fatal and recovered cases of coronavirus disease 2019 in Wuhan, China: a retrospective study. *Chin Med J (Engl)* 2020; **133**: 1261-1267 [PMID: 32209890 DOI: 10.1097/CM9.0000000000000824]

117 **Parvathaneni V**, Gupta V. Utilizing drug repurposing against COVID-19 - Efficacy, limitations, and challenges. *Life Sci* 2020; **259**: 118275 [PMID: 32818545 DOI: 10.1016/j.lfs.2020.118275]

World Journal of Gastroenterology

Submit a Manuscript: https://www.f6publishing.com

World J Gastroenterol 2021 February 14; 27(6): 470-486

DOI: 10.3748/wjg.v27.i6.470

ISSN 1007-9327 (print) ISSN 2219-2840 (online)

ORIGINAL ARTICLE

Basic Study

Demethylation of miR-34a upregulates expression of membrane palmitoylated proteins and promotes the apoptosis of liver cancer cells

Fu-Yong Li, Ting-Yong Fan, Hao Zhang, Yu-Min Sun

ORCID number: Fu-Yong Li 0000-0002-0017-2529; Ting-Yong Fan 0000-0002-3614-2292; Hao Zhang 0000-0002-1774-7325; Yu-Min Sun 0000-0003-0396-2283.

Author contributions: Li FY conceived the idea; Fan TY conducted the analyses; Zhang H and Sun YM provided the data; All authors contributed to the writing and revisions.

Institutional review board statement: The study was reviewed and approved by the Shandong Cancer Hospital affiliated to Shandong University.

Conflict-of-interest statement: All the Authors have no conflict of interest related to the manuscript.

Data sharing statement: No additional data are available.

Open-Access: This article is an open-access article that was selected by an in-house editor and fully peer-reviewed by external reviewers. It is distributed in accordance with the Creative Commons Attribution NonCommercial (CC BY-NC 4.0) license, which permits others to distribute, remix, adapt, build upon this work non-commercially,

Fu-Yong Li, Department of Interventional Radiology, Jinan City People's Hospital, Jinan 271100, Shandong Province, China

Ting-Yong Fan, Department of Radiation Oncology, Shandong Cancer Hospital affiliated to Shandong University, Jinan 250117, Shandong Province, China

Hao Zhang, Department of Endoscopy, Shandong Cancer Hospital affiliated to Shandong University, Jinan 250117, Shandong Province, China

Yu-Min Sun, Department of Cardiology, Jinan City People's Hospital, Jinan 271100, Shandong Province, China

Corresponding author: Ting-Yong Fan, MD, Chief Physician, Department of Radiation Oncology, Shandong Cancer Hospital affiliated to Shandong University, No. 440 Jiyan Road, Jinan 250117, Shandong Province, China. fantcwq50216@163.com

Abstract

BACKGROUND

Liver cancer is a common cancer and the main cause of cancer-related deaths worldwide. Liver cancer is the sixth most common cancer in the world. Although miR-34a and palmitoyl membrane palmitoylated protein (MPP2) are reportedly involved in various cell processes, their precise roles in liver cancer are still unclear.

AIM

To investigate the expression of micro RNA 34a (miR-34a), methylation of the miR-34a promoter and the expression of MPP2 in liver cancer cells and their related mechanisms.

METHODS

Together, 78 cases of liver cancer tissues and 78 cases of adjacent tissues were collected. The methylation degree of miR-34a promoter in liver cancer/paracancerous tissue and liver cancer cells/normal liver cells, and the expression levels of miR-34a and MPP2 in the above samples were detected. Demethylation of liver cancer cells or transfection of liver cancer cells with miR-34a mimetic was performed. The MPP2 overexpression vector was used to transfect liver cancer

and license their derivative works on different terms, provided the original work is properly cited and the use is non-commercial. See: http://creativecommons.org/Licenses/by-nc/4.0/

Manuscript source: Unsolicited manuscript

Specialty type: Gastroenterology and hepatology

Country/Territory of origin: China

Peer-review report's scientific quality classification
Grade A (Excellent): 0
Grade B (Very good): 0
Grade C (Good): C, C
Grade D (Fair): D
Grade E (Poor): 0

Received: October 20, 2020
Peer-review started: October 20, 2020
First decision: December 8, 2020
Revised: December 21, 2020
Accepted: December 29, 2020
Article in press: December 29, 2020
Published online: February 14, 2021

P-Reviewer: Gassler N, Gupta S, Zhang X
S-Editor: Zhang L
L-Editor: Filipodia
P-Editor: Wang LL

cells, and the changes in proliferation, invasion, apoptosis, migration, and other biological functions of liver cancer cells after the above interventions were observed. Double luciferase reporter genes were used to detect the targeting relationship between miR-34a and MPP2.

RESULTS
Clinical samples showed that the expression levels of miR-34a and MPP2 in liver cancer tissues were lower than those in the normal tissues. The methylation degree of miR-34a promoter region in liver cancer cells was higher than that in normal liver cells. After miR-34a demethylation/mimetic transfection/MPP2 overexpression, the apoptosis of liver cancer cells was increased; the proliferation, invasion and migration capabilities were decreased; the expression levels of caspase 3, caspase 9, E-cadherin, and B-cell lymphoma 2 (Bcl-2)-associated X protein were increased; and the expression levels of Bcl-2, N-cadherin, and β-catenin were decreased. Double luciferase reporter genes confirmed that MPP2 is targeted by miR-34a. Rescue experiments showed that small interfering MPP2 could counteract the promoting effect of miR-34a demethylation on apoptosis and the inhibitory effect on cell proliferation, invasion, and migration.

CONCLUSION
miR-34a demethylation upregulates the expression level of MPP2 in liver cancer cells and promotes the apoptosis of liver cancer cells. miR-34a demethylation is a potential method for liver cancer treatment.

Key Words: Liver cancer; miR-34a; Membrane palmitoylated proteins; Methylation; Cell apoptosis; Caspase 3

©The Author(s) 2021. Published by Baishideng Publishing Group Inc. All rights reserved.

Core Tip: This study confirmed the relationship of microRNA 34a (miR-34a) hypermethylation with membrane palmitoylated protein (MPP2) expression by investigating the changes of biological function and MPP2 expression level of liver cancer cells after miR-34a demethylation. miR-34a can inhibit the occurrence of liver cancer by upregulating MPP2, and its demethylation in liver cancer cells is a potential method of liver cancer treatment. In essence, miR-34a methylation is located upstream of its binding site with p53. Therefore, it is valuable to study the role of miR-34a methylation/demethylation on the expression level of upstream regulatory factors such as p53, and to explore its function in the future.

Citation: Li FY, Fan TY, Zhang H, Sun YM. Demethylation of miR-34a upregulates expression of membrane palmitoylated proteins and promotes the apoptosis of liver cancer cells. *World J Gastroenterol* 2021; 27(6): 470-486
URL: https://www.wjgnet.com/1007-9327/full/v27/i6/470.htm
DOI: https://dx.doi.org/10.3748/wjg.v27.i6.470

INTRODUCTION

Liver cancer is the sixth most common cancer and second cause of cancer-related deaths worldwide[1]. In China, the population with a higher incidence of liver cancer is aged 50 or above[2]. Hepatitis B virus and hepatitis C virus are the main factors causing liver cancer[3]. The occurrence of liver cancer is a cumulative process. For example, liver cirrhosis mass develops from low to high, which can be regarded as the possible occurrence of liver cancer[4]. In the early stage of liver cancer, tumor resection, liver transplantation, local ablation and other treatment methods have relatively optimistic curative effects, but the recurrence rate of the above treatment in 5 years is relatively high[5]. MicroRNA (miRNA) influences the occurrence of tumors by mediating post-transcriptional regulation of gene expression[4], so targeted administration of miRNA has considerable prospects in tumor treatment.

miRNA is a key member of the non-coding RNA family[6], and can bind to the 3'-

untranslated region (UTR) of mRNA to regulate the expression of mRNA[7]. miR-34a plays an important role in cell apoptosis. Inhibition of miR-34a can promote cell proliferation[8]. Yamakuchi *et al*[9] found that miR-34a binds to the 3'-UTR segment of sirtuin 1 (SIRT1) in human colon cancer cells to inhibit SIRT1 expression and ultimately regulate cell apoptosis. Chang *et al*[10] believed that p53 trans-activates miR-34a, thus causing gene re-expression and promoting cell apoptosis. miR-34a is involved in the development of liver cancer. Cui *et al*[11] proved that the low expression of miR-34a is related to the large tumor of liver cancer patients and the high serum alpha-fetoprotein level. miR-34a was considered a predictor of early recurrence of liver cancer. In liver cancer, miR-34 was upregulated by enhancing emodin protein[12].

Membrane palmitoylated protein (MPP) contains many domains for cell-cell interaction[13]. MPP promotes the polarization of epithelial cells and the formation of tight junctions by forming complexes with human Discs Large 1[14]. At the same time, MPP also interconnects the cell membrane-cytoskeleton[15]. MPP may be a specific exosome accessory factor required for the maturation of ribosomal RNA[16], indicating that MPP may affect protein synthesis. Moreover, MPP2 can control cell growth and interfere with intracellular protein by enhancing E7 protein[17].

Comparing the expression levels of miR-34a in cancer tissues and paracancerous tissues, we found that miR-34a expression is low in liver cancer. Since abnormal DNA methylation at promoters is frequently involved in tumorigenesis, we explored the methylation of miR-34a promotor. Methprimer predicted that the promoter region of miR-34a has CpG binding sites. Methylation-specific polymerase chain reaction (PCR) found that miR-34a is hypermethylated in liver cancer. Based on this, we speculated that methylation may be the cause of low miR-34a expression in liver cancer, and we designed experiments for confirmation. miRDB and TargetScan databases revealed that MPP2 is downstream of miR-34a through exploration of the molecular mechanism of miR-34a methylation and MPP2 in liver cancer cells.

MATERIALS AND METHODS

Collection of tissue samples

Tissue samples were collected from 78 patients with liver cancer in Shandong Cancer Hospital affiliated to Shandong University (Shandong, China), including 42 males and 36 females. Inclusion criterion was as follows[4]: Liver cancer was confirmed using blood tests, imaging tests, and liver biopsy. Exclusion criteria were as follows[4]: mentally ill patients; patients with other tumors; patients with a treatment history of surgery, chemotherapy, radiotherapy or antibiotic treatment; and patients who did not cooperate with the treatment. The patients were fully informed of the study, and the study was approved by the Shandong Cancer Hospital affiliated to Shandong University Ethics Committee. Tissue samples and sections were stored in liquid nitrogen for later use.

Cell culture, transfection, and demethylation

Hepatocellular carcinoma cell lines (HepG2, Hep3B, PLC/PRG/5) and human normal hepatocytes (THLE-2) were purchased from ATCC (Manassas, VA, United States). The cells were cultured in a cell incubator in 37 ℃ with 5% CO_2. The culture medium system was as follows: Dulbecco's Modified Eagle Medium (DMEM; Hyclone, Logan, UT, United States) + 10% fetal bovine serum (FBS) solution (Gibco, Gaithersburg, MD, United States) + 1% penicillin/streptomycin solution (100X, Solarbio, Beijing, China). Subsequent experiments were carried out when the cell fusion reached 80%-90%.

Before transfection, the medium was replaced without FBS to eliminate interference. Transfected cells were inoculated into 6-well plates with 1 × 10^5 cells per well. MPP2 small interfering RNA (siRNA) (siMPP2), MPP2-short hairpin RNA (shRNA) (sh-MPP2), negative control (NC) shRNA, miR-34a mimics (pre-miR 34a), and NC mimics (NC pre) were all purchased from Shanghai Sangon Biotech (Shanghai, China). Lipofectamine 2000 Transfection Kit (Invitrogen, Carlsbad, CA, United States) was used for cell transfection. After transfection for 8 h, fresh culture medium was applied and cultured in a humidity incubator including 5% CO_2 with constant temperature for 48 h at 37 ℃.

Another group of cells with good growth status were treated with 5-Aza methylation inhibitor (10 mol/L). After 48 h, fresh culture medium was applied. The culture condition was 37 ℃ and 5% CO_2.

Extraction of total RNA and reverse transcription reaction

The tissue sample was cut, milled, and prepared into a cell suspension. Then 1 mL Trizol was added to the cell suspension, and a pipette was used for repeated inhalation, and blow-out of cell suspension was performed to facilitate full cell lysis and extract total RNA from the tissue samples. The concentration and purity of total RNA at 260-280 nm were detected using an ultraviolet spectrophotometer, and those with OD260/OD280 more than 1.8 were used in subsequent experiments. The FastQuant RT Super Mix (KR108) kit (Tiangen Biotech, Beijing, China) was selected for reverse transcription. Then 5 μL of 4 × FQ-RT Super Mix, 1 μg total RNA, and RNase-Free ddH_2O were used to replenish the system to 20 μL. Reverse transcription reaction was carried out for 15 min at 42 ℃ and enzyme inactivation was carried out for 3 min at 95 ℃.

Detection of methylation of miR-34a by methylation-specific PCR method

Methprimer was used to predict the CpG site of miR-34a promoter. DNA was treated with sulfite using EZ DNA Methylation-GoldTM Kit (Zymo Research, Irvine, CA, United States). Methylation-specific PCR (MSP) detection was carried out using the MSP Kit (Tiangen). The miR-34a MSP primer was designed and synthesized by Shanghai Sangon Biotech. Upstream primer of miR-34a-MSP (5' to 3'): TGTTAGTTTTTTCGGGGAGTTTTCGG; downstream primer of miR-34a-MSP (5' to 3'): ACGCCAACTCCTCCCCCGTCCCGAAC; upstream primer of miR-34a-UMSP (5' to 3'): TAGTTTTTTTGGGGAGTTTTTGGTTT; downstream primer of miR-34a-UMSP (5' to 3'): TAACACCAACTCCTCCCCCATCCCAA.

qPCR detection of miR-34a, MPP2 mRNA

miR-34a and MPP2 mRNA were quantified using FastFire qPCR PreMix SYBR Green Kit (Tiangen) and ABI PRISM 7000 (Applied Biosystems, Foster City, CA, United States) instruments. The primers were designed and synthesized by Shanghai Sangon Biotech. The upstream primer of miR-34a (5' to 3'): TCCTTCCTACTCG TACCACCAAA, and the downstream primer of miR-34a (5' to 3'): AGGTGAGGAGATGTCGTTGT; upstream primer of MPP2 mRNA (5' to 3'): AGATCT TCTTCTTCAAGGACCGGTT; downstream primer of MPP2 mRNA (5' to 3'): GGCTGGTCA GTGGCTTGGGGTA. The reaction system referred to the kit specification (50 μL). The reaction system was as follows: 1.5 μL upstream primer, 1.5 μL downstream primer, 25 μL of 2 × FastFire qPCR PreMix, 5 μL cDNA template, 5 μL of 50 × ROX Reference Dye, and RNase-Free ddH2O was added to make the total reaction system to 50 μL. The reaction process was as follows: pre-denaturation at 95 ℃ for 3 min, for 1 cycle; denaturation at 95 ℃ for 15 s, annealing at 60 ℃ for 15 s, for a total of 40 cycles. The results were analyzed by ABI PRISM 7000 instrument. The internal reference genes were U6 and GAPDH, which were standardized by $2^{-\Delta\Delta CT}$ method. The upstream primer of GAPDH (5' to 3'): GTCTCCTCTGACTTCAACAGCG, downstream (5' to 3'): GTCTCCTCTGACTTCAACAGCG. The upstream primer of U6 (5' to 3'): CGCTTCGGCAGCACATATAC, downstream (5' to 3'): AAAATA TGGAACGCTTCACGA.

Determination of protein expression by Western blotting

The protein was extracted and separated by sodium dodecyl sulfate-polyacrylamide gel electrophoresis, electrotransferred to nitrocellulose filter membrane, and placed at room temperature for 1 h (closed with 5% of skim milk -phosphate-buffered solution [PBS] solution). MPP2 (at 2 g/mL), caspase 3 (1:5000), caspase 9 (1:10000), E-cadherin (1:10000), B-cell lymphoma 2 (Bcl-2)-associated X protein (Bax) (1:10000), Bcl-2 (1:2000), N-cadherin (1:10000), β-catenin (1:10000) and β-actin (1:10000) primary antibodies were added and placed overnight at 4 ℃. The nitrocellulose membrane was washed with PBS solution for three times, then goat anti-rabbit secondary antibody (horseradish peroxidase [HRP] cross-linked) was added, and the mixture was placed for 1h at room temperature. Finally, the nitrocellulose membrane was washed with PBS solution and visualized using enhanced chemiluminescence method. The internal reference protein was β-actin, and the relative expression level of the protein to be detected was normalized to the intensity of β-actin band.

Caspase 9, caspase 3, E-cadherin, Bax, Bcl-2, N-cadherin, β-catenin, β-actin primary antibody and secondary antibody goat anti-rabbit (HRP cross-linked) were purchased from Shanghai Abcam Company (Shanghai, China).

Detection of cell survival by the MTT assay

Trypsin enzymolysis was added to cells, centrifugation was performed to remove

trypsin solution, fresh culture medium was added, and repeated inhalation and blow-out of cell suspension were carried out to prepare the cell suspension. Four 96-well plates were taken and cells were inoculated into the well (5×10^3 cells/100 μL per well), with three wells in each group. One well plate was taken out every 24 h, 5 mg/mL MTT solution was added with 10 μL/well, the cells were continued to culture for 1 h, then the culture medium was removed, and the OD value was measured at 570 nm with a microplate reader. Since the number of living cells is proportional to the absorbance, the absorbance value is applied as the cell activity. The experiment was repeated three times to visualize the cell activity-time curve.

Evaluation of cell migration and invasion by the Transwell method

Trypsin enzymolysis was carried out to prepare the cell suspension. Cells were inoculated into the migration upper chamber (containing 200 μL 10% FBS +1% DMEM) with 2×10^4 cells/well, and DMEM (containing 10% FBS with a total volume of 500 μL) was added into the lower chamber. After 24 h of cell culture, the upper chamber fluid was removed and the cells on the chamber wall were wiped off. A 4% of polymethanol was used to fix the Transwell opposite cells for 20 min. Crystal violet was used for staining for 15 min, and PBS was used to wash the Transwell chamber. Images of cell migration were collected under a 200-fold microscope. The cell number was calculated by randomly selecting three fields of view, and the average value was taken as the number of transmembrane cells. The experiment was repeated three times. Invasion was paved with 8% matrix glue on the above steps, and the number of cells per well was increased to 5×10^4.

Double luciferase reporter of gene determination

After amplification, MPP2 was cloned into pmirGLO vector to construct pmirGLO-MPP2-wt, and GeneArt TM Site-Directed Mutagenesis PLUS System (Thermo Fisher Scientific, Waltham, MA, United States) to construct pmirGLO-MPP2-mut vector, which was co-transfected with miR-34a, Ncmics, NC pre and pre-miR-34a into cells respectively. After 48 h of transfection, the luciferase intensity was detected using double luciferase reporter genes (Promega, Madison, WI, United States). The operation steps were carried out strictly in accordance with the instructions.

Statistics and analysis

SPSS 20.0 (AsiaAnalytics, Shanghai, China) was applied for index data analysis, and GraphPad Prism 6.0 was used for statistical analysis. Each experiment was repeated three times. The measurement data were expressed by mean ± SD. The comparison between groups was performed using one-way analysis of variance and *t*-test. Pearson correlation analysis was applied to discuss the correlation between miR-34a and MPP2. All data were tested using two-tailed test. The value of 95% was taken as confidence interval, and the difference was considered statistically significant at $^aP < 0.05$.

RESULTS

Low expression of miR-34a and MPP2 in hepatocellular carcinoma

In this study, 78 cases of liver cancer tissues and adjacent normal tissues were randomly selected as research objects. qPCR and Western blotting were used to determine the expression of miR-34a and MPP2 (Figure 1). Compared with adjacent normal tissues, miR-34a and MPP2 were lower in liver cancer tissues. Subsequently, the expression levels of miR-34a and MPP2 in three liver cancer cells (HepG2, Hep3B, PLC/PRG/5) and human normal liver cells (THLE-2) were detected. Compared with THLE-2, miR-34a and MPP2 were poorly expressed in liver cancer cells. The above results indicate that miR-34a and MPP2 are expressed at lower levels in liver cancer.

Low miR-34a expression in hepatocellular carcinoma due to methylation

To determine the cause of low expression of miR-34a in liver cancer, methylation of the miR-34a promoter was studied. First, Methprimer was used to predict the CpG site in the miR-34a promoter region. The results showed that there was a CpG site near the promoter 500 bp (Figure 2A). Then the MSP method was used to detect the methylation of miR-34a in tissue samples and cells. The results showed that methylated PCR bands appeared in liver cancer tissues and cells (Figure 2B). Based on this, we speculate that miR-34a expression is low in liver cancer due to methylation.

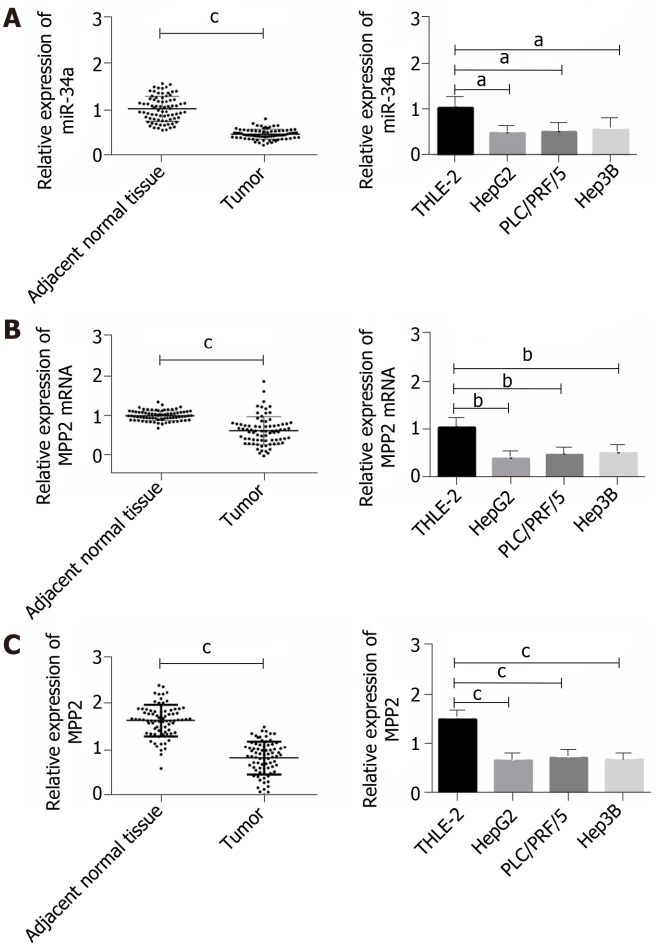


Figure 1 Low expression of microRNA 34a and membrane palmitoylated proteins in liver cancer. A: Low expression of microRNA 34a (miR-34a) in liver cancer tissues and cells; B: The mRNA expression of membrane palmitoylated protein (MPP2) was low in liver cancer tissues and cells; and C: The protein expression of MMP2 in liver cancer tissues and cells; a indicates $^{a}P < 0.05$, $^{b}P < 0.01$, $^{c}P < 0.001$).

Upregulation of miR-34a promotes cell apoptosis and MPP2 expression, and inhibits cell proliferation, invasion, and migration

DNA methylation inhibitor 5-Aza was used to demethylate liver cancer cells, the MSP method was applied to detect the methylation of miR-34a, qPCR was applied to detect the expression level of miR-34a, and Western blotting was applied to detect the expression levels of MPP2, caspase 3, caspase 9, E-cadherin, Bax, Bcl-2, N- cadherin, and β-catenin. The MTT method was used to detect the changes in cell activity at different time points and concentrations. The Transwell method was used to detect the invasion and migration ability of cells. The specific results are shown in Figure 3 and Supplementary Figures 1 and 2. After 5-Aza intervention, the methylation level of miR-34a in cells was decreased and the expression level was increased. Compared with the NC demethylation group, the cell activity, cell migration, and proliferation were decreased; the expression of Bcl-2, N-cadherin and β-catenin was downregulated; and the expression levels of caspase 9, caspase 3, E-cadherin, and Bax were upregulated. Compared with the NC pre-group, the pre-miR-34a group also showed a similar change trend in miR-34a demethylation. After miR-34a demethylation or promotion of miR-34a expression level, MPP2 expression level was upregulated in liver cancer cells. The above results indicated that miR-34a expression level is upregulated after miR-34a demethylation, which promotes the expression and apoptosis of MPP2, caspase 9, caspase 3, E-cadherin, Bax, and Bcl-2 and inhibits cell proliferation, migration, and invasion.

Upregulation of MPP2 promotes cell apoptosis and inhibits cell proliferation, migration, and invasion

Since upregulation of miR-34a can change the expression level of MPP2, the effect of MMP2 overexpression on the biological function of liver cancer cells was studied. The MPP2 results showed that overexpression of MPP2 did not change the methylation

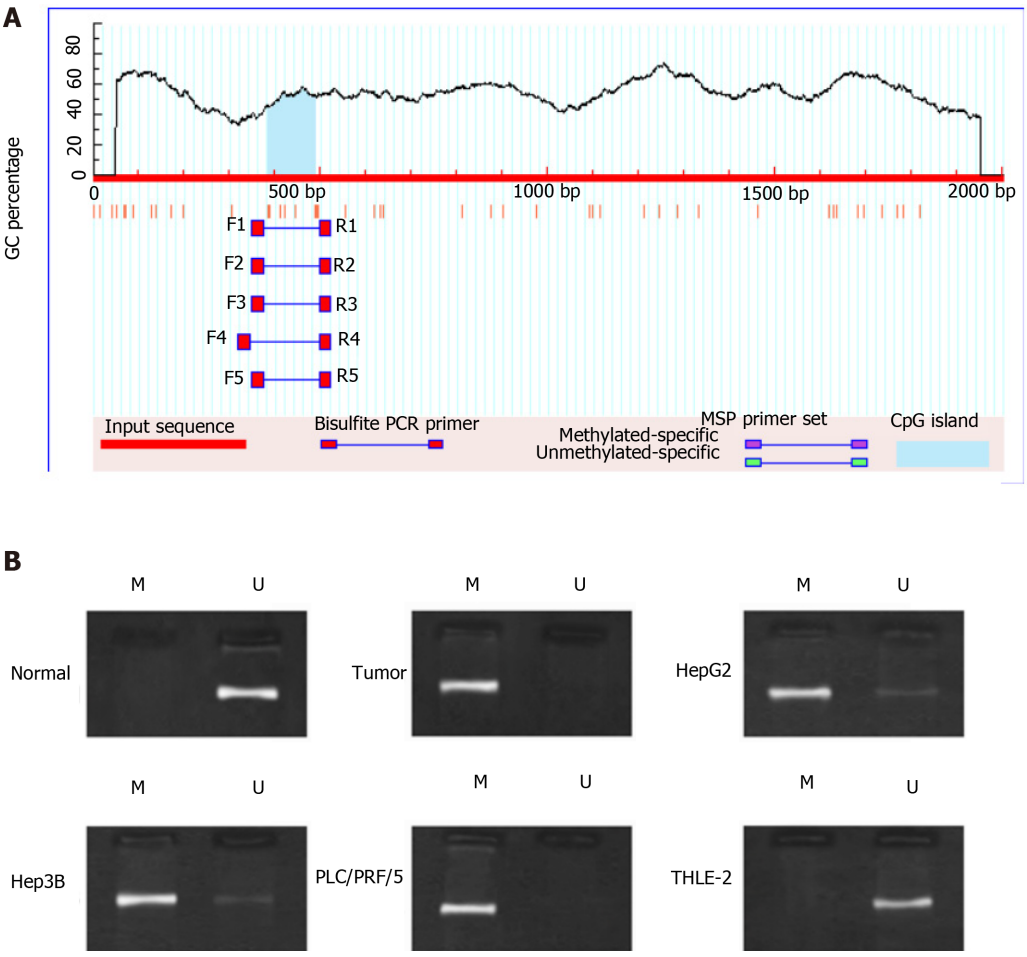


Figure 2 Highly methylated miR-34a in liver cancer. A: Methylation site prediction; B: Methylation of miR-34a in liver cancer. MSP: Methylation-specific polymerase chain reaction.

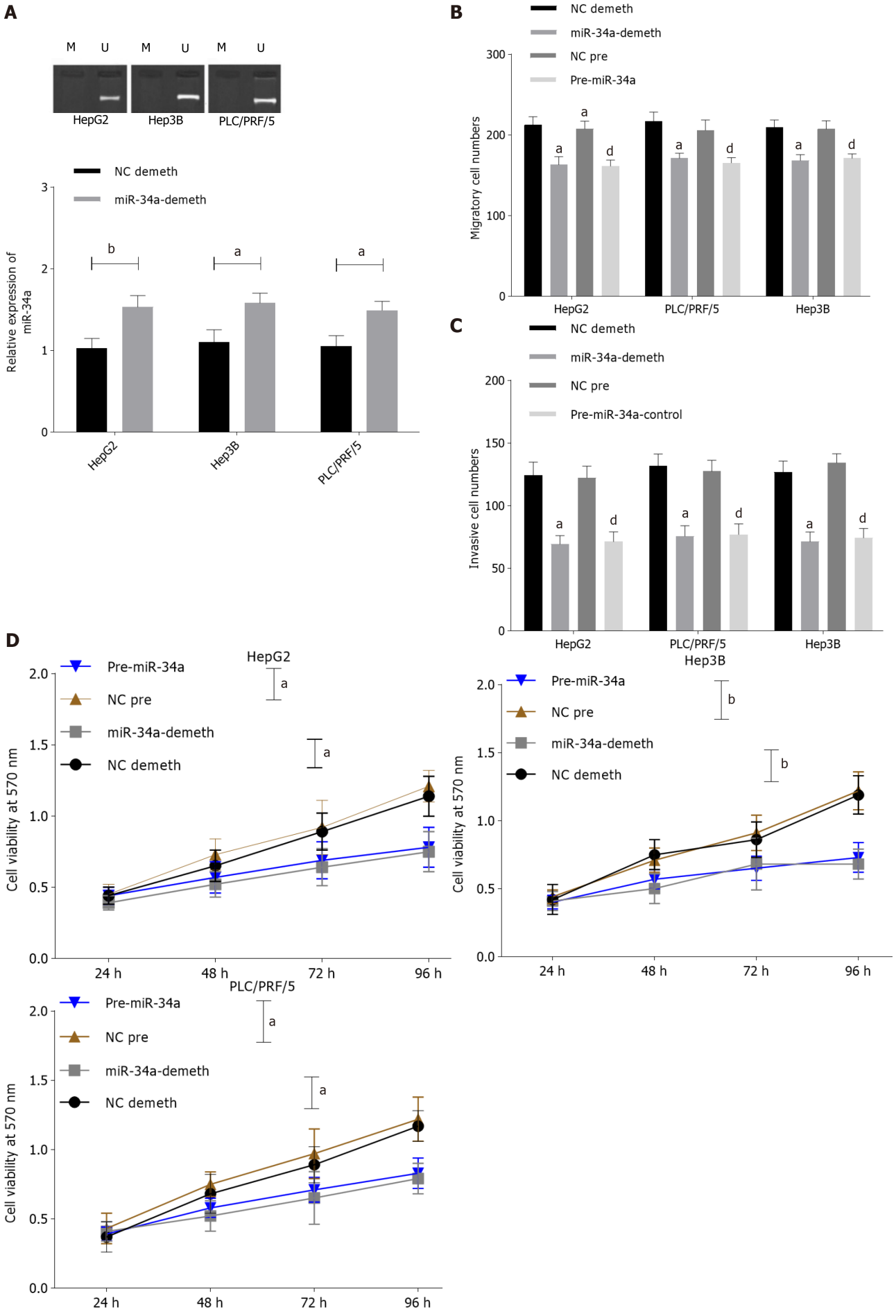
and expression level of miR-34a (Figure 4A). However, the Transwell experiment showed that compared with the NC-sh group, the cell migration number (Figure 4B) and invasion number (Figure 4C) of the sh-MPP2 group decreased significantly. The MTT assay showed that compared with the NC-sh group, the sh-MPP2 group showed a decrease in cell activity (Figure 4D). Western blot analysis showed that compared with the N- sh group, the expression levels of Bcl-2, N-cadherin, and β-catenin in the sh-MPP2 group were downregulated, whereas the expression levels of caspase 9, caspase 3, E-cadherin, Bax, and Bcl-2 were upregulated (Figure 4E). The above results indicate that upregulation of MPP2 promotes cell apoptosis and inhibits cell proliferation, migration, and invasion.

MPP2 is the target of miR-34a

Both the Targetscan and miRDB databases predicted that MPP2 was the target gene of miR-34a (Figure 5A). The upregulation or downregulation of MPP2 expression level was closely related to the upregulation or downregulation of miR-34a expression level (Figure 5B and C). Pearson analysis showed that there was a positive correlation between miR-34a and MPP2 (Figure 5D). To verif the targeted relationship between inflammatory miR-34a and MPP2, a double luciferase reporting experiment was carried out. The results showed that when miR-34a mimics and pmirGLO-MPP2-wt were co-transfected, fluorescence was decreased (Figure 5E). Therefore, miR-34a it appears can target and promote MPP2 expression.

Rescue experiment

The liver cancer cells were transfected with miR-34a demethylation and miR-34a demethylation + si MMP2 respectively, and corresponding MTT, Western blot analysis, and Transwell experiments were conducted (Figure 6, Supplementary Figures 3-5). Compared with the miR-34a demethylation group, cell migration and proliferation in the miR-34a demethylation + si MPP2 group were increased; cell


A
M U M U M U
HepG2 Hep3B PLC/PRF/5
NC demeth
miR-34a-demeth
Relative expression of miR-34a
b a a
HepG2 Hep3B PLC/PRF/5
B
NC demeth
miR-34a-demeth
NC pre
Pre-miR-34a
Migratory cell numbers
HepG2 PLC/PRF/5 Hep3B
C
NC demeth
miR-34a-demeth
NC pre
Pre-miR-34a-control
Invasive cell numbers
HepG2 PLC/PRF/5 Hep3B
D
HepG2
Pre-miR-34a
NC pre
miR-34a-demeth
NC demeth
Cell viability at 570 nm
24 h 48 h 72 h 96 h
Hep3B
PLC/PRF/5

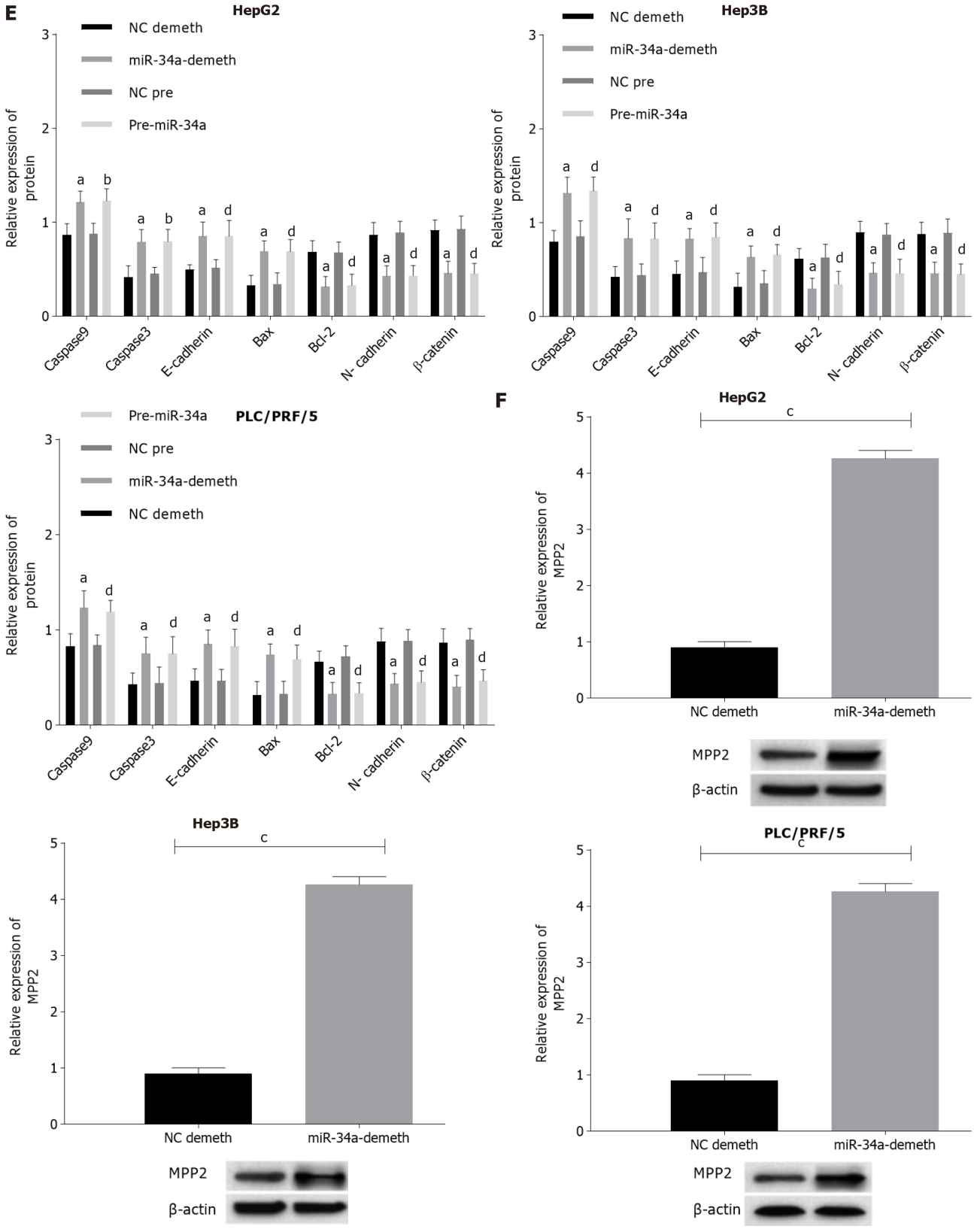


Figure 3 Upregulation of microRNA 34a promotes cell apoptosis and membrane palmitoylated protein expression, and inhibits cell proliferation, invasion, and migration. A: Image of microRNA 34a (miR-34a) demethylation results; B: Upregulation of miR-34a inhibits cell migration; a indicates that compared with negative control (NC) demethylation group, $^{a}P < 0.05$; $^{b}P < 0.01$, and d indicates compared with the NC pre group, $^{d}P < 0.05$; C: miR-34a upregulated the number of cell invasions; a indicates compared with the NC demethylation group, $^{a}P < 0.05$; d indicates compared with the NC pre group, $^{d}P < 0.05$; D: miR-34a upregulated and inhibited cell activity; a indicates $^{a}P < 0.05$, $^{b}P < 0.01$; E: Upregulation of miR-34a inhibited the downregulation of B-cell lymphoma 2 (Bcl-2), N- cadherin and β-catenin expression, while promoting caspase 9, caspase 3, E-cadherin and Bcl-2-associated X protein; a indicates compared with the NC demethylation group, $^{a}P < 0.05$; and d indicates compared with the NC pre group, $^{d}P < 0.05$; and F: Upregulation of miR-34a promoted the expression of membrane palmitoylated proteins, c indicates $^{c}P < 0.001$.

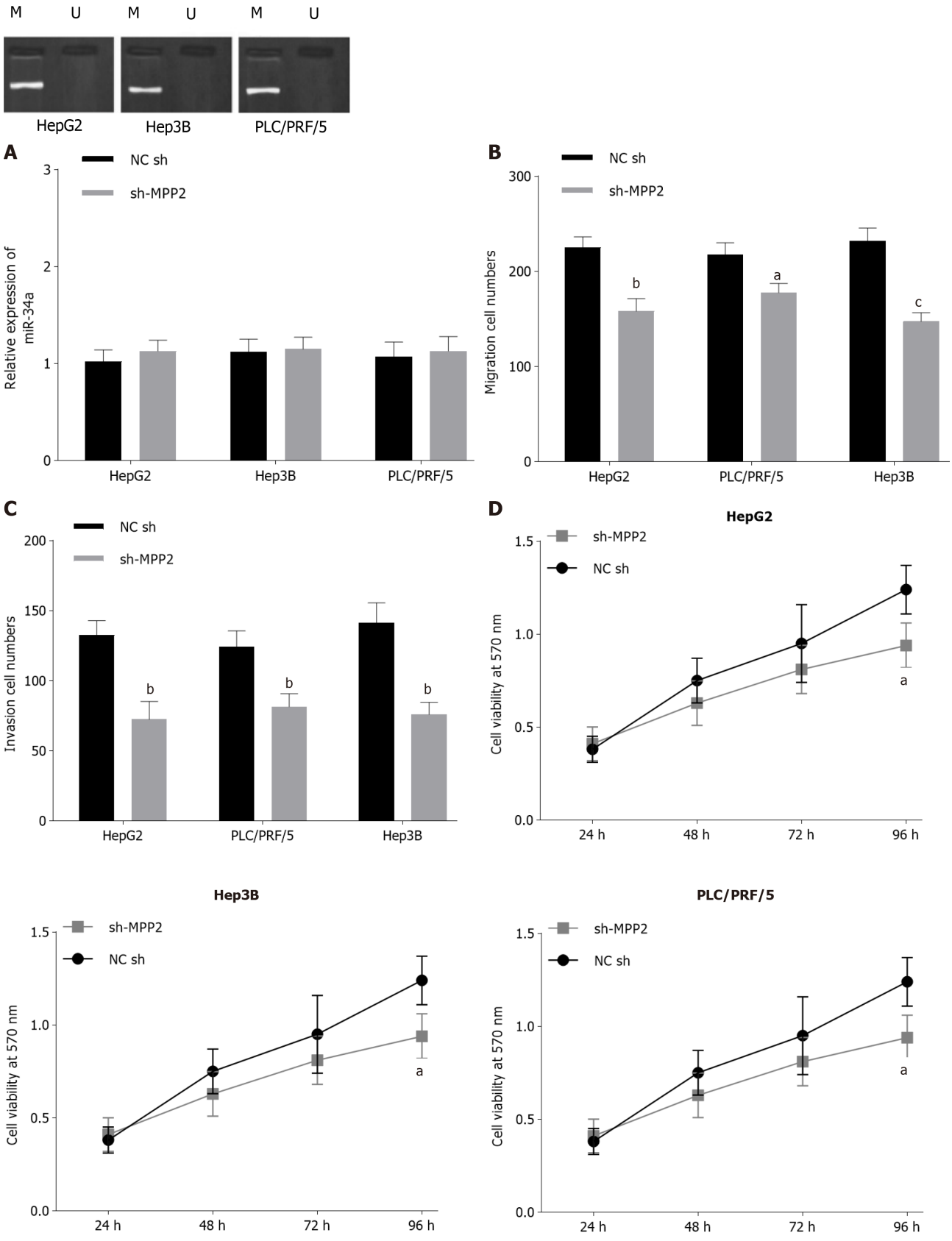
activity was increased; the expression levels of Bcl-2, N-cadherin, and β-catenin were upregulated; and the expression levels of caspase 9, caspase 3, E-cadherin, and Bax were downregulated. The miR-34a demethylation + si MPP2 group had no significant difference with the control group. The above results show that inhibition of MPP2 can counteract the effect of miR-34a demethylation on cell biological function.

DISCUSSION

miRNA plays an important role in the process of cell biology, and also affects cell processes such as cell proliferation, differentiation, apoptosis, and growth by regulating the expression level of many genes[18]. miRNA shows dynamic changes in different stages of cells. The high expression level of miRNA has specificity in different stages of cell development, thus playing a specific function in a certain period[19]. As the expression level of miRNA in normal tissues and tumor tissues is quite different[18] and can reflect the development and differentiation of tumor[20], how to regulate miRNA expression level has become a new research direction in cancer therapy. Some studies have claimed that miRNA is strictly regulated by DNA methylation[21]. Oshima *et al*[22] found that DNA methylation could downregulate miRNA encoded by 14q32 gene, thus inhibiting tumor development. Ning *et al*[23] showed that DNA (cytosine-5)-methyltransferase 1 and enhancer of zeste homolog 2 mediate DNA methylation and silence miR-200b, miR-200a and miR429, eventually promoting the development of gastric cancer and glioblastoma. Due to the reversibility of methylation and the amplification effect of miRNA, methylated miRNA can be used as a diagnostic index for cancer[24].

The miR-34a promoter has a CpG site near 400 bp to 500 bp (Figure 1B), so its expression level may be regulated by DNA methylation. The results showed that the expression level of miR-34a in liver cancer cells was lower than that in normal liver cells, whereas the methylation degree was higher than that in normal liver cells. After DNA demethylation, the expression level of miR-34a in liver cancer cells was increased; the apoptosis of cells was increased; and the migration, invasion, and proliferation ability were decreased. Many studies[25,26] have suggested that miR-34a can inhibit the proliferation and invasion of liver cancer cells and promote cell apoptosis by acting on different target proteins. The above results indicate that miR-34a is regulated by downregulation or silencing of CpG methylation[27], thus leading to the occurrence of liver cancer. The expression level of miR-34a in liver cancer cells was increased after demethylation, thus playing the role of tumor suppressor to prevent the subsequent development of liver cancer.

The essential action mechanism of miR-34a was to bind with downstream target protein mRNA, thus regulating transcription and translation of target gene and ultimately affecting cell biological function. To discuss the molecular mechanism of miR-34a on regulating cell biological functions, downstream studies of miR-34a were carried out. It was found that miR-34a had an MPP2 mRNA-binding site (Figure 5A), so miR-34a was considered a target on MPP2. The results showed that miR-34a could promote MPP2 expression in a targeted manner, thus causing increased apoptosis and decreased proliferation, migration and invasion of liver cancer cells. MPP2 belongs to the membrane-associated guanylate kinase p55 subgroup and plays an important role in cell-cell interaction[28]. The deletion and downregulation of MPP2 can lead to disorder of the SK2 channel and destroy Ca^{2+}/K^{+} diffusion, thus affecting cell signal transmission[29]. Baumgartner *et al*[30] showed that MPP2 plays a role as a tumor suppressor in tumorigenesis, which can inhibit the expression level of c-Src and affect cell proliferation, migration and invasion. Many studies[31-33] have confirmed that the miRNA regulation of genes is not limited to inhibitory effects, as miRNA can also promote gene expression by binding with mRNA. In this study, the effect of miR-34a on liver cancer may be that miR-34a binds to MPP2 mRNA, enhances mRNA transcription, and upregulates MPP2 expression. Upregulation of MPP2 will inhibit the expression level of downstream proteins such as c-Src, promote the recovery of pathways such as SK2, lead to changes in cytoskeleton of liver cancer cells, and eventually lead to weakening of malignant functions such as proliferation, migration and invasion. Cell adhesion plays an important role in cell migration and invasion, that is, cell adhesion inhibits epithelial-mesenchymal transition, which is the basis of cancer cell migration and invasion. MPP2 is a protein closely related to cell adhesion. In this study, the expression levels of intercellular adhesion molecules E-cadherin and N-cadherin were detected, which can be used to evaluate cell adhesion. Cancer cells are often accompanied by downregulation of E-cadherin and upregulation of N-


M
U
M
U
M
U
HepG2
Hep3B
PLC/PRF/5
A
NC sh
sh-MPP2
Relative expression of miR-34a
HepG2
Hep3B
PLC/PRF/5
B
NC sh
sh-MPP2
Migration cell numbers
b
a
c
HepG2
PLC/PRF/5
Hep3B
C
NC sh
sh-MPP2
Invasion cell numbers
b
b
b
HepG2
PLC/PRF/5
Hep3B
D
HepG2
sh-MPP2
NC sh
Cell viability at 570 nm
a
24 h
48 h
72 h
96 h
Hep3B
sh-MPP2
NC sh
Cell viability at 570 nm
a
24 h
48 h
72 h
96 h
PLC/PRF/5
sh-MPP2
NC sh
Cell viability at 570 nm
a
24 h
48 h
72 h
96 h

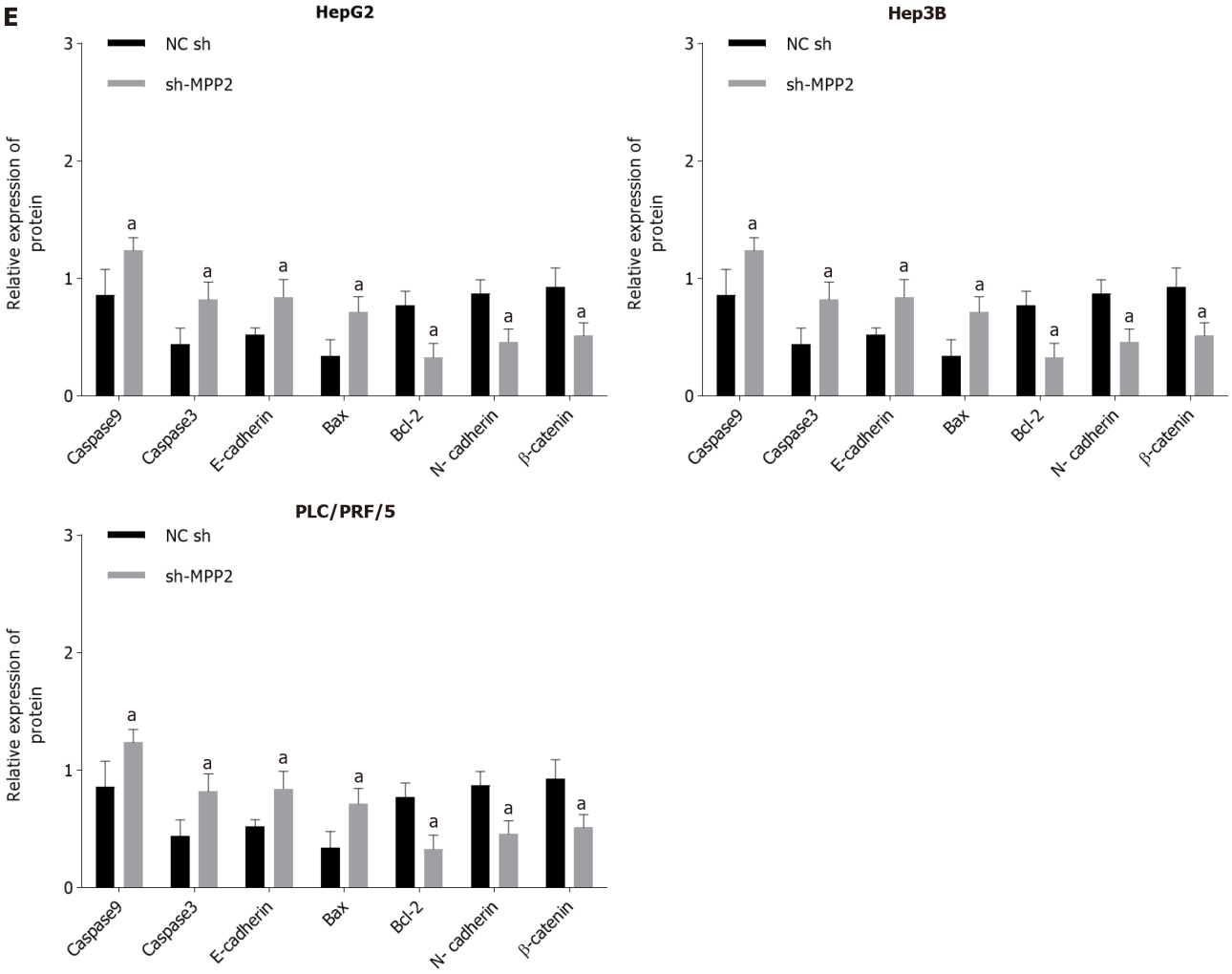


Figure 4 Membrane palmitoylated proteins promote cell apoptosis and inhibits cell proliferation, invasion, and migration. A: Overexpression of membrane palmitoylated proteins (MPP2) did not affect methylation and the expression level of microRNA 34a (miR-34a); B: MPP2 inhibited cell migration; compared with the negative control-short hairpin (NC-sh) group, a indicates $^{a}P < 0.05$, $^{b}P < 0.01$, $^{c}P < 0.001$; C: MPP2 inhibited cell invasion, compared with the NC-sh group, b indicates $^{b}P < 0.01$; D: MPP2 inhibited cell activity compared with the NC-sh group, a indicates $^{a}P < 0.05$; and E: MPP2 inhibited the downregulation of B-cell lymphoma 2 (Bcl-2), N-cadherin and β-catenin expression, but promoted caspase 9, caspase 3, E-cadherin, Bcl-2-associated X protein compared with the NC-sh group, a indicates $^{a}P < 0.05$).

cadherin. In this paper, the demethylation of miR-34a or the upregulation of MPP2 could lead to the upregulation of E-cadherin and downregulation of N-cadherin. However, when miR-34a is demethylated and MPP2 is down-regulated, E-cadherin is downregulated and N-cadherin is upregulated. The above results indicate that demethylated miR-34a may promote cell adhesion through MPP2, and finally inhibit cell migration and invasion. Therefore, the relationship between miR-34a methylation and MPP2 expression can be used as a research point for liver cancer treatment. For the development of miR-34a, demethylation drugs are expected to become a potential treatment for hepatocellular carcinoma. Due to time and cost reasons, this paper failed to launch a suitable in vivo tumor experiment to further study the regulation of demethylated miR-34a/MPP2 axis in solid hepatocellular carcinoma. In addition, miRDB and TargetScan databases predicted that MPP2 might be the downstream target protein of miR-34a, and the double luciferase reporter gene verified that there was a targeting relationship between the two. However, other downstream target genes of miR-34a were not mentioned in this study. This is also the limitation of this paper. Other downstream targets of miR-34a will be discussed in future studies. According to Figure 1, miR-34a and MPP2 are statistically different between normal adjacent tissues and tumor tissues, indicating that miR-34a and MPP2 expression seem to be related to the distance between them and tumor. The lack of exploration on this point is the deficiency of this paper. Therefore, this "expression-distance" relationship will be discussed in depth in future research.

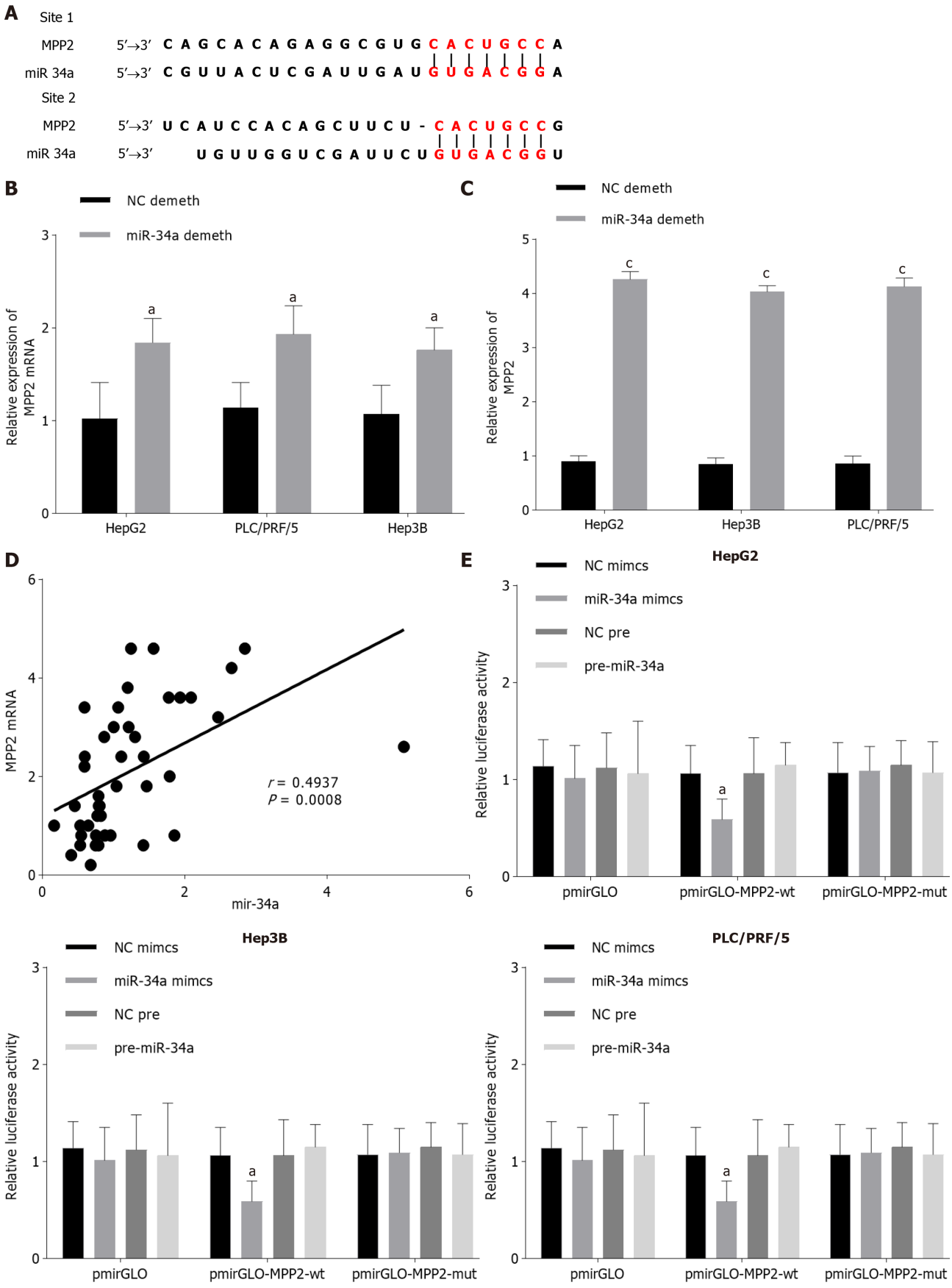
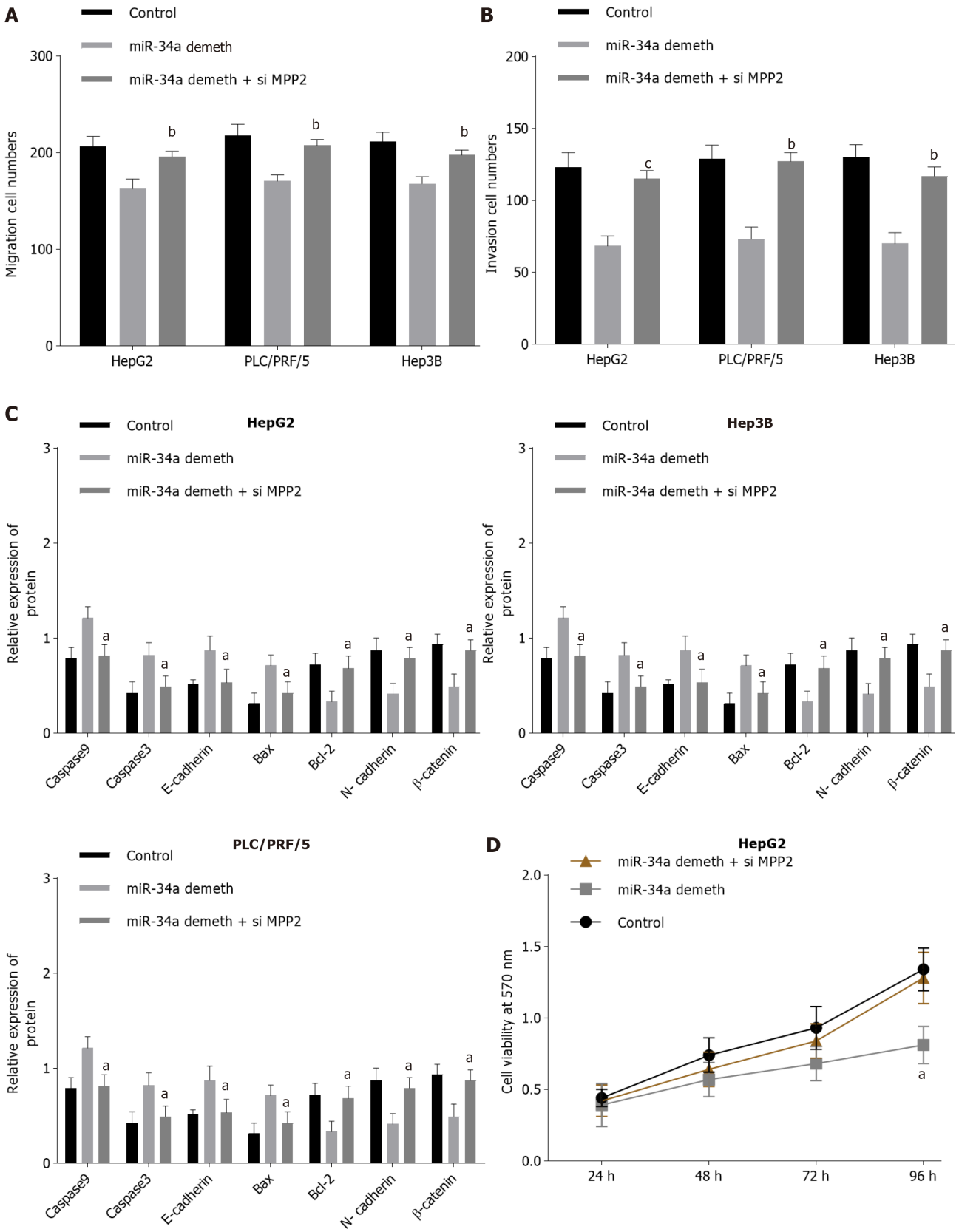


Figure 5 Membrane palmitoylated protein is the target of miR-34a. A: MicroRNA 34a (miR-34a) and membrane palmitoylated protein (MPP2) mRNA had binding sites; B and C: Effect of miR-34a expression change on MPP2 compared with the negative control (NC) demethylation group, a indicates $^{a}P < 0.05$; D: miR-34a had a positive correlation with MPP2 mRNA, $^{a}P < 0.05$, $^{c}P < 0.001$; and E: Double luciferase reporter gene verified the targeting relationship of miR-34a/MPP2; compared with NC mimics, a indicates $^{a}P < 0.05$.


A
Control
miR-34a demeth
miR-34a demeth + si MPP2
Migration cell numbers
300
200
100
0
b
b
b
HepG2
PLC/PRF/5
Hep3B
B
Control
miR-34a demeth
miR-34a demeth + si MPP2
Invasion cell numbers
200
150
100
50
0
c
b
b
HepG2
PLC/PRF/5
Hep3B
C
HepG2
Control
miR-34a demeth
miR-34a demeth + si MPP2
Relative expression of protein
3
2
1
0
a
Caspase9
Caspase3
E-cadherin
Bax
Bcl-2
N- cadherin
β-catenin
Hep3B
Control
miR-34a demeth
miR-34a demeth + si MPP2
Relative expression of protein
PLC/PRF/5
Control
miR-34a demeth
miR-34a demeth + si MPP2
Relative expression of protein
D
HepG2
miR-34a demeth + si MPP2
miR-34a demeth
Control
Cell viability at 570 nm
2.0
1.5
1.0
0.5
0.0
a
24 h
48 h
72 h
96 h

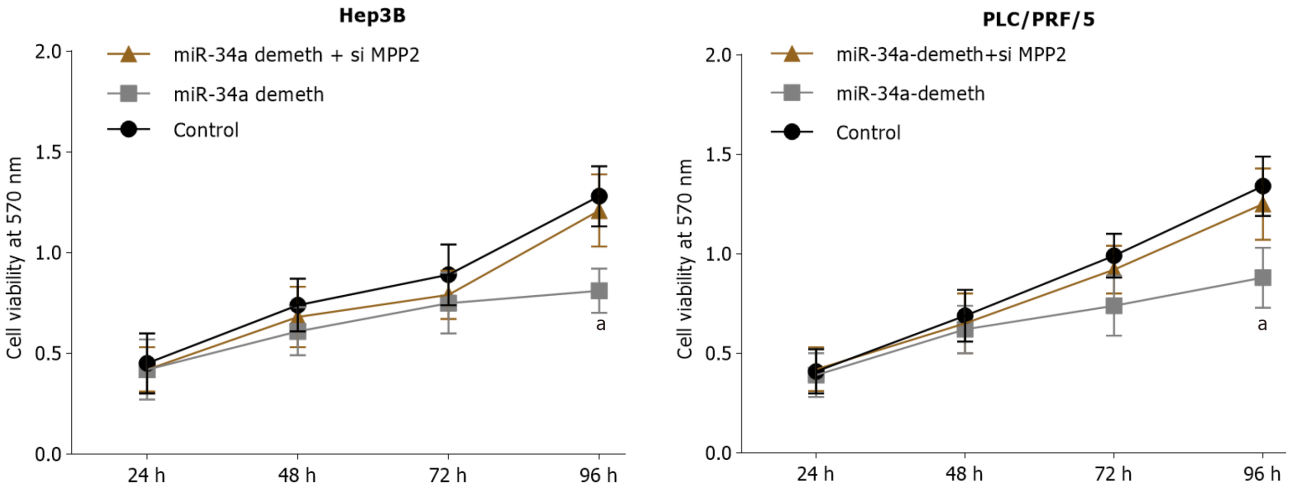


Figure 6 Rescue experiment. A: Small interfering membrane palmitoylated proteins (si-MPP2) can counteract the effect of microRNA 34a (miR-34a) demethylation on cell migration; B: si-MPP2 counteracts the effect of miR-34a demethylation on cell invasion, $^{b}P < 0.01$, $^{c}P < 0.001$; C: si-MPP2 counteracts the effect of miR-34a demethylation on cell activity; and D: si-MPP2 counteracts the effect of miR-34a demethylation on related proteins, a indicates $^{a}P < 0.05$).

CONCLUSION

This study identified the relationship of miR-34a hypermethylation with MPP2 expression by studying the changes of biological function and MPP2 expression of liver cancer cells after miR-34a demethylation. It was shown that miR-34a can inhibit the occurrence of liver cancer by upregulating MPP2, and its demethylation in liver cancer cells is a potential method for liver cancer treatment. In essence, the miR-34a methylation site is located on the upstream of its binding site with p53[27]. Therefore, it is valuable to study the role of miR-34a methylation/demethylation on the expression of upstream regulatory factors such as p53, and to explore its function in the future.

ARTICLE HIGHLIGHTS

Research background

Liver cancer is the sixth most common cancer in the world. Although miR-34a and palmitoyl membrane protein (MPP2) are reportedly involved in various cell processes, their precise roles in liver cancer are unknown.

Research motivation

miR-34a expression is low in liver cancer. The promoter region of miR-34a has CpG-binding sites and miR-34a is hypermethylated in liver cancer. MPP2 was downstream of miR-34a *via* miRDB and TargetScan databases prediction.

Research objectives

This study investigated the expression of miR-34a, the methylation of miR-34a promoter, and the expression of MPP2 in liver cancer cells and their related mechanisms.

Research methods

The methylation degree of miR-34a promoter and the expression levels of miR-34a and MPP2 in the above samples were detected. miR-34a was demethylated by 5′-Za. miR-34a or MPP2 was upregulated by miR-34a mimics or MPP2 shRNA. The changes in proliferation, invasion, apoptosis, migration and other biological functions of liver cancer cells were observed. Double luciferase reporter genes were used to detect the targeting relationship between miR-34a and MPP2.

Research results

miR-34a and MPP2 were downregulated in liver cancer and miR-34a was highly methylated in liver cancer. After miR-34a demethylation/mimetic transfection/MPP2 overexpression, liver cancer cells apoptosis was increased, but the proliferation,

invasion and migration capabilities were decreased. MPP2 was targeted by miR-34a.

Research conclusions

miR-34a demethylation upregulates the expression of MPP2 in liver cancer cells and promotes the apoptosis of liver cancer cells.

Research perspectives

The demethylation of miR-34a is a potential method for liver cancer treatment.

REFERENCES

1 **Ferlay J**, Soerjomataram I, Dikshit R, Eser S, Mathers C, Rebelo M, Parkin DM, Forman D, Bray F. Cancer incidence and mortality worldwide: sources, methods and major patterns in GLOBOCAN 2012. *Int J Cancer* 2015; **136**: E359-E386 [PMID: 25220842 DOI: 10.1002/ijc.29210]

2 **Bosch FX**, Ribes J, Díaz M, Cléries R. Primary liver cancer: worldwide incidence and trends. *Gastroenterology* 2004; **127**: S5-S16 [PMID: 15508102 DOI: 10.1053/j.gastro.2004.09.011]

3 **Tunissiolli NM**, Castanhole-Nunes MMU, Biselli-Chicote PM, Pavarino EC, da Silva RF, da Silva RC, Goloni-Bertollo EM. Hepatocellular Carcinoma: a Comprehensive Review of Biomarkers, Clinical Aspects, and Therapy. *Asian Pac J Cancer Prev* 2017; **18**: 863-872 [PMID: 28545181 DOI: 10.22034/APJCP.2017.18.4.863]

4 **Sulas P**, Di Tommaso L, Novello C, Rizzo F, Rinaldi A, Weisz A, Columbano A, Roncalli M. A Large Set of miRNAs Is Dysregulated from the Earliest Steps of Human Hepatocellular Carcinoma Development. *Am J Pathol* 2018; **188**: 785-794 [PMID: 29248455 DOI: 10.1016/j.ajpath.2017.10.024]

5 **Xu X**, Tao Y, Shan L, Chen R, Jiang H, Qian Z, Cai F, Ma L, Yu Y. The Role of MicroRNAs in Hepatocellular Carcinoma. *J Cancer* 2018; **9**: 3557-3569 [PMID: 30310513 DOI: 10.7150/jca.26350]

6 **Rupaimoole R**, Calin GA, Lopez-Berestein G, Sood AK. miRNA Deregulation in Cancer Cells and the Tumor Microenvironment. *Cancer Discov* 2016; **6**: 235-246 [PMID: 26865249 DOI: 10.1158/2159-8290.CD-15-0893]

7 **Shukla GC**, Singh J, Barik S. MicroRNAs: Processing, Maturation, Target Recognition and Regulatory Functions. *Mol Cell Pharmacol* 2011; **3**: 83-92 [PMID: 22468167]

8 **Zhu M**, Wu J, Ma X, Huang C, Wu R, Zhu W, Li X, Liang Z, Deng F, Zhu J, Xie W, Yang X, Jiang Y, Wang S, Geng S, Xie C, Zhong C. Butyl benzyl phthalate promotes prostate cancer cell proliferation through miR-34a downregulation. *Toxicol In Vitro* 2019; **54**: 82-88 [PMID: 30243731 DOI: 10.1016/j.tiv.2018.09.007]

9 **Yamakuchi M**, Ferlito M, Lowenstein CJ. miR-34a repression of SIRT1 regulates apoptosis. *Proc Natl Acad Sci* 2008; **105**: 13421-13426 [PMID: 18755897 DOI: 10.1073/pnas.0801613105]

10 **Chang TC**, Wentzel EA, Kent OA, Ramachandran K, Mullendore M, Lee KH, Feldmann G, Yamakuchi M, Ferlito M, Lowenstein CJ, Arking DE, Beer MA, Maitra A, Mendell JT. Transactivation of miR-34a by p53 broadly influences gene expression and promotes apoptosis. *Mol Cell* 2007; **26**: 745-752 [PMID: 17540599 DOI: 10.1016/j.molcel.2007.05.010]

11 **Cui X**, Wu Y, Wang Z, Liu X, Wang S, Qin C. MicroRNA-34a expression is predictive of recurrence after radiofrequency ablation in early hepatocellular carcinoma. *Tumour Biol* 2015; **36**: 3887-3893 [PMID: 25596083 DOI: 10.1007/s13277-014-3031-5]

12 **Bai J**, Wu J, Tang R, Sun C, Ji J, Yin Z, Ma G, Yang W. Emodin, a natural anthraquinone, suppresses liver cancer *in vitro* and *in vivo* by regulating $VEGFR_2$ and miR-34a. *Invest New Drugs* 2020; **38**: 229-245 [PMID: 30976957 DOI: 10.1007/s10637-019-00777-5]

13 **Conte I**, Lestingi M, den Hollander A, Miano MG, Alfano G, Circolo D, Pugliese M, Testa F, Simonelli F, Rinaldi E, Baiget M, Banfi S, Ciccodicola A. Characterization of MPP4, a gene highly expressed in photoreceptor cells, and mutation analysis in retinitis pigmentosa. *Gene* 2002; **297**: 33-38 [PMID: 12384283 DOI: 10.1016/s0378-1119(02)00872-7]

14 **Stucke VM**, Timmerman E, Vandekerckhove J, Gevaert K, Hall A. The MAGUK protein MPP7 binds to the polarity protein hDlg1 and facilitates epithelial tight junction formation. *Mol Biol Cell* 2007; **18**: 1744-1755 [PMID: 17332497 DOI: 10.1091/mbc.e06-11-0980]

15 **Stöhr H**, Stojic J, Weber BH. Cellular localization of the MPP4 protein in the mammalian retina. *Invest Ophthalmol Vis Sci* 2003; **44**: 5067-5074 [PMID: 14638699 DOI: 10.1167/iovs.03-0702]

16 **Schilders G**, Raijmakers R, Raats JM, Pruijn GJ. MPP6 is an exosome-associated RNA-binding protein involved in 5.8S rRNA maturation. *Nucleic Acids Res* 2005; **33**: 6795-6804 [PMID: 16396833 DOI: 10.1093/nar/gki982]

17 **Lüscher-Firzlaff JM**, Westendorf JM, Zwicker J, Burkhardt H, Henriksson M, Müller R, Pirollet F, Lüscher B. Interaction of the fork head domain transcription factor MPP2 with the human papilloma virus 16 E7 protein: enhancement of transformation and transactivation. *Oncogene* 1999; **18**: 5620-5630 [PMID: 10523841 DOI: 10.1038/sj.onc.1202967]

18 **Lujambio A**, Calin GA, Villanueva A, Ropero S, Sánchez-Céspedes M, Blanco D, Montuenga LM, Rossi S, Nicoloso MS, Faller WJ, Gallagher WM, Eccles SA, Croce CM, Esteller M. A microRNA DNA methylation signature for human cancer metastasis. *Proc Natl Acad Sci* 2008; **105**: 13556-

13561 [PMID: 18768788 DOI: 10.1073/pnas.0803055105]
19 **Neilson JR**, Zheng GX, Burge CB, Sharp PA. Dynamic regulation of miRNA expression in ordered stages of cellular development. *Genes Dev* 2007; **21**: 578-589 [PMID: 17344418 DOI: 10.1101/gad.1522907]
20 **Lu J**, Getz G, Miska EA, Alvarez-Saavedra E, Lamb J, Peck D, Sweet-Cordero A, Ebert BL, Mak RH, Ferrando AA, Downing JR, Jacks T, Horvitz HR, Golub TR. MicroRNA expression profiles classify human cancers. *Nature* 2005; **435**: 834-838 [PMID: 15944708 DOI: 10.1038/nature03702]
21 **Han L**, Witmer PD, Casey E, Valle D, Sukumar S. DNA methylation regulates MicroRNA expression. *Cancer Biol Ther* 2007; **6**: 1284-1288 [PMID: 17660710 DOI: 10.4161/cbt.6.8.4486]
22 **Oshima G**, Poli EC, Bolt MJ, Chlenski A, Forde M, Jutzy JMS, Biyani N, Posner MC, Pitroda SP, Weichselbaum RR, Khodarev NN. DNA Methylation Controls Metastasis-Suppressive 14q32-Encoded miRNAs. *Cancer Res* 2019; **79**: 650-662 [PMID: 30538122 DOI: 10.1158/0008-5472.CAN-18-0692]
23 **Ning X**, Shi Z, Liu X, Zhang A, Han L, Jiang K, Kang C, Zhang Q. DNMT1 and EZH2 mediated methylation silences the microRNA-200b/a/429 gene and promotes tumor progression. *Cancer Lett* 2015; **359**: 198-205 [PMID: 25595591 DOI: 10.1016/j.canlet.2015.01.005]
24 **Ezzat WM**, Amr KS, Elhosary YA, Hegazy AE, Fahim HH, Eltaweel NH, Kamel RR. Detection of DNA methylated microRNAs in hepatocellular carcinoma. *Gene* 2019; **702**: 153-157 [PMID: 30922710 DOI: 10.1016/j.gene.2019.02.080]
25 **Zhou Y**, Liu K, Liu Y, Tan L. MicroRNA-34a inhibit hepatocellular carcinoma progression by repressing hexokinase-1. *J Cell Biochem* 2018 [PMID: 30474301 DOI: 10.1002/jcb.27988]
26 **Han R**, Chen X, Li Y, Zhang S, Li R, Lu L. MicroRNA-34a suppresses aggressiveness of hepatocellular carcinoma by modulating *E2F1, E2F3*, and Caspase-3. *Cancer Manag Res* 2019; **11**: 2963-2976 [PMID: 31114344 DOI: 10.2147/CMAR.S202664]
27 **Lodygin D**, Tarasov V, Epanchintsev A, Berking C, Knyazeva T, Körner H, Knyazev P, Diebold J, Hermeking H. Inactivation of miR-34a by aberrant CpG methylation in multiple types of cancer. *Cell Cycle* 2008; **7**: 2591-2600 [PMID: 18719384 DOI: 10.4161/cc.7.16.6533]
28 **Rademacher N**, Schmerl B, Lardong JA, Wahl MC, Shoichet SA. MPP2 is a postsynaptic MAGUK scaffold protein that links SynCAM1 cell adhesion molecules to core components of the postsynaptic density. *Sci Rep* 2016; **6**: 35283 [PMID: 27756895 DOI: 10.1038/srep35283]
29 **Kim G**, Luján R, Schwenk J, Kelley MH, Aguado C, Watanabe M, Fakler B, Maylie J, Adelman JP. Membrane palmitoylated protein 2 is a synaptic scaffold protein required for synaptic SK2-containing channel function. *Elife* 2016; **5** [PMID: 26880549 DOI: 10.7554/eLife.12637]
30 **Baumgartner M**, Weiss A, Fritzius T, Heinrich J, Moelling K. The PDZ protein MPP2 interacts with c-Src in epithelial cells. *Exp Cell Res* 2009; **315**: 2888-2898 [PMID: 19665017 DOI: 10.1016/j.yexcr.2009.07.028]
31 **Roberts AP**, Lewis AP, Jopling CL. miR-122 activates hepatitis C virus translation by a specialized mechanism requiring particular RNA components. *Nucleic Acids Res* 2011; **39**: 7716-7729 [PMID: 21653556 DOI: 10.1093/nar/gkr426]
32 **Ørom UA**, Nielsen FC, Lund AH. MicroRNA-10a binds the 5'UTR of ribosomal protein mRNAs and enhances their translation. *Mol Cell* 2008; **30**: 460-471 [PMID: 18498749 DOI: 10.1016/j.molcel.2008.05.001]
33 **Huang V**, Place RF, Portnoy V, Wang J, Qi Z, Jia Z, Yu A, Shuman M, Yu J, Li LC. Upregulation of Cyclin B1 by miRNA and its implications in cancer. *Nucleic Acids Res* 2012; **40**: 1695-1707 [PMID: 22053081 DOI: 10.1093/nar/gkr934]

World Journal of Gastroenterology

Submit a Manuscript: https://www.f6publishing.com

World J Gastroenterol 2021 February 14; 27(6): 487-500

DOI: 10.3748/wjg.v27.i6.487

ISSN 1007-9327 (print) ISSN 2219-2840 (online)

ORIGINAL ARTICLE

Basic Study

Circular RNA circVAPA promotes chemotherapy drug resistance in gastric cancer progression by regulating miR-125b-5p/STAT3 axis

Peng Deng, Ming Sun, Wen-Yan Zhao, Bin Hou, Kai Li, Tao Zhang, Feng Gu

ORCID number: Peng Deng 0000-0001-8147-1098; Ming Sun 0000-0003-1452-5660; Wen-Yan Zhao 0000-0001-7123-7126; Bin Hou 0000-0002-8427-4716; Kai Li 0000-0002-6683-517X; Tao Zhang 0000-0002-6720-1355; Feng Gu 0000-0003-0625-7897.

Author contributions: Deng P and Sun M performed the majority of experiments and analyzed the data; Zhao WY performed the molecular investigations; Hou B and Gu F designed and coordinated the research; Li K and Zhang T wrote the paper.

Supported by Natural Science Foundation of Liaoning Province, No. 2019-MS-385.

Institutional review board statement: This study was reviewed and approved by the First Affiliated Hospital of China Medical University.

Institutional animal care and use committee statement: The animal study was reviewed and approved by the First Affiliated Hospital of China Medical University.

Conflict-of-interest statement: The authors declare no conflict of interest related to this manuscript.

Data sharing statement: No additional data are available.

Peng Deng, Bin Hou, Kai Li, Department of Surgical Oncology and General Surgery, Key Laboratory of Precision Diagnosis and Treatment of Gastrointestinal Tumors, Ministry of Education, The First Affiliated Hospital of China Medical University, Shenyang 110001, Liaoning Province, China

Ming Sun, Department of Urology, Shengjing Hospital of China Medical University, Shenyang 110004, Liaoning Province, China

Wen-Yan Zhao, Department of General Surgery, Shengjing Hospital of China Medical University, Shenyang 110004, Liaoning Province, China

Tao Zhang, Department of Stem Cells and Regenerative Medicine, China Medical University, Shenyang 110122, Liaoning Province, China

Feng Gu, Department of Ophthalmology, The First Affiliated Hospital of China Medical University, Shenyang 110001, Liaoning Province, China

Corresponding author: Feng Gu, PhD, Chief Physician, Department of Ophthalmology, The First Affiliated Hospital of China Medical University, No. 155 Nanjing North Street, Heping District, Shenyang 110001, Liaoning Province, China. fenggu78186069@163.com

Abstract

BACKGROUND

Gastric cancer (GC) is a prevalent malignancy, leading to a high incidence of cancer-associated death. Cisplatin (DDP)-based chemotherapy is the principal therapy for clinical GC treatment, but DDP resistance is a severe clinical challenge and the mechanism remains poorly understood. Circular RNAs (circRNAs) have been identified to play crucial roles in modulating the chemoresistance of gastric cancer cells.

AIM

To explore the effect of circVAPA on chemotherapy resistance during GC progression.

METHODS

The effect of circVAPA on GC progression and chemotherapy resistance was analyzed by MTT assay, colony formation assay, Transwell assay, wound healing assay, and flow cytometry analysis in GC cells and DDP resistant GC cell lines,

ARRIVE guidelines statement: The authors have read the ARRIVE guidelines, and the manuscript was prepared and revised according to the ARRIVE guidelines.

Open-Access: This article is an open-access article that was selected by an in-house editor and fully peer-reviewed by external reviewers. It is distributed in accordance with the Creative Commons Attribution NonCommercial (CC BY-NC 4.0) license, which permits others to distribute, remix, adapt, build upon this work non-commercially, and license their derivative works on different terms, provided the original work is properly cited and the use is non-commercial. See: http://creativecommons.org/Licenses/by-nc/4.0/

Manuscript source: Unsolicited manuscript

Specialty type: Gastroenterology and hepatology

Country/Territory of origin: China

Peer-review report's scientific quality classification

Grade A (Excellent): 0
Grade B (Very good): B
Grade C (Good): C, C
Grade D (Fair): 0
Grade E (Poor): 0

Received: December 6, 2020
Peer-review started: December 6, 2020
First decision: December 17, 2020
Revised: December 21, 2020
Accepted: January 7, 2021
Article in press: January 7, 2021
Published online: February 14, 2021

P-Reviewer: Mohamed SY, Ying G
S-Editor: Fan JR
L-Editor: Wang TQ
P-Editor: Liu JH

and tumorigenicity analysis in nude mice *in vivo*. The mechanism was investigated by luciferase reporter assay, quantitative real-time PCR, and Western blot analysis.

RESULTS

CircVAPA expression was up-regulated in clinical GC tissues compared with normal samples. CircVAPA depletion inhibited proliferation, migration, and invasion and increased apoptosis of GC cells. The expression of circVAPA, STAT3, and STAT3 downstream genes was elevated in DDP resistant SGC7901/DDP cell lines. CircVAPA knockdown attenuated the DDP resistance of GC cells. Mechanically, circVAPA was able to sponge miR-125b-5p, and miR-125b-5p could target STAT3 in the GC cells. MiR-125b-5p inhibitor reversed circVAPA depletion-enhanced inhibitory effect of DDP on GC cells, and STAT3 knockdown blocked circVAPA overexpression-induced proliferation of DDP-treated SGC7901/DDP cells. The depletion of STAT3 and miR-125b-5p inhibitor reversed circVAPA depletion-induced GC cell apoptosis. Functionally, circVAPA contributed to the tumor growth of SGC7901/DDP cells *in vivo*.

CONCLUSION

CircVAPA promotes chemotherapy resistance and malignant progression in GC by miR-125b-5p/STAT3 signaling. Our findings present novel insights into the mechanism by which circVAPA regulates chemotherapy resistance of GC cells. CircVAPA and miR-125b-5p may be considered as the potential targets for GC therapy.

Key Words: Gastric cancer; Progression; Chemoresistance; CircVAPA; miR-125b-5p; STAT3

©The Author(s) 2021. Published by Baishideng Publishing Group Inc. All rights reserved.

Core Tip: We concluded that circVAPA contributed to chemotherapy resistance and malignant progression in gastric cancer (GC) by miR-125b-5p/STAT3 signaling. Our findings present novel insights into the mechanism that circVAPA regulates chemotherapy resistance of GC cells. CircVAPA and miR-125b-5p may be considered as potential targets for GC therapy.

Citation: Deng P, Sun M, Zhao WY, Hou B, Li K, Zhang T, Gu F. Circular RNA circVAPA promotes chemotherapy drug resistance in gastric cancer progression by regulating miR-125b-5p/STAT3 axis. *World J Gastroenterol* 2021; 27(6): 487-500
URL: https://www.wjgnet.com/1007-9327/full/v27/i6/487.htm
DOI: https://dx.doi.org/10.3748/wjg.v27.i6.487

INTRODUCTION

Gastric cancer (GC) is a prevalent malignancy and the second cause of tumor-associated mortality in the world[1]. Chemotherapy is a favored strategy toward advanced-stage GC cases, in which oxaliplatin, cisplatin (DDP), and 5-FU are usually admitted as first-line therapies[2-4]. Although the improved chemotherapy effectiveness, the GC patients' survival is still unsatisfactory, and chemotherapy always attains a low response rate[5,6]. Whether intrinsic or acquired, chemoresistance is a significant challenge for GC treatment efficiency in the clinic[7]. The mechanism for GC chemotherapy resistance development is not well-understood, in which micro-environmental and genetic contributors are able to result in chemoresistance[8]. Hence, understanding the molecular mechanism of chemotherapy resistance in GC is urgently needed.

Circular RNAs (circRNAs), as an emerging class of non-coding RNAs, present various functions in the regulation of gene expression at the post-transcriptional and transcriptional levels[9]. It has been identified that circRNAs are able to serve as the competitive endogenous sponge for microRNAs (miRNAs) and thereby inhibit

miRNAs, providing a new manner for modulating miRNAs and indicating a promising mechanism of circRNA function[10,11]. Meanwhile, previous studies have reported that circVAPA is elevated in tumors and contributes to cancer progression, such as liver cancer and breast cancer[12,13]. MiRNAs are short non-coding RNAs with a length of about 22nt and can target various genes by pairing with the mRNAs at the post-transcriptional level[14,15]. MiR-125b-5p is a well-investigated tumor suppressor in multiple cancer models, including bladder cancer, laryngeal squamous cell carcinoma, and colon cancer[16-18]. Furthermore, it has been well-identified that circRNAs and miRNAs are involved in the chemotherapy resistance in GC[8,19-21]. However, the role of circVAPA and miR-125b-5p in modulating chemotherapy resistance of GC cells is still unreported.

It has been recognized that STAT3 serves as a critical regulator in tumorigenesis[22]. As an important transcriptional factor, STAT3 is able to mediate multiple gene expression in modulating cell survival response to different stimulations[23]. Furthermore, STAT3 remarkably promotes chemoresistance as a crucial indicator in GC cells by various mechanisms, such as increasing the expression of vacuolar ATPase pump and oncogenes as well as the apoptotic factors[24]. Nevertheless, the impact of circVAPA and miR-125b-5p on STAT3 in the regulation of GC cells chemotherapy resistance is still unclear.

In this study, we were interested in the function of circVAPA in the progression of chemotherapy resistance of GC cells. We found an unreported role of circVAPA in enhancing chemotherapy resistance and promoting the malignant progression of GC by modulating miR-125b-5p/STAT3 signaling.

MATERIALS AND METHODS

GC clinical samples

The clinical GC tissue samples (n = 50) and adjacent normal tissues (n = 50) were obtained from the First Affiliated hospital of China Medical University. The diagnosis of cases was performed by two clinicians based on histopathological analysis. The samples were collected and immediately stored at -80 °C followed by further analysis. The samples were written-approved by the patients. This study conformed to the experimental guidelines of the World Medical Association and the Ethics Committee of the First Affiliated Hospital of China Medical University.

Cell culture and treatment

The SGC7901, HGC27, and SGC7901/DDP cell lines were maintained in the laboratory. The cells were incubated in an incubator at 5% CO_2 and 37 °C in the Dulbecco's modified Eagle's medium (DMEM) medium (Hyclone, United States) with fetal bovine serum (10%, Hyclone, United States), streptomycin (0.1 mg/mL, Hyclone, United States), and penicillin (100 units/mL, Hyclone, United States). DDP was obtained from Sigma (United States). The circVAPA shRNA, pcDNA3.1-circVAPA, pcDNA3.1-STAT3, STAT3 siRNA, miR-125b-5p mimic, and miR-125b-5p inhibitor were purchased from GenePharma (China). The transfection in the cells was performed with Liposome 2000 (Invitrogen, United States).

MTT assay

The cell viability was assessed by MTT assays at various time points in 6-well dishes. Briefly, the MTT solution (Solarbio, China) was added into the cells and cultured at the condition of 5% CO_2 and 37 °C for 4 h. After that, dimethyl sulfoxide (DMSO; 100 μL, 10 min; Sigma, United States) was used to terminate the reaction. The cell viability was analyzed at the absorbance of 490 nm by applying a microplate reader (Thermo, United States).

Colony formation assay

About 1 × 10^3 cells were plated in 6-well dishes and cultured in DMEM at the condition of 5% CO_2 and 37 °C. After 2 wk, cells were washed with phosphate buffered saline (PBS) buffer, made in methanol about 30 min, and dyed with 1% crystal violet dye solution, after which the number of colonies was calculated.

Transwell assay

Transwell assays were performed to analyze cell invasion and migration using a Transwell plate (Corning, United States) according to the manufacturer's instructions.

Briefly, the upper chamber was plated with around 1 × 10^5 cells. The cells were then fixed with 4% paraformaldehyde and dyed with crystal violet. The invaded and migrated cells were recorded and calculated.

Wound healing assay

Cells were plated in a 24-well plate at 3 × 10^5/well and cultured overnight to reach full confluence as a monolayer. A 20 μL pipette tip was applied to slowly cut a straight line across the well. Then the well was washed with PBS three times and changed with the serum-free medium and continued to culture. The wound healing percentage was calculated.

Analysis of cell apoptosis

Cell apoptosis was measured by applying the Annexin-V-FITC apoptosis kit (BD, United States) based on flow cytometry analysis using a FACSCalibur flow cytometer, followed by the quantification analysis using FlowJo software.

Luciferase reporter gene assay

SGC7901 and HGC27 cells were plated in 24-well dishes followed by treatment with miR-125b-5p mimic. After 48 h of the treatment, the luciferase activities were analyzed by utilizing the luciferase reporter assays (Promega, United States). The relative luciferase activities were analyzed by the Renilla luciferase activities.

Quantitative real-time PCR

RNA isolation was performed by applying TRIzol reagent (Solarbio, China) and the first-strand cDNA was synthesized (Solarbio, China). Quantitative real-time PCR was carried out by applying SYBR-Green (Takara, China). The primer sequences are as follows: circVAPA forward: 5′-TGGATTCCAAATTGAGATGCGTATT-3′, reverse: 5′-CACTTTTCTATCCGATGGATTTCGC-3′; miR-125b-5p forward: 5′-TCCCTGAGACCCTAACTTGTGA-3′, reverse: 5′- AGTCTCAGGGTCCGAGGTATTC-3′; STAT3 forward: 5′-CTGGCCTTTGGTGTTGAAAT-3′, reverse: 5′-AAGGCACCC ACAGAAACAAC-3′; GAPDH forward: 5′-AAGAAGGTGGTGAAGCAGGC-3′, reverse: 5′-TCCACCACCCAGTTGCTGTA-3′.

Western blot analysis

Total proteins were extracted from the cells using radioimmunoprecipitation assay buffer (CST, United States) and quantified using the BCA Protein Quantification Kit (Abbkine, United States). The proteins at the same concentration were subjected to sodium dodecyl sulfate- polyacrylam-ide gel electrophoresis and transferred to polyvinylidene fluoride membranes (Millipore, United States), followed by incubation with 5% milk and with the primary antibodies at 4 °C overnight. The corresponding second antibodies (BOSTER, China) were used for incubating the membranes for 1 h at room temperature, followed by visualization using a chemiluminescence detection kit (Beyyotime, China). The primary antibodies applied in this study comprised STAT3 (Abcam, United States), p-STAT3 (Abcam, United States), Survivin (Abcam, United States), Mcl-1 (Abcam, United States), Bcl-xl (Abcam, United States), and β-actin (Abcam, United States).

Analysis of tumorigenicity in nude mice

The tumor growth of GC cells *in vivo* was tested in nude Balb/c mice (4-week-old, male, n = 5). And about 1 × 10^7 SGC7901/DDP cells were subcutaneously injected in the mice. Five days after injection, we measured tumor growth every 5 d. We sacrificed the mice 30 d after injection, and tumors were scaled. Tumor volume (V) was observed by estimating the length (L) and width (W) with calipers and calculated as (L × W^2) × 0.5. Animal care and method procedure were authorized by the Animal Ethics Committee of the First Affiliated Hospital of China Medical University.

Statistical analysis

Data are presented as the mean ± SD, and statistical analyses were performed with GraphPad Prism 7. The unpaired Student's t-test was applied for comparing the difference between two groups, and one-way ANOVA was applied for comparing among multiple groups. $^aP < 0.05$ were considered statistically significant.

RESULTS

CircVAPA enhances proliferation and represses apoptosis of GC cells

To identify the clinical association of circVAPA with GC, we analyzed the expression of circVAPA in the clinical GC samples. Our data showed that circVAPA expression was elevated in the GC tissue samples (n = 50) relative to that in the adjacent normal tissues (n = 50), implying the potential correlation of circVAPA with GC (Figure 1A). The cell viability was reduced by the depletion of circVAPA in the SGC7901 and HGC27 cell lines (Figure 1B and C). Similarly, colony formation assays revealed that circVAPA shRNA treatment remarkably decreased the colony numbers of SGC7901 and HGC27 cells (Figure 1D and E). Furthermore, apoptosis of SGC7901 and HGC27 cells was induced by circVAPA knockdown (Figure 1F and G). These findings indicated that circVAPA is able to increase proliferation and attenuate apoptosis of GC cells

CircVAPA promotes invasion and migration of GC cells

Next, the function of circVAPA in modulating migration and invasion of GC cells was assessed. Transwell assays demonstrated that migration and invasion of SGC7901 and HGC27 cells were alleviated by circVAPA shRNA (Figure 2A and B). Besides, wound healing assays showed that circVAPA depletion remarkably increased wound proportion in SGC7901 and HGC27 cell lines (Figure 2C and D). These data indicated that circVAPA contributes to migration and invasion of GC cells.

Elevation of circVAPA enhances chemotherapy drug resistance of GC cells

Next, we were interested in the impact of circVAPA on the chemoresistance of GC cells. To this end, we first explored the expression of circVAPA in SGC7901 and DDP resistant SGC7901/DDP cell lines. Significantly, the expression of circVAPA was up-regulated in SGC7901/DDP cells compared with that in SGC7901 cells (Figure 3A). Meanwhile, STAT3 phosphorylation, STAT3 expression, and STAT3 downstream gene (including Survivin, Mcl-1, and Bcl-xl) expression were elevated in the SGC7901/DDP cells relative to those in SGC7901 cells (Figure 3A and B). Importantly, depletion of circVAPA remarkably reduced the IC_{50} value of DDP for the inhibition of SGC7901/DDP cells (Figure 3C). In addition, DDP was able to induce apoptosis of SGC7901/DDP cells, and circVAPA depletion notably reinforced this effect in the system (Figure 3D). Together, these findings suggested that circVAPA contributes to chemotherapy drug resistance of GC cells.

CircVAPA is able to sponge miR-125b-5p in gastric cancer cells

Next, we explored the mechanism of circVAPA-mediated GC progression and chemotherapy resistance. The bioinformatic analysis revealed the potential interaction of circVAPA and miR-125b-5p (Figure 4A). The SGC7901 and HGC27 cells were treated with miR-125b-5p mimic and the enhancement of miR-125b-5p was confirmed in the cells (Figure 4B). Treatment with miR-125b-5p mimic was able to decrease luciferase activities of wild type circVAPA, but not circVAPA mutant in the cells (Figure 4C and D). Moreover, the expression of miR-125b-5p was up-regulated by circVAPA shRNA in the SGC7901 and HGC27 cells. These findings indicated that circVAPA spongs miR-125b-5p in the GC cells (Figure 4E and F).

MiR-125b-5p targets STAT3 in GC cells

Furthermore, we identified the binding site of miR-125b-5p within the 3′ untranslated region of the *STAT3* gene through bioinformatic analysis (Figure 5A). Treatment with miR-125b-5p mimic repressed luciferase activities of STAT3, but not STAT3 mutant in the SGC7901 and HGC27 cells (Figure 5B). Consistently, the mRNA and protein levels of STAT3 were inhibited by the miR-125b-5p mimic in the cells (Figure 5C and D). Moreover, circVAPA knockdown down-regulated STAT3 in the SGC7901 and HGC27 cells, while miR-125b-5p inhibitor was able to reverse this effect in the cells (Figure 5E).

CircVAPA promotes chemotherapy drug resistance of GC cells by modulating miR-125b-5p/STAT3 axis

We then investigated whether circVAPA mediates chemotherapy drug resistance of GC cells by modulating the miR-125b-5p/STAT3 axis. Significantly, depletion of circVAPA enhanced the inhibitory effect of DDP on SGC7901 and HGC27 cell viability, while miR-125b-5p inhibitor rescued this phenotype in the cells (Figure 6A and B). In addition, overexpression of circVAPA promoted the proliferation of DDP-

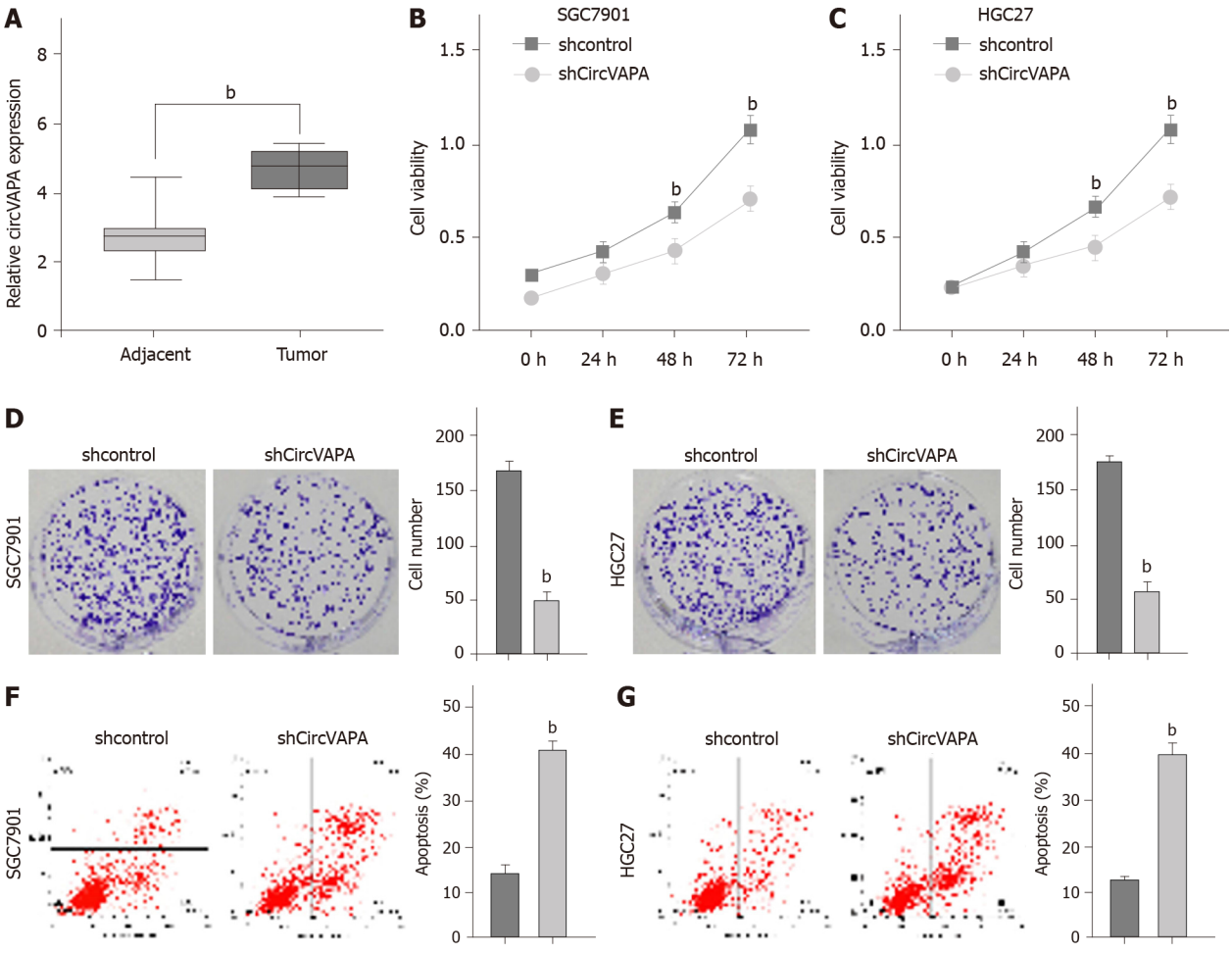


Figure 1 CircVAPA enhances proliferation and represses apoptosis of gastric cancer cells. A: The expression of circVAPA was measured by qPCR in the gastric cancer tissues (n = 50) and adjacent normal tissues (n = 50); B-G: SGC7901 and HGC27 cells were treated with the circVAPA shRNA or control shRNA. Cell viability was tested by MTT assay (B and C), cell proliferation was measured by colony formation assay (D and E), and cell apoptosis was analyzed by flow cytometry (F and G). Data are presented as the mean ± SD. $^{b}P < 0.01$.

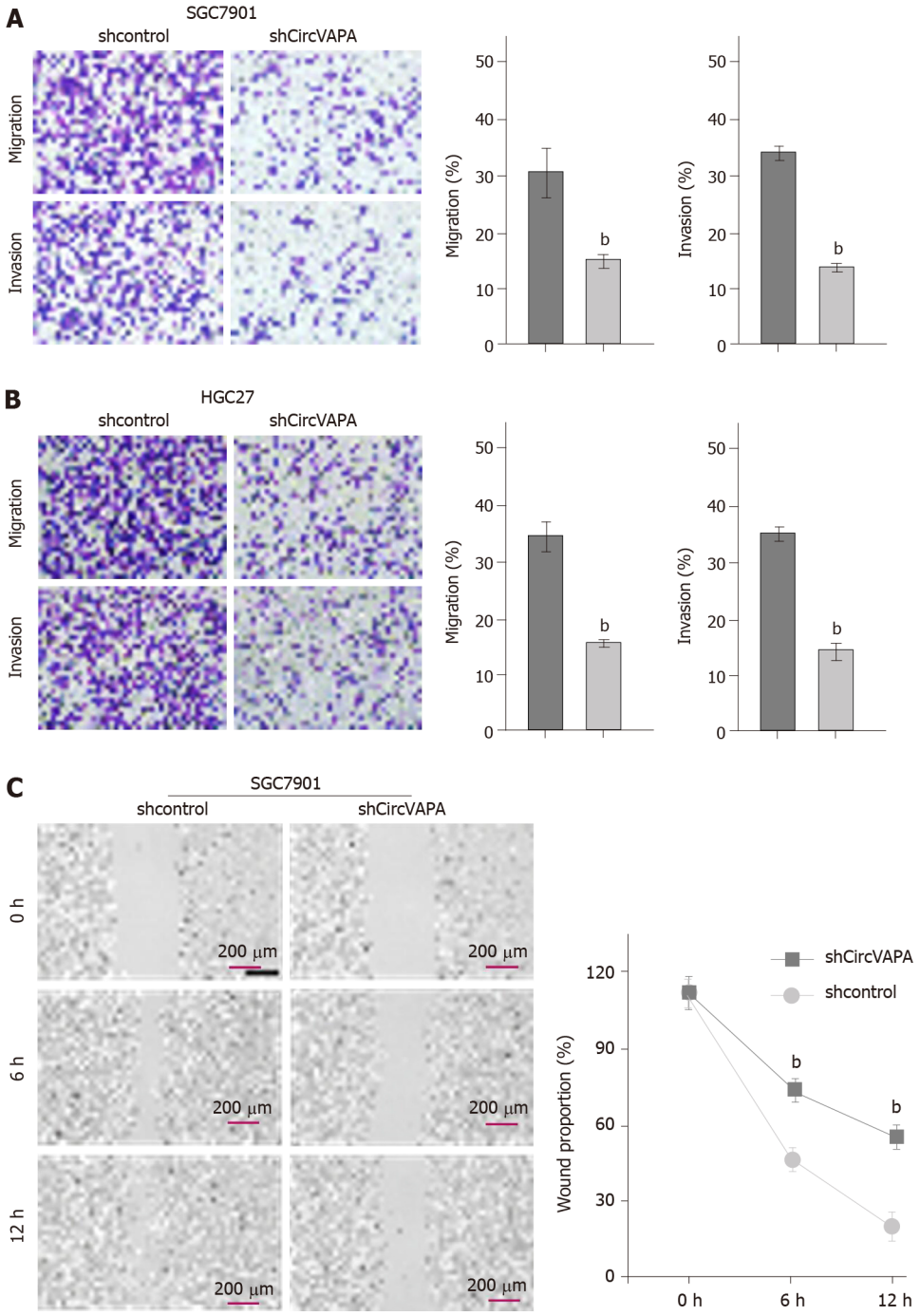
treated SGC7901/DDP cells, while STAT3 siRNA could reduce this effect in the system (Figure 6C). Meanwhile, circVAPA knockdown reinforced DDP-induced apoptosis of SGC7901 and HGC27 cells, whereas miR-125b-5p inhibitor or STAT3 overexpression could reverse this effect (Figure 6D). These results suggested that circVAPA promotes chemotherapy resistance of GC cells by modulating the miR-125b-5p/STAT3 axis (Figure 6E).

CircVAPA promotes the tumor growth of chemoresistant gastric cancer cell in vivo

Next, the circVAPA function in GC cell growth was analyzed by tumorigenicity analysis *in vivo*. The tumor growth of GC cells was inhibited by circVAPA knockdown, as presented by the decreased tumor size, tumor volume, and tumor weight in the nude mice (Figure 7A-C). Meanwhile, we validated that miR-125b-5p expression was up-regulated while STAT3 expression was down-regulated by circVAPA depletion in the tumor tissues (Figure 7D and E). Together, these data indicated that circVAPA contributes to the tumor growth of chemoresistant GC cells *in vivo*.

DISCUSSION

The chemotherapy resistance in GC patients is a severe clinical challenge, and the molecular mechanism is still poorly understood[7]. CircRNAs have been identified to participate in the modulation of GC progression[25]. Nevertheless, the specific functions of circVAPA in the modulation of GC development remain obscure. In the present study, we uncovered that circVAPA contributed to chemotherapy resistance and promoted the malignant progression in GC by modulating miR-125b-5p/STAT3


A
SGC7901
shcontrol
shCircVAPA
Migration
Invasion
Migration (%)
Invasion (%)
b
B
HGC27
shcontrol
shCircVAPA
Migration
Invasion
Migration (%)
Invasion (%)
b
C
SGC7901
shcontrol
shCircVAPA
0 h
6 h
12 h
200 μm
Wound proportion (%)
shCircVAPA
shcontrol
b
0 h
6 h
12 h

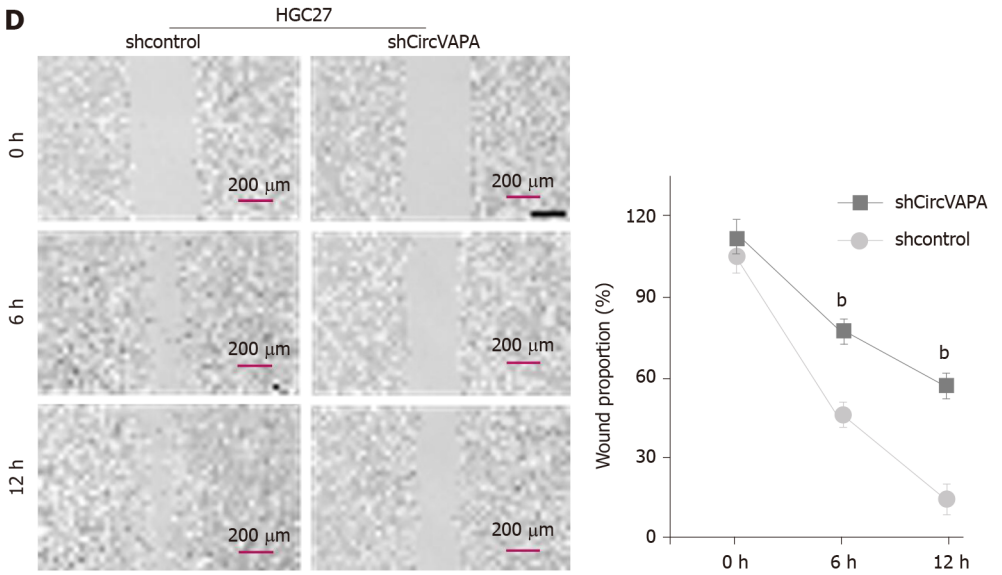


Figure 2 CircVAPA promotes invasion and migration of gastric cancer cells. A-D: SGC7901 and HGC27 cells were treated with the circVAPA shRNA or control shRNA. Cell migration and invasion were tested by transwell assay (A and B), and migration and invasion were analyzed by wound healing assay (C and D). The wound healing proportion is shown. Data are presented as the mean ± SD. $^{b}P < 0.01$.

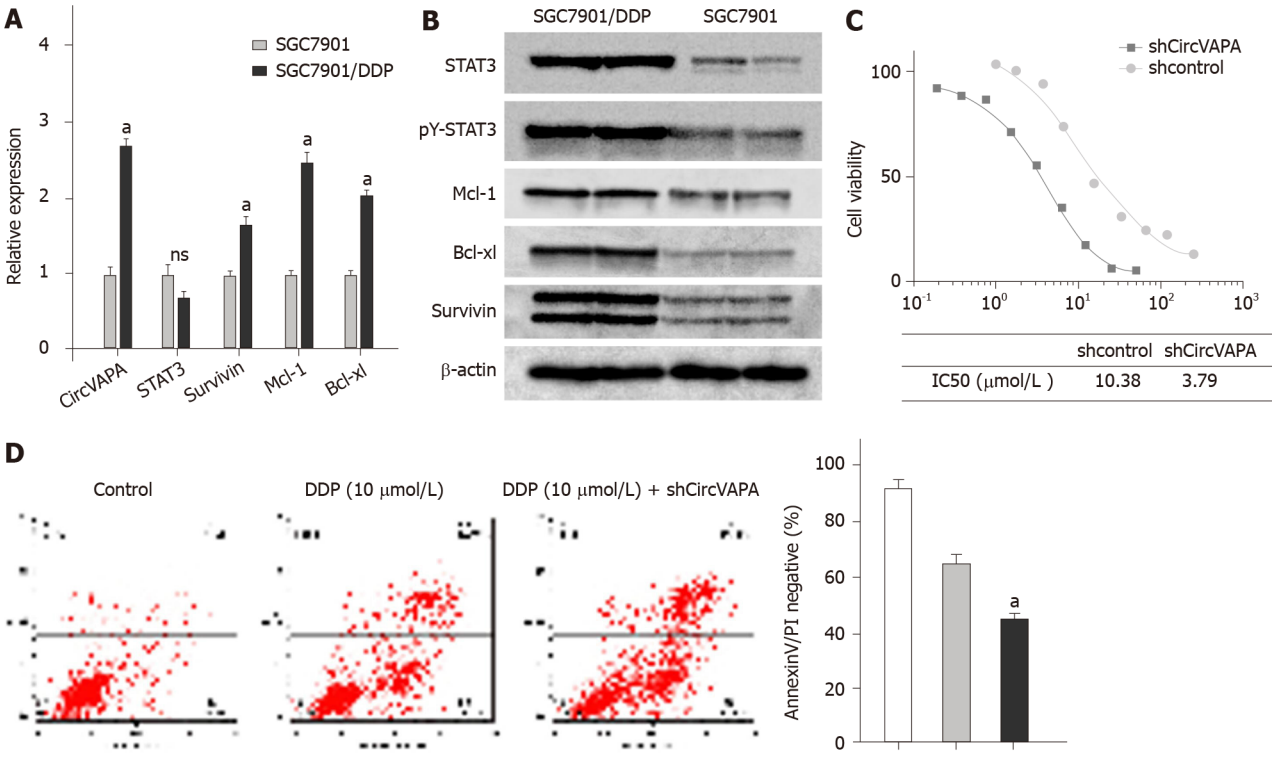


Figure 3 Elevation of CircVAPA enhances chemotherapy drug resistance of gastric cancer cells. A: The expression of circVAPA, STAT3, Survivin, Mcl-1, and Bcl-xl was measured by qPCR in the SGC7901 and SGC7901/cisplatin (DDP) cells; B: STAT3 phosphorylation and levels of STAT3, Survivin, Mcl-1, and Bcl-xl were tested by Western blot analysis; C: SGC7901/DDP cells were initially treated with DDP at indicated doses and then with control shRNA or circVAPA shRNA. Cell viability was analyzed by MTT assay; D: SGC7901/DDP cells were treated with DDP or co-treated with DDP and circVAPA shRNA. Cell apoptosis was analyzed by flow cytometry. Data are presented as the mean ± SD. $^{a}P < 0.05$.

signaling.

As a critical cancer regulator, several circRNAs have been identified in the modulation of chemotherapy resistance during GC progression. It has been reported that circ-PVT1 promotes paclitaxel resistance by regulating miR-124-3p/ZEB1 in GC cells[26]. Circ0026359 increases the DDP resistance of GC cells by modulating the miR-1200/POLD4 axis[27]. CircAKT3 promotes DDP resistance by up-regulating PIK3R1

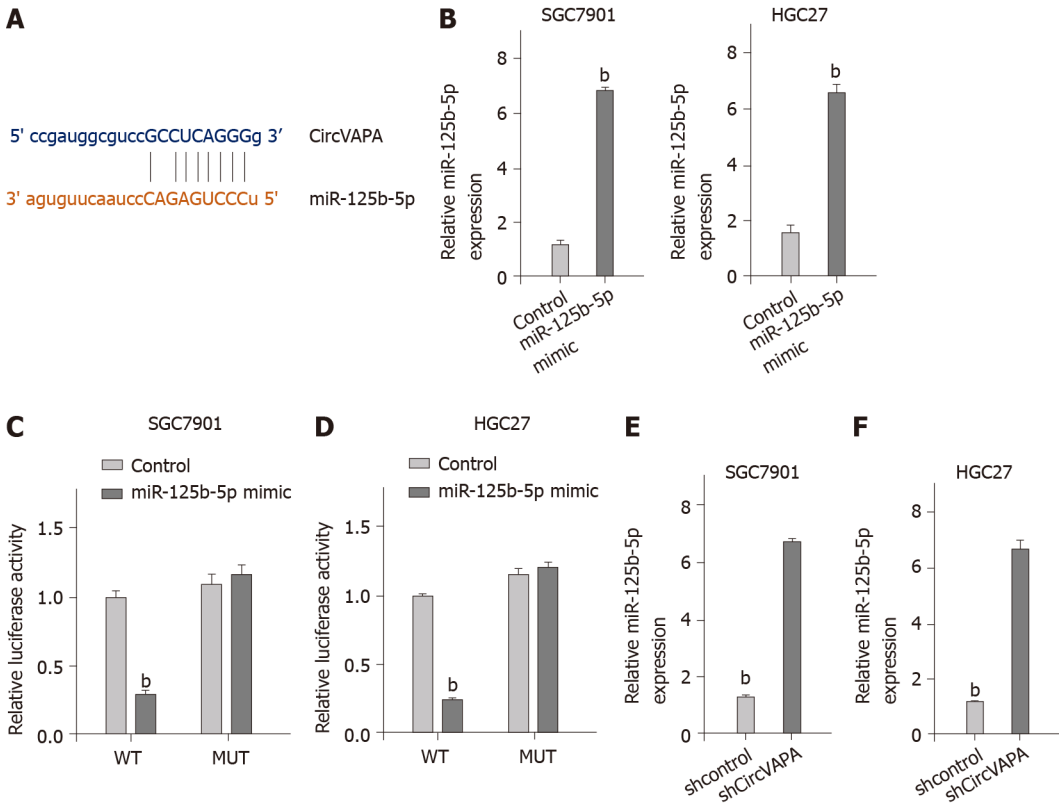


Figure 4 CircVAPA is able to sponge miR-125b-5p in gastric cancer cells. A: The interaction of CircVAPA and miR-125b-5p was analyzed by bioinformatic analysis based on ENCORI (http://starbase.sysu.edu.cn/index.php); B-D: SGC7901 and HGC27 cells were treated with control mimic or miR-125b-5p mimic. The expression levels of miR-125b-5p were tested by qPCR in the cells (B), and luciferase activities of wild type CircVAPA and CircVAPA with the miR-125b-5p-binding site mutant were examined by luciferase reporter gene assay (C and D); E and F: SGC7901 and HGC27 cells were treated with the circVAPA shRNA or control shRNA. The expression of miR-125b-5p was analyzed by qPCR assay. Data are presented as the mean ± SD. $^{b}P < 0.01$. MUT: Mutant; WT: Wild type.

through targeting miR-198 in GC cells[28]. CircFN1 contributes to DDP resistance of GC cells by targeting miR-182-5p[29]. CircMCTP2 attenuates DDP resistance by miR-99a-5p/MTMR3 signaling in GC cells[30]. Moreover, circVAPA presents oncogenic properties in cancers, including liver cancer and colorectal cancer[13,31]. In this study, circVAPA expression was elevated in the clinical GC samples. CircVAPA depletion inhibited proliferation, migration, and invasion, and increased apoptosis of GC cells. CircVAPA knockdown reduced tumor growth of GC cells *in vivo*. CircVAPA contributed to chemotherapy drug resistance of GC cells. These findings present a novel function of circVAPA in modulating chemotherapy drug resistance and malignant progression of GC cells, indicating valuable evidence of circRNA function in GC development.

MiRNAs are the essential contributor for regulating chemotherapy drug resistance of GC cells. It has been reported that miR-625 inhibits chemotherapy resistance by regulating ALDH1A1 in GC cells[32]. MiR-21-5p regulates doxorubicin resistance of GC cells *via* modulating TIMP3 and PTEN expression[33]. MiR-187 affects DDP resistance by targeting transforming growth factor-β signaling in GC cells[34]. Moreover, constitutive activation of STAT3 contributes to chemotherapy resistance of GC cells[35]. STAT3 signaling is involved in fibroblasts-mediated chemoresistance of GC cells[36]. Suppression of STAT3 inhibits drug resistance of GC cells to chemotherapeutic drugs[37]. In the mechanistic study, we found that circVAPA sponged miR-125b-5p and miR-125b-5p targeted STAT3 in the GC cells. MiR-125b-5p inhibitor rescued circVAPA depletion-enhanced inhibitory effect of DDP on GC cells, and STAT3 knockdown blocked circVAPA overexpression-induced proliferation of DDP-treated SGC7901/DDP cells. Depletion of STAT3 and miR-125b-5p inhibitor reversed circVAPA depletion-induced GC cell apoptosis. These data demonstrate an unreported regulation axis associated circVAPA with STAT3 and miR-125b-5p, revealing a new mechanism involving the circVAPA/miR-125b-5p/STAT3 axis in GC development.

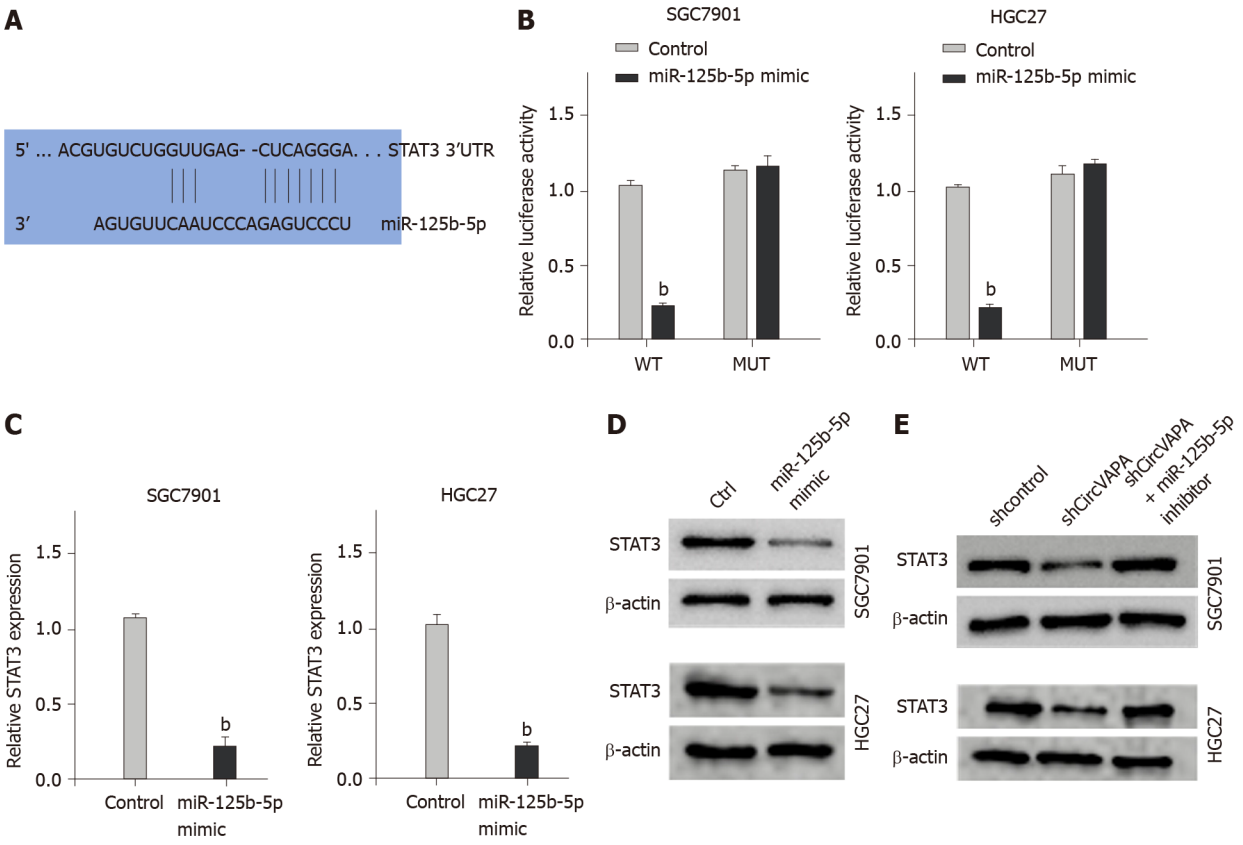


Figure 5 MiR-125b-5p targets STAT3 in gastric cancer cells. A: The binding of miR-125b-5p and the 3' untranslated region of *STAT3* was identified by bioinformatic analysis based on Targetscan (http://www.targetscan.org/vert_72/); B-D: SGC7901 and HGC27 cells were treated with control mimic or miR-125b-5p mimic. The luciferase activities of wild type STAT3 and STAT3 with the miR-125b-5p-binding site mutant were examined by luciferase reporter gene assay (B), the mRNA expression of STAT3 was analyzed by qPCR assay (C), and the protein expression of STAT3 was determined by Western blot analysis (D); E: SGC7901 and HGC27 cells were treated with control shRNA or circVAPA shRNA, or co-treated with circVAPA shRNA and miR-125b-5p inhibitor. The protein expression of STAT3 was tested by Western blot analysis. Data are presented as the mean ± SD. $^{b}P < 0.01$. MUT: Mutant; WT: Wild type.

CONCLUSION

CircVAPA promotes chemotherapy resistance and the malignant progression in GC by modulating miR-125b-5p/STAT3 signaling. Our findings present novel insights into the mechanism by which circVAPA regulates chemotherapy resistance of GC cells. CircVAPA and miR-125b-5p may be considered as potential targets for GC therapy.

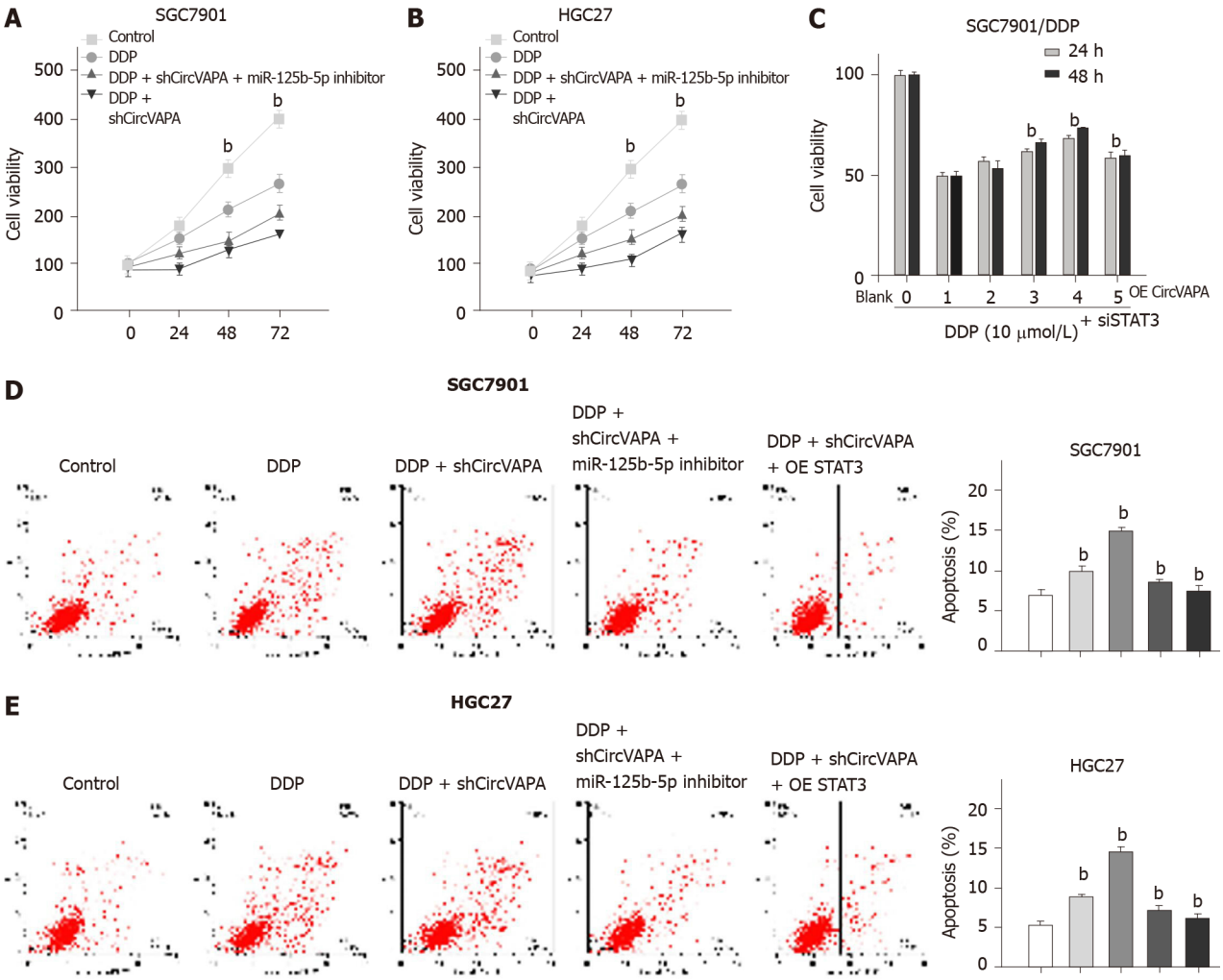


Figure 6 CircVAPA promotes chemotherapy drug resistance of gastric cancer cells by modulating miR-125b-5p/STAT3 axis. A and B: SGC7901 and HGC27 cells were treated with cisplatin (DDP), DDP, and circVAPA shRNA, or co-treated with DDP, circVAPA shRNA, and miR-125b-5p inhibitor. Cell viability was measured by MTT assay; C: SGC7901/DDP cells were treated with DDP or co-treated with DDP and pcDNA3.1-circVAPA at the indicated dose, or co-treated with DDP, pcDNA3.1-circVAPA, and STAT3 siRNA. Cell viability was measured by MTT assay; D and E: SGC7901 and HGC27 cells were treated with DDP, DDP, and circVAPA shRNA, or co-treated with DDP, circVAPA shRNA, and miR-125b-5p inhibitor or pcDNA3.1-STAT3. Cell apoptosis was analyzed by flow cytometry. Data are presented as the mean ± SD. $^{b}P < 0.01$. DDP: Cisplatin.

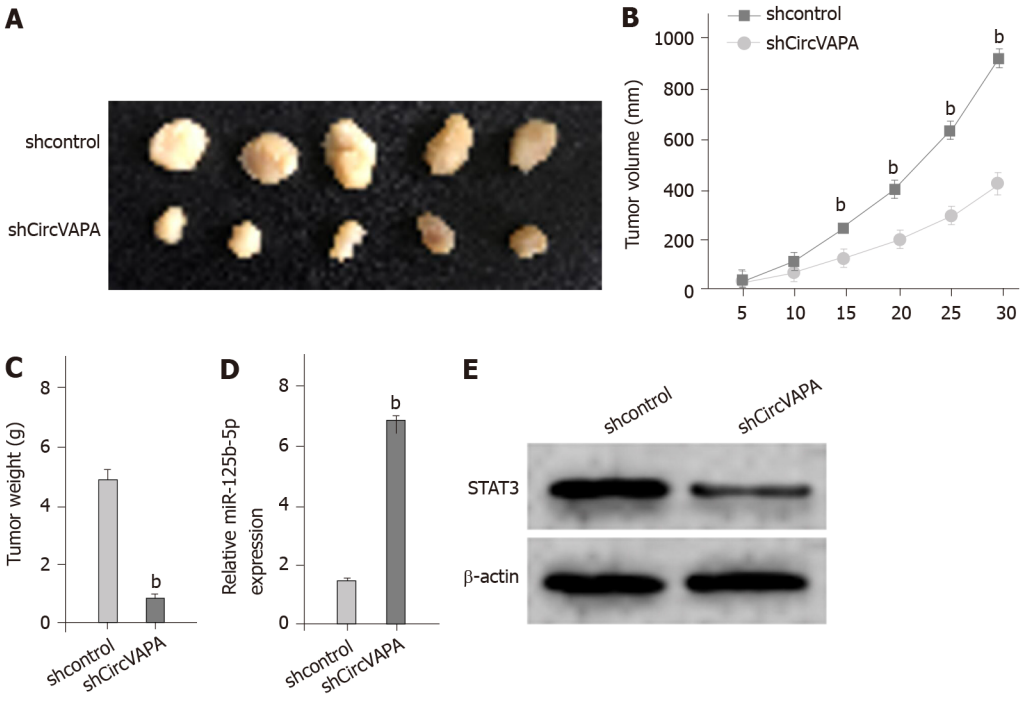


Figure 7 CircVAPA promotes tumor growth of chemoresistant gastric cancer cells *in vivo*. A-D: The impact of circVAPA on tumor growth of melanoma cells *in vivo* was analyzed by nude mice tumorigenicity assay (n = 5). SGC7901/cisplatin cells were treated with control shRNA or circVAPA shRNA. Representative images of dissected tumors from nude mice are shown (A). The average tumor volume (B) and weight (C) were calculated and presented. The expression of miR-125b-5p was measured by qPCR in the tumor tissues of the mice (D); E: The expression of STAT3 was tested by Western blot analysis in the tumor tissues of the mice. Data are presented as the mean ± SD. $^{b}P < 0.01$.

ARTICLE HIGHLIGHTS

Research background

Gastric cancer (GC) is a common malignant tumor and causes a high incidence of cancer-associated death. Cisplatin (DDP)-based chemotherapy is the main therapy for clinical GC treatment, but the mechanism of chemotherapy resistance is still poorly understood, which is a severe clinical challenge. CircRNAs have been identified to play a vital role in regulating the chemoresistance of gastric cancer cells. The development process of GC chemotherapy resistance is not well-understood. In addition, it is well known that circRNAs and miRNAs are involved in chemotherapy resistance of GC cells. However, the role of circVAPA and miR-125b-5p in regulating the chemotherapy resistance of GC cells has not been reported yet.

Research motivation

To investigate the impact of circVAPA on chemotherapy resistance during the progression of GC.

Research objectives

We collected the clinical GC tissue samples (n = 50) and the adjacent normal tissues (n = 50) and analyzed the effect of circVAPA on GC progression and chemotherapy resistance.

Research methods

The role of circVAPA in chemotherapy resistance and GC progression was analyzed by transwell assay, MTT assay, colony formation assay, healing assay, and wound flow cytometry analysis in GC cells and DDP resistant GC cell lines, and *in vivo* tumorigenicity analysis in nude mice. The mechanism was investigated by quantitative real-time PCR, luciferase reporter assay, and Western blot analysis.

Research results

CircVAPA depletion inhibited proliferation, migration, and invasion and increased apoptosis of GC cells. CircVAPA knockdown reduced tumor growth of GC cells *in vivo*. CircVAPA promoted the chemotherapy resistance of GC cells. We found that

circVAPA targeted miR-125b-5p and miR-125b-5p to STAT3 in GC cells. MiR-125b-5p inhibitor rescued the depletion of circVAPA and enhanced the inhibitory effect of DDP on GC cells, while STAT3 knockdown prevented the proliferation of DDP-treated SGC7901/DDP cells induced by circVAPA overexpression. Depletion of STAT3 and miR-125b-5p inhibitor reversed circVAPA depletion-induced GC cell apoptosis.

Research conclusions

CircVAPA promotes chemotherapy resistance and the malignant progression of GC cells by modulating miR-125b-5p/STAT3 signaling. CircVAPA and miR-125b-5p may be considered as potential targets for GC therapy.

Research perspectives

CircRNA circVAPA promotes chemotherapy drug resistance in the progression of gastric cancer by regulating the miR-125b-5p/STAT3 axis.

REFERENCES

1 **Marin JJ**, Al-Abdulla R, Lozano E, Briz O, Bujanda L, Banales JM, Macias RI. Mechanisms of Resistance to Chemotherapy in Gastric Cancer. *Anticancer Agents Med Chem* 2016; **16**: 318-334 [PMID: 26234359 DOI: 10.2174/1871520615666150803125121]

2 **Ham IH**, Oh HJ, Jin H, Bae CA, Jeon SM, Choi KS, Son SY, Han SU, Brekken RA, Lee D, Hur H. Targeting interleukin-6 as a strategy to overcome stroma-induced resistance to chemotherapy in gastric cancer. *Mol Cancer* 2019; **18**: 68 [PMID: 30927911 DOI: 10.1186/s12943-019-0972-8]

3 **Zhai J**, Shen J, Xie G, Wu J, He M, Gao L, Zhang Y, Yao X, Shen L. Cancer-associated fibroblasts-derived IL-8 mediates resistance to cisplatin in human gastric cancer. *Cancer Lett* 2019; **454**: 37-43 [PMID: 30978440 DOI: 10.1016/j.canlet.2019.04.002]

4 **Zheng P**, Chen L, Yuan X, Luo Q, Liu Y, Xie G, Ma Y, Shen L. Exosomal transfer of tumor-associated macrophage-derived miR-21 confers cisplatin resistance in gastric cancer cells. *J Exp Clin Cancer Res* 2017; **36**: 53 [PMID: 28407783 DOI: 10.1186/s13046-017-0528-y]

5 **Guo W**, Deng L, Chen Z, Chen Z, Yu J, Liu H, Li T, Lin T, Chen H, Zhao M, Zhang L, Li G, Hu Y. Vitamin B12-conjugated sericin micelles for targeting CD320-overexpressed gastric cancer and reversing drug resistance. *Nanomedicine (Lond)* 2019; **14**: 353-370 [PMID: 30328369 DOI: 10.2217/nnm-2018-0321]

6 **Xu Z**, Chen L, Xiao Z, Zhu Y, Jiang H, Jin Y, Gu C, Wu Y, Wang L, Zhang W, Zuo J, Zhou D, Luan J, Shen J. Potentiation of the anticancer effect of doxorubicinin drug-resistant gastric cancer cells by tanshinone IIA. *Phytomedicine* 2018; **51**: 58-67 [PMID: 30466628 DOI: 10.1016/j.phymed.2018.05.012]

7 **Min A**, Kim JE, Kim YJ, Lim JM, Kim S, Kim JW, Lee KH, Kim TY, Oh DY, Bang YJ, Im SA. Cyclin E overexpression confers resistance to the CDK4/6 specific inhibitor palbociclib in gastric cancer cells. *Cancer Lett* 2018; **430**: 123-132 [PMID: 29729292 DOI: 10.1016/j.canlet.2018.04.037]

8 **Yuan L**, Xu ZY, Ruan SM, Mo S, Qin JJ, Cheng XD. Long non-coding RNAs towards precision medicine in gastric cancer: early diagnosis, treatment, and drug resistance. *Mol Cancer* 2020; **19**: 96 [PMID: 32460771 DOI: 10.1186/s12943-020-01219-0]

9 **Kristensen LS**, Hansen TB, Venø MT, Kjems J. Circular RNAs in cancer: opportunities and challenges in the field. *Oncogene* 2018; **37**: 555-565 [PMID: 28991235 DOI: 10.1038/onc.2017.361]

10 **He J**, Xie Q, Xu H, Li J, Li Y. Circular RNAs and cancer. *Cancer Lett* 2017; **396**: 138-144 [PMID: 28342987 DOI: 10.1016/j.canlet.2017.03.027]

11 **Wang Y**, Mo Y, Gong Z, Yang X, Yang M, Zhang S, Xiong F, Xiang B, Zhou M, Liao Q, Zhang W, Li X, Li X, Li Y, Li G, Zeng Z, Xiong W. Circular RNAs in human cancer. *Mol Cancer* 2017; **16**: 25 [PMID: 28143578 DOI: 10.1186/s12943-017-0598-7]

12 **Zhou SY**, Chen W, Yang SJ, Li J, Zhang JY, Zhang HD, Zhong SL, Tang JH. Circular RNA circVAPA regulates breast cancer cell migration and invasion *via* sponging miR-130a-5p. *Epigenomics* 2020; **12**: 303-317 [PMID: 31920104 DOI: 10.2217/epi-2019-0124]

13 **Liu C**, Zhong X, Li J, Xu F. Circular RNA circVAPA Promotes Cell Proliferation in Hepatocellular Carcinoma. *Hum Gene Ther Clin Dev* 2019; **30**: 152-159 [PMID: 31368365 DOI: 10.1089/humc.2019.079]

14 **Esquela-Kerscher A**, Slack FJ. Oncomirs - microRNAs with a role in cancer. *Nat Rev Cancer* 2006; **6**: 259-269 [PMID: 16557279 DOI: 10.1038/nrc1840]

15 **Di Leva G**, Garofalo M, Croce CM. MicroRNAs in cancer. *Annu Rev Pathol* 2014; **9**: 287-314 [PMID: 24079833 DOI: 10.1146/annurev-pathol-012513-104715]

16 **Liu S**, Chen Q, Wang Y. MiR-125b-5p suppresses the bladder cancer progression *via* targeting HK2 and suppressing PI3K/AKT pathway. *Hum Cell* 2020; **33**: 185-194 [PMID: 31605287 DOI: 10.1007/s13577-019-00285-x]

17 **Hui L**, Zhang J, Guo X. MiR-125b-5p suppressed the glycolysis of laryngeal squamous cell carcinoma by down-regulating hexokinase-2. *Biomed Pharmacother* 2018; **103**: 1194-1201 [PMID: 29864898 DOI: 10.1016/j.biopha.2018.04.098]

18 **Shi H**, Li K, Feng J, Liu G, Feng Y, Zhang X. LncRNA-DANCR Interferes With miR-125b-5p/HK2 Axis to Desensitize Colon Cancer Cells to Cisplatin vis Activating Anaerobic Glycolysis. *Front Oncol* 2020; **10**: 1034 [PMID: 32766131 DOI: 10.3389/fonc.2020.01034]

19 **Yang W**, Ma J, Zhou W, Cao B, Zhou X, Yang Z, Zhang H, Zhao Q, Fan D, Hong L. Molecular mechanisms and theranostic potential of miRNAs in drug resistance of gastric cancer. *Expert Opin Ther Targets* 2017; **21**: 1063-1075 [PMID: 28994330 DOI: 10.1080/14728222.2017.1389900]

20 **Dehghanzadeh R**, Jadidi-Niaragh F, Gharibi T, Yousefi M. MicroRNA-induced drug resistance in gastric cancer. *Biomed Pharmacother* 2015; **74**: 191-199 [PMID: 26349984 DOI: 10.1016/j.biopha.2015.08.009]

21 **Wei L**, Sun J, Zhang N, Zheng Y, Wang X, Lv L, Liu J, Xu Y, Shen Y, Yang M. Noncoding RNAs in gastric cancer: implications for drug resistance. *Mol Cancer* 2020; **19**: 62 [PMID: 32192494 DOI: 10.1186/s12943-020-01185-7]

22 **Deng J**, Liu Y, Lee H, Herrmann A, Zhang W, Zhang C, Shen S, Priceman SJ, Kujawski M, Pal SK, Raubitschek A, Hoon DS, Forman S, Figlin RA, Liu J, Jove R, Yu H. S1PR1-STAT3 signaling is crucial for myeloid cell colonization at future metastatic sites. *Cancer Cell* 2012; **21**: 642-654 [PMID: 22624714 DOI: 10.1016/j.ccr.2012.03.039]

23 **Levy DE**, Lee CK. What does Stat3 do? *J Clin Invest* 2002; **109**: 1143-1148 [PMID: 11994402 DOI: 10.1172/JCI15650]

24 **Lee HJ**, Zhuang G, Cao Y, Du P, Kim HJ, Settleman J. Drug resistance *via* feedback activation of Stat3 in oncogene-addicted cancer cells. *Cancer Cell* 2014; **26**: 207-221 [PMID: 25065853 DOI: 10.1016/j.ccr.2014.05.019]

25 **Shan C**, Zhang Y, Hao X, Gao J, Chen X, Wang K. Biogenesis, functions and clinical significance of circRNAs in gastric cancer. *Mol Cancer* 2019; **18**: 136 [PMID: 31519189 DOI: 10.1186/s12943-019-1069-0]

26 **Liu YY**, Zhang LY, Du WZ. Circular RNA circ-PVT1 contributes to paclitaxel resistance of gastric cancer cells through the regulation of ZEB1 expression by sponging miR-124-3p. *Biosci Rep* 2019; **39** [PMID: 31793989 DOI: 10.1042/BSR20193045]

27 **Zhang Z**, Yu X, Zhou B, Zhang J, Chang J. Circular RNA circ_0026359 Enhances Cisplatin Resistance in Gastric Cancer *via* Targeting miR-1200/POLD4 Pathway. *Biomed Res Int* 2020; **2020**: 5103272 [PMID: 32855967 DOI: 10.1155/2020/5103272]

28 **Huang X**, Li Z, Zhang Q, Wang W, Li B, Wang L, Xu Z, Zeng A, Zhang X, Zhang X, He Z, Li Q, Sun G, Wang S, Li Q, Wang L, Zhang L, Xu H, Xu Z. Circular RNA AKT3 upregulates PIK3R1 to enhance cisplatin resistance in gastric cancer *via* miR-198 suppression. *Mol Cancer* 2019; **18**: 71 [PMID: 30927924 DOI: 10.1186/s12943-019-0969-3]

29 **Huang XX**, Zhang Q, Hu H, Jin Y, Zeng AL, Xia YB, Xu L. A novel circular RNA circFN1 enhances cisplatin resistance in gastric cancer *via* sponging miR-182-5p. *J Cell Biochem* 2020 [PMID: 31898357 DOI: 10.1002/jcb.29641]

30 **Sun G**, Li Z, He Z, Wang W, Wang S, Zhang X, Cao J, Xu P, Wang H, Huang X, Xia Y, Lv J, Xuan Z, Jiang T, Fang L, Yang J, Zhang D, Xu H, Xu Z. Circular RNA MCTP2 inhibits cisplatin resistance in gastric cancer by miR-99a-5p-mediated induction of MTMR3 expression. *J Exp Clin Cancer Res* 2020; **39**: 246 [PMID: 33198772 DOI: 10.1186/s13046-020-01758-w]

31 **Li XN**, Wang ZJ, Ye CX, Zhao BC, Huang XX, Yang L. Circular RNA circVAPA is up-regulated and exerts oncogenic properties by sponging miR-101 in colorectal cancer. *Biomed Pharmacother* 2019; **112**: 108611 [PMID: 30797148 DOI: 10.1016/j.biopha.2019.108611]

32 **Gong X**, Xu B, Zi L, Chen X. miR-625 reverses multidrug resistance in gastric cancer cells by directly targeting ALDH1A1. *Cancer Manag Res* 2019; **11**: 6615-6624 [PMID: 31410057 DOI: 10.2147/CMAR.S208708]

33 **Chen J**, Zhou C, Li J, Xiang X, Zhang L, Deng J, Xiong J. miR215p confers doxorubicin resistance in gastric cancer cells by targeting PTEN and TIMP3. *Int J Mol Med* 2018; **41**: 1855-1866 [PMID: 29393355 DOI: 10.3892/ijmm.2018.3405]

34 **Zhu QL**, Li Z, Lv CM, Wang W. MiR-187 influences cisplatin-resistance of gastric cancer cells through regulating the TGF-β/Smad signaling pathway. *Eur Rev Med Pharmacol Sci* 2019; **23**: 9907-9914 [PMID: 31799659 DOI: 10.26355/eurrev_201911_19556]

35 **Song S**, Min H, Niu M, Wang L, Wu Y, Zhang B, Chen X, Liang Q, Wen Y, Wang Y, Yi L, Wang H, Gao Q. S1PR1 predicts patient survival and promotes chemotherapy drug resistance in gastric cancer cells through STAT3 constitutive activation. *EBioMedicine* 2018; **37**: 168-176 [PMID: 30316864 DOI: 10.1016/j.ebiom.2018.10.005]

36 **Ma J**, Song X, Xu X, Mou Y. Cancer-Associated Fibroblasts Promote the Chemo-resistance in Gastric Cancer through Secreting IL-11 Targeting JAK/STAT3/Bcl2 Pathway. *Cancer Res Treat* 2019; **51**: 194-210 [PMID: 29690750 DOI: 10.4143/crt.2018.031]

37 **Huang S**, Chen M, Shen Y, Shen W, Guo H, Gao Q, Zou X. Inhibition of activated Stat3 reverses drug resistance to chemotherapeutic agents in gastric cancer cells. *Cancer Lett* 2012; **315**: 198-205 [PMID: 22104727 DOI: 10.1016/j.canlet.2011.10.011]

World Journal of Gastroenterology

Submit a Manuscript: https://www.f6publishing.com

World J Gastroenterol 2021 February 14; 27(6): 501-512

DOI: 10.3748/wjg.v27.i6.501

ISSN 1007-9327 (print) ISSN 2219-2840 (online)

ORIGINAL ARTICLE

Retrospective Cohort Study

Validation of serum tumor biomarkers in predicting advanced cystic mucinous neoplasm of the pancreas

Li-Qi Sun, Li-Si Peng, Jie-Fang Guo, Fei Jiang, Fang Cui, Hao-Jie Huang, Zhen-Dong Jin

ORCID number: Li-Qi Sun 0000-0002-1151-3931; Li-Si Peng 0000-0002-8891-782X; Jie-Fang Guo 0000-0002-7005-2880; Fei Jiang 0000-0001-7620-6185; Fang Cui 0000-0002-7395-8442; Hao-Jie Huang 0000-0002-3100-5301; Zhen-Dong Jin 0000-0002-9358-7351.

Author contributions: Sun LQ, Peng LS, and Guo JF contributed equally to this study and should be regarded as co-first authors; Sun LQ, Peng LS, and Guo JF were responsible for study design/planning, study conduct, data analysis, and writing and revising the paper; Jiang F and Cui F assisted with data collection and analysis; Jin ZD and Huang HJ designed the study and they shared co-corresponding authorship; all authors have read and approved the final manuscript.

Supported by National Natural Science Foundation of China, No. 81770642; the Shanghai Association for Science and Technology, China, No. 19411951602.

Institutional review board statement: The study was reviewed and approved by the Shanghai Changhai Hospital Ethics Committee (CHEC No. 2019-081).

Conflict-of-interest statement: The authors declare no conflicts of

Li-Qi Sun, Li-Si Peng, Jie-Fang Guo, Fei Jiang, Fang Cui, Hao-Jie Huang, Zhen-Dong Jin, Department of Gastroenterology, Changhai Hospital, Second Military Medical University, Shanghai 200433, China

Corresponding author: Zhen-Dong Jin, MD, PhD, Director, Professor, Department of Gastroenterology, Changhai Hospital, Second Military Medical University, No. 168 Changhai Road, Yangpu District, Shanghai 200433, China. zhendongjin@163.com

Abstract

BACKGROUND

Early detection of advanced cystic mucinous neoplasms [(A-cMNs), defined as high-grade dysplasia or malignancy] of the pancreas is of great significance. As a simple and feasible detection method, serum tumor markers (STMs) may be used to predict advanced intraductal papillary mucinous neoplasms (IPMNs) and mucinous cystic neoplasms (MCNs). However, there are few studies on the usefulness of STMs other than carbohydrate antigen (CA) 19-9 for early detection of A-cMNs.

AIM

To study the ability of five STMs-CA19-9, carcinoembryonic antigen (CEA), CA125, CA724, and CA242 to predict A-cMNs and distinguish IPMNs and MCNs.

METHODS

We mainly measured the levels of each STM in patients pathologically diagnosed with cMNs. The mean levels of STMs and the number of A-cMN subjects with a higher STM level than the cutoff were compared respectively to identify the ability of STMs to predict A-cMNs and distinguish MCNs from IPMNs. A receiver operating characteristic curve with the area under curve (AUC) was also created to identify the performance of the five STMs.

RESULTS

A total of 187 patients with cMNs were identified and 72 of them showed A-cMNs. We found that CA19-9 exhibited the highest sensitivity (SE) (54.2%) and accuracy (76.5%) and a moderate ability (AUC = 0.766) to predict A-cMNs. In predicting high-grade dysplasia IPMNs, the SE of CA19-9 decreased to 38.5%. The ability of CEA, CA125, and CA724 to predict A-cMNs was low (AUC = 0.651, 0.583, and 0.618, respectively). The predictive ability of CA242 was not identified. The combination of STMs improved the SE to 62.5%. CA125 may be specific to the

interest.

Data sharing statement: No additional data are available.

Open-Access: This article is an open-access article that was selected by an in-house editor and fully peer-reviewed by external reviewers. It is distributed in accordance with the Creative Commons Attribution NonCommercial (CC BY-NC 4.0) license, which permits others to distribute, remix, adapt, build upon this work non-commercially, and license their derivative works on different terms, provided the original work is properly cited and the use is non-commercial. See: http://creativecommons.org/licenses/by-nc/4.0/

Manuscript source: Unsolicited manuscript

Specialty type: Gastroenterology and hepatology

Country/Territory of origin: China

Peer-review report's scientific quality classification

Grade A (Excellent): 0
Grade B (Very good): 0
Grade C (Good): C
Grade D (Fair): 0
Grade E (Poor): 0

Received: December 12, 2020
Peer-review started: December 12, 2020
First decision: December 17, 2020
Revised: December 30, 2020
Accepted: January 12, 2021
Article in press: January 12, 2021
Published online: February 14, 2021

P-Reviewer: Viswanath YK
S-Editor: Zhang L
L-Editor: Wang TQ
P-Editor: Liu JH

diagnosis of advanced MCNs.

CONCLUSION
CA19-9 has a moderate ability, and CEA, CA125, and CA724 have a low ability to predict A-cMNs. The combination of STM testing could improve SE in predicting A-cMNs.

Key Words: Serum tumor markers; Diagnosis; Advanced cystic mucinous neoplasms; Mucinous cystic neoplasms; Intraductal papillary mucinous neoplasms

©The Author(s) 2021. Published by Baishideng Publishing Group Inc. All rights reserved.

Core Tip: The value of serum tumor markers (STMs) in predicting advanced cystic mucinous neoplasms (A-cMNs) has not been well studied except for carbohydrate antigen (CA) 19-9. Our study illustrates for the first time the potential value of multiple STMs in the diagnosis of A-cMNs. CA19-9 was the most accurate STM in predicting A-cMNs with a moderate ability. CEA, CA125, and CA724 showed a low ability to predict A-cMNs. CA125 may be specific to the diagnosis of advanced mucinous cystic neoplasms. CA242 was not identified as a useful STM in predicting A-cMNs in our study. The combination of STMs could improve sensitivity in predicting A-cMNs.

Citation: Sun LQ, Peng LS, Guo JF, Jiang F, Cui F, Huang HJ, Jin ZD. Validation of serum tumor biomarkers in predicting advanced cystic mucinous neoplasm of the pancreas. *World J Gastroenterol* 2021; 27(6): 501-512
URL: https://www.wjgnet.com/1007-9327/full/v27/i6/501.htm
DOI: https://dx.doi.org/10.3748/wjg.v27.i6.501

INTRODUCTION

Pancreatic cystic lesions (PCLs) are being detected more frequently due to advancements in radiological technologies. Their prevalence ranges from 1.9% to 49.1% in different races[1-3]. The primary management goal of PCLs is to correctly identify malignant and invasive PCLs. Serum tumor markers (STMs) may play an adjunct role to imaging features in the evaluation of PCLs.

Cystic mucinous neoplasms (cMNs) of the pancreas, including mucinous cystic neoplasms (MCNs) and intraductal papillary mucinous neoplasms (IPMNs), have the potential to undergo malignant transformation, which is a cause for concern. Early detection of cMNs with high-grade dysplasia or invasive cancer [advanced cMNs (A-cMNs)] is important for improving prognoses.

MCN and IPMN have different biological behaviors and originate from different embryonic layers[4]. Although they may have similar imaging presentations, especially branch duct IPMN and MCN, they are different tumor types. Theoretically, they may also show different specific STMs. However, there is little available data demonstrating the difference.

STM testing is accessible in routine health checkups. It is more suitable as a screening modality than cross-imaging technologies. Several STMs, including carbohydrate antigen (CA) 19-9, carcinoembryonic antigen (CEA), CA125, CA724, and CA242, have been reported to be associated with the presence, metastasis, and recurrence of pancreatic adenocarcinoma[5-9]. However, the value of these STMs for PCLs is not well studied except for CA19-9 and CEA. CA19-9 is considered an independent predictor of malignancy in PCLs by many guidelines[10-12]. The value of CEA is mostly based on evidence of cyst fluid analyses, and it has the ability to distinguish mucinous from non-mucinous PCLs[13]. The sensitivity (SE) of CEA in serum is considered relatively low in predicting advanced IPMNs[14-16]. No previous studies have reported the value of CA125, CA724, or CA242 in predicting A-cMNs.

To evaluate the ability of CA19-9, CEA, CA125, CA724, and CA242 in predicting A-cMNs and whether the STM levels vary in MCNs and IPMNs, we conducted a retrospective cohort study of 187 patients diagnosed with PCLs and assessed their STM levels. Although we have obtained some promising findings, as a retrospective

study with incomplete data, these findings need to be further confirmed by multi-center prospective studies.

MATERIALS AND METHODS

Patients

We conducted a retrospective study at Changhai Hospital affiliated to Second Military Medical University, one of the largest pancreatic disease research centers in Shanghai, China. Patients who underwent surgical resection for an identified pancreatic cyst and whose final pathological outcomes were identified with cMNs were included in our study. A-cMNs were defined as MCNs and IPMNs with high-grade dysplasia or malignancy identified by pathological outcomes. Patient demographics, pathologic data, and STMs were extracted. The Institutional Review Board of Changhai Hospital approved the study.

The decision regarding surgical treatment was made by our multidisciplinary hepato-pancreatobiliary team for the vast majority of patients according to the FG guidelines of 2006 and 2012[17,18]; the decisions for the remaining cases were made according to the patients' own wishes.

Serum tumor marker analyses

Serum CA19-9, CA125, CA724, CA242, and CEA were measured by using electrochemiluminescence immunoassays on a Roche Cobas E601 immunoassay analyzer (Roche Diagnostics, Mannheim, Germany) equipped with dedicated reagents, according to the manufacturer's instructions. All of the assays were carried out at the Department of Laboratory Medicine, Changhai Hospital.

In our center, the cutoff values for STMs were: CA19-9, 37.0 U/mL; CEA, 5.0 ng/mL; CA125, 35.0 U/mL; CA724, 9.8 U/mL; and CA242, 20.0 U/mL. The mean levels of STMs and the number of A-cMN subjects with a higher STM level than the cutoff were compared to identify the ability of STMs to predict A-cMNs. STMs with a significant difference between A-cMNs and non-A-cMNs for both the mean level and number of subjects were considered to have the ability to predict A-cMNs. A receiver operating characteristic curve was created to identify the true ability of these STMs in predicting A-cMNs. STMs with areas under curve (AUCs) higher than 0.9, 0.7-0.9, and lower than 0.7 were considered to have strong, moderate, and low abilities in predicting A-cMNs, respectively. The SE, specificity (SP), and accuracy (AC) were also calculated to measure performance of the five STMs. For combination analysis, if any of these STM levels were elevated (higher than the cutoff level) in one subject, the combination was considered positive.

Statistical analysis

Categorical data were reported as frequencies or percentages. Continuous data are reported as the mean ± SD. Two-tailed Student's *t* tests for continuous variables and chi-square tests for categorical variables were used to identify predictors of A-cMNs. The *Z* test was calculated to determine whether the AUCs are significantly different between STMs. $P < 0.05$ was considered statistically significant. Data were analyzed with IBM Statistic Package for Social Science Statistics version 22.0 (IBM Corp., Armonk, NY, United States).

RESULTS

Patient selection and characteristics

From January 2013 to June 2019, 187 patients were identified with cMNs by surgical resection specimens in our center and were included in our study. Of the 187 patients, 151 (80.7%) had IPMNs, and 36 (19.3%) had MCNs. Of the 151 IPMN subjects, 46 IPMNs with invasive cancer and 13 IPMNs with high-grade dysplasia were identified. Of the 36 MCN subjects, 12 MCNs with invasive cancer and one MCN with high-grade dysplasia (HGD) were identified. In total, 72 advanced-cMNs were included in our study. The mean age of the overall study cohort was 60.2 ± 11.9 years, and males (109, 58.3%) were slightly more predominant than females (78, 41.7%). The median cyst size (interquartile range) of the study cohort was 28.5 mm (19-42 mm). The number of patients with cysts located in the pancreatic head/body/tail/whole pancreas was 111, 31, 30, and 15, respectively (Table 1). Male sex ($P = 0.001$), aging ($P = 0.014$), and large

Table 1 Baseline characteristics and performance of each serum tumor maker in predicting advanced cystic mucinous neoplasms

	Overall	Benign	Advanced	*P* value[1]
Patients characteristics (*n* = 187)				
Male (*n*, %)	109 (58.3)	63 (54.8)	46 (63.9)	0.007
Age (Median, IQR)	62 (54-68)	61 (51-68)	63.5 (56-70)	0.014
Cyst size (Median, IQR, mm)	28.5 (19-42)	24.5 (15-37)	38.5 (28-59.5)	< 0.0001
Location (H/B/T/D)	111/31/30/15	63/20/20/10	48/11/10/5	
CA19-9 (*n* = 187)				
Median, IQR (U/mL)	10.11(4.4-52.9)	7.1(3.4-16.3)	55.5 (9.3-319.3)	< 0.0001
≥ 37/< 37 U/mL	50/137	11/104	39/33	< 0.0001
CEA (*n* = 187)				
Median, IQR (ng/mL)	2.37 (1.54-3.98)	2.23 (1.5-3.3)	3.1 (2.02-5.2)	< 0.0001
≥ 5/< 5 ng/mL	27/160	9/106	18/54	0.001
CA125 (*n* = 135)				
Median, IQR (U/mL)	12.2 (8.2-18.8)	12.1 (7.0-16.8)	12.75 (8.9-23.4)	0.002
≥ 35 /< 35 U/mL	10/125	1/82	9/43	0.002
CA724 (*n* = 116)				
Median, IQR (U/mL)	1.6 (1.025-3.15)	1.44 (1.0-2.66)	2.4 (1.07-6.8)	0.014
≥ 9.8/< 9.8 U /mL	10/106	3/70	7/36	0.05
CA242 (*n* = 31)				
Median, IQR (U/mL)	7.13 (3.6-12.7)	5.35 (2.7-7.9)	11.1 (6.95-31.7)	0.136
≥ 20/< 20 U/mL	6/25	1/15	5/10	0.08

[1]*P* values were based on student's *t* test comparing mean values of each serum tumor maker. cMN: Cystic mucinous neoplasm; IQR: Interquartile range; CEA: carcinoembryonic antigen; CA: Carbohydrate antigen.

cyst size ($P < 0.0001$) were associated with the malignant transformation of MNs.

Performance of each STM in predicting advanced cystic mucinous neoplasms

Receiver operating characteristic curves are demonstrated in Figure 1. The baseline characteristics and performance of each STM, including the overall characteristics and the classification of benign *vs* malignant by surgical pathology, are shown in Table 1. The SE, SP, positive predictive value, negative predictive value, AC, and AUC of each STM and their combination in predicting A-cMNs are presented in Table 2.

Serum CA19-9 tests were available for all 187 subjects. The mean CA19-9 level was 121.3 ± 10.11 U/mL, and CA19-9 ≥ 37 U/mL was observed in 50 subjects, including 39 advanced cases. Serum CEA tests were also available for all 187 subjects. The mean CEA level was 3.46 ± 3.75 ng/mL, and CEA ≥ 5 ng/mL was observed in 27 subjects, including 18 advanced cases. Serum CA125 tests were available for 135 (72.2%) subjects, and the mean level was 17.65 ± 21.56 U/mL. An elevated CA125 level ≥ 35 U/mL was observed in ten subjects, including nine advanced cases. Serum CA724 tests were available for 116 (62%) subjects, and the mean level was 5.46 ± 17.56 U/mL. An elevated CA724 level ≥ 9.8 U/mL was observed in ten subjects, including seven advanced cases. Serum CA242 tests were available for 31 (16.6%) subjects, and the mean level was 32.12 ± 92.2 U/mL. An elevated CA242 Level ≥ 20 U/mL was observed in six subjects, including five advanced cases (Table 1).

CA19-9 (both $P < 0.0001$), CEA ($P < 0.0001$ and 0.001), CA125 (both $P = 0.002$), and CA724 ($P = 0.014$ and 0.05) all had the ability to predict A-cMNs because they showed significant differences in mean levels between the benign and advanced groups and in the number of advanced cases with a higher STM level than the cutoff (Table 1). These STMs had relatively high SP (90.4%, 92.17%, 98.8%, and 95.9%). However, their SE was suboptimal (54.2%, 25%, 17.3%, and 16.3%) (Table 2). Comparing their AUCs, CA19-9

Table 2 Performance of five serum tumor makers in predicting advanced cystic mucinous neoplasms

	SE (95%CI)	SP (95%CI)	PPV (95%CI)	NPV (95%CI)	AC	AUC	*P* value
CA19-9 (%)	54.2 (42.1-65.8)	90.4 (83.2-94.5)	78 (63.6.7-88)	75.9 (67.7-82.6)	76.5	0.766	
CEA (%)	25 (15.9-45.9)	92.17 (85.26-96.13)	66.67 (46-82.8)	66.3 (58.3-73.4)	66.31	0.651	0.04
CA125 (%)	17.3 (8.7-30.8)	98.8 (92.54-99.9)	90 (54.1-99.5)	65.5 (56.5-73.7)	67.4	0.583	0.004
CA724 (%)	16.3 (7.3-31.3)	95.9 (87.7-98.9)	70 (35.4-91.9)	66 (56.1-74.8)	66.4	0.618	0.03
CA242 (%)	31.25 (12.1-58.5)	93.3 (66-99.7)	83.3 (36.5-99.1)	56 (35.3-75)	61.3	0.758	0.81
CA199 ± any one of other STMs	62.5 (50.3-73.4)	83.5 (75.1-89.5)	70.3 (57.4-80.8)	78 (69.5-84.8)	75.4	0.715	0.32

P value: Comparison results of areas under curves for carbohydrate antigen 19-9 and other serum tumor makers in predicting advanced-cystic mucinous neoplasms. SE: Sensitivity; SP: Specificity; PPV: Positive predictive value; NPV: Negative predictive value. AC: Accuracy; AUC: Area under curve; CA: Carbohydrate antigen; STM: Serum tumor maker.

had a significantly better performance (0.766) than CEA (0.651, $P = 0.04$), CA125 (0.583, $P = 0.004$), and CA724 (0.618, $P = 0.03$). CEA, CA125, and CA724 had comparable performances in predicting A-cMNs ($P > 0.05$ for all) (Table 3).

The ability of CA242 to predict A-cMNs was not identified by our study. We found no significantly higher mean level nor any significantly greater number of subjects with a higher STM level than the cutoff in the advanced groups ($P = 0.136$ and 0.08) despite the comparable AUC to CA19-9 (0.758, $P = 0.81$). The combination of STMs increased the SE to 62.5%, but the SP decreased to 83.5%. However, the diagnostic AC remained high (75.4%) (Table 2). The AUC was comparable to that of CA19-9 alone ($P = 0.32$).

Performance of STMs in predicting advanced IPMNs and MCNs

In all 151 IPMN subjects, both CA19-9 and CEA were available. CA125, CA724, and CA242 were available in 109, 96, and 28 subjects, respectively. CA19-9, CEA, and CA724 were identified as having definite abilities in predicting advanced IPMNs (Table 4).

In all 36 MCN subjects, both CA19-9 and CEA were available. CA125, CA724, and CA242 were available in 26, 20, and 3 subjects, respectively. CA19-9, CEA, and CA125 were identified as having definite abilities in predicting advanced MCNs. Moreover, the subjects with advanced MCN were much older than those with non-advanced MCN ($P = 0.005$) (Table 5).

The mean level and elevated number of subjects for CA19-9, CEA, CA724, and CA242 were not significantly different between advanced MCNs and IPMNs. However, the mean CA125 Level in advanced MCNs was 74.4 ± 60.3 U/mL, which was much higher than that in advanced IPMNs (17.3 ± 16.4 U/mL, $P < 0.0001$). CA125 tests were available in 7 of 13 advanced MCNs, and five (71.4%) subjects had elevated CA125 Levels. Meanwhile, CA125 tests were available in 45 of 59 advanced IPMNs, and four (8.9%) subjects had elevated CA125 levels. The number of subjects with elevated CA125 levels in advanced MCNs was also higher than that in IPMNs ($P < 0.0001$) (Table 6). The SE, SP, AC, and AUC of the standard serum CA125 cutoff level (35 U/L) in differentiating advanced MCNs and advanced IPMNs were 71.4%, 91.1%, 88.5%, and 0.779, respectively. Therefore, in addition to the ability to predict A-cMNs, serum CA125 testing may be useful to differentiate advanced MCNs and advanced IPMNs.

Performance of each STM in predicting high-grade dysplasia IPMN

Thirteen cases of IPMN and one case of MCN with high-grade dysplasia were identified in our study. Due to the small number of MCNs with HGD, we only assessed the performance of STMs in predicting IPMN with HGD. CA19-9 and CEA were both available in all 13 HGD IPMNs. The mean levels of CA19-9 and CEA were 182.5 ± 356.5 U/mL and 3.77 ± 2.17 ng/mL for HGD IPMNs, respectively. There were five cases with CA19-9 levels > 37 U/mL and three cases with CEA levels > 5 ng/mL. In addition, seven patients with HGD IPMNs were tested for CA125 (mean level 10.9 ± 2.17 U/mL), five for CA724 (mean level 3.09 ± 2.4 U/mL), and three for CA242 (mean level 172.7 ± 283.5 U/mL). Comparison of levels of the five STMs between benign and HGD IPMN patients showed that only CA19-9 had the ability to predict HGD IPMNs.

Table 3 Receiver operating characteristic curve comparison analyses of each serum tumor marker

ROC curve	ΔAUC[1]	Standard error	*Z* statistic	*P* value
CA19-9 *vs* CEA	0.115	0.038 and 0.042	2.03	0.04
CA19-9 *vs* CA125	0.183	0.038 and 0.051	2.88	0.004
CA19-9 *vs* CA724	0.148	0.038 and 0.058	2.14	0.03
CA19-9 *vs* CA242	0.008	0.038 and 0.090	0.08	0.81
CEA *vs* CA125	0.068	0.042 and 0.051	1.03	0.30
CEA *vs* CA724	0.033	0.042 and 0.058	0.46	0.62
CA125 *vs* CA724	0.035	0.051 and 0.058	0.45	0.63

[1]ΔAUC: The gap between the two areas under the curves. CA: Carbohydrate antigen; CEA: Carcinoembryonic antigen; ROC: Receiver operating characteristic; AUC: Area under curve.

Table 4 Performance of each serum tumor maker in predicting advanced intraductal papillary mucinous neoplasms

	Overall	Benign	Advanced	*P* value[1]
CA19-9 (*n* = 151)				
Median, IQR (U/mL)	9.7 (3.75-46.3)	6.05 (3.1-15.2)	46.3 (9.0-166.4)	< 0.0001
≥ 37/< 37 U/mL	40/111	9/83	31/8	< 0.0001
CEA (*n* = 151)				
Median, IQR (ng/mL)	2.7 (1.85-4.16)	2.46 (1.67-3.44)	3.1 (2.05-5.3)	0.002
≥ 5/< 5 ng/mL	24/127	9/83	15/44	0.01
CA125 (*n* = 109)				
Median, IQR (U/mL)	11.9 (8.0-17.35)	11.65 (6.8-16.6)	12.1 (8.7-18.8)	0.051
≥ 35 /< 35 U/mL	5/104	1/63	4/41	0.182
CA724 (*n* = 96)				
Median, IQR (U/mL)	1.64 (1.04-3.17)	1.44 (1.02-2.7)	2.5 (1.16-6.8)	0.022
≥ 9.8/< 9.8 U /mL	9/87	2/56	7/31	0.035
CA242 (*n* = 28)				
Median, IQR (U/mL)	7.44 (4.1-12.7)	5.7 (3.6-8.23)	9.8 (6.9-20.7)	0.174
≥ 20/< 20 U/mL	5/23	1/12	4/11	0.416

[1]*P* values were based on student's *t* test comparing mean values of each serum tumor maker. CA: Carbohydrate antigen; CEA: Carcinoembryonic antigen; IQR: Interquartile range.

The SE, SP, AC, and AUC values of CA199 for differentiating HGD IPMNs and benign IPMNs were 38.5%, 90.2%, 83.8%, and 0.643, respectively.

DISCUSSION

Due to the absence of reliable standards for distinguishing advanced PCLs from non-advanced PCLs, the clinical management of PCLs remains difficult. PCLs, especially cMNs, have the potential to undergo carcinogenesis, and malignant transformation may take a relatively long time[3]. Therefore, early detection of A-cMNs is key to the management of PCLs. Current guidelines recommend long-term, routine yearly surveillance by magnetic resonance imaging (MRI)/magnetic resonance cholangiopancreatography (MRCP), and/or endoscopic ultrasound (EUS)[10-12]. The benefit of

Table 5 Performance of each serum tumor maker in predicting advanced mucinous cystic neoplasms

	Overall	Benign	Advanced	*P* value[1]
CA19-9 (*n* = 31)				
Median, IQR (U/mL)	14.7 (7.3-108.1)	7.73 (5.63-24.2)	157 (15.7-1100)	0.001
≥ 37/< 37 U/mL	10/26	2/21	8/5	0.003
CEA (*n* = 31)				
Median, IQR (ng/mL)	1.5 (1.05-2.58)	1.5 (1.0-1.87)	2.56 (1.31-5.57)	0.004
≥ 5/< 5 ng/mL	3/33	0/23	3/10	0.04
CA125 (*n* = 26)				
Median, IQR (U/mL)	14.5 (10.0-25.7)	14.4 (9.2-20.1)	68.6 (11.9-125)	< 0.0001
≥ 35 /< 35 U/mL	5/21	0/19	5/2	< 0.0001
CA724 (*n* = 20)				
Median, IQR (U/mL)	1.5 (0.96-2.7)	1.52 (0.99-2.24)	1.53 (0.8-6.8)	0.538
≥ 9.8/< 9.8 U /mL	1/19	1/14	0/5	1.00
CA242 (*n* = 3)				
Median, IQR (U/mL)	2.39 (0.1)	1.25 (0.1)	35.35	Not applicable
≥ 20/< 20 U/mL	1/2	0/2	1/0	0.333

[1]*P* values were based on student's *t* test comparing mean values of each serum tumor maker. CA: Carbohydrate antigen; CEA: Carcinoembryonic antigen; IQR: Interquartile range.

Table 6 Comparison of serum carbohydrate antigen 125 levels in mucinous cystic neoplasms and intraductal papillary mucinous neoplasms

	Overall	Benign	Advanced
mean ± SD (U/mL) (IPMN)	14.6 ± 12.2	12.7 ± 7.56	17.3 ± 16.4
mean ± SD (U/mL) (MCN)	30.5 ± 40.5	14.3 ± 6.4	74.4 ± 60.3
Comparison *P* value	0.001	0.69	< 0.0001
≥ 35/< 35 U/mL (IPMN)	5/104	1/63	4/41
≥ 35/< 35 U/mL (MCN)	5/21	0/19	5/2
Comparison *P* value	0.03	1.00	< 0.0001

MCN: Mucinous cystic neoplasm; SD: Standard deviation; IPMN: Intraductal papillary mucinous neoplasm.

yearly surveillance in reducing pancreatic cancer-related mortality remains to be established. Further, routine surveillance may impose psychological and economic burdens[19]. STMs are much more accessible than MRI/MRCP/EUS, which can be obtained during health checkups. The value of STMs in predicting advanced PCLs remains to be fully elucidated.

The role of STMs in the early detection of pancreatic ductal adenocarcinoma (PDA) is doubtful due to their low SE. However, as a tumor progresses, the level of STMs increases[14]. Moreover, the 5-year survival rate after surgical resection of A-MNS was much higher than that of PDA[20-23]. In other words, although STMs may not be able to detect early A-MNs, they can contribute to finding late A-MNs that are more indolent than PDA, and the prognosis is still satisfactory[24]. Thus, unlike the role of STMs in PDA, STM testing may play a more active role in the management of PCLs.

CA19-9 was widely acknowledged as the most accurate STM for predicting A-cMNs, and the value of CA19-9 was also identified in our study. Although false negative results and false positive results (caused by biliary tract obstruction and inflammation, pancreatitis, and other digestive cancers)[9] limit its clinical application,

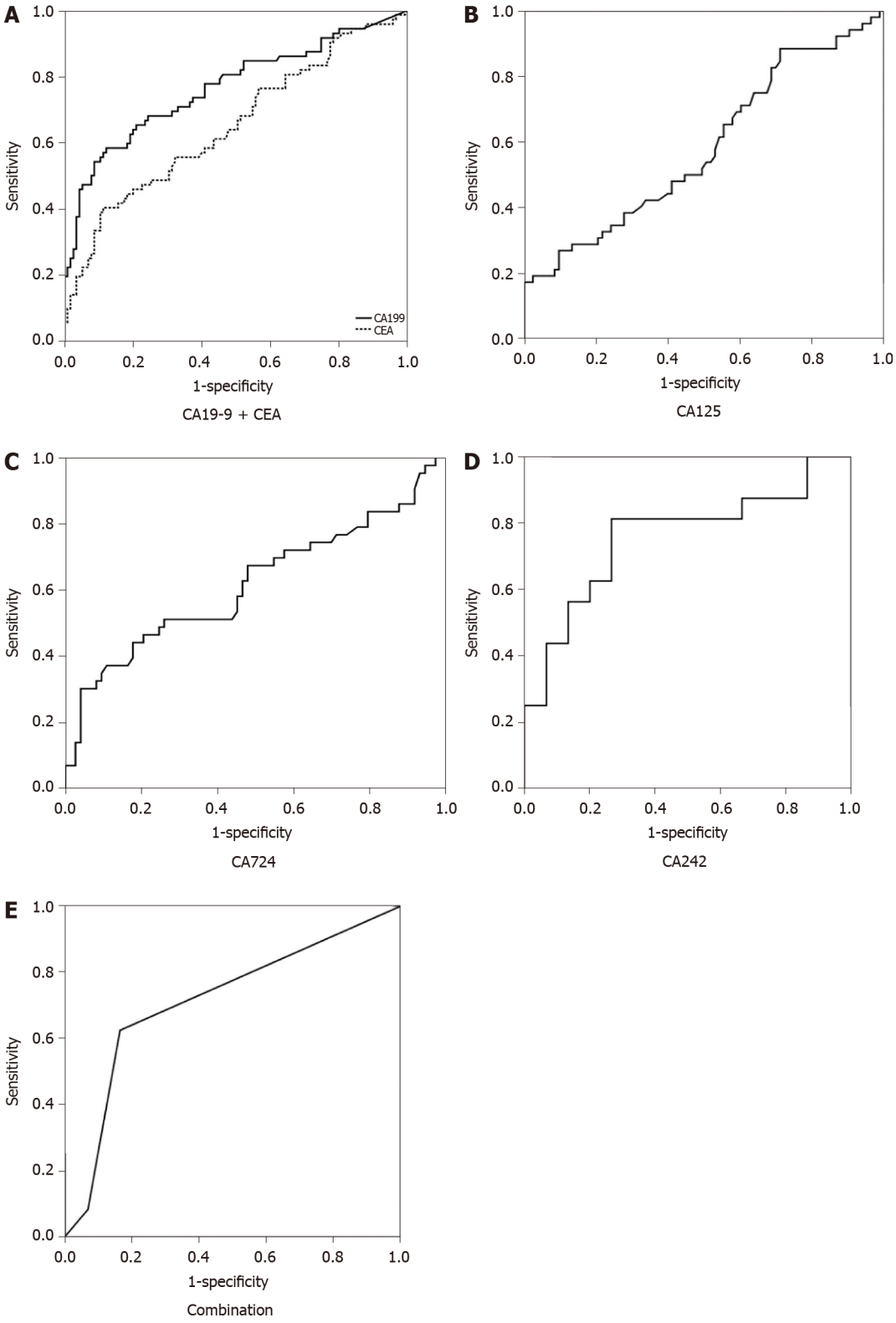


Figure 1 Receiver operating characteristic curves. A: Carbohydrate antigen (CA) 19-9 + carcinoembryonic antigen; B: CA125; C: CA724; D: CA242; and E: Their combination in the diagnosis of advanced cystic mucinous neoplasms of the pancreas.

it is still widely used in the management of PCLs. The pooled SE for CA19-9 in predicting advanced PCLs was approximately 40% by a meta-analysis[14]. As our study showed, although the best performances were observed in all analysis groups, the SE was suboptimal, and the AUC for CA19-9 was 0.766, which indicated that the ability of CA19-9 to predict A-cMNs was moderate. Moreover, if merely based on the commonly used cutoff (37 U/mL), up to 33/72 (45.8%) malignant subjects would be considered negative, and 11/115 (9.6%) benign subjects would be considered positive.

Furthermore, we for the first time report that CA19-9 was still a useful diagnostic tool for predicting HGD IPMNs, but the SE and AUC decreased as expected.

The reported SE and SP of CEA for IPMNs were 18% and 93%, respectively[14]. In our study, serum CEA detection had the ability to distinguish A-cMNs from non-A-cMNs. However, the AUC for CEA was 0.651, and the SE was 25%. Both indicators performed worse than CA19-9. The results indicated that the predictive value of CEA for A-cMNs was low. Therefore, it is essential to explore other biomarkers to supplement CA19-9 and CEA to improve the diagnosis of A-cMNs.

Our study identified CA125 and CA724 as useful STMs in predicting A-cMNs with a relatively low SE (17.3% and 16.3%) and low AUC (0.583 and 0.618), which indicated that both STMs were weak predictors of A-cMNs. Therefore, CA125 and CA724 could not be identified as valuable screening markers for A-cMNs alone despite their relatively high SP (98.8% and 95.9%). Nevertheless, we identified that serum CA125 was more likely a predictor of advanced MCN than advanced IPMN. The results were similar to those of two recently published studies[25,26]. The possible reason may be the tissue histogenesis of MCN. Elevated CA125 levels are common in serous ovarian tumors. However, for mucinous ovarian tumors, an increase in serum CA125 levels is not uncommon[27]. MCNs and mucinous ovarian tumors both originate from primordial germ cells[4], and ovarian-like stroma can be obtained from the tissue of advanced MCNs[28]; thus, advanced MCNs may theoretically have an increased CA125 level as well as ovarian tumors. If a patient's serum CA125 level is elevated, it may be necessary to examine the pancreas to exclude advanced MCNs after an ovarian examination. However, the result was concluded from a small sample size, and the true value of CA125 in the management of A-cMNs needs to be further studied.

We did not find that CA242 showed predictive value. This may be due to our study's small sample size. The recognition of CA242 has not been established until recent years in our hospital. As a result, there were fewer patients who underwent CA242 testing in our hospital than those who were tested for other STMs. However, CA242 had a comparable AUC to CA19-9 (0.758 *vs* 0.766, $P = 0.81$). The value of CA242 in PCLs may be verified by enlarging the sample size.

The combination of multiple STMs can improve their diagnostic AC in pancreatic cancer[5]. However, no one has explored this field in PCLs. In our study, the combination of STMs slightly increased the SE of CA19-9 to 62.5%. However, the SP decreased to 83.5%, and the AUC decreased to 0.715. The bias may exist due to the incomplete data for CA125, CA724, and CA242. Overall, the more data from these incomplete STMs that were included in our study, the more positive subjects were associated with combined results, and the SE was improved. Since STMs are the modalities for screening, the high SE of the combination will lead to more subjects undergoing further imaging evaluation to avoid missed diagnosis of advanced cases, which we deem justified. In addition, the reported AC of CT for identifying benign from malignant cysts was 71%–80%, and the AC of MRI or MRCP for differentiating a benign from a malignant cyst ranged from 55% to 76%[12]. The diagnostic accuracies were very similar to the AC of STMs that we reported in this research. Although imaging modalities can provide more information, we still believe that as a screening tool, serum STM detection may play a role in the management of PCLs.

Our study has limitations that merit discussion. First, this work was designed to be a retrospective, single-center study; hence, selection bias could not be completely avoided. Thus, the results of this study might not be applicable to other medical settings. Second, the CA125, CA724, and CA242 data were incomplete, which might influence the statistical results and decrease the AC of the combination analysis. Third, our analysis focused on cMNs. The application of our study might be limited in clinical practice due to the difficulty of making a definitive diagnosis preoperatively. Fourth, due to the lack of data, other STMs associated with pancreatic cancer, such as CA50, were not included.

CONCLUSION

In conclusion, this is the first study to illustrate the potential value of multiple STMs for the diagnosis of A-cMNs. CA19-9 is the most accurate STM for predicting A-cMNs, showing a moderate ability. CEA, CA125, and CA724 present a low ability to predict A-cMNs. CA125 may be specific to the diagnosis of advanced-MCNs. CA242 is not identified as a useful STM for predicting A-cMNs in our study; however, the AUC for CA242 is comparable to that for CA19-9. Thus, a greater sample size will be necessary to identify the true value of CA242. A combination of the five STMs could improve SE

in predicting A-cMNs.

ARTICLE HIGHLIGHTS

Research background

Early detection of advanced cystic mucinous neoplasms (A-cMNs) of the pancreas is key to the management of pancreatic cystic lesions (PCLs) in relation to the carcinogenic potential of cMNs. However, the long-term, routine yearly surveillance by imaging methods recommended by the current guidelines will impose heavy psychological and economic burdens on patients.

Research motivation

As an economical and feasible detection method, serum tumor markers (STMs) can be obtained during ordinary health checkups. However, the role of STMs in predicting advanced PCLs remains elusive. In view of the consistency between the increasing level of STMs and tumor progression, STM detection may play an important role in the early diagnosis of advanced PCLs.

Research objectives

This study aimed to evaluate the ability of five common serum tumor markers to predict A-cMNs separately and in combination. The relevant research results may be beneficial to the management of PCLs and the optimization of guidance or consensus.

Research methods

This retrospective cohort study mainly measured the levels of serum carbohydrate antigen (CA) 19-9, carcinoembryonic antigen (CEA), CA125, CA724, and CA242 in patients pathologically diagnosed with cMNs to identify the ability of these STMs to predict A-cMNs and distinguish mucinous cystic neoplasms (MCNs) from intraductal papillary mucinous neoplasms. A receiver operating characteristic curve with an area under curve and the sensitivity (SE), specificity (SP), and accuracy were also created to identify the performance of the five STMs.

Research results

CA19-9 showed the highest SE and accuracy and a moderate ability to predict A-cMNs. The ability of CEA, CA125, and CA724 to predict A-cMNs was low. The predictive ability of CA242 was not identified. A combination of STMs could improve SE. CA125 was more likely a predictor of advanced MCNs than advanced intraductal papillary mucinous neoplasms.

Research conclusions

CA19-9 showed a moderate ability, and CEA, CA125, and CA724 showed a low ability to predict A-cMNs. Detection of multiple STMs could improve SE in predicting A-cMNs, which has great potential to improve the early diagnosis rate of advanced PCLs in clinical practice. CA125 may be specific to the diagnosis of advanced MCNs and can be used as a reminder for physicians not to ignore pancreatic examination in patients with elevated CA125.

Research perspectives

A multicenter prospective study that monitors PCL patients with detailed data on serum tumor markers should be performed.

REFERENCES

1 **Sun L**, Wang Y, Jiang F, Qian W, Shao C, Jin Z. Prevalence of pancreatic cystic lesions detected by magnetic resonance imaging in the Chinese population. *J Gastroenterol Hepatol* 2019; **34**: 1656-1662 [PMID: 30883900 DOI: 10.1111/jgh.14658]

2 **Zerboni G**, Signoretti M, Crippa S, Falconi M, Arcidiacono PG, Capurso G. Systematic review and meta-analysis: Prevalence of incidentally detected pancreatic cystic lesions in asymptomatic individuals. *Pancreatology* 2019; **19**: 2-9 [PMID: 30503370 DOI: 10.1016/j.pan.2018.11.014]

3 **Kromrey ML**, Bülow R, Hübner J, Paperlein C, Lerch MM, Ittermann T, Völzke H, Mayerle J, Kühn JP. Prospective study on the incidence, prevalence and 5-year pancreatic-related mortality of

pancreatic cysts in a population-based study. *Gut* 2018; **67**: 138-145 [PMID: 28877981 DOI: 10.1136/gutjnl-2016-313127]

4 **Elias KM**, Tsantoulis P, Tille JC, Vitonis A, Doyle LA, Hornick JL, Kaya G, Barnes L, Cramer DW, Puppa G, Stuckelberger S, Hooda J, Dietrich PY, Goggins M, Kerr CL, Birrer M, Hirsch MS, Drapkin R, Labidi-Galy SI. Primordial germ cells as a potential shared cell of origin for mucinous cystic neoplasms of the pancreas and mucinous ovarian tumors. *J Pathol* 2018; **246**: 459-469 [PMID: 30229909 DOI: 10.1002/path.5161]

5 **Zhang Y**, Yang J, Li H, Wu Y, Zhang H, Chen W. Tumor markers CA19-9, CA242 and CEA in the diagnosis of pancreatic cancer: a meta-analysis. *Int J Clin Exp Med* 2015; **8**: 11683-11691 [PMID: 26380005]

6 **Dong D**, Jia L, Zhang L, Ma N, Zhang A, Zhou Y, Ren L. Periostin and CA242 as potential diagnostic serum biomarkers complementing CA19.9 in detecting pancreatic cancer. *Cancer Sci* 2018; **109**: 2841-2851 [PMID: 29945294 DOI: 10.1111/cas.13712]

7 **Liu P**, Zhu Y, Liu L. CA724 is a novel factor for predicting the unresectability in pancreatic adenocarcinoma. *Int J Clin Exp Pathol* 2015; **8**: 15112-15117 [PMID: 26823852]

8 **Liu L**, Xu HX, Wang WQ, Wu CT, Xiang JF, Liu C, Long J, Xu J, Fu de L, Ni QX, Houchen CW, Postier RG, Li M, Yu XJ. Serum CA125 is a novel predictive marker for pancreatic cancer metastasis and correlates with the metastasis-associated burden. *Oncotarget* 2016; **7**: 5943-5956 [PMID: 26745601 DOI: 10.18632/oncotarget.6819]

9 **Luo G**, Liu C, Guo M, Cheng H, Lu Y, Jin K, Liu L, Long J, Xu J, Lu R, Ni Q, Yu X. Potential Biomarkers in Lewis Negative Patients With Pancreatic Cancer. *Ann Surg* 2017; **265**: 800-805 [PMID: 28267695 DOI: 10.1097/SLA.0000000000001741]

10 **Tanaka M**, Fernández-Del Castillo C, Kamisawa T, Jang JY, Levy P, Ohtsuka T, Salvia R, Shimizu Y, Tada M, Wolfgang CL. Revisions of international consensus Fukuoka guidelines for the management of IPMN of the pancreas. *Pancreatology* 2017; **17**: 738-753 [PMID: 28735806 DOI: 10.1016/j.pan.2017.07.007]

11 **European Study Group on Cystic Tumours of the Pancreas**. European evidence-based guidelines on pancreatic cystic neoplasms. *Gut* 2018; **67**: 789-804 [PMID: 29574408 DOI: 10.1136/gutjnl-2018-316027]

12 **Elta GH**, Enestvedt BK, Sauer BG, Lennon AM. ACG Clinical Guideline: Diagnosis and Management of Pancreatic Cysts. *Am J Gastroenterol* 2018; **113**: 464-479 [PMID: 29485131 DOI: 10.1038/ajg.2018.14]

13 **Brugge WR**, Lewandrowski K, Lee-Lewandrowski E, Centeno BA, Szydlo T, Regan S, del Castillo CF, Warshaw AL. Diagnosis of pancreatic cystic neoplasms: a report of the cooperative pancreatic cyst study. *Gastroenterology* 2004; **126**: 1330-1336 [PMID: 15131794]

14 **Wang W**, Zhang L, Chen L, Wei J, Sun Q, Xie Q, Zhou X, Zhou D, Huang P, Yang Q, Xie H, Zhou L, Zheng S. Serum carcinoembryonic antigen and carbohydrate antigen 19-9 for prediction of malignancy and invasiveness in intraductal papillary mucinous neoplasms of the pancreas: A meta-analysis. *Biomed Rep* 2015; **3**: 43-50 [PMID: 25469245 DOI: 10.3892/br.2014.376]

15 **Jang JY**, Park T, Lee S, Kim Y, Lee SY, Kim SW, Kim SC, Song KB, Yamamoto M, Hatori T, Hirono S, Satoi S, Fujii T, Hirano S, Hashimoto Y, Shimizu Y, Choi DW, Choi SH, Heo JS, Motoi F, Matsumoto I, Lee WJ, Kang CM, Han HS, Yoon YS, Sho M, Nagano H, Honda G, Kim SG, Yu HC, Chung JC, Nagakawa Y, Seo HI, Yamaue H. Proposed Nomogram Predicting the Individual Risk of Malignancy in the Patients With Branch Duct Type Intraductal Papillary Mucinous Neoplasms of the Pancreas. *Ann Surg* 2017; **266**: 1062-1068 [PMID: 27607098 DOI: 10.1097/SLA.0000000000001985]

16 **Kim JR**, Jang JY, Kang MJ, Park T, Lee SY, Jung W, Chang J, Shin Y, Han Y, Kim SW. Clinical implication of serum carcinoembryonic antigen and carbohydrate antigen 19-9 for the prediction of malignancy in intraductal papillary mucinous neoplasm of pancreas. *J Hepatobiliary Pancreat Sci* 2015; **22**: 699-707 [PMID: 26178866 DOI: 10.1002/jhbp.275]

17 **Tanaka M**, Chari S, Adsay V, Fernandez-del Castillo C, Falconi M, Shimizu M, Yamaguchi K, Yamao K, Matsuno S; International Association of Pancreatology. International consensus guidelines for management of intraductal papillary mucinous neoplasms and mucinous cystic neoplasms of the pancreas. *Pancreatology* 2006; **6**: 17-32 [PMID: 16327281 DOI: 10.1159/000090023]

18 **Tanaka M**, Fernández-del Castillo C, Adsay V, Chari S, Falconi M, Jang JY, Kimura W, Levy P, Pitman MB, Schmidt CM, Shimizu M, Wolfgang CL, Yamaguchi K, Yamao K; International Association of Pancreatology. International consensus guidelines 2012 for the management of IPMN and MCN of the pancreas. *Pancreatology* 2012; **12**: 183-197 [PMID: 22687371 DOI: 10.1016/j.pan.2012.04.004]

19 **Andermann A**, Blancquaert I, Beauchamp S, Déry V. Revisiting Wilson and Jungner in the genomic age: a review of screening criteria over the past 40 years. *Bull World Health Organ* 2008; **86**: 317-319 [PMID: 18438522 DOI: 10.2471/blt.07.050112]

20 **Hirono S**, Shimizu Y, Ohtsuka T, Kin T, Hara K, Kanno A, Koshita S, Hanada K, Kitano M, Inoue H, Itoi T, Ueki T, Shimokawa T, Hijioka S, Yanagisawa A, Nakamura M, Okazaki K, Yamaue H. Recurrence patterns after surgical resection of intraductal papillary mucinous neoplasm (IPMN) of the pancreas; a multicenter, retrospective study of 1074 IPMN patients by the Japan Pancreas Society. *J Gastroenterol* 2020; **55**: 86-99 [PMID: 31463655 DOI: 10.1007/s00535-019-01617-2]

21 **Antoñanzas J**, Cienfuegos JA, Hurtado-Pardo L, Panadero P, Benito A, Pardo F, Rotellar F, Martí-Cruchaga P, Zozaya G, Valentí V, Hernández Lizoain JL. Intraductal papillary mucinous neoplasm

(IPMN) of the pancreas: clinicopathological features and long-term outcomes following a pancreatectomy. *Rev Esp Enferm Dig* 2018; **110**: 768-774 [PMID: 30168337 DOI: 10.17235/reed.2018.5646/2018]

22 **Al Efishat M**, Attiyeh MA, Eaton AA, Gönen M, Basturk O, Klimstra D, D'Angelica MI, DeMatteo RP, Kingham TP, Balachandran V, Jarnagin WR, Allen PJ. Progression Patterns in the Remnant Pancreas after Resection of Non-Invasive or Micro-Invasive Intraductal Papillary Mucinous Neoplasms (IPMN). *Ann Surg Oncol* 2018; **25**: 1752-1759 [PMID: 29589164 DOI: 10.1245/s10434-018-6445-2]

23 **Marchegiani G**, Mino-Kenudson M, Ferrone CR, Morales-Oyarvide V, Warshaw AL, Lillemoe KD, Castillo CF. Patterns of Recurrence After Resection of IPMN: Who, When, and How? *Ann Surg* 2015; **262**: 1108-1114 [PMID: 25793719 DOI: 10.1097/SLA.0000000000001008]

24 **Li Y**, Zhu Z, Peng L, Jin Z, Sun L, Song B. The pathological features and prognoses of intraductal papillary mucinous neoplasm and mucinous cystic neoplasm after surgical resection: a single institution series. *World J Surg Oncol* 2020; **18**: 287 [PMID: 33148260 DOI: 10.1186/s12957-020-02063-8]

25 **Deng S**, Fan Z, Gong Y, Cheng H, Jin K, Qian Y, Xiao Z, Liu Y, Wang R, Zheng Y, Ni Q, Yu X, Liu C, Luo G. Clinical implication of serum CA125 for the prediction of malignancy in mucinous cystic neoplasms of the pancreas. *Exp Ther Med* 2020; **20**: 158 [PMID: 33093896 DOI: 10.3892/etm.2020.9287]

26 **Zhao ZM**, Jiang N, Gao YX, Yin ZZ, Zhao GD, Tan XL, Xu Y, Liu R. Clinical diagnosis and management of pancreatic mucinous cystadenoma and cystadenocarcinoma: Single-center experience with 82 patients. *World J Gastrointest Oncol* 2020; **12**: 642-650 [PMID: 32699579 DOI: 10.4251/wjgo.v12.i6.642]

27 **Moss EL**, Hollingworth J, Reynolds TM. The role of CA125 in clinical practice. *J Clin Pathol* 2005; **58**: 308-312 [PMID: 15735166 DOI: 10.1136/jcp.2004.018077]

28 **Crinò SF**, Bernardoni L, Gabbrielli A, Capelli P, Salvia R, Rusev BC, Scarpa A, Manfrin E. Beyond Pancreatic Cyst Epithelium: Evidence of Ovarian-Like Stroma in EUS-Guided Through-the-Needle Micro-Forceps Biopsy Specimens. *Am J Gastroenterol* 2018; **113**: 1059-1060 [PMID: 29899433 DOI: 10.1038/s41395-018-0124-6]

World Journal of Gastroenterology

Submit a Manuscript: https://www.f6publishing.com

World J Gastroenterol 2021 February 14; 27(6): 513-522

DOI: 10.3748/wjg.v27.i6.513

ISSN 1007-9327 (print) ISSN 2219-2840 (online)

ORIGINAL ARTICLE

Retrospective Study

Washed microbiota transplantation reduces proton pump inhibitor dependency in nonerosive reflux disease

Ya-Mei Zheng, Xian-Yun Chen, Jie-Yi Cai, Yu Yuan, Wen-Rui Xie, Jia-Ting Xu, Harry Hua-Xiang Xia, Min Zhang, Xing-Xiang He, Li-Hao Wu

ORCID number: Ya-Mei Zheng 0000-0001-6622-2616; Xian-Yun Chen 0000-0002-9068-2660; Jie-Yi Cai 0000-0001-5355-6422; Yu Yuan 0000-0002-9536-3167; Wen-Rui Xie 0000-0001-7180-5090; Jia-Ting Xu 0000-0001-8685-7416; Harry Hua-Xiang Xia 0000-0002-7952-9200; Min Zhang 0000-0002-3792-8668; Xing-Xiang He 0000-0003-2075-9527; Li-Hao Wu 0000-0003-4674-8287.

Author contributions: Zheng YM contributed to the study design, performed the experiments, and wrote the paper; Wu LH contributed to the study design, provided critical revision of the article for important intellectual content, and made final approval of the article; Chen XY, Cai JY, Zhang M, and Xia HHX designed the study and contributed to the analysis and interpretation of the data; Yuan Y, Xie WR, He XX, and Xu JT provided clinical advice and supervised the report.

Institutional review board statement: This retrospective study was approved by the Ethics Committee of Guangdong Pharmaceutical University (Approval No. Yilun Shen[2019] No. 93 01).

Conflict-of-interest statement: The authors have no conflicts of

Ya-Mei Zheng, Xian-Yun Chen, Jie-Yi Cai, Yu Yuan, Wen-Rui Xie, Jia-Ting Xu, Xing-Xiang He, Li-Hao Wu, Department of Gastroenterology, The First Affiliated Hospital of Guangdong Pharmaceutical University, Research Center for Engineering Techniques of Microbiota-Targeted Therapies of Guangdong Province, Guangzhou 510030, Guangdong Province, China

Harry Hua-Xiang Xia, Department of Science and Education, The First Affiliated Hospital of Guangdong Pharmaceutical University, Guangzhou 510030, Guangdong Province, China

Min Zhang, Department of Epidemiology and Health Statistics, Guangdong Pharmaceutical University, Guangzhou 510220, Guangdong Province, China

Corresponding author: Li-Hao Wu, MD, Associate Professor, Department of Gastroenterology, The First Affiliated Hospital of Guangdong Pharmaceutical University, Research Center for Engineering Techniques of Microbiota-Targeted Therapies of Guangdong Province, No. 19 Nonglinxia Road, Yuexiu District, Guangzhou 510030, Guangdong Province, China. wulihao888@126.com

Abstract

BACKGROUND

The pathogenesis of gastroesophageal reflux disease (GERD) is closely associated with the intestinal bacteria composition and their metabolites.

AIM

To investigate whether washed microbiota transplantation (WMT) improves symptoms of nonerosive reflux disease (NERD) with proton pump inhibitor (PPI) dependency.

METHODS

Patients with recurrent NERD and PPI dependency at the First Affiliated Hospital of Guangdong Pharmaceutical University from 2017 to 2018 were included and divided into a WMT or PPI group treated with PPI with/without WMT. The endpoint was NERD symptom frequency evaluated 1 mo after WMT using reflux disease questionnaire (RDQ) and GERD questionnaire (GERDQ) scores, remission time, PPI dose, and the examination of intestinal mucosal barrier function.

RESULTS

In the WMT (n = 15) and PPI (n = 12) groups, the total remission rate at 1 mo after

interest to declare.

Data sharing statement: No additional data are available.

Open-Access: This article is an open-access article that was selected by an in-house editor and fully peer-reviewed by external reviewers. It is distributed in accordance with the Creative Commons Attribution NonCommercial (CC BY-NC 4.0) license, which permits others to distribute, remix, adapt, build upon this work non-commercially, and license their derivative works on different terms, provided the original work is properly cited and the use is non-commercial. See: http://creativecommons.org/Licenses/by-nc/4.0/

Manuscript source: Unsolicited manuscript

Specialty type: Gastroenterology and hepatology

Country/Territory of origin: China

Peer-review report's scientific quality classification
Grade A (Excellent): 0
Grade B (Very good): B
Grade C (Good): C
Grade D (Fair): 0
Grade E (Poor): 0

Received: November 29, 2020
Peer-review started: November 29, 2020
First decision: December 8, 2020
Revised: December 20, 2020
Accepted: January 12, 2021
Article in press: January 12, 2021
Published online: February 14, 2021

P-Reviewer: Maslennikov R
S-Editor: Fan JR
L-Editor: Wang TQ
P-Editor: Li JH

treatment was 93.3% *vs* 41.7%. Compared with the PPI group, the WMT group showed better results in GERDQ (P = 0.004) and RDQ (P = 0.003) and in remission months (8 *vs* 2, P = 0.002). The PPI dose was reduced to some extent for 80% of patients in the WMT group and 33.3% in the PPI group. In 24 patients, intestinal mucosal barrier function was examined before treatment, and changes in the degree of damage were observed in 13 of these patients after treatment. Only one of the 15 patients had minor side effects, including a mushy stool two or three times a day, which resolved on their own after 1 wk.

CONCLUSION
This study is the first to demonstrate that WMT may be safe and effective for relieving NERD symptoms and reducing PPI dependency and recurrence.

Key Words: Nonerosive reflux disease; Washed microbiota transplantation; Proton pump inhibitor dependency; Intestinal bacteria; Lipopolysaccharide; Small intestinal bacterial overgrowth

©The Author(s) 2021. Published by Baishideng Publishing Group Inc. All rights reserved.

Core Tip: In this study, we demonstrated for the first time that washed microbiota transplantation (WMT) is safe and effective for treating patients with nonerosive reflux disease (NERD) and proton pump inhibitor (PPI) dependency compared with PPI treatment. WMT significantly relieved the symptoms of NERD in patients, reduced PPI dependency, prolonged the duration of symptom remission, and reduced symptom recurrence.

Citation: Zheng YM, Chen XY, Cai JY, Yuan Y, Xie WR, Xu JT, Xia HHX, Zhang M, He XX, Wu LH. Washed microbiota transplantation reduces proton pump inhibitor dependency in nonerosive reflux disease. *World J Gastroenterol* 2021; 27(6): 513-522
URL: https://www.wjgnet.com/1007-9327/full/v27/i6/513.htm
DOI: https://dx.doi.org/10.3748/wjg.v27.i6.513

INTRODUCTION

Gastroesophageal reflux disease (GERD) is divided into nonerosive reflux disease (NERD), reflux esophagitis, and Barrett's esophagus, and more than 70% of GERD cases are NERD[1]. The current treatment for GERD is proton pump inhibitors (PPIs)[2]. However, due to the chronic nature and recurrence of GERD, current PPI treatments for GERD do not provide satisfactory effects, especially in patients with NERD, who have a poorer response to PPIs than patients with reflux esophagitis[3-7]. In addition, many patients need to take PPIs for a long time[8], potentially leading to changes in their intestinal microbiota, such as increases in *Enterococcus*, *Streptococcus*, *Staphylococcus*, and potentially pathogenic *Escherichia coli*[6,9]. *Escherichia coli* is a Gram-negative bacterium, and a component of its cell wall, lipopolysaccharide, can cause lower esophageal sphincter (LES) relaxation and gastric empty-out delay and lead to the occurrence of GERD[6]. Many studies have also found that long-term use of PPIs can result in small intestinal bacterial overgrowth (SIBO)[9-11], which can cause chronic inflammation; immune reactions may give rise to reduced reactivity of esophageal smooth muscle[12]. At the same time, SIBO leads to the production of excess amounts of methane gas by the intestinal bacteria, which inhibits contractile activity, slows intestinal transit, and, consequently, affects gastric emptying and induces gastroesophageal reflux[13,14]. These studies suggest that the recurrence of symptoms and long-term use of PPI in patients with GERD (including NERD) may be related to changes in the intestinal microbiota and SIBO induction after previous PPI use.

In recent years, research on the application of fecal microbiota transplantation (FMT) in clinical diseases has developed rapidly. Good clinical effects of FMT have been observed for many diseases, including refractory *Clostridium difficile* infection[15], irritable bowel syndrome[16], inflammatory bowel disease[17], and constipation[18]. FMT reconstructs the balance of the intestinal flora in patients by using healthy donor feces,

reducing the colonization of pathogenic bacteria, and leading to a treatment effect by regulating metabolism and immunity[19]. The latest study showed that the method of generating bacterial solutions through automatic purification systems is very popular among doctors and patients; therefore, FMT is also called washed microbiota transplantation (WMT)[20].

Since our hospital launched WMT to treat diseases such as GERD, ulcerative colitis, irritable bowel syndrome, constipation, non-alcoholic fatty liver, and autism for two years and obtained good clinical results, more than 2500 times have been treated. This study mainly assessed the therapeutic effects of WMT in patients with PPI-dependent NERD.

MATERIALS AND METHODS

Subjects

Patients with a clear diagnosis of NERD and dependency on PPIs who were admitted to the Department of Gastroenterology of the First Affiliated Hospital of Guangdong Pharmaceutical University from January 1, 2017 to November 30, 2018 and had poor curative effects and recurrent symptoms after PPI use were included and divided into WMT and PPI groups. Patients who received WMT treatment provided informed consent.

Inclusion criteria

The age of the included patients was 18-85 years old. Consistent with the diagnosis of GERD, endoscopy excluded reflux esophagitis and Barrett's esophagus. The patients had a history of disease for more than 6 mo with PPI dependency, and no antibiotics were used 1 wk before treatment and during treatment. PPI dependency was defined that after standard PPI treatment, complete remission of GERD symptoms was not achieved or the symptoms recurred after the drug was stopped. The inclusion criteria of the WMT group were to meet both the above criteria and the following criteria: Patients had consented to WMT treatment, if they were not included in the PPI group.

Exclusion criteria

Patients were excluded if they had severe heart and lung disease, liver and kidney failure, malignant tumors, pregnancy, or other diseases that significantly affect quality of life, or they refused or failed to complete the follow-ups.

Treatment plan

The PPI group was treated with a previous treatment plan (mainly PPI treatment), while WMT treatment was added in the WMT group. The source of the bacterial suspension for WMT was mixed multidonor feces. All donors were healthy people aged 18 to 25 years, and they were required to undergo health examinations to exclude digestive tract diseases, tumors, infectious diseases, metabolic diseases, genetic diseases, and other related diseases and not to take antibiotics, as well as drugs that affect digestive tract dynamics and/or cause intestinal microecological disorders, for the last 3 mo. Two hundred milliliters of fresh fecal liquid was separated using an automatic purification system (GenFMTer; FMT Medical, Nanjing, China), and the prepared bacteria were injected into the patient's intestine *via* the middle or lower digestive tract within half an hour. There were two transplantation routes. One was the middle-gut route: Transendoscopic enteral tubing was placed in the jejunum under gastroscopy, and PPIs (such as lansoprazole 30 mg + normal saline 100 mL) were administered intravenously 1 h before injection of bacteria (to reduce the inactivation of bacteria when moving through the stomach). Metoclopramide hydrochloride (10 mg) was injected intramuscularly (to reduce adverse reactions such as vomiting or abdominal distension caused by irritation of the gastrointestinal tract by the bacterial fluid). The patients were placed in a sitting position when injecting the bacterial solution. The injection process was slow, requiring an injection time of at least 30 min for 200 mL of bacterial solution. After the injection, the patient was asked to remain sitting or standing for at least 2 h. The other route was the lower gut route: Transendoscopic enteral tubing was placed into the caecum *via* enteroscopy. When injecting the bacterial solution, the patient was in the right lateral position, and the time of injection was 30 min. After the injection was completed, the patient was instructed to rest in the right lateral position for at least 2 h. One course was administered once daily for 3 d. Four courses were administered, with one course per

month given in the first month, second month, third month, and sixth month.

Outcome measurement

The main outcome measure was NERD symptom frequency evaluated 1 mo after WMT. The reflux disease questionnaire (RDQ) and GERD questionnaire (GERDQ) were administered to the patient before and 1 mo after treatment and reviewed. The RDQ integrates the severity and frequency of heartburn, chest pain, acid regurgitation, and regurgitation over the past 4 wk. The GERDQ measures the frequency of symptoms, such as reflux, heartburn, nausea, upper abdominal pain, sleep disturbance, additional antacids, and other symptoms during the past 7 d.

Other outcome measures included remission, relapse after remission, monosymptomatic remission, and biochemical coupling examination of intestinal barrier function. Remission was defined as RDQ and GERDQ scores reduced by 30% at 1 mo posttreatment. Relapse after remission was defined as: After WMT treatment, the patient's symptoms of NERD reached remission but then worsened to a level observed prior to WMT treatment; the RDQ and GERDQ scores increased by 30% from the previous period, and the duration of this increase exceeded 1 mo. Monosymptomatic remission was defined when the RDQ or GERDQ scores of heartburn, acid regurgitation, chest pain, regurgitation, and sleep disturbance declined posttreatment compared with pretreatment. Biochemical coupling examination of intestinal barrier function was performed by determining serum levels of diamine oxidase (DAO), D-lactic acid (DLA), and lipopolysaccharide[21] according to the test developed by the Institute of Biophysics, Chinese Academy of Sciences (Beijing, China), and the manufacturer's protocol. DAO > 10 U/L indicated intestinal mucosal damage and increased intestinal permeability; DLA > 15 mg/L indicated abnormal intestinal permeability; and lipopolysaccharide > 20 U/L indicated intestinal bacterial translocation[22]. Thus, abnormal levels of any of these indicators reflect intestinal mechanical barrier dysfunction. PPI medication status, side effects of WMT treatment, and WMT course were also determined.

Statistical analysis

SPSS version 20.0 or GraphPad Prism version 5.0 was used for data analyses. The data are described as frequencies, percentages, medians, and interquartile ranges. Comparisons of lipopolysaccharide values and scores of RDQ and GERDQ were performed by applying the non-parametric Wilcoxon signed-rank test or Mann-Whitney test, and a two-tailed P value of < 0.05 was considered statistically significant.

Ethics statement

This retrospective study was approved by the Ethics Committee of Guangdong Pharmaceutical University (Approval No. Yilun Shen [2019] No. 93 01).

RESULTS

Of the 61 patients with NERD who were screened, 51 were eligible according to the inclusion criteria, and 27 completed the follow-ups (Figure 1). The WMT group included 15 patients, and the PPI group comprised 12 patients. There were no significant differences in the characteristics of the two study groups at enrolment (Table 1).

At 1 mo after treatment, the total remission rate in the WMT and PPI groups was 93.3% *vs* 41.7%. Compared with the PPI group, the WMT group showed better results in the GERDQ scores (7 *vs* 11, $P = 0.004$) and RDQ scores (8 *vs* 20.5, $P = 0.003$), as well as in the remission months [8 (3, 17) *vs* 2 (0, 4), $P = 0.002$] (Table 2); nine patients showed sustained remission for more than 6 mo in the WMT groups, while there were only two in the PPI group. Furthermore, the patients in the WMT group achieved better improvements in heartburn (9/10 *vs* 7/11), acid regurgitation (12/14 *vs* 7/11), chest pain (5/6 *vs* 1/5), regurgitation (9/12 *vs* 4/8), and sleep disturbance (9/11 *vs* 5/5) than the PPI group. However, 13.3% (2/15) of patients in the WMT group relapsed after remission (Table 3).

The PPI dose was reduced to some extent in 80% (12/15) of the patients in the WMT group and 33.3% (4/12) in the PPI group. After receiving the WMT treatment, 72.7% (8/11) of the patients who continued using PPIs reduced their PPI doses, and all four patients with on-demand PPI use were also reduced. In addition, 33.3% (5/15) of the patients maintained symptomatic relief and stopped taking PPIs in the WMT group, while the percentage was 16.7% (2/12) in the PPI group (Table 4).

Table 1 Basic information of patients with nonerosive reflux disease

Item	PPI	WMT	*P* value
Female	6	8	
Age (median; IQR, yr)	58.5 (53, 67.25)	62 (55, 67)	0.526
Duration (median; IQR, mo)	48 (15, 144)	24 (6, 60)	0.218
BMI (median; IQR, kg/m^2)	21.63 (19.13, 24.38)	24.24 (22.58, 25.43)	0.079

WMT: Washed microbiota transplantation; PPI: Proton pump inhibitors; BMI: Body mass index; IQR: Interquartile range.

Table 2 Symptom scores and remission time before and after treatment in the two groups

Group	PPI (*n* = 12)	WMT (*n* = 15)	*P* value[1]
Pre-GERDQ (median; IQR)	12 (9, 13.75)	12 (10, 12)	0.746
Post-GERDQ (median; IQR)	11 (8.25, 13.5)	7 (7, 8)	0.004
Intra-group, *P* value[2]	0.477	0.003	
Pre-RDQ (median, IQR)	26 (18, 33)	23 (16, 25)	0.203
Post-RDQ (median, IQR)	20.5 (12.75, 26)	8 (6, 12)	0.003
Intra-group, *P* value	0.005	0.002	
Remission time (median, IQR; mo)	2 (0, 4)	8 (3, 17)	0.002

[1]The RDQ and GERDQ scores between two groups were analyzed by non-parametric Mann-Whitney test.
[2]The intra-group RDQ and GERDQ scores were analyzed by non-parametric Wilcoxon signed-rank test.
WMT: Washed microbiota transplantation; PPI: Proton pump inhibitors; RDQ: Reflux disease questionnaire; GERDQ: Gastroesophageal reflux disease questionnaire; IQR: Interquartile range.

Table 3 Clinical responses to washed microbiota transplantation in patients with nonerosive reflux disease

Item		WMT, *n* = 15
Remission[1], *n*		14 (93.3)
Remission after the first course of WMT, *n*		13 (86.7)
Remission after the first course of FMT until the end of the study, *n*		10 (66.7)
No remission after the first course of WMT, *n*		2 (13.3)
Recurrence after remission, *n*		2 (13.3)
Side effects of WMT treatment[2], *n*	No	14 (93.3)
	Yes	1 (6.70)

[1]The scores of the reflux disease questionnaire or gastroesophageal reflux disease questionnaire at 1 mo post-washed microbiota transplantation (WMT) were reduced by 30%.
[2]Only one of the 15 patients had minor side effects, with a mushy stool two or three times a day, which resolved on their own after 1 wk, but no abdominal pain, black stool, fever, or serious WMT-related side effects were observed.
WMT: Washed microbiota transplantation; FMT: Fecal microbiota transplantation.

With regard to the relationship between courses of WMT and remission in patients with NERD symptoms (Figure 2), ten people who completed three or more WMT courses achieved an 80% symptom remission rate. With increasing courses of WMT treatment, the remission rate increased.

Twenty-four patients had the function of the intestinal mucosal barrier examined before treatment, which showed that over half of the patients (13/24) had different degrees of intestinal mucosal barrier function damage, such as the change of epithelial permeability (8/24), the damage of intestinal epithelial cells (4/24), intestinal mucosal

Table 4 Use of proton pump inhibitors in nonerosive reflux disease patients

Items		PPI	WMT
Continuous use before treatment (*n*)	No reduction after treatment	3	4
	Reduction after treatment	5	0
	Withdrawal after treatment	3	0
Usage as needed before treatment (*n*)	No reduction after treatment	0	4
	Reduction after treatment	2	2
	Withdrawal after treatment	2	2

WMT: Washed microbiota transplantation; PPI: Proton pump inhibitors.

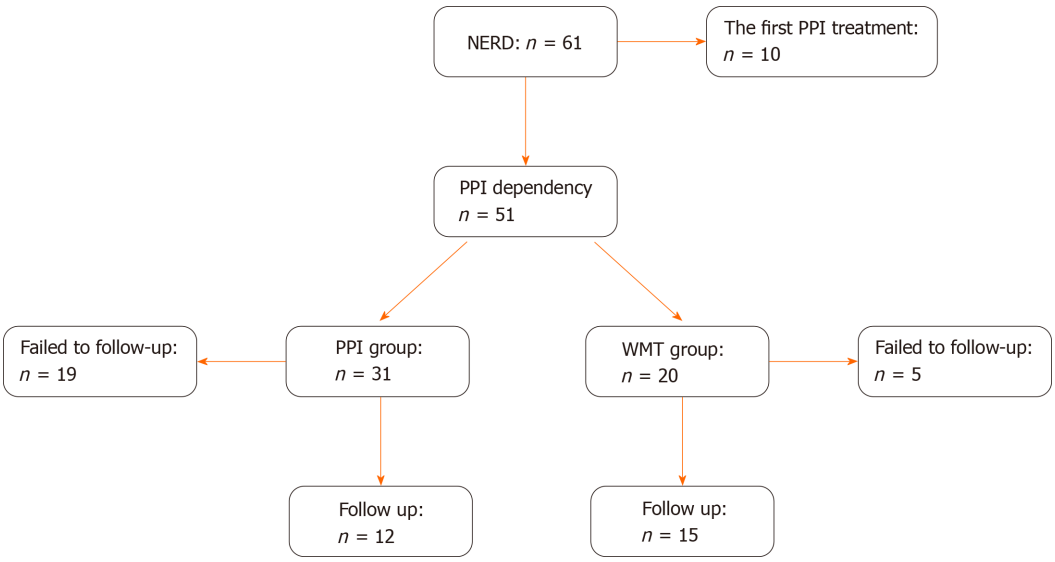


Figure 1 Flow chart for the inclusion of patients. NERD: Nonerosive reflux disease; WMT: Washed microbiota transplantation; PPI: Proton pump inhibitor dependency.

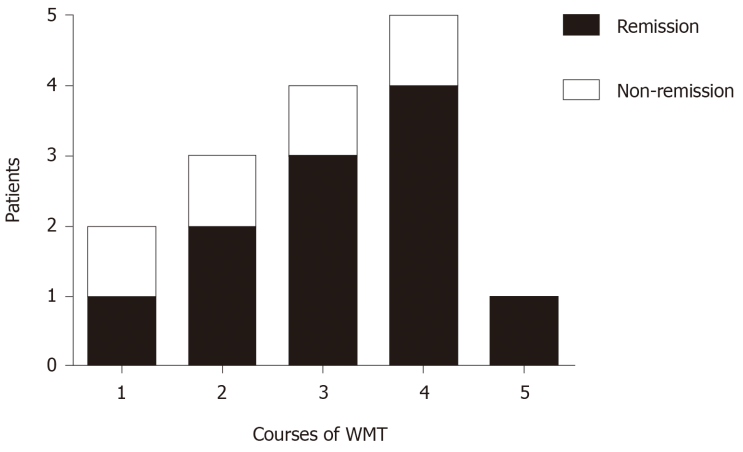


Figure 2 Relationship between courses of washed microbiota transplantation and remission of nonerosive reflux disease. WMT: Washed microbiota transplantation.

ischaemia (4/24), and intestinal bacterial translocation (2/24). However, in the WMT group, eight samples were analyzed, and the function of the intestinal mucosal barrier observed as being worse in the post-treatment than pre-treatment, two patients before treatment with intestinal mucosal damage were positive to negative, while six patients with intestinal mucosal barrier damage were negative to positive. Wilcoxon signed-rank test showed that the numeric values of lipopolysaccharide, diamine oxidase, and D-lactate had no significant difference between before and after WMT treatment (Table 5).

Only one of the 15 patients had minor side effects, including a mushy stool two or three times a day, which resolved on their own after 1 wk, but no abdominal pain, black stool, fever, or serious WMT-related side effects were observed.

DISCUSSION

PPIs are currently the first-line treatment for GERD. NERD, which accounts for most GERD cases, ruins patients' quality of life and is more difficult to treat than reflux esophagitis[23]. However, not all patients with NERD can achieve good treatment effects because PPIs are less effective in patients with NERD than in those with reflux esophagitis, and its chronic and recurrent nature means that some patients need to take PPIs for a long time. In addition, potential side effects of long-term use of PPIs are gradually being revealed, including SIBO, lack of micronutrients, and dementia[9,11,24]. A study with population-based follow-up for 10 years in Hong Kong, China in 2018 showed that long-term PPI use could increase the risk of gastric cancer[25]. Therefore, new challenges are arising for NERD treatment, and the results of our study show that WMT can solve this problem. This study confirmed that WMT had a significant clinical effect on NERD in patients with PPI dependency compared to PPI alone. It can reduce the PPI dose and the NERD recurrence rate. Our results showed that WMT, combined with PPI treatment, resulted in remission in 93.3% (14/15) of the patients, and 80% (12/15) of the patients reduced the PPI dose, which was far better than that of the PPI group (33.3%). Compared with the PPI group, the WMT group showed better results in the GERDQ scores and RDQ scores as well as in the remission months, which had obvious statistical significance.

It is widely believed that GERD usually occurs through the following four mechanisms[26]: Transient LES relaxation, low LES pressure, swallowing-associated LES relaxation, and straining during periods with low LES pressure. Recently, new findings related to the pathogenesis of GERD showed that lipopolysaccharide, a component of Gram-negative cell walls, is involved in the mechanism of GERD. Research has shown that the state of esophageal diseases (oesophagitis, Barrett's esophagus, *etc*.) is mainly dominated by type II Gram-negative bacteria. We know that lipopolysaccharide is the main structure of the outer membrane in Gram-negative bacteria; it can activate Toll-like receptor 4 and the downstream nuclear factor kB pathway to induce an inflammatory response and upregulate the expression of inducible nitrous oxide synthase, which relaxes the LES, and COX-2, which delays gastric emptying[27]. In this retrospective study, 24 patients had the function of the intestinal mucosal barrier examined before treatment, which showed that over half of the patients (13/24) had different degrees of intestinal mucosal barrier function damage, which may be involved in the pathogenesis of GERD. We also analyzed the values of lipopolysaccharide, diamine oxidase, and D-lactate before and after WMT treatment for 8 patients. The results showed that the medians were increased after treatment compared with those before treatment, but there was no significant difference. This seems to be contrary to evidence from a previous study. However, this may be due to the small number of samples, and the test was not performed at the same time. This result gives us good inspiration to focus on researching this aspect in the future.

The results of this trial indicate that as the number of courses of WMT treatment increases, the remission rate increases. The response rate of patients who completed more than four courses of WMT reached 83.3%, but the results may have some limitations due to the small sample size in this study. Although WMT is increasingly used in clinical treatment, there is no uniform treatment course or dosage. According to previous reports, multiple fresh fecal transplants can improve clinical efficacy[28]. We recommend that WMT for GERD be administered in four courses at 1, 2, 3, and 6 mo (1 course is a continuous fecal treatment for 3 d, with 200 mL of fecal separated solution injected into the jejunum or caecum *via* the middle or lower digestive tract per day). The four courses of treatment recommended in this study are feasible, and it seems

Table 5 Results of examining the function of the intestinal mucosal barrier in the washed microbiota transplantation group

Item	Lipopolysaccharide	Diamine oxidase	D-lactate
Pre-treatment (median, IQR)	7.5 (3.6, 10.4)	4.1 (3.2, 6.5)	8.9 (7.6, 11.8)
Post-treatment (median, IQR)	10.1 (1.0, 23.6)	7.7 (2.3, 13.54)	16.3 (7.7, 18.3)
P value[1]	0.401	0.263	0.208

[1]The results were analyzed by nonparametric Wilcoxon signed-rank test.
IQR: Interquartile range.

that increasing the treatment course can increase the rate of remission. The poor WMT responses observed in this study may be related to the existence of organic lesions that cause GERD, such as hiatal hernia, in some patients, and some may be related to failure to complete the recommended courses.

Because this is a retrospective study, its limitations are that the accuracy and completion of the relevant data and questionnaires could not be improved during follow-up. Memory bias may have affected the questionnaires. The analysis of related test items had a small sample size, which affects the analysis of the experimental results.

CONCLUSION

In conclusion, this study for the first time demonstrated that WMT is safe and effective in treating patients with NERD and PPI dependency. Compared to the PPI group, it can significantly relieve the symptoms of NERD patients, reduce PPI dependency, prolong the duration of remission in symptoms, and reduce recurrence. It can also increase the diversity and evenness of the bacterial community. The next step is to expand the sample size and perform further studies to confirm the role of WMT in the treatment of NERD and elucidate its mechanism.

ARTICLE HIGHLIGHTS

Research background

The pathogenesis of gastroesophageal reflux disease (GERD) is closely associated with the intestinal bacteria composition and their metabolites.

Research motivation

At present, the treatment of GERD has not achieved satisfactory clinical results.

Research objectives

To investigate whether washed microbiota transplantation (WMT) improves symptoms of nonerosive reflux disease (NERD) with proton pump inhibitor (PPI) dependency.

Research methods

Patients with recurrent NERD and PPI dependency at the First Affiliated Hospital of Guangdong Pharmaceutical University from 2017 to 2018 were included and divided into a WMT or PPI group treated with PPI with/without WMT. The endpoint was NERD symptom frequency evaluated 1 mo after WMT using reflux disease questionnaire (RDQ) and GERD questionnaire (GERDQ) scores, remission time, PPI dose, and the examination of intestinal mucosal barrier function.

Research results

In the WMT (n = 15) and PPI (n = 12) groups, the total remission rate at 1 mo after treatment was 93.3% *vs* 41.7%. Compared with the PPI group, the WMT group showed better results in GERDQ (P = 0.004) and RDQ (P = 0.003) and in remission months (8 *vs* 2, P = 0.002). The PPI dose was reduced to some extent for 80% of patients in the WMT group and 33.3% in the PPI group. In 24 patients, intestinal mucosal barrier function

was examined before treatment, and changes in the degree of damage were observed in 13 of these patients after treatment. Only one of the 15 patients had minor side effects, including a mushy stool two or three times a day, which resolved on their own after 1 wk.

Research conclusions

This study is the first to demonstrate that WMT may be safe and effective for relieving NERD symptoms and reducing PPI dependency and recurrence.

Research perspectives

WMT could be a new treatment for NERD.

ACKNOWLEDGEMENTS

We acknowledge Professor Fa-Ming Zhang and his team at the Second Affiliated Hospital of Nanjing Medical University of China for technical guidance on washed microbiota transplantation. We also acknowledge the patients and donors for their participation in this study.

REFERENCES

1 **Savarino E**, de Bortoli N, De Cassan C, Della Coletta M, Bartolo O, Furnari M, Ottonello A, Marabotto E, Bodini G, Savarino V. The natural history of gastro-esophageal reflux disease: a comprehensive review. *Dis Esophagus* 2017; **30**: 1-9 [PMID: 27862680 DOI: 10.1111/dote.12511]

2 **Hunt R**, Armstrong D, Katelaris P, Afihene M, Bane A, Bhatia S, Chen MH, Choi MG, Melo AC, Fock KM, Ford A, Hongo M, Khan A, Lazebnik L, Lindberg G, Lizarzabal M, Myint T, Moraes-Filho JP, Salis G, Lin JT, Vaidya R, Abdo A, LeMair A; Review Team:. World Gastroenterology Organisation Global Guidelines: GERD Global Perspective on Gastroesophageal Reflux Disease. *J Clin Gastroenterol* 2017; **51**: 467-478 [PMID: 28591069 DOI: 10.1097/MCG.0000000000000854]

3 **Kinoshita Y**, Ashida K, Hongo M; Japan Rabeprazole Study Group for NERD. Randomised clinical trial: a multicentre, double-blind, placebo-controlled study on the efficacy and safety of rabeprazole 5 mg or 10 mg once daily in patients with non-erosive reflux disease. *Aliment Pharmacol Ther* 2011; **33**: 213-224 [PMID: 21083596 DOI: 10.1111/j.1365-2036.2010.04508.x]

4 **Labenz J**, Labenz G, Stephan D, Willeke F; LOPA-Studiengruppe. [Insufficient symptom control under long-term treatment with PPI in GERD - fact or fiction? *MMW Fortschr Med* 2016; **158** Suppl 4: 7-11 [PMID: 27221555 DOI: 10.1007/s15006-016-8303-0]

5 **Jovov B**, Que J, Tobey NA, Djukic Z, Hogan BL, Orlando RC. Role of E-cadherin in the pathogenesis of gastroesophageal reflux disease. *Am J Gastroenterol* 2011; **106**: 1039-1047 [PMID: 21448147 DOI: 10.1038/ajg.2011.102]

6 **Imhann F**, Bonder MJ, Vich Vila A, Fu J, Mujagic Z, Vork L, Tigchelaar EF, Jankipersadsing SA, Cenit MC, Harmsen HJ, Dijkstra G, Franke L, Xavier RJ, Jonkers D, Wijmenga C, Weersma RK, Zhernakova A. Proton pump inhibitors affect the gut microbiome. *Gut* 2016; **65**: 740-748 [PMID: 26657899 DOI: 10.1136/gutjnl-2015-310376]

7 **Khan Z**, Alastal Y, Khan MA, Khan MS, Khalil B, Shrestha S, Kamal F, Nawras A, Howden CW. On-Demand Therapy with Proton Pump Inhibitors for Maintenance Treatment of Nonerosive Reflux Disease or Mild Erosive Esophagitis: A Systematic Review and Meta-Analysis. *Gastroenterol Res Pract* 2018; **2018**: 6417526 [PMID: 30158966 DOI: 10.1155/2018/6417526]

8 **Yadlapati R**, DeLay K. Proton Pump Inhibitor-Refractory Gastroesophageal Reflux Disease. *Med Clin North Am* 2019; **103**: 15-27 [PMID: 30466671 DOI: 10.1016/j.mcna.2018.08.002]

9 **Jackson MA**, Goodrich JK, Maxan ME, Freedberg DE, Abrams JA, Poole AC, Sutter JL, Welter D, Ley RE, Bell JT, Spector TD, Steves CJ. Proton pump inhibitors alter the composition of the gut microbiota. *Gut* 2016; **65**: 749-756 [PMID: 26719299 DOI: 10.1136/gutjnl-2015-310861]

10 **Freedberg DE**, Kim LS, Yang YX. The Risks and Benefits of Long-term Use of Proton Pump Inhibitors: Expert Review and Best Practice Advice From the American Gastroenterological Association. *Gastroenterology* 2017; **152**: 706-715 [PMID: 28257716 DOI: 10.1053/j.gastro.2017.01.031]

11 **Naito Y**, Kashiwagi K, Takagi T, Andoh A, Inoue R. Intestinal Dysbiosis Secondary to Proton-Pump Inhibitor Use. *Digestion* 2018; **97**: 195-204 [PMID: 29316555 DOI: 10.1159/000481813]

12 **Tugtepe H**, Tugay M, Bozkurt S, Yildiz F, Utkan T, Yegen BC, Dagli TE. Esophageal smooth muscle reactivity is impaired in chronic reflux esophagitis by both receptor- and nonreceptor-mediated mechanisms. *J Pediatr Surg* 2007; **42**: 641-646 [PMID: 17448759 DOI: 10.1016/j.jpedsurg.2006.12.048]

13 **Suri J**, Kataria R, Malik Z, Parkman HP, Schey R. Elevated methane levels in small intestinal bacterial overgrowth suggests delayed small bowel and colonic transit. *Medicine (Baltimore)* 2018;

97: e10554 [PMID: 29794732 DOI: 10.1097/MD.0000000000010554]
14 **Pimentel M**, Lin HC, Enayati P, van den Burg B, Lee HR, Chen JH, Park S, Kong Y, Conklin J. Methane, a gas produced by enteric bacteria, slows intestinal transit and augments small intestinal contractile activity. *Am J Physiol Gastrointest Liver Physiol* 2006; **290**: G1089-G1095 [PMID: 16293652 DOI: 10.1152/ajpgi.00574.2004]
15 **Mullish BH**, Quraishi MN, Segal JP, McCune VL, Baxter M, Marsden GL, Moore D, Colville A, Bhala N, Iqbal TH, Settle C, Kontkowski G, Hart AL, Hawkey PM, Williams HR, Goldenberg SD. The use of faecal microbiota transplant as treatment for recurrent or refractory Clostridium difficile infection and other potential indications: joint British Society of Gastroenterology (BSG) and Healthcare Infection Society (HIS) guidelines. *J Hosp Infect* 2018; **100** Suppl 1: S1-S31 [PMID: 30173851 DOI: 10.1016/j.jhin.2018.07.037]
16 **Wen W**, Zhang H, Shen J, Wei L, Shen S. Fecal microbiota transplantation for patients with irritable bowel syndrome: A meta-analysis protocol. *Medicine (Baltimore)* 2018; **97**: e12661 [PMID: 30290648 DOI: 10.1097/MD.0000000000012661]
17 **Ianiro G**, Bibbò S, Scaldaferri F, Gasbarrini A, Cammarota G. Fecal microbiota transplantation in inflammatory bowel disease: beyond the excitement. *Medicine (Baltimore)* 2014; **93**: e97 [PMID: 25340496 DOI: 10.1097/MD.0000000000000097]
18 **Ding C**, Fan W, Gu L, Tian H, Ge X, Gong J, Nie Y, Li N. Outcomes and prognostic factors of fecal microbiota transplantation in patients with slow transit constipation: results from a prospective study with long-term follow-up. *Gastroenterol Rep (Oxf)* 2018; **6**: 101-107 [PMID: 29780597 DOI: 10.1093/gastro/gox036]
19 **Zhang F**, Cui B, He X, Nie Y, Wu K, Fan D; FMT-standardization Study Group. Microbiota transplantation: concept, methodology and strategy for its modernization. *Protein Cell* 2018; **9**: 462-473 [PMID: 29691757 DOI: 10.1007/s13238-018-0541-8]
20 **Zhang T**, Lu G, Zhao Z, Liu Y, Shen Q, Li P, Chen Y, Yin H, Wang H, Marcella C, Cui B, Cheng L, Ji G, Zhang F. Washed microbiota transplantation vs. manual fecal microbiota transplantation: clinical findings, animal studies and in vitro screening. *Protein Cell* 2020; **11**: 251-266 [PMID: 31919742 DOI: 10.1007/s13238-019-00684-8]
21 **Li HC**, Fan XJ, Chen YF, Tu JM, Pan LY, Chen T, Yin PH, Peng W, Feng DX. Early prediction of intestinal mucosal barrier function impairment by elevated serum procalcitonin in rats with severe acute pancreatitis. *Pancreatology* 2016; **16**: 211-217 [PMID: 26804005 DOI: 10.1016/j.pan.2015.12.177]
22 **Shen S**, Zhao J, Dai Y, Chen F, Zhang Z, Yu J, Wang K. Methamphetamine-induced alterations in intestinal mucosal barrier function occur *via* the microRNA-181c/ TNF-α/tight junction axis. *Toxicol Lett* 2020; **321**: 73-82 [PMID: 31862507 DOI: 10.1016/j.toxlet.2019.12.020]
23 **Savarino E**, Marabotto E, Bodini G, Pellegatta G, Coppo C, Giambruno E, Brunacci M, Zentilin P, Savarino V. Epidemiology and natural history of gastroesophageal reflux disease. *Minerva Gastroenterol Dietol* 2017; **63**: 175-183 [PMID: 28215067 DOI: 10.23736/S1121-421X.17.02383-2]
24 **Vaezi MF**, Katzka D, Zerbib F. Extraesophageal Symptoms and Diseases Attributed to GERD: Where is the Pendulum Swinging Now? *Clin Gastroenterol Hepatol* 2018; **16**: 1018-1029 [PMID: 29427733 DOI: 10.1016/j.cgh.2018.02.001]
25 **Cheung KS**, Chan EW, Wong AYS, Chen L, Wong ICK, Leung WK. Long-term proton pump inhibitors and risk of gastric cancer development after treatment for *Helicobacter pylori*: a population-based study. *Gut* 2018; **67**: 28-35 [PMID: 29089382 DOI: 10.1136/gutjnl-2017-314605]
26 **Tack J**, Pandolfino JE. Pathophysiology of Gastroesophageal Reflux Disease. *Gastroenterology* 2018; **154**: 277-288 [PMID: 29037470 DOI: 10.1053/j.gastro.2017.09.047]
27 **Yang L**, Francois F, Pei Z. Molecular pathways: pathogenesis and clinical implications of microbiome alteration in esophagitis and Barrett esophagus. *Clin Cancer Res* 2012; **18**: 2138-2144 [PMID: 22344232 DOI: 10.1158/1078-0432.CCR-11-0934]
28 **He Z**, Li P, Zhu J, Cui B, Xu L, Xiang J, Zhang T, Long C, Huang G, Ji G, Nie Y, Wu K, Fan D, Zhang F. Multiple fresh fecal microbiota transplants induces and maintains clinical remission in Crohn's disease complicated with inflammatory mass. *Sci Rep* 2017; **7**: 4753 [PMID: 28684845 DOI: 10.1038/s41598-017-04984-z]

World Journal of Gastroenterology

Submit a Manuscript: https://www.f6publishing.com

World J Gastroenterol 2021 February 14; 27(6): 523-533

DOI: 10.3748/wjg.v27.i6.523

ISSN 1007-9327 (print) ISSN 2219-2840 (online)

ORIGINAL ARTICLE

Prospective Study

Prevalence of advanced liver fibrosis and steatosis in type-2 diabetics with normal transaminases: A prospective cohort study

Jasbir Makker, Hassan Tariq, Kishore Kumar, Madhavi Ravi, Danial Haris Shaikh, Vivien Leung, Umar Hayat, Muhammad T Hassan, Harish Patel, Suresh Nayudu, Sridhar Chilimuri

ORCID number: Jasbir Makker 0000-0002-1673-8515; Hassan Tariq 0000-0002-9178-0342; Kishore Kumar 0000-0002-9768-5354; Madhavi Ravi 0000-0001-6580-5721; Danial Haris Shaikh 0000-0002-5798-9046; Vivien Leung 0000-0003-2548-6986; Umar Hayat 0000-0003-3484-1994; Muhammad T Hassan 0000-0001-6982-8250; Harish Patel 0000-0003-3638-9495; Suresh Nayudu 0000-0002-7829-4024; Sridhar Chilimuri 0000-0001-9866-4785.

Author contributions: Makker J and Tariq H designed and performed the study, analyzed the data, and drafted the manuscript; Kumar K and Ravi M collected the clinical data and performed Liver elastography; Hayat U and Patel H performed the bio statistical analysis; Shaikh DH, Hassan MT, Patel H and Leung V made critical revisions to the manuscript; Nayudu S and Chilimuri S supervised the study performance, reviewed the manuscript and gave final approval of the version of the article to be published.

Institutional review board statement: The study protocol conformed to the ethical guidelines of the 1975 Declaration of Helsinki, as reflected in the Bronx Care Health System Institutional Review Board's approval (IRB #05 10 18

Jasbir Makker, Hassan Tariq, Kishore Kumar, Madhavi Ravi, Danial Haris Shaikh, Vivien Leung, Harish Patel, Suresh Nayudu, Sridhar Chilimuri, Division of Gastroenterology, Department of Medicine, BronxCare Health System, Bronx, NY 10457, United States

Umar Hayat, KU School of Medicine-Wichita, University of Kansas, Wichita, KS 67214, United States

Muhammad T Hassan, Department of Medicine, BronxCare Health System, Bronx, NY 10457, United States

Corresponding author: Jasbir Makker, MD, Attending Physician, Division of Gastroenterology, Department of Medicine, BronxCare Health System, 1650 Selwyn Avenue, Suite 10C, Bronx, NY 10457, United States. jmakker@bronxcare.org

Abstract

BACKGROUND

Nonalcoholic fatty liver disease (NAFLD) and type-2 diabetes mellitus (T2DM) have an intricate bidirectional relationship. Individuals with T2DM, not only have a higher prevalence of non-alcoholic steatosis, but also carry a higher risk of progression to nonalcoholic steatohepatitis. Experts still differ in their recommendations of screening for NAFLD among patients with T2DM.

AIM

To study the prevalence of NAFLD and advanced fibrosis among our patient population with T2DM.

METHODS

During the study period (November 2018 to January 2020), 59 adult patients with T2DM and 26 non-diabetic control group individuals were recruited prospectively. Patients with known significant liver disease and alcohol use were excluded. Demographic data and lab parameters were recorded. Liver elastography was performed in all patients.

RESULTS

In the study group comprised of patients with T2DM and normal alanine aminotransferase levels (mean 17.8 ± 7 U/L), 81% had hepatic steatosis as diagnosed by elastography. Advanced hepatic fibrosis (stage F3 or F4) was

04).

Informed consent statement: All study participants provided written informed consent prior to study enrollment.

Conflict-of-interest statement: All authors report no conflicts of interest.

Data sharing statement: No additional data are available.

Open-Access: This article is an open-access article that was selected by an in-house editor and fully peer-reviewed by external reviewers. It is distributed in accordance with the Creative Commons Attribution NonCommercial (CC BY-NC 4.0) license, which permits others to distribute, remix, adapt, build upon this work non-commercially, and license their derivative works on different terms, provided the original work is properly cited and the use is non-commercial. See: http://creativecommons.org/licenses/by-nc/4.0/

Manuscript source: Unsolicited manuscript

Specialty type: Gastroenterology and hepatology

Country/Territory of origin: United States

Peer-review report's scientific quality classification

Grade A (Excellent): 0
Grade B (Very good): 0
Grade C (Good): C, C
Grade D (Fair): 0
Grade E (Poor): 0

Received: November 7, 2021
Peer-review started: November 7, 2020
First decision: December 3, 2020
Revised: December 12, 2020
Accepted: December 27, 2020
Article in press: December 27, 2020
Published online: February 14, 2021

P-Reviewer: Malnick SD, Zhang LL
S-Editor: Zhang L
L-Editor: A
P-Editor: Liu JH

present in 12% of patients with T2DM as compared to none in the control group. Patients with T2DM also had higher number of individuals with grade 3 steatosis [45.8% *vs* 11.5%, (P < 0.00001) and metabolic syndrome (84.7% *vs* 11.5%, P < 0.00001)].

CONCLUSION

A significant number of patients with T2DM, despite having normal transaminase levels, have NAFLD, grade 3 steatosis and advanced hepatic fibrosis as measured by liver elastography.

Key Words: Advanced liver fibrosis; Diabetes; Steatosis; Normal transaminases; Fatty liver disease; Metabolic syndrome

©The Author(s) 2021. Published by Baishideng Publishing Group Inc. All rights reserved.

Core Tip: Individuals with type 2 diabetes mellitus (T2DM) have a higher prevalence of non-alcoholic steatosis and a higher risk of progression to non-alcoholic steatohepatitis and cirrhosis. Experts differ in their screening recommendations for nonalcoholic fatty liver disease among patients with T2DM. We prospectively recruited and performed liver elastography on 59 diabetics and 26 non-diabetic control patients. Patients with known liver disease and alcohol use were excluded. Our study shows advanced fibrosis is prevalent among patients with T2DM as compared to non-diabetics, even with normal liver enzymes. Screening for liver fibrosis in all patients with T2DM should be considered, regardless of liver enzyme levels.

Citation: Makker J, Tariq H, Kumar K, Ravi M, Shaikh DH, Leung V, Hayat U, Hassan MT, Patel H, Nayudu S, Chilimuri S. Prevalence of advanced liver fibrosis and steatosis in type-2 diabetics with normal transaminases: A prospective cohort study. *World J Gastroenterol* 2021; 27(6): 523-533
URL: https://www.wjgnet.com/1007-9327/full/v27/i6/523.htm
DOI: https://dx.doi.org/10.3748/wjg.v27.i6.523

INTRODUCTION

Nonalcoholic fatty liver disease (NAFLD) encompasses a spectrum of clinico-pathological conditions ranging from simple fatty liver disease to nonalcoholic steatohepatitis (NASH). The risk of progression of NASH to cirrhosis has previously been estimated at 21%-26% over a mean follow up of 8.2 years[1]. With the globalization of western diets and increasingly sedentary lifestyles, obesity rates have skyrocketed to epidemic proportions. In parallel with obesity, the prevalence of NAFLD has dramatically increased. The prevalence of NAFLD worldwide ranges from 6% to 35% depending on the method used for diagnosis and the study population[2]. The prevalence in United States has ranged between 11%-34% with the most recent study reporting a prevalence of 46%[3]. As a result of its increasing prevalence, NAFLD has now become the leading cause of liver disease in the western countries[2]. With the rising rates of NAFLD, and the availability of effective durable treatment options for other chronic liver diseases like chronic hepatitis C, experts have predicted NAFLD to become the leading cause of liver transplantation in the near future.

NAFLD and type-2 diabetes mellitus (T2DM) are intricately related to each other and this relationship is bidirectional. Development of insulin resistance is a key phenomenon underlying NAFLD as well as T2DM and as a result, these two disorders commonly occur together. Individuals with T2DM have a higher prevalence of NAFLD[4]. Individuals with T2DM who develop non-alcoholic steatosis also carry a higher risk of progression to NASH[5]. Development of NASH is characterized by progressive hepatocyte necroinflammation which is an important harbinger of cirrhosis and its associated complications such as hepatocellular cancer. In a study from the United States involving 1249 patients with T2DM and biopsy proven NAFLD, prevalence of NASH and advanced liver fibrosis was 69.2% and 41% respectively[6]. A Canadian study with a 12-year follow-up involving nearly 2.5 million

participants, among which nearly one-fifth had newly diagnosed T2DM, found more than two-fold risk of incident liver cirrhosis in patients with newly diagnosed T2DM[7].

Despite the alarming rise in NAFLD prevalence among patients with T2DM, major societies differ in their recommendations about screening for NAFLD among patients with T2DM. The American Association for the Study of Liver Diseases does not recommend NAFLD screening in individuals with T2DM due to its unknown long-term benefits and cost-effectiveness[8]. On the other hand, American Diabetes Association recommends assessment of liver fibrosis in patients with T2DM and elevated transaminases[9]. Our study was conducted to explore the prevalence of NAFLD and advanced fibrosis among our minority inner city population with T2DM who had normal transaminases.

MATERIALS AND METHODS

Study group

From November 2018 to January 2020, all patients aged 18 years and above with T2DM attending the endocrine clinic at our hospital were offered enrollment in this prospective cohort study. All patients who agreed, provided a written and informed consent for their participation. Patients with a known diagnosis of cirrhosis, chronic hepatitis B, chronic hepatitis C, autoimmune hepatitis, drug induced hepatitis, cholestatic liver disease, hemochromatosis and alcoholic liver disease were excluded. Patients with significant alcohol use defined as more than 20 g of daily alcohol use were excluded. Furthermore, any patient with alanine transaminase (ALT) level more than 40 (upper limit of normal at our lab) was excluded.

The study protocol conformed to the ethical guidelines of the 1975 Declaration of Helsinki, as reflected in the Bronx Care Health System Institutional Review Board's approval (IRB #05 10 18 04).

Control group

The control group comprised of patients without T2DM and normal ALT level (< 40 U/L) as defined by our lab. Patients were recruited from the gastroenterology clinic at our hospital. These patients had no known history of fatty liver disease. Exclusion criteria similar to the study group were applied.

Clinical and laboratory parameters

Demographic data including age, gender and ethnicity were collected. All comorbid medical conditions and a complete drug history were recorded *via* patient interviews. A physical examination including measurement of waist circumference, weight, height and body mass index (BMI) was performed at the time of inclusion. Laboratory data including liver enzymes, hemoglobin A1c, lipid profile available within one year of enrollment were recorded.

Assessment of hepatic steatosis and fibrosis using transient elastography

All patients were required to fast for three hours prior to elastography. Liver elastography was performed using the M or XL probe from Fibroscan 502 touch model (Echosens). The probe is automatically selected by the software based on thoracic perimeter and skin capsule distance measurements. Liver stiffness measurement and controlled attenuation parameter (CAP) which estimates the amount of liver fat was obtained. Elastography examination was considered reliable if at least 10 measurements were taken with an interquartile range interval per median LS less than 30%. Liver stiffness and CAP are calculated as a median over minimum 10 validated measurements and expressed in kilopascals (Kpa) and decibel per meter (db/m), respectively. Cut off for stage F0-1, F2, F3 and F4 fibrosis were ≤ 7 Kpa, ≥ 7.5 Kpa, ≥ 10 Kpa and ≥ 14.0 Kpa, respectively[10]. Cut off for CAP to diagnose hepatic steatosis grade 1 (5%-33% steatosis), grade 2 (34%-66% steatosis) and grade 3 (> 66% steatosis) were 238 db/m, 259 db/m and 290 db/m respectively[11].

Metabolic syndrome

Metabolic syndrome was defined by the National Cholesterol Education Program's Adult Treatment Panel III criteria. It is defined as presence of at least three of the following criteria: Waist circumference > 102 cm in men or > 88 cm in women, plasma triglycerides ≥ 150 mg/dL, high density lipoprotein cholesterol < 40 mg/dL in men or < 50 mg/dL in women, blood pressure ≥ 130/85 mmHg, and fasting plasma glucose ≥

110 mg/dL[12].

Sample size and statistical analysis

Sample size estimation was based on the assumption that prevalence of advanced fibrosis among patients with T2DM is around 20%. For a power of 80% at 5% significance level, 57 patients were required in the study group.

Statistical analysis was performed using statistical analysis system software, version 9.4 and graphpad prism software version 8.4.3. Frequencies and percentages were reported for categorical variables. Mean and standard deviations were reported for numerical continuous variables. Dichotomous variables were compared by chi-square analysis using the pearson test. A two-tailed value of < 0.05 was considered statistically significant. Bivariate analysis was done using analysis of variance to determine predictors of advanced fibrosis.

RESULTS

The study group comprised of 59 patients, whereas the control group had 26 patients. Demographics and baseline characteristics of both the groups were compared as shown in Table 1. The mean duration of T2DM in the study group was 15 ± 9 years. Diabetic microvascular complications including retinopathy, nephropathy, and neuropathy were prevalent in 22%, 30% and 17% of study patients, respectively. 41% of these patients were on insulin, 59% on metformin, 17% on sulfonylureas, 20% on glucagon-like peptide 1 receptor agonists, 8% on pioglitazone, 12% on sodium-glucose cotransporter-2 inhibitors, and 19% on dipeptidyl peptidase 4 inhibitors. Mean BMI of patients in the study group was significantly higher as compared to those in the control group (33.1 ± 8.4 *vs* 27.6 ± 4.7, $P = 0.0002$). A total of 7 patients in the study group were not obese and had BMI < 25, 18 patients were with BMI: 25-29.9, 11 had a BMI: 30-34.9, 14 had a BMI: 35-39.9, and 9 patients had a BMI of > 40.

Prevalence of hepatic fibrosis

Elastography revealed that 76% of our study group patients had absent or low-grade (F0-1) fibrosis, 12% had F2 stage fibrosis, 5% had F3 stage fibrosis, and 7% had F4 stage fibrosis. Advanced fibrosis stage (F3 or F4) was diagnosed in a total of seven (12%) patients from the study group (Figure 1). In the control group none of the patients had advanced stage fibrosis, 2 (8%) patients had F2 fibrosis and 24 (92%) patients had F0-1 stage fibrosis (Figure 2).

Prevalence of hepatic steatosis

Eighty-one percent of our study group patients with T2DM had hepatic steatosis as diagnosed by liver elastography. Steatosis grade 3 was prevalent in 27 (46%) patients as compared to 3 (12%) patients in the control group (P value < 0.00001). Steatosis stage 0, 1, and 2 were diagnosed in 11 (19%), 8 (13%), and 13 (22%) patients respectively in the study group (Figure 3). In comparison, the control group had 11 (42%), 7 (27%), and 5 (19%) patients with steatosis stage 0, 1, and 2 respectively.

Prevalence of metabolic syndrome

Metabolic syndrome was more prevalent among the study group patients. Fifty (85%) patients were diagnosed with metabolic syndrome in the study group and on the contrary only three (12%) patients in the control group had metabolic syndrome (P < 0.00001). Among the 27 (46%) patients in the study group who had S3 steatosis, 26 (96%) had metabolic syndrome. Twenty-eight out of the 59 (48%) patients who had metabolic syndrome in the study group met three criteria for metabolic syndrome, 13 (22%) patients met four criteria and remaining 9 (15%) patients met all the five criteria for metabolic syndrome (Figure 4).

Bivariate analysis was performed using analysis of variance to determine predictors of advanced fibrosis. Duration of T2DM was found to be a significant predictor (P < 0.05) of advanced fibrosis. Age ($P = 0.29$), BMI ($P = 0.30$), and waist circumference ($P = 0.46$) had no association with advanced fibrosis.

DISCUSSION

With the prevalence rate of obesity and T2DM reaching epidemic proportions, NAFLD

Table 1 Comparison of characteristics between control and study group

Variate	Control group, *n* = 26	Study group, *n* = 59	*P* value
Age (yr)	53 ± 12.3	62 ± 11.7	0.0014
Gender, *n* (%)			0.8099
Male	9 (35)	23 (39)	
Female	17 (65)	36 (61)	
Ethnicity, *n* (%)			0.5005
Hispanic	21 (81)	41 (69.5)	
African American	3 (12)	13 (22)	
Others	2 (7)	5 (8.5)	
Waist circumference (cm)	97.5 ± 8.4	98. 6 ± 18.5	0.7595
BMI (kg/m^2)	27.6 ± 4.7	33.1 ± 8.4	0.0002
Hypertension, *n* (%)	15 (58)	43 (73)	0.2083
Hyperlipidemia, *n* (%)	10 (38)	35 (59)	0.0999
ALT (U/L)	17 ± 7	17.8 ± 7	0.7189
Platelet count (10^9/L)	258 ± 81	237 ± 61	0.2007
Albumin (g/L)	4.4 ± 0.3	4.3 ± 0.3	0.0687
HDL (mg/dL)	57.7 ± 18.2	49.7 ± 15.5	0.0588
LDL (mg/dL)	106.3 ± 33.6	87.4 ± 35.5	0.0231
TG (mg/dL)	122.5 ± 79.3	154.7 ± 77.9	0.0883
HbA1c	5.4 ± 0.3	7.9 ± 1.8	< 0.0001
Liver stiffness using elastography (kPa)	5.2 ± 1.6	7.5 ± 9.6	0.2138
CAP (dB/m)	230 ± 70	284 ± 64	0.0008

BMI: Body mass index; ALT: Alanine transaminase; HbA1c: Hemoglobin A1c; CAP: Controlled attenuation parameter.

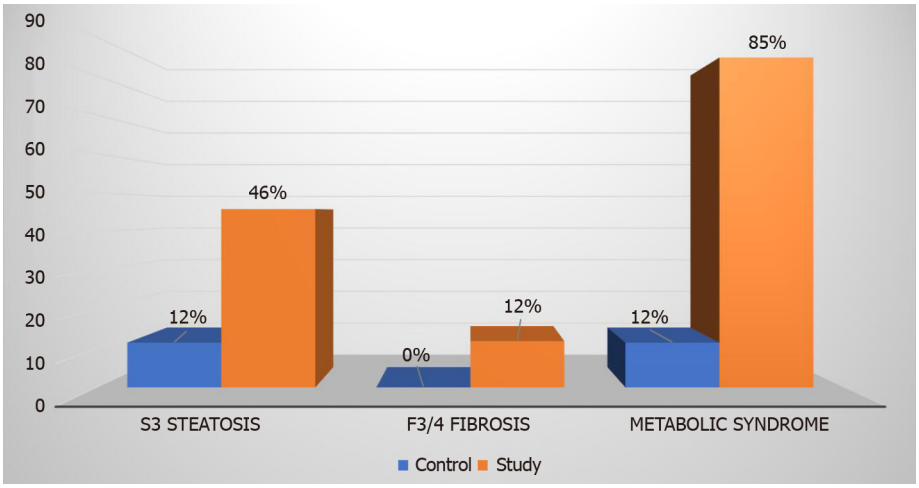


Figure 1 Comparison of S3 steatosis, F3/4 fibrosis and metabolic syndrome among control (non-diabetic) and study (diabetic) group.

has become a health crisis. NAFLD is seen frequently in T2DM with prevalence reported as high as 74% reported in one of the studies[13]. The pathophysiology of NAFLD and T2DM are intricately intertwined with insulin resistance serving as the common mediator. Severe hepatic necro-inflammation can progress to cirrhosis, especially more so in patients with T2DM. A study conducted by McPherson[14] has previously shown an alarmingly high rate of fibrosis progression not only in patients

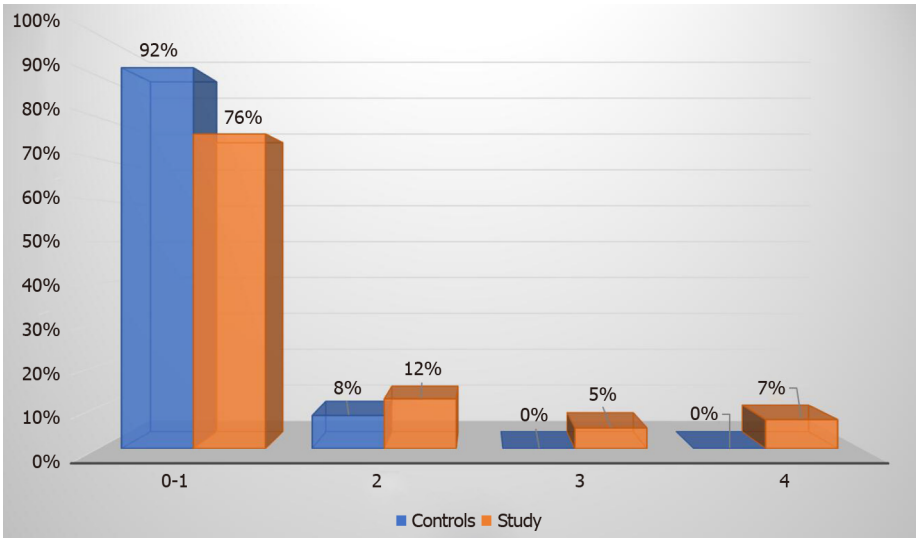


Figure 2 Control and study group patients stratified according to fibrosis stage.

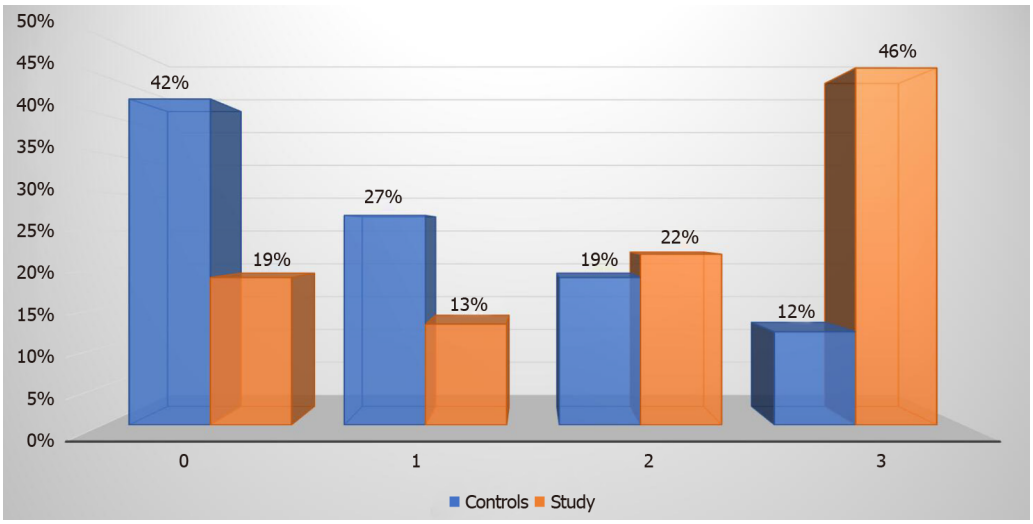


Figure 3 Control and study group patients stratified according to steatosis stage.

with NASH but also in individuals with NAFLD. The same study also showed that 22% of their patients who had NAFLD at their index liver biopsy showed progression to advanced fibrosis on their follow-up biopsy. Co-occurrence of NAFLD and T2DM poses a heightened risk of extrahepatic morbidity and mortality from cardiovascular disease, chronic kidney disease and hepatocellular cancer[15]. Despite these findings, guidelines from the expert societies differ in their opinion regarding the utility of screening for hepatic fibrosis in patients with NAFLD.

The prevalence of NAFLD in our study patients was higher than in previous reports, ranging from 40% to 70% in patients with T2DM[16]. Eighty-one percent of our patients with T2DM were found to have hepatic steatosis and nearly half of them had S3 steatosis. The prevalence of NAFLD in patients with T2DM previously reported in literature varies depending on the ethnicity and method used to diagnose NAFLD. Hispanics have been reported to have highest prevalence of non-alcoholic fatty liver disease[13] and more than 80% of our study patients were of Hispanic ethnicity.

Our study demonstrated that even patients with T2DM who had normal ALT levels were at risk of severe progressive liver disease. Twelve percent of our patients with T2DM had undiagnosed advanced fibrosis. Importantly, these patients who were noted to have advanced fibrosis had normal transaminases (mean ALT = 17.8 ± 7 U/L). Thus, based on current guidelines, these patients without clinically obvious cirrhosis would have gone undiagnosed for years. Among the seven study patients with BMI less than 25, five patients met criteria for metabolic syndrome, four patients

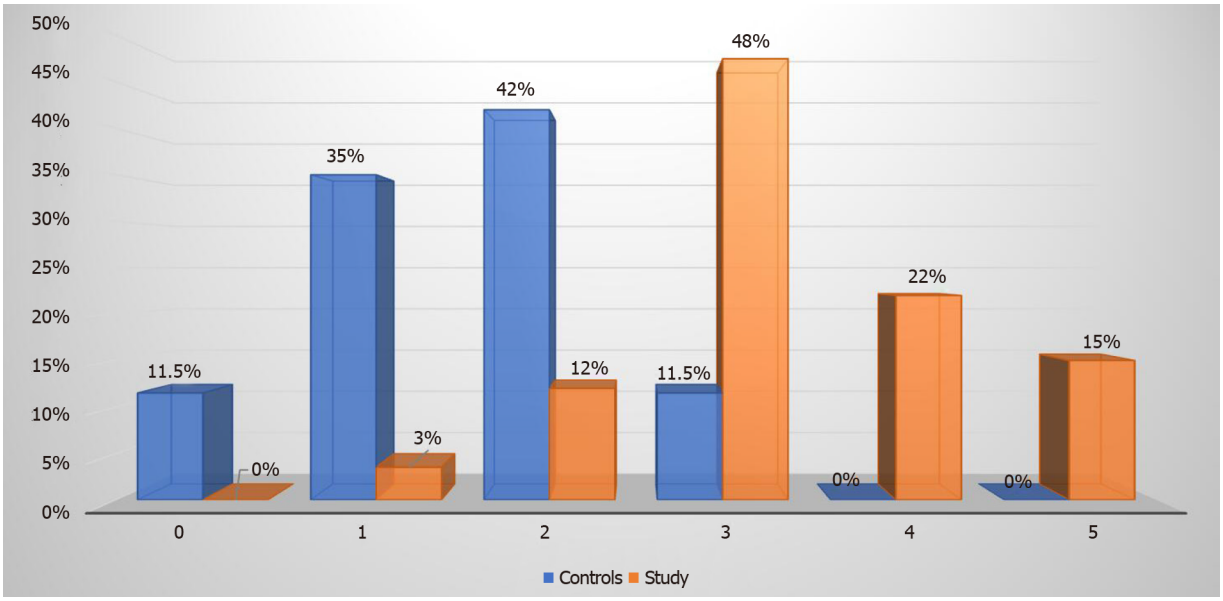


Figure 4 Control and study group patients stratified according to number of criteria met for metabolic syndrome.

had hepatic steatosis and one patient had advanced stage hepatic fibrosis. Thus, even non-obese patients with T2DM and normal transaminases could not be assumed to have a safer metabolic profile.

A cross sectional study done by Tuong *et al*[17] similarly studied the prevalence of hepatic fibrosis among patients with T2DM and found 73.3% of their diabetic patients to have NAFLD. The prevalence of F3 and F4 in their study group was 5.9% and 3.6% respectively, but they included patients with elevated transaminases as well, with a mean ALT of 60.6 U/L in the advanced fibrosis group. Another cross-sectional study by Lai *et al*[18] using transient elastography in patients with T2DM, showed a prevalence of cirrhosis and advanced fibrosis in 13.5% and 21% of patients, respectively. This study also included patients with elevated transaminases with a mean ALT of 38 U/L in patients with cirrhosis. A Turkish study found prevalence of advanced fibrosis of 16.9% and cirrhosis of 8% in their patients with T2DM. The mean ALT in their patients with F3 fibrosis was 39 U/L[19]. In a large prospective cohort study from Hong Kong involving 1918 patients with T2DM, increased liver stiffness suggestive of F3 or F4 fibrosis was found in 18.8% of their diabetic patients with normal ALT, defined as ALT less than 30 U/L in men and less than 19 U/L in women. This data is predominantly from an Asian population and does not reflect our study population[20]. In a study from Australia, prevalence of significant fibrosis, defined by the study as stage F2 and above, was 35% in diabetics. The mean ALT level was 38 U/L among these patients with significant fibrosis[21]. In a prospective French study, significant fibrosis defined as liver stiffness > 8.7 kPa was found in 12.9% of patients with T2DM. However, this study did not exclude patients with significant alcohol use and some of their patients found to have cirrhosis reported > 70 drinks of alcohol per week[22]. Prevalence of F4 stage fibrosis defined as liver stiffness > 9.5 kPA in another study from Romania was 18.6%. However, like most of the other studies, they too included patients with elevated ALT, with a significant number of patients having an ALT more than 40 U/L[23]. Currently, it is not the standard of care to assess liver fibrosis using liver biopsy in patients with normal ALT levels. However, it has been shown before that ALT is not a reliable criterion to exclude patients for assessment of liver fibrosis[24]. In this Italian study involving 458 liver biopsy confirmed NAFLD patients, 63 patients had normal ALT. NASH was demonstrated in 27% of those who had ALT levels less than 30 U/L in men and 19 U/L in women.

Liver biopsy is considered a gold standard diagnostic method for evaluating chronic liver diseases. In patients with NAFLD, it is particularly useful to assess for the presence of steatohepatitis which may progress to the development of cirrhosis. However, liver biopsy is an imperfect tool that is costly and invasive. It is associated with complications including pain in up to 50% of patients, serious bleeding in 0.6%, injury to other internal organs in about 0.08% and rarely death in 0.1% of patients[25]. Considering the enormous burden of NAFLD in our communities and the invasive nature of liver biopsy, it is not practically feasible to subject all patients with NAFLD

to liver biopsy. Surrogate non-invasive methods of liver fibrosis assessment have been developed and are widely available. Vibration controlled liver elastography is one such tool, that is commonly available in United States. It is a quick office-based procedure with acceptable intra-observer and inter-observer variability which has been validated worldwide[26].

We noticed striking gender differences in our study population. In general, higher prevalence of NAFLD has been reported in males as compared to female patients. However, when age specific gender differences are explored further, post-menopausal women have a higher prevalence of NAFLD as compared to men[27]. Our study results are consistent with these findings, demonstrating that 86% of all female patients as compared to 78% of all male patients had NAFLD. Among the 23 male patients in the study group (mean age of 63 years) only one (4%) patient had advanced fibrosis. In comparison, 36 patients were females (mean age of 62 years) and a total of six (17%) had advanced fibrosis. Female patients not only had higher prevalence of NAFLD, but also had a higher prevalence of grade 3 steatosis which was observed in 55% of females as compared to 30% of males. Although gender has been consistently shown to be a significant modifier, gender specific personalized therapy for NAFLD has not been explored and further research is needed to investigate this area.

Clinical implication

Considering the high prevalence of T2DM and NAFLD in our modern world, the burden of undiagnosed cirrhosis is enormous. Diagnosing these patients in a timely fashion would provide the opportunity to adopt intensive lifestyle modifications, and consequently avoid or at the least delay the progression to advanced hepatic fibrosis. Thus, it is important to recognize these patients early on, emphasize the progression of untreated NAFLD to liver cirrhosis, and potentially reduce morbidity, mortality and its related health care burden.

Study limitations

Our study has several limitations. Firstly, the number of overall patients in our study group is small and hence further studies with larger sample sizes are needed to validate our results. Second, we utilized liver elastography to diagnose NAFLD and liver biopsy was not performed in our patients, hence, we do not know the prevalence of NASH, which is the main driver for cirrhosis. However, it is not only unethical but risky too, to perform a liver biopsy in all T2DM patients especially with normal transaminase levels. Thirdly, the inclusion criteria in our study required a normal ALT level, defined as less than 40 U/L by our lab, which is higher than the current accepted standard. Nevertheless, the mean ALT level in the control and study group was 17 and 17.8 U/L, respectively. Fourthly, patients in our study group are older than the control group. Multiple studies have explored the influence of age on liver stiffness, and the results have been conflicting so far, reporting no difference across age groups[28,29], higher liver stiffness measurement in younger[30] or older[31] age. Lastly, our study and control group populations comprised predominantly of Hispanics and African Americans and hence these results cannot be generalized.

CONCLUSION

In conclusion, our study data shows that significant liver disease is prevalent among patients with T2DM, even with normal ALT levels. Measuring ALT levels in our study as a predictor of significant liver disease was unreliable. Timely work up with non-invasive techniques for estimation of liver fibrosis is warranted to prevent presentation at advanced stages of fibrosis. Primary care physicians and endocrinologists should be aware of this complication and should consider screening for liver fibrosis in all patients with T2DM, regardless of liver enzyme levels. Larger studies involving other ethnic groups are needed to validate our results.

ARTICLE HIGHLIGHTS

Research background

With the current obesity epidemic, prevalence of non-alcoholic fatty liver disease (NAFLD) has increased. Individuals with type 2 diabetes mellitus (T2DM) have a higher prevalence of non-alcoholic steatosis, may carry a higher risk of progression to

nonalcoholic steatohepatitis and eventually cirrhosis.

Research motivation

Experts still differ in their recommendations of screening for NAFLD among patients with T2DM.

Research objectives

To study the prevalence of NAFLD and advanced fibrosis among our patient population with T2DM with normal transaminases and without known liver disease.

Research methods

Prospective cohort study assessing hepatic steatosis and fibrosis using transient elastography in 59 patients with T2DM, compared to 26 non-diabetic control group patients.

Research results

In our study group, 81% of patients had hepatic steatosis and 12% had advanced fibrosis on liver elastography. In the control group none of the patients had advanced stage fibrosis. Grade 3 steatosis was prevalent in 46% of patients in the study group as compared to 12% patients in the control group (P value < 0.00001).

Research conclusions

A significant number of patients with T2DM, despite having normal transaminase levels, have advanced fibrosis or steatosis as measured by liver elastography.

Research perspectives

Physicians should be aware of prevalence of significant liver disease among patients with T2DM, even with normal liver enzymes and should consider earlier screening to prevent presentation at advanced stages of fibrosis. Larger studies are needed to confirm and validate our results.

REFERENCES

1 **Matteoni CA**, Younossi ZM, Gramlich T, Boparai N, Liu YC, McCullough AJ. Nonalcoholic fatty liver disease: a spectrum of clinical and pathological severity. *Gastroenterology* 1999; **116**: 1413-1419 [PMID: 10348825 DOI: 10.1016/s0016-5085(99)70506-8]

2 **Vernon G**, Baranova A, Younossi ZM. Systematic review: the epidemiology and natural history of non-alcoholic fatty liver disease and non-alcoholic steatohepatitis in adults. *Aliment Pharmacol Ther* 2011; **34**: 274-285 [PMID: 21623852 DOI: 10.1111/j.1365-2036.2011.04724.x]

3 **Younossi ZM**, Koenig AB, Abdelatif D, Fazel Y, Henry L, Wymer M. Global epidemiology of nonalcoholic fatty liver disease-Meta-analytic assessment of prevalence, incidence, and outcomes. *Hepatology* 2016; **64**: 73-84 [PMID: 26707365 DOI: 10.1002/hep.28431]

4 **Williamson RM**, Price JF, Glancy S, Perry E, Nee LD, Hayes PC, Frier BM, Van Look LA, Johnston GI, Reynolds RM, Strachan MW; Edinburgh Type 2 Diabetes Study Investigators. Prevalence of and risk factors for hepatic steatosis and nonalcoholic Fatty liver disease in people with type 2 diabetes: the Edinburgh Type 2 Diabetes Study. *Diabetes Care* 2011; **34**: 1139-1144 [PMID: 21478462 DOI: 10.2337/dc10-2229]

5 **Bian H**, Zhu X, Xia M, Yan H, Chang X, Hu X, Pan B, Guo W, Li X, Gao X. Impact of Type 2 Diabetes on Nonalcoholic Steatohepatitis and Advanced Fibrosis in Patients with Nonalcoholic Fatty Liver Disease. *Endocr Pract* 2020; **26**: 444-453 [PMID: 31968197 DOI: 10.4158/EP-2019-0342]

6 **Bazick J**, Donithan M, Neuschwander-Tetri BA, Kleiner D, Brunt EM, Wilson L, Doo E, Lavine J, Tonascia J, Loomba R. Clinical Model for NASH and Advanced Fibrosis in Adult Patients With Diabetes and NAFLD: Guidelines for Referral in NAFLD. *Diabetes Care* 2015; **38**: 1347-1355 [PMID: 25887357 DOI: 10.2337/dc14-1239]

7 **Porepa L**, Ray JG, Sanchez-Romeu P, Booth GL. Newly diagnosed diabetes mellitus as a risk factor for serious liver disease. *CMAJ* 2010; **182**: E526-E531 [PMID: 20566726 DOI: 10.1503/cmaj.092144]

8 **Chalasani N**, Younossi Z, Lavine JE, Charlton M, Cusi K, Rinella M, Harrison SA, Brunt EM, Sanyal AJ. The diagnosis and management of nonalcoholic fatty liver disease: Practice guidance from the American Association for the Study of Liver Diseases. *Hepatology* 2018; **67**: 328-357 [PMID: 28714183 DOI: 10.1002/hep.29367]

9 **American Diabetes Association**. 4. Comprehensive Medical Evaluation and Assessment of Comorbidities: *Standards of Medical Care in Diabetes-2020*. *Diabetes Care* 2020; **43**: S37-S47 [PMID: 31862747 DOI: 10.2337/dc20-S004]

10 **Bonder A**, Afdhal N. Utilization of FibroScan in clinical practice. *Curr Gastroenterol Rep* 2014; **16**:

372 [PMID: 24452634 DOI: 10.1007/s11894-014-0372-6]
11 **Wang Y**, Fan Q, Wang T, Wen J, Wang H, Zhang T. Controlled attenuation parameter for assessment of hepatic steatosis grades: a diagnostic meta-analysis. *Int J Clin Exp Med* 2015; **8**: 17654-17663 [PMID: 26770355]
12 **Expert Panel on Detection**, Evaluation, and Treatment of High Blood Cholesterol in Adults. Executive Summary of The Third Report of The National Cholesterol Education Program (NCEP) Expert Panel on Detection, Evaluation, And Treatment of High Blood Cholesterol In Adults (Adult Treatment Panel III). *JAMA* 2001; **285**: 2486-2497 [PMID: 11368702 DOI: 10.1001/jama.285.19.2486]
13 **Williams CD**, Stengel J, Asike MI, Torres DM, Shaw J, Contreras M, Landt CL, Harrison SA. Prevalence of nonalcoholic fatty liver disease and nonalcoholic steatohepatitis among a largely middle-aged population utilizing ultrasound and liver biopsy: a prospective study. *Gastroenterology* 2011; **140**: 124-131 [PMID: 20858492 DOI: 10.1053/j.gastro.2010.09.038]
14 **McPherson S**, Hardy T, Henderson E, Burt AD, Day CP, Anstee QM. Evidence of NAFLD progression from steatosis to fibrosing-steatohepatitis using paired biopsies: implications for prognosis and clinical management. *J Hepatol* 2015; **62**: 1148-1155 [PMID: 25477264 DOI: 10.1016/j.jhep.2014.11.034]
15 **Byrne CD**, Targher G. NAFLD: a multisystem disease. *J Hepatol* 2015; **62**: S47-S64 [PMID: 25920090 DOI: 10.1016/j.jhep.2014.12.012]
16 **Lazo M**, Clark JM. The epidemiology of nonalcoholic fatty liver disease: a global perspective. *Semin Liver Dis* 2008; **28**: 339-350 [PMID: 18956290 DOI: 10.1055/s-0028-1091978]
17 **Tuong TTK**, Tran DK, Phu PQT, Hong TND, Dinh TC, Chu DT. Non-Alcoholic Fatty Liver Disease in Patients with Type 2 Diabetes: Evaluation of Hepatic Fibrosis and Steatosis Using Fibroscan. *Diagnostics (Basel)* 2020; **10** [PMID: 32183383 DOI: 10.3390/diagnostics10030159]
18 **Lai LL**, Wan Yusoff WNI, Vethakkan SR, Nik Mustapha NR, Mahadeva S, Chan WK. Screening for non-alcoholic fatty liver disease in patients with type 2 diabetes mellitus using transient elastography. *J Gastroenterol Hepatol* 2019; **34**: 1396-1403 [PMID: 30551263 DOI: 10.1111/jgh.14577]
19 **Demir M**, Deyneli O, Yılmaz Y. Screening for hepatic fibrosis and steatosis in Turkish patients with type 2 diabetes mellitus: A transient elastography study. *Turk J Gastroenterol* 2019; **30**: 266-270 [PMID: 30411703 DOI: 10.5152/tjg.2018.18559]
20 **Kwok R**, Choi KC, Wong GL, Zhang Y, Chan HL, Luk AO, Shu SS, Chan AW, Yeung MW, Chan JC, Kong AP, Wong VW. Screening diabetic patients for non-alcoholic fatty liver disease with controlled attenuation parameter and liver stiffness measurements: a prospective cohort study. *Gut* 2016; **65**: 1359-1368 [PMID: 25873639 DOI: 10.1136/gutjnl-2015-309265]
21 **Casey SP**, Kemp WW, McLean CA, Topliss DJ, Adams LA, Roberts SK. A prospective evaluation of the role of transient elastography for the detection of hepatic fibrosis in type 2 diabetes without overt liver disease. *Scand J Gastroenterol* 2012; **47**: 836-841 [PMID: 22519948 DOI: 10.3109/00365521.2012.677955]
22 **de Lédinghen V**, Vergniol J, Gonzalez C, Foucher J, Maury E, Chemineau L, Villars S, Gin H, Rigalleau V. Screening for liver fibrosis by using FibroScan(®) and FibroTest in patients with diabetes. *Dig Liver Dis* 2012; **44**: 413-418 [PMID: 22285146 DOI: 10.1016/j.dld.2011.12.005]
23 **Sima A**, Sporea I, Timar R, Vlad M, Braha A, Popescu A, Nistorescu S, Mare R, Sirli R, Albai A, Albai O, Diaconu L, Sorescu T, Popescu S, Sima L. Non-Invasive Assessment of Liver Steatosis and Fibrosis using Transient Elastography and Controlled Attenuation Parameter in Type 2 Diabetes Patients. *Acta Endocrinol (Buchar)* 2018; **14**: 394-400 [PMID: 31149289 DOI: 10.4183/aeb.2018.394]
24 **Fracanzani AL**, Valenti L, Bugianesi E, Andreoletti M, Colli A, Vanni E, Bertelli C, Fatta E, Bignamini D, Marchesini G, Fargion S. Risk of severe liver disease in nonalcoholic fatty liver disease with normal aminotransferase levels: a role for insulin resistance and diabetes. *Hepatology* 2008; **48**: 792-798 [PMID: 18752331 DOI: 10.1002/hep.22429]
25 **Tapper EB**, Lok AS. Use of Liver Imaging and Biopsy in Clinical Practice. *N Engl J Med* 2017; **377**: 756-768 [PMID: 28834467 DOI: 10.1056/NEJMra1610570]
26 **Fraquelli M**, Rigamonti C, Casazza G, Conte D, Donato MF, Ronchi G, Colombo M. Reproducibility of transient elastography in the evaluation of liver fibrosis in patients with chronic liver disease. *Gut* 2007; **56**: 968-973 [PMID: 17255218 DOI: 10.1136/gut.2006.111302]
27 **Lonardo A**, Nascimbeni F, Ballestri S, Fairweather D, Win S, Than TA, Abdelmalek MF, Suzuki A. Sex Differences in Nonalcoholic Fatty Liver Disease: State of the Art and Identification of Research Gaps. *Hepatology* 2019; **70**: 1457-1469 [PMID: 30924946 DOI: 10.1002/hep.30626]
28 **Ling W**, Lu Q, Quan J, Ma L, Luo Y. Assessment of impact factors on shear wave based liver stiffness measurement. *Eur J Radiol* 2013; **82**: 335-341 [PMID: 23116805 DOI: 10.1016/j.ejrad.2012.10.004]
29 **Mulabecirovic A**, Mjelle AB, Gilja OH, Vesterhus M, Havre RF. Liver elasticity in healthy individuals by two novel shear-wave elastography systems-Comparison by age, gender, BMI and number of measurements. *PLoS One* 2018; **13**: e0203486 [PMID: 30216377 DOI: 10.1371/journal.pone.0203486]
30 **Colombo S**, Belloli L, Zaccanelli M, Badia E, Jamoletti C, Buonocore M, Del Poggio P. Normal liver stiffness and its determinants in healthy blood donors. *Dig Liver Dis* 2011; **43**: 231-236 [PMID: 20817625 DOI: 10.1016/j.dld.2010.07.008]
31 **Roulot D**, Costes JL, Buyck JF, Warzocha U, Gambier N, Czernichow S, Le Clesiau H, Beaugrand

M. Transient elastography as a screening tool for liver fibrosis and cirrhosis in a community-based population aged over 45 years. *Gut* 2011; **60**: 977-984 [PMID: 21068129 DOI: 10.1136/gut.2010.221382]

World Journal of Gastroenterology

Submit a Manuscript: https://www.f6publishing.com

World J Gastroenterol 2021 February 14; 27(6): 534-544

DOI: 10.3748/wjg.v27.i6.534

ISSN 1007-9327 (print) ISSN 2219-2840 (online)

CASE REPORT

Pancreaticoduodenectomy after neoadjuvant chemotherapy for gastric cancer invading the pancreatic head: A case report

Masahiro Yura, Kiminori Takano, Kiyohiko Adachi, Asuka Hara, Keita Hayashi, Yuki Tajima, Yasushi Kaneko, Yoichiro Ikoma, Hiroto Fujisaki, Akira Hirata, Kumiko Hongo, Kikuo Yo, Kimiyasu Yoneyama, Reiko Dehari, Kazuo Koyanagi, Motohito Nakagawa

ORCID number: Masahiro Yura 0000-0003-4150-2085; Kiminori Takano 0000-0003-0366-8367; Kiyohiko Adachi 0000-0002-7952-6616; Asuka Hara 0000-0002-3295-9094; Keita Hayashi 0000-0002-4022-7627; Yuki Tajima 0000-0002-9121-0227; Yasushi Kaneko 0000-0003-4854-7673; Yoichiro Ikoma 0000-0001-5061-4092; Hiroto Fujisaki 0000-0002-3719-4924; Akira Hirata 0000-0001-6836-1177; Kumiko Hongo 0000-0001-5150-7838; Kikuo Yo 0000-0002-1971-0390; Kimiyasu Yoneyama 0000-0001-5715-7365; Reiko Dehari 0000-0003-0812-9549; Kazuo Koyanagi 0000-0002-8010-8630; Motohito Nakagawa 0000-0003-0507-444X.

Author contributions: Yura M and Takano K performed the surgery and wrote the paper; Koyanagi K and Nakagawa M reviewed the manuscript; Dehari R contributed to pathological diagnosis; All other authors equally contributed to medical treatment; All authors were responsible for the revision of the manuscript and final approval for submission.

Informed consent statement: Written informed consent was obtained from the patient for publication of this case report and any accompanying images.

Conflict-of-interest statement: All

Masahiro Yura, Kiminori Takano, Kiyohiko Adachi, Asuka Hara, Keita Hayashi, Yuki Tajima, Yasushi Kaneko, Yoichiro Ikoma, Hiroto Fujisaki, Akira Hirata, Kumiko Hongo, Kikuo Yo, Kimiyasu Yoneyama, Motohito Nakagawa, Department of Surgery, Hiratsuka City Hospital, Hiratsuka 2540065, Kanagawa, Japan

Reiko Dehari, Department of Surgical Pathology, Hiratsuka City Hospital, Hiratsuka 2540065, Kanagawa, Japan

Kazuo Koyanagi, Department of Gastroenterological Surgery, Tokai University School of Medicine, Isehara 259193, Kanagawa, Japan

Corresponding author: Masahiro Yura, MD, Doctor, Surgeon, Department of Surgery, Hiratsuka City Hospital, 1-19-1, Mihamihara, Hiratsuka 2540065, Kanagawa, Japan. myura@ncc.go.jp

Abstract

BACKGROUND

Pancreaticoduodenectomy (PD) for advanced gastric cancer is rarely performed because of the high morbidity and mortality rates and low survival rate. However, neoadjuvant chemotherapy for advanced gastric cancer has improved, and chemotherapy combined with trastuzumab may have a preoperative tumor-reducing effect, especially for human epidermal growth factor receptor 2 (HER2)-positive cases.

CASE SUMMARY

We report a case of successful radical resection with PD after neoadjuvant S-1 plus oxaliplatin (SOX) and trastuzumab in a patient (66-year-old male) with advanced gastric cancer invading the pancreatic head. Initial esophagogastroduodenoscopy detected a type 3 advanced lesion located on the lower part of the stomach obstructing the pyloric ring. Computed tomography detected lymph node metastasis and tumor invasion to the pancreatic head without distant metastasis. Pathological findings revealed adenocarcinoma and HER2 positivity (immunohistochemical score of 3 +). We performed staging laparoscopy and confirmed no liver metastasis, no dissemination, negative lavage cytological findings, and immobility of the distal side of the stomach due to invasion to the pancreas. Laparoscopic gastrojejunostomy was performed at that time. One

authors declare no conflicts of interest.

CARE Checklist (2016) statement: The authors have read the CARE Checklist (2016), and the manuscript was prepared and revised according to the CARE Checklist (2016).

Open-Access: This article is an open-access article that was selected by an in-house editor and fully peer-reviewed by external reviewers. It is distributed in accordance with the Creative Commons Attribution NonCommercial (CC BY-NC 4.0) license, which permits others to distribute, remix, adapt, build upon this work non-commercially, and license their derivative works on different terms, provided the original work is properly cited and the use is non-commercial. See: http://creativecommons.org/Licenses/by-nc/4.0/

Manuscript source: Unsolicited manuscript

Specialty type: Gastroenterology and hepatology

Country/Territory of origin: Japan

Peer-review report's scientific quality classification

Grade A (Excellent): A
Grade B (Very good): B, B
Grade C (Good): C
Grade D (Fair): 0
Grade E (Poor): 0

Received: December 4, 2020
Peer-review started: December 4, 2020
First decision: December 24, 2020
Revised: January 6, 2021
Accepted: January 26, 2021
Article in press: January 26, 2021
Published online: February 14, 2021

P-Reviewer: Lu J, Zhou ZH
S-Editor: Zhang L
L-Editor: Filipodia
P-Editor: Liu JH

course of SOX and three courses of SOX plus trastuzumab were administered. Preoperative computed tomography showed partial response; therefore, PD was performed after neoadjuvant chemotherapy, and pathological radical resection was achieved.

CONCLUSION

We suggest that radical resection with PD after neoadjuvant chemotherapy plus trastuzumab is an option for locally advanced HER2-positive gastric cancer invading the pancreatic head in the absence of non-curative factors.

Key Words: Pancreaticoduodenectomy; Gastric cancer; Neoadjuvant chemotherapy; Trastuzumab; Human epidermal growth factor receptor 2; Case report

©The Author(s) 2021. Published by Baishideng Publishing Group Inc. All rights reserved.

Core Tip: Because of the high surgical risk and poor prognosis, pancreaticoduodenectomy (PD) is rarely performed for gastric cancer. However, due to advances in surgery and improvements in perioperative management, PD may be considered for gastric cancer to improve long-term survival. We present the successful case of radical resection with PD after neoadjuvant chemotherapy combined with trastuzumab for human epidermal growth factor receptor 2-positive locally advanced gastric cancer invading the pancreatic head without postoperative severe complication. This case suggests that radical resection with PD after neoadjuvant chemotherapy combined with trastuzumab is an option for locally advanced human epidermal growth factor receptor 2-positive gastric cancer invading the pancreatic head in the absence of non-curative factors.

Citation: Yura M, Takano K, Adachi K, Hara A, Hayashi K, Tajima Y, Kaneko Y, Ikoma Y, Fujisaki H, Hirata A, Hongo K, Yo K, Yoneyama K, Dehari R, Koyanagi K, Nakagawa M. Pancreaticoduodenectomy after neoadjuvant chemotherapy for gastric cancer invading the pancreatic head: A case report. *World J Gastroenterol* 2021; 27(6): 534-544
URL: https://www.wjgnet.com/1007-9327/full/v27/i6/534.htm
DOI: https://dx.doi.org/10.3748/wjg.v27.i6.534

INTRODUCTION

Gastric cancer is the fifth most frequent cancer and the third most frequent cause of cancer death worldwide, according to the global cancer statistics presented in 2018[1]. Curative resection of gastric cancer is essential to achieve long-term survival. In patients with locally advanced gastric cancer invading adjacent organs, extended multivisceral resection is required to achieve an R0 resection. Pancreaticoduodenectomy (PD) is theoretically needed to achieve an R0 resection for locally advanced gastric cancer with invasion to the head of the pancreas and duodenum. This procedure has rarely been performed for gastric cancer because of the significant morbidity and mortality and poor prognosis[2,3]; however, some recent studies have shown that resection combined with PD is associated with improved survival in patients with locally advanced gastric cancer[4-7]. Li *et al*[8] described in their recent systematic review that PD is a feasible option for locally advanced gastric cancer invading the duodenum and/or pancreas, with acceptable surgical risk, and offers survival benefits for selected patients. In addition, several randomized controlled studies showed that postoperative adjuvant chemotherapy for gastric cancer has improved the prognosis of advanced cases[9-11], and preoperative chemotherapy is also expected to be effective, with several clinical trials currently underway[12,13]. Therefore, multidisciplinary treatment is considered important especially for advanced cases, and the indications for PD to achieve an R0 resection for locally advanced gastric cancer invading the pancreas should be reconsidered.

However, there are no reports showing the therapeutic effect of PD on advanced gastric cancer after neoadjuvant chemotherapy especially in combination with trastuzumab. Our case is the successful report of radical resection with PD after

neoadjuvant S-1 plus oxaliplatin (SOX) combined with trastuzumab in a patient with locally advanced gastric cancer invading the pancreatic head.

CASE PRESENTATION

Chief complaints

A 66-year-old man had symptoms of abdominal pain, distension, and weight loss (from 62 to 47 kg within 6 mo).

History of present illness

The patient complained of abdominal distension and weight loss and had visited the hospital previously. Esophagogastroduodenoscopy (EGD) was performed, and an advanced type 3 lesion was detected on the lower part of the gastric body with stenosis, causing resistance to passage of the scope. He was then admitted to our hospital and underwent a detailed medical examination and treatment.

History of past illness

He had no specific past illness but had a current active smoking status [Brinkman Index: 920 (20 × 46 years)].

Personal and family history

No family history to note.

Physical examination

Mild tenderness was noted in the upper abdomen.

Laboratory examinations

Initial laboratory data revealed a hemoglobin level of 11.0 g/dL, white blood cell count of 9700 cells/μL, and platelet count of 3.17 × 10^5/μL. The creatinine level was 0.81 mg/dL, total bilirubin level was 0.3 mg/dL, direct bilirubin level was 0.1 mg/dL, aspartate aminotransferase level was 43 IU/L, alanine aminotransferase level was 72 IU/L, and albumin level was 3.5 g/dL. Tumor marker level of the carcinoembryonic antigen was 23.00 ng/mL, and carbohydrate antigen 19-9 level was 53.20 U/mL.

Imaging examinations

EGD identified stenosis caused by a large tumor (Figure 1). Computed tomography (CT) showed lymph node (LN) metastases at the station of the lesser curvature (#3 LN; 11.8 mm × 8.5 mm, Figure 2A), right greater curvature nodes along the right gastroepiploic artery (#4d LN; 10.3 mm × 8.4 mm, Figure 2B), infrapyloric nodes (#6 LN; 21.6 mm × 14.7 mm, Figure 2C), anterosuperior LNs along the common hepatic artery (#8a; 14.0 mm × 13.4 mm, Figure 2D), and suspicion of metastatic #6 LN invasion to the pancreatic head (the names of the LN station are provided in Table 1). There were no findings of distant metastasis.

Biopsies were taken, and the histological examination led to a diagnosis of adenocarcinoma (papillary and well-differentiated adenocarcinoma; Figure 3A). Additional pathological examination revealed human epidermal growth factor receptor 2 (HER2) positivity based on an immunohistochemical score of 3 + (Figure 3B).

The clinical diagnosis was gastric cancer LD circ cType3 cT4b (panc) N2M0 cStageIVA according to the Union for International Cancer Control Tumor, Node Metastasis Classification of Malignant Tumors, Eighth Edition[14]. The lymph node station was defined according to the Japanese Classification of Gastric Cancer, 15th Edition[15].

FINAL DIAGNOSIS

Pathological examination and classification

Pathological examination of the resected specimen revealed that the primary tumor was mixed-type adenocarcinoma (papillary adenocarcinoma, moderately differentiated adenocarcinoma > poorly differentiated adenocarcinoma non-solid type, mucinous adenocarcinoma) and subserosal invasion (35 mm × 30 mm) with lymphatic

Table 1 Lymph node station

Station No.	Definition
1	Right paracardial nodes
3	Lesser curvature nodes
4sb	Left greater curvature nodes along the left gastroepiploic artery
4d	Right greater curvature nodes along the right gastroepiploic artery
5	Suprapyloric nodes
6	Infrapyloric nodes
7	Nodes at the root of the left gastric artery
8a	Anterosuperior LNs along the common hepatic artery
8p	Posterior LNs along the common hepatic artery
9	Nodes at the celiac artery
11p	Nodes along the proximal splenic artery
12a	Hepatoduodenal ligament LNs along the proper hepatic artery
12b	Hepatoduodenal ligament LNs along the bile duct
12p	Hepatoduodenal ligament LNs along the portal vein
14v	Nodes along the superior mesenteric vein
13a	Superior posterior pancreatoduodenal lymph nodes
13b	Inferior posterior pancreatoduodenal lymph nodes
17a	Superior anterior pancreatoduodenal lymph nodes
17b	Inferior anterior pancreatoduodenal lymph nodes

LNs: Lymph node.

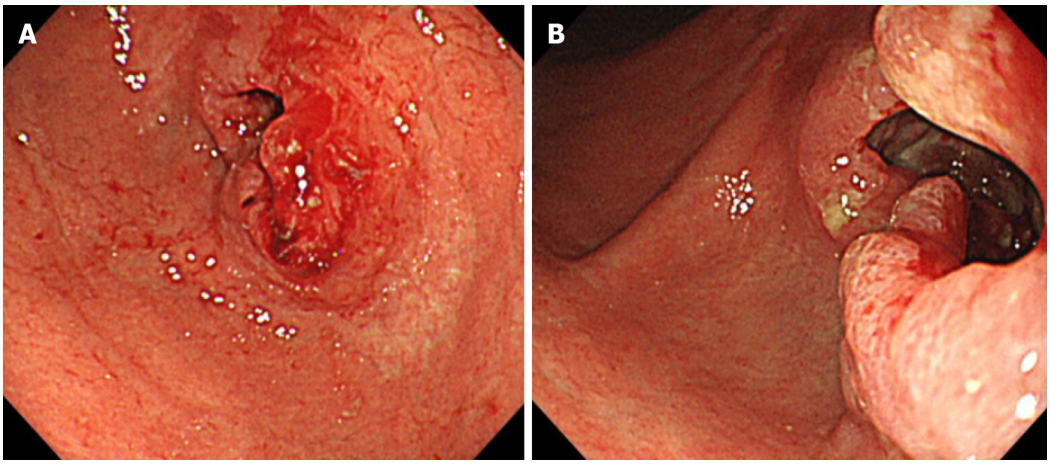


Figure 1 Initial endoscopic findings. A and B: Type 3 primary tumor located on the lower part of the stomach.

and venous infiltration (Ly1a, V1a). The horizontal and vertical surgical margins were negative, and all dissected LNs were negative for metastasis (0/54). Pathological findings also suggested pancreatic infiltration. The cancer cells infiltrating the pancreas may have invaded along the lymph nodes or nerves on the surface of the pancreas. (Figure 4). The pathological diagnosis was gastric cancer LD Circ ypType3, ypT4b (panc) N0M0, ypStage IIIA. Degeneration of cancer cells was limited, and the pathological therapeutic effect was classified as grade 1a according to the Japanese Classification of Gastric Cancer, 15th Edition[15].

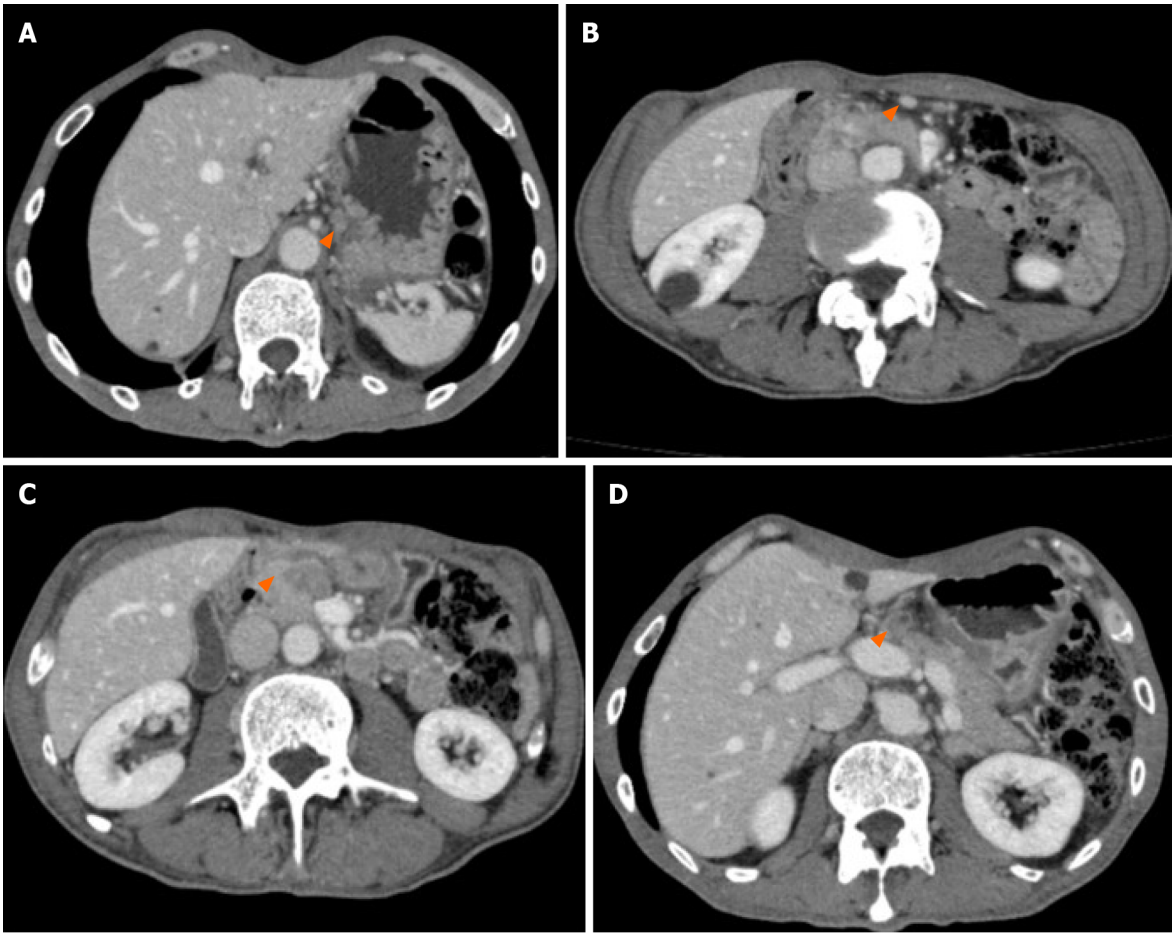


Figure 2 Initial computed tomography findings, computed tomography showed lymph node swelling. A: Swelling of #3 lymph node (LN) (orange triangle; 11.8 mm × 8.5 mm); B: Swelling of #4d LN (orange triangle; 10.3 mm × 8.4 mm); C: Swelling of #6 LN, suspected to be invasion to the pancreatic head (orange angle; 21.6 mm × 14.7 mm); D: Swelling of #8a LN (orange triangle; 14.0 mm × 13.4 mm).

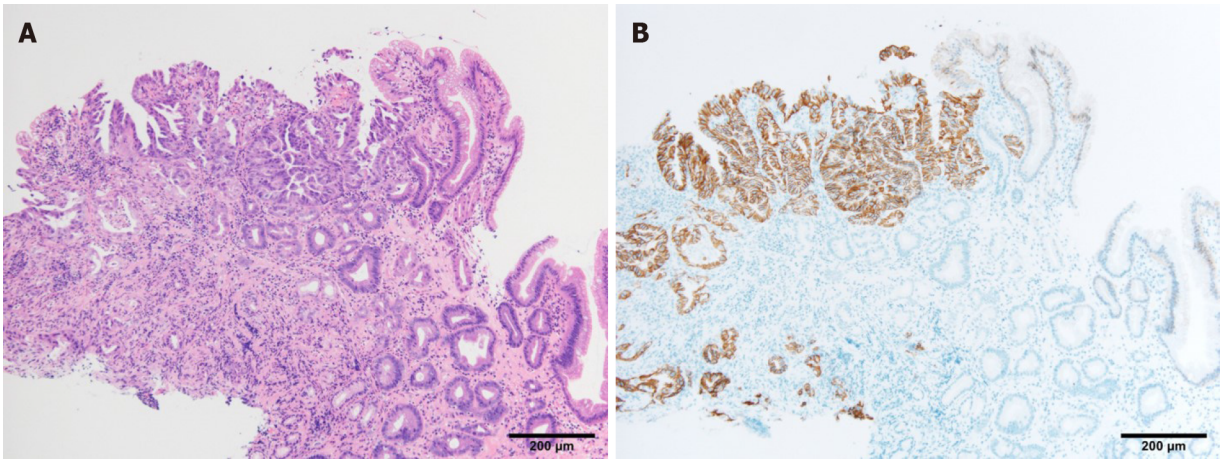


Figure 3 Pathological findings from endoscopic biopsy. Pathological examination of the endoscopic biopsy revealed a papillary and well-differentiated adenocarcinoma. A: Hematoxylin and eosin staining results; × 10; B: Human epidermal growth factor receptor 2 positivity was detected by an immunohistochemical staining; × 10.

TREATMENT

As the patient was undernourished, we inserted a double elemental diet tube to administer enteral nutrition and drain food residue from the stomach. After 10 d of continuous enteral nutrition, we performed staging laparoscopy and confirmed no liver metastasis, no dissemination, and negative lavage cytological results. In addition,

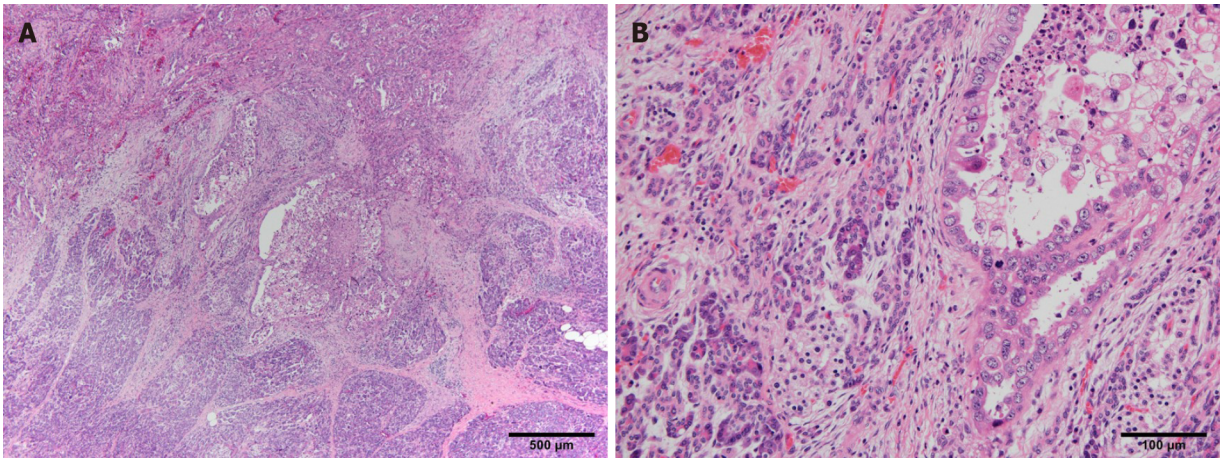


Figure 4 Pathological findings from resected specimens showing pancreatic infiltration of cancer cells. A: Hematoxylin and eosin staining results; × 4; B: Hematoxylin and eosin staining results; × 20.

immobility of the lower part of the stomach body due to cancerous invasion to the pancreatic head was confirmed. Thus, laparoscopic ante-colic gastrojejunostomy (GJ) and half-cut of the gastric body at the distal side of the anastomosis were performed.

Considering the clinical and intraoperative findings, it was a locally advanced gastric cancer with pancreatic head invasion without non-curative factors such as dissemination and distant metastasis. As a treatment strategy, preoperative chemotherapy was given first, and in the case of stable disease or partial response, R0 resection with PD could be adopted.

Neoadjuvant chemotherapy and toxicities

After laparoscopic GJ, one course of SOX (S-1 120 mg/d on days 1-14, oxaliplatin 100 mg/m^2 on day 1) was performed during one continuous hospitalization stay after surgery, and three courses of SOX with trastuzumab (S-1 120 mg/d on days 1-14, oxaliplatin 100 mg/m^2 on day 1, trastuzumab 8 mg/kg during the first cycle and 6 mg/kg during the second and third cycles) was performed in an outpatient setting. For this regimen, only grade 2 elevations in aspartate aminotransferase and alanine aminotransferase levels (84 and 96 IU/L, respectively) were observed, and no grade 3 or more severe adverse events were detected according to the National Cancer Institute Common Terminology Criteria for Adverse Events version 5.0[16].

Radiological evaluation

After neoadjuvant chemotherapy, EGD showed shrinkage of the primary tumor, but the scope could not pass through (Figure 5A and B), while CT showed marked reduction of the primary tumor and metastatic LNs. The #3 (Figure 6A) and #4d (Figure 6B) LNs could not be detected, and #6 LN, which had been suspected of invading the pancreatic head before chemotherapy, was scarred and could not be measured (Figure 6C). The #8a LN had shrunk (from 14.0 mm × 13.4 mm to 9.2 mm × 7.0 mm; Figure 6D). The clinical therapeutic effect was classified as a partial response on radiological examination according to the Response Evaluation Criteria in Solid Tumors criteria version 1.0.

Although the invasion of the pancreas was not clear on CT, magnetic resonance imaging showed that most of the boundary between the stomach or lymph nodes around the stomach and pancreas had fatty tissue, but some of the boundaries were unclear; thus, the invasion could not be denied. Thus, the preoperative diagnosis was ycT4b (panc) N1M0 ycStage IVA.

Preoperative medical examination

The surgical risks for this patient included his age (66 years), obstructive pulmonary dysfunction [vital capacity (%), 101.5; forced expiratory volume in 1 s (%), 69.5; forced expiratory volume in 1 s (L), 2.48], current heavy smoker status [Brinkman Index: 920 (20 × 46 years)], undernutrition (total protein level 5.8 g/dL, albumin level 3.2 g/dL), a history of GJ, and the patient's clinical state after four courses of neoadjuvant chemotherapy. Cardiac function was normal (normal wall motion, ejection fraction of 72.8%) after neoadjuvant chemotherapy with trastuzumab, and the brain natriuretic

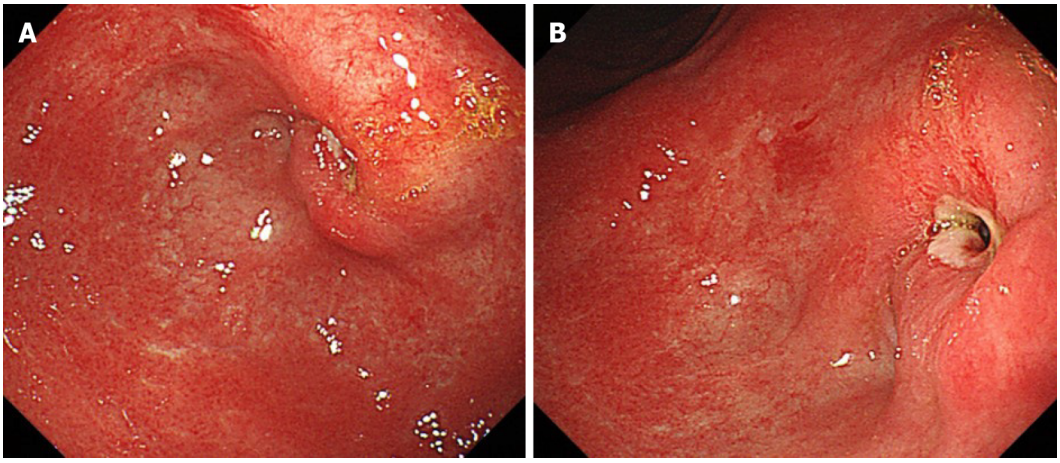


Figure 5 Endoscopic findings after neoadjuvant chemotherapy. A and B Shrinkage of the primary tumor.

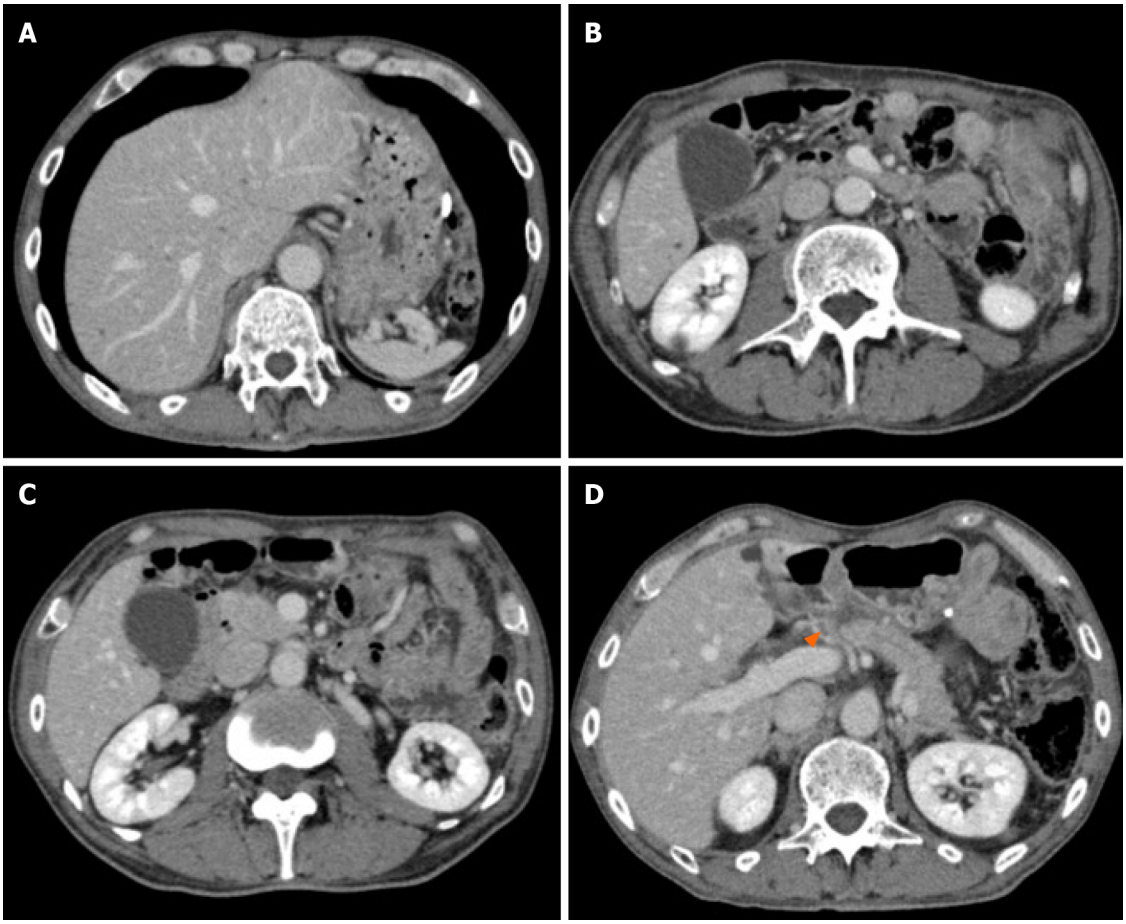


Figure 6 Computed tomography findings after neoadjuvant chemotherapy. A: #3 lymph node (LN) became smaller and could not be detected; B: #4d LN became smaller and could not be detected; C: #6 LN became smaller and could not be detected; D: #8a LN became smaller (orange triangle; 14.0 mm × 13.4 mm to 9.2 mm × 7.0 mm).

peptide level was 33.3 pg/mL. Tumor marker levels were decreased compared with initial blood tests, and the carcinoembryonic antigen level improved from 23.00 to 11.00 ng/mL and the carbohydrate antigen 19-9 level from 53.20 to 26.80 U/mL. The therapeutic strategy was explained to the patient, who decided to undergo surgical treatment.

Pancreaticoduodenectomy with D2 lymph node dissection for distal gastric cancer

After detachment of adhesions between the omentum and abdominal wall, we

confirmed no liver metastasis or dissemination. Rapid lavage cytology revealed no cancer cells in the ascites (Class I). We first performed omentectomy to expose the layer of the colic vein and superior mesenteric vein and performed Kocher mobilization until the inferior vena cava could be identified; the layers were continued up to the layer of the omentectomy. Near the right gastroepiploic artery and vein, the metastatic LN and/or tissues with desmoplastic and inflammatory reactions near the primary lesion invaded the pancreatic head and could not be separated. Therefore, PD was required to achieve R0 resection. We made a jejunum incision at the proximal and distal sides of the anastomosis, which was bypassed in a previous surgery, and performed D2 lymphadenectomy (#1, #3a, #3b, #4sb, #4d, #5, #6, #7, #8a, #9, #11p, #12a) with #8p and #14v LN dissection. The gastric body was cut using an Endo GIA 60 mm stapler (Covidien, Mansfield, MA, United States). After regional LN dissection of the gastric cancer, the gastroduodenal artery was ligated. The dorsal side of the pancreas was tunneled in front of the portal vein. We decided that resection of the tumor could be performed if the pancreas was cut at the line just on the portal vein.

The vein branches of the superior mesenteric vein (first jejunal vein, inferior pancreaticoduodenal vein, gastrocolic trunk, posterior superior pancreatoduodenal vein) were processed, and the artery branches (first jejunal artery, inferior pancreaticoduodenal artery, dorsal pancreatic artery) were processed outside the plexus of the superior mesenteric artery. After excision of the gallbladder, the common bile duct was dissected, and PD was completed (#13a, #13b, #17a, #17b, #12b, and #12p were taken together with the specimen).

Reconstruction

Reconstruction of modified Child's method with Braun enteroenterostomy was performed. First, pancreaticojejunostomy and cholangiojejunostomy were performed, followed by antecolic reverse peristaltic GJ. Jejunum of the afferent loop was sutured to the gastric body to prevent reflux to the afferent loop. Finally, jejunostomy was performed distal to the GJ, and Braun enteroenterostomy was made. The total operation time was 11 h and 16 minutes, and total blood loss was 490 mL.

OUTCOME AND FOLLOW-UP

On the day after the operation, the patient started drinking water and using a jejunostomy tube for enteral nutrition, and he resumed eating on the second day. Surgical complications included aspiration pneumonia, pancreatic fistula, and intraabdominal abscess, each of which was cured with antibiotics and defined as Clavien-Dindo grade 2[17]. The patient was discharged on postoperative day 16 without the need for enteral nutrition. Adjuvant S-1 (100 mg/body) was started 2 mo after the surgery and SOX (S-1; 120 mg/d on days 1-14, oxaliplatin; 100 mg/m^2 on day 1) was started 3 mo after the surgery. Postoperative SOX chemotherapy was performed for three courses. There are no recurrences 8 mo after surgery. The timeline was showed in Table 2.

DISCUSSION

We present the successful case of radical resection with PD after neoadjuvant chemotherapy combined with trastuzumab for HER2-positive locally advanced gastric cancer invading the pancreatic head.

The principle of surgical oncology with curative intent is *en bloc* resection of organs potentially invaded by the cancer. In cases of pancreatic head invasion, PD with gastrectomy is required. Because of the high surgical risk and poor prognosis, PD is rarely performed for gastric cancer. However, due to advances in surgery and improvements in perioperative management, PD may be considered for gastric cancer to improve long-term survival. Recent reports from two Japanese high-volume cancer centers reported morbidity rates of 45.1% (14/31) and 73.9% (17/23) and mortality rates of 0% and 12.9% (4/31), respectively, after PD for gastric cancer[5,7]. Pancreatic fistula was the most common complication in these studies (12.9% and 43.5%). Saka *et al*[7] reported that early detection of pancreatic fistulas and drain discharge management are important to prevent fatal complications, such as an intraabdominal abscess leading to rupture of pseudoaneurysms, and emphasized that medical staff (including the surgeon and nursing staff) should be trained in drain management.

Table 2 Timeline from the onset of symptoms to the completion of treatment

Time series	Symptoms and treatment details
5 mo ago	He had symptoms of abdominal pain, distension and weight loss (from 62 to 47 kg within 6 mo) and visited hospital
	Double elemental diet tube was inserted to administer enteral nutrition and drain food residue from the stomach
4 mo ago	Staging laparoscopy confirmed no liver metastasis, no dissemination, and negative lavage cytological results
	Laparoscopic ante-colic gastrojejunostomy and half-cut of the gastric body at the distal side of the anastomosis were performed
1-4 mo ago	SOX 1
	SOX + Trastuzumab 2-4
The date of surgery	Pancreaticoduodenectomy with D2 lymph node dissection for distal gastric cancer was done
	Adjuvant S1 1
2-8 mo after surgery	Adjuvant SOX 1-3
	CT shows no recurrence (7 mo after surgery)

CT: Computed tomography; SOX: S-1 plus oxaliplatin.

Therefore, those authors recommended that PD should be performed only at institutions comfortable with PD management.

In our institution, PD is typically performed for pancreatic cancer by hepatobiliary-pancreatic surgeons and appropriate drainage treatment can be performed by radiologists if necessary. Thus, in this case, upper gastrointestinal surgeon and hepatobiliary-pancreatic surgeon performed the surgery in collaboration, allowing us to perform adequate regional LN dissection of the stomach and provide safe surgery and postoperative management for PD. In the present case, although severe inflammatory reactions around the tumor and degeneration and desmoplastic changes due to neoadjuvant chemotherapy were observed, the intraoperative blood loss was 490 mL, blood transfusion was not required, the intensive care unit stay was 1 d, postoperative complications did not exceed grade 2, and the patient was discharged 16 d after surgery. In addition, from an oncological perspective, R0 resection was achieved, and the number of LNs dissected was 54.

Li *et al*[8] reported a 5-year overall survival (OS) rate of gastric cancer patients after PD of 39.3%, which is comparable with that of patients with stage IIIB (34.8%) gastric cancer, as is registered nationally by the Japanese Gastric Cancer Society[18]. Katai *et al*[18] also reported, in a nationwide study, a rate of PD performed for gastric cancer of 0.1% (120/12202) and a 5-year OS rate of 41.4%. These findings suggest that PD is a beneficial technique under the correct indications. Saka *et al*[7] reported that the 5-year OS rate was 0% in patients with non-curative factors [such as para-aortic LN (PAN) metastasis, positive lavage cytological results, and peritoneal dissemination] and 47.4% in patients those without these factors. Nunobe *et al*[5] reported that the 5-year OS rate after R0 resection with PD was significantly better in the ≤ pN2 group (50.0%) compared with the ≥ pN3 group (7.7%). In our case, we confirmed negative lavage cytological results, no PAN, no dissemination during surgery, and no detected LN metastasis pathologically after surgery. All of these factors may affect survival after PD. According to these studies, PD is considered to be required in gastric cancer surgery in about 1 in 500 to 1000 cases[7,18], of which about one-third may have incurable factors[7]. Combining neoadjuvant chemotherapy may reduce the proportion of incurable cases and increase the rate of radical resection with PD.

Several randomized studies have shown a survival benefit of postoperative adjuvant chemotherapy for advanced gastric cancer[9-11]. However, no reports have described the efficacy or completion rate of adjuvant chemotherapy after PD. The completion rate of adjuvant chemotherapy after routine gastrectomy was reported to be 65.8% for S-1[9], 67% for capecitabine plus oxaliplatin[10], and 49% for docetaxel plus S-1[11]. This indicates that 33%-51% of patients do not benefit from chemotherapy. Adjuvant chemotherapy may be inadequate if the procedure becomes more invasive because of major surgical complications combined with organ resection and loss of appetite or physical fitness. Thus, preoperative chemotherapy is considered to have benefits in these patients compared with postoperative chemotherapy. Clinical trials of neoadjuvant chemotherapy for gastric cancer with extensive nodal metastasis (bulky and/or PANs) reported high completion rates of 65%-81%[19-21]. Despite the inclusion of

double or triple chemotherapy regimens in these trials, compliance was greater compared with single-agent postoperative adjuvant chemotherapy. Considering the effects of preoperative chemotherapy and the highly invasive postoperative situation, patients with locally advanced gastric cancer who require PD for radical resection are thought to be good candidates for neoadjuvant chemotherapy. We used SOX plus trastuzumab as preoperative chemotherapy because, at our facility, we typically use the SOX regimen as preoperative chemotherapy for advanced gastric cancer with multiple LN metastases, according to a recent ongoing randomized clinical trial (JCOG1509)[13]. Furthermore, preoperative and perioperative chemotherapies combined with trastuzumab for HER2-positive gastric cancer are currently underway[12,22]. Thus, we think that SOX plus trastuzumab combination is expected as effective preoperative chemotherapy for HER-2 positive advanced gastric cancer.

Another problem is that invasion of adjacent organs cannot always be confirmed pathologically[7]. Desmoplastic and inflammatory reactions surrounding the tumor cannot be differentiated from tumor invasion during surgery; thus, PD cannot be avoided in such cases. However, neoadjuvant chemotherapy has a possibility to differentiate between cases of true tumor invasion and inflammatory reactions and may even avoid PD in some cases.

There were some limitations to this case report. First, the long-term survival benefit of neoadjuvant chemotherapy combined with trastuzumab in this patient was unknown, and a longer observation time is required. However, we achieved R0 resection with PD after this regimen and confirmed no LN metastasis pathologically. Previous reports have reported a survival benefit in such cases. Second, we use SOX combined with trastuzumab, for which no clear evidence has been established. However, the therapeutic effects of neoadjuvant SOX (JCOG1509; UMIN000024065) and neoadjuvant chemotherapy combined with trastuzumab for advanced gastric cancer (JCOG1301; UMIN000016920[12]) are currently being verified in clinical trials in Japan.

CONCLUSION

We suggest that radical resection with PD after neoadjuvant chemotherapy combined with trastuzumab is one option for locally advanced HER2-positive gastric cancer invading the pancreatic head in the absence of non-curative factors.

REFERENCES

1 **Bray F**, Ferlay J, Soerjomataram I, Siegel RL, Torre LA, Jemal A. Global cancer statistics 2018: GLOBOCAN estimates of incidence and mortality worldwide for 36 cancers in 185 countries. *CA Cancer J Clin* 2018; **68**: 394-424 [PMID: 30207593 DOI: 10.3322/caac.21492]

2 **Ohashi I**. Combined resection of adjacent organs for advanced cancer of the stomach: pancreatoduodenectomy and left upper abdominal evisceration (in Japanese). *Surg Ther* 1985; **52**: 173-180

3 **Shchepotin IB**, Chorny VA, Nauta RJ, Shabahang M, Buras RR, Evans SR. Extended surgical resection in T4 gastric cancer. *Am J Surg* 1998; **175**: 123-126 [PMID: 9515528 DOI: 10.1016/S0002-9610(97)00268-7]

4 **Wang XB**, Yang LT, Zhang ZW, Guo JM, Cheng XD. Pancreaticoduodenectomy for advanced gastric cancer with pancreaticoduodenal region involvement. *World J Gastroenterol* 2008; **14**: 3425-3429 [PMID: 18528942 DOI: 10.3748/wjg.14.3425]

5 **Nunobe S**, Hiki N, Ohyama S, Fukunaga T, Seto Y, Yamaguchi T. Survival benefits of pancreatoduodenectomy for gastric cancer: relationship to the number of lymph node metastases. *Langenbecks Arch Surg* 2008; **393**: 157-162 [PMID: 18060424 DOI: 10.1007/s00423-007-0248-4]

6 **Chan WH**, Cheow PC, Chung AY, Ong HS, Koong HN, Wong WK. Pancreaticoduodenectomy for locally advanced stomach cancer: preliminary results. *ANZ J Surg* 2008; **78**: 767-770 [PMID: 18844905 DOI: 10.1111/j.1445-2197.2008.04646.x]

7 **Saka M**, Mudan SS, Katai H, Sano T, Sasako M, Maruyama K. Pancreaticoduodenectomy for advanced gastric cancer. *Gastric Cancer* 2005; **8**: 1-5 [PMID: 15747167 DOI: 10.1007/s10120-004-0298-z]

8 **Li DB**, You J, Wang SJ, Zhou YM. Pancreaticoduodenectomy for locally advanced gastric cancer: Results from a pooled analysis. *Asian J Surg* 2019; **42**: 477-481 [PMID: 30316667 DOI: 10.1016/j.asjsur.2018.09.005]

9 **Sakuramoto S**, Sasako M, Yamaguchi T, Kinoshita T, Fujii M, Nashimoto A, Furukawa H, Nakajima T, Ohashi Y, Imamura H, Higashino M, Yamamura Y, Kurita A, Arai K; ACTS-GC Group. Adjuvant chemotherapy for gastric cancer with S-1, an oral fluoropyrimidine. *N Engl J Med* 2007; **357**: 1810-

1820 [PMID: 17978289 DOI: 10.1056/NEJMoa072252]
10 **Bang YJ**, Kim YW, Yang HK, Chung HC, Park YK, Lee KH, Lee KW, Kim YH, Noh SI, Cho JY, Mok YJ, Kim YH, Ji J, Yeh TS, Button P, Sirzén F, Noh SH; CLASSIC trial investigators. Adjuvant capecitabine and oxaliplatin for gastric cancer after D2 gastrectomy (CLASSIC): a phase 3 open-label, randomised controlled trial. *Lancet* 2012; **379**: 315-321 [PMID: 22226517 DOI: 10.1016/S0140-6736(11)61873-4]
11 **Yoshida K**, Kodera Y, Kochi M, Ichikawa W, Kakeji Y, Sano T, Nagao N, Takahashi M, Takagane A, Watanabe T, Kaji M, Okitsu H, Nomura T, Matsui T, Yoshikawa T, Matsuyama J, Yamada M, Ito S, Takeuchi M, Fujii M. Addition of Docetaxel to Oral Fluoropyrimidine Improves Efficacy in Patients With Stage III Gastric Cancer: Interim Analysis of JACCRO GC-07, a Randomized Controlled Trial. *J Clin Oncol* 2019; **37**: 1296-1304 [PMID: 30925125 DOI: 10.1200/JCO.18.01138]
12 **Kataoka K**, Tokunaga M, Mizusawa J, Machida N, Katayama H, Shitara K, Tomita T, Nakamura K, Boku N, Sano T, Terashima M, Sasako M; Stomach Cancer Study Group/Japan Clinical Oncology Group. A randomized Phase II trial of systemic chemotherapy with and without trastuzumab followed by surgery in HER2-positive advanced gastric or esophagogastric junction adenocarcinoma with extensive lymph node metastasis: Japan Clinical Oncology Group study JCOG1301 (Trigger Study). *Jpn J Clin Oncol* 2015; **45**: 1082-1086 [PMID: 26355164 DOI: 10.1093/jjco/hyv134]
13 **Terashima M**, Yoshikawa T, Boku N, Ito S, Tsuburaya A, Iwasaki Y, Fukagawa T, Tokunaga M, Sano T, Sasako M; Stomach Cancer Study Group; Japan Clinical Oncology Group. Current status of perioperative chemotherapy for locally advanced gastric cancer and JCOG perspectives. *Jpn J Clin Oncol* 2020; **50**: 528-534 [PMID: 32134452 DOI: 10.1093/jjco/hyaa005]
14 **Brierley**, James D, Gospodarowicz, MK, Wittekind, C. TNM classification of malignant tumors: International union against cancer. 8th ed. Oxford: Wiley; 2017
15 **Japanese Gastric Cancer Association**. Japanese classification of gastric carcinoma: 3rd English edition. *Gastric Cancer* 2011; **14**: 101-112 [PMID: 21573743 DOI: 10.1007/s10120-011-0041-5]
16 **Common Terminology Criteria for Adverse Events (CTCAE) v5.0**. Available from: https://ctepcancergov/protocolDevelopment/electronic_applications/ctchtm#ctc_50
17 **Clavien PA**, Barkun J, de Oliveira ML, Vauthey JN, Dindo D, Schulick RD, de Santibañes E, Pekolj J, Slankamenac K, Bassi C, Graf R, Vonlanthen R, Padbury R, Cameron JL, Makuuchi M. The Clavien-Dindo classification of surgical complications: five-year experience. *Ann Surg* 2009; **250**: 187-196 [PMID: 19638912 DOI: 10.1097/SLA.0b013e3181b13ca2]
18 **Katai H**, Ishikawa T, Akazawa K, Isobe Y, Miyashiro I, Oda I, Tsujitani S, Ono H, Tanabe S, Fukagawa T, Nunobe S, Kakeji Y, Nashimoto A; Registration Committee of the Japanese Gastric Cancer Association. Five-year survival analysis of surgically resected gastric cancer cases in Japan: a retrospective analysis of more than 100,000 patients from the nationwide registry of the Japanese Gastric Cancer Association (2001-2007). *Gastric Cancer* 2018; **21**: 144-154 [PMID: 28417260 DOI: 10.1007/s10120-017-0716-7]
19 **Yoshikawa T**, Sasako M, Yamamoto S, Sano T, Imamura H, Fujitani K, Oshita H, Ito S, Kawashima Y, Fukushima N. Phase II study of neoadjuvant chemotherapy and extended surgery for locally advanced gastric cancer. *Br J Surg* 2009; **96**: 1015-1022 [PMID: 19644974 DOI: 10.1002/bjs.6665]
20 **Tsuburaya A**, Mizusawa J, Tanaka Y, Fukushima N, Nashimoto A, Sasako M; Stomach Cancer Study Group of the Japan Clinical Oncology Group. Neoadjuvant chemotherapy with S-1 and cisplatin followed by D2 gastrectomy with para-aortic lymph node dissection for gastric cancer with extensive lymph node metastasis. *Br J Surg* 2014; **101**: 653-660 [PMID: 24668391 DOI: 10.1002/bjs.9484]
21 **Takahari D**, Ito S, Mizusawa J, Katayama H, Terashima M, Sasako M, Morita S, Nomura T, Yamada M, Fujiwara Y, Kimura Y, Ikeda A, Kadokawa Y, Sano T; Stomach Cancer Study Group of the Japan Clinical Oncology Group. Long-term outcomes of preoperative docetaxel with cisplatin plus S-1 therapy for gastric cancer with extensive nodal metastasis (JCOG1002). *Gastric Cancer* 2020; **23**: 293-299 [PMID: 31515693 DOI: 10.1007/s10120-019-01007-w]
22 **Wagner AD**, Grabsch HI, Mauer M, Marreaud S, Caballero C, Thuss-Patience P, Mueller L, Elme A, Moehler MH, Martens U, Kang YK, Rha SY, Cats A, Tokunaga M, Lordick F. EORTC-1203-GITCG - the "INNOVATION"-trial: Effect of chemotherapy alone *vs* chemotherapy plus trastuzumab, *vs* chemotherapy plus trastuzumab plus pertuzumab, in the perioperative treatment of HER2 positive, gastric and gastroesophageal junction adenocarcinoma on pathologic response rate: a randomized phase II-intergroup trial of the EORTC-Gastrointestinal Tract Cancer Group, Korean Cancer Study Group and Dutch Upper GI-Cancer group. *BMC Cancer* 2019; **19**: 494 [PMID: 31126258 DOI: 10.1186/s12885-019-5675-4]

Published by **Baishideng Publishing Group Inc**
7041 Koll Center Parkway, Suite 160, Pleasanton, CA 94566, USA
Telephone: +1-925-3991568
E-mail: bpgoffice@wjgnet.com
Help Desk: https://www.f6publishing.com/helpdesk
https://www.wjgnet.com

© 2021 Baishideng Publishing Group Inc. All rights reserved.

ISSN 1007-9327 (print)
ISSN 2219-2840 (online)

World Journal of *Gastroenterology*

World J Gastroenterol 2021 February 21; 27(7): 545-665



Published by Baishideng Publishing Group Inc

World Journal of Gastroenterology

Contents

Weekly Volume 27 Number 7 February 21, 2021

REVIEW

545 *Helicobacter pylori*: Commensal, symbiont or pathogen?

Reshetnyak VI, Burmistrov AI, Maev IV

561 Digestive system involvement of infections with SARS-CoV-2 and other coronaviruses: Clinical manifestations and potential mechanisms

Zhan GF, Wang Y, Yang N, Luo AL, Li SY

ORIGINAL ARTICLE

Basic Study

576 Xiangbinfang granules enhance gastric antrum motility *via* intramuscular interstitial cells of Cajal in mice

Chen QC, Jiang Z, Zhang JH, Cao LX, Chen ZQ

592 Sinapic acid ameliorates D-galactosamine/lipopolysaccharide-induced fulminant hepatitis in rats: Role of nuclear factor erythroid-related factor 2/heme oxygenase-1 pathways

Ansari MA, Raish M, Bin Jardan YA, Ahmad A, Shahid M, Ahmad SF, Haq N, Khan MR, Bakheet SA

Clinical and Translational Research

609 Quantitative multiparametric magnetic resonance imaging can aid non-alcoholic steatohepatitis diagnosis in a Japanese cohort

Imajo K, Tetlow L, Dennis A, Shumbayawonda E, Mouchti S, Kendall TJ, Fryer E, Yamanaka S, Honda Y, Kessoku T, Ogawa Y, Yoneda M, Saito S, Kelly C, Kelly MD, Banerjee R, Nakajima A

Retrospective Study

624 Clinicopathological features and prognostic factors associated with gastroenteropancreatic mixed neuroendocrine non-neuroendocrine neoplasms in Chinese patients

Huang YC, Yang NN, Chen HC, Huang YL, Yan WT, Yang RX, Li N, Zhang S, Yang PP, Feng ZZ

641 Effect of liver inflammation on accuracy of FibroScan device in assessing liver fibrosis stage in patients with chronic hepatitis B virus infection

Huang LL, Yu XP, Li JL, Lin HM, Kang NL, Jiang JJ, Zhu YY, Liu YR, Zeng DW

Clinical Trials Study

654 Simultaneous partial splenectomy during liver transplantation for advanced cirrhosis patients combined with severe splenomegaly and hypersplenism

Jiang WT, Yang J, Xie Y, Guo QJ, Tian DZ, Li JJ, Shen ZY

ABOUT COVER

Emilio De Raffele, MD, PhD, Consultant Surgeon, Division of Pancreatic Surgery, Department of Digestive Diseases, Azienda Ospedaliero-Universitaria di Bologna, IRCCS, Policlinico S.Orsola-Malpighi, Università degli Studi di Bologna, Via Albertoni 15, Bologna 40138, Italy. e.deraffele@aosp.bo.it

AIMS AND SCOPE

The primary aim of *World Journal of Gastroenterology* (*WJG*, *World J Gastroenterol*) is to provide scholars and readers from various fields of gastroenterology and hepatology with a platform to publish high-quality basic and clinical research articles and communicate their research findings online. *WJG* mainly publishes articles reporting research results and findings obtained in the field of gastroenterology and hepatology and covering a wide range of topics including gastroenterology, hepatology, gastrointestinal endoscopy, gastrointestinal surgery, gastrointestinal oncology, and pediatric gastroenterology.

INDEXING/ABSTRACTING

The *WJG* is now indexed in Current Contents®/Clinical Medicine, Science Citation Index Expanded (also known as SciSearch®), Journal Citation Reports®, Index Medicus, MEDLINE, PubMed, PubMed Central, and Scopus. The 2020 edition of Journal Citation Report® cites the 2019 impact factor (IF) for *WJG* as 3.665; IF without journal self cites: 3.534; 5-year IF: 4.048; Ranking: 35 among 88 journals in gastroenterology and hepatology; and Quartile category: Q2. The *WJG*'s CiteScore for 2019 is 7.1 and Scopus CiteScore rank 2019: Gastroenterology is 17/137.

RESPONSIBLE EDITORS FOR THIS ISSUE

Production Editor: *Yu-Jie Ma*; **Production Department Director:** *Xiang Li*; **Editorial Office Director:** *Ze-Mao Gong*.

NAME OF JOURNAL
World Journal of Gastroenterology

ISSN
ISSN 1007-9327 (print) ISSN 2219-2840 (online)

LAUNCH DATE
October 1, 1995

FREQUENCY
Weekly

EDITORS-IN-CHIEF
Andrzej S Tarnawski, Subrata Ghosh

EDITORIAL BOARD MEMBERS
http://www.wjgnet.com/1007-9327/editorialboard.htm

PUBLICATION DATE
February 21, 2021

COPYRIGHT
© 2021 Baishideng Publishing Group Inc

INSTRUCTIONS TO AUTHORS
https://www.wjgnet.com/bpg/gerinfo/204

GUIDELINES FOR ETHICS DOCUMENTS
https://www.wjgnet.com/bpg/GerInfo/287

GUIDELINES FOR NON-NATIVE SPEAKERS OF ENGLISH
https://www.wjgnet.com/bpg/gerinfo/240

PUBLICATION ETHICS
https://www.wjgnet.com/bpg/GerInfo/288

PUBLICATION MISCONDUCT
https://www.wjgnet.com/bpg/gerinfo/208

ARTICLE PROCESSING CHARGE
https://www.wjgnet.com/bpg/gerinfo/242

STEPS FOR SUBMITTING MANUSCRIPTS
https://www.wjgnet.com/bpg/GerInfo/239

ONLINE SUBMISSION
https://www.f6publishing.com

© 2021 Baishideng Publishing Group Inc. All rights reserved. 7041 Koll Center Parkway, Suite 160, Pleasanton, CA 94566, USA
E-mail: bpgoffice@wjgnet.com https://www.wjgnet.com

World Journal of Gastroenterology

Submit a Manuscript: https://www.f6publishing.com

World J Gastroenterol 2021 February 21; 27(7): 545-560

DOI: 10.3748/wjg.v27.i7.545

ISSN 1007-9327 (print) ISSN 2219-2840 (online)

REVIEW

Helicobacter pylori: Commensal, symbiont or pathogen?

Vasiliy Ivanovich Reshetnyak, Alexandr Igorevich Burmistrov, Igor Veniaminovich Maev

ORCID number: Vasiliy Ivanovich Reshetnyak 0000-0003-3614-5052; Alexandr Igorevich Burmistrov 0000-0001-8853-3394; Igor Veniaminovich Maev 0000-0001-6114-564X.

Author contributions: All authors have equally contributed to the conception and design of the study, literature review and analysis, drafting critical revision and editing, and final approval of the final version.

Conflict-of-interest statement: No potential conflicts of interest.

Open-Access: This article is an open-access article that was selected by an in-house editor and fully peer-reviewed by external reviewers. It is distributed in accordance with the Creative Commons Attribution NonCommercial (CC BY-NC 4.0) license, which permits others to distribute, remix, adapt, build upon this work non-commercially, and license their derivative works on different terms, provided the original work is properly cited and the use is non-commercial. See: http://creativecommons.org/Licenses/by-nc/4.0/

Manuscript source: Invited manuscript

Specialty type: Gastroenterology and hepatology

Country/Territory of origin: Russia

Vasiliy Ivanovich Reshetnyak, Alexandr Igorevich Burmistrov, Igor Veniaminovich Maev, Department of Propaedeutic of Internal Diseases and Gastroenterology, A.I. Yevdokimov Moscow State University of Medicine and Dentistry, Moscow 127473, Russia

Corresponding author: Vasiliy Ivanovich Reshetnyak, DSc, MD, PhD, Full Professor, Department of Propaedeutic of Internal Diseases and Gastroenterology, A.I. Yevdokimov Moscow State University of Medicine and Dentistry, p. 1, 20 Delegatskaya Street, Moscow 127473, Russia. vasiliy.reshetnyak@yandex.ru

Abstract

This review considers the data on *Helicobacter pylori* (*H. pylori*), which have been accumulated over 40 years since its description as an etiological factor in gastrointestinal diseases. The majority of modern publications are devoted to the study of the pathogenic properties of the microorganism in the development of chronic gastritis, peptic ulcer disease, and gastric cancer, as well as methods for its eradication. However, in recent years, there have been more and more studies which have suggested that *H. pylori* has a beneficial, or potentially positive, effect on the human body. The authors have attempted to objectively analyze the information accumulated in the literature on *H. pylori*. Some studies consider it as one of the recently identified human bacterial pathogens, and special attention is paid to the evidence suggesting that it is probably part of the composition of the human microbiome as a commensal (*commensal* from French to English is a table companion) or even a symbiont. The presented data discussing the presence or absence of the effect of *H. pylori* on human health suggest that there is an apparent ambiguity of the problem. The re-assessment of the data available on *H. pylori* infection is important in order to answer the question of whether it is necessary to create a program of mass *H. pylori* eradication or to apply a more personalized approach to treating patients with *H. pylori*-associated gastrointestinal diseases and to perform eradication therapy.

Key Words: *Helicobacter pylori*; Pathogen; Commensal; Microbiome; Peptic ulcer; Gastric cancer; Asthma; Inflammatory bowel diseases

©The Author(s) 2021. Published by Baishideng Publishing Group Inc. All rights reserved.

Core Tip: This review provides data on *Helicobacter pylori* (*H. pylori*) as one of the recently identified human bacterial pathogens. On the one hand, its role as a human

Peer-review report's scientific quality classification
Grade A (Excellent): 0
Grade B (Very good): B, B
Grade C (Good): C, C, C, C
Grade D (Fair): 0
Grade E (Poor): 0

Received: December 5, 2020
Peer-review started: December 5, 2020
First decision: December 27, 2020
Revised: December 28, 2020
Accepted: January 21, 2021
Article in press: January 21, 2021
Published online: February 21, 2021

P-Reviewer: Chivu-Economescu M, Keikha M, Lombardo L, Romano M
S-Editor: Fan JR
L-Editor: Webster JR
P-Editor: Liu JH



pathogenic bacterium that is commonly found in patients with chronic gastritis, peptic ulcer disease, and gastric cancer is discussed. On the other hand, the high prevalence of *H. pylori* in the population and its asymptomatic coexistence with humans in most of the world's population indicates its persistence in the body as a representative of the microbiome and as a nonpathogenic microorganism. The presented data suggest that there is an apparent ambiguity of the problem and a need for an analytically developed, comprehensive approach to study the effect of *H. pylori* infection on human health and to perform eradication therapy.

Citation: Reshetnyak VI, Burmistrov AI, Maev IV. *Helicobacter pylori*: Commensal, symbiont or pathogen? *World J Gastroenterol* 2021; 27(7): 545-560
URL: https://www.wjgnet.com/1007-9327/full/v27/i7/545.htm
DOI: https://dx.doi.org/10.3748/wjg.v27.i7.545

INTRODUCTION

Over four decades, the problem of studying *Helicobacter pylori* (*H. pylori*) has occupied the minds of many scientists around the world. *H. pylori* is a bacterium that is commonly found in patients with chronic gastritis, peptic ulcer disease (PUD) and gastric cancer (GC), as well as among the healthy population. *H. pylori* was first reported in 1875, when Bottcher and Letulle observed it on the margins of peptic ulcers[1]. Despite the high prevalence of the microorganism demonstrated later, its discovery occurred only at the beginning of the 1980s[2]. It is obvious that since 1983 *H. pylori* has been colonizing more than half of the world population[3]. This event has produced a major multidisciplinary interest including gastroenterologists, microbiologists, and infectious disease specialists among others. The role of *H. pylori* as a true pathogen has been the center of major discussions for many years. *H. pylori* infection has been linked to gastric and duodenal ulcers (in 1%-10% of infected patients), gastric carcinoma (0.1%-3%), and gastric mucosa-associated lymphoid tissue (MALT) lymphoma (less than 0.01%)[4,5]. However, the vast majority of the infected population will never develop symptoms related to *H. pylori* infection.

H. pylori colonization of the human stomach occurs early in life and persists indefinitely unless treated[3]. At the same time, transmission of *H. pylori* is mainly in a family setting[6].

The decline in *H. pylori* prevalence with time was first reported in 1997[7], and later confirmed in two large population-based studies in the United States[8]. As a result of *H. pylori's* gradual decline, a series of negative consequences have been described[2]. There has been an alarming increase in asthma[9,10], as well as a potential increase in the susceptibility to diarrheal diseases[11]. However, a more serious consequence related to the decline of *H. pylori* is the escalation of esophageal diseases, such as gastroesophageal reflux disease (GERD), Barrett's esophagus, and adenocarcinoma of the esophagus[12,13]. We do not know if the decline in *H. pylori* infections is the cause of these emerging diseases or if it is just an indicator of the hygiene hypothesis[2]. Due to its low virulence and the fact that disease is observed mostly in elderly infected individuals, *H. pylori* could be considered a commensal organism and only an opportunistic pathogen.

GENERAL CHARACTERISTICS OF *H. PYLORI*

Basic facts

H. pylori is a gram-negative, S-shaped, or helical microaerophilic bacterium belonging to the genus *Helicobacteraceae*[14,15]. In 1979, R. Warren identified *Campylobacter pylori* and suggested that this microorganism was an etiological agent of gastritis. In 1982, B.J. Marshall isolated a culture of *H. pylori* and showed the relationship between its persistence and PUD development[16].

According to the modern concepts, the predominant habitat (life, growth, and reproduction) of *H. pylori* is the supraepithelial mucus layer in the region of the gastric pits and in the first parts of the duodenum[16]. *H. pylori* is generally not detected neither

in the subepithelial space of the stomach nor in the epithelium of gastric glands[13]. The motility of the microorganism through the mucus layer occurs due to the presence of several mobile flagella, which contributes to the migration of the bacterium to areas with suitable conditions for existence[17].

The most favorable conditions for bacterial life have been found to be the optimum temperature of 37°C, pH 4.0-6.0, microaerophilic conditions, the presence of water and nutrients[15]. *H. pylori* does not contain enzymes that metabolize carbohydrates. The metabolism of a bacterial cell is provided by the energy released during the utilization of amino acids obtained from the host[18]. The microorganism is characterized by its possible persistence in the human body as S-shaped, C(U)-shaped, and coccoid forms[2,15,16]. The similar mechanism of transition from one form to another is an adaptation to survival during adverse environmental conditions (temperature or pH shifts, long intervals between meals, and antibiotic therapy)[15].

Epidemiology and routes of transmission

The data currently available suggest that there is a high prevalence of *H. pylori* in the population. The detection rates of *H. pylori* vary from 35% to 90% in representatives of the population in different regions[15,19-22]. A large variation of the indicator depends on a number of factors, including the socio-economic state of the country, age, the method of detecting *H. pylori* and other factors[20]. Thus, in their article, Mentis *et al*[19] reported the detection of *H. pylori* in 71.6% of the population in Italy and in 84.2% of those surveyed in Poland. Luzza *et al*[20] reported that in Italy among 518 subjects who were evaluated by both the ^{13}C-urea breath test (UBT) and serology, 310 (59.8%) were UBT positive, 479 (92.4%) *vacA*-positive, and 369 (71.2%) *cagA*-positive. Similar indicators for Africa and Asia were distributed in the following order: Ethiopia (72.2%) and Rwanda (75.3%), China 83.4%, Japan (39.9%), and Taiwan (72.1%)[19]. Burucoa *et al*[21] established the largest proportion of *H. pylori*-positive patients in Africa (70.1%) [95% confidence interval (CI): 62.6%-77.6%], South America (69.4%) (95%CI: 63.9%-74.9%), and West Asia (66.6%) (95%CI: 56.1%-77.0%). The regions with least occurrence were Oceania (24.4%) (95%CI: 18.5%-30.4%), Western Europe (34.3%) (95%CI: 31.3%-37.2%), and North America (37.1%) (95%CI: 32.3%-41.9%). In Russia, the prevalence of *H. pylori* in children aged 5–10 and 11–14 years and in adults was 29%, 50%, and 70%-92%, respectively[13,23].

To date, the main route of transmission of *H. pylori* is not known. Infection most often occurs from person to person; in this case this generalized mechanism can be divided into vertical (that is, transmission of the pathogen within one family), and horizontal (contact with people outside the family or infection with environmental objects-environmental contamination)[19]. Possible transmission routes, such as fecal-oral, oral-oral, and gastro-oral, have been comprehensively studied in recent years[21,24,25]. *H. pylori* can be isolated from different body fluids. The pathogen was detected in the dental plaque, saliva, tonsil tissue, root canals, and on the oral mucosa (including on the surface of the tongue), using a polymerase chain reaction assay[21]. Particular attention is paid to the environmental contamination associated with the consumption of *H. pylori*-containing water and food[26].

The majority of authors consider the intrafamilial transmission of the pathogen to be the predominant and most significant route. This opinion is confirmed by factors, such as close interpersonal contacts in the family, the single socioeconomic status of family members, and genetic predisposition to *H. pylori* persistence[24,27].

PATHOGENIC PROPERTIES OF *H. PYLORI*

H. pylori virulence factors and its role in systemic diseases

To survive the unfavorable, hyperacid conditions of the stomach, *H. pylori* synthesizes a number of virulence factors that both improve conditions for vital activity in an acidic environment and have a damaging effect on the gastric mucosa.

In their work, Kao *et al*[28] noted that on entry into the host stomach, *H. pylori* uses urease activity to neutralize hydrochloric acid that is one of the protective factors and has a pronounced antimicrobial effect. Regulation of urease synthesis is encoded by a number of genes called the *urease gene cluster*. This set of genes includes catalytic units (*urea A/B*), an acid-gated urea channel (*ureI*), and accessory assembly proteins (*ure E-H*)[29].

Of interest is the fact that urease synthesis depends on the pH surrounding the bacterium: The ureI-channels are tightly closed at pH 7.0 and are completely open at pH 5.0[28,30]. That is, when the external conditions change, namely, when stomach

lumen acidity increases, *H. pylori* releases urease that hydrolyzes urea into CO_2 and ammonia (NH_3) that in turn binds to water and forms unstable ammonium hydroxide. This sequence of biochemical reactions leads to medium alkalization[28]. This mechanism of overcoming the acid barrier is extremely important for the survival of the bacterium along with a spiral shape, a smooth cell wall, and helicoidal movements. Schoep *et al*[31] demonstrated that urease-negative bacteria were unable to colonize the gastric mucosa of gnotobiotic piglets.

Another important virulence factor promoting the spread of the bacterium to the gastric epithelium is its motility due to the presence of 4-7 mobile sheathed flagella. The flagellum is a complex organ that is composed of several types of protein subunits and consists of the basal body, hook, and filament[32,33]. There are several types of flagella-driven motility: "Swimming motility", "spreading motility'', and ''swarming motility"[33]. Along with urease activity, flagellar motility has been shown to be an essential factor for colonization of the gastric mucosa[34]. There are also studies which demonstrate the utmost importance of flagella in the formation of microbial biofilms on the surface of the gastric mucosa[35,36].

Bacterial adhesion is the key stage of colonization, which determines a whole set of processes of gastric *H. pylori* persistence. The literature describes adhesion molecules (outer membrane proteins), such as blood-antigen-binding protein A, sialic acid-binding adhesin, neutrophil-activating protein, heat shock protein (Hsp) 60, adherence-associated proteins (AlpA and AlpB), *H. pylori* outer membrane protein, and LacDiNAc binding adhesin[28,37-40]. Among the key factors of colonization, virulence factors that have a direct damaging effect on the gastric mucosal epithelium can be separated out; these are cagA, γ-glutamine transferase, high-temperature requirement A, and vacuolating cytoxin A (vacA)[38,39].

CagA is a highly antigenic protein with a molecular weight of 120-145 kDa[41,42]. The locus of a gene responsible for the synthesis of cagA and a type IV secretion system (T4SS) is named *the cag pathogenicity island*[38]. CagA acts intracellularly through the epithelial cells *via* the T4SS: The latter forms a syringe-like pilus structure, through which the cagA molecule enters the host epithelial cell[40]. After translocation into the cell, cagA undergoes phosphorylation on the inner side of the cytoplasmic membrane of an epithelial cell and thus acquires biochemical activity[43]. It was found experimentally that cagA phosphorylation-competent mice developed cancers, such as gastrointestinal adenocarcinoma, myeloid leukemia, and B-cell lymphoma. Moreover, these pathogenic processes were not observed in phosphorylation-resistant forms[44]. The main pathogenetic effect of cagA is to enhance the mitotic activity of gastric epithelial cells, which contributes to malignancy if the microbe persists long-term[43,45].

VacA is a protein with a molecular weight of 88 kDa, which consists of two subunits (p33 and p55) and has multiple pathogenetic effects[43]. After protein internalization, large pores are formed in the cytoplasmic membrane of gastric epithelial cells, which makes the cells more susceptible to the effects of bacterial urease[46]. Beyond that point, the launch of a cascade of biochemical reactions promotes the accumulation of large vacuoles inside the cells, which leads to the functional inferiority of epithelial cells. Through the intracellular transporter system, vacA is able to enter the mitochondria, where it disrupts the integrity of the inner mitochondrial membrane. This induces a drop in the mitochondrial transmembrane potential ($\Delta\Psi m$) with the subsequent release of cytochrome C and the activation of the proapoptotic factor Bcl-2 associated X protein[47]. There are data showing that vacA is involved in avoiding a pronounced immune response to the entry of an infectious agent. This is achieved by both the reduction in the activation of T lymphocytes in the lamina propria and disruption of the autophagy process[48].

Immune response to H. pylori invasion

When entering the human body, *H. pylori* is constantly controlled by the immune system. The inflammatory response is well-known to be a marker for a developing immune response. In *H. pylori* persistence, the focus of inflammation primarily affects gastric epithelial cells; in this case the inflammatory reaction involves neutrophils, lymphocytes, macrophages, and dendritic cells (DCs), which migrate to the site of infection through the systemic circulation[49,50].

The contact of DCs with *H. pylori* antigenic determinants results in autocrine activation of the pool of immature $CD4^+$ T cells, followed by their differentiation into T-helper (Th) 1 lymphocytes through interleukin (IL)-12 production[51]. There are Th1 lymphocytes that are the major inflammatory effector cells for *H. pylori* invasion[52]. In addition, proinflammatory cytokines, such as IL-1, IL-6, tumor necrosis factor (TNF)-α, and interferon (IFN)-γ, are involved in the immune response[53].

The initial Th1 cell immune response is aimed at completely eradicating the

infectious agent. However, it has been shown experimentally that vacA is able to exert an immunosuppressive effect on the cells of the immune system, by inhibiting the production of IL-23 by DCs[54]. Furthermore, *H. pylori* HspB is capable of inhibiting the proliferation of mitogen-stimulated T cells, by enhancing the suppressive effects of regulatory T (Treg) cells in both innate and adaptive immune responses[55,56].

The interaction of *H. pylori* with Th2 lymphocytes is not obvious. Due to the activation of the Th1 cellular component of the immune system, the Th2 cellular pathway for differentiation of immature lymphocytes is not believed to play a considerable role in the immune response[52]. At the same time, it has been proven that the level of immunoglobulin G (IgG) is a reliable indicator of *H. pylori* persistence. In infected individuals, a Th2 response induces IgG1 production while a Th1 response contributes to a significant increase in the overall levels of IgG2 through IL-2 and IFN-γ production. IgG2 titers are higher than IgG1 titers in *H. pylori*-infected patients, particularly in those with ulcer disease[57].

Thus, the persistence of *H. pylori* in the human body is accompanied by the pronounced immune response to bacterial invasion, which is subsequently replaced by immune tolerance. This fact may suggest that the relationship between *H. pylori* and the host is symbiotic.

H. pylori-associated diseases

The currently available data may suggest that *H. pylori* persistence in the stomach is associated with the development of gastroduodenal diseases, such as chronic gastritis, PUD, gastric adenocarcinoma, and gastric MALT lymphoma[3,28,58,59]. Recent data show a statistically significant relationship between *H. pylori* detection and pancreatic cancer development[60,61].

The risk of developing symptoms of a gastrointestinal disease depends on the degree of pathogenic properties in a persistent strain, the genetic characteristics of the host, environmental factors, and the pattern of diet[62,63]. The researchers emphasize the fact that the persistence of *H. pylori* in the gastric mucosa is constantly controlled by the immune system, as a result of which the pathogenic properties of *H. pylori* and, as a consequence, the symptoms of the disease manifest in the presence of favorable factors. Beyond that point, more and more attention is paid to the implication of *H. pylori* in the pathogenesis of extragastric diseases. Thus, the role of the microorganism in developing a number of neurological, cardiovascular, hematological, skin, and metabolic diseases is being actively investigated[62-66]. The results of the available studies are undoubtedly quite contradictory and require a more thorough study.

The meta-analysis by Wang *et al*[67] demonstrated that chronic *H. pylori* infection is a predictor for the possible development of ischemic brain injury. Reports suggesting a relationship between *H. pylori* detection and Alzheimer's disease development have been published[68,69]. Huang *et al*[70] were able to establish that the risk of Parkinson's disease was significantly higher in the *H. pylori*-positive group than in the *H. pylori*-negative (HPN) group (adjusted hazard ratio: 2.29, 95%CI: 1.44–3.66; $P < 0.001$).

Little experience has been accumulated in studying the effects of *H. pylori* on the development of cardiovascular diseases. Some studies confirm a significant relationship between the detection of *H. pylori*, the development of atherosclerotic vascular lesions, and, as a consequence, a higher risk of coronary heart disease[71-74]. Jukic *et al*[73] found that *H. pylori*-positive patients more often suffered from hypertension ($P = 0.014$), had higher systolic ($P = 0.043$) and diastolic ($P = 0.005$) blood pressure, as well as elevated plasma triglyceride levels ($P = 0.013$) and a low antiatherogenic high-density lipoprotein level ($P = 0.01$). At the same time, there was no significant difference in the severity of the disease between the two groups.

Vijayvergiya *et al*[75] described the considered hypotheses on the mechanisms of endothelial dysfunction in *H. pylori* infection. Some hypotheses state that pathophysiological changes in the microvascular bed result from a secondary increase in homocysteine levels: *H. pylori* induces vitamin B_{12} and folic acid malabsorption, by elevating the homocysteine level that negatively affects the endothelium[76,77]. The theory of cytokine-induced vascular wall injury, which in turn is the first stage of atherosclerotic changes, should also be actively studied. The work by Rasmi *et al*[78] confirmed that *H. pylori cagA*-positive patients with cardiac syndrome X were found to have increased IL-1 and TNF-α levels. The experimental data obtained by de Jesus Souza *et al*[79] showed that urease is a potent stimulus for endothelial cell production of reactive oxygen species and NO, which also leads to the enhanced production of nuclear factor kappa B, activation and upregulated expression of cyclooxygenase-2, heme oxygenase-1, IL-1β, and intercellular adhesion molecule-1. Such experimentally established changes in the pro-inflammatory molecule profile can indirectly indicate the possible pathogenetic features of *H. pylori*-induced injury to the vascular bed.

An association between *H. pylori* infection and skin diseases is being actively studied. Yu *et al*[80] provided evidence that the detection rate of *H. pylori* was 49.5% among 1038 representatives in a study group (patients diagnosed with psoriasis), while the rate was 38.8% in a control group (n = 703) (the pooled OR was 1.70; 95%CI: 1.15-2.52; P = 0.008). Onsun *et al*[81] concluded that *H. pylori* was detected in 184 (61.3%) individuals among 300 patients with psoriasis and in 89 (59.3%) representatives in a control group (among 150 healthy people). At the same time, it was noted that the disease severity, as assessed by the Psoriasis area and severity index scores, was noted to be significantly higher in *H. pylori*-positive patients. The literature provides a large number of reports on *H. pylori* detection in patients who, in addition to psoriasis, have lichen ruber planus, scabies, rosacea, Sweet's syndrome, Behcet's disease, and Schönlein-Henoch purpura[82].

It should be noted that antibacterial drug manufacturers have an impact on more attention to the pathogenic properties of *H. pylori* and mass (program) eradication therapy[3].

IS EVERYTHING SO CLEAR?

Rare development of symptoms with high prevalence in the population

Following the discoveries by R. Warren and B.J. Marshall, the concept of pathogenesis and treatment regimens for PUD implied mainly the identification and eradication of *H. pylori*. It is currently known that the occurrence of *H. pylori* is high in the healthy population (about 50% of the population worldwide and more than 70% of that in developing countries)[2]. *H. pylori* infection is usually acquired in childhood and generally persists lifelong. Thus *H. pylori* has infected the majority of the world's population for the majority of their lifetime and in most cases causes no symptoms[3,83]. The infectious process in *H. pylori* is chronic and only one in ten colonized individuals; most commonly the elderly, develop clinical manifestations years later[2]. Tsimmerman[13] reported that less than 1% of individuals infected with *H. pylori* develop various diseases and about 70% of people who are found to have the bacterium are healthy bacterial carriers. The available data show that only 5%-10% of those infected develop symptoms of gastritis or PUD[84-87]. Moreover, the review data (Araújo *et al*[88]) indicate that the detection rate of *H. pylori* infection in patients diagnosed with PUD does not differ from that of *H. pylori* in the general population. The authors also noted that in 20%-50% of cases of PUD, they are unable to identify the overarching etiological factor of an ulcerative lesion, that is to say, an idiopathic ulcer (*H. pylori* negative, non-steroidal anti-inflammatory drug-negative peptic ulcer/NSAIDs). Sidorenko[89] stated that the given facts provide a strong argument that refutes the leading role of *H. pylori* in the development of gastroduodenal diseases. The wide spread of *H. pylori* infection among individuals without signs of pathology and the low incidence rate during chronic colonization of the gastric mucosa clearly indicate that *H. pylori* is more likely to be an opportunistic or latent pathogen than a truly pathogenic bacterium.

The presented data suggest that the infectious theory of chronic gastritis, PUD, and GC seems to be rather an exception to the rule. In addition, the severity of chronic gastritis and/or PUD appears to be directly related to other etiological factors, along with the density of *H. pylori* contamination.

H. pylori and PUD

PUD is a chronic multifactorial disease characterized by an imbalance between the aggressive components of the gastroduodenal contents and the protective mechanisms of the gastric mucosa. A significant role in the pathophysiological changes characteristic of PUD is played by important components, such as hereditary predisposition, psychoemotional and psychosocial stress effects, autonomic dysfunction, local pathogenetic effects (acidity of the stomach contents), immunodeficiency state, oxidative stress, smoking, excessive alcohol consumption, and the use of steroid drugs and nonsteroidal anti-inflammatory drugs[87,90]. In their review, Malfertheiner *et al*[87] focused on the fact that the development of PUD depends on the complex influence and/or a combination of both exo- and endogenous factors. In addition to the above described exogenous factors, the most important endogenous components of ulcerogenesis are the level and adequate function of enteric hormones (gastrin, somatostatin), genetic predisposing factors (the number of parietal cells, the basal level of gastric hydrochloric acid secretion, and defects in bicarbonate secretion). Such observations show that the presence of *H. pylori* infection may be only one (but

far short of being single) component in the genesis of ulcerative disorders.

It is essential to also recall the fact that in the case of *Helicobacter* etiology, the risk of developing the disease depends on the genotype of *H. pylori*: The patients with a confirmed diagnosis of PUD were found to have *vacA*-positive and *cagA*-positive genotypes[91,92]. At the same time, the genotypes containing the *vacA* gene are known to account for about 60% of all detected forms of *Helicobacter*[93].

In addition to *H. pylori*-associated ulcers, the current classification identifies tumor ulcers, ulcerative lesions in Zollinger-Ellison syndrome, Crohn's disease, eosinophilic gastroduodenitis, radiation damage, and viral infections (cytomegalovirus or herpesvirus infection in immunocompromised patients). The idiopathic form occupies a separate place[87].

Interestingly, epidemiological studies in recent years demonstrate a progressive increase in the idiopathic forms of PUD with a decrease in the global prevalence of *H. pylori* infection[94,95]. Thus, Indian researchers have shown that 45.9% of cases of peptic ulcers of the stomach and 29.6% of those of the duodenum are idiopathic (they are unassociated with either *H. pylori* detection or a history of steroid/NSAID intake)[96].

Reshetnyak *et al*[97] presented data on the role of *H. pylori* and drugs in the development of gastric mucosal (GM) lesions in patients with systemic lupus erythematosus (SLE) and antiphospholipid syndrome (APS). Endoscopic examinations of patients with SLE and APS revealed the following GM changes: antral gastritis (82.4%), erosion (24.7%), hemorrhages (8.2%), and pangastritis (8.2%). The rate of *H. pylori* infection in patients with SLE and APS corresponded to that in the general population. The authors' data showed that there was no direct correlation between the observed GM changes and *H. pylori* infection. However, therapy with glucocorticoid, low-dose acetylsalicylic acid, NSAIDs, and anticoagulants was in this case responsible for GM damage in patients with SLE and APS.

There is evidence suggesting the most favorable course of *H. pylori*-associated ulcers compared with other diagnosed types. Kanno *et al*[98] established that among 382 examinees diagnosed with PUD, the patients with a confirmed diagnosis of *H. pylori*-positive ulcer had a statistically significant increase in healing rates. In the study, the patients were divided into 4 groups: A simple *H. pylori* group; a *H. pylori* (+)/NSAIDs (+) group; a simple NSAIDs group; and an idiopathic ulcer (IPU) group. Indicators, such as healing rates at 3 mo, treatment course, and recurrence rates, were estimated. According to the data presented, the healing rates in these groups were distributed as follows: 95.0%, 94.9%, 73.3%, and 77.4%, respectively. This indicator for idiopathic forms was statistically significantly different ($P < 0.01$). The recurrence rate in the IPU group was also much higher: 13.9% in the IPU group and 2.1% in the simple *H. pylori* group ($P < 0.01$). The cumulative recurrence rates estimated by the Kaplan-Meier method were also significantly higher in the IPU group than those in the simple *H. pylori* group ($P = 0.015$).

Rasane *et al*[99] demonstrated that patients with HPN PUD had a more pronounced severe course of the disease and a more negative prognosis than those with *H. pylori*-associated forms. Thus, albumin levels in the HPN group were higher than those in the *H. pylori*-positive group: 2.97-0.96 *vs* 3.86-0.91, $P = 0.0001$. The same pattern was observed when evaluating the patients' state on admission to hospital: In the HPN group, the scores of scales, such as the American Society of Anesthesiologists scoring system and the Charlson comorbidity index, were much higher: 3.11-0.85 *vs* 2.60-0.73 ($P = 0.005$) and 4.81-2.74 *vs* 2.98-2.71 ($P = 0.004$), respectively. There were also significant differences in indicators, such as hospital length of stay: 20.20-13.82 *vs* 8.48-7.24; $P = 0.0001$) and 30 d readmission rate (11; 29.73% *vs* 5; 11.91%; $P = 0.049$).

The diversity of causes that lead to the ulcerative process allows PUD to be considered as a polyetiological and polypathogenetic disease. When *H. pylori* was discovered, there were many theories of PUD development: Vascular, stomach inflammatory, allergic, hormonal, motor-primacy, corticovisceral, neurogenic, psychosomatic, and acidopeptic theories. Each of them deserves attention, as it reflects one of the facets of this complex problem. The above data suggest that for people who are predisposed to this pathology, the emergence of an infectious theory has become an important and significant addition to the already existing etiological factors. Also, not in all cases, but only in a certain state of the macroorganism, *H. pylori* becomes a pathogen and is an additional cause of chronic gastritis, PUD, and even GC.

H. pylori and GC

GC occupies one of the leading places in the pattern of cancers. Epidemiological studies have demonstrated that GC develops in *H. pylori*-infected people 1.4-4.2 times more often than in the general population[100-102]. At the same time it should be noted that GC develops only in 1%-2% of cases with a 50% or more frequency of gastric

colonization with *Helicobacter* worldwide[13,103]. Among the population of India and Africa, where the *H. pylori* infection rates reach 90%-95%, GC is diagnosed much less frequently than in Western Europe and the United States, where the prevalence of *H. pylori* does not exceed 35%-50%[104]. The carcinogenic potential of *H. pylori* is rather ambiguous: It has been found that *H. pylori* toxins do not exert a direct mutagenic effect on gastric epithelial cells[105]. Virulence factors have been described in *H. pylori*, but the presence or absence of these factors is not critical in disease development[2]. In addition, there is evidence that *H. pylori* persistence increases the risk of developing only distal (pyloroantral) GC, whereas proximal (cardiac) GC is unassociated with *H. pylori*. Moreover, antral colonization with *H. pylori*, especially with its *cagA*-positive strains, somehow prevents the development of cardiac GC and carcinoma of the lower third of the esophagus, performing a protective function[106]. Rokkas *et al*[107] called the relationship between *H. pylori* infection and subsequent GC development an unclear epidemiological paradox.

Blaser[108] has stated his belief that there is a certain balance between the negative and positive effects of *H. pylori* on humans. Some authors consider that *H. pylori* shows its pathogenicity, by regulating the expression of different genes to the extent that is dictated by the response of a macroorganism[109,110]. Thus, the microorganism and the macroorganism create a finely tuned balance system, the resulting impairment of which develops a specific disease with certain clinical signs and prognosis[111]. In the vast majority of cases, long-lasting *H. pylori* infection induces chronic gastritis, while only some patients develop PUD and GC. For this reason, the bacterium is considered to be a risk factor for the development and recurrence of PUD and GC[112,113]. Therefore, *H. pylori* is assigned to the group of pathogenic bacteria. However, it would be more correct to treat only those individuals at high risk for GC or to establish programs for early detection of GC without implementing massive eradication programs for this bacterium that may be important to colonize the gastric stomach of young humans[2].

BENEFICIAL "PROTECTIVE ROLE" OF *H. PYLORI*

H. pylori and asthma

The literature in recent years has enough works, the results of which suggest that there is an inverse correlation between the persistence of *H. pylori* and the detection of asthma cases[8,114-117].

Chen *et al*[8] reported that the detection of *H. pylori* in young and middle-aged patients (mean age 25 years) is inversely correlated not only with asthma, but also with other atopic diseases (dermatitis, atopic rash, and eczema). These researchers found a strong inverse relationship between the detection of *H. pylori* and the early onset of asthma (≤ 5 years old): OR = 0.58; 95%CI: 0.38-0.88. The difference in the patients' current status was also statistically significant: Asthma was observed less frequently in patients with detected *H. pylori* infection (P = 0.03). Elias *et al*[115] showed that 25% and 40% of children were seropositive for IgG in the study and control groups, respectively (P = 0.03) (the children's age ranged from 4.8 to 17.3 years). Interestingly, *cagA* IgG seropositivity was associated with a low risk of asthma [adjusted OR 0.30 (95%CI: 0.10-0.87)]. However, this pattern was not found for *cagA*-negative serology [adjusted OR = 0.64 (95%CI: 0.30-1.37)]. As in a previous study, *H. pylori* seropositive children had a lower likelihood of asthma than seronegative children [adjusted OR = 0.29 (95%CI: 0.10- 0.82)].

Greek colleagues found that the detection rate of *H. pylori* was 11.1% in children aged 8.6 ± 4.5 years with asthma symptoms, while it was 29.6% in the control group of the same age without bronchial obstruction symptoms (OR = 0.1; 95%CI: 0.039-0.305; P = 0.026)[109]. This correlation has been confirmed by a number of other earlier studies[118,119].

Oertli *et al*[120] investigated in detail and described the mechanism of anti-atopic action of *Helicobacter*. Their study indicated that immune tolerance could be acquired due to the immune system's constant response to bacterial γ-glutamyl transpeptidase (GGT) and vacA. At the same time, there was a gradual maturation of DCs and their more targeted interaction with Treg cells, which contributed to the more targeted autoactivation of the lymphocyte pool to various antigens. Such mechanisms ultimately result in immune tolerance to benign antigens (allergens). Special attention should also be paid to the fact that isogenic *H. pylori* mutants lacking either GGT or vacA are incapable of preventing DC maturation and fail to drive DC tolerization as assessed by induction of Treg properties in cocultured naive T cells.

Pachathundikandi *et al*[121] associated the phenomenon of tolerance with the ability

of *H. pylori* antigens to activate inflammasomes and to stimulate the production of cytokines, such as IL-1b and IL-18. The authors argue that such cytokine regulation assists in reducing the hyper-reactivation of the immune system and, as a consequence, prevents the development of both asthma and inflammatory bowel diseases.

H. pylori and inflammatory bowel diseases

The negative association between *H. pylori* persistence and inflammatory bowel diseases (IBD) development has also been studied for a long time. *H. pylori* persistence may be supposed to be a potentially beneficial factor against the development of IBD. Several large meta-analyses have concluded that the risk of IBD is higher in HPN patients[122]. Wu *et al*[123] showed that 24.9% of IBD patients had *H. pylori* infection *vs* 48.3% of the controls. The pooled risk ratio for *H. pylori* infection in IBD patients compared with the controls was 0.48 (95%CI: 0.43-0.54; $P < 0.001$). Rokkas *et al*[124] obtained similar results: 26.5% (95%CI: 25.2-27.8) of IBD patients were positive for *H. pylori* infection, compared to 44.7% (43.3%-46.1%) of individuals in the control group. In the literature, there are also studies proving that *H. pylori* eradication leads to the development of intestinal lesions[125]. However, there is also a contradiction in the accumulated data, since existing studies link *H. pylori* infection with the development of colorectal cancer[126].

H. pylori and GERD

In addition to the impact of *H. pylori* infection on the development of atopic reactions, considerable attention has been paid to the detection of *H. pylori* in patients with GERD. There remain a number of controversial points around the question of how eradication therapy affects the development or progression of GERD symptoms. The available data are rather contradictory and do not give a general insight into the problem. In their studies, a number of authors prove that there is no significant difference between *H. pylori*-positive and HPN patients and the development of GERD symptoms in these patients[127,128]. Thus, on the basis of their study, Bor *et al*[127] have come to the conclusion that the detection of *H. pylori* does not affect either the development of GERD symptoms or the severity of the disease course. The detection rate of *H. pylori* was 77.1% in asymptomatic patients *vs* 71.4% in GERD patients ($\chi^2 = 2.6$; $P = 0.27$). Xue *et al*[129] believe that eradication therapy fails to affect esophageal mucosal changes; therefore, there is no association with *H. pylori*. In their study, the investigators divided patients with endoscopically confirmed GERD into 2 groups (*H. pylori*-positive and HPN patients, respectively). The *H. pylori*-positive group received eradication therapy before treatment with proton pump inhibitors (10 d eradication, then esomeprazole 20 mg bid for 46 d). The other group was treated only with proton pump inhibitors (esomeprazole 20 mg bid therapy for 8 wk). As a result, there were 176 *H. pylori*-positive cases (with 92 eradication cases) and 180 negative cases. The healing rates in the *H. pylori*-positive eradicated group and the *H. pylori*-positive non-eradicated group reached 80.4% and 79.8%, respectively ($P = 0.911$), with reflux symptom scores of 0.22 and 0.14 ($P = 0.588$). The healing rates of esophagitis in the *H. pylori*-positive non-eradicated group and the *H. pylori*-negative group were 79.8 and 82.2%, respectively ($P = 0.848$); the reflux symptom scores were 0.14 and 0.21 ($P = 0.546$).

At the same time, contrary cases have been also described. The meta-analysis by Zhao *et al*[130] demonstrated that eradication therapy can lead to erosive GERD: The OR for the development of erosive GERD after *H. pylori* eradication was 1.67 (95%CI: 1.12-2.48; $P = 0.01$). Chung *et al*[131] revealed a clear inverse relationship between the detection of *H. pylori* and GERD: The prevalence of *H. pylori* infection was lower in cases with reflux esophagitis than in the controls (38.4% *vs* 58.2%, $P < 0.001$). The severity of esophagitis was also found to be inversely correlated with the detection of *H. pylori*. It is anticipated that *H. pylori* urease activity contributes to the neutralization of gastric acidity and, therefore, reduces the risk of acid reflux disease[132].

There are studies indicating the possible positive effect of *H. pylori* on the human body. In this connection, *H. pylori* in the majority of bacteria carriers can probably be attributed to bacteria that colonize the human body and constitute a population of commensal bacteria that use the host for their vital activity, but do not exhibit their pathogenic properties (as their persistence is under strict control by the host immune system). Such relationships between commensal bacteria and humans are typified by co-evolution, co-adaptation, and interactions[133]. Taking into account immune tolerance to *H. pylori* in the presence of long-term persistence in the host, the microorganism can also be considered as a symbiont[13].

CONCLUSION

The presented data suggest that there is clear ambiguity related to the problem of studying the mechanisms of ulcerogenesis, and the role of *H. pylori* in the processes of ulceration and carcinogenesis. On this basis, the management strategies for these inpatients are extremely difficult for clinicians. It is evident that a complete understanding of the mechanisms of inflammatory gastroduodenal mucosal injuries requires a more thorough approach, by considering the infectious and noninfectious, exogenous and endogenous factors, and an evaluation of the pathogenic and positive effects of *H. pylori* on human vital processes. Given the discussions surrounding the active eradication of *H. pylori* from the human population[134], it is more important than ever to critically assess its role within the microbiome. There is no coordinated attempt to eradicate these organisms from the human population; Malnick *et al*[3] suggested that there should not be a similar effort to eradicate *H. pylori*. Considering the growing number of publications on the potentially positive effects of the microorganism on the human body, it is not improbable that *H. pylori* is one of the bacteria in the healthy microbiome for the majority of the human population. There is a complex biological relationship between humans and commensal bacteria that is only now beginning to be understood. To better understand the mutualistic (*mutual* from Latin) role of *H. pylori* in cohorts at low risk for *H. pylori*-associated diseases, more investigations are needed to qualitatively and quantitatively estimate its benefits in healthy humans[132].

The manifestation of the pathogenic properties of *H. pylori*, which is characteristic of a smaller proportion of the human population having a genetic predisposition to develop gastrointestinal diseases, requires a reassessment of the available data on *H. pylori* infection. The "test and treat" approach to *H. pylori* does not address this issue at all[3]. It may be that the more correct way is an individualized approach to the patient according to the *H. pylori* endemic region, the presence of gastrointestinal diseases among relatives, or the impossibility of excluding nonmodifiable risk factors. Therefore, the most correct approach will be used to consider *H. pylori* persistence in terms of the possible positive role of the bacterium in the body and, therefore, to perform more individualized eradication therapy in the context of assessment of additional risk factors. Answers to such considerations should be obtained during further research.

ACKNOWLEDGEMENTS

The authors would like to express their gratitude to Aglaya Svyatoslavovna Yakovleva for technical assistance in preparing this article.

REFERENCES

1 **Fernandes YC**, Bonatto Gda R, Bonatto MW. Recurrence rate of Helicobacter pylori in patients with peptic ulcer five years or more after successful eradication. *Arq Gastroenterol* 2016; **53**: 152-155 [PMID: 27438419 DOI: 10.1590/S0004-28032016000300006]

2 **Li J**, Perez-Perez GI. Helicobacter pylori the Latent Human Pathogen or an Ancestral Commensal Organism. *Front Microbiol* 2018; **9**: 609 [DOI: 10.3389/fmicb.2018.00609]

3 **Malnick SD**, Melzer E, Attali M, Duek G, Yahav J. Helicobacter pylori: friend or foe? *World J Gastroenterol* 2014; **20**: 8979-8985 [PMID: 25083071 DOI: 10.3748/wjg.v20.i27.8979]

4 **McColl KE**. Clinical practice. Helicobacter pylori infection. *N Engl J Med* 2010; **362**: 1597-1604 [PMID: 20427808 DOI: 10.1056/NEJMcp1001110]

5 **Crowe SE**. *Helicobacter pylori* Infection. *N Engl J Med* 2019; **380**: 1158-1165 [PMID: 30893536 DOI: 10.1056/NEJMcp1710945]

6 **Everhart JE**. Recent developments in the epidemiology of Helicobacter pylori. *Gastroenterol Clin North Am* 2000; **29**: 559-578 [PMID: 11030073 DOI: 10.1016/s0889-8553(05)70130-8]

7 **Haruma K**, Okamoto S, Kawaguchi H, Gotoh T, Kamada T, Yoshihara M, Sumii K, Kajiyama G. Reduced incidence of Helicobacter pylori infection in young Japanese persons between the 1970s and the 1990s. *J Clin Gastroenterol* 1997; **25**: 583-586 [PMID: 9451667 DOI: 10.1097/00004836-199712000-00006]

8 **Chen Y**, Blaser MJ. Helicobacter pylori colonization is inversely associated with childhood asthma. *J Infect Dis* 2008; **198**: 553-560 [PMID: 18598192 DOI: 10.1086/590158]

9 **Eder W**, Ege MJ, von Mutius E. The asthma epidemic. *N Engl J Med* 2006; **355**: 2226-2235 [PMID: 17124020 DOI: 10.1056/NEJMra054308]

10 **Holster IL**, Vila AM, Caudri D, den Hoed CM, Perez-Perez GI, Blaser MJ, de Jongste JC, Kuipers

EJ. The impact of Helicobacter pylori on atopic disorders in childhood. *Helicobacter* 2012; **17**: 232-237 [PMID: 22515362 DOI: 10.1111/j.1523-5378.2012.00934.x]

11 **Rothenbacher D**, Blaser MJ, Bode G, Brenner H. Inverse relationship between gastric colonization of Helicobacter pylori and diarrheal illnesses in children: results of a population-based cross-sectional study. *J Infect Dis* 2000; **182**: 1446-1449 [PMID: 11015236 DOI: 10.1086/315887]

12 **Hunt RH**, Yaghoobi M. The Esophageal and Gastric Microbiome in Health and Disease. *Gastroenterol Clin North Am* 2017; **46**: 121-141 [PMID: 28164846 DOI: 10.1016/j.gtc.2016.09.009]

13 **Tsimmerman YS**. [Critical analysis of the Helicobacter pylori-infection leading role in the development of gastroduodenal diseases]. *Clin Pharmacol Ther* 2019; **28**: 19-27

14 **Kanizaj TF**, Kunac N. Helicobacter pylori: future perspectives in therapy reflecting three decades of experience. *World J Gastroenterol* 2014; **20**: 699-705 [PMID: 24574743 DOI: 10.3748/wjg.v20.i3.699]

15 **Reshetnyak VI**, Reshetnyak TM. Significance of dormant forms of *Helicobacter pylori* in ulcerogenesis. *World J Gastroenterol* 2017; **23**: 4867-4878 [PMID: 28785141 DOI: 10.3748/wjg.v23.i27.4867]

16 **Christopher JA**, Abiodun OJ. Helicobacter pylori infection: past, present and future. *Pan Afr Med J* 2016; **23**: 216 [DOI: 10.11604/pamj.2016.23.216.8852]

17 **de Bernard M**, Josenhans C. Pathogenesis of Helicobacter pylori infection. *Helicobacter* 2014; **19** Suppl 1: 11-18 [PMID: 25167940 DOI: 10.1111/hel.12160]

18 **Stark RM**, Suleiman MS, Hassan IJ, Greenman J, Millar MR. Amino acid utilisation and deamination of glutamine and asparagine by Helicobacter pylori. *J Med Microbiol* 1997; **46**: 793-800 [PMID: 9291892 DOI: 10.1099/00222615-46-9-793]

19 **Mentis A**, Lehours P, Mégraud F. Epidemiology and Diagnosis of Helicobacter pylori infection. *Helicobacter* 2015; **20** Suppl 1: 1-7 [PMID: 26372818 DOI: 10.1111/hel.12250]

20 **Luzza F**, Suraci E, Larussa T, Leone I, Imeneo M. High exposure, spontaneous clearance, and low incidence of active Helicobacter pylori infection: the Sorbo San Basile study. *Helicobacter* 2014; **19**: 296-305 [PMID: 24758553 DOI: 10.1111/hel.12133]

21 **Burucoa C**, Axon A. Epidemiology of Helicobacter pylori infection. *Helicobacter* 2017; **22** Suppl 1 [PMID: 28891138 DOI: 10.1111/hel.12403]

22 **Hooi JKY**, Lai WY, Ng WK, Suen MMY, Underwood FE, Tanyingoh D, Malfertheiner P, Graham DY, Wong VWS, Wu JCY, Chan FKL, Sung JJY, Kaplan GG, Ng SC. Global Prevalence of Helicobacter pylori Infection: Systematic Review and Meta-Analysis. *Gastroenterology* 2017; **153**: 420-429 [PMID: 28456631 DOI: 10.1053/j.gastro.2017.04.022]

23 **Tsimmerman IaS**. [The problem of growing resistance of microorganisms to antibiotic therapy and prospects for Helicobacter pylori eradication]. *Klin Med (Mosk)* 2013; **91**: 14-20 [PMID: 24417061]

24 **Kayali S**, Manfredi M, Gaiani F, Bianchi L, Bizzarri B, Leandro G, Di Mario F, De' Angelis GL. Helicobacter pylori, transmission routes and recurrence of infection: state of the art. *Acta Biomed* 2018; **89**: 72-76 [PMID: 30561421 DOI: 10.23750/abm.v89i8-S.7947]

25 **Mladenova I**, Durazzo M. Transmission of Helicobacter pylori. *Minerva Gastroenterol Dietol* 2018; **64**: 251-254 [PMID: 29458239 DOI: 10.23736/S1121-421X.18.02480-7]

26 **Zamani M**, Vahedi A, Maghdouri Z, Shokri-Shirvani J. Role of food in environmental transmission of *Helicobacter pylori*. *Caspian J Intern Med* 2017; **8**: 146-152 [PMID: 28932364 DOI: 10.22088/cjim.8.3.146]

27 **Sgambato D**, Visciola G, Ferrante E, Miranda A, Romano L, Tuccillo C, Manguso F, Romano M. Prevalence of *Helicobacter pylori* infection in sexual partners of *H. pylori*-infected subjects: Role of gastroesophageal reflux. *United European Gastroenterol J* 2018; **6**: 1470-1476 [PMID: 30574317 DOI: 10.1177/2050640618800628]

28 **Kao CY**, Sheu BS, Wu JJ. Helicobacter pylori infection: An overview of bacterial virulence factors and pathogenesis. *Biomed J* 2016; **39**: 14-23 [DOI: 10.1016/j.bj.2015.06.002]

29 **Marcus EA**, Sachs G, Scott DR. Acid-regulated gene expression of Helicobacter pylori: Insight into acid protection and gastric colonization. *Helicobacter* 2018; **23**: e12490 [PMID: 29696729 DOI: 10.1111/hel.12490]

30 **Weeks DL**, Eskandari S, Scott DR, Sachs G. A H+-gated urea channel: the link between Helicobacter pylori urease and gastric colonization. *Science* 2000; **287**: 482-485 [PMID: 10642549 DOI: 10.1126/science.287.5452.482]

31 **Schoep TD**, Fulurija A, Good F, Lu W, Himbeck RP, Schwan C, Choi SS, Berg DE, Mittl PR, Benghezal M, Marshall BJ. Surface properties of Helicobacter pylori urease complex are essential for persistence. *PLoS One* 2010; **5**: e15042 [PMID: 21124783 DOI: 10.1371/journal.pone.0015042]

32 **Lowenthal AC**, Hill M, Sycuro LK, Mehmood K, Salama NR, Ottemann KM. Functional analysis of the Helicobacter pylori flagellar switch proteins. *J Bacteriol* 2009; **191**: 7147-7156 [PMID: 19767432 DOI: 10.1128/JB.00749-09]

33 **Gu H**. Role of Flagella in the Pathogenesis of Helicobacter pylori. *Curr Microbiol* 2017; **74**: 863-869 [PMID: 28444418 DOI: 10.1007/s00284-017-1256-4]

34 **Gupta N**, Maurya S, Verma H, Verma VK. Unraveling the factors and mechanism involved in persistence: Host-pathogen interactions in Helicobacter pylori. *J Cell Biochem* 2019; **120**: 18572-18587 [PMID: 31237031 DOI: 10.1002/jcb.29201]

35 **Hathroubi S**, Zerebinski J, Ottemann KM. Helicobacter pylori Biofilm Involves a Multigene Stress-Biased Response, Including a Structural Role for Flagella. *mBio* 2018; **9**: e01973-18 [PMID: 30377283 DOI: 10.1128/mBio.01973-18]

36 **García A**, Salas-Jara MJ, Herrera C, González C. Biofilm and Helicobacter pylori: from environment to human host. *World J Gastroenterol* 2014; **20**: 5632-5638 [PMID: 24914322 DOI: 10.3748/wjg.v20.i19.5632]

37 **Matsuo Y**, Kido Y, Yamaoka Y. Helicobacter pylori Outer Membrane Protein-Related Pathogenesis. *Toxins (Basel)* 2017; **9**: 101 [PMID: 28287480 DOI: 10.3390/toxins9030101]

38 **Chang WL**, Yeh YC, Sheu BS. The impacts of H. pylori virulence factors on the development of gastroduodenal diseases. *J Biomed Sci* 2018; **25**: 68 [PMID: 30205817 DOI: 10.1186/s12929-018-0466-9]

39 **Ricci V**, Giannouli M, Romano M, Zarrilli R. Helicobacter pylori gamma-glutamyl transpeptidase and its pathogenic role. *World J Gastroenterol* 2014; **20**: 630-638 [PMID: 24574736 DOI: 10.3748/wjg.v20.i3.630]

40 **Javed S**, Skoog EC, Solnick JV. Impact of Helicobacter pylori Virulence Factors on the Host Immune Response and Gastric Pathology. *Curr Top Microbiol Immunol* 2019; **421**: 21-52 [PMID: 31123884 DOI: 10.1007/978-3-030-15138-6_2]

41 **Tohidpour A**. CagA-mediated pathogenesis of Helicobacter pylori. *Microb Pathog* 2016; **93**: 44-55 [PMID: 26796299 DOI: 10.1016/j.micpath.2016.01.005]

42 **Ansari S**, Yamaoka Y. Survival of Helicobacter pylori in gastric acidic territory. *Helicobacter* 2017; **22**: 10.1111/hel.12386 [PMID: 28402047 DOI: 10.1111/hel.12386]

43 **Maleki Kakelar H**, Barzegari A, Dehghani J, Hanifian S, Saeedi N, Barar J, Omidi Y. Pathogenicity of Helicobacter pylori in cancer development and impacts of vaccination. *Gastric Cancer* 2019; **22**: 23-36 [PMID: 30145749 DOI: 10.1007/s10120-018-0867-1]

44 **Ohnishi N**, Yuasa H, Tanaka S, Sawa H, Miura M, Matsui A, Higashi H, Musashi M, Iwabuchi K, Suzuki M, Yamada G, Azuma T, Hatakeyama M. Transgenic expression of Helicobacter pylori CagA induces gastrointestinal and hematopoietic neoplasms in mouse. *Proc Natl Acad Sci USA* 2008; **105**: 1003-1008 [PMID: 18192401 DOI: 10.1073/pnas.0711183105]

45 **Romano M**, Ricci V, Zarrilli R. Mechanisms of disease: Helicobacter pylori-related gastric carcinogenesis--implications for chemoprevention. *Nat Clin Pract Gastroenterol Hepatol* 2006; **3**: 622-632 [PMID: 17068500 DOI: 10.1038/ncpgasthep0634]

46 **De Falco M**, Lucariello A, Iaquinto S, Esposito V, Guerra G, De Luca A. Molecular Mechanisms of Helicobacter pylori Pathogenesis. *J Cell Physiol* 2015; **230**: 1702-1707 [PMID: 25639461 DOI: 10.1002/jcp.24933]

47 **Rassow J**, Meinecke M. Helicobacter pylori VacA: a new perspective on an invasive chloride channel. *Microbes Infect* 2012; **14**: 1026-1033 [DOI: 10.1016/j.micinf.2012.07.002]

48 **Raju D**, Hussey S, Ang M, Terebiznik MR, Sibony M, Galindo-Mata E, Gupta V, Blanke SR, Delgado A, Romero-Gallo J, Ramjeet MS, Mascarenhas H, Peek RM, Correa P, Streutker C, Hold G, Kunstmann E, Yoshimori T, Silverberg MS, Girardin SE, Philpott DJ, El Omar E, Jones NL. Vacuolating cytotoxin and variants in Atg16L1 that disrupt autophagy promote Helicobacter pylori infection in humans. *Gastroenterology* 2012; **142**: 1160-1171 [PMID: 22333951 DOI: 10.1053/j.gastro.2012.01.043]

49 **McGee DJ**, Mobley HL. Pathogenesis of Helicobacter pylori infection. *Curr Opin Gastroenterol* 2000; **16**: 24-31 [PMID: 17024012]

50 **Suzuki T**, Kato K, Ohara S, Noguchi K, Sekine H, Nagura H, Shimosegawa T. Localization of antigen-presenting cells in Helicobacter pylori-infected gastric mucosa. *Pathol Int* 2002; **52**: 265-271 [PMID: 12031081]

51 **Figueiredo CA**, Marques CR, Costa Rdos S, da Silva HB, Alcantara-Neves NM. Cytokines, cytokine gene polymorphisms and Helicobacter pylori infection: friend or foe? *World J Gastroenterol* 2014; **20**: 5235-5243 [PMID: 24833853 DOI: 10.3748/wjg.v20.i18.5235]

52 **D'Elios MM**, Codolo G, Amedei A, Mazzi P, Berton G, Zanotti G, Del Prete G, de Bernard M. Helicobacter pylori, asthma and allergy. *FEMS Immunol Med Microbiol* 2009; **56**: 1-8 [PMID: 19220467 DOI: 10.1111/j.1574-695X.2009.00537.x]

53 **Bimczok D**, Clements RH, Waites KB, Novak L, Eckhoff DE, Mannon PJ, Smith PD, Smythies LE. Human primary gastric dendritic cells induce a Th1 response to H. pylori. *Mucosal Immunol* 2010; **3**: 260-269 [PMID: 20237463 DOI: 10.1038/mi.2010.10]

54 **Altobelli A**, Bauer M, Velez K, Cover TL, Müller A. *Helicobacter pylori* VacA Targets Myeloid Cells in the Gastric Lamina Propria To Promote Peripherally Induced Regulatory T-Cell Differentiation and Persistent Infection. *mBio* 2019; **10** [PMID: 30890606 DOI: 10.1128/mBio.00261-19]

55 **Hsu WT**, Ho SY, Jian TY, Huang HN, Lin YL, Chen CH, Lin TH, Wu MS, Wu CJ, Chan YL, Liao KW. Helicobacter pylori-derived heat shock protein 60 increases the induction of regulatory T-cells associated with persistent infection. *Microb Pathog* 2018; **119**: 152-161 [PMID: 29660522 DOI: 10.1016/j.micpath.2018.04.016]

56 **Lehours P**, Ferrero RL. Review: Helicobacter: Inflammation, immunology, and vaccines. *Helicobacter* 2019; **24** Suppl 1: e12644 [PMID: 31486236 DOI: 10.1111/hel.12644]

57 **Watanabe M**, Kato J, Inoue I, Yoshimura N, Yoshida T, Mukoubayashi C, Deguchi H, Enomoto S, Ueda K, Maekita T, Iguchi M, Tamai H, Utsunomiya H, Yamamichi N, Fujishiro M, Iwane M, Tekeshita T, Mohara O, Ushijima T, Ichinose M. Development of gastric cancer in nonatrophic stomach with highly active inflammation identified by serum levels of pepsinogen and Helicobacter pylori antibody together with endoscopic rugal hyperplastic gastritis. *Int J Cancer* 2012; **131**: 2632-2642 [PMID: 22383377 DOI: 10.1002/ijc.27514]

58 **Sokic-Milutinovic A**, Alempijevic T, Milosavljevic T. Role of Helicobacter pylori infection in gastric carcinogenesis: Current knowledge and future directions. *World J Gastroenterol* 2015; **21**: 11654-11672 [PMID: 26556993 DOI: 10.3748/wjg.v21.i41.11654]

59 **Huang JQ**, Sridhar S, Hunt RH. Role of Helicobacter pylori infection and non-steroidal anti-inflammatory drugs in peptic-ulcer disease: a meta-analysis. *Lancet* 2002; **359**: 14-22 [PMID: 11809181 DOI: 10.1016/S0140-6736(02)07273-2]

60 **Ertz-Archambault N**, Keim P, Von Hoff D. Microbiome and pancreatic cancer: A comprehensive topic review of literature. *World J Gastroenterol* 2017; **23**: 1899-1908 [PMID: 28348497 DOI: 10.3748/wjg.v23.i10.1899]

61 **Xiao M**, Wang Y, Gao Y. Association between Helicobacter pylori infection and pancreatic cancer development: a meta-analysis. *PLoS One* 2013; **8**: e75559 [PMID: 24086571 DOI: 10.1371/journal.pone.0075559]

62 **Otero LL**, Ruiz VE, Perez GIP. Helicobacter pylori: The balance between a role as colonizer and pathogen. *Best Pract Res Clin Gastroenterol* 2014; **28**: 1017-1029 [DOI: 10.1016/j.bpg.2014.09.003]

63 **Mentis AFA**, Boziki M, Grigoriadis N, Papavassiliou AG. Helicobacter pylori infection and gastric cancer biology: tempering a double-edged sword. *Cell Mol Life Sci* 2019; **76**: 2477-2486 [DOI: 10.1007/s00018-019-03044-1]

64 **Gravina AG**, Zagari RM, De Musis C, Romano L, Loguercio C, Romano M. *Helicobacter pylori* and extragastric diseases: A review. *World J Gastroenterol* 2018; **24**: 3204-3221 [PMID: 30090002 DOI: 10.3748/wjg.v24.i29.3204]

65 **German SV**, Bobrovnitsky IP. [New aspects of Helicobacter pylori infection: Association with metabolic disturbances]. *Ter Arkh* 2017; **89**: 102-107 [PMID: 29171479 DOI: 10.17116/terarkh20178910102-107]

66 **Maev IV**, Samsonov AA, Andreev DN, Grechushnikov VB, Korovina TI. [Clinical significance of helicobacter pylori infection]. *Clin Med* 2013; **91**: 4-12 [PMID: 24437177]

67 **Wang ZW**, Li Y, Huang LY, Guan QK, Xu DW, Zhou WK, Zhang XZ. Helicobacter pylori infection contributes to high risk of ischemic stroke: evidence from a meta-analysis. *J Neurol* 2012; **259**: 2527-2537 [PMID: 22688569 DOI: 10.1007/s00415-012-6558-7]

68 **Kountouras J**, Boziki M, Zavos C, Gavalas E, Giartza-Taxidou E, Venizelos I, Deretzi G, Grigoriadis N, Tsiaousi E, Vardaka E. A potential impact of chronic Helicobacter pylori infection on Alzheimer's disease pathobiology and course. *Neurobiol Aging* 2012; **33**: e3-e4 [PMID: 22325590 DOI: 10.1016/j.neurobiolaging.2012.01.003]

69 **Franceschi F**, Covino M, Roubaud Baudron C. Review: Helicobacter pylori and extragastric diseases. *Helicobacter* 2019; **24** Suppl 1: e12636 [PMID: 31486239 DOI: 10.1111/hel.12636]

70 **Huang HK**, Wang JH, Lei WY, Chen CL, Chang CY, Liou LS. Helicobacter pylori infection is associated with an increased risk of Parkinson's disease: A population-based retrospective cohort study. *Parkinsonism Relat Disord* 2018; **47**: 26-31 [PMID: 29174171 DOI: 10.1016/j.parkreldis.2017.11.331]

71 **Izadi M**, Fazel M, Sharubandi SH, Saadat SH, Farahani MM, Nasseri MH, Dabiri H, SafiAryan R, Esfahani AA, Ahmadi A, Jonaidi Jafari N, Ranjbar R, Jamali-Moghaddam SR, Kazemi-Saleh D, Kalantar-Motamed MH, Taheri S. Helicobacter species in the atherosclerotic plaques of patients with coronary artery disease. *Cardiovasc Pathol* 2012; **21**: 307-311 [PMID: 22104005 DOI: 10.1016/j.carpath.2011.09.011]

72 **Park MJ**, Choi SH, Kim D, Kang SJ, Chung SJ, Choi SY, Yoon DH, Lim SH, Kim YS, Yim JY, Kim JS, Jung HC. Association between Helicobacter pylori Seropositivity and the Coronary Artery Calcium Score in a Screening Population. *Gut Liver* 2011; **5**: 321-327 [PMID: 21927661 DOI: 10.5009/gnl.2011.5.3.321]

73 **Jukic A**, Bozic D, Kardum D, Becic T, Luksic B, Vrsalovic M, Ljubkovic M, Fabijanic D. *Helicobacter pylori* infection and severity of coronary atherosclerosis in patients with chronic coronary artery disease. *Ther Clin Risk Manag* 2017; **13**: 933-938 [PMID: 28794636 DOI: 10.2147/TCRM.S142193]

74 **Sharma V**, Aggarwal A. Helicobacter pylori: Does it add to risk of coronary artery disease. *World J Cardiol* 2015; **7**: 19-25 [PMID: 25632315 DOI: 10.4330/wjc.v7.i1.19]

75 **Vijayvergiya R**, Vadivelu R. Role of Helicobacter pylori infection in pathogenesis of atherosclerosis. *World J Cardiol* 2015; **7**: 134-143 [PMID: 25810813 DOI: 10.4330/wjc.v7.i3.134]

76 **Cárdenas VM**, Boller F, Román GC. *Helicobacter pylori*, Vascular Risk Factors and Cognition in U.S. Older Adults. *Brain Sci* 2019; **9**: 370 [PMID: 31842501 DOI: 10.3390/brainsci9120370]

77 **Santarelli L**, Gabrielli M, Cremonini F, Santoliquido A, Candelli M, Nista EC, Pola P, Gasbarrini G, Gasbarrini A. Atrophic gastritis as a cause of hyperhomocysteinaemia. *Aliment Pharmacol Ther* 2004; **19**: 107-111 [PMID: 14687172 DOI: 10.1046/j.1365-2036.2003.01820.x]

78 **Rasmi Y**, Raeisi S, Seyyed Mohammadzad MH. Association of inflammation and cytotoxin-associated gene a positive strains of helicobacter pylori in cardiac syndrome x. *Helicobacter* 2012; **17**: 116-120 [PMID: 22404441 DOI: 10.1111/j.1523-5378.2011.00923.x]

79 **de Jesus Souza M**, de Moraes JA, Da Silva VN, Helal-Neto E, Uberti AF, Scopel-Guerra A, Olivera-Severo D, Carlini CR, Barja-Fidalgo C. Helicobacter pylori urease induces pro-inflammatory effects and differentiation of human endothelial cells: Cellular and molecular mechanism. *Helicobacter* 2019; **24**: e12573 [PMID: 30907046 DOI: 10.1111/hel.12573]

80 **Yu M**, Zhang R, Ni P, Chen S, Duan G. *Helicobacter pylori* Infection and Psoriasis: A Systematic

Review and Meta-Analysis. *Medicina (Kaunas)* 2019; **55** [PMID: 31561576 DOI: 10.3390/medicina55100645]
81 **Onsun N**, Arda Ulusal H, Su O, Beycan I, Biyik Ozkaya D, Senocak M. Impact of Helicobacter pylori infection on severity of psoriasis and response to treatment. *Eur J Dermatol* 2012; **22**: 117-120 [PMID: 22063790 DOI: 10.1684/ejd.2011.1579]
82 **Yorulmaz A**, Kulcu SC. Helicobacter pylori and inflammatory skin diseases. *World J Dermatol* 2015; **4**: 120-128 [DOI: 10.5314/wjd.v4.i3.120]
83 **Atherton JC**, Blaser MJ. Coadaptation of Helicobacter pylori and humans: ancient history, modern implications. *J Clin Invest* 2009; **119**: 2475-2487 [PMID: 19729845 DOI: 10.1172/JCI38605]
84 **Stein M**, Ruggiero P, Rappuoli R, Bagnoli F. Helicobacter pylori CagA: From Pathogenic Mechanisms to Its Use as an Anti-Cancer Vaccine. *Front Immunol* 2013; **4**: 328 [PMID: 24133496 DOI: 10.3389/fimmu.2013.00328]
85 **Walker MM**, Talley NJ. Review article: bacteria and pathogenesis of disease in the upper gastrointestinal tract--beyond the era of Helicobacter pylori. *Aliment Pharmacol Ther* 2014; **39**: 767-779 [PMID: 24612362 DOI: 10.1111/apt.12666]
86 **Calvet X**, Ramírez Lázaro MJ, Lehours P, Mégraud F. Diagnosis and epidemiology of Helicobacter pylori infection. *Helicobacter* 2013; **18** Suppl 1: 5-11 [PMID: 24011238 DOI: 10.1111/hel.12071]
87 **Malfertheiner P**, Chan FK, McColl KE. Peptic ulcer disease. *Lancet* 2009; **374**: 1449-1461 [PMID: 19683340 DOI: 10.1016/S0140-6736(09)60938-7]
88 **Araújo MB**, Borini P, Guimarães RC. Etiopathogenesis of peptic ulcer: back to the past? *Arq Gastroenterol* 2014; **51**: 155-161 [PMID: 25003270 DOI: 10.1590/s0004-28032014000200016]
89 **Sidorenko SV**. [Diagnosis and treatment of infections caused by Helicobacter pylori]. *Antibiot Khimioter* 2001; **46**: 23-31 [PMID: 11871316]
90 **Rosenstock S**, Jørgensen T, Bonnevie O, Andersen L. Risk factors for peptic ulcer disease: a population based prospective cohort study comprising 2416 Danish adults. *Gut* 2003; **52**: 186-193 [PMID: 12524398 DOI: 10.1136/gut.52.2.186]
91 **Figura N**, Guglielmetti P, Rossolini A, Barberi A, Cusi G, Musmanno RA, Russi M, Quaranta S. Cytotoxin production by Campylobacter pylori strains isolated from patients with peptic ulcers and from patients with chronic gastritis only. *J Clin Microbiol* 1989; **27**: 225-226 [PMID: 2913034 DOI: 10.1128/JCM.27.1.225-226.1989]
92 **Atherton JC**, Cao P, Peek RM Jr, Tummuru MK, Blaser MJ, Cover TL. Mosaicism in vacuolating cytotoxin alleles of Helicobacter pylori. Association of specific vacA types with cytotoxin production and peptic ulceration. *J Biol Chem* 1995; **270**: 17771-17777 [PMID: 7629077 DOI: 10.1074/jbc.270.30.17771]
93 **Atherton JC**. The clinical relevance of strain types of Helicobacter pylori. *Gut* 1997; **40**: 701-703 [PMID: 9245920 DOI: 10.1136/gut.40.6.701]
94 **Iijima K**, Kanno T, Koike T, Shimosegawa T. Helicobacter pylori-negative, non-steroidal anti-inflammatory drug: negative idiopathic ulcers in Asia. *World J Gastroenterol* 2014; **20**: 706-713 [PMID: 24574744 DOI: 10.3748/wjg.v20.i3.706]
95 **Charpignon C**, Lesgourgues B, Pariente A, Nahon S, Pelaquier A, Gatineau-Sailliant G, Roucayrol AM, Courillon-Mallet A; Group de l'Observatoire National des Ulcères de l'Association Nationale des HépatoGastroentérologues des Hôpitaux Généraux (ANGH). Peptic ulcer disease: one in five is related to neither Helicobacter pylori nor aspirin/NSAID intake. *Aliment Pharmacol Ther* 2013; **38**: 946-954 [PMID: 23981105 DOI: 10.1111/apt.12465]
96 **Goenka MK**, Majumder S, Sethy PK, Chakraborty M. Helicobacter pylori negative, non-steroidal anti-inflammatory drug-negative peptic ulcers in India. *Indian J Gastroenterol* 2011; **30**: 33-37 [PMID: 21424697 DOI: 10.1007/s12664-011-0085-9]
97 **Reshetnyak TM**, Doroshkevich IA, Seredavkina NV, Nasonov EL, Maev IV, Reshetnyak VI. The Contribution of Drugs and *Helicobacter pylori* to Gastric Mucosa Changes in Patients with Systemic Lupus Erythematosus and Antiphospholipid Syndrome. *Int J Rheumatol* 2019; **2019**: 9698086 [PMID: 31191660 DOI: 10.1155/2019/9698086]
98 **Kanno T**, Iijima K, Abe Y, Yagi M, Asonuma S, Ohyauchi M, Ito H, Koike T, Shimosegawa T. Helicobacter pylori-negative and non-steroidal anti-inflammatory drugs-negative idiopathic peptic ulcers show refractoriness and high recurrence incidence: Multicenter follow-up study of peptic ulcers in Japan. *Dig Endosc* 2016; **28**: 556-563 [PMID: 26866510 DOI: 10.1111/den.12635]
99 **Rasane RK**, Horn CB, Coleoglou Centeno AA, Fiore NB, Torres Barboza M, Zhang Q, Bochicchio KM, Punch LJ, Bochicchio GV, Ilahi ON. Are Patients with Perforated Peptic Ulcers Who are Negative for *Helicobacter pylori* at a Greater Risk? *Surg Infect (Larchmt)* 2019; **20**: 444-448 [PMID: 30939075 DOI: 10.1089/sur.2018.249]
100 **Tsimmerman YS**. [Gastric cancers: a modern approach to the problem]. *Vestnik chirurgicheskoj gastroenterologii* 2011; **2**: 77-88
101 **Laine L**, Hopkins RJ, Girardi LS. Has the impact of Helicobacter pylori therapy on ulcer recurrence in the United States been overstated? *Am J Gastroenterol* 1998; **93**: 1409-1415 [PMID: 9732917 DOI: 10.1111/j.1572-0241.1998.452_a.x]
102 **Leodolter A**, Kulig M, Brasch H, Meyer-Sabellek W, Willich SN, Malfertheiner P. A meta-analysis comparing eradication, healing and relapse rates in patients with Helicobacter pylori-associated gastric or duodenal ulcer. *Aliment Pharmacol Ther* 2001; **15**: 1949-1958 [PMID: 11736726 DOI: 10.1046/j.1365-2036.2001.01109.x]
103 **Lamb A**, Chen LF. Role of the Helicobacter pylori-induced inflammatory response in the

development of gastric cancer. *J Cell Biochem* 2013; **114**: 491-497 [PMID: 22961880 DOI: 10.1002/jcb.24389]

104 **Correa P**. Human gastric carcinogenesis: a multistep and multifactorial process--First American Cancer Society Award Lecture on Cancer Epidemiology and Prevention. *Cancer Res* 1992; **52**: 6735-6740 [PMID: 1458460]

105 **Danesh J**. Helicobacter pylori infection and gastric cancer: systematic review of the epidemiological studies. *Aliment Pharmacol Ther* 1999; **13**: 851-856 [PMID: 10383517 DOI: 10.1046/j.1365-2036.1999.00546.x]

106 **Hansen S**, Melby KK, Aase S, Jellum E, Vollset SE. Helicobacter pylori infection and risk of cardia cancer and non-cardia gastric cancer. A nested case-control study. *Scand J Gastroenterol* 1999; **34**: 353-360 [PMID: 10365894 DOI: 10.1080/003655299750026353]

107 **Rokkas F**. [Helicobacter pylori infection as risk factor of a carcinoma of the stomach: current evidence]. *Russ J Gastroenterol Hepatol Coloproctol* 2002; **3**: 66-70

108 **Blaser MJ**. Helicobacter pylori: Balance and inbalance. *Europ J Gastroenterol Hepatol* 1998; **10** Suppl 1: 15-18 [DOI: 10.1097/00042737-199806001-00004]

109 **Cover TL**, Blaser MJ. Helicobacter pylori in health and disease. *Gastroenterology* 2009; **136**: 1863-1873 [PMID: 19457415 DOI: 10.1053/j.gastro.2009.01.073]

110 **Blaser MJ**. Helicobacter pylori and the pathogenesis of gastroduodenal inflammation. *J Infect Dis* 1990; **161**: 626-633 [PMID: 2181029 DOI: 10.1093/infdis/161.4.626]

111 **Bardakhch'ian EA**, Kharlanova NG, Kamneva NV, Lomov SIu, Saiamov SR, Golubev BP. [Coccoid forms of Helicobacter pylori and their role in human pathology]. *Eksp Klin Gastroenterol* 2003; **(6)**: 11-15, 153 [PMID: 15065521]

112 **Yamaoka Y**. Pathogenesis of Helicobacter pylori-Related Gastroduodenal Diseases from Molecular Epidemiological Studies. *Gastroenterol Res Pract* 2012; **2012**: 371503 [PMID: 22829807 DOI: 10.1155/2012/371503]

113 **Liu J**, He C, Chen M, Wang Z, Xing C, Yuan Y. Association of presence/absence and on/off patterns of Helicobacter pylori oipA gene with peptic ulcer disease and gastric cancer risks: a meta-analysis. *BMC Infect Dis* 2013; **13**: 555 [PMID: 24256489 DOI: 10.1186/1471-2334-13-555]

114 **Miftahussurur M**, Nusi IA, Graham DY, Yamaoka Y. *Helicobacter*, Hygiene, Atopy, and Asthma. *Front Microbiol* 2017; **8**: 1034 [PMID: 28642748 DOI: 10.3389/fmicb.2017.01034]

115 **Elias N**, Nasrallah E, Khoury C, Mansour B, Abu Zuher L, Asato V, Muhsen K. Associations of Helicobacter pylori seropositivity and gastric inflammation with pediatric asthma. *Pediatr Pulmonol* 2020; **55**: 2236-2245 [PMID: 32543787 DOI: 10.1002/ppul.24905]

116 **Tsigalou C**, Konstantinidis TG, Cassimos D, Karvelas A, Grapsa A, Tsalkidis A, Panopoulou M, Tsakris A. Inverse association between *Helicobacter pylori* infection and childhood asthma in Greece: a case-control study. *Germs* 2019; **9**: 182-187 [PMID: 32042724 DOI: 10.18683/germs.2019.1174]

117 **Ierardi E**, Losurdo G, Giorgio F, Di Leo A. Might helicobacter pylori play a role in allergic or cross-reaction related disorders? *Expert Rev Gastroenterol Hepatol* 2020; **14**: 643-646 [PMID: 32510247 DOI: 10.1080/17474124.2020.1780119]

118 **Amberbir A**, Medhin G, Erku W, Alem A, Simms R, Robinson K, Fogarty A, Britton J, Venn A, Davey G. Effects of Helicobacter pylori, geohelminth infection and selected commensal bacteria on the risk of allergic disease and sensitization in 3-year-old Ethiopian children. *Clin Exp Allergy* 2011; **41**: 1422-1430 [PMID: 21831135 DOI: 10.1111/j.1365-2222.2011.03831.x]

119 **Zevit N**, Balicer RD, Cohen HA, Karsh D, Niv Y, Shamir R. Inverse association between Helicobacter pylori and pediatric asthma in a high-prevalence population. *Helicobacter* 2012; **17**: 30-35 [PMID: 22221613 DOI: 10.1111/j.1523-5378.2011.00895.x]

120 **Oertli M**, Noben M, Engler DB, Semper RP, Reuter S, Maxeiner J, Gerhard M, Taube C, Müller A. Helicobacter pylori γ-glutamyl transpeptidase and vacuolating cytotoxin promote gastric persistence and immune tolerance. *Proc Natl Acad Sci USA* 2013; **110**: 3047-3052 [PMID: 23382221 DOI: 10.1073/pnas.1211248110]

121 **Pachathundikandi SK**, Müller A, Backert S. Inflammasome Activation by Helicobacter pylori and Its Implications for Persistence and Immunity. *Curr Top Microbiol Immunol* 2016; **397**: 117-131 [PMID: 27460807 DOI: 10.1007/978-3-319-41171-2_6]

122 **Kyburz A**, Müller A. Helicobacter pylori and Extragastric Diseases. *Curr Top Microbiol Immunol* 2017; **400**: 325-347 [PMID: 28124160 DOI: 10.1007/978-3-319-50520-6_14]

123 **Wu XW**, Ji HZ, Yang MF, Wu L, Wang FY. Helicobacter pylori infection and inflammatory bowel disease in Asians: a meta-analysis. *World J Gastroenterol* 2015; **21**: 4750-4756 [PMID: 25914487 DOI: 10.3748/wjg.v21.i15.4750]

124 **Rokkas T**, Gisbert JP, Niv Y, O'Morain C. The association between Helicobacter pylori infection and inflammatory bowel disease based on meta-analysis. *United European Gastroenterol J* 2015; **3**: 539-550 [PMID: 26668747 DOI: 10.1177/2050640615580889]

125 **Jovanovic IR**, Milosavjevic TN, Jankovic GP, Micev MM, Dugalic PD, Saranovic D, Ugljesic MM, Popovic DV, Bulajic MM. Clinical onset of the Crohn's disease after eradication therapy of Helicobacter pylori infection. Does Helicobacter pylori infection interact with natural history of inflammatory bowel diseases? *Med Sci Monit* 2001; **7**: 137-141 [PMID: 11208510]

126 **Papamichael K**, Konstantopoulos P, Mantzaris GJ. Helicobacter pylori infection and inflammatory bowel disease: is there a link? *World J Gastroenterol* 2014; **20**: 6374-6385 [PMID: 24914359 DOI: 10.3748/wjg.v20.i21.6374]

127 **Bor S**, Kitapcioglu G, Kasap E. Prevalence of gastroesophageal reflux disease in a country with a high occurrence of *Helicobacter pylori*. *World J Gastroenterol* 2017; **23**: 525-532 [PMID: 28210089 DOI: 10.3748/wjg.v23.i3.525]

128 **Mungan Z**, Pınarbaşı Şimşek B. Gastroesophageal reflux disease and the relationship with Helicobacter pylori. *Turk J Gastroenterol* 2017; **28**: S61-S67 [PMID: 29199171 DOI: 10.5152/tjg.2017.16]

129 **Xue Y**, Zhou LY, Lin SR, Hou XH, Li ZS, Chen MH, Yan XE, Meng LM, Zhang J, Lu JJ. Effect of Helicobacter pylori eradication on reflux esophagitis therapy: a multi-center randomized control study. *Chin Med J (Engl)* 2015; **128**: 995-999 [PMID: 25881589 DOI: 10.4103/0366-6999.155049]

130 **Zhao Y**, Li Y, Hu J, Wang X, Ren M, Lu G, Lu X, Zhang D, He S. The Effect of Helicobacter pylori Eradication in Patients with Gastroesophageal Reflux Disease: A Meta-Analysis of Randomized Controlled Studies. *Dig Dis* 2020; **38**: 261-268 [PMID: 32396919 DOI: 10.1159/000504086]

131 **Chung SJ**, Lim SH, Choi J, Kim D, Kim YS, Park MJ, Yim JY, Kim JS, Cho SH, Jung HC, Song IS. Helicobacter pylori Serology Inversely Correlated With the Risk and Severity of Reflux Esophagitis in Helicobacter pylori Endemic Area: A Matched Case-Control Study of 5,616 Health Check-Up Koreans. *J Neurogastroenterol Motil* 2011; **17**: 267-273 [PMID: 21860818 DOI: 10.5056/jnm.2011.17.3.267]

132 **Lin D**, Koskella B. Friend and foe: factors influencing the movement of the bacterium Helicobacter pylori along the parasitism-mutualism continuum. *Evol Appl* 2015; **8**: 9-22 [PMID: 25667600 DOI: 10.1111/eva.12231]

133 **Blaser MJ**, Falkow S. What are the consequences of the disappearing human microbiota? *Nat Rev Microbiol* 2009; **7**: 887-894 [PMID: 19898491 DOI: 10.1038/nrmicro2245]

134 **Lee YC**, Chen TH, Chiu HM, Shun CT, Chiang H, Liu TY, Wu MS, Lin JT. The benefit of mass eradication of Helicobacter pylori infection: a community-based study of gastric cancer prevention. *Gut* 2013; **62**: 676-682 [PMID: 22698649 DOI: 10.1136/gutjnl-2012-302240]

World Journal of Gastroenterology

Submit a Manuscript: https://www.f6publishing.com

World J Gastroenterol 2021 February 21; 27(7): 561-575

DOI: 10.3748/wjg.v27.i7.561

ISSN 1007-9327 (print) ISSN 2219-2840 (online)

REVIEW

Digestive system involvement of infections with SARS-CoV-2 and other coronaviruses: Clinical manifestations and potential mechanisms

Gao-Feng Zhan, Yue Wang, Ning Yang, Ai-Lin Luo, Shi-Yong Li

ORCID number: Gao-Feng Zhan 0000-0003-3002-9333; Yue Wang 0000-0002-0456-1273; Ning Yang 0000-0002-7977-1128; Ai-Lin Luo 0000-0003-0152-1628; Shi-Yong Li 0000-0001-7442-1826.

Author contributions: Zhan GF, Wang Y, and Yang N reviewed the literature and drafted the manuscript; Luo AL and Li SY checked and revised the manuscript; all authors contributed to the conception and design of the review and approved the final manuscript for submission.

Conflict-of-interest statement: All the authors declare no conflict of interest related to this manuscript.

Open-Access: This article is an open-access article that was selected by an in-house editor and fully peer-reviewed by external reviewers. It is distributed in accordance with the Creative Commons Attribution NonCommercial (CC BY-NC 4.0) license, which permits others to distribute, remix, adapt, build upon this work non-commercially, and license their derivative works on different terms, provided the original work is properly cited and the use is non-commercial. See: http://creativecommons.org/License

Gao-Feng Zhan, Yue Wang, Ai-Lin Luo, Shi-Yong Li, Department of Anesthesiology, Tongji Hospital, Tongji Medical College, Huazhong University of Science and Technology, Wuhan 430030, Hubei Province, China

Ning Yang, Department of Anesthesiology, Union Hospital, Tongji Medical College, Huazhong University of Science and Technology, Wuhan 430030, Hubei Province, China

Corresponding author: Shi-Yong Li, MD, PhD, Doctor, Department of Anesthesiology, Tongji Hospital, Tongji Medical College, Huazhong University of Science and Technology, No. 1095 Jiefang Avenue, Wuhan 430030, Hubei Province, China. shiyongli@hust.edu.cn

Abstract

Although coronavirus (CoV) infection is often characterized by respiratory symptoms, the virus can also result in extrapulmonary symptoms, especially the symptoms related to the digestive system. The outbreak of coronavirus disease 2019 (COVID-19) is currently the world's most pressing public health threat and has a significant impact on civil societies and the global economy. The occurrence of digestive symptoms in patients with COVID-19 is closely related to the development and prognosis of the disease. Moreover, thus far, there are no specific antiviral drug or vaccine approved for the treatment or prevention of COVID-19. Therefore, we elaborate on the effects of CoVs on the digestive system and the potential underlying mechanisms.

Key Words: SARS-CoV-2; Gastrointestinal diseases; Liver dysfunction; COVID-19; Coronavirus; Mechanisms

©The Author(s) 2021. Published by Baishideng Publishing Group Inc. All rights reserved.

Core Tip: In this review, it is reported that coronavirus infections can cause a series of digestive diseases, and may also be accompanied by digestive manifestations and abnormal digestive function. Furthermore, the potential mechanisms of coronavirus disease 2019 on the digestive system, such as angiotensin-converting enzyme 2, immune injury, gut microbiota, hypoxemia, and psychological stress, are also

s/by-nc/4.0/

Manuscript source: Unsolicited manuscript

Specialty type: Gastroenterology and hepatology

Country/Territory of origin: China

Peer-review report's scientific quality classification
Grade A (Excellent): 0
Grade B (Very good): B, B
Grade C (Good): 0
Grade D (Fair): 0
Grade E (Poor): 0

Received: December 11, 2020
Peer-review started: December 11, 2020
First decision: December 27, 2020
Revised: December 28, 2020
Accepted: January 13, 2021
Article in press: January 13, 2021
Published online: February 21, 2021

P-Reviewer: Dogrul AB, Galloro G
S-Editor: Fan JR
L-Editor: Wang TQ
P-Editor: Liu JH

discussed. This review provides a new perspective for the prevention and treatment of infections with severe acute respiratory syndrome coronavirus 2 and other coronaviruses.

Citation: Zhan GF, Wang Y, Yang N, Luo AL, Li SY. Digestive system involvement of infections with SARS-CoV-2 and other coronaviruses: Clinical manifestations and potential mechanisms. *World J Gastroenterol* 2021; 27(7): 561-575
URL: https://www.wjgnet.com/1007-9327/full/v27/i7/561.htm
DOI: https://dx.doi.org/10.3748/wjg.v27.i7.561

INTRODUCTION

In December 2019, an outbreak of coronavirus disease 2019 (COVID-19) caused by severe acute respiratory syndrome coronavirus 2 (SARS-CoV-2; previously called 2019-nCoV), initially emerged in Wuhan, China. It has posed a serious threat to human health worldwide. The World Health Organization has declared that COVID-19 is a public health emergency of pandemic proportions[1]. As of December 9, 2020, a total of 67780361 laboratory-confirmed cases including 1551214 deaths have been reported in 220 countries, areas, and territories[1]. The COVID-19 pandemic is currently the world's most pressing public health threat and has a significant impact on civil societies and the global economy.

It is well established that most individuals with COVID-19 present with fever and typical respiratory symptoms, such as cough and dyspnea, similar to those of SARS and Middle East respiratory syndrome (MERS)[2-5]. Therefore, nasopharyngeal and oropharyngeal swabs are the suitable samples for reverse transcriptase-polymerase chain reaction detection of SARS-CoV-2. However, concurrent extra-pulmonary symptoms, such as gastrointestinal manifestations, mainly including diarrhea, nausea, vomiting, abdominal pain, and anorexia, have also been reported in recent studies[6,7]. In addition, rectal swabs and stool specimens of patients with COVID-19 have shown to be positive for SARS-CoV-2, and the virus remained detectable even after the clearance of the virus in the respiratory tract[7-10]. Furthermore, Pan *et al*[11] demonstrated that patients with digestive symptoms have a longer time from onset to admission and a worse prognosis than that of patients without digestive symptoms[11]. Together, these indicate that SARS-CoV-2 can infect and replicate in the gastrointestinal tract, and it may also have potential to cause digestive system damage. With the ongoing COVID-19 pandemic, those studies are of great guiding significance for disease prevention, control, and management. The present review aims to summarize data regarding epidemiology, gastrointestinal characteristics, possible mechanisms, and potential therapeutic strategy in patients infected with coronaviruses (CoVs) from the perspective of the digestive system (Figure 1).

EFFECTS OF COVS ON THE DIGESTIVE SYSTEM

CoVs are a group of enveloped, positive-sense, single-stranded RNA viruses (+ssRNA) with a crown-like appearance, which belongs to the family Coronaviridae of order Nidovirales[12,13]. CoVs harbor the largest genome among those known RNA viruses, with a genome length ranging from 26-32 kilobases (kb) and a diameter in the range of 120-160 nm[14-16]. CoVs are genetically classified into four genera: *Alpha-coronavirus*, *Beta-coronavirus*, *Gamma-coronavirus*, and *Delta-coronavirus*[12,17]. *Alpha-coronavirus* and *Beta-coronavirus* primarily infect mammals, whereas *Gamma-coronavirus* and *Delta-coronavirus* usually infect birds[16]. To date, seven coronavirus species under two genera have been identified to cause diseases in human: *Alpha-coronavirus* (HCoV-NL63 and HCoV-229E) and *Beta-coronavirus* (HCoV-OC43, HCoV-HKU1, SARS-CoV, MERS-CoV, and SARS-CoV-2)[18].

HCoV-NL63, HCoV-229E, HCoV-OC43, and HCoV-HKU1 cause mild common cold symptoms, whereas the other three highly pathogenic CoVs have caused large-scale pandemic since the beginning of the 21st century: SARS-CoV in 2002 and 2003, MERS-CoV in 2012, and the newly emerged SARS-CoV-2[19]. The three highly contagious pathogens are zoonotic in origin and have crossed the species barrier to human.

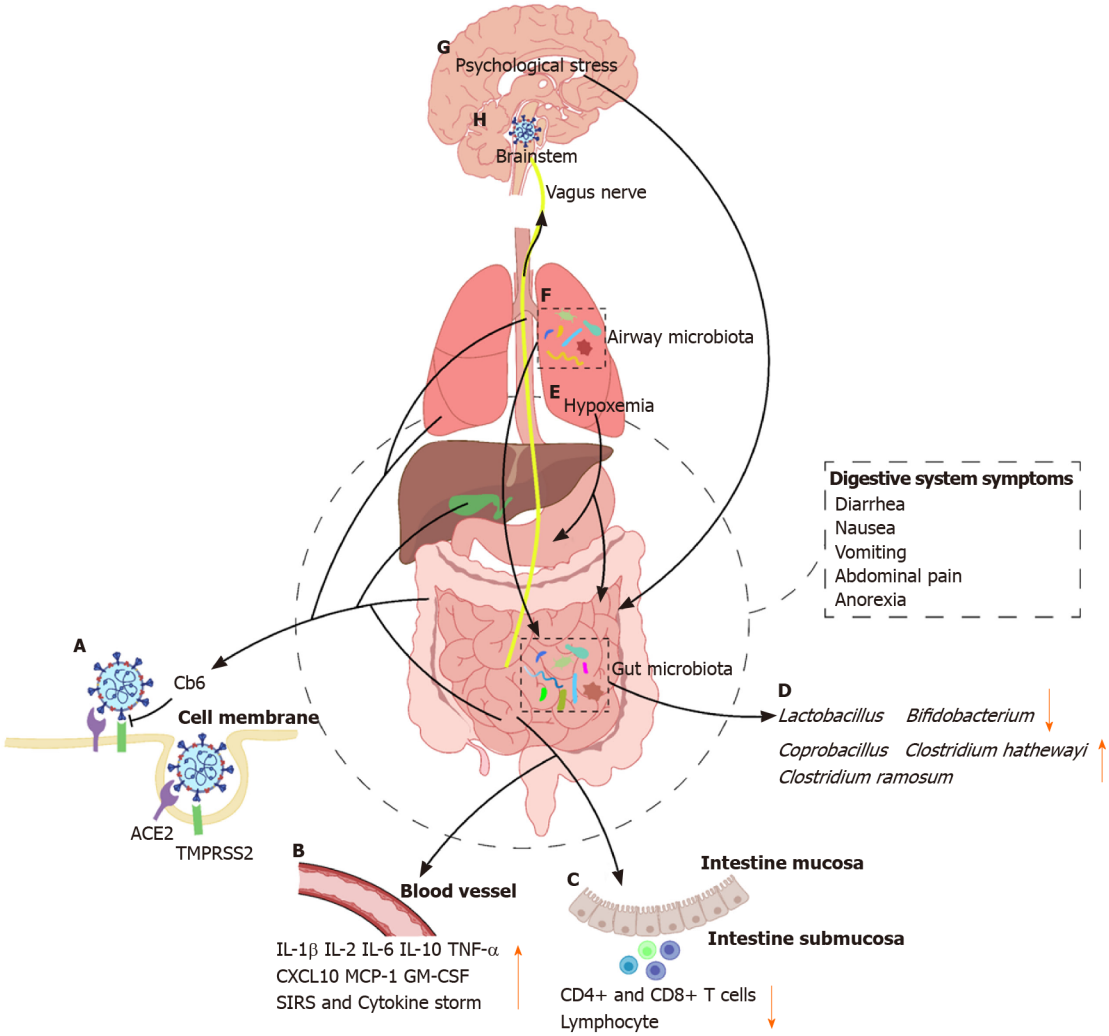


Figure 1 Possible mechanisms of coronavirus disease 2019 on the digestive system. ACE2: Angiotensin-converting enzyme 2; CXCL10: Interferon-gamma-inducible protein-10; GM-CSF: Granulocyte-macrophage colony stimulating factor; IL: Interleukin; MCP: Monocyte chemoattractant protein; SIRS: Systemic inflammatory response syndrome; TMPRSS2: Transmembrane serine protease 2; TNF: Tumour necrosis factor.

Furthermore, these three viruses are known to cause digestive symptoms.

CoVs and digestive manifestations

SARS-CoV: SARS-CoV has a large RNA genome length of 27.9 kb, emerged in the Guangdong Province of China, and had spread to 29 countries and areas worldwide. By July 2003, there were a total of 8098 laboratory-confirmed cases including 774 deaths (case-fatality rate: 9.6%) of SARS[20]. SARS-CoV has been considered to originate from bats, and market palm civets and racoon dogs have been unequivocally considered the intermediate hosts[21].

SARS is characterized by fever and respiratory complications, and it may also lead to acute respiratory distress syndrome and multiple organ failure in severe cases. Moreover, gastrointestinal manifestations are frequently observed in patients with SARS-CoV infection[22]. The tropism of SARS-CoV in the digestive system is commonly known to occur, and a retrospective study demonstrated that 38.4% of patients with SARS had diarrhea, usually within the first week of the disease course[23]. It was also demonstrated that up to 60% of patients with SARS suffered from liver impairment, and SARS-CoV was detected in liver tissue although viral inclusions were not observed[24]. In addition, the rate of SARS-CoV RNA positivity in collected stool specimens increased progressively and peaked at day 11 of the illness, with viral RNA remaining detectable in a stool sample in a patient even 73 d after symptom onset[23,25]. Furthermore, the presence of SARS-CoV RNA in the gastrointestinal tract may indicate a poor prognosis, and the viral load in the stool is correlated with death[26].

MERS-CoV: MERS-CoV has a large RNA genome length of 30.1 kb, emerged in the Saudi Arabia, and then spread to 27 countries and areas with a total of 2468 confirmed

cases and including 851 associated deaths (case-fatality rate: 34.4%) by the end of September 2019[27]. MERS-CoV has originated from bats, but dromedary camels has been considered the intermediate host[28].

Human-to-human transmission of MERS-CoV occurred mainly through nosocomial transmission[29]. Although most patients with MERS present with nonspecific respiratory symptoms, such as fever, cough, and shortness of breath, approximately one third of patients have gastrointestinal symptoms, such as diarrhea, vomiting, and abdominal pain, which were the most commonly demonstrated extrapulmonary clinical features[30]. In addition, MERS-CoV RNA was detected in 14.6% of stool specimens from patients with MERS, but the positive rate of virus detection was lower than that of SARS[31,32]. Moreover, an *in vitro* study has shown that MERS-CoV can successfully replicate in human primary intestinal epithelial cells[33].

SARS-CoV-2: SARS-CoV-2 has a genome length of 29.9 kb, shares an approximately 79% sequence identity to the SARS-CoV and the similarity of the whole-genome to BatCoV RaTG13 (a bat coronavirus detected in *Rhinolophus affinis*) is up to 96.2%[34]. Recent studies have suggested that bats may be the natural reservoir of SARS-CoV-2, and that there may be multiple potential intermediate hosts, such as pangolins, minks, and snakes[35-37]. In terms of the current pandemic situation, the case fatality of COVID-19 may not reach as high as that of SARS and MERS.

The majority of patients with COVID-19 exhibit mild to moderate pulmonary symptoms, and SARS-CoV-2 can extend to multiple extra-pulmonary organs including the heart, brain, kidneys, liver, and gut. Based on the data presented in Table 1, 6.7% of the total patients with SARS-CoV-2 infection have diarrhea and there are a great number of patients who had abnormal liver function with a paucity of concurrent or isolated pre-existing digestive system comorbidities. It was reported that COVID-19 patients with diarrhea presented severe symptoms of pneumonia compared to those without diarrhea, and COVID-19 patients with gastrointestinal manifestations or liver injury are more likely to require mechanical ventilation and hospitalization in the intensive care unit than those without gastrointestinal manifestations or liver injury[7,38-40]. Followed by the detection of SARS-CoV-2 RNA in the stool of the first case of COVID-19 in the United States, it was recently reported that viral RNA was detected in 59% of patients with COVID-19 in stool samples and the SARS-CoV-2 lasts significantly longer in stool samples than in respiratory and serum specimens[41,42]. In addition, To and colleagues demonstrated that SARS-CoV-2 was detected in the self-collected saliva specimens in 91.7% patients with COVID-19[43]. Furthermore, autopsy studies have demonstrated varying degrees of degeneration, necrosis, and shedding in the gastrointestinal mucosa and segmental dilatation and stenosis in the small intestine of patients with COVID-19[44,45]. Taken together, it is therefore likely that SARS-CoV-2 poses a serious threat to the digestive system.

Digestive diseases related to CoV infections

Digestive diseases include a series of disorders that affect the oropharynx and digestive tract, liver and biliary system, and pancreas, affecting human lives commonly. At the beginning of the COVID-19 outbreak, more medical resources were freed up to control the spread of the virus so that more individuals can be protected. Meanwhile, it is safe for most patients with pre-existing diseases. However, it may also increase the relative risk of complications caused by delayed screening, diagnosis, and treatment, and being afraid of seeking medical attention[46]. Challenges encountered regarding the most common pre-existing digestive diseases during the ongoing COVID-19 pandemic are described below.

Liver diseases

Hepatitis refers to inflammation of the liver caused by multiple pathogens (viruses, bacteria, drugs, autoimmune factors, and so on), which can progress to fibrosis, cirrhosis, and even liver cancer, posing a great threat to human health. The most common causes of hepatitis are the five main hepatitis virus types (A, B, C, D, and E)[47]. In a number of studies, hepatitis was noted in patients with SARS and COVID-19[7,11,48,49]. SARS patients with hepatitis B are more likely to develop severe hepatitis than in those without. Similarly, severe cases of COVID-19 were more prone to infect HBV than non-severe cases[48,50]. Collectively, these findings show that CoVs might play a significant role in hepatitis, although detailed studies are needed to confirm this.

Fatty liver disease is a spectrum of disorders characterized predominantly by macrovesicular hepatic steatosis, and it presents a condition of excess fat stored in the

Table 1 Presentation of gastrointestinal symptoms, abnormal liver function, and pre-existing digestive diseases in patients with severe acute respiratory syndrome coronavirus 2 infection

Ref.	Patients with COVID-19	Gastrointestinal symptoms			Patients with abnormal biochemical indicators of liver function	Patients with pre-existing digestive diseases	Patients testing positive for SARS-CoV-2 in stool or rectal swab specimens
		Diarrhoea	Nausea and vomiting	Abdominal pain			
Guan *et al*[7]	1099	42 (3.8%)	55 (5.0%)	NA	Abnormal AST: 168/757 (22.2%). Abnormal ALT: 158/741 (21.3%). Abnormal TBIL: 76/722 (10.5%)	CHB: 23 (2.1%)	Stool specimens: 4/NA. Rectal swab: 4/NA
Wang *et al*[6]	138	14 (10.1%)	19 (13.7%)	3 (2.2%)	Mild elevation of AST and ALT	4 (2.9%)	NA
Huang *et al*[40]	41	1/38 (2.6%)	NA	NA	Abnormal AST: 15 (31.0%)	Chronic liver disease: 1 (2%)	NA
Fan *et al*[116]	148	6 (4.1%)	3 (2.0%)	NA	Abnormal AST: 32 (21.6%). Abnormal ALT: 27 (18.2%). Abnormal TBIL: 9 (6.1%)	9 (6.1%)	NA
Cai *et al*[49]	298	9 (3.0%)	NA	NA	Abnormal AST: 25 (8.4%). Abnormal ALT: 39 (13.1%). Abnormal TBIL: 24 (8.1%)	CHB: 5 (1.7%). NAFLD: 14 (4.7%). ALD: 9 (3.0%)	NA
Chen *et al*[3]	99	2 (2.0%)	1 (1.0%)	NA	Abnormal AST: 35 (35.0%). Abnormal ALT: 28 (28.0%). Abnormal TBIL: 18 (18.0%). Abnormal albumin: 97 (98.0%)	NA	NA
Holshue *et al*[41]	1	1	1	NA	Abnormal AST: 1. Abnormal ALT: 1. Abnormal TBIL: 1. Abnormal albumin: 1	NA	Stool specimens: 1/1
Zhang *et al*[117]	140	18/139 (12.9%)	31/139 (22.3%)	8/139 (5.8%)	NA	FLD and abnormal liver function: 8 (5.7%). Chronic gastritis and gastric ulcer: 7 (5.0%). Cholelithiasis: 6 (4.3%)	NA
Xiao *et al*[10]	73	26 (35.6%)	NA	NA	NA	NA	Stool specimens: 39/73 (53.4%)
Zhou *et al*[118]	191	9 (4.7%)	7 (3.7%)	NA	Abnormal ALT: 59/189 (31.2%)	NA	NA
Zhang *et al*[119]	82 (Deaths)	10 (12.2%)	2 (2.3%)	NA	Abnormal AST: 44/72 (61.1%). Abnormal ALT: 22/72 (30.6%). Abnormal TBIL: 22/72 (30.6%). Abnormal albumin: 56/72 (77.8%)	Liver disease: 2/82 (2.4%)	NA
Xu *et al*[120]	62	3 (4.8%)	NA	NA	Abnormal AST: 10 (16.1%)	Liver disease: 7 (11.3%)	NA
Chen *et al*[121]	21	4/20 (20.0%)	NA	NA	Abnormal AST: 6 (28.6%). Abnormal albumin: 8 (38.1%)	NA	NA
Pan *et al*[11]	204	29 (14.2%)	8 (3.9%)	4 (2.0%)	Abnormal AST: NA. Abnormal albumin: NA	CHB: 1 (0.5%). FLD: 1 (0.5%). Gastritis: 1 (0.5%)	NA
Luo *et al*[122]	1141	68 (5.9%)	Nausea: 134 (11.7%). Vomiting: 119 (10.4%)	45 (3.9%)	Mild elevation of AST and ALT	NA	NA
Total	3738	174/2592					

	(6.7%)

ALD: Alcoholic fatty liver disease; ALT: Alanine transaminase; AST: Aspartate aminotransferase; CHB: Chronic hepatitis B; COVID-19: Coronavirus disease 2019; FLD: Fatty liver disease; NAFLD: Non-alcoholic fatty liver disease; SARS-CoV-2: Severe acute respiratory syndrome coronavirus 2; TBIL: Total bilirubin.

liver, including non-alcoholic fatty liver disease (NAFLD) and alcoholic fatty liver disease (ALD). Patients with hypertension, diabetes, obesity, and old age have a high risk of developing severe COVID-19[51]. These comorbidities also increase the risk of NAFLD, thus leading to liver injury. The ongoing COVID-19 pandemic has several negative effects on individuals, especially those encountering job loss, financial strain, death of a loved one, and so on. Under these stressors, an individual's alcohol consumption is likely to increase[52]. Therefore, COVID-19 is likely to have a long-lasting impact on the development of ALD.

Given that patients with liver cirrhosis and cancer have a high risk of infection due to the immunocompromised status[53], measures to prevent SARS-CoV-2 infection are needed. Xiao and colleagues designed a study showing that none of the participants who undertook precautionary and protective measures had clinical symptoms suggestive of SARS-CoV-2 infection, whereas 17 of 101 patients with decompensated cirrhosis who did not undertake these measures were diagnosed with COVID-19[54]. This research suggests that more strategies should be implemented to prevent SARS-CoV-2 infection in patients with liver cirrhosis and cancer, such as online health education and medication guidance.

The outbreaks of SARS and MERS might potentially increase the risk of transmission of viral infection from donors to recipients and thus even lead to death[40,55]. Tzedakis *et al*[56] reported that a local liver transplant center decreased transplant activity by 60% since the COVID-19 pandemic and that it is crucial and necessary to balance costs and benefits while performing liver transplant[56]. During the COVID-19 pandemic, all donors and recipients of liver transplant must be screened for the presence of SARS-CoV-2 to ensure the safety and success of the liver transplantation.

Gastrointestinal diseases

Ulcerative colitis and Crohn's disease are two major idiopathic inflammatory bowel disorders (IBDs) that could cause prolonged inflammation of the gastrointestinal tract[57]. Patients with IBD who use immunosuppressive and biological agents are more susceptible to opportunistic and severe infections than those who do not[58,59]. Therefore, it is reasonable to assume that patients with IBD have more severe COVID-19, although there has been no direct clinical evidence to prove it. An and colleagues showed that none of the 318 patients with IBD (204 with ulcerative colitis and 114 with Crohn's disease)developed SARS-CoV-2 infection with early effective warning and protective measures[60]. In addition, patients with cancer also have an increased risk of infection[61]. Furthermore, it was demonstrated that individuals with cancer may have a

high risk of severe COVID-19 and a poorer prognosis[62]. Although the risk of SARS-CoV-2 infection in patients with gastrointestinal cancer remains unknown, effective precautionary approaches are necessary to better protect patients.

POSSIBLE MECHANISMS OF COVID-19 ON THE DIGESTIVE SYSTEM

It has been commonly known that respiratory droplets and direct contact are the two major transmission pathways of SARS-CoV-2. However, a recent study performed by Liu and colleagues has shown a possibility of aerosol transmission[63]. A large number of studies have reported gastrointestinal symptoms and liver dysfunction in patients with SARS-CoV-2 infection. At the same time, SARS-CoV-2 could be detected in rectal swabs and stool specimens in patients with COVID-19[7,10]. Moreover, biopsy and autopsy reports have revealed that COVID-19 caused pathological changes in the digestive system. In addition, high airborne concentration of SARS-CoV-2 was detected in toilet room of Fangcang Hospital where patients with COVID-19 were treated[63]. Taken together, these research findings provide a theoretical basis for the spread of COVID-19 through the faecal-oral route, although there is no direct evidence for the transmission pathway thus far.

The digestive tract communicates with the outside world directly, similar to the respiratory tract. Therefore, SARS-CoV-2 has the opportunity to enter the gastrointestinal tract and cause a direct cytopathic effect by local replication. In addition, systemic responses to excessive immune inflammation induced by SARS-CoV-2 infection may also cause damage to the digestive system indirectly. However, the mechanisms of how COVID-19 affects the digestive system remain poorly known. Furthermore, there is also no specific antiviral drug or vaccine approved to treat or prevent COVID-19 to date. Hence, it is particularly urgent to identify the potential therapeutic strategies for COVID-19.

Angiotensin-converting enzyme 2 and transmembrane serine protease 2

Angiotensin-converting enzyme 2 (ACE2) is a well-known receptor located on cells of various organs for regulating cardiovascular function through the renin-angiotensin system, playing a major role in regulating hypertension and anti-atherosclerosis mechanisms[64,65]. In recent two decades, the role of ACE2 in SARS-CoV and influenza virus infection as a target functional receptor has attracted widespread attention[66-68]. It has been reported that the entry of SARS-CoV-2 into the host cell depends on the binding of viral spike (S) proteins to the SARS-CoV receptor ACE2 followed by the transmembrane serine protease 2 (TMPRSS2) for the S protein priming[69]. Therefore, human cells co-expressing ACE2 and TMPRSS2 are susceptible to SARS-CoV-2 infection[70]. A recent study performed by Zhang and colleagues has demonstrated that type II alveolar cells have higher expression of ACE2 and TMPRSS2 than type I alveolar cells in the lung. Besides, co-expression of ACE2 and TMPRSS2 has also been found in the glandular cells of upper esophageal and absorptive enterocytes of the ileum and colon[70,71]. Intestinal epithelial cells can act as a barrier and help to coordinate immune responses in microbial infections[72]. A number of studies have reported that absorptive enterocytes can be damaged or developed malabsorption and intestinal secretion abnormalities due to coronavirus or rotavirus infection, thus resulting in diarrhea and vomiting[73,74]. Therefore, gastrointestinal manifestations in patients with COVID-19 might be associated with infected enterocytes co-expressing ACE2 and TMPRSS2. Moreover, co-expression of ACE2 and TMPRSS2 has been observed in cholangiocytes, but not in hepatocytes[75]. Cholangiocytes play a pivotal role in liver regeneration and immune responses, and injury of cholangiocytes may cause a variety of diseases and even lead to liver failure[76]. Therefore, we can preliminarily conclude that the abnormal liver function in patients with COVID-19 may not be directly caused by the damage to hepatocytes, but it may be caused by damage to cholangiocytes. Liver damages may also be caused by other factors, such as drugs used in the treatment or systemic inflammatory response.

Compared with control mice, ACE2 knockout mice are more susceptible to induced colitis upon treatment with chemical irritants[77]. The expression of ACE2 protein is downregulated after virus entry, which may worsen the digestive symptoms. Recently, studies have demonstrated that the fusion protein of human recombinant ACE2 (hrACE2) with the Fc fragment of the human immunoglobulin IgG1 showed high affinity to the receptor-binding domain (RBD) of SARS-CoV-2 and potently neutralized SARS-CoV-2 *in vitro*[78,79]. A newly online published report in *Nature* demonstrated that CB6, a neutralizing monoclonal antibody (mAb) isolated from a

patient with convalescent COVID-19, can block the binding of soluble SARS-CoV-2 RBD with ACE2 receptor and showed inhibitory effect to SARS-CoV-2 infection *in vitro* and in rhesus monkeys[80]. Additionally, a recent *in vivo* study has reported that hrACE2 can block the early stages of SARS-CoV-2 infection at the organoid level in engineered human blood vessels, kidneys, and small intestinal enterocytes[78,81]. Moreover, a serine protease TMPRSS2 inhibitor has been approved for clinical use to block the entry of CoVs[69]. Taken together, it is therefore likely that ACE2 and TMPRSS2 may be the potential targets for prevention and treatment of the COVID-19 patients with digestive symptoms.

Immune injury

Immune injury plays an important role in the occurrence, development, and prognosis of digestive diseases[82-84]. A growing body of evidence suggests that severe SARS-CoV-2 infection can activate innate and adaptive immune responses, increase serum levels of pro-inflammatory cytokines and chemokines including interleukin (IL)-6, IL-1β, IL-2, IL-10, tumor necrosis factor α (TNF-α), interferon-gamma-inducible protein-10 (CXCL10), monocyte chemoattractant protein-1, and granulocyte-macrophage colony stimulating factor, and even induce systemic inflammatory response syndrome (SIRS) and cytokine storm, thus leading to local and systemic tissue damage[40,85,86]. Concentrations of IL-6 were significantly different between patients with mild and severe COVID-19, and elevated IL-6 was found to be a stable indicator of adverse outcomes for severe COVID-19 patients. A clinical trial (ChiCTR2000029765) that explored the potential therapeutic effect of IL-6 receptor-targeted mAb in patients with severe COVID-19, has shown the effectiveness of controlling fever and improving respiratory function quickly[87]. It has been reported that vagus nerve stimulation (VNS) can exert anti-inflammatory effects *via* activation of the cholinergic anti-inflammatory pathway[88,89]. Based on preliminary observations and available scientific and clinical data, it is speculated that VNS may play a vital role in improving the prognosis of patients with COVID-19[90]. Additionally, patients with severe COVID-19 more frequently have lymphopenia, and drastically decreased numbers of $CD4^+$ and $CD8^+$ T cells than moderate cases. Furthermore, inflammation-mediated gastrointestinal tissue damage in patients with COVID-19 is supported by the histopathological evidence of diffuse endothelial inflammation in the small intestine submucosa[91]. It has also been confirmed by the presence of numerous infiltrating plasma cells and lymphocytes with interstitial edema in the lamina propria of the stomach, duodenum, and rectum of patients with COVID-19[10].

Gut microbiota

The human intestine harbors nearly 100 trillion microorganisms, which are composed of more than 1000 different bacterial species, including but not limited to bacteria, fungi, and viruses[92,93]. It is known that gut microbiota plays a vital role in a variety of diseases, including digestive, metabolic, respiratory, and even neuropsychiatric diseases[94-96]. Additionally, many studies have reported that chronic respiratory diseases and pneumonia can not only change the airway microbiota, but also alter the gut microbiota indirectly through the circulatory and lymphatic systems[97-100]. SARS-CoV-2 can down-regulate the expression of ACE2 in the intestine, which affects the absorption of tryptophan, resulting in damage to the gut microbiota and possibly influencing intestinal inflammation[101,102]. Xu *et al*[103] indicated that some patients with COVID-19 showed gut microbial dysbiosis with decreased abundance of *Lactobacillus* and *Bifidobacterium*[103]. Zuo *et al*[104] showed that the increased levels of *Coprobacillus*, *Clostridium hathewayi*, and *Clostridium ramosum* were positively correlated with the susceptibility and severity of COVID-19[104]. Furthermore, studies have shown that short-chain fatty acids, the most critical metabolites of the gut microbiota, play an important role in reducing the intestinal pH, maintaining the integrity of the intestinal epithelium, and enhancing the host systemic immunity[105-107]. Antibiotics are commonly prescribed in patients with COVID-19, however, it can also profoundly perturb the composition of the human gut microbiota[108]. Guidance from China's National Health Commission and National Administration of Traditional Chinese Medicine suggested that the use of probiotics has a good curative effect in patients with severe SARS-CoV-2 infection. Taken together, improvement of the composition of the gut microbiota and its metabolites may be a potential strategy for the treatment of COVID-19.

Hypoxemia

After SARS-CoV-2 infects the lungs, it causes inflammation and edema of the

pulmonary parenchyma and interstitium, which in turn affect alveolar gas exchange and thereby lead to hypoxemia[109]. Hypoxemia can cause metabolism and normal physiological dysfunctions in various tissues and organs including the digestive system. Long-term hypoxemia can cause cell necrosis, which in turn leads to damage of the gastrointestinal mucosal cells, thus leading to gastrointestinal ulceration and bleeding.

Psychological stress

Psychological stress has a profound influence on the digestive system, it can alter the intestinal motility, increase the gastrointestinal permeability, and change the composition of intestinal microbiota[110]. A study on active Weibo users showed that individuals were more concerned about their health and showed more negative emotions, such as anxiety and depression, after the outbreak of the COVID-19[111]. Quarantine is an effective measure to protect individuals from contagious patients and those who are at risk of infection, however, it may also increase negative psychological stress[112]. Taken together, digestive diseases and symptoms in patients with COVID-19 may be partially caused by psychological stress.

Others

Multiple lines of evidence has shown that some patients with COVID-19 have digestive system symptoms, such as nausea, vomiting, and anorexia, which indirectly reflect the impairment of the dorsal vagal complex[6,113,114]. One of the possible mechanisms is that the neurotropic virus retrogrades along the vagus nerve once the virus enters the vagal nerve endings, thus damaging the brainstem[115]. Moreover, the virus may reach the brainstem through the circulatory system with or without crossing the blood–brain barrier[113].

CONCLUSION

CoV infections can cause a series of digestive diseases, and may also be accompanied by digestive manifestations and abnormal digestive function. Although it is still unknown whether the SARS-CoV-2, which causes abnormalities in the digestive system, enters the digestive system directly or indirectly affects the digestive system, it is necessary to undertake early measures to prevent the spread of the virus through the fecal-oral transmission. In addition to ACE2 and immune injury, gut microbiota, hypoxemia, and psychological stress may also be targets for future intervention and treatment of digestive system damage caused by SARS-CoV-2 infection. Further research is warranted to elucidate the relationship between the COVID-19 and the digestive system.

REFERENCES

1 World Health Organization. WHO Coronavirus Disease (COVID-19) situation Dashboard. 2020 [cited 9 December 2020]. Available from: https://www.who.int/

2 **Young BE**, Ong SWX, Kalimuddin S, Low JG, Tan SY, Loh J, Ng OT, Marimuthu K, Ang LW, Mak TM, Lau SK, Anderson DE, Chan KS, Tan TY, Ng TY, Cui L, Said Z, Kurupatham L, Chen MI, Chan M, Vasoo S, Wang LF, Tan BH, Lin RTP, Lee VJM, Leo YS, Lye DC; Singapore 2019 Novel Coronavirus Outbreak Research Team. Epidemiologic Features and Clinical Course of Patients Infected With SARS-CoV-2 in Singapore. *JAMA* 2020; **323**: 1488-1494 [PMID: 32125362 DOI: 10.1001/jama.2020.3204]

3 **Chen N**, Zhou M, Dong X, Qu J, Gong F, Han Y, Qiu Y, Wang J, Liu Y, Wei Y, Xia J, Yu T, Zhang X, Zhang L. Epidemiological and clinical characteristics of 99 cases of 2019 novel coronavirus pneumonia in Wuhan, China: a descriptive study. *Lancet* 2020; **395**: 507-513 [PMID: 32007143 DOI: 10.1016/S0140-6736(20)30211-7]

4 **Zumla A**, Hui DS, Perlman S. Middle East respiratory syndrome. *Lancet* 2015; **386**: 995-1007 [PMID: 26049252 DOI: 10.1016/S0140-6736(15)60454-8]

5 **Cheng VC**, Lau SK, Woo PC, Yuen KY. Severe acute respiratory syndrome coronavirus as an agent of emerging and reemerging infection. *Clin Microbiol Rev* 2007; **20**: 660-694 [PMID: 17934078 DOI: 10.1128/CMR.00023-07]

6 **Wang D**, Hu B, Hu C, Zhu F, Liu X, Zhang J, Wang B, Xiang H, Cheng Z, Xiong Y, Zhao Y, Li Y, Wang X, Peng Z. Clinical Characteristics of 138 Hospitalized Patients With 2019 Novel Coronavirus-Infected Pneumonia in Wuhan, China. *JAMA* 2020; **323**: 1061-1069 [PMID: 32031570 DOI: 10.1001/jama.2020.1585]

7 **Guan WJ**, Ni ZY, Hu Y, Liang WH, Ou CQ, He JX, Liu L, Shan H, Lei CL, Hui DSC, Du B, Li LJ, Zeng G, Yuen KY, Chen RC, Tang CL, Wang T, Chen PY, Xiang J, Li SY, Wang JL, Liang ZJ, Peng YX, Wei L, Liu Y, Hu YH, Peng P, Wang JM, Liu JY, Chen Z, Li G, Zheng ZJ, Qiu SQ, Luo J, Ye CJ, Zhu SY, Zhong NS; China Medical Treatment Expert Group for Covid-19. Clinical Characteristics of Coronavirus Disease 2019 in China. *N Engl J Med* 2020; **382**: 1708-1720 [PMID: 32109013 DOI: 10.1056/NEJMoa2002032]

8 **Xu Y**, Li X, Zhu B, Liang H, Fang C, Gong Y, Guo Q, Sun X, Zhao D, Shen J, Zhang H, Liu H, Xia H, Tang J, Zhang K, Gong S. Characteristics of pediatric SARS-CoV-2 infection and potential evidence for persistent fecal viral shedding. *Nat Med* 2020; **26**: 502-505 [PMID: 32284613 DOI: 10.1038/s41591-020-0817-4]

9 **Tang A**, Tong ZD, Wang HL, Dai YX, Li KF, Liu JN, Wu WJ, Yuan C, Yu ML, Li P, Yan JB. Detection of Novel Coronavirus by RT-PCR in Stool Specimen from Asymptomatic Child, China. *Emerg Infect Dis* 2020; **26**: 1337-1339 [PMID: 32150527 DOI: 10.3201/eid2606.200301]

10 **Xiao F**, Tang M, Zheng X, Liu Y, Li X, Shan H. Evidence for Gastrointestinal Infection of SARS-CoV-2. *Gastroenterology* 2020; **158**: 1831-1833. e3 [PMID: 32142773 DOI: 10.1053/j.gastro.2020.02.055]

11 **Pan L**, Mu M, Yang P, Sun Y, Wang R, Yan J, Li P, Hu B, Wang J, Hu C, Jin Y, Niu X, Ping R, Du Y, Li T, Xu G, Hu Q, Tu L. Clinical Characteristics of COVID-19 Patients With Digestive Symptoms in Hubei, China: A Descriptive, Cross-Sectional, Multicenter Study. *Am J Gastroenterol* 2020; **115**: 766-773 [PMID: 32287140 DOI: 10.14309/ajg.0000000000000620]

12 **Zumla A**, Chan JF, Azhar EI, Hui DS, Yuen KY. Coronaviruses - drug discovery and therapeutic options. *Nat Rev Drug Discov* 2016; **15**: 327-347 [PMID: 26868298 DOI: 10.1038/nrd.2015.37]

13 **Woo PC**, Huang Y, Lau SK, Yuen KY. Coronavirus genomics and bioinformatics analysis. *Viruses* 2010; **2**: 1804-1820 [PMID: 21994708 DOI: 10.3390/v2081803]

14 **Schoeman D**, Fielding BC. Coronavirus envelope protein: current knowledge. *Virol J* 2019; **16**: 69 [PMID: 31133031 DOI: 10.1186/s12985-019-1182-0]

15 **Wu Y**, Xu X, Chen Z, Duan J, Hashimoto K, Yang L, Liu C, Yang C. Nervous system involvement after infection with COVID-19 and other coronaviruses. *Brain Behav Immun* 2020; **87**: 18-22 [PMID: 32240762 DOI: 10.1016/j.bbi.2020.03.031]

16 **Tang Q**, Song Y, Shi M, Cheng Y, Zhang W, Xia XQ. Inferring the hosts of coronavirus using dual statistical models based on nucleotide composition. *Sci Rep* 2015; **5**: 17155 [PMID: 26607834 DOI: 10.1038/srep17155]

17 **Li F**. Structure, Function, and Evolution of Coronavirus Spike Proteins. *Annu Rev Virol* 2016; **3**: 237-261 [PMID: 27578435 DOI: 10.1146/annurev-virology-110615-042301]

18 **Wu A**, Peng Y, Huang B, Ding X, Wang X, Niu P, Meng J, Zhu Z, Zhang Z, Wang J, Sheng J, Quan L, Xia Z, Tan W, Cheng G, Jiang T. Genome Composition and Divergence of the Novel Coronavirus (2019-nCoV) Originating in China. *Cell Host Microbe* 2020; **27**: 325-328 [PMID: 32035028 DOI: 10.1016/j.chom.2020.02.001]

19 **Singh A**, Shaikh A, Singh R, Singh AK. COVID-19: From bench to bed side. *Diabetes Metab Syndr* 2020; **14**: 277-281 [PMID: 32283498 DOI: 10.1016/j.dsx.2020.04.011]

20 **World Health Organization**. Summary of probable SARS cases with onset of illness from 1 November 2002 to 31 July 2003. Available from: https://www.who.int/csr/sars/

21 **Kan B**, Wang M, Jing H, Xu H, Jiang X, Yan M, Liang W, Zheng H, Wan K, Liu Q, Cui B, Xu Y, Zhang E, Wang H, Ye J, Li G, Li M, Cui Z, Qi X, Chen K, Du L, Gao K, Zhao YT, Zou XZ, Feng YJ, Gao YF, Hai R, Yu D, Guan Y, Xu J. Molecular evolution analysis and geographic investigation of severe acute respiratory syndrome coronavirus-like virus in palm civets at an animal market and on farms. *J Virol* 2005; **79**: 11892-11900 [PMID: 16140765 DOI: 10.1128/JVI.79.18.11892-11900.2005]

22 **Peiris JS**, Lai ST, Poon LL, Guan Y, Yam LY, Lim W, Nicholls J, Yee WK, Yan WW, Cheung MT, Cheng VC, Chan KH, Tsang DN, Yung RW, Ng TK, Yuen KY; SARS study group. Coronavirus as a possible cause of severe acute respiratory syndrome. *Lancet* 2003; **361**: 1319-1325 [PMID: 12711465 DOI: 10.1016/s0140-6736(03)13077-2]

23 **Leung WK**, To KF, Chan PK, Chan HL, Wu AK, Lee N, Yuen KY, Sung JJ. Enteric involvement of severe acute respiratory syndrome-associated coronavirus infection. *Gastroenterology* 2003; **125**: 1011-1017 [PMID: 14517783 DOI: 10.1016/s0016-5085(03)01215-0]

24 **Chau TN**, Lee KC, Yao H, Tsang TY, Chow TC, Yeung YC, Choi KW, Tso YK, Lau T, Lai ST, Lai CL. SARS-associated viral hepatitis caused by a novel coronavirus: report of three cases. *Hepatology* 2004; **39**: 302-310 [PMID: 14767982 DOI: 10.1002/hep.20111]

25 **Chan KH**, Poon LL, Cheng VC, Guan Y, Hung IF, Kong J, Yam LY, Seto WH, Yuen KY, Peiris JS. Detection of SARS coronavirus in patients with suspected SARS. *Emerg Infect Dis* 2004; **10**: 294-299 [PMID: 15030700 DOI: 10.3201/eid1002.030610]

26 **Hung IF**, Cheng VC, Wu AK, Tang BS, Chan KH, Chu CM, Wong MM, Hui WT, Poon LL, Tse DM, Chan KS, Woo PC, Lau SK, Peiris JS, Yuen KY. Viral loads in clinical specimens and SARS manifestations. *Emerg Infect Dis* 2004; **10**: 1550-1557 [PMID: 15498155 DOI: 10.3201/eid1009.040058]

27 **World Health Organization**. Middle East respiratory syndrome coronavirus (MERS-CoV). Available from: https://www.who.int/emergencies/mers-cov/

28 **Haagmans BL**, Al Dhahiry SH, Reusken CB, Raj VS, Galiano M, Myers R, Godeke GJ, Jonges M, Farag E, Diab A, Ghobashy H, Alhajri F, Al-Thani M, Al-Marri SA, Al Romaihi HE, Al Khal A,

Bermingham A, Osterhaus AD, AlHajri MM, Koopmans MP. Middle East respiratory syndrome coronavirus in dromedary camels: an outbreak investigation. *Lancet Infect Dis* 2014; **14**: 140-145 [PMID: 24355866 DOI: 10.1016/S1473-3099(13)70690-X]

29 **Chowell G**, Abdirizak F, Lee S, Lee J, Jung E, Nishiura H, Viboud C. Transmission characteristics of MERS and SARS in the healthcare setting: a comparative study. *BMC Med* 2015; **13**: 210 [PMID: 26336062 DOI: 10.1186/s12916-015-0450-0]

30 **Assiri A**, McGeer A, Perl TM, Price CS, Al Rabeeah AA, Cummings DA, Alabdullatif ZN, Assad M, Almulhim A, Makhdoom H, Madani H, Alhakeem R, Al-Tawfiq JA, Cotten M, Watson SJ, Kellam P, Zumla AI, Memish ZA; KSA MERS-CoV Investigation Team. Hospital outbreak of Middle East respiratory syndrome coronavirus. *N Engl J Med* 2013; **369**: 407-416 [PMID: 23782161 DOI: 10.1056/NEJMoa1306742]

31 **Poon LL**, Guan Y, Nicholls JM, Yuen KY, Peiris JS. The aetiology, origins, and diagnosis of severe acute respiratory syndrome. *Lancet Infect Dis* 2004; **4**: 663-671 [PMID: 15522678 DOI: 10.1016/S1473-3099(04)01172-7]

32 **Corman VM**, Albarrak AM, Omrani AS, Albarrak MM, Farah ME, Almasri M, Muth D, Sieberg A, Meyer B, Assiri AM, Binger T, Steinhagen K, Lattwein E, Al-Tawfiq J, Müller MA, Drosten C, Memish ZA. Viral Shedding and Antibody Response in 37 Patients With Middle East Respiratory Syndrome Coronavirus Infection. *Clin Infect Dis* 2016; **62**: 477-483 [PMID: 26565003 DOI: 10.1093/cid/civ951]

33 **Zhou J**, Li C, Zhao G, Chu H, Wang D, Yan HH, Poon VK, Wen L, Wong BH, Zhao X, Chiu MC, Yang D, Wang Y, Au-Yeung RKH, Chan IH, Sun S, Chan JF, To KK, Memish ZA, Corman VM, Drosten C, Hung IF, Zhou Y, Leung SY, Yuen KY. Human intestinal tract serves as an alternative infection route for Middle East respiratory syndrome coronavirus. *Sci Adv* 2017; **3**: eaao4966 [PMID: 29152574 DOI: 10.1126/sciadv.aao4966]

34 **Zhou P**, Yang XL, Wang XG, Hu B, Zhang L, Zhang W, Si HR, Zhu Y, Li B, Huang CL, Chen HD, Chen J, Luo Y, Guo H, Jiang RD, Liu MQ, Chen Y, Shen XR, Wang X, Zheng XS, Zhao K, Chen QJ, Deng F, Liu LL, Yan B, Zhan FX, Wang YY, Xiao GF, Shi ZL. A pneumonia outbreak associated with a new coronavirus of probable bat origin. *Nature* 2020; **579**: 270-273 [PMID: 32015507 DOI: 10.1038/s41586-020-2012-7]

35 **Ji W**, Wang W, Zhao X, Zai J, Li X. Cross-species transmission of the newly identified coronavirus 2019-nCoV. *J Med Virol* 2020; **92**: 433-440 [PMID: 31967321 DOI: 10.1002/jmv.25682]

36 **Cheng ZJ**, Shan J. 2019 Novel coronavirus: where we are and what we know. *Infection* 2020; **48**: 155-163 [PMID: 32072569 DOI: 10.1007/s15010-020-01401-y]

37 **Wu D**, Wu T, Liu Q, Yang Z. The SARS-CoV-2 outbreak: What we know. *Int J Infect Dis* 2020; **94**: 44-48 [PMID: 32171952 DOI: 10.1016/j.ijid.2020.03.004]

38 **Wan Y**, Li J, Shen L, Zou Y, Hou L, Zhu L, Faden HS, Tang Z, Shi M, Jiao N, Li Y, Cheng S, Huang Y, Wu D, Xu Z, Pan L, Zhu J, Yan G, Zhu R, Lan P. Enteric involvement in hospitalised patients with COVID-19 outside Wuhan. *Lancet Gastroenterol Hepatol* 2020; **5**: 534-535 [PMID: 32304638 DOI: 10.1016/S2468-1253(20)30118-7]

39 **Jin X**, Lian JS, Hu JH, Gao J, Zheng L, Zhang YM, Hao SR, Jia HY, Cai H, Zhang XL, Yu GD, Xu KJ, Wang XY, Gu JQ, Zhang SY, Ye CY, Jin CL, Lu YF, Yu X, Yu XP, Huang JR, Xu KL, Ni Q, Yu CB, Zhu B, Li YT, Liu J, Zhao H, Zhang X, Yu L, Guo YZ, Su JW, Tao JJ, Lang GJ, Wu XX, Wu WR, Qv TT, Xiang DR, Yi P, Shi D, Chen Y, Ren Y, Qiu YQ, Li LJ, Sheng J, Yang Y. Epidemiological, clinical and virological characteristics of 74 cases of coronavirus-infected disease 2019 (COVID-19) with gastrointestinal symptoms. *Gut* 2020; **69**: 1002-1009 [PMID: 32213556 DOI: 10.1136/gutjnl-2020-320926]

40 **Huang C**, Wang Y, Li X, Ren L, Zhao J, Hu Y, Zhang L, Fan G, Xu J, Gu X, Cheng Z, Yu T, Xia J, Wei Y, Wu W, Xie X, Yin W, Li H, Liu M, Xiao Y, Gao H, Guo L, Xie J, Wang G, Jiang R, Gao Z, Jin Q, Wang J, Cao B. Clinical features of patients infected with 2019 novel coronavirus in Wuhan, China. *Lancet* 2020; **395**: 497-506 [PMID: 31986264 DOI: 10.1016/S0140-6736(20)30183-5]

41 **Holshue ML**, DeBolt C, Lindquist S, Lofy KH, Wiesman J, Bruce H, Spitters C, Ericson K, Wilkerson S, Tural A, Diaz G, Cohn A, Fox L, Patel A, Gerber SI, Kim L, Tong S, Lu X, Lindstrom S, Pallansch MA, Weldon WC, Biggs HM, Uyeki TM, Pillai SK; Washington State 2019-nCoV Case Investigation Team. First Case of 2019 Novel Coronavirus in the United States. *N Engl J Med* 2020; **382**: 929-936 [PMID: 32004427 DOI: 10.1056/NEJMoa2001191]

42 **Zheng S**, Fan J, Yu F, Feng B, Lou B, Zou Q, Xie G, Lin S, Wang R, Yang X, Chen W, Wang Q, Zhang D, Liu Y, Gong R, Ma Z, Lu S, Xiao Y, Gu Y, Zhang J, Yao H, Xu K, Lu X, Wei G, Zhou J, Fang Q, Cai H, Qiu Y, Sheng J, Chen Y, Liang T. Viral load dynamics and disease severity in patients infected with SARS-CoV-2 in Zhejiang province, China, January-March 2020: retrospective cohort study. *BMJ* 2020; **369**: m1443 [PMID: 32317267 DOI: 10.1136/bmj.m1443]

43 **To KK**, Tsang OT, Yip CC, Chan KH, Wu TC, Chan JM, Leung WS, Chik TS, Choi CY, Kandamby DH, Lung DC, Tam AR, Poon RW, Fung AY, Hung IF, Cheng VC, Chan JF, Yuen KY. Consistent Detection of 2019 Novel Coronavirus in Saliva. *Clin Infect Dis* 2020; **71**: 841-843 [PMID: 32047895 DOI: 10.1093/cid/ciaa149]

44 **Hanley B**, Lucas SB, Youd E, Swift B, Osborn M. Autopsy in suspected COVID-19 cases. *J Clin Pathol* 2020; **73**: 239-242 [PMID: 32198191 DOI: 10.1136/jclinpath-2020-206522]

45 **Tian Y**, Rong L, Nian W, He Y. Review article: gastrointestinal features in COVID-19 and the possibility of faecal transmission. *Aliment Pharmacol Ther* 2020; **51**: 843-851 [PMID: 32222988 DOI: 10.1111/apt.15731]

46 **Tapper EB**, Asrani SK. The COVID-19 pandemic will have a long-lasting impact on the quality of cirrhosis care. *J Hepatol* 2020; **73**: 441-445 [PMID: 32298769 DOI: 10.1016/j.jhep.2020.04.005]

47 **World Health Organization**. Hepatitis. Available from: https://www.who.int/health-topics/hepatitis

48 **Fiore C**, Eisenhut M, Krausse R, Ragazzi E, Pellati D, Armanini D, Bielenberg J. Antiviral effects of Glycyrrhiza species. *Phytother Res* 2008; **22**: 141-148 [PMID: 17886224 DOI: 10.1002/ptr.2295]

49 **Cai Q**, Huang D, Ou P, Yu H, Zhu Z, Xia Z, Su Y, Ma Z, Zhang Y, Li Z, He Q, Liu L, Fu Y, Chen J. COVID-19 in a designated infectious diseases hospital outside Hubei Province, China. *Allergy* 2020; **75**: 1742-1752 [PMID: 32239761 DOI: 10.1111/all.14309]

50 **Musa S**. Hepatic and gastrointestinal involvement in coronavirus disease 2019 (COVID-19): What do we know till now? *Arab J Gastroenterol* 2020; **21**: 3-8 [PMID: 32253172 DOI: 10.1016/j.ajg.2020.03.002]

51 **Stefan N**, Birkenfeld AL, Schulze MB, Ludwig DS. Obesity and impaired metabolic health in patients with COVID-19. *Nat Rev Endocrinol* 2020; **16**: 341-342 [PMID: 32327737 DOI: 10.1038/s41574-020-0364-6]

52 **Keyes KM**, Hatzenbuehler ML, Hasin DS. Stressful life experiences, alcohol consumption, and alcohol use disorders: the epidemiologic evidence for four main types of stressors. *Psychopharmacology (Berl)* 2011; **218**: 1-17 [PMID: 21373787 DOI: 10.1007/s00213-011-2236-1]

53 **Strnad P**, Tacke F, Koch A, Trautwein C. Liver - guardian, modifier and target of sepsis. *Nat Rev Gastroenterol Hepatol* 2017; **14**: 55-66 [PMID: 27924081 DOI: 10.1038/nrgastro.2016.168]

54 **Xiao Y**, Pan H, She Q, Wang F, Chen M. Prevention of SARS-CoV-2 infection in patients with decompensated cirrhosis. *Lancet Gastroenterol Hepatol* 2020; **5**: 528-529 [PMID: 32197093 DOI: 10.1016/S2468-1253(20)30080-7]

55 **Kumar D**, Tellier R, Draker R, Levy G, Humar A. Severe Acute Respiratory Syndrome (SARS) in a liver transplant recipient and guidelines for donor SARS screening. *Am J Transplant* 2003; **3**: 977-981 [PMID: 12859532 DOI: 10.1034/j.1600-6143.2003.00197.x]

56 **Tzedakis S**, Jeddou H, Houssel-Debry P, Sulpice L, Boudjema K. COVID-19: Thoughts and comments from a tertiary liver transplant center in France. *Am J Transplant* 2020; **20**: 1952-1953 [PMID: 32282972 DOI: 10.1111/ajt.15918]

57 **Baumgart DC**, Sandborn WJ. Inflammatory bowel disease: clinical aspects and established and evolving therapies. *Lancet* 2007; **369**: 1641-1657 [PMID: 17499606 DOI: 10.1016/S0140-6736(07)60751-X]

58 **Toruner M**, Loftus EV Jr, Harmsen WS, Zinsmeister AR, Orenstein R, Sandborn WJ, Colombel JF, Egan LJ. Risk factors for opportunistic infections in patients with inflammatory bowel disease. *Gastroenterology* 2008; **134**: 929-936 [PMID: 18294633 DOI: 10.1053/j.gastro.2008.01.012]

59 **Kucharzik T**, Maaser C. Infections and Chronic Inflammatory Bowel Disease. *Viszeralmedizin* 2014; **30**: 326-332 [PMID: 26288602 DOI: 10.1159/000366463]

60 **An P**, Ji M, Ren H, Su J, Kang J, Yin A, Zhou Q, Shen L, Zhao L, Jiang X, Xiao Y, Tan W, Lv X, Li J, Liu S, Zhou J, Chen H, Xu Y, Liu J, Chen M, Cao J, Zhou Z, Shen L, Tan S, Yu H, Dong W, Ding Y. Protection of 318 inflammatory bowel disease patients from the outbreak and rapid spread of COVID-19 infection in Wuhan, China. *Soc Sci Elec Publishing* 2020 [DOI: 10.2139/ssrn.3543590]

61 **Mao R**, Liang J, Shen J, Ghosh S, Zhu LR, Yang H, Wu KC, Chen MH; Chinese Society of IBD; Chinese Elite IBD Union; Chinese IBD Quality Care Evaluation Center Committee. Implications of COVID-19 for patients with pre-existing digestive diseases. *Lancet Gastroenterol Hepatol* 2020; **5**: 425-427 [PMID: 32171057 DOI: 10.1016/S2468-1253(20)30076-5]

62 **Liang W**, Guan W, Chen R, Wang W, Li J, Xu K, Li C, Ai Q, Lu W, Liang H, Li S, He J. Cancer patients in SARS-CoV-2 infection: a nationwide analysis in China. *Lancet Oncol* 2020; **21**: 335-337 [PMID: 32066541 DOI: 10.1016/S1470-2045(20)30096-6]

63 **Liu Y**, Ning Z, Chen Y, Guo M, Liu Y, Gali NK, Sun L, Duan Y, Cai J, Westerdahl D, Liu X, Xu K, Ho KF, Kan H, Fu Q, Lan K. Aerodynamic analysis of SARS-CoV-2 in two Wuhan hospitals. *Nature* 2020; **582**: 557-560 [PMID: 32340022 DOI: 10.1038/s41586-020-2271-3]

64 **Patel VB**, Zhong JC, Grant MB, Oudit GY. Role of the ACE2/Angiotensin 1-7 Axis of the Renin-Angiotensin System in Heart Failure. *Circ Res* 2016; **118**: 1313-1326 [PMID: 27081112 DOI: 10.1161/CIRCRESAHA.116.307708]

65 **Miller AJ**, Arnold AC. The renin-angiotensin system in cardiovascular autonomic control: recent developments and clinical implications. *Clin Auton Res* 2019; **29**: 231-243 [PMID: 30413906 DOI: 10.1007/s10286-018-0572-5]

66 **Kuba K**, Imai Y, Rao S, Gao H, Guo F, Guan B, Huan Y, Yang P, Zhang Y, Deng W, Bao L, Zhang B, Liu G, Wang Z, Chappell M, Liu Y, Zheng D, Leibbrandt A, Wada T, Slutsky AS, Liu D, Qin C, Jiang C, Penninger JM. A crucial role of angiotensin converting enzyme 2 (ACE2) in SARS coronavirus-induced lung injury. *Nat Med* 2005; **11**: 875-879 [PMID: 16007097 DOI: 10.1038/nm1267]

67 **Wrapp D**, Wang N, Corbett KS, Goldsmith JA, Hsieh CL, Abiona O, Graham BS, McLellan JS. Cryo-EM structure of the 2019-nCoV spike in the prefusion conformation. *Science* 2020; **367**: 1260-1263 [PMID: 32075877 DOI: 10.1126/science.abb2507]

68 **Yang P**, Gu H, Zhao Z, Wang W, Cao B, Lai C, Yang X, Zhang L, Duan Y, Zhang S, Chen W, Zhen W, Cai M, Penninger JM, Jiang C, Wang X. Angiotensin-converting enzyme 2 (ACE2) mediates influenza H7N9 virus-induced acute lung injury. *Sci Rep* 2014; **4**: 7027 [PMID: 25391767 DOI:

10.1038/srep07027]
69 **Hoffmann M**, Kleine-Weber H, Schroeder S, Krüger N, Herrler T, Erichsen S, Schiergens TS, Herrler G, Wu NH, Nitsche A, Müller MA, Drosten C, Pöhlmann S. SARS-CoV-2 Cell Entry Depends on ACE2 and TMPRSS2 and Is Blocked by a Clinically Proven Protease Inhibitor. *Cell* 2020; **181**: 271-280. e8 [PMID: 32142651 DOI: 10.1016/j.cell.2020.02.052]
70 **Zhang H**, Kang Z, Gong H, Xu D, Wang J, Li Z, Li Z, Cui X, Xiao J, Zhan J, Meng T, Zhou W, Liu J, Xu H. Digestive system is a potential route of COVID-19: an analysis of single-cell coexpression pattern of key proteins in viral entry process. *Gut* 2020; gutjnl-2020 [DOI: 10.1136/gutjnl-2020-320953]
71 **Van Pelt J**, Van Kuik JA, Kamerling JP, Vliegenthart JF, Van Diggelen OP, Galjaard H. Storage of sialic acid-containing carbohydrates in the placenta of a human galactosialidosis fetus. Isolation and structural characterization of 16 sialyloligosaccharides. *Eur J Biochem* 1988; **177**: 327-338 [PMID: 3142773 DOI: 10.1111/j.1432-1033.1988.tb14380.x]
72 **Haber AL**, Biton M, Rogel N, Herbst RH, Shekhar K, Smillie C, Burgin G, Delorey TM, Howitt MR, Katz Y, Tirosh I, Beyaz S, Dionne D, Zhang M, Raychowdhury R, Garrett WS, Rozenblatt-Rosen O, Shi HN, Yilmaz O, Xavier RJ, Regev A. A single-cell survey of the small intestinal epithelium. *Nature* 2017; **551**: 333-339 [PMID: 29144463 DOI: 10.1038/nature24489]
73 **Desmarets LMB**, Theuns S, Roukaerts IDM, Acar DD, Nauwynck HJ. Role of sialic acids in feline enteric coronavirus infections. *J Gen Virol* 2014; **95**: 1911-1918 [PMID: 24876305 DOI: 10.1099/vir.0.064717-0]
74 **Crawford SE**, Ramani S, Tate JE, Parashar UD, Svensson L, Hagbom M, Franco MA, Greenberg HB, O'Ryan M, Kang G, Desselberger U, Estes MK. Rotavirus infection. *Nat Rev Dis Primers* 2017; **3**: 17083 [PMID: 29119972 DOI: 10.1038/nrdp.2017.83]
75 **Seow J**, Pai R, Mishra A, Shepherdson E, Lim T, Goh B, Chan J, Chow P, Ginhoux F, DasGupta R, Sharma A. scRNA-seq reveals ACE2 and TMPRSS2 expression in TROP2+ Liver Progenitor Cells: Implications in COVID-19 associated Liver Dysfunction. *bioRxiv* 2020 [DOI: 10.1101/2020.03.23.002832]
76 **Banales JM**, Huebert RC, Karlsen T, Strazzabosco M, LaRusso NF, Gores GJ. Cholangiocyte pathobiology. *Nat Rev Gastroenterol Hepatol* 2019; **16**: 269-281 [PMID: 30850822 DOI: 10.1038/s41575-019-0125-y]
77 **Hashimoto T**, Perlot T, Rehman A, Trichereau J, Ishiguro H, Paolino M, Sigl V, Hanada T, Hanada R, Lipinski S, Wild B, Camargo SM, Singer D, Richter A, Kuba K, Fukamizu A, Schreiber S, Clevers H, Verrey F, Rosenstiel P, Penninger JM. ACE2 links amino acid malnutrition to microbial ecology and intestinal inflammation. *Nature* 2012; **487**: 477-481 [PMID: 22837003 DOI: 10.1038/nature11228]
78 **Monteil V**, Kwon H, Prado P, Hagelkrüys A, Wimmer RA, Stahl M, Leopoldi A, Garreta E, Hurtado Del Pozo C, Prosper F, Romero JP, Wirnsberger G, Zhang H, Slutsky AS, Conder R, Montserrat N, Mirazimi A, Penninger JM. Inhibition of SARS-CoV-2 Infections in Engineered Human Tissues Using Clinical-Grade Soluble Human ACE2. *Cell* 2020; **181**: 905-913. e7 [PMID: 32333836 DOI: 10.1016/j.cell.2020.04.004]
79 **Lei C**, Qian K, Li T, Zhang S, Fu W, Ding M, Hu S. Neutralization of SARS-CoV-2 spike pseudotyped virus by recombinant ACE2-Ig. *Nat Commun* 2020; **11**: 2070 [PMID: 32332765 DOI: 10.1038/s41467-020-16048-4]
80 **Shi R**, Shan C, Duan X, Chen Z, Liu P, Song J, Song T, Bi X, Han C, Wu L, Gao G, Hu X, Zhang Y, Tong Z, Huang W, Liu WJ, Wu G, Zhang B, Wang L, Qi J, Feng H, Wang FS, Wang Q, Gao GF, Yuan Z, Yan J. A human neutralizing antibody targets the receptor-binding site of SARS-CoV-2. *Nature* 2020; **584**: 120-124 [PMID: 32454512 DOI: 10.1038/s41586-020-2381-y]
81 **Lamers MM**, Beumer J, van der Vaart J, Knoops K, Puschhof J, Breugem TI, Ravelli RBG, Paul van Schayck J, Mykytyn AZ, Duimel HQ, van Donselaar E, Riesebosch S, Kuijpers HJH, Schipper D, van de Wetering WJ, de Graaf M, Koopmans M, Cuppen E, Peters PJ, Haagmans BL, Clevers H. SARS-CoV-2 productively infects human gut enterocytes. *Science* 2020; **369**: 50-54 [PMID: 32358202 DOI: 10.1126/science.abc1669]
82 **Adams DH**, Ju C, Ramaiah SK, Uetrecht J, Jaeschke H. Mechanisms of immune-mediated liver injury. *Toxicol Sci* 2010; **115**: 307-321 [PMID: 20071422 DOI: 10.1093/toxsci/kfq009]
83 **Zhou JA**, Jiang M, Yang X, Liu Y, Guo J, Zheng J, Qu Y, Song Y, Li R, Qin X, Wang X. Unconjugated bilirubin ameliorates the inflammation and digestive protease increase in TNBS-induced colitis. *Mol Med Rep* 2017; **16**: 1779-1784 [PMID: 28656252 DOI: 10.3892/mmr.2017.6825]
84 **Lohse AW**, Weiler-Normann C, Tiegs G. Immune-mediated liver injury. *J Hepatol* 2010; **52**: 136-144 [PMID: 19913936 DOI: 10.1016/j.jhep.2009.10.016]
85 **Qin C**, Zhou L, Hu Z, Zhang S, Yang S, Tao Y, Xie C, Ma K, Shang K, Wang W, Tian DS. Dysregulation of Immune Response in Patients With Coronavirus 2019 (COVID-19) in Wuhan, China. *Clin Infect Dis* 2020; **71**: 762-768 [PMID: 32161940 DOI: 10.1093/cid/ciaa248]
86 **Tan M**, Liu Y, Zhou R, Deng X, Li F, Liang K, Shi Y. Immunopathological characteristics of coronavirus disease 2019 cases in Guangzhou, China. *Immunology* 2020; **160**: 261-268 [PMID: 32460357 DOI: 10.1111/imm.13223]
87 **Cao X**. COVID-19: immunopathology and its implications for therapy. *Nat Rev Immunol* 2020; **20**: 269-270 [PMID: 32273594 DOI: 10.1038/s41577-020-0308-3]
88 **Tracey KJ**. Physiology and immunology of the cholinergic antiinflammatory pathway. *J Clin Invest*

2007; **117**: 289-296 [PMID: 17273548 DOI: 10.1172/JCI30555]
89 **Tracey KJ**. The inflammatory reflex. *Nature* 2002; **420**: 853-859 [PMID: 12490958 DOI: 10.1038/nature01321]
90 **Staats P**, Giannakopoulos G, Blake J, Liebler E, Levy RM. The Use of Non-invasive Vagus Nerve Stimulation to Treat Respiratory Symptoms Associated With COVID-19: A Theoretical Hypothesis and Early Clinical Experience. *Neuromodulation* 2020; **23**: 784-788 [PMID: 32342609 DOI: 10.1111/ner.13172]
91 **Varga Z**, Flammer AJ, Steiger P, Haberecker M, Andermatt R, Zinkernagel AS, Mehra MR, Schuepbach RA, Ruschitzka F, Moch H. Endothelial cell infection and endotheliitis in COVID-19. *Lancet* 2020; **395**: 1417-1418 [PMID: 32325026 DOI: 10.1016/S0140-6736(20)30937-5]
92 **Feng T**, Elson CO. Adaptive immunity in the host-microbiota dialog. *Mucosal Immunol* 2011; **4**: 15-21 [PMID: 20944557 DOI: 10.1038/mi.2010.60]
93 **Sender R**, Fuchs S, Milo R. Revised Estimates for the Number of Human and Bacteria Cells in the Body. *PLoS Biol* 2016; **14**: e1002533 [PMID: 27541692 DOI: 10.1371/journal.pbio.1002533]
94 **Selber-Hnatiw S**, Rukundo B, Ahmadi M, Akoubi H, Al-Bizri H, Aliu AF, Ambeaghen TU, Avetisyan L, Bahar I, Baird A, Begum F, Ben Soussan H, Blondeau-Éthier V, Bordaries R, Bramwell H, Briggs A, Bui R, Carnevale M, Chancharoen M, Chevassus T, Choi JH, Coulombe K, Couvrette F, D'Abreau S, Davies M, Desbiens MP, Di Maulo T, Di Paolo SA, Do Ponte S, Dos Santos Ribeiro P, Dubuc-Kanary LA, Duncan PK, Dupuis F, El-Nounou S, Eyangos CN, Ferguson NK, Flores-Chinchilla NR, Fotakis T, Gado Oumarou H D M, Georgiev M, Ghiassy S, Glibetic N, Grégoire Bouchard J, Hassan T, Huseen I, Ibuna Quilatan MF, Iozzo T, Islam S, Jaunky DB, Jeyasegaram A, Johnston MA, Kahler MR, Kaler K, Kamani C, Karimian Rad H, Konidis E, Konieczny F, Kurianowicz S, Lamothe P, Legros K, Leroux S, Li J, Lozano Rodriguez ME, Luponio-Yoffe S, Maalouf Y, Mantha J, McCormick M, Mondragon P, Narayana T, Neretin E, Nguyen TTT, Niu I, Nkemazem RB, O'Donovan M, Oueis M, Paquette S, Patel N, Pecsi E, Peters J, Pettorelli A, Poirier C, Pompa VR, Rajen H, Ralph RO, Rosales-Vasquez J, Rubinshtein D, Sakr S, Sebai MS, Serravalle L, Sidibe F, Sinnathurai A, Soho D, Sundarakrishnan A, Svistkova V, Ugbeye TE, Vasconcelos MS, Vincelli M, Voitovich O, Vrabel P, Wang L, Wasfi M, Zha CY, Gamberi C. Human Gut Microbiota: Toward an Ecology of Disease. *Front Microbiol* 2017; **8**: 1265 [PMID: 28769880 DOI: 10.3389/fmicb.2017.01265]
95 **Schirmer M**, Franzosa EA, Lloyd-Price J, McIver LJ, Schwager R, Poon TW, Ananthakrishnan AN, Andrews E, Barron G, Lake K, Prasad M, Sauk J, Stevens B, Wilson RG, Braun J, Denson LA, Kugathasan S, McGovern DPB, Vlamakis H, Xavier RJ, Huttenhower C. Dynamics of metatranscription in the inflammatory bowel disease gut microbiome. *Nat Microbiol* 2018; **3**: 337-346 [PMID: 29311644 DOI: 10.1038/s41564-017-0089-z]
96 **Jiang C**, Li G, Huang P, Liu Z, Zhao B. The Gut Microbiota and Alzheimer's Disease. *J Alzheimers Dis* 2017; **58**: 1-15 [PMID: 28372330 DOI: 10.3233/JAD-161141]
97 **Rutten EPA**, Lenaerts K, Buurman WA, Wouters EFM. Disturbed intestinal integrity in patients with COPD: effects of activities of daily living. *Chest* 2014; **145**: 245-252 [PMID: 23928850 DOI: 10.1378/chest.13-0584]
98 **Wang J**, Li F, Wei H, Lian ZX, Sun R, Tian Z. Respiratory influenza virus infection induces intestinal immune injury *via* microbiota-mediated Th17 cell-dependent inflammation. *J Exp Med* 2014; **211**: 2397-2410 [PMID: 25366965 DOI: 10.1084/jem.20140625]
99 **Yildiz S**, Mazel-Sanchez B, Kandasamy M, Manicassamy B, Schmolke M. Influenza A virus infection impacts systemic microbiota dynamics and causes quantitative enteric dysbiosis. *Microbiome* 2018; **6**: 9 [PMID: 29321057 DOI: 10.1186/s40168-017-0386-z]
100 **Budden KF**, Gellatly SL, Wood DL, Cooper MA, Morrison M, Hugenholtz P, Hansbro PM. Emerging pathogenic links between microbiota and the gut-lung axis. *Nat Rev Microbiol* 2017; **15**: 55-63 [PMID: 27694885 DOI: 10.1038/nrmicro.2016.142]
101 **Ma C**, Cong Y, Zhang H. COVID-19 and the Digestive System. *Am J Gastroenterol* 2020; **115**: 1003-1006 [PMID: 32618648 DOI: 10.14309/ajg.0000000000000691]
102 **Perlot T**, Penninger JM. ACE2 - from the renin-angiotensin system to gut microbiota and malnutrition. *Microbes Infect* 2013; **15**: 866-873 [PMID: 23962453 DOI: 10.1016/j.micinf.2013.08.003]
103 **Xu K**, Cai H, Shen Y, Ni Q, Chen Y, Hu S, Li J, Wang H, Yu L, Huang H, Qiu Y, Wei G, Fang Q, Zhou J, Sheng J, Liang T, Li L. [Management of corona virus disease-19 (COVID-19): the Zhejiang experience]. *Zhejiang Da Xue Xue Bao Yi Xue Ban* 2020; **49**: 147-157 [PMID: 32096367 DOI: 10.3785/j.issn.1008-9292.2020.02.02]
104 **Zuo T**, Zhang F, Lui GCY, Yeoh YK, Li AYL, Zhan H, Wan Y, Chung ACK, Cheung CP, Chen N, Lai CKC, Chen Z, Tso EYK, Fung KSC, Chan V, Ling L, Joynt G, Hui DSC, Chan FKL, Chan PKS, Ng SC. Alterations in Gut Microbiota of Patients With COVID-19 During Time of Hospitalization. *Gastroenterology* 2020; **159**: 944-955. e8 [PMID: 32442562 DOI: 10.1053/j.gastro.2020.05.048]
105 **Jung TH**, Park JH, Jeon WM, Han KS. Butyrate modulates bacterial adherence on LS174T human colorectal cells by stimulating mucin secretion and MAPK signaling pathway. *Nutr Res Pract* 2015; **9**: 343-349 [PMID: 26244071 DOI: 10.4162/nrp.2015.9.4.343]
106 **Fukuda S**, Toh H, Hase K, Oshima K, Nakanishi Y, Yoshimura K, Tobe T, Clarke JM, Topping DL, Suzuki T, Taylor TD, Itoh K, Kikuchi J, Morita H, Hattori M, Ohno H. Bifidobacteria can protect from enteropathogenic infection through production of acetate. *Nature* 2011; **469**: 543-547 [PMID: 21270894 DOI: 10.1038/nature09646]

107 **Li M**, van Esch BCAM, Wagenaar GTM, Garssen J, Folkerts G, Henricks PAJ. Pro- and anti-inflammatory effects of short chain fatty acids on immune and endothelial cells. *Eur J Pharmacol* 2018; **831**: 52-59 [PMID: 29750914 DOI: 10.1016/j.ejphar.2018.05.003]

108 **Dethlefsen L**, Huse S, Sogin ML, Relman DA. The pervasive effects of an antibiotic on the human gut microbiota, as revealed by deep 16S rRNA sequencing. *PLoS Biol* 2008; **6**: e280 [PMID: 19018661 DOI: 10.1371/journal.pbio.0060280]

109 **Duan J**, Wu Y, Liu C, Yang C, Yang L. Deleterious effects of viral pneumonia on cardiovascular system. *Eur Heart J* 2020; **41**: 1833-1838 [PMID: 32383765 DOI: 10.1093/eurheartj/ehaa325]

110 **Konturek PC**, Brzozowski T, Konturek SJ. Stress and the gut: pathophysiology, clinical consequences, diagnostic approach and treatment options. *J Physiol Pharmacol* 2011; **62**: 591-599 [PMID: 22314561]

111 **Li S**, Wang Y, Xue J, Zhao N, Zhu T. The Impact of COVID-19 Epidemic Declaration on Psychological Consequences: A Study on Active Weibo Users. *Int J Environ Res Public Health* 2020; **17** [PMID: 32204411 DOI: 10.3390/ijerph17062032]

112 **Brooks SK**, Webster RK, Smith LE, Woodland L, Wessely S, Greenberg N, Rubin GJ. The psychological impact of quarantine and how to reduce it: rapid review of the evidence. *Lancet* 2020; **395**: 912-920 [PMID: 32112714 DOI: 10.1016/S0140-6736(20)30460-8]

113 **Chigr F**, Merzouki M, Najimi M. Autonomic Brain Centers and Pathophysiology of COVID-19. *ACS Chem Neurosci* 2020; **11**: 1520-1522 [PMID: 32427468 DOI: 10.1021/acschemneuro.0c00265]

114 **Cholankeril G**, Podboy A, Aivaliotis VI, Tarlow B, Pham EA, Spencer SP, Kim D, Hsing A, Ahmed A. High Prevalence of Concurrent Gastrointestinal Manifestations in Patients With Severe Acute Respiratory Syndrome Coronavirus 2: Early Experience From California. *Gastroenterology* 2020; **159**: 775-777 [PMID: 32283101 DOI: 10.1053/j.gastro.2020.04.008]

115 **Tassorelli C**, Mojoli F, Baldanti F, Bruno R, Benazzo M. COVID-19: what if the brain had a role in causing the deaths? *Eur J Neurol* 2020; **27**: e41-e42 [PMID: 32333819 DOI: 10.1111/ene.14275]

116 **Fan Z**, Chen L, Li J, Cheng X, Yang J, Tian C, Zhang Y, Huang S, Liu Z, Cheng J. Clinical Features of COVID-19-Related Liver Functional Abnormality. *Clin Gastroenterol Hepatol* 2020; **18**: 1561-1566 [PMID: 32283325 DOI: 10.1016/j.cgh.2020.04.002]

117 **Zhang JJ**, Dong X, Cao YY, Yuan YD, Yang YB, Yan YQ, Akdis CA, Gao YD. Clinical characteristics of 140 patients infected with SARS-CoV-2 in Wuhan, China. *Allergy* 2020; **75**: 1730-1741 [PMID: 32077115 DOI: 10.1111/all.14238]

118 **Zhou F**, Yu T, Du R, Fan G, Liu Y, Liu Z, Xiang J, Wang Y, Song B, Gu X, Guan L, Wei Y, Li H, Wu X, Xu J, Tu S, Zhang Y, Chen H, Cao B. Clinical course and risk factors for mortality of adult inpatients with COVID-19 in Wuhan, China: a retrospective cohort study. *Lancet* 2020; **395**: 1054-1062 [PMID: 32171076 DOI: 10.1016/S0140-6736(20)30566-3]

119 **Zhang B**, Zhou X, Qiu Y, Song Y, Feng F, Feng J, Song Q, Jia Q, Wang J. Clinical characteristics of 82 cases of death from COVID-19. *PLoS One* 2020; **15**: e0235458 [PMID: 32645044 DOI: 10.1371/journal.pone.0235458]

120 **Xu XW**, Wu XX, Jiang XG, Xu KJ, Ying LJ, Ma CL, Li SB, Wang HY, Zhang S, Gao HN, Sheng JF, Cai HL, Qiu YQ, Li LJ. Clinical findings in a group of patients infected with the 2019 novel coronavirus (SARS-Cov-2) outside of Wuhan, China: retrospective case series. *BMJ* 2020; **368**: m606 [PMID: 32075786 DOI: 10.1136/bmj.m606]

121 **Chen G**, Wu D, Guo W, Cao Y, Huang D, Wang H, Wang T, Zhang X, Chen H, Yu H, Zhang X, Zhang M, Wu S, Song J, Chen T, Han M, Li S, Luo X, Zhao J, Ning Q. Clinical and immunological features of severe and moderate coronavirus disease 2019. *J Clin Invest* 2020; **130**: 2620-2629 [PMID: 32217835 DOI: 10.1172/JCI137244]

122 **Luo S**, Zhang X, Xu H. Don't Overlook Digestive Symptoms in Patients With 2019 Novel Coronavirus Disease (COVID-19). *Clin Gastroenterol Hepatol* 2020; **18**: 1636-1637 [PMID: 32205220 DOI: 10.1016/j.cgh.2020.03.043]

World Journal of Gastroenterology

Submit a Manuscript: https://www.f6publishing.com

World J Gastroenterol 2021 February 21; 27(7): 576-591

DOI: 10.3748/wjg.v27.i7.576

ISSN 1007-9327 (print) ISSN 2219-2840 (online)

ORIGINAL ARTICLE

Basic Study

Xiangbinfang granules enhance gastric antrum motility *via* intramuscular interstitial cells of Cajal in mice

Qi-Cheng Chen, Zhi Jiang, Jun-Hong Zhang, Li-Xing Cao, Zhi-Qiang Chen

ORCID number: Qi-Cheng Chen 0000-0001-5852-3056; Zhi Jiang 0000-0001-5261-1493; Jun-Hong Zhang 0000-0003-0611-9478; Li-Xing Cao 0000-0001-6602-7730; Zhi-Qiang Chen 0000-0001-7658-2746.

Author contributions: Chen QC, Cao LX and Chen ZQ designed the research study; Chen QC, Jiang Z and Zhang JH performed the research; Chen QC analyzed the data and wrote the manuscript; all authors have read and approved the final manuscript.

Supported by The Specific Research Fund for TCM Science and Technology of Guangdong Provincial Hospital of Chinese Medicine, No. YN10101902; and the National Regional Traditional Chinese Medicine (Specialist) Clinic Construction, No. (2018)205.

Institutional review board statement: The study was reviewed and approved by the Institutional Animal Care and Ethics Committee of Guangdong Provincial Hospital of Traditional Chinese Medicine (approval No. 2018003).

Institutional animal care and use committee statement: All animal procedures were conducted according to the Regulations for the Care and Use of Laboratory

Qi-Cheng Chen, Zhi Jiang, Li-Xing Cao, Zhi-Qiang Chen, The Research Team of TCM Applications of Perioperative, The Second Affiliated Hospital of Guangzhou University of Chinese Medicine, Guangdong Provincial Hospital of Traditional Chinese Medicine, Guangzhou 510120, Guangdong Province, China

Jun-Hong Zhang, Department of Research Public Service Center, The Second Affiliated Hospital of Guangzhou University of Chinese Medicine, Guangdong Provincial Hospital of Traditional Chinese Medicine, Guangzhou 510120, Guangdong Province, China

Corresponding author: Zhi-Qiang Chen, MD, Professor, The Research Team of TCM Applications of Perioperative, The Second Affiliated Hospital of Guangzhou University of Chinese Medicine, Guangdong Provincial Hospital of Traditional Chinese Medicine, No. 111 Dade Road, Guangzhou 510120, Guangdong Province, China. wssq@gzucm.edu.cn

Abstract

BACKGROUND

Interdigestive migrating motor complexes (MMC) produce periodic contractions in the gastrointestinal tract, but the exact mechanism of action still remains unclear. Intramuscular interstitial cells of Cajal (ICC-IM) participate in gastrointestinal hormone and neuromodulation, but the correlation between ICC-IM and MMC is also unclear. We found that xiangbinfang granules (XBF) mediated the phase III contraction of MMC. Here, the effects of XBF on gastric antrum motility in *W/W*^{v} mice and the effects of ICC-IM on gastric antrum MMC are reported.

AIM

To observe the effects of ICC-IM on gastric antrum motility and to establish the mechanism of XBF in promoting gastric antrum motility.

METHODS

The density of c-kit-positive ICC myenteric plexus (ICC-MP) and ICC-IM in the antral muscularis of *W/W*^{v} and wild-type (WT) mice was examined by confocal microscopy. The effects of XBF on gastric antrum slow waves in *W/W*^{v} and WT mice were recorded by intracellular amplification recording. Micro-strain-gauge force transducers were implanted into the gastric antrum to monitor the MMC and the effect of XBF on gastric antrum motility in conscious *W/W*^{v} and WT mice.

RESULTS

In the gastric antrum of *W/W*^{v} mice, c-kit immunoreactivity was significantly reduced, and no ICC-IM network was observed. Spontaneous rhythmic slow waves also appeared in the antrum of *W/W*^{v} mice, but the amplitude of the antrum slow wave decreased significantly in *W/W*^{v} mice (22.62 ± 2.23 mV *vs* 2.92 ± 0.52 mV, $P < 0.0001$). MMCs were found in 7 of the 8 WT mice but no complete MMC cycle was found in *W/W*^{v} mice. The contractile frequency and amplitude index of the gastric antrum were significantly increased in conscious WT compared to *W/W*^{v} mice (frequency, 3.53 ± 0.18 cpm *vs* 1.28 ± 0.12 cpm; amplitude index, 23014.26 ± 1798.65 mV·20 min *vs* 3782.16 ± 407.13 mV·20 min; $P < 0.0001$). XBF depolarized smooth muscle cells of the gastric antrum in WT and *W/W*^{v} mice in a dose-dependent manner. Similarly, the gastric antrum motility in WT mice was significantly increased after treatment with XBF 5 mg ($P < 0.05$). Atropine (0.1 mg/kg) blocked the enhancement of XBF in WT and *W/W*^{v} mice completely, while tetrodotoxin (0.05 mg/kg) partially inhibited the enhancement by XBF.

CONCLUSION

ICC-IM participates in the regulation of gastric antrum MMC in mice. XBF induces MMC III-like contractions that enhance gastric antrum motility *via* ICC-IM in mice.

Key Words: Interstitial cells of Cajal; Migrating motor complex; *W/W*^{v}; Gastric antrum motility; Xiangbinfang granules; Chinese medicine

©The Author(s) 2021. Published by Baishideng Publishing Group Inc. All rights reserved.

Core Tip: This study shows that intramuscular interstitial cells of Cajal (ICC-IM) play crucial roles in regulating the activity of gastric antral migrating motor complexes (MMC). This may be an important bridge between the vagus, enteric nervous system and motilin to regulate smooth muscle contraction. Through the muscarinic receptor pathway on ICC-IM, the Chinese medicine Xiangbinfang granules depolarize smooth muscle cells and initiates an action potential, changing the periodic motion of MMC into a phase III-like contraction pattern in the gastric antrum of mice.

Citation: Chen QC, Jiang Z, Zhang JH, Cao LX, Chen ZQ. Xiangbinfang granules enhance gastric antrum motility *via* intramuscular interstitial cells of Cajal in mice. *World J Gastroenterol* 2021; 27(7): 576-591
URL: https://www.wjgnet.com/1007-9327/full/v27/i7/576.htm
DOI: https://dx.doi.org/10.3748/wjg.v27.i7.576

INTRODUCTION

Interdigestive migrating motor complexes (MMC) induce periodic contractions of the gastric, small intestine, or colon smooth muscle, propagating along the gastrointestinal (GI) tract. Although the exact mechanism of MMC action still remains unclear, MMC have been classified into four stages. The MMC phase III consists of a high-frequency, high-amplitude rhythmic contraction, which has important physiological significance in normal GI motility and digestion[1]. Interstitial cells of Cajal (ICC), which are electrically coupled to smooth muscle cells (SMCs), produce slow waves that function as pacemaker activity[2]. There are several ICC subtypes based on their anatomical locations, morphology, and function in the GI tract. ICC associated with the myenteric plexus (ICC-MP) are responsible for producing slow waves. Intramuscular ICC (ICC-IM), which are located in muscle bundles between muscle cells, mediate information transmission from autonomic nerves to SMCs[3]. In the small intestine of *W/W*^{v} mice lacking ICC-MP, there are no rhythmic slow waves and there are irregular contractions of longitudinal and circular muscles[4]. However, the MMC cycle still exists in the isolated intestine of *W/W*^{v} mice, suggesting that MMC do not require ICC-MP[5]. Other studies have shown that with the depletion of gastric ICC, disorders of the MMC cycle are common in diabetic gastroparesis[6,7]. This seems to indicate that ICC, especially ICC-IM, may also be involved in regulating the movement of MMC.

Animals in Guangzhou University of Chinese Medicine.

Conflict-of-interest statement: The authors declare that there is no conflict of interest in this study.

Data sharing statement: Technical appendix, statistical code, and dataset are available from the corresponding author at wssq@gzucm.edu.cn.

ARRIVE guidelines statement: The authors have read the ARRIVE guidelines, and the manuscript was prepared and revised according to the ARRIVE guidelines.

Open-Access: This article is an open-access article that was selected by an in-house editor and fully peer-reviewed by external reviewers. It is distributed in accordance with the Creative Commons Attribution NonCommercial (CC BY-NC 4.0) license, which permits others to distribute, remix, adapt, build upon this work non-commercially, and license their derivative works on different terms, provided the original work is properly cited and the use is non-commercial. See: http://creativecommons.org/licenses/by-nc/4.0/

Manuscript source: Unsolicited manuscript

Specialty type: Gastroenterology and hepatology

Country/Territory of origin: China

Peer-review report's scientific quality classification
Grade A (Excellent): 0
Grade B (Very good): B
Grade C (Good): C
Grade D (Fair): 0
Grade E (Poor): 0

Received: October 27, 2020
Peer-review started: October 27, 2020
First decision: December 13, 2020
Revised: December 24, 2020
Accepted: January 13, 2021
Article in press: January 13, 2021
Published online: February 21, 2021

P-Reviewer: Baker SA, Huizinga JD
S-Editor: Chen XF
L-Editor: Webster JR
P-Editor: Ma YJ

The Chinese herbal medicine xiangbinfang granules (XBF) is an effective treatment for promoting the post-surgical recovery of GI function[8,9]. Previous studies have shown that XBF significantly enhanced MMC activity in the antrum, pylorus, duodenum, jejunum, and the colon in beagles[10]. XBF was also found to promote contraction of the stomach, duodenum, and jejunum in healthy volunteers[11]. However, the mechanism of XBF in enhancing MMC activity in the GI tract is still unclear.

In this study, we observed the MMC activity of the gastric antrum in *W/W*^{v} mice that lacked ICC-IM and analyzed the effects of the traditional Chinese medicine XBF in promoting gastric antrum motility.

MATERIALS AND METHODS

Animals

This study included 36 *W/W*^{v} and 36 wild-type (WT) mice. *W/W*^{v} mice were obtained from Jackson Laboratory (Bar Harbor, ME, United States) and bred in Guangdong Provincial Experimental Animal Center. The *W/W*^{v} and WT mice (weighing 18-25 g) were allowed free access to a standard laboratory chow diet and water and housed at a temperature of 22-24°C under a 12:12 h light/dark cycle. The study protocol was approved by the Institutional Animal Care and Ethics Committee of Guangdong Provincial Hospital of Traditional Chinese Medicine (No. 2018003). All animal procedures were conducted according to the Regulations for the Care and Use of Laboratory Animals in Guangzhou University of Chinese Medicine.

Tissue preparation

The mice were initially anesthetized with isoflurane before being killed by cervical dislocation. The whole stomach was placed in Krebs-Ringer buffer that was constantly perfused with oxygen. A cut was made along the lesser curvature of the stomach, the stomach was washed with ice-cold Krebs with the mucosa facing upward, and then the mucosa and submucosa were carefully removed.

Immunofluorescence staining of the gastric antrum

Ten *W/W*^{v} and 10 WT mice were used for immunofluorescence staining of the gastric antrum. The immunolabeling of mouse tissues was carried out on whole tissue mounts devoid of mucosa and submucosa. The whole mounts were stained with the primary antibodies for 1:100 c-kit (SC-168; Santa Cruz, CA, United States) and incubated for 1 h with 1:400 donkey anti-Rb IgG and Alexa Fluor 594. All immunostaining was imaged with a confocal microscope (Zeiss LSM 710; Göttingen, Germany) at an excitation wavelength of 594 nm. The c-kit-positive cells were observed under a 20 × objective lens. The confocal micrographs shown are digital composites of the Z-series with a depth of 6-10 μm for ICC-MP and 15-30 μm for ICC-IM. The density of ICC-MP and ICC-IM was estimated by scanning through a 6-μm thickness of tissue area, counting the number of positive cells. The area of each micrograph was 424.3 μm × 424.3 μm = 0.18 mm^{2}. The unit volume was 424.3 μm × 424.3 μm × 6 μm = 0.0011 mm^{3}. The immunofluorescence staining of the gastric antrum was performed as previously described[12].

Intracellular microelectrode recording

Eighteen *W/W*^{v} and 18 WT mice were used for intracellular microelectrode recording. Full-thickness muscle strips (8 mm × 4 mm) were cut from the gastric antrum and pinned onto the base of a silica layer and continuously perfused with oxygenated Krebs-Ringer buffer at 37°C. Before recording, the strips were incubated for 2 h. The glass microelectrodes with resistance ranging between 50 and 80 MΩ were filled with 1 mol/L KCl for penetrating cells. The electrical response was recorded and amplified using a high input impedance amplifier (AXON 210B; Molecular Devices, San Jose, CA, United States). The data were recorded on a computer using Clampfit 10.4 software.

Recording of MMC in the gastric antrum

When the 8 *W/W*^{v} and 8 WT mice were anesthetized by isoflurane inhalation, the limbs were fixed on the Baoding frame, and the abdominal hair was shaved with a razor and disinfected with iodophor. The abdominal cavity was carefully opened and the gastric antrum fully exposed. Then the micro-strain-gauge force transducers (J2A-

06-S108N-10C; Micro-Measurements, Raleigh, NC, United States) were sutured to the gastric serosa with a needle and nylon thread. The electrode leads were drawn from the back of the neck through the subcutaneous layer before closing the abdomen. After monitoring the animal's wakefulness for more than 15 min, the micro-strain-gauge force transducers were connected to the Porti physiological recorder (TMSI, Netherlands) to measure the gastric contractile motion. The first 30 min were recorded for baseline control and the next 30 min for treatment. The gastric contractile frequency and amplitude index (sum of amplitudes within 20 min) were analyzed.

Solutions and drugs

XBF was produced by Hunan Academy of Chinese Medicine and contains *Areca catechu L.* (*Binlang*), *Ginseng* (*Renshen*), *Fructus amomi* (*Sharen*), *Radix linderae* (*Wuyao*) and *Prunus persica Batsch* (*Taoren*). Atropine (Lot A0132), tetrodotoxin (TTX, Lot T8024) and other chemicals were all acquired from Sigma (Sigma-Aldrich, St. Louis, MO, United States) unless indicated otherwise. The XBF, atropine, and TTX were dissolved in dH_2O and further diluted in Krebs-Ringer buffer to the final concentration. Krebs buffer consisted of 121.9 mmol/L NaCl, 15.5 mmol/L $NaHCO_3$, 5.9 mmol/L KCl, 1.2 mmol/L $MgSO_4$, 1.2 mmol/L KH_2PO_4, 11.5 mmol/L glucose, and 2.5 mmol/L $CaCl_2$. The pH of the Krebs buffer was 7.3-7.4 when bubbled with 95% O_2-5% CO_2 at 37 ± 0.5 °C.

Statistical analysis

The data are shown as mean ± SD. Welch's *t*-test was used to compare the difference between WT and *W/W*^{v} mice. The paired *t*-test was used to analyze the data before and after administration. The number of MMC was compared by Fisher's exact test. A P value < 0.05 was considered significant. Data statistics were calculated with GraphPad Prism 5 (GraphPad Software, La Jolla, CA, United States).

RESULTS

Immunogenicity of c-kit-positive cells in the gastric antrum of WT and W/W^v mice

Immunofluorescence showed that there were many c-kit-positive ICC in the myenteric plexus of the gastric antrum in WT mice. The c-kit-positive cells were connected to form a rich and dense ICC-MP network (Figure 1Aa). In *W/W*^{v} mice, the c-kit immunogenicity of ICC-MP decreased (Figure 1Ab). Compared with WT mice, the density of ICC-MP in the gastric antrum of *W/W*^{v} mice was significantly decreased (Figure 1B; P < 0.001). A large number of bipolar ICC were found in the longitudinal and circular muscles of the gastric antrum in WT mice (Figure 1Ac). Although sparse c-kit immunoreactivity was visible occasionally, no ICC-IM network was found in the antrum of *W/W*^{v} mice (Figure 1Ad). There was a significant difference in ICC-IM density between WT and *W/W*^{v} mice (Figure 1C; P < 0.001).

Characteristics of the gastric antrum slow waves in WT and W/W^v mice

The spontaneous periodic depolarization slow wave of the gastric antrum was observed in WT mice (Figure 2A). In WT mice, the resting membrane potential (RMP) was –(56.49 ± 3.58) mV, the amplitude was 22.62 ± 2.23 mV, and the frequency was 6.16 ± 1.12 cpm. Spontaneous periodic depolarization slow waves with low amplitude were also observed in the antrum of *W/W*^{v} mice (Figure 2B). In *W/W*^{v} mice, the RMP was –(52.95 ± 2.34) mV, the amplitude was 2.92 ± 0.52 mV, and the frequency was 7.48 ± 0.66 cpm. The difference determined was statistically significant between WT and *W/W*^{v} mice (Figure 2C-E; ^aP < 0.05, ^cP < 0.0001).

Effect of XBF on the gastric antrum slow wave in WT and W/W^v mice

With perfused XBF at the concentration of 10^{-2} g/L, the slow waves of the gastric antrum began to depolarize in WT and *W/W*^{v} mice (Figure 3A and B). After treatment with concentrations of 10^{-2} g/L, 5 × 10^{-2} g/L, and 10^{-1} g/L XBF, RMP decreased from −(56.49 ± 0.53) mV to −(52.31 ± 0.82) mV, −(51.08 ± 0.61) mV, and −(49.87 ± 1.58) mV, respectively. The frequency changed from 5.99 ± 0.18 cpm to 5.95 ± 0.44 cpm, 6.47 ± 0.37 cpm, and 6.79 ± 0.14 cpm, respectively, and the amplitude decreased from 21.78 ± 0.65 mV to 20.85 ± 0.90 mV, 19.56 ± 1.60 mV, and 18.15 ± 0.65 mV, respectively in WT mice. The differences in RMP and amplitude were significantly different at all XBF concentrations between the control and treatment groups (P < 0.05 or 0.01), and the frequency increased significantly except at the concentration of 10^{-2} g/L (Figure 3C-E).

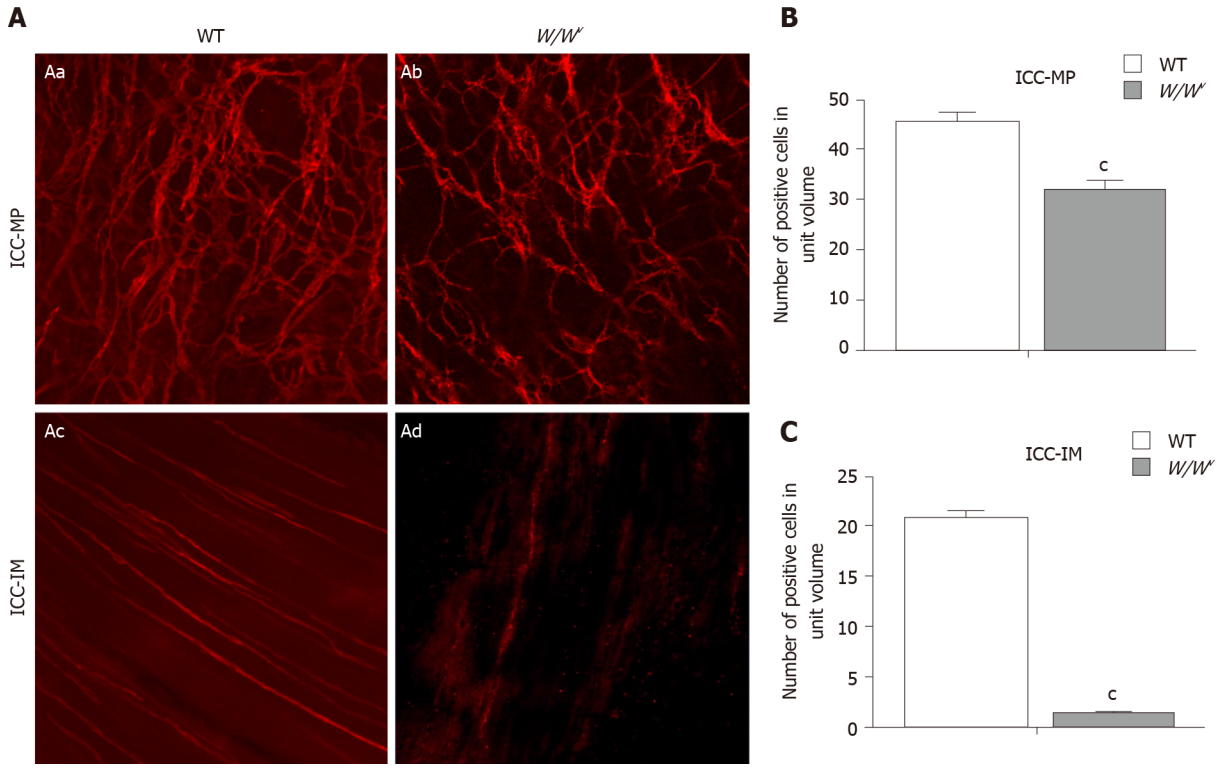


Figure 1 Immunogenicity of c-kit positive cells in the gastric antrum of wild-type and *W/W*^{v} mice. The c-kit positive cells were observed under a confocal microscope. The unit volume was 424.3 μm × 424.3 μm × 6 μm ≈ 0.0011 mm^3. A: Immunostaining images showing the networks of interstitial cells of Cajal myenteric plexus (ICC-MP) and intramuscular interstitial cells of Cajal (ICC-IM), respectively: The abundant c-kit positive ICC-MP network of gastric antrum in wild-type (WT) mice (Aa); the sparse c-kit positive ICC-MP network of the gastric antrum in *W/Wv* mice (Ab); c-kit positive ICC-IM network of the gastric antrum in WT mice (Ac); no ICC-IM network distribution in the antrum of *W/Wv* mice (Ad); B and C: The number of c-kit positive cells in ICC-MP and ICC-IM was compared in the gastric antrum of WT and *W/W*^{v} mice under unit volume (424.3 μm × 424.3 μm) (n = 10, ^{c}P < 0.001). ICC-MP: Interstitial cells of Cajal myenteric plexus; ICC-IM: Intramuscular interstitial cells of Cajal; WT: Wild-type.

In *W/W*^{v} mice, the RMP decreased from −(53.13 ± 0.53) mV to −(49.47 ± 0.79) mV, −(48.41 ± 1.24) mV, and −(46.98 ± 1.40) mV, respectively. The frequency changed from 7.55 ± 0.12 cpm to 8.02 ± 0.19 cpm, 8.25 ± 0.18 cpm, and 7.65 ± 0.15 cpm, respectively, and the amplitude decreased from 2.84 ± 0.08 mV to 2.71 ± 0.11 mV, 2.87 ± 0.10 mV, and 2.66 ± 0.21 mV, respectively, at concentrations of 10^{-2} g/L, 5 × 10^{-2} g/L, and 10^{-1} g/L. Compared to the WT controls, the differences in RMP were statistically significant at all concentrations (P < 0.01). At concentrations of 10^{-2} g/L and 5 × 10^{-2} g/L, the slow-wave frequency increased significantly (P < 0.05). However, the amplitude was not significantly altered at any XBF concentration in *W/W*^{v} mice.

Effects of atropine and TTX on gastric antral slow waves induced by XBF

The results of intracellular recording showed that atropine could completely abolish the effect of XBF on gastric antrum slow waves in WT and *W/W*^{v} mice (Figure 4A and B). After pretreatment with 0.5 mmol/L atropine, perfusion of XBF at a concentration of 10^{-1} g/L did not alter the RMP, frequency, or amplitude of the gastric antrum slow waves in WT and *W/W*^{v} mice (Figure 4C-E). In the presence of TTX 10^{-7} M, perfusion of XBF at a concentration of 10^{-1} g/L was able to decrease the RMP of gastric antrum slow waves in WT and *W/W*^{v} mice (Figure 4F and G). TTX did not block the enhancement of gastric antrum slow waves in WT and *W/W*^{v} mice (Figure 4H-J).

Characteristics of gastric antrum motility in WT and W/W^{v} *mice*

The MMCs in the gastric antrum were recorded by a micro-strain-gauge force transducer for 30 min. As shown in Figure 5, it was very difficult to distinguish between MMC phase I and phase II in WT. With the increase of irregular contraction frequency, regular contractions with the frequency 3.53 ± 0.18 cpm and amplitude index 23014.26 ± 1798.65 mV·20 min occurred in the antrum of WT mice. In the 30 min recording, there were only sporadic contractions in the gastric antrum of *W/W*^{v}. Occasionally, there was a strong paroxysmal contraction with a frequency of 1.28 ± 0.12 cpm and an amplitude index of 3782.16 ± 407.13 mV·20 min. The differences in the frequency and amplitude index were all statistically significant (P < 0.0001). We

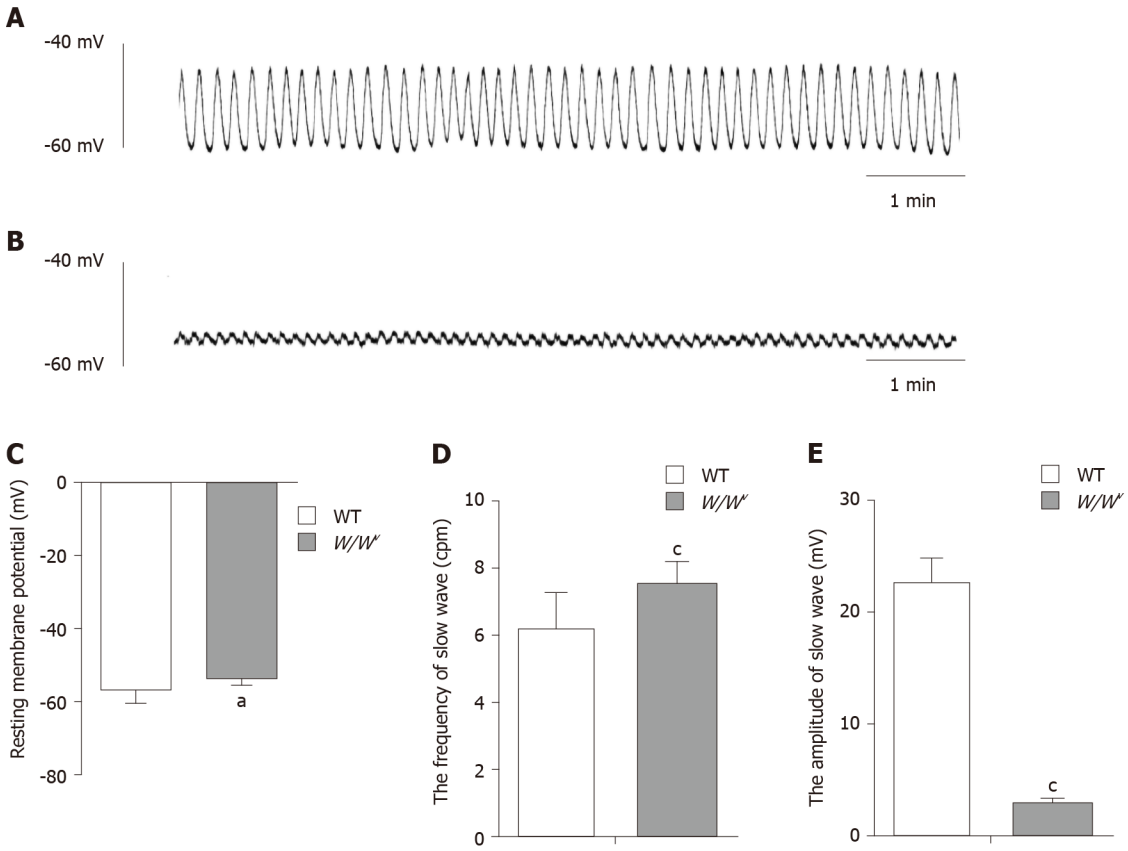
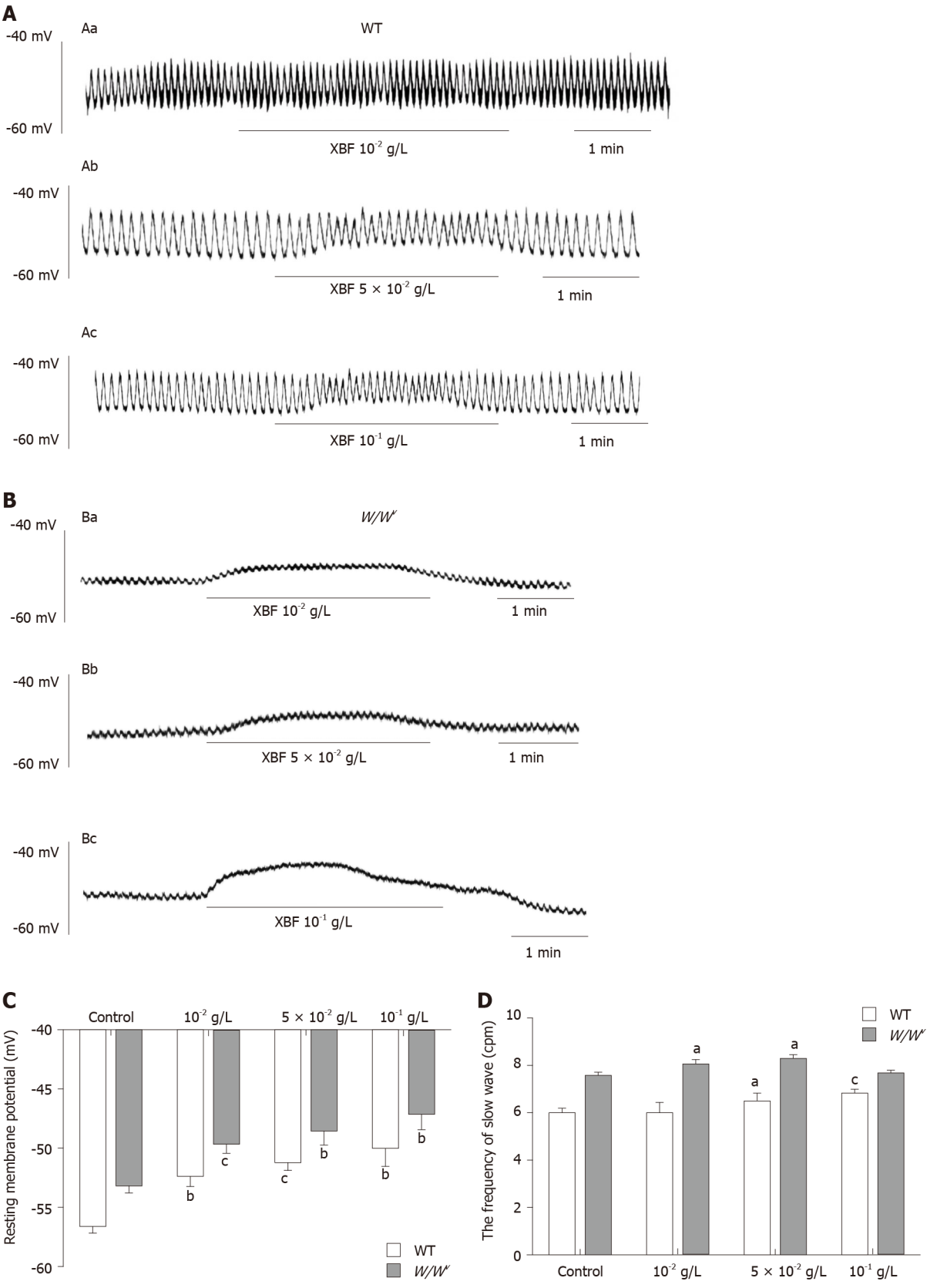


Figure 2 Characteristics of the gastric antrum slow waves in wild-type and *W/W*^{v} mice. A: Spontaneous rhythmic slow waves in the antrum of wild-type (WT) mice; B: Spontaneous rhythmic slow waves with the lower amplitude in the antrum of *W/Wv* mice; C-E: Comparison of resting membrane potential, frequency and amplitude of the gastric antrum slow waves between WT and *W/W*^{v} mice (n = 18, Welch's t-test, $^{a}P < 0.05$, $^{c}P < 0.0001$). WT: Wild-type.

observed that 7 out of 8 WT mice developed a total of 13 MMC III phase contractions, while in the 8 *W/W*^{v} mice, only 2 developed 3 MMC phase III-like contractions of shorter duration, lower amplitude, and lower frequency. There was a significant difference in the number of MMCs between both groups (Fisher's exact test, P = 0.0406). For the gastric antrum of WT mice, the duration of the MMC phase III was 151.08 ± 8.87 s, the amplitude was 315.45 ± 5.55 mV, and the interval between MMCs was 10.75 ± 0.61 min. In the gastric antrum of *W/W*^{v} mice, the duration of the MMC phase III-like contractions was 123.67 ± 2.96 s, the amplitude was 194.12 ± 4.76 mV, and during the 30 min observation, no phase III-like contractions were found twice in the same *W/W*^{v} mice. Compared to WT mice, the duration and amplitude of the MMC III phase in the gastric antrum was significantly reduced in *W/W*^{v} mice (P = 0.0117 and 0.0020, respectively), suggesting there was no typical MMC cycle in the gastric antrum of *W/W*^{v} mice.

Effect of XBF on gastric antrum motility in WT and W/W^{v} *mice*

After the administration of XBF (5 mg), strong contractions in the antrum of WT mice were observed instantaneously (Figure 6). The periodic MMC movement turned into a high frequency and high amplitude MMC III phase contraction. However, XBF did not significantly enhance the contraction of the gastric antrum in *W/W*^{v} mice (Figure 6). After treatment in turn with 0.6 mg, 1.25 mg, and 5 mg of XBF, the frequency index of the gastric antrum in WT mice was 3.16 ± 0.39 cpm, 3.30 ± 0.26 cpm, and 5.58 ± 0.62 cpm and the amplitude index was 13415.25 ± 1694.38 mV·20 min, 24537.89 ± 2406.33 mV·20 min, and 51807.48 ± 9255.04 mV·20 min, respectively, while the frequency index of the gastric antrum in *W/W*^{v} mice was 1.85 ± 0.48 cpm, 1.93 ± 0.37 cpm, and 1.99 ± 0.37 cpm and the amplitude index was 6488.43 ± 1490.04 mV·20 min, 7733.07 ± 1469.27 mV·20 min, and 6901.26 ± 807.34 mV·20 min, respectively. These results demonstrated that with high-dose XBF treatment, there was a significant difference in the frequency and amplitude indices of the gastric antrum between WT and *W/W*^{v} mice (all $P < 0.05$ or 0.01).


A
Aa
WT
-40 mV
-60 mV
XBF 10-2 g/L
1 min
Ab
XBF 5 × 10-2 g/L
Ac
XBF 10-1 g/L
B
Ba
W/W^v
Bb
Bc
C
Control
10-2 g/L
5 × 10-2 g/L
10-1 g/L
Resting membrane potential (mV)
WT
W/W^v
D
The frequency of slow wave (cpm)

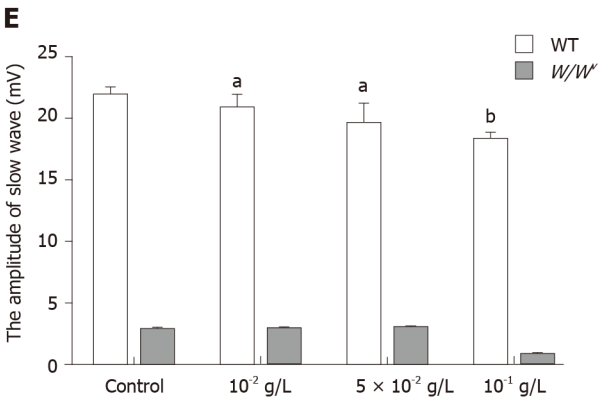


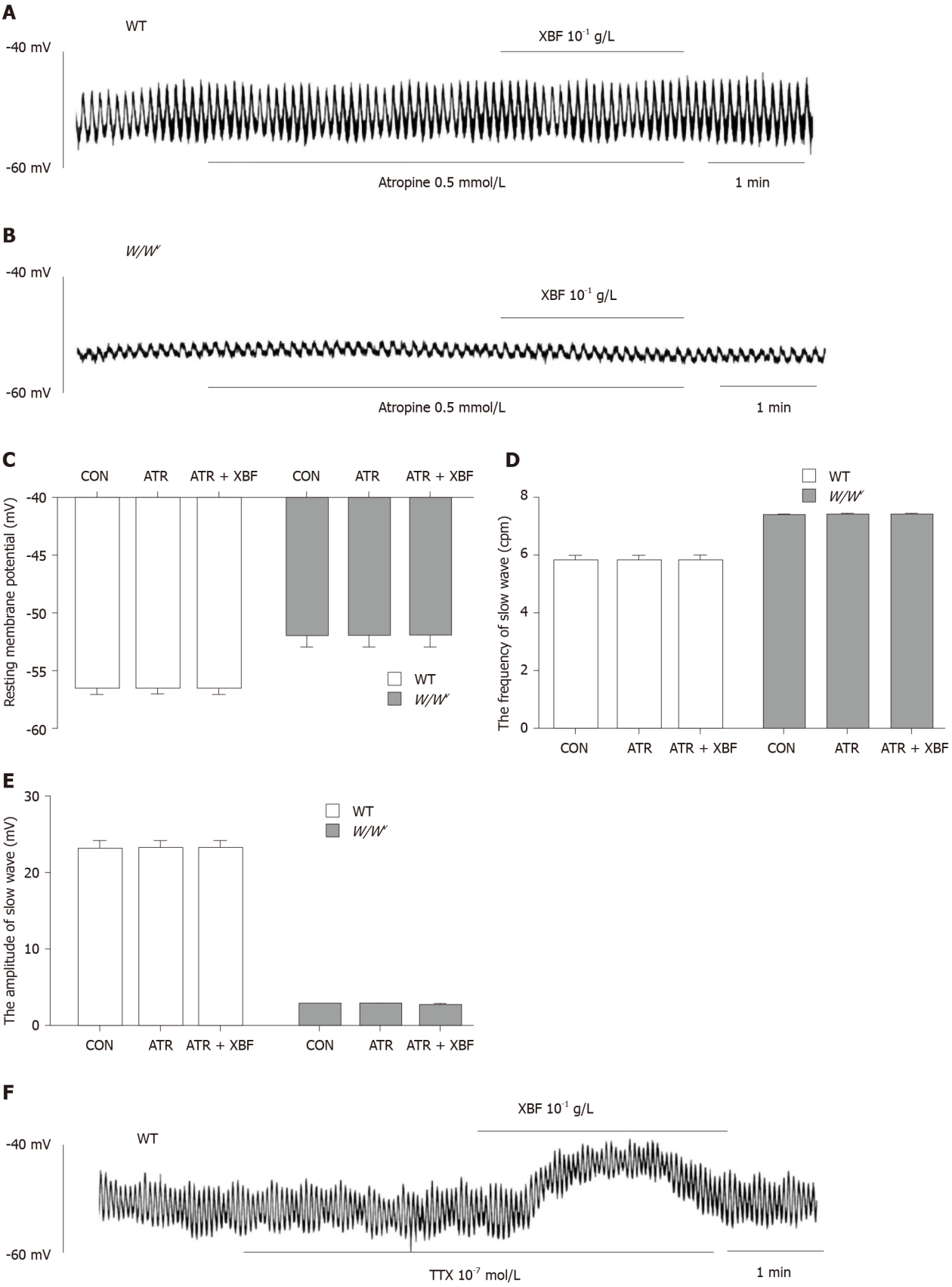
Figure 3 Effect of Xiangbinfang granule on gastric antrum slow wave in wild-type and *W/W*^{v} mice. A: Representative trace of the effect of different concentrations of Champaign formula on gastric antrum slow waves in wild-type (WT) mice. After infusion of Xiangbinfang granule (XBF) at the concentration of 10^{-2} g/L (Aa), 5 × 10^{-2} g/L (Ab) and 10^{-1} g/L (Ac), the slow waves resting membrane potential (RMP) decreased, frequency increased and amplitude decreased; B: Representative trace of the effect of different concentrations of Champaign formula on gastric antrum slow waves in *W/W*^{v} mice. Infused XBF at the concentrations of 10^{-2} g/L (Ba), 5 × 10^{-2} g/L (Bb) and 10^{-1} g/L (Bc) decreased the RMP in *W/W*^{v} gastric antrum slow waves; C-E: Histogram of XBF for gastric slow wave RMP (C), frequency (D) and amplitude (E) in WT and *W/W*^{v} mice. (Control, n = 18; treatment, n = 6. Paired t-test was used to compare the difference before and after administration, $^{a}P < 0.05$, $^{b}P < 0.001$, $^{c}P < 0.0001$). WT: Wild type; XBF: Xiangbinfang granule.

Effects of atropine and TTX on the gastric antrum motility induced by XBF

To clarify the mechanism of XBF in promoting antral motility, atropine and TTX were injected intraperitoneally, and then XBF was administered by gavage. The results indicated that contractions were inhibited in the antrum of WT and *W/W*^{v} mice after intraperitoneal injection of 0.1 mg/kg of atropine, and subsequent treatment with 5 mg of XBF did not increase the contractile activity of the gastric antrum (Figure 7A and C). These results suggest that atropine could completely eliminate the motility-promoting effect of XBF in both WT and *W/W*^{v} mice (Figure 7E). The frequency and amplitude of gastric antral contractions were abolished by 0.05 mg/kg of TTX. Subsequent treatment with 5 mg of XBF induced a contraction enhancement in WT and *W/W*^{v} mice (Figure 7B and D). In comparison with XBF without TTX, TTX pretreatment could partially reduce the gastric antrum motility-promoting effect mediated by XBF (Figure 7F).

DISCUSSION

C-kit is a necessary condition for the development of a GI pacemaker system[13]. Previous studies have shown that the W-mutation causes loss of the ICC network in the GI tract of *W/W*^{v} mice, such as the disappearance of ICC-MP and decreased ICC-MP in the jejunum and ileum[4]. In the *W/W*^{v} colon, the density of c-kit positive ICC-MP was reduced by 50%-60% compared to that of WT mice[12]. While a normal ICC-MP network was observed, the ICC-IM disappeared completely in the gastric antrum of *W/W*^{v} mice[14]. We scanned whole muscle specimens to obtain a more accurate number of ICC and compared them to WT mice; about 60% of ICC-MP was retained in the antrum of *W/W*^{v} mice, and no ICC-IM network was observed. GI slow waves are mainly produced by ICC-MP[2], and ICC-IM is responsible for the regenerative component of the slow wave[15]. Our immunofluorescent staining showed that the ICC-MP network density decreased but did not disappear, and the slow-wave activity in *W/W*^{v} mice was preserved. However, due to the lack of an ICC-IM network in the antrum of *W/W*^{v} mice, there is no regenerative component in the *W/W*^{v} antrum slow wave. Therefore, *W/W*^{v} mice showed a low-amplitude slow wave and disturbed movement in the antrum. ICC-IM were also innervated and provided mechanisms for neural signal transduction to the gastric musculature[16]. ICC-IM were densely innervated by excitatory and inhibitory enteric motor neurons and in close contact with nerve terminals. ICC-IM played a role in both nitrergic inhibitor and cholinergic excitatory motor neurotransmission in the gastric antrum[17,18]. Excitatory junctional potential and inhibitory junctional potential after intrinsic nerve stimulation were greatly attenuated in the antrum of *W/W*^{v} mice, and the reduced density of ICC-IM leads to reduced neural regulation in the *W/W*^{v} antrum[19]. Hirst *et al*[19] have shown that excitatory vagal stimulation response resembles the regenerative response which


A
WT
XBF 10-1 g/L
-40 mV
-60 mV
Atropine 0.5 mmol/L
1 min
B
W/W^v
-40 mV
XBF 10-1 g/L
-60 mV
Atropine 0.5 mmol/L
1 min
C
CON
ATR
ATR + XBF
CON
ATR
ATR + XBF
Resting membrane potential (mV)
-40
-45
-50
-55
-60
WT
W/W^v
D
WT
W/W^v
The frequency of slow wave (cpm)
8
6
4
2
0
CON
ATR
ATR + XBF
CON
ATR
ATR + XBF
E
The amplitude of slow wave (mV)
30
20
10
0
WT
W/W^v
CON
ATR
ATR + XBF
CON
ATR
ATR + XBF
F
XBF 10-1 g/L
WT
-40 mV
-60 mV
TTX 10-7 mol/L
1 min

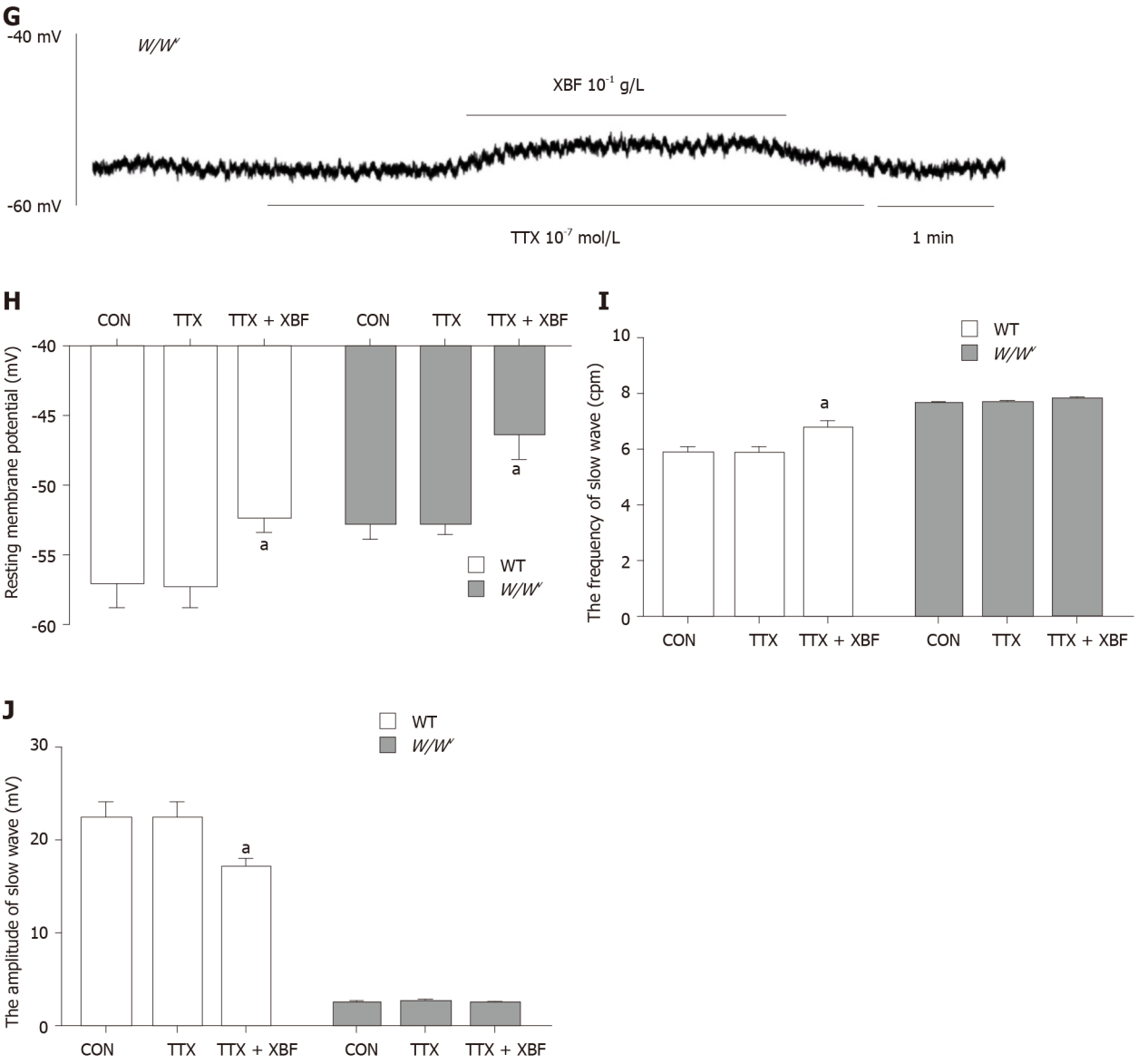


Figure 4 Effects of atropine and tetrodotoxin on the enhancement of gastric antrum slow wave by Xiangbinfang granule. A and B: Representative trace of the effect of Xiangbinfang granule (XBF) 10^{-1} g/L on slow waves of the gastric antrum pretreated with atropine 5 mmol/L in wild-type (WT) (A) and *W/W*^{v} mice (B); C-G: Histogram of atropine blocking the effect of XBF on the enhancement of resting membrane potential (C), frequency (D) and amplitude (E) of antral slow waves. Representative trace of the effect of 10^{-1} g/L of XBF on slow waves of the gastric antrum pretreated with 10^{-7} M of tetrodotoxin (TTX) in WT (F) and *W/W*^{v} (G) mice; H-J: Histogram of TTX blocking the effect of XBF on the enhancement of the resting membrane potential (H), frequency (I) and amplitude (J) of antral slow waves. (Compared with pretreatment, $n = 3$, $^{a}P < 0.05$). WT: Wild-type; XBF: Xiangbinfang granule; TTX: Tetrodotoxin; CON: Basic control; ATR: Atropine.

was initiated in this tissue by ICC-IM. Regenerative responses were the dominant responses produced by neural stimulation. This suggested that ICC-IM is regulated by vagus nerve.

The MMC has been found to be a complex system that may be regulated by motilin[20], the enteric nervous system, and the vagus nerve. Mondal *et al*[21] found that treatment with motilin induced phase III contractions *in vivo* and *in vitro*, while motilin antagonists can abolish the occurrence of spontaneous gastric phase III contractions. Their other experiment showed that motilin-induced gastric contractions were mediated through the myenteric plexus in a vagus-independent manner[22]. ICC-IM may play an important role in this process.

The MMC have a temporally coordinated cyclic motor pattern during the interdigestive state of the stomach and small intestine in many animals. In the human and dog gastrointestinal tracts, the occurrence of MMC is regulated at 90-120-min intervals[23,24]. Because of motilin and motilin receptor pseudogenes[25], mice and rats have shown different MMC patterns. Strain-gauge force transducer implantation is a crucial technique for recording GI MMC movement in conscious animals[23,24,26,27]. Takayama *et al*[26] examined the gastrointestinal motility of W-mutant rats by an

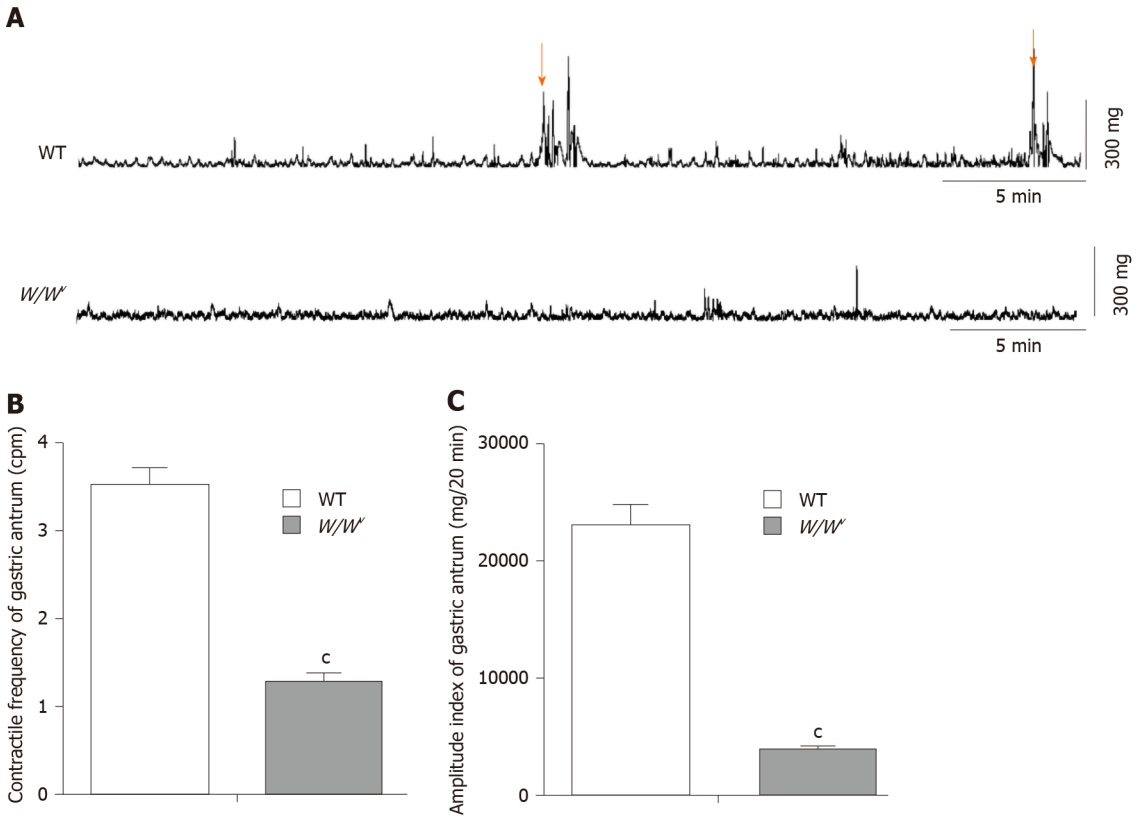


Figure 5 Characteristics of gastric antrum motility in conscious wild-type and *W/Wv* mice. Micro strain-gauge force transducers were implanted into the gastric antrum to observe the migrating motor complex (MMC). A: Representative trace of the gastric antrum contractions in conscious wild-type (WT) and *W/Wv* mice. The black arrow shows the MMC III phase contraction; B and C: The histograms of the comparison of the contractile frequency (B) and amplitude index (C) of the gastric antrum in WT and *W/Wv* mice. (n = 8, Welch's t-test, $^cP < 0.0001$). WT: Wild-type.

extraluminal strain-gauge force transducer method. They found the duration of MMC was 2.5 ± 2.3 min and the interval of MMC was 5.4 ± 2.9 min. Similar results were observed by Taniguchi *et al*[27] in their study, spontaneous phase III contractions were observed every 13-16 min. It was difficult to record the gastrointestinal motor pattern of the mice *in situ*. Spencer *et al*[5] tried to record MMC in the isolated small intestine of mice. They found the interval between MMCs in the mouse small intestine was 5 ± 1 min, and the durations of MMC contractions were about 30 s. The MMC was regulated by motilin, the enteric nervous system, and the vagus nerve. Motilin-induced contractions are much less potent than those of MMC *in vivo*[28]. The complex regulatory system of MMC was not complete *in vitro*. Therefore, we miniaturized the strain-gauge force transducer to facilitate MMC recording in the gastric antrum of conscious mice. In this study, we found that the duration of the MMC phase III was 151.08 ± 8.87 s, the amplitude was 315.45 ± 5.55 mV, and the interval between MMCs was 10.75 ± 0.61 min in WT mice. There was no complete MMC cycle in the gastric antrum of *W/W*^{v} mice. The gastric antrum of *W/W*^{v} mice lacked ICC-IM and the corresponding motor nerve conduction was inhibited[29]. The typical MMC disappeared in *W/W*^{v} mice, suggesting that ICC-IM is an important factor in regulating the MMC activity.

In this study, we found that XBF enhanced the contractions of the gastric antrum in WT mice through slow-wave depolarization of SMCs. The effect of XBF on enhancing the antral motility was greatly reduced in *W/W*^{v} mice. ICC specifically express calcium-activated chloride channels (CACC), which are regulated by anoctamine 1 (Ano1). Exogenous nerve stimulation or GI hormones could act on ICC to produce slow waves by CACC[30]. SMCs respond to slow waves to generate action potentials by activating voltage-dependent L-type calcium channels[31]. Under physiological conditions, cell-membrane potential depolarization increased the probability of the L-type calcium channels opening, allowing calcium influx to induce SMCs to generate action potentials and contractions[32-34]. In Ano1-knockout mice, the excitability of smooth muscle contraction induced by carbachol was decreased. This is caused by cholinergic nerve stimulation that first activates muscarinic receptors on ICC-IM and then stimulates the CACC channel, thereby causing the SMCs to depolarize and

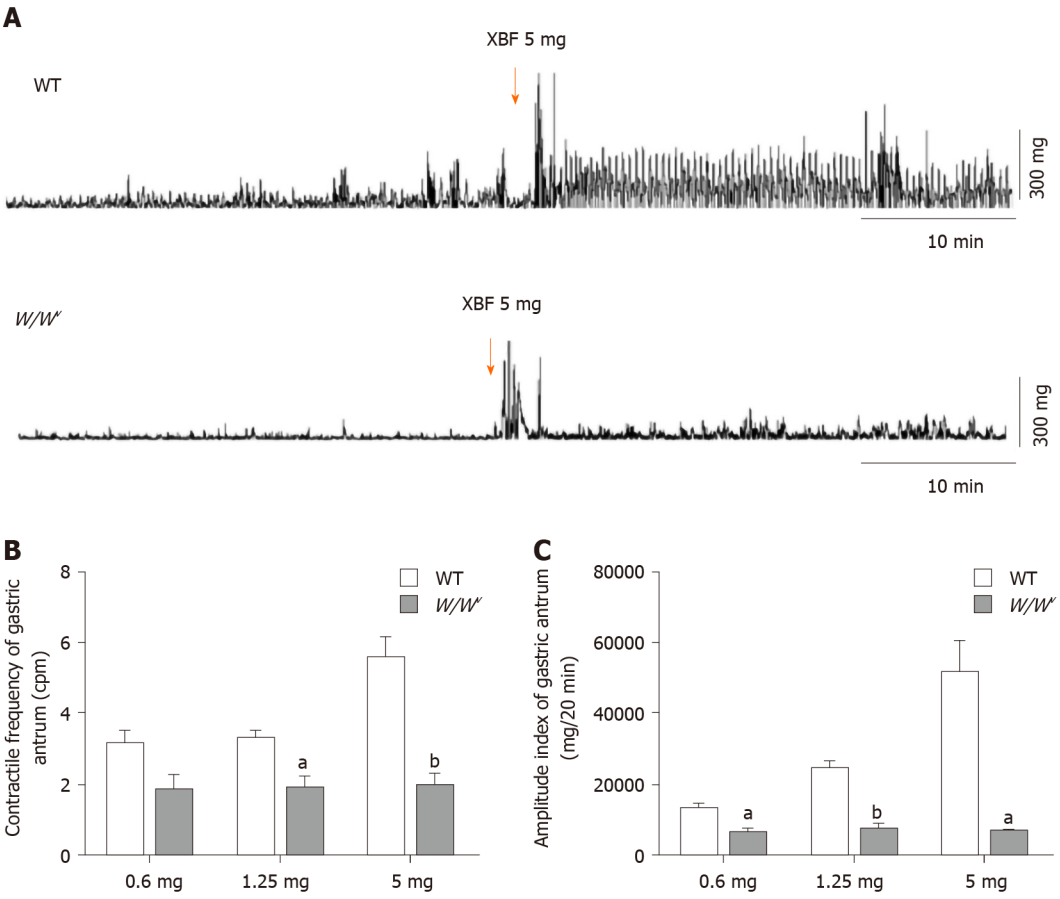


Figure 6 Effect of Xiangbinfang granule on gastric antrum motility in wild-type and *W/W*^{v} mice. A: Representative trace of the enhancement of the gastric antrum motility in wild-type (WT) and *W/W*^{v} by Xiangbinfang granule (XBF); B: Comparison of the antral contractile frequency of WT and *W/W*^{v} mice after intragastric administration of 0.6 mg, 1.25 mg and 5 mg XBF; C: Comparison of antral contractile amplitude index of WT and *W/W*^{v} mice after intragastric administration of 0.6 mg, 1.25 mg and 5 mg XBF (n = 8, Welch's t-test, $^{a}P < 0.05$, $^{b}P < 0.01$). WT: Wild-type; XBF: Xiangbinfang granule.

generate action potentials through gap junctions[35]. Thus, the response of the distal stomach to cholinergic stimulation was weakened and blocked the neural activation of regenerative potentials in *W/W*^{v} mice deficient in ICC-IM, and the low level of potential depolarization during the slow-wave plateau period reduced the probability of L-type calcium channels opening. Therefore, XBF depolarized the SMCs slow waves (Figure 3) but did not significantly enhance the mechanical contraction (Figure 6) of the gastric antrum in *W/W*^{v} mice. Our study showed that atropine completely blocked the gastric antral motility induced by XBF, but TTX just partially reduced the effect of XBF in both WT and *W/W*^{v} mice (Figure 7). This suggested that XBF enhances the smooth muscle contraction of the gastric antrum through the cholinergic pathway of ICC-IM and the enteric nervous system.

The Chinese medicine XBF, composed of *Areca catechu L.*, *Ginseng*, *Fructus amomi*, *Radix linderae*, and *Prunus persica Batsch*, promotes entire GI motility in the treatment of postoperative ileus[8-11]. Previous studies have shown that *Areca catechu L.* enhances gastric motility in healthy people[36]. Arecoline, the main active component of *Areca*, with an XBF content of 0.112 mg/g[37], promoted GI motility through the M3 receptor[38,39]. Ginsenoside RF, an extract of *Ginseng*, induced membrane depolarization of ICC[40] and *Fructus amomi* promoted the contraction of the antrum and duodenum in beagle dogs[41]. The promotion of GI motility by XBF is the result of the interaction of these Chinese herbs, and the most important active components still need to be further characterized.

CONCLUSION

Our study shows that ICC-IM play a crucial role in regulating gastric antral MMC activity. They may be an important bridge between the vagus nerve, the enteric nervous system, and motilin in regulating smooth muscle contraction. Through the

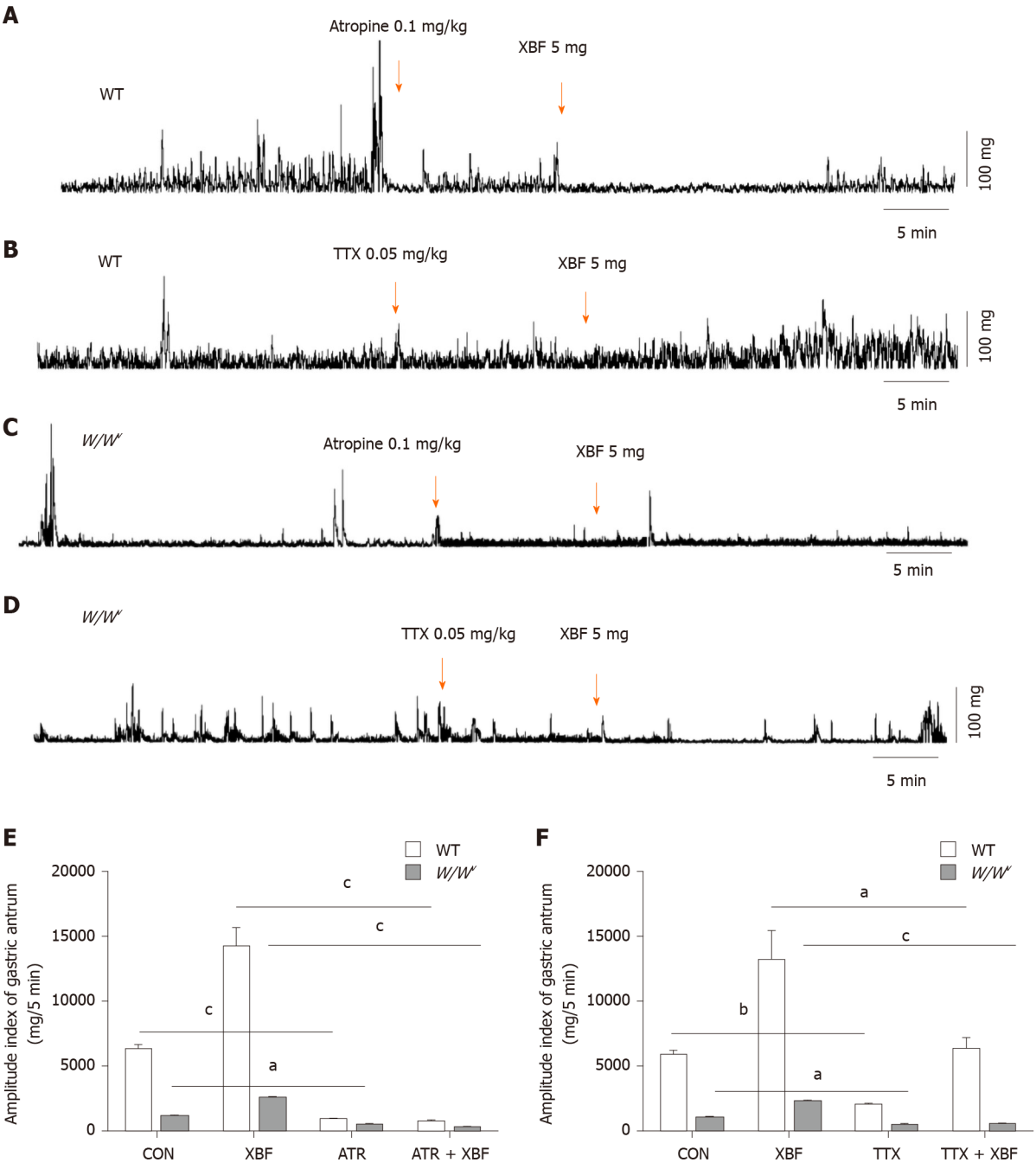


Figure 7 Atropine and tetrodotoxin block the enhancement of antrum motility induced by Xiangbinfang granule. A-D: Intraperitoneal injection of 0.1 mg/kg atropine (ATR) completely blocked the enhancement effect of Xiangbinfang granule (XBF, 5 mg) on gastric antrum in wild-type (WT) (A) and *W/W*^{v} (C) mice. Tetrodotoxin (TTX) partially reduced the gastric antrum motility enhancement mediated by XBF in WT (B) and *W/W*^{v} (D) mice; E-F: Comparison of the effect of XBF 5 mg of antral contractile amplitude index in WT and *W/W*^{v} mice after pretreatment with ATR 0.1 mg/kg (E) and TTX 0.05 mg/kg (F). (n = 4, Welch's t-test, ^{a}P < 0.05, ^{b}P < 0.01, ^{c}P < 0.001). WT: Wild-type; XBF: Xiangbinfang granule; TTX: Tetrodotoxin; CON: Basic control; ATR: Atropine.

muscarinic receptor pathway on ICC-IM, XBF depolarizes SMCs and initiates an action potential, changing the periodic motion of MMC into a phase III-like contraction pattern in the gastric antrum of mice.

ARTICLE HIGHLIGHTS

Research background

The Chinese medicine Xiangbinfang granule (XBF) is an effective prescribed treatment for promoting the recovery of gastrointestinal (GI) function post-surgery. In previous studies, we found that XBF mediated the phase III contraction of migrating motor

complexes (MMC). However, the mechanism of XBF in enhancing MMC activity in the GI tract is still unclear.

Research motivation

In this study, we observed the MMC activity of gastric antrum in *W/W*^{v} mice that lack intramuscular interstitial cells of Cajal (ICC-IM) and analyzed the effect of the traditional Chinese medicine XBF in promoting gastric antrum movement. From this study, we will further understand the role of ICC-IM in MMC activities. Meanwhile, the mechanism of XBF promoting gastrointestinal motility through ICC-IM was discussed, so as to provide the basis for the development and application of XBF.

Research objectives

W/W^{v} mice were used to observe the effects of ICC-IM on gastric antrum motility and to establish the mechanism of XBF in promoting gastric antrum motility. We further investigated the correlation between ICC-IM and MMC in mouse gastric antrum.

Research methods

The density of c-kit positive ICC myenteric plexus and ICC-IM in the antral muscularis of *W/W*^{v} and wild-type (WT) mice was examined by confocal microscopy. The effects of XBF on the gastric antrum slow waves in *W/W*^{v} and WT mice were recorded by intracellular amplification recording. The micro-strain-gauge force transducers were implanted into the gastric antrum to monitor the MMC and the effect of XBF on gastric antrum motility in conscious *W/W*^{v} and WT mice.

Research results

In the gastric antrum of *W/W*^{v} mice, no ICC-IM network was observed. Spontaneous rhythmic slow waves with the low amplitude also appeared in the antrum of *W/W*^{v} mice. In this study, we found that the duration of MMC phase III was 151.08 ± 8.87 s, the amplitude was 315.45 ± 5.55 mg, and the interval between MMCs was 10.75 ± 0.61 min in the gastric antrum of WT mice. There was no complete MMC cycle in *W/W*^{v} gastric antrum lacking ICC-IM. The gastric antrum motility in WT and *W/W*^{v} antrum was significantly increased after treatment with XBF. Atropine blocked the enhancement of XBF completely, while tetrodotoxin partially inhibited the enhancement of XBF.

Research conclusions

In this study, we first examined the gastrointestinal motility of W-mutant mice by an extraluminal strain-gauge force transducer method. It showed that ICC-IM plays an important role in the regulation of gastric antrum MMC.

Research perspectives

In this study, MMC were recorded only at a single site in the gastric antrum. It was impossible to describe the propulsion of gastrointestinal movement. Therefore, recording at multiple gastrointestinal sites is important to further clarify the motility of gastrointestinal MMC in mice.

REFERENCES

1 **Singaram K**, Gold-Smith FD, Petrov MS. Motilin: a panoply of communications between the gut, brain, and pancreas. *Expert Rev Gastroenterol Hepatol* 2020; **14**: 103-111 [PMID: 31996050 DOI: 10.1080/17474124.2020.1718492]

2 **Parsons SP**, Huizinga JD. Slow wave contraction frequency plateaux in the small intestine are composed of discrete waves of interval increase associated with dislocations. *Exp Physiol* 2018; **103**: 1087-1100 [PMID: 29860720 DOI: 10.1113/EP086871]

3 **Yadak R**, Breur M, Bugiani M. Gastrointestinal Dysmotility in MNGIE: from thymidine phosphorylase enzyme deficiency to altered interstitial cells of Cajal. *Orphanet J Rare Dis* 2019; **14**: 33 [PMID: 30736844 DOI: 10.1186/s13023-019-1016-6]

4 **Der-Silaphet T**, Malysz J, Hagel S, Larry Arsenault A, Huizinga JD. Interstitial cells of cajal direct normal propulsive contractile activity in the mouse small intestine. *Gastroenterology* 1998; **114**: 724-736 [PMID: 9516393 DOI: 10.1016/s0016-5085(98)70586-4]

5 **Spencer NJ**, Sanders KM, Smith TK. Migrating motor complexes do not require electrical slow waves in the mouse small intestine. *J Physiol* 2003; **553**: 881-893 [PMID: 14514874 DOI: 10.1113/jphysiol.2003.049700]

6 **Hayashi Y**, Toyomasu Y, Saravanaperumal SA, Bardsley MR, Smestad JA, Lorincz A, Eisenman ST,

Cipriani G, Nelson Holte MH, Al Khazal FJ, Syed SA, Gajdos GB, Choi KM, Stoltz GJ, Miller KE, Kendrick ML, Rubin BP, Gibbons SJ, Bharucha AE, Linden DR, Maher LJ 3rd, Farrugia G, Ordog T. Hyperglycemia Increases Interstitial Cells of Cajal *via* MAPK1 and MAPK3 Signaling to ETV1 and KIT, Leading to Rapid Gastric Emptying. *Gastroenterology* 2017; **153**: 521-535. e20 [PMID: 28438610 DOI: 10.1053/j.gastro.2017.04.020]

7 **Park KS**, Cho KB, Hwang IS, Park JH, Jang BI, Kim KO, Jeon SW, Kim ES, Park CS, Kwon JG. Characterization of smooth muscle, enteric nerve, interstitial cells of Cajal, and fibroblast-like cells in the gastric musculature of patients with diabetes mellitus. *World J Gastroenterol* 2016; **22**: 10131-10139 [PMID: 28028361 DOI: 10.3748/wjg.v22.i46.10131]

8 **Gan H**, Lin J, Jiang Z, Chen Q, Cao L, Chen Z. Xiangbin prescription for the recovery of gastrointestinal function after abdominal surgery (the XBPRS trial): study protocol for a randomized controlled trial. *Trials* 2018; **19**: 146 [PMID: 29486765 DOI: 10.1186/s13063-018-2484-z]

9 **Wen SL**, Feng X, Chen ZQ, Xiao J, Zhang WX. Effect of XiangBin granules on post-operative gastrointestinal function and brain-gut peptides after transabdominal gynecological surgery. *Eur J Obstet Gynecol Reprod Biol* 2016; **205**: 1-6 [PMID: 27552171 DOI: 10.1016/j.ejogrb.2016.07.496]

10 **Chen ZQ**, Cao LX, Shang WF, Yang RX, Ye F, Chen QC, Pang FS, Jiang Z, Liu WP, Zhou L. The effect of xiangbin fang on gastrointestinal motility of dogs after abdominal operation. *Zhongyi Zazhi* 2015; **56**: 1953-1957 [DOI: 10.13288/j.11-2166/r.2015.22.018]

11 **Jiang Z**, Cao LX, Liu B, Chen QC, Shang WF, Zhou L, Li DY, Guo DA, Chen ZQ. Effects of Chinese herbal medicine Xiangbin prescription on gastrointestinal motility. *World J Gastroenterol* 2017; **23**: 2987-2994 [PMID: 28522917 DOI: 10.3748/wjg.v23.i16.2987]

12 **Wang XY**, Chen JH, Li K, Zhu YF, Wright GW, Huizinga JD. Discrepancies between c-Kit positive and Ano1 positive ICC-SMP in the W/Wv and wild-type mouse colon; relationships with motor patterns and calcium transients. *Neurogastroenterol Motil* 2014; **26**: 1298-1310 [PMID: 25039457 DOI: 10.1111/nmo.12395]

13 **Klüppel M**, Huizinga JD, Malysz J, Bernstein A. Developmental origin and Kit-dependent development of the interstitial cells of cajal in the mammalian small intestine. *Dev Dyn* 1998; **211**: 60-71 [PMID: 9438424 DOI: 10.1002/(SICI)1097-0177(199801)211:1<60::AID-AJA6>3.0.CO;2-5]

14 **Dickens EJ**, Edwards FR, Hirst GD. Selective knockout of intramuscular interstitial cells reveals their role in the generation of slow waves in mouse stomach. *J Physiol* 2001; **531**: 827-833 [PMID: 11251061 DOI: 10.1111/j.1469-7793.2001.0827h.x]

15 **Edwards FR**, Hirst GD. An electrical description of the generation of slow waves in the antrum of the guinea-pig. *J Physiol* 2005; **564**: 213-232 [PMID: 15613372 DOI: 10.1113/jphysiol.2004.077123]

16 **Wright GW**, Parsons SP, Loera-Valencia R, Wang XY, Barajas-López C, Huizinga JD. Cholinergic signalling-regulated KV7.5 currents are expressed in colonic ICC-IM but not ICC-MP. *Pflugers Arch* 2014; **466**: 1805-1818 [PMID: 24375291 DOI: 10.1007/s00424-013-1425-7]

17 **Lies B**, Gil V, Groneberg D, Seidler B, Saur D, Wischmeyer E, Jiménez M, Friebe A. Interstitial cells of Cajal mediate nitrergic inhibitory neurotransmission in the murine gastrointestinal tract. *Am J Physiol Gastrointest Liver Physiol* 2014; **307**: G98-106 [PMID: 24833707 DOI: 10.1152/ajpgi.00082.2014]

18 **Blair PJ**, Bayguinov Y, Sanders KM, Ward SM. Relationship between enteric neurons and interstitial cells in the primate gastrointestinal tract. *Neurogastroenterol Motil* 2012; **24**: e437-e449 [PMID: 22805588 DOI: 10.1111/j.1365-2982.2012.01975.x]

19 **Hirst GD**, Dickens EJ, Edwards FR. Pacemaker shift in the gastric antrum of guinea-pigs produced by excitatory vagal stimulation involves intramuscular interstitial cells. *J Physiol* 2002; **541**: 917-928 [PMID: 12068050 DOI: 10.1113/jphysiol.2002.018614]

20 **Deloose E**, Vos R, Corsetti M, Depoortere I, Tack J. Endogenous motilin, but not ghrelin plasma levels fluctuate in accordance with gastric phase III activity of the migrating motor complex in man. *Neurogastroenterol Motil* 2015; **27**: 63-71 [PMID: 25393165 DOI: 10.1111/nmo.12470]

21 **Mondal A**, Xie Z, Miyano Y, Tsutsui C, Sakata I, Kawamoto Y, Aizawa S, Tanaka T, Oda S, Sakai T. Coordination of motilin and ghrelin regulates the migrating motor complex of gastrointestinal motility in Suncus murinus. *Am J Physiol Gastrointest Liver Physiol* 2012; **302**: G1207-G1215 [PMID: 22383491 DOI: 10.1152/ajpgi.00379.2011]

22 **Mondal A**, Kawamoto Y, Yanaka T, Tsutsui C, Sakata I, Oda SI, Tanaka T, Sakai T. Myenteric neural network activated by motilin in the stomach of Suncus murinus (house musk shrew). *Neurogastroenterol Motil* 2011; **23**: 1123-1131 [PMID: 22029733 DOI: 10.1111/j.1365-2982.2011.01801.x]

23 **Itoh Z**, Honda R, Hiwatashi K, Takeuchi S, Aizawa I, Takayanagi R, Couch EF. Motilin-induced mechanical activity in the canine alimentary tract. *Scand J Gastroenterol Suppl* 1976; **39**: 93-110 [PMID: 1069368]

24 **Vantrappen G**, Janssens J, Peeters TL, Bloom SR, Christofides ND, Hellemans J. Motilin and the interdigestive migrating motor complex in man. *Dig Dis Sci* 1979; **24**: 497-500 [PMID: 456236 DOI: 10.1007/BF01489315]

25 **He J**, Irwin DM, Chen R, Zhang YP. Stepwise loss of motilin and its specific receptor genes in rodents. *J Mol Endocrinol* 2010; **44**: 37-44 [PMID: 19696113 DOI: 10.1677/JME-09-0095]

26 **Takayama I**, Seto E, Zai H, Ohno S, Tezuka H, Daigo Y, Fujino MA. Changes of *in vivo* gastrointestinal motor pattern in pacemaker-deficient (WsRC-Ws/Ws) rats. *Dig Dis Sci* 2000; **45**: 1901-1906 [PMID: 11117558 DOI: 10.1023/a:1005612109863]

27 **Taniguchi H**, Ariga H, Zheng J, Ludwig K, Takahashi T. Effects of ghrelin on interdigestive contractions of the rat gastrointestinal tract. *World J Gastroenterol* 2008; **14**: 6299-6302 [PMID: 19009642 DOI: 10.3748/wjg.14.6299]

28 **Mizumoto A**, Sano I, Matsunaga Y, Yamamoto O, Itoh Z, Ohshima K. Mechanism of motilin-induced contractions in isolated perfused canine stomach. *Gastroenterology* 1993; **105**: 425-432 [PMID: 8335198 DOI: 10.1016/0016-5085(93)90716-p]

29 **Kito Y**. The functional role of intramuscular interstitial cells of Cajal in the stomach. *J Smooth Muscle Res* 2011; **47**: 47-53 [PMID: 21757854 DOI: 10.1540/jsmr.47.47]

30 **Gomez-Pinilla PJ**, Gibbons SJ, Bardsley MR, Lorincz A, Pozo MJ, Pasricha PJ, Van de Rijn M, West RB, Sarr MG, Kendrick ML, Cima RR, Dozois EJ, Larson DW, Ordog T, Farrugia G. Ano1 is a selective marker of interstitial cells of Cajal in the human and mouse gastrointestinal tract. *Am J Physiol Gastrointest Liver Physiol* 2009; **296**: G1370-G1381 [PMID: 19372102 DOI: 10.1152/ajpgi.00074.2009]

31 **Kim YC**, Suzuki H, Xu WX, Hashitani H, Choi W, Yun HY, Park SM, Youn SJ, Lee SJ, Lee SJ. Voltage-dependent Ca Current Identified in Freshly Isolated Interstitial Cells of Cajal (ICC) of Guinea-pig Stomach. *Korean J Physiol Pharmacol* 2008; **12**: 323-330 [PMID: 19967074 DOI: 10.4196/kjpp.2008.12.6.323]

32 **Thornbury KD**, Hollywood MA, McHale NG, Sergeant GP. Cajal beyond the gut: interstitial cells in the urinary system--towards general regulatory mechanisms of smooth muscle contractility? *Acta Gastroenterol Belg* 2011; **74**: 536-542 [PMID: 22319963]

33 **McClain JL**, Fried DE, Gulbransen BD. Agonist-evoked Ca^{2+} signaling in enteric glia drives neural programs that regulate intestinal motility in mice. *Cell Mol Gastroenterol Hepatol* 2015; **1**: 631-645 [PMID: 26693173 DOI: 10.1016/j.jcmgh.2015.08.004]

34 **Sanders KM**, Koh SD, Ro S, Ward SM. Regulation of gastrointestinal motility--insights from smooth muscle biology. *Nat Rev Gastroenterol Hepatol* 2012; **9**: 633-645 [PMID: 22965426 DOI: 10.1038/nrgastro.2012.168]

35 **Sung TS**, Hwang SJ, Koh SD, Bayguinov Y, Peri LE, Blair PJ, Webb TI, Pardo DM, Rock JR, Sanders KM, Ward SM. The cells and conductance mediating cholinergic neurotransmission in the murine proximal stomach. *J Physiol* 2018; **596**: 1549-1574 [PMID: 29430647 DOI: 10.1113/JP275478]

36 **Sun J**, Cao LX, Chen QC, Jiang Z, Chen ZQ, Zhou L. Effect of semen arecae on multichannel electrogastrogram and motilin and corticotropin-releasing hormone levels of healthy people. *Zhongyao Xinyao Yu Linchuang Yaoli* 2016; **27**: 281-285 [DOI: 10.3969/j.issn.1003-9783.2016.02.028]

37 **Xu FF**, Qi R, Jiang SW, Wang W, Chen ZQ, Guo DA, Liu B. Simultaneous determination of ten compounds in xiangbin fang by LC-MRM-MS. *Zhonghua Zhongyiyao Zazhi* 2017; **32**: 2226-2229

38 **Xie DP**, Chen LB, Liu CY, Zhang CL, Liu KJ, Wang PS. Arecoline excites the colonic smooth muscle motility *via* M3 receptor in rabbits. *Chin J Physiol* 2004; **47**: 89-94 [PMID: 15481791]

39 **Zhang JH**, Cao LX, Deng SG, Chen QC, Jiang Z, Chen ZQ, Zhou L. Effects of arecoline hydrobromide on the motility of isolated gastric smooth muscle strips in rats. *Guangdong Yixue* 2016; **37**: 2881-2885 [DOI: 10.3969/j.issn.1001-9448.2016.19.011]

40 **Han S**, Kim JS, Jung BK, Han SE, Nam JH, Kwon YK, Nah SY, Kim BJ. Effects of ginsenoside on pacemaker potentials of cultured interstitial cells of Cajal clusters from the small intestine of mice. *Mol Cells* 2012; **33**: 243-249 [PMID: 22350744 DOI: 10.1007/s10059-012-2204-6]

41 **Chen QC**, Pang FS, Cao LX, Jiang Z, Zhou L, Chen ZQ. Effect of Chinese herbs on gastrointestinal motility of chronic experimental beagle model. *Guangzhou Zhongyiyao Daxue Xuebao* 2016; **33**: 674-678 [DOI: 10.13359/j.cnki.gzxbtcm.2016.05.014]

World Journal of Gastroenterology

Submit a Manuscript: https://www.f6publishing.com

World J Gastroenterol 2021 February 21; 27(7): 592-608

DOI: 10.3748/wjg.v27.i7.592

ISSN 1007-9327 (print) ISSN 2219-2840 (online)

ORIGINAL ARTICLE

Basic Study

Sinapic acid ameliorates D-galactosamine/lipopolysaccharide-induced fulminant hepatitis in rats: Role of nuclear factor erythroid-related factor 2/heme oxygenase-1 pathways

Mushtaq Ahmad Ansari, Mohammad Raish, Yousef A Bin Jardan, Ajaz Ahmad, Mudassar Shahid, Sheikh Fayaz Ahmad, Nazrul Haq, Mohammad Rashid Khan, Saleh A Bakheet

ORCID number: Mushtaq Ahmad Ansari 0000-0002-9106-0978; Mohammad Raish 0000-0002-6015-6125; Yousef A Bin Jardan 0000-0002-9106-0970; Ajaz Ahmad 0000-0001-6295-8685; Mudassar Shahid 0000-0003-3714-4772; Sheikh Fayaz Ahmad 0000-0002-8282-3726; Nazrul Haq 0000-0003-0666-808X; Mohammad Rashid Khan 0000-0002-9106-09784; Saleh A Bakheet 0000-0003-2322-9732.

Author contributions: Ansari MA and Raish M conceptualized the study; Ahmad A, Bin Jardan YA and Shahid M helped in the methodology; Shahid M did the formal analysis; Ahmad SF, Khan MR and Haq N helped in managing resources; Ansari MA, Raish M and Bakheet SA wrote the original first draft and supervised the study and the project was administered by Ansari MA; Shahid M and Raish M did the review, editing, and finalized the manuscript draft; Ansari MA acquired funding for this research.

Supported by Deanship of Scientific Research at King Saud University, No. RG-1439-083.

Institutional review board statement: The experiment

Mushtaq Ahmad Ansari, Sheikh Fayaz Ahmad, Mohammad Rashid Khan, Saleh A Bakheet, Department of Pharmacology and Toxicology, College of Pharmacy, King Saud University, Riyadh 11451, Saudi Arabia

Mohammad Raish, Yousef A Bin Jardan, Mudassar Shahid, Nazrul Haq, Department of Pharmaceutics, College of Pharmacy, King Saud University, Riyadh 11451, Saudi Arabia

Ajaz Ahmad, Department of Clinical Pharmacy, College of Pharmacy, King Saud University, Riyadh 11451, Saudi Arabia

Corresponding author: Mushtaq Ahmad Ansari, PhD, Associate Professor, Department of Pharmacology and Toxicology, College of Pharmacy, King Saud University, King Khalid Road, Riyadh 11451, Saudi Arabia. muansari@ksu.edu.sa

Abstract

BACKGROUND

Sinapic acid (SA) has been shown to have various pharmacological properties such as antioxidant, antifibrotic, anti-inflammatory, and anticancer activities. Its mechanism of action is dependent upon its ability to curb free radical production and protect against oxidative stress-induced tissue injuries.

AIM

To study the hepatoprotective effects of SA against lipopolysaccharide (LPS)/D-galactosamine (D-GalN)-induced acute liver failure (ALF) in rats.

METHODS

Experimental ALF was induced with an intraperitoneal (i.p.) administration of 8 μg LPS and 800 mg/kg D-GalN in normal saline. SA was administered orally once daily starting 7 d before LPS/D-GalN treatment.

RESULTS

Data showed that SA ameliorates acute liver dysfunction, decreases serum levels of alanine transaminase (ALT), and aspartate aminotransferase (AST), as well as malondialdehyde (MDA) and NO levels in ALF model rats. However, pretreatment with SA (20 mg/kg and 40 mg/kg) reduced nuclear factor kappa-

proposal was authorized by the Ethics Committee of the Experimental Animal Care Society, King Saud University, Saudi Arabia (No. KSU-SE-20-13).

Institutional animal care and use committee statement: The experiment proposal was authorized by the Ethics Committee of the Experimental Animal Care Society, King Saud University, Saudi Arabia (No. KSU-SE-20-13).

Conflict-of-interest statement: The author declares that there are no conflicts of interest.

Data sharing statement: No additional data are available.

ARRIVE guidelines statement: The authors have read the ARRIVE Guidelines, and the manuscript was prepared and revised according to the ARRIVE Guidelines.

Open-Access: This article is an open-access article that was selected by an in-house editor and fully peer-reviewed by external reviewers. It is distributed in accordance with the Creative Commons Attribution NonCommercial (CC BY-NC 4.0) license, which permits others to distribute, remix, adapt, build upon this work non-commercially, and license their derivative works on different terms, provided the original work is properly cited and the use is non-commercial. See: http://creativecommons.org/licenses/by-nc/4.0/

Manuscript source: Unsolicited manuscript

Specialty type: Gastroenterology and hepatology

Country/Territory of origin: Saudi Arabia

Peer-review report's scientific quality classification

Grade A (Excellent): 0
Grade B (Very good): B
Grade C (Good): C, C
Grade D (Fair): 0
Grade E (Poor): 0

light-chain-enhancer of activated B cells (NF-κB) activation and levels of inflammatory cytokines (tumor necrosis factor-α and interleukin 6). Also, SA increased the activity of the nuclear factor erythroid-related factor 2/heme oxygenase-1 (Nrf2/HO-1) signaling pathway.

CONCLUSION

In conclusion, SA offers significant protection against LPS/D-GalN-induced ALF in rats by upregulating Nrf2/HO-1 and downregulating NF-κB.

Key Words: Sinapic acid; D-galactosamine/lipopolysaccharide; Oxidative stress; Fulminant hepatitis; Antioxidant; Nuclear factor erythroid-related factor 2/heme oxygenase-1 pathways

©The Author(s) 2021. Published by Baishideng Publishing Group Inc. All rights reserved.

Core Tip: This work demonstrated for the first time that the sinapic acid (SA) has hepatoprotective effects in the D-galactosamine/lipopolysaccharide (D-GalN/LPS)-induced rat model through its ability to suppress oxidative stress, inflammation, and apoptosis. The protective mechanism of SA depends on the downregulation of nuclear factor kappa-light-chain-enhancer of activated B cells and the restoration of antioxidant enzyme levels through the activation of the Nrf2/HO-1 pathway. Thus, SA could be applied to treat or prevent D-GalN/LPS-induced acute liver failure in the future.

Citation: Ansari MA, Raish M, Bin Jardan YA, Ahmad A, Shahid M, Ahmad SF, Haq N, Khan MR, Bakheet SA. Sinapic acid ameliorates D-galactosamine/lipopolysaccharide-induced fulminant hepatitis in rats: Role of nuclear factor erythroid-related factor 2/heme oxygenase-1 pathways. *World J Gastroenterol* 2021; 27(7): 592-608
URL: https://www.wjgnet.com/1007-9327/full/v27/i7/592.htm
DOI: https://dx.doi.org/10.3748/wjg.v27.i7.592

INTRODUCTION

Naturally occurring phenolic compounds play a significant role in disease prevention and treatment[1]. Natural phenols from plants include phenolic acids, tannins, flavonoids, stilbenes, coumarins, curcuminoids, quinones, lignans, and others. Sinapic acid (SA) Hydroxycinnamic acids (HCAs) are a group of naturally occurring phenolic acid and highly abundant in the human diet, such as fruits, vegetables, and grains[2]. Previous studies demonstrate that SA is a bioactive phenolic acid and has the potential to attenuate various chemically induced toxicities[3]. Fulminant hepatitis is a life-threatening clinical syndrome that is associated with overwhelming inflammation, hepatic encephalopathy, liver injury, and eventually liver failure[4]. Several studies have identified various etiologies for acute liver failure such as viral infections, bacterial infections, alcohol, and drugs[5-7]. Lipopolysaccharide (LPS) contains endotoxin prompted inflammation, and D-galactosamine (D-GalN) consequences in lipid peroxidation *via* promoting the release of reactive oxygen species (ROS) in liver cells[8]. There is an urgent need for the development of novel hepatoprotective therapies. The pathogenesis of fulminant hepatitis is currently under extensive investigation using LPS/D-GalN-prompted acute liver failure (ALF) model. This is a well-known model to probe the mechanism, pathogenesis, and agents for human liver injury[9,10]. D-GalN, a well-established hepatotoxic agent, produces hepatic necrosis by inhibiting mRNA translation[11]. LPS is known to stimulate Kupffer cells and promote the release of inflammatory cytokines such as tumor necrosis factor-α and interleukin 6 (TNF-α and IL-6), that successively produce hepatonecrosis and ALF. Furthermore, ROS-induced mitochondrial dysfunction was identified as a probable mechanism in LPS/D-GalN-induced ALF[12,13].

Several reports indicated that decreasing inflammation and oxidative stress could mitigate liver damage[14]. The homeostasis of metabolism, redox equilibrium and production of ROS are easily apparent at the mitochondrial level in which superoxide is generated as a result of the electron transport chain and Kerb's cycle reaction. The

Received: October 26, 2020
Peer-review started: October 26, 2020
First decision: November 25, 2020
Revised: November 30, 2020
Accepted: January 21, 2021
Article in press: January 21, 2021
Published online: February 21, 2021

P-Reviewer: Marickar F, Valenzuela R
S-Editor: Gao CC
L-Editor: A
P-Editor: Ma YJ

recent data demonstrate that nutritional intake, energy metabolism is also associated at nuclear level *via* the nuclear factor erythroid-related factor-2 (Nrf2)/antioxidant response element (ARE) pathway[15]. Several genes that contribute to oxidative stress are controlled by the key Nrf2. Before elevation in ROS, the Nrf2 transcription factor present in cytoplasm causes it to translocate to the nucleus. Activated, Nrf2 binds to the promoter region cis-acting enhancer ARE sequence (core sequence: TGAG/CNNNGC) of antioxidant genes to increase their expression of 500 genes including *Gsts*, *Nqo1*, *Ugts*, *Gclc*, *Gclm*, and *Ho-1 etc*. referred to as the "Nrf2 regulon"[16], which enhanced the capacity of the cellular radical-scavenging systems which decrease oxidative stress and activate pro-inflammatory pathways[17,18]. NRF2/ARE pathway predominantly involves in phase-II detoxification organs including liver, kidney, heart, intestine *etc*. A link between liver diseases and oxidative stress is indispensable. Nrf2 is a key regulator of cytodefence *via* mediation of antioxidant response, anti-inflammatory and chemoprotective activity[19]. The capacities of Nrf2 to enhance the expressions of antioxidant proteins and suppress oxidative stress-related injury have been broadly studied[14,20]. Therefore, implication of Nrf2/ARE activating regimens may be used for liver diseases. The generation of ROS devastates the antioxidant capacity, which contributes to the pathogenesis of several diseases, including fulminant hepatitis[10,21]. SA, also known as 3,5-dimethoxy-4-hydroxycinnamic acid, is a key phytoconstituent of citrus fruits, spices, berries, cereals, vegetables and oilseed crops commonly used in food and beverages[22]. SA is known to possess activities, such as antimicrobial, antioxidant, anti-inflammatory, anticancer, antidiabetic, antihypertensive, anti-anxiety, neuroprotective and hepatoprotective activities[3,22-26]. SA is a prominent member of the Brassicaceae family[24]. Literature reveals that SA is a bioactive phenolic acid and has the potential to attenuate various chemically induced toxicities[3]. SA is a potent scavenger of ROS; this property allows it to protect against tissue injuries[3,25,26]. SA induced NRF2/HO-1 has been reported in various disease models[25-29]. The amolearation of LPS/D-GalN-induced fulminant hepatitis through NRF2/HO-1 activation have been previously documented[30-32]. However, the hepatoprotective effects of SA in LPS/D-GalN-induced fulminant hepatitis has not been previously investigated. To identify the detailed mechanisms of action for SA, we tested its antioxidant and anti-inflammatory activities in a rat model of LPS/D-GalN-induced fulminant hepatitis. Thus, the purpose of the current study was to explore the underlying hepatoprotective mechanism of SA against LPS/D-GalN-induced ALF in rats. We also aimed to identify its effects on ROS production, inflammation and apoptosis and the roles of Nrf2/heme oxygenase 1 (HO-1) and NF-κB pathways.

MATERIALS AND METHODS

Drugs and chemicals

SA, LPS, and D-GalN were acquired from Sigma-Aldrich (Switzerland). The following primary antibodies were purchased from Santa Cruz Biotechnology (Dallas, TX, United States): transforming growth factor (TGF-β), Nrf2, HO-1, B-cell lymphoma 2 (Bcl-2), Caspase 3, Bcl2-Associated X, Apoptosis Regulator (Bax), nuclear factor of kappa light polypeptide gene enhancer in B cells inhibitor alpha (IκBα), NF-κB, and beta-actin (β-actin). HRP-conjugated secondary antibodies were also purchased from Santa Cruz Biotechnology (Dallas, TX, United States). A nuclear and cytoplasmic protein NE-PER kit was purchased from Pierce Biotechnology (Rockford, IL, United States). Enzyme-linked immunosorbent assay (ELISA) kits for rat TNF-α, IL-6, and myeloperoxidase (MPO) were purchased from R&D Systems, Inc. (MN, United States).

Animals

Wistar adult male rats (weight, 212-226 g) were taken from the animal facility of King Saud University, Riyadh, Saudi Arabia. The experiment proposal was authorized by the Ethics Committee of the Experimental Animal Care Society, King Saud University, Saudi Arabia (KSU-SE-20-13). They were kept under standard conditions 24 ± 2 °C, 12 h light/dark cycle, and received water and food *ad libitum*. The studies were performed according to the protocols that were approved by the Animal Ethics Committee of King Saud University, College of Pharmacy, Riyadh, Saudi Arabia.

Experimental design

The total forty-two rats were arbitrarily categorized into four groups: The control group (n = 6), the D-GalN/LPS treated (ALF) group (n = 12), the ALF + SA (20 mg/kg)

group (n = 12), and the ALF + SA (40 mg/kg) group (n = 12), To induce ALF, rats were injected intraperitoneally (i.p.) with 8 μg/kg LPS and 800 mg/kg D-GalN in 800 μL sterile normal saline. SA (20 and 40 mg/kg) solution in normal saline were administered *via* gavage once per day starting seven days before LPS/D-GalN treatment. The normal control group was injected i.p. with an equal volume of normal saline. Rats were anesthetized with ketamine (55 mg/kg) and xylazine (7 mg/kg) and euthanized 72 h after the D-GalN/LPS injection. Both serum and liver samples were collected and stored at -80 °C for further analysis. The dose of SA was selected based on preliminary and published data[3,23,33].

Survival rate and liver function activity

The rate of survival was observed for 48 h after the injection with D-GalN/LPS. Rats were witnessed for morbidity every hour after the injection of D-GalN/LPS. Assay kits to measure levels of aspartate aminotransferase (AST), alanine transaminase (ALT) and the ratio of bilirubin to alkaline phosphatase were purchased from Human Diagnostic Worldwide (Wiesbaden, Germany), using a spectrophotometer (Shimadzu – Model UV 2401, Kyoto, Japan)."

Histological evaluation

Hepatic tissue from each rat was fixed in 12% formalin for histopathological evaluation. The hepatic tissues were gradually dehydrated, embedded in paraffin, cut into 5-μm sections, and stained with hematoxylin and eosin for histological inspection. Briefly, the severity of liver damage was evaluated by a blinded pathologist using four-point scale from 0 to 3 as follows: 0, l, 2, and 3 represent no damage, mild damage, moderate damage, and very severe damage, scoring system in 20 random fields at 400 × magnification per animal (n = 6) for each group. A light microscope (Olympus, Japan) examined the histological anomalies.

Preparation of nuclear and total protein extracts

Total hepatic protein was extracted by homogenizing (T 25 Digital ULTRA-TURRAX®) tissue in cold RIPA buffer (Pierce Biotechnology, United States) and the supernatant was collected after centrifuging at 2500 × g for 20 min at 4 °C. Similarly, cytosolic and nuclear proteins were prepared using the NE-PER Kit (Pierce Biotechnology, United States) following the kit instructions. The protein concentration was examined using (Pierce Biotechnology, United States) the method bicinchoninic acid (Pierce™ BCA) assay[34].

Oxidative stress indices

The levels of malondialdehyde (MDA) and NO were examined in hepatic tissues using commercially available colorimetric assay kit (Sigma-Aldrich, St. Louis, MO, United States).

Antioxidant enzyme indices

Hepatic superoxide dismutase (SOD), catalase (CAT), and glutathione peroxidase (GP_x) activities in homogenized hepatic tissues were examined using commercial kits (Cayman Chemical, Ann Arbor, MI, United States).

Cytokine and inflammatory marker

TNF-α, IL-6, and MPO levels in the hepatic tissue were measured using ELISA kits according to the kit instructions. Absorbance was read at 450 nm.

Western blot analysis

Protein expression was performed using western blot analysis using a previously described protocol[35]. Precisely, 30-40 μg of protein was separated *via* sodium dodecyl sulfate-polyacrylamide gel electrophoresis (SDS-PAGE), electrophoretically transferred to nitrocellulose membranes, blocked with 4% casein and BSA in TBS containing 1% Tween-20 (TBST), and incubated at 4 °C overnight with the primary antibodies. The next day, membranes were washed five times with TBST and incubated with secondary antibodies for 2 h at room temperature. Bands were observed using Luminata™ Western Chemiluminescent HRP Substrates (Millipore, Billerica, MA, United States). Densitometric analysis of the immunoblots was also performed using a LI-COR C-Di-Git Blot Scanner (Lincoln, NE, United States).

Statistical analysis

All results are presented as arithmetic means ± SE. Data were analyzed using a one-way analysis of variance followed by Dennett's test by using Graph Pad V6.

RESULTS

Effects of SA on the survival rate of animals with D-GalN/LPS-induced ALF

The effect of SA pretreatment (20 and 40 mg/kg) on the 96 h survival rate is shown in Figure 1. After the administration of D-GalN/LPS, five rats died before 12 h with a survival rate of 58.33% after 96 h. Pretreatment with 20 and 40 mg/kg SA increased the survival rate by 66.66% and 75%, respectively, compared to the ALF group.

Effect of SA pretreatment on liver failure serum markers in D-GalN/LPS-induced ALF

The administration of D-GalN/LPS to rats caused ALF, as demonstrated by the significant increase in ALT, AST, and bilirubin levels (1485.73%, 774.10%, and 374.28%, respectively) compared with the normal controls ($P < 0.05$, $P < 0.05$, $P < 0.05$). Nevertheless, pretreatment with 20 and 40 mg/kg SA prevented ALF, as demonstrated by the 51.93% and 69.65% decreases in ALT levels ($P < 0.05$, $P < 0.05$), 44.29% and 73.66% decreases in AST levels ($P < 0.05$, $P < 0.05$) and 48.67% and 56.22% decreases in bilirubin levels ($P < 0.01$, $P < 0.01$) compared to the ALF rats (Table 1). Moreover, the histological examination of liver tissues showed that D-GalN/LPS caused focal central vein congestion, massive changes in lipid accumulation, ballooning formation, loss of cellular boundaries, and necrosis with inflammation. SA pretreatment, especially the 40 mg/kg dose, improved liver architecture in comparison to the ALF rats.

Effect of SA pretreatment on oxidative stress markers in the hepatic tissue of ALF rats

Liver tissue from the D-GalN/LPS-induced ALF animals showed significantly higher levels of MDA (122.90%) ($P < 0.05$) (Figure 2A) and NO_2^-content (230.01%) ($P < 0.05$) (Figure 2B) compared with the liver tissue from the control animals. However, the oral administration of 20 and 40 mg/kg SA significantly and dose-dependently reduced the MDA levels by 35.24% and 41.22%, respectively ($P < 0.05$; Figure 2A) and NO_2^- levels by 39.05% and 51.82%, respectively ($P < 0.05$; Figure 2B).

Effect of SA pretreatment on the activity of antioxidant enzyme markers in hepatic tissue of D-GalN/LPS-induced ALF rats

Hepatic tissue from D-GalN/LPS-induced ALF rats show 55.14% ($P < 0.05$), 70.01% ($P < 0.05$), and 73.37% ($P < 0.05$) reduction in the activities of GPx, SOD, and CAT, respectively (Figure 3). The oral administration of 20 and 40 mg/kg SA significantly restored the activity of GPx by 29.23% and 78.81%, respectively ($P < 0.05$); the activity of SOD by 117.64% and 185.87%, respectively ($P < 0.05$); and CAT activity by 123.41% and 198.41%, respectively ($P < 0.05$).

Effect of SA pretreatment on cytokines and inflammatory markers in hepatic tissue of D-GalN/LPS-induced ALF

The data suggested that TNF-α, IL-6 and MPO levels were significantly augmented in the D-GalN/LPS-induced ALF that is 524.61 %, 154.57 % and 118.56 % respectively ($P < 0.05$) as compared to control rats. SA at 20 and 40 mg/kg pretreatment significantly and dose-dependently downregulate these effects of TNF-α, IL-6 and MPO ($P < 0.05$; Figure 4) that is 29.69% and 50.39% for TNF-α, 37.03%, 46.53% for IL-6 and 23.52% and 32.72% for MPO as compared to D-GalN/LPS –induced ALF rats.

SA downregulates NF-κB (p65) in ALF

To examine the probable mechanism by which SA blocks TGFβ and IL-6 generation, we analyzed the activity of 20 and 40 mg/kg SA on NF-κB activation. As illustrated in Figure 5, the protein expression of IκB-α in the ALF group declined compared to the control group; however, this decrease was reversed by 20 and 40 mg/kg SA in a dose-dependent fashion. Moreover, In the ALF group, we detected increased nuclear NF-κB (p65) relative to the control group. However, 20 and 40 mg/kg treatment with SA reduced NF-κB (p65) during ALF in dose-dependent manner. The data proposed that SA may inhibit D-GalN/LPS -induced TGFβ generation by blocking NF-κB activation. Induction with D-GalN/LPS encouraged the translocation of p65 into the nucleus, and

Table 1 Effect of sinapic acid pretreatment on liver function serum markers in D-galactosamine/lipopolysaccharide-induced acute liver failure

Serum	Control	D-GalN/LPS	SA 20 mg/kg + D-GalN/LPS	SA 40 mg/kg + D-GalN/LPS
Total protein (mg/dL)	121.98 ± 1.45	82.48 ± 1.84	92.70 ± 1.17[a,b]	104.96 ± 2.24[a,b]
AST (U/L)	85.78 ± 3.26	749.83 ± 36.99	417.67 ± 23.46[a,b]	197.50 ± 18.25[a,b]
ALT (U/L)	60.75 ± 4.18	963.33 ± 45.73	463.00 ± 22.41[a,b]	292.33 ± 23.76[a,b]
Bilirubin (mg/dL)	0.35 ± 0.04	1.66 ± 0.15	0.85 ± 0.03[a,b]	0.73 ± 0.02[a,b]

The results are presented as the mean ± SE of six animals per group.
[a]Denotes significant differences to the in D-galactosamine/lipopolysaccharide–induced acute liver failure group ($P < 0.05$).
[b]Denotes significant differences to the normal control. SA: Sinapic acid; D-GalN/LPS: D-galactosamine/lipopolysaccharide; ALT: Alanine transaminase; AST: Aspartate aminotransferase.

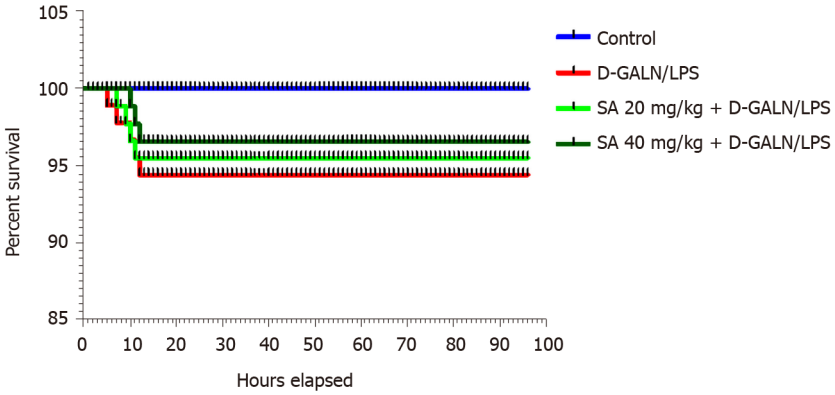


Figure 1 Effect of sinapic acid (20 and 40 mg/kg bodyweight) pretreatment on the survival rate of D-galactosamine/lipopolysaccharide-induced acute liver failure. SA: Sinapic acid; D-GalN/LPS: D-galactosamine/lipopolysaccharide.

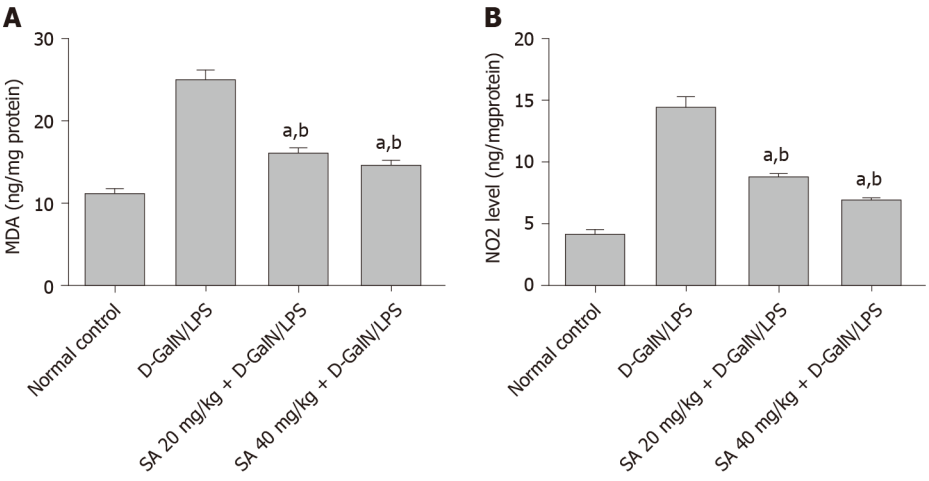


Figure 2 Effect of sinapic acid pretreatment on oxidative stress markers in hepatic tissue of D-galactosamine/lipopolysaccharide-induced acute liver failure. The results are presented as mean ± SE with six animals per group. [a]Denotes significant differences compared to the control group ($P < 0.05$); [b]Denotes significant differences compared to the D-galactosamine/lipopolysaccharide group ($P < 0.05$). MDA: Malondialdehyde; SA: Sinapic acid; D-GalN/LPS: D-galactosamine/lipopolysaccharide.

induced the inflammatory response through the NF-κB signaling pathway. As illustrated in Figure 5, D-GalN/LPS apparently upregulated the expression of Bax, caspase 3, and downregulated the expression of Bcl-2, which indicated apoptosis. On the contrary, dose-dependent downregulation of Bax, caspase 3 and upregulation of Bcl-2 was observed after pretreatment with 20 and 40 mg/kg SA in the D-GalN/LPS

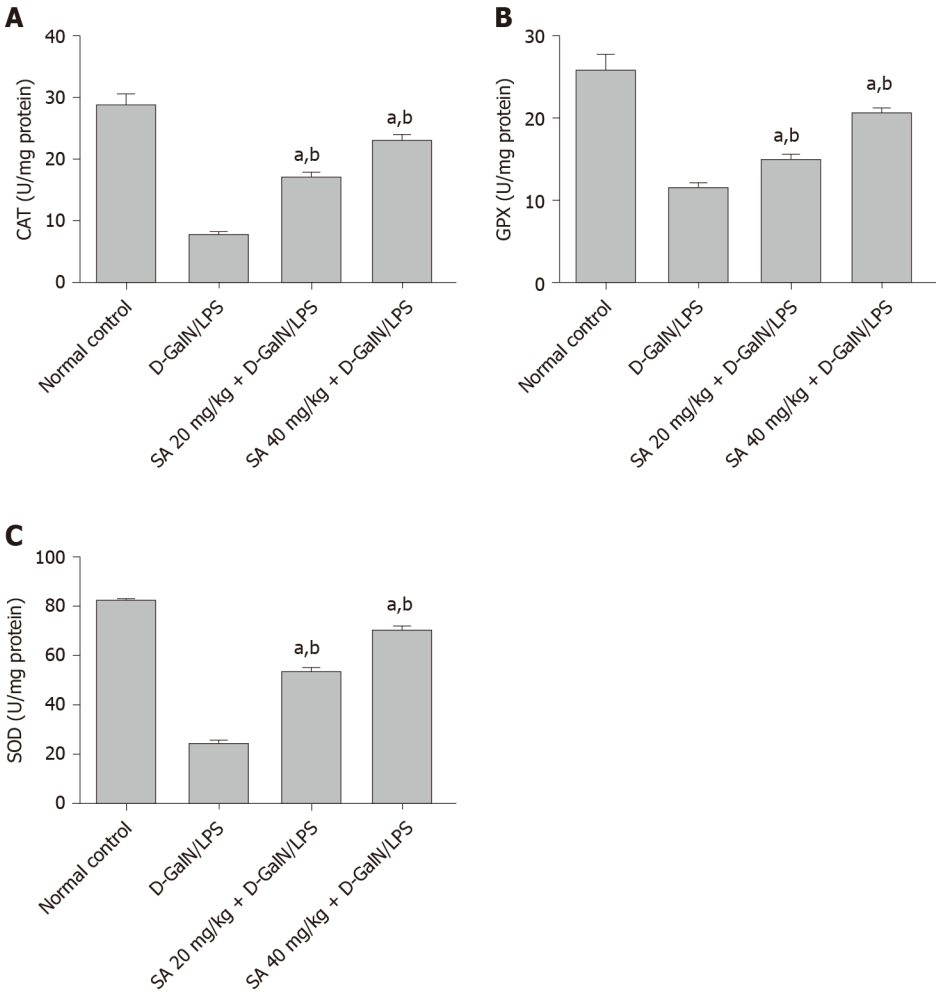


Figure 3 Effect of sinapic acid pretreatment on antioxidant enzyme activity in hepatic tissue from D-galactosamine/lipopolysaccharide-induced acute liver failure rats. The results are presented as mean ± SE with six animals per group. [a]Denotes significant differences compared to the control group ($P < 0.05$); [b]denotes significant differences compared to the D-galactosamine/lipopolysaccharide group ($P < 0.05$). CAT: Catalase; SA: Sinapic acid; D-GalN/LPS: D-galactosamine/lipopolysaccharide.

group. These results indicate that SA inhibited LPS/D-GalN-induced hepatocyte apoptosis by affecting the expression of apoptosis-related factors. D-GalN/LPS administration induced iNOS expression compared to the normal control. Pretreatment with 20 and 40 mg/kg SA significantly and dose-dependently inhibits iNOS expression, thus suggestive its potent anti-inflammatory effects. The antioxidant activity of SA is controlled *via* the modulation of the Nrf2/HO-1 pathway. Hepatic tissue from D-GalN/LPS-induced ALF show lower levels of Nrf2 and HO-1 expression as compared to the normal control rats. However, treatment with 20 mg/kg and 40 mg/kg SA significantly and dose-dependently upregulated the expression of Nrf2 and HO-1 compared with tissues from D-GalN/LP -induced animals ($P < 0.05$).

Effects of SA on histoarchitecture of liver tissues in ALF

As illustrated in Figure 6A, the hepatic tissues from the normal control group exhibited normal cellular and lobular architecture. Hepatic tissue from the ALF group exhibited prominent pathological alterations comprising widespread portal inflammation, hepatic cell necrosis, and infiltration of inflammatory cells (Figure 6B). However, pretreatment with 20 mg/kg and 40 mg/kg SA significantly ameliorated the D-GalN/LPS-induced pathological alterations in a dose-dependent manner as demonstrated by the reduced cell infiltration and restored lobular architecture. The severity of liver damage score has been illustrated in Figure 7.

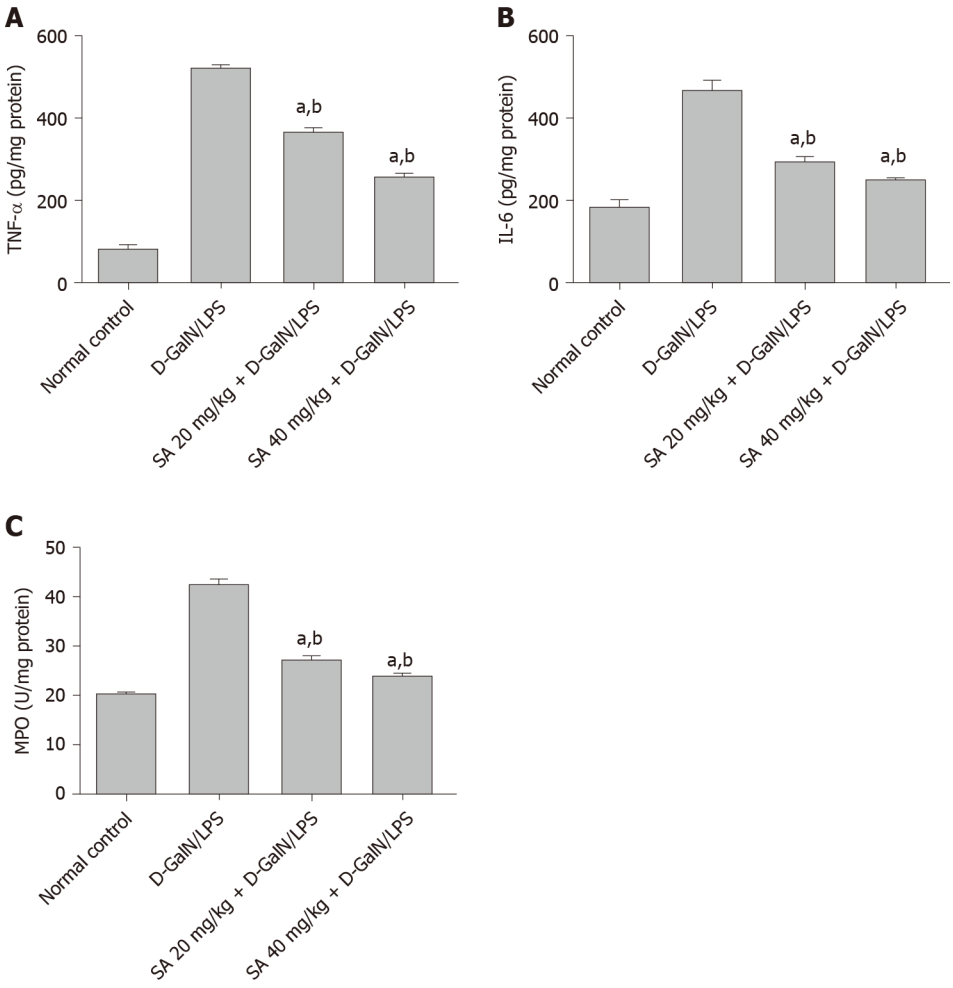
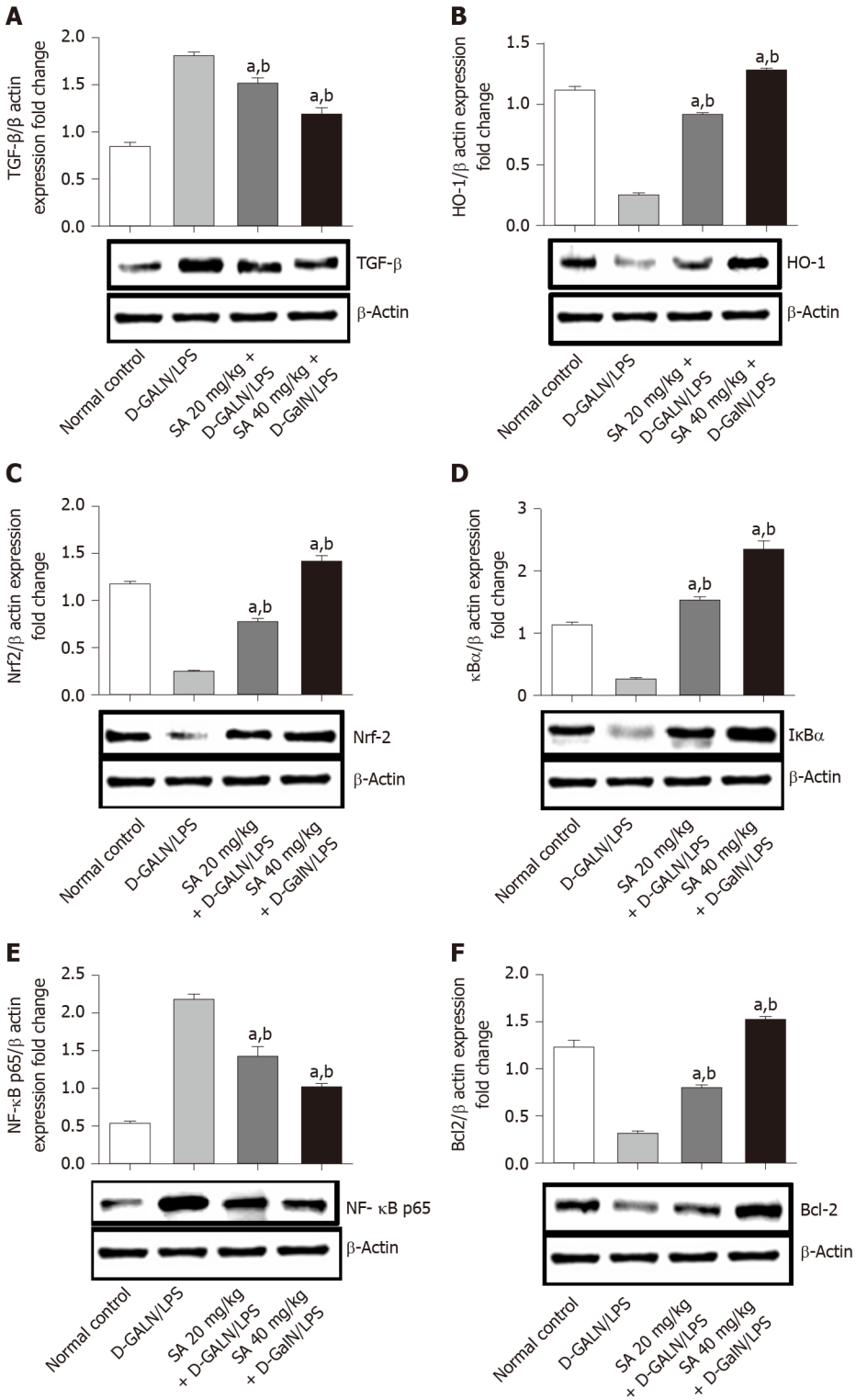


Figure 4 Effect of sinapic acid pretreatment on cytokines and inflammatory markers in hepatic tissue of D-galactosamine /lipopolysaccharide-induced acute liver failure. The results are presented as mean ± SE with six animals per group. [a]Denotes significant differences compared to the control group ($P < 0.05$); [b]denotes significant differences compared to the D-galactosamine/lipopolysaccharide group ($P < 0.05$). TNF-α: Tumor necrosis factor-α; IL-6: Interleukin 6; MPO: Myeloperoxidase; SA: Sinapic acid; D-GalN/LPS: D-galactosamine/lipopolysaccharide.

DISCUSSION

There is an overwhelming amount of evidence showing that SA protects against liver damage in animal models *via* various mechanisms, such as its antioxidant activity, anti-inflammatory activity, and ability to downregulate NF-κB p65. Therefore, SA has potential as a hepatoprotective agent for decreasing inflammation in CCL_4 and dimethyl nitrosamine-induced acute liver fibrosis[23]. The fulminant hepatitis rodent model was not investigated, and more detailed mechanisms remain unclear. Since SA has potent anti-inflammatory and antioxidant functions, we hypothesized that SA could also have hepatoprotective effects against D-GalN/LPS-induced fulminant hepatitis. The D-GalN/LPS-induced animal model of ALF is widely used to check the efficacy of hepatoprotective agents[36,37]. To examined the hepatoprotective effect of SA, serum levels of AST and ALT were analyzed to study the extent of liver damage. Several reports have shown that SA decreased AST and ALT[23]. AST and ALT are two known serum biomarkers of liver dysfunction[38,39]. Elevated levels of AST are indicative of tissue necrosis[40]. D-GalN/LPS-induced ALF rats exhibit enhanced serum levels of AST and ALT that were accompanied by enhanced inflammatory infiltration, hemorrhage, hepatocyte necrosis, and the loss of hepatic architecture. Pretreatment with SA (20 and 40 mg/kg) dose-dependently downregulated the AST and ALT levels and helped restore liver functions and structures. These results are consistent with previous reports[3,23,24,41,42]. Mitochondrial dysfunction and oxidative stress are two linked cellular events[43]. The dysfunction of mitochondrial dynamics leads to accumulation ROS and encourages induction of DNA damage, up or down regulation of apoptotic/anti-apoptotic factors, phosphatases and apoptotic/antiapototic factors leading to redox imbalance leading to wide range of disease including fulminant


A
TGF-β/β actin expression fold change
2.0
1.5
1.0
0.5
0.0
a,b
a,b
TGF-β
β-Actin
Normal control
D-GALN/LPS
SA 20 mg/kg + D-GALN/LPS
SA 40 mg/kg + D-GalN/LPS
B
HO-1/β actin expression fold change
1.5
1.0
0.5
0.0
a,b
a,b
HO-1
β-Actin
Normal control
D-GALN/LPS
SA 20 mg/kg + D-GALN/LPS
SA 40 mg/kg + D-GalN/LPS
C
Nrf2/β actin expression fold change
2.0
1.5
1.0
0.5
0.0
a,b
a,b
Nrf-2
β-Actin
Normal control
D-GALN/LPS
SA 20 mg/kg + D-GALN/LPS
SA 40 mg/kg + D-GalN/LPS
D
κBα/β actin expression fold change
3
2
1
0
a,b
a,b
IκBα
β-Actin
Normal control
D-GALN/LPS
SA 20 mg/kg + D-GALN/LPS
SA 40 mg/kg + D-GalN/LPS
E
NF-κB p65/β actin expression fold change
2.5
2.0
1.5
1.0
0.5
0.0
a,b
a,b
NF- κB p65
β-Actin
Normal control
D-GALN/LPS
SA 20 mg/kg + D-GALN/LPS
SA 40 mg/kg + D-GalN/LPS
F
Bcl2/β actin expression fold change
2.0
1.5
1.0
0.5
0.0
a,b
a,b
Bcl-2
β-Actin
Normal control
D-GALN/LPS
SA 20 mg/kg + D-GALN/LPS
SA 40 mg/kg + D-GalN/LPS

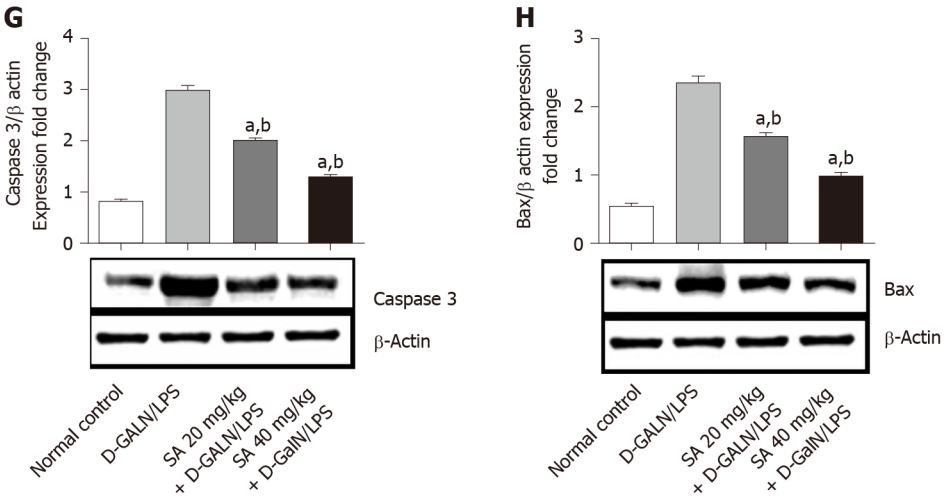


Figure 5 Sinapic acid downregulates nuclear factor kappa B in acute liver failure. A-H: Effect of sinapic acid on the protein expression of transforming growth factor-β1 (A), heme oxygenase-1 (B), nuclear factor erythroid 2-related factor 2 (C), nuclear factor of kappa light polypeptide gene enhancer in B cells inhibitor alpha protein (D), nuclear factor kappa B (E), anti-apoptotic protein BCl2 (F), caspase 3 (G), and Bax in D-galactosamine/lipopolysaccharide (D-GalN/LPS)-induced acute liver failure (ALF) (H). The results are presented as the mean ± SE of six animals per group. [a]Denotes significant differences to the D-GalN/LPS-induced ALF group ($P < 0.05$); [b]denotes significant differences compared to the normal control. TGF-β1: Transforming growth factor-β1; HO-1: Heme oxygenase-1; Nrf2: Nuclear factor erythroid 2-related factor 2; IkBα: Nuclear factor of kappa light polypeptide gene enhancer in B cells inhibitor alpha; NF-κb: Nuclear factor kappa B; SA: Sinapic acid; D-GalN/LPS: D-galactosamine/lipopolysaccharide.

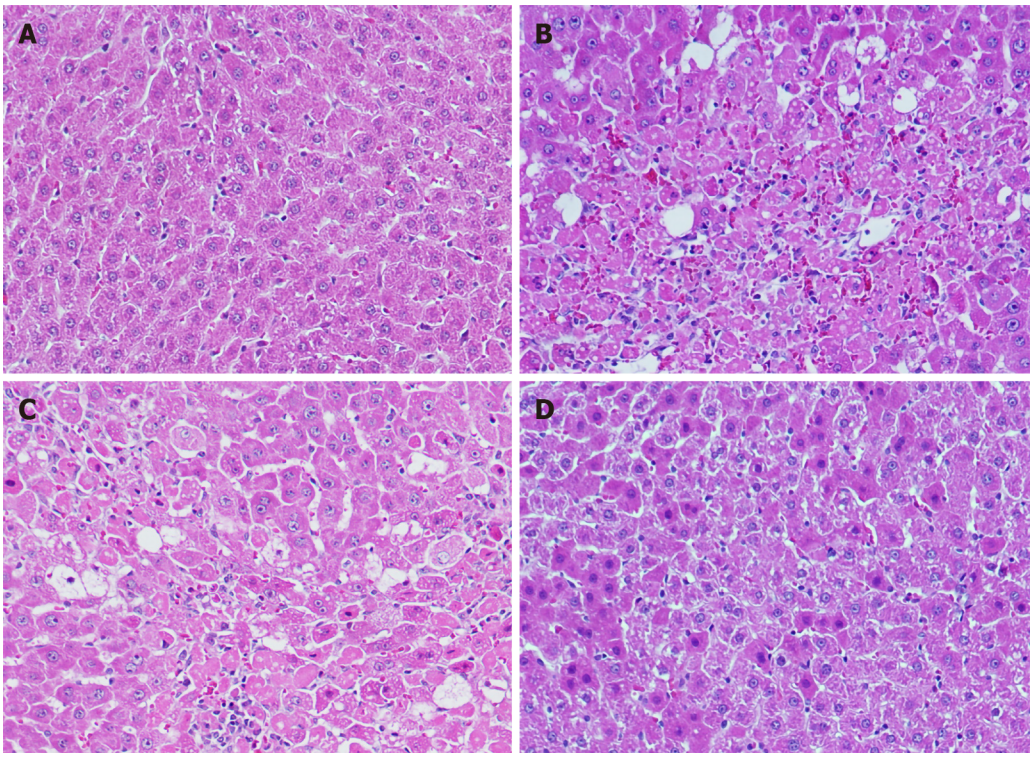


Figure 6 Light photomicrographs of hepatic tissues. Hematoxylin and eosin stains, magnification 100 ×. A: Hepatic section of normal control rat exhibits normal architecture of hepatic cord of cells; B: Hepatic section of D-galactosamine/lipopolysaccharide (D-GalN/LPS) treated rats exhibiting massive fatty changes, focal central vein congestion, ballooning formation, necrosis with inflammation, and loss of cellular boundaries, massive cellular infiltration; C: Hepatic section of rats treated D-GalN/LPS and 20 mg/kg of sinapic acid (SA) showing mild central vein congestion, mild fatty changes, ballooning, necrosis with sinusoidal dilatation, mild cellular infiltration; D: Hepatic section of rats treated D-GalN/LPS and 40 mg/kg of SA exhibiting the absence of ballooning, inflammatory cells, and regeneration of hepatocytes around central vein toward near-normal liver architecture but slight congestion in the central vein.

hepatic disease[42,44,45]. Previous evidence indicate that mitochondrial defects contribute to liver damage *via* a number of pathways[46,47], involving inhibition of mitochondrial β-oxidation and respiratory chain activity, failure of mitochondrial membrane potential and damage to the antioxidant protection mechanism.

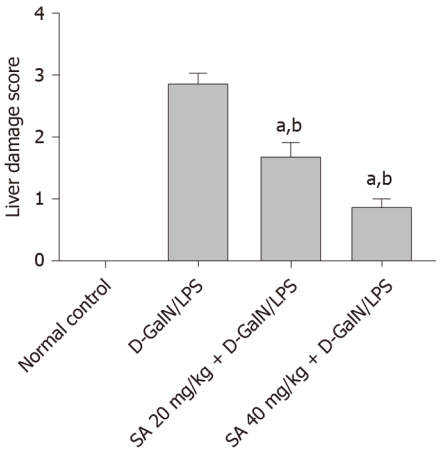


Figure 7 The liver damage score was examned using four-point scale from 0 to 3. 0, I, 2, and 3 represent no damage, mild damage, moderate damage, and very severe damage, scoring system in 20 random fields at 400 × magnification per animal (n = 6 per group). [a]Denotes significant differences compared to the control group (P < 0.05); [c]Denotes significant differences compared to the D-galactosamine/lipopolysaccharide group (P < 0.05). SA: Sinapic acid; D-GalN/LPS: D-galactosamine/lipopolysaccharide.

ROS play a significant role in the pathogenesis of ALF[21,48]. Reactive nitrogen species (RNS) and ROS can react with polyunsaturated fatty acids (PUFAs) to cause lipid peroxidation; this process may further damage the cellular membrane and trigger apoptosis[49,50]. Kupffer cells and neutrophils undergo apoptosis during vascular oxidative stress, which leads to ALF[51]. Several reports have implicated oxidative stress in D-GalN/LPS-induced ALF[52]. MDA is the end product of lipid peroxidation and the accumulation of ROS/RNS. It is also an excellent marker for oxidative stress[53]. The level of MDA and NO increased significantly in D-GalN/LPS-induced ALF rats as compared to normal control rats. The pretreatment with 20 and 40 mg/kg SA pretreatment substantially and dose-dependently curbed the oxidative stress as indicated by reduced MDA and NO levels. Therefore, SA might have potent antioxidant activity through its ability to inhibit ROS/RNS production induced by D-GalN/LPS. There are several reports that SA has potent antioxidant activity[3]. D-GalN/LPS-induced oxidative stress leads to the accumulation of hepatic lipid peroxides and the depletion of antioxidant enzymes such as GPx, SOD, and CAT.

D-GalN/LPS-induced ALF rats exhibit lower levels of GPx, SOD, and CAT as compared to normal control animals. SA (20 and 40 mg/kg) pretreatment significantly restored levels of GPx, SOD, and CAT in hepatic tissues, which is possibly an adaptive response to oxidative stress. SA has been previously shown to restore levels of GPx, SOD and CAT in a CCL4 and dimethyl nitrosamine-induced model of acute liver injury[23]. D-GalN/LPS-induced liver failure caused the production of TNF-α and IL-6, which triggered an inflammatory cascade in hepatocytes causing ALF[54,55]. Several natural polyphenols have been reported to prevent liver injuries[52,56]. Thus, levels of TNF-α and IL-6 in the liver were analyzed in the study. Pretreatment with SA reduced levels of these cytokines in a dose-dependent fashion. This finding may partially explain the hepatoprotective activity of SA. NF-κB is activated by D-GalN/LPS through the phosphorylation and degradation of IκB-α; this allows NF-κB to translocate to the nucleus and increase the gene expression of cytokines such as TNF-α and IL-6[57]. Out data indicate that SA downregulated NF-κB activation by decreasing IκB-α degradation in a dose-dependent fashion.

Nrf2, a crucial transcription factor, controls these enzymes such as SOD, CAT, GPx, and HO-1 by binding to the elements of antioxidant response, inducing adaptive cytoprotective responses, and having a strong influence on the response to oxidative stress[58]. Several antioxidant genes are controlled by Nrf2. Upon activation by oxidative stress, Nrf2 translocates to the nucleus and binds to antioxidant transcription elements of Phase II to increase the expression of antioxidant genes[13,52,59]. The restoration of antioxidant enzymes SOD, CAT, GPx, and HO-1 and down regulation of TNF-α and IL-6 due to upregulation of NRF2 and down regulation of NF-kB indicates towards cytoprotective effect due to its antioxidant and antinflamatory nature[58]. The data indicates SA mediates Nrf2 nucleus translocation as evident upregulation of NRF2 expression in nucleus that cause upregulation in antioxidant enzyme SOD, CAT, GPx, and HO-1 that performing a defending role against D-Gal/LPS induced inflammation and oxidative stress[58,60]. Down regulation of NRF2 is linked with

enhanced inflammation, while its upregulation reduces transcriptionally mediated NF-kB, pro-inflammatory and immune responses[44,61]. HO-1 is a rate-limiting enzyme that translates heme into equimolar amounts of iron, carbon monoxide, and biliverdin. HO-1 has cytoprotective and antioxidant activities and is activated in D-GalN/LPS-induced hepatitis[6,52]. The pretreatment of D-GalN/LPS-induced ALF rats with SA induced the expression of HO-1 through increased Nrf2 expression. Several studies have shown that there is a reduction in the expression of HO-1 and Nrf2 in D-GalN/LPS-induced ALF, which is similar to our results (Figure 2)[23,48,52]. Our data show that HO-1 and Nrf2 were downregulated in liver tissue after D-GalN/LPS administration, but SA pretreatment enhanced their expression in a dose-dependent manner. These outcomes showed that the Nrf2/HO-1 signaling pathways are implicated in the protective mechanism of SA. Apoptosis plays a key role in the pathogenesis of D-GalN/LPS-induced ALF[62]. Our data showed that D-GalN/LPS treatment may increase apoptotic and necrotic hepatocellular death through the upregulation of Bax and caspase-3 and the downregulation of Bcl-2. SA pretreatment significantly downregulates the expression of Bax and caspase-while upregulating Bcl2 in a dose-dependent manner, thus reducing apoptotic cell damage in hepatocytes. The aforesaid data is consistent with previously published studies[63,64].

CONCLUSION

This work demonstrated for the first time that the SA has hepatoprotective effects in the D-GalN/LPS-induced rat model through its ability to suppressing oxidative stress, inflammation, and apoptosis. The protective mechanism of SA depends on the downregulation of NF-κB and the restoration of antioxidant enzyme levels through the activation of the Nrf2/HO-1 pathway. Thus, SA could be applied to treat or prevent D-GalN/LPS -induced ALF in the future (Figure 8).

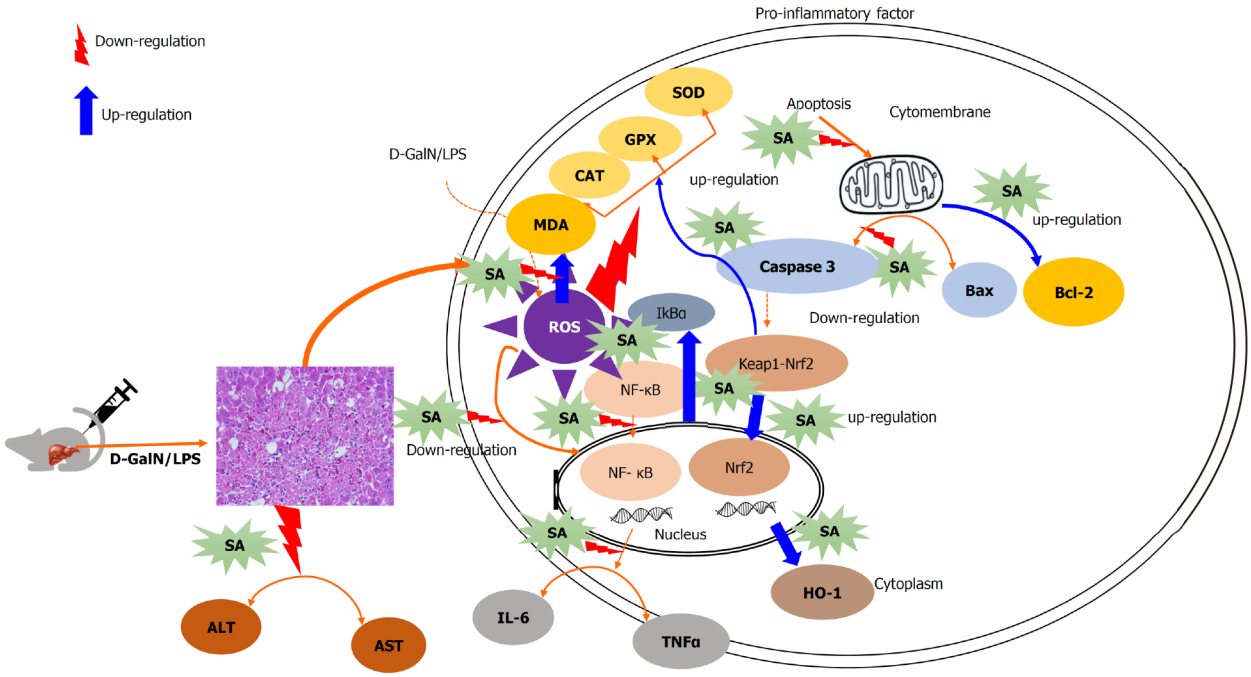


Figure 8 Graphical abstract. SA: Sinapic acid; D-GalN/LPS: D-galactosamine/lipopolysaccharide; ALT: Alanine transaminase; AST: Aspartate aminotransferase; TNF-α: Tumor necrosis factor-α; IL-6: Interleukin 6; TGF-β1: Transforming growth factor-β1; HO-1: Heme oxygenase-1; Nrf2: Nuclear factor erythroid 2-related factor 2; IkBα: Nuclear factor of kappa light polypeptide gene enhancer in B cells inhibitor alpha; NF-κb: Nuclear factor kappa B; ROS: Reactive oxygen species; CAT: Catalase; MDA: Malondialdehyde; GPX: Glutathione peroxidase; SOD: Superoxide dismutase.

ARTICLE HIGHLIGHTS

Research background

Sinapic acid (SA) has been shown to have various pharmacological properties such as antioxidant, antifibrotic, anti-inflammatory, and anticancer activities. Its mechanism of action is dependent upon its ability to curb free radical production and protect against oxidative stress-induced tissue injuries.

Research motivation

In the current study, the hepatoprotective effects of SA against lipopolysaccharide (LPS)/D-galactosamine (D-GalN)-induced acute liver failure (ALF) in rats were studied.

Research objectives

In the current study, the hepatoprotective effects of SA against LPS/D-GalN-induced acute liver failure (ALF) in rats were studied.

Research methods

Experimental ALF was induced with an intraperitoneal (i.p.) administration of 8 μg LPS and 800 mg/kg D-GalN in normal saline. SA was administered orally once daily starting 7 d before LPS/D-GalN treatment.

Research results

Data showed that SA ameliorates acute liver dysfunction, decreases serum levels of alanine transaminase (ALT), and aspartate aminotransferase (AST), as well as malondialdehyde (MDA) and NO levels in ALF model rats. However, pretreatment with SA (20 mg/kg and 40 mg/kg) reduced nuclear factor kappa-light-chain-enhancer of activated B cells (NF-κB) activation and levels of inflammatory cytokines (tumor necrosis factor-α and interleukin 6). Also, SA increased the activity of the nuclear factor erythroid-related factor 2/heme oxygenase-1 (Nrf2/HO-1) signaling pathway.

Research conclusions

In conclusion, SA offers significant protection against LPS/D-GalN-induced ALF in rats by upregulating Nrf2/HO-1 and downregulating NF-κB.

Research perspectives

The amolearation of LPS/D-GalN-induced fulminant hepatitis through NRF2/HO-1 activation have been previously documented. However, the hepatoprotective effects of SA in LPS/D-GalN-induced fulminant hepatitis has not been previously investigated. To identify the detailed mechanisms of action for SA, we tested its antioxidant and anti-inflammatory activities in a rat model of LPS/D-GalN-induced fulminant hepatitis. Thus, the purpose of the current study was to explore the underlying hepatoprotective mechanism of SA against LPS/D-GalN-induced ALF in rats. We also aimed to identify its effects on ROS production, inflammation and apoptosis and the roles of Nrf2/HO-1 and NF-κB pathways.

ACKNOWLEDGEMENTS

The authors thank the Deanship of Scientific Research for the funding of this work through the Research Group Number, RG-1439-083 and RSSU for their technical support at King Saud University.

REFERENCES

1 **Huang WY**, Cai YZ, Zhang Y. Natural phenolic compounds from medicinal herbs and dietary plants: potential use for cancer prevention. *Nutr Cancer* 2010; **62**: 1-20 [PMID: 20043255 DOI: 10.1080/01635580903191585]
2 **Herrmann K**. Occurrence and content of hydroxycinnamic and hydroxybenzoic acid compounds in foods. *Crit Rev Food Sci Nutr* 1989; **28**: 315-347 [PMID: 2690858 DOI: 10.1080/10408398909527504]
3 **Chen C**. Sinapic Acid and Its Derivatives as Medicine in Oxidative Stress-Induced Diseases and Aging. *Oxid Med Cell Longev* 2016; **2016**: 3571614 [PMID: 27069529 DOI: 10.1155/2016/3571614]
4 **Ndekwe P**, Ghabril MS, Zang Y, Mann SA, Cummings OW, Lin J. Substantial hepatic necrosis is prognostic in fulminant liver failure. *World J Gastroenterol* 2017; **23**: 4303-4310 [PMID: 28694671 DOI: 10.3748/wjg.v23.i23.4303]
5 **Rolando N**, Harvey F, Brahm J, Philpott-Howard J, Alexander G, Gimson A, Casewell M, Fagan E, Williams R. Prospective study of bacterial infection in acute liver failure: an analysis of fifty patients. *Hepatology* 1990; **11**: 49-53 [PMID: 2295471 DOI: 10.1002/hep.1840110110]
6 **Wang YY**, Diao BZ, Zhong LH, Lu BL, Cheng Y, Yu L, Zhu LY. Maslinic acid protects against lipopolysaccharide/d-galactosamine-induced acute liver injury in mice. *Microb Pathog* 2018; **119**: 49-53 [PMID: 29627448 DOI: 10.1016/j.micpath.2018.04.002]
7 **Yang X**, Fujisawa M, Yoshimura T, Ohara T, Sato M, Mino M, San TH, Gao T, Kunkel SL, Matsukawa A. Spred2 Deficiency Exacerbates D-Galactosamine/Lipopolysaccharide -induced Acute Liver Injury in Mice *via* Increased Production of TNFα. *Sci Rep* 2018; **8**: 188 [PMID: 29317674 DOI: 10.1038/s41598-017-18380-0]
8 **Morikawa A**, Kato Y, Sugiyama T, Koide N, Chakravortty D, Yoshida T, Yokochi T. Role of nitric oxide in lipopolysaccharide-induced hepatic injury in D-galactosamine-sensitized mice as an experimental endotoxic shock model. *Infect Immun* 1999; **67**: 1018-1024 [PMID: 10024538 DOI: 10.1128/IAI.67.3.1018-1024.1999]
9 **Tuñón MJ**, Alvarez M, Culebras JM, González-Gallego J. An overview of animal models for investigating the pathogenesis and therapeutic strategies in acute hepatic failure. *World J Gastroenterol* 2009; **15**: 3086-3098 [PMID: 19575487 DOI: 10.3748/wjg.15.3086]
10 **Zhang L**, Li HZ, Gong X, Luo FL, Wang B, Hu N, Wang CD, Zhang Z, Wan JY. Protective effects of Asiaticoside on acute liver injury induced by lipopolysaccharide/D-galactosamine in mice. *Phytomedicine* 2010; **17**: 811-819 [PMID: 20171071 DOI: 10.1016/j.phymed.2010.01.008]
11 **Sathivel A**, Balavinayagamani, Hanumantha Rao BR, Devaki T. Sulfated polysaccharide isolated from Ulva lactuca attenuates d-galactosamine induced DNA fragmentation and necrosis during liver damage in rats. *Pharm Biol* 2013; : [PMID: 24329421 DOI: 10.3109/13880209.2013.846915]
12 **Hoek JB**, Pastorino JG. Ethanol, oxidative stress, and cytokine-induced liver cell injury. *Alcohol* 2002; **27**: 63-68 [PMID: 12062639 DOI: 10.1016/s0741-8329(02)00215-x]
13 **Ma Q**. Role of nrf2 in oxidative stress and toxicity. *Annu Rev Pharmacol Toxicol* 2013; **53**: 401-426 [PMID: 23294312 DOI: 10.1146/annurev-pharmtox-011112-140320]
14 **Li S**, Tan HY, Wang N, Zhang ZJ, Lao L, Wong CW, Feng Y. The Role of Oxidative Stress and Antioxidants in Liver Diseases. *Int J Mol Sci* 2015; **16**: 26087-26124 [PMID: 26540040 DOI: 10.3390/ijms161125942]
15 **Vomhof-Dekrey EE**, Picklo MJ Sr. The Nrf2-antioxidant response element pathway: a target for regulating energy metabolism. *J Nutr Biochem* 2012; **23**: 1201-1206 [PMID: 22819548 DOI: 10.1016/j.jnutbio.2012.03.005]
16 **Kobayashi M**, Yamamoto M. Nrf2-Keap1 regulation of cellular defense mechanisms against electrophiles and reactive oxygen species. *Adv Enzyme Regul* 2006; **46**: 113-140 [PMID: 16887173

DOI: 10.1016/j.advenzreg.2006.01.007]
17 **Dreger H**, Westphal K, Wilck N, Baumann G, Stangl V, Stangl K, Meiners S. Protection of vascular cells from oxidative stress by proteasome inhibition depends on Nrf2. *Cardiovasc Res* 2010; **85**: 395-403 [PMID: 19679681 DOI: 10.1093/cvr/cvp279]
18 **Nioi P**, McMahon M, Itoh K, Yamamoto M, Hayes JD. Identification of a novel Nrf2-regulated antioxidant response element (ARE) in the mouse NAD(P)H:quinone oxidoreductase 1 gene: reassessment of the ARE consensus sequence. *Biochem J* 2003; **374**: 337-348 [PMID: 12816537 DOI: 10.1042/BJ20030754]
19 **Alam J**, Stewart D, Touchard C, Boinapally S, Choi AM, Cook JL. Nrf2, a Cap'n'Collar transcription factor, regulates induction of the heme oxygenase-1 gene. *J Biol Chem* 1999; **274**: 26071-26078 [PMID: 10473555 DOI: 10.1074/jbc.274.37.26071]
20 **Cichoż-Lach H**, Michalak A. Oxidative stress as a crucial factor in liver diseases. *World J Gastroenterol* 2014; **20**: 8082-8091 [PMID: 25009380 DOI: 10.3748/wjg.v20.i25.8082]
21 **Lingappan K**. NF-κB in Oxidative Stress. *Curr Opin Toxicol* 2018; **7**: 81-86 [PMID: 29862377 DOI: 10.1016/j.cotox.2017.11.002]
22 **Andreasen MF**, Landbo AK, Christensen LP, Hansen A, Meyer AS. Antioxidant effects of phenolic rye (Secale cereale L.) extracts, monomeric hydroxycinnamates, and ferulic acid dehydrodimers on human low-density lipoproteins. *J Agric Food Chem* 2001; **49**: 4090-4096 [PMID: 11513715 DOI: 10.1021/jf0101758]
23 **Shin DS**, Kim KW, Chung HY, Yoon S, Moon JO. Effect of sinapic acid against dimethylnitrosamine-induced hepatic fibrosis in rats. *Arch Pharm Res* 2013; **36**: 608-618 [PMID: 23435910 DOI: 10.1007/s12272-013-0033-6]
24 **Niciforovic N**, Abramovic H. Sinapic Acid and Its Derivatives: Natural Sources and Bioactivity. *Compr Rev Food Sci Food Saf* 2014; **13**: 34-51 [DOI: 10.1111/1541-4337.12041]
25 **Ansari MA**. Sinapic acid modulates Nrf2/HO-1 signaling pathway in cisplatin-induced nephrotoxicity in rats. *Biomed Pharmacother* 2017; **93**: 646-653 [PMID: 28686978 DOI: 10.1016/j.biopha.2017.06.085]
26 **Raish M**, Ahmad A, Ahmad Ansari M, Ahad A, Al-Jenoobi FI, Al-Mohizea AM, Khan A, Ali N. Sinapic acid ameliorates bleomycin-induced lung fibrosis in rats. *Biomed Pharmacother* 2018; **108**: 224-231 [PMID: 30219680 DOI: 10.1016/j.biopha.2018.09.032]
27 **Li X**, Lin J, Ding X, Xuan J, Hu Z, Wu D, Zhu X, Feng Z, Ni W, Wu A. The protective effect of sinapic acid in osteoarthritis: In vitro and *in vivo* studies. *J Cell Mol Med* 2019; **23**: 1940-1950 [PMID: 30604480 DOI: 10.1111/jcmm.14096]
28 **Scapagnini G**, Vasto S, Abraham NG, Caruso C, Zella D, Fabio G. Modulation of Nrf2/ARE pathway by food polyphenols: a nutritional neuroprotective strategy for cognitive and neurodegenerative disorders. *Mol Neurobiol* 2011; **44**: 192-201 [PMID: 21499987 DOI: 10.1007/s12035-011-8181-5]
29 **Ansari MA**, Raish M, Ahmad A, Alkharfy KM, Ahmad SF, Attia SM, Alsaad AMS, Bakheet SA. Sinapic acid ameliorate cadmium-induced nephrotoxicity: In vivo possible involvement of oxidative stress, apoptosis, and inflammation *via* NF-κB downregulation. *Environ Toxicol Pharmacol* 2017; **51**: 100-107 [PMID: 28233699 DOI: 10.1016/j.etap.2017.02.014]
30 **Luo JF**, Shen XY, Lio CK, Dai Y, Cheng CS, Liu JX, Yao YD, Yu Y, Xie Y, Luo P, Yao XS, Liu ZQ, Zhou H. Activation of Nrf2/HO-1 Pathway by Nardochinoid C Inhibits Inflammation and Oxidative Stress in Lipopolysaccharide-Stimulated Macrophages. *Front Pharmacol* 2018; **9**: 911 [PMID: 30233360 DOI: 10.3389/fphar.2018.00911]
31 **Lim DW**, Choi HJ, Park SD, Kim H, Yu GR, Kim JE, Park WH. Activation of the Nrf2/HO-1 Pathway by *Amomum villosum* Extract Suppresses LPS-Induced Oxidative Stress *In Vitro* and *Ex Vivo* . *Evid Based Complement Alternat Med* 2020; **2020**: 2837853 [PMID: 32454852 DOI: 10.1155/2020/2837853]
32 **Lv H**, Yang H, Wang Z, Feng H, Deng X, Cheng G, Ci X. Nrf2 signaling and autophagy are complementary in protecting lipopolysaccharide/d-galactosamine-induced acute liver injury by licochalcone A. *Cell Death Dis* 2019; **10**: 313 [PMID: 30952839 DOI: 10.1038/s41419-019-1543-z]
33 **Cherng YG**, Tsai CC, Chung HH, Lai YW, Kuo SC, Cheng JT. Antihyperglycemic action of sinapic acid in diabetic rats. *J Agric Food Chem* 2013; **61**: 12053-12059 [PMID: 24261449 DOI: 10.1021/jf403092b]
34 **Smith PK**, Krohn RI, Hermanson GT, Mallia AK, Gartner FH, Provenzano MD, Fujimoto EK, Goeke NM, Olson BJ, Klenk DC. Measurement of protein using bicinchoninic acid. *Anal Biochem* 1985; **150**: 76-85 [PMID: 3843705 DOI: 10.1016/0003-2697(85)90442-7]
35 **Towbin H**, Staehelin T, Gordon J. Electrophoretic transfer of proteins from polyacrylamide gels to nitrocellulose sheets: procedure and some applications. *Proc Natl Acad Sci USA* 1979; **76**: 4350-4354 [PMID: 388439 DOI: 10.1073/pnas.76.9.4350]
36 **Galanos C**, Freudenberg MA, Reutter W. Galactosamine-induced sensitization to the lethal effects of endotoxin. *Proc Natl Acad Sci USA* 1979; **76**: 5939-5943 [PMID: 293694 DOI: 10.1073/pnas.76.11.5939]
37 **Silverstein R**. D-galactosamine lethality model: scope and limitations. *J Endotoxin Res* 2004; **10**: 147-162 [PMID: 15198850 DOI: 10.1179/096805104225004879]
38 **Johnston DE**. Special considerations in interpreting liver function tests. *Am Fam Physician* 1999; **59**: 2223-2230 [PMID: 10221307]
39 **McGill MR**. The past and present of serum aminotransferases and the future of liver injury

biomarkers. *EXCLI J* 2016; **15**: 817-828 [PMID: 28337112 DOI: 10.17179/excli2016-800]
40 **Gowda S**, Desai PB, Hull VV, Math AA, Vernekar SN, Kulkarni SS. A review on laboratory liver function tests. *Pan Afr Med J* 2009; **3**: 17 [PMID: 21532726]
41 **George J**, Rao KR, Stern R, Chandrakasan G. Dimethylnitrosamine-induced liver injury in rats: the early deposition of collagen. *Toxicology* 2001; **156**: 129-138 [PMID: 11164615 DOI: 10.1016/s0300-483x(00)00352-8]
42 **Valenzuela R**, Videla LA. Impact of the Co-Administration of N-3 Fatty Acids and Olive Oil Components in Preclinical Nonalcoholic Fatty Liver Disease Models: A Mechanistic View. *Nutrients* 2020; **12** [PMID: 32075238 DOI: 10.3390/nu12020499]
43 **Brinkkoetter PT**, Song H, Lösel R, Schnetzke U, Gottmann U, Feng Y, Hanusch C, Beck GC, Schnuelle P, Wehling M, van der Woude FJ, Yard BA. Hypothermic injury: the mitochondrial calcium, ATP and ROS love-hate triangle out of balance. *Cell Physiol Biochem* 2008; **22**: 195-204 [PMID: 18769046 DOI: 10.1159/000149797]
44 **Valenzuela R**, Illesca P, Echeverría F, Espinosa A, Rincón-Cervera MÁ, Ortiz M, Hernandez-Rodas MC, Valenzuela A, Videla LA. Molecular adaptations underlying the beneficial effects of hydroxytyrosol in the pathogenic alterations induced by a high-fat diet in mouse liver: PPAR-α and Nrf2 activation, and NF-κB down-regulation. *Food Funct* 2017; **8**: 1526-1537 [PMID: 28386616 DOI: 10.1039/c7fo00090a]
45 **Ortiz M**, Soto-Alarcón SA, Orellana P, Espinosa A, Campos C, López-Arana S, Rincón MA, Illesca P, Valenzuela R, Videla LA. Suppression of high-fat diet-induced obesity-associated liver mitochondrial dysfunction by docosahexaenoic acid and hydroxytyrosol co-administration. *Dig Liver Dis* 2020; **52**: 895-904 [PMID: 32620521 DOI: 10.1016/j.dld.2020.04.019]
46 **Pessayre D**, Fromenty B, Berson A, Robin MA, Lettéron P, Moreau R, Mansouri A. Central role of mitochondria in drug-induced liver injury. *Drug Metab Rev* 2012; **44**: 34-87 [PMID: 21892896 DOI: 10.3109/03602532.2011.604086]
47 **McGill MR**, Sharpe MR, Williams CD, Taha M, Curry SC, Jaeschke H. The mechanism underlying acetaminophen-induced hepatotoxicity in humans and mice involves mitochondrial damage and nuclear DNA fragmentation. *J Clin Invest* 2012; **122**: 1574-1583 [PMID: 22378043 DOI: 10.1172/JCI59755]
48 **Sayed RH**, Khalil WK, Salem HA, Kenawy SA, El-Sayeh BM. Sulforaphane increases the survival rate in rats with fulminant hepatic failure induced by D-galactosamine and lipopolysaccharide. *Nutr Res* 2014; **34**: 982-989 [PMID: 25439027 DOI: 10.1016/j.nutres.2014.10.003]
49 **Lundgren CAK**, Sjöstrand D, Biner O, Bennett M, Rudling A, Johansson AL, Brzezinski P, Carlsson J, von Ballmoos C, Högbom M. Scavenging of superoxide by a membrane-bound superoxide oxidase. *Nat Chem Biol* 2018; **14**: 788-793 [PMID: 29915379 DOI: 10.1038/s41589-018-0072-x]
50 **Que X**, Hung MY, Yeang C, Gonen A, Prohaska TA, Sun X, Diehl C, Määttä A, Gaddis DE, Bowden K, Pattison J, MacDonald JG, Ylä-Herttuala S, Mellon PL, Hedrick CC, Ley K, Miller YI, Glass CK, Peterson KL, Binder CJ, Tsimikas S, Witztum JL. Oxidized phospholipids are proinflammatory and proatherogenic in hypercholesterolaemic mice. *Nature* 2018; **558**: 301-306 [PMID: 29875409 DOI: 10.1038/s41586-018-0198-8]
51 **Jaeschke H**, Farhood A. Neutrophil and Kupffer cell-induced oxidant stress and ischemia-reperfusion injury in rat liver. *Am J Physiol* 1991; **260**: G355-G362 [PMID: 2003603 DOI: 10.1152/ajpgi.1991.260.3.G355]
52 **Xie YL**, Chu JG, Jian XM, Dong JZ, Wang LP, Li GX, Yang NB. Curcumin attenuates lipopolysaccharide/d-galactosamine-induced acute liver injury by activating Nrf2 nuclear translocation and inhibiting NF-kB activation. *Biomed Pharmacother* 2017; **91**: 70-77 [PMID: 28448872 DOI: 10.1016/j.biopha.2017.04.070]
53 **Diesen DL**, Kuo PC. Nitric oxide and redox regulation in the liver: Part I. General considerations and redox biology in hepatitis. *J Surg Res* 2010; **162**: 95-109 [PMID: 20444470 DOI: 10.1016/j.jss.2009.09.019]
54 **Nakama T**, Hirono S, Moriuchi A, Hasuike S, Nagata K, Hori T, Ido A, Hayashi K, Tsubouchi H. Etoposide prevents apoptosis in mouse liver with D-galactosamine/lipopolysaccharide-induced fulminant hepatic failure resulting in reduction of lethality. *Hepatology* 2001; **33**: 1441-1450 [PMID: 11391533 DOI: 10.1053/jhep.2001.24561]
55 **Pathil A**, Warth A, Chamulitrat W, Stremmel W. The synthetic bile acid-phospholipid conjugate ursodeoxycholyl lysophosphatidylethanolamide suppresses TNFα-induced liver injury. *J Hepatol* 2011; **54**: 674-684 [PMID: 21146893 DOI: 10.1016/j.jhep.2010.07.028]
56 **Zhou RJ**, Zhao Y, Fan K, Xie ML. Protective effect of apigenin on d-galactosamine/LPS-induced hepatocellular injury by increment of Nrf-2 nucleus translocation. *Naunyn Schmiedebergs Arch Pharmacol* 2020; **393**: 929-936 [PMID: 31758207 DOI: 10.1007/s00210-019-01760-w]
57 **Gilmore TD**. Introduction to NF-kappaB: players, pathways, perspectives. *Oncogene* 2006; **25**: 6680-6684 [PMID: 17072321 DOI: 10.1038/sj.onc.1209954]
58 **Soto-Alarcón SA**, Ortiz M, Orellana P, Echeverría F, Bustamante A, Espinosa A, Illesca P, Gonzalez-Mañán D, Valenzuela R, Videla LA. Docosahexaenoic acid and hydroxytyrosol co-administration fully prevents liver steatosis and related parameters in mice subjected to high-fat diet: A molecular approach. *Biofactors* 2019; **45**: 930-943 [PMID: 31454114 DOI: 10.1002/biof.1556]
59 **Wang W**, Zhang Y, Li H, Zhao Y, Cai E, Zhu H, Li P, Liu J. Protective Effects of Sesquiterpenoids from the Root of Panax ginseng on Fulminant Liver Injury Induced by Lipopolysaccharide/d-Galactosamine. *J Agric Food Chem* 2018; **66**: 7758-7763 [PMID: 29974747 DOI:

10.1021/acs.jafc.8b02627]
60 **Wen T**, Wu ZM, Liu Y, Tan YF, Ren F, Wu H. Upregulation of heme oxygenase-1 with hemin prevents D-galactosamine and lipopolysaccharide-induced acute hepatic injury in rats. *Toxicology* 2007; **237**: 184-193 [PMID: 17587481 DOI: 10.1016/j.tox.2007.05.014]
61 **Wardyn JD**, Ponsford AH, Sanderson CM. Dissecting molecular cross-talk between Nrf2 and NF-κB response pathways. *Biochem Soc Trans* 2015; **43**: 621-626 [PMID: 26551702 DOI: 10.1042/BST20150014]
62 **Gao K**, Liu F, Chen X, Chen M, Deng Q, Zou X, Guo H. Crocetin protects against fulminant hepatic failure induced by lipopolysaccharide/D-galactosamine by decreasing apoptosis, inflammation and oxidative stress in a rat model. *Exp Ther Med* 2019; **18**: 3775-3782 [PMID: 31616509 DOI: 10.3892/etm.2019.8030]
63 **Zhang Z**, Tian L, Jiang K. Propofol attenuates inflammatory response and apoptosis to protect d-galactosamine/lipopolysaccharide induced acute liver injury *via* regulating TLR4/NF-κB/NLRP3 pathway. *Int Immunopharmacol* 2019; **77**: 105974 [PMID: 31735662 DOI: 10.1016/j.intimp.2019.105974]
64 **Wu YL**, Lian LH, Wan Y, Nan JX. Baicalein inhibits nuclear factor-κB and apoptosis *via* c-FLIP and MAPK in D-GalN/LPS induced acute liver failure in murine models. *Chem Biol Interact* 2010; **188**: 526-534 [PMID: 20850421 DOI: 10.1016/j.cbi.2010.09.008]

World Journal of Gastroenterology

Submit a Manuscript: https://www.f6publishing.com

World J Gastroenterol 2021 February 21; 27(7): 609-623

DOI: 10.3748/wjg.v27.i7.609

ISSN 1007-9327 (print) ISSN 2219-2840 (online)

ORIGINAL ARTICLE

Clinical and Translational Research

Quantitative multiparametric magnetic resonance imaging can aid non-alcoholic steatohepatitis diagnosis in a Japanese cohort

Kento Imajo, Louise Tetlow, Andrea Dennis, Elizabeth Shumbayawonda, Sofia Mouchti, Timothy J Kendall, Eve Fryer, Shogi Yamanaka, Yasushi Honda, Takaomi Kessoku, Yuji Ogawa, Masato Yoneda, Satoru Saito, Catherine Kelly, Matt D Kelly, Rajarshi Banerjee, Atsushi Nakajima

ORCID number: Kento Imajo 0000-0002-1931-6326; Louise Tetlow 0000-0001-6285-4878; Andrea Dennis 0000-0002-0152-6528; Elizabeth Shumbayawonda 0000-0003-0351-2063; Sofia Mouchti 0000-0002-3169-5242; Timothy J Kendall 0000-0002-4174-2786; Eve Fryer 0000-0003-1385-6433; Shogi Yamanaka 0000-0001-8882-3981; Yasushi Honda 0000-0002-1624-5462; Takaomi Kessoku 0000-0002-5587-1386; Yuji Ogawa 0000-0001-7033-088X; Masato Yoneda 0000-0001-7815-549X; Satoru Saito 0000-0002-5666-5218; Catherine Kelly 0000-0002-5834-1234; Matt D Kelly 0000-0002-5834-635X; Rajarshi Banerjee 0000-0003-2022-5218; Atsushi Nakajima 0000-0002-6263-1436.

Author contributions: Imajo K and Nakajima A developed the study concept, protocols and initiated the project; Kelly MD and Banerjee R assisted in the further development of the protocol and drafting the clinical study protocol; Imajo K, Nakajima A, Fryer E, Kendall TJ, Yamanaka S, Honda Y, Kessoku T, Ogawa Y, Yoneda M and Saito S contributed to the data collection; Tetlow L, Dennis AM, Shumbayawonda E to the data analysis; Imajo K, Tetlow L, Nakajima A, Dennis AM, Shumbayawonda E, Kelly C, Kelly

Kento Imajo, Yasushi Honda, Takaomi Kessoku, Yuji Ogawa, Satoru Saito, Atsushi Nakajima, Department of Gastroenterology and Hepatology, Yokohama City University School of Medicine, Yokohama 236-0004, Japan

Louise Tetlow, Andrea Dennis, Elizabeth Shumbayawonda, Sofia Mouchti, Catherine Kelly, Matt D Kelly, Rajarshi Banerjee, Innovation, Perspectum, Oxford OX4 2LL, United Kingdom

Timothy J Kendall, Centre for Inflammation Research, University of Edinburgh, Edinburgh, United Kingdom, Edinburgh EH16 4TJ, United Kingdom

Eve Fryer, Department of Cellular Pathology, Oxford University Hospitals NHS Foundation Trust, Oxford OX3 9DU, United Kingdom

Shogi Yamanaka, Anatomic and Clinical Pathology Department, Yokohoma City University Hospital, Yokohoma 236-0004, Japan

Masato Yoneda, Department of Gastroenterology, Yokohama City University Graduate School of Medicine, Yokohama 236-0004, Japan

Corresponding author: Andrea Dennis, PhD, Research Scientist, Innovation, Perspectum, Gemini One, 5520 John Smith Drive, Oxford OX4 2LL, United Kingdom.
andrea.dennis@perspectum.com

Abstract

BACKGROUND

Non-invasive assessment of non-alcoholic steatohepatitis (NASH) is increasing in desirability due to the invasive nature and costs associated with the current form of assessment; liver biopsy. Quantitative multiparametric magnetic resonance imaging (mpMRI) to measure liver fat (proton density fat fraction) and fibroinflammatory disease [iron-corrected T1 (cT1)], as well as elastography techniques [vibration-controlled transient elastography (VCTE) liver stiffness measure], magnetic resonance elastography (MRE) and 2D Shear-Wave elastography (SWE) to measure stiffness and fat (controlled attenuated parameter, CAP) are emerging alternatives which could be utilised as safe surrogates to liver biopsy.

MD and Banerjee R drafted and completed the manuscript. All authors contributed to the final manuscript.

Institutional review board statement: The study was conducted in accordance with the ethical principles of the Declaration of Helsinki 2013, was approved by the Ethics Committee of Yokohama City University Hospital and was registered as a clinical trial (UMIN Clinical Trials Registry: UMIN000026145).

Conflict-of-interest statement: Perspectum Ltd is a privately funded commercial enterprise that develops medical devices to address unmet clinical needs, including LiverMultiScan®. LT, ES, AD, MK are all employees of Perspectum. RB is CEO of Perspectum. KI, and AN have no relevant disclosures to this study. TK and EF undertake consultancy work for Perspectum.

Data sharing statement: No additional data are available.

Open-Access: This article is an open-access article that was selected by an in-house editor and fully peer-reviewed by external reviewers. It is distributed in accordance with the Creative Commons Attribution NonCommercial (CC BY-NC 4.0) license, which permits others to distribute, remix, adapt, build upon this work non-commercially, and license their derivative works on different terms, provided the original work is properly cited and the use is non-commercial. See: http://creativecommons.org/Licenses/by-nc/4.0/

Manuscript source: Unsolicited manuscript

Specialty type: Gastroenterology and hepatology

Country/Territory of origin: Japan

Peer-review report's scientific quality classification

Grade A (Excellent): A
Grade B (Very good): B
Grade C (Good): C

AIM

To evaluate the agreement of non-invasive imaging modalities with liver biopsy, and their subsequent diagnostic accuracy for identifying NASH patients.

METHODS

From January 2019 to February 2020, Japanese patients suspected of NASH were recruited onto a prospective, observational study and were screened using non-invasive imaging techniques; mpMRI with Liver*MultiScan*®, VCTE, MRE and 2D-SWE. Patients were subsequently biopsied, and samples were scored by three independent pathologists. The diagnostic performances of the non-invasive imaging modalities were assessed using area under receiver operating characteristic curve (AUC) with the median of the histology scores as the gold standard diagnoses. Concordance between all three independent pathologists was further explored using Krippendorff's alpha (a) from weighted kappa statistics.

RESULTS

N = 145 patients with mean age of 60 (SD: 13 years.), 39% females, and 40% with body mass index ≥ 30 kg/m^2 were included in the analysis. For identifying patients with NASH, MR liver fat and cT1 were the strongest performing individual measures (AUC: 0.80 and 0.75 respectively), and the mpMRI metrics combined (cT1 and MR liver fat) were the overall best non-invasive test (AUC: 0.83). For identifying fibrosis ≥ 1, MRE performed best (AUC: 0.97), compared to VCTE-liver stiffness measure (AUC: 0.94) and 2D-SWE (AUC: 0.94). For assessment of steatosis ≥ 1, MR liver fat was the best performing non-invasive test (AUC: 0.92), compared to controlled attenuated parameter (AUC: 0.75). Assessment of the agreement between pathologists showed that concordance was best for steatosis (a = 0.58), moderate for ballooning (a = 0.40) and fibrosis (a = 0.40), and worst for lobular inflammation (a = 0.11).

CONCLUSION

Quantitative mpMRI is an effective alternative to liver biopsy for diagnosing NASH and non-alcoholic fatty liver, and thus may offer clinical utility in patient management.

Key Words: Corrected T1; Fibro-inflammation; Non-invasive imaging; Non-alcoholic steatohepatitis; Multiparametric magnetic resonance imaging; Non-alcoholic fatty liver disease

©The Author(s) 2021. Published by Baishideng Publishing Group Inc. All rights reserved.

Core Tip: There is growing interest in the utility of non-invasive tests in the management of non-alcoholic steatohepatitis (NASH). We explored how magnetic resonance imaging technology can stratify patients with simple fatty liver disease from those with NASH. Our results showed that quantitative magnetic resonance imaging derived metrics showed the strongest correlations to the histological pathological components of NASH with very few technical failures. We also observed very high levels of inter-reader disagreement in histopathological biopsy reads, highlighting the pressing need for alternative diagnostic tests for NASH. Our work therefore supports the use of this non-invasive technology in day-to-day practice.

Citation: Imajo K, Tetlow L, Dennis A, Shumbayawonda E, Mouchti S, Kendall TJ, Fryer E, Yamanaka S, Honda Y, Kessoku T, Ogawa Y, Yoneda M, Saito S, Kelly C, Kelly MD, Banerjee R, Nakajima A. Quantitative multiparametric magnetic resonance imaging can aid non-alcoholic steatohepatitis diagnosis in a Japanese cohort. *World J Gastroenterol* 2021; 27(7): 609-623
URL: https://www.wjgnet.com/1007-9327/full/v27/i7/609.htm
DOI: https://dx.doi.org/10.3748/wjg.v27.i7.609

Grade D (Fair): 0
Grade E (Poor): 0

Received: August 28, 2020
Peer-review started: August 28, 2020
First decision: November 3, 2020
Revised: November 17, 2020
Accepted: December 28, 2020
Article in press: December 28, 2020
Published online: February 21, 2021

P-Reviewer: Lei YC, Xu CF, Wu B
S-Editor: Zhang H
L-Editor: A
P-Editor: Wang LL

INTRODUCTION

Non-alcoholic fatty liver disease (NAFLD) is the most common cause of chronic liver disease, affecting approximately 25% of the general population worldwide[1] and up to 30% of the general population in Japan[2]. Additionally, up to 19% of individuals in south east Asia with body mass index (BMI) ≤ 25 kg/m^2 have "lean" or "non-obese" NAFLD[3,4]. The scope of disease aetiologies within NAFLD differ in both clinical significance and prognosis[1,5-7] on a continuum that encompasses "simple steatosis" or NAFL (hepatic steatosis without inflammation), to non-alcoholic steatohepatitis (NASH) and NASH cirrhosis. NASH results when fat accumulation in the liver triggers inflammatory signals and reactive oxygen species that can amplify liver injury and stimulate fibrosis[8]. NASH is predicted to become the leading cause of liver transplant over the coming decade[1] as NASH patients have a greater tendency to develop advanced liver fibrosis, cirrhosis, and hepatocellular carcinoma[9-11].

Liver biopsy is the current gold standard for differentiating simple steatosis from NASH as well as staging the severity of fibrosis in patients with NAFLD[12]. However, due to the limitations associated with biopsy[13], high procedure costs, high levels of discordance between readers, and poor acceptability by patients, there has been an increase in the use of non-invasive imaging biomarkers to diagnose and monitor the disease.

Vendor-neutral and scalable multiparametric magnetic resonance imaging (mpMRI) measurements of liver fat proton density fat fraction (PDFF) with IDEAL and iron corrected T1-mapping (cT1) are emerging as promising quantitative imaging biomarkers for NASH. MRI liver fat correlates strongly with histologically graded steatosis across the clinical range seen in NASH[14] and has high diagnostic accuracy in stratifying all grades of liver steatosis[15-17]. cT1 correlates with ballooning[18], and has been shown to predict clinical outcomes in patients with chronic liver disease[19,20]. Both metrics have good technical validity with high repeatability and reproducibility across MRI manufacturers and field strengths[21]. Additionally, due to their sensitivity to subtle changes in hepatic fat and fibro-inflammation, mpMRI techniques are increasingly used as inclusion criteria endpoints in NASH clinical trials and are included in the FDA Biomarker Qualification Program.

Magnetic resonance elastography (MRE) is an alternative MR based approach that can be used to stage fibrosis. MRE has shown utility in identifying patients with NASH from those with simple steatosis[22] whilst also being able to detect the presence of advanced fibrosis in patients with chronic liver disease[23]. However, MRE has not demonstrated sufficient utility for the longitudinal monitoring of fibrosis progression or regression[14,24].

Ultrasound based methods such as vibration-controlled transient elastography (VCTE) liver stiffness measure (LSM) have shown good utility in identifying patients with advanced fibrosis[25,26], however they may be less reliable in patients who are morbidly obese; a high-risk group for NASH[25]. VCTE controlled-attenuation parameter (CAP) has been shown to be sensitive to early changes in liver fat albeit with a low ability to differentiate steatosis levels.

The aim of this study was to evaluate the diagnostic performance of quantitative mpMRI, MRE, and transient elastography (VCTE and 2D shear-wave elastography) to identify patients with suspected NASH and to report on the correlations between these non-invasive technologies and histology.

MATERIALS AND METHODS

This was an observational trial conducted and sponsored by the Yokohoma City University Hospital between January 2019 and February 2020. *N* = 151 adult participants who underwent a liver biopsy for suspected NASH were included in this interim analysis. Participants were invited to undergo core liver biopsy if there was evidence of steatosis (Proton density fat fraction ≥ 5.2% or CAP ≥ 236)[16]. Patients were excluded if there was contraindication to MRI, history of alcoholism, or evidence of other chronic liver disease (Figure 1). The study was conducted in accordance with the ethical principles of the Declaration of Helsinki 2013, was approved by the Ethics Committee of Yokohama City University Hospital and was registered as a clinical trial (UMIN Clinical Trials Registry: UMIN000026145).

Histopathological evaluations

Liver biopsy samples were obtained using a 16-gauge needle biopsy kit with an

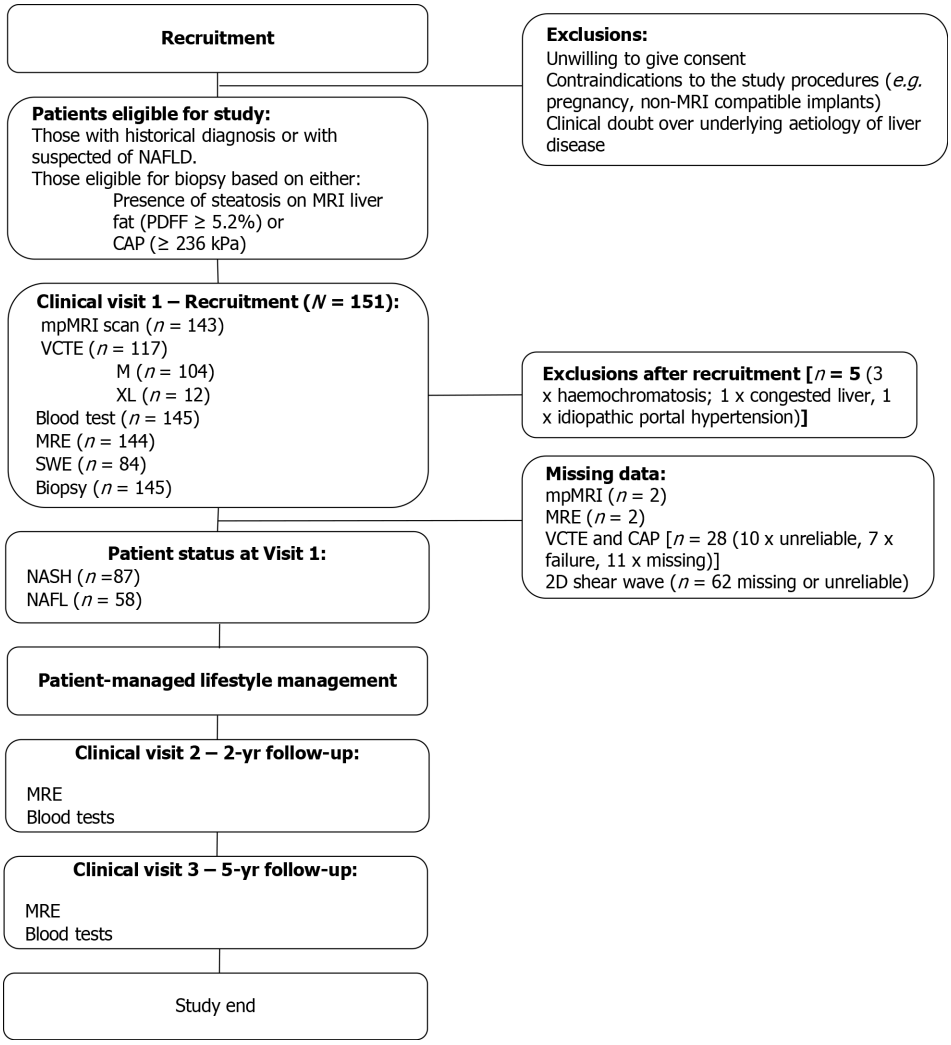


Figure 1 CONSORT diagram of patient pathway and inclusion into the study. mpMRI: Quantitative multiparametric magnetic resonance imaging; CAP: Controlled-attenuation parameter; MRE: Magnetic resonance elastography; NASH: Non-alcoholic steatohepatitis; NAFLD: Non-alcoholic fatty liver disease; VCTE: Vibration-controlled transient elastography.

adequate liver biopsy defined as being ≥ 20 mm in length and/or with ≥ 10 portal tracts. Biopsy samples were assessed independently by three histopathologists, one at YCUH at the time of collection and then later by a further two pathologists using digitalised biopsy slides. Histological scoring of fibrosis, steatosis, lobular inflammation, and hepatocyte ballooning was performed by all pathologists, and overall disease activity was graded according to the NAFLD activity score [NASH Clinical Research Network (NAS)]. NASH was defined as NAS ≥ 4, ballooning ≥ 1 and inflammation ≥ 1 as described in AASLD guidelines[12]. All scores were taken from the median score for each component from the three pathologists.

Non-invasive biomarkers

MR liver fat and cT1 measurements were made using the non-contrast Liver*MultiScan*® mpMRI protocol (Perspectum, Oxford, United Kingdom), performed with the patient in the supine position using a 3 Tesla GE Discovery 750W scanner system (GE Healthcare, Milwaukee, WI, United States). The average scan time for this protocol was 10 min. Four single transverse slices were captured through the liver centered on the porta hepatis. Anonymised mpMRI data were analysed off-site by image analysts trained in abdominal anatomy and artefact detection, who were blinded to the clinical data and risk grouping. For MR liver fat, three 15 mm diameter circular regions of interest (ROIs) were selected on the transverse maps to cover a representative sample of the liver parenchyma. For cT1 (ms), three ROIs were placed on the central slice within the typical percutaneous biopsy region. Median values from all pixels within the ROIs were calculated and used as the representative score.

MRE examinations were performed using the same MRI scanner and following a 2-

dimensional MRE protocol[27]. Interpretation of MRE images to obtain stiffness values was performed by abdominal radiologists[22]. VCTE-LSMs were obtained by one operator using either 3.5 MHz M-probe and/or 2.5 MHz XL-probe dependent upon suitability (waste-hip circumference and BMI) and through use of the automatic probe selection tool embedded within the Fibroscan operating software[28]. VCTE-LSM measures with at least 10 valid shots and a success rate of ≥ 60% were considered reliable and used for statistical analysis. Hepatic steatosis was assessed using the CAP value provided by the device. 2D shear-wave elastography (2D-SWE) measurements were obtained using a Logiq S8 system (GE Healthcare)[29]. Example images are shown in Figure 2 for all methods.

Statistical analysis

Descriptive statistics were used to summarise baseline participant characteristics. Continuous variables were reported as mean and standard deviation, categorical variables were reported as frequency and percentage, and confidence intervals (CI) were reported at the 95% level. Mean difference in biomarker values between those with NAFL and those with NASH were compared using independent t-tests or Wilcoxon signed-rank tests, depending on distribution. Diagnostic performance of non-invasive biomarkers was assessed using area under receiver operator characteristic curve (AUC) with multivariate logistic regressions utilised to assess performance of combined biomarkers. Correlations between median scores from the 3 pathology reads and image-derived markers (MR liver fat, cT1, MRE, VCTE-LSM and CAP) were assessed using Spearman's rank correlation coefficient.

Inter-rater variability analysis between the pathology scores given by the 3 pathologists were performed using tri-variate weighted kappa statistic, with the overall variability seen for each of the histological metrics assessed by Krippendorff's alpha[30].

Statistical analysis was performed using R software version 3.6.1 with $P < 0.05$ considered to be statistically significant. Case-wise deletion was employed to include only complete cases for MR metrics, VCTE-LSM and CAP for each analysis as appropriate rather than imputing any missing values.

RESULTS

Of the initial 151 patients who underwent liver biopsy, 145 were eligible for the study. The average age was 60 (± 13) years, 61% patients were male, 40% BMI ≥ 30 kg.m^{-2} and 60% of patients had NASH (NAS ≥ 4 with ballooning ≥ 1 and inflammation ≥ 1; Table 1). There was a broad range of histology scores across all aspects of the key histopathological hallmarks of NASH (Table 2). From the entire cohort, one had missing MRE data, two had missing Liver*MultiScan*® data, 28 missing or uninterpretable Fibroscan data, and 61 had missing or uninterpretable 2D-SWE data. Investigation into potential causes of failure for the ultrasound based methods revealed BMI to be significantly higher in the cases in which VCTE-LSM was unreported (31.7 kg/m^2 *vs* 28.1 kg/m^2, $P < 0.05$), and similarly was elevated in those with missing 2D-SWE (29.5 kg/m^2 *vs* 27.9 kg/m^2).

Diagnostic accuracy of non-invasive imaging markers for differentiation of disease activity

Steatosis (NAFL): MR Liver fat [AUC: 0.92 (CI: 0.87-0.98)], and CAP [AUC: 0.75 (CI: 0.58-0.92)] both discriminated between steatosis ≥ 1, while the other imaging markers were unable to [cT1 AUC: 0.64 (CI: 0.46-0.82), MRE AUC: 0.53 (CI: 0.33-0.72), VCTE-LSM AUC: 0.60 (CI: 0.37-0.82), 2D-SWE AUC: 0.53 (CI: 0.22-0.84)]. For steatosis ≥ 2, MR liver fat again showed the best performance [MR liver fat: AUC: 0.86 (CI: 0.80-0.93); *vs* CAP AUC: 0.68 (CI: 0.59-0.78)]. 7 patients had CAP technical failure and 10 patients were not able to gain reliable results.

NASH: To diagnose steatohepatitis (NAS ≥ 4 with at least one in both ballooning and inflammation), MR liver fat [AUC: 0.80 (CI: 0.73-0.87)], cT1 [AUC: 0.75 (CI: 0.67-0.84)], and CAP [AUC: 0.71 (CI: 0.62-0.80)] all had good discriminatory performance, while VCTE-LSM [AUC: 0.56 (CI: 0.45-0.66)], MRE [AUC: 0.57 (CI: 0.47-0.67)] and 2D-SWE [AUC: 0.58 (CI: 0.45-0.71)] were not as effective (Figure 3). Multivariate analysis to explore the potential for increased diagnostic performance of biomarkers used in combination for identifying those with NASH, revealed the combination of cT1 and MR liver fat [AUC: 0.83 (CI: 0.76-0.90)] was superior to the individual markers and to

Table 1 Participant demographics

	Total (*n* = 145), mean ± SD (% of cohort)	NASH	NAFL
Total cohort (*n*)	145	87	58
Sex (male)	88 (60.7%)	46	42[a]
Age	60.2 ± 13.1	60.9 ± 13.2	59 ± 12.9
BMI average	28.8 ± 4.7	29.9 ± 4.4	27.1 ± 4.8[c]
Normal BMI (≥ 18.5 ≤ 22.9)	21.4 ± 1.6 (*n* = 17)	*n* = 6	*n* = 12
Overweight (≥ 23.0 ≤ 27.9)	25.6 ± 1.1 (*n* = 43)	*n* = 26	*n* = 26
Obese (≥ 27.5)	32.1 ± 3.2 (*n* = 82)	*n* = 55	*n* = 20
Blood serum tests			
AST (IU/L)	47.8 ± 27.5	56.4 ± 29.8	34.8 ± 17.1[c]
ALT (IU/L)	59.8 ± 49.3	71.3 ± 51.5	42.6 ± 41.4[c]
GGT	85.9 ± 78.4	97.8 ± 85.8	69.3 ± 62.9[b]
Total bilirubin (mg/dL)	0.86 ± 0.4	0.8 ± 0.3	0.9 ± 0.4
Platelets ($\times 10^4$/μL)	19.4 ± 7.3	19.9 ± 7.5	18.8 ± 7
HbA1C (%)	6.5 ± 1.1	6.6 ± 1.0	6.5 ± 1.1
Fasting insulin (mU/mL)	20 ± 14.2	20.6 ± 11.6	19 ± 17.4
Fasting blood glucose (mg/dL)	124 ± 34.7	126.1 ± 32.5	120.8 ± 37.8
Albumin (g/dL)	4.3 ± 0.5	4.3 ± 0.4	4.2 ± 0.5
Non-invasive test			
cT1	871 ± 102 (*n* = 143)	907 ± 90 (*n* = 87)	817 ± 96[c] (*n* = 56)
MR liver fat	11.4 ± 6.1 (*n* = 143)	13.6 ± 5.8 (*n* = 87)	8.1 ± 5.1[c] (*n* = 56)
CAP	294.3 ± 47.4 (*n* = 117)	309.1 ± 37.1 (*n* = 74)	268.9 ± 52.7[c] (*n* = 43)
VCTE-LSM	12.8 ± 9.5 (*n* = 117)	13 ± 8.4 (*n* = 74)	12.5 ± 11.1 (*n* = 43)
MRE	4.2 ± 1.7 (*n* = 144)	4.3 ± 1.5 (*n* = 88)	4.1 ± 1.9 (*n* = 56)
SE	9.3 ± 2.7 (*n* = 84)	9.6 ± 2.4 (*n* = 50)	8.8 ± 3.1 (*n* = 33)
Reported pre-existing conditions			
Hypertensive	*n* = 71	*n* = 45	*n* = 26
Dyslipidaemic	*n* = 111	*n* = 72	*n* = 39
Reported as diabetic	*n* = 97	*n* = 59	*n* = 38

Non-alcoholic steatohepatitis (NASH) were patients with NASH clinical research network ≥ 4 with ballooning ≥ 1. Stars denote significance difference between those with NASH and non-alcoholic fatty liver these levels:

[a]$P < 0.05$.

[b]$P < 0.01$.

[c]$P < 0.001$. MRE: Magnetic resonance elastography; CAP: Controlled-attenuation parameter; VCTE: Vibration-controlled transient elastography; cT1: Corrected T1; BMI: Body mass index; NASH: Non-alcoholic steatohepatitis; NAFL: Non-alcoholic fatty liver.

the combination of VCTE-LSM and CAP in combination [AUC: 0.71 (CI: 0.66-0.8)] (Figure 4).

Fibrosis: To measure fibrosis alone, MRE [AUC: 0.97 (CI: 0.94-1.0)], VCTE-LSM [AUC: 0.94 (CI: 0.9-0.99)] and 2D-SWE [AUC: 0.94 (CI: 0.86-1.0)] were all excellent at discriminating for any fibrosis (≥ 1) whilst MR liver fat [AUC: 0.68 (CI: 0.44-0.92)], cT1 [AUC: 0.63 (CI: 0.3-0.97)] and CAP [AUC: 0.6 (CI: 0.39-0.81)] were not as effective. These performances were maintained for discriminating those with more advanced fibrosis (≥ 2): MRE [AUC: 0.92 (CI: 0.87-0.97)]; VCTE-LSM [AUC: 0.88 (CI: 0.81-0.95)]; 2D-SWE [AUC: 0.87 (CI: 0.76-0.99)] compared to cT1 [AUC: 0.62 (CI: 0.49-0.74)] MR liver fat [AUC: 0.60 (CI: 0.48-0.72)] and CAP [AUC: 0.57 (CI: 0.45-0.70)]. VCTE-LSM,

Table 2 Range of histology scores reported across the entire cohort

Histology scores from biopsy (*n* = 144)				
	Score	**Total**	**NASH**	**NAFL**
Steatosis (Brunt)	0	13	0	13
	1	74	36	37
	2	35	30	5
	3	21	20	1
Lobular inflammation	0	13	0	1
	1	91	48	51
	2	35	35	9
	3	4	3	0
Ballooning	0	39	0	39
	1	72	55	16
	2	32	31	1
	3	0	0	0
Fibrosis (Kleiner)	0	5	1	0
	1	24	10	14
	2	27	16	11
	3	55	39	15
	4	31	19	12
NAS	0	0	0	0
	1	5	0	5
	2	23	0	22
	3	26	0	26
	4	25	25	1
	5	37	35	2
	6	16	16	0
	7	8	8	0
	8	2	2	0

NASH: Non-alcoholic steatohepatitis; NAFL: Non-alcoholic fatty liver.

and to an even greater extent 2D-SWE, however both had high levels of missing data (20% and 42% respectively), likely to be related to elevated obesity.

Advanced NASH: To identify those with NASH and fibrosis (NAS ≥ 4 with F ≥ 2), both cT1 [AUC: 0.74 (CI: 0.66-0.82)] and MR liver fat [AUC: 0.71 (CI: 0.63-0.80)] outperformed the other measures; MRE [AUC 0.66 (CI: 0.57-0.75)], VCTE-LSM [AUC: 0.64 (CI: 0.54-0.74)], CAP [AUC: 0.68 (CI: 0.59-0.78)], and 2D-SWE [AUC: 0.62 (CI: 0.49-0.75)]. Combining cT1 and MR liver fat improved the performance [AUC: 0.76 (CI: 0.69-0.84)] and was superior to the combination of VCTE-LSM and CAP [AUC: 0.70 (CI: 0.61-0.79)], (Figure 4).

Correlations between image derived biomarkers and histological markers of disease

MRI cT1 correlated significantly with all key aspects of histology [fibrosis, steatosis, ballooning and lobular inflammation (r_s = 0.24, r_s = 0.29, r_s = 0.39, r_s = 0.31, respectively)] and with overall NAS (r_s = 0.58). MR liver fat was positively correlated with steatosis (r_s = 0.70), and with inflammation (r_s = 0.28), ballooning (r_s = 0.29) and overall NAS (r_s = 0.64) but was negatively correlated with fibrosis (r_s = -0.25). MRE was significantly

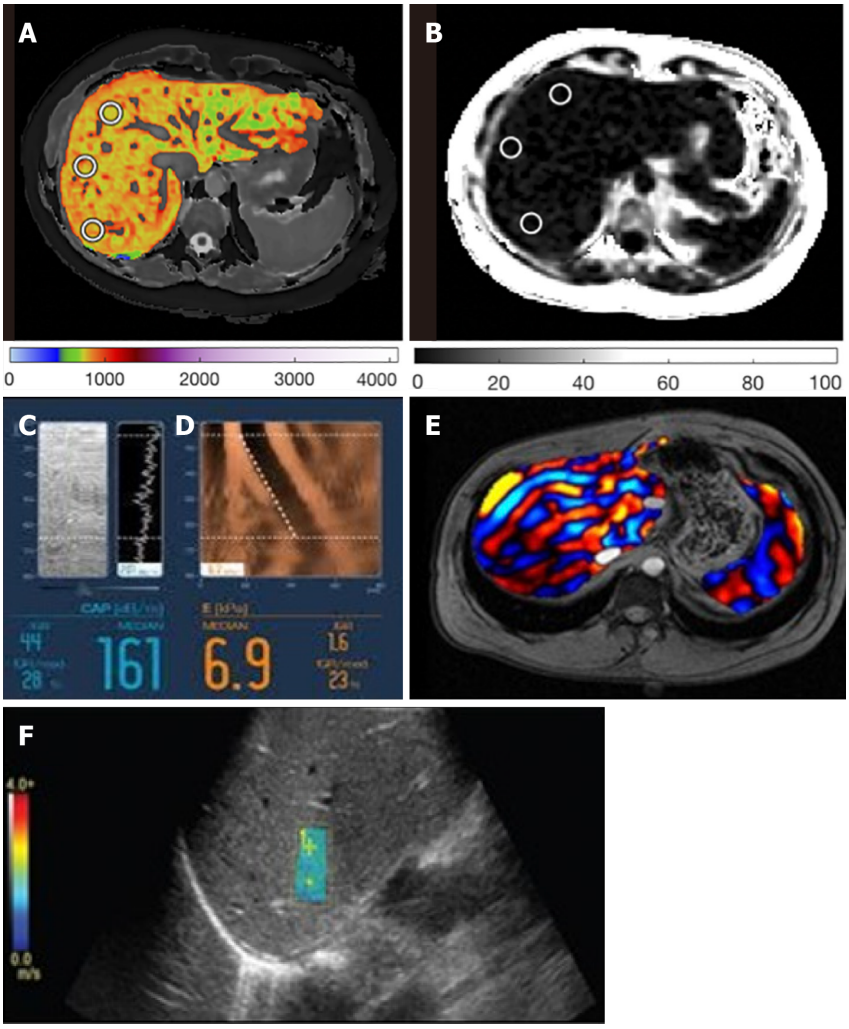


Figure 2 Example images from each technology. A: Corrected T1 map; B: Magnetic resonance liver fat map; C: Fibroscan controlled-attenuation parameter; D: Fibroscan Liver Stiffness; E: magnetic resonance elastography liver stiffness map; and F: 2D Shear-wave elastography.

correlated with fibrosis (r_s = 0.75) as well as ballooning and lobular inflammation (r_s = 0.32, r_s = 0.16 respectively) and negatively correlated with steatosis (r_s = -0.23). VCTE-LSM correlated significantly with fibrosis (r_s = 0.69) and ballooning (r_s = 0.29), and CAP with steatosis (r_s = 0.39), inflammation (r_s = 0.26), ballooning (r_s = 0.33) and NAS (r_s = 0.49). 2D shear-wave elastography was positively correlated with fibrosis (r_s = 0.72) and ballooning (r_s = 0.34; Table 3).

Concordance between pathologists

Assessment of the overall agreement (Krippendorff's alpha) of the pathologists for each histological marker showed that there was moderate agreement for indicators of steatosis (a = 0.58) and NAS (a = 0.42), fair agreement for ballooning and fibrosis (a = 0.40 for both), and none to slight agreement on lobular inflammation (a = 0.11). Assessment of the trivariate weighted kappa scores from individual pathologists for each metric showed no reoccurring pattern of agreement between any two pathologists (Table 4).

DISCUSSION

The diagnosis of NASH is important as it provides prognostic information indicating an increased risk of fibrosis progression and liver-related mortality but has hitherto been limited because of the need for histological verification. In clinical practice, distinguishing between NAFL, NASH, and NASH with fibrosis is highly desirable for risk stratification. Patients with steatosis can be educated about future cardiovascular risk, and lifestyle measures to prevent them, while those with NASH, or NASH and

Table 3 Spearman's correlation coefficients for all variables

	cT1, (*n* = 143)	MR liver fat (*n* = 143)	MRE (*n* = 144)	VCTE-LSM (*n* = 117)	CAP (*n* = 117)	2D SWE (*n* = 84)
Fibrosis	0.24, $P < 0.01$	-0.25, $P < 0.01$	0.75, $P < 0.001$	0.69, $P < 0.001$	0.05, $P = 0.58$	0.72, $P < 0.001$
Steatosis	0.29, $P < 0.001$	0.70, $P < 0.001$	-0.23, $P < 0.01$	-0.09, $P = 0.23$	0.39, $P < 0.001$	-0.07, $P = 0.53$
Lobular inflammation	0.31, $P < 0.001$	0.28, $P < 0.001$	0.16, $P < 0.01$	0.15, $P = 0.10$	0.26, $P < 0.01$	0.16, $P = 0.15$
Ballooning	0.39, $P < 0.001$	0.29, $P < 0.001$	0.32, $P < 0.01$	0.29, $P < 0.01$	0.33, $P < 0.001$	0.34, $P < 0.001$
NAS	0.58, $P < 0.001$	0.64, $P < 0.001$	0.06, $P = 0.44$	0.13, $P = 0.13$	0.49, $P < 0.001$	0.16, $P = 0.13$

$P < 0.05$: Correlations with statistical significance. MRE: Magnetic resonance elastography; CAP: Controlled-attenuation parameter; VCTE: Vibration-controlled transient elastography; cT1: Corrected T1; SWE: Shear-Wave elastography; NASH: Non-alcoholic steatohepatitis; LSM: Liver stiffness measure.

Table 4 Inter-rater variability between the three pathologists for each histology metric

Histological metric	Pathologists	Kappa weighted	Lower CI	Upper CI	ASE	*P* value	Overall inter-rater variability (Krippendorff's alpha)
Steatosis	1 *vs* 2	0.609	0.517	0.7	0.0467	< 0.0001	0.584
	1 *vs* 3	0.483	0.388	0.579	0.0489	< 0.0001	
	2 *vs* 3	0.585	0.485	0.686	0.0513	< 0.0001	
Lobular inflammation	1 *vs* 2	0.118	0.0631	0.173	0.0281	< 0.0001	0.109
	1 *vs* 3	0.0376	0.00574	0.0695	0.0163	0.02	
	2 *vs* 3	0.179	0.0699	0.288	0.0556	0.001	
Ballooning	1 *vs* 2	0.297	0.205	0.389	0..047	< 0.0001	0.398
	1 *vs* 3	0.459	0.344	0.573	0.0583	< 0.0001	
	2 *vs* 3	0.27	0.18	0.36	0.0453	< 0.0001	
Fibrosis	1 *vs* 2	0.719	0.65	0.788	0.0353	< 0.0001	0.398
	1 *vs* 3	0.571	0.496	0.647	0.0386	< 0.0001	
	2 *vs* 3	0.597	0.521	0.672	0.0385	< 0.0001	
NAS	1 *vs* 2	0.279	0.202	0.357	0.0398	< 0.0001	0.421
	1 *vs* 3	0.244	0.172	0.316	0.0366	< 0.0001	
	2 *vs* 3	0.434	0.35	0.518	0.043	< 0.0001	

CI: Confidence intervals.

fibrosis, can be monitored and treated (pioglitazone, cevoglitazar) to reduce the risk of cardiovascular and liver clinical complications. In this study, we were able to identify and differentiate patients with steatosis, NASH, and NASH with fibrosis with good diagnostic performance using non-invasive technologies which characterise liver tissue accurately.

The diagnosis of NASH is based, at present, on the histological presence of steatosis and either lobular inflammation or ballooning, with the presence of fibrosis highlighting disease progression. Currently, the only biomarkers shown to predict outcomes in patients are histological fibrosis and cT1[19,20,31]. However, cT1 is sensitive to ballooning, inflammation, steatosis as well as fibrosis, and so cannot be considered a pure fibrosis biomarker. When measuring just fibrosis, MRE had greater correlations to histology and greater sensitivity than other methods but could not by itself distinguish NAFL from NASH or NASH with fibrosis. Whilst ultrasound methods are also effective for staging advanced fibrosis, in line with reported literature[32-35], they can be less reliable in obese patients with higher BMI as observed in the patients in this cohort with missing VCTE and 2D-SWE data. In contrast BMI has not been shown to systematically affect the failure rate for MRE[23] or of mpMRI[36,37], except for the very

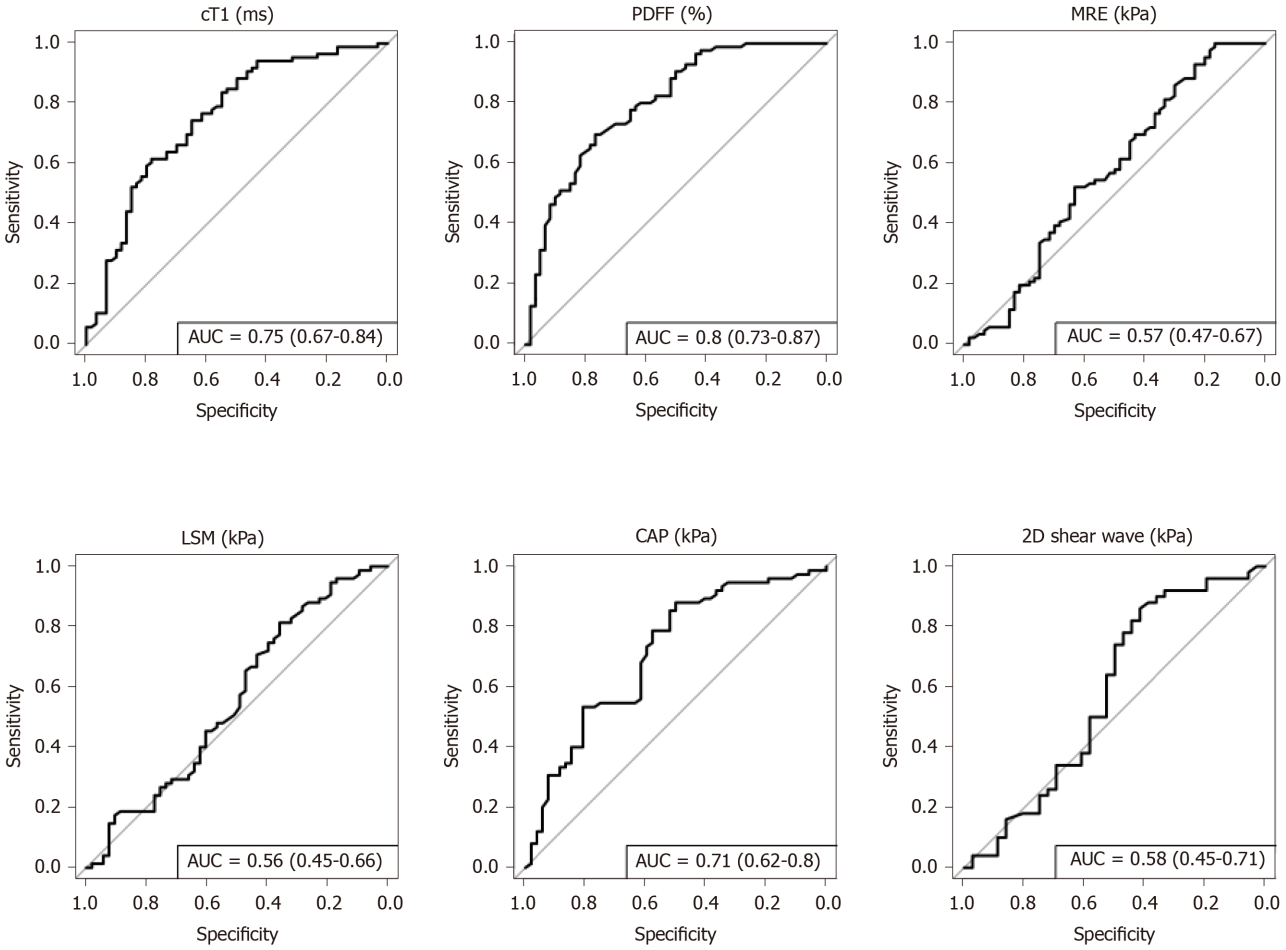


Figure 3 Receiver operator characteristic curves for discriminating those with non-alcoholic steatohepatitis (NAS ≥ 4 and ballooning > 1 or inflammation > 1) from those without. Area under the curve and confidence intervals displayed in the legend for each non-invasive measure. MRE: Magnetic resonance elastography; CAP: Controlled-attenuation parameter; cT1: Corrected T1; LSM: Liver stiffness measure; PDFF: Proton density fat fraction.

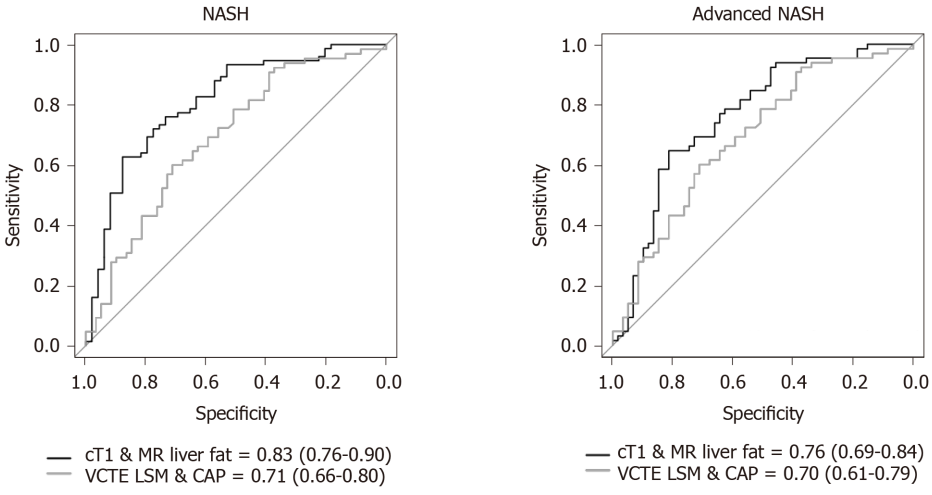


Figure 4 Receiver operator characteristic curves for discriminating those with non-alcoholic steatohepatitis (left) and those with non-alcoholic steatohepatitis with fibrosis (right). Area under the curve and confidence intervals displayed in the legend for each non-invasive measure. CAP: Controlled-attenuation parameter; VCTE: Vibration-controlled transient elastography; cT1: Corrected T1; NASH: Non-alcoholic steatohepatitis.

unusual circumstances when a participant is simply too large to fit into the scanner. All elastography measures however have been shown to be confounded by iron, steatosis and inflammation[38] in the measure of fibrosis.

The assessment of steatosis is important as the accumulation of liver fat is linked with the progression of hepatocyte injury that can ultimately result in fibrosis[39]; the downstream consequence of NASH which is linked to poor clinical outcomes[31]. In this study, MR liver fat demonstrated better performance than CAP for the detection and differentiation of steatosis grades. As a result, this makes MR liver fat a good marker of NAFL and NASH. However, where cT1 appears to have an advantage over MR liver fat as a non-invasive biomarker for NASH is in the detection and diagnosis of patients with both NASH and fibrosis. Both cT1, and uncorrected T1 have been reported to be elevated in those with advanced liver fibrosis[40-43]. A key limitation of MR liver fat as a solo biomarker of NASH is that patients with advanced fibrosis and cirrhosis have lower acclimations of liver fat than those at earlier stages of disease[44,45]. Our results, in line with those reported in the literature, demonstrate a negative association between MR liver fat and advanced fibrosis[44,45]. This is an important consideration and is reflected in the superior diagnostic accuracy of cT1 when compared to MR liver fat for identifying those with NASH and fibrosis ≥ 2, with the composite marker of cT1 and MR liver fat showing the greatest diagnostic accuracy.

New diagnostic tools are evaluated by comparison to histological measures to evaluate their utility. Nevertheless, recent studies on the reproducibility of histology[46] have established that biopsy, as the de facto benchmark, is not perfect. We also observed discordance between different pathologists across the four cardinal pathological features (steatosis, ballooning, lobular inflammation and fibrosis), with no common pattern of concordance seen between any two pathologists. Previous literature discusses the subjective nature of histological grading systems[47] which is evident in these findings, demonstrating that subjectivity as well as potential sampling and human error can affect results[48-50]. This analysis highlights the need for more robust endpoints with which to evaluate the performance of non-invasive diagnostics. The gold standard would be a tool that predicts clinical outcomes and can thus provide prognosis. Whilst such studies are both time-consuming and costly in order to generate the necessary evidence, encouragingly, initial work in this space has demonstrated potential for cT1 to predict clinical outcomes in patients with chronic liver disease[19,20]. It is hoped that further validation of these observations in patients with NASH specifically will aid in the development of a clinical pathway that does not rely on invasive liver biopsy.

This study was not without its limitations, with the pre-screening step prior to liver biopsy likely truncating the correlations that would be observed across the full disease spectrum. While this may also impact the diagnostic accuracy evaluated, this pre-screening approach is representative of clinical practice. Observed failure rates for the ultrasound-based methods also have the potential to skew the results given its dependence on BMI, with patients with high BMI less likely to be included in the study. In practice this has a bearing on the value proposition of such technologies for screening and monitoring as failed measurements will result in necessary further clinical tests for patients.

CONCLUSION

In summary, this study demonstrates the clinical utility of mpMRI for the stratification of NAFLD, and encourages mpMRI use as a non-invasive alternative to biopsy in the clinical care pathway. Quantitative mpMRI metrics showed the strongest overall correlations to the histological components of NASH with fewer technical failures. mpMRI also out-performed MRE and ultrasound-based elastography methods in the identification of patients with NASH and fibrosis. The ability to risk stratify patients in a single non-invasive test is a particular strength of mpMRI, offering a safe and cost-effective alternative to liver biopsy.

ARTICLE HIGHLIGHTS

Research background

Non-alcoholic fatty liver disease affects 25% of the population worldwide and up to 30% in the Japanese population, and in some can progress to non-alcoholic

steatohepatitis (NASH), a leading cause of liver transplant due to its strong propensity to develop into cirrhosis and hepatocellular carcinoma.

Research motivation

Liver biopsy is the current reference standard for a clinical diagnosis of NASH, a method that is expensive, invasive and suffers from great observer variability. Non-invasive and scalable alternatives are required in order to meet the burgeoning demands of the disease on clinical caseloads across the globe.

Research objectives

The main objectives of the study were to evaluate the diagnostic performance of non-invasive, image derived metrics to identify patients with suspected NASH. The metrics under investigation included two quantitative multi-parametric magnetic resonance imaging (MRI) measures, iron corrected T1 mapping [(cT1), a marker of fibro-inflammation] and proton density liver fat fraction (a marker of liver fat), magnetic resonance elastography and ultrasound based transient elastography (vibration-controlled transient elastography and 2D shear-wave elastography), both markers of liver stiffness.

Research methods

In an observational study of patients who were being screened clinically on suspicion of NASH, n = 145 individuals underwent liver biopsy and concomitant imaging measures of liver health. Diagnosis of NASH was based on histology, graded using the NAS- Clinical Research Network scoring system and diagnostic accuracy of the image-derived metrics assessed using area under receiver operator characteristic curve. In addition, the biopsy slides were read by 2 further pathologists and comparisons made to explore the level of agreement on diagnosis between individual doctors.

Research results

In this study assessing the ability of different non-invasive biomarkers to detect NASH, MR liver fat and cT1 were superior to the other metrics investigated. Crucially however, the composite marker of cT1 and MR liver fat showed the greatest diagnostic accuracy for identifying those with NASH and also those with NASH with fibrosis. These measures also had very few technical failures. This is the first assessment and direct comparison of these technologies in a Japanese cohort. We also observed discordance between different pathologists across the four cardinal pathological features (steatosis, ballooning, lobular inflammation and fibrosis), with no common pattern of agreement seen between any two pathologists.

Research conclusions

These results demonstrate the clinical utility of quantitative multiparametric magnetic resonance imaging (mpMRI) for the identification and stratification of patients with NASH from those with evidence of NAFLD and encourages mpMRI use as a non-invasive alternative to biopsy in the clinical care pathway. Quantitative mpMRI metrics showed the strongest correlation to the histological components of NASH with fewer technical failures. mpMRI also out-performed magnetic resonance elastography and ultrasound-based elastography methods in the identification of patients with NASH and fibrosis. Liver biopsy suffered from high levels of inter-reading disagreement, highlighting the pressing need for alternative diagnostic tests for NASH.

Research perspectives

The ability to risk stratify patients in a single non-invasive test is a particular strength of mpMRI, offering a safe and cost-effective alternative to liver biopsy. Future work should be focused on validating these findings further and on longer term outcomes studies to investigate the prognostic natures of these measurements in a Japanese population.

REFERENCES

1 **Younossi Z**, Anstee QM, Marietti M, Hardy T, Henry L, Eslam M, George J, Bugianesi E. Global burden of NAFLD and NASH: trends, predictions, risk factors and prevention. *Nat Rev Gastroenterol Hepatol* 2018; **15**: 11-20 [PMID: 28930295 DOI: 10.1038/nrgastro.2017.109]

2 **Fan JG**, Kim SU, Wong VW. New trends on obesity and NAFLD in Asia. *J Hepatol* 2017; **67**: 862-873 [PMID: 28642059 DOI: 10.1016/j.jhep.2017.06.003]

3 **Albhaisi S**, Chowdhury A, Sanyal AJ. Non-alcoholic fatty liver disease in lean individuals. *JHEP Rep* 2019; **1**: 329-341 [PMID: 32039383 DOI: 10.1016/j.jhepr.2019.08.002]

4 **Younes R**, Bugianesi E. NASH in Lean Individuals. *Semin Liver Dis* 2019; **39**: 86-95 [PMID: 30654392 DOI: 10.1055/s-0038-1677517]

5 **Angulo P**. Long-term mortality in nonalcoholic fatty liver disease: is liver histology of any prognostic significance? *Hepatology* 2010; **51**: 373-375 [PMID: 20101746 DOI: 10.1002/hep.23521]

6 **Singh S**, Allen AM, Wang Z, Prokop LJ, Murad MH, Loomba R. Fibrosis progression in nonalcoholic fatty liver *vs* nonalcoholic steatohepatitis: a systematic review and meta-analysis of paired-biopsy studies. *Clin Gastroenterol Hepatol* 2015; **13**: 643-54. quiz e39-40 [PMID: 24768810 DOI: 10.1016/j.cgh.2014.04.014]

7 **Seki Y**, Kakizaki S, Horiguchi N, Hashizume H, Tojima H, Yamazaki Y, Sato K, Kusano M, Yamada M, Kasama K. Prevalence of nonalcoholic steatohepatitis in Japanese patients with morbid obesity undergoing bariatric surgery. *J Gastroenterol* 2016; **51**: 281-289 [PMID: 26314837 DOI: 10.1007/s00535-015-1114-8]

8 **Marra F**, Lotersztajn S. Pathophysiology of NASH: perspectives for a targeted treatment. *Curr Pharm Des* 2013; **19**: 5250-5269 [PMID: 23394092 DOI: 10.2174/13816128113199990344]

9 **Wong SW**, Ting YW, Chan WK. Epidemiology of non-alcoholic fatty liver disease-related hepatocellular carcinoma and its implications. *JGH Open* 2018; **2**: 235-241 [PMID: 30483595 DOI: 10.1002/jgh3.12070]

10 **Angulo P**, Keach JC, Batts KP, Lindor KD. Independent predictors of liver fibrosis in patients with nonalcoholic steatohepatitis. *Hepatology* 1999; **30**: 1356-1362 [PMID: 10573511 DOI: 10.1002/hep.510300604]

11 **Ekstedt M**, Nasr P, Kechagias S. Natural History of NAFLD/NASH. *Curr Hepatol Rep* 2017; **16**: 391-397 [PMID: 29984130 DOI: 10.1007/s11901-017-0378-2]

12 **Chalasani N**, Younossi Z, Lavine JE, Charlton M, Cusi K, Rinella M, Harrison SA, Brunt EM, Sanyal AJ. The diagnosis and management of nonalcoholic fatty liver disease: Practice guidance from the American Association for the Study of Liver Diseases. *Hepatology* 2018; **67**: 328-357 [PMID: 28714183 DOI: 10.1002/hep.29367]

13 **Piccinino F**, Sagnelli E, Pasquale G, Giusti G. Complications following percutaneous liver biopsy. A multicentre retrospective study on 68,276 biopsies. *J Hepatol* 1986; **2**: 165-173 [PMID: 3958472 DOI: 10.1016/s0168-8278(86)80075-7]

14 **Harrison SA**, Dennis A, Fiore MM, Kelly MD, Kelly CJ, Paredes AH, Whitehead JM, Neubauer S, Traber PG, Banerjee R. Utility and variability of three non-invasive liver fibrosis imaging modalities to evaluate efficacy of GR-MD-02 in subjects with NASH and bridging fibrosis during a phase-2 randomized clinical trial. *PLoS One* 2018; **13**: e0203054 [PMID: 30192782 DOI: 10.1371/journal.pone.0203054]

15 **Caussy C**, Reeder SB, Sirlin CB, Loomba R. Noninvasive, Quantitative Assessment of Liver Fat by MRI-PDFF as an Endpoint in NASH Trials. *Hepatology* 2018; **68**: 763-772 [PMID: 29356032 DOI: 10.1002/hep.29797]

16 **Imajo K**, Kessoku T, Honda Y, Tomeno W, Ogawa Y, Mawatari H, Fujita K, Yoneda M, Taguri M, Hyogo H, Sumida Y, Ono M, Eguchi Y, Inoue T, Yamanaka T, Wada K, Saito S, Nakajima A. Magnetic Resonance Imaging More Accurately Classifies Steatosis and Fibrosis in Patients With Nonalcoholic Fatty Liver Disease Than Transient Elastography. *Gastroenterology* 2016; **150**: 626-637. e7 [PMID: 26677985 DOI: 10.1053/j.gastro.2015.11.048]

17 **Jayakumar S**, Middleton MS, Lawitz EJ, Mantry PS, Caldwell SH, Arnold H, Mae Diehl A, Ghalib R, Elkhashab M, Abdelmalek MF, Kowdley KV, Stephen Djedjos C, Xu R, Han L, Mani Subramanian G, Myers RP, Goodman ZD, Afdhal NH, Charlton MR, Sirlin CB, Loomba R. Longitudinal correlations between MRE, MRI-PDFF, and liver histology in patients with non-alcoholic steatohepatitis: Analysis of data from a phase II trial of selonsertib. *J Hepatol* 2019; **70**: 133-141 [PMID: 30291868 DOI: 10.1016/j.jhep.2018.09.024]

18 **Eddowes PJ**, McDonald N, Davies N, Semple SIK, Kendall TJ, Hodson J, Newsome PN, Flintham RB, Wesolowski R, Blake L, Duarte RV, Kelly CJ, Herlihy AH, Kelly MD, Olliff SP, Hübscher SG, Fallowfield JA, Hirschfield GM. Utility and cost evaluation of multiparametric magnetic resonance imaging for the assessment of non-alcoholic fatty liver disease. *Aliment Pharmacol Ther* 2018; **47**: 631-644 [PMID: 29271504 DOI: 10.1111/apt.14469]

19 **Jayaswal ANA**, Levick C, Selvaraj EA, Dennis A, Booth JC, Collier J, Cobbold J, Tunnicliffe EM, Kelly M, Barnes E, Neubauer S, Banerjee R, Pavlides M. Prognostic value of multiparametric magnetic resonance imaging, transient elastography and blood-based fibrosis markers in patients with chronic liver disease. *Liver Int* 2020 [PMID: 32730664 DOI: 10.1111/Liv.14625]

20 **Pavlides M**, Banerjee R, Sellwood J, Kelly CJ, Robson MD, Booth JC, Collier J, Neubauer S, Barnes E. Multiparametric magnetic resonance imaging predicts clinical outcomes in patients with chronic liver disease. *J Hepatol* 2016; **64**: 308-315 [PMID: 26471505 DOI: 10.1016/j.jhep.2015.10.009]

21 **Bachtiar V**, Kelly MD, Wilman HR, Jacobs J, Newbould R, Kelly CJ, Gyngell ML, Groves KE, McKay A, Herlihy AH, Fernandes CC, Halberstadt M, Maguire M, Jayaratne N, Linden S, Neubauer S, Banerjee R. Repeatability and reproducibility of multiparametric magnetic resonance imaging of the liver. *PLoS One* 2019; **14**: e0214921 [PMID: 30970039 DOI: 10.1371/journal.pone.0214921]

22 **Chen J**, Talwalkar JA, Yin M, Glaser KJ, Sanderson SO, Ehman RL. Early detection of nonalcoholic

steatohepatitis in patients with nonalcoholic fatty liver disease by using MR elastography. *Radiology* 2011; **259**: 749-756 [PMID: 21460032 DOI: 10.1148/radiol.11101942]

23 **Singh S**, Venkatesh SK, Wang Z, Miller FH, Motosugi U, Low RN, Hassanein T, Asbach P, Godfrey EM, Yin M, Chen J, Keaveny AP, Bridges M, Bohte A, Murad MH, Lomas DJ, Talwalkar JA, Ehman RL. Diagnostic performance of magnetic resonance elastography in staging liver fibrosis: a systematic review and meta-analysis of individual participant data. *Clin Gastroenterol Hepatol* 2015; **13**: 440-451. e6 [PMID: 25305349 DOI: 10.1016/j.cgh.2014.09.046]

24 **Castera L**, Friedrich-Rust M, Loomba R. Noninvasive Assessment of Liver Disease in Patients With Nonalcoholic Fatty Liver Disease. *Gastroenterology* 2019; **156**: 1264-1281. e4 [PMID: 30660725 DOI: 10.1053/j.gastro.2018.12.036]

25 **Kwok R**, Tse YK, Wong GL, Ha Y, Lee AU, Ngu MC, Chan HL, Wong VW. Systematic review with meta-analysis: non-invasive assessment of non-alcoholic fatty liver disease--the role of transient elastography and plasma cytokeratin-18 fragments. *Aliment Pharmacol Ther* 2014; **39**: 254-269 [PMID: 24308774 DOI: 10.1111/apt.12569]

26 **Cosyns B**, Lancellotti P. Normal reference values for echocardiography: a call for comparison between ethnicities. *Eur Heart J Cardiovasc Imaging* 2016; **17**: 523-524 [PMID: 26976356 DOI: 10.1093/ehjci/jev353]

27 **Yin M**, Talwalkar JA, Glaser KJ, Manduca A, Grimm RC, Rossman PJ, Fidler JL, Ehman RL. Assessment of hepatic fibrosis with magnetic resonance elastography. *Clin Gastroenterol Hepatol* 2007; **5**: 1207-1213. e2 [PMID: 17916548 DOI: 10.1016/j.cgh.2007.06.012]

28 **Sandrin L**, Fourquet B, Hasquenoph JM, Yon S, Fournier C, Mal F, Christidis C, Ziol M, Poulet B, Kazemi F, Beaugrand M, Palau R. Transient elastography: a new noninvasive method for assessment of hepatic fibrosis. *Ultrasound Med Biol* 2003; **29**: 1705-1713 [PMID: 14698338 DOI: 10.1016/j.ultrasmedbio.2003.07.001]

29 **Ferraioli G**, Tinelli C, Lissandrin R, Zicchetti M, Dal Bello B, Filice G, Filice C. Point shear wave elastography method for assessing liver stiffness. *World J Gastroenterol* 2014; **20**: 4787-4796 [PMID: 24782633 DOI: 10.3748/wjg.v20.i16.4787]

30 **Landis JR**, Koch GG. An application of hierarchical kappa-type statistics in the assessment of majority agreement among multiple observers. *Biometrics* 1977; **33**: 363-374 [PMID: 884196 DOI: 10.2307/2529786]

31 **Angulo P**, Kleiner DE, Dam-Larsen S, Adams LA, Bjornsson ES, Charatcharoenwitthaya P, Mills PR, Keach JC, Lafferty HD, Stahler A, Haflidadottir S, Bendtsen F. Liver Fibrosis, but No Other Histologic Features, Is Associated With Long-term Outcomes of Patients With Nonalcoholic Fatty Liver Disease. *Gastroenterology* 2015; **149**: 389-97. e10 [PMID: 25935633 DOI: 10.1053/j.gastro.2015.04.043]

32 **Castéra L**, Foucher J, Bernard PH, Carvalho F, Allaix D, Merrouche W, Couzigou P, de Lédinghen V. Pitfalls of liver stiffness measurement: a 5-year prospective study of 13,369 examinations. *Hepatology* 2010; **51**: 828-835 [PMID: 20063276 DOI: 10.1002/hep.23425]

33 **Petta S**, Di Marco V, Cammà C, Butera G, Cabibi D, Craxì A. Reliability of liver stiffness measurement in non-alcoholic fatty liver disease: the effects of body mass index. *Aliment Pharmacol Ther* 2011; **33**: 1350-1360 [PMID: 21517924 DOI: 10.1111/j.1365-2036.2011.04668.x]

34 **Tapper EB**, Lok AS. Use of Liver Imaging and Biopsy in Clinical Practice. *N Engl J Med* 2017; **377**: 756-768 [PMID: 28834467 DOI: 10.1056/NEJMra1610570]

35 **Cassinotto C**, Boursier J, de Lédinghen V, Lebigot J, Lapuyade B, Cales P, Hiriart JB, Michalak S, Bail BL, Cartier V, Mouries A, Oberti F, Fouchard-Hubert I, Vergniol J, Aubé C. Liver stiffness in nonalcoholic fatty liver disease: A comparison of supersonic shear imaging, FibroScan, and ARFI with liver biopsy. *Hepatology* 2016; **63**: 1817-1827 [PMID: 26659452 DOI: 10.1002/hep.28394]

36 **Mojtahed A**, Kelly CJ, Herlihy AH, Kin S, Wilman HR, McKay A, Kelly M, Milanesi M, Neubauer S, Thomas EL, Bell JD, Banerjee R, Harisinghani M. Reference range of liver corrected T1 values in a population at low risk for fatty liver disease-a UK Biobank sub-study, with an appendix of interesting cases. *Abdom Radiol (NY)* 2019; **44**: 72-84 [PMID: 30032383 DOI: 10.1007/s00261-018-1701-2]

37 **Wilman HR**, Kelly M, Garratt S, Matthews PM, Milanesi M, Herlihy A, Gyngell M, Neubauer S, Bell JD, Banerjee R, Thomas EL. Characterisation of liver fat in the UK Biobank cohort. *PLoS One* 2017; **12**: e0172921 [PMID: 28241076 DOI: 10.1371/journal.pone.0172921]

38 **Thomaides-Brears HB**, Lepe R, Banerjee R, Duncker C. Multiparametric MR mapping in clinical decision-making for diffuse liver disease. *Abdom Radiol (NY)* 2020; **45**: 3507-3522 [PMID: 32761254 DOI: 10.1007/s00261-020-02684-3]

39 **Kleiner DE**, Brunt EM. Nonalcoholic fatty liver disease: pathologic patterns and biopsy evaluation in clinical research. *Semin Liver Dis* 2012; **32**: 3-13 [PMID: 22418883 DOI: 10.1055/s-0032-1306421]

40 **Heye T**, Yang SR, Bock M, Brost S, Weigand K, Longerich T, Kauczor HU, Hosch W. MR relaxometry of the liver: significant elevation of T1 relaxation time in patients with liver cirrhosis. *Eur Radiol* 2012; **22**: 1224-1232 [PMID: 22302503 DOI: 10.1007/s00330-012-2378-5]

41 **Thomsen C**, Christoffersen P, Henriksen O, Juhl E. Prolonged T1 in patients with liver cirrhosis: an *in vivo* MRI study. *Magn Reson Imaging* 1990; **8**: 599-604 [PMID: 2082130 DOI: 10.1016/0730-725x(90)90137-q]

42 **Bradley CR**, Cox EF, Scott RA, James MW, Kaye P, Aithal GP, Francis ST, Guha IN. Multi-organ assessment of compensated cirrhosis patients using quantitative magnetic resonance imaging. *J Hepatol* 2018; **69**: 1015-1024 [PMID: 29886155 DOI: 10.1016/j.jhep.2018.05.037]

43 **Banerjee R**, Pavlides M, Tunnicliffe EM, Piechnik SK, Sarania N, Philips R, Collier JD, Booth JC, Schneider JE, Wang LM, Delaney DW, Fleming KA, Robson MD, Barnes E, Neubauer S. Multiparametric magnetic resonance for the non-invasive diagnosis of liver disease. *J Hepatol* 2014; **60**: 69-77 [PMID: 24036007 DOI: 10.1016/j.jhep.2013.09.002]

44 **Permutt Z**, Le TA, Peterson MR, Seki E, Brenner DA, Sirlin C, Loomba R. Correlation between liver histology and novel magnetic resonance imaging in adult patients with non-alcoholic fatty liver disease - MRI accurately quantifies hepatic steatosis in NAFLD. *Aliment Pharmacol Ther* 2012; **36**: 22-29 [PMID: 22554256 DOI: 10.1111/j.1365-2036.2012.05121.x]

45 **Wildman-Tobriner B**, Middleton MM, Moylan CA, Rossi S, Flores O, Chang ZA, Abdelmalek MF, Sirlin CB, Bashir MR. Association Between Magnetic Resonance Imaging-Proton Density Fat Fraction and Liver Histology Features in Patients With Nonalcoholic Fatty Liver Disease or Nonalcoholic Steatohepatitis. *Gastroenterology* 2018; **155**: 1428-1435. e2 [PMID: 30031769 DOI: 10.1053/j.gastro.2018.07.018]

46 **Davison BA**, Harrison SA, Cotter G, Alkhouri N, Sanyal A, Edwards C, Colca JR, Iwashita J, Koch GG, Dittrich HC. Suboptimal reliability of liver biopsy evaluation has implications for randomized clinical trials. *J Hepatol* 2020; **73**: 1322-1332 [PMID: 32610115 DOI: 10.1016/j.jhep.2020.06.025]

47 **Sanai FM**, Keeffe EB. Liver biopsy for histological assessment: The case against. *Saudi J Gastroenterol* 2010; **16**: 124-132 [PMID: 20339187 DOI: 10.4103/1319-3767.61244]

48 **Kleiner DE**, Brunt EM, Van Natta M, Behling C, Contos MJ, Cummings OW, Ferrell LD, Liu YC, Torbenson MS, Unalp-Arida A, Yeh M, McCullough AJ, Sanyal AJ; Nonalcoholic Steatohepatitis Clinical Research Network. Design and validation of a histological scoring system for nonalcoholic fatty liver disease. *Hepatology* 2005; **41**: 1313-1321 [PMID: 15915461 DOI: 10.1002/hep.20701]

49 **Merriman RB**, Ferrell LD, Patti MG, Weston SR, Pabst MS, Aouizerat BE, Bass NM. Correlation of paired liver biopsies in morbidly obese patients with suspected nonalcoholic fatty liver disease. *Hepatology* 2006; **44**: 874-880 [PMID: 17006934 DOI: 10.1002/hep.21346]

50 **Pournik O**, Alavian SM, Ghalichi L, Seifizarei B, Mehrnoush L, Aslani A, Anjarani S, Eslami S. Inter-observer and Intra-observer Agreement in Pathological Evaluation of Non-alcoholic Fatty Liver Disease Suspected Liver Biopsies. *Hepat Mon* 2014; **14**: e15167 [PMID: 24497882 DOI: 10.5812/hepatmon.15167]

World Journal of Gastroenterology

Submit a Manuscript: https://www.f6publishing.com

World J Gastroenterol 2021 February 21; 27(7): 624-640

DOI: 10.3748/wjg.v27.i7.624

ISSN 1007-9327 (print) ISSN 2219-2840 (online)

ORIGINAL ARTICLE

Retrospective Study

Clinicopathological features and prognostic factors associated with gastroenteropancreatic mixed neuroendocrine non-neuroendocrine neoplasms in Chinese patients

Yu-Chen Huang, Ning-Ning Yang, Hong-Chun Chen, Yuan-Li Huang, Wen-Tian Yan, Ru-Xue Yang, Nan Li, Shan Zhang, Pan-Pan Yang, Zhen-Zhong Feng

ORCID number: Yu-Chen Huang 0000-0002-7740-5634; Ning-Ning Yang 0000-0003-0691-7293; Hong-Chun Chen 0000-0002-7751-5390; Yuan-Li Huang 0000-0001-9899-811X; Wen-Tian Yan 0000-0001-5260-4701; Ru-Xue Yang 0000-0001-8818-2272; Nan Li 0000-0002-5522-4252; Shan Zhang 0000-0001-7891-6906; Pan-Pan Yang 0000-0003-3633-6844; Zhen-Zhong Feng 0000-0001-9385-3157.

Author contributions: Huang YC collected the clinical data and prepared the manuscript; Huang YC and Yang NN designed the study and supervised the statistical data; Huang YC and Chen HC designed the research and contributed to the analyses; Huang YL, Yan WT, Yang RX, Li N, Zhang S, and Yang PP provided clinical advice; Feng ZZ made the pathologic diagnosis and supervised the report.

Supported by The Natural Science Foundation of Anhui Province, No. 1908085MH275; the Key Project of Science and Technology Development Foundation of Bengbu Medical College, No. BYKF201710; and the Graduate Innovation Program of Bengbu Medical College, No. Byycx20064.

Yu-Chen Huang, Ning-Ning Yang, Hong-Chun Chen, Yuan-Li Huang, Wen-Tian Yan, Nan Li, Zhen-Zhong Feng, Department of Pathology, The First Affiliated Hospital of Bengbu Medical College, Bengbu 233000, Anhui Province, China

Yu-Chen Huang, Ning-Ning Yang, Hong-Chun Chen, Yuan-Li Huang, Wen-Tian Yan, Nan Li, Zhen-Zhong Feng, Department of Pathology, Bengbu Medical College, Bengbu 233000, Anhui Province, China

Ru-Xue Yang, Department of Pathology, The First Affiliated Hospital of Anhui Medical University, Hefei 230000, Anhui Province, China

Shan Zhang, Department of Pathology, The Second People's Hospital of Hefei, Hefei 230000, Anhui Province, China

Pan-Pan Yang, Department of Pathology, The Second Affiliated Hospital of Anhui Medical University, Hefei 230000, Anhui Province, China

Corresponding author: Zhen-Zhong Feng, PhD, Professor, Department of Pathology, First Affiliated Hospital of Bengbu Medical College, No. 287 Changhuai Road, Longzihu District, Bengbu 233000, Anhui Province, China. fzz18297301626@163.com

Abstract

BACKGROUND

The incidence of mixed neuroendocrine-non-neuroendocrine neoplasms (MiNEN) is low. To improve our understanding of this rare tumor type and optimally guide clinical treatment, associated risk factors, clinical manifestations, and prognosis must be explored.

AIM

To identify risk factors that influence the prognosis of patients with gastroenteropancreatic MiNEN (GEP-MiNEN).

METHODS

We retrospectively analyzed the clinical data of 46 patients who were diagnosed with GEP-MiNEN at the First Affiliated Hospital of Bengbu Medical College

Institutional review board statement: This study was reviewed and approved by the Ethics Committee of the First Affiliated Hospital of Bengbu Medical College.

Informed consent statement: All patients provided written informed consent.

Conflict-of-interest statement: We have no financial relationships to disclose.

Data sharing statement: No additional data are available.

Open-Access: This article is an open-access article that was selected by an in-house editor and fully peer-reviewed by external reviewers. It is distributed in accordance with the Creative Commons Attribution NonCommercial (CC BY-NC 4.0) license, which permits others to distribute, remix, adapt, build upon this work non-commercially, and license their derivative works on different terms, provided the original work is properly cited and the use is non-commercial. See: http://creativecommons.org/Licenses/by-nc/4.0/

Manuscript source: Unsolicited manuscript

Specialty type: Gastroenterology and hepatology

Country/Territory of origin: China

Peer-review report's scientific quality classification
Grade A (Excellent): A
Grade B (Very good): 0
Grade C (Good): 0
Grade D (Fair): 0
Grade E (Poor): 0

Received: November 15, 2020
Peer-review started: November 15, 2020
First decision: December 17, 2020
Revised: December 24, 2020
Accepted: January 13, 2021
Article in press: January 13, 2021
Published online: February 21, 2021

P-Reviewer: Tonelli F
S-Editor: Zhang L

(Anhui, China) between January 2013 and December 2017. Risk factors influencing the prognosis of the patients were assessed using Kaplan-Meier curves and cox regression models. We compared the results with 55 randomly selected patients with gastroenteropancreatic GEP neuroendocrine tumors, 47 with neuroendocrine carcinomas (NEC), and 58 with poorly differentiated adenocarcinoma.

RESULTS
Among the 46 patients with GEP-MiNEN, thirty-five had gastric tumors, nine had intestinal tumors (four in the small intestine and five in the colon and rectum), and two had pancreatic tumors. The median age of the patients was 66 (41-84) years, and the male-to-female ratio was 2.83. Thirty-three (71.7%) patients had clinical stage III and IV cancers. Distant metastasis occurred in 14 patients, of which 13 had metastasis to the liver. The follow-up period was 11-72 mo, and the median overall survival was 30 mo. Ki-67 index ≥ 50%, high proportion of NEC, lymph node involvement, distant metastasis, and higher clinical stage were independent risk factors affecting the prognosis of patients with GEP-MiNEN. The median overall survival was shorter for patients with NEC than for those with MiNEN (14 mo *vs* 30 mo, $P = 0.001$), but did not significantly differ from those with poorly differentiated adenocarcinoma and MiNEN (30 mo *vs* 18 mo, $P = 0.453$).

CONCLUSION
A poor prognosis is associated with rare, aggressive GEP-MiNEN. Ki-67 index, tumor composition, lymph node involvement, distant metastasis, and clinical stage are important factors for patient prognosis.

Key Words: Mixed neuroendocrine non-neuroendocrine neoplasm; Mixed adenoneuroendocrine carcinoma; Prognosis; Gastro-entero-pancreatic tract

©The Author(s) 2021. Published by Baishideng Publishing Group Inc. All rights reserved.

Core Tip: A poor prognosis is associated with gastroenteropancreatic mixed neuroendocrine-non-neuroendocrine neoplasms, a rare, aggressive type of tumor. Ki-67 index, tumor composition, lymph node involvement, distant metastasis, and clinical stage are important factors for patient prognosis.

Citation: Huang YC, Yang NN, Chen HC, Huang YL, Yan WT, Yang RX, Li N, Zhang S, Yang PP, Feng ZZ. Clinicopathological features and prognostic factors associated with gastroenteropancreatic mixed neuroendocrine non-neuroendocrine neoplasms in Chinese patients. *World J Gastroenterol* 2021; 27(7): 624-640
URL: https://www.wjgnet.com/1007-9327/full/v27/i7/624.htm
DOI: https://dx.doi.org/10.3748/wjg.v27.i7.624

INTRODUCTION

Mixed neuroendocrine-non-neuroendocrine neoplasms (MiNEN) comprise a group of extremely rare heterogeneous tumors, accounting for > 5% of all gastrointestinal neuroendocrine tumors[1]. However, their prevalence might be largely underestimated due to diagnostic limitations and insufficient scientific understanding[2]. This type of tumor is characterized by a mixture of neuroendocrine and non-neuroendocrine components, each accounting for > 30% of the tumor. The most common combination is a mixture of adenocarcinomas and neuroendocrine carcinomas, defined as mixed adeno-neuroendocrine carcinoma (MANEC) in the 2010 version of the World Health Organization (WHO) digestive system tumor classification. Although non-neuroendocrine components are usually adenocarcinomas, they can also be squamous cell carcinomas, sarcomas, or other types of tumors[3-5]. The 2019 edition of the WHO digestive system classification categorizes MANEC as MiNEN, which comprises a mixture of other types of tumors and neuroendocrine neoplasms, and thus

L-Editor: Wang TQ
P-Editor: Ma YJ

comprehensively describes the potential biological entities that constitute this tumor[4].

MiNEN have been identified in the stomach, intestines, pancreas, biliary tract, appendix, and cervix. The clinical manifestations, treatment, and prognosis of this type of tumor are not clear due to a dearth of reports[4,6-8]. We retrospectively analyzed the clinicopathological data of 46 patients with gastroenteropancreatic MiNEN (GEP-MiNEN) and identified risk factors that influence prognosis. We also compared prognostic differences between GEP-MiNEN and gastroenteropancreatic neuroendocrine tumors (NET), neuroendocrine carcinomas (NEC), and poorly differentiated adenocarcinoma to improve the understanding of GEP-MiNEN and to guide future clinical treatment.

MATERIALS AND METHODS

Patient selection

We searched the pathological databases of the First Affiliated Hospital of Bengbu Medical College (Bengbu, China) using the following keywords: Mixed adenoneuroendocrine carcinoma, MANEC, mixed neuroendocrine non-neuroendocrine tumor, and MiNEN between January 2013 and December 2017, and limited the tumor site to the gastrointestinal tract and the pancreas. We retrieved data on 46 patients who matched the diagnostic criteria. Two senior pathologists reviewed and categorized these patients according to the current diagnostic criteria for MiNEN as defined by the WHO (2019). This study was approved by the Ethics Committee of The First Affiliated Hospital of Bengbu Medical College (No. 2020057). All patients provided written informed consent to use their clinical data.

Inclusion criteria

The WHO (2019) classifies MiNEN as tumors of the digestive system characterized by presence of neuroendocrine and non-neuroendocrine components, each accounting for > 30% of the tumor[4]. The inclusion criteria were as follows: All patients were treated surgically, including by endoscopy and laparotomy; the postoperative pathology was diagnosed as MiNEN by two senior doctors; the tumor was in the stomach, intestine, or pancreas, and the patient had no history of other malignant tumors; and preoperative radiotherapy or chemotherapy had not been administered.

Methods

Tumor tissues were fixed with 10% neutral formaldehyde, embedded in paraffin, sliced into 4 μm-thick sections, and then stained with hematoxylin and eosin. The sections were histologically analyzed using a light microscope. Tumors were clinically staged according to the American Joint Committee on Cancer (8th edition).

Sections were immunohistochemically analyzed using the EnVision method with the following primary monoclonal antibodies for Ki-67 (mouse anti-human antibody, clone MIB-1), cluster of differentiation (CD) 56 (mouse anti-human antibody, clone 56C04), synaptophysin (rabbit anti-human antibody, clone SP11), and chromogranin A (CgA; rabbit anti-human antibody, clone SP12) (all from Maixin Biotechnology Co., Ltd., Fuzhou, China). Ki-67 staining revealed brownish-yellow granules in the nuclei of tumor cells, and ≥ 20%, 21%-50%, and ≥ 51% stained nuclei were regarded as immunohistochemically positive, low expression, and high expression, respectively. The CD56 signal was observed on cell membranes, whereas Syn and CgA signals were located in the cytoplasm. Overall survival (OS) was defined as the time elapsed from the date of surgery to the date of death or the end of follow-up.

Follow-up

Follow-up was conducted for 46 patients by either reviewing their information files, making phone calls, or sending out e-mails from the date of diagnosis until December 31, 2019. The OS of the patients who survived or were lost to follow-up was excluded at the date of their last follow-up.

Statistical analysis

Data were statistically analyzed using statistic package for social science 25.0 (IBM Corp., Armonk, NY, United States). Categorical and continuous variables were analyzed using chi-square tests and independent-sample *t*-test, respectively. Survival was assessed using univariate Kaplan-Meier analysis and survival curves. Survival rates between groups were compared using log-rank tests, and OS rates were analyzed

using multivariate Cox regression models. Values with $P < 0.05$ were considered statistically significant. The statistical methods were reviewed by Lian-Guo Fu from Bengbu Medical College.

RESULTS

Clinicopathological information of patients

The clinicopathological data of 46 patients (males, $n = 34$; male-to-female ratio, 2.83: 1; average age, 65 (41-84) years; median age, 66 years) with GEP-MiNEN were analyzed. Among the forty-six patients, thirty-five patients had gastric tumors, nine had intestinal tumors, and two had pancreatic tumors. The tumor diameter was ≥ 5 and < 5 cm in 29 and 17 patients, respectively. Microscopy revealed a significant proportion of tumors categorized as NEC and as adenocarcinoma in 28 (60.9%) and 18 (39.1%) patients, respectively. Nerve invasion and vascular tumor thrombus were evident in 27 (58.7%) and 26 (56.5%) of the 46 patients, respectively. Furthermore, 34 (74.0%) of the 46 patients had lymph node involvement, and 14 (30.4%) had distant metastasis. Tumors metastasized to the liver in thirteen of these fourteen patients (three tumors were discovered during surgery), and to the ovary in one patient (Table 1).

Microscopic and immunohistochemical features

The 46 patients exhibited GEP-MiNEN comprising medium or poorly differentiated adenocarcinoma combined with neuroendocrine carcinoma (Figure 1A). Among them, thirty-three had poorly differentiated adenocarcinoma and four had mucinous adenocarcinomas. In 13 patients with moderately differentiated adenocarcinoma, the neuroendocrine component was NEC G3. The adenocarcinoma in these patients had an irregular papillary, adenoid, sieve, or nested distribution, and cells had round or oval nuclei, and coarse and granular chromatin (Figure 1B). The neuroendocrine carcinomas were nested, with an organoid-like distribution, and comprised small cubic or cylindrical tumor cells with round nuclei, reduced cytoplasm, an increased nucleoplasm ratio, and fine nuclear chromatin (Figure 1C).

The adenocarcinoma components expressed cytokeratin (Figure 1D), and most did not express neuroendocrine cancer markers. The neuroendocrine cancer components expressed CgA, Syn, and CD56. All patients were positive for CgA (Figure 1E), 35 were positive for Syn (76.1%) (Figure 1F), and 32 were positive for CD56 (69.6%). The Ki-67 proliferation index was > 50% (high expression) and < 50% (low expression) in 29 and 17 patients, respectively.

Follow-up and survival analysis

Follow-up was conducted for the patients for a median of 39 (11-72) mo. As of December 31, 2019, a total of forty-two cases were subjected to follow-up and four cases were lost to the follow-up process (8.7%). By the end of the follow-up process, 27 patients had succumbed to tumor-related death. The average and median survivals were 28.60 ± 15.14 and 30 mo, respectively (range, 12-43 mo). Univariate analysis using log-rank tests indicated that the age of the patients, tumor size, Ki-67 index, tumor composition (proportion of neuroendocrine and non-neuroendocrine tumor), degree of adenocarcinoma differentiation, lymph node involvement, vascular tumor thrombus, neurological recidivism, distant metastasis, and clinical stage were associated with OS ($P < 0.05$). Table 2 and Figure 2A-J respectively show the results of univariate analysis of survival and survival curves. Patients aged ≥ 65 years with a tumor diameter ≥ 5 cm, a Ki-67 index ≥ 50, high NEC, poorly differentiated adenocarcinoma, lymph node involvement, vascular tumor thrombus, nerve invasion, distant metastasis, and high clinical stage had a reduced OS. Sex ($P = 0.464$) and tumor location ($P = 0.056$) were not significantly associated with OS.

Meaningful indicators in the univariate analysis were included in the Cox regression analysis, and the results showed that Ki-67 index ≥ 50% ($P = 0.008$), lymph node involvement (95%CI: 1.667-25.197, $P = 0.007$), distant metastasis (95%CI: 0.037-0.540, $P = 0.004$), increased proportion of NEC ($P = 0.039$), and clinical stage ($P = 0.024$) were independent risk factors that affected the OS of patients with GEP-MiNEN (Figure 2K and Table 3).

Comparative analysis of GEP-MiNEN, NET, and NEC

We selected 55 patients [males, $n = 24$; average age at diagnosis, 49 (11-85) years] with gastrointestinal pancreatic neuroendocrine tumors (GEP-NET) in the intestine ($n = 39$),

Table 1 Patients' characteristics

Variable	Frequency (*n*)	Ratio (%)
Gender		
Male	34	73.9
Female	12	26.1
Age (yr)	66 (41-84)	
< 65	20	43.5
≥ 65	26	56.5
Location		
Stomach	35	76.1
Intestine	9	19.6
Pancreas	2	4.3
Size (cm)	5.4 (0.5-18)	
< 5 cm	25	54.3
≥ 5 cm	21	45.7
Ki- 67 index		
< 50%	17	37.0
≥ 50%	29	63.0
Proportions of two components		
NEC higher	28	60.9
AC higher	18	39.1
Histological grade of adenocarcinoma		
Moderately differentiated	13	28.3
Poorly differentiated	33	71.7
Neuroendocrine component		
NET	0	0
NEC	46	100
Lymph node metastasis		
Presence	34	73.9
Absence	12	26.1
Vascular tumor thrombus		
Presence	26	56.5
Absence	20	43.5
Neurological recidivism		
Presence	27	58.7
Absence	19	41.3
Distant metastasis		
Presence	14	30.4
Absence	32	69.6
Clinical TNM stage		
I + II	13	28.3
III	23	50.0
IV	10	21.7

NET: Neuroendocrine tumors; NEC: Neuroendocrine carcinomas.

pancreas (n = 9), and stomach (n = 7). The average tumor size was 1.7 cm. Lymph nodes were involved in 13 patients, and two had distant metastasis (the small intestine was the primary site of all tumors; one case metastasized to the liver and the other to the pancreas). Eight of the fifty-five patients were lost to follow-up. Tumor location, lymph node involvement, and distant metastasis significantly differed between patients with GEP-NET and MiNEN. By the end of the follow-up period, the median OS was significantly longer in the patients with NET than in the patients with MiNEN (50 mo *vs* 30 mo, $P < 0.001$).

We selected 47 patients [males, n = 34; average age at diagnosis, 64 (range, 40-83 years)] with gastrointestinal pancreatic neuroendocrine carcinoma (GEP-NEC) tumors located in the stomach (n = 26), intestine (n = 15), and pancreas (n = 6). The average tumor size was 5.2 cm. Lymph nodes were involved in 33 cases, and 21 patients had distant metastasis. Tumors metastasized to the pancreas (n = 1), to both the liver and rectum (n = 1), abdominal cavity (n = 4), and liver (n = 15). Six patients were lost to follow-up. The effects of sex, age, tumor size, tumor location, lymph node involvement, and distant metastasis on OS did not significantly differ between GEP-NEC and MiNEN ($P > 0.05$ for all). The median OS was significantly shorter in the patients with GEP-NEC than in those with MiNEN (14 *vs* 30 mo, $P = 0.001$; Table 4).

Comparative analysis of GEP-MiNEN and poorly differentiated adenocarcinoma

We selected 58 patients [average age, 61 (31-81) years; male, n = 37] with poorly differentiated gastrointestinal pancreatic adenocarcinoma located in the stomach (n = 42), intestines (n = 12), and pancreas (n = 4). The tumors were < 5 and ≥ 5 cm in 25 and 33 patients, respectively. Lymph node involvement and distant metastasis were found in 47 and 16 patients, respectively. Sex, age, tumor size, tumor location, lymph node involvement, and distant metastasis did not significantly differ between the two groups ($P > 0.05$ for all); median OS did not differ either (30 mo *vs* 18 mo, $P = 0.453$; Table 5).

DISCUSSION

In the 2010 WHO classification of digestive diseases, MANEC is defined as "a tumor with the morphologically recognizable glandular epithelial and neuroendocrine phenotype and is defined as cancer because both components are malignant." A mixture of squamous cell carcinoma and neuroendocrine components has also been identified in some esophageal and anal tumors[4]. At least 30% of malignancies are deemed eligible for classification as MANEC[9]. For instance, a typical adenocarcinoma without the morphological characteristics of a neuroendocrine tumor, in which immunohistochemical staining reveals scattered neuroendocrine markers, should not be diagnosed as "adenocarcinoma with neuroendocrine differentiation". In 2017, the classification of pancreatic neuroendocrine tumors was modified by the WHO and classified together with digestive tumors. The previous term, MANEC, was replaced by MiNEN[10]. The WHO stipulated in 2019 that the term MiNEN is applicable to all digestive tract and neuroendocrine tumors of the digestive system and that these tumors are classified as NET, NEC, and MiNEN. The MiNEN comprise non-neuroendocrine (mostly adenomas or adenocarcinomas, and rarely squamous cell carcinomas) and neuroendocrine components (NETG1, NETG2, NEC), either of which must account for at least 30% of the tumor[11,12]. While MiNEN have been found in most organs, they are usually found in the gastrointestinal tract and pancreas[5,13,14].

The diagnosis of MiNEN is primarily based on tumor cytology and structure, and neuroendocrine components can be confirmed by immunolabeling with synaptophysin, chromogranin A, and CD56[7]. The recent widespread application of immunohistochemistry has shown that MiNEN tumors are not as rare as previously hypothesized, and the morbidity and mortality rates of gastrointestinal MiNEN are constantly increasing at an alarming pace[15]. However, knowledge of MiNEN remains limited. The two cellular components of MiNEN are difficult to distinguish, especially when both are poorly differentiated, and they are often misdiagnosed as adenocarcinomas or grade 3 neuroendocrine tumors[16]. We identified MiNEN as a combination of moderately or poorly differentiated adenocarcinoma and NEC. Therefore, in addition to NET, our control group comprised patients with NEC and

Table 2 Univariate analysis of overall survival

Variable	*n*	Log-rank	*P* value
Gender		0.537	0.464
Male	31		
Female	11		
Age (yr)		4.815	0.028
< 65	17		
≥ 65	25		
Location		5.747	0.056
Stomach; Intestine	32; 8		
Pancreas	2		
Size (cm)		5.106	0.024
< 5 cm	22		
≥ 5 cm	20		
Ki-67 index		9.349	0.002
< 50%	17		
≥ 50%	25		
Proportion of the two components		9.421	0.002
NEC higher	26		
AC higher	16		
Histological grade of adenocarcinoma		11.303	0.001
Moderately differentiated	13		
Poorly differentiated	29		
Lymph node metastasis		8.800	0.003
Presence	32		
Absence	10		
Vascular tumor thrombus		12.250	< 0.001
Presence	25		
Absence	17		
Neurological recidivism		11.056	0.001
Presence	26		
Absence	16		
Distant metastasis		44.917	< 0.001
Presence	10		
Absence	32		
Clinical TNM stage		48.942	< 0.001
I + II	13		
III	19		
IV	10		

NEC: Neuroendocrine carcinomas; TNM: Tumor node metastasis.

poorly differentiated adenocarcinoma.

Most MiNEN cases develop slowly and manifest as nonspecific clinical symptoms like those of traditional adenocarcinoma. The disease, for many patients, is usually in its advanced stages by the time when a physician is consulted, and most demonstrate lymph node and distant metastasis, indicating that most conventional adenocarcinoma cases with MiNEN are characterized by aggressive behavior and a poor prognosis[7,16]. The GEP-MiNEN tumors analyzed herein were most prevalent in the stomach of the 46 patients, followed by the intestine and pancreas. We found that 58.7%, 56.5%, 74.0%, and 30.4% of the patients had nerve invasion, vascular tumor thrombus, lymph node involvement, and distant metastasis, respectively. The most common site of distant metastasis was the liver [13 (28.3%) of 46]. Lymph node involvement (P = 0.007) and distant metastasis (P = 0.004) were independent risk factors for the OS of patients. These results suggest that MiNEN cases have significant invasive potential.

Nie *et al*[17] suggested that the degree of differentiation of the adenocarcinoma and the neuroendocrine cancer cells of gastric MANEC affect prognosis. A lower degree of cancer cell differentiation was associated with a worse prognosis. The prognosis of patients with gastrointestinal MANEC largely depends on the stage and type of neuroendocrine components of the tumor, suggesting that NEC components comprise a key prognostic indicator[7,14,18-20]. Park *et al*[21] have suggested that gastric cancer with neuroendocrine differentiation indicates a poor prognosis, and the degree of such differentiation can serve as an independent prognostic indicator.

The neuroendocrine components of the 46 analyzed GEP-MiNEN were NEC G3, and the adenocarcinomas were either moderately differentiated or poorly differentiated. The median OS was significantly shorter for patients with poorly differentiated adenocarcinoma, compared to that observed in those with moderately differentiated adenocarcinoma (20 mo *vs* 40 mo, P = 0.001). Furthermore, the median OS was significantly shorter in patients with major NEC compared to that in patients with major adenocarcinoma (20 mo *vs* 43 mo, P = 0.002). Multivariate analysis selected major NEC as an independent risk factor for OS (95%CI: 1.065-11.286, P = 0.039). This further shows that the degree of adenocarcinoma differentiation and the proportion of NEC severely impact the survival and prognosis of patients, which is consistent with the findings of previous studies[2,17,18,22,23].

Xie *et al*[19] examined 80 patients with gastric MANEC and associated a Ki-67 index ≥ 60% with poor survival and higher recurrence rates. Milione *et al*[23] have reported that the Ki-67 index of the NEC component is the most powerful prognostic indicator, and that the risk of death is 8 -fold higher in patients with Ki-67 ≥ 55% than in those with Ki-67 < 55%. The median OS of our patients was significantly shorter for patients with a Ki-67 index ≥ 50% than for those with a Ki- 67 index < 50% (25 mo *vs* 43 mo, P = 0.002). In line with previous studies, we also identified the Ki-67 index as an independent prognostic indicator of OS (95%CI: 1.466-12.459, P = 0.008).

Among the 46 patients examined herein, 33 (71.7%) had clinical stages III and IV GEP-MiNEN at the time of diagnosis. By the end of the follow-up, 22 of these 33 patients succumbed (within an average of 20.13 mo). The median OS was significantly shorter for patients with stages III and IV, compared to that in patients with stage I + II tumors (20 mo *vs* 40 mo, P < 0.001). Multivariate analysis showed that clinical stage was an independent risk factor for the OS of the patients (95%CI: 0.077-0.837, P = 0.024), which was consistent with the findings of the study by Song *et al*[24]. Our findings were in line with those of a previous study in which a prognostic model based on tumor node metastasis staging combined with tumor composition ratio and Ki-67 index achieved a similar discriminative ability[19].

Brathwaite *et al*[16] found that the prognosis was worse for MANEC than conventional adenocarcinoma and low-grade neuroendocrine tumors. Others[22] have suggested that the prognosis of gastric MANEC is worse than that of gastric adenocarcinoma. However, whether the prognosis is better for patients with gastric MANEC than NEC patients is not clear. One study found no significant differences in survival between patients with gastric and colorectal MANEC and NEC[25]. Watanabe *et al*[26] found that disease-free survival and OS rates were significantly lower among patients with MANEC than patients with adenocarcinoma. The prognosis of patients, especially those with stage III MANEC, is as poor as that of NEC patients compared with colorectal adenocarcinoma. La Rosa *et al*[27] suggested that MANEC tumors containing well-differentiated NET and adenocarcinoma components should be regarded as adenocarcinomas, while MANEC tumors containing poorly differentiated NEC components should be regarded as NEC.

We found that 34 (74.0%) of the 46 patients with MiNEN had lymph node involvement, which was slightly more than the 33 (70.2%) of the 47 patients with NEC. However, distant metastasis was more prevalent in patients with NEC than in those

Table 3 Multivariate Cox regression analysis results of overall survival

Variable	B	SE	Wald χ^2	*P* value	HR	95%CI
Ki-67 index	1.452	0.546	7.078	0.008	4.273	1.466-12.459
Lymph node metastasis	1.869	0.693	7.277	0.007	6.481	1.667-25.197
Distant metastasis	-1.962	0.686	8.171	0.004	0.141	0.037-0.540
NEC/AC proportion	1.243	0.602	4.262	0.039	3.467	1.065-11.286
Clinical stage	-1.374	0.610	5.070	0.024	0.253	0.077-0.837

NEC: Neuroendocrine carcinomas; CI: Confidence interval; HR: Hazard ratio.

with MiNEN [21 (44.7%) of 47 *vs* 14 (30.4%) of 46], which was consistent with previous findings[6,28]. Furthermore, the metastatic behavior of the two types of tumors might differ; MiNEN usually involve regional lymph nodes, while NEC frequently exhibit distant metastasis, suggesting that NEC are more aggressive. We found that the median OS was significantly longer for patients with MiNEN than those with NEC (30 mo *vs* 14 mo, $P = 0.001$).

Few reports have described the prognosis of patients with MiNEN and poorly differentiated adenocarcinoma. Among forty-two of the forty-six patients with GEP-MiNEN who had complete follow-up data, fourteen had distant, thirteen had liver, and one had ovarian metastases. Among the 50 out of the 58 patients with poorly differentiated adenocarcinoma who had complete follow-up data, 16 developed distant metastases to the liver ($n = 10$), abdominal cavity ($n = 4$), and ovaries ($n = 2$), where a Klugenberg tumor formed. Sex, age, tumor size, tumor location, Ki-67 index, lymph node involvement, distant metastasis, and clinical stage did not significantly differ between patients with MiNEN and those with poorly differentiated adenocarcinoma ($P > 0.05$ for all). Furthermore, median OS did not significantly differ between these patients (30 mo *vs* 18 mo, $P = 0.453$).

Although the histological origin and molecular mechanism of MiNEN remain controversial, the findings of the existing molecular and genetic studies on MiNEN of the digestive system have shown that neuroendocrine and non-neuroendocrine components share a common monoclonal origin[29-32]. The origin of MiNEN is associated with mutations in MiNEN-related genes, including *TP53*, *BRAF*, and *KRAS* [2,16,25], of which the *TP53* mutation is the most common[29]. Milione *et al*[23] showed a higher frequency of chromosomal and genetic abnormalities in neuroendocrine, compared to that in non-neuroendocrine components, indicating that non-neuroendocrine progression to a neuroendocrine cellular phenotype was more frequent than previously thought. Microsatellite instability might be a driving factor for the development of gastrointestinal neuroendocrine tumors[16]. Conventional colorectal adenocarcinomas and MANEC might have a common genetic profile[25], and might respond to chemotherapy for colorectal adenocarcinoma, revealing a genetic connection between most colorectal MANEC and NET and the adenocarcinoma family.

In the absence of contraindications, the main treatment following a diagnosis of GEP-MiNEN is radical surgery. Chemotherapy is the treatment of choice for poorly differentiated, or rapidly progressing advanced tumors. Cisplatin/5-FU combined with etoposide is the most common chemotherapeutic regimen applied to treat MiNEN and is similar to those used to treat adenocarcinomas[12,31,33]. Neoadjuvant chemotherapy significantly improves the OS of patients with locally advanced NEC and MANEC in the stomach with an acceptable level of toxicity[34]. Surgical removal of each metastasis combined with systemic chemotherapy can significantly improve the prognosis of patients with colorectal MiNEN tumors that have already metastasized to distant locations[35]. An optimal combination of systemic chemotherapy and somatostatin analogs such as octreotide and lanreotide can prolong the progression-free survival of patients with metastatic neuroendocrine tumors[12].

CONCLUSION

Overall, GEP-MiNEN are rare and heterogeneous tumors with a highly variable prognosis for which there are no clear treatment guidelines. Although we found a

Table 4 Comparative of mixed neuroendocrine-non-neuroendocrine neoplasms, neuroendocrine tumors, and neuroendocrine carcinomas

Variable	NET (*n* = 55)	NEC (*n* = 47)	MiNEN (*n* = 46)	*P* value	
				NET *vs* MiNEN	NEC *vs* MiNEN
Male/female	24/31	34/13	34/12	0.004	0.864
Age [yr, mean (range)]	49 (11-85)	64 (40-83)	65 (41-84)	< 0.001	0.857
Location				< 0.001	0.162
Stomach	7	26	35		
Intestine	39	15	9		
Pancreas	9	6	2		
Size [cm, mean (range)]	1.7 (0.2-11)	5.2 (1.5-16.0)	5.4 (0.5-18)	< 0.001	0.742
Ki-67 index				< 0.001	0.051
< 2%	15	2	0		
2%-20%	39	5	1		
> 20%	1	40	45		
Lymph node metastasis				< 0.001	0.691
Presence	13	33	34		
Absence	42	14	12		
Distant metastasis				< 0.001	0.156
Presence	2	21	14		
Absence	53	26	32		
Survival time (mo)				< 0.001	0.001
Median	50	14	30		
Mean	49.3	34	28.6		
Follow-up				< 0.001	0.054
Dead	3	34	27		
Alive	44	7	15		

MiNEN: Mixed neuroendocrine-non-neuroendocrine neoplasms; NET: Neuroendocrine tumors; NEC: Neuroendocrine carcinomas.

worse prognosis for patients with MiNEN than for those with NEC, it did not significantly differ from that of patients with poorly differentiated adenocarcinoma. Thus, patients with GEP-MiNEN and those with adenocarcinoma should be similarly treated. Furthermore, the treatment of any suspected or diagnosed GEP-MiNEN patient should be discussed at a multidisciplinary expert meeting to determine optimal personalized treatment for individual patients. The number of patients in the present retrospective study was limited by the rarity of GEP-MiNEN, and they were sourced from a single institution. Therefore, further multicenter, larger-cohort studies are warranted to clarify the clinicopathological features and biological behavior of GEP-MiNEN.

Table 5 Comparison between patients with mixed neuroendocrine-non-neuroendocrine neoplasms and those with poorly differentiated adenocarcinoma

Variable	Poorly differentiated adenocarcinoma (*n* = 58)	MiNEN (*n* = 46)	*P* value
Male/female	37/21	34/12	0.271
Mean age, years, (range)	61 (31-81)	65 (41-84)	0.055
Location			0.836
Stomach	42	35	
Intestine	12	9	
Pancreas	4	2	
Size (cm)			0.254
< 5	25	25	
≥ 5	33	21	
Ki- 67 index			0.104
< 50%	13	17	
≥ 50%	45	29	
Lymph node metastasis			0.385
Presence	47	34	
Absence	11	12	
Distant metastasis			0.750
Presence	16	14	
Absence	42	32	
Clinical TNM stage			0.402
I + II	10	13	
III	34	23	
IV	14	10	
Survival time (mo)			0.453
Median	18	30	
Mean	24.3	28.6	
Follow-up			0.863
Dead	33	27	
Alive	17	15	

MiNEN: Mixed neuroendocrine-non-neuroendocrine neoplasms; TNM: Tumor node metastasis.

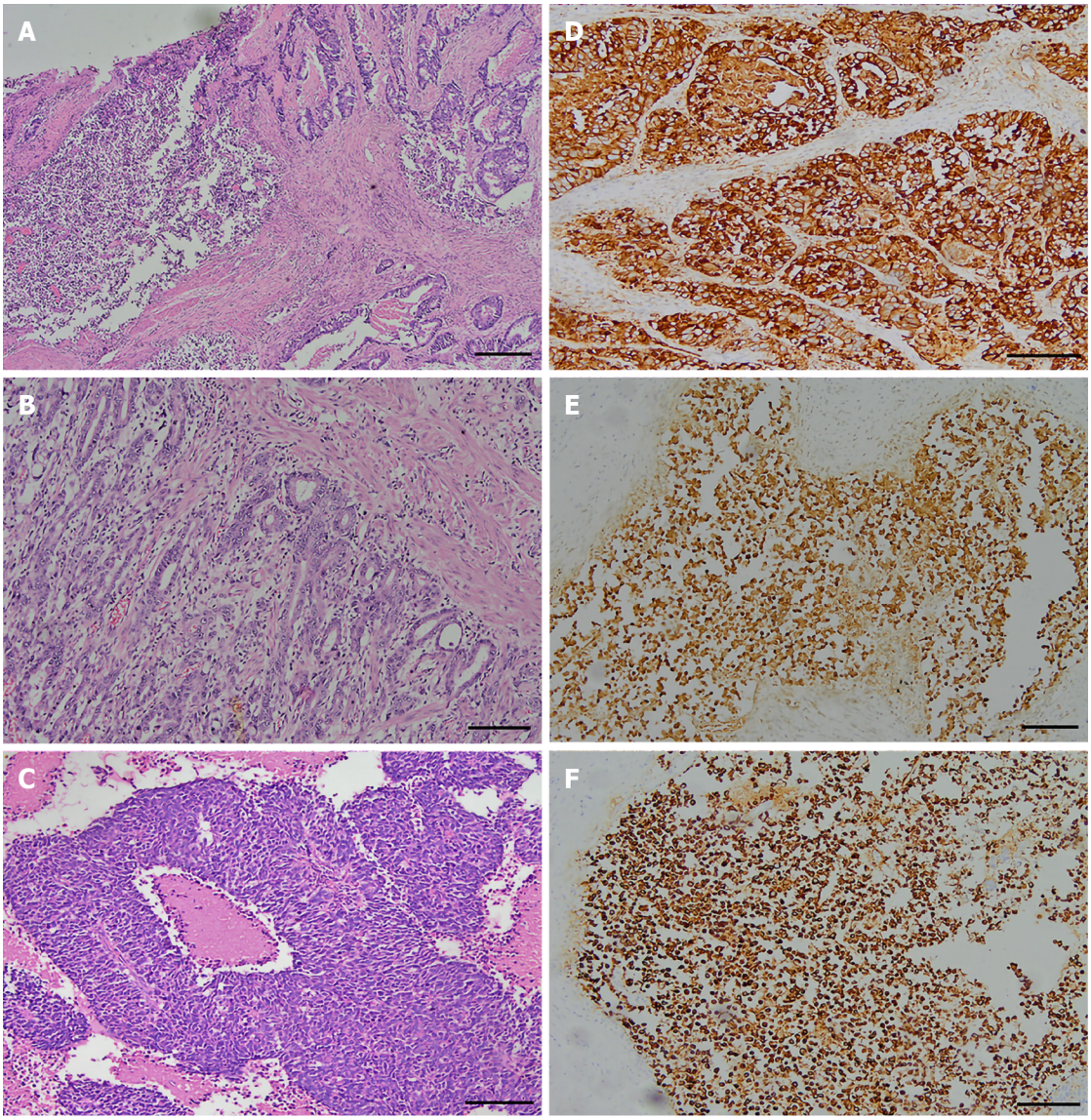
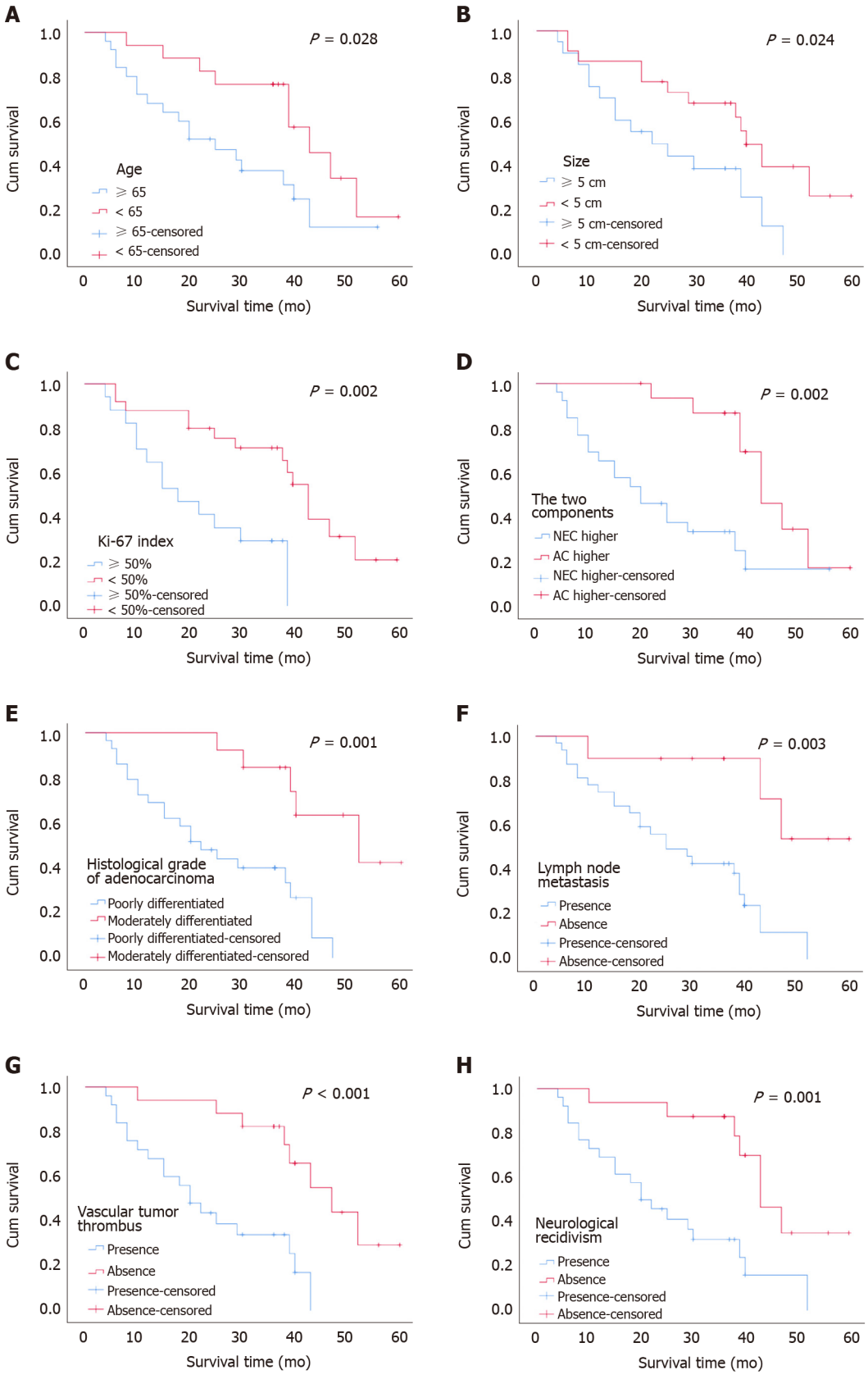


Figure 1 Histopathological and immunohistochemical findings of gastroenteropancreatic mixed neuroendocrine-non-neuroendocrine neoplasms. A: Neuroendocrine carcinoma (left) and adenocarcinoma (right) (Hematoxylin-eosin staining, scale bar 200 μm); B: Adenocarcinoma component (Hematoxylin-eosin staining, scale bar 200 μm); C: Neuroendocrine component (Hematoxylin-eosin staining, scale bar 100 μm); D: Cytokeratin-positive adenocarcinoma (EnVision, scale bar 100 μm); E: CgA-positive neuroendocrine (EnVision, scale bar 100 μm); F: Syn-positive neuroendocrine (EnVision, scale bar 100 μm).


A
P = 0.028
Age
⩾ 65
< 65
⩾ 65-censored
< 65-censored
B
P = 0.024
Size
⩾ 5 cm
< 5 cm
⩾ 5 cm-censored
< 5 cm-censored
C
P = 0.002
Ki-67 index
⩾ 50%
< 50%
⩾ 50%-censored
< 50%-censored
D
P = 0.002
The two components
NEC higher
AC higher
NEC higher-censored
AC higher-censored
E
P = 0.001
Histological grade of adenocarcinoma
Poorly differentiated
Moderately differentiated
Poorly differentiated-censored
Moderately differentiated-censored
F
P = 0.003
Lymph node metastasis
Presence
Absence
Presence-censored
Absence-censored
G
P < 0.001
Vascular tumor thrombus
Presence
Absence
Presence-censored
Absence-censored
H
P = 0.001
Neurological recidivism
Presence
Absence
Presence-censored
Absence-censored
Cum survival
Survival time (mo)

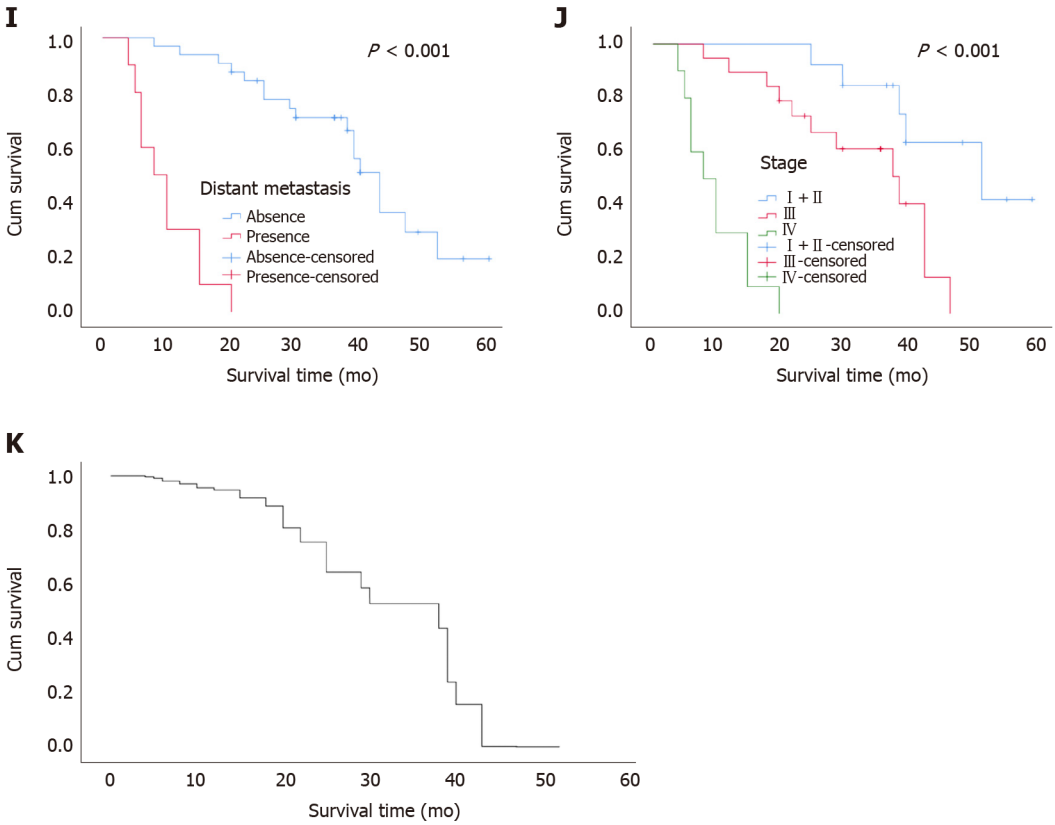


Figure 2 Kaplan-Meier curves of overall survival among 46 patients with gastroenteropancreatic mixed neuroendocrine-non-neuroendocrine neoplasms. Overall survival grouped by A: Age (P = 0.028); B: Tumor size (P = 0.024); C: Ki-67 index (P = 0.002); D: Proportions of NEC and adenocarcinoma (P = 0.002); E: Adenocarcinoma differentiation (P = 0.001); F: Lymph node metastasis (P = 0.003); G: Vascular tumor thrombus (P < 0.001); H: Nerve invasion (P = 0.001); I: Distant metastasis (P < 0.001); and J: Clinical stage (P < 0.001); K: Overall survival of 46 patients with gastroenteropancreatic mixed neuroendocrine-non-neuroendocrine neoplasms.

ARTICLE HIGHLIGHTS

Research background

Mixed neuroendocrine-non-neuroendocrine neoplasms (MiNEN) are a rare tumor type. However, their prevalence might be largely underestimated due to diagnostic limitations and insufficient scientific understanding. The clinical manifestations, treatment, and prognosis of this type of tumor are still poorly understood. Our research on the risk factors, clinical manifestations, and prognosis related to this rare tumor type is of great significance for optimizing clinical treatment.

Research motivation

MiNEN associated risk factors, clinical manifestations, and prognosis must be explored to improve our understanding of this rare tumor type and optimize clinical treatment.

Research objectives

We have identified the risk factors that influence the prognosis of patients with gastroenteropancreatic MiNEN (GEP-MiNEN). We also compared prognostic differences between GEP-MiNEN and gastroenteropancreatic neuroendocrine tumors, neuroendocrine carcinomas (NEC), and poorly differentiated adenocarcinoma to improve the understanding of GEP-MiNEN and to guide future clinical treatment.

Research methods

This is a single-center, retrospective study. We retrospectively analyzed the clinical data of patients who were diagnosed with GEP-MiNEN. Risk factors influencing patient prognosis were assessed using Kaplan-Meier curves and Cox regression models. We compared the results with randomly selected patients with gastroenteropancreatic neuroendocrine tumors, NEC, and poorly differentiated adeno-

carcinomas.

Research results

Most GEP-MiNEN in our study were gastric tumors, a few were intestinal tumors, and a minority, pancreatic tumors. The median overall survival was 30 mo. Ki- 67 index ≥ 50%, high proportion of NEC, lymph node involvement, distant metastasis, and higher clinical stage were independent risk factors affecting the prognosis of patients with GEP-MiNEN. The median overall survival was shorter for patients with NEC than for those with MiNEN but did not significantly differ from those with poorly differentiated adenocarcinoma and MiNEN. Thus, patients with GEP-MiNEN and those with adenocarcinoma should be similarly treated. Furthermore, the treatment of any suspected or diagnosed GEP-MiNEN patient should be discussed at a multidisciplinary expert meeting to determine optimal personalized treatment. However, the number of patients in the present retrospective study was limited by the rarity of GEP-MiNEN, and they were sourced from a single institution. Therefore, further multicenter, larger-cohort studies are warranted to clarify the clinicopathological features and biological behavior of GEP-MiNEN.

Research conclusions

A poor prognosis is associated with GEP-MiNEN. Ki-67 index, tumor composition, lymph node involvement, distant metastasis, and clinical stage are important factors for patient prognosis.

Research perspectives

In view of the limited number of patients and the short-term follow-up of our study, a larger prospective study with long-term follow-up is needed to confirm our results.

ACKNOWLEDGEMENTS

We would like to thank Dr. Lian-Guo Fu for significant contributions to data analysis.

REFERENCES

1 **de Mestier L**, Cros J, Neuzillet C, Hentic O, Egal A, Muller N, Bouché O, Cadiot G, Ruszniewski P, Couvelard A, Hammel P. Digestive System Mixed Neuroendocrine-Non-Neuroendocrine Neoplasms. *Neuroendocrinology* 2017; **105**: 412-425 [PMID: 28803232 DOI: 10.1159/000475527]

2 **Frizziero M**, Chakrabarty B, Nagy B, Lamarca A, Hubner RA, Valle JW, McNamara MG. Mixed Neuroendocrine Non-Neuroendocrine Neoplasms: A Systematic Review of a Controversial and Underestimated Diagnosis. *J Clin Med* 2020; **9** [PMID: 31963850 DOI: 10.3390/jcm9010273]

3 **Merola E**, Zandee WT, de Mestier L, Klumpen HJ, Makulik K, Geboes K, van Velthuysen ML, Couvelard A, Cros J, van Eeden S, Hoorens A, Stephenson T, Zajęcki W, de Herder W, Munir A. Histopathological Revision for Gastro-Entero-Pancreatic Neuroendocrine Neoplasms in Expert Centers: Does it Make the Difference? *Neuroendocrinology* 2020 [DOI: 10.1159/000507082]

4 **Assarzadegan N**, Montgomery E. What is New in 2019 World Health Organization (WHO) Classification of Tumors of the Digestive System: Review of Selected Updates on Neuroendocrine Neoplasms, Appendiceal Tumors, and Molecular Testing. *Arch Pathol Lab Med* 2020 [PMID: 32233993 DOI: 10.5858/arpa.2019-0665-RA]

5 **La Rosa S**, Sessa F, Uccella S. Mixed Neuroendocrine-Nonneuroendocrine Neoplasms (MiNENs): Unifying the Concept of a Heterogeneous Group of Neoplasms. *Endocr Pathol* 2016; **27**: 284-311 [PMID: 27169712 DOI: 10.1007/s12022-016-9432-9]

6 **Oneda E**, Liserre B, Bianchi D, Rota L, Savelli G, Zorzi F, Zaniboni A. Diagnosis of Mixed Adenoneuroendocrine Carcinoma (MANEC) after Neoadjuvant Chemotherapy for Pancreatic and Gastric Adenocarcinoma: Two Case Reports and a Review of the Literature. *Case Rep Oncol* 2019; **12**: 434-442 [PMID: 31275134 DOI: 10.1159/000501200]

7 **Pham QD**, Mori I, Osamura RY. A Case Report: Gastric Mixed Neuroendocrine-Nonneuroendocrine Neoplasm with Aggressive Neuroendocrine Component. *Case Rep Pathol* 2017; **2017**: 9871687 [PMID: 28626594 DOI: 10.1155/2017/9871687]

8 **Qiu S**, Pellino G, Warren OJ, Mills S, Goldin R, Kontovounisios C, Tekkis PP. Mixed adenoneuroendocrine carcinoma of the colon and rectum. *Acta Chir Belg* 2018; **118**: 273-277 [PMID: 29911510 DOI: 10.1080/00015458.2018.1482697]

9 **Bosman FT**. International Agency for Research on Cancer: WHO Classification of Tumours of the Digestive System, 4th ed. Lyon. IARC, 2010

10 **Inzani F**, Petrone G, Rindi G. The New World Health Organization Classification for Pancreatic

Neuroendocrine Neoplasia. *Endocrinol Metab Clin North Am* 2018; **47**: 463-470 [PMID: 30098710 DOI: 10.1016/j.ecl.2018.04.008]

11 **Nagtegaal ID**, Odze RD, Klimstra D, Paradis V, Rugge M, Schirmacher P, Washington KM, Carneiro F, Cree IA; WHO Classification of Tumours Editorial Board. The 2019 WHO classification of tumours of the digestive system. *Histopathology* 2020; **76**: 182-188 [PMID: 31433515 DOI: 10.1111/his.13975]

12 **Skalický A**, Vištejnová L, Dubová M, Malkus T, Skalický T, Troup O. Mixed neuroendocrine-non-neuroendocrine carcinoma of gallbladder: case report. *World J Surg Oncol* 2019; **17**: 55 [PMID: 30902091 DOI: 10.1186/s12957-019-1598-4]

13 **Di Palma S**, Mufaddal M, Iyer V, Sciarra A, La Rosa S. Does Mixed Neuroendocrine-Nonneuroendocrine Neoplasm (MiNEN) of the Parathyroid Gland Exist? *Head Neck Pathol* 2020 [PMID: 32506375 DOI: 10.1007/s12105-020-01178-4]

14 **Frizziero M**, Wang X, Chakrabarty B, Childs A, Luong TV, Walter T, Khan MS, Morgan M, Christian A, Elshafie M, Shah T, Minicozzi A, Mansoor W, Meyer T, Lamarca A, Hubner RA, Valle JW, McNamara MG. Retrospective study on mixed neuroendocrine non-neuroendocrine neoplasms from five European centres. *World J Gastroenterol* 2019; **25**: 5991-6005 [PMID: 31660035 DOI: 10.3748/wjg.v25.i39.5991]

15 **Wang J**, He A, Feng Q, Hou P, Wu J, Huang Z, Xiao Z, Sun C, Liao W, Wu L. Gastrointestinal mixed adenoneuroendocrine carcinoma: a population level analysis of epidemiological trends. *J Transl Med* 2020; **18**: 128 [PMID: 32169074 DOI: 10.1186/s12967-020-02293-0]

16 **Brathwaite SA**, Smith SM, Wai L, Frankel W, Hays J, Yearsley MM, Abdel-Misih S. Mixed adenoneuroendocrine carcinoma: A review of pathologic characteristics. *Hum Pathol* 2018; **73**: 184-191 [PMID: 29288693 DOI: 10.1016/j.humpath.2017.12.009]

17 **Nie L**, Li M, He X, Feng A, Wu H, Fan X. Gastric mixed adenoneuroendocrine carcinoma: correlation of histologic characteristics with prognosis. *Ann Diagn Pathol* 2016; **25**: 48-53 [PMID: 27806846 DOI: 10.1016/j.anndiagpath.2016.09.004]

18 **Harada K**, Sato Y, Ikeda H, Maylee H, Igarashi S, Okamura A, Masuda S, Nakanuma Y. Clinicopathologic study of mixed adenoneuroendocrine carcinomas of hepatobiliary organs. *Virchows Arch* 2012; **460**: 281-289 [PMID: 22358181 DOI: 10.1007/s00428-012-1212-4]

19 **Xie JW**, Lu J, Wang JB, Lin JX, Chen QY, Cao LL, Lin M, Tu RH, Huang ZN, Lin JL, Zheng CH, Li P, Huang CM. Prognostic factors for survival after curative resection of gastric mixed adenoneuroendocrine carcinoma: a series of 80 patients. *BMC Cancer* 2018; **18**: 1021 [PMID: 30348122 DOI: 10.1186/s12885-018-4943-z]

20 **Zheng SL**, Yip VS, Pedica F, Prachalias A, Quaglia A. Intrahepatic bile duct mixed adenoneuroendocrine carcinoma: a case report and review of the literature. *Diagn Pathol* 2015; **10**: 204 [PMID: 26589730 DOI: 10.1186/s13000-015-0439-1]

21 **Park JY**, Ryu MH, Park YS, Park HJ, Ryoo BY, Kim MG, Yook JH, Kim BS, Kang YK. Prognostic significance of neuroendocrine components in gastric carcinomas. *Eur J Cancer* 2014; **50**: 2802-2809 [PMID: 25201164 DOI: 10.1016/j.ejca.2014.08.004]

22 **Sun L**, Zhang J, Wang C, Zhao S, Shao B, Guo Y, Liu Y, Sun Y. Chromosomal and molecular pathway alterations in the neuroendocrine carcinoma and adenocarcinoma components of gastric mixed neuroendocrine-nonneuroendocrine neoplasm. *Mod Pathol* 2020; **33**: 2602-2613 [PMID: 32461621 DOI: 10.1038/s41379-020-0579-z]

23 **Milione M**, Maisonneuve P, Pellegrinelli A, Grillo F, Albarello L, Spaggiari P, Vanoli A, Tagliabue G, Pisa E, Messerini L, Centonze G, Inzani F, Scarpa A, Papotti M, Volante M, Sessa F, Fazio N, Pruneri G, Rindi G, Solcia E, La Rosa S, Capella C. Ki67 proliferative index of the neuroendocrine component drives MANEC prognosis. *Endocr Relat Cancer* 2018; **25**: 583-593 [PMID: 29592868 DOI: 10.1530/ERC-17-0557]

24 **Song LJ**, Yuan L. Comparative analysis of colorectal mixed adenoneuroendocrine carcinoma and adenocarcinoma with neuroendocrine differentiation: a population-based study. *Int J Clin Exp Pathol* 2019; **12**: 922-932 [PMID: 31933902]

25 **Jesinghaus M**, Konukiewitz B, Keller G, Kloor M, Steiger K, Reiche M, Penzel R, Endris V, Arsenic R, Hermann G, Stenzinger A, Weichert W, Pfarr N, Klöppel G. Colorectal mixed adenoneuroendocrine carcinomas and neuroendocrine carcinomas are genetically closely related to colorectal adenocarcinomas. *Mod Pathol* 2017; **30**: 610-619 [PMID: 28059096 DOI: 10.1038/modpathol.2016.220]

26 **Watanabe J**, Suwa Y, Ota M, Ishibe A, Masui H, Nagahori K, Tsuura Y, Endo I. Clinicopathological and Prognostic Evaluations of Mixed Adenoneuroendocrine Carcinoma of the Colon and Rectum: A Case-Matched Study. *Dis Colon Rectum* 2016; **59**: 1160-1167 [PMID: 27824701 DOI: 10.1097/DCR.0000000000000702]

27 **La Rosa S**, Marando A, Sessa F, Capella C. Mixed Adenoneuroendocrine Carcinomas (MANECs) of the Gastrointestinal Tract: An Update. *Cancers (Basel)* 2012; **4**: 11-30 [PMID: 24213223 DOI: 10.3390/cancers4010011]

28 **Zhang P**, Wang W, Lu M, Zeng C, Chen J, Li E, Tan H, Wang W, Yu X, Tang Q, Zhao J, Shen L, Li J. Clinicopathological features and outcome for neuroendocrine neoplasms of gastroesophageal junction: A population-based study. *Cancer Med* 2018; **7**: 4361-4370 [PMID: 30062861 DOI: 10.1002/cam4.1702]

29 **Scardoni M**, Vittoria E, Volante M, Rusev B, Bersani S, Mafficini A, Gottardi M, Giandomenico V, Malleo G, Butturini G, Cingarlini S, Fassan M, Scarpa A. Mixed adenoneuroendocrine carcinomas of

the gastrointestinal tract: targeted next-generation sequencing suggests a monoclonal origin of the two components. *Neuroendocrinology* 2014; **100**: 310-316 [PMID: 25342539 DOI: 10.1159/000369071]

30 **Paniz Mondolfi AE**, Slova D, Fan W, Attiyeh FF, Afthinos J, Reidy J, Pang Y, Theise ND. Mixed adenoneuroendocrine carcinoma (MANEC) of the gallbladder: a possible stem cell tumor? *Pathol Int* 2011; **61**: 608-614 [PMID: 21951672 DOI: 10.1111/j.1440-1827.2011.02709.x]

31 **Gurzu S**, Fetyko A, Bara T, Banias L, Butiurca VO, Bara T Jr, Tudorache V, Jung I. Gastrointestinal mixed adenoneuroendocrine carcinoma (MANEC): An immunohistochemistry study of 13 microsatellite stable cases. *Pathol Res Pract* 2019; **215**: 152697 [PMID: 31704155 DOI: 10.1016/j.prp.2019.152697]

32 **Nassereddine H**, Poté N, Théou-Anton N, Lamoureux G, Fléjou JF, Couvelard A. A gastric MANEC with an adenocarcinoma of fundic-gland type as exocrine component. *Virchows Arch* 2017; **471**: 673-678 [PMID: 28653202 DOI: 10.1007/s00428-017-2178-z]

33 **Zhang M**, Zhao P, Shi X, Zhao A, Zhang L, Zhou L. Clinicopathological features and prognosis of gastroenteropancreatic neuroendocrine neoplasms in a Chinese population: a large, retrospective single-centre study. *BMC Endocr Disord* 2017; **17**: 39 [PMID: 28705205 DOI: 10.1186/s12902-017-0190-6]

34 **Ma F**, Wang B, Xue L, Kang W, Li Y, Li W, Liu H, Ma S, Tian Y. Neoadjuvant chemotherapy improves the survival of patients with neuroendocrine carcinoma and mixed adenoneuroendocrine carcinoma of the stomach. *J Cancer Res Clin Oncol* 2020; **146**: 2135-2142 [PMID: 32306127 DOI: 10.1007/s00432-020-03214-w]

35 **Kanazawa Y**, Kikuchi M, Imai Y, Katakami N, Kaihara S, Shinohara S. Successful Treatment of a Mixed Neuroendocrine-Nonneuroendocrine Neoplasm of the Colon with Metastases to the Thyroid Gland and Liver. *Case Rep Otolaryngol* 2020; **2020**: 5927610 [PMID: 32099708 DOI: 10.1155/2020/5927610]

World Journal of Gastroenterology

Submit a Manuscript: https://www.f6publishing.com

World J Gastroenterol 2021 February 21; 27(7): 641-653

DOI: 10.3748/wjg.v27.i7.641

ISSN 1007-9327 (print) ISSN 2219-2840 (online)

ORIGINAL ARTICLE

Retrospective Study

Effect of liver inflammation on accuracy of FibroScan device in assessing liver fibrosis stage in patients with chronic hepatitis B virus infection

Ling-Ling Huang, Xue-Ping Yu, Ju-Lan Li, Hui-Ming Lin, Na-Ling Kang, Jia-Ji Jiang, Yue-Yong Zhu, Yu-Rui Liu, Da-Wu Zeng

ORCID number: Ling-Ling Huang 0000-0001-9307-9181; Xue-Ping Yu 0000-0002-1157-2501; Ju-Lan Li 0000-0003-4222-2966; Hui-Ming Lin 0000-0002-1312-8703; Na-Ling Kang 0000-0001-6923-5754; Jia-Ji Jiang 0000-0003-0637-7653; Yue-Yong Zhu 0000-0002-0746-4911; Yu-Rui Liu 0000-0003-0553-846X; Da-Wu Zeng 0000-0003-3818-0062.

Author contributions: Huang LL, Liu YR, Yu XP, Li JL contributed equally to this work; Huang LL, Zeng DW and Liu YR conceived and designed the experiments; Huang LL, Jiang JJ and Zeng DW performed the experiments; Huang LL, Yu XP, Zeng DW and Zhu YY analyzed the data; Li JL, Lin HM and Kang NL contributed the reagents/materials/analysis tools; Huang LL and Zeng DW wrote the manuscript; all authors approved the final version of the manuscript.

Supported by Science and Technology Department of Fujian Province, China, No. 2019Y0015 and No. 2019J01432; Chinese National 13th Five-Year Plan's Science and Technology Projects, No. 2017ZX10202201; Quanzhou Science and Technology Project of Fujian Province, China, No.

Ling-Ling Huang, Hui-Ming Lin, Na-Ling Kang, Jia-Ji Jiang, Yue-Yong Zhu, Yu-Rui Liu, Da-Wu Zeng, Department of Hepatology, Hepatology Research Institute, The First Affiliated Hospital, Fujian Medical University, Fuzhou 350005, Fujian Province, China

Xue-Ping Yu, Ju-Lan Li, Department of Infectious Diseases, The First Hospital of Quanzhou Affiliated to Fujian Medical University, Quanzhou 362000, Fujian Province, China

Yue-Yong Zhu, Fujian Key Laboratory of Precision Medicine for Cancer, Fujian Key Laboratory of Laboratory Medicine, The First Affiliated Hospital, Fujian Medical University, Fuzhou 350005, Fujian Province, China

Corresponding author: Da-Wu Zeng, MD, PhD, Associate Chief Physician, Doctor, Department of Hepatology, Hepatology Research Institute, The First Affiliated Hospital, Fujian Medical University, No. 20 Chazhong Road, Taijiang District, Fuzhou 350005, Fujian Province, China. zengdw1980@fjmu.edu.cn

Abstract

BACKGROUND

Transient elastography (FibroScan) is a new and non-invasive test, which has been widely recommended by the guidelines of chronic hepatitis B virus (HBV) management for assessing hepatic fibrosis staging. However, some confounders may affect the diagnostic accuracy of the FibroScan device in fibrosis staging.

AIM

To evaluate the diagnostic value of the FibroScan device and the effect of hepatic inflammation on the accuracy of FibroScan in assessing the stage of liver fibrosis in patients with HBV infection.

METHODS

The data of 416 patients with chronic HBV infection who accepted FibroScan, liver biopsy, clinical, and biological examination were collected from two hospitals retrospectively. Receiver operating characteristic (ROC) curves were used to analyze the diagnostic performance of FibroScan for assessing the stage of liver fibrosis. Any discordance in fibrosis staging by FibroScan and pathological scores was statistically analyzed. Logistic regression and ROC analyses were used to

2018Z074.

Institutional review board statement: This study was approved by the Institutional Review Board of Fujian Medical University.

Informed consent statement: The need for informed consent was waived due to the retrospective nature of the study.

Conflict-of-interest statement: We have no financial relationships to disclose.

Open-Access: This article is an open-access article which was selected by an in-house editor and fully peer-reviewed by external reviewers. It is distributed in accordance with the Creative Commons Attribution Non Commercial (CC BY-NC 4.0) license, which permits others to distribute, remix, adapt, build upon this work non-commercially, and license their derivative works on different terms, provided the original work is properly cited and the use is non-commercial. See: http://creativecommons.org/licenses/by-nc/4.0/

Manuscript source: Unsolicited manuscript

Specialty type: Gastroenterology and hepatology

Country/Territory of origin: China

Peer-review report's scientific quality classification

Grade A (Excellent): 0
Grade B (Very good): 0
Grade C (Good): C
Grade D (Fair): 0
Grade E (Poor): 0

Received: November 26, 2020
Peer-review started: November 26, 2020
First decision: December 21, 2020
Revised: December 30, 2020
Accepted: January 13, 2021
Article in press: January 13, 2021
Published online: February 21, 2021

P-Reviewer: Izumi N
S-Editor: Fan JR
L-Editor: Webster JR

analyze the accuracy of FibroScan in assessing the stage of fibrosis in patients with different degrees of liver inflammation. A non-invasive model was constructed to predict the risk of misdiagnosis of fibrosis stage using FibroScan.

RESULTS

In the overall cohort, the optimal diagnostic values of liver stiffness measurement (LSM) using FibroScan for significant fibrosis (≥ F2), severe fibrosis (≥ F3), and cirrhosis (F4) were 7.3 kPa [area under the curve (AUC) = 0.863], 9.7 kPa (AUC = 0.911), and 11.3 kPa (AUC = 0.918), respectively. The rate of misdiagnosis of fibrosis stage using FibroScan was 34.1% (142/416 patients). The group of patients who showed discordance between fibrosis staging using FibroScan and pathological scores had significantly higher alanine aminotransferase and aspartate aminotransferase levels, and a higher proportion of moderate to severe hepatic inflammation, compared with the group of patients who showed concordance in fibrosis staging between the two methods. Liver inflammation activity over 2 (OR = 3.53) was an independent risk factor for misdiagnosis of fibrosis stage using FibroScan. Patients with liver inflammation activity ≥ 2 showed higher LSM values using FibroScan and higher rates of misdiagnosis of fibrosis stage, whereas the diagnostic performance of FibroScan for different fibrosis stages was significantly lower than that in patients with inflammation activity < 2 (all $P < 0.05$). A non-invasive prediction model was established to assess the risk of misdiagnosis of fibrosis stage using FibroScan, and the AUC was 0.701.

CONCLUSION

Liver inflammation was an independent risk factor affecting the diagnostic accuracy of FibroScan for fibrosis stage. A combination of other related non-invasive factors can predict the risk of misdiagnosis of fibrosis staging using FibroScan.

Key Words: Liver stiffness measurement; Fibrosis stage; Liver inflammation; Hepatitis B virus; FibroScan; Predictive model

©The Author(s) 2021. Published by Baishideng Publishing Group Inc. All rights reserved.

Core Tip: Transient elastography (FibroScan) is a recommended non-invasive test for evaluation of liver fibrosis in patients with chronic hepatitis B virus (HBV) infection. In this study, we demonstrated the good performance of FibroScan in predicting liver fibrosis staging. However, we found discordance between Fibroscan fibrosis staging and pathological score. Liver inflammation was an independent risk factor affecting the accuracy of FibroScan assessing HBV-related liver fibrosis staging. The combination of other related non-invasive factors can predict the risk of FibroScan staging misdiagnosis, and may be helpful for guiding the diagnosis and therapy of chronic HBV infection.

Citation: Huang LL, Yu XP, Li JL, Lin HM, Kang NL, Jiang JJ, Zhu YY, Liu YR, Zeng DW. Effect of liver inflammation on accuracy of FibroScan device in assessing liver fibrosis stage in patients with chronic hepatitis B virus infection. *World J Gastroenterol* 2021; 27(7): 641-653
URL: https://www.wjgnet.com/1007-9327/full/v27/i7/641.htm
DOI: https://dx.doi.org/10.3748/wjg.v27.i7.641

INTRODUCTION

Approximately 248 million individuals worldwide have been infected with chronic hepatitis B virus (HBV)[1], which can develop into hepatic failure, cirrhosis, and tumorigenesis, causing nearly 650000 deaths every year[2]. Hepatic fibrosis is an intermediate stage in the progression of chronic hepatic disease from mild hepatitis to decompensated cirrhosis[2,3]. Therefore, timely and accurate assessment of hepatic

P-Editor: Ma YJ

fibrosis stage is helpful to determine the optimal treatment plan, so as to minimize and delay the progression of liver injury[3,4]. Although liver biopsy is the gold standard for evaluating the stage of liver fibrosis, it is invasive, expensive, and accompanied by potential complications and sampling errors[5]. Transient elastography (FibroScan) is a new non-invasive test[3,6] that can replace biopsy, and it has been widely recommended by the guidelines on HBV management for assessing the stage of hepatic fibrosis[4]. Therefore, considering liver biopsy only in patients at a high fibrosis stage could minimize unnecessary biopsies.

The Society of Radiologists in Ultrasound consensus statement on liver elastography indicated that liver stiffness measurement (LSM) obtained using ultrasound elastography is associated with the degree of hepatic fibrosis[7]. However, increased LSM values as per transient elastography in acute hepatitis do not actually reflect the grade of liver fibrosis. During an acute attack of chronic liver disease, LSM values are affected by liver inflammatory activity indices such as serum total bilirubin (TBIL) and alanine aminotransferase (ALT), which may overestimate the liver fibrosis stage. The 2019 Chinese guidelines for chronic hepatitis B and the non-invasive liver fibrosis guidelines of the European Society and Latin American Society of Hepatology indicated that the diagnostic cutoffs of LSM should be adapted to ALT levels that assess the stage of HBV-related fibrosis[8,9]. In clinical practice, elevated ALT levels in many patients with chronic hepatic disease reflect hepatic inflammatory injury. Many studies have suggested that the cutoff value of LSM tends to increase and its diagnostic accuracy tends to decrease with elevated ALT level[10,11]; however, whether pathological hepatic inflammation would similarly affect cutoff values and the diagnostic accuracy of LSM in assessing the stage of hepatic fibrosis remains unclear.

In this study, we aimed to investigate in detail the impact of liver inflammation on LSM values and the diagnostic performance of FibroScan in assessing the stage of fibrosis in patients with chronic HBV infection.

MATERIALS AND METHODS

Research population

The study protocol was approved by the Institutional Review Board of Fujian Medical University, Fuzhou, China, and the need for written informed consent from patients was waived owing to the retrospective nature of the study. As shown in Figure 1, a total of 416 patients aged 18 years and above with chronic HBV infection who consented to undergo FibroScan and liver biopsy were enrolled in The First Affiliated Hospital of Fujian Medical University, and The First Hospital of Quanzhou Affiliated to Fujian Medical University between January 2014 and December 2019. Chronic HBV infection was defined as the persistent presence of hepatitis B surface antigen (HBsAg) and HBV-DNA in the serum for more than 6 mo. Patients with other types of hepatitis virus infections; those with body mass index (BMI) > 28 kg/m^2; those with fatty liver disease, alcoholic liver disease, drug-induced liver disease, autoimmune liver disease, genetic, or metabolic disease; those with decompensated cirrhosis, malignant tumors, or severe extrahepatic disease or pregnancy; and those with unreliable LSM values by FibroScan were excluded. Patients with hepatic steatosis by histology of liver biopsy were also excluded. All patients were examined using FibroScan, and fasting venous blood samples were collected for routine clinical examination within 1 wk of liver biopsy.

Clinical and laboratory parameters

Information regarding the following clinical parameters was collected: Patient age, sex, weight, height, status of alcohol consumption, and history of HBV infection. The BMI was calculated as weight (kg)/height^2 (m^2). Serum samples were collected after the patients fasted for 8 h at night, for the following measurements: HBsAg, hepatitis B envelope antigen (HBeAg), HBV-DNA, TBIL, ALT, aspartate aminotransferase (AST), albumin (ALB), prothrombin time (PT), platelet (PLT), and alpha-fetoprotein.

Liver stiffness measurement by FibroScan

LSM was performed using FibroScan 502 (Echosens, Paris, France). The detection method was followed as per the user manual, and the monitoring points were selected from the right anterior axillary line to the axillary midline 7, 8 or 8, 9 intercostals of the patient. The LSM values could be considered reliable when at least 10 valid measurements yielded a success rate of more than 60% and the interquartile range/median was less than 30%. The median value was determined as the final result

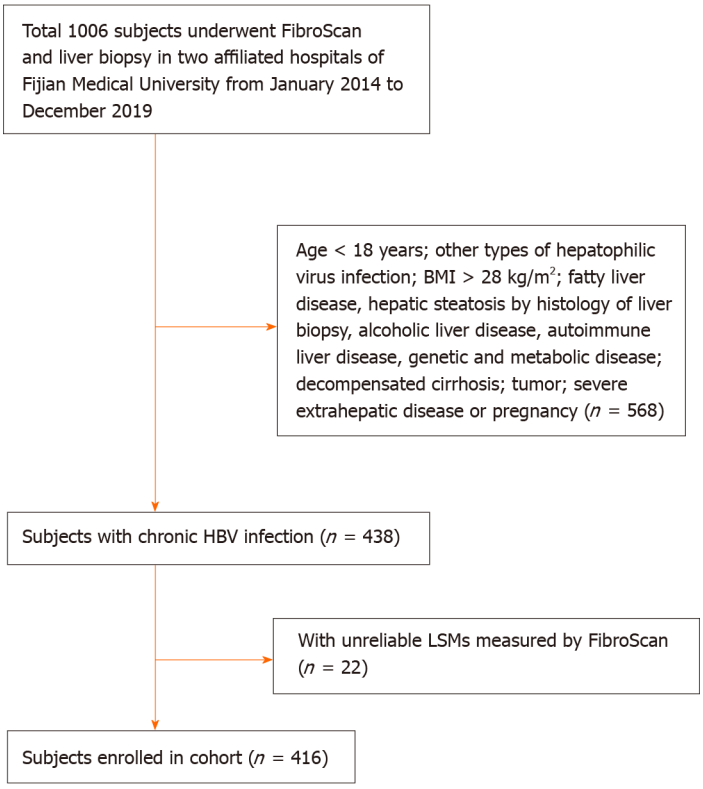


Figure 1 Flowchart of patient enrolment. BMI: Body mass index; HBV: Hepatitis B virus; LSM: Liver stiffness measurements; FibroScan: Transient elastography.

of liver stiffness, and its unit was kPa. FibroScan was performed by an expert certified technician.

Liver histology assessment

Percutaneous liver biopsy was performed using 16-gauge modified aspiration needles (ACUSON; Siemens, United States) under ultrasound guidance. Qualified liver specimens with a minimum length of 1.5 cm and having more than six portal veins were fixed in 4% neutral formalin, embedded in paraffin, and stained with hematoxylin and eosin (H&E) and Masson's trichrome by two experienced pathologists who were blinded to the LSM values of FibroScan and clinical data. The pathological diagnosis was graded according to the METAVIR score standard[12], as follows: F0, no fibrosis; F1, fibrous enlargement in the manifold area without septa; F2, fibrous enlargement in the manifold area and few septa; F3, plentiful septa without cirrhosis; and F4, early cirrhosis. Significant fibrosis was defined as ≥ F2; advanced fibrosis, as ≥ F3; and cirrhosis, as F4. Hepatic inflammation activity according to the degree of piecemeal necrosis (PN) was graded as A0, none; A1, mild PN; A2, moderate PN; and A3, severe PN[12].

Statistical analysis

Measurement and enumeration data were expressed as the means with standard deviation or median and ratio or composition ratio, respectively. Student's *t*-test, Chi-squared test, and Mann-Whitney *U* test were performed for comparative analysis, and the Spearman test was performed for correlation analyses. Receiver operating characteristic (ROC) curves were used to analyze the diagnostic performance and obtain the optimal cut-off value of FibroScan for assessing the stage of liver fibrosis. Multivariate regression analyses were employed to select the independent risk factors related to the misdiagnosis of the stage of fibrosis using FibroScan, and a non-invasive risk prediction model was constructed. To compare the area under the curves (AUCs) of the prediction model with that of other single related factors, the DeLong test was applied. Statistical analyses were performed using SPSS v23.0 (SPSS Inc. Chicago, IL, United States) and MedCalc v19.1 (MedCalc Software Bvba, Ostend, Belgium). A two-sided $P < 0.05$ was considered statistically significant.

RESULTS

Demographic and clinical characteristics

In total, 416 patients were enrolled in this study (Table 1). All patients were HBsAg positive, and most of them were male (73.3%) and HBeAg positive (57.0%). The mean age, BMI, TBIL, ALB, ALT, AST, PLT, HBV DNA, PT, and LSM values were 38.67 years, 22.90 kg/m^2, 17.11 μmoL/L, 42.50 g/L, 95.25 IU/L, 58.46 IU/L, 187.46 × 10^9/L, 4.98 log IU/mL, 12.20 s, and 9.83 kPa, respectively. According to the METAVIR score, the distribution of the stage of liver fibrosis was as follows: F0-F1 = 175 (42.1%), F2 = 106 (25.5%), F3 = 67 (16.1%), and F4 = 68 (16.3%). The distribution of liver inflammation activity was as follows: A0 = 17 (4.1%), A1 = 236 (56.7%), A2 = 119 (28.6%), and A3 = 44 (10.6%).

Diagnostic value of FibroScan for staging of liver fibrosis

Using hepatic pathology and METAVIR fibrosis stages as a reference, the LSM values of FibroScan were positively associated with hepatic fibrosis (r = 0.732). In the overall cohort, the optimal diagnostic LSM values of FibroScan for significant fibrosis (≥ F2), severe fibrosis (≥ F3), and cirrhosis (F4) were 7.3 kPa (AUC = 0.863), 9.7 kPa (AUC = 0.911), and 11.3 kPa (AUC = 0.918), respectively (Table 2).

Discordance in stage of liver fibrosis between FibroScan and pathological scores

Misdiagnosis of the stage of fibrosis using FibroScan was defined when at least one stage of liver fibrosis was discordant with that observed using pathological staging in the METAVIR scoring system. The 416 patients were accordingly divided into the concordance group (n = 274) and discordance group (n = 142). Figure 2 shows the distribution of predicted fibrosis stage by FibroScan in different pathological stages of liver fibrosis. The rate of misdiagnosis using FibroScan was 34.1% (142/416 patients), and 8.2% (34/416) of the patients showed a discordance between the values obtained using the two methods for two stages. In total, 81 patients showed discordance (19.5%) attributed to overstaging by FibroScan, and the remaining 61 patients showed discordance (14.7%) attributed to understaging. There were no significant differences in the demography, HBV virology, and LSM values obtained using FibroScan between the two groups. However, in the discordance group, ALT and AST levels, the proportion of liver inflammation activity over 2, and significant fibrosis were significantly higher than the levels in the concordance group (P < 0.001) (Table 1).

Factors related to misdiagnosis of liver fibrosis stage by FibroScan

Univariate analysis revealed that ALT levels ≥ 5 times the upper limit of normal (5 ULN), AST levels ≥ 2 ULN, and liver inflammation activity over 2 (A ≥ 2) were significantly related to misdiagnosis of the stage of liver fibrosis by FibroScan (P < 0.001). Subsequently, these variables were subjected to multiple regression analyses. Finally, liver inflammation activity ≥ 2 (OR = 3.53, 95%CI: 2.11-5.92, P < 0.001) was considered an independent risk factor for mis-staging of liver fibrosis using FibroScan (Table 3).

Effect of liver inflammation on diagnostic accuracy of FibroScan staging

Figure 3 shows the effect of liver inflammation on LSM values obtained using FibroScan for different stages of fibrosis. Within each fibrosis stage, namely F0-1, F2, F3, and F4, the LSM values of patients with inflammation activity ≥ 2 (A ≥ 2) were significantly higher than those of patients with inflammation activity < 2 (A < 2) (all P < 0.05).

Figure 4 shows the prevalence of misdiagnosis of the stage of liver fibrosis using FibroScan staging in patients with different liver inflammation activities. Patients with inflammation activity ≥ 2 had higher rates of FibroScan mis-staging (55.8% *vs* 20.2%, P < 0.001), over-staging (36.8% *vs* 8.3%, P < 0.001), and under-staging (19.0% *vs* 11.9%, P = 0.044), compared with patients with inflammation activity < 2.

Figure 5 shows the effect of liver inflammation activity on the diagnostic performance of FibroScan for different fibrosis stages. In patients with inflammation activity < 2, the diagnostic performance of FibroScan for significant fibrosis (≥ F2), advanced fibrosis (≥ F3), and cirrhosis (F4) were significantly better than that in patients with inflammation activity ≥ 2 (0.831 *vs* 0.702, 0.903 *vs* 0.815, and 0.941 *vs* 0.836, all P < 0.05), as observed by comparing the AUCs.

Table 1 Demographic characteristics and clinical features of our patient cohort

	All (*n* = 416)	Concordance group (*n* = 274)	Discordance group (*n* = 142)	*P* value
Age (yr)	38.67 ± 10.47	38.41 ± 10.63	39.18 ± 10.18	0.467
Male, *n*	305 (73.3)	209 (76.3)	96 (67.6)	0.058
BMI (kg/m^2)	22.90 ± 2.64	22.88 ± 2.49	22.94 ± 2.92	0.833
TBIL (μmoL/L)	17.11 ± 21.56	17.70 ± 23.30	15.98 ± 17.73	0.402
Albumin (g/L)	42.50 ± 5.02	42.57 ± 5.05	42.37 ± 5.00	0.706
ALT (IU/L)	95.25 ± 52.0	78.90 ± 99.89	126.10 ± 118.46	< 0.001
AST (IU/L)	58.46± 108.85	49.05 ± 55.44	76.61 ± 62.80	< 0.001
PLT (10^9/L)	187.46 ± 56.53	186.36 ± 56.86	189.59 ± 56.04	0.916
HBsAg (Log IU/mL)	3.42 ± 0.97	3.38 ± 1.04	3.50 ± 0.80	0.258
HBeAg positive (%)	237 (57.0)	155 (56.6)	82 (57.7)	0.818
HBV-DNA (Log IU/mL)	4.98 ± 2.18	4.95 ± 2.16	5.05 ± 2.23	0.641
PT (s)	12.20 ± 0.98	12.17 ± 1.03	12.25 ± 0.88	0.387
AFP (ng/mL)	11.37 ± 34.59	11.98 ± 36.80	10.20 ± 29.95	0.597
LSM (kPa)	9.83 ± 7.70	9.75 ± 7.21	9.97 ± 5.14	0.751
Fibrosis stage[1], *n*				< 0.001
F0-1	175 (42.1)	143 (52.2)	32 (22.5)	
F2	106 (25.5)	49 (17.9)	57 (40.1)	
F3	67 (16.1)	23 (8.4)	44 (31.0)	
F4	68 (16.3)	59 (21.5)	9 (6.3)	
Inflammation grade[1], *n*				< 0.001
A0	17 (4.1)	15 (5.5)	2 (1.4)	
A1	236 (56.7)	187 (68.2)	49 (34.5)	
A2	119 (28.6)	49 (17.9)	70 (49.3)	
A3	44 (10.6)	23 (8.4)	21 (14.8)	

[1]According to METAVIR system, the liver fibrosis stage ranged from 0 to 4, and liver inflammation grade ranged from 0 to 3. BMI: Body mass index; TBIL: Total bilirubin; ALT: Alanine aminotransferase; AST: Aspartate aminotransferase; PLT: Platelet count; HBV: Hepatitis B virus; PT: Prothrombin time; AFP: Alpha fetoprotein; LSM: Liver stiffness measurements; HBsAg: Hepatitis B surface antigen; HBeAg: Hepatitis B envelope antigen.

Table 2 Accuracy of liver stiffness measurement values by transient elastography in diagnosing ≥ F2, ≥ F3, and F4, as measured by area under the receiver operating characteristic curve (*n* = 416)

Fibrosis stage	AUC (95%CI)	Sensitivity (%)	Specificity (%)	PPV (%)	NPV (%)	Cut-off point
≥ F2	0.863 (0.826-0.895)	83.40	81.71	86.01	78.49	≥ 7.3
≥ F3	0.911 (0.880-0.937)	80.74	87.19	76.59	89.72	≥ 9.7
F4	0.918 (0.887-0.942)	86.76	89.08	61.47	97.10	≥ 11.3

AUC: Area under the receiver operating characteristic curve; NPV: Negative predictive value; PPV: Positive predictive value; ≥ F2: Significant fibrosis; ≥ F3: Advanced fibrosis; F4: Cirrhosis.

Development of a non-invasive prediction model for misdiagnosis of liver fibrosis stage using FibroScan

The ALT and AST levels were positively correlated with hepatic inflammation (r = 0.534 and 0.527, P < 0.001) by the Spearman's test, and these were significantly related with misdiagnosis of fibrosis stage using FibroScan (all P < 0.001) (Table 3). Using

Table 3 Univariate and multivariate regression analyses of risk of misdiagnosis of fibrosis stage by transient elastography in all patients

Variables	Univariate analyses		Multivariate analyses	
	OR (95%CI)	*P* value	OR (95%CI)	*P* value
Age (yr)	1.00 (0.99-1.03)	0.472		
Male, *n*	0.65 (0.42-1.02)	0.059		
BMI (kg/m^2)	1.01 (0.93-1.09)	0.832		
TBIL > 2 ULN (μmoL/L)	0.68 (0.24-1.92)	0.464		
Albumin (g/L)	0.99 (0.95-1.03)	0.707		
ALT[1] (IU/L)				
< 2 ULN	Reference	Reference	Reference	Reference
2-5 ULN	2.16 (1.31-3.56)	0.003	1.00 (0.52-1.93)	0.996
≥ 5 ULN	4.93 (2.66-9.12)	< 0.001	1.11 (0.44-2.76)	0.996
AST[1] ≥ 2 ULN (IU/L)	4.42 (2.73-7.16)	< 0.001	2.05 (0.97-4.34)	0.059
PLT (10^9/L)	1.00 (0.99-1.01)	0.580		
HBsAg (Log IU/mL)	1.13 (0.91-1.40)	0.258		
HBeAg positive	1.05 (0.70-1.58)	0.818		
HBV-DNA (Log IU/mL)	1.02 (0.93-1.12)	0.636		
PT (s)	1.09 (0.89-1.34)	0.408		
AFP (ng/mL)	1.00 (0.99-1.01)	0.622		
Inflammation activity[2]				
A < 2	Reference	Reference	Reference	Reference
A ≥ 2	5.01 (3.24-7.74)	< 0.001	3.53 (2.11-5.92)	< 0.001

[1]Normal alanine aminotransferase and aspartate aminotransferase levels are 40 U/L for women and men.
[2]Inflammation activity was calculated as a range of 0-3 according to the METAVIR system. BMI: Body mass index; TBIL: Total bilirubin; ALT: Alanine aminotransferase; AST: Aspartate aminotransferase; PLT: Platelet count; HBV: Hepatitis B virus; PT: Prothrombin time; AFP: Alpha fetoprotein; ULN: Upper limit of normal; HBsAg: Hepatitis B surface antigen; HBeAg: Hepatitis B envelope antigen.

these related factors, a non-invasive prediction model was developed to identify the risk of misdiagnosis using FibroScan, as follows: logit (P) = -1.477 + (0.139, 0.732) × ALT levels (2-5, ≥ 5 ULN) + 1.310 × AST levels (> 2 ULN) + (1.056, 0.815, −0.154) × FibroScan-predicted fibrosis staging (F2, F3, and F4).

We compared the prediction performance of the model with that of other single related factors to evaluate the misdiagnosis of the stage of liver fibrosis using FibroScan (Figure 6). The AUC value of the prediction model was 0.701 (95%CI: 0.655-0.745), which was significantly higher than that of ALT levels (0.636, 95%CI: 0.588-0.683), AST levels (0.639, 95%CI: 0.590-0.685) and FibroScan-predicted fibrosis stages (0.611, 95%CI: 0.562-0.658) (all $P < 0.001$). The cut-off point, sensitivity, and specificity of the model were 0.340, 63.38%, and 67.52%, respectively.

DISCUSSION

Accurate evaluation of the stage of hepatic fibrosis is important in patients with chronic HBV infection for determining the initiation of antiviral therapy and is an important index for evaluating the efficacy of antiviral therapy. FibroScan is a recommended non-invasive test for evaluation of liver fibrosis in patients with chronic HBV infection[4,13]. In the present study, we confirmed that LSM values obtained using FibroScan were positively correlated with hepatic fibrosis and demonstrated the good performance of FibroScan in predicting the stage of liver fibrosis. We found that the optimal diagnostic LSM values of FibroScan for significant fibrosis (≥ F2), severe fibrosis (≥ F3), and cirrhosis (F4) were 7.3 kPa (AUC = 0.863), 9.7 kPa (AUC = 0.911),

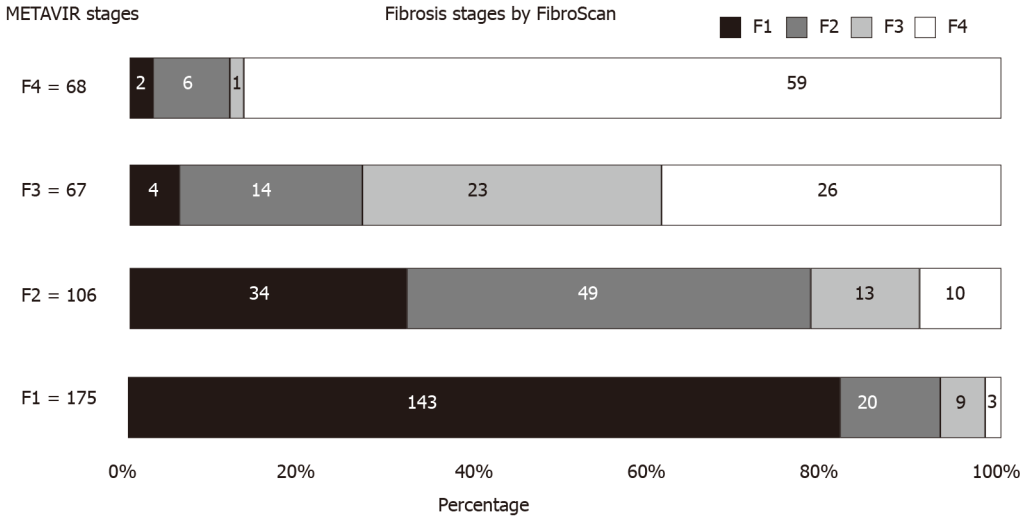


Figure 2 Distribution of predicted fibrosis stages by transient elastography according to different METAVIR liver fibrosis stages. FibroScan: Transient elastography.

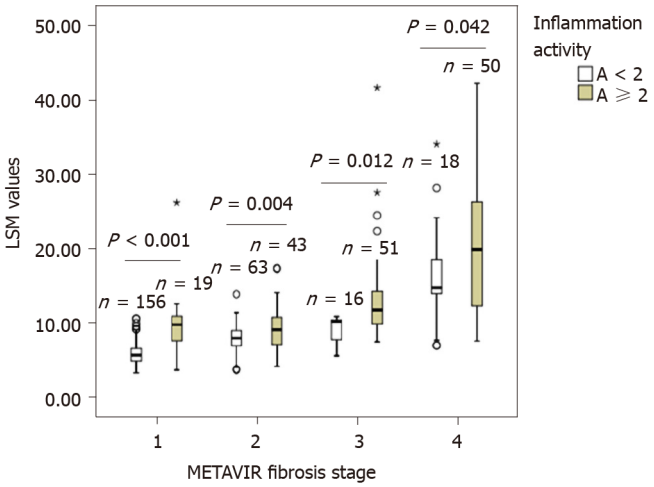


Figure 3 Comparison of liver stiffness measurement values by transient elastography in patients with different liver inflammation activities in different METAVIR fibrosis stages. LSM: Liver stiffness measurements.

and 11.3 kPa (AUC = 0.918), respectively. Our results are consistent with those of previous studies[6,14,15].

Although LSM values measured by ultrasound elastography are related to the stage of fibrosis, they could be affected by acute hepatitis, high ALT and/or AST levels, obstructive cholestasis, and infiltrative hepatic disease[7,16,17]. We explored the relationship between various anthropometric, biochemical, and pathological parameters and the diagnostic accuracy of FibroScan for determining the stage of liver fibrosis. A discordance between the fibrosis stage determined using FibroScan and that determined by pathological examination was observed in 34.1% of the patients (142/416), with 19.5% of patients (81/416) over-staged and 14.7% of patients (61/416) under-staged in our study. Compared with patients who showed concordance between values obtained using the two methods, those who showed discordance had significantly higher ALT and AST levels, and a higher proportion of moderate to severe liver inflammatory activity. Furthermore, multivariate analysis showed that liver inflammatory activity over 2 was an independent risk factor for misdiagnosis of fibrosis stage using FibroScan.

However, the bias caused by liver inflammation in the assessment of liver fibrosis stage using FibroScan is still unclear. The changes occurring in liver enzymes during inflammatory degeneration, necrosis, and fibrosis of hepatic cells are strong indicators of inflammation, in which ALT and AST are the most valuable serum biochemical indices for the detection of liver injury. Many studies have shown that elevated LSM

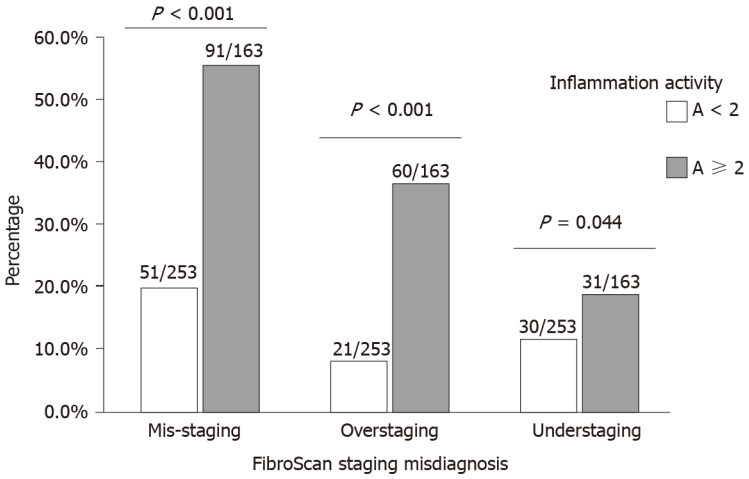


Figure 4 Prevalence of misdiagnosis of stage of liver fibrosis by transient elastography in patients with different inflammatory activities.

values were related to increased ALT levels, and have proposed a variety of dual cut-offs of LSM values adapted to ALT levels, which may improve the diagnostic performance of FibroScan in evaluating the stage of hepatic fibrosis in patients with chronic HBV infection[10,11,18]. The elevated baseline LSM values due to liver inflammation in patients with elevated ALT levels could lead to inappropriate overestimation of the stage of liver fibrosis. We found that patients with inflammation activity ≥ 2 had higher LSM values in each fibrosis stage among F0-1, F2, F3, and F4 (all $P < 0.05$), and a higher percentage of mis-staging (55.8% *vs* 20.2%, $P < 0.001$), over-staging (36.8% *vs* 8.3%, $P < 0.001$), and under-staging (19.0% *vs* 11.9%, $P = 0.044$) using FibroScan, compared with patients with inflammation activity < 2. Other studies reported a lack of these correlations and indicated that mildly increased ALT levels did not affect the performance of LSM in assessing hepatic fibrosis in patients with chronic HBV infection[19,20]. A recent study reported that the sensitivity and specificity of LSM values for assessing the stage of liver fibrosis were significantly lower in patients with ALT levels ≥ 2 times the ULN[11]. Our study findings are consistent with this result. We found that FibroScan was significantly better in predicting significant fibrosis (≥ F2), advanced fibrosis (≥ F3), and cirrhosis (F4) in patients with inflammation activity < 2 than in patients with inflammation activity ≥ 2, by comparing the AUCs (0.831 *vs* 0.702, 0.903 *vs* 0.815, and 0.941 *vs* 0.836, all $P < 0.05$). Therefore, we concluded that the diagnostic accuracy of LSM was mainly influenced by significantly elevated ALT levels (ALT > 2 ULN), acute viral hepatitis, HBV flares, and the severity of liver fibrosis.

At present, many non-invasive models have been developed to diagnose liver fibrosis. The WHO guidelines on chronic HBV infection recommended that LSM and APRI are the most helpful detection methods to evaluate hepatic fibrosis with limited resources[21]. The accuracy of LSM values could be affected by inflammation and other influencing factors. FibroScan may yield low LSM values and underestimate or misdiagnose the stage of liver fibrosis in patients with mild hepatic inflammation, and it may show elevated LSM values and overestimate or misdiagnose cirrhosis in patients with severe inflammation. In our study, the severity of liver inflammation was an independent risk factor for misdiagnosis of the stage of liver fibrosis using FibroScan; however, the measurement of severity entailed an invasive procedure. Therefore, we used other relevant non-invasive factors to predict the risk of misdiagnosis using FibroScan, which may be of great significance in determining the fibrosis stage or performing liver biopsy, and may guide the diagnosis of and therapy of chronic HBV infection. Our model consisted of three routinely assessed parameters (ALT levels, AST levels, and FibroScan-predicted fibrosis staging), which showed better performance than those of other single related factors in predicting the risk of misdiagnosis of the stage of hepatic fibrosis using FibroScan staging by ROC analysis. According to this model, more attention should be paid to patients at a high risk of being misdiagnosed using FibroScan, a comprehensive evaluation of the degree of hepatic fibrosis should be conducted, and further liver biopsy should be performed, if necessary, to determine whether antiviral therapy needs to be initiated immediately.

This study has several limitations. First, the effects of controlled attenuation parameters and histological steatosis on the diagnostic performance of FibroScan were

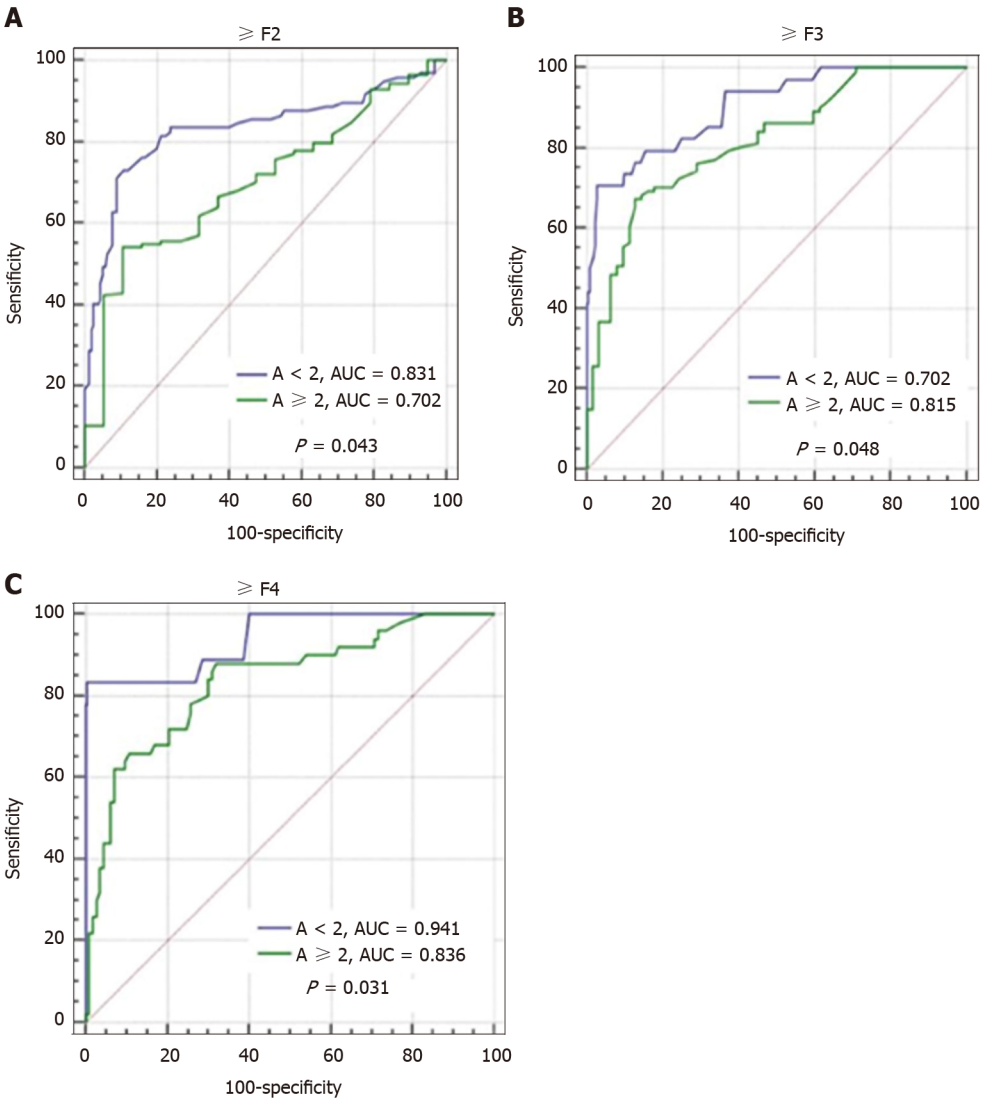


Figure 5 Comparison of effects of different liver inflammatory activities on diagnostic performance of transient elastography in assessing different fibrosis stages. A: ≥ F2; B: ≥ F3; C: F4. AUC: Area under the curve; ≥ F2: Significant fibrosis; ≥ F3: Advanced fibrosis; F4: Cirrhosis.

not discussed. Second, the sample size of the study was very small. An extensive liver biopsy database should be established to comprehensively evaluate the reliable cut-off value of FibroScan for assessing the stage of liver fibrosis. Third, the results of our study warrant further verification in large-scale, multicenter cohort studies.

CONCLUSION

In conclusion, liver inflammation is an independent risk factor that affects the accuracy of FibroScan in assessing the stage of HBV-related liver fibrosis. A combination of other related non-invasive factors can help predict the risk of misdiagnosis of the stage of liver fibrosis using FibroScan, which may help to decide whether liver biopsy is required and guide the diagnosis of and therapy of chronic HBV infection.

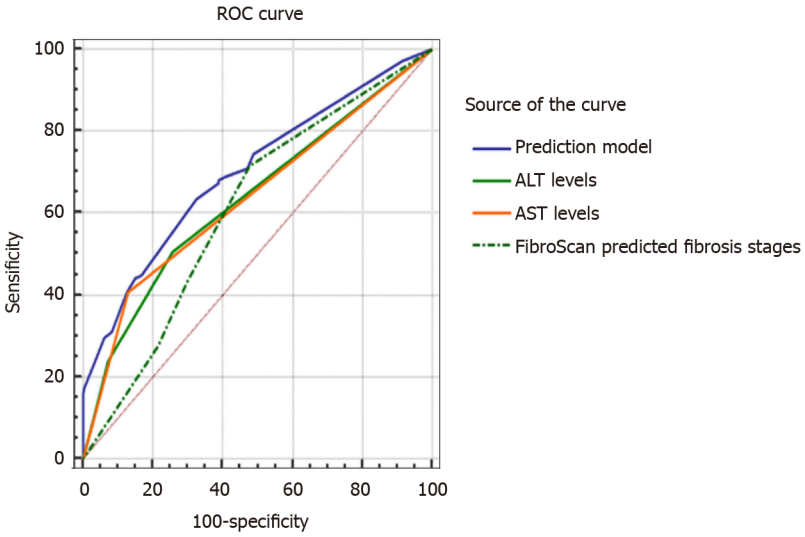


Figure 6 Comparison of receiver operating characteristic curves in prediction model and single related factors with regard to misdiagnosis of the stage of liver fibrosis using transient elastography. ALT: Alanine aminotransferase; AST: Aspartate aminotransferase; ROC: Receiver operating characteristic; FibroScan: Transient elastography.

ARTICLE HIGHLIGHTS

Research background

Transient elastography (FibroScan) is a new and non-invasive test, which can replace biopsy and has been widely recommended by the guidelines of chronic hepatitis B virus (HBV) management for assessing hepatic fibrosis staging. Liver stiffness measurement (LSM) by FibroScan is associated with the degree of hepatic fibrosis, but can also be confounded by liver necroinflammation, alanine aminotransferase (ALT), cholestasis, portal hypertension, hepatic congestion, and body mass index (BMI) and other factors, which may affect the diagnostic accuracy of the FibroScan device in fibrosis staging.

Research motivation

Many studies suggested that the cutoff value of LSM tends to increase with elevated ALT level, and its diagnostic accuracy tends to decrease with elevated ALT level, but it is not clear whether pathological hepatic inflammation would similarly affect LSM values and diagnostic accuracy of FibroScan assessing hepatic fibrosis.

Research objectives

We aimed to evaluate the diagnostic value of FibroScan and the effect of hepatic inflammation on the accuracy of FibroScan assessing liver fibrosis staging in patients with chronic HBV infection, and to develop a predictive model combining other related non-invasive confounders to predict the risk of FibroScan staging misdiagnosis.

Research methods

The data of 416 patients with chronic HBV infection who accepted FibroScan, liver biopsy, clinical, and biological examination were retrospectively collected between January 2014 and December 2019 from two affiliated hospitals of Fujian Medical University. Receiver operating characteristic (ROC) curves were used to analyze the data. The diagnostic performance of FibroScan for the stage of liver fibrosis was analyzed using ROC curves. Any discordance in fibrosis staging by FibroScan and pathological scores was statistically analyzed. The accuracy of FibroScan in assessing the stage of fibrosis in patients with different degrees of liver inflammation was analyzed using Logistic regression and ROC curves. A non-invasive model was constructed to predict the risk of misdiagnosis of fibrosis stage using FibroScan.

Research results

We confirmed that LSM values obtained using FibroScan were positively correlated with hepatic fibrosis and demonstrated the good performance of FibroScan in

predicting the stage of liver fibrosis. However, discordance between the fibrosis stage determined using FibroScan and that determined by pathological examination was observed in some patients. Furthermore, we found that liver inflammatory activity over 2 was an independent risk factor for misdiagnosis of fibrosis stage using FibroScan. Patients with liver inflammation activity ≥ 2 showed higher LSM values using FibroScan and higher rates of misdiagnosis of fibrosis stage, whereas the diagnostic performance of FibroScan for different fibrosis stages was significantly lower than that in patients with inflammation activity < 2. A non-invasive prediction model was established to assess the risk of misdiagnosis of fibrosis stage using FibroScan, and the area under the curve was 0.701, which was superior to that observed using other single related factors.

Research conclusions

Liver inflammation was an independent risk factor affecting the diagnostic accuracy of FibroScan for HBV-related fibrosis staging. The combination of other related non-invasive factors can predict the risk of misdiagnosis of fibrosis staging using FibroScan, and may be helpful for making decisions on liver biopsy and guiding the diagnosis and therapy of chronic HBV infection.

Research perspectives

This multi-center cross-sectional study developed and evaluated a noninvasive model to predict the risk of misdiagnosis of fibrosis staging using FibroScan, thus an extensive liver biopsy database should be established to comprehensively evaluate the reliable cut-off value of FibroScan for assessing the stage of liver fibrosis and further verify the diagnostic performance of this model in future prospective studies.

REFERENCES

1 **Schweitzer A**, Horn J, Mikolajczyk RT, Krause G, Ott JJ. Estimations of worldwide prevalence of chronic hepatitis B virus infection: a systematic review of data published between 1965 and 2013. *Lancet* 2015; **386**: 1546-1555 [PMID: 26231459 DOI: 10.1016/S0140-6736(15)61412-X]

2 **Wu JF**, Chang MH. Natural history of chronic hepatitis B virus infection from infancy to adult life - the mechanism of inflammation triggering and long-term impacts. *J Biomed Sci* 2015; **22**: 92 [PMID: 26487087 DOI: 10.1186/s12929-015-0199-y]

3 **Shiha G**, Ibrahim A, Helmy A, Sarin SK, Omata M, Kumar A, Bernstien D, Maruyama H, Saraswat V, Chawla Y, Hamid S, Abbas Z, Bedossa P, Sakhuja P, Elmahatab M, Lim SG, Lesmana L, Sollano J, Jia JD, Abbas B, Omar A, Sharma B, Payawal D, Abdallah A, Serwah A, Hamed A, Elsayed A, AbdelMaqsod A, Hassanein T, Ihab A, GHaziuan H, Zein N, Kumar M. Asian-Pacific Association for the Study of the Liver (APASL) consensus guidelines on invasive and non-invasive assessment of hepatic fibrosis: a 2016 update. *Hepatol Int* 2017; **11**: 1-30 [PMID: 27714681 DOI: 10.1007/s12072-016-9760-3]

4 **European Association for the Study of the Liver**. EASL 2017 Clinical Practice Guidelines on the management of hepatitis B virus infection. *J Hepatol* 2017; **67**: 370-398 [PMID: 28427875 DOI: 10.1016/j.jhep.2017.03.021]

5 **Ilic I**, Milovanovic T. The risk-benefit assessment of liver biopsy in times of non-invasive screening for liver fibrosis. *J Hepatol* 2020; **73**: 701-702 [PMID: 32546400 DOI: 10.1016/j.jhep.2020.05.017]

6 **Jia J**, Hou J, Ding H, Chen G, Xie Q, Wang Y, Zeng M, Zhao J, Wang T, Hu X, Schuppan D. Transient elastography compared to serum markers to predict liver fibrosis in a cohort of Chinese patients with chronic hepatitis B. *J Gastroenterol Hepatol* 2015; **30**: 756-762 [PMID: 25353058 DOI: 10.1111/jgh.12840]

7 **Dietrich CF**, Bamber J, Berzigotti A, Bota S, Cantisani V, Castera L, Cosgrove D, Ferraioli G, Friedrich-Rust M, Gilja OH, Goertz RS, Karlas T, de Knegt R, de Ledinghen V, Piscaglia F, Procopet B, Saftoiu A, Sidhu PS, Sporea I, Thiele M. EFSUMB Guidelines and Recommendations on the Clinical Use of Liver Ultrasound Elastography, Update 2017 (Long Version). *Ultraschall Med* 2017; **38**: e48 [PMID: 30176678 DOI: 10.1055/a-0641-0076]

8 **Chinese Society of Infectious Diseases**, Chinese Medical Association, Chinese Society of Hepatology Chinese Medical Association. [The guidelines of prevention and treatment for chronic hepatitis B (2019 version)]. *Zhonghua Gan Zang Bing Za Zhi* 2019; **27**: 938-961 [PMID: 31941257 DOI: 10.3760/cma.j.issn.1007-3418.2019.12.007]

9 **European Association for Study of Liver**, Asociacion Latinoamericana para el Estudio del Higado. EASL-ALEH Clinical Practice Guidelines: Non-invasive tests for evaluation of liver disease severity and prognosis. *J Hepatol* 2015; **63**: 237-264 [PMID: 25911335 DOI: 10.1016/j.jhep.2015.04.006]

10 **Song ZZ**. Acute viral hepatitis increases liver stiffness values measured by transient elastography. *Hepatology* 2008; **48**: 349-50; author reply 350 [PMID: 18571790 DOI: 10.1002/hep.22385]

11 **Zeng J**, Zheng J, Jin JY, Mao YJ, Guo HY, Lu MD, Zheng HR, Zheng RQ. Shear wave elastography for liver fibrosis in chronic hepatitis B: Adapting the cut-offs to alanine aminotransferase levels

improves accuracy. *Eur Radiol* 2019; **29**: 857-865 [PMID: 30039224 DOI: 10.1007/s00330-018-5621-x]

12 **Bedossa P**, Poynard T. An algorithm for the grading of activity in chronic hepatitis C. The METAVIR Cooperative Study Group. *Hepatology* 1996; **24**: 289-293 [PMID: 8690394 DOI: 10.1002/hep.510240201]

13 **Sarin SK**, Kumar M, Lau GK, Abbas Z, Chan HL, Chen CJ, Chen DS, Chen HL, Chen PJ, Chien RN, Dokmeci AK, Gane E, Hou JL, Jafri W, Jia J, Kim JH, Lai CL, Lee HC, Lim SG, Liu CJ, Locarnini S, Al Mahtab M, Mohamed R, Omata M, Park J, Piratvisuth T, Sharma BC, Sollano J, Wang FS, Wei L, Yuen MF, Zheng SS, Kao JH. Asian-Pacific clinical practice guidelines on the management of hepatitis B: a 2015 update. *Hepatol Int* 2016; **10**: 1-98 [PMID: 26563120 DOI: 10.1007/s12072-015-9675-4]

14 **Chon YE**, Choi EH, Song KJ, Park JY, Kim DY, Han KH, Chon CY, Ahn SH, Kim SU. Performance of transient elastography for the staging of liver fibrosis in patients with chronic hepatitis B: a meta-analysis. *PLoS One* 2012; **7**: e44930 [PMID: 23049764 DOI: 10.1371/journal.pone.0044930]

15 **Verveer C**, Zondervan PE, ten Kate FJ, Hansen BE, Janssen HL, de Knegt RJ. Evaluation of transient elastography for fibrosis assessment compared with large biopsies in chronic hepatitis B and C. *Liver Int* 2012; **32**: 622-628 [PMID: 22098684 DOI: 10.1111/j.1478-3231.2011.02663.x]

16 **Ferraioli G**, Filice C, Castera L, Choi BI, Sporea I, Wilson SR, Cosgrove D, Dietrich CF, Amy D, Bamber JC, Barr R, Chou YH, Ding H, Farrokh A, Friedrich-Rust M, Hall TJ, Nakashima K, Nightingale KR, Palmeri ML, Schafer F, Shiina T, Suzuki S, Kudo M. WFUMB guidelines and recommendations for clinical use of ultrasound elastography: Part 3: liver. *Ultrasound Med Biol* 2015; **41**: 1161-1179 [PMID: 25800942 DOI: 10.1016/j.ultrasmedbio.2015.03.007]

17 **Barr RG**, Wilson SR, Rubens D, Garcia-Tsao G, Ferraioli G. Update to the Society of Radiologists in Ultrasound Liver Elastography Consensus Statement. *Radiology* 2020; **296**: 263-274 [PMID: 32515681 DOI: 10.1148/radiol.2020192437]

18 **Chan HL**, Wong GL, Choi PC, Chan AW, Chim AM, Yiu KK, Chan FK, Sung JJ, Wong VW. Alanine aminotransferase-based algorithms of liver stiffness measurement by transient elastography (Fibroscan) for liver fibrosis in chronic hepatitis B. *J Viral Hepat* 2009; **16**: 36-44 [PMID: 18673426 DOI: 10.1111/j.1365-2893.2008.01037.x]

19 **Li Q**, Chen L, Zhou Y. Diagnostic accuracy of liver stiffness measurement in chronic hepatitis B patients with normal or mildly elevated alanine transaminase levels. *Sci Rep* 2018; **8**: 5224 [PMID: 29588489 DOI: 10.1038/s41598-018-23646-2]

20 **Seo YS**, Kim MY, Kim SU, Hyun BS, Jang JY, Lee JW, Lee JI, Suh SJ, Park SY, Park H, Jung EU, Kim BS, Kim IH, Lee TH, Um SH, Han KH, Kim SG, Paik SK, Choi JY, Jeong SW, Jin YJ, Lee KS, Yim HJ, Tak WY, Hwang SG, Lee YJ, Lee CH, Kim DG, Kang YW, Kim YS; Korean Transient Elastography Study Group. Accuracy of transient elastography in assessing liver fibrosis in chronic viral hepatitis: A multicentre, retrospective study. *Liver Int* 2015; **35**: 2246-2255 [PMID: 25682719 DOI: 10.1111/liv.12808]

21 Guidelines for the Prevention, Care and Treatment of Persons with Chronic Hepatitis B Infection. Geneva: World Health Organization; 2015 [PMID: 26225396]

World Journal of Gastroenterology

Submit a Manuscript: https://www.f6publishing.com

World J Gastroenterol 2021 February 21; 27(7): 654-665

DOI: 10.3748/wjg.v27.i7.654

ISSN 1007-9327 (print) ISSN 2219-2840 (online)

ORIGINAL ARTICLE

Clinical Trials Study

Simultaneous partial splenectomy during liver transplantation for advanced cirrhosis patients combined with severe splenomegaly and hypersplenism

Wen-Tao Jiang, Jian Yang, Yan Xie, Qing-Jun Guo, Da-Zhi Tian, Jun-Jie Li, Zhong-Yang Shen

ORCID number: Wen-Tao Jiang 0000-0002-6592-4322; Jian Yang 0000-0001-9481-0407; Yan Xie 0000-0002-7812-8632; Qing-Jun Guo 0000-0002-9108-489X; Da-Zhi Tian 0000-0002-6664-041X; Jun-Jie Li 0000-0001-8318-3372; Zhong-Yang Shen 0000-0001-8536-3780.

Author contributions: Jiang WT is the first author; Yang J and Xie Y are the co-first authors; Jiang WT contributed to study conception; Yang J and Xie Y contributed to data collection; Yang J contributed to manuscript drafting; Jiang WT, Yang J, Xie Y, Guo QJ, Tian DZ, Li JJ and Shen ZY contributed critical revision of the manuscript for important intellectual content.

Supported by National Natural Science Foundation of China, No. 81870444; Tianjin Natural Science Foundation, No. 19JCQNJC10300; and Spring Bud Plan of Tianjin First Central Hospital, No. TFCHCL201801.

Institutional review board statement: This study was approved by the Ethics Committee of Tianjin First Central Hospital (Approval No. 2019N168KY).

Clinical trial registration statement: This study is registered at Chinese

Wen-Tao Jiang, Jian Yang, Yan Xie, Qing-Jun Guo, Da-Zhi Tian, Jun-Jie Li, Zhong-Yang Shen, Department of Liver Transplantation, Tianjin First Center Hospital, First Clinical Institute of Tianjin Medical University, Tianjin 300192, China

Wen-Tao Jiang, Yan Xie, Qing-Jun Guo, Da-Zhi Tian, Jun-Jie Li, Zhong-Yang Shen, Organ Transplantation Center, Tianjin First Center Hospital, Tianjin 300192, China

Jian Yang, Department of Hepatological Surgery, Zibo Central Hospital, Zibo 255000, Shandong Province, China

Corresponding author: Zhong-Yang Shen, MD, Dean, Doctor, Department of Liver Transplantation, Tianjin First Center Hospital, First Clinical Institute of Tianjin Medical University, No. 24 Fukang Road, Nankai District, Tianjin 300192, China.
yangjian06281@126.com

Abstract

BACKGROUND

The most effective treatment for advanced cirrhosis and portal hypertension is liver transplantation (LT). However, splenomegaly and hypersplenism can persist even after LT in patients with massive splenomegaly.

AIM

To examine the feasibility of performing partial splenectomy during LT in patients with advanced cirrhosis combined with severe splenomegaly and hypersplenism.

METHODS

Between October 2015 and February 2019, 762 orthotopic LTs were performed for patients with end-stage liver diseases in Tianjin First Center Hospital. Eighty-four cases had advanced cirrhosis combined with severe splenomegaly and hypersplenism. Among these patients, 41 received partial splenectomy during LT (PSLT group), and 43 received only LT (LT group). Patient characteristics, intraoperative parameters, and postoperative outcomes were retrospectively analyzed and compared between the two groups.

RESULTS

Clinical Trial Registry. The registration identification number is ChiCTR-TRC-10001070.

Informed consent statement: All study participants, or their legal guardian, provided informed written consent prior to study enrollment.

Conflict-of-interest statement: The authors declare no conflicts of interest.

Data sharing statement: Participants gave informed consent for data sharing.

CONSORT 2010 statement: The authors have read the CONSORT 2010 statement, and the manuscript was prepared and revised according to the CONSORT 2010 statement.

Open-Access: This article is an open-access article that was selected by an in-house editor and fully peer-reviewed by external reviewers. It is distributed in accordance with the Creative Commons Attribution NonCommercial (CC BY-NC 4.0) license, which permits others to distribute, remix, adapt, build upon this work non-commercially, and license their derivative works on different terms, provided the original work is properly cited and the use is non-commercial. See: http://creativecommons.org/Licenses/by-nc/4.0/

Manuscript source: Unsolicited manuscript

Specialty type: Gastroenterology and hepatology

Country/Territory of origin: China

Peer-review report's scientific quality classification

Grade A (Excellent): 0
Grade B (Very good): 0
Grade C (Good): C
Grade D (Fair): 0
Grade E (Poor): 0

Received: November 25, 2020
Peer-review started: November 25, 2020
First decision: December 8, 2020

The incidence of postoperative hypersplenism (2/41, 4.8%) and recurrent ascites (1/41, 2.4%) in the PSLT group was significantly lower than that in the LT group (22/43, 51.2%; 8/43, 18.6%, respectively). Seventeen patients (17/43, 39.5%) in the LT group required two-stage splenic embolization, and further splenectomy was required in 6 of them. The operation time and intraoperative blood loss in the PSLT group (8.6 ± 1.3 h; 640.8 ± 347.3 mL) were relatively increased compared with the LT group (6.8 ± 0.9 h; 349.4 ± 116.1 mL). The incidence of postoperative bleeding, pulmonary infection, thrombosis and splenic arterial steal syndrome in the PSLT group was not different to that in the LT group, respectively.

CONCLUSION
Simultaneous PSLT is an effective treatment and should be performed in patients with advanced cirrhosis combined with severe splenomegaly and hypersplenism to prevent postoperative persistent hypersplenism.

Key Words: Liver transplantation; Partial splenectomy; Hypersplenism; Splenomegaly; Liver cirrhotic; Megalosplenia

©The Author(s) 2021. Published by Baishideng Publishing Group Inc. All rights reserved.

Core Tip: In this article, for the first time, we describe partial splenectomy during liver transplantation (PSLT) in patients with advanced cirrhosis combined with severe splenomegaly and hypersplenism. PSLT can effectively alleviate the severity of postoperative hypersplenism and ascites in megalosplenia patients.

Citation: Jiang WT, Yang J, Xie Y, Guo QJ, Tian DZ, Li JJ, Shen ZY. Simultaneous partial splenectomy during liver transplantation for advanced cirrhosis patients combined with severe splenomegaly and hypersplenism. *World J Gastroenterol* 2021; 27(7): 654-665
URL: https://www.wjgnet.com/1007-9327/full/v27/i7/654.htm
DOI: https://dx.doi.org/10.3748/wjg.v27.i7.654

INTRODUCTION

Liver cirrhosis is the leading cause of liver disease related morbidity and mortality worldwide and is often accompanied by portal hypertension and splenomegaly[1]. The most effective treatment for advanced cirrhosis and portal hypertension is liver transplantation (LT)[2]. Splanchnic hemodynamics change dramatically after LT, including improved portal outflow resistance, decreased portal vein pressure, and movement of accumulated blood from viscera to the systemic circulation. These changes significantly increase portal vein flow, gradually improve spleen congestion, and further ameliorate splenomegaly and hypersplenism[3].

However, splenomegaly and hypersplenism can persist even after LT in patients with massive splenomegaly[4]. Persistent hypersplenism-related pancytopenia may interfere with the management of immunosuppressive therapy[5]. Splenomegaly may further result in excessive portal pressure or splenic artery steal syndrome. The resulting decrease in hepatic arterial inflow can then affect liver graft function[6]. The most common therapies for splenomegaly and hypersplenism are total splenectomy during LT (TSLT) and selective splenic artery embolization (SAE) after LT[7], but they have considerable limitations.

TSLT is associated with increased operative time and additional blood loss[6]. Furthermore, TSLT increases the risk of postoperative complications, such as overwhelming post-splenectomy infection syndrome (OPIS), reactive thrombocytosis, and portal venous system thrombosis[8,9]. It remains controversial whether simultaneous splenectomy during LT is beneficial in these patients.

SAE after LT is a secondary treatment used in addition to surgery to manage hypersplenism in patients with cirrhosis and portal hypertension[7]. However, SAE after LT results in a high risk of infection[10]. Patients with cirrhosis are often debilitated and may have compromised immunity. The immune-compromised nature of a transplant recipient magnifies the risk of major infectious complications. Serious

Revised: December 20, 2020
Accepted: January 13, 2021
Article in press: January 13, 2021
Published online: February 21, 2021

P-Reviewer: Gelmini R
S-Editor: Gao CC
L-Editor: Webster JR
P-Editor: Ma YJ

complications may occur after SAE, such as abdominal infection, pancreatitis, splenic abscess, and splenic rupture. Post-embolization syndrome, characterized by fever and/or abdominal pain, occurs in up to 78% of patients following SAE[11]. Other disadvantages of SAE include high recurrence rates, and difficulty accessing the embolic area[12].

Cirrhosis with severe splenomegaly and hypersplenism is common, yet satisfactory treatment is lacking[13]. In our center, splenectomy during LT has been used for more than ten years, but was abandoned due to uncontrollable postoperative complications, such as portal vein thrombosis, insufficient portal vein flow, and OPIS[6,8,9]. Later, we performed LT without intraoperative intervention[8]. If hypersplenism or portal hypertension persisted after surgery, then we performed SAE[7]. However, we found that this process increased the risk of infection due to extensive splenic infarction and prolonged the patient's discharge time. A method that limits the extent of splenectomy and spares splenic function is necessary.

To realize this need, we first proposed and designed the procedure of partial splenectomy during LT (PSLT), which is an all-in-one treatment for post-LT complications. In this article, we demonstrate the role of PSLT in the treatment of advanced cirrhosis with severe splenomegaly and hypersplenism.

MATERIALS AND METHODS

Patient selection

Between October 2015 and February 2019, 762 cases of classic orthotopic LT were performed at our institution. Among these, there were 84 cases of advanced cirrhosis combined with severe splenomegaly (Figure 1) and hypersplenism. Forty-one cases received PSLT (PSLT group), and 43 cases received only LT with no intervention (LT group). Patient characteristics, intraoperative parameters, and postoperative outcomes were compared between the LT and PSLT groups and retrospectively analyzed. All patients were followed-up regularly by the same surgical team. No patients were lost during follow-up. The last census date for the study was October 31, 2020. All grafts used for LT were obtained from deceased donors, and no organs from executed prisoners were used. All deceased donations complied with the China Organ Donation Program. This study was approved by the ethics committee of Tianjin First Central Hospital.

The inclusion criteria for the 2 groups were the same and are as follows: (1) Indication for LT; (2) The primary disease was benign liver disease or liver cancer meeting the Milan criteria; (3) Model for End-Stage Liver Disease (MELD) score < 25 and the patient was in a stable condition; and (4) Severe splenomegaly (spleen volume > 1000 mL) and hypersplenism (platelet count < 50×10^9/L). In our previous studies, hypersplenism persisted after LT in most patients with a spleen volume >1000 mL and platelet count < 50×10^9/L[14]. The exclusion criteria included: (1) MELD score > 25; (2) Severe perisplenic adhesions; (3) Accompanying splenic tumor; and (4) Spleen volume < 1000 mL or platelet count > 50×10^9/L.

Surgical procedure of PSLT

Partial splenectomy was performed after classic orthotopic LT (caval replacement) as follows: The primary splenic artery was isolated, exposed, and prepared for clamping to prevent uncontrolled bleeding (Figure 2A and B). According to the anatomic classification of the spleen vessels evaluated by preoperative spiral computed tomography (CT) three-dimensional reconstruction, hilar vessels from the lower pole of the spleen were selectively closed with a vascular clamp (usually, half or one third of the spleen was removed as shown in Figure 3; and the cutting planes defined for spleen resection should be maintained above the costal margin; meanwhile, adjusted as per the intraoperative flow by Doppler ultrasound: portal vein flow should be more than 100 mL/100 g/min and hepatic artery blood flow should be more than 35 mL/100 g/min). The relevant ischemic demarcation line was then observable (Figure 2E), and the resection was performed along the demarcation line (Figure 2F). A Cavitron ultrasonic surgical aspirator and bipolar coagulation forceps were used to split the spleen. Hemostasis was performed along the resection line using surgical, bipolar coagulation, and argon beam (Figure 2G). Segmental hilar vessels were allowed to remain with the splenic remnant. Bleeding should be carefully avoided ensuring safety. The splenic artery was clamped with conventional forceps during the splenic incision, and the tube structure was clipped with titanium clamps. After repeated hemostasis, the splenic artery was opened again to assess the presence of

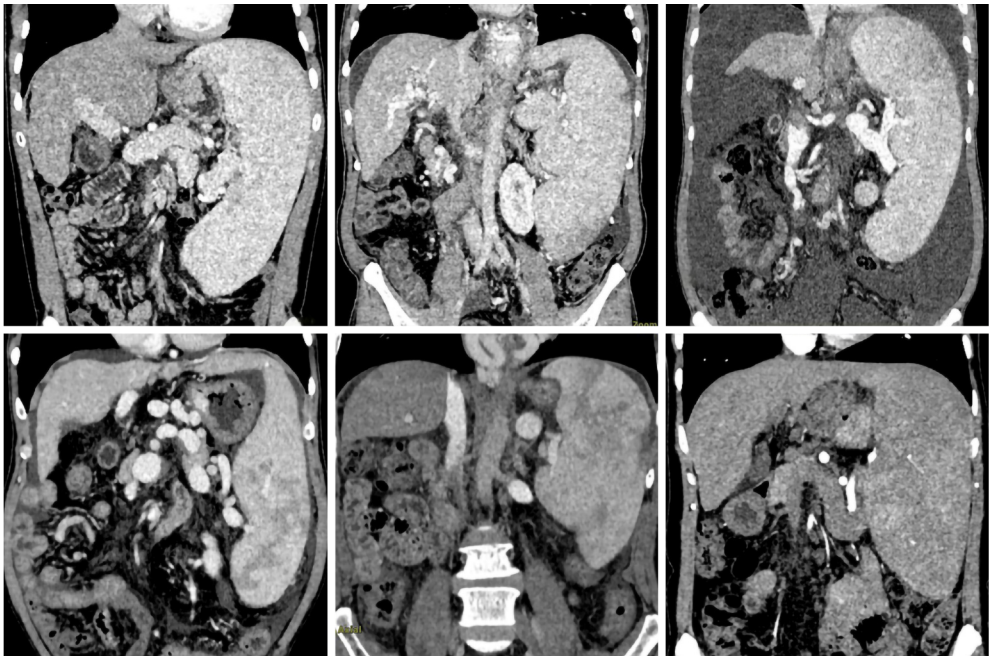


Figure 1 Preoperative computed tomography scan of patients with advanced cirrhosis combined with severe splenomegaly.

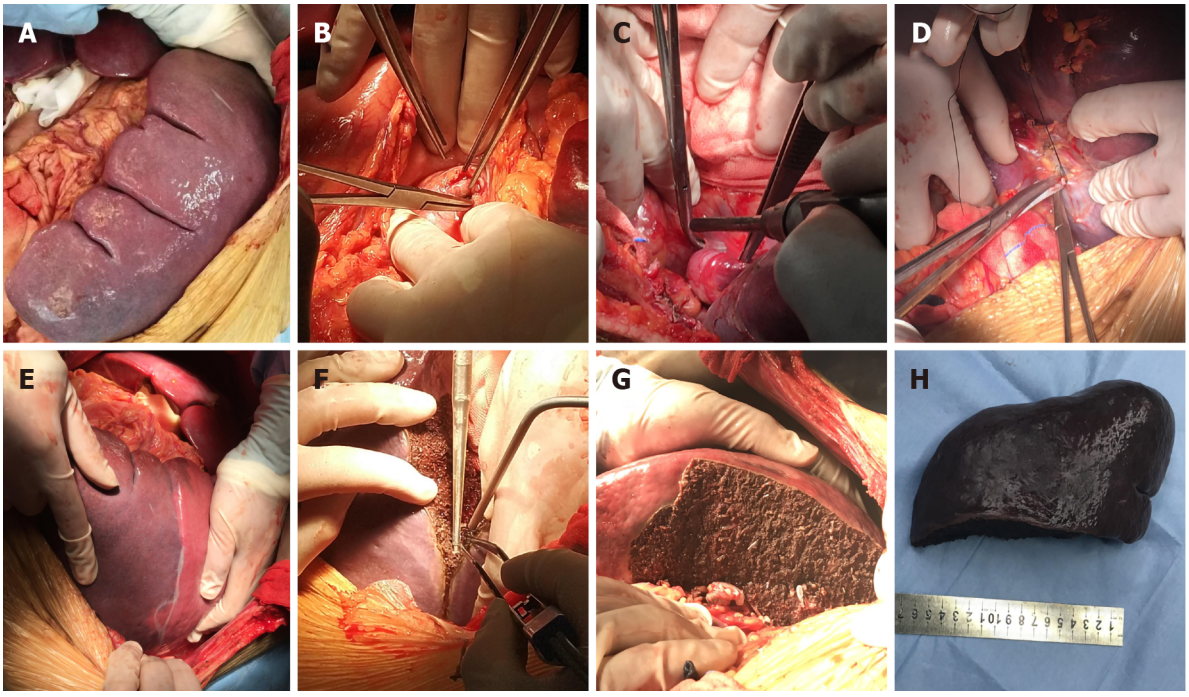


Figure 2 Surgical procedure of partial splenectomy during liver transplantation. A: Partial splenectomy for severe hypersplenism was performed after classic orthotopic liver transplantation; B: The main splenic artery was isolated and exposed; C: The hilar vessels from the lower pole of the spleen were selectively ligated; D: The main collateral circulation of the spleen was isolated and ligated; E: Ischemic demarcation line became observable; F: The spleen was resected along the ischemic line using a Cavitron ultrasonic surgical aspirator and bipolar coagulation forceps; G: The segmental hilar vessels were allowed to remain with the splenic remnant; H: The spleen specimen.

hemostasis, and the drainage tube and hemostatic gauze were placed last.

Perioperative management and assessment

After LT, blood biochemistry was performed regularly to monitor liver function. Color Doppler ultrasound was reviewed every day for one week and every three days for one month to monitor the dynamic flow of the hepatic artery, portal vein, and vena cava. All patients were analyzed by the same senior color Doppler ultrasound operator. Enhanced CT was reexamined preoperatively and postoperatively at 1, 6,

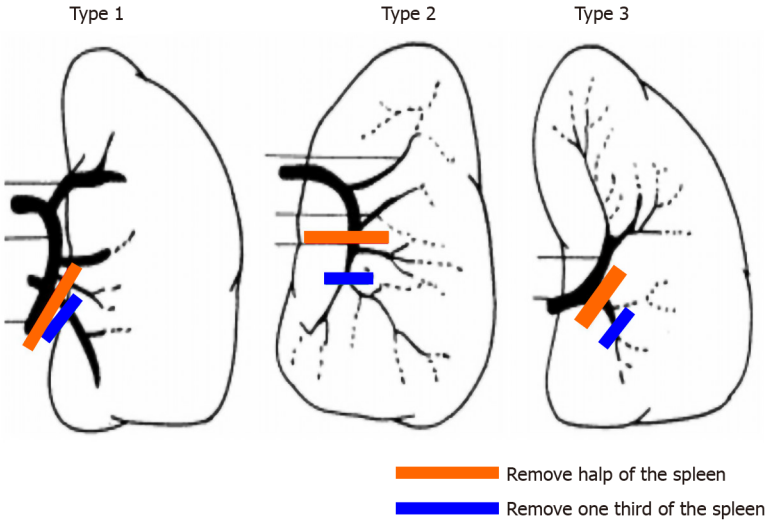


Figure 3 Removal of half or one third of the spleen according to the splenic hilum vessel anatomy. The red line represents half splenectomy, and the green line represents one-third splenectomy.

and 12 mo to measure spleen volume.

The Chi-square test, Fisher exact test, and paired t-test were used to compare patient characteristics, intraoperative parameters, and postoperative results in the LT group and PSLT group. All quantitative data were expressed as mean ± SD. SPSS 21.0 was used for statistical analysis, and $P < 0.05$ was considered statistically significant.

RESULTS

Preoperative characteristics

As shown in Tables 1 and 2, there was no difference in preoperative characteristics between the two groups. The MELD scores in the LT group and PSLT group were 19.4 ± 4.9 and 20.7 ± 4.6 points, respectively, and the Graft /Recipient Weight Ratios (%) were 1.4 ± 0.5 and 1.4 ± 0.6, respectively. Preoperative spleen volumes in the LT group and PSLT group were 1665 ± 611 cm^3 and 1711 ± 682 cm^3, respectively, and platelet counts were 38.6 ± 14.7 × $10^3/mm^3$ and 36.9 ± 14.1 × $10^3/mm^3$, respectively. Preoperative portal vein blood flow in the LT and PSLT groups was 12.4 ± 3.9 and 11.8 ± 3.7 cm/s, respectively, and preoperative hepatic arterial blood flow in the two groups was 40.3 ± 22.1 and 40.9 ± 21.7 cm/s, respectively.

Operative characteristics

As summarized in Table 3, the total operation time in the PSLT group (8.6 ± 1.3 h) was longer than that in the LT group (6.8 ± 0.9 h), and the time required for partial splenectomy was 1.8 ± 0.3 h (range 1.6 to 2.1 h). Intraoperative blood loss in the PSLT group (640.8 ± 347.3 mL) was more than that in the LT group (349.4 ± 116.1 mL), and blood loss during partial splenectomy was 85.6 ± 79.2 mL (range 50 to 350 mL). The weight of excised spleen in the PSLT group was 787 ± 371.4 g (range 342 to 1806 g). The mean portal flow in the LT group and PSLT group increased from 12.4 ± 3.9 cm/s and 11.8 ± 3.7 cm/s preoperative to 47.6 ± 14.1 cm/s and 42.7 ± 13.8 cm/s postoperative, respectively. The mean hepatic artery blood flow in the PSLT group (49.3 ± 13.6 cm/s) was higher than that in the LT group (42.6 ± 11.4 cm/s).

Postoperative outcome

As shown in Figure 4A, spleen volume in the LT group and PSLT group decreased from 1665 ± 611 cm^3 and 1711 ± 682 cm^3 preoperative to 1316 ± 397 cm^3 and 745 ± 189 cm^3 at postoperative 1 mo, 1157 ± 361 cm^3 and 668 ± 174 cm^3 at postoperative 6 mo, and 1041 ± 364 cm^3 and 581 ± 179 cm^3 at postoperative 12 mo, respectively. Postoperative blood flow in the hepatic artery and portal vein were monitored by color Doppler ultrasound. Compared with the LT group, hepatic artery flow increased in the PSLT group and portal vein flow decreased (Figure 4B and C).

In the PSLT group, platelet counts increased to the peak level at postoperative day 14, and leukocyte counts increased to the peak value at postoperative day 7. Both

Table 1 Preoperative characteristics

	LT group (*n* = 43)	PSLT group (*n* = 41)	*P* value
Gender (male/female)	27/16	28/13	0.651
Age, yr	49.2 ± 12.8	52.7 ± 13.1	0.219
Indication for transplantation			
Hepatitis B cirrhosis	19	21	0.662
Hepatic malignancy	10	8	0.792
Alcoholic cirrhosis	8	6	0.772
Autoimmune liver disease	2	3	0.672
etc.	4	3	> 0.99
MELD score at transplantation	19.4 ± 4.9	20.7 ± 4.6	0.214
PreOP biology			
Total bilirubin (μmol/L)	133.0 ± 106.9	128.5 ± 97.2	0.841
Serum creatinine (μmol/L)	96.1 ± 72.6	82.6 ± 66.3	0.377
INR	1.6 ± 0.6	1.7 ± 0.6	0.447
Plasma ammonia (μmol/L)	59.7 ± 21.5	57.6 ± 23.4	0.669
PreOP platelet count, $10^3/mm^3$	38.6 ± 14.7	36.9 ± 14.1	0.590
PreOP spleen volume, cm^3	1665 ± 611	1711 ± 682	0.745
PreOP PV flow, cm/s	12.4 ± 3.9	11.8 ± 3.7	0.472
PreOP HA flow, cm/s	40.3 ± 22.1	40.9 ± 21.7	0.453

LT: Liver transplantation; PSLT: Partial splenectomy during liver transplantation; HA: Hepatic artery; PV: Portal vein; MELD: Model for End-Stage Liver Disease; INR: International normalized ratio; PreOP: Preoperative.

Table 2 Donors' characteristics

	LT group (*n* = 43)	PSLT group (*n* = 41)	*P* value
Gender (male/female)	31/12	28/13	> 0.99
Age, yr	42.6 ± 16.3	44.5 ± 15.9	0.665
Cause of death			
Cerebral trauma	24	22	> 0.99
Cerebrovascular accident	10	8	0.792
Brain tumor (glioma)	4	5	0.735
Hypoxic brain injury	2	3	0.672
etc.	3	3	> 0.99
ICU stay, d	2.71 ± 2.05	2.83 ± 2.24	0.798

LT: Liver transplantation; PSLT: Partial splenectomy during liver transplantation; ICU: Intensive care unit.

platelet counts and leukocyte counts in the PSLT group increased faster than those in the LT group, resulting in a significant difference between the groups. Platelet count was 139.4 ± 72.4 × $10^3/mm^3$ in the PSLT group and 84.1 ± 51.5 × $10^3/mm^3$ in the LT group at postoperative 12 mo ($P < 0.001$). Leukocyte count was 3.6 ± 1.4 × $10^3/mm^3$ in the PSLT group and 1.9 ± 0.8 × $10^3/mm^3$ in the LT group at postoperative 12 mo ($P < 0.001$).

Postoperative complications in the two groups are summarized in Table 4. The incidence of postoperative hypersplenism (2/41, 4.8%) and recurrent ascites (1/41,2.4%) in the PSLT group were significantly lower than that in the LT group

Table 3 Operative characteristics

	LT group (*n* = 43)	PSLT group (*n* = 41)	*P* value
Operating time, h	6.8 ± 0.9	8.6 ± 1.3	< 0.001
Time for PS		1.8 ± 0.3	
Blood loss, mL	349.4 ± 116.9	440.8 ± 141.3	0.002
During PS		85.6 ± 79.2	
PostOP HA flow, cm/s	42.6 ± 11.4	49.3 ± 13.6	0.016
PostOP PV flow, cm/s	47.6 ± 14.1	42.7 ± 13.8	0.022
Weight of PS, g		787 ± 371.4	
Percentage of PS, (*n*)			
Half of spleen		23	
Third of spleen		18	

LT: Liver transplantation; PSLT: Partial splenectomy during liver transplantation; HA: Hepatic artery; PV: Portal vein; PreOP: Preoperative.

Table 4 Postoperative complications, *n* (%)

	LT group (*n* = 43)	PSLT group (*n* = 41)	*P* value
Postoperative hypersplenism	22 (51.1)	2 (4.8)	< 0.001
Recurrent ascites	8 (18.6)	1 (2.4)	0.029
Reoperation due to post-op bleeding	2 (4.6)	3 (7.3)	0.672
Postoperative pulmonary infection	5 (11.6)	4 (9.7)	> 0.99
Post-op thrombosis	1 (2.3)	1 (2.4)	> 0.99
Splenic arterial steal syndrome	4 (9.3)	0	0.116
Two-stage splenic embolization	17 (39.5)	0	< 0.001
Further splenectomy	6 (13.9)	0	0.026

LT: Liver transplantation; PSLT: Partial splenectomy during liver transplantation.

(22/43,51.2%; 8/43, 18.6%, respectively). Seventeen patients (17/43, 39.5%) in the LT group required multiple partial splenic embolization (PSE) to relieve postoperative persistent hypersplenism in 15 and refractory ascites in 2. Six of them required further splenectomy after PSE, 2 patients due to persistent severe splenic infarction syndrome, 2 patients due to persistent hypersplenism despite embolization, 1 patient due to splenic abscess with repeated infection after PSE, and 1 patient due to hypersplenism and persistent abdominal pain after PSE. In the PSLT group, no patient underwent two-stage splenic embolization or surgery for postoperative persistent hypersplenism.

Other postoperative complications requiring reoperation were postoperative bleeding (n = 3), pulmonary infection (n = 4), thrombosis (n = 1) and splenic arterial steal syndrome (n = 0) in the PSLT group, which were similar to those (n = 2, n = 5, n = 1, n = 4, respectively) in the LT group. In-hospital mortality did not occur in either group.

DISCUSSION

Partial splenectomy can be used to treat severe splenomegaly and hypersplenism, and its safety and efficacy have been confirmed[15,16]. Partial splenectomy reduces spleen volume and alleviates the symptoms of hypersplenism while maintaining the immunological functions of the spleen. These beneficial effects have also been confirmed in animal models. However, so far there are no reports on the application of partial splenectomy in LT.

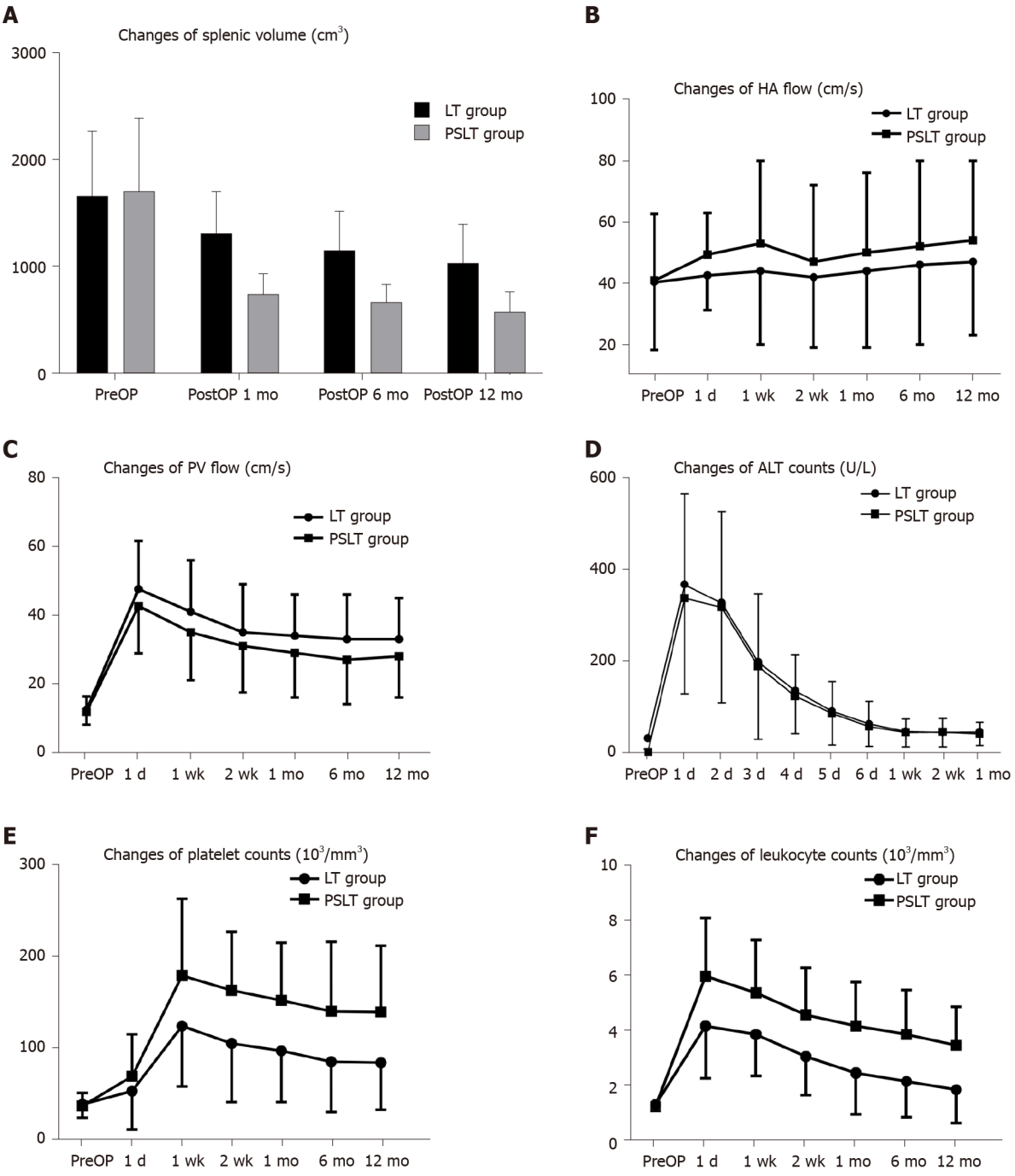


Figure 4 Postoperative changes in the two groups. A: Spleen volume; B: Hepatic artery flow; C: Portal vein flow; D: Alanine transaminase; E: Platelet count; F: Leukocyte count. HA: Hepatic artery; PV: Portal vein; ALT: Alanine transaminase; PreOP: Preoperative.

In this article, we described the PSLT procedure for advanced cirrhosis with severe splenomegaly and hypersplenism. Hypersplenism/splenomegaly can lead to post-LT complications and PSLT could offer an all-in-one intervention to mitigate these clinically-relevant issues. As our data showed, although partial splenectomy took 1.5-2 h and resulted in blood loss of 50-350 mL, the PSLT group showed significant improvement in ascites and hypersplenism after transplantation, and no recurrence of splenomegaly or hypersplenism was observed during follow-up. In the LT group, the average spleen volume after 12 mo is still greater than 1000 cm^3, and 51% of the patients will continue to have hypersplenism. Most of them must undergo the second stage of splenic embolization or splenectomy to improve hematological parameters to allow the use of other myelosuppressive drugs.

Most previous studies on partial splenectomy in patients with cirrhosis advocated subtotal splenectomy and reported that approximately 90% of the spleen can be removed to ensure a curative effect[16,17]. However, the magnitude of PSLT was far less,

and the therapeutic effect was also significant. In our study, we usually remove half or one third of the spleen according to the splenic hilum vessel anatomy, as shown in Figure 3. We also try to maintain the cutting planes of spleen resection above the costal margin to protect the spleen section. In addition, we found that intraoperative resection ratio and splenic volume reduction ratio reassessed by CT scan after surgery were significantly different (Figure 5). The reduction degree of spleen volume varies by patient, and may be related to the history of liver disease and the severity of splenic hyperplasia. Patients with a long history of cirrhosis and severe splenic hyperplasia are more likely to have poor relief of hypersplenism after LT.

However, the present study is retrospective and only included relatively few patients from a single center. Large multicenter studies with long-term follow-up are necessary. In addition, we have not applied this procedure in living donor LT patients. Further studies are needed to investigate whether partial splenectomy during living donor LT can reduce portal vein perfusion and prevent small spleen syndrome, as well as treat hypersplenism.

CONCLUSION

In conclusion, PSLT solves a series of problems such as end-stage liver disease, hypersplenism, splenomegaly and hemodynamic disorder all at once, so patients do not need to receive two-stage splenic embolization or splenectomy. However, PSLT requires up to 25% longer operation time and the need for blood products, which would raise concerns in transplant surgeons. Appropriate patient selection is necessary to ensure that the benefits outweigh the risks. According to our experience, patients with preoperative severe splenomegaly (spleen volume > 1000 mL) and hypersplenism (platelet count < 50 × 10^9/L) are more likely to have intractable hypersplenism after LT, and PSLT is recommended. PSLT is not recommended when the patient has a MELD score > 25, severe perisplenic adhesions, accompanied by splenic tumor, splenic volume < 1000 mL or platelet count > 50 × 10^9/L.

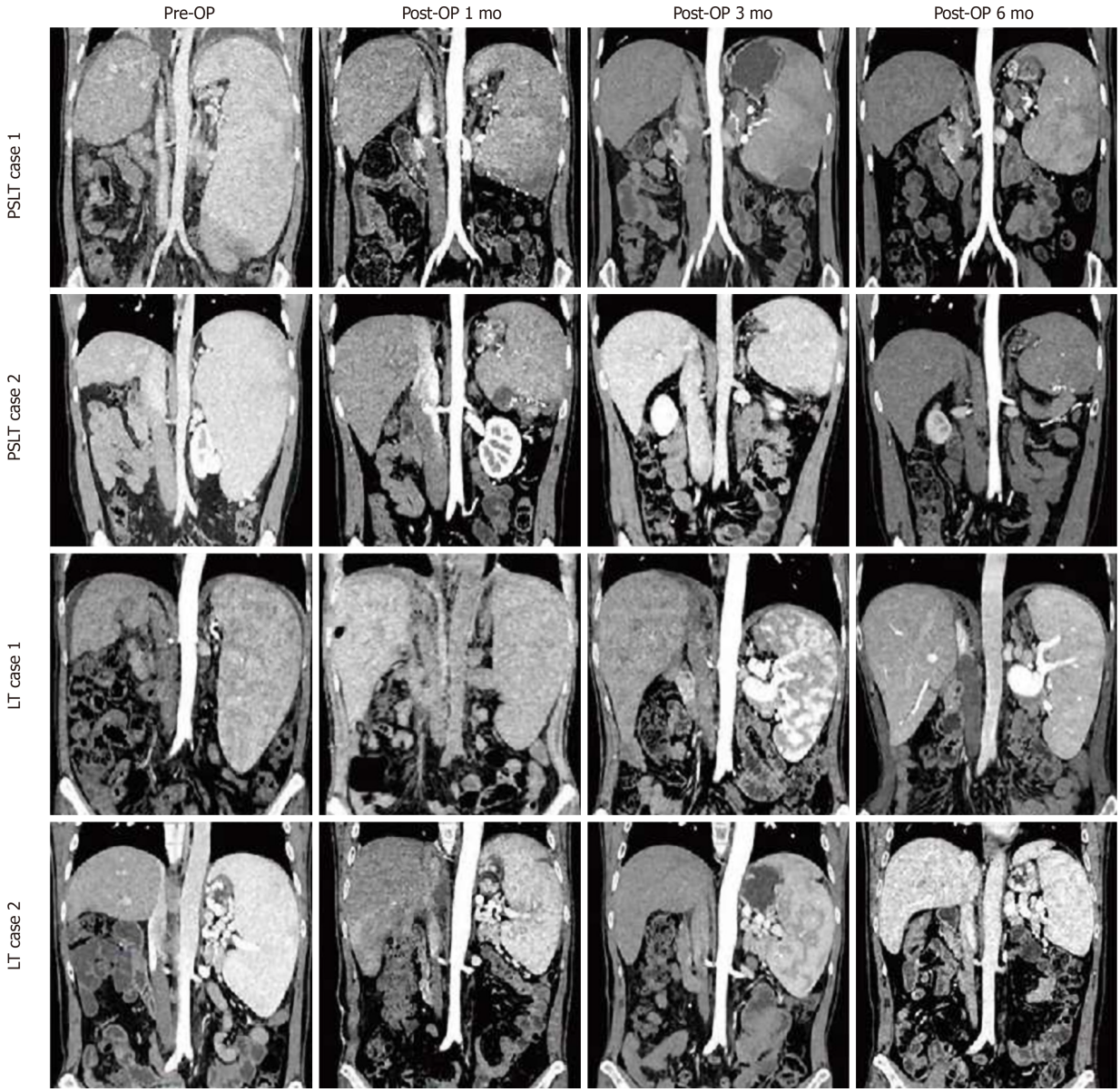


Figure 5 Chronologic changes in the splenic volume after liver transplantation or partial splenectomy during liver transplantation. PreOP: Preoperative; LT: Liver transplantation; PSLT: Partial splenectomy during liver transplantation.

ARTICLE HIGHLIGHTS

Research background

The most effective treatment for advanced cirrhosis and portal hypertension is liver transplantation (LT). However, splenomegaly and hypersplenism can persist even after LT in patients with massive splenomegaly. Persistent hypersplenism-related pancytopenia may interfere with the management of immunosuppressive therapy. Splenomegaly may further result in excessive portal pressure or splenic artery steal syndrome. The resulting decrease in hepatic arterial inflow can then affect liver graft function.

Research motivation

The most common therapies for splenomegaly and hypersplenism are total splenectomy during LT and selective splenic artery embolization after LT, but they have considerable limitations. Cirrhosis with severe splenomegaly and hypersplenism is common, yet satisfactory treatment is lacking. To realize this need, we first proposed and designed the procedure of partial splenectomy during LT (PSLT), which is an all-in-one treatment for post-LT complications.

Research objectives

To examine the feasibility of performing partial splenectomy during LT in patients with advanced cirrhosis combined with severe splenomegaly and hypersplenism.

Research methods

Between October 2015 and February 2019, 762 cases of classic orthotopic LT were performed at our institution. Among these, there were 84 cases of advanced cirrhosis combined with severe splenomegaly and hypersplenism. Forty-one cases received PSLT (PSLT group), and 43 cases received only LT with no intervention (LT group). Patient characteristics, intraoperative parameters, and postoperative outcomes were compared between the LT and PSLT groups and retrospectively analyzed.

Research results

The incidence of postoperative hypersplenism and recurrent ascites in the PSLT group was significantly lower than that in the LT group. Seventeen patients in the LT group required two-stage splenic embolization, and further splenectomy was required in 6 of them. The operation time and intraoperative blood loss in the PSLT group were relatively increased compared with the LT group. The incidence of postoperative bleeding, pulmonary infection, thrombosis and splenic arterial steal syndrome in the PSLT group was similar to that in the LT group, respectively.

Research conclusions

PSLT can reduce the incidence of postoperative hypersplenism and recurrent ascites, and reduce the risk of secondary splenic embolization and splenectomy, but the operation time and intraoperative blood loss were increased.

Research perspectives

According to our experience, patients with preoperative severe splenomegaly and hypersplenism are more likely to have intractable hypersplenism after LT, and PSLT is recommended.

REFERENCES

1 **Khanna R**, Sarin SK. Noncirrhotic Portal Hypertension: Current and Emerging Perspectives. *Clin Liver Dis* 2019; **23**: 781-807 [PMID: 31563222 DOI: 10.1016/j.cld.2019.07.006]

2 **Kockerling D**, Nathwani R, Forlano R, Manousou P, Mullish BH, Dhar A. Current and future pharmacological therapies for managing cirrhosis and its complications. *World J Gastroenterol* 2019; **25**: 888-908 [PMID: 30833797 DOI: 10.3748/wjg.v25.i8.888]

3 **Mukhtar A**, Dabbous H. Modulation of splanchnic circulation: Role in perioperative management of liver transplant patients. *World J Gastroenterol* 2016; **22**: 1582-1592 [PMID: 26819524 DOI: 10.3748/wjg.v22.i4.1582]

4 **Kawano F**, Ishizaki Y, Yoshimoto J, Fujiwara N, Kawasaki S. Factors Affecting Persistent Splenomegaly After Adult-to-Adult Living Donor Liver Transplantation Using a Left Lobe. *Transplant Proc* 2019; **51**: 1946-1949 [PMID: 31279408 DOI: 10.1016/j.transproceed.2019.02.033]

5 **Molina Perez E**, Fernández Castroagudín J, Seijo Ríos S, Mera Calviño J, Tomé Martínez de Rituerto S, Otero Antón E, Bustamante Montalvo M, Varo Perez E. Valganciclovir-induced leukopenia in liver transplant recipients: influence of concomitant use of mycophenolate mofetil. *Transplant Proc* 2009; **41**: 1047-1049 [PMID: 19376423 DOI: 10.1016/j.transproceed.2009.02.033]

6 **Chezmar JL**, Redvanly RD, Nelson RC, Henderson JM. Persistence of portosystemic collaterals and splenomegaly on CT after orthotopic liver transplantation. *AJR Am J Roentgenol* 1992; **159**: 317-320 [PMID: 1632346 DOI: 10.2214/ajr.159.2.1632346]

7 **DuBois B**, Mobley D, Chick JFB, Srinivasa RN, Wilcox C, Weintraub J. Efficacy and safety of partial splenic embolization for hypersplenism in pre- and post-liver transplant patients: A 16-year comparative analysis. *Clin Imaging* 2019; **54**: 71-77 [PMID: 30553121 DOI: 10.1016/j.clinimag.2018.11.012]

8 **Golse N**, Mohkam K, Rode A, Pradat P, Ducerf C, Mabrut JY. Splenectomy during whole liver transplantation: a morbid procedure which does not adversely impact long-term survival. *HPB (Oxford)* 2017; **19**: 498-507 [PMID: 28233673 DOI: 10.1016/j.hpb.2017.01.020]

9 **Badawy A**, Hamaguchi Y, Satoru S, Kaido T, Okajima H, Uemoto S. Evaluation of safety of concomitant splenectomy in living donor liver transplantation: a retrospective study. *Transpl Int* 2017; **30**: 914-923 [PMID: 28512755 DOI: 10.1111/tri.12985]

10 **Ricci K**, Asharf EH. The use of splenic artery embolization to maintain adequate hepatic arterial inflow after hepatic artery thrombosis in a split liver transplant recipient. *Int J Surg Case Rep* 2018; **51**: 241-243 [PMID: 30218820 DOI: 10.1016/j.ijscr.2018.09.003]

11 report on dracunculiasis cases, January–October 2014. *Wkly Epidemiol Rec* 2014; **89**: 587-588

[PMID: 25538996]

12 **Koconis KG**, Singh H, Soares G. Partial splenic embolization in the treatment of patients with portal hypertension: a review of the english language literature. *J Vasc Interv Radiol* 2007; **18**: 463-481 [PMID: 17446537 DOI: 10.1016/j.jvir.2006.12.734]

13 **Gangireddy VG**, Kanneganti PC, Sridhar S, Talla S, Coleman T. Management of thrombocytopenia in advanced liver disease. *Can J Gastroenterol Hepatol* 2014; **28**: 558-564 [PMID: 25222481 DOI: 10.1155/2014/532191]

14 **He J**, Guo QJ, Xie Y, Zhang L, Tian DZ, Wang HH, Chen CY, Jiang WT. Application of image post -processing technique to measure spleen volume and evaluate the effect of orthotopic liver transplantation on relieving hypersplenism. *Zhonghua Qiguan Yizhi Zazhi* 2019; **40**: 107-11 [DOI: 10.3760/cma.j.issn.0254-1785.2019.02.010]

15 **Guan YS**, Hu Y. Clinical application of partial splenic embolization. *ScientificWorldJournal* 2014; **2014**: 961345 [PMID: 25538966 DOI: 10.1155/2014/961345]

16 **Chu H**, Han W, Wang L, Xu Y, Jian F, Zhang W, Wang T, Zhao J. Long-term efficacy of subtotal splenectomy due to portal hypertension in cirrhotic patients. *BMC Surg* 2015; **15**: 89 [PMID: 26205377 DOI: 10.1186/s12893-015-0077-2]

17 **Radević B**, Jesić R, Sagić D, Perisić V, Nenezić D, Popov P, Ilijevski N, Dugalić V, Gajin P, Vucurević G, Radak Dj, Trebjesanin Z, Babić D, Kastratović D, Matić P. [Partial resection of the spleen and spleno-renal shunt in the treatment of portal hypertension with splenomegaly and hypersplenism]. *Acta Chir Iugosl* 2002; **49**: 93-98 [PMID: 12587456 DOI: 10.2298/aci0203093r]

Published by **Baishideng Publishing Group Inc**
7041 Koll Center Parkway, Suite 160, Pleasanton, CA 94566, USA
Telephone: +1-925-3991568
E-mail: bpgoffice@wjgnet.com
Help Desk: https://www.f6publishing.com/helpdesk
https://www.wjgnet.com

© 2021 Baishideng Publishing Group Inc. All rights reserved.

ISSN 1007-9327 (print)
ISSN 2219-2840 (online)

World Journal of *Gastroenterology*

World J Gastroenterol 2021 February 28; 27(8): 666-759



Published by Baishideng Publishing Group Inc

World Journal of Gastroenterology

Contents

Weekly Volume 27 Number 8 February 28, 2021

OPINION REVIEW

666 New therapeutic options for persistent low-level viremia in patients with chronic hepatitis B virus infection: Increase of entecavir dosage

Yin GQ, Li J, Zhong B, Yang YF, Wang MR

REVIEW

677 G protein-coupled receptors as potential targets for nonalcoholic fatty liver disease treatment

Yang M, Zhang CY

ORIGINAL ARTICLE

Basic Study

692 Fork head box M1 regulates vascular endothelial growth factor-A expression to promote the angiogenesis and tumor cell growth of gallbladder cancer

Wang RT, Miao RC, Zhang X, Yang GH, Mu YP, Zhang ZY, Qu K, Liu C

708 Effect of berberine on hyperglycaemia and gut microbiota composition in type 2 diabetic Goto-Kakizaki rats

Zhao JD, Li Y, Sun M, Yu CJ, Li JY, Wang SH, Yang D, Guo CL, Du X, Zhang WJ, Cheng RD, Diao XC, Fang ZH

Prospective Study

725 Endoscopic full-thickness resection using an over-the-scope device: A prospective study

Guo JT, Zhang JJ, Wu YF, Liao Y, Wang YD, Zhang BZ, Wang S, Sun SY

META-ANALYSIS

737 Risk factors for lymph node metastasis in T1 esophageal squamous cell carcinoma: A systematic review and meta-analysis

Jiang KY, Huang H, Chen WY, Yan HJ, Wei ZT, Wang XW, Li HX, Zheng XY, Tian D

CASE REPORT

751 Septic shock due to *Granulicatella adiacens* after endoscopic ultrasound-guided biopsy of a splenic mass: A case report

Cho SY, Cho E, Park CH, Kim HJ, Koo JY

World Journal of Gastroenterology

Weekly Volume 27 Number 8 February 28, 2021

Contents

ABOUT COVER

Marco Milone, MD, PhD, FACS, Professor, Surgeon, Department of Clinical Medicine and Surgery, University of Naples "Federico II", Via Pansini 5, Naples 80131, Italy. milone.marco.md@gmail.com

AIMS AND SCOPE

The primary aim of *World Journal of Gastroenterology* (*WJG*, *World J Gastroenterol*) is to provide scholars and readers from various fields of gastroenterology and hepatology with a platform to publish high-quality basic and clinical research articles and communicate their research findings online. *WJG* mainly publishes articles reporting research results and findings obtained in the field of gastroenterology and hepatology and covering a wide range of topics including gastroenterology, hepatology, gastrointestinal endoscopy, gastrointestinal surgery, gastrointestinal oncology, and pediatric gastroenterology.

INDEXING/ABSTRACTING

The *WJG* is now indexed in Current Contents®/Clinical Medicine, Science Citation Index Expanded (also known as SciSearch®), Journal Citation Reports®, Index Medicus, MEDLINE, PubMed, PubMed Central, and Scopus. The 2020 edition of Journal Citation Report® cites the 2019 impact factor (IF) for *WJG* as 3.665; IF without journal self cites: 3.534; 5-year IF: 4.048; Ranking: 35 among 88 journals in gastroenterology and hepatology; and Quartile category: Q2. The *WJG*'s CiteScore for 2019 is 7.1 and Scopus CiteScore rank 2019: Gastroenterology is 17/137.

RESPONSIBLE EDITORS FOR THIS ISSUE

Production Editor: *Ji-Hong Liu*; **Production Department Director:** *Yun-Xiaojian Wu*; **Editorial Office Director:** *Ze-Mao Gong*.

NAME OF JOURNAL
World Journal of Gastroenterology

ISSN
ISSN 1007-9327 (print) ISSN 2219-2840 (online)

LAUNCH DATE
October 1, 1995

FREQUENCY
Weekly

EDITORS-IN-CHIEF
Andrzej S Tarnawski, Subrata Ghosh

EDITORIAL BOARD MEMBERS
http://www.wjgnet.com/1007-9327/editorialboard.htm

PUBLICATION DATE
February 28, 2021

COPYRIGHT
© 2021 Baishideng Publishing Group Inc

INSTRUCTIONS TO AUTHORS
https://www.wjgnet.com/bpg/gerinfo/204

GUIDELINES FOR ETHICS DOCUMENTS
https://www.wjgnet.com/bpg/GerInfo/287

GUIDELINES FOR NON-NATIVE SPEAKERS OF ENGLISH
https://www.wjgnet.com/bpg/gerinfo/240

PUBLICATION ETHICS
https://www.wjgnet.com/bpg/GerInfo/288

PUBLICATION MISCONDUCT
https://www.wjgnet.com/bpg/gerinfo/208

ARTICLE PROCESSING CHARGE
https://www.wjgnet.com/bpg/gerinfo/242

STEPS FOR SUBMITTING MANUSCRIPTS
https://www.wjgnet.com/bpg/GerInfo/239

ONLINE SUBMISSION
https://www.f6publishing.com

© 2021 Baishideng Publishing Group Inc. All rights reserved. 7041 Koll Center Parkway, Suite 160, Pleasanton, CA 94566, USA
E-mail: bpgoffice@wjgnet.com https://www.wjgnet.com

World Journal of Gastroenterology

Submit a Manuscript: https://www.f6publishing.com

World J Gastroenterol 2021 February 28; 27(8): 666-676

DOI: 10.3748/wjg.v27.i8.666

ISSN 1007-9327 (print) ISSN 2219-2840 (online)

OPINION REVIEW

New therapeutic options for persistent low-level viremia in patients with chronic hepatitis B virus infection: Increase of entecavir dosage

Guo-Qing Yin, Jun Li, Bei Zhong, Yong-Fong Yang, Mao-Rong Wang

ORCID number: Guo-Qing Yin 0000-0002-8972-3752; Jun Li 0000-0002-1961-7188; Bei Zhong 0000-0002-5460-7428; Yong-Fong Yang 0000-0002-3214-0038; Mao-Rong Wang 0000-0002-5044-1643.

Author contributions: Yin GQ and Zhong B proposed the views to the infectious disease academic community; all the authors participated in the conception, plan, writing, question-and-answer, and modification of the manuscript; all authors contributed equally to this work.

Conflict-of-interest statement: The authors declare no conflict of interests.

Open-Access: This article is an open-access article that was selected by an in-house editor and fully peer-reviewed by external reviewers. It is distributed in accordance with the Creative Commons Attribution NonCommercial (CC BY-NC 4.0) license, which permits others to distribute, remix, adapt, build upon this work non-commercially, and license their derivative works on different terms, provided the original work is properly cited and the use is non-commercial. See: http://creativecommons.org/Licenses/by-nc/4.0/

Manuscript source: Invited

Guo-Qing Yin, Department of Infectious Diseases, Nanjing Zhong-Da Hospital, Southeast University School of Medicine, Nanjing 210009, Jiangsu Province, China

Jun Li, Department of Infectious Diseases, The First Affiliated Hospital with Nanjing Medical University, Nanjing 210029, Jiangsu Province, China

Bei Zhong, The Sixth Affiliated Hospital, Guangzhou Medical University/Qingyuan People's Hospital, Qingyuan 511518, Guangdong Province, China

Yong-Fong Yang, Department of Liver Disease, The Second Hospital of Nanjing, Nanjing University of Chinese Medicine, Nanjing 210003, Jiangsu Province, China

Mao-Rong Wang, Department of Infectious Diseases and Liver Disease Center, The Affiliated Nanjing Jinling Hospital, Nanjing University, Nanjing 210002, Jiangsu Province, China

Corresponding author: Guo-Qing Yin, MD, PhD, Chief Doctor, Chief Physician, Department of Infectious Diseases, Nanjing Zhong-Da Hospital, Southeast University School of Medicine, No. 87 Dingjiaqiao, Nanjing 210009, Jiangsu Province, China. yingq62@sina.com

Abstract

Chronic hepatitis B virus (HBV) infection (CHB) is a public health concern worldwide. Current therapies utilizing nucleos(t)ide analogs (NA) have not resulted in a complete cure for CHB. Furthermore, patients on long-term NA treatment often develop low-level viremia (LLV). Persistent LLV, in addition to causing the progression of liver disease or hepatocellular carcinoma, may shed light on the current plight of NA therapy. Here, we review the literature on LLV, NA treatment, and various doses of entecavir to find a strategy for improving the efficacy of this antiviral agent. For LLV patients, three therapeutic options are available, switching to another antiviral monotherapy, interferon-α switching therapy, and continuing monotherapy. In real-world clinical practice, entecavir overdose has been used in antiviral therapy for CHB patients with NA refractory and persistent LLV, which encouraged us to conduct further in-depth literature survey on dosage and duration related entecavir studies. The studies of pharmacodynamics and pharmacokinetics show that entecavir has the maximal selected index for safety, and has great potential in inhibiting HBV replication, in all of the NAs. In the particular section of the drug approval package published by the United States Food and Drug Administration, entecavir doses 2.5-20 mg/d do not increase adverse events, and entecavir doses higher than 1.0 mg/d might improve the antiviral efficacy. The literature survey led us to two suggestions: (1)

manuscript

Specialty type: Gastroenterology and hepatology

Country/Territory of origin: China

Peer-review report's scientific quality classification

Grade A (Excellent): 0
Grade B (Very good): B, B
Grade C (Good): 0
Grade D (Fair): 0
Grade E (Poor): 0

Received: October 21, 2020
Peer-review started: October 21, 2020
First decision: December 3, 2020
Revised: December 25, 2020
Accepted: January 21, 2021
Article in press: January 21, 2021
Published online: February 28, 2021

P-Reviewer: Farag N, Romano L
S-Editor: Fan JR
L-Editor: Wang TQ
P-Editor: Ma YJ

Increasing entecavir dose to 1.0 mg/d for the treatment of NA naïve patients with HBV DNA >2 × 10^6 IU/mL is feasible and would provide better prognosis; and (2) Further research is needed to assess the long-term toxic effects of higher entecavir doses (2.5 and 5.0 mg/d), which may prove beneficial in treating patients with prior NA treatment, partial virological response, or LLV state.

Key Words: Chronic hepatitis B virus infection; Low-level viremia; Therapeutic options; Entecavir; Dose; Efficacy

©The Author(s) 2021. Published by Baishideng Publishing Group Inc. All rights reserved.

Core Tip: Persistent low-level viremia (LLV), in addition to causing the progression of liver disease or hepatocellular carcinoma, may shed light on the current plight of nucleos(t)ide analog (NA) therapy. Since 2006, the authors focused on NA-refractory and participated in treating LLV patients. We presented the interferon-α switching therapy to treat LLV patient with failure of combined nucleoside plus nucleotide therapy. The current study scoured the literature to shed light on the possibility of improving the antiviral effect of entecavir by increasing the dose. Here, we recommend that clinical trials involving entecavir should trial doses over more 1.0 mg/d for treating NA-refractory patients.

Citation: Yin GQ, Li J, Zhong B, Yang YF, Wang MR. New therapeutic options for persistent low-level viremia in patients with chronic hepatitis B virus infection: Increase of entecavir dosage. *World J Gastroenterol* 2021; 27(8): 666-676
URL: https://www.wjgnet.com/1007-9327/full/v27/i8/666.htm
DOI: https://dx.doi.org/10.3748/wjg.v27.i8.666

INTRODUCTION

Hepatitis B virus (HBV) can lead toa debilitating liver infection; chronic HBV infection (CHB) is a public health concern worldwide, affecting about 240 million people. Current therapies for CHB include nucleos(t)ide analogs (NA) and interferon (INF). However, while these therapies are effective treatments, they cannot cure HBV. Since 2016, four significant articles regarding the treatment of CHB have been published by the following authors, Terrault NA *et al*, Kim JH *et al*, Terrault NA *et al*, and Lok AS *et al*, respectively[1-4]. These articles shed light on the current plight of treating CHB and the efforts of clinicians and researchers.

Recently, it was shown that the incidence of persistent low-level viremia (LLV)(HBV DNA < 2 × 10^3 IU/mL) gradually increased in some patients during NA treatment, contributing to the progression of liver disease. The American Association for the Study of Liver Diseases (AASLD) 2016 guidelines suggest that LLV patients on entecavir or tenofovir monotherapy should continue monotherapy, regardless of alanine aminotransferase status[1]. This suggestion is different from the previous NA therapy strategy and a bit confounding to researchers. Subsequently, Kim *et al*[2] reported that persistent LLV patients on continued entecavir monotherapy were at a higher risk of hepatocellular carcinoma (HCC)[2]. Their results were contrary to the AASLD recommendation. However, the 2018 AASLD recommendation upheld its 2016 recommendation[3].

While the recommendations and reports may differ, these articles do confirm that the current problem for patients is the entecavir refractory HBV. Currently, several researchers are developing novel antiviral therapies for HBV. Unfortunately, these newly developed therapies cannot eradicate the intrahepatic covalently closed circular DNA (cccDNA) or integrated HBV DNA. In a report by Lok AS *et al*, a complete HBV cure was defined as "undetectable hepatitis B surface antigen in the serum and eradication of HBV DNA in the hepatocytes, including intrahepatic cccDNA and integrated HBV DNA". Thus, the current therapies relying on NAs and/or INF cannot achieve a complete HBV cure[3,4].

The molecular mechanisms of LLV or NA refractoriness have been partially discovered. In an important investigation regarding NA mediated development of

resistance, Coffin CS and colleagues analyzed the prevalence of HBV DNA, cccDNA, HBV resistant mutations, and gene diversity in different tissues including plasma, peripheral blood mononuclear cells (PBMCs), and liver explants in patients undergoing NA treatment and liver explants. The results showed 100% and 83% wild type HBV in the plasma and PBMCs. Moreover, 66% of drug-resistant mutations were observed in the liver explants. Notably, the adefovir-treated patients who exhibited adefovir resistant mutation received the combination lamivudine plus tenofovir rescue therapy. While this rescue treatment resulted in undetectable HBV DNA and 100% wild type HBV in the plasma, detectable HBV DNA, cccDNA, and HBV resistant mutations correlating with adefovir and lamivudine were retained in the liver explants. Thus, the rescue lamivudine plus tenofovir therapy could not eradicate the previous adefovir drug-resistant virus and instead induced the new lamivudine-resistant mutation, in the liver of these patients[5]. Hence, the presence of this mutation in the liver suggested that the LLV patients possessed intrahepatic viruses that were resistant or less sensitive to NAs.

Molecular evolutionary analysis can reconstruct phylogenetic trees and infer phylogenetic histories[6,7]. The evolutionary patterns of HBV resistant mutations during NA treatment have been studied by combining molecular phylogenetic analysis with the NA resistant mutation profile[5,8-12]. These studies indicate that prolonged entecavir or tenofovir treatment leads to development of LLV status, NA resistance, virology breakthrough, and biochemical breakthrough resulting in progression of liver disease or HCC in the majority of patients. Thus, LLV should be considered as the early stage of NA resistance.

Currently, the primary goals of NA therapy are to suppress HBV replication for as long as possible and to avoid the progression of liver disease; and the ultimate goal of antiviral treatment is to prolong survival of CHB patients and to provide them with better quality of life[1,3,4]. Therefore, prolonged treatment with NAs could result in life-extending goals in most patients. Moreover, carefully balancing between the risks and benefits required for prolonging life and reducing the HCC risk, support the AASLD statement.

Here, we investigate the literature on persistent LLV patients receiving NA combination therapy (nucleoside plus nucleotide analogs). The regimens of IFN-α therapy, namely, switching from NAs to INF-α and subsequent re-treatment with IFN -α, were applied to treat these patients. IFN -α switching therapy resulted in safe NA cessation, and IFN-α re-treatment caused sustained immune controls[13]. However, IFN-α therapy caused stronger adverse effects and was not suitable for cirrhosis patients. Moreover, our previous study and the research by Reijnders *et al* indicated that increasing the entecavir dose when treating persistent LLV patients resulted in no observed side effects[14,15]. Therefore, the current study scoured the literature to shed light on the possibility of improving the antiviral effect of entecavir by increasing the dose and prolonging the treatment time.

LITERATURE SEARCH STRATEGY

All HBV treatment articles available since 1995 on the MEDLINE/PUBMED database and United States Food and Drug Administration (FDA) website were searched. In addition, information on prescriptions of the NA drugs entecavir, lamivudine, adefovir, telbivudine, tenofovir, and tenofovir alafenamide (TAF) was also retrieved. Furthermore, all available literature relating to LLV, partial virological response, virological breakthrough, and NA resistance were collated together to find the optimum therapy strategy for LLV.

The aim was to find the correlation between entecavir doses and efficacy. Here, search terms applied to enable identification of doses and antiviral efficacy were chronic hepatitis B, entecavir, tenofovir, adefovir, telbivudine, lamivudine, and tenofovir alafenamide. The articles retrieved by this strategy included the studies on pharmacokinetics, pharmacodynamics, pre-marketing randomized, placebo-controlled trials, as well as case reports and real-world clinical observation, randomized, contrast studies, and the therapy guidelines for CHB. In addition, to compare the antiviral efficacy of entecavir with newly developed drugs, the literature on the novel CHB therapeutic agents was retrieved.

THERAPY FOR PERSISTENT LLV

Persistent LLV and partial virological response in NA therapy

Persistent LLV and partial virological response are common phenomena and may be found in all types of NA therapy. In studies prior to 2016, LLV was referred to as a partial virological response, when primarily detectable HBV DNA was < 2×10^3 IU/mL following 48 wk of treatment. However, LLV in entecavir and tenofovir therapy was defined when detectable HBV DNA was < 2×10^3 IU/mL during therapy[2,8]. The AASLD guidelines defined LLV in entecavir and tenofovie therapy as < 2×10^3 IU/mL detectable HBV DNA, with or without viral rebound during therapy[1,3]. These definitions were examined in the paper by Zoutendijk *et al*[16] who, in a cohort of 333 HBV patients (293 naïve and 90 experienced) treated with entecavir at standard doses, showed that by weeks 48, 96, and 144 of entecavir treatment (standard doses without changes in therapy), NA-naïve patients reached 48%, 76%, 90% and 89%, 98%, 99% of hepatitis B e antigen (HBeAg)-positive and HBeAg-negative virological response, respectively.

LLV patients have two types, those with partial virological response and those with viral breakthrough. The incentives of LLV are caused by the following: (1) Patients with high basal viremia may show a slow decline of plasma HBV-DNA under antiviral treatment; (2) Patients exposed previously to lamivudine ± adefovir may harbor resistance mutations and are more prone to develop resistance to entecavir or tenofovir; and (3) Suboptimal adherence to treatment. Resistance testing in LLV patients might not be technically possible because of low viral levels[1,3]. Therefore, the LLV patients evaluated included patients treated with NAs that were resistant to NA therapy, and a few patients with detectable resistance mutations.

Incidence of LLV

The incidence of LLV with entecavir and tenofovir treatment is similar. Previous studies showed that the incidences of partial virological response during entecavir monotherapy were 45% at week 48 in the Liu *et al*'s study[8], 17% at year 2 in Chang *et al*'s paper[17] and 23.6%, 11.3%, and 22% at 96 wk in studies by Lok AS *et al*, Zoutendijk R *et al*, and Choi HN *et al*, respectively[16,18,19]. Kim *et al*[2] presented an article in Seoul, Korea, in which the total proportion of LLV was 43% (377/875)[2]. Kim's data is similar to Liu's results in Shanghai, China[8], but different from other studies[16-20]. In addition, the incidence of partial virological response to tenofovir monotherapy ranged from 18.1% to 45.3%[21-24], similar to that of entecavir.

Current therapeutic options for LLV

For patients with partial virological response to NAs, or LLV, three therapeutic options are available: (1) Traditional treatment, which is switching to another antiviral monotherapy with a high genetic barrier, or the addition of a second antiviral with a complementary resistance profile. The disadvantage of this traditional treatment is that it results in the failure of combined therapy with nucleoside plus nucleotide, which shortens the total course of the NA treatment; (2) The AASLD guidelines recommend continued monotherapy for LLV patients who received entecavir or tenofovir monotherapy[1,3]. Continuation of monotherapy prolongs the period of NA therapy. However, prolonged treatment with entecavir or tenofovir increases the LLV incidence, resulting in HBV DNA > 2×10^3 IU/mL and the emergence of detectable drug-resistant mutations, which ultimately leads to the progression of liver disease[2]; and (3) The use of the IFN-α therapy as used by Yin GQ and Zhong B to treat the failure of the combined nucleoside plus nucleotide therapy and subsequent virological breakthrough in LLV patients (HBV DNA < 2×10^3 IU/mL)[13]. The IFN-α therapy freed the patients from the predicament of multidrug resistance. However, IFN-α therapy in LLV or NA-refractory patients is problematic as it causes significant adverse events. Moreover, most patients have to undergo IFN-α re-treatment twice or more to achieve immune control. Twelve years ago, we started using IFN-α on patients with a focus of alleviating LLV in NA-refractory patients. However, we found that some patients were not suitable candidates for IFN-α therapy. Thus, the focus was shifted to treating LLV by increasing the entecavir dose.

ATTEMPTS TO INCREASE THE DOSE OF ENTECAVIR IN CLINICAL THRERAPY

Entecavir overdose has been used in antiviral therapy for CHB patients with NA refractoriness and persistent LLV. In real-world clinical practice, Reijnders *et al*[14] and we, in previous works, increased the entecavir dose in excess of the Baraclude prescribing information recommended dose to treat the LLV patients. Reijnders *et al*[14] increased the entecavir dose to 2.0 mg/d to treat patients with NA refractoriness and LLV, which resulted in a decline of HBV DNA and was tolerated well[14]. In our clinical work, we used the entecavir at a dose higher than that recommended by Baraclude to treat HBV patients with NA complications such as multidrug-resistant mutations and renal impairment, resulting in a decrease of viral load and stable creatinine clearance[15]. The 2015 WHO CHB guidelines stated that 'in unstable persons with deteriorating renal function, entecavir can be used at a recommended dosage of 1 mg daily and the patient should be monitored for lactic acidosis'[25]. The doses of entecavir utilized in the Reijnders *et al*' clinical study and our clinical report, as well as the dose recommended by the 2015 WHO CHB guidelines, were higher than the Baraclude recommended dosage. This information of entecavir overdose has been noted by Bristol-Myers Squibb Company and the FDA. Baraclude prescribing information (2015) states that "there is limited experience of entecavir overdosage reported in patients. Healthy subjects who received single entecavir doses up to 40 mg or multiple doses up to 20 mg/d for up to 14 d did not experience unexpected or adverse events. If an overdose occurs, the patient must be monitored for evidence of toxicity, and standard supportive treatment applied as necessary"[26]. The results of the clinical investigation encouraged us to conduct further in-depth literature survey on studies of the pharmacodynamics, pharmacokinetics, and treatment dosage and duration of entecavir.

PHARMACOKINETICS AND PHARMACODYNAMICS OF ENTECAVIR

Generally, NA incorporation into the mitochondrial DNA (mtDNA) *via* mitochondrial polymerase γ results in host mitochondrial dysfunction and morphological changes. However, entecavir triphosphate is a poor substrate for mitochondrial polymerase γ and does not significantly inhibit the mitochondrial respiratory function or alter the mtDNA synthesis[27]. In the cell line HepG2 and the HBV-transfected cell lines 2.2.15, entecavir showed efficacy at a 50% effective concentration (EC_{50}) of 3.8 ± 1.4 nmol/L (1.1 ± 0.41ng/mL), and 50% cytotoxic concentration (CC_{50}) of 30 μmol/L. The CC_{50}/EC_{50} ratio of entecavir was 8000, which was the maximal selected index for safety in all of the NAs[28]. The poor binding of entecavir to mitochondrial polymerase γ leads to the selected index.

An *in vitro* investigation by Liu *et al*[29] showed that the NA concentration varied between the cells and the supernatant samples; thus, the variability in entecavir and lamivudine concentrations encompasses a wide linear range of measurements[29]. Therefore, the plasma entecavir concentration was generally thought to predict the antiviral efficacy in the pharmacokinetic studies. The pharmacokinetic parameters of the entecavir dose were reported by Yan *et al*. For a 0.1mg dose, the mean steady-state (day 14) peak plasma concentration (C_{max}) was 0.60 ng/mL, and the area under the concentration-time curve (AUC) was 2.51 ng/h/mL. For doses of 0.5mg and 1.0 mg, the corresponding C_{max} and AUC values were 4.23 ng/mL and 14.78 ng/h/mL, and 8.24 ng/mL and 26.38 ng/h/mL, respectively. In addition, steady-state (drug-input/clearance) entecavir plasma concentrations were approximately 0.2 ng/mL and 0.4 ng/mL for the 0.5 mg dose and 1.0 mg dose, respectively[30]. As the entecavir dose increased from 0.1 mg to 1.0 mg, the AUC increased, suggesting that an increase in entecavir dose was associated with an increase in efficacy.

Yurdaydin *et al*[31] compared the EC_{50} of entecavir with that of lamivudine, adefovir, telbivudine, and tenofovir. They found that the EC_{50} of entecavir was lower than that of other NAs (Table 1). TAF is a pro-drug of tenofovir and has been used to treat CHB. The EC_{50} of TAF was lower than that of tenofovir but higher than that of entecavir[32]. Tenofovir conjugating a lipid moiety (CMX-157), a lipid conjugated tenofovir moiety, is in development for treating CHB. The EC_{50} of CMX-157 is 1.6 μmol/L, which is nearly a 5-fold increase in potency over tenofovir, but 1/420 of the efficacy for entecavir[33]. Thus, entecavir is the most effective treatment among all of the current and developing therapies (Table 1).

The pharmacokinetics and pharmacodynamics data indicate that entecavir is the

Table 1 Relative potencies of various nucleos(t)ide analogs for inhibiting hepatitis B virus

Drug	EC_{50} (nM), mean ± SD	Difference (fold) from entecavir EC_{50}	Ref.
Entecavir	5.3 ± 2.5	1	Yurdaydin *et al*[31], 2008
TAF	86.6	16	Gibson *et al*[32], 2016
Lamivudine	1491 ± 1033	281	Yurdaydin *et al*[31], 2008
CMX-157	1600	420	Pei *et al*[33], 2017
Tenofovir	2482 ± 1938	468	Yurdaydin *et al*[31], 2008
Adefovir	2636 ± 1549	497	Yurdaydin *et al*[31], 2008
Telbivudine	8950 ± 4803	1689	Yurdaydin *et al*[31], 2008

EC_{50}: Effective concentration of nucleos(t)ide analogs that results in 50% inhibition of HBV DNA production; TAF: Tenofovir alafenamide; CMX-157: Tenofovir conjugated with a lipid moiety.

safest treatment and has great potential in inhibiting HBV replication.

EFFICACY AND SAFETY OF ENTECAVIR AT VARIOUS DOSES (0.1-20 MG/D) IN CLINICAL STUDIES FROM BERGMAN'S REVIEW

Bergman KL and Zheng JH presented a review entitled "Clinical pharmacology and biopharmaceutics review 021797/S-000", which was published in the United States FDA website in 2005[34]. In this particular section of the drug approval package published by the FDA, the authors submitted 37 placebo-controlled phases 1, 2, or 3 clinical trials of entecavir, with the registration numbers A1436001-A1436066 (Table 2). Some of main findings in Bergman's review are:

FDA has approved using entecavir at doses of 0.5 mg/d and 1.0 mg/d to treat nucleoside-naïve patients and lamivudine refractory patients

Prior to determining the pivotal entecavir dose required for treating CHB, researchers first investigated the characteristics of the exposure-response relationship for safety. The incidence of headache and nausea after taking the medicine (which were the most common treatment emergent adverse events) was defined as the index of safety in the clinical studies A1463004 and A1463005. According to these safety indicators, the incidence of adverse events was greater as the dose of entecavir increased, ranging from 0.5 mg to 40 mg (Table 2a). Considering the greater antiviral activity *vs* the 0.1 mg dose, superiority over lamivudine for antiviral activity response, reduction of HBV DNA to < 0.7MEq/mL after 22 wk, and an acceptable safety profile, entecavir 0.5 mg/d was selected for treating nucleoside-naïve patients. According to the observation that 1.0 mg/d entecavir exhibited significantly greater antiviral activity than the 0.5 mg/d, with the reduction of HBV DNA to < 400 copies/mL after 24 wk, and an acceptable safety profile, entecavir 1.0 mg/d was determined to treat lamivudine refractory patients. Researchers, however, chose the lower limit of the effective dose to treat CHB (Table 2b and c).

Increase in entecavir dose from 0.1 mg/d to 20 mg/d entails increased efficacy (higher AUC value)

Researchers investigated the pharmacokinetic parameters for multiple doses of entecavir (0.1, 0.5, 1.0, 2.5, 5, 10, and 20 mg/d) in healthy volunteers, for up to 14 d; or single doses up to 40 mg/d in the clinical studies. The trough concentrations were used for analysis. Thus, during a 14-d course of treatment with multiple dosing, a steady-state was attained approximately 9 to 10 d following once-daily dosing (Table 2d). The doses of 0.1, 0.5, 1.0, 2.5, 5.0, 10, and 20 mg per day, and their AUC values are depicted in Table 3. The AUC for the 2.5-5.0 mg dose was significantly higher than the 1.0 mg dose. In addition, the AUC for 10-20 mg/d was significantly higher than that of the 2.5-5.0 mg/d (Table 2d).

Table 2 Summary of principal findings from Bergman's review on the Food and Drug Administration website

Research project in Bergman's review	Content of research project	Registration number of clinic studies	Page in Bergman's review
(a) Treatment of emergent adverse events	Treatment of emergent adverse events in the clinical studies in which entecavir doses from 0.5 to 40 mg/d were used to select the pivotal doses of entecavir	A 1463004, A1463005	Pages 17 and18
(b) Entecavir 0.5 and 1.0 mg/d for current treatment	The dose and dose regimen of 0.5 mg/d for NA naïve patients and 1 mg/d for lamivudine refractory patients were determined to treat CHB	A1463002, A1463005, A1463014, A1463022, A1463027	Pages 23 and 24
(c) Exposure-response: HBV DNA changes for 0.1 up to 1.0 mg/d	HBV DNA changes for 0.1, 0.5, and 1.0 mg/d were reported	A1463004, A143005, A1463014, A1463017	Pages 11-17
(d) Pharmacokinetics of multiple doses	Entecavir multiple dose pharmacokinetic parameters from 0.5 to 20 mg/d were presented	A1463002, A1463033	Page 25
(e) Overall incidence of adverse events for doses 0.5 and 1.0 mg/d	No apparent dose-response relationship in the overall incidence of adverse events for doses of 0.5 and 1.0 mg/dwasfound	A 1463004, A1463005, A1403014,	Pages 18 and 19
(f) Doses and adverse events for multiple dose therapy, 0.5 mg up to 20 mg/d	The dose and adverse events with entecavir multiple doses, 0.5 mg up to 20 mg daily, were reported in nine clinical trials	A 1463001, A1463002, A1463003, A 1463004, A1463005, A1463010, A1463033, A1463034, A1463041	Pages 17, 21, and 23
(g) Cardiovascular safety	The studies for cardiovascular safety included *in vitro* investigations and six clinical studies, in which the safety of entecavir was assessed at doses of 0.5 mg/d to 20 mg/d and a single dose of 40 mg	A1463001, A1463002, A1463010, A1463033, A1463034, A1463041	Pages 21 and 23

NA: Nucleos(t)ide analogs; CHB: Chronic hepatitis B virus infection; HBV: Hepatitis B virus.

Table 3 Pharmacokinetic parameters of entecavir multiple doses in Bergman's review

Dose (mg/d)	AUC (ng/h/mL)	C_{max} (ng/mL)	T_{max} (h)	$T_{1/2}$ (h)
20	545.6 ± 57.9	179.8 ± 34.8	1.0	142.5 ± 55.5
10	304.3 ± 35.6	99.9 ± 13.7	0.75	127.5 ± 41.8
5.0	145.8 ± 28.4	46.2 ± 6.4	0.88	91.3 ± 57.9
2.5	71.6 ± 10.3	22.8 ± 5.7	0.75	115.7 ± 37.2
1.0	26.38 ± 12	8.24 ± 16	0.75	148.89 ± 39.5
0.5	14.78 ± 17	4.23 ± 9	1.0	129.9 ± 17.28
0.1	2.5 ± 21	0.6 ± 29	1.0	127.69 ± 91.44

Data are presented as the mean ± SD. Source: A1463002 and A1463033 clinical studies; AUC: Area under the concentration-time curve.

Dosage related adverse events in entecavir multiple-dose studies (0.5 mg up to 20 mg)

Researchers have assessed the integrated safety data of the entecavir treatment. In the clinical studies A1463001, A1463002, A1463003, A 1463004, A1463005, A1463010, A1463033, A1463034, and A1463041, no relationship between the doses administered and the severity of the adverse events was observed (Table 2e and f), which was different from the data regarding the treatment of emergent adverse events in the clinical studies A 1463004 and A1463005 (Table 2a); and no relationship between the predicted entecavir exposure (C_{max}, AUC, or C_{min}) and the severity of adverse events was found for the central nervous system, gastrointestinal, or the digestive system. The overall incidence of adverse events with an oral entecavir dose of 0.5 mg or 1.0 mg was comparable to that of the placebo, for example, 40% in the entecavir treatment *vs* 38% in the placebo group. In addition, no apparent dose-response relationship was found for the overall incidence of adverse events observed in this double-blind, randomized clinical study (Table 2e). In addition to the 0.5 mg or 1.0 mg dose data, entecavir retained a wide margin of safety at a much higher dose (2.5-20 mg/d;

Table 2f). Surprisingly, in the clinical studies A1463004 and A1463005, the subjects participated in both the trials (1) most common treatment emergency adverse event study; and (2) the overall incidence of adverse events research. This indicated that the emergency adverse event only occurred at the initial stage of entecavir treatment, and it disappeared with continued entecavir treatment.

Further studies focused on cardiovascular adverse events during entecavir treatment. First, researchers conducted *in vitro* studies to assess the cardiovascular safety of entecavir. The researchers evaluated the possibility of entecavir to interfere with cardiac calcium and potassium currents or the electrophysiological parameters. Entecarir (30 μmol/L, > 10000 × the steady-state human plasma concentrations[30]) did not have any significant biological effect on the L-type calcium currents or the Purkinje fiber action potential parameters[including the resting membrane potential, overshoot, maximal upstroke velocity, or 50%–90% repolarization (APD_{50} and APD_{90})].

Furthermore, researchers carried out clinical trials using entecavir doses to evaluate untoward cardiac effects (Table 2f). Electrocardiogram (ECG) parameters were evaluated over a range of entecavir doses (0.1-40 mg). The retrospective ECG analysis parameters were used to evaluate the effects of entecavir. The results were as follows: (1) No dose-or concentration-dependent relationships between the QT interval or changes in the QTc were observed for entecavir doses of 0.5-20 mg for up to 14 d or as a single dose of 0.5-40 mg; and (2) For each additional 10 ng/mL of plasma concentration, an estimated increase in the change in QTcB ranged from-1.22 to 0.22 msec. The estimated slope of the linear regression at day 1 was slightly greater than zero, whereas the estimated slope on days 7 and 14 was negative (Table 2g). The *in vitro* data and the ECG data from six clinical studies suggested that QT or QTc interval prolongation potential of entecavir was minimal. Thus, entecavir therapy was considered safe for the cardiovascular system.

In 2005, 0.5 mg/d entecavir for nucleoside-naïve patients and 1.0 mg/d for lamivudine-refractory patients were approved by the FDA for treating CHB, and these doses have been used to this day.

Insights from Bergman's review

Double-blind, randomized clinical studies showed that entecavir doses 2.5-20 mg/d for 14 d did not increase adverse events. In addition, three main findings were presented: (1) The researchers had completed phases 1 and 2 clinical studies for entecavir over a range of doses (0.1 up to 20 mg/d); (2) The correlation between AUC values in the plasma and the entecavir doses of 0.1, 0.5, 1.0, 2.5, 5, 10, and 20 mg/d implied that using doses higher than 1.0 mg/d might improve the antiviral efficacy; and (3) The maximum dose of entecavir can exceed 20 mg/d.

Thus, Bergman's review indicated that increasing the dose of entecavir to 2.5-20 mg/d may improve its antiviral efficacy, and its use was safe over a broad range of doses (0.5 up to 20 mg/d).

INCREASING DOSE OF ENTECAVIR IN LLV PATIENTS

In summary, data from clinical, pharmacokinetics, and pharmacodynamics studies and the Bergman's review showed that entecavir doses at over 1.0 mg/d improved efficacy and were safe. We hypothesized that patients with prior NA treatment, partial virological response, or LLV should continue monotherapy, at higher doses of 2.5-5.0 mg/d.

The goal of increasing the dose was to maximally inhibit HBV replication during entecavir treatment for 15 years or longer. Compared to the approved NAs and NAs being newly developed[4,31-33], entecavir has the strongest ability to inhibit HBV and the broadest safety range. The clinical trials for multiple doses of entecavir, 0.1 mg/d up to 20 mg/d (Tables 2 and 3), have been conducted[34]. The long-term safety of 1.0 mg/d entecavir has been determined in the clinical treatment of patients with lamivudine refractoriness or cirrhosis[1,3,25]. However, no controlled clinical trials have been conducted to assess the long-term toxicity of ingesting entecavir at doses above 1.0 mg/d. Thus, we recommend that clinical trials assessing the long-term toxic effects of entecavir at doses of 2.5 and 5.0 mg/d should be conducted to determine if these doses could improve the efficacy of entecavir. Moreover, compared to the development of novel NAs and the HBV inhibitors[3,33], utilizing an available treatment is cost-effective and potentially a more viable option. However, these views should be evaluated by researchers.

Liu and colleagues demonstrated that rapid suppression of HBV within 12 wk of

entecavir treatment reduced the incidence of drug-resistant mutations and prolonged the duration of entecavir therapy (seeing the Figure 1 in Liu's paper)[8]. In addition, NA naïve patients with cirrhosis or hepatic decompensation were treated with entecavir at a dose of 1.0 mg/d to improve the entecavir response and to reduce drug-resistant mutations[25,35]. Inspired by the above research, we suggest that the entecavir dose should be increased to 1.0 mg/d for the treatment of NAs naïve patients with HBV DNA > 2×10^6 IU/mL.

NAs have been used to treat CHB for the last 20 years. Approximately 150 NA derivatives have been examined, including17 NAs (such as lamivudine, telbivudine, entecavir, adefovir, tenofovir, TAF, and GS-7340)[33]. Entecavir, tenofovir, and TAF are the most commonly used drugs and are recommended as the first-line therapy based on their highest potency and lowest frequency of developing resistance[1,3,4,32]. Because NAs cannot eradicate cccDNA, half of the patients with entecavir or tenofovir monotherapy will eventually present with LLV. Therefore, increased doses of entecavir could be a viable option for treating the patients with prior NA treatment, partial virological response, or LLV, and could be used in over 50% of the population requiring entecavir treatment. We deduce that increasing the dose of entecavir is appropriate for patients on entecavir monotherapy. However, increasing the tenofovir or TAF doses is not a suitable option as their doses could not be safely increased[32,36].

CONCLUSION

Persistent LLV sheds light on the current plight of NA therapy. The majority of patients on long-term entecavir or tenofovir treatment eventually reach LLV status resulting in progression of liver disease or HCC. For patients with partial virological response to NA, or LLV, three therapeutic options are available, namely, switching to another antiviral monotherapy, IFN-α switching therapy, and continuing monotherapy.

Literature survey indicates that entecavir possesses a strong capacity for inhibiting HBV and a broad dose-range safety. Moreover, entecavir overdose has been used in antiviral therapy in limited patients; thus, an increased dose could be utilized to treatLLV or NA refractory patients. The results of placebo-controlled phase 1, 2, or 3 clinical trials indicate that increasing the dose of entecavir to 2.5-20 mg/d might improve the antiviral efficacy, and higher entecavir doses (up to 20 mg/d) were considered safe. To decrease the incidence of LLV, we suggest increasing entecavir dose to 1.0 mg/d for the treatment of NA naïve patients with HBV DNA > 2×10^6 IU/mL. In addition, clinical trials should be conducted to assess the long-term toxic effects of entecavir at doses of 2.5-5.0 mg/d in patients with prior NA treatment, partial virologic response, or LLV state.

ACKNOWLEDGEMENTS

We are very grateful to Professor Yun Chen at School of Pharmacy, Nanjing Medical University for the comprehensive evaluation of the manuscript and valuable advice on pharmacokinetics and pharmacodynamics. The authors thank Mc. Jing Zhong, Medical Science Manager, Virology from Bristol-Myers Squibb China Medical Affairs for literature search and pharmaceutical professional advice, and Dr. Cun Shan at the Department of Infectious Diseases, Nanjing Zhong-Da Hospital for language modification in the writing of the manuscript.

REFERENCES

1 **Terrault NA**, Bzowej NH, Chang KM, Hwang JP, Jonas MM, Murad MH; American Association for the Study of Liver Diseases. AASLD guidelines for treatment of chronic hepatitis B. *Hepatology* 2016; **63**: 261-283 [PMID: 26566064 DOI: 10.1002/hep.28156]

2 **Kim JH**, Sinn DH, Kang W, Gwak GY, Paik YH, Choi MS, Lee JH, Koh KC, Paik SW. Low-level viremia and the increased risk of hepatocellular carcinoma in patients receiving entecavir treatment. *Hepatology* 2017; **66**: 335-343 [PMID: 28012257 DOI: 10.1002/hep.28916]

3 **Terrault NA**, Lok ASF, McMahon BJ, Chang KM, Hwang JP, Jonas MM, Brown RS Jr, Bzowej NH, Wong JB. Update on prevention, diagnosis, and treatment of chronic hepatitis B: AASLD 2018 hepatitis B guidance. *Hepatology* 2018; **67**: 1560-1599 [PMID: 29405329 DOI: 10.1002/hep.29800]

4 **Lok AS**, Zoulim F, Dusheiko G, Ghany MG. Hepatitis B cure: From discovery to regulatory approval. *Hepatology* 2017; **66**: 1296-1313 [PMID: 28762522 DOI: 10.1002/hep.29323]

5 **Coffin CS**, Mulrooney-Cousins PM, Peters MG, van Marle G, Roberts JP, Michalak TI, Terrault NA. Molecular characterization of intrahepatic and extrahepatic hepatitis B virus (HBV) reservoirs in patients on suppressive antiviral therapy. *J Viral Hepat* 2011; **18**: 415-423 [PMID: 20626626 DOI: 10.1111/j.1365-2893.2010.01321.x]

6 **Tamura K**, Stecher G, Peterson D, Filipski A, Kumar S. MEGA6: Molecular Evolutionary Genetics Analysis version 6.0. *MolBiolEvol* 2013; **30**: 2725-2729 [PMID: 24132122 DOI: 10.1093/molbev/mst197]

7 **Nei M**, Gojobori T. Simple methods for estimating the numbers of synonymous and nonsynonymous nucleotide substitutions. *MolBiolEvol* 1986; **3**: 418-426 [PMID: 3444411 DOI: 10.1093/oxfordjournals.molbev.a040410]

8 **Liu F**, Chen L, Yu DM, Deng L, Chen R, Jiang Y, Chen L, Huang SY, Yu JL, Gong QM, Zhang XX. Evolutionary patterns of hepatitis B virus quasispecies under different selective pressures: correlation with antiviral efficacy. *Gut* 2011; **60**: 1269-1277 [PMID: 21292683 DOI: 10.1136/gut.2010.226225]

9 **Rawbone RG**. Switching to low tar cigarettes: are the tar league tables relevant? *Thorax* 1984; **39**: 657-662 [PMID: 6474400 DOI: 10.1371/journal.pone.0140070]

10 **Gao S**, Duan ZP, Chen Y, van der Meer F, Lee SS, Osiowy C, van Marle G, Coffin CS. Compartmental HBV evolution and replication in liver and extrahepatic sites after nucleos/tide analogue therapy in chronic hepatitis B carriers. *J ClinVirol* 2017; **94**: 8-14 [PMID: 28709006 DOI: 10.1016/j.jcv.2017.06.009]

11 **Coffin CS**, Mulrooney-Cousins PM, van Marle G, Roberts JP, Michalak TI, Terrault NA. Hepatitis B virus quasispecies in hepatic and extrahepatic viral reservoirs in liver transplant recipients on prophylactic therapy. *Liver Transpl* 2011; **17**: 955-962 [PMID: 21462295 DOI: 10.1002/lt.22312]

12 **Chen L**, Zhang Q, Yu DM, Wan MB, Zhang XX. Early changes of hepatitis B virus quasispecies during lamivudine treatment and the correlation with antiviral efficacy. *J Hepatol* 2009; **50**: 895-905 [PMID: 19304333 DOI: 10.1016/j.jhep.2008.12.018]

13 **Yin GQ**, Zhong B. Efficacy of interferon for chronic hepatitis B in patients with nucleoside and nucleotide combination therapy failure. *J Gastroenterol Hepatol* 2016; **31**: 248-255 [PMID: 26456953 DOI: 10.1111/jgh.13191]

14 **Reijnders JG**, Pas SD, Schutten M, de Man RA, Janssen HL. Entecavir shows limited efficacy in HBeAg-positive hepatitis B patients with a partial virologic response to adefovir therapy. *J Hepatol* 2009; **50**: 674-683 [PMID: 19231002 DOI: 10.1016/j.jhep.2008.10.033]

15 **Shan C**, Yin GQ, Wu P. Efficacy and safety of tenofovir in a kidney transplant patient with chronic hepatitis B and nucleos(t)ide multidrug resistance: a case report. *J Med Case Rep* 2014; **8**: 281 [PMID: 25146249 DOI: 10.1186/1752-1947-8-281]

16 **Zoutendijk R**, Reijnders JG, Brown A, Zoulim F, Mutimer D, Deterding K, Petersen J, Hofmann WP, Buti M, Santantonio T, van Bömmel F, Pradat P, Oo Y, Luetgehetmann M, Berg T, Hansen BE, Wedemeyer H, Janssen HL; VIRGIL Surveillance Study Group. Entecavir treatment for chronic hepatitis B: adaptation is not needed for the majority of naïve patients with a partial virological response. *Hepatology* 2011; **54**: 443-451 [PMID: 21563196 DOI: 10.1002/hep.24406]

17 **Chang TT**, Lai CL, Kew Yoon S, Lee SS, Coelho HS, Carrilho FJ, Poordad F, Halota W, Horsmans Y, Tsai N, Zhang H, Tenney DJ, Tamez R, Iloeje U. Entecavir treatment for up to 5 years in patients with hepatitis B e antigen-positive chronic hepatitis B. *Hepatology* 2010; **51**: 422-430 [PMID: 20049753 DOI: 10.1002/hep.23327]

18 **Choi HN**, Song JE, Lee HC, Jo HH, Lee CH, Kim BS. Efficacy of prolonged entecavir monotherapy in treatment-naïve chronic hepatitis B patients exhibiting a partial virologic response to entecavir. *Clin Mol Hepatol* 2015; **21**: 24-31 [PMID: 25834799 DOI: 10.3350/cmh.2015.21.1.24]

19 **Lok AS**, Trinh H, Carosi G, Akarca US, Gadano A, Habersetzer F, Sievert W, Wong D, Lovegren M, Cohen D, Llamoso C. Efficacy of entecavir with or without tenofovirdisoproxil fumarate for nucleos(t)ide-naïve patients with chronic hepatitis B. *Gastroenterology* 2012; **143**: 619-628. e1 [PMID: 22643350 DOI: 10.1053/j.gastro.2012.05.037]

20 **Zoutendijk R**, Reijnders JG, Zoulim F, Brown A, Mutimer DJ, Deterding K, Hofmann WP, Petersen J, Fasano M, Buti M, Berg T, Hansen BE, Sonneveld MJ, Wedemeyer H, Janssen HL; VIRGIL Surveillance Study Group. Virological response to entecavir is associated with a better clinical outcome in chronic hepatitis B patients with cirrhosis. *Gut* 2013; **62**: 760-765 [PMID: 22490523 DOI: 10.1136/gutjnl-2012-302024]

21 **Du Jeong I**, Jung SW, Park BR, Lee BU, Park JH, Kim BG, Bang SJ, Shin JW, Park NH. Clinical Course of Partial Virologic Response with Prolonged Tenofovir Therapy in Nuclos(t)ides-Naïve Patients with Chronic Hepatitis B. *Dig Dis Sci* 2017; **62**: 2908-2914 [PMID: 28871337 DOI: 10.1007/s10620-017-4737-1]

22 **Perry CM**, Simpson D. Tenofovir disoproxil fumarate: in chronic hepatitis B. *Drugs* 2009; **69**: 2245-2256 [PMID: 19852527 DOI: 10.2165/10482940-000000000-00000]

23 **Song JE**, Lee CH, Kim BS. Efficacy of long-term tenofovir disoproxil fumarate therapy in chronic hepatitis B patients with partial virologic response in real practice. *Korean J Intern Med* 2019; **34**: 802-810 [PMID: 30959583 DOI: 10.3904/kjim.2019.037]

24 **Lovett GC**, Nguyen T, Iser DM, Holmes JA, Chen R, Demediuk B, Shaw G, Bell SJ, Desmond PV, Thompson AJ. Efficacy and safety of tenofovir in chronic hepatitis B: Australian real world experience. *World J Hepatol* 2017; **9**: 48-56 [PMID: 28105258 DOI: 10.4254/wjh.v9.i1.48]

25 Guidelines for the Prevention, Care and Treatment of Persons with Chronic Hepatitis B Infection. Geneva: World Health Organization; 2015 Mar [PMID: 26225396]

26 Baraclude® prescribing information. Available from: https://www.drugs.com/pro/baraclude.html

27 **Innaimo SF**, Seifer M, Bisacchi GS, Standring DN, Zahler R, Colonno RJ. Identification of BMS-200475 as a potent and selective inhibitor of hepatitis B virus. *Antimicrob Agents Chemother* 1997; **41**: 1444-1448 [PMID: 9210663 DOI: 10.1128/AAC.41.7.1444]

28 **Rivkin A**. A review of entecavir in the treatment of chronic hepatitis B infection. *Curr Med Res Opin* 2005; **21**: 1845-1856 [PMID: 16307706 DOI: 10.1185/030079905X65268]

29 **Liu YT**, Liu W, Zhu GY, Wang FL, Chen Q. Involvement of multidrug resistance protein 4 in the hepatocyte efflux of lamivudine and entecavir. *Mol Med Rep* 2018; **17**: 7113-7121 [PMID: 29568871 DOI: 10.3892/mmr.2018.8779]

30 **Yan JH**, Bifano M, Olsen S, Smith RA, Zhang D, Grasela DM, LaCreta F. Entecavir pharmacokinetics, safety, and tolerability after multiple ascending doses in healthy subjects. *J ClinPharmacol* 2006; **46**: 1250-1258 [PMID: 17050790 DOI: 10.1177/0091270006293304]

31 **Yurdaydin C**. Entecavir: a step forward in combating hepatitis B disease. *Expert OpinPharmacother* 2008; **9**: 3095-3109 [PMID: 19006481 DOI: 10.1517/14656560802515546]

32 **Gibson AK**, Shah BM, Nambiar PH, Schafer JJ. Tenofovir Alafenamide. *Ann Pharmacother* 2016; **50**: 942-952 [PMID: 27465879 DOI: 10.1177/1060028016660812]

33 **Pei Y**, Wang C, Yan SF, Liu G. Past, Current, and Future Developments of Therapeutic Agents for Treatment of Chronic Hepatitis B Virus Infection. *J Med Chem* 2017; **60**: 6461-6479 [PMID: 28383274 DOI: 10.1021/acs.jmedchem.6b01442]

34 **Bergman KL**, Zheng JH. Clinical pharmacology and biopharmaceutics review 021797/S-000. Availablefrom: https://www.accessdata.fda.gov/drugsatfda_docs/nda/2005/21797_BARACLUDE_biopharmr.PDF

35 **Kearney BP**, Flaherty JF, Shah J. Tenofovir disoproxil fumarate: clinical pharmacology and pharmacokinetics. *ClinPharmacokinet* 2004; **43**: 595-612 [PMID: 15217303 DOI: 10.2165/00003088-200443090-00003]

36 **Liaw YF**, Raptopoulou-Gigi M, Cheinquer H, Sarin SK, Tanwandee T, Leung N, Peng CY, Myers RP, Brown RS Jr, Jeffers L, Tsai N, Bialkowska J, Tang S, Beebe S, Cooney E. Efficacy and safety of entecavir *vs* adefovir in chronic hepatitis B patients with hepatic decompensation: a randomized, open-label study. *Hepatology* 2011; **54**: 91-100 [PMID: 21503940 DOI: 10.1002/hep.24361]

World Journal of Gastroenterology

Submit a Manuscript: https://www.f6publishing.com

World J Gastroenterol 2021 February 28; 27(8): 677-691

DOI: 10.3748/wjg.v27.i8.677

ISSN 1007-9327 (print) ISSN 2219-2840 (online)

REVIEW

G protein-coupled receptors as potential targets for nonalcoholic fatty liver disease treatment

Ming Yang, Chun-Ye Zhang

ORCID number: Ming Yang 0000-0002-4895-5864; Chun-Ye Zhang 0000-0003-2567-029X.

Author contributions: Yang M and Zhang CY designed, collected data, wrote, revised, and finalized the manuscript and contributed equally.

Supported by University of Missouri, Postdoctoral Research Award.

Conflict-of-interest statement: The authors declare no conflicts of interest.

Open-Access: This article is an open-access article that was selected by an in-house editor and fully peer-reviewed by external reviewers. It is distributed in accordance with the Creative Commons Attribution NonCommercial (CC BY-NC 4.0) license, which permits others to distribute, remix, adapt, build upon this work non-commercially, and license their derivative works on different terms, provided the original work is properly cited and the use is non-commercial. See: http://creativecommons.org/Licenses/by-nc/4.0/

Manuscript source: Unsolicited manuscript

Specialty type: Gastroenterology

Ming Yang, Department of Surgery, University of Missouri, Columbia, MO 65212, United States

Chun-Ye Zhang, Department of Veterinary Pathobiology, University of Missouri, Columbia, MO 65212, United States

Corresponding author: Ming Yang, DVM, PhD, Postdoctoral Fellow, Department of Surgery, University of Missouri, One Hospital Dr. Medical Science Building, Columbia, MO 65212, United States. yangmin@health.missouri.edu

Abstract

Nonalcoholic fatty liver disease (NAFLD) is a broad-spectrum disease, ranging from simple hepatic steatosis to nonalcoholic steatohepatitis, which can progress to cirrhosis and liver cancer. Abnormal hepatic lipid accumulation is the major manifestation of this disease, and lipotoxicity promotes NAFLD progression. In addition, intermediate metabolites such as succinate can stimulate the activation of hepatic stellate cells to produce extracellular matrix proteins, resulting in progression of NAFLD to fibrosis and even cirrhosis. G protein-coupled receptors (GPCRs) have been shown to play essential roles in metabolic disorders, such as NAFLD and obesity, through their function as receptors for bile acids and free fatty acids. In addition, GPCRs link gut microbiota-mediated connections in a variety of diseases, such as intestinal diseases, hepatic steatosis, diabetes, and cardiovascular diseases. The latest findings show that gut microbiota-derived acetate contributes to liver lipogenesis by converting dietary fructose into hepatic acetyl-CoA and fatty acids. GPCR agonists, including peptides and natural products like docosahexaenoic acid, have been applied to investigate their role in liver diseases. Therapies such as probiotics and GPCR agonists may be applied to modulate GPCR function to ameliorate liver metabolism syndrome. This review summarizes the current findings regarding the role of GPCRs in the development and progression of NAFLD and describes some preclinical and clinical studies of GPCR-mediated treatment. Overall, understanding GPCR-mediated signaling in liver disease may provide new therapeutic options for NAFLD.

Key Words: Nonalcoholic fatty liver disease; G protein-coupled receptors; Metabolism; Bile acids; Short-chain fatty acids; Gut microbiota

©The Author(s) 2021. Published by Baishideng Publishing Group Inc. All rights reserved.

and hepatology

Country/Territory of origin: United States

Peer-review report's scientific quality classification
Grade A (Excellent): 0
Grade B (Very good): B
Grade C (Good): 0
Grade D (Fair): 0
Grade E (Poor): 0

Received: November 11, 2020
Peer-review started: November 11, 2020
First decision: December 17, 2020
Revised: December 24, 2020
Accepted: January 21, 2021
Article in press: January 21, 2021
Published online: February 28, 2021

P-Reviewer: Chen Y
S-Editor: Zhang L
L-Editor: Filipodia
P-Editor: Ma YJ

Core Tip: Nonalcoholic fatty liver disease (NAFLD) is the most common chronic liver disease. Without effective treatment, NAFLD can progress to fibrosis, cirrhosis, and liver cancer. Currently, there is no effective treatment option. G protein-coupled receptors (GPCRs) have been shown to play essential roles in metabolic disorders, such as NAFLD, through their function as receptors for bile acids and free fatty acids. Therapies such as probiotics and GPCR agonists could be applied to modulate GPCR function to ameliorate liver metabolism syndrome. Herein, this review summarizes the current findings regarding the role of GPCRs in the development and progression of NAFLD.

Citation: Yang M, Zhang CY. G protein-coupled receptors as potential targets for nonalcoholic fatty liver disease treatment. *World J Gastroenterol* 2021; 27(8): 677-691
URL: https://www.wjgnet.com/1007-9327/full/v27/i8/677.htm
DOI: https://dx.doi.org/10.3748/wjg.v27.i8.677

INTRODUCTION

Nonalcoholic fatty liver disease (NAFLD) is a broad-spectrum disease characterized by pathological severity ranging from simple hepatic steatosis to nonalcoholic steatohepatitis (NASH)[1]. NAFLD patients with progressive liver fibrosis have a high incidence of developing cirrhosis and hepatocellular carcinoma (HCC)[2]. NAFLD is often associated with other metabolic disorders, including obesity, diabetes, and insulin resistance[3]. Abnormal accumulation of hepatic lipids is the main manifestation of NAFLD. Lipotoxicity caused by toxic free fatty acids, such as palmitic acid, cholesterol, and ceramides, contributes to early-stage NAFLD progression to advanced NASH and advanced liver disease[4]. However, there is still no approved treatment for NAFLD[5]. G protein-coupled receptors (GPCRs) play important roles in metabolic disorders and can respond to various extracellular signals, including fatty acids (FAs)[6,7]. Data are increasingly showing that GPCRs and their signaling pathways are promising targets for NAFLD treatment.

Studies on the gut–liver axis are rapidly contributing to mounting evidence that dysbiosis of gut microbiota contributes to NAFLD progression *via* multiple mechanisms, including the secondary bile acid-induced senescence-associated secretory phenotype of hepatic stellate cells (HSCs)[8], bacterial product-induced proinflammatory responses through Toll-like receptors and toxic products[9,10]. In addition, bile acids (BAs), primarily produced in the liver and metabolized by gut microbiota, have pleiotropic roles in metabolism, including glucose homeostasis, digestion and absorption of dietary lipids, intestinal bacterial growth, and liver regeneration[11]. One of the molecular mechanisms for this BA interaction is with Takeda GPCR 5 and G protein-coupled bile acid receptor-1 (TGR5/GPBAR1) to regulate lipid and glucose metabolism[12,13].

In this review, we focus on the role of GPCRs in NAFLD development and progression by regulating nutrient metabolism. First, we introduce the role of GPCRs in liver metabolism and discuss how GPCR-mediated signaling impacts lipid synthesis, lipid and glucose metabolism, and production of extracellular matrix (ECM) proteins. Then, we summarize the role of GPCRs in NAFLD and advanced liver disease, followed by further discussion on current GPCR-targeted treatments in cellular and animal models for liver disease. Finally, we look to the therapeutic potential of GPCR-mediated signaling in liver disease and current preclinical and clinical trials.

EFFECT OF GPCRS ON LIVER METABOLISM

GPCRs, the largest family of membrane proteins, mediate cellular responses to various stimuli and play essential roles in most patho/physiological processes[14]. Some GPCRs can be activated by energy metabolites, such as FAs, saccharides, lactates, and ketone bodies[15]. Increasing evidence indicates that GPCRs play pivotal roles in liver metabolism by modulating diverse signaling pathways[16,17], including the Hedgehog,

Wnt, Notch, and transforming growth factor-β pathways[18]. GPCRs are receptors of short-, medium-, and long-chain FAs and can regulate the secretion of gut hormones, lipid and glucose metabolism, and generation of ECM proteins (Figure 1). Herein, we discuss how GPCRs mediate liver metabolism *via* these ligands.

Medium-chain fatty acids and long-chain fatty acids

Long-chain fatty acids (LCFAs) with more than 16 carbons are the most common fatty acids in Western diets and are commonly associated with inflammation and lipid accumulation[19]. In contrast, consuming diets rich in medium-chain fatty acids with 8-12 carbons can increase energy expenditure and decrease fatty acid accumulation. Oleate, an unsaturated (18:1) LCFA, can stimulate glucagon-like peptide 1 (GLP-1) secretion from an immortalized murine enteroendocrine cell line of GLUTag cells through their receptors *via* upregulating GPR40 (FFAR1) and GPR41 (FFAR3)[20]. Another study showed that GPR120 (FFA4) functions as a receptor for LCFA to regulate the secretion of GLP-1 from the gastrointestinal tract[21]. GLP-1 shows anti-inflammatory activity, including suppression of inflammatory cytokine expression in macrophages[22]. Accumulating evidence indicates that GLP-1 receptor agonists, GLP-1, and glucagon receptor co-agonists are treatment options for NAFLD[23,24]. The GPR40 agonist GW9508 decreased oleic acid-induced lipid accumulation in liver cancer cell line HepG2 cells *via* activating mitogen-activated protein kinase signaling, to downregulate the expression of sterol regulatory element-binding protein 1[25]. The effect of GW9508 on sterol regulatory element-binding protein 1 was diminished in GPR40-knockdown HepG2 cells. Moreover, GW9508 attenuated liver X receptor-induced hepatic lipid accumulation *via* activating the mitogen-activated protein kinase signaling pathway[26]. Another report showed that GPR40-deficient mice were protected against conjugated linoleic acid-induced accumulation of triglycerides in the liver[27], which might be associated with the secretion of insulin from the pancreas[28]. GPR120, as a receptor for unsaturated LCFAs, plays an essential role in liver metabolism. Ichimura *et al*[29] reported that GPR120-deficient mice showed a marked increase in hepatic lipids with a 10% greater bodyweight increase than wild-type mice[29]. Gpr43$^{-/-}$ mice were obese compared to wild-type mice with an increase in short-chain fatty acid (SCFA)-producing bacteria in the gut and increased concentrations of fecal SCFA and plasma acetate[30]. In addition, a specific deficiency of GPR43 in the adipose tissue attenuated high-fat diet (HFD)-induced liver steatosis.

SCFAs

SCFAs, including acetate, propionate, and butyrate, are the main metabolites of gut microbiota under an anaerobic microenvironment. SCFAs fuel intestinal cells and modulate the gut immune response *via* activating GPCRs (*e.g.*, GPR41/FFAR3 and GPR43/FFAR2) and inhibiting histone deacetylase[31]. In addition, GPCRs modulate SCFA-mediated inflammatory responses. For example, an antagonist of GPR41 or GPR43 alone as well as in combination were able to recover the inhibiting effect of acetate on lipopolysaccharides/tumor necrosis factor alpha-induced interleukin (IL)-6 and IL-8 production in human umbilical vein endothelial cells[32]. GPR41/43 are also involved in the effect of butyrate and propionate on IL-6 production but not IL-8 production. A new finding showed that microbial acetate contributed to liver lipogenesis by converting dietary fructose into hepatic acetyl-CoA and fatty acids[33]. SCFAs are also associated with the ameliorating effect of fructo-oligosaccharides on steatohepatitis and chronic inflammation[34].

Bile acids

Toxic BAs can cause hepatocyte death by directly activating cell death receptors or inducing oxidative damage, resulting in mitochondrial dysfunction, endoplasmic reticulum stress, and cell death[35]. Conversely, BAs can activate nuclear farnesoid X receptor and GPCR signaling to protect against liver and gastrointestinal inflammation[36,37]. TGR5 is widely expressed in different nonparenchymal liver cells, altering expression in response to BAs like lithocholic acid. TGR5 deletion increased the sensitivity of cholic acid feeding and bile duct ligation-induced liver injury in the endothelin-1 associated signaling pathway[38]. Administration of parenteral nutrition increased liver weight, the infiltration of macrophages, and inflammatory cytokine IL-6 expression[39] in TGR5$^{-/-}$ mice compared to wild-type mice. Meanwhile, unconjugated primary BAs and secondary BAs were increased due to the elevated abundance of *Bacteroides* and *Parabacteriodes* in the gut. Another study showed that BA-activated Mas-related GPCR4 played a critical role in cholestatic itch[40].

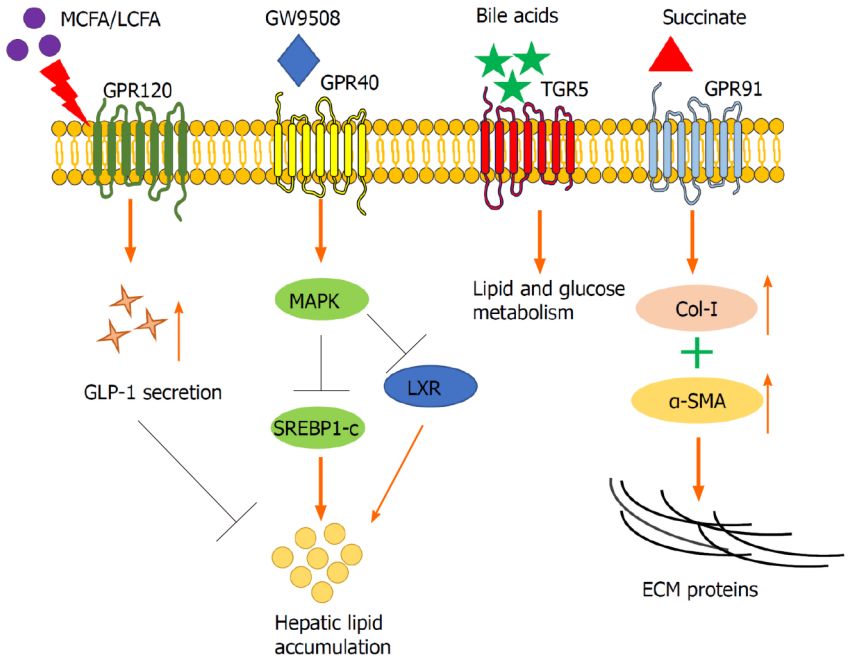


Figure 1 The role of G protein-coupled receptors in liver metabolism and the generation of extracellular matrix proteins. G protein-coupled receptors are receptors of diverse molecules, such as fatty acids, bile acids, and other agonists (*e.g.*, GW9508). They can regulate hepatic lipid and glucose metabolism and extracellular matrix (ECM) production *via* directly modulating hepatic cells (hepatocytes and hepatic stellate cells), and indirectly regulating gut hormones (*e.g.*, glucagon-like peptide-1, GLP-1). α-SMA: α-smooth muscle actin; Col-I: Collagen type I; LCFA: Long-chain fatty acid; LXR: Liver X receptor; MAPK: Mitogen-activated protein kinase; MCFA: Medium-chain fatty acid; SREBP1-c: Sterol regulatory element-binding protein 1.

Gut hormones

Gut hormones, such as peptide-YY and GLP-1, can be modulated through GPCRs to regulate insulin secretion in obese subjects[21,41]. For instance, SCFAs can stimulate incretin hormone GLP-1 secretion *via* GPR43 in the intestinal L cells to impact insulin sensitivity and appetite[42]. GLP-1 can regulate hepatic steatosis by preventing HFD-induced very-low-density lipoprotein overproduction and insulin resistance[43], accompanying the reduction in the mRNA and protein expression of sterol regulatory element-binding protein 1c, stearoyl-CoA desaturase-1, and fatty acid synthase.

Others

Conditional deletion of GPRC6a in hepatocytes by cross-breeding Alb-Cre and Gprc6a$^{flox/flox}$ mice resulted in abundant liver fat accumulation and glycogen depletion[44]. In addition, GPRC6a depletion altered the production of FGF-21 and its release, which controlled systemic energy homeostasis. Exposure of succinate upregulated the expression of GPR91 in primary and immortalized HSCs accompanying the increased expression of ECM proteins. Inhibiting GPR91 expression by lentivirus harboring shRNA reduced succinate-mediated HSC activation[45].

EFFECT OF GPCRS IN NAFLD, NASH, AND HCC

GPCRs

To date, some GPCRs have been shown to play critical roles in liver diseases (Table 1). Herein, we summarize some crucial GPCRs with potential clinical value at different stages of liver diseases, ranging from NAFLD to HCC. For instance, GPR120 is a functional receptor for ω-3 fatty acids that show strong anti-inflammatory and anti-insulin resistance effects. Oh *et al*[46] reported that GPR120 agonist cpdA treatment increased insulin sensitivity and glucose tolerance and decreased hepatic steatosis in HFD-induced obese mice[46].

GPR49, an orphan GPCR with unknown ligands, is highly expressed in human HCC cell lines PLC/PRF/5 and HepG2[47]. In addition, overexpression of GPR49 has been shown in HCC tissue with a mutation of beta-catenin exon three. Another orphan GPCR receptor, GPR137, is also broadly expressed in human liver cancer cell lines,

Table 1 The role of G protein-coupled receptors in nonalcoholic fatty liver disease, nonalcoholic steatohepatitis, and hepatocellular carcinoma

Liver disease	GPCRs	Expression	Ref.
NAFLD/Steatosis	GPR120	GPR120 agonist cpdA treatment increased insulin sensitivity and glucose tolerance and decreased hepatic steatosis in HFD-induced obese mice	[46]
HCC	GPR49	GPR49 is highly expressed in human HCC cell lines PLC/PRF/5 and HepG2; overexpression of GPR49 in HCC tissue with a mutation of beta-catenin exon 3 was also shown	[47]
HCC	GPR137	Knockdown of GPR137 in HepG2 cells induced cell cycle arrest and cell apoptosis. Additionally, low expression of GPR137 indicated the progression of human HCC and a low survival rate	[49]
NAFLD/Steatosis	GPR132	GPR132 was involved in hepatic lipid metabolism and gallstone formation in mice because GPR132-deficient mice fed a lithogenic diet quickly developed gallstones and had a high cholesterol saturation index	[51]
NAFLD/Steatosis	GPR55	GPR55-deficient (GPR55$^{-/-}$) mice showed impaired insulin signaling and had a significant increase in total body fat and liver fatty acid synthase, resulting in the development of hepatic steatosis	[53]
NASH/Fibrosis	GPR91	Succinate in the fatty liver can activate HSC *via* GPR91 receptor, resulting in NASH progression	[45]
Liver injury/Fibrosis	GPBAR1	GPBAR1 is an upstream regulator of the axis expression of chemokine CCL2 and its receptor CCR2 in the interface of liver sinusoidal cells	[54]

GPCRs: G protein-coupled receptors; HCC: Hepatocellular carcinoma; HFD: High-fat diet; HSC: Hepatic stellate cell; NAFLD: Nonalcoholic fatty liver disease; NASH: Nonalcoholic steatohepatitis.

such as HepG2 and Bel7404. The depletion of GPR137 by lentivirus-mediated RNA interference in these two cell lines remarkably inhibited the proliferation and colony formation capacity[48]. Knockdown of GPR137 in HepG2 cells resulted in cell cycle arrest and cell apoptosis, suggesting that targeting GPR137 can inhibit cancer growth. Moreover, low expression of GPR137 indicated the progression of human HCC and low survival rates[49].

GPR132 or G2A receptor is a proton-sensing GPCR and plays an important role in cell cycle and proliferation, oncogenesis, and the immune response[50]. GPR132 is also involved in hepatic lipid metabolism and gallstone formation in mice because GPR132-deficient mice fed a lithogenic diet quickly developed gallstones and had a high cholesterol saturation index[51].

Not all GPCRs have a protective effect against liver disease. Succinate was increased in fatty liver cells of high fat/calorie diet plus high fructose and glucose in drinking water-fed mice[45]. Exposure of succinate upregulated the expression of GPR91 in primary and immortalized HSCs and increased the expression of ECM proteins of these cells. Inhibiting GPR91 expression by lentivirus harboring shRNA reduced succinate-mediated HSC activation. Meanwhile, the expression of GPR91 was correlated with the severity of fibrosis in human NASH biopsy specimens[45]. GPR55 and its endogenous ligand, l-α-lysophosphatidylinositol are positively correlated with obesity and type 2 diabetes (T2D)[52]. Moreover, GPR55-deficient (GPR55$^{-/-}$) mice showed impaired insulin signaling evidenced by reduced phosphorylation of protein kinase B and its downstream targets and had a significant increase in total body fat and liver fatty acid synthase, which can result in the development of hepatic steatosis[53]. In the same study, the author also found that lysophosphatidylinositol activated rat H4IIE liver cells and human HepG2 liver cells *via* GPR55 to enhance insulin-dependent protein kinase B phosphorylation. Deletion of GPBAR1, a GPCR for secondary BAs, accelerated the severity of liver injury caused by acetaminophen[54]. Further, GPBAR1 agonism mediated the axis expression of chemokine CCL2 and its receptor CCR2 in the interface of liver sinusoidal cells.

GPCR signaling and regulatory proteins

Generally, GPCRs are linked to distinct families of G proteins, including Gs, Gi, and Gq[55]. For example, the glucagon receptor most highly expressed in hepatocytes is linked to the stimulatory G proteins, Gs. Heterotrimeric G proteins are involved in the signaling of approximately 800 GPCR family members[56]. Some of these signaling pathways play an important role in liver metabolism. For instance, $G\alpha_{12}$ protein ($G\alpha_{12}$) ablation significantly increases fasting-induced fat accumulation in the liver of mice, and $G\alpha_{12}$ expression is also decreased in liver biopsies of NAFLD patients[16]. A mechanistic study showed that $G\alpha_{12}$ regulated mitochondrial respiration through modulating sirtuin 1 and peroxisome proliferator-activated receptor alpha expression. Moreover, the expression of $G\alpha_{12}$ has been associated with the overall survival of HCC

patients[57]. Understanding the role of G proteins in the liver also helps unlock the role of GPCRs in liver metabolism and disease progression.

Regulators of G protein signaling (RGS) proteins negatively regulate GPCR signaling. RGS5 can protect against NAFLD and NASH. In the liver, RGS5 is an essential molecule that protects against the progression of NAFLD. RGS5 directly binds to transforming growth factor beta-activated kinase 1 (TAK1) and inhibits its phosphorylation and the subsequent c-Jun N-terminal kinase/p38 pathways. RGS5 is a promising target molecule for fine-tuning the activity of transforming growth factor beta-activated kinase 1 and NAFLD treatment[58].

Activated HSCs are one of the major sources of myofibroblasts in many types of liver injury[59], which produce ECM proteins. GPCR-mediated signaling plays an important role in HSC contraction, migration, and activation. Bahrami *et al*[60] reported that RGS5 can regulate GPCR signaling in HSCs and modulate HSC activation and hepatic fibrogenesis[60]. RGS6$^{-/-}$ mice showed reduced alcohol consumption when given free access to alcohol. RGS6$^{-/-}$ mice were also protected from alcohol-induced hepatic steatosis, cardiac toxicity, dysfunction of the gut barrier, and endotoxemia when they were forced to consume alcohol[61]. Another study showed that overexpression of RGS16, specifically in the liver, displayed fatty liver after overnight fasting but low blood glucose levels compared with wild-type mice[62]. In contrast, RGS16-knockout mice showed a higher rate of fatty acid oxidation in liver extracts compared with wild-type mice, suggesting that RGS16 inhibits GPCR-mediated fatty acid oxidation. Therefore, RGS is a group of therapeutic candidates for modulating GPCRs to treat liver disease.

The signaling of most GPCRs *via* G proteins is regulated by GPCR kinases (GRKs)[63], which also function in the pathogenesis of liver injury. For instance, GRK2 hemizygous (GRK2$^{+/-}$) mice showed a reduced level of triglycerides and a reduced liver-to-body weight ratio compared to wild-type mice when fed a methionine and choline-deficient diet[64]. Increased GRK2 protein and mRNA levels were also detected in human liver biopsies of steatosis and NASH patients. Moreover, high GRK2 expression exaggerated palmitic acid-triggered lipid accumulation in human hepatocytes[64].

Gut microbiota-mediated GPCR expression

The gut–liver axis plays a critical role in the development of liver diseases[65,66]. Gut microbiota-derived metabolites and their associated signaling pathways play important roles in NAFLD development[67]. Rau *et al*[68] reported that SCFA-producing bacteria were dominant in the fecal bacteria of NAFLD patients, accompanying high acetate and propionate in fecal metabolites[68]. These metabolites are associated with immunological features in NAFLD progression. Manipulation of gut microbiota is a promising preventive and therapeutic strategy for NAFLD. For instance, administration of a bacterial cocktail, consisting of three strains of *Bifidobacterium adolescentis* and three strains of *Lactobacillus rhamnosus*, alleviated a high-fat, high-cholesterol diet-induced NAFLD symptom in mice by increasing the concentration of intestinal SCFAs[69]. Similar findings have also been achieved in clinical trials for human patients[70,71]. Gut microbiota-derived metabolites contribute to the development of NAFLD, including SCFAs[68], endogenous alcohol[72,73], and BAs[74,75]. Gut microbiota in the colon is the main source of the production of SCFAs[76,77], which affect lipid and glucose metabolism. It has been demonstrated that both BAs[78] and SCFAs[79] can activate GPCRs to modulate immune responses. Hence, modulating gut microbiota is an attractive strategy to interfere with liver disease.

For example, farnesoid X receptor agonist fexaramine-induced lithocholic acid-producing bacteria *Acetatifactor* and *Bacteroides* impact liver bile acid synthesis, which in turn can enhance the expression of intestinal farnesoid X receptor targeted genes[80]. In hepatocytes, palmitate can be metabolized to sphingosine 1-phosphate (S1P), which binds to different types of S1P receptors (S1PRs) like S1PR1-3 to activate HSCs to myofibroblasts[81]. In addition, S1P can increase the recruitment of bone marrow mesenchymal stem cells *via* activating S1PRs to produce proinflammatory cytokines IL-1β, tumor necrosis factor alpha, and IL-6, resulting in acceleration of the pathophysiological process of liver disease[82]. The S1P-S1PR1 axis is also associated with chronic intestinal inflammation and colitis-associated cancer by modulating IL-6 and transcription factor STAT3[83].

In addition to liver disease, gut microbiota-associated products affect other diseases, such as inflammatory bowel disease, diabetes, autoimmune disease, and cardiovascular disease, through GPCRs[84-86]. For example, tryptamine, a tryptophan-derived monoamine produced by gut bacteria like *Bacteroides thetaiotaomicron* can activate the serotonin 5-HT$_4$ receptor, which is uniquely expressed in colonic epithelial

cells to increase ionic flux across colonic epithelium, altering the host gut transmit[87]. Increasing evidence shows that the microbiota plays a crucial role in influencing host appetite and eating-relative behavior[88]. Of note, the gut–liver axis is bidirectional[10,89] because the liver also impacts the components of gut microbiota (Figure 2) by primary BAs, which may result in a change of appetite[90].

GPCR-BASED THERAPIES FOR LIVER DISEASES

GPCRs are a promising therapy for NAFLD treatment (Table 2). Recently, Pi *et al*[44] reported that Gprc6a$^{Liver\text{-}cko}$ mice (a strain with conditional depletion of GPRC6A in mouse hepatocytes) on a normal diet had excessive liver fat accumulation and impaired glucose and pyruvate tolerance without insulin resistance[44]. Intraperitoneal or oral administration of a peptide hormone metabolitin that binds to GPRC6A significantly ameliorated NAFLD symptoms and inhibited gut triglyceride and cholesterol absorption and insulin resistance *via* activating the 5′ AMP-activated protein kinase signaling pathway[91]. Metabolitin treatment was able to stimulate the expression of GLP-1, which further validated the metabolitin-GPRC6A interaction because the GPRC6A receptor functions as an amino acid sensor mediating GLP-1 secretion in the intestinal L cells[92].

Oral administration of a GPR39 agonist, TC-G1008, inhibited liver injury marker glutamic-pyruvic transaminase expression and reduced hepatic cell necrosis in concanavalin A-induced hepatitis liver in mice[93]. Another study showed that an acute dose of TC-G1008 reduced ethanol intake in mice without affecting total fluid intake[94]. GPR40 deficiency was associated with hepatic inflammation and steatosis in low-fat diet-fed mice[95]. Oral administration of a GPR40 full agonist, SCO-267, reduced liver weight, triglyceride and collagen production, and serum alanine amino-transferase without affecting food intake or glucose levels in choline-deficient, L-amino acid-defined, high-fat diet-fed mice[96]. Furthermore, SCO-267 improved mitochondrial function and beta-oxidation, while inhibiting lipogenesis, inflammation, and generation of reactive oxygen species in the liver.

GPR120 agonist III significantly suppressed macrophage infiltration and reactive oxygen species production and reversed hepatic inflammation, endoplasmic reticulum stress, and apoptosis in high-fat, high-cholesterol diet or methionine and choline-deficient-induced steatohepatitis[97]. In addition, GPR120 agonist TUG-891 inhibited lipid accumulation in hepatocytes[98].

Treatment with docosahexaenoic acid, an omega-3 fatty acid, inhibited lipid droplets by interacting with GPR40 in primary hepatocytes *via* reduced expression of lipogenic enzymes, such as fatty acid synthase, acetyl-CoA carboxylase, and stearoyl-CoA desaturase-1[99]. PBI-4547, a fatty acid mimetic, is a GPR84 antagonist. In a mouse model of diet-induced obesity, PBI-4547 treatment ameliorated NAFLD-associated metabolic dysregulation and hepatic steatosis and ballooning, which was depleted in GPR84$^{-/-}$ mice[100]. PBI-4547 increased liver fatty acid oxidation and gene expression of mitochondrial uncoupling proteins. Another study showed that inhibition of GPR84 with antagonists CpdA and CpdB significantly reduced myeloid cell infiltration and ameliorated inflammation and fibrosis in acute liver injury[101]. GPR43-deficient mice became obese when fed a normal diet. In contrast, mice with GPR43 overexpressed specifically in adipose tissue remained lean even on a high-fat diet[30]. Oral administration of compound probiotics ameliorated HFD-induced gut microbe dysbiosis and chronic metabolic inflammation in NAFLD rats *via* GPR43[102].

URGENT NEED FOR CLINICAL TRIALS

GPCRs, as the largest group of transmembrane receptors[103], play important roles in various diseases, including inflammatory bowel diseases[104,105], kidney diseases[106], liver diseases[107], bone disease[6], central nervous system disorders[108], heart diseases[109], and respiratory diseases[110]. To date, about fifty GPCR targeting peptides have been approved to treat metabolic diseases and tumors[111]. With the analysis of public databases, Sriram and Insel[112] reported that about 35% of approved drugs target GPCRs[112]. GPCRs and GPCR-associated proteins consist of about 17% of all protein targets for approved drugs. The application of GPCRs has been tested in clinical trials for metabolic disorders[113,114], including obesity and diabetes.

For example, T2D patients aged 20 or older orally received 75 mg of GPR119 agonist DS-8500a daily for 4 wk, resulting in enhanced insulin secretory capacity compared to

Table 2 G protein-coupled receptor-mediated treatment in nonalcoholic fatty liver disease

GPCRs	Treatment	Study	Effect	Ref.
GPRC6A	Metabolitin, a peptide hormone	Mice	Specifically deleting Gprc6a in mouse hepatocytes caused hepatic fat accumulation. Metabolitin can significantly ameliorate NAFLD symptoms and inhibit gut triglyceride and cholesterol absorption and insulin resistance *via* GPRC6A-mediated activation of the 5′ AMP-activated protein kinase signaling pathway	[44,91]
GPR39	Agonist TC-G1008	Mice	Oral administration of TC-G1008 inhibited hepatic cell necrosis in concanavalin A-induced hepatitis liver in mice. In addition, acute administration of TC-G1008 reduced ethanol intake	[93,94]
GPR40	Agonist SCO-267	Mice	GPR40 deficiency was associated with hepatic inflammation and steatosis in low-fat diet-fed mice. Oral administration of SCO-267 reduced HFD-induced increase in liver weight, triglyceride and collagen production, and serum alanine aminotransferase	[95,96]
GPR40	Docosahexaenoic acid	Primary hepatocytes, HFD-fed mice	Treatment with DHA, an omega-3 fatty acid, inhibited lipid droplets by interacting with GPR40 in primary hepatocytes *via* reduced expression of lipogenic enzymes. In addition, it significantly reduced the HFD-induced liver steatosis score in mice	[99]
GPR43	Compound probiotics	Rats	Overexpressing GPR43 in adipose tissue kept mice lean on a HFD diet. Compound probiotics can modulate gut microbiota dysbiosis, SCFAs, and their receptors, like GPR43, in NAFLD rats	[30,102]
GPR84	Antagonist PBI-4547GPR84 Antagonists CpdA and CpdB	$Gpr84^{-/-}$ mice; Wild-type mice	PBI-4547 treatment ameliorated NAFLD-associated metabolic dysregulation, hepatic steatosis and ballooning, which was depleted in $Gpr84^{-/-}$ mice. Inhibition of GPR84 with antagonists CpdA and CpdB significantly reduced myeloid cell infiltration and ameliorated inflammation and fibrosis in acute liver injury	[100,101]
GPR120	TUG-891Agonist III	Hepatocytes; Mice	Agonist TUG-891 inhibited lipid accumulation in hepatocytes. Agonist III significantly suppressed macrophage infiltration, ROS production, hepatic inflammation, ER stress, and steatohepatitis	[97,98]

DHA: Docosahexaenoic acid; ER: endoplasmic reticulum; GPCRs: G protein-coupled receptors; HFD: High-fat diet; NAFLD: Nonalcoholic fatty liver disease; NASH: Nonalcoholic steatohepatitis; ROS: Reactive oxygen species; SCFA: Short-chain fatty acid.

placebo treatment[114]. In addition, DS-8500a significantly reduced total cholesterol, low-density lipoprotein cholesterol, and triglyceride concentrations and significantly increased high-density lipoprotein cholesterol concentrations compared to placebo treatment. No significant treatment-associated adverse events occurred in this trial. Another phase 2 clinical trial showed that daily treatment of GPR40 agonist Fasiglifam for 12 wk significantly improved glycemic control in T2D patients who were not responsible to diet or metformin treatment compared to placebo treatment, evidenced by the reduction of hemoglobin A(1c) from baseline[115]. In addition, Fasiglifam did not cause a higher risk of hypoglycemic events in patients.

However, our current knowledge about the function of GPCRs in liver metabolism disorders is still limited. When considering potential drugs for treatments, even fewer candidates have been tested in clinical trials. Some experimental trials in rodents have been investigated to explore the role of GPCRs in liver diseases, such as GPR40[99] and GPR43[102]. Some of the GPCRs, such as prostaglandin E2 receptors[116] and beta-2 adrenergic receptor[117], have been investigated in preclinical studies using tissue biopsies of human patients. Meanwhile, the side effects of GPCR-targeted molecules need to be considered when designing new therapeutic agents. For example, Fasiglifam increased the ratio of liver enzymes aspartate aminotransferase/alanine transaminase in T2D patients compared to placebo treatment while being evaluated for cardiovascular safety in a phase 3 trial[118].

CONCLUSION

Many GPCRs have critical roles in metabolic disorders, including NAFLD, through their function as receptors for metabolites, such as SCFAs and BAs. GPCR-mediated signaling pathways are involved in hepatic lipid accumulation and fibrogenesis and can also modulate the secretion of gut hormones (*e.g.*, GLP-1), which further impacts liver function, suggesting that GPCRs play a pivotal role in the gut–liver axis. Furthermore, GPCRs and their associated molecules are candidates as biomarkers for NAFLD diagnosis. Overall, GPCRs and their regulating factors provide potential pharmacological targets for NAFLD treatment.

There are several advantages to targeting GPCRs to treat NAFLD compared with other NAFLD therapeutics. First, therapeutic candidates or drugs can be easily found.

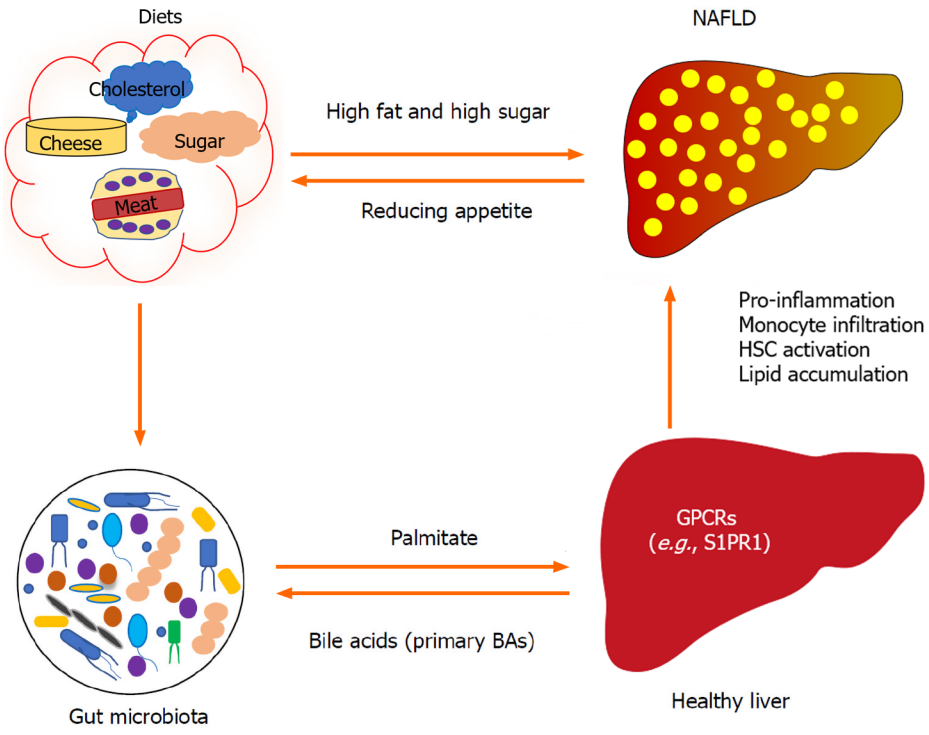


Figure 2 G protein-coupled receptor-mediated interaction of the gut and liver. Gut microbiota-derived metabolites or molecules (*e.g.*, palmitate) impact liver function by being metabolized to sphingosine 1-phosphate in hepatocytes, which can stimulate the activation of hepatic stellate cells (HSCs) and proinflammation *via* sphingosine 1-phosphate receptor 1 (S1PR1). In turn, primary bile acids (BAs) are synthesized in the liver, which can also influence the components of gut microbiota. A high fat and high sugar diet can induce nonalcoholic fatty liver disease (NAFLD) and change gut microbiota. Gut microbiota has been shown to impact appetite, and the progression of NAFLD may also impact the appetite. GPCRs: G protein-coupled receptors.

The data from public databases (ChEMBL, Guide to PHARMACOLOGY/GtoPdb, and DrugBank) show that about 35% of approved drugs target GPCRs[112]. Second, functional selection of GPCR ligands helps minimize the potential side effects of selected treatment[119]. Third, GPCRs are implicated in the development and progression of NAFLD, including lipid metabolism, proinflammation, and fibrosis. Therefore, targeting GPCR can be applied to different stages of NAFLD therapy, ranging from simple steatosis to NASH. However, current GPCR-mediated treatments in hepatic steatosis, liver fibrosis, and liver cancer are mainly performed either in cells or animals. Few preclinical and clinical trials in humans have been carried out so far. More work is needed to unmask the role of GPCRs in the clinic.

The structures of GPCRs are critically important for de novo design of GPCR targeting drugs. However, only about 60 GPCR structures have been resolved with the advanced technologies like X-ray crystallography and cryo-electron microscopy[120]. A new protocol has optimized the precrystallization process for resolving GPCR structures *via* X-ray crystallography[121]. Some technologies such as cell-based electrical impedance also help identify GPCR-targeting molecules[122]. In addition, computer-based design of GPCR allosteric receptors helps reveal the unknown GPCR signaling pathways and the relative molecular mechanism[123]. In conclusion, advanced technologies help unravel the clear role of each GPCR in both physiological and pathological environment to accelerate GPCR-mediated therapy.

REFERENCES

1 **Aron-Wisnewsky J**, Vigliotti C, Witjes J, Le P, Holleboom AG, Verheij J, Nieuwdorp M, Clément K. Gut microbiota and human NAFLD: disentangling microbial signatures from metabolic disorders. *Nat Rev Gastroenterol Hepatol* 2020; **17**: 279-297 [PMID: 32152478 DOI: 10.1038/s41575-020-0269-9]

2 **Friedman SL**, Neuschwander-Tetri BA, Rinella M, Sanyal AJ. Mechanisms of NAFLD development and therapeutic strategies. *Nat Med* 2018; **24**: 908-922 [PMID: 29967350 DOI: 10.1038/s41591-018-0104-9]

3 **Lindenmeyer CC**, McCullough AJ. The Natural History of Nonalcoholic Fatty Liver Disease-An Evolving View. *Clin Liver Dis* 2018; **22**: 11-21 [PMID: 29128051 DOI: 10.1016/j.cld.2017.08.003]

4 **Marra F**, Svegliati-Baroni G. Lipotoxicity and the gut-liver axis in NASH pathogenesis. *J Hepatol* 2018; **68**: 280-295 [PMID: 29154964 DOI: 10.1016/j.jhep.2017.11.014]

5 **Gottlieb A**, Canbay A. Why Bile Acids Are So Important in Non-Alcoholic Fatty Liver Disease (NAFLD) Progression. *Cells* 2019; **8** [PMID: 31671697 DOI: 10.3390/cells8111358]

6 **Luo J**, Sun P, Siwko S, Liu M, Xiao J. The role of GPCRs in bone diseases and dysfunctions. *Bone Res* 2019; **7**: 19 [PMID: 31646011 DOI: 10.1038/s41413-019-0059-6]

7 **Peng WT**, Sun WY, Li XR, Sun JC, Du JJ, Wei W. Emerging Roles of G Protein-Coupled Receptors in Hepatocellular Carcinoma. *Int J Mol Sci* 2018; **19** [PMID: 29734668 DOI: 10.3390/ijms19051366]

8 **Yoshimoto S**, Loo TM, Atarashi K, Kanda H, Sato S, Oyadomari S, Iwakura Y, Oshima K, Morita H, Hattori M, Honda K, Ishikawa Y, Hara E, Ohtani N. Obesity-induced gut microbial metabolite promotes liver cancer through senescence secretome. *Nature* 2013; **499**: 97-101 [PMID: 23803760 DOI: 10.1038/nature12347]

9 **Zhang C**, Yang M, Ericsson AC. Antimicrobial Peptides: Potential Application in Liver Cancer. *Front Microbiol* 2019; **10**: 1257 [PMID: 31231341 DOI: 10.3389/fmicb.2019.01257]

10 **Tripathi A**, Debelius J, Brenner DA, Karin M, Loomba R, Schnabl B, Knight R. The gut-liver axis and the intersection with the microbiome. *Nat Rev Gastroenterol Hepatol* 2018; **15**: 397-411 [PMID: 29748586 DOI: 10.1038/s41575-018-0011-z]

11 **de Aguiar Vallim TQ**, Tarling EJ, Edwards PA. Pleiotropic roles of bile acids in metabolism. *Cell Metab* 2013; **17**: 657-669 [PMID: 23602448 DOI: 10.1016/j.cmet.2013.03.013]

12 **Chiang JYL**, Ferrell JM. Bile acid receptors FXR and TGR5 signaling in fatty liver diseases and therapy. *Am J Physiol Gastrointest Liver Physiol* 2020; **318**: G554-G573 [PMID: 31984784 DOI: 10.1152/ajpgi.00223.2019]

13 **Donepudi AC**, Boehme S, Li F, Chiang JY. G-protein-coupled bile acid receptor plays a key role in bile acid metabolism and fasting-induced hepatic steatosis in mice. *Hepatology* 2017; **65**: 813-827 [PMID: 27351453 DOI: 10.1002/hep.28707]

14 **Rosenbaum DM**, Rasmussen SG, Kobilka BK. The structure and function of G-protein-coupled receptors. *Nature* 2009; **459**: 356-363 [PMID: 19458711 DOI: 10.1038/nature08144]

15 **Blad CC**, Tang C, Offermanns S. G protein-coupled receptors for energy metabolites as new therapeutic targets. *Nat Rev Drug Discov* 2012; **11**: 603-619 [PMID: 22790105 DOI: 10.1038/nrd3777]

16 **Kim TH**, Yang YM, Han CY, Koo JH, Oh H, Kim SS, You BH, Choi YH, Park TS, Lee CH, Kurose H, Noureddin M, Seki E, Wan YY, Choi CS, Kim SG. Gα12 ablation exacerbates liver steatosis and obesity by suppressing USP22/SIRT1-regulated mitochondrial respiration. *J Clin Invest* 2018; **128**: 5587-5602 [PMID: 30300140 DOI: 10.1172/JCI97831]

17 **Li X**, Millar JS, Brownell N, Briand F, Rader DJ. Modulation of HDL metabolism by the niacin receptor GPR109A in mouse hepatocytes. *Biochem Pharmacol* 2010; **80**: 1450-1457 [PMID: 20655299 DOI: 10.1016/j.bcp.2010.07.023]

18 **Gu YJ**, Sun WY, Zhang S, Wu JJ, Wei W. The emerging roles of β-arrestins in fibrotic diseases. *Acta Pharmacol Sin* 2015; **36**: 1277-1287 [PMID: 26388156 DOI: 10.1038/aps.2015.74]

19 **Montgomery MK**, Osborne B, Brown SH, Small L, Mitchell TW, Cooney GJ, Turner N. Contrasting metabolic effects of medium- versus long-chain fatty acids in skeletal muscle. *J Lipid Res* 2013; **54**: 3322-3333 [PMID: 24078708 DOI: 10.1194/jlr.M040451]

20 **Thombare K**, Ntika S, Wang X, Krizhanovskii C. Long chain saturated and unsaturated fatty acids exert opposing effects on viability and function of GLP-1-producing cells: Mechanisms of lipotoxicity. *PLoS One* 2017; **12**: e0177605 [PMID: 28520810 DOI: 10.1371/journal.pone.0177605]

21 **Hirasawa A**, Tsumaya K, Awaji T, Katsuma S, Adachi T, Yamada M, Sugimoto Y, Miyazaki S, Tsujimoto G. Free fatty acids regulate gut incretin glucagon-like peptide-1 secretion through GPR120. *Nat Med* 2005; **11**: 90-94 [PMID: 15619630 DOI: 10.1038/nm1168]

22 **Guo C**, Huang T, Chen A, Chen X, Wang L, Shen F, Gu X. Glucagon-like peptide 1 improves insulin resistance in vitro through anti-inflammation of macrophages. *Braz J Med Biol Res* 2016; **49**: e5826 [PMID: 27878229 DOI: 10.1590/1414-431X20165826]

23 **Patel V**, Joharapurkar A, Kshirsagar S, Sutariya B, Patel M, Patel H, Pandey D, Patel D, Ranvir R, Kadam S, Bahekar R, Jain M. Coagonist of GLP-1 and Glucagon Receptor Ameliorates Development of Non-Alcoholic Fatty Liver Disease. *Cardiovasc Hematol Agents Med Chem* 2018; **16**: 35-43 [PMID: 29357809 DOI: 10.2174/1871525716666180118152158]

24 **Valdecantos MP**, Pardo V, Ruiz L, Castro-Sánchez L, Lanzón B, Fernández-Millán E, García-Monzón C, Arroba AI, González-Rodríguez Á, Escrivá F, Álvarez C, Rupérez FJ, Barbas C, Konkar A, Naylor J, Hornigold D, Santos AD, Bednarek M, Grimsby J, Rondinone CM, Valverde ÁM. A novel glucagon-like peptide 1/glucagon receptor dual agonist improves steatohepatitis and liver regeneration in mice. *Hepatology* 2017; **65**: 950-968 [PMID: 27880981 DOI: 10.1002/hep.28962]

25 **Ou HY**, Wu HT, Lu FH, Su YC, Hung HC, Wu JS, Yang YC, Wu CL, Chang CJ. Activation of free fatty acid receptor 1 improves hepatic steatosis through a p38-dependent pathway. *J Mol Endocrinol* 2014; **53**: 165-174 [PMID: 25008074 DOI: 10.1530/JME-14-0003]

26 **Li M**, Meng X, Xu J, Huang X, Li H, Li G, Wang S, Man Y, Tang W, Li J. GPR40 agonist ameliorates liver X receptor-induced lipid accumulation in liver by activating AMPK pathway. *Sci Rep* 2016; **6**: 25237 [PMID: 27121981 DOI: 10.1038/srep25237]

27 **Sartorius T**, Drescher A, Panse M, Lastovicka P, Peter A, Weigert C, Kostenis E, Ullrich S, Häring HU. Mice Lacking Free Fatty Acid Receptor 1 (GPR40/FFAR1) are Protected Against Conjugated

Linoleic Acid-Induced Fatty Liver but Develop Inflammation and Insulin Resistance in the Brain. *Cell Physiol Biochem* 2015; **35**: 2272-2284 [PMID: 25895678 DOI: 10.1159/000374031]

28 **Schmidt J**, Liebscher K, Merten N, Grundmann M, Mielenz M, Sauerwein H, Christiansen E, Due-Hansen ME, Ulven T, Ullrich S, Gomeza J, Drewke C, Kostenis E. Conjugated linoleic acids mediate insulin release through islet G protein-coupled receptor FFA1/GPR40. *J Biol Chem* 2011; **286**: 11890-11894 [PMID: 21339298 DOI: 10.1074/jbc.C110.200477]

29 **Ichimura A**, Hirasawa A, Poulain-Godefroy O, Bonnefond A, Hara T, Yengo L, Kimura I, Leloire A, Liu N, Iida K, Choquet H, Besnard P, Lecoeur C, Vivequin S, Ayukawa K, Takeuchi M, Ozawa K, Tauber M, Maffeis C, Morandi A, Buzzetti R, Elliott P, Pouta A, Jarvelin MR, Körner A, Kiess W, Pigeyre M, Caiazzo R, Van Hul W, Van Gaal L, Horber F, Balkau B, Lévy-Marchal C, Rouskas K, Kouvatsi A, Hebebrand J, Hinney A, Scherag A, Pattou F, Meyre D, Koshimizu TA, Wolowczuk I, Tsujimoto G, Froguel P. Dysfunction of lipid sensor GPR120 leads to obesity in both mouse and human. *Nature* 2012; **483**: 350-354 [PMID: 22343897 DOI: 10.1038/nature10798]

30 **Kimura I**, Ozawa K, Inoue D, Imamura T, Kimura K, Maeda T, Terasawa K, Kashihara D, Hirano K, Tani T, Takahashi T, Miyauchi S, Shioi G, Inoue H, Tsujimoto G. The gut microbiota suppresses insulin-mediated fat accumulation *via* the short-chain fatty acid receptor GPR43. *Nat Commun* 2013; **4**: 1829 [PMID: 23652017 DOI: 10.1038/ncomms2852]

31 **Vinolo MA**, Rodrigues HG, Nachbar RT, Curi R. Regulation of inflammation by short chain fatty acids. *Nutrients* 2011; **3**: 858-876 [PMID: 22254083 DOI: 10.3390/nu3100858]

32 **Li M**, van Esch BCAM, Henricks PAJ, Folkerts G, Garssen J. The Anti-inflammatory Effects of Short Chain Fatty Acids on Lipopolysaccharide- or Tumor Necrosis Factor α-Stimulated Endothelial Cells *via* Activation of GPR41/43 and Inhibition of HDACs. *Front Pharmacol* 2018; **9**: 533 [PMID: 29875665 DOI: 10.3389/fphar.2018.00533]

33 **Zhao S**, Jang C, Liu J, Uehara K, Gilbert M, Izzo L, Zeng X, Trefely S, Fernandez S, Carrer A, Miller KD, Schug ZT, Snyder NW, Gade TP, Titchenell PM, Rabinowitz JD, Wellen KE. Dietary fructose feeds hepatic lipogenesis *via* microbiota-derived acetate. *Nature* 2020; **579**: 586-591 [PMID: 32214246 DOI: 10.1038/s41586-020-2101-7]

34 **Takai A**, Kikuchi K, Ichimura M, Tsuneyama K, Moritoki Y, Matsumoto K, Tsunashima H, Onda T, Kuniyoshi N, Nariyama T, Ohyatsu S, Kubota J, Nagumo K, Sato S, Hara M, Miyakawa H. Fructo-oligosaccharides ameliorate steatohepatitis, visceral adiposity, and associated chronic inflammation *via* increased production of short-chain fatty acids in a mouse model of non-alcoholic steatohepatitis. *BMC Gastroenterol* 2020; **20**: 46 [PMID: 32103741 DOI: 10.1186/s12876-020-01194-2]

35 **Perez MJ**, Briz O. Bile-acid-induced cell injury and protection. *World J Gastroenterol* 2009; **15**: 1677-1689 [PMID: 19360911 DOI: 10.3748/wjg.15.1677]

36 **Chiang JY**. Bile acid metabolism and signaling. *Compr Physiol* 2013; **3**: 1191-1212 [PMID: 23897684 DOI: 10.1002/cphy.c120023]

37 **Jia W**, Xie G, Jia W. Bile acid-microbiota crosstalk in gastrointestinal inflammation and carcinogenesis. *Nat Rev Gastroenterol Hepatol* 2018; **15**: 111-128 [PMID: 29018272 DOI: 10.1038/nrgastro.2017.119]

38 **Klindt C**, Reich M, Hellwig B, Stindt J, Rahnenführer J, Hengstler JG, Köhrer K, Schoonjans K, Häussinger D, Keitel V. The G Protein-Coupled Bile Acid Receptor TGR5 (Gpbar1) Modulates Endothelin-1 Signaling in Liver. *Cells* 2019; **8** [PMID: 31752395 DOI: 10.3390/cells8111467]

39 **Willis KA**, Gomes CK, Rao P, Micic D, Moran ER 3rd, Stephenson E, Puchowicz M, Al Abdallah Q, Mims TS, Gosain A, Yin D, Talati AJ, Chang EB, Han JC, Pierre JF. TGR5 signaling mitigates parenteral nutrition-associated liver disease. *Am J Physiol Gastrointest Liver Physiol* 2020; **318**: G322-G335 [PMID: 31905022 DOI: 10.1152/ajpgi.00216.2019]

40 **Meixiong J**, Vasavda C, Snyder SH, Dong X. MRGPRX4 is a G protein-coupled receptor activated by bile acids that may contribute to cholestatic pruritus. *Proc Natl Acad Sci U S A* 2019; **116**: 10525-10530 [PMID: 31068464 DOI: 10.1073/pnas.1903316116]

41 **Larraufie P**, Martin-Gallausiaux C, Lapaque N, Dore J, Gribble FM, Reimann F, Blottiere HM. SCFAs strongly stimulate PYY production in human enteroendocrine cells. *Sci Rep* 2018; **8**: 74 [PMID: 29311617 DOI: 10.1038/s41598-017-18259-0]

42 **Tolhurst G**, Heffron H, Lam YS, Parker HE, Habib AM, Diakogiannaki E, Cameron J, Grosse J, Reimann F, Gribble FM. Short-chain fatty acids stimulate glucagon-like peptide-1 secretion *via* the G-protein-coupled receptor FFAR2. *Diabetes* 2012; **61**: 364-371 [PMID: 22190648 DOI: 10.2337/db11-1019]

43 **Khound R**, Taher J, Baker C, Adeli K, Su Q. GLP-1 Elicits an Intrinsic Gut-Liver Metabolic Signal to Ameliorate Diet-Induced VLDL Overproduction and Insulin Resistance. *Arterioscler Thromb Vasc Biol* 2017; **37**: 2252-2259 [PMID: 29074588 DOI: 10.1161/ATVBAHA.117.310251]

44 **Pi M**, Xu F, Ye R, Nishimoto SK, Williams RW, Lu L, Darryl Quarles L. Role of GPRC6A in Regulating Hepatic Energy Metabolism in Mice. *Sci Rep* 2020; **10**: 7216 [PMID: 32350388 DOI: 10.1038/s41598-020-64384-8]

45 **Liu XJ**, Xie L, Du K, Liu C, Zhang NP, Gu CJ, Wang Y, Abdelmalek MF, Dong WY, Liu XP, Niu C, Yang C, Diehl AM, Wu J. Succinate-GPR-91 receptor signalling is responsible for nonalcoholic steatohepatitis-associated fibrosis: Effects of DHA supplementation. *Liver Int* 2020; **40**: 830-843 [PMID: 31903720 DOI: 10.1111/liv.14370]

46 **Oh DY**, Walenta E, Akiyama TE, Lagakos WS, Lackey D, Pessentheiner AR, Sasik R, Hah N, Chi TJ, Cox JM, Powels MA, Di Salvo J, Sinz C, Watkins SM, Armando AM, Chung H, Evans RM,

Quehenberger O, McNelis J, Bogner-Strauss JG, Olefsky JM. A Gpr120-selective agonist improves insulin resistance and chronic inflammation in obese mice. *Nat Med* 2014; **20**: 942-947 [PMID: 24997608 DOI: 10.1038/nm.3614]

47 **Yamamoto Y**, Sakamoto M, Fujii G, Tsuiji H, Kenetaka K, Asaka M, Hirohashi S. Overexpression of orphan G-protein-coupled receptor, Gpr49, in human hepatocellular carcinomas with beta-catenin mutations. *Hepatology* 2003; **37**: 528-533 [PMID: 12601349 DOI: 10.1053/jhep.2003.50029]

48 **Shao X**, Liu Y, Huang H, Zhuang L, Luo T, Huang H, Ge X. Down-regulation of G protein-coupled receptor 137 by RNA interference inhibits cell growth of two hepatoma cell lines. *Cell Biol Int* 2015; **39**: 418-426 [PMID: 25490967 DOI: 10.1002/cbin.10412]

49 **Liu F**, Zhu C, Huang X, Cai J, Wang H, Wang X, He S, Liu C, Yang X, Zhang Y, Zhang T. A low level of GPR37 is associated with human hepatocellular carcinoma progression and poor patient survival. *Pathol Res Pract* 2014; **210**: 885-892 [PMID: 25169131 DOI: 10.1016/j.prp.2014.07.011]

50 **Murakami N**, Yokomizo T, Okuno T, Shimizu T. G2A is a proton-sensing G-protein-coupled receptor antagonized by lysophosphatidylcholine. *J Biol Chem* 2004; **279**: 42484-42491 [PMID: 15280385 DOI: 10.1074/jbc.M406561200]

51 **Johnson LE**, Elias MS, Bolick DT, Skaflen MD, Green RM, Hedrick CC. The G protein-coupled receptor G2A: involvement in hepatic lipid metabolism and gallstone formation in mice. *Hepatology* 2008; **48**: 1138-1148 [PMID: 18821587 DOI: 10.1002/hep.22433]

52 **Moreno-Navarrete JM**, Catalán V, Whyte L, Díaz-Arteaga A, Vázquez-Martínez R, Rotellar F, Guzmán R, Gómez-Ambrosi J, Pulido MR, Russell WR, Imbernón M, Ross RA, Malagón MM, Dieguez C, Fernández-Real JM, Frühbeck G, Nogueiras R. The L-α-lysophosphatidylinositol/GPR55 system and its potential role in human obesity. *Diabetes* 2012; **61**: 281-291 [PMID: 22179809 DOI: 10.2337/db11-0649]

53 **Lipina C**, Walsh SK, Mitchell SE, Speakman JR, Wainwright CL, Hundal HS. GPR55 deficiency is associated with increased adiposity and impaired insulin signaling in peripheral metabolic tissues. *FASEB J* 2019; **33**: 1299-1312 [PMID: 30148676 DOI: 10.1096/fj.201800171R]

54 **Biagioli M**, Carino A, Fiorucci C, Marchianò S, Di Giorgio C, Bordoni M, Roselli R, Baldoni M, Distrutti E, Zampella A, Fiorucci S. The Bile Acid Receptor GPBAR1 Modulates CCL2/CCR2 Signaling at the Liver Sinusoidal/Macrophage Interface and Reverses Acetaminophen-Induced Liver Toxicity. *J Immunol* 2020; **204**: 2535-2551 [PMID: 32213564 DOI: 10.4049/jimmunol.1901427]

55 **Rossi M**, Zhu L, McMillin SM, Pydi SP, Jain S, Wang L, Cui Y, Lee RJ, Cohen AH, Kaneto H, Birnbaum MJ, Ma Y, Rotman Y, Liu J, Cyphert TJ, Finkel T, McGuinness OP, Wess J. Hepatic Gi signaling regulates whole-body glucose homeostasis. *J Clin Invest* 2018; **128**: 746-759 [PMID: 29337301 DOI: 10.1172/JCI94505]

56 **Yang YM**, Kuen DS, Chung Y, Kurose H, Kim SG. $G\alpha_{12/13}$ signaling in metabolic diseases. *Exp Mol Med* 2020; **52**: 896-910 [PMID: 32576930 DOI: 10.1038/s12276-020-0454-5]

57 **Yang YM**, Lee CG, Koo JH, Kim TH, Lee JM, An J, Kim KM, Kim SG. Gα12 overexpressed in hepatocellular carcinoma reduces microRNA-122 expression *via* HNF4α inactivation, which causes c-Met induction. *Oncotarget* 2015; **6**: 19055-19069 [PMID: 25965999 DOI: 10.18632/oncotarget.3957]

58 **Wang J**, Ma J, Nie H, Zhang XJ, Zhang P, She ZG, Li H, Ji YX, Cai J. Hepatic Regulator of G Protein Signaling 5 Ameliorates Nonalcoholic Fatty Liver Disease by Suppressing Transforming Growth Factor Beta-Activated Kinase 1-c-Jun-N-Terminal Kinase/p38 Signaling. *Hepatology* 2020 [PMID: 32191345 DOI: 10.1002/hep.31242]

59 **Kisseleva T**. The origin of fibrogenic myofibroblasts in fibrotic liver. *Hepatology* 2017; **65**: 1039-1043 [PMID: 27859502 DOI: 10.1002/hep.28948]

60 **Bahrami AJ**, Gunaje JJ, Hayes BJ, Riehle KJ, Kenerson HL, Yeung RS, Stempien-Otero AS, Campbell JS, Mahoney WM Jr. Regulator of G-protein signaling-5 is a marker of hepatic stellate cells and expression mediates response to liver injury. *PLoS One* 2014; **9**: e108505 [PMID: 25290689 DOI: 10.1371/journal.pone.0108505]

61 **Stewart A**, Maity B, Anderegg SP, Allamargot C, Yang J, Fisher RA. Regulator of G protein signaling 6 is a critical mediator of both reward-related behavioral and pathological responses to alcohol. *Proc Natl Acad Sci U S A* 2015; **112**: E786-E795 [PMID: 25646431 DOI: 10.1073/pnas.1418795112]

62 **Pashkov V**, Huang J, Parameswara VK, Kedzierski W, Kurrasch DM, Tall GG, Esser V, Gerard RD, Uyeda K, Towle HC, Wilkie TM. Regulator of G protein signaling (RGS16) inhibits hepatic fatty acid oxidation in a carbohydrate response element-binding protein (ChREBP)-dependent manner. *J Biol Chem* 2011; **286**: 15116-15125 [PMID: 21357625 DOI: 10.1074/jbc.M110.216234]

63 **Gurevich VV**, Gurevich EV. GPCR Signaling Regulation: The Role of GRKs and Arrestins. *Front Pharmacol* 2019; **10**: 125 [PMID: 30837883 DOI: 10.3389/fphar.2019.00125]

64 **Cruces-Sande M**, Vila-Bedmar R, Arcones AC, González-Rodríguez Á, Rada P, Gutiérrez-de-Juan V, Vargas-Castrillón J, Iruzubieta P, Sánchez-González C, Formentini L, Crespo J, García-Monzón C, Martínez-Chantar ML, Valverde ÁM, Mayor F Jr, Murga C. Involvement of G protein-coupled receptor kinase 2 (GRK2) in the development of non-alcoholic steatosis and steatohepatitis in mice and humans. *Biochim Biophys Acta Mol Basis Dis* 2018; **1864**: 3655-3667 [PMID: 30261289 DOI: 10.1016/j.bbadis.2018.09.027]

65 **Ohtani N**, Kawada N. Role of the Gut-Liver Axis in Liver Inflammation, Fibrosis, and Cancer: A Special Focus on the Gut Microbiota Relationship. *Hepatol Commun* 2019; **3**: 456-470 [PMID: 30976737 DOI: 10.1002/hep4.1331]

66 **Quesada-Vázquez S**, Aragonès G, Del Bas JM, Escoté X. Diet, Gut Microbiota and Non-Alcoholic Fatty Liver Disease: Three Parts of the Same Axis. *Cells* 2020; **9** [PMID: 31936799 DOI: 10.3390/cells9010176]

67 **Chu H**, Duan Y, Yang L, Schnabl B. Small metabolites, possible big changes: a microbiota-centered view of non-alcoholic fatty liver disease. *Gut* 2019; **68**: 359-370 [PMID: 30171065 DOI: 10.1136/gutjnl-2018-316307]

68 **Rau M**, Rehman A, Dittrich M, Groen AK, Hermanns HM, Seyfried F, Beyersdorf N, Dandekar T, Rosenstiel P, Geier A. Fecal SCFAs and SCFA-producing bacteria in gut microbiome of human NAFLD as a putative link to systemic T-cell activation and advanced disease. *United European Gastroenterol J* 2018; **6**: 1496-1507 [PMID: 30574320 DOI: 10.1177/2050640618804444]

69 **Wang G**, Jiao T, Xu Y, Li D, Si Q, Hao J, Zhao J, Zhang H, Chen W. Bifidobacterium adolescentis and Lactobacillus rhamnosus alleviate non-alcoholic fatty liver disease induced by a high-fat, high-cholesterol diet through modulation of different gut microbiota-dependent pathways. *Food Funct* 2020; **11**: 6115-6127 [PMID: 32573567 DOI: 10.1039/c9fo02905b]

70 **Malaguarnera M**, Vacante M, Antic T, Giordano M, Chisari G, Acquaviva R, Mastrojeni S, Malaguarnera G, Mistretta A, Li Volti G, Galvano F. Bifidobacterium longum with fructo-oligosaccharides in patients with non alcoholic steatohepatitis. *Dig Dis Sci* 2012; **57**: 545-553 [PMID: 21901256 DOI: 10.1007/s10620-011-1887-4]

71 **Alisi A**, Bedogni G, Baviera G, Giorgio V, Porro E, Paris C, Giammaria P, Reali L, Anania F, Nobili V. Randomised clinical trial: The beneficial effects of VSL#3 in obese children with non-alcoholic steatohepatitis. *Aliment Pharmacol Ther* 2014; **39**: 1276-1285 [PMID: 24738701 DOI: 10.1111/apt.12758]

72 **Zhu L**, Baker SS, Gill C, Liu W, Alkhouri R, Baker RD, Gill SR. Characterization of gut microbiomes in nonalcoholic steatohepatitis (NASH) patients: a connection between endogenous alcohol and NASH. *Hepatology* 2013; **57**: 601-609 [PMID: 23055155 DOI: 10.1002/hep.26093]

73 **Yuan J**, Chen C, Cui J, Lu J, Yan C, Wei X, Zhao X, Li N, Li S, Xue G, Cheng W, Li B, Li H, Lin W, Tian C, Zhao J, Han J, An D, Zhang Q, Wei H, Zheng M, Ma X, Li W, Chen X, Zhang Z, Zeng H, Ying S, Wu J, Yang R, Liu D. Fatty Liver Disease Caused by High-Alcohol-Producing Klebsiella pneumoniae. *Cell Metab* 2019; **30**: 675-688. e7 [PMID: 31543403 DOI: 10.1016/j.cmet.2019.08.018]

74 **Puri P**, Daita K, Joyce A, Mirshahi F, Santhekadur PK, Cazanave S, Luketic VA, Siddiqui MS, Boyett S, Min HK, Kumar DP, Kohli R, Zhou H, Hylemon PB, Contos MJ, Idowu M, Sanyal AJ. The presence and severity of nonalcoholic steatohepatitis is associated with specific changes in circulating bile acids. *Hepatology* 2018; **67**: 534-548 [PMID: 28696585 DOI: 10.1002/hep.29359]

75 **Janssen AWF**, Houben T, Katiraei S, Dijk W, Boutens L, van der Bolt N, Wang Z, Brown JM, Hazen SL, Mandard S, Shiri-Sverdlov R, Kuipers F, Willems van Dijk K, Vervoort J, Stienstra R, Hooiveld GJEJ, Kersten S. Modulation of the gut microbiota impacts nonalcoholic fatty liver disease: a potential role for bile acids. *J Lipid Res* 2017; **58**: 1399-1416 [PMID: 28533304 DOI: 10.1194/jlr.M075713]

76 **Morrison DJ**, Preston T. Formation of short chain fatty acids by the gut microbiota and their impact on human metabolism. *Gut Microbes* 2016; **7**: 189-200 [PMID: 26963409 DOI: 10.1080/19490976.2015.1134082]

77 **Holmes ZC**, Silverman JD, Dressman HK, Wei Z, Dallow EP, Armstrong SC, Seed PC, Rawls JF, David LA. Short-Chain Fatty Acid Production by Gut Microbiota from Children with Obesity Differs According to Prebiotic Choice and Bacterial Community Composition. *mBio* 2020; **11** [PMID: 32788375 DOI: 10.1128/mBio.00914-20]

78 **Fiorucci S**, Biagioli M, Zampella A, Distrutti E. Bile Acids Activated Receptors Regulate Innate Immunity. *Front Immunol* 2018; **9**: 1853 [PMID: 30150987 DOI: 10.3389/fimmu.2018.01853]

79 **Zhan K**, Gong X, Chen Y, Jiang M, Yang T, Zhao G. Short-Chain Fatty Acids Regulate the Immune Responses *via* G Protein-Coupled Receptor 41 in Bovine Rumen Epithelial Cells. *Front Immunol* 2019; **10**: 2042 [PMID: 31555273 DOI: 10.3389/fimmu.2019.02042]

80 **Pathak P**, Xie C, Nichols RG, Ferrell JM, Boehme S, Krausz KW, Patterson AD, Gonzalez FJ, Chiang JYL. Intestine farnesoid X receptor agonist and the gut microbiota activate G-protein bile acid receptor-1 signaling to improve metabolism. *Hepatology* 2018; **68**: 1574-1588 [PMID: 29486523 DOI: 10.1002/hep.29857]

81 **Kleuser B**. Divergent Role of Sphingosine 1-Phosphate in Liver Health and Disease. *Int J Mol Sci* 2018; **19** [PMID: 29510489 DOI: 10.3390/ijms19030722]

82 **Rohrbach T**, Maceyka M, Spiegel S. Sphingosine kinase and sphingosine-1-phosphate in liver pathobiology. *Crit Rev Biochem Mol Biol* 2017; **52**: 543-553 [PMID: 28618839 DOI: 10.1080/10409238.2017.1337706]

83 **Liang J**, Nagahashi M, Kim EY, Harikumar KB, Yamada A, Huang WC, Hait NC, Allegood JC, Price MM, Avni D, Takabe K, Kordula T, Milstien S, Spiegel S. Sphingosine-1-phosphate links persistent STAT3 activation, chronic intestinal inflammation, and development of colitis-associated cancer. *Cancer Cell* 2013; **23**: 107-120 [PMID: 23273921 DOI: 10.1016/j.ccr.2012.11.013]

84 **Melhem H**, Kaya B, Ayata CK, Hruz P, Niess JH. Metabolite-Sensing G Protein-Coupled Receptors Connect the Diet-Microbiota-Metabolites Axis to Inflammatory Bowel Disease. *Cells* 2019; **8** [PMID: 31091682 DOI: 10.3390/cells8050450]

85 **Zhang C**, Yang M. The Role and Potential Application of Antimicrobial Peptides in Autoimmune Diseases. *Front Immunol* 2020; **11**: 859 [PMID: 32457759 DOI: 10.3389/fimmu.2020.00859]

86 **Maslowski KM**, Vieira AT, Ng A, Kranich J, Sierro F, Yu D, Schilter HC, Rolph MS, Mackay F, Artis D, Xavier RJ, Teixeira MM, Mackay CR. Regulation of inflammatory responses by gut microbiota and chemoattractant receptor GPR43. *Nature* 2009; **461**: 1282-1286 [PMID: 19865172 DOI: 10.1038/nature08530]

87 **Bhattarai Y**, Williams BB, Battaglioli EJ, Whitaker WR, Till L, Grover M, Linden DR, Akiba Y, Kandimalla KK, Zachos NC, Kaunitz JD, Sonnenburg JL, Fischbach MA, Farrugia G, Kashyap PC. Gut Microbiota-Produced Tryptamine Activates an Epithelial G-Protein-Coupled Receptor to Increase Colonic Secretion. *Cell Host Microbe* 2018; **23**: 775-785. e5 [PMID: 29902441 DOI: 10.1016/j.chom.2018.05.004]

88 **van de Wouw M**, Schellekens H, Dinan TG, Cryan JF. Microbiota-Gut-Brain Axis: Modulator of Host Metabolism and Appetite. *J Nutr* 2017; **147**: 727-745 [PMID: 28356427 DOI: 10.3945/jn.116.240481]

89 **Rowland I**, Gibson G, Heinken A, Scott K, Swann J, Thiele I, Tuohy K. Gut microbiota functions: metabolism of nutrients and other food components. *Eur J Nutr* 2018; **57**: 1-24 [PMID: 28393285 DOI: 10.1007/s00394-017-1445-8]

90 **Frost G**, Sleeth ML, Sahuri-Arisoylu M, Lizarbe B, Cerdan S, Brody L, Anastasovska J, Ghourab S, Hankir M, Zhang S, Carling D, Swann JR, Gibson G, Viardot A, Morrison D, Louise Thomas E, Bell JD. The short-chain fatty acid acetate reduces appetite *via* a central homeostatic mechanism. *Nat Commun* 2014; **5**: 3611 [PMID: 24781306 DOI: 10.1038/ncomms4611]

91 **Teng B**, Huang C, Cheng CL, Udduttula A, Yu XF, Liu C, Li J, Yao ZY, Long J, Miao LF, Zou C, Chu J, Zhang JV, Ren PG. Newly identified peptide hormone inhibits intestinal fat absorption and improves NAFLD through its receptor GPRC6A. *J Hepatol* 2020; **73**: 383-393 [PMID: 32147363 DOI: 10.1016/j.jhep.2020.02.026]

92 **Oya M**, Kitaguchi T, Pais R, Reimann F, Gribble F, Tsuboi T. The G protein-coupled receptor family C group 6 subtype A (GPRC6A) receptor is involved in amino acid-induced glucagon-like peptide-1 secretion from GLUTag cells. *J Biol Chem* 2013; **288**: 4513-4521 [PMID: 23269670 DOI: 10.1074/jbc.M112.402677]

93 **Muneoka S**, Goto M, Nishimura T, Enomoto K, Kadoshima-Yamaoka K, Tomimori Y. G Protein-Coupled Receptor 39 Agonist Improves Concanavalin A-Induced Hepatitis in Mice. *Biol Pharm Bull* 2019; **42**: 1415-1418 [PMID: 31167986 DOI: 10.1248/bpb.b18-00982]

94 **Cuzon Carlson VC**, Ford MM, Carlson TL, Lomniczi A, Grant KA, Ferguson B, Cervera-Juanes RP. Modulation of Gpr39, a G-protein coupled receptor associated with alcohol use in non-human primates, curbs ethanol intake in mice. *Neuropsychopharmacology* 2019; **44**: 1103-1113 [PMID: 30610192 DOI: 10.1038/s41386-018-0308-1]

95 **Lu Z**, Li Y, Syn WK, Li AJ, Ritter S, Wank SA, Lopes-Virella MF, Huang Y. GPR40-Deficiency Is Associated with Hepatic FAT/CD36 Upregulation, Steatosis, Inflammation and Cell Injury in C57BL/6 Mice. *Am J Physiol Endocrinol Metab* 2020 [PMID: 33103454 DOI: 10.1152/ajpendo.00257.2020]

96 **Ookawara M**, Matsuda K, Watanabe M, Moritoh Y. The GPR40 Full Agonist SCO-267 Improves Liver Parameters in a Mouse Model of Nonalcoholic Fatty Liver Disease without Affecting Glucose or Body Weight. *J Pharmacol Exp Ther* 2020; **375**: 21-27 [PMID: 32719069 DOI: 10.1124/jpet.120.000046]

97 **Chen X**, Liu C, Ruan L. G-Protein-Coupled Receptors 120 Agonist III Improves Hepatic Inflammation and ER Stress in Steatohepatitis. *Dig Dis Sci* 2020 [PMID: 32372191 DOI: 10.1007/s10620-020-06280-9]

98 **Park S**, Kang S, Im D. TUG-891, an agonist of GPR120, inhibits lipid accumulation in hepatocytes. *FASEB J* 2017; **31**: 992-995 [DOI: 10.1096/fasebj.31.1_supplement.992.5]

99 **On S**, Kim HY, Kim HS, Park J, Kang KW. Involvement of G-Protein-Coupled Receptor 40 in the Inhibitory Effects of Docosahexaenoic Acid on SREBP1-Mediated Lipogenic Enzyme Expression in Primary Hepatocytes. *Int J Mol Sci* 2019; **20** [PMID: 31142011 DOI: 10.3390/ijms20112625]

100 **Simard JC**, Thibodeau JF, Leduc M, Tremblay M, Laverdure A, Sarra-Bournet F, Gagnon W, Ouboudinar J, Gervais L, Felton A, Letourneau S, Geerts L, Cloutier MP, Hince K, Corpuz R, Blais A, Quintela VM, Duceppe JS, Abbott SD, Blais A, Zacharie B, Laurin P, Laplante SR, Kennedy CRJ, Hébert RL, Leblond FA, Grouix B, Gagnon L. Fatty acid mimetic PBI-4547 restores metabolic homeostasis *via* GPR84 in mice with non-alcoholic fatty liver disease. *Sci Rep* 2020; **10**: 12778 [PMID: 32728158 DOI: 10.1038/s41598-020-69675-8]

101 **Puengel T**, De Vos S, Hundertmark J, Kohlhepp M, Guldiken N, Pujuguet P, Auberval M, Marsais F, Shoji KF, Saniere L, Trautwein C, Luedde T, Strnad P, Brys R, Clément-Lacroix P, Tacke F. The Medium-Chain Fatty Acid Receptor GPR84 Mediates Myeloid Cell Infiltration Promoting Steatohepatitis and Fibrosis. *J Clin Med* 2020; **9** [PMID: 32316235 DOI: 10.3390/jcm9041140]

102 **Liang Y**, Liang S, Zhang Y, Deng Y, He Y, Chen Y, Liu C, Lin C, Yang Q. Oral Administration of Compound Probiotics Ameliorates HFD-Induced Gut Microbe Dysbiosis and Chronic Metabolic Inflammation *via* the G Protein-Coupled Receptor 43 in Non-alcoholic Fatty Liver Disease Rats. *Probiotics Antimicrob Proteins* 2019; **11**: 175-185 [PMID: 29353414 DOI: 10.1007/s12602-017-9378-3]

103 **Bebelman MP**, Crudden C, Pegtel DM, Smit MJ. The Convergence of Extracellular Vesicle and GPCR Biology. *Trends Pharmacol Sci* 2020; **41**: 627-640 [PMID: 32711926 DOI: 10.1016/j.tips.2020.07.001]

104 **Zeng Z**, Mukherjee A, Varghese AP, Yang XL, Chen S, Zhang H. Roles of G protein-coupled

receptors in inflammatory bowel disease. *World J Gastroenterol* 2020; **26**: 1242-1261 [PMID: 32256014 DOI: 10.3748/wjg.v26.i12.1242]

105 **Włodarczyk M**, Sobolewska-Włodarczyk A, Cygankiewicz AI, Jacenik D, Krajewska WM, Stec-Michalska K, Piechota-Polańczyk A, Wiśniewska-Jarosińska M, Fichna J. G protein-coupled receptor 55 (GPR55) expresses differently in patients with Crohn's disease and ulcerative colitis. *Scand J Gastroenterol* 2017; **52**: 711-715 [PMID: 28272905 DOI: 10.1080/00365521.2017.1298834]

106 **Asico LD**, Rozyyev S, Crusan AM, Jose PA, Villar VAM. Elucidating the Role of Lipid Rafts on G Protein-Coupled Receptor Function in the Mouse Kidney: An In Vivo Approach. *Methods Mol Biol* 2021; **2187**: 187-206 [PMID: 32770507 DOI: 10.1007/978-1-0716-0814-2_10]

107 **Keitel V**, Häussinger D. Role of TGR5 (GPBAR1) in Liver Disease. *Semin Liver Dis* 2018; **38**: 333-339 [PMID: 30357770 DOI: 10.1055/s-0038-1669940]

108 **Chang J**, Mancuso MR, Maier C, Liang X, Yuki K, Yang L, Kwong JW, Wang J, Rao V, Vallon M, Kosinski C, Zhang JJ, Mah AT, Xu L, Li L, Gholamin S, Reyes TF, Li R, Kuhnert F, Han X, Yuan J, Chiou SH, Brettman AD, Daly L, Corney DC, Cheshier SH, Shortliffe LD, Wu X, Snyder M, Chan P, Giffard RG, Chang HY, Andreasson K, Kuo CJ. Gpr124 is essential for blood-brain barrier integrity in central nervous system disease. *Nat Med* 2017; **23**: 450-460 [PMID: 28288111 DOI: 10.1038/nm.4309]

109 **Wang J**, Gareri C, Rockman HA. G-Protein-Coupled Receptors in Heart Disease. *Circ Res* 2018; **123**: 716-735 [PMID: 30355236 DOI: 10.1161/CIRCRESAHA.118.311403]

110 **Dhyani V**, Gare S, Gupta RK, Swain S, Venkatesh KV, Giri L. GPCR mediated control of calcium dynamics: A systems perspective. *Cell Signal* 2020; **74**: 109717 [PMID: 32711109 DOI: 10.1016/j.cellsig.2020.109717]

111 **Davenport AP**, Scully CCG, de Graaf C, Brown AJH, Maguire JJ. Advances in therapeutic peptides targeting G protein-coupled receptors. *Nat Rev Drug Discov* 2020; **19**: 389-413 [PMID: 32494050 DOI: 10.1038/s41573-020-0062-z]

112 **Sriram K**, Insel PA. G Protein-Coupled Receptors as Targets for Approved Drugs: How Many Targets and How Many Drugs? *Mol Pharmacol* 2018; **93**: 251-258 [PMID: 29298813 DOI: 10.1124/mol.117.111062]

113 **Terauchi Y**, Yamada Y, Watada H, Nakatsuka Y, Shiosakai K, Washio T, Taguchi T. Efficacy and safety of the G protein-coupled receptor 119 agonist DS-8500a in Japanese type 2 diabetes mellitus patients with inadequate glycemic control on sitagliptin: A phase 2 randomized placebo-controlled study. *J Diabetes Investig* 2018; **9**: 1333-1341 [PMID: 29607623 DOI: 10.1111/jdi.12846]

114 **Watada H**, Shiramoto M, Irie S, Terauchi Y, Yamada Y, Shiosakai K, Myobatake Y, Taguchi T. G protein-coupled receptor 119 agonist DS-8500a effects on pancreatic β-cells in Japanese type 2 diabetes mellitus patients. *J Diabetes Investig* 2019; **10**: 84-93 [PMID: 29624887 DOI: 10.1111/jdi.12849]

115 **Burant CF**, Viswanathan P, Marcinak J, Cao C, Vakilynejad M, Xie B, Leifke E. TAK-875 versus placebo or glimepiride in type 2 diabetes mellitus: a phase 2, randomised, double-blind, placebo-controlled trial. *Lancet* 2012; **379**: 1403-1411 [PMID: 22374408 DOI: 10.1016/S0140-6736(11)61879-5]

116 **Cusimano A**, Foderà D, Lampiasi N, Azzolina A, Notarbartolo M, Giannitrapani L, D'Alessandro N, Montalto G, Cervello M. Prostaglandin E2 receptors and COX enzymes in human hepatocellular carcinoma: role in the regulation of cell growth. *Ann N Y Acad Sci* 2009; **1155**: 300-308 [PMID: 19250221 DOI: 10.1111/j.1749-6632.2009.03701.x]

117 **Wu FQ**, Fang T, Yu LX, Lv GS, Lv HW, Liang D, Li T, Wang CZ, Tan YX, Ding J, Chen Y, Tang L, Guo LN, Tang SH, Yang W, Wang HY. ADRB2 signaling promotes HCC progression and sorafenib resistance by inhibiting autophagic degradation of HIF1α. *J Hepatol* 2016; **65**: 314-324 [PMID: 27154061 DOI: 10.1016/j.jhep.2016.04.019]

118 **Menon V**, Lincoff AM, Nicholls SJ, Jasper S, Wolski K, McGuire DK, Mehta CR, Rosenstock J, Lopez C, Marcinak J, Cao C, Nissen SE; GRAND 306 Investigators. Fasiglifam-Induced Liver Injury in Patients With Type 2 Diabetes: Results of a Randomized Controlled Cardiovascular Outcomes Safety Trial. *Diabetes Care* 2018; **41**: 2603-2609 [PMID: 30459247 DOI: 10.2337/dc18-0755]

119 **Bosier B**, Hermans E. Versatility of GPCR recognition by drugs: from biological implications to therapeutic relevance. *Trends Pharmacol Sci* 2007; **28**: 438-446 [PMID: 17629964 DOI: 10.1016/j.tips.2007.06.001]

120 **Li Y**, Sun Y, Song Y, Dai D, Zhao Z, Zhang Q, Zhong W, Hu LA, Ma Y, Li X, Wang R. Fragment-Based Computational Method for Designing GPCR Ligands. *J Chem Inf Model* 2020; **60**: 4339-4349 [PMID: 31652060 DOI: 10.1021/acs.jcim.9b00699]

121 **Audet M**, Villers K, Velasquez J, Chu M, Hanson C, Stevens RC. Small-scale approach for precrystallization screening in GPCR X-ray crystallography. *Nat Protoc* 2020; **15**: 144-160 [PMID: 31784719 DOI: 10.1038/s41596-019-0259-y]

122 **Doijen J**, Van Loy T, Landuyt B, Luyten W, Schols D, Schoofs L. Advantages and shortcomings of cell-based electrical impedance measurements as a GPCR drug discovery tool. *Biosens Bioelectron* 2019; **137**: 33-44 [PMID: 31077988 DOI: 10.1016/j.bios.2019.04.041]

123 **Chen KM**, Keri D, Barth P. Computational design of G Protein-Coupled Receptor allosteric signal transductions. *Nat Chem Biol* 2020; **16**: 77-86 [PMID: 31792443 DOI: 10.1038/s41589-019-0407-2]

World Journal of Gastroenterology

Submit a Manuscript: https://www.f6publishing.com

World J Gastroenterol 2021 February 28; 27(8): 692-707

DOI: 10.3748/wjg.v27.i8.692

ISSN 1007-9327 (print) ISSN 2219-2840 (online)

ORIGINAL ARTICLE

Basic Study

Fork head box M1 regulates vascular endothelial growth factor-A expression to promote the angiogenesis and tumor cell growth of gallbladder cancer

Rui-Tao Wang, Run-Chen Miao, Xing Zhang, Gang-Hua Yang, Yi-Ping Mu, Zi-Yun Zhang, Kai Qu, Chang Liu

ORCID number: Rui-Tao Wang 0000-0003-0487-0575; Run-Chen Miao 0000-0003-1651-3970; Xing Zhang 0000-0001-9568-8124; Gang-Hua Yang 0000-0002-9347-5771; Yi-Ping Mu 0000-0001-9155-5973; Zi-Yun Zhang 0000-0003-1272-3268; Kai Qu 0000-0002-1138-3727; Chang Liu 0000-0002-7318-1004.

Author contributions: Wang RT, Miao RC and Zhang X contributed equally to this work; Wang RT and Liu C designed the research; Wang RT, Miao RC and Zhang X wrote the paper; Yang GH, Mu YP and Miao RC collected the patient's clinical data; Yang GH, Zhang ZY and Qu K analyzed the data; Zhang X revised the paper; all authors read and approved the final manuscript.

Supported by Scientific and Technological Development Research Project Foundation of Shaanxi Province of China, No. 2020SF-069.

Institutional review board statement: The study was reviewed and approved by the First Affiliated Hospital of Xi'an Jiaotong University College of Medicine Institutional Review Board.

Rui-Tao Wang, Run-Chen Miao, Xing Zhang, Zi-Yun Zhang, Kai Qu, Chang Liu, Department of Hepatobiliary Surgery, The First Affiliated Hospital of Xi'an Jiaotong University, Xi'an 710061, Shaanxi Province, China

Run-Chen Miao, Chang Liu, Department of SICU, The First Affiliated Hospital of Xi'an Jiaotong University, Xi'an 710061, Shaanxi Province, China

Gang-Hua Yang, Department of Geriatric Surgery, The First Affiliated Hospital of Xi'an Jiaotong University, Xi'an 710061, Shaanxi Province, China

Yi-Ping Mu, Department of Medical Information Management Office, The First Affiliated Hospital of Xi'an Jiaotong University, Xi'an 710061, Shaanxi Province, China

Corresponding author: Chang Liu, MD, PhD, Chief Doctor, Professor, Department of Hepatobiliary Surgery, The First Affiliated Hospital of Xi'an Jiaotong University, No. 277 West Yanta Road, Xi'an 710061, Shaanxi Province, China. liuchangdoctor@163.com

Abstract

BACKGROUND

Gallbladder cancer (GBC) is an aggressive type of biliary tract cancer that lacks effective therapeutic targets. Fork head box M1 (FoxM1) is an emerging molecular target associated with tumor progression in GBC, and accumulating evidence suggests that vascular endothelial growth factor (VEGF) promotes various tumors by inducing neoangiogenesis.

AIM

To investigate the role of FoxM1 and the angiogenesis effects of VEGF-A in primary GBC.

METHODS

Using immunohistochemistry, we investigated FoxM1 and VEGF-A expression in GBC tissues, paracarcinoma tissues and cholecystitis tissues. Soft agar, cell invasion, migration and apoptosis assays were used to analyze the malignant phenotype influenced by FoxM1 in GBC. Kaplan-Meier survival analysis was performed to evaluate the impact of FoxM1 and VEGF-A expression in GBC patients. We investigated the relationship between FoxM1 and VEGF-A by

Institutional animal care and use committee statement: This study was reviewed and approved by the Ethics Committee of the Xi'an Jiaotong University.

Conflict-of-interest statement: The authors declared no conflicts of interest.

Data sharing statement: No additional data are available.

ARRIVE guidelines statement: The authors have read the ARRIVE guidelines, and the manuscript was prepared and revised according to the ARRIVE guidelines.

Open-Access: This article is an open-access article that was selected by an in-house editor and fully peer-reviewed by external reviewers. It is distributed in accordance with the Creative Commons Attribution NonCommercial (CC BY-NC 4.0) license, which permits others to distribute, remix, adapt, build upon this work non-commercially, and license their derivative works on different terms, provided the original work is properly cited and the use is non-commercial. See: http://creativecommons.org/licenses/by-nc/4.0/

Manuscript source: Unsolicited manuscript

Specialty type: Gastroenterology and hepatology

Country/Territory of origin: China

Peer-review report's scientific quality classification

Grade A (Excellent): 0
Grade B (Very good): B
Grade C (Good): C
Grade D (Fair): 0
Grade E (Poor): 0

Received: September 9, 2020
Peer-review started: September 9, 2020
First decision: December 4, 2020
Revised: December 16, 2020
Accepted: January 21, 2021
Article in press: January 21, 2021
Published online: February 28, 2021

regulating the level of FoxM1. Next, we performed MTT assays and Transwell invasion assays by knocking out or overexpressing VEGF-A to evaluate its function in GBC cells. The luciferase assay was used to reveal the relationship between FoxM1 and VEGF-A. BALB/c nude mice were used to establish the xenograft tumor model.

RESULTS

FoxM1 expression was higher in GBC tissues than in paracarcinoma tissues. Furthermore, the high expression of Foxm1 in GBC was significantly correlated with a malignant phenotype and worse overall survival. Meanwhile, high expression of FoxM1 influenced angiogenesis; high expression of FoxM1 combined with high expression of VEGF-A was related to poor prognosis. Attenuated FoxM1 significantly suppressed cell proliferation, transfer and invasion *in vitro*. Knockdown of FoxM1 in GBC cells reduced the expression of VEGF-A. Luciferase assay showed that FoxM1 was the transcription factor of VEGF-A, and knockdown VEGF-A in FoxM1 overexpressed cells could partly reverse the malignancy phenotype of GBC cells. In this study, we found that FoxM1 was involved in regulation of VEGF-A expression.

CONCLUSION

FoxM1 and VEGF-A overexpression were associated with the prognosis of GBC patients. FoxM1 regulated VEGF-A expression, which played an important role in the progression of GBC.

Key Words: Gallbladder neoplasms; Fork head box M1; Vascular endothelial growth factor-A; Angiogenesis; Progression; Prognosis

©The Author(s) 2021. Published by Baishideng Publishing Group Inc. All rights reserved.

Core Tip: Fork head box M1 (FoxM1) is an emerging molecular target associated with early metastasis, drug resistance and poor patient survival in gallbladder cancer. Accumulating evidence suggests that vascular endothelial growth factor (VEGF) plays important roles in many kinds of tumors by inducing neoangiogenesis. In the present study, we found that VEGF-A overexpression was correlated with proliferation, invasion and poor prognosis. The results of Kaplan-Meier analysis showed that both FoxM1 and VEGF-A were associated with survival in gallbladder cancer. VEGF-A expression was regulated by FoxM1, which was the mechanism of FoxM1 enhancing the angiogenesis of gallbladder cancer.

Citation: Wang RT, Miao RC, Zhang X, Yang GH, Mu YP, Zhang ZY, Qu K, Liu C. Fork head box M1 regulates vascular endothelial growth factor-A expression to promote the angiogenesis and tumor cell growth of gallbladder cancer. *World J Gastroenterol* 2021; 27(8): 692-707
URL: https://www.wjgnet.com/1007-9327/full/v27/i8/692.htm
DOI: https://dx.doi.org/10.3748/wjg.v27.i8.692

INTRODUCTION

Gallbladder cancer (GBC), a frequent and aggressive type of biliary tract cancer, is now the sixth most common gastrointestinal cancer. The vast majority (65% to 90%) of GBCs are adenocarcinomas followed by squamous cell or adenosquamous cell carcinomas (5% to 10%) and undifferentiated carcinomas (5%)[1]. The incidence rate is 2.2 per 100000 per year worldwide[1]. Surgery combined with adjuvant chemotherapy and radiotherapy is the general therapy for patients with GBC. However, GBC is known to have an occult onset, rapid progression and abysmal prognosis, with a mean 6-mo survival time and a 5-yr survival rate of 5%[2]. Furthermore, a low diagnosis rate of GBC has been demonstrated in Japan, with only a 0.011% detection rate from mass screening[3]. Thus, accurate and specific diagnosis of GBC at the early stage is still urgently needed to improve therapeutic efficacy.

Cancer cells achieve invasion and metastasis through extracellular proteolysis,

P-Reviewer: Merigo F, Zhang L
S-Editor: Gao CC
L-Editor: Filipodia
P-Editor: Liu JH

which affects cell proliferation, adhesion, migration and angiogenesis. In addition, Fork head box M1 (FoxM1) is characterized as a critical proliferation-associated transcription factor in cell cycle progression[4]. Inhibiting FoxM1 expression has been reported to induce the loss of the mitotic spindle, resulting in failed cell division. FoxM1 is widely expressed in normal proliferating cells and is also overexpressed in cancer cells, such as ovarian cancer cells, renal cell carcinoma cells, pancreatic cancer cells, breast cancer cells, laryngeal squamous carcinoma cells, glioma cells, prostate carcinoma cells and gastric cancer cells[5]. Moreover, the overexpression of FoxM1 has an impact on poor patient prognosis and can be regarded as an independent predictor of low survival[4]. However, in patients with GBC, the clinical correlation of FoxM1 expression remains unclear.

In recent research, investigators have found that the downregulation of FoxM1 inhibits the activity of vascular endothelial growth factor (VEGF), matrix metalloproteinase (MMP)-2, MMP-9, Cyclin B1, CDC25, p21 and p27 proteins, affecting cancer cell proliferation, migration and invasion[6]. Moreover, FoxM1 was proven to be upregulated at both the mRNA and protein levels[7]. In glioma, with the increase in FoxM1, cancer cell invasiveness and tumorigenicity are also promoted[8]. These investigations indicate that FoxM1 plays an important role in the progression of carcinoma and could have the same function in GBC cells. Two investigations also found a correlation between lymph node metastasis and FoxM1. However, the correlation between elevated levels of FoxM1 and clinical specimens has been controversial.

We found that FoxM1 overexpression promoted tumor cell migration and invasion, while FoxM1 downregulation led to an increase in cell apoptosis rates, indicating that FoxM1 might play a key role in disease progression of GBC. Moreover, we found that FoxM1 could be directly involved in the regulation of VEGF-A expression by combining with the VEGF-A promoter and activating VEGF-A transcription. Therefore, we indicated that FoxM1 could promote GBC *progression via* VEGF-A.

MATERIALS AND METHODS

Patient tissues and information

After surgery, 48 cases of fresh frozen GBC tumor tissue were collected from the First Affiliated Hospital of Xi'an Jiaotong University, together with paired tumor-free liver tissue (at least 2 cm from the tumor) from September 2015 to February 2017. GBC was confirmed by histopathological examination, and the study was approved by the Ethics Staff of the First Affiliated Hospital of Xi'an Jiaotong University.

Cell culture and treatment

The human GBC cell line SGC-996 was purchased from the Cell Bank of the Chinese Academy of Sciences (Shanghai branch) and was cultured in RPMI 1640 medium containing 10% fetal bovine serum (Gibco, Grand Island, NY, United States) at 37 °C with 5% CO_2.

shRNA transfection

At 24 h after cell seeding in the culture dish, the recombinant adenovirus vector containing specific shRNA was transfected into SGC-996 cells with Lipofectamine 2000 (Invitrogen, United States) at different multiplicities of infection. Recombinant lentiviruses containing FoxM1 shRNA and VEGF-A shRNA were purchased from GenePharma (Shanghai, China). A negative control carrying green fluorescent protein, which expresses a scrambled RNA, was constructed as a control. The virus containing the construct was isolated using plaque screening, purification and amplification. The protocol for lentivirus infection was according to the GenePharma Recombinant Lentivirus Operation Manual (http://www.genepharma.com).

The overexpression of VEGF-A and FoxM1 by lentiviral transfection

A FoxM1 expression plasmid was purchased from Sino Biological Inc. (Beijing, China). SGC-996 cells were transfected with the FoxM1 expression vector or an empty control vector (400 ng/well) using HiPerFect. After 48 h of transfection, the cells were collected, and protein levels were analyzed by Western blotting and quantitative reverse transcription (qRT)-PCR. The overexpression of VEGF-A was performed as described above.

Western blot analysis

Western blot analysis was performed as previously reported. Briefly, the membranes were probed with the following primary antibodies: FoxM1 (1:1000, Proteintech, Wuhan, China), VEGF-A (1:1000, Proteintech, Wuhan, China) and β-actin (1:3000, Abways, Shanghai, China). After being washed with TBS-T, the membranes were incubated with horseradish peroxidase-conjugated anti-rabbit or anti-mouse secondary antibody (1:10000, Proteintech, Wuhan, China). Mouse anti-β-actin (1:1000, Proteintech, Wuhan, China) with goat anti-mouse (1:10000, Proteintech, Wuhan, China) antibodies were used as a loading control. Chemiluminescence detection was performed with ChemiGlow detection reagents (Bio-Rad Western ECL Substrate). The blots were visualized with a Bio-Rad ChemiDoc MP and quantified with a densitometer using the imager application program (Alpha Innotech, San Leandro, CA, United States).

RNA isolation and RT-PCR

RNA isolation and RT-PCR analysis were performed as previously described. The cDNA for FoxM1, VEGF-A and β-actin were amplified using the Platinum Taq DNA Polymerase kit (Life Technologies) with specific primers. β-actin was used as an internal control. Primer sequences were as follows: FoxM1 Forward, 5′-CAC CCC AGT GCC AAC CGC TAC TTG-3′; FoxM1 Reverse, 5′-AAA GAG GAG CTA TCC CCT CCT CAG-3′; VEGF-A Forward, 5′- CAG ATT ATG CGG ATC AAA CCT CA -3′; VEGF-A Reverse, 5′-CAA GGC CCA CAG GGA CTG CAA -3′.

Immunohistochemical staining

Tissue specimens were fixed in neutral buffered formalin (10% vol/vol formalin in water, pH 7.4) and embedded in paraffin wax. Serial sections of 5 mm thickness were cut and mounted on charged glass slides. Conditions for FoxM1 and VEGF-A were optimized and evaluated by two independent pathologists. The goat monoclonal antibodies against FoxM1 (sc-26688; Santa Cruz Biotechnology, Santa Cruz, CA, United States) and VEGF-A (sc-152; Santa Cruz Biotechnology, Santa Cruz, CA, United States) were used at dilutions of 1:200. The streptavidin–peroxidase kit (SP-9000 Golden Bridge Int., Beijing, China) was used in accordance with the manufacturer's instructions. An irrelevant goat antiserum served as a negative control. Sections were counterstained with Mayer's hematoxylin. The immunohistochemical score and analysis were described as previously reported.

Soft agar cloning assay

Experiments with soft agar were carried out on 6-well plates. Agar was used for the bottom (0.8%) and top (0.4%) containing cells and fed every 4 d in a complete DMEM medium. After 20 d, colonies with diameters greater than 150 μm were scored under a 10-fold fluorescence microscope.

Apoptosis assay

The SGC-996 cells were inoculated into a 6-well plate with a density of 1 x 10^6 cells per well. Cells at logarithmic growth stage were digested by 0.25% trypsin, and the supernatant was discarded after 800 rpm centrifugation for 5 min. The mixture was resuspended with PBS, centrifuged at 800 rpm for 5 min, and washed twice with PBS. Annexin V (10 μL) was added at a concentration of 50 μg/mL and left standing for 40min (Bender Medsystems, Australia). Flow cytometry was used to detect apoptosis (Beckman, United States).

MTT assay for cell viability

SGC-996 cells were seeded at 5 × 10^3 cells per well in 96-well flat-bottom plates before transfection. For the assay, 20 μL of MTT solution (5 g/L) was added to each well, and the cells were incubated for 4 h. Then, supernatants were removed, and formazan crystals were dissolved in 200 mL dimethyl sulfoxide. After the insoluble crystals were completely dissolved, the absorbance values at 490 nm were measured using a microplate reader (Bio-Rad, Hercules, CA, United States).

Cell invasion and migration assays

Cell invasion and migration assays were performed using Transwell permeable supports with 8 μm pore size (Costar, Cambridge, MA, United States). Cells were suspended in serum-free medium and seeded into Transwell inserts either uncoated (for the migration assay) or coated (for the invasion assay) with growth factor-reduced

Matrigel (BD Biosciences, Bedford, MA, United States). Bottom wells were filled with complete medium. After 24 h, the invaded cells were fixed with methanol and stained with a crystal violet solution. The number of cells that penetrated the membrane was determined by counting the mean cell number in five randomly selected high-power fields.

Clone formation assay

For the clonogenic assay, cells were plated in the 6-well plate with 1000 cells per well. The samples were fixed with 4% paraformaldehyde for 30 min and stained with 0.05% crystal violet for 20 min. Representative photos were collected and more than 40 colonies were counted.

Endothelial cell tube formation assay

The pre-cooled 96 well plates were coated with matrix gel (35 μL/well) and then placed in the humidified CO_2 incubator at 37 degrees Celsius for 1 h to solidify the coating. HUVEC cells were starved overnight under 1% bovine serum albumin. Then, the cells were digested with trypsin and collected and inoculated on a 96 well plate with a density of 2.5×10^4 cells per well. SGC-996 cells were cocultured with HUVEC for 4 h. The tube formation of HUVECs was observed at 4 h by a microscope.

Luciferase assay

A pmirGLO Dual luciferase miRNA Target Expression Vector (E1330; Promega Corporation) contained the fragment of FOXM1 3'UTR and VEGF 3'UTR was used to establish luciferase reporter plasmids: WT-FOXM1; MUT-FOXM1; WT-VEGF; and MUT-VEGF. HEK293T cells were cultured in 24-well plates. When the cells reached 70% confluence, cells were transfected with 2 μg WT-FOXM1 or MUT-FOXM1 and 2 μg WT-VEGF or MUT-VEGF using Lipofectamine® 3000 (Invitrogen, Thermo Fisher Scientific, Inc). After 48 h, luciferase activity was detected by the dual-enzyme reporter assay kit (Promega).

Xenotransplantation model in nude mice

Animal experiments were approved by the Animal Ethics Committee of the Medical College of Xi'an Jiaotong University. BALB/c nude mice aged 4-6 wk were purchased from Medical Laboratory Animal Center of Xi'an Jiaotong University. Mice weighing 16 to 20 g were randomly divided into three groups: (1) Lenti-FoxM1-shRNA; (2) cDNA-FoxM1; or (3) control (1×10^7 SGC-996 cells were injected into the back of mice to establish xenograft tumor model). After 1 mo, the mice were killed, and the tumors were collected.

Statistical analysis

All data are expressed as the mean ± SD. To compare the means of normally distributed variables, analysis of variance or Student's *t* test was applied. *P* value less than 0.05 was considered significant in all tests. All analyses were performed using SPSS software version 19.0 (SPSS Inc., Chicago, IL, United States).

RESULTS

FoxM1 was overexpressed in GBC tissues

First, the expression of FoxM1 was higher than that in paracarcinoma tissues or cholecystitis tissues (Figure 1A). Moreover, we compared the levels of FoxM1 expression in four paired GBC clinical samples by qRT-PCR and Western blot analysis. The results revealed that the expression of FoxM1 in GBC was significantly higher than that in paracarcinoma tissue (Figure 1B and 1C). Western blot results showed that the protein level of FoxM1 in GBC tissues was higher than the expression of FoxM1 in paracarcinoma tissues (Figure 1D and 1E). This suggested that FoxM1 expression was closely related to the development of GBC.

Overexpression of FoxM1 promoted proliferation and metastasis of GBC cells in vitro

To investigate the function of FoxM1 in GBC, the expression of FoxM1 was suppressed by lenti-FoxM1 shRNA and was elevated by lenti- FoxM1 in the SGC-996 cell line. The protein and mRNA levels of FoxM1 were significantly decreased after lenti-FoxM1 shRNA transfection (Figure 2A-D). The protein and mRNA levels of FoxM1 were

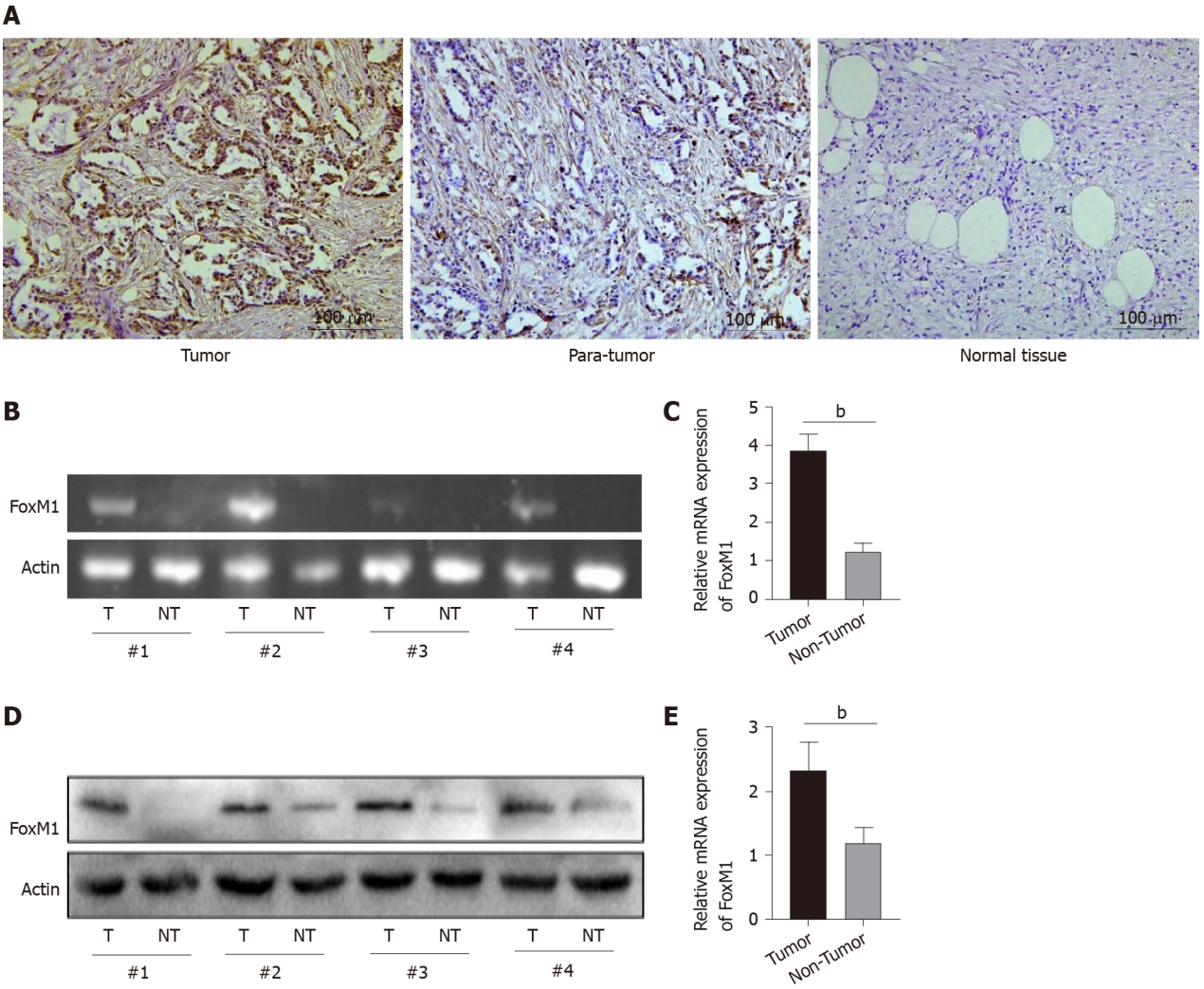


Figure 1 The expression of fork head box M1 in gallbladder cancer. A: The expression of fork head box M1 in gallbladder cancer tissues (immunohistochemical staining, scale bars: 100 μm); B and C: Relative mRNA expression of fork head box M1; D and E: Relative protein expression of fork head box M1. $^{a}P < 0.05$, $^{b}P < 0.01$. FoxM1: Fork head box M1.

significantly increased after lenti- FoxM1 transfection (Figure 2E-H).

As demonstrated by the soft agar cloning assay, lenti-FoxM1 shRNA significantly decreased proliferation in SGC-996 cells. Conversely, lenti-FoxM1 significantly increased SGC-996 cell proliferation (Figure 2I and 2J). To determine the potential metastatic-promoting effect of FoxM1 in GBC cells, we investigated cell migration and invasion abilities. Compared with that in SGC-996 cells, less cell penetration was observed in lenti-FoxM1 shRNA-transfected cells. However, lenti-FoxM1-transfected cells had stronger invasion abilities in the presence of Matrigel (Figure 3A-D). As shown in the apoptosis assay, knockdown-FoxM1 cells increased apoptotic levels (Figure 3E and 3F). Tube formation also showed that in FoxM1 up-regulated cells vessel generation ability was significantly enhanced (Figure 3G and 3H). These data suggested that FoxM1 plays important roles in GBC progression.

FoxM1 promoted GBC cell proliferation and metastasis via VEGF-A

As shown in Figure 3G and 3H, the high expression level of FoxM1 influenced vessel generation in GBC. Meanwhile, research revealed that VEGF-A was associated with endothelial cell proliferation, division, migration and lumen formation. Therefore, we examined the correlation between FoxM1 and VEGF-A. As shown in Figure 3, FoxM1 and VEGF-A were both associated with GBC, and the expression of VEGF-A was obviously decreased in FoxM1 siRNA-transfected SGC-996 cells. We detected the expression of FoxM1 and VEGF-A by consecutive section immunohistochemistry in 48 GBC tissues. A positive correlation between FoxM1 and VEGF-A was observed (Figure 4A-D). Thus, we hypothesized that VEGF-A is regulated by FoxM1 to promote GBC cell migration and invasion.

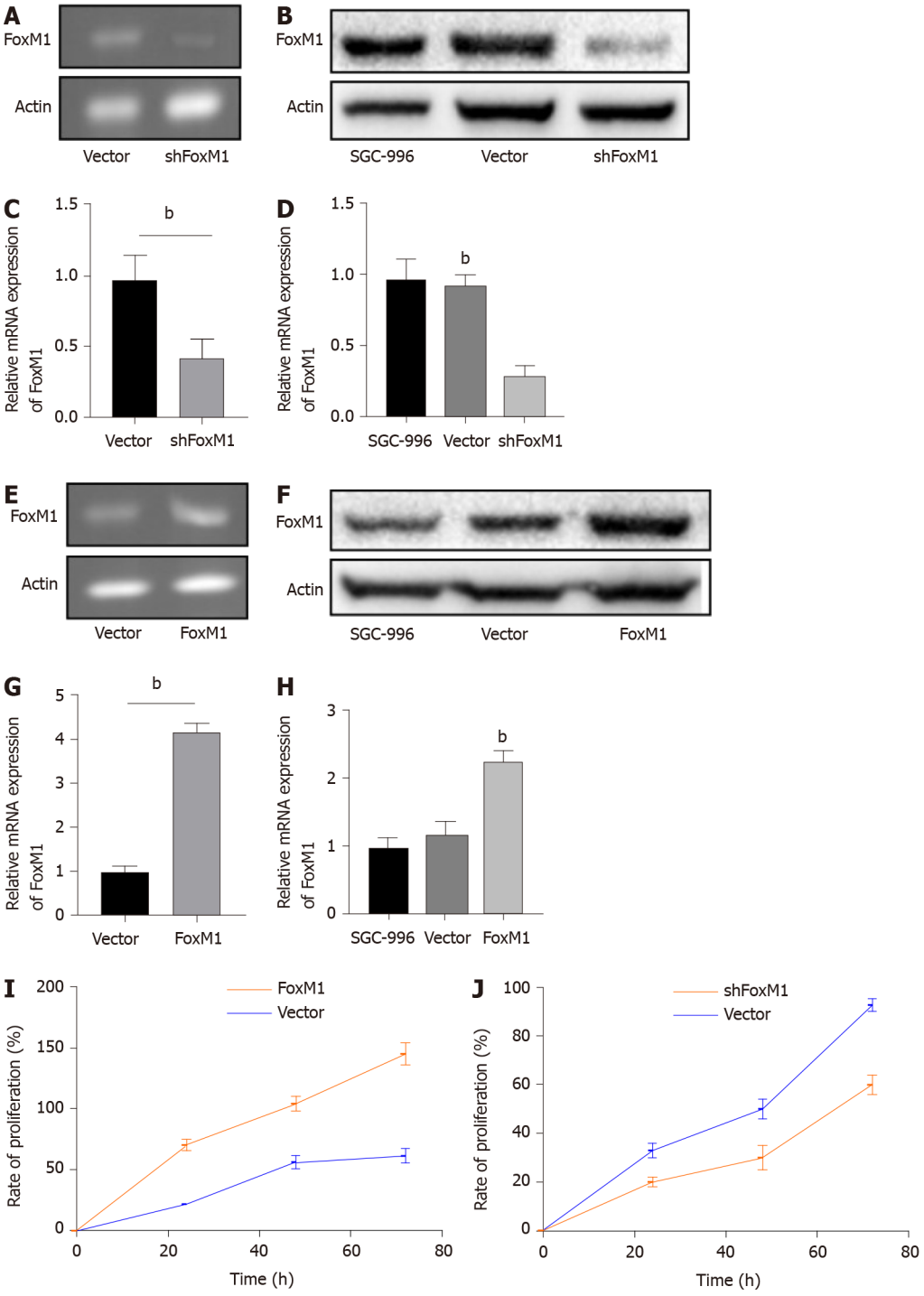


Figure 2 Fork head box M1 influenced proliferation of gallbladder cancer cells *in vitro*. A-H: Relative mRNA and protein expression of fork head box M1; I: Rate of proliferation after overexpression of fork head box M1; J: Rate of proliferation after inhibition of fork head box M1. $^{a}P < 0.05$, $^{b}P < 0.01$. FoxM1: Fork head box M1.

First, we investigated whether FoxM1 regulated the protein and mRNA levels of VEGF-A in GBC cells. Therefore, we determined the VEGF-A protein and mRNA expression levels after silencing FoxM1 by Western blot and RT-PCR analyses, respectively. We found that FoxM1 knockdown led to significant downregulation of VEGF-A protein and mRNA expression levels in SGC-996 cells (Figure 4E and 4G). To further prove the link between FoxM1 and VEGF-A expression, we overexpressed FoxM1 by transfecting lenti-FoxM1 in SGC-996 cells and found that VEGF-A expression was significantly increased at the transcriptional and translational levels (Figure 4F and 4H). Moreover, the luciferase assay showed that FoxM1 was the transcription factor of VEGF-A (Figure 4I). Nevertheless, knockdown VEGF-A in FoxM1 overexpressed cells could partly reverse the malignant phenotype of GBC cells

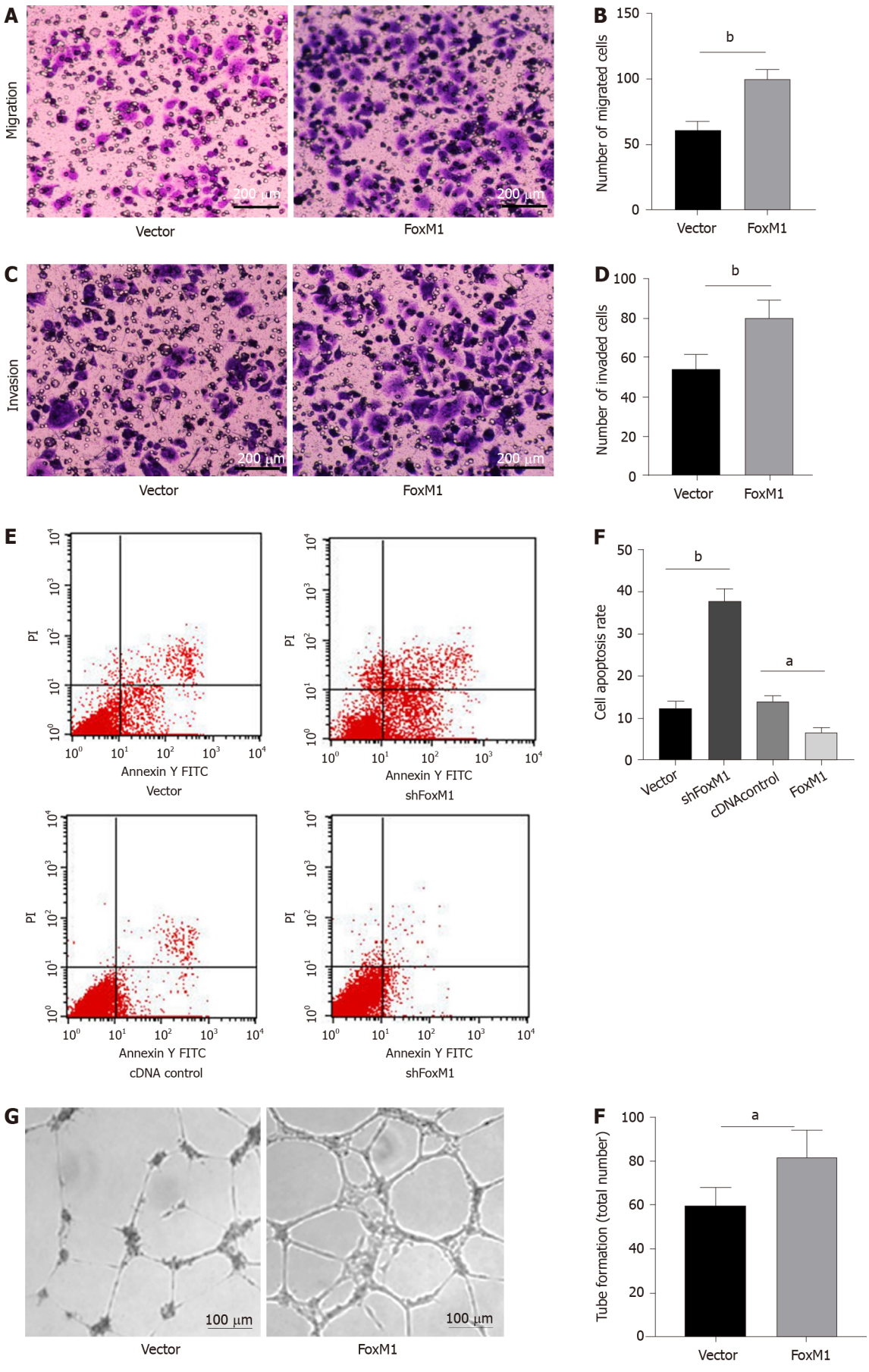


Figure 3 Fork head box M1 influenced migration and invasion of gallbladder cancer cells *in vitro*. A-D: Lenti-fork head box M1-transfected cells had stronger migration and invasion abilities (cell invasion and migration assays, scale bars: 200 μm); E and F: Knockdown-fork head box M1 cells increased

apoptotic levels (apoptosis assay); G and H: Upregulated fork head box M1 significantly enhanced vessel generation ability (endothelial cell tube formation assay, scale bars: 100 μm). [a]*P* < 0.05, [b]*P* < 0.01. FoxM1: Fork head box M1.

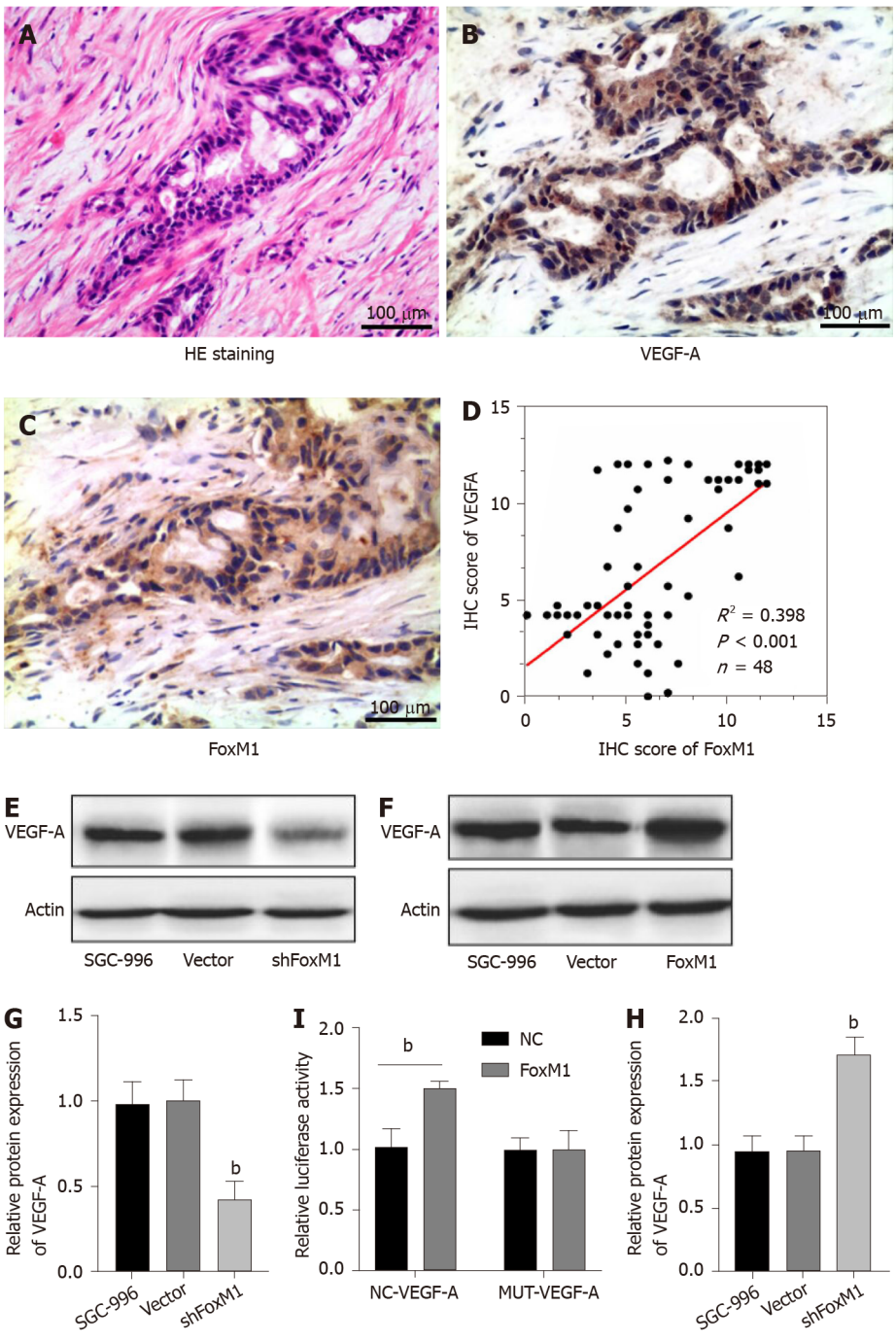


Figure 4 Fork head box M1 promoted gallbladder cancer cell proliferation and metastasis *via* vascular endothelial growth factor-A. A-C: Hematoxylin-eosin staining, immunohistochemical staining of fork head box M1 and vascular endothelial growth factor-A (VEGF-A) in gallbladder cancer tissues (scale bars: 100 μm); D: Correlation between fork head box M1 and VEGF-A analyzed according to fluorescence score; E-H: Relative protein expression of VEGF-A; I: Luciferase assay of fork head box M1 and VEGF-A. [a]*P* < 0.05, [b]*P* < 0.01. FoxM1: Fork head box M1; VEGF-A: Vascular endothelial growth factor-A; NC: Normal control.

(Figure 5A-I). These results indicated that FoxM1 was involved in the regulation of VEGF-A expression.

FoxM1 enhanced the angiogenesis of GBC by regulating VEGF-A in vivo

Because the *in vitro* study showed that VEGF-A, a potent vascular active molecule, promoted proliferation, invasion and metastasis regulated by FoxM1, we further

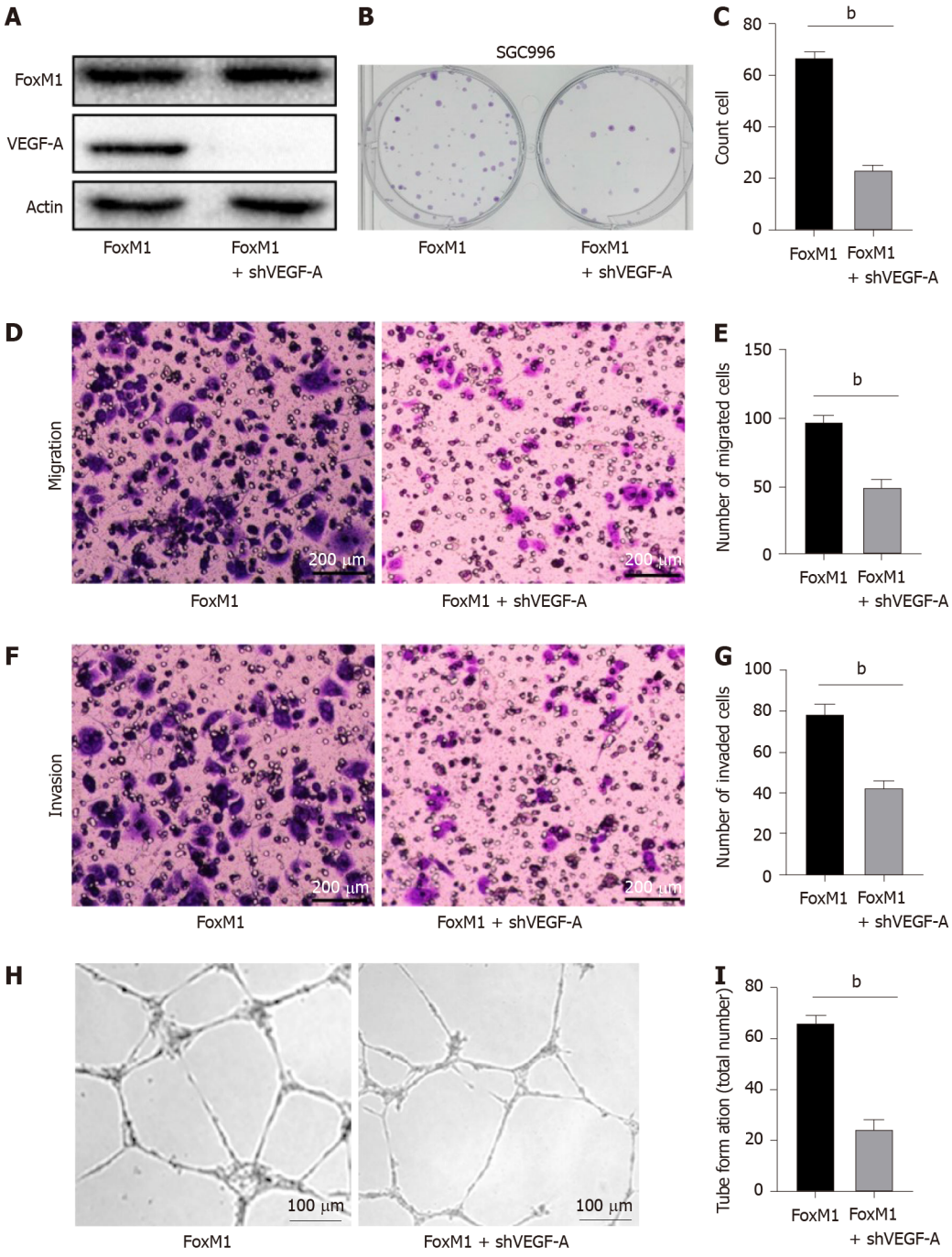
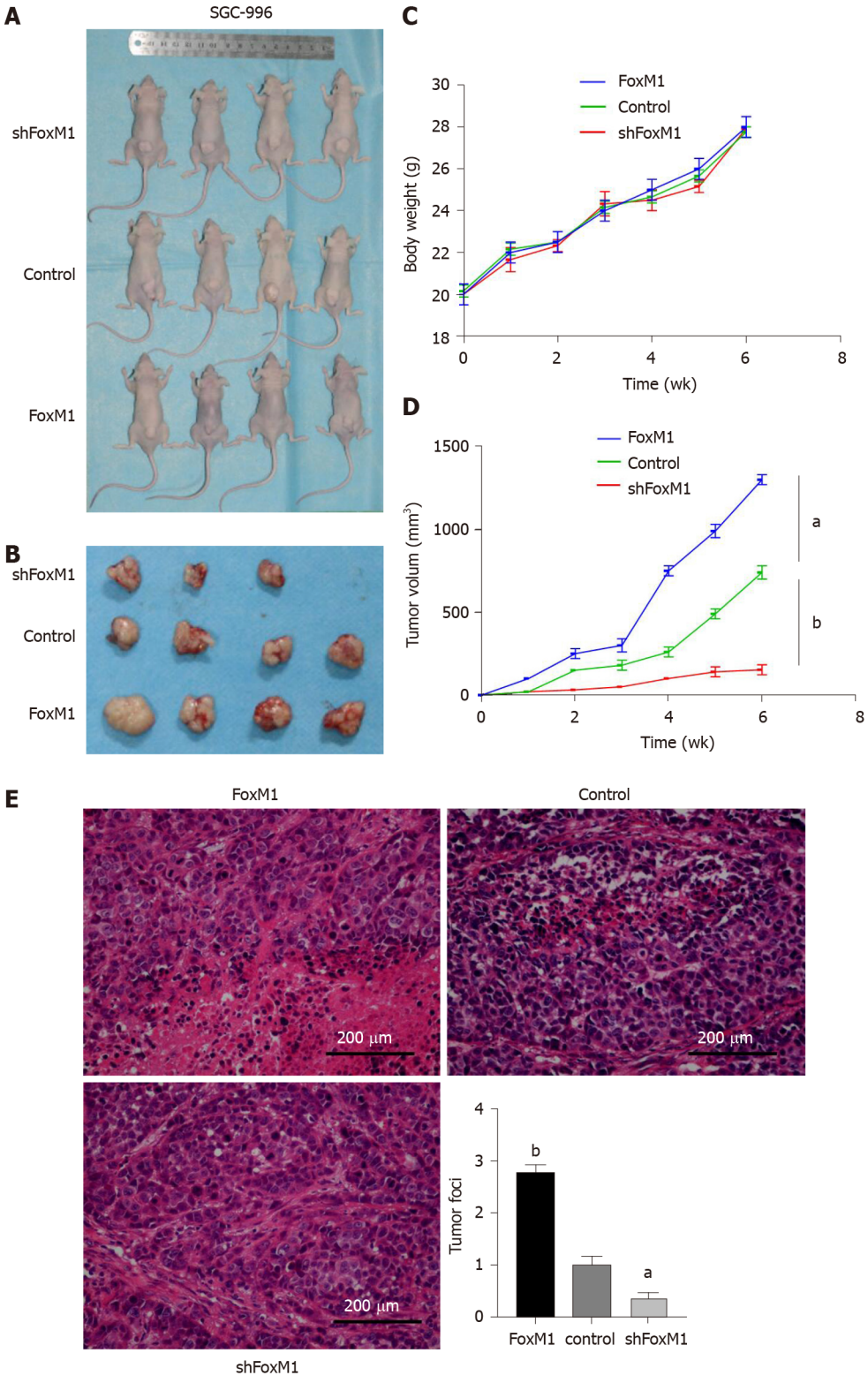


Figure 5 Knockdown vascular endothelial growth factor-A in fork head box M1 overexpressed cells could partly reverse the malignant phenotype of gallbladder cancer cells. A: Relative protein expression of fork head box M1 and vascular endothelial growth factor-A; B and C: Clone formation of gallbladder cancer cells; D-G: Knockdown vascular endothelial growth factor-A in fork head box M1 overexpressed cells influenced migration and invasion abilities (cell invasion and migration assays, scale bars: 200 μm); H and I: Knockdown vascular endothelial growth factor-A in fork head box M1 overexpressed cells suppressed vessel generation ability (endothelial cell tube formation assay, scale bars: 100 μm). $^{a}P < 0.05$, $^{b}P < 0.01$. FoxM1: Fork head box M1; VEGF-A: Vascular endothelial growth factor-A.

investigated the function of the FoxM1-VEGF-A axis on angiogenesis in GBC. As a result, the tumor volume and weight of mice transfected with lenti-FoxM1-shRNA or lenti-FoxM1 were determined (Figure 6A-D). The tumors of mice transfected with lenti-FoxM1 were larger than the control group, and the tumors of mice transfected with lenti-FoxM1-shRNA were smaller than the control group. Next, analysis of hematoxylin-eosin staining was performed to detect the number of tumor foci (Figure 6E). The most tumor foci were in tumor tissues of mice overexpressing FoxM1. Additionally, microvascular density, CD31 and VEGF-A were measured to investigate the angiogenic ability (Figure 6F and 6G). The above results showed that FoxM1 can improve the angiogenesis of GBC by regulating the expression of VEGF-A. Kaplan-


A
SGC-996
shFoxM1
Control
FoxM1
B
shFoxM1
Control
FoxM1
C
FoxM1
Control
shFoxM1
Body weight (g)
Time (wk)
D
FoxM1
Control
shFoxM1
Tumor volum (mm3)
Time (wk)
a
b
E
FoxM1
Control
200 μm
200 μm
200 μm
shFoxM1
Tumor foci
b
a
FoxM1 control shFoxM1

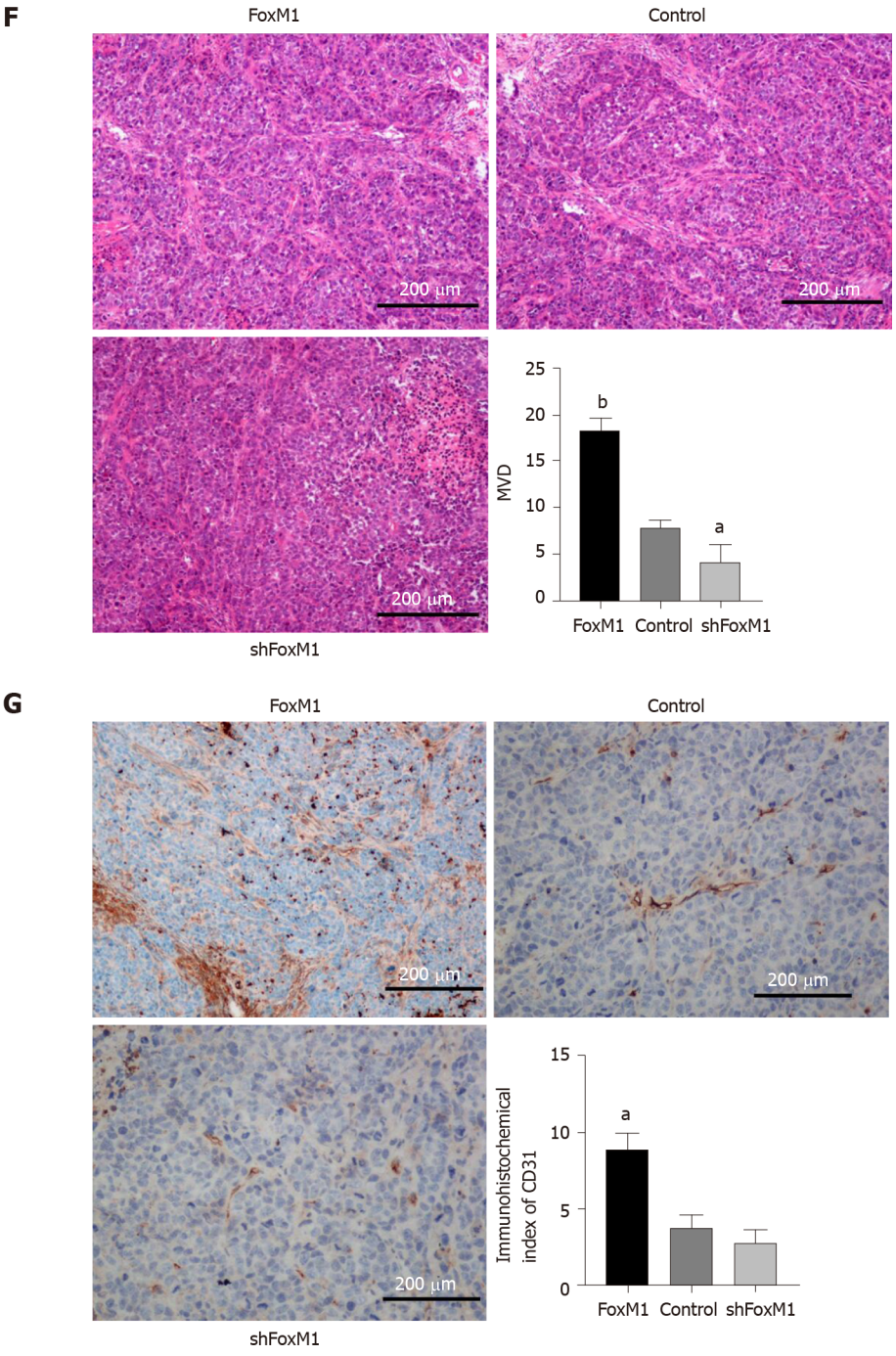


Figure 6 Fork head box M1 enhanced the angiogenesis of gallbladder cancer by regulating vascular endothelial growth factor-A *in vivo*. A: Tumor-bearing mice [(1) Lenti-fork head box M1 (FoxM1)-shRNA, (2) cDNA-FoxM1, (3) control: xenotransplantation model]; B: Tumor from the three groups; C: Body weight of tumor-bearing mice; D: Tumor volume of tumor-bearing mice; E: Hematoxylin-eosin staining of tumor foci; F: Hematoxylin-eosin staining of microvascular density; G: Immunohistochemistry staining of CD31. Five fields per sample were counted; four samples in the control and FoxM1 groups and three samples in the shFoxM1 group were analyzed. Scale bars: 200 μm. $^{a}P < 0.05$, $^{b}P < 0.01$. FoxM1: Fork head box M1.

Meier analysis was used to assess the impact of FoxM1 and VEGF-A on survival. The results showed that the group with high expression of FoxM1 or VEGF-A showed poor survival compared with the patients with low expression of FoxM1 and VEGF-A (Figure 7).

DISCUSSION

GBC is still a frequent malignancy with a dismal prognosis. Because of the rapid progression and low diagnosis rate of GBC, it is necessary to explore the inherent mechanisms of tumorigenesis. The essential interrelation between FoxM1 and VEGF-A

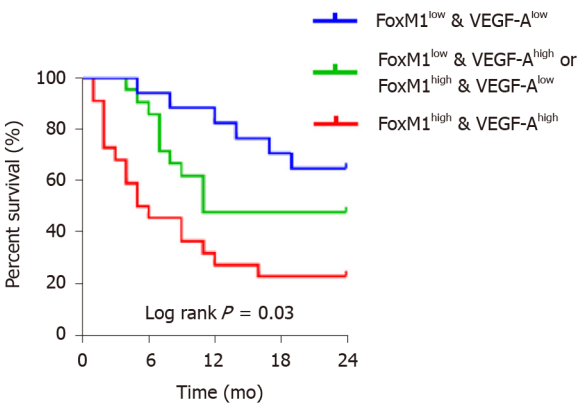


Figure 7 High expression of fork head box M1 and vascular endothelial growth factor-A were associated with poor prognosis of gallbladder cancer patients. Kaplan-Meier analysis, n = Blue: 12, Green: 14, Red: 20. FoxM1: Fork head box M1; VEGF-A: Vascular endothelial growth factor-A.

provided us with a broader approach to malignancy therapy. In this investigation, we found that FoxM1 played an essential role in the expression of VEGF. Previous studies have indicated that high expression levels of FoxM1 are relevant to adverse prognosis in multiple malignancies[9]. We proved that the upregulation of FoxM1 in GBC cells influenced the expression of VEGF-A *in vivo* and *in vitro*. In GBC patients, VEGF-A expression was closely related to the overexpression of FoxM1 and was highly expressed to promote vascularization. FoxM1 could directly regulate the activity of the VEGF gene promoter to induce its expression. We detected the opposite results in GBC cells with inhibited FoxM1. Our conclusions could provide a novel strategy for treating GBC.

The contribution of FoxM1 on numerous kinds of malignancies has been demonstrated by previous investigations[8,10-13]. As an important factor of poor prognosis, the expression level of FoxM1 has a negative correlation with survival duration[14-16]. In our previous study, we found that FoxM1 was upregulated in GBC tissues compared with normal tissues and as a prognostic biomarker had greater relevance to prognosis and survival[17]. Likewise, in this study, the role of VEGF-A in the progression of GBC was investigated. The same tumor-promoting function through enhanced proliferation, invasion and metastasis was observed in GBC cells. The function of VEGF-A in promoting cancer was also shown in other investigations[18,19]. A significant decrease in the expression of VEGF-A was detected after knocking down the expression of FoxM1.

Angiogenesis is indispensable to the proliferation of tumor cells, auxesis, migration and invasion. In addition, directly controlling angiogenesis could inhibit the progression of tumors. Angiogenesis is influenced by various factors, which has been shown in many studies[20]. Oxygen deficiency is one such factor. VEGF expression could be promoted by oxygen deficiency in a mouse model, especially in the adjacent areas of the necrotic regions[18-20]. For example, as glioma is a hypoxic tumor, the overexpression of VEGF in glioma is associated at least with hypoxia and has been observed in many studies[21-23]. Moreover, the following two observations were made in our research. The expression of VEGF in GBC cells was significantly higher than that in paracarcinoma tissue. The expression of VEGF in the adjacent areas of the necrotic regions was significantly related to the cells in other normal areas ($P < 0.001$).

In addition to VEGF, MMP-2, MMP-9 and uPAR are thought to participate in the migration and invasion of tumor cells[24]. It is generally accepted that VEGF is a predominant facilitator of angiogenesis and the angiogenic signaling cascade[25]. VEGF-A, a member of the VEGF family, is also considered to be critical for tumor growth, invasion and metastasis[26,27]. The direct interaction of FoxM1 with the VEGF-A promoter was discovered in our study, which could prove the direct regulation between FoxM1 and VEGF-A. First, the participation of FoxM1 in the regulation of the VEGF promoter was evidenced by our results, and the expression of FoxM1 could activate the VEGF promoter-mediated luciferase expression. Then, we selected two consensus binding sequences on the VEGF-A promoter to which FoxM1 could bind both *in vivo* and *in vitro*. After destroying them, the promoter of VEGF-A could not mediate its transcription. The activity of the FoxM1 binding areas could be evaluated.

It is also widely accepted that FoxM1 is a crucial mediator in the cell cycle[28]. FoxM1 is accumulated in the late G1 and S phases during the cell cycle. It could also be

downregulated by many tumor suppressors, such as p53. FoxM1-siRNA has been used to decrease the proliferation and division of cells by suppressing mRNA and protein related to the cell cycle. As essential components of tumor progression, MMP-2, MMP9, uPA and uPAR were reduced by decreasing FoxM1, which has been proven in numerous studies[6].

Previous investigations have shown that as a consequence of downregulating FoxM1 with FoxM1-siRNA, the colonies of tumor cells decrease significantly[29]. Other studies also revealed that downregulation of FoxM1 could decrease the average number of cells crossing the Matrigel-coated membrane in one high power field and the migrating distance[5,30]. This evidence suggests that FoxM1 plays an essential role in tumor progression. In the present study, we also found that the downregulation of FoxM1 could suppress the viability, migration and invasion of tumor cells. Moreover, decreased FoxM1 has been shown to be relevant to prognosis and survival.

In conclusion, this study indicated that FoxM1 could be directly involved in the regulation of VEGF-A expression by activating and regulating the VEGF-A promoter. The overexpression of FoxM1 leading to excess VEGF-A and angiogenesis was proven to be enhanced in the adjacent areas of the necrotic regions. Therefore, it is conceivable that controlling the expression of FoxM1 could inhibit the angiogenesis and growth of GBC cells with the possibility of decreasing the invasion and metastasis of cancer cells, indicating that FoxM1 may play a key role in the pathogenesis and disease progression of GBC. This is the first work on the effects of FoxM1 and VEGF-A on GBC cells, and we hope the data can offer some reference and evidence to other studies or promote further discussion.

CONCLUSION

In conclusion, FoxM1 and VEGF-A overexpression were associated with prognosis of GBC patients. FoxM1 regulated VEGF-A expression, which played an important role in the progression of GBC.

ARTICLE HIGHLIGHTS

Research background

Gallbladder cancer (GBC), with low detectable diagnosis and high metastasis, has a short survival time and a low 5-yr survival rate. Fork head box M1 (FoxM1) is relevant to poor prognosis and malignant behaviors, including proliferation, invasion and metastasis. Vascular endothelial growth factor-A (VEGF-A) plays an important role in angiogenesis. In GBC, it is meaningful to investigate the functional correlation between FoxM1 and VEGF-A.

Research motivation

FoxM1 is relevant to poor prognosis and malignant behaviors including proliferation, invasion and metastasis. VEGF-A plays an important role in angiogenesis. However, it is unclear whether FoxM1 could regulate VEGF-A.

Research objectives

This study aimed to investigate whether FoxM1 enhanced the angiogenesis of GBC *via* regulating VEGF-A.

Research methods

Using immunohistochemistry, we investigated FoxM1 and VEGF-A expression in GBC tissues, paracarcinoma tissues and cholecystitis tissues. Soft agar, cell invasion, migration and apoptosis assays were used to analyze the malignant phenotype influenced by FoxM1 in GBC. Kaplan-Meier survival analysis was performed to evaluate the impact of FoxM1 and VEGF-A expression in GBC patients. We investigated the relationship between FoxM1 and VEGF-A by regulating the level of FoxM1. Next, we performed MTT assays and Transwell invasion assays by knocking out or overexpressing VEGF-A to evaluate its function in GBC cells. The luciferase assay was used to reveal the relationship between FoxM1 and VEGF-A. BALB/c nude mice were used to establish the xenograft tumor model.

Research results

FoxM1 expression was higher in GBC tissues than in paracarcinoma tissues. Furthermore, the high expression of FoxM1 in GBC was significantly correlated with the malignant phenotype and worse overall survival. Meanwhile, high expression of FoxM1 influenced angiogenesis. Attenuated FoxM1 significantly suppressed cell proliferation, transfer and invasion *in vitro*. Knockdown of FoxM1 in GBC cells reduced the expression of VEGF-A. The luciferase assay showed that FoxM1 was the transcription factor of VEGF-A. Knockdown VEGF-A in FoxM1 overexpressed cells could partly reverse the malignant phenotype of GBC cells. High expression of FoxM1 combined with high expression of VEGF-A was related to poor prognosis. In this study, we found that FoxM1 was involved in regulation of VEGF-A expression.

Research conclusions

FoxM1 and VEGF-A overexpression were associated with prognosis of GBC patients. FoxM1 upregulated VEGF-A expression, which played an important role in the progression of GBC.

Research perspectives

By comprehending the way FoxM1 induced angiogenesis through regulating VEGF-A in GBC, the present study showed a possible method for treatment strategy of GBC patients with metastasis and in late stage.

ACKNOWLEDGEMENTS

We are indebted to the individuals who have participated in or have helped with this article.

REFERENCES

1 **Mehrotra R**, Tulsyan S, Hussain S, Mittal B, Singh Saluja S, Singh S, Tanwar P, Khan A, Javle M, Hassan MM, Pant S, De Aretxabala X, Sirohi B, Rajaraman P, Kaur T, Rath GK. Genetic landscape of gallbladder cancer: Global overview. *Mutat Res* 2018; **778**: 61-71 [PMID: 30454684 DOI: 10.1016/j.mrrev.2018.08.003]

2 **Montalvo-Jave EE**, Rahnemai-Azar AA, Papaconstantinou D, Deloiza ME, Tsilimigras DI, Moris D, Mendoza-Barrera GE, Weber SM, Pawlik TM. Molecular pathways and potential biomarkers in gallbladder cancer: A comprehensive review. *Surg Oncol* 2019; **31**: 83-89 [PMID: 31541911 DOI: 10.1016/j.suronc.2019.09.006]

3 **Hickman L**, Contreras C. Gallbladder Cancer: Diagnosis, Surgical Management, and Adjuvant Therapies. *Surg Clin North Am* 2019; **99**: 337-355 [PMID: 30846038 DOI: 10.1016/j.suc.2018.12.008]

4 **Choi HJ**, Jhe YL, Kim J, Lim JY, Lee JE, Shin MK, Cheong JH. FoxM1-dependent and fatty acid oxidation-mediated ROS modulation is a cell-intrinsic drug resistance mechanism in cancer stem-like cells. *Redox Biol* 2020; **36**: 101589 [PMID: 32521504 DOI: 10.1016/j.redox.2020.101589]

5 **Nandi D**, Cheema PS, Jaiswal N, Nag A. FoxM1: Repurposing an oncogene as a biomarker. *Semin Cancer Biol* 2018; **52**: 74-84 [PMID: 28855104 DOI: 10.1016/j.semcancer.2017.08.009]

6 **Liao GB**, Li XZ, Zeng S, Liu C, Yang SM, Yang L, Hu CJ, Bai JY. Regulation of the master regulator FOXM1 in cancer. *Cell Commun Signal* 2018; **16**: 57 [PMID: 30208972 DOI: 10.1186/s12964-018-0266-6]

7 **Song X**, Fiati Kenston SS, Zhao J, Yang D, Gu Y. Roles of FoxM1 in cell regulation and breast cancer targeting therapy. *Med Oncol* 2017; **34**: 41 [PMID: 28176242 DOI: 10.1007/s12032-017-0888-3]

8 **Kim H**, Park KJ, Ryu BK, Park DH, Kong DS, Chong K, Chae YS, Chung YG, Park SI, Kang SH. Forkhead box M1 (FOXM1) transcription factor is a key oncogenic driver of aggressive human meningioma progression. *Neuropathol Appl Neurobiol* 2020; **46**: 125-141 [PMID: 31179553 DOI: 10.1111/nan.12571]

9 **Liu L**, Wu J, Guo Y, Xie W, Chen B, Zhang Y, Li S, Hua Y, Peng B, Shen S. Overexpression of FoxM1 predicts poor prognosis of intrahepatic cholangiocarcinoma. *Aging (Albany NY)* 2018; **10**: 4120-4140 [PMID: 30580327 DOI: 10.18632/aging.101706]

10 **Wang H**, Li H, Hu L, Wang J, Liu Q, Wang D, Sun X. Overexpression of FoxM1 in Sinonasal Inverted Papilloma and Associated Squamous Cell Carcinoma. *Am J Rhinol Allergy* 2019; **33**: 706-715 [PMID: 31333047 DOI: 10.1177/1945892419863193]

11 **Zhou W**, Yu X, Sun S, Zhang X, Yang W, Zhang J, Zhang X, Jiang Z. Increased expression of MMP-2 and MMP-9 indicates poor prognosis in glioma recurrence. *Biomed Pharmacother* 2019; **118**: 109369 [PMID: 31545229 DOI: 10.1016/j.biopha.2019.109369]

12 **Hu G**, Yan Z, Zhang C, Cheng M, Yan Y, Wang Y, Deng L, Lu Q, Luo S. FOXM1 promotes hepatocellular carcinoma progression by regulating KIF4A expression. *J Exp Clin Cancer Res* 2019; **38**: 188 [PMID: 31072351 DOI: 10.1186/s13046-019-1202-3]

13 **Marchand B**, Pitarresi JR, Reichert M, Suzuki K, Laczkó D, Rustgi AK. PRRX1 isoforms cooperate with FOXM1 to regulate the DNA damage response in pancreatic cancer cells. *Oncogene* 2019; **38**: 4325-4339 [PMID: 30705403 DOI: 10.1038/s41388-019-0725-6]

14 **Cai H**, Chen J, He B, Li Q, Li Y, Gao Y. A FOXM1 related long non-coding RNA contributes to gastric cancer cell migration. *Mol Cell Biochem* 2015; **406**: 31-41 [PMID: 25907137 DOI: 10.1007/s11010-015-2421-3]

15 **Huang W**, Chen Z, Zhang L, Tian D, Wang D, Fan D, Wu K, Xia L. Interleukin-8 Induces Expression of FOXC1 to Promote Transactivation of CXCR1 and CCL2 in Hepatocellular Carcinoma Cell Lines and Formation of Metastases in Mice. *Gastroenterology* 2015; **149**: 1053-67. e14 [PMID: 26065367 DOI: 10.1053/j.gastro.2015.05.058]

16 **Okada K**, Fujiwara Y, Takahashi T, Nakamura Y, Takiguchi S, Nakajima K, Miyata H, Yamasaki M, Kurokawa Y, Mori M, Doki Y. Overexpression of forkhead box M1 transcription factor (FOXM1) is a potential prognostic marker and enhances chemoresistance for docetaxel in gastric cancer. *Ann Surg Oncol* 2013; **20**: 1035-1043 [PMID: 23054116 DOI: 10.1245/s10434-012-2680-0]

17 **Wang R**, Song Y, Xu X, Wu Q, Liu C. The expression of Nek7, FoxM1, and Plk1 in gallbladder cancer and their relationships to clinicopathologic features and survival. *Clin Transl Oncol* 2013; **15**: 626-632 [PMID: 23359173 DOI: 10.1007/s12094-012-0978-9]

18 **Wang Y**, Huang Q, Liu J, Wang Y, Zheng G, Lin L, Yu H, Tang W, Huang Z. Vascular endothelial growth factor A polymorphisms are associated with increased risk of coronary heart disease: a meta-analysis. *Oncotarget* 2017; **8**: 30539-30551 [PMID: 28430629 DOI: 10.18632/oncotarget.15546]

19 **Marisi G**, Scarpi E, Passardi A, Nanni O, Ragazzini A, Valgiusti M, Casadei Gardini A, Neri LM, Frassineti GL, Amadori D, Ulivi P. Circulating VEGF and eNOS variations as predictors of outcome in metastatic colorectal cancer patients receiving bevacizumab. *Sci Rep* 2017; **7**: 1293 [PMID: 28465540 DOI: 10.1038/s41598-017-01420-0]

20 **Xie Y**, Mansouri M, Rizk A, Berger P. Regulation of VEGFR2 trafficking and signaling by Rab GTPase-activating proteins. *Sci Rep* 2019; **9**: 13342 [PMID: 31527750 DOI: 10.1038/s41598-019-49646-4]

21 **Wei Y**, Sun Q, Zhao L, Wu J, Chen X, Wang Y, Zang W, Zhao G. LncRNA UCA1-miR-507-FOXM1 axis is involved in cell proliferation, invasion and G0/G1 cell cycle arrest in melanoma. *Med Oncol* 2016; **33**: 88 [PMID: 27389544 DOI: 10.1007/s12032-016-0804-2]

22 **Engeland K**. Cell cycle arrest through indirect transcriptional repression by p53: I have a DREAM. *Cell Death Differ* 2018; **25**: 114-132 [PMID: 29125603 DOI: 10.1038/cdd.2017.172]

23 **Jin H**, Li XJ, Park MH, Kim SM. FOXM1-mediated downregulation of uPA and MMP9 by 3,3'-diindolylmethane inhibits migration and invasion of human colorectal cancer cells. *Oncol Rep* 2015; **33**: 3171-3177 [PMID: 25962429 DOI: 10.3892/or.2015.3938]

24 **Elaimy AL**, Mercurio AM. Convergence of VEGF and YAP/TAZ signaling: Implications for angiogenesis and cancer biology. *Sci Signal* 2018; **11** [PMID: 30327408 DOI: 10.1126/scisignal.aau1165]

25 **Ramjiawan RR**, Griffioen AW, Duda DG. Anti-angiogenesis for cancer revisited: Is there a role for combinations with immunotherapy? *Angiogenesis* 2017; **20**: 185-204 [PMID: 28361267 DOI: 10.1007/s10456-017-9552-y]

26 **Frezzetti D**, Gallo M, Maiello MR, D'Alessio A, Esposito C, Chicchinelli N, Normanno N, De Luca A. VEGF as a potential target in lung cancer. *Expert Opin Ther Targets* 2017; **21**: 959-966 [PMID: 28831824 DOI: 10.1080/14728222.2017.1371137]

27 **Liang L**, Yue Z, Du W, Li Y, Tao H, Wang D, Wang R, Huang Z, He N, Xie X, Han Z, Liu N, Li Z. Molecular Imaging of Inducible VEGF Expression and Tumor Progression in a Breast Cancer Model. *Cell Physiol Biochem* 2017; **42**: 407-415 [PMID: 28558368 DOI: 10.1159/000477485]

28 **Zhang J**, Niu Y, Huang C. Role of FoxM1 in the Progression and Epithelial to Mesenchymal Transition of Gastrointestinal Cancer. *Recent Pat Anticancer Drug Discov* 2017; **12**: 247-259 [PMID: 28440206 DOI: 10.2174/1574892812666170424144352]

29 **O'Regan RM**, Nahta R. Targeting forkhead box M1 transcription factor in breast cancer. *Biochem Pharmacol* 2018; **154**: 407-413 [PMID: 29859987 DOI: 10.1016/j.bcp.2018.05.019]

30 **Laissue P**. The forkhead-box family of transcription factors: key molecular players in colorectal cancer pathogenesis. *Mol Cancer* 2019; **18**: 5 [PMID: 30621735 DOI: 10.1186/s12943-019-0938-x]

World Journal of Gastroenterology

Submit a Manuscript: https://www.f6publishing.com

World J Gastroenterol 2021 February 28; 27(8): 708-724

DOI: 10.3748/wjg.v27.i8.708

ISSN 1007-9327 (print) ISSN 2219-2840 (online)

ORIGINAL ARTICLE

Basic Study

Effect of berberine on hyperglycaemia and gut microbiota composition in type 2 diabetic Goto-Kakizaki rats

Jin-Dong Zhao, Yan Li, Min Sun, Chan-Juan Yu, Jia-Yun Li, Si-Hai Wang, Di Yang, Cheng-Lin Guo, Xue Du, Wen-Jin Zhang, Ruo-Dong Cheng, Xiao-Chuan Diao, Zhao-Hui Fang

ORCID number: Jin-Dong Zhao 0000-0003-0005-1820; Yan Li 0000-0002-7640-7216; Min Sun 0000-0002-8528-0050; Chan-Juan Yu 0000-0002-4897-4109; Jia-Yun Li 0000-0003-2471-8669; Si-Hai Wang 0000-0003-3526-7867; Di Yang 0000-0002-9253-5293; Cheng-Lin Guo 0000-0003-3884-1035; Xue Du 0000-0002-6573-8060; Wen-Jin Zhang 0000-0003-4554-4653; Ruo-Dong Cheng 0000-0002-0861-7748; Xiao-Chuan Diao 0000-0002-0884-2144; Zhao-Hui Fang 0000-0002-3197-1534.

Author contributions: Zhao JD, Li Y and Fang ZH designed the study and wrote the manuscript; Sun M, Yu CJ, Li JY, Diao XC, Guo CL, Yang D, Du X, and Zhang WJ conducted the experiments; Wang SH and Cheng RD helped complete the data analysis and provided language modification; all authors read and approved the final manuscript.

Supported by National Natural Science Foundation of China, No. 81603574 and No. 81774286; National Key Research and Development Program, No. 2018YFC1704202 and No. 2020YFE0201800; University Scientific Research Projects of Anhui, No. KJ2020A0401 and No. KJ2019A0442; and Province Science Foundation of Anhui, No.

Jin-Dong Zhao, Chan-Juan Yu, Jia-Yun Li, Si-Hai Wang, Di Yang, Cheng-Lin Guo, Xue Du, Wen-Jin Zhang, Ruo-Dong Cheng, Xiao-Chuan Diao, Zhao-Hui Fang, Department of Endocrinology, The First Affiliated Hospital of Anhui University of Chinese Medicine, Hefei 230031, Anhui Province, China

Yan Li, Department of Infectious Diseases, The First Affiliated Hospital of Anhui University of Chinese Medicine, Hefei 230031, Anhui Province, China

Min Sun, School of Life Sciences, Anhui University, Hefei 230039, Anhui Province, China

Corresponding author: Zhao-Hui Fang, PhD, Chief Doctor, Department of Endocrinology, The First Affiliated Hospital of Anhui University of Chinese Medicine, No. 117 Meishan Road, Hefei 230031, Anhui Province, China. fangzhaohui1111@163.com

Abstract

BACKGROUND

A recent investigation showed that the prevalence of type 2 diabetes mellitus (T2DM) is 12.8% among individuals of Han ethnicity. Gut microbiota has been reported to play a central role in T2DM. Goto-Kakizaki (GK) rats show differences in gut microbiota compared to non-diabetic rats. Previous studies have indicated that berberine could be successfully used to manage T2DM. We sought to understand its hypoglycaemic effect and role in the regulation of the gut microbiota.

AIM

To determine whether berberine can regulate glucose metabolism in GK rats *via* the gut microbiota.

METHODS

GK rats were acclimatized for 1 wk. The GK rats were randomly divided into three groups and administered saline (Mo), metformin (Me), or berberine (Be). The observation time was 8 wk, and weight, fasting blood glucose (FBG), insulin, and glucagon-like peptide-1 (GLP-1) were measured. Pancreatic tissue was observed for pathological changes. Additionally, we sequenced the 16S rRNA V3-V4 region of the gut microbiota and analysed the structure.

RESULTS

1708085QH213.

Institutional review board statement: The Institutional Review Board approval is not applicable in this study because it did not involve human beings.

Institutional animal care and use committee statement: All animal experiments were performed in accordance with the guidelines approved by the Animal Ethics Committee of Diabetes Institute, Anhui Academy Chinese Medicine (approval No. 2017AH-06).

Conflict-of-interest statement: None of the authors have any conflicts of interest to declare.

Data sharing statement: No additional data are available.

ARRIVE guidelines statement: The authors have read the ARRIVE guidelines, and the manuscript was prepared and revised according to the ARRIVE guidelines.

Open-Access: This article is an open-access article that was selected by an in-house editor and fully peer-reviewed by external reviewers. It is distributed in accordance with the Creative Commons Attribution NonCommercial (CC BY-NC 4.0) license, which permits others to distribute, remix, adapt, build upon this work non-commercially, and license their derivative works on different terms, provided the original work is properly cited and the use is non-commercial. See: http://creativecommons.org/Licenses/by-nc/4.0/

Manuscript source: Unsolicited manuscript

Specialty type: Gastroenterology and hepatology

Country/Territory of origin: China

Peer-review report's scientific quality classification

Grade A (Excellent): 0
Grade B (Very good): 0
Grade C (Good): C, C
Grade D (Fair): 0

Compared with the Mo group, the Me and Be groups displayed significant differences in FBG ($P < 0.01$) and GLP-1 ($P < 0.05$). A significant decrease in weight and homeostatic model assessment-insulin resistance was noted in the Be group compared with those in the Me group ($P < 0.01$). The pancreatic islets of the Me- and Be-treated rats showed improvement in number, shape, and necrosis compared with those of Mo-treated rats. A total of 580 operational taxonomic units were obtained in the three groups. Compared to the Mo group, the Me and Be groups showed a shift in the structure of the gut microbiota. Correlation analysis indicated that FBG was strongly positively correlated with Clostridia_UCG-014 ($P < 0.01$) and negatively correlated with *Allobaculum* ($P < 0.01$). Body weight showed a positive correlation with *Desulfovibrionaceae* ($P < 0.01$) and a negative correlation with *Akkermansia* ($P < 0.01$). Importantly, our results demonstrated that Me and Be could significantly decrease *Bacteroidetes* ($P < 0.01$) and the *Bacteroidetes*/*Firmicutes* ratio ($P < 0.01$). Furthermore, *Muribaculaceae* ($P < 0.01$; $P < 0.05$) was significantly decreased in the Me and Be groups, and *Allobaculum* ($P < 0.01$) was significantly increased.

CONCLUSION

Berberine has a substantial effect in improving metabolic parameters and modulating the gut microbiota composition in T2DM rats.

Key Words: Type 2 diabetes mellitus; Amelioration of hyperglycaemia; Modulation of gut microbiota; Berberine; Metformin; Goto-Kakizaki rats

©The Author(s) 2021. Published by Baishideng Publishing Group Inc. All rights reserved.

Core Tip: Recent studies suggested that the gut microbiota has an essential role in type 2 diabetes mellitus. Our study verifies the effects of berberine in regulating glucose metabolism and reducing pancreas injury in Goto-Kakizaki rats. Berberine also provides an alternative means of modulating the gut microbiota. The results revealed evidence of a decrease in *Desulfobacterota*, *Desulfovibrionaceae,* and Clostridia_UCG-014 and an increase in *Verrucomicrobiota*, *Akkermansia*, and *Allobaculum*. Correlation analysis indicated that fasting blood glucose was strongly positively correlated with Clostridia_UCG-014 and negatively correlated with *Allobaculum*.

Citation: Zhao JD, Li Y, Sun M, Yu CJ, Li JY, Wang SH, Yang D, Guo CL, Du X, Zhang WJ, Cheng RD, Diao XC, Fang ZH. Effect of berberine on hyperglycaemia and gut microbiota composition in type 2 diabetic Goto-Kakizaki rats. *World J Gastroenterol* 2021; 27(8): 708-724
URL: https://www.wjgnet.com/1007-9327/full/v27/i8/708.htm
DOI: https://dx.doi.org/10.3748/wjg.v27.i8.708

INTRODUCTION

Type 2 diabetes mellitus (T2DM) has become a critical and urgent human health concern worldwide. A recent epidemiological investigation shows that the prevalence of T2DM is 12.8% among individuals of Han ethnicity[1]. T2DM is a metabolic disorder and affects patients' quality of life. Its physiological hallmarks are insulin resistance and β-cell failure[2]. Accumulating evidence has suggested that diabetes is also associated with gut microbiota composition and homeostasis[3].

Goto-Kakizaki (GK) rats, which provide an elevated blood glucose and non-obese T2DM experimental model, have been widely used to study T2DM[4,5]. When GK rats are 28 d of age, basal hyperglycaemia, impaired insulin secretion by pancreatic β-cells, and increased hepatic glucose production are observed[6,7]. Typical T2DM characteristics are more obvious in 8-week-old rats[8].

T2DM patients and animals show significant differences in gut microbiota composition compared to their non-diabetic counterparts[9-11]. Hence, regulators of gut microbiota may become potential alternative targets for diabetes treatment. Metformin is a first-line oral agent used to treat T2DM. Metformin therapy for T2DM has been extensively used for 70 years[12]. Its main effect involves decreasing hepatic glucose

Grade E (Poor): 0

Received: October 24, 2020
Peer-review started: October 24, 2020
First decision: November 23, 2020
Revised: December 17, 2020
Accepted: January 13, 2021
Article in press: January 13, 2021
Published online: February 28, 2021

P-Reviewer: Li H, Olt S
S-Editor: Gao CC
L-Editor: Wang TQ
P-Editor: Ma YJ

production and improving glucose uptake and insulin sensitivity[13,14]. Some studies also suggest that metformin treatment modulates the gut microbiota, thus contributing to the anti-diabetic effect[15-17].

For many years, studies have shown that tradition Chinese medicine (TCM) exhibits an effect against the development of T2DM and treats T2DM by decreasing fasting blood glucose (FBG) and glycated haemoglobin A1c, improving insulin resistance, and protecting β-cells and pancreatic islet function[18-20]. Berberine has been used as a TCM or an alternative treatment for T2DM. Berberine is derived from *Rhizoma Coptidis*, *Cortex Phellodendri Amurensis*, *Radix Scutellariae Baicalensis*, and others. Recently, many scholars have demonstrated that berberine is an effective, potent anti-diabetic agent[21,22]. At present, there are many reports indicating that berberine can regulate blood glucose, improve blood lipids, and reduce insulin resistance[19,23,24]. Some studies have reported that berberine repairs the gut barrier structure and alters the diversity of the gut microbiota[25,26], suggesting that its effects are exerted *via* modulation of the gut bacteria.

More information regarding the influence of berberine on T2DM hyperglycaemia and gut microbiota composition is needed. In this study, we evaluated the effects of berberine in regulating glucose metabolism and its influence on imbalanced gut microbiota in T2DM GK rats to elucidate the hypoglycaemic mechanism of berberine.

MATERIALS AND METHODS

Chemicals

Berberine chloride hydrate was purchased from Shanghai Macklin Biochemical Co., Ltd. (Shanghai, China). Metformin was purchased from Sino-American Shanghai Squibb Pharmaceuticals Ltd., (Shanghai, China). Plasma insulin and stimulate glucagon-like peptide-1 (GLP-1) concentrations were measured with a Mercodia ELISA kit (Uppsala, Sweden). The assay kits for FBG, total cholesterol (TC), and triglycerides (TG) were provided by Nanjing Jiancheng Bioengineering Institute (Nanjing, China).

Animals and experimental design

Thirty male GK rats (6 wk old) were obtained from the Shanghai Laboratory Animal Center (Shanghai, China; certificate No. 2015000535026). The animals were acclimated in a specific pathogen-free animal laboratory at 22 ± 2 °C with 50%-70% relative humidity under a 12/12 h light/dark cycle. They were fed standard laboratory chow and provided with water *ad libitum*.

Following acclimatization for 1 wk, GK rats with high FBG levels exceeding 11.1 mmol/L were randomly divided into three groups (n = 10): A model group (Mo), which received an equal volume of saline intragastrically once daily; a metformin group (Me), which received 100 mg/kg intragastrically once daily; and a berberine group (Be), which received 200 mg/kg intragastrically once daily. The course of treatment was 8 wk, and body weight was measured every 2 wk. One rat from each of the three groups (3 total) died during the experiment; we speculate that the cause may be related to high blood glucose, infection, or other conditions.

Sample collection and biochemical analysis

At the end of the observation period, 27 rats were weighed and deeply anaesthetized with intraperitoneal pentobarbital sodium (30 mg/kg, Merck, United States). Blood samples were collected in non-heparinized tubes, incubated on ice for 30-60 min, and centrifuged at 4000 rpm for 10 min at 4 °C, and the entire contents of the colon were carefully removed and placed in Eppendorf tubes. The serum, pancreas, and colon contents were then collected and stored at -80 °C. The FBG and lipid parameters were analysed using an automatic biochemistry analyser (AU 7600, HITACHI, Japan). Serum insulin and GLP-1 were measured using a Multi-Mode Microplate Reader (Synergy Neo2, Biotek, United States) according to the manufacturer's instructions. Isolated pancreas tissues were fixed in a tube containing 4% paraformaldehyde solution for 24 h.

Histology

Pancreatic tissues were washed with phosphate-buffered saline, embedded in paraffin wax, sliced into 5-μm sections, and stained with haematoxylin and eosin (H&E). The sections were observed using a Zeiss Axioskop 2 plus upright light microscope and

camera (Zeiss, Oberkochen, Germany; × 100 magnification).

Illumina MiSeq pyrosequencing of the gut microbiota

Total bacterial DNA was extracted using a TIANamp Stool DNA kit (Tiangen Biotech Co., Ltd., Beijing, China) following the manufacturers' instructions and stored at -20 °C prior to further analysis. The 16S rRNA gene from DNA samples was amplified using the conventional barcoded universal bacterial primers F338/R806 targeting the V3-V4 region, which were selected to analyse the taxonomic composition of the gut microbiota. Sequencing of polymerase chain reaction products was performed using the Illumina HiSeq platform (Illumina, San Diego, CA, United States) for pair-end reads with an average length of 451 bp. The trimmed sequences were de-multiplexed and quality-filtered to the Quantitative Insights Into Microbial Ecology (QIIME, v1.9.1) and R software (v3.3.1)[10,27]. The acquired data were analysed by the Majorbio Biopharm Technology Co., Ltd. (Shanghai, China)[28].

The results of the shared and unique classification of operational taxonomic units (OTUs) were determined using the Greengenes Database (http://greengenes.secondgenome.com/) following the 97% homology cut-off value[29]. Taxonomic annotation of OTUs was performed using the RDP Classifier (https://sourceforge.net/projects/rdp-classifier/) against the SILVA 16S rRNA database (https://www.arb-silva.de/), which was performed using R software. Venn diagrams, community bar charts, unweighted UniFrac-based principal coordinates analysis (PCoA), and correlation heat-maps were generated using R software.

Statistical analysis

All data are expressed as the mean ± SD for each group. The data were analysed by one-way analysis of variance (ANOVA) followed by the least significant differences test or Tamhane's T2 and Spearman's correlation with SPSS 23.0 software (NY, United States). P values < 0.05 were considered indicative of statistical significance. GraphPad Prism 5.0 software and Multi Experiment Viewer software (v4.9.0) were used to perform the statistical analyses.

RESULTS

Body weight and metabolic parameter levels after treatment

Before treatment, body weight was not significantly different (P > 0.05) among the three groups. Compared with the Mo and Me groups, the Be group had a significantly lower weight from 4 to 9 wk (P < 0.01). However, the body weight of Me rats was not significantly different from that of the Mo group (Figure 1).

The FBG levels were also not significantly different (P > 0.05) before the experiment. Compared with those of the Mo group, the FBG levels of the Me and Be groups were notably lower. Moreover, the Be group exhibited a marked reduction compared with the Me group (P < 0.01) (Figure 2A). The fasting insulin level was significantly different between the Mo and Me groups (P < 0.05), and it was close to being significantly different in the Be group (P = 0.058) (Figure 2B). In addition, homeostatic model assessment-insulin resistance (HOMA-IR) showed a greater reduction in insulin resistance after treatment in the Be group than in the Mo or Me groups (P < 0.01) (Figure 2C). Compared with that in the Mo group, the GLP-1 levels of the Me and Be groups were notably increased (P < 0.05). There were no significant differences in fasting insulin or GLP-1 between the Me and Be groups (P > 0.05) (Figure 2B and D).

Interestingly, the Be group showed lower TC values than the Mo group (P < 0.01). There was no significant difference between the Be and Me groups (P > 0.05); however, both showed a similar trend in blood lipid regulation. In addition, the TG levels were not significantly different after treatment (Figure 2E).

Pathological changes in the pancreas after treatment

As expected, H&E staining revealed that the pancreatic islet β cells in the Mo group were reduced, and the pancreatic islets had mild amyloidosis. The size of the β cells was decreased, the nuclei showed pyknosis, endocrine granules were significantly reduced, and lipids were deposited in the cell cytoplasm (Figure 3A). In the Me and Be groups, the shape of the pancreatic islets was still regular, the number of pancreatic islet β cells was slightly increased, the nucleus was enlarged and rounded, the H&E staining was lighter, and the capillaries in the pancreatic islets were proliferated (Figure 3B and C).

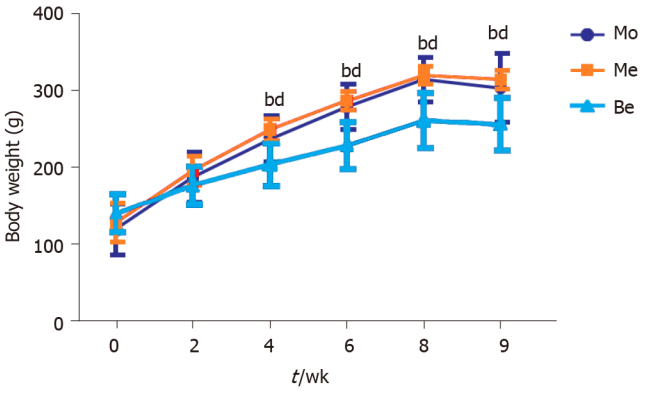


Figure 1 Comparison of body weight. $^{b}P < 0.01$ *vs* the Mo group; $^{d}P < 0.01$ *vs* the Me group. Mo: Model group; Me: Metformin group; Be: Berberine group.

Community structure of the gut microbiota

To characterize the composition of the gut microbiota, a total of 1505750 clean reads were generated from 27 samples, providing a total of 580 OTUs. Notably, eight unique OTUs were found in the Be group, one was found in the Me group, and there were no unique OTUs in the Mo group (Figure 4).

PCoA score plots based on phylogenetic statistical analysis methods indicated clustering of the gut microbiota within groups. PCoA of both unweighted UniFrac distances showed a clear separation in the three groups [the first principal component 47.56%, the second principal component (PC2) 26.95%]. The gut microbiota structure of the Me and Be groups showed the same trend, particularly an obvious shift along PC2 with Be treatment (Figure 5).

Modulation of the key community of gut microbiota

The dominant gut bacteria were of the phylum *Firmicutes* and *Bacteroidetes*. The composition of each sample is listed in detail (Figure 6). The abundance of *Firmicutes* in the Me group (85.62% ± 4.85%) was significantly higher than that in the Mo group (73.21% ± 4.63%) ($P < 0.01$). The proportion of *Firmicutes* showed an increasing trend in the Be group (78.30% ± 12.39%), but there was no significant difference compared with that in the Mo and Me groups ($P > 0.05$). In contrast, the composition of *Bacteroidetes* was significantly lower in the Me and Be groups (6.30% ± 2.56%, 8.38% ± 5.51%) than in the Mo group (14.65% ± 4.01%) ($P < 0.01$) (Figure 7). The gut microbiota of the Mo group was characterized by an increased *Bacteroidetes*/*Firmicutes* ratio (20.10 ± 5.66), and this ratio showed significant differences with lower proportions in the Me and Be groups (7.48 ± 3.24, 12.15 ± 11.66) ($P < 0.01$) (Figure 7). There were no significant differences in *Firmicutes*, *Bacteroidetes*, or the *Bacteroidetes*/*Firmicutes* ratio between the Me and Be groups ($P > 0.05$) (Figure 7).

Desulfobacterota abundance in the Be group (1.36% ± 2.63%) was significantly lower than that in the Mo and Me groups (9.93% ± 6.37%, 6.64% ± 4.00%) ($P < 0.01$ or $P < 0.05$). The proportion of *Desulfobacterota* showed a decreasing trend in the Me group, but there was no significant difference compared with that in the Mo group ($P > 0.05$) (Figure 7). Furthermore, *Verrucomicrobiota* in the Be group (8.59% ± 8.87%) was significantly higher than that in the Mo and Me groups ($P < 0.01$), but these changes were not significantly different between the Mo and Me groups. The mean did not exceed 0.05% in the Me and Be groups (Figure 7).

At the genus level, the microbiota composition varied greatly among the three groups (Figure 8). The relative abundance of *Allobaculum* contributed to 24.36% of the total faecal microbiota population. A higher proportion of *Allobaculum* was observed in the Be and Me groups (37.76% ± 10.35%, 28.49% ± 9.55%) than in the Mo group (7.07% ± 7.81%) ($P < 0.01$). Moreover, the Be group exhibited a remarkable increment compared with the Me group ($P < 0.05$) (Figure 9). Reductions in *Muribaculaceae*, *Lachnospiraceae*, *Desulfovibrionaceae*, and Clostridia_UCG-014 were detected in the Be group compared with those in the Mo group ($P < 0.01$, $P < 0.05$). Furthermore, the advantages of the Be group were more prominent than those in the Me group at *Desulfovibrionaceae* and Clostridia_UCG-014 ($P < 0.01$) (Figure 9). The Be group exhibited a significant increase in the relative abundance of *Akkermansia* compared with that in the Mo and Me groups ($P < 0.01$) (Figure 9).

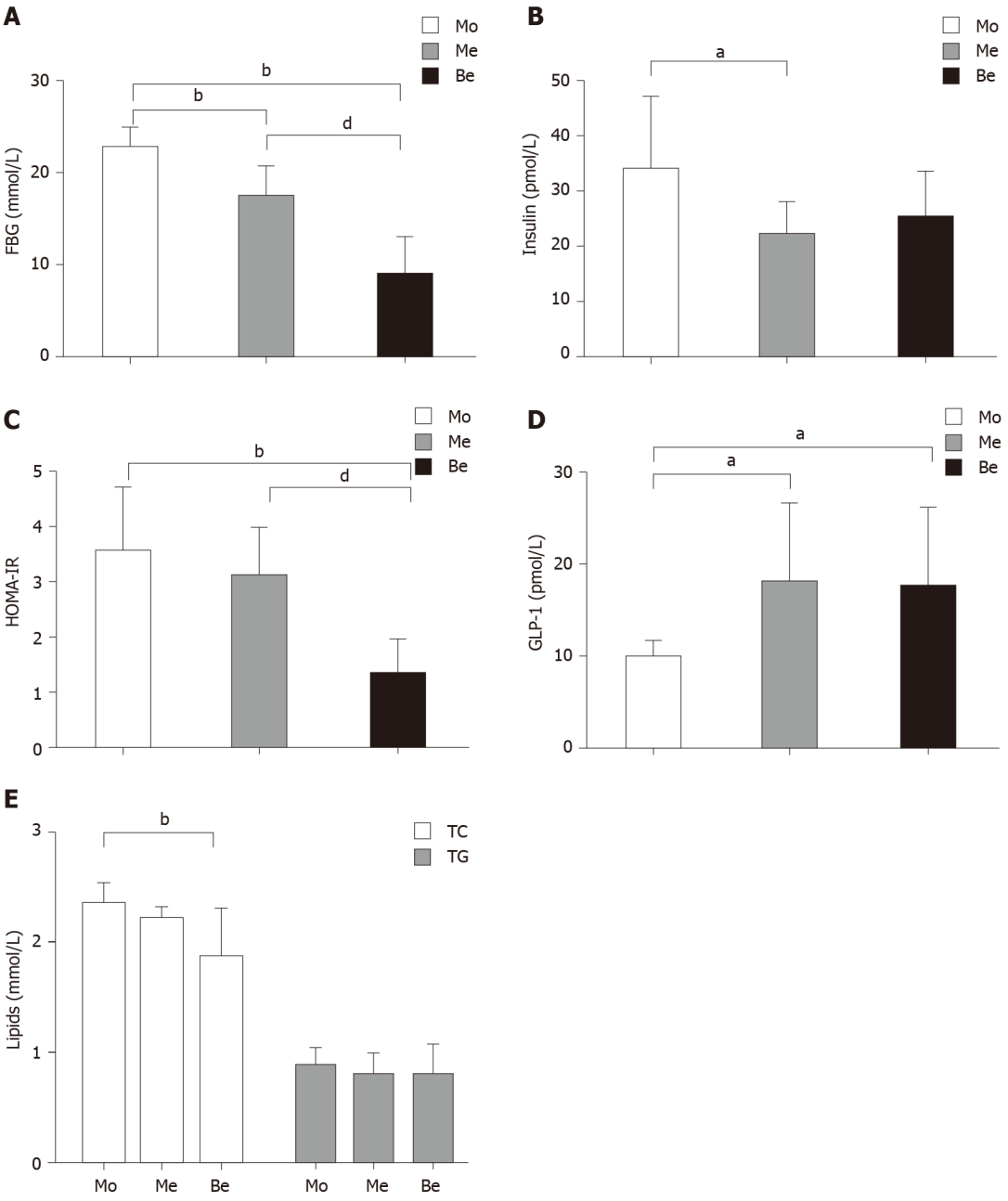


Figure 2 Body weight and metabolic parameter levels after treatment. A: Comparison of the fasting FBG levels. $^{b}P < 0.01$ *vs* the model (Mo) group; $^{d}P < 0.01$ *vs* the metformin (Me) group; B: Comparison of the insulin levels. $^{a}P < 0.05$ *vs* the Mo group; C: Comparison of the homeostatic model assessment-insulin resistance levels. $^{b}P < 0.01$ *vs* the Mo group; $^{d}P < 0.05$ *vs* the Me group; D: Comparison of the glucagon-like peptide-1 levels. $^{a}P < 0.05$ *vs* the Mo group; E: Comparison of the lipid levels. $^{b}P < 0.01$ *vs* the Mo group. FBG: Fasting blood glucose; HOMA-IR: Homeostatic model assessment-insulin resistance; GLP-1: Glucagon-like peptide-1; TC: Total cholesterol; TG: Triglycerides; Mo: Model group; Me: Metformin group; Be: Berberine group.

Correlations between T2DM-related factors and gut microbiota

Correlation heat-map analysis was applied to investigate T2DM-related factors that significantly affected gut microbiota at the genus level (Figure 10). Based on the heat map, we found that *Desulfovibrionaceae*, *Lachnospiraceae*, and Clostridia_UCG-014 were positively correlated with the FBG levels, while *Allobaculum* and *Akkermansia* were negatively associated with the FBG concentration ($P < 0.05$, $P < 0.01$). Among them, a strong correlation with Clostridia_UCG-014 and *Allobaculum* was observed. HOMA-IR and Clostridia_UCG-014 were significantly positively correlated, and HOMA-IR was negatively correlated with *Akkermansia* ($P < 0.05$). In addition, both FBG and TC levels showed positive correlations with *Desulfovibrionaceae* and Clostridia_UCG-014 and negative correlations with *Allobaculum* and *Akkermansia* ($P < 0.05$). Body weight showed a positive correlation with *Desulfovibrionaceae*, *Lachnospiraceae*, and Clostridia_UCG-014 and a negative correlation with *Akkermansia* ($P < 0.05$) (Figure 11).

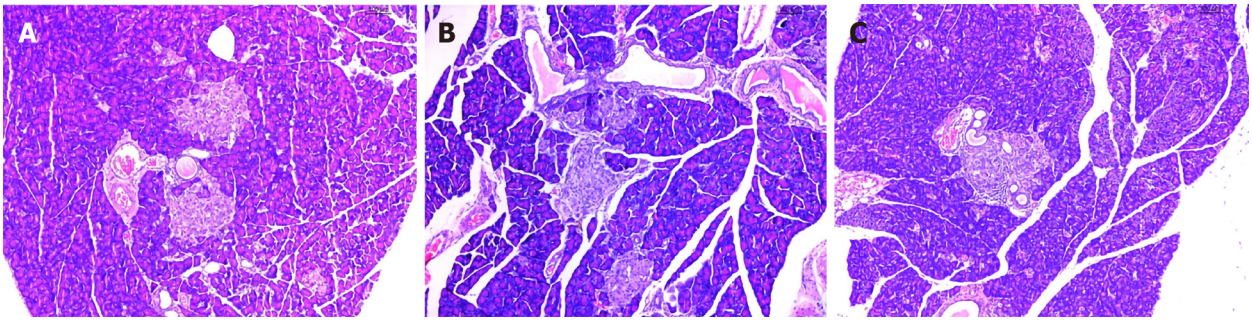


Figure 3 Histopathological images of the pancreas. Hematoxylin and eosin staining (original magnification × 100). A: Model group; B: Metformin group; C: Berberine group.

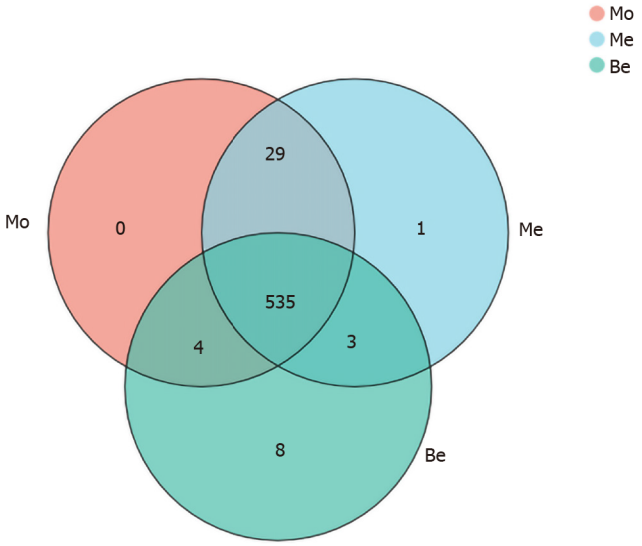


Figure 4 Comparison of the operational taxonomic units. Mo: Model group; Me: Metformin group; Be: Berberine group.

Correlation network built with Networkx

Networkx analysis was performed to build a species correlation network and between-species and T2DM-related factors correlation network (Figures 11 and 12). In the single-factor correlation network comparisons, we found that *Allobaculum* had a direct negative correlation with Clostridia_UCG-014 and *Muribaculaceae*. Clostridia_UCG-014 had a direct negative correlation with *Akkermansia* but not with *Allobaculum*. Meanwhile, a positive correlation with *Lactobacillus* was shown. In addition, there were certain associations among seven of the eight most abundant bacterial species (Figure 13). Based on the 16 most abundant bacteria and seven indicators related to T2DM, a two-factor correlation network diagram was formed and involved eight bacterial species and three indicators (Figure 12). FBG was positively correlated with five bacterial species and negatively correlated with two bacterial species. HOMA-IR was positively correlated with four bacterial species and negatively correlated with one bacterial species. TC was positively correlated with four bacterial species and negatively correlated with two bacterial species.

DISCUSSION

In the present study, we found that administration of metformin for 8 wk did not effectively lower body weight compared with saline. In previous research, the results indicated that metformin treatment improved markers of metabolic disorders and that body weight of T2DM patients or animals remained constant[10,30]. The main reasons may be as follows: GK rats are not obese and do not show significant weight gain. Furthermore, standard rodent feed was used in this study. In addition, although metformin can reduce weight, the effect is not obvious in non-obese subjects. It has

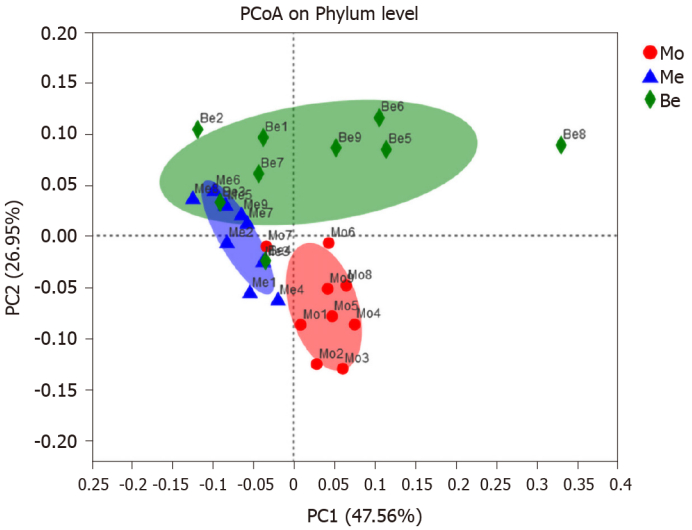


Figure 5 Comparison of gut microbiota structure using principal coordinates analysis. PCoA: Principal coordinates analysis; PC1: The first principal component; PC2: The second principal component; Mo: Model group; Me: Metformin group; Be: Berberine group.



Figure 6 Comparison of the composition abundance in gut bacterial phylum.

been demonstrated that metformin could modulate FBG and insulin in our study, and the same results were obtained in previous studies[31,32]. We did not observe a significant improvement in HOMA-IR with metformin treatment, which may be because of the short-term treatment or because normal feed was used in the present study unlike that in other research. Therefore, we need to conduct long-term observation in further studies.

Although metformin is a powerful drug in T2DM, berberine showed the best hypoglycaemic and body weight-lowering effect in this research. Body weight has positive and negative correlations with gut microbiota; adjustment of the gut microbiota has an effect on body weight. Moreover, Chinese medicine theory believes that berberine has the characteristics of bitterness and coldness; thus, it may reduce food intake and energy intake, which leads to a significant reduction in body weight and FBG. In addition, berberine improves HOMA-IR, thus exerting a strong anti-glycaemic effect. These findings are similar to those of a previous systematic review[22]. In addition, our current results show that berberine treatment provided a beneficial effect on elevated levels of TC compared with saline. This may be due to the means by which berberine promotes lipid metabolism, improves antioxidant capacity, and

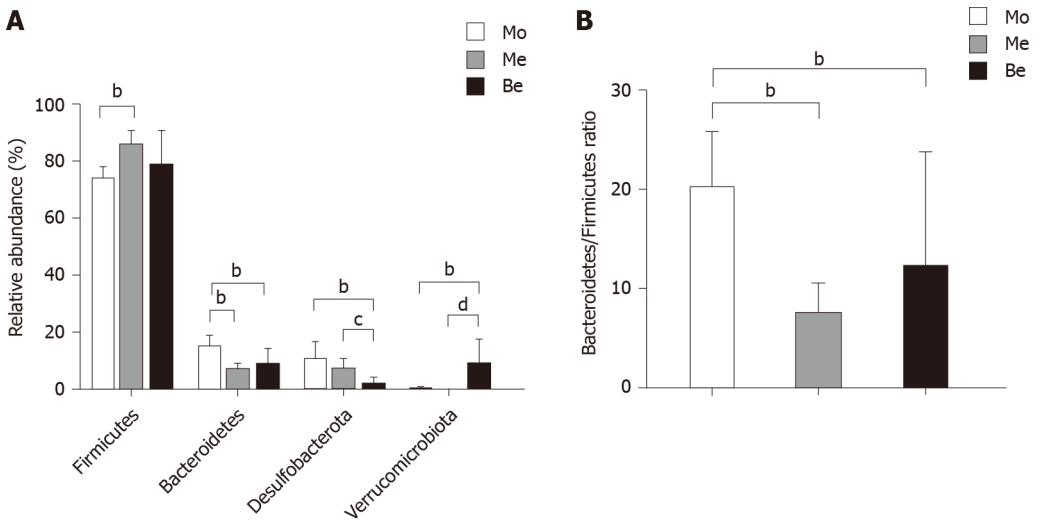


Figure 7 Relative abundance of gut bacterial phylum and the *Bacteroidetes*/*Firmicutes* ratio. A: Comparison of the relative abundance of gut bacterial phylum; $^{b}P < 0.01$ *vs* the model group; $^{c}P < 0.05$, $^{d}P < 0.01$ *vs* the metformin group; B: Comparison of the *Bacteroidetes*/*Firmicutes* ratio; $^{b}P < 0.01$ *vs* the model group. Mo: Model group; Me: Metformin group; Be: Berberine group.

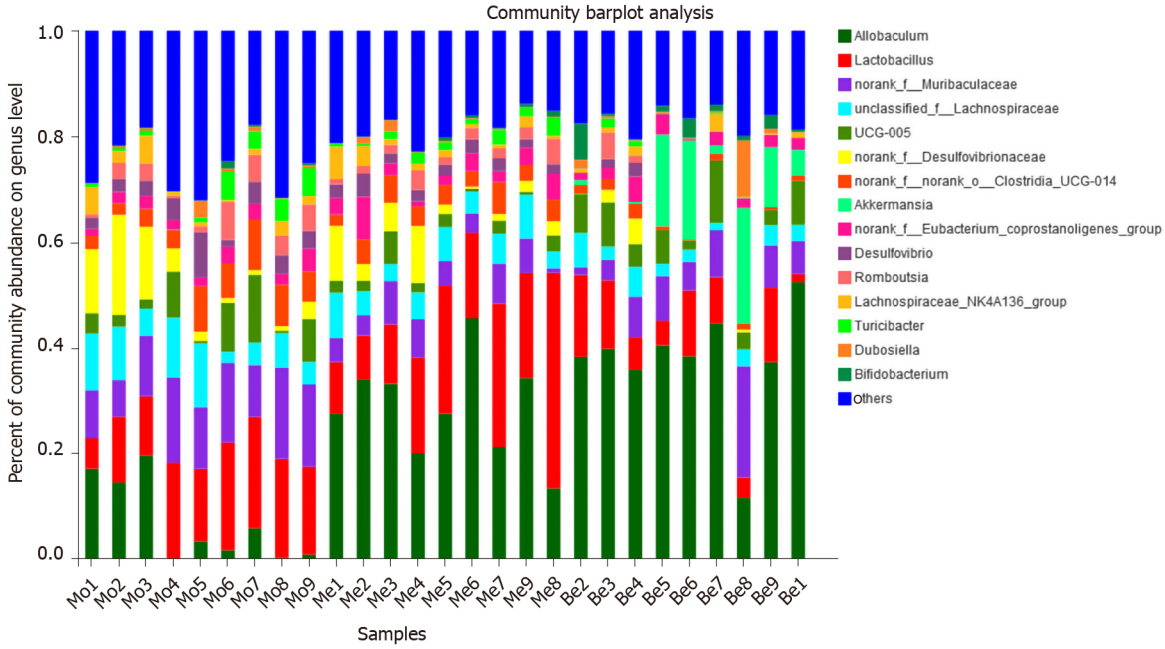


Figure 8 Comparison of the composition abundance in gut bacterial genera.

inhibits preadipocyte differentiation[33].

Short chain fatty acids (SCFAs) as fermentation products of gut microbiota are involved in stimulating the secretion of a number of gut peptide hormones, including PYY, GLP-1, and GLP-2[34]. GLP-1 has an effect on insulin secretion following meal consumption. It is also involved in the regulation of β-cell proliferation and protection of β-cells in the pancreatic islets[35]. It is well known that the insulin-producing β-cells are important in maintaining balance in glucose metabolism. The pancreatic islets of rats in the Mo group displayed severe pathology, including fewer cells, smaller size of cells, and necrosis. The pancreatic islets of rats in the Me and Be groups showed improvement compared with those in the Mo group. These results agree with the findings of Cui *et al*[36].

A previous study showed that the secretion of GLP-1 was lower in T2DM mice[37]. In the present study, we found that the administration of metformin and berberine for 8 wk was effectively anti-diabetic, and we also observed an increase in GLP-1 secretion when rats were supplemented with metformin or berberine because these compounds

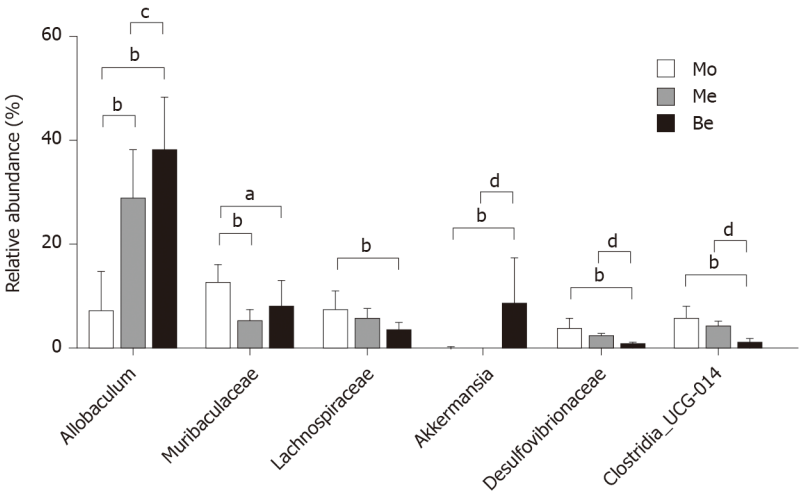


Figure 9 Comparison of the relative abundance in gut bacterial genera. $^{a}P < 0.05$, $^{b}P < 0.01$ *vs* the model group; $^{c}P < 0.05$, $^{d}P < 0.01$ *vs* the metformin group. Mo: Model group; Me: Metformin group; Be: Berberine group.

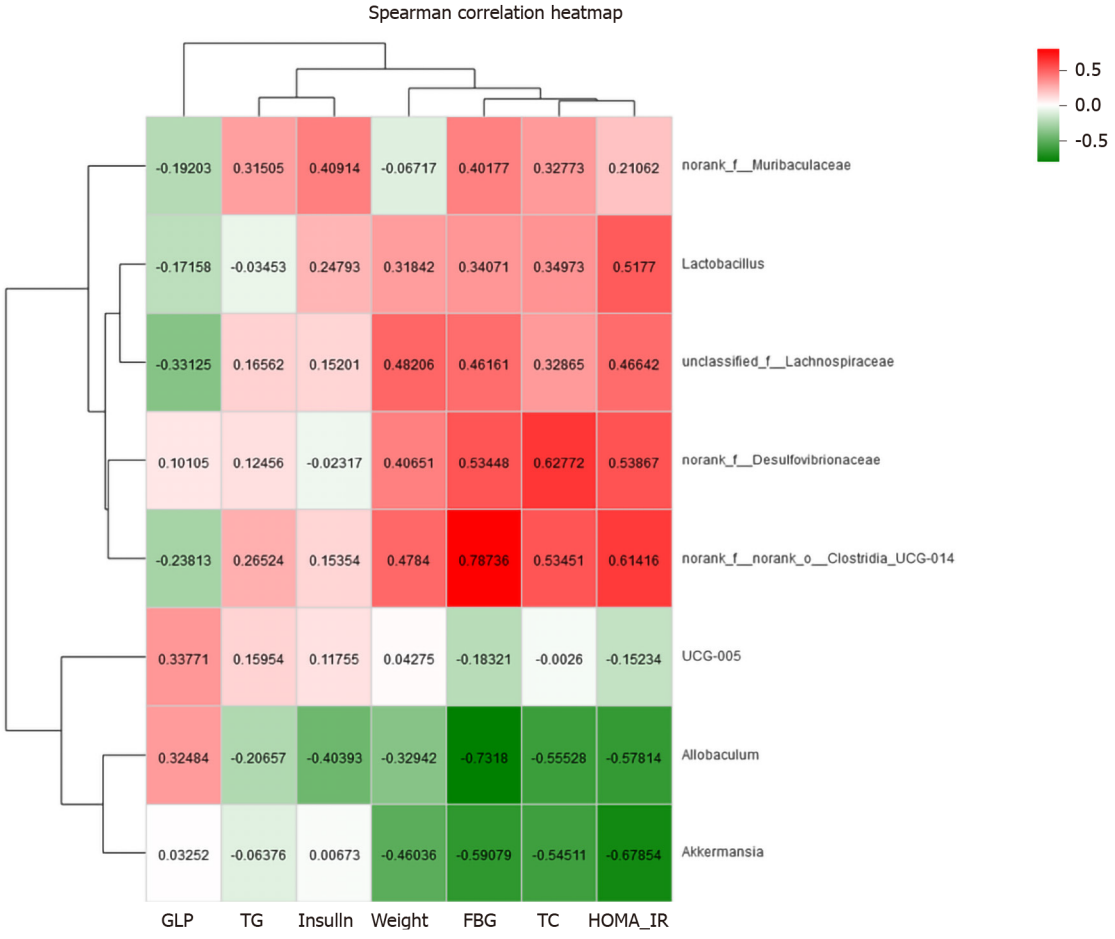


Figure 10 Correlation analysis between type 2 diabetes mellitus-related biochemical factors and gut microbiota at the genus level. The colours ranged from green (negative correlation) to red (positive correlation). Statistical significance was based on a *P* value of 0.05 (Spearman's correlation coefficient). *r* values are indicated. GLP: Glucagon-like peptide-1; TG: Triglycerides; FBG: Fasting blood glucose; TC: Total cholesterol; HOMA-IR: Homeostatic model assessment-insulin resistance.

can increase the proliferation of L cells and enhance glucagon and prohormone invertase synthesis[38].

Gut microbiota plays an important role in the regulation of multiple host metabolic pathways (*e.g.*, glucose and lipid homeostasis). Berberine can notably change the composition of the gut microbiota in T2DM rats and can particularly influence certain bacteria correlated with SCFAs production and anti-inflammatory activity, further contributing to its biological effects through the modulation of gut farnesoid X receptor and/or the G-protein-coupled receptor activity[39,40]. *Firmicutes* and *Bacteroidetes* were the two main bacterial phylum in the gut microbiota. The present study showed that *Firmicutes* and *Verrucomicrobiota* distinctly decreased and that *Bacteroidetes*, the *Bacteroidetes*/*Firmicutes* ratio, and *Desulfobacterota* significantly increased in T2DM. At the phylum level, current studies identified that the *Firmicutes, Bacteroidetes,* and *Bacteroidetes*/*Firmicutes* ratio were modified after oral administration of berberine. Similar results[41] were observed in studies by Zhao *et al*[40] and Tian *et al*[42]. Berberine led to changes in proteins involved in microbial defense and stress responses and enrichment of proteins from the *Verrucomicrobiota* phylum[43]. For instance, *Desulfovibrionaceae* was enriched in patients with T2DM. Our results are supported by research that indicated a negative correlation between the abundance of *Desulfovibrionaceae* and mRNA expression of interleukin-6 and tumor necrosis factor α[44].

The data suggested that berberine mainly reversed the decrease in the proportions of *Muribaculaceae*, *Lachnospiraceae*, *Desulfovibrionaceae*, and Clostridia_UCG-014 and the increase in the relative abundance of *Allobaculum* and *Akkermansia* in T2DM rats. Correlation analysis indicated that these bacteria were significantly associated with the levels of FBG, TC, HOMA-IR, and body weight. These results suggest that OTUs of the gut microbiota are associated with specific metabolic biomarkers. The control of blood glucose is the most important observation indicator for the treatment of diabetes, especially FBG. Therefore, we need to up-regulate *Akkermansia* and *Allobaculum* and down-regulate *Romboutsia*, *Turicibacter*, *Desulfovibrio*, *Desulfovibrionaceae*, and Clostridia_ UCG-014 to balance the microbiota, allowing FBG to return to normal levels as these bacteria are closely related to FBG.

We did not find a relationship between *Muribaculaceae* and berberine in previous T2DM studies. *N. sativa* is an annual herb, and it significantly increases the abundance of *Muribaculaceae*[45], which is inconsistent with our research results. However, further studies are needed to probe the controversy regarding this genus[46]. Berberine reduced the populations of *Lachnospiraceae* and *Desulfovibrionaceae* in our study. These results agree with the research by Cui *et al*[36]. The abundances of certain SCFAs-producing *Lachnospiraceae* were significantly increased in T2DM patients[10]. *Desulfovibrionaceae* induced abnormal proliferation and metabolism of epithelial cells, which impaired the gut barrier function[27,47]. Although our data illustrated that Clostridia_UCG-014 might play a significantly positive role in improvements and has a strong positive correlation with FBG levels, the role of this genus in T2DM has not yet been explored. However, its appearance in the results of our analyses suggests that it might be a future target of interest. The Clostridia_UCG-014 and *Clostridium spp* belong to the *Clostridiaceae* family. A study suggested that berberine reduced *Clostridium spp* by altering bile acid metabolism and activating FXR signalling[48].

In this study, *Allobaculum* is the most abundant bacterial species. Because *Allobaculum* was strongly negatively associated with FBG, the relative abundance of *Allobaculum* was reduced. *Allobaculum* belonging to putative SCFAs-producing bacteria was markedly increased by berberine. In agreement with previous studies, we showed that the selective modulations of specific gut microbial phylotypes, particularly the enrichment of SCFAs-producing *Allobaculum*, may participate in the actions of berberine in alleviating the T2DM[25,49].

These may participate in the actions of berberine in alleviating hyperglycaemia. Some other studies also demonstrated that berberine increased the abundance of probiotic *Akkermansia* in T2DM mice[48,50]. *Akkermansia* can reduce systemic inflammation and improve insulin resistance[17,51], which may contribute to the metabolic protective effects of berberine. We have observed that berberine regulates T2DM associated with the gut microbiota by increasing the number of SCFAs-producing bacteria and probiotics, and reducing opportunistic pathogens. Berberine mixture was more effective than metformin in altering features of the gut microbiota.

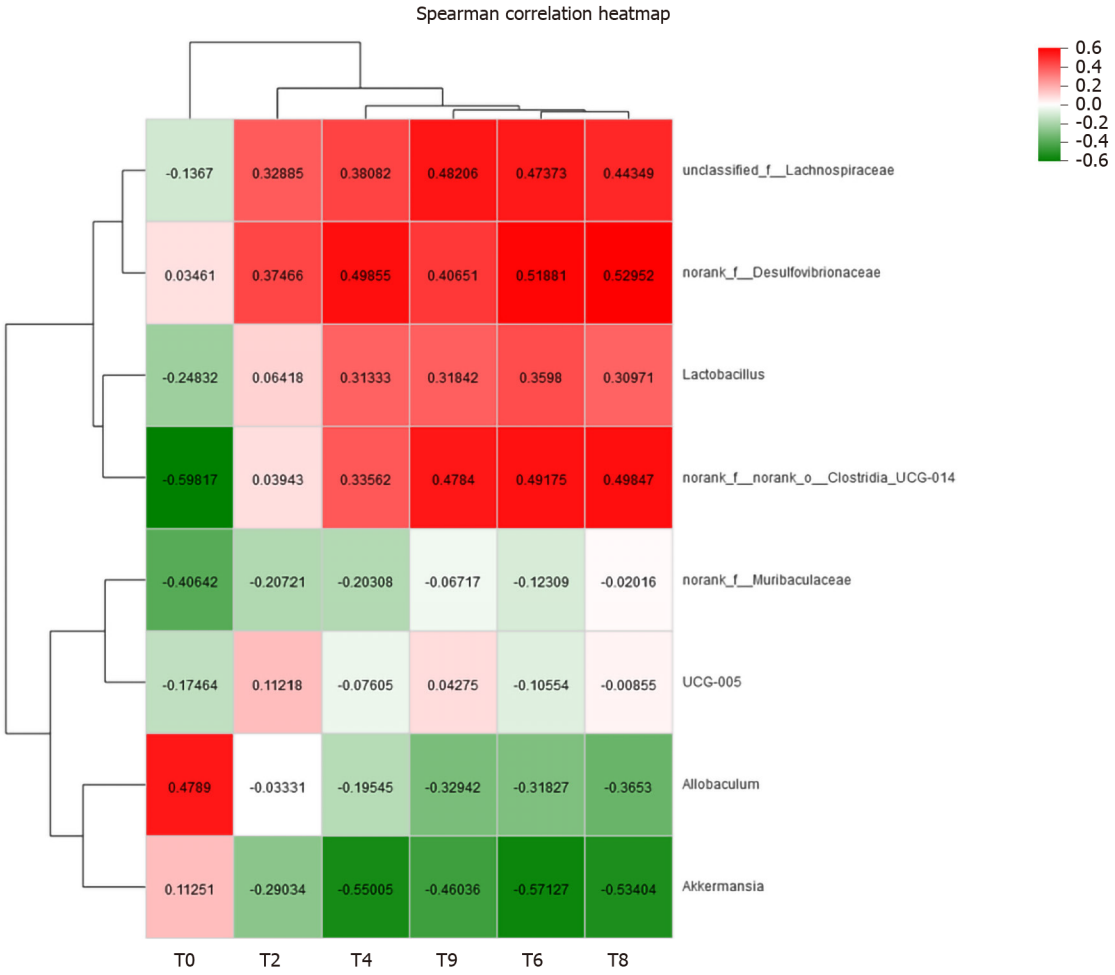


Figure 11 Correlation analysis between type 2 diabetes mellitus-related body weight and gut microbiota at the genus level. The colours range from green (negative correlation) to red (positive correlation). Statistical significance was based on a *P* value of 0.05 (Spearman's correlation coefficient). *r* values are indicated.

CONCLUSION

In summary, the gut microbiota plays crucial roles in fighting T2DM. GK rats have been shown to have altered gut microbiota composition. Disturbance of the gut microbiota can directly or indirectly lead to insulin resistance or T2DM. As expected, our results showed that berberine could effectively promote insulin secretion, gut hormone secretion, and pancreatic islet β cells and improve the symptoms of body weight, hyperglycaemia, and insulin resistance; intestinal barrier; inflammation; and lipid metabolism disorders resulting from T2DM. Thus, it can promote the achievement of diabetes treatment and reduce the various complications of diabetes. We demonstrated that gut microbiota is a pharmacological target to exert a hypoglycaemic effect after berberine treatment of T2DM rats, but the mechanism is not yet entirely clear. Gut microbiota may also have a potential signalling function that needs to be studied for wider clinical and experimental usage[52].

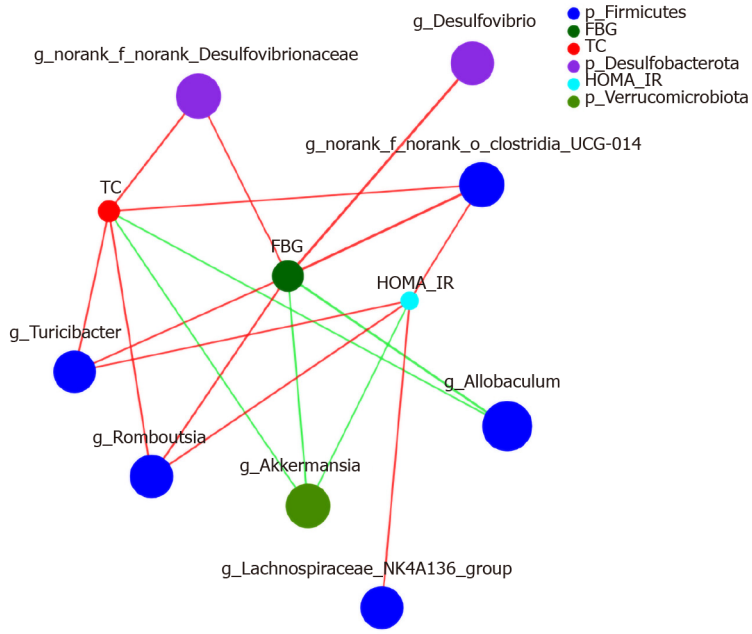


Figure 12 Construct of a species and type 2 diabetes mellitus biochemical factors-related network at the genus level. The colours range from green (negative correlation) to red (positive correlation). Statistical significance was based on a *P* value of 0.05 (Networkx). The size of the node represents the abundance of species. The thickness of the line indicates the size of the correlation coefficient. The thicker the line, the higher the correlation between species; the more lines, the closer the relationship between the species and other species. FBG: Fasting blood glucose; HOMA-IR: Homeostatic model assessment-insulin resistance.

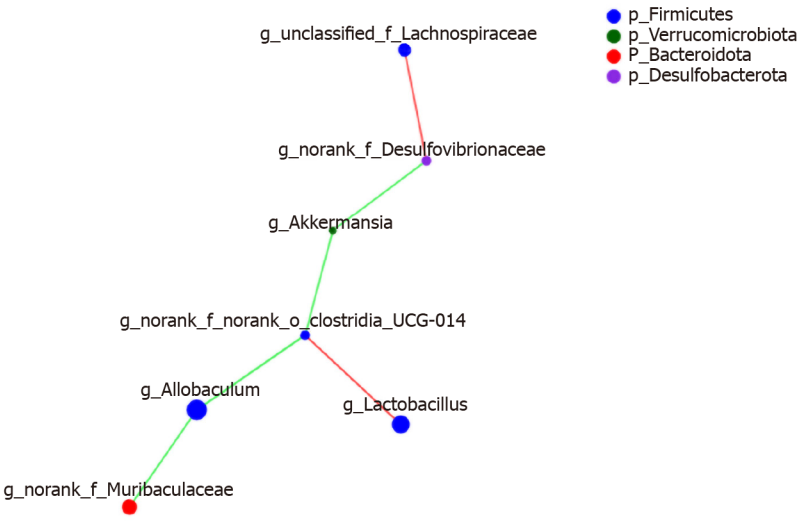


Figure 13 Construct of a species-related network at the genus level. The colours range from green (negative correlation) to red (positive correlation). Statistical significance was based on a *P* value of 0.05 (Networkx). The size of the node represents the abundance of species. The thickness of the line indicates the size of the correlation coefficient. The thicker the line, the higher the correlation between species; the more lines, the closer the relationship between the species and other species.

ARTICLE HIGHLIGHTS

Research background

Type 2 diabetes mellitus (T2DM) has become a critical and urgent human health concern worldwide. Accumulating evidence has suggested that diabetes is also associated with gut microbiota composition and homeostasis. Hence, regulators of gut microbiota may become potential alternative targets for diabetes treatment. For many years, studies have shown that traditional Chinese medicine (TCM) exhibits an effect against the development of T2DM and can be used to treat T2DM. Thus, exploring a TCM monomer that can effectively regulate gut microbiota could benefit the prognosis

of T2DM.

Research motivation

Goto-Kakizaki (GK) rats have been widely used to study T2DM, and berberine has been used for T2DM. At present, there are many reports indicating that berberine can regulate blood glucose, improve blood lipids, and reduce insulin resistance. Some studies have reported that berberine repairs the gut barrier structure and alters the diversity of the gut microbiota. Therefore, this study aimed to verify the effect of berberine treatment in GK rats and explore the underlying mechanism about gut microbiota.

Research objectives

To determine whether berberine can regulate the glucose metabolism in GK rats *via* regulating the gut microbiota.

Research methods

Male GK rats were randomly divided into a saline (Mo), metformin (Me), or berberine (Be) group, with ten rats in each group. The observation time was 8 wk, and weight, fasting blood glucose (FBG), insulin, and glucagon-like peptide-1 (GLP-1) were measured. The pathology of the pancreatic tissue was observed. We also sequenced the 16S rRNA V3-V4 region of the gut microbiota and analysed the relationship to metabolic parameters.

Research results

The FBG, GLP-1, and homeostatic model assessment-insulin resistance (HOMA-IR) levels and pancreatic islets in the Me and Be groups were significantly different from those of the Mo group. Correlation analysis indicated that FBG was strongly positively correlated with Clostridia_UCG-014 and negatively correlated with *Allobaculum*. Importantly, our results demonstrated that Me and Mo could significantly decrease *Bacteroidetes* and the *Bacteroidetes*/*Firmicutes* ratio. Furthermore, *Muribaculaceae* ($P < 0.01$; $P < 0.05$) was significantly decreased in the Me and Be groups, and *Allobaculum* ($P < 0.01$) was significantly increased.

Research conclusions

Berberine has a substantial effect in regulating the gut microbiota to improve metabolic parameters in GK rats.

Research perspectives

We observed that berberine might decrease FBG, reduce HOMA-IR, and increase GLP-1 in GK rats. Further investigation of the underlying molecular mechanisms of berberine in regulating the gut farnesoid X receptor and/or the G-protein-coupled receptor is required to provide experimental evidence for wider clinical and experimental usage.

REFERENCES

1 **Li Y**, Teng D, Shi X, Qin G, Qin Y, Quan H, Shi B, Sun H, Ba J, Chen B, Du J, He L, Lai X, Li Y, Chi H, Liao E, Liu C, Liu L, Tang X, Tong N, Wang G, Zhang JA, Wang Y, Xue Y, Yan L, Yang J, Yang L, Yao Y, Ye Z, Zhang Q, Zhang L, Zhu J, Zhu M, Ning G, Mu Y, Zhao J, Teng W, Shan Z. Prevalence of diabetes recorded in mainland China using 2018 diagnostic criteria from the American Diabetes Association: national cross sectional study. *BMJ* 2020; **369**: m997 [PMID: 32345662 DOI: 10.1136/bmj.m997]

2 **Kahn SE**. The relative contributions of insulin resistance and beta-cell dysfunction to the pathophysiology of Type 2 diabetes. *Diabetologia* 2003; **46**: 3-19 [PMID: 12637977 DOI: 10.1007/s00125-002-1009-0]

3 **Burcelin R**, Serino M, Chabo C, Blasco-Baque V, Amar J. Gut microbiota and diabetes: from pathogenesis to therapeutic perspective. *Acta Diabetol* 2011; **48**: 257-273 [PMID: 21964884 DOI: 10.1007/s00592-011-0333-6]

4 **Movassat J**, Calderari S, Fernández E, Martín MA, Escrivá F, Plachot C, Gangnerau MN, Serradas P, Alvarez C, Portha B. Type 2 diabetes - a matter of failing beta-cell neogenesis? *Diabetes Obes Metab* 2007; **9** Suppl 2: 187-195 [PMID: 17919193 DOI: 10.1111/j.1463-1326.2007.00786.x]

5 **Portha B**, Lacraz G, Kergoat M, Homo-Delarche F, Giroix MH, Bailbé D, Gangnerau MN, Dolz M, Tourrel-Cuzin C, Movassat J. The GK rat beta-cell: a prototype for the diseased human beta-cell in type 2 diabetes? *Mol Cell Endocrinol* 2009; **297**: 73-85 [PMID: 18640239 DOI:

10.1016/j.mce.2008.06.013]
6 **Goto Y**, Suzuki K, Ono T, Sasaki M, Toyota T. Development of diabetes in the non-obese NIDDM rat (GK rat). *Adv Exp Med Biol* 1988; **246**: 29-31 [PMID: 3074659 DOI: 10.1586/17446651.2.6.785]
7 **Portha B**, Giroix MH, Serradas P, Gangnerau MN, Movassat J, Rajas F, Bailbe D, Plachot C, Mithieux G, Marie JC. beta-cell function and viability in the spontaneously diabetic GK rat: information from the GK/Par colony. *Diabetes* 2001; **50** Suppl 1: S89-S93 [PMID: 11272210 DOI: 10.2337/diabetes.50.2007.s89]
8 **Ehses JA**, Lacraz G, Giroix MH, Schmidlin F, Coulaud J, Kassis N, Irminger JC, Kergoat M, Portha B, Homo-Delarche F, Donath MY. IL-1 antagonism reduces hyperglycemia and tissue inflammation in the type 2 diabetic GK rat. *Proc Natl Acad Sci USA* 2009; **106**: 13998-14003 [PMID: 19666548 DOI: 10.1073/pnas.0810087106]
9 **Larsen N**, Vogensen FK, van den Berg FW, Nielsen DS, Andreasen AS, Pedersen BK, Al-Soud WA, Sørensen SJ, Hansen LH, Jakobsen M. Gut microbiota in human adults with type 2 diabetes differs from non-diabetic adults. *PLoS One* 2010; **5**: e9085 [PMID: 20140211 DOI: 10.1371/journal.pone.0009085]
10 **Qin J**, Li Y, Cai Z, Li S, Zhu J, Zhang F, Liang S, Zhang W, Guan Y, Shen D, Peng Y, Zhang D, Jie Z, Wu W, Qin Y, Xue W, Li J, Han L, Lu D, Wu P, Dai Y, Sun X, Li Z, Tang A, Zhong S, Li X, Chen W, Xu R, Wang M, Feng Q, Gong M, Yu J, Zhang Y, Zhang M, Hansen T, Sanchez G, Raes J, Falony G, Okuda S, Almeida M, LeChatelier E, Renault P, Pons N, Batto JM, Zhang Z, Chen H, Yang R, Zheng W, Li S, Yang H, Wang J, Ehrlich SD, Nielsen R, Pedersen O, Kristiansen K, Wang J. A metagenome-wide association study of gut microbiota in type 2 diabetes. *Nature* 2012; **490**: 55-60 [PMID: 23023125 DOI: 10.1038/nature11450]
11 **Zhang C**, Wu W, Xin X, Li X, Liu D. Extract of ice plant (Mesembryanthemum crystallinum) ameliorates hyperglycemia and modulates the gut microbiota composition in type 2 diabetic Goto-Kakizaki rats. *Food Funct* 2019; **10**: 3252-3261 [PMID: 31089648 DOI: 10.1039/c9fo00119k]
12 **Miller RA**, Birnbaum MJ. An energetic tale of AMPK-independent effects of metformin. *J Clin Invest* 2010; **120**: 2267-2270 [PMID: 20577046 DOI: 10.1172/JCI43661]
13 **Graham GG**, Punt J, Arora M, Day RO, Doogue MP, Duong JK, Furlong TJ, Greenfield JR, Greenup LC, Kirkpatrick CM, Ray JE, Timmins P, Williams KM. Clinical pharmacokinetics of metformin. *Clin Pharmacokinet* 2011; **50**: 81-98 [PMID: 21241070 DOI: 10.2165/11534750-000000000-00000]
14 **Ferrannini E**, Fonseca V, Zinman B, Matthews D, Ahrén B, Byiers S, Shao Q, Dejager S. Fifty-two-week efficacy and safety of vildagliptin vs. glimepiride in patients with type 2 diabetes mellitus inadequately controlled on metformin monotherapy. *Diabetes Obes Metab* 2009; **11**: 157-166 [PMID: 19125777 DOI: 10.1111/j.1463-1326.2008.00994.x]
15 **Lee H**, Ko G. Effect of metformin on metabolic improvement and gut microbiota. *Appl Environ Microbiol* 2014; **80**: 5935-5943 [PMID: 25038099 DOI: 10.1128/AEM.01357-14]
16 **de la Cuesta-Zuluaga J**, Mueller NT, Corrales-Agudelo V, Velásquez-Mejía EP, Carmona JA, Abad JM, Escobar JS. Metformin Is Associated With Higher Relative Abundance of Mucin-Degrading Akkermansia muciniphila and Several Short-Chain Fatty Acid-Producing Microbiota in the Gut. *Diabetes Care* 2017; **40**: 54-62 [PMID: 27999002 DOI: 10.2337/dc16-1324]
17 **Shin NR**, Lee JC, Lee HY, Kim MS, Whon TW, Lee MS, Bae JW. An increase in the Akkermansia spp. population induced by metformin treatment improves glucose homeostasis in diet-induced obese mice. *Gut* 2014; **63**: 727-735 [PMID: 23804561 DOI: 10.1136/gutjnl-2012-303839]
18 **Tong XL**, Wu ST, Lian FM, Zhao M, Zhou SP, Chen XY, Yu B, Zhen Z, Qi LW, Li P, Wang CZ, Sun H, Yuan CS. The safety and effectiveness of TM81, a Chinese herbal medicine, in the treatment of type 2 diabetes: a randomized double-blind placebo-controlled trial. *Diabetes Obes Metab* 2013; **15**: 448-454 [PMID: 23231379 DOI: 10.1111/dom.12051]
19 **Dai P**, Wang J, Lin L, Zhang Y, Wang Z. Renoprotective effects of berberine as adjuvant therapy for hypertensive patients with type 2 diabetes mellitus: Evaluation *via* biochemical markers and color Doppler ultrasonography. *Exp Ther Med* 2015; **10**: 869-876 [PMID: 26622407 DOI: 10.3892/etm.2015.2585]
20 **Jung CH**, Seog HM, Choi IW, Choi HD, Cho HY. Effects of wild ginseng (Panax ginseng C.A. Meyer) leaves on lipid peroxidation levels and antioxidant enzyme activities in streptozotocin diabetic rats. *J Ethnopharmacol* 2005; **98**: 245-250 [PMID: 15814255 DOI: 10.1016/j.jep.2004.12.030]
21 **Lan J**, Zhao Y, Dong F, Yan Z, Zheng W, Fan J, Sun G. Meta-analysis of the effect and safety of berberine in the treatment of type 2 diabetes mellitus, hyperlipemia and hypertension. *J Ethnopharmacol* 2015; **161**: 69-81 [PMID: 25498346 DOI: 10.1016/j.jep.2014.09.049]
22 **Wang Y**, Yan A, Li S, Liu B, Li H, Yan Y. Efficacy and safety of berberine in the treatment of type 2 diabetes with insulin resistance: Protocol for a systematic review. *Medicine (Baltimore)* 2019; **98**: e16947 [PMID: 31464934 DOI: 10.1097/MD.0000000000016947]
23 **Turner N**, Li JY, Gosby A, To SW, Cheng Z, Miyoshi H, Taketo MM, Cooney GJ, Kraegen EW, James DE, Hu LH, Li J, Ye JM. Berberine and its more biologically available derivative, dihydroberberine, inhibit mitochondrial respiratory complex I: a mechanism for the action of berberine to activate AMP-activated protein kinase and improve insulin action. *Diabetes* 2008; **57**: 1414-1418 [PMID: 18285556 DOI: 10.2337/db07-1552]
24 **Martínez N**, White V, Kurtz M, Higa R, Capobianco E, Jawerbaum A. Activation of the nuclear receptor PPARα regulates lipid metabolism in foetal liver from diabetic rats: implications in diabetes-induced foetal overgrowth. *Diabetes Metab Res Rev* 2011; **27**: 35-46 [PMID: 21218506 DOI:

10.1002/dmrr.1151]
25 **Zhang X**, Zhao Y, Zhang M, Pang X, Xu J, Kang C, Li M, Zhang C, Zhang Z, Zhang Y, Li X, Ning G, Zhao L. Structural changes of gut microbiota during berberine-mediated prevention of obesity and insulin resistance in high-fat diet-fed rats. *PLoS One* 2012; **7**: e42529 [PMID: 22880019 DOI: 10.1371/journal.pone.0042529]
26 **Xie W**, Gu D, Li J, Cui K, Zhang Y. Effects and action mechanisms of berberine and Rhizoma coptidis on gut microbes and obesity in high-fat diet-fed C57BL/6J mice. *PLoS One* 2011; **6**: e24520 [PMID: 21915347 DOI: 10.1371/journal.pone.0024520]
27 **Karlsson FH**, Tremaroli V, Nookaew I, Bergström G, Behre CJ, Fagerberg B, Nielsen J, Bäckhed F. Gut metagenome in European women with normal, impaired and diabetic glucose control. *Nature* 2013; **498**: 99-103 [PMID: 23719380 DOI: 10.1038/nature12198]
28 **Liu DQ**, Tong C. Bacterial community diversity of traditional fermented vegetables in China, LWT Food Sci Technol 2017; 86: 40-48 [DOI: 10.1016/j.lwt.2017.07.040]
29 **Amato KR**, Yeoman CJ, Kent A, Righini N, Carbonero F, Estrada A, Gaskins HR, Stumpf RM, Yildirim S, Torralba M, Gillis M, Wilson BA, Nelson KE, White BA, Leigh SR. Habitat degradation impacts black howler monkey (Alouatta pigra) gastrointestinal microbiomes. *ISME J* 2013; **7**: 1344-1353 [PMID: 23486247 DOI: 10.1038/ismej.2013.16]
30 **Wu H**, Esteve E, Tremaroli V, Khan MT, Caesar R, Mannerås-Holm L, Ståhlman M, Olsson LM, Serino M, Planas-Fèlix M, Xifra G, Mercader JM, Torrents D, Burcelin R, Ricart W, Perkins R, Fernàndez-Real JM, Bäckhed F. Metformin alters the gut microbiome of individuals with treatment-naive type 2 diabetes, contributing to the therapeutic effects of the drug. *Nat Med* 2017; **23**: 850-858 [PMID: 28530702 DOI: 10.1038/nm.4345]
31 **Gao K**, Yang R, Zhang J, Wang Z, Jia C, Zhang F, Li S, Wang J, Murtaza G, Xie H, Zhao H, Wang W, Chen J. Effects of Qijian mixture on type 2 diabetes assessed by metabonomics, gut microbiota and network pharmacology. *Pharmacol Res* 2018; **130**: 93-109 [PMID: 29391233 DOI: 10.1016/j.phrs.2018.01.011]
32 **Shin NR**, Bose S, Wang JH, Ansari A, Lim SK, Chin YW, Choi HS, Kim H. *Flos Lonicera* Combined with Metformin Ameliorates Hepatosteatosis and Glucose Intolerance in Association with Gut Microbiota Modulation. *Front Microbiol* 2017; **8**: 2271 [PMID: 29204141 DOI: 10.3389/fmicb.2017.02271]
33 **Li JW**, Yuan K, Shang SC, Guo Y. A safer hypoglycemic agent for type 2 diabetes–Berberine organic acid salt. *J Functional Foods* 2017; **38**: 399-408 [DOI: 10.1016/j.jff.2017.09.031]
34 **Lü F**, Jin T, Drucker DJ. Proglucagon gene expression is induced by gastrin-releasing peptide in a mouse enteroendocrine cell line. *Endocrinology* 1996; **137**: 3710-3716 [PMID: 8756537 DOI: 10.1210/endo.137.9.8756537]
35 **Tanaka T**, Yano T, Adachi T, Koshimizu TA, Hirasawa A, Tsujimoto G. Cloning and characterization of the rat free fatty acid receptor GPR120: *in vivo* effect of the natural ligand on GLP-1 secretion and proliferation of pancreatic beta cells. *Naunyn Schmiedebergs Arch Pharmacol* 2008; **377**: 515-522 [PMID: 18320172 DOI: 10.1007/s00210-007-0250-y]
36 **Cui HX**, Hu YN, Li JW, Yuan K. Hypoglycemic Mechanism of the Berberine Organic Acid Salt under the Synergistic Effect of Intestinal Flora and Oxidative Stress. *Oxid Med Cell Longev* 2018; **2018**: 8930374 [PMID: 30662584 DOI: 10.1155/2018/8930374]
37 **Sogin EM**, Anderson P, Williams P, Chen CS, Gates RD. Application of 1H-NMR metabolomic profiling for reef-building corals. *PLoS One* 2014; **9**: e111274 [PMID: 25354140 DOI: 10.1371/journal.pone.0111274]
38 **Wang ZK**, Yang YS, Chen Y, Yuan J, Sun G, Peng LH. Intestinal microbiota pathogenesis and fecal microbiota transplantation for inflammatory bowel disease. *World J Gastroenterol* 2014; **20**: 14805-14820 [PMID: 25356041 DOI: 10.3748/wjg.v20.i40.14805]
39 **Wang LL**, Guo HH, Huang S, Feng CL, Han YX, Jiang JD. Comprehensive evaluation of SCFA production in the intestinal bacteria regulated by berberine using gas-chromatography combined with polymerase chain reaction. *J Chromatogr B Analyt Technol Biomed Life Sci* 2017; **1057**: 70-80 [PMID: 28505492 DOI: 10.1016/j.jchromb.2017.05.004]
40 **Zhao L**, Zhang Q, Ma W, Tian F, Shen H, Zhou M. A combination of quercetin and resveratrol reduces obesity in high-fat diet-fed rats by modulation of gut microbiota. *Food Funct* 2017; **8**: 4644-4656 [PMID: 29152632 DOI: 10.1039/c7fo01383c]
41 **Li T**, Chiang JY. Nuclear receptors in bile acid metabolism. *Drug Metab Rev* 2013; **45**: 145-155 [PMID: 23330546 DOI: 10.3109/03602532.2012.740048]
42 **Tian Y**, Cai J, Gui W, Nichols RG, Koo I, Zhang J, Anitha M, Patterson AD. Berberine Directly Affects the Gut Microbiota to Promote Intestinal Farnesoid X Receptor Activation. *Drug Metab Dispos* 2019; **47**: 86-93 [PMID: 30409838 DOI: 10.1124/dmd.118.083691]
43 **Li L**, Chang L, Zhang X, Ning Z, Mayne J, Ye Y, Stintzi A, Liu J, Figeys D. Berberine and its structural analogs have differing effects on functional profiles of individual gut microbiomes. *Gut Microbes* 2020; **11**: 1348-1361 [PMID: 32372706 DOI: 10.1080/19490976.2020.1755413]
44 **Liu G**, Bei J, Liang L, Yu G, Li L, Li Q. Stachyose Improves Inflammation through Modulating Gut Microbiota of High-Fat Diet/Streptozotocin-Induced Type 2 Diabetes in Rats. *Mol Nutr Food Res* 2018; **62**: e1700954 [PMID: 29341443 DOI: 10.1002/mnfr.201700954]
45 **Dong J**, Liang Q, Niu Y, Jiang S, Zhou L, Wang J, Ma C, Kang W. Effects of Nigella sativa seed polysaccharides on type 2 diabetic mice and gut microbiota. *Int J Biol Macromol* 2020; **159**: 725-738 [PMID: 32437806 DOI: 10.1016/j.ijbiomac.2020.05.042]

46 **Zhao J**, Li Y, Sun M, Xin L, Wang T, Wei L, Yu C, Liu M, Ni Y, Lu R, Bao T, Zhang L, Wu Y, Fang Z. The Chinese Herbal Formula Shenzhu Tiaopi Granule Results in Metabolic Improvement in Type 2 Diabetic Rats by Modulating the Gut Microbiota. *Evid Based Complement Alternat Med* 2019; **2019**: 6976394 [PMID: 31275416 DOI: 10.1155/2019/6976394]

47 **Roediger WE**, Moore J, Babidge W. Colonic sulfide in pathogenesis and treatment of ulcerative colitis. *Dig Dis Sci* 1997; **42**: 1571-1579 [PMID: 9286219 DOI: 10.1023/a:1018851723920]

48 **Zhang W**, Xu JH, Yu T, Chen QK. Effects of berberine and metformin on intestinal inflammation and gut microbiome composition in db/db mice. *Biomed Pharmacother* 2019; **118**: 109131 [PMID: 31545226 DOI: 10.1016/j.biopha.2019.109131]

49 **Zhang X**, Zhao Y, Xu J, Xue Z, Zhang M, Pang X, Zhang X, Zhao L. Modulation of gut microbiota by berberine and metformin during the treatment of high-fat diet-induced obesity in rats. *Sci Rep* 2015; **5**: 14405 [PMID: 26396057 DOI: 10.1038/srep14405]

50 **Zhu L**, Zhang D, Zhu H, Zhu J, Weng S, Dong L, Liu T, Hu Y, Shen X. Berberine treatment increases Akkermansia in the gut and improves high-fat diet-induced atherosclerosis in Apoe$^{-/-}$ mice. *Atherosclerosis* 2018; **268**: 117-126 [PMID: 29202334 DOI: 10.1016/j.atherosclerosis.2017.11.023]

51 **Everard A**, Belzer C, Geurts L, Ouwerkerk JP, Druart C, Bindels LB, Guiot Y, Derrien M, Muccioli GG, Delzenne NM, de Vos WM, Cani PD. Cross-talk between Akkermansia muciniphila and intestinal epithelium controls diet-induced obesity. *Proc Natl Acad Sci USA* 2013; **110**: 9066-9071 [PMID: 23671105 DOI: 10.1073/pnas.1219451110]

52 **Zhao J**, Li Y, Xin L, Sun M, Yu C, Shi G, Bao T, Liu J, Ni Y, Lu R, Wu Y, Fang Z. Clinical Features and Rules of Chinese Herbal Medicine in Diabetic Peripheral Neuropathy Patients. *Evid Based Complement Alternat Med* 2020; **2020**: 5795264 [PMID: 32724325 DOI: 10.1155/2020/5795264]

World Journal of Gastroenterology

Submit a Manuscript: https://www.f6publishing.com

World J Gastroenterol 2021 February 28; 27(8): 725-736

DOI: 10.3748/wjg.v27.i8.725

ISSN 1007-9327 (print) ISSN 2219-2840 (online)

ORIGINAL ARTICLE

Prospective Study

Endoscopic full-thickness resection using an over-the-scope device: A prospective study

Jin-Tao Guo, Jing-Jing Zhang, Yu-Fan Wu, Ye Liao, Yi-Dan Wang, Bao-Zhen Zhang, Sheng Wang, Si-Yu Sun

ORCID number: Jin-Tao Guo 0000-0001-5722-6359; Jing-Jing Zhang 0000-0003-1357-9384; Yu-Fan Wu 0000-0003-4290-8263; Ye Liao 0000-0001-9026-8438; Yi-Dan Wang 0000-0003-1566-3459; Bao-Zhen Zhang 0000-0001-7871-8213; Sheng Wang 0000-0002-1531-7655; Si-Yu Sun 0000-0002-7308-0473.

Author contributions: Guo JT and Zhang JJ were involved in the study conception and design; Guo JT, Wang S, and Sun SY performed the research; Liao Y, Wu YF, Zhang BZ, and Wang YD analyzed the data; Guo JT wrote the manuscript; Guo JT and Sun SY performed critical revision of the article for important intellectual content; all authors approved the final version of the article.

Supported by National Natural Science Foundation of China, No. 81900601; Innovative Talent Support Program of Liaoning Province, No. LR2019073; and Outstanding Scientific Fund of Shengjing Hospital, No. 201701 and No. 201702.

Institutional review board statement: This study was reviewed and approved by the Internal Review Board and Ethics Committee of China Medical University.

Jin-Tao Guo, Jing-Jing Zhang, Yu-Fan Wu, Ye Liao, Yi-Dan Wang, Bao-Zhen Zhang, Sheng Wang, Si-Yu Sun, Department of Gastroenterology, Shengjing Hospital of China Medical University, Shenyang 110004, Liaoning Province, China

Corresponding author: Si-Yu Sun, MD, PhD, Chief Doctor, Director, Professor, Department of Gastroenterology, Shengjing Hospital of China Medical University, No. 36 Sanhao Street, Shenyang 110004, Liaoning Province, China. sun-siyu@163.com

Abstract

BACKGROUND

Endoscopic submucosal dissection to treat mucosal and submucosal lesions sometimes results in low rates of microscopically margin-negative (R0) resection. Endoscopic full-thickness resection (EFTR) has a high R0 resection rate and allows for the definitive diagnosis and treatment of selected mucosal and submucosal lesions that are not suitable for conventional resection techniques.

AIM

To evaluate the efficacy and safety of EFTR using an over-the-scope clip (OTSC).

METHODS

This prospective, single-center, non-randomized clinical trial was conducted at the endoscopy center of Shengjing Hospital of China Medical University. The study included patients aged 18-70 years who had gastric or colorectal submucosal tumors (SMTs) (≤ 20 mm in diameter) originating from the muscularis propria based on endoscopic ultrasound (EUS) and patients who had early-stage gastric or colorectal cancer (≤ 20 mm in diameter) based on EUS and computed tomography. All lesions were treated by EFTR combined with an OTSC for wound closure between November 2014 and October 2016. We analyzed patient demographics, lesion features, histopathological diagnoses, R0 resection (negative margins) status, adverse events, and follow-up results.

RESULTS

A total of 68 patients (17 men and 51 women) with an average age of 52.0 ± 10.5 years (32-71 years) were enrolled in this study, which included 66 gastric or colorectal SMTs and 2 early-stage colorectal cancers. The mean tumor diameter was 12.6 ± 4.3 mm. The EFTR procedure was successful in all cases. The mean EFTR procedure time was 39.6 ± 38.0 min. The mean OTSC defect closure time was 5.0 ± 3.8 min, and the success rate of closure for defects was 100%.

Clinical trial registration statement: The clinical trial is registered with Chinese Clinical Trial Registry, using identifier ChiCTR-OPC-14005459.

Informed consent statement: All study participants, or their legal guardian, provided written consent prior to study enrollment.

Conflict-of-interest statement: The authors of this manuscript having no conflicts of interest to disclose.

Data sharing statement: No additional data are available.

CONSORT 2010 statement: The authors have read the CONSORT 2010 statement, and the manuscript was prepared and revised according to the CONSORT 2010 statement.

Open-Access: This article is an open-access article that was selected by an in-house editor and fully peer-reviewed by external reviewers. It is distributed in accordance with the Creative Commons Attribution NonCommercial (CC BY-NC 4.0) license, which permits others to distribute, remix, adapt, build upon this work non-commercially, and license their derivative works on different terms, provided the original work is properly cited and the use is non-commercial. See: http://creativecommons.org/Licenses/by-nc/4.0/

Manuscript source: Invited manuscript

Specialty type: Gastroenterology and hepatology

Country/Territory of origin: China

Peer-review report's scientific quality classification

Grade A (Excellent): 0
Grade B (Very good): B
Grade C (Good): C
Grade D (Fair): 0
Grade E (Poor): 0

Received: November 10, 2020
Peer-review started: November 10, 2020
First decision: December 3, 2020

Histologically complete resection (R0) was achieved in 67 (98.5%) patients. Procedure-related adverse events were observed in 11 (16.2%) patients. The average post-procedure length of follow-up was 48.2 ± 15.7 mo. There was no recurrence during follow-up.

CONCLUSION

EFTR combined with an OTSC is an effective and safe technique for the removal of select subepithelial and epithelial lesions that are not amenable to conventional endoscopic resection techniques.

Key Words: Endoscopic full-thickness resection; Over-the-scope clip; Early gastric cancer; Early colorectal cancer; Submucosal tumor; Gastrointestinal stromal tumor

©The Author(s) 2021. Published by Baishideng Publishing Group Inc. All rights reserved.

Core Tip: A prospective study of endoscopic full-thickness resection (EFTR) combined with an over-the-scope clip (OTSC) was conducted to assess the treatment of mucosal and submucosal lesions that are not amenable to conventional endoscopic resection techniques. The study had a long follow-up period and included a large number of cases, thus providing statistical strength. We found that EFTR combined with an OTSC was a safe and effective treatment modality for mucosal and submucosal lesions that cannot be treated using conventional endoscopic resection techniques.

Citation: Guo JT, Zhang JJ, Wu YF, Liao Y, Wang YD, Zhang BZ, Wang S, Sun SY. Endoscopic full-thickness resection using an over-the-scope device: A prospective study. *World J Gastroenterol* 2021; 27(8): 725-736
URL: https://www.wjgnet.com/1007-9327/full/v27/i8/725.htm
DOI: https://dx.doi.org/10.3748/wjg.v27.i8.725

INTRODUCTION

While endoscopic submucosal dissection (ESD) is an established treatment method for gastrointestinal adenomas and early-stage cancer[1], it occasionally results in low rates of microscopically margin-negative (R0) resections. ESD remains controversial for the treatment of submucosal tumors (SMTs) arising from the muscularis propria, because this method has a higher risk of perforation[2-4]. In addition, when lesions are situated at anatomical locations that are difficult to access, ESD can result in high rates of adverse events. Therefore, endoscopic full-thickness resection (EFTR) is the preferred resection technique for this subgroup of tumors.

Closure of the gastrointestinal wall after EFTR is also important. The over-the-scope clip (OTSC) is a metal clip system introduced in Germany in 2008. It has good elasticity, a wingspan of 11-14 mm, strong fastening force and stability, and the ability to grip the full-thickness of the gastrointestinal tract to close more tissues. Previous studies have shown that OTSC can effectively close gastrointestinal wall defects caused by EFTR, but most of these studies had used retrospective data[5,6]. This study aimed to prospectively evaluate the efficacy and safety of EFTR combined with an OTSC for resection of these lesions.

MATERIALS AND METHODS

Study design and patient selection

A prospective, single-center, non-randomized clinical trial was conducted at the endoscopy center of Shengjing Hospital of China Medical University between November 2014 and October 2016. This study was approved by the Institutional Review Board and Ethics Committee of China Medical University. The trial registration number is ChiCTR-OPC-14005459.

Revised: December 13, 2020
Accepted: January 21, 2021
Article in press: January 21, 2021
Published online: February 28, 2021

P-Reviewer: Imaeda H
S-Editor: Gao CC
L-Editor: Wang TQ
P-Editor: Liu JH

Inclusion criteria

Patients aged 18-70 years who had gastrointestinal SMTs ≤ 20 mm originating from the muscularis propria based on endoscopic ultrasound (EUS), or early gastric and colorectal cancer lesions ≤ 20 mm without evidence of lymph node metastasis based on EUS and computed tomography (CT) were included in the study. The largest diameter of the tumor was evaluated using EUS before the procedure.

Exclusion criteria

The exclusion criteria included contraindications for endoscopy examination, coagulation disorders, and refusal to provide informed consent.

Primary endpoints

The primary endpoints included macroscopically complete resection (*i.e.*, the endoscopist determined that there was no evidence of macroscopic residual lesions) and histologically complete resection (R0 resection defined as tumor-free lateral and deep resection margins).

Secondary endpoints

The secondary endpoints were procedure-related adverse events, EFTR time, OTSC closure time, necessity of surgical therapy, evidence of residual or recurrent lesions during follow-up, and other long-term complications associated with OTSC.

Endoscopic equipment and accessories

A standard single-channel gastroscope (EG29-i10, Pentax, Tokyo, Japan) or colonoscope (EC38-i10M, Pentax, Tokyo, Japan) with a transparent cap was used for the endoscopic procedure. A linear array echoendoscope (EG3870UT; Pentax, Tokyo, Japan) or EUS microprobe (UM-2R, Olympus Corporation, Tokyo, Japan) was used for the evaluation of tumor size, echo characteristics, and the originating layer. A triangle-tipped knife (TT knife, Olympus Corporation, Tokyo, Japan) and insulation-tipped knife (IT knife, Olympus Corporation, Tokyo, Japan) were used for the dissection and resection of tumors, while hot coagulation forceps (FD- 410LR, Olympus Corporation, Tokyo, Japan) were used for gastric or colorectal wall hemostasis. Twin graspers (Ovesco Endoscopy GmbH, Tuebingen, Germany) were used for clamping the two sides of the gastric defect, and metal clips (Boston Resolution, Boston, United States) and the OTSC system (Ovesco Endoscopy GmbH, Tuebingen, Germany) were used to close the defect.

Procedure and patient management

All EFTR procedures were performed in an inpatient setting under general anesthesia with endotracheal intubation with propofol. All patients received prophylactic medication 6 h before surgery with a single dose of an intravenous antibiotic (ceftriaxone, intravenous 1 g). Patients on anticoagulants (clopidogrel, heparin, warfarin, or direct oral anticoagulants) were instructed to discontinue these medications. All patients provided written informed consent.

EFTR procedure

EFTR for SMTs: The gastric or colorectal mucosa and submucosa surrounding the tumor were incised with a triangle tip (TT) knife. EFTR was performed, involving the tumor and surrounding tissues, with an insulated tip (IT) knife. An iatrogenic perforation was created. Hot coagulation forceps were used to stop any bleeding.

EFTR for early cancer: Each patient first underwent a gastroscopy or colonoscopy in order to identify the lesion and to mark its lateral margins with argon plasma coagulation (APC; Erbe APC 300, 25 W; ERBE Elektromedizin GmbH; Germany). The gastric or colorectal mucosa and submucosa surrounding the tumor were incised with a TT knife. EFTR was performed, involving the tumor and surrounding tissues, with an IT knife. An iatrogenic perforation was created. Hot coagulation forceps were used to stop any bleeding.

Wound closure with the OTSC system

The gastric or colorectal tissue on either side of the iatrogenic perforation was held with a double clamp or forceps and pulled into the transparent cap of the OTSC device. When both side of the defect were fully absorbed into the transparent cap, the OTSC was released to close the defect. If the defect closure was incomplete, metal clips were used to close the remainder (Figures 1 and 2).

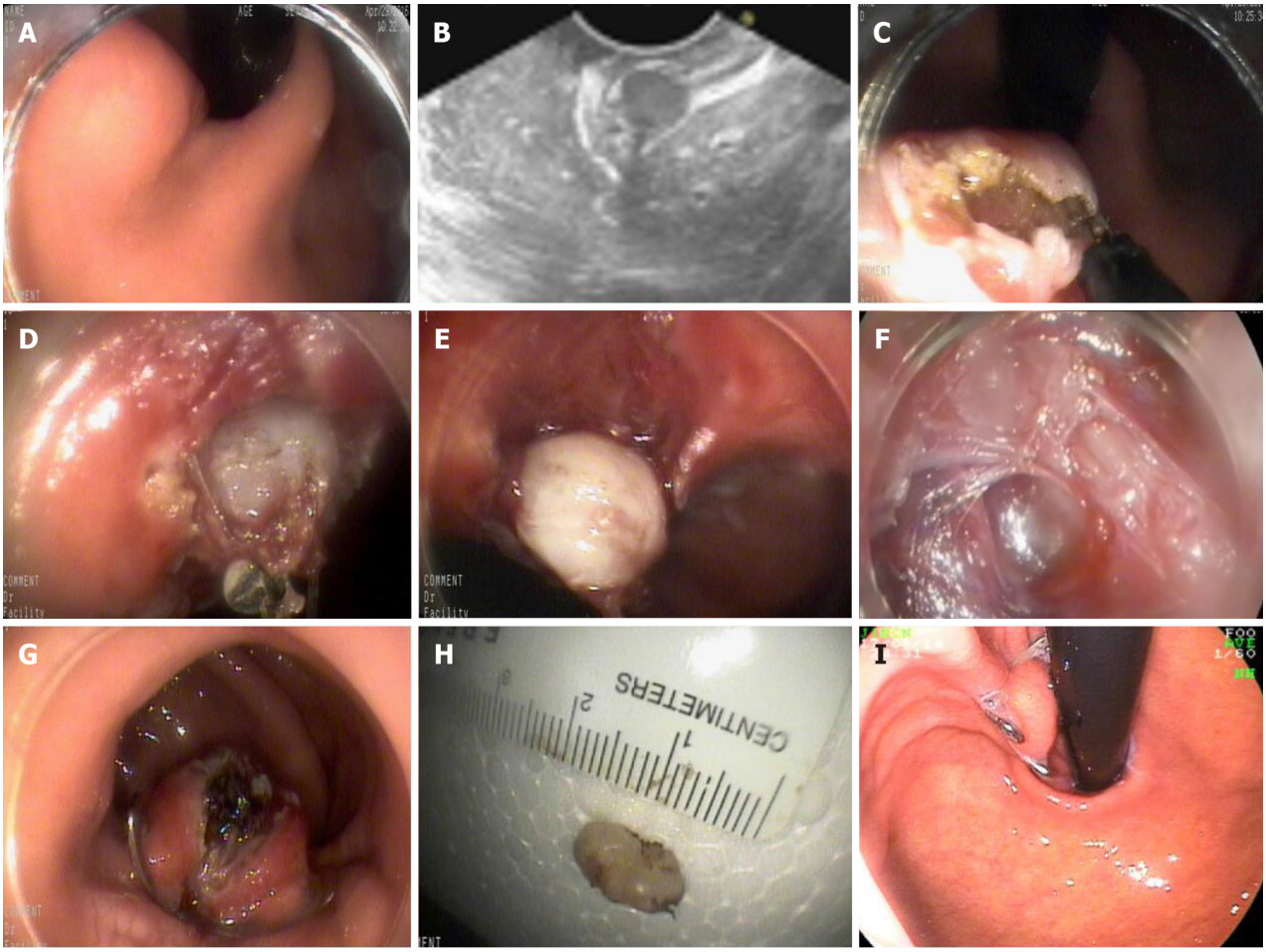


Figure 1 Wound closure with the over-the-scope clip system. A and B: A protruding tumor with a smooth surface in the cardia. The tumor originated from the muscularis propria based on endoscopic ultrasound; C-E: Full-thickness resection was performed; F: Gastric defect formed after full-thickness tumor resection; G: The over-the-scope clip was released to approximate the gastric wall at the defect; H: The tumor; I: Gastroscopic re-examination 6 mo post-procedure revealed a nearly normal gastric wall.

Carbon dioxide was injected throughout the procedure. A 20-mL syringe was used to aspirate free gas from the abdomen during or after the procedure.

Patient management

All patients were closely observed in the hospital. The postoperative treatment included 24 h of fasting (both food and water) as well as routine administration of antibiotics within 24 h of the procedure. Proton pump inhibitors were needed for patients with upper gastrointestinal resections. If significant hemorrhage occurred, hemostasis was obtained endoscopically or surgically. If peritonitis symptoms were observed, a gastric or intestinal decompression tube was placed. If conservative or endoscopic treatment was unsuccessful, surgical treatment was performed. On postoperative day 2, patients without postoperative bleeding or peritonitis were advanced to a liquid diet.

Follow-up

Patients were scheduled for endoscopy follow-up at 3 mo and at 1, 2, and 3 years after the initial EFTR, in order to observe local healing and determine if the OTSC had disintegrated. The excision site was examined for visual residual or recurrent lesions. If there was evidence of residual or recurrent lesions, a biopsy was performed.

RESULTS

Patient characteristics and indications for EFTR

Between November 2014 and October 2016, a total of 79 patients were screened for

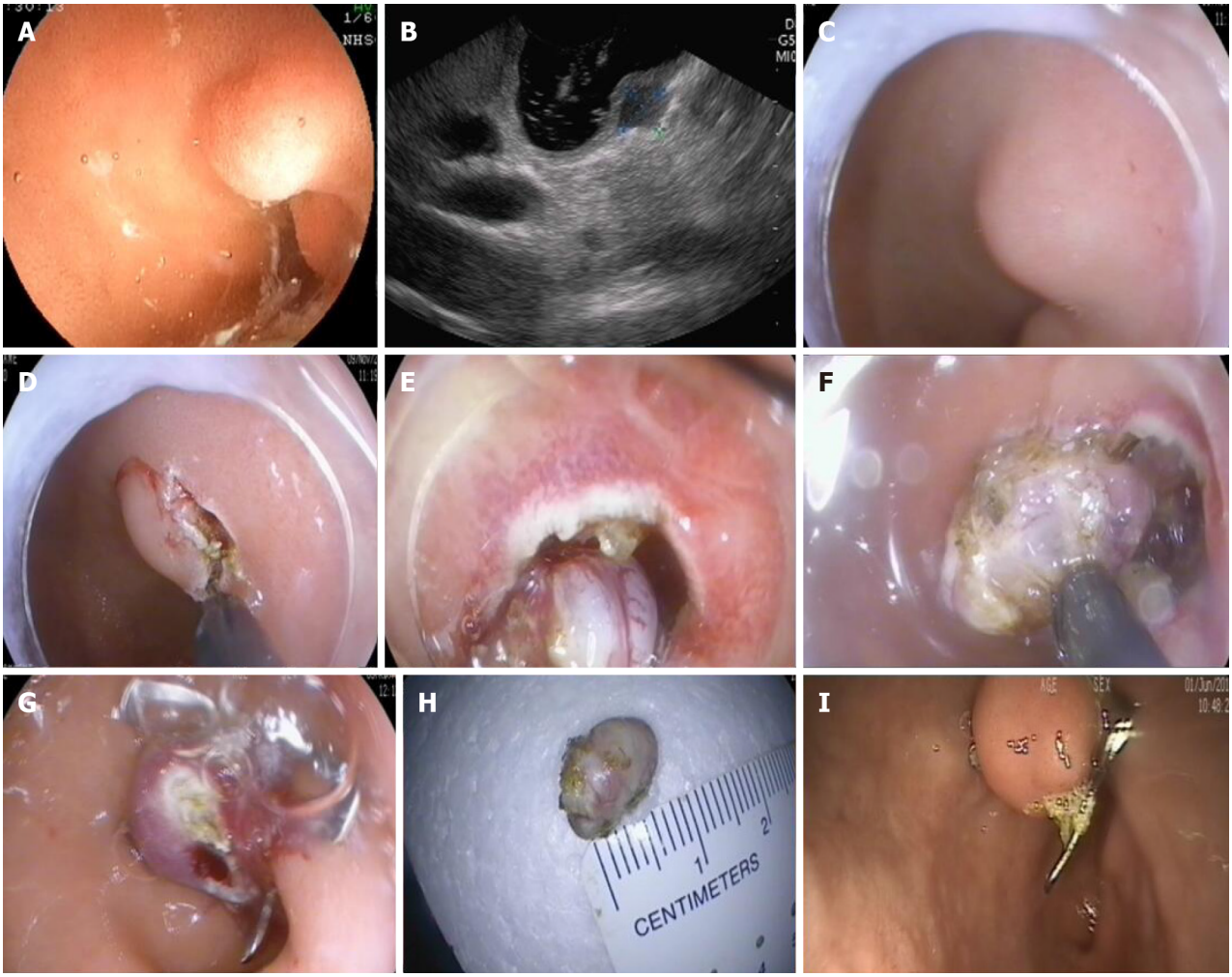


Figure 2 Wound closure with the over-the-scope clip system. A and B: A protruding tumor with a smooth surface in the duodenal area. The tumor originated from the muscularis propria based on endoscopic ultrasound; C-E: Full-thickness resection was performed; F: Gastric defect formed after full-thickness tumor resection; G: The over-the-counter clip was released to approximate the duodenal wall at the defect; H: The tumor; I: Gastroscopic re-examination 6 mo post-procedure revealed a nearly normal duodenal wall.

eligibility at our endoscopy center. Eleven patients were not included in the study. Among them, nine patients chose regular follow-up and two chose surgical operation. We enrolled 68 patients (17 men and 51 women) with an average age of 52 ± 10.5 years (range, 32-71 years). The mean diameter of the tumors was 12.6 ± 4.3 mm (range, 3-20 mm) measured by preoperative EUS. The patient and lesion characteristics are shown in Table 1.

Procedural data and technical success

In our study, EFTR had a success rate of 100% (68/68). No patients were excluded due to unsuccessful advancement of the endoscope. The average EFTR procedure time was 39.6 ± 38.0 min (range, 5-236 min). The success rate of the defect closure was 100% (68/68). The average OTSC defect closure time was 5.0 ± 3.8 min (range, 2-26 mi). In 67 patients, complete closure of the defect required only one OTSC, and one patient required two OTSCs. Procedural data are shown in Table 2.

Histology/R0 resection

Histologically complete resection (R0) was achieved in 67 (98.5%) patients. Of the 68 lesions included in the study, 66 had gastric or colorectal SMTs, and two had early colorectal cancer. Detailed histology results are shown in Table 3.

Of the patients with SMTs, 63.6% (42/66) had gastrointestinal stromal tumors (GISTs). Of the patients with GISTs, 95.2% (40/42) exhibited a low or very low risk mitotic index. The remaining two cases had a moderate risk. Other histological findings in patients with SMTs included leiomyoma (21.2%, 14/66), schwannoma (6.1%, 4/66), and ectopic pancreas (3.0%, 2/66). R0 resection was achieved in all

Table 1 Patient and lesion characteristics

Patient characteristics (*n* = 68)	
Sex, *n* (%)	
Male	17 (25)
Female	51 (75)
Age, median (range)	52 ± 10.5 (32-71)
Indication for EFTR, *n* (%)	
Submucosal tumor	66 (97.1)
Early cancer	2 (2.9)
Location of lesion, *n* (%)	
Cardia	5 (7.3)
Gastric fundus	41 (60.2)
Gastric body	12 (17.6)
Antrum	6 (8.8)
Duodenum	1 (1.4)
Rectum	4 (4.4)
Maximum diameter of lesion, mean, mm (range)	20, 12.6 ± 4.3 (3-20)

EFTR: Endoscopic full-thickness resection.

Table 2 Procedural data (entire cohort)

Median procedure time, min (range)	
Total procedure time	53.7 ± 41.5 (12-263)
EFTR time	39.6 ± 38.0 (5-236)
OTSC defect closure time	5.0 ± 3.8 (2-26)
Technical success, *n* (%)	68 (100)
R0 resection, *n* (%)	67 (98.5)

EFTR: Endoscopic full-thickness resection; OTSC: Over-the-scope clip; R0 resection: Histologically complete resection, defined as tumor-free lateral and deep resection margins.

patients with SMTs (100%). Two patients who underwent EFTR had early colorectal cancer. One of these patients underwent additional surgery due to a diagnosis of rectal adenocarcinoma with submucosal infiltration > 2 mm.

Adverse events

Mild adverse events including tolerable abdominal pain, discomfort, and elevated body temperature were observed in 26 (38.2%) patients. Procedure-related adverse events were observed in 11 (16.2%) patients (Table 4). In one patient, delayed bleeding at the resection site occurred on postoperative day 2. The patient was hemodynamically stable, and a blood transfusion was not required. The patient was successfully treated by endoscopic hemostasis with standard clips. Eight patients had a fever > 37.5 °C, and all recovered after the administration of antibiotics. Two patients with upper gastrointestinal EFTR developed localized peritonitis, which was resolved after the placement of a gastric decompression tube.

Follow-up outcomes

The average post-procedure length of follow-up was 48.2 ± 15.7 mo. During follow-up, 24 patients (including 22 with stomach lesions and two with lesions in the colorectum) shed their OTSC; one patient developed upper gastrointestinal bleeding, which was

Table 3 Lesion characteristics

Pathological diagnosis, *n* (%)	
GIST	42 (61.7)
Leiomyoma	14 (20.5)
Schwannoma	4 (5.8)
Ectopic pancreas	2 (2.9)
Endometriosis	1 (1.4)
Fibrolipomatous hyperplasia	1 (1.4)
Colorectal adenocarcinoma	2 (2.8)
Inflammatory myofibroblastic tumor like hyperplasia	1 (1.4)
Hyaline degeneration with calcification	1 (1.4)

GIST: Gastrointestinal stromal tumor.

Table 4 Adverse events

Procedure-related adverse events, *n* (%)	
Mild adverse events[1]	
Abdominal pain	18 (26.5)
Discomfort	1 (1.4)
Elevated body temperature	7 (10.3)
Moderate adverse events[2]	
Bleeding	1 (1.5)
Fever	8 (11.8)
Local peritonitis	2 (2.9)
Severe adverse events[3]	0
Perforation	0
Persistent peritonitis	0

[1]Mild adverse events: Not requiring medical or repeated endoscopic intervention and did not prolong hospital admission.
[2]Moderate adverse events: Requiring medical or repeated endoscopic intervention and/or prolonging hospital admission.
[3]Severe adverse events: Requiring surgical therapy and/or potentially life threatening.

stopped using endoscopic therapy. An OTSC of the rectum was removed during an operation in one case. The remaining patients did not shed their OTSCs. There was no recurrence during the follow-up period.

DISCUSSION

Surgical resection of gastrointestinal tumors is often associated with a high incidence of complications and mortality. The continuous innovation of endoscopic resection techniques has largely led to it replacing surgery as the primary treatment strategy for early gastrointestinal tumors. In surgically resected specimens, the risk of lymph node metastasis from intramucosal carcinoma is very small. Therefore, endoscopic resection is an option for the treatment of intramucosal carcinoma that does not require lymph node dissection.

ESD has recently become a standard therapy[7-9]. However, ESD is not always effective for specific lesions, such as some mucosal lesions with adhesion caused by pathological biopsy or repeated inflammatory stimuli and some SMTs with tight connections to the muscularis propria or exogenous SMTs. EFTR is especially

beneficial in the treatment of such types of mucosal and submucosal lesions.

EFTR of early gastric cancer is mainly used for non-lifting lesions due to fibrosis or scarring as well as for lesions with challenging locations that make the ESD procedure difficult. The exposure of the lumen to the abdominal cavity during EFTR for cancerous lesions is controversial due to the potential risk of tumor cell seeding. Maehata *et al*[10] predicted that cancer cells, including cancer stem cells in early gastric cancers, could easily detach from the source by contact with the cancer surface. To avoid the potential risk of iatrogenic cancer cell seeding into the peritoneum, a non-exposure approach may be optimal in EFTR. The combination of laparoscopic and endoscopic approaches to neoplasia with a non-exposure technique is the most widely reported technique due to concerns about intraperitoneal metastasis[10-12]. Since ESD or laparoscopy is often used in the treatment of early gastric cancer at Shengjing Hospital of China Medical University, no case of early gastric cancer met the inclusion criteria of this study.

Current international guidelines recommend endoscopic therapy for early colorectal cancer with a low risk of lymphatic metastasis[13-15]. For lesions at difficult anatomical sites or lesions that are non-lifting due to scarring, EFTR is an alternative resection technique that expands the possibilities of endoscopic resection[16-21]. A study by Kuellmer *et al*[22] included 64 cases undergoing EFTR after incomplete resection of a malignant polyp (group 1) and 92 non-lifting lesions (group 2). Technical success was achieved in 144 (92.3%) out of 156 cases with an average procedural time of 42 min. R0 resection was achieved in 112 (71.8%) of 156 patients. Subgroup analysis showed an R0 resection rate of 87.5% in group 1 and 60.9% in group 2 ($P < 0.001$). They reported that EFTR is technically feasible and safe for the treatment of early colorectal cancers[22]. In our study, EFTR was performed in two patients with early colorectal cancer. One of these patients underwent an additional surgery due to a diagnosis of rectal adenocarcinoma with submucosal infiltration > 2 mm. However, low-risk *vs* high-risk lesions are difficult to discern before resection, as the criteria are based on histologic features. EFTR is also one method to remove lesions locally in order to provide further pathological diagnosis.

In our study, most cases were SMTs. SMTs originating from the muscularis propria are a good indication for EFTR. Endoscopic resection not only enables sufficient tissue to be obtained for pathological diagnosis but is also curative, as it involves resection of the tumor. EFTR is inevitable for deep or muscularis propria SMTs that are tightly connected. Ye *et al*[23] evaluated the safety and efficacy of EFTR ($n = 51$) with defect closure using clips and an endoloop for the resection of gastric subepithelial tumors of the muscularis propria. EFTR was successfully carried out in 50 (98%) patients, with a mean operation time of 52 min[23]. In our preliminary study[24], 23 cases of exposed EFTR were reported. EFTR was successfully carried out in 100% of the cases, and delayed perforation was not observed during follow-up. The average tumor size was 12.1 ± 4.7 mm (range, 6-20 mm)[24]. Li *et al*[25] reported 28 EFTR procedures for cases of gastric GIST originating from the muscularis propria. The average tumor size was 1.6 ± 0.4 cm, and the *en bloc* resection rate was 92.9%. In the study, the average EFTR time was 39.6 min (range, 5-236 min). The success rate of defect closure was 100% (68/68), and the R0 resection rate was also 100%. EFTR lasted 236 min in one case. The specific reasons are as follows: (1) The case was at the beginning of the learning curve; (2) The location of the lesion was difficult to operate; and (3) Intraoperative hemostasis took a long time.

EFTR can also be used to treat duodenal SMTs. In a study by Kappelle *et al*[5], EFTR was performed on 13 lesions in 12 patients: Seven gastric and six duodenal SMTs. Technical success was achieved in 11 (85%) cases. In all the 11 cases, R0 resection was achieved[5]. Ren *et al*[26] investigated 32 patients with non-ampullary duodenal SMTs who underwent EFTR. The complete resection rate was 100%, and neither delayed bleeding nor fistulas were observed[26]. In our study, a case of duodenal bulb SMT was included, and R0 resection was achieved. The histopathologic diagnosis of this lesion was a low-risk GIST.

There are also retrospective studies with small sample sizes that confirm the efficacy of EFTR in the treatment of colorectal SMTs originating from the muscularis propria. In a study by Albrecht *et al*[16], R0 resection was achieved in all colorectal SMTs, and 3-mo follow-up data showed no residual tumor. In our study, a case of rectal SMT was included. The histopathologic diagnosis of this lesion was endometriosis.

In our study, pre-procedure evaluation by EUS was necessary. EUS can assess the origin of lesions, invasion depth, size, echogenic characteristics, and the presence of enlarged lymph nodes, as well as help make a preliminary judgment about the nature of the lesion to assess the feasibility of EFTR[27-32].

To carry out EFTR safely, reliable endoscopic suturing devices are necessary to close

the resected openings. There are several methods for closure after EFTR including OTSC. The defect in the wall can be closed with endoclips, clips combined with an endoloop, or a suturing device. In a study conducted by Li *et al*[25], the purse-string suture method with metal clips and nylon suture snares was used for the closure of gastric wall defects. The mean closure time was 54.5 ± 27.5 min[25]. In our study, the success rate of the defect closure was 100% (68/68). The average OTSC defect closure time was 5.01 ± 3.83 min (range, 2-26 min). The closure time was much shorter than that in previous reports. Several studies report OTSC-assisted EFTR, which included OTSC closure prior to EFTR[6,22,33,34]. This method is time saving, but can only be used on small lesions.

The use of an OTSC to close a 2-cm (diameter) gastric wall defect has been proven to be safe and effective. Thus, we chose the lesions with a diameter of less than 2 cm in the study.

Whether small GISTs require endoscopic resection remains controversial. The National Comprehensive Cancer Network guidelines recommend that in the case of small GISTs (≤ 2 cm) lacking high-risk EUS features [*e.g.*, irregular border, lobulation, internal heterogeneous echogenicity, anechoic (cystic) spaces, hyperechoic foci, and tumor extraluminal growth], conservative follow-up should be performed. However, the European Society for Medical Oncology indicates that surgery should be the standard treatment for small histologically confirmed GISTs. Furthermore, some researchers have even proposed that all GISTs have malignant potential and, thus, surgical or endoscopic resection should be performed on detected GISTs.

Since endoscopic resection is a simple and minimally invasive method of obtaining histological samples, this method is recommended even for small gastric tumors originating from the muscularis propria. In this way, patients not only avoid the burden of survival and follow-up with a tumor, but also obtain an accurate diagnosis.

In our study, the average post-procedure follow-up time was 48.2 mo. During follow-up, 24 patients (including 22 with lesions in the stomach and two with lesions in the rectum) shed the OTSC. One of those 24 patients developed upper gastrointestinal bleeding due to OTSC loss. The bleeding was successfully treated using endoscopic therapy. OTSC of the rectum was removed during an operation in one case. The rest of the patients did not shed OTSC and remain in follow-up. OTSC can spontaneously fall off, but according to the current literature, the fall off time varies according to the location[35,36]. Li *et al*[35] found that 80% of intestinal OTSCs could spontaneously fall off within 3 mo. Shoar *et al*[37] reported cases of long-term attachment of OTSC in the stomach and found that 27.8% of all OTSCs would spontaneously fall off and that the possibility of falling off was significantly related to the original position of the clamp.

Long-term gastric attachment appears to be safe even if no spontaneous detachment occurs. However, removal of the clamp is necessary when complications associated with the clip (such as localized inflammation, ulcers, or luminal obstruction) occur, or when the patient strongly requests it. Several techniques can now be used to remove selective clamps, including argon arc beam, YAG laser, bipolar cutting equipment, and cold salt solution technology[36].

This study had some limitations regarding the study design. It was a single center study, and had a small sample size for early colorectal cancer. This new technique must be further investigated in larger, multicenter, randomized, controlled studies.

CONCLUSION

In conclusion, our study demonstrated that EFTR combined with OTSC is a safe and effective technique for the resection of small SMTs and early gastrointestinal cancers that are not suitable for ESD, with excellent R0 resection rates.

ARTICLE HIGHLIGHTS

Research background

Endoscopic submucosal dissection to treat mucosal and submucosal lesions often results in low rates of microscopically margin-negative (R0) resection. Endoscopic full-thickness resection (EFTR) has a high R0 resection rate and allows for the definitive diagnosis and treatment of selected mucosal and submucosal lesions that are not suitable for conventional resection techniques. The aim of the study was to evaluate

the efficacy and safety of EFTR using an over-the-scope clip (OTSC).

Research motivation

Data on the safety and efficacy of EFTR combined with OTSC in the treatment of gastrointestinal epithelial and subepithelial lesions have been lacking in high-level prospective studies.

Research objectives

We prospectively investigated the safety and efficacy of EFTR combined with OTSC in the treatment of epithelial and subepithelial tumors, as well as OTSC shedding during long-term follow-up, in order to provide a high level of clinical basis for the further use of this method.

Research methods

A single-center prospective study was performed.

Research results

A total of 68 patients (17 men and 51 women) with an average age of 52.0 ± 10.5 years (range, 32-71 years) were enrolled in this study, which included 66 gastric or colorectal submucosal tumors and 2 early-stage colorectal cancers. The mean tumor diameter was 12.6 ± 4.3 mm. The EFTR procedure was successful in all cases. The mean EFTR procedure time was 39.6 ± 38.0 min. The mean OTSC defect closure time was 5.0 ± 3.8 min, and the success rate of closure for defects was 100%. Histologically complete resection (R0) was achieved in 67 (98.5%) patients. Procedure-related adverse events were observed in 11 (16.2%) patients. The average post-procedure length of follow-up was 48.2 ± 15.7 mo. There was no recurrence during follow-up.

Research conclusions

EFTR combined with OTSC is an effective and safe technique for the removal of select subepithelial and epithelial lesions that are not amenable to conventional endoscopic resection techniques.

Research perspectives

EFTR combined with OTSC is an effective and safe technique for the removal of select subepithelial and epithelial lesions that are not amenable to conventional endoscopic resection techniques.

ACKNOWLEDGEMENTS

We thank all the doctors who participated in this study.

REFERENCES

1 **Chung IK**, Lee JH, Lee SH, Kim SJ, Cho JY, Cho WY, Hwangbo Y, Keum BR, Park JJ, Chun HJ, Kim HJ, Kim JJ, Ji SR, Seol SY. Therapeutic outcomes in 1000 cases of endoscopic submucosal dissection for early gastric neoplasms: Korean ESD Study Group multicenter study. *Gastrointest Endosc* 2009; **69**: 1228-1235 [PMID: 19249769 DOI: 10.1016/j.gie.2008.09.027]

2 **Chun SY**, Kim KO, Park DS, Lee IJ, Park JW, Moon SH, Baek IH, Kim JH, Park CK, Kwon MJ. Endoscopic submucosal dissection as a treatment for gastric subepithelial tumors that originate from the muscularis propria layer: a preliminary analysis of appropriate indications. *Surg Endosc* 2013; **27**: 3271-3279 [PMID: 23519491 DOI: 10.1007/s00464-013-2904-9]

3 **He Z**, Sun C, Wang J, Zheng Z, Yu Q, Wang T, Chen X, Liu W, Wang B. Efficacy and safety of endoscopic submucosal dissection in treating gastric subepithelial tumors originating in the muscularis propria layer: a single-center study of 144 cases. *Scand J Gastroenterol* 2013; **48**: 1466-1473 [PMID: 24131359 DOI: 10.3109/00365521.2013.845796]

4 **Białek A**, Wiechowska-Kozłowska A, Pertkiewicz J, Polkowski M, Milkiewicz P, Karpińska K, Ławniczak M, Starzyńska T. Endoscopic submucosal dissection for treatment of gastric subepithelial tumors (with video). *Gastrointest Endosc* 2012; **75**: 276-286 [PMID: 22032850 DOI: 10.1016/j.gie.2011.08.029]

5 **Kappelle WFW**, Backes Y, Valk GD, Moons LMG, Vleggaar FP. Endoscopic full-thickness resection of gastric and duodenal subepithelial lesions using a new, flat-based over-the-scope clip. *Surg Endosc* 2018; **32**: 2839-2846 [PMID: 29282573 DOI: 10.1007/s00464-017-5989-8]

6 **Al-Bawardy B**, Rajan E, Wong Kee Song LM. Over-the-scope clip-assisted endoscopic full-thickness resection of epithelial and subepithelial GI lesions. *Gastrointest Endosc* 2017; **85**: 1087-1092 [PMID: 27569858 DOI: 10.1016/j.gie.2016.08.019]

7 **Gincul R**, Ponchon T, Napoleon B, Scoazec JY, Guillaud O, Saurin JC, Ciocirlan M, Lepilliez V, Pioche M, Lefort C, Adham M, Pialat J, Chayvialle JA, Walter T. Endoscopic treatment of sporadic small duodenal and ampullary neuroendocrine tumors. *Endoscopy* 2016; **48**: 979-986 [PMID: 27494453 DOI: 10.1055/s-0042-112570]

8 **Facciorusso A**, Antonino M, Di Maso M, Muscatiello N. Endoscopic submucosal dissection *vs* endoscopic mucosal resection for early gastric cancer: A meta-analysis. *World J Gastrointest Endosc* 2014; **6**: 555-563 [PMID: 25400870 DOI: 10.4253/wjge.v6.i11.555]

9 **Pimentel-Nunes P**, Dinis-Ribeiro M, Ponchon T, Repici A, Vieth M, De Ceglie A, Amato A, Berr F, Bhandari P, Bialek A, Conio M, Haringsma J, Langner C, Meisner S, Messmann H, Morino M, Neuhaus H, Piessevaux H, Rugge M, Saunders BP, Robaszkiewicz M, Seewald S, Kashin S, Dumonceau JM, Hassan C, Deprez PH. Endoscopic submucosal dissection: European Society of Gastrointestinal Endoscopy (ESGE) Guideline. *Endoscopy* 2015; **47**: 829-854 [PMID: 26317585 DOI: 10.1055/s-0034-1392882]

10 **Maehata T**, Goto O, Takeuchi H, Kitagawa Y, Yahagi N. Cutting edge of endoscopic full-thickness resection for gastric tumor. *World J Gastrointest Endosc* 2015; **7**: 1208-1215 [PMID: 26566427 DOI: 10.4253/wjge.v7.i16.1208]

11 **Goto O**, Shimoda M, Sasaki M, Kiguchi Y, Mitsunaga Y, Akimoto T, Ochiai Y, Fujimoto A, Maehata T, Nishizawa T, Takeuchi H, Kitagawa Y, Kameyama K, Yahagi N. Potential for peritoneal cancer cell seeding in endoscopic full-thickness resection for early gastric cancer. *Gastrointest Endosc* 2018; **87**: 450-456 [PMID: 28890117 DOI: 10.1016/j.gie.2017.08.036]

12 **Niimi K**, Aikou S, Kodashima S, Yagi K, Oya S, Yamaguchi D, Yamashita H, Yamamichi N, Fujishiro M, Koike K, Seto Y. Video of the Month: A Novel Endoscopic Full-Thickness Resection for Early Gastric Cancer. *Am J Gastroenterol* 2015; **110**: 1535 [PMID: 26618417 DOI: 10.1038/ajg.2015.226]

13 **ASGE Standards of Practice Committee**. , Fisher DA, Shergill AK, Early DS, Acosta RD, Chandrasekhara V, Chathadi KV, Decker GA, Evans JA, Fanelli RD, Foley KQ, Fonkalsrud L, Hwang JH, Jue T, Khashab MA, Lightdale JR, Muthusamy VR, Pasha SF, Saltzman JR, Sharaf R, Cash BD. Role of endoscopy in the staging and management of colorectal cancer. *Gastrointest Endosc* 2013; **78**: 8-12 [PMID: 23664162 DOI: 10.1016/j.gie.2013.04.163]

14 **Ferlitsch M**, Moss A, Hassan C, Bhandari P, Dumonceau JM, Paspatis G, Jover R, Langner C, Bronzwaer M, Nalankilli K, Fockens P, Hazzan R, Gralnek IM, Gschwantler M, Waldmann E, Jeschek P, Penz D, Heresbach D, Moons L, Lemmers A, Paraskeva K, Pohl J, Ponchon T, Regula J, Repici A, Rutter MD, Burgess NG, Bourke MJ. Colorectal polypectomy and endoscopic mucosal resection (EMR): European Society of Gastrointestinal Endoscopy (ESGE) Clinical Guideline. *Endoscopy* 2017; **49**: 270-297 [PMID: 28212588 DOI: 10.1055/s-0043-102569]

15 **Tanaka S**, Kashida H, Saito Y, Yahagi N, Yamano H, Saito S, Hisabe T, Yao T, Watanabe M, Yoshida M, Kudo SE, Tsuruta O, Sugihara KI, Watanabe T, Saitoh Y, Igarashi M, Toyonaga T, Ajioka Y, Ichinose M, Matsui T, Sugita A, Sugano K, Fujimoto K, Tajiri H. JGES guidelines for colorectal endoscopic submucosal dissection/endoscopic mucosal resection. *Dig Endosc* 2015; **27**: 417-434 [PMID: 25652022 DOI: 10.1111/den.12456]

16 **Albrecht H**, Raithel M, Braun A, Nagel A, Stegmaier A, Utpatel K, Schäfer C. Endoscopic full-thickness resection (EFTR) in the lower gastrointestinal tract. *Tech Coloproctol* 2019; **23**: 957-963 [PMID: 31368009 DOI: 10.1007/s10151-019-02043-5]

17 **Ahlenstiel G**, Hourigan LF, Brown G, Zanati S, Williams SJ, Singh R, Moss A, Sonson R, Bourke MJ; Australian Colonic Endoscopic Mucosal Resection (ACE) Study Group. Actual endoscopic *vs* predicted surgical mortality for treatment of advanced mucosal neoplasia of the colon. *Gastrointest Endosc* 2014; **80**: 668-676 [PMID: 24916925 DOI: 10.1016/j.gie.2014.04.015]

18 **Jayanna M**, Burgess NG, Singh R, Hourigan LF, Brown GJ, Zanati SA, Moss A, Lim J, Sonson R, Williams SJ, Bourke MJ. Cost Analysis of Endoscopic Mucosal Resection *vs* Surgery for Large Laterally Spreading Colorectal Lesions. *Clin Gastroenterol Hepatol* 2016; **14**: 271-8. e1-2 [PMID: 26364679 DOI: 10.1016/j.cgh.2015.08.037]

19 **Ono H**, Yao K, Fujishiro M, Oda I, Nimura S, Yahagi N, Iishi H, Oka M, Ajioka Y, Ichinose M, Matsui T. Guidelines for endoscopic submucosal dissection and endoscopic mucosal resection for early gastric cancer. *Dig Endosc* 2016; **28**: 3-15 [PMID: 26234303 DOI: 10.1111/den.12518]

20 **Zhao B**, Mei D, Luo R, Lu H, Bao S, Xu H, Huang B. Clinicopathological features, risk of lymph node metastasis and survival outcome of synchronous multiple early gastric cancer. *Clin Res Hepatol Gastroenterol* 2020; **44**: 939-946 [PMID: 32122791 DOI: 10.1016/j.clinre.2020.02.004]

21 **Horiuchi Y**, Ida S, Yamamoto N, Nunobe S, Ishizuka N, Yoshimizu S, Ishiyama A, Yoshio T, Hirasawa T, Tsuchida T, Kumagai K, Ohashi M, Sano T, Fujisaki J. Feasibility of further expansion of the indications for endoscopic submucosal dissection in undifferentiated-type early gastric cancer. *Gastric Cancer* 2020; **23**: 285-292 [PMID: 31486980 DOI: 10.1007/s10120-019-01003-0]

22 **Kuellmer A**, Mueller J, Caca K, Aepli P, Albers D, Schumacher B, Glitsch A, Schäfer C, Wallstabe I, Hofmann C, Erhardt A, Meier B, Bettinger D, Thimme R, Schmidt A; FTRD study group. Endoscopic full-thickness resection for early colorectal cancer. *Gastrointest Endosc* 2019; **89**: 1180-1189. e1 [PMID: 30653939 DOI: 10.1016/j.gie.2018.12.025]

23 **Ye LP**, Yu Z, Mao XL, Zhu LH, Zhou XB. Endoscopic full-thickness resection with defect closure

using clips and an endoloop for gastric subepithelial tumors arising from the muscularis propria. *Surg Endosc* 2014; **28**: 1978-1983 [PMID: 24619327 DOI: 10.1007/s00464-014-3421-1]

24 **Guo J**, Liu Z, Sun S, Liu X, Wang S, Ge N, Wang G, Qi Y. Endoscopic full-thickness resection with defect closure using an over-the-scope clip for gastric subepithelial tumors originating from the muscularis propria. *Surg Endosc* 2015; **29**: 3356-3362 [PMID: 25701060 DOI: 10.1007/s00464-015-4076-2]

25 **Li J**, Meng Y, Ye S, Wang P, Liu F. Usefulness of the thread-traction method in endoscopic full-thickness resection for gastric submucosal tumor: a comparative study. *Surg Endosc* 2019; **33**: 2880-2885 [PMID: 30456512 DOI: 10.1007/s00464-018-6585-2]

26 **Ren Z**, Lin SL, Zhou PH, Cai SL, Qi ZP, Li J, Yao LQ. Endoscopic full-thickness resection (EFTR) without laparoscopic assistance for nonampullary duodenal subepithelial lesions: our clinical experience of 32 cases. *Surg Endosc* 2019; **33**: 3605-3611 [PMID: 31240477 DOI: 10.1007/s00464-018-06644-3]

27 **Antonini F**, Delconte G, Fuccio L, De Nucci G, Fabbri C, Armellini E, Frazzoni L, Fornelli A, Magarotto A, Mandelli E, Occhipinti P, Masci E, Manes G, Macarri G. EUS-guided tissue sampling with a 20-gauge core biopsy needle for the characterization of gastrointestinal subepithelial lesions: A multicenter study. *Endosc Ultrasound* 2019; **8**: 105-110 [PMID: 29770781 DOI: 10.4103/eus.eus_1_18]

28 **Pesenti C**, Bories E, Caillol F, Ratone JP, Godat S, Monges G, Poizat F, Raoul JL, Ries P, Giovannini M. Characterization of subepithelial lesions of the stomach and esophagus by contrast-enhanced EUS: A retrospective study. *Endosc Ultrasound* 2019; **8**: 43-49 [PMID: 30264741 DOI: 10.4103/eus.eus_89_17]

29 **Cazacu IM**, Singh BS, Luzuriaga Chavez AA, Koduru P, Ejaz S, Weston BR, Ross WA, Lee JH, Roy-Chowdhuri S, Bhutani MS. EUS and EUS-guided FNA/core biopsies in the evaluation of subepithelial lesions of the lower gastrointestinal tract: 10-year experience. *Endosc Ultrasound* 2020; **9**: 329-336 [PMID: 32913150 DOI: 10.4103/eus.eus_51_20]

30 **Okuwaki K**, Masutani H, Kida M, Yamauchi H, Iwai T, Miyata E, Hasegawa R, Kaneko T, Imaizumi H, Watanabe M, Kurosu T, Tadehara M, Adachi K, Tamaki A, Koizumi W. Diagnostic efficacy of white core cutoff lengths obtained by EUS-guided fine-needle biopsy using a novel 22G franseen biopsy needle and sample isolation processing by stereomicroscopy for subepithelial lesions. *Endosc Ultrasound* 2020; **9**: 187-192 [PMID: 32584314]

31 **Fabbri C**, Fornelli A, Fuccio L, Giovanelli S, Tarantino I, Antonini F, Liotta R, Frazzoni L, Gusella P, La Marca M, Barresi L, Macarri G, Traina M, De Biase D, Fiorino S, Jovine E, Larghi A, Cennamo V. High diagnostic adequacy and accuracy of the new 20G procore needle for EUS-guided tissue acquisition: Results of a large multicentre retrospective study. *Endosc Ultrasound* 2019; **8**: 261-268 [PMID: 31115386 DOI: 10.4103/eus.eus_14_19]

32 **Hu J**, Ge N, Wang S, Liu X, Guo J, Wang G, Sun S. The Role of Endoscopic Ultrasound and Endoscopic Resection for Gastric Glomus: A Case Series and Literature Review. *J Transl Int Med* 2019; **7**: 149-154 [PMID: 32010601 DOI: 10.2478/jtim-2019-0030]

33 **Andrisani G**, Pizzicannella M, Martino M, Rea R, Pandolfi M, Taffon C, Caricato M, Coppola R, Crescenzi A, Costamagna G, Di Matteo FM. Endoscopic full-thickness resection of superficial colorectal neoplasms using a new over-the-scope clip system: A single-centre study. *Dig Liver Dis* 2017; **49**: 1009-1013 [PMID: 28539229 DOI: 10.1016/j.dld.2017.04.015]

34 **Lagoussis P**, Soriani P, Tontini GE, Neumann H, Pastorelli L, de Nucci G, Vecchi M. Over-the-scope clip-assisted endoscopic full-thickness resection after incomplete resection of rectal adenocarcinoma. *Endoscopy* 2016; **48** Suppl 1 UCTN: E59-E60 [PMID: 26890543 DOI: 10.1055/s-0042-100197]

35 **Li P**, Ma B, Gong S, Zhang X, Li W. Efficacy and safety of endoscopic full-thickness resection in the colon and rectum using an over-the-scope device: a meta-analysis. *Surg Endosc* 2021; **35**: 249-259 [PMID: 31953724 DOI: 10.1007/s00464-020-07387-w]

36 **Hu J**, Yang Y, Ge N, Wang S, Guo J, Liu X, Wang G, Sun S. Long-term assessment of over-the-scope clip (OTSC) behavior after gastric application. *Minim Invasive Ther Allied Technol* 2020; **29**: 86-89 [PMID: 31144550 DOI: 10.1080/13645706.2019.1590417]

37 **Shoar S**, Poliakin L, Khorgami Z, Rubenstein R, El-Matbouly M, Levin JL, Saber AA. Efficacy and Safety of the Over-the-Scope Clip (OTSC) System in the Management of Leak and Fistula After Laparoscopic Sleeve Gastrectomy: a Systematic Review. *Obes Surg* 2017; **27**: 2410-2418 [PMID: 28353180 DOI: 10.1007/s11695-017-2651-4]

World Journal of Gastroenterology

Submit a Manuscript: https://www.f6publishing.com

World J Gastroenterol 2021 February 28; 27(8): 737-750

DOI: 10.3748/wjg.v27.i8.737

ISSN 1007-9327 (print) ISSN 2219-2840 (online)

META-ANALYSIS

Risk factors for lymph node metastasis in T1 esophageal squamous cell carcinoma: A systematic review and meta-analysis

Kai-Yuan Jiang, Heng Huang, Wei-Yang Chen, Hao-Ji Yan, Zhen-Ting Wei, Xiao-Wen Wang, Hao-Xuan Li, Xiang-Yun Zheng, Dong Tian

ORCID number: Kai-Yuan Jiang 0000-0002-4859-646X; Heng Huang 0000-0003-1966-3763; Wei-Yang Chen 0000-0002-6665-0618; Hao-Ji Yan 0000-0003-4420-4657; Zhen-Ting Wei 0000-0001-7192-3951; Xiao-Wen Wang 0000-0001-5053-2708; Hao-Xuan Li 0000-0003-2873-8085; Xiang-Yun Zheng 0000-0002-2175-9257; Dong Tian 0000-0002-4145-8638.

Author contributions: Jiang KY, Huang H and Tian D designed the research; Jiang KY and Huang H performed the research and drafted the article; Chen WY, Yan HJ and Wei ZT screened the literature and collected the data; Wang XW, Li HX and Zheng XY analyzed the data and interpreted the data; Tian D revised the article; All authors have read and approved the final manuscript; Jiang KY and Huang H contributed equally to this work.

Conflict-of-interest statement: The authors have no conflicts of interest to declare.

PRISMA 2009 Checklist statement: The authors have read the PRISMA 2009 Checklist, and the manuscript was prepared and revised according to the PRISMA 2009 Checklist.

Open-Access: This article is an

Kai-Yuan Jiang, Heng Huang, Wei-Yang Chen, Hao-Ji Yan, Zhen-Ting Wei, Xiao-Wen Wang, Hao-Xuan Li, Xiang-Yun Zheng, College of Clinical Medicine, North Sichuan Medical College, Nanchong 637000, Sichuan Province, China

Kai-Yuan Jiang, Dong Tian, Department of Thoracic Surgery, Affiliated Hospital of North Sichuan Medical College, Nanchong 637000, Sichuan Province, China

Corresponding author: Dong Tian, MD, PhD, Doctor, Department of Thoracic Surgery, Affiliated Hospital of North Sichuan Medical College, No. 63 Wenhua Road, Shunqing District, Nanchong 637000, Sichuan Province, China. 22tiandong@163.com

Abstract

BACKGROUND

Lymph node metastasis (LNM) affects the application and outcomes of endoscopic resection in T1 esophageal squamous cell carcinoma (ESCC). However, reports of the risk factors for LNM have been controversial.

AIM

To evaluate risk factors for LNM in T1 ESCC.

METHODS

We searched Embase, PubMed and Cochrane Library to select studies related to LNM in patients with T1 ESCC. Included studies were divided into LNM and non-LNM groups. We performed a meta-analysis to examine the relationship between LNM and clinicopathologic features. Odds ratio (OR), mean differences and 95% confidence interval (CI) were assessed using a fixed-effects or random-effects model.

RESULTS

Seventeen studies involving a total of 3775 patients with T1 ESCC met the inclusion criteria. After excluding studies with heterogeneity based on influence analysis, tumor size (OR = 1.93, 95%CI = 1.49-2.50, $P < 0.001$), tumor location (OR = 1.46, 95%CI = 1.17-1.82, $P < 0.001$), macroscopic type (OR = 3.17, 95%CI = 2.33-4.31, $P < 0.001$), T1 substage (OR = 6.28, 95%CI = 4.93-8.00, $P < 0.001$), differentiation (OR = 2.11, 95%CI = 1.64-2.72, $P < 0.001$) and lymphovascular invasion (OR = 5.86, 95%CI = 4.60-7.48, $P < 0.001$) were found to be significantly associated with LNM. Conversely, sex, age and infiltrative growth pattern were not identified as risk factors for LNM.

open-access article that was selected by an in-house editor and fully peer-reviewed by external reviewers. It is distributed in accordance with the Creative Commons Attribution NonCommercial (CC BY-NC 4.0) license, which permits others to distribute, remix, adapt, build upon this work non-commercially, and license their derivative works on different terms, provided the original work is properly cited and the use is non-commercial. See: http://creativecommons.org/Licenses/by-nc/4.0/

Manuscript source: Unsolicited manuscript

Specialty type: Gastroenterology and hepatology

Country/Territory of origin: China

Peer-review report's scientific quality classification

Grade A (Excellent): 0
Grade B (Very good): B
Grade C (Good): 0
Grade D (Fair): 0
Grade E (Poor): 0

Received: November 28, 2020
Peer-review started: November 28, 2020
First decision: January 17, 2021
Revised: January 20, 2021
Accepted: February 1, 2021
Article in press: February 1, 2021
Published online: February 28, 2021

P-Reviewer: Spartalis E
S-Editor: Gao CC
L-Editor: Filipodia
P-Editor: Liu JH

CONCLUSION

A tumor size > 2 cm, lower location, nonflat macroscopic type, T1b stage, poor differentiation and lymphovascular invasion were associated with LNM in patients with T1 ESCC.

Key Words: Risk factors; Lymph node metastasis; T1; Esophageal squamous cell carcinoma; Meta-analysis; Review

©The Author(s) 2021. Published by Baishideng Publishing Group Inc. All rights reserved.

Core Tip: No consensus is available in the literature about risk factors for lymph node metastasis (LNM) in T1 esophageal squamous cell carcinoma. This meta-analysis is the first to comprehensively evaluate LNM only in esophageal squamous cell carcinoma patients with T1 stage. We investigated the relationship between LNM and the factors of demographic and clinicopathological characteristics. The results showed that risk factors associated with LNM were tumor size, tumor location, T1 substage, tumor differentiation, lymphovascular invasion and macroscopic type.

Citation: Jiang KY, Huang H, Chen WY, Yan HJ, Wei ZT, Wang XW, Li HX, Zheng XY, Tian D. Risk factors for lymph node metastasis in T1 esophageal squamous cell carcinoma: A systematic review and meta-analysis. *World J Gastroenterol* 2021; 27(8): 737-750
URL: https://www.wjgnet.com/1007-9327/full/v27/i8/737.htm
DOI: https://dx.doi.org/10.3748/wjg.v27.i8.737

INTRODUCTION

The morbidity and mortality of esophageal cancer (EC) rank 7th and 6th among cancers globally[1]. In the last few decades, there has been great progress in the early diagnosis, surgical techniques and comprehensive treatment of EC. However, long-term efficacy remains poor, and the 5-yr survival rate is only 10%-30%[2]. In general, the opportunity for a cure in cancer is determined by early screening and intervention.

Esophageal squamous cell carcinoma (ESCC) is the most common histological type of EC in Asia[3]. T1 EC are stratified into T1a (mucosal layer) and T1b (submucosal layer) based on the 8th edition EC tumor, node, metastasis staging. For patients with T1a or T1b tumors, the 5-yr survival rate can be higher than 85%[4]. Although radical esophagectomy with lymphadenectomy is still the gold standard, endoscopic imaging with resection offers a new model for the treatment of early ESCC. In addition, evaluation of the clinical stage, disease extent, tumor grade and risk of lymph node metastasis (LNM) is critical when determining eligibility for endoscopic treatment of T1 ESCC[5]. LNM rates in T1a and T1b are reportedly 7.0%-16.0% and 16.0%-41.1%, respectively[6-8], and thus endoscopic resection (ER) for the treatment of T1 ESCC should be considered carefully[9]. Furthermore, LNM may be regarded as the most important prognostic factor in ESCC[10], and accurate assessment of the risk of LNM in T1 ESCC is particularly important.

Risk factors for LNM in T1 ESCC have been reported without consensus. We previously demonstrated that clinicopathological and hematological parameters can predict the risk of LNM in T1 ESCC, though some features were not included and the sample size in that study was limited. Herein, we present a meta-analysis to evaluate risk factors of LNM alone in stage T1 ESCC.

MATERIALS AND METHODS

This meta-analysis was performed in accordance with the guidelines proposed by the preferred reporting items for systematic reviews and meta-analyses (PRISMA) statement (http://www.prisma-statement.org/)[11].

Literature search strategy

To select relevant studies for the meta-analysis, we searched the following electronic databases: PubMed, EMBASE, and the Cochrane Library. The last search was performed on July 1, 2020. The search terms were "T1," "early," "mucosal," "submucosal," "superficial," "intramucosal," "esophageal," "esophagus," "squamous," "cancer" and "carcinoma." Two authors (Tian D and Jiang KY) independently performed the selection and evaluation of references. When necessary, a third author (Huang H) independently resolved any discrepancies between the two review authors. The full text of studies meeting the inclusion criteria were reviewed to identify whether they contained useful information.

Inclusion and exclusion criteria

The criteria for inclusion in this meta-analysis were as follows: (1) A case-control study of risk factors for LNM in stage T1 ESCC; (2) All patients underwent 2- or 3-field lymphadenectomy; (3) Published in English; (4) Contained original data, odds ratio (OR), mean difference and 95% confidence intervals (CI); (5) The definition and classification standard of tumors were basically the same; and (6) When overlapping data resources were presented in several articles, only the study with the highest quality and largest sample size was selected. Studies were excluded from the meta-analysis for the following reasons: (1) References were abstracts, comments, reviews and editorials; (2) Patients with esophagogastric junction adenocarcinoma or esophageal adenocarcinoma; or (3) Low reliability and poor quality Newcastle-Ottawa Scale score ≤ 5).

Literature selection and data extraction

According to the above criteria, qualified literature was selected by reading the title, abstract and full text. The following data were extracted: first author, publication year, location, research period, study design, case number, operation protocol, lymph node status (LNM/non-LNM), age, sex, tumor size, tumor location, macroscopic type, T1 substage, tumor differentiation, lymphovascular invasion (LVI) and infiltrative growth pattern (INF). A structured table was employed to help extract relevant data from the included studies. We used the Newcastle-Ottawa Scale for evaluating the quality of references. The scale includes three aspects (selection, comparability and outcome) ranging from 0 to 9 stars, and studies with a score of 6 were considered to have adequate methodologic quality for inclusion[12].

Definitions

Patients in the literature included underwent open esophagectomy or thoracoscopy-assisted esophagectomy or ER and 2- or 3-field lymph node dissection. Postoperative pathological results confirmed that the tumor invaded the mucosa or submucosa. T1 ESCC was stratified as T1a, which included T1a-carcinoma in situ, T1a-lamina propria mucosa, T1a-MM (muscularis mucosa), and T1b, which include SM1 (the upper third of the submucosal layer), SM2 (the middle third of the submucosal layer) and SM3 (the lower third of the submucosal layer). Tumor locations were classified as upper, middle and lower. Tumor differentiation was stratified into well differentiated, moderately differentiated and poorly differentiated. Macroscopic type was divided into flat and nonflat types based on visual observation. LVI (absent/present) and INF (a/b/c) were determined by postoperative immunohistochemistry or hematoxylin-eosin staining. The INF division was as follows: INF-a (expansive growth of tumor nests with a well-demarcated border from the surrounding tissue), INF-b (growth pattern intermediate between that of INF-a and INF-c) and INF-c (infiltrative growth of tumor nests with an ill-defined border from the surrounding tissue).

Statistical analysis

Statistical software Review Manager 5.3 and Stata 15.0 were used for data analyses. Dichotomous data were analyzed using the OR with 95%CI. For continuous data, the mean difference and 95%CI were calculated. The Mantel-Haenszel method and inverse variance method were applied for dichotomous and continuous data, respectively. Heterogeneity among the included studies was preliminarily examined by a Galbraith plot. If heterogeneity was detected, influence analysis was performed to explore individual studies with heterogeneity. After excluding studies with heterogeneity, data were graphically plotted using forest plots to evaluate the treatment effects and heterogeneity of the trials. Heterogeneity was quantified with the χ^2 (Cochrane Q) test and the I^2 statistic, whereby low, moderate and high degrees of heterogeneity corresponded to I^2 values of 25%, 50% and 75%, respectively. When $P > 0.1$ and $I^2 <$

50%, a fixed-effects model was utilized; otherwise, a random-effects model was applied. After the heterogeneity test of outcome indicators, the *P* value, OR value and 95%CI of the combined statistics were then calculated. Funnel plots were used to evaluate the presence of publication bias.

RESULTS

Study selection

A flow chart of the selection process for the studies included in this meta-analysis is presented in Figure 1. The search strategy identified 1527 records from all sources (Embase, *n* = 911; PubMed, *n* = 562; and Cochrane, *n* = 54). Of these, 537 duplicate records, 21 non-English articles and 226 non-full texts were excluded. In addition, 666 studies were excluded after scanning the article types, titles and abstracts, including 79 case reports/reviews and 587 title/abstract clearly irrelevant articles; thus, 80 studies remained for full-text assessment. Thereafter, 33 studies were included for qualitative synthesis. Seven studies had duplicate data sources, eight studies included patients with esophagogastric junction adenocarcinoma or esophageal adenocarcinoma, and one study included some patients without lymphadenectomy. Ultimately, 17 studies meeting all inclusion criteria were selected for the meta-analysis.

Study characteristics and quality assessment

Table 1 shows the baseline characteristics and quality assessment scores of the 17 included retrospective studies. Three[13-15] were multicenter studies, and fourteen[16-29] were single-center studies. All studies were conducted in Asian countries, including seven in China[14,15,20,21,23,26,29], seven in Japan[16,18,19,22,24,27,28] and three in South Korea[13,17,25]. All patients underwent open esophagectomy/thoracoscopy-assisted esophagectomy/ER and 2- or 3-field lymphadenectomy. Moreover, postoperative pathological results confirmed T1 ESCC in all cases. A total of 3775 patients were enrolled, of whom 914 had LNM and 2861 were non-LNM, with a metastasis rate of 24.2%. In terms of the assessment of the Newcastle-Ottawa Scale, 11 studies[8,13,16-22,25,27] scored 6, and 6 studies[14,15,23,24,26,28] scored 7.

Risk factors for LNM

The results for the relationship between LNM and clinicopathological factors in T1 ESCC patients after excluding studies with heterogeneity in all analyses are provided in Table 2. Galbraith plots are depicted in Supplementary Figures 1-3, plots of influence analyses in Supplementary Figure 4, forest plots in Figure 2-4, and funnel plots in Supplementary Figures 5-7.

Age and sex

Six studies[16,17,19,20,23,28] reporting continuous age of patients were analyzed in this meta-analysis. The mean age in the LNM and non-LNM groups ranged from 57.5-67.3 and 58.0-63.7 years, respectively. Thirteen studies[13-17,19-21,23-25,28,29] recorded the rate of LNM in males *vs* females (14.4%-39.6% *vs* 0%-66.7%). The Galbraith plot and influence analysis indicated no heterogeneity in the studies including age analysis, though one study (Chiba *et al*[24]) with sex analysis exhibited strong heterogeneity (Supplementary Figures 1 and 4A). No significant difference between LNM and age was observed (OR = -0.81, 95%CI = -1.75-0.14, P = 0.10; heterogeneity: I^2 = 22%, P = 0.27) (Figure 2A). After excluding the study by Chiba *et al*[24], the results indicated that the rate of LNM according to sex was not significantly different (OR = 1.16, 95%CI = 0.91-1.48, P = 0.23; heterogeneity: I^2 = 0%, P = 0.78) (Figure 2B).

Tumor size, location and macroscopic type

Six studies[13-15,17,21,26] including 1482 patients, twelve studies[13-16,19-23,25,26,29] including 2751 patients, and six studies[13,18,21,22,25,27] including 1213 patients analyzed the relationship between LNM and tumor size, location and macroscopic type, respectively. The rates of LNM for tumor size ≤ 2 cm *vs* tumor size > 2 cm, upper-middle ESCC *vs* lower ESCC and nonflat type *vs* flat type were 8.9%-28.4% *vs* 17.5%-42.6%, 6.9%-41.5% *vs* 15.6%-36.8% and 23.5%-68.2% *vs* 8.2%-25.0%, respectively. Although no heterogeneity regarding tumor size analysis or macroscopic type analysis (Supplementary Figures 2A and C) was detected, influence analysis suggested heterogeneities for tumor location in the studies of Wang *et al*[29] and Wu *et al*[20] (Supplementary Figures 2B and 4B). Moreover, the rate of LNM in patients with tumor size ≤ 2 cm was 1.93 times

Table 1 Baseline characteristics of included studies

Reference	Location	Period	Design	Case	Operation protocol	Lymphadenectomy strategy	LNM/non-LNM	Quality assessment
Aoyama *et al*[16] (2019)	Japan	2012-2016	SR	50	Esophagectomy	2- or 3-field lymphadenectomy	13/37	6
Chiba *et al*[24] (2010)	Japan	1992-2008	SR	110	Esophagectomy	Lymphadenectomy	33/77	7
Huh *et al*[25] (2018)	South Korea	1996-2015	SR	275	Esophagectomy	Lymphadenectomy	40/235	6
Li *et al*[26] (2013)	China	2006-2011	SR	189	Esophagectomy	Lymphadenectomy	47/95	7
Makuuchi *et al*[27] (1997)	Japan	1974-1995	SR	133	Esophagectomy	Lymphadenectomy	35/98	6
Min *et al*[17] (2020)	South Korea	2001-2014	SR	501	Esophagectomy	2-field lymphadenectomy: 462; 3-field lymphadenectomy: 39	140/361	6
Mitobe *et al*[18] (2013)	Japan	1990-2009	SR	110	Esophagectomy: 106; ER + esophagectomy: 4	Lymphadenectomy	37/73	6
Moon *et al*[13] (2014)	South Korea	2009-2012	MR	104	Esophagectomy	Lymphadenectomy	15/89	6
Ozawa *et al*[19] (2016)	Japan	1986-2013	SR	167	Esophagectomy; VATS	2- or 3-field lymphadenectomy	46/121	6
Shen *et al*[14] (2018)	China	2014-2016	MR	221	Esophagectomy	Lymphadenectomy	53/168	7
Tian *et al*[15] (2020)	China	2013-2019	MR	243	Esophagectomy	3-field lymphadenectomy	46/197	7
Tomita *et al*[28] (2008)	Japan	1998-2006	SR	115	Esophagectomy	2- or 3-field lymphadenectomy	52/63	7
Wang *et al*[29] (2016)	China	2002-2014	SR	228	Esophagectomy	2- or 3-field lymphadenectomy	90/138	6
Wu *et al*[20] (2018)	China	2002-2010	SR	240	Esophagectomy	2-field lymphadenectomy	39/201	6
Xue *et al*[21] (2012)	China	1990-2004	SR	271	Esophagectomy	Lymphadenectomy	53/218	6
Yachida *et al*[22] (2020)	Japan	1986-2010	SR	320	Esophagectomy	3-field lymphadenectomy	93/227	6
Zhou *et al*[23] (2016)	China	2008-2015	SR	498	Esophagectomy	Lymphadenectomy	87/411	7

ER: Endoscopic resection; LNM: Lymph node metastasis; MR: Multicenter retrospective; SR: Single-center retrospective; VATS: Video-assisted thoracoscopic surgery.

higher than that in patients with tumor size ≤ 2 cm (OR = 1.93, 95%CI = 1.49-2.50, P < 0.001; heterogeneity: I^2 = 0%, P = 0.74) (Figure 3A). Additionally, the rate of LNM differed significantly with respect to tumor location (OR = 1.46, 95%CI = 1.17-1.82, P < 0.001; heterogeneity: I^2 = 0%, P = 0.57) (Figure 3B) and macroscopic type (OR = 3.17, 95%CI = 2.33-4.31, P < 0.001; heterogeneity: I^2 = 35%, P = 0.17, Figure 3C).

T1 substage, differentiation, LVI and INF

The relationship between T1 substage and LNM was analyzed in 17 studies[13-29], involving 3775 patients, and the relationship between differentiation and LNM was analyzed in 13 studies[13-15,18-21,23-26,28,29], involving 2599 patients. The rates of LNM in T1a *vs* T1b and well differentiated/moderately differentiated *vs* poorly differentiated were 1.5%-23.5% *vs* 20.9%-57.3% and 12.6%-43.3% *vs* 23.8%-63.6%, respectively. Based on heterogeneity and influence analyses, studies with heterogeneity by Aoyama *et al*[16] and Ozawa *et al*[19] were excluded from the T1 substage analysis, and those of Shen *et al*[14] and Zhou *et al*[23] were excluded from the differentiation analysis (Supplementary Figures 3A, 3B, 4C and 4D). Nonetheless, pooled analysis suggested that the rate of LNM differed significantly for T1 substage (OR = 6.28, 95%CI = 4.93-

Table 2 Meta-analysis results for the relationship between lymph node metastasis and clinicopathological factors in T1 esophageal squamous cell carcinoma patients

Factors	Studies	Patients	Heterogeneity I^2 (*P* value)	Pooled OR (95%CI)	*P* value
Age (continuous) (yr)	6	1571	22% (0.27)	-0.81 (-1.75-0.14)	0.10
Sex (male/female)	12	2913	0% (0.78)	1.16 (0.91-1.48)	0.23
Tumor size (> 2/≤ 2) (cm)	6	1482	0% (0.74)	1.93 (1.49-2.50)	< 0.001[a]
Tumor location (L/U-M)	10	2291	0% (0.57)	1.46 (1.17-1.82)	< 0.001[a]
T1 substage (T1b/T1a)	15	3558	0% (0.87)	6.28 (4.93-8.00)	< 0.001[a]
Differentiation (G3/G1-2)	11	1966	0% (0.49)	2.11 (1.64-2.72)	< 0.001[a]
LVI (present/absent)	11	2226	40% (0.08)	5.86 (4.60-7.48)	< 0.001[a]
Macroscopic type (nonflat/flat)	6	1213	35% (0.17)	3.17 (2.33-4.31)	< 0.001[a]
INF (present/absent)	3	591	0% (0.66)	1.82 (0.89-3.73)	0.10

[a]$P < 0.05$. CI: Confidence interval; ESCC: Esophageal squamous cell carcinoma; G1-2: Well differentiated-moderately differentiated; G3: Poorly differentiated; INF: Infiltrative growth pattern; L: Lower; LNM: Lymph node metastasis; LVI: Lymphovascular invasion; OR: Odds ratio; U-M: Upper-middle.

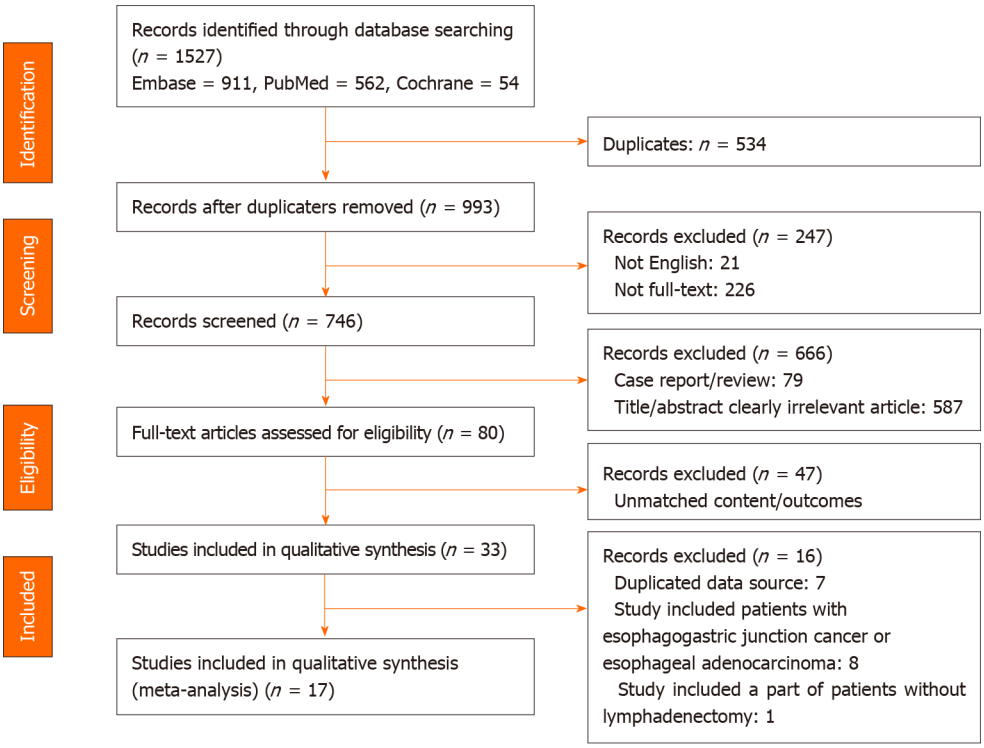


Figure 1 The flow chart of the selection process for the studies included in this meta-analysis. In total, 1527 records were identified from all sources (Embase, PubMed, and Cochrane Library). Only 17 studies involving 3775 patients met all inclusion criteria and were selected for the meta-analysis.

8.00, $P < 0.001$; heterogeneity: $I^2 = 0\%$, $P = 0.87$, Figure 4A) and differentiation (OR = 2.11, 95%CI = 1.64-2.72, $P < 0.001$; heterogeneity: $I^2 = 0\%$, $P = 0.49$, Figure 4B).

Fourteen studies[13,14,16-19,21-26,28,29] involving 3112 patients reported rates of LNM in LVI present and LVI absent cases, at 35.3%-86.5% and 8.8%-32.2%, respectively. Three studies[18,19,22] involving 1213 patients reported rates of LNM in INF-c and INF-a/b cases, at 28.6%-60.0% and 28.1%-32.4%, respectively. Studies by Huh *et al*[25], Min *et al*[17] and Mitobe *et al*[18] with heterogeneity were excluded from the LVI analysis due to the results of heterogeneity and influence analyses (Supplementary Figures 3C and 4E). However, no heterogeneity in the analysis of INF was found (Supplementary Figure 3D). Additionally, pooled analysis showed that the rate of LNM was significantly different in LVI (OR = 5.86, 95%CI = 4.60-7.48, $P < 0.001$; heterogeneity: $I^2 = 40\%$, $P =$

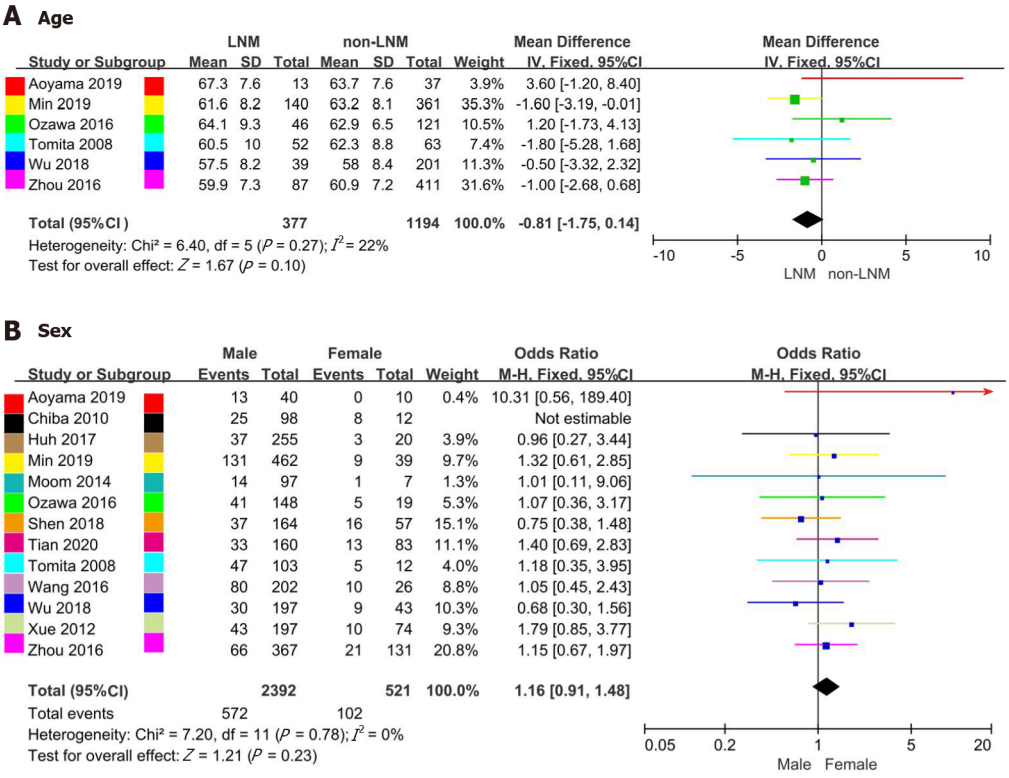


Figure 2 Forest plot. A: Forest plot evaluating the association between age (> 60/≤ 60) and lymph node metastasis (LNM); B: Forest plot evaluating the association between sex (male/female) and LNM. CI: Confidence interval; IV: Inverse-Variance; M-H: Mantel-Haenszel.

0.08, Figure 4C), with no difference for INF (OR = 1.82, 95%CI = 0.89-3.73, P = 0.010; heterogeneity: I^2 = 0%, P = 0.66, Figure 4D).

Assessment of publication bias

Funnel plots of the studies were used in the meta-analysis for age, sex, tumor size, tumor location, macroscopic type, T1 substage, differentiation, LVI and INF. According to the results, the distribution of each study was concentrated and symmetrical (Supplementary Figures 5-7). There was no evidence of publication bias.

DISCUSSION

In some institutions, ER is the preferred treatment for patients with stage T1 ESCC because of its minimally invasive nature[30,31]. However, ER can only remove local lesions, and the lymph nodes cannot be dissected. A portion of early ESCC cases with noncurative resection after ER treatment has been identified, and additional radical esophagectomy with lymph node dissection is usually recommended[32]. Wang *et al*[33] reported no statistical significance in recurrence-free survival and overall survival of T1 EC patients in ER + esophagectomy and esophagectomy groups; thus, ER can be accepted for patients with stage T1 cancer even if esophagectomy is eventually warranted due to LNM. Overall, lymph node status plays an important role in surgical strategy selection and prognosis[34]. The LNM rate of T1 ESCC has been reported to be 12.9%-45.0%, with a large deviation[18,28,35]. The results of this meta-analysis showed an LNM rate of 24.2%, and risk factors associated with LNM were tumor size, tumor location, T1 substage, tumor differentiation, LVI and macroscopic type.

T1 substage, tumor differentiation and tumor size have been indicated as predictors of LNM in several studies, and our study verified these results. Previous studies reported LNM rates in MM1, MM2, MM3, SM1, SM2 and SM3 of 0%, 1.5%-3.7%, 5.3%-30.8%, 8.7%-42.1%, 12.7%-40.7% and 28.4%-66.7%, respectively[14,16-18,21-23,35]. Submucosal tumors have a high risk of LNM, and there is no safe area for ER of T1b tumors[6]. Because T1a substage (MM1, MM2 and MM3) and T1b substage (SM1, SM2 and SM3) are difficult to distinguish during surgery, further staging of T1a and T1b is not necessary. In this meta-analysis, the rates of LNM in T1a and T1b were 5.4% and 33.7%, respectively. Moreover, the LNM rate increased significantly when the tumor

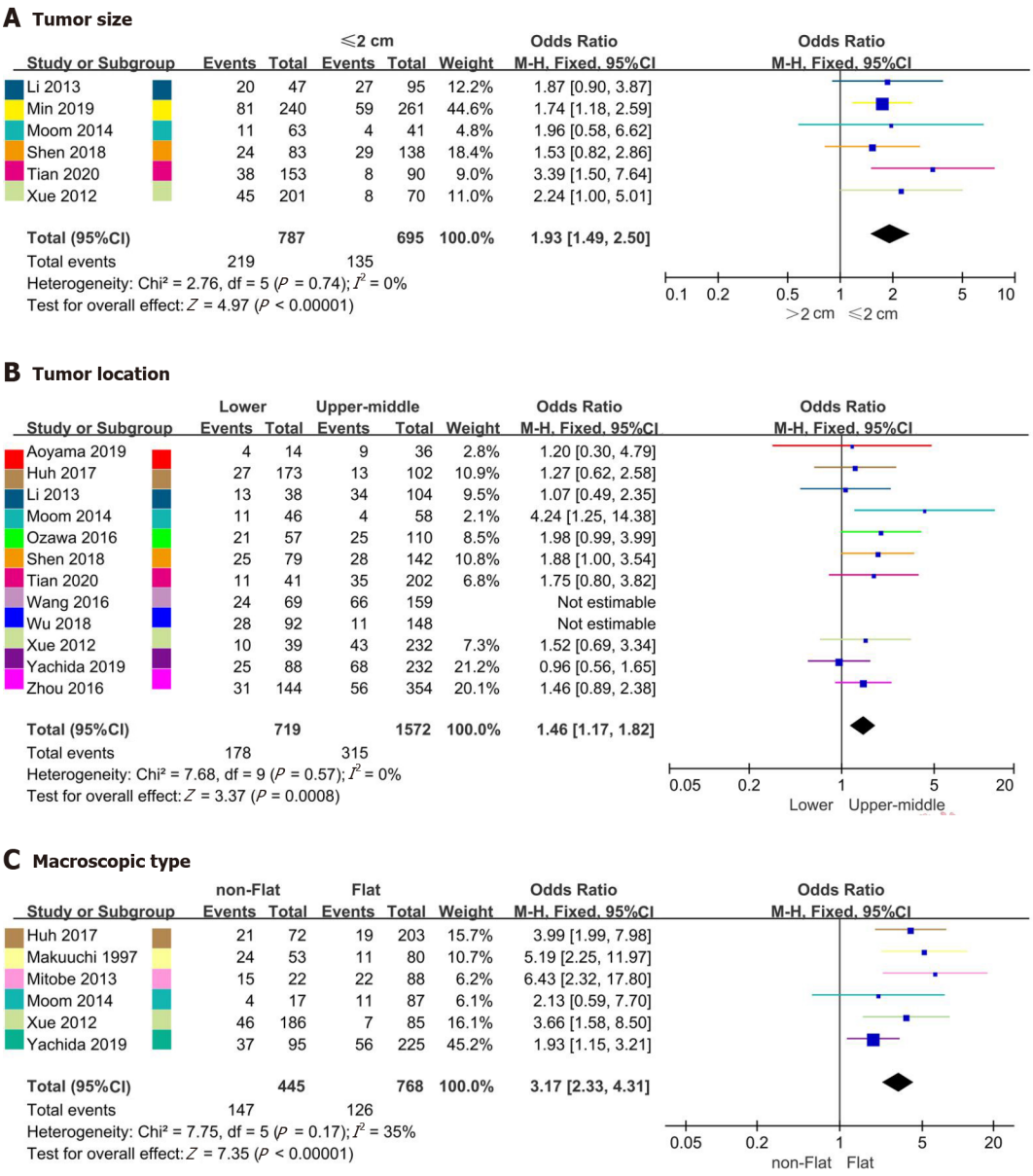


Figure 3 Forest plot. A: Forest plot evaluating the association between tumor size (> 2/≤ 2) and lymph node metastasis (LNM); B: Forest plot evaluating the association between tumor location (lower/upper-middle) and LNM; C: Forest plot evaluating the association between macroscopic type (nonflat/flat) and LNM. CI: Confidence interval; M-H: Mantel-Haenszel.

infiltrated the submucosa, and the risk of LNM was 2.11 times higher in patients with poorly differentiated tumors than in patients with well differentiated/moderately differentiated tumors. Furthermore, well-differentiated tumor cells were closer to the mature form of the tissue, where the tumor grows slowly and has a lower risk of metastasis; poorly differentiated tumor cells were closer to the immature form of the tissue, where the tumor grows fast and is highly malignant. In the case of the lymphatic drainage network, poorly differentiated cancer cells are prone to LNM[36,37].

Tumor size > 2 cm is helpful for predicting LNM in superficial ESCC. Friedland *et al*[38] suggested that lesions with a size > 2 cm can be resected using endoscopic mucosal resection and if larger, by expanded endoscopic submucosal dissection. We found that the risk of metastasis was still high in larger tumors and that endoscopic submucosal dissection should be carefully selected. In addition, although tumor size is used in the tumor, node, metastasis staging system of breast, lung, and liver cancers, among others, the EC staging system does not consider the pathological features of tumor size. We believe that it is necessary to identify the cut-off value of tumor size and incorporate it into the staging system for more accurate preoperative and postoperative assessment.

In contrast to a previous meta-analysis that included both ESCC and adenocarcinoma of the esophagogastric junction, we found that tumors at a lower location

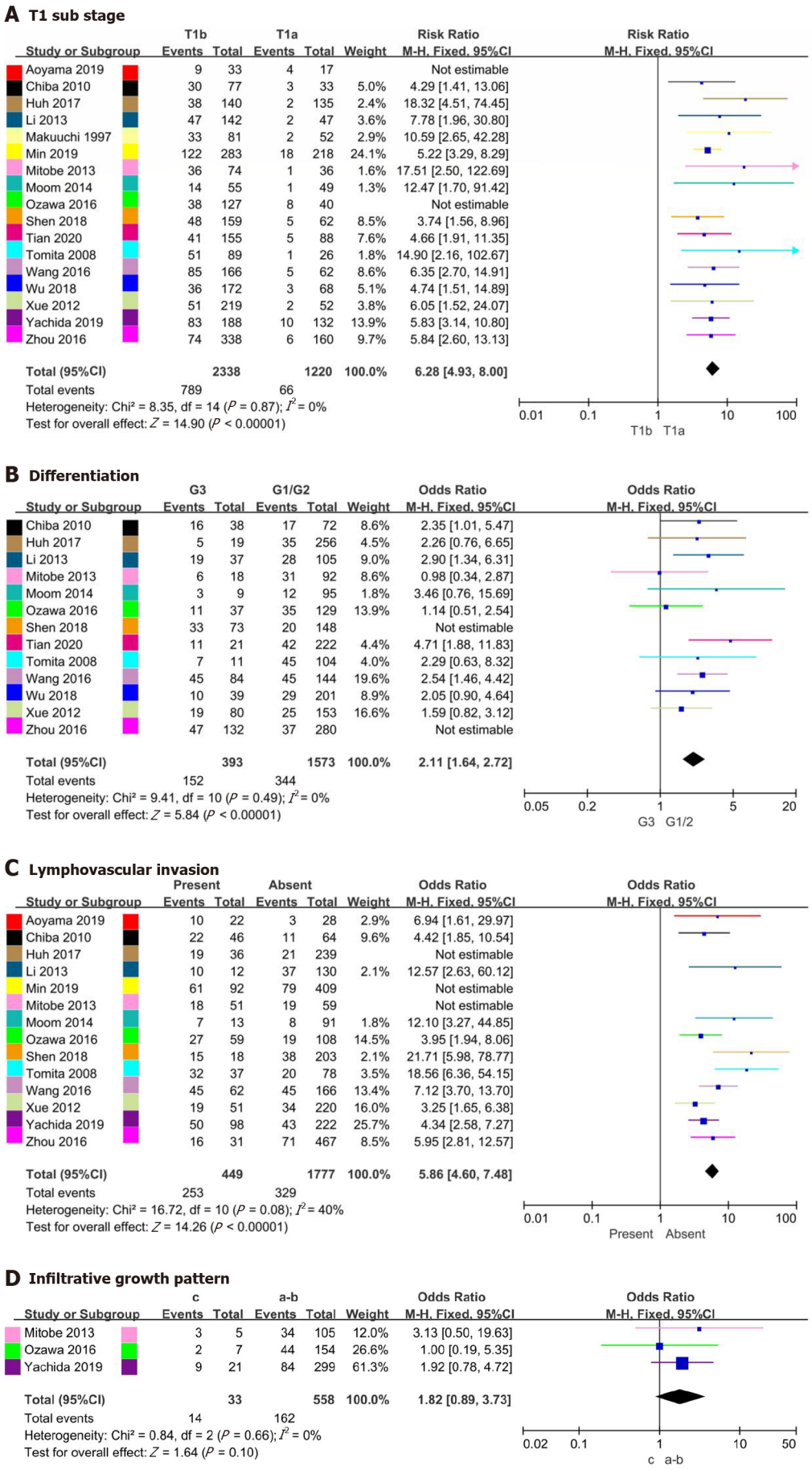


Figure 4 Forest plot. A: Forest plot evaluating the association between T1 substage (T1a/T1b) and lymph node metastasis (LNM); B: Forest plot evaluating the

association between differentiation (poorly differentiated/well differentiated-moderately differentiated) and LNM; C: Forest plot evaluating the association between lymphovascular invasion (present/absent) and LNM; D: Forest plot evaluating the association between infiltrative growth pattern (c/a-b) and LNM. CI: Confidence interval; G1/2: Well differentiated/moderately differentiated; G3: Poorly differentiated; M-H: Mantel-Haenszel.

had a higher risk of LNM in ESCC[39]. The relationship between tumor location and LNM mainly manifests by lymphatic drainage. Because of the network of longitudinal and transverse lymphatic vessels of the esophagus, lymphatic drainage is extensive, presenting as adjacent LNM and skip metastasis[40]. Thus, tumors in the upper esophagus mainly metastasize to the superior mediastinal lymph nodes, especially the recurrent laryngeal nerve and the superior parietal esophagus lymph nodes[30]. In contrast, LNM of middle ESCC and lower ESCC mainly occurs in the mediastinal lymph nodes and celiac lymph nodes, respectively[31]. Most studies have shown that tumor location is not a risk factor for LNM[22,25,26]. Nevertheless, Ozawa *et al*[19] and Wu *et al*[20] reported that lower ESCC had a higher risk of LNM. The middle and lower part of the esophagus stretches as the lymphatic networks develop in the submucosal layer during embryonal growth[41], which provides anatomical conditions for skip metastasis of the lymph nodes in lower esophageal carcinoma. Furthermore, the incidence of metastasis of upper mediastinal nodes can be as high as that of lower mediastinal nodes in lower ESCC[42,43]. Therefore, skip metastasis of lower ESCC is not negligible.

Macroscopic tumor type is divided into I (protruded type), II (flat type) and III (excavated type) by visual observation. Because the protruded type and excavated type have similar outcomes and prognoses, previous studies further classified the macroscopic type as a flat type (II) and nonflat type (I and III)[13,18,22,35,44,45]. It has been reported that macroscopic type correlates with invasion depth and LNM[22,27]. Additionally, tumors of type II have lower rates of LNM, malignancy and postoperative recurrence[46]. According to the present meta-analysis, the rates of LNM in nonflat ESCC and flat ESCC were 33.0% and 16.4%, respectively. Although esophagectomy is the preferred choice for tumors of macroscopic type I or III, ER is the first treatment for flat-type tumors, and excised specimens can be evaluated to decide whether esophagectomy should be performed[18].

LVI has been proven to be an independent risk factor for LNM in patients with ESCC[6,14,17,21,22,44]. Tumor cells become isolated from the tumor assembly at the primary lesion and then spread through the lymphatic or blood vessels, possibly invading lymphatic or blood vessels in the process[47], which is considered the initial step of LNM and distant metastasis[48]. Endoscopic ultrasonography and other imaging technologies can partially predict the depth of invasion and regional distribution of LNM, but LVI can only be detected after ER or surgery. If LVI is detected in a resected specimen after ER, additional surgical therapy with lymph node dissection should be considered[25,49]. Hsu *et al*[50] reported 5-yr overall survival rates of 28.2% and 61.1% in a positive LVI group and negative LVI group, respectively. This suggests that for patients with LVI, postoperative treatment should be the focus for improving prognosis. Additionally, hematoxylin-eosin staining and immunohistochemistry for the detection of LVI may provide a more reliable result[18].

In this meta-analysis, sex, age and INF were not risk factors for LNM in T1 ESCC patients. Nevertheless, due to the limited number of studies included (only three studies), more studies are needed to evaluate the relationship of INF with LNM. Xu *et al*[39] analyzed the risk factors for LNM in superficial EC with similar results. Their study included a small number of patients with esophageal adenocarcinoma, whereas all the patients in our study had ESCC. Furthermore, our inclusion criteria were stricter, and the quality of the studies was higher. For each analysis of clinicopathological features, we performed influence analysis to exclude studies with heterogeneity for more reliable results. In general, heterogeneity may be due to the number of included cases, surgical procedures, lymph node dissection and other factors.

There were some limitations in the present meta-analysis that should be considered. First, as all+ the included studies were retrospective, selection bias was inevitable. Second, the guidelines of EC staging in the included literature differed slightly and were revised several times during the study period, which may lead to inconsistent tumor staging. Third, all included studies were performed in Asian countries (China, Japan and South Korea), and the results may therefore be influenced by ethnicity.

CONCLUSION

This meta-analysis is the first to comprehensively evaluate LNM only in ESCC patients with T1 stage. We identified that patients with tumor size > 2 cm, lower tumor location, nonflat macroscopic type, T1b stage, poor differentiation and LVI had a significant risk of LNM. For these patients, radical esophagectomy may be a better choice than ER.

ARTICLE HIGHLIGHTS

Research background

Endoscopic resection has been increasingly used in patients with T1 esophageal squamous cell carcinoma (ESCC). However, lymph node metastasis (LNM) has been widely reported in patients with T1 ESCC, and some studies have even found higher rates of metastasis. Endoscopic resection for T1 ESCC should be carefully considered.

Research motivation

Endoscopic resection is not appropriate for patients with a potential risk of LNM and the risk of metastasis must be assessed in advance to make the right decision. In addition, reports of the risk factors for LNM have been controversial.

Research objectives

The purpose of this meta-analysis was to assess risk factors of LNM for patients with T1 ESCC.

Research methods

We conducted a comprehensive search of multiple electronic databases including PubMed, EMBASE and the Cochrane Library to select studies related to the topics. Statistical analysis was conducted *via* comprehensive meta-analysis software.

Research results

A total of 3775 patients with T1 ESCC from 17 studies were included. The rates of LNM in T1a and T1b were 5.4% and 33.7%, respectively. Tumor size > 2 cm, lower tumor location, nonflat macroscopic type, T1b stage, poor differentiation and lymphovascular invasion were found to be significantly associated with LNM. Conversely, sex, age and infiltrative growth pattern were not identified as risk factors for LNM.

Research conclusions

This meta-analysis is the first to comprehensively evaluate LNM only in ESCC patients with T1 stage. For patients with a potential high risk of LNM, radical esophagectomy is superior to endoscopic resection, and potential metastatic lymph nodes can be dissected.

Research perspectives

All included studies were performed in Asian countries (China, Japan and South Korea), and the results may therefore be influenced by ethnicity. There is still a need to include data from other continents.

REFERENCES

1 **Heymach J**, Krilov L, Alberg A, Baxter N, Chang SM, Corcoran RB, Dale W, DeMichele A, Magid Diefenbach CS, Dreicer R, Epstein AS, Gillison ML, Graham DL, Jones J, Ko AH, Lopez AM, Maki RG, Rodriguez-Galindo C, Schilsky RL, Sznol M, Westin SN, Burstein H. Clinical Cancer Advances 2018: Annual Report on Progress Against Cancer From the American Society of Clinical Oncology. *J Clin Oncol* 2018; **36**: 1020-1044 [PMID: 29380678 DOI: 10.1200/JCO.2017.77.0446]

2 **Allemani C**, Matsuda T, Di Carlo V, Harewood R, Matz M, Nikšić M, Bonaventure A, Valkov M, Johnson CJ, Estève J, Ogunbiyi OJ, Azevedo E Silva G, Chen WQ, Eser S, Engholm G, Stiller CA, Monnereau A, Woods RR, Visser O, Lim GH, Aitken J, Weir HK, Coleman MP; CONCORD Working Group. Global surveillance of trends in cancer survival 2000-14 (CONCORD-3): analysis of individual records for 37 513 025 patients diagnosed with one of 18 cancers from 322 population-

based registries in 71 countries. *Lancet* 2018; **391**: 1023-1075 [PMID: 29395269 DOI: 10.1016/S0140-6736(17)33326-3]
3 **Chen W**, Zheng R, Baade PD, Zhang S, Zeng H, Bray F, Jemal A, Yu XQ, He J. Cancer statistics in China, 2015. *CA Cancer J Clin* 2016; **66**: 115-132 [PMID: 26808342 DOI: 10.3322/caac.21338]
4 **Plum PS**, Hölscher AH, Pacheco Godoy K, Schmidt H, Berlth F, Chon SH, Alakus H, Bollschweiler E. Prognosis of patients with superficial T1 esophageal cancer who underwent endoscopic resection before esophagectomy-A propensity score-matched comparison. *Surg Endosc* 2018; **32**: 3972-3980 [PMID: 29536160 DOI: 10.1007/s00464-018-6139-7]
5 **Naveed M**, Kubiliun N. Endoscopic Treatment of Early-Stage Esophageal Cancer. *Curr Oncol Rep* 2018; **20**: 71 [PMID: 30058019 DOI: 10.1007/s11912-018-0713-y]
6 **Duan XF**, Tang P, Shang XB, Jiang HJ, Yu ZT. The prevalence of lymph node metastasis for pathological T1 esophageal cancer: a retrospective study of 143 cases. *Surg Oncol* 2018; **27**: 1-6 [PMID: 29549895 DOI: 10.1016/j.suronc.2017.11.002]
7 **Weksler B**, Kennedy KF, Sullivan JL. Using the National Cancer Database to create a scoring system that identifies patients with early-stage esophageal cancer at risk for nodal metastases. *J Thorac Cardiovasc Surg* 2017; **154**: 1787-1793 [PMID: 28867381 DOI: 10.1016/j.jtcvs.2017.07.036]
8 **Endo M**, Yoshino K, Kawano T, Nagai K, Inoue H. Clinicopathologic analysis of lymph node metastasis in surgically resected superficial cancer of the thoracic esophagus. *Dis Esophagus* 2000; **13**: 125-129 [PMID: 14601903 DOI: 10.1046/j.1442-2050.2000.00100.x]
9 **Ancona E**, Rampado S, Cassaro M, Battaglia G, Ruol A, Castoro C, Portale G, Cavallin F, Rugge M. Prediction of lymph node status in superficial esophageal carcinoma. *Ann Surg Oncol* 2008; **15**: 3278-3288 [PMID: 18726651 DOI: 10.1245/s10434-008-0065-1]
10 **Dubecz A**, Kern M, Solymosi N, Schweigert M, Stein HJ. Predictors of Lymph Node Metastasis in Surgically Resected T1 Esophageal Cancer. *Ann Thorac Surg* 2015; **99**: 1879-85; discussion 1886 [PMID: 25929888 DOI: 10.1016/j.athoracsur.2015.02.112]
11 **Moher D**, Liberati A, Tetzlaff J, Altman DG; PRISMA Group. Preferred reporting items for systematic reviews and meta-analyses: the PRISMA statement. *BMJ* 2009; **339**: b2535 [PMID: 19622551 DOI: 10.1136/bmj.b2535]
12 **Sterne JA**, Sutton AJ, Ioannidis JP, Terrin N, Jones DR, Lau J, Carpenter J, Rücker G, Harbord RM, Schmid CH, Tetzlaff J, Deeks JJ, Peters J, Macaskill P, Schwarzer G, Duval S, Altman DG, Moher D, Higgins JP. Recommendations for examining and interpreting funnel plot asymmetry in meta-analyses of randomised controlled trials. *BMJ* 2011; **343**: d4002 [PMID: 21784880 DOI: 10.1136/bmj.d4002]
13 **Moon JY**, Kim GH, Kim JH, Kim HH, Ryu KD, Park SO, Lee BE, Song GA. Clinicopathologic factors predicting lymph node metastasis in superficial esophageal squamous cell carcinoma. *Scand J Gastroenterol* 2014; **49**: 589-594 [PMID: 24641315 DOI: 10.3109/00365521.2013.838604]
14 **Shen W**, Shen Y, Tan L, Jin C, Xi Y. A nomogram for predicting lymph node metastasis in surgically resected T1 esophageal squamous cell carcinoma. *J Thorac Dis* 2018; **10**: 4178-4185 [PMID: 30174862 DOI: 10.21037/jtd.2018.06.51]
15 **Tian D**, Jiang KY, Huang H, Jian SH, Zheng YB, Guo XG, Li HY, Zhang JQ, Guo KX, Wen HY. Clinical nomogram for lymph node metastasis in pathological T1 esophageal squamous cell carcinoma: a multicenter retrospective study. *Ann Transl Med* 2020; **8**: 292 [PMID: 32355736 DOI: 10.21037/atm.2020.02.185]
16 **Aoyama J**, Kawakubo H, Mayanagi S, Fukuda K, Irino T, Nakamura R, Wada N, Suzuki T, Kameyama K, Kitagawa Y. Discrepancy Between the Clinical and Final Pathological Findings of Lymph Node Metastasis in Superficial Esophageal Cancer. *Ann Surg Oncol* 2019; **26**: 2874-2881 [PMID: 31209674 DOI: 10.1245/s10434-019-07498-2]
17 **Min BH**, Yang JW, Min YW, Baek SY, Kim S, Kim HK, Choi YS, Shim YM, Choi YL, Zo JI. Nomogram for prediction of lymph node metastasis in patients with superficial esophageal squamous cell carcinoma. *J Gastroenterol Hepatol* 2020; **35**: 1009-1015 [PMID: 31674067 DOI: 10.1111/jgh.14915]
18 **Mitobe J**, Ikegami M, Urashima M, Takahashi H, Goda K, Tajiri H. Clinicopathological investigation of lymph node metastasis predictors in superficial esophageal squamous cell carcinoma with a focus on evaluation of lympho-vascular invasion. *Scand J Gastroenterol* 2013; **48**: 1173-1182 [PMID: 23971724 DOI: 10.3109/00365521.2013.832365]
19 **Ozawa Y**, Kamei T, Nakano T, Taniyama Y, Miyagi S, Ohuchi N. Characteristics of Postoperative Recurrence in Lymph Node-Negative Superficial Esophageal Carcinoma. *World J Surg* 2016; **40**: 1663-1671 [PMID: 26908240 DOI: 10.1007/s00268-016-3454-9]
20 **Wu J**, Chen QX, Shen DJ, Zhao Q. A prediction model for lymph node metastasis in T1 esophageal squamous cell carcinoma. *J Thorac Cardiovasc Surg* 2018; **155**: 1902-1908 [PMID: 29233596 DOI: 10.1016/j.jtcvs.2017.11.005]
21 **Xue L**, Ren L, Zou S, Shan L, Liu X, Xie Y, Zhang Y, Lu J, Lin D, Dawsey SM, Wang G, Lu N. Parameters predicting lymph node metastasis in patients with superficial esophageal squamous cell carcinoma. *Mod Pathol* 2012; **25**: 1364-1377 [PMID: 22627741 DOI: 10.1038/modpathol.2012.89]
22 **Yachida T**, Oda I, Abe S, Sekiguchi M, Nonaka S, Suzuki H, Yoshinaga S, Taniguchi H, Sekine S, Masugata H, Masaki T, Daiko H, Saito Y. Risk of Lymph Node Metastasis in Patients with the Superficial Spreading Type of Esophageal Squamous Cell Carcinoma. *Digestion* 2020; **101**: 239-244 [PMID: 30909271 DOI: 10.1159/000499017]
23 **Zhou Y**, Du J, Li H, Luo J, Chen L, Wang W. Clinicopathologic analysis of lymph node status in

superficial esophageal squamous carcinoma. *World J Surg Oncol* 2016; **14**: 259 [PMID: 27729036 DOI: 10.1186/s12957-016-1016-0]

24 **Chiba T**, Kawachi H, Kawano T, Kumagai J, Kitagaki K, Sekine M, Uchida K, Kobayashi M, Sugihara K, Eishi Y. Independent histological risk factors for lymph node metastasis of superficial esophageal squamous cell carcinoma; implication of claudin-5 immunohistochemistry for expanding the indications of endoscopic resection. *Dis Esophagus* 2010; **23**: 398-407 [PMID: 19903192 DOI: 10.1111/j.1442-2050.2009.01023.x]

25 **Huh CW**, Jung DH, Kim JH, Ma DW, Youn YH, Park H. Clinical implication of endoscopic gross appearance in superficial esophageal squamous carcinoma: revisited. *Surg Endosc* 2018; **32**: 367-375 [PMID: 28664436 DOI: 10.1007/s00464-017-5685-8]

26 **Li B**, Chen H, Xiang J, Zhang Y, Kong Y, Garfield DH, Li H. Prevalence of lymph node metastases in superficial esophageal squamous cell carcinoma. *J Thorac Cardiovasc Surg* 2013; **146**: 1198-1203 [PMID: 23988285 DOI: 10.1016/j.jtcvs.2013.07.006]

27 **Makuuchi H**, Shimada H, Mizutani K, Chino O, Nishi T, Tanaka H, Machimura T, Mitomi T, Osamura Y. Clinical pathological analysis of surgically resected superficial esophageal carcinoma to determine criteria for deciding on treatment strategy. *Diagn Ther Endosc* 1997; **3**: 211-220 [PMID: 18493439 DOI: 10.1155/dte.3.211]

28 **Tomita N**, Matsumoto T, Hayashi T, Arakawa A, Sonoue H, Kajiyama Y, Tsurumaru M. Lymphatic invasion according to D2-40 immunostaining is a strong predictor of nodal metastasis in superficial squamous cell carcinoma of the esophagus: algorithm for risk of nodal metastasis based on lymphatic invasion. *Pathol Int* 2008; **58**: 282-287 [PMID: 18429826 DOI: 10.1111/j.1440-1827.2008.02224.x]

29 **Wang S**, Chen X, Fan J, Lu L. Prognostic Significance of Lymphovascular Invasion for Thoracic Esophageal Squamous Cell Carcinoma. *Ann Surg Oncol* 2016; **23**: 4101-4109 [PMID: 27436201 DOI: 10.1245/s10434-016-5416-8]

30 **Yang AJ**, Choi SH, Byun HK, Kim HJ, Choi J, Lee YC, Lee SK, Park KR, Lee CG. Management of Clinical T1N0M0 Esophageal Cancer. *Gut Liver* 2019; **13**: 315-324 [PMID: 30600672 DOI: 10.5009/gnl18254]

31 **Chu JN**, Choi J, Tramontano A, Morse C, Forcione D, Nishioka NS, Abrams JA, Rubenstein JH, Kong CY, Inadomi JM, Hur C. Surgical *vs* Endoscopic Management of T1 Esophageal Adenocarcinoma: A Modeling Decision Analysis. *Clin Gastroenterol Hepatol* 2018; **16**: 392-400. e7 [PMID: 29079222 DOI: 10.1016/j.cgh.2017.10.024]

32 **Dermine S**, Leconte M, Leblanc S, Dousset B, Terris B, Berger A, Berger A, Rahmi G, Lepilliez V, Plomteux O, Leclercq P, Coriat R, Chaussade S, Prat F, Barret M. Outcomes of esophagectomy after noncurative endoscopic resection of early esophageal cancer. *Therap Adv Gastroenterol* 2019; **12**: 1756284819892556 [PMID: 31839807 DOI: 10.1177/1756284819892556]

33 **Wang S**, Huang Y, Xie J, Zhuge L, Shao L, Xiang J, Zhang Y, Sun Y, Hu H, Chen S, Lerut T, Luketich JD, Zhang J, Chen H. Does delayed esophagectomy after endoscopic resection affect outcomes in patients with stage T1 esophageal cancer? *Surg Endosc* 2018; **32**: 1441-1448 [PMID: 28916920 DOI: 10.1007/s00464-017-5830-4]

34 **Ho HJ**, Chen HS, Hung WH, Hsu PK, Wu SC, Chen HC, Wang BY. Survival Impact of Total Resected Lymph Nodes in Esophageal Cancer Patients With and Without Neoadjuvant Chemoradiation. *Ann Surg Oncol* 2018; **25**: 3820-3832 [PMID: 30284131 DOI: 10.1245/s10434-018-6785-y]

35 **Jia R**, Luan Q, Wang J, Hou D, Zhao S. Analysis of Predictors for Lymph Node Metastasis in Patients with Superficial Esophageal Carcinoma. *Gastroenterol Res Pract* 2016; **2016**: 3797615 [PMID: 27799939 DOI: 10.1155/2016/3797615]

36 **Rice TW**, Ishwaran H, Hofstetter WL, Schipper PH, Kesler KA, Law S, Lerut EM, Denlinger CE, Salo JA, Scott WJ, Watson TJ, Allen MS, Chen LQ, Rusch VW, Cerfolio RJ, Luketich JD, Duranceau A, Darling GE, Pera M, Apperson-Hansen C, Blackstone EH. Esophageal Cancer: Associations With (pN+) Lymph Node Metastases. *Ann Surg* 2017; **265**: 122-129 [PMID: 28009736 DOI: 10.1097/SLA.0000000000001594]

37 **Ishihara R**, Oyama T, Abe S, Takahashi H, Ono H, Fujisaki J, Kaise M, Goda K, Kawada K, Koike T, Takeuchi M, Matsuda R, Hirasawa D, Yamada M, Kodaira J, Tanaka M, Omae M, Matsui A, Kanesaka T, Takahashi A, Hirooka S, Saito M, Tsuji Y, Maeda Y, Yamashita H, Oda I, Tomita Y, Matsunaga T, Terai S, Ozawa S, Kawano T, Seto Y. Risk of metastasis in adenocarcinoma of the esophagus: a multicenter retrospective study in a Japanese population. *J Gastroenterol* 2017; **52**: 800-808 [PMID: 27757547 DOI: 10.1007/s00535-016-1275-0]

38 **Friedland S**, Triadafilopoulos G. Can endoscopic resection for Barrett's dysplasia and early cancer be curative? *Ann N Y Acad Sci* 2018; **1434**: 54-58 [PMID: 29752721 DOI: 10.1111/nyas.13715]

39 **Xu W**, Liu XB, Li SB, Yang ZH, Tong Q. Prediction of lymph node metastasis in superficial esophageal squamous cell carcinoma in Asia: a systematic review and meta-analysis. *Dis Esophagus* 2020; **33** [PMID: 32399558 DOI: 10.1093/dote/doaa032]

40 **Wang Y**, Zhu L, Xia W, Wang F. Anatomy of lymphatic drainage of the esophagus and lymph node metastasis of thoracic esophageal cancer. *Cancer Manag Res* 2018; **10**: 6295-6303 [PMID: 30568491 DOI: 10.2147/CMAR.S182436]

41 **Tachimori Y**. Pattern of lymph node metastases of squamous cell esophageal cancer based on the anatomical lymphatic drainage system: efficacy of lymph node dissection according to tumor location. *J Thorac Dis* 2017; **9**: S724-S730 [PMID: 28815068 DOI: 10.21037/jtd.2017.06.19]

42 **Tachimori Y**, Nagai Y, Kanamori N, Hokamura N, Igaki H. Pattern of lymph node metastases of

esophageal squamous cell carcinoma based on the anatomical lymphatic drainage system. *Dis Esophagus* 2011; **24**: 33-38 [PMID: 20626450 DOI: 10.1111/j.1442-2050.2010.01086.x]

43 **Tachimori Y**, Ozawa S, Numasaki H, Matsubara H, Shinoda M, Toh Y, Udagawa H, Fujishiro M, Oyama T, Uno T; Registration Committee for Esophageal Cancer of the Japan Esophageal Society. Efficacy of lymph node dissection by node zones according to tumor location for esophageal squamous cell carcinoma. *Esophagus* 2016; **13**: 1-7 [PMID: 26752982 DOI: 10.1007/s10388-015-0515-3]

44 **Ma DW**, Jung DH, Kim JH, Park JJ, Youn YH, Park H. Predicting lymph node metastasis for endoscopic resection of superficial esophageal squamous cell carcinoma. *J Thorac Cardiovasc Surg* 2019; **157**: 397-402. e1 [PMID: 30143376 DOI: 10.1016/j.jtcvs.2018.07.034]

45 **Shimada H**, Nabeya Y, Matsubara H, Okazumi S, Shiratori T, Shimizu T, Aoki T, Shuto K, Akutsu Y, Ochiai T. Prediction of lymph node status in patients with superficial esophageal carcinoma: analysis of 160 surgically resected cancers. *Am J Surg* 2006; **191**: 250-254 [PMID: 16442955 DOI: 10.1016/j.amjsurg.2005.07.035]

46 **Xue LY**, Qin XM, Liu Y, Liang J, Lin H, Xue XM, Zou SM, Zhang MY, Zhang BH, Hui ZG, Zhao ZT, Ren LQ, Zhang YM, Liu XY, Yuan YL, Ying JM, Gao SG, Song YM, Wang GQ, Dawsey SM, Lu N. Clinicopathological parameters predicting recurrence of pT1N0 esophageal squamous cell carcinoma. *World J Gastroenterol* 2018; **24**: 5154-5166 [PMID: 30568392 DOI: 10.3748/wjg.v24.i45.5154]

47 **Schiefer AI**, Schoppmann SF, Birner P. Lymphovascular invasion of tumor cells in lymph node metastases has a negative impact on survival in esophageal cancer. *Surgery* 2016; **160**: 331-340 [PMID: 27085684 DOI: 10.1016/j.surg.2016.02.034]

48 **Zhao B**, Zhang J, Zhang J, Luo R, Wang Z, Xu H, Huang B. Risk Factors Associated with Lymph Node Metastasis for Early Gastric Cancer Patients Who Underwent Non-curative Endoscopic Resection: a Systematic Review and Meta-analysis. *J Gastrointest Surg* 2019; **23**: 1318-1328 [PMID: 30187319 DOI: 10.1007/s11605-018-3924-5]

49 **Newton AD**, Predina JD, Xia L, Roses RE, Karakousis GC, Dempsey DT, Williams NN, Kucharczuk JC, Singhal S. Surgical Management of Early-Stage Esophageal Adenocarcinoma Based on Lymph Node Metastasis Risk. *Ann Surg Oncol* 2018; **25**: 318-325 [PMID: 29147928 DOI: 10.1245/s10434-017-6238-z]

50 **Hsu CP**, Chuang CY, Hsu PK, Chien LI, Lin CH, Yeh YC, Hsu HS, Wu YC. Lymphovascular Invasion as the Major Prognostic Factor in Node-Negative Esophageal Cancer After Primary Esophagectomy. *J Gastrointest Surg* 2020; **24**: 1459-1468 [PMID: 31273552 DOI: 10.1007/s11605-019-04310-0]

World Journal of Gastroenterology

Submit a Manuscript: https://www.f6publishing.com

World J Gastroenterol 2021 February 28; 27(8): 751-759

DOI: 10.3748/wjg.v27.i8.751

ISSN 1007-9327 (print) ISSN 2219-2840 (online)

CASE REPORT

Septic shock due to *Granulicatella adiacens* after endoscopic ultrasound-guided biopsy of a splenic mass: A case report

Seo-Yeon Cho, Eunae Cho, Chang-Hwan Park, Hee-Joon Kim, Joo-Yeon Koo

ORCID number: Seo-Yeon Cho 0000-0003-0779-394X; Eunae Cho 000-0001-5931-4643; Chang-Hwan Park 0000-0002-2995-8779; Hee-Joon Kim 0000-0002-8636-5726; Joo-Yeon Koo 000-0003-0551-5954.

Author contributions: Cho SY contributed to analysis and interpretation of the data and drafting of the article; Park CH, Kim HJ and Koo JY contributed to technical and material support; Cho E contributed to critical revision and final approval of this article.

Informed consent statement: The study participant provided informed consent for this manuscript and its publication.

Conflict-of-interest statement: The authors have no conflicts of interest to declare.

CARE Checklist (2016) statement: The authors have read the CARE Checklist (2016), and the manuscript was prepared and revised according to the CARE Checklist (2016).

Open-Access: This article is an open-access article that was selected by an in-house editor and fully peer-reviewed by external reviewers. It is distributed in accordance with the Creative Commons Attribution

Seo-Yeon Cho, Eunae Cho, Chang-Hwan Park, Division of Gastroenterology, Department of Internal Medicine, Chonnam National University Hospital, Gwangju 61469, South Korea

Hee-Joon Kim, Department of Surgery, Chonnam National University Hospital, Gwangju 61469, South Korea

Joo-Yeon Koo, Department of Pathology, Chonnam National University Hospital, Gwangju 61469, South Korea

Corresponding author: Eunae Cho, MD, Associate Professor, Division of Gastroenterology, Department of Internal Medicine, Chonnam National University Hospital, 42 Jebong-ro, Donggu, Gwangju 61469, South Korea. cea202@cnuh.com

Abstract

BACKGROUND

Endoscopic ultrasound-guided fine needle aspiration or biopsy (EUS-FNA or FNB) has become a popular method for diagnosing various lesions of the gastrointestinal tract and surrounding tissue due to the accuracy and safety. To the best of our knowledge, no case report of severe infection after EUS-FNB of a solid lesion in the spleen has been described. Herein, we report a rare case of septic shock after EUS-FNB of a splenic mass.

CASE SUMMARY

A 45-year-old male patient presented to the outpatient clinic due to an incidentally detected splenic mass. A definitive diagnosis could not be established based on the abdominal magnetic resonance imaging. EUS of the spleen showed a 6 cm-sized, relatively well-demarcated, heterogeneous mass, and EUS-FNB with a 22G needle was performed. Ten days after the procedure patient developed septic shock and a splenic abscess was identified. Blood culture revealed growth of *Granulicatella adiacens*. After the treatment with antibiotics the patient underwent surgical resection, and the pathological examination showed diffuse large B-cell lymphoma. The patient received chemotherapy and he is in complete remission.

CONCLUSION

Infection of a splenic mass after EUS-FNB is a rare complication and prophylactic antibiotics might be considered.

Key Words: Endoscopic ultrasound; Endoscopic ultrasound-guided fine needle biopsy;

NonCommercial (CC BY-NC 4.0) license, which permits others to distribute, remix, adapt, build upon this work non-commercially, and license their derivative works on different terms, provided the original work is properly cited and the use is non-commercial. See: http://creativecommons.org/Licenses/by-nc/4.0/

Manuscript source: Unsolicited manuscript

Specialty type: Gastroenterology and hepatology

Country/Territory of origin: South Korea

Peer-review report's scientific quality classification

Grade A (Excellent): 0
Grade B (Very good): B, B
Grade C (Good): C, C
Grade D (Fair): D
Grade E (Poor): 0

Received: November 23, 2020
Peer-review started: November 23, 2020
First decision: December 21, 2020
Revised: January 18, 2021
Accepted: February 11, 2021
Article in press: February 11, 2021
Published online: February 28, 2021

P-Reviewer: Carrara S, Kawashima H, Yumoto T
S-Editor: Gao CC
L-Editor: A
P-Editor: Li JH



Splenic neoplasms; Lymphoma; Septic shock; Case report

©The Author(s) 2021. Published by Baishideng Publishing Group Inc. All rights reserved.

Core Tip: As the risk of infection after endoscopic ultrasound (EUS)-guided sampling of a solid organ is very low, prophylactic antibiotics are generally not recommended. However, our patient developed an abscess after EUS-guided fine needle biopsy of a splenic tumor. To the best of our knowledge, this is the first case of septic shock after EUS-guided fine needle biopsy of a splenic large B cell lymphoma and of an infection caused by *Granulicatella adiacens* during this procedure. Therefore, we suggest considering prophylactic antibiotic usage for EUS-guided sampling of splenic tumors.

Citation: Cho SY, Cho E, Park CH, Kim HJ, Koo JY. Septic shock due to *Granulicatella adiacens* after endoscopic ultrasound-guided biopsy of a splenic mass: A case report. *World J Gastroenterol* 2021; 27(8): 751-759
URL: https://www.wjgnet.com/1007-9327/full/v27/i8/751.htm
DOI: https://dx.doi.org/10.3748/wjg.v27.i8.751

INTRODUCTION

Endoscopic ultrasound (EUS)-guided fine needle aspiration or biopsy (FNA or FNB) has emerged as a popular and safe method for accurate diagnosis of various lesions of the gastrointestinal tract and adjacent organs. Splenic tumors are relatively rare and encompass a variety of benign and malignant diseases. Traditionally, percutaneous biopsies under ultrasound guidance have been performed for the diagnosis of these lesions. However, when the lesion is invisible by external ultrasonography, the procedure is impossible, and the complication rate of 5.3% has been reported[1]. EUS has an advantage of providing a clear image of the spleen through the gastric wall, and tissue sampling can be done with no intervening organs under real-time guidance with color Doppler, reducing major complications such as hemorrhage[2].

The incidence of infectious adverse events after EUS-FNA is less than 1%[3], and most of the severe infectious adverse events occur after EUS-FNA of cystic lesions. Therefore, current guidelines suggest antibiotic prophylaxis for the EUS-guided sampling of cystic lesions but for the sampling of solid lesions due to the very low risk of infection after the procedure[4].

Granulicatella adiacens (*G. adiacens*) is a catalase-negative, gram-positive coccus. It is a part of the normal flora of oral cavity, genitourinary and gastrointestinal tract rarely causing any disease. Reported infectious cases by *G. adiacens* include endocarditis and sepsis in immunocompromised patients and peritonitis, abscess, and severe infections in patients with prosthetic devices[5].

To the best of our knowledge, no case of severe infection after EUS-FNB of a splenic tumor and no case of sepsis by *G. adiacens* after EUS has been reported. We herein report the first case of septic shock due to *G. adiacens* after EUS-FNB of a splenic mass.

CASE PRESENTATION

Chief complaints

A 45-year-old male patient presented with an incidentally detected, 6 cm-sized splenic mass in the abdominal computed tomography (CT) after a traffic accident (Figure 1A).

History of present illness

He denied fever, night sweat, weight loss and abdominal pain but complained of mild low back pain due to the accident.

History of past illness

The patient had no previous medical history.

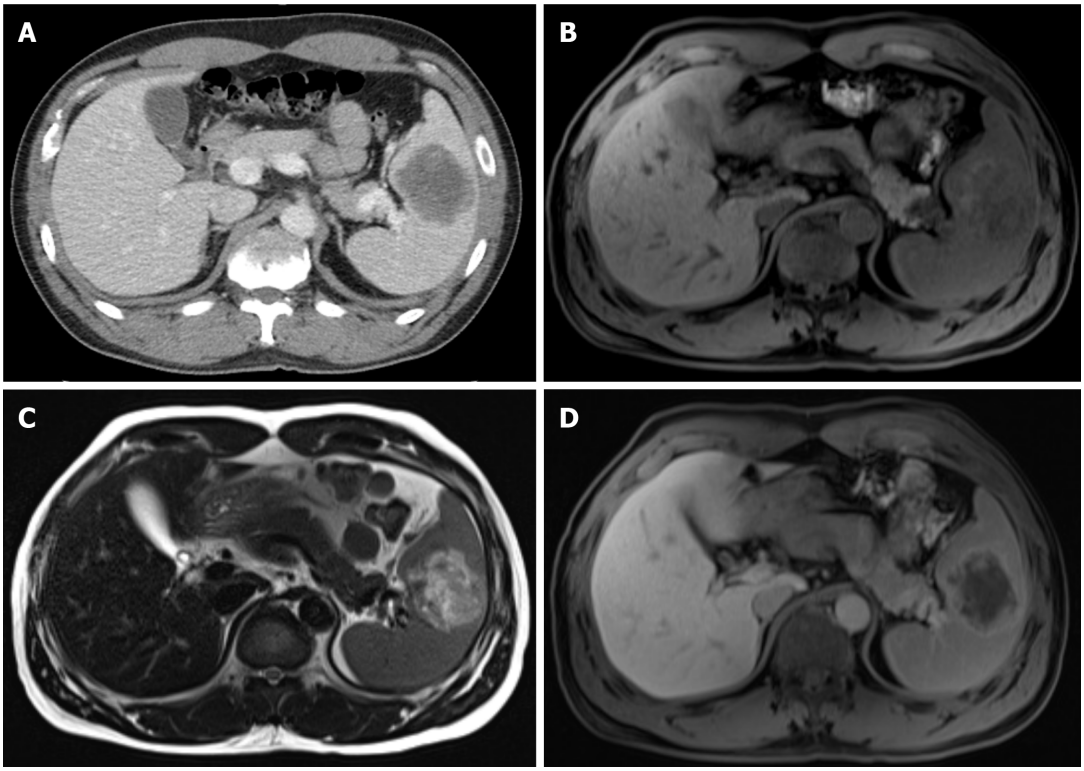


Figure 1 Initial abdominal computed tomography and magnetic resonance imaging findings. A: Post-contrast phases of abdominal computed tomography showed a 6 cm-sized hypodense mass with peripheral enhancing rim in the spleen; B: T1-weighted abdominal magnetic resonance imaging showed a 6 cm-sized heterogeneously hypointense splenic mass; C: T2-weighted image showed heterogeneous hyperintense signal of this lesion; D: Gadolinium-enhanced T1-weighted image showed peripheral enhancement and a central hypo-enhancing lesion.

Personal and family history

The patient had no family history.

Physical examination

Physical examination revealed an enlarged spleen, two finger breadths below the left costal margin and no palpable lymph node enlargement.

Laboratory examinations

Laboratory findings showed slightly elevated aspartate aminotransferase (AST) of 54 U/L (normal 10-37 U/L) but normal lactate dehydrogenase (LDH), alanine aminotransferase (ALT), alkaline phosphatase (ALP), and bilirubin levels. Other examinations including complete blood count, C-reactive protein (CRP), coagulation profiles, and renal function tests were within normal limits.

Imaging examinations

Abdominal CT showed a 6 cm-sized hypodense mass with peripheral enhancing rim in the spleen (Figure 1A). Abdominal magnetic resonance imaging (MRI) revealed a 6 cm-sized splenic mass, which was heterogeneously hypointense on T1-weighted image (Figure 1B), hyperintense T-2 weighted image (Figure 1C) and peripheral enhancement with a central hypo-enhancing lesion on gadolinium-enhanced T1-weighted image (Figure 1D), which was considered as a rare splenic tumor such as sclerosing angiomatoid nodular transformation (SANT) of the spleen.

Further diagnostic work-up

EUS-FNB using a 22G needle (EchoTip Procore®, Cook medical, Limerick, Ireland) was performed for pathologic diagnosis. EUS without contrast medium of the lesion demonstrated a 6 cm-sized, relatively well-demarcated, heterogeneously hypoechoic lesion in the spleen without any necrotic changes (Figure 2). Three needle passes were performed and three biopsy specimens and 8 cytology slides were made. No adverse events occurred during the one-day hospitalization for the procedure. The patient did not receive prophylactic antibiotics, due to the solid nature of the lesion. Histopathology revealed mostly blood clots and a few inflammatory cells and

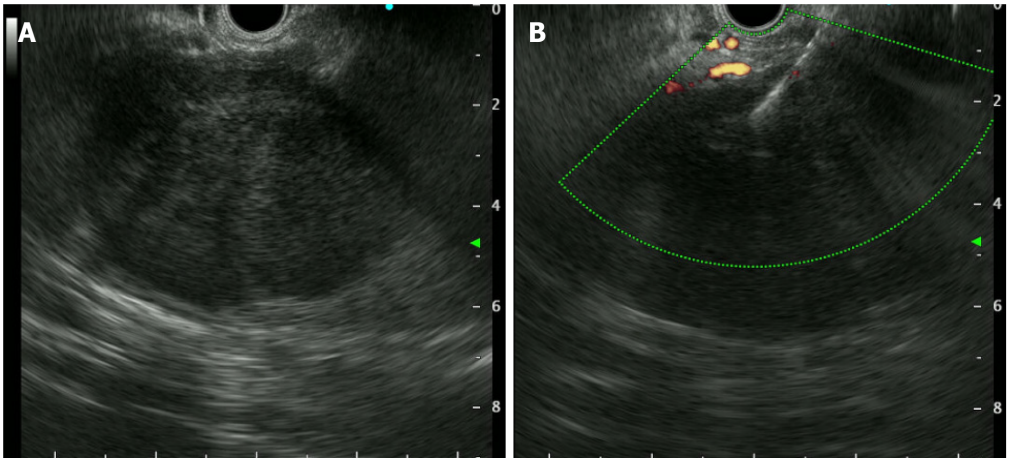


Figure 2 Endoscopic ultrasound finding of the splenic mass. A: Endoscopic ultrasound showed a well-demarcated, heterogeneously hypoechoic mass without evidence of necrosis in the spleen; B: Endoscopic ultrasound-guided fine needle biopsy using a 22G needle was performed.

cytopathology was suspicious for poorly differentiated malignancy. Further laboratory exams were performed and splenectomy was planned. Laboratory findings showed elevated soluble interleukin-2 receptor of 3891 U/mL (normal 158-623 U/mL), decreased complement 3 of 69.1 mg/dL (normal 90-180 mg/dL), but normal immunoglobulin E of 15.6 IU/mL (normal 1.5-158 IU/mL) and complement 4 of 27.5 mg/dL (normal 10-40 mg/dL).

Clinical course

Ten days after the procedure the patient was readmitted due to pain in the left upper quadrant. He complained of nausea, vomiting and fever. He had suffered from chills for three days before readmission. On admission, his blood pressure was 70/40 mmHg, heart rate was 86/min, respiratory rate was 20/min, and body temperature was 38.4 °C. Laboratory findings showed leukocytosis of 19200/μL, hemoglobin 12.0 g/dL, platelet count 34000/μL, AST 102 U/L, ALT 55 U/L, ALP 426 U/L, total bilirubin 14.73 mg/dL, LDH 1300 U/L, and CRP 31.08 mg/dL (normal < 0.3 mg/dL).

Abdominal CT and MRI, compared to previous results, revealed slightly increased splenic lesion. Abdominal CT revealed a 7 cm-sized low-density lesion (Figure 3A), MRI revealed a low signal lesion on T1-weighted image (Figure 3B) compared to initial MRI, much higher signal lesion on T2-weighted image with non-enhancing debris or necrotic portions inside (Figure 3C) and much lower signal with minimal peripheral enhancement showing a capsule development on gadolinium-enhanced T1-weighted image (Figure 3D), suggestive for abscess formation.

The blood culture revealed *G. adiacens* three days after readmission. The blood sample was cultivated in a liquid medium and it was identified by matrix-assisted laser desorption/ionization time-of-flight mass spectrometry.

FINAL DIAGNOSIS

Diagnosis of septic shock due to a splenic abscess caused by *G. adiacens* after EUS-FNB of a splenic tumor was made.

TREATMENT

Intravenous piperacillin/tazobactam was initially started to cover broad-spectrum antimicrobials due to his septic condition. After identifying the pathogen, *G. adiacens*, and piperacillin/tazobactam was changed to ampicillin/sulbactam. Patient's condition, vital signs and laboratory findings improved. Intravenous antibiotics were administered for 12 d and the patient was discharged. After recovery from the infection, he got vaccination to reduce the risk of infections with encapsulated organisms after splenectomy. Splenectomy was performed 4 wk after vaccination, 40 d after the septic shock event.

Pathological finding of the resected splenic mass was consistent with diffuse large

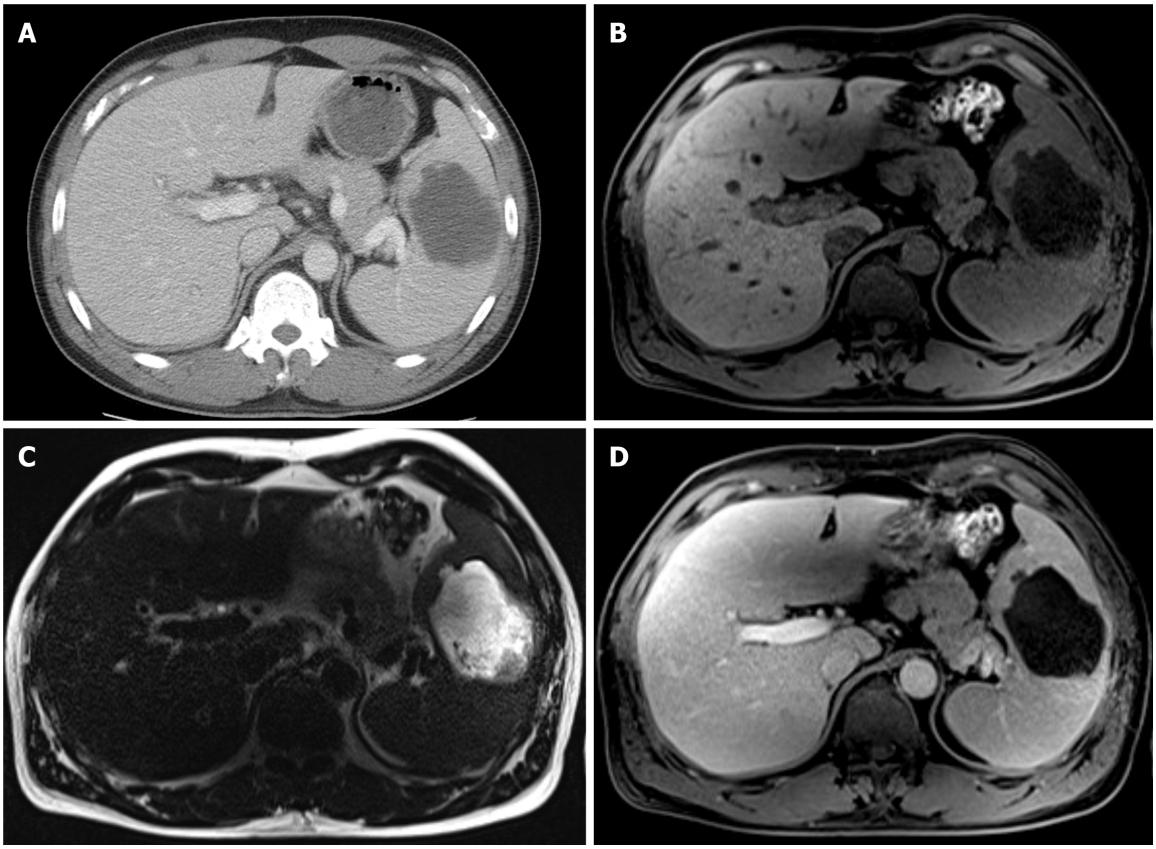


Figure 3 Abdominal computed tomography and magnetic resonance imaging at the readmission. A: Abdominal computed tomography revealed a 7 cm-sized low-density lesion; B: T1-weighted magnetic resonance imaging (MRI) revealed a 7cm-sized hypointense mass with a lower signal compared to the initial MRI; C: T2-weighted MRI revealed much higher signal intensity of this lesion compared to the initial MRI with non-enhancing debris or necrotic portions inside; D: Gadolinium-enhanced T1-weighted image revealed a much lower signal lesion with minimal peripheral enhancement suspecting a capsule development, suggestive for abscess formation.

B-cell lymphoma (DLBCL) (Figure 4). ^{18}F-Fluorodeoxyglucose (FDG)-positron emission tomography (PET) (Figure 5) and bone marrow biopsy were examined for staging, and there was no other organ involvement of lymphoma. Our patient was in Ann Arbor stage I with non-bulky (< 7.5 cm) mass and international prognostic index was 0 (age < 60 years, normal serum LDH, performance status 0, Ann Arbor stage I, and no extranodal disease)[6]. He underwent 4 cycles of chemotherapy with rituximab, cyclophosphamide, doxorubicin, vincristine, and prednisolone (R-CHOP) after splenectomy[6].

OUTCOME AND FOLLOW-UP

He has followed up blood exams and CT every 6 mo and he is in complete remission until now, 20 mo after chemotherapy.

DISCUSSION

Our patient underwent EUS-FNB of a splenic mass and developed septic shock due to a splenic abscess. To the best of our knowledge, this is the first case of septic shock after EUS-FNB of a splenic lymphoma. Also, EUS-related infections caused by *G. adiacens*, rarely causing any disease, have never been reported before.

Conclusive diagnosis of a splenic mass by radiology is difficult because splenic tumors are relatively uncommon and different splenic tumors often share similar radiologic findings[7]. The most common primary malignant tumor of the spleen is lymphoma[8]. More often, lymphomatous involvement of the spleen is secondary and primary splenic lymphoma (PSL), defined as lymphomatous involvement of the spleen without peripheral lymph node involvement, is rare (< 1%)[9]. Imaging findings

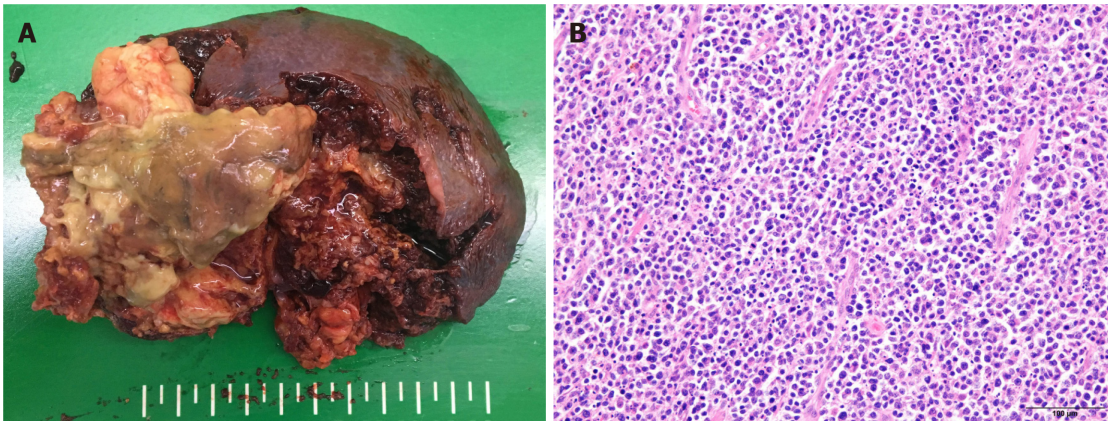


Figure 4 Gross and microscopic findings of the resected splenic mass. A: Laparoscopic splenectomy showed about 6 cm-sized mass with central necrosis and abscess formation; B: Microscopic findings showed diffuse large B-cell lymphoma (hematoxylin-eosin staining, × 200).

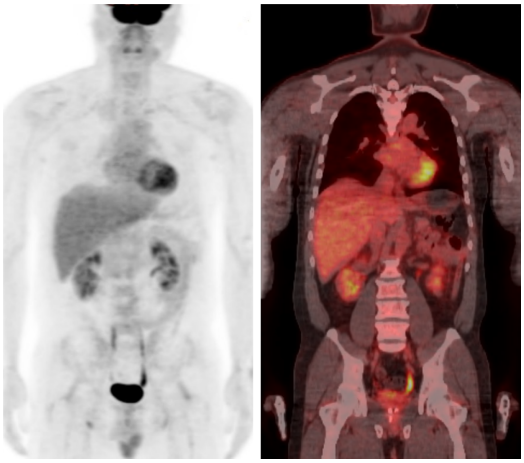


Figure 5 ^{18}F-fluorodeoxyglucose-positron emission tomography after splenectomy showed no other organ involvement of lymphoma.

of splenic lymphomas (in the order of most to least frequent) are homogeneous splenomegaly, diffuse infiltration with miliary lesions, multiple tumoral foci, and a large solitary mass[10]. Splenic lymphomas present with hypodense in plain CT and hypo-enhancement in post-contrast CT[11]. Significant necrosis is observed often, especially in large tumors and large cell lymphomas[12]. In MRI, primary lymphomas show hypointense or nearly isointense on T1-weighted images, hyperintense on T2-weighted images, and mild or absent enhancement on gadolinium enhanced images[9].

SANT of the spleen is a benign vascular lesion consisting of multiple angiomatoid nodules surrounded by a dense fibrous tissue[13]. It commonly presents as a solitary and well-circumscribed splenic mass with smooth borders. SANT rarely cause symptoms and therefore, most SANT lesions are found incidentally[14]. MRI of the SANT shows heterogeneously hypointense on T1 and T2-weighted images and progressive enhancement with peripheral and septal enhancement in "spoke wheel" pattern in gadolinum-enhanced T1-weighted images[13]. We suspected SANT of the spleen in our patient because there was a solitary mass in the spleen without any other organ involvement and the splenic lesion showed peripheral enhancement in contrast enhanced T1 weighted image. Also, the splenic mass was found incidentally after a traffic accident and he had no subjective symptoms such as fever, night sweat, or bodyweight loss, which are known as the B symptoms of lymphoma[11]. However, conclusive diagnosis of the splenic lesion based on the radiologic studies was impossible and pathological confirmation was needed.

EUS-guided splenic biopsy has become popular due to the advantage of providing a clear image of the spleen through the gastric wall and safety and effectiveness for diagnosis of splenic tumors[2]. Until now, there has been no report of serious infection after EUS-FNB of splenic lesion. Therefore, we decided to perform EUS-FNB of the splenic mass in our patient.

The risk of infection associated with EUS-guided sampling of solid organs is low, compared with cystic lesions[3]. In a retrospective analysis of 16 cases of EUS-guided FNA of a focal splenic lesion, no infectious events were found[15]. Recent guidelines do not recommend prophylactic antibiotics for the FNA or FNB of solid masses and lymph nodes[3]. Based on the recommendations, we did not prescribe prophylactic antibiotics at the time of EUS-FNB of the splenic mass; however, our patient developed septic shock due to the splenic abscess 10 days after the procedure.

The risk factors of infection after EUS-guided sampling are cystic lesions regardless of the location, ascites, and pleural fluid around the lesions[16]. CT or MRI findings of the splenic mass in our patient had none of these risk factors. Necrosis is also a well-known risk factor for infection[17]. However, initial EUS of the spleen in our patient showed a solid mass without necrotic changes. Also, he had no other risk factors for infection such as diabetes mellitus. Laboratory findings before EUS-FNB showed no elevation of inflammatory markers. However, septic shock developed and a new splenic abscess was found in MRI obtained at readmission. Therefore, the splenic abscess and sepsis in our patient was likely due to EUS-FNB and his immunocompromised status, later proven as lymphoma.

Patients with hematologic malignancies usually have weak immunity and are vulnerable to bacterial infections, due to immunoglobulin abnormalities and complement system dysfunction[18]. Our patient also had decreased complement 3 level. Patients with advanced hematologic malignancies have high risk of bacteremia and sepsis after the gastrointestinal endoscopy[19]. As our patient was diagnosed with DLBCL, he had the susceptibility for a bacterial infection and sepsis after the EUS-FNB, and, consequently, a splenic abscess and septic shock developed.

Limited data are available regarding the incubation period for infection after EUS-guided sampling due to the rarity of this complication. In a systematic review and meta-analysis, infectious events after EUS-FNA of the pancreatic cystic lesions were reported to be 0.44% (19/5124 patients), and symptoms to suspect infection developed about 2 d to 7 d after EUS-FNA of pancreatic cystic lesions[20-23]. In several case series, mediastinal infection including abscess developed 2 d to 15 d after EUS-FNA of mediastinal masses or lymph nodes[24-27]. Our patient felt chillness 7 d after EUS-FNB and septic shock developed after 10 d of the procedure. Initial evaluation of the splenic lesion including CT, MRI, and EUS showed no abscess formation, but MRI obtained on readmission showed a new abscess in the splenic mass. Therefore, it is likely that the splenic abscess was the infectious complication of EUS-FNB in our patient.

G. adiacens, formerly known as nutritionally variant streptococci (NVS), is present in the normal flora of the oral cavity, gastrointestinal and genitourinary tract and rarely causes any infection. When the infection occurs, it is most commonly presented as endocarditis or bacteremia, although meningitis, osteomyelitis, peritonitis, and infections of foreign bodies such as prosthetic devices have been reported[5]. So far, no case of splenic abscess or bacteremia due to *G. adiacens* after the EUS-FNB has been reported.

G. adiacens is associated with bacteremia in immunocompromised patients, especially, with hematologic malignancies. In a retrospective study that included 13 patients with NVS bacteremia, 77% of the them had hematologic malignancy[28]. Our patient had DLBCL of the spleen, and he might have been contaminated with the *G. adiacens* during the EUS-guided sampling of the splenic mass, leading to the splenic abscess, bacteremia, and septic shock.

The protective effect of prophylactic antibiotics in patients with hematologic malignancy has not been studied. No large scale, prospective studies on the effects of prophylactic antibiotics for the EUS-FNB of splenic tumors have been conducted, and further research is necessary. However, our case showed that prophylactic antibiotic usage might be considered in splenic tumor patients, taking into account lymphoma as the most common primary tumor of the spleen, to avoid severe infection after the EUS-guided sampling. In our patient, there was no other organ involvement of lymphoma and biopsy had to be performed at the spleen. However, because most splenic lymphomas are secondary and PSL is rare, looking for other organ involvement using various imaging studies including CT, FDG-PET and laboratory tests is important before EUS-FNB. If other organ involvement such as peripheral lymph nodes are found, biopsy can be performed at these sites to decrease the risk of infection.

Studies regarding bacteremia and infectious complication following EUS revealed that blood cultures were positive for various pathogens including viridans group streptococci, coagulase negative staphylococcus, and Gram negative bacilli[16,29]. There is no prospective randomized study in which antibiotics should be administered before the EUS-guided sampling. In the studies for antibiotic prophylaxis of EUS-guided sampling of pancreatic cystic lesions, fluoroquinolones or beta-lactams were

used most often, because these antibiotics can cover both gram positive and gram negative organisms[4]. The optimal duration or dosage of antibiotic therapy has not been studied adequately as well. Most studies used prophylactic antibiotics intravenously at first, followed by orally for 3-5 d[4]. Therefore, although the effectiveness of antibiotics differs as local patterns of resistance, obtaining the susceptibility and source of infection, fluoroquinolones or beta-lactam antibiotics as prophylaxis, intravenously at first followed by oral administration could be used before EUS-guided sampling of a splenic mass. Further large scale, prospective studies are needed regarding the antibiotic prophylaxis of EUS-guided sampling.

CONCLUSION

Although EUS-FNB is considered a safe method and the risk of infection in the solid lesions is low, severe infection can occur after EUS-FNB of a splenic lymphoma. Therefore, prophylactic antibiotics for EUS-guided sampling of splenic tumors should be considered.

REFERENCES

1 **Civardi G**, Vallisa D, Bertè R, Giorgio A, Filice C, Caremani M, Caturelli E, Pompili M, De Sio I, Buscarini E, Cavanna L. Ultrasound-guided fine needle biopsy of the spleen: high clinical efficacy and low risk in a multicenter Italian study. *Am J Hematol* 2001; **67**: 93-99 [PMID: 11343380 DOI: 10.1002/ajh.1085]

2 **Iwashita T**, Yasuda I, Tsurumi H, Goto N, Nakashima M, Doi S, Hirose Y, Takami T, Moriwaki H. Endoscopic ultrasound-guided fine needle aspiration biopsy for splenic tumor: a case series. *Endoscopy* 2009; **41**: 179-182 [PMID: 19214901 DOI: 10.1055/s-0028-1119474]

3 **ASGE Standards of Practice Committee**, Early DS, Acosta RD, Chandrasekhara V, Chathadi KV, Decker GA, Evans JA, Fanelli RD, Fisher DA, Fonkalsrud L, Hwang JH, Jue TL, Khashab MA, Lightdale JR, Muthusamy VR, Pasha SF, Saltzman JR, Sharaf RN, Shergill AK, Cash BD. Adverse events associated with EUS and EUS with FNA. *Gastrointest Endosc* 2013; **77**: 839-843 [PMID: 23684089 DOI: 10.1016/j.gie.2013.02.018]

4 **Polkowski M**, Jenssen C, Kaye P, Carrara S, Deprez P, Gines A, Fernández-Esparrach G, Eisendrath P, Aithal GP, Arcidiacono P, Barthet M, Bastos P, Fornelli A, Napoleon B, Iglesias-Garcia J, Seicean A, Larghi A, Hassan C, van Hooft JE, Dumonceau JM. Technical aspects of endoscopic ultrasound (EUS)-guided sampling in gastroenterology: European Society of Gastrointestinal Endoscopy (ESGE) Technical Guideline - March 2017. *Endoscopy* 2017; **49**: 989-1006 [PMID: 28898917 DOI: 10.1055/s-0043-119219]

5 **Gardenier JC**, Hranjec T, Sawyer RG, Bonatti H. Granulicatella adiacens bacteremia in an elderly trauma patient. *Surg Infect (Larchmt)* 2011; **12**: 251-253 [PMID: 21524203 DOI: 10.1089/sur.2010.059]

6 **Zelenetz AD**, Gordon LI, Abramson JS, Advani RH, Bartlett NL, Caimi PF, Chang JE, Chavez JC, Christian B, Fayad LE, Glenn MJ, Habermann TM, Lee Harris N, Hernandez-Ilizaliturri F, Kaminski MS, Kelsey CR, Khan N, Krivacic S, LaCasce AS, Mehta A, Nademanee A, Rabinovitch R, Reddy N, Reid E, Roberts KB, Smith SD, Snyder ED, Swinnen LJ, Vose JM, Dwyer MA, Sundar H. NCCN Guidelines Insights: B-Cell Lymphomas, Version 3.2019. *J Natl Compr Canc Netw* 2019; **17**: 650-661 [PMID: 31200358 DOI: 10.6004/jnccn.2019.0029]

7 **Lee HJ**, Kim JW, Hong JH, Kim GS, Shin SS, Heo SH, Lim HS, Hur YH, Seon HJ, Jeong YY. Cross-sectional Imaging of Splenic Lesions: RadioGraphics Fundamentals | Online Presentation. *Radiographics* 2018; **38**: 435-436 [PMID: 29528823 DOI: 10.1148/rg.2018170119]

8 **Siewert B**, Millo NZ, Sahi K, Sheiman RG, Brook OR, Sun MRM, Kane RA. The Incidental Splenic Mass at CT: Does It Need Further Work-up? *Radiology* 2018; **287**: 156-166 [PMID: 29369753 DOI: 10.1148/radiol.2017170293]

9 **Giovagnoni A**, Giorgi C, Goteri G. Tumours of the spleen. *Cancer Imaging* 2005; **5**: 73-77 [PMID: 16154823 DOI: 10.1102/1470-7330.2005.0002]

10 **Saboo SS**, Krajewski KM, O'Regan KN, Giardino A, Brown JR, Ramaiya N, Jagannathan JP. Spleen in haematological malignancies: spectrum of imaging findings. *Br J Radiol* 2012; **85**: 81-92 [PMID: 22096219 DOI: 10.1259/bjr/31542964]

11 **Li M**, Zhang L, Wu N, Huang W, Lv N. Imaging findings of primary splenic lymphoma: a review of 17 cases in which diagnosis was made at splenectomy. *PLoS One* 2013; **8**: e80264 [PMID: 24278265 DOI: 10.1371/journal.pone.0080264]

12 **Nakashima A**, Nakashima K, Seto H, Kamei T, Kakishita M, Kitagawa M. Primary splenic lymphoma presenting as a large cyst. *Radiat Med* 1994; **12**: 42-45 [PMID: 8016404]

13 **Lewis RB**, Lattin GE Jr, Nandedkar M, Aguilera NS. Sclerosing angiomatoid nodular transformation of the spleen: CT and MRI features with pathologic correlation. *AJR Am J Roentgenol* 2013; **200**: W353-W360 [PMID: 23521478 DOI: 10.2214/AJR.12.9522]

14 **Martel M**, Cheuk W, Lombardi L, Lifschitz-Mercer B, Chan JK, Rosai J. Sclerosing angiomatoid nodular transformation (SANT): report of 25 cases of a distinctive benign splenic lesion. *Am J Surg Pathol* 2004; **28**: 1268-1279 [PMID: 15371942 DOI: 10.1097/01.pas.0000138004.54274.d3]

15 **Rana SS**, Sharma V, Sharma R, Srinivasan R, Gupta R. Safety and utility of endoscopic ultrasound-guided fine-needle aspiration of focal splenic lesions: a retrospective analysis. *Ann Gastroenterol* 2017; **30**: 559-563 [PMID: 28845112]

16 **Jenssen C**, Alvarez-Sánchez MV, Napoléon B, Faiss S. Diagnostic endoscopic ultrasonography: assessment of safety and prevention of complications. *World J Gastroenterol* 2012; **18**: 4659-4676 [PMID: 23002335 DOI: 10.3748/wjg.v18.i34.4659]

17 **Beger HG**, Bittner R, Block S, Büchler M. Bacterial contamination of pancreatic necrosis. A prospective clinical study. *Gastroenterology* 1986; **91**: 433-438 [PMID: 3522342 DOI: 10.1016/0016-5085(86)90579-2]

18 **Safdar A**, Armstrong D. Infections in patients with hematologic neoplasms and hematopoietic stem cell transplantation: neutropenia, humoral, and splenic defects. *Clin Infect Dis* 2011; **53**: 798-806 [PMID: 21890754 DOI: 10.1093/cid/cir492]

19 **ASGE Standards of Practice Committee**. , Khashab MA, Chithadi KV, Acosta RD, Bruining DH, Chandrasekhara V, Eloubeidi MA, Fanelli RD, Faulx AL, Fonkalsrud L, Lightdale JR, Muthusamy VR, Pasha SF, Saltzman JR, Shaukat A, Wang A, Cash BD. Antibiotic prophylaxis for GI endoscopy. *Gastrointest Endosc* 2015; **81**: 81-89 [PMID: 25442089 DOI: 10.1016/j.gie.2014.08.008]

20 **de Jong K**, Poley JW, van Hooft JE, Visser M, Bruno MJ, Fockens P. Endoscopic ultrasound-guided fine-needle aspiration of pancreatic cystic lesions provides inadequate material for cytology and laboratory analysis: initial results from a prospective study. *Endoscopy* 2011; **43**: 585-590 [PMID: 21611945 DOI: 10.1055/s-0030-1256440]

21 **Guarner-Argente C**, Shah P, Buchner A, Ahmad NA, Kochman ML, Ginsberg GG. Use of antimicrobials for EUS-guided FNA of pancreatic cysts: a retrospective, comparative analysis. *Gastrointest Endosc* 2011; **74**: 81-86 [PMID: 21704808 DOI: 10.1016/j.gie.2011.03.1244]

22 **Williams DB**, Sahai AV, Aabakken L, Penman ID, van Velse A, Webb J, Wilson M, Hoffman BJ, Hawes RH. Endoscopic ultrasound guided fine needle aspiration biopsy: a large single centre experience. *Gut* 1999; **44**: 720-726 [PMID: 10205212 DOI: 10.1136/gut.44.5.720]

23 **Zhu H**, Jiang F, Zhu J, Du Y, Jin Z, Li Z. Assessment of morbidity and mortality associated with endoscopic ultrasound-guided fine-needle aspiration for pancreatic cystic lesions: A systematic review and meta-analysis. *Dig Endosc* 2017; **29**: 667-675 [PMID: 28218999 DOI: 10.1111/den.12851]

24 **Valli PV**, Gubler C, Bauerfeind P. Severe Infectious Complications after Endoscopic Ultrasound-Guided Fine Needle Aspiration of Suspected Mediastinal Duplication Cysts: A Case Series. *Inflamm Intest Dis* 2017; **1**: 165-171 [PMID: 29922673 DOI: 10.1159/000464327]

25 **von Bartheld M**, van der Heijden E, Annema J. Mediastinal abscess formation after EUS-guided FNA: are patients with sarcoidosis at increased risk? *Gastrointest Endosc* 2012; **75**: 1104-1107 [PMID: 22365439 DOI: 10.1016/j.gie.2012.01.002]

26 **Aerts JG**, Kloover J, Los J, van der Heijden O, Janssens A, Tournoy KG. EUS-FNA of enlarged necrotic lymph nodes may cause infectious mediastinitis. *J Thorac Oncol* 2008; **3**: 1191-1193 [PMID: 18827619 DOI: 10.1097/JTO.0b013e3181872752]

27 **Savides TJ**, Margolis D, Richman KM, Singh V. Gemella morbillorum mediastinitis and osteomyelitis following transesophageal endoscopic ultrasound-guided fine-needle aspiration of a posterior mediastinal lymph node. *Endoscopy* 2007; **39** Suppl 1: E123-E124 [PMID: 17440855 DOI: 10.1055/s-2007-966157]

28 **Yacoub AT**, Krishnan J, Acevedo IM, Halliday J, Greene JN. Nutritionally variant streptococci bacteremia in cancer patients: a retrospective study, 1999-2014. *Mediterr J Hematol Infect Dis* 2015; **7**: e2015030 [PMID: 25960858 DOI: 10.4084/MJHID.2015.030]

29 **Janssen J**, König K, Knop-Hammad V, Johanns W, Greiner L. Frequency of bacteremia after linear EUS of the upper GI tract with and without FNA. *Gastrointest Endosc* 2004; **59**: 339-344 [PMID: 14997128 DOI: 10.1016/s0016-5107(03)02707-x]

Published by **Baishideng Publishing Group Inc**
7041 Koll Center Parkway, Suite 160, Pleasanton, CA 94566, USA
Telephone: +1-925-3991568
E-mail: bpgoffice@wjgnet.com
Help Desk: https://www.f6publishing.com/helpdesk
https://www.wjgnet.com

© 2021 Baishideng Publishing Group Inc. All rights reserved.